CUMULATIVE INDEX

Volumes 16–20

NUCLEAR SCIENCE ABSTRACTS

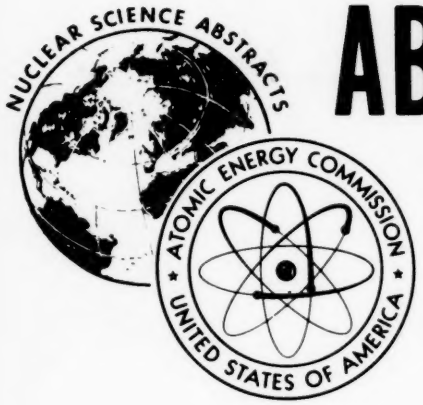

Volumes 16 through 20

1962 – 1966

SUBJECTS (S)

UNITED STATES ATOMIC ENERGY COMMISSION
Division of Technical Information

USAEC DEPOSITORY LIBRARIES

Collections of USAEC reports are maintained in the libraries of the organizations listed below for reference use by the general public. Facilities for making photocopies are available. The USAEC also makes available through these libraries atomic energy reports of countries other than the U. S. that are abstracted in *Nuclear Science Abstracts*.

ALABAMA
Auburn, Auburn University
ALASKA
College, University of Alaska
ARIZONA
Tucson, University of Arizona
ARKANSAS
Fayetteville, University of Arkansas
CALIFORNIA
Berkeley, University of California
Davis, University of California
Los Angeles, University of California
San Diego, Public Library
Stanford, Stanford University
COLORADO
Boulder, University of Colorado
Denver, Public Library
CONNECTICUT
New Haven, Yale University
DELAWARE
Newark, University of Delaware
DISTRICT OF COLUMBIA
Washington, Library of Congress
FLORIDA
Coral Gables, University of Miami
Gainesville, University of Florida
Tallahassee, The Florida State University
GEORGIA
Atlanta, Georgia Institute of Technology
HAWAII
Honolulu, University of Hawaii
IDAHO
Pocatello, Idaho State University
ILLINOIS
Chicago, John Crerar Library
Chicago, University of Chicago
Evanston, Northwestern University
Urbana, University of Illinois
INDIANA
Bloomington, Indiana University
Lafayette, Purdue University
IOWA
Ames, Iowa State University
KANSAS
Manhattan, Kansas State University
KENTUCKY
Lexington, University of Kentucky
Louisville, University of Louisville
LOUISIANA
Baton Rouge, Louisiana State University
New Orleans, Tulane University
MARYLAND
Baltimore, Johns Hopkins University
College Park, University of Maryland
MASSACHUSETTS
Cambridge, Harvard University
Cambridge, Massachusetts Institute of Technology
MICHIGAN
Ann Arbor, University of Michigan
Detroit, Public Library
East Lansing, Michigan State University
MINNESOTA
Minneapolis, University of Minnesota
MISSISSIPPI
State College, Mississippi State University
MISSOURI
Kansas City, Linda Hall Library
Rolla, University of Missouri School of Mines and Metallurgy
St. Louis, Washington University
MONTANA
Bozeman, Montana State College
NEVADA
Las Vegas, Nevada Southern University
Reno, University of Nevada
NEW JERSEY
Princeton, Princeton University
Teaneck, Fairleigh Dickinson University
NEW MEXICO
Albuquerque, University of New Mexico
NEW YORK
Albany, The University of the State of New York
Buffalo, State University of New York at Buffalo
Ithaca, Cornell University
New York, Atomic Industrial Forum, Inc.
New York, Columbia University
New York, New York University
Rochester, University of Rochester
Schenectady, Union College
Syracuse, Syracuse University
Troy, Rensselaer Polytechnic Institute
NORTH CAROLINA
Charlotte, Public Library of Charlotte and Mecklenburg County
Durham, Duke University
Raleigh, North Carolina State College
NORTH DAKOTA
Grand Forks, University of North Dakota
OHIO
Cincinnati, University of Cincinnati
Cleveland, Public Library
Columbus, Ohio State University
Toledo, University of Toledo
Youngstown, Youngstown University
OKLAHOMA
Norman, University of Oklahoma
Stillwater, Oklahoma State University
OREGON
Corvallis, Oregon State University
Portland, Reed College
PENNSYLVANIA
Philadelphia, University of Pennsylvania
Pittsburgh, Carnegie Library
University Park, Pennsylvania State University
PUERTO RICO
Rio Piedras, University of Puerto Rico
RHODE ISLAND
Providence, Brown University
SOUTH CAROLINA
Columbia, University of South Carolina
TENNESSEE
Knoxville, University of Tennessee
Memphis, Public Library
Nashville, Joint University Libraries
Oak Ridge, Oak Ridge Associated Universities
TEXAS
Austin, University of Texas
College Station, Texas A & M University
Dallas, Southern Methodist University
Houston, Rice University
Lubbock, Texas Technological College
San Antonio, Public Library
UTAH
Salt Lake City, University of Utah
VIRGINIA
Blacksburg, Virginia Polytechnic Institute
Charlottesville, University of Virginia
Norfolk, Old Dominion College
WASHINGTON
Pullman, Washington State University
Seattle, University of Washington
WEST VIRGINIA
Morgantown, West Virginia University
WISCONSIN
Madison, University of Wisconsin
Milwaukee, Public Library
WYOMING
Laramie, University of Wyoming

UNITED STATES ATOMIC ENERGY COMMISSION

NUCLEAR SCIENCE ABSTRACTS

Cumulative Index

Volumes 16 through 20
1962 - 1966

SUBJECTS (S)

Division of Technical Information

This eleven-volume set is for sale by the
Superintendent of Documents, U. S. Government Printing Office
Washington, D. C. 20402 Price $36.00

STAFF OF NUCLEAR SCIENCE ABSTRACTS

John W. Norris
Managing Editor

Donald D. Davis
Assistant Managing Editor

David E. Bost
Production Manager

Robert E. Upchurch
Subject Heading Specialist

J. Paul Meredith
Descriptive Cataloging Specialist

Clara L. Fox
Corporate Author Specialist

Mary H. Newman
Reports Evaluator

Brainard L. Patton
Scheduling and Publishing Coordinator

Section Editors

Everett J. Hoffman
Chemistry

Robert C. Kelly
Engineering; Earth Sciences

Lee M. Thompson
General Physics

Charles E. Stuber
High Energy Physics

Hugh E. Voress
Life Sciences

Lawrence T. Whitehead
Nuclear Data

James M. Jacobs
Reactor Technology; Metals and Ceramics

Abstractors

F. S. Armstrong*
Mary M. Brown
Jane G. Buchanan
D. Lamar Cason
Bennie G. Di Bona
Helen G. Donald
James R. Dulaney
Wells L. Green
Bernard O. Griggs
Harry G. Grisham
Mary C. Grissom
Miriam P. Guthrie
Fernando Hamilton
Phyllis C. Hansen
Thomas F. Heagerty
Carolyn D. Houston
Rose V. Jermain
Sidney F. Lanier
Betty L. McDowell
William D. Matheny
John H. Mitchell
Dora H. Moneyhun
Luther Norene
Carol Oen
Jean F. Peckham
Henry D. Raleigh
Mona H. Raridon
Julia S. Redford
Ned W. Rizzardi
Francis L. Sachs
Lila B. Smith
Polly C. Summers
Anne G. Ward
Helen L. Ward
David C. West
Milton O. Whitson
Juanita Wilson

*Atomic Energy of Canada, Ltd.

Acknowledgments

Agreements between the United States Atomic Energy Commission and the following organizations with regard to providing continuing services and specific literature coverage for *Nuclear Science Abstracts* are gratefully acknowledged:

American Institute of Physics; Atomic Energy of Canada Limited; Atomic Energy Research Establishment, United Kingdom; Aktiebolaget Atomenergi, Sweden; European Atomic Energy Community (EURATOM); Gmelin Institute, International Atomic Energy Agency; Japan Atomic Energy Bureau—Japan Atomic Energy Research Institute; Netherlands Patent Office; Reactor Centrum Nederland.

Communication concerning the editorial policy and content of *NSA* should be addressed to the Managing Editor, *Nuclear Science Abstracts*, AEC Division of Technical Information Extension, P. O. Box 62, Oak Ridge, Tennessee 37830.

Use of funds for printing this publication approved by the Director of the Bureau of the Budget, June 28, 1966.

Cumulative Index
Volumes 16-20, Subjects, 1962-1966

NUCLEAR SCIENCE ABSTRACTS

A semimonthly publication of the USAEC Division of Technical Information, Edward J. Brunenkant, Director. Published by the USAEC Division of Technical Information Extension, Robert L. Shannon, Extension Manager.

Nuclear Science Abstracts provides the only comprehensive abstracting and indexing coverage of the international literature on nuclear science and technology. *NSA* covers scientific and technical reports of the U. S. Atomic Energy Commission and its contractors, those of other U. S. Government agencies, and those of other governments, universities, industrial, and research organizations. It also covers patents, books, and journal literature on a worldwide basis. A list of the journals scanned appears in Issues 1 and 13 of each volume. Nearly 400,000 abstracts have appeared in *NSA* through Volume 20. The subject matter covered in *NSA* is described in Issue 1 of each volume and in TID-4552, *Subject Scope of Nuclear Science Abstracts*. The latter is available free from the U. S. Atomic Energy Commission, Division of Technical Information Extension, P. O. Box 62, Oak Ridge, Tennessee 37830.

Abstracts are arranged according to subject categories which are defined in Issue 1 of each volume. If the language of the original item is not English, the language is indicated. Translations are not abstracted if an abstract of the original item has appeared in *NSA*.

AVAILABILITY OF PUBLICATIONS ABSTRACTED

The public availability of all U. S. Atomic Energy Commission reports is indicated in the report number indexes. The availability of other reports, when known, is also indicated. The availability of some unnumbered reports is given in the abstract.

Dissertations abstracted in *Dissertation Abstracts* and included in *NSA* are available from University Microfilms, Inc., 315 N. First Street, Ann Arbor, Michigan 48103.

Information on the availability of the published literature and unpublished conference papers abstracted in *NSA* may be obtained from the Division of Technical Information Extension, P. O. Box 62, Oak Ridge, Tennessee 37830.

HOW TO OBTAIN NUCLEAR SCIENCE ABSTRACTS

NSA is available to the general public on a subscription basis from the Superintendent of Documents, U. S. Government Printing Office, Washington, D. C. 20402, as follows:

For the 24 regular issues, $30.00 domestic, $37.00 foreign. A single issue costs $1.75, plus 25 percent for foreign mailing. Domestic rates apply to the United States, Canada, Mexico, and Central and South American countries except Argentina, Brazil, Guyana, French Guiana, Surinam, and British Honduras. Foreign rates apply to the countries excepted above and to all other countries throughout the world.

For the quarterly, semiannual, and annual indexes, $22.00 domestic, $25.00 foreign.

Multivolume subject and author indexes are available as follows:

Vols. 1-4 (1948-1950). Johnson Reprint Corporation, 111 Fifth Avenue, New York, N. Y. 10003, $30.00.

Vols. 5-10 (1951-1956). Superintendent of Documents, U. S. Government Printing Office, Washington, D. C. 20402, $5.25.

Vols. 11-15, Subjects. Superintendent of Documents, U. S. Government Printing Office, Washington, D. C. 20402, $19.00.

Vols. 11-15, Personal Authors. Superintendent of Documents, U. S. Government Printing Office, Washington, D. C. 20402, $14.25.

Vols. 11-15, Corporate Authors. Superintendent of Documents, U. S. Government Printing Office, Washington, D. C. 20402, $2.50.

Vols. 16-20. (To be issued in 1967.)

Cumulative Report Number Index, Vols. 1—15 Revised, is available from the Superintendent of Documents, U. S. Government Printing Office, Washington, D. C. 20402, $4.00.

Cumulative Report Number Index, Vols. 16—20, is available from the Superintendent of Documents, U. S. Government Printing Office, Washington, D. C. 20402, $4.25.

Annual indexes are available separately from the Superintendent of Documents, U. S. Government Printing Office, Washington, D. C. 20402, as follows:

Vol. 16, Subjects and Authors, $9.75.
Vol. 17, Subjects and Authors, $12.25.
Vol. 18, Subjects and Authors, $12.50.
Vol. 19, Subjects and Authors, $12.50.

Annual indexes for Vol. 20 were not issued since they are a part of the cumulation for Vols. 16–20.

NSA is available on an exchange basis to universities, research institutions, industrial firms, and publishers of scientific information. Inquiries should be directed to the U. S. Atomic Energy Commission, Division of Technical Information Extension, P. O. Box 62, Oak Ridge, Tennessee 37830.

Government agencies may obtain *NSA* free of charge.

INTRODUCTION

Subject entries in this index are generally specific materials, things, and processes. These are followed by modifiers that describe the properties of, and processes applied to, the entries.

The number preceding the colon is the *NSA* volume number, and the number following is the abstract number. The designation (R) following the abstract number indicates that the abstract is of a progress report; (P) indicates a patent; and (T) indicates a translation. Abstracts for reports other than progress reports carry no letter designation. References to report numbers, where appropriate, are included after the abstract number of the citation. Published literature (journal article or book) is identifiable by the absence of a report number.

Special characters are added to modifiers in the field of physics; if the modifier does not establish the experimental or theoretical character of a reference, a symbol (E), (T), or (E/T) is placed immediately after the modifying phrase and before the journal reference number. The value of this identification has been established by the American Institute of Physics.

The user should bear in mind that the ideas presented in the original literature, rather than key words, have been indexed. The indexers have tried to select what seemed the most probable and logical place to look for typical information. Since it is not possible to anticipate where a user would look for information, numerous cross references are included.

Experience in using an index of this type will be the best guide in obtaining the desired information, and a consideration of synonymous or closely related terms as well as recent developments in scientific terminology will prove valuable.

Information must be so indexed as to be of the greatest use to the greatest number of users. This requires that a topic be indexed to headings that most specifically describe it and not ordinarily to the headings that describe its ultimate use, nor to the general class headings that include the specific headings. For example, information on the treatment of thyroid disease with I-131 would be indexed under Thyroid Gland and under Iodine Isotopes I-131, but not necessarily under Radiotherapy. A study of the effects of x radiation on hair would be indexed under both X Radiation and Hair.

The broad, general class headings are used only for general information or for comprehensive reports or articles.

Subject Heading Styles

Generally, the direct form of subject entry is used rather than inverted headings, e.g., Amino Acids rather than Acids, Amino; Helium Isotopes He-4 rather than Helium — isotopes He-4 or Helium — He-4 isotopes. Note, however, that in some cases parenthetic modifying terms or inverted headings of the form Neutrons, Fast are used in preference to a direct entry that would result in the scattering of information. Organic compounds are usually entered in the index in the inverted form so that substituted compounds can be listed near the parent compound; e.g., Benzene, Bromo- rather than Bromobenzene. Subject headings were chosen from TID-5001(5th Rev.) "Subject Headings used by the USAEC Division of Technical Information."

Alphabetization

Subject headings are alphabetized word-by-word. A parenthetic qualifier following a subject heading is disregarded in alphabetizing unless there are two or more headings identical except for the parenthetic qualifier, in which case the qualifier determines the order. Headings involving Greek letters are arranged as if the names of the letters were spelled out.

Examples:

M-Capture
  see Electron Capture
Magnesium
Magnesium Alloys
Manganese Fluorides
Manganese(II) Fluorides
Mesons
Mesons (π)
Mesons (ρ)
3-Pentanol, 2,4-Dimethyl-
2-Pentanol, 2-Methyl-
2-Pentanol, 4-Methyl-

Nomenclature of Inorganic Compounds

Inorganic compounds are indexed in the direct form, listing cations in the order of increasing valence in the case of polycationic salts of varying valence and in alphabetic order for polycationic salts in which all cations have the same valence; e.g., Sodium Aluminum Silicates and Potassium Sodium Sulfates.

Multicomponent Alloys and Other Systems

Multicomponent alloys, except well-known trade names, are indexed under a heading in the form "element alloy" for each element in the alloy. The modifier begins with element symbols for each component arranged alphabetically as if the English name for the element were spelled out.

Example: Copper–Gold Alloy is indexed
  Copper Alloys
    Cu–Au ...
  Gold Alloys
    Cu–Au ...

Well-known alloys such as Zircaloy-2 are indexed directly to the trade name; cross references referring from each component of the alloy to the entry for the trade name are included.

Multicomponent systems of nonmetallic elements are indexed in a manner similar to alloys except the main heading used contains the word "Systems" in place of "Alloys."

Example: Silicon–Tungsten Systems are indexed
Silicon Systems
Si–W...
Tungsten Systems
Si–W...

Multicompound systems and mixtures of compounds are indexed under the main heading for each component compound; the modifiers begin with an alphabetical listing of compound formulas.

Example: Lead Titanate–Lead Zirconate is indexed
Lead Titanates
$PbTiO_3$–$PbZrO_3$...
Lead Zirconates
$PbTiO_3$–$PbZrO_3$...

A mixed system of compounds and elements is indexed using a combined form of the above conventions, e.g., a dispersion of copper and alumina would be indexed

Aluminum Oxides
Al_2O_3–Cu...
Copper Systems
Al_2O_3–Cu...

Physical States and Configurations of Materials

Specification of the physical state, if other than normal, or geometric configuration of the material is included in the modifying phrase, i.e., liquid metals would be indexed to the metal with "liquid" in the modifier, and carbon crucibles would be indexed to Carbon with "crucibles" appropriately placed in the modifier and also to Crucibles if appropriate.

Modifying Phrases

The modifiers appearing under a subject heading are written specifically to describe the relation of the item being indexed to that heading. Effort is exerted to begin the modifier with the word judged to be of greatest use to the greatest number of users: this, however, does not obviate the need to consider all modifiers under the main heading(s) of interest.

Modifiers are usually intended to form a meaningful phrase when combined with the main heading. Some are intended to be read following the main heading, e.g., the entry Hydrogen—sorption by charcoal is read "hydrogen sorption by charcoal"; however, as a result of placing the important word first, many modifiers must be arranged for smooth reading, e.g., Formaldehyde—yields in radiolysis of ethyl ether, effects of deuterium on is read "effects of deuterium on formaldehyde yields in radiolysis of ethyl ether" and Uranium—crystal structure of, effect of cooling rate on allotropic transformations in is read "effect of cooling rate on allotropic transformations in crystal structure of uranium." Prepositions are sometimes omitted if no ambiguity results.

SUBJECTS (S)

S

S1C
see *Submarine Reactors (S1C)*
S3G
see *Submarine Advanced Reactor*
S4G
see *Submarine Advanced Reactor*
S5G
see *Submarine Reactors (S5G)*
S3W
see *Submarine Fleet Reactor*
S4W
see *Submarine Fleet Reactor*
S PARTICLES
see also Mesons
see also V Particles
decay, use in analysis of lepton electromagnetic properties, 16: 29707
production and properties, having hypercharge = ±1, 17: 19044 (TID-16612)
role in meson (K) decay, 18: 22756
S-Process
see *Dual-Temperature Process*
SABUGALITES
crystal properties, 16: 25638
SACCHARIC ACID
complexes with rare earths, preparation of, 20: 33216
complexes with thorium, preparation and structure of, 19: 401
reactions with dysprosium, 20: 43140
uses in determination of ytterbium, 20: 14490
SACCHARIN
radiation effects on rat response to, x, 18: 19667
radiation effects on conditioned aversion to, in rats, 19: 17598
radiation effects on rat aversion to, humoral factor in, 20: 5303 (USNRDL-TR-925)
radioinduced avoidance of, in rats, effects of postirradiation fluids on x, 18: 23290
radioinduced avoidance in rats of, x, 18: 29311
Saccharose
see *Sucrose*
SACLAY PROTON SYNCHROTRON
beam control for Saturn, design and performance of system for, 20: 44048
beam injection in, high-brilliance ion source for, 19: 47172
bus bar design, auxiliary, 16: 9489
description and operations of, review, 18: 10704
design of, and radiation control at, 16: 29875 (CEA-1500)
electronic complex for, description of fast transistorized, 18: 24266
injector for, description of increased-energy, 18: 32307 (CEA-R-2425)
neutron energies and fluxes near, fast, 17: 42009 (CEA-2303)
performance for production of 1-Bev/c meson (K^+) beams, (E), 19: 10017 (NP-14472)
radiation dosimetry of, methods for, 20: 29845 (CONF-651109, pp 117-42)
SACLAY REACTORS
design of OSIRIS, 20: 18181
design of Osiris, for testing reactor structural materials, 19: 27824
design of RAPSODIE, 16: 26569
environs monitoring, 1961 and 1962, 18: 20209 (CEA-2397)
fuel element testing, design of alpha-beta-gamma laboratory for, 18: 1310
prompt-neutron decay in ALECTO, statistical study of, 19: 3508 (CEA-R-2454)
reactivity of RUBEOLE and ULYSSES, source excitation measurement of, 19: 3772 (CEA-R-2377)
use in CEA research program, 18: 15618
SACLAY REACTORS (AQUILON)
criticality studies with enriched fuels in (E/T), 19: 3511 (CEA-R-2477)
description and summary of experimental work, 18: 6532
fuel composition changes in lattices of same geometry in, 18: 6533
fuel element fabrication for substitution experiments in, 18: 8782(T) (EURAEC-891)
fuel element testing in, 18: 15606(R) (EURAEC-889)
fuel elements in, testing uranium carbide, (E), 19: 17254 (CEA-R-2615)
kinetics of Aquilon-II, 18: 38297 (A/CONF.28/P/76)
kinetics studies in, 19: 35378(R) (EANDC(E)-57(U))
neutron diffusion in, measurement of radial, 20: 24788 (CEA-R-2889)
neutron flux measurements in, macroscopic and microscopic flux interaction in, 17: 42227
neutron leakage due to moderator poisoning in, measurement for uranium oxide cluster and gas tube lattices, 18: 6533
neutron multiplication factors, 16: 15772 (CEA-2077)
neutron spectra in lattices of, (E/T), 20: 3582 (CEA-R-2482)
operation, 1964, 19: 17255(R) (EURAEC-1199(Suppl.))
properties of uranium oxide clusters in tubes of gas in, measurements of, 18: 6533
SACLAY REACTORS (EL-2)
design and performance of, 16: 26626
design and performance, 18: 4863
development and uses of, 18: 38572 (A/CONF.28/P/33)
fuel element design and performance, review, 16: 16669
fuel element processing for, headend process for, 18: 39370 (NP-10416)
fuel element rupture detection in, 17: 9869
fuel element rupture in, detection system for, 20: 10288 (CEA-R-2784)
fuel elements for, 18: 15496(T) (AEC-tr-6329)
neutron flux distributions in, 17: 10158
operation experience, 20: 18181
radiation heating of materials in, (E), 19: 26628 (CEA-R-2581)
release of radioactive gaseous effluents, methods for control of, 18: 41701
SACLAY REACTORS (EL-3)
auxiliaries, design of cryogenic device for production of cold neutron beam, 16: 26193 (CEA-2012)
charging and discharging of, design, maintenance, and operation of cask for, 16: 31279(T) (AEC-tr-5304)
core of, study of snowflake version of, 18: 11480 (CEA-2344)
design and operation, 18: 15613
design and performance of, 16: 26626
design and research program using, 20: 18181
development and uses of, 18: 38572 (A/CONF.28/P/33)
experimental facilities for cold-neutron-scattering studies, 16: 18449
fission products ionization losses to water vapor in, conversion to electric energy, 18: 18630
fuel element burn-up, 16: 19928
fuel element design and development, 17: 41364(T,R) (EURAEC-562)
fuel element development for, 17: 41365(T,R) (EURAEC-645)
fuel element development and testing, 18: 10456(T,R) (EURAEC-733)
fuel element development and testing, 18: 32064(T,R) (EURAEC-1064)
fuel element processing for, headend process for, 18: 39370 (NP-10416)
fuel element radiological inspection after irradiation, 18: 15619
fuel element testing in, 18: 15606(R) (EURAEC-889)
fuel element testing in, 19: 13874(R) (EURAEC-1179)
fuel element testing for, 19: 17255(R) (EURAEC-1199(Suppl.))
fuel element welding, electron beam equipment and techniques for, 16: 19271
fuel element welding, 18: 32114(T) (AI-Trans-48)
fuel elements for, 18: 15496(T) (AEC-tr-6329)
fuel elements for, analysis by Armor process, 18: 11413(T,R) (EURAEC-815)
fuel-element testing in, 18: 14387(T,R) (EURAEC-860)
in-pile loop in, for irradiation of fuel samples, 18: 4871
neutron distributions in biological exposure chamber of, 17: 34283
neutron flux distributions in, 17: 10158
neutron flux measurements in, cold, 16: 32380
operation and experimental program, 18: 4864
operation during irradiation of plutonium recycling fuels, 17: 39679(T)

(EURAEC-610)
radiation heating of materials in, (E), 19: 26628 (CEA-R-2581)
radioisotope production in, 17: 35203
release of radioactive gaseous effluents, methods for control of, 18: 41701

SACLAY REACTORS (OSIRIS)
automation of, centralized data processing equipment for, 20: 1536
description, 20: 18148

SACLAY REACTORS (PROSERPINE)
criticality and reactivity measurements on, 18: 1229 (CEA-2309)
reactivity, and effectiveness of delayed neutrons, 16: 21739

SAFARI
see South African Research Reactor

SAFETY
see also Reactor Safety
accident prevention in government-sponsored activities, 19: 34401 (N64-24119)
accident rate in radioactive materials shipment, 17: 18335 (TID-7651 (p.3-17))
accidents and injuries at ORNL, 1965, 20: 33557(R) (ORNL-3969)
accidents in handling radioactive materials, survey of, 17: 27618
accidents in U. S. nuclear facilities, 1961 and 1962, 18: 43859
accidents in well logging, 20: 41216
activities and program at Goodyear Atomic Corp., 1965, 20: 23372(R) (GAT-R-379)
activities at Goodyear Atomic Corp., Portsmouth, Ohio, 1961, 16: 16605 (GAT-R-281)
activities at Goodyear Atomic Corp., 1964, 19: 30438(R) (GAT-R-359)
activities at Idaho Operations Office, 1963, 19: 4398(R) (IDO-12037)
activities at Nuclear Safety Information Center, Jan.–June 1965, 20: 4186(R) (ORNL-3843, pp 235-44)
administration at Argonne National Lab., 19: 24780
administration of, at Argonne National Lab., 20: 14800
administrative policies for nuclear, in British processing plants, 16: 7802
administrative policies for nuclear, in U.S. processing plants, 16: 7803
administrative policies for, in French processing plants, 16: 7801
aerospace systems prelaunch factors, meteorological studies of, 18: 8908 (SC-DC-3553(p.209-18))
air particulate radioactivity measurements on nuclear submarines, 18: 10299 (AD-401763)
airspace closure during Sedan event of Plowshare Project, 17: 19730 (PNE-205F)
analysis in vessels for storage of fissile materials, 18: 44976
analysis of low-level radioactive waste containers in accident environment, 19: 20196 (CONF-650103-6)
analysis of methods for transporting research reactor fuel elements to radiochemical processing plants, 17: 28562 (EUR-185.f,d,e)
analysis of radioactive shipment accidents, 17: 18336 (TID-7651(p.18-30))
analysis of shielded cask for shipping irradiated HFIR fuel, 19: 7736 (ORNL-TM-959)
analysis of soluble neutron absorber in gaseous diffusion plant, 19: 6127 (K-1624)
analysis of spent fuel processing plant, 19: 42599 (NP-15312)
analysis of 5-watt radiostrontium-fueled generator for meteorological station, 20: 39311 (MND-SR-2586)
apparatus for serious radioactive accidents at Marcoule Center for Plutonium Production, 16: 16597 (CEA-2113)
applications and devices for laboratory, summary of, 16: 30682(R) (UCRL-6936)
aspects of, in radiography, 17: 30769
assessment of radiation hazards, 17: 6330
at AEC facilities, 1961 and 1962, accident report on, 18: 1957 (TID-5360(Suppl.4))
at nuclear power plants, 18: 10314
bibliography of UKAEA publications available to public, 16: 17339 (NP-11504)
bibliography on, 18: 22175 (VDDIT-86)
bibliography on, 20: 27207 (ORNL-NSIC-16)
bibliography on chemical detectors for, 18: 19847 (LAMS-2378(Vol.II))
bibliography on nuclear, 19: 26578 (ORNL-NSIC-8)
bibliography on nuclear, 19: 42659 (ORNL-NSIC-9)
bibliography on nuclear, 20: 18945 (ORNL-NSIC-14)
birdcage container for shipping fisaile materials, 19: 13665 (LA-3203-MS)
blanket dispensing device for clothing fires, 16: 7654(P)
book: *Dictionary of Nuclear Science and Techniques* (E/T), 19: 1985
book: *High-Efficiency Air Filtration*, 19: 18226
book: *Industrial Health in Handling Thorium*, 18: 12397
book: *Industrial Safety in Work with Beryllium and Its Alloys*, 19: 13956(T) (JPRS-27976)
book: *Introduction to Radiological Health*, 18: 14153
book: *Ionizing Radiation Hazards*, 19: 9425
book: *Nuclear Glossary. English-French, French-English* (E/T), 19: 1984
book: *Problems of Radiation Safety in Space Flights. Physical and Biological Studies with High-Energy Protons*, 20: 10604(T) (NASA-TT-F-353)
book: *Radioisotope Techniques*, 20: 33742
book: *Safety Measures in Chemical Laboratories*, 19: 22648
book: *Safety Standard for Non-Medical X-Ray and Sealed Gamma-Ray Sources*. Part I. *General*, 19: 15818
book: *Standards for the Transport of Radioactive Materials*, in Italian, 19: 32494
book: *The Radiochemical Manual*. Second Edition, 20: 36924
book: *Ventilation During Operations Using Radioactive Substances*, in Russian, 19: 15820
British nuclear installations act, 18: 20247
civil liability for nuclear damage, international conference on, 19: 7758
civil liability for nuclear, 20: 609
code of practice against radiation hazards, 16: 20902
comparison of radiation hazards with other risks, 19: 675 (AHSB(A)-R-8(p.89-108))
compressed air system, bibliography on, 18: 9757 (KAPL-M-TL-1)
conference on air cleaning, ORNL, Oak Ridge, Oct. 22 to 25, 1963, 18: 14116 (TID-7677)
conference on safety for electrical instrumentation in hazardous areas, Wilmington, Delaware, May 2 and 3, 1960, 16: 27349
consideration in plutonium metallurgy technology at Los Alamos, 16: 4472
control of isolation locks in nuclear plants, 19: 11425
control of nuclear, in chemical processing facilities of Savannah River Plant, 20: 431 (CONF-651103-7)
control program for industrial, 18: 39530 (HW-SA-3631)
criteria for design and use of nuclear devices in space, 20: 32855
criteria for handling uranium-233 alloy during fabrication of fuel elements, 17: 39289 (NAA-SR-Memo-8915)
criteria for handling infectious agents in laboratories, 19: 31635 (ORNL-TM-1162)
criteria for shipment of radioactive materials on toll facilities, 19: 20239
criteria for, in handling and shipping sealed radioisotope sources, 19: 40802 (CONF-650616-5)
critical mass control in laboratory hood, 17: 30749 (HW-76553(Rev.))
criticality accidents in nuclear industry, prevention of, 20: 35704
criticality control, 17: 10528 (ANL-6637(p.43-57))
criticality control in chemical processing department at Hanford, administration of, 19: 46433 (RL-SA-43)
criticality control in handling of fissionable material, conference on, 20: 35669 (STI-PUB-114)
criticality control in French industrial installations, 20: 35694
criticality control in systems of fissionable material, design criteria for, 20: 35695
criticality control in facilities handling fissionable material, multiple-contingency principle for, 20: 35696
criticality control at Harwell Research Establishment, 20: 35699
criticality control in USAEC facilities and plants, 20: 35700
criticality control in fuel-element fabrication at Savannah River Plant, 20: 35702
criticality control in processing of fissionable material, administrative procedures for, 20: 35697
criticality control in Hanford radiochemical processing plants, 20: 35701
criticality detection and alarm systems, review of design principles of, 20: 2075 (AHSB(S)R-92)
criticality evaluation of packages for transport of fissile materials, 19: 40828 (SC-RR-65-98, pp 679-90)
criticality studies on water-reflected systems of fissionable material, 20: 35684
criticality studies on plutonium solutions and uranium solutions in cylindrical geometry, French program of, 20: 35688
criticality studies for processing of irradiated MTR-type, 20: 35703
danger indicating and warning equipment for Nuclear Research Center at Julich, 18: 20257
design criteria for, in line of hot cells, 17: 2752
design of device for, in radioactive measuring apparatus, 20: 29515(P)
development and research projects in nuclear, summary of, 20: 46974
development of I.C.C. regulations for radioactive shipments, 17: 18338 (TID-7651(p.45-54))
development of radiological protection standards, 19: 677 (AHSB(A)-R-8 (p.113-21))
developments in, at Marcoule Center, 17: 41042
developments in nuclear, review, 16: 3303
developments in nuclear, review of, 17: 34185
developments in nuclear, review on, 19: 32495
developments in, *Technical Progress Review*, Fall 1963, 18: 464

developments in, *Technical Progress Review*, Winter 1964-1965, 19: 24778
diffusion and mixing of tritium in air, 16: 15023 (LA-2671)
documentation and reporting procedures for radiation accidents, 19: 22645
dosimetry aspects of nuclear accidents, 17: 37370
dosimetry investigation summary for Recuplex criticality accident, 17: 18325(HW-SA-2730)
during accidents involving radioactive materials, organization plan for, 19: 20197 (COO-281)
during handling and laundering of beryllium-contaminated protective clothing, 17: 32291 (UCRL-7311)
during transport of high-level wastes and irradiated fuel elements, container development, 17: 3222 (TID-7635(p.97-111))
during transport of radioactive materials, 19: 666 (AHSB(A)-R-8(p.19-24))
during transport of radioisotopes in Great Britain, 19: 668 (AHSB(A)-R-8 (p.31-5))
during transport of radioactive materials by commercial air carrier, 19: 11419 (ORNL-P-745)
during transportation of highly radioactive materials by truck, 17: 3214 (TID-7635(p.10-21))
during transportation of highly radioactive materials by truck, 17: 3215 (TID-7635(p.21-8))
during transportation of radioactive materials, 17: 3219 (TID-7635 (p.78-80))
during transportation of high explosives and nuclear materials, 17: 3223 (TID-7635(p.112-15))
education in university atomic energy programs for, 19: 11437
emergency planning for radiation accidents, 19: 22646
evaluation of flash units for photographing explosives, 20: 16739(R) (UCRL-14534, pp 44-9)
evaluation of nuclear excavation of sea-level Isthmian canal, 20: 1985 (PNE-2003)
evaluation of pilot plant for strontium-90 processing, 19: 30631 (MND-3137)
evaluation of projects for nuclear, 19: 13671(R) (WASH-1052)
evaluation of respiratory protection program at National Reactor Testing Station, 16: 27464 (IDO-12020)
evaluation of shipping containers for radioisotopes, 18: 22289
experience at Marcoule irradiated fuel reprocessing plant, 18: 37421 (A/CONF.28/P/83)
experience at Marcoule irradiated fuel reprocessing plant, 19: 20037 (CEA-R-2654)
fire and explosion protection of glove-box facilities, bibliography on, 18: 39414 (TID-3578)
fire hazards to occupants of shelters, 18: 31740 (FMRC-15328)
fire prevention and control in glove boxes for handling highly radioactive materials in the presence of volatile solvents, 18: 35766 (ORNL-TM-923)
fire testing of radioisotope shipping containers, 17: 3688
for fuel for multi-region lattice critical experiments, 16: 5857 (WCAP-1409)
for plants using gaseous fluorine, 16: 15034
for workers using radioactive materials, 17: 8432(T) (AEC-tr-5445)
guide for, in shipping irradiated nuclear fuel, 20: 33582
handling of radioactive materials in processing plants, auxiliary equipment for, 16: 27514(P)
handling of toxic materials, design of facility for, 17: 18742(R) (DCAS-TDR-62-62)
handling radioactive materials, equipment for, 17: 25495
hazards evaluation in use of radioactivity, regulations for, 19: 11465
hazards evaluation of in-tank waste solidification unit, 19: 19427 (RL-SEP-65)
hazards in cryogenic operations, 17: 36027 (LADC-5863)
hazards of cesium-137 thermoelectric cells, 19: 13843(R) (SAN-366-1)
hazards of coal-driven power plants, 20: 610
hazards of sealed radiation sources in Poland, 20: 35681
hazards of various radioactive materials, 18: 16241
hazards reduction techniques for nuclear space isotope power systems, 20: 33755
hazards review of promethium purification demonstration facility, 19: 18050 (HW-83299)
hazards summary of pilot plant for studying fission product release from containment vessel, 17: 41028 (ORNL-TM-683)
hearings on AEC regulatory problems before Eighty-seventh Congress, 17: 12518
heat transfer in liquid hydrocarbon fuel fires, 18: 13367 (SC-DR-320-63)
in AEC 1964 operations, nuclear incident related to, 20: 11051
in aerospace nuclear program, review of considerations for, 18: 8552 (SC-DC-3553(p.9-16))
in aerospace nuclear systems, NASA philosophy of, 18: 8554 (SC-DC-3553(p.33-7))
in aerospace nuclear systems, USAF philosophy of, 18: 8555 (SC-DC-3553(p.47-51))
in aerospace nuclear power, outline of standards and evaluation of, 19: 20206 (TID-7698(Pt.I)(p.31-2))
in atomic energy facilities, 19: 20209
in atomic energy program, 1965 Report to Congress on, 20: 24825
in beryllium machining, 17: 41035
in design of glove boxes, 16: 10294 (AHSB(S)R-18)
in Dutch reactor stations, medical aspects of, 19: 9423
in fabrication and shipping of enriched fuel rods, 16: 32036 (NAA-SR-Memo-7538)
in fabrication and use of radioisotopic sources, 20: 16914(R) (ORNL-3900, pp 182-93)
in fabrication of massive enriched uranium–molybdenum core components for Super Kukla, 19: 46967 (Y-KB-62)
in fission-product containment, pilot plant for, 19: 7731(R) (ORNL-3691(p.77-85))
in fissionable materials processing plants, bibliography, 17: 3236 (VDIT-64)
in fuel and process tube handling, engineering drawings of carriage for, 18: 32982
in handling and shipping radioactive materials, proposed IAEA regulations, 17: 3253
in handling and shipping fissionable material, 20: 3370 (CONF-651103-2)
in handling and shipping fissionable material, 20: 47002
in handling and storage of liquid hydrogen, 20: 9191
in handling beryllium, 19: 13903(T) (JPRS-27980)
in handling gaseous and liquid hydrogen, development of room inerting system for, 18: 33804 (LADC-6432)
in handling of chemicals, guide for, 17: 25475 (HW-SA-3015)
in handling of fissionable materials, criticality, 20: 35691
in handling of liquid hydrogen, 20: 9192
in handling of radioactive materials, 16: 3262 (JAERI-6008)
in handling of radioactive material, bibliography, 16: 17908 (AERE-BIB-122(Suppl.I))
in handling of radioactive materials, 18: 31830
in handling plutonium alloys and compounds, 20: 43578 (HW-59541)
in handling uranium by using neutron absorbers, 20: 20975
in handling zirconium and its alloys, 17: 10863 (RSPP-20(Issue 1))
in handling zirconium and its alloys, recommendations for, 18: 8542 (AHSB(S)R-59)
in hydrolysis and polymerization of plutonium in nitric acid and uranyl nitrate solutions, 17: 23435 (ORNL-TM-580)
in industrial use of radioactive sources, 18: 20253
in industrial uses of radioactive tracers, 18: 25725
in Kilorod program for production of thorium–uranium-233 rods, changes in solvent extraction flowsheet in, 17: 39176 (ORNL-TM-676)
in laboratories and facilities handling fission products and plutonium, 16: 3261 (HW-69587(Rev.))
in launch and re-entry of aerospace vehicles, research in U. S. on, 20: 33558 (ORNL-NSIC-10)
in milling and mining of uranium, 17: 2532
in mining radioactive minerals, 18: 4035
in nuclear industrial plants, 19: 11452
in nuclear industries, 19: 24776
in nuclear materials management, 18: 33799 (CONF-620-2)
in nuclear medicine laboratories, 19: 6132
in nuclear plants and peaceful uses of nuclear energy, Italian laws for, 18: 27729
in nuclear plants, industrial, 20: 33598
in nuclear power plants, economics of, 17: 8477
in nuclear rocket flight operations, environmental aspects of, 18: 1987
in observations in radiation fields, use of television systems for, 18: 14168
in occupational uses of radiation, 19: 9417
in operation of glove boxes and containment enclosures, 16: 29063 (TID-16020)
in operation of plutonium anion-exchange contactor, 19: 22629
in plants for production of fast-reactor fuel, 20: 35693
in plants with large amounts of fissionable materials, 18: 14135
in plutonium fuel element fabrication facility, 18: 23824 (HW-81363)
in plutonium handling, 16: 33311 (HW-SA-2740)
in plutonium handling, *Plutonium Abstracts*, Vol. 4, No. 3, April 1, 1964, 18: 23138 (HW-68600-37)
in plutonium handling, review on, 18: 43857
in preparation and recovery of reactor fuels, 19: 23996(R) (ORNL-3650(p.1-110))
in preparation of strontium-90-labeled glass, 18: 39830
in processing irradiated fuels, 17: 18186
in processing of cold enriched uranium, 16: 15030 (Y-A2-191(Del.))
in production of cobalt radioapplicators, 17: 25497
in Project Gnome, comparison of observed and predicted effects, 16: 17342 (PNE-128P)
in radiochemical plants, 19: 7732(R) (ORNL-3691(p.101-3))

in radiochemical processing plants, 19: 22428
in radioisotope applications, data and principles for insurance premium calculations for, 18: 20250
in radiotherapy, design of radiology departments in Soviet Union for, 16: 15031(T) (JPRS-13372)
in science, desirable degrees of, 18: 8553 (SC-DC-3553(p.19-21))
in shipment of explosives, 20: 594 (LA-DC-7469)
in shipping and handling radioactive materials, 19: 665 (AHSB(A)-R-8 (p.13-17))
in shipping and storage of irradiated reactor fuels prior to reprocessing, 16: 29273
in shipping nuclear materials, 17: 33433 (TID-7660(p.155-63))
in shipping of irradiated fuel from NS *Savannah* reactor for reprocessing, 18: 440 (NP-13235)
in shipping of irradiated magnox fuel elements in United Kingdom, 20: 9200
in shipping of radioactive materials by truck, economical control of risks in, 17: 27599 (NYO-9773)
in shipping of radioactive material in 1962, 18: 1958 (TID-16764(Suppl.1))
in shipping of radioactive materials, vehicle-collision problem in, 19: 7652 (NYO-2539-3)
in shipping reactor fuel elements, 17: 16317 (NAA-SR-Memo-8151)
in space flight, health and nuclear technology, 16: 4411
in transport of radioactive materials, testing programs for containers, 17: 3213 (TID-7635)
in transport of radioactive materials, 17: 3227 (TID-7635(p.128-33))
in transport of radioactive materials in Great Britain, regulations for, 19: 670 (AHSB(A)-R-8(p.47-51))
in transport of radioactive materials in Great Britain, regulations for, 19: 671 (AHSB(A)-R-8(p.53-8))
in transportation of radioactive materials, design of containers for, 19: 22610
in uranium mines in France, 19: 9411
in uranium ore processing plant, 16: 22470
in uranium ore processing plants in Yugoslavia, 17: 41170
in use of fissile materials, control systems for, 19: 15809
in use of gas cylinders, model safeguards and regulations for, 19: 28572 (AHSB(S)R-84)
in use of glove boxes, development of air balance monitor for, 19: 687(R) (HW-81746(p.5.25-8))
in use of nuclear power in space flight, 18: 6513 (CONF-311-8)
in use of water on fires involving plutonium, 18: 41676 (HW-82254(Rev.))
in waste disposal, 18: 45158
incidents at Dow Chemical Co., Freeport, Texas, 19: 32452 (CONF-650201(p.20-2))
incidents related to nuclear, in AEC facilities, 20: 45990
industrial accidents in USAEC facilities, summary, 16: 2062 (TID-5360 (Suppl.3))
industrial hygiene, 17: 4751
information center for nuclear, establishment at ORNL, 17: 38437(R) (ORNL-3483)
information center for nuclear, operation of, 19: 22600(R) (ORNL-3776 (p.129-32))
instrumentation for nuclear chemical plant, 18: 22367
insurance for liability in industrial and medical uses of, 18: 35798
insurance problems in shipping of fuels by sea, 19: 7726 (EUR-1639.f)
insurance view of non-nuclear and nuclear plants, 19: 32453 (CONF-650201(p.23-31))
isotope and radiation technology, *Technical Progress Review*, Winter, 1964–1965, 19: 13824
launch abort environment studies, review, 19: 24749 (SC-RR-64-1651)
licensing regulations for, proposed amendments to, 18: 470
liquid hydrogen handling and storage for research equipment, 20: 33560 (UCRL-16730)
listing of accidents in AEC installations during 1959 and 1960, 16: 5610 (TID-5360(Suppl.3)(Rev.))
loss, recovery, and activity control of radium capsule, 17: 18408
manual, 18: 8547 (IDO-12028)
manual, 19: 26582 (Y-1401(Rev.))
manual for radiation, 19: 46685
manual for radiobiology, 19: 6124 (COO-119-230)
manual of analytical procedures of Radiological Safety Laboratory, Nevada Test Site, 16: 28874 (TID-15916)
manual on radiological, 18: 37431 (AD-438147)
materials management relation to, 20: 20974
method for analysis of nuclear systems, graphic, 20: 34873
method for estimation of number of uranium-bearing fuel elements required for criticality, 16: 22848
methods for handling beryllium, 20: 21341 (MAB-205-M)
methods in uranium mines, 18: 12403
natural pollutant-removal processes in the atmosphere, 17: 37364 (HW-SA-3144)
neutron multiplication in storage capsules of plutonium-238-enriched plutonium dioxide, 20: 45955 (MLM-1340)
nuclear energy accidents and incidents, review, 19: 6121 (CEA-Bib-48)
nuclear, handbook, 17: 32293 (Y-1272)
Nuclear Safety Information Center at ORNL, operation in first two years, 19: 30442 (ORNL-TM-1136)
nuclear weapon accident prevention program of USAF, 18: 8558 (SC-DC-3553(p.361-5))
nuclear, bibliography on, 20: 7317 (ORNL-NSIC-12)
nuclear, standardization at the international level, 18: 18065 (HW-SA-3310)
of aerospace nuclear power sources, program at Sandia Corporation, 19: 27812 (SC-DC-65-1420)
of chemicals, manual on, 19: 5761 (TID-21344)
of Dribble Project, 19: 18174 (TID-21630)
of EBR-II fuel reprocessing facility, 18: 31651 (A/CONF.28/P/280)
of experiments operated in reactors, 18: 33149 (ORNL-TM-745)
of fuel reprocessing in U. S., 18: 31650 (A/CONF.28/P/278)
of glove boxes in Plutonium Reclamation Facility, 17: 23545 (HW-64888)
of nuclear aerospace power supplies, impact effects studies in assessment of, 18: 14114 (SC-DR-316-63)
of nuclear auxiliary power systems for space, 20: 18949 (SC-DC-66-1369)
of Nuclear Fuel Services plant for power fuel reprocessing, 18: 31652 (A/CONF.28/P/281)
of nuclear space vehicles, (E/T), 19: 10656
of old cobalt-60 teletherapy sources, 18: 4940 (ORNL-TM-712)
of radioactive shipments, operational decision making for, 17: 18337 (TID-7651(p.31-44))
of radioactive shipments, Canadian regulations on, 17: 18341 (TID-7651(p.99-102))
of radioisotope sources, AEC testing program on, 19: 2678 (ORNL-P-657)
of SNAP-3 thermoelectric generator, tests, 19: 30625 (MND-P-2358)
of stocks of radioactive materials, emergency planning for, 18: 43844
of storage and transportation of fissile materials, 18: 41681 (TID-7700(p.47-9))
of storage of SRE Core III elements in cell, evaluation of, 18: 12847 (NAA-SR-Memo-9349)
of uranium materials handling at Oak Ridge Gaseous Diffusion Plant, 18: 41682 (TID-7700(p.54-6))
of x-ray equipment in physician's offices, 18: 35793
off-site radiological monitoring procedures for missile test ranges, 18: 8556 (SC-DC-3553(p.255-8))
ordinance on control of radioisotopes and safeguards against radiation hazards, 17: 10857 (NP-12427)
organization and planning for management of radiation accidents, 19: 22644
packaging design for transport of radioactive materials, 19: 673 (AHSB(A)-R-8(p.63-80))
parameters for determination of safe quantities of radioactive materials for manipulation or transportation, 18: 35782
personnel-exposure and contamination control at the ORNL Research Reactor, 16: 25654 (ORNL-TM-278)
personnel protection in plutonium extraction plant in 4 yr of operation, 17: 41044
planning for emergencies at Chalk River, 17: 25492
plutonium criticality limits in equipment at Rocky Flats, Colorado, 18: 37445 (RFP-363)
plutonium materials management at Rocky Flats, Colo., 20: 18948 (RFP-720)
plutonium oxidation using steam in inert atmospheres, 20: 43854 (HW-66431)
plutonium release due to overheating or fires, 19: 20200 (HW-83668)
policies and programs of, Eurochemic, 20: 4048(R) (NP-15406)
preventive maintenance in chemical and mining industries, bibliography on, 20: 1976 (VDDIT-94)
problems in fabrication of uranium and its compounds, 17: 34167
problems in handling plutonium, 20: 27199 (JAERI-4036)
problems of, in transport of radioactive material by rail in Germany, 17: 41039
problems of, in design of pilot plants for irradiated fuel processing by fluoride volatility, 20: 20810(T) (ANL-Trans-250)
problems on atomic-powered naval vessels, 18: 37423 (A/CONF.28/P/378)
procedures for criticality control, 19: 40807 (RL-SEP-389(Rev.))
procedures for fuel element preparation and handling, 20: 4194
procedures for handling radium, 19: 22640
procedures for, in transport of radioactive materials, 17: 41038
procedures for, in transport of irradiated nuclear fuels, 17: 41040
procedures for plutonium handling, 18: 41672 (ANL-6884)
procedures for pressurized cryogenics, 18: 15044 (LADC-5956)
procedures for radiological emergency, 18: 37468
procedures for radioisotope handling at Lawrence Radiation Laboratory, 19: 7739 (UCRL-11700)

procedures for radiation accidents, 19: 22633
procedures for receiving and shipping fissionable materials, 20: 29450 (ISO-270)
procedures for, at U. S. nuclear test sites, 18: 27714
procedures in radiation accidents, 18: 33817
program at CERN, 16: 9043
program at National Institute of Radiological Sciences, Japan, 20: 5672
program for Operation HENRE, 20: 11930 (CEX-65.03)
program for radioisotope and reactor systems in space, review of, 17: 23569
program for tritium hazards at NRU reactor, 17: 14541
program for, in nuclear device detonation, 20: 39149 (NVO-28)
program in India, 18: 37427 (A/CONF.28/P/788)
program of AEC, review, 20: 4188 (TID-22268)
program of British Atomic Energy Authority, 16: 27483
programs at ORNL, Jan. to June 1962, 16: 30678(R) (ORNL-3319)
programs for radioisotope handling and reactor monitoring in Canada, 19: 15817
programs on, report to Congress on, 1962, 17: 40439
progress in aerospace nuclear, review, 18: 43850
progress review of nuclear, 17: 23567
progress review of nuclear, 18: 43849
protective measures for electromagnetic separation of plutonium at Oak Ridge National Lab., 16: 7787
public health problems of irradiated pet meat, 18: 29909
radiation accidents in AEC facilities, 1942 to 1961, 19: 24768
radiation accidents review, 19: 34414
radiation and health in Japan, industrial, 18: 31823
radiation doses to Mexican family exposed to unshielded 5-C cobalt-60 source for 4 months, 18: 18080
radiation emergency drill, 19: 22601 (ORNL-TM-1068)
radiation exposure to man by television sets and luminous dials, 17: 32309
radiation exposure records in program for, legal aspects of, 20: 14801
radiation hazard from surface contamination of jet aircraft, 16: 24022
radiation hazards in use of promethium-147-activated luminous paints, 17: 27619
radiation hazards to public, 17: 39344
radiation hazards in space flights, 18: 141
radiation in universities, code of practice for, 18: 20245
radiation monitoring for, development of integrating multipoint remote-area equipment for, 18: 41792
radiation protection of personnel at nuclear power station of icebreaker *Lenin*, 17: 42365
radiation protection problems in large electrical engineering company, 18: 8600
radiation protection guides, regulations, and standards for, Federal Radiation Council views on, 19: 9431
radiation regulations, review, 17: 18418
radiation safety and control at ORNL, 1960–62, 17: 18330 (ORNL-TM-507)
radiation safety and control, 19: 710
radiation, manual on, 18: 18129
radioisotope handling, in Canada, 20: 43763
radiological assistance team organization and operation, 18: 6969 (ANL-6786)
radiological assistance plan of AEC for emergencies involving radioactive materials, 18: 14104 (CONF-277-6)
radiological data on, 18: 22257
radiological emergency procedures for laymen involved in accidents involving radioactive materials, 18: 20273
radiological protection guide for nuclear reactor fuel fabrication plants, 18: 31827
radiological, in mining and milling of nuclear materials, conference on, Vienna 1963, 18: 18114
radiological, program for Salmon Event, 20: 5667 (TID-1020)
rapid method for estimating radiation hazard from radon decay products in the air, 16: 19192
re-entry hazards from nuclear engine materials, source term program analysis of, 18: 8557 (SC-DC-3553(p.351-60))
re-entry ablation of strontium-90 fuel capsules for space power plants, 20: 11189 (MND-3062-25)
re-entry flight test (RFD-2), stability analysis of vehicle for, 19: 34344 (SC-RR-65-129)
reactor shield plug-coffin design for safe handling of irradiated materials, 18: 13223(P)
reactor site selection with regard to protection of drinking waters from radioactive contamination, 19: 2546
recommendations for, in diagnostic radiography, 17: 8473
record of atomic energy industry, 19: 36742
reduction of human errors in man-machine systems, 18: 21719 (SC-R-748)
regulation of atomic energy by states, 17: 13725
regulations and procedures of Pakistan Atomic Energy Commission, 17: 3210 (NP-12227)
regulations and standards for nuclear, development of, 20: 45987
regulations for design, construction, and operation of electric accelerators, 17: 34171
regulations for fissile material containers and shipping procedures, 17: 18340 (TID-7651(p.88-98))
regulations for gamma defectoscopy in Bulgaria, 20: 11036(T) (JPRS-33502)
regulations for international rail transport of radioisotopes, 18: 43847
regulations for protection from ionizing radiations, 19: 38898
regulations for radioactive material containers, IAEA, 16: 25672
regulations for radioisotope handling and shipping in United Kingdom, 16: 25673
regulations for radioactive materials, lecture, 17: 14552
regulations for radioisotope uses in Great Britain, 18: 8697
regulations for radiation use, 18: 20249
regulations for radiation protection, 19: 2566
regulations for radioisotopes, 19: 11464
regulations for shipping radioactive materials, 16: 2090
regulations for shipping fissionable materials, I.A.E.A., 16: 7799
regulations for shipping fissionable materials, I.A.E.A., 16: 7800
regulations for shipping and handling radioactive materials in Russia, 16: 16612(T) (JPRS-12823)
regulations for shipping spent fuels, 20: 2084 (EURAEC-374(Vol.2))
regulations for shipping radioactive materials, 20: 18940 (EUR-2747.f)
regulations for transport of radioactive materials, 18: 27748
regulations for transport of radioactive materials in Great Britain, 19: 664 (AHSB(A)-R-8(p.7-11))
regulations for transport of nuclear fuel materials and reactor fuel elements in Great Britain, 19: 669 (AHSB(A)-R-8(p.37-45))
regulations for transport of fissionable materials, 19: 672 (AHSB(A)-R-8 (p.59-62))
regulations for transport of radioactive materials, IAEA, 19: 32496
regulations governing radiodiagnostic equipment, 17: 29125 (SCPRI(A)-87)
regulations governing clinical uses of radioactive drugs, 18: 31831
regulations in radioactive material shipping, review, 16: 25671
regulations on shipment of radioactive materials, handbook of Federal, 19: 30475
regulations preparation and evaluation, 19: 24773
regulatory programs for handling sealed radium and other radiation sources, 19: 42403
relation to radiation protection regulations, 17: 32317
requirements for industrial radiography using radioisotopes, 16: 24029
requirements for radiation, 17: 37385
requirements for, in reprocessing irradiated fuels, review of, 20: 16577
research and development program for nuclear, AEC, 18: 15435
research and development by the U.S.A.E.C., 18: 32962 (A/CONF.28/P/282)
research on, review of 1964 Geneva papers on, 19: 24779
research programs on, at ORNL, July to December 1962, 17: 16321(R) (ORNL-3401)
research programs on nuclear, at ORNL, 19: 22595(R) (ORNL-3776)
research programs on nuclear, 20: 4182(R) (ORNL-3843)
research programs on nuclear, at ORNL, 20: 18020(R) (ORNL-3900, pp 2-81)
research programs on nuclear, 20: 29470
research progress on, June to December 1963, 18: 14112(R) (ORNL-3547)
research progress on, *Technical Progress Review*, Fall 1964, 19: 11438
research progress on nuclear, 1964, 19: 30066(R) (ORNL-3789)
respirator program for uranium mills, 17: 32311
review of, at Oak Ridge Critical Experiments Facility, 17: 4742 (ORNL-TM-349)
review of Hanford program for, 20: 11046
review of nuclear industry, 19: 713
review of progress on nuclear, 20: 608
review of progress on nuclear, 20: 46972
review of, for health physics trainees, 20: 35667 (IDO-17182)
role of health physicists in radiation programs, 19: 4399 (LA-DC-6679)
role of health physicist in radiation protection, 19: 18205
shielding design for temporary use in installation of tube inlets into contaminated rooms, 19: 715(P)
shipment and storage of spent fuel, 16: 15019 (APAE-Memo-310)
SNAP 10A Prelaunch Test Facility safeguards, 18: 45075 (NAA-SR-Memo-8685)
standards for fissionable materials handling, 19: 40840
standards for industrial uses of radiation, 19: 44307
standards for irradiated fuel element shipping casks, 17: 18343 (TID-7651(p.126-31))
standards for radiation protection, 17: 14573
standards for radium control, 18: 22305
standards for radiation protection of ICRP, 20: 5663 (NP-15451)
statistical analysis of frequency and severity of accidents to potential

highway carriers of radioactive materials, 17: 8431 (NYO-9771)
status of developments, reactor and general, 1961, 16: 2087
status of meteorological knowledge as factor in pollution control, 17: 10843 (BNL-6538)
summary of data on 60 nuclear accidents, 1945 through 1961, 18: 31804(T) (NP-tr-1153)
supervision of radiation-exposed personnel, 18: 29403
survey of criticality incidents, 16: 7804
survey of radiation facilities and hygiene in dental offices, 17: 10871
systems design for, 20: 2085 (SC-R-65-991)
technician training for, manual for, 19: 40801 (ANL-6991)
techniques for, in shipping spent fuel elements, 18: 37422 (A/CONF.28/P/184)
testing of nonslip floor finishes, 18: 5548(R) (UCRL-7450)
testing of radiation source containers for, 18: 22278(R) (ORNL-TM-630)
testing program for radioisotope devices and sealed sources, 16: 9058
training courses in radiological protection, 19: 9427
training exercise for emergency procedures, 16: 22427 (AEEW-M-201)
training programs, 17: 10854 (HW-SA-2565)
uranium contamination of water supplies, 19: 36743
use of soluble poison in processing of irradiated reactor fuels, 20: 33426
use of urethan spray foam for containment, 20: 41200 (ORNL-TM-1551)

SAFETY HAZARDS

see also Dust Hazards
see also Health Physics
see also Radiation Detection Instruments
see also Radiation Protection
see also Remote-Control Equipment

accidents in fuel fabrication and radioisotope processing plants, theoretical possibilities and consequences of, 18: 25711 (ORNL-3441)
airborne plutonium contamination in production areas, 20: 43595
analyses during abort and re-entry of SNAP-10A, testing program for, 17: 28573 (NAA-SR-8304)
analysis for out-of-pile fuels, (E/T), 19: 17244
analysis for RFD-2, (E), 19: 17352 (SC-RR-65-13)
analysis for rupture of secondary coolant system of ESCR, 16: 5028 (NAA-SR-Memo-4823)
analysis for sealed radiation sources and radioisotopes, 18: 27745
analysis for space nuclear power plants, ground-based, 18: 1955 (SC-DC-3248)
analysis in RIFT flight, 18: 1985
analysis in site selection for waste-processing plants, 17: 41087
analysis in siting high-flux experimental reactors, 16: 21744
analysis of agricultural, from atomic installations, 17: 41089
analysis of discharge of waste solutions to Clinch River, 18: 19448(R) (ORNL-TM-757)
analysis of downwind regions from 10-kMw reactor following vaporization of core, 16: 4400 (NP-11116)
analysis of fission gas release from AE-6 Reactor on March 25, 1959, 16: 5071 (NAA-SR-Memo-3757)
analysis of fission product contamination in power-reactor accidents, 18: 40879
analysis of, for nuclear facility in Netherlands, 17: 41099
analysis of, in nuclear-facility siting, 17: 41105
analysis of, in nuclear rocket re-entry, 18: 4836 (SC-DC-3249)
analysis of, in siting nuclear facilities, 17: 41081
analysis of nuclear facility, by public health officials, 17: 41098
analysis of off-site in Project Gnome, 16: 18718 (PNE-132F)
analysis of, from accidents in processing plants, 18: 27744
analysis of, from solar flares during manned space missions, (T), 19: 20873 (D2-11608)
assessment of Atlas-Centaur abort, 20: 4187 (SC-RR-65-333)
book: *Atmospheric Pollution*, 17: 18292(T) (JPRS-18455)
book: *Reactor Safeguards*, 17: 9896
code of practice against radiation, 17: 34187
containment of reactor accidents, review, 17: 34192
control, developments in, 16: 15028(R) (UCRL-6658(Rev.))
control, development of equipment and methods for, 16: 20875(R) (UCRL-6818)
control in and around nuclear power stations, 17: 34162
control in nuclear reactors, 18: 43868
control of industrial, from use of radioisotopes, 20: 41208
control of liquid hydrogen, at experimental facilities, 19: 38875 (HASL-160)
control of, progress at Lawrence Radiation Lab. on, Oct. to Dec. 1962, 17: 29129(R) (UCRL-7254)
control of radiographic, 19: 36127
control reports on, index to UCRL quarterly, 19: 40833 (UCRL-14116)
cosmic proton doses in manned spacecraft on months-long missions, 18: 28904
cosmic ray particles for space flight, 20: 41187 (BNL-9468)
criticality control program at Savannah River Plant, formulation and implementation, 16: 1989
criticality studies on plutonium-containing vessels in cubic and square arrays, (E/T), 19: 37512(R) (HW-84608(p.81-90))
criticality, at Hanford Chemical Processing Department, (E), 19: 30974 (HW-81460)
determination of, from radioactive consumer products, 20: 14792
environmental exposures from sources near ground, data from Green Glow Program on, 19: 1033(R) (HW-81746(p.1.1-19))
environmental radioactive contamination of nuclear plants, effects on siting criteria, 17: 14527 (HW-SA-2809)
evaluation of aerospace nuclear systems, 19: 10632
evaluation of industrial, use of direct-reading instruments in, 18: 434 (LADC-5967)
evaluation of, involving lead-210 in uranium mines, 17: 41169
evaluation of radiation, in England, 17: 311
evaluation of, from rocket reactor tests, 20: 38525(R) (NUS-208)
evaluation of, in shipping cask for irradiated PM-1 and PM-3A cores, 18: 16225 (MND-M-1856)
evaluation of, in transport of radioactive materials, 19: 46663
evaluation of, in radiological containment systems, 20: 4214
evaluation of, in peaceful uses of atomic energy, 20: 14802
evaluation of, in reactor fuel reprocessing, 20: 16582
evaluation of, in booster rocket altitude aborts, 20: 47092 (SC-CR-66-2047)
experiments for evaluation of radiological, 20: 41178 (AD-635547)
fall-out, 16: 9040
fallout, assessment in New Zealand of, 19: 35892 (NP-15082)
fire damage in shipping containers, requirements for simulation, 18: 23827 (NYO-2539-1)
from accidental release of radioactive materials in hospitals, 18: 8586
from cosmic radiation in solar system, (T), 19: 29014 (NASA-CR-151)
from disposal of radioactive wastes in fresh water, 19: 12858
from explosion in plutonium waste, 18: 43843
from fallout, evaluation by Public Health Service, 18: 22295
from hospital radioactive waste disposal, 18: 22290
from ignition and combustion of reactor materials, 19: 11441
from industrial radioactivity, review, 18: 18077
from internally deposited radioisotopes, 18: 43321 (ORNL-P-350)
from iodine-131 used clinically, 18: 41259
from irrigation using water containing radioactive wastes, 19: 10666
from medical radiation, 18: 27157
from mercury-203 kidney localization, 18: 29482
from mobile image intensifier x-ray machines, 18: 39001
from pediatric radiodiagnosis, 18: 22282
from radiation, 18: 22297
from radiation in industry, 18: 29397
from radiation sources, British regulations for, 18: 20242
from radiation sources, 18: 22311
from radiation, comparison with other hazards, 18: 22298
from radioactive contamination, health aspects of, 18: 22284
from radioactive contamination, health aspects of, 18: 22285
from radioactive contamination, health aspects of, 18: 22286
from radioactive materials, 16: 33322
from radioactive waste disposal, 19: 1947
from radioactive waste disposal in municipal sewage systems, 20: 41217
from radiodiagnosis in general practice, 18: 21938
from radioisotope, preventive measures for, 18: 29903
from resuspension of radioactive particulate matter from surfaces, 19: 13696
from rocket reactor debris, dose models for evaluating, 20: 2091
from tritium diffusion in atmosphere, 19: 30462
from tritium in hydrogeologic studies, 19: 18183
from tritium release by electron-capture detectors, 19: 46670
from use of nuclear energy, review of, 19: 11440
from x-ray equipment in Mississippi, 18: 22303
gamma source loss in field work, exposure hazard from, 20: 16764
improved method for determining the active concentration of naturally radioactive aerosols, 16: 22466
in accidents involving radioisotopes, 1945-1962, 19: 13679
in americium and curium processing, 16: 8808 (MND-P-1972)
in arc melting of thorium, 16: 17911 (BM-RI-5969)
in Canada, relation to economy, 18: 1963
in collision of nuclear-powered ship, 19: 3768
in EURATOM, status of insurance and liability programs for, 18: 43109(R) (EUR-1850.e(p.179-82))
in fallout shelters from water shortage, 18: 25714
in filtered ventilation systems, 18: 14117 (TID-7677(p.56-72))
in fuel element shipping, 16: 25647(R) (EURAEC-164)
in German uranium mines, 18: 18115
in handling thorium, 16: 16593 (AEET/HP/SM-5)
in handling, shipping, and storage of irradiated fuel elements, 18: 16238
in industrial use of radiation sources, 20: 23545(T) (AEC-tr-6466/1, pp 106-10)
in laser use, 17: 29131(R) (UCRL-7254(p.6-16))

in nuclear plants, review of, 18: 41695
in operation of hot cells, 19: 11445
in operation of ICPP Waste Calcining Facility, analysis of, 18: 26977 (IDO-14620)
in ORNL Kilorod Facility for fabrication of uranium-233-enriched thorium dioxide–uranium dioxide fuel, 19: 26600
in plutonium processing, 16: 19179 (LAMS-2660)
in preparation and use of radioisotopes, 19: 13678
in processing rare earths, 16: 30690
in production of uranium alloys, 18: 1953 (NP-13261(p.297-320))
in radiochemical processing plants, 19: 9410
in radiochemical processing plants, 19: 11443
in radiodiagnosis, review, 16: 20892
in radiological wear measurements on refractory materials, review, 16: 16066
in Remote Split-Table Machine operation in plutonium critical mass experiments, 18: 10302 (HW-66266(Suppl.1, Rev.))
in research on radioactivity content in human diet, 16: 33332
in Salmon event of Vela Uniform Program, 20: 33561 (VUF-1025)
in shipping radioactive materials by trucks, 16: 33324
in transportation of radioactive materials, 17: 308 (NYO-9772)
in uranium mines in Japan, 19: 9421
in use of uranium in commercial alloys, 16: 25664
insurance problems, 16: 24025
laboratory guides for radiotoxicity of isotopes, 20: 41199 (ORNL-TM-626)
manual, 18: 8547 (IDO-12028)
manual on hazardous research equipment, 16: 11979 (UCRL-9711)
noise control in industrial plants, 19: 40806 (RL-SA-37)
of atomic energy, 18: 31782 (A/CONF.28/P/288)
of fission product release from power reactors, trends in assessment of, 18: 39561
of iodine-131-therapy of hyperthyroidism, 18: 43338
of microwaves, 19: 85
of nuclear disaster, role of public health offices in, 18: 20252
of nuclear origin in space flight, 17: 22949 (LADC-5765)
of radiation, review, 17: 3196
of radiation, evaluation of source contribution to, 18: 31807
of radioactive contamination of surface waters to animals and plants, 20: 43598
of radioactive detectors in gas chromatography, 16: 33330
of radioactive luminous materials, 17: 16338
of radioactivity from nuclear explosions, 18: 35769 (TID-7695(p.161-8))
of radioactivity release, review, 16: 19206
of radiodiagnosis, evaluation of, 18: 31348
of radiography, survey of oral, 20: 3846
of radon-222 in underground mines, effects of positive-pressure ventilation on, 20: 6694(R) (MIT-952-2)
of selenium vapors from rectifiers, 20: 7322 (SC-DC-65-1790)
of space flight, 18: 25045
of waste disposal and nuclear accidents, 18: 37429 (A/CONF.28/P/870)
of x radiation to children, 18: 20263
postattack research methods, 20: 45952 (HI-647-RR)
protection against radiological, at Brookhaven AGS, (E), 19: 25090 (BNL-8972)
protection against, for handling and storage of spent reactor fuels, (E), 19: 40837
protection against plutonium, at Rocky Flats plant, 20: 154 (RFP-621)
protective measures against tritium oxide, 20: 41185 (AECL-2594)
public health evaluation of, from operation of nuclear power plants, 20: 43632
public health planning in British Columbia for, 18: 27726
radiation damage to flight crew and ground personnel of jet aircraft, evaluation, 16: 22465
radiation exposure, assessment of occupational, 19: 38474
radiation, evaluation of, 18: 31813
radioactive gas production in operation of linear accelerator, 18: 14683 (TID-7677(p.208-21))
radioactive waste disposal, in Canada, 20: 45942 (AECL-2478)
radioactivity monitoring near nuclear installations, 17: 41083
radioinduced eye defects at French Atomic Energy Commission, 20: 45972
radioinduced human, evaluation of, 18: 22296
review of assessment of radiation, 16: 20898
review of radiation, 18: 5161
review of, to individuals and populations from use of radioisotopes, 20: 46003
siting facilities at NRTS, 17: 41101
supervision of internal contamination at Atomic Energy Commission at Marcoule, France, 20: 45973
testing RFD-2 re-entry vehicle for, (E), 19: 21763 (SC-DR-64-1741)
tests, evaluations and special equipment development at NASA Manned Spacecraft Center, 20: 41219
to chemical engineers from irradiation, review of, 17: 23559(T) (CEA-tr-X-499)
to population in maximum credible reactor accident, limitation of, 19: 22607
toxicology of epoxy resins, 16: 9813(T) (AEC-tr-4996)
Safety Rods
see Reactor Control Rods

SAINT LAURENT-DES-EAUX REACTOR (EDF-4)
construction of, use of prefabricated sections in, 19: 48021
containment design and performance for, 20: 35028(T) (ORNL-tr-1230)
containment for, design and construction of prestressed concrete, 20: 45127(T) (ORNL-tr-1228)
cooling system design for, 18: 38402 (A/CONF.28/P/94)
description and performance of, (E), 19: 45614
design, 18: 24920
design, 18: 38388 (A/CONF.28/P/38)
design and development, 19: 38202
development, 19: 33641
fuel element design and development, 18: 38355 (A/CONF.28/P/60)
pressure vessel design, 18: 38394 (A/CONF.28/P/52)
pressure vessel of, design of prestressed concrete, 19: 5499
pressure vessel thermal insulation in, use of pumice concrete for, 19: 38209

ST. LOUIS
strontium-90 content of teeth of children born in, 20: 32913

SALADO FORMATION (N. MEX.-TEX.)
atomic-explosion effects on, in Gnome underground shot, 17: 14514

SALAMANDERS
calcium–strontium discrimination during renal tubular reabsorption in newt, 19: 31672(R) (NIRS-3(p.65-77))
cell division in *Axolotl* and *Tritos punctatus* larvae, effects of electric and uv light on, 19: 17511
cell growth and differentiation in, 19: 2070(R) (ORNL-3700(p.69-76))
cell growth and differentiation in, 20: 6697(R) (ORNL-3853, pp 78-87)
cell growth and differentation in, 19: 2070(R) (ORNL-3700(p.69-76))
crystalline structure of lens of, 20: 6697(R) (ORNL-3853, pp 78-87)
ectoderm morphology of, effects of RNA fractions from rat liver on, 20: 6697(R) (ORNL-3853, pp 78-87)
gamma crystallins in, lens nuclei of, during Wolfian lens regeneration, 20: 40499(R) (ORNL-3922, pp 69-79)
iodine-131 metabolism in, 18: 38748
irradiated embryos, toxic effect on non-irradiated embryos, 17: 33743
lens regeneration in, 18: 27006(R) (ORNL-3601(p.69-82))
lens regeneration in, effects of actinomycin on, 19: 45738
lens regeneration in, effects of *in vitro* growth on, 20: 40499(R) (ORNL-3922, pp 69-79)
migratory behavior of *Ambystoma*, 20: 12568(R) (TID-22639)
nucleic acid synthesis in iris epithelium of, effects of lens removal on, 20: 40499(R) (ORNL-3922, pp 69-79)
oöcyte nucleoli membrane in Triturus, 20: 6697(R) (ORNL-3853, pp 78-87)
radiation effects on regenerative ability and nucleic acid content of normal, amputated, and DNA-treated extremities, 17: 7834
radiation effects on developing eyes, 17: 7848
radiation effects on skin epithelium of young, 17: 14000
radiation effects on hematopoietic cells in, microcinematography method for determination of, 17: 21542
radiation effects on cornea in, 18: 1418
radiation effects on cell regeneration in, 18: 19553(R) (TID-20513)
radiation effects on auditory organs in, protective effects of parabiosis against, x, 18: 25148
radiation effects on eggs of Triturus, beta, 18: 31161
radiation effects on developing ear of *Amblystoma punctatum*, 19: 8864
radiation effects on response of, to tissue transplants, 19: 13013
radiation effects on mitosis in cornea of *Axolotl* and *Triton punctatus* larvae, 19: 15044
radiation effects on inhibition of homogenate of regeneration blastemas in, 19: 15076
radiation effects on loss of regeneration capacity in extremities of, 19: 19544
radiation effects on DNA and RNA variations in regeneration of extremities, 19: 19546
radiation effects on extremities and life span of, protective effects of DNA and RNA against, 19: 26118
radiation effects on extremities of, cell regenerative effects of RNA in, 19: 26137
radiation effects on nucleic acid contents in extremities of larval, 19: 25942
radiation effects on neuroblasts in *Amblystoma punctatum* embryos, 19: 28026
radiation effects on breakage of lampbrush chromosomes in oocytes of, 19: 29961
radiation effects on morphology of erythrocytes in, 19: 43730
radiation effects on response to tissue grafts, 19: 45897

radiation effects on development of axial skeleton and spinal cord in, x, 20: 5312
radiation effects on regenerative growth in, x, 20: 6837
radiation effects on regeneration in Axolotl, x, 20: 18337
radiation effects on limb regeneration in, role of normal epidermis in recovery from x, 20: 20465
radiation effects on reproduction of, 20: 26663
radiation effects on regenerative capacity of axolotl limbs, effects of RNA on recovery from, 20: 29038
radiation injuries and recovery in, 18: 38969
radiation injuries of, regeneration induced by testicle grafts, 19: 21899
radioinduced breakage of lampbrush chromosomes in Triturus oocytes, 18: 27005(R) (ORNL-3601(p.60-8))
radioinduced suppression of regenerative capacity of extremities, restorative effects of nucleic acids and proteins, 16: 26794
radioinduced suppression of regenerative capacity of extremities of, effects of DNA, protein, and RNA on, 17: 33665
radioresistance of lens of, 19: 21866(T) (JPRS-28782(p.36-41))
radiosensitivity of forelimb and hindlimb of *Amblystoma punctatum* embryos, 17: 19851
radiosensitivity of, 19: 2060 (BNL-7596)
radiosensitivity of melanophores in head and tail of, 19: 8812
radiosensitivity of olfactory epithelium of *Siredon mexicanum*, effects of age, 19: 35965
radiosensitivity of cornea in *Siredon mexicanum*, effects of age, 20: 82
resistance of lens to trauma, 19: 21866(T) (JPRS-28782(p.36-41))
Salamine
see Protamines
SALICYL PHOSPHATE
hydrolysis, catalytic effects of metal ions and complexes, 16: 28949
radiation effects on hydrolysis of, background, 20: 20744
SALICYLALDEHYDE
chelate formation effects on cobalt-60 distribution in rat, 16: 12873
complexes with calcium, copper, lanthanum, yttrium, and zinc, association constants for, 20: 33276
complexes with cobalt, magnetic moments of, 20: 36823
complexes with cobalt, radiation effects on, annealing of recoil damage in neutron, 20: 38965
complexes with ethylenediamine, solvent properties for copper, iron, nickel, and uranium, 18: 22181
complexes with iron, magnetic moments of, 20: 36823
complexes with iron, Moessbauer spectra of, at +23, −78, and −195°C, 20: 36823
complexes with nickel, magnetic moments of, 20: 36823
complexes with triethylenetetramine cobalt chloride, radiation effects on, neutron, 20: 25173
oxidation by hydrogen peroxide, tracer study of, 17: 2710
triethylenetetramine cobalt chloride, radiation damage annealing in, 17: 7135 (NP-12330(p.422-8))
use of alcoholic solution with *p*-dimethylaminoaniline for colorimetric determination of uranium, 18: 21965
yields in gamma radiolysis of oxygenated benzyltrimethylammonium hydroxide solutions, 19: 22299
5-nitro-, chelates with europium, fluorescence and lifetimes, 17: 35730
SALICYLATE COMPLEXES
fluorescence of, effects of cations on, 17: 33879
with antipyrine and rare earths, benzene solvent extraction studies on, 20: 43256
with rare earths, preparation and properties, 19: 7422
with uranium, preparation and composition of, 20: 29197
with uranyl nitrate, composition and stability of, spectrophotometric studies of, 20: 29202
SALICYLATES
reactions with hydroxyl radicals from irradiated benzoic acid solutions, 19: 32224
SALICYLIC ACID
see also Acetylsalicylic Acid
analysis for oxygen, activation, 18: 37092
chelates with beryllium, ion exchange studies of, 17: 28781
complex with beryllium, preparation and stability of, 17: 1358 (AAEC/E-94)
complex with beryllium, stability constant of, 18: 39150 (AAEC/TM-240)
complexes with copper and a,a′-dipyridyl, formation constants and structure of, 20: 10465 (COO-1020-8)
complexes with neodymium, preparation and stability of, 18: 13825
complexes with niobium and amines, formation and stability, 17: 25250
complexes with vanadium, properties, 16: 18915
complexing with beryllium, dissociation and stability constants, 16: 4174
diiodo-, metabolism of iodine-131-labeled, 18: 38775(R) (ORO-624)
dissociation constants in heavy water and light water, 20: 7088
effects on cesium-137 uptake by wheat roots, 19: 50
effects on hydrogen-tritium exchange in benzene, 18: 31553
effects on radioinduced vulcanization of butadiene–styrene rubber, 19: 36507
effects on radioinduced graft polymerization of polypropene to acrylonitrile, 2-methyl-5-vinylpyridine, and styrene, 18: 25505(T) (AEC-tr-6372(p.363-9))
effects on strontium-90 excretion in rats, 20: 37025(R) (PG-Report-705)
labeling with carbon-14, 20: 10868
labeling with iodine-131 and tritium, 18: 43589
preparation of tritium-labeled, by charcoal sorption and gas exposure, 16: 17379
preparation of tritium-labeled, substituent effects on hydrogen-tritium exchange in platinum catalyzed, 18: 31553
production by gamma radiolysis of benzoic acid, 17: 8146
protective effects against radiation, metabolic factors in, 17: 15794
radioinduced production in calcium benzoate, 19: 834
radiolysis of, kinetics of gamma, 17: 8146
reactions with aqueous beryllium nitrate solutions, 16: 4126(T) (AAEC/Trans-8)
reactions with enzymes, 19: 5723
reactions with plutonium in aqueous solutions, 19: 2464(P)
reactions with rare earths in presence of pyridine for their separation from aqueous solutions, 19: 20079
reactions with uranyl ions, spectrophotometric studies of complex formation in, 19: 19903
reactions with uranyl ions, stability of complexes formed in, 19: 19904
reactions with uranyl ions, 20: 29197
separation from radiolysis products of *o*-iodobenzoic acid by chromatography, 19: 24434
solvent properties for beryllium in presence of amyl alcohol, 16: 8706 (AAEC/E-81)
solvent properties for thorium, 17: 8224
use as liquid scintillator for counting americium-241 and polonium-210 in aqueous and non-aqueous media, 20: 22866 (CONF-651214-1)
use for therapy of beryllium disease in animals, 20: 42754
yields in radiolysis of concentrated aqueous solutions of sodium benzoate, mechanism of, 18: 43536
3-oximinomethyl-, analytical use for thorium, 17: 27263
3,5-diiodo-, effects on iodine metabolism in lactating cows, 19: 45781
SALICYLIC ACID, 4-AMINO-
complexes with thorium, infrared spectra of, 19: 11057
effects on iodine-131 metabolism in human thyroid, 20: 32911
SALICYLIC ACID, ESTERS
p-octylphenyl, protective effects against radiation damage in polymethyl methacrylate, 19: 15646
SALICYLIC ACID, PHENYL ESTER
reactions with foreign particles in ice-water system, 18: 15722 (TID-20332)
Salicylic Acid, Sodium Salts
see Sodium Salicylates
SALICYLIC ACID, SULFO-
see also Sulfosalicylate Complexes
complexes with copper or iron and triethylenetetraminehexaacetic acid, 20: 10466 (COO-1020-11)
complexes with copper and a,a′-dipyridyl, formation constants and structure of, 20: 10465 (COO-1020-8)
complexes with EDTA or nitrilotriacetic acid and uranium in aqueous solutions, 20: 8879 (COO-1020-7)
complexes with gadolinium, potentiometric and spectrophotometric studies of, 20: 45652
complexes with rare earths, composition of, fluorometric and spectrophotometric studies of, 20: 40926
reactions with thorium ions, 16: 27004
sodium salt, analytical use of, in titrimetric determination of beryllium, 17: 6011
use for therapy of beryllium disease in animals, 20: 42754
use of, as making agent in solvent extraction of rare earths using butyric acid, 20: 45612
Antarox DM-970–sodium hexametaphosphate–sodium dodecyl sulfate–$NaNO_3$–sulfosalicylic acid, efficiency of, as radioactivity decontamination solution for cotton protective clothing, 20: 29477
SALICYLIC ACID, THIO-
analytical use of, for gravimetric determination of zirconium, 17: 21639
analytical uses in determination of metal ions, 19: 19812
complexes with thorium, infrared spectra of, 19: 11057
Salicylic Acid, Thorium Salts
see Thorium Salicylates
Salicylic Acid, Uranyl Salts
see Uranyl Salicylates
SALICYLOHYDROXAMIC ACID
analytical uses in determination of cerium, 19: 22127
SALINA FORMATION (U. S.)
geology and hydrology of, for potential use for radioactive waste disposal, 19: 14894 (SAN-413-2)

SALIVA
see also Salivary Glands
calcium-45 secretion in human, 19: 17479
calcium-47 content in man, after intravenous administration, 19: 21846
cesium-131 secretion in human, as compared to potassium-39, 19: 19486
effects of protein from, on radioinduced leukopenia, 18: 31289
iodine-131 excretion in, in thyroid diseased persons, 18: 29498
iodine-131 uptake by human, effects of gastrointestinal cycle on, 19: 14983
iodine-131 uptake by human, ratio of, to blood plasma uptake, 19: 14973
parotin A, antigenicity of, 19: 31670(R) (NIRS-3(p.19-56))
radiation effects on sodium content, 17: 15719
radiation effects on secretion of rubidium-86 in, in rats, 17: 37143
strontium-85 secretion in human, 19: 17479
trace element content in, neutron activation analysis method for, 19: 33765
tritium excretion in man, 19: 7206(R) (ORNL-3697(p.173-7))
use in calcium metabolism studies, 19: 6926

SALIVARY GLANDS
calcium-45 uptake and loss by rat, effects of acetylcholine and pilocarpine on, 17: 13889
calcium-45 transfer in rat, regulation of, 19: 8747
gold-198 incorporation by, 17: 33501
iodine metabolism in hamsters, tracer study, 19: 27915
iodine-131 concentration in mice, effects of sex, 17: 1202
iodine-131 concentration in mice, endocrine factors, 17: 1203
iodine-131 concentration by, in mice, 19: 33771
iodine-131 content of mouse, 18: 38766
iodine-131 retention by, effects of potassium perchlorate on, 19: 246
iodine-131 uptake by mouse, effects of thyroidectomy on, 18: 43191
iodine-131 uptake by, 20: 31160
mercury-203 uptake by rat, after repeated vapor inhalation, 19: 3860
nucleic acid synthesis in chromosomes, from *Chironomus tentans*, 16: 17401
photoscanning of, after injection of labeled colloidal albumin, 18: 19813 (CONF-164-11)
radiation damage to, in rats, effects of cortisone on, 17: 10470
radiation effects on secretion of sodium and potassium by, 17: 1293
radiation effects on masculinization of submaxillary, in rats, 17: 5800
radiation effects on zinc-65 content of mouse, x, 17: 33725
radiation effects on morphology and secretory function of, 18: 122(T)
radiation effects on cholesterol and fatty acid synthesis in, from calcium-45 deposited in, 18: 29346
radiation effects on rat, histochemical study, 18: 36960
radiation effects on metabolism of sodium and rubidium in rat, 18: 43247
radiation effects on secretory functions, effects of cysteamine in dogs, 19: 13053
radiation effects on function of, in rabbits, 19: 15110
radiation effects in rat, histochemical, 19: 21932
radiation effects on mouse submandibular, gamma, 20: 22684
radiation injuries induced by dental radiography, 19: 28092
radiation injuries to, in experimental animals following subcutaneous injection of radionuclides, 20: 42967
radiation of, histological modifications in testicles induced by, 16: 20216
radiation of, histological modifications in ovaries induced by, 16: 20217
radiation sickness effects on parotid in rats, 16: 8633(T) (JPRS-11848 (p.25-33))
radioactivity contained in, of experimental animals following subcutaneous injection of radionuclides, 20: 42967
radioinduced chromosome breakage in, in Drosophila, 17: 10403
radioinduced complications in, following facial radiotherapy, alpha, beta, and gamma, 20: 22652
radioinduced cytologic and functional changes in human, following cobalt-60 radiotherapy, 20: 40644
radioinduced tumors, 16: 26826
radiosensitivity of, 19: 34024
radiosensitivity of, 20: 18523
radiotherapy of human, clinical study of short term effects from, 19: 28140
radiotherapy of Mikulicz's disease of, x, 20: 16316
radiotherapy of postoperative parotitis, γ and x, 20: 45535
radiotherapy of skull base metastases from malignancies of, 20: 45562
radium-224 content in rat, after intravenous injection, 19: 40315
sodium-22 uptake by cell nuclei in Chironomus, 20: 24850
strontium excretion by, 18: 27051
strontium-85 transfer in rat, regulation of, 19: 8747
tumors of, histology and treatment of, 17: 38882
uptake of bromomercurihydroxypropane, tracer study, 20: 22817
uptake of iodine-131-labeled iodide, 19: 10756

SALMONELLA
chemically induced pyrimidine mutations in, *S. typhimurium*, genetic analysis of, 19: 45878
control of, in foods by radiation processing, 18: 14320
cross-linking of desoxyribonucleic acid strands induced by ultraviolet radiation in *Salmonella typhimurium*, 16: 31482
episomic element in *Salmonella typhosa*, 17: 1193
gene differentiation in, 19: 21756 (BNL-8934)
genetic linkage map of *S. typhimurium*, 19: 21817(R) (BNL-867(p.119-50))
genetic map of *S. typhimurium*, 19: 38291 (BNL-8825)
genetic map of *Salmonella typhimurium*, 19: 14899 (BNL-7909)
genetic map of *Salmonella typhimurium*, 19: 14899 (BNL-7909)
infections in food, 18: 14321
mutants of, 18: 4
mutations in *Salmonella typhimurium* induced by wild-type recombinations, 17: 1196
radiation effects on transduction by bacteriophage in, 18: 6617(R) (TID-19843)
radiation effects on, potentiation effects of chloral hydrate and other halogenated compounds on, 19: 33893
radiation effects on phosphorus-32 labeling of RNA in typhimurium, 19: 43743
radiation effects on morphology of, x, 20: 6854
radiation effects on biochemical properties of, x, 20: 6854
radiation effects on, effects of colicine factor on uv, 20: 12677
radiation effects on, effects of temperature and vitamin K_5 on γ, 20: 14395
radiation effects on populations of, in swine meal, γ, 20: 41394
radiation effects on synthesis of deoxyribonucleic acid in *Salmonella typhimurium*, ultraviolet, 16: 4065
radiation effects on, in frozen egg, gamma, 18: 522
radiation effects on dehydrase activity of, uv, 18: 9861
radiation effects on microcolony formation in *Salmonella typhimurium*, 18: 13556
radiation effects on *Salmonella typhimurium*, gamma, 18: 15854
radiation effects on *Pseudomonas sp.*, 18: 19627
radiation effects on mouse immunity to *Salmonella typhimurium*, gamma, 19: 33946
radiation effects on, 19: 44557 (NYO-3426-1)
radiation effects on microcolony formation in, 18: 13556
radioinduced elimination from frozen whole eggs, 16: 3993 (AERE-R-3811)
radioinduced elimination from frozen whole eggs, 16: 3993 (AERE-R-3811)
radioinduced inactivation of, synergistic effects of phosphorus-32 beta particles and ultraviolet radiation on, 18: 29340
radioinduced mutations in, uv, 19: 10844
radioinduced mutations in *S. typhimurium*, genetic analysis of, 19: 45878
radioinduced mutations of, uv, 20: 28977
radiopreservation of food contaminated with, review, 20: 41390
radiopreservation of food infected with, 18: 14325
radiosensitivity of, 19: 26722
radiosensitivity of *Salmonella typhi*, 19: 7046
radiosensitivity of *Salmonella typhimurium*, effects of heat on gamma, 18: 41127
radiosensitivity of, ultraviolet, 19: 45963
radiosensitivity of, effects of oxygen on, 17: 33682
radiosensitivity of, in eggs, 17: 31889
radiosensitivity of, ultraviolet, 19: 24314
radiosterilization in foods, 19: 26733
sulfur metabolism in, 18: 3407(R) (NYO-10710)

Salt Baths
see Liquid Baths

SALT DEPOSITS
actinide recovery from debris formed by nuclear explosion in, 19: 44156 (DP-956)
atomic-explosion effects on, in Gnome underground shot, 17: 14514
bibliography on waste disposal in, 18: 31041 (KFK-205)
cavity behavior in Tatum Dome, Mississippi, 18: 12337 (TID-20083)
cavity wall response to tamped nuclear explosions in (T), 19: 2473 (UCRL-7916)
closure rates of mine openings, convergence and laboratory model studies of, 18: 41638 (ORNL-P-302)
fission product storage in, dimensioning for maximum credible accident in, (T), 20: 16722 (BMwF-FBK-65-03)
geology in United States, summary, 17: 4705
geology of Hutchinson salt member of Carey Salt Co. Mine, Lyons, Kansas, 17: 36009 (ORNL-TM-597)
in Eddy County, New Mexico, geology, 16: 31959(R) (PNE-130F)
in United States, location, 16: 25067 (TID-7628(p.469-76))
nuclear explosion in, grout mixtures and instrument holes for, 20: 9138 (VUF-3019)
nuclear explosion in, decoupling in Salmon, 20: 14664 (UCRL-14487 (Rev.1))
nuclear explosion in Tatum, Salmon, 20: 36962
nuclear explosion in Tatum, calculations of free-field motion for Salmon,

20: 36963
nuclear explosions in domes, activation of media from (T), 19: 679 (HNS-1229-54)
nuclear explosions in, environment created by Gnome event, 19: 22454 (PNE-107F)
nuclear explosions in, iron mineral formation in, 20: 7253
nuclear explosions in, ground-water safety in, 20: 9094 (VUF-1027)
nuclear explosions in, full and partial decoupling in, (T), 20: 36964
permeability measurements of rock salt, 16: 3252
radiation and temperature effects on mine stability and plastic flow in, 20: 18897 (ORNL-P-2006)
radioactive waste disposal in, 16: 25040 (TID-7628(p.12-16))
radioactive waste disposal in, 16: 25067 (TID-7628(p.469-76))
radioactive waste disposal in, 16: 25068 (TID-7628(p.477-90))
radiometric prospecting for, methods used in, 18: 5525
seismic effects of Pre-Dribble detonations in, 18: 371 (NP-13279)
seismic profiling study of Tatum Salt Dome in Mississippi, 19: 6888 (NP-14517)
seismic profiling of southeast flank of Tatum Salt Dome, Mississippi, 19: 7717 (NVO-977-2)
seismic signal decoupling in, from underground nuclear explosions, (T), 19: 26553 (UCRL-12327)
seismic wave propagation from domes, 18: 37357 (NP-14227)
shock measurements in, from Gnome event, 17: 31089 (PNE-104F)
shock wave propagation by nuclear explosion in Salmon event, calculations on, 20: 23323 (UCRL-12326)
spherical cavity formation in, feasibility studies of, 17: 20198(R) (TID-18502)
triaxial compression and deformation tests of cores from Tatum Dome, 19: 12883 (TID-21592)
underground thermonuclear explosions in, effects on earth deformation, 16: 23357 (PNE-109F)
use of Lyons, Kansas, mine for demonstration disposal of high-level radioactive solids, 18: 7982 (ORNL-TM-734)
waste disposal in natural, 16: 2808(R) (ORNL-TM-15)
waste disposal in natural, 17: 2654
waste disposal in, 17: 39298(R) (ORNL-3492(p.19-37))
waste disposal in natural, operations summary of, 18: 19448(R) (ORNL-TM-757)
waste disposal in, 19: 3802
waste disposal in, 19: 8675(R) (ORNL-3697(p.19-31))
waste disposal in Lyons, Kansas, mine, field experiment, 19: 21751 (ORNL-P-1064)
waste disposal in, 20: 30943(R) (ORNL-TM-1465)
waste disposal in, problems in, 19: 40272
waste disposal in, economics and safety of, 20: 8478(R) (KFK-357)
waste disposal in, concept and field demonstration for high-level, 20: 8483
waste disposal in, demonstration of high-level, 20: 18169
waste disposal in, design and operation of Project Salt Vault for, 20: 20347 (ORNL-P-2058)
waste disposal in, laboratory studies of, 20: 45217 (ORNL-P-2126)
waste disposal in, demonstration of, 20: 45571(R) (ORNL-3945, pp 248-55)
waste solid disposal in mine, demonstration of, 19: 45689 (ORNL-P-1568)
waste storage experiment in Lyons, Kansas, mine, 19: 42195 (ORNL-P-1479)
waste storage in, 18: 6537(R) (ORNL-TM-603)
waste storage in German, geological study of, 19: 19429(T) (AEC-tr-6544)
waste storage in, mechanisms of, 17: 26932(R) (ORNL-TM-516)
waste storage in, in Europe, 18: 38687 (A/CONF.28/P/783)
waste storage in, equipment for, 20: 18165 (ORNL-P-1987)

SALT DEPOSITS (N. MEX.)
analysis of Project Coach excavation site, chemical, 18: 41304(R) (ORNL-TM-775)

SALT WASH MEMBER (COLO.)
geochemistry of Frenchy Incline uranium deposit in, 16: 27438

SALT WASH MEMBER (COLO.–UTAH)
localization of uranium–vanadium deposits by sedimentation, 17: 1647

Salting-out Agents
see Solvent Extraction Processes

SALTS
(See also specific classes of salts by name of metal.)
see also Ammonium Salts
see also Fused Salts
see also Paramagnetic Salts
activity coefficients at various concentrations and 25°C, tables, 19: 11048 (IA-1004)
age estimation of deposits of, using chlorine-36, 20: 25308
analysis for cerium using sodium molybdate, titrimetric, 18: 25287
analysis for impurities by infrared spectroscopy, 19: 17781(R) (ORNL-3750)
analysis for nitrides and oxides by high-temperature fluorination, 16: 23638 (TID-7629(p.295-307))
analysis of Project Coach excavation site, chemical, 18: 41304(R) (ORNL-TM-775)
chemical properties of metal-salt systems at high temperatures, 17: 4249(R) (NAA-SR-7400(Sect.VII))
chemical reactions in molten, 18: 3298(R) (ORNL-2221(Pts.1-5)(Del.))
conversion of radioactive solutions of, into compact solids, 17: 4620(P)
counting in liquid scintillators, losses in, 18: 39118
deposition on electric insulators, x-ray fluorescent method for measuring, 20: 29103
design of level indicators for molten, 20: 41233(R) (ORNL-3875, pp 101-24)
determination in sea water, 20; 40523(R) (RLO-1750-8(Vol.1))
determination in solution using pulsed neutrons, 20: 43163(P)
diffusion in, thermodynamic analysis of, 20: 23736
dissolution in underground domes, formation of spherical cavities by, 17: 16179(R) (TID-18074)
distribution in Pacific Ocean near mouth of Columbia River, 20: 18902 (RLO-1725-41)
effects of sodium, on growth of Clostridium in fish, 20: 9313 (CONF-651024, pp 3-6)
effects on cellophane filter performance, 19: 46237(R) (ORNL-3832, pp 76-99)
effects on excretion and skeletal retention of strontium in mice, 18: 31102
effects on infrared spectra of water–water-d_2 solutions, 20: 45643
effects on intestinal sorption of heavy and light water in rats, 20: 22568
effects on radioinduced graft copolymerization, 20: 7183(P)
effects on radiolysis of water, 20: 8981 (CEA-R-2794)
electrochemistry of molten, review, 16: 27025
electrochemistry of molten, review on, 18: 31537
electron spin resonance of ion radical, 20: 1935
excess free energy of reciprocal solutions of, calculation by perturbation method, 18: 3748
infrared spectra effects on phosphoryl group and water in tributyl phosphate solutions, 16: 10015
isotope effects on ion exchange in liquid and solid, 17: 23339
metal ion sequestration in aqueous solutions of, tracer studies of, 17: 27320(R) (ORO-602)
preparation and properties of poly-(vinylbenzyltrimethylammonium) poly-(styrenesulfonate), 16: 104
purification by crystallization and precipitation, tracer studies, 16: 3335(T) (AEC-tr-4497(p.251-60))
purification of magnesium chloride-base, equipment and methods for, 20: 31314(R) (ANL-7175, pp 1-41)
radiation effects on, in electron microscopy, 19: 36490
radiation effects on, review of, 20: 4464
radiosensitivity effects of inorganic, on barley seeds, 20: 16297(R) (EUR-2548.f)
separation by extraction chromatography using organic phosphorus compounds, 20: 10759 (INP-427/C)
separation by solvent extraction, effects of ion charge magnitude on, 18: 35482
separation from low-level wastes by electrodialysis, 20: 26563
separation from sea water using magnetohydrodynamic effect, 19: 44578(P)
separation from water by electrodialysis, 16: 16603 (ERDL-1671-TR)
separation of boron cage-acid, by solvent extraction, 19: 36220(R) (MIT-2098-142)
surface phenomena in melts of, 18: 32078
thermal conductivity of molten, design of device for measuring, 19: 729(R) (ORNL-P-532)
thermodynamic properties of molten, 17: 2945 (ORNL-3293)
tracer study of balance of, with water in human body, 20: 42782
vapor pressure above aqueous, at high temperatures, 19: 23163(R) (ORNL-3650(p.111-86))
x-ray-diffraction properties of fatty-acid and phthalic-acid, 18: 2097

SAMARIUM
see also Rare Earths
abundance determination in stellar atmospheres, 20: 46279
abundance in meteorites and terrestrial matter, 18: 10753
abundance in meteoritic, terrestrial, and solar matter, review on, 19: 13620
abundance in sun, (E), 20: 17237
alloying characteristics with transition metals, 18: 41924(R) (IITRI-578P19-13)
alpha emission spectra from thick sources, 16: 9449
alpha reactions (α,xny) at 27 to 52 Mev, gamma spectra from, (E), 20: 6348
alpha reactions at 24 Mev, isomer production in, (E), 20: 46717

analysis for oxygen by neutron activation, 20: 3863(R) (IS-1200(Sect. C))
analysis of, x-ray spectrographic, 19: 5794
atomic M states in, widths of, 17: 32724(R) (PR-P-57(p.21-36))
binding by sodium amalgam, 16: 14756
bremsstrahlung reactions (γ,n) at 8 to 16 Mev, spectra from, (E), 20: 15723 (MIT-2098-162)
bremsstrahlung reactions (γ,n) with, neutron emission in, (E), 20: 15724 (MIT-2098-224)
burnup in reactors, 16: 24486
cohesive energy and ionization of, relation between, (T), 19: 47062
conductivity of, electric and thermal, (E), 19: 18510
content and distribution in beef heart, 19: 45753 (AE-191)
content and relative abundances in terrestrial materials, 18: 20202
content in African pitchblende, estimation of induced fission vs spontaneous fission from, 20: 37994
content in common rock types, 20: 41068 (PNE-5006)
content in eclogites from Nowa Wies in Snieznik Klodzki, Poland, 20: 18900
content in Gulf of Mexico surface water, 20: 43087(R) (TID-23295, Sect. 4)
content in human heart, neutron activation determination of, 18: 33457 (AE-146)
content in igneous rocks, meteorites, and sediments, variation in, 17: 25435
content in Japanese hot springs, activation determination of, 19: 42443
content in sea water and sediment, 17: 30719
content in standard diabase W-1 and standard granite G-1, 19: 26529
content of, in marine organisms, 17: 15604
corrosion by atmosphere at high temperatures, 16: 5315 (WADD-TR-61-123)
crystal-field splittings in lanthanum chloride, inclusion of J mixing in, 17: 8050
crystal structure of, phase transformation in, 18: 18393
crystallization and precipitation of, separation factors in fractional, 17: 8064
determination as extracted nitrate complex, spectrophotometric, 19: 9070
determination as impurity in natural fluorites by activation methods, 19: 17835
determination at controlled potential, coulometric method development, 16: 11523(R) (TID-15106)
determination by carrier distillation, spectrographic, 18: 9985
determination by complexometric titration using acetic acid compounds, 18: 43417
determination by paper chromatography and fluorescence, 17: 37158
determination by precipitation as diliturate, gravimetric, 18: 31447
determination by precipitation as normal tellurite, 20: 1760
determination by radioactivation on chromatographic paper, 18: 39120
determination by spectrophotometry, effects of complexing reagents on, 19: 11026
determination by spectrochemical methods, voltage-fluctuation patterns in, 19: 40416
determination by spectrometry using 4,5-dihydroxy-3-[(*p*-sulfophenyl)azo]-2,7-naphthalenedisulfonic acid, 20: 12806
determination by thermal-neutron activation methods, sensitivity for, 19: 9071
determination by titration with sodium tungstate, 19: 26270
determination in aluminum as trace impurity, activation, 17: 10546
determination in artificial graphite, 18: 9584
determination in aluminum by activation and gamma spectrometry, 18: 31391
determination in americium by emission spectrography, 20: 8835 (RFP-414)
determination in aqueous solutions, effects of sodium tungstate on spectrofluorometric, 20: 12787
determination in cerium oxide, spectrophotometric, 16: 12981
determination in concentrates, spectrophotometric, 17: 30495
determination in cerium oxide, spectrographic, 19: 15339 (AEET/Spec./7)
determination in chromium–nickel steels and nickel-based alloys, 19: 40445
determination in carbonatites by ion exchange chromatography and oxalate precipitation, 20: 16346
determination in conductive tissue of beef heart, activation, 20: 31176
determination in complexes with diketones, spectrofluorometric, 20: 36722
determination in diabase and granite by spark source mass spectrography, 19: 11406
determination in europium oxide, spectrographic, 17: 2931
determination in EDTA complexes, spectrophotometric, 17: 6010
determination in erbium, mass spectrographic, 19: 2232
determination in enriched uranium fuels, neutron-capture gamma rays for, 19: 2258
determination in fluorite, gravimetric, photometric, and titrimetric, 18: 13704
determination in gadolinium oxide, spectrographic, 19: 22089 (AEET/Spec/14)
determination in glass, emission spectrographic, 20: 12810
determination in high-purity aluminum, activation, 17: 29954
determination in hydrochloric acid or methanol–nitric acid media, spectrophotometric, 20: 3888 (TID-22402)
determination in highly purified graphite by emission spectrography, 20: 26783
determination in human heart tissue, activation, 20: 31175
determination in hydrochloric acid solutions, spectrographic carrier-distillation, 20: 36729
determination in irradiated lanthanum, ytterbium, and yttrium by gamma spectral analysis, 16: 132(T) (AEC-tr-4686)
determination in iron–yttrium garnet powders, spectrographic, 17: 34431
determination in minerals and rocks, spectrographic, 17: 6008
determination in minerals by neutron activation followed by gamma spectrometry, 18: 43430
determination in minerals by neutron activation, 19: 30424
determination in minerals and rocks, activation, 20: 22950
determination in minerals by neutron activation, 20: 33178(T) (AEC-tr-6639, pp 86-91)
determination in magnesium alloys by successive potentiometric titration, 20: 38830
determination in nuclear fuels by isotope dilution, 18: 21970
determination in neodymium mixtures by absorption spectra of their dichlorooxinates, 19: 11027
determination in presence of other rare earths, spectrophotometric, 17: 32002
determination in promethium-147, 18: 35450 (ORNL-TM-922)
determination in purified uranium compounds by chromatography and spectrography, 19: 19800
determination in reactor graphite, spectrochemical, 16: 26932
determination in rare earth mixtures, spectrographic, 17: 127
determination in rare earth mixtures, activation, 20: 20562 (LYCEN-6538)
determination in rare earth mixtures, polarographic, 20: 26792
determination in rocks, chemical spectrographic method for, 20: 29083(R) (UCRL-14767)
determination in rare earths using acetonitrile, controlled-potential coulometric, 20: 38812
determination in sodium rare earth sulfates, spectrochemical, 18: 1527
determination in standard silicate rocks, activation, 18: 39128
determination in solutions by spectrophotometry using arsenazo III, 19: 17781(R) (ORNL-3750)
determination in standard igneous rocks G-1, W-1, and G-B by x-ray fluorescence, 20: 29101
determination in thorium by spectral analysis, 17: 6021
determination in thorium dioxide, isotope dilution, 18: 1547
determination in thorium and uranium, spectrographic, 20: 26746 (ISO-SA-13)
determination in TBP extracts, spectrophotometric, 20: 29125
determination in uranium thermal neutron fission products by ion exchange, 16: 12965
determination in uranium, spectrographic and spectrophotometric, 16: 25266 (CNEN-135)
determination in uranium, spectrographic, 16: 28867 (IEA-46)
determination in uranium compounds, spectral, 16: 32934
determination in uranium, spectrographic, 18: 9752 (IA-900)
determination in uranium and zirconium, direct spectrochemical, 18: 37076 (IA-925)
determination in uranium, spectrochemical, 19: 7307
determination in uranium and zirconium, spectrographic, 20: 2520(R) (IA-920)
determination in uranium compounds, spectrographic, 20: 29129
determination in uranium dioxide fuel pellets, 20: 41112 (IITRI-578P11-54)
determination in yttrium and samarium oxides, activation, 16: 25292
determination of, in lanthanum oxide, spectrographic, 17: 15932
determination of, in residues by iron flux method, spectrographic, 17: 19942 (PG-Report-157)
determination of, in rice plant and soil by activation and focusing chromatography, 17: 30219
determination of, review on x-ray spectrographic, 17: 23252 (IS-550)
determination of traces of, by electrochemical stripping, 19: 7331
determination of trace amounts of, by reactor neutron activation methods, 20: 26760
determination of, coulometric, 18: 41354
determination of, effects of tiron on spectrophotometric, 19: 7325
determination of, in SAP by spectrography, 19: 38553
determination of, in rare earth mixtures, photometric, 20: 252
determination of, in uranium by neutron activation methods, 20: 40832
determination of, in standard rocks by neutron activation and gamma

spectrometric methods, 20: 45587
determination using xylenol orange, spectrophotometric, 17: 25126
determination using hexamethylenetetramine and vanadic acid, indirect, 18: 1558
determination using 4-(2-pyridylazo)resorcinol, spectrophotometric, 18: 19895
determination using Xylenol Orange, spectrophotometric, 18: 25285
determination using 4-(2-pyridylazo)resorcinol, spectrophotometric, 18: 35461
determination using 2-(*p*-sulfophenylazo)-1,8-dihydroxynaphthalene-3,6-disulfonic acid, spectrophotometric, 18: 41341
determination using xylenol orange, spectrophotometric, 18: 43394
determination using *p*-(2-azo-pyridine)-resorcinol, spectrophotometric, 19: 2236
determination using Chromotrope 2B, photometric, 20: 1772
determination using thenoyltrifluoroacetone, photometric, 20: 8859
determination using Xylenol Orange, photometric and titrimetric, 20: 22949
determination using *N*-methylanabasine-α′-azo-β-naphthol, photometric, 20: 26801
determination with thorium in monazites, thorium phosphates, and xenotimes, 18: 19885
diffusion in germanium, (E), 19: 11755(T)
diffusion in uranium, 19: 16062 (CEA-R-2446)
dissolution and ion exchange in ammonium and potassium carbonate solutions, 17: 12240
dissolution and ion exchange behavior in ammonium and potassium carbonate solutions, 17: 39035
distribution between lead and zinc at 500°C, 18: 42089
distribution in aqueous chloride systems with TBP, 20: 7004 (IS-T-42)
distribution in tissues of mice of ionic and chelated form, tracer study, 17: 10308 (TID-17542)
effects as coactivator with cerium on emission spectra of borate phosphors, 19: 40494(T)
effects on crystal structure of cobalt, iron, and nickel intermetallic compounds, 20: 37243
effects on dielectric constant and electric conductivity of cerium aluminate, 19: 15535(T)
effects on diffusion of niobium, 17: 23876(R) (USBM-U-1031)
effects on flash mechanism in phosphors, 17: 5049(T) (UCRL-Trans-853(L))
effects on neutron spectra in benzene, polyethylene, and water, 18: 15157
effects on oxidation of chromium at 2300°F, 16: 18079(P)
effects on performance of alkaline earth sulfide luminescent dosimeters, 18: 35773(R) (UCRL-7811)
effects on properties of electrorefined vanadium, 19: 2795 (BM-RI-6653)
effects on radiation damage in calcium fluoride crystals, 16: 22662
effects on spectrophotometric determination of thorium, 19: 24408
electric conductivity of, pressure and temperature dependence of, 18: 7238
electric conductivity and Hall coefficient, effects of magnetic ordering and temperature on, 18: 27993
electric conductivity at low temperatures, (E), 20: 35920
electrochemical characteristics of, in phosphoric acid, 17: 25165 (TID-18697)
electrochemical properties in phosphoric acid, 17: 32034 (CONF-20-22)
electron binding energies of, K- and L-shell, 20: 46603 (UCRL-16798)
electron interactions in, s-f, 18: 1667
electron phototransfer with europium in calcium fluoride, 19: 26325
emission spectra of, isotope shift in, (E), 20: 10045
energy levels in $f^6(^7F)sp$ subconfiguration of, 20: 31919
energy levels of, intermediate coupling effects on low-lying, 17: 25932
energy levels of, ionization energies from, (T), 20: 37439
evaporation during urania reduction to uranium carbide, 20: 10272(R) (NAA-SR-9339)
evaporation from irradiated fuel, 19: 32282 (NAA-SR-10738)
fluorescence emission of, effects of aromatic carbonyl compounds on, 20: 26761
fluorescence in borate phosphors, 19: 34184(T)
fluorescence in cerium dioxide, concentration effects on, 19: 34180
fluorescence in yttrium, gadolinium, and lutetium orthovanadates, 19: 36392
fluorescence of, preparation of targets for studies of L-shell, 17: 36664 (UCRL-6989)
friction and wear properties of, in vacuum, effects of crystal structure on, 20: 21365
friction characteristics in vacuum, 19: 6255 (NASA-TN-D-2513)
gamma incoherent scattering by K-shell electrons of, at 320 kev, (E), 20: 11514
gamma resonant scattering by, 17: 29879(R) (IA-822)
gamma scattering at 8.997 Mev, cross sections for, 17: 35253(R) (IA-775)
gamma scattering cross sections of, resonant, 18: 36622
gamma spectra from 14-Mev neutron activation, determination by, 19: 26241
Hall effect in, at 2.4 to 350°K, (E), 20: 24624(T)
heat of solution in liquid tin at 750°K, 18: 24183
heat of solution in liquid tin at 828°K, 20: 11304
heat of sublimation and surface energy of, calculation of, 18: 626
heat of sublimation, 18: 23439 (CONF-405-36)
heat of sublimation, 19: 2315
heat of vaporization and vapor pressure of, 17: 22156 (ARL-63-15)
helium-3 elastic scattering at 20 Mev, differential cross sections, 18: 26681
hydridation of, kinetic studies of, 16: 31366
ion exchange and solubility in potassium carbonate solutions, 18: 31453
ion exchange behavior in hydrochloric acid–organic solvent media, 18: 39124
ionization and oxidation on rhenium and tungsten in oxygen atmosphere, 20: 757
ionization on rhenium and tungsten surfaces, effects of adsorbed oxygen on, 20: 31225
ionization potentials of, 18: 43527
ionization potentials of, electron-impact method for measuring, 20: 43235
liquid, solubility of tungsten in, at high temperatures, 20: 41412(R) (IS-1500(Sect. M))
luminescence in zinc borate glass, 19: 46269
luminescence spectra of, in magnesium oxide, 20: 7098
magnetic field at nuclei of, implanted in iron, 20: 40342
magnetic fields at lattice sites of, in iron, following Coulomb excitation implantation, (E), 20: 26372
magnetic moment of ions of, in crystalline state and in solution, 18: 25350
magnetic properties at low temperatures, 16: 10585
magnetic properties at 4.2–300°K, 17: 37710
magnetic properties of, effects of crystalline field and structure on, 18: 24186
magnetic properties, 20: 11340
magnetic properties, 20: 21414
magnetic properties at 2 to 300°K, 20: 43939
magnetic susceptibility of pure metallic, at 77 to 300°K, 20: 7590
magnetic transitions in, initial susceptibility and thermal hysteresis investigation of, 20: 7565 (IS-T-59)
melt technology and non-cutting shaping of, 19: 13969
meson (μ^-) capture by, probability for, (T), 20: 28456
neutron absorption cross section, 17: 14740 (TID-11295(2nd Ed.))
neutron absorption cross sections for natural, multigroup library of, 17: 24394 (NAA-SR-Memo-8274)
neutron absorption properties of, burnup effects on, (E), 19: 40163
neutron absorption by, gamma spectra from, 20: 13966 (UNC-5140)
neutron absorption cross section in pitchblende, thermal, 20: 37994
neutron capture cross sections, 16: 26509
neutron capture gamma spectra, 16: 19745(R) (ARF-1193-9)
neutron capture gamma spectrum, 16: 28024(R) (ARF-1193-12)
neutron capture, gamma spectra following, 16: 29750 (ANL-6589)
neutron cross sections, 18: 7696(R) (ORNL-TM-761)
neutron cross sections for, thermal, 18: 28562 (AE-143)
neutron cross sections of, shell effects on thermal, (E), 19: 47618
neutron cross sections at 0.025 ev to 10 Mev, 20: 8074 (KFK-352)
neutron cutoff energies for 1/v detector filters, effective, 16: 18219
neutron effective cutoff energies for filters of, for spherical, cylindrical, and slab geometries, 17: 3787
neutron effective cutoff energies, 17: 10506(R) (ORNL-3320(p.1-15))
neutron elastic scattering at 0.3 to 1.5 Mev, differential cross sections for (E), 19: 3381
neutron elastic scattering at 0.3 to 2.2 Mev, angular distributions from, (E), 19: 19095 (WASH-1053)
neutron filters of, effective cutoff energies as a function of thickness for, 16: 28014 (ORNL-TM-236)
neutron flux perturbation measurements of pellets of, 17: 36347(R) (NARF-62-18P)
neutron radiative capture cross sections, 16: 14059
neutron radiative capture cross sections, 17: 4037
neutron radiative capture cross sections at 30 and 65 kev, 18: 34274(R) (NIRS-2(p.3-15))
neutron reaction rates in light and heavy water, (T), 19: 33227
neutron reactions with, effects of burn-up on thermal absorption cross sections for, 17: 15214 (GEAP-4017)
neutron reactions (n,γ) at thermal energies, low-energy gamma rays from, 17: 36408 (NP-13020(p.160-5))
neutron reactions (n,γ) at 10 to 20 ev, spectra from, 18: 20388
neutron reactions (n,γ) with, spectra from thermal, 18: 40529
neutron scattering on resonant nuclei of, complex scattering amplitudes for coherent Bragg resonance, 17: 37798
neutron scattering by, cross sections for, 17: 41873 (WASH-1044)

neutron spectra effects of, in graphite, 18: 2817
neutron spectra effects in graphite, 18: 11145 (GA-4812)
neutron spectra for solutions of, 17: 24369(R) (GA-3542)
neutron total cross section of, fast, 17: 20982 (HW-SA-2875)
neutron total cross section at 0.7 to 14 ev, (E), 19: 21285
neutron transmission, 16: 18460
nuclear magnetic moments, spin-orbit coupling, and hyperfine fields, 16: 16831
nuclear relaxation time in calcium fluoride crystals doped with, 19: 13381
optical properties in ferrite garnets, spectra of, 17: 37231(T)
oxidation at high temperatures, 17: 14773(R) (TID-18063)
oxidation at 600 to 1300°C, rate of, 18: 35961
oxidation by air at 300 to 500°C, 17: 34330(R) (USBM-U-1057)
oxidation in dry and moist air at 100 to 800°C, rate of, 20: 21265 (RPI-2714-8)
oxidation kinetics of, effects of moisture and temperature on, 20: 35854
oxidation of, heats of reaction for, (E), 20: 757
oxidation of, kinetics of high-temperature, 20: 5859
oxygen-16 reactions with natural, multiple Coulomb excitation in, 17: 38284
paramagnetism of polycrystalline, 16: 1686
partition coefficients and reciprocal ionic radii, 17: 27562 (INSJ-54)
performance in aerosols, as reactor control, 19: 43505
performance of neutron filters of, effective cutoff energies for, (T), 20: 17663
phase transformation temperature, 16: 5315 (WADD-TR-61-123)
phase transformations at 6 to 65 kbar, solid-liquid and solid-solid, 19: 40095
photon reactions (γ,n) with, energy spectra from, (E), 20: 42165(R) (MIT-2098-251, pp 16-20)
poisoning efficiency in radiochemical processes, 16: 25415 (ORNL-3309)
polarographic behavior in tetraethylammonium bromide at dropping mercury electrode, 18: 23463
polarographic behavior in dimethylformamide and dimethylsulfoxide, 19: 40681
polarography of, in acetone solution, 17: 14253
precipitation by benzenephosphinic and benzenephosphonic acids, 18: 27308
precipitation with cerium–cadmium intermetallic compounds from liquid cadmium, 18: 34192
preparation and purification, 19: 40948 (IS-1195)
preparation of pure, 16: 22086
preparation of ultra-high purity, by zone refining, 17: 23863(R) (AFCRL-63-36)
production in Shippingport Pressurized Water Reactor, 16: 7298 (WAPD-PWR-TE-116)
properties as neutron filters, 18: 2841(R) (ORNL-3488(p.1-17))
properties as phosphor activator, 16: 25974
properties for use in reactor control rods, 18: 44959(P)
properties, physical and thermodynamic, 19: 40948 (IS-1195)
proton inelastic scattering at 25 to 1700 kev, x-ray yields from, (E), 19: 39881
proton reactions (p,γpxn) at 660 Mev, production of neutron-deficient radioactive rare earths in, 18: 24691
proton reactions (p,n) at 20.5 Mev, Coulomb displacement energies from, (E), 19: 23755
proton reactions at 660 Mev, 18: 7713
proton reactions at 25 to 100 kev, x-ray production in, 18: 28259
proton scattering by, L- and M-shell ionization yields from, (E), 19: 8067 (UCRL-12136)
purification, industrial methods, 16: 482
purification of fission-produced, in feed materials from promethium-147 separations, 19: 44116 (ORNL-TM-1062)
purification techniques, 19: 30338
radioactivity, natural, 16: 2508
radioinduced production of helium and hydrogen in, neutron, 19: 26901
radioinduced reduction of trivalent to divalent, in fluorite crystals, 16: 7945
reactions with cerimolybdic acid and its salt in chloride and nitrate solutions, precipitations in, 19: 2287
reactions with dichalcogenides and powdered graphite, preparation of intercalation compounds by, 20: 20648 (AD-621029)
reactions with external magnetic field, calculation of matrix elements in, 18: 4408(T)
reactions with samarium oxide in silica capsules, formation of samarium silicates by, 20: 13260(R) (NP-15852)
reactor criticality effects on very high-flux reactors, kinetics of, 18: 19311 (CEA-2389)
reactor criticality effects in VVR-S, (T), 20: 24803
reduction and deposition potentials, 19: 7362(T) (UCRL-Trans-1153(L))
reduction in acetonitrile solutions, color production in controlled-potential coulometric, 20: 38813
samarium-149 hyperfine interactions in, (E/T), 19: 8465
scattering on beryllium–copper alloy at 5 kev, secondary electrons from, 20: 41620 (NIJS-R-471)
separation by anion exchange in acetic acid–nitric acid medium, 18: 16131
separation by anion exchange in EDTA, effects of temperature on, 18: 20110
separation by anion exchange in acid-organic solvent media, 18: 23707(R) (TID-20609)
separation by continuous countercurrent ion method, 18: 31679
separation by electrophoresis on zirconium phosphate paper, 17: 4467
separation by extraction using alkali metal amalgams, 17: 40939
separation by partition chromatography with reversed phases, 17: 29025 (AERE-R-4358)
separation by partition chromatography using di-(2-ethylhexyl)-orthophosphoric acid as column material, 18: 3889
separation by reversed-phase partition chromatography using organophosphorus compounds, 18: 25614
separation by solvent extraction using TBP, effects of trilon B, 16: 275
separation by solvent extraction using amines, 17: 14375 (BM-RI-6205)
separation by solvent extraction from nitric acid solutions using organophosphorus compounds, 19: 4244 (IS-942)
separation by solvent extraction using TBP, computer program for cascade calculations for, 19: 22092 (IS-T-6)
separation from aqueous solutions by solvent extraction using bis(dihexylphosphinyl)-methane, 19: 24619
separation from aqueous solutions of organic acids by solvent extraction using high-molecular-weight amines, 19: 40657
separation from aqueous solutions by solvent extraction using monomerized and dimerized bis(2-ethylhexyl) phosphate, 20: 27051
separation from beryllium fluorides and lithium fluorides, 20: 32804(R) (ORNL-3936, pp 122-71)
separation from cadmium by coprecipitation with cadmium–cerium alloy, 16: 16464
separation from cerium, lanthanum, neodymium and praseodymium by ion exchange, 17: 1567
separation from cerium, lanthanum, neodymium, and praseodymium by ion exchange, 18: 349
separation from europium by ion exchange, 17: 20105
separation from europium by distillation of bromides, 19: 38765
separation from europium, radiochemical, 20: 27056
separation from fission products by solvent extraction and ion exchange, 20: 7203
separation from gadolinium and ytterbium by zone crystallization in nitrate medium and by precipitation using ammonium oxalate, 18: 16137
separation from lanthanum by zone crystallization in nitrate medium and by precipitation using ammonium sulfate, 18: 16137
separation from lanthanum and uranium using ammonium nitrate–trioctylamine, chromatographic, 19: 2234
separation from lithium beryllium fluorides by solvent extraction using bismuth–lithium alloys, 20: 45790(R) (ORNL-3945, pp 72-8)
separation from magnesium–thorium alloy by transfer to liquid scrub alloy in fused salt, 19: 20066
separation from methanol-nitric acid systems using anion exchange resins, 16: 25280 (TID-15598)
separation from metal ions by ion exchange in isopropyl alcohol, 18: 20104
separation from neodymium by displacement chromatography, band distribution in, 17: 6004
separation from neodymium, electrolytic, 18: 13773
separation from neodymium and promethium by ion exchange, 18: 21707(R) (MLM-1177)
separation from neodymium, 18: 21708(R) (MLM-1178)
separation from neodymium by ion exchange, 19: 22411
separation from neodymium by solvent extraction using bis(2-ethylhexyl) phosphate, 20: 27052
separation from nitrate solutions using alkyl amines, 17: 3873
separation from nitric acid solutions by solvent extraction using TBP, effects of ammonium nitrate on, 18: 31665
separation from nitric or sulfuric acid solutions, ion exchange selectivity scales for, 19: 9257
separation from nitrate solutions by solvent extraction using long-chain tertiary amines, 20: 27063
separation from other rare earths, 18: 5434(P)
separation from other rare earths by ion exchange, 19: 18057
separation from other light lanthanides by partition chromatography following production by proton bombardment of erbium, 19: 20078
separation from other rare earths by paper electromigration and focusing chromatography, 19: 30327
separation from other rare earths and ores by ion exchange using citric acid and EDTA elutants, 19: 46438
separation from other rare earths by thin-layer chromatography, 20: 7202
separation from other elements by solvent extraction using TBP, 20: 10952

separation from other inorganic ions by paper chromatography, 20: 12939
separation from other rare earths by paper chromatography, 20: 27049
separation from other rare earths by cation exchange in ammonium lactate solutions, 20: 26800
separation from perchloric acid solutions by ion exchange materials, 20: 20823
separation from promethium by electrolysis, 18: 3811 (NP-13165(Vol.2) (p.133-42))
separation from praseodymium, electrolytic, 18: 13773
separation from promethium by ion exchange, 19: 38772
separation from promethium in fission product solutions, eluting agents for ion-exchange, 20: 43411 (BNWL-SA-677)
separation from rare earths by electrolysis, 16: 11737
separation from rare earths using di-(2-ethylhexyl) orthophosphoric acid, chromatographic, 16: 14660
separation from rare earths, 17: 6019
separation from rare earth mixtures by chromatography using di-(2-ethylhexyl) phosphoric acid on Kel-F, 17: 34060
separation from rare earths by ion exchange centrifuge chromatography, 18: 17940
separation from rare earths by reverse-phase paper chromatography, 19: 7298
separation from rare earths by cation exchange using ammonium α-hydroxyisobutyrate and lactate, 19: 24432
separation from rare earths by reversed phase partition chromatography using 2-ethylhexyl phenylphosphonate, 19: 24431
separation from rare earths, thorium, and uranium by reversed-phase chromatography using methylenebis(di-n-hexylphosphine oxide), 20: 18599
separation from rare earths by solvent extraction using diisoamyl ester of methylphosphonic acid, 20: 27065
separation from rare earths by thin-layer chromatography, 20: 45597
separation from scandium by cation exchange chromatography, 18: 25613
separation from scandium and thorium by reversed-phase chromatography, 19: 44125
separation from scandium by ion exchange chromatography, 20: 20821
separation from sulfuric acid by diisobutylphosphoric acid, 18: 1829
separation from thorium tetrafluoride, 17: 19966
separation from thorium by solvent extraction using 2,4-pentanedione, 18: 20106
separation from thorium and uranium by paper chromatography, 18: 33505
separation from transplutonium elements by ion exchange using EDTA, 20: 35596
separation from uranium by anion exchange using carbonate solutions, 18: 361
separation from uranium by anion exchange, 19: 2451
separation from uranium by combined ion exchange-solvent extraction using nitric acid–tetrahydrofuran solutions, 20: 20811
separation from yttrium by solubility of carbonates in water, 20: 7019(T) (LA-tr-65-24)
separation from ytterbium using organic acids, 20: 14490
separation of, from rare earth concentrates by solvent extraction using amalgams, 17: 16157
separation of microgram amounts, high-efficiency electromagnetic, 16: 9118
shock compression of, 20: 39425(T)
solubility and ion-exchange properties in potassium carbonate solutions, 19: 13536
solubility in bismuth at 300 to 700°C, 16: 24216
solubility in cadmium at 400°C, 17: 40421(R) (ANL-6766)
solubility in gold, solid, 20: 17016 (IS-1175)
solubility in liquid cadmium at 325 to 550°C, 16: 32059
solvent distribution in diisoamyl methylphosphonate–nitric acid, 20: 45819
solvent effects in thorium–uranium fuel processing systems, 16: 3080
solvent extraction from nitric acid solutions by TBP, calculated cascade equilibria for, 18: 25624
solvent extraction by bidentate organophosphorus compounds, 19: 277 (IS-827)
solvent properties for tantalum, 20: 13180(R) (IS-RD-4)
sorption by n-butanol–nitric acid mixture, 16: 14738
sorption from nitric acid by ion exchange paper, 19: 24435
specific heat at 0.4 to 4°K, 16: 21189
specific heat at 0.4 to 4°K, 16: 32121 (TID-16704)
specific heats at 200 to 900°K, 16: 16746
spectra, flame, 16: 30400
spectra in alkali-halide single crystals, absorption and luminescence, 17: 27372(T)
spectra in dioxane–water and deuterium solutions, near infrared, 18: 17825
spectra in labeled perchloric acid and nitrate solutions, near-infrared and visible, 17: 2932
spectra in lithium nitrate–potassium nitrate system at 0.35 to 2.6 microns, absorption, 16: 17598
spectra in oxides, fine structure of L_m absorption, 18: 39195
spectra in thorium oxide at 100°K, nephelauxetic effects on reflection, 18: 25423
spectra of, differentiation between atom and ion, 18: 8913 (IA-841)
spectra of, effect of transitions in 4f shell on absorption, 17: 6099
spectra of, emission and x-ray fluorescence, 18: 183
spectra of, infrared, 17: 32739
spectra of, isotope shifts in, 17: 22327
spectra of minerals, effects of temperature on infrared, 17: 33880
spectra of singly ionized atomic, isotopic shifts in, 18: 40138(T)
spectra of solutions of, infrared, 17: 2983
spectra of, analytical applications of flame, 18: 11982
spectra of, assignments of furnace absorption, 19: 22160 (IA-964)
spectra of, atomic absorption, 18: 31513
spectra of, determination of $K\alpha$ x-ray, 18: 22693
spectra of, electron-transfer, 20: 23033
spectra of, isotopic shifts in, 18: 32763
spectra of, use of fuel-rich premixed oxyacetylene flame for emission, 18: 25278
spectral properties in rare earth oxide matrices, 18: 13869
sputtering at 50 to 600 ev by rare gas ions, 17: 8931(R) (NP-12389)
thermal conductivity at 80 to 460°K, 18: 42079(T)
thermal conductivity at low temperatures, (E), 20: 35920
thermal expansion at 77 to 300°K, 20: 7590
thermal hysteresis of magnetic transitions in polycrystalline, 20: 851
thermodynamic properties, 18: 10107
toxic effects on adenosine triphosphate metabolism in mitochondria, 17: 13928
use as activator for strontium sulfide crystals, 16: 15314(T)
use as dopant in luminescent materials, 19: 24537(P)
use in reactor control, 18: 33090 (A/CONF.28/P/274)
valence states of, x-ray spectroscopic analysis of, 20: 32720(T)
vapor pressure, 18: 8382
vapor pressure, 19: 2315
vapor pressure, 20: 33303
vapor pressure of, saturated, 19: 34728
vapor pressures at 1033 to 1302°K, 18: 23439 (CONF-405-36)
x-ray-diffraction patterns of, effects of cold working on, 20: 39421

SAMARIUM ACETATES

complexes with thiourea, solubility in water, 20: 1869
thermal decomposition of, study of products from, 20: 45658

SAMARIUM ALLOYS

formation and structure of $R(Me,X)_2$ type compounds in, 19: 30767
oxidation of, effects of non-rare earth additions on, 17: 3389(R) (USBM-U-978)
phase studies, 17: 23876(R) (USBM-U-1031)
Al–Sm, crystal structure, 19: 7950
Al–Sm, crystal structure of intermetallic compound SmAl in, 19: 14020
Al–Sm, crystal structure of Laves phases in, 19: 47052
Al–Sm, crystal structure and stability of intermetallic compounds in, 20: 21415
Al–Sm, Curie temperature and magnetic moments for, 17: 37775
Al–Sm, magnetic hyperfine interactions in samarium-149 in, 20: 15992
Al–Sm, magnetic properties of intermetallic compounds of, 20: 39433
Al–Sm, oxidation by air at 500°C, 17: 34330(R) (USBM-U-1057)
Al–Sm, phase studies, 19: 20596
Al–Sm, phase studies of, atomic size effects in, 19: 23111
Al–Sm, physical properties, (E), 19: 16188
Al–Sm, preparation and crystal structure of SmAl, 19: 7934
Al–Sm, properties of intermetallic compounds in, tabulation of, 20: 43972
Au–Sm, oxidation of, kinetics of high-temperature, 20: 5859
Au–Sm, phase studies of solid solutions in, 19: 41062
Be–Sm, crystal structure, 17: 36330
Be–Sm, crystal structure of, 18: 18399(T)
Be–Sm, structure of $SmBe_{13}$, 19: 23009(T) (JPRS-28849(p.195-6))
Bi–Sm, magnetic properties at 4 to 300°K, 19: 30743(R) (NYO-3454-1)
Bi–Sm, magnetic properties of LnBi type compound in, 19: 42867
Cd–Sm, crystal structure of intermetallic compound $SmCd_6$, 19: 16162
Cd–Sm, decomposition pressures, 19: 32279(R) (ANL-7020(p.3-99))
Cd–Sm, eutectic temperature in SmCd–Sm region, 19: 32279(R) (ANL-7020(p.3-99))
Cd–Sm, phase studies, 18: 36751 (ANL-6912)
Cd–Sm, phase studies, 20: 27546
Co–Sm, crystal structure of Laves phases in, 19: 47052
Co–Sm, crystal structure of intermetallic compounds in, 20: 37243
Co–Sm, crystal structure of intermetallic compound, 20: 43920
Co–Sm, ferrimagnetism of intermetallic compounds of, (E), 20: 24656
Co–Sm, magnetic properties of, antiferromagnetic effects on, 16: 22624
Co–Sm, magnetic properties of cubic Laves phase in, 19: 13399
Co–Sm, magnetic properties, 19: 38049
Co–Sm, magnetic properties of intermetallic compounds in, 20: 9511
Co–Sm, magnetization of, 18: 5804

Co–Sm, magneto-optic properties of intermetallic compound $SmCo_5$ in, 19: 41084
Co–Sm, thermomagnetic properties of, down to liquid helium temperatures, 16: 16742
Cr–Ni–Sm, fabrication of reactor control rods of, 19: 28803(P)
Cr–Sm, oxidation by air at 500°C, 17: 34330(R) (USBM-U-1057)
Cr–Sm, physical properties, (E), 19: 16188
Cu–Sm, analysis for AlB_2 and $CeCu_2$ type intermetallic compounds, 17: 29335
Cu–Sm, crystal structure, 18: 5791
Cu–Sm, crystal structure studies, 19: 44678(R) (ANL-7000, pp 186-200)
Cu–Sm, magnetic properties and crystal structure of intermetallic compounds in, 19: 9695
Cu–Sm, oxidation by air at 500°C, 17: 34330(R) (USBM-U-1057)
Cu–Sm, physical properties, (E), 19: 16188
Cu–Sm, structure of SmCu, 17: 36304 (TID-19337)
Dy–Sm, electric conductivity at 4.2, 77, and 296°K, 20: 22312(R) (AD-622796)
Dy–Sm, electric conductivity of, conduction-electron impurity-scattering effects on, (E), 20: 24644
Fe–Sm, crystal structure of $SmFe_7$, 20: 21400
Fe–Sm, crystal structure of intermetallic compounds in, 20: 37243
Fe–Sm, crystal structure of intermetallic compound, 20: 39409
Fe–Sm, hyperfine interactions of samarium-149 in, (E/T), 19: 8465
Fe–Sm, isomer shift of iron-57 in $SmFe_2$ at 300 and 800°K, 19: 44678(R) (ANL-7000, pp 186-200)
Fe–Sm, magnetic properties, 19: 38049
Fe–Sm, Mössbauer effect measurements of hyperfine interactions in Laves phase in, 19: 4683
Fe–Sm, oxidation by air at 500°C, 17: 34330(R) (USBM-U-1057)
Fe–Sm, physical properties, (E), 19: 16188
Ga–Sm, crystal structure studies, 19: 44678(R) (ANL-7000, pp 186-200)
Ga–Sm, preparation and properties of MX_3-type compounds in, 18: 37723
Ge–Sm, crystal structure of intermetallic compounds in, 19: 11762
Ge–Sm, crystal structure, 20: 7591
Ge–Sm, crystal structure of, at or near equiatomic proportions, 20: 19225
Ge–Sm, crystal structure of intermetallic compound SmGe in, 20: 33886 (UCRL-14152)
Ge–Sm, crystal structure of intermetallic compound Sm_5Ge_4 in, 20: 33910
Ge–Sm, crystal structure and magnetic properties, 20: 38369
Ge–Sm, preparation and crystal structure of SmGe, 20: 19224
Ge–Sm, structure of germanide, 19: 23006(T) (JPRS-28849(p.184-7))
Hg–Sm, preparation and structure of intermetallic compounds of, (E), 19: 4666
Hg–Sm, thermodynamic properties and vapor pressure measurements, 20: 21384
In–Sm, crystal structure of $SmIn_3$, 20: 17060
In–Sm, preparation and properties of MX_3-type compounds in, 18: 37723
La–Sm, electric conductivity, magnetic susceptibility, and superconducting transition temperatures of, 20: 29753
Mg–Sm, phase studies at 400 to 1100°C, 17: 34330(R) (USBM-U-1057)
Mg–Sm, phase studies, 18: 2174(R) (USBM-U-1082)
Mg–Sm, thermodynamic properties, 19: 41013 (IS-T-25)
Mg–Sm, thermodynamics of formation of intermetallic compounds, 20: 41412(R) (IS-1500(Sect. M))
Mn–Hg–Sm, preparation, 18: 34027 (AD-428772)
Mn–Sm, amalgam studies, 18: 34026 (AD-428771)
Mn–Sm, analysis by x-ray fluorescence, 18: 27340
Mn–Sm, crystal structure of intermetallic compound Sm_6Mn_{23} in, size-factor limitation in, 19: 23079
Mn–Sm, crystal structure of Sm_6Mn_{23} in, 20: 17096(T)
Mn–Sm, crystal structure and magnetic properties of intermetallic compounds of, 20: 21403
Mn–Sm, existence of Sm_6Mn_{23} compound in, 19: 14074
Mn–Sm, magnetic moments of intermetallic compound Sm_6Mn_{23} in, 19: 23109
Mn–Sm, magnetic properties of intermetallic compound $SmMn_5$ in, at 80 to 1400°K, 20: 7610
Mn–Sm, phase studies by differential thermal, thermomagnetic, and x-ray analysis of, 19: 46989 (AD-614466)
Mn–Sm, preparation, phase studies, and properties of, 19: 46987 (AD-614462)
Mn–Sm, preparation by sinter process using mercury, 19: 46908 (AD-614464)
Mn–Sm, preparation and structure, 20: 15110
Ni–Sm, crystal structure of equiatomic intermetallic compound in, 19: 24994
Ni–Sm, crystal structure of intermetallic compounds in, 20: 37243
Ni–Sm, fabrication of control rods of, 19: 28802(P)
Ni–Sm, magnetic and structural characteristics of intermetallic compound of type LnNi in, 18: 37697
Ni–Sm, magnetic properties of, antiferromagnetic effects on, 16: 22624
Ni–Sm, magnetic properties of $SmNi_5$ at 4–300°K, 17: 37713
Ni–Sm, magnetic properties of cubic Laves phase in, 19: 13399
Ni–Sm, magnetic properties, 19: 38049
Ni–Sm, magnetic properties of intermetallic compounds in, 20: 9511
Ni–Sm, oxidation by air at 500°C, 17: 34330(R) (USBM-U-1057)
Ni–Sm, physical properties, (E), 19: 16188
Pb–Sm–Zn, component distribution in recrystallized, 20: 39435
Pd–Sm, phase studies, 19: 47051
Pd–Sm, preparation and properties, 19: 16068 (EUR-1894.i)
Po–Sm, preparation and properties of, 20: 35909
Pt–Sm, crystal structure of equiatomic intermetallic compound in, 19: 24994
Pt–Sm, magnetic properties, 19: 38049
Re–Sm, magnetic properties, 19: 38049
Rh–Sm, crystal structure of equiatomic intermetallic compound in, 19: 24994
Ru–Sm, process for improving workability of, 19: 40999(P)
Sm–Ag, crystal structure, 17: 16658 (TID-18197)
Sm–Ag, crystal structure of intermetallic compounds AgSm and Ag_3Sm in, 20: 4447
Sm–Ag, crystal structure, 17: 16658 (TID-18197)
Sm–Ag, magnetic properties of intermetallic compound with CsCl structure in, 19: 2814
Sm–Ag, phase diagrams, 19: 7941
Sm–Sn, magnetic properties of $SmSn_3$ at 2 to 300°K, 19: 30743(R) (NYO-3454-1)
Sm–Sn, magnetic properties of, at 2 to 300°K, 20: 4423
Sm–Sn, temperature dependence of tin Knight shift and magnetic susceptibility in, 20: 861
Sm–Sn, tin Knight shift and magnetic susceptibility of $SmSn_3$, 20: 12324
Sm–Tl, preparation and properties of MX_3-type compounds in, 18: 37723
Sm–V, oxidation by air at 500°C, 17: 34330(R) (USBM-U-1057)
Sm–V, physical properties, (E), 19: 16188
Sm–Zn, crystal structure, 18: 5791
Sm–Zn, crystal structure of intermetallic compounds in, 20: 9515
Sm–Zn, crystal structure of intermetallic compound $SmZn_{12}$ in, 20: 39417
Sm–Zn, crystallographic and thermodynamic data on intermetallic compound, 20: 41412(R) (IS-1500(Sect. M))
Sm–Zn, magnetic susceptibility of AB_2-type compound in, 20: 24589(R) (NYO-3560-3)
Sm–Zn, melting point of $SmZn_2$, 20: 31743
Sm–Zn, phase diagrams, 20: 4297(R) (IS-1200(Sect.M))
Sm–Zn, structure of SmZn, 17: 36304 (TID-19337)
Sm–Zr, oxidation by air at 500°C, 17: 34330(R) (USBM-U-1057)
Sm–Zr, physical properties, (E), 19: 16188

SAMARIUM ALUMINATES
crystal structure, 19: 11754(T)
dielectric constant, 19: 15534(T)
physical properties, 20: 45639
preparation and properties, 20: 8915
preparation of monocrystals of, with perovskite structure, 20: 40920
$CeAlO_3$–$SmAlO_3$, properties and structure, 17: 20015

SAMARIUM ARSENIDES
electric properties and uses of, 18: 34158
preparation, semiconducting properties, and structure of, 19: 22965 (AL-TDR-64-239)
thermoelectric properties, 17: 11296 (AD-278352)

SAMARIUM AZIDES
preparation and spectra of, 19: 13389
thermal decomposition of, differential thermal analysis of, 18: 25446

SAMARIUM BORATES
crystal structure, 17: 27837
crystal structure of vaterite-type, polymorphism in, 20: 12837
polymorphism, x-ray analysis, 16: 162
preparation and properties, 19: 7498
spectra of, infrared, 20: 35519
$LaBO_3$–$SmBO_3$, structural polymorphism of, 17: 32124
$NdBO_3$–$SmBO_3$, structural polymorphism of, 17: 32124

SAMARIUM BORIDES
boron-11 NMR in hexavalent, 17: 676
electric conductivity of hexa-, 17: 16726
electric resistance, 19: 6356
electron structure and physical properties of crystals of, 17: 27875
fabrication by hot pressing, 19: 11710
mechanical properties, 19: 11710
performance as control materials for high-temperature reactors, 18: 22519
physical properties of hexa-, 16: 12154
preparation and decomposition, 17: 1509
preparation and purification, 19: 46941 (NP-15514(Vol.3))
preparation and reactions, 19: 15502
preparation and thermal decomposition, 16: 93(R) (TID-14090)
preparation and thermodynamic properties, 20: 5551

preparation, properties, and uses, 17: 2959(T) (AEC-tr-5264)
radiation sintering of, 17: 20512 (GEAP-3743(Pt.II))
spectra of, valence state determination from x-ray absorption, 19: 30194
testing for use as reactor absorber material, 16: 32072
thermal conductivity, 17: 28843
thermionic emission of, on iridium and tungsten substrates, (E), 20: 5532(T) (K-Trans-10)
thermodynamics of formation of, 19: 40524
x-ray absorption by, edge structure in, 19: 22185
x-ray absorption spectra of, (E/T), 19: 23975(T)

SAMARIUM BROMIDES
density of aqueous solutions of, 20: 40796(R) (IS-1500(Sect.C))
electric conductivity of methanol solutions of anhydrous, at 20 and 45°C, 20: 22991
spectra of, electron-transfer, 20: 25104
thermal decomposition of hydrates of, mechanisms of, 19: 46271

SAMARIUM CARBIDES
electric conductivity and thermoelectric power at room temperature to 4°K, 18: 23511
eutectic temperature between carbon and dicarbide, 19: 41014 (LA-DC-6819)
lattice parameters and phase transformation temperatures in, 19: 41014 (LA-DC-6819)
microhardness, 19: 41014 (LA-DC-6819)
properties of, chemical and physical, 18: 23517

SAMARIUM CARBONATES
complexes of, composition in solution of, 20: 10824
crystal structure of, x-ray diffraction studies of, 20: 38869(R) (COO-1109-22, Paper 8)
preparation by heating aqueous solution of rare earth chlorides and ammonium trichoroacetate, 19: 36399
preparation by precipitation, 17: 15951 (LADC-5579)
preparation from acetates and propionates, 20: 26911
preparation, properties, and structure, 17: 15950 (LADC-5566)
spectra of solid, electron transfer, 20: 35506
spectra of, electron-transfer, 20: 25104
thermal decomposition of, compound formations in, 17: 15951 (LADC-5579)
thermal decomposition at 25 to 1400°C, thermogravimetric analysis of, 18: 25354

SAMARIUM CHLORIDES
chlorine-35 and -37 quadrupole frequency in, 20: 24591(R) (TID-22848)
complexes with phenanthroline, preparation and properties, 19: 40514
complexes with 1,10-phenanthroline, structure and thermal stability of, 18: 25387
crystal field parameters for, 19: 15545
cyclopentadienyl-, magnetic susceptibility, 18: 1712(R) (TID-19613)
cyclopentadienyl-, synthesis, 18: 1712(R) (TID-19613)
entropy of formation and vapor pressure over, 18: 25426
fluorescence of aqueous solutions of, effects of heavy water on, 20: 25102
fluorescence of, in aqueous solutions, deuterium effects on, 19: 22206
formation and stability, 17: 35834
heat of dilution of aqueous, at 25°C, 20: 38903
heat of vaporization and vapor pressure of, above melting point, 17: 37185
magnetic phases, (T), 20: 20143
magnetic transitions at 0.2 to 4.2°K, 19: 15522
melting point and vapor pressure of, 18: 8387
melting points and vapor pressure, 18: 8386
neutron attenuation by aqueous solutions, 16: 15612 (GA-2544)
neutron spectra for solutions of, 17: 24369(R) (GA-3542)
pharmacological and toxicological effects, 16: 2877 (UCLA-492)
preparation and vapor pressure at 1200 to 1400°C, 18: 8382
preparation of, method for, 18: 6832
properties of aqueous solutions of, thermodynamic and transport, 20: 22968 (IS-1344)
properties of di- and trivalent, review on, 19: 22229
properties of, magnetic and thermal, 20: 43176 (NP-16302)
reactions with gaseous alkali and alkaline earth metals and hydrogen, thermodynamics of, 20: 43222
reactions with isopropylamine, thermogravimetric study of, 20: 36853
reactions with trimethylamine hydrochloride, 19: 42515
solubility of gypsum in aqueous solutions of, 18: 23536
specific gravity and apparent molal volume of aqueous solutions of, at 25°C, 20: 38905
spectra, absorption maxima for calibrating spectrophotometers, 16: 31534
spectra in molten chloride eutectic, near-infrared, 19: 17870
spectra of hydrated, absorption, 16: 31609 (UCRL-6564-T)
spectra of, Zeeman effect in absorption and fluorescence, 17: 8049
spectra of, diffuse reflectance, 18: 13689
spectra of, effects of organic solvents on oscillation absorption bands in, 19: 22192
spectra of, electron-transfer, 20: 25104
structural properties of trichloride, 17: 14210 (NBS-MON-25(Sect.1))
thermodynamic properties of aqueous solutions, 16: 31584 (IS-417)
thermodynamic properties, 18: 10108
vapor pressure, 17: 32118
vapor pressure, 18: 31525
vapor pressure and heat of sublimation, 17: 18086
viscosity of aqueous solutions of, at 25°C, 20: 38904
alkyl aluminum–$SmCl_3$, catalytic effects of, on directional polymerization of 1,3-butadiene in nitrogen, 19: 2318
CsCl–$SmCl_3$, phase diagrams, 18: 43523
HCl–$NdCl_3$–$SmCl_3$–TBP–H_2O, solvent distribution of neodymium and samarium in, 20: 7004 (IS-T-42)
KCl–$SmCl_3$, phase diagrams, 18: 17844
KCl–$SmCl_3$, phase diagram, 18: 17844
KCl–$SmCl_3$, phase diagrams, 18: 43523
KCl–$SmCl_3$–H_2O, phase studies, 17: 35841
KCl–$SmCl_3$–NaCl, phase studies, 19: 40517
KCl–$SmCl_3$, vapor pressure, 18: 25435
$LaCl_3$–$SmCl_3$, phase studies, 20: 8938
RbCl–$SmCl_3$, phase diagrams, 18: 43523
$SmCl_3$–NaCl, phase diagrams, 18: 43523
$SmCl_3$–UO_2Cl_2, fluorescence spectra of, 19: 15548
Sm–$SmCl_3$, phase studies and properties of, 18: 6832

SAMARIUM CHROMATES
preparation and structure, 17: 37238

SAMARIUM CHROMITES
phase studies, 20: 36812
spectra of, infrared, 20: 36807

SAMARIUM COMPLEXES
chloride, stability of, potentiometric determination of, 19: 17904
effects on liver in rats, 18: 13390(R) (ORINS-43)
hexanitrocobaltate, preparation and composition of, effects of temperature on, 20: 29209
luminescence decay times and spectra of, 17: 31980 (CONF-37-4)
luminescence properties of trivalent, 19: 7588
properties as laser material, 17: 25843(R) (AD-282296)
spectra and stability constants, 19: 5873
thiocyanate, solubility and thermal stability of, 20: 45692
trimethylamine chloride, preparation and properties, 19: 42515
with [(2-hydroxyethyl)imino]diacetic acid, dissociation constant of, 19: 38671
with acetic acid chelates, preparation of mixed, 17: 14259
with acetonitrile, pyridinium salts, and triphenylphosphonium, preparation and properties of, 20: 43231
with acetylacetone and dibenzoylmethane, energy transfer and luminescence quenching in, 20: 25052
with α-hydroxyglycolate, isobutyrate, and lactate, formation constants, 16: 11635
with α-hydroxyisobutric acid, ion exchange determination of stability, constants of, 18: 35521
with α-picolinic acid and α-picolinic acid *N*-oxide, stability constants, 19: 13307
with antipyrine-salicylates, benzene solvent extraction studies on, 20: 43256
with benzoylacetonate and dibenzoylmethide, fluorescence decay times of, 17: 12843
with beta-diketones, preparation, 19: 5866
with butyl phosphates, formation and stability of, 20: 26883
with cadmium, cobalt, or zinc and complexone(III), solubility in water and thermal stability, 19: 22239
with citric acid, thermal dissociation of, 17: 1485
with citric acid, preparation and properties of, 18: 41460
with citric and tartaric acids, formation, 16: 193
with dibenzoylmethide, preparation and thermal stability of, 18: 12088
with dibenzoylmethide and hexafluoroacetylacetonate, fluorescence quantum efficiency of, 18: 41428
with dicyclopentadienyl acetate, amide, benzoate, formate, methoxide, and phenoxide, synthesis, 16: 25321(R) (TID-16224)
with diethylenetriaminepentaacetic acid, formation and stability constants of, 17: 16001
with diglycolic acid, stability constant for, 18: 8338
with diglycolic and dipicolinic acids, thermodynamic properties of, 18: 13733
with diketones, spectrofluorometric analysis for, 20: 36722
with dilactic, mandelic, and quinic acids, formation and stability constants of, 20: 12817 (IS-1311)
with dimethyl formamide, preparation and properties of, 20: 35491
with dimethyl formamide, preparation and properties of, 20: 35510
with dimethyl sulfoxide, preparation and composition of, 20: 25051
with DTPA, formation and stability constants of, 17: 32110
with EDTA, heat of formation, 18: 1681

with EDTA, crystal structure of, 18: 12121 (AEET/CD/16)
with EDTA, preparation, composition, and stability of, 20: 29222
with EDTA, structure of, 18: 35547
with Eriochrome Violet B, dropping mercury electrode and polarographic behavior, 16: 14707
with ethylenediaminetetraacetic acid, 16: 5341
with ethylenediaminetetraacetic acid, complex formation and properties, 17: 28913
with gluconic acid in aqueous solution, 16: 9993
with gluconic acid, stability of, 18: 1697
with gluconic acids, stability constants, 19: 40508
with glycine, stability constants for, 19: 22227
with glycolic and lactic acids, thermodynamic properties of, 20: 43215
with glyoxylic acid, formation constant of, 18: 22101
with HEDTA, stability constants of, 16: 32054 (IS-304)
with hydroxycitrate, structure, 18: 43525
with isobutyrate and α-hydroxy- and α,β,β′-trihydroxyisobutyrate ligands, stability constants of, 18: 10124
with kojic acid and 2,4-pentanedione, stability constants of, 19: 2294
with mandelic acid and α-methylmandelic acid, stability of, 20: 40902
with methoxyacetic, propionic, and thioglycolic acids, formation constants of, 18: 17859
with methylethyl and methylpropyl glycolates, stability of, 18: 22095
with nicotinic acid and hexathiocyanatochromium in aqueous solutions, formation and stability of, 17: 18080
with nicotinic acid, formation and stability, 17: 35832
with nitric acid, formation and stability, 16: 31627
with nitrilotriacetic acid, enthalpy and entropy of formation, 16: 11601
with phenanthroline, infrared spectra of, 20: 16437
with phthalocyanine, synthesis and purification of, 18: 17841
with potassium carbonate, distribution coefficient and structure, 16: 22055 (TID-16027)
with S-ethylthioglycolate and mercaptopropionate ions, stability constants of, 17: 25102
with serine, stability and composition, 19: 19874
with serine, stability of, 20: 29208
with sodium triphosphate, preparation, 19: 17880
with tartaric acid and trihydroxyglutaric acid, stability constants for, 20: 36838
with terpyridine, composition and spectra of, 19: 30193
with thenoyltrifluoroacetone, effects of Lewis bases on fluorescence yields of, 19: 7551
with thenoyltrifluoroacetone, magnetic susceptibilities of, 20: 16416(R) (NYO-906-68)
with triphenylphosphine oxide, properties and spectra of, 19: 42466
with triphosphate, stability constants, 17: 2963
with trisbenzoylacetonate and trisbenzoylmethide chelates, luminescence, 16: 14739
with 1,10-phenanthroline, formation and solubility of, 18: 1685
with 1-hydroxycyclopentanecarboxylic acid, stability of, 20: 26910
with 1-hydroxycyclopentanecarboxylic acid, preparation, properties, and structure of, 20: 26837
with 1,10-phenanthroline, magnetic properties and structure of acetate and nitrate, 19: 36405
with 1,10-phenanthroline–thenoyltrifluoroacetone, preparation and luminescence of, 20: 29221
with 2-hydroxybenzophenone, emission spectra of, 17: 6085
with 2,2′-bipyridyl, infrared spectra of, 20: 16437
with 2,2′-dipyridyl, preparation and fluorescence and infrared spectra of, 18: 23500
with 2,2,6,6-tetramethyl-3,5-heptanedione, preparation and volatility of, 20: 7074
with 2,4-pentanedione and bipyridine or 1,10-phenanthroline, spectra and structure of, 20: 26887
with 2,4-pentanedione, luminescence spectra of, (E), 20: 29238
with 2,4-pentanedione, preparation, properties, and solvates, 16: 10016
with 2,4-pentanedione, solubilities of, in solvents, 17: 23446
with 8-quinolinol, composition and thermal stability of, 18: 17784

SAMARIUM COMPOUNDS
analysis for trace elements, spectrographic, 16: 28869 (JEN-107-DQ/I-33)
hyperfine interactions of samarium-149 in samarium iron garnet, (E/T), 19: 8465
magnetic fields in, temperature dependence of effective, 20: 2520(R) (IA-920)
preparation and properties of argentocyanide, 16: 8747
preparation of dicyclopentadienyl chlorides, 16: 9980(R) (TID-15018)
preparation of organic, 17: 3014(R) (TID-17309)
solubility in water and thermolysis of dilitrurate, 18: 31447
with organic acids, preparation and properties, 19: 44028

SAMARIUM ETHYL SULFATES
crystal field cleavage in, 17: 8087
crystal field parameters for, 19: 15545
samarium ion energy levels in, Orbach relaxation mechanism for excited, 20: 30758
spin-lattice relaxation time, 16: 21188
thermal decomposition, effects of atmosphere, particle size, and upheat rate on, 16: 13048

SAMARIUM FERRATES
hyperfine interactions of samarium-149 in, (E/T), 19: 8465
iron-57 magnetic resonance in, 16: 18481
radiation effects on magnetic properties of, neutron, 17: 2042
rare earth ion hyperfine constants in, 18: 22000(R) (AROD-3006:6)
samarium-149 hyperfine interactions in, 19: 39265(R) (IA-1021)

SAMARIUM FERRATES(III)
crystal structure, 19: 46256

SAMARIUM FERROCYANIDES
preparation and properties, 19: 22246
thermal decomposition, 19: 22247

SAMARIUM FLUORIDES
complexes with alkali metal fluorides, formation of, 18: 6798(T) (AEC-tr-6232)
density from melting point to 2500°K, 16: 8740
effects on freezing point depression in sodium fluoride, 18: 5284
optical properties, 16: 26996
preparation and magnetic moments, 20: 7089
preparation, properties, and structure, 17: 15950 (LADC-5566)
solubility in beryllium nitrate solutions, 19: 40670
solubility in molten fluoride mixtures, 16: 23595
structural properties of trifluoride, 17: 14210 (NBS-MON-25(Sect.1))
$LiF–SmF_3$, phase studies, 19: 30149(R) (ORNL-3789(p.3-35))
$NH_4F–SmF_3$, chemical properties and crystal structure, 18: 16013
$SmF_3–NaF$, phase diagrams at 300 to 1300°C, 20: 33278
$SmF_3–NaF$, phase studies, 19: 30149(R) (ORNL-3789(p.3-35))

SAMARIUM FORMATES
decomposition thermograms, 16: 22067(T) (AEC-tr-4460(p.157-62)
preparation and properties, 19: 30163
preparation of, microscopical identification of spherulites in, 18: 10055
structure, 16: 33001

SAMARIUM GALLATES
structural properties of $Sm_3Ga_5(GaO_4)_3$, 17: 14210 (NBS-MON-25(Sect.1))

SAMARIUM GERMANATES
crystal structure of, ir spectral studies on, 20: 43218

SAMARIUM GERMANIUM SULFIDES
preparation and structure of, 20: 23680

SAMARIUM HYDRIDES
crystal structure, 16: 7567
dissociation pressure of, effects of temperature on, 20: 35471 (AWRE-O-31/66)
magnetic moments, 16: 24173(R) (TID-15819)
magnetic properties at 4.2–300°K, 17: 37710
mass spectra of volatile, 17: 6791 (IS-424)
properties and structure, 20: 16453
spectra of, effects of organic solvents on oscillation absorption bands in, 19: 22192
$LiH–SmH_2$, phase studies, 19: 19881

SAMARIUM HYDROXIDES
preparation and properties of, 19: 34153(T) (ORNL-tr-661)
preparation and structure of, 19: 42865
solubility of, photocolorimetric determination of, 17: 1478
thermal decomposition, 17: 32109
thermal decomposition of, thermographic and x-ray studies on, 20: 25061

SAMARIUM HYPOPHOSPHITES
spectra of, infrared and Raman, 18: 35533

SAMARIUM IODATES
solubility of, in water, 20: 45656

SAMARIUM IODIDES
preparation and structure of tri-, 18: 29602 (LADC-6087)
preparation of hydrates of, 18: 39227

SAMARIUM IONS
crystalline electric field for, origin of, (T), 19: 15545
effects on spectrophotometric determination of erbium, holmium, and neodymium, 20: 43100
electrofluorescence of di- and trivalent, in aluminum oxide, 16: 19500
electron energy level schemes and energy matrices, 16: 19499
electron energy levels, 17: 29422
electron paramagnetic resonance in calcium fluorides, relaxation in, 18: 23526
electron paramagnetic resonance of trivalent, in calcium tungstate crystals, (E/T), 19: 34189
electron spin resonance of trivalent, hyperfine structure constants from, 17: 37785
electron spin resonance in calcium fluorides, spectra of, 18: 23524
energy levels in lanthanum chlorides, Orbach relaxation mechanism for excited, 20: 30758
energy levels in samarium ethyl sulfates, Orbach relaxation mechanism for excited, 20: 30758

energy transfer from 4,4′-dimethoxybenzophenone to, effects of terbium ions on two-step, 19: 7387
fluorescence decay in lanthanum chloride crystals, 20: 30782
fluorescence in barium fluoride and strontium fluoride crystals, vibronic spectra of, 18: 10094
fluorescence of divalent, in lanthanum trichloride, 20: 26344 (N-65-34948)
fluorescence of trivalent, in sodium tungstate solution, 20: 43211
fluorescence of trivalent, in potassium oxalate solution, 20: 43212
hydrolysis in aqueous solutions of sodium perchlorate at 25°C, constants for, 20: 43221
hyperfine constants for, in europium and samarium iron garnets, 18: 22000(R) (AROD-3006:6)
hyperfine interactions in tetravalent, constants for, 17: 37686
luminescence of, in aqueous solutions, effects of heavy water on, 20: 26849
magnetic hyperfine interactions and relaxation times, in europium iron garnet, 16: 33628
magnetic properties of, in the iron garnets, 17: 31186
paramagnetic resonance linewidth of trivalent, in lanthanum magnesium nitrate, (E), 19: 5891
polarographic reduction at mercury electrode, reversible and irreversible processes in, 16: 32962
polarography at mercury electrode, derivative, 16: 32963
radiationless transition probability for, in fluorite, 17: 39791(T)
radioinduced fluorescence and reduction in calcium fluorides, impurity effects on, 20: 34831
reactions with Arsenazo III, 18: 6755
reduction in calcium fluoride, yttrium ion effects on, (E), 19: 38595
spectra in acetophenone, energy transfer in, 19: 40504
spectra in alkali halide crystals at low temperatures, absorption and emission, 18: 25406(T)
spectra in alkali halides, emission, 19: 2331
spectra in alkali-earth fluoride crystals, Zeeman effect in, (E/T), 19: 4145(T)
spectra in alkaline earth fluorides, absorption and luminescence, 16: 27803(T)
spectra in alkaline earth titanates as crystal field probe, 18: 31459
spectra in barium fluoride crystals, effects of light on, 16: 27805(T)
spectra in barium, calcium, and strontium fluorides, absorption and luminescence, 19: 19854
spectra in calcination products of magnesium chloride, nitrate, and sulfate, luminescence, 18: 6803
spectra in calcium fluoride, pressure effects, 16: 28954
spectra in lanthanum chlorides, far i-r, 18: 44455
spectra in potassium chloride and sodium chloride crystals, luminescence, 18: 30423(T)
spectra in rubidium chlorides, pseudolocalized vibrational frequencies in, 19: 28319
spectra in silicate glass, fluorescence, 19: 47886(T) (N64-21857, pp 1-6)
spectra of, calculation of nephelauxetic parameters in, 20: 33291
spectra of, effects of chemical bonding and transitions on, 20: 36845
spin-lattice relaxation rates at 1.4 to 5°K for, in double nitrates, 16: 27813
spin-lattice relaxation rate of trivalent, in lanthanum double nitrate at 1.4 to 5°K, 18: 2484
spin-lattice relaxation of trivalent, in lanthanum double nitrate at $T \leq 1.5$°K, direct phonon bottleneck process in, 18: 2485
spin lattice relaxation in rare earth salts at 1.2 to 5°K, (E), 20: 28644
spin-lattice relaxation rate in lanthanum ethyl sulfate crystals, 19: 14121 (AD-608278)
spin-lattice relaxation rates in single crystals of anhydrous lanthanum trichloride, (E), 20: 6542
spin-lattice relaxation of trivalent, in lanthanum chlorides, (E), 20: 12292
spin-lattice relaxation in yttrium ethyl sulfates, (E), 20: 12300
spin-lattice relaxation in lanthanum ethyl sulfates, (E), 20: 12300
spin-lattice relaxation in magnesium lanthanum nitrates, (E), 20: 12300
spin-lattice relaxation time in lanthanum trichloride, angular and temperature effects on, 20: 40350
spin-lattice relaxation of, in lanthanum fluorides, 20: 42540
Stark effect in barium chlorofluoride crystals, 19: 43475
transitions in strontium chloride and strontium fluoride, selection rules and spectra for divalent, 17: 18064
valency in calcium fluoride crystals, electrolytic method for controlling, 18: 22026
valency in calcium fluoride crystals, effects of oxygen on, 19: 41993(T)

SAMARIUM ISOPROPOXIDE
reactions with methyl acetoacetate, 20: 10846

SAMARIUM ISOTOPES
abundance of, mass spectrographic determination of, 18: 8298
alpha decay systematics for, 17: 7199
buildup in reactors, (E), 20: 6589
content in Arkansas rain water in Oct. 1964, 20: 16685
content in meteorites, 17: 25468
decay of compound nucleus of, excitation functions from, (E), 20: 17784
deuteron reactions (d,p), energy levels from, 17: 31482
effects of even, on samarium emission spectra, (E), 20: 10045
energy level structure of odd-A, (E), 19: 41778
energy levels, interactions, nuclear moments, and transitions in, 17: 24381 (AD-403411)
energy levels of even-even, collective, (E), 20: 42265
energy levels of, rotational, (T), 20: 44843
excitation of even-even, by oxygen ions to 65 Mev, (E), 20: 12110
excited states in even, first, 16: 12518
gamma reactions on, cross sections for, 19: 12496
mass differences of, (E), 20: 22153
neutron capture cross sections at 30 kev, 19: 23163(R) (ORNL-3650 (p.111-86))
neutron capture in, 17: 15285
neutron cross sections at 0.025 ev to 10 Mev, 20: 8074 (KFK-352)
neutron resonance integrals for, 17: 22566 (TID-18590)
neutron resonances in, 18: 11195(R) (EANDC(E)-49(L))
nuclear compressibility, 16: 18531
nuclear gyromagnetic ratios and quadrupole moments, 16: 21446
preparation of self-supporting foils of, 20: 31696
production in fission of uranium-233 and -235, poisoning from, 18: 15473 (ORNL-TM-781)
production in plutonium-239 fission, 18: 38085(T) (AEC-tr-6398(p.288-95))
production in thermal-neutron fission of uranium-235, (E), 19: 45260(R) (IDO-14660)
proton reactions (p,p′), energy levels from, 17: 31482
spectra of, volume effects on shifts in, 17: 22580
spectra of, shifts in x-ray, 18: 17064(T)
yields in thorium-232 helium-ion fission, 17: 22567 (UCRL-10673)
yields in uranium-233 thermal fission, (E), 20: 3010(R) (IDO-14663)
yields of, in proton spallation of tantalum at 660 Mev, 18: 4576 (NP-13165(Vol.2)(p.87-100))

SAMARIUM ISOTOPES Sm-140
production and identification of, (E), 20: 28274 (JINR-P-2647)

SAMARIUM ISOTOPES Sm-141
production and identification of, (E), 20: 28274 (JINR-P-2647)

SAMARIUM ISOTOPES Sm-142
penetration range distributions in aluminum from heavy ion-induced reactions, 18: 15274
penetration range distributions in aluminum from heavy ion-induced reactions, 18: 15273
production in heavy-ion induced reactions, recoil range properties of, 17: 33094
production in heavy ion reactions with nuclei, angular momentum effects on excitation functions for, (E), 20: 17784

SAMARIUM ISOTOPES Sm-143
gamma spectra, 20: 44634(R) (IDO-17188)
gamma transitions in, effects of radial matrix elements on probabilities of M4, 18: 2861
half life, 20: 28446
isomeric transition in, 17: 7237
production of isomeric states in yttrium-89 (n,n′γ) reactions at 14 Mev, cross sections for, (E), 19: 41781

SAMARIUM ISOTOPES Sm-144
alpha inelastic scattering at 3 and 4 Mev, K x-ray yield from, (E), 20: 36264
decay of, quasi-particle, 18: 32745(R) (UCRL-11213(p.1-48))
deuteron reactions (d,p), ground-state Q values of, 17: 26628
deuteron reactions (d,3n) at 26 Mev, (E), 19: 14606
deuteron reactions (d,d′γ) at 12 Mev, 0+ states from, 19: 41747
deuteron reactions (d,p) at 12 Mev, samarium-145 energy level from, (E), 19: 41778
deuteron reactions (d,p) at 15 Mev, samarium-145 levels from, (E), 20: 26179
deuteron reactions (d,xn) with, europium-142, -143, and -144 production in, 20: 28446
energy levels, 17: 26628
energy levels from (p,p′γ) and (d,d′γ) reactions at 12 Mev, 0+, (E), 19: 41747
energy levels of, properties of first 2+, (T), 20: 10044
fluorine-19 reactions (F-19, 7n) and (F-19,8n) with, alpha activities from, (E), 19: 16982
gamma scattering by, resonance, 18: 11175 (ANL-6797(p.275-87))
ionization in K-shell by alpha particles at 3 to 4 Mev, x-ray yields from, (E), 20: 2625
mass difference of neodymium-144 and, 18: 32825
neon-20 reactions (Ne-20,6n) and (Ne-20,7n) with, alpha activities from, (E), 19: 16982
neutron capture cross section, thermal, 16: 29840
neutron radiative capture cross sections at 30 kev, 18: 34274(R)

(NIRS-2(p.3-15))
neutron radiative capture cross sections, (T), 19: 19106
neutron reactions (n,2n), isomeric yields, 16: 6253 (ARGMA-TN-2H1N-30)
neutron reactions (n,2n), cross sections for, 16: 7072
neutron reactions (n,2n), cross section for, 17: 7237
neutron reactions (n,2n) at 14 Mev, shell effects in, (T), 19: 12536
neutron reactions (n,2n) at 14 Mev, cross sections for samarium-143 isomeric states from, (E), 19: 41781
neutron reactions (n,2n) at 3 Mev above threshold, cross section for, (E), 20: 46614
nitrogen ion reactions at 44 and 52 Mev, Coulomb excitation in, 18: 7718
oxygen-16 scattering at 31 to 45 Mev, B(E2) values for transitions from, (E), 20: 17734
production in stars, 16: 12308
proton elastic scattering at 10.0 to 10.4 Mev, proton polarization in, (E), 20: 38068
proton inelastic scattering by, isobaric analog states in, 20: 46580(R) (BMwF-FBK-66-05)
proton reactions (p,p'γ) at 12 Mev, 0⁺ states from, (E), 19: 41747
proton reactions (p,n) and (p,p) at 9.2 to 10.8 Mev, isobaric analog states from, (E), 20: 3084
proton reactions (p,n) at 10 Mev, europium-144 production from, (E), 20: 4887
proton spallation products, 16: 15625 (JINR-P-483(Pt.III))
separation from neutron-deficient europium-144, 20: 43067(R) (IDO-14679, pp 6-46)
spectra, isotopic shifts, 16: 19513(T)
spectra of, isotope effects in, 18: 32763
triton reactions (t,p) at 12 Mev, samarium-146 energy levels from, (E), 20: 38052

SAMARIUM ISOTOPES Sm-145
alpha decay energy, 18: 13071
Auger K-electron spectra, 16: 15655
core isomerism in, (T), 19: 17051
decay, auger electron spectra from, 16: 15625 (JINR-P-483(Pt.III))
energy level at 0.90 Mev, spin of, (E), 20: 38068
energy level transitions from europium-145 decay, (E), 20: 22003 (JINR-P-2581)
energy levels, 16: 4824
energy levels, 17: 26628
energy levels from deuteron reactions (d,p) with samarium-144 at 15 Mev, (E), 20: 26179
energy levels from europium-145 decay, spins for, (E), 20: 28291
energy levels from beta decay of europium-145, (E), 20: 44845
energy levels of, from europium-145 decay, (E), 19: 27832 (JINR-P-2052)
energy levels of, parity and spin of, (E), 20: 4838 (JINR-P-2314)
gamma dose constants for, 20: 46617
gamma emission, 16: 24583
gamma spectra, 18: 12498
neutron capture cross section, thermal, 16: 29840
properties for use in radiography of teeth, evaluation of, 19: 13176

SAMARIUM ISOTOPES Sm-146
age estimations using, 20: 33536
alpha activity (E), 19: 1574
alpha decay of, data review on, 18: 13071
alpha decay of, energies and rates for, 18: 26640
alpha decay of, half life and alpha energy in, (E), 20: 46760
buildup in reactors, compensation for, 18: 24853(P)
energy levels, 17: 40040
energy levels, 18: 30760
energy levels and gamma spectra of, 17: 9547
energy levels at 1381 kev from decay of europium-146 and promethium-146, 20: 12081
energy levels of, from europium-146 decay, (E), 20: 3075
energy levels of, properties of first 2⁺, (T), 20: 10044
energy levels of, spin and parity of, (E), 20: 38052

SAMARIUM ISOTOPES Sm-147
alpha decay and half life, 16: 2508
alpha decay energy, 17: 21003
alpha decay energy of, 19: 35615(R) (NP-15037)
alpha decay of, data review on, 18: 13071
alpha decay of, half life and atomic stopping cross sections for, (E), 20: 3028
alpha emission spectra from thick sources, 16: 9449
Coulomb excitation at levels to 1.8 Mev, 18: 9335
Coulomb excitation of, gamma angular distribution in, (E), 19: 16896
determination in uranium-233 and -235 fission products, (E), 20: 11960(R) (IDO-14667)
deuteron reactions (d,p), ground-state Q values of, 17: 26628
deuteron reactions (d,p) at 12 Mev, samarium-148 energy levels from, 18: 6236
energy levels, 17: 26628
energy levels, 20: 6396
energy levels and gamma spectra, 16: 12491
energy levels and gamma spectra, 16: 23095
energy levels and gamma spectra of, from Coulomb excitation, 18: 21350
energy levels and gamma spectra of, 18: 42671
energy levels from europium-147 decay, 16: 28106
energy levels from europium-147 positron decay, (E), 19: 35385 (JINR-P-2166)
energy levels from europium-147 decay, multipolarity and spin of, (E), 20: 30362
energy levels of, parity and spin of, (E), 19: 45267 (JINR-P-2161)
energy levels, probability of transitions between low-lying, 16: 15662
gamma reactions (γ,n) in stars, 16: 12308
gamma spectra from Coulomb excitation of, 17: 31501
half life, 18: 19004
half life, (E), 19: 14613
hyperfine structure and nuclear moments of, 20: 37459
neutron capture at thermal energies, alpha spectra and branching ratios from, 16: 28124
neutron capture cross sections at 10^3 to 10^8 ev, 16: 26518
neutron cross sections at 0.414 ev to 10 Mev, 16: 9427 (GA-2451 (Vol.III))
neutron cross section of, thermal, (E), 20: 46598(R) (RPI-328-68)
neutron radiative capture cross sections at 30 kev, 18: 34274(R) (NIRS-2(p.3-15))
neutron radiative capture cross sections, (T), 19: 19106
neutron reactions (n,α), cross section and Qα for, 19: 35615(R) (NP-15037)
neutron reactions (n,γ), gamma spectra of 3.4-ev resonance of, 19: 39781 (JAERI-1073)
neutron reactions (n,α) up to 200 ev, alpha decay of samarium-148 in, (E), 20: 38072
neutron resonance scattering by, spin of low-energy resonances from, 18: 11183 (ANL-6797(p.363-8))
neutron resonance scattering by spin determination from, (E), 19: 35378(R) (EANDC(E)-57(U))
nuclear magnetic moments, 16: 16831
proton elastic scattering at 55 Mev, effects of nuclear deformation on, 18: 24665
proton elastic scattering at 55 Mev, 19: 29312
proton reactions (p,p') at 4 Mev, energy levels from, (E), 19: 41778
reactions with helium-3 at 15 Mev, cross sections radioisotope produced in, 18: 28743
sorption by humic acids and peat, 16: 11591
spin, 16: 17128
yields from uranium-235 fission by thermal neutrons, 16: 23079
yields from uranium-235 thermal fission, 19: 29313
yields in plutonium-241 thermal fission, (E), 19: 8495
yields in thermal neutron fission of uranium-233 and -235, 20: 43067(R) (IDO-14679, pp 6-46)

SAMARIUM ISOTOPES Sm-148
alpha decay and half life, 16: 2508
alpha decay of excited, lifetime for, (E/T), 20: 28273 (JINR-P-2625)
alpha decay of excited, (E), 20: 38072
alpha decay of, data review on, 18: 13071
decay scheme of excited states, 16: 14025
deuteron reactions (d,p), ground-state Q values of, 17: 26628
deuteron reactions (d,p) at 12 Mev, samarium-149 energy levels from, (E), 19: 41778
energy level at 1.46 Mev, parity and spin of, 18: 21262
energy level de-excitation characters for, experimental 1⁻, 17: 17201
energy levels, 16: 13984
energy levels, 17: 26628
energy levels, 17: 40040
energy levels from europium-148 and promethium-148 decays, 17: 7181
energy levels from promethium-148 beta decay, 17: 26515
energy levels from europium-148 beta decay, 17: 26516
energy levels in, from promethium-148 decay, 16: 28133
energy levels in, from europium-148 decay, 16: 28106
energy levels in, negative parity, (T), 19: 39845
energy levels of, populated by decay of promethium-148, K/L+M conversion ratios of transitions among, 18: 1089
energy levels of, spin assignments for 1.90, 2.09, and 2.19 Mev, 17: 19351
energy levels of, lifetimes of, (E), 19: 16977
energy levels of, properties of first 2⁺, (T), 20: 10044
energy levels of, E1 transition from and lifetime of octupole, (T), 20: 19979
energy levels of, collective, (E), 20: 42265
gamma reactions (γ,n) in stars, 16: 12308
neutron binding energies in, anomalies in, (T), 19: 14523 (JINR-E-1924)
neutron cross sections at 0.414 ev to 10 Mev, 16: 9427 (GA-2451

(Vol.III))
neutron radiative capture cross sections at 30 kev, 18: 34274(R) (NIRS-2(p.3-15))
neutron radiative capture cross sections, (T), 19: 19106
oxygen-16 scattering at 31 to 45 Mev, B(E2) values for transitions from, (E), 20: 17734
production in neutron capture by samarium-147, spin and parity from, 16: 28124
proton inelastic scattering at 12 Mev, energy levels from, 18: 6236
proton scattering at 9.98 to 10.50 Mev, europium-149 analog states from elastic and inelastic, (E), 20: 30430
spectra, isotopic shifts, 16: 19513(T)
spectra of, isotope effects in, 18: 32763
triton reactions (t,p) at 12 Mev, samarium-150 energy levels from, (E), 20: 38052
yields in plutonium-241 thermal fission, (E), 19: 8495

SAMARIUM ISOTOPES Sm-149

abundance in meteorites, 17: 12465
alpha decay and half life, 16: 2508
alpha decay of, data review on, 18: 13071
buildup and decay in natural-uranium fueled gas-cooled graphite-moderated reactors, reactivity controlled by, 18: 1271
concentration by A.W.R.E. isotope separator, 19: 34608
Coulomb excitation at levels to 1.8 Mev, 18: 9335
determination in irradiated uranium rod, mass spectrometric, 17: 33833
determination in uranium-233 and -235 fission products, (E), 20: 11960(R) (IDO-14667)
deuteron reactions (d,p), ground-state Q values of, 17: 26628
deuteron reactions (d,p) at 12 Mev, samarium-150 energy levels from, 18: 6236
energy level at 22 kev, decay and natural width, 16: 12430 (JINR-P-846)
energy level at 22 kev, lifetime of, 18: 1064
energy levels, 17: 26628
energy levels and gamma spectra, 16: 12490
energy levels from europium-149 decay, 16: 12459
energy levels of, spin assignments for low-energy, 17: 855
energy levels of, spin assignments for, 17: 40109
energy levels of, lifetimes of (E), 19: 3300
energy levels of, determination from europium- and promethium-149 decay, 20: 45046(R) (IDO-17192)
energy-level transitions from beta decay of europium-149 and promethium-149, (E), 20: 46751
energy-levels of, hyperfine interactions of, in ferrimagnetic samarium compounds, (E/T), 19: 8465
excited states of, gamma cascade position of 22-kev, 17: 9562
gamma emission at 22 kev, Mössbauer spectra, 16: 23144
gamma reactions (γ,n) in stars, 16: 12308
gamma resonance absorption in, without recoil, 17: 38068 (JINR-P-1231 (p.52-4))
hyperfine interactions of ground- and 22-kev-state in samarium ferrites, 19: 39265(R) (IA-1021)
hyperfine structure and nuclear moments of, 20: 37459
interactions of ground state with 22-kev excited state in, (E), 19: 5569(R) (MIT-2098-64)
internal conversion spectra at 5.2 to 8.0 and 0.3 to 1.4 Mev, 18: 24959 (NP-13910)
magnetic hyperfine interactions in $SmAl_2$, 20: 15992
Mössbauer effect in, 18: 1015 (JINR-P-1370)
Mössbauer effect in, bibliography on, 18: 14650
Mössbauer effect on, use of europium for studies on, 20: 20622
neutron binding energies in, anomalies in, (T), 19: 14523 (JINR-E-1924)
neutron capture at thermal energies, alpha spectra and branching ratios from, 16: 28124
neutron capture by, conversion electron and gamma spectra for thermal, 17: 28305
neutron capture by, gamma spectra from, 18: 24959 (NP-13910)
neutron capture by, thermal, 18: 42622(R) (ANL-6879(p.2-20))
neutron capture by, gamma spectrum from thermal, (E), 19: 23784
neutron capture by, neutron separation energy determination from, (E), 20: 30366
neutron capture by, samarium-150 energy-level spins and transitions from thermal, (E), 20: 46744
neutron capture in, gamma spectrum for thermal, 17: 41527(R) (ANL-6720(p.2-15))
neutron cross sections at 0.414 ev to 10 Mev, 16: 9427 (GA-2451 (Vol.III))
neutron cross section uncertainty, 20: 45193 (CONF-660303, pp 204-9)
neutron effective activation cross section, 16: 9653 (KAPL-2000-16)
neutron radiative capture cross sections at 30 kev, 18: 34274(R) (NIRS-2(p.3-15))
neutron radiative capture cross sections, (T), 19: 19106
neutron reactions (n,α), cross sections for thermal, 16: 33881
neutron reactions (n,γ) with, rotational-vibrational effects on spectra from, 18: 11162 (ANL-6797(p.89-110))
neutron reactions at 0.1 to 0.9 ev, resonances in, 18: 17037
neutron reactions at 0.4 to 8 ev, cross sections for, 18: 36585
neutron reactions (n,α) at 0.004 to 0.1 ev, spectra from, (E), 19: 35378(R) (EANDC(E)-57(U))
neutron reactions (n,α), cross section Qα for, 19: 35615(R) (NP-15037)
neutron reactions (n,γ), gamma spectra of 0.096- and 0.89-ev resonance of, 19: 39781 (JAERI-1073)
neutron reactions (n,α) with, cross sections for thermal, (E), 19: 41809(T)
neutron reactions (n,α) at 0.004 to 0.1 ev, spins of resonances from, (E), 20: 28370
neutron reactions (n,γ) with, conversion electron spectra from, (E), 20: 34637
neutron reactions (n,γ) with, gamma angular correlations from thermal, 20: 36215
neutron reactions (n,α) up to 200 ev, alpha decay of samarium-150 in, (E), 20: 38072
neutron resonance scattering by, spin of low-energy resonances from, 18: 11183 (ANL-6797(p.363-8))
neutron resonance scattering by, spin determination from, (E), 19: 35378(R) (EANDC(E)-57(U))
neutron scattering on resonant nuclei of, complex scattering amplitudes for coherent Bragg resonance, 17: 37798
poisoning efficiency in radiochemical processes, 16: 25415 (ORNL-3309)
production in reactor, equation for calculation as function of time, 16: 15900 (FXM-1484)
proton elastic scattering at 55 Mev, effects of nuclear deformation on, 18: 24665
proton elastic scattering at 55 Mev, 19: 29312
proton reactions (p,xn) with, cross sections, 19: 16840(R) (IDO-17050)
reactor criticality effects of, tables for calculating transients from, 20: 12352 (DP-958)
separation from homogeneous reactor fuel, 17: 9892
spin, 16: 17128
yields from uranium-235 fission by thermal neutrons, 16: 23079
yields from uranium-235 thermal fission, 19: 29313
yields in plutonium-241 thermal fission, (E), 19: 8495
yields in thermal neutron fission of uranium-233 and -235, 20: 43067(R) (IDO-14679, pp 6-46)

SAMARIUM ISOTOPES Sm-150

alpha decay energy, 18: 13071
alpha decay of excited, lifetime for, (E/T), 20: 28273 (JINR-P-2625)
alpha decay of excited, (E), 20: 38072
conversion electron spectra and energy levels from neutron reactions (n,γ) with samarium-149, (E), 20: 34637
decay scheme, 18: 42622(R) (ANL-6879(p.2-20))
decay scheme, 20: 18174(R) (NP-15771)
deuteron reactions (d,p), ground-state Q values of, 17: 26628
deuteron reactions (d,p) at 12 Mev, samarium-151 energy levels from, (E), 19: 41778
deuteron reactions (d,p) with, deformed and spherical nuclei from, (E), 19: 45359
electron conversion in, after neutron capture, (E), 19: 23794
energy level at 1360 kev, spin of, 18: 32864
energy levels, 16: 21396
energy levels, 17: 26628
energy levels, 17: 40040
energy levels, 17: 41873 (WASH-1044)
energy levels, 17: 41527(R) (ANL-6720(p.2-15))
energy levels, 18: 7684 (NP-13420)
energy levels, 18: 11162 (ANL-6797(p.89-110))
energy levels and gamma transitions for, 17: 28305
energy levels at 5 to 8 Mev, transition electron spectra from, (E), 19: 35378(R) (EANDC(E)-57(U))
energy levels from samarium-149 (n,γ) reactions, parity and spin of, (E), 20: 36215
energy levels of, vibrations in low-lying, 18: 18970
energy levels of, parity and spin of, (E), 19: 23674
energy levels of, vibration-rotation interactions in, (T), 19: 41818
energy levels of, rotational, (E), 20: 6348
energy levels of, properties of first 2⁺, (T), 20: 10044
energy levels of, E1 transition from and lifetime of octupole, (T), 20: 19979
energy levels of, spin and parity of, (E), 20: 38052
energy levels of, parity and spin of, (E), 20: 40069(R) (EANDC(E)-66(U))
energy levels of, collective, (E), 20: 42265
energy-level spins and transitions from thermal-neutron capture by samarium-149, (E), 20: 46744
gamma cascade from 440-337 kev transition in, 17: 22651
gamma reactions (γ,n) in stars, 16: 12308
gamma transitions, 18: 24959 (NP-13910)
mass difference of neodymium-150 and, 18: 32825

neutron average effective cross section of, thermal, 17: 3778
neutron binding energies in, anomalies in, (T), 19: 14523 (JINR-E-1924)
neutron capture by, spectra from, 17: 7273
neutron cross sections at 0.414 ev to 10 Mev, 16: 9427 (GA-2451 (Vol.III))
neutron cross sections and resonance integrals, 17: 10506(R) (ORNL-3320(p.1-15))
neutron radiative capture cross sections at 30 kev, 18: 34274(R) (NIRS-2(p.3-15))
neutron radiative capture cross sections, (T), 19: 19106
neutron reactions (n,γ) gamma energy from, 16: 7124
neutron reactions (n,γ), excited energy levels and gamma energies from, 17: 26494
neutron reactions (n,γ) with, rotational-vibrational effects on spectra from, 18: 11162 (ANL-6797(p.89-110))
neutron reactions (n,γ) with, conversion-electron spectrum from, 18: 11165 (ANL-6797(p.148-55))
neutron resonance integral of, 17: 3778
nuclear spin of second excited state of, 17: 22651
oxygen-16 scattering at 31 to 45 Mev, B(E2) values for transitions from, (E), 20: 17734
production from neutron capture by samarium-149, neutron separation energy determination from, (E), 20: 30366
production in neutron capture by samarium-149, spin and parity from, 16: 28124
proton inelastic scattering at 12 Mev, energy levels from, 18: 6236
proton reactions (p,t) at 40 Mev, spectra from, (E), 20: 36176(R) (TID-22971, pp 41-140)
proton reactions (p,γ) in stars, 16: 12308
proton scattering at 10.30 to 10.55 Mev, europium-151 analog states from elastic and inelastic, (E), 20: 30430
spectra, isotopic shifts, 16: 19513(T)
spectra of, isotope effects in, 18: 32763
triton reactions (t,p) at 12 Mev, energy level excitation in, (E), 19: 10323
triton reactions (t,p) at 12 Mev, samarium-152 energy levels from, (E), 20: 38052
yields from uranium-235 fission by thermal neutrons, 16: 23079
yields in plutonium-241 thermal fission, (E), 19: 8495

SAMARIUM ISOTOPES Sm-151

analysis for impurities, spectrographic, 19: 17781(R) (ORNL-3750)
content in rain water, Fayetteville, Arkansas, Oct. 1964, 20: 16663 (TID-21470)
determination in atmosphere, 19: 4375
determination in irradiated uranium rod, mass spectrometric, 17: 33833
determination in uranium-233 and -235 fission products, (E), 20: 11960(R) (IDO-14667)
determination in waste solutions by isotope dilution mass spectrometry, 20: 43068(R) (IDO-14679, pp 47-50)
electron energy level widths for, M, (E/T), 20: 15241 (CONF-233(Vol.3), pp 454-64)
energy level transitions in, multipolarity of 4.821-kev, (E/T), 20: 15241 (CONF-233(Vol.3), pp 454-64)
energy level widths of, transition properties of, 18: 2885
energy levels, 17: 26628
energy levels, 18: 11162 (ANL-6797(p.89-110))
energy levels and decay schemes, 16: 5973
energy levels and gamma spectra, 16: 19800
energy levels from promethium-151 decay, 17: 847
energy levels from promethium-151 decay, 18: 19014
energy levels from beta decay of promethium-151, (E), 20: 46672
energy levels in, 17: 11652
energy levels of, parity and spin for, (E), 19: 31279
gamma emission by, internal conversion coefficients for, (E), 19: 10251 (NP-14498)
gamma reactions (γ,n) in stars, 16: 12308
gamma transition multipolarities, (E), 19: 27452
gamma transitions in, internal conversion spectra from, 18: 17017
ground water contamination by, in Shoal Event, hazards from, 20: 16742 (VUF-1014)
half life of, determination by direct decay, (E), 19: 37847
neutron binding energies in, anomalies in, (T), 19: 14523 (JINR-E-1924)
neutron cross sections at 0.414 ev to 10 Mev, 16: 9427 (GA-2451 (Vol.III))
neutron reactions (n,γ) with, rotational-vibrational effects on spectra from, 18: 11162 (ANL-6797(p.89-110))
neutron resonance integrals for dilute solutions of, (T), 19: 29260 (TID-21744)
neutron total cross sections in thermal energy range, 16: 18460
neutron total cross section measurements on, 18: 2891
preparation of gamma source of, 19: 42775
production in deuteron reactions (d,p) with samarium-150, deformed and spherical shapes from, (E), 19: 45359
sorption by humic acids and peat, 16: 11591
yields from uranium-235 fission by thermal neutrons, 16: 23079
yields from uranium-235 thermal fission, 19: 29313
yields in plutonium-241 thermal fission, (E), 19: 8495
yields in thermal neutron fission of uranium-233 and -235, 20: 43067(R) (IDO-14679, pp 6-46)

SAMARIUM ISOTOPES Sm-152

abundance in meteorites and terrestrial matter, 18: 10753
alpha decay energy, 18: 13071
alpha inelastic scattering at 3 and 4 Mev, K x-ray yield from, (E), 20: 36264
alpha reactions (α,2n) at 18 to 20.5 Mev, gadolinium-154 energy-level transitions from, (E), 20: 44735
axial asymmetry in, 16: 11001
beta-transition probabilities and spectra of, 17: 24389 (JINR-P-1209)
decay of, E2 and K conversion coefficients in, 17: 7203
determination in uranium-233 and -235 fission products, (E), 20: 11960(R) (IDO-14667)
deuteron reactions (d,p), ground-state Q values of, 17: 26628
deuteron reactions (d,p) at 12 Mev, samarium-153 energy levels from, (E), 19: 41778
electron internal conversion coefficients for, total and K-shell, 17: 13552
electron (K) internal conversion coefficient at 122 kev, measurement of, 17: 9501 (IS-590)
electron scattering by, excitation cross sections for, (T), 19: 31290
electron transmission for, Auger, 19: 7539(R) (ORNL-3697(p.131-43))
energy level (4^+) excitation in, double coulomb, 18: 28601
energy level at 122 kev, lifetime of, (E), 20: 40110
energy level at 1576 kev, properties of, 18: 2904
energy level de-excitation characters for, experimental I^-, 17: 17201
energy level decay, 16: 17097
energy level densities and thermodynamic functions for, (T), 19: 33361
energy level lifetime, 122-kev, 16: 5983
energy level transitions in, E2 conversion coefficients of rotational, (T), 19: 21308
energy level transitions in, M1-M3 mixing in gamma angular correlations of 3-2-0, (T), 20: 8116
energy level transitions in, conversion coefficients for E2, (E), 20: 15698 (CONF-233(Vol.2), pp 109-16)
energy level transitions in, conversion coefficients for E2, (E), 20: 15705 (CONF-233(Vol.2), pp 177-90)
energy level transitions in, K and L conversion coefficients for, (E), 20: 36236
energy level transitions in, E2 conversion coefficients for 245-kev, (E), 20: 36239
energy level transitions in, L subshell ratios for E2, (E), 20: 36260
energy levels, 16: 2515
energy levels, 16: 17081
energy levels, 17: 26628
energy levels, 17: 40040
energy levels, 18: 32777
energy levels, (E), 19: 10323
energy levels, (E), 19: 39928
energy levels, 18: 11162 (ANO-6797(p.89-110))
energy levels, (E), 20: 4476(R) (IS-1200(Sect.P))
energy levels from europium-152 decay, (E), 20: 15832
energy levels, g values of first excited states, 16: 21505
energy levels of, electric monopole transitions between, 18: 6252
energy levels of, magnetic moments of 2+, 17: 831
energy levels of, properties of first-excited 2^+, 17: 15289
energy levels of, rotation-vibration, 18: 15206 (TID-20224)
energy levels of, vibrations in low-lying, 18: 18970
energy levels of, properties of octupole, 18: 21172 (JINR-E-1561)
energy levels of, collective, 18: 34913
energy levels of, vibration-rotation interactions in, 18: 34846
energy levels of, gamma vibrational, (T), 19: 14597
energy levels of, lifetimes of, (E), 19: 16977
energy levels of, lifetime of 122-kev, (E), 19: 23781
energy levels of, quadrupole moment for 2^+, (T), 19: 33304
energy levels of, vibration-rotation interactions in, (T), 19: 41818
energy levels of, rotational, (E), 20: 6348
energy levels of, properties of first 2^+, (T), 20: 10044
energy levels of, high-spin rotational, (E/T), 20: 19953
energy levels of, spin and parity of, (E), 20: 38052
energy levels of, collective, (E), 20: 42265
energy levels of, octupole vibrational, (T), 20: 44825
energy states, calculation of collective excitations in, 16: 15674
energy-level transitions from neodymium-150 (α,2n) reactions at 18 to 20.5 Mev, (E), 20: 44735
excitation of rotational levels in, by oxygen ions at 18 to 42 Mev, 17: 41859 (CONF-62-15)
excited state spectrum, first, 16: 17108
gamma angular correlation measurements of, in liquid and solid sources,

18: 1078
gamma decay, angular distribution coefficients, 17: 11647 (UCRL-10202)
gamma reactions (γ,n) in stars, 16: 12308
gamma spectra, E2 emission parameters, 16: 21444
gamma transitions in, particle parameters of, 19: 14641
gyromagnetic ratio of, (E), 20: 8062(R) (COO-720-058)
half life of, (E), 20: 8062(R) (COO-720-058)
half life of first excited state of, 18: 16986
half lives of metastable states of, (E), 19: 31219 (IS-1071)
internal conversion coefficients, 16: 11032
internal conversion coefficients of 2^+–0^+ E2 transitions of, 17: 7079 (IS-272)
ionization in K-shell by alpha particles at 3 to 4 Mev, x-ray yields from, (E), 20: 2625
magnetic hyperfine interactions and relaxation times of ionized, in europium iron garnet, 16: 33628
magnetic properties in europium ferrates, 16: 16832
Mössbauer effect in, bibliography on, 18: 14650
neutron activation of bare and cadmium-clad foils of, 17: 36347(R) (NARF-62-18P)
neutron binding energies in, anomalies in, (T), 19: 14523 (JINR-E-1924)
neutron cross sections at 0.414 ev to 10 Mev, 16: 9427 (GA-2451 (Vol.III))
neutron radiative capture cross sections at 30 kev, 18: 34274(R) (NIRS-2(p.3-15))
neutron radiative capture cross sections, (T), 19: 19106
neutron reactions (n,γ) with, rotational-vibrational effects on spectra from, 18: 11162 (ANL-6797(p.89-110))
neutron reactions (n,γ), activation integral for resonance, (E), 19: 31244 (ZfK-RN-23)
neutron reactions (n,γ), gamma spectra of 8.2-ev resonance of, 19: 39781 (JAERI-1073)
neutron resonance parameters at 8.036 ev, 16: 13999
neutron resonance integrals for dilute solutions of, (E), 19: 29260 (TID-21744)
nitrogen ion scattering at 11 Mev, Coulomb excitation in, 18: 38128
nitrogen-14 inelastic scattering by, Coulomb excitation from, (E), 20: 30488
nitrogen-14 scattering at 52 Mev, interference effects in 2^+ level excitation in, (T), 20: 15768
nuclear deformation parameters, (T), 19: 16952
nuclear magnetic resonance fluorescence in europium, hydrated europium chloride, and europium oxide, (E), 20: 46795
nuclear octupole deformation, 16: 3745
nuclear shape parameters for, 18: 11221
nuclear strength parameter correlation with beta bands in, (T), 20: 38180
nuclear vibrational-rotational interactions in, 18: 34950
oxygen ion reactions with, double Coulomb excitation in, 17: 801 (TID-16963)
oxygen ion reactions at 65 Mev, conversion electron spectra from, 20: 27309
oxygen ion scattering by, Coulomb excitation of 2^+ state in, (T), 19: 33304
oxygen-16 reactions at 65 Mev, multiple Coulomb excitation in, 17: 38284
oxygen-16 reactions at 36.5 to 64.0 Mev, band mixing from multiple Coulomb excitation in, 18: 1072
oxygen-ion scattering at 35 Mev, lifetime of 2^+ levels from, (E), 20: 12020
oxygen-16 inelastic scattering at 43.5 Mev, vibrational-state excitation in, (E), 19: 45321
oxygen-16 reactions at 18 to 42 Mev, level excitation in, 18: 24727
oxygen-16 scattering at 38 to 48 Mev, level excitation in, 18: 24729
oxygen-16 scattering at 57 Mev, level excitation in, 18: 24730
oxygen-16 scattering by, excitation of rotational states in, (T), 19: 33367
performance of activation detectors of, for neutron flux measurements, 20: 33636
proton reactions (p,t) at 40 Mev, spectra from, (E), 20: 36176(R) (TID-22971, pp 41-140)
proton reactions (p,γ) in stars, 16: 12308
proton scattering at 3 Mev, energy spectra of, (E), 20: 8062(R) (COO-720-058)
proton scattering at 10.3 to 10.6 Mev, europium-153 analog states from elastic, 20: 30430
reactions with oxygen-16, gamma spectra from, 18: 32777
rotation states of deformed axial symmetry in, 17: 19282
scattering resonances in, interference between, 17: 7109 (NP-12330 (p.147-51))
spectra, isotopic shifts, 16: 19513(T)
spectra of, isotope effects in, 18: 32763
transitions in, conversion coefficients of E2, 18: 42769
transitions in, particle parameters of E2, (E), 19: 21399
triton reactions (t,p) at 12 Mev, samarium-154 energy levels from, (E), 20: 38052
x-ray spectra from μ^- mesic atoms of, (E/T), 20: 42310
yields from uranium-235 fission by thermal neutrons, 16: 23079
yields from uranium-235 thermal fission, 19: 29313
yields in plutonium-241 thermal fission, (E), 19: 8495
yields in thermal neutron fission of uranium-233 and -235, 20: 43067(R) (IDO-14679, pp 6-46)
Zeeman splitting, g values, 16: 5824

SAMARIUM ISOTOPES Sm-153

beta decay of, gamma spectrum from, 18: 21271
beta emission, 16: 8197
beta spectra, 18: 42781
beta transitions in, polarization from, (E), 20: 4880
content in rain water, Fayetteville, Arkansas, Oct. 1964, 20: 16663 (TID-21470)
conversion lines of 70-kev gamma ray of, K and L, (E), 19: 33353
decay, (E), 20: 1178
decay, europium K-Auger-spectrum from, 16: 7030
decay, europium-153 levels from, 16: 7031
decay half life, from (n,γ) reactions, (E), 19: 31244 (ZfK-RN-23)
decay of, gamma transitions in, (E), 20: 15795
determination by autoradiographic measurement of half life using ring oven methods, 20: 18584
determination by neutron activation, in ceramic-coated fuel elements, 19: 28255
diffusion in irradiated artificial graphite, 18: 632
distribution and volatility in air-burst debris, 20: 9184 (USNRDL-TR-933)
distribution from nuclear excavation in basalt, 20: 613
energy levels, 17: 26628
energy levels, 18: 11162 (ANL-6797(p.89-110))
energy levels, 18: 42622(R) (ANL-6879(p.2-20))
energy levels of, single quasiparticle, (T), 19: 17052
energy levels of, spectra from, 19: 35615(R) (NP-15037)
gamma dose constants for, 20: 46617
gamma emission, 16: 24583
gamma spectra, 17: 34966
gamma spectra, (E), 20: 15734 (ZfK-PhA-18)
half life, 16: 2541
half life, 17: 38111
half life, (E), 20: 14461(R) (ORNL-3889, pp 48-70)
neutron binding energies in, anomalies in, (T), 19: 14523 (JINR-E-1924)
neutron reactions (n,γ) gamma energy from, 16: 7124
production in neon-22 and oxygen-18 reactions with thorium-232, 18: 24690
properties for steam density measurement in boilers, 18: 14305
radioactivity, 19: 17368
use of portable sources of, for diagnostic radiography, 18: 3634
yields in proton fission of uranium-238 at 7.1, 9.4, and 12.0 Mev, 20: 37995

SAMARIUM ISOTOPES Sm-154

alpha inelastic scattering at 3 and 4 Mev, K x-ray yield from, (E), 20: 36264
alpha reactions (α,4n) at 40 Mev, conversion electron anisotropy from, (E), 19: 45352
alpha reactions (α,2n) at 18 to 20.5 Mev, gadolinium-156 energy-level transitions from, (E), 20: 44735
determination in uranium-233 and -235 fission products, (E), 20: 11960(R) (IDO-14667)
deuteron reactions (d,p), ground-state Q values of, 17: 26628
deuteron reactions (d,p) at 12 Mev, samarium-155 energy levels from, (E), 19: 41778
deuteron scattering at 11 Mev, 16: 21504
electron tunneling in, quantum mechanical fluctuation effects on, 20: 38408
energy level (4^+) excitation in, double coulomb, 18: 28601
energy level transitions in, E2 conversion coefficients of rotational, (T), 19: 21308
energy levels, 17: 26628
energy levels, 18: 18956
energy levels of, vibrations in low-lying, 18: 18970
energy levels of, properties of octupole, 18: 21172 (JINR-E-1561)
energy levels of, collective, 18: 34913
energy levels of, quadrupole, 18: 36684
energy levels of, gamma vibrational, (T), 19: 14597
energy levels of, corrections in Bohr-Mottelson model for rotational, 19: 17048
energy levels of, properties of first 2^+, (T), 20: 10044
energy levels of, quadrupole motion in, (T), 20: 28289 (UCRL-16768)
energy levels of, spin and parity of, (E), 20: 38052
energy levels of, properties of, 20: 38408
energy levels of, collective, (E), 20: 42265
energy levels with spin and parity 4^+ and 6^+ produced by cascade Coulomb excitation with nitrogen-14 ions at 50 Mev, 17: 7290

gamma reactions (γ,p) on, promethium-153 from, 17: 9543
gamma spectra, E2 emission parameters, 16: 21444
gyromagnetic ratio of, (E), 20: 8062(R) (COO-720-058)
internal conversion coefficients, 16: 11032
ionization in K-shell by alpha particles at 3 to 4 Mev, x-ray yields from, (E), 20: 2625
neutron binding energies in, anomalies in, (T), 19: 14523 (JINR-E-1924)
neutron cross sections at 0.414 ev to 10 Mev, 16: 9427 (GA-2451 (Vol.III))
neutron radiative capture cross sections at 30 kev, 18: 34274(R) (NIRS-2(p.3-15))
neutron radiative capture cross sections, (T), 19: 19106
neutron reactions (n,2n), cross sections for, 16: 7072
neutron reactions (n,2n) at 14 Mev, shell effects in, (T), 19: 12536
nitrogen ion scattering at 11 Mev, Coulomb excitation in, 18: 38128
nuclear rotations, 16: 11042
oxygen ion reactions with, double Coulomb excitation in, 17: 801 (TID-16963)
oxygen-16 inelastic scattering at 43.5 Mev, vibrational-state excitation in, (E), 19: 15321
proton reactions (p,γ) in stars, 16: 12308
proton scattering at 11 Mev, 16: 21504
spectra, isotopic shifts, 16: 19513(T)
spectra of, isotope effects in, 18: 32763
triton reactions (t,p) at 12 Mev, samarium-156 energy levels from, (E), 20: 38052
yields from uranium-235 fission by thermal neutrons, 16: 23079
yields from uranium-235 thermal fission, 19: 29313
yields in plutonium-241 thermal fission, (E), 19: 8495
yields in thermal neutron fission of uranium-233 and -235, 20: 43067(R) (IDO-14679, pp 6-46)

SAMARIUM ISOTOPES Sm-155

beta and conversion electron spectra, 17: 21023
beta decay of, coincidence measurements for, (E), 19: 31276
beta spectra, (E), 20: 35741 (CEA-R-2950)
decay of, europium-155 energy-level transitions from, (E), 20: 44736
energy levels, 17: 26628
energy levels of, single quasiparticle, (T), 19: 17052
gamma dose constants for, 20: 46617
gamma spectra, 17: 34966
gamma spectra, 18: 1050

SAMARIUM ISOTOPES Sm-156

beta decay of, europium-156 levels from, (E), 20: 28392
beta decay scheme, 16: 13957(R) (NP-11403)
beta decay scheme, (E), 19: 21350
decay of, half life from beta and gamma, 17: 26587
decay scheme, 19: 32680(R) (IDO-17052)
energy levels of, spin and parity of, (E), 20: 38052
production in neon-22 and oxygen-18 reactions with thorium-232, 18: 24690

SAMARIUM ISOTOPES Sm-157

book: *Isobaric Nuclei with Mass Number A = 157*, 20: 26232
half life, (E), 20: 46628

SAMARIUM ISOTOPES Sm-158

half-life, (E), 20: 46628

SAMARIUM LACTATES

preparation, 20: 22998

SAMARIUM MOLYBDATES

physical properties at 600 to 1325°C, 16: 13003(R) (NP-11299)
preparation and crystal structure of, 20: 31740

SAMARIUM NIOBATES

distribution in strontium molybdate single crystals, coefficients of, 20: 29746
preparation and properties of ortho-, 18: 5307
preparation and structure of, 18: 12673
preparation and structure of perovskite type, 20: 844
$CaMoO_4$–$SmNbO_4$, fluorescence spectra, 18: 26017
$CaMoO_4$–$SmNbO_4$, preparation and spectra of, 18: 26017
$CaWO_4$–$SmNbO_4$, preparation, luminescent properties, and structure of, 18: 26017

SAMARIUM NITRATES

analysis of, for gadolinium, 17: 21661
binding energies in, infrared spectral studies of, 20: 40886
complex formation with dipyridine, 18: 1686
neutron spectra for solutions of, 17: 24369(R) (GA-3542)
nitrogen-14 NMR, (E), 20: 12325
preparation and properties of crystalline hexahydrate, 19: 7375
radiosensitivity and toxic effects in rats, 16: 18763(R) (NP-11660(p.59-66))
separation by solvent extraction using TBP, calculation of cascade stagewise conditions for, 18: 20098 (IS-780)
separation by solvent extraction using organophosphorus compounds, 19: 24629
separation from aqueous solutions by solvent extraction using TBP-nitric acid system, 17: 37307
solubility in TBP, 18: 13927
solubility polytherms of systems with other ceric earths, 18: 20108
solvent extraction behavior in nitric acid–TBP–water systems, 16: 87 (IS-335)
specific gravity of aqueous solutions of, 20: 40796(R) (IS-1500(Sect.C))
spectra in solution, absorption, 17: 35684 (IA-809)
spectra of solid, electron transfer, 20: 35506
thermal decomposition at 25 to 1500°C, 17: 145 (BM-RI-6060)
thermal decomposition at 25 to 1400°C, thermogravimetric analysis of, 18: 25354
toxic effects in rats with and without whole-body x irradiation, effects of saline-sucrose solution on, 16: 26657(R) (NP-11966(p.27-35))
toxic effects on rats, 16: 14463(R) (NP-11359(p.97-105)
toxicity in mice and rats, 18: 17458

SAMARIUM NITRIDES

magnetic properties, 19: 38067
magnetic properties at 2 to 300°K, 20: 43939
properties of, electric and magnetic, 17: 32081

SAMARIUM OXALATES

carbon-14 exchange between, and alkali metal oxalates, 20: 45634
crystal structure of monoclinic decahydrate of, 20: 36835
dynamic decomposition of, effects of air, carbon dioxide, and nitrogen on, 18: 23507
magnetic susceptibility of hydrated, (E), 20: 3930
solubility in EDTA at 25 and 40°C, 19: 9149
spectra of hydrate of, infrared, 20: 8898
spectra of solid, electron transfer, 20: 35506
spectra of, electron-transfer, 20: 25104
thermal decomposition at 340 to 440°C, 16: 11633
thermal decomposition at 25 to 1500°C, 17: 145 (BM-RI-6060)
thermal decomposition of hydrated, 18: 8377
thermal decomposition at 25 to 1400°C, thermogravimetric analysis of, 18: 25354
thermal dissociation of hydrates of, 20: 35509

SAMARIUM OXIDES

analysis, neutron activation, 16: 25292
atomic charge and permittivity of, (E/T), 19: 47901(T)
catalytic effects on dehydrogenation of cyclohexane, 16: 110
catalytic effects on dehydrogenation of cyclohexane at 515 to 590°C, 19: 30222
catalytic properties, 17: 2991
compatibility and encapsulation with alloys and metals, 20: 11267 (BNWL-SA-488)
composition of, prepared by heating at 1100 to 1250°C in sealed silica capsules, 20: 26340(R) (AD-631987)
content in mckelveyite uranium mineral, 19: 40799
crystal structure of, effects of pressure on polymorphism in, 19: 17885
crystal structure of sesqui-, modifications and phase transformations, 19: 30727 (BM-RI-6616)
crystal structure and petrography of, 20: 24590 (ORNL-P-1158)
crystalline parameters and transformations of, stable above 2000°C, 20: 23679
crystallographic modifications and phase transformations of, 20: 16489
determination by neutron activation, in ceramic-coated fuel elements, 19: 28255
determination in uranium dioxide fuel pellets, 20: 41112 (IITRI-578P11-54)
diffusion of oxygen in, tracer studies for determining activation energies for, 20: 38865(R) (COO-1109-22, Paper 4)
effects on conversion reactions of butane, catalytic, 19: 26373
effects on hydrogen oxidation, catalytic, 19: 26343
effects on optical properties of silicate glasses, 19: 44030
electric properties, 19: 28825
electronegativity and ion radii of, prediction of phases in binary systems with other oxides from, 19: 23061
entropy and heat content at high temperatures, 16: 30356 (BM-RI-6033)
fabrication, 18: 35932(R) (HW-81600(p.2.1-23))
hardness and melting point, 20: 5845
heat of formation on hot metal surfaces, 20: 31225
neutron absorption by strips of, in reactor control systems, 18: 28943
oxygen-18 exchange between molecular oxygen and, 19: 46266
performance with photographic film as slow-neutron detector, 17: 3332
phase studies at 400 to 2200°C, 20: 25048
phase studies of, at 2200 to 2300°C, 20: 1827
phase transformations in, 17: 32058
phase transformations in, at 1800 to 2400°C, 19: 44731
phase transformations in, at 50 to 1500°C, 20: 5536
phase transformations in, at high pressure and 550 to 1450°C, 20: 26833
physical properties at 600 to 1325°C, 16: 13003(R) (NP-11299)
polymorphism, 16: 3014
polymorphism of trivalent, 17: 28905

preparation and crystal structure of SmO, 20: 26907
preparation by thermal decomposition of carbonates, nitrates, oxalates, and sulfates, 17: 145 (BM-RI-6060)
preparation of concentrated, by fractional crystallization, 18: 8449
preparation of divalent, 20: 13260(R) (NP-15852)
preparation of lower, 20: 38867(R) (COO-1109-22, Paper 6)
preparation of pure, by fractional crystallization, 18: 8450
preparation of samarium phosphide from, at high temperatures, 20: 25046
preparation of, methods for, 20: 17007(R) (AD-627468)
properties for use with lead oxide and silicate as neutron-trapping material, 19: 23941
properties of, 18: 35932(R) (HW-81600(p.2.1-23))
properties of, chemical and physical, 19: 11120
properties of, effects of temperature on mechanical and physical, 17: 16760
proton reactions at 590 Mev and 18 Bev, yields of iodine isotopes from, (E), 20: 22045
radiation effects, 17: 8886 (NAA-SR-6514)
radiation effects on catalytic activity of, in decomposition of hydrogen peroxide, 20: 43364
radiation effects on mechanical and physical properties of, 17: 16760
reactions with alkali metal salts(liquid), 16: 18917
reactions with barium carbonates, ternary oxide formation, 19: 46242(R) (TID-22207, Paper B)
reactions with boron, 19: 15502
reactions with boron oxides at high temperatures, 20: 16489
reactions with calcium fluoride, 16: 32050
reactions with melted fluorides, 17: 32111
reactions with rhodium oxides, 17: 39044
reactions with samarium in silica capsules, formation of samarium silicates by, 20: 13260(R) (NP-15852)
reactions with sodium metaphosphate, spectra of compound formed in, 19: 38668
reactions with uranium dioxides, 18: 26896(R) (ANL-6868(p.133-74))
reduction by lanthanum, 16: 22086
reduction by lanthanum, thermal, 20: 25087
reduction of, by cerium at 1200°C, 20: 33303
refraction of, calculation of molar and specific, 19: 13395
samarium absorption spectra in, fine structure of L_{III}, 18: 39195
samarium-149 gamma resonance absorption in, 17: 38068 (JINR-P-1231 (p.52-4))
separation from europium, polarographic, 17: 10572
separation of, from silicon oxides in liquid state, 17: 14287
solubility in boiling water, 17: 32058
solubility in ethyl, isopropyl, methyl, and propyl alcohols in presence of ammonia, 20: 20686
spectra at 200 to 1600°C, emission, 17: 30510 (IS-578)
spectra in low frequency region, infrared, 18: 23549
spectra of, infrared absorption, 17: 27840
spectra of, x-ray absorption, 19: 30194
spectral properties of rare earth-activated, 18: 13868
structure of B-form, at 1260 to 2100°C, 17: 35817
thermal expansion at 25 to 1000°C, 17: 14813 (BM-RI-6180)
thermodynamic properties, 16: 96 (TID-14101)
thermodynamic properties, 16: 25386
thermodynamic properties at 10 to 350°K, 16: 26963 (TID-16400)
toxicity in mice and rats, 18: 17458
use as neutron absorber in glasses, 20: 12273(P)
use as thermal-neutron absorber in paints, 18: 13184(P)
actinide oxides–Sm_2O_3, preparation of sols of, 20: 39341(P)
Al–Cr–Ni–Sm_2O_3–Ti, properties as reactor control material, 18: 42889
Al_2O_3–Sm_2O_3, phase studies, 16: 27642(T) (FTD-TT-62-505)
Al_2O_3–Sm_2O_3, phase studies, 20: 25053
Al_2O_3–Sm_2O_3, phase studies, 20: 45639
BaO–Sm_2O_3, optical properties of compounds formed in, 20: 13278
BaO–Sm_2O_3, phase studies, 20: 302
BeO–Sm_2O_3, fabrication, 16: 25734 (NAA-SR-7293)
BeO–Sm_2O_3, phase studies, 16: 27642(T) (FTD-TT-62-505)
B_2O_3–Sm_2O_3, liquid immiscibility in, 20: 40910
CaO–Sm_2O_3–UO_2–ZrO_2, corrosion and surface properties of, 20: 16089(R) (WAPD-MRP-114)
CeO_2–Sm_2O_3, equilibrium phase studies on, 18: 23509
CeO_2–Sm_2O_3, fluorescence properties of, 20: 16466(T)
Cr_2O_3–Sm_2O_3, phase diagrams, 20: 8937
Cr–Sm_2O_3, phase studies, 20: 8937
Eu_2O_3–Sm_2O_3–UO_2, preparation for burnable poison fuel elements, 19: 2779
Fe_2O_3–PbF_2–PbO–Sm_2O_3, crystal growth in, composition diagrams for, 19: 17902
Fe_2O_3–Sm_2O_3, crystal structure and magnetic properties, 20: 4411
Ga_2O_3–MoO_3–Sm_2O_3, crystal growth in, composition diagrams for, 19: 17902
Ga_2O_3–PbF_2–PbO–Sm_2O_3, crystal growth in, composition diagrams for, 19: 17902
IrO_2–Sm_2O_3, phase studies in air, 19: 32751
La_2O_3–Sm_2O_3–SiO_2, phase studies, 16: 18870
Nb_2O_5–Sm_2O_3, properties and structure of compounds formed in, 18: 34199
Nd_2O_3–Sm_2O_3, phase transformation in, x-ray study of, 16: 10566
$PaO_{2.5}$–$SmO_{1.5}$, fluorite phase in, 19: 24511
PbO–Sm_2O_3, phase studies on, 19: 14011
PrO_2–Sm_2O_3, preparation and phase studies of, 20: 26908
ReO_2–Sm_2O_3, magnetic properties and structure of compounds formed in, 20: 36784(R) (AD-636054)
ReO_2–Sm_2O_3, preparation and ferromagnetic properties of phases in, 20: 13260(R) (NP-15852)
Sm_2O_3–SiO_2, phase diagram, 16: 6736
SmO–SiO_2, preparation and crystal structure, 19: 38621
Sm_2O_3–SiO_2, preparation, properties, and structure of $Sm_4(SiO_4)_3$ in, 20: 36784(R) (AD-636054)
SmO–SiO_2, spectra and crystal structure of, infrared, 19: 38622
Sm_2O_3–SrO, optical properties of compounds formed in, 20: 13278
Sm_2O_3–SrO, phase studies, 20: 302
Sm_2O_3–Ta_2O_5, crystal structure, preparation, and properties, 19: 32749
Sm_2O_3–Ta_2O_5, properties and structure of compounds formed in, 18: 34199
Sm_2O_3–TiO_2, phase studies, 19: 32752
Sm_2O_3–TiO_2, phase studies, 19: 42464
Sm_2O_3–UO_2, corrosion by steam at 650°C and water at 360°C, 18: 25919(R) (ANL-6868(p.190-200))
Sm_2O_3–UO_2, preparation by pneumatic impaction, 18: 29001(R) (HW-79280(p.5.1-25))
Sm_2O_3–UO_2, samarium oxide distribution in impacted, 18: 12547(R) (HW-76303(p.3.1-37))
SmO–W, fabrication and properties, 17: 34330(R) (USBM-U-1057)
Sm_2O_3–WO_3, phase studies, 19: 5858
Sm_2O_3–WO_3, phase studies at 800 to 1700°C, 20: 25586
Sm_2O_3–W–WO_3, phase diagrams at 1400 and 1700°C, 20: 25586
Sm_2O_3–ZrO_2, electric conductivity, 19: 37094
Sm_2O_3–ZrO_2, phase studies, 19: 42464
Sm_2O_3–ZrO_2, phase transformations in, fluorite, 19: 358(T) (ORNL-tr-201)

SAMARIUM OXYBROMIDES
preparation and crystal structure, 20: 1834
preparation and structure of, 20: 869

SAMARIUM OXYCHLORIDES
spectra of, electron-transfer, 20: 25104
structural properties, 17: 14210 (NBS-MON-25(Sect.1))

SAMARIUM OXYFLUORIDES
preparation and properties, 18: 17839

SAMARIUM OXYSULFIDES
properties of crystals of, chemical and physical, 17: 8080

SAMARIUM OXYTELLURIDES
preparation and properties, 17: 2975
preparation and properties, and crystalline structure, 17: 6068

SAMARIUM PERCHLORATES
crystal structure of hydrated, 17: 19995
magnetic susceptibility of hydrated, (E), 20: 3930
reactions of, with *N,N*-dimethylacetamide, adduct formation in, 19: 36397
spectra of, effects of organic solvents on oscillation absorption bands in, 19: 22192
stability constants of, thermal, 19: 40509
thermal decomposition of, differential thermal analysis and thermogravimetric studies on, 18: 25396
dioxane–$Sm(ClO_4)_3$, magnetic susceptibility of hydrated, (E), 20: 3930

SAMARIUM PERRHENATES
preparation and properties of, 20: 43217

SAMARIUM PHOSPHATES
preparation and single crystal growth of ortho-, 18: 25356
preparation and ultraviolet absorption spectra, 19: 22172
spectra of solid, electron transfer, 20: 35506
spectra of, electron-transfer, 20: 25104
structure, 19: 42458 (NP-15162)

SAMARIUM PHOSPHIDES
preparation and physicochemical properties of, 20: 45686
preparation from oxide at high temperatures, 20: 25046

SAMARIUM PYROPHOSPHATES
preparation and properties, 18: 41454
preparation and properties, 19: 38616

SAMARIUM SELENIDES
crystal structure, 17: 32125
crystal structure, 18: 1628
crystal structure of, reflection spectra for zonal, (E), 20: 40339
electric conduction in, 18: 37115 (ANL-6856)
electric conductivity and properties of, 18: 42068
electron structure of mono-, electric conductivity and magnetic sus-

ceptibility from, 17: 32082
preparation and properties of Sm_2Se_4, 20: 45689
preparation of, by selenite reduction, 19: 36426
preparation, semiconducting properties, and structure of, 19: 22965 (AL-TDR-64-239)
properties, 16: 32068
reactions with gallium selenides, 18: 41384
structure and electric properties, 16: 15260(R) (AD-262215)
thermoelectric properties of sesqui-, 17: 11292 (AD-277043)
thermoelectric properties, 17: 11296 (AD-278352)
NdSe–SmSe, electric conductivity and properties of, 18: 42068
CaSe–Sm_2Se_3, phase studies, 20: 10857

SAMARIUM SILICATES
crystal structure, 20: 26356
preparation of $Sm_2O(SiO_4)$ monocrystals, 20: 40919

SAMARIUM SILICIDES
crystal structure, 19: 11125
crystal structure, 19: 32755
crystal structure, 19: 40477
oxidation by air at 500°C, 17: 34330(R) (USBM-U-1057)
preparation and crystal structure of, 20: 19224
preparation of lower, 20: 38867(R) (COO-1109-22, Paper 6)

SAMARIUM SULFATES
see also Ammonium Samarium Sulfates
crystal structure of, infrared spectral studies on, 20: 43219
dissociation in water, constants and spectra of, 18: 23501
heat of dehydration, 16: 1783
paramagnetic resonance of trivalent gadolinium ions in octohydrate, zero-field, 16: 16384
preparation, properties, and structure, 17: 15950 (LADC-5566)
reduction of anhydrous, by carbon monoxide, 18: 25427
spectra of solid, electron transfer, 20: 35506
spectra of, electron-transfer, 20: 25104
thermal decomposition, 16: 26993
thermal decomposition at 25 to 1500°C, 17: 145 (BM-RI-6060)
thermal decomposition at 25 to 1400°C, thermogravimetric analysis of, 18: 25354
$Sm_2(SO_4)_3$–Na_2SO_4, thermal stability, 19: 40511

SAMARIUM SULFIDES
crystal structure, 18: 1628
crystal structure of, reflection spectra for zonal, (E), 20: 40339
crystal structure, 17: 32125
electric properties at 80 to 1700°K, 18: 37719(T)
electric properties of, 19: 32171
electric properties and transport mechanism, (E), 20: 15981(T)
electron structure of mono-, electric conductivity and magnetic susceptibility from, 17: 32082
magnetic susceptibility at 290 to 1300°K, 19: 41060(T)
preparation and structure of poly-, 18: 10063
preparation by sulfonation of oxide using carbon disulfide, 19: 19927
properties of crystals of, chemical and physical, 17: 8080
properties of, electric and magnetic, 17: 32081
samarium valence states in, x-ray spectroscopic studies of, 20: 32720(T)
semiconductor properties, 16: 1691
spectra of, nephalauxetic effect in reflection, 19: 36390
thermal conductivity at 80 to 460°K, 18: 42079(T)
Ce_2S_3–SmS, compound formation in, 20: 16431
Dy_2S_3–SmS, compound formation in, 20: 16431
EuS–Sm_2S_3, compound formation in, 20: 16431
Gd_2S_3–SmS, compound formation in, 20: 16431
La_2S_3–SmS, compound formation in, 20: 16431
Nd_2S_3–SmS, compound formation in, 20: 16431
Pr_2S_3–SmS, compound formation in, 20: 16431
Sm_2S_3–Ag_2S, crystal structure, 20: 26829
SmS–Tb_2S_3, compound formation in, 20: 16431
Sm_2S_3–YbS, compound formation in, 20: 16431

SAMARIUM SYSTEMS
CeO_2–La_2O_3–Sm, fluorescence properties of, 20: 16466(T)
CeO_2–Sm–ThO_2, samarium fluorescence in, 20: 16466(T)
O–Sm, phase studies and atmospheric corrosion of, 16: 5315 (WADD-TR-61-123)
O–Sm–Ti, reactions in gases, properties of compounds formed by, 20: 45640
O–Sm–W, phase studies, 20: 5851
O–Sm–W, phase studies at 1400 to 1700°C, 20: 25586
Sm–H_2O, neutron reactions with, 18: 7656 (AE-125)
Sm–H_2O, neutron spectra in, 18: 34733
Sm–H_2O, neutron spectra in, thermal, 19: 42037 (BNWL-95, pp 4-17)
Sm–Se, preparation, phase studies, and properties of compounds in, 19: 5862
Sm–Si, physical properties, (E), 19: 16188
Sm–$SmCl_3$, phase studies and properties of, 18: 6832
Sm–Te, preparation, phase studies, and properties of compounds in, 19: 5862

SAMARIUM TANTALATES
fluorescence spectra, 18: 26017
preparation and structure of, 18: 12673
preparation and structure of perovskite type, 20: 844
preparation, properties, and structure of, 18: 1691

SAMARIUM TELLURIDES
composition and crystalline parameters of, 17: 20008
crystal structure, 17: 32125
crystal structure, 18: 1628
electric conductivity and properties of, 18: 42068
electron structure of mono-, electric conductivity and magnetic susceptibility from, 17: 32082
preparation and crystallographic parameters of, 17: 18023
preparation, properties, and stability of, 20: 26844
preparation, semiconducting properties, and structure of, 19: 22965 (AL-TDR-64-239)
properties, 16: 32068
structure and electric properties, 16: 15260(R) (AD-262215)
Ga_2Te_3–Sm_2Te_3, compound formation and semiconductor properties in, 20: 27503

SAMARIUM, TRISCYCLOPENTADIENYL-
preparation by reaction of samarium fluoride with magnesium cyclopentadienide, 20: 35493

SAMARIUM TUNGSTATES
preparation and crystal structure of, 20: 31740
preparation and properties of single-crystal bronze, 20: 33281

SAMARIUM VANADATES
preparation and properties, 19: 22245

SAMARSKITES
age estimation by complete lead method, 16: 27458
age estimation of, by uranium–krypton and uranium–xenon methods, 19: 46598
analysis for niobium and tantalum by ion exchange, 16: 16312
analysis of, for niobium and tantalum by column extraction, 20: 43131
chemical properties, comparison with ampangabeites, 17: 32270
krypton and xenon contents of, 19: 46598
separation of niobium, tantalum, and uranium from, by solvent extraction, 17: 20110

SAMPLING
adsorption effects in instruments for radioisotope, 18: 35773(R) (UCRL-7811)
at high altitude, design of air ejector pump for, 17: 1709 (TID-16973)
bottle-handling sealing methods for uranium concentrate, 16: 16474 (MCW-1455)
card holder design for air, 20: 39253
collector design for atmospheric, 20: 14815 (COO-401-139)
design and calibration of cascade impactor for field survey, 16: 1957
design and calibration of continuous proportional sampler for rivers and streams, 16: 10217
design of apparatus for flow along large channels, 18: 12431(P)
design of automatic changer, 16: 5442
design of automatic changing mechanism for gamma spectrometer, 17: 25624
design of automatic zone scraper and sample collector for radioassay of thin-layer chromatograms, 19: 4044 (ORINS-47)
design of battery-operated instruments for high-volume air, 18: 35773(R) (UCRL-7811)
design of selector valve for gas, 16: 28453(P)
design of turntable for thin-layer chromatography, engineering drawings for, 19: 28216
development of filter and impactor media for high-altitude, 19: 4404 (TLW-1092)
development of high-altitude methods, 16: 14923 (TID-15430)
development of sample holder for, of neutron scattering from light water, 17: 18551 (TID-18427)
development of self-contained air sampler, 16: 10122 (AEEW-M-102)
device design for raindrops, 16: 20565 (HW-73119)
device for continuous air, design and performance of, 19: 36826
device for fluid, design of, 17: 12410(P)
device for, in fluidized-bed chemical processes, 17: 37295(T,R) (EURAEC-665)
device for radioactive liquids at various depths, 16: 14868(P)
device for sodium from circuit for impurity analysis, 18: 11975(T) (AEC-tr-6304)
device with electrostatic precipitator for aerosols, 16: 19027(P)
electrostatic precipitator development for stratospheric, 19: 44801(R) (NYO-2363-3)
equipment and methods for solid material, coring, 19: 24640 (BNWL-66)
equipment and method of, for Gulliver program, 19: 33738(R) (N64-22756)
equipment and methods for fallout, review on, 20: 2086(T) (BNL-tr-42)
equipment and method for atmospheric sodium, 20: 4148 (AD-623515)

equipment and methods for, in marine ecosystems, 20: 16175(R) (RT/BIO(65)-1)
equipment and method for cold trap analyses, 20: 25567(R) (MSAR-66-71)
equipment and methods for fallout, 20: 38743
equipment and method for continuous surface water, 20: 43523
equipment and techniques of sea water and estuary silts, 20: 40523(R) (RLO-1750-8(Vol.I))
equipment design and performance for estimating respirable dust concentrations, 16: 17931
equipment design for stream water, 17: 6398 (KY-423)
equipment for air at high altitudes, 16: 27420(R) (TID-16015)
equipment for air at high altitudes, development of cryogenic, 20: 2045 (UCRL-13162)
equipment for air, calibration of, 19: 2554 (HW-73341)
equipment for air, calibration facility for, 20: 13077 (Y-1503)
equipment for atmospheric, engineering drawings of intermittent rotoslide, 18: 17987
equipment for atmosphere, engineering drawings of, 19: 22650
equipment for atmospheric radioactive aerosol, electric hand ventilator, 19: 30457
equipment for atmospheric, for pollution, 20: 9185 (Y-KB-64)
equipment for atmospheric fallout, 20: 9241(P)
equipment for atmospheric, engineering drawings of, 20: 23244
equipment for automatic, of river water, 16: 30673 (HW-SA-2126)
equipment for collecting carbon dioxide in troposphere, design of, 18: 42149
equipment for continuous, evaporator-collector, 20: 1757
equipment for dry or precipitated fallout, 18: 41707
equipment for dust and rainfall, 17: 3169
equipment for enclosure for atmospheric, engineering drawings of, 20: 23245
equipment for fission-gas, 17: 21610 (DP-814)
equipment for fission-product transport in NSPP containment systems, 19: 29481
equipment for fission products released in Nuclear Safety Pilot Plant, 19: 36709 (ORNL-P-1034)
equipment for flowing gas, 19: 24832(P)
equipment for gas collection in Project Gnome, 17: 14613(R) (ORNL-3378(p.47-62))
equipment for graphite ball fuel elements, 19: 38792 (JUL-250-RW)
equipment for high-altitude nuclear debris, flight tests, 19: 26537 (SC-RR-64-1793)
equipment for high-altitude, 20: 620 (COO-401-118)
equipment for, in graphite reactor core, 17: 42314(P)
equipment for liquid sodium, 20: 25474(R) (BNL-954, pp 122-67)
equipment for multi-coil magnetic probe signals, design of, 20: 19998 (CLM-R-50)
equipment for nuclear safety pilot plant, 20: 4184(R) (ORNL-3843, pp 71-135)
equipment for organic drift material in streams, 19: 14908 (HW-SA-3385)
equipment for potassium–sodium alloy corrosion loops, 19: 20477(R) (ORNL-3604)
equipment for preparation of samples from Molten Salt Reactor Experiment, 19: 44168 (ORNL-P-1532)
equipment for preparation and transfer of samples for oxygen trace analysis, 19: 43933 (LA-3344)
equipment for radioactive-liquid, 19: 20101(T) (ORNL-tr-442)
equipment for reactor graphite, 19: 33546(P)
equipment for reactor containment test facilities, 20: 20940(R) (ORNL-3915)
equipment for river-water, 20: 39185
equipment for sodium sample preparation for Second Round Carbon-in-Sodium Analysis program, 18: 37065 (NAA-SR-Memo-9294(Rev.))
equipment for sodium, engineering drawings of, 20: 1799
equipment for stratospheric, 17: 18291(R) (NYO-9677)
equipment for stratospheric, design of balloon-borne direct-flow filter, 18: 43752
equipment for stratosphere particle, design and development of air ejector sampler, 19: 720(R) (COO-401-105)
equipment for taking debris and gas samples from atomic cloud, design of plane-released, 19: 2533 (UCRL-13126)
equipment for tritium, on surfaces, 20: 7323 (USNRDL-TR-913)
equipment for, during nuclear mining of ores, 20: 45570(R) (ORNL-3945, pp 189-94)
equipment for, of uranium concentrates, 20: 10978 (RMO-3006)
equipment for, performance of May pack, 19: 7730(R) (ORNL-3691(p.46-74))
errors in subisokinetic, of aerosol particles in air stream, 20: 20927 (BNWL-217)
fallout in air, water, soil, and milk in New Zealand, 20: 40521(R) (NP-16270)
filters for atmospheric, Sand program studies on efficiency of, 20: 23377 (SC-RR-65-491(Vol.2))
for mass spectrometric analyses, specimen-bonding technique for surface ionization filaments, 16: 29316 (IDO-14590)
for radioactivity in liquid scintillation medium, 20: 43748(P)
graphite from reactors, apparatus for, 17: 7593(P)
high-altitude gas and particles, equipment design, 17: 3158 (TID-16988 (Paper 1))
in ecological studies, 17: 7683 (HW-SA-2853)
indexing of radioactive samples for, 20: 43748(P)
isokinetic, of particles in air streams, use of nozzles in, 20: 39103(R) (BNWL-235-3, pp 51-69)
jet device for, development of hypervelocity, 20: 9093(R) (ORNL-3830, pp 271-4)
manipulator equipment for hot cells, 18: 17977(R) (ORNL-TM-793)
marking system for materials exposed to nuclear blast environment, 20: 18176 (SCL-DR-66-6)
materials for airborne iodine isotope, 17: 5754 (PG-Report-408)
measurements on, of enriched uranium-235 fluid in cylindrical storage tanks, 20: 25198 (Y-1502)
method for cesium, in sea water, 20: 39147 (CONF-660401-6)
method for iodine analysis in atmosphere, 19: 40402 (BMI-X-10137)
method for quality control, during reactor component fabrication, 20: 21308
method for radionuclide, at NRTS, 20: 45219
method for recovering specimens irradiated near nuclear explosion, 19: 40706 (ORNL-TM-1191)
method for stack effluent, using activated charcoal, 20: 4179 (LA-3363)
method for surface radioactive contamination, 18: 18101
methods for air, during reactor fuel manufacture, 20: 43630
methods for determination of uranium texture gradients in fuel cores, 16: 33470 (HW-74429(p.14-25))
methods for, in beta radiometric analysis, 17: 1412
methods for radioactivity assay in man, 19: 30474
methods for radioiodine vapor, diffusion-tube, 20: 4185(R) (ORNL-3843, pp 169-234)
methods for solubility of elements in liquid plutonium, evaluation, 19: 38580 (LA-3303)
methods for taking microsamples of irradiated fuel cores, using ultrasonics, 18: 35146(R) (GEAP-4601)
methods for two-stage, comparison of, 19: 30639 (LADC-6484)
methods in AOQ concept, equations for, 18: 31737
methods of adaptive, in digital control, 19: 13860 (IS-995)
methods of continuous, of surface water, 20: 43624
methods of, for atmosphere analysis, 17: 39313(R) (ORNL-3492 (p.185-93))
methods of, for determining radioactive dusts, 17: 32310
methods of, for gravel at potential waste disposal sites, 17: 21373 (IDO-12027)
methods of, for monitoring process-waste effluents, 18: 465
methods of, for uranium concentrates, 17: 33427 (TID-7660(p.91-100))
methods of, development for MSRE, 19: 35772(R) (ORNL-3812(p.27-53))
methods of, for liquid sodium, 18: 13612 (CEA-2369)
methods used in France for nuclear materials management, 20: 20973
micro-, techniques of, for irradiated ceramic materials, 18: 673
of air, directional dependence of filters, 16: 29125
of air, fabrication of high-volume apparatus for, 16: 30682(R) (UCRL-6936)
of air for aerosols, comparison of laboratory techniques used in, 19: 15785 (LADC-5923)
of air for iodine-131, design of equipment, 16: 32915 (AEET/HP/TM/2)
of air for particulate alpha emitters, data analysis, 19: 17791 (UR-658)
of air for radioactive particulates, 18: 8595
of air for radioactive particles, use of log-normal distribution in, 19: 26570 (AERE-M-1469(Rev.))
of air in radiochemical laboratories, evaluation of sample reliability in, 18: 37438 (AERE-R-4680)
of air, marking of filters for, 17: 18235
of air, design of portable battery-operated high volume equipment for, 19: 30492 (UCRL-7894)
of air, diaphragm pump for, 19: 30366(P)
of air, equipment for, 19: 28576(R) (UCRL-12167)
of airborne radioactivity, nomographs for, 18: 5548(R) (UCRL-7450)
of atmosphere for particulates, probe for airplane, 18: 36076(P)
of atmosphere, engineering drawings of enclosure for equipment for, 19: 22649
of atomic clouds, drone for, 19: 4283 (UCRL-13129)
of effluents from ion exchange columns, development of automatic swivel-funnels for use with fraction collector for simultaneous use with several columns, 18: 29593
of fallout, development of electrostatic precipitator for, 17: 10856 (NP-12351)
of fallout, development of devices for, 19: 7731(R) (ORNL-3691(p.77-85))
of fallout, dry and wet methods for, 19: 36732
of fallout, in high-altitude balloon flights, 1963, 18: 16203(R) (NYO-

10496)
of gases from loss-of-fluid test for analysis, 19: 32059(R) (IDO-14655)
of gases, design of cell for, 19: 22101 (RFP-456)
of granular material, design of apparatus for, 17: 8524 (GAT-T-927)
of ions in plasma diagnostics, 20: 46852
of microarthropods inhabiting leaf litter, litter-bag method, 17: 7761
of near-bottom sea water off California, 20: 35183 (UCSD-34P127-1)
of particles in gaseous streams, turbulent deposition in lines for, 16: 29223 (TID-7627(p.127-37))
of potassium–sodium alloys from engineering test rigs for oxide analysis, 17: 33802 (TIM-711)
of radioactive liquids, design of centrifugal pump system for, 16: 33112(P)
of radioactive liquids, system for, 18: 20134(R) (ORNL-TM-792)
of radioactive waste sludge from underground tanks, core drill for, 18: 15654 (HW-74040)
of raindrops, design and performance of sampler, 17: 3263 (HW-SA-2751)
of sea foods for bacteriological studies, 20: 41384(R) (TID-22833)
of stratospheric aerosols, development of multiple-jet impactor for, 17: 29127 (TID-18624)
of stratospheric aerosols, balloon flight record on, 19: 14115(R) (NYO-2363-2)
of the stratosphere, design of electrostatic precipitator for, 17: 16319(R) (NYO-9674)
of the upper atmosphere, design of apparatus for, 17: 16320(R) (NYO-9675)
of upper atmosphere for nuclear debris, dynamic analysis of SAND flight, 19: 44142 (SC-RR-65-286)
of uranium concentrates, minimum sample size for, 18: 22171 (MCW-1454)
of uranium concentrates, evaluation of falling-stream reference system, 18: 43133 (TID-7700(p.145-60))
of uranium hexafluoride from cylinders for analysis, 19: 36230 (K-P-3248)
one-sided tolerance limits and variable sampling plans, 17: 23849 (SCR-607)
optimum use of subgrouping certain 100% inspection situations, 16: 32540 (HW-SA-2119)
performance and stability of multichannel systems for process control, 16: 14858
permissible limits for small lots, 16: 3384 (KAPL-M-GLB-6)
precipitator for aerosol, electrostatic, 17: 36115 (LF-7)
principles and types of, 19: 44296 (NYO-4700(Rev.)(Suppl.II))
problems in atmosphere, 18: 10616
program for milk, in France, 20: 33567
radiometric devices for on-line, 18: 2122
reconstruction of analog signal from nonuniformly spaced samples, 19: 31643 (SC-TM-65-3)
rocket design for cloud, 18: 37313 (UCRL-13116)
sample changer design, 19: 18098 (KAPL-3074)
signals from nonuniformly spaced samples, reconstruction of analog, 19: 44809 (SC-DR-65-291)
simulation of fixed-frequency, computer program for, 20: 4288 (SC-DR-65-312)
stations for Clinch River, automatic, 20: 8479(R) (ORNL-3849, pp 1-42)
statistical analysis of methods for collection of dried milk for fall-out monitoring studies, 16: 22459 (TID-7632(p.415-24))
statistical methods estimating design data, 16: 7642
statistical method for obtaining optimum allocation of total sample size, 20: 42698(R) (ANL-7136, pp 80-94)
statistical techniques for, 20: 42695 (TRG-Report-1200)
subisokinetic, of particles in air streams, 20: 39103(R) (BNWL-235-3, pp 51-69)
system design for fission gas, 19: 24078(R) (GA-4710)
system for falling stream, engineering drawings of, 20: 1797
system for jet, of material in vicinity of nuclear detonation, 20: 14662(R) (ORNL-TM-1394)
system for process solutions at Eurochemic process plant, 20: 1955 (NP-15403)
system for radioactive aerosol, design and performance of automatic, 20: 45950 (HASL-178)
system for radioisotopes in biological and medical fields, automatic, 16: 10232
system for reactor coolant, 19: 35645(P)
systems for air, development of, 18: 10308(R) (UCRL-7571)
systems for flowing liquid wastes, 16: 3295
tubes for gas-cooled reactor effluent, design of device for removal of obstacles from, 17: 40320(P)

SAN FRANCISCO BAY AREA (CALIF.)
radioisotope distribution in sediments of waters of, 17: 40527 (TID-7664 (p.149-59))
radium-228 monitoring in foods in, 20: 148(R) (NYO-3086-1 Pt.IV)
uranium content of diets in, 20: 8740 (CONF-727, pp 136-41)

SAN GABRIEL ANORTHOSITE MASSIF (CALIF.)
titaniferous magnetite deposits, 16: 14994 (BM-RI-5962)

SAN JUAN BASIN (N. MEX.)
geology and hydrology of, for potential use for radioactive waste disposal, 19: 14894 (SAN-413-2)

SAN ONOFRE POWER REACTOR
boiler model for, 19: 45601(R) (WCAP-3750)
control systems for, design of, 20: 28759 (NYO-3270-2(Vol.2))
coolant injection system for, 19: 40195(R) (WCAP-3269-5)
coolant loss accidents in, flow analysis of, (T), 20: 12418(R) (WCAP-3739)
cooling system for, design of, 20: 28758 (NYO-3279-2(Vol.1))
core lattice parameters for, optimization of, 19: 45599 (WCAP-3269-49)
design and safeguards for, regulatory action relative to, 19: 12795
design features, 20: 14157
design of, 20: 28758 (NYO-3270-2(Vol.1))
engineered safeguards of, effects on distance requirements, 19: 33594 (CONF-650201(p.98-101))
fuel assembly design and testing for, 20: 12418(R) (WCAP-3739)
fuel assembly for, mechanical testing of, 20: 12418(R) (WCAP-3739)
fuel handling and transfer system for, design of, 20: 28758 (NYO-3270-2(Vol.1))
hazards analysis for, 20: 28760 (NYO-3270-2(Vol.3))
instrumentation for, in-core, 20: 6630 (WCAP-3269-46)
instrumentation for, design of, 20: 28759 (NYO-3270-2(Vol.2))
power generation system of, design of, 20: 28759 (NYO-3270-2(Vol.2))
site description of, 20: 28758 (NYO-3270-2(Vol.1))
waste disposal system for, design of, 20: 28758 (NYO-3270-2(Vol.1))
xenon oscillations in, calculations of, 19: 40195(R) (WCAP-3269-5)

SAND DOLLARS
carbon isotope variations in, 20: 36549
carbon isotopic variations in, environmental and genetic factors, 20: 36550
oxygen isotope variations in, 20: 36549

SANDIA CORP., ALBUQUERQUE, N. MEX.
aerospace nuclear safety program, 19: 27812 (SC-DC-65-1420)
air radioactivity from Jan. to June 1964, 19: 6101 (SC-RR-64-1679)
atmospheric radioactivity, Jan. to June 1965, 19: 46648(R) (SC-RR-65-464)
bibliography of civilian application releases through 1962, 17: 26947 (SCR-600)
bibliography on public releases through 1963, 18: 29152 (SC-R-64-104)
environs monitoring for beta-gamma activity in air, 16: 3264 (SC-4610(RR))
environs monitoring for beta-gamma activity, July to Dec. 1962, 17: 34152 (SC-4774(RR))
environs monitoring for beta-gamma activity in air, July to December, 1963, 18: 14074 (SC-RR-64-70)
fallout monitoring, 1963, 17: 34153 (SC-4926(RR))
fallout monitoring July to Dec. 1964, 19: 26538(R) (SC-RR-65-184)
radioactivity in air at, Jan. thru June 1962, 16: 29183 (SC-4722(RR))
standard environmental test methods used at, 18: 31056 (SC-4452C(M))

SANDIA ENGINEERING REACTOR
design, 16: 674
design, 19: 48062 (SC-4522(RD))
experimental facilities for, description of, 19: 48062 (SC-4522(RD))
experimental facilities for, design of neutron radiographic, 20: 35152 (SC-RR-66-203)
hazards analysis for, 19: 48062 (SC-4522(RD))
operation procedures for, 19: 48062 (SC-4522(RD))
radiation flux maps, 19: 12845 (SC-RR-64-1757)
reactivity worths in, measurement of, 18: 33150 (SC-RR-64-524A)
site description, 19: 48062 (SC-4522(RD))

SANDIA PULSED REACTOR
components of, ion plating of, 20: 8466 (SC-DR-65-530)
design and construction, 16: 679
design and performance for fast burst production, (E), 19: 31607 (LA-DC-6786)
laboratory facility for, design of, 17: 2621 (SC-4737(M))
neutron dosimetry using phantoms and nuclear emulsion, 18: 31917 (UCRL-10907)
neutron flux measurements in facility, 16: 15788 (SCR-463)
neutron pulse timing, 18: 3354
neutron spectra in, 19: 849(R) (FDL-TDR-64-30)
power recording instrumentation calibration, 17: 26902 (SCTM-284-62(53))
radiation from, 18: 14348(R) (RTD-TDR-63-3051)
shock forces in, inertial, 20: 3592
start-up and operation, health physics aspects of, 16: 23335 (SC-4680(M))

SANDIA PULSED REACTOR II
criticality calculations for, 19: 48063 (SC-RR-65-344)

SANDS

see also Beaches
see also Black Sands
see also Monazites
see also Quartz
see also Silicon Oxides
age estimation of, in marine Pleistocene deposits in Palos Verdes Hills, Calif., from thorium-230 to uranium-234 ratio, 19: 22563
analysis for alpha-emitting radioisotopes, by autoradiography, 19: 30101
analysis for manganese and sodium, activation, 18: 43401
analysis for moisture, development of cadmium probe for, 16: 22504
analysis for moisture by neutron reactions, development of scintillator probe for, 17: 30867
analysis for moisture by neutron absorption, 17: 32018
analysis for moisture by neutron flux attenuation method, 18: 31384
analysis for moisture, activation, 18: 39105
analysis for moisture, radiometric, 19: 7767 (IFA-MR-24)
analysis for moisture by neutron thermalization, 20: 3913(P)
analysis for radionuclides, gamma-spectrometric, 16: 20323 (PG-Report-312)
analysis for ruthenium-103 and ruthenium-106, radiochemical method, 16: 16309 (PG-Report-308)
analysis for water using neutron probes, 20: 16926
analysis of grains of, for alpha-emitting radioisotopes, by autoradiography, 19: 30102
analysis of Taiwan River, for micro-amounts of thorium, colorimetric, 16: 1708
analysis, spectrochemical, 16: 4379
beta activity measurement from, 17: 5972 (PG-Report-403)
cesium-137 gamma spectra in, (E), 20: 22308 (HASL-167)
coating grains with carbon by pyrolysis of hydrocarbons in fluidized bed, 16: 500 (PAN-232/IV)
contents of potassium, thorium, and uranium in beach, at Atlantic and Gulf Coasts, 18: 35732
distribution of radioisotopes in, 17: 2643 (UCRL-13048)
drift measurement in Denmark using chromium-51, 16: 23995
drift measurements in, using tracer techniques, 20: 33541
drift measurement on Japanese coasts, tracer study, 16: 24003
drift measurement on Portugal seacoasts, tracer study, 16: 24005
drift measurements in sea and on shore, tracer techniques for, 18: 1919
drift measurements on sea bed in Japanese harbors, tracer study using Geiger-Mueller tube, 19: 24736
drift movement on Thyborn Inlet, Denmark, tracer study, 16: 25641
effects of medium of, on gamma energy spectra, (E), 20: 40290
efficiency of alluvial, for decontamination of drinking water from radioisotopes, 19: 24424
erosion and displacement by surf, tracer studies, 20: 510 (EUR-2167.d)
fluidization of, effects of electrostatic phenomena on, 17: 11202(T) (AEC-tr-5621)
gamma and neutron attenuation in serpentine, reactor, (E), 20: 6524
gamma attenuation coefficients at 0.03 to 10 Mev, 19: 35569
gamma attenuation coefficients, 16: 23246
gamma energy distributions at 320 kev in, 18: 9559
gamma scattering by quartz, energy spectra from, 19: 14741
gamma scattering by quartz, energy distributions from, (E), 19: 31429
gamma scattering by, energy distribution from, (E), 20: 30728
gamma shielding by, in basement fallout shelters, (E), 20: 7298 (CEX-59.7B(Pt.3))
geochemistry of thorium and uranium in, in Lower Triassic deposits, Pripyat Basin, USSR, 20: 11026
humidity of fine-grain, equipment for measuring, 20: 46022
impact loads on rigid-body cone in, 19: 10692 (SCL-DR-64-144)
ion equilibria in Eurochemic site, in Belgium, 16: 34144(T,R) (EURAEC-275)
migration of, radioactive tracer study of, 17: 12455(T) (NP-tr-943)
migration of salt in columns wetted by water, 16: 6517 (IA-687)
mixtures with epoxy resins, weathering effects on, 16: 15028(R) (UCRL-6658(Rev.))
moisture content in, apparatus for measuring, 16: 30670
moisture content of, in mixtures with sugar, neutron gage for determining, 20: 5819
moisture content of, neutron recoil methods of measuring, 20: 31627
movement in rivers, use of chromium-51 tracer to study, 20: 43549 (NP-16200)
movement in Yugoslav river, tracer studies, 19: 13618 (NP-14667)
movement of Japanese estuary and coastal, tracer study, 18: 4010
movement of sea, tracer study, 16: 16586
movement of, tracer techniques for measurement of, 18: 1917
performance as reactor shielding, (E/T), 19: 14759
phosphorus-32 uptake by, in water basin, 17: 15622
potassium content of, effects of chemical processes, origin, and transport on, 20: 33514
preparation of gold-198-labeled, 17: 31982
preparation of silver-110-labeled, for tracer application, 19: 2676 (CONF-188-2)
processing titanium–zirconium, 17: 25452
properties as water fallout filter, 19: 15754 (NP-14781)
radioactivity in, effects on activity of rats, 19: 29868
radioactivity of Brazilian, environmental contamination from, 18: 31768
radioactivity of, in Central Asia, gamma scanning methods of surveying, 20: 33514
radioactivity of, used in Roorkee University buildings, India, 20: 43533
radioisotope movement in, Belgian studies on, 19: 10659(R) (EURAEC-703)
radioisotope permeability and retention in, device for measuring, 18: 16215
ruthenium-106 sorption by, 20: 10855
scavenging of fission products from water by, 17: 30765
seepage of liquid wastes in, 17: 36993(R) (TID-19164)
seepage of liquid wastes in, 17: 36994(R) (TID-19186)
seepage of liquid wastes in, 17: 36995(R) (TID-19187)
seepage of liquid wastes in, 17: 36996(R) (TID-19188)
seepage of liquid wastes in, 17: 36997(R) (TID-19189)
sorption of cesium and strontium from Purex-type wastes by, 16: 11343 (ORNL-TM-127)
sorptive properties for strontium-90, 16: 27013
sorptive properties of calcium carbonate mixtures of, for calcium–strontium systems, 17: 19711 (TID-7644(p.187-99))
sorptive properties for radioactive wastes, 17: 29982
sorptive properties for waste solutions, 18: 24980(T,R) (EURAEC-300)
sorptive properties for thorium and uranium from solutions, 18: 37060 (A/CONF.28/P/814)
sorptive properties for strontium, ruthenium, cesium, and cerium, 18: 37288 (A/CONF.28/P/813)
sorptive properties for fission products, 19: 36560
sorptive properties for strontium-90 in ground water, 19: 46602
sorptive properties for radioruthenium in different solutions, 20: 40890
stress propagation in, methods for predicting, 19: 34361(R) (AD-609555)
strontium-90 migration rate in, 18: 5475 (UCRL-13010)
surface labeling with chromium-51, 17: 117
thorium and uranium abundances in, 20: 2052
thorium content of, effects of chemical processes, origin, and transport on, 20: 33514
transport in rivers, use of radioisotopes for measurement, 16: 16588
transport of surf coast, tracer methods for measuring, 20: 2060
uranium content of, effect of chemical processes, origin, and transport on, 20: 33514
use for filtration of research reactor feed solutions, 20: 43426 (ORNL-TM-1650)
use in laminated shielding panels, 20: 14680(P)
use in mixtures with ion exchangers for water decontamination, 20: 40484
use of, for disposal of waste solutions, 17: 10221(T,R) (EURAEC-443)
x-ray attenuation coefficients, 16: 23246

SANDSTONE
analysis for gold, activation, 18: 27326
analysis for potassium, thorium, and uranium in Arkansas and Oregon, 18: 11523(R) (TID-19927)
diffusion of radioisotopes in deep permeable formations of, 19: 8673(R) (ORNL-3697(p.3-10))
geochemistry of thorium and uranium in, in Lower Triassic deposits, Pripyat Basin, USSR, 20: 11026
neutron distribution in, Monte Carlo calculations on, 20: 35658
permeability and radon diffusion in synthetic, 20: 1878
radioactivity of, Braunschweig, Germany, 20: 20890
radioisotope sorption by, in deep permeable formations, 17: 39296(R) (ORNL-3492(p.3-12))
rock matrix effect in, theory of neutron logging for, 20: 18932
sorptive properties of Berea, for iodine vapors, 20: 8479(R) (ORNL-3849, pp 1-42)
thorium and uranium content of graywackes and orthoquartzites, 19: 9373
uranium ore formation in, 17: 34119

SANDSTONE DEPOSITS
(See also headings of the form Sandstone Deposits (Wyo.))
analysis for radioactivity in Erlangen, Germany, gamma-spectrometric, 18: 43809
determination of phosphorites in, by natural gamma well logging, 18: 5504
geology and lithology of uranium-bearing, in Erlangen, Germany, 18: 43829
mineralogy of asphaltic, at Mas Alary, Herault, France, 19: 9390
oxidation-reduction properties of uraniferous, 18: 6967
radioactivity monitoring and paleogeography in Lower Keuper, Germany, 19: 24708
radioactivity of pelitic, in Vindhyan formations of India, 17: 39273
thorium and uranium contents in, 18: 23144(R) (TID-20506)
uranium isotope fractionation in, Gas Hills, Wyoming, 20: 2057

uranium isotopic fractionation in, 17: 8418

SANDSTONE DEPOSITS (COLO.)

analysis for protactinium-231 and thorium-230, spectrometric, 19: 24742
uranium equilibrium and migration in, 19: 24742
uranium isotopic fractionation in, 19: 20187

SANDSTONE DEPOSITS (WYO.)

analysis for protactinium-231 and thorium-230, spectrometric, 19: 24742
carbon, oxygen, and sulfur isotopic ratios in, in Gas Hills district, 19: 22587
ecology of plankton in, 16: 4029 (TID-12946(App.I,Vol.I))
protactinium-231 and thorium-230 contents in Shirley Basin, 18: 31778
uranium equilibrium and migration in, 19: 24742
uranium isotope fractionation in Shirley Basin, 18: 31777
uranium isotopic fractionation in, Wyoming Wind River Basin, 18: 39525
uranium isotopic fractionation in, 19: 20187

SANITARY ENGINEERING

following thermonuclear attack, 18: 25720
radiation dosimeters for, 16: 25665
radiation protection of environment in Soviet Union, evaluation of problems in, 18: 37424 (A/CONF.28/P/379)
specification guides at HAPO for, 18: 3921 (TID-15244(Rev.))
specification guides at HAPO for, 18: 3922 (TID-15245(Rev.))
thermonuclear warfare effects on, 18: 18107

Santobrite

see Sodium, (Pentachlorophenoxy)-

Santowax OM

see Terphenyl

Santowax OMP

see Polyphenyl Systems

Santowax R

see Polyphenyl Systems

SAP (SINTERED ALUMINUM PRODUCTS)

analysis for aluminum, 18: 15949 (EUR-585.i)
analysis for aluminum oxide, 19: 15344 (EUR-2207.i)
analysis for aluminum, carbon, iron, silicon, and zinc at different laboratories, statistics on, 19: 19750 (EUR-2286.f)
analysis for components and impurities, methods for, 20: 45574 (EUR-3064.f)
analysis for impurities, x-ray spectrographic, 17: 27226 (EUR-21.f)
analysis for impurities, spectrographic, 17: 27271
analysis for iron inclusions, electron-beam, 18: 39058 (EUR-1643.e (p.275-300))
analysis for oxide content in commercial, 19: 22993 (RISO-96)
analysis for rare earths by chromatography and spectrography, 18: 13655
analysis for rare earths, spectrographic, 19: 38553
analysis of, use of microprobe automatic spectrometer for elemental and structural, 18: 5225
bonding by silver diffusion, study using electron microprobe, 19: 30077 (EUR-1819.e(p.27-36))
bonding methods for, 17: 25753
bonding of, by various techniques, 16: 32092 (BMI-1594)
bonding of, for fuel element cladding, 16: 26642(R) (BMI-1577(Del.))
compatibility with fissionable materials, 17: 29255 (ZFK-WF-13)
compatibility with uranium dioxide, 18: 37671 (A/CONF.28/P/421)
compatibility with uranium and uranium carbides, 18: 40827 (EUR-1830.e(Pt.II))
compatibility with liquid lead, 18: 40827 (EUR-1830.e(Pt.II))
compatibility with uranium dioxide to 525°C, 20: 5838(R) (RISO-110)
compatibility with uranium carbide to 600°C, 20: 5838(R) (RISO-110)
corrosion by biphenyl, 20: 25491(T) (AECL-2330, pp 179-95)
corrosion by organic liquids, 19: 2847
corrosion by terphenyls, 17: 36954
corrosion by terphenyls at 400 to 450°C, 17: 37478 (EUR-379.e)
corrosion by terphenyl, 18: 13233(R) (BNL-823(p.1-19))
corrosion by terphenyl at 400°C, fretting, 20: 43843
corrosion by water at 290°C, 17: 35079(R) (ANL-6749)
corrosion by water at 260 to 350°C, 18: 16438 (ANL-6785)
corrosion in terphenyl at 450°C, 18: 40827 (EUR-1830.e(Pt.II))
corrosion of M-257 by terphenyls, 18: 11366 (BNL-7650)
corrosion of Trefimetaux, by water at 290 and 315°C, 18: 25919(R) (ANL-6868(p.190-200))
corrosion of type 930, by Santowax R at 400°C, 17: 4302(R) (RISÖ-49)
corrosion resistance at high temperatures, 18: 8723(R) (IDO-16934)
creep, 16: 26642(R) (BMI-1577(Del.))
creep of, at 700, 800, and 900°F, 16: 28642(R) (BMI-1581(Del.))
creep properties, 17: 15466(R) (SRO-77)
creep properties, 20: 19220 (RT/MET-(65)2)
creep properties, 18: 13354(R) (BMI-1657(Del.))
creep properties of type 930, effects of hydrogen on, 20: 5838(R) (RISO-110)
creep rupture at 700 to 900°F, long-term, 19: 16061 (BMI-X-10113)
creep rupture of M-257, M-583, SAP-895 and SAP-915, at 700 to 900°F, 20: 5851
creep-rupture properties, 17: 3378(R) (BMI-1583(Del.))
creep-rupture properties of, at 700 to 900°F, 17: 22159(R) (BMI-X-221)
creep-rupture properties of M-257, M-583, and 895 at 700, 800, and 900°F, 17: 23864(R) (BMI-1619(Del.))
creep-rupture properties, 17: 22966(R) (BMI-1614(Del.))
creep-rupture properties of M-257, M-583, and M-895 at 700 to 900°F, 17: 25685(R) (BMI-1624(Del.))
creep-rupture properties, 17: 26944(R) (BMI-1630(Del.))
creep-rupture properties of M-257, M-583, and 895, at 800 and 900°F, 17: 28533(R) (SRO-83)
creep-rupture properties of M-257, M-583, and 895, at 700 to 900°F, 17: 29314(R) (BMI-X-238)
creep-rupture properties of, research program on long-term, 17: 37507(R) (BMI-X-257)
creep-rupture properties of M-257 and -895, at 800 and 900°F, 17: 42352(R) (SRO-94)
creep-rupture properties at 700 to 900°F, 17: 40423(R) (BMI-1639(Del.))
creep-rupture properties at 700 to 900°F, 17: 40424(R) (BMI-1642(Del.))
creep-rupture properties of M-257 and 895, at 700 and 900°F, 18: 3190(R) (SRO-95)
creep-rupture properties at 700 to 900°F, 18: 2157(R) (BMI-1644(Del.))
creep-rupture properties at 700 to 900°F and 1 to 1000 hr, 18: 5772(R) (BMI-X-266)
creep-rupture properties at 700 to 900°F, long-term, 18: 7985(R) (BMI-1650(Del.))
creep-rupture properties of 895, at 900°F, 18: 9652(R) (SRO-97)
creep-rupture studies, 17: 14727(R) (BMI-1600(Del.))
creep-rupture testing, 17: 4305(R) (SRO-74)
creep-rupture testing, 17: 24687(R) (SRO-82)
creep-rupture testing of M-257 and 895 at 800 and 900°F, 17: 31733(R) (SRO-84)
creep-rupture testing, 17: 35154(R) (SRO-92)
creep-rupture testing of, -895, M-583, and M-257 at 700 to 900°F, 17: 35251(R) (BMI-1632(Del.))
creep rupture testing of SAP-895 at 900°F and 7500 to 7700 psi, 18: 30998(R) (SRO-102)
creep rupture testing at 800 to 1000°F, 18: 35153(R) (SRO-103)
creep rupture testing of 895 and 915, 18: 36809(R) (SRO-105)
creep testing, 17: 38551(R) (SRO-93)
creep tests, 17: 17546(R) (SRO-80)
creep-rupture, 16: 24149(R) (BMI-X-204)
creep-rupture at 700 to 900°F, long-term, 18: 34032(R) (BMI-1668(Del.))
creep-rupture at 700 to 1000°F, long-term, 18: 34034(R) (BMI-1672(Del.))
creep-rupture properties of 895 and 915, at 700 to 900°F, 18: 13292(R) (SRO-98)
creep-rupture properties of M-257, -583, -895, and -915, at 700, 800, and 900°F, 18: 15664(R) (BMI-1655(Del.))
creep-rupture properties of M-257, M-583, 895, and 915, at 700, 800, and 900°F, 18: 16467(R) (BMI-X-277)
creep-rupture properties at 700 to 900°F, long-term, 18: 20450(R) (BMI-1661(Del.))
creep-rupture properties of M-257, 583, 895, and 915, at 700, 800, and 900°F, 18: 24988(R) (BMI-1665(Del.))
creep-rupture properties of M-257, M-538, 895, and 915, at 700, 800, and 900°F, 18: 32135(R) (BMI-X-296)
creep-rupture properties at 700, 800, 900, and 1000°F, 18: 40970(R) (BMI-1674(Del.))
creep-rupture properties of, long-term testing of, 16: 32031(R) (BMI-X-207)
creep-rupture testing, 18: 15537(R) (SRO-99)
creep-rupture testing, 18: 17351(R) (BMI-1659(Del.))
creep-rupture testing of, 18: 24910(R) (SRO-101)
creep-rupture testing at 800 to 1000°F, 18: 35153(R) (SRO-103)
crystal orientation in rolled and extruded, effect of alumina content on, 19: 28820
crystal structure of, effects of iron-rich inclusions on, 18: 20562
crystal structure and properties of, effects of heat treatments above melting point on, 20: 842
defects at room temperature, origin and development of cup and cone, 18: 27933
deformation mechanisms in, 20: 35898 (UCRL-16803)
deformation of, electron microscopic study of dislocation structures in tensile, 19: 46996 (EUR-2479.e)
deformation of, mechanisms of plastic, 19: 11682
deposition on uranium carbides, 18: 40827 (EUR-1830.e(Pt.II))
development, 17: 1049(R) (SRO-73)
development, 17: 19634(R) (SRO-81)
development and properties, 17: 29317 (EUR-272.f)
development and properties of, 16: 28542(R) (SRO-68)
development as reactor material, 18: 44075
development for use as cladding on uranium dioxide fuel, 18: 13259
development of, 17: 7609(R) (SRO-75)
development of tubes of, for use in canning uranium dioxide pellets,

19: 7855(R) (RISO-90)
diffusion in cobalt, Inconel, and uranium carbide, 19: 13938 (EUR-2158.f)
diffusion of silver in, 18: 5225
dissolution in nitric acid solution containing mercury catalyst, 18: 17938 (RT/CHI(63)-34)
dissolution in sulfuric acid solutions using mercury catalyst, 19: 26474
dissolution of, by caustic solutions in recirculation dissolver, 19: 40655 (RT/CHI(65)-1)
ductility properties at 25 to 500°C, 20: 5838(R) (RISO-110)
elastic modulus, 18: 4242 (EUR-402.i)
electric conductivity, effects of alumina content on, 20: 13306
extrusion and magnetic pulse swaging, 19: 11711
extrusion of vacuum-sintered SAP930 finned tubes, 18: 12598 (NAA-SR-Memo-9057)
fabrication, 17: 36954
fabrication, 18: 37671 (A/CONF.28/P/421)
fabrication and mechanical properties of, 16: 14375(R) (BMI-1557(Del.))
fabrication and properties of Frittoxal, 17: 27757 (EUR-273.f)
fabrication and properties of, 18: 37656 (A/CONF.28/P/733)
fabrication and properties of, 17: 24605(R) (ACNP-63012)
fabrication and properties of, 17: 33236(R) (ACNP-63022)
fabrication and properties of, 16: 17299(R) (SRO-66)
fabrication and properties of, 20: 39359 (RISO-113)
fabrication and properties of APM alloys for organic reactor fuel cladding, 16: 4521
fabrication and testing for reactor cooling channels, 20: 18174(R) (NP-15771)
fabrication and testing capsules of, 20: 43812(R) (BNWL-269, pp 4.1-9)
fabrication by extrusion and cold work, 18: 41977 (EUR-1844.f)
fabrication for nuclear uses, 20: 37210
fabrication into reactor fuel cladding, (E), 19: 40172
fabrication of APM by extrusion for organic reactors, 18: 24893(R) (NAA-SR-8888(Sect.III))
fabrication of cylinders of, using magnetic fields, 20: 19199 (RT/EL-(65)9)
fabrication of end-cap bonding process development for, 16: 28642(R) (BMI-1581(Del.))
fabrication of fuel tubes of, 20: 8398(R) (NAA-SR-11450, Sect.6)
fabrication of hexagonal APM process tubes for organic reactors, 18: 21569 (NAA-SR-Memo-8121)
fabrication of thin-walled tubes of, by drawing and extrusion, 18: 2213
fabrication of, effects of hydrogen content and large inclusions on, 19: 27789
fabrication processes for, development of, 20: 32796(R) (AI-CE-3)
fusion with aluminum oxide, property changes from, 19: 18493
hardening of, isochronal recovery of, 20: 2375
hardness of types 865, 895, and 930, 20: 5838(R) (RISO-110)
heat of combustion of powders of, 16: 24139(R) (AD-269265)
hydrogen uptake from terphenyl at 450°C, 19: 7855(R) (RISO-90)
inclusions in tubing of, size and type of, 20: 5630 (NAA-SR-Memo-11562)
internal friction, 18: 4242 (EUR-402.i)
internal friction of, low-frequency, 20: 17065
joining of APM, for reactor applications, 18: 578 (NAA-SR-8578)
joining of APM, for organic reactors, 18: 24893(R) (NAA-SR-8888(Sect.III))
joining to aluminum by ultrasonic fusion, 17: 39499 (DP-306)
joining to stainless steel by hot-pressing, 19: 24089(R) (SRO-114)
machining of, equipment and methods for electric discharge, 20: 33851
magnetic pulse swaging of uranium dioxide fuel rods coated with APM, 17: 37491 (NAA-SR-8263)
mechanical properties and degree of dispersion of, effects of cold-working processes on, 18: 7205 (EUR-433.d)
mechanical properties of, effects of cyclic thermal treatment on, 18: 10547(T) (JPRS-22697(p.124-38))
mechanical properties, 19: 7855(R) (RISO-90)
mechanical properties of APM, 19: 10675(R) (NAA-SR-9999)
mechanical properties, studies of metallurgical factors in, 19: 16067 (EUR-1846.f)
mechanical properties of, effects of cold work, notches, and strain rate on, 19: 27789
mechanical properties of APM-M768, effects of temperature on, 20: 19178(R) (IDO-17154)
mechanical properties, 20: 32796(R) (AI-CE-3)
metallurgical defects in APM, 18: 22487 (NAA-SR-8262)
metallurgy of APM M-257 and XAP-001, mechanical and physical, 17: 535 (NAA-SR-Memo-7354)
microscopic examination of, techniques for electron, 19: 7855(R) (RISO-90)
microstructure of annealed and ion bombarded foils of, 18: 34038 (EUR-1833.e)
microstructure of, effects of alumina content and cold-working on, 20: 19220 (RT/MET-(65)2)
microstructure of, use of ionic bombardment for determining, 20: 31765
microstructures of SAP-930 and XAP-005, electron microscopic studies of, 18: 12649 (NAA-SR-Memo-8598)
performance as cladding for thorium-bearing reactor fuel elements, (E), 19: 31551(R) (SRO-115)
performance as cladding on uranium carbide fuel elements, 20: 46220 (AECL-2571)
performance in organic-cooled reactors, (E), 19: 40218
performance of APM-M768, in-pile, 20: 19178(R) (IDO-17154)
phase studies, 19: 11682
phase transformations in, effects of liquid aluminum on alumina, 20: 13296
plastic deformation mechanisms, 18: 14459 (EUR-550.f)
plastic deformation of, effects of grain dimension and tempering on, 18: 42060
plasticity of dispersed-phase, mechanisms of, 20: 11269 (EUR-2483.f)
preparation for fuel cladding, 19: 33622
processing uranium carbide fuels coated with, method for, 20: 45788(R) (ORNL-3945, pp 27-47)
properties and technology of aluminum–aluminum oxide, 20: 13213 (EUR-2447.f)
properties as uranium fuel cladding, 19: 27735(R) (NAA-SR-10850)
properties for cladding uranium carbide fuels, 19: 35778(R) (SRO-116)
properties for organic-cooled uranium-dioxide-fueled reactors, 18: 37671 (A/CONF.28/P/421)
properties for organic-cooled-reactor fuel sheathing and coolant tubes, 18: 38265 (A/CONF.28/P/23)
properties for use as fuel element jacket, 18: 44232(P)
properties for use as fuel cladding material in reactors, 19: 39206
properties in organic-cooled power reactors, 19: 27789
properties of, effects of thermal cycling on, 17: 36295 (EUR-378.f)
properties of welded sheaths, sheets, and tubes of, corrosion, mechanical, and physical, 18: 7172
properties of, methods for determining, 20: 13319
quality control of tubes of, mechanical radiographic methods for, 20: 20861 (EUR-2443.f)
radiation damage induced by oxygen and inert gas bombardment, 19: 47080 (EUR-2478.e)
radiation effects on mechanical properties of types 865, 895, and 930, 17: 4302(R) (RISO-49)
radiation effects on sheathed uranium dioxide, 18: 38265 (A/CONF.28/P/23)
radiation effects on mechanical properties of, fast-neutron, 19: 7855(R) (RISO-90)
radiation effects on tensile properties of types 865, 895, and 930, effects of test temperature on fast neutron, 20: 5838(R) (RISO-110)
reactions with uranium at 600°C, 20: 37203
reactions with uranium at 450 to 600°C, 20: 43835 (RISO-91)
reactions with uranium monocarbide at 450 to 600°C, 20: 43835 (RISO-91)
recrystallization, 20: 5838(R) (RISO-110)
rupture life of rods and tubes of type 930, at 500°C, 20: 5838(R) (RISO-110)
rupture life, effects of oxide content on, 20: 5839(R) (RISO-110)
solubility in mercury-catalyzed nitric acid, 19: 22429
solubility in mercury-catalyzed sulfuric acid, 20: 25207
sorptive properties for hydrogen from Progil OM2 terphenyl at 400 and 450°C of type 895, 20: 5838(R) (RISO-110)
strain fields around aluminum oxide particles in, 19: 26842
stress-rupture properties of 895 and 915, at 700 to 900°F, 18: 6493(R) (SRO-96)
structural properties, 19: 2847
structure and density of oxide phase of, 19: 7855(R) (RISO-90)
structure of, distribution of constituents and inclusions in, 17: 25802
structure of, dispersed-phase, 18: 14461 (EUR-589.f)
structure of, effects of thermal treatments above melting point, 19: 16069 (EUR-2205.f)
subgrain size in extruded bars of, effects of heat treatment on, 19: 6247 (EUR-1847.i)
tensile properties, 18: 8723(R) (IDO-16934)
tensile properties of, effects of hydrogen on, 18: 42105(P)
tensile properties of commercial, at room temperature and 400°C, 19: 22993 (RISO-96)
tensile properties at 25 and 400°C, effects of oxide content on, 20: 5838(R) (RISO-110)
tensile properties at −196 to 25°C, 20: 19204 (EUR-2648.i)
tensile strength of SAP alloy XAP-001 and -005 tubing, 20: 8398(R) (NAA-SR-11450, Sect.6)
tensile tests on, computer analyses of, 20: 4371 (EUR-2514.e)
testing cladding of, nondestructive methods for, 20: 14712
testing finned cladding of, eddy-current method for, 20: 14703
testing of finned APM tubing, eddy-current, 17: 35999 (NAA-SR-Memo-7769)
testing tubes of, low-voltage radiographic methods for, 20: 14706

texture of extruded, 20: 5838(R) (RISO-110)
thermal conductivity, effects of alumina content on, 20: 13306
thermal expansion of, with various oxide contents, 18: 20517 (EUR-1613.i)
thermal stability at 600°C, 17: 30984 (RISÖ-58)
uses in fuel element end caps to reduce creep, 18: 42102(P)
wear against SAP and steels, 20: 15998 (EUR-2117.n)
wear in vibration against antimony tellurides, 20: 43843
wear testing for reactor pressure tubes, 19: 8634 (EUR-1816.e)
welding, 18: 40827 (EUR-1830.e(Pt.II))
welding and forming of channels of, in ORGEL reactor, 18: 41976 (EUR-1818-i)
welding fuel element end caps, pressure, 17: 23931
welding of, evaluation of cold pressure methods of, 17: 36248 (NAA-SR-Memo-7748)
welding of, for use for nuclear fuel cladding, 19: 39131
welding of, magnetic-force butt upset methods of, 18: 10509
welding of, magnetic force techniques for, 16: 16699 (HW-72379)
welding sheaths, sheets, and tubes of, techniques for, 18: 7172
welding sintered compacts of, electron beam guns and method for, 16: 19283

SAPHIR (Switzerland)
see Swimming Pool Reactors

SAPPHIRES
brazing to alumina, 20: 24490(R) (AD-624927)
corrosion by barium vapor at 800 to 1000°C, 18: 44498(R) (MND-2812-3)
corrosion by cesium, 17: 21835
corrosion by cesium at 400°C, 20: 4337
crystal defects in, electron microscopy of, 19: 31456
crystal growth using induction plasma torch, 16: 5661
crystal structure of synthetic, 16: 20380
crystal structure, 18: 24065(R) (GEMP-34A)
degassing of, 20: 43815(R) (NASA-CR-54356)
diffusion of krypton from, at 1100 and 1200°C, 19: 44599(R) (GEMP-50A)
diffusion of krypton in, at 1100 and 1200°C, 20: 27587(R) (GEMP-400A, pp 279-81)
elastic modulus and internal friction of, development of measuring apparatus for, 18: 44931(R) (ANL-6936(p.39-72))
elastic properties at high temperatures, 16: 7921
electric properties as capacitor material, 20: 43815(R) (NASA-CR-54356)
electron transmission at 1 to 8 Mev, 18: 17244 (NASA-SP-3008)
europium sulfide epitaxial growth on crystals of, 19: 11079
friction coefficient with titanium-base alloy *in vacuo*, 20: 7571 (NAA-SR-9644)
Kapitza resistance in, at superconducting temperature, 17: 18892 (ASD-TDR-62-1111)
machining rods of synthetic, technique for, 17: 37497
mechanical properties, 19: 11682
nuclear magnetic resonance spectrum, 16: 13776
phonon detection in, bolometer for, 20: 4479(R) (TID-22179, pp 1-83)
properties for use as fuel-propellant partition in gaseous fuel rocket reactors, 19: 40229 (LA-3229, pp 116-36)
radiation damage in synthetic, 16: 567 (AD-256732L)
radiation effects on thermoluminescence of, gamma, 17: 4997
radiation effects, 17: 22222 (MMPP-NPC-1-3)
radiation effects on thermoluminescence of, effects of high pressure on, 17: 31032
radiation effects on thermoluminescence of, gamma, 17: 38616(R) (MDL-Q2)
radiation effects on spectral properties of, gamma, 18: 18442
radiation effects on optical transmission properties of, electron, 19: 18537 (NASA-TN-D-2620)
radioinduced cavities and exfoliation in, helium-ion and proton, 18: 2313
radioinduced defects in, electron spin resonance studies of, 18: 14543(R) (TID-20237)
radioinduced dislocation loops in, oxygen-ion, 20: 31793
sealing of synthetic, to refractory metals, 17: 6676(R) (RADC-TDR-62-401)
solidification of molten particles of, liquid-solid transformation kinetics in, 18: 45195 (UCRL-11513)
sputtering by argon ions at 2 kev, 19: 31456
thermal contact resistance of normal and superconducting, 17: 645
thermal expansion at room temperature to 1000°C, 16: 4476
thermal expansion at low temperatures, 19: 9767(R) (IS-900(Sect.P))
thermal properties, 16: 22597 (WADD-TR-60-924)
thermal resistance at normal and superconducting indium boundaries with, at 1.1 and 2.1°K, 18: 34699
thermoluminescence of alumina, seeded with magnesium and nickel impurities, 16: 13060
use in vacuum systems, seals for, 20: 9135 (CONF-650512, pp 14-17)
wear characteristics, 16: 30518

SAR
see Submarine Advanced Reactor

Saran
see Ethylene, Dichloro- Polymers

SARCOLYSINE
effects on developmental phases of L-strain cells, 19: 31849

SARCOMAS
(See also specific sarcomas, organs, tissues, animals, etc.)
see also Carcinomas
acid phosphatase in Yoshida ascites, effects of nitromin on, 16: 8607
antigenic specificity of chemically-induced mouse, 18: 29318
chemically induced osteogenic, in rats, 20: 5334
chemotherapy of lymphosarcomas, 20: 5485
chromosome aberrations induced by nitrogen mustard and triethylene-amine, with and without added nicotinic amide, in, 20: 40550
clinical aspects and etiology of bone, 18: 29488
cytology of lympho-, 19: 29847 (ACRH-103(p.48-61))
development in radiation dermatitis, case history of, 19: 167
development in rats, effects of whole-body x irradiation on, 17: 5860
development in thyroid gland, following x irradiation, 17: 27184
development of abdominal, in man 20 years after thorotrast application, 17: 15711
effects of combined radiation and actinomycin D therapy on mouse, 20: 40762
effects of inoculations of, on iodine-131 metabolism in rat thyroid, 18: 9881
effects of lympho-, on tuberculosis incidence in Hiroshima, 20: 12639 (TID-21517)
effects of osteogenic, on fluoride, lead, lead-210, radium-226, and radium-228 content in bones, 18: 13406(R) (ANL-6769(p.66-74))
effects of osteogenic, on lead-210 and radium-226 and -228 content in human bones, 18: 29229
effects of porphyrins on radiosensitivity of rhabdomyo-, 20: 40657
effects of 3-methylcholanthrene and nitromin on virus production in chicken, 20: 35303
effects of 3,3',5-L-triiodothyronine on growth of rat, 19: 45943
effects on DNA metabolism in rats, 20: 26690
growth of x-irradiated viruses of Rous, on chick embryo chorioallantoic membrane, 20: 103
histology of transplanted radioinduced, in rats, 19: 36001
immunity transfer to homographs of, effects of hyperimmune liquids on, 19: 17574
immunogenic effects of irradiated Sarcoma I ascites tumor on mice, 16: 25108
in beagles fed strontium-90, 17: 38646(R) (UCD-108(p.150-9))
incidence in Canada of, 19: 43655
incidence in dogs, 19: 10721(R) (COO-119-231(p.70-5))
induction by injected fluids from, in irradiated mice, 18: 41073 (COO-1038-4)
induction by 3,4-benzopyrene in mice, immunological properties of, 19: 12895
induction of immunoresistance in mouse, by irradiation of cells in suspension before injection, 20: 10634
induction, two-stage mechanism in rats, 17: 17659
leukemogenic properties of myxofibro-, after serial passage in mice, 20: 40502(R) (ORNL-3922, pp 115-27)
lipid metabolism in rat, 19: 25906(R) (ORINS-49(p.9-39))
lympho-, effects of lipopolysaccharides on rat, 20: 5436(R) (UR-668, pp 149-60)
metastatic rate of injected epitheliomas in irradiated rats, 18: 23264
morphology of cells in irradiated, in human bone, 19: 245
niobium-90 metabolism in rat, 20: 1595
niobium-95 metabolism in rat, 20: 1595
pathological manifestations of leukemic reticulo-, induced by chemotherapy or x rays, 20: 42729
pathology of pelvic osteogenic, after radiation therapy, 16: 18771
pathology of tumors related to Kaposis visceral, 19: 15046
radiation dose distribution in Yoshida, empirical method for estimating gamma, 19: 42336
radiation effects on lipoproteins in, 16: 1497(T) (JPRS-10440)
radiation effects on time of mitosis in Yoshida cells, 16: 4078
radiation effects combined with prednisolone on mitosis in MTK, 16: 8603
radiation effects combined with maleic acid on mitosis of MTK, in mice, 16: 8604
radiation effects combined with igrocin on chromosomes and mitosis in rat, 16: 14556
radiation effects combined with citric acid on mitosis in rat, 16: 14557
radiation effects and effects of various chemicals on electrokinetic potential of cells, 16: 21963
radiation effects on Yoshida ascites, in rats, 16: 25220
radiation effects on development, growth, and sensitivity of Yoshida ascites, 16: 25221
radiation effects combined with the sodium salt of arsphenamine on mitosis in MTK, 16: 8594

radiation effects on frequency of, in lymph system of mice, 17: 2844
radiation effects combined with dehydroascorbic acid on Yoshida, in rats, 17: 17905
radiation effects on growth of radioinduced bone, x, 17: 30367
radiation effects on oxygen content of cells of, radioprotectant assay by, 17: 35575
radiation effects on mouse, protective effects of testosterone against, 17: 38823
radiation effects on cells of, in tissue culture, deuteron, 18: 15829
radiation effects on DPN distribution in cells of, x, 18: 29378
radiation effects on cells of rat Yoshida ascites, effects of hypothermia on x, 18: 29500
radiation effects on, protective effects of protoporphyrins against, 18: 41250
radiation effects on growth of transplanted, in mice, 19: 124
radiation effects on transplanted rat, in chicks, x, 19: 5647
radiation effects on development of, in guinea pig, 19: 8891
radiation effects on mouse Crockers, effects of AET and cysteamine on, 19: 8969
radiation effects on nucleic acid content of Yoshida, x, 19: 13031
radiation effects on onset of, in rats, 19: 13042
radiation effects on mouse, effects of nicotinic acid on x, 19: 13113
radiation effects on development of, in mouth of monkey, 19: 17599
radiation effects on nuclear ATP synthesis in mouse lympho-, x, 19: 26062
radiation effects on development of extraskeletal osteogenic, therapeutic, 19: 26169
radiation effects on electrophoretic properties of rat, 19: 28088
radiation effects on electrophoretic properties of proteins of rat, 19: 28089
radiation effects on electrophoretic properties of proteins of ascites fluid induced by, 19: 28090
radiation effects on enzyme activity in cell homogenates of, 19: 36013
radiation effects on development of cranial, from therapy of retinoblastoma, 19: 38486
radiation effects on growth of transplanted, in mice, 19: 43763
radiation effects on proliferation of, mechanisms for, 19: 45923
radiation effects on immune reactions to transplanted ultraviolet-induced, in mice, 19: 45827
radiation effects on growth of transplanted, in mice, effects of sodium cysteinethiosulfonate on, 20: 131
radiation effects on DNA synthesis in rat Yoshida, tracer study, 20: 3701
radiation effects on tritiated-thymidine metabolism in Yoshida ascites, 20: 3702
radiation effects on immune reactions to transplanted, in mice, 20: 5413
radiation effects on cell survival in mouse, effects of oxygen inhalation on x, 20: 12725
radiation effects on DPN content in, x, 20: 14370
radiation effects on distribution of cells of phosphorus-32-labeled Yoshida, in rat tissues, 20: 16188
radiation effects on incidence and latency of mouse lympho-, x, 20: 18317
radiation effects on DNA synthesis in, x, 20: 18271
radiation effects on antigenicity of spontaneous rat, y, 20: 33006
radiation effects on virus production in chicken, mechanism of x, 20: 35303
radiation effects with resins on growth of transplanted fibro-, in rats, gamma, 20: 35314
radiation effects on rat lymphoblastic lympho-, electromagnetic, 20: 40661
radiation effects on growth of cells from, x, 20: 42888
radiation effects on transplants of mouse, x, 20: 42889
radiation effects on growth of Yoshida ascites, in rats, x, 20: 42962
radiation effects on development of, in rat bones, variations with mode of administration of strontium-90, 20: 45423
radiation effects on acid phosphatase in Yoshida ascites, 16: 8607
radiation effects on immunity transfer to homografts of, in newborn mice, 19: 17574
radiodiagnosis by photoscanning, 19: 5745
radiodiagnosis in bones using calcium-47, 20: 8(R) (STI/DOC/10/42, pp 23-43)
radiodiagnosis of parathyroid, using selenium-75-selenomethionine, 18: 43341
radioinduced, 19: 12986
radioinduced bone, following radiation therapy, 18: 5103
radioinduced by injected plutonium-239, in dogs, 19: 40382
radioinduced by ingested strontium-90, in dogs, 19: 43727(R) (UCD-472-112, pp 126-40)
radioinduced by injected Thorotrast, 19: 43850
radioinduced by phosphorus-32 in bones of rats, 19: 43772
radioinduced by radiotherapy, 19: 36154
radioinduced chromosome aberrations in MN lymphocytic, in mice, 16: 14583
radioinduced chromosomal aberrations in rat, protective effects of Serotonin and 5-methoxytryptamine against, 18: 31305
radioinduced immunity to grafted J, in CBA mice, x, 20: 42890
radioinduced in bone, by strontium-90 and chemical carcinogens, 20: 10627
radioinduced in bone, latent period for, 20: 22853(R) (ANL-7060)
radioinduced in children, by radiotherapy of benign tumor, 19: 34022
radioinduced in frontal bone by cerebral tumor therapy, 16: 20171
radioinduced in hematopoietic system in mice, dose rate relation to, 18: 9854
radioinduced in human liver by Thorotrast, 18: 27077
radioinduced in human pituitary, x, 19: 24294
radioinduced in human bone by therapy, 19: 26168
radioinduced, in jaws of rabbits, beta, 17: 37080
radioinduced in long bones, radium-224, 18: 5057
radioinduced in lymph system in hamsters, 17: 14012
radioinduced in man, 19: 28038
radioinduced in mice, beta and x, 18: 23231(R) (ANL-6823(p.20-43))
radioinduced in mice, relation of ovarian tumors, 19: 7134
radioinduced in mice, 19: 28045
radioinduced in mouse lymph system, radiosensitivity of, 19: 45977
radioinduced in organs in rats, 17: 35533
radioinduced in rats, osteogenic, 18: 8169
radioinduced in rats, 19: 25973
radioinduced in rats by injected phosphorus-32, 19: 36001
radioinduced in rats by yttrium-90, 20: 8654
radioinduced in rats, 20: 22696
radioinduced in rabbit jaws, x, 20: 45354(R) (COO-119-234, pp 227-50)
radioinduced in skeleton in man by therapy, 17: 21538
radioinduced in swine, by beta particles from ingested strontium-90, 20: 10597(R) (BNWL-122, pp 37-45)
radioinduced liver, by deposited Thorotrast, 20: 6949
radioinduced lympho-, chromosome complements in x, 19: 45911
radioinduced mouse lymph and lung, frequency of x, 19: 31817
radioinduced mouse lympho-, etiology of x, 20: 18359
radioinduced mouse, growth of transplants of, 20: 22631
radioinduced on guinea pig skin, 19: 15066
radioinduced on human skin, case study of, 19: 15066
radioinduced osteogenic, 17: 35562
radioinduced osteogenic, in man, 19: 31846
radioinduced osteogenic, in rats, 20: 5334
radioinduced radioresistant mouse, induction by exposure of cells in suspension before injection, 20: 10634
radioinduced transplantable fibro-, in rats, gamma, 20: 35314
radioinduced uterine, after therapy, 20: 8790
radioinduced uterine, 20: 14300
radioinduced uterine, following pelvic irradiation, 20: 14301
radioinduced, by radiotherapy of carcinomas, 20: 211
radioinduced, etiology of, 19: 31962
radioinduced, following therapy for exchondromas, 19: 36183
radioinduced, in guinea pigs, x, 20: 6814
radioinduced, in rats, 20: 5296(R) (NP-15585)
radioinduced, pathology of, 19: 33802
radioisotope content of bones of patients with, 20: 41191(R) (HUX-3170-1)
radioisotope uptake by rat brain, 18: 1471
radiosensitivity of Jensen and Yoshida, effects of hypermetabolic state on, 17: 35542
radiosensitivity of, effects of tumor autografting on, 18: 21877
radiosensitivity of, immunological method for increasing, 18: 29483
radiosensitivity of, effects of immunization on x, 18: 38864
radiosensitivity of cells from rat, effects of growth phase on, 18: 41145
radiosensitivity of, in human bone, 19: 245
radiosensitivity of rat, x-ray, 19: 3936
radiosensitivity of osteogenic, in man, 19: 12987
radiosensitivity of, effects of anoxia in rats, 19: 24309
radiosensitivity of, in mice, 19: 29928
radiosensitivity of cells of fibro-, in mice, 20: 5362
radiosensitivity of rat, effects of anoxia on x, 20: 22776
radiosensitivity to local irradiation, immunological method of increasing, 19: 128
radiotherapeutic effects on induction of, 18: 13473
radiotherapy effects combined with Actihaemyl in mouse, histology of, 19: 46123
radiotherapy of chondral, using sulfur-35, 19: 36139
radiotherapy of cutaneous and uterine, 16: 20092
radiotherapy of diffuse reticulum cell, using gold-198, 18: 3669
radiotherapy of facial bone, 19: 36154
radiotherapy of, fractionation effects on, 17: 40618
radiotherapy of, high-energy electron, 18: 3658
radiotherapy of human limb, production of anoxia by tourniquet application prior to, 20: 45517
radiotherapy of Kaposi's, 16: 21928
radiotherapy of lympho-, pneumonitis induction by x, 18: 19566
radiotherapy of lymphomas, relation between dose and recurrence,

18: 29521
radiotherapy of lympho-, protective effects of bone marrow after, 19: 32015
radiotherapy of lymphosarcoma, 19: 36200
radiotherapy of lymphosarcomas, 20: 5485
radiotherapy of lympho-, effects of bone marrow transplants on x, 20: 6971
radiotherapy of lympho- and reticulum-cell-, review of, 20: 45537
radiotherapy of lymphosarcoma in dogs, effects of hematopoietic grafts from normal or immunized donors or splenectomy on, 20: 45551
radiotherapy of mediastinum, late pathological effects, 20: 18519
radiotherapy of mouse, synergistic effects of x radiation and chemotherapeutic agents on, 19: 10963
radiotherapy of osteogenic, in children, 20: 6941
radiotherapy of retinal, effects of, on facial structure, 18: 11659
radiotherapy of testicular, 18: 41277
radiotherapy of transplanted, effects of fractionated local and whole-body exposure in mice, 19: 2199
radiotherapy of, using Mev-range x radiation, 17: 27000
radiotherapy of uterine, efficiency of, 20: 14301
radiotherapy of, complications from, 18: 29449
radiotherapy of, combined with use of carcinostatic agents, 20: 22831
radiotherapy of, low-dose x, 20: 36698
radiotherapy of, occurrence x-ray induced carcinoma 20 years after, 18: 27169
radiotherapy of, with massive doses of sulfur-35, contamination control during, 18: 37036
radiotherapy of, x, 20: 16312
radiotherapy, whole-body gamma, 18: 13390(R) (ORINS-43)
research on, at Argonne Cancer Research Hospital, April to Sept. 1962, 17: 24818(R) (ACRH-18)
research programs on, Great Britain, 1964, 19: 45744
strontium-85 and -90 uptake, 18: 11578
succinic dehydrogenase activity in Yoshida, effects of fatty acid extracts from irradiated rabbits on, 16: 25225
surgery of lymphosarcomas, 20: 5485
surgical treatment of osteogenic, in children, 20: 6941
technetium-99 uptake by rat, 19: 33763
therapy of malignant vascular after radiation treatment and surgery, neutron capture, 16: 2880
therapy of nonresectable abdominal lympho-, occurrence of acute radiation nephritis in, 17: 27203
therapy of reticulum cell skin, use of laser and x radiation for, 20: 45568
therapy of thyroid, with radioiodine, 17: 7736
therapy of, using strontium-89 in dog, 18: 29436(R) (COO-119-229(p.152-69))
thorium dioxide effects on development of, in liver in man, 17: 27081
thorium dioxide effects on development of hemangioendothelial, in liver in man, 17: 27190
thorium dioxide effects on development of, in rat lungs, 18: 31103
Thorotrast-induced rat, 18: 17518
transplantation of radioinduced, in rats, 19: 43772
transplanted Yoshida, effects of fatty acid extracts from irradiated rabbits on DNA and mitosis in, 16: 25228
treatment with bone marrow infusion after massive supressive therapy, 16: 8656
uptake of radioinduced fatty acids in rats, tracer study on, 19: 12937
virus injections, effects on phosphorus-32 uptake by nucleic acids in chicken thymus gland, 16: 12867
virus-induced in monkeys, 19: 21806
yttrium-90 injections in mouse, distribution in organs from colloidal intratumoral, 17: 30213

SARCOSINE
radiation effects on poly-, electron spin resonance spectra of, 17: 23413
radiolysis of, electron spin relaxation times at 4.2°K of radicals from, 20: 26997

Sarcosine, N-Amidino-
see Creatine

SARGASSO SEA
biochemical circulation and composition of nutrients in, 18: 17382(R) (NYO-3140-1A)
biochemical circulation of nutrients in, role of phytoplankton on, 18: 19471(R) (NYO-3140-1)
properties of, annual and seasonal variations in biological, chemical, and physical, 18: 21711 (NYO-3140-1B)
salinity, temperature, and analysis, 16: 4031 (TID-12946(App.2))
strontium content and variable strontium-chlorinity relation of, 19: 614

SASKATCHEWAN
ages of clausthalite, galena, and pitchblende from Lake Athabaska Area, 16: 29194
ages of uranium minerals in Lake Athabaska Area, 16: 29197
anomalous uranium-lead ages of pitchblendes from Lake Athabaska Area, 16: 29193

SATELLITES
aerodynamic re-entry of Task-2 thermoelectric generator, 16: 3965 (MND-P-2291)
argon-37 content in iron and lead of recovered, 16: 16080
atmospheric density studies by Cosmos 3 and Cosmos 5, 18: 5903
bibliographies on, 17: 11457
bibliography on nuclear energy for, 16: 23345 (NP-11732)
bibliography on Soviet, 16: 12790 (TID-15207)
biological phenomena in, 16: 15507
book: *Advances in Space Technology*, 18: 20673
book: *Artificial Satellites in a Rarefied Plasma*, 18: 30930
book: *Satellite Environment Handbook*, 19: 21157
book: *Space Physics with Artificial Satellites*, 20: 2863(T)
charge accumulation and secondary electron emission by, 17: 5644 (ZPh-084)
communication systems of, inflatable solar turboelectric generator for, 17: 30643
conference, 19: 14202
conference on communication and manned, 19: 13610
control and stationing of, using magnetic-expansion plasma engines, 19: 6905
control of earth, design and performance of ion-engine systems for orbit, (E/T), 20: 5638
control of stationary, ion propulsion system for, (T), 19: 9315
control of stationary, radioisotope thruster for, 19: 42631
control of, ion engine systems for, 18: 33699
control of, performance of ion engines for, 20: 39092
control system for synchronous, use of ion thrust devices for, 18: 16582
control system for, performance of cesium ion engine, 19: 44227
cosmic γ-ray detection, 17: 13005
cosmic photon data from Sputnik III for May 15, to Aug. 16, 1958, 17: 34716
cosmic radiation background for, 17: 24231
cosmic radiation data from Russian, 18: 28274(T) (JPRS-25029)
cosmic radiation measurements from Explorer VI and Pioneer V with proportional counter telescope, 16: 20626 (AD-269307)
cosmic radiation studies from nuclear emulsions recovered from polar orbits, 16: 2293 (AFCRL-285)
cosmic-ray experiments for Explorer XII and Orbiting Geophysical Observatory, 18: 7452
cosmic ray reactions with, radioisotope production in, 19: 3008
cosmic-ray studies by Cosmos 3 and Cosmos 5, 18: 5947
cosmic-electron survey by Explorer XIV, 19: 20900
cosmic-radiation interference in communication with, at 20 Mc, (E), 19: 20879
cosmic-ray detectors aboard TRAAC, design of, 18: 32505
cosmic-ray experiments of Cosmos 3 and 5, 18: 24327
cosmic-ray studies of Cosmos 3 and 5, 18: 24328
description of Orbital Solar Observatory, 17: 16471
description of Orbital Geophysical Observatory, 17: 42410
design and development of Navigator, 17: 38573(R) (63SD760)
design and development of Navigator, 18: 6510(R) (63SD886)
design and development of Navigator, 18: 35197(R) (64SD700)
design and instrumentation of Injun 3, 18: 7073
design and performance of Explorer XVII, 19: 39679
design description of Solar Electric Test Satellite, 17: 31779
design of listening post for solar radiation, 18: 10338 (LNF-63/54 (p.15-17))
design of mission-support components for (E), 19: 2919
design study of flare-activated, for studying hazards of radiation belts and solar flares, 19: 6006 (AFWL-TDR-64-67)
detection by tracking stations near trajectories, (E), 19: 21767 (SC-TM-65-44)
development and properties of, review, 17: 17610
development for Vela Project, 19: 2471 (SC-DC-64-1591)
development of manned orbiting station with SNAP-8 power plant (E/T), 19: 3712 (64SD647)
development of, NASA Semiannual Report to Congress, Jan. 1 to June 30, 1964, 19: 19453
development of, review of programs for (E), 19: 2918
devices on, for on-board development of exposed nuclear emulsions, 18: 23957
disposal of orbiting SNAP, techniques for ocean burial, 20: 20302 (SC-RR-65-472)
drag and sputtering characteristics, 16: 10400 (ASD-TR-61-322(p.1-7))
drag forces on, correlation to Forbush decreases of cosmic radiation, 18: 5951
drag forces on, due to charged particles, 18: 40055
drag on charged, in plasma, 16: 14136 (AFOSR-1159)
effects of artificial, on ionosphere and interplanetary media, 17: 16863
effects on charged-particle intensity in Van Allen belts, 20: 30223(T) (NASA-TT-F-389, pp 817-21)

electric drag forces on, in earth's upper atmosphere, 17: 13864
electric potential of, effects of ionized regions on, 17: 3908 (RM-3096-PR)
electric power for manned orbital space station, use of SNAP-2 for, 17: 24724 (AI-7950)
electric power system for SYNCOM 2, 18: 33700
electromagnetic radiation environment of, review, 16: 32252 (NASA-TN-D-1360)
electromagnetic radiation environment of, review, 16: 32253 (NASA-TN-D-1361)
electron density and temperature near, ionospheric, (E), 19: 5070
electron density, magnetic field, and spread echoes from Alouette, 17: 11451
electron density profiles around, 17: 9007
electron density perturbation by Alouette, local, 17: 11451
electron detection and measurement by Lincoln Experimental, equipment for, 20: 6184 (AD-619977)
electron spectra measurements by Discoverers 29 and 31, 17: 9171 (UCRL-6902-T)
electron spectra observations by Discoverers 29 and 31, 17: 6917 (UCRL-6792-T)
energetic particle studies by Explorer XII, data summary, 16: 20851
equipment for Agena 626, radiation hardening of impedance probe, 18: 12412 (AFCRL-63-753)
Explorer XII observations on electron distribution in outer radiation zone and magnetosphere boundary, 18: 26246
flight-control systems for, development of radiation-resistant, 17: 41484(R) (AD-292307)
flight of Discoverer XVIII, radiobiological experiments, 16: 25173 (NP-11784)
flights of Vostok 3 and 4, radiation dose rates for, 18: 2557(T) (FTD-TT-63-968(p.308-15))
galactic and solar cosmic rays observed by Explorer VII, from Oct. 1959 to Feb. 1961, 18: 28301
gamma detection and measurement by Explorer XI, 18: 30436 (CONF-320-4)
gamma detection and measurement by, vidicon spark chamber system for, 18: 31877 (CERN-64-30(p.95-104))
geomagnetic field measurements by Electron 2, 19: 35316
heat transfer from, heat pipe design for, 19: 35613(R) (LA-3316)
helium-3 content in Discoverer-17, 18: 44400
helium-3 content in Discoverer XVII, origin of, 19: 21438
instrumentation, 17: 24230
instrumentation for gamma-ray astronomy in space, 16: 1979
instrumentation for measuring space radiation, 16: 9711 (LMSD-288084)
instrumentation for radiation measurement, 16: 18699 (TID-15480)
instrumentation for cosmic-ray studies, 18: 23988
instrumentation for measurement of auroral phenomena, 18: 33935
instrumentation for detection of nuclear explosions in space, 19: 774 (LAMS-3074)
instrumentation for, 19: 2585
instrumentation for Cosmos-12 and -15, for measuring electrons and ions, 19: 29016
instrumentation for Injun 1 and Solar Radiation 3, 20: 34073
instrumentation of Explorer VIII for ionosphere measurements, 16: 17316 (NASA-TN-D-414)
instrumentation of Cosmos 3 and Cosmos 5 for detection of charged particles in ionosphere, 18: 5946
instrumentation of UK1 for solar x-ray measurements, 18: 7088
instrumentation of Explorer XVII, performance of vacuum, 18: 8634
instrumentation of, radiation effects on, 19: 36866 (N65-20670)
instruments for, 18: 20412
instruments for, cosmic-ray, 18: 20828
interactions with nuclear explosion shock waves, 19: 9756 (TO-B-64-10)
ion acoustic wave emission in ionosphere by, attenuation of, (T), 20: 28107(T)
launch of Ranger RA-1 in Aug. 1961, 16: 3976(R) (NP-11109)
magnetic field and plasma measurements by Explorer 10, relation, 17: 31590
magnetosphere studies by Interplanetary Monitoring Platform IMP-1, 19: 16762
maintenance of orbiting, design of service module for, 19: 2488
mass spectrometer for use in, 17: 10945
materials evaluation for, use of vacuum chambers in, 16: 31782
materials for, optical and infrared properties of, 17: 15953 (NASA-TN-D-1523)
measurements of high-energy gamma rays from solar flares by Orbiting Solar Observatory, 17: 22407
measurements of trapped particles by 1958ε, 17: 5182
metallographic studies of Sputnik 4 fragment, 17: 37470
meteoroid penetration experiments in Explorers XIII and XVI, 18: 741
meteorological observations by, conference on, 17: 27563 (NP-12932)
motion in elliptical orbits, (T), 19: 4783(T) (FTD-TT-64-1077)
motion in interplanetary space and ionosphere, electromagnetic effects from, (T), 19: 39683
motion in tenuous plasma, scaling conditions for sheaths from simulated, (E), 20: 17546
motion of, perturbations in, 19: 27353
nuclear power plants for, 16: 20236
nuclear power plants, effects of space radiation on, 16: 24547
nuclear-powered, re-entry destruction of reactor for, 16: 5087 (RAD-TR-61-28)
nuclear safety aspects of TRANSIT-4A, 18: 9069 (SC-DC-3553(p.91-102))
orbital decay of, semi-annual effects in, 19: 45158 (NP-15424)
orbital variations of, causes of, 18: 6097
orbits about celestial bodies as tests of general relativity, precession of, (T), 20: 11883
orbits of, geophysical effects on, 17: 7679
orbits of, relativity theory for perihelion precession of, 20: 1116
orientation in space, determination of, 19: 38957(P)
orientation of Explorer 11, analysis of, 17: 3594
origin of the planetary, 17: 6908
particle and field investigations by U. S., 18: 21090
performance for ionospheric electron temperature determination, (E), 19: 45177
performance of Alouette II, experiments and results from, 20: 32247
plasma flow over charged, (T), 19: 27674
plasma probe instrumentation on Explorer X, 18: 7012
plasma sheath around, radio-wave propagation effects of, (T), 19: 39517 (AD-610009)
power generator ejection from NIMBUS-B, dynamic analysis of mechanism for SNAP-19, 19: 39071 (MND-3169-68)
power plant development for, 19: 32655(R) (MND-P-3005)
power plant development for, 19: 32656(R) (MND-P-3006)
power plant failure aboard SNAP-10A-powered Snapshot, 20: 10417 (NAA-SR-Memo-11635)
power plant for communications, Rankine steam-cycle, (T), 19: 10624
power plant for, torque production by SNAP-10A, (T), 20: 1528 (NAA-SR-11207)
power plants for communications, survey of, 20: 29608
power plants for manned space stations, development of nuclear, (E), 19: 29730 (64SD-913)
power plants for manned, efficiency of thermally integrated electric-power/life-support, (E/T), 20: 5820 (NASA-CR-316)
power plants for, development of radioisotope, 19: 32657(R) (MND-P-3007)
power plants for, design studies of, 20: 4299(R) (ORNL-2711)
power requirements of communication-type, use of SNAP reactors for fulfilling, 16: 34126 (NAA-SR-7408)
power requirements and development for communications, survey, 17: 4363
power sources for, impact testing of capsules for radioisotopic, 19: 44298(R) (SC-RR-65-9)
power sources in, heat pipe for radioisotope, 19: 36885 (LA-3278)
power supplies for, requirements through 1976, 17: 7680
power supplies for, design and performance of lithium-cooled uranium carbide-fueled 300-kw(e) advanced reactor for, 18: 9716 (SC-DC-3553 (p.103-27))
power supply design for Telstar, 17: 9118
power supply for International Ionospheric, 17: 9127
power supply performance in, radioisotope-thermoelectric, 17: 2637
power supply systems for Surveyor and Transit, 17: 31767
power system for Orbiting Astronomical Observatory, 17: 37322
power systems, effects of weightlessness on, 16: 21852
power units, survey of materials problems for auxiliary, 16: 7325 (MAB-177-M)
propulsion of, comparison of solar-thermal and solar-electric-thermal, 17: 16196
propulsion of stationary, ion systems for, 17: 7648
propulsion of, effect of Alfvèn waves on, (T), 19: 36645
propulsion of, performance of low power pulsed resistojet for, 19: 22523
propulsion systems for, review of low-thrust, 17: 22959
propulsion systems for, launching and orbit transfer parameters for electrothermal arc-jet, 17: 32219
propulsion systems for control of stationary, electric, 17: 32220
propulsion using Alfvèn waves, (T), 19: 37728
radar reflection by, plasma sheath effects on, 17: 36745(R) (AD-295198)
radiation detection and telemetering systems for, 18: 485
radiation detection equipment for, abstracts on, 19: 14420 (ATD-P-64-51)
radiation detection equipment for Cosmos 17, design of, 19: 20343
radiation detectors for, performance of emulsion, 19: 44436 (CERN-65-4 (Vol.II), pp X13-18)
radiation detectors for, performance of emulsion, 19: 44437 (CERN-65-4 (Vol.II), pp X19-32)
radiation dose measurements in space by recoverable, using thermo-luminescent detectors, 17: 41247 (NRL-5938)

radiation dose measurements in space using, 18: 31228
radiation dose measurements at 200 to 400 km, 1960–1963, 19: 700
radiation dose rates in Vostok 3 and 4, 18: 2556(T) (FTD-TT-63-968(p.316-20))
radiation doses to, in various orbits, 20: 11840
radiation dosimetry in Vostok-3 and -4, 18: 41691
radiation dosimetry in Vostok-5 and -6, 19: 9951
radiation effects of Van Allen belts, 16: 34133
radiation effects on electronic systems of, 17: 2628 (TID-17210)
radiation effects on electric components of, electron, 17: 16875
radiation effects on ECHO II skin material, cosmic electron, 17: 18368 (TID-7652(p.260-8))
radiation effects on transistor performance in, 17: 36360
radiation effects on Echo II laminate, electron, 19: 37168 (NASA-TN-D-2207)
radiation effects on, 19: 39059
radiation effects on electronic equipment in flashing light, 20: 4262 (NP-15610)
radiation effects on telemetry circuits in, 20: 5806 (AD-619387)
radiation effects on temperature distribution in rotating cylindrical, 20: 13349
radiation experiments on Telstar, 19: 23511
radiation intensity measurements by Sputnik II, 18: 18828(T)
radiation monitoring on Kosmos and Vostok, 19: 40841
radiation protection for Explorer XVII power supply, 17: 37638
radiation protection in Vostok-3 and -4, 18: 42336
radiation shielding of solar cells in, evaluation of quartz for, 17: 42404
radio signals from, Faraday effect in, 17: 26265
radio signals from, comparison with Jupiter radio emission, 20: 21510
radio wave transmission from, signal scintillation in, (E), 19: 31145
radio wave transmission from, amplitude scintillation in, (E), 19: 31151
radio wave transmission from, geographical distribution of amplitude scintillation in, (E), 19: 31152
radioactivities of recovered, argon-37, tritium, and xenon-127, 17: 4708
radioactivity induced in Discoverer 17 by solar protons, 17: 5098
radioactivity of Cosmos-3, after July 9, 1962, explosion, (E), 20: 30234
radioactivity of Sputnik 4 fragment, 18: 13666
radioactivity of Sputnik 4 fragment, 18: 26127
radiobiology studies in Discoverer XVII, 16: 32723 (AF-SAM-62-67)
radioisotope production in Sputnik 4 by cosmic rays, 17: 37919
re-entry and disposal phenomena for nuclear powered, (E/T), 19: 14878 (RTD-TDR-63-3003)
re-entry and impact of polar orbit, probability distributions of latitudes of, (T), 20: 20361 (SC-RR-66-41)
re-entry behavior of Nimbus/SNAP 19, analysis, 19: 34342 (MND-3169-67)
scintillations of, geomagnetic control for radio-star study, 17: 23534
Scout I instrumentation for primary cosmic ray spectrum measurements, 16: 33181
search procedures for finding, in noisy sky, 16: 1275(R) (NP-10832)
self-erecting structures for use in, radioinduced memory of polyethylene for possible application to, 18: 12728 (RAI-308)
semiconductor radiation detectors for Telstar, 17: 32458
shielding against solar protons, aluminum, 19: 30009
shielding for Advanced Orbiting Solar Observatory, (T), 19: 25618
shielding for manned, (T), 20: 5673
solar cell degradation in space, 17: 39671 (NASA-SP-3003)
solar plasma data from Mariner II, 18: 44399
solar x-ray intensity measurements by Russian, 17: 15065(T)
solar x-ray measurements by Russian, 18: 7450
sputtering under solar wind bombardment, rate of material loss from, 17: 41694
studies of upper atmosphere and space, bibliography of Soviet, 19: 37200(T) (JPRS-30925)
television broadcast from, power requirements for direct, 17: 10211
testing of Nuclear Test Detection, solar simulation, 20: 29440
thermal design and performance of near-earth ANNA, (E), 19: 18967 (NP-14826)
torque operating on SNAP reactor generated fields in, time equations for electromagnetic, 17: 24730
tracking of, British program for, 18: 21091
tritium content of iron and lead in recovered, 16: 16080
tritium content of Discoverer-17, 18: 44400
tritium content of Discoverer-17, origin of, 19: 21438
use during IGY, survey, 16: 16817
use for measurement of electron content of ionosphere, comparison of methods for, 17: 37899
use for measurement of solar x rays, 19: 9833
use for nuclear-explosion detection, replenishment statistics for, (T), 20: 15600
use for radiation measurements from high-altitude explosions, (E), 19: 5054(T) (FTD-TT-64-1077(p.173-90))
use in detection and identification of high-altitude nuclear explosions, 16: 20854
use in detection and identification of high-altitude nuclear explosions, 16: 20855
use in detection of atomic explosions in space, 17: 1167 (LADC-5489)
use in detection of atomic weapons testing in-space, 17: 42408
use in electron-density measurements using r-f plasma probe, 17: 37405
use of artificial, in estimating ionospheric electron distribution, 16: 912
use to detect electromagnetic signal from low- and intermediate-altitude nuclear explosions, 19: 33117 (RM-4542(RAND))
uses for measurement of diurnal variations of ionospheric electron content, (E), 19: 23509 (AD-606701)
uses for radio astronomy, 17: 7677
uses in research on ionosphere, review of results from, 19: 25431
x-ray spectrometer for, scanning mechanism for, 17: 4808 (NASA-TN-D-1097)
Saturable Reactors
see Electronic Equipment
Saturne Accelerator
see Saclay Proton Synchrotron
Sausage Instability
see Pinch Effect
Savannah Merchant Ship Reactor
see Maritime Pressurized Water Reactor
SAVANNAH RIVER
biological survey, near Savannah River Plant, 16: 9029 (TID-14772)
biological survey on selected tributary, 1961, 16: 33317 (TID-16777)
cesium-137 content in fish in Lower Three Runs of, compared with Clinch River, Tenn., 20: 33581
ecology of catfish in, 19: 33733 (TID-21791)
Estuary, hydraulics, 17: 29151
Estuary, radiobiological monitoring, 17: 29151
strontium-90 content in fish in Lower Three Runs of, 20: 33581
SAVANNAH RIVER AREA (S. C.)
aeroradioactivity survey and areal geology, 16: 11933 (CEX-58.4.2)
ecological study of catfish in rivers of, 19: 33733 (TID-21791)
environs monitoring, 1963, 18: 37383
environs monitoring, Jan. to July 1964, 19: 22557
environs monitoring, 1964, 20: 18915
geology and hydrology of basement rock, 18: 29135 (DP-844)
iodine-131 release to atmosphere at, 19: 24782
monitoring environs, 1962, 17: 36085
monitoring of environs, 1961, 17: 18456
radium content of drinking water, 17: 20239 (DPSPU 63-30-10)
SAVANNAH RIVER COMPONENTS TEST REACTOR
characteristics for fuel testing, 18: 45126 (TID-7697(p.3.9.1-21))
components development and operations in, 17: 38551(R) (SRO-93)
construction, 16: 2730(R) (DP-655)
construction, 16: 2731(R) (DP-665)
construction progress, October 1961, 16: 5015(R) (DP-675)
containment, 16: 18679
containment and control systems performance, 19: 43619
containment building for, performance of iodine absorber units for, 18: 15611 (TID-7677(p.248-58))
containment building for, leak testing of, 20: 2037 (DP-968)
control and safety rod drive systems for, 17: 29841 (TID-19001)
control and safety rod drive systems for, performance of, 20: 5194 (DP-971)
coolant baffle repairs in situ, 19: 43602
cooling system corrosion evaluation, 19: 43603
cooling system, corrosion of mild steel components in, 19: 16014 (CONF-446-81)
corrosion in, three-year record of, 19: 38262 (DP-964)
corrosion of mild steel equipment in, during preconstruction and checkout periods, 18: 13331 (DP-801)
corrosion of mild steel in, 18: 28073
critical experiments in, analysis using HERESY code, 18: 42884(R) (NYO-3194-1)
criticality and startup testing of, (E), 20: 5193 (DP-967)
criticality, preparations for initial approach, 16: 17290(R) (DP-715)
criticality studies, 16: 21810(R) (DP-725)
design and construction, 16: 2740(R) (SRO-60)
design and construction, 16: 8365(R) (SRO-63)
design modifications and operation, 16: 28542(R) (SRO-68)
development, 16: 6221(R) (SRO-61)
development, 16: 15896(R) (DP-705)
development, 16: 17299(R) (SRO-66)
development, 16: 28543(R) (SRO-69)
development and operation of, 16: 31253(R) (DP-765)
development and operation, 16: 33989(R) (SRO-72)
development and operation of, 16: 34065(R) (DP-775)
development and operation of, 17: 7609(R) (SRO-75)
development and operation, 17: 13672(R) (DP-815)

development and operations of, summary, 18: 24882(R) (DP-905)
development and pre-startup operation, 16: 9641(R) (DP-685)
development, summary for SRL during Jan. 1962, 16: 9667(R) (SRO-64)
driver tube fabrication, 16: 4514 (NMI-ABB-1)
driver tube quality and uniformity, 16: 17995 (DP-691)
effects on dimensional changes in tubular uranium fuel elements, 20: 25615 (DP-1019)
fabrication and irradiation testing of Zircaloy-clad thorium–uranium fuel tubes, 20: 782 (DP-943)
fuel assemblies for, for hydraulic testing of bayonet loops, 16: 28542(R) (SRO-68)
fuel bundle testing in, for CANDU Reactor, 18: 40751(R) (DPST-64-83-7)
fuel driver tubes for, fabrication processes for concentric, 19: 24953 (NMI-7262)
fuel element design for, 18: 36809(R) (SRO-105)
fuel element development and fabrication for, 18: 45031(R) (SRO-106)
fuel element development and fabrication for, 18: 45032(R) (SRO-107)
fuel element fabrication, 16: 9660(R) (NMI-7241)
fuel element fabrication, development of extrusion methods for, 17: 14737(R) (NMI-7258)
fuel element fabrication, 17: 25758
fuel element fabrication for, development summary, 18: 15537(R) (SRO-99)
fuel element failure in, detection of, 18: 3383
fuel element failure in, design of detection device, 20: 40458 (DP-1049, pp 21-31)
fuel-element radiation testing, 16: 7865 (NMI-7204)
fuel element testing, 16: 33454 (NMI-7218-1)
fuel element testing in, for CANDU reactor, 18: 15537(R) (SRO-99)
fuel element testing in, 19: 1874(R) (DP-925)
fuel failure detection in, 17: 40404 (CONF-243-2)
fuel failure location determination and moderator helium release in, 16: 30065(R) (DP-755)
fuel tube fabrication for, braze end capping techniques development for, 17: 25775(R) (NMI-7246)
fuel tube fabrication for, driver, 19: 27781 (NMI-7263)
fuel tube fabrication for, 19: 45569 (DP-976)
fuel tubes, braze end capping techniques development, 16: 12748(R) (NMI-7245)
fuel tubes, fabrication, 16: 12747(R) (NMI-7244)
fuel tubes for, brazing of end caps on, 17: 23957(R) (NMI-7247)
fuel tubes for, evaluation of Zircaloy-clad uranium as, 17: 22096 (NMI-7218-2)
fuel tubes for, irradiation testing of uranium–zirconium alloy, 20: 2466
hazards evaluation of, 17: 17592 (DP-600)
hydraulics tests, 16: 11220(R) (DP-695)
inspection and status of, 19: 33601(R) (DP-965)
instrumentation for activity monitoring, 17: 1067
irradiation programs, 18: 13292(R) (SRO-98)
maintenance and modifications on, radiation exposure during, *in-situ*, 20: 47069
moderator, control of dissolved helium in, 17: 40405 (CONF-243-3)
moderator of, control of dissolved gases in, 20: 6673 (DP-988)
modification of, review of procedures, 20: 40429
neutron flux and reactivity measurements on mockup lattice, 16: 8310 (DP-457)
neutron flux distributions in, calculation of, 20: 45203 (DP-1045)
operating program, 20: 40456 (DP-1049)
operation, 16: 12750(R) (SRO-65)
operation, 16: 19996(R) (SRO-67)
operation, 16: 30064(R) (DP-745)
operation, 17: 1049(R) (SRO-73)
operation, 17: 4305(R) (SRO-74)
operation, 17: 7597(R) (DP-785)
operation, 17: 15466(R) (SRO-77)
operation, 17: 17546(R) (SRO-80)
operation, 17: 19611(R) (DP-825)
operation, 17: 19634(R) (SRO-81)
operation, 17: 22851(R) (DP-835)
operation, 17: 28526(R) (DP-845)
operation and shutdown in Nov. to Dec. 1964, 19: 11668(R) (DP-945)
operation, Dec. 1962, 17: 10059(R) (SRO-76)
operation, Dec. 1963, 18: 9652(R) (SRO-97)
operation in Nov. 1962, 17: 11979(R) (DP-805)
operation, July and August 1963, 18: 3171(R) (DP-865)
operation, June 1963, 17: 31733(R) (SRO-84)
operation, May–June 1963, 17: 38540(R) (DP-855)
operation, May 1963, 17: 28533(R) (SRO-83)
operation, Nov. 1963, 18: 6493(R) (SRO-96)
operation, Oct. 1963, 18: 3190(R) (SRO-95)
operation of, April 1963, 17: 24687(R) (SRO-82)
operation of, July 1963, 17: 35154(R) (SRO-92)
operation of, Apr. 1964, 18: 24910(R) (SRO-101)
operation, Sept. 1963, 17: 42352(R) (SRO-94)
operation, Aug. 1964, 18: 45031(R) (SRO-106)
operation, Dec. 1964, 19: 10571(R) (SRO-111)
operation, Feb. 1954, 18: 15537(R) (SRO-99)
operation, Jan. 1964, 18: 13292(R) (SRO-98)
operation, Jan.–Feb. 1964, 18: 15520(R) (DP-895)
operation, July-Aug. 1964, 19: 1874(R) (DP-925)
operation, May 1964, 18: 30998(R) (SRO-102)
operation, Nov. 1964, 19: 14843(R) (SRO-110)
operation, Nov.-Dec. 1963, 18: 15605(R) (DP-885)
operation, Oct. 1961–Dec. 1964, 20: 32859 (DP-991)
operation, Sept. and Oct. 1964, 19: 8633(R) (DP-935)
operation, Sept. 1964, 18: 45032(R) (SRO-107)
operational physics data, 18: 3364
operations, 18: 35143(R) (DP-915)
operations, 18: 35153(R) (SRO-103)
operations, 18: 36809(R) (SRO-105)
operations and performance, (E), 19: 40267
operations of, summary, 18: 11432(R) (DP-875)
physics data for, low-power, 17: 40263 (CONF-243-1)
preparation for standby status, 19: 24088(R) (SRO-112)
radiation effects on Zircaloy-2-clad uranium–zirconium fuel elements in, 20: 9572 (DP-994)
reactor vessel stress analysis, 16: 2675
research program, 17: 11097(R) (NMI-7257)
safety analysis of maximum credible accident in, 20: 14183 (DP-1037)
safety systems performance, 20: 40457 (DP-1049, pp 1-19)
shutdown and standby condition, 19: 35846 (CONF-650602-23)
shutdown of, standby condition after, 19: 29792
shutdown status of, 19: 46917(R) (DP-975)
startup of, with test fuel elements, 17: 10127(R) (DP-795)
startup program physics tests, 16: 23269(R) (DP-735)
steel corrosion by heavy water coolant-moderator in, 20: 29654
testing, 16: 30093(R) (SRO-71)

SAVANNAH RIVER PLANT

analysis of Purex Process at, 18: 6896
basin facility for disassembling and inspecting irradiated fuels, 19: 9304 (DP-922)
biological survey of Savannah River near, 16: 9029 (TID-14772)
biological survey of selected environs sites, 1961, 16: 33317 (TID-16777)
chemical processing facilities of, nuclear safety control in, 20: 431 (CONF-651103-7)
contamination and radiation control in plutonium processing plant at, 16: 29045
contamination control in high-level caves at, 17: 23556 (TID-16181)
control of personnel actions in, procedures for, 17: 39172 (DPSPU-62-30-12A)
criticality control program, formulation and implementation, 16: 1989
description of hot Metallography Facility at, 17: 21808 (TID-18566)
diversification potential survey, 1964, 19: 10693 (SRO-109)
dosimetry system for use in event of accidents at, 20: 11029 (DP-1006)
ecology of, 19: 35887 (TID-21713)
ecology of large vertebrate population at, 18: 11568 (TID-19562)
environmental radioactivity monitoring, July to Dec. 1963, 19: 7725(R) (DPSPU-64-30-1)
environs monitoring, results of eleven-year program, 17: 18321 (DPSPU-63-30-8)
environs monitoring, 1964, 18: 41643(R) (DPSPU-64-30-2)
environs monitoring for radioactivity, biological, 19: 11416 (DPSPU-64-30-4)
environs monitoring, July through Dec. 1965, 20: 27195(R) (DPST-66-30-1)
environs monitoring, Jan. to July 1965, 20: 29431
environs monitoring, January to June 1966, 20: 43577(R) (DPST-66-30-2)
fuel element handling, health physics aspects of spent, 16: 17933
fuel processing and storage facilities at, (E), 19: 40837
fuel-element fabrication at, criticality control in, 20: 35702
fuels reprocessing, performance of 3 and 30% TBP processes for, 19: 46423 (DPSPU-64-30-28)
geology and hydrology of area, 16: 25044 (TID-7628(p.115-29))
geology of site, 16: 25061 (TID-7628(p.380-95))
heavy water production capacity at, 18: 28916(R) (DPST-64-83-4)
manual on stainless steel properties, 19: 887 (DP-860(Vol.I))
monitoring of environs, 1961, 16: 20905
publications by DuPont in 1951-1963, bibliography, 19: 12863 (DP-929)
publications in 1964, bibliography, 19: 27843 (DP-929(Suppl.1))
radiation monitoring instruments for, calibration of, 17: 20346 (DPSPU-63-30-9)
radiation monitoring at, Jan. to June 1965, 19: 44288(R) (DPST-65-30-2)
radioactivity confinement system for, performance of airborne, 20: 35608 (DP-MS-66-52)
stainless steel fabrication manual, 19: 9632 (DP-860(Vol.II))

transplutonium element production at, 20: 5822 (DP-1000)
tritium assimilations at, 17: 33785 (DP-831(p.38-45))
waste disposal by burial at, during 10-yr period, 17: 24733 (DPSPU-63-30-2)
waste disposal in ground, 16: 25044 (TID-7628(p.115-29))
waste disposal in basement rock, 18: 29135 (DP-844)
waste disposal sites of, hydrology and lithology of, 17: 2639 (DPSPU-62-30-21B)
waste handling at, low- and medium-level liquid, 20: 1548 (DPSPU-65-30-30)

SAVANNAH RIVER PRODUCTION REACTORS
containment filter system for, performance of carbon-bed, 20: 22463(R) (DP-1028)
containment filtration system, 18: 1279 (CONF-255-6)
control of, on-line computer, 19: 43583
control rod actuator system for, design of, 20: 45190 (DP-670)
control using on-line computers, 20: 24777 (DPSPU-66-30-6)
coolant burnout heat fluxes in high-flux, 20: 47034
coolant purification by miniature ion exchange columns, 17: 19556(R) (DP-806)
cooling system ion-exchange resin radiolysis in, 18: 22198 (CONF-179-3)
core design and operation for high-flux, 19: 45637 (DP-999)
core design for high fluxes, 19: 29720
core design for high-flux, 19: 45638 (DP-999, pp 7-17)
core design for high-flux, engineering aspects of, 19: 45641 (DP-999, pp 43-64)
core development for, high-flux, 19: 29722
core development for, high-flux, 19: 29723
core development for high-flux, 19: 45640 (DP-999, pp 29-42)
decontamination of heat exchangers, 16: 27158 (DP-703)
design and operation of high-flux, 19: 31588
fuel element dimensional stability and textures, Mark VB, 17: 26889 (TID-18744)
fuel element fabrication, Mark VB and VIIA, 17: 25347 (NLCO-872)
fuel element stress-corrosion cracking in (E), 19: 3711
heavy water reconcentration, performance criterion for process unit for, 16: 27533 (DP-652)
irradiation techniques in high flux, 20: 8455 (BNL-9654)
isotope production in high-flux, 19: 45639 (DP-999, pp 19-28)
moderator purity in, monitoring of, 19: 21711 (DPSPU-63-30-40)
moderator quality control, 19: 14864 (DPSPU-63-30-39)
neutron flux density in, computer control of, 19: 43584
operation control by computer, 19: 42129 (DPSPU-65-30-27)
operation of, computer system for axial power monitoring, 20: 42661 (DPSPU-66-30-2)
operation with high-flux cores, (E), 19: 29721
operation with high-flux core, 19: 45643 (DP-999, pp 73-86)
performance of high-flux core in, (E), 19: 29725
power monitoring using on-line computers, axial, 20: 34875
radioisotope production in, 20: 21212 (CONF-660305-19)
reactivity in high-flux core of, temperature coefficients of, (E/T), 19: 29724
reactivity in high-flux, temperature coefficients of, 19: 45642 (DP-999, pp 65-71)
resin depletion in heavy water purification system of, 20: 2419 (DP-973)
safety practices, 16: 22473
shutdown of, gadolinium nitrate injection system for, 19: 43585
shutdown system using injection of gadolinium nitrate, 20: 30920(P)

SAVANNAH RIVER REACTOR MOCKUP
buckling measurements for natural uranium tubular fuel assemblies in, 18: 4740 (CONF-187-24)
coolant, void reactivity coefficients, 16: 17234 (DP-641)
critical substitution measurements in, 16: 28542(R) (SRO-68)
fuel element burnup testing in, 18: 13292(R) (SRO-98)
mixed lattice experiments in, analysis using HERESY code, 18: 42884(R) (NYO-3194-1)
neutron buckling measurements in, in heavy water-moderated lattices of natural uranium, 16: 4678 (DP-640)
neutron flux and reactivity measurements on HWCTR lattice, 16: 8310 (DP-457)

Saws
see Cutting Tools

SAXTON POWER REACTOR
(General Public Utilities)
boiler corrosion testing in, 20: 30884(R) (WCAP-3269-16)
control of, boric-acid shim, 18: 21652
control of, chemical studies of soluble-poison, 20: 5134(R) (WCAP-3269-12)
control of, chemical shim experiment for, 20: 6629 (WCAP-3269-24)
control rod cladding for, corrosion testing of, 20: 12418(R) (WCAP-3739)
coolant fission product activity levels in, 19: 40196(R) (WCAP-3269-6)
coolant fission product levels in, (E/T), 20: 5134(R) (WCAP-3269-12)
coolant loss accidents in, (T), 20: 10382(R) (WCAP-3269-13)
coolant sampling in, chemical and radiochemical analysis of, 20: 12418(R) (WCAP-3739)
core design for, (E), 19: 17241
core fouling in, effects on boron hideout, 19: 45601(R) (WCAP-3750)
core II design, 20: 18095 (WCAP-3385-52)
core II design calculations, 19: 38193 (WCAP-5495)
critical experiments for plutonium partial core, 20: 28768 (WCAP-3385-54)
criticality studies of plutonium dioxide–uranium dioxide fueled, 20: 28766 (WCAP-3385-51)
criticality studies for, analysis of single-region, 20: 28769 (WCAP-3385-54, App.A)
criticality studies for, analysis of multi-region, 20: 28770 (WCAP-3385-54, App.B)
description, 17: 2595
description and experimental testing program for, 18: 829
design and development, 19: 29651(R) (WCAP-3269-3)
design and engineering test program, 16: 11279
design and operation of, review on, 20: 1508
design of plutonium dioxide–uranium dioxide fueled Core II, 20: 28766 (WCAP-3385-51)
development of in-pile supercritical-pressure loop for, 19: 29671
development of partial core using plutonium dioxide-uranium dioxide fuel, 20: 35082
electrical design of, economic factors of, 17: 10108
fuel assemblies for, in-pile testing of, 19: 29651(R) (WCAP-3269-3)
fuel assemblies for, design of removable, 19: 40198(R) (WCAP-3721)
fuel assemblies for, fabrication and loading of RCC test, 19: 45601(R) (WCAP-3750)
fuel assemblies for, design of, 19: 48000(R) (WCAP-3738)
fuel assemblies for, irradiation proof testing of, 20: 12417(R) (WCAP-3269-15)
fuel assembly design for irradiation testing in, 20: 12418(R) (WCAP-3739)
fuel element cladding corrosion in, analysis of products from, 20: 8429
fuel element design specifications, 19: 24094(R) (WCAP-3385-2)
fuel element fabrication, 20:7531(R) (BNWL-150, pp 4.1-17)
fuel element irradiation testing, 19: 2882
fuel element irradiation testing in, Zircaloy clad, 20: 10382(R) (WCAP-3269-13)
fuel element irradiation testing in, 20: 30884(R) (WCAP-3269-16)
fuel element performance (E), 19: 3688
fuel element testing in, 19: 10517(R) (WCAP-3385-1)
fuel element testing in, 19: 45600(R) (WCAP-3385-4)
fuel element thermal testing, 19: 41006(R) (CEND-3107-238)
fuel elements for, fabrication of, 19: 39125(R) (BNWL-91)
fuel elements for, fabrication and testing of, 20: 28767 (WCAP-3385-53)
fuel elements of, corrosion product deposition in, (E), 20: 10382(R) (WCAP-3269-13)
fuel elements of, crud testing of, (E), 20: 10382(R) (WCAP-3269-13)
fuel elements of, power sharing of plutonia–urania, 20: 28772 (WCAP-3385-54, App.D)
fuel pellet temperature for Doppler broadening of uranium-238 resonance, 20: 5135 (WCAP-3269-40)
fuel performance testing in, 19: 31521(R) (WCAP-3385-3)
fuel rod irradiation performance, thin-walled stainless steel-clad, 19: 17269 (CONF-654-41)
fuel rod testing in-pile, Zircaloy-4 clad, 20: 5134(R) (WCAP-3269-12)
fuel rods for, fabrication costs of plutonium, 19: 46962 (BNWL-131C)
fuel-pellet temperature for Doppler broadening of uranium-238 resonance, 19: 29659
instrumentation for, nuclear and process, 17: 34216
kinetic experiments on, (E), 19: 8643 (WCAP-3269-28)
kinetic experiments in, instrumentation development for, 20: 12418(R) (WCAP-3739)
kinetic experiments on Core II of, 20: 47017(R) (WCAP-3385-8)
kinetics of Core II of, 19: 29691
kinetics of, effects of chemical sham control on, (E/T), 19: 45598 (WCAP-3269-44)
kinetics of, measurement using random perturbations (E/T), 19: 3678
licensing activities for, 18: 1267
neutron flux and multiplication in subcritical, thermal, 20: 12418(R) (WCAP-3739)
neutron flux distribution in, calculation of, 20: 35003 (BNWL-232)
neutron noise analysis in, 20: 28774 (WCAP-3385-54, App.F)
noise analysis in, (E), 19: 40164
noise measurements for, 18: 35156 (TID-7679(p.427-47))
operation and safeguards of, regulatory actions relative to, 19: 12795
operation experience, 18: 33070 (A/CONF.28/P/202)

operation of, component performance during first-year, (E), 19: 5490(R) (WCAP-3269-2)
operation of, effects of crud deposits on, 19: 45601(R) (WCAP-3750)
operation of, Jan. to July 1966, 20: 47017(R) (WCAP-3385-8)
operation of, review, 19: 19395
operation of, using chemical shim control, 19: 3698
performance of partial plutonium dioxide-uranium dioxide core during startup tests, 20: 35083
performance of, reliability of, 20: 45181
power disturbances in, local, (E/T), 20: 5134(R) (WCAP-3269-12)
pressure vessel leak testing, 19: 43576
pressure vessel, manufacture and performance of multi-layer, 16: 9675 (WCAP-1391(Rev.))
pressure vessel, manufacture and performance of multi-layer, 16: 9676 (WCAP-1620)
pressure vessel multilayer shell design and fabrication, 16: 19021
radiation dose rates from components of, 19: 48000 (WCAP-3738)
reactivity and kinetic parameters at power, measurement of (E/T), 19: 3677
reactivity of, effects of coolant heat transfer and radioactive corrosion products on, 19: 40196(R) (WCAP-3269-6)
reactivity of, void effects on, 20: 28773 (WCAP-3385-54, App.E)
reactivity of, zero-power, (E/T), 20: 20271(R) (WCAP-3385-6)
reactivity tests and zero power experiments with core II of, 20: 14148(R) (WCAP-3385-5)
reactivity transfer functions of, measurement of, (E), 19: 17282 (WCAP-5496)
shutdown of, neutron decay constants from, 20: 28775 (WCAP-3385-54, App.G)
Zircaloy-4 corrosion and hydriding in, under conditions of heat transfer, 20: 4331
Scabbing
see Rupture
SCALERS
circuit design and performance for 20-Mc/s transistorized decade, 16: 3213
circuit design and testing for fast, hybrid bistable, 19: 38307 (TID-21930)
circuit design for transistorized dekatron, 16: 8926
circuit design for high-speed pulse frequency, 17: 23721
circuit developments, review of fast transistor, 16: 33183
circuits for fast transistorized, 17: 3285
control unit for automatic normalization of foil counting, 16: 13292 (NAA-SR-Memo-6283)
counting losses for, Laplace transforms for calculating, 20: 31594
counting rates from small set of binary, computation from periodic observations, 19: 26670 (UCRL-7798)
counting rates of, dead-time corrections to, 18: 37553
data printout system for, design of, 19: 34528
data recording system design for Harwell solid-state, 18: 16275 (AERE-M-1332)
data recording systems with paper tape output for nuclear data, 19: 36794
data recording systems for experimental reactor physics, 19: 38088
data scanning and punch out device for, 18: 29922 (KFK-201)
description of binary-quinary difference counter, 20: 46020
description of fast, 17: 27660
description of, for 10^9-cps bidirectional counters, 18: 7005
description of preset count, for nucleonic measurements, 17: 14702
design, 18: 7056(R) (ORNL-3499(Vol.II)(p.127-40))
design, 18: 23895
design, 18: 29940
design and characteristics, 17: 14634
design and characteristics of 100 MH_3 pre-, 19: 20380
design and development of fast, 18: 9752 (IA-900)
design and development of, summary, 18: 34752(R) (CU(PNPL)-234)
design and operation of high-speed decade, 16: 10173 (DC-59-5-16)
design and performance for recording nuclear data, 16: 16636
design and performance of combined scintillation-, detection system, 16: 17902
design and performance using transistor-driven decade counter tubes, 16: 20801
design and performance, 17: 23686
design and performance of 10-Mc, with print-out facilities, 17: 25550 (NP-12803)
design and performance of fast and slow, (E), 20: 5680 (ELI-91)
design and performance of portable, 20: 16846
design for electron detection by Lincoln Experimental Satellite, 20: 6184 (AD-619977)
design for ORIC beam monitoring, 20: 39507
design for ring counter having luminous indicator and printer control, 17: 1747 (NP-12182)
design for tracer experiments, 17: 373
design for use with Geiger-Mueller counter tubes, 16: 27336
design of advanced multi, 20: 23427(R) (UCRL-16580, pp 219-50)
design of automatic, 18: 33884 (RT/EL(64)-7)
design of beam pulse, for cyclotron time-of-flight system, 17: 361 (NYO-9360)
design of bi-directional decade counter with anti-coincidence network and digital display, 18: 16313
design of binary and octal, 18: 20301
design of d-c to 100 Mc, 20: 41269(R) (ORNL-3875, pp 4-12)
design of decimal, 18: 43908
design of digital decimal pulse ratemeter, 19: 20295
design of electronic timing circuit, 17: 18560
design of fast decade transistorized, 17: 18541 (RT/EL(62)18)
design of fast remote read-off for, 16: 33246
design of fast scale-of-five circuit, 19: 20296
design of fast transistorized, for automatic operation, 16: 16534
design of portable transistorized, with decatron readout, 17: 8628
design of pulse, 16: 23845 (NP-11734)
design of reversible binary, 19: 34531
design of transistorized decade, using a cold-cathode indicator tube display, 16: 11847 (CREL-957)
design of transistorized microsecond, 16: 25563 (NP-11735)
design of transistorized decade-type, with resolution time of 10^{+7} sec, 16: 27255 (JINR-P-895)
design of transistorized 10-Mc decade, 18: 7000 (UCRL-7567)
design of transistorized decade, 18: 43883 (IAE-616)
design of transistorized bidirectional decade, (E), 19: 20319 (IDO-17059)
design of tunnel-diode binary, with 1.2-Gc counting rate, 19: 9525
design of type-3009 fast, 17: 25551 (NP-12870)
design of, using tunnel diodes, 17: 21982(T) (NP-tr-994)
design of, using tunnel diodes, 17: 23685
design of, with multi-stable system, 16: 33166(T) (AEC-tr-5403)
design of 10-Mc decade, 19: 11599
design of 10-Mc, engineering drawings for, 19: 20306
design of 10-nsec resolution-time pre-, 18: 24030
design of 100-Mc, in biquinary tunnel diode mode, 20: 16775 (DESY-65/17)
design of 180-Mcps binary, 18: 41821
design of 25-Mc, with print-punch facilities, 17: 23687
design of 50-kc transistorized decade, 16: 20676
design of, for use in radiometric analysis, 20: 7043
design using tunnel-diode multivibrators, 18: 29919 (EUR-528.e)
design with central core memory, 18: 41733
design with readout system, engineering drawings for, 20: 14899
design with 10-nsec resolution, decade, 18: 1991 (PPAD-480-D)
development in Japan, 19: 36829
development of fast decimal, 19: 18320
development of high-speed transistorized, 17: 8516 (AERE-R-4074)
development of magnetic memory, 17: 10968
development of multipurpose readout type, 16: 23842 (CREL-952)
development of multiple-input binary, with feedback, 18: 41741
development of portable 12-v, 17: 14610(R) (ORNL-3378(p.28-36))
development of serial binary, 19: 18243
development of storage circuits with scaling ratios of 2 and 5, 16: 29105 (JINR-P-897)
development of 10-Mc time-gated sequential multichannel, 16: 12211(R) (CU(PNPL)-208)
development of 50 Mc decade, 18: 33956
engineering drawing for 100 Mc decade, 18: 31974
engineering drawings for decade, 18: 39699
maintenance, 18: 35854
micrologic elements for, 18: 23850
modifications to, for rate studies, 18: 33868
noise filter for, 20: 29556
output from, time distribution of, (T), 20: 35714 (CEA-R-2907)
performance of, evaluation of, 19: 36815 (ORNL-P-1383)
performance of, used for scintillation scanning, 19: 17763
power supplies for, engineering drawings, 17: 21998
printout circuitry for, design of, (E), 19: 44351 (SGAE-E-4/1965)
pulse resolving circuit using tunnel diodes for reducing counting losses, 16: 16549
read-out systems for, design of serial digital, 19: 2572 (ELI-85)
read-out systems for binary, decimal, 19: 2619
readout and scaling system for, design of, 19: 811
registration of state of decatron, design of transistorized electronic system for, 20: 39178
resolving power of, using fast prescaler, 17: 14698
resolving time of binary, 20: 16802
service manual for AAEC Type 2A, 17: 39407 (AAEC/M-66)
time coding with binary, 16: 20769
use for environmental monitoring, 20: 38735(R) (NYO-1704-13)
use of decade, in radiation detection instruments, 18: 39653
use of fast circuitry, in nuclear physics, 18: 24014

use of fast, with pulse-height analyzer, 18: 25810 (NAS-NRC-Pub-1184 (p.184-5))
use of 100-channel kicksorters as, 16: 19067 (CREL-1061)

SCANDATES
see also Calcium Scandates
see also Strontium Scandates

SCANDIUM
abundance and distribution in rocks, 20: 29436
abundance in meteorites and terrestrial matter, 18: 10753
abundance in meteoritic, terrestrial, and solar matter, review on, 19: 13620
abundance in solar atmosphere, 16: 29599 (AFOSR-3024)
abundance in sun, (E), 20: 17237
abundance in 3 Centauri A, 17: 32851
alloying characteristics with transition metals, 18: 41924(R) (IITRI-578P19-13)
alloying effects on lattice constant of cerium, 16: 32056
alloying effects on phase transformation of cerium, 16: 1694
alloying effects on alpha-gamma phase transformation of cerium, 17: 565
analysis for tantalum, spectrophotometric, 19: 32059(R) (IDO-14655)
analytical chemistry review, 16: 32945
atomic Slater-Condon parameters for, 17: 2426
behavior in separation of rare earths using anion-exchange resins and EDTA, 16: 20549
bibliography, 16: 12116 (WADD-TR-60-864)
book: *Scandium: Its Geochemistry and Mineralogy*, 17: 6301
book: *The Technology of Scandium, Yttrium, and the Rare Earth Metals*, 18: 4189
bremsstrahlung reactions with, isomer production in, (E), 20: 46733
compressibility at room temperature, 18: 20553
compressibility of, isothermal coefficients of volume, 19: 9710
conductivity of, electric and thermal, (E), 19: 18510
content and distribution in beef heart, 19: 45753 (AE-191)
content in high-velocity A stars, 18: 36135
content in human heart, neutron activation determination of, 18: 33457 (AE-146)
content in Japanese hot springs, activation determination of, 19: 42443
content in meteorites and terrestrial specimens, 17: 30690
content in meteoritic chondrules, (E), 19: 28536
content in schlieren granite segregations, 19: 24699
content in snow, use of, as tracer in studying atmospheric precipitation phenomena, 20: 27144 (BNWL-SA-650)
content in volcanic rocks, 17: 30691
content of, in marine organisms, 17: 15604
contents in meteoritic and terrestrial matter, 19: 37428(R) (N64-32896)
corrosion by manganese–plutonium–uranium alloy at 900°C, 16: 22549
crystal structure of, x-ray absorption spectral studies of, 17: 32589
crystallization with thionalid, tracer study of, 16: 12961 (USNRDL-TR-551)
determination after separation as iodide complex using diantipyrilmethane, 18: 13702
determination as impurity in natural fluorites by activation methods, 19: 17835
determination as trace in standard rocks G-1 and W-1, spectrographic, 16: 20831
determination as trace impurity in plutonium–thorium–uranium and thorium–uranium alloys, 19: 17798
determination by amperometric titration using *N*-benzoylphenylhydroxylamine, 18: 13695
determination by activation and isotope dilution, substoichiometric, 18: 21997
determination by calculation of weight from activities and neutron fluxes measured after irradiation, 18: 27297
determination by complex formation with diantipyrinylmethane, 19: 20080
determination by charged-particle reactions at 2 Mev, 20: 43097
determination by complexometric methods, evaluation of azo derivatives of chromotropic acid for indicators in, 18: 39138
determination by flame spectroscopy, 16: 32975
determination by neutron activation methods, 20: 16383
determination by reactions with xylenol orange, 18: 5221
determination by thermal-neutron activation methods, sensitivity for, 19: 9071
determination by titration, suitability of tetraethylenepentaminehepta-acetic acid for, 19: 19813
determination, fluorimetric, 16: 28896
determination in aluminum as trace impurity, activation, 17: 10546
determination in aluminum, activation, 18: 21993
determination in aluminum by activation and gamma spectrometry, 18: 31391
determination in aluminum by solvent extraction and activation methods, 19: 9082
determination in aluminosilicates, carbon ash, and minerals, colorimetric, 19: 9091
determination in aluminum, activation, 19: 28224 (SGAE-CH-13/1964)
determination in asbestos using ion exchange, activation, 20: 16336(R) (NYO-10175)
determination in animals, minerals, plants, rocks, sediments, and soils, activation, 20: 22886
determination in aluminum, activation, 20: 22896
determination in beryllium, activation, 17: 25123
determination in biological materials by ion exchange and gamma spectrometry, 18: 13660
determination in beryllium, neutron activation technique for, 18: 27352
determination in beryllium by activation, 19: 24415
determination in clay, acetic acid leachates, sand, and silt, spectrochemical, 16: 4379
determination in coal and rocks using sulfonazo, photometric, 16: 31576
determination in complex minerals by combination of neutron activation and paper chromatography, 16: 27436
determination in coal ash, chromatographic and colorimetric, 17: 15920
determination in copper using xylenol orange, spectrophotometric, 17: 33805
determination in cerium, erbium, and lutetium, mass spectrographic, 19: 2232
determination in copper by activation, 19: 40422
determination in cigarette tobacco, activation, 20: 14439(R) (GA-5556)
determination in carbonatites by ion exchange chromatography and oxalate precipitation, 20: 16346
determination in conductive tissue of beef heart, activation, 20: 31176
determination in compounds by neutron activation, use of TTA extraction in, 20: 33157 (UJV-1512)
determination in diabase W-1 and granite G-1, spectrographic, 16: 17895
determination in drugs, activation, 19: 24400 (KR-91)
determination in dark and light meteorites by neutron activation methods, 20: 26788
determination in europium oxide, spectrographic, 17: 2931
determination in graphite, activation, 18: 13676
determination in glass samples, activation, 20: 14439(R) (GA-5556)
determination in high-purity aluminum, activation, 17: 29954
determination in hydrochloric acid or methanol–nitric acid media, spectrophotometric, 20: 3888 (TID-22402)
determination in human heart tissue, activation, 20: 31175
determination in iron, activation, 19: 10980 (EURAEC-1273)
determination in iron–rare earth alloys and medium alloyed steels, 19: 40445
determination in minerals and sea water, spectrophotometric, 17: 33829
determination in minerals and rocks by activation, use of paper chromatography and computers in, 19: 7338
determination in meteorites, activation, 19: 7349
determination in minerals by neutron activation, 19: 30424
determination in marine plants and animals, neutron activation, 19: 36314
determination in meteorites, ores, and rocks by neutron activation methods, 19: 36254
determination in niobium by activation, 19: 24416
determination in oxide mixtures with lanthanum and yttrium, photometric, 16: 28899
determination in polyphenyls by activation analysis, 17: 38945
determination in presence of rare earths, consecutive chelatometric, 18: 43413
determination in presence of thorium, titrimetric, 19: 4089
determination in presence of lanthanum, chelatometric, 19: 7300
determination in pure aluminum by neutron activation methods, 19: 36251
determination in presence of aluminum and beryllium by gas chromatography of trifluoroacetylacetonates, 20: 14486
determination in paper samples in criminal cases, activation, 20: 14439(R) (GA-5556)
determination in presence of lanthanum, thorium, and uranium on paper chromatograms, colorimetric, 20: 22910
determination in plutonium by carrier distillation methods, spectrographic, 20: 40814 (RFP-664)
determination in rare earth ores, soils, and yttrium oxide, activation and spectrometric, 16: 2975
determination in rare earths and thorium using mandelic acid, gravimetric, 16: 12988
determination in rocks, activation, 18: 41327
determination in rocks and soils in Norway, activation, 19: 308
determination in river silts, soils, and tobacco, activation, 20: 1739(R) (GA-4297)
determination in rare earths by precipitation by 2,5-dihydroxy-1,4-benzoquinone, 20: 26771
determination in silicate rocks, combined cation exchange-spectrochemical, 16: 25287
determination in soil and rocks, 17: 6019
determination in sulfuric acid solutions, spectrographic, 19: 7308

determination in sea water by neutron activation methods, 19: 22574
determination in sea water and silts, spectroscopic, 19: 36315
determination in soils, activation, 20: 1738(R) (GA-4041)
determination in silicate ores, activation, 20: 2056
determination in soils, activation, 20: 14439(R) (GA-5556)
determination in silts in water, activation, 20: 14439(R) (GA-5556)
determination in silicates, activation, 20: 26782
determination in seawater, activation, 20: 40834
determination in seawater by activation and gamma spectrometry, 20: 43059 (BNWL-SA-674)
determination in terphenyls, activation, 17: 28813
determination in thorium mixtures using *m*-nitrobenzoic acid, gravimetric, 18: 17751
determination in thorium mixtures using quinaldic acid, thermogravimetric, 18: 17753
determination in uranium compounds by reversed-phase partition chromatography, 16: 23636 (TID-7629(p.276-84))
determination in uranium compounds, spectrophotometric, 17: 14169
determination in zirconium by activation, 19: 24418
determination of, in residues by iron flux method, spectrographic, 17: 19942 (PG-Report-157)
determination of, in uranium using Xylenol Orange, 17: 38944
determination of, spectrophotometric, 17: 35628 (IS-612)
determination of trace amounts of, in iron, activation, 20: 14471
determination of trace amounts of, by reactor neutron activation methods, 20: 26760
determination of, paper chromatographic methods for, 18: 29600
determination of, evaluation of reagents for spectrophotometric, 18: 43425
determination of, comparative evaluation of 18 reagents for complexometric and photometric, 19: 5796
determination of, titrimetric methods for, 20: 3863(R) (IS-1200(Sect. C))
determination of, in ores, by activation analysis, 20: 33209
determination of, using Arsenazo III, photometric, 20: 36778
determination of, evaluation of titrimetric EDTA method with visual indicator end points for, 20: 43067(R) (IDO-14679, pp 6-46)
determination of, in standard rocks by neutron activation and gamma spectrometric methods, 20: 45587
determination of, using Arsenazo III, photometric, 20: 45591
determination, photometric, 16: 23657
determination, spectrophotometric, 17: 19962
determination, spectrophotometric, 17: 19965
determination, spectrophotometric, 17: 19987
determination, tracer techniques for, 16: 23736
determination using α-(2,4-dihydroxyphenylazo)-pyridine, photometric, 16: 12993
determination using arsenazo III, absorptiometric, 16: 14653
determination using tiron, ultraviolet spectrophotometric, 16: 26937
determination using chlorphosphonazo III, photometric, 17: 6016
determination using arsenazo III, 17: 14192
determination using Pontachrome Azure Blue B, spectrophotometric, 18: 1562
determination using Eriochrome cyanine R, spectrophotometric, 18: 1564
determination using chlorophosphonazo III, photometric, 18: 1588
determination using arsenazo III, method for, 18: 10005
determination using arsenazo, photometric, 18: 27598
determination using chromotrope 2B, photometric, 19: 328
determination using Xylenol Orange, colorimetric, 19: 7296
determination using EDTA titrations, complexometric, 19: 28245
determination using derivatives of resorcylaldehyde and salicylaldehyde and 3-methyl-1-butanol, fluorometric, 20: 1773
determination using pyrocatechol violet, spectrophotometric, 20: 7034
determination using stilbazochrome, photometric, 20: 7037
determination using azo-derivatives of 8-quinolinol, spectrophotometric, 20: 8858
determination using Chromotrope 2B, photometric, 20: 1772
determination using salicylaldehyde semicarbazone, spectrofluorimetric, 20: 14476
determination using 2-(2′-thiazoleazo)-5-diethylaminophenol, spectrophotometric, 20: 24999
determination, use of pulsed neutrons in activation, 19: 36323
development for low-weight high-temperature uses, 16: 10419 (ASD-TR-61-322(p.563-86))
discovery and development of, review on, 17: 10618
dissociation energy of gaseous and heat of vaporization of solid, correlation of, 17: 6095
dissociation energies at high temperatures, 18: 3795
dissociation energy of gaseous molecule Sc_2, 18: 7218 (WADD-TR-60-782(Pt.XIX))
dissociation energy and free energy functions of, calculation of, 18: 8357
dissolution and ion exchange in ammonium and potassium carbonate solutions, 17: 12240
distribution coefficient between fused bismuth and fused salt eutectic, 17: 21683
distribution in tissues of mice of ionic and chelated form, tracer study, 17: 10308 (TID-17542)
distribution of, between nitric acid and ion-exchange resin, synergistic effects of thorium on, 17: 15948 (LA-2836)
effects on ductility of iodide chromium, 18: 32189
effects on extraction of calcium and strontium, 18: 1811
effects on oxidation resistance of cerium, 18: 43537(P)
elastic properties at 25°C, 20: 31748
electric conductivity of, 17: 8840
electric conductivity, paramagnetic susceptibility and Hall effect of, 18: 10549
electric conductivity of, effects of pressure on, 18: 42069
electric conductivity at 2 to 20°K, 19: 37084
electric conductivity of single crystals of, in magnetic fields, 19: 42878
electric conductivity at 1.5 to 300°K, 20: 4297(R) (IS-1200(Sect.M))
energy level transitions in, Coster-Kronig, (T), 20: 15238 (CONF-233 (Vol.3), pp 398-418)
energy level widths for, K, (T), 20: 15239 (CONF-233(Vol.3), pp 419-39)
fabrication, ore processing, properties, and uses of, 18: 35949
gamma spectra from neutron capture by, 16: 8162(R) (ARF-1193-6)
geochemical behavior in lavas of Chaine des Puys, 18: 41669
geochemistry and mineralogy, 16: 24000
geochemistry and mineralogy of, in Cherry Mountains (Urals), USSR, book, 19: 20190
Hartree-Fock potential of neutral atoms of, analytical expressions for, 18: 16656
heats of combustion and solution, 17: 37209
hydrolysis constant of, measurement of, by chelate solvent extraction, 20: 38925
ion exchange distribution between acid solutions and sulfonic acid resins, 18: 31494
ion exchange in concentrated hydrochloric and perchloric acids, distribution coefficients of, 18: 17759
ion exchange on zirconium-base and clay-mineral ion exchangers, 17: 25364
liquid, solubility of tantalum in, at high temperatures, 20: 41412(R) (IS-1500(Sect. M))
magnetic properties of single crystals of, 17: 32640
magnetic properties of, effects of crystalline field and structure on, 18: 24186
magnetic properties of polycrystals and single crystals of, 19: 23001(T) (JPRS-28849(p.81-5))
magnetic susceptibility at 10 to 293°K, 19: 20595
magnetic susceptibility of, 19: 38045
magnetic susceptibility of, pressure effects on, (E), 20: 13312(T)
magnetic susceptibility at 1.5 to 4.2°K and at 14 to 20°K, (E), 20: 21381
microhardness of single crystals of, anisotropy in, 19: 23002(T) (JPRS-28849(p.86-97))
microstructure, metallographic study of impurities in, 19: 23003(T) (JPRS-28849(p.143-7))
neon ion reactions with, 18: 18872 (JINR-P-1521)
neutron capture by, gamma spectra from thermal, (E), 20: 15787
neutron capture gamma spectrum, 16: 28024(R) (ARF-1193-12)
neutron capture gamma spectra, 18: 24625 (WASH-1046)
neutron inelastic scattering by, fast, (E/T), 20: 19805(R) (ANL-7110, pp 1-28)
neutron reactions (n,γ) with, gamma transition intensities from, 17: 40045
nuclear magnetic resonance in, 19: 9767(R) (IS-900(Sect.P))
nuclear magnetic resonance of, Knight shifts and relaxation times in, (E), 19: 9141
nuclear magnetic resonance in, (E), 20: 4476(R) (IS-1200(Sect.P))
oxidation, 19: 23002(T) (JPRS-28849(p.86-97))
oxidation by air at 300 to 900°C, 20: 16985
oxidation in air, kinetics and products of, 19: 7372
oxidation kinetics at 600 to 1200°C, 19: 36988
oxidation of coating of, at 20 to 900°C in air, 18: 4204
oxygen ion reactions with, 18: 18872 (JINR-P-1521)
partition coefficients and reciprocal ionic radii, 17: 27562 (INSJ-54)
photonuclear reactions, production of short-lived isomers, 16: 12530
positron mean life in, 17: 25944
precipitation from hydrochloric acid solutions by sodium silicofluoride, 20: 14566
precipitation using calcium oxalate, 17: 19931
precipitation with cerium–cadmium intermetallic compounds from liquid cadmium, 18: 34192
precipitation with aluminum tris-(8-hydroxyquinolate), 18: 39255
preparation and magnetic properties, 17: 16723
preparation and properties, 16: 1692
preparation and properties of high-purity, 16: 27653
preparation and properties of crystals of, 17: 36211
preparation and purification, 19: 40948 (IS-1195)
preparation as radiation target materials, methods development for,

18: 27815(R) (ORNL-TM-718)
preparation by zone refining and vacuum distillation and properties of crystals of, 17: 41395
preparation of self-supporting radiation targets of, 20: 17218
pressure-volume variations below 300°K, magnetic effects in, (E), 19: 23054
production, 18: 3798(P)
production in supernova interiors, rapid nuclear processes for, 17: 39835
properties, 16: 29410
properties, 19: 23002(T) (JPRS-28849(p.86-97))
properties and structure of monocrystals, 18: 34147
properties and uses of, review of, 20: 43203
properties of, chemical and physical, 17: 18071
properties of, chemical and physical, 17: 32648
proton reactions (p,n) at 18.5 Mev, angular distributions of quasielastic, 18: 40587
proton reactions with, titanium-44 production in, 19: 19134
purification, 19: 22999(T) (JPRS-28849(p.31-46))
purification of, radiochemical method for, 20: 8838 (UCRL-14258)
quantum defect for ^2S state, 17: 20736
radiation effects on microstructure of, 20: 33941 (DP-MS-66-9)
reactions of, with propylfluorone, 17: 18084
reactions with chlorine and nitrate ions, mechanisms of, 19: 22223
reactions with hydrogen, 19: 15466(T) (LA-tr-65-2)
reduction and deposition potentials, 19: 7362(T) (UCRL-Trans-1153(L))
scandium-45 NMR in, Knight shift and quadrupole coupling in, (E), 19: 16976
scandium-45 nuclear magnetic relaxation in, 18: 16563
separation by anion exchange in acetic acid–nitric acid medium, 18: 16131
separation by anion exchange in EDTA, effects of temperature on, 18: 20110
separation by anion exchange in potassium sulfate, 19: 11283
separation by reversed-phase partition chromatography using organophosphorus compounds, 18: 25614
separation by solvent extraction using hydrogen 2-ethylhexyl phenacyl phosphonate, steric effects in, 16: 16366
separation from acid solutions by solvent extraction using alkyl phosphates or sorption on cellulose phosphates, 19: 40689
separation from aqueous solutions by solvent extraction, uses of diketones in, 19: 7630
separation from aqueous solutions by complex formation and solvent extraction using 8-quinolinol and chloroform, 19: 7642
separation from aqueous solutions by ion exchange, 19: 18062
separation from aqueous solutions by solvent extraction using alcohols, 20: 9087
separation from aqueous solutions by ion exchange, tracer studies of, 20: 18831
separation from beryllium, cassiterite, and tungstate, 17: 6019
separation from cadmium by coprecipitation with cadmium–cerium alloy, 16: 16464
separation from calcium by solvent extraction using TBP, 17: 25316
separation from calcium by thin-layer chromatography, 18: 17949
separation from calcium by ion exchange, 20: 43430
separation from chloride solutions by solvent extraction using amines, 17: 3070(R) (ORNL-TM-265)
separation from cobalt, manganese, nickel, and zinc by precipitation using cinnamic acid, 18: 43426
separation from concentrates and slags by solvent extraction using alkyl phosphoric acids, 19: 20082
separation from cobalt, manganese, nickel, and zinc by precipitation using ammonium cinnamate, 20: 25012
separation from hafnium and titanium by selective iodate precipitation, 16: 17695
separation from hydrochloric acid solutions by solvent extraction using alkyl esters of phosphoric acid, 19: 7631
separation from hydrochloric acid solutions by solvent extraction using ethyl ether, 19: 36357
separation from hydrochloric acid solutions by solvent extraction using 2-ethylhexanol, 19: 36252
separation from hydrochloric acid solutions by solvent extraction using dialkyl alkylphosphonates, 20: 36941
separation from iron by solvent extraction, 16: 3092(P)
separation from lanthanides and other metals by paper chromatography using alcohols, 16: 27140
separation from lanthanum, chromatographic, 19: 7300
separation from methanol-nitric acid systems using anion exchange resins, 16: 25280 (TID-15598)
separation from metal ions by ion exchange in isopropyl alcohol, 18: 20104
separation from metallic ions by ion exchange chromatography, 19: 533
separation from metal ions by ion exchange chromatography, 20: 20821
separation from nitric or sulfuric acid solutions, ion exchange selectivity scales for, 19: 9257
separation from other metals by ion exchange, 17: 21791
separation from other metal ions on silica columns treated with dinonyl naphthalenesulfonic acid, 19: 15691
separation from other elements by solvent extraction of dianthipyrinylmethane complex, 19: 20080
separation from other elements by electrophoresis in glycolic acid, 19: 40671
separation from other elements by electrophoresis and chromatography, 20: 9070
separation from other inorganic ions by paper chromatography, 20: 12939
separation from other metals by ion exchange chromatography, 20: 16574
separation from other rare earths by ion exchange using triisooctylamine, 20: 43439
separation from perchlorate–chloride and perchlorate–nitrate solutions, 20: 18832
separation from perchloric acid solutions by ion exchange materials, 20: 20823
separation from pitchblende residues, leaching processes for, 20: 43420 (NCW-1508)
separation from potassium by carrier precipitation, 17: 2242 (TID-16949)
separation from pyroxenites by solvent extraction, precipitation of oxalate, and reduction, 19: 20081
separation from rare earths and yttrium by solvent extraction, 17: 27369
separation from rare earths and thorium by solvent extraction using thiocyanate-tributyl phosphate, 18: 1807
separation from rare earths and thorium by ion exchange in chloride–thiocyanate media, 18: 20113
separation from rare earths and yttrium by cation exchange chromatography, 18: 25613
separation from rare earths and thorium by paper chromatography, 20: 20825
separation from solutions by sorption on iron hydroxide, 19: 32307
separation from thorium and zirconium by selective iodate precipitation, 16: 17695
separation from thorium, solvent-extraction, 17: 35654
separation from thorium by solvent extraction using 5,7-dichloro-8-quinolinol, 18: 5221
separation from thorium in uranium ore processing, 18: 37300(P)
separation from thorium and uranium by ion exchange in nitrate solutions, 19: 38770
separation from thorium and other rare earths by reversed-phase chromatography, 19: 44125
separation from thorium and other rare earths by ion exchange in ammonium thiocyanate–organic solvent–water systems, 20: 1959
separation from titanium by cation exchange chromatography, 17: 32054
separation from titanium by solvent extraction, 19: 18067
separation from uranium by anion exchange using carbonate solutions, 18: 361
separation from uranium by cation exchange chromatography, 19: 13245
separation from uranium plant iron sludge and wolframite concentrates, 19: 9248 (BM-RI-6580)
separation from waste water, methods for, 19: 40276
separation of carrier-free calcium from, by reversed-phase partition chromatography, 16: 5406 (PAN-262/V)
separation of, from uranium ore leach, spectrographic, 17: 16164
separation of, from thorium using m-nitrobenzoic, quinoline-2-carboxylic, or tetrachlorophthalic acids, 17: 15909
separation of, from thiocyanate solutions by solvent extraction using 4-methyl-2-pentanone, 17: 20122
separation of trace elements from, by precipitation ion exchange, 20: 1958
separation of, from other elements by extraction using thenoyltrifluoroacetone, 20: 33157 (UJV-1512)
separation of, from zinc, in hydrochloric acid solutions by ion-exchange chromatography, 20: 45809
separation using cerium and zirconium pyrophosphates, 18: 17953
Slater-Condon parameters of, determined from spectral data, 17: 31118
solubility in delta-plutonium, 18: 18291(R) (LAMS-3057)
solubility in liquid cadmium, 17: 1985
solubility in liquid cadmium, 17: 7655(R) (ANL-6600)
solubility in liquid scandium trichloride, 19: 9046(R) (IS-900(Sect.C))
solvent extraction by synergic mixtures of phosphonates and thenoyltrifluoroacetone, steric effects, 17: 14382
solvent partition in hydrochloric acid–4-methyl-2-pentanone–8-quinolinol with dibutyl ester of butylphosphonic acid and trioctylphosphine oxide, 18: 16134
solvent partition between hydrochloric or nitric acids and di- or monobutyl phosphates, 18: 35483
solvent properties for tantalum, thermodynamics of, 20: 11306
sorption from nitric acid by ion exchange paper, 19: 24435

specific heat at low temperatures, 16: 1797
spectra, flame, 16: 30400
spectra in oxides, emission, 18: 39196
spectra of, absorption, 18: 1489(R) (IS-700(Sect. C))
spectra of, atomic absorption, 17: 10549
spectra of, analytical applications of flame, 18: 11982
spectra of, Ohlin structure near limit of continuous x-ray, (E), 19: 44940
spectra of, use of fuel-rich premixed oxyacetylene flame for emission, 18: 25278
structural effects on lanthanum and praseodymium orthoferrites, 18: 12711(T)
superconductivity of, 20: 40047
thermal conductivity at 5 to 320°C, 18: 24182
thermal conductivity at 2 to 20°K, 19: 37084
thermodynamic properties and vapor pressure at 298 to 1800°K, 17: 37206
thermodynamic properties at 0°C to melting point, 20: 29743
thermodynamic properties of, at 0°C to melting point, 20: 41412(R) (IS-1500(Sect. M))
thermoelectric voltage of polycrystals and single crystals of, 19: 23002(T) (JPRS-28849(p.86-97))
vapor pressure, 16: 10003
vapor pressure, measurements using tracers, 16: 25778
x-ray mass absorption at 1.49 to 15.77 kev, (E), 19: 25146(R) (TID-21542)

SCANDIUM ACETATES

preparation and crystal structure of ammoniated, 19: 40507
spectra of, infrared absorption, 18: 41446

SCANDIUM ALLOYS

nuclear magnetic resonance in, (E/T), 20: 4476(R) (IS-1200(Sect. P))
properties of, chemical and physical, 17: 32648
structure of intermetallic compounds with group VIII and IB metals, 17: 1988
Al–Co–Sc, crystal structure of intermetallic compound ScCoAl in, 19: 30701
Al–Cu–Sc, crystal structure of ternary phases in, 20: 17097(T)
Al–Ni–Sc, crystal structure of intermetallic compound ScNiAl in, 19: 30701
Al–Sc, crystal structure of stoichiometric, 19: 9712(T)
Al–Sc, crystal structure of AB type compound in, 19: 37063
Al–Sc, phase diagram, 20: 11297
Al–Sc, properties of intermetallic compounds in, tabulation of, 20: 43972
Al–Sc, structure of intermetallic compounds of, 19: 32755
Al–Sc, tensile properties, effects of composition on, 20: 11297
Au–Sc, crystal structure, 17: 41333(R) (ANL-6677)
Au–Sc, crystal structure studies, 19: 44678(R) (ANL-7000, pp 186-200)
Au–Sc, phase studies of solid solutions in, 19: 41062
Be–Sc, crystal structure of intermetallic compound $ScBe_3$ in, 18: 39960(T)
Be–Sc, phase studies, 20: 31667
Be–Sc, structure, effects of ultra-rapid quenching on, 17: 14812(R) (ASD-TDR-62-181)
Be–Sc, structure of intermetallic phase $ScBe_{13}$ in, 18: 18390
Be–Sc, structure of intermetallic compounds in, 19: 23011(T) (JPRS-28849(p.199-200))
Bi–Sc, structure of intermetallic compound ScBi in, 17: 1983(T)
Cd–Sc, crystal structure, 17: 1359(R) (ANL-5469)
Cd–Sc, crystal structure and phase studies, 17: 40421(R) KANL-6766)
Cd–Sc, preparation and structure of, 17: 39587
Cd–Sc, structure of $ScCd_3$, 18: 2232 (TID-18374)
Ce–Sc, phase studies, 19: 7969
Ce–Sc, preparation and oxidation resistance, 18: 43537(P)
Co–Ni–Sc, crystal structure of Laves phases in, 20: 41412(R) (IS-1500 (Sect. M))
Co–Ni–Sc, scandium-45 NMR in cubic Laves-phase intermetallic compounds of, Knight shift and linewidth in, (E), 20: 24654
Co–Sc, cobalt ion EPR in intermetallic compounds of, 20: 15963
Co–Sc, crystal structure, 17: 41333(R) (ANL-6677)
Co–Sc, crystal structure of, 18: 24157
Co–Sc, crystal structure of intermetallic compounds of, 18: 39927
Co–Sc, structure of intermetallic compounds in, 19: 23011(T) (JPRS-28849(p.199-200))
Cr–Sc, crystal structure and phase studies, 18: 12623 (ASD-TDR-63-204)
Cr–Sc, phase studies of solid solution formation in, 19: 41050
Cu–Sc, crystal structure, 17: 41333(R) (ANL-6677)
Cu–Sc, crystal structure of, 18: 24157
Cu–Sc, crystal structure of intermetallic compounds of, 18: 39927
Cu–Sc, structure of intermetallic compounds in, 19: 23011(T) (JPRS-28849(p.199-200))
Er–Sc, magnetic properties, 19: 32743
Er–Sc, phase studies, 19: 7969
Er–Sc, phase studies, 19: 32743
Er–Sc, temperature effects on magnetic properties of, 20: 23682
Fe–Ni–Sc, crystal structure of Laves phases in, 20: 41412(R) (IS-1500 (Sect. M))
Fe–Sc, isomer shift of iron-57 in $ScFe_2$ at 300 and 800°K, 19: 44678(R) (ANL-7000, pp 186-200)
Fe–Sc, magnetic moments in, determination of, using Moessbauer effect, 20: 26819 (NML-64-2)
Fe–Sc, structure of intermetallic compounds in, 19: 23911(T) (JPRS-28849(p.199-200))
Ga–Sc, crystal structure of AB type compound in, 19: 37063
Ga–Sc, crystallization of Sc_3Ga_5 with $D8_8$ structure, 18: 42027
Ga–Sc, structure of intermetallic compounds of, 19: 32755
Gd–Sc, magnetic ordering in, gadolinium-content effects on g factor for, (E), 20: 32716
Gd–Sc, magnetic properties, 19: 4682
Gd–Sc, phase studies of samarium-type intermediate phases in, 19: 44672 (AD-619201)
Gd–Sc, scandium-45 hyperfine interactions in, 20: 9658 (IS-T-38)
Gd–Sc, thermal analysis and x-ray-diffraction studies of, 18: 22509
Ge–Sc, crystal structure of AB type compound in, 19: 37063
Ge–Sc, preparation and crystal structure of intermetallic compounds in, 19: 28835
Ge–Sc, structure of intermetallic compounds of, 19: 32755
Hg–Sc, crystal structures of HgSc and Hg_3Sc, 18: 12708
In–Sc, scandium-45 NMR in, magnetic properties from, 19: 16119
In–Sc, structure of intermetallic compounds of, 19: 32755
Ir–Sc, crystal structure, 17: 41333(R) (ANL-6677)
La–Sc, phase studies of samarium-type intermediate phases in, 19: 44672 (AD-619201)
Mg–Sc, crystal structure of AB type compound in, 19: 37063
Mg–Sc, phase diagrams, 20: 41412(R) (IS-1500(Sect. M))
Mg–Sc, phase studies, 19: 7495
Mg–Sc, structure of intermetallic compounds of, 19: 32755
Mn–Ni–Sc, crystal structure of Laves phases in, 20: 41412(R) (IS-1500 (Sect. M))
Mn–Sc, crystal structure of, 18: 24157
Mn–Sc, crystal structure of intermetallic compounds of, 18: 39927
Mn–Sc, structure of intermetallic compounds in, 19: 23011(T) (JPRS-28849(p.199-200))
Mo–Sc, phase studies, 18: 12623 (ASD-TDR-63-204)
Mo–Sc, phase studies of solid solution formation in, 19: 41050
Nb–Sc, critical current density of superconducting, in transverse field of 30 kgauss, 18: 6128
Nb–Sc, crystal structure and phase studies, 18: 12623 (ASD-TDR-63-204)
Nb–Sc, phase studies of solid solution formation in, 19: 41050
Nd–Sc, phase diagram, 18: 20520 (IS-841)
Ni–Sc, crystal structure, 17: 41333(R) (ANL-6677)
Ni–Sc, structure of intermetallic compounds in, 19: 23011(T) (JPRS-28849(p.199-200))
Pb–Sc, structure of Sc_5Pb_3 in, 19: 37066
Pd–Sc, crystal structure, 17: 41333(R) (ANL-6677)
Pt–Sc, crystal structure, 17: 41333(R) (ANL-6677)
Pu–Sc, crystal structure lattice parameters of delta- and epsilon-phase, 18: 27998
Pu–Sc, crystal structure and phase studies, 18: 30975(R) (LAMS-3096)
Pu–Sc, crystal structure and phases of, 20: 1534(R) (LA-3370)
Pu–Sc, phase studies, 17: 22855(R) (LAMS-2875)
Pu–Sc, phase studies, 18: 7125(R) (LAMS-3021)
Pu–Sc, phase studies, 19: 13886(R) (LA-3208-MS)
Pu–Sc, phase studies, 20: 5843
Pu–Sc, phase studies, 20: 5848
Pu–Sc, phase studies, 20: 11224
Re–Sc, crystal structure of $ScRe_3$ and Sc_5Re_{24}, 17: 29347
Re–Sc, structure of intermetallic compounds in, 19: 23011(T) (JPRS-28849(p.199-200))
Rh–Sc, crystal structure, 17: 41333(R) (ANL-6677)
Rh–Sc, crystal structure of equiatomic intermetallic compound in, 19: 24994
Rh–Sc–Ti, superconductivity, 18: 21112
Ru–Sc, crystal structure, 17: 41333(R) (ANL-6677)
Sb–Sc, structure of intermetallic compound ScSb in, 17: 1983(T)
Sc–Ag, crystal structure, 17: 41333(R) (ANL-6677)
Sc–Ag, crystal structure studies, 19: 44678(R) (ANL-7000, pp 186-200)
Sc–Sn, structure of Sc_5Sn_3 in, 19: 37066
Sc–Ta, phase studies, 18: 12623 (ASD-TDR-63-204)
Sc–Ta, phase studies of solid solution formation in, 19: 41050
Sc–Tb, magnetic ordering temperature and structure of, from liquid helium temperatures to 300°K, 20: 24660
Sc–Tb, magnetic structure properties of, 20: 2338 (ORNL-P-1735)
Sc–Tc, phase studies on, 17: 11220
Sc–Tc, structure, 16: 3504
Sc–Ti, magnetic susceptibility of, 19: 38045
Sc–Ti, phase diagram, 16: 29409
Sc–Ti, phase studies, 16: 25824 (IS-310)
Sc–Ti, properties, 16: 29410

Sc–V, superconductivity in, (E), 19: 5108
Sc–W, phase studies, 18: 12623 (ASD-TDR-63-204)
Sc–W, phase studies of solid solution formation in, 19: 41050
Sc–Y, nuclear magnetic resonance in, 18: 2401(R) (IS-700(Sect.P))
Sc–Y, phase studies, 17: 27785 (IS-569)
Sc–Y, phase studies, 18: 18307
Sc–Y, phase studies and structure, 18: 42092
Sc–Y, scandium-45 hyperfine interactions in, 20: 9658 (IS-T-38)
Sc–Zn, preparation and structure of, 17: 39587
Sc–Zr, electronic properties, 18: 44150(R) (ORNL-3670(p.44-53))
Sc–Zr, phase studies, 17: 27785 (IS-569)
Sc–Zr, phase studies, 18: 18307
Sc–Zr, scandium-45 hyperfine interactions in, 20: 9658 (IS-T-38)
Sc–Zr, superconductivity, 20: 40047
Sc–Zr, superconducting transition temperature and electronic specific heat of, 20: 42121

SCANDIUM BORATES
spectra of, infrared, 20: 35519

SCANDIUM BORIDES
crystal structure of, x-ray absorption spectral studies of, 17: 32589
nuclear magnetic resonance of boron-11 in hexavalent, 17: 676
preparation and properties of di- and tetra-, 19: 23014(T) (JPRS-28849 (p.213-16))
preparation and structure of dodeca-, 17: 14266
preparation, properties, and uses, 17: 2959(T) (AEC-tr-5264)
stability of, chemical and thermal, 20: 14531
thermal expansion of, x-ray diffraction analysis of, 19: 22221
thermionic properties, 16: 13626
thermoelectric emission, 19: 6357
thermoemission properties of, 17: 39799

SCANDIUM BROMIDES
complexes of, stability constants of, 18: 35537
complexes with ammonia and water, infrared spectra of, 17: 35823
crystal lattice energy of, relation of self energy of gaseous ions to, 18: 16017
preparation and crystal lattice of, 18: 41458
preparation and thermal stability of ammoniated, 17: 25248
thermal stability of ammines, 17: 35824

SCANDIUM CARBIDES
crystal structure of, x-ray absorption spectral studies of, 17: 32589
dissociation energies at high temperatures, 18: 3795
hydrolysis of, methane production in, 20: 26890
preparation and properties, 16: 29400
preparation and properties, 19: 356(T) (JPRS-26877(p.1-24))
preparation and properties of, 19: 18472(T) (JPRS-28739)
preparation, properties, and structure of, 20: 26890
ScC–TiC, physical properties, 19: 18472(T) (JPRS-28739)
ScC–TiC, properties, 16: 29400
ScC–TiC–WC, preparation and hardness, 20: 15017

SCANDIUM CARBONATES
complexes of, composition in solution of, 20: 10824
compound formation with oxalate, electric conductivity and structure of, 19: 38672
decomposition of, mechanism of thermal, 17: 4553
preparation and thermal decomposition, 18: 17774 (LADC-6082)
solubility in complexone III, 20: 23026
solubility of, in water charged with carbon dioxide, 20: 45636

SCANDIUM CHLORIDES
complexes with ammonia and water, infrared spectra of, 17: 35823
crystal lattice energy of, relation of self energy of gaseous ions to, 18: 16017
dissolution in liquid scandium trichloride, phases in, 19: 9046(R) (IS-900(Sect.C))
preparation, 19: 13309
preparation and thermal stability of ammoniated, 17: 25248
preparation and thermodynamic properties, 18: 6832
properties of di- and trivalent, review on, 19: 22229
properties, chemical and physical, 16: 17615 (IS-300)
reactions with ethylendiamine, mechanism, 17: 32147
reactions with nitrogen oxides, 20: 29214
separation by reversed-phase partition chromatography using organophosphorus compounds, 18: 25614
solubility in hydrochloric acid at 25°C, 19: 40520
solvent properties of liquid, for scandium, 19: 9046(R) (IS-900(Sect.C))
stability constants of complexes of, 18: 31486
thermal stability of ammines, 17: 35824
thermodynamic properties, 18: 10108
toxic effects in rats, 16: 28670(R) (UCLA-507)
toxicology and pharmacology, 16: 14426 (TID-15406)
CsCl–$ScCl_3$, phase diagram, 16: 11641
KCl–$ScCl_3$, phase diagrams, 19: 26308
$ScCl_3$–NaCl, phase diagrams, 18: 17796
Sc–$ScCl_3$, phase studies and properties of, 18: 6832
Sc–$ScCl_3$, phase studies, 19: 13309

SCANDIUM COMPLEXES
acetate and sulfate, formation constants, 19: 18062
chloride and nitrate, stability of, extraction and ion exchange studies of, 19: 22223
chloride and nitrate, formation and stability of, 20: 18831
equilibrium quotients and stability of bromide and chloride, 16: 25356
gluconate, stability and acid dissociation constants of, 19: 36422
preparation and stability of ammoniated chloride and bromide, 17: 25248
spectra of organophosphorus-trifluorothenoylacetone, infrared, stability of, equations for, 20: 8934
with Alizarin Red S, composition, nature, and stability of, 18: 16039
with Aluminon, composition and stability of, spectrophotometric studies of, 20: 29180
with arsenazo III, formation mechanism of, 17: 6007
with arsenazo, composition of, 18: 19948
with arsenazo, composition and stability, 19: 36379
with ascorbic acid, absorption spectra of, 18: 31527
with benzoylacetone, dibenzoylmethane, and TTA, preparation and properties of, 20: 26830
with chromotrope 2B, composition and stability of, 18: 35542
with dialkyl phosphoric acids, preparation and properties, 18: 25429
with ethylenediaminetetraacetic acid, chemical and physical properties of, 16: 17615 (IS-300)
with organophosphorus esters and TTA, proton magnetic resonance spectra of, 18: 12132
with oxalate, properties and stability of, 18: 31515
with phenanthroline, infrared spectra of, 20: 16437
with quercetin, 17: 19962
with substituted 8-quinolinols, thermodynamics of dissociation of solvated, 17: 23243
with substituted 8-quinolinols, structure and thermal decomposition of solvated, 17: 23244
with thenoyltrifluoroacetone and 1,10-phenanthroline, preparation, 20: 45690
with tropolone, preparation, properties, and structure, 20: 5538
with TTA, solvent distribution in organic systems, 19: 24441
with xylenol orange, spectra of, 18: 13703
with Xylenol Orange, composition and chemical properties of, 20: 38924
with 2,2′-bipyridyl, infrared spectra of, 20: 16437
with 2,2′-dipyridyl and thenoyltrifluoroacetone, preparation, 20: 45690
with 2,2,6,6-tetramethyl-3,5-heptanedione, preparation and volatility of, 20: 7074
with 5,7-dihalo-8-quinolinols and 8-quinolinol, chemistry of, 18: 3789

SCANDIUM COMPOUNDS
organic, preparation and properties of scandium chloroacetates, 20: 16427
preparation and crystal structure, 19: 13364
preparation, properties, and uses of, review of, 20: 43203
solubility in water and thermolysis of diliturate, 18: 31447

SCANDIUM FLUORIDES
crystal structure, 19: 30149(R) (ORNL-3789(p.3-35))
effects on freezing point depressions in sodium fluorides, 18: 5284
equilibrium distribution in complex, 18: 6800
heat of sublimation and vapor pressure of, 20: 26874
heat of sublimation and sublimation pressure of, mass spectrometric studies of, 20: 29183
reactions with ammonia, 17: 25248
reduction using magnesium, 19: 7495
rotational states, 18: 43502
spectra of, in neon matrices at 4°K, Franck-Condon factors in visible and near-infrared absorption, 20: 45665
spectra of, rotational analysis of, 18: 23531
spectrum of, 17: 21685(T)
thermal stability, 17: 23321
thermodynamic functions of interactions with water, 17: 40798
KF–ScF_3, preparation and properties of K_3ScF_6, 19: 40512
KF–ScF_3–NaF, phase studies, 19: 40512
MgF_2–ScF_3, phase diagram, 17: 23321
ScF_3–NaF, crystal structure of Na_3ScF_6 and $NaScF_4$ in, 20: 22856(R) (ORNL-3913, pp 1-51)
ScF_3–NaF, phase diagram, 18: 37126
ScF_3–NaF, phase diagrams, 20: 22856(R) (ORNL-3913, pp 1-51)
ScF_3–NaF, phase studies, 19: 30149(R) (ORNL-3789(p.3-35))
ScF_3–NaF, preparation and properties of Na_3ScF_6, 19: 40512

SCANDIUM FORMATES
thermal decomposition of, composition of products in, 17: 25162 (LADC-5486)

SCANDIUM HYDRIDES
dissociation pressure, 18: 31417 (AWRE-O-22/64)
formation in hydrogen–scandium systems, 20: 322
preparation, 16: 12097(R) (LAR-1)
preparation and properties of, 19: 15466(T) (LA-tr-65-2)

preparation from scandium metal and hydrogen, 18: 43539(P)
pressure-temperature-composition relations, 16: 12104(R) (LAR-10)
scandium NMR in, Knight shifts and relaxation times in, (E), 19: 9141
LiH–ScH_2, phase studies, 19: 19681

SCANDIUM HYDROXIDES
precipitation by ammonium and sodium hydroxides solutions, 17: 25247
solubility and precipitation of, determination of pH for, 19: 36379
thermal decomposition of, analysis of products of, 20: 45695

SCANDIUM HYPOPHOSPHITES
preparation and properties of, 20: 16426

SCANDIUM IODIDES
preparation and crystal structure, 18: 22084
reactions with ammonia, 17: 25248
stability and thermodynamic properties, 18: 1675
thermal stability of ammines, 17: 35824

SCANDIUM IONS
complex formation by, optimum conditions for, 19: 13374
effects on spectrophotometric determination of erbium, holmium, and neodymium, 20: 43100
entropy and heat of formation in aqueous solution, equation for calculation of, 18: 22066
exchange on natural and synthetic exchangers, 16: 20356 (JÜL-32-RC)
radioprotective effects in mice, 18: 13567
reactions with derivatives of Arsenazo III, spectrophotometric studies of, 19: 40426
separation by thin-layer ionophoresis, 18: 10185
separation of, parameters for cation-exchange, 17: 32092
Slater-Condon parameters of, determined from spectral data, 17: 31118
sorption from perchloric acid solutions by cellulose and resin sulfonic acid exchangers, 18: 35473
spectra of, optical, (T), 19: 22218
stability constants and structure, effects of ligand fields, 17: 28911
toxicity of, in mouse, determination by LD_{50} on thirtieth day of, 17: 17719
van der Waals radii of, relation of hydration energy to, 18: 16016

SCANDIUM ISOTOPES
binding energies and spectra of, from residual two-body interaction theory, 18: 4605
decay of isomeric, energy and half life for, (E), 19: 10329
deuteron reactions at 15 Mev, isomeric states from, (E), 20: 15856
energy levels, 17: 41530(R) (ANL-6720(p.43-7))
energy levels, 18: 24625 (WASH-1046)
energy levels of, weak-coupling model for $d_{3/2}$-hole states in, 20: 15852
transitions in, M2, (T), 19: 19207
wave functions for two-particle $1f_{7/2}$ shell, 18: 30733 (NYO-9891)

SCANDIUM ISOTOPES Sc-40
beta decay of, branching ratios and gamma transitions in, (T), 20: 10021
beta decay of, energy levels and gamma spectra from, (E), 20: 10020
beta decay of, gamma spectra from, (E), 20: 34640
beta decay of, ground state spin from, (E), 19: 39850
mass difference of calcium-40 and, (E), 19: 39850
mass from threshold energy for calcium-40 (p,n) reactions, (E), 20: 44812
positron spectra, 16: 23069

SCANDIUM ISOTOPES Sc-41
beta decay of, mesonic exchange effect in, 19: 21348
core deformability and electric quadrupole moments, 16: 7026
energy levels, 17: 41873 (WASH-1044)
energy levels, 18: 21338
energy levels, (E), 19: 39874
energy levels from calcium-40 (p,γ) reactions at 0.6 to 5.2 Mev, 20: 15849
energy levels of, figures of merit for low lying, 17: 26592
energy levels of, even-parity-hole states in $f_{7/2}$, 18: 36646
energy levels of, lifetime and radiative width of first excited, (E), 19: 45344
energy-level transition probabilities of, E2, (T), 20: 3115
half life and mass of, (E), 19: 14590
nuclear density distributions of, from calcium-40 (p,γ) reactions at 0.25–1.52 Mev, 17: 31473
nuclear magnetic moment corrections for, perturbation theory for, 20: 13838
positron emission, decay scheme and spectra, 16: 24836

SCANDIUM ISOTOPES Sc-42
beta decay, 17: 34932
beta decay of, maximum energy and half life of, 17: 29636
beta decay of, conserved vector current hypothesis and ft values for, (E/T), 19: 39859
decay of, 16: 30930(R) (NYO-2669)
decay, one-minute positron activity in, 16: 21636
decay schemes, 17: 17218
energy level population in (α,d) reactions, 18: 34779 (UCRL-11341)
energy level scheme, (E), 20: 12061
energy level structure, (E), 19: 5167
energy levels, 18: 34960
energy levels, 18: 32747(R) (UCRL-11213(p.64-86))
energy levels from helium-3 reactions (He-3,p) and (He-3,pγ) with calcium-40 at 10, 12, and 15 Mev, (E), 20: 22073
energy levels from calcium-40 (α,d) reactions at 24.8 Mev, (E), 20: 43717
energy levels, inversion of lowest T = 0,1 states in, 16: 13997
energy levels of, $(f_{7/2})^3$, 18: 16933 (ANL-6848(p.182-7))
energy levels of, even-parity-hole states in $f_{7/2}$, 18: 36646
energy levels of, symplectic symmetry in $f_{7/2}$, (T), 19: 6670
energy levels of, from calcium-40 (He-3,p) reactions, (E/T), 19: 17031
energy levels of, central and tensor potentials in shell model calculations of, 20: 28360
energy levels of, shell-model potential parameters for low-lying, (T), 20: 38145
isomeric behavior, 16: 14378(R) (NYO-2302)
nucleon-nucleon interactions in, core polarization effects in two-body, (T), 20: 1186
positron decay, 17: 5325 (PUC-1962-62)
positron decay, maximum energy and half life, 16: 12529

SCANDIUM ISOTOPES Sc-43
beta decay and energy levels, 18: 22912
beta decay of, log ft values for, (T), 20: 19932
decay spectrum of, beta and gamma, (E), 19: 5258
energy levels, (E), 20: 42253
energy levels from proton reactions (p,γ) with calcium-42, (E), 19: 41738
energy levels from titanium (α,p) reactions at 9 to 10 Mev, (E), 19: 43317
energy levels from proton reactions (p,γ) with calcium-42, spins and parities of, (E), 20: 26118
energy levels from alpha reactions (α,p) with calcium-40 at 9 and 10 Mev, (E), 20: 28345
energy levels of, lifetime of $d_{3/2}$ hole, 18: 34923
energy levels of, even-parity-hole states in $f_{7/2}$, 18: 36646
energy levels of, lifetimes of, 18: 42624(R) (ANL-6879(p.35-63))
energy levels of, lifetime of metastable, (E), 19: 12512
energy levels of, lifetime of $d_{3/2}$ hole, (E/T), 19: 19095 (WASH-1053)
energy levels of, M2 lifetimes of, (T), 19: 19207
energy levels of, lifetime of low-lying hole, 19: 47115(R) (ANL-6983)
energy levels of, odd-parity, (T), 20: 46700
gamma spectra and half life of isomeric, (E), 19: 41802(T)
isomeric transition in, 435-μsec, 18: 38112
isomeric transitions, (E), 20: 46242(R) (TID-23239)
nuclear moments and spins of, determination, (E/T), 20: 6299 (PUC-1965-158)
nuclear moments of, E2 and M1, (E), 20: 12070
production in nitrogen-14 reactions with chlorine-35, cross section for, 17: 24053(R) (ORNL-3432)
production in nitrogen-14 reactions with phosphorus-31 and sulfur-32, 17: 38108
production in nitrogen-14 reactions with chlorine-35, phosphorus-31, and sulfur-32, (E), 19: 21392
production in proton reactions with silver at 2.9 Bev, range studies of, 18: 26648
production of isomeric, (E), 19: 41802(T)
yields in proton spallation of copper at 24 Bev, 16: 24859

SCANDIUM ISOTOPES Sc-44
beta decay, beta-gamma circular-polarization correlation parameters in, 16: 15683
beta decay, isospin conservation in, 16: 17084
beta decay of isomeric, calcium-44 energy levels from, (E), 20: 44682
beta decay of, asymmetry parameters and isotopic spin impurity coefficients for, (E), 19: 8447
beta decay of, charge dependence of nuclear forces in ΔT = ±1, 18: 19024
beta decay of, circular polarization of gamma radiation following, 18: 21309
beta decay of, Coulomb matrix elements and impurity coefficients in, 18: 28665
beta decay of, Fermi matrix elements for, (T), 19: 35389 (KFK-313)
beta decay of, log ft values for, (T), 20: 19932
beta decay of, transitions to vibrational levels in, 18: 36625
beta emission from, hindrance phenomena in, 16: 23073
decay, beta-gamma circular-polarization correlation and isospin conservation in, 16: 21616
decay of, ratio of electron capture to positron emission in, 18: 2886
decay scheme, 17: 2244 (TID-17183)
decay scheme and gamma spectra of ground- and isomeric-state, 18: 18971
decay scheme of 2.4-day isomer, 17: 2244 (TID-17183)
energy level density in, spin dependence of, (E), 19: 47596(R) (TID-22141, pp 94-7)
energy levels, 17: 28249 (UCOL-P-518)
energy levels, (E), 19: 23355(R) (BNL-867(p.1-117))
energy levels of, low-lying, 18: 19104

energy levels of, parameters for, 18: 19046
energy levels of, even-parity-hole states in $f_{7/2}$, 18: 36646
gamma spectra, (E), 19: 16840(R) (IDO-17050)
gyromagnetic factor of first excited state, 17: 11612 (AFOSR-2975)
half life, 20: 16331 (GA-6568)
half life measurements from 440-Mev proton reactions with stone meteorites, 17: 28943(R) (TID-18961)
isomeric ratios from proton reactions (p,n) with calcium-44 at 40 Mev, 16: 11694(R) (TID-15020(p.35-6))
isomeric transition in, 50-μsec, 18: 38112
nuclear g-factor and magnetic moment of first excited state of, 17: 2259
nuclear magnetic dipole moments for, (T), 20: 19932
nuclear magnetic moments of the two long-lived states of, measurement using the atomic-beam magnetic resonance method, 17: 38123
nuclear spins and hyperfine structure, 17: 7137 (PUC-1962-59)
nuclear structure of, determination of, 18: 21339
photoproduction of isomeric, yield ratios for, (E/T), 20: 1246
photoproduction of isomeric, (E), 20: 46733
preparation of isomers in alpha reactions (α,n), effects of alpha energy, 16: 23030
production by potassium-41(α,n) reactions, isomeric cross section ratios for, (E), 19: 41820
production in (He-3,α) reactions at 27.5 Mev, ratio of ground- and isomeric-state, 18: 18971
production in heavy ion reactions, cross sections for isomer-pair, 17: 34877 (JINR-P-1277)
production in nitrogen-14 reactions with chlorine-35, cross section for, 17: 24053(R) (ORNL-3432)
production in nitrogen-14 reactions with phosphorus-31 and sulfur-32, 17: 38108
production in potassium (α,n) reactions to 42 Mev, isomeric cross section ratios for, (E), 19: 41695
production in potassium-44 (α,n) reactions, isomeric cross section ratios for, (T), 19: 41696
production in potassium-41 (α,n) reactions, isomeric cross section ratios for, 20: 4922
production in proton reactions with silver at 2.9 Bev, range studies of, 18: 26648
production method for, 19: 36452(R) (BNL-900(p.105-20))
production method for, 20: 20177(R) (BNL-929, pp 83-105)
production of ground-state and isomeric, in alpha reactions (α,n) with potassium-41 at 8 to 19 Mev, 18: 36673
production of isomeric pair of, ratio of cross sections for heavy-ion, 18: 6261
production of isomers of, in scandium-45 (p,pn) reactions, 18: 32859
production of isomer pairs of, in heavy ion reactions, 18: 34948
production of isomeric, cross section for (d,t) reaction for, 18: 44734 (NP-14266)
production of isomer pairs of, in nitrogen-14 reactions with chlorine-35, phosphorus-31, and sulfur-32, (E), 19: 21392
production of isomer pairs of, in potassium-41 (α,n) reactions, (E), 20: 28352
yield ratios for isomeric, from (γ,n), (γ,np), and (n,2n) reactions, (E), 20: 17777
yields in proton spallation of copper at 24 Bev, 16: 24859
yields of isomeric pair of, in deuteron reactions with scandium-45, 19: 41714
yields of metastable, in proton spallation of copper at 24 Bev, 16: 24859

SCANDIUM ISOTOPES Sc-45

abundance in meteorites and terrestrial matter, 18: 10753
alpha reactions (α,αn), (α,n), (α,2n), (α,2p), and (α,2pn) at 15 to 40 Mev, excitation functions for, 18: 26649
alpha reactions (α,p) at 22 Mev, angular distributions from, 17: 28288
alpha reactions in, excitation functions and cross sections for, 17: 11624 (NYO-10386)
beta decay of, circular polarization of gamma radiation following, 18: 21309
bremsstrahlung reactions (γ,n), (γ,2n), and (γ,2p) at 45 Mev, yield ratios for, 19: 23209(R) (RPI-328-20)
bremsstrahlung reactions (γ,n) at 48 Mev, (E), 19: 47596(R) (TID-22141, pp 94-7)
bremsstrahlung reactions at 45 Mev, (E), 19: 47596(R) (TID-22141, pp 94-7)
bremsstrahlung reactions (γ,n) at 24, 36, and 48 Mev, scandium-44 isomeric yield ratio from, (E), 20: 17777
Coulomb excitation of, gamma angular distribution from, (E), 19: 16896
determination in human urine and waste solutions, 16: 2980
deuteron reactions (d,p) with, compound nucleus formation effects in, 17: 38222
deuteron reactions (d,p) with, excited states from, 18: 15294
deuteron reactions (d,α) and (d,p) at 3 to 4.3 Mev, energy levels from, 18: 19046
deuteron reactions (d,t) at 26 Mev, cross sections for isomer formation in, 18: 44734 (NP-14266)
deuteron reactions (d,t) at 19 to 28.6 Mev, yields of scandium-44 isomer pairs in, 19: 41714
energy level at 1.660 Mev, gamma spectrum from, 18: 18894
energy level at 12.4 kev, K-conversion coefficient for, (E), 20: 38087
energy level density, 16: 19797
energy levels, 18: 18894
energy levels, 18: 22911
energy levels, 18: 40560
energy levels, (E), 20: 42253
energy levels from titanium (α,p) reactions at 9 to 10 Mev, (E), 19: 43317
energy levels from calcium-45 beta decay, (E), 20: 1206
energy levels from electron capture decay of titanium-45, 20: 3128
energy levels from calcium-44 (He-3,d) reactions, parity and spin of 378-kev, (E/T), 20: 30429
energy levels from beta decay of titanium-45, (E), 20: 30456
energy levels from titanium-48 (p,α) reactions, (E), 20: 34639
energy levels of, parameters for, 18: 19046
energy levels of, lifetime of $d_{5/2}$ hole, 18: 34923
energy levels of, even-parity-hole states in $f_{7/2}$, 18: 36646
energy levels of, lifetime of $d_{3/2}$ hole, (E/T), 19: 19095 (WASH-1053)
energy levels of, M.2 transitions of $d_{3/2}$, (T), 19: 19173
energy levels of, M2 lifetimes of, (T), 19: 19207
energy levels of, M2 transitions of $d_{3/2}$, (T), 19: 19173
energy levels of, lifetime of low-lying hole, 19: 47115(R) (ANL-6983)
gamma reactions (γ,n) at 48 Mev, isomer ratios in, 19: 23209(R) 19: 23209(R) (RPI-328-20)
helium-3 reactions (He-3,α) at 27.5 Mev, ground- and isomeric-state production in, 18: 18971
helium-3 reactions (He-3,d) at 24.4 Mev, momentum spectra from, (E), 20: 13345(R) (NP-15772)
hyperfine interactions in scandium-rich alloys, 20: 9658 (IS-T-38)
hyperfine structure of, analysis by exchange polarization, 19: 27580
neon-22 reactions at 60 to 160 Mev, production of scandium-44 isomer pairs in, 18: 34948
neutron activation cross sections, 17: 10139
neutron capture by, scandium-46 levels from thermal, (E), 20: 28373
neutron capture by, gamma spectra from, 20: 29078(R) (AD-633252)
neutron capture cross sections and radiation widths, (E), 19: 41806(T)
neutron capture cross section at 14.7 Mev, (E), 20: 46614
neutron capture in, gamma energies from, 16: 28162
neutron reactions (n,p) at 14 Mev, direct and evaporation mechanisms, 16: 4850
neutron reactions (n,2n) at 14.8 Mev, cross sections for, 16: 7072
neutron reactions (n,α) and (n,p) at 7.0 to 19.8 Mev, cross sections for, 16: 19782
neutron reactions (n,2p) at 14.8 Mev, cross section limit, product half life, and Q value for, 17: 2242 (TID-16949)
neutron reactions (n,α) at 14.8 Mev, cross sections for, 17: 2242 (TID-16949)
neutron reactions (n,2n) at 14.8 Mev, cross sections for, 17: 2242 (TID-16949)
neutron reactions (n,helium-3) at 14.8 Mev, cross section limit, product half life, and Q value for, 17: 2242 (TID-16949)
neutron reactions (n,p) at 14.8 Mev, separation energies for, 17: 2242 (TID-16949)
neutron reactions (n,αγ), (n,αn), (n,pγ), and (n,pn) at 14.8 Mev, cross sections for, 17: 2242 (TID-16949)
neutron reactions (n,2n) at 14.1 Mev, cross sections for, 17: 15299
neutron reactions (n,2n) with, product half life for, 17: 25857(R) (PR-P-56(p.4-18))
neutron reactions (n,α) with, product half life for, 17: 25857(R) (PR-P-56(p.4-18))
neutron reactions (n,d) at 14 Mev, cross sections for ground-state transitions in, 17: 34920
neutron reactions (n,2p) at 14.7 Mev, cross-section limits for, 17: 36707
neutron reactions (n,He^3) at 14.7 Mev, cross-section limits for, 17: 36707
neutron reactions (n,γ) at 0.15 to 14.65 Mev, cross sections for, 18: 1037
neutron reactions (n,2p) at 14.8 Mev, cross-section limits for, 18: 1077
neutron reactions (n,He^3) at 14.8 Mev, cross-section limits for, 18: 1077
neutron reactions (n,2n) with, cross sections for positron production in, 18: 13061
neutron reactions (n,α) at 14 Mev, 18: 17057
neutron reactions (n,γ) at thermal energy, gamma spectra from, 18: 28569 (MITNE-37)
neutron reactions (n,2n) at 14 Mev, shell effects in, (T), 19: 12536
neutron reactions (n,γ) with, cascade transitions in, (E), 19: 16897
neutron reactions (n,2n), isomer ratios in, 19: 23209(R) (RPI-328-20)
neutron reactions (n,γ) with, levels populated in thermal, (E), 19: 25526
neutron reactions (n,2n) at 14 Mev, (E), 19: 47596(R) (TID-22141, pp 94-7)
neutron reactions (n,α) with, cross sections for, 20: 1947

neutron reactions (n,γ) with, isomeric cross sections for, (E/T), 20: 6301 (TID-22165)
neutron reactions (n,γ) with, gamma spectra from thermal, (E), 20: 9981 (WASH-1064)
neutron reactions (n,2n) at 14 Mev, scandium-44 isomeric yield ratio from, (E), 20: 17777
neutron reactions (n,γ) with, thermal, (E), 20: 34574
neutron reactions (n,γ) at thermal energies, gamma spectra from, (E), 20: 42382
neutron reactions (n,p) at 14.7 Mev, cross section for, (E), 20: 46614
neutron reactions (n,2n) at 3 Mev above threshold, cross section for, (E), 20: 46614
neutron reactions (n,α) with, ratio of forward to backward recoil-nuclei yields for, (E), 20: 46614
nitrogen-14 reactions (N-14,N-15) at 27.5 Mev, excitation functions for, 18: 24716
nitrogen-14 reactions (N-14,N-15) at 27.5 Mev, excitation functions for, 18: 28573(R) (ORNL-3630(p.1-17))
nitrogen-14 reactions (N-14,N-15) with, scandium-44 isomeric state from, (E), 19: 37823(R) (ORNL-3800(p.1-49))
nitrogen-14 reactions with, excitation functions for one-neutron-transfer, (E/T), 19: 47586 (ORNL-TM-1218)
nitrogen-14 reactions at 20 to 42 Mev, excitation functions for, (E), 19: 47667
nuclear magnetic dipole moments for, (T), 20: 19932
nuclear magnetic relaxation in scandium metal, 18: 16563
nuclear magnetic resonance in scandium nitrides, Knight shift and relaxation in, 18: 19980
nuclear magnetic resonance in indium–scandium alloys, 19: 16119
nuclear magnetic resonance in scandium, Knight shift anisotropy in, (E), 19: 16976
nuclear magnetic resonance in cubic Laves-phase cobalt–nickel–scandium alloy, Knight shift and linewidth in, (E), 20: 24654
oxygen-16 reactions at 20 to 80 Mev, production of scandium-44 isomer pairs in, 18: 34948
photon reactions at 300 Mev peak, isomer production in, (E/T), 20: 1246
proton inelastic scattering at 3 to 4.3 Mev, energy levels from, 18: 19046
proton reactions (p,d) at 17.5 Mev, energy spectra for, 18: 19104
proton reactions (p,n) with, excitation of isobaric analog state in, 18: 28574(R) (ORNL-3630(p.18-30))
proton reactions (p,2p) at 150 Mev, 18: 32824
proton reactions (p,n) and (p,pn) at 120 to 670 Mev, 18: 32859
proton reactions (p,d) with, analytical uses of, 19: 14494 (ANL-6878 (p.249-75))
proton reactions (p,α) with, models for, (T), 19: 14496 (ANL-6878(p.335-50))
proton reactions (p,n) at 3.5 to 6.75 Mev, total cross sections for, (E), 19: 23682
proton reactions (p,α) and (p,p) at 6.75, cross sections for, (E), 19: 23682
proton reactions (p,n) with, neutron production for activation analysis in, 20: 16332 (GA-6691)
proton reactions (p,n) at 100 to 400 Mev, excitation functions for, 20: 30464
proton reactions (p,α) at 8.5 to 9.4 Mev, statistical fluctuations in cross sections for, 20: 40065(R) (BMwF-FB-K-66-01)
proton reactions (p,n) at 15.25 Mev, angular distributions for quasi-elastic, (E), 20: 42169(R) (UCRL-14744, pp 1-18)
proton reactions (p,α), statistical fluctuations in, 20: 46580(R) (BMwF-FBK-66-05)
proton reactions (p,n), 16: 2492(R) (TID-14186)
proton reactions (p,γ), excitation energies, 16: 19797
proton reactions (p,α) at 18 Mev, seniority wave function effects on angular distributions and cross sections, 16: 21578
proton reactions (p,pn) at 370 Mev, cross sections for, 17: 796 (NEVIS-109)
proton reactions (p,n), cross section relations with energy, 17: 7144 (TID-17357(Pt.III))
proton reactions (p,n) at 6.75 Mev with, cross section for, 17: 22618
proton reactions (p,n) with, excitation function for, 17: 28247(R) (TID-18788)
proton reactions (p,γ) at 1.3–2.5 Mev, gamma decay from resonances in, 17: 31422
proton reactions (p,γ) at 900–1400 kev, resonances in, 17: 31426
proton reactions (p,n) and (p,np) with, cross sections for, 18: 4539 (JINR-E-1384)
proton scattering spectra, 16: 2492(R) (TID-14186)
proton scattering by, energy levels from, 18: 30867

SCANDIUM ISOTOPES Sc-46

activity measurements in fragment of Sputnik IV, 17: 28943(R) (TID-18961)
activity of, method for determining gamma, 20: 9196
beta decay, beta-gamma circular-polarization correlation parameters in, 16: 15683
beta decay, beta gamma circular polarization anisotropy in, 16: 28034 (PUC-1962-71)
beta decay of, chemical effects on gamma angular correlations in, 17: 41946
beta decay of, angular correlations in, 18: 34752(R) (CU(PNPL)-234)
beta decay of, asymmetry parameters and isotopic spin impurity coefficients for, (E), 19: 8447
beta decay of, β-γ circular polarization correlation in, (E), 20: 6391
beta decay of, β-γ circular polarization in, (E), 20: 32457
beta decay of, β–γ circular polarization correlation in, (E), 20: 34649
beta decay of, Coulomb matrix elements and impurity coefficients in, 18: 28665
beta decay of, log ft values for, (T), 20: 19932
beta decay of, polarized correlations in (E), 19: 1680
beta-gamma circular-polarization correlation of, in various chemical forms, 17: 40018
calibration of, by sum peak method using sodium iodide crystal, 19: 32276
content and motion in soil, 19: 36661
content in meteorites, 18: 10756
content in particles suspended in Columbia River, 19: 622(R) (HW-81746 (p.3.84-6))
content in reactor effluent, effect of SiO_2 on, 20: 45215 (BNWL-282)
content in Sputnik 4 fragment, 18: 13666
content in stone meteorites, gamma spectrometric study of, 18: 2515
cross sections for, production in 1-Bev proton reactions with iron, 17: 28943(R) (TID-18961)
decay, beta-gamma circular-polarization correlation and isospin conservation in, 16: 21616
decay, gamma circular polarization from, 16: 23076
decay of, beta-gamma circular polarization correlation in, 17: 28296
decay of, beta-gamma circular polarization correlation in, (E), 19: 14636
decay of, gamma angular correlations in, (E), 19: 19213
decay of, gamma transitions in, (E), 19: 39866
decay scheme, 18: 2962
detection and measurement of, by 4π-liquid scintillation counting, 19: 11595
detection in gastrointestinal tract from drinking water, continuous monitoring system for, 20: 27191 (BNWL-SA-212)
determination in Columbia River, 20: 8980(R) (BNWL-36, pp 3.1-122)
determination in crushed oil shales, activation, 20: 23236(R) (ORNL-TM-1496)
determination in irradiated materials by extraction and precipitation, gamma spectrometric, 20: 16336(R) (NYO-10175)
determination in meteorites, 17: 12452 (LA-2765)
determination in neutron-irradiated clays and soils, 20: 43607
determination in urine, gamma spectrometric, 19: 32 (HW-SA-3641)
determination in water, radiochemical, 17: 10850(R) (HW-73337(p.77-157))
determination of ratio with scandium-48 in titanium oxide targets, spectrometric, 18: 25298
electron conversion, 18: 18911
energy levels, 18: 19010
energy levels, (E), 19: 16897
energy levels, (E), 20: 34574
energy levels, (E), 20: 42382
energy levels, 18: 42622(R) (ANL-6879(p.2-20))
energy levels from scandium-45 (n,γ) reactions, 18: 28569 (MITNE-37)
energy levels from scandium-45 thermal neutron capture, parities and spins for, (E), 20: 28373
energy levels of 7-Mev deuteron bombarded, 16: 30930(R) (NYO-2669)
energy levels of, even-parity-hole states in $f_{7/2}$, 18: 36646
energy levels of, symplectic symmetry in $f_{7/2}$, (T), 19: 6670
energy levels of, low-lying excited, (E), 19: 25526
energy levels up to 7.6 Mev, 18: 15294
excretion by man, effects of chelating agents on, 20: 1691
excretion by man, effects of DIPA and EDTA on, 20: 31
gamma dose constants for, 20: 46617
gamma emission by, 18: 8313
gamma emission by, methods of measuring, 20: 8870
gamma emission of, 17: 7116 (NP-12330(p.186-92))
gamma spectra, 16: 4751 (JAERI-4019)
gamma spectra, 16: 12265
gamma spectra, 16: 11883
gamma spectra, 17: 34966
gamma spectra, 19: 4474 (TID-7705(p.113-23))
gamma spectra, 19: 28639 (TID-21830)
gamma spectra between 0 and 350 kev, 16: 28162
gamma spectra of, multidimensional measurement of, 18: 8642 (HW-SA-3225)
gamma spectra of, computer program for determination of, 19: 18387
gamma transitions in, design of spectrometer for study of angular correla-

tions of, 18: 2044
gastrointestinal transit time of ceramic spheres containing, 20: 42740 (LA-DC-7764)
half life, 20: 8076 (NP-15663)
half life measurements from 440-Mev proton reactions with stone meteorites, 17: 28943(R) (TID-18961)
incorporation in solid cracking catalyst, process for, 20: 38993(P)
incorporation in tetrahydrated ammonium thallium sulfates, mixed crystal formation in, 20: 43252
internal conversion coefficients of the E2 transitions, 16: 29798
metabolism in man, 17: 7750 (TID-17547)
metabolism in man, 19: 43692
neutron capture by, gamma spectra from, 20: 29078(R) (AD-633252)
nuclear magnetic dipole moments for, (T), 20: 19932
nuclear properties, 17: 863
production by neutron reactions (n,γ), 18: 37592
production in Canada, 18: 14338
production in reactor, 17: 1176(R) (HW-70050(p.78-142))
production of isomeric pairs of, in scandium-45 (n,γ) reactions, (E/T), 20: 6301 (TID-22165)
sensitivity for activation analysis using beta-gamma-gamma sum-coincidence gamma spectrometer, 20: 16335(R) (NBS-TN-276)
separation and purification for medical use, 18: 37581 (A/CONF.28/P/457)
separation from zirconium-95 by anion exchange, 19: 26224 (AERE-R-4872)
sorption by Columbia River particulate material, 18: 35761 (HW-79279)
sorption from reactor effluent by particles in Columbia River, 19: 215(R) (HW-81746(p.3.81))
sorption on sediments in Columbia River, 19: 15784(R) (HW-83614)
standardization using a thallium-activated sodium iodide crystal, 17: 25292
tracer applications in sedimentation, 16: 17898
tracer applications in coal processing, 17: 12519(R) (NYO-9852)
tracer use for determination of scandium, 16: 23736
tracer use in measurement of sedimentation drift, 16: 24001
tracer use in sedimentation measurements in Bombay Harbor, 16: 24002
tracer uses in clay movement in porous media, 19: 20183
transport in Columbia River, 20: 25290
use as tracer for ground water research, 20: 39155
use as tracer in studies on erosion and sand transport on surf coasts, 20: 2060
use in silt movement analysis, 20: 4166 (AERE-R-4980)
use in tracer studies of sand erosion and displacement by surf, 20: 510 (EUR-2167.d)
use of, in microspheres for cancer therapy in animals and man, 17: 10288
yields in proton spallation of copper at 24 Bev, 16: 24859

SCANDIUM ISOTOPES Sc-47
beta decay of, log ft values for, (T), 20: 19932
decay of, beta-gamma correlations in, 18: 19027
decay scheme, (E), 19: 31217 (IDO-17042(p.11-47))
energy levels, (E), 20: 22010(R) (NYO-72-28)
energy levels and gamma spectra of, (E), 19: 31217 (IDO-17042(p.11-47))
energy levels from titanium (α,p) reactions at 9 to 10 Mev, (E), 19: 43317
energy levels from titanium-48 (p,2p) reactions at 155 Mev, (E), 20: 6330
energy levels from titanium-50 (p,α) reactions, (E), 20: 34639
energy levels of, mean life-times and mixing ratios of, 17: 40067
energy levels of, lifetime of $d_{3/2}$ hole, 18: 34923
energy levels of, even-parity-hole states in $f_{7/2}$, 18: 36646
energy levels of, lifetime of $d_{3/2}$ hole, (E/T), 19: 19095 (WASH-1053)
energy levels of, M2 lifetimes of, (T), 19: 19207
energy levels of, lifetime of low-lying hole, 19: 47115(R) (ANL-6983)
energy levels of, lifetime of metastable hole state in, (E), 20: 42192
energy levels of, from titanium (γ,p) reactions at 0.16 to 0.51 Mev, 20: 43102
gamma dose constants for, 20: 46617
half life measurements from 440-Mev proton reactions with stone meteorites, 17: 28943(R) (TID-18961)
measurement in samples containing calcium-47, 19: 7612
metabolism and fecal excretion by man after intravenous and oral administration, 20: 12612
metabolism in rat bones, 20: 40545
metabolism of, use of scanner for measuring, 19: 6927
nuclear magnetic dipole moments for, (T), 20: 19932
nuclear moments of, E2 and M1, (E), 20: 12070
production in reactors, 17: 3022 (BNL-6407)
production in 1- and 3-Bev proton reactions with simulated stone meteorites, 17: 28943(R) (TID-18961)
properties and uses of, produced at Brookhaven, 19: 22853 (ORNL-TM-1047(p.113-16))
spin of 160-kev level in, 17: 26480
standardization in calcium-47 solutions, method for, 20: 9027 (AERE-R-4886)
yields in proton spallation of copper at 24 Bev, 16: 24859

SCANDIUM ISOTOPES Sc-48
beta decay of, asymmetry parameters and isotopic spin impurity coefficients for, (E), 19: 8447
beta decay of, Coulomb matrix elements and impurity coefficients in, 18: 28665
beta decay of, energy levels from, (E), 19: 23677
beta decay scheme, 17: 22575
beta spectra, 17: 2463(R) (BNL-731(p.53-8))
decay, 17: 31797(R) (BNL-782(p.51-9))
decay scheme, 17: 13584
decay scheme, 20: 43550(R) (NYO-844-67)
determination of ratio with scandium-46 in titanium oxide targets, spectrometric, 18: 25298
energy levels, (E), 20: 19273(R) (BNL-929, pp 3-43)
energy levels from calcium-48 (p,nγ) reactions at 3.25 Mev, 19: 43357
energy levels from proton reactions (p,nγ) with calcium-48 at 1 to 1.35 Mev, 20: 26117
energy levels of, even-parity-hole states in $f_{7/2}$, 18: 36646
gamma dose constants for, 20: 46617
neutron reactions (n,α) at 14 Mev, nuclear shell effects in cross sections for, 18: 18977
production by scandium fixation in ion exchanger and neutron irradiation, 19: 32666(P)
production by vanadium (n,α) reactions, (E), 20: 46242(R) (TID-23239)
production of, techniques for, 18: 41892 (BNL-864)
separation and purification for medical use, 18: 37581 (A/CONF.28/P/457)
separation and purification of carrier-free, by ion exchange and solvent extraction, 18: 37101
yields in proton spallation of copper at 24 Bev, 16: 24859

SCANDIUM ISOTOPES Sc-49
beta decay of, log ft values for, (T), 20: 19932
energy levels, 18: 42624(R) (ANL-6879(p.35-63))
energy levels, 19: 1562(R) (ORNL-3679(p.1-18))
energy levels and ground-state mass, (E), 20: 38063
energy levels from calcium-48 (p,γ) reactions at 0.8 to 1.4 Mev, 18: 19078
energy levels from helium-3 reactions (He-3,d) with calcium-48 at 12 Mev, (E), 20: 13854
energy levels from proton reactions with calcium-48 at 800 to 1400 kev, (E), 20: 26111
energy levels from proton elastic scattering by calcium-48 at 1.3 to 7.0 Mev, isobaric-analog, 20: 26174
energy levels of, isobaric-spin splitting of single-particle and single-hole, 17: 9572
energy levels of, splitting of single-particle, 18: 30798
energy levels of, even-parity-hole states in $f_{7/2}$, 18: 36646
energy levels of, density and yield curves for, (E), 19: 23677
energy-level transition probabilities of, E2, (T), 20: 3115
separation from irradiated calcium, 17: 32164

SCANDIUM ISOTOPES Sc-50
beta decay scheme of isomers, 17: 22575
decay scheme, 17: 13530
decay scheme, 17: 19310
energy levels of, even-parity-hole states in $f_{7/2}$, 18: 36646
nucleon interactions in, properties from effective, (T), 20: 17735
nucleon residual interactions in, effective, (T), 19: 35472
production of isomeric, in neutron reactions with titanium-50 at 14–15 Mev, 17: 40079

SCANDIUM LACTATES
preparation and solubility, 20: 22998

SCANDIUM MANGANATES
crystal structure of $ScMnO_3$, x-ray-diffraction studies of, 19: 44005
magnetic properties and manganese ion moment configurations of, 18: 24128 (CONF-405-34)
magnetic structures, 18: 23523

SCANDIUM MINERALS
book: *Scandium: Its Geochemistry and Mineralogy*, 17: 6301

SCANDIUM MOLYBDATES
crystal structure, 20: 7056

SCANDIUM NIOBATES
distribution in strontium molybdate single crystals, coefficients of, 20: 29746
preparation and structure of, 18: 12673

SCANDIUM NITRATES
oxidation at 1000°C to scandium oxide, 19: 36988
preparation and properties of complex, 17: 32172
preparation and properties of, 20: 29214
properties, chemical and physical, 16: 17615 (IS-300)
reactions with strong base in aqueous solution, 19: 11069
separation by reversed-phase partition chromatography using organophosphorus compounds, 18: 25614
separation from nitric acid solutions by solvent extraction using

tributyl phosphate, 20: 9076
solubility in water and in nitric acid and organic solvents, 17: 32115

SCANDIUM NITRIDES
corrosion of, by acids, alkalis, and water, effects of temperature on, 17: 3434
crystal structure of, x-ray absorption spectral studies of, 17: 32589
figure of merit and atomic characteristics, 19: 2284
oxidation of, in air, effects of temperature on, 17: 3434
preparation and properties, 19: 356(T) (JPRS-26877(p.1-24))
preparation and properties, 18: 3782
properties, electric and optical, 17: 32652
properties, electric and optical, 18: 18472
scandium-45 NMR in, Knight shifts and relaxation in, 18: 19980
superconducting properties, 19: 20572
thermal conductivity of, ratio of electron and lattice parts of, 19: 5852

SCANDIUM OXALATES
carbon-14 exchange between, and alkali metal oxalates, 20: 45634
compound formation with carbonate, electric conductivity and structure of, 19: 38672
decomposition of, mechanism of thermal, 17: 4553
formation and properties of, 18: 31515
precipitation by ammonium and sodium hydroxides solutions, 17: 25247
precipitation with uranium oxalate, 17: 1421 (TID-17033)
precipitation with uranium(IV) oxalate, 17: 25235
properties and stability of, 18: 31515
thermal decomposition, 17: 1494
thermal decomposition of, composition of products in, 17: 25162 (LADC-5486)

SCANDIUM OXIDES
see also Lithium Scandium Molybdenum Oxides
determination in thorium oxide by emission spectroscopy, 20: 16393
dissociation energies at high temperatures, 18: 3795
dissociation energy of, mass spectrographic study of, 19: 30171
electron spectra of, 20: 31219(R) (UCRL-16658, pp 11-20)
electronegativity and ion radii of, prediction of phases in binary systems with other oxides from, 19: 23061
electronic spectra of mono-, 19: 36345 (UCRL-11927)
electronic symmetry determination in, by electric deflection, (E), 19: 42493
entropy, 17: 32031 (BM-RI-6245)
formation of, in thermal decomposition of scandium formate and oxalate, 17: 25162 (LADC-5486)
formation on scandium in air, 19: 7372
heat of formation of, calculation from heats of combustion and solution, 17: 37209
molecular constants and thermodynamic properties of, 18: 12075
preparation of, from low-grade thortveitites, 19: 36357
radiation effects on microstructure of, 20: 33941 (DP-MS-66-9)
reactions with hydrochloric acid, product formation in, 20: 43259
scandium emission spectra in, 18: 39196
sintering of, effects of environment and temperature on, 16: 30168(R) (ORNL-3313(p.65-132))
solubility in complexone III, 20: 23026
spectra in blue-green and orange regions, emission, 17: 1432
spectra in low frequency region, infrared, 18: 23549
spectra of gaseous, ground state and hyperfine-structure separation in optical, (E), 19: 42495
spectra of, infrared absorption, 17: 27840
spectra of monocrystals of, at 80°K and room temperature, uv absorption, 20: 31240
spectra of, parameters for emission, 17: 1433
spectra of, optical energy gap in, 18: 19986
structural effects on beryllium oxides, 16: 5689 (ORNL-TM-94)
structure at 20 and 880°C, 18: 39934
thermal capacity at 50 to 298°K, 17: 32031 (BM-RI-6245)
thermal expansion coefficients at 25 to 1000°C, 16: 16715(R) (CAL-PI-1273-M-10)
thermodynamic properties at 300 to 2000°K, 17: 14203 (BM-RI-6198)
vaporization from tungsten extrusion chambers at 2550°K, mass spectroscopic study of, 20: 8947
wavefunctions for, calculation for ground-state assignment, (T), 19: 44020
Al_2O_3–Sc_2O_3, phase studies, 18: 5270
BaO–Sc_2O_3, optical properties of compounds formed in, 20: 13278
BaO–Sc_2O_3, preparation, phase studies, and properties of, 20: 26898
B_2O_3–Sc_2O_3, liquid immiscibility in, 20: 40910
CaO–Sc_2O_3, phase diagram, 20: 841
CaO–Sc_2O_3, preparation, phase studies, and properties of, 20: 26898
CdO–Sc_2O_3, phase studies, 20: 29168
CoO–Sc_2O_3, phase studies, 20: 29168
CrO_3–Sc_2O_3, phase diagrams, 20: 29167
Fe_2O_3–MnO_x–Sc_2O_3, phase studies of solid solutions in, 20: 36839
Ga_2O_3–Sc_2O_3, phase diagram, 17: 12274
In_2O_3–Sc_2O_3, crystal structure of, 20: 46215
IrO_2–Sc_2O_3, phase studies in air, 19: 32751
La_2O_3–Sc_2O_3, analysis of, for lanthanum and scandium, photometric, 16: 28899
MgO–Sc_2O_3, electric properties of solid solutions, 19: 36338(R) (NP-15160)
MgO–Sc_2O_3, phase studies, 18: 7239
MgO–Sc_2O_3, phase studies on, 18: 23529
Mn_2O_3–Sc_2O_3, magnetic susceptibility, 20: 29168
Mn_2O_3–Sc_2O_3, phase studies, 20: 29168
MnO–Sc_2O_3, phase studies, 20: 29168
Nb_2O_5–Sc_2O_3, properties and structure of compounds formed in, 18: 34199
Nb_2O_5–Sc_2O_3, properties and structure of compounds formed in, 18: 34199
NiO–Sc_2O_3, phase studies, 20: 29168
Sc_2O_3–SiO_2, phase studies and properties of scandium silicates in, 16: 20444
Sc_2O_3–SiO_2, phase studies and structure of, 17: 1993
Sc_2O_3–SrO, optical properties of compounds formed in, 20: 13278
Sc_2O_3–SrO, preparation, phase studies, and properties of, 20: 26898
Sc_2O_3–ThO_2, phase diagram, 20: 839
Sc_2O_3–UO_2, phase diagram, 20: 839
Sc_2O_3–Y_2O_3, analysis of, for scandium and yttrium, photometric, 16: 28899
Sc_2O_3–Y_2O_3, phase diagram, 20: 840
Sc_2O_3–ZnO, phase studies, 20: 29168
Sc_2O_3–ZrO_2, electric conductivity, 19: 37094
$ScO_{1.5}$–ZrO_2, electric conductivity of, 20: 19243
Sc_2O_3–ZrO_2, phase studies, 18: 10113
Sc_2O_3–ZrO_2, phase studies, 19: 11753
Sc_2O_3–ZrO_2, phase studies, 19: 42464
Sc_2O_3–ZrO_2, phase transformations in, fluorite, 19: 358(T) (ORNL-tr-201)
Sc_2O_3–ZrO_2, preparation of sols of, 20: 8958(P)

SCANDIUM PERCHLORATES
properties, chemical and physical, 16: 17615 (IS-300)
reactions with chromium(III)–neptunium(V) complex in perchloric acid, spectra of, 17: 6074
separation by reversed-phase partition chromatography using organophosphorus compounds, 18: 25614

SCANDIUM PERRHENATES
synthesis and properties of, 19: 28305

SCANDIUM PHOSPHIDES
preparation and crystal structure of, 17: 12673
properties of, chemical and physical, 20: 8910

SCANDIUM SELENIDES
crystal structure, 18: 1628
crystal structure and stability, 19: 36365

SCANDIUM SILICATES
preparation of $Sc_2O(SiO_4)$ monocrystals, 20: 40919
structure of, polymorphic, 20: 14537

SCANDIUM SILICIDES
crystal structure, 19: 32755
crystal structure, 19: 40479
preparation and properties, 19: 357(T) (JPRS-26877(p.25-47))
preparation and properties, 19: 42513
preparation of, method for, 20: 37176
preparation using arc smelting, 20: 46168
production of, conditions for, 17: 27736
properties of, physicochemical, 20: 17047
structure of, 17: 27736

SCANDIUM SULFATES
solubility in sulfuric acid solutions, 19: 30196
thermal stability of anhydride and pentahydrate of, 19: 30196

SCANDIUM SULFIDES
crystal structure, 18: 1628
crystal structure, 19: 44010
preparation and properties, 18: 39186

SCANDIUM SYSTEMS
Al–C–Sc, phase studies of, atomic size effects in, 19: 23111
B–C–Sc, crystal structure of ScB_2C_2, 19: 46258
Co–Sc–Si, crystal structure, G phases in, 17: 14876
Ge–Ni–Sc, crystal structure, G phases in, 17: 14876
H–Sc, phase studies by x-ray powder methods, 19: 42510(T)
H–Sc, phase studies and thermodynamics of, 20: 322
H–Sc, phase studies and thermodynamics of, at 700 to 900°C, 20: 26817 (LA-3473)
H–Sc–Y, phase studies, 20: 5909
I–4,4'-methylenediantipyrine–Sc, complex formation in, 19: 38670
Ni–Sc–Si, crystal structure, G phases in, 17: 14876
Sc–$ScCl_3$, phase studies and properties of, 18: 6832
Sc–$ScCl_3$, phase studies, 19: 13309
Sc–Si, crystal structure of AB type compound in, 19: 37063

Sc–Si, crystal structure, 18: 13795
Sc–Si, preparation and crystal structure, 19: 28835
SCANDIUM TANTALATES
fluorescence spectra, 18: 26017
preparation and structure of, 18: 12673
SCANDIUM TELLURIDES
crystal structure, 18: 1628
crystal structure, 19: 44010
crystal structure, 20: 7071
SCANDIUM TUNGSTATES
SCANDIUM THIOCYANATES
preparation and properties, 18: 17845
SCANDIUM, TRISCYCLOPENTADIENYL-
preparation by reaction of scandium fluoride with magnesium cyclopentadienide, 20: 35493
SCANDIUM VANADATES
structure of, x ray diffraction analysis of, 17: 10663
SCARS
see also Burns
see also Trauma
examination of post operative, for keloids, 16: 1563
formation on skin wounds, tracer studies, 16: 29(R) (TID-14100)
in mouse brain, due to goldthioglucose, 19: 35879
radioinduced carcinomas near nuclear blast burn, 17: 38754
radioinduced in mice and rats, x, 20: 28946
surgical repair of burn, of residents of Hiroshima exposed to thermal radiation from atomic explosion, 19: 28007
therapy of delayed formation of, using Padutin, 20: 45356 (EUR-2752.e)
SCATTERING
(Limited to theoretical studies of scattering processes of particles in general composite systems.)
absorption effects in peripheral interactions, (T), 19: 4922
absorption effects in high-energy, (T), 19: 37585
acnode singularities in Feynman diagrams, Mandelstam representation breakdown for, 17: 31303
amplitude absorptive analytic properties, 16: 17039
amplitude analytical properties, conformal mapping approach to, 16: 12427 (JINR-D-832)
amplitude analyticity in complex angular momentum of relativistic S-matrix, 16: 21698 (AFOSR-2400)
amplitude, analyticity of general unitarity term of three-momentum transfers, 16: 17019
amplitude analytic continuation in angular momentum, 16: 24743 (UCRL-10116)
amplitude analyticity domain, holomorphy domain of, 17: 22460
amplitude analyticity and unitarity of double-dispersion, Regge poles from, 17: 24281
amplitude analyticity for four-point function in momentum space, geometric analytic completion for, 18: 21037
amplitude and diffraction peak in, unitarity bounds on, 18: 34560
amplitude and trajectories in lambda plane, nonrelativistic partial wave, 20: 32187
amplitude asymptotic behavior, analytic properties of partial wave amplitudes and, 16: 22947
amplitude at high energy, (T), 19: 16565
amplitude attenuation in, 17: 6894
amplitude behavior in high-energy, perturbation theory of, 17: 26344
amplitude behavior in, perturbation theory of, 17: 28176
amplitude behavior at large angular momentum, 18: 931
amplitude behavior in high-energy for negative momentum transfer, 18: 36392
amplitude bounds for fixed-momentum-transfer, for spin-½ particles, 18: 18682
amplitude bounds in ladder graph approximation for, 18: 32590
amplitude continuation to second sheet using N/D method on one sheet, 16: 15565
amplitude determination for low-energy, 16: 8296
amplitude determination by interpolation for complex angular momenta, 16: 19900
amplitude expansion in relativistic spherical functions, 16: 28345
amplitude for crossed-box ladder graphs in the Bethe-Salpeter equation, 20: 2818
amplitude for elastic, high-energy bounds for (T), 19: 1466
amplitude for high-energy, partial-wave contribution from analyticity to, 18: 21043
amplitude for high-energy, (T), 19: 16495
amplitude for high-energy, asymptotic behavior of, (T), 19: 16572
amplitude for high-energy elastic, forward peak in, 20: 17459
amplitude for high-energy, analyticity and unitarity restrictions on, (T), 20: 24173
amplitude for high-energy, forward, (T), 20: 30109
amplitude for inelastic atomic electron, 18: 24307
amplitude for low-energy, plane wave approximation for, 18: 28587
amplitude for meson (π)-nucleon S-wave, 18: 20937
amplitude for neutron-proton, N/D analysis of, 18: 44577
amplitude for nonlocal potential, lambda plane of nonrelativistic partial-wave, 20: 32188
amplitude for partial-wave, in N/D method (T), 19: 1291
amplitude for potential, retarded functions for, 17: 4215
amplitude for production processes in quantum field theory, (T), 19: 20961
amplitude for proton–proton, at finite angles, 18: 30597
amplitude for quasiclassical, in a centrally symmetric field, 18: 5879
amplitude for relativistic multichannel, analytical properties of, 20: 39911
amplitude for three-body, in complex angular momentum (T), 19: 3132
amplitude for three-body, one-particle singularities of, (T), 19: 20953
amplitude for three-body, variational principle for Faddeev equations for, (T), 20: 11692 (UCRL-11768)
amplitude for three-body, Lippman-Schwinger equation for, 20: 25929
amplitude for three-body rearrangement, distorted-wave Born approximation for, 20: 30120
amplitude for three-body, solution in distorted-wave formalism for, 20: 30121
amplitude for three-particle inelastic, analytical properties of, 20: 42019
amplitude for two-particle single-channel, Hilbert-space formulation of, 18: 14872
amplitude for two-particle, Bethe-Salpeter equation for, (T), 19: 32950
amplitude for, complex singularity in analytic continuation of four-point, (T), 19: 31068
amplitude for, determination of off-the-energy-shell, 18: 30642
amplitude for, equations for classical and quantal, 19: 20825
amplitude for, in field theory, 18: 36385
amplitude, high energy limits from analyticity in Lehmann ellipses, 16: 6972
amplitude high-energy behavior at fixed angle in perturbation theory, 18: 30624
amplitude imaginary component, channel-spin contribution analyticity, 16: 21294
amplitude in complex angular momentum plane, partial-wave, (T), 19: 14357
amplitude in left half-plane of complex angular momentum, asymptotic behavior of, 20: 11710
amplitude in relativistic quantum field theory, analyticity properties of, 19: 16496
amplitude in two-particle, S-matrix existence from probability, 20: 4687
amplitude, invariant parametrization of relativistic matrix, 16: 12393
amplitude of approximation to N/D solution for (T), 19: 1458
amplitude of Coulomb, analyticity in the complex angular momentum plane of, 16: 28353 (UCRL-9972)
amplitude of elastic, high-energy, 18: 26322
amplitude of, expansion in relativistic spherical functions, 17: 7521
amplitude of forward, asymptotic properties and zeros of, 17: 20852
amplitude of forward, sum rules for, (T), 19: 16608
amplitude of forward, univalent functions for analytic properties of, 20: 1065
amplitude of $g\,\phi^4$ lagrangian interaction, analytical properties of, 20: 44396
amplitude of, in two-dimension theory, 17: 40237
amplitude of nonrelativistic, analyticity properties and asymptotic behavior of, 20: 7930
amplitude of, quasipotential character of, 17: 22420 (JINR-D-1191)
amplitude of relativistic, scale transformation and Regge behavior of, 17: 19123
amplitude of, singularities in angular momentum of, 17: 754
amplitude of two-body, Mandelstam representation constraint by unitarity in, 17: 9254
amplitude of, upper bound on growth of, 18: 7481
amplitude of, essential singularities in complex angular momentum plane for, (T), 19: 12313
amplitude of, generalized Regge representation of, 20: 19588
amplitude of, low-energy expansion for long-range quadrupole potentials, 18: 22684
amplitude of, N/D equations with nonunique solutions for, 19: 18846
amplitude of, solution of singular N/D equations for, 20: 6130
amplitude of, wave-packet derivation of field-theoretic, 20: 44318
amplitude parameterization from singularities in complex j-plane for, 19: 1415 (NP-14404(p.102-12))
amplitude perturbation expansion in, inequality in Feynman integrands for, 17: 24345
amplitude phase in, intensity correlations for, 18: 2707
amplitude properties of local non-causal current operators in S-matrix theories, 16: 17022
amplitude representation, containing bound states and resonances, 16: 18603
amplitude residues for non-relativistic two-channel process at bound-state

energies, 17: 24346
amplitude singularities at high energies, explicit, 16: 22962
amplitude singularities at isolated real points, 16: 24732
amplitude singularities in single field theoretic model, 17: 26318
amplitude singularities in, Regge, 17: 26343
amplitude singularities at $l = -1$ in the Bethe–Salpeter equations, 18: 6076
amplitude singularities arising from the third double-spectral function, partial-wave, 18: 18765
amplitude singularities for elastic, 18: 24395 (NP-13872)
amplitude singularities on unphysical Riemann sheets, (T), 19: 8236
amplitude singularities in complex j plane, partial, (T), 19: 16648
amplitude vertex parts for direct-process, 17: 5360
amplitudes above the Bev region, "multicenter" peripheral model for, 16: 26116
amplitudes, analytic property proofs for relativistic, 16: 998
amplitudes, analytic and group theoretical properties, 16: 1175
amplitudes, analytics of potential, 16: 18342
amplitudes, analytic behavior in complex plane, 16: 31195
amplitudes and crossing matrices in isospin, 17: 22465
amplitudes and cross section calculations for, using crossing symmetry and holomorphy, 20: 32106 (AD-634706)
amplitudes and cross sections for high-energy, equations for, 20: 44301
amplitudes and dispersion relations, analyticity of, 16: 23251
amplitudes and matrix for many-channel potential, 16: 33713
amplitudes and phase shifts in, analytic properties and asymptotic behavior of, (T), 19: 12265
amplitudes and polarizations at high energies, asymptotic relations among, 18: 14808 (JINR-E-1520)
amplitudes and Regge pole trajectories for nonrelativistic, partial, 20: 25931
amplitudes and singularities in complex momentum plane of inelastic, 18: 28406
amplitudes and triple angular correlations for inelastic, 18: 40625
amplitudes, asymptotic forms of Regge, 17: 17046
amplitudes, asymptotic forms and holomorphy domains of, 17: 20877
amplitudes, asymptotic behavior of photon, 17: 34927
amplitudes at high energies, real and imaginary parts, 16: 10838
amplitudes at high energies, spin structure, 16: 19713
amplitudes at high energies, 16: 22943
amplitudes at high energies, moving-pole hypothesis in, 16: 22960
amplitudes at high energies and fixed angles, asymptotic, 16: 26446
amplitudes at high energies, moving pole in hypothesis of, 16: 27909 (NP-11775)
amplitudes at high energies, in complex l-plane, 16: 33775
amplitudes at high energies, asymptotic behavior of, 17: 9241
amplitudes at high energies, real part of, (T), 19: 32991
amplitudes at high energies, behavior of real parts of forward, (T), 19: 41376
amplitudes at high energies, integral representation for, (T), 20: 11736
amplitudes at high momentum transfers, asymptotic behavior of, (T), 20: 13546 (JINR-P-2519)
amplitudes at high energy, ladder approximation for asymptotic behavior of, 20: 15501
amplitudes at high energies, (T), 20: 15519
amplitudes at high energies for elastic, restrictions on imaginary part of, 20: 25928
amplitudes at high energies, review of forward, (T), 20: 42028
amplitudes below elastic threshold of, Regge asymptotic representation of, 18: 9136
amplitudes, Born series of non-relativistic elastic, 17: 6973
amplitudes, boundary-curve intersections for 4-point function in, 16: 22894
amplitudes, class of solvable potentials for s-wave Schrödinger equation for, 16: 22728 (NYO-10134)
amplitudes corresponding to Feynman diagrams in, analytical properties of, 19: 21054
amplitudes for, analyticity domain of, 17: 16956 (NYO-10239)
amplitudes for arbitrary-spin, construction of invariant, 17: 17035
amplitudes for arbitrary-spin particles, energy dispersion relations for complex J partial-wave, 18: 10889
amplitudes for arbitrary-spin particles for potential, Born approximation for, 18: 10890
amplitudes for arbitrary-spin particles, crossing relations for helicity, 18: 14825
amplitudes for arbitrary-spin nonzero-mass two-body, construction of invariant scalar, (T), 19: 10109
amplitudes for charged particles, analytic properties of, 17: 11572
amplitudes for charged-particle, analytical properties of partial-wave, 17: 22502
amplitudes for, complex angular momentum effects on, 17: 2435
amplitudes for Compton, asymptotic behavior of, 18: 18640 (JINR-P-1525)
amplitudes for complex particles on force centers, properties of, 20: 34261 (JINR-P-2697)
amplitudes for Coulomb and screened-Coulomb, 19: 1283
amplitudes for Dirac potentials, 16: 3809
amplitudes for, effects of removal of background integrals from, 17: 19087
amplitudes for elastic, boundedness properties of, 17: 20889
amplitudes for elastic, effects of reggeon production on, 18: 42431
amplitudes for elastic, analyticity and causality in (T), 19: 3114 (NP-14346)
amplitudes for elastic nucleon-nucleon, unitarity of, (T), 19: 37550
amplitudes for elastic, correlation of asymptotic values of total cross section and, 20: 25935
amplitudes for elastic, three-particle contributions to, 20: 30129
amplitudes for elastic, imaginary-mass representations of Poincare group for, 20: 32154
amplitudes for elementary particles in nonlinear field theory, analytic properties of, 18: 30617 (JINR-P-1638)
amplitudes for final-state interactions in, Aitchison equation for, 20: 12016
amplitudes for finite-range-potential, analyticity properties of, 20: 30131
amplitudes for forward, high-energy lower bounds for, (T), 19: 16666 (JINR-P-1928)
amplitudes for four-body, (T), 20: 2791
amplitudes for, from complex Yukawa potentials, 17: 2422
amplitudes for, from Yukawa potentials, 17: 19178
amplitudes for highly singular potential in, Regge asymptotic behavior in, 18: 2678
amplitudes for high-energy elastic, relativistic approximation for Dirac particles, 18: 15285
amplitudes for high-energy, with symmetry-breaking interaction, 19: 1239
amplitudes for high-energy, in local quantum field, (T), 19: 5016 (JINR-P-1793)
amplitudes for high-energy elastic, impact-parameter expansion of, 19: 8191
amplitudes for highly singular and nonregional potentials, Regge behavior of, 19: 37548(T) (JPRS-29641(p.1-22))
amplitudes for high-energy nucleon-nucleon, (T), 20: 7876
amplitudes for high-energy, analyticity in energy variables for, (T), 20: 15520
amplitudes for high-energy elastic, 20: 44384
amplitudes for hyperon-nucleon and nucleon-nucleon, relations between, 18: 20913 (TID-20483)
amplitudes for, in complex-angular-momentum theory, 16: 33738
amplitudes for, in fixed-fermion field theory, 17: 5210
amplitudes for inelastic, spectral representations of, 17: 28209
amplitudes for inelastic, effects of S-matrix unitarity on, (T), 20: 6105 (ISS-65/14)
amplitudes for inelastic, threshold behavior of partial, 20: 15500
amplitudes for isotopic spin exchange contribution to, 17: 22481
amplitudes for large-angle proton-proton, asymptotic decrease of, (T), 19: 8196
amplitudes for large-angle, 19: 47430
amplitudes for large angular momenta, effect of Coulomb forces on partial-wave, 20: 32141
amplitudes for lepton-lepton, (T), 19: 16694
amplitudes for many-body, discontinuity equations for, (T), 20: 13531 (IC/65/17)
amplitudes for massless particles with gauge invariance in S-matrix theory, 18: 9174
amplitudes for meson (π-π), double spectral functions of Mandelstam representation of, 18: 32574
amplitudes for meson (π)–meson (π), 19: 1264
amplitudes for meson–nucleon, asymptotic, (T), 19: 37657
amplitudes for multi-channel, pole residues of, 17: 9276
amplitudes for multi-channel threshold branch-point of, 18: 7545
amplitudes for multichannel, with unstable particles, 18: 24433
amplitudes for multichannel, approximate solution of N/D equations for, (T), 20: 6063
amplitudes for multichannel quasi-potential, asymptotic behavior of, 20: 39905
amplitudes for n strongly coupled two-body channels, uncoupled phase method for relating, 18: 9244
amplitudes for n-body system, separation of total angular momentum for, 20: 39897
amplitudes for neutral mesons, Chew-Mandelstam equations for, 16: 29988
amplitudes for nonrelativistic three-body problem, analytic properties of, 18: 30509 (JINR-E-1659)
amplitudes for nonrelativistic three-body problem, analytic properties of, 18: 30512 (JINR-P-1662)
amplitudes for nucleons, field theoretical derivation, 16: 21402
amplitudes for nucleon Compton, Regge-pole analysis of, 17: 36623
amplitudes for particles with spin, continuation in total angular momentum

of partial-wave, 18: 6060
amplitudes for particle production in inelastic, asymptotic behavior of, 18: 30514 (NP-14048)
amplitudes for partial-wave, generalized Cauchy representation for resonance phenomena in, 20: 24118
amplitudes for particles with unequal mass, Bethe-Salpeter equations for, (T), 20: 34299
amplitudes for, photon Regge pole contribution to, 17: 31329
amplitudes for potential, asymptotic behavior of, (T), 20: 4849(R) (UCRL-14360, pp 1-50)
amplitudes for potential, 20: 17438
amplitudes for potential, S-matrix for low- and high-energy, 20: 17491
amplitudes for potential and field-theoretical, asymptotic behavior of, 20: 24151
amplitudes for production processes in, (T), 19: 20925 (ICTP-64/3)
amplitudes for relativistic Dirac and Klein-Gordon particles, (T), 19: 4902
amplitudes for s-wave, on fixed centers, (T), 19: 35023 (JINR-P-2111)
amplitudes for Schroedinger- and Dirac-potential, asymptotic expansion of, 18: 9103
amplitudes for singular, generalized Lippmann-Schwinger equations for, 20: 27994
amplitudes for singular potential, iterative method for partial wave, 20: 30136
amplitudes for spin-wave, by magnetic defects, 17: 34657
amplitudes for spinless-particle, 18: 840 (JINR-P-1318)
amplitudes for spinning particles, effects of "nonsense" channels on, 19: 1267
amplitudes for spinning particles in Treiman-Yang criterion for, 19: 3286
amplitudes for spinless massive, perturbation theory for, 20: 24131
amplitudes for strong, field theoretical models for, 18: 916
amplitudes for SU_3 multiplets, mass breaking in $\ddot{U}_{12}$ for, 20: 24136
amplitudes for system of fixed centers, 20: 21710 (JINR-P-2554)
amplitudes for three-body, from two-body amplitudes, 16: 27786
amplitudes for three-particle production, 17: 2295
amplitudes for three-particle two-body Yukawa potential, continuation to complex total angular momentum, 18: 21041
amplitudes for three-body, with complex total angular momentum, 18: 34518 (UCRL-11546)
amplitudes for three-body, (T), 19: 6535
amplitudes for three-body, p-wave, (T), 19: 18812
amplitudes for three-body, S-matrix elements for, 19: 37530 (JINR-E-2108)
amplitudes for three-body, in complex momentum, (T), 19: 39596
amplitudes for three-body, threshold behavior of, 20: 21747
amplitudes for three-particle, dispersion relations for, 20: 30132
amplitudes for two fermions, Bethe-Salpeter equation for, with massless vector particle mediation, 18: 10929
amplitudes for two-scalar-particle, (T), 19: 6708
amplitudes for two-particle, representation of, 19: 16468 (JINR-P-1918)
amplitudes for two-body, threshold sheet structure of, (T), 20: 4668
amplitudes for two- and three-particle, reduced, 20: 41959
amplitudes for vector mesons, 17: 11509
amplitudes for Yukawa potential, in determinantal and N/D methods (T), 19: 3067
amplitudes for Yukawa potential, use of N/D method in, 19: 21067
amplitudes for Yukawa potential, 20: 30128
amplitudes for, ambiguities in, 20: 25889 (RHEL/R-108)
amplitudes for, Amati-Fubini-Stanghellini approximation for, 20: 46391 (UCRL-17068)
amplitudes for, analyticity and unitarity of, (T), 20: 15518
amplitudes for, analyticity and unitarity of, (T), 20: 19595
amplitudes for, analyticity of, (T), 20: 19605
amplitudes for, asymptotic relations between, 18: 20907 (JINR-P-1564)
amplitudes for, bootstrap method for calculating, 20: 34295
amplitudes for, calculation using bootstrap method, 20: 34215
amplitudes for, Coulomb-wave, 18: 16910 (ANL-6848(p.38-42))
amplitudes for, construction of separable hamiltonians from, 19: 41546
amplitudes for, compositeness conditions for partial-wave, 20: 32137
amplitudes for, crossing relations of two-body, 20: 24164
amplitudes for, differential properties for Feynman, (T), 20: 15525
amplitudes for, dynamical calculation of, (T), 20: 25894
amplitudes for, general quantum field theory for analytic properties of, 20: 41936
amplitudes for, identity in, 18: 26287
amplitudes for, involving massless particles, invariant, (T), 20: 24163
amplitudes for, iteration method for determining partial-wave, 19: 3094
amplitudes for, Kronecker-delta singularities in angular momentum plane, (T), 20: 15521
amplitudes for, limitations on locations of Regge poles in, (T), 19: 5035
amplitudes for, mass-splitting effects on symmetry relations between, (T), 19: 41430
amplitudes for, N/D calculations of p-wave, (T), 20: 30158
amplitudes for, normalization integrals of Bethe-Salpeter, (T), 19: 41434
amplitudes for, normalization of Bethe-Salpeter bound-state, 19: 45078
amplitudes for, production, (T), 19: 18917
amplitudes for, representations of n-angular diagrams in, (T), 19: 6519 (JINR-P-1814)
amplitudes for, representation of, (T), 19: 20955
amplitudes for, Regge-pole representation of, (T), 20: 6062
amplitudes for, real part of forward, (T), 20: 25945
amplitudes for, single- and multi-channel N/D equations for, 19: 18889
amplitudes for, singularities in three-particle, (T), 20: 11701
amplitudes for, structure of physical sheet and discontinuities across unitary cuts for two- and three-particle production, 18: 24455
amplitudes for, three-particle unitarity conditions for partial-wave, (T), 19: 37632
amplitudes, forward peak appearance in, 17: 42184
amplitudes having complex singularities, integral representations of, 16: 33969
amplitudes in, analyticity and unitarity in complex energy plane of, 18: 9145
amplitudes in angular momentum plane, Regge poles in nonrelativistic, 17: 41841
amplitudes in angular momentum representation, partial, (T), 19: 33079
amplitudes in, asymptotic behavior and quasioptical model of, 17: 26381
amplitudes in, Bohr approximation calculations of, 17: 7184
amplitudes in bound-state, analyticity of, (T), 19: 18821
amplitudes in complex angular momentum plane, 17: 6974
amplitudes in complex angular momentum plane, singularities of relativistic, 17: 41808
amplitudes in Compton, 18: 28332 (UJV-1021/63)
amplitudes in complex angular momentum plane of, Feynman diagrams for, (T), 19: 8278
amplitudes in complex angular momentum plane of, analytic continuation of p-wave, (T), 19: 16587
amplitudes in complex z plane, singularity of, 19: 21055
amplitudes in complex plane of coupling constant, poles of p-wave, 19: 23386
amplitudes in complex K-plane, effective range parameter in S-matrix theory for, 19: 47390
amplitudes in complex angular momentum plane, partial wave, (T), 20: 11693 (UCRL-12016-T)
amplitudes in complex angular momentum plane, analyticity test for, 20: 19567
amplitudes in complex lambda plane, singularities of partial-wave, 20: 32189
amplitudes in coupled-channel, with complex angular momentum, (T), 19: 23418
amplitudes in, crossing-symmetric Watson-Sommerfeld transformation, power series, and Regge poles for partial, 17: 39929
amplitudes in dispersion theory, approximation scheme for calculating, 17: 19536
amplitudes in elastic, adiabatic switching for transition, 17: 34740
amplitudes in elastic, high-energy behavior of real part of, (T), 19: 31047
amplitudes in elementary particle, natural boundary and singularities of partial-wave, 17: 15090 (UCRL-10615)
amplitudes in, exchange effects on, 17: 28194
amplitudes in fixed-fermion model for, redundant poles and zeros on unphysical sheet for, 17: 34742
amplitudes in, high-energy behavior of Feynman, 17: 26355
amplitudes in high-energy, upper bound at fixed angles, 17: 26377
amplitudes in, high-energy behavior of Feynman, 17: 35075
amplitudes in, high-energy behavior of production, 17: 39921
amplitudes in high energy, renormalization method for, 18: 20983
amplitudes in high-energy diffraction, 18: 32534 (NP-13989)
amplitudes in high-energy, upper bounds for, 18: 36396
amplitudes in high energy, forward, (T), 19: 27151 (JINR-P-2022)
amplitudes in high-energy, properties of forward, (T), 20: 2762
amplitudes in high-energy elastic, real and imaginary, 20: 32179
amplitudes in, imaginary parts of spin-dependent, 17: 26309
amplitudes in inelastic, analytical properties of, 17: 32942
amplitudes in, integral representation for, 17: 2166 (JINR-P-1060)
amplitudes in, Khuri representations and Legendre transforms for, 17: 39928
amplitudes in local field theory, (T), 19: 12380
amplitudes in local field theory, restrictions on forward, 19: 45039 (TPJU-10/65)
amplitudes in mass-shell, 18: 26410
amplitudes in, model for asymptotic nonforward, 18: 2694
amplitudes in multichannel, N/D method for, 20: 32181
amplitudes in nonlocal theory of, analytical properties of forward, 17: 41839
amplitudes in nonphysical region, integral representation of relativistic,

20: 24156
amplitudes in nonrelativistic quantum mechanics, analytic properties of, 17: 42174
amplitudes in, parameterization in space-time theory, 17: 2052
amplitudes in perturbation theory of, high-energy behavior of, 17: 28164
amplitudes in perturbation theory of, high-energy behavior of, 17: 28166
amplitudes in, perturbation-theoretical integral representation of high-energy behavior of, 18: 6032
amplitudes in, perturbation theory for high-energy behavior of, 18: 7501
amplitudes in perturbation theory, singularities of, 19: 47412
amplitudes in, poles in coupled, 18: 7489
amplitudes in potential, Watson-Sommerfeld transformation for many-particle, 18: 21040
amplitudes in potential theory, singularities in, (T), 19: 41550
amplitudes in potential, analyticity of, 20: 7947
amplitudes in quantum field theory, crossing property for two-body, 20: 24107
amplitudes in quantum field theory, analyticity of, 20: 34312
amplitudes in, quasioptical quantum field theory of, 17: 13349 (JINR-P-1149)
amplitudes in, quasi-classical approximation, 17: 36618
amplitudes in quasi-potential, analytic properties of, 18: 6054
amplitudes in, Regge trajectory and resonant partial wave, 17: 11530
amplitudes in, Regge pole hypothesis for imaginary to real part ratio of forward, 17: 26356
amplitudes in, Regge poles and zeros of Hankel functions for, 17: 31301
amplitudes in, Regge-pole approximation to, 17: 35073
amplitudes in Regge pole theory of, exact form of, 18: 2606
amplitudes in relativistic velocity space, properties of spiral, 17: 41830
amplitudes in, rotation matrices corresponding to complex angular momenta for, 18: 2604
amplitudes in s-channel in quantum field theory, Regge pole effects on threshold behavior of inelastic, 17: 41831
amplitudes in, S-matrix theory for unstable-particle, 17: 28195
amplitudes in S-matrix theory with generalized potential, asymptotic behavior of partial-wave, 20: 32140
amplitudes in static approximation for elastic, SU(n)-invariant, 20: 32136
amplitudes in three-body, non-Regge singularities in, (T), 19: 12339
amplitudes in three-body, model for, (T), 19: 35092
amplitudes in two-meson approximation, 16: 29991
amplitudes in two-particle, propagator ghosts and Regge poles in, 17: 31298
amplitudes in two-body, boson radiative corrections to, 18: 32539
amplitudes in, analytic continuation in angular momentum variable of, 18: 12984
amplitudes in, analytic continuation of, 18: 24440
amplitudes in, analyticity of compound-particle, 18: 32582
amplitudes in, analyticity of absorptive part of, (T), 19: 4982
amplitudes in, analyticity for optical potentials from, 19: 25324
amplitudes in, analyticity properties of, 20: 21733
amplitudes in, angular momentum separation in three-body, 18: 26336
amplitudes in, asymptotic behavior and discontinuity of, 18: 36390
amplitudes in, asymptotic behavior of p-wave and total, 18: 36381
amplitudes in, asymptotic behavior of, (T), 19: 14403 (JINR-P-1916)
amplitudes in, asymptotic behavior of, (T), 19: 37552
amplitudes in, asymptotic behavior of, (T), 20: 9828
amplitudes in, asymptotic behavior of inelasticity parameter for, 20: 39894
amplitudes in, axiomatic quantum field theory for, 20: 13565
amplitudes in, Bethe-Salpeter calculations, 18: 22744
amplitudes in, bootstrap solution of solvable model for, 19: 31053
amplitudes in, boundary conditions for partial-wave, 18: 12897 (EFINS-63-67)
amplitudes in, Cutkosky rule for Feynman graphs for, 20: 11687 (JINR-P-2485)
amplitudes in, dispersion relations for p-wave, 18: 37944
amplitudes in, equations for, 18: 18742
amplitudes in, exponential decreasing of fixed-angle, (T), 19: 8283
amplitudes in, harmonic analysis in three-dimensional Lorentz group, 19: 25323
amplitudes in, high energy behavior of real part of forward, 19: 23399
amplitudes in, impact parameter formalism for, 20: 13610
amplitudes in, inequalities for forward, 18: 12898 (EFINS-63-72)
amplitudes in, inelastic effects in N/D method for p-wave, (T), 19: 10141
amplitudes in, integral representations for, (T), 20: 15451
amplitudes in, invariant expansions of relativistic, 18: 14807 (JINR-E-1503)
amplitudes in, Jost functions for, (T), 19: 14336
amplitudes in, Kronecker-delta-type singularities and Regge poles in, (T), 20: 15465
amplitudes in, Landau singularities in, 18: 36393
amplitudes in, Lee model for production and elastic, 20: 41986
amplitudes in, Lorentz and spin invariance for, (T), 19: 33012
amplitudes in, Mandelstam and optical-model representations for, (T), 19: 12338
amplitudes in, modified Born approximation for, (T), 19: 10117
amplitudes in, motion of poles of Bethe-Salpeter p-wave, (T), 19: 21111
amplitudes in, moving branch points in j plane and Regge-pole unitarity conditions for, (T), 19: 33017
amplitudes in, multichannel effective-range theory from N/D formalism for, 19: 23414
amplitudes in, N/D approach in bootstrap solutions for, 19: 39463 (IC/65/62)
amplitudes in, nonrelativistic invariant functions for, 18: 18709
amplitudes in, non-dynamical formalism of, (T), 20: 9795 (UCRL-14582-T)
amplitudes in, one-variable dispersion relations for analyticity of, (T), 19: 25307
amplitudes in, one-channel N/D method with inelastic unitarity for, 19: 32995
amplitudes in, optical models for, 20: 13601
amplitudes in, phase representation and high-energy behavior of forward, (T), 19: 27242
amplitudes in, physical sum rule for forward, (T), 20: 11696
amplitudes in, physical region decoupling method for coupled channel, 20: 11711
amplitudes in, polarization and zeros of, 20: 25938
amplitudes in, real part of, (T), 19: 12214
amplitudes in, relativistic generalization of dynamic equation for Jost function for, 20: 11703
amplitudes in, removal of kinematic singularities from helicity, (T), 20: 15482
amplitudes in, resonance poles in multichannel, 18: 24432
amplitudes in, singular potentials in Lippman-Schwinger equation for p-wave, (T), 19: 10142
amplitudes in, singular N/D equations for, 20: 6131
amplitudes in, single-collision approximation for, (T), 20: 11742
amplitudes in, threshold behavior of p-wave, 18: 30613
amplitudes in, two-dimensional representations of, 18: 32677
amplitudes in, two-particle unitary approximation for, 19: 35086
amplitudes in, unitarity condition for Regge representation of, 17: 34751
amplitudes in, unitarity condition for Nakanishi representation of, 19: 35085
amplitudes in, unitarity conditions for off-shell two-particle p-wave, 20: 21756
amplitudes, integral representations, 16: 9402
amplitudes, integral representations for, 16: 12376
amplitudes, kinematic branch points of n-line graphs, 16: 21208
amplitudes, multiperipheral model for, 17: 20888
amplitudes near singular lines, 16: 10925
amplitudes of, analytical properties of Feynman, 17: 15077 (JINR-P-1106)
amplitudes of, analytic continuation by three-particle cut, 17: 39869
amplitudes of, as functions of complex angular momentum, 17: 9408
amplitudes of, as function of angular momentum, 17: 9411
amplitudes of, asymptotic behavior of Schroedinger, 18: 932
amplitudes of boson-fermion, in model field theory, 20: 6116
amplitudes of charged particle, determination of real part of forward, (T), 19: 45048(T) (ANL-Trans-217)
amplitudes of, complex angular momentum plane of, 17: 11495 (TID-17731)
amplitudes of, double phase representation of elastic, 17: 34737 (TID-19142)
amplitudes of elastic, imaginary character of, 18: 2699
amplitudes of elastic, use of convergent series in calculating partial-wave, 18: 7522
amplitudes of elastic, analytic properties of partial wave, 18: 26383
amplitudes of elastic, calculation of inelastic scattering from, 19: 33256
amplitudes of elastic, three theoretical approaches to, 19: 37638
amplitudes of elastic, analytic properties of unitarity integral of quantum field theory for, 20: 6114
amplitudes of elastic, effects of inelastic channels on partial-wave, 20: 34266
amplitudes of elastic, at high energies, (T), 20: 44374
amplitudes of, external-mass singularities in, 18: 2689
amplitudes of, for spin-½-particle–field interactions, 17: 11508
amplitudes of forward, dispersion relations for real parts of, 18: 2697
amplitudes of forward elastic, Regge behavior of, 18: 10919
amplitudes of forward, current-commutator constraints on three- and four-point functions for, 20: 32163
amplitudes of forward, Bethe-Salpeter equation for absorptive parts of, 20: 44310
amplitudes of high-energy elastic, 17: 5217

amplitudes of, high-energy behavior of, 17: 9418
amplitudes of high-energy, perturbation theory of, 18: 2706
amplitudes of high-energy, perturbation theory for, 18: 12939
amplitudes of inelastic, 17: 16949 (JINR-E-1156)
amplitudes of, Khuri series for partial-wave, convergence for single Yukawa potential, 18: 9243
amplitudes of, limitations imposed by unitarity on imaginary part of, 17: 9421
amplitudes of, Mandelstam representation for construction of, 17: 3965 (NP-12262)
amplitudes of, modified Regge formula for, 17: 17033
amplitudes of nonrelativistic two-particle, integral representation for, 20: 19549
amplitudes of, parametric representations of, 17: 6965
amplitudes of particles with spin, Regge boson pole contributions to, 17: 41835
amplitudes of production processes in, dispersion relations for partial, 17: 39927
amplitudes of, rate of decrease of, 17: 9412
amplitudes of, Regge poles in, 17: 9410
amplitudes of, Regge pole applications to, 17: 9414
amplitudes of, Regge behavior of high-energy, renormalization group method for, 18: 2700
amplitudes of Schroedinger, analyticity properties of, 16: 32309
amplitudes of, spin effect on Regge poles in, 17: 19167
amplitudes of three-body, Lehmann ellipse for, (T), 19: 8164
amplitudes of two and three-particle states, singularities in the unphysical sheet reached by, 17: 26345
amplitudes of two-body, equation for, (T), 19: 45123
amplitudes of, analytic properties of, (T), 19: 8221
amplitudes of, analytic continuation to second sheet in crossed channels, 19: 29058 (ICTP-64/14)
amplitudes of, analytic properties and logarithmic potential in $g\phi^4$ theory for, 19: 32944 (JINR-P-2073)
amplitudes of, analyticity test for, 20: 32149
amplitudes of, asymptotic behavior of partial-wave, 18: 14875
amplitudes of, asymptotic behavior of, 18: 14913
amplitudes of, asymptotic and threshold values in static models for, (T), 20: 2763
amplitudes of, calculation method using phenomenological, 20: 2804
amplitudes of, causality principle for asymptotic behavior of, (T), 19: 12263
amplitudes of, causality condition in momentum space for off-mass-shell, 20: 27971
amplitudes of, Chew-Low and pseudoscalar-static models for, 19: 27150 (JINR-P-2021)
amplitudes of, crossing relations for helicity, 18: 18657
amplitudes of, crossing symmetric Regge representation for invariant, 20: 6115
amplitudes of, decomposition of analytic relativistic S-matrix elements into Lorentz invariant, 18: 26294
amplitudes of, dispersion relations in, 18: 24383 (JINR-E-1646)
amplitudes of, effects of vacuum Regge trajectory on, (T), 20: 39925
amplitudes of, generalization of Pomeranchuk–Okun theorem for, 20: 7889 (NYO-3399-03)
amplitudes of, Greenberg-Low bound on, 20: 24124
amplitudes of, integral representations of relativistic, (T), 20: 1053 (JINR-P-2321)
amplitudes of, Legendre transforms for crossing symmetry in, 18: 18764
amplitudes of, Mandelstam representation for, 19: 29067 (LA-DC-6390)
amplitudes of, many-particle unitarity relations and analyticity in S-matrix theory for, 19: 32966
amplitudes of, Mandelstam and angular-momentum analyticity of, 20: 32164
amplitudes of, N/D equations with finite strip for elastic p-wave, 20: 7928
amplitudes of, probability functional with off-mass-shell generalization for transition, 20: 27970
amplitudes of, properties of N/D, 20: 41961
amplitudes of, relativistic equations for three-particle, 20: 39914
amplitudes of, representations of, 18: 12921
amplitudes of, representation of, 19: 35051
amplitudes of, singular-potential Bethe-Salpeter, 18: 30544
amplitudes of, solutions of N/D equations for, 20: 44307
amplitudes of, theorem on high-energy, 20: 41963
amplitudes of, truncation of unitary sum for, 19: 45093
amplitudes of, unitarity condition for analytic properties of, 20: 13631
amplitudes of, unitarity extension of analyticity domain of, 20: 24125
amplitudes of, unphysical unitarity of p-wave, (T), 19: 35105
amplitudes of, with unstable particles, 18: 34605
amplitudes on Mandelstam's boundary curves, elliptic-integral representation of, 18: 9112
amplitudes on physical boundary in, singularities in Feynman, 19: 35089
amplitudes on unphysical sheets and resonance poles in, 18: 16786
amplitudes, perturbation expansion integral representation for, 16: 26437
amplitudes, pole position relation to pole residue, 16: 4956
amplitudes, properties of high-energy elastic, 16: 29992
amplitudes, Regge-pole application effects on, 16: 26128
amplitudes, Regge-pole effects on asymptotic, 17: 32957
amplitudes, unitarity theories for singularities in, 16: 33746
amplitudes, unitarity and behavior of, 17: 11912
amplitudes, unitary symmetry of strong-interaction, 16: 29989
amplitudes with complex singularities, integral representations for, 17: 31302
amplitudes without kinematic singularities for two-body, scalar, 18: 9088 (UCRL-11113)
amplitudes, analyticity in angular momentum and energy (T), 19: 1461
analysis by invariant-imbedding approach to random-walk method, (T), 19: 20660 (P-1113(RAND))
analysis in meson (π)–meson (π) interactions at high energies, 19: 1270
analysis of, chamber design for, 17: 39416 (UCRL-7427)
analysis of Chandrasekhar functions for isotropic, 16: 19894
analysis of dissimilar-particle, Reggeian, 17: 15082 (NYO-9289)
analysis of, double bent-crystal monochromator for, 18: 7058 (TID-19849)
analysis of elastic, multilevel and multichannel, 17: 9182 (AFOSR-2871)
analysis of elastic complex, quasi-classical, 17: 22558 (JINR-P-1244)
analysis of elastic spin-zero, computer program for, 18: 18878 (NASA-TN-D-2120)
analysis of heavy-ion, equivalence of optical model and phase shift, 17: 27949 (UCRL-10769)
analysis of high-energy diffraction, using Regge poles, 16: 26154
analysis of high-energy, phenomenological, 17: 11566
analysis of laws of, for neutrons, 17: 17623(R) (IDO-16827)
analysis of proton-proton, 18: 14590(R) (NIRL/R/60)
analysis of three-body potential, 19: 16483 (UCRL-11866)
analysis of 3-body, 16: 22918
analysis of, for spin-l_1 particles on spin-l_2 particles, 19: 23359 (JINR-P-1965)
analysis of, integro-differential equation solutions for, 18: 13180 (RM-3575-PR)
analysis of, integrals for, 18: 14815 (NP-13616)
analytic approximation to the low-energy solutions of inverse amplitude dispersion relations, 17: 7510
analytic continuation of the S-matrix in angular momentum, 17: 5552
analytic continuation of the partial-wave amplitude, 17: 36856
analytic functions in, asymptotic behavior of phase representation of, 17: 22496
analytic Lorentz-covariant functions in, 17: 31296
analytic properties in potential, 16: 13889
analytic properties of the S-matrix in, Mandelstam's work on, 17: 11483 (NP-12436)
analytic properties of iterated cross box diagram in complex angular momentum plane, (T), 19: 43062
analyticity and causality in nonrelativistic, 17: 42167
analyticity and iteration in Yukawa-potential, 18: 10902
analyticity and unitarity effects on perturbation-theoretical elementary particle models, 16: 23252
analyticity and unitarity conditions in, consequences of, 17: 16955 (NYO-10238)
analyticity as fundamental principle in, 19: 37673 (UCRL-11921)
analyticity in angular momentum of the relativistic many-channel S matrix from dispersion relations and unitarity, 17: 998
analyticity in complex angular momentum of S-matrix for nonlocal potential, 18: 44638
analyticity in, effects on Regge trajectories, 17: 19179
analyticity of positions and residues of Regge poles in, 16: 33773
analyticity of S-matrix for potential, 18: 4444
analyticity of single Regge-pole terms in, 18: 4471 (UCRL-10700)
analyticity of two-channel S matrix in, 16: 33774
analyticity properties of amplitudes, 16: 29654 (NP-11950(Vol.II)(p.275-354))
analyticity properties of complex angular momentum planes in, 16: 33968
angular correlation data in, analysis of, 17: 15088 (UCRL-6994)
angular correlations in, static electric quadrupole perturbations in, 17: 19120
angular correlations for E2 and E3 transitions in Coulomb excitation, (T), 20: 38032
angular distribution analysis, chamber design for, 16: 367
angular distribution of inelastically scattered particles in Coulomb excitation, 16: 28332
angular distributions from, method for measuring, 18: 30767
angular distributions from, criteria for measuring, (T), 20: 9788(R) (ANL-7029, pp 25-7)
angular momenta in potential, determinantal method for complex,

17: 19531
angular momenta in relativistic, complex, (T), 20: 4636
angular momenta in, group theoretical properties of complex, (T), 20: 4700
angular momenta in, Born series for Jost function for large complex, 20: 19565
angular momentum analyticity in potential, 18: 11005
angular momentum and many-particle states in (T), 19: 1366
angular momentum continuation in three-body problem without branch points in, 18: 14989
angular momentum continuation in inelastic N/D problems in, 19: 27311
angular momentum in, maximum analyticity application to, 16: 21306
angular momentum in, reduction of algebra of complex, 17: 20841 (JINR-E-1208)
angular momentum in nonrelativistic potential, 18: 7476
angular momentum in, Clebsch-Gordon coefficients for, 18: 20991
angular momentum in, group properties of complex, 18: 28412
angular momentum in inelastic, complex, (T), 19: 37653
angular momentum in, complex, (T), 19: 37654
angular momentum in Lobachevskii space of relativistic velocities, (T), 19: 37692(T)
angular momentum in, complex, (T), 20: 4697
angular momentum in, complex, (T), 20: 19596
angular momentum poles of S matrix for spin ½ particles, 17: 11913
angular momentum poles for, S matrix representations of, 17: 11914
angular momentum plane in high-energy, singularities in, 17: 17021
angular momentum plane in, discontinuities across cuts in complex, 17: 19114
angular momentum planes in, moving Regge cuts in, 18: 6017
angular-momentum plane of, cuts in, 18: 9131
angular-momentum plane of, cuts in, 18: 9132
angular momentum plane of, cuts and poles in, 18: 10936
angular momentum transport in quantum statistical mechanics of, 17: 11917
anisotropic multiple, calculation by parallel plane dispersion methods, 16: 32270 (DASA-1257)
anisotropy in integral transport theory, approximation for, 19: 33202
anisotropy of in-pile neutron, magnetized ferromagnetic slab calculation of, 18: 19276
anomalous thresholds in unitary theories, 17: 5562
approximation for strongly interacting particles, determinantal, 18: 10840 (ARL-63-76)
approximation method for Regge trajectories and the Chew-Frautschi diagram, 17: 24273 (UCRL-10584(Rev.))
approximation methods for high-energy, (T), 20: 30086 (CONF-640509(Pt.1), Paper 4)
approximation method, 16: 21706
asymmetry in FORTRAN program for analysis of left-right, 16: 938 (ANL-6420)
asymptotic absorptive amplitude in multiperipheral model for, Bethe-Salpeter equation in, 18: 18766
asymptotic behavior in high-energy elastic, 16: 3653
asymptotic behavior of Coulomb, classical and quantum analyses of, 16: 29970
asymptotic behavior of phase shift for large λ, 18: 7478
asymptotic behavior of particle-production amplitudes of inelastic, 18: 30513 (NP-14047)
asymptotic behavior of complex phase shifts in, (T), 19: 21079 (IC/65/2)
asymptotic collision matrix for strong interactions at multi- Bev, 16: 27964
asymptotic condition in local relativistic quantum field theory, 18: 7565
asymptotic limits in potential, 17: 19533
asymptotic propagators and vertex functions for three-particle interactions, 19: 1282
asymptotic properties of multiperipheral model for, 17: 19096
atom-atom, errors in total cross section measurements for, 19: 23280
atomic beam, extrema velocities of total elastic cross sections for, 17: 5090
atomic, dispersion corrections for factors, 17: 3649
axiomatic frame for nonrelativistic potential, 18: 7482
axiomatic S-matrix theory, 17: 5569
axioms for S-matrix, search for, 18: 30620 (UCRL-11392)
baryon number conservation in field theory of, 17: 5270
Bethe-Salpeter equation for, (T), 20: 11746
Bethe-Salpeter equation in, Fredholm method for solving, 20: 11757
Bethe-Salpeter equation for, Wick rotation in, 20: 36083
Bethe–Salpeter equations for three-particle, solutions to, 20: 39900
Bethe–Salpeter equations for three-particle, solutions to, 20: 39901
Bethe-Salpeter structure of three-nucleon potential problem in, with analyticity and unitarity, 18: 20930
binary collision expansion of quantum statistical pair propagator, 16: 2455
Boltzmann equation for, explicit solution of one-velocity multi-dimensional, 19: 3195
Boltzmann transport equation exact solution, 16: 5875
book: *Collision Theory*, 18: 28419
book: *Complex Angular Momenta and Particle Physics*, 19: 3109
book: *Contribution to the Study of β Back Scattering*, 17: 783
book: *Dispersion Relations*, 16: 995
book: *Dispersion Relations and Causal Description*, 16: 2375
book: *Dispersion Relations and Their Connection with Causality*, 19: 18912
book: *Introduction to Field Theory and Dispersion Relations*, 19: 37698
book: *Mandelstam Theory and Regge Poles*, 19: 3107
book: *Modern Quantum Theory*, 18: 15011
book: *Potential Scattering*, 20: 15566
book: *Quantum Mechanics. I.*, 16: 15355
book: *Quantum Scattering Theory. Selected Papers*, a collection of reprints, 18: 24512
book: *Quantum Theory of Scattering*, 17: 7053
book: *Regge Poles and S-Matrix Theory*, 19: 10112
book: *S-Matrix Theory of Strong Interactions*, 16: 21329
book: *Scattering Theory of Waves and Particles*, 20: 46424
book: *The Complex j-Plane. Complex Angular Momentum in Nonrelativistic Quantum Scattering Theory*, 18: 32670
book: *The Inverse Problem of Scattering Theory*, 19: 5053(T)
book: *The Optical Model in Nuclear and Particle Physics*, 17: 33108
book: *The Two-Nucleon Interaction*, 18: 909
book: *Variational Principles in the Theory of Collisions*, 18: 15010(T)
bootstrap calculations in soluble model of, 18: 14987
bootstrap calculations on, approximation method for, 18: 34562
bootstrap solutions in, uniqueness of, 17: 22473
Borchers' theorem for scattering matrix localization, 17: 40244
Born series convergence for, acceleration and continuation of, 17: 24083
bound states and renormalization in potential, 18: 26413
bound states in, (T), 19: 16520
bound states in central potential, (T), 19: 43061
bound states in multichannel and single-channel, (T), 19: 39600
boundary condition for nonrelativistic Schrödinger equation, outgoing-wave, 18: 34597
bounds on momentum dependence of phase shifts and magnitude of coupling constants, 17: 11922
by complex nuclear-potential, semi-classical treatment, 16: 19790
by nuclear magnetic moments, electron bremsstrahlung in, 18: 42773
by screened Coulomb potential, 16: 2457
by singular potential $-gr^{-4}\ln r$ (T), 19: 3134
by thermodynamic systems, Van Hove function for, (T), 19: 30853
calculation of Regge poles by continued fractions, 17: 5550
calculations and measurements of atomic, 16: 22806
calculations for elastic, approximation methods for, 18: 44296
calculations for medium-energy projectiles using distorted wave Born approximation, 16: 23043
calculations for nonstationary multiple Compton, 18: 20920
calculations of cross sections of, formulas for, 16: 33962
calculations of Mössbauer-resonance, for nuclei Z-30, -40, -50, -60, -70, -80, and -90, (E/T), 19: 36220(R) (MIT-2098-142)
calculations using variational principles, 16: 2635
canonical transformation effects on s-matrix singularities, 16: 19897
causality in nonrelativistic, R-matrix for, (T), 19: 10095
chamber for studying, using junction counters, 17: 25892
charge exchange in neutron-proton, 19: 25268
charge independence in low-energy, 19: 37639
Chew-Mandelstam equation in, inverse amplitude and N/D method for, 17: 20923
chiral symmetries in, 16: 33707
classical theory of elastic atomic, truncated matching potentials for, 18: 14741
Clebsch-Gordan coefficients in, expressions of, 18: 10996
cluster decomposition properties of the S matrix for zero-spin bosons, 18: 2708
coefficients in degenerate systems, 16: 10738
coherence of radiation emitted by current distributions and random charge, 16: 5806
collective enhancement effects in inelastic, 16: 3701
collision lifetimes in many-body processes, 17: 17030
collision matrix in, unitarity of one-level approximation of, 17: 22578
collision probabilities in cuboids and cylinders, 18: 24377 (AEEW-M-442)
collision probabilities in, solution of multigroup equations in, 18: 24378 (AEEW-R-326)
collisions of alkali atoms with rare gas atoms, cross sections for transitions in, 17: 31119
complex angular momentum in S-matrix theory, 16: 29975
complex angular momenta and unitarity in crossed channels, 17: 4219
complex angular momentum in many-channel potential, 17: 11501

(UCRL-10209)
complex angular momentum, dispersion relations and Regge poles in, 17: 20594(R) (UCRL-10572)
complex angular momentum in perturbation theory, 17: 31659
complex angular momentum in spinor Bethe-Salpeter equation for, 17: 31661
complex angular momentum in many-channel problems in (T), 19: 1373
complex energy and complex relation pulse in noncentral potentials, 18: 7483
complex-potential, inequalities in, 16: 18343
constants for atomic factors, analytical, 18: 2524
constants for multiple, calculation by Moliere formulation, 16: 11899
convergence behavior of Born series for rearrangement, (T), 20: 41642
correspondence principle in indefinite-metric, 16: 17046
Coulomb, amplitude of a Klein-Gordon particle, 17: 31232
Coulomb, decay of ultrahigh-energy particles in condensed matter as as result of, 17: 17056
Coulomb excitation, effects of elastic scattering resonances, 16: 19798
Coulomb Green's function in closed order, 17: 31356
Coulomb T matrix in two-body, anomalous behavior of, 18: 14991
Coulomb wave functions for, nonrelativistic, 16: 9557 (LAMS-2616)
Coulomb wave functions for, 17: 24314
Coulomb, effects of distortion and noise on measurement in nuclear emulsion, 19: 2965
Coulomb, effects of distortion and noise on measurement of multiple, 19: 9936
Coulomb, inelastic effects in multiple, (E/T), 19: 25274
Coulomb, nonrelativistic limit of, 18: 24500
coupling constant and spectral functions for high-energy, conformal mapping for, 17: 17054
coupling constant relations in S-matrix theory, 19: 41382
coupling constants and unsubtracted dispersion relations, 17: 5560
coupling constants in, effects of S-matrix on, 17: 19157
coupling constants for three-particle, upper bound for, 18: 899
cross section for molecular, determination of Lennard-Jones parameters from total, 18: 22046
cross section for high-energy, phenomenological analysis of, (T), 19: 14368
cross section for back-, lower limit of, (T), 20: 7954
cross section for, in crossed-beam experiment, method for calculating total, 19: 27080
cross section for, high-energy behavior of total, 17: 9421
cross section relations with target velocity, derivation of expression for, 16: 1019 (AROD-2188:2)
cross sections, analytical properties of elastic, 16: 15647
cross sections, analytic properties of partial differential, 16: 21290
cross sections at high energies, effects of Regge poles on, 17: 9274
cross sections at high energies, behavior of, 16: 26447
cross sections for elastic, of particles with spin, 16: 28005
cross sections for classical, from repulsive potentials, 17: 618
cross sections for classical, for repulsive potentials, 17: 639
cross sections for final-state, 17: 5356
cross sections for molecular beams at high velocities, total elastic, 17: 12841
cross sections for backscatter in inhomogeneous media, 17: 19144
cross sections for heavy nuclei, probability distributions of, 17: 24499
cross sections for elastic, one-meson (π) approximation of Regge pole method for asymptotic behavior of, 17: 29520
cross sections for, asymptotic relations between high-energy, 17: 37938 (JINR-P-1353)
cross sections for, calculations of resonance behavior of, 17: 37878
cross sections for high-energy, lower bound for elastic, 18: 2603
cross sections for atom-molecule, 18: 10779
cross sections for, relation of electric transitions and quadrupole moment of nuclei to, 18: 18941
cross sections for, approximation method based on R-matrix theory, 18: 21304
cross sections for particles and antiparticles, 18: 24382 (JINR-E-1623)
cross sections for atomic and molecular, 18: 36718 (ORNL-3113(Rev.))
cross sections for elastic, status of, 18: 40370
cross sections for gas–ion, with charge exchange, 18: 42325
cross sections for molecular beam, nonadiabatic elastic, Coriolis shifts in, (T), 19: 6454
cross sections for elastic, higher-order stationary-phase approximations for classical and semiclassical expressions for, (T), 19: 23382
cross sections for radiation damage calculations, approximation of, (T), 20: 901
cross sections for elastic and inelastic, temperature dependence of, 20: 3435
cross sections for, infrared singularities in, 20: 2754 (JINR-P-2309)
cross sections for two-body, moment relations for Schroedinger, 20: 17483
cross sections for, compound elastic and doorway state, (T), 20: 24352 (MIT-2098-149)
cross sections for quasielastic, diffraction model for, 20: 26148
cross sections for high-energy, functional integration method for infrared singularities of, 20: 25934
cross sections for high-energy, complex moment method for nonvanishing total, 18: 6039
cross sections in polarized-particle–polarized-target, total, 17: 39911
cross sections in high-energy potential, partial-wave summation for, (T), 19: 10042
cross sections in high-energy, (T), 19: 12269
cross sections in diffraction peak region, restrictions on elastic, (T), 20: 11764
cross sections near thresholds, in attractive Coulomb fields, 17: 33083
cross sections near threshold of, resonances in, (T), 19: 27512
cross sections of atom-atom, resonance behavior of, 18: 20765
crossing matrices, methods for evaluating, (T), 19: 41381
cusp effects near unstable-particle production thresholds, 16: 18366
data analysis, 16: 26071 (JINR-P-817)
density matrix for two-particle, 20: 37829
depolarization of electrons and positrons in Bhabha and Møller, 17: 39849
description at high energies, 18: 10909
description of "almost-logical" S-matrix theories, (T), 19: 6575
description of, from liquid-like binary, 17: 28137 (BNL-6364)
description of projection operators and quasiparticles in, (T), 19: 6579
diagram technique and Regge poles in, 17: 40235
diagrams containing multi-particle intermediate states, method for summing, 19: 41429
differential equations in many-body problems in, solutions for set of coupled second-order, 20: 6120
diffraction, nonshrinking, 17: 20902
diffraction of charged particles by optical inhomogeneities, 20: 41523
diffraction patterns in high-energy elastic, 17: 9238
diffraction peak in elastic, bounds to width of, 17: 29545
diffraction peak shrinkage in proton-proton, 18: 32581
diffraction peak width at high energy, lower bound on, (T), 19: 16571
diffraction peaks and forces at small distances in (T), 19: 1379
diffraction width in high-energy, 18: 28377
diffuse reflection of parallel rays, 17: 39852
diffusion approximation for multiple, Fokker-Planck, 18: 20924
dipole-quadrupole and retardation effects in atom-atom, at low energies, 18: 20733 (WIS-TCI-41)
Dirac equation for high-energy attractive Coulomb, quasiclassical solution to, 20: 15559
Dirac equation with Yukawa potential for, 17: 16990
Dirac-Coulomb integrals for charged-particle, evaluation of zero-energy-loss, 18: 12982
discontinuities in, unitarity of, 17: 5543
discontinuities in, unitarity of, 17: 42168
dispersion calculations for, effects of singularities of 5-point function on, 16: 33966
dispersion equations for, bootstrap approximation in soluble model of partial-wave, 18: 14996
dispersion relation techniques and applications, 16: 996
dispersion relations for square diagram with nonzero masses, 16: 987
dispersion relations and diffraction, 16: 2446
dispersion relations, causality condition and, 16: 8114
dispersion relations, scattering matrices, and spectral functions, 16: 10924
dispersion relations for potential, 16: 10881
dispersion relations and stability conditions, 16: 17023
dispersion relations for nucleon Compton amplitudes, 16: 18516
dispersion relations, axiomatic formulation of, 16: 21307
dispersion relations, probabilistic indefinite metric in, 16: 22858
dispersion relations in, proof of partial-wave, 16: 22916
dispersion relations in, 17: 7010
dispersion relation proofs in, 17: 13377
dispersion relations for potential, double, 17: 13380
dispersion relation in the Lee model with second order pole production, 17: 20850
dispersion relations in, prediction of interaction symmetry from, 17: 20905
dispersion relations in multi-channel, subtraction of, 17: 20920
dispersion relations and resonance, S-matrix and amplitudes for, 17: 21214
dispersion relations and spectral representations in perturbation theory, 17: 22423 (JINR-P-1205)
dispersion relations for, with arbitrary mass ratios, 17: 28213
dispersion relations for pseudoscalar-meson elastic, 17: 32951
dispersion relations for, integration of, 17: 33229
dispersion relations in unphysical region, physical interpretation of, 17: 39854
dispersion relations for sum of chain diagrams, spectral functions for,

17: 42182
dispersion relations for stable- and unstable-particle, 18: 876
dispersion relations in, analysis of partial-wave, 18: 886
dispersion relations for zero momentum-transfer elastic, removal of divergences by conformal mapping in, 18: 7522
dispersion relations for, variational technique for partial-wave, 18: 9176
dispersion relations in multiple, 18: 9210
dispersion relations, solution to N/D equations in, 18: 16813
dispersion relations for, review of relativistic, 18: 18720
dispersion relations for, one-variable, 18: 24427
dispersion relations for, 18: 30614 (AERE-R-4646)
dispersion relations in, subtractions in fixed-momentum-transfer, 18: 36391
dispersion relations for nonlocal potentials, 19: 10150
dispersion relations of amplitude of relativistic, (T), 19: 12302
dispersion relations for, proof of, 19: 18913
dispersion relations for, (T), 19: 18915
dispersion relation for elastic, (T), 19: 41363
dispersion relations in, solubility of partial-wave, 20: 11699
dispersion relations for πN, partial-wave, (T), 20: 30073
dispersion-theoretic impulse approximation for potential, 17: 7512
dispersion theories for low-energy, 16: 22900
dispersion theory of strong interactions for high-energy, 18: 16747 (BNL-7534(p.49-80))
dispersion theory for high-energy, 19: 18918
dispersion theory of low-energy, 19: 45051
dispersion theory of low-energy, 20: 15522
dispersion theory for, perturbation methods in, 20: 30124
dispersive formulation of Levinson theorem for, 17: 5228
distorted-wave expansion, 16: 4701
distorted-wave Born approximation expansions in, perturbation technique with convergence for, 18: 24502
distribution for large momentum transfer, calculation of, 17: 22551 (CERN-63-9)
distribution functions for the wavefunction phase at a boundary in elastic, 18: 933
distributions from multiple, in nuclear emulsion, 18: 2065
distributions from, computer analysis using Hauser-Feshbach theory, (T), 19: 31232 (ORNL-TM-1117)
distributions from light-nucleus–heavy-nucleus, 20: 3013 (JINR-P-2331)
distributions from one-dimensional, from two-particle targets, 20: 7888 (JINR-P-2418)
domains of analyticity for contributions from diagrams, determination from selection rules for particles of unequal masses, 17: 22504
domination of high-energy, by Gribov-Pomeranchuk singularity, 18: 32565
double-dispersion relations, 16: 8121
dynamical description of physical systems by S-matrix theory, 17: 36857
effect of target density on, 20: 46351
effective collision cross sections, 16: 19538
effective-core shrinkage at high energies, 18: 21043
effective-range approximation with Regge representation in low-energy, 19: 1415 (NP-14404(p.102-12))
effects of anisotropic, in Boltzmann transport equation, 18: 24565 (LA-3051)
effects of final-state interactions on, 17: 29503 (UCRL-10762)
effects of final-state interactions on, 18: 26379
effects of multiple, on transition radiation, 18: 40415
effects of nucleons on diffraction, 18: 32580
effects of reactions on elastic, 16: 29811
effects of shell closure on angular distributions of elastically scattered particles, 18: 4603
effects of slit on, theory, 17: 9594
eigenvalue condition for V + N potential in, dispersion theory calculation of, 17: 13370
elastic and inelastic high-energy, 18: 16747 (BNL-7534(p.49-80))
elastic, at high energies and Regge predictions, 17: 31272 (CONF-22-6)
elastic, high-energy behavior of amplitudes in, 17: 7003
elastic, of heavy ions, 17: 20989 (TID-18505)
elastic, of mesons (μ^-) in nuclear emulsions, 17: 31383
elastic, statistical model for large-angle high-energy, 17: 13389
elastic-inelastic discrimination in high-momentum-transfer elementary-particle, 18: 44517 (CERN-64-38)
electrodynamics of, method for writing quantum, 17: 11468 (JINR-D-1108)
electromagnetic form factors in, asymptotic behavior of, 18: 14894
electromagnetic structure functions in, Mott effect on, 19: 21073
electromagnetic-wave, by plane layers of turbid matter, 17: 9014(T)
electron elastic-scattering form factors for d-shell nuclei, (T), 20: 42376
elementary particle descriptions as Regge poles in, 19: 1229 (JINR-P-1780)
elementary particle production in quantum field theory, 20: 30157
elementary-particle three-body, Regge cuts in nonrelativistic, 18: 28346
endpoint method generalization for, 18: 35056
energy exchange in Maxwellian gases, 17: 5128
energy level excitation of deformed nuclei by multiple Coulomb processes, 17: 26483
energy-momentum conservation in, restrictions imposed by Boltzmann equation on, 17: 5205 (UCRL-6559-T)
energy-momentum conservation laws in, deviations from, 17: 22510
energy spectrum and determinant method in quantized field theory, 16: 12373
energy transfer cross section for laws of, model for differential, 17: 41566(T) (EURAEC-779)
enhancement factors for final-state, 16: 17027
equation for solution of inelastic neutron magnon, in crystals, 19: 14260
equation, formulation of nonlinear singular integral Low, 16: 24913 (JINR-P-890)
equation, operators connected with nonlinear singular integral Low, 16: 24914 (JINR-P-901)
equations for, Euclidean approach to Bethe-Salpeter, 18: 40320
equations for inverse-square-field, derivation of, 16: 29497
equations for, linear, 16: 26085 (NP-11632)
equations for meson-nucleon, algebraic, 17: 28142 (JINR-E-1262)
equations for one-channel, general solution of singular integral, 20: 36071 (IFA-FT-58)
equipment and techniques for studying 100-Bev, 17: 23626
equipment for measuring multiple, 16: 6600
exchange amplitudes in elastic, 18: 32554
exchange contributions to high-energy, 18: 2699
excitation in inelastic, distorted-wave theory of double, 17: 736
excitations in nuclear, Fermi-liquid model for collective, 18: 26612
expansions for nonrelativistic, 18: 28383
experiments on Compton, using low-activity sources, 20: 19049
explicit forms and recursion relations for T-matrices in, 17: 26011
expressions for 3-j symbols, 17: 16957 (ORNL-TM-514)
extension of Levinson's theorem to the relativistic case, 17: 31657
extension of the Regge formula, 16: 28318
extrapolation of S matrix to complex angular momenta, representations for, (T), 19: 21080 (IC/65/9)
factorization of the residues of Regge poles, 16: 29979 (UCRL-10115)
factors for 208 atoms and ions, wave-function computation of, 18: 22670 (LAMS-3056)
Fano's theory of homogeneity, 19: 3129
fermion Regge pole description of meson (π)–nucleon scattering, 18: 6040
fermion Regge trajectories for nucleon-pseudoscalar meson interactions in, 18: 34558
Feynman amplitudes for, U-functions of, (T), 19: 16637
Feynman amplitudes of, analytic property of, 19: 21113
Feynman diagram majorization, 16: 10826
Feynman diagram majorization, generalization of Symanzik's theorem for, 16: 22951
Feynman diagrams for, calculation using isobar approximation with Regge pole, 17: 22421 (JINR-E-1210)
Feynman diagrams for, prevention of essential singularities by, 18: 14874
Feynman diagrams for, properties of Landau curves of, 18: 34668
Feynman diagrams for, pole contribution to multi-loop, (T), 19: 16503
Feynman diagrams for, method for calculating, 20: 44294
Feynman diagrams in, leading Landau curves of, 18: 7504
Feynman diagrams in, homology groups for sixth-order, 19: 32970
Feynman diagrams in, singularities of, 19: 33106
Feynman diagrams in, Schwinger's formula for propagators of, 19: 35078
Feynman diagrams in, analytic property of fifth-order, 20: 13593
Feynman diagrams in, Landau curves of, 20: 21732
Feynman diagrams in, uniformization of Riemann surface for, (T), 20: 15495
Feynman diagrams in, complex singularities of, 20: 44343
Feynman diagrams in, 20: 46403
Feynman diagrams with three-particle intermediate states, Mandelstam representation for, (T), 19: 37676
Feynman–Gell-Mann equation in spinor space, finite dimensional representations of Lorentz group for solution of, 17: 34744
Feynman graph behavior in, asymptotic, 18: 839 (JINR-P-1305)
Feynman graphs for, discontinuities of, (T), 20: 19582
Feynman graphs for, majorization of, 20: 39867
Feynman graphs in, singularities of, 18: 18665
Feynman graphs in, asymptotic behavior of, 19: 39465 (JINR-E-2125)
Feynman integrals in, perturbation method for high-energy behavior of ladder diagrams from, 18: 12983
Feynman integrals in, analytic properties of, 20: 15523
Feynman, diagrams in, parametric representation for diverging, 19: 37696
field theory for boson, 17: 2440

field theory for, S-matrix reduction by asymptotic conditions in, 18: 30636
field theory in, convergent and renormalization, 18: 32673
first-order approximations for central potential, equivalence of Brysk and determinantal methods for, 17: 17011
focusing singularity in p-space of constant curvature, 20: 2813
forces in, approximation for long-range, 17: 9580
forces in, velocity dependent, 17: 13417
form factors for proton-proton, nonlocal, (T), 19: 16533
formalism for multichannel, Lorentz-invariant, 18: 44611
formalism for spin-one particles, 17: 26461 (PAN-241)
formulas of, for shielded Coulomb potential, 18: 15300
formulation of problems in high-energy nuclear, two-body, 18: 21337
frequency distribution function of, sum rules for generalized, 20: 42092
frequency redistribution of, from moving atoms, 17: 16973
from compound systems, soluble problems in, 17: 38424
generalization of Boltzmann collision integral, 16: 19722
Green function for, multiple poles in, 20: 4662
Green function for multiparticle, asymptotic of virtual part of, 20: 46405
Green's function for, binary collision expansion of double-time-temperature-dependent, 20: 11760
Green's functions in, analytic expression for class of, 20: 44368
hamiltonian in hard-core potential, point transformations for, (T), 19: 8153
Hamiltonians, use of rotating coordinates in, 17: 4104
hard-core potential, Regge poles for, 17: 16992
Hartree-Fock-Slater factors for atoms, 18: 26234
Heisenberg nonlinear theory of, consistency problem in spectral formulas in, 19: 45094
helicity amplitudes, 17: 22422 (JINR-E-1227)
high-energy $\bar{N}N\omega$ coupling from Regge trajectories, 17: 13410
higher Born approximations for Coulomb, of a spinless particle, 17: 5558
Hilbert space functional analysis in potential theory of, 18: 44603 (UCRL-11566)
hypervirial relations for distorted Coulomb, (T), 20: 6146
hypervirial theorem for collisions between electrons and atoms, 17: 31209
identification of composite and elementary particle, 17: 22473
impulse approximation in, 17: 4217
impulse approximation derivation, 16: 26441
in K = 0 band of odd-odd deformed nuclei, 17: 7146 (UCRL-9764)
in nonadiabatic atomic collisions, cross sections for, 18: 12834(T)
inelastic, by nuclei with monopole and quadrupole excitations, 16: 14023
inelastic contribution in N/D solutions, elimination, 16: 5890
inelastic cross sections, calculations for, 16: 3874(R) (ORNL-3193 (p.254-8))
inelastic, description of peripheral model for, 17: 13373
inelastic deuteron, compilation of data on, 18: 18983
inelastic diffraction processes at high energies, 17: 7522
inelastic, excitation of collective states of nuclei by proton, 17: 17276
inelastic, forward and backward selection rule in parity-unfavored, 17: 35072
inelastic, interference between the amplitudes of, 16: 17055
influence of fixed centers of, on approach to equilibrium, 18: 21030
interaction potentials for composite systems, (T), 20: 42236
interactions in, dynamics of field theory for nonlocal, 17: 37967
interactions of competing particle resonances in, 18: 7521
interactions of quantized fields, effects on Wick products, 16: 8128
interference between nuclear resonant and Rayleigh, in crystals, 17: 4013
interference between Raleigh and resonance, 17: 7109 (NP-12330(p.147-51))
interference of Rayleigh and nuclear-resonant, in crystals, 18: 26656
into rearranged channel, coupled equations for, 18: 34643
intrinsic parity from the S-matrix viewpoint, 17: 999
inverse problem of, in quantum theory, 17: 13366(T)
inverse, quantum mechanical inversion of eigenvalues in, 18: 6059
ion–atom charge exchange, model for, 20: 41624 (UCRL-17034)
irreducible representations in, reduction of 8-dimensional representations into, 17: 5545
irreversible quantum mechanical processes in, 18: 38004
isospin splitting of meson (π)-nucleon interactions by inelasticity in, 18: 18690
isotropic, of point-source radiation, 18: 16796
iteration-variation method for atomic, 17: 5565
Jost functions and S-matrix for short-range potentials, (T), 19: 16519
Jost functions for, derivation from amplitude properties, 18: 11008
K matrix in inelastic, truncation bounds on, 18: 30563
kinematics of multiparticle, relativistic and nonrelativistic, 19: 31225 (NIJS-R-429)
Landau curve of single-loop scattering diagram with internal diagonal line, 20: 44342
lectures on theory, 16: 31007 (CERN-62-18)
Lee field model for, 16: 33704
Levinson theorem in, generalization of, 20: 44293
lifetime matrix in, relativistic formulation of, (T), 20: 9830
limit of Thomson, high-intensity, 17: 31149
limits for large-angle elastic, lower, 18: 10946
Lorentz covariant Lee model for, 17: 13446
Lorentz-invariant Hamiltonian models of interacting particles, 17: 34732 (NYO-10276)
low-angle, use to determine specific area of scatterers, 16: 22878
Low equation in, solutions of, 17: 24343
Low equations for, solutions of 2-dimensional, 18: 22781
lower bound for the leading Regge trajectory, 17: 13669
Mandelstam representation and unitarity conditions in, 16: 27912 (NYO-10232)
Mandelstam representation and Regge poles in, 17: 761
Mandelstam representation in, 17: 20845 (JINR-P-1195)
Mandelstam, scalar variables for S-matrix, (T), 19: 35108
Mandelstam's boundary curves for, periods of, 18: 9112
many-body problems in, 17: 11481 (NP-12435(Pt.I))
many-body problems in, 17: 11482 (NP-12435(Pt.II))
many-fermion problem of, graphical resummation for rearrangement of adiabatic perturbation expansion for energy in, 18: 18669
mass formula for S-wave unitary multiplet, 18: 44586
mass-1 thermal gas, program for calculating, 18: 10766 (KAPL-M-FDF-4)
mathematical analysis of break-up processes, 16: 2485 (NP-10958)
mathematical analysis of two-body unitarity relation, 16: 2625 (AFOSR-1176)
mathematical analysis of, 17: 13339 (JEN-111-DF/132)
mathematical methods in (T), 19: 1090
mathematics of multiple, discussion of uniqueness problems in, 17: 11490 (RM-3221-PR)
matrices in inverse, pathological (T), 19: 1442
matrices leaving angular distributions invariant in, transformation group for, 18: 44597
matrices, use to interpret interpolating fields, 16: 12562
matrix analytic structure in neutral pseudoscalar theory, 16: 18350
matrix axioms for, electromagnetism and S-, (T), 19: 8204
matrix calculation from Schroedinger equation, computer program for, 16: 29664 (UCRL-10384)
matrix construction without divergences, 16: 26181
matrix construction for, axiomatic, (T), 19: 33108
matrix development in quantized field theory, 17: 757
matrix development in relativistically invariant field theory, 18: 6075
matrix development quantum electrodynamics, 18: 28430
matrix element for, distorted-wave approximation to Humblet-Rosenfeld, (T), 19: 27197
matrix element growth, restrictions, 16: 4954
matrix elements at high energies, 19: 1279
matrix elements for, with incoming-wave final state, 18: 14975
matrix elements for three-body, (T), 19: 31011 (TID-21784)
matrix elements for inelastic, (T), 20: 1054 (JINR-P-2328)
matrix elements for, of complex systems, upper and lower bounds on, 17: 36849
matrix elements in quantum field theory, 17: 19081
matrix elements in, local-operator, 18: 10966
matrix elements in nonlocal field theory, diagram technique for, 18: 11022
matrix elements in relativistic three-body problem, equations for, 20: 30148
matrix for, in quantum field theory, 17: 19156
matrix for, in static meson theories, 17: 19089
matrix for nonlocal separable potentials in, analytic properties of, (T), 19: 5000
matrix for nonrelativistic spinless compound-particle, 19: 14350
matrix for nonrelativistic spin-dependent, analytic properties of, 20: 13633
matrix for potential, complex-angular-momentum effects on, 17: 2441
matrix for potential, at large complex angular momenta, 18: 21036
matrix for relativistic-particle, spatial cluster decomposition properties of, 19: 16497
matrix for spinless-particle, in relativistic field theory, 18: 42508
matrix for, coupled N/D equations for, 19: 37561
matrix for, effects of interaction range on structure of, (T), 19: 25266 (UCRL-11961)
matrix for, inversion of R, (T), 20: 13538 (IDO-17142)
matrix formulation for, statistical model for completely reduced, 18: 10910
matrix N/D method with arbitrary inelasticity for, 20: 30130
matrix of, mathematical-physics methods in quantum field theory for, 19: 41540
matrix reconstruction near threshold, 16: 22946
matrix reduction formalism modification for, 18: 28339
matrix representation in quantum field theory, 19: 29118
matrix theory and dynamic properties of elementary particles, 16: 15608

matrix theory of, langrangian form of, 20: 11762
measurement in nuclear emulsions, 17: 18527 (CERN-63-3(p.245-74))
measurement of, background reduction using cyclotron D voltage regulator, 16: 33254
measurement of elastic, at very high energies, techniques for, 18: 20897 (CERN-64-6(p.31-48))
measurement of multiple in nuclear emulsions, digitally controlled device for, 16: 19108
measurement of small-angle elastic, techniques for, 17: 18532 (CERN-63-3(p.339-59))
measurement of spurious, in emulsions, 16: 8122
measurements of proximity, cross-sections for unstable particles, 16: 8222
measurements on aluminum-copper alloys, diffuse x-ray, 18: 32158
mechanisms of high-energy, diffraction-peak shrinkage in, 18: 14917
meson (ρ) trajectories in high-energy, 18: 12945
method for studying elastic, at high energies, 16: 4873
Milne problem for non-absorbing medium with linearly anisotropic, 16: 31006 (BNL-5151)
misalignment effects in molecular, analysis of, 18: 8914 (K-1584)
model for calculating energy distribution in thermal neutron, 19: 47557
model for elastic and multiple-production, at high energies, 17: 13375
model for elastic and inelastic, dressed-particle operators for Lee, 17: 22449
model for elastic proton–proton, validity of optical, 18: 10885 (TID-20109)
model for elastic, statistical (T), 19: 1413 (NP-14404(p.59-79))
model for high-energy proton–proton and proton–antiproton, 18: 14864
model for high-energy, nonlocal, 18: 16784
model for high-energy two-particle, multiperipheral, 19: 1414 (NP-14404 (p.80-101))
model for high-energy, multiperipheral, (T), 20: 19598
model for high-energy, modified single-particle exchange, 20: 37862
model for large-angle high-energy elastic, statistical, (T), 19: 10088
model for, Markovian stochastic, 17: 13353 (RM-2936-ARPA)
model for neutron elastic, optical, 18: 7678 (CONF-346-5)
model for nonrelativistic particles, nonunique solutions for, 20: 11763
model for potential, absorption effects in single-particle-exchange model for, (T), 20: 24078
model for, production and scattering in Lee, 17: 36581 (TID-19331)
model for, Regge poles in one-pion exchange, 17: 19537
model for strong absorption in elastic, for charged and neutral particles interacting with complex nuclei, 18: 6186
model for two-body relativistic, optical, 20: 34594
model for Van Hove's $G_s(r,t)$, simple binary, 18: 26421
model for, complex angular momentum method in multichannel, 18: 42461
model for, one-dimensional, 18: 32569
model for, tests of one-pion-exchange, 18: 20935
model of high-energy, ladder, 17: 13402
model of two-body, composite particles in relativistic, (T), 19: 16506
model of 30-Mev proton, optical, 19: 28962(R) (MIRL/R/81)
models for, compound particle, 17: 19540
models for elastic, diffraction, (T), 20: 24080
models for high-energy, comparisons between, 17: 32952
models for high-energy, consistency problems in, 18: 2692
models for high-energy, diffraction, 20: 25942
models for many-body, 17: 19101
models for, relation between Lee and optical potential, 17: 36579 (TID-17868)
models for spinless particle, amplitude bounds in ladder-graph, 19: 3078
models for strong, peripheral, inelastic, 17: 15079 (NP-12566)
models for three-body, 19: 1260
models for two-nucleon, comparison of, 18: 14884
models of very-high-energy, restriction on, 20: 24102
modification of S-matrix reduction formulas (T), 19: 3058
molecular beam, computer program for calculating, 20: 39321(R) (MLM-1312)
molecular, comparison of approximations of total elastic cross sections, 17: 29439
momentum spectra in, at high energies, (T), 19: 37616
momentum transfer in inelastic, (T), 19: 42992
Monte Carlo method in, principles and uses of, 20: 9800
multichannel reaction analysis, for strongly coupled channels, 16: 18604
multichannel theory of, field theory formulation of nonrelativistic, 18: 15301
multipion-exchange contribution for proton-proton phase shifts, comparison to ALV theory, 18: 9172
multiple, calculation by means of second difference sums of deflections measured on trajectories in nuclear emulsions, 17: 14971
multiple-channel problems, solution method, 16: 5895
multiple, corrections to the optical potential for, 16: 28104
multiple dispersion relations in, 17: 9825
multiple, in the presence of energy losses, 17: 6954 (NP-12259)
multiple, in the problems of nuclear physics, 17: 36412 (NP-13020 (p.186-200))
multiple method of second difference sums in nuclear emulsions, 17: 16815
multiple, of fast charged particles, theory of small-angle, 17: 40249
multiple scattering effects in small-angle proton-nucleus, 18: 21242
multiple, theory for particles traversing a finite body, 18: 6078
n-vertex loops, analytic properties, 16: 5888
N/D equations for, iterative solution of, 18: 44615
N/D equations for, exact solution of one-photon-exchange, (T), 20: 34292
N/D method for p-wave meson (π)–meson (π) (T), 19: 1286
N/D method in, inelasticity in one-channel, 20: 19566
non-perturbative solution for small-angle problems, 17: 22429 (LNF-63/19)
non-relativistic time-dependent theory of, Coulomb interactions in, 18: 28268
nonlocal effects of Moeller and Bhabha, at high energies, 18: 26289
nonrelativistic dispersion formulas, 16: 11128
nuclear reaction theory, effects of physical properties on channel radii, 16: 19786
nuclear surface diffuseness effects on particle-nucleus diffraction, (T), 19: 10289
of Dirac and Schrödinger particles, potential, 18: 32559
of Dirac particles on central scalar potentials, amplitude for, 18: 32553
of Dirac particles by compound system, rearrangement, (T), 19: 14386
of Dirac particles by scalar potential, elastic, (T), 19: 41510
of equal-mass particles, dispersion relations for, 18: 14913
of free particles by identical bound particles, 17: 19111
of neutral particles by crystals, theory of momentum exchange in elastic, 18: 21342
of nonrelativistic systems with arbitrary spin, 17: 710 (LAMS-2740)
of nuclear reaction products, chamber for observing, 17: 32393(P)
of particle by bound two-particle system, (T), 19: 12179
of particles at high energies, formulas for elastic, 18: 44531
of particles at very high energy, elastic, (T), 19: 31023
of particles by nuclei, diffraction, (T), 19: 37899
of particles by superposed Yukawa potentials, relativistic, (T), 19: 39598
of particles on singular potentials, (T), 19: 37581
of particles with arbitrary spin on spinless targets, phase shift statistical description of, (T), 19: 4993
of particles, asymptotic wave behavior in, (T), 19: 37549
of polarized spin-½ particles by particles with spin 1 and 0, (T), 19: 32962
of relativistic particles, quantum theory of, 19: 20950
of spinless neutral bosons in one space dimension with unitarity and crossing symmetry, 18: 14983
of spinless particles with equal masses, unitarity of amplitudes for elastic, (T), 19: 37550
of wave packets, resonance, (T), 20: 25799
Omnes singular integral equation for, iteration of, 20: 7898
on energy-dependent exponential potentials, cross sections for, (T), 19: 37625
operator for classical gases, applicability of Green function form of three-particle, 17: 15144
operator for gases, three-particle, 17: 11513
operator for, spectrum of, 20: 27979
operator in classical gases, structure of three-particle, 17: 20685
operators for, in Lee model of field theory (T), 19: 3122
operators in two dimensions for, divergence of ternary, (T), 20: 2786
operators in, equations of motion for radiative, 18: 36404
operators in, Feynman graphs for truncated time-ordered Green's functions for, 19: 23501
operators in, resolvent of the sum of two commuting, (T), 19: 8286
opposite boundary values in axiomatic theory, 17: 22332
optical-potential renormalization, 16: 22898
optical potential in inelastic, relation between optical model and direct interaction theory for, 17: 731
optical potential method for atomic, generalized, 17: 36456 (UCRL-10878)
origin of heavy-particle stripping, 17: 5397
orthogonality-constraint method for rearrangement, (T), 19: 10079
parametric dispersion relations, 16: 10869
parity changes in inelastic, (T), 19: 5252
parity rule for small-angle, 18: 16921 (ANL-6848(p.118-22))
partial amplitudes at low-energies, 16: 978
partial-wave amplitude determination using analyticity, crossing symmetry, and unitarity, 16: 5883
partial-wave amplitudes from N/D method, 16: 26132
partial wave amplitudes, analytic continuation of, 17: 5548
partial wave amplitudes in second Riemann sheet, existence of poles for, 17: 24351
partial wave amplitudes in, dispersion relations for, 18: 7480

partial wave analysis for relativistic Coulomb, for charged spinless particles, 17: 22451
partial wave and scattering amplitudes, high-energy, 16: 12564
partial waves in multi-particle-production interactions, 16: 1078
particle collision probabilities in, approximations for, 18: 18654
particle formation in quasi-elastic, 18: 14816 (NP-13618)
particle model of, from collective states of nuclei, 17: 11699
path integrals in Feynman representation of, functional, 18: 26427
peripheral collision theory based on the S matrix, 17: 20584 (UCRL-10022(p.191-3))
permissible rate of decrease in amplitude of forward, at high energies, (T), 20: 2810
permutation symmetries of two-body amplitudes in, (T), 19: 6553
perturbation expansion of S-matrix, 16: 31186
perturbation expansion in high-energy, partial summation of, 17: 13387
perturbation of resonant states in potential, 18: 44606
perturbation theory for three-particle system, 18: 26432
perturbation theory for partial waves in, 19: 16667 (TID-20517)
perturbation theory for, high-energy behavior of five-point function for ladder diagrams in, 19: 21096
perturbation theory for, time-dependent, 20: 2776
perturbation theory for, hierarchial principle in, 20: 27995
phase approximation in high-energy, N/D method in random, (T), 19: 8161
phase calculations for, method of, (T), 19: 31076
phase in single-channel, truncation bounds on, 18: 30563
phase matrix, variational principle for, (T), 20: 41991
phase of analytic two-channel S-matrix in, resonance effects on behavior of, (T), 19: 31054
phase relations for nonlocal potentials, 18: 36286
phase relations in nuclear, 17: 41532(R) (ANL-6720(p.59-66))
phase shift analysis, 16: 4727
phase-shift analysis of single channel, 17: 26484
phase shift analysis of spin-independent, 20: 44337
phase shift and angle of deflection in, numerical formulas for, 18: 24468
phase shift and resonance equations for elastic, 19: 39487 (UCRL-14193)
phase shift approximation for, 17: 24271 (TID-16793)
phase shifts and bound state energies in, method of evaluation, 17: 13393
phase shifts and existence of anions in potential, at zero energy, 18: 18568
phase shifts and transport cross sections in, effects of three turning points on, (T), 19: 20957
phase-shifts at low energies, Born approximation for small elastic, 17: 20869
phase shifts for, ambiguity problems in, 17: 33234
phase shifts for electron, on screened Coulomb potential, 18: 34528
phase shifts for long-range potentials in low-energy expansion of, 17: 13365
phase shifts for low-energy, 18: 7494
phase shifts for molecular beam, calculation of intermolecular potential parameters from, 18: 4338
phase shifts for meson (π)-nucleon, inelastic effects on, 18: 32575
phase shifts for many-channel, differential equations for, 18: 32577
phase shifts for nucleon-nucleon, singlet-state, 18: 34546
phase shifts for potential, nonrelativistic, 17: 2443
phase shifts for potential, of Dirac particles, 17: 19102
phase shifts for proton-proton, electromagnetic corrections to p-wave, (T), 19: 16632
phase shifts for potential-well, quantum mechanical, (T), 19: 20956
phase shifts for proton–proton, at 435 Mev, (T), 19: 37622
phase shifts for screened Coulomb potential, 16: 3775
phase shifts for single-channel, 17: 747
phase shifts for singular nucleon-nucleon potential, 17: 40032
phase shifts for S-wave, for $l = 0$, 18: 6020
phase shifts for S-wave, by square well potential, (T), 19: 25516
phase shifts for two-nucleon, 16: 24708
phase shifts for, moment relations of, (T), 19: 8303
phase shifts from differential cross sections, determination of molecular beam, 18: 4337
phase shifts in, approximation for, 18: 7491
phase shifts in, asymptotic, 18: 9123
phase shifts in, distorted wave approximation for, 17: 31295
phase shifts in, extension of Born approximation for, 17: 24316
phase shifts in inverse, 18: 44533
phase shifts in low-energy, negative energy moments of partial-wave, 18: 21054
phase shifts in multichannel, bound states of hamiltonian operator in, 17: 24283
phase shifts in nonrelativistic, energy moments of, 17: 13445
phase shifts in, partition function for energy moments of, 18: 2710
phase shifts in potential, Regge-pole effects on, 17: 32956
phase shifts in potential and multichannel, NYU research on, 18: 30299 (AFCRL-63-925)
phase shifts in presence of metastable states, semi-classical, 20: 28032
phase shifts in, relation between Dirac and Schroedinger equations for, 17: 31314
phase shifts in singular-potential, heuristic Feynman-integral cutoff for weak-coupling limit of, 18: 21049
phase shifts in spin-½–spin-0 elastic, 17: 11570
phase shifts in, variational calculations of, 17: 19098
phase shifts in, approximations for, 18: 14883
phase shifts in, effect of $^3S_1$–$^3D_1$ coupling on $^3D_1$, 20: 27969 (UCRL-14885-T)
phase shifts in, field-theory proof of Levison's theorem for, 20: 24123
phase shifts in, Levinson's theorem for, 18: 42476
phase shifts in, separable potentials from, 20: 10074
phase shifts, macroscopic causality relation to energy derivative, 16: 8294
phase studies for elastic and inelastic, from heavy nuclei, 17: 31463
phase-shift representations in, validity of, (T), 19: 35155
phase-space integral in statistical model for multiple-production, classical, 20: 8113
phases in potential field, quasi-classical approximation for, 19: 16554(T)
phases of, Chew-Low equations and isospin dependence of, 19: 27144 (JINR-P-1964)
photon emission in potential, infrared divergence effects in, 17: 19546
photon exchanges and radiative corrections in, 17: 19097
polarization changes in potential, (T), 19: 5030
polarization change in potential, classical approximation for, (T), 19: 41501
polarization in elastic, S-matrix for bound state systems, 16: 13914
polarization in elastic, strong-absorption model for, 18: 24636
polarization in elastic, 19: 19181
polarization in high-energy inelastic, distortion due to elastic scattering in, 18: 15289
polarization phenomena in, 17: 36413 (NP-13020(p.201-13))
Pomeranchuk trajectory for nonisotopic-spin-flip scattering length, second, 17: 34768
Pomeranchuk-Okun rule for inelastic, (T), 19: 29099
Pomeranchuk's theorem for high-energy limits of total cross sections, 18: 2647
potential, amplitudes for high-energy elastic, 16: 22882
potential, amplitude double dispersion relation for nonlocal, 17: 26328
potential, analytic properties of off-energy-shell amplitudes, 16: 6020
potential, analyticity in angular momentum, coupling constant, and energy of S-matrix for, 17: 34810
potential, angular momentum analyticity in hard core, 17: 24333
potential, application of Regge poles to Mandelstam representation of, 17: 22453
potential, Born approximation and transport theory application to low-energy, 17: 22454
potential, bound-state solution of Bethe-Salpeter equations for, 18: 9236
potential, complex angular momentum in many-channel, 18: 4435
potential, continuation to complex l values, 16: 27957 (UCRL-10033)
potential, convergence of Born series and existence of bound states in, 17: 36850
potential, cross sections, energy moments, and phase shifts for Gaussian, 18: 2711
potential, derivation of fundamental relations for, 17: 7506
potential, derivation of complex angular momentum by Fredholm method for, 17: 36836
potential determination using spectral measure function, 16: 8118
potential, determinantal method and Jost functions in, 17: 26314
potential, effects of kinetic properties of scatterers, 16: 26440
potential, equations for S-wave, 16: 31182
potential for Coulomb, with hard core and attractive well, (T), 19: 23392
potential for nucleon-nucleon, 18: 11219 (TID-20105)
potential for scatterer with closely coupled states, optical model, 16: 18262
potential for singular, infinity of strength of, (T), 20: 42027
potential, Green's function for spherical symmetry in, 17: 26317
potential in nucleon-nucleon, soft-core, (T), 19: 14387
potential, Jost function and its spectral function for, 16: 28344
potential, Mandelstam representation in, 17: 34721 (CERN-63-26)
potential, nonadiabaticity in, 17: 32967
potential, partial wave amplitudes for branch cuts and Regge poles in, 17: 22452
potential, perturbative expansion for large angular momenta in, 18: 7580
potential, phase shift maxima and minima in, 17: 24323
potential, phase shift series for, 17: 26349
potential, properties of relativistic two-body, 17: 32928
potential, Regge trajectories for square-well, 17: 24324
potential, Regge trajectories at negative angular momenta in, 17: 41775

potential, Regge trajectories for weak short-range, 18: 2608
potential, regularity of T matrix in Dirac, 17: 32926
potential, S-matrix behavior for large imaginary angular momentum, 17: 26325
potential, S-matrix properties of Schroedinger equation for, 17: 29559
potential, solution of Bethe-Salpeter equations for, 18: 9235
potential theory of, principle of maximum and minimum in, 20: 44300
potential, three-particle unitarity in, 17: 28188
potential, uncoupled phase shifts from high-energy WKB approximation in, 17: 40032
potential, unitary impulse approximation for multichannel three-body, 17: 28193
potential, variational principles for vector wave equation solution of electromagnetic, 17: 26351
potential, wave operators for spherically symmetric, 17: 29528
potential, with complex angular momentum and energy, 16: 24310
potential with n bound states, 16: 29673
potential, amplitudes in, 20: 19551
potential, amplitudes and resonance poles in three-dimensional, 20: 34271
potential, analyticity for solution of, 20: 32162
potential, angular momentum and energy properties in, (T), 19: 16511
potential, approximation for spherically symmetric, 18: 18666
potential, approximation method for phase shifts in, 20: 37852
potential, arbitrary phase shift differences in, (T), 20: 6127
potential, asymptotic convergence in, 18: 26301
potential, asymptotic approximation for monotonic, (T), 19: 27540
potential, asymptotic behavior in angular momentum for, (T), 19: 31293
potential, asymptotic expansion for Green function of nonrelativistic, (T), 20: 19565
potential, Born approximation and large-momentum transfer in, 20: 17460
potential, Born series for bound states in, 18: 28641
potential, calculation by determinantal and N/D methods, 20: 39927
potential, completeness, dispersion relations, and unitarity in, 20: 22464 (IC-66/29)
potential, compositeness condition in, 19: 35014 (BNL-8245)
potential, contiguous Dirac phase shifts in, (T), 20: 6126
potential, convergence and error bounds of Born expansion for, (T), 19: 35158
potential, distance determination for high-energy, (T), 20: 6108 (NP-15600)
potential, double spectral function in, 19: 21093
potential, energy gap equation for soft core, 19: 41662 (JINR-P-2176)
potential, equivalence of Fredholm and multichannel N/D methods in, 19: 35084
potential, field theory for singular, 18: 26415
potential, for relativistic spinless particles, 20: 28036
potential, Fourier series expansion for kernel continuity in generalized, 20: 32118
potential, Fredholm equation for, 18: 40389
potential, Fredholm method for amplitudes in, (T), 19: 12382
potential, Green function for barriers in, 18: 21025
potential, lifetime matrix in, (T), 19: 27188
potential, Mandelstam representation in hard-core, 18: 28351
potential, modified determinantal method for Yukawa, 20: 32135
potential, Moeller operators for singular, 20: 37831
potential, momentum transfer in, (T), 19: 39543
potential, N/D method in, 19: 25314
potential, N/D method in, 20: 6129
potential, nonrelativistic Coulomb Green's function in momentum space for, 18: 40390
potential, off-shell structure of partial T matrix in, 20: 24134
potential, osymptotic expansions of tan δ in singular, 20: 7926
potential, partial wave amplitudes in many-channel, 18: 28347
potential, perturbation theory for strong repulsive, 18: 26302
potential, perturbed bound-state poles in, 20: 15480
potential, phase method for multichannel, (T), 19: 8279
potential, property of vertex function in, (T), 19: 20964
potential, R-matrix approach to complex angular momentum and three-particle, (T), 20: 11691 (ORNL-3914)
potential, Regge poles in quasi-classical, 18: 19119
potential, Regge poles in nonrelativistic, (T), 19: 47320
potential, Regge representation for, 18: 30559
potential, Regge trajectories in, 18: 36399
potential, Regge trajectories in nonrelativistic, (T), 19: 43153
potential, Regge trajectory for complex angular momentum in, 20: 7949
potential, regularization method in, 20: 44330
potential, repulsive core in effective nonlocal energy-independent, (T), 20: 11653
potential, S-matrix for, (T), 19: 44995 (COO-30-97)
potential, S-matrix theory for, 20: 17490
potential, Schwinger variational principle for, (T), 20: 11747
potential, short range interaction without strong singularity for kernel continuity in generalized, 20: 32117
potential, singular inverse-power, 19: 35090
potential, space-time properties for particle wave packet, 20: 21761
potential, subtractions in, (T), 19: 27195
potential, sum rules in nonrelativistic, (T), 20: 9806
potential, sum rules in, 20: 11739
potential, theory for nonrelativistic, 18: 40344
potential, theory for, 20: 4701
potential, three-body, 20: 17430 (JINR-P-2565)
potential, time evolution of wave packet in, 19: 29283
potential, upper bound for the double spectral function in, (T), 19: 35058
potential, variational bounds for multichannel, 20: 2815
potential, wave-packet formalism for, 19: 32951
potential, with inverse-square attraction, 18: 21055
potentials and Regge poles in, separable nonlocal, 18: 2605
potentials, determination from singularities of Jost functions, 16: 18191
potentials for classical radiation damage, cut-off radius for, 19: 1007 (RISÖ-83)
potentials for hard-core, pseudo-, 20: 9819
potentials for many-channel s-wave, Bargmann, 18: 34532
potentials for multiparticle, separable two-body, (T), 20: 34296
potentials for rearrangement collisions, optical theory, 16: 18263
potentials for, in systems with arbitrary angular momenta, 18: 14981
potentials for, in complex angular momentum plane, inversion in, 19: 47361
potentials for, inversion in lambda plane for singular, 20: 32152
potentials for, optical, 18: 13098
potentials for, phase shifts in stochastic fields for, (T), 20: 44393
potentials in asymptotic phase and amplitude for modified Coulomb, (T), 20: 11689 (LA-DC-6912)
potentials in complex angular momentum plane, separable, 17: 22495
potentials in, construction from many-channel S-matrix, 17: 26748
potentials in coordinate space, Jost functions for singular, 19: 47360
potentials in coordinate space, singular logarithmic, 20: 6121
potentials in elastic, S-matrix formalism for optical model, 20: 12021
potentials in elastic, phase-shift analysis of, (T), 20: 15463
potentials in elementary-particle, separable, 19: 1417 (NP-14404(p.128-39))
potentials in inverse, asymptotic properties of, 20: 44321
potentials in nucleon-nucleon, 19: 1552 (JINR-P-1728)
potentials in Padé approximant for short-range, 19: 41407
potentials in, relation between hard-core and velocity-dependent, 17: 762
potentials in, analyticity in angular momentum for singular, 18: 40273
potentials in, approximation for scattering length produced by repulsive singular, 19: 25331
potentials in, approximations of Regge, 20: 13603
potentials in, asymptotic properties of S matrix for, (T), 19: 27261
potentials in, asymptotic Regge behavior for nonlocal, 19: 31078
potentials in, asymptotic form of phase shift for strongly singular, (T), 20: 11712
potentials in, asymptotic amplitude and phase for modified Coulomb, 20: 24112
potentials in, asymptotic behavior of S-matrix in complex angular momentum for singular, 20: 25895
potentials in, Born approximation and dispersion relations for singular, 20: 25937
potentials in, bound states for attractive, (T), 19: 10043
potentials in, bound states of nonlocal separable, 20: 17495
potentials in, correlation and quantum corrections to Thomas-Fermi, (T), 19: 8257
potentials in, eigenvalues of Lippmann-Schwinger kernel for Yukawa and nucleon-nucleon, (T), 20: 13836
potentials in, expansions in classical collision theory for, 20: 2808
potentials in, expansions for long-range effective, (T), 20: 9832
potentials in, Green's function for quasi-, (T), 19: 12381
potentials in, high-energy limit for singular repulsive, (T), 19: 31292
potentials in, high-energy approximation for nonlocal, 20: 19573
potentials in, kernels of non-local, (T), 20: 13586
potentials in, Laplace transforms for Jost functions for singular repulsive, 19: 35104
potentials in, limiting procedures for singular and nonsingular cut-off, 20: 32134
potentials in, minimum principle for effective, (T), 19: 27249
potentials in, non-Born phase shifts for long and short range, (T), 19: 31055
potentials in, nonuniqueness of N/D solutions for singular, 20: 44347
potentials in, one-region two-center expansions of generalized Coulomb, 18: 40408
potentials in, perturbative expansion for gr^{-2} ln (R/r), (T), 19: 8280
potentials in, pentization technique for highly singular repulsive, (T), 19: 10139
potentials in, Perey effect in wave functions for, (T), 19: 12342

potentials in, peratization theory for exponentially singular, 19: 25332
potentials in, peratization technique for singular logarithmic, 19: 35055
potentials in, phase shifts from repulsive, 18: 32842
potentials in, phase-shift determination of, 18: 34635
potentials in, quasi-Born treatment of square-well, 20: 19559
potentials in, Regge poles for Z^{-4} repulsive, 18: 37950
potentials in, Regge behavior for higher order singularities in, (T), 19: 8306
potentials in, Regge poles for velocity-dependent, (T), 19: 27283
potentials in, Regge trajectories and S-matrix for singular, 20: 11706
potentials in, renormalization of Schroedinger equation solutions for, 19: 35217
potentials in, S-matrix elements for nonlocal, (T), 19: 8307
potentials in, S-matrix representation for highly singular, 19: 31077
potentials in, S-matrix and cut-off procedures for singular, 19: 37564
potentials in, Schroedinger equation for inverse fourth-power, 18: 40387
potentials in, separable, (T), 19: 39949
potentials in, short-range singular, 18: 28443
potentials in, singular, 19: 31064
potentials in, wave operators for strongly singular and not spherically symmetric, (T), 19: 16539
potentials in, zero-energy parameters for, 18: 18648 (UCRL-7155-T)
potentials, tables of classical integrals for Bohr, Born-Mayer, and Thomas-Fermi, 17: 38088 (ORNL-3493)
potentials with bound states in, attractive, 19: 35201
potentials with hard cores in, 17: 9541
production amplitudes in, representations for single-particle, 17: 9222
propagation of single-scattering distribution in multiple, 17: 17228
properties of high angular momentum partial wave amplitudes, 16: 4705
properties of Landau curves in, 18: 42506
properties of s-amplitude, 16: 33717
properties of S-wave, 17: 5227
quantum effects in elastic molecular, 18: 30616 (COO-1328-7)
quantum-electrodynamic treatment of electrons, mesons(μ), and photons as Regge poles in, 17: 40239
quantum field theory for elastic proton-proton, with high momentum cut-off, (T), 19: 23478
quantum mechanical relations for, 17: 11932
quantum theory for elastic, space structure and relativistic, 20: 15629
quasi-classical treatment of elastic, for heavy ions, 17: 17115 (JINR-P-1153)
quasiparticle method for binding energies, cross sections, and scattering lengths in potential theory, 18: 14880
radiation diffusion in semi-infinite medium with nonisotropic, 18: 2679
radiative corrections to high-energy, 17: 19142
radiative corrections to, unified theory for, 18: 12888 (AFOSR-4742)
radiative corrections to high-energy electron-electron, 19: 31073
radiative transfer in, equation of, 20: 2930 (AD-614636)
radius in, calculation of lower limit for, 16: 24740
random phase approximation for N/D method in high-energy, 20: 7927
range of high-energy interactions, 17: 31339
ranges of high-energy, energy variation of, 20: 6153
rearrangement collisions in, integral equation for uniqueness of, 17: 5204 (UCRL-6558-T)
rearrangement, theory, 16: 19557
recurrence relations for Appell functions in, calculation of matrix elements in angular momentum representation, 17: 16962
reduction formula for vertex function, extended, 17: 31325
redundant poles of S-matrix, 16: 17045
Regge behavior of amplitude of, for highly singular potential, 18: 6061
Regge cuts and three-particle states in a nonrelativistic model, 17: 36838
Regge cuts in angular momentum plane of high-energy, (T), 20: 30160
Regge exponent in high-energy, expression for, 17: 15121
Regge method in relativistic amplitude of, (T), 19: 12306
Regge parameters in many-channel relativistic, dynamical equations for, 17: 39931
Regge parameters in potential, 18: 9087 (UCRL-11096)
Regge parameters in potential, numerical study of, 19: 10110
Regge parameters in potential, approximation methods for, 20: 39923
Regge pole analysis of three-body, difficulties in, 18: 34518 (UCRL-11546)
Regge pole and fixed branch cut domination of high-energy, theory based on simple vacuum pole trajectories, 17: 37958
Regge pole behavior in diffraction, 17: 24340
Regge pole behavior in, validity of renormalization group equations for, 17: 34769
Regge pole contributions in elastic, 18: 7477
Regge pole dominance in high-energy, at low momentum transfer (T), 19: 3068
Regge pole hypothesis in high-energy, with multiple-particle production, 18: 7479
Regge pole kinematics in, (T), 19: 10061
Regge pole-like high-energy behavior in perturbation theory, 18: 930
Regge pole parameters in, dynamical determination of, 17: 28167
Regge pole parameters in, formulation and numerical solution of dynamical equations for, 18: 942
Regge pole parameters in, integral equations for, (T), 19: 12230
Regge pole phenomenological applications in, 20: 46388 (ANL-7173)
Regge pole positions in, calculation of, 17: 9409
Regge pole theory in high-energy, 18: 40360
Regge pole threshold motion in, 17: 22493
Regge pole trajectory for elastic, removal of the meaningless state on vaccum, 17: 11486 (NP-12479)
Regge pole trajectories in, analytic properties of, 17: 20942
Regge-pole trajectories for Yukawa potential, perturbative expansions of, 17: 40236
Regge pole trajectories in, restrictions on, 18: 2600
Regge pole trajectories in, as functions of coupling constants and energies, 18: 6077
Regge pole trajectories for hard-core potential, 18: 12977
Regge pole trajectories in nonrelativistic two-channel, (T), 19: 12257
Regge pole trajectories in Coulomb-well type potential, (T), 19: 47311 (NP-15454)
Regge poles and asymptotic values of scattering matrix in the complex momentum plane, positions of, 18: 5879
Regge poles and complex singularities in, 17: 31663
Regge poles and cuts in field theory model for, (T), 20: 2768
Regge poles and fixed branch cuts in angular momentum plane for diffraction, analyticity in, 18: 18687
Regge poles and Landau singularities in, 17: 7526
Regge poles and perturbation theory in, 17: 11905 (JINR-E-1095)
Regge poles and perturbative expansion in, 18: 10871 (LNF-63/47 (p.118-21))
Regge poles and polarization in, hypothesis of, 17: 9247
Regge poles and trajectories in high-energy, (T), 20: 34322
Regge poles at zero energy in, 20: 44344
Regge poles for δ-potential, (T), 19: 12311
Regge poles for, on δ potentials, 17: 37972
Regge poles for velocity-dependent potentials in, 19: 29101
Regge poles in, (T), 19: 14375
Regge poles in, 20: 30163
Regge poles in analysis of high-energy, 17: 9417
Regge poles in, application and theory, 17: 24276 (UCRL-10677)
Regge poles in backward, at high energy, (T), 19: 12305
Regge poles in bootstrap dynamic pseudoscalar meson, SU(3) octet of even-signature, 18: 21042
Regge poles in cut-off Coulomb potential, (T), 19: 33056
Regge poles in electromagnetic and weak, 19: 1416 (NP-14404(p.113-27))
Regge poles in Froissart-Gribov continuation, unitary conditions for, 20: 11724
Regge poles in high-energy potential, 17: 37949
Regge poles in high-energy inelastic, 17: 7513
Regge poles in, Levinson's theorem, 17: 42170
Regge poles in, observable effects of singularities on left half-plane Re $l < -1$, 17: 40245
Regge poles in, of electrons at high energies, 17: 3991
Regge poles in potential at high energy, 17: 758
Regge poles in potential, review, 17: 19535
Regge poles in potential, localization of, 18: 32570
Regge poles in potential, (T), 19: 10156
Regge poles in quantum field theory, 17: 22775
Regge poles in relativistic, on Coulomb potential, 19: 27173
Regge poles in velocity-dependent potential, (T), 19: 33077
Regge poles in Yukawa-potential, perturbation theory for, 19: 12310
Regge poles in, at high energies, 18: 18677
Regge poles in, calculation by continued fractions, (T), 19: 10054
Regge poles in,effective-range expansion from threshold, 18: 40315
Regge poles in, lectures on, 18: 22731 (NP-13880)
Regge poles, method of calculating, 16: 31029
Regge poles near thresholds in multichannel, (T), 19: 25326
Regge-Pomeranchuk pole approximation for high-energy elastic, experimental verification of, 17: 20895
Regge surfaces and singularities in a relativistic theory, 17: 13668
Regge trajectories for single attractive Yukawa potential, 16: 21268 (UCRL-10140)
Regge trajectories in relativistic Schrödinger theory, 16: 28334
Regge trajectories in, use of perturbation theory in evaluating, 17: 2420 (JINR-E-1061)
Regge trajectories for the square-well potential, 17: 5554
Regge trajectories in, dispersion relations for crossing of, 17: 19147
Regge trajectories in potential, equations for, 17: 19534
Regge trajectories in, 17: 20840 (JINR-E-1194)
Regge trajectories in, weak-coupling limit of, 17: 40243
Regge trajectories in $\lambda\phi^4$ theory, 17: 42182

Regge trajectories in, perturbation theory calculation of, 18: 18655
Regge trajectories for cross sections for nucleon-nucleon, 18: 20936
Regge trajectories for baryons and nucleons in, model for, 18: 20940
Regge trajectories for boson-fermion cross sections with domination by complex conjugate pairs of u-channel trajectories, 18: 20942
Regge trajectories of fermions, 18: 22723 (JINR-P-1592)
Regge trajectories for Coulomb potential, 18: 24430
Regge trajectories in, signatures of, 18: 32572
Regge trajectories in high-energy elementary-particle, 18: 40251 (UCRL-11516)
Regge trajectories and Lippmann-Schwinger equation in, (T), 19: 8277
Regge trajectories in potential, calculation by W.K.B. approximation, (T), 19: 8299
Regge trajectories in, threshold behavior of, (T), 19: 12224
Regge trajectories with right-hand cut in, formula for, (T), 19: 18875
Regge trajectories in, principle of maximum analyticity for properties of, 19: 21061
Regge trajectories in, analytic properties of, (T), 19: 25300
Regge trajectories in, modification by contact potential, 19: 32960
Regge trajectories in, nonrelativistic, 19: 45028 (NP-15207)
Regge trajectories for Coulomb potential cuts in, 20: 46404
Regge trajectory in field theory, 17: 11919
Regge trajectory in low-energy alpha-alpha, 17: 13405
Regge trajectory on high-energy, 17: 9250
Regge trajectory of deuteron, properties of, 18: 9116
Regge type solutions in renormalizable field theories of, condition for, 17: 26366
Regge 6-j symbols, recursion relations and simplified expressions for, 17: 22436 (ORNL-3440)
Regge-pole model for high-energy pp and $\bar{p}p$, 18: 14893
Regge-pole parameters for, self-consistent determination of, 18: 14882
Regge-pole theory of high-energy, 20: 19597
Regge-pole theory in, status of, 20: 32185
Reggeon unitarity conditions in Froissart-Gribov continuation for, 19: 29049 (IC/65/41)
relation between binding energy and coupling constant in, 17: 6943 (BNL-5517)
relation of coupling constants to S-matrix zeros, 16: 27950
relations for two-body, 18: 858 (PAN-436/XVIII)
relativistic model, 16: 10852
relativistic theory of, complex angular momentum in, 17: 11521
relativistic two-body equation solution, 16: 18348
renormalization in potential, (T), 19: 20945
representation for, polynomial boundedness in Mandelstam, 18: 44614
representation of near-threshold and resonance effects in, 18: 9199
representation of high-order poles in S matrix, (T), 19: 6577
representations for, properties of perturbation-theoretical integral, 18: 44618
representations of SU(3), irreducible, 18: 10874(R) (NP-13571(p.1-5))
representations of SU(3), structure of irreducible, 18: 10875(R) (NP-13571(p.6-12))
representations of SU(3), 18: 26355
representations of cross sections for high-energy interactions, 18: 42417
representations of semisimple Lie groups, (T), 19: 8263
representations of semisimple Lie groups, (T), 19: 8264
research at Oxford on, 17: 2058(R) (NP-12207)
research facilities for, 19: 47327
research on, monthly summary, 17: 19510(R) (TID-18344)
research on 1 to 3 Mev, survey on, 17: 41855 (AFCRL-62-162)
research on >3 Bev quasi-elastic, review of, 17: 13374
research programs at Lyman Laboratory, Harvard University, 16: 29660 (TID-16119)
research progress at Tufts University, 17: 37661(R) (TID-19415)
research progress on, 18: 10628(R) (TID-20068)
resonance and high-energy limit of amplitude for, 19: 21000
resonance energies and widths for compound states of given J and T in elastic, cross-section calculation from, 18: 18890
resonance model for multiplets of SU(3) scheme under broken symmetry, 18: 4481
resonance overlapping in three-particle final states in S-wave, dispersion theory of, 18: 21044
resonance poles and shadow poles in many-channel S-matrix, 18: 14877
resonance widths in elastic cross sections, effects of target thickness and beam straggling on, 17: 15288
resonance widths in multichannel, formula for, 19: 1238
resonance-pole motion in two-body, S-matrix theory for, 19: 23371
resonances and bound states in nonrelativistic, distributions of, 18: 12992
resonances in nucleon-nuclear, coupled-channel and single-particle (T), 19: 1566 (PUC-1964-154)
resonances in, theory of, 18: 4445
reverse quantum mechanical problem in, 16: 12341
Riccati equation in, upper and lower bounds for solution of, 17: 22456
role of short-range three-particle forces in processes with the generation of three particles near threshold, 17: 7518
Rosenbluth formulas for differential cross sections in, 18: 9211
s-matrix as analytic function of angular momentum in potential, 17: 22462
S matrix continuation into second Riemann sheet, 16: 18389
S-matrix for complex angular momentum and energy in, real unitary representation of many-channel, 17: 32927
S matrix for high angular momentum, asymptotic behavior of, 17: 17023
S matrix for many-channel, 18: 26283
S-matrix for one-dimensional Schrödinger equation, 16: 2483 (JINR-D-690)
S matrix for, method for calculating, (T), 20: 34272
S matrix holomorphy domain in potential, 16: 21295
S matrix in complex angular momentum space of, quasi-classical solutions for, 17: 41836
S matrix in wave packet description for spinless-particle elastic, (T), 19: 12175
S matrix left-hand cut discontinuity and equivalent potentials, 16: 21297
S-matrix, removal of ultraviolet divergences from, 17: 22463
S-matrix, stochastic field theory and, 17: 13394
S-matrix theory for joining radius independent formulation of resonant, 17: 41787
S-matrix theory, group-theoretical basis of, 16: 28349 (UCRL-9963)
S-matrix theory, lectures on, 16: 9560 (UCRL-9875(Vol.I))
S-matrix theory of strong interactions without elementary particles, 17: 5570
S-matrices in, Padé approximant for unitary, 20: 15363
S-matrix analyticity for singular potentials in, 18: 34637 (NP-14076)
S-matrix asymptotic behavior in nonrelativistic Yukawa-potential, P-wave, 20: 9802
S-matrix convergence in nonlocal quantum electrodynamics, 20: 24259
S-matrix determination from elastic, (T), 19: 18761
S-matrix dynamics in, variational principle in, (T), 19: 35150
S-matrix element for nonlocal potential, (T), 19: 18901
S-matrix elements in, unitarity and on-mass-shell analyticity in, (T), 19: 32964
S-matrix elements for, cluster decomposition of, 20: 15484
S-matrix elements in, reduction formulas in axiomatic quantum field theory for, 20: 15502
S-matrix elements for, cluster expansions of causal, 20: 39858 (JINR-P-2760)
S-matrix equations with Regge behavior, dynamical, 18: 12917 (UCRL-11125)
S-matrix experiment and theory, 18: 30614 (AERE-R-4646)
S-matrix for finite times in interacting-particle wave-function space, 20: 11761
S-matrix for high-energy, (T), 20: 30108
S-matrix for large angular momentum, asymptotic form of, 20: 21754
S-matrix for long-range potential, poles of, 20: 39868
S-matrix for low-energy, threshold poles for, 20: 13588
S-matrix for multichannel, unitarity of, 20: 39866
S-matrix for potential, in complex angular momentum plane, analytic properties of, 20: 32186
S-matrix for potential, completeness, unitarity, and dispersion relations for, 20: 46395
S-matrix for quantum, structure of, 20: 37854
S-matrix for screened Coulomb potential, poles of, 20: 36081
S-matrix for singular potentials of, properties of, (T), 20: 4640 (IC/65/75)
S-matrix for strongly singular potentials in, asymptotic behavior of, 20: 24132
S-matrix for strongly singular potentials in, analytic structure in, 20: 30100
S-matrix for superposition of singular exponential potentials, 18: 36288
S-matrix for two-body, singularities in effective range approximation for, 20: 25920
S-matrix for two-channel, analytic properties of, (T), 19: 18760
S-matrix for, consistency of unitarity condition with broken U(12) symmetry, (T), 19: 45018 (JINR-P-2283)
S-matrix for, equation of motion for half, 20: 17493
S-matrix for, experimental test of substitution law in, 20: 19516
S-matrix for, hamiltonian hermicity of effects on energy dependence of, 20: 46419
S-matrix for, higher-order poles in, 20: 41943
S-matrix for, implications of isospin I^2 and I_3 conservation for, 20: 19575
S-matrix for, invariants of simple Lie groups for, 20: 46407
S-matrix for, most general Clebsch-Gordan coefficients for, 20: 41944
S-matrix for, relativistic combination of internal and spin symmetries in, (T), 20: 11755
S-matrix for, relativistic Lee model for, 20: 41948
S-matrix for, U(12) symmetry and unitarity condition for, 20: 37855

S-matrix for, unitarity and on-mass-shell analyticity in, (T), 19: 32965
S-matrix formalism in perturbation theory, 20: 15526
S-matrix gauge transformations in quantum electrodynamics, 19: 35211
S-matrix in angular momentum plane, (T), 19: 18916
S-matrix in axiomatic field theory, causal, (T), 20: 15515
S-matrix in complex plane under reflection and unitarity restrictions, 18: 32573
S-matrix in complex angular momentum plane for, Sommerfeld-Watson transformation and dispersion relations for, (T), 20: 11732
S-matrix in complex angular momentum plane, dispersion relations for, (T), 20: 37836
S-matrix in Heisenberg representation for, 20: 30104
S-matrix in many-channel, analytic properties of, 20: 15505
S-matrix in potential, analyticity of, (T), 19: 16532
S-matrix in quantum field theory, one-particle singularities of, 20: 6122
S-matrix in unified theories of, singularities of, (T), 20: 4639 (IC/65/73)
S-matrix in, computation of multichannel, (T), 19: 25313
S-matrix in, conditions of macroscopic causality for, (T), 20: 13539 (JINR-E-2500)
S-matrix in, crossing principle in, 20: 41803(R) (UCRL-16863)
S-matrix in, extraction of singularities from, 20: 44319
S-matrix in, gauges and invariance of, 20: 44303
S-matrix in, integral equations for one-channel relativistic case including CDD poles, 20: 25919
S-matrix in, Jost functions, Levinson theorem, and multichannel problems in relativistic, 20: 44386
S-matrix in, Regge pole representation of, 20: 21755
S-matrix invariance under complex inhomogeneous Lorentz group, complex angular momentum in, (T), 20: 11758
S-matrix potential in one-dimensional Schroedinger equation, (T), 20: 30248
S-matrix representation from Neumann series expansion of the Schroedinger equation, 18: 14985
S-matrix singularities in, 20: 15524
S-matrix theory, 20: 19594
S-matrix theory, 20: 19606
S-matrix theory for, 19: 18914
S-matrix theory for, causality in, 19: 20943
S-matrix theory for, isospin and spin in, 20: 11720
S-matrix theory for, N/D method for mass shifts in, 20: 15466
S-matrix theory for coupling constant bounds, unitarity and analyticity in, 20: 17477
S-matrix theory for, substitution law in, 20: 19586
S-matrix theory for strongly interacting particles, 20: 21774
S-matrix theory for, symmetries in first-approximation, 20: 42169(R) (UCRL-14744, pp 1-18)
S-matrix theory for, physical-region singularities in, 20: 41954
S-matrix theory in, lectures on analytic, 19: 1408 (NP-14403)
S-matrix theory in, causality in, 20: 32112
S-matrix theory in, unitarity in, 20: 42020
S-matrix theory of, dispersion theory for, 19: 32979
S-matrix theory of, SU(6) invariance in, (T), 19: 43185
S-matrix theory of, Hilbert space in, 19: 43206
S-matrix theory of, variational principles for coupled-channel N/D, method in, 19: 43211
S-matrix theory of, relativistic, 20: 19593
S-matrix theory of, discontinuity formula for physical-region singularities in, 20: 34276
S-matrix theory of, relativistic U(6,6) symmetry group for, 20: 39888
S-matrix theory of, macroscopic causality conditions in, 20: 41962
S-matrix theory of, cross-discontinuity condition in, 20: 41966
S-matrix theory of, normal thresholds in subenergy variables in, 20: 44305
S-matrix theory of, icecream-cone singularity, 20: 44306
S-matrix theory of, spin and statistics in, 20: 44332
S-matrix with inelasticity in, Levinson's theorem for, 20: 17452
S-matrix with noncompact symmetry groups in, 20: 39854 (JINR-E-2754)
scaling law for high-energy elastic, 18: 28330 (TID-20722)
scatterer size effects in, 16: 943
Schrödinger equation solution in inhomogeneous media for limiting absorption and amplitudes, 16: 5802
self-consistent S matrix with Regge asymptotic behavior, 17: 13670
semi-classical approach to high-energy, 17: 11925
simulation of the hard core by a velocity dependence, 17: 11921
single-channel, improved minimum principle for, 17: 17029
singular potentials and peratization in, 18: 12972 (TID-20113)
singular wave function operator application in, 16: 21279
singularities at vanishing coupling constant, model for, 17: 15127
singularities in angular momentum plane in high-energy, 17: 37958
singularities in Feynman diagrams in, method for determining, 18: 6074
singularities in, representation of non-Landau, 17: 19099
singularities of Feynman graph in, in k-space, 17: 2444
singularities of Feynman graphs, 17: 31278 (JINR-P-1272)
singularities of partial-wave amplitude, in angular momentum plane, (T), 19: 37652
singularities of Regge trajectories associated with asymptotes to Landau curves, 18: 929
singularities of s-matrix after a canonical transformation, 17: 16978
singularities of unstable and virtual particle, 17: 22467
singularities on Landau surfaces in, 17: 9220
singularity in partial-wave amplitude, essential, 17: 29554
singularity of Jost functions and potentials in, 18: 44529
singularity of partial-wave amplitude, in J-plane at negative integers, 18: 9158
Slater integrals in inelastic nuclear computer program for, 19: 1565 (ORNL-TM-964)
solution of Boltzmann transport equation, 17: 5539
solution of kinetic equations in, application of the stationary phase method in, 17: 11308 (JINR-P-1113)
solutions for multiparticle problems in, 18: 6034
solutions of symmetric Dirac–Coulomb hamiltonian, 18: 34576
space-like intervals in S-matrix, contribution of, 16: 32340
space-time dilation in high-energy, 18: 37895
spectra calculations by asymptotic self-consistency method, 16: 13882
spectra from, propagation of approximation errors in, 17: 8947 (TID-15543)
spectra of, zeros of causal transforms of folded, (T), 19: 8285
spectral functions, from extrapolation of amplitudes, 16: 24312
spectral functions in, dispersion relations for imaginary part of, 18: 10641
spectral representations of products of Heisenberg operators, 16: 18398
spectral representations of integral operators in, 18: 4899 (BNL-6915)
spectrum of integral operator for, in the physical sheet, 16: 32310 (BNL-5894)
spin density matrix formalism for polarized thermal-neutron, 18: 14813 (KR-65)
spin effects in, triangle inequalities for, 17: 5544
spin flip and substate excitation in proton inelastic, 18: 21252
spinors in, transition operator for plane-wave, 19: 25396
S-states in potential, 3-body Green's function for, 16: 24733
statistical mechanics of moderately dense fluids in, theory of irreversible, 18: 20633 (TID-20512)
statistical theory of nuclear collision cross sections, 18: 32837
strength of coupling constant in strong interactions, 17: 11924
strip approximation of, artificial singularities in N/D equations in, 17: 19146
strip approximation for, revision of, 18: 28384
strip approximation for, consistency of, 18: 28385
strong absorption model for elastic nuclear, 18: 1032
structure of S-matrix singularities, analyticity and unitarity, 16: 17021
Sturmian functions in Schroedinger three-body problem, 16: 28319
sum rules relating coherent x-ray scattering data to diamagnetic nuclear shielding constant, 17: 18940
surface corrections to the high-energy optical potential, 17: 13434
surface divergences in the Bogolyubov method, 17: 7516
symmetric expansion of one- and two-center Coulomb potentials, 16: 5804
symmetrical matrix of 6j symbols, definition, 16: 12350
symmetries in high-energy, 17: 13378
symmetries in, inhomogeneous Lorentz group, 17: 5229
symmetries in, spin and spin-orbit effects in, (T), 20: 15547
symmetry breaking in, eightfold-way, 18: 21045
symmetry breaking mechanism in pseudoscalar octet-baryon octet, (T), 19: 12335
symmetry group (SU3) in, generators of, 18: 24422
symmetry properties of 3-j symbols in, 17: 19094
symmetry properties of S matrix, Jost function method for, (T), 20: 2790
symmetry theory of, mathematics of, 18: 14998
T-matrices for, calculation of explicit forms and recursion relations for elements in, 17: 32919 (WAPD-T-1579)
T-matrix in, limiting forms of screened Coulomb, 20: 21731
targets, device for producing atomic beam, 16: 6573
TCP invariance of matrix of, interpolation by weakly local fields, 17: 22446
testing of SU(3) symmetry by, (T), 20: 15532
theoretical analysis of dispersion relations, 16: 10923
theory, 17: 29493 (CERN-63-14)
theory, 17: 32910 (TID-7668(Sect.II))
theory for anisotropic and isotropic multiple, one-velocity infinite-homogeneous-medium, 18: 30334
theory for Dirac equation and Regge poles in, 19: 18909
theory for elastic, nonelastic processes in, 19: 47330
theory for existence of bound states in, 19: 16706
theory for high energy, 20: 4636
theory for many-body, 20: 28015
theory for multichannel, derivation of effective-range in, 16: 32433
theory for multiparticle, projection operators in unified, 20: 13850

theory for neutral scalar fields, Haag theorem for, 20: 34267
theory for neutron reactions below 5 Mev, 16: 23145
theory for nonrelativistic, Fredholm, 20: 41993
theory for particles of arbitrary spin, non-dynamical, (T), 20: 9795 (UCRL-14582-T)
theory, for polarization analysis of spin 1 particles, 16: 28003
theory for relativistic two-body, 20: 28005
theory for strong interactions, evaluation of S-matrix, 18: 14936
theory for strong-interaction, S-matrix, 19: 10157
theory for strongly interacting particles, 20: 21773
theory for system of identical particles, nonrelativistic time-dependent, 20: 4655
theory for time-dependent, 18: 9427
theory for two-plane wave, (T), 20: 21716 (JINR-P-2603)
theory for very high-energy phenomena, summary of CERN conference on, 17: 20566 (UCRL-10022(p.3-7))
theory, for 2-body final-state effects on strong, 16: 32318
theory for, analytic continuation of coupling constant in Chew-Low equation for, 19: 31027
theory for, Coulomb problem in, 20: 21702 (AD-621385)
theory for, high-energy behavior of Feynman integrals in, 18: 44626
theory for, Jost function in s-matrix, 18: 37931
theory for, large momentum transfer, optical model, 18: 37979
theory for, lectures on, 20: 25889 (RHEL/R-108)
theory for, nonrelativistic finite system of particles with local two-body interactions in, 20: 27983
theory for, normal products in terms of functional integrals in S-matrix, 20: 2765
theory for, research on, 20: 13463(R) (UCRL-16511, pp 1-53)
theory for, statistical contribution to elastic, 20: 46418
theory for, unitary relation in S-matrix, 18: 30590
theory for, variational principle in s-matrix, 19: 1457
theory, lectures on non-relativistic, 16: 21260 (AFOSR-2409)
theory of accidental degeneracies, contributions to, 17: 13383
theory of, analyticity and phase retrieval in, 18: 9144
theory of arbitrary-spin, optical, 18: 10852 (JINR-P-1484)
theory of backward, at high energies, 17: 4051 (JINR-E-1064)
theory of, bound states embedded in continuum of, 17: 24287
theory of, breakdown of rotating coordinate system in, 18: 5873
theory of complex angular momenta, review of recent developments, 18: 19061
theory of, consisting in S-matrix, 18: 6022
theory of, constructing polarization potential in, 16: 32348
theory of Coulomb, Fourier integrals in, 18: 26280
theory of critical, at small angles, 17: 2430
theory of, crossing symmetry in S-matrix, 17: 17034
theory of, crossing-symmetric Watson-Sommerfeld transformation in, 17: 26370
theory of deep penetration of charged particles, 17: 3981
theory of, developments in, 17: 31091(R) (UCRL-10862)
theory of, development, 18: 5841(R) (AROD-2800.12)
theory of diffraction-type, extension of Pomeranchuk's theorem to, 17: 35071
theory of diffraction, with excitation of collective nuclear states, 20: 38143
theory of dispersion relations in, 17: 9197 (NP-12449)
theory of, double dispersion relation for class of nonlocal potentials in, 17: 37991
theory of double, S-matrix, 20: 2774
theory of elastic, for nonzero-mass vector particles, 16: 29702
theory of elastic and inelastic, 16: 33798
theory of elastic small-angle multiple, information loss in, 20: 30151
theory of elastic, derivation of formal, 19: 39821
theory of elastic, unitarity and bound-state problem in, 20: 7916
theory of energy-time wave-packet, 18: 22753
theory of Fermi coupling S matrices in, 19: 25286
theory of, fundamental properties of perturbation-theoretical integral representations in, 16: 29978
theory of, hard-core model for, 17: 22363
theory of heavy-particle, two-term approximation in, 18: 2552
theory of high-energy potential, 16: 31194
theory of high-energy, 17: 9419
theory of high-energy, (T), 20: 4696
theory of high-energy, 20: 15438
theory of high-energy, analyticity and large-momentum-transfer processes in, 20: 17461
theory of high-energy, review on, 20: 19609
theory of high-energy, lectures on, 20: 37826 (NP-16231)
theory of, hypervirial theorem in, 17: 11908
theory of, hypervirial theorem in, 17: 11909
theory of, impulse approximation in, 18: 6049
theory of inelastic, moving poles in, 18: 10971
theory of inelastic, matrix elements and parity rules for, 18: 26651
theory of inelastic, near-threshold behavior in, 18: 32624
theory of inelastic, 18: 36699
theory of inelastic diffraction, with excitation of collective nuclear states, 20: 38142
theory of, integral operators in, 18: 9105
theory of, intermediate scattering function in, 17: 22475
theory of, introduction to, 17: 21212
theory of large momentum transfer, 17: 26360
theory of many-body potential, review of, 20: 44654 (PUC-937-227)
theory of many-particle relativistic, 20: 34293
theory of, microcausality and microcovariance in, 18: 9222
theory of, minimum variational principles in, 17: 21208
theory of, moving-pole, 17: 7004
theory of multi-channel, time-dependent, 18: 2715
theory of multichannel, bounds on parameters in, 18: 18704
theory of multichannel, minimum principle formulation in, 18: 21050
theory of multichannel, Ehrenfest theorem for, 20: 9816
theory of multichannel, determinantal formulation of, 20: 19599
theory of multichannel potential, long-range perturbations in, (T), 20: 44802
theory of multichannel, four-fermion and Yukawa coupling equivalence for, 20: 44377
theory of multiple small-angle, relativistic correction to, 17: 11573
theory of multiple, extension of transport operator, 17: 19047 (UCRL-6990-T)
theory of multiple, projected and spatial angles in, 17: 26347
theory of multiple, 18: 26307
theory of multiple, 19: 23470
theory of multiple, 20: 13163(R) (ANL-7129)
theory of, new approximation in, 17: 11492 (TID-16044)
theory of non-shrinking diffraction, Regge-Pomeranchuk vacuum pole trajectories in, 18: 2675
theory of non-relativistic, classical and quantum cross sections in, 18: 42464 (AD-433256)
theory of non-relativistic one-dimensional potential, 18: 42465 (AD-433257)
theory of nonlocal separable-potential, effects of exclusion principle on, 18: 37874 (64-RL-3604-M)
theory of nonrelativistic, 18: 12992
theory of nucleon, strip approximation to Mandelstam, 17: 11498 (UCRL-10028)
theory of, of highly singular potentials, 17: 5553
theory of, optical-model representation of, 17: 17067
theory of particles and resonances in, matrix, 18: 2683
theory of particle polarization in high-energy physics, 18: 20893 (AFOSR-5287)
theory of, peripheral interaction expansion in, 17: 9420
theory of phonon, by point defects, 19: 40109
theory of planar three-particle, 17: 28177
theory of potential, 16: 29648 (NP-11950(Vol.I)(p.1-66))
theory of potential, converging, 18: 14997
theory of potential, Regge poles and Mandelstam representation in, 20: 9789 (CEA-R-2753)
theory of potential, Born approximation in, 20: 24113
theory of pre-local, 17: 22777
theory of proton, parametric correlations in effective range, 17: 20867
theory of quasi-free, 19: 28962(R) (NIRL/R/81)
theory of radiation damping, 17: 11916
theory of radiation, by random aggregates, 17: 29514
theory of Regge poles in, non-relativistic, 19: 12171 (UCRL-7874(A)-T)
theory of relativistic Coulomb, 17: 7520
theory of relativistic, Regge poles in Schroedinger, 17: 15074 (EFINS-62-17)
theory of relativistic, by fixed-point scatterer, 17: 34796
theory of relativistic, causality in, 18: 10939
theory of relativistic, 18: 16769
theory of relativistic, 18: 22732 (NP-13890)
theory of relativistic, quantum, 18: 42627(R) (ANL-6879(p.88-113))
theory of, research progress on, 18: 8920(R) (TID-19940(p.119-39))
theory of resonance, by atomic systems, 16: 16886
theory of resonance, 16: 17008
theory of resonance, 18: 44571
theory of, review, 17: 9475
theory of S-matrix, 17: 10240(R) (NP-12208)
theory of S-matrix, 19: 9775(R) (UCRL-11466)
theory of S-matrix in terms of current operator, 19: 27170
theory of slow neutron, in magnetic crystals, 17: 32987
theory of spatial three-body, 18: 42373 (NASA-CR-53233)
theory of spherical-particle, application of Rayleigh-Gans, 17: 25889
theory of spin wave–spin wave, in Heisenberg ferromagnet, (T), 19: 47874 (AD-613606)
theory of strong and weak, book on, 17: 29561
theory of, strong coupling analysis in, 17: 40081

theory of strong interactions at high energies, Regge-pole, 18: 16748 (BNL-7534(p.81-2))
theory of strong interactions, review, 18: 40364
theory of, SU, representation in Pomeranchuk, 17: 39908
theory of, three-body problem with separable potentials in, 17: 31330
theory of, transmission-line, 16: 27942
theory of two-particle, Whiteman-type functional for, 20: 17496
theory of, adiabatic switching in Schroedinger, 20: 27974
theory of, analyticity test for complex angular momentum in, 18: 30551
theory of, analyticity, discontinuity and unitarity in s-matrix, 18: 37896
theory of, analytical S-matrix, 19: 3115 (UCRL-10843)
theory of, analytic S-matrix, 20: 15512
theory of, approximation techniques in three-body, 18: 32591
theory of, approximate dynamical symmetries for, 20: 15483
theory of, axiomatics of S-matrix, 18: 14935
theory of, comparison of field and S-matrix, 18: 24483 (SUI-63-21)
theory of, comparison of field theory and S-matrix, 19: 8311
theory of, completeness of set of eigenstates of non-Hermitian operators in, 20: 44707
theory of, consequences of Bethe-Salpeter equation for, 20: 25932
theory of, continuity theorem and Mandelstam representations in, 18: 18738
theory of, coupling constants, propagators, and vertex functions in, 19: 12340
theory of, coupling constants and crossed channels in, 19: 18833
theory of, determination of subtraction terms in S-matrix, 19: 16589
theory of, determinantal method for N/D equations in, (T), 20: 11700
theory of, Dirac magnetic poles in S-matrix, 19: 12204
theory of, discontinuities and unitarity in S-matrix, 19: 31037
theory of, distorted-wave and dispersion, 18: 30737 (UCRL-7478-T)
theory of, dominance theorem in crossing matrices in, 19: 18828
theory of, double spectral functions and single integrals of Mandelstam representation in, 18: 36406
theory of, Ehrenfest's theorem in, 19: 33046
theory of, exposition of formal, 19: 12170 (UCRL-7874-T)
theory of, extremal properties of approximate methods in, 18: 36405
theory of, Feynman amplitudes and graphs in, 18: 40392
theory of, Fokker-Planck coefficients for inverse square law force in, 19: 8287
theory of, gauge invariance in S-matrix, 18: 24497
theory of, generalized phase approach to, 18: 32559
theory of, general and relativistic, 20: 4475(R) (ANL-7081, pp 95-119)
theory of, hermitian analyticity and extended unitarity in S-matrix, 18: 40272
theory of, high-energy asymptotic behavior of Feynman diagrams in, 19: 5050
theory of, identities from Ehrenfest theorem and Lippman-Schwinger equation in, (T), 20: 2785
theory of, in relativistic quantum field theory, 18: 40402
theory of, interaction-region model for quantum, 20: 36207
theory of, Jost functions in, 18: 26304
theory of, lectures on, 18: 12908 (NP-13602(Vol.II))
theory of, local operators in s-matrix, 18: 34541
theory of, loosely bound systems in relativistic, 19: 45110
theory of, Lorentz-invariant variables for many-body systems in, 20: 24133
theory of, lower bounds on inverse reactance matrix in, 19: 33019
theory of, Mandelstam representation for sixth-order ladder diagram in, 18: 40414
theory of, matrix analytic regularization and divergences in, 18: 16808
theory of, multichannel bootstrap calculation method in, 19: 16553
theory of, N/D method for extinct bound states in, 20: 41975
theory of, Nakanishi's inequality for, (T), 20: 2767
theory of, non-Landau singularities in, 19: 27196
theory of, non-Regge terms in vector-spinor, 19: 12219
theory of, optical-model, 18: 15268
theory of, parametric integral formulas in, 18: 14999
theory of, properties of bound states in, 18: 12920
theory of, properties of S-matrix, 18: 32663
theory of, quantum, 18: 42323
theory of, quantum mechanics for Feynman diagrams in, 19: 12341
theory of, radial wave equations for nonrelativistic quantum, 19: 41360
theory of, reciprocity in, 18: 12971 (NASA-TN-D-1985)
theory of, Regge behavior of spinor channel in vector-spinor, 18: 37887 (UCRL-11500)
theory of, relativistic, 18: 14817 (NP-13644)
theory of, research at Univ. of Maryland on, 18: 30505 (AFOSR-4514)
theory of, research summary on, 20: 19169(R) (BNL-929, pp 106-11)
theory of, resonances in, 18: 42638 (KFKI-20/1963)
theory of, review of S-matrix, 19: 14382
theory of, review of, 19: 33084
theory of, S-matrix, 18: 10988
theory of, S-matrix, 18: 12907 (NP-13602(Vol.I))
theory of, s-matrix, 18: 16552(R) (UCRL-11132)
theory of, S-matrix, 18: 38003
theory of, S-matrix, 18: 40343
theory of, S-matrix (T), 19: 3113 (CAR-882-1)
theory of, S-matrix singularities in, 19: 10056
theory of, S-matrix operator in, 19: 12379
theory of, S-matrix, 19: 25478
theory of, S-matrix, 19: 25265(R) (UCRL-11776)
theory of, solution of singular integral equation in, 18: 40265
theory of, solutions for N and D equations in, 19: 16586
theory of, space and time in S-matrix, 19: 33020
theory of, spectral function in terms of amplitude in physical region in, 18: 40416
theory of, structure of g-plane in relativistic Schroedinger, 19: 21053
theory of, time duration in S-matrix, 18: 36322
theory of, uses for studying decaying states (T), 19: 3123
theory of, variational N/D method in S-matrix, 19: 29094
theory of, vector-spinor bootstrap in S-matrix, 18: 28361
theory of, wave functions in quantum, 18: 40385
theory of, wave packets in quantum, 19: 21092
theory of, wave-packet, 19: 27274
theory of, with singular potentials, 19: 18796
theory, poles in low energy, 16: 24912 (AD-270903)
theory, quantum mechanical analysis, 16: 21146
theory, renormalization using U-matrix axiomatics, 16: 28342
theory, reverse problem in, 16: 9410
theory, Schrödinger equation solution for limiting absorption and amplitude, 16: 5801
three body operator in nonequilibrium statistical mechanics, 17: 38423
three-body problem for short-range forces in the linear approximation in the force range, 17: 7517
three spin-zero particle problem in nonrelativistic, total angular momentum plane in, 17: 42169
three-particle partial amplitudes and unitarity conditions for complex values of angular momenta, (T), 20: 2811
three-particle scattering operator in generalized Boltzmann equation for homogeneous gases, 18: 14835
threshold effect in elastic, according to the optical model, 17: 4092
threshold effects in average cross sections according to R-matrix theory, 17: 7236
threshold of resonance, origin of, (T), 19: 6525
time-duration concept in S-matrix theory, 16: 33777
topological methods in S-matrix theory, 19: 18924 (UCRL-11346)
trajectories in, two Pomeranchuk-Regge, 17: 11915
trajectories of Regge poles from Yukawa potential, weak coupling case of, 17: 17277
transformation of two particles into two particles at high energies, 17: 9244
transition amplitudes in inelastic, threshold anomalies, 16: 7233
transition amplitudes in, analyticity and unitarity of general, 17: 5547
transition complex theory of rearrangement collisions in bimolecular chemical reactions, 16: 28956
transition matrix for scattering of free particles by systems of identical bound particles, 16: 21312
transition operator for many-body, in presence of hard core, 17: 41752
transport and multiplicative processes in, theory of first-passage distributions in, 20: 20101
transport coefficients in, generalized master equation and t-matrix expansion for, 17: 24297
transport equation for radiation beam, 17: 2182
transport equation for, exponential transformation of Boltzmann, 18: 12909 (NP-13627)
transport equation with plane symmetry in isotropic, (T), 19: 10094
transport in, transformation of equations for, 17: 5206 (WAPD-T-1305)
transport theory, singular integral method for isotropic medium, 16: 9420
transport theory, time lag in, 16: 10700
two-particle, amplitude variation with energy and momentum transfer in, 17: 5264
two Regge poles in high-energy, 17: 31319
two-electron exchange processes in, 18: 18585
uncertainty relation weakening in high-energy proton-proton, 17: 31651 (NP-12975(p.144-61))
uniqueness of the partial wave amplitude, 17: 32904 (EFINS-63-40)
unitarity condition for high-energy, 17: 13408
unitarity effects in nucleon-nucleon, inelastic (T), 19: 3083
unitarity integral for, anomalous threshold effects on three-particle, 17: 39930
unitarity integral for three-body, (T), 20: 4647 (TID-22274)
unitarity properties, for case of two possible reactions, 16: 21702
unitarity relations in elastic, 16: 33742
unitarity requirement of high-energy inelastic, 16: 31190
unitarity restrictions on Regge asymptotic behavior in, 18: 28320 (EFINS-73-3)

unitary amplitudes for, in one-dimensional worlds, 19: 20924 (ICTP-64/2)
unitary integral in, three-particle, 18: 30585
unitary symmetry effects on strong interactions, 16: 26156
unitary transformations in, (T), 19: 8304
unsubtracted dispersion relation and pion-nucleon forward charge exchange, 16: 27946
use of gamma resonance, for determination of nuclear level lifetimes, (E), 19: 6643
use of WKB method in three dimensions for, 18: 30621
vacuum boundary conditions for P_N approximation for, variational, 20: 30116
validity of the Rosenbluth formula in implication of Regge poles, 17: 5555
variation principles for an arbitrary operator for, 17: 33230
variational calculations for nonrelativistic elastic, 17: 7507
variational method for nonrelativistic, modification of integral form of, 17: 24279
variational principles for multi-channel, 16: 14016
variational principle for potential, 16: 15573
variational principle for Brueckner theory, 16: 28331
variational principles for multi-channel systems, 16: 10840
vector mesons as Regge poles in perturbation theory, 17: 32902 (EFINS-63-35)
velocity-dependent nuclear potentials in, 16: 2497 (UCRL-6552)
velocity-dependent nucleon–nucleon Green potential in, 17: 11527
velocity dependent potentials in low-energy, 19: 12190
vertex function in "one-logarithmic" approximation, calculation of, 17: 9459
vertex functions, absorptive part in anomalous region, 16: 18606
vertex functions in, asymptotic values of relativistic, 17: 28216
vertex functions in, integral representations for, 18: 7488
vertex functions in, Levinson's theorem for zeros of, 20: 32172
wave amplitudes for inelastic, high-energy behavior of partial, 18: 32588
wave equations for nonlocal solvable interactions in, Schroedinger, 18: 26404
wave equations for metastable states and resonances in, 18: 42749
wave flux in, decay laws and S-matrix pole multiplicity for, 19: 45070
wave function for, 16: 22875
wave function spectral representation in momentum space in potential, 18: 21035
wave functions for three-body interaction, 16: 12554
wave functions for particle scattering by identical bound particles, 16: 19510
wave functions for particle in central r^{-3} potential, 16: 32307
wave functions for three-body interactions, two-body methods for, 17: 32922
wave functions for, analyticity and bound states in, 18: 4430 (JINR-E-1400)
wave functions for S-wave, by potentials, 18: 7528
wave functions for, by arbitrary nonphysical potentials, 19: 37565
wave functions for bound-state, in nonlocal solvable potential, 20: 6119
wave functions in repulsive fields, Bessel function expansion for radial Coulomb, 17: 24344
wave packets in nonrelativistic, time delay in, 20: 1067
weak interaction mediated by Regge particles, 17: 36588
Weyl-Wigner formulation for, 18: 22787 (TID-20515)
Wick's theorem in, 18: 26398
Yukawa interactions with hard cores, uncoupled phase method with p- and s-wave orbital angular momenta and closed channel, 18: 9244

Scattering Chambers
see Radiation Target Chambers

Scattering Cross Sections
see Cross Sections

Scattering Cross Sections (Electron)
see Electron Scattering Cross Sections

Scattering Cross Sections (Gamma)
see Gamma Scattering Cross Sections

Scattering Cross Sections (Neutron)
see Neutron Scattering Cross Sections

Scattering Cross Sections (Proton)
see Proton Scattering Cross Sections

Sceptre
see Pinch Devices

SCHIFF BASES
analytical use for determination of thorium by spectrophotometric method, 19: 46206
analytical use of glyoxal bis(2-hydroxy-5-chloranil) for determination of uranyl ions, 19: 24421
complexes with copper(II), spectra of, 20: 289 (TID-21358)
complexes with uranyl ions, 17: 25233
complexes with uranyl nitrate, solubilities in ethanol, 19: 9113
hydrolysis of, deuterium isotope effects in, 19: 22268
oxidation by *m*-chloroperoxybenzoic acid, kinetics of, 20: 1571(R) (TID-22186)
reactions with uranium tetrachloride, 19: 11122
solvent properties of, in chloroform for metals, 20: 10759 (INP-427/C)
use of alcoholic solution of *p*-dimethylaminoaniline with salicylaldehyde for determination of uranium, 18: 21965

SCHISTOSOMA
effects of egg purification in, on cercariae infectivity, 20: 14304
effects on blood serum of monkeys, 19: 8937
immune reactions of mice to irradiated cercariae of, 20: 42947
immune reactions to normal and irradiated cercaria of, in monkeys and rats, 20: 24917
immunization against, produced by irradiated cercaria in rhesus monkey, 16: 14402
immunization against, with irradiated cercariae, 19: 8937
immunization against, in rhesus monkeys, effects of irradiated cercariae on, 19: 36045
labeling with iron-59, 19: 33734
preparation of irradiated vaccines against parasitic, 19: 7175
radiation effects on *S. masoni* cercariae, use to immunize monkeys, 16: 20202
radiation effects on host-parasite relationships of, gamma, 19: 8944
radiation effects on infectivity of cercariae of, in mice, 19: 43848
radiation effects on growth of cercariae of, in mice, γ, 20: 5313
radiation effects on infectivity of cercariae of, γ, 20: 8591
radiation effects on infectivity of cercariae of, γ, 20: 14304
radiation effects on reactions in mice, gamma, 20: 20360(R) (PRNC-73)
radiation effects on infectivity of, in mice, gamma, 20: 20446

SCHOEPITES
synthesis, 18: 16009

SCHROECKINGERITES
occurrence in Mieszko coal mine, Walbrzych, Poland, 20: 23331

SCHWARTZWALDER MINE (COLO.)
mineralogy of uranium deposits in, 20: 33546
radon decay product inhalation hazards in, 20: 43617

SCINTILLATION
book: *The Scintillation Technique in Radiometry*, 17: 14704
collection of carbon dioxide for, design of vial reaction tube for, 18: 33478
Compton edges and backscatter peaks in, 19: 33704
counting errors due to oxygen-quenching in liquid, effects of sample preparation on, 19: 7597
decay time measurement, use of photomultiplier tubes, 16: 3529(R) (ANL-6432)
decay time, measurement from organic crystals, plastics, and solutions excited by α particles, β particles, or ultraviolet radiation, 17: 25588(R) (ANL-6646(p.30-1))
decay time of, in liquid phosphors, 19: 24864
developments in liquid, review on, 20: 22883
electric field effects on rare-gas, 19: 816
electron-ion recombination effects in alpha-induced, in liquid helium, 19: 11241
inhibition by organic solvents, 19: 15558
mechanisms of, in organic solids, 19: 46399
of metal salts, counting losses in, 18: 39118
processes in, theory of, 17: 6444(T) (AEC-tr-5259)
properties of thallium dimer in sodium iodide (thallium) process, (E/T), 20: 28609(R) (NYO-3408-6)
pulse amplitude of, device for measuring, 18: 43918
pulse forms in radioinduced, method of determining, 17: 16421 (CEA-2194)
spectra from alpha reactions with argon–nitrogen mixtures, 20: 22853(R) (ANL-7060)
spectra from point sources in scattering medium, 20: 5760
spectra shapes, gamma, 19: 30581
theory of organic-crystal, 18: 31607
use in fallout evaluation from air filters and rain samples, 19: 18225
use of, for studying metastases of thyroid adenocarcinoma, 17: 26996
used for measuring radiation intensity variations in cardiovascular studies, 18: 25051

Scintillation Counters
see Radiation Detection Instruments (Pulse Type)

SCINTILLATION DETECTORS
see also Phosphors
adaptation of liquid-sample, for directional counting, 17: 18632
alpha energy resolution of liquid, 18: 2025 (TID-18358)
amplification-channel stabilization in, reference light pulse for, 19: 40870 (IAE-695)
amplifiers for, design of temperature compensating, 20: 35729 (AD-635882)
background and noise in, for beta spectrometer, 17: 23782
background of samples containing quenchers in liquid counting, measurement of, 17: 25606

background reduction in liquid, use of glass light filter for, 18: 16307 (TID-7689(p.31-3))
beta counting in, from carbon-14 decay, balanced quenching method for, 20: 18594
book: *Organic Scintillation Detectors. Counting of Low-Energy Beta Emitters*, 17: 14705
book: *Scintillation Counters in High Energy Physics*, 19: 46856(T)
book: *The Theory and Practice of Scintillation Counting*, 19: 2651
cable system for power supply and pulse transmission, 20: 14876
calibration for gamma counting facility, 19: 31460(R) (ANL-7010 (p.179-233))
calibration for gamma rays, computer corrections for, 19: 36822 (USNRDL-TR-832)
calibration for measuring radon-222 in air, 17: 16417 (AERE-R-4165)
calibration for neutrons, absolute, 17: 14648 (IKF-6)
calibration for neutrons, 18: 35859
calibration for slow neutrons for measuring water content in Leda clay, 18: 33897
calibration of, 18: 7697(R) (TID-19931)
calibration of crystal and 4π, for determination of potassium in body, 17: 1748 (LADC-5447)
calibration of crystalline, 19: 7274(R) (IDO-14636)
calibration of, design of pulse-size Wheatstone bridge for, 17: 37421
calibration of flow-through, using control sources, 17: 28805
calibration of, for energy measurements of beta and gamma radiation, 16: 27311
calibration of, for cosmic-shower detection, 17: 13052
calibration of Geiger-Müller counters with, 17: 4842
calibration of human whole-body counter, for measurements of cesium-137, potassium-40, and iodine-131 content in man, 18: 29975(R) (COO-119-229(p.186-98))
calibration of liquid, for low-energy beta particles, 16: 31853
calibration of liquid, 20: 23494
calibration of organic, for fast neutron spectroscopy, 19: 13735 (ORNL-P-993)
calibration of scintillation gamma spectrometers, 19: 4519
calibration of single and multi-crystal, for whole-body counting, 16: 16138
calibration of sodium iodide, measurements on distributed gamma sources, 20: 43668(R) (ANL-7136, pp 1-16)
calibration of specific ionization by, 18: 37547
calibration of thallium-activated sodium iodide, for determining gamma energies, 19: 11423(R) (UCRL-12004)
calibration of thallium-activated sodium iodide, for atmospheric fallout measurements, 20: 27196 (HASL-170)
calibration of, apparatus for, 19: 36863(P)
calibration of, nitrogen light source for, 18: 31964
camera using multichannel collimators with, 18: 33940
camera with eleven-inch crystal for, 18: 22344(R) (UCRL-11184(p.69-85))
characteristics and performance of, for thermal neutrons, 17: 30869
characteristics and use in gamma spectrometry, 17: 34259
characteristics of Donner Laboratory whole-body, 16: 9771(R) (UCRL-9897(p.201-21))
characteristics of glass, for gamma dosimetry, 17: 39409(R) (AD-296591)
characteristics, statistical evaluation of, 16: 23848 (SCTM-326-61(14))
charged-particle scattering losses in plastic and sodium iodide in, 20: 31542
circuit development suppression of pulse rates from, 20: 21086
circuit for canceling background radiation in Hornyak buttons, 16: 23916 (UAC-6092)
circuit systems for whole-body liquid, design and performance of, 16: 23875
circuitry for, 17: 3348(P)
coincidence circuits for slow, design of transistorized, 17: 14668
coincidence circuit for, design of fast transistorized, 18: 10397
coincidence circuits for, design of transistorized, 19: 22753
coincidence circuits for, development of fast multiple, 20: 7361 (INR-594/1A/PL)
coincidence counting with, design of tunnel diode circuit for, 16: 13347
collimator design for, 19: 34068
collimator development for, 18: 5641 (TID-7673(p.25-65))
collimator resolution for radiodiagnostic, 18: 39045
collimator selections for image intensification in gamma scintigraphy, 18: 27799
collimator system for, with sodium iodide well-type crystals, 16: 27274
collimators for, used in radiodiagnosis, 20: 19051
color coding of radioisotope scans made using, 18: 2046
color translation apparatus for, 19: 42761
Compton spectra measurements using, 16: 31854
conference, 16: 23876
conference, 20: 33646
conference on, 18: 33900
construction and operation, 17: 41306
construction and performance of threshold ultrafast-neutron, 19: 34576
construction of gas, for neutron counter, 20: 37127
construction, performance, and testing of stack of, for cosmic-ray measurements underground, 20: 11527
conversion of signals to color, design of electronic gating circuit for, 18: 35896
conversion of signals to color, 18: 35897
cooling, 18: 14235
cooling of photomultiplier tubes in, 17: 4824
cooling system for well-logging, 20: 39140(P)
correction factors for distortions in, 18: 5649
cosmic-radiation momentum spectra using, 18: 41851
counters for use with thallium-activated sodium iodide, design of compact, 20: 46032 (AERE-R-5225)
counting data analysis, computer program for, 20: 39226
counting efficiencies of thallium-activated sodium iodide crystals, 17: 34261
counting gamma and x radiations by, interpretation of readings in, 17: 14566
counting vials for tritium, performance of, 19: 31696
coupling between photomultiplier and scintillator in, flexible light pipe for, 18: 18236
crystal preparation for, anthracene, 19: 26697
current-pulse center of gravity in, determination of, (T), 19: 20336
data analysis from, using computers, (E), 19: 13725 (LNF-64/51)
data analysis from low-resolution measurements of beta and conversion-electron spectra, (T), 20: 5768
data analysis of capture gamma measurements by, 20: 46038 (CEA-R-3034)
data analysis of gamma spectra from, computer programs for, 20: 39237
data from, color display of, 19: 17761
data from, color display of, 19: 17762
data recording systems for hodoscopes of, 20: 33690
data tabulation and calculation for, computer programs for, 19: 36528
decay time studies of, for improving coincidence measurements, 19: 24864
delay time and resolution of fast coincidence, 16: 5527
description, 18: 10978
description and performance, employing amplitude-insensitive pulse-shape discrimination system, 16: 5531
description and response of stop, for mesons, 17: 14683
description for air shower measurements, 18: 36217
description of alpha- and beta-spectrometer, 18: 18220
description of combined sodium iodide-plastic, for fast coincidence measurements with good energy resolution, 17: 23771
description of double sodium iodide, for small samples, 16: 1330(R) (LAMS-2627(p.234-7))
description of glass, for continuous measurement of gas diffusion coefficients in liquids, 16: 16351
description of large-area liquid, for cosmic-neutrino experiments, 20: 33689
description of low-background, for radon measurements, 17: 32459
description of mobile automatic alpha, beta, and gamma counting facility, 18: 29981 (NDL-TM-12)
description of neutron, for use above the atmosphere, 17: 16922
description of rare-gas, with very short resolving times, 17: 20352
description of scintillation cameras, 17: 29998
description of scintiscanners for scintigrams, 17: 29999
description of small, linear, wide-range, 16: 29148
description of, used as particle detector, 17: 12562
description of vise-configuration, for beta counting, 17: 27694
description of 4π liquid, for fast neutron bursts, 16: 23921
description of, for charged and neutral particles, (E), 19: 44499
design, 19: 34583(P)
design and calibration of multiplate shower counter for high-energy gamma rays, 18: 18235
design and development of, 17: 6132(R) (TID-17272)
design and development of, summary, 18: 34752(R) (CU(PNPL)-234)
design and efficiency of coincidence, for β counting, 20: 23475
design and operation of automatic and semi-automatic, 16: 25940 (NP-11977(p.116-20))
design and operation of high-pressure helium–xenon, for neutron spin polarization analysis, 17: 8600 (UCRL-6878)
design and operation of 4000-liter liquid, 17: 15253(R) (GA-3874)
design and operation of nanosecond, 17: 21104 (ANL-6700)
design and operation of transistorized, for radon monitoring, 20: 21067
design and performance of plastic, for measurement of iron-59 absorption in rats, 16: 7390
design and performance in particle-interaction measurements at high energies, 16: 10213
design and performance of continuous flow, for alpha and beta measurements in streams, 16: 14961

design and performance of high-pressure gas, 16: 16544
design and performance, 16: 17851
design and performance of liquid, for whole-body counting, 16: 19075 (TID-15659)
design and performance of liquid, for whole-body counting, 16: 19172(R) (AD-266007)
design and performance, system for indicating particle entry, 16: 20737
design and performance using organic scintillators, 16: 20708
design and performance of liquid, for neutrons, 16: 20709
design and performance of spectrometer for solar gamma radiation, 16: 23926
design and performance of liquid, for neutrons, 16: 30603(T) (AEC-tr-5368)
design and performance of, for indicating particle entry, 16: 33165(T) (AEC-tr-5402)
design and performance of low-background beta, using thin plastic phosphors, 16: 6579
design and performance of 4π, for measuring low beta activity, 17: 1743 (CEA-2182)
design and performance for gamma correlation measurements, 17: 2255
design and performance for gamma correlation measurements, 17: 2256
design and performance of thallium-activated sodium iodide, for neutrons, 17: 6474
design and performance of, for fast neutron dosimetry, 17: 9491
design and performance of, review, 17: 10964
design and performance of glass, 17: 10965
design and performance of gaseous, 17: 14645 (DP-800)
design and performance of, for beta counting, 17: 16430 (TRG-Report-464)
design and performance of, for space uses, 17: 16892
design and performance of microwave discharge chamber, 17: 23669
design and performance of gas-amplified, 17: 23670
design and performance of, for elastic scattering measurements, 17: 23671
design and performance of gaseous, 17: 29209
design and performance of liquid organic, 17: 30099
design and performance of, using current mode impedance matching, 17: 30100
design and performance of liquid, with single photomultiplier tube, 17: 30101
design and performance of 400-liter liquid, for (n,γ) reaction cross sections, 17: 30876
design and performance of high efficiency, for thermal neutrons, 17: 30879
design and performance, 17: 34307(P)
design and performance of large-area, for cosmic ray detection, 17: 39436
design and performance for low energy ions, 18: 513
design and performance for auroral particle fluxes, 18: 6096
design and performance for gamma rays, use in neutron-capture cross section measurements, 18: 8659
design and performance of large-area plastic, 18: 10371 (CERN-64-4)
design and performance of phosphor-photodiode radiation-burst sensor, 18: 14348(R) (RTD-TDR-63-3051)
design and performance, 18: 18199
design and performance of large-area, 18: 18210
design and performance using liquid scintillators, 18: 20335 (NP-13840)
design and performance for measuring soft beta particles from radioisotopes, methods of improving, 18: 30003
design and performance of, for gamma and fast neutron spectra, 18: 39690
design and performance for alpha, beta, and gamma radiation, 19: 13782
design and performance of whole-body plastic, for gamma rays, 19: 20377
design and performance of large-area, 19: 22712
design and performance, 19: 22785
design and performance of sandwich type high energy gamma, 19: 24854
design and performance in neutron time-of-flight spectrometers, 19: 28642
design and performance of automatic gamma, 19: 39003
design and performance of scintillating fibers, for low-energy beta particles, 19: 44451 (IITRI-578P26-8)
design and performance of large liquid, 19: 46775
design and performance of zinc sulfide (silver) for alpha counting, 20: 2152
design and performance of argon-gas, for fission fragments, 20: 2163
design and performance for neutron pulse intensity measurements, 20: 7436
design and performance of, for use in high-radiation background areas, 20: 7454
design and performance of, for detecting plutonium-239 in wounds, 20: 9262
design and performance of, for assaying large samples, 20: 9271
design and performance of shadow-shielded whole-body, 20: 13074 (SRRC-11/65)
design and performance of scintillation camera, 20: 19085
design and performance of, for measuring thermal neutrons in soil–water systems, 20: 19092
design and performance for whole-body facility, 20: 21075
design and performance for nuclear debris analysis, 20: 20881 (DASA-1704)
design and performance for coincidence studies, 20: 23458 (CEA-R-2901)
design and performance of Hamburg 4π, 20: 25401
design and performance of slow ion counter, 20: 27336
design and performance for use in magnetic beta spectrometer, 20: 27292
design and performance of, based on medicinal paraffin, 20: 37112
design and performance of diamond, for gamma rays and neutrons, 20: 41290
design and performance of two-impulse neutron, with plastic scintillator, 20: 41337
design and performance of thin plastic and sodium iodide nanosecond, for x-ray lifetime determinations, 20: 41325
design and performance for aerial survey of gamma activity, 20: 43513 (CEX-59.4.26)
design and performance for alpha particles, 20: 46070
design and use for absolute determination of gamma-emitting radioisotopes, 18: 1498 (CEA-2352)
design and use of 4π liquid, 16: 23871
design characteristics of pulse-counting-type survey meter, 16: 11967(R) (JAERI-5003(p.184-7))
design for alpha counting of smear samples, engineering drawings for, 18: 27804
design for alpha particles using large zinc sulfide phosphors, 19: 42715(R) (ORNL-3782, pp 35-51)
design for alpha particles, 20: 43750
design for alpha–beta surface contamination monitoring, 20: 9248 (EUR-2577.i)
design for antineutrino reactions, 18: 33901
design for automatic sample counters, 18: 14267
design for beta emitters in atmosphere, 18: 14203 (CEA-2356)
design for beta particles, 19: 2637
design for beta-emitting aqueous solutions, 20: 46072
design for continuous scanning of paper chromatograms, 16: 17856(P)
design, for cosmic particle detection in space, 17: 16893
design for cosmic neutron monitoring, 20: 23906 (N-65-10044)
design for Cosmos 17, 19: 20343
design for delayed neutrons, 20: 9290
design for depth dose measurements, 19: 22761
design for detection and measurement of cosmic showers at Ootacamund, India, 16: 8077 (NP-11232(p.431-5))
design for detecting neutrinos, 16: 31925
design for detection and measurement of beta activity in powdered samples, 18: 7066
design for detection of alpha, beta, and gamma radiations, 18: 7084
design for detecting hot spots in reactors, 18: 27809(P)
design for detecting beta particles emitted from movable member, 18: 33976(P)
design for determination of neutron spectra from measurements of moderated foils, 16: 8903 (HW-71710)
design for determination of plutonium in nitric acid solution by x-ray counting, 17: 1379 (DP-734)
design for determining argon-41 in air, 18: 5211 (CRRD-1171)
design for determining spectrum of alpha source, 18: 5690(P)
design for determining radioisotope distribution in living organisms, 19: 18285
design for deuteron spectra, 19: 14533(R) (NYO-1082-1)
design for discrimination between particles of differing ionization power, 17: 32426
design for discriminating between electrons and pions, 19: 7790 (TID-21338(p.193-8))
design for dose and dose-rate indicators, 17: 16473(P)
design for dosimetry at plane beta emitters, 19: 22796
design for dosimetry of radium implants, 20: 22814
design for dosimetry of beta applicators in tissues, 20: 38777
design for electron and photon spectroscopy up to 10 Bev, (E), 19: 46805
design for epithermal neutrons used in well logging, 20: 39138(P)
design for extensive air showers, 19: 44529
design for fast electrons and soft x rays, 16: 12633
design for fast neutron spectrometry, 19: 30574
design for fast-neutron dosimetry, (E), 19: 20312 (AERE-R-4525)
design for fast-neutron fission, 19: 42715(R) (ORNL-3782, pp 35-51)
design for fission product monitoring in reactor gaseous coolant, 18: 37556(P)
design for fluid material with transparent walls of solid scintillation material, 18: 7092(P)
design for gamma activity measurements in geological surveys, 20: 11087 (AE-203)
design for gamma cameras, 20: 668

design for gamma detection in intense charged-particle flux, 18: 41852
design for gamma spectrometry, engineering drawings for, 17: 34304
design for high energy electrons, 18: 23895
design for *in vivo* determination of plutonium in lungs, 19: 25(R) (HW-81746(p.2.9-12))
design for inner Van Allen electrons, 18: 2747
design for internal conversion coefficient determinations, (E), 19: 44501
design for liquid, 18: 16375(P)
design for low beta activity in liquids, 20: 5798(P)
design for low-level beta activity, 17: 32410
design for low-background beta measurements, 20: 9296(P)
design for low-background beta measurements, 20: 9298(P)
design for low-background beta measurements, 20: 9297(P)
design for low-background beta counting without lead shielding, 20: 14873
design for low-energy γ and x radiations, 20: 19089
design for low-level counting, optimum window setting in, 19: 36834
design for measurement of low alpha activity, 16: 364
design for measurement of atmospheric radon, 18: 2049
design for measurement of cosmic gamma radiation, 19: 30571
design for measuring radioactivity of fluids, 16: 13432(T) (AEC-tr-4492 (p.99-103))
design for measuring atmospheric mesons (μ), 19: 9537
design for measuring radiation dose in bone, 19: 13056
design for measuring beta activity of gas or liquid samples, 19: 13810(P)
design for measuring gamma radiation from stars, 19: 26917(R) (IA-984)
design for meson (K^+) detection, 20: 16826 (PPAD-574E)
design for metabolic studies using gamma emitters, 18: 20346
design for monitoring airborne alpha activity, 17: 16476(P)
design for monitoring plutonium in process streams in presence of americium, 19: 9053 (AERE-R-4498)
design for monitoring plutonium in wounds, 20: 39267
design for negative halogen ions, 20: 43735
design for neutron capture cross section measurements, 16: 14084
design for neutron counting using helium-3 (n,p) reactions, 16: 27402(R)
design for neutron resonance scattering detection, 17: 30877
design for neutron time-of-flight spectrometry, 19: 20355
design for neutron capture studies, 20: 19035 (NIJS-R-470)
design for neutrons, 20: 43750
design for on-line alpha and gamma activity monitoring, 16: 29048
design for plutonium aerosol monitoring, 19: 18288
design for positrons in space, 16: 23924
design for producing color scintigrams, 19: 13150
design for radiation monitoring in accelerator areas, 19: 30565
design for radon-222 determinations, 19: 2208 (CLOR-28)
design for reactor transfer function measurement, 20: 6682 (SGAE-R-1/1965)
design for reduced light losses, 16: 16562(P)
design for slow neutrons and insensitive to gamma radiation, 16: 20718
design for small animal scanning system, 18: 15763 (ACRH-20(p.136-43))
design for studies of positronium in gases, 18: 4397 (NP-13327)
design for studying extensive air showers, 19: 22751
design for thoron monitoring in human breath, 17: 14652 (UR-619)
design for triggering photography of mesons(K^+) in hydrogen bubble chamber, 16: 23919
design for tritium-in-air monitoring, 20: 4235 (AECL-2283)
design for tumor localization and organ visualization after administration of radioisotopes, 16: 25097(R) (TID-16081)
design for two-dimensional scanning and automatically recorded scintigram, 20: 11161(P)
design for underwater use, 19: 22660(R) (HW-83298(p.7.1-30))
design for use in column chromatography, 16: 1934 (AD-255935)
design for use in space, 16: 23927
design for use in radiation protection, 20: 5762
design for well logging, 20: 5658(P)
design for well logging, 20: 39139(P)
design for whole-body counting, 16: 27348 (HASL-100)
design for whole-body counter, 17: 23013
design for whole-body counting, 19: 22685(R) (ANL-6839(p.12-17))
design for whole-body counting, 19: 22802
design for whole-body counter facility, 20: 7325
design for whole-body scanning, 20: 39265
design for x-ray scanning of fuel plates, 19: 11598
design for 0.1- to 2-Mev gamma spectrometer, 18: 20411
design for 1- to 15-Mev cosmic electrons, 20: 7367 (NASA-TN-D-3108)
design modifications for measurement of absorbed electron dose, 16: 20688
design modifications for cost reduction of, for alpha counting of smear samples, 17: 14610(R) (ORNL-3378(p.28-36))
design modification, for improvement of quality of scintigrams, 18: 4113
design modification of liquid, for carbon-14 determination, 20: 16862
design of alpha, for rock analyses, 19: 40432
design of alpha, using 72-in.^{2} phosphor, 20: 39257
design of anticoincidence, for gamma spectroscopy of molten-plutonium fuel elements, 19: 44453 (LA-DC-7316)
design of balloon-borne cosmic-ray telescope, 16: 23925
design of beta-gamma coincidence, 18: 22359
design of Bologna, for whole-body measurements, 19: 4503
design of boron-loaded liquid, 17: 4839
design of bubble-chamber, for neutrons, 18: 18204
design of collimator for, 18: 4114
design of collimated, for radioactive clouds, 20: 33633 (UCRL-14633)
design of controlled scintillation chamber having 2500 cm^3 operational scintillating volume, 16: 22338
design of dE/dx, with photomultiplier, 17: 4833
design of directional proton-recoil, for cosmic neutrons, 20: 21117
design of dosimeter, 18: 30006
design of double pulse, for neutrons, 18: 43989
design of fiber type for low-energy beta counting, 16: 696
design of filament, for weak-interaction detection and measurement, 16: 27352
design of flexible probe with, for dose measurements from radioactive implants, 19: 36149
design of, for alpha particle detection, 17: 37012(R) (NYO-9505 (p.80-6))
design of, for analysis of fecal samples, 17: 5734
design of, for beta measurement in fluids, 17: 16482(P)
design of, for counting carbon-14 and tritium in gas-liquid chromatographic effluents, 17: 11027
design of, for fast neutrons, 17: 6381 (AD-254402)
design of, for monitoring PRTR cooling system effluent, 17: 14647 (HW-SA-2849)
design of, for potassium monitoring in crude and refined ores, 16: 33340(R) (JLI-2748-0-5)
design of, for radon monitoring, engineering drawings for, 17: 32375
design of, for simultaneous counting of carbon-14 and tritium, 17: 22026
design of, for slow neutrons, 17: 23761
design of gain stabilization system for gamma spectrometers using, 20: 7457
design of gamma-insensitive, slow-neutron, 16: 31837(T) (AEC-tr-5370)
design of gamma probe for field use in water, 18: 10403
design of gamma spectrometer for studying lunar composition, 16: 23930
design of gas chamber for stable pulse heights, 17: 3341
design of gas scintillator, 16: 33219
design of gas-filled, for neutron polarization measurements, 18: 30054
design of gas, for alpha particles and electrons, 19: 20361
design of gaseous, for uranium-233 fission cross-section studies, 16: 14081
design of gaseous, for measuring fission cross sections, (E), 19: 9485 (NP-14488)
design of helium (liquid), as neutron polarimeter, 16: 13337
design of helium-3, for neutrons, 17: 3313 (UCRL-7068)
design of high-sensitivity portable, for river monitoring, 17: 18597 (HW-54676)
design of horizontally directional, for well logging, 20: 11024
design of large, 16: 33220
design of large-area, 16: 23937
design of large single-photomultiplier, for high-reliability cosmic-particle detection, 20: 23482
design of large sodium iodide crystal, for gamma radiation, 20: 27353
design of large-area liquid, 18: 39697
design of linear, nanosecond-range, noble-gas, 16: 13276 (CEA-2073)
design of liquid, 16: 23920
design of liquid, for counting fluids, 16: 17877(P)
design of liquid, for use with a Cherenkov system to study meson (μ) interactions with nuclei, 17: 4809 (NP-12248)
design of liquid, for measurement of carbon-14-labeled compounds, 17: 4821
design of liquid, for thermal neutrons, 18: 33953
design of liquid, for neutron-capture cross section measurements, 19: 4517
design of liquid, for slow neutrons, 19: 32585
design of liquid, for beta counting, (E), 19: 44506
design of liquid, for slow neutrons, 20: 5746 (ZFK-RN-18)
design of liquid, for gamma measurements and phototube testing, 20: 11128
design of lithium-6-iodide activation, for neutrons, 20: 16819 (LA-3435)
design of low-background, for beta rays, 18: 14261
design of low-weight, with focusing collimator, 19: 42727
design of miniature, 17: 1178(R) (HW-70050(p.220-88))
design of NaI luminescent chamber system, 16: 31918
design of neutron–gamma, for well logging, 20: 33723(P)
design of organic liquid, for fast neutrons, 20: 46048(R) (ORNL-3973 (Vol.1), pp 60-4)
design of phosphor-phototube, 19: 842(P)
design of plastic, for alpha particles, 19: 11574
design of portable probe, 16: 17871(P)

design of portable, 17: 4715
design of portable alpha, with flat large-area probe for surface monitoring, 18: 12493(P)
design of portable, transistorized, for weak beta and gamma measurement, 20: 25416
design of portable, for radioisotope scanning, 20: 33142(P)
design of pulse analyzing circuit for phoswich-type, 16: 7725
design of sample changer for liquid, 17: 20380(P)
design of shock-resistant luminophore-photomultiplier tube assembly, 17: 8680(P)
design of silver-activated zinc sulfide sandwiched, for fast neutrons, 20: 41335
design of sodium iodide, 19: 29506(R) (GEAP-4845)
design of solid angle silver-activated zinc sulfide, for alpha particles, 20: 46056(T) (NP-tr-1428)
design of spark-chamber, for electrons, with discrimination against mesons (π), 19: 44522
design of stabilized, 17: 23801(P)
design of standard luminophore, 16: 14982(P)
design of stilbene, for neutrons, 20: 14900
design of stilbene, for neutrons, 20: 31532
design of sturdy, for alpha counting, 18: 35898(P)
design of telescope of, for proton spectrometry, 19: 30562
design of total-absorption, for high-energy photons, 17: 4854
design of transistorized, for airborne radiometric monitoring, 16: 30588 (RISO-36)
design of transistorized, 16: 33150 (ISS-61/30)
design of transistorized, with pulse-height analyzer, 18: 14240
design of transistorized for monitoring radiation in kilns, 19: 11601
design of tunnel-diode time-marker circuit for, 19: 11564
design of two-dimensional coordinate, 16: 31943
design of, using semiconductor triodes, 16: 33211
design of wedge-shaped, for magnetic spectrometer, 20: 14822(R) (RHEL/R-112, pp 99-128)
design of well-logging apparatus with sodium iodide crystal at liquid nitrogen temperature, 16: 27409(P)
design of well-type, for annular counting of low γ activity in large liquid volumes, 20: 3817
design of whole-body counter using, 20: 38753
design of, with compensating reflector for crystal, 18: 5688(P)
design of, with window of tube optically coupled to crystal, 17: 41313(P)
design of x-ray, for 1–12 Å range, 20: 43726
design of xenon–helium-filled, 16: 20715
design of zinc sulfide, for detection and measurement of uranium-emitted alpha particles, 17: 6434 (HW-73155)
design of 1.25-meter liquid, 16: 14059
design of 2π scintillating-fiber, for low-energy beta counting, 16: 11846(R) (ARF-1192-3)
design of 30-channel system of, for studying proton reactions, 19: 22731
design of 4-m³, for primary cosmic gamma rays, 16: 13338
design of 4π, for beta counting, 18: 20380
design of 4π, for gases, 18: 43980
design of 4π plastic beta, 17: 6459
design of, for dosimetric control of liquid flow, 18: 16374(P)
design of, for measurement of thoron in breath, 18: 14130 (UR-640)
design of, for measurement of plutonium-239 in lungs of man, 20: 7456
design of, for mobile whole-body counter, 20: 7455
design of, for monitoring air for alpha and beta particles, 20: 39269
design of, for neutron-gamma well logging, 20: 29445(P)
design of, for renal scanning, 19: 26198
design of, for tomographic gamma scanning, 20: 33103 (UCRL-16899)
design of, used with fission chamber, 20: 39256
design of, using plastics, 18: 16366
design of, with high spatial resolution, 18: 20353
design of, with magnetic memory for studying radioisotope distributions, 19: 13795
design of, with plastic filament scintillator, 19: 34546
design to distinguish between gamma rays and neutrons for well logging, 17: 25662(P)
design using epoxy cement to couple the scintillator and photomultiplier tube, 17: 25661(P)
design using silicon photodiodes, 16: 695
design using two phosphors, 19: 24872(P)
design using universal modules, 19: 9520
design with continuous sensitivity variation compensation, 20: 11167(P)
design with multiple arrangement of photomultipliers, 19: 36861(P)
design with photomultiplier cooling for neutron detection, 19: 42748
design, calibration, and performance of plastic, for carbon-14-labeled amino acids, 18: 10175
design, calibration, and performance, 18: 43936(R) (MIT-952-1(p.163-95))
design, for use in gamma cameras, 20: 8763
determination of chemical and radiochemical purity of sodium iodide-131, 17: 35651
development, 17: 39438
development, 20: 2177
development, 20: 35771
development, 18: 27753(R) (ORNL-3578(p.6-36))
development and dosimetric performance, 17: 25651
development and evaluation for fast neutrons, 16: 1005(T) (UCRL-Trans-689)
development and operation characteristics, 16: 14939
development and operation of, review of, 17: 6444(T) (AEC-tr-5259)
development and operation of gaseous, review of, 17: 41264
development and performance of lithium glass and zinc sulfide, for neutron detection, 16: 31874
development and performance for nuclear particle research, 20: 27328
development for auroral phenomena, 18: 33935
development for beta spectra with digital-computer analysis, 19: 2641
development for beta counting using plastic sandwich phosphors, 20: 5783
development for clinical scanning using iodine-131, 20: 20535
development for counting simultaneously positrons emitted from 20 sources, 16: 25571 (TID-16268)
development for counting soft beta emitters, 17: 25637
development for color scintigraphy, 19: 13151
development for detection of slow positive ions, 16: 11891
development for detection of beta particles from tritium, 18: 19887
development for determination of radioisotopes in biological materials, 18: 39630(T) (AEC-tr-6390(p.553-7))
development for determination of absolute activity of radioactive solutions, 19: 28425
development for discrimination against gamma background in fast neutron detection, 18: 18181
development for dosimetry of gamma and x radiation, 17: 41269
development for fast neutron detection by evaluation of solvents, 16: 30180(R) (ANL-6474(p.11-13))
development for fuel rupture monitoring, 19: 34425(R) (HW-84384 (p.7.1-27))
development for gamma dosimetry, 18: 30050
development for gamma- and x-ray detection and dosimetry, review of, 19: 18261 (NP-14685)
development for gamma rays, 19: 20356
development for heavy ions, 18: 5662
development for high-energy particle detection, (E), 19: 36804 (BNL-9218)
development for in-line analysis of process streams for plutonium, 19: 9059 (HW-84251)
development for low-level counting, 20: 21042 (SGAE-E-6/1966)
development for measurements of capture gamma rays from natural elements, 16: 8162(R) (ARF-1193-6)
development for measuring cosmic neutron background, 18: 14756(R) (ANL-6769(p.34-9))
development for mesons (π^+), 18: 39671
development for measuring beta absorption in liquids, 20: 31521
development for monitoring tritiated water vapor in air, 20: 25411
development for neutron radiative capture reactions, review of, 17: 41995
development for neutrons with fast cancellation of gamma background, 18: 41867
development for neutron cross section measurements, 18: 42646 (ORNL-TM-954)
development for neutron fission and radiative capture studies, 19: 42747
development for neutron dose rates in mixed gamma-neutron fields, 20: 31505(R) (BNWL-235-4, pp 30-4)
development for neutron dosimetry, 20: 35758 (PG-Report-711)
development for particle detection, 19: 13746
development for radon counting, 18: 37535
development for radioisotope scanning, 19: 17743
development for radioisotope scanning, 19: 17744
development for radioisotope scanning, 19: 17745
development for radioisotope scanning, 19: 17746
development for radiodiagnosis, review of, 20: 16855
development for thermal neutrons, 16: 8918(T) (FTD-TT-61-261)
development for thermal neutron time-of-flight studies, 19: 18296
development for uranium-235 enrichment measurement in fuels, 20: 39335
development for use in area radiation monitors, 16: 17817 (HW-69879 (Rev.))
development for use in image intensification of weak beams, 16: 20642 (NP-11663)
development for use in difference method of counting small pulses, 18: 39646
development for uv radiation, 18: 33908
development for whole-body counting, 19: 2191 (ORNL-P-658)
development for whole-body counter, 19: 22705
development for whole-body counting, 19: 33704

development in Japan, 19: 36829
development of alpha, for measuring uranium contamination on reactor fuel elements, 20: 27120 (BNWL-SA-646)
development of anticoincidence shielded multidimensional, for gamma spectrometers, 19: 15897
development of anticoincidence system of, for meson (π^0) energy and flight direction determination, 19: 30566
development of anticoincidence, for suppressing Compton background in gamma spectrograms, 19: 36243(R) (X64-17610)
development of balloon-borne, for fallout monitoring in upper atmosphere, 20: 43512(R) (ANL-7136, pp 315-27)
development of beta-gamma, 17: 32399 (HW-SA-2932)
development of boron-containing and lithium-containing glass, 16: 25877(R) (ANL-6534)
development of boron-loaded liquid, for neutrons, 19: 18327
development of bulk liquid, using anticoincidence shielding, 18: 27794
development of cadmium-loaded, for neutrinos, 20: 4847 (UCRL-12085(Pt.1))
development of cerium-activated glass, for alpha counting, 17: 11003 (HW-72512)
development of cylindrical, for slow neutrons, 19: 13791
development of dE/dx plastic, for pulsed accelerators, 18: 23993
development of directional, for measuring gamma rays from stars, 19: 15905
development of dispersion, for slow neutrons, 19: 13790
development of, for dosimetry, 16: 31989(T) (FTD-TT-62-678)
development of, for measuring plutonium-239 in wounds, 17: 1741 (AERE-M-595)
development of, for scanning in solid propellant radiography, 17: 10188 (AD-275297(p. 70-4))
development of, for use in radioisotope scanning, 18: 5640 (TID-7673 (p.3-24))
development of gas-filled, for x rays, 18: 30049
development of high-efficiency fast-neutron, with gamma-background cut-off by photomultiplier space charge, 19: 34572
development of high-efficiency fast-neutron, with gamma discrimination, 19: 34571
development of immersible gamma probe for direct measurement of activity in sea water, 20: 41147
development of inorganic and organic, 20: 39233
development of large-volume, for radioisotope process control, 18: 14205 (CONF-187-86)
development of liquid terphenyl–boron, 16: 19079 (TID-15701)
development of liquid, using transient excited dimers, 17: 18602 (TID-16601)
development of liquid benzene, for determination of carbon-14, 18: 8687
development of liquid, review on, 18: 13854
development of liquid, for carbon-14 dioxide counting, 18: 31396
development of liquid, of soft beta particles, 19: 39002
development of liquid, for measurement of neutron inelastic scattering cross sections, 19: 46766(R) (TID-22141, pp 67-79)
development of liquid, for measurement of neutrino-proton interaction cross sections, 20: 21027 (CERN-65-32, pp 41-4)
development of liquid, 20: 23527 (CONF-651207)
development of lithium-6-loaded, for neutrons, 16: 27382
development of lithium-glass, for neutron detection, 17: 32405 (ZFK-RN-19)
development of low background liquid, for low specific activity tritiated water, 16: 16093
development of low-background, for alpha particles, 18: 33933
development of plastic, for beta detection with reduced gamma sensitivity, 17: 1775
development of plastic-well-type, for gamma activities in large-volume samples, 18: 41854
development of plastic–phosphor, for beta detection, 20: 14874
development of plastic, for cosmic particles, 20: 21028 (CERN-65-32, pp 65-70)
development of praseodymium-doped fluoride lattices for infrared quanta, 18: 2070
development of resonant, 18: 39638
development of sodium iodide, for high-energy gammas, 19: 11568
development of spectrometers of, for charged particles, 19: 15894
development of stilbene, for fast neutrons, 19: 22798
development of telescopes of, for deuterons and protons, 19: 15891
development of two-phase, for counting aqueous solutions, 17: 18479
development of ultrasensitive, for ocean monitoring, 20: 13056 (AD-627000)
development of water-rich emulsions for, 17: 29216
development of whole-body, 16: 11956(R) (JAERI-5003(p.107-11))
development of zinc sulfide particle counting, 16: 332 (HW-55917)
development of, for measurement of pulsed x radiation from radar, 18: 12442(R) (AD-412461)
development of, for visualization of isotope distribution on colored scintigrams, 18: 33968
development of, for use in radioscanning of man, 19: 30012 (ACRH-103 (p.76-103))
development of, for clinical scanning, 20: 8777
development of, for measurement of absorbed dose from high energy electrons, 20: 40746(R) (NYO-3510-2)
development of, review of, 19: 42725
development, physical principles, and technical methods of scanning by, 17: 8636
development, review, 17: 23673
development status, 16: 20641 (NP-11616)
development, for use in radioisotope scanning, 19: 30045
development, for use as neutron dosimeters, 20: 37025(R) (PG-Report-705)
developments for low-level tritium counting, 16: 16094
developments in, 17: 22051
diffusion chamber design for use in, rotating, 18: 39633
discrimination characteristics of organic, 17: 14349
discrimination characteristics of, for different particles, 17: 32444
discrimination efficiencies of, 19: 4516
discrimination of spurious events in, method for, 18: 14214 (LNF-63/65)
discriminator for, design of pulse-shape, 19: 808
distributions of random sum photopeaks in spectrometers using, 19: 4512
dose sensitivity of gamma, 18: 30013
dose sensitivity of, energy dependence of, 18: 39684
effects of geometry on xenon-filled, 19: 6198
efficiencies and photofractions of cylindrical thallium-activated sodium iodide, Monte Carlo calculations of, 17: 32416
efficiencies of alkali-halide, for gamma radiation, 17: 14351
efficiencies of cylindrical sodium-iodide (thallium) gamma-ray, table of, (T), 20: 29562
efficiencies of, for plane gamma sources, 17: 14667
efficiencies of thallium-doped sodium iodide, 19: 6180 (AAEC/TM-268)
efficiency and peak-to-peak ratio for sodium iodide crystal, absolute, 20: 41307
efficiency and resolving time of, statistical limits on, (T), 19: 34549
efficiency and resolution of thin crystal, for actinides, 20: 18562(R) (EUR-2640.e)
efficiency and statistical aspects of liquid, by internal standard technique, 17: 23751
efficiency and transparency of liquid, for gamma radiation, 19: 7799
efficiency, effects of temperature, 16: 23858(T) (AEC-tr-5120)
efficiency for assaying iodine-125, 18: 23390
efficiency for beta counting, effects of sample volume on, 20: 5510
efficiency for carbon-14 and tritium, discriminator ratio method for determining, 19: 24464
efficiency for collimated gamma rays, 20: 21056
efficiency for copper Kα emission, 18: 33896
efficiency for counting aqueous cylindrical gamma sources, 19: 6193
efficiency for determination of radioiodine, 19: 32068
efficiency for fast neutrons at 1 to 20 Mev, 18: 41778
efficiency for fast neutron detection, Monte-Carlo calculations of, 19: 35368
efficiency for fission neutrons of varying energies, 17: 26541
efficiency for fluorescent beta-excited x rays, 16: 22507
efficiency for fluorine-18, 18: 12008
efficiency for gamma counting, 17: 38995
efficiency for gamma detection, computer program for calculating, 19: 11582
efficiency for gamma radiation using well-type crystals, geometrical effects on, 20: 2169
efficiency for gamma radiation, calculation of, 20: 14897
efficiency for iodine-125 determination in clinical applications, 18: 15915 (TID-7689(p.15-16))
efficiency for low-energy beta counting, 20: 11122
efficiency for neutrons, effects of gamma background on, 16: 33217
efficiency for neutron detection in presence of gamma radiation, 18: 41794
efficiency for neutrons in Bev range, 20: 13109
efficiency for simultaneous determination of calcium-45 and phosphorus-32 in inorganic salts, 20: 20584
efficiency for x ray detection, 20: 16836
efficiency for x-ray counting, (E), 20: 13092
efficiency improvement by use of frosted vials, 17: 34257
efficiency in detection of high-energy neutrons from pulsed source, 16: 19725 (SCR-467)
efficiency in gamma-ray telescopes, Monte Carlo calculations for, 20: 31554
efficiency measurement in organic, for high-energy neutrons, 17: 4836
efficiency measurement in liquid, using external gamma sources, 17: 6454
efficiency measurement of liquid, channels ratio method for, 17: 27689
efficiency of boron- and lithium-loaded, for thermal neutrons,

17: 29197 (EUR-133.i)
efficiency of crystal, liquid, and plastic, for gamma radiation, 19: 39009
efficiency of cylindrical gamma, formulas for absolute, 18: 37525
efficiency of drilled-hole scintillometer, embedded in plastic, 20: 29546
efficiency of fast-neutron, 18: 41850
efficiency of gas, for neutron detection, 19: 9771(R) (PR-P-63)
efficiency of large-area liquid, 20: 41339
efficiency of liquid, for quenched liquids, 17: 141
efficiency of liquid, for tritium counting, 17: 29986
efficiency of liquid, determination of, 17: 30086
efficiency of liquid, for absolute beta counting, 19: 22743
efficiency of liquid, 19: 24860
efficiency of liquid, for beta particles, 20: 10902
efficiency of liquid, for low-energy beta emitters, 20: 33637
efficiency of liquid, methods for determining, 20: 43675
efficiency of liquid, for separation of beta spectra of carbon-14 and tritium, 20: 43098
efficiency of lithium iodide crystal for neutrons, calculations for, (T), 19: 29172 (LADC-6488)
efficiency of long scintillator rods in gamma detectors, 18: 30068
efficiency of medicinal, paraffin-based, liquid whole-body, 20: 29541
efficiency of neutron, at 20 to 70 Mev, 20: 31584
efficiency of photodiodes, 18: 10416
efficiency of plastic-type, for neutrons at 4 to 76 Mev, 16: 19125
efficiency of plastic, for 1- to 10-kev photons, 18: 25845
efficiency of plastic, for 21- to 29-Mev neutrons, 18: 35873
efficiency of plastic, for 14-Mev neutrons, 19: 22696 (IKF-D-32)
efficiency of plastic, for x-ray flux at 1.8 to 4.5, 20: 19066
efficiency of sodium iodide, for gamma rays, 19: 20358
efficiency of sodium iodide, for gamma radiation, 20: 11127
efficiency of thallium-activated sodium iodide, for gamma radiation, 18: 18231
efficiency of thallium-activated sodium iodide crystal, 18: 25865
efficiency of thallium-activated sodium iodide, for gamma radiation, 19: 32581
efficiency of thallium-doped sodium iodide crystal, for gamma radiation, 20: 31553
efficiency of unshielded whole-body, in man, 20: 9266
efficiency of well-type crystals in, for gamma measurements, 19: 39039
efficiency of well-type, for absolute counting, 20: 2170
efficiency of 4π, for source calibration, 18: 39654
efficiency of, crystals and collimator design for, 19: 42740
efficiency of, in extended gamma fields, 18: 33941
efficiency of, using sodium iodide crystals for gamma detection, 18: 22345(R) (UCRL-11184(p.86-90))
efficiency of, using liquid scintillators, 19: 2630
efficiency of, using larger parabolic phosphors, 20: 16849
electron ionization loss at 20 to 150 Mev in Ne 102A, 20: 44232
electron photoproduction in, energy for, 18: 33860
energy dependence compensation in, method for, 18: 18245(P)
energy dependence of, method for compensating, 18: 22378(P)
energy resolution and light yield, effect of filling gas, 16: 11917
energy resolution, dependence on activator distribution in sodium iodide phosphors, 16: 15340
energy resolution of, device for measuring, 18: 30047
energy resolution in liquid, factors affecting, 19: 20351
energy response of gas-type, factors affecting linearity, 16: 7728
energy transfer in, by beta particles, 20: 2189
engineering drawing for portable alpha, 18: 41876
engineering drawings for portable, 18: 41877
evaluation for clinical studies, 20: 26723
evaluation for whole-body counting, 18: 39632
evaluation of boron--zinc sulfide, for detection of thermal neutrons, 16: 351(T) (AEC-tr-4702)
fabrication of high pressure helium-3 gas, for gammas and neutrons, 20: 43733
fabrication of zinc sulfide screens for, 20: 7441
feasibility of cadmium sulfide, using matched pairs of crystals, (E), 19: 40598
gamma absorption in well-type, (T), 19: 28684
gamma backscattering in, 19: 15864 (NP-14690)
gamma detection efficiencies of annular and well type sodium iodide crystals at 0.1 to 6 Mev, 17: 37419 (TID-17630)
gamma detection photo fractions for cylindrical thallium-activated sodium iodide, effects of gamma collimation on, 18: 29978 (KFK-188)
gamma detection using thallium-activated sodium iodide, angular resolution correction in, (E), 19: 34492
gamma-ray attenuation factors for angular correlation and angular distribution measurements, 16: 19135
gamma-ray efficiencies of well-type sodium iodide (thallium) crystals, 17: 36150 (IS-606)
gamma resolution of, energy dependence of, 17: 11627 (TID-15088)
gamma total absorption in well-type, probability for, 20: 676
gas circulation pump for, 18: 10420
glass for, development and evaluation of, 20: 5585
glasses for, development and properties of, 20: 21044(T) (ANL-Trans-285)
image contrast intensification for, 17: 11046
image intensifier systems for, efficiency of, 17: 23666
insulation and refrigeration of, in well logging, 18: 5689(P)
iron-55 and -59 counting in blood samples with liquid, 19: 32250(R) (UCRL-11833(p.112-20))
light attenuation in, 20: 31546
light collection by, variance in, 17: 34221 (ANL-6737)
light collection efficiency of, methods of increasing, 17: 18606 (UCRL-7067)
light collection efficiency of, methods for increasing, 17: 27703
light-collection variance in, computer program for calculating, 17: 8596 (TID-15541)
light pipe for coupling to photomultiplier tube, 19: 7814
light pipes for, development of, 18: 37536
light pipes for, efficiency of, 18: 20399
light pipes for, fabrication of, 18: 31965
light source for, engineering drawings of triggered nanosecond, 18: 31973
light systems for, efficiency of elliptical cylinder, 18: 30052
light-pipe materials for alpha, 16: 11860(R) (ORNL-3191(p.19-35))
liquid, comparison of glass and polyethylene vials for, 17: 23756
liquid, efficiency for calcium-45 counting, 16: 16316
liquid, method for measuring low-level tritium using benzene, 16: 16097
liquid, performance of for whole-body counting, 16: 16136
liquid, performance of single phototube for measurement of tritium in biological materials, 16: 16098
liquid, relation between counting efficiency and fluorescence intensity, 16: 7699
liquid, review, 17: 4818
liquid, control circuits for, 20: 43749(P)
localization of spark in, from magnetopinch effect in electrode, 18: 10378 (LNF-63/54(p.1-4))
logic of, circuit for test display lamp for, 20: 41314
luminescence decay in organic, 17: 25646
luminescence decay in organic, means for hastening, (E), 19: 17959 (SC-TM-64-1742)
luminescence response of Pilot B plastic, to electrons and protons, (E), 19: 40916
measurements of low-level radioactive contamination of elements by, 18: 35441
medical use of, review, 20: 5487
meson (μ) production in large plastic, by background neutrals, 20: 21028 (CERN-65-32, pp 65-70)
meson (μ) production in liquid, by cosmic rays, (E), 20: 21029 (CERN-65-32, pp 71-2)
method for simultaneous carbon-14 and tritium measurement using, 18: 17743
modification for improved sensitivity at high elevations, 16: 10780
modification of large fission gamma counter (H-4), 16: 1317(R) (LAMS-2627(p.145-9))
neutron detection process in plastic, computer program for simulation of, 20: 39196 (AE-236)
neutron polarization measurements using liquid-helium, 16: 27355
neutron pulse amplitude distribution in, calculation of, 17: 8644
noise-pulse-elimination circuits for, 16: 22358
nuclear particle discrimination using, 17: 8663(P)
operation of alarm systems of, maintenance of, 19: 22711
operation of, efficiency and principles of, 17: 30860
operation of medical scanner of, maintenance of, 19: 22711
operation of, reduction of pile-up contamination in pulse-height spectra, 17: 18604 (TID-18300)
operation of sensitive hardness-compensated gamma dosimeter, 19: 34568
operation parameters of xenon dE/dx, 19: 42724
operation under conditions of rapidly changing radiation flux, 17: 1746 (KAPL-M-FTG-1)
optical characteristics of ion detectors, (T), 20: 7397
optical piping systems for, 18: 10419
particle detection in background energy range, statistical method for, 17: 37429
particle discrimination by thallium-activated potassium iodide, effects of crystal temperature and thallium content, 16: 23956
particle discrimination in, pulse-shape, (E/T), 19: 4458 (ISS-64/23)
particle discrimination in, circuit for, 19: 43392
particle identification and range measurement in plate-loaded filamentary, 17: 23672
particle identification by pulse shape discrimination, method for, 19: 34515
particle range spectrum in, 19: 795
particle velocity measurements using filamentary, 16: 31919
performance and calibration of array, in whole-body gamma counting

facility, 16: 8532(R) (ACRH-16(p.126-35))
performance and preparation of thallium-activated cesium iodide, (E), 19: 28679
performance as anticoincidence shields for germanium gamma spectrometers, (E), 19: 44519
performance as beam profile scanners, 18: 724 (AERE-R-4402)
performance as cosmic-ray monitors, atmospheric effects on, 20: 6004 (AD-619508)
performance as dosimeters in mixed gamma and neutron fields, 19: 20330(T) (AEC-tr-6547)
performance as dosimeters for fast neutrons, 20: 7446
performance as fuel-cladding-failure monitor in sodium-cooled reactors, (E), 19: 8575 (NAA-SR-6463)
performance as 4π beta spectrometers, 18: 20360
performance at high temperatures, using highly ruggedized photomultiplier tubes, 20: 41374
performance, effect of proton-induced radioactivity, 17: 28686(R) (UCRL-10683(p.1-14))
performance evaluation of, computer program for, 18: 33232(R) (NYO-910-3)
performance for absolute fast-neutron flux measurements, 18: 4089 (EANDC-33U(p.136-49))
performance for absolute beta counting, 18: 31911 (NP-13998)
performance for absolute radioactivity measurements, 20: 15690 (CEA-R-2813)
performance for alpha detection, 18: 39685
performance for analysis of biological materials for beta-emitting isotopes, 16: 22391
performance for analysis of complex gamma spectra, 20: 36217
performance for beta spectroscopy, 17: 41289
performance for beta particles, effects of discrimination and dead times on, 19: 39014
performance for beta dosimetry, 19: 44491(T) (CEA-tr-R-1866)
performance for Bev-range neutrons, 20: 11106 (NP-15786)
performance for beta and gamma spectroscopy, 20: 36186
performance for beta dosimetry of skin, 20: 41274 (ORNL-TM-1581)
performance for carbon-14 and tritium counting, evaluation of various solvents for, 18: 33938
performance for charged-particle discrimination in mass spectroscopy, 17: 32428
performance for charged particles, mass discrimination in, 19: 9513
performance for charged-particles mass discrimination, 19: 9518
performance for counting weak beta emitters in bacterial cells, 18: 36931
performance for cosmic radiation, (T), 19: 4863(T) (FTD-TT-64-1077(p.100-72))
performance for counting one, two, and three γ-emitting isotopes in man, 20: 22933
performance for detection of low energy beta rays, 16: 14965
performance for detection of low energy beta rays, 16: 33170(T) (NP-tr-920)
performance for detection of air fluorescence from nuclear explosions, (T), 20: 15608
performance for detection of γ and x radiation from deposited plutonium-239 in dogs, 20: 30968 (BNWL-SA-11)
performance for determination measurement of cobalt-60 deposited in lungs, 20: 41190 (CONF-660621-4)
performance for fast neutrons, 18: 501
performance for fast neutrons, 18: 41772 (KFKI-1491/A)
performance for fast neutron dosimetry, 19: 763(R) (HW-81746(p.2.19-23))
performance for fast neutron absolute flux determinations, using organic compounds, 20: 39223
performance for gamma radiations, experimental determination of summing distributions, 16: 11883
performance for gamma counting by integral and differential systems, 16: 21876
performance for gamma counting, 17: 3316 (Y-1402)
performance for gamma detection at doses of 10^4 to 10^8 r, 18: 18201
performance for gamma spectra, compensation for instabilities in, 18: 33926
performance for gamma detection, effects of additions of organometallic compounds to plastics on, 18: 33939
performance for gamma rays, effects of backscattering on, 19: 13789
performance for gamma spectroscopy, (E), 19: 16840(R) (IDO-17050)
performance for gamma radiation, plateau curves for, 19: 15869 (NP-14715)
performance for γ point sources in scattering media, 20: 5760
performance for gammas, from 31 to 1836 kev, 20: 8075 (NP-15648)
performance for gamma dosimetry near reactor pipes, 20: 21047
performance for identification of nuclear radiation, 18: 41823
performance for in-pile gamma and neutron detection, (E), 20: 5728 (IBM-65-825-1487)
performance for leak detection in containers for radioactive materials, 20: 41197(R) (NP-16172)
performance for liquid scintillation counting, dispensing of radioactive solutions for, 19: 30514 (AERE-M-1574)
performance for low-level beta radiation, effects of sample-holder material on, 17: 16458
performance for low-level gamma dosimetry, 19: 44528
performance for low-energy gamma radiation, effects of collimator design on, 19: 46119
performance for mass discrimination of protons, deuterons, and tritons, 16: 27304
performance for measurement of electron spectra in tissue, 16: 17853
performance for measuring gamma spectra, 18: 18232
performance for measuring uranium 235/238 ratios in fuels, 19: 4454 (HW-81486)
performance for measurement of gamma radiation from positron annihilation, 20: 38745(R) (NYO-3267-3)
performance for measuring carbon-14 uptake during photosynthesis, 20: 45311
performance for monitoring air, 16: 25542 (AEEW-R-150)
performance for neutron spectroscopy at 0.5 to 15 Mev, 17: 8626
performance for neutron detection in gamma background, 18: 10406
performance for neutron spectrometry, 18: 14285
performance for neutron dosimetry, 18: 38732
performance for neutron dosimetry, 19: 2628
performance for neutrino detection, 20: 4848 (UCRL-12085(Pt.2))
performance for neutron spectroscopy, 20: 19790
performance for neutron flux measurements, Monte Carlo corrections for, 20: 26062 (CEA-R-2971)
performance for particle detection, comparison with photographic emulsions, 18: 23906
performance for radiation dosimetry, 19: 46851
performance for scanning liver for radioactive materials, 16: 25098
performance for scanning liver for radioactive materials, 16: 25099
performance for secondary-electron detection, 20: 5757
performance for slow neutrons, 19: 42749
performance for soft x-ray counting, 18: 2097
performance for triple-coincidence gamma spectroscopy, (E), 20: 5770
performance for tritium monitoring in radiochemical laboratories, 20: 23365 (CONF-640413, pp 87-90)
performance for tritium beta dosimetry, 20: 23367 (CONF-640413, pp 98-102)
performance for tritium beta dosimetry, 20: 23368 (CONF-640413, pp 103-6)
performance for whole-body counting, 16: 16140
performance for whole-body counting, 16: 16145
performance for whole-body counting, 16: 16146
performance for whole-body gamma counting, 18: 37545
performance for whole-body γ counting of man, 20: 46031(R) (AERE-PR-HPM-9, pp 17-26)
performance for zero-thickness sources, valley-to-peak ratios for, 20: 41312
performance in aerosol monitor, 19: 13753
performance in analysis of beta-active biological materials, 19: 40436
performance in anti-Compton, gamma spectrometers, 20: 13098
performance in anticoincidence gamma spectrometers, 20: 14865
performance in beta spectroscopy, 18: 18211
performance in coincidence, for gamma spectroscopy, 18: 20331 (KR-64(Sect.X))
performance in coincidence counters using fast PM tubes, 19: 4511
performance in counting sulfur-35-labeled hydrogen sulfide, 16: 7588
performance in delayed-coincidence applications, 16: 21434
performance in detection of iodine-131 rose bengal and colloidal gold-198 in liver, 16: 25190
performance in detection of thermal neutrons, 18: 14246
performance in fast neutron spectrometry, 18: 41789
performance in gamma spectrometer system, 16: 3841(R) (ORNL-3193 (p.29-44))
performance in gamma spectrometer, 16: 20628 (ANL-6499)
performance in gamma spectrometer, 18: 43935(R) (LA-3132-MS(p.142-3))
performance in gamma–gamma angular-correlation spectrometers, 19: 835
performance in gamma cameras, 19: 17756
performance in gamma camera, 19: 17757
performance in gamma camera, 19: 17758
performance in gamma cameras, 19: 17759
performance in gamma spectrometers for low-intensity complex spectra, 19: 34577
performance in gamma spectrometers, 19: 34578
performance in identification of beta emitters by Le Gallic method, 18: 39099
performance in identification of low-energy beta emitters, 18: 39100
performance in image separation radioisotope scanning, 17: 17693
performance in localization of brain tumors after administration of arsenic-74, 16: 25102
performance in magnetic fields, 20: 5736 (NP-15597)

performance in measuring charged particle mass, 16: 11905
performance in measurement of low-energy beta particles, 18: 29989
performance in molybdenum-99 liver scanning in man, 19: 46139
performance in Mössbauer effect spectrometer, 19: 46831
performance in nanosecond range, spark pulse generators in improving, 17: 11037
performance in neutron time-of-flight spectrometers, 18: 16323
performance in neutron spectroscopy, 18: 29993
performance in nitrogen-14 measurement, comparison with Cherenkov detectors, 19: 30081(R) (NBL-216)
performance in nuclear spectrometry, review of, 19: 18262 (NP-14686)
performance in photoproton telescopes, 17: 32440
performance in point source gamma detection, 20: 46042 (HASL-177)
performance in radiological flaw-detection systems, 17: 8384
performance in radioisotope diagnostics, 18: 27251
performance in radioisotope scanning, 19: 17765
performance in Russian Cosmos 3 and 5 satellites, 18: 24327
performance in simultaneous measurement of strontium-85 and zinc-65 in rats, 18: 43175(R) (LA-3132-MS(p.42-8))
performance in small animal counter, 18: 43934(R) (LA-3132-MS(p.76-83))
performance in space vehicles for measuring soft corpuscular radiation, 16: 27870
performance in spectrometers, 19: 13804
performance in telescope, for photonuclear reactions, 19: 34543
performance in time-of-flight neutron spectrometers, 18: 34752(R) (CU(PNPL)-234)
performance in whole-body counting of cesium-137, 17: 23054
performance in whole-body counter, 19: 12910 (DPSPU-64-30-7B)
performance in whole-body counter, 20: 35357
performance in x-ray diffractometers, effects of window width on, 18: 41783
performance of airborne, for radiation measurements over ground surface, 16: 19196
performance of air-filled, for alpha particles, 18: 23972
performance of annular-crystal, for neutron-capture gamma spectrometry, (E), 19: 40896
performance of boron and lithium glasses and stilbene crystals for neutrons, 17: 34869
performance of cesium iodide and sodium iodide, for underwater use, 20: 31499 (AD-633752)
performance of coincidence, for decay-rate measurements, 19: 2614
performance of crystal, 17: 4841
performance of cyanoplatinate(II) salts as, 17: 14352
performance of europium-activated lithium iodide, for fast-neutron spectrometry, 17: 34291
performance of europium-activated lithium iodide, for fast neutron spectroscopy, 19: 13731 (NP-14722)
performance of europium-activated lithium iodide, for neutron spectra, 20: 11116
performance of flat slow, for thermal neutrons, 17: 8640
performance of, for cosmic-ray detection, 17: 20355
performance of, for deuterons, nuclear interaction correction for, 17: 23768
performance of, for counting beta particles from iodine-131 in blood plasma, 18: 1577
performance of gallium arsenide, as charged-particle spectrometer, 20: 41313
performance of gas, 17: 11005 (IKF-5)
performance of gaseous, for measuring α and neutron fission rates, 19: 47567 (CEA-R-2775)
performance of helium-filled, for neutrons, 18: 20398
performance of helium-filled, effects of impurities and outgassing on, 20: 7424
performance of Hornyak button-type, for fast neutrons and gamma radiation, 19: 30559
performance of immersible, for radiometric analysis of urine, 19: 46083
performance of internal-source, in spectroscopic uses, 17: 41287
performance of large liquid, parameter effects, 16: 8958
performance of large plastic, 17: 3326
performance of large liquid, 17: 23680
performance of large liquid, for neutron-capture studies, 18: 4534 (EANDC-33U(p.114-35))
performance of large, in multicount hodoscope system, 19: 34565
performance of large plastic, for gamma aerial monitoring, 20: 5761
performance of large-area organic, (E), 20: 7419
performance of large-volume liquid-organic, for gamma radiation, 20: 13079
performance of large-volume, for radioisotope process control, 20: 23455 (ALO-1355-1)
performance of LiI(Eu), for measurement of neutron flux density and dose, 19: 20375
performance of liquid-helium, for alpha detection, 16: 7729
performance of liquid, for carbon-14 beta counting, 17: 377
performance of liquid, for determination of carbon-14 and tritium, 17: 7957 (PAN-330/XIII)
performance of liquid, for tritium counting, 17: 30023
performance of liquid, for analysis of clay and soil suspensions for carbon-14, 18: 29599
performance of liquid, for assaying carbon-14 dioxide in Warburg flasks, 19: 4084
performance of liquid, for thermal neutrons, 19: 18297
performance of liquid, for fast neutron flux measurements, 19: 28641
performance of liquid, for analysis of antineutrino-proton interactions, 20: 993 (COO-818-70)
performance of liquid-organic, for beta particles, effect of added sodium naphthylamine sulfonate on, 20: 13080
performance of liquid, phosphorescence effects of glass containers on, 20: 16863
performance of liquid, effects of phosphor solutions on, 20: 23493
performance of liquid, for measurement of beta particles from carbon-14 and tritium, 20: 23495
performance of liquid, 20: 37107
performance of lithium-6 salicylate, for neutron detection, 18: 16308 (TID-7689(p.103-5))
performance of lithium-6-glass, for neutron counting, (E), 20: 13090
performance of NE 150 plastic, for fast neutrons, 20: 27307
performance of neutron time-of-flight, 19: 11542
performance of organic, for fast neutrons, 17: 14350
performance of organic phosphors and sodium iodide crystals as, for gamma radiation, 17: 34858
performance of organic, for discriminating between charged particles, 18: 16324
performance of organic, for discrimination of gamma rays and neutrons, 18: 20350
performance of organic, effects of high voltage on, 19: 34482
performance of organic, for fast neutrons, 19: 46774
performance of organic plastic, for whole-body counting of man, 20: 1710
performance of organic, for pulsed gamma radiation dosimetry, 20: 11137
performance of organic, for fast neutrons, 20: 33630 (ORNL-3888)
performance of plastic, 16: 6594
performance of plastic phosphor well-type, for counting biological samples, 16: 20658
performance of plastic-phosphor, in measuring beta spectra, 16: 31855
performance of plastic, optimization of light collection in, 17: 32396 (AERE-R-3972)
performance of plastic, for mesons (μ), 19: 42751
performance of plastic well-type, for determining absolute photoelectric cross sections, 20: 11496
performance of plastic, for electrons, 20: 23504
performance of portable, for gamma monitoring of large soil areas for plutonium-239, 19: 22641
performance of rare gas, effects of electric fields on, (E/T), 19: 26379 (NP-14813)
performance of rate meters and scalers used with, for radioisotope scanning, 19: 17763
performance of resonance gamma, 19: 11543
performance of scintillator-semiconductor photodiode, 18: 8658
performance of shadow shield, for whole-body counting of man, 18: 2021(R) (HW-77609(Sect.2))
performance of silver-doped zinc sulfide crystals, for alpha particles, electrons, and protons, 20: 23505
performance of single channel, for gamma spectra, 20: 27264 (NP-15379)
performance of sodium iodide, for gamma spectroscopy, (T), 19: 30520 (IDO-17017)
performance of sodium-iodide, for beta bremsstrahlung in man, 19: 30582
performance of sodium iodide, for ground contamination isopleths, 20: 7358(R) (EGG-1183-2057)
performance of sodium iodide, for absolute gamma activity measurements, 20: 16858
performance of sodium iodide, in determining phosphorus-32 *in vivo*, 20: 25328
performance of, statistical analysis of, 17: 11041
performance of stilbene, for neutron flux measurements, 19: 28628 (EUR-1815.e(Rev.)(p.246-53))
performance of thallium-activated sodium iodide, for gamma spectroscopy, 20: 13067 (JUL-308-RB)
performance of thallium-activated sodium iodide, for measuring radionuclide transfer in cows, 20: 16160 (UCRL-14739(Pt.2))
performance of thallium-activated cesium iodide, for determining composition of primary cosmic rays, 20: 41667(R) (MIT-2098-251, pp 1-13)
performance of thin, for beta emitters, 17: 3049
performance of total-absorption, for Bev particles, 17: 14680
performance of two-crystal, scanning-bed, whole-body, 19: 30580
performance of unactivated cesium iodide crystals, 20: 35791

performance of wedge-shaped, for magnetic spectrometer, 20: 41289
performance of well-type sodium iodide-crystal, for gamma detection, 20: 19090
performance of, whole-body dog counting system, 17: 17756 (HW-55856)
performance of whole-body, 19: 46836
performance of, with calcium fluoride crystals, 17: 11044
performance of zinc sulfide, for alpha particles, 20: 9260
performance of, as x radiation dosimeters, 20: 2157
performance of, effects of color quenching variables due to sample preparation, 19: 20324 (ORNL-P-1094)
performance of, error statistics for, 20: 19053
performance of, error-statistics calculations for, 20: 19054
performance of, evaluation standards for, 20: 42738(R) (ANL-7136, pp 255-65)
performance of, for zonal scanning of thin-layer chromatograms, 18: 27041
performance of, for beta counting, 19: 9500
performance of, for radioisotope scanning, 19: 17748
performance of, for radioisotope scanning, 19: 17749
performance of, for radioisotope scanning, 19: 17750
performance of, for radioisotope scanning, 19: 17751
performance of, for radioisotope scanning, 19: 17752
performance of, for cylindrical and sectional radioisotope scanning, 19: 17753
performance of, for scanning man, 19: 26667(R) (ORINS-49(p.111-26))
performance of, for scanning of skeleton using strontium-85, 19: 42396
performance of, for whole-body counting of man, 20: 3805
performance of, for whole-body counting of man, 20: 6992
performance of, for whole-body counting of man, 20: 6993
performance of, for whole-body counting, 20: 6754
performance of, for detection of activity from iron-55 and iron-59 in mixed sample, 20: 8580
performance of, for radiation detection in activation analysis, 20: 35767
performance of, for measuring beta activity in tritiated surface films, 20: 36738
performance of, for measurement of γ activity from potassium-40 in soils, 20: 39280
performance of, in field use, 18: 10402
performance of, in whole-body counters, 19: 9501
performance of, in radioisotope scanning, 19: 17764
performance of, in low-level gamma counters, 19: 28152
performance of, review of, 19: 38995 (NP-15259)
performance of, steep-rise method for analyzing, 20: 7435
performance of, using bundles of plastic scintillating fibers, for low-energy beta counting, 18: 22356
performance, reduction of errors, 16: 13440(T) (AEC-tr-4492(p.144-51))
performance, separation of gamma pulses from neutron pulses, 16: 24579
performance, temperature dependence, 16: 13307(T) (AEC-tr-5062)
performance, temperature effects on, 16: 20714
performance using liquid scintillation solutions, 17: 1185
performance with anticoincidence guard for cosmic-ray studies, 18: 14277
performance with light pipe, 17: 14697
performance with on-line computers for analyzing nuclear events, (E), 19: 46806
performance with photographic film in slow neutron flux measurement, 17: 3331
performance with pulse-height analyzer for gamma spectrometry, 18: 14250
performance with sonic spark chambers for proton detection at 20 Bev, (E), 19: 46800
phosphor selection for gamma, 20: 31574
phosphors for, preparation of silver-doped zinc sulfide, 20: 9260
photofraction of cylindrical thallium-activated sodium iodide, for 0.32- to 2.76-Mev gamma radiation, 17: 32415
photography of images produced in, 17: 30106
photography of light from, 17: 23665
photomultiplier amplification coefficients for, effects of load on, 19: 42755
photomultiplier current for, pulsed, 19: 30578
photomultiplier design and performance for use with, 20: 43746
photomultiplier efficiency in coincidence, 19: 815
photomultiplier fatigue in, effects of bremsstrahlung, 16: 5582
photomultiplier gain in thallium-activated sodium iodide, temperature dependence of, (E), 19: 28650
photomultiplier gain in, effect of source intensity variation on, 19: 44374 (AROD-3347:6)
photomultiplier performance with, for n-γ coincidence methods, 17: 34864
photomultiplier performance for use with fast, XP 1021, 20: 46075
photomultiplier socket assembly for organic, 20: 25422
photomultiplier tubes for, description of, 17: 32451
photomultiplier tubes for, using cesium potassium antimonide photocathode, (E), 19: 28653
photomultiplier tubes for, use of antimony–cesium cathodes in, 20: 33653
photomultipliers for, 17: 12573
photon reflection coatings for, preparation and properties of, 20: 21136
photopeak efficiencies of thallium-activated sodium iodide crystals, 17: 34262
photopeak efficiencies of thallium-activated sodium iodide, (E), 19: 44515
physical phenomena in, 18: 14226(T) (AEC-tr-6345)
plastic block 3-unit, design and performance for whole-body counting, 16: 16137
plastic, performance as gamma detectors for whole-body counters, 16: 16143
plastic, performance of for environs monitoring, 16: 16614
positron annihilation in, absorption of photon pairs from, 19: 792
power supplies for, engineering drawings of 600- to 1800-v, 17: 34305
preamplifiers for, design of, 19: 22757
precision and reliability of, effects of stability on, 19: 18274
preparation and performance of sandwiched plastic, 16: 2335
preparation and properties of boron-containing, for slow neutrons, 18: 7064
preparation and scintillation efficiency of plastic, for thermal neutrons, 16: 20717
preparation and scintillation efficiency of plastic, for thermal neutrons, 16: 33164(T) (AEC-tr-5401)
preparation for radon-222 determination, 20: 14881
preparation of, by deposition of zinc sulfide layer on plexiglas, 17: 4847
preparation of discs for, by compression, 17: 32406
preparation of vacuum-sealed liquid-phosphor, 20: 5785
properties and uses of liquid, 16: 24337
properties and uses, 18: 39641
properties as neutron detectors, 18: 31937
properties for alpha activity of fuel element surfaces, 18: 12459 (HW-78268)
properties for mean gamma energy determination, 18: 13595
properties in gamma- and x-ray dosimetry, 19: 30557
properties of glass-loaded liquid, 18: 13636(R) (ORNL-3537(p.71-105))
properties of, having thallium-activated sodium iodide crystals, 16: 33205
properties of large-volume liquid and plastic, 18: 2091
properties of liquid, for low-level beta counting, 17: 41292
properties of lithium-drifted germanium, 18: 20375
properties of organic, for fast neutrons, 20: 27307
properties of Plexiglas, for use in, 17: 16418 (BNL-6865)
properties of polystyrene, nuclear magnetic resonance study, 17: 30551
properties of total absorption, for 1- to 10-Bev particles, 17: 23681
properties of 4π beta and neutron, 18: 31939
properties of, review, 19: 28681
proton losses in plastic and sodium iodide scintillators in, (E), 19: 30567
pulse amplifiers and modifiers for, design of, 20: 5780
pulse amplifiers for, 20: 7393
pulse amplitude discriminators with tunnel diodes for, 18: 35864
pulse analyzers for, time-to-pulse height, 19: 13733 (NRS-23)
pulse analyzers for, pulse matching and resolution in, (T), 19: 13734 (NRS-25)
pulse analyzers for, time sorter linearity in, 19: 18312
pulse contours, method of recording, 16: 30181(R) (ANL-6474(p.14-21))
pulse discriminator for proton-recoil, design of fast zero-crossing, 20: 21114
pulse forms of scintillations of fluorescent liquids in, method of determining, 17: 16421 (CEA-2194)
pulse-height distributions in, use of Monte Carlo code for calculating, 16: 23006(R) (ORNL-3268(p.99-100))
pulse-height distribution asymmetry from, for monoenergetic x radiation, 17: 1778
pulse height distribution at output of, methods for calculating, 20: 29542
pulse height distribution from, evaluation of, 20: 31555
pulse-height response to gamma radiation, Monte Carlo calculation for determination, 16: 5497 (ORNL-3169)
pulse-height spectra analysis in, by gain scanning, 17: 14700
pulse height spectra in gamma spectrometers, analysis of, 19: 15899
pulse height spectra from, computer analysis for gamma, 20: 41292
pulse height variation in instruments using, 19: 18278
pulse initiation by preceding pulse in radioactivity measurements in, 19: 32562
pulse line width of, effects of integration time constant on, 17: 23774
pulse pile-up rejection circuitry for gamma spectrometers of, 20: 651 (EGG-1183-2055)
pulse properties in NaI(Tl) crystal, 16: 27342
pulse shape discrimination in background noise, optimum linear filter for, 16: 17841
pulse shape discrimination, survey, 16: 23913
pulse-shape discrimination circuits for, at high gamma background,

17: 29219
pulse shape discriminator for, 19: 18306
pulse shape discriminator design for zinc sulfide, 19: 44368 (AERE-M-833)
pulse shape discrimination in fast neutron dosimetry, 20: 29524 (CONF-651109, pp 647-52)
pulse shape discrimination for, 20: 31535
pulse spectra from gamma, computer analysis of, 18: 10377 (IKF-10)
pulse timing for, optimum filter for, 20: 13104
pulse yield relations for heavy ions in, 20: 21084
pulse-analyzer channel utilization in spectrometers using sodium iodide, 20: 25423
pulse-height analyzers for, fast single-channel, 19: 18329
pulse-height distributions from, unfolding of, (T), 19: 28732 (ORNL-3743)
pulse-height distribution from neutron capture and inelastic scattering, 20: 4999(R) (ORNL-2599)
pulse-height distribution unfolding in gamma, 20: 27313
pulse-height spectra of, analysis of, 18: 33925
pulse-height spectra transmission from, over large dynamic range, 19: 4436
pulse-shape determination by sampling individual photons, nanosecond, 18: 23978
pulse-shape discriminator for, for rejection of gamma events in fast neutron spectroscopy, transistorized, 18: 23994
pulse-shape discrimination for phototube noise pulse separation, 19: 18308
pulse-shape discriminator for dual-crystal Compton reduction, 20: 2167
pulse-shape discrimination in dual-crystal, for gamma radiation, 20: 14844 (AD-620395)
pulse-shape discrimination in organic, circuits for, 20: 16839
pulse-shape discrimination of, for cosmic ray studies, 20: 37111
pulses from cosmic ray, design and sensitivity of system for measuring amplitude of, 20: 43687
pulses from, photo-peak analysis program for, 20: 19014 (AD-616703)
quantum counting efficiency, 16: 7711
quenching corrections for, in counting of doubly labeled organic compounds, 19: 4067
quenching corrections for liquid, in sample counting, 19: 20332
quenching corrections for liquid, exponential function in, 20: 2168
quenching of liquid, use x and γ sources for, 18: 20352
quenching of, reduction of oxygen, 20: 18712
radiation background of sodium iodide, cosmic, 20: 11132
radiometric properties of, 20: 16865
research program on low-background liquid-solid, 17: 20350(R) (ORO-490)
resolution, 16: 23881
resolution, 16: 23915 (UCRL-9976)
resolution, effect of photomultiplier single-electron statistics and line shape on, 16: 30626
resolution, effects of dislocations, 16: 23882
resolution for spectrometry of soft x radiation, 18: 41872
resolution for 160-Mev protons, 17: 40436(R) (NYO-10063(p.105-15))
resolution in, theory of time, 19: 805
resolution of, corrections for, 18: 495 (ZFK-PHA-7)
resolution of, effects of photomultiplier electron noise on, 17: 25640
resolution of lead-sandwich shower, 20: 31587
resolution of neutron plastic-phosphor, 18: 41839
resolution of noble-liquid, 17: 32449
resolution of organic-phosphor beta spectrometers, corrections for, 20: 7400
resolution of sodium iodide (thallium activated) non-proportional effects on, 16: 27354
resolution of thallium-activated sodium iodide crystal for soft x and gamma radiation, 19: 36849
resolution of, determination of overall spatial, 19: 7807
resolution of, relations for time, 18: 30027
resolving time and stability, 16: 22928
resolving time of thallium-activated sodium iodide, nanosecond, 18: 23979
resolving time of, digital time-interval analyzer for, 19: 18328
resolving time of, in coincidence with lithium-drifted germanium detector, 20: 46079
response functions of gamma, 20: 5181(R) (ORNL-3029)
response of alpha, in gamma and neutron backgrounds, 20: 41271(R) (ORNL-3875, pp 44-52)
response of anthracene and terphenyl, to fast neutrons, (E), 20: 7158
response of Electron-2, to cosmic-ray nuclear component, 20: 23963
response of europium-activated lithium iodide, to neutrons, 18: 14269
response of gamma, Monte Carlo calculation of, 18: 30063
response of gas-filled low-pressure, to alpha particles in electric fields, 19: 28678
response of liquid helium, to alpha and beta particles, 19: 11571
response of neutron, sources for calibrating, 20: 35756 (LA-DC-7702)
response of organic, to fast neutrons, (T), 19: 38997 (UCRL-16149)
response of partially shielded, 16: 13305 (USNRDL-TR-543)
response of silver-activated zinc sulfide, to electrons, (E), 19: 44520
response of sodium iodide crystals to electrons and x rays, 20: 25373 (AD-631709)
response of thallium-activated sodium iodide crystals to gamma rays and electrons, nonproportional, 16: 20713
response of thallium-activated sodium iodide, to electrons, 18: 7042 (CONF-340-4)
response of, effects of fast neutrons on, 18: 18219
response of, formulas for, 18: 35881
response of, method for determining, 18: 18246(P)
response, statistical approach, 16: 3842(R) (ORNL-3193(p.44-52))
response theory of collimated, spatial, 16: 5508
response times in cadmium sulfide, 18: 2067
response to alpha particles and fission products, use of thallium-activated cesium iodide foils, 16: 20669
response to beta particles, corrections for, 19: 35615(R) (NP-15037)
response to electrons at 450 to 1450 Mev, 18: 10379 (LNF-63/54(p.8-15))
response to electron beams, 18: 32289
response to fast neutrons, 17: 34855
response to gamma radiation, energy dependence of, 18: 2034 (UCRL-10986)
response to high-energy cosmic particles, (T), 19: 18726
response to low-energy x radiation, equipment and methods for studying, 20: 21107
response to 150-Mev protons, measurement of ionization curves from, 20: 14891
responses to neutrons and photons at 0.1 to 14 Mev, (T), 19: 9495 (UCRL-12150)
review, 16: 23874
review, 16: 23942
review, 17: 8653
review, 18: 33967
review, 19: 830
review of solid, 17: 20600
sample changer for gamma-well, automatic, 18: 23873 (HW-80798)
sample changer for automatic gamma, design of, 19: 7808
sample changer for, automatic, 19: 7313
sample conveyor for, light-tight, 19: 24878(P)
sample handling and indexing for, 20: 43748(P)
scintillation absorption in long plastic, effective coefficient for, 20: 23503
scintillation decay times of naphthalene, 19: 13764
scintillation decay of organic phosphors in, at 0 to 100 nsec, (E), 20: 7157
scintillation intensity of thallium-doped sodium iodide crystal, angular dependence of, 20: 23502
scintillation mechanisms in helium-filled, 19: 18330
scintillation output of liquid, automatic quench determination for, 19: 2636
scintillation response and stopping power for electrons and positrons in thallium-activated sodium iodide, 19: 15914
sensitivity and origin of background in sodium iodide crystals, 16: 16135
sensitivity and resolution of collimators for medical scanning, 16: 22353
sensitivity for beta-emitting solutions, 18: 29967 (AERE-R-4638)
sensitivity for neutrons, 18: 486(R) (AD-297107)
sensitivity improvement by efficient light collection, 16: 24578
sensitivity of, for evaluation of biological radiation damage, 17: 18614
sensitivity of, for oceanography studies, 20: 16828 (TID-22763)
shielding for, silver-110 contamination in lead, 20: 33708
signal amplitudes from, temperature effects on, 19: 34574
spectra from, computer program for analysis of, 20: 16344
spectra from, construction of sum, 19: 812
stability of, circuit for improving, 20: 31575
stabilization, 19: 22756
stabilization circuits for, 18: 499
stabilization circuits for, 18: 33934
stabilization in gamma spectrometers, device for, 18: 18216
stabilization of gain of gamma spectrometers using, electronics design for, (E), 20: 7410
stabilization system for sodium iodide, design of, 20: 7358(R) (EGG-1183-2057)
stabilizer for, design of automatic gain, 19: 11553
standardization of liquid, method for external, 20: 37085
standards for, dispersion for addition of internal, 20: 16834
standards in heterogeneous counting with internal, 17: 40499
support in thyroid radioiodine uptake studies, construction of trolley for, 17: 6213
survey of, using gaseous scintillators, 18: 41811
telemetering systems for balloon-borne, pulse-height, 19: 13763

temperature effect compensation in, 18: 23964
temperature effects on counting-rate of, determination of, 19: 4522
testing of cerium-activated glass as, 17: 4806 (HW-SA-2191)
testing of remote-use γ-detection instrument, 16: 1935 (AFSWC-TN-61-5)
time-delay spectrum of coincidence pairs in, analytic expression for, 16: 30571 (BNL-4950)
time resolution, 17: 18636
time resolution in, 16: 27353
time resolution limits, 19: 782 (SGAE-PH-5/1964)
time resolution of sodium iodide, for gamma rays, 19: 26699
time resolution reduction in, for fast neutron energy measurements, 17: 34254
time resolution using thallium-activated sodium iodide, 20: 23456(R) (ANL-7108, pp 5-16)
time resolution using thallium-activated sodium iodide crystals, 20: 33662
timing coincidence, light-pulse system design for, 16: 31888
use as spectrometers in space, 16: 23928
use for aerial surveying, 19: 788 (USAELRDL-TR-2397)
use for charged-particle and gamma spectrometry, 20: 35798
use for contour brain scanning with iodine-131-labeled serum albumin, 19: 34062
use for counting β activity in biological materials, 20: 16177
use for counting root uptake of radioactivity, 18: 41056
use for CP-5 reactor fuel quality evaluation, 20: 1533 (CONF-650532-2)
use for detecting thyroid diseases, 19: 5743
use for detection of gamma radiation from isotopes deposited in glands or organs, by external scanning, 20: 5447
use for determining human calcium-47 uptake, 18: 23226
use for determining calcium-47 and scandium-47 retention, 19: 6927
use for diagnosis of heart diseases, 19: 5748
use for dosimetry in nuclear catastrophes, 20: 35786
use for environmental gamma measurement, (E), 19: 22692 (HASL-150)
use for external scanning of children, after injection of radioisotopes, 20: 6947
use for extracorporeal monitoring of circulating blood, design of shielded coil for, 20: 38558
use for gamma angular correlation measurements, correction factors for, 19: 9482 (NASA-TN-D-2549)
use for gamma counting, 20: 11201(R) (NYO-3136-2)
use for gamma counting, 20: 11204(R) (NYO-3136-2, App. 3)
use for high-energy-particle registration, 18: 39691
use for linear and logarithmic radiation monitoring, 19: 24842 (HW-63247)
use for low-level plutonium determination, comparison of autoradiography with, 20: 3877 (LA-DC-7483)
use for measurement of gastrointestinal absorption of cobalt-58-labeled vitamin B_{12}, 18: 15799
use for measuring iodine-131 in rat thyroid gland, 20: 16179
use for monitoring fuel element failure, 18: 1206(P)
use for radioactivity measurements of uranium mine dust, 18: 18126
use for screening for unilateral renal hypertension, 17: 35367
use for simultaneous glycolysis and phosphate transport studies, 18: 11579
use for whole-body counting in humans, 16: 4313 (A/AC.82/G/L.692)
use for whole-body measurements of strontium-90 in man, 20: 16303(R) (AD-626384)
use for whole-body counting of calcium-47 and strontium-85 in bone metabolism studies, 20: 42744(R) (UCRL-16246, pp 19-35)
use for whole-body measurements of plutonium in dogs and rats, 20: 9166(R) (BNWL-36, pp 2.1-58)
use in absolute beta measurement in layered preparations, 18: 33659
use in absolute determination of gamma background, 20: 35743 (CLOR-46/D)
use in aerial prospecting for radioactive minerals, 16: 20822
use in aerial surveys for determination of potassium, radium, and thorium in rocks, 16: 33281
use in angular-correlation polarimeter for study of gamma-gamma cascades, 17: 32400 (KFK-129)
use in beta-decay measurements, 19: 26694
use in beta-particle measurements, 20: 2180(P)
use in bone density gamma radiography, 20: 43049
use in boundary localization between radioactive and inactive solutions, 19: 13715
use in burst slug detection system in reactors, 18: 1204(P)
use in burst slug detection system in reactors, 18: 1205(P)
use in calibration and standardization of gamma sources, 17: 6822
use in cameras, for radiodiagnosis, 20: 25389 (UCRL-16724)
use in carbon-14 determination, 18: 25293
use in chemistry, 20: 33649
use in clinical medicine, conference on, 19: 5739
use in comparing human body weight and motor aptitude, 18: 31078
use in cosmic-ray detection, (T), 19: 18281
use in counting doubly labeled samples, 18: 2092
use in counting tritiated thymidine transferred to females by labeled Drosophila males, 20: 40625(R) (ORNL-3922, pp 59-64)
use in detecting bone metastases, 19: 5745
use in determination of small amounts of radium-226, 19: 9092
use in determination of radioisotopes in biomedical samples, 19: 43659
use in determining amount of characteristic radiation in continuous spectra of x-ray beam, 16: 19677 (TID-15698)
use in determining mass of charged particles, 16: 33730
use in determining decay rate of carbon-14-labeled compounds, 17: 27453
use in determining isotope gamma activity, 18: 18187
use in determining human potassium-40 burden, 18: 31948
use in determining transmutation of carbon-14-labeled fructose in liver, 20: 3684
use in determining activity of technetium-99m and iodine-125, 20: 40547
use in diagnosing parathyroid tumors, 19: 5744
use in diagnosing pulmonary embolism, 19: 5750
use in diagnosing pulmonary infarcts in dogs, 19: 5751
use in diagnosis of intracranial tumors, 19: 5754
use in diagnosis of renal diseases, 19: 5756
use in diagnostic x-ray dosimetry, 19: 46858
use in extended-source gamma spectroscopy, 18: 1942 (CEA-2231)
use in gamma spectrometers, 18: 39650
use in helicopter signaling system, 20: 41221(R) (COO-1471-1)
use in helium-3-neutron coincidence system, 19: 15893
use in high-level whole-body counter, 18: 33937
use in iron-55 and iron-59 simultaneous assay, 18: 21978
use in liver scanning, 19: 5753
use in liver scanning, 16: 25100
use in localizing functioning bone marrow, 20: 45523
use in measurements on beta backscattering, 19: 16959
use in measurement of collimated radiations, 19: 22722
use in measurement of carbon-14 and tritium, 19: 28420(R) (NP-14825)
use in measurement of alpha contaminated surfaces, 19: 39045(P)
use in measuring activity of iodine-125, 20: 46068
use in measuring slowing-down time of neutrons to cadmium edge, 18: 21148
use in measuring sediment density and concentration, 20: 41156
use in measuring time intervals, problems in, 16: 1956
use in medical diagnosis, design of pulse analyzer for suppressing background during, 20: 41318
use in medical radiodiagnosis, review, 20: 20531
use in medical scanning, phantoms for determining parameters in, 19: 5742
use in medicine, development and future of, 19: 5757
use in metabolism studies, techniques for, 19: 36848
use in monitoring gamma emitters in PRTR effluent, 18: 8606(R) (HW-78388(p.7.1-10))
use in monitoring of surface contamination by beta-emitting isotopes, 20: 23467(T) (AEC-tr-6466/1, pp 135-7)
use in multidimensional gamma spectrometer, 19: 36229 (BNWL-SA-137)
use in myocardial scanning, 19: 5747
use in neutron dose rate measurements over broad energy range, 19: 4465 (NP-14358)
use in neutron dosimetry, 20: 43671 (ORNL-P-2467)
use in pancreas scanning, 19: 5746
use in plasma jet density diagnostics, (E), 19: 5300(T) (AEC-tr-6518 (p.241-7))
use in plasmoid electron measurements, (E), 19: 5299(T) (AEC-tr-6518 (p.235-40))
use in probes for moisture measurements, 17: 30867
use in proton scattering polarization analysis, 18: 20383
use in radiation quality control of manufactured articles, 16: 13484(T) (AEC-tr-4492(p.362-8))
use in radiocarbon dating, 17: 14656
use in radiochemistry, 20: 9038
use in radiodiagnosis, 18: 9949
use in radiodiagnosis and research, 19: 7236
use in radiodiagnosis, clinical evaluation of, 19: 26213
use in radiodiagnosis, comparison of 8 inch with 3 inch crystal, 20: 40779
use in radiodiagnosis, radioisotope scanning, information capacity of, 19: 36838
use in radiodiagnosis, practical and theoretical aspects of, 18: 21940
use in radiography, 20: 41116(P)
use in remote control of several cranes, 19: 11330 (SGAE-IB/IA-4/1964)
use in renal scanning, 19: 5755
use in renography for kidney function studies, 20: 40775(T)
use in roentgen fluorescence analysis, 18: 12016
use in scanning Neohydrin labeled with mercury-197 or -203 or albumin labeled with iodine-131, 19: 22051

use in soft x-ray spectrometer, 19: 34476 (IPP-1/32)
use in spleen scanning, methods for, 19: 5752
use in testing reactor fuel elements for uranium-235 distribution, 17: 29085 (TID-17097)
use in toroid-sector type beta spectrometers, 16: 5520
use in two-crystal x-ray pair spectrometers, 18: 7075
use in void fraction detection in potassium flow, 20: 41111
use in x-ray fluorescence analysis of uranium solutions, 19: 36324
use of alpha scintillation chambers for determination of radium isotopes by the emanation method, 16: 22339
use of car-mounted, in natural radioactivity survey in Japan, 20: 45894
use of car-mounted, in natural radioactivity survey in Japan, 20: 45895
use of car-mounted, in natural radioactivity survey in Japan, 20: 45896
use of car-mounted, in natural radioactivity survey in Japan, 20: 45897
use of color scheme for beta-gamma discrimination, 17: 27704
use of continuous-flow column, for beta emitters in solution, 17: 6446
use of dimethyl sulfoxide in, 20: 9278
use of dual-probe, for placenta localization using iodine-131, 20: 20527
use of, for detection of pericardial effusion of heart, 17: 15582
use of gas-filled, for electron diffusion and recombination measurements, 18: 10789
use of image intensifier system with, 16: 20720
use of, in diagnosis of thyroid diseases, 17: 19754
use of internal liquid, for calibration of beta sources, 19: 15369
use of large-volume liquid, in radioisotope identification, 18: 1769
use of liquid-benzene, for naturally occurring carbon-14 counting, 17: 23280
use of liquid coincidence, in determination of barium-137, 18: 19891
use of liquid, for absolute activity measurements, 17: 10966
use of liquid, for simultaneous carbon-14–tritium counting, 17: 16457
use of liquid, for counting carbon-14, 17: 18481
use of liquid, for determination of sulfur-35 in biological materials, 17: 18482
use of liquid, for counting of carbon-14-labeled paper chromatograms, 17: 18483
use of liquid, for counting tritium in suspended materials, 17: 18480
use of liquid, for assay of radioactive paper chromatographs, 17: 27275
use of liquid, in absolute beta activity measurements, 17: 14662
use of liquid, in whole-body radioactivity measurements, 18: 4949
use of liquid scintillation, in determination of tritium, 18: 19890
use of liquid, for determination of tritium in form of hydrocarbon and water, 18: 25301
use of liquid, for biological and medical research, 18: 33220
use of liquid, for counting high-energy beta-emitters, 19: 10722
use of liquid, for measuring carbon-14-labeled carbon dioxide, 20: 18999
use of liquid, for low-energy beta particles, 20: 27343
use of liquid, for urinary tritium measurements, 20: 45983
use of liquid, in radiometric tool wear studies, 19: 9472 (AD-602717)
use of liquid, in tritiated blood plasma studies, 19: 17740
use of liquid, in neutron spectrometers, 20: 4249 (UCRL-16311)
use of plastic, in cosmic-meson monitors, 19: 28643
use of plastic, in thyroid carcinoma therapy, 20: 19084
use of scintillating fiber bundles for low energy beta counting, 16: 31811 (ARF-1192-6)
use of sodium iodide (thallium), for high-energy gamma detection, 20: 35746 (IEA-108)
use of thallium-activated, in measuring scandium-47 in samples containing calcium-47, 19: 7612
use of thallium-activated sodium iodide, in detection and measurement of low-energy gamma radiation, 20: 33661
use of thallium-activated sodium iodide, in multidimensional gamma spectrometers, 20: 33714
use of whole-body liquid, in pharmacological studies, 17: 18486
use of 4π, for absolute activity measurement of beta sources, 18: 33946
use of, factors affecting clinical, 19: 5740
use of, in scanning thyroid gland for iodine-131 deposition, 18: 27252
use to measure radioactivity of atomic cloud from SULKY cratering experiment, 20: 25232 (PNE-701F)
use to obtain starting pulses for time-of-flight measurements, 20: 31579
use with attachments to provide Polaroid color scanning of placenta, 20: 35371
use with image intensifier in beam profile detector, 16: 10191 (PPAD-435D)
use with light pipes in radiometric instruments, 18: 33850(T) (AEC-tr-6399(p.163-72))
use with magnetic analyzers, for charged particles, 20: 16859
use with neutron sources in moisture gages, 17: 29887
use with photographic film for fast neutron dosimetry, 20: 16861
uses and instrumentation for, review of, 20: 43096
uses for Compton spectroscopy of gamma radiation, 20: 5775
uses for counting sulfur-35-labeled hydrogen sulfide from radiolysis of labeled thiosulfates, 19: 17818
uses for detecting helium-5 energy levels from neutron-helium scattering, (E), 20: 6335
uses for determination of thyroid volume, 17: 30011
uses for determination of soft-beta-emitting radioisotopes, 18: 41340
uses for determination of radioisotopes, preparation of samples for, 19: 24461
uses for neutron dosimetry, (E), 19: 22697 (JUL-213-ST)
uses for radioactivity counting of tritium-labeled nucleic acids, 19: 9072
uses for whole-body counting in radiodiagnosis, 19: 269
uses for whole-body counting in clinical studies, 19: 31692
uses in beta-gamma coincidence method for absolute counting of radioisotopes, 19: 30305
uses in betatron gammascopy, 16: 13483(T) (AEC-tr-4492(p.357-61))
uses in color scanner for radiation dosimetry, 19: 46819
uses in detecting leaks in fuel element cans, 19: 21626(P)
uses in determination of radioactivity of labeled carbon dioxide, diffusion apparatus, 18: 27314
uses in determination of colored carbon-14-labeled nitro compounds, 19: 9088
uses in determination of tritium, 19: 22138
uses in determining absolute activity of weak beta emitters, 18: 29988
uses in gamma detection, reduction of Compton distribution in, 18: 39647
uses in *in vivo* determination of phosphorus-32, 19: 26(R) (HW-81746 (p.2.12-16))
uses in luciferin-luciferase determination of adenosine triphosphate, 19: 7295
uses in magnetic short-lens spectrometer, 18: 39640
uses in measurement of thorium and uranium content of rocks, 19: 7724
uses in measurement of soft beta emitters, 20: 29084
uses in medicine, review of, 20: 5487
uses in photoscanner for image of distribution of radioactive materials in spatial unit, 19: 844(P)
uses in portable dosimeter for intermediate neutrons, 19: 30577
uses in preparation of oscillographs of geometric deposition of radioisotopes, 19: 4533(P)
uses in radiometric equipment to control distances between loading cranes, 19: 22834
uses in scattering chambers, (E), 19: 40907
uses in spectrometry of dual-labeled samples, computer program for data analysis in, 20: 31177
uses in tracer studies of pancreatic lipase activity, 19: 14964
uses in well logging, 19: 7722(P)
utilization in nuclear technology, 17: 41304
vacuum chambers for, design of, (E), 20: 7415
voltage supply for, design of stable high, 17: 11022

Scintillators
see Phosphors

Scintillogs
see Radiation Detection Instruments (Ion Current Type)

Scooter Project
see Plowshare Project

SCOTLAND
age estimation of igneous rocks from Assynt and Scourie areas in, isotopic, 19: 6115
age estimation of tertiary igneous rocks on Isle of Skye in northwest, 19: 36683
environs monitoring of Hunterston reactor environment, pre-operational, 18: 8249
environs monitoring of Hunterston reactor area, 18: 8250
radiation dose rates in Aberdeen, Dundee, and Edinburgh, environmental 18: 35750
radiobiological research in Edinburgh, 19: 33823
rocks in, estimation of ages of, 20: 37016
silt movement in ebb channel, Firth of Forth, 20: 11022 (AERE-R-5080)
strontium-86 and -87 and rubidium-87 content in granophyre and tertiary granite from Skye, 19: 4365
strontium-90 content in human bones in, 20: 18922

SCOTT-R
see Supercritical Once-Thru Tube Reactor

SCREENING
see also Particles

SCREENS
(Including sieves.)
see also Filters
design of fluorescent, for ZGS beam diagnostics, 20: 27671
development and use of intensifying, for reducing radiation dose in radiography, 20: 33130
effects of sorptive properties of, on hydrogen yields in beta radiolysis of water, 20: 45714(R) (ORNL-3945, pp 218-20)
efficiency for water entrainment removal by, method of predicting, 16: 26470 (KAPL-2000-18)
fabrication of lead, for use with reactor cores, 20: 10314(P)
iodine retention on silver-plated copper, 20: 43067(R) (IDO-14679,

pp 6-46)
performance testing of sieve trays for GS heavy water process, 20: 37160 (DP-1025)
properties of wire gauze, flow friction, geometric, and heat transfer, 20: 35624(R) (TUBIK-1, pp 34-72)
radiation effects on electroluminescent, 16: 22248
radiation protection, calculations for, 20: 35347
testing capacity of, in heavy water production plant, 18: 23137(R) (DPST-64-83-3)
trays, capacity testing of, 18: 15537(R) (SRO-99)
use in cylindrical beta counters, 20: 31536
use of kryptonated molecular, for determining water in organic liquids, 20: 18570(R) (NYO-2757-5)
use of reinforcing, for diminution of x-ray dose and image intensification in radiodiagnosis, 17: 25487
Screw-Dynamic Pinch
see Pinch Devices
SCRUBBERS
see also Extraction Apparatus
see also Spray Columns
condensate removal system for gas fields, design of radiometric, 20: 23549(T) (AEC-tr-6466/1, pp 256-9)
design and development of wet cyclone, for collection of carbon black, 20: 16740(R) (UCRL-14534, pp 50-3)
design and instrumentation, 16: 14815(R) (EURAEC-23)
design and tests of dry, for cave facilities, 17: 39224 (UCRL-10953)
design for facility for separation of plutonium from leachable residues, 19: 20083
design for processing reactor coolant water, 20: 26406
design for removal of halogen-acid off-gases, 17: 5648
design of dry, for use in air conditioning systems of facilities for separation of transcurium elements, engineering drawings for, 17: 39232
development for ruthenium tetroxide in air, 18: 34006(R) (ORNL-TM-889)
development of liquid-jet fume for off-gas in calcination of wastes, 16: 29247 (TID-7627(p.557-80))
for removal of radioiodine, 16: 11342(R) (EURAEC-83)
for removal of radioiodine, 16: 17332(R) (EURAEC-25)
for removal of radioiodine, 16: 26636(R) (EURAEC-84)
performance of BEPO, for iodine removal, 17: 15491 (AERE-M-1163)
performance of electrostatic bubble, 17: 37003(R) (HW-78118)
testing electrostatic, 18: 8445(R) (HW-78388(p.4.1-15))
tests with incinerator for combustion of plutonium wastes, 18: 3386 (HW-68788)
use in gas purification system in plutonium-processing facility, 20: 25199(T) (ORNL-tr-1121)
SCRUGHAM PEAK QUADRANGLE (NEV.)
geologic map, 18: 35704 (TEI-849)
geologic map of, 17: 4724
SCRUP Process
see Purex Process
Scylla
see Magnetic Mirror Machines
Scyllac (Scylla-closed) Theta Pinch
see Pinch Devices
SDR Reactor (Alaska)
see Chugach Power Reactor
SEA URCHINS
analysis for potassium and sodium in eggs of, activation, 19: 32103
calcium metabolism, tracer study, 17: 33604
carbon isotope variations in, 20: 36549
carbon isotopic variations in, environmental and genetic factors, 20: 36550
deuterium effects on hydrostatic pressure sensitivity in, 19: 27929
development of, effects of adenosine nucleotides on, 18: 33270(R) (NIRS-2(p.23-6))
effects of actinomycin D and heavy water on macromolecule synthesis in developing eggs of, 19: 43709
effects of deuterium oxide on mitosis in eggs of, effects of pressure and temperature on, 20: 32917
egg cleavage in, effects of heat on, 18: 11674
embryology of, 19: 33686 (CALT-51-3)
enzyme synthesis in embryo of, during development, 20: 8508(R) (EUR-2589.e)
heavy water effects on morphology of eggs, 17: 26975
metabolism of nucleic acids and proteins in anucleate and nucleate eggs of, 20: 8508(R) (EUR-2589.e)
metabolism of radionuclides by, 19: 43669(R) (NP-15159)
mitosis in eggs of, effects of deuterium oxide and hydrostatic pressure on, 19: 35996
nucleic acids in embryos of, methods for analysis and separation of, 20: 8508(R) (EUR-2589.e)
ovarian phagocytes of, intranuclear crystals in, 19: 31675(R) (ORNL-3768(p.70-84))
oxygen isotope variations in, 20: 36549
oxygen isotopic variations in, environmental and genetic factors, 20: 36550
parthenogenesis of unfertilized eggs of, by heavy water, 16: 28707
phosphorus-32 uptake by eggs of, 18: 27042
photoreactivating enzyme in eggs, 20: 40543
photoreactivation in gametes and zygotes of sand dollar, 16: 17364
potassium content of eggs of, 18: 21801
potassium content and transport in eggs of, 17: 33503
protein synthesis in eggs of, during deuterium parthenogenesis, 18: 24
radiation effects on mitosis in eggs of, 18: 9835 (UCRL-10979)
radiation effects on sperm of, 18: 23339
radiation effects on zygote cell division in, gamma, 19: 19496(R) (ANL-6938(p.49-56))
radiation effects on egg development in, gamma, 19: 31670(R) (NIRS-3(p.19-56))
radiation effects on egg development in, beta, 19: 31670(R) (NIRS-3(p.19-56))
radiation effects on morphogenesis in, ultraviolet, 19: 45840
radiation effects on sulfhydryl groups in eggs of, thermal and uv, 20: 12624
radiation effects on protein synthesis in eggs of, 20: 16160 (UCRL-14739(Pt.2))
radiation effects on eggs of, effects of AET on x, 20: 40619(R) (NYO-2740-3, pp 216-57)
radiation effects on egg cleavage in, uv, 18: 11674
radiation injuries of eggs of, protective effects of aminoethylisothiuronium, 19: 28116
radioinduced cleavage delay in *Arbacia punctulata* eggs, *in vitro* and *in vivo* recovery of, 17: 1324
radioinduced cleavage delay in gametes in *Arbacia punctulata*, recovery from, 17: 5895
radioinduced mitosis delay in, mechanisms for, 20: 6861
RNA synthesis in embryos of, 19: 31675(R) (ORNL-3768(p.70-84))
RNA synthesis in eggs of, during deuterium parthenogenesis, 18: 24
sodium content and transport in eggs of, 17: 33503
sodium content of eggs of, 18: 21801
SEA WATER
age of, tracer study, 20: 18934
alkaline earth separation from, 19: 5569(R) (MIT-2098-64)
ammonia content, 16: 4030 (TID-12946(App.I,Vol.II))
analysis and sampling of Israel-shore, 20: 2520(R) (IA-920)
analysis for barium, cesium, and rubidium content and distribution, activation, 18: 41329
analysis for barium and strontium, flame photometric, 20: 22871(R) (MIT-905-52, pp 42-73)
analysis for beryllium, spectrophotometric, 18: 1546
analysis for bromine in sediments in, activation, 20: 40811 (ORO-2670-13)
analysis for calcium-48/calcium ratio, activation, 18: 8529
analysis for calcium, use of calcium-45 as tracer in, 20: 3902
analysis for carbon dioxide and salts, 20: 40523(R) (RLO-1750-8(Vol.I))
analysis for cerium-144, cesium-137, and strontium-90, radiochemical, 18: 8287(T) (AEC-tr-6049(p.47-74))
analysis for cerium-141 and -144, method for, 19: 2228
analysis for cerium-144, cesium-137, cobalt-60, plutonium-144, and strontium-90, method for, 20: 35405
analysis for cesium-137 and strontium-90, 16: 4132 (CNI-93)
analysis for cesium-137 and strontium-90, radiochemical, 16: 7760
analysis for cesium-137, 17: 14168
analysis for cesium-137, 17: 37156
analysis for cesium-132 using ammonium molybdophosphate, gamma spectrometric, 18: 187
analysis for cesium by ammonium phosphomolybdate adsorption-flame photometry method, 18: 13633(R) (ORNL-3537(p.60-4))
analysis for cesium, 18: 13668
analysis for cesium-137 and strontium-90, method for, 19: 36724
analysis for cesium-137, large-volume, 19: 44296 (NYO-4700(Rev.) (Suppl.II))
analysis for cesium-137 by ion exchange and gamma spectroscopy, 20: 16342
analysis for cesium-137 and strontium-90, radiometric, 20: 18592
analysis for cesium-137, 20: 23305
analysis for cesium by flame photometry, use of permanganate as precipitant in, 20: 24972 (AD-632283)
analysis for cesium-137 and trace elements by activation and gamma spectrometry, 20: 43059 (BNWL-SA-674)
analysis for chlorine and sodium, activation, 19: 10983(R) (TEES-2671-3)
analysis for chlorine, chlorophyll, dissolved oxygen, inorganic nutrients, and silicates, methods for, 20: 28877 (NYO-1918-124)
analysis for cobalt, potassium, and uranium, 19: 22543
analysis for copper, manganese, and copper, activation, 20: 18576(R)

(TID-22660)
analysis for copper, manganese, and zinc, activation, 20: 43085(R) (TID-23295, Sect.2)
analysis for dissolved oxygen, radiometric, 19: 17782 (ORO-592)
analysis for dissolved oxygen, thallium-204 beta source and Geiger-Mueller counter for use in, 20: 31171 (ORO-596)
analysis for fall-out fission products, 16: 6643 (DASA-1300(Vol.4))
analysis for fallout radioactivity, radiochemical, 18: 8281 (NYO-4700 (Rev.))
analysis for fallout fission products in, 19: 9367 (IAEA-R-1)
analysis for fission products, methods for, 17: 21464
analysis for fission products and trace elements, 18: 19837(R) (MIT-905-1)
analysis for fission products, methods for, 20: 1749 (USNRDL-TR-912)
analysis for gold by neutron activation methods, 19: 5788
analysis for manganese, iron, and zinc in Chesapeake Bay, 16: 14998(R) (NYO-8100)
analysis for manganese and zinc, activation, 17: 4469
analysis for mixed fission products in Ligurian, method for, 19: 19790
analysis for nickel-63, liquid scintillation method for, 20: 12779 (USNRDL-TR-924)
analysis for niobium-95 and zirconium-95, spectrographic, 17: 32005
analysis for nuclear explosion debris, radiochemical, 19: 24716
analysis for oxygen, radiometric, 16: 24577
analysis for phosphorus-32, radiochemical, 16: 22500 (NS-7)
analysis for plutonium using cupferron, 16: 17605
analysis for plutonium, 18: 39108
analysis for radioactivity from fallout fission products, 17: 30766
analysis for radioisotopes, development of method for, 17: 40748
analysis for radioactivity in France, 18: 16204(R) (SCPRI(RM)-XII-1963)
analysis for radioruthenium by ion exchange on ferric hydroxide resin, 18: 33449(R) (NIRS-2(p.15-19))
analysis for radioactivity, 19: 4076
analysis for radium in France, 16: 31966
analysis for radium, 19: 9080
analysis for radium-226, method for shipboard, 20: 7259(R) (TID-22411, App.D)
analysis for rare gases, mass spectrometric, 19: 2247
analysis for rare earth elements by cation exchange, 20: 43087(R) (TID-23295, Sect.4)
analysis for residual chlorine, spectrophotometric, 16: 31562
analysis for rubidium, strontium, and uranium, isotope dilution, 18: 1547
analysis for rubidium by direct flame photometry and mass spectrometry, 19: 28241
analysis for ruthenium, activation, 20: 43086(R) (TID-23295, Sect.3)
analysis for scandium, spectrophotometric, 17: 33829
analysis for silver using thionalid, 16: 12961 (USNRDL-TR-551)
analysis for stable strontium, activation, 20: 25007
analysis for strontium-90, method for, 16: 26935
analysis for strontium, spectrophotometric, 18: 29574
analysis for strontium-90, large-volume, 19: 44296 (NYO-4700(Rev.) (Suppl.II))
analysis for strontium-90 by precipitation with manganese dioxide, 20: 24973 (AD-632528)
analysis for sulfur-35, method for, 19: 40431
analysis for tantalum, activation, 17: 40749
analysis for thorium, spectrophotometric, 16: 26927
analysis for tin traces, activation, 18: 21963
analysis for titanium, polarographic, 20: 14455(R) (ORNL-3889, pp 25-32)
analysis for trace elements, 18: 21712(R) (NYO-10065)
analysis for trace elements, 18: 43790(R) (TID-21137)
analysis for trace elements by solvent extraction and spectrography, 19: 28253
analysis for trace elements, spectroscopic, 19: 36315
analysis for trace amounts of uranium by controlled-potential polarography, 20: 16389
analysis for trace elements, activation, 20: 40834
analysis for trace elements, activation, 20: 45880(R) (YALE-2912-12)
analysis for tritium in New Zealand, 1956 to 1960, 16: 16078
analysis for tritium, in northern Europe, 1957 to 1962, 16: 25619(R) (TID-16272)
analysis for uranium, fluorometric, 19: 30085(R) (TID-21853)
analysis for uranium by ion exchange separation and fluorimetry, 19: 46223
analysis for uranium, luminescent method for, 20: 33523
analysis for vitamin B_{12}, microbiological, 18: 19486(R) (TID-20433)
analysis for yttrium-90, method for, 20: 43688
analysis for zirconium, fluorimetric, 18: 43406
analysis for zirconium and zirconium-95, spectrophotometric, 20: 43088(R) (TID-23295, Sect.5)
analysis for 18 trace elements by activation methods, 19: 22574
analysis in Long Island Sound and Antarctic region, 18: 43790(R) (TID-21137)
analysis of Copenhagen harbor specimens of, for strontium-90, 17: 12498 (RISO-51)
analysis of, for radioactive materials in Germany, 16: 32721
analysis of, for strontium, spectrometric, 17: 17990
analysis of north Atlantic, for strontium isotopes, 18: 3984(R) (NYO-10517(p.39-42))
analysis of silt-containing, for radionuclides, gamma-spectrometric, 16: 20323 (PG-Report-312)
analysis of, for dissolved organic carbon, 18: 17382(R) (NYO-3140-1A)
bacteria in, studies on, 20: 16175(R) (RT/BIO(65)-1)
beta activity of, in Italy, 1962, 18: 18040 (BIO/03/63)
biological conditions in North Sea, 18: 17334 (NP-13756(Vol.I))
book: *Advances in Water Pollution Research*, Vol. 1, 2, and 3, 20: 20982
boron content in silt solutions in, 17: 3175
boron isotopic abundances in, 17: 36553
buoy dynamics in, submerged, (T), 20: 6686(R) (NVO-98-12)
calcium content in, around Egypt, 16: 4020 (A/AC.82/G/L.665)
calcium content of, effects on uptake of strontium-90 by fish, 20: 24836 (AE-224)
calcium-to-strontium ratio in, effects of morphological form on, 20: 43534
carbon distribution in, mixing rates and residence times of radioactive, 18: 12361
carbon-12/14 content in surface, ratio of, 17: 25464
carbon-14 content in subsurface samples from Caribbean, 16: 22411 (TID-15914)
carbon-14 activity in New Zealand, interpretation of, 19: 20238
carbon-14 content in, 19: 32419
carbon-14 content in, 19: 44267
carbon-14 content of, 19: 32437
carbon-14 content and distribution in, 1963 to 1966, 20: 31397(R) (RLO-1776-2)
carbon-14 content of, methods for determining, 20: 31433
carbon-14 content of deep and surface, of north Indian Ocean, 20: 41127
carbon-14 content, vertical mixing anomaly from, 17: 25465
carbon-14 distribution in, 19: 28420(R) (NP-14825)
carbon-14 separation from, 20: 18934
carbonate formation by marine mollusks and bacteria in, 18: 19520(R) (TID-20499)
cesium-137 content in, determination of, by estimation from content in marine organisms, 16: 17900
cesium-137 content off Cape of Good Hope, Aug. and Sept. 1961, 16: 18756
cesium-137 content in Osaka Bay, Japan, 16: 20123
cesium-137 content in Osaka Bay, Japan, 17: 7775
cesium-137 and strontium-90 vertical distribution in, 20: 27153
cesium-137 content, vertical mixing anomaly from, 17: 25465
cesium-137 content to 5,000 m in Western North Pacific, 16: 5551 (A/AC.82/G/L.697)
cesium-137 distribution in, sampling method for measuring, 20: 39147 (CONF-660401-6)
cesium-137 precipitation from, 17: 30726
characteristics of Niantic Bay, Rhode Island, 18: 45192(R) (TID-21157)
chemical composition of, 19: 24258
chemical composition of sediments of Bay of Roquebrune, 20: 36553
chemical properties of, effects of depth and temperature on, 20: 40523(R) (RLO-1750-8(Vol.1))
chemical reactions in, 20: 18633 (NYO-3450-1, pp 203-11)
chemistry and plankton distribution in, 16: 9745(R) (TID-14965)
chemistry and plankton distribution between Woods Hole, Mass. and Bermuda, 16: 9746(R) (TID-14965(Appl.))
chemistry of Sargasso Sea, 16: 4030 (TID-12946(App.I,Vol.II))
chemistry of, research on, 19: 31696
chromium-51 in, uptake by clams of, 20: 40575
chromium-51 uptake by particles in, 19: 10767
circulation of, methods for studying, 17: 8390(R) (TID-16991)
collection, storage, and analysis of, method for, 17: 23259 (USNRDL-TR-637)
contamination by accidents at IRR-1, estimates of, 19: 39265(R) (IA-1021)
contamination by radioactive waste of, 19: 24809
contamination by radioactive wastes, 19: 27837
contamination by waste disposal, effects on human and marine life and problems in, 16: 17921
contamination by waste from nuclear ships, 20: 23396
contamination of, by fallout, pollution, and waste disposal, effects on marine life in, 17: 15526
contamination of Irish Sea near Windscale, 17: 24737
contamination of northern Pacific, by radioactive waste, 19: 27838
contamination of, around Japan 1957 to 1961, 18: 11503
contamination of, by radioactive waste, 18: 14145
content of trace elements in, effects of removal, supply, and transport mechanisms on, 20: 18892 (NYO-3450-1, pp 41-89)

corrosive effects on chromium–iron–nickel alloys at 550°F, 17: 27749 (KAPL-M-CC-3)
corrosive effects on magnesium alloys, 19: 6271(T) (JPRS-27451)
corrosive effects on concrete reinforcements, 19: 30676(T) (ORNL-tr-515)
corrosive effects on molybdenum and tungsten coupled with aluminum, copper, or magnesium, galvanic, 20: 11230 (BM-RI-6715)
corrosive effects on Haynes 25, Hastelloy C and N, effects of aeration on, 20: 35851 (USNRDL-TR-1036)
corrosive effects on steel in evaporator environments, review, 20: 43834 (ORNL-TM-1612)
cosmic meson (μ) energy spectra in, to depth of 1400 m, (E), 20: 27778
current analysis in, tracer techniques for, 19: 13830
currents in, near-bottom measurements off California of, 20: 35183 (UCSD-34P127-1)
decomposition, distribution, and production of organic compounds in, 20: 28878 (NYO-1918-138)
decontamination using microscopic marine algae, 16: 26677
desalination by distillation, survey of large-scale processes for, 19: 11302 (AERE-M-1504)
desalination by electrochemonuclear processes, 20: 36506 (BNL-959)
desalination for Northeast U. S. water supplies, potential, 20: 45186 (NP-16148)
desalination in nuclear-powered ships, apparatus for ion exchange resin replacement for, 20: 23041(P)
desalination of, fuel cycle costs for reactors for, 17: 39201(R) (ORNL-3452(p.240-51))
desalination of, theory on, 18: 6138(R) (ORNL-3499(Vol.I))
desalination of, use of nuclear reactors for, 18: 4828 (ORNL-TM-735)
desalination of, abstracts from conference on, 20: 28812 (ORNL-3962)
desalination of, bibliography on, 18: 31662 (ORNL-TM-892)
desalination of, bibliography on, 20: 14510 (NP-15834)
desalination of, bibliography on economics of nuclear, 20: 24738 (PEL-97)
desalination of, BWR development for, 20: 32849
desalination of, CANDU-type reactors for, 19: 38216
desalination of, computer code for design of evaporator plant for, 19: 44140 (ORNL-TM-1244)
desalination of, comparison of organic-cooled and water-cooled power reactors for, 19: 45620
desalination of, computer program for cost, heat, and material balance calculations for conversion plants for, 20: 3923 (ORNL-TM-1299)
desalination of, computer codes for flash evaporator, 20: 10474 (ORNL-TM-1321)
desalination of, conference on, 20: 16157
desalination of, chemical research on, 20: 17158(R) (ORNL-3900, pp 82-149)
desalination of, cost of nuclear and fossil fueled plants for, 20: 22461
desalination of, cost of nuclear and fossil fuel plants for, 20: 45187
desalination of, development of nuclear power for, 18: 35178
desalination of, development of reactors for, 18: 38517 (A/CONF.28/A/824)
desalination of, development of reactors for, 18: 45045
desalination of, development of reactors for, 19: 1914
desalination of, design of dual-purpose plants for, (E), 19: 29649 (PB-181694)
desalination of, dual purpose nuclear power plants for, 19: 33631
desalination of, development of nuclear power for, 19: 33638
desalination of, developments in nuclear program on, 19: 38212
desalination of, design and economics of sodium cooled fast breeder reactor for, 19: 40190 (ORNL-TM-784)
desalination of, development of dual-purpose nuclear power plants for, 19: 42124
desalination of, deep-pool reactor development for, 19: 45631 (COO-283)
desalination of, design of organic-cooled dual-purpose reactor for, 19: 45618
desalination of, development of single-purpose reactors for, 19: 45634
desalination of, design of dual-purpose nuclear power plants for, 19: 45635
desalination of, development of dual purpose nuclear power plants for, 20: 6650
desalination of, development of nuclear systems for, 20: 18020(R) (ORNL-3900, pp 2-81)
desalination of, development of dual-purpose nuclear power plants for, 20: 28815
desalination of, dual purpose nuclear plant dynamic behavior analysis for, 20: 40438
desalination of, dual purpose nuclear plant optimization for, 20: 40439
desalination of, design of dual-purpose plant for, 20: 47038
desalination of, design of nuclear dual-purpose plant for, 20: 47045
desalination of, design and economics of dual-purpose nuclear plant for, 20: 47053
desalination of, design and economic aspects of heavy water-moderated power reactors for, 17: 38550 (SL-2008)
desalination of, design of small nuclear reactor for use in plant for, 19: 17334
desalination of, economic implications of nuclear energy for, 18: 21665
desalination of, economics of dual-purpose reactors for, 18: 45036(T) (JPRS-26497)
desalination of, economics of nuclear, 19: 1916
desalination of, economics of combined desalination–electric-power plants for, (E), 19: 10551 (NYO-3316-1)
desalination of, engineering evaluation of large evaporator plants for nuclear, 19: 13556 (K-D-1780)
desalination of, evaluation of nuclear, 19: 21708 (ORNL-TM-465)
desalination of, economics of nuclear-powered electrodialysis for, 19: 24109
desalination of, economics of dual-purpose plant for, (E), 19: 29646 (NP-14617)
desalination of, economic aspects of nuclear, 19: 38185 (ORNL-P-1278)
desalination of, economic comparison of two evaporators for, 19: 40699 (ORNL-TM-826)
desalination of, economics of low-temperature reactors for, 19: 42097 (ORNL-TM-1152)
desalination of, economics of dual-purpose reactor for, 19: 45606
desalination of, environmental factors for nuclear, 20: 20288 (BNWL-SA-596)
desalination of, evaluation of potential energy sources for, 20: 18704
desalination of, economics of nuclear power reactors for, 20: 24740
desalination of, economics of nuclear dual-purpose for, 20: 26514(T) (ORNL-tr-1173)
desalination of, economics of dual purpose plants for, 20: 32846
desalination of, economics of dual-purpose heavy water reactor for, 20: 32847
desalination of, energy requirements and processes for, 20: 31192
desalination of, economics for nuclear, 20: 35102(T) (AEC-tr-6733)
desalination of, economics of small dual-purpose nuclear plants for, 20: 35105
desalination of, economics of fossil- and nuclear-fired units for, 20: 36541
desalination of, economics of large-scale nuclear plants for, 20: 38524
desalination of, evaluation for New Jersey–New York City area, 20: 42658 (NP-16250)
desalination of, economic and technical advantages of dual-purpose nuclear power plants in Israel, 20: 45188
desalination of, economics of nuclear, 20: 47051
desalination of, economics of nuclear, 20: 47052
desalination of, evaluation of fast oxide breeder reactors for, 17: 1043 (LA-2733)
desalination of, feasibility study of dual-purpose power reactor for Florida Keys for, 18: 24906 (NYO-10719)
desalination of, feasibility of dual-purpose power plants for, 19: 31571
desalination of, feasibility of offshore power plants for, 20: 10413 (ORNL-TM-1329)
desalination of, feasibility of nuclear plant for, 20: 14166 (TID-22330(Vol.3))
desalination of, for agriculture, 20: 24775 (ORNL-P-2071)
desalination of, hearings before Joint Committee on Atomic Energy on, 20: 24827
desalination of, Low-pressure Steam Reactor Review Group report on, 18: 36833 (TID-20039)
desalination of, laser interferometric studies of electrodialytic, 20: 31220(R) (UCRL-16658, pp 39-72)
desalination of, methods for, 18: 36834
desalination of, methods for, 19: 31573
desalination of, nuclear power program for, 19: 17327
desalination of, nuclear power development for, 20: 24776
desalination of, nuclear power plant design for, 20: 47042(P)
desalination of, nuclear power development for, 20: 47096
desalination of, objectives of United Kingdom program for, 20: 18705
desalination of, potential of boiling water reactors in, 19: 31572
desalination of, performance of NPR for, 19: 40219 (RL-SA-21)
desalination of, properties of concrete evaporator shells for, 20: 10475 (ORNL-TM-1373)
desalination of, properties of flash distillation for, 20: 31193
desalination of, properties of electrodialysis, 20: 31194
desalination of, reactor economics for, 18: 19394
desalination of, reactor methods for, 18: 19402
desalination of, reactor program for, 19: 21709
desalination of, reactor design and economics for, 19: 35776 (ORNL-TM-1143)
desalination of, review, 19: 34293 (BNWL-SA-134)
desalination of, reactor fuel element fabrication cost estimates for, 20: 5173(R) (ORNL-3870, pp 191-3)
desalination of, reactor design and economic feasibility for, 20: 10414

(TID-22330(Vol. 1))
desalination of, review of methods of, 20: 8903
desalination of, review of nuclear, 20: 32845
desalination of, reactor design and economic feasibility for, 20: 47048
desalination of, steam cycles for, 20: 20291
desalination of, structural engineering aspects of dual-purpose plants for, 20: 35104
desalination of, thermal efficiency of power reactors for, 20: 36507(T) (AEC-tr-6744)
desalination of, uses of nuclear reactors in, 18: 33121 (A/CONF.28/P/220)
desalination of, uses of heat from nuclear reactors for, 19: 24142
desalination of, using process heat reactors, 19: 38227
desalination of, uses of nuclear reactors in, 19: 45619
desalination of, use of nuclear reactors for, 19: 45636
desalination of, using reactor heat, in Soviet Union, 19: 48014
desalination of, using nuclear reactors, 20: 1422
desalination of, use of reactor as heat source in, 20: 8903
desalination of, use of evaporation plants and reactor heat for, 20: 10415
desalination of, using nuclear energy, California Water Plan, for, 20: 43195
desalination of, 1964 report from Department of Interior, 19: 44154
desalination of, 10,000-Mw(t) fast breeder reactor for, 20: 26394(R) (ANL-7193)
desalination plants for, turbine development for large dual-purpose (E/T), 19: 1890 (SL-2158)
desalination plant for, computer program for determining cost, geometry, and operating characteristics of, 20: 30953 (ORNL-TM-1542)
desalination studies on, 19: 15415(R) (ORNL-3714(Vol.I)(p.87-9))
desalination, using nuclear energy, cost factors, 17: 31675 (CONF-14-6)
desalination using conventional and nuclear energy, review, 18: 19499
desalination using reactors, cost aspects of, 19: 8651
desalination using nuclear energy, economics of, 19: 21707 (ORNL-TM-432)
desalination using nuclear-powered osmosis plants, 19: 42120
desalination using nuclear energy, abstracts of publications on, 19: 45590 (TID-3584)
desalination using nuclear energy, 19: 48111
desalination using nuclear reactors, 20: 1481
desalination using reactors, economic aspects of, 20: 6649
desalination using offshore nuclear power plant, feasibility of, 20: 12453 (TID-22330(Vol.2))
desalination using small organic-cooled reactors, 20: 12454(T) (JPRS-33480)
desalination using dual-purpose reactors of Beloyarsk type, 20: 16107(T) (JPRS-33406)
desalination using dual-purpose fast reactors, 20: 16108(T) (JPRS-33459)
desalination using nuclear power plants, economics of, 20: 20292
desalination using nuclear power plants, 20: 28813
desalination using reactors, design of plants for, 20: 35103
desalination using reactors, economics of, 20: 42659
desalinization of, costs of thermal energy from reactor for, 18: 9615(R) (HW-78388(p.3.1-15))
desalinization of, use of nuclear reactors for, 18: 39394
desalinization plant for, reference design of nuclear, 17: 28499
desalinization, economics of, 18: 15585
deuterium and oxygen-18 content and distribution in, effects of atmospheric processes on, 20: 9156
deuterium content in, calculations of, 19: 28538
deuterium distribution in, factors affecting, 20: 18201 (NYO-3450-1, pp 149-68)
diffusion and movement in, in New York Harbor, hydraulic and mathematical models for, 17: 7684(R) (NYO-8103)
diffusion from instantaneous point-source in, horizontal turbulent, 18: 3406 (NYO-8104)
diffusion in, at Tokai-mura, 16: 11975(R) (JAERI-5003(p.256-8))
diffusion in, equations for, 17: 7684(R) (NYO-8103)
diffusion in, mathematical analysis, 16: 11973(R) (JAERI-5003 (p.246-50))
diffusion of soluble contaminants in, 20: 43541
diffusion of strontium-90 in, from strontium titanate heat sources, (E), 19: 28716
diffusion processes in, analysis of dye patch experiments on, 18: 11534 (TID-20115)
diffusion processes in, 20: 33502
dispersion and movement in Cape Kennedy area, physical processes of, 20: 20359 (NYO-2973-1)
distillation during fertilizer production in power reactor, economics of, 17: 29799 (ORNL-TM-609)
distillation of, cost aspects of nuclear power for, 17: 19633(R) (PB-161062)
distillation of, economic aspects of use of power reactors for energy for, 17: 36930 (TID-19267)
distillation of, using large reactors, 17: 9886
distillation of, uses of power reactors as source of heat in, 17: 29801 (SL-1998)
distillation of, use of nuclear reactors in, 17: 36882
distillation of, design study of heavy-water reactors for, 18: 21632 (DP-866)
distillation of, economic assessment of large dual-purpose nuclear power plants for, 18: 19403
distillation of, economic assessment of large dual-purpose nuclear power plants for, 18: 36834
distillation of, economics of conventional and nuclear power for, 18: 38547 (A/CONF.28/P/548)
distillation of, survey of status of, 19: 44153(T) (JPRS-31361)
distribution of trace elements in, 18: 39478 (TID-21067)
drift at Cape Canaveral, non-tidal, 18: 15715 (TID-20322)
ebb and flow in Solway Firth and Irish Sea, 19: 10662 (PG-Report-605)
ecology of marine mammals in, in northwest Alaska, 1961, 19: 33694 (PNE-466)
effects of movement on climate, 20: 43505(R) (COO-689-60, App.A-5)
effects on carbon dioxide content of atmosphere, 17: 30712
effects on fallout from nuclear explosions, 19: 24719
effects on fatigue crack propagation in nickel–chromium–molybdenum–vanadium steel, 20: 11273(R) (NRL-6364)
effects on formation of corrosion-resistant films on titanium and zirconium oxides, 18: 20481
fallout contamination in, 18: 10278(T) (AEC-tr-6128(p.312-28))
fallout content of, 1962 to 1964, 19: 9370 (NP-14556(p.11-80))
fallout cycling and levels of, 16: 22455 (TID-7632(p.348-59))
fallout diffusion in, from vertical exchange data, 18: 37363 (A/CONF.28/P/766)
fallout dispersion in, 20: 37037
fallout distribution in, 17: 19746 (TID-18468(p.311-52))
fallout monitoring in France, July 1963, 17: 41031(R) (SCPRI(RM)VII-1963)
fallout monitoring in, in France, Oct. 1963, 18: 6949(R) (SCPRI(RM)X-1963)
fallout monitoring in, 20: 7255(R) (TID-22411)
fallout radionuclide distribution in deep offshore, of Japan, 20: 16681
fission product accumulation coefficients of marine organisms in, 18: 21780(T) (JPRS-24227)
fission product content in, 1960 and 1961, 20: 31419
fission product contamination of, from nuclear plants, 20: 46001
fission product distribution from fall-out or flow-out, 16: 10349
fission product dispersion in, 19: 24715
fission product distribution in, natural carriers for, 20: 31422
fission product metabolism by plankton in, 19: 22(T) (JPRS-25966(p.28-41))
fission product movement in, 16: 10348
fission product separation from, by coprecipitation with carriers, 19: 34277
fission product uptake from, by marine animals, 20: 26549(R) (NP-15915)
flow measurements in Magothy Estuary, Round Bay, and Severn Estuary using Deep Water Isotopic Current Analyzer, 17: 34195(R) (JLI-2748-0-7)
gamma activity in, direct measurement using immersible scintillation probe, 20: 41147
gamma detection and measurement in, instrument for deep-sea, 18: 29985(T) (AEC-tr-6433)
gamma monitoring near Thresher accident, 18: 41678 (NOLTR-64-21)
gamma spectrometric analysis for fallout fission products, 20: 41145
gamma spectrometry of English Channel, in May 1961, *in situ*, 17: 19973
gas exchange with atmosphere, tracer studies of, 18: 7592(R) (TID-19900)
heat of evaporation of, at 125 to 200°C, 19: 17848 (AERE-M-1534)
heavy water separation from, MHD method for, 18: 22192(P)
iron content, 16: 4030 (TID-12946(App.I,Vol.II))
iron/manganese distribution in environments of, 20: 18895 (NYO-3450-1, pp 217-76)
isotopic exchange between, and macrophytic algae, kinetics of, 20: 45899
isotopic variations of deuterium and oxygen-18 in, 20: 18896 (NYO-3450-1, pp 277-374)
isotopic variations of deuterium and oxygen-18 in, 20: 43509
krypton content of deep, 19: 2530
lead content in Mediterranean Sea, 17: 32274
lead content profiles in, 18: 12344
lead isotopes in, in Los Angeles basin, California, effects of automobile exhausts on, 19: 11453
lead-210 content in, 17: 30736
level of Pleistocene, determination of, from fossil coral age, 20: 37014
light absorption in, visible-region, 17: 30543

manganese content, 17: 33602
manganese sedimentation mechanisms in, in open ocean, 18: 36897(R) (TID-20887)
manganese-54 content in Tyrrhenian Sea, 19: 29845
measurement of deep ocean tsunami waves in, testing of taut-line buoy system for, 19: 17415(R) (NVO-98-4)
measurement of deep ocean tsunami waves in, design and operation of taut-line buoy system for, 19: 17414(R) (NVO-98-3)
measurement of salinity and saturation in, 18: 43787 (CU-2663-12(p.52-4))
mesopelagic organisms in deep scattering layers of, distribution of migrating, 20: 14235 (SAN-584-1)
microbiological assays in, tracer techniques for, 20: 20368 (CONF-640309-1)
mixing of deep ocean, tracer study, 20: 18934
model of oceans in Northern Hemisphere, 20: 4153(R) (UCRL-14360, pp 73-85)
monitoring after radioactive waste disposal operations, procedures for, 16: 9726
monitoring for radioactivity after waste disposal, 19: 8677
movement and mixing of, research on, 20: 18198
movement in Chukchi Sea area, 19: 29810(R) (PNE-457)
movement in Suruga Bay, Japan, 19: 5601 (IAEA-R-19)
movement of surface, south of Iceland, 20: 12541 (NYO-2929-1)
neutron activation of, gamma dose curves from, (T), 19: 46589 (UCRL-14332)
nitrogen fixation by marine algae in, 19: 2020
oceanographic survey of Yokohama Harbor for waste disposal from nuclear-powered ships, 18: 15657 (NP-13685)
oceanographical conditions in North Sea, 18: 17334 (NP-13756(Vol.I))
osmotic behavior of simulated, 20: 22857(R) (ORNL-3913, pp 111-32)
oxygen gradients in Mediterranean, 20: 41128
oxygen-18 enrichment of, effect of evaporation on, 20: 43509
phosphate distribution in, 16: 4029 (TID-12946(App.I,Vol.I))
physical dispersion in coastal and estuarine, fluorescent die tracer studies, 16: 14998(R) (NYO-8100)
plankton distributions and metabolism in, 16: 4029 (TID-12946 (App.I,Vol.I))
plankton distribution and metabolism in, 16: 4030 (TID-12946 (App.I,Vol.II))
plankton distribution in ecosystem of, 20: 16175(R) (RT/BIO(65)-1)
plankton distribution in, 16: 4029 (TID-12946(App.I,Vol.I))
potassium-40 background activity in, sensitivity of gamma spectrometer and scintillation detectors for, 20: 16828 (TID-22763)
processing for cesium and strontium removal, method for shipboard, 20: 7256(R) (TID-22411, App.A)
processing for deuterium and salt recovery, magnetohydrodynamic, 19: 44578(P)
processing for heavy water production, 18: 22406(P)
processing for trace-element separation by cation exchange, 19: 18084(P)
processing for uranium extraction, 19: 13660
processing for uranium separation using basic zinc carbonate, 19: 24634(P)
processing for uranium recovery, ion exchanger for, 19: 24635(P)
processing for yttrium-90 separation, 20: 31249
promethium-147 content in Tyrrhenian Sea, 19: 29845
properties of, tracer studies of, 18: 43996
properties, chemical and physical, 16: 4031 (TID-12946(App.2))
quark content in, (E), 20: 34236
radiation effects on marine life in, natural β, 20: 38741
radiation in, cosmic and nuclear, 17: 32718(R) (NP-12996(p.36-7))
radiation monitoring in France, September 1963, 18: 1956(R) (SCPRI(RM)IX-1963)
radiation monitoring at waste disposal sites, 19: 24767
radiation monitoring of, sample preparation for, 19: 26588
radiation processing of, effects on fish, 20: 13152
radio wave scattering by surface of disturbed, structure effects on spatial characteristics of, (E), 20: 20908
radioactive contamination of Inner Oslofjord, dispersion factors in, 19: 24810
radioactive contamination by waste disposal, 19: 36702 (EUR-2407.f)
radioactive contamination of, review on, 20: 23312
radioactive contamination of organisms inhabiting, 20: 43596
radioactive contamination of, Japan, 1961–64, 20: 43615
radioactive decay of strontium-85-labeled strontium titanate in, 20: 43592 (USNRDL-TR-1042)
radioactive waste disposal in, legal aspects, 16: 11348
radioactive waste disposal in, relation to marine ecology, 16: 9835
radioactive waste disposal in, by Marcoule establishment, 17: 15526
radioactive waste disposal in, problems in, 18: 11503
radioactive waste disposal in, safety precautions for, 19: 40277
radioactive waste disposal in, biological, chemical, and physical processes affecting, 20: 32883
radioactivity distributions in, studies of dispersion and mixing processes for, 17: 21463
radioactivity distribution in, from nuclear rocket accidents, 17: 38445 (TID-7653(Pt.I)(p.52-68))
radioactivity equilibrium in, thorium and uranium, 19: 9380
radioactivity from Columbia River effluent, 19: 46680
radioactivity from cesium-137 and strontium-90 in Faeroe Islands, 1964, 20: 7320 (RISO-108)
radioactivity from cesium-137 and strontium-90 in Greenland, 1964, 20: 7321 (RISO-109)
radioactivity from gamma emitters in Gulf of Mexico, 20: 18200 (NYO-3450-1, pp 109-29)
radioactivity from trace elements in, Swordfish Program studies on, 20: 18576(R) (TID-22660)
radioactivity in Atlantic Ocean, Black and Caspian Seas, 19: 7704
radioactivity in Atlantic, 1962, 20: 23392
radioactivity in Irish Sea near Windscale, 18: 8597
radioactivity in Japan from April to June 1962, 17: 18311
radioactivity in Sea of Constance area, 19: 30454
radioactivity in Sea of Constance precipitations, tributaries, and alpha and beta, 19: 30455
radioactivity in, use of biological samples for determination of, 17: 19753(T) (JPRS-18633)
radioactivity in 1958, 1959, and 1960 at Ispra, 16: 4983 (NP-10731 (p.129-44))
radioactivity in, from fallout in Baltic Bay of Tvären, 1957 to 1963, 19: 22532 (AE-171)
radioactivity in, IGY program for measuring, 19: 24705
radioactivity in, data on, 19: 40792
radioactivity in, equipment and method for detecting and measuring, 20: 25375 (AD-632284)
radioactivity induced by neutron sources in, calculations, 19: 32422 (UCRL-12407)
radioactivity, maximum permissible concentrations, 17: 23546 (HW-77690)
radioactivity measurements in, detector for, 20: 13056 (AD-627000)
radioactivity monitoring of, in France, 18: 6950(R) (SCPRI(RM)XI-1963)
radioactivity monitoring of, review of methods for, 19: 26276
radioactivity of, along Italian coast, 18: 1903
radioactivity of, determination from plankton analysis, 17: 2814
radioactivity of, IGY observations on, 18: 6946 (NP-13423)
radioactivity of Italian, network for monitoring, 19: 30467
radioactivity of Japanese, 18: 37428 (A/CONF.28/P/849)
radioactivity of, measurements in Federal Republic of Germany, April to June 1962, 17: 15625
radioactivity of, methods of determining, 17: 21464
radioactivity of marine organisms in, survey, 18: 17335 (NP-13756 (Vol.II))
radioactivity of Northeast Pacific Ocean, effects of Hanford waste solutions on, 20: 40523(R) (RLO-1750-8(Vol.1))
radioactivity of Osaka Bay, Japan, 1961, 16: 20121
radioactivity of Suruga Bay, Japan, 1960 and 1961, 19: 30417
radioactivity of, in Germany, 3rd quarter 1962, 18: 12357
radioactivity of, in Federal Republic of Germany, 4th quarter, 1962, 18: 11898
radioactivity of, in Federal Republic of Germany, 3rd quarter 1962, 18: 14091
radioactivity of, in Pacific Ocean, 131° 57′E to 164° 00′W longitude and 52° 57′ to 08° 45′N latitude, 1961, 18: 25690
radioactivity of, from Gulf of Naples and Pacific Ocean, 1959, 18: 31752 (BLG-243)
radioactivity of, from naturally occurring radioisotopes, 18: 31757(T) (JPRS-25068(p.16-29))
radioactivity of, along Italian coast, 18: 37362 (A/CONF.28/P/558)
radioactivity of, in vicinity of Christmas Island, 1962, 19: 24378 (UWFL-88)
radioactivity of, method for measuring, 19: 34277
radioactivity of, effects on radioactivity of invertebrates and fishes, 19: 42669
radioactivity of, from Adriatic and Ligurian Seas, 19: 15757(R) (TID-21521)
radioactivity of, in Kobe Harbor, Japan, 1962-65, 20: 7271
radioactivity of, model for predicting mixing rates of, 20: 7258(R) (TID-22411, App.C)
radioactivity of, radium-228 and thorium-228, 20: 7260(R) (TID-22411, App.E)
radioactivity of, effects of waste disposal practices on, 20: 11054
radioactivity of, effects on radioactivity of sea foods, 20: 11054
radioactivity of, correlation of high-yield surface from Operation Hardtack for, 20: 27211 (USNRDL-TR-991)
radioactivity of, effects of fallout fission products on, 1945 to 1963, 20: 41144
radioactivity of, effects of fallout fission product accumulation by plankton on, 20: 41146
radioisotope behavior in, JRR-1 coolant, 19: 33668

radioisotope concentrations in, maximum permissible, 16: 10318
radioisotope concentration in, using ferric hydroxide ion exchange material, 20: 22923
radioisotope contents in, review, 17: 3188
radioisotope content around British Isles, programs for monitoring, 18: 8603
radioisotope content in Tyrrhenian, 19: 30411
radioisotope content in, ferric hydroxide resins for measuring, 19: 32787(R) (NIRS-3(1-17))
radioisotope content of, effects on radioactivity of edible marine organisms, 19: 43669(R) (NP-15159)
radioisotope content of, effects on development of fish spawn of strontium-90 and yttrium-90, 20: 20445(T) (TRG-Inf. Ser.-166)
radioisotope content of, effects of plankton on, 20: 33502
radioisotope content in animals and plants in, effects and source of artificial and natural, 19: 20226
radioisotope diffusion in interstitial water of sediments in, 20: 45910
radioisotope distribution in Atlantic Ocean from fall-out, 16: 26731
radioisotope distribution in, 19: 22545
radioisotope distribution between suspended materials and Indian Ocean, 20: 41140
radioisotope lifetimes and paths in, from aerospace nuclear system contamination, 18: 8062 (SC-DC-3553(p.195-207))
radioisotope production in, by cosmic radiation, 17: 41009
radioisotope sinking in, acceleration of rates of, 18: 8526
radioisotope sorption by sedimentary particles in, 17: 31830 (TID-19127)
radioisotopes distribution in, after fixation on ion-exchange resins, 20: 47089
radioisotopes in, dietary contamination in Japan by, 19: 40309(R) (NP-15180)
radioisotopes in, permissible concentrations of, 19: 42669
radioisotopes in, chemical properties of, 20: 33502
radiological monitoring in France, May 1963, 17: 32289(R) (SCPRI(RM)V-1963))
radiological monitoring in France, June 1963, 17: 34154(R) (SCPRI(RM)VI-1963)
radionuclide content in, 19: 3885
radionuclide distribution in coastal and offshore, of Oregon and Washington, 19: 27910 (UWFL-86)
radionuclides in, permissible concentrations of, 16: 29261
radium uptake by mollusks from, (E), 19: 35889
radium-226 content in Tyrrhenian Sea, 19: 29845
radium-226 content and distribution in, 19: 13638
rare earths content in, 17: 30719
reactions with sodium, use as hydrogen generator for recovering deeply submerged objects, 20: 1567 (SC-RR-65-380)
rubidium-87/strontium-86 ratio in North Atlantic, age estimation from, 20: 45916(R) (MIT-1381-12)
ruthenium-106 solvent extraction from, using polyvinyl chloride, 18: 10186
salinity and temperature, seasonal and anomalous variations, 16: 4029 (TID-12946(App.I,Vol.I))
salt separation from, for Arizona, feasibility of nuclear facilities for, 18: 29102
sampling, container for, 16: 4030 (TID-12946(App.I,Vol.II))
sand drift measurements in and on shore of, tracer techniques for measurement of, 18: 1919
separation of fission products from, ion exchange, 20: 22872(R) (NIRS-4, pp 12-17)
separation of iron-55 and -59 from, by precipitation, 20: 3891(T) (CEA-tr-A-1838)
separation of radioisotopes from, methods for, 20: 18576(R) (TID-22660)
separation of radioisotopes from, by sorption by metal sulfide-ion exchange resins, 20: 29345
separation of thorium from, by precipitation as tannate of gelatin, 20: 27067
silicon-32 content in marine samples, 17: 30739
silicon-32 content of, at various depths, 18: 39488 (NP-14127)
solvent properties for rare gases at 0 to 25°C, 17: 21705
solvent properties for strontium titanate, strontium-85 studies of, 18: 31363 (USNRDL-TR-745)
solvent properties for fission products, 19: 24813
solvent properties for strontium-90-labeled strontium titanate, rates of solution, 19: 32124 (TID-21020)
solvent properties for gases, effects of physicochemical factors on measurements of, 20: 18632 (NYO-3450-1,pp 91-107)
sorption of manganese-54 and zinc-65 from, by montmorillonite clay, 20: 18576(R) (TID-22660)
sorption of radioisotopes from, by bottom silts, 17: 37021(T) (JPRS-20795(p.1-6))
sorptive properties for carbon dioxide from troposphere, 17: 25469
spectra of, visible absorption, 18: 3791
strontium content and variable strontium-chlorinity relation of Sargasso, 19: 614
strontium content in, estimation of, from content in aragonite oolites, 20: 18631 (NYO-2266-1)
strontium content of, effects on uptake of strontium-90 by fish, 20: 24836 (AE-224)
strontium isotopic ratio, 16: 22426
strontium isotopic composition in, age estimation from, 20: 16711(R) (MIT-1381-13)
strontium-90 content in surface, 17: 10835
strontium-90 circulation in, 20: 45258(R) (IAEA-2607-12)
strontium-90 content of surface, in Atlantic Ocean, North Sea, and Baltic Sea, 18: 22248(T) (JPRS-24281)
strontium-90 content in southern Pacific, 1961, 19: 18149(J) (JPRS-28558)
strontium-90 content in Norwegian, 1962 and 1963, 19: 24722
strontium-90 content in, 1965, 19: 45748(R) (TID-22193)
strontium-90 content in, 20: 23291
strontium-90 content above and below surfaces of, 20: 31421
strontium-90 content in, errors in analysis for, 20: 31423
strontium-90 content in, estimate of total, 20: 43517(T) (AEC-tr-6798, Paper 2)
strontium-90 content in, vertical mixing anomaly from, 17: 25465
strontium-90 content to 5,000 m in Western North Pacific, 16: 5551 (A/AC.82/G/L.697)
strontium-90 content in, around Egypt, 16: 4020 (A/AC.82/G/L.665)
strontium-90 distribution and uptake in Japanese, 20: 7269
strontium-90 distribution in, 1960 and 1961, 20: 31420
strontium-90 distribution in, effects of hydrographic processes on, 20: 33526
strontium-90 distribution on surfaces of, 20: 43516(T) (AEC-tr-6798, Paper 1)
strontium-90 removal from, by Acantharia, 19: 24723
strontium-90 secretion by *Cystoseira barbata* in, 19: 14997
strontium-90 uptake by *Cystoseira barbata* from, 19: 14997
strontium-90 uptake from, by *Nerita forskali* Reclus, 20: 218(R) (STI/DOC/10/42, pp 1-22)
sulfur isotope ratios in, 16: 2028
sulfur isotopic composition, 16: 5569
sulfur isotopic contents in, biogeochemical studies on, 20: 18893 (NYO-3450-1, pp 131-48)
sulfur-34 distribution in ancient, variations in, 20: 41135
tantalum separation from, by solvent extraction, 17: 40749
thorium content and distribution in, 19: 13638
thorium isotope abundances in, 20: 29412
thorium series equilibrium in, 19: 22537(R) (TID-21522)
trace element separation from, by sorption on ferric hydroxide gel, 18: 37083
trace elements in Indian Ocean by marine organisms, 20: 40572
trace elements in, research program on, 19: 42634(R) (YALE-2912-10)
tritium content in New Zealand in 1956 to 1963, review of measurements of, 19: 6093 (INS-R-24)
tritium content of upper layer of North Pacific, depth and residence time of, 17: 30698
uptake of fallout fission products by marine organisms from, 20: 40546
uranium content and distribution in Indian and Antarctic, 20: 25300
uranium content and uranium-234/-238 activity ratio in western North Pacific, 20: 33524
uranium content and distribution in, 19: 13638
uranium distribution in Antarctic, 19: 4372
uranium isotope abundances in, 20: 29412
uranium isotope ratio in, from Sagami Bay, Japan, 20: 512
uranium occurrence in, 20: 21243
uranium separation from, economics of, 18: 26917 (DM-72)
uranium separation from, 18: 43722
uranium series equilibrium in, 19: 22537(R) (TID-21522)
uranium uptake by mollusks from, (E), 19: 35889
uranium-235/-238 ratio in US coastal, 19: 44263
uranium-234/-238 ratios in, 20: 39133
vapor pressure, 19: 348(R) (ORNL-3679(p.117-26))
vapor pressure of, at 125 to 200°C, 19: 17848 (AERE-M-1534)
vitamin B_{12} in, 16: 4030 (TID-12946(App.I,Vol.II))
waste disposal in, problems of, 17: 29873
waste disposal in, control and evaluation of radioactive, 18: 36860
water currents in Solway Firth, Scotland, 18: 12336 (PG-Report-550)
xenon content of deep, 19: 2530

SEAFOOD

cesium-137 content of, effects on radiation levels of food chain, 19: 17453(T) (JPRS-28-560)
food poisoning incidents attributed to, 20: 43775
radiation effects on microbial populations on fillets of yellow perch, following refrigerated storage, gamma, 20: 43793
radiation effects on chemical, microbiological, and physical properties of crab meat, 19: 30597(R) (TID-21404)

radiation pasteurization of shrimp, gamma, 18: 21810 (TID-7684(p.28-31))
radiation pasteurization of raw shrimp, effects of chlortetracycline and low temperature on, 19: 34602
radiation processing of Gulf oysters and shrimp, effects on storage life and wholesomeness, 20: 39288(R) (ORO-636)
radiation processing of, effects on storage life and wholesomeness, 20: 41384(R) (TID-22833)
radiation processing of fish fillets and clam and lobster meats, 20: 41384(R) (TID-22833)
radiation processing of, effects on refrigerated storage life, 17: 33618(R) (TID-17557)
radiation processing of shrimp, effect on storage life, 18: 21807(R) (ORO-615)
radiation processing of crab, effect on wholesomeness, 18: 41091(R) (TID-21116)
radiation processing of Dungeness and king crab, effects on refrigerated storage life, 19: 15943 (CONF-640909-10)
radiation processing of shrimp, effects on wholesomeness, 19: 15949 (CONF-641002(p.23-8))
radiation processing of shrimp, effects on storage life, 19: 20407(R) (ORO-626)
radiation processing of, effects on wholesomeness, 19: 32626(R) (NYO-3461-1)
radiation processing of shrimp, effects on refrigerated storage life, 19: 34599
radiation processing of crab and shrimp, effects on quality and storage life, 16: 33350
radiation processing of Pacific crab, procedures for, 17: 30782(R) (TID-18036)
radiation processing of crab, optimal conditions for, 18: 21811 (TID-7684(p.32-7))
radiation processing of King crab meat, effect on storage life, 19: 18355
radiation processing of King crab, bacterial count, total volatile base, and trimethylamine production in, 19: 18356
radiopreservation of pacific coast, gamma, 20: 29583(R) (TID-22515)
radiopreservation of, using gamma radiation, 20: 43774
radiopreservation of fresh, pickled, salted, smoked, and cooked, effects on taste and storage life, gamma, 20: 43776
radiosensitivity of *Clostridium botulinum* type E spores on homogenates of haddock, γ, 20: 40699
sampling for bacteriological studies, 20: 41384(R) (TID-22833)
strontium-90 content of, effects on radiation levels of food chain, 19: 17453(T) (JPRS-28560)

SEALING MATERIALS
bibliography on space environmental effects on, 16: 5722 (NP-11194)
development and evaluation for space electric power systems, 18: 41928(R) (NASA-CR-54089)
development and testing for space power systems, 18: 34046(R) (NASA-CR-54041)
development for underground explosion instrument holes, grout, 20: 9138 (VUF-3019)
development for use with sheathed thermocouples, 18: 28937(R) (ORNL-3578(p.100-21))
development for use in space vehicles, 20: 4312
development of, for magnetic materials, 20: 29366(R) (TID-22970, pp 375-91)
effects on ground-water permeation of on-grade concrete, 17: 29137 (UCRL-7254(p.43-5))
evaluation of polyurethan as, for environmental sealing of connectors on military cables, 18: 13369 (SC-TM-64-26)
performance and selection of, for use in space vehicles, 20: 16944 (NASA-SP-3025)
performance of silicone resin GE SR-82 in glass and metal ultrahigh vacuum systems, 18: 8511
preparation of potting compound with nuclear radiation shielding properties, 19: 3475(P)
properties, effects of low pressure at elevated temperature, 16: 6245 (NP-11181)
radiation effects at cryogenic temperatures, 16: 15982
radiation effects of O-ring, 17: 36347(R) (NARF-62-18P)
radiation effects on mechanical properties of, at low temperatures, 17: 37567(R) (FZK-161-2(Vol.II))
radiation effects on, 17: 39666 (HW-76263)
radiation effects on strength properties of high-temperature tank sealants, 17: 41482 (AD-288562)
radiation effects on physical properties of fuel tank and pressure sealants, 17: 41483 (AD-288936)
radiation effects on, in vacuum, 18: 2293(R) (FZK-161-1)
radiation effects on, in vacuum and at cryotemperatures, 18: 20581(R) (FZK-172)
radiation effects on O-rings, 18: 33839 (RTD-TDR-63-4287(Vol.II))
radiation effects on, 18: 36052
radiation effects on, at low temperatures, 19: 6360(R) (FZK-188-2)
radiation effects in space on engineering properties of organic, research program on, 19: 9730(R) (FZK-217)
radiation effects on, in combination with cryotemperature and vacuum, 19: 18535(R) (FZK-188-1)
radiation effects on O-ring elastomer compounds, gamma, 19: 18536 (FZK-196)
radiation effects on, review, 19: 18539 (REIC-21(Add.))
radiation effects on, in combination with cryotemperature and vacuum, 19: 42902(R) (FZK-243)
radiation effects on, at cryogenic temperatures in vacuum, 20: 23794
radiation effects on, in combination with cryotemperatures and vacuum, 20: 43994(R) (FZK-290)
reliability of ceramic-to-metal, statistical evaluation of, 17: 23906(R) (RADC-TDR-63-43)
space environmental effects on plastic potting compounds, 18: 42117 (RSIC-150(Vol.I)(App.G))
specifications for silicone rubber, primers, and adhesives, 19: 18399 (TID-21513)
testing for high-pressure pump uses, 17: 35959(R) (NYO-9800)
testing of, for use in structural openings of Plutonium Recycle Test Reactor, 17: 10121 (HW-64972)
thermal stability of elastomeric, 18: 44160 (WAPD-TM-432)
weathering effects on epoxy and thiokos, in linoleum joints, 16: 15028(R) (UCRL-6658(Rev.))

SEALS AND GLANDS
see also Ceramic Bonding
see also Gaskets
see also Rotary Seals
see also Vacuum Seals
analysis of fluid flow through concentric and eccentric cylindrical, with and without annular grooves, 16: 7664(T) (AEC-tr-4905)
bibliography on dynamic shaft, 19: 6028 (TID-21379)
closure of pressure vessel openings using, 17: 4654(P)
closure system design, explosively driven, 19: 20100 (UCRL-12203)
compression forces, load monitoring device for measurement, 16: 19011 (KAPL-M-JOS-1)
corrosion of ceramic-to-metal, by barium vapor, 18: 44497(R) (MND-2812-2)
corrosion of ceramic-to-metal, by barium vapor, 18: 44498(R) (MND-2812-3)
corrosion of ceramic-to-metal, by barium vapor, 18: 44499(R) (MND-2812-4)
corrosion of K-seals by ammoniated water at 600°F, 18: 8753 (KAPL-M-SFB-1)
design and development, for superheater steam pipes in BONUS reactor, 16: 9649 (GNEC-192)
design and operation of liquid-metal, 18: 27647
design and performance of mechanical face-type, 19: 42026
design and properties of nonbolted closure for reactor pressure vessels, 18: 11388
design and testing of pressure-type, for reactor mechanical drives, 16: 13189
design and testing for high-pressure pumps, 17: 35959(R) (NYO-9800)
design combining fluid bearing and vacuum pump, 19: 5426(P)
design criteria for plenum to reflector block seal in HTGR, 16: 17294 (GAMD-1375)
design development of dynamic seals for gases, 16: 27163 (TID-16358)
design for adjacent blocks in reactor core structure, for reduced coolant leakage, 18: 26848(P)
design for air-tight supply line wall lead-in for hot cells, 18: 22215(P)
design for bubble chamber, for wide pressure and temperature ranges, 20: 25439(P)
design for coaxial tubes, 19: 38785(P)
design for concentric pair of ducts, 17: 16201(P)
design for connecting handling hood to loading channel, 19: 33558(P)
design for coupling fueling machine to reactor standpipe, 18: 21587(P)
design for coupling refueling machine to reactors, 19: 33541(P)
design for EGCR coolant blower shafts, 16: 28385 (TID-7631(p.15-25))
design for emergency sealing of apertures in reactors, 18: 13194(P)
design for fluid-tight intercommunication between two superposed chambers, 18: 8471(P)
design for fluid-tight coupling for pressure vessel to anchoring structure, 19: 36598(P)
design for gas-cooled reactor channels, 17: 13752(P)
design for glove-box windows, 19: 34310(P)
design for helium systems, 18: 15524 (HW-76008)
design for hot-cell wall apertures, 20: 12953(P)
design for inspection window on pressure vessels, 20: 45062
design for insulated tube coupling, 19: 42621(P)
design for leak-tight movement transmission through walls, 20: 2005(P)
design for multi-tube connections through wall, 17: 13744(P)
design for pipe plugs, 18: 31707(P)
design for pipes of different thermal expansion coefficients, 16: 19024(P)

design for piston-cylinder type pressure vessel, 17: 40970(P)
design for pressure vessels, 16: 31788(P)
design for pressure vessels, 16: 33107(P)
design for pressure vessels, 16: 33116(P)
design for pressure vessel openings, 17: 9991(P)
design for pressure vessels, 20: 10301(P)
design for reactor control mechanical drives, 17: 42276(P)
design for reactor void gages, 19: 31542(R) (HPR-59)
design for reactor moderator block assembly, 20: 1380(P)
design for remotely plugging open-ended bores, 17: 1589(P)
design for respirators, 19: 10718(P)
design for rotatable shaft in casing, 16: 1898(P)
design for shafts passing through gas enclosures, 19: 22469(P)
design for shielding wall lead-through tubes for manipulators, 19: 30365(P)
design for standpipes of Dungeness Calder Hall Reactor, 19: 33618
design for thermocouple connections in pressure vessel cover, 18: 26840(P)
design for tubes, 20: 9109(P)
design for tubular elements, 19: 40705(P)
design for tubular members, 20: 41100(P)
design for two tubular elements, 18: 33708(P)
design for two tubular elements, 19: 37018(P)
design for use with weighing apparatuses, 19: 10717(P)
design for water-cooled and -moderated maritime reactors, 18: 24946(P)
design of barrier seal assembly for remote-control manipulator, 19: 34308(P)
design of closure for access holes in boiler, 17: 27528(P)
design of closure for reactor pressure vessels, 19: 25663(P)
design of compression, 17: 12416(P)
design of corrosion-resistant, using elastomer with fluorinated compound, 19: 36584(P)
design of coupling device for plug in reactor standpipe, 16: 16487(P)
design of detachable flanged joints for coaxially extended pipes, 18: 22214(P)
design of diaphragm, for rotary shaft, 19: 42620(P)
design of double, with means for detecting leaks, 17: 16206(P)
design of fitting for passage of electrical elements through pressure vessels, 16: 14866(P)
design of flat plate and plug, for reactor vessels, 20: 10313(P)
design of flexible, for leak tight vessels, 19: 34317(P)
design of fluid pressure resistant, 18: 31704(P)
design of fluid-tight hole closure seals, 16: 28500(P)
design of fluid-tight, for reactor control drive mechanisms, 16: 28503(P)
design of fluid-tight deformable passage, for control rods, 17: 40326(P)
design of fluid-tight, 19: 28486(P)
design of fluid-tight, for movable parts, 20: 12949(P)
design of, for EGCR core, 17: 17551 (TID-18099)
design of, for HTGR cooling system compressor, 16: 28388 (TID-7631 (p.40-5))
design of, for HTGR cooling system circulator shafts, 16: 28386 (TID-7631(p.26-32))
design of gastight, for kilocurie gamma shielding window, 16: 3156
design of insulating, for heated test sections in tubes, 19: 44134 (EUR-2434.d)
design of interchangeable, for ports in alpha-beta-gamma cells, 18: 389
design of leading-in plate for passing cables into reactor vessels, 17: 17512(P)
design of liquid-ring, for rotatable covers, 16: 31786(P)
design of liquid, to allow force transmission, 19: 10716(P)
design of low-temperature, for plastic window, 18: 34685
design of mechanical, for organic fluids, 17: 14416 (HW-57581(Del.))
design of mechanical coupling, for pressure vessels, 20: 1374(P)
design of metal-metal oxide, for refractory vessel containing radioactive wastes, 20: 5209(P)
design of O-ring, for high-pressure applications, 18: 25015 (UCRL-7359)
design of plug and extractor for reactor fuel channels, 18: 13209(P)
design of plug and insertion means for apertures in reactor pressure vessels, 19: 45510(P)
design of plug for reactor access holes, 16: 15853(P)
design of plug for reactor access holes, 16: 15857(P)
design of plug for reactor standpipes, 16: 28591(P)
design of plug for reactor standpipes, 17: 16211(P)
design of plug for reactor standpipes, 18: 13215(P)
design of plug for reactor standpipes, 19: 38113(P)
design of reactor pump shaft-, 19: 17316
design of replaceable gastight utility plug for shielded facility, 16: 3132
design of replaceable two-piece gas-tight plugs for hot cells, 20: 7226
design of shielded plug for reactor access holes, 16: 15831(P)
design of sleeve coupling for closure of access holes in pressure vessel, 17: 29753(P)
design of static seal for liquid hydrogen, 17: 26
design of thermally compensated, for autoclaves, 20: 4087 (ORNL-TM-1293)
design of welded-metal-bellows, 18: 24823 (TID-7690(p.176-88))
development and testing of high-pressure, 17: 14423(R) (TID-16291)
development and testing for mercury-vapor turbine in SNAP-8, 19: 29748 (NASA-CR-54234(Vol.IV))
development for EGCR loading machine actuating cylinders, 20: 20244 (ORNL-TM-1419)
development for gas-cooled power reactors, 16: 19992 (NYO-9792)
development for gas cooled reactors, 18: 23743 (TID-7690(p.121-42))
development for heavy-water boiling reactor (E), 19: 3644 (HPR-35 (Vol.II)(Sect.11))
development for high-pressure pumps, 17: 37316(R) (TID-16966)
development for high-pressure pumps, 17: 37317(R) (TID-17608)
development for high-pressure circulating pumps, 19: 4281 (NYO-2682-1)
development for liquid metal cooled reactors, 17: 7606(R) (ORNL-1515)
development for nuclear space propulsion systems, 18: 35216
development for potassium-driven turbines for space power plants, 20: 18881(R) (N-65-18742)
development for shafts in potassium space power systems, materials testing in, 20: 2242
development for SNAP-50, 19: 29732(R) (APS-5152-R2)
development for ultrahigh vacuum systems, 20: 9134 (CONF-650512, pp 10-13)
development for volatility separation processes, 20: 7192(R) (K-1649)
development of ceramic-to-metal, for high-temperature thermionic converters, 17: 34369(R) (RBESO-3404-3)
development of ceramic-to-metal, for high-temperature thermionic converters, 18: 4179 (RTD-TDR-63-4109)
development of ceramic-to-metal, for thermionic cells, 18: 42348 (GEST-2035)
development of ceramic-to-metal, for thermionic cells, 19: 39070(R) (GEST-2046)
development of ceramic-metal, for nuclear-thermionic cells, 19: 44979(R) (NP-15419)
development of ceramic-metal, for thermionic cells, 19: 44980(R) (NP-15433)
development of ceramic-to-metal, for nuclear thermionic generating system, 20: 6023(R) (AD-619379)
development of ceramic-metal bore, for use with alkali metals, 20: 43815(R) (NASA-CR-54356)
development of ceramic-to-metal bore, for advanced space power systems, 20: 46145 (NASA-CR-54093)
development of cryogenic, for electrical leads, 18: 22576
development of cylindrical, for EGCR charge machine, 20: 36491(R) (ORNL-3951, pp 197-216)
development of dynamic, for rotary shafts, 16: 28393 (TID-7631(p.85-103))
development of dynamic shaft, for space applications, 16: 31692(R) (NP-12020)
development of, for use in pressurized water reactors, 16: 33978(R) (BMI-X-10008)
development of, for molten fluoride pumps, 17: 252 (ORNL-TM-386)
development of, for nuclear technological uses, 17: 4973
development of, for high-pressure pumps, 17: 10778(R) (NYO-9742)
development of, for high-pressure pumps, 17: 10779(R) (NYO-9743)
development of, for rotary calciners, 17: 19727 (BNL-759(p.78-80))
development of, for transuranium processing equipment, 17: 21594(R) (ORNL-TM-355)
development of frozen electrolyte–silicone rubber, 20: 6024(R) (ANL-6925(p.235-47))
development of high-pressure pump seal, 17: 16183(R) (NYO-9801)
development of high-pressure pump, 18: 20133(R) (NYO-9802)
development of large-diameter metal, for pressure vessels in nuclear rockets, 18: 43748 (ACF-1)
development of liquid-vapor, for SNAP-8, 19: 29747 (NASA-CR-54234(Vol.III))
development of mechanical, demountable seal for beryllium window of x-ray tubes, 19: 15703
development of mercury-oil, for SNAP-8, 19: 29745 (NASA-CR-54234(Vol.I))
development of rotating-shaft helium, 16: 8835 (NP-11243)
development of rotating-shaft and valve-stem, for liquid metals, 17: 7606(R) (ORNL-1515)
development of solidified-metal, sump-type, 16: 14843 (ORNL-TM-179)
drive mechanism sealing from liquid reactor coolant, 18: 7877(P)
engineering drawings of, for force transmission, 18: 41605
fabrication of ceramic-to-metal, for high-temperature operation, 17: 34366 (LAMS-2917)
fabrication of manipulator gauntlets of, 20: 5612 (ORNL-TM-1326)
fabrication of metal-to-ceramic, for use to 1500°C, 19: 2790
fabrication of omega, using high-energy-rate process, (E), 19: 22450 (KAPL-3094)

fabrication of pump, by hot pressing, 17: 7606(R) (ORNL-1515)
failure of rotating-plug, 18: 6411(R) (ANL-6706)
fatigue strength of omega seal welds in chromium–iron–nickel Alloy 600, 18: 27860 (KAPL-2000-21(p.I.1-11))
fluid flow through, 16: 19049(T) (AEC-tr-5109)
friction in, dry, 18: 23742 (TID-7690(p.106-20))
gastight, for shielding windows, 16: 687
heat sensitive, for radioisotope heat source safety, 20: 46128(P)
leak detection, development of methods and equipment for, 16: 29379 (RADC-TDR-62-66)
leak testing of seals on blister drive shafts for EGCR charge machine, 17: 16180 (TID-18233)
leak testing of, for containers of radioactive materials, 19: 34421
leakage of gastight, for conduits and cables, 17: 18219 (NAA-SR-Memo-8035)
load-deflection and stress-deflection characteristics of metallic, photoelastic determination of, 17: 16170 (AECL-1662)
materials for liquid-metal pump, development and testing of, 19: 40718 (TIM-909)
materials requirements for, in thermionic energy converters, 17: 1916(R) (ARF-2215-6)
performance for SNAP-8, 18: 40932 (NP-14234)
performance in heavy water pumps, 16: 20564 (DP-666)
performance of boron-free, radiation-resistant, insulating vitreous, 20: 15131(P)
performance of ceramic-to-metal, at high temperatures, 18: 29928(R) (NP-13979)
performance of face-type mechanical shaft seals in high-pressure water, effects of seal ring deflection on, 19: 26489 (AECL-2242)
performance of inflatable, for enclosures containing high-purity atmospheres, 18: 390
performance of metal "O" rings for sealing reactor pressure vessels, 19: 22467
performance of silicone GE SR-82, in sealing leaks in glass and metal ultrahigh vacuum systems, 18: 8511
performance of silver chloride, in cesium vapor devices, 18: 31699
performance tests of self-tightening Dome nozzle closure, 18: 10216 (HW-79205)
permeability of O-rings to helium in reactors, 18: 44950
plug design for irradiation capsules, 20: 10294(P)
plug design for pipe, 18: 31708
plug design for pressurized reactor tubes, 18: 35107(P)
potential of visco seal for use on compressors and turbines of gas cooled reactors, 16: 25506 (TID-15987)
preparation of ceramic-refractory metal, for space power systems, 20: 2292
preparation of devitrified glass, for metals, 20: 46181(P)
preparation of liquefiable bismuth–tin alloy, for reactor pressure vessels and covers, 19: 44658(P)
production of bakeable ceramic-to-metal, for C Stellarator, 18: 10495 (MATT-228)
properties of labyrinth seals, 16: 8879(T) (AEC-tr-4960)
radiation and temperature effects on silicone rubber O-rings, 16: 15245 (DC-59-10-15)
radiation effects on, in vacuum, 18: 2293(R) (FZK-161-1)
radiation effects on, in vacuum and at cryotemperatures, 18: 20581(R) (FZK-172)
radiation effects on elastomer, gamma and neutron, 18: 24937 (APEX-917)
radiation effects on NERVA flange, under dynamic operation conditions, 19: 14867 (FZK-170-2)
radiation effects on, in rotary pumps, 20: 4299(R) (ORNL-2711)
radiation effects on, at cryogenic temperatures, 20: 23794
radiation effects on, in combination with cryotemperatures and vacuum, 20: 43994(R) (FZK-290)
ring deflection effects on characteristics of face-type shaft, in high-pressure water, 19: 28468 (CRE-1176)
shield plug design for reactor access tubes, 20: 10296(P)
solder method for metal tubing, 19: 15696 (K-L-6018)
space environmental effects on, 18: 42118 (RSIC-150(Vol.I)(App.H))
specification for confinement seals in Hanford buildings, 19: 11326 (HWS-6574(Rev.1))
specification guides at HAPO for, 18: 3923 (TID-15246(Vol.I)(Rev.))
stress analysis of ceramic, 18: 44041 (MATT-293)
survey on design of labyrinth, 16: 25505 (TID-15986)
survey on theory of interface conditions in mechanical, 16: 25507 (TID-15988)
test of NMPO blower shaft, duration, 19: 40701 (TID-22007)
testing aluminum wire, 17: 33159(R) (ORNL-3472(p.107-18))
testing elastomeric, for spacecraft, 20: 29366(R) (TID-22970, pp 375-91)
testing for organic coolant pumps, 18: 24893(R) (NAA-SR-8888(Sect.III))
testing for Pathfinder reactor vessel, 17: 2573 (ACNP-62002)
testing for Prototype Organic Power Reactor coolant pump, 19: 9309 (NAA-SR-Memo-6918)
testing of dome-type, for pressure tube closure, 17: 24687(R) (SRO-82)
testing of dome-type, for pressure tube closure, 17: 35154(R) (SRO-92)
testing of elliptical primary coolant pump seals for NPD reactor, twisting-deflection, 18: 33096 (AECL-1988)
testing of face-type shaft, for high-temperature pumps, 20: 4299(R) (ORNL-2711)
testing of, for use on EGCR charge machine blister drives, 17: 17427 (TID-18234)
testing of stainless steel boss at 3000 psig and −65 to 600°F, 16: 10514 (DC-60-2-112)
tests of dynamic centrifugal shaft, for liquid metal pumps, 19: 40702 (TIM-914)
tests of labyrinth, for back diffusion, 16: 3101 (TID-14183)
torque transmission through gas-tight, 19: 6065(P)
welding of omega, evaluation of welding power source for automatic, 18: 27916 (KAPL-2000-21(p.VIII.1-7))

Seaweed
see Algae

SEBACIC ACID
radioinduced inclusions in compound with urea, 16: 3047
thermodynamic dissociation constants and solubilities of rare earth and thorium salts, 16: 11563

SEBACIC ACID, BIS(2-ETHYLHEXYL) ESTERS
effects on gamma radiolysis of polyvinyl chloride, 20: 25154

SEBACIC ACID, ESTER POLYMERS
radiation effects on physicochemical properties of, 20: 43343

Second Virial Coefficients
see Virial Coefficients

SECURININE
therapeutic effects of, on radiation sickness in rats, 18: 5139(T) (JPRS-22123)

SEDIMENTARY DEPOSITS
accumulation rates of marine, determination by protactinium-231/thorium-230 and thorium-230/thorium-232 ratios, 19: 22539(R) (TID-21522(B1-14))
age and deposition rate estimation on marine, by protactinium-231/thorium-230 and thorium-230/thorium-232 ratios, 19: 22537(R) (TID-21522)
age and deposition rate estimation on ocean-floor, by protactinium-231/thorium-230 ratio, 19: 22538(R) (TID-21522(A1-19))
age determination of, using lead–uranium method, 17: 21918
age estimation of marine, by protactinium-231/thorium-230 ratio, 18: 43601(R) (TID-21007)
age estimation of pelagic, from uranium-234/uranium-238 ratio, (E/T), 19: 38866
analysis for gold by neutron activation, 20: 33170(T) (AEC-tr-6639, pp 55-9)
analysis for potassium, thorium, and uranium by scintillation counting and x-ray fluorescence, 20: 20613
analysis for potassium by scintillation counting, 20: 37012
analysis for thorium and uranium in carbon, by gamma spectroscopy, 18: 41351
analysis of, from Chukchi Sea, 19: 29810(R) (PNE-457)
chemistry of marine, research on, 19: 31696
distribution of heavy radioelements in, in Florida, 18: 35735
prospecting for uranium, bibliography on, 16: 13371 (VDIT-54)
radioelement dispersion in, effects on uranium exploration, 18: 18059
rare-earth contents in oceanic, (E), 19: 36670
seismic effects of Pre-Dribble detonations in, 18: 371 (NP-13279)

SEDIMENTATION
age estimation in deep-sea, 17: 28943(R) (TID-18961)
calculation of density and viscosity of sucrose solutions for, 19: 32187 (K-1635)
coefficients of particles in zonal ultracentrifuge, computer program for calculating, 18: 41301 (K-DP-356)
determination in South Atlantic, 18: 43794
drift measurement using radioisotopes, 16: 24001
drift measurement at Europoort using radioisotopes, 16: 24004
effects of X agent on neutral red, effects of color on, 19: 11230
effects of X agent on neutral red, effects of aluminum foil shielding on, 19: 11231
effects of X agent on neutral red, 19: 11232
in cells, parameters of, 17: 19751 (UCRL-10640)
in ultracentrifuge, equation for describing, 19: 15486
measurement of, radiation gage for, 19: 24836(P)
profile of North Atlantic, mineral and ionium/thorium analysis of, 18: 33790
prognostic value of erythrocyte, in cervical radiotherapy, 17: 38786
radiation effects on sewage, 17: 16057(R) (TID-18262)
radiation effects on rate of bismuth chloride, 20: 18792
rate of coastal, as indicated by cerium-144 : promethium-147 ratio, 20: 45258(R) (IAEA-2607-12)
sulfur-34 distribution in, variations in, 20: 41135

transport studies using scandium-46 as tracer, 16: 17898
use in studies of radioactive aerosols, 20: 16655
see also Precipitation (Chemical)

SEDIMENTATION APPARATUS
design of, for particle separation, 17: 8316(P)
design of recording balance for particle-size analysis, 16: 261(R) (MCW-1465)
use of centrifugal photosedimentometer for particle size analysis in sub-sieve range, 19: 6143 (AWRE-O-76/64)

Sediments
see Silts

SEED
(See also specific plants.)
adaptation and dissemination in γ-irradiated forests, 20: 6821
alterations in, by atmospheric agent, 17: 7694
analysis for calcium and magnesium, activation, 18: 23418
analysis for lead-210, radiochemical, 20: 5505
analysis of corn, for moisture, neutron moderation method, 16: 26900 (ORO-485)
analysis of, activation, 19: 19771(R) (TEES-2671-4(Chap.9))
ascorbic acid content in Gramineae, 20: 38583
book: *Pre-Sowing Irradiation of Agricultural Seeds*, 19: 15202
chemically induced mutations in presoaked Arabidopsis, 20: 5357
cold sensitivity of cacao, 18: 27016(R) (TID-20708(p.6-28))
cold sensitivity of cacao, factors affecting, 19: 33717(R) (NYO-2043-108(p.5-32))
development of Quercus, 18: 3396 (BNL-6895)
effects of alkylating chemicals on *Lakota durum*, biological and mutagenic, 20: 33064
effects of chemical mutagens in *Zea mays*, 19: 15010 (BNL-7815)
effects of chemicals on barley, 16: 7413 (BNL-675(p.128-57))
effects of diethyl pyrocarbonate on cells and growth of barley, 20: 36589
effects of EMS mutagen on, genetic, 20: 22679
effects of ethyl methanesulfonate in maize, mutagenic, 20: 1656
effects of ethyleneimine and gamma radiation, 16: 6316(T) (JPRS-11322(p.447-57))
effects of ethylenimine on wheat, genetic, 20: 1655
effects of ethylenimine and x radiation on morphology of jute, 20: 33048
effects of exposure to low-dose x radiation or soaking in distilled water on growth and development of plants from, 18: 23253(T) (OTS-61-11326)
effects of free lipid fraction from irradiated seedling bean leaves on wheat, toxic, 20: 36598
effects of gases at 3 to 45°C on maize, biological, 20: 14216 (BNL-9859)
effects of gibberellic acid on normal and irradiated embryos, 16: 28801
effects of heavy cosmic-ray particles on corn, 18: 3474 (BNL-6857)
effects of irradiation of pollen on production, 17: 1304
effects of irradiation on growth of plants of carrot, flax, radish, and tomato, α, β, γ, and thermal neutron, 20: 45453
effects of irradiation on yield and food value of corn, 20: 45455
effects of Myleran on *Vicia faba*, combined with radiomimetic compounds and x rays, 16: 1595
effects of nitrosoamides on, chemical inhibition of radiomimetic, 19: 43870
effects of radiation and diethyl sulfate on barley, 20: 14384
effects of soaking and redrying on germination of, 20: 6787(R) (ORNL-3853, pp 177-81)
effects of space flight conditions on, genetic, 17: 17775(T) (JPRS-18395(p.161-72))
effects of space flight environment on, genetic, 20: 1649
effects of space flight on plant, 17: 35282(T) (FTD-MT-62-78(p.344-9))
effects of temperature and packaging on stored irradiated, 19: 45817(R) (ORO-631, pp 145-71)
effects of x radiation combined with chemical mutagens on tobacco, 16: 25193 (CNEN-118)
electric conductivity of barley, effects of temperature on, 18: 11602
enzyme reactions, 16: 11452(R) (ANL-6464(p.128-32))
evolution of carbon-14-labeled dioxide from, technique for measuring, 18: 6857
free radicals induced in, by various physical treatments, 20: 6786(R) (ORNL-3853, pp 155-60)
genetic effects of space flight on pine and wheat, 20: 42912
genetics of, effects of radiation-processed fruit juices on, 17: 23141
genetics of, effects of ethylenimine on, 16: 14491
genetics of, effects of chemical mutagens on, 16: 28775
germination of cotton, effects of irradiated infusoria on, 18: 3502(T) (JPRS-21996)
germination of, in *Zea mays*, 17: 35272 (BNL-6547)
germination of lettuce, effects of storage on, 19: 2009(R) (ORNL-3700 (p.176-9))
germination of, role of lipoxidase in, 17: 40445 (TID-18185)
gibberellic acid effects on subsequent growth of irradiated maize, 19: 33968
irradiation facility, 16: 14248
irradiation of watermelon, effects of, on harvest, 18: 14311
irradiation of, design of transportable gamma facility for, 18: 39743(T) (AEC-tr-6390(p.193-201))
irradiation of, physical aspects of, 20: 45360 (ORNL-P-2435)
metabolism in wheat, effects of cysteine and quinone on, 20: 31002
mitosis in dormant, 20: 6787(R) (ORNL-3853, pp 177-81)
mutation analysis of, methods for, 19: 45737
mutation frequency in dormant rice, effects of chemicals on, 19: 8855
mutation induction by chemicals and radiation in rice, 16: 1608
mutations in chlorophyll of, frequency of chemically induced, 17: 38689
mutations in maize, frequency of chemically induced, 17: 38690
mutations in maize, induced by x-rays and ethyl methanesulfonate, 20: 45361 (TID-22622)
mutations induced in barley, by gamma rays, sulfates, and sulfonates, 16: 1588
mutations induced by irradiation, 16: 31515
neutron dosimetry in, fast, 20: 38693
nuclei in wheat, microspectrophotometric study of properties of, 20: 40631(R) (ORNL-3922, pp 161-6)
nucleic acid synthesis in barley, 18: 17361(R) (TID-20353)
phosphate metabolism in germinating lettuce, effects of monochromatic light on, 16: 31404(R) (ANL-6535(p.147-54))
phosphorus-32 effects on barley, during germination, 17: 24996
physiology, effects of various treatments, 16: 15046(R) (TID-15341)
polymer grafting on irradiated, protective effects, 16: 1519
preparation of lipoxidase from leguminous and other, 17: 40445 (TID-18185)
protein synthesis in pea, tracer study, 16: 11451(R) (ANL-6464 (p.116-27))
radiation control of insect pests of stored grains, 17: 20289
radiation dosage for lethality in dormant Guar, 19: 40376
radiation dose level effects on relative biological effectiveness and elimination of chromosomal aberrations, 16: 1603
radiation dose measurements for, 18: 17595
radiation effect on wheat, effects of oxygen tension and storage temperature on neutron, 18: 31221
radiation effects, 16: 1580
radiation effects, 16: 1617
radiation effects, 16: 1571
radiation effects, biological traits affecting, 16: 1577
radiation effects on morphophysiological characteristics of wheat, 16: 1609
radiation effects on mutation rates in first and later formed sprouts in barley, 16: 1578
radiation effects on phosphorylation and red spectrum photomorphogenesis of mitochondria in lettuce, 16: 1583
radiation effects on germination of lettuce, at 26°C, 16: 1584
radiation effects on growth of wheat, 16: 1598
radiation effects on growth of seedlings, 16: 1525
radiation effects on metabolic reactions in corn, 16: 1492(T) (JPRS-10170(p.405-17))
radiation effects on oat, 16: 1515
radiation effects, protection by partial hydration, 16: 5158(R) (TID-14316)
radiation effects on *Vicia faba*, 16: 1575
radiation effects on oxygen-saturated and dry barley, 16: 9885
radiation effects on germination, sprouting, and survival, 16: 12884(T) (AEC-tr-5052)
radiation effects on production, pollen exposure, 16: 12931
radiation effects on stored chestnuts, 16: 14564
radiation effects, 16: 15046(R) (TID-15341)
radiation effects of cotton, on chemical composition and accumulation of cottonseed oil, 16: 10369(T) (JPRS-12305)
radiation effects on rice, 16: 9852
radiation effects on soybean, genetic, 16: 8572
radiation effects on, application to crop protection, 16: 16110
radiation effects on genetics in barley, 16: 17526
radiation effects on aging of onion, 16: 17482
radiation effects on survival and germination, 16: 20167
radiation effects on dormant flax, measurement by iodine number, oil quality, and seed yield, 16: 21934
radiation effects, genetic, 16: 26682 (BNL-5899)
radiation effects, genetic, 16: 28790
radiation effects on chimeric formation of X, panicle in dormant rice, 16: 30253
radiation effects on cytology and genetics of rice, thermal neutron and x, 16: 32763
radiation effects on growth and viability of sweet clover, 16: 1600
radiation effects, genetic, 17: 15682
radiation effects, genetic, 17: 23144
radiation effects, genetic, 17: 24894(R) (TID-18673)

radiation effects on ascorbic acid content in *Vicia faba*, beta, 17: 15716
radiation effects on barley, 17: 25012
radiation effects on chromosomes in barley, oxygen effect, 17: 30391
radiation effects on corn, from satellite flights, 17: 31947
radiation effects on development of corn, 17: 3260
radiation effects on electron spin resonance signals, 17: 10850(R) (HW-73337(p.77-157))
radiation effects on, electron spin resonance studies of effects of oxygen on, 17: 40570
radiation effects on enzyme activity of *Pisum sativum* L., 17: 7828
radiation effects on, environmental factors in, 17: 31869
radiation effects on, environmental factors in, 17: 31951
radiation effects on fertility of rice, 17: 35578
radiation effects on frequency and types of chromosome aberrations and mutations in wheat, 17: 40588
radiation effects on germination of Nicotiana, 17: 30314
radiation effects on germination of Fraxinus, beta, 17: 37070
radiation effects on germination and survival of oat, effects of storage on, 17: 38845
radiation effects on growth and reproduction of dormant, of *Sorghum vulgare* Pers., 17: 12171
radiation effects on growth of grain and vegetable, 17: 34202
radiation effects on growth of, effects of environment on, 17: 33578
radiation effects on Lupinus, x, 17: 35481
radiation effects on maize, neutron and x, 17: 10380
radiation effects on maturation, 17: 23199
radiation effects on meiosis of *L. esculentum* and *L. peruvianum*, 17: 19833
radiation effects on metabolism of sprouting, 17: 30330
radiation effects on oak and pine, 17: 2819 (BNL-6466)
radiation effects on phytoncidal activity of white mustard, 17: 30373
radiation effects on soybean, genetic, 17: 27071(T) (OTS-62-11755/2 (p.99-100))
radiation effects on coffee, genetic, 17: 15565
radiation effects on Delphinium, genetic, 17: 19763
radiation effects on rice, genetic, 17: 24893 (TID-18672)
radiation effects on tomato, genetic, 17: 30374
radiation effects on wheat, genetic, 17: 28714
radiation effects on wheat, genetic, 17: 28715
radiation effects on dry, of *Arabidopsis thaliana*, 18: 63
radiation effects on Quercus, gamma, 18: 1368 (BNL-6893)
radiation effects in maize, genetic, 18: 1374 (BNL-7367)
radiation effects on germination of dry and wet, x, 18: 1378(T) (CEA-tr-X-490)
radiation effects on genetics of rice, gamma and neutrons, 18: 1388
radiation effects on barley, protective effects of tyramine and tryptamine against x, 18: 3589
radiation effects on Quercus, gamma, 18: 3477 (BNL-6892)
radiation effects on germination of barley, 18: 5038
radiation effects on germination of *Phacelia tanacetifolia*, uv and visible, 18: 9840
radiation effects on respiration of buckwheat, after soaking in boron-containing water, 18: 9849
radiation effects on wheat, plant sensitivity from gamma, 18: 9850
radiation effects on *Solanum nigrum*, 18: 11668
radiation effects on genetics of barley, post-treatment of fast neutron and x, 18: 11842
radiation effects on oat and wheat, gamma, neutron, and x, 18: 13494
radiation effects on tomato, effects on plant genetics, 18: 13533
radiation effects on wheat, 18: 17590
radiation effects on nicotine content of tobacco plants from gamma-irradiated, 18: 17591
radiation effects on development of nicotiana, 18: 19690
radiation effects on, protective effects of cysteine and sodium hydrosulfite against, 18: 21923
radiation effects on grain yield from wheat, 18: 21833(T) (OTS-63-11453/2(p.87-98))
radiation effects on diseases carried by, gamma, 18: 21843
radiation effects on germination of cotton, gas plasma, 18: 21911
radiation effects on cytology in bean, gamma, 18: 23252(T) (ORNL-tr-84)
radiation effects on nucleic acid metabolism in, 18: 25175
radiation effects in grass, genetic, 18: 25177
radiation effects on dimensions of cells in leaves of sugar beets, 18: 25136
radiation effects on barley and lily, proton and x, 18: 27083
radiation effects on meristematic cells of rye and wheat, 18: 27125
radiation effects on red balsam, effects on anthocyanin production of, 18: 29277
radiation effects on yield of alfalfa, gamma, 18: 31169
radiation effects on Lilium, x, 18: 31215
radiation effects in cotton, 18: 33313
radiation effects on extracts of cellular structure of sugar beet leaves by exposure of, 18: 33314
radiation effects on cotton, gamma, 18: 33333
radiation effects on barley, combined with mutagens, 18: 33375
radiation effects on potato production of, x, 18: 33376
radiation effects on barley, effects of chlorides of calcium, magnesium, and sodium on, 18: 33409
radiation effects in stored barley, 18: 35349
radiation effects on *Lupinus termis*, 18: 36990
radiation effects on, of *Crotalaria intermedia*, genetic, 18: 36994
radiation effects on germination of tobacco, 18: 38897
radiation effects on amino acids in cotton, gamma, 18: 38943
radiation effects on free radicals in cotton, 18: 38944
radiation effects on pea, 18: 38946
radiation effects on, effects on anatomic structure of plants, 18: 41188
radiation effects on germination and harvest of maize, uv, 18: 41209
radiation effects on chromosomes in barley, 18: 41210
radiation effects on wheat, genetic, 18: 41115
radiation effects on germination of maize, gamma, 18: 41126
radiation effects in *Zea mays*, meson (μ^-) and (π^-), 18: 41157
radiation effects on *Vicia faba*, 18: 41171
radiation effects on Triticum, neutron and x, 18: 43218(R) (EUR-1882.e(p.7-26))
radiation effects on *Phaseolus vulgaris* viability, 19: 67 (AAEC/TM-263)
radiation effects on jute, genetic, 19: 116
radiation effects on jute, genetic, 19: 165
radiation effects on, gas-plasma, 19: 185
radiation effects on, genetic, 19: 3896(R) (ORO-625(p.109-29))
radiation effects on Luzula, x, 19: 3929
radiation effects on, genetic, 19: 3982
radiation effects on *Allium cepa*, protective effects of aminothioamides against, 19: 5677
radiation effects on germination of jute, gamma and x, 19: 5716
radiation effects on amylase activity and germination of groundnut, gamma, 19: 7167
radiation effects on tomato, 19: 8858
radiation effects combined with chemicals on growth and mutation frequency of rice, 19: 8854
radiation effects in, genetic, 19: 12992
radiation effects in *Glycine max*, 19: 15011 (BNL-7890)
radiation effects in pea, genetic, 19: 43770
radiation effects in wheat, biological, 19: 43781
radiation effects in rice, biological, 19: 43781
radiation effects in *Zea mays*, genetic, 19: 15010 (BNL-7815)
radiation effects on cotton, effects on plant growth and fiber texture, 19: 8860
radiation effects on germination of Pinus, gamma, 19: 10829
radiation effects on development of *Triticum aestivum*, 19: 10887
radiation effects on nucleic acid metabolism in, 19: 12959 (TID-21460)
radiation effects on chromosomes of *Sorghum vulgare*, neutron and x, 19: 13085
radiation effects on germination of Arabidopsis, x, 19: 15157
radiation effects on germination of Pinus, gamma, 19: 15165
radiation effects on growth inhibitors in wheat, x, 19: 15171
radiation effects on barley and wheat, gamma and x, 19: 15173
radiation effects on germination of Pinus, environmental factors affecting gamma, 19: 15177
radiation effects on lipid metabolism in germinating and maturing cotton, 19: 17519(T)
radiation effects on mutagenesis of rye grass, gamma and x-ray, 19: 17527
radiation effects on chromosome aberrations in barley, protective effects of animal compounds against, 19: 17686
radiation effects from fission products in soil on, of grain crops, 19: 19508(T) (JPRS-28977)
radiation effects on germination and plant growth from maize, 19: 19528
radiation effects on chromosome aberrations in *Crepis capillaris*, moisture effects on fast neutron post-, 19: 19581
radiation effects on chromosome rearrangements in barley, partial recovery from, 19: 19639
radiation effects on, 19: 21792(R) (ORNL-3650(p.187-219))
radiation effects on development of maize, 19: 21870
radiation effects during storage of clover and barley, effects of moisture on, 19: 21946
radiation effects on germination of *Brassica juncea*, 19: 21884
radiation effects in wheat, genetic, 19: 24261(R) (TID-21649)
radiation effects on germination of wheat, x, 19: 25935
radiation effects on chromosomes of barley, aberrant gamma, 19: 25946
radiation effects on germination and growth of *Papaver somniferum*, 19: 25947
radiation effects on germination and growth of *Artemisia kurramensis*, 19: 25948
radiation effects on germination and growth of *Atropa belladonna*, 19: 25949
radiation effects on germination of *Papaver somniferum*, 19: 25950

radiation effects on morphine production by *Papaver somniferum* plants grown from, 19: 25951
radiation effects in *Arabidopsis thaliana*, genetic, 19: 27971
radiation effects on barley, aberrant and mutagenic gamma, 19: 27996
radiation effects on growth and development of plants grown from exposed, of *Rauwolfia serpentina*, 19: 27999
radiation effects on growth and metabolism in, 19: 29893(R) (ANL-6971 (p.166-205))
radiation effects on *Pisum sativum*, genetic, 19: 29897 (EUR-2218.e)
radiation effects on bacterial resistance of prunus seedlings, 19: 33887
radiation effects on growth of embryos from wheat, 19: 33888
radiation effects on growth and metabolism of sunflower, relation between, 19: 33894
radiation effects on yields from, gamma, 19: 36008
radiation effects on germination and plant growth, 19: 36051
radiation effects on wheat, effects of water content on, 19: 38412
radiation effects on content of ascorbic acid and ascorbic acid oxidase in *Momordica charantia*, 19: 40371
radiation effects on fat content in cabbage, γ, 19: 42282
radiation effects on lipoxidase activity in, gamma, 19: 42323
radiation effects on interaction of induced chromosome breaks in barley, neutron and x-ray, 19: 42343
radiation effects in wheat, genetic, 19: 42260 (TID-22115)
radiation effects on nitrogenous bases in DNA in bean, fast neutron and gamma, 19: 42322
radiation effects on production of pine, gamma, 19: 43722(R) (TID-22108)
radiation effects on *Digitalis lanata EHRH*, 19: 43746
radiation effects on Pinus, physiological, 19: 45855
radiation effects on *Acer negundo*, genetic, 19: 45865
radiation effects on red clover, genetic, 19: 45882
radiation effects on barley, genetic, 19: 45819(R) (TID-22176)
radiation effects in corn, on seedling growth, 19: 45836
radiation effects on pea, genetic, 20: 81
radiation effects on growth of seedlings from *Zea mays*, 20: 109
radiation effects on, genetic, 20: 1649
radiation effects on wheat, genetic, γ, 20: 1655
radiation effects in oat, genetic, 20: 1665
radiation effects on barley, biological, 20: 1667
radiation effects on, genetic, 20: 1622 (WT-820)
radiation effects on wheat, genetic, fast neutron, 20: 1655
radiation effects on wheat, genetic, 20: 3762
radiation effects on barley, effects of dimethyl sulfoxide and nitric oxide on oxygen effect in, 20: 5298(R) (RLO-353-4)
radiation effects on rice, 20: 5393
radiation effects on wheat, x, 20: 5403
radiation effects on rice, genetics, γ, 20: 8693
radiation effects on *Pisum sativum*, x, 20: 8660
radiation effects on rice, γ, 20: 8693
radiation effects on growth and development of maize, gamma, uv, and x-ray, 20: 10613(T) (NP-tr-1344)
radiation effects on germination of grass, γ, 20: 10646
radiation effects on germination of conifer, gamma, 20: 12671
radiation effects on *Vigna sinensis*, neutron and x, 20: 14341
radiation effects on germination of *Phleum pratense*, γ and x, 20: 14349
radiation effects on germination of *Rauwolfia serpentina*, γ, 20: 16249
radiation effects on barley, protective effects of inorganic salts against, 20: 16297(R) (EUR-2548.f)
radiation effects combined with magnetic fields on barley, x, 20: 18387
radiation effects on barley, effects of seed water on oxygen effect on gamma, 20: 18389
radiation effects on rice, genetic γ, 20: 18416
radiation effects on rice, genetic γ, 20: 18417
radiation effects on barley, genetic x, 20: 18418
radiation effects on bean and soybean, genetic x, 20: 18419
radiation effects on barley, protective effects of carbonates and phosphates against x, 20: 18435
radiation effects on Southern Pine, effects of moisture content and stratification on x, 20: 22744
radiation effects on enzymatic activity and germination in Pisum, x, 20: 22606
radiation effects on pea, factors affecting x, 20: 22676
radiation effects on barley, genetic x, 20: 22679
radiation effects on pea, γ, 20: 28909
radiation effects on chromosomal bridges at anaphase in barley, fast-neutron and x, 20: 29031
radiation effects on corn and wheat, γ, 20: 31110
radiation effects on corn and wheat, γ, 20: 31113
radiation effects on development of pea, γ, 20: 31114
radiation effects on wheat, metabolic γ, 20: 31002
radiation effects on DNA from cotton, γ, 20: 31019
radiation effects on biochemical properties of, effects of storage on γ, 20: 31024
radiation effects on jute, genetic γ, 20: 31027 (AECD/AG-14)
radiation effects on maize, genetic fast-neutron and x, 20: 31092
radiation effects on carbohydrate synthesis in cotton, γ, 20: 32955
radiation effects on growth and morphology of *Vicia sativa* and *V. villosa*, fast-neutron, 20: 32988
radiation effects on, effects of oxygen pressure and temperature during storage on γ, 20: 33045
radiation effects on *Lakota durum*, biological and mutagenic, 20: 33064
radiation effects on *Vigna sinensis*, γ and fast-neutron, 20: 32969(R) (ORO-648, pp 123-58)
radiation effects on cotton, 20: 32969(R) (ORO-648, pp 123-58)
radiation effects from phosphorus-32 on wheat, effects of feed solution additives on, 20: 35226
radiation effects on sprouting of maize, 20: 35250
radiation effects on gladiolus, fast-neutron, gamma, and x, 20: 35290
radiation effects on mutations and survival of dry *Arabidopsis thaliana*, gamma and heavy particle, 20: 35298
radiation effects on, research summary for India, 20: 36539(R) (NP-16171)
radiation effects on summer wheat, γ, thermal neutron, uv, and x, 20: 35317
radiation effects on chromosomes in barley, effects of diethyl pyro-carbonate on fast-neutron and gamma, 20: 36589
radiation effects in cotton species *Gossypium barbadense*, 20: 36623
radiation effects on ascorbic acid content in germinating, 20: 38583
radiation effects on apple, genetic, fast neutron and γ, 20: 38692
radiation effects on barley, effects of centrifugation on γ, 20: 38618
radiation effects on barley, γ, 20: 38691
radiation effects on chromosomes of *Vicia faba*, repair mechanisms for, 20: 40609 (CONF-660418-1)
radiation effects on jute, gamma, 20: 40681
radiation effects on rice, chlorophyll mutations from β, thermal neutron, or x, 20: 40641
radiation effects on maize, fast-neutron and x, 20: 42843 (BNL-10358)
radiation effects on cotton, gamma, 20: 42896
radiation effects on, of pure and hybrid winter wheat, gamma, 20: 42897
radiation effects on mutagenesis in dry *Vicia faba*, 20: 42920
radiation effects on rice growth following sulfur-35 irradiation of, varietal differences in, 20: 42949
radiation effects on cabbage, high-energy proton, 20: 42898
radiation effects on starch hydrolysis of barley endosperms, γ, 20: 45422
radiation effects on barley, genetic, 20: 45464
radiation effects on germination of, 20: 45264(R) (UCLA-12-595, pp 72-89)
radiation effects on growth of barley, γ, 20: 45328
radiation effects on oat, genetic, 20: 45369
radiation effects on microflora of winter rye, uv, 20: 45389
radiation effects on storage time for sunflower, gamma, 20: 45416
radiation effects on soybean, thermal neutron and x, 20: 45388
radiation effects on *Sorghum arundinaceum*, gamma, 18: 25131
radiation effects on barley, 16: 7413 (BNL-675(p.128-57))
radiation effects on viability and aberrations in potato, 17: 31938
radiation effects on mutation frequency in dormant rice, 19: 8855
radiation effects on genetics of, x, 16: 14491
radiation effects on genetics of Triticinoe, 16: 23454
radiation effects on genetics of tomato, 16: 25197 (CNEN-119)
radiation effects on genetics of, γ, 16: 28775
radiation effects, genetic, 18: 11645(R) (ORO-614)
radiation injuries in barley, effects of oxygen, 16: 1579
radiation injuries in barley, effects of dormant state on, 18: 5140(T) (JPRS-22147)
radiation injuries in barley, protective effects of cysteine against, 18: 5140(T) (JPRS-22147)
radiation injuries in dry, relation to free radical production and decay, 20: 8588 (BNL-9537)
radiation injury to radish, protective effects of erioglaucine against, 19: 186(R) (HW-81746(p.3.111-13))
radiation lethal dose measurements for red clover, 16: 8573
radiation processing of stored, effects on germination and fungi growth, 19: 15946 (CONF-641002(p.4-7))
radiation processing of *Musa balbisiana*, for fungus control, 19: 25923
radioinduced and spontaneous mutations in tomato, quantitative comparison of, 17: 10391
radioinduced chlorophyll mutations in, frequency of, 17: 38689
radioinduced chromosome aberrations in barley, effects of intensity on frequency of, 17: 31902
radioinduced chromosome aberrations in dry wheat, 18: 5027
radioinduced chromosomal aberrations in radicals of wheat, 19: 7096
radioinduced chromosome aberrations in *Vicia faba*, role of free radicals in, 19: 8877
radioinduced chromosome aberrations in barley, gamma, 19: 15069
radioinduced chromosome aberrations in, 20: 97
radioinduced chromosome aberrations of tomato, 20: 1638
radioinduced chromosome aberrations in barley, x, 20: 8702

radioinduced chromosome aberrations in barley and *Vicia faba*, effects of Myleran on neutron, 20: 31136
radioinduced chromosome breaks in *Vicia faba*, effects of dinitrophenol on, 20: 42913
radioinduced double kernels in rice, 17: 35579
radioinduced electron spin resonance signals in lettuce, effects of hydration on γ, 20: 40631(R) (ORNL-3922, pp 161-6)
radioinduced free radicals in lettuce, formation and decay, 16: 1574
radioinduced free radicals, 16: 7440
radioinduced free radicals in, effects of oil and protein content on, 17: 15763
radioinduced free radicals in, 17: 25028
radioinduced free radicals in mustard, effects of water and AET on, 18: 31165
radioinduced free radicals in, 19: 5668
radioinduced free radicals in, effects of water content on, 19: 5687
radioinduced free radicals in, effects on oxygen and nitric oxide on, 19: 5688
radioinduced free radicals in, ESR spectra of, 19: 15168
radioinduced free radicals in, ESP measurements of fission neutron, γ, and x, 20: 8588 (BNL-9537)
radioinduced genetic variation in a diploid selfing line of, 17: 33630
radioinduced genetic variability in oat, effects of ploidy on, 19: 26053
radioinduced grafting of vinylpyrrolidone on, biological effects, 16: 1460
radioinduced injuries and mutations in rice, protective effects of cysteine and sodium hydrosulfite against, 19: 26121
radioinduced mutations in polyploids, effects of diplontic selection on frequency and spectrum radioinduced, 16: 1592
radioinduced mutations in barley, scoring of, 17: 33720
radioinduced mutations in *Vicia sativa* L., 17: 10395
radioinduced mutations in cabbage, 17: 35527
radioinduced mutations in barley, effects of pre-treatment on, uv, 17: 35539
radioinduced mutations in, method for producing gamma, 18: 29189
radioinduced mutations in barley, effects of temperature on gamma, 18: 31218
radioinduced mutations in rice, methods for determining, 19: 2118
radioinduced mutations in barley, protective effects of aminoethylisothiuronium, 19: 36105
radioinduced mutations in jute, γ, 20: 16217 (AECD-AG-7)
radioinduced mutations in barley, x, 20: 18411
radioinduced mutations for variegation in Einkorn wheat, beta, fast neutron, gamma, and thermal neutron, 20: 20497
radioinduced mutations in wheat, x, 20: 20501
radioinduced mutations in cotton, beta, 20: 22664
radioinduced mutations in barley and rice seeds, γ and x, 20: 31050
radioinduced mutations in barley, x, 20: 40711
radioinduced mutations in rice, beta, thermal neutron, or x, 20: 40640
radioinduced mutations in wheat, x, 20: 42846 (IAEA-2466-13)
radioinduced mutations in, factors affecting frequency of beta, 20: 45432
radioinduced mutations in maize, frequency of, 17: 38690
radioinduced photoconductivity in barley, 18: 13532
radioinduced sterility in, γ, 19: 43767
radiosensitivity, 16: 18788
radiosensitivity, 16: 28740 (BNL-5039)
radiosensitivity, 17: 31816(R) (ORO-605)
radiosensitivity, 18: 13484
radiosensitivity, 18: 25133
radiosensitivity, effects of oxygen, 16: 1533
radiosensitivity, effects of physiological state, 16: 1535
radiosensitivity, effects of water content, oxygen supply, storage period, and light, 16: 12917
radiosensitivity, effects of paramagnetic ions, 17: 23142
radiosensitivity, effects of humidity and dose rate, 17: 23143
radiosensitivity effects of water content and calcium chloride solutions on barley, x, 20: 38736
radiosensitivity, factors affecting, 16: 23469
radiosensitivity, factors affecting, 16: 23369
radiosensitivity, genetic factors, 16: 26819
radiosensitivity, modifying factors, 16: 31516
radiosensitivity of pasture type rye grass, 16: 1610
radiosensitivity of barley, effects of water content and x-ray wave length on, 16: 1619
radiosensitivity of wheat and barley, effect of variety, 16: 9848(T) (JPRS-11485(p.158-63))
radiosensitivity of pine, effects of water content on, 16: 17470
radiosensitivity of crimson clover, 16: 21932
radiosensitivity of lespedeza, 16: 31488
radiosensitivity of *Haplopappus gracilis*, 17: 7825
radiosensitivity of chromosomes during germination, 17: 15650
radiosensitivity of, effects of moisture content on, 17: 15799
radiosensitivity of tomato, 17: 17765(R) (TID-18414)
radiosensitivity of germinating rice, effects of soaking on, 17: 30371
radiosensitivity of germinating rice, effects of gibberellic and indoleacetic acids on, 17: 30372
radiosensitivity of tree, 17: 33575
radiosensitivity of, effects of ploidy on, 17: 38879
radiosensitivity of, mechanism of humidity effects on, 17: 38880
radiosensitivity of, effects of protective compounds on, 17: 38881
radiosensitivity of *Allium L.*, 18: 11712
radiosensitivity of pea, effects of water content on, 18: 17577
radiosensitivity of tree, 18: 23312
radiosensitivity of rye, effects of moisture, temperature treatment, radiation wave length, and ascorbic acid content on, 18: 25126
radiosensitivity of onion, effects of aging on, 18: 25179
radiosensitivity of castorbean, 18: 25180
radiosensitivity of oat, effects of moisture content on, 18: 25181
radiosensitivity of barley, 18: 25182
radiosensitivity of tropical plant, 18: 27070(R) (TID-20708(p.28-41))
radiosensitivity of, constant for predicting, 18: 33384
radiosensitivity of papaya, 18: 33389
radiosensitivity of tomato, effects of hydration on, 18: 35377
radiosensitivity of buckwheat, effects of ploidy on, 18: 41189
radiosensitivity of chromosomes in maize, 19: 2062 (BNL-8462)
radiosensitivity of, review on, 19: 7155
radiosensitivity of dry barley, effects of oxygen on, 19: 8947
radiosensitivity of barley, effects of water soaking on, 19: 15089
radiosensitivity of sprouting maize, effects of 2,4-dinitrophenol on fast neutron and gamma, 19: 19582
radiosensitivity of *Arabidopsis thaliana*, 19: 21914
radiosensitivity of rice and wheat, 19: 21917
radiosensitivity of barley, correlation of temperature and water content effects on, 19: 24316
radiosensitivity of barley, environmental effects on, 19: 26042
radiosensitivity of, effects of nitric oxide or water on, 19: 29886(R) (ANL-6971(p.29-46))
radiosensitivity of prunus species, 19: 33887
radiosensitivity of, 19: 33956
radiosensitivity of *Avena strigosa* and *Triticum monococcum*, 19: 33843
radiosensitivity of rice and wheat, effects of age, 19: 36075
radiosensitivity of barley, effects of treatment with cysteamine, ethyl sulfonate, or oxygen, 19: 36122
radiosensitivity of, 19: 45884
radiosensitivity of, species differences in, 19: 45817(R) (ORO-631, pp 145-71)
radiosensitivity of rice, effects of moisture content and variety, 20: 1669
radiosensitivity of *Phaseolus mungo*, post- and pre-irradiation heat treatment effects on, 20: 1690
radiosensitivity of *Crotalaria intermedia*, effects of nitric oxide on, 20: 3759
radiosensitivity of cotton, γ, 20: 6874
radiosensitivity of barley and bean, γ, 20: 6873
radiosensitivity of wheat, effects of ploidy on, 20: 6897
radiosensitivity of, effects of dose fractionation on γ and x, 20: 6827
radiosensitivity of *Melandrium album*, γ and x, 20: 8647
radiosensitivity of barley, effects of hydrogen ion content on γ, 20: 8696
radiosensitivity of Phalaris, effects of ploidy, 20: 8697
radiosensitivity of *Trifolium subterraneum*, 20: 8704
radiosensitivity of, effects of chromosome volume on γ, 20: 8705
radiosensitivity of *Vicia sativa*, effects of moisture on, 20: 16276
radiosensitivity of *Vicia faba*, effects of infrared radiation on x, 20: 16278
radiosensitivity of wheat, γ and x, 20: 16285
radiosensitivity of wheat, x, 20: 16286
radiosensitivity of medicinal plant, γ, 20: 16290
radiosensitivity of *Lolium perenne*, effects of water content on, 20: 18382
radiosensitivity of rice, x, 20: 18414
radiosensitivity of *Oenothera berteriana*, 20: 22764
radiosensitivity of pea, effects of chemical and biological compounds on, 20: 29049
radiosensitivity of wheat, effects of age on, 20: 32978
radiosensitivity of Hibiscus and Vigna, fission-neutron, 20: 32969(R) (ORO-648, pp 123-58)
radiosensitivity of dormant, fast-neutron, 20: 32969(R) (ORO-648, pp 123-58)
radiosensitivity of *Lupinus angustifolius* L., effect of moisture content on γ, 20: 36646
radiosensitivity of deciduous tree, effects of physiological state and water content on γ and neutron, 20: 38594(R) (ORO-2066-10)
radiosensitivity of sprouting barley, γ, 20: 40716
radiosensitivity of tobacco, factors affecting, 20: 40613 (N-66-18147)
radiosensitivity of Pinus, γ, 20: 42850(R) (NYO-2043-130)
radiosterilization of grain, apparatus and dose calculations for, 19: 42783

RNA metabolism in aleurone cells of, effects of gibberellic acid on, 19: 48102(R) (TID-22175)
sampling in oak-pine forest, 19: 12903 (BNL-7837)
sensitivity of barley, to ethyl methanesulfonate, 18: 25182
sensitivity of castorbean, to ethyl methanesulfonate, 18: 25180
space flight effects on, 18: 1326(T) (FTD-TT-63-968(p.326-31))
strontium accumulation in barley and wheat, 18: 21789
strontium-85 uptake by barley, oat, rye, and wheat, 19: 33753
strontium-90 content in plant, 20: 18906(T)
sulfur metabolism in cacao, 18: 27016(R) (TID-20708(p.6-28))
sulfur metabolism in cacao, 20: 42850(R) (NYO-2043-130)
viability and aberrations in potato, effects of chemicals on, 17: 31938
X-agent effects on growth of, 17: 38668

SEEDLINGS

calcium metabolism, replacement of calcium by strontium, tracer study, 17: 28653
calcium-45 uptake and transport by oat, 19: 11535
cation metabolism in wheat, 20: 38548(R) (ORO-2410-1)
cesium-137 metabolism by rice, effects of fertilizers and irrigation on, 19: 12912 (NP-14761)
cesium-137 uptake by wheat, cultured with ammonia, 19: 29878
chemical effects on potato, 19: 3965
desoxyribonucleic acid synthesis by primary root of *Glycine max*, 20: 14215 (BNL-8643)
development in *Pinus lambertiana*, 19: 43643(R) (TID-22143)
development of Pinus, role of cotyledons in, 19: 31625 (BNL-8203)
development of Vicia, effects of chemicals on, 17: 38691
effects of arginine and cysteine on mutations in onion, 19: 17481
effects of chemical growth inhibitors on rice, 19: 45794
effects of deuterium on root development in corn and pea, 18: 19662
effects of ethyl methanesulfonate in maize, mutagenic, 20: 1656
effects of irradiation of seed on height, in barley, 16: 17526
effects of irradiation of seeds on growth of oak and pine, 17: 2819 (BNL-6466)
effects of irradiation of seeds on growth of oak and pine, 17: 2820 (BNL-6467)
effects of light on metabolism in squash, 20: 42842(R) (ANL-7136, pp 290-301)
effects of seed irradiation on ribonucleic acid metabolism in corn, 16: 17452
fertilizer absorption by rice, tracer study of foliar, 20: 14240 (NP-15670)
growth, effects of post-irradiation storage on chromosomal aberrations and, 16: 1581
growth of bean, effects of temperature on, 20: 45248(R) (NYO-2043-129)
growth of *Pisum*, effects of chelated nutrient solution on, 18: 36868 (BNL-7246)
growth of rough lemon and trifoliate orange, effects of iron and zinc chelates on, 19: 29813 (TID-20741)
growth of wheat, effects of radiation and weightlessness on, 19: 43717 (NASA-CR-303)
growth of, from irradiated pea seeds, 20: 81
growth of, relation of geoelectric effect and geotropic curvature, 19: 29893(R) (ANL-6971(p.166-205))
incorporation of carbon-14-labeled glucosides of chalcone in red cabbage, 19: 15660
lipoxidase activity in maize, 18: 15704 (TID-18662)
morphology of Vicia, effects of seed exposure to chemicals on, 17: 38692
mutation induction in, diepoxybutane, 16: 1602
nucleic acid synthesis in, effects of light on, 16: 26816
oxidative phosphorylation of root and shoot mitochondria in corn, temperature effects on, 19: 6920
photomorphogenesis, control of development and growth by visible radiation, 16: 1582
radiation effects, 17: 23143
radiation effects on morphophysiological characteristics of wheat seed, 16: 1609
radiation effects on growth of wheat, 16: 1612
radiation effects on wheat, in relation to polyploidy, 16: 1613
radiation effects on germination and growth, with and without embryo transplantation, 16: 1573
radiation effects on diploid wheat, comparison of beta and gamma, 16: 12932
radiation effects on roots of *Zea mays*, 17: 1321
radiation effects on nucleic acid distribution and metabolism in *Zea mays*, 17: 1322
radiation effects on ribonuclease activity in *Zea mays*, 17: 1323
radiation effects on nucleic acid and protein metabolism in barley, 17: 10456
radiation effects on cell division, 17: 10359 (HW-SA-2606)
radiation effects on, of grain, maize, and potatoes, 17: 17806
radiation effects on peroxide formation in barley and bean, 17: 23129
radiation effects on einkorn wheat, acute and chronic, 17: 30224
radiation effects on peroxidase activity in corn, gamma, 17: 30357
radiation effects on growth of Fraxinus, beta, 17: 37070
radiation effects on roots of *Vicia faba*, x, 17: 40607
radiation effects on pea, mitotic cycle duration effects on chromosome breakage in gamma, 18: 1417
radiation effects on Quercus, gamma, 18: 3477 (BNL-6892)
radiation effects on root meristems of maize, x, 18: 5016
radiation effects on leaf growth, effects of kinetin on, 18: 8134
radiation effects on cell permeability in *Allium cepa* L., 18: 11675
radiation effects on oat and wheat, gamma, neutron, and x, 18: 13494
radiation effects on cotton, gamma, 18: 20418
radiation effects on barley, protective effects of chlorides of barium, beryllium, and strontium against, 18: 23368
radiation effects on pea, genetic, 18: 35308 (BNL-7316)
radiation effects on, of *Crotalaria intermedia*, genetic, 18: 36994
radiation effects on pea, 18: 38946
radiation effects on *Pinus thunbergii*, gamma, 19: 3944
radiation effects on potato, gamma and fast neutron, 19: 3965
radiation effects on catalase activity and peroxide content of cotton, 19: 8934
radiation effects on nucleic acid metabolism in, 19: 12959 (TID-21460)
radiation effects on growth of Pinus, gamma, 19: 15165
radiation effects on, gamma, 19: 15166
radiation effects on barley and wheat, gamma and x, 19: 15173
radiation effects on maize, gamma, 19: 15178
radiation effects on growth of *Vicia faba*, dose-rate effects on, 19: 17561
radiation effects on growth of *Vicia faba*, theoretical calculations of acute and protracted, 19: 17562
radiation effects on development of maize, 19: 19528
radiation effects on *Brassica juncea*, 19: 21884
radiation effects on carbon dioxide exchange in spine, 19: 24346
radiation effects on bean, protective effects of compressed nitrogen against, 19: 26139
radiation effects on, small-dose, 19: 25931
radiation effects on growth and development of *Rauwolfia serpentina*, grown from exposed seed, 19: 27999
radiation effects on bacterial resistance of prunus, 19: 33887
radiation effects from incorporated phosphorus-32 in *Vicia faba*, 19: 33827
radiation effects on cytology and morphology in Pinus, 19: 43722(R) (TID-22108)
radiation effects on growth in Pinus and Quercus, gamma, 19: 43722(R) (TID-22108)
radiation effects on growth of corn, 19: 45836
radiation effects on respiration in corn, 19: 45836
radiation effects in seed on growth of Pinus, 19: 45855
radiation effects on ascorbic acid content in legume, beta and gamma, 19: 45938
radiation effects on growth of *Zea mays*, from irradiated seed, 20: 109
radiation effects on development of wheat, 20: 1666
radiation effects on growth of barley, 20: 1667
radiation effects on growth of bean and pea, γ, 20: 5388
radiation effects on cells in roots of pea, γ, 20: 5390
radiation effects on growth of corn, in contaminated soil, β, 20: 5305
radiation effects on cell division in wheat, γ, 20: 6787(R) (ORNL-3853, pp 177-81)
radiation effects on *Ricinus communis*, γ, 20: 8703
radiation effects on growth and pH in maize, effects of dose on β, 20: 10683
radiation effects on barley, x, 20: 10619
radiation effects on survival of conifer, gamma, 20: 12671
radiation effects on pine, effects of water stress on γ, 20: 12674
radiation effects on development of *Vigna sinensis*, neutron and x, 20: 14341
radiation effects on corn and pea, from tritiated water and tritiated thymidine, 20: 16227(R) (NYO-3561-2)
radiation effects on lipid metabolism in cotton, γ, 20: 18374
radiation effects combined with magnetic fields on barley, x, 20: 18387
radiation effects combined with magnetic fields on development of, x, 20: 18388
radiation effects on barley, x, 20: 18411
radiation effects on DNA synthesis in pea, γ and neutron, 20: 28989
radiation effects on metabolism in, x, 20: 31115
radiation effects on cytology and growth of *Pinus rigida*, chronic gamma, 20: 31077
radiation effects on fatty acid content in free lipid fraction of leaves of bean, x, 20: 36598
radiation effects on Gramineae, β and γ, 20: 38583
radiation effects on development of barley, γ, 20: 38691
radiation effects on growth of barley, x, 20: 38736
radiation effects on density and diversity of, in tropical rain forest, γ, 20: 42853(R) (ORO-3299-1)

radiation effects on height of barley, grown at low and high altitudes, 20: 42894
radiation effects on diurnal variations in mitotic frequency in root tips of Pinus, gamma, 20: 42953
radiation effects on, protective effects of inert gases and low molecular narcotics on x, 20: 43007
radiation effects on growth of wheat, γ, 20: 45452
radiation effects on height of soybean, following seed exposure to thermal neutrons, 20: 45358(R) (NP-16208)
radiation effects on morphology of Vicia, exposed as seeds, 17: 38692
radiation effects on development of Vicia, 17: 38691
radiation processing of stored onion, *Allium cepa*, effects on plant viability and vigor, 19: 42781
radiation processing of stored onion, *Allium cepa*, effects on plant viability and vigor, 19: 42782
radioinduced chromosome aberrations in diploid and tetraploid cells in roots of *Vicia faba*, 16: 1590
radioinduced chromosome rearrangements in *Crepis capillaris*, reproduction and structure of, 19: 17610
radioinduced chromosome aberrations in roots of tomato, 20: 1638
radioinduced chromosome aberrations in root tips of, 20: 1649
radioinduced chromosome aberrations in *Vicia faba*, 20: 6776(R) (ORNL-3853, pp 50-3)
radioinduced genetic effects in barley, 16: 1572
radioinduced germination, root growth, and sprout growth of Pinus, 18: 38807
radioinduced growth inhibition, following exposure of seeds, 16: 1525
radioinduced growth inhibition in cereal, effects of oxygen tension on gamma, 19: 38418
radioinduced mutations in maize, rate of artificial, 17: 38694
radioinduced mutations in *Haplopappus gracilis*, 18: 29246 (TID-20784)
radioinduced mutations in barley, characteristics of, 19: 8856
radioinduced mutations in presoaked Arabidopsis, x, 20: 5357
radioinduced mutations in, x, 16: 1602
radioinduced somatic mutations in maize, effects of temperature on, 16: 28765 (RT/BIO(62)44)
radioinduced tumors in tobacco, 17: 23147
radiosensitivity, genetic factors, 16: 26819
radiosensitivity in tomato, genetic control of, 17: 33677
radiosensitivity of roots in *Vicia faba*, dose-response relationship, 16: 20153
radiosensitivity of crimson clover, 16: 21932
radiosensitivity of white pine, 17: 33723
radiosensitivity of tree, 17: 33575
radiosensitivity of *Vicia faba*, oxygen effects on, 19: 42326
radiosensitivity of pea, effects of chemical and biological compounds on, 20: 29049
radiosensitivity of deciduous tree, γ and neutron, 20: 38594(R) (ORO-2066-10)
respiration in cacao, 18: 27016(R) (TID-20708(p.6-28))
root growth in wheat, 19: 2009(R) (ORNL-3700(p.176-9))
rubidium uptake by isolated cells of bean, effects of chemicals, light, and temperature on, 20: 14217 (COO-888-43)
selenium-75 sorption and exchange by *Astragalus preussii* root, 16: 30201
sodium-22 uptake and transport by oat, 19: 11535
strontium metabolism by barley, effects of genotype, 19: 42244 (TID-22106)
strontium-89 metabolism by rice, effects of fertilizers and irrigation on, 19: 12912 (NP-14761)
sulfur-35 uptake and incorporation by radish, 17: 37048
survival of wheat, following gamma radiation, 20: 36650
translocation of phosphorus-32, nitrogen-15, and carbon-14 in soybean, 17: 24871

SEFOR
see Southwest Experimental Fast Oxide Reactor

Segregation
see Phase Studies

Seignette Salts
see Potassium Sodium Tartrates

SEIGNETTOELECTRIC MATERIALS
analysis of, neutron-diffraction, 17: 6647 (BNL-5747)
Cherenkov emission from electric and magnetic moments in transparent uniaxial, energy losses from, 18: 885(T)
Cherenkov losses in transparent uniaxial, 17: 20706(T)
conference on ferroelectricity, 20: 2526
conference on ferroelectricity, 20: 20171
crystal structure of hydrogen-bonded, neutron scattering study of vibrational, 18: 39155 (EUR-1643.e(p.181-7))
crystal structure of hydrogen-bonded, thermal effects on, 19: 26917(R) (IA-984)
crystal structure, 19: 26915(R) (AD-609133)
electronic dipoles and internal electric fields in, 17: 27393(T)
fabrication of ferroelectric ceramics by hot pressing, 19: 44644 (SC-TM-65-276)
frequency modulation in cyclotrons with, 17: 7413
lead-207 chemical shifts in perovskite, 18: 12081
lithium NQR in, 16: 29571
magnetic resonance of irradiated, effects of water of hydration on, 17: 24023
Mössbauer effect in, relation to homogeneous modes of lattice vibrations, 17: 10639
Mössbauer effect in, 17: 38071 (JINR-P-1231(p.107-11))
performance in direct energy conversion devices, 16: 22751
performance of barium titanates and lead zirconates, in ferroelectric transducers, 20: 41684
phase transitions in deuterated potassium acid phosphates, theory for, 18: 5864
phase transitions in, microscopic theory for, 19: 43482
polarization and Curie temperature of, effects of crystal structure on, 11: 6678 (TID-14508)
preparation and properties of, 18: 29151(R) (SC-DC-64-890)
preparation and properties of crystalline perovskite, 19: 9115
properties of, hysteresis bridge for measurement of, 18: 25738 (BNL-8006)
proton dynamics in hydrogen-bonded, (E), 19: 42491
proton-lattice interactions in hydrogen-bonded crystals of, 17: 22358
radiation effects on dielectric properties of ceramic, 16: 3518 (AFCRL-351)
radiation effects on hysteresis loop of guanidinium aluminum sulfate crystals, 16: 25456
radiation effects on lithium hydrazinium sulfate, electron spin resonance studies, 17: 22250
radiation effects on, 17: 23862(R) (AD-286036)
radiation effects on dielectric properties, 18: 16545
radiation effects on tri-hydrogen lithium selenites, EPR studies of gamma, 18: 39325
radiation effects on sodium selenite, gamma, 19: 26884 (NIJS-R-442)
radiation effects on electric properties of, fast-neutron and gamma, 20: 11352 (NP-15707)
radiation effects on triglycine sulfate, gamma, 20: 35560
radiation excitation of anomalous surface layers on perovskite-type, 17: 23993
research program on, 19: 7843(R) (AD-420637)
review, 19: 1083
shock wave effects on behavior of, 18: 44154 (SC-DC-64-348)
spectra of hydrogen-bonded, infrared absorption, 19: 26917(R) (IA-984)
spectra of, cold-neutron-scattering analysis of low-frequency vibrational, 19: 45241
thermoelectric measurements on single-crystal bismuth strontium titanate, 19: 24989(R) (TID-21673)
use as radiation detectors, 20: 31539
use in gamma detection, (E), 19: 28687
use of ceramic, in gamma dosimetry, 18: 31914 (SC-R-64-197)

SEISMIC WAVES
air-blast coupling to prograde and retrograde surface waves, 17: 37900
amplitude and travel-time spectra of, analysis of, for Salmon explosion, 20: 36968
amplitude equalization of surface, for determination of source parameters of underground nuclear explosions, 19: 36676 (VESIAC-8422VU)
amplitude modulation by crust curvature in Sahara event and Italian underwater explosions, 19: 36677(R) (VESIAC-5155)
amplitude of BUFF-event, 20: 41149 (AD-632956)
amplitude ratios for differentiation of earthquakes and underground nuclear explosions, 19: 18176 (VESIAC-4992-VU)
amplitudes and travel times from Salmon explosion, 20: 36967
amplitudes for decoupled sources, first-zone P, 20: 36966
amplitudes from nuclear explosions, 18: 35706 (TID-7695(p.195-206))
amplitudes of, from nuclear explosions in four media, 17: 16286
amplitudes of, from Project Gnome, 17: 21915
amplitudes of, source size estimation from, 19: 46615 (AD-612033)
analysis from HANDCAR event, 20: 25305 (PNE-801F)
analysis of earthquake- and nuclear-test-produced, 18: 43824
analysis of, for discrimination of earthquake-nuclear explosion data, 18: 12763 (AFCRL-63-672)
analysis, performance of horizontal and vertical arrays for, (E/T), 19: 26552(R) (NP-14823)
arrival times and magnitudes of, at Canadian stations, from Project-Long-Shot underground explosion, 20: 33533
attenuation in geologic discontinuity, acceleration, stresses, and velocity in, 19: 46580 (AD-613287)
correlation of earthquake and explosion, 17: 14516
coupling in spherical underground cavities, 16: 25633 (UCRL-6086(Rev.))
coupling in underground cavities, 17: 17626 (NOTS-TP-2986)
coupling to media, shotpoint effects on, 16: 25632 (UCRL-6059)
decoupling of, from underground nuclear explosions in salt, (T), 19: 26553 (UCRL-12327)

detection and analysis of, from PALANQUIN event, 20: 25306 (PNE-913F)
detection and comparison of, from earthquakes and underground nuclear explosions, 20: 20906
detection and discrimination 2000 to 6000 miles from source, 19: 20177
detection and discrimination of underground explosion, 20: 14768
detection and measurement by horizontal and vertical arrays, (E/T), 19: 26552(R) (NP-14823)
detection and recording of, design of stations for, 20: 27178
detection and recording of, from Salmon Event, 20: 43551 (VUF-3015)
detection by "black-box" systems, 17: 8399
detection of, design of equipment for, 17: 41002
detection of nuclear-blast-produced, by statistical analysis of seismometer data, (T), 19: 18172 (NP-14809)
detection of P-waves from weak sources at great distances, 18: 18792
detection of T-phase in Hawaii, May 11, 1962, from underwater explosion, 18: 39522
detection of tsunami, equipment development and installation for, 19: 13619(R) (NVO-98-1)
detection of tsunami, equipment development and installation for, 19: 17414(R) (NVO-98-3)
detection of tsunami, equipment development and installation for, 19: 17415(R) (NVO-98-4)
detection of tsunami, equipment development and installation for, 19: 34362(R) (NVO-98-6)
detection of tsunami, equipment development and installation for, 19: 33691(R) (NVO-98-7)
detection of tsunami, operational and support requirements plan for, 20: 543(R) (NVO-98-9)
detection of tsunami, system design and development for, 20: 2058(R) (NVO-98-10)
detection of underground-nuclear-explosion produced, instrumentation for, 20: 39134
detection of, development of well methods for, 19: 26557(R) (VESIAC-7724VU)
detection of, effect of focus depth on, 20: 23317(R) (AD-627373)
detection of, large-aperture detector array for, 20: 20909
detection of, motion product seismograms for, 18: 18146
detection of, process for, 18: 18793
detection on ocean bottom, 18: 16198
diffraction at crustal discontinuities, calculation of, 17: 39274
displacement amplitude and energy variations with distance by, 20: 41169
distribution around source, model studies of, 19: 26558(R) (VESIAC-7373VU)
effects of, from underground nuclear explosions, on content of radon and thoron in surface soil layers, 17: 36008 (EGG-B-2516)
effects of underground explosion on structures, 18: 20127 (UCRL-7773)
energy content of, use for evaluating source size, 19: 46615 (AD-612033)
energy flow from earthquakes and underground atomic explosions, (T), 20: 547
excitation by atmospheric nuclear explosions, 18: 21081
excitation by earthquakes and underground explosions, 17: 25444
focal depth determination for earthquake, delay time method for, 19: 28554 (AD-607491)
focal depth of earthquake, delay time method for determining, 19: 28554 (AD-607491)
from explosion in buried spherical cavity, (T), 19: 24733 (VESIAC-8580VU)
from high-explosive cratering teats at Nevada Test Site, 17: 37350 (SC-4693(RR))
from TENDRAC event, measurement of, 18: 10263 (AD-404012)
interactions of, Feynman diagrams and rules for, 20: 18936
measurement from CHASE IV test, 20: 23319 (AD-631052)
measurement in Project Gnome, 16: 31694 (PNE-150F)
measurement in southern Mississippi, crustal structure determinations from, 20: 36965
measurement of tsunami, pressure sensors for, 20: 2059(R) (NVO-98-11)
measurements from CHARCOAL test, 20: 23318 (AD-631043)
measurements of Gnome explosion, 19: 6107 (NP-14516)
monitoring in Salmon explosion, volunteer team program, 19: 28555 (AD-612711)
observations on Project Gnome, 18: 10215
patterns for underground nuclear explosions and earthquakes, 17: 37901
production by atmospheric motion, solar activity effects on, 20: 46489
production by nuclear explosions in cavities, 20: 4167 (RM-3727(RAND))
production by 1962 Christmas Island nuclear explosions, 18: 16546 (AWRE-O-87/63)
production from cavity explosions, 19: 13561(R) (AD-439079)
production of, computer code for source mechanism determination for, 20: 20912
propagation by nuclear explosions, 17: 16901
propagation from atmospheric atomic explosions, (E), 19: 18179
propagation from Bilby underground nuclear explosion, 20: 454
propagation from cylindrical media about point sources, (T), 19: 30418 (VESIAC-6796VU)
propagation from earthquakes and underground explosions, comparison of, 17: 23526
propagation from explosions, model studies of, 19: 26559(R) (VESIAC-8746VU)
propagation from earthquakes and explosions, 20: 542 (NP-15557)
propagation from Long Shot underground nuclear explosion, surface, 20: 45923
propagation from nuclear explosions, amplitudes and travel times of, 17: 41006
propagation from nuclear explosions, 18: 35705 (TID-7695(p.181-94))
propagation from nuclear explosions in salt formations, 20: 14663 (UCRL-14463(Rev.1))
propagation from nuclear explosions in overdriven cavities, 20: 20898 (AD-624016)
propagation from nuclear and high-explosive detonations through geologic materials, 20: 45879 (SC-M-66-451)
propagation from Project Gnome, phase-velocity reinterpretation from, 17: 21912
propagation from Soviet explosions, properties of, 18: 41667
propagation from Salmon explosion, 20: 36962
propagation from Salmon explosion, time dependence of, (T), 20: 36963
propagation from thermonuclear explosions, analysis of, 20: 20907
propagation from underground explosions, 16: 11944
propagation from underground nuclear explosions, 17: 16905
propagation from underground explosions, use in determining ground crust structure, 17: 21911
propagation from underground explosions, ground particle acceleration from, 17: 21914
propagation from underground explosions, crustal structure in Nevada and southern Idaho from, 17: 41001
propagation from underground explosions, crustal structure in eastern Colorado from refraction measurements of, 17: 41002
propagation from underground explosions, crustal structure of California and Nevada from refraction measurements of, 17: 41004
propagation from underground and underwater explosions, crustal structure of California and Nevada from refraction measurements of, 17: 41007
propagation from underground and underwater explosions, crustal structure of California coast from refraction measurements of, 17: 41003
propagation from underground explosions, analysis of, 18: 18790
propagation from underground explosion in salt dome, 18: 37357 (NP-14227)
propagation from underground atomic explosions, 20: 23324 (UCRL-12328)
propagation from underground explosions, 17: 16287
propagation in elastic half-space, from explosions in spherical cavities, (T), 19: 6384 (NP-14508)
propagation in rock from surface nuclear explosions, 20: 4143 (AD-619969)
propagation in underground explosions, structure of crust and upper mantle in western U. S. from, 17: 41000
propagation of elastic, abstracts on, 20: 20896 (AD-623592)
propagation of nuclear-explosion, in earth crust, 20: 45912(R) (AD-628385)
propagation of primary, by underground explosions, review of mechanism of, 19: 26554 (VESIAC-4410-48-X)
propagation of second Rayleigh and second and third Love modes in, from high-altitude explosions, (E), 20: 32269
propagation of surface, from Hardhat explosion, 18: 16197
propagation of surface, from high-altitude explosions, 18: 21081
propagation of surface and underground, models of, 19: 20172(R) (NP-14877)
propagation of, model for, 18: 18794
propagation through rocks, 16: 29189 (UCRL-13039)
shape of, from underground nuclear explosions, 17: 20196 (NP-12700)
shapes of, from underground explosions, 17: 32271
signals in deep wells, 19: 7716(R) (AFCRL-62-878)
source identification using long- and intermediate-period, 19: 26550(R) (AD-607946)
spectra of, from underwater explosions, 19: 20175
surface radiation patterns for underground nuclear explosions and earthquakes, 17: 37901
travel time from thermonuclear explosions, statistical treatment, 20: 45919
travel time from underground explosions, measurement of, 17: 21398 (PNE-235F)
travel time of, from thermonuclear explosions, 20: 45918
travel times from central Pacific nuclear explosions, 19: 40779
travel times of principal body phases of, from Project Gnome, 17: 21915
use of micro-, for crustal structure studies, 18: 18789

velocity of Pn, regional variations and effects on epicenter location, 17: 21913
velocity of, from SULKY underground nuclear explosion, 20: 31393 (PNE-711F)

SEISMOLOGY

advances in, survey of recent, 19: 15765 (AEET/NP/11)
aftershock measurements in CIMARRON event, 17: 10242 (NP-12339)
air-blast coupling to prograde and retrograde surface waves, 17: 37900
air-blast-induced ground motions, method of simulating, 19: 20184
analysis of earth motion accelerograms, 18: 31747 (UCRL-13109)
analysis of ocean-bottom data from Pacific, 19: 26551 (AFCRL-64-666)
analysis of seismic data, methods development for, 20: 9136(R) (AD-626380)
analysis of seismic data, methods development for, 20: 9137(R) (AD-626382)
analysis of strong-motion seismograms, for nuclear test detection, 19: 9384(R) (AD-442907)
apparatus and principles for, 17: 23539
bibliography on Soviet, 16: 25608 (AD-265437)
bibliography on, for VELA-UNIFORM project, 19: 18171 (AD-422423)
borehole research in, Vela Uniform project, 19: 20173 (VESIAC-4410-83-X)
Colona earthquake measurements, 17: 14476 (NP-12594)
comparison of data from SHOAL and HARDHAT explosions and FALLON earthquake, 18: 39476 (NP-14283)
conference on, 17: 20195 (NP-12678)
conference on high-frequency seismic energy, Lakewood, Colorado, October 15 and 16, 1962, 18: 23784 (NP-13956)
conference on soil-underground protective structure interaction, Univ. of Arizona, Tucson, Ariz., June 8 to 11, 1964, 19: 13607
coupling of underwater and underground high-explosive events, 19: 36677(R) (VESIAC-5155)
crustal studies of the earth using nuclear explosions, 20: 45912(R) (AD-628385)
data for amplitudes and travel times from STILLWATER event, 17: 10244 (NP-12444)
data for amplitudes and travel times from Gnome event, 19: 6886 (NP-14510)
data for CLEARWATER event, long-range, 18: 16189 (AD-427125(Rev.))
data for Hardhat event, 19: 6885 (NP-14507)
data for on-site inspection, Vela Project, 17: 10238(R) (AD-278378)
data for SHOAL event, local, 18: 16190 (NP-13757)
data from Antler event, analysis of, 18: 10264 (AD-407430)
data from BILLIKEN calibration explosion in southeast Missouri, 19: 20171 (AFCRL-64-659)
data from Coast and Geodetic Survey in nuclear detonation series, 1961 to 1963, 18: 20201 (NP-13867)
data from Fisher and Gnome events, long-range, 19: 26555 (VESIAC-5197VU)
data from HARDHAT event, 19: 26556 (VESIAC-5439VU)
data from MISSISSIPPI Event, 18: 18025 (NP-13775)
data from PALANQUIN underground explosion, 20: 37010 (AD-631340)
data from Project SHOAL, volunteer team program for compilation of, 19: 22575
data from RED HOT explosion, long range, 20: 39124 (AD-632957)
data from SALMON nuclear explosion, long-range, 19: 11403 (NP-14678)
data from STONES event, long-range, 18: 16191 (NP-13586(Rev.))
data from STONES nuclear underground test, 18: 10265 (NP-13586)
data on BUFF event, analysis of, 20: 41149 (AD-632956)
data processing in, noise correlations for multichannel, 20: 14763
data processing methods for detection and interpretation of teleseismic signals, (E/T), 20: 14762
data recording in, using magnetic tape, 20: 23316 (AD-625199)
decoupling in Salmon nuclear detonation, 20: 14664 (UCRL-14487 (Rev.1))
deep boreholes, 17: 3142 (AD-274106)
detection and measurement of underground nuclear explosions, 17: 16262 (AD-297344)
detection of nuclear explosions, mathematical development of discrete filters for, 17: 37354
detection of nuclear explosions by seismic arrays, theory, 19: 22569 (VESIAC-8859VU)
detection of underground explosions and distinguishing from earthquakes, feasibility of methods for, 17: 1165 (AD-273825)
detection systems in, three-dimensional, 18: 18145
detonation effects in salts and sedimentary deposits in Operation Pre-Dribble, 18: 371 (NP-13279)
development for underground explosion discrimination, 20: 14768
development of broadband, conference, (E), 19: 22568 (VESIAC-4410-77-X)
development of, conference on, 20: 28140
developments in, for distinguishing underground explosions from earthquakes, 19: 20177
developments in, for using nuclear explosions in determining internal structure of earth, 20: 5610
discrimination between earthquakes and explosions, research program on, 19: 24734(R) (VESIAC-8754VU)
discrimination of signals from earthquakes and explosions, auditory, 18: 33765 (AD-437784)
earth motion from underground nuclear explosion, 17: 16265 (PNE-111F)
earth motion in noise trains, analysis, 19: 36677(R) (VESIAC-5155)
earth movement recording using geophones, 19: 9385(R) (NP-14531)
earthquake and underground explosion discrimination in, methods of, 20: 35659
earthquake hypocenter location, computer program for, 19: 24733 (VESIAC-8580VU)
effects from Danny Boy explosion, 19: 26561 (WT-1813)
effects of decoupling on spectra, 17: 12457
energy source depth determination in, theoretical studies of, 19: 6106 (AFCRL-64-750)
equipment and techniques for, 17: 20199(T) (FTD-TT-62-269)
equipment for nuclear test detection, development of multiple array processor, 19: 24728(R) (NP-14956)
error determination in seismic event location, 19: 20172(R) (NP-14877)
focal depth determinations for distinguishing underground blasts from earthquakes, 17: 14475 (NP-12255)
generation of shear waves by underground explosions, 17: 5107
ground motion induced by underground nuclear explosions, calculation, 19: 15767 (UCRL-12219)
ground motion predictions for nuclear explosions at Pahute Mesa and Yucca Flat, 19: 11404 (NVO-1163-24)
ground motion predictions for 100- and 1500-kt detonations at Yucca Flat, 19: 13648 (NVO-1163-16)
ground shock from small-scale cratering detonations in hard rock, measurements of, 20: 25231 (PNE-504F)
ground-water flow-path determination by inhole well logging, refraction seismic methods, and rotary drilling, 19: 647(R) (HW-81746(p.4.61-3))
hypocenter computation for Sahara explosion of May 1, 1962, 19: 6887 (NP-14513)
instrumentation design for, 20: 7283 (SC-M-65-330)
instrumentation for up-hole-velocity surveys, 20: 43551 (VUF-3015)
interpretation of seismograms from thermonuclear explosions, 20: 45918
long-range measurements of Dormouse prime shot, 17: 11321 (NP-12418)
long-range seismic measurements of New Madrid, event on Feb. 2, 1962, 17: 10825 (NP-12465)
measurements for comparing earthquakes and underground explosions, 20: 20900 (AD-627039)
measurements for comparing earthquakes and underground explosions, 20: 20901 (AD-627040)
measurements for comparing earthquakes and underground explosions, 20: 20902 (AD-627051)
measurements in Vela Project, 20: 20876 (NP-15949)
measurements in, interpretation of data in long-range, 19: 24731 (VESIAC-7378VU)
measurements of Dugout row-charge cratering experiments, strong-motion, 20: 1981 (PNE-605F)
method for detecting remote explosions, 19: 6112(T) (FTD-MT-64-407)
methods for geophysical study of Hanford Works area, 18: 9751 (HW-SA-3280)
noise in two French stations, 19: 36677(R) (VESIAC-5155)
of AARDVARK shot, 17: 6267 (NP-12328)
of DANNY BOY shot, 17: 6268 (NP-12419)
of Gnome event, 18: 31045 (AD-428227)
of Hyrax event, 17: 6269 (NP-12420)
of Shoal shot, measurements, 19: 5591 (VUF-1011)
of underwater explosions, 19: 20175
performance for detection of underground nuclear explosions, 17: 16905
performance of gravity meters and vertical seismographs for measurement of normal mode oscillations of the earth, 16: 33298
problems in, for design of nuclear power plants, 19: 17315
profiling study of Tatum Salt Dome in Mississippi, 19: 6888 (NP-14517)
records of GNOME event, compilation, 19: 18175 (VESIAC-4260)
reduction of seismic effect of explosions by short-delay blasting, 19: 9386(T) (UCRL-Trans-1106(L))
refraction survey of Porpoise area in Nevada Test Site, 19: 6586 (NP-14518)
refraction survey of Tatum Salt Dome, Mississippi, 19: 7717 (NVO-977-2)
seismic effects from underground thermonuclear explosion, measurement, 17: 21395 (PNE-213F)
seismic signals from nuclear explosions in overdriven cavities, 20: 27176
seismic wave source mechanism, computer code for determining, 20: 20912
seismic wave travel times, measurement of, 20: 45919
seismograms compilation for Project GNOME, 17: 10824 (NP-12462)
signals from Gnome, 17: 14486
simulation of seismic disturbances, computer program for, 20: 14755

(UCRL-7929)
stability of Lucas Heights area, review, 20: 41148 (AAEC-TM-316)
station design and performance, Eskdalemuir, Scotland, 20: 39128
station operational magnification and physical environment, 18: 18791
studies of earthquakes and explosions, 19: 24732 (VESIAC-7542VU)
surface particle motion in Shoal explosion, 19: 7718 (VUF-1013)
telluric current micropulsations, comparison between high-altitude-explosion and natural, 17: 12859
travel times to Australian stations from 1958 Pacific nuclear explosions, 17: 12467
underground explosion detection in, teleseismic record evaluation for, 20: 20911
underground nuclear explosion detection using, 17: 6265 (NP-12297)
use for detection of atmospheric and underground nuclear explosions, 19: 46620
use in detecting nuclear underground explosions and geological studies, 20: 41152
use in detection and identification of underground nuclear explosions, 16: 20854
use in detection and identification of underground nuclear explosions, 16: 20855
use in detection of underground nuclear explosions, 19: 11409
use in geophysical studies on liquid waste discharge to ground, 20: 14753 (BNWL-47)
use in on-site inspection of underground nuclear explosions, 16: 30658 (NP-12000)
use of crustal phases in focal depth discrimination for nuclear explosions, 18: 12335 (IDA/HQ-63-1345)
use of nuclear explosions in studies of earth, 18: 35707 (TID-7695 (p.229-38))
use of nuclear explosions in, bibliography on, 20: 18855 (CEA-Bib-66)
uses with probabilistic methods, for nuclear-blast detection, (T), 19: 18172 (NP-14809)
VELA-UNIFORM program, measurement of signals from Fisher detonation in, 17: 6259 (NP-12279)
VELA-UNIFORM program, measurement of signals from Small Boy in, 17: 6260 (NP-12280)
VELA-UNIFORM program, measurement of signals from Sedan shot in, 17: 6261 (NP-12281)
VELA-UNIFORM program, measurements of signals from Merrimac shot in, 17: 6262 (NP-12282)
VELA-UNIFORM program, measurement of signals from Antler shot in, 17: 6264 (NP-12284)
VELA-UNIFORM program, measurement of signals from Chinchilla shot in, 17: 6266 (NP-12298)
VELA-UNIFORM studies of Project SHOAL, 18: 22261 (AD-434785)
wave equation development, 19: 20172(R) (NP-14877)

SEISMOMETERS
array design, information theory uses in, 19: 39269(R) (SU-SEL-64-133)
arrays of, for investigating earthquake mechanism, 20: 41152
bibliography, 20: 23419 (AD-626405)
coherence measurements with time-sampling ocean-bottom, 20: 14766
data processing and recording for large-aperture arrays, 20: 14761
description of array of, in southern Scotland, 20: 39128
design, 16: 10258
design, 18: 18792
design and performance of three-dimensional, 18: 18145
design and performance of, with leaf-spring suspension, 20: 4216 (AWRE-O-70/65)
design and performance of large aperture, 20: 20899(R) (AD-626777)
design and performance of Large Aperture Seismic Array, 20: 45911 (AD-628148)
design and signal handling system of large-aperture arrays, 20: 14760
design and use of, in recording stations, 20: 27178
design for detection and discrimination of underground explosions, 20: 14769
design of large array of, for earthquakes and nuclear explosions, 19: 34377 (AD-609851)
design of large array of, for detection of distant underground nuclear explosions, 20: 20913
design of large-aperture array of, 20: 20909
design of linear cross array of, for detecting underground nuclear explosions, 20: 39134
design, installation, and operation of large-aperture arrays, 20: 14759
development and performance of ocean-bottom, 20: 14765
development and performance of large-aperture arrays, 20: 41155
development and testing of unattended, 20: 14764
development of arrays of, review of, 20: 14757
development of broadband, conference, (E), 19: 22568 (VESIAC-4410-77-X)
development of direction-indicating, 18: 18146
development of horizontal air-bearing, 17: 8534 (SCTM-74-62(13))
effects of Soviet nuclear tests on gravimeter, 16: 12822
operation and performance of large-aperture arrays, 20: 14758
operation and performance of ocean-bottom, (E/T), 20: 14767
performance of horizontal and vertical arrays of, (E/T), 19: 26552(R) (NP-14823)
performance of laser interferometer, 20: 25304 (BNWL-241)
response of Yellowknife array of, signal processing techniques for, 20: 27172
signal-to-noise ratios, summing technique, 16: 3251
wave frequency data, method for moving-spectrum analysis, 16: 5578

SELACHYL ALCOHOL
effects on radiation sickness in animals, therapeutic, 20: 38731
protective effects of, against radiation injury of hematopoietic system, 18: 31264
radiosensitivity effects on rat erythropoiesis, 18: 5146
use in therapy of radiation sickness in rats, condition of maxillodental system during, 19: 8976

SELENATES
see also Barium Selenates
see also Gadolinium Selenates
radiolysis of aqueous solutions of, at 77°K, yields of hydrogen from gamma, 20: 18748

SELENIDES
see also Barium Selenides
see also Bismuth Selenides
see also Cadmium Selenides
see also Calcium Selenides
see also Carbonyl Selenides
see also Cerium Selenides
see also Erbium Selenides
see also Europium Selenides
see also Gadolinium Selenides
see also Hydrogen Selenides
see also Indium Selenides
see also Iron Selenides
see also Lanthanum Selenides
see also Lead Selenides
see also Magnesium Selenides
see also Manganese Selenides
see also Methyl Selenides
see also Molybdenum Selenides
see also Neodymium Selenides
see also Nickel Selenides
see also Niobium Selenides
see also Oxyselenides
see also Plutonium Selenides
see also Praseodymium Selenides
see also Rare Earth Selenides
see also Scandium Selenides
see also Strontium Selenides
see also Tantalum Selenides
see also Thorium Selenides
see also Tungsten Selenides
see also Uranium Selenides
see also Ytterbium Selenides
see also Yttrium Selenides
see also Zinc Selenides
see also Zirconium Selenides
conference on, 18: 37115 (ANL-6856)
formation of, paragenesis with pitchblendes in, 20: 20918
preparation and crystal structure of three-component, 19: 9152
preparation of actinide, by exothermic reactions, 19: 24538(P)
properties of mixed alkaline-earth–rare-earth, 19: 372
semiconductivity and superconductivity in cobaltite- and pyrite-type phases of, 17: 34590
thermoelectric properties, 17: 24049(R) (NRL-Memo-1404)

SELENIOUS ACID
analytical use in qualitative analysis of tetravalent and trivalent cerium mixtures, 20: 43122
determination using sulfatoceric acid, 18: 41355
solvent properties for niobium and zirconium, 17: 6022
uses in conductometric titration of lanthanum, 20: 14484

SELENITES
see also Hafnium Selenites
see also Lithium Selenites
see also Rare Earth Selenites
see also Sodium Selenites
see also Thorium Selenites
radiation effects on reactions of, with hydroxyl ions, 19: 44090
radiolysis of aqueous solutions of, at 77°K, yields of hydrogen from gamma, 20: 18748

SELENIUM
abundance in 3 Centauri A, upper limit, 16: 4659
analysis for antimony and sulfur by neutron activation, 20: 35444

analysis for arsenic, copper, iron, and zinc, activation, 18: 21988
analysis for arsenic by activation methods, 19: 15391
analysis for chlorine, phosphorus and sulfur by activation methods, 19: 19798
analysis for chlorine traces by neutron activation, 20: 35443
analysis for impurities, activation, 18: 13676
analysis for trace impurities, activation, 17: 32020
analysis for trace impurities, activation, 18: 39103
analysis for traces of chlorine and sodium by neutron activation, 20: 1769
analysis of, self-shielding effects in neutron activation, 18: 31387
bibliography on, 16: 3510 (SB-438)
book: *Chemistry of Selenium, Tellurium, and Polonium*, 20: 29235
bremsstrahlung reactions (γ,α) at 32.5 Mev, alpha spectra and yields in, (E), 20: 26231
chemistry, inorganic, 16: 8752
content and distribution in beef heart, 19: 45753 (AE-191)
content in chondrites, 20: 4526
content in horse heart cytochrome c, 16: 9831
content in human heart, neutron activation determination of, 18: 33457 (AE-146)
content in lead-zinc deposits in Klitchkin region, 16: 27451
content in meteorites, 20: 42064
crystal structure powder diffraction patterns, 19: 17795
crystallization with thionalid, tracer study of, 16: 12961 (USNRDL-TR-551)
determination by activation methods, rapid separation process for, 20: 8867
determination by charged-particle reactions at 2 Mev, 20: 43097
determination by thermal-neutron activation methods, sensitivity for, 19: 9071
determination in animal tissue by activation, 19: 46172 (KR-95)
determination in biological material, activation, 17: 38941
determination in biological materials by ion exchange and gamma spectrometry, 18: 13660
determination in biological materials, activation, 18: 33464 (NASA-CR-52997)
determination in biological samples using neutron activation analysis, 19: 2249
determination in biological materials, use of automated gamma spectrometers in activation, 20: 38843
determination in copper by activation, 19: 40422
determination in copper by neutron activation, 20: 17822
determination in conductive tissue of beef heart, activation, 20: 31176
determination in food and other biological materials, activation, 17: 39011
determination in hair by activation methods for identification of individuals, 19: 17824
determination in hair, activation, 19: 26225 (AERE-R-4881)
determination in human heart tissue, activation, 20: 31175
determination in iron, minerals, and platinum by activation methods, 19: 22148
determination in liver and milk, activation, 19: 19771(R) (TEES-2671-4(Chap.9))
determination in minerals by neutron activation, 19: 30424
determination in meteorites by neutron activation, 20: 23859
determination in nicotinic acid, activation, 16: 22021
determination in polonium, 17: 30583 (MLM-1158)
determination in plants by fluorimetric method using diaminonaphthalene, isotope dilution methods in, 18: 27306
determination in petroleum, activation, 20: 29139
determination in rare earth selenides, 20: 16395
determination in solutions, spectrographic, 16: 8672 (AERE-R-3875)
determination in sulfur, activation, 17: 15917
determination in silicon, activation, 18: 33502
determination in sea water, activation, 18: 43790(R) (TID-21137)
determination in sea water by neutron activation methods, 19: 22574
determination in steel, activation, 20: 22940
determination in silicates, activation, 20: 26782
determination in seawater, activation, 20: 40834
determination in solution, colorimetric, 20: 43071 (IDO-14679, pp 75-191)
determination in tissue, after neutron activation, 17: 31813 (AERE-R-4309)
determination of traces in platinum, activation, 17: 21645
determination of trace amounts of, by reactor neutron activation methods, 20: 26760
determination of trace amounts in biological materials, using neutron activation analysis, 20: 33223
determination of traces of, in biological materials, activation, 20: 38837
determination of, in water by neutron activation analysis using freezing, 20: 45602
determination on polystyrene filters, colorimetric, 20: 43069(R) (IDO-14679, pp 51-9)
determination, use of pulsed neutrons in activation, 19: 36323
deuteron elastic scattering at 6.5 Mev, polarization in, 17: 38157
deuteron reactions (d,p) at 13.6 Mev, proton spectra from, 16: 26356
diffusion in selenium, radioactive-tracer study of, 18: 37688(T) (AEC-tr-6398(p.334-7))
diffusion in thallium selenides, tracer study of, 18: 37687(T) (AEC-tr-6398(p.328-33))
diffusion of impurities in polycrystalline, tracer study of, 18: 37687(T) (AEC-tr-6398(p.328-33))
diffusion of impurities in, tracer study of, 18: 37688(T) (AEC-tr-6398 (p.334-7))
displacement in zinc selenides by electron bombardment, 17: 11320 (NP-12360)
distribution in sea water, effects of depth on, 20: 18892 (NYO-3450-1, pp 41-89)
distribution in tissues in chick, effects of vitamin E, tracer study, 17: 23064
distribution in tissues and teeth of rats, tracer study of, 18: 38757
distribution in tissues, 16: 1397
distributions in sea water, geographical and vertical, 19: 22574
effects on chick embryos, 18: 38775(R) (ORO-624)
effects on determination of iridium in ores by neutron activation analysis, 20: 36751
effects on growth of beryllium oxide crystals, 17: 30511 (NAA-SR-8235)
effects on phosphorus metabolism in rats and sheep, 18: 27060
effects on radioinduced crosslinking and decomposition of polyethylene, 20: 31279
effects on selenium-75 uptake by sheep blood cells, 18: 3468
electron and hole drift mobilities and space-charge-limited currents in, effects of arsenic, 16: 21018 (AFOSR-1416)
electron energy loss spectra at 0.8 and 1.5 Mev, 16: 12274
electron secondary emission by, 19: 27101
electron spectra of, 20: 31219(R) (UCRL-16658, pp 11-20)
energy level transitions in, Coster-Kronig, (T), 20: 15238 (CONF-233 (Vol.3), pp 398-418)
energy level widths for, K, (T), 20: 15239 (CONF-233(Vol.3), pp 419-39)
excretion of, 16: 1397
explosibility of powders of, 19: 36698 (BM-RI-6516)
fabrication, ore processing, properties, and uses of, 18: 35949
fission product stopping in, ionization of inner electron shells, 16: 13834
fluorescence yields in proportional and scintillation detectors, 18: 3796
gamma scattering by, resonance, 18: 11175 (ANL-6797(p.275-87))
gamma spectra from 14-Mev neutron activation of, determination by, 19: 26241
geochemistry and mineralogy of, in Cherry Mountains (Urals), USSR, book, 19: 20190
Hartree-Fock wave functions, 16: 18162 (MRL-103)
Hartree-Fock potential of neutral atoms of, analytical expressions for, 18: 16656
incorporation in styrene polymers using phenyl selenium, 19: 7526
incorporation into polystyrene for use as scintillator, 19: 13406(T) (JPRS-28565)
ion exchange in concentrated hydrochloric and perchloric acids, distribution coefficients of, 18: 17759
metabolic effects of, 18: 43316
metabolism by plants, tracer study, 17: 17657
metabolism in domestic animals, tracer study, 17: 31816(R) (ORO-605)
metabolism in liver, tracer study, 16: 30199
metabolism in mice, 17: 12111
metabolism in rats and sheep, 18: 27060
metabolism in sheep, tracer study of, 19: 6969
neutron activation of, for measurements of neutron flux in reactors, 17: 38996
neutron activation of, shielding effects during thermal, 18: 6184(T) (SC-T-523)
neutron capture cross sections at 30 and 65 kev, 16: 33792(R) (ORNL-TM-383)
neutron capture gamma spectrum, 16: 28024(R) (ARF-1193-12)
neutron elastic scattering at 400 kev, cross section for, 18: 38074(T) (AEC-tr-6398(p.64-9))
neutron elastic scattering at 3.3 Mev, asymmetry in polarized, (E/T), 19: 10343
neutron elastic scattering at 0.8 Mev, angular distributions from, (T), 19: 37884
neutron elastic scattering at 1 Mev, differential cross sections for, (E/T), 20: 9981 (WASH-1064)
neutron elastic scattering at 0.8 Mev, cross sections for, (T), 20: 15770
neutron elastic scattering at 0.68 to 1.25 Mev, (E/T), 20: 19805(R) (ANL-7110, pp 1-28)
neutron elastic scattering at 3.2 Mev, (E/T), 20: 46644
neutron radiative capture cross sections at 30 and 65 kev, 18: 34274(R) (NIRS-2(p.3-15))
neutron reactions at 3.7 Mev, cross-section measurements, 16: 8224
neutron reactions (n,γ) at high energies, gamma spectra for,

17: 26419(R) (ARF-1193-23)
neutron resonance parameters and total cross section of, 17: 22568 (WASH-1041)
neutron resonance absorption integral of, (E), 20: 14008(R) (ANL-7122, pp 42-69)
neutron scattering at 1 Mev, 16: 3662
neutron scattering angular distribution, 16: 12419 (ANL-5567(Rev.))
neutron scattering by, measurement of polarization in, 17: 2243(R) (TID-17083)
neutron scattering by, crystal structure effects on, 17: 38045(T) (AEC-tr-5734(p.267-9))
neutron scattering at 0.4 to 1.2 Mev, cross sections for, 18: 9331
neutron scattering cross sections at 0.5 to 0.8 Mev, 18: 26571
neutron thermal, self-shielding effects in activation, 18: 33488
neutron total cross sections at 0.003 to 0.008 ev, 16: 24811
neutron total cross sections at 0.003 to 0.008 ev, 16: 28032 (NP-11631)
neutron total cross section at 14 Mev, 17: 36676
neutron transmission resonances below 2 kev, 16: 28054
neutron transmission by, 17: 41527(R) (ANL-6720(p.2-15))
nitrogen ion reactions, Coulomb excitation of energy levels in, 16: 33826
pair distribution function for, 20: 29623(R) (TID-22970, pp 121-256)
performance as electrophotographic material for particle track coordinates in spark chambers, 20: 21037 (JINR-P-2594)
performance of rectifiers of, in Cockcroft-Walton voltage multipliers, 19: 11878
photoconductivity of, sensitivity to x radiation, 20: 4999(R) (ORNL-2599)
positron annihilation in, angular correlations from, (E), 19: 41285
properties of, as Rankine-cycle fluid, 18: 14513
properties of, review on chemical and nuclear, 20: 1744 (NAS-NS-3030 (Rev.))
proton reactions (p,n) at 18.5 Mev, angular distributions of quasielastic, 18: 40587
proton reactions at 30 to 150 kev, L x-ray emission following, 18: 30322(T) (UCRL-Trans-1056(L))
proton reactions (p,n) at 14.8 Mev, neutron spectra from, 16: 26326 (UCRL-6733)
proton reactions (p,n) on, spectra from, 17: 17226
proton reactions (p,n) with, time-of-flight neutron spectrum from, 17: 20994 (UCRL-7233)
purification of, radiochemical method for, 20: 8838 (UCRL-14258)
radiation effects on K absorption spectrum, neutron, 17: 14319
radiation effects on crystals of, 18: 8882
radiation effects on crystallization of, 18: 16540
radiation effects on electric conductivity of crystalline reactor, gamma, 19: 20644
radiation effects on distribution of radioactive, between red and gray allotropic modifications, neutron, 20: 38961
radiation effects on thermal conductivity of amorphous, electron, 20: 46211
radiochemistry of, review on, 20: 1744 (NAS-NS-3030(Rev.))
radioinduced formation of crystallization centers in amorphous, 17: 33990
radiosensitivity effects on catalase, 20: 18449
reactions with actinides to form binary compounds, 19: 24538(P)
reactions with cerium dioxide, 19: 23015(T) (JPRS-28849(p.217-26))
reactions with sodium in liquid ammonia, saline compound production in, 18: 23149(T) (ANL-Trans-8)
reactions with sulfur, tracer studies, 16: 3341(T) (AEC-tr-4497 (p.308-19))
semiconductor properties of, effects of chlorine and sodium on, 20: 1769
separation by solvent extraction, 17: 6132(R) (TID-17272)
separation from arsenic and germanium, tracer studies of, 20: 8867
separation from basic media, flocculating agent for, 19: 34288(P)
separation from carbonate leach solutions of uranium ores, 20: 25219(P)
separation from carbonate leach solutions of uranium ores, 20: 25220(P)
separation from chloride solutions by solvent extraction using amines, 18: 1799(R) (ORNL-3496)
separation from irradiated strontium oxide targets by partition chromatography on teflon, 18: 23731
separation from nitric acid solutions by solvent extraction using trilaurylamine in toluene, 18: 27615(R) (MITNE-43)
separation from nitric acid solutions by solvent extraction using tridodecylamine in toluene, 19: 5991(R) (MITNE-54)
separation from nitric or sulfuric acid solutions, ion exchange selectivity scales for, 19: 9257
separation from other inorganic ions by paper chromatography, 20: 12939
separation from pitchblende residues, leaching processes for, 20: 43420 (MCW-1508)
separation from rhenium by anion exchange chromatography, 19: 24433
separation from solutions by solvent extraction, review of methods for, 19: 13543
separation from tellurium, tracer studies, 16: 3340(T) (AEC-tr-4497 (p.297-307))
separation from tellurium by anion exchange, 16: 31659
separation from tellurium, methods for, 17: 27401
separation of bromine from activated, by solvent extraction and ion exchange, 18: 31566 (TID-18567(p.2-6))
separation of bromine from irradiated, by ion exchange, carrier-free, 18: 31568 (TID-18567(App.VI))
separation of, radiochemical procedure for, 17: 6132(R) (TID-17272)
Slater-Condon parameters of, determined from spectral data, 17: 31118
solubility in liquid sodium, effects of free energy gradient on, 18: 22488 (NAA-SR-8381)
sorption by cellulose ion exchangers from acetone and ethanol mixtures with hydrochloric acid, 18: 16140
sorption from hydrochloric acid by cellulose and resin paper ion exchangers, 18: 16139
spectra of, analysis of visible, 17: 35263(R) (UCRL-10706(p.1-110))
superconductivity under high pressure, (E), 19: 39736
thermal conductivity of amorphous, effect of cadmium, phosphorus, and manganese admixtures on, 20: 46211
thermodynamic properties of amorphous and hexagonal, at 0°C, 17: 29328(R) (TID-19007)
toxic effects in animals, reaction mechanisms, 16: 14442
toxic effects in animals, 18: 27060
toxic effects on chick embryos, comparison of sulfur-35 with, 19: 14999
toxic effects on chickens, 19: 45761(R) (ORO-631, pp 122-31)
tracer applications, survey, 16: 1359
transition probabilities of forbidden lines of, 18: 14736
uptake by microorganisms, tracer studies of, 19: 6962
use as catalyst in destruction of radioactive celluloses using sulfuric acid, 20: 5208(P)
use in diagnosis of gastrointestinal diseases, 19: 43886
vapor pressure, 20: 331
volatilization, tracer analysis of, 16: 22583 (BM-RI-6004)

SELENIUM COMPLEXES
with cyanates, formation and hydrolysis of, 18: 3672(R) (BNL-799 (p.64-73))
with diaminobenzene, preparation of free radical from, 18: 12521(R) (BNL-823(p.57-65))
with diethyldithiophosphate, solvent extraction from mineral acids using carbon tetrachloride, 16: 28926(T) (AEC-tr-5202)
with protactinium, preparation and properties, 19: 17890
with 1,2-diaminobenzene, reactions with sodium in tetrahydrofuran, 19: 15332(R) (BNL-841(p.52-62))

SELENIUM COMPOUNDS
analysis of, colorimetric, 18: 3672(R) (BNL-799(p.64-73))
cell dimensions and magnetic susceptibilities of rare earth, 16: 1681
dialkyl, protective effects against radiation damage to silicone oils and diesters of silicic acids, 19: 24561
geochemistry and thermodynamic properties, with selenium-76 and -82, 16: 9991
isotope exchange reactions in cyanides, 16: 14746
organic, synthesis of radioprotective analogs of 2-aminoethanethiol and 2-aminoethylisothiouronium salts, 17: 14047
organic, preparation and reactions of, for biomedical studies, 20: 26903
phenyl-, radioprotective activity in mice, 17: 40666
preparation of selenium-75-labeled guanine, purine, and cystine, 16: 21873
synthesis of radioprotective analogs of 2-aminoethylthiouronium salts, 16: 23515(R) (AD-269983)

SELENIUM CYANATES
formation and hydrolysis of, 18: 3672(R) (BNL-799(p.64-73))

SELENIUM FLUORIDES
electron attachment cross section for, as function of impact energy, 17: 3566 (AFCRL-62-419)
enthalpy of formation of SeF_6, 20: 20650(R) (ANL-7055, pp 167-76)
enthalpy of formation of, 20: 31213(R) (ANL-7175, pp 119-58)
fluorine NMR in, selenium isotope effects on, 18: 43474
heat of formation of hexa-, 19: 32118(R) (ANL-7020(p.165-74))
molecular force constants of hexavalent, calculation of, 17: 25174
molecular force constants of SeF_6, 20: 26865
molecular structure of, mean-square amplitudes of interatomic distances in hexavalent, 18: 1639
molecular structure of, mean amplitudes of vibration at 0 and 298°K in, 20: 38897
preparation of fluorine-18-labeled, 20: 41020
reactions with vanadium pentafluoride, 20: 36804
spectra, Raman, 17: 25236

Selenium Hydrides
see Hydrogen Selenides

SELENIUM IONS
chromatography on acetylated filter paper, 16: 6379
electron spin resonance of molecular, in alkali halide single crystals, (E/T), 20: 18005

Slater-Condon parameters of, determined from spectral data, 17: 31118
van der Waals radii of, relation of hydration energy to, 18: 16016

SELENIUM ISOTOPES
atomic mass comparisons for, 18: 15228
energy levels, interactions, nuclear moments, and transitions in, 17: 24381 (AD-403411)
gamma reactions on, cross sections for, 19: 12496
isomeric transitions of E_3 type, 16: 31066 (NP-11746)
isotope effects on fluorine nuclear magnetic resonance spectra in selenium fluorides, 18: 43474
neutron resonance absorption at 0.1 to 5 kev, 19: 1637
production in secondary reactions in copper, (E), 19: 37895
proton reactions (p,n) at 17 Mev on even, effects of excited isobaric states, 16: 26333 (UCRL-6830)
separation by isotopic exchange, 19: 18369
separation by thermodiffusion concentration distribution in tubes for, 17: 11059
spectra in hydrogen selenide, analysis of near-infrared, 18: 25437

SELENIUM ISOTOPES Se-72
proton reactions at 2.9 Bev, isobaric yields from, 16: 23126

SELENIUM ISOTOPES Se-73
book: *Isobaric Nuclei with the Mass Number A = 73*, 18: 7784
decay of, arsenic-73 double isomerism from, 17: 28319
decay scheme, 17: 31073(R) (ANL-6719)
decay scheme, 17: 41925
gamma spectra, 18: 24585(R) (IDO-16969)

SELENIUM ISOTOPES Se-74
book: *Isobaric Nuclei with Mass Number A = 74*, 18: 2959
energy levels and transition probabilities of second 2^+ states, 16: 23142
energy levels from bromine-74 decay, (E), 20: 28464
neutron reactions (n,p) arsenic-74 production in, 16: 11037
neutron reactions (n,p), separation energies for, 17: 2242 (TID-16949)
neutron reactions (n,$\alpha\gamma$), (n,αn), (n,2n), (n,np), (n,2p), (n,pγ), and (n,pn) at 14.8 Mev, cross sections for, 17: 2242 (TID-16949)
neutron reactions (n,p), preparation of arsenic-74 by, in reactor, 17: 24508
neutron reactions (n,2n) at 14 Mev, shell effects in, (T), 19: 12536
neutron reactions (n,p) with, cross sections for, 19: 15391
neutron reactions (n,2n) and (n,p) at 14.4 Mev, cross sections for, (E), 20: 40079 (ORO-3346-2)
production in stars, 16: 12308
proton reactions (p,p'γ) at 4.2 and 4.6 Mev, second 2+ level properties, 16: 3714

SELENIUM ISOTOPES Se-75
analytical uses, 16: 22583 (BM-RI-6004)
binding to serum lipoproteins in dogs and rats, 16: 28716
content in polonium process waste stream, 18: 13358(R) (MLM-1151)
decay of, gamma spectra from, (E), 20: 12022
decay of, internal conversion coefficient ratios from, (E), 19: 23711
decay of, local energy deposition due to electron-capture and internal conversion, 20: 18958
decay of, probability for electron-capture, (E), 20: 28328
decay scheme, 16: 9465
decay scheme, 18: 29145(R) (MLM-1185)
determination in irradiated polyphenyls, 16: 7496
diagnostic and therapeutic use, review of various aspects for, 18: 17693
diagnostic use for tumors of parathyroid gland or pancreas, 19: 34054
diagnostic use for pancreatic scanning in selenomethionine, 19: 36194
diagnostic use in thyroid scanning, 18: 17703
diagnostic use in parathyroid gland, 19: 4026
diagnostic use of selenomethionine-incorporated, 18: 43341
diagnostic use of selenomethionine-incorporated, in pancreas scanning, 19: 5746
diagnostic use of methionine-incorporated, in parathyroid tumor scanning, 19: 5744
diagnostic uses of, 19: 24391
dosimetry of, at various source distances, 20: 19091
dosimetry of, in nuclear medicine, 20: 26713
energy from, determination of total, 19: 38878 (ORNL-P-1405)
exchange reactions in cyanides, 16: 14746
excretion and retention in gravid and normal rats, effects of atoxic and toxic doses on, 16: 30198(R) (TID-16577)
excretion in urine, 18: 41052
fixation to protein-polysaccharides of bovine cartilage, 20: 40544
gamma dose constants for, 20: 46617
gamma spectra, 16: 11883
gamma spectra, 17: 34966
gamma spectra, 18: 12498
gamma spectra, (E), 20: 25393
incorporation in amino acids in microbes, 19: 6962
incorporation in cystine of, 20: 3661 (NP-15594)
incorporation in methionine of, 20: 3661 (NP-15594)
incorporation in selenocystine by neutron activation, 20: 14630
incorporation into blood proteins, 20: 5262
localization and translocation in leaves, roots, and stems of *A. racemosus*, 16: 30201
metabolism by chickens, effects of parathyroid hormones on, 19: 3837(R) (ORO-625(p.86-92))
metabolism by chickens, effects of dietary selenium and age on, 19: 10773
metabolism in cock sperm, 19: 35925
metabolism in dogs, 20: 5262
metabolism in domestic animals, 18: 11645(R) (ORO-614)
metabolism in mice, 18: 17426
metabolism in parathyroid gland of chickens, 19: 45761(R) (ORO-631, pp 122-31)
metabolism in sheep and swine, 19: 45759(R) (ORO-631, pp 77-82)
production by neutron reactions (n,γ), 18: 37592
radiation effects on metabolism of, in chicks and rats, 17: 38742(R) (NYO-10602)
radiation effects on chick metabolism of, gamma, 18: 38882
separation from fission products by amalgam exchange, radiochemical, 18: 16148
separation from neutron-irradiated biological materials, use of Szilard-Chalmers effect in, 20: 18583
sorption and exchange by root seedlings of *Astragalus preussii*, 16: 30201
stability and storage of organic compounds labeled with, review on, 20: 35574
tracer use in mouse immunological studies, 20: 40503(R) (ORNL-3922, pp 137-45)
tracer uses in studying intestinal transport of selenomethionine, 16: 14445
transfer of, across pericardium in dogs, 18: 15804
uptake and retention by microorganisms, 19: 6962
uptake by brain, measurement techniques for, 18: 17419
uptake by chick serum proteins, 18: 3470
uptake by sheep blood cells of, 18: 3468
uptake by swine blood cells in vitro, effects of dietary calcium, zinc, and corn oil on, 20: 40556
uptake in cytochrome c in rats, 16: 9831
use as tracer for impurity diffusion processes, 18: 37687(T) (AEC-tr-6398(p.328-33))
use for tumor localization, 20: 26722
use in determining life span of porcine and sheep erythrocytes, 20: 32907(R) (ORO-648, pp 62-70)
use in gamma backscattering density measurements, 20: 41257
use in pancreas scanning, 19: 19722
use in pancreas scanning, 20: 40748
use in photoscanning of pancreas, 19: 19723
use in radiodiagnosis of pancreatic diseases, 18: 23392
use in scanning for parathyroid tumors, 20: 22810
use in scintiscanning, review, 20: 22828
use in study of diffusion in selenium, 18: 37688(T) (AEC-tr-6398 (p.334-7))
use of compounds labeled with, in medicine, 20: 43051
use of methionine-incorporated, in pancreatic diagnosis, 20: 22828
use with gold-198 in subtractive gamma scanning of pancreas, 20: 33140

SELENIUM ISOTOPES Se-76
alpha reactions at 3 to 10 Mev, gamma yields from, 16: 23065
deuteron elastic scattering and stripping reactions (d,p) at 7.8 Mev, cross sections for, 16: 26300
deuteron inelastic scattering at 15 Mev, energy levels from, (E), 19: 47642
deuteron reactions (d,p) with, angular distributions for, 17: 31452
deuteron reactions (d,d) at 7.8 Mev, distorted waves approximation in, 17: 38182
deuteron reactions (d,p) and (d,t) at 15 Mev, level structure from, (E), 19: 35488
energy level lifetime, 0.559-Mev, 17: 17211
energy level transitions in, M1-M2 mixing ratios as test of purity of vibrational, (T), 19: 25503
energy level widths, (E/T), 20: 30360 (WASH-1068)
energy levels, 16: 5988
energy levels, 16: 17081
energy levels, 16: 23073
energy levels, 17: 800 (TID-16960)
energy levels and transition probabilities of second 2^+ states, 16: 23142
energy levels from arsenic-76 decay, 18: 28599
energy levels from decay of arsenic-76, 18: 32741 (TID-18567(App.I))
energy levels from decay of bromine-76, 18: 32742 (TID-18567(App.II))
energy levels in, structure of low-lying 2^+, 17: 11698
energy levels of, determination by Coulomb excitation, 17: 34982
energy levels of, electric monopole transitions between, 18: 6252
energy levels of, second excited 2^+, 18: 38147

energy levels of, properties of 2+, (E), 19: 33322
energy levels of, structure of first and second excited, 20: 10092
energy levels, second 2+ state at 1.1 to 1.5 Mev, 16: 18496
excited state spectrum, first, 16: 17108
gamma scattering at 10 to 27 Mev, structure of giant dipole resonance in, (T), 19: 8442
gamma transition at 559.3 kev following Coulomb excitation, (E), 20: 3043
geochemistry and thermodynamic properties of compounds, 16: 9991
isotope effects in reduction of sodium selenates and selenites, 20: 18642
neutron potential scattering cross sections, 18: 2849
neutron reactions (n,γ) with, activation cross sections for short-lived isomers in, 18: 15219
neutron reactions (n,p) with, cross sections for, 19: 15391
neutron reactions (n,2n) and (n,p) at 14.4 Mev, cross sections for, (E), 20: 40079 (ORO-3346-2)
oscillations and transition probabilities, 18: 18921
oxygen-ion inelastic scattering at 37 Mev, Coulomb excitation in, 18: 26610
proton inelastic scattering at 12 Mev, collective states excited in, 17: 38268
proton inelastic scattering on, excitation of collective states in, 18: 2898
proton reactions (p,p'γ) at 5.0 Mev, second 2+ level properties, 16: 3714
proton reactions (p,γ) in stars, 16: 12308
proton reactions (p,pn) at 2.9 Bev with, cross section for, 17: 22621
surface oscillations of, 18: 13114

SELENIUM ISOTOPES Se-77

bremsstrahlung reactions at 0.8 Mev, excitation of isomeric states in, 18: 2945
Coulomb excitation of, gamma angular distribution in, (E), 19: 16896
determination of metastable, in blood, body fluids, urine, and water, activation, 19: 10983(R) (TEES-2671-3)
deuteron (d,p) reaction with, 19: 3267
deuteron inelastic scattering at 15 Mev, energy levels from, (E), 19: 47642
deuteron reactions (d,p) and (d,t) at 15 Mev, level structure from, (E), 19: 35488
electron conversion coefficients and neutron activation cross sections for metastable, 16: 26351
energy level at 248 kev, g-factor for, 18: 34895
energy level structure, (E), 19: 35488
energy levels, 16: 5988
energy levels, 17: 41528(R) (ANL-6720(p.16-28))
energy levels from Coulomb excitation and gamma de-excitation, 16: 14011
energy levels in, near 245 kev, 17: 22264(R) (ANL-6679)
energy levels of, parity and spin of excited-state, 18: 9366
energy levels of, spin of 987-ev, 17: 41873 (WASH-1044)
energy levels of, effects of collective vibrational motion on anomalous coupling, (T), 20: 28420
energy-level transitions from beta decay of arsenic-77, (E), 20: 46757
gamma dose constants for metastable, 20: 46617
gamma emission by, 18: 8313
gamma spectra, 16: 4751 (JAERI-4019)
gamma spectra, 17: 34966
gamma spectra following Coulomb excitation, (E), 20: 3043
gamma spectra from Coulomb excitation of, (E), 19: 37817(R) (ORNL-3778(p.116-19))
gamma transitions following Coulomb excitation, (E), 20: 3043
half life, 16: 26213 (AE-78)
half life of metastable state of, 17: 5352
neutron capture cross sections at 10^3 to 10^5 ev, 16: 26518
neutron capture resonances in, 18: 42622(R) (ANL-6879(p.2-20))
neutron inelastic scattering by, strength function and spin for, 18: 28675
neutron potential scattering cross sections, 18: 2849
neutron reactions (n,p), separation energies for, 17: 2242 (TID-16949)
neutron reactions (n,αγ), (n,αn), (n,2n), (n,np), (n,2p), (n,pγ), and (n,pn) at 14.8 Mev, cross sections for, 17: 2242 (TID-16949)
neutron reactions on, widths of resonances in, 17: 13557
neutron reactions (n,γ) with, partial radiation widths of, 18: 11179 (ANL-6797(p.322-3))
neutron reactions (n,γ) with, sum-coincidence studies of gamma cascades from, 18: 21329
neutron reactions (n,p) with, cross sections for, 19: 15391
neutron reactions with, resonances in, (E), 19: 45296
neutron resonance capture gamma spectra of, partial widths for radiative transitions in, 18: 1055
nitrogen ion reactions at 16.5 and 18.3 Mev, angular distribution of gamma radiation from excited levels from, 16: 33827
nitrogen-ion scattering at 16.2 and 17.7 Mev, gamma polarization from, (E), 20: 15759
nuclear properties of isomeric, 18: 13626(R) (NYO-10174)
photoactivation of isomeric, cross sections for, 18: 7705
production of metastable isomeric, by reactor irradiation, (E), 19: 33295
production of short-lived isomer of, by thermal neutron reactions (n,γ), cross sections for, 18: 15219
proton elastic scattering at 13 Mev, cross sections for, 16: 26300
proton reactions (p,n) at 1.5 to 6.0 Mev, threshold measurements on, 18: 6200
proton scattering at 13 Mev, distorted waves approximation in, 17: 38182

SELENIUM ISOTOPES Se-78

alpha reactions at 3 to 10 Mev, gamma yields from, 16: 23065
deuteron inelastic scattering at 15 Mev, energy levels from, (E), 19: 47642
deuteron reactions (d,p) and (d,t) at 15 Mev, level structure from, (E), 19: 35488
deuteron scattering at 11 Mev, 16: 21504
energy level structure, (E), 19: 35488
energy levels, 16: 5988
energy levels, 16: 23073
energy levels, 19: 3267
energy levels and transition probabilities of second 2+ states, 16: 23142
energy levels of, 17: 13557
energy levels of, determination by Coulomb excitation, 17: 34982
energy levels of, electric monopole transitions between, 18: 6252
energy levels, second 2+ state at 1.1 to 1.5 Mev, 16: 18496
gamma transition at 614.2 kev following Coulomb excitation, (E), 20: 3043
neutron reactions (n,α) and (n,p) at 14.4 Mev, cross sections for, (E), 20: 40079 (ORO-3346-2)
nitrogen-14 scattering at 36 Mev, interference effects in 2+ level excitation in, (T), 20: 15768
oscillations and transition probabilities, 18: 18921
oxygen-ion inelastic scattering at 37 Mev, Coulomb excitation in, 18: 26610
proton inelastic scattering at 12 Mev, collective states excited in, 17: 38268
proton reactions (p,p'γ) at 4.1 Mev, second 2+ level properties, 16: 3714
proton reactions (p,n) at 1.5 to 6.0 Mev, threshold measurements on, 18: 6200
proton scattering at 11 Mev, 16: 21504

SELENIUM ISOTOPES Se-79

electron conversion coefficients and neutron activation cross sections for metastable, 16: 26351
energy level structure, (E), 19: 35488
energy levels of, effects of collective vibrational motion on anomalous coupling, (T), 20: 28420
gamma dose constants for metastable, 20: 46617
gamma emission by, 18: 8313
gamma spectra, 17: 34966
gamma spectra, 18: 1050
gamma spectra, 20: 44634(R) (IDO-17188)

SELENIUM ISOTOPES Se-80

alpha reactions at 3 to 10 Mev, gamma yields from, 16: 23065
deuteron inelastic scattering at 15 Mev, energy levels from, (E), 19: 47642
deuteron reactions (d,p) and (d,t) at 15 Mev, level structure from, (E), 19: 35488
deuteron reactions (d,p) at 15 Mev, isomeric yield ratios for, 20: 16508(R) (NYO-2771-13)
effects on rotation-vibration bands in spectra of hydrogen selenide, 19: 11100
energy levels, 16: 23073
energy levels and transition probabilities of second 2+ states, 16: 23142
energy levels below 1.47 Mev and gamma spectra, 16: 18498
energy levels of, electric monopole transitions between, 18: 6252
energy levels of, power functions for, 17: 38003(T) (AEC-tr-5734(p.25-6))
energy levels, second 2+ state at 1.1 to 1.5 Mev, 16: 18496
gamma transition at 666.2 kev following Coulomb excitation, (E), 20: 3043
neutron activation cross section at 24 kev, (E), 20: 12135
neutron capture by, isomer ratios for, 18: 44786
neutron elastic scattering at 4 Mev, polarized, 18: 40511 (NP-14205)
neutron elastic scattering by, cross sections for, 18: 44760
neutron potential scattering cross sections, 18: 2849
neutron reactions (n,γ), isomeric cross section ratios, 16: 2477 (ANL-6405)
neutron reactions (n,np), cross sections, 16: 14028
neutron reactions (n,γ), activation measurements for, 16: 24787 (NP-11793)
neutron reactions (n,np) at 14 Mev, cross sections for, 17: 2242 (TID-16949)
neutron reactions with, determination of mass-flow function from, 17: 33027
neutron reactions (n,2n) at 14.8 Mev, isomeric cross section ratios in, (E), 19: 27517
neutron reactions (n,α) and (n,2n) at 14.4 Mev, cross sections for, (E),

20: 40079 (ORO-3346-2)
neutron scattering at 4.0 Mev, polarization angular distributions from, (E), 20: 30360 (WASH-1068)
neutron total cross sections, 16: 14072
oscillations and transition probabilities, 18: 18921
proton inelastic scattering at 12 Mev, collective states excited in, 17: 38268
proton reactions (p,n) with, thresholds for, (E), 19: 6704
proton reactions (p,n) at 14.2 Mev, angular distributions, Q values, and spectra from, 20: 13345(R) (NP-15772)
proton reactions (p,n) at 14.2 Mev, Q-values and differential cross sections for, (E/T), 20: 34520 (INSJ-97)
proton reactions (p,γ) in stars, 16: 12308
proton reactions (p,n) at 1.5 to 6.0 Mev, threshold measurements on, 18: 6200

SELENIUM ISOTOPES Se-81
decay data, 17: 17298
decay of, gamma spectra from, 19: 45679(R) (NYO-1859-11)
decay scheme, 17: 805 (TID-16984)
decay scheme, 17: 20564(R) (TID-18442)
energy level densities in, effects of spin on, 16: 33853
energy level structure, (E), 19: 35488
energy levels of, effects of collective vibrational motion on anomalous coupling, (T), 20: 28420
gamma dose constants for metastable, 20: 46617
isomeric-pair production by neutron activation, yield ratios of, 17: 7248
production of isomer pairs of, in (n,2n) reactions, (E), 19: 27517
production of isomeric, in deuteron reactions (d,p) at 15 Mev, 20: 16508(R) (NYO-2771-13)
yield from neutron fission of uranium-235, 16: 21347 (AWRE-0-58/61)
yields from thermal neutron fission of plutonium-239, 17: 41898
yields from uranium-233 and -235 neutron and proton fission, 16: 32414

SELENIUM ISOTOPES Se-82
alpha reactions at 3 to 10 Mev, gamma yields from, 16: 23065
deuteron inelastic scattering at 15 Mev, energy levels from, (E), 19: 47642
deuteron reactions (d,p) and (d,t) at 15 Mev, level structure from, (E), 19: 35488
energy levels and transition probabilities of second 2^+ states, 16: 23142
gamma reactions (γ,n) on, nuclear excited states from, 16: 33853
gamma transition at 655.4 kev following Coulomb excitation, (E), 20: 3043
geochemistry and thermodynamic properties of compounds, 16: 9991
isotope effects in reduction of sodium selenates and selenites, 20: 18642
neutron reactions (n,2n), cross sections for, 16: 7072
neutron reactions (n,2n) at 14 Mev, shell effects in, (T), 19: 12536
neutron reactions (n,2n) at 14.8 Mev, isomeric cross section ratios in, (E), 19: 27517
neutron reactions (n,2n) at 14.4 Mev, cross sections for, (E), 20: 40079 (ORO-3346-2)
neutron reactions (n,γ) with, isomer ratios from, 20: 44816
neutron reactions (n,2n) at 3 Mev above threshold, cross section for, (E), 20: 46614
proton reactions (p,n) with, thresholds for, (E), 19: 6704

SELENIUM ISOTOPES Se-83
energy level structure, (E), 19: 35488
gamma dose constants for, 20: 46617
gamma emission by, 18: 8313
gamma spectra, 16: 4751 (JAERI-4019)
gamma spectra, 17: 34966
spectra and energy levels, beta and gamma, 16: 17148
yields from thermal neutron fission of plutonium-239, 17: 41898
yields from uranium-233 and -235 neutron and proton fission, 16: 32414

SELENIUM OXIDES
arsenic-76 distribution in, 16: 11761
oxidizing effects on olefins, 19: 32048(R) (NP-15073)
radiation effects on mechanical properties, 18: 16542
separation by thin-layer ionophoresis, 18: 10185
sorption on anion exchange papers in hydrobromic and hydrochloric acids and lithium chloride, 18: 25374

SELENIUM SYSTEMS
properties of intermetallic compounds with rare earths, 16: 1689
As–Se, electron secondary emission by, 19: 27101
As–Se–S, viscosity of, effects of sintering on, 20: 35886 (IS-T-80)
As–Se–Te, radiation effects on electric conductivity of, 18: 16541
As–Se–Te, radiation effects on, 19: 2862
As–Se–Te–Tl, thermoelectric properties, 18: 37115 (ANL-6856)
As–Se–Tl, radiation effects on electric conductivity of, 18: 16541
As–S–Se, sintering mechanism of, 20: 41064(R) (IS-1500(Sect.E))
Au–Se, electron transfer in dilute, 17: 37189
Ba–Ce–Se, electric properties, 17: 34469
Ba–rare earths–Se, crystal structure, 19: 13298
Bi–Se, thermodynamic properties at 300 to 390°C, 17: 29328(R) (TID-19007)
Bi–Se, thermoelectric properties, review, 18: 32511 (GIC-3362-1)
Bi–Se–Te, electric properties of semiconducting, effect of oxygen on, 19: 33520(T) (AEC-tr-6585)
Bi–Se–Te, performance of power generation thermocouple of, 17: 36280(R) (AD-291456)
Bi–Se–Te, thermoelectric properties, review, 18: 32511 (GIC-3362-1)
CdSe–Se, radiation effects on electric properties of, 17: 14912
CdS–Se, radiation effects on electric properties of, 17: 14912
Ce–Se, phase diagrams, 17: 4886(R) (AD-275610)
Ce–Se, preparation, phase studies, and properties of compounds in, 19: 5862
Ce–Se–Sr, electric properties, 17: 34469
Cr–Se, crystal and magnetic structure of, 17: 37826
Cr–Se, magnetic and crystal structure of, 16: 18445
Cr–Se, magnetic structure of, temperature effects on, 16: 16834
Er–Se, crystal chemistry and phase studies of, 18: 23506
Er–Se, phase equilibria and crystal chemistry, 19: 19879
Er–Se, phase studies of compounds in, 18: 37115 (ANL-6856)
Er–Se, phase studies, 20: 7622
Ga–La–Se, chemical properties, 19: 38598
Gd–Se, phase diagrams, 17: 4886(R) (AD-275610)
Gd–Se, phase studies of, between Gd : Se = 1 : 1.6 and Gd : Se = 1 : 2.0, 20: 45648
Hg–Se, performance as indicator electrode, 20: 22871(R) (MIT-905-52, pp 42-73)
In–Se, phase studies, 17: 22208
In–Se, phase studies and microhardness, 17: 36325
La–Se, preparation, phase studies, and properties of compounds in, 19: 5862
Nb–Se, phase studies, 19: 7932
Nd–Se, preparation, phase studies, and properties of compounds in, 19: 5862
Pb–O–Se, crystal structure powder diffraction pattern of phases in, 19: 17795
Pr–Se, preparation, phase studies, and properties of compounds in, 19: 5862
rare earths–Se–Sr, crystal structure, 19: 13298
Re–Se, crystal structure of compound $ReSe_2$ in, 19: 23026
Sb–As–Se–Tl, thermoelectric properties, 18: 37115 (ANL-6856)
Sb–Bi–Se–Te, thermoelectric properties, review, 18: 32511 (GIC-3362-1)
Sb–Cr–Se, thermoelectric properties, 16: 18017(R) (AD-266019)
Sb–Se, electron secondary emission by, 19: 27101
Sb–Se, thermoelectric properties, review, 18: 32511 (GIC-3362-1)
Se–S–Te–U, thermoelectric properties, 17: 14856 (WCAP-1866)
Se–Ta, phase studies, 19: 7932
Se–Te, performance as electrophotographic material for particle track coordinates in spark chambers, 20: 21037 (JINR-P-2594)
Se–Te, thermoelectric capacities of liquid, 19: 44712
Se–Te–Sn, properties for thermoelectric power generation, 17: 36280(R) (AD-291456)
Se–Te–U, thermoelectric properties, 17: 24064(R) (WCAP-1865)
Se–Th, phase studies, 16: 30877
Se–Tl, diffusion in, 18: 37687(T) (AEC-tr-6398(p.328-33))
Sm–Se, preparation, phase studies, and properties of compounds in, 19: 5862
2-Selenoylacetone
see Acetone, 2-(Selenoyl)-

SELF-DIFFUSION
activation energy prediction for, 17: 35264(R) (UCRL-10706(p.111-203))
activation in alpha-uranium, thermodynamics of, 20: 43928
coefficients for ionic cesium and sodium in agar gels, 20: 25099
in liquids, neutron study, 16: 6870
in metals, model for, 19: 11682
in metals, prediction of activation energies of, 18: 14478 (UCRL-10581)
in solids, measurement by self-absorption of beta particles in samples of finite thickness, 17: 23589
measurement for radioisotopes in dilute solutions, apparatus for, 19: 395
measurement for radioisotopes in dilute solutions, methods for, 19: 396
mechanisms of, in water, effects of ions on, 19: 32159
of liquid metals, measurement by tracer methods, 16: 27657
of pure gases in tubes, 17: 35992(T) (AERE-Trans-946)
radiation effects on, 18: 22016(R) (ORNL-3591(p.115-23))
SELNI Power Reactor
see Trino Power Reactor

SEMEN
see also Sperm
radiation effects on goat, prenatal gamma exposure, 18: 41212
radiation effects on bull, x, 20: 40610(R) (COO-895-9)
Semi-Homogeneous Experiment (SHE)
see Critical Assemblies

SEMICARBAZIDE
complexes with uranyl ions, preparation of, 17: 35699 (TID-17418)
complexes with uranyl chlorides, polarographic behavior of, 20: 20677
reaction of hydrochloride with cerium, complex formation, 17: 4544
reactions with aldehydes, carbon-14 and tritium isotope effects, 16: 23577

SEMICONDUCTOR DETECTORS
amplifier and shaping circuit for, design for electronic timing, 18: 4129
amplifier circuit designs for, review, (E), 19: 40899
amplifier design for helium-3 and lithium-6 sandwich-type, for reactor environment, 18: 24024
amplifier design for, transistorized low-noise pre-, 18: 25789 (NAS-NRC-Pub-1184(p.61-4))
amplifier design for, fast, 20: 46080
amplifier for, description of transistorized low-noise, 18: 23997
amplifier for, design of high-pulse-rate, 20: 4243 (LAL-1102)
amplifier for, design of low-noise charge-sensitive transistorized pre-, 20: 21072
amplifier for, design of charge-sensitive, 20: 27319
amplifier for, development of low-noise, 19: 18267 (NP-14729)
amplifier for, performance of transistorized pre-, 20: 2154
amplifier signal-to-noise ratio for, effects of input resistance on, 19: 44489 (ZFK-PHA-12, pp 219-23)
amplifier systems for, (E), 20: 46049(R) (ORNL-3973(Vol.2), pp 96-103)
amplifiers for, design of fast-coincidence pre-, 18: 20356
amplifiers for, design of low-noise, 18: 20366
amplifiers for, design of cascode, 18: 33898
amplifiers for, development of low-noise charge-sensitive, 18: 33927
amplifiers for, development of low-noise vacuum-tube, 18: 33928
amplifiers for, design of, 18: 39662
amplifiers for, design of, 19: 9522
amplifiers for, design of charge-sensitive, 19: 24857
amplifiers for, design of fast, 19: 26662 (KFK-257)
amplifiers for, design of stable, 19: 28666
amplifiers for, development of low noise, 19: 44483 (ZFK-PHA-12, pp 172-88)
amplifiers for, design and performance of charge-sensitive, 19: 44484 (ZFK-PHA-12, pp 189-95)
amplifiers for, development of, 19: 46643(R) (LAL-1136)
amplifiers for, design of charge-sensitive pre-, 20: 14851 (BNL-9980)
amplifiers for, design and performance of pre-, 20: 16806 (CLOR-44/D)
amplifiers for, design of integrated-circuit charge-sensitive pre-, 20: 21112
amplifiers for, design of 5-kev resolution, 20: 23427(R) (UCRL-16580, pp 219-50)
amplifiers for, design of charge-sensitive pre-, using field-effect transistors, 20: 33694
amplifiers for, design of, 20: 33695
amplifiers for, fast, 20: 46082
angular distribution measurements with, target chamber for, 18: 41804
arrays of, identification of individual detectors in multidetector, 17: 3344
background count in silicon surface-barrier, 18: 22331 (CLOR/IBJ-II-22)
barrier layer depth in n-i-p silicon, 20: 43742
behavior of np, in presence of pp^+, 16: 16546
beta spectroscopy by, corrections for backscattering and energy resolution in, 18: 41788
bibliography, 16: 17825 (TID-3907(Rev.I))
bibliography, 17: 1780
bibliography on, 20: 35757 (PAEC(A)IN-658)
book: *Semiconductor Counters for Nuclear Radiations*, 18: 23969
book: *Semiconductor Particle Detectors*, 18: 25848
book: *Semiconductor Counters for Nuclear Radiations*, 20: 41352
calibration, 17: 12802(R) (PR-P-55)
calibration for fission fragments, 19: 19095 (WASH-1053)
calibration of coincidence telescopes of, gallium arsenide light sources for, 19: 42711 (JINR-P-2262)
calibration of p-n junction, 17: 3322
calibration of pulse-height response of, to protons, 17: 30856 (SAM-TDR-63-21)
calibration of silicon surface-barrier, for neutron dosimetry, 19: 26669 (TID-21844)
calibration of silicon, for fission fragments and heavy ions, 19: 30526 (ORNL-P-1089)
calibration of, accuracy of techniques for, 19: 20371
capacitance of, beat-frequency method for measuring, 19: 34474 (INR-584/II/PS)
carrier collection time and equivalent circuit of surface-barrier, (E/T), 19: 34494
characteristics and production of ion-drifted p-i-n type, 16: 11855 (NP-11377)
characteristics and performance, 17: 7655(R) (ANL-6600)
characteristics and response, 17: 11045
characteristics of gold-silicon surface barrier as alpha particle, 16: 7708
characteristics of, review, 17: 11009 (TID-16206)
characteristics of solid-state materials as, 18: 4102
charge carrier lifetime and resistivity in silicon, thermal cycling effects on, 20: 30785
charge carrier trapping in lithium-drifted germanium, (E), 19: 40919
charge collection efficiency in, (T), 19: 22805
charge collection time in, relation of particle impact angle and range to, (T), 19: 34495
charge collection in, properties of, (T), 20: 16885
charge collection time of lithium-compensated silicon, 20: 43703
charge collection efficiency of silicon surface-barrier, 20: 43705
charge collection in junction and lithium-drifted, 20: 46033 (ANL-7226)
charge production in lithium-drifted germanium and silicon, 20: 5784
charge transport time in, effect of non-constant carrier mobility on, 19: 20366
charge-carrier collection of p-n, for 4.98-Mev alpha particles, 20: 29550
charged particle discrimination, 16: 3217
charged particle events in, optical simulation of, 19: 22766
charged particle energy-loss spectra in, fluctuations of, (E/T), 20: 29531 (UCRL-16715)
charged particle spectrometry with, 18: 14590(R) (NIRL/R/60)
circuit design and performance of low-current threshold, employing uni-tunnel diode, 17: 23744 (TID-15831)
circuit design for time-energy measurement with, 20: 27289
circuit design for lithium-drifted germanium, 20: 46081
circuitry for identifying charged particles from energy and time-of-flight, 18: 25794 (NAS-NRC-Pub-1184(p.96-103))
coating with lithium-6 and uranium-235 by electrospraying, 19: 44635 (INR-595/IA/PL)
coincidence circuits for, efficiency of, 19: 44485 (ZFK-PHA-12, pp 196-200)
coincidence circuits for, efficiency for low-amplitude pulses, 19: 44486 (ZFK-PHA-12, pp 201-5)
collection time of p-n and p-i-n, 20: 46077
concepts and operation of, for charged particles, 19: 4526
conference, 20: 1345
conference, 20: 33646
conference on, 18: 33900
construction and performance review, 17: 1754
construction and performance of thin-silicon, 17: 4852
construction and performance of lithium-drifted and silicon-junction, 17: 30093
construction of gold–silicon surface-barrier counters of very high resistivity, 16: 19086
contacts for surface-barrier, metal-semiconductor, 18: 39663
cryostat design for gamma, engineering drawings for, 19: 44539
cryostat for, design of liquid nitrogen, 19: 28629 (INR-583/II/PL)
cryostats for germanium, development of, 19: 11580
cryostats for lithium-drifted germanium, for gamma rays, 19: 26704
current in high-resistivity n-silicon, reverse, 20: 41300
current leakage and noise in lithium-drifted silicon, geometric control of, 19: 46754 (BNL-9535)
current pulses produced in, direct recording of, 20: 46078
data analysis of gamma spectra from lithium-drifted germanium, computer programs for, 20: 39237
defects in silicon surface-barrier, pulse-height, 19: 13771
defects in silicon p-i-n, determination of, 20: 11103 (JINR-P-2489)
depletion depth of lithium-ion-drifted germanium, 19: 15909
description and performance of multi-guard-ring gold–silicon surface-barrier, for beta spectrometers, 19: 30519 (CLOR/IBJ-II-36/D)
description of gold-silicon-gold surface-barrier, 16: 30610
description of lithium-drifted, for alpha particles, 19: 32566
description of silicon p-n junction microplasma, for gamma rays, 17: 20369
description of vacuum-encapsulated lithium-drifted silicon, for telescope counters, 20: 33668
design and development, 17: 4807 (MITNE-8)
design and development of contoured, for charged particle detection, 18: 41773(R) (NYO-3246-1)
design and development of contoured, 18: 41774(R) (NYO-3246-2)
design and fabrication of silicon surface-barrier-type, for charged-particle spectrometry, 17: 36418 (NP-13020(p.260-4))
design and operation characteristics, 18: 20349
design and operation of long-tube, for reactor in-core measurements, 19: 44450(R) (IBK-120a)
design and operation of gamma, based on germanium with radioinduced defects, 20: 23472
design and performance of p–n junction, 16: 11896
design and performance, 16: 17851
design and performance of surface-barrier-type, for nuclear reaction studies, 16: 20744
design and performance for detection and mass identification of

protons, deuterons, tritons, helium-3, and alpha particles, 16: 20746
design and performance for neutrons, 16: 20755
design and performance for measurement of dE/dx and total energy of nuclear reactions, 16: 20747
design and performance of solid-state fission counters, 16: 24553
design and performance of gallium arsenides and silicon, 16: 27357
design and performance of p-n diffusion and surface barrier, 16: 29134
design and performance of silicon junction, for measurement for neutron flux, 17: 1757
design and performance of, review of, 17: 4849
design and performance of thin, 17: 6440 (UCRL-10030)
design and performance of helium-3-filled, for fast neutron spectra, 17: 6481
design and performance of silicon, for alpha-active elements in solution, 17: 30886
design and performance of silicon p-n junction, for Telstar, 17: 32458
design and performance of silicon surface-barrier, for charged-particle spectrometry, 18: 4092 (PAN-463/IA,II)
design and performance of, review of, 18: 4130
design and performance for inner Van Allen zone protons, 18: 7087
design and performance of, review of, 18: 10424
design and performance of reversed-biased-diode radiation-burst sensor, 18: 14348(R) (RTD-TDR-63-3051)
design and performance, 18: 15202 (NP-13678)
design and performance of lithium-drifted silicon surface barrier type, with guard ring, 18: 16314
design and performance of silicon, for spectrometry of charged particles, 18: 23962
design and performance of counter telescope for 14-Mev neutrons, 18: 23985
design and performance of position-sensitive, 18: 25784 (NAS-NRC-Pub-1184(p.42-5))
design and performance for electronic functions, 18: 41710(R) (AL-TDR-64-46)
design and performance for *in vivo* measurements of beta activity, 19: 9473 (AE-162)
design and performance of, 19: 11513
design and performance of gold-silicon surface barrier, for fission products, 19: 11516
design and performance of lithium-drifted and p-i-n junction, 19: 13738 (UCRL-13106)
design and performance of anticoincidence lithium-drifted germanium, 19: 20322 (LA-DC-6397)
design and performance of p-i-n diode, for gamma spectroscopy, 19: 22717
design and performance, 19: 22785
design and performance for proton scattering measurements, 19: 28962(R) (NIRL/R/81)
design and performance of germanium p-i-n, for gamma radiation, 19: 36827
design and performance of germanium, for gamma spectrometry, 19: 42715(R) (PRNL-3782, pp 35-51)
design and performance of silicon, for beta and gamma rays, 19: 44472 (ZFK-PHA-12, pp 52-63)
design and performance of lithium-drifted, for beta and gamma spectroscopy, 20: 664
design and performance of field-effect transistor, 20: 4250 (UCRL-16446)
design and performance of silicon, for particle impact position finding, 20: 5747(T) (NP-tr-1302)
design and performance of silicon, for energetic electron and proton measurements from rockets, 20: 7386
design and performance of surface-barrier, for alpha spectrometry, 20: 9276
design and performance for measuring electron and proton spectra during auroral storms, 20: 11853
design and performance of silicon, for charged particle identification, 20: 13076 (UR-875-117)
design and performance of lithium-6-silicon, for fast neutrons, 20: 21034 (EUR-2712.e)
design and performance of lithium-drifted silicon-diode, 20: 21064
design and performance of silicon, 20: 23427(R) (UCRL-16580, pp 219-50)
design and performance of silicon, for beta spectroscopy, 20: 23457 (CEA-R-2839)
design and performance of lithium-drifted germanium, 20: 31500(R) (BNWL-235-4, pp 4-10)
design and performance of, for use in 4π beta spectrometers, 20: 37125
design and performance, 20: 41369(P)
design and performance of lithium-drifted silicon, for charged particle identification, 20: 43717
design and performance of surface-barrier silicon, for charged particle identification, 20: 43717
design and performance of surface-contoured, 20: 46046(R) (NYO-3246-8)
design and preparation of multiple-junction, for high-energy particles, 18: 20417(P)
design and production of, standards for, 19: 44474 (ZFK-PHA-12, pp 66-9)
design and response to high-intensity transient gamma pulses, 16: 27265 (UCRL-13041)
design and response of, for stratospheric x-ray measurement, 20: 23479
design and testing of germanium n-i-p, 18: 31924
design and use for measuring reactor neutron flux distribution, 16: 20754
design and use for intracavitary dosimetry in radium therapy, 20: 41377
design and uses of germanium and silicon lithium-drifted, 20: 7359 (EUR-2580.e)
design and uses of, review on, 20: 16869
design feasibility as personnel dosimeter for fast neutrons, 17: 23746(R) (TID-18552)
design for alpha detection and discrimination in aerosols, 20: 691(P)
design for alpha particles, 16: 1977
design for alpha spectrometry, 18: 29987
design for beta spectroscopy below 4.2°K, 18: 2076
design for charged particles, 18: 2099(P)
design for charged-particle analyses in aurorae, 18: 20364
design for charged-particle identification, 20: 29526 (INP-444/PL)
design for complex nuclear reaction analysis, 18: 30016
design for continuous recording of neutrons, 16: 13320
design for detection and measurement of low-energy electrons, 20: 21138
design for determining energy of charged particles, 16: 30633(P)
design for determination of radiation energy and impinging position, 20: 687(P)
design for deuterons and protons, 19: 11520
design for energy discrimination of charged particles, 16: 27397(P)
design for fissiochemical experiments, 19: 40547(R) (AGN-8137(Vol.I))
design for flux mapping in inaccessible reactor core regions, 17: 10988
design for magnetic spectrometer, 18: 8649(R) (TID-19940(p.77-118))
design for neutron counting, 18: 27791(R) (WCAP-2596)
design for reactor power level and period, 18: 22334 (HW-74913)
design for Z = 1 and 2 particles, 18: 14224 (UCRL-11245)
design in combination with amplifier, 18: 16373(P)
design of amplifying, 20: 41361(P)
design of, based on Hall effect, 16: 27327
design of computer-controlled bistabilized system of, for studying mesic gamma spectra at 184 in. cyclotron, 20: 46052 (UCRL-16814)
design of cooled lithium-drifted, using hybrid preamplifier, 19: 13777
design of dE/dx, using p-n junctions, 18: 30069
design of dE/dx, with particle position indication, 20: 33667
design of deep-depletion-layer diode, 18: 35884
design of discriminating, 20: 5802(P)
design of dosimeter for fast and slow neutrons, 17: 20386(P)
design of fast-response p-n junction, for gamma radiation, 19: 42768(P)
design of, for alpha counting, engineering drawings for, 17: 32378
design of, for alpha particle detection, 17: 37012(R) (NYO-9505 (p.80-6))
design of linear junction, 18: 25858(P)
design of lithium-drifted germanium, 18: 43936(R) (MIT-952-1(p.163-95))
design of lithium-drifted silicon, 20: 11170(P)
design of lithium-drifted germanium, engineering drawings for, 20: 14904
design of lithium-drifted germanium, 20: 33712
design of lithium-drifted silicon high-voltage, 20: 46051 (UCRL-16718)
design of low-inertia silicon n-p and n-i-p, for pulsed x radiation, 18: 31925
design of multiple coincidence, 19: 9521
design of multiple-junction, for high energy radiations, 20: 14909(P)
design of oscillating-circuit type, 17: 16483(P)
design of oxide-passivated silicon p-n junction, for alpha particles, 20: 21077
design of photoconductive, with improved response, 18: 10431(P)
design of silicon-gold-lithium-6 fluoride, for fast neutrons, 16: 3853(R) (ORNL-3193(p.116-19))
design of silicon-gold-lithium-6 fluoride, for fast neutrons, 16: 3854(R) (ORNL-3193(p.119-23))
design of silicon charged-particle, nomograph, 16: 29541
design of silicon junction, 17: 3330
design of silicon n-p-p junction rectifier, for fast neutrons, 17: 32411
design of silicon p-n, 20: 31604(P)
design of single crystal silicon n-i-p, 18: 31922
design of small, for alpha particles, 17: 4840
design of small needle-type, 20: 8805
design of solar-cell-type, 17: 3684
design of surface barrier counters for heavy particles, 16: 13755
design of thick-depletion-zone p-n type, for neutrons, 20: 13116(P)
design of threshold, for position and energy determinations, 17: 23779
design of total-absorption lithium-drifted germanium, for protons, 20: 33676

design of surface-barrier, for thermal neutron detection, 18: 5654
design of system of, for energy and position determination, 20: 16878
design, performance, and uses of, 17: 25598 (ISS-63/20)
design of, for analysis of accelerator-beam pulses, 19: 4515
design of, with heat eliminator, 18: 14289(P)
design of, with uranium-235-coated p-n junction diodes, for neutron flux mapping in reactors, 19: 30592(P)
design, operation, theory, and uses of, review of, 17: 18635
design, performance, and uses, 17: 22021
design using lithium-drifted germanium crystals, for gamma spectrometry, 19: 34524
design with alpha particle energy resolution, for detecting plutonium and uranium, 18: 41880(P)
design with alpha particle energy resolution, for monitoring air, 18: 41881(P)
design with capability of distinguishing alphas, electrons, and protons, (E), 20: 5732 (KFK-335)
design with protective electrode, 18: 18193
design with separate ohmic contacts to reduce leakage current, 18: 8693(P)
design with surface field stability, 18: 2078
design, fabrication, and performance of vacuum encapsulated lithium-drift telescope, 20: 41376
design, performance, and uses, 18: 25837
development, 16: 11860(R) (ORNL-3191(p.19-35))
development, 16: 17816(R) (EURAEC-107)
development, 17: 2051(R) (CU(PNPL)-219)
development, 17: 15251(R) (CU(PNPL)-220)
development, 17: 14653(R) (WCAP-2175)
development, 17: 25858(R) (PR-P-56(p.19-33))
development, 17: 35253(R) (IA-775)
development, 17: 41873 (WASH-1044)
development, 18: 2585(R) (ISS-63/37)
development, 18: 8918(R) (PR-P-59(p.21-36))
development, 18: 14271
development, 19: 36870
development, 19: 46820
development, 20: 2143
development, 20: 2177
development, 20: 18198
development, 20: 35773
development, 19: 31460(R) (ANL-7010(p.179-233))
development, 20: 21026 (BNL-948, pp 704-17)
development, 20: 2520(R) (IA-920)
development, 19: 46643(R) (LAL-1136)
development, 20: 25383(R) (N-66-15632)
development, 19: 35615(R) (NP-15037)
development, 18: 27753(R) (ORNL-3578(p.6-36))
development, 20: 18988(R) (ORNL-929, pp 58-66)
development and fabrication, 20: 6694(R) (MIT-952-2)
development and operation of guard-ring, 17: 14608(R) (ORNL-3378 (p.18-21))
development and performance for neutrons, 16: 3186 (UCRL-6505)
development and performance of silicon surface-barrier-type, 17: 29189 (AERE-R-4122)
development and performance for neutron detection, 17: 36145 (ASD-TDR-62-838)
development and performance of silicon carbide diodes for neutron detection, 17: 36155(R) (WCAP-2346)
development and performance for fission products and neutrons, 19: 44450(R) (IBK-120a)
development and performance for nuclear particle research, 20: 27328
development and performance of lithium-drifted germanium, 20: 35726 (AD-634718)
development and testing of gamma-transient, 19: 11499 (UCRL-13128)
development and theory, 17: 367
development and uses of silicon-junction, 17: 36171
development and uses of, conference on, 19: 44467 (ZFK-PHA-12)
development and uses of, review of, 20: 7389
development and use, review of, 20: 41287
development at Chalk River, 17: 32724(R) (PR-P-57(p.21-36))
development for airborne radiation, 19: 40834(R) (UCRL-14151)
development for alpha particles, 17: 3302(R) (AD-276079)
development for discrimination between heavy particles, 20: 25409
development for dosimetry under military tactical conditions, 16: 11844 (AD-259711)
development for fast neutrons, for SNAP 10A, 20: 20298 (NAA-SR-11762)
development for fission fragments, 18: 33955
development for fission studies, 20: 39242
development for high-temperature neutron counting, 18: 2035(R) (WCAP-2403)
development for high energy physics, future, 18: 7028 (BNL-7393)
development for high-energy particle detection, (E), 19: 36804 (BNL-9218)
development for *in vivo* dosimetry, 19: 33704
development for in-pile flux measurements, 19: 36824 (WCAP-5482)
development for in-line determination of actinide separation from lanthanides, 20: 35764 (UCRL-16869)
development for krypton-85 counting, 19: 24611(R) (MLM-1227)
development for low-level krypton-85, 19: 28717(R) (MLM-1221)
development for measurement of charge-exchange neutral particles, 19: 21482(R) (ORNL-3760(p.23-9))
development for monitoring air for plutonium, 17: 11012 (UCRL-6692)
development for neutron dosimetry, 16: 1943(R) (ORNL-3189(p.166-71))
development for neutrons, 16: 16524(R) (EURAEC-185)
development for neutron dosimetry, 17: 3207 (HW-SA-2785)
development for neutron detection, 17: 32404(R) (WCAP-2274)
development for neutron detection and measurement, 20: 7459(P)
development for neutron dose rates in mixed gamma-neutron fields, 20: 31505(R) (BNWL-235-4, pp 30-4)
development for neutron dosimetry, 20: 35758 (PG-Report-711)
development for particle discrimination by time-of-flight methods, 18: 33932
development for scattering experiments, 16: 3671(R) (TID-14241)
development for use in shielding experiments, 18: 32949(R) (EUR-534.d(Pt.II))
development for use in neutron dosimetry, 19: 767(R) (HW-81746(p.5.46-53))
development for use in gamma spectrometers, 20: 23527 (CONF-651206)
development for uv radiation, 18: 37539
development in Japan, 19: 36829
development in USSR, 16: 25567 (NP-11947)
development of, and applications in radiobiological studies, 17: 39414 (SAM-TDR-63-25)
development of cadmium sulfide, 17: 11006 (NP-12376)
development of dE/dx silicon surface-barrier, 19: 30568
development of dewar assembly for, 20: 24351(R) (MIT-905-52, pp 1-41)
development of E and dE/dx, 18: 23984
development of encapsulated surface-barrier, 16: 14901 (ANL-6526)
development of fast-response, for alpha particles, 19: 11519
development of fast-neutron dosimeters using, (E), 20: 2134 (TID-22335)
development of fission chamber-, for neutron detection, 19: 22716
development of, for neutrons, 17: 358(R) (EURAEC-51)
development of, for use in identification of high-energy particles, 17: 4141 (BNL-6512(p.134-47))
development of, for use at cryogenic temperatures, 17: 10900(R) (NP-12363)
development of, for airborne alpha particles, 17: 16332(R) (UCRL-7143)
development of gallium arsenide, for gamma detection, 18: 7091(P)
development of germanium, 19: 1053(R) (PR-P-62)
development of germanium, 20: 23427(R) (UCRL-16580, pp 219-50)
development of germanium, for gamma rays, 20: 26396(R) (IDO-17140)
development of highly linear, for space uses, 17: 16895
development of high-sensitivity fast neutron dosimeter, 17: 41250(R) (TID-19491)
development of high-resistivity, 18: 30008
development of high-temperature, for nuclear particles, 18: 33918
development of high-sensitivity fast neutron dosimeter, 18: 39623(R) (TID-21077)
development of large-active-volume thin-entry-window, 17: 30849 (CONF-. 35-1)
development of lithium drifted p-i-n silicon, for dosimetry, 17: 31058
development of lithium-drifted silicon, 18: 2401(R) (IS-700(Sect.P))
development of lithium-drifted germanium and silicon, 18: 14592(R) (PR-P-60)
development of lithium-compensated diode, 19: 11517
development of lithium-drifted germanium, for gamma radiation, 19: 21792(R) (ORNL-3650(p.187-219))
development of lithium-drifted germanium, for high resolution spectroscopy, 20: 16160 (UCRL-14739(Pt.2))
development of lithium-drifted silicon, for whole-body dosimetry, 20: 33626(R) (N-65-32043)
development of lithium-drifted germanium, for gamma spectroscopy, 20: 35785
development of lithium-6 fluoride-sandwiched silicon, for neutron spectrometry, 20: 43718
development of miniature silicon carbide, for neutron detection, 16: 22333(R) (WCAP-1874)
development of miniature silicon carbide, for neutron detection, 16: 22334(R) (WCAP-1929)
development of miniature silicon carbide, for alpha particles, 16: 25573(R) (WCAP-1989)
development of miniature, for reactor uses, 16: 33162(R) (WCAP-2053)
development of miniature, for neutron monitoring, 17: 30859 (WCAP-2128)
development of miniature silicon carbide, 17: 37420(R) (WCAP-2382)
development of nuclear-compensated silicon n-i-p junction, 18: 33920

development of oxide-passivated silicon-junction-type, 18: 39672
development of p-i-n junction-type for beta, gamma, and minimum ionizing particle detection, 16: 15955
development of p-i-n junction type, 17: 18587(R) (AD-283836)
development of pile-up detection circuits for, 18: 39675
development of proton recoil telescope of, for neutron flux and spectra measurements, 19: 11533
development of sensitive fast neutron dosimeter, 19: 11498(R) (TID-21446)
development of silicon n–p junctions for spectroscopy, 16: 1961
development of silicon carbide diodes for neutrons, 17: 8601(R) (WCAP-2117)
development of silicon carbide, for high neutron fluxes, 17: 22005 (EURAEC-587)
development of silicon-junction fast-neutron dosimeter, 17: 36137(R) (AD-289692)
development of silicon carbide, 18: 489(R) (EURAEC-287)
development of silicon carbide junction, for neutron detection, 18: 18179(R) (WCAP-2562)
development of silicon junction, by ion implantation doping, 18: 33921
development of silicon spectrometric, 18: 41847
development of silicon diodes for gamma monitoring (E/T), 19: 776 (NP-14332)
development of silicon p-i-n fast neutron dosimeters, 19: 38992 (COO-1226-8)
development of silicon, 19: 44468 (ZFK-PHA-12, pp 10-15)
development of silicon surface barrier, for charged-particle spectrometers, 20: 21054
development of solar cell, 18: 14331
development of solid-state gamma, 18: 43114(R) (NP-14236)
development of surface-field-controlled, (E), 19: 20323(R) (NYO-3246-4)
development of telescopes of, 19: 11526
development of telescope, 20: 19813 (IKF-14)
development of uranium-235-coated silicon carbide surface junctions for neutron detection, 19: 30536(R) (WCAP-2666)
development of uranium-235-coated silicon carbide diodes for neutron detection, 19: 30535(R) (WCAP-2644)
development of, for dosimetry, 18: 39683
development of, for dosimetry in radiotherapy, 19: 34066
development of, for measurement of gamma and x radiation, 19: 34098
development of, for gamma spectroscopy, 20: 29078(R) (AD-633252)
development of, for measurement of absorbed electron dose, 20: 40746(R) (NYO-3510-2)
development of, review of, 19: 11512
development of, review of, 19: 42725
development, review, 17: 23673
development survey, 16: 31916
development using cascade production mechanism for particle counting, 20: 5793
development, properties, and use of, 20: 2155
development, properties, and use for nuclear spectrometry, 20: 39231
developments in, angular and spatial resolution for, 17: 22051
dewar vessel design for lithium-drifted germanium, (E), 19: 44511
discriminator circuits for, using tunnel diodes, 18: 24031
distribution from pulse-shape gamma rays in lithium-drifted germanium, 20: 33674
drifting of, automatic apparatus for lithium-, 18: 20344 (UCRL-11261)
efficiencies of lithium-drifted germanium, for gamma radiation, (T), 20: 7407
efficiency and properties of thermal-neutron, 17: 25599 (PAN-377/I–B, IX)
efficiency for alpha particles, 17: 7119 (NP-12330(p.202-8))
efficiency of germanium, for gammas at 500 to 1500 kev, 20: 41288
efficiency of lithium-drifted germanium for analysis of aluminum by neutron activation method, 19: 36251
efficiency of lithium-drifted germanium, for gamma rays, 20: 32564
efficiency of lithium-drifted germanium, for gamma radiation, (T), 20: 39271
efficiency of p-n junction, 19: 26665 (NP-14875)
efficiency of sandwich, as fission-neutron spectrometer, (E), 20: 4238 (EUR-2487.e)
efficiency of silicon *p–n* junction, for x-ray measurements, 20: 29540
electric circuitry for multiple systems of, high-stability, modular, 18: 33936
electric current pulses in, formation and shape of, 18: 35871
electric current rectification in silicon surface-barrier, (E), 19: 28662
electric currents in silicon barrier, reverse, 19: 11514
electric field strength relations for silicon surface-barrier, 18: 33954
electrodes for surface-barrier, use of conducting oxide, 16: 13343
electron lifetime in silicon p-i-n, 20: 33671
energy resolution in, electrical limitations to, 16: 20756
energy resolution of, in counting heavy ions, 17: 22022
energy resolution for nuclear particles, 18: 20395
energy resolution of, dependence on preamplifier parameters, (E/T), 19: 34522
energy resolution of, preamplifiers, bipolar and FET transistors, and tubes for optimum, 20: 16871
energy resolution with internal carrier multiplication, 20: 33666
energy resolution of lithium-drifted germanium, for gamma radiation, 20: 33673
energy resolving power of p-i-n, recombination less effects on, 20: 41283
etching surfaces of lithium-drifted, cells for, (E), 20: 5776
fabrication, 16: 14378(R) (NYO-2302)
fabrication and characteristics of lithium-drifted germanium diodes for gamma spectrometry, 19: 44371 (AERE-R-4921)
fabrication and performance, 16: 23838 (BNL-737)
fabrication and performance of thin diffused-junction $\Delta E/\Delta x$, 16: 23898
fabrication and performance of lithium-drifted p^+-i-n^+ diode, 16: 23900
fabrication and performance of encapsulated p-n junction-type, 17: 23784
fabrication and performance, 17: 37444
fabrication and performance of double-barrier gold–silicon, 18: 41809
fabrication and performance of lithium-drifted silicon, 19: 13772
fabrication and performance of lithium-drifted germanium, for gamma spectrometry, (E), 19: 28658
fabrication and performance of lithium-drifted germanium surface-barrier, (E), 19: 28659
fabrication and performance of high-voltage silicon surface-barrier, (E), 19: 28663
fabrication and performance of silicon-wafer, 19: 30630(R) (MLM-1245)
fabrication and performance of p-i-n junction, for gamma dosimeters, 19: 34468 (AECL-2252)
fabrication and performance of windowless lithium-drifted germanium, 19: 39018
fabrication and performance of germanium-silicon, 20: 2182(P)
fabrication and performance of thick-surface-barrier, 20: 13093
fabrication and performance of lithium-drifted germanium, for gamma radiation, 20: 16890
fabrication and performance of large-volume lithium-drifted germanium, for gamma radiation, 20: 19072
fabrication and performance of large-volume lithium-drifted germanium, 20: 21104
fabrication and performance of coaxial lithium-drifted germanium and silicon, as gamma spectrometers, 20: 33680
fabrication and performance of lithium compensated silicon focal plane, for beta spectrometers, 20: 41326
fabrication and performance of lithium-drifted germanium diode, for gamma spectroscopy, 20: 46034 (AWRE-NR-3/66)
fabrication and performance of uranium-235-coated silicon carbide, for reactor neutrons, 20: 46073
fabrication and properties of n^+-i-p^+, 16: 23896
fabrication and properties of boron-10-diffused silicon junction, 16: 23903 (UAC-6130)
fabrication and properties, 18: 39622 (SSI-9)
fabrication and properties of silicon surface-barrier, 19: 6197
fabrication by neutron transmutation methods, 20: 16505 (BNL-949)
fabrication of compensated oxide-passivated silicon-junction-type, 17: 27695
fabrication of compensated p-i-n germanium-diode, (E), 20: 5702
fabrication of diffused and lithium-drifted silicon, 19: 20328(R) (UCRL-11828(p.225-6))
fabrication of germanium and silicon, for nuclear spectroscopy, 20: 32373(R) (COO-1530-1)
fabrication of high-voltage PIN, 19: 11499 (UCRL-13128)
fabrication of lithium-drifted, 17: 31077(R) (CU(PNPL)-228)
fabrication of lithium-drifted germanium, 19: 5569(R) (MIT-2098-64)
fabrication of lithium-drifted silicon-junction, 19: 9484 (NP-14473)
fabrication of lithium-drifted germanium p-i-n, 19: 9771(R) (PR-P-63)
fabrication of lithium-ion-drift, 19: 11499 (UCRL-13128)
fabrication of lithium-drifted germanium gamma, 19: 11549
fabrication of lithium-drifted diodes, 19: 13744
fabrication of lithium-drifted position-sensitive, 19: 39027
fabrication of lithium-drifted germanium, temperature control system for, 19: 39029
fabrication of lithium-drifted silicon, 19: 42720 (UCRL-16190)
fabrication of lithium-drifted germanium, 20: 13058 (AD-627930)
fabrication of lithium-drifted surface-barrier silicon, 20: 19079
fabrication of lithium-drifted germanium, 20: 22010(R) (NYO-72-28)
fabrication of lithium-drifted p-i-n junction, for gamma or x rays, 20: 25433(P)
fabrication of lithium-drifted germanium, 20: 36155(R) (COO-1420-124)
fabrication of lithium-drifted germanium, 20: 35734 (AERE-R-5206)
fabrication of lithium-drifted germanium, 20: 41367(P)
fabrication of p-n junction, using ion implantation technique, 20: 20125
fabrication of position-sensitive, from web silicon, (E), 19: 28657
fabrication of silicon diode, 19: 32600(P)

fabrication of silicon, with plasma-oxidized surfaces, 20: 5740 (TID-
fabrication of p-type silicon, 20: 41363(P)
22407)
fabrication of silicon junctions using ion implantation, 20: 21098
fabrication of surface-barrier, 19: 11606(P)
fabrication of surface barrier, technique for, 20: 13072 (RT/EL(65)7)
fabrication of thin-window germanium, method for, 20: 19043 (UCRL-
16480)
fabrication of 70- to 25-μ, 19: 781 (PAN-516/II)
fabrication techniques for large-volume lithium-drift germanium,
20: 31513 (UCRL-14561)
fabrication, operation, and uses of, review of, 20: 5763
fabrication, testing, properties, and uses of silicon surface-barrier,
20: 19078
fission fragment detection in, multiplication in pulse-height response
to, 18: 33915
gain stabilization in, use of variable-gain amplifier for, 17: 24750(R)
(UCRL-10624)
gain stabilization in, 18: 32281(R) (UCRL-11213(p.139-53))
gamma absorption, effects of orientation and shape, 16: 5751 (AERE-
R-3869)
gamma response of lithium-drifted germanium, temperature dependence of,
20: 46049(R) (ORNL-3973(Vol.2), pp 96-103)
gamma spectra discrimination by, 18: 31962
gamma spectra from lithium-drifted p-i-n junction in germanium, 16: 10241
heat effects on amplitude spread of silicon surface-barrier, 18: 43981
housings and mountings for lithium-drifted germanium and silicon,
19: 22700 (UCRL-11946)
induced charge calculation in, 17: 14682
lifetime and homogeneity of p-i-n, methods for measuring, 20: 41283
lifetime of lithium-drifted silicon, effects of fabrication techniques on,
20: 7450
lifetime under in-pile conditions of fission fragment bombardment,
18: 15673(R) (IDO-16932)
measurement of energy and line width of 6.8- to 18-Mev monochromatic
neutron beams with silicon, 16: 25589
meson (π) and proton energy loss distributions in silicon, (E), 20: 7418
meson (π) energy losses in silicon, at 50 to 365 Mev, (E), 20: 7411
neutron detection and measurement with silicon-junction, 16: 24846
neutron detection and spectroscopy with, 17: 41238 (AD-289566)
neutron detection using coated silicon-carbide, in-pile, (E), 19: 28690
neutron-induced background processes in, 16: 21527
neutron reactions with silicon in, 18: 24599 (NP-13930(p.26-38))
neutron reactions with silicon at 5 to 9 Mev in, 18: 24600 (NP-13930
(p.39-40))
neutron reactions (n,α) and (n,p) with silicon-28 at 13.5 to 14.4 Mev in,
(E), 20: 1163
neutron spectrometer using silicon surface-barrier, proton-recoil,
19: 28691
noise characteristics in ion-drifted p-i-n, 18: 14278
operation, 16: 20629 (BNL-699)
operation and performance of gold-doped silicon, for high resolution nu-
clear spectroscopy, 16: 7716
operation and performance for measuring neutron fluxes, 16: 8943
operation and performance, 16: 10242
operation and performance of silicon surface-barrier type, for measuring
fast-neutron fluxes, 16: 14964
operation and performance, 17: 372
operation mechanisms of, 19: 44450(R) (IBK-120a)
operation of lithium-drifted silicon junction, effects of forward ion drift,
17: 4832
operation of lithium-drifted germanium, for gamma rays, 20: 33718
operation principles and uses, 16: 13315
operation principles and characteristics, 18: 25836
operational modes of gold-silicon surface-barrier rectifiers, 18: 23991
oscillations in silicon diode, electron beam-induced, 18: 10399
particle emission angle and energy measurements in, simultaneous,
17: 39432
particle identification by energy losses in, signal-to-noise ratio in, (T),
19: 34497
particle simulators for silicon, fast infrared emitting diodes as,
18: 41860
performance, 16: 20743
performance, 16: 20750
performance, 17: 18646
performance, 18: 23981
performance, 19: 5572(R) (PPAD-525-D)
performance, 19: 19091 (UCRL-11871)
performance and preparation of silicon, 16: 11903
performance and properties of, 19: 32566
performance and properties, 20: 14907
performance and uses of lithium-drifted p-i-n junctions, 17: 41309
performance and use of, optical theory of, 18: 10390
performance and uses of lithium-drifted germanium, in gamma
spectrometry, 19: 22742
performance and uses, 19: 33704
performance and uses for electron and gamma spectroscopy, 20: 9255
(UCRL-16307)
performance as alpha spectrometer, 16: 23840 (CEA-2138)
performance as charged-particle and neutron spectrometers, 16: 20752
performance as counters for magnetic beta spectrometer, 19: 34486
performance as dosimeters in mixed gamma and neutron fields,
19: 20330(T) (AEC-tr-6547)
performance as gamma spectrometers, 18: 18214
performance as gamma and x-ray dosimeter, 18: 23967
performance as gamma spectrometers, 18: 27788(R) (ORNL-3578(p.1-5))
performance as gamma spectrometers for scanning irradiated fuel elements,
20: 19080
performance as spectrometers, 16: 4349
performance, for alpha energy measurements, 17: 10850(R) (HW-73337
(p.77-157))
performance for alpha particles and electrons, 19: 13730 (NP-14721)
performance for alpha particles, effects of dead layer on, 19: 18310
performance for alpha dosimetry, 19: 31930 (NYO-3267-2)
performance for alpha and helium-3 particles, 19: 44476 (ZFK-PHA-12,
pp 123-5)
performance for alpha detection in presence of deuterons, 19: 45289
(ZFK-PHA-12, pp 99-105)
performance for alpha particles, 19: 45291 (ZFK-PHA-12, pp 117-22)
performance for alpha, beta, and gamma dosimetry, (E), 20: 7406
performance for analysis of 10-Bev elastic p-p interactions, (E),
19: 16467 (JINR-E-1898)
performance for beta spectra, backscattering and resolution corrections
for, 20: 16867
performance for charged particle angular distributions from neutron-
induced reactions, 20: 25376 (AECD/EP-9)
performance for detecting cosmic particles, on TRAAC satellite,
18: 32505
performance for determining deuteron/proton ratios in cyclotron beams,
19: 44482 (ZFK-PHA-12, pp 154-62)
performance for dosimetry of high-energy protons, 18: 37515(R) (ORNL-
TM-931)
performance for dosimetry of α and proton beams, 20: 18190(R) (UCRL-
16613)
performance for elastic proton-proton scattering at high energies,
19: 31087
performance for fast neutron dosimetry, 16: 30581 (HW-SA-2624)
performance for fast-neutron spectral measurements, 17: 34290
performance for fast-neutron spectroscopy, 18: 23960
performance for fission fragments, pulse-height defect in, 19: 11524
performance for fission fragments, pulse-height defect in, 19: 26700
performance for γ dosimetry, 20: 38771
performance for heavy fission particles, 19: 44481 (ZFK-PHA-12,
pp 149-53)
performance for heavy ions, energy dispersion and pulse height defect in,
(T), 20: 11138
performance for high-resolution gamma spectroscopy, 18: 20374
performance for inpile measurements, 18: 7853(R) (KR-58)
performance for internal conversion measurements, 19: 40880 (UCRL-
16035)
performance for in-pile gamma and neutron detection, (E), 20: 5728
(IBM-65-825-1487)
performance for light pulses, 18: 14213 (JINR-P-1526)
performance for low-energy gamma spectroscopy, 18: 20373
performance for measurement of x-ray beam quality, 18: 22364
performance for measurement of absorbed energy distributions for 20-Mev
electrons, 18: 35848(R) (TID-20918)
performance for measurement of alpha range-energy relation in air,
20: 19069
performance for measuring alpha particles from polonium-210 and
neptunium-237, 20: 29552
performance for neutron spectroscopy at 0.5 to 15 Mev, 17: 8626
performance for neutron spectroscopy, 17: 41994
performance for neutron spectrometry, 18: 2098
performance for neutron counting, (E), 19: 18256(R) (EURAEC-1215)
performance for neutron spectrometry in shielding rigs, (E), 20: 4997(R)
(EUR-2494.d)
performance for neutron detection and spectroscopy, (E), 20: 5714 (AD-
623722)
performance for nuclear spectrometry, lectures on, 19: 44466 (UCRL-
16231)
performance for particle detection, comparison with photographic
emulsions, 18: 23906
performance for personnel dosimetry, 20: 35777
performance for proton polarization measurements, 19: 44477 (ZFK-PHA-
12, pp 126-32)

performance for prompt neutrons and fission fragments, 20: 17864
performance for radiation dosimetry, 19: 46850
performance for residual-nucleus distributions from reactions, 18: 7078
performance for recoil analysis of nuclear reactions, 18: 18222
performance for soft x-ray counting, 18: 2097
performance for solar protons, 18: 14707
performance for thermal neutrons in intense gamma background, 19: 44480 (ZFK-PHA-12, pp 144-6)
performance for time-resolution measurements, 19: 32547 (EUR-2274.e)
performance for triton discrimination, 19: 44475 (ZFK-PHA-12, pp 84-97)
performance in alpha spectrometers, 18: 18192
performance in alpha spectrometers, 18: 29974 (CLOR/IBJ-II-25)
performance in alpha spectrometers, 19: 11521
performance in alpha spectrometers, 19: 11530
performance in alpha monitoring, 20: 23499
performance in anticoincidence gamma spectrometers, 20: 14865
performance in beta spectrometers, 19: 15898
performance in β-spectrometers for conversion coefficient measurements, 20: 3019 (ORNL-P-1657)
performance in charged particle elastic scattering studies, 19: 40962
performance in coincidence-anticoincidence schemes, 19: 9517
performance in Compton-recoil gamma spectrometers, 18: 7077
performance in Compton-electron measurement, 19: 32551(R) (NP-14962)
performance in current generating mode in medium dose rate radiation fields, 17: 3301(R) (AD-275139)
performance in cyclotron scattering chambers, 18: 20688
performance in detection of fast and slow neutrons, 18: 43991
performance in dosimetry, 19: 18289
performance in fast-neutron recoil spectrometers, 18: 20365
performance in fast-neutron spectrometer, 18: 43942 (TID-21202)
performance in fission fragment and neutron dosimetry, 20: 5719 (CEA-R-2846)
performance in gamma measurements, 19: 22718
performance in high-intensity neutron fluxes in reactors, 17: 34282
performance in internal conversion coefficient spectrometers, 19: 11577
performance in mapping radiation fields of linear accelerator and pulsed reactor, 17: 1744 (DASA-1275)
performance in neutron time-of-flight spectrometers, 18: 16323
performance in neutron spectrometers using lithium-6 (n,t) reactions, 19: 11534
performance in neutron spectrometers, (E), 19: 17156(R) (EUR-2197.d)
performance in neutron spectrometers, 19: 44478 (ZFK-PHA-12, pp 132-9)
performance in nuclear pulse-height spectroscopy, 16: 20753
performance in nuclear power plants, 17: 41227
performance in proton-recoil neutron spectrometers, 19: 7781 (AERE-R-4686)
performance in radiodiagnosis, 16: 16556
performance in radiographic inspection systems, 19: 6190
performance in x-ray emission spectrography, 20: 16887
performance of anticoincidence-shielded germanium, as gamma spectrometers, (E), 19: 44519
performance of bulk ionization silicon, for 10- and 30-Mev protons, 17: 4837
performance of Compton spectrometer, for nondestructive burnup determination of fuel elements, 20: 21050
performance of cuprous oxide for gamma radiation, 18: 37503 (A/CONF.28/P/815)
performance of encapsulated lithium-drifted germanium, as gamma spectrometers, 20: 33682
performance of gallium arsenide, for alpha particles, 17: 41257
performance of gamma, 19: 34585(P)
performance of germanium, for gamma spectroscopy, (E), 19: 22684 (AE-174)
performance of germanium, for gamma rays, 19: 44473 (ZFK-PHA-12, pp 64-5)
performance of germanium, for gamma spectroscopy of fast-neutron inelastic scattering, (E), 20: 7414
performance of germanium, in gamma spectrometers, 20: 11095 (CRGP-1224)
performance of germanium, in applied gamma spectrometry, 20: 11134
performance of germanium, for high-energy protons, 20: 23427(R) (UCRL-16580, pp 219-50)
performance of germanium, for measuring gamma energies, 20: 26396(R) (IDO-17140)
performance of germanium, for muonic x-ray spectra, 20: 29525 (CONF-660209-9)
performance of germanium, for determining monazite and pitchblende gamma spectra, 20: 29079 (AERE-M-1736)
performance of germanium, for gamma angular correlations, 20: 36155(R) (COO-1420-124)
performance of germanium, for measuring gamma angular correlations, 20: 38184
performance of gold-silicon surface-barrier, for electrons, 18: 30026
performance of gold–silicon, for beta particles, 19: 26701
performance of gold-silicon surface-barrier, for alpha activity measurement, 19: 26652 (CLOR/IBJ-II-33)
performance of gold–silicon, with multi-gard-ring for beta spectroscopy, 20: 665
performance of guard-ring silicon surface-barrier, for beta spectrometry, 17: 4855
performance of high resistivity silicon surface barrier, 19: 18307
performance of, in measurement of D-D branching ratios, 17: 8937(R) (NP-12415(p.40-5))
performance of junction, for alpha monitoring, 20: 11092 (CLOR-39/D)
performance of lithium-silicon p-i-n junction as, 16: 22317(R) (AD-269972)
performance of lithium-drifted, for beta and gamma spectrometry, 17: 4857
performance of lithium-ion-drifted junctions in silicon as, 17: 8597 (TID-15552)
performance of lithium-drift, for 3- to 4-Bev particle detection, 17: 23683
performance of lithium-charged, for fast-neutron spectroscopy, 17: 34284
performance of lithium-drifted p-i-n, 18: 2403(R) (PR-P-58)
performance of lithium-drifted silicon, for electrons, 18: 12443(R) (AD-413449)
performance of lithium-drifted, for assaying fuel elements, 18: 15494(R) (SWRI-1321-1)
performance of lithium-drifted germanium diodes for gamma spectrometers, 18: 29966 (AECL-1960)
performance of lithium-6-coated surface barrier junctions in neutron spectrometry, 18: 29992
performance of lithium-drifted diode, as gamma pair spectrometers, 18: 33912
performance of lithium-drifted germanium, in gamma spectroscopy, 19: 800
performance of lithium-doped silicon junction, for high-energy particles, 19: 11528
performance of lithium fluoride-silicon sandwich, in neutron spectrometers, 19: 11531
performance of lithium-drifted germanium diode, as gamma spectrometers, 19: 17781(R) (ORNL-3750)
performance of lithium-drifted germanium, in Compton-rejection spectrometer, 19: 18313
performance of lithium-drifted, in beta spectrometers, 19: 20360
performance of lithium-drifted germanium, in gamma spectrometers, 19: 32561
performance of lithium-drifted germanium, for gamma assay, 19: 32594
performance of lithium-drifted silicon, in thermal-vacuum environment, (E), 19: 40902
performance of lithium-drifted germanium, as gamma spectrometers, (E), 19: 44510
performance of lithium-drifted silicon, for particle identification, (E), 19: 44517
performance of lithium-compensated silicon, for deuterons and protons, 19: 44471 (ZFK-PHA-12, pp 30-2)
performance of lithium-6-loaded, in neutron spectrometers, 19: 44457 (NP-15475)
performance of lithium-drifted silicon, for alpha particles and protons, 19: 46770 (UCRL-16354)
performance of lithium-drifted germanium, for electron and gamma spectroscopy, 20: 9255 (UCRL-16307)
performance of lithium-drifted germanium, in coincidence measurements, 20: 9243 (AECL-2505)
performance of lithium-drifted germanium, for 30- and 40-Mev protons, 20: 9282
performance of lithium-drifted, temperature dependence of, 20: 9250(R) (NYO-3510-14)
performance of lithium-drifted silicon, for α and β particles, 20: 11097 (INR-621/XV/I)
performance of lithium-drifted germanium p-i-n, for gamma spectrometry, 20: 19061
performance of lithium-drifted germanium, for high-resolution gamma spectrometry, 20: 19087
performance of lithium-drifted germanium, for short-lived radioisotopes, (E), 20: 19273(R) (BNL-929, pp 3-43)
performance of lithium-drifted surface-barrier silicon, for conversion electrons, 20: 19079
performance of lithium-drifted germanium, for nondestructive activation analysis, 20: 22875 (ORO-2670-10)
performance of lithium-drifted silicon, in gamma spectrometers, 20: 25393
performance of lithium-drifted silicon, for, 20: 27301
performance of lithium-drifted germanium, for gamma spectrometry, 20: 27329

performance of lithium-drifted germanium, for gammas, 20: 31514(R) (UCRL-14881)
performance of lithium-drifted silicon, as beta and gamma spectrometer, 20: 31519
performance of lithium-drifted germanium, for gamma spectroscopy, 20: 35730 (AECL-2569)
performance of lithium-drifted germanium, for gamma rays, 20: 13095
performance of n-p silicon solar-cell, as gamma-ray dose meter, 18: 4080 (BNL-7310)
performance of n-type silicon, for alpha particles and protons, 17: 376
performance of p-i-n electron junction, 16: 19059(R) (AD-265759)
performance of p-n junction, for x-ray spectrometry, 17: 6458
performance of p-i-n, at low temperatures, 18: 41806
performance of p-n junctions for alphas, deuterons, electrons, and fission fragments, 18: 29969(R) (AFOSR-4920(Paper 2))
performance of p-n silicon, for fast neutron dosimetry, 20: 25374 (AD-631742)
performance of phosphorus-diffused silicon, in kinetic energy measurements of fission fragments, 19: 31236 (SGAE-PH-10/1964)
performance of position-sensitive surface barrier, for alpha particles, 20: 27314
performance of sandwich type, for fast neutrons, 20: 33620 (EUR-2793.e)
performance of scintillator-semiconductor photodiode, 18: 8658
performance of silicon-gold diodes for fission detection, 16: 3845(R) (ORNL-3193(p.58-62))
performance of silicon, 16: 4346
performance of silicon junction, for gamma dosimetry, 17: 3345
performance of silicon, in vacuum, 17: 16896
performance of silicon carbide, for neutrons at high temperatures, 17: 34300
performance of silicon surface-barrier, 18: 6161 (NP-13346)
performance of silicon-junction, 18: 6163 (NP-13349)
performance of silicon-junction, in beta spectrometers, 18: 12470
performance of silicon surface-barrier, 18: 20354
performance of silicon surface-barrier, 18: 20355
performance of silicon and germanium, for fast neutrons and gamma rays, 18: 20413
performance of silicon, for electron spectrometry, 18: 34752(R) (CU(PNPL)-234)
performance of silicon surface-barrier, for thermal neutrons, 18: 43954
performance of silicon p-n junction, 19: 7803
performance of silicon, with multiple barriers, 19: 11518
performance of silicon solar cells for gamma dosimetry, (E), 19: 18254 (BNL-902)
performance of silicon surface barrier, with guard rings, 19: 44469 (ZFK-PHA-12, pp 16-24)
performance of silicon-array, as cosmic-proton dosimeters, (E), 20: 2133 (NASA-SP-71, pp 245-50)
performance of silicon, for neutron spectrometry in shielding rigs, (E), 20: 4997(R) (EUR-2494.d)
performance of silicon, 20: 7422
performance of silicon surface-barrier, for fission fragments, 20: 7438
performance of silicon surface-barrier, for particle spectra from 10 to 200 kev, 20: 11115
performance of silicon, for recording protons, α particles, and nuclei ($Z > 2$), 20: 11124(T)
performance of silicon, for neutron total cross section measurements, 20: 13101
performance of silicon, for hydrogen and nitrogen ion detection, 20: 17253(R) (ORNL-3908, pp 90-9)
performance of silicon surface-barrier, in studies of recoil nuclei, 20: 17820
performance of silicon, for energy measurements on fission fragments, 20: 19070
performance of silicon, as fast-neutron dosimeter, 20: 21095
performance of silicon, for proton spectroscopy in nuclear reactions, 20: 26226
performance of silicon diode, for gamma and neutron dosimetry, 20: 29518 (BNWL-SA-27)
performance of silicon, for beta spectra measurements on strontium-90–yttrium-90, 20: 29520 (CLOR-45/D)
performance of silicon, for low-background counting of alpha and beta particles, 20: 31540
performance of silicon E(dE/dx), for particle discrimination, 20: 33643
performance of silicon telescope, for charge and energy spectrometry of cosmic particles, 20: 37575
performance of silicon, for neutral atom detection, 20: 39580(R) (ORNL-3989, pp 78-88)
performance of silicon carbide, for alpha particles and fission fragments, 20: 46073
performance of surface-barrier, for charged-particle spectrometry, 18: 41810
performance of surface-barrier, in spectrometers, 19: 9515
performance of surface-barrier p-type silicon, for alpha particles, 19: 42757
performance of surface barrier, at 4.2°K, 20: 5790
performance of, equations for charge carrier motion and collection for, (T), 20: 9256
performance of, equations for, 20: 14875
performance of, for solid body dosimetry for radiotherapy, 20: 5479
performance of, for radiation detection in activation analysis, 20: 35767
performance of, space charge calculations for, 20: 7373
performance optimization of silicon junction, 17: 18630
performance status of silicon junction, 16: 20674
photoconduction measurements on doped cadmium sulfide, 20: 23461 (LNF-66/3)
photoeffects in silicon surface-barrier diodes, 16: 8924
preamplifier design for, linear low-noise, 16: 22359
preamplifier design for, 18: 41787
preamplifier design optimization of, (E/T), 19: 28638 (ORNL-TM-1055)
preamplifier for cooled, field-effect transistor, 20: 29548
preamplifier for silicon surface barrier, design of, 19: 22769
preamplifier for, design of low-noise charge-sensitive, 18: 10409
preamplifier for, design of, 18: 43966
preamplifier for, design of stable and low-noise charge sensitive, 19: 32553 (ZfK-PhA-16)
preamplifiers for, design of low-noise charge-sensitive, 19: 2602 (CRGP-1182)
preamplifiers for, design and performance of, 19: 36842
preamplifiers for, design of high-resolution transistorized, (E), 20: 5772
preparation and application to the detection of relativistic particles, 16: 20748
preparation and performance of ionization chamber using, 16: 20749
preparation and performance of silicon-junction, 18: 5637 (PAN-444/Ia,II,IX)
preparation and performance of 11-micron dE/dx surface barrier, 18: 23987
preparation and performance of homogeneous silicon minimum-ionizing-particle, 19: 9488 (PPAD-529-E)
preparation and performance of depleted surface-barrier, 20: 16818 (KFK-328)
preparation and performance of p-i-n junction, 20: 31537
preparation and properties of silicon surface-barrier, with deep sensitive volume, 18: 29999
preparation and properties of lithium-drifted germanium, (E), 19: 22701 (UCRL-12245)
preparation and properties of shallowly diffused silicon junctions, 20: 21099
preparation and use of lithium-drifted planar germanium, 20: 33681
preparation by deep lithium-ion-drifting, 18: 23982
preparation by doping of crystals by ion bombardment, 16: 19132
preparation of diffused and drifted, 18: 32281(R) (UCRL-11213 (p.139-53))
preparation of germanium, 16: 32404 (UCRL-10362)
preparation of germanium n-i-p, for gamma detection, 19: 34499
preparation of lithium-drifted, 17: 14676
preparation of lithium-drifted, 17: 16898
preparation of lithium-drifted silicon, 18: 27790(R) (ORNL-3578(p.46-59))
preparation of lithium-drifted germanium, with proper current-voltage characteristics, 18: 37543
preparation of lithium-drifted silicon junction, 19: 6187
preparation of lithium-drifted germanium, 20: 33672
preparation of silicon, by lithium ion drift method, 17: 4804 (ARL-62-406)
preparation of silicon, 18: 22341 (PAN-484/II)
preparation of silicon surface-barrier, method for, 19: 34502
preparation of silicon surface-barrier, sealed in epoxy resin, 19: 34548
preparation of silicon p-i-n, (E), 20: 43741
preparation of surface-barrier diodes for nuclear particle detection, 16: 5526
preparation of thin-window germanium, gold-plating procedure for, 19: 42763
preparation of, use of radioisotopes in, 18: 25846
preparation with lithium-diffused junctions with surface barrier, 17: 23754
processing lithium-drifted germanium, 19: 7783 (GPI-57)
production and encapsulation of lithium-drifted germanium, 20: 41271(R) (ORNL-3875, pp 44-52)
production and properties of lithium-drifted p-i-n, 16: 29141
production of silicon, with wide sensitivity range, 19: 44470 (ZFK-PHA-12, pp 25-9)
properties and theory of, review on, 19: 828
properties and uses outline, 16: 23870
properties and uses of, at Central Institute of Nuclear Physics, Rossendorf, 17: 22032

properties and uses, review, 17: 41446
properties and uses, 18: 10391
properties and uses, 18: 20376
properties and uses, 19: 4495
properties and uses of, review on, 20: 11126
properties and uses of, 20: 35800
properties and use of germanium and silicon, for gamma and electron spectroscopy, 20: 39232
properties as spectrometer, 17: 30850 (EUR-222.f)
properties for alpha particles, 17: 41243 (EUR-429.e)
properties for detection of transient gamma rays, 16: 3185 (UCRL-6298)
properties for fission product energy measurements, 18: 7696(R) (ORNL-TM-761)
properties for in-core neutron flux measurements, 18: 38345 (A/CONF. 28/P/858)
properties for isotopic age determinations, 17: 41010
properties for measurement of in-pile neutrons, 18: 31938
properties for neutron cross section measurements, 17: 38061 (AE-115)
properties for use in detecting fast neutrons, 16: 23899 (AERE-R-3874)
properties in fast neutron spectrometer, 18: 18177 (TID-20418)
properties in fission fragment energy measurements, 18: 2848 (UCRL-11006)
properties in high-energy particle spectrometry, 18: 20410
properties in secondary beam profile measurement, 18: 20327 (BNL-7880)
properties of cadmium sulfide as, 18: 14208 (GNE/Phys/63-9)
properties of cadmium telluride p-n junction, 20: 31523
properties of commercial, 18: 20377
properties of, for in-pile neutron flux measurements, 17: 8627
properties of, for alpha spectrometry, 17: 29195 (CEA-2272)
properties of germanium, with radiation defects, 18: 43990
properties of germanium and silicon, 20: 39230
properties of gold-silicon surface barrier as alpha particle, 16: 27270(T) (FTD-TT-62-863)
properties of high resistivity silicon, 20: 4259(P)
properties of internally amplifying gallium-diffused junctions, 20: 21100
properties of large lithium-drifted germanium, mounting and storage, 20: 5741 (UCRL-14263)
properties of lithium-drifted germanium, 18: 20375
properties of nuclear-compensated silicon, 19: 36807 (CEA-R-2722)
properties of p-n junction-type, effects of environment on, 18: 31963
properties of photoconductivity, for detecting single gamma photons, 17: 16451
properties of silicon surface-barrier, as fast neutron spectrometers, 16: 27263 (TID-16326)
properties of silicon surface-barrier, 16: 27359
properties of silicon, for neutron flux measurements and spectroscopy, 17: 34884 (TID-19047)
properties of silicon surface-barrier, for alpha particles, 18: 2019 (CLOR-I-B-IBJ-18)
properties of silicon, in gamma dosimetry, 18: 2068
properties of silicon carbide, for neutrons, 18: 22347(T,R) (EURAEC-1008)
properties of silicon-n-gold, 18: 27805
properties of, survey, 18: 20334 (KR-64(Sect. XXXI))
proton channeling in silicon, at 2.1 Mev, 18: 33917
pulse amplification in silicon junction, internal, 18: 33959
pulse amplifier for, low-noise, 18: 25790 (NAS-NRC-Pub-1184(p.65-9))
pulse amplifiers for, time resolution of nanosecond, 18: 24028
pulse amplifiers for, design of nanosecond, 18: 41855
pulse amplifiers for, design of fast, charge-sensitive, 19: 11579
pulse amplitude and polarity of charged-particle entrance effects on, 20: 31498 (AD-632527)
pulse amplitudes and waveforms from alpha-excited, temperature and voltage bias effects on, 18: 25786 (NAS-NRC-Pub-1184(p.49-52))
pulse analyzers for, time-to-pulse height, 19: 44488 (ZFK-PHA-12, pp 215-18)
pulse dividers for, design of high-speed analog, 18: 33929
pulse enhancement in silicon p-n junction, 18: 10418
pulse-height analysis, servo-stabilized analog-to-digital converter for high resolution, 16: 15959
pulse height defect for aluminum-27 and magnesium-24 ions in silicon, 19: 30561
pulse-height spectrum expansion for kicksorter, bias unit, 17: 32355
pulse modifiers for p-i-n, with RC networks, 19: 11522
pulse output of, time resolution limits in, 18: 25787 (NAS-NRC-Pub-1184 (p.53-8))
pulse preamplifiers for, transistorized, 19: 11523
pulse preamplifiers for, design and performance of, 19: 11527
pulse quenching in silicon, by magnetic fields, (E), 19: 24847
pulse rise time in silicon, electron mobility effects on, 19: 20359
pulse rise times in, charged-particle discrimination by, 19: 20369
pulse rise times in detection and measurement of charged particles, 20: 21137
pulse rise-time for gold-silicon surface-barrier, 18: 23983
pulse shape analysis for particle identification in p-i-n, 17: 25638
pulse shape discrimination circuit for, 16: 23901 (PUC-1962-69)
pulse-shape discrimination in, 17: 23775
pulse time and amplitude measuring system for, 18: 23995
pulse time-to-amplitude converter circuit for, 18: 24017
pulse-height analyzers for, fast single-channel, 19: 18329
pulse-shape discrimination in lithium-drifted germanium, 19: 9771(R) (PR-P-63)
pulse-shape discrimination between alpha particles and protons, system for, 20: 16900
radiation absorption in, charge separation from, 20: 7374
radiation damage effects on performance of silicon, alpha, 18: 30255
radiation damage effects in lithium-drifted silicon, alpha, fast neutron, and proton, 18: 33913
radiation damage effects in lithium-drifted silicon, gamma, 18: 33914
radiation damage in, 18: 30031
radiation detection with, review on, 18: 25850
radiation dosimetry using, 16: 27275
radiation effects on behavior, 16: 5489 (EURAEC-161)
radiation effects on properties of components, 16: 19072(R) (EURAEC-246)
radiation effects on, gamma, 16: 29437 (GA-2984)
radiation effects on pn junction type, for gamma-ray detection, 17: 357 (CRRD-1102)
radiation effects, 17: 360 (NP-12159)
radiation effects on determination of energy spectra of short-lived particles, 17: 8607
radiation effects on silicon-junction, in space, 17: 16885
radiation effects on diode, 17: 22215 (AFSWC-TDR-62-118)
radiation effects on resolution of, fast neutron, 17: 34244
radiation effects on silicon, electron and neutron, 18: 20357
radiation effects on response of, alpha and fission fragment, 18: 30256
radiation effects on, 19: 1956(R) (IDO-16994)
radiation effects on, 19: 6213(R) (EURAEC-1113)
radiation effects on performance of, 19: 11610
radiation effects on diffused silicon, low-rate proton, 19: 11611
radiation effects on, methods of evaluating, 19: 15939
radiation effects on satellite, in Van Allen belts, 19: 23511
radiation effects on satellite-carried, 19: 23512
radiation effects on silicon carbide, neutron, 19: 34592(R) (EURAEC-1384)
radiation effects on diffusion-drift, high-energy proton, 20: 7461
radiation effects on lithium-drifted germanium, 1- to 16-Mev neutron, (E), 20: 7462
radiation effects on current output of lithium-drifted, 20: 9250(R) (NYO-3510-14)
radiation effects on p-i-n, electron, gamma, and x, 20: 11173 (D2-84071-1)
radiation effects on, neutron, 20: 46099
radiation noise in silicon, measurement of, 20: 693 (NP-15172)
radiation surface-barrier, proton, 18: 14212 (JINR-P-1516)
radioinduced noise in silicon, electromagnetic, (E), 20: 14923
research on, 19: 41678(R) (PR-P-65)
resolution curve for, prompt, 20: 46083
resolution for fission fragments, (T), 19: 39033
resolution for heavy charged particles, (E), 20: 33670
resolution in, electrical limitations to, 16: 30600 (UCRL-9529)
resolution of germanium and silicon, (T), 20: 19063
resolution of lithium-drifted surface-barrier, 17: 24750(R) (UCRL-10624)
resolution of silicon n-i-p, for heavy intermediate-energy charged particles, 18: 31923
resolution time, 19: 2620
resolving time for, 20: 46081
resolving time of lithium-drifted germanium, in coincidence with scintillation detectors, 20: 46079
response and sensitivity of silicon p-i-n, in high-dose-rate gamma fields, (E), 20: 5743 (UCRL-14405)
response characteristics of germanium and silicon, to gamma rays, Monte Carlo calculation of, 20: 43701
response of contoured silicon, to electrons and protons, 19: 7787 (NYO-3246-3)
response of lithium-compensated silicon junction, to gamma rays at low temperatures, 19: 11529
response of lithium-drifted silicon, to conversion electrons in bismuth-207 and cesium-137, 20: 14444(R) (MLM-1268)
response of lithium-drifted silicon p-i-n, to beta particles, 20: 14886
response of lithium-drifted germanium and silicon, temperature dependence of, 20: 21102
response of lithium-drifted germanium, to gamma rays, (T), 20: 29528 (LA-3456)
response of lithium-drifted germanium, to gamma radiation, temperature

dependence of, 20: 33683
response of lithium-drifted germanium, for gamma rays, 20: 37126
response of lithium-drifted germanium, to gamma rays, temperature dependence of, 20: 41273 (ORNL-TM-1295)
response of p-i-n junction, to low-energy beta emitters, 20: 25407
response of silicon surface barrier, to hydrogen ions, 16: 23904 (SCDC-2522)
response of silicon lithium-drifted p-i-n, 18: 41755(R) (AD-600253)
response of silicon, at low temperatures, 19: 28664
response of silicon, optical method for monitoring, 19: 28669
response of silicon surface-barrier, to fission fragments, 20: 21101
response of silicon surface-barrier to conversion electrons, fission fragments, and alpha particles, 20: 33665
response of silicon, to argon-40 and iodine-127 ions, 20: 39470(R) (ORNL-3924)
response of stacked silicon, effects of crystallographic orientation on, 19: 6182 (BNL-8623)
response of surface-barrier, to fission fragments, 18: 33945
response of surface-barrier, to protons at 50 to 160 Mev, (E/T), 19: 28665
response of surface-barrier, to fission fragments, (E), 19: 40901
response of surface-barrier p-n, to heavy ionizing particles, (T), 20: 5758
response to alpha and beta particles, temperature dependence of, 18: 33916
response to alpha particles and electrons, 19: 2630
response to alpha particles, analysis of, 19: 35615(R) (NP-15037)
response to bromine-79 and iodine-127 ion beams, (E), 19: 36814(R) (ORNL-3778(p.125-7))
response to electrons and gamma rays, 18: 32777
response to electrons, transient, 18: 33919
response to electrons below 30 kev, 20: 17168
response to fast neutrons, relations with radiation damage in reactor materials, 16: 33574
response to fission fragments, 16: 23005(R) (ORNL-3268(p.94-7))
response to fission fragments, 17: 18637
response to fission fragments, multiplication phenomenon in, 17: 27702
response to fission fragments, energy losses by atomic collisions in, 17: 32792
response to fission fragments, non-linear, 19: 26917(R) (IA-984)
response to gamma radiation, Monte Carlo analysis of, (T), 19: 28683
response to heavy ions, 18: 14207 (CONF-354-4)
response to intense gamma pulses, 19: 19095 (WASH-1053)
response to low-energy x radiation, equipment and methods for studying, 20: 21107
response to transient ionizing flux (E), 19: 2604 (LA-DC-6500)
review, 16: 23894
review, 16: 23944
review, 16: 33202
review, 17: 379
review, 17: 10957
review, 17: 17643
review, 18: 41808
review, 19: 18324
review, 19: 24867
review for beta and gamma detection, 17: 30889
review of applications and limitations of, 18: 14225 (UCRL-11302)
review on, 20: 2138
scattering chamber for use with, 18: 43950
scattering chamber for use with, design of, 18: 43969
scattering chamber for use with, 20: 16883
sensitive region in germanium p-i-n determination of width of, 20: 11102 (JINR-P-2487)
sensitivity of surface-barrier, gamma and neutron, 17: 21315(R) (GEAP-4162)
sensitivity of surface-barrier, for beta particles, 19: 22709
sensitivity of, for fast and thermal neutrons and fission fragments, 18: 18183
sensitivity to gamma rays and neutrons, 20: 21059
sensitivity to 30- to 600-kev pulsed x radiation, 19: 6205
silicon-recoil spectra from neutron irradiation of diodes in, 17: 37256
solid angles for proton-recoil, 17: 36140 (AE-116)
spectrum expander for, 16: 27295
spectrum expander for spectroscopy using, charge-compensation, 19: 13769
stability of lithium-drifted silicon, 20: 5767
stabilization of lithium-drifted silicon junction, 18: 33922
stabilization using reference spectra, 19: 4520
status, 19: 32559
surface contouring of silicon diffused junction, 20: 46044(R) (NYO-3246-6)
surface contouring of, 20: 46045(R) (NYO-3246-7)
surface contours of p-n junctions in, properties of, 20: 14858(R) (NYO-3246-5)
surface effects in lithium-drifted silicon, 18: 20326 (BNL-7853)
surface potential of lithium-drifted germanium, 20: 21096
system for heavy particle detection using, 18: 41816
telescope design using, 18: 2840 (NYO-9766)
temperature effects in, 16: 27360
testing of silicon carbide, for neutron detection, 18: 39614(R) (EURAEC-1027)
time resolution of silicon-junction, 18: 24023
time resolution of p-i-n, in γ-γ coincidence measurements, 20: 33679
time response of indium antimonide photodetectors, nanosecond, 17: 25275
timing aspects of, collection times and rise-time in, 18: 25788 (NAS-NRC-Pub-1184(p.59-60))
timing circuits for, design of nsec-resolution, 18: 18226
timing circuits for, design of, 20: 38161
transistor counting circuit for, 17: 1772
use as alpha and neutron counters in column separation of transplutonic elements, 18: 20101 (UCRL-11300)
use as beta spectrometers, 16: 13360
use as spectrometers for charged particles, 17: 366(T) (AEC-tr-5369)
use for alpha particles at 25 Mev (E), 19: 1234 (PAN-347)
use for alpha spectrometry, 18: 4095
use for analysis of fission fragments, 17: 41904
use for coincidence beta spectroscopy, 17: 32421
use for fast neutron flux distribution measurement, 16: 7696
use for fast neutron spectroscopy, 17: 23766
use for measurement of fission fragment energy, 16: 13313
use for measuring density of liquid hydrogen, 20: 31494
use for spectral analysis of fast and intermediate neutrons, 19: 11532
use in a scattering chamber, 17: 25892
use in alpha spectroscopy, 16: 33244
use in angular correlation measurements, geometrical corrections for, (T), 19: 36845
use in angular distribution measurements, data handling in, 19: 11570
use in associated particle techniques, 16: 21130(R) (NP-11643)
use in beta and gamma spectroscopy, 18: 23989
use in beta spectroscopy, 18: 23990
use in biological and medical research, 19: 11535
use in charged-particle spectroscopy, background reduction in, 20: 33697
use in chemistry, 20: 33649
use in detection and measurement of hydrogen ions, 20: 28504
use in detection of charged particles and neutrons, 16: 5492 (JÜL-20-RE)
use in determination of isotopic content of alpha emitters, 19: 42427
use in determination of radioisotopes in biomedical samples, 19: 43659
use in dosimetry, review, 17: 20371
use in fast-neutron spectrometers, 18: 18206
use in fission fragment distribution analyses, (E), 19: 5126 (CEA-R-2408)
use in fission rate measurements, (E), 19: 17312
use in fission-fragment detection and measurement, 18: 44736 (ORNL-3692)
use in fission-fragment detection, pulse-height defects in, 19: 40892
use in gamma coincidence spectrometer, 18: 43927 (AAEC/TM-265)
use in gamma intensity measurement, 19: 24877(P)
use in gamma spectrometric determinations of fission products, 20: 22889
use in gas density measurement, 19: 28624(P)
use in health physics monitoring instruments, 17: 10960
use in heavy particle beam analyzer, 16: 33245
use in helium-3-neutron coincidence system, 19: 15893
use in high-energy accelerator experiments, 20: 4243 (LAL-1102)
use in high-resolution coincidence circuits, 18: 31907 (ISS-64/11)
use in hygrometers, 20: 14840
use in investigating resonance reactions, 19: 11525
use in low-energy nuclear physics, 20: 33650
use in magnetic spectrometers for alpha particles and deuterons, 20: 27286
use in measurement of gaseous diffusion coefficients, 20: 29510
use in measuring lifetimes of ultra-shortlived nuclear isomers, 18: 24025
use in medicine, 17: 28753
use in neutron spectrometer for (n,p) reactions with helium-3, 18: 37510 (BRL-Memo-1545)
use in nuclear medicine and biology, 19: 11581
use in nuclear physics, conference on, 19: 11511
use in nuclear physics experiments, 19: 26680
use in nuclear research, 20: 43737
use in particle identification, system for, 19: 34530
use in particle spectrometer, 18: 20330 (CEA-2388)
use in pocket-size radiac, 17: 36139(R) (AD-295747)
use in proton recoil neutron spectrometer, 17: 3308 (NP-12226)
use in proton-recoil neutron spectrometer, 20: 19018(R) (ANL-7110, pp 231-310)
use in radiation dosimetry, 20: 31560

use in radiation target chambers for particle correlation measurements, 20: 31556
use in radiochemistry, 20: 9038
use in series-parallel combinations for detection of fission events, 17: 15251(R) (CU(PNPL)-220)
use in x-ray emission spectrography, 20: 22859(R) (UCRL-16580, pp 149-205)
use instead of emulsions in nuclear spectroscopy, 16: 33243
use of cadmium sulfide, for gamma dose rate determinations, 18: 20351
use of coaxial germanium, in gamma spectrometers, 20: 33677
use of germanium lithium-drifted diode for gamma spectroscopy, 17: 25645
use of gold-doped silicon, to control bubble chamber photography, 16: 23905 (PPAD-437E)
use of gold-silicon, in α spectrometry, 16: 4327 (PAN-242/1-B)
use of junction-type, in radiometric well logging, 19: 13658(P)
use of lithium-coated solid-state, for thermal neutron flux measurements, 17: 35253(R) (IA-775)
use of lithium-drifted germanium, in high-resolution gamma spectrometry, 18: 32281(R) (UCRL-11213(p.139-53))
use of lithium-drifted germanium, for gamma spectroscopy, (E), 19: 5215
use of lithium-drifted germanium, in coincidence measurements, 19: 9771(R) (PR-P-63)
use of lithium-drifted germanium, in activation analysis, 19: 19775(R) (UCRL-11828(p.197-9))
use of lithium-drifted germanium, in determination of hafnium in zirconium oxide by activation analysis, 19: 34129
use of lithium-drifted germanium, in neutron activation analysis, 20: 2166
use of lithium-drifted germanium, for precision gamma energy measurements, 20: 3043
use of lithium-drifted germanium, in gamma detection and measurement, 20: 14845 (AD-620434)
use of lithium-drifted germanium, in neutron activation analysis, 20: 16888
use of lithium-drifted silicon, in dosimetry, 20: 19031(R) (N-65-19766)
use of lithium-drifted germanium, in anti-Compton gamma spectrometers, 20: 27300
use of lithium-drifted germanium, in gamma spectrometers, 20: 27316
use of lithium-drifted germanium, in high-resolution gamma spectrometry, instrument requirements for, 20: 33692
use of lithium-drifted germanium, in γ-γ coincidence measurements, 20: 33678
use of lithium-drifted germanium, in neutron capture gamma spectroscopy, 20: 37072 (KFK-429)
use of lithium-drifted germanium, in γ-γ coincidence experiments, 20: 39197 (AECL-2565)
use of lithium-drifted germanium, for gamma spectroscopy, 20: 39243
use of lithium-6, for measuring fast neutron spectra in reactors, 20: 34911
use of multiple arrays in magnetic spectrometer image planes, 16: 8935
use of pairs of, for analyzing distributions from nuclear reactions, 18: 21250
use of photosensitive, for accelerator beams, 18: 41770 (JINR-P-1695)
use of silicon diode, for neutron diffraction analysis, 20: 43730
use of silicon p-n junction to monitor 14-Mev neutrons, 16: 5539
use of silicon p-n junction as dosimeter, 17: 20372
use of silicon p-n, in dosimeter for beta particles and gamma radiation, 20: 21133
use of silicon solar cell to measure intense radiation, 16: 13359
use of silicon surface-barrier, in detecting plutonium penetration through capsules, 19: 36750 (LA-DC-6973)
use of silicon surface-barrier, in fast-neutron spectrometers, 20: 5181(R) (ORNL-3029)
use of silicon, for spectrometric analysis of beta source mixtures, 19: 32111
use of silicon, for wide-range gamma dosimetry, 20: 19015 (AD-629511)
use of silicon, in gamma rate meters, 20: 33699
use of single crystals of cadmium telluride in gamma spectrometers, 20: 13073(R) (SAN-549-1)
use of spaced, in fast neutron spectrometer, 18: 18243(P)
use of thin-window lithium-drifted germanium, in detection and measurement of high-energy protons, 20: 33675
use of transistorized preamplifier, signal-to-noise ratio, 17: 8544
use of tunnel diodes with charge-multiplying, 20: 21113
use of, for analysis of gas mixtures, 20: 33190(T) (SLAC-Trans-43)
use of, in LET measurements and neutron dosimetry, 20: 43671 (ORNL-P-2467)
use, review, 16: 23895
use to detect alpha particles in chemical process streams, 16: 23902
use with alpha sources as timing devices, 20: 21021 (AD-622629)
use with uranium salts for thermal neutron detection, 19: 44479 (ZFK-PHA-12, pp 140-3)
uses, 18: 23902
uses for measuring fast neutron spectra, 19: 24181
uses for neutron spectrometry, 18: 23884 (NP-13930(p.159-77))
uses in a Compton spectrometer, 19: 4496
uses in aerospace research, 20: 31605
uses in arrangement for discriminating x rays of different hardnesses, 19: 2658(P)
uses in determining alpha emitters in isotopic mixtures, 17: 25121
uses in measuring neutron fluxes responsible for radiation damage to reactor shielding, 18: 29996
uses in measuring thickness of thin polymer films, 19: 46888
uses in proton-recoil fast-neutron spectrometer, 18: 41795
uses in radioisotopic age estimation, 19: 33704
uses in scattering chambers, 19: 40907
uses of, low-level, 17: 16056(R) (TID-18261(p.73-4))
vacuum chambers for, design of, (E), 20: 7415
volume of lithium-drifted germanium, method for increasing active, (T), 19: 32550(R) (N64-18291)
window thickness of diffusion junctions, reduction, 16: 23897
window thickness variations as function of bias voltage in diffused p-n junction, 18: 5674

SEMICONDUCTORS

(See also specific materials.)
see also Electric Conductivity
see also Semiconductor Detectors
see also Transistors
abstracts on materials and uses, 1958, 16: 2842
amplifiers for, design of pulse, 19: 42714(R) (ORNL-3782, pp 11-19)
analysis for admixtures, radioactivation, 16: 5296
analysis for impurities, activation, 16: 3325(T) (AEC-tr-4497(p.169-78))
analysis for impurities, radiochemical methods for, 17: 133
analysis for impurities, survey of activation methods for, 18: 31408
analysis for trace carbon, fluorine, and oxygen, activation, 19: 5817
analysis in production, activation, 20: 22879(T) (AEC-tr-6466/1, pp 260-7)
band structure and electron-phonon interactions in, thermionic and thermomagnetic study of, 18: 18490
band structure, study by cyclotron resonance methods, 16: 15444
behavior in space, 16: 30726
bistability model, 16: 337(R) (NP-10868)
bibliography, 17: 32338 (NP-12989)
bibliography on radiation effects on, 17: 22224 (NP-12732)
bibliography on radiation effects on, 16: 25842 (LAMS-2706)
bombardment conductivity pulse variation in non-uniform electric field distribution in zinc sulfide, 16: 18185
bonding thin metallic films to, methods for, 19: 20520 (SC-DC-65-1256)
book: *Effects of Radiation on Materials and Components*, 18: 37783
book: *Effects of Radiation on Semiconductors*, 19: 20651(T)
book: *Electron-Hole Transitions in Semiconductors*, 17: 29476
book: *Electron Radiation Damage in Semiconductors and Metals*, 20: 41508
book: *Electronic Devices*, 2nd ed., 16: 17828(T) (FTD-TT-61-102)
book: *Fluctuation Phenomena in Solids*, 19: 18623
book: *Radiation Effects on Semiconductors*, 19: 34766
book: *Solid State Physics. XIII.*, 16: 21221
book: *Solid State Physics. XI.*, 16: 21222
book: *Solid State Physics*, Vol. 16, 19: 14065
book: *Thermoelectricity: Science and Engineering*, 16: 3595
book: *Wave Mechanics of Crystalline Solids*, 16: 15350
carrier capture probability in nonmetallic, 17: 5036(R) (ORNL-3364 (p.1-26))
carrier interactions in, hyperfine, (T), 19: 34729
carrier lifetimes in, in magnetic traps, 18: 30305 (D1-82-0340)
carrier transport in, with nonconstant electric fields, (T), 20: 42546
carriers in P-type germanium, energy of, 19: 32048(R) (NP-15073)
catalytic properties of, effects of radioactive impurities on, 19: 11187
characteristics and uses, 16: 18183
characteristics of diodes, high-frequency, 16: 14898 (AERE-M-983)
charge carrier disorder in, (T), 19: 44844
charge transport, mathematical analysis, 16: 9202(4) (MND-2584-2)
charge-carrier lifetime in p-i-n junctions of, method for measuring, 20: 33671
charged-particle binding energy in, effect of magnetic field on, 19: 47143
charged-particle passage through, electromagnetic radiation emission from, (T), 20: 17494
chemisorption of gases by, 18: 25033(T) (SC-T-64-901)
cleaning of surfaces of, methods for, 19: 31642 (SC-TM-64-963)
coating with phosphorus, method for, 19: 33708(P)
conference on physics of failures in, 18: 29964
conference on transport phenomena in, 18: 42158 (NP-14281)
conference, Prague, Aug. 29 to Sept. 2, 1960, 16: 10648
cooling of high-current, design of water heatsink for, 18: 41721 (UCRL-11048)

crystal lattice atom displacement energy in, measurement by electron collision, 18: 13386(T) (AI-Trans-36)
crystal lattice dynamics of, 18: 18488
crystal lattice vibrations in, review of, 20: 34807 (BNL-940, pp 29-43)
crystal lattice vibrations in, review, (T), 20: 40344
crystal structure, 16: 25547 (AROD-2302.8)
crystal structure of, neutron spectrometric studies of lattice dynamics in, 16: 32107 (AECL-1571)
crystal structure of, analysis using inelastic scattering of thermal neutrons, 20: 20170
current carriers in, Coulomb relaxation of, (T), 19: 18589
current density calculation, 16: 19468 (NASA-TN-D-1176)
current rectification processes at metal contacts with, 20: 29569
current-voltage characteristics of tunnel junctions of, second harmonic detection system for, 19: 38944
cyclotron resonance of, theoretical analysis of Azhel-Kamer, 17: 8948(R) (TID-17398)
cyclotron resonance in, classical and quantum mechanical, 18: 18489
cyclotron resonance and magneto-optical effects in, 18: 40084
cyclotron resonance and magneto-optical properties, (T), 19: 11862
defect formation thresholds for, 18: 30219
design and performance of Hall-type, for magnetic field measurements, 16: 22332 (USNRDL-TR-559)
design and performance of p-n junction, for solar cells, 17: 30642
design of, for production of electrical energy, 17: 41665(P)
design of fuel-element, for reactors, 19: 10527(P)
design of lithium-drifted silicon p-i-n, for beta particles, 20: 21077
development, 16: 4422(R) (MND-2584)
development, 17: 4885 (AD-274971)
development by crystallochemical methods, 20: 29623(R) (TID-22970, pp 121-256)
development for radiation counting systems, 18: 14271
development of diode, with low noise characteristic, 18: 4076(P)
development of, for direct energy conversion above 800°K, 17: 16775(R) (GACD-2813)
development of high-temperature broad-band, 16: 10185 (GACD-2495)
development of high-temperature, for thermoelectric power generation, 16: 12090(R) (EOS-1592-2M-5)
development of large-area silicon hot electron emitter, 16: 19462(R) (AD-268422)
development of lithium-drifted silicon, 19: 11515
development of radioresistant, for converting solar energy, 16: 29478(R) (NP-11930)
diffusion of impurities in, tracer study of, 18: 37687(T) (AEC-tr-6398 (p.328-33))
diffusion of lithium into, by drifting method, 17: 16898
diffusion theory, negative temperature states of p–n junctions, 16: 869
donor ground state energies in, corrections to shallow, 17: 36479
doping of oxide, mechanisms of, 20: 41458(R) (TID-23268)
doping of, by rare-earth ion bombardment, 20: 20122
doping of, using ion implantation techniques, 20: 35863 (ORNL-TM-1495)
Doppler and Cherenkov effect in anisotropic ferrites for electric dipole source, 18: 22560
effects on catalysis of radioinduced decomposition of carbon dioxide, 20: 413
effects on gamma radiolysis of methanol, catalytic, 20: 18744
effects on life of cutting tools during uranium machining by cooling, 20: 14689(R) (NLCO-970, pp 5.1-7)
effects on microcircuits including, 19: 18347
effects on radiolysis of water vapor, 20: 9002
efficiency, effects of impurities on, 17: 5638 (AFCRL-62-148)
electric conductivity in varying magnetic field, 16: 7222
electric conductivity and electron flux in, 16: 30901(R) (GACD-3178)
electric conductivity of organic, 17: 18895 (ISS-62/16)
electric conductivity of, calculation of high-frequency, 17: 34601
electric conductivity of, effects of magnetic fields on, (T), 19: 8013(T) (UCRL-Trans-1088(L))
electric conductivity in microwave resion, magnetic field effects on, (T), 19: 8014(T) (UCRL-Trans-1089(L))
electric conductivity dispersion in, thermodynamical model of, 19: 21495
electric conductivity of, transient, 19: 21496
electric conductivity of, measuring methods for, 19: 23164(R) (SU-SEL-64-103)
electric conductivity in ohmic contact with normal metal at low temperatures, (E), 19: 39734
electric conductivity measurements on, methods and uses of, 20: 2345 (UCRL-11030)
electric conductivity of magnesium-base, effects of pressure on, (E/T), 20: 4476(R) (IS-1200(Sect.P))
electric conductivity of organic, review, 20: 46244
electric current lifetimes in, measurement of, 18: 23756
electric properties of organic, 16: 15352
electric properties of diffused junctions, 16: 30983
electric properties of anomalously composed daltonides, prediction of, 17: 20492
electric properties of heat-treated polyacrylonitrile, 18: 24149(T,R) (AEC-tr-6316(p.226-31))
electric properties of diffused silicon, effects of processes and treatments on, 19: 46727 (UCRL-16197)
electric transport phenomena and interband electron–electron scattering in, 16: 30901(R) (GACD-3178)
electromagnetic wave conductivity of, in a-c fields, 16: 32515
electromagnetic wave reflection from moving plasma in, 17: 5513
electromagnetic-wave absorption in heavily doped, 17: 34601
electromagnetic wave propagation in, kinetic theory of, (T), 19: 8538
electromagnetic wave excitation in electron-hole plasma of, in constant electric and magnetic fields, 20: 28621
electromagnetic wave propagation in, (E/T), 20: 30735(R) (TID-22970, pp 331-73)
electromagnetic wave propagation in, nonlinear theory of, 20: 44966
electromagnetic-wave propagation in, (T), 19: 23869
electromagnetic-wave propagation in plasma of, in stationary electric fields, (T), 20: 18013
electromagnetic, plasma, and spin wave interactions in antiferromagnetic, coupling of, 20: 43982
electron attenuation in silicon, energy losses and spectra in, 18: 28148
electron band structure of, high-pressure determination of, 20: 14221 (COO-1198-230)
electron beam interactions in, voltage induction by, (E/T), 20: 42533
electron bombardment of diodes of, enhancement of reverse current by, 17: 18564
electron conduction dynamics in, lectures on, 17: 13195
electron emission from electrodes of, 18: 20152
electron emission from, time dependence of Schottky effect in, 20: 46946
electron energy-loss interactions and surface effects in, 16: 19456(R) (AD-263112)
electron energy losses in, characteristic, (T), 20: 5015
electron gas at high temperatures in, perturbative effects, 16: 21217
electron interactions in, effects of interband, 16: 15322
electron interactions in, effects on effective-mass equation, (T), 19: 4761
electron interband transport in, quantum theory of, 20: 30735(R) (TID-22970, pp 331-73)
electron momentum distribution in germanium and silicon, positron annihilation method for determining, 20: 37736 (COO-1297-7)
electron motion in, effects of magnetic fields on, (T), 19: 11828 (NP-14645)
electron reactions with, electron-hole recombination radiation from, 18: 32285
electron recombination with donors in, 20: 29623(R) (TID-22970, pp 121-256)
electron structure and wave functions for, 17: 2058(R) (NP-12207)
electron susceptibility in, effect of resonance radiation field on valence, (T), 20: 12312
electron temperature in, effect of electric fields on, 18: 16882
electron transport in, kinetic approach to thermal (T), 19: 1060
electron tunneling in, 18: 36155(R) (TID-20873)
electron tunneling in, many-particle theory of, 19: 18931
electron work function for, a-c method for measuring, 20: 13025 (IPP-2/37)
electron-hole generation and recombination in, lifetime intervening in, (T), 19: 35589
electron-hole plasma in, helical and two-stream oscillations in, (E/T), 19: 29383 (AD-606186)
electron-hole plasma instabilities in longitudinal magnetic fields, 19: 29424
electron-hole plasma of, h-f stabilization of screw instability in, (T), 20: 12252
electronic bistability and harmonic oscillation, 16: 14915(R) (NP-11265)
electronic properties of single-crystal, effects of ion-bombardment on, 20: 17151
electronic transport properties for mixed-valence, model, 16: 18141(R) (AD-266220)
electrotransport in, review of theory of, 18: 2256
energy distribution of current carriers in, in presence of fast electrons, 17: 39793(T)
energy gaps in, calculation from atomic radii, 16: 33608
energy levels of, band structure of, 18: 36155(R) (TID-20873)
energy loss in, problems from, 19: 7804
etching by selective radiation, process for photosensitive gas phase, 17: 29277(P)
etching of, design of cells for, (E), 20: 5776
fabrication, 17: 23587 (BNL-790)
fabrication and oxide coating of diffused, method for, 17: 29276(P)
fabrication and properties of sintered, for use as thermoelectric cooling

plates and generators, 20: 29690
fabrication by neutron transmutation doping, 16: 27262(R) (NYO-10086)
fabrication by neutron transmutation doping, 18: 2116
fabrication by neutron transmutation doping, 18: 37662 (BNL-874 (p.10-11))
fabrication of, by neutron transmutation doping, 17: 14944(R) (NYO-10088)
fabrication of lithium-drifted silicon p-i-n junctions, 20: 1580(P)
fabrication of p-n junction, using ion implantation technique, 20: 20125
failure analysis, procedure for, 19: 25814 (SC-RR-65-137)
Faraday effect in, theory of, 17: 32701 (AERE-R-4341)
field effect theory, 16: 15765
fission-fragment damage in, (E), 19: 39245
galvanomagnetic properties, in presence of anisotropic electron scattering, 16: 24331
heat transport in, mathematical analysis of, 16: 9202(R) (MNO-2584-2)
heating by ion bombardment, apparatus for study of, 18: 28109
hypersonic waves in, energy conservation of, 18: 15711(R) (TID-20256)
impurity problems in, use of radiotracers in study of, 18: 16385 (TID-7688(p.38-40))
infrared absorption by, (E), 20: 30734(R) (TID-22970, pp 1-63)
infrared radiation modulation in, by free carrier absorption, 17: 32729 (SCR-636)
instabilities of transverse electromagnetic waves in, 17: 29680
interactions in, many-body theory for, 19: 18597
interactions in, quantum-statistical Green-function method for many-body, 19: 23507(T)
ion reactions with surfaces of, Auger neutralization in, (E/T), 19: 37219
ion reactions with, doping effect in, (E), 20: 12280
ion recombination in plasma in, impedance of, (T), 20: 24584 (AD-626197)
ionized impurity scattering in degenerate, application of variational technique in the partial-wave method, 16: 21195
irradiation of p-n junction, electric power generation from, 17: 39368(P)
junction theory of, review of, 20: 39230
krypton-85 content in, permissible limits of, 20: 8493 (SZS-7(1965))
lectures on, 18: 18487
light detection by, research on, 19: 39269(R) (SU-SEL-64-133)
light effects on surface properties of, 18: 41557
light effects on, device for measuring, 18: 20307
magnetic coefficients for, tables, 16: 23835 (AFOSR-2665)
magnetic field effects on Pippard, gauge-invariant nonlocal theory for, 20: 19740
magnetic field effects on, device for measuring, 18: 20307
magnetic properties in high fields, 16: 15442
magnetic properties of, Hall effect and magnetoresistance, 17: 983(T)
magnetic properties of tantalum, (E), 19: 47524
magnetic susceptibility, 18: 18491
magneto-optical effects in, intraband, interband, and Zeeman, 18: 18489
magnetoresistance of inhomogeneous, (T), 19: 8517
magnetoresistance of inhomogeneous, high-field, (T), 19: 8518
magnetoresistance of, high-field, (T), 19: 18593
meson (μ^+) stopping in, depolarization and quenching in, (E), 20: 13498
microwave field interactions with, 16: 5776(R) (NP-11141)
microwave–plasma interactions in, (E/T), 20: 3157 (AD-614654)
minority-carrier diffusion lengths in, 17: 8963
mobility and thermoelectric power in many-valley polar, 17: 3605
molecular structure, 20: 6551
neutron capture in, transmutation doping and defect formation by, 18: 30278
neutron reactions, recoil and transmutation, 16: 6817(R) (ORNL-3213 (p.57-80))
neutron transmutation doping, 18: 14331
noise generation in, low-frequency, 17: 10936
noise in, survey and evaluation of literature on, 19: 36760 (TID-21902)
nuclear dynamic polarization near paramagnetic impurity in, 18: 34334
nuclear polarization in indium–antimony, effects of d-c current on, 17: 13161
nuclear polarization by hot electrons, 18: 37780(T)
nuclear polarization by direct currents in, (T), 20: 8311
nuclear polarization in, effects of hot carrier flow on, 20: 34846
nuclear spin polarization in, effects of electron interactions on, (T), 20: 24623(T)
operation and response of solar energy converters, 17: 6552
optical properties of metal precipitates in, 16: 29485 (TID-16383)
oscillation frequency and stability in p-type, effects of thermal carriers on, 16: 29902 (D1-82-0183)
oscillations in, circuit-independent spontaneous, 16: 337(R) (NP-10868)
oxidation of silicon surfaces in oxygen plasma, (E), 20: 5740 (TID-22407)
performance as gamma spectrometers, 19: 42706
performance evaluation in Nernst effect thermomagnetic generators, 16: 22343
performance for gamma spectroscopy, 20: 13067 (JUL-308-RB)
performance for radiation dosimetry during therapy, 17: 29147
performance in circuits, computer program for network analysis of, 18: 43888 (LA-3119)
performance in direct-energy-conversion devices, 18: 30475(R) (AFCRL-63-940)
performance in reactor startup instrumentation, 19: 33536
performance of bolometers of, 18: 18238
performance of diode, in flow measurement, 17: 12528 (KAPL-M-RFS-3)
performance of diode, as photomultiplier element, 20: 19042 (UCRL-14445)
performance of Josephson-junction, in superconducting galvanometer, (E/T), 20: 25356
performance of large coaxial lithium-drifted germanium, for gamma spectroscopy, (E), 20: 11086 (AAEC/TM-299)
performance of redrift-treated lithium-drifted silicon, 20: 41311
performance of silicon surface-barrier for α dosimetry, 20: 5721 (CLOR/IBJ-II-37/D)
performance of surface-field-controlled, (E), 19: 20323(R) (NYO-3246-4)
phonon modes in, amplification of transverse optical, (T), 19: 31452
phonon processes in, theory of Franz-Keldysh effect on, 20: 29709(R) (TID-22970, pp 65-119)
photoconductivity of sensitizing effects of eosin on, 19: 22388
photocurrent noise spectra in, design of analyzer for l-f, 20: 43653
photoeffect from, theory of external, 17: 24066(T) (JPRS-19316)
photon absorption by, effects of crossed electric and magnetic fields on, (E/T), 20: 30735(R) (TID-22970, pp 331-73)
piezoelectric properties of, apparatus for measuring, (E), 20: 5883 (IS-1263)
plasma and spin wave interactions in, 20: 26392
plasma collective behavior in, 16: 6854
plasma effects in, conference on, 20: 1346
plasma instabilities in, theory for any injection level, 17: 2360 (D1-82-0198)
plasma instabilities in, review, 17: 7490
plasma magnetic moment of, optical-induced, 17: 25846(R) (AD-405168)
plasma of, stability of electron-hole, (E), 19: 29466
plasma oscillations in, collective excitation of, (T), 20: 8310
plasma oscillations in, strong magnetic field effects on electron-hole, (T), 20: 30677
plasma oscillations in, spin-orbital interaction effects on, 20: 40227
plasma phenomena in, correlation with gases, 19: 45383 (D1-82-0419)
plasma pinch effect in, 18: 42789 (D1-82-0356)
polaron band model application to cerium sulfides, 16: 606
potential energy for, 18: 20829(R) (AD-429503)
preparation and properties, 16: 12028(R) (NP-11410)
preparation and properties of refractory metal, 16: 21111(R) (AD-265106)
preparation and properties, 17: 25690(R) (NYO-10472)
preparation and properties of crystalline perovskite, 19: 9115
preparation by irradiation of oxides, 18: 5410(P)
preparation by neutron transmutation doping, 19: 7769(R) (NYO-3124-1)
preparation for thermoelectric power generation, 17: 24049(R) (NRL-Memo-1404)
preparation of cesium-doped silicon, 17: 39476
preparation of radiation-resistant thin-film diodes, 20: 19096(R) (N-65-17884)
preparation with controlled amounts of interstitial atoms and vacancies, 17: 16581(P)
production by radioinduced graft polymerization of glass backing thread with phenylacetylene vapor, 19: 443
production of diamond, by ion bombardment, (E), 19: 16234
production of p-n junctions by proton irradiation, 16: 7950(P)
production of silicon p-n junctions by ion bombardment, 17: 10773 (ASD-TDR-62-428)
production of silicon junctions by positive ion bombardment, 17: 22311
production of, use of radiochemical techniques in, 19: 42812
properties, 18: 30218
properties, 19: 11512
properties, 20: 31620
properties, 19: 9767(R) (IS-900(Sect.P))
properties and uses in instrumentation, 16: 33211
properties at high temperatures, 16: 18043 (WADD-TR-60-266)
properties, determination by microwaves, 16: 21010(R) (AD-264878)
properties evaluation for use in solar cells, 17: 4354 (ASD-TR-61-242)
properties for gamma spectrometry, 20: 39231
properties for use in thermionic converters, 17: 3464 (ARA-1029)
properties for use in thermionic converters, 18: 811(R) (AD-289355)
properties for use in radiation detection, 19: 33704
properties in space uses, survey, 16: 30826
properties of chemically reactive thin films of, vacuum tube for measurement of electric and optical, 18: 29158 (UCRL-7406)
properties of cobaltite- and pyrite-type compounds as, 17: 34590
properties of electron-hole plasmas in, sustaining helical instability, 18: 32886 (D1-82-0339)
properties of gallium-selenium, dielectric constants and infrared

absorption, 20: 36359(R) (TID-22992)
properties of narrow-band, as thermoelectric elements, 17: 11294(R) (AD-277223)
properties of uranium dioxide, 19: 16139
properties of, effects of low temperature on, 20: 4417
properties of, electric and metallurgical, 19: 32048(R) (NP-15073)
properties of, transmuted center Fermi level spectroscopy, for determining, (T), 20: 38407
properties, effects of dispersed colloidal phase on electric and optical, 16: 5779 (TID-14396)
properties, electric and optical, 16: 21010(R) (AD-264878)
radiation and environmental effects in space, 18: 34235
radiation damage, 16: 13316
radiation damage by high-energy electrons and protons, research on, (E), 20: 11346(R) (NP-15611)
radiation damage in, proton, 17: 18366 (TID-7652(p.230-42))
radiation damage in, correlation of neutron and proton, 17: 32678
radiation damage in, mechanisms of partial annealing of, 18: 12750
radiation damage in, electron, 18: 24996(R) (NAA-SR-8888(Sect.VI))
radiation damage in space, equivalence of particle and photon, 18: 39991 (D2-90407)
radiation damage in silicon, comparison of gamma and neutron, 19: 32615 (NAA-SR-10856)
radiation damage in, electron and neutron, 20: 908
radiation damage to, in solar cells by 96-Mev protons, 17: 34489 (NP-13031)
radiation damage to, 18: 30251
radiation-defect annihilation in, theory for, 17: 27928(T)
radiation effects in space, 16: 2786 (JPL-TR-32-150)
radiation effects on electrical properties, in-pile measurement, 16: 7730
radiation effects, 16: 10416 (ASD-TR-61-322(p.505-13))
radiation effects on electronic properties, review, 16: 12188
radiation effects mechanisms, 16: 12196
radiation effects on surface wettability, gamma, 16: 12201
radiation effects on adsorptive and catalytic properties, 16: 13665
radiation effects, 16: 15980
radiation effects on carrier life-times and mobilities, proton, 16: 12175 (CERN-62-5)
radiation effects in engineering uses, 16: 16625
radiation effects on p-n germanium diodes, gamma, 16: 18091
radiation effects, 16: 19440(T) (FTD-TT-62-414)
radiation effects on, coated with antimony-activated tin dioxide films, 16: 21107
radiation effects on, gamma, 16: 29437 (GA-2984)
radiation effects on conductivity and permittivity of spheroidal inhomogeneities in, 16: 30911 (TID-16560)
radiation effects, 16: 32152 (SCR-532)
radiation effects on adsorption and catalytic properties of, 16: 32160
radiation effects on, 16: 32145 (FZM-1943)
radiation effects, 16: 33522 (REIC-24)
radiation effects on, 16: 33377 (PAN-319/I-B)
radiation effects on, permanent and transient, 17: 3555
radiation effects on, permanent and transient, 17: 3556
radiation effects on catalytic properties of, 17: 6738 (ASD-TDR-62-233)
radiation effects on, in space, 17: 8910
radiation effects, 17: 11267 (TID-15959)
radiation effects on, prediction of, 17: 12723 (TID-17933)
radiation effects, 17: 16763
radiation effects on digital computer circuits of, gamma, 17: 20510(R) (BSC-37051)
radiation effects on, 17: 20515 (REIC-26)
radiation effects at 4.2°K, design of cryostat for electron, 17: 28091
radiation effects of electrons and protons on, 17: 29269
radiation effects on, review, 17: 34513
radiation effects on, 17: 34554(R) (ORNL-3480(p.79-94))
radiation effects on, proton, 17: 34524
radiation effects on electric current characteristics of, 17: 36343(R) (EGG-B-2462)
radiation effects on, neutron, 17: 36355
radiation effects on, surface, 17: 39685
radiation effects on, 17: 39007
radiation effects on, 17: 41227
radiation effects on silicon diode, effects of neutron-gamma ratio on transient, 18: 647 (D2-9878-3(Sect.E))
radiation effects on diamond-lattice, review on, 18: 2303
radiation effects on, 18: 2306
radiation effects on properties of, 18: 2318
radiation effects on, 18: 8872 (NP-13504)
radiation effects on, permanent, 18: 12751
radiation effects on, for space applications, 18: 12757
radiation effects on, literature survey on, 18: 14539(R) (RADC-TDR-63-226)
radiation effects on, review of, 18: 14564
radiation effects on electric conductivity of, gamma, 18: 16541
radiation effects on, comparison of proton and neutron, 18: 22527(R) (NASA-CR-40)
radiation effects on thermal conductivity of, 18: 28059
radiation effects on, electron and proton, 18: 30235(R) (N64-20726)
radiation effects on, electron and proton, 18: 30236(R) (NASA-CR-62)
radiation effects on NERVA electronic components, neutron, 18: 30237 (NP-14069)
radiation effects on, 18: 30276
radiation effects of, alpha, 18: 32061(R) (UCRL-11317(p.198-203))
radiation effects on, fast-neutron and gamma, 18: 33825 (AD-435095)
radiation effects on performance of, in telemetry electronics, 18: 33838 (RTD-TDR-63-4287(Vol.I))
radiation effects on performance of, in telemetry electronics, 18: 33839 (RTD-TDR-63-4287(Vol.II))
radiation effects on thermoelectric properties of, 18: 34237
radiation effects on electric properties of, effects of radiolytic absorbent material on, 18: 36053
radiation effects on, 18: 35805(R) (BSR-847)
radiation effects on oxide electrodes of, heterogeneous sensitization, 18: 37769(T) (AEC-tr-6398(p.495-504))
radiation effects on, review on, 18: 37787
radiation effects on, review of, 18: 39579
radiation effects on, in space environment, 18: 44275
radiation effects on, 19: 849(R) (FDL-TDR-64-30)
radiation effects on, 19: 2665 (SC-R-64-1324)
radiation effects on cryogenic temperature-sensor, (E), 19: 4538 (LA-DC-6649)
radiation effects on electron-hole pair production in, transient gamma, 19: 4540
radiation effects on, computer program and model for simulating, 19: 4546
radiation effects on impurity photoconductivity in germanium, electron, (E), 19: 4549(T)
radiation effects on, hardening against, 19: 9547
radiation effects on, research program on, 19: 9727 (ARL-64-151)
radiation effects on electric conductivity and Hall effect of, apparatus for galvanomagnetic measurements of in-reactor, 19: 11790
radiation effects on metal-oxide, gamma, 19: 11607
radiation effects on, interaction mechanisms in, 19: 11608
radiation effects on surfaces of transistors and diodes, gamma, 19: 13816
radiation effects on, methods of evaluating, 19: 15939
radiation effects on properties and structure of, 19: 18545
radiation effects on defects in, review of energy spectrum and nature of, 19: 18553
radiation effects on, transient, (E/T), 19: 18554
radiation effects on conductivity of silicon-diode, neutron, (E), 19: 22811
radiation effects on catalytic activity in conversion of cyclohexane, 19: 26417
radiation effects on triodes, (E), 19: 26714
radiation effects on aluminum–silicon dioxide–silicon capacitors, electron, 19: 26713
radiation effects on, simulation by irasers, (E), 19: 32778 (SC-DC-65-1421)
radiation effects on minority carrier diffusion length and lifetime in base region of p-n junction, proton, 19: 32616 (NASA-TN-D-2817)
radiation effects on metal-oxide, electron, 19: 32622
radiation effects of radioactive impurities on catalytic and chemosorption properties, 19: 37194
radiation effects on, electron, 19: 40286(R) (NAA-SR-11200)
radiation effects on silicon, gamma, 19: 39269(R) (SU-SEL-64-133)
radiation effects on, in space environment, 19: 39059
radiation effects on, electron-hole pair production in high-energy particle, (T), 19: 39250
radiation effects on photoconductivity in silicon, electron, 19: 40933(R) (NP-15300)
radiation effects on photoconductivity of silicon, electron, 19: 40934(R) (NP-15301)
radiation effects on germanium, neutron, 19: 40939
radiation effects on thermally stimulated conductivity of silicon, neutron, (E), 19: 41985
radiation effects on, 19: 47076 (AD-612090)
radiation effects on, system performance predictions from, 19: 46874
radiation effects on, in space vehicles, 19: 46875
radiation effects on, 20: 695
radiation effects of cosmic radiation on, 20: 3239 (NASA-SP-71)
radiation effects on, conference on, 20: 2480
radiation effects on, 20: 2481
radiation effects on, at 0 to 140°K, 20: 2482
radiation effects on, 20: 2497
radiation effects on double acceptor defects in n-type, 20: 2499
radiation effects on silicon carbide, 20: 2503
radiation effects on, threshold energy for, 20: 2513

radiation effects on, surface design effects on, 20: 2411(R) (AD-618078)
radiation effects on, model for predicting transient, 20: 2412(R) (AD-618079)
radiation effects on, review of, 20: 4464
radiation effects on electric properties of, role of doping in, 20: 4265
radiation effects on MOS, gamma, 20: 7463
radiation effects on, homogeneity measurements from electron, 20: 11361
radiation effects on, transient, 20: 13130 (SC-DC-65-1892)
radiation effects on, instrumentation for analyzing, 20: 14918(R) (ECOM-01313-1)
radiation effects on, nuclear-explosion, 20: 14921
radiation effects on, 20: 17158(R) (ORNL-3900, pp 82-149)
radiation effects on junctions of, proton, 20: 16907(R) (N-65-17517)
radiation effects on, review of, 20: 16911
radiation effects on, 20: 20365
radiation effects on, gamma and neutron, 20: 19098(R) (N-65-17953)
radiation effects on electric properties of germanium and silicon, neutron, 20: 21150 (HMI-B-45)
radiation effects on, review of, 20: 21156
radiation effects on, review of, 20: 21160
radiation effects on, conference on, 20: 21164
radiation effects on, generalized model analysis of ionizing, (T), 20: 21167
radiation effects on, modeling of, 20: 21173
radiation effects on, photovoltaic theory for, 20: 21437
radiation effects on, design effects in, 20: 23515(R) (AD-624509)
radiation effects on MOS, electron, 20: 23523
radiation effects on diodes and transistors, model for, 20: 23763(R) (AD-625341)
radiation effects on surface of, 20: 25447(R) (N-66-15448)
radiation effects on sorptive properties of surfaces of, (T), 20: 29815
radiation effects on silicon, transient annealing from neutron, 20: 31613 (SC-DC-66-1443)
radiation effects on MOS, x, 20: 31615
radiation effects on, defect annealing in, 20: 33731(R) (N-66-13174)
radiation effects on devices of, pulsed, 20: 33735
radiation effects on antimony–indium, gamma and neutron, 20: 37295
radiation effects on physical properties of, 20: 46966(R) (NAA-SR-12010)
radiation effects on, in integrated MOS circuit, 20: 46097(R) (AD-630344)
radiation effects on, review of, 20: 46098
radiation processing of components of, commercial applications of, 18: 31987 (CONF-568-1)
radiation resistance of, review, 19: 6214 (HMI-B-28)
radiation response of, generalized model for, (T), 20: 23519(R) (AD-631367)
radiation- and stress-induced defects in germanium-diode, 20: 4264
radioinduced conductivity in films of, performance of chamber for measuring x, 20: 39179
radioinduced current and voltage pulses in, 18: 44276
radioinduced damage in n- and p-type silicon, transient electron, (E), 20: 11176(R) (NP-15835)
radioinduced damage in silicon, gain degradation from neutron, 20: 21169
radioinduced defects in diamond-lattice, review on, 19: 11811
radioinduced defects in germanium and silicon, 20: 904
radioinduced defects in, structural properties of, 20: 2486
radioinduced defects in, fluorescence studies of, 20: 2498
radioinduced defects in, 20: 2516
radioinduced defects in, model for annealing, 20: 21153(R) (N-65-25593)
radioinduced defects in, fast electron, 20: 40332
radioinduced doping in, neutron, 18: 18156
radioinduced electron-cavity pair formation in, 17: 27932
radioinduced electron-hole pairs in n-type silicon, formation energy for alpha, (E), 20: 2362
radioinduced inhomogeneities in, 17: 37607
radioinduced leakage current of MOS field-effect transistors of, 20: 9304
radioinduced phase conversion in, processes for, 20: 9309(P)
radioinduced regeneration effects in p-n junction, in isolated circuits, 20: 21168
radioinduced transmutation doping, 19: 13439
radioinduced variations of direct characteristic of diode, in pulsed reactor, 20: 35809
radiosensitivity levels for types of, fast-neutron, 20: 16911
reactions of recoils from neutron (n,γ) reactions in, 19: 46398
recombination of electrons and donors in, 18: 34280(R) (NYO-2680-1)
relaxation time of recombination radiation in, 20: 8302
research in Japan on, 19: 23550
research program on wires and solenoids, 17: 11335 (TID-17827)
research programs of U. S. Army on, 1962 summary, 17: 33413(R) (NP-12967)
sorptive properties of, effects of radioactive impurities on, 19: 11187
sound amplification by conduction electrons in, magnetic field dependence of, 17: 36492
sputtering by mercury and rare gas ions, yields from, 16: 31727
sputtering of single-crystal, atom-ejection patterns, (E), 20: 40305
stability of lithium-drifted silicon, 20: 21103
superconducting transitions in, 18: 21102
superconducting transition in, induction using field effect, (T), 20: 11901(T)
superconductivity in polar and nonpolar, 16: 24332
superconductivity of, theory for, 18: 15103
superconductivity in many-valley, 18: 16887
superconductivity in strong magnetic fields, (T), 19: 37751
superconductivity in, (T), 20: 4781
superconductivity in films of, lower temperature limit for, (T), 20: 8010
superconductivity in pure undoped, production by laser illumination, (T), 20: 8026(T)
superconductivity in degenerate p-n junction, electron and hole, (T), 20: 9936(T)
superconductivity of ionic, high-current, (T), 20: 21889
superconductivity of thin films of, (T), 20: 32338(T)
superconductivity of thin nondegenerate films of, factors affecting, (T), 20: 46525(T)
surface contamination of, use of radioisotopes for detection of, 18: 20420
surface phenomena in melts of, 18: 32078
surface physics of, use of field emission microscopy in study of, 20: 32742
surface properties, 20: 29623(R) (TID-22970, pp 121-256)
switching characteristics of series-connected tunnel diodes, analog study of, 18: 41719 (SCL-DC-64-57)
switching time of tunnel diodes, 17: 362 (RISO-42)
synthesis by radioinduced reactions, 16: 27034 (NYO-9864)
synthesis in radiation induced reactions, 16: 8667(R) (NYO-9862)
synthesis of high-polymeric, 17: 12185(T) (SCL-T-462)
testing of commercial microelectronic circuits, 18: 29918 (CONF-567-1)
theory, 18: 4332(T) (NASA-TT-F-73)
thermal conductivity, modification of three-phonon processes by isotopic scattering, 16: 21196
thermal conductivity of liquid, 18: 11529(R) (TID-20066)
thermal conductivity in, existence of super-, (T), 20: 18014
thermal conductivity of, effect of heat transport by radiation on, 20: 22329
thermal conductivity at low temperatures, (T), 20: 24592 (TRG-Report-977)
thermal diffusivity measurements, 16: 16708(R) (AD-266128)
thermal effects in, compensation of, 20: 20992
thermionic work functions of cesium–antimony, cesium–silicon, and cesium–tellurium films in cesium vapor, 17: 32830
thermoelectric and thermomagnetic effects in, 18: 18490
thermoelectric effects in non-linear junctions of, 17: 11294(R) (AD-277223)
thermoelectric properties, bibliography, 16: 13514 (NAA-SR-Memo-7079)
thermoelectric properties, 18: 818(R) (NP-13266)
thermomagnetic properties, density-matrix analysis, 16: 22808
thermomagnetic properties, 17: 9101
transitions in silicon, electric properties of p–n, (E), 19: 23954 (JINR-P-2002)
transport coefficients for, variational Boltzmann calculation with optical-mode scattering for, (T), 19: 4829 (TID-21325)
transport effects in, research on, 20: 2519(R) (AD-615152)
transport phenomena in, 16: 15322
transport properties of mixed-valence, effects of magnetic fields on, 17: 30982(R) (NP-12969(Paper V))
transport properties of n-type, theory of high-field, 19: 23164(R) (SU-SEL-64-103)
transport properties of n-type, theory of high-field, 19: 39269(R) (SU-SEL-64-133)
tunneling between Josephson junctions, quantum interference effects in, 18: 12789
ultrasonic wave propagation in strong magnetic field, attenuation oscillations and velocity of, 20: 34862
ultrasound extinction in, effects of drift motion of carriers on, 17: 4982
use as modulators for d-c amplifiers, survey of, 17: 334 (JAERI-4022)
use as pressure transducers, (E), 20: 5216 (SC-TM-65-457)
use in absorbed-dose measurements, (E), 19: 28674
use in cavity resonators for detection of particles, 20: 46065
use in circuits for nuclear instrumentation, 17: 10957
use in cooling systems for in-pile television equipment, 18: 32984(P)
use in ion chamber detectors, 18: 43957
use in maritime reactor control instrumentation, 19: 10630
use in promethium-147 nuclear battery, 18: 27827
use in reactor safety systems, 20: 22360
use in static energy conversion, 17: 34531 (ASD-TDR-63-723)
use of, for dosimetry of penetrating radiation, 17: 8660
use of niobium–tin, for high field magnets, 19: 47526

uses in cooling television cameras in reactors by Peltier effect, 18: 44951(P)
uses of organic, review, 20: 46244
SENA POWER REACTOR
description, 20: 24763
description and performance of, (E), 19: 45614
design and construction, 18: 38540(T,R) (TID-20953)
design and construction, 19: 3656(T,R) (TID-21280)
design and construction, 19: 31552(R) (TID-21757)
design and construction, 19: 42087(R) (EUR-2428.f)
design and construction of, 18: 9663
design and development in 1963, 18: 26920(R) (EUR-1804.f)
design and development, 19: 24091(R) (TID-21500)
design and development, Jan.–Mar. 1965, 19: 40192(R) (TID-22003)
design and economics, 20: 1480
design and operation characteristics of, 20: 47021
design and status of Sena power plant, 19: 3708
design and testing, 18: 38510 (A/CONF.28/P/770)
design, construction, and improvements, 19: 40209
development and economic aspects, 18: 38457 (A/CONF.28/P/514)
development of, review, 19: 19395
development of, review of, 20: 18104
development of, 1965, 20: 36465(R) (EUR-2962.f)
development status, 20: 12412(R) (TID-22516)
development, April–June 1965, 20: 3484(R) (TID-22329)
development, Oct.–Dec. 1963, 18: 31001(T,R) (TID-20700)
development, 1–3/66, 20: 45124(R) (TID-23339)
development, 10–12/65, 20: 45123(R) (TID-23338)
electric system of, design review, 20: 1507
fuel cycle for, analysis of plutonium, 20: 47006(R) (EURAEC-1666)
fuel element shipping from, to United States, 18: 5544 (EUR-112.e,f (Vol.1))
fuel element shipping from, to United States, 18: 5545 (EUR-112.e,f (Vol.3))
fuel rods for, plutonium distribution in, 20: 47006(R) (EURAEC-1666)
instrumentation for, (E), 19: 24006 (CONF-640607(Vol.I)(Paper A-2))
SENN Reactor
see Garigliano Power Reactor
SEPARATION PROCESSES
see also Adsorption Separation Process
see also Alloy Separation Processes
see also Amex Process
see also Amine Extraction Process
see also Butex Process
see also Citriflex Process
see also Countercurrent Separation Processes
see also CSREX Process
see also Electrolytic Separation Processes
see also Electromagnetic Separation
see also Electromigration Separation
see also Electrostatic Separation
see also Fluoride Volatility Processes
see also Hermex Process
see also High Temperature Separation Processes
see also Ion Exchange Processes
see also Isotope Separation Methods
see also Neuflex Process
see also Purex Process
see also Radioactive Gas Separation Processes
see also RaLa Process
see also Recuplex Process
see also Redox Process
see also Solvent Extraction Processes
see also TBP Process
see also Thermox Process
see also Thorex Process
see also Tramex Process
see also Tributyl Phosphate Process (Canada)
see also 25 Process
see also 25-TBP Process
see also Volatility Separation Processes
see also Zircex Process
see also Zirflex Process
analysis in, in-line, 16: 30630
analytical procedures for, 17: 27231(R) (IDO-14605)
analytical procedures for, 19: 7274(R) (IDO-14636)
bibliography on, for irradiated fuels, 17: 3 (ORNL-2971(Vol.6))
bibliography on reprocessing of irradiated fission reactor fuel and breeding elements, 16: 1859 (TID-3529(Rev.2))
bibliography on reprocessing of irradiated fuel and breeding materials, 18: 35646 (TID-3312(Suppl.1))
book: *Chemical Processing of Reactor Fuels*, 16: 277
book: *Chemical Processing in the Atomic Energy Industry*, 18: 39398
book: *Chemical Technology of Prepared Radioactive Elements*, 16: 247
book: *Designs and Means for Automatization of Radiochemical Installations*, 18: 13953
book: *Extractive Recovery of Irradiated Nuclear Fuel*, 16: 1870
book: *Ion Exchange Technology*, 19: 30141
book: *Ion Flotation*, 18: 43726
book: *Rare Metal Extraction by Chemical Engineering Techniques*, 18: 13952
book: *Research and Determination of Trace Elements*, 17: 25158
book: *Separation Processes in Practice*, 16: 18997
book: *Technology of Uranium*, 20: 45801(T) (AEC-tr-6638)
collector control device for fractionation column, design of automatic, 18: 12277(P)
conceptual study of demonstration of chop-leach process, 17: 40928 (IDO-14610)
conference on instrumentation in plants for chemical reprocessing of irradiated fuels, Paris, Nov. 22 and 23, 1963, 19: 2436 (NP-14343)
cost evaluations and flowsheets, 17: 23450
cost factors, 17: 8232 (BNL-5479)
criticality control in, for zirconium fuel, effects of boric acid on, 20: 43067(R) (IDO-14679, pp 6-46)
criticality of plutonium metal dissolvers in, the "always safe" conditions for, 17: 26195
crystallization in, effects of complexing on, 16: 8816
decontamination of penta- and tetra-complexes of ruthenium nitrosyl in fuel processing plant, countercurrent computation of, 17: 40944
description for trivalent actinides, 18: 37290 (A/CONF.28/P/819)
description of head-end, for reprocessing of thorium fuels, 19: 30324 (ORNL-TM-1139)
description of large-scale, for fission products, 18: 31649 (A/CONF.28/252)
description of, for determining fission yields, 19: 28450
description of, mathematical, 18: 37258 (A/CONF.28/P/346)
design and construction of air-water, for use in fog-cooling studies, 16: 17794 (EURAEC-49)
design and control of dodecyl benzenesulfonate foam, 19: 46429 (ORNL-P-1522)
design for actinides using complexing and electrodialysis or molecular filtration, 19: 28459(P)
design for alkali metals, alkaline earth metals, and ruthenium, (E), 19: 45260(R) (IDO-14660)
design for carbon-14-labeled carbon dioxide and monoxide, 19: 538
design for low-grade uranium ores, 18: 37414 (A/CONF.28/P/844)
design for rare earth and thorium ores, 19: 24639(P)
development, 16: 2669(R) (ANL-6454)
development, 16: 20297(R) (ANL-6477(p.29-105))
development, 16: 28358(R) (ANL-6580)
development, 17: 11936(R) (ANL-6672)
development, 17: 22783(R) (ANL-6705)
development, 18: 23701(R) (NAA-SR-8888(Sect.V))
development and use of rapid radiochemical, review of, 20: 20826
development at Argonne National Laboratory, 16: 26455(R) (ANL-6573)
development for fast reactor breeding and fuel elements, 20: 6600(R) (ANL-7105, pp 1-35)
development for fuel reprocessing in Czechoslovakia, 19: 15685
development for irradiated fuel elements, review, 16: 16670
development for irradiated reactor fuels, 17: 4248(R) (NAA-SR-7400 (Sect.VI))
development for production of zirconium sponge from Indian zircon, 19: 34266 (AEET-201)
development for processing finely divided reactor fuels, series mixer-settler apparatus for, 19: 44127(P)
development for processing of thorium-bearing fuels for gas-cooled high-temperature reactors, 20: 33428
development for purification of organic moderators and coolants, 19: 15690
development for removal of radioactive krypton from effluent gases from fuel element processing plants, 18: 8451
development for reactor fuel processing, Technical Progress Review, Fall 1963, 18: 8452
development for reprocessing clad fuel elements, 18: 37299(P)
development for reactor fuel processing, *Technical Progress Reviews*, Spring 1964, 19: 11290
development for reclamation of plutonium and uranium from fast reactor fuels, 19: 35604(R) (ANL-7045(p.1-23))
development for spent fuel reprocessing, survey of Czech, 18: 37277 (A/CONF.28/P/760)
development for spent power reactor fuels, 20: 4069
development for treatment of irradiated fuel elements, 18: 35247(R) (NAA-SR-9700)
development for use in activation analysis, 20: 12803
development, Nov. 1961, 16: 4959(R) (ANL-6473)
development of, 16: 32882(R) (ORNL-3314)

development of adsorption methods, review, 16: 20316
development of aqueous, for irradiated fuels, review of, 20: 36947
development of burn-leach, for graphite-base fuels, 19: 22406 (ORNL-TM-1096)
development of carrier-free, for study of complex beta spectra, 18: 31566 (TID-18567(p.2-6))
development of chlorination-column sorption, for irradiated uranium or uranium–plutonium fuels, 18: 22194(P)
development of chlorination-fluorination, for irradiated fuels, 19: 31462(R) (ANL-7028)
development of close-coupled, for decontamination of remotely handled fuels, 20: 9044(R) (ORNL-3830, pp 30-68)
development of combined chloride volatility-aqueous processing method for spent uranium–zirconium alloy fuels, 18: 1801 (ORNL-TM-645)
development of dry, for processing irradiated fuel elements, review of, 19: 40667
development of equilibrium density gradient sedimentation method for labeled and unlabeled enzymes, 17: 5710
development of fluidized-bed, for reactor fuels, 17: 23439(T) (AEC-tr-5786)
development of foam, 16: 22269(R) (TID-15919)
development of foam, 16: 29039(R) (RAI-101)
development of foam, 17: 10219(R) (ORNL-TM-343)
development of foam-column, for removal of cesium and strontium from waste solutions, 17: 12366(R) (RAI-104)
development of foam, 17: 17619(R) (ORNL-TM-482)
development of foam, 17: 21594(R) (ORNL-TM-355)
development of foam-type, for low-level wastes, 17: 26931(R) (ORNL-TM-453)
development of foam, for low-level waste solutions, 17: 26932(R) (ORNL-TM-516)
development of foam, for waste solutions, 17: 28584(R) (RAI-113)
development of foam-extraction, 18: 1797 (NYO-10038)
development of foam, for low-level waste solutions, 18: 6537(R) (ORNL-TM-603)
development of foam, for decontaminating low-level process-waste water, 18: 19448(R) (ORNL-TM-757)
development of foam, 18: 34007(R) (ORNL-TM-890)
development of headend, 18: 10198
development of improved aqueous, for uranium–zirconium alloy fuels, 18: 10181 (IDO-14619)
development of ionophoresis, 18: 25612(T) (ORNL-tr-128)
development of MHD, for electrically conducting fluids, 18: 22192(P)
development of nonaqueous, for fuel processing, review, 19: 34284
development of oxidative-slagging method for reactor fuel elements, 17: 25374(P)
development of phosfluor process for ceramic fuels, 16: 24645
development of pyrometallurgical, 19: 11293
development of pyrochemical, for fast breeder reactor fuels, 19: 32279(R) (ANL-7020(p.3-99))
development of pyrochemical, for fuel reprocessing, 20: 25208
development of qualitative semimicro, use of tracer techniques in, 17: 21774 (NP-12726)
development of radiochemical, 18: 20044
development of reductive chlorination, for low-grade ores, 20: 4072(P)
development of salt cycle, engineering, 18: 27279(R) (HW-80284(p.4.1-23))
development of salt-cycle, 19: 13524(R) (HW-81984(p.4.1-20))
development of salt cycle, engineering, 19: 34302(R) (HW-84384 (p.4.1-9))
development of shear-leach, for clad fuel elements, 20: 20808(R) (ORNL-3916)
development of thin-layer chromatography, 19: 9267
development of, for processing high-purity materials, 19: 7625
development of, for purification of 48 elements, 20: 8838 (UCRL-14258)
development of, for use in radiochemistry, review of, 20: 16557
development of, for use in activation analysis, 20: 29120
development of, for reactor fuel processing, *Technical Progress Reviews*, Summer 1966, 20: 45813
development review, 16: 6515
development, efficiency, and uses of Sol-Gel, 19: 15674
developments and economics of aqueous, 18: 13973
developments at Ames Lab., 16: 11352(R) (IS-348)
developments in salt-cycle, for plutonium dioxide–uranium dioxide fuels, 19: 46422 (BNWL-SA-205)
developments using foam-liquid column, 16: 10102(R) (ORNL-TM-65)
differential electrolysis methods evaluation for, 18: 27813(R) (ORNL-TM-428)
dissolution of uranium–zirconium reactor fuels in, effects on titanium equipment, 17: 14378 (ORNL-TM-395)
distillation column design and efficiency for, 19: 38766
economic aspects, 18: 6901
economics, 16: 29057
economics of aqueous, pyrochemical, and volatility, for carbide, metal, and oxide fast-breeder reactor fuels, 20: 43410 (ANL-7137)
efficiency of dry, for irradiated fissionable materials, 19: 24615
efficiency of foam, 18: 16129(R) (RAI-116)
efficiency of ion flotation, for separation of zirconium from aqueous solutions, 19: 22413
equipment and flowsheets for shear-leach, 20: 9044(R) (ORNL-3830, pp 30-68)
equipment for Eurex, testing of, 20: 14644
equipment for rapid radiochemical, utilizing precipitation with carrier, 19: 22421
equipment for sedimentation extraction, 20: 25211
equipment for thermal diffusion, 16: 31688(P)
fission-product removal in nitric-acid-leach process in reprocessing uranium dioxide-dispersed graphite fuels, 17: 32200
flooding in perforated-plate extraction columns, geometry, operating variables, and physical properties of, 20: 14462 (ORNL-3890)
flow rate control by vacuum spillways for mixers-decanters in, 19: 2439 (NP-14343(p.Id1-4))
flowsheets for waste treatment at Eurochemic, 18: 40957 (NP-8519)
foam column for, performance of 24-inch-diameter, 17: 40684(R) (ORNL-TM-608)
foam columns in, dynamic properties of, 18: 17939 (TID-20461)
foam, model for flow of liquid in, 17: 40931(R) (ORNL-TM-613)
foam separation and scavenging-precipitation for low-level radioactive wastes, 20: 10438(R) (ORNL-3830, pp 96-139)
foam separation in, centrifugal foam breaker for, 17: 33768(R) (ORNL-TM-541)
foam separation of metals, studies of factors of, 18: 17939 (TID-20461)
foam, engineering drawings of column for use in, 18: 31682
for azeotropic mixture separation by extractive distillation, 16: 3093(P)
for cerium purification, 20: 36936
for chemical isomers, 19: 32048(R) (NP-15073)
for deuterium enrichment featuring chemical exchange, 19: 18374(P)
for enriched uranium, criticality control in, 17: 19035 (RFP-104)
for fission products in waste solutions, 20: 27039 (NP-15946)
for gas-iodine systems, 19: 32495
for ions in low-activity radioactive effluents, review on, 18: 35648
for irradiated uranium fuels, chlorination method, 16: 20552
for metals, by cation exchange, 17: 10733 (IS-466)
for preparation of reactor fuels, 19: 17441
for reactor fuels, corrosion in, 17: 39178(R) (ORNL-3452(p.1-25))
for separating non-surface-active ions from solutions, 16: 30510(P)
for separation of film-forming impurities from organic coolants, 16: 29037 (NAA-SR-6905)
fuel reprocessing costs, 16: 8817
in-line analysis of electrolytic dissolver solutions for nitric acid and salt concentrations, 17: 18176 (IDO-14603)
in-line plutonium monitor for, 17: 332 (HW-57662)
instrumentation for, in reprocessing fuel elements, 19: 2438 (NP-14343 (p.Ic1-23))
instrumentation for, for fuel element reprocessing, 20: 16559
isotopic fractionation during analytical, 20: 42738(R) (ANL-7136, pp 255-65)
materials management during, at Windscale, 20: 20972
mechanism of foam, 16: 32898(R) (ORNL-3314(p.190-4))
mechanisms of foam, 16: 7475(R) (ORNL-TM-81)
mechanisms of foam, 16: 20537(R) (ORNL-TM-177)
method for separating uranium from uranium–zirconium alloy, 17: 245(P)
method for, in radioactivation analysis, 20: 33214
methods for fission product recovery, review on developments in, 20: 14436 (BNWL-SA-504)
methods for transplutonium elements, review on, 20: 16402
nuclear materials management in, 18: 39367 (HW-SA-3672)
performance of flash-evaporation, for sea-water desalination, (E), 19: 29649 (PB-181694)
performance of freezing, for processing uranium wastes, 18: 38684 (A/CONF.28/P/609)
performance of halide- and oxide-reduction, for reactive metals, 17: 32504
plutonium determination by oxidation-reduction titrations in, 18: 11963 (HW-53368(Suppl.1))
radiation monitoring equipment for, 20: 14853 (CNEA-159)
radiochemical, methods in, 17: 35922
radiochemical, automation developments in, 19: 6001
radiochemical, for use with activation analysis of biological matter, 20: 33182(T) (AEC-tr-6639, pp 108-13)
radiochemical, for use with activation analysis of biological materials, 20: 38842
radiometric techniques and instrumentation for in-line process monitoring, 18: 8669
recent advances in aqueous, 16: 624
research on chemical, 19: 4250(R) (ORNL-3627(p.177-208))

research on chemical, review, 19: 34101
research progress at Argonne National Lab., October to December 1961, 16: 20296(R) (ANL-6477)
review, 17: 28792
review of aqueous, for reactor fuels, 18: 33058 (A/CONF.28/P/249)
review of, for reactor fuels, 17: 34063
review of gas, liquid, and solid, for traces of inorganic ions in aqueous solutions, 16: 3071
review of wet, 16: 285
shape factors for thermal diffusion columns, 20: 10949 (K-1469)
shielded cells for radioactive, leak detection in, 20: 14788 (JAERI-1089)
survey of halogenation methods for irradiated reactor fuels, 17: 32199
testing of cesium nickel ferrocyanide process in Purex Plant equipment, 17: 3066 (HW-75051)
tracer study of, method for, 17: 1696(P)
transformation theory of separation cascade, 18: 13933
transformation theory of cascades, 18: 13934
transformation theory for rectangular cascade, (T), 20: 448
use in trace analysis, 20: 40850
use of AIROX, in reprocessing and refabrication of second-cycle irradiated uranium dioxide fuel, 19: 44114 (NAA-SR-11375)
waste disposal, 16: 287

SEPARATORS

see also Cascade Impactors
see also Cascades
see also Cyclone Separators
see also Electrostatic Precipitators
see also Entrainment Separators
see also Magnetic Separators
design and development of steam, 19: 45574(R) (GEAP-4914)
design and operation of fluidized-bed coal gasifier, 19: 17333(R) (TID-21596)
design and performance of A.W.R.E., 19: 34608
design and testing of stacked-clone, for solvent extraction, 20: 9053(R) (CRNL-3830, pp 252-60)
design of immiscible liquids, 19: 28465(P)
design of phase, 19: 34315(P)
design of radial vane, for water and steam, 20: 39019(R) (GEAP-5149)
design of SGAE electromagnetic isotope, 19: 34614
design of, for isopropylbiphenyl, 20: 40449(R) (SAN-650-1)
development and testing of steam–water, 19: 32344(R) (ACNP-65001)
development for separation of steam from water, 19: 44131 (ACNP-65003)
development of horizontal and upcomer, for steam, 19: 38801(R) (ACNP-65004)
development of steam–water, 20: 28696(R) (GEAP-5084)
ion beam formation in Pretoria isotope, 19: 34613
ion beam reactions in electromagnetic isotope, 20: 21219
performance of electromagnetic isotope separator RISC at CERN, 19: 35511
performance of radioisotope, at CERN, 19: 34612
performance of radioisotope, at Institute for Nuclear Study, Japan, 20: 16928(R) (INSJ-92)
theory for rectangular cascade, transformation, 20: 23574
use of Orsay, for spallation and spectroscopic studies, 20: 33764

SER

see Systems for Nuclear Auxiliary Power

SERF

see Sandia Engineering Reactor

SERINE

analysis for carbon-14 by continuous scintillation counting, 17: 5709
carbon-14 uptake by, in algae proteins during photosynthesis, 19: 24244
complexes with lanthanum, stability of, 19: 36421
complexes with rare earths and yttrium, stability of, 20: 26896
complexes with rare earths, stability of, 20: 29208
determination in protein hydrolyzates using carbon-14- or tritium-labeled 1-fluoro-2,4-dinitrobenzene, 16: 16089
determination of, in rabbit urine, design of photometer for, 17: 30214
effects on enzyme activity, 19: 21817(R) (BNL-867(p.119-50))
hydrolysis by hydrochloric acid in tritiated water, hydrogen exchange in free and protein-combined, 19: 9243
nitrogen-15 content in, significance of excess, 17: 23043
photolysis of, transformation of amino acids in uv, 18: 23204(T) (JPRS-24164(p.19-42))
preparation of carbon-14-labeled, method for, 19: 36526
radiation effects on spectra of solid crystalline, 17: 12741
radiation effects on content of, in mouse tissues, 17: 30377
radiation effects on content of, in nervous system of guinea pigs exposed prenatally, 19: 5673
radiation effects on content of, in kidneys and liver of mice, 19: 7149
radiation effects on incorporation of, by blood cells, x, 20: 28922
radioinduced decarboxylation in solid state, yields in, 19: 13438
radioinduced radicals in, 16: 30452
radiosensitivity effects on pea seeds, 17: 38881
reactions with rare earths, composition and stability of complexes formed in, 19: 19874
synthesis and transformation in uv photolysis of organic compounds in mixtures with ammonium compounds, 18: 23204(T) (JPRS-24164 (p.19-42))

Serotonin

see 5-Indolol, 3-(2-Aminoethyl)-

SERUMS

see also Blood Serum
analysis for bromine in human, spectrometric, 17: 17990
analysis for bromine-82, potassium-42, and sodium-24 simultaneously, method for, 18: 9998
analysis for calcium, copper, magnesium, and manganese, activation, 20: 16347
analysis for protein-bound iodine by automatic reaction rate method, 18: 1522
content in culture, effects of, on radiosensitivity of mammalian cells, 20: 16298
content of β-glucuronidase of carcinoma patients during radium therapy, 20: 43025
contents of bromine, iron, and zinc in human, 16: 20098
denaturation of BSA by slow neutron inelastic scattering, 20: 45268 (AD-638991)
effects of cancer radiotherapy on beta-glucuronidase activity, 16: 20258
effects of hyperimmune, on transfer of immunity to sarcoma I homografts in newborn mice, 19: 17574
effects of injection with cytotoxic, on gamma irradiated guinea pigs, 17: 38892
effects of irradiated, on liver catalase activity in mice, 16: 8606
effects of irradiated, on kidneys and liver in rats, 18: 11612
effects of radiophosphorus on denatured and whole, in rats, 19: 38368
effects on radiation midlethal dose killing effect in mice, 20: 33074
effects on radioinduced heme synthesis in peripheral blood, in hens, 16: 2893
iodine content in human, protein-bound, 16: 20331
preparation and metabolism of iodine-131 labeled albumins in rabbits and rats, 16: 2854
preparation of iodine-131-labeled sterile pyrogen-free human, 19: 40639
protective effects, from irradiated animals against radiation sickness in recipient, 16: 5222
protective effects against radiation sickness in guinea pigs, 18: 17651
protective effects on leptospirosis antibody formation in irradiated rabbits, 18: 25228
radiation effects on test reactions, in malignant tumors, 16: 4064
radiation effects on protein levels in rat, whole-body, 16: 20287
radiation effects on cattle, protection against, 17: 17943
radiation effects on globulin isoelectric point in cattle, 17: 17872
radiation effects on protein synthesis in, in mouse/rat chimeras, 17: 19843
radiation effects on electrophoretic pattern of proteins of, 17: 30411
radiation effects on proteins of, gamma, 18: 3582
radiation effects on proteins of, in Hiroshima bomb survivors, 19: 38377
radiation effects on properdin of human and bovine, uv, 20: 42823
radiosensitivity effects of, 17: 38895
radiosensitivity effects of Bogomoletz, 17: 38910
radiosterilization of antitoxin and toxoid, 16: 32684

SERVOMECHANISMS

see also Cybernetics
see also Feedback Systems
see also Laboratory Equipment
see also Reactor Control Rods
see also Remote-Control Equipment
aided tracking system, analysis of parameters in, 18: 15696 (SC-TM-366-63(72))
amplifier design for reactor control, 16: 6537 (DC-58-10-44)
analysis for power regulation in reactors, 16: 4990(T) (JPRS-10815)
analysis, use of computer techniques for, 16: 10383 (DC-58-4-128)
bibliography on hot gas servomechanism theory and technology, 16: 5434 (NP-11192)
control motor design for, 18: 478 (NP-13201)
description of hydraulic, for reactor control systems, 17: 36916(P)
design, 19: 36772
design and operation of acceleration-responsive switch, 17: 30843(P)
design and operation of fluid-circuit, 20: 8442 (NASA-CR-54758)
design and performance for Deep Water Isotopic Current Analyzer, 17: 34195(R) (JLI-2748-0-7)
design and performance of two-state, 17: 35260(R) (TID-19135)
design for automatic reactor control by moving detectors, 18: 1196
design for automatic control of light source position, 19: 24664(P)
design for continuous measurement of solid propellant burning rates, 20: 9131
design for control of power level in reactors, 16: 6099 (DCL-57-1-129)

design for gas-cooled reactor loading, 17: 13760(P)
design for high-precision Mössbauer spectrometer for constant-velocity scanning, 18: 5671
design for improved stowage, 17: 17480(P)
design for loading gas-cooled reactors, 17: 13759(P)
design for regulating magnetic fields, 17: 26253(P)
design for remote-control milling machine, 17: 4334(R) (IDO-16805 (p.36-43))
design for use in master-slave electric manipulators, 19: 2487
design of amplifier for shim rod, 16: 13284 (DC-59-1-23)
design of constant-spill, for Brookhaven AGS magnet power supply, 19: 30878 (BNL-9080)
design of core servicing mechanism for gas-cooled reactors, 18: 12820(P)
design of electro-pneumatic linear type actuator, 17: 339 (TID-16885)
design of electromagnetic repositioning, for precision balance, 17: 8560(P)
design of electromagnetic, for displacement of reactor control rods, 18: 6433(P)
design of electronically controlled manipulator, 16: 654
design of electronically controlled manipulator, 16: 3124
design of flexible, for electric master-slave manipulator, 19: 6038
design of, for control of Cosmotron flat-top beam spill-out, 17: 9631 (BNL-6424)
design of, for reactor loading, 17: 13753(P)
design of, for reactor control rod drive, 17: 26079
design of GEL-II "Handyman", 17: 23456 (59GL235)
design of high precision and velocity servomultiplier, 16: 4982 (NP-10731(p.126-8))
design of hydraulic, 16: 16493(P)
design of hydraulic, for control-rod positioning, 18: 3082
design of master-slave, with through-ceiling operation, 18: 385
design of Mobot Mark II, 16: 652
design of redundant, for reactor control, 18: 28996 (AEEW-R-283)
design of room-temperature pneumatic rack actuator, 17: 338 (TID-16884)
design of servomechanical function generator for kinetic reactor analog, 17: 1725
design of slow-speed saturating, with coulomb friction, (T), 19: 30481 (AEET/ED/SG/17)
design of solenoid-actuated step-by-step linear-motion, with gripper and load transfer magnet, 18: 10222(P)
design of transistorized system for master-slave electric manipulators, 16: 3125
development, for handling irradiated aircraft power plants, 16: 7624 (APEX-911)
development for high-energy accelerator requirements, 19: 47159 (BNL-9388)
development for modified Brookhaven AGS, 19: 28934 (BNL-8937)
development for radiological containment systems, 20: 4214
development for use in radiation-resistant pneumatic power systems for space vehicles, 17: 32208(R) (GDC-63-140)
development of fluid amplifier, 16: 10123 (APEX-666(Pt.2))
development of manipulators for high-energy accelerators, 20: 2551
development of restraint system for anti-G protection, 19: 46485 (CONF-640508, pp 210-23)
dynamics of, with backlash, 17: 22282(T) (JPRS-18823)
equations of, with moving detectors for reactor control, 18: 17263
failure modes of Automatic Distribution Control System, 18: 36758 (HW-76885)
for radioisotope scanning, 19: 17753
maintenance, guide for HTRE 1, 16: 9678 (XDC-55-11-101)
operation of, in DRAGON charging machine, 17: 28539
performance and stability in multichannel data–sampling process control systems, 16: 14858
performance characteristics for control rod positioning, 16: 15971
performance criterion for linear and type-0 and -2, 19: 30480 (AEET/ED/SG/16)
performance evaluation of gear type pneumatic servo motor combined with 4-way servo valve, 16: 10126 (DC-59-12-28)
radiation effects on, 17: 36347(R) (NARF-62-18P)
radiation effects on hydraulic, for space vehicles, 20: 11181
research facilities for, Casaccia, Italy, 20: 36540
research programs on reactor, 19: 33530(R) (RT/ING(64)-10)
use for correction of phase changes between deflectors in r-f separator, 20: 21467 (CERN-66-8)

Set Theory
see Topology

Settled Bed Reactors
see Pebble Bed Reactors

710 Reactor
see Systems for Nuclear Auxiliary Power

SEWAGE
see also Waste Disposal
see also Waste Processing
analysis for beryllium, colorimetric, 18: 9995
analysis for radioisotopes, spectrometric, 17: 36063
analysis for radioactive ruthenium, 18: 41357
cesium-137 content in treatment plant for, from fallout, 17: 16299
conference on water pollution research, London, Sept. 1962, 20: 20982
decontamination, 16: 25677
dilution and flow of, tracer studies on, 18: 24043 (INS-R-14)
dilution by sea water, tracer study, 16: 22500 (NS-7)
disposal of, review of, 18: 9743
disposal of, after nuclear attack, 19: 15788 (NP-14835)
disposal of, in radioisotope hospital wards, 20: 38790
disposal of, tracer studies of, 20: 2201
distributions in large natural waters from planned outlets, tracer studies of, 17: 25534
effects of carbon-14 and strontium-90 on anaerobic digestion, 17: 36064
flow through treatment plants of, tracer study, 20: 5432
gamma-radiation tagging of, in treatment plants, 17: 4371 (TID-16466 (Pt.B))
labeling using gold-198, 20: 12545(R) (PAEC(A)AR651)
monitor system for, 17: 36039(R) (UCRL-7355)
monitoring equipment and methods, direct continuous, 16: 16613
monitoring for carbon-14 activity in, from surface waters, 18: 14310
monitoring of, using labeled bacteria, 18: 11565
neutralization of radioactive, 16: 2065(T) (JPRS-10498)
processing of, effects of strontium-89 on nitrifying bacteria in biological, 18: 27732
radiation control of *Entamoeba histolytica* in, 20: 5366
radiation effects on sedimentation, 16: 15047(R) (TID-15389)
radiation effects on sedimentation of, 17: 2007(R) (TID-16998)
radiation effects on sedimentation of, 17: 16057(R) (TID-18262)
radiation effects on colloidal properties and sedimentation of, 18: 5362(R) (COO-275)
radiation effects on, 18: 17612
radiation effects on sedimentation and alkylbenzenesulfonate decomposition in, gamma, 19: 6223
radiation effects on growth of microorganisms in, 19: 24196
radiation effects on growth of microorganisms in, 19: 24197
radiation monitoring in Bonn and Cologne, 19: 42665
radioactive contamination of, hygienic aspects of, 18: 18106
radioactive processing of, 19: 38288
radioactivity, 18: 33805(R) (NIRS-2(p.57-67))
radioactivity, from Los Angeles County, Calif., 16: 29249 (TID-16466)
radioactivity from fallout in sludges of, in Exeter, England, 19: 36723
radioactivity in, device for detection and measurement of, 17: 12565
radioactivity in disposal systems for, from fallout and industrial and medical wastes, 18: 18090
radioactivity in sludge from, in Japan in 1964, 20: 29455
radioactivity of, due to fallout, 20: 5432
radioactivity of, effects of fallout cesium-137 and strontium-90 on, 20: 23374(R) (NIRS-4, pp 81-7)
radioactivity of, from radioisotope hospital wards, 20: 38790
radiological monitoring of, 19: 36726
separation of radioactive materials from, by adsorption by peat soils, 19: 22412
sludge density measurement, 17: 8672(P)
sludge density measurements in, configuration effects on radiometric gages for, 19: 36595
sterilization of, use of heat and radiation from reactors for, 17: 23542 (AD-286432)
tracer techniques for determining coliform microorganisms in, 18: 29181
treatment by activated sludge plants, effects of radioisotopes on, 20: 218(R) (STI/DOC/10/42, pp 1-22)
treatment of radioactive, by oxidation, 18: 19454

SEWAGE SYSTEMS
construction for waste-solution discharge, into Escaut River in Belgium, proposal for, 20: 22515(T) (ORNL-tr-965)
flow through treatment plant, tracer study, 20: 5432
mixing of radioactive wastes in, 19: 36726
radiation doses received by sewer workers, calculation of, 17: 36061
radioactive waste disposal in, hazards from, 20: 36533 (BMWF-FBK-66-04)
radioactive waste discharge in municipal, hazards from, 20: 41217

SEX
effects of paternal irradiation on ratio of, in swine, 20: 45362(R) (TID-23311)
effects of, on critical organ exposure in patients undergoing fluoroscopy, 20: 43050
effects on behavior and learning ability of rats irradiated *in utero*, 19: 38361(R) (TID-21951)
effects on calcium-45 elution in rat blood plasma, 18: 27038
effects on ecology of Dover sole and sablefish, 20: 24831(R) (RLO-1731-5)
effects on human blood picture, 20: 6810

effects on incidence of proton-induced tumors in rats, 20: 6885
effects on learning capacity of Rhesus monkeys, 20: 92
effects on organ weight in man, 20: 20374
effects on radioinduced and spontaneous leukemia in mice, 20: 22738
effects on serum iodine extractable with butanol in Japanese children, 20: 6832
frequency of liver metastases from Yoshida ascites sarcoma in male and female rats, 20: 42962
radiation effects on, of viviparous lizards exposed while embryos, x, 20: 5324
radiation effects on, of mealy bugs, 20: 12715
radiation effects on ratios of rat, prenatal exposure, 20: 28952
radiation effects on *Ascaridia galli*, x, 20: 42968
radiation effects on ratios of, in frogs, 20: 45256
radioinduced mutation in Ecballium for reversal of, fast-neutron, 20: 8690
radiosensitivity differences in chickens depending on, γ, 20: 40693
radiosensitivity effects of, in hamsters, 20: 1676
radiosensitivity effects on leukemogenesis in mice, 20: 5367
ratio in offspring of x-ray technicians in Japan, 19: 26598
ratio of offspring of women irradiated during pregnancy, 20: 10657
Sex Hormones
see Gonadal Hormones
SEXIPHENYL
properties of methyl-, and methoxyl-, as scintillator solute, 16: 31634
synthesis and properties, 17: 37248 (EUR-295.f)
SF MATERIALS ACCOUNTING
AEC audit of, 18: 1951 (IDO-16925(p.111-18))
analytical methods for plutonium and uranium in nuclear fuel cycle, handbook on, 18: 8283 (TID-7029)
Atomics International application of statistical techniques, 16: 3267 (TID-7615(p.7-13))
calorimetry applications in, 17: 33434 (TID-7660(p.166-95))
chemical uranium bias check program for, 17: 33429 (TID-7660(p.112-19))
coding and numbering systems in, 17: 33425 (TID-7660(p.65-71))
computer applications in, 17: 33421 (TID-7660(p.34-7))
computer applications in, 17: 33422 (TID-7660(p.38-41))
computer processing of uranium core data at Hanford, 18: 43130 (TID-7700(p.85-97))
conference on, Chicago, Oct. 3 to 5, 1962, 17: 33417 (TID-7660)
conference on management of nuclear materials, Idaho Falls, Idaho, Oct. 16 to 18, 1963, 18: 3399 (IDO-16925)
control of uranium fuel element fabrication, systems for, 19: 39130 (RFP-507)
control system development, 16: 3269 (TID-7615(p.22-56))
data processing by random-access electronic equipment, 18: 43131 (TID-7700(p.98-109))
data processing in, 16: 3277 (TID-7615(p.128-9))
description of automated accounting system at Hanford, 17: 41327 (HW-SA-3163)
equipment and measurements for, of uranium compounds, 20: 43065 (GAT-T-1403)
in coating wastes, 17: 33431 (TID-7660(p.133-46))
in EBR-II fuel cycle, 17: 33420 (TID-7660(p.20-33))
management by reactor operators, 17: 33269
management conference, 16: 3265 (TID-7615)
manual for, 17: 7657 (IDO-16817)
manual for NRTS, 17: 18326 (IDO-16846)
methods, 17: 33418 (TID-7660(p.1-5))
methods for inventories and materials management at Albuquerque, 16: 3275 (TID-7615(p.120-4))
methods for, review of, 19: 18210
methods of, in fabrication of uranium dioxide powders, 17: 33419 (TID-7660(p.6-19))
methods of, review of, 18: 1950 (IDO-16925(p.101-9))
methods of, use of binomial distribution in, 18: 2145 (IDO-16925(p.67-75))
methods of, using automatic data processing system, 18: 1949 (IDO-16925(p.41-8))
methods of, at Windscale New Separation Plant, 20: 20830
methods of, review of UKAEA, 20: 22528
nuclear materials control system development, 17: 37015(R) (WCAP-6015)
nuclear materials automated accounting system used at Hanford, 18: 29812 (HW-SA-3546)
procedures for, in fuel processing, 16: 25479 (ORNL-TM-288)
procedures for Kilorod program, 17: 39504 (ORNL-TM-675)
programs for, AEC and private, 17: 33442
punched-card machine method, 16: 11353 (LA-2662)
ramjet propulsion program, 16: 3266 (TID-7615(p.1-6))
ratio method for plutonium, evaluation, 16: 3271 (TID-7615(p.65-77))
report preparation, IBM equipment in, 16: 3276 (TID-7615(p.125-7))
safeguards, definition and history, 16: 3268 (TID-7615(p.14-21))
sampling and weight control in, of uranium hexafluoride, 20: 43062 (CONF-661011-1)
sampling of enriched uranium hexafluoride for analysis, 19: 36230 (K-P-3248)
techniques used in Y-12 plant, 18: 43132 (TID-7700(p.110-19))
use of IBM 650 and 1410 computers in Goodyear gaseous diffusion plant, 18: 43129 (TID-7700(p.72-84))
SFR
see Submarine Fleet Reactor
SGHWR
see Steam Generating Heavy Water Moderated Reactor
SGR
see Sodium Graphite Reactors
Shadow Shielding
see Gamma Shielding
Shadowgraph Photography
see Spark Shadowgraph Photography
SHALE DEPOSITS
uranium occurrence in, in Japan, 19: 9396
waste disposal at depth of 900 ft in, equipment for, 19: 21753
SHALE DEPOSITS (INDIA)
geochemistry at Nagarjunasagar dam site, 16: 27441
SHALES
see also Bituminous Shales
see also Black Shales
see also Carbonaceous Shales
see also Oil Shales
age determinations on, radiogenic strontium effects on rubidium-strontium, 18: 3988(R) (NYO-10517(p.55-64))
age estimation of, rubidium–strontium method for, 17: 3176
age of Michigan, rubidium-87/strontium-86 estimation of, 20: 45916(R) (MIT-1381-12)
analysis for beryllium, fluorometric, 17: 4698
analysis for gold, activation, 18: 27326
analysis for isoprenoid alkanes, methods for, 20: 16633 (UCRL-16605)
carbon, potassium, thorium, and uranium content in black, from South Wales coalfield, 18: 37416
ion exchange properties for cesium in waste solutions, 16: 12798
neutron emission by, 18: 16209
oil recovery from, use of nuclear explosions for, 20: 16589 (UCRL-12224-T)
potassium, thorium, and uranium distribution in Cretaceous Mancos, 17: 4696
potassium-39 to -41 ratios in, 19: 28551
radioactive waste disposal in, by hydraulic fracturing, 19: 12859
radioactive waste disposal in, hydraulic-fracturing method for, 20: 28856
radioactive waste disposal in, by hydraulic fracturing, 20: 38538
radioactivity in sedimentary, in gas and oil fields in Japan, 17: 27579
radioactivity of siliceous, elemental content dependence of, 17: 39272
radioisotope movement in Conasauga, 19: 8676(R) (ORNL-3697 (p.54-61))
rare earth abundance and distribution in, 20: 23278
retorting of oil-bearing, in chimneys from nuclear explosions, 20: 33441
separation of aluminum, iron, and uranium from, by chloride volatility, 16: 5416(P)
separation of thorium from, method for chemical, 19: 46190
sorption of cesium and strontium from Purex-type wastes by, 16: 11343 (ORNL-TM-127)
sorptive properties for strontium, 18: 43091(R) (ORNL-TM-830)
sorptive properties of Conasauga, for strontium, 19: 7617(R) (ORNL-3697(p.49-53))
uranium distribution between organic and mineral parts of uraniferous, 17: 14488
waste disposal in, by hydraulic fracturing, 17: 39297(R) (ORNL-3492 (p.13-18))
waste disposal in, by hydraulic fracturing, 19: 8674(R) (ORNL-3697 (p.10-19))
waste disposal in, hydraulic fracturing methods for, 20: 28857
SHAPED CHARGES
see also Explosions
use in reactor poisoning, 18: 24876 (APEX-142)
SHE (Semi-Homogeneous Experiment)
see Critical Assemblies
SHEEP
analysis of organs, tissues, and wastes of, for plutonium, tracer technique for, 19: 4079
analysis of wool fleece for radioactivity, 17: 23025
body water content and turnover in, tracer study, using T_2O, 20: 40541(R) (UCD-34P104-3)
cadmium metabolism in, effects of zinc on, 18: 41039(R) (HW-80500 (p.140-3))
cadmium metabolism in, tracer study, 19: 8739 (HW-SA-3746)
cadmium-115 secretion in milk of, 20: 10527(R) (BNWL-122, pp 94-8)

calcium metabolism in, 18: 11559(R) (TID-19977)
calcium-45 uptake and specific activity in plasma and urine in, 19: 31736
carbon-14 respiration in, apparatus for studies on, 19: 4435
cerium-144 toxicity in, following chronic intravenous injection, 20: 32907(R) (ORO-648, pp 62-70)
cerium-144 toxicity in, 20: 32967(R) (ORO-648, pp 36-55)
cerium-144 toxicology in, 19: 45759(R) (ORO-631, pp 77-82)
cesium content, 17: 30268
cesium-137 contents, 17: 34173
cesium-137 dosimetry and metabolism in male, 16: 17409 (HW-72511)
cesium-137 dosimetry, use of whole-body dose as indicator of gonad dose, 16: 20105
cesium-137 content of rumen of, effects of cesium content in diet, 20: 10520(R) (BNWL-122, pp 64-6)
cesium-137 content in browsing, effects of food-chain on, 20: 40541(R) (UCD-34P104-3)
cesium-137 content in Icelandic, 1958 to 1964, 20: 45908
cesium-137 metabolism in, 18: 41035(R) (HW-80500(p.102-8))
cesium-137 metabolism in adults and lambs, after oral administration, 19: 40334
cesium-137 retention in, 20: 42739(R) (COO-1339-3)
cesium-144 metabolism, 19: 3835(R) (ORO-625(p.64-9))
development in, effects of maternal nutrition on embryonic and fetal, 18: 38775(R) (ORO-624)
distance traveled by, on winter range, 19: 35870 (ORNL-P-1340)
dosimetry of gamma radiation from ingested cesium-137 in, performance of *in vivo* thermoluminescent detector for, 20: 11091(R) (BNWL-122, pp 67-72)
ecology of, on winter range, 19: 35870 (ORNL-P-1340)
effects of chronic, low-level ingestion of iodine-125 and -131 in, 17: 35295(R) (HW-76000(p.45-55))
effects of ingested cesium-137 in, pathological, 19: 40334
effects of injected bone marrow from, in irradiated mice, 18: 43324
effects of irradiated blood transfusions on tumor induction in, 20: 32968(R) (ORO-648, pp 56-61)
enzyme activity in intestinal mucosa cells of, 20: 32907(R) (ORO-648, pp 62-70)
erythrocyte life span in, tracer study, 19: 38343
erythrocyte life span in, tracer study, 19: 45759(R) (ORO-631, pp 77-82)
erythrocyte life span in, tracer study on, 20: 32907(R) (ORO-648, pp 62-70)
etiology and pathology of glomerulonephritis in, 20: 42855(R) (TID-23203)
fallout fission product contamination of, 18: 38993 (HW-SA-3693)
fallout uptake by, effects of biological and environmental factors on cesium-137 and strontium-90, 20: 20388 (SAN-34-2)
fatty acid metabolism in digestive tract of, 18: 15708 (TID-20218)
fission product metabolism in, 18: 11645(R) (ORO-614)
fission product metabolism by, after fallout exposure, 19: 11390 (AWRE-T-57/58)
fission product metabolism in, 20: 18188(R) (ORO-635)
forage intake by grazing, 19: 35869 (ORNL-P-1339)
function tests in, use of iodine-131-hippuran renogram in, 18: 41274(R) (HW-80500(p.167-72))
gamma and x-ray dosimetry determination using phantoms, 20: 38625
gastrointestinal absorption of magnesium, tracer study, 17: 5737
gastrointestinal function in, preparation of chromium-51-labeled EDTA for studies on, 19: 20026
immune reactions of, to irradiated and normal nematodes, 18: 43231 (TID-21203)
immune reactions to irradiated pantothenic acid in, 19: 8914
immunization against *Dictyocaulus filaria*, using irradiated larvae, 19: 42275
immunization against *Dictyocaulus fileria*, using γ or x irradiated larvae, 20: 8653
iodine metabolism, tracer study, 17: 23020
iodine metabolism in tissue cultures of thyroid cells of, 18: 43194
iodine-125 and -131 uptake by thyroid of, effects of administration mode on, 18: 8084
iodine-131 content of thyroids, Egypt, 1956 to 1957, 16: 20125
iodine-131 content of thyroid of, after grazing on contaminated forage, 17: 35297(R) (HW-76000(p.60-2))
iodine-131 content of thyroidal lymph in, 17: 38721
iodine-131 content in tissues of, long-term ingestion study, 20: 10516(R) (BNWL-122, 49-51)
iodine-132 uptake and distribution in organs of lactating, 18: 8085
iron-59 content in young, after natural exposure, 20: 14243(R) (TID-22626)
iron-59 metabolism in, 18: 11559(R) (TID-19977)
irradiation of, holding apparatus for, 18: 12759(P)
lipid function in membranes of, 20: 16160 (UCRL-14739(Pt.2))
lipid metabolism in, 18: 9783(R) (TID-20028)
lipid metabolism in, tracer studies on, 18: 33213 (ST1/DOC/10/28(p.79-103))
liver function tests in, using iodine-131-labeled rose bengal dye blood-clearance method, 17: 35316(R) (HW-76000(p.174-7))
liver function tests in, 19: 40350 (HW-SA-3723)
meat composition of lambs, evaluation by potassium-40 measurements in carcasses and live animals, 18: 31070
metabolism in, tracer studies of, 20: 12609
metabolism of gonadal hormones in ovaries in, tracer study on, 20: 38547(R) (NYO-918-15)
milk production by, tracer study, 20: 10517(R) (BNWL-122, pp 52-4)
molybdenum-99 metabolism in, 20: 32907(R) (ORO-648, pp 62-70)
mucopolysaccharide content in kidneys and intestinal mucosa cells of, 20: 32907(R) (ORO-648, pp 62-70)
neutron dose measurements in, 18: 38728
ova transfers in, effects on offspring, 19: 8942
parasitic blood loss in, use of iron-59 in measurement of, 18: 21752
phosphorus metabolism in, tracer studies, 16: 12862(R) (TID-15299)
phosphorus metabolism in lambs, 18: 9776 (TID-20003)
physiology of digestion in, 20: 40541(R) (UCD-34P104-3)
placental transfer of fluorine-18 in, 19: 8761
placental transfer of iodine-131 in pregnant, 19: 12942
plutonium deposition and retention in, inhaled, 19: 36697 (AWRE-O-29/65)
potassium content, 17: 30268
potassium-40 content in tissues of, internal radiation dose from, 20: 42940
potassium-40 measurements in, for use as growth index, 20: 42739(R) (COO-1339-3)
potassium-42 metabolism in, 18: 41035(R) (HW-80500(p.102-8))
praseodymium-144 toxicity in, following chronic intravenous injection, 20: 32907(R) (ORO-648, pp 62-70)
protection against fallout, 19: 46700
radiation dose measurements in phantoms of, gamma and x, 19: 36823 (USNRDL-TR-842)
radiation dose to gastrointestinal tract in, from ingested insoluble radioisotopes, 18: 25142
radiation dosimetry of cesium-137 in, use of thermoluminescent detector for, 20: 5285 (BNWL-SA-172)
radiation dosimetry of cesium-137 in, use of thermoluminescent detector for, 20: 11091(R) (BNWL-122, pp 67-72)
radiation effects on Purkinje fibers of heart, 16: 16279
radiation effects on renal transplantation in, x, 17: 30380
radiation effects on, mixed neutron and gamma, 18: 8109 (RTD-TDR-63-3077)
radiation effects on, prolonged or single-exposure iodine-131, 18: 8159
radiation effects on reproduction in, prolonged or single-exposure iodine-131, 18: 8160
radiation effects on thyroid of, iodine-131 and x, 18: 8162
radiation effects on, high-level gamma, neutron, or mixed, 18: 11645(R) (ORO-614)
radiation effects on reproduction of, 18: 11645(R) (ORO-614)
radiation effects on mouse immunity to erythrocytes of, continuous gamma, 18: 19623
radiation effects on testes of, x, 18: 23338
radiation effects on reproductive potential in, x, 18: 23342
radiation effects on plasma iron clearance time in, 18: 31179
radiation effects on lymph nodes and lymphocyte production in, x, 18: 35352
radiation effects on cerebrospinal fluid production in, 18: 38775(R) (ORO-624)
radiation effects on morphological development in young, prenatal, 18: 38775(R) (ORO-624)
radiation effects on, pathological, 18: 38775(R) (ORO-624)
radiation effects on, fission-neutron and x, 18: 41222
radiation effects from ingested iodine-131 in ewes and lambs, 18: 41022(R) (HW-80500(p.1-5))
radiation effects on, 19: 3891(R) (ORO-625(p.1-27))
radiation effects on reproductive system of, 19: 3892(R) (ORO-625 (p.28-37))
radiation effects on, pathological, 19: 3893(R) (ORO-625(p.38-55))
radiation effects on, physiological, 19: 3894(R) (ORO-625(p.56-63))
radiation effects on, air and *in vivo* dosimetry of gamma and neutron, 19: 8951
radiation effects on limb development of fetuses of, exposed *in utero*, 19: 15096
radiation effects on molybdenum-99 metabolism in, 19: 45759(R) (ORO-631, pp 77-82)
radiation effects on tungsten-185 metabolism in, 19: 45759(R) (ORO-631, pp 77-82)
radiation effects on, delayed pathological, 19: 45812(R) (ORO-631, pp 1-35)
radiation effects on, pathological, 19: 45814(R) (ORO-631, pp 45-66)
radiation effects on, physiological, 19: 45815(R) (ORO-631, pp 67-76)

radiation effects on copper and zinc content and enzyme activity in blood serum of, 20: 16222 (AFWL-TR-65-112)
radiation effects on, pathological γ and neutron, 20: 18188(R) (ORO-635)
radiation effects, 20: 18198
radiation effects on blood–brain barrier permeability in, neutron, 20: 20489
radiation effects on, γ, 20: 31026 (AD-633606)
radiation effects of prenatal exposure on embryos of, fast neutron, 20: 32966(R) (ORO-648, pp 26-35)
radiation effects on mortality of, patterns in, 20: 32967(R) (ORO-648, pp 36-55)
radiation effects on Dische-positive material in blood and urine in, gamma, 20: 36604
radiation effects on, fission-neutron, 20: 38637
radiation hazards to, from fallout in event of nuclear war, 17: 34184
radiation injuries, correlation of systemic and hematological recovery, 17: 15804 (USNRDL-TR-606)
radiation injuries of liver of, induced by injected neptunium-237, 19: 40350 (HW-SA-3723)
radiation lethal dose determinations for, fission neutron, 18: 31228
radiation lethal dose determinations for, x, 18: 31228
radiation lethality in, dose determinations for γ and x, 20: 20487
radiation sickness in, diagnosis of, 20: 128
radiation syndrome in, compared to other large animals, 20: 8729
radioactivity from cesium-137 and strontium-90 in Faeroe Islands, 1964, 20: 7320 (RISO-108)
radiodiagnosis of amniotic fluid in pregnant, by isotope dilution and scanning, 20: 45527
radioinduced skeletal anomalies in, exposed *in utero*, γ, 20: 14337
radionuclide transfer from plasma to milk in, 17: 35304(R) (HW-76000(p.98-108))
recovery from radiation injury as evaluated by split-dose technique, 20: 42996
rubidium-86 metabolism in, 18: 41035(R) (HW-80500(p.102-8))
selenium metabolism in, tracer study of, 18: 27060
selenium metabolism in, tracer study of, 19: 6969
selenium-75 uptake by blood cells of, 18: 3468
selenium-75 metabolism in, 19: 45759(R) (ORO-631, pp 77-82)
selenium-75 uptake by milk of, 18: 17426
sodium content, 17: 30268
spleen of, protective factor for radioinduced mouse leukemia in, 18: 27222
strontium and strontium-90 contents in bone ash from ewes and fetuses, 16: 17430 (A/AC.82/G/L.756)
strontium-90 distribution in bones, 17: 5741
strontium-90 content in bones of, 18: 33240
strontium-90 content in bone tissues in, 19: 15001
strontium-90 content in bones of Australian, 1961 through 1963, 20: 31403
strontium-90 content in browsing, effects of food-chain on, 20: 40541(R) (UCD-34P104-3)
strontium-90 content in Icelandic, 1958 to 1964, 20: 45908
strontium-90 distribution in bones of, in Portugal, 20: 22540
strontium-90 metabolism in fetuses and newborn, after intravenous or oral administration to mother, 19: 40331
strontium-90 metabolism in, 19: 45759(R) (ORO-631, pp 77-82)
strontium-90 metabolism as phytate or chloride in, 20: 35215
strontium-90 metabolism by, 19: 3835(R) (ORO-625(p.64-9))
strontium-90 toxicity in, 20: 35318
strontium-90 uptake by, compared with calcium, 18: 31104
tellurium-127 metabolism in, 19: 45759(R) (ORO-631, pp 77-82)
tellurium-132 uptake and distribution in organs of lactating, 18: 8085
thyroid tumors induced in, by chronic ingestion of iodine-131, 17: 5768
thyroid uptake of iodine-125 by, 17: 35296(R) (HW-76000(p.56-9))
toxic effects of chronic ingestion of low levels of iodine-131 by, 17: 40482 (HW-SA-3085)
toxic effects of neptunium-237 in, 17: 35292(R) (HW-76000(p.31-5))
transfer to transuranic elements from plasma to milk, tracer study, 17: 10326
transplantation of ovaries in, method for auto-, 20: 38547(R) (NYO-918-15)
tungsten-185 metabolism in, 20: 32907(R) (ORO-648, pp 62-70)
uptake of cerium-144, cesium-137, and strontium-90, 16: 9907
uptake of iodine-131-labeled triiodothyronine by, 19: 27934
uranium content in meat from grazing, 19: 21830
urea nitrogen content in blood of, 20: 40541(R) (UCD-34P104-3)
vaccine for lungworm in, preparation from irradiated larvae, 19: 43750
zinc metabolism in, effects of cadmium on, 18: 41039(R) (HW-80500 (p.140-3))
zinc metabolism in, tracer study, 19: 8739 (HW-SA-3746)
zinc metabolism in, effects of cadmium on, 19: 5604 (HW-SA-3729)
zinc-65 uptake and distribution in, dosimetry of, 16: 28712 (HW-SA-2338)
zinc-65 secretion in milk of, 20: 10527(R) (BNWL-122, pp 94-8)

SHEETS
see also Films
see also Foils
see also Plates
see also Reactor Fuel Sheets
angular distribution of crystal planes in, pole figure facility for measuring, 20: 29083(R) (UCRL-14767)
conference on behavior of sheet materials, New York, August 16 to 19, 1960, 16: 6696 (NP-11199)
cuttability of thin, tool activation for determination of, 19: 4561
development of refractory alloy, 17: 6517 (MAB-188-M)
effects of pretreatment on adherence of ground-coat porcelain enamel and surface roughness of metal, 18: 16457(T) (AI-Trans-41)
electromagnetic field propagation through infinite, 17: 24054 (SCR-623)
electromagnetic wave scattering by turbid matter in plane, 17: 9014(T)
extrusion from compacted tungsten powders, equipment and methods for, 20: 39352 (BM-RI-6817)
fabrication of lead, methods for, 18: 32953
fabrication of metal strips, 19: 30711(P)
fabrication of projections on Zircaloy, 19: 28773 (BMI-X-10096)
fabrication of refractory metal, methods and problems of, 18: 34103
forming of refractory metal, methods and problems of, 18: 34107
gamma transport in finite, Monte Carlo analysis of, 18: 4684 (NRL-5981)
heat flow in two-layer composite, 17: 1619
hole detection in moving, 18: 22236(P)
irradiation of, facility for, 19: 30620(P)
magnetization of iron, by step-increased magnetic fields, (T), 19: 25625(T) (AI-Trans-84)
neutron transport in infinite, operator equations for, 17: 9485
production from refractory metals, development of methods for, 16: 3420 (DMIC-161)
properties of RMSP tungsten, 18: 35979(R) (AD-437255)
radiation processing of, design of apparatus for, 19: 26737(P)
refractory metal, evaluation test methods for, 17: 22095 (MAB-192-M)
rolling techniques for refractory materials, 17: 6597(R) (DMIC-176)
testing of metal, electromagnetic pulse method for, 19: 28523(P)
thickness control using radiometric gages, 20: 23548(T) (AEC-tr-6466/1, pp 124-7)
welding by vertical ascending method, stress distributions from, 18: 35973(T,R) (EURAEC-1023)
welding of, Hanford procedures for, 19: 20524 (TID-20625(Vol.IV)(Rev.I))
welding to tubes in boiler, technique for internal, 19: 24951 (NAA-SR-8541)
Sheldon Nuclear Facility
see Hallam Power Reactor
Shell Nuclear Models
see Nuclear Models (Shell)

SHELLS (GEOMETRY)
acceleration of spherical, analysis of steady-state, 18: 36905 (UCRL-13063)
analysis and design of, 19: 32048(R) (NP-15073)
analysis of bellows, design charts and formulas for, 18: 36886 (NAA-SR-9848)
analysis of cylindrical, clamped along oblique contour, 18: 21733(T) (ORNL-tr-19)
behavior of underwater, reactor containment, 16: 12800 (BRL-1153)
blast effects on cylindrical, 18: 12280 (ASD-TDR-62-475)
blast effects on reactor containment vessel models, internal, 18: 17258 (BRL-Memo-1530)
blast effects on thin water-submerged, 18: 39403 (BRL-1231)
book: *Non-Classical Shell Problems*, 19: 24648
book: *Post-Buckling Behavior of Cylindrical Shells*, 18: 29814(T) (NASA-TT-F-90)
buckling of spherical, 18: 37306 (TID-20950)
bursting strength of cylinder with hemispherical cap, 18: 35655 (IITRI-528-20)
conference on simplified calculation methods, 17: 16192
contour specification in, computer program in, 18: 13372 (SCL-TM-64-26)
contours for toroidal, method for determining meridional, 18: 16164 (ERR-AN-174)
creep effects in pressurized copper, analytical method for, 20: 39391 (CONF-660629-1)
creep in thin spherical, effects of temperature on primary, 19: 18088
creep-buckling of thin metal, at 1500°F, 20: 4299(R) (ORNL-2711)
creep-buckling of hemispherical copper, 20: 4299(R) (ORNL-2711)
deflection and stresses in thin cylindrical, measurement, and theory, 16: 7629 (DC-59-7-129)
deformation and stress stability of shallow spherical, nonlinear, 19: 21620
deformation of cylindrical, from internal static pressure loadings, 17: 39227
deformation of rigid-plastic hollow, effects of axial tension and external pressure on, 20: 31335

deformation, stability, and vibration of, bibliography on, 20: 4079 (UCRL-13187)
deformations and stability of shallow and deep spherical, 16: 16472 (AROD-2465.1)
design and load carrying capacity of shallow anisotropic plastic, 19: 28473
design and testing of prestressed concrete spherical, for containing explosions, 18: 8462 (LA-2901)
design of minimum-weight closure heads for pressure vessels, 17: 6211
dynamic buckling of elastically supported, under dynamic axial load and lateral pressure, 19: 26483 (SCL-DR-65-28)
dynamic loading of cylindrical, (T), 19: 10691 (SCL-DR-64-113)
dynamic response of axisymmetric, 18: 43122 (SCL-DR-64-64)
dynamic response of cylindrical, to lateral loads, (T), 19: 45711 (SC-TM-65-81)
elastic behavior of, 17: 13706
elastic properties, 20: 4299(R) (ORNL-2711)
elastic response of thin spherical, to internal explosions, 18: 8461 (BRL-Memo-1520)
elastic wave propagation in open-end cylinder, analog model of, (T), 20: 3630 (SC-DC-65-1697)
electromagnetic field propagation into, 17: 24054 (SCR-623)
gas flow along cylindrical, supersonic streamlined, 19: 13591
heat transfer analysis of rotating spherical, in plane-wave radiation energy flux, 19: 11351 (UCRL-7960)
heat transfer from internally heated thin, convective and radiative, 16: 25536
impact effects on spherical, research program on, 20: 463(R) (SC-DC-65-1634)
impact testing of spherical, 18: 20195(R) (SC-DC-64-383)
impact testing of spherical, development of equipment and methods for, 18: 29813(R) (SC-DC-64-1034)
impact testing of spherical, development of equipment and methods for, 19: 557(R) (SC-DC-64-1509)
impact testing of spherical, equipment and methods for, 19: 26482(R) (SC-DC-65-1305)
limit pressure of radial nozzle in spherical, 19: 9288 (WAPD-T-1636)
nozzles in pressurized spherical, stress at, 20: 43467 (TID-23343)
nozzles in spherical, flexibility of, 20: 43468 (TID-23344)
plastic deformation of membrane, under internal pressure, 18: 1185(R) (ARF-8262-3)
plastic deformation of dynamic- and static-loaded, 18: 7865(R) (TID-19871)
plastic deformation of dynamic- and static-loaded, 18: 32980(R) (IITRI-8262-6)
plastic instability of cylindrical, under internal pressure, 19: 556 (IITRI-528-19)
radiation effects on strength of, 17: 6754(T) (FTD-TT-62-719)
radiation effects on plastic expansion of spherical, 19: 14106
response of buried aluminum cylindrical, to quasi-static overpressures, 19: 20136 (AFWL-TDR-64-13)
response of thin-walled cylindrical, to dynamic internal pressures, 17: 40955 (CONF-39-100)
response to high-intensity dynamic pressure pulse loading, 16: 12209 (AFSWC-TR-61-31(II))
shock effects on elastic cylindrical, (T), 20: 23267 (AD-627597)
stiffness of laterally loaded conical, (T), 19: 45712 (SC-TM-65-82)
strain energy stored in cylindrical, from tension wires, analysis, 19: 36580 (UCRL-13160(Pt.2))
strength of spherical, subjected to internal pressure, effects of time factor in, 19: 13559(T) (RISLEY-Trans-280)
strength of steel, for reactor containment, 20: 30813
stress analysis in axisymmetric thin, computer program for, 17: 6507
stress analysis in perforated cylindrical, subjected to boundary and surface forces, 18: 18453 (IMM-NYU-320)
stress analysis of joined revolving, computer program for, 16: 29304 (KAPL-M-EC-19)
stress analysis of cylindrical, computer program for, 16: 30514 (KAPL-M-EC-20)
stress analysis of thin spherical, 17: 16664 (UCRL-13064)
stress analysis of spherical, with rigidly reinforced opening, 18: 1185(R) (ARF-8262-3)
stress analysis of, computer program for, 18: 1882 (KAPL-2292)
stress analysis of cylindrical and spherical, with rigidly reinforced openings, 18: 7865(R) (TID-19871)
stress analysis of hemispherical lightweight cellular core with flexible support shell, 18: 8021 (UCRL-7473)
stress analysis of, computer program for, 18: 13987 (WAPD-TM-398)
stress analysis of filament-wound laminated structures, 18: 26115 (SCL-TM-64-53)
stress analysis of cylindrical and spherical, with rigidly reinforced openings, 18: 32980(R) (IITRI-8262-6)
stress analysis of concentric spherical, under heating, 18: 33755
stress analysis of spherical, with rigidly reinforced opening, 19: 1825(R) (IITRI-578P22-11)
stress analysis of axisymmetric thin, subjected to pressure and high temperatures, 19: 9282 (LAMS-3083)
stress analysis of, with rigidly reinforced openings, 19: 14774(R) (IITRI-578P22-12)
stress analysis of axisymmetric intersecting, 19: 36582
stress analysis of cascade spherical, 19: 38170 (AFOSR-65-0315)
stress analysis of axisymmetric thin, 19: 44219 (ACF-8)
stress analysis of, derivation of equations for, 20: 4100 (BW-67-2(a))
stress analysis of spherical, from impacts, (T), 20: 26589(R) (SC-CR-66-2025)
stress analysis of shallow visco-elastic, with elastic reinforcement, (T), 20: 25591
stress analysis of circular cylindrical, with oblique edge, (E/T), 20: 27124
stress and deflection of axisymmetric thin, computer program for calculating, 19: 1948 (ACF-2)
stress and strain analysis for pyrolytic carbon spheres, 18: 27964 (ORNL-3553)
stress distributions in, 20: 4999(R) (ORNL-2599)
stress distribution in heated spherical, theoretical analysis, 20: 36957 (DRI-2327)
stress in thick-walled long conical, for nozzle design, (T), 20: 30928
stress patterns of attachment region of hemispherical, with radially attached nozzles, 19: 44144 (TID-22134)
stress-strain distribution in magnesium and steel lap-jointed thin, 18: 18355 (UCRL-7304)
stresses on nozzles attached to, analysis of, 19: 25761(R) (ORNL-3731(p.229-35))
structural analysis of cylindrical and spherical reactor-containment, (E/T), 19: 8574 (IITRI-578P22-9)
structural stability of toroidal, bibliography on, 18: 5440 (AD-423823)
support of sphere by tension wires in cylindrical, model studies, 19: 36581 (UCRL-13160(Pt.3))
thermal loading of cylindrical, dynamic response of, (T), 20: 18852 (SCL-DR-65-144)
thermal stability of thin-metal, 20: 4999(R) (ORNL-2599)
thermal stress analysis of, 16: 28646(R) (ORNL-2247(Pts.1-5))
thermal stress analysis, 17: 13708
thermal stress analysis of conical, 19: 30350
thermal stress and temperature distributions in plane, for reactors, (T), 19: 21618
thermal stress and temperature distributions in cylindrical, (T), 19: 21619
thermal stresses in cylindrical, temperature effects on, 16: 28390 (TID-7631(p.62-71))
thermal stresses in, (E/T), 19: 10466(T)
vibrations of concentric spherical, thermally induced, 18: 27634 (UCRL-7402)

SHELLSOL

Shellsol T–TBP, radiation effects on clarification and coalescence time of reactor fuel solutions in, 20: 29333 (RT-CHI-(65)33)

SHELTERS

see also Field Fortifications
see also Structures

air cooling and ventilation in, 20: 39074
air intake stack and filter cartridge for fallout, 20: 14722(P)
air shafts and emergency exits of, self-closing cover plate for, 18: 6941(P)
analysis for protection against fallout, 17: 2734
analysis of data from survey of, 18: 37430 (AD-431995)
assessment of deep underground sites for military command centers, geologic, 19: 9353 (ESD-TDR-64-134)
availability of, for urban and rural populations, mathematical analysis of, 18: 14101 (AD-427995)
bibliography on construction of, for military use, 18: 3970 (AD-299189(Suppl.1))
blast detection and alarm system for, 20: 33614(P)
blast effects, effects of earth covering, 16: 12816 (WT-1128)
blast effects from atomic explosions on communal, instruments for measuring, 16: 23856 (WT-790)
blast effects on animals and dummies in group, 16: 24017 (WT-798)
blast effects on cylindrical underground, 19: 20659 (AD-606490)
blast effects on family defense, experimental, 16: 25657 (WT-359)
blast effects on underground, 16: 12815 (WT-1127)
blast effects on underground and basement-type home, 17: 29880 (WT-801)
blast effects on, from nuclear explosions, computer program for calculating, 19: 32400
blast load reduction on above-ground, for aircraft, 18: 1886 (AD-422046(p.151-68))
blast pressure measurements in, 17: 29884 (WT-1501)
book: *The Architect in the Nuclear Age*, 20: 1577

communications systems of fallout, specifications of radio equipment for, 18: 33840 (TGGM-642)
conference, 20: 39054
conference on blast effects on, 18: 1937 (AD-422046)
construction and management of industrial, 16: 11988
cooling and heating systems for municipal emergency, 16: 13394
cooling techniques for 100-man, analysis of, 18: 12328 (AD-416490)
cost factors for, 19: 46671
cost-effectiveness of fallout, 20: 23264 (AD-624701)
design analysis, 18: 10259 (AD-405709)
design and analysis of reinforced-concrete arches for underground, 17: 2656 (AD-274727L)
design and construction for protection against fallout in Sweden, 19: 18223
design and cost data for family and small-group protection against fall-out, 16: 4406 (UCRL-6654)
design and cost factors for, to accommodate 100 persons for 14 days, 17: 6324 (USNRDL-TR-582)
design and cost of tunnel-grid, for urban populations, 19: 20202 (ORNL-P-1093)
design and costs of tunnel grid blast, 19: 40759 (ORNL-TM-1183)
design and economics of rock, 16: 33323
design and operation of fallout, protective and environmental aspects of, 19: 36707 (NP-15266)
design considerations for protection from nuclear weapons, 18: 27691 (R-425-PR)
design, construction, and cost of deep-rock and normal, in Sweden, 16: 27486
design, construction, and habitability of home basement, 17: 2657 (AD-276392)
design criteria for animal, 20: 29392
design for cast-in-place concrete, 17: 6313 (NP-12349)
design for personnel in nuclear energy surface mining operations, 16: 11368(T) (UCRL-Trans-768(L))
design for protection from fall-out, 16: 6652
design for protection from atomic bombs, 16: 27495
design for protection from fall-out, regulations in, 16: 10310(T) (AEC-tr-4964)
design for protection against fall-out, 17: 321
design for protection against fallout gamma radiation, 17: 29121 (NP-12762)
design for protection against biological, chemical, and radiological warfare agents, 19: 46651(T) (JPRS-30979)
design for protection against nuclear weapons effects in schools, evaluation of, 20: 20868 (AD-626770)
design for protection from window-collimated ceiling-scattered fallout radiation, 20: 34801
design for target community, 20: 39089
design fundamentals, 17: 30634 (NP-12961)
design of blast-resistant tunnel for large cities, 20: 39088
design of buildings including fallout, case studies of, 20: 39086
design of concrete, computer program for, 20: 7246 (GA-6697)
design of dual-purpose group, 18: 41629 (AD-412342)
design of dual-use military, 18: 20197 (NAVDOCKS-P-310)
design of fallout, 18: 14155
design of fallout, 18: 25681(P)
design of family, 16: 5625(P)
design of fire-safe, criteria for, 20: 39065
design of fireproof, with secured ventilation systems, 20: 39066
design of fireproof, Swedish, 20: 39067
design of foldable fallout, 18: 3972(P)
design of foldable, tent-like, 20: 5632(P)
design of, for protection against blast and fallout, 17: 12494 (MMPP-S-1)
design of, for radiation and blast protection, 17: 18221 (NAS-NRC-Pub-992)
design of ground-shock resistant, 20: 39084
design of opening and entrance for buried, 18: 6940 (NP-13459)
design of openings for buried, 17: 39291 (NP-13087)
design of personnel, 16: 3263 (NAVDOCKS-TP-PL-8)
design of portable or fixed, 20: 41118(P)
design of precast fallout, 20: 41119(P)
design of prefabricated roof structure for fallout, 20: 2039(P)
design of prefabricated fallout, 20: 2040(P)
design of prefabricated fallout, 20: 14723(P)
design of prefabricated, blast-resistant, 20: 39075
design of public, in Denmark, 20: 39079
design of rectangular underground, 16: 17907 (AD-264553)
design of seven-man, 200 psi blast-resistant, 20: 39077
design of simple bomb shelter, 18: 33758(P)
design of Swiss, 20: 39082
design of tunnel-grid, for urban populations, 20: 16159(R) (ORNL-3900, pp 150-81)
design of underground, in hospital, 19: 15732
design of underground, in hospital, 19: 15733
design of underground, effects of soil dynamics on, 20: 39070
design of, distribution and magnitude of weapon effects for, 20: 16620 (AD-624370)
design of, effect of apertures and ceiling-shine on, 20: 43526
design of, engineering approach to, 20: 39069
design of, for emergency operating center, 18: 35702 (NP-14108)
design of, for protection against blast effects, 20: 2083 (CEX-65.4)
design of, under highways, 19: 46669
design optimization of blast, 19: 9355 (HI-361-RR/2)
design specifications for Austrian, 20: 39081
design study for atomic explosions, 20: 23339 (AD-625752)
design study for atomic explosions, 20: 23340 (AD-625753)
design study of tunnel-grid blast, for portion of Detroit, 19: 46568 (ORNL-TM-1223)
design, economics, and suitability of partially underground, for single family use, 19: 22517 (USNRDL-TR-647)
development of blast-closure valve for ventilation systems, 17: 10776 (NP-12454)
development of private cooperative, 20: 39085
development of radiation-absorbing glass for, 20: 23761(R) (AD-624874)
development status in Netherlands, 20: 39076
diet for occupants of fallout, 18: 27739
distortion of tunnels by blast loading, analysis of static and dynamic, 18: 1885 (AD-422046(p.92-105))
distribution and types of, in Houston, Texas and Durham, N. C., statistical analysis of, 18: 14101 (AD-427995)
doors and valves for Canadian blast, use of plastic, 20: 39080
doors for blast, design of, 20: 39073
dynamic loading of strip footing of flexible arch structure in sand, simulation tests, 19: 46567 (NP-15396)
effectiveness during radiological warfare, 16: 19191
effectiveness of fallout, evaluation of, 20: 23265 (AD-624702)
effectiveness of fallout, evaluation of, 20: 23266 (AD-624703)
effectiveness of various types of, for protection against multi-megaton nuclear weapons, 18: 12385 (NP-13568)
effectiveness of, public attitudes toward, 1963, 18: 12380 (AD-404511)
effectiveness of, public attitudes toward, 1963, 18: 12381 (AD-404512)
effectiveness of, in protection against nuclear explosions, 19: 15207
effectiveness of, for protection against radiation hazards from thermonuclear explosions, 19: 46671
effects of atomic explosions on AEC prototype communal, 16: 23359 (WT-360)
efficiency of nuclear blast, model analysis of, 20: 39071
electric and mechanical services for, integrated systems for, 16: 27500
engineering data on design and construction of, 17: 39290 (NAVDOCKS-P-290)
environment of, effects of fire in internal, 20: 39059
environmental control in closed, techniques and cost analysis of, 18: 12383 (AD-413416)
environmental control system for emergency use in, 19: 15789 (ORNL-TM-1067)
environmental monitoring in civil defense, evaluation of instrument packages for, 18: 39526 (AD-600759)
environmental studies of 100-man underground, under occupancy conditions, 19: 15731 (USNRDL-TR-618)
evaluation for shielding against fall-out from nuclear weapons, 16: 29967
evaluation of basements in public buildings, mines, and home basements, 17: 2657 (AD-276392)
evaluation of buildings for use as, 20: 7326
evaluation of earth-covered, for fall-out protection, 16: 9730 (CEX-60.6)
evaluation of family and personnel type, for protection during atomic explosion, 16: 24018 (WT-1161)
evaluation of kill probability in basement and underground family, in target area, 17: 6345
evaluation of protection afforded by various types of, 18: 14102 (AD-428008)
evaluation of protection afforded by wood-frame houses and civil defense, 18: 23826 (NP-13942)
evaluation of residential structure for protection against fallout radiation, 20: 43496 (CEX-59.7B(Pt.1))
evaluation of types of blast, categories and variables for, 19: 24693 (ORNL-TM-1089)
evaluation of, for postattack protection, 20: 41177 (AD-632211)
evaluation of, for waterworks personnel, 20: 45940 (AD-639710)
existing in basements, mines, and in boats on bodies of water in U. S., 1961 survey, 17: 2657 (AD-276392)
fallout, attitudes and knowledge concerning, in Austin, Texas, 17: 37362 (AD-286933)
fallout measurement device for, 18: 18081
fallout, efficiency of, 18: 22279 (URS-638-2)
fallout, physiology and psychology in overloaded, 19: 6120 (AD-420449)

fallout, protective lightway for, 20: 29483(P)
fallout, sensitivity analysis of components and systems of, 20: 20922 (AD-624704)
family adoption of public fallout, study in Des Moines, Iowa, 19: 9350 (AD-602854)
feasibility of doubly curved shell, for nuclear explosions, 20: 23341 (AD-625782)
feasibility of nuclear explosion, 19: 44215 (ORNL-3865)
filtration system design for personnel protection in, 17: 12490 (ACR-72)
financing nationwide systems of, alternative approaches, 20: 45938 (AD-635930)
fire hazards to occupants of, 18: 31740 (FMRC-15328)
food and medical supplies for, 19: 24753
food and water management for, of 50 or more occupants, 18: 12379 (AD-403714)
food evaluation for rations in fallout, 20: 2067 (AD-614824)
food for fallout, 18: 18067
food supplies for, problems in provisioning, 17: 8441
food supplies for fallout, 19: 36725
foods for, criteria for, 17: 8443
foods for, packaging and storage of, 17: 8442
for hospitals, 18: 18079
for protection against fall-out, 16: 26733
foundations for underground, design of, 20: 39068
furnishings design for, 20: 18946 (ORNL-TM-1428)
gamma attenuation by ducts and entrances, 16: 13388 (AD-264022)
gamma attenuation in ducts with two right-angle bends, 16: 15756 (ARF-1158A02-7)
gamma distribution in entranceways, 16: 708
gamma dose attenuation in two-legged concrete ducts of, first- and second-order contributions to, 20: 27126
gamma dose rate in test, from simulated contaminated field, 19: 32399 (PSDC-TR-14)
gamma dosimetry at right-angle bends in entrances of, 17: 3798
gamma radiation in basement, distributions of air-scattered, (E), 20: 7298 (CEX-59.7B(Pt.3))
gamma radiation streaming through air pipes, review of, 20: 39060
gamma ray measurements in, 17: 29883 (WT-1174)
gamma shielding by cylindrical steel structures, floor-barrier reduction factors for, 20: 34800
gamma streaming through air ducts in concrete, 18: 29860 (AD-430603)
gamma streaming through air duct in concrete, 19: 21594 (AD-424387)
ground motion effects on contents of buried, 19: 40758 (AD-426249)
ground shock measurements, from nuclear detonations, 16: 2837 (WT-1487)
habitability, effect of oxygen depletion and fire gases, 16: 10308 (NP-11303)
habitability of fallout, under fire exposure, 20: 41184 (AD-637806)
health care of populations in, 18: 12382 (AD-411787)
importance in radiological defense, 19: 32471(T) (FTD-TT-64-1352)
location of communal, effect of population mobility, 16: 15025 (ORO-SP-30)
management factors for efficient operation of, 19: 46637 (AD-612254)
materials evaluation for hardened, 18: 29859 (AD-429134)
medical care in, manual for, 19: 12892 (AD-423696)
medical care of occupants of, 18: 14100 (AD-415614)
moisture sources and control in, 18: 37433 (AD-600423)
moisture sources and control in, 18: 37434 (AD-600437)
monitor system for fallout, engineering drawings for, 20: 14903
national program for fallout, medical aspects of, 18: 22294
neutron distribution in concrete entranceways, 16: 708
neutron dosimetry at right-angle bends in entrances of, 17: 3798
neutron flux distribution in multi-legged entranceways in, 17: 26220
neutron measurements in, 17: 29883 (WT-1174)
neutron transmission through ducts in concrete, (E/T), 19: 23939 (NP-14882)
nuclear weapons effects, 16: 18713 (AFSWC-TN-61-26)
occupancy after nuclear explosions, rule for, 20: 23385(T) (ORNL-tr-970)
occupancy tests in simulated community fallout, environmental and organizational factors in, 20: 2070 (AD-615004)
occupancy tests in simulated fallout, 20: 2071 (AD-615005)
occupancy tests of, under austerity conditions, 18: 37432 (AD-439251)
oxygen supply in small fallout, testing of potassium superoxide canisters for production of, 19: 18221
performance of basements as fallout gamma shielding, (T), 19: 29460
personnel, evaluation of buried conduits as, 16: 9031 (WT-1421)
personnel, evaluation of buried steel-arch structures, 16: 9032 (WT-1422)
plans for area-wide, in city community, 20: 41183 (AD-635931)
population assignment to, punched-card method for, 18: 14111 (OAD-RM-105)
population assignment and traffic to, plans for, 19: 46635 (AD-611764)
population direction to and management in, 19: 46636 (AD-611765)
power plants for, evaluation of small auxiliary, 19: 9352 (AD-603227)
power supplies for, review of, 18: 36222 (AD-431610)
power systems for community, evaluation of auxiliary, 19: 9351 (AD-603068)
properties of fallout, for domestic animals, 19: 46700
protection afforded against blast effects, 16: 21870(R) (DASA-1271)
protection afforded by, cost factors, 16: 33314 (SC-4689(RR))
protection afforded by trench-type, against nuclear explosions, 17: 2667 (WT-560)
protection afforded by above-ground and below-ground, from fallout, 18: 8509 (CEX 59.7b(Part II))
protection afforded by, against close-in fallout, 19: 34397 (BNL-9188)
protection factor for fallout, calculation of, 20: 16733 (ORNL-P-1098)
protection of air traffic control system from chemical–biological–radiological warfare agents, equipment for, 19: 9354 (GDC-64-026)
protective criteria for, 18: 18072
protective effects of typical S.W. stucco and frame house against fall-out, 16: 10298 (CEX-60.5)
protective effects of fallout, in the Los Angeles area, 17: 12492 (CEX-61.4)
protective effects of, against chemical and radiological warfare agents, 18: 1961(T) (FTD-TT-63-585)
protective effects of, in radiological warfare, 18: 1978
psychologic and social aspects of occupation, 17: 1674
psychologic discomfort survey, 17: 27611
public opinion survey, 1963, 19: 32446 (AD-609202)
radiation dose estimates for underground reinforced concrete, 17: 2656 (AD-274727L)
radiation dose rate in multistory windowless, effects of limited strips of contamination on, 17: 26216
radiation dose rates in, from simulated fallout field, effects of interior partitions on, 17: 26217
radiation dose rates in ground holes, from overhead irradiation, 18: 5473(R) (ORNL-3499(Vol.I)(p.147-52))
radiation dose rates in concrete bunkers, 18: 5474(R) (ORNL-3499(Vol.I)(p.153-5))
radiation dose rates in underground concrete-lined, 18: 14060 (ORNL-3513)
radiation dose rates in compartmentalized, gamma and neutron, 18: 25712 (USNRDL-TR-722)
radiation hazard from fallout particles captured by air filter in, 19: 13605 (AD-605502)
radiation monitoring, rate meters for, 16: 13395
radiation monitoring systems for, 18: 14099 (AD-412431)
radiation monitoring in basement of two-story wood-frame house, 20: 7358(R) (EGG-1183-2057)
rations for, development of cereal wafer for, 17: 8444
rations in, storage life of, 18: 35758(R) (AD-431930)
residential basement, review of 1960 data on, 18: 14101 (AD-427995)
response of buried hollow cylinders to quasi-static overpressures, 19: 20136 (AFWL-TDR-64-13)
role in protection of populations from fall-out radiation, 16: 33315 (TID-16741)
role in radiological defense of, 19: 19554
role in radiological defense of, 20: 5416
shielding against nuclear-explosion initial radiations, problems in, 20: 39061
shielding calculations for fallout, shape factors in, 19: 44217
shielding calculations for, errors in, (E), 20: 39062
shielding characteristics of various structures used as, 18: 37430 (AD-431995)
shielding from radioactive fallout by core, in typical British house, 20: 39083
shielding parameters of, after nuclear attack, 20: 18938 (AD-629784)
shielding properties of roof slab and structures against fallout, calculation of, 20: 43568 (AD-636787)
shielding protection factors for fall-out, 16: 19198
shielding-analysis methods for, status of, 20: 39063
shock isolation methods, 18: 29858 (AD-428009)
shock isolation systems for underground fallout, response spectra of multi-degree-of-freedom, 20: 23342 (AD-627516)
shock wave propagation in ducts and entrance structures of, 20: 39072
shock waves in tunnels, designs for protection against, 20: 27125 (UCRL-14848-T)
social aspects of civilian-defense, 18: 39545
specifications for fallout, equivalent residual dose concept in evaluation of, 17: 37363 (CDRP-182-106)
stress distribution around deep underground, 18: 1884 (AD-422046 (p.55-85))
support systems for civil defense, 18: 5568
survey of fallout, comparison of aerial photographic and documentary methods, 17: 6302 (AD-276119)
survey of public opinion on, 18: 37435 (AD-600751)
survey of public opinion on fallout, 18: 39475 (AD-600752)

survey of underground, 19: 30396 (SC-DC-65-1424)
survival in fallout, without trained manager, 20: 2069 (AD-615003)
survival ration, nutritional evaluation, 17: 27612
testing for habitability, 17: 27598 (NRL-5882)
testing French underground, in Plumbbob operation, 16: 24019 (WT-1453)
testing reinforced concrete dual-purpose underground, 16: 29250 (WT-1449)
thermal transient response of underground, scale model tests on, 20: 20920 (AD-621377)
types for fallout protection, 19: 42675
underground in rock, construction problems, 17: 2658 (AFSWC-TDR-61-93)
underground, uses of light from nuclear reactors in clearing space for, 19: 21710
use of ships and boats as, 18: 1960 (USNRDL-TR-659)
use of underground highway and parking garage for Manhattan Island fallout, engineering study on, 20: 16623 (ORNL-TM-1381)
use of underground structures as, 20: 39078
value of, in protection of population from effects of thermonuclear explosions, 17: 35258 (P-2665(RAND))
ventilating system for fallout, 19: 38833(P)
ventilating system for fallout, 20: 27127(P)
ventilation design for blast and fall-out, 16: 13393
ventilation, development of lithium hydroxide canisters for, 16: 2054 (NP-10935)
ventilation of crowded outside-air-cooled, manual punkah-pump for, 19: 30395 (ORNL-TM-1154)
ventilation of fallout, by induced draft, 20: 20921(R) (AD-621998)
ventilation of, durability tests of punkah-pump for, 19: 38832 (ORNL-TM-1155)
ventilation systems for, performance of gravity, 19: 22594 (NP-14976)
ventilation valves for blast, 20: 39073
water supply for fallout, 18: 25714
water supply production from wastes, evaluation of processes for, 18: 16228 (NP-13740)
windows for fallout, design of, 19: 44218(P)

SHERWOOD PROJECT

see also Thermonuclear Reactors

coils for use in, development of epoxy potting system for, 17: 14420 (LAMS-2797)
cryogenic aspects, 16: 4904(R) (NBS-7207)
cryogenic aspects, research summary, 16: 24888(R) (NBS-7244)
cryogenic aspects of, developments in, 17: 13620(R) (NBS-7644)
cryogenic aspects of, progress on, 17: 14941(R) (NBS-7608)
cryogenic developments in, 17: 21137(R) (NBS-7677)
cryogenics, 17: 33149(R) (NBS-7919)
cryogenics developments in, 18: 13133(R) (NBS-8212)
cryogenics developments in, 18: 24544(R) (NBS-8253)
cryogenics developments in, 19: 31331(R) (NBS-8797)
cryogenics of, developments in, 18: 1126(R) (NBS-7973)
development, 16: 12612(R) (NBS-7218)
development of, review of, 19: 43413 (LA-3253(Rev.))
developments in Astron research, 17: 29660 (UCRL-7083)
diffusion pump fluid evaluation in, 16: 31735 (UCRL-6577-T)
magnet refrigeration development, 20: 1265 (NBS-3346)
magnets for, development of cryogenic, 20: 1264 (NBS-8843)
research in, 19: 12637(R) (LA-3202-MS)
research in, 18: 30886(R) (LAMS-3085)
research programs in, summary of, 16: 29906(T) (NYO-9191)
research programs on, at LRL in fiscal year 1963, 18: 15729 (UCRL-Pub-48)
research programs through 1966, projection of, 18: 30887(R) (LAMS-3085(p.5-16))
research status summary, 16: 14139 (NP-11573)
status, 18: 7789 (NP-13428)
status, 20: 13916 (MATT-412)
status, 18: 24755 (NP-13895)
status report for Aug. to Nov. 1961, 16: 9498(R) (LAMS-2651)
vacuum system development for, 16: 17584(R) (ORNL-3262(p.199-205))

Shield Ducts

see Reactor Shield Voids

SHIELD TEST AIR REACTOR

design and development, 16: 23332 (DC-60-2-230)

SHIELD TEST POOL REACTOR

gamma and neutron dose rates from, calorimetric determination of, 18: 3043 (TID-19678)
neutron flux measurements in, 17: 27423(R) (TID-18195)
radiation heat in east and north faces of, 16: 28652(R) (TID-16374)
testing facilities of, design of hot wire thermal stability rig for, 16: 28652(R) (TID-16374)

Shield Testing Reactor

see Bulk Shielding Facility

Shield Voids

see Reactor Shield Voids

SHIELDED CONTAINERS

catalog of engineering equipment for, 16: 30515 (TID-4100(1st Rev. Index 2))
catalog of, Atomic Energy of Canada Ltd., 20: 32891
construction of low-background counting facility, evaluation of Portland cements for use in, 17: 11903 (UCRL-10475)
container for steel–lead–steel, design of plywood, 20: 39164
cooling fuel-element, 18: 40808 (GEAP-4704)
criticality analysis for fissile material, 20: 31514(R) (UCRL-14881)
criticality of arrays of, for storage of plutonium nitrate solution, 19: 18733 (BNWL-19)
criticality studies, 16: 12841
density measurements on wood for, interpretation, 16: 20861 (AHSB(S)R-36)
description of, 20: 10963
description of, for handling cobalt-60, 17: 29974
description of package range for radioactive loads up to 20,000-C cobalt-60, 19: 26572 (AERE-M-1512)
design, 17: 6244 (HW-SA-2807)
design, 20: 43475(P)
design, 20: 23350 (CF-52-10-230(Del.))
design and construction of lead, 18: 16227 (NP-13691)
design and development for EBR-II fuel cycle facility, 19: 15662(R) (ANL-6900(p.45-142))
design and development for irradiated fuel element shipment, 19: 32495
design and development for radioactive biological materials, 20: 6694(R) (MIT-952-2)
design and fabrication for irradiated fuel elements, 19: 5405(R) (WCAP-3374-2)
design and hazards analysis for shipping cerium-144 and associated impurities from Purex waste, 18: 23823 (HW-65268)
design and testing, for radioactive material shipping, 16: 25672
design and testing of, for fuel transfer, 18: 43359(R) (ANL-6800(p.43-196))
design and tests of Class I, for shipping fissile materials, 19: 18193 (HW-SA-3995)
design and use in replacing radiation sources in exposure devices, 19: 32340(P)
design for cobalt-60 source for insect studies, 19: 36714
design for depleted fuel elements, 18: 12406(P)
design for dry enriched uranium, engineering drawings for, 19: 28607
design for fuel element transfer, 18: 36770(P)
design for gamma sources, 19: 18098 (KAPL-3074)
design for handling plutonium solutions, engineering drawings of, 18: 5570
design for handling and shipping of spent fuel elements, 20: 9209
design for heating solid waste materials, 18: 33171(P)
design for irradiated fuel elements, 20: 24757
design for long-term storage of radioisotopes, 17: 36065
design for neutron sources, 17: 23592
design for neutron auto-radiography of encapsulated irradiated fuels, 18: 26068 (ANL-6799)
design for plutonium shipping, 17: 10862 (RFP-290)
design for plutonium dioxide shipping, 19: 30443 (RFP-501)
design for point radiation sources, 18: 11365(P)
design for radiation sources, 19: 38905(P)
design for radioactive pencils used in pipe weld inspection, 17: 1588(P)
design for radioactive materials, 19: 30479(P)
design for radioisotopes, 17: 16355(P)
design for radioisotope storage and transportation, 19: 13688
design for radiology departments of cancer hospitals, 16: 8844(T)
design for shipment of dry uranium-235 compounds, 18: 22280 (Y-1460)
design for shipment of radioisotopes, 19: 15942 (ORNL-P-920)
design for shipment of radioactive material, 19: 46665
design for shipment of radioactive materials, 20: 43492 (ORNL-TM-1312(Vol.2))
design for shipping radioactive materials, 16: 2090
design for shipping strontium-90, 16: 3260 (HW-68081)
design for shipping and loading cobalt-60 sources, 16: 20586(P)
design for shipping strontium-90 and cerium-144, 16: 30695 (HW-SA-2295)
design for shipping of spent fuel elements, 17: 3762
design for shipping irradiated fuel elements, 17: 29717 (NAA-SR-Memo-7844)
design for shipping radioactive materials, 17: 29153(P)
design for shipping spent fuel elements from Elk River and Piqua Reactors, 17: 30756 (TID-18813)
design for shipping uranium hexafluoride, engineering drawings for, 17: 30777
design for shipping spent fuel elements from Elk River and Piqua Reactors, engineering drawings for, 17: 30778
design for shipping irradiated fuel elements, 17: 32303

design for shipping radioactive waste, 17: 35245 (NP-12997)
design for shipping radioisotopes, engineering drawings for, 18: 5569
design for shipping fission products, evaluation of, 18: 25707 (HW-65268 (Rev.1))
design for shipping spent reactor fuels, computer code for, 18: 35659 (ORNL-3648)
design for shipping spent BR2 and HFR fuel elements, 18: 37309 (A/CONF.28/P/448)
design for shipping spent fuel elements from Elk River and Piqua Reactors, 19: 569 (TID-21246)
design for shipping plutonium, engineering drawings of, 19: 4426
design for shipping irradiated EGCR fuel, 19: 7665 (ORNL-TM-1001)
design for shipping radioactive materials, 19: 9435(P)
design for shipping irradiated fuel assemblies, 19: 19392 (WCAP-6062)
design for shipping radioactive materials, review, 19: 40823 (SC-RR-65-98, pp 450-72)
design for shipping irradiated Yankee fuel elements, evaluation of, 19: 46650 (WCAP-1859(Rev.))
design for shipping and handling radioactive materials, 20: 616(P)
design for shipping spent fuels, 20: 2084 (EURAEC-374(Vol.2))
design for shipping spent fuel elements, 20: 14678(P)
design for shipping and storage of spent fuel elements, 20: 14679(P)
design for shipping irradiated nuclear fuel, 20: 33582
design for shipping high-level waste, 20: 40476(R) (BNWL-267)
design for shipping radioactive waste, 20: 40481 (WAPD-T-1851)
design for shipping tritium, 20: 41196 (LA-DC-7996)
design for source storage with means for source removal, 18: 12408(P)
design for storage of plugs and experimental devices from reactors, 16: 17331 (CEA-2084)
design for storage of damaged fuel elements, 16: 31241(P)
design for storage of radium needles, 19: 9356
design for storage and shipping of radioactive materials, 20: 43476(P)
design for storing and shipping radiation sources, 16: 11825(P)
design for storing radioisotopes, 18: 5695(P)
design for storing radiation sources, 18: 18130(P)
design for storing and transporting radioactive materials, 19: 6140(P)
design for storing defective or depleted fuel elements, 19: 35625(P)
design for studying properties of actinides, 20: 15038 (CONF-660305-12)
design for temporary storage of irradiated fuel elements, 19: 38908(P)
design for therapeutic syringe, 16: 25
design for therapeutic irradiation, 17: 1590(P)
design for transferring fuel elements to water tank, 17: 20277(P)
design for transferring EBR-II fuel from reactor to cycle facility, 19: 9300 (ANL-6934)
design for transporting radioactive materials, 18: 4050(P)
design for transporting thermally hot highly radioactive material, 18: 12407(P)
design for transportation of radioactive materials, 19: 22610
design for transporting fissile cartridges, 19: 32500(P)
design for transporting used fuel elements, 19: 42662(T) (ORNL-tr-600)
design for transporting irradiated specimens, 20: 9107(P)
design for transporting spent reactor fuel rods, 20: 10985(P)
design for treatment of radioactive fluids, 17: 35975(P)
design for use in charging nuclear reactors, 18: 33007(P)
design for waste disposal, 16: 26641 (TID-15431)
design for withdrawing radioactive wire from cell, 18: 27650(P)
design modification for fuel-transfer, 18: 17922(R) (ANL-6725(p.88-99))
design of air-cooled, for spent fuel elements, 18: 4049(P)
design of, British regulations on., 17: 18342 (TID-7651(p.103-25))
design of cask for shipping irradiated fuel, 17: 8429 (NP-12393)
design of cooled shipping cask for spent reactor fuel, 16: 27184(P)
design of cylindrical capped metallic, for portable isotope pencil, 19: 32335(P)
design of, development of regulations for, 17: 18340 (TID-7651(p.88-98))
design of double-walled, for storage of radioactive materials, 20: 39040(P)
design of drum type, 19: 34312(P)
design of, for handling and transport of radioactive liquids, 18: 472
design of, for heat-evolving radiation sources, 17: 4756(P)
design of, for shipping fuel elements, 17: 8488(P)
design of impact-resistant, for fission products, 17: 6362
design of lead, 20: 32680
design of light, for radiation sources, 19: 44179(P)
design of liquid-filled, for transfer of fuel elements from reactors, 17: 40316(P)
design of quick-opening lids for, 19: 42716(R) (ORNL-3782, pp 52-64)
design of radiation source holder, 16: 27187(P)
design of, regulation-compliance problems in, 17: 18344 (TID-7651(p.132-44))
design of reinforced concrete, for nuclear reactor experiments, 17: 19508 (ANL-6664)
design of shipping cask for irradiated fuel elements, 16: 33095
design of shipping cask and protective buffer, 18: 22273 (HW-68274)
design of, to I.A.E.A. standards, 17: 18352 (TID-7651(p.331-93))
design of, to I.A.E.A. regulations, 17: 41036
design of transport cask using liquid metal coolant, 18: 23759(P)
design of, use of safety standards in evaluation of, 17: 18343 (TID-7651(p.126-31))
design of 4-liter, for dissolver solutions, 17: 16194
design specifications for, using cadmium and wood shielding, 18: 14103 (AHSB(S)R-63)
design with remotely operated shutter, 18: 33728(P)
design with safety latch, 18: 16274(P)
design with wheels, 18: 25736(R)
development for radioactive materials, 20: 18020(R) (ORNL-3900, pp 2-81)
development for shipping spent fuel, 18: 33822
development for shipping spent reactor fuel, 19: 23996(R) (ORNL-3650(p.1-110))
development for shipping failed fuel, 19: 31521(R) (WCAP-3385-3)
development for shipping and storage of fissile materials, 20: 20840(R) (BNWL-193, pp 57-67)
development for use during shipment of high-level wastes and irradiated fuel elements, 17: 3222 (TID-7635(p.97-111))
development of fire-impact shield for radioisotope shipping carriers, 19: 11420 (ORNL-P-856)
development of improved, for shipment of plutonium and uranium, 20: 35671 (UCRL-14903)
development of lead-clad steel, 18: 32952
drop tests for strain and cavity deflection for 8 models, 17: 3221 (TID-7635(p.83-96))
drop tests on Types F and G, 19: 38546(R) (RFP-552)
economic comparison of lead, steel, and uranium shielding in, for shipping spent fuel elements, 20: 33559 (ORNL-P-2161)
economics of lead, steel, and uranium, comparison of, 20: 16622 (ORNL-3918)
effects of fire on tinplate cans for radioisotope containment, 20: 11028 (AERE-M-1664)
engineering drawing for, 18: 1983
engineering drawings for cobalt-60, 18: 1984
engineering drawings of, shipping plutonium, 19: 34422
fabrication of rhenium, for radioisotopes, 19: 894(R) (GEMP-39A)
fire damage studies for, modeling requirements for, 18: 23827 (NYO-2539-1)
fire resistance of lead-lined casks, analysis, 19: 40813 (SC-RR-65-98, pp 107-13)
fire resistance of lead, 19: 40831 (SC-RR-65-98, pp 723-31)
fire test of lead cask, calculations, 19: 40832 (SC-RR-65-98, pp 732-5)
fire test of 15-ton lead-lined, 19: 40827 (SC-RR-65-98, pp 631-50)
fire testing, 17: 3217 (TID-7635(p.32-45))
fire testing of shipping, 18: 27811(R) (ORNL-TM-198)
fire testing of, for shipping radioactive materials, 19: 24817
fire tests of packagings for radioactive materials, 19: 40814 (SC-RR-65-98, pp 114-18)
for fissionable material, safety, 20: 3370 (CONF-651103-2)
for radiation sources, safety tests for effects of age, mechanical damage, fire, and radiation on, 18: 22278(R) (ORNL-TM-630)
for radium storage, 19: 9317
for shipping of radioactive materials, vehicle-collision problem in, 19: 7652 (NYO-2539-3)
for storage of wastes in radioisotope hospitals, volume and number calculations for, 20: 38790
for transport of radioactive materials, testing programs, 17: 3213 (TID-7635)
for transport of radioactive materials, 17: 3253
handling reactor fuel casks, equipment for, 19: 20099 (TID-21644)
hazards evaluation of shipping cask for irradiated PM-1 and PM-3A cores, 18: 16225 (MND-M-1856)
heat generation rates in, for irradiated fuel elements, 17: 35103 (NAA-SR-Memo-2658)
heat generation rates in, for irradiated fuel elements, 17: 35104 (NAA-SR-Memo-3034)
heat removal from spring-loaded dry shipping cask, 18: 14028 (KAPL-M-6106)
heat removal from, for shipping irradiated fuel elements, 19: 46667
heat transfer by, 16: 839
heat transfer from spent reactor fuels during shipping in, 17: 25411 (ORNL-3439)
heat transfer in shipping containers for cobalt-60, 17: 3218 (TID-7635 (p.59-77))
impact resistance of, for radioactive material transport, 19: 22591 (CONF-641201-16)
impact testing, 17: 6244 (HW-SA-2807)
impact testing, 17: 26197
impact tests of casks for irradiated fuel, 19: 40818 (SC-RR-65-98, pp 261-82)
impact tests of steel shells of casks, 18: 6934 (ORNL-TM-680)

impact tests on scale model of cask, 17: 36000 (ORNL-TM-629)
laboratory and service tests, 17: 3219 (TID-7635(p.78-80))
leak detection in, at reprocessing facility, 20: 14788 (JAERI-1089)
leak detection in, autoradiographic and radiometric methods for, 20: 41197(R) (NP-16172)
leak rates of, methods of establishing, 19: 11383
leak testing of sealed, 19: 34421
legal requirements for, for shipping radioactive materials, 16: 25671
materials transfer from, to hot cells, 20: 4208
neutron surface multiplication for, adjoint-problem solution for, 18: 34726 (AWRE-O-21/64)
pressure venting device for, for shipping spent fuel elements, 19: 24815
production of lead, methods for, 18: 32953
requirements for shipping radioisotopes, 17: 27586 (AHSB(RP)R-23)
safety analysis for shipping of irradiated fuel from NS *Savannah*, 18: 440 (NP-13235)
safety analysis of cask for shipping irradiated HFIR fuel, 19: 7736 (ORNL-TM-959)
safety aspects for spent-fuel transport, 18: 31780 (A/CONF.28/P/279)
safety evaluation of 20-inch-cube birdcage, 19: 13665 (LA-3203-MS)
scattering outside cylindrical, sky-shine, 20: 40288
shutter design for, 19: 18230(P)
spent fuel shipping cask criticality analysis, 20: 38486 (ACNP-66551)
standards for, for shipping irradiated fuel elements, 19: 24814
stress analysis of radioisotope, from internal pressures, 20: 14667 (ORNL-TM-1312(Vol.1))
structural integrity of shipping casks, factors affecting, 17: 3220 (TID-7635(p.81-2))
structural integrity in transport, research program for evaluation of, 17: 10780 (NYO-9859)
survey of testing programs for shipping radioactive materials, 18: 10306 (NYO-9774)
temperature measurements on, for spent fuel elements, 20: 25332
test standard for, for radioisotope sealed sources, 19: 40802 (CONF-650616-5)
testing, 19: 22818(R) (ORNL-3650(p.221-38))
testing by exposure to standard fires, 17: 18350 (TID-7651(p.304-14))
testing for fire-resistivity, 17: 30068
testing for fission product shipping, drop, 18: 25708 (HW-77962)
testing in fire, 17: 3688
testing lead shipping casks, impact, 19: 18208
testing of bird cage type, for plutonium shipping, 17: 18345 (TID-7651(p.145-60))
testing of buffered, for fission-product shipping, 17: 30751 (HW-77963)
testing of cadmium-lined steel dividers of casks for shipping fuel elements, 16: 8902 (DP-373)
testing of designs for enriched uranium shipping, 17: 18346 (TID-7651(p.161-86))
testing of filter cask for shipment of strontium carbonate, 16: 8834 (HW-72295)
testing of, for enriched uranium, 17: 4745 (Y-KB-22)
testing of lead-filled steel, by impact and puncture, 17: 18348 (TID-7651(p.211-37))
testing of lead-filled casks and wooden fire and impact shields, 18: 1981
testing of lead-shielded steel, for shipping irradiated fuel, 18: 10301 (DP-843)
testing of lead, gamma radiographic, 20: 29388
testing of shipping cask for fission products, 19: 4395 (HW-71744)
testing of structural integrity, 17: 3227 (TID-7635(p.128-33))
testing of, use of scale models for, 17: 18349 (TID-7651(p.238-64))
testing of 15-ton lead-steel, by impact and static compression, 17: 18347 (TID-7651(p.197-210))
testing of, fire, 19: 34419
testing of, for fuel shipping, electric analog computer for fire, 19: 36731
testing of, for radioactive materials, 19: 30436 (AERE-R-4810)
testing of, for transport of radioactive materials, 19: 11467
testing of, for use in shipment of enriched uranium, 19: 24816
tests on ORNL casks, nondestructive and fire, 17: 3216 (TID-7635 (p.28-32))
thermal insulation for cobalt-60, testing of unventilated and ventilated, 19: 26571 (AERE-M-1511)
thermal tests of shipping cask for spent Piqua-Elk River fuel, 18: 29810 (COO-1028-2)

SHIELDING

see also Aircraft Shield Test Reactor
see also Beta Shielding
see also Bremsstrahlung Shielding
see also Bulk Shielding Facility
see also Electromagnetic Shielding
see also Gamma Shielding
see also Ground Shield Test Reactor
see also Reactor Shielding
see also Shielding Materials
see also Thermal Radiation Shielding
see also Tower Shielding Facility
see also X-Ray Shielding
activities of ORNL Radiation Shielding Information Center, 20: 46929(R) (ORNL-3973(Vol.1), pp 48-51)
against accelerator radiation, 18: 730 (JINR-P-1349)
against cosmic rays, role of nuclear reactions in, 16: 33960
against electrons and protons in space, 18: 658 (REIC-32)
against electrons in space, calculations for (T), 19: 3460
against fall-out from nuclear weapons, structure evaluation for, 16: 29967
against fallout contamination, provided by structures, 17: 20245(R) (TO-B-62-58)
against gamma and neutron emission, analysis of two-component materials weight efficiency for, 19: 31426
against light flashes from nuclear explosions, 19: 8806
against neutron and protons in space, 18: 802 (AFCRL-63-214)
against neutrons in activation analysis, 17: 19939 (IA-756)
against nuclear-explosion initial radiations, problems in, 20: 39061
against protons during space flight, 17: 27596 (NP-12905)
against radiation environment in space, calculation of thicknesses for, 17: 19696
aggregates for concrete, 19: 29447
analysis and development of cosmic-radiation, conference, 20: 3239 (NASA-SP-71)
analysis, description of computer programs for, 16: 11116 (DC-57-11-77)
analysis for radioisotope, computer program for, 20: 40285 (BNWL-236)
analysis for space vehicles, cross sections for, 20: 5181(R) (ORNL-3029)
analysis methods for, status of, 20: 39063
analysis of accelerator, 20: 4514 (UCRL-16445)
analysis of Apollo spacecraft, computer code for sector, 19: 38015 (N64-29365)
analysis of, computer programs for, 17: 15405 (NP-12557)
analysis of electronic equipment, 16: 10609 (DC-58-5-179)
analysis of, for burst slug detection equipment for EGCR, 17: 17562 (TID-18241)
analysis of, in Fontenay-aux-Roses Reactors, 17: 19588
analysis of laminated configurations tested in GE Outside Test Tank, 16: 14201 (DC-61-4-15)
analysis of performance of, in real fallout field, 20: 41201 (RRA-T55 and Summary)
analysis of physics problems of, 16: 29965(T) (FTD-TT-62-832)
analysis of SNAP requirements, computer program for IBM-7094, 18: 28920 (NAA-SR-Memo-8968)
analysis of space-environment, computer, 18: 35048 (AMRL-TDR-64-11)
analysis of space-vehicle, 19: 22651
analysis of spherically symmetric, Boltzmann transfer equation solution, 16: 10938 (NARF-61-43T)
analysis of, computer program for, 18: 13176 (NAA-SR-Memo-9327)
analysis of, computer program for, 19: 3453 (NAA-SR-Memo-9327(Add.))
analysis of, for manned orbiting space station, (T), 19: 23944
analysis of, integrals for, 18: 14815 (NP-13616)
analysis of, provided by Japanese houses, 19: 7204(R) (ORNL-3697 (p.155-9))
analysis using cyclotron beams, 18: 27790(R) (ORNL-3578(p.46-59))
analysis, spherical harmonics equations for, 16: 10395 (WAPD-T-1182(Rev.1))
bibliography, 16: 9552 (TID-3303(Suppl.1))
bibliography of literature examined by Radiation Shielding Information Center at ORNL, 17: 28409 (ORNL-RSIC-1)
bibliography of literature examined by Radiation Shielding Information Center at ORNL, 18: 7846 (ORNL-RSIC-2)
bibliography of literature examined by Radiation Shielding Information Center, 19: 19330 (ORNL-RSIC-5)
bibliography on, 20: 1305 (AED-C-01-10)
bibliography on accelerator and space vehicle, 20: 13965 (ORNL-RSIC-11)
bibliography on accelerator and space vehicle, 20: 20098 (ORNL-RSIC-12(Vol.1))
bibliography on, annotated, 16: 17222 (NP-11466)
bibliography on computer codes for, 20: 46934 (ORNL-RSIC-15)
bibliography on, Soviet-literature, 20: 43666 (AD-623557)
book: *Concrete for Radiation Shielding*, 16: 24220 (NP-11837)
book: *Concrete for Shielding Nuclear Installations*, 20: 46171
book: *Principles of Radiation Protection Engineering*, 19: 46683(T)
book: *Shielding Equipment for Individual Protection and Protective Materials for Work with Radioactive Materials, Planned for Production in 1965. Catalog*, 20: 33599
book: *The Propagation of Gamma Quanta in Matter*, 19: 40071
calculation for irradiated fuels, rapid, 18: 11360 (CEA-2288)
calculation methods for, 18: 13175 (ESD-TDR-63-231)
calculation of charged-particle diffusion and penetration, 18: 30941

calculation of, for hot cells, 18: 6410
calculations for cylindrical gamma sources, 20: 32678
calculations for extended-source, 16: 29968
calculations for fallout shelters, shape factor in, 19: 44217
calculations for high energy accelerators, 20: 935 (ORNL-TM-1298)
calculations for, method and results of, 17: 22695
calculations for manned space vehicles, 19: 35563
calculations for manned space vehicles, effective residual dose concept for, 19: 45470
calculations for personnel protection, slide rule for, 19: 32499
calculations for space, experiments for checking, 17: 18377 (TID-7652(p.523-94))
calculations for space vehicle, 19: 17159(R) (ORNL-3714(Vol.II) (p.97-118))
calculations for space vehicle, computer programs for, 19: 41954 (NP-15338)
calculations for space radiation, methods for, 19: 45463 (NP-15425)
calculations for SNAP-7, 20: 4278 (MND-P-2229)
calculations for space vehicles, 20: 17965
calculations for space vehicles, 20: 23417
calculations for shelters, errors in, (E), 20: 39062
calculations for, use of Monte Carlo Method in, 17: 24602
calculations for 45-Bev electron accelerator, nucleon-meson, 19: 17159(R) (ORNL-3714(Vol.II)(p.97-118))
calculations for 400-Mev Frascati linac, (T), 19: 26975 (LNF-65/4)
calculations for, exponential transformation in Monte Carlo, 20: 15937
calculations in, graphs of exponential integral function $E_1(x)$ and $E_2(x)$ in, 17: 38417 (JAERI-6012)
calculations of, equations for, 17: 40224
calculations of, for Hanford Pot Calcination Demonstration, 17: 33397 (ORNL-TM-595)
calculations of, slide rule for, 17: 2418(P)
calculations of, from bremsstrahlung and electrons in earth's radiation belt, 20: 28599
calculations, computer use for, 20: 38350 (ORNL-P-2310)
cascade calculations for 4.5-Bev electron accelerator, nucleon-meson, 18: 7360(R) (ORNL-3499(Vol.II)(p.24-5))
cascade shower calculations for, effects of mathematical errors on, (T), 20: 30725 (ORNL-3786)
cascades in, method for solving equations for meson-nucleon, 17: 31281 (ORNL-3467)
cascades in, calculation of meson–nucleon, (T), 19: 18751 (ORNL-3734)
comparison of theory and experimentation of, from structures for radiation protection against fallout, 20: 43568 (AD-636787)
computer programs for parameters of, abstracts on, 20: 22310 (ORNL-RSIC-13)
computer programs for $^{238}PuO_2$ neutron, computation comparisons of, 20: 46936 (ORNL-TM-1632)
conference on accelerator, 17: 22688
constants for concretes, 16: 6072 (ANL-6443)
construction factors, determination, 16: 7227
construction of, for highly sensitive gamma spectrography, 17: 25558
cooling of lead, for gamma radiation and neutrons, 16: 18593 (TIM-80)
cosmic proton reactions in aluminum, radiation dose from, 17: 3811
cosmic proton reactions with carbon, gamma dose from, 17: 3812
data for high-energy electron accelerator, 19: 17170
data on, against radiation transport in air from atomic explosions, 19: 38893
design, 17: 2743
design analyses for Army Reactors (SM-1)
design and development for Navigator space vehicles, 18: 6510(R) (63SD886)
design and development for space vehicles, conference on, 19: 32495
design and economics of doors for, 19: 23940 (UCRL-11810)
design and evaluation for irradiation facilities, 19: 11457
design calculations for nuclear space vehicle, methods for, 18: 9714 (NP-13468)
design, computer program SPAN-3 for, 16: 15116 (WAPD-TM-235)
design considerations for 500-Mev to 1-Bev linear accelerator, 17: 7318 (BNL-6511(p.110-23))
design criteria for earth satellites, 19: 23946
design criteria for space vehicles, 19: 24268
design criteria for 800-Mev proton linear accelerators, 20: 5940 (LA-DC-7522)
design criteria for LAMPF 800-Mev proton linac, (T), 20: 7674 (LA-DC-7318)
design curves for gamma sources, 19: 33704
design for Advanced Orbiting Solar Observatory, (T), 19: 25618
design for Apollo, 18: 3033
design for Apollo mission space vehicle, 19: 21992
design for β-γ monitor, 20: 39262
design for body counters, shadow, 20: 659
design for Cambridge Synchrotron, 18: 34367 (CEAL-1000)
design for cobalt-60 teletherapy units, 19: 36193
design for driving mechanisms, 17: 40329(P)
design for ductwork in radiation facilities, 18: 35049
design for electron and proton accelerators, calculation of, 17: 22696
design for electron microscope, 20: 39038
design for facility for 160,000-C cobalt-60 gamma source, 20: 9018
design for fuel-handling facilities, computer program for, 20: 46930(R) (ORNL-3973(Vol.1), pp 52-9)
design for gamma source for inspection of weldments, 18: 43775
design for gamma spectrometer, 20: 39260
design for gloveboxes for handling curium-244, 20: 45960 (RFP-811)
design for handling ALRR components, 20: 42681(R) (IS-1500(Sect. R))
design for high-energy accelerators, 16: 28220 (TID-7636(p.409-13))
design for high-energy electron accelerators, (T), 20: 2555
design for irradiation chamber adjacent to reactor core, movable, 18: 7878(P)
design for KEMA Suspension Test Reactor (KSTR), biological and thermal, 19: 10653
design for laboratory for work with 1000°C neutron sources, 18: 12294
design for low-level radiation counters, 19: 40834(R) (UCRL-14151)
design for manned space vehicle, 17: 22769
design for manned space vehicles, (T), 20: 5673
design for manned space vehicles using nuclear rocket propulsion, 20: 20093 (N-65-22849)
design for meson (π) production facility using proton linear accelerator, 20: 2559
design for NRL 60-Mev electron linear accelerator, 20: 2556
design for nuclear-powered space vehicles utilizing radiation scattering, 18: 13183(P)
design for nuclear-powered airplanes, 19: 5537(P)
design for photographic film in space, 18: 12720 (D2-90037-9)
design for point radiation sources, 18: 11365(P)
design for protection against radioactive materials in operating room, 19: 7246
design for protection of male abdominal region during pelvic radiology, 19: 30007
design for protection of male gonads during diagnostic radiography, 20: 16321
design for proton linear accelerators, 20: 33982 (BNL-10244)
design for radiation belt particles, 16: 24910
design for radioisotopes, attenuation factors in, 18: 22984 (NYO-10721)
design for radioisotopic storage device, 20: 45849(P)
design for radium needles, 20: 9186
design for space vehicles, 18: 3034
design for space vehicles, 19: 3457
design for spacecraft, ionization loss and Monte Carlo calculations for, 17: 18383 (TID-7652(p.682-97))
design for spent reactor fuel, computer program for, 19: 23943
design for tandem accelerators, (T), 20: 2558
design for whole-body counter, 20: 38753
design for 1000-Bev proton accelerator, 17: 19409 (BNL-772)
design for 20-Mev electron linac (E), 19: 1093 (JAERI-1063)
design for 45-Bev electron accelerator, nucleon-meson cascade calculations for, 17: 29418 (ORNL-3412)
design for 80-C strontium-90 beta source, engineering drawings of, 19: 20134
design of accelerator, methods for, 17: 22693
design of accelerator, skyshine calculations for, (E), 20: 44057
design of active, for manned space vehicles, 17: 4212
design of, analytic methods of, 17: 4281
design of array of, for chlorine logging apparatus, 20: 29443(P)
design of barricades for hazardous pressure systems, 19: 26518 (KAPL-M-6446)
design of cadmium, for fission product neutron cross section determinations, 19: 36217(R) (IDO-14656)
design of collapsible, 17: 20143(P)
design of collapsible or fixed, for personnel, 20: 41118(P)
design of concrete, using boron carbide aggregate, 20: 11229(P)
design of cubicle for, from patients with implanted radioisotopes, 17: 16345
design of door for megavoltage radiotherapy room, 19: 36153
design of equipment for personnel, 20: 35351
design of flexible, 20: 12272(P)
design of, for EGCR service machine, 17: 17549 (TID-18097)
design of, for gold-198 infusion in cancer patients, 17: 17682
design of, for protection of ovaries during radiotherapy, 17: 40462
design of, for protection of testes during radium therapy of penis, 17: 40463
design of formable, for neutrons, 17: 16731(P)
design of gonad, for hip radiography, 18: 37046
design of high-energy, calculations on meson-nucleon cascade for, 17: 9646 (ORNL-3289)
design of interlocking slabs which can be removed individually,

17: 31639(P)
design of labyrinth for reduced radiation scattering in biological, for package irradiation plant, 18: 41593(P)
design of LCBWR, 20: 5106 (ACNP-65544(Vol.II))
design of lead, 20: 32680
design of lead, for coil circulating radioactive solutions during scintillation counting, 20: 38558
design of magnetic, for space vehicles, 20: 40291
design of minimum-weight proton, for spacecraft, 17: 18388 (TID-7652 (p.773-93))
design of, neutron cross sections for, 17: 39976 (NARF-62-17T)
design of, nucleon-meson cascade calculations for, 17: 18384 (TID-7652(p.698-712))
design of Orsay linear accelerator, 17: 22703
design of portable, for personnel during diagnostic radiography, 19: 46036
design of radiation source, for irradiating natural animal populations, 20: 40518 (CEX-63.10)
design of shielded vehicles for work in radiation areas of high-energy accelerators, (E), 20: 2542 (UCRL-16236)
design of spherical, for radiation sources, 20: 25450(P)
design of temporary, for use in installation of tube inlets into radioactively contaminated rooms, 19: 715(P)
design of water, of whole-body gamma spectrometer, 18: 10427
design of window, 16: 27182(P)
design of zinc bromide filled windows for, 17: 7498 (USNRDL-TR-594)
design of, calculation validation method for, (T), 19: 17157(R) (ORNL-3714(Vol.I)(p.43-67))
design of, for installation in homes, 20: 33102(P)
design of, for protection of gonads of children during radiographic examination, 18: 39003
design of, for protection of anesthesiologists, 19: 31925
design of, methods and tables for, 20: 11058(T)
design of, use of dimensional analysis and model theory in, 20: 30730
design optimization for space power plant, 16: 14365
design optimization for gamma and neutron, 19: 32615 (NAA-SR-10856)
design optimization for laminated, computer program for, 20: 6518 (NAA-SR-Memo-11516)
design requirements for concrete, (E), 19: 29445
design requirements for, of underground structures against nuclear explosions, 20: 25230 (HN-183)
design studies on, damage detectors, 18: 31935
development at Ispra Research Center, 17: 28407 (EUR-142.d)
development for accelerators, 20: 26611
development for Apollo, instrumentation for, 17: 14607(R) (ORNL-3378 (p.1-17))
development for Cockcroft-Walton accelerators, 18: 5548(R) (UCRL-7450)
development for d-c magnetic fields, 18: 30940
development for fission sources, 20: 10439(R) (ORNL-3830, pp 285-98)
development for gamma spectrometer, 18: 43952
development for high-energy radiation, 19: 23163(R) (ORNL-3650(p.111-86))
development for Intense Neutron Generator, 19: 39761 (AECL-2177, Paper 8))
development for manned space vehicles, 19: 40063 (NP-15125)
development for pipes from reactor vessel through thermal shield, 16: 28315(P)
development for radiation detection equipment, 18: 25835
development for radiological containment systems, 20: 4214
development for space vehicles, straightahead approximation in, (T), 19: 17161 (ORNL-P-786)
development for space radiation, calculations for, 19: 21242 (NP-14837)
development for Stanford Linear Accelerator, 17: 35000(R) (SLAC-10)
development for Stanford Linear Accelerator, 20: 13366(R) (SLAC-53)
development for subcritical thermal assemblies, 19: 17368
development for use in high-energy radiation, 19: 16820(R) (ORNL-3714(Vol.II))
development for whole-body counter facility, 20: 16737(R) (UCRL-14534, pp 13-18)
development of active electrostatic and magnetic, for spacecraft, 17: 10200 (NP-12371)
development of cement-iron mixtures for accelerator, 20: 4998 (JINR-P-2359)
development of cesium-137 thermoelectric cells, 19: 13843(R) (SAN-366-1)
development of electromagnetic pulse, for communication systems, 18: 26819
development of, for space vehicles, 17: 15376 (N62-11035)
development of lead-ore, 18: 42875(P)
development of space-vehicle, problems in, 18: 26816
development of split scatter type for space applications, 16: 11111 (AD-259663)
development of suspended, for human chest films, 17: 30237
development of, for space applications, 20: 41219
development of, with neutron-absorbing particles distributed in organic binder, 19: 1819(P)
development problems in cosmic radiation, 16: 20232
dimensioning of, scattering effects of gamma and x rays on, 17: 15379
dimensions and weights for aircraft reactors, 16: 7226 (NEPA-1079)
doors, design, 16: 28313 (BNL-5262)
dose build-up factor in infinite, for line isotropic gamma source, 20: 1316
dose buildup factor for finite slabs, gamma, 18: 38240 (TO-B-64-44)
ducts and voids in, effects of, approximate method for determining, 17: 4282
effectiveness for protection from a number of radiation sources, optimum, 17: 40221
effectiveness for 12.5-Mev tandem Van de Graaff accelerators, 20: 23820 (ANL-7139)
effectiveness in space vehicles, gamma attenuation measurements of, 18: 16231 (TID-7689(p.76-80))
effectiveness of, at Lawrence Radiation Laboratory Bevatron and synchrocyclotron, 17: 22700
effectiveness of, against radioinduced tumors in mice, 18: 1430
effectiveness of gonad, during diagnostic radiology, 19: 46145
effectiveness of iron, in various arrangements and thicknesses, 18: 40737 (TO-B-64-49)
effectiveness of, for liquid scintillation spectrometers, 18: 35855
effects in irradiated rabbits of abdominal, 19: 33953
effects of abdominal, on survival in γ- and proton-irradiated rats, 20: 18441
effects of intestinal, on hematopoiesis in mice, 20: 18432
effects of partial, on development of enzyme systems in liver of irradiated rats, 17: 33482(R) (NP-13010(p.11-22))
effects of partial-body, on distribution of x radiation in dogs, 20: 35276
effects of self-, in neutron activation analysis, 20: 12794
effects of terrain and vegetation, 17: 33577
effects of wedge-shaped filters on geometry of cobalt-60 gamma beams used for therapy, 19: 42397
effects of, of abdomen of rats during x irradiation of Yoshida sarcoma, 20: 42962
effects on adsorption dose factor of cylindrical source, 16: 24909
effects on bone marrow in astronauts, 20: 31029 (BNL-10221)
effects on neutral red sedimentation in sunlight, 19: 11232
effects on whole-body counting in man, 20: 9266
efficiency of core shelters in typical British house for radioactive fallout, 20: 39083
efficiency of lead-polyethylene combinations for gamma, (E), 19: 6824
electron beam diocotron instabilities in, (T), 20: 3252 (NP-15578)
electron dose rates behind spherical multilayer, computer program for calculation of, 19: 40064 (NP-15132)
electron-photon cascade showers in accelerator, calculations of, 17: 22694
electron reactions in space vehicle, bremsstrahlung from, 19: 40062 (N64-29366)
electron transmission through, calculation of space radiation dose from, 19: 38016 (N64-29368)
electron transmission through spacecraft, isotropically incident, (E), 20: 42520
electronic, of rare earths, recoilless gamma absorption studies of, 20: 37161
electrostatic, for space vehicles, 17: 17395
empirical constants in calculations, 16: 19886
evaluation for promethium sources, 17: 29155 (HW-77375)
evaluation for ships, 16: 31179 (USNRDL-TR-373)
evaluation of, for interelectrode space in plasma cells, 17: 11311(R) (LAMS-2796)
evaluation of, for facility used in whole-body radioactivity counting, 17: 27516
evaluation of shadow geometries for space nuclear systems in Outside Test Tank, 16: 15993
evaluation of 2π covers, 16: 11115 (DC-57-10-46)
fabrication of flexible, for protective garments, 18: 21547(P)
fabrication of flexible lead, 18: 21548(P)
fabrication of heat-resistant, 17: 2419(P)
fabrication of lead bricks, 16: 30766(P)
fabrication of lead bricks for, 17: 29702
fabrication of massive high-density walls, 17: 18730(P)
fabrication of plastic, for Centaur vehicle, 20: 36349 (N-66-18473)
fabrication of pliable sheeting, 18: 25909(P)
fabrication of protective walls using distance rods, 17: 39521(P)
fabrication using cement and depleted uranium, 20: 41435(P)
facility description for studies at Battelle, 18: 21543 (BMI-1384)
fallout attenuation parameters for concrete block structures, 18: 27690 (NRL-TR-43)
feasibility of electromagnetic, for space vehicles, 17: 31633 (ASD-

TDR-63-194)
filters for dosimetry in cobalt-60 teletherapy, 19: 33997
for dental installations, 17: 6344
for low-level gamma counting facilities, 16: 33318 (TID-16825)
for radiation detectors, 17: 6486(P)
for space vehicles, combination of active and passive, 17: 18390 (TID-7652(p.819-28))
for space vehicles, 18: 31824
for space vehicles, 19: 31803(T) (UCRL-Trans-1225)
for space vehicles, 19: 31810
for whole-body counting room, comparison of water and lead, 17: 25592(R) (ANL-6646(p.66-7))
for whole-body counting room, 18: 20337 (NYO-2553-1)
for whole-body radiation counters, 18: 37551
form stone, casting for, 19: 9358(P)
from radiation in space vehicles, 18: 20240
gamma and fast neutron penetration from disk source in homogeneous, 20: 26335
gamma attenuation in ducts with two right-angle bends, 16: 15756 (ARF-1158A02-7)
gamma attenuation in two-legged 11-in. rectangular concrete duct, 16: 21692 (NP-11657)
gamma attenuation in slab, computer program for calculation, 16: 24907 (WAPD-T-1464)
gamma attenuation in concrete above-ground blockhouse, 17: 42158
gamma attenuation in circular concrete duct with two right-angle bends, 18: 1169 (AD-289349)
gamma attenuation by concrete blockhouse, 18: 44917 (NUC-E-15)
gamma attenuation by barriers, air-scattered, (E), 19: 29439 (CEX-63.3)
gamma attenuation by boron-containing blocks, 19: 35570
gamma attenuation by horizontal concrete slabs, from finite plane source, (E/T), 20: 3271
gamma attenuation in hollow cylindrical, (T), 20: 8279
gamma attenuation in lithium hydride–heavy metal, 20: 34791
gamma attenuation in, computer code for calculating, 16: 19236 (HW-73381)
gamma attenuation in massive laminated, calculational method for, 19: 3450 (AE-157)
gamma backscattering by infinite concrete plane, 17: 26230
gamma buildup factors for, empirical functions for, 20: 20097 (ORNL-RSIC-10)
gamma dose attenuation in concrete ducts, energy dependence of, (E/T), 19: 45457 (AD-462614)
gamma dose from 1.25-Mev plane source behind, (T), 19: 17171
gamma dose rate behind laminated slabs, computer program for, 20: 20095 (ORNL-3805)
gamma dose rate distribution in compartmented steel, 18: 42868 (TO-B-64-1)
gamma dose rates from neutron capture in crew shields, 16: 12645 (DC-60-4-172)
gamma dose rates in cylindrical and rectangular steel structures from fallout, 20: 15931 (TO-B-65-27)
gamma dose rates in, computer program for calculating, 16: 11117 (DC-57-11-101)
gamma heating in stratified lead and water slabs, 20: 4999(R) (ORNL-2599)
gamma penetration of complex configurations, use of model experiments for studying, 17: 2417
gamma penetration in slab geometry and infinite media, solution of transport equation for, 18: 9561
gamma penetration in slabs (E/T), 19: 3455 (USNRDL-TR-730)
gamma penetration of bulb, comparison of calculated and experimental, 16: 714
gamma-ray transmission through slabs, 16: 24601
gamma scattering from concrete, from point isotropic source at slab surface, 20: 40284 (AD-637125)
gamma streaming in ducts in, 17: 3800
gamma streaming through air duct in concrete, 19: 21594 (AD-424387)
gamma transmission by multilayer, (T), 20: 12271
gamma transmission by lead and polyethylene slab, 18: 13177 (NARE-62-16T)
gamma transmission in beryllium–Herimet slabs, 19: 29438 (APEX-502)
gamma transport from distributed sources in laminated, Monte Carlo analysis of, 18: 22859
gamma transport in, solutions using Tschebyscheff polynomial expansions and method of moments, 18: 13181
gamma transport in, exponential transform for, 20: 20099 (ORNL-RSIC-14)
gamma transport in compartmented, Monte Carlo computer code for, 20: 44987 (AD-637685)
gamma-ray backscatter and transmission in slabs, Monte Carlo code for, 19: 8559 (TO-B-63-73)
geometry, analysis of point kernel concept, 16: 3882(R) (ORNL-3193 (p.310-14))
heat production in concrete pressure vessel, 17: 7500
heat transfer in space-vehicle fuel tanks, 16: 1269 (AD-256894)
improvements to prevent radiation leakage in radiodiagnosis and radiotherapy, 18: 27271
information center on, operation of ORNL, 19: 17158(R) (ORNL-3714 (Vol.I)(p.68-9))
information centers for problems of, 19: 47908 (ANL-7050, pp 125-39)
information on, center for, 18: 6406(R) (ORNL-3499(Vol.I)(p.165))
information on, retrieval system for, 18: 6407(R) (ORNL-3499(Vol.I) (p.166-7))
information on, center for, 19: 23996(R) (ORNL-3650(p.1-110))
integrity tests of hot cells in Naval High-Level Radiation Laboratory, 19: 26492 (NRL-6205)
magnetic coils for, of space vehicles, 20: 40292
magnetic-field, for space vehicles, 17: 18389 (TID-7652(p.808-18))
magnetic-field, Liouville theorem for problems in, (T), 19: 23945
magnetic, charged particle motion around superconducting solenoid, 20: 42521
magnetic, theory and experiments on, for space vehicles, 18: 26107 (ERR-FW-210)
mass calculations for cosmic-ray, for manned space vehicles, (T), 20: 3245 (NASA-SP-71, pp 407-14)
materials and processes for, review of, 16: 30119
materials for nuclear power plant, 20: 30815
materials for reactor environmental test chambers, 20: 478
measurements in 2π solid angle shield cover experiments, 16: 19883 (XDC-59-5-78)
mechanical properties of concretes as, effects of high temperatures on, (E), 19: 29451
meson (μ) flux in neutrino, measurement of, 20: 22306 (CERN-65-32, pp 147-52)
meson (μ) ionization energy losses in, (T), 20: 3238 (JINR-P-2354)
method of filtration, x-ray equipment, 20: 16844
method of, in waste disposal, 20: 38539(P)
methods and principles of, 17: 7499
neutron albedo on slab, transport solution for, 18: 21134 (TID-20540)
neutron angular distributions behind iron, fast, 20: 40286
neutron attenuation in concrete and iron, from alpha reactions with tantalum, (E), 20: 2554
neutron attenuation in air-filled ducts through water, (T), 20: 10221 (NP-15692)
neutron attenuation in water, verification of geometrical transformation of, 20: 46935 (ORNL-TM-1603)
neutron attenuation in, computer code for calculation, 16: 19236 (HW-73381)
neutron attenuation in massive laminated, calculational methods for, 19: 3450 (AE-157)
neutron cross section calculations, computer program for, 16: 21691 (DC-60-7-9)
neutron cross sections for, library preparation of, 20: 26333 (CONF-660303-2)
neutron distributions in hydrogen-free, (T), 19: 5392
neutron dose rates in, first-collision moments method for calculating, fast, 16: 1024 (NARF-61-12T)
neutron dose rates in, computer program for calculating, 16: 11117 (DC-57-11-101)
neutron doses behind space-vehicle, from cosmic proton reactions, 18: 28538
neutron flux distributions in, development of hand calculations for, 16: 26432 (APEX-652)
neutron flux distributions in concrete-walled ducts in, calculation of thermal, 18: 9557 (ORNL-3507)
neutron flux distributions and spectra in iron–water, (E/T), 20: 40287
neutron penetration in, Monte Carlo calculation of deep, 18: 15424 (NP-13719)
neutron penetration in thin iron and polyethylene, (E), 19: 35571
neutron penetration of bulk, comparison of calculated and experimental, 16: 714
neutron removal cross sections, fast, 16: 19884 (XDC-60-1-215)
neutron scattering by cylindrical volume of, computer program for analysis of, 17: 31634 (NAA-SR-Memo-8516)
neutron slowing down in, calculation method for, 17: 12776(R) (ORNL-3360(p.96-7)))
neutron spectra in aluminum and iron, measurement of fast, 17: 34287
neutron spectra in paraffin, fast, (E/T), 20: 3257
neutron spectra outside pulsed-accelerator, 20: 2553
neutron transmission in, 17: 37993(R) (GA-4426)
neutron transmission by, angular distributions in, 20: 5181(R) (ORNL-3029)
neutron transmission by lead and polyethylene slabs, 18: 13177 (NARF-62-16T)
neutron transmission by beryllium-Hevimet slabs, 19: 29438 (APEX-502)

neutron transport in plate layers of, solution of Boltzmann equation for, 19: 3196
neutron transport in heterogeneous, with anisotropic scattering, (T), 20: 2989
neutron transport in, exponential transform for, 20: 20099 (ORNL-RSIC-14)
neutron transport calculations for, cross section library for, 20: 30723 (NAA-SR-11831)
neutron transport in slab geometry, numerical integration of equations for, 19: 17168
nucleon transport through, IBM-7090 Monte Carlo codes for, 17: 18379 (TID-7652(p.608-18))
nucleon-meson cascade equations for accelerator, solutions of, 19: 35564 (ORNL-P-299)
nucleon-meson cascade equations for accelerator, numerical solution for, 20: 24576 (ORNL-TM-951)
of contaminated patients, during transport and medical care, 17: 41020 (HW-SA-2859)
of ducts through shielding walls, 19: 23952(P)
of electronic equipment using special potting mixtures, 19: 3475(P)
of fallout by structures, mobile radiological unit for measuring, 19: 18142 (CEX-63.11)
of fallout shelters, use of highways for, 19: 46669
of gonads, during diagnostic radiography, 20: 1703
of infants in pelvic examinations, protective effects of, 19: 19677
of isotopic power sources, handbook on, 19: 21595 (TID-7698(Pt.I)(p.33-248))
of radioisotopic power sources, 19: 2690
of spinal cord, during radiotherapy of spinal tumors, 20: 6976
optical, for thermal radiation, 20: 614
optimization for army reactor (PL-1), 16: 28522 (APAE-Memo-315)
optimization for radiation mixtures, 20: 34788
optimization for SNAP manned vehicles, fast-neutron weighting factors, 20: 43580 (NAA-SR-Memo-11901)
particle transport, invariant imbedding theory, 16: 14202 (NARF-61-41T)
passages in, for cables or pipes, 16: 6079(P)
penetration by simulated nuclear weapon radiation, 17: 12781(R) (ORNL-3360(p.122-33))
penetration for remote-control equipment, design of tubes for, 19: 30365(P)
performance and requirements in space vehicles, 17: 16876
performance and stressing of hardened-concrete, (E), 19: 29448
performance evaluation of space-vehicle, 18: 28903
performance for 2-Mev to 100-Bev alpha particles, tabulations of, 20: 12265 (NP-15697(Vol.1))
performance in space vehicles, calculation of (E/T), 19: 2190
performance of accelerator and space vehicle, methods of calculating, (E/T), 20: 17158(R) (ORNL-3900, pp 82-149)
performance of charged-particle, (E/T), 19: 9886 (NAS-NRC-PUB-1133)
performance of concrete blocks and poured concrete, (E), 19: 8562
performance of concretes as, effects of temperature on, (E), 19: 29452
performance of copper for cosmic-ray, on manned space vehicles, (T), 20: 3240 (NASA-SP-71, pp 183-8)
performance of cosmic-ray, on Apollo Command/Service Module, (T), 20: 3244 (NASA-SP-71, pp 365-75)
performance of crushable, analysis of, 17: 1000(R) (ARF-4267-2)
performance of space-vehicle, against solar-flare protons, 18: 28295
performance of superconducting-magnet dynamic, for space vehicles, (T), 20: 3241 (NASA-SP-71, pp 199-209)
performance of, analysis using CHARGE computer program, (T), 19: 29462
performance of, use of radioisotopes for studying, 19: 20417
photon streaming around offset holes in, 17: 19509 (NAA-SR-Memo-5001)
photon transport in slab geometry, numerical integration of equations for, 19: 17168
physics of radiation, results of research in, 18: 38062 (A/CONF.28/P/377)
pipe leads through, design of, 19: 10458(P)
plug design for, 19: 35644(P)
plug design for gastight facility, 16: 3132
preparation of, for experiments at ORNL isochronous cyclotron, 18: 7363(R) (ORNL-3499(Vol.II)(p.104-5))
principles and uses, 18: 17375
problems in cosmic radiation, 16: 16187
problems in, listing and discussion, 16: 11125 (TID-14558)
problems in space-vehicle, 19: 40072
production of steel doors, 17: 7504
properties of ceramic, 20: 27615
properties of concrete, 16: 24221
properties of concrete, effects of aggregate on, 19: 18488
properties of concretes as, symposium, 19: 29444
properties of dwellings in Hiroshima and Nagasaki, 20: 39064
properties of Japanese residences as, 19: 42655 (CEX-62.11)
properties of magnetic-field cosmic-particle shields for space vehicles, 16: 15432
properties of multi-story windowless structure as, against strips of contamination from nuclear explosion fallout, 18: 35771 (TO-B-63-76)
properties of ponds for fuel element storage and unloading, 18: 40812 (NP-10375)
properties of steel, for mesons (μ), 18: 26165 (BNL-837(p.91-113))
properties of structures for, against fallout, 19: 11414 (AD-420472)
properties of umbrella-type, for solar-flare protons, 18: 3035
properties of underground structures as, against nuclear explosions, 18: 3971 (WT-1723)
properties of, for silicon solar cells, 19: 40931 (AD-609424)
protective effects of lead, against radiation injuries in dogs, 17: 21581
protective effects of intestinal, against x radiation effects on rat enzymes, 17: 38762
protective effects of, against radiation injuries in embryos of rats and mice, 18: 33423
protective effects of local, against radiation injuries in rats, 18: 39021
protective effects of, against radiation injury of rat placenta, 19: 19557
protective effects of, in man against chronic low doses of radiation, 20: 42865
proton attenuation by thick concrete, 6.2-Bev, (E), 19: 5389 (UCRL-11331)
proton dose in complex-configuration, code system for calculation of, (T), 19: 17173
proton dose rates at center of spherical-shell, formula for calculation of, 17: 26224
proton dose rates behind spherical multilayer, calculation, (T), 19: 17172
proton dose rates behind spherical multilayer, computer program for calculation of, 19: 40064 (NP-15132)
proton reactions in graphite and nickel at 660 Mev, secondary neutron production in, (E), 19: 38018
proton reactions with, code for calculation at <400 Mev, 17: 12785(R) (ORNL-3360(p.204-13))
proton shield optimization theory for spherical geometry, minimum-weight (T), 19: 1817 (UNC-5086)
radiation absorbed dose rates in, calorimetric measurement of reactor, 19: 45467
radiation absorption and dose distribution in, from uniformly distributed isotropic sources, 19: 31437
radiation attenuation by proton accelerator, 20: 2552
radiation attenuation by vertical, (E/T), 20: 6516 (AD-617524)
radiation distributions in, in space vehicles, 19: 30010
radiation dose accumulation in, from point isotropic source, 19: 31432
radiation dose build-up factors for concrete, 19: 1818
radiation dose rates in cylindrical volume source, source function coefficient evaluation, 16: 11118 (DC-57-11-103)
radiation dose rates in compartmentalized shelters, gamma and neutron, 18: 25712 (USNRDL-TR-722)
radiation doses in space vehicle, computer programs for calculating, 20: 15930 (NP-15697(Vol.2))
radiation effects on windows, 16: 686
radiation flux from cylindrical and spherical sources with slab, 19: 40068
radiation flux from cylindrical or spherical sources with shell-shaped, 19: 41960
radiation hazards in supersonic jet aircraft from solar flares, 20: 46932(R) (ORNL-3973(Vol.2), pp 71-84)
radiation heating in laminated, 20: 4299(R) (ORNL-2711)
radiation intensities from 4-Bev photons on concrete, 17: 34993 (CEAL-1004)
radiation levels in and about systems, instruments and techniques for measuring, 16: 10169 (DC-57-2-76)
radiation scattering in multibend ducts in, Monte Carlo calculation of, 17: 21201 (NARF-62-13T)
radiation streaming in cylindrical ducts in, 17: 3801
radiation streaming in annular and ordinary ducts, geometrical attenuation of, (T), 19: 12726
radiation streaming through voids in, 19: 27707
radiation streaming through single-bend aluminum ducts in, 19: 47863 (AD-613480)
radiation transport in, conservative finite-difference approximations to, (T), 20: 8273 (LA-3401)
radioinduced heating, neutron, 16: 23959
radiosensitivity effects on rat intestine, x, 19: 5697
radiosensitivity effects on thymic lymphocytes of adrenal gland and splenic, 20: 142
recommendations for concrete structures, 17: 14762
regulations on, for sealed radiation sources, 17: 8484
requirements for accelerator facility, 17: 7393
requirements for electronic components in space, 18: 10358
requirements for high-intensity proton linac, 18: 22620 (TID-7691(p.333-60))
requirements for isochronous cyclotrons, 17: 7395

requirements for large isochronous cyclotron, 17: 7396
requirements for LRL 184-inch cyclotron, 17: 7401
requirements for manned space vehicles, 17: 16877
requirements for manned space vehicles, 17: 35333 (NP-13060(p.339-64))
requirements for moderate-energy electron accelerators, 18: 10708
requirements for manned space vehicles, 18: 19265
requirements for manned military space missions, (T), 20: 2656 (NASA-SP-71, pp 265-86)
requirements for nuclear thermionic converter-space radiator against micrometeoroids, 18: 12852(R) (AD-409570)
requirements for Plutonium Reclamation Facility, 16: 23780 (HW-68021)
requirements for protecting astronauts from solar flares, (T), 20: 2655 (NASA-SP-71, pp 85-96)
requirements for radiation sources carried by space vehicles, 16: 20236
requirements for space radiations, 16: 10418 (ASD-TR-61-322(p.532-8))
requirements for space vehicles, 16: 20235
requirements for space vehicles, 16: 20241
requirements for space flight, conference, 17: 18353 (TID-7652)
requirements for space flight, 17: 18382 (TID-7652(p.662-81))
requirements for space radiation, 17: 26741 (ORNL-TM-552)
requirements for, at 200-Bev proton synchrotron, (T), 20: 5945 (UCRL-16464)
requirements in spacecraft, for solar-flare protons, 16: 30992
requirements of, in space, 17: 18354 (TID-7652(p.vii-xvii))
requirements of, for isotopic power sources in space missions, 18: 11362
requirements of, for neutron generators, 20: 41215
research, (T), 20: 6521(R) (ORNL-3858(Vol.2), pp 73-81)
research, (E), 20: 6297(R) (ORNL-3858(Vol.2), pp 82-90)
research for SNAP, review of, 20: 5183 (ORNL-P-1736)
research on, 19: 16819(R) (ORNL-3714(Vol.I))
research on gamma and neutron, (E), 20: 6520(R) (ORNL-3858(Vol.1), pp 42-6)
research on, review of, 20: 34778 (N-65-32252)
research programs on, in Japan, 17: 17624(R) (JAERI-5006)
research programs on, Reactor Station Geesthacht, Germany, 1961, 18: 32948(R) (EUR-534.d(Pt.I))
research programs on, Reactor Station Geesthacht, Germany, 1962, 18: 32949(R) (EUR-534.d(Pt.II))
research progress on high-energy, 20: 46931(R) (ORNL-3973(Vol.2))
review, 20: 23418
roof-reduction factors in, comparison of Monte Carlo and moment methods for calculating, 17: 26214
scattering functions for slabs, 18: 13180 (RM-3575-PR)
secant integrals of first and second kinds, 17: 4881
shape of, for disc radiation source, 18: 26818
shock crushing studies, 16: 30004(R) (ARF-4267-1)
simulation using photons, 16: 15758 (DC-61-1-116)
slowing-down equation for, constant solution of, 18: 34747
solar proton reactions in, secondary radiation dose from, 17: 18378 (TID-7652(p.595-607))
solar-flare proton dose to tissue behind slab, secondary particle contribution to, (T), 20: 35350
standards for, in radiodiagnosis, 18: 35404
stress analysis of prestressed concrete, finite element method for, 19: 20086 (GAMD-5926)
studies in Japan, 19: 3452 (JAERI-4029)
survey, 16: 7773 (TID-14742)
test facilities design, 16: 9628 (DC-58-4-152)
testing in air of porous, calculations and data analysis, 16: 23244 (DC-61-2-101)
theory, generalization to non-isotopic sources, 16: 1161
theory of magnetic, for space vehicles, 18: 42867 (MTP-RP-64-1)
thermal effects of fire on cobalt-60 teletherapy heads, 17: 18350 (TID-7651(p.304-14))
thermal stress in spherical concrete, calculation of, 17: 36354
thermal stresses in annular concrete, computer analysis of, 17: 26223
thermal stresses in concrete and steel annular, computer program for calculating, 19: 29478
thick-walled concrete, pressure and leakage-rate testing of, 17: 19508 (ANL-6664)
thicknesses of, for strontium-90–yttrium-90–lead bremsstrahlung sources, 19: 8563
threaded panel design for interchangeable manipulating devices, 19: 2529(P)
transport calculations for proton, 17: 4211 (UCRL-10440)
transport equation for inhomogeneous, 18: 38234 (A/CONF.28/P/363)
use of chalk bricks as structural material, 17: 33644
use of chalk in bags, as portable, 17: 33643
use of collimated neutron beam sources in studying, 16: 19885
use of lead grating during x radiotherapy of stomach carcinomas, 20: 38763
use of lead, for Paramecium growth studies, 20: 42886
use of lead, for protection of gonads during electron beam therapy, 20: 43012 (BMwF-FBK-66-03)
use of water, for personnel protection, 20: 43613
use of wedge-shaped lead, for gamma dose distribution measurements in phantoms, 20: 38762
weight optimization of laminated, use of method of steepest descent in, 17: 24600 (NAA-SR-Memo-8181)
weight reduction methods, 16: 6121
whole-body, effectiveness as protection of man against radiation injuries, 16: 20242
windows for, cleaning of clouded oil-filled, 17: 3707
windows for, design of liquid-filled, 19: 35580(P)
windows in, procedure for cleaning clouded oil-filled, 17: 2758

SHIELDING MATERIALS

(See also specific materials.)

ablation measuring system for spacecraft, feasibility of radioisotope, 20: 36353
analysis of concrete, petrographic, 19: 29446
attenuation factors for, radioisotope and fission-product, 18: 22984 (NYO-10721)
attenuation of gamma radiation by, 17: 4280
attenuation of gamma radiation by, 17: 7502
attenuation of neutrons by, 17: 4279
availability of battleship armor plate for, 19: 22823 (ORNL-TM-1047 (p.106-8))
bibliography on, 20: 10220 (AED-C-01-11)
bibliography on concrete, 18: 22983 (CEA-Bib-40)
bibliography on gamma and neutron, 19: 25615 (AED-C-01-08)
bibliography on hydrogenous, 16: 9550 (DC-51-11-26)
book: *Nuclear Technology in Construction*, 19: 38828
bremsstrahlung production from electron and photon reactions in, 20: 34779 (N-66-12185)
buildup factors for, at various gamma energies, 17: 22767
cascade showers in high-energy accelerator, 20: 935 (ORNL-TM-1298)
cascade showers in, (T), 20: 6521(R) (ORNL-3858(Vol.2), pp 73-81)
composition and properties of refractory, 19: 26761(P)
composition of, 17: 9816(P)
criteria for, 20: 1314
density of cast iron, radiographical methods for determination of, 19: 47039
description of polymer-dispersion, for neutrons, 17: 41375(P)
design and fabrication of clothing with lead-mercury amalgam, 19: 18228(P)
design of flexible, for personnel, 17: 5529(P)
design of laminated, for gamma radiation and neutrons, 18: 38236 (A/CONF.28/P/684)
design of laminated, 20: 14680(P)
design of multilayer, response matrix method for, 18: 38235 (A/CONF.28/P/657)
development and fabrication of plastic-clad metal plates for, 18: 7850(P)
development and testing for aerospace uses, 17: 36347(R) (NARF-62-18P)
development for hot-cell window, 16: 3884(R) (ORNL-3193(p.318-19))
development for space uses, 18: 11512(R) (NARF-63-9p)
development of boron-impregnated plastic, literature search on, 17: 9812(R) (AD-272874L)
development of cement filler of ferromagnetic spinel crystallites dispersed in aluminum silicates, 18: 41479(P)
development of elastomeric, 17: 2415 (RIA-62-654)
development of, for nuclear technological uses, 17: 4973
development of hydride, for space reactor, 18: 32955
development of lead-brick, 18: 31742
development of lead-clad steel, 18: 32952
development of lead brick as, 18: 40742
development of lead as, 18: 40743
development of light-weight boron, 16: 21690(R) (AD-267561L)
development of Marbolite, for gamma rays, 17: 35065
development of polyethylene particles in an organic binder as, 17: 31638(P)
effective cutoff energies for boron, cadmium, gadolinium, and samarium, 16: 28014 (ORNL-TM-236)
efficiency of concrete, in criticality incident of 10^{17} fissions, 20: 43421 (NP-16216)
efficiency of two-component, for gamma rays and neutrons, 19: 31426
electron range-energy relations in, tables, 19: 8004 (NASA-SP-3012)
electron ranges in, as function of atomic number and energy, 19: 17169
electron transport through thick layers of, similarity principles for, (T), 20: 8276
evaluation for high-energy accelerators, thickness-energy curves for, 16: 29878 (NP-11931)
evaluation for reactor uses, (E/T), 19: 17156(R) (EUR-2197.d)
evaluation for space vehicles, 16: 14203 (NARF-62-1T)
evaluation of depleted uranium for, 16: 11195 (DC-55-12-110)

evaluation of, for use in TRU Facility at ORNL, 17: 12183(R) (ORNL-3375)
evaluation of microwave, 20: 9188
evaluation of multilayer, for aircraft reactors, 18: 15594 (NARF-58-29R)
evaluation of multilayer, for aircraft reactors, 18: 15595 (NARF-58-40R)
evaluation of reactor, (E/T), 19: 14753
evaluation of refractory concretes, 20: 44005
fabrication and forming of flexible film, 19: 44670(P)
fabrication and properties of concrete blocks for, for reactor walls, 17: 24651
fabrication for accelerators and reactors, 16: 30757
fabrication of calcium boride bricks, 17: 25767(P)
fabrication of cast, flexible, polyvinyl chloride plastisol, 17: 15375 (LAMS-2800)
fabrication of cementitious building materials, 17: 12643(P)
fabrication of ceramic lead-containing structures, 18: 35977 (P)
fabrication of chemical complex-containing, 16: 30774(P)
fabrication of concrete containing carbon and lead, 20: 2306(P)
fabrication of ferrous-carbon type, process for, 20: 2301(P)
fabrication of flexible plastic film, 16: 20587(P)
fabrication of glass fiber-reinforced polyester, containing iodides of heavy metals, 20: 9481(P)
fabrication of lead bricks, 17: 29702
fabrication of lead, methods for, 18: 32953
fabrication of metal-coated textiles, 19: 28608(P)
fabrication of multi-layer, for neutron and gamma radiation, 20: 28601(P)
fabrication of phosphate glass, 16: 27618(P)
fabrication of porous refractory, 17: 41398(P)
fabrication of powdered lead–silicone rubber–fiber flock flexible, 20: 25338(P)
for accelerators, 17: 36086
for diagnostic x-ray departments, 16: 17920
for gamma sources, nomograms for determining thicknesses for, 19: 21598
for photographic film detectors, 16: 27248 (AHSB(RP) R-19)
for professional office buildings, efficiencies of, 17: 6720
for remote-handling facilities, survey of, 17: 2748
for remote-handling facilities, survey of, 17: 3695
gamma absorption by heterogeneous, effective atomic numbers for, 19: 40069
gamma and neutron flux in, P_3 method for calculating, 20: 32673 (NAA-SR-Memo-11872)
gamma attenuation factors for, 17: 7501
gamma attenuation by, Monte Carlo calculation of, (T), 19: 8561
gamma attenuation and heating in, calculation of, 19: 25617
gamma attenuation in lead alloy, (E), 20: 6523
gamma attenuation calculations for, build-up factor effects on, 20: 40289
gamma attenuation coefficients for, cobalt-60, 20: 42518
gamma attenuation in, tables of equivalent thickness of, 20: 44989
gamma attenuation in, accuracy of calculations for, 19: 43464
gamma backscattering on, effect of material properties on, 20: 8283
gamma buildup factors for, 18: 26814(T) (ORNL-tr-80)
gamma buildup factors for heterogeneous layered, 20: 8280
gamma contamination of steel and lead sheet, 18: 43801(R) (LA-3132-MS(p.145-52))
gamma scattering and transport in, Monte Carlo methods for calculating, 18: 20932
gamma scattering by concrete and lead, 19: 5390
gamma secondary radiation in light-weight, 18: 3032
gamma transmission through cylinders and spheres of, Monte Carlo calculations for, 18: 35052
gamma transmission through slab, Monte Carlo calculations of, 19: 14733 (WAPD-BT-31(p.43-9))
gamma transport, 16: 32520 (XDC-60-2-28)
hydrogenous, properties and radiation stability, 16: 9550 (DC-51-11-26)
neutron albedo measurement on, thermal, 19: 40065 (NP-15152)
neutron attenuation in hydrogenous, 16: 6076 (XDC-57-1-32)
neutron attenuation by, 17: 11900 (NARF-62-16T)
neutron attenuation in, 19: 30895
neutron attenuation in, accuracy of calculations for, 19: 43464
neutron diffusion in laminated, Monte Carlo computer program for, 18: 42866 (ML-TDR-64-52)
neutron penetration, calculations, 16: 3880(R) (ORNL-3193(p.299-304))
neutron penetration in, calculations on, 20: 10439(R) (ORNL-3830, pp 285-98)
neutron removal cross sections for, 18: 34888
neutron spectra in, foil-activation measurement of (E/T), 19: 3771 (AE-155)
neutron transmission at 4.5 and 14.5 Mev by, asymptotic, 19: 1812(R) (HW-81746(p.2.36-8))
neutron transmission by hydrogenless, 19: 47870
neutron transmission through iron–water mixtures, 20: 34784
neutron transport in, analysis of fast, (E), 19: 21199 (CEX-65.02)
neutron transport in finite slab, source functions for, (T), 20: 2930 (AD-614636)
neutron transport, 16: 32520 (XDC-60-2-28)
nuclear cascades in, for accelerators, 16: 9555
nucleon cascades in, computer program for calculating, 20: 8274 (LNF-65/30)
nucleon transport in, calculations for (E/T), 19: 3461
particle dose and spectra calculations behind proton, computer program for, 20: 36348 (N-66-17566)
particle multiplication and transport in, solution to Milne problem for, (T), 19: 47865 (ANL-7061)
performance against isotropically incident electrons, (E), 19: 29459
performance for cosmic alpha particles and protons, tabulations of, 20: 12265 (NP-15697(Vol.1))
performance of barium and zinc chloride solutions as transparent, (E), 20: 10226
performance of borated-graphite and -iron oxides, for fast neutrons, 20: 14180 (COO-1430-1)
performance of laminar, (E/T), 19: 14755
performance of reinforced chamotte and chromite, for reactor thermal shielding, (T), 20: 12340
positron range-energy relations in, tables, 19: 8004 (NASA-SP-3012)
preparation and properties of concrete with dispersed ores, 16: 17223(P)
preparation and properties of phosphate glass, 19: 7595(P)
preparation and properties of boron–glycerin–litharge cement, 19: 18441
preparation and uses of asphalt, 20: 2248(P)
preparation of flexible film for use as clothing and coating, 16: 30764(P)
preparation of hydrated metal borate structural material or cement, 17: 30934(P)
preparation of mixtures of bitumen and heavy material for, 17: 1914(P)
preparation of olefinically unsaturated hydrocarbon polymer, for neutrons, 20: 30732(P)
preparation of, containing ground lead minerals and neutron absorbers, 19: 19337(P)
production of lead brick, methods for, 18: 32954
production of polymeric, 19: 24546(P)
properties, 18: 35050
properties and testing of concrete and steel, 20: 1312
properties and uses, 16: 30844
properties for gamma and thermal radiation, 19: 18507
properties for space vehicles, 16: 14351(R) (LNP-NR-140)
properties for space vehicles as function of atomic mass, 17: 26741 (ORNL-TM-552)
properties for space applications, calculation of, 19: 31443
properties of boron steel as, 16: 21034 (HW-SA-2583)
properties of boron- and cadmium-containing plastics, 19: 17963
properties of combinations of, 18: 40740
properties of concrete, metals, and soils as irradiation facility, 19: 11423(R) (UCRL-12004)
properties of conventional building supplies as, in dental roentgenographic installations, 17: 29703
properties of filled plastics as, 19: 46354
properties of high-density lead-slag concretes, 19: 18508
properties of lead-containing, 17: 8721
properties of lead as, effects of impurities on, 17: 33256
properties of lead glycerolates as reactor, 18: 1171
properties of lead concrete extra-high-density, 20: 27523
properties of titanium, yttrium, and zirconium hydrides for use as space, 19: 37104
properties of, for fast neutrons, 20: 35570(R) (MLM-1299, pp 17-21)
properties of, gamma and neutron counters and dosimeters for determining, 18: 33886(T) (JPRS-25467(p.9-24))
properties, protective and thermal, 16: 25031 (JPL-TR-32-232)
proton beam scattering by accelerator, secondary particle production by, 20: 27683
proton interactions at 10 to 1000 Bev in, cascade showers from, (T), 19: 10452 (CERN-64-47)
proton reactions at high energies, neutron diffusion from, (T), 20: 10223 (ORNL-P-1787)
proton transmission at 100 and 400 Mev, current to dose conversion factors for, (T), 19: 17162 (ORNL-P-801)
radiation absorption by, calculation of lead equivalents for, 18: 1172
radiation critical energies and units for, 17: 38420
radiation effects on hydrogenous, 16: 17221 (DC-52-5-41)
radiation effects, design of SNAP Shield Test Experiment for evaluation, 16: 32519 (NAA-SR-7432)
radiation effects on organic-fluid, 17: 16107
radiation effects on color and electric properties of glass, 17: 36364
radiation effects on cadmium, 19: 47576(R) (IDO-17081, pp 49-76)
radiation effects on glass, charge accumulation from gamma, 20: 30727

radiation transport by, high-energy, 17: 22694
radiation transport in, non-equilibrium diffusion equation for, (T), 19: 45460 (LA-3377)
radiation transport in, formulation of, (T), 20: 1303 (AD-614250)
radiation transport in, stopping power for, 20: 9166(R) (BNWL-36, pp 2.1-58)
radioactivity in concrete, y, 20: 8742(R) (COO-119-233, pp 97-100)
radioactivity in cement raw materials, 20: 43514 (UCRL-16878)
radioactivity induced in cyclotron, 17: 7395
radiological use of zinc bromide, 19: 15301
radiological use of, evaluation of, 19: 15301
radiolysis of water, around high-power gamma facility, 20: 5670
requirements for high-energy accelerators, review of, 17: 5057
requirements for nuclear-powered space vehicles, 17: 35333 (NP-13060(p.339-64))
requirements for reactor beam tubes, 17: 7503
research at Geesthacht Reactor Station, (E), 20: 4997(R) (EUR-2494.d)
selection for low-background, 18: 35260(R) (AERE-PR/HPM-5)
specific activity of lead, 17: 31637
stress analysis of reactor, 18: 36759 (IITRI-578P21-6)
survey of earth materials, 16: 29964 (UCRL-9970)
technology of concrete, 17: 35064
temperature distribution in gamma-radiation, (T), 20: 5002
testing at Dubna proton synchrocyclotron, 18: 34374
testing of high-density slag concrete as, 17: 33222 (ORNL-3473)
testing of, ESTAKOS experiment for, 18: 32949(R) (EUR-534.d(Pt.II))
transmission factors for uranium-235 fission products, 18: 15197 (LAMS-2963)
use of boric acid esters of monoaliphatic alcohols as neutron, 17: 9815(P)
use of concrete mixed with brown iron ores as, in nuclear engineering, 17: 19596
use of densified wood laminates as neutron, 20: 33777
use of lead as, at Trawsfynydd nuclear power station, 18: 28902
use of lead sulfide in plastic matrix as, 19: 35579(P)
use of lead–uranium dioxide as, 19: 46916 (BNWL-IR-3)
use of Plastilin for electron therapy discrimination, 20: 36700
use of tungsten–uranium alloys as, 16: 21006(P)
use of waste from lead processing as, 18: 4687(P)
x radiation produced in, 16: 431(T) (CEA-tr-A-971)
x-ray scattering in, J-discontinuity in, (T), 20: 8277

SHIKIMIC ACID
labeling with carbon-14, 19: 46312
preparation of uniformly C^{14}-labeled, 16: 13029(T)

Shims
see Reactor Control Rods

SHIPPING
analysis of air, for nuclear materials, (T), 19: 24065 (AFWL-TDR-64-81)
book: *Standards for the Transport of Radioactive Materials*, in Italian, 19: 32494
book: *The Transport of Radioactive Materials*. UKAEA, 19: 9426
cask design and regulations for spent fuel, 20: 2084 (EURAEC-374 (Vol.2))
cask design evaluation for fission product, 18: 25707 (HW-65268(Rev.1))
cask design for irradiated EGCR fuel, 19: 7665 (ORNL-TM-1001)
cask design for liquid waste, 20: 40476(R) (BNWL-267)
cask design for radioactive material, 19: 46665
cask for irradiated fuels, testing of 15-ton lead-shielded, 17: 18347 (TID-7651(p.197-210))
cask for irradiated reactor fuel, testing of, 18: 39528 (APED-4522)
cask for irradiated HFIR fuel, safety analysis, 19: 7736 (ORNL-TM-959)
cask for spent fuel elements from Elk River and Piqua Reactors, 19: 569 (TID-21246)
cask for spent Piqua-Elk River fuel, thermal tests of, 18: 29810 (COO-1028-2)
cask for, heat removal from spring-loaded dry, 18: 14028 (KAPL-M-6106)
cask testing for fission product, 18: 25708 (HW-77962)
casks for fuel, electric analog computer for fire tests of, 19: 36731
casks for irradiated fuel, impact tests on, 19: 40818 (SC-RR-65-98, pp 261-82)
casks for radioactive materials, structural analysis of, 20: 43492 (ORNL-TM-1312(Vol.2))
casks for spent BR2 and HFR fuel elements, 18: 37309 (A/CONF.28/P/448)
casks for spent fuel, economics of lead, steel, and uranium-shielded, 20: 16622 (ORNL-3918)
casks for, impact resistance of, 19: 22591 (CONF-641201-6)
container and equipment for radioactive materials, design of, 20: 18165 (ORNL-P-1987)
container and packaging for uranium hexafluoride, development and testing of, 20: 20936 (K-1661)
container design for parts at Y-12 plant, 19: 8717 (Y-OA-21)
container design for radioactive materials, review, 19: 40823 (SC-RR-65-98, pp 450-72)
container design for plutonium nitrate and oxide, 19: 40825 (SC-RR-65-98, pp 609-19)
container design for fissionable material, 20: 27210(R) (UCRL-14680)
container design for radioactive materials, 20: 616(P)
container development for mixed-oxide fuels, 19: 31521(R) (WCAP-3385-3)
container development and tests for radioactive materials, 19: 40816 (SC-RR-65-98, pp 141-86)
container drop tests for uranium hexafluoride, 10-ton capacity, 19: 40824 (SC-RR-65-98, pp 580-608)
container fire damage studies, modeling requirements for, 18: 23827 (NYO-2539-1)
container fire tests, modeling of, 19: 40815 (SC-RR-65-98, pp 133-40)
container fire test, 15-ton, 19: 40827 (SC-RR-65-98, pp 631-50)
container for dry uranium-235 compound, evaluation of, 18: 22280 (Y-1460)
container for dry enriched uranium, engineering drawings for Foamglas-insulated, 19: 28607
container for fissile materials, tests of, 18: 6972 (LAMS-2983)
container for fissile materials, safety evaluation of, 19: 13665 (LA-3203-MS)
container for fissile materials, design and tests of Class I, 19: 18193 (HW-SA-3995)
container for fissionable materials, impact tests of, 19: 26491 (LAMS-2983(Suppl.))
container for fuel cores, fire resistance tests of wood, 20: 37024 (NLCO-899)
container for irradiated fuels from power stations in United Kingdom, 19: 40829 (SC-RR-65-98, pp 711-18)
container for low-assay uranium compounds, tests of, 19: 40819 (SC-RR-65-98, pp 330-56)
container for radioisotopes, fire-impact shield for, 19: 11420 (ORNL-P-856)
container for radiocesium thermoelectric cell, design of, 19: 13843(R) (SAN-366-1)
container for radioactive material, design of, 19: 22610
container for radioactive materials, safety regulations for, 20: 32680
container for radioactive materials, design of, 20: 40481 (WAPD-T-1851)
container for radioisotope, design and testing of plywood, 20: 39164
container for spent fuel-element, 20: 14678(P)
container for transferring EBR-II fuel from reactor to cycle facility, 19: 9300 (ANL-6934)
container for uranium hexafluoride, engineering drawings, 17: 21859
container for used fuel element, 19: 42662(T) (ORNL-tr-600)
container response to vehicle collisions, analysis, 19: 40817 (SC-RR-65-98, pp 243-60)
container safety regulations for radioactive materials, IAEA, 16: 25672
container standardization for radioactive materials, 19: 40822 (SC-RR-65-98, pp 442-9)
container tests for uranium hexafluoride, 19: 13557 (K-D-1845)
container tests for slightly enriched uranium fuel cores, 19: 40820 (SC-RR-65-98, pp 357-76)
container tests for plutonium nitrate solutions, 19: 40821 (SC-RR-65-98, pp 423-41)
containers for fission-product, testing of buffered, 17: 30751 (HW-77963)
containers for fissionable materials, impact tests of birdcage-type, 19: 6129 (ORNL-3735)
containers for fissile materials, impact tests of drum-type birdcage, 19: 15697 (ORNL-P-869)
containers for, of fission products, 17: 6362
containers for radioactive fuel elements, design and properties of, 18: 14139
containers for radioactive materials, fire testing of, 19: 15790 (SC-R-64-1366)
containers for radioactive materials, tests of, 19: 30436 (AERE-R-4810)
containers for radioisotopes, stress analysis from internal pressures in, 20: 14667 (ORNL-TM-1312(Vol.1))
containers for radioactive materials, classification system for, 20: 14789 (ORNL-P-1910)
containers for radioactive materials, dynamic response of tiedowns for, 20: 23375 (NYO-2539-2)
containers for radioactive materials, leak detection in, 20: 41197(R) (NP-16172)
containers for spent fuel element, temperature measurements on, 20: 25332
containers for uranium hexafluoride, destructive tests of ten-ton, 20: 593 (KY-500)
containers for, drop tests on Types F and G, 19: 38546(R) (RFP-552)
containers for, plutonium, engineering drawings of, 19: 34422
cost calculations for spent reactor fuels, computer code for, 18: 35659 (ORNL-3648)

cost estimation for nuclear fuels, 20: 28686 (ORNL-3943)
cost of spent fuel-element, 18: 37420 (A/CONF.28/P/64)
decay-heat analysis for fuel-element, 18: 40808 (GEAP-4704)
economic analysis of, of spent domestic and foreign reactor fuels to reprocessing plant in USA, 17: 28446 (ORNL-TM-590)
economic and safety aspects of irradiated-fuel-element, 17: 39198(R) (ORNL-3452(p.233-5))
economics of irradiated fuel, 19: 46664
equipment for strontium-90, design testing, 16: 31985 (HW-SA-2655)
facilities for radioisotope, in United Kingdom, 16: 25673
fire codes for, national, 20: 23397
fissionable material, criticality studies, 16: 12841
fuel element, safety in, 20: 45571(R) (ORNL-3945, pp 248-55)
hazards in solidified high-level waste, 20: 24809(R) (BNWL-213)
hazards in solidified high-level waste, 20: 40476(R) (BNWL-267)
hazards in, of solidified high-level waste, 20: 12517(R) (BNWL-170)
heat removal in irradiated fuel element, 19: 46667
heat transfer from spent reactor fuels during, 17: 25411 (ORNL-3439)
licensing procedure for radioactive material, 19: 46666
materials management in, of uranium compounds, 20: 43065 (GAT-T-1403)
methods for fission-product, in large quantities, 18: 31649 (A/CONF.28/P/252)
methods for plutonium, at Rocky Flats, Colo., 20: 18948 (RFP-720)
of Army ML-1 Reactor by air, tiedown system for, 17: 13774 (AGN-TM-379)
of cerium fission products, tests of cask for, 19: 4395 (HW-71744)
of enriched uranium, testing of containers for, 17: 18346 (TID-7651(p.161-86))
of enriched uranium, testing of containers for, 19: 24816
of fissile materials, regulation of containers and procedures for, 17: 18340 (TID-7651(p.88-98))
of fission products, design of cask for, 18: 23823 (HW-65268)
of fissionable material in Great Britain, regulations for, 19: 672 (AHSB(A)-R-8(p.59-62))
of fissionable material, safety measures for, 20: 47002
of fuel elements to Piqua reactor site, 19: 24087 (NAA-SR-Memo-10529)
of fuels and fuel elements in Great Britain, regulations for, 19: 669 (AHSB(A)-R-8(p.37-45))
of fuels by sea, review of insurance problems in, 19: 7726 (EUR-1639.f)
of irradiated fuel in Europe, review, 17: 8429 (NP-12393)
of irradiated fuel elements, evaluation of casks for, 17: 18343 (TID-7651(p.126-31))
of irradiated fuel elements, cask design for, 17: 29717 (NAA-SR-Memo-7844)
of irradiated fuel from NS *Savannah* reactor for reprocessing, 18: 440 (NP-13235)
of irradiated fuel from SENN in Italy to U. S., 18: 448(T) (EURAEC-215)
of irradiated fuels from European power reactors to United States, 18: 5544 (EUR-112.e,f(Vol.1))
of irradiated fuels from European power reactors to United States, 18: 5545 (EUR-112.e,f(Vol.3))
of irradiated fuel elements, impact and static tests of 15-ton cask for, 18: 10301 (DP-843)
of irradiated fuels on European continent, economics of, 18: 37425 (A/CONF.28/P/422)
of irradiated fuels in EURATOM, procedures for, 18: 41675(R) (EUR-1850.e(p.195-200))
of irradiated fuel assemblies from Yankee reactor, experience in, 19: 19392 (WCAP-6062)
of irradiated fuel elements, economics and safety in, 19: 22428
of irradiated fuels from nuclear power plants, 19: 31622
of irradiated fuels, review, 19: 34282
of irradiated HNPF fuel elements, permissible heat generation rates in cask for, 17: 35104 (NAA-SR-Memo-3034)
of irradiated nuclear fuels, 18: 29912
of irradiated OMRE fuel elements, permissible heat generation rates in cask for, 17: 35103 (NAA-SR-Memo-2658)
of irradiated reactor fuels prior to reprocessing, 16: 29273
of irradiated reactor fuels, mechanics of, 17: 17450
of irradiated reactor fuels, review of problems in, 19: 9413
of irradiated research reactor fuel, 17: 28562 (EUR-185.f,d,e)
of low-level radioactive wastes, structural integrity of containers for, 19: 20196 (CONF-650103-6)
of plutonium, deceleration testing of bird cages for, 17: 18345 (TID-7651(p.145-60))
of plutonium dioxide, study of heat generation due to decay in wood containers, 19: 9406 (RFP-418)
of plutonium nitrate, design of containers for, 19: 4402 (RFP-437)
of plutonium oxide, study of shipper-receiver differences in, 19: 42425 (RFP-502)
of plutonium, engineering drawings of containers for, 19: 4426
of plutonium, measurement problems in, 19: 38535 (RFP-508)
of radiation sources, safety tests on containers for, 18: 22278(R) (ORNL-TM-630)
of radioactive cesium, containment in glass for, 19: 4428(P)
of radioactive materials by ocean, conference on, in New York, Jan. 1962, 16: 19212
of radioactive materials, review of national and international regulations, 16: 25671
of radioactive materials, containers and safety regulations for, 16: 29257
of radioactive materials by truck, accident hazards and economics of, 16: 33324
of radioactive materials, evaluation of accidents in, 17: 308 (NYO-9772)
of radioactive materials, evaluation of containers for, 17: 10780 (NYO-9859)
of radioactive materials, testing of packaging for, 17: 18317 (AHSB(S)R-19)
of radioactive materials, conference on, 17: 18334 (TID-7651)
of radioactive materials, accident experience in, 17: 18335 (TID-7651 (p.3-17))
of radioactive materials, effects of accidental release, 17: 18336 (TID-7651(p.18-30))
of radioactive materials, development of I.C.C. regulations for, 17: 18338 (TID-7651(p.45-54))
of radioactive materials, summary of Federal interagency committee work on, 17: 18339 (TID-7651(p.55-87))
of radioactive materials, Canadian regulations for, 17: 18341 (TID-7651(p.99-102))
of radioactive materials, British regulations on, 17: 18342 (TID-7651 (p.103-25))
of radioactive materials, problems of container design, 17: 18344 (TID-7651(p.132-44))
of radioactive materials by truck, economical control of risks in, 17: 27599 (NYO-9773)
of radioactive materials, container for, 17: 29153(P)
of radioactive materials, effects of packaging on radiation fields from, 17: 34150 (CRRD-1110)
of radioactive materials, bibliography on, 17: 34155 (TID-3552(Rev.2))
of radioactive materials, testing of packaging for conformance to I.A.E.A. regulations for, 17: 41036
of radioactive materials in Germany, accidents during, 18: 460
of radioactive materials, accidents in, 18: 469
of radioactive material in 1962, accidents in, 18: 1958 (TID-16764 (Suppl.1))
of radioactive materials, design of casks for, 18: 4050(P)
of radioactive materials, survey of container testing programs for, 18: 10306 (NYO-9774)
of radioactive materials, economic and legal aspects of, 18: 35797
of radioactive materials in Great Britain, 18: 41694
of radioactive materials, conference on, 19: 663 (AHSB(A)-R-8)
of radioactive materials in Great Britain, safety regulations for, 19: 664 (AHSB(A)-R-8(p.7-11))
of radioactive materials, radiation hazards during, 19: 665 (AHSB(A)-R-8 (p.13-17))
of radioactive materials, radiation hazards during, 19: 666 (AHSB(A)-R-8(p.19-24))
of radioactive materials in Great Britain, legislation relevant to, 19: 667 (AHSB(A)-R-8(p.25-30))
of radioactive materials in Great Britain, regulations for, 19: 671 (AHSB(A)-R-8(p.53-8))
of radioactive materials, packaging design for, 19: 673 (AHSB(A)-R-8 (p.63-80))
of radioactive materials in Great Britain, liability and indemnity policies for, 19: 674 (AHSB(A)-R-8(p.81-7))
of radioactive materials in Great Britain, organization for emergencies during, 19: 676 (AHSB(A)-R-8(p.109-12))
of radioactive materials in Great Britain, regulations for, 19: 670 (AHSB(A)-R-8(p.47-51))
of radioactive materials, transportation standards for, 19: 714
of radioactive materials, vehicle-collision problem in, 19: 7652 (NYO-2539-3)
of radioactive materials by commercial air carrier, separation distance calculations for, 19: 11419 (ORNL-P-745)
of radioactive materials, developments in containers for, 19: 11467
of radioactive materials, packaging and regulatory problems in, 19: 13666 (LA-DC-6866)
of radioactive materials, containers, economics, and regulations for, 19: 15793
of radioactive materials, fire testing of container for, 19: 24817
of radioactive materials, handbook of Federal regulations on, 19: 30475
of radioactive materials, IAEA safety regulations for, 19: 32496
of radioactive materials, standards for, 19: 36730
of radioactive materials, international conference on, 19: 40808 (SC-RR-65-98)
of radioactive materials, review of research on, 19: 40809 (SC-RR-65-

98, pp 17-31)
of radioactive materials, aspects of, 19: 40812 (SC-RR-65-98, pp 74-8)
of radioactive materials, regulatory packaging standards for, 19: 40811 (SC-RR-65-98, pp 45-54)
of radioactive materials, special problems in, 19: 40826 (SC-RR-65-98, pp 625-9)
of radioactive materials, incidents during, 20: 25324 (TID-16764 (Suppl.2))
of radioisotopes and radiation sources, fire tests of containers, 17: 20238 (COO-274)
of radioisotopes, engineering drawings of containers for, 18: 5569
of radioisotopes for agricultural research, safety measures in, 17: 27627
of radioisotopes, import regulations for, 17: 40438
of radioisotopes in Great Britain, 19: 668 (AHSB(A)-R-8(p.31-5))
of radioisotopes, evaluation of cardboard-box-steel-can containers for, 18: 22289
of radioisotopes, radiation protection during, 19: 13688
of radioisotopes, container designs for, 19: 15942 (ORNL-P-920)
of SNAP systems by highway, shock and vibration tests on, 17: 24744 (NAA-SR-Memo-8074)
of solution of americium, curium, and fission product isotopes from Savannah River Plant to ORNL, 19: 7650 (CONF-641201-2)
of spent fuel elements, containers for, 17: 3762
of spent fuel elements, air-cooled container for, 18: 4049(P)
of spent fuel elements, development of casks for, 18: 33822
of spent fuel elements, convective heat transfer in vertical channels of cask for, 18: 35641(R) (ORNL-TM-785)
of spent fuel elements, safety and economics of, 19: 5451(R) (ORNL-3627(p.249-55))
of spent reactor fuel elements, 16: 19177(R) (EURAEC-167)
of spent reactor fuels, safety aspects of casks for, 18: 31780 (A/CONF.28/P/279)
of strontium-90, containment in phosphate glass for, 19: 4427(P)
of strontium-90, design of cask and protective buffer for, 18: 22273 (HW-68274)
of uranium hexafluoride, engineering drawings of containers for, 17: 30777
package development for plutonium dioxide, 19: 30443 (RFP-501)
packages for fissile materials, criticality evaluation of, 19: 40828 (SC-RR-65-98, pp 679-90)
packaging of radioactive materials for, development of standards for, 19: 40810 (SC-RR-65-98, pp 32-44)
problems and safety aspects for spent magnox fuel elements, 20: 9200
procedures and regulations for spent fuel elements, 17: 16313(R) (EURAEC-292)
radiation effects on storage properties of fruits and vegetables, 17: 30026
radioactive materials, design of casks for, 16: 30695 (HW-SA-2295)
radioisotope, fire tests on container for, 18: 22271 (COO-277)
reactor fuel element, pressure venting device for casks for, 19: 24815
regulations and permits for safe interstate, of explosives, 20: 594 (LA-DC-7469)
regulations and standards for radioactive materials, 20: 45985
regulations for beryllium-containing materials, 20: 43629
regulations for fissionable materials, IAEA, 16: 7800
regulations for fissionable materials, IAEA, 16: 7799
regulations for fissionable material, revised EAEA, 20: 27217
regulations for irradiated fuel element, 19: 24814
regulations for radioactive materials in USSR, 16: 3293(T) (JPRS-10599)
regulations for radioactive materials, IAEA, 16: 2090
regulations for radioactive materials in Russia, 16: 16612(T) (JPRS-12823)
regulations for, radioactive material in USSR, 17: 4752
regulations for, radioactive material in USSR, 17: 4753
regulations for radioisotopes, 17: 27586 (AHSB(RP)R-23)
regulations for radioactive material, 18: 20248
regulations for radioactive materials, 20: 18940 (EUR-2747.f)
regulations for radioactive materials, key to IAEA 1964, 20: 20945 (TRG-Report-1073)
regulations for, of radioactive materials, 20: 4181 (NP-15620)
regulations for, of nuclear material, 20: 46002
regulations for, radioactive materials, 18: 27748
review of radioisotope, in United States, 20: 11035 (TID-8541, pp 249-319)
safety criteria for, of sealed radioisotope sources, 19: 40802 (CONF-650616-5)
safety for radioactive materials, operational decision making methods, 17: 18337 (TID-7651(p.31-44))
safety hazards analysis for sealed radiation sources and radioisotopes, 18: 27745
safety hazards in radioactive-material, 19: 46663
safety hazards in, for reactor fuels, (E), 19: 35624
safety measures for fissionable materials, 20: 3370 (CONF-651103-2)
safety precautions for fuel-element, 18: 37422 (A/CONF.28/P/184)
safety regulations for radioisotope, description of international, 18: 43847
safety regulations for irradiated fuel elements, 20: 24757
safety standards for, of fissionable materials, 19: 40840
sampling and weight control in, of uranium hexafluoride, 20: 43062 (CONF-661011-1)
shielded container design for tritium, 20: 41196 (LA-DC-7996)
shipper-receiver differences in, 17: 32315
standards for irradiated nuclear fuel, 20: 33582
standards for radioactive materials, 16: 3299
standards for radioactive materials, 20: 25322 (ORNL-NSIC-11)
statistical analysis of frequency and severity of accidents to potential highway carriers of radioactive materials, 17: 8431 (NYO-9771)

SHIPPINGPORT ATOMIC POWER STATION, PENNA.
environs monitoring for radioactivity, June 1962 to July 1963, 18: 18048
environs monitoring, July through Dec. 1963, 19: 18165
environs monitoring, 1964, 20: 18915
environs monitoring, Jan. to July 1965, 20: 29431
environs monitoring, 1965, 20: 37026 (PNRO-SMD-137)
monitoring of environs, 1961, 16: 20906

SHIPPINGPORT PRESSURIZED WATER REACTOR
(Duquesne Light Company)
boiler corrosion in, causes and extent of, 19: 46913(R) (BMI-1733(Del.))
boiler sludge accumulation and composition, 17: 40346 (WAPD-PWR-TE-149)
boiler transients, comparison of test data with model, 19: 28505 (WAPD-T-1648)
catalog of document abstracts, 16: 7296 (WAPD-PWR-1606(Rev.))
catalog of document abstracts, 17: 36933 (WAPD-PWR-1606(Add.1))
computing and data logging system performance test, 16: 5487 (DLCS-4000101)
container air cooling system butterfly valve integrity testing for, 17: 26851 (DLCS-3570401)
container air cooling system testing, 16: 26590 (DLCS-3960101)
container air lock integrity test, 16: 9640 (DLCS-3570104)
container airlock integrity testing for, 17: 26849 (DLCS-3570107)
container integrity test, 16: 8359 (DLCS-3570302)
container integrity test, 16: 20000 (TID-15627)
container integrity testing of butterfly valve hydraulic system test, 18: 24880 (DLCS-3570501)
container integrity in, airlock tests of, 18: 33101 (DLCS-3570110)
container integrity test of butterfly valve hydraulic system, 19: 27777 (DLCS-5680301)
container integrity test, 16: 21809 (DLCS-3570105)
container tightness integrity testing for, 17: 26850 (DLCS-3570303)
containers for, leak detection in, 18: 1231 (DLCS-1010102)
containment leak rate testing, 20: 6628 (WAPD-PWR-TE-201)
containment system for, testing of, 18: 6485 (DLCS-3570108)
contamination levels during refueling, 16: 21806 (DLCS-3170101)
control and instrumentation of, bibliography on, 20: 47044
control and transient plant response during Seed-1 depletion in, 17: 10066 (WAPD-PWR-TE-74)
control of, nuclear protection system description, 20: 42640 (WAPD-PWR-2210(Vol.1))
control rod drive mechanism test, 16: 9631 (DLCS-1480116)
control rod drive analysis, 16: 32534 (DANATOM-06-61)
control rod drive mechanism testing, 17: 40347 (WAPD-PWR-TE-153)
control rod position and control equipment, instruction manual for Core 2, 20: 42643 (WAPD-PWR-2217)
control rod power supply for, instruction manual, 20: 42642 (WAPD-PWR-2216)
control rod withdrawal transients in, analog simulation and testing, 16: 25000 (WAPD-PWR-TE-99)
control rods, calibration, 16: 21797 (DLCS-1500103)
control rods for, corrosion of, 17: 10074 (WAPD-TM-337)
control rods, radiation effects on, 17: 10074 (WAPD-TM-337)
control rods testing for evaluation of radiation effects on hafnium in, 16: 25854 (WAPD-TM-336)
control system design and performance, 18: 9658
control systems for, development of, 20: 28764(R) (WAPD-MRP-116)
coolant filters for, instruction manual for motor-operated valve loop, 20: 47016 (WAPD-PWR-2220)
coolant flow and pressure drop in Core-1, Seed 2, 16: 24999 (WAPD-PWR-TE-98)
coolant flow and pressure drop, 17: 29779 (DLCS-1470108)
coolant flow distribution in core 1 seed 4, 20: 5133 (WAPD-PWR-TS-151)
coolant flow in, analysis of mixing behavior of, 17: 11992 (WAPD-PWR-TE-93)
coolant flow in core 2 fuel assemblies, 18: 13354(R) (BMI-1657(Del.))
coolant flow in core-2 fuel assemblies of, 19: 18421(R) (BMI-1697(Del.))
coolant flow in core-2 fuel assemblies, 19: 18420(R) (BMI-1694(Del.))
coolant flow in core-2 seed and blanket fuel assemblies, model studies of,

19: 25720 (BMI-1720)
coolant flow in, determination of, for core 2 design by scale model tests, 16: 30054 (BMI-1582)
coolant flow instrumentation calibration, 16: 9635 (DLCS-3370103)
coolant flow instrumentation for core 1 seed 4, calibration of, 20: 5133 (WAPD-PWR-TS-151)
coolant level instrumentation calibration, 16: 9638 (DLCS-3430102)
coolant loop and purification system relief valve tests, 16: 8358 (DLCS-3070202)
coolant loop relief valve testing for, 18: 45011 (DLCS-3070203)
coolant pump power supply check, 16: 11218 (DLCS-3590601)
coolant pumps for Core 2, instruction manual, 20: 42644 (WAPD-PWR-2219)
coolant purification system demineralizer recharging, 16: 21802 (DLCS-1800102)
coolant radioactivity in Seed 1, 16: 26599 (WAPD-PWR-TE-79)
coolant radionuclide distribution, core 1 seed 2, 16: 21824 (WAPD-PWR-TE-89)
coolant, radionuclide base levels for Core 1, Seed 3, 17: 17573 (WAPD-PWR-TE-128(Rev.))
coolant radionuclide base levels in, Core 1 Seed 4, 18: 1259 (WAPD-PWR-TE-157)
coolant stop valve testing, 16: 30101 (WAPD-PWR-TE-142)
coolant, transient fission product activity in, 17: 15474 (WAPD-PWR-TE-147(Rev.))
coolant tritium content in, reduction of, by use of lithium-7 resin, 17: 17572 (WAPD-PWR-TE-103)
coolant water level instrumentation calibration, 16: 9639 (DLCS-3430103)
cooling system decontamination, 17: 21261 (WAPD-PWR-TE-148(Rev.))
cooling system, demineralizer test, 16: 21804 (DLCS-2130102)
cooling system, evaluation of hydrogen distribution and leak rate from, 16: 20002 (TID-15631)
cooling system, governor valve opening test, 16: 21801 (DLCS-1740405)
cooling system of, testing components in, 18: 6486 (DLCS-4140101)
cooling system pressure drop evaluation for Core 1, Seed 3, 16: 11217 (DLCS-1470107)
cooling system pressure drop tests, 16: 24979 (DLCS-1470107(Rev.))
cooling system, radiation levels during seed 2 power operations, 16: 18671 (TID-14885)
cooling system radiation levels in, determination of, from cobalt-60 activity in, 16: 30099 (WAPD-PWR-TE-86)
cooling system testing, Cooldown System performance in, 18: 24881 (DLCS-4140301)
core design for, (E), 19: 17241
core flow instrumentation calibration, 16: 9636 (DLCS-3380102)
core fuel assembly flow rates, Core 1 Seed 2, 17: 10068 (WAPD-PWR-TE-92)
core hydraulic and thermal data analysis, 16: 30100 (WAPD-PWR-TE-140)
core II boron capture fraction measurements, 16: 792
core II depletion, 16: 6226 (WAPD-T-1387(Rev.1))
core II design and operating characteristics, 16: 784
core II nuclear properties, 16: 785
core II self-shielded boron representation, 16: 791
core life, effects of plutonium on, 16: 12769
core materials for, metallurgy of, 20: 18094(R) (WAPD-MRP-115)
core materials for, metallurgy of, 20: 28764(R) (WAPD-MRP-116)
core removal cooling system tests, 16: 9632 (DLCS-2150201)
core thermocouple calibration, 20: 6627 (WAPD-PWR-TE-141)
core-1 seed-1 depletion analysis, three-dimensional diffusion theory, 16: 12770
core 1 seed 2 physics test results, analysis of, 17: 11991 (WAPD-PWR-TE-81)
core 2 analytic model description, 16: 12756 (WAPD-T-1386)
core 2 design and performance evaluation, 16: 6225 (WAPD-T-1378 (Rev.1))
core-2 power distribution, mock-up, 17: 11993 (WAPD-T-1369(Rev.))
core 2 thermal performance, 16: 6223(R) (WAPD-MRP-94)
core-2", self-shielded boron representation for neutron diffusion calculations, 16: 5918 (WAPD-T-1384)
corrosion in 1B boiler of, causes and extent of, 19: 46912(R) (BMI-1727 (Del.))
corrosion in 1B boiler of, 20: 7490(R) (BMI-1745, Sect.A)
criticality of core 1, seed 3, 16: 6223(R) (WAPD-MRP-94)
criticality predictions for core-2, 17: 11994 (WAPD-T-1370)
criticality studies of core II, 16: 789
crud deposition in control rod mechanism region, radioactive, 18: 40875 (WAPD-PWR-TE-145)
data acquisition, description of on-line digital computer system for, 16: 20016
data acquisition system design for, 17: 10920 (WAPD-T-1447)
data logging and computing system performance test, 16: 19240 (TID-15630)
data logging and computing system calibration tests, 16: 26591 (DLCS-4000301(Rev.))
data recording and computing system calibration test, 16: 23316 (DLCS-4000301)
decontamination of, 20: 16088 (WAPD-299)
description, 17: 5611
design and development of, 20: 28764(R) (WAPD-MRP-116)
design and operation, 18: 33076 (A/CONF.28/P/208)
design of, mechanical and thermal, 20: 18094(R) (WAPD-MRP-115)
development, 16: 24998(R) (WAPD-MRP-97)
development, 16: 34080(R) (WAPD-MRP-99)
development and engineering summary for 10–64 to 1–65, 19: 24093(R) (WAPD-MRP-111)
development and engineering summary for April 24–July 23, 1965, 20: 5132(R) (WAPD-MRP-113)
development and engineering of, 20: 18094(R) (WAPD-MRP-115)
development and operation, summary for Dec. 1961 to Feb. 1962, 16: 15924(R) (WAPD-MRP-96)
development and operation of, 17: 1113(R) (DLCS-5000862)
development and operation, 17: 7614(R) (WAPD-MRP-100)
development and operation, Feb. 24–Apr. 23, 1963, 17: 26870(R) (WAPD-MRP-103)
development and operation, June 24–Aug. 23, 1963, 17: 36931(R) (WAPD-MRP-93)
development and operation, Apr. 24–June 23, 1963, 17: 36932(R) (WAPD-MRP-104)
development and operation, June 24–Aug. 23, 1963, 17: 42362(R) (WAPD-MRP-105)
development and operation, Aug. 24,-Oct. 23, 1963, 18: 7932(R) (WAPD-MRP-106)
development and operation, Oct. 24, 1963–Jan. 23, 1964, 18: 21643(R) (WAPD-MRP-107)
development and operation, Jan. 24–Apr. 23, 1964, 18: 29060(R) (WAPD-MRP-108)
development and operation of Core 2, 18: 40913
development and operation, Apr. 24–July 23, 1964, 18: 45034(R) (WAPD-MRP-109)
development and operation, Jan. 24–Apr. 23, 1965, 19: 31556(R) (WAPD-MRP-112)
development and operation, July 24–Oct. 23, 1964, 19: 12785(R) (WAPD-MRP-110)
development and operations of Core 1 and 2, 20: 16089(R) (WAPD-MRP-114)
development and physics studies, 17: 15473(R) (WAPD-MRP-101)
development of, abstracts and indexes on, 19: 42101 (WAPD-PWR-1606 (Add.2))
development progress on, Dec. 24, 1962 to Feb. 23, 1963, 17: 19638(R) (WAPD-MRP-102)
developments, future plans, and performance of, 18: 9676
emergency plan, 16: 24010 (DLCS-5020100)
emergency plan drill for major personal injury in nuclear portion of station involving contamination, 16: 5605 (DLCS-3810301)
environmental radioactivity measurements in 1962, 17: 41029 (PNROO-DEV-125)
environs monitoring, July to September 1961, 16: 5611 (TID-14424)
environs monitoring, 16: 6647(R) (TID-13523)
environs monitoring, July to September, 1962, 17: 10867(R) (TID-17769)
environs monitoring around, 18: 31793 (PNROO-DEV-129)
fall-out monitoring, 16: 19185(R) (TID-15632)
fission product poisoning, 16: 787
flow coastdown tests of primary coolant, Core 1, 17: 10069 (WAPD-PWR-TE-95)
flow instrumentation in, calibration of, 17: 29781 (DLCS-3370104)
fuel blanket assembly for core-2, design of MELBA, 20: 20270 (WAPD-TM-483)
fuel blanket, chemical analysis, 16: 5270 (WAPD-T-1221)
fuel blanket for, experimental and theoretical isotopic composition of irradiated Core 1, 18: 9624 (WAPD-T-1608)
fuel burnup in, 20: 5132(R) (WAPD-MRP-113)
fuel depletion in, development of mass spectrometric and radiochemical determination methods for, 18: 3140 (WAPD-T-1615)
fuel depletion in, calculation of, 18: 3220
fuel depletion studies for core II, 16: 788
fuel element analysis for uranium and plutonium isotopic content, 16: 28568 (WAPD-TM-265)
fuel element burnup testing, 19: 25068
fuel element density, gage for radiation-attenuation measurement of, 17: 24638 (WAPD-BT-28(p.45-52))
fuel element design and performance, review, 16: 16669
fuel element detection and location system performance during start-up, evaluation, 16: 1240 (DLCS-3500257)
fuel element dissolution and depletion analysis, 16: 33999 (WAPD-BT-26(p.63-70))

fuel element fabrication and impurities, 16: 6698 (WAPD-251)
fuel element fabrication, 16: 24626
fuel element fabrication for, development of nondestructive testing methods for, 17: 27560 (WAPD-T-1530)
fuel element fabrication for Core 2 Seed 1, 18: 9654 (WAPD-BT-29 (p.29-43))
fuel element fabrication for, 19: 14846 (WAPD-BT-31(p.19-25))
fuel element failure during station start-up, tests for, 16: 8367 (TID-12966)
fuel element failure detection system for, performance of, 17: 10073 (WAPD-TM-330)
fuel element failure monitors for, performance of, (E), 19: 8632 (DLCS-3990312)
fuel element failure detection systems for, feasibility of chemical, 20: 14847 (BMwF-FBK-65-01)
fuel element fission product release, (E), 19: 14848 (WAPD-BT-31 (p.75-85))
fuel element irradiation testing for, 20: 28764(R) (WAPD-MRP-116)
fuel element processing for, 18: 31658(R) (IDO-14635)
fuel element reprocessing facility for blanket elements, safety in, (E), 19: 36711 (RL-SEP-466)
fuel elements, analysis of irradiated, 17: 17574 (WAPD-T-1461)
fuel elements for, coating of, with pyrolytic carbon, 17: 10063 (WAPD-272)
fuel elements, location of failed, 16: 21823 (WAPD-PWR-TE-70)
fuel handling tool for Core 2, instruction manual, 20: 42641 (WAPD-PWR-2213)
fuel heat treatment in beta-field structure in molten salt bath, 16: 11157 (WAPD-243)
fuel performance for, boron capture fraction in mockup measurements of, 17: 11995 (WAPD-T-1371(Rev.))
fuel plate fabrication, 16: 28474(P)
fuel plate fabrication by gas pressure bonding, Core 2, 17: 36254 (WAPD-245)
fuel plate fabrication for core 2, gas pressure bonding quality in, 18: 29058 (WAPD-BT-30(p.65-79))
fuel plate frictional pressure drop tests for Core II, 16: 14319 (WAPD-R(TH)-604)
fuel plate thermal expansions, 16: 33995 (WAPD-BT-26(p.9-18))
fuel plates for core 2, bonding mechanisms for Zircaloy-2 cladding on, 20: 39361 (WAPD-305)
fuel process development for, 20: 28764(R) (WAPD-MRP-116)
fuel rod fabrication defects observed from core 1 blanket, 17: 1130 (WAPD-TM-321)
fuel rod from Core 1 blanket changes after exposure to two seed lives, 16: 6115 (WAPD-TM-308)
fuel rod isotopic composition after irradiation, 16: 24493
fuel rods for core I, examination of in-pile failure during testing, 16: 1253 (WAPD-BT-23(p.53-74))
fuel rods from blanket region of Core I, inspection of, 20: 3495
fuel rods from Core 1 Seed 3 blanket, metallurgical examination of spent, 19: 1894 (WAPD-TM-433)
fuel rods of Core 1 Seed 2, metallurgical examination of spent, 17: 36934 (WAPD-TM-326)
fuel-temperature measurements, 16: 8370 (WAPD-T-1367)
fuel wafer manufacture for core 2, porosity control in uranium-zirconium dioxide, 18: 29059 (WAPD-BT-30(p.81-7))
heat exchanger, radiation levels in 1-B after shutdown, 16: 21803 (DLCS-1840402)
heat transfer in Core 2, effects of multipass hydraulic core configurations, 16: 27223 (WAPD-T-1365)
inspection of boiler from, 20: 29616(R) (BMI-1738)
instrumentation, calibration of differential pressure type, 16: 9637 (DLCS-3420104)
instrumentation calibration for coolant flow, 16: 21807 (DLCS-3370103(Rev.))
instrumentation for water level determinations, calibration tests, 16: 23315 (DLCS-3430103(Rev.))
instrumentation for transient behavior of, 17: 10064 (WAPD-PWR-TE-65)
instrumentation for, calibration during Core 1 Seed 4 operation, (E), 19: 17271 (DLCS-3430106)
instrumentation for, calibration of differential pressure, 17: 29782 (DLCS-3420105)
instrumentation of, testing BF, source-range detectors, 17: 10067 (WAPD-PWR-TE-78)
loading (1963) seed portion of reactor core, third, 17: 42379
loading, comparison of first and second, 16: 15939
loading Core I, 16: 34079 (WAPD-260)
loading of, radiation dosage control in, 17: 29784 (DLCS-3970101)
loading, radiation contamination levels during Core 1 Seed 2-Seed 3, 16: 9634 (DLCS-3170102)
materials development and selection for, review of, 17: 7615 (WAPD-T-1545)
monitoring during Core 1 Seed 3 operation by FEDAL system, 17: 26852 (DLCS-3990105)
monitoring during Core 1 Seed 3 operation by FEDAL system, 17: 26854 (DLCS-3990306)
monitoring during Core 1 Seed 3 startup by FEDAL system, 17: 26853 (DLCS-3990243)
monitoring of waste effluents, Nov. 1961, 16: 28635 (DLCS-2180102)
neutron axial and radial flux perturbation and samarium transient tests, 16: 7298 (WAPD-PWR-TE-116)
neutron diffusion in, development of computer program for simulating, 17: 9859 (TID-17473)
neutron diffusion theory for, control rod representation of, (T), 20: 16090 (WAPD-T-1841)
neutron flux distribution inside pressure vessel of, 17: 1129 (WAPD-PWR-TE-144)
neutron flux distribution in, 20: 3519
neutron flux measurements in shield tank of, fast, 18: 43039 (WAPD-PWR-TE-161)
neutron flux measurements in Core 2, system description for, 20: 42647 (WAPD-PWR-2226)
neutron flux wire measurements in core 2 seed 1, 20: 45125 (WAPD-PWR-TE-203)
neutron monitoring outside pressure vessel of, 18: 29065
neutron poison plate spacer design, 19: 14845 (WAPD-BT-31(p.1-17))
operating experience, 16: 634
operating experience, 17: 33361
operation, 16: 8368(R) (TID-13198)
operation, 16: 9668(R) (TID-13028)
operation, 16: 9669(R) (TID-13436)
operation, 16: 21821(R) (TID-15502)
operation, 16: 23317(R) (DLCS-5000462)
operation, 16: 30062(R) (DLCS-5000662)
operation, 16: 30098(R) (WAPD-MRP-98)
operation, 16: 31293
operation, 16: 31296
operation, 17: 2601
operation, 17: 13777(R) (DLCS-5001262)
operation, Aug. 1963, 18: 1232(R) (DLCS-5000863)
operation characteristics, 16: 3950
operation, December 1961, 16: 9671(R) (TID-14687)
operation, December 1961, 16: 23323(R) (TID-15438)
operation experience, developments, and future plans, 16: 9674 (WAPD-T-1429)
operation experience during Seed 2 lifetime, 17: 15450 (DLCS-36402)
operation experience, performance, and future plans, 17: 40348 (WAPD-TM-390)
operation experience during Seed 1 lifetime, 18: 9658
operation experience, 18: 33070 (A/CONF.28/P/202)
operation experience, 18: 33071 (A/CONF.28/P/203)
operation, February 1962, 16: 24995(R) (TID-15224)
operation, hydraulic and thermal characteristics, 16: 6224 (WAPD-T-1318)
operation, January 1962, 16: 14318(R) (TID-15063)
operation, July 1963, 17: 36925(R) (DLCS-5000763)
operation, June 1963, 17: 35139(R) (DLCS-5000663)
operation kinetics and stability, 17: 35108 (WAPD-T-1601)
operation, May 1962, 16: 24980(R) (DLCS-5000562)
operation, May 1963, 17: 29785(R) (DLCS-5000563)
operation, Nov. 1963, 18: 9642(R) (DLCS-5001163)
operation, November 1961, 16: 9670(R) (TID-14629)
operation, October 1961, 16: 6222(R) (TID-14419)
operation, October 1963, 18: 4792(R) (DLCS-5001063)
operation of, 16: 30063(R) (DLCS-5000762)
operation of, January 1963, 17: 17534(R) (DLCS-5000163)
operation of, March 1963, 17: 24675(R) (DLCS-5000363)
operation of, November 1962, 17: 10049(R) (DLCS-5001162)
operation of, October 1962, 17: 10048(R) (DLCS-5001062)
operation of, summary for February 1963, 17: 21312(R) (DLCS-5000263)
operation of, economics and technical aspects of, 19: 38186 (ORNL-TM-1145)
operation performance at steady state loads, 16: 8973 (DLCS-1650102)
operation review, 17: 38559
operation, Sept. 1963, 18: 1233(R) (DLCS-5000963)
operation, September 1961, 16: 3947 (TID-14088)
operation, September 1962, 17: 1114(R) (DLCS-5000962)
operation summary, April 1963, 17: 28525(R) (DLCS-5000463)
operation without primary system purification, 16: 33998 (WAPD-BT-26 (p.49-62))
operation, Apr. 1964, 18: 26916(R) (DLCS-5000464)
operation, Aug. 1964, 18: 45014(R) (DLCS-5000864)
operation, Dec. 1963, 18: 13283(R) (DLCS-5001263)
operation, Dec. 1957-Mar. 1963, 18: 40912
operation, Dec. 1964, 19: 29631(R) (DLCS-5001264)

operation, Feb. 1964, 18: 23053(R) (DLCS-5000264)
operation, Jan. 1964, 18: 15519(R) (DLCS-5000164)
operation, July 1964, 18: 45013(R) (DLCS-5000764)
operation, June 1964, 18: 45012(R) (DLCS-5000664)
operation, Mar. 1964, 18: 26915(R) (DLCS-5000364)
operation, May 1964, 18: 35142(R) (DLCS-5000564)
operation, Nov. 1964, 19: 17272(R) (DLCS-5001164)
operation, Oct. 1964, 19: 12773(R) (DLCS-5001064)
operation, Oct. 24, 1961 to Jan. 30, 1963, 19: 5470(R) (DLCS-36403)
operation, Sept. 1964, 19: 5471(R) (DLCS-5000964)
operational experience through three seeds, 16: 24492
operations, survey of experience, 16: 5038
operator training program, 17: 1143
performance during Seed-1 depletion, steady state tests, 17: 10065 (WAPD-PWR-TE-71)
performance of, reliability of, 20: 45181
physics research program, 18: 43034 (TID-7050(p.1-14))
poisoning, development of boron-10-enriched alloys for, 16: 12666 (WAPD-BT-24(p.65-84))
poisoning of, by fission products, 17: 10072 (WAPD-T-1528)
power coastdown in, during scram of core 1, 16: 30102 (WAPD-PWR-TE-143)
power distributions in core II mockup, 16: 790
power distribution measurements in, 17: 21322 (WAPD-T-1496)
power distribution measurements in Core 1, 18: 9655 (WAPD-BT-29 (p.59-68))
power distribution across fuel subassemblies of core 1 seed 4 blanket, thermocouple performance for, 20: 1477 (WAPD-PWR-TE-166)
power-xenon oscillations in, analysis of (E), 19: 3667
pressure instrumentation calibration, 16: 8909 (TID-14883)
pressure instrumentation for, calibration of, 17: 29780 (DLCS-3360304)
pressurizer level instrumentation for, calibration of, 17: 29783 (DLCS-3430104)
radiation levels during Core 1 Seed 4, external, 19: 8631 (DLCS-3410122)
radiation levels in coolant loop piping and purification demineralizers of, 17: 31723 (DLCS-3410114)
radiation levels in reactor coolant loop piping and purification demineralizers of, 17: 31724 (DLCS-3410117)
radiation monitoring of cooling system heat exchangers, 17: 35138 (DLCS-3410204)
radiation survey of reactor vessel head, core 1, seed 3, 17: 33306 (DLCS-3050123)
radioisotope production in, economic and technical feasibility of, 19: 28723
reactivity calculations for core 2 assemblies, 20: 18094(R) (WAPD-MRP-115)
reactivity coefficients at 5532.3 EFPH, 16: 21798 (DLCS-1510108)
reactivity coefficients at OEFPH, core I seed 2, 16: 21799 (DLCS-1510109)
reactivity coefficients at power, core I seed 2, 16: 21800 (DLCS-1510205)
reactivity lifetime in core 1 seed 4, 20: 5133 (WAPD-PWR-TS-151)
reactivity lifetime thermal performance, 20: 6627 (WAPD-PWR-TE-141)
reactivity of, blanket-seed relations in Core I and II, 17: 18998
reactivity of core 2 seed 1, 20: 5132(R) (WAPD-MRP-113)
reactivity of core-2 seed 1, 20: 3502
reactivity of seed-4, xenon-free temperature coefficient of, 18: 40876 (WAPD-PWR-TE-164)
reactivity temperature coefficient measurements at power, 16: 8366 (TID-12965)
relief valve operation, evaluation of self-actuated, 16: 19998 (TID-15625)
relief valve operation, evaluation of self-actuated, 16: 19999 (TID-15626)
safety analysis of core-2, 19: 29650 (WAPD-SC-501(Del.))
safety injection system modification, 16: 6223(R) (WAPD-MRP-94)
Seed 2 nuclear properties, physics tests, 16: 7297 (WAPD-PWR-TE-84)
shielding construction inside containment vessels, 16: 24232
shutdown, effects of rapid, 16: 21808 (DLCS-3440103)
startup of, control rod withdrawal transients calculations for, 18: 29057 (WAPD-BT-30(p.1-22))
startup, operation of FEDAL system, 16: 18670 (TID-14884)
station performance during unscheduled power transient, 16: 8369 (TID-14640)
steam generator blowdown sludge removal rate, evaluation, 16: 25001 (WAPD-PWR-TE-118)
steam generator for, metallographic inspection of, 20: 22408 (BMI-1764)
steam generator for Core 2, description and operation of, 20: 42645 (WAPD-PWR-2222)
steam generator for Core 2, description and operation of, 20: 42646 (WAPD-PWR-2223)
temperature detectors for, calibration of, 18: 24918 (WAPD-PWR-TE-159(Rev.))
temperature sensing element intercalibration, 16: 7288 (DLCS-2430104)
testing of automatic data logging and computing system, 16: 11219 (DLCS-4000201)
testing of automatic data logging and computing system for, 17: 28524 (DLCS-4000201(Rev.))
testing of butterfly valves in air cooling system, 18: 3170 (DLCS-3570204)
thermal operating performance, 18: 15434 (TID-7669)
thermocouple elements for core 1 seed 4, periodic calibration of, 20: 5133 (WAPD-PWR-TS-151)
thermodynamic characteristics, 16: 838
valve testing in primary plant, self-actuated relief, 16: 9633 (DLCS-3070103)
waste disposal, area monitoring, 16: 21860 (DLCS-1690203)
waste disposal at, 20: 40481 (WAPD-T-1851)
waste disposal from, environmental monitoring of, 18: 31793 (PNROO-DEV-129)
waste disposal from, 20: 3521
waste disposal operation during cooldown for refueling, 16: 21805 (DLCS-2390301)
waste disposal system, performance, 16: 7332
waste disposal system effluents, characterization of nuclides in, 16: 9724 (DLCS-2180101)
waste disposal system incinerator tests, 16: 16025 (TID-14871)
waste disposal system performance evaluation, 17: 4372 (WAPD-T-1280)
waste processing, hydrogen burner testing for, 17: 15520 (DLCS-3670101)
waste processing, modification proposals for ion exchange process for, 16: 1281 (WAPD-BT-23(p.75-81))
water purification equipment for, engineering drawings for, 17: 29049
weld cutting machines for Core 2 vessel ports, instruction manual, 20: 42649 (WAPD-PWR-2230)
weld cutting machine for Core 2 vessel seal, instruction manual, 20: 42650 (WAPD-PWR-2232)
welding machine for Core 2 omega seal, instruction manual, 20: 42648 (WAPD-PWR-2229)
xenon oscillations in, small perturbation analysis of operator-induced, 18: 9653 (WAPD-BT-29(p.1-18))

SHIPS
design of Japanese nuclear-powered, 20: 12462 (CONF-640810, pp 122-37)
nuclear-powered, apparatus for replacing ion exchange resin in, 20: 23041(P)
nuclear-powered, bibliography on, 20: 40444 (AED-C-22-06)
nuclear-powered, development of oceanographic research, 20: 18129
nuclear-powered, design of Japanese, 20: 24783
nuclear-powered, effectiveness of collision barrier, 20: 47061
nuclear-powered, Japanese classification guide, 20: 40448 (NP-16217)
nuclear-powered, licensing of, 20: 12464 (CONF-640810, pp 156-65)
nuclear-powered, research on collision-resisting sides of, 19: 46464(T) (NSJ-tr-30)
nuclear-powered, role of, 20: 12460 (CONF-640810, pp 7-21)
nuclear, legal aspects of entry into foreign ports, 20: 2088
propulsion of, bibliography on nuclear, 20: 26516 (AED-C-22-05)
speed of, measurement of, using neutron activation of oxygen in water, 20: 25368(P)
waste disposal from nuclear, marine contamination from, 20: 23396

Ships (Commercial)
see Merchant Vessels

Ships (Naval)
see Naval Vessels

SHIRLEY BASIN AREA (WYO.)
geochemical fronts and geologic mapping of, 18: 41671
protactinium-231 and thorium-230 contents in sandstone deposits of, 18: 31778
uranium isotope fractionation in sandstone deposits of, 18: 31777
uranium occurrence, paleotopographic control of mineral belt, 16: 5584

SHOCK
see also Blast Effects
see also Impact Shock
see also Thermal Rupture
see also Trauma
development from radiotherapy of carcinoma of uterine cervix, 17: 10496
effects on recovery of dogs and rats from radiation injuries, 19: 8781(R) (AD-422394)
induced by burns in dogs, 16: 31492
induced by irradiation and trauma in rabbits, 18: 3503(T) (JPRS-22001)
induced in irradiated rabbits by gamma globulin, 19: 19535
radiation effects on pattern and threshold of seizures of electro-16: 75
radiation effects on electro-shock seizure responses to reserpine and

iproniazid in rats, 17: 73
radiation effects on electro-shock seizure response in rats, whole-body exposure, 17: 30299
radiation effects on guinea pig anaphylactic, x, 18: 5055
radiation effects on seizures of electro-, in rats, 18: 9885
radiation effects on electroshock seizures in rat cysteine and dose effects on, 19: 19514
radiation effects on suppression of lethal anaphylactic, in mice, 19: 26050
study methods for, following atomic explosions, 20: 45952 (HI-647-RR)

SHOCK TUBES

axial field effects in magnetically driven annular, 17: 19458 (RLE-TR-408)
bibliography on, 18: 40982 (MLM-1189)
bibliography on, 19: 28918 (MLM-1189(Suppl.))
calibration for overpressure measurements, 16: 12813 (WT-1101)
cesium vapor ionization in, 16: 23178 (NP-11610)
characteristics of H-type, containing two gases, 18: 19231
chlorine recombination rate in, direct measurement of atomic, 17: 27373
collisionless plasma and shock production in annular, 17: 9789
construction and design of electric-discharge-driven, 16: 4897 (D1-82-0077)
current distribution in magnetic annular, 16: 18241
curvature of shock wave in circular, (T), 20: 44890
data from, extrapolation to structures, 16: 11359 (WT-59)
description and operation of water, for coolant decompression studies, 19: 25640(R) (IITRI-578P21-12)
description of large explosive-driven plywood, (E), 19: 19433 (LA-3089)
design, 18: 20119 (ARL-64-5)
design and performance of large, 16: 24275 (CLM-R-18)
design and performance for atomic property measurements, 16: 26029
design and performance of stepped, for simulating air blast, 19: 13555 (AWRE-E6/64)
design and performance of electromagnetic, 19: 44857
design and performance, 20: 619 (AWRE-O-59/65)
design and properties of electric-arc driven, 17: 25916
design and use of, 17: 37873
design for nuclear blast simulation, 20: 29371 (AWRE-E-1/66)
design for plasma production, 18: 24743 (ANL-6802(p.29-36))
design for plasma diagnostics, nonuniform, 19: 41855 (NP-15142)
design for plasma production, 20: 26330(P)
design of argon–cesium, for MHD generators, 20: 41703
design of explosive-driven, 20: 25226
design of impulse tubes, 18: 32304
development, 18: 36759 (IITRI-578P21-6)
development and operation of inductive-hydrodynamic, 18: 40691
development for plasma diagnostics, 20: 22170 (AD-622701)
development for production of sharp-rising overpressures of 400 milliseconds duration for biomedical studies, 16: 18732(R) (DASA-1246)
development of electromagnetic, for high-temperature, dense plasma production, 20: 38335
discharge current in electromagnetic, (T), 19: 23843
driving force in electromagnetic, origin of, 17: 20713
electric conductivity of ionized air in, 16: 18189
electric current shortcircuiting in, snowplow model for, 18: 34330
electric currents in magnetic annular, (E), 19: 5342
electric power generation in, MHD, 18: 12870
electrodes in, electric resistance and sheath potential between, 17: 42056
electron density and temperature in electromagnetic, (E), 19: 21515
electron density distribution in, microwave probing technique for measuring, 20: 38305
electron temperatures in, double-probe measurements of, 17: 29684
energy losses due to radiation in, (E), 20: 41750
evaluation for use in studies on dynamically loaded underground structures, 17: 5666 (AD-274294)
flow characteristics in electromagnetically driven tee, (E/T), 19: 9795
flow from open end of rectangular, model study of, 20: 912 (AWRE-O-61/65)
flow in magnetic annular, analysis of non-uniform, 16: 16803 (AFOSR-2194)
flow model for magnetic annular, large-radius-ratio, 16: 18242
flow of high-enthalpy ionized air in, 16: 32476 (CAL-AF-1500-A-1)
flow phenomena, testing time and contact-zone characteristics, 16: 7989
flow properties in explosive-driven, for blast simulation, 20: 4708(R) (UCRL-14360, pp 50-73)
gas flow in electric, modes of, (E), 20: 6173
gas ionization in, magnetically induced, 18: 7423
heat transfer to end wall in, convective, 18: 8474 (BSD-TDR-63-47)
helium ionization in, kinetics of, 20: 9853
helium ionization in, from uv radiation, 20: 44980
ion density profile of plasma flow in electric, (E), 19: 27646
ionization in, measurement by stagnation-point Langmuir probes, 18: 42181
luminescence front in electromagnetic, (E), 19: 27681
luminous and shock fronts in, photographic studies of, 17: 22750
luminous front and shock waves in electromagnetic, (E), 19: 12683
luminous fronts preceeding shock waves in electromagnetic, (T), 19: 12666
luminous phenomena in electromagnetic, interpretation of, 17: 25917
magnetic field distortion by flow in, 16: 5796
magnetic field effects in conical, 17: 36519
magnetic flux transport by plasma in, 18: 35007
magnetohydrodynamic experiments in low-attenuation electromagnetic, 20: 37882
magnetohydrodynamic flow in, boundary layer, 20: 42037 (UTIAS-115)
microwave diagnostics of plasma in, 17: 15031
performance, effects of nuclear explosions, 16: 18713 (AFSWC-TN-61-26)
performance of coaxial and tee types, 19: 40849 (TID-22061)
performance of double-driver, (E), 19: 41162
plasma acceleration in magnetic annular, 16: 25912 (NP-11848)
plasma acceleration in magnetic annular, 17: 5466
plasma acceleration in electromagnetic, snowplow theory of, 17: 42064
plasma acceleration in electromagnetic, mechanisms of, 18: 19216
plasma acceleration in coaxial, snowplow model for, (E), 19: 5317
plasma behavior and properties in magnetically driven, (E), 19: 41936
plasma behavior in, in magnetic field, 18: 19240
plasma clouds in electromagnetically driven, production and structure of, 18: 19232
plasma diagnostics in, optical interferometry, 17: 11853
plasma diagnostics in, (E), 19: 23825 (NP-14917)
plasma discharge and shock fronts with two-gas systems, 16: 11091
plasma flow modes in electric, (E), 20: 38345
plasma front velocity and preionization in, microwave measurements of, 18: 15391
plasma front velocities in, 18: 19234
plasma heating in electrically driven, 18: 42827
plasma heating in, by pinch effects, (E), 19: 21473 (IPP-1/28)
plasma insulation in, magnetic, 17: 29659 (SSD-TDR-63-72)
plasma ionization phenomena in, microwave diagnostics of, 18: 32919
plasma ionization equilibrium in electric, deviations from, (E), 19: 31388
plasma ionization in, potassium-seeded argon, (E), 20: 41715
plasma luminosity in electromagnetic, 18: 42848
plasma precursor ionization in, (E/T), 19: 21471 (IPP-1/24)
plasma production, 16: 1104 (AFOSR-1173)
plasma production and properties in, in air, 16: 12610 (CAL-AF-1441-A-4)
plasma production in T-type electromagnetic, luminosity structures in, 18: 19233
plasma production in conical electromagnetic, thermodynamics of argon, 18: 40685
plasma production in inductive hydrodynamic, argon, 20: 6478
plasma properties in MHD, (E), 19: 10434
plasma thermodynamics in conical electromagnetic, 18: 38226
plasma-stream and shock production and propagation in discharge, (E), 20: 20089
plasmas in electromagnetic, production and properties of shock-heated, 20: 38344
precursor afterglow ionization in hydromagnetic, 17: 7422 (AWRE-O-11/62)
precursor effects in electrically driven, 19: 7673
precursor wave motion in, electron densities in, 17: 37839
pressure wave measurement from, technique for, (E), 20: 2822 (AWRE-O-60/65)
properties and uses, 17: 11424
properties and uses of electric and electromagnetic, 17: 39813
radiation emission from, (E), 19: 33402(R) (AFCRL-65-315)
sheath formation on, during generation of cesium plasma, 17: 4163(R) (AD-275015)
shock compression in, maximum, (T), 19: 14132 (LGI-63/18)
shock front detection in magnetically driven, method for, 19: 43442
shock front shape in, (E/T), 19: 6800
shock front visualization in electromagnetic, 17: 28041
shock fronts in, curvature of, 17: 28038
shock fronts in electromagnetic, self-luminescence, (E), 20: 13949
shock production in electromagnetic, ionizing switch-on, 20: 25971
shock propagation with precursor arc in, 18: 28143
shock reflection against end plate in high-explosive, 18: 34332
shock separation from driven gas in electromagnetic, 18: 25645
shock structure in electromagnetic, (E), 19: 37983
shock velocity attenuation in, radiation effects on, 17: 8917 (AFOSR-1101)
shock velocity in, electric contactor pins for measuring, 19: 9458
shock velocity in, thin film thermometer for measuring, 20: 618 (AWRE-O-58/65)

shock wave attenuation in, boundary layer effects on, (T), 20: 46444
shock wave diagnostics in magnetically driven, (E), 19: 20661 (RLE-TR-428)
shock wave electric conductivity in coaxial, 18: 18459 (TID-20415)
shock wave propagation and structure in electric-discharge, (E), 19: 27676
shock wave reflection, effects of boundary-layer growth on, 16: 7990
shock-wave seeding effects on inert-gas electric conductivity in, (E/T), 19: 35526 (NRC-7884)
spectra in electromagnetic, using air, (E), 19: 37984
temperature measurement in, transition probabilities for argon lines for, 20: 42483
theory of magnetically driven, having varying driving field, 16: 33614
use as vacuum ultraviolet radiation source, 17: 39722 (NRL-5967)
use for determinations of helium oscillator strengths, 17: 31613
use for studying magnetically-induced ionization in magnetohydrodynamic generator, (E/T), 19: 9959(R) (AD-421896)
use in gaseous state studies, 16: 9528(T) (FTD-TT-61-196)
use in recombination rate measurements, 17: 8094
use in spectroscopy, 18: 28168
use in study of exchange reactions between deuterium and hydrogen, 18: 3724
use in study of high-temperature gases, 19: 32825
use in study of plasma dynamics, (T), 20: 44167
use in testing overpressure effects on small animals, 16: 20864(R) (DASA-1242)
use of explosive-driven, in simulation of nuclear blast effects on re-entry vehicles, 18: 31687 (LADC-6458)
use of T tube for verification of equation of state of hydrogen, 18: 18497
uses of water-filled, for analyses of reactor coolant-loss accidents, (E), 20: 5023(R) (IITRI-578P21-15)
vaporization and wave propagation of water in, 16: 13735
wave attenuation in, effect of radiative losses on, 17: 2389
wave attenuation in, effects of radiation on, 17: 19442(R) (AD-283512)
wave generation in electromagnetic, precursor, (E), 20: 34766
wave propagation in magnetically driven, switch-on, 18: 7422
wave propagation in conical, analysis of, 18: 20647

SHOCK WAVES

see also Detonation Waves
see also Impact Shock
see also Seismic Waves

acceleration at fronts of, model for Fermi, 20: 11437
acceleration in constant-area ducts, electromagnetic, 16: 18237
acceleration in hydrogen, 18: 1160
acceleration in plasma, 17: 26682
acceleration of, by d-c crossed-field magnetohydrodynamic device, 17: 4169 (MIT-28-T-P)
air velocity in, from TNT explosions, 18: 28467
analysis from HANDCAR event, 20: 25305 (PNE-801F)
analysis of, computer program for, 17: 39724 (SC-4796(RR))
analysis of magnetic, in plasma at Alfven-Mach numbers to 20, 16: 4907(R) (UCRL-9777)
analytical uses in reactor accidents, 17: 26110
arrival time measurements in Project Scooter, 16: 5109 (UCRL-6605)
attenuation and transmission in tubes, 19: 25071(R) (TID-21667)
attenuation in earth, 16: 2836 (WT-1406)
attenuation in electromagnetic shock tubes, radiation effects on, 17: 8917 (AFOSR-1101)
attenuation in ionized gas in transverse magnetic field, 18: 26802
attenuation in plasma of electromagnetically driven, 17: 2389
attenuation in shock tubes, boundary layer effects on, (T), 20: 46444
attenuation in tubes, radiation effects on, 17: 19442(R) (AD-283512)
attenuation in tunnels, nomograms, 16: 17349(T) (AEC-tr-5025)
attenuation of nuclear-explosion, by underground structures, 18: 3971 (WT-1723)
base pressure analysis under conditions of missile flight through, 17: 32730 (TID-19116)
behavior at remote distances from explosion points, 17: 301
behavior in clayey soils, 16: 3584
behavior in flow over a wedge, 17: 2105
behavior in high-altitude shot, use of smoke puffs to study, 16: 2824 (WT-1108)
behavior in T-shaped tubes, 18: 8924
behavior of high-altitude, analysis of hydrodynamic and radiation aspects of, 16: 29473 (DASA-1291)
behavior of large-amplitude, in gases, 16: 3540(T) (AEC-tr-3973(Pt.II and Add.)(p.834-74))
behavior of switch-on, in one-dimensional hydromagnetic flows, (T), 20: 2834
bibliography of Soviet studies on, 19: 9762 (AID-P-64-44)
biological effects of, from atomic explosion, 18: 25722
blast from Dugout row-charge cratering experiment, measurements of close-in air, 19: 38790 (PNE-608F)
Boltzmann equation for, solution of, 17: 25874
book: *Action of Shock and Explosion in Deformable Media*, 16: 9301(T) (UCRL-Trans-777(L))
book: *Electrically Energized Shock Tubes*, 17: 28402
book: *Magnetohydrodynamic Shock Waves*, 18: 34360
book: *Non-linear Wave Propagation*, 19: 19319
book: *Physics of Heat Exchange and Gas Dynamics*, 17: 12437
book: *Physics of Shock Waves and High-Temperature Hydrodynamic Phenomena*, 19: 42955
book: *The Shock Wave of an Atomic Explosion*, translated from the Russian language, 16: 9736(T) (JPRS-11811)
boundary conditions in finite-difference calculations for, 19: 874 (NYO-1480-4)
boundary layer behind strong, insulation thickness of, 17: 9794
boundary layers and sheath potentials in, in air, 17: 6899
calculation for Hardhat explosion in granite, 18: 45193 (UCRL-7762 (Rev.I))
cesium ionization behind, in argon, 18: 28163
characteristics of hydromagnetic, used for ionization of gases, 17: 36475
charged-particle scattering and transmission by, in plasma, (T), 20: 8218
chemical effects on alkali metal compounds, 16: 22051 (ORNL-TM-256)
chemical species distribution in air, 16: 33938
collision integrals for, in ionized gas, 17: 39801
collision term for plasma, 19: 31335(R) (UCRL-12303)
collisionless, in a two-fluid system, 17: 9698
collisions with equal-strength shock waves in rail gun, 18: 19229
compression of lanthanides by, 20: 39425(T)
compression of uranium by, dynamic adiabatic curve, 20: 836(T) (UCRL-Trans-1213(L))
compression of, maximum, (T), 19: 14132 (LGI-63/18)
compression shock form in freely expanding gas jets, 16: 22735(T) (AEC-tr-5196)
compression, in transition between gas dynamic and molecular flow, 18: 42165(T) (AEC-tr-6480)
condensation processes behind, feasibility of optical studies, 16: 24889 (NP-11601)
conference on soil-underground protective structure interaction, Univ. of Arizona, Tucson, Ariz., June 8 to 11, 1964, 19: 13607
configuration in conducting gas in uniform magnetic field, 16: 5809
curvature of, in circular shock tubes, (T), 20: 44890
decay of magnetohydrodynamic piston-produced, 18: 7410
deformation effects on metals, conference, 16: 19277
density measurements, design of beta-ray densitometer for, 16: 5512
density measurement in atmospheric, design of gage using beta attenuation for, 18: 8618
density-pressure ratios across, in krypton and xenon, (T), 19: 14709
detection and measurement, 16: 11356 (WT-1)
detection and measurement, 16: 18713 (AFSWC-TN-61-26)
detection, performance of radiological defense warning system, 16: 2827 (WT-1112)
detonation of explosives by, 18: 45171 (LADC-5611)
detonation of liquid explosives by, pressure transducer studies of, 18: 43111 (LADC-6179)
development and theory of Lamb, 16: 14988(R) (ANL-6329)
diagnostics, in preionized gases, 16: 12604 (AFCRL-62-240)
diagnostics of, use of microwave techniques for, 20: 4934 (AD-619093)
diffraction by structures, 16: 14993 (WT-786)
diffraction in elastic medium by cylindrical cavity with elastic liner, 17: 1581 (NP-12181)
diffraction in gases, analysis of, 18: 26123
diffraction, interaction, and reflection, 16: 11359 (WT-59)
diffraction of cylindrical elastic and weak, 18: 26141
dissipation in collisionless plasma, mechanisms for, (T), 19: 47828
dissipation of hydromagnetic, magnetic field damping effects on, 18: 7387
dissociation behind a magnetically driven shock front in hydrogen, thermal, 18: 19223
dissociation effects of, in hydrogen, 17: 8945 (RISO-46)
dynamic pressure, from nuclear explosions, measurement, 16: 2820 (WT-714)
effect of solar-wind, on geomagnetic storms, (T), 20: 4745
effect of topography on, in air, 17: 6276 (WT-502)
effect on charged-particle motion in magnetic fields, (T), 19: 30971
effect on spall gaps in subsurface layers of earth, 20: 41126
effects of blast, on axisymmetric supersonic missile, (E/T), 19: 36574 (SC-TM-65-218)
effects of electric discharge, on human ear, 19: 44283 (AWRE-E-1/65)
effects of explosion-produced, on h-f, uhf, and vhf antennas, (E), 19: 20109(R) (CER-D1703)
effects of geo-, on approaching solar plasma, 18: 28201 (NP-13988)
effects of hydromagnetic, on solar proton events, (T), 19: 41230
effects of hydromagnetic, on gas state transitions, 20: 34340

effects of interplanetary, on cosmic radiation, 18: 30442(T) (NASA-TT-F-127(p.41-7))
effects of interplanetary, on sudden impulse pairs in magnetic storms, 19: 39681
effects of ionizing, in cylindrical plasmas, (T), 20: 3201
effects of low pressure, on plasma ionization, 20: 13921(R) (NP-15703, pp 52-63)
effects of MHD, on charged-particle motion in plasma, (T), 19: 31413
effects of nuclear-explosion, on biotites, 19: 26530
effects of solar wind, on geomagnetic storms, (T), 20: 4744
effects of solar-flare, on geomagnetic disturbances, (T), 19: 45163
effects on arches, domes, and spheres, 17: 2659 (AFSWC-TR-61-90)
effects on argon diffusion in stony meteorites, 18: 18031
effects on argon diffusion in stony meteorites, 18: 18032
effects on blast loading of structure, 17: 29882 (WT-1162)
effects on calcite and quartz, 17: 3150 (NP-12194)
effects on circular cylinders, (E/T), 20: 4132 (AWRE-O-93/65)
effects on complex tunnel model, 19: 34290 (AD-609289)
effects on coolant expulsion in reactor accidents, 20: 22348
effects on crushable reactor shields, 18: 36759 (IITRI-578P21-6)
effects on crystal structure of bismuth and potassium bromide, 20: 4708(R) (UCRL-14360, pp 50-73)
effects on electric conductivity of aluminum oxide and carbon tetrachloride, 20: 4708(R) (UCRL-14360, pp 50-73)
effects on eyes of nuclear explosion observers, 20: 45451
effects on geomagnetic storm sudden commencement, (T), 20: 11811(T)
effects on hard rocks and underground structures, 20: 496
effects on hardness of metals, 19: 898 (HW-SA-3738)
effects on human eyes in Japan, atomic bomb, 19: 13039
effects on interferometric density determination in supersonic gas flow, 17: 20683
effects on ionic composition of ionospheric D region (T), 19: 3159
effects on magnetic properties of plasma, 16: 2597(T) (AEC-tr-4729)
effects on magnetic properties of nickel ferrite, 20: 4708(R) (UCRL-14360, pp 50-73)
effects on man following nuclear air blast, tolerance to, 20: 2083 (CEX-65.4)
effects on man, pathological, 20: 2083 (CEX-65.4)
effects on mineral phases in Gnome explosion, 19: 281 (PNE-112F (Pt.III))
effects on molecular beam production by nozzles, 18: 40158
effects on phase transformations in matter, one-dimensional model for, (T), 19: 30848(R) (UCRL-12473(p.31-63))
effects on photoviscoelastic plates, 20: 43495(R) (AD-628806)
effects on piezoelectricity of Z-cut tourmalines, (E), 20: 5011
effects on plasma, 18: 30873 (AFCRL-63-577)
effects on spherical models, studies in Operation Teapot, 16: 2828 (WT-1114)
effects on structures, 16: 11359 (WT-59)
effects on structure of graphite, 18: 39250
effects on structure of magnesium oxide crystals, 19: 16060 (AROD-4434:2)
effects on sugar-pine wood and reactor pressure vessels, (E), 20: 5023(R) (IITRI-578P21-15)
effects on symmetric flow of conducting gas, (T), 20: 34341
effects on underground structures, 19: 46569
effects on underground structures, design procedures for minimizing, 20: 23267 (AD-627597)
effects on underground structures, isolation systems for minimizing, (T), 20: 23268 (AD-627870)
electric conductivity of plasma produced by, 17: 4190
electric conductivity of, in coaxial tube, 18: 18459 (TID-20415)
electric current sheets in inverse-pinch, (E), 19: 6380 (AD-608147)
electric currents in, in magnetic annular shock tubes, (E), 19: 5342
electric discharge production by, 16: 19552
electrical "precursor" phenomena ahead of advancing fronts, 16: 27808
electrode performance in plasma, boundary-layer resistance and sheath potential of, 17: 42056
electromagnetic, in nonlinear line, 17: 24066(T) (JPRS-19316)
electron and ion density ahead of air, 20: 44403(R) (AD-628143)
electron density and continuum radiation behind, 18: 16648 (NP-13739)
electron density and temperature behind, in helium, (E), 19: 23901
electron density and velocity behind, laser beam diagnostics of, 20: 6490
electron density ionization rate and thermal equilibrium behind, 20: 4934 (AD-619093)
electron-plasma oscillations by, 18: 7823
electron propagation from strong, in shock tubes, 17: 37839
emission from dielectric breakdown in gases, 17: 665
energy density in converging, stability of, (T), 20: 2839
energy transfer in, 19: 32825
equations for, in classical and relativistic MHD, 20: 19627
equations of state in, 20: 38433 (ANL-7120, pp 641-53)
equilibrium behind, mathematical analysis, 16: 12300
evolutionality conditions for, 16: 326
excitation, electrodynamic, 16: 15349
excitation in conducting fluid, resonance, 17: 22392
excitation in plasma, (E), 19: 41911
excitation of acoustical, in plasma, 16: 18557 (PIBMRI-893-61)
excitation of argon and xenon in, to corresponding states, (E), 19: 14143 (UCRL-7907(Rev.I))
excitation of, effects of magnetic fields on, 17: 36519
exothermic processes, 16: 9528(T) (FTD-TT-61-196)
experimental techniques in, conference on, 18: 5442
extinction in inhomogeneous media, 16: 3583
flow by conical, power series solution for compressible, 17: 40977 (NYO-10432)
flow in shock tubes, testing-time and contact-zone characteristics, 16: 7989
flow of two-dimensional axisymmetric, Newtonian approximation for, 16: 27809
flows behind strong cylindrical magnetohydrodynamic, 17: 5130
fluid dynamics of axial-symmetric, from nuclear explosion, 18: 40050 (RM64TMP-17)
fluid-dynamics calculations of pseudo-viscosity for, (T), 19: 47119 (UCRL-14244)
formation and propagation through ionosphere after thermonuclear explosion, 16: 33297
formation and propagation in gases, (E/T), 19: 4334(T) (FTD-MT-63-197)
formation by exploding wires, 17: 13214
formation by supersonic flow past two-dimensional blunt body, (T), 19: 5570 (NYO-1480-1)
formation in gas-flow tube, kinetic theory of, 18: 34279 (NP-14186)
formation in magnetogasdynamic flow, 18: 16560
formation in plasmas, theory, 16: 3768 (R61SD089)
formation in plasma by piston expansion with a weak magnetic field, 17: 36774
formation in shock tubes in two-gas systems, 16: 11091
formation in steam-water flow through overexpanded nozzles, 16: 7663 (UCRL-6676)
formation of imploding, by exploding films, 17: 13212
formation of magnetogasdynamic, with electric conductivity as dissipative mechanism, 20: 39944
forms from underground explosions at 96 to 714 km distances, 16: 17899
from Dugout cratering experiment, 19: 28474 (PNE-600F)
from exploding wires at low ambient densities, 16: 24273 (BRL-1152)
from multi-megaton nuclear weapon, prevention and management of casualties from, 18: 12385 (NP-13568)
from nuclear explosion, effects on drag loading of structures and structural panels, 16: 2829 (WT-1124)
front analysis, effects of Joule heating on electron density level and microwave properties downstream, 16: 12234(R) (USCEC-75-3)
front structure in atomic hydrogen, effects of Lyman continuum radiation on, 17: 32744
front structure of plane, mathematical analysis, 17: 689
fronts in two-dimensional unsteady hydrodynamic flow, 16: 21210
gas acceleration by, density restrictions on, 18: 15726 (UCRL-7672-T)
gas and isotope separation in, from compression shocks in free-expanding gas, 20: 27064
gas density behind, electron beam measurement of, 18: 14654
gas dissociation behind, 18: 44478
gas flow past fronts, dissociating, 16: 22709 (AD-271032)
gas flows across, in carbon dioxide, (T), 19: 42926 (NASA-SP-3018)
gas state behind strong, excitation and relaxation of, (T), 19: 40040
gas states, 16: 9528(T) (FTD-TT-61-196)
gas temperatures behind, 18: 24236
generation by water impacts on liquid aluminum in vacuum, 20: 18050(R) (STL-372-22)
ground motions induced by air-blast, simulation of, 19: 20184
ground shock spectra for underground structures, 18: 1887 (AD-422046(p.169-87))
hazards from, from underwater nuclear explosions, 20: 29481
hazards of, to populations during nuclear wars, 20: 43566 (AD-625251)
heating rates for cylinders in laminar hypersonic, 20: 20857 (SC-DC-65-1907)
hydrodynamic characteristics, analysis, 16: 24286 (UCRL-6797)
hydrodynamic, one-dimensional solution for, 17: 20712
hydrodynamic properties of, technique for observing, 19: 41118 (LA-DC-6996)
hydrodynamics of, tensor artificial viscosity for two-dimensional Lagrangian system, 18: 20635 (UCRL-7205-T)
hydrogen atom formation behind, spectrophotometric studies of, 19: 23282
hydrogen dissociation behind, at 2950 to 5330°K, 16: 18200
hydromagnetic disturbance in collisionless plasma, 16: 14170
hydromagnetic, research program, 16: 15715(R) (AFCRL-62-230)
hydroxy radical production by, in argon–hydrogen–oxygen mixtures, 18: 43478

in fluid flow, numerical calculations of, 18: 13362 (NYO-10433)
in granite from Hardhat event, calculation, 18: 20125 (UCRL-7762)
instabilities of collision-free magnetohydrodynamic, in plasma, 16: 29962
interaction with magnetic field in conducting fluid, 17: 5459
interaction with void in nitromethane, analysis of, 18: 27656 (LA-3077)
interactions in air and argon, analysis of, 17: 41656
interactions in elastic medium with shifting boundaries, 17: 8420
interactions in nitromethane-filled corners, hydrodynamics of, (E/T), 20: 21784 (LA-3450)
interactions in space, effects on geomagnetic storms, 17: 19017
interactions of crossflow, flow field analysis of, (T), 20: 30167 (SC-DC-65-1916)
interactions of laser-driven imploding, in plasma, 20: 22245
interactions of magnetically driven, in rail gun, 18: 32279 (RISÖ-79)
interactions of MHD-supported, with magnetic fields, 19: 41120 (N64-30509)
interactions of nuclear-explosion, with re-entry vehicle, computer analysis of, 19: 9756 (TO-B-64-10)
interactions of oblique, with turbulent boundary layer, temperature measurements in, 18: 6558 (SC-DC-3565)
interactions of symmetric, 18: 5883
interactions with hydromagnetic waves, 16: 1104 (AFOSR-1173)
interactions with bubbles, configurations from, 16: 20608
interactions with nova envelope, luminescence caused by, 17: 20811
interactions with magnetic fields, 17: 25918
interactions with hydrogen atoms, electric polarizability from, 17: 34653
interactions with pyrolytic graphite, Hugoniot equation of state at 0–300 k bars from, 17: 37680
interactions with metals, thermodynamic parameters from mirror-image approximation for particle velocity and pressure in, 17: 37676
interactions with aluminum at 0 to 31 k bars, Hugoniot equation of state from, 17: 37533
interactions with boundary layers, pressure probe for, 18: 3410 (SC-TM-83-62(71))
interactions with solar chromosphere, gas-dynamic model for, 18: 18541
interactions with electromagnetic waves in d-c magnetic fields, 18: 26125
interactions with cylindrical cavity, stresses from, 18: 30313 (RTD-TDR-63-3021)
interactions with electromagnetic fields, magnetic field diffusion in, 18: 34333
interactions with magnetic fields, (E/T), 19: 5333
interactions with axi-symmetric supersonic missile, transient base pressure study of, 19: 8008 (SC-DC-64-1595)
interactions with microwaves, (E), 19: 12640 (R63SD91)
interactions with gas in magnetic fields, (T), 19: 18585
interactions with plasma in pinch devices, heating effects of, (E), 19: 21473 (IPP-1/28)
interactions with cylindrical cavities in elastic media, 19: 20659 (AD-606490)
interactions with solar corona, magnetic-field effects in heating by, (T), 19: 23252
interactions with magnetosphere, (T), 19: 25426(T)
interactions with discontinuities in inhomogeneous explosives, theoretical study, 19: 36218 (LA-3235)
interactions with supersonic conical missiles, patterns, (T), 19: 43636 (SC-TM-65-217)
interactions with plasma, heating effects of, (E), 19: 45434
interactions with supersonic missiles, transient base pressure from, 20: 9850
interactions with electromagnetic fields, properties of, (T), 20: 13637 (IPP-3/28)
interactions with magnetic fields, 20: 15882(R) (NP-15868)
interactions with stationary cone, transient flow field analysis of, (T), 20: 30168 (SC-DC-66-1329)
interactions with gases, effect of line radiation on precursor ionization in, 20: 37881
interactions with impure argon, mass spectroscopy of, 20: 43123
interactions with electromagnetic waves in ionized medium, 16: 19840 (GCA-TR-61-38A)
ionization equilibrium behind, in atomic gas, 18: 9040
ionization fronts from exploding wires, 17: 13211
ionization in, determination of photoinduced, 18: 44432
ionization of air by, electric conductivity, 16: 18189
ionization of air behind, at 0.02 to 0.2 torr, 17: 5131
ionization of air, electrostatic probe measurement of, 19: 20841
ionization of argon by normal, 18: 35042
ionization of argon plasma by, 19: 38008
ionization of argon, (T), 19: 43431
ionization of gas by, with oblique fields, basic equations for, 17: 37840
ionization of gas before, microwave, 18: 1131 (R63SD78)
ionization of gases by, 17: 35027 (R63SD60)
ionization of gases by, far-flow approximations for precursor, 18: 34288
ionization of gases in electromagnetic fields, (T), 19: 43432
ionization of rare gases by, 17: 36539
ionization of xenon by, impurity effects on, 18: 34361
ionization rate behind, in air, 17: 6773 (AFCRL-62-751)
ionization rates in xenon, effects of impurities on, 18: 42785(R) (AD-600531)
ionization relaxation for, in monatomic gases, 18: 29855
ionization upstream from, 19: 41935
kinetic theory, 16: 7960(T) (AEC-tr-4741)
kinetics of interactions with crushable foamglass, 20: 16023(R) (IITRI-578P21-16)
lethal pressures for mice, rats, guinea pigs, and rabbits, 17: 22977(R) (DASA-1325)
location in time and space by photographic techniques, 16: 2821 (WT-1102)
luminescence front in electromagnetic, (E), 19: 27681
luminescence of cylindrically converging, in impact with chamber walls, effects of external short-circuit ring on, 18: 11326
luminescence of, in plasma acceleration, 17: 38409
luminosity from, 17: 664
luminosity structures of plasmas from electromagnetically driven, 18: 19233
luminous fronts preceding, in electromagnetic shock tubes, (T), 19: 12666
magnetogasdynamic flow with, 17: 20714
magnetohydrodynamic, evolutionarity, 16: 2590(T) (AEC-tr-4703)
magnetohydrodynamic, relations for, 16: 22716(R) (AFSWC-TDR-62-12(Vol.II)(Chap.6))
magnetohydrodynamic structure in gas with anisotropic conductivity, 16: 33957
magnetohydrodynamically supported hypersonic, 17: 6783 (BSD-TDR-62-337)
magnetohydrodynamics of, evolutionary, 17: 9068
magnetohydrodynamic, perturbations in non-uniform ducts by, 17: 24168
magnetohydrodynamics of oblique, (T), 19: 4767
magnetohydrodynamic detonation in, 19: 44837
magnetohydrodynamic, in nonaligned flow in perfect gases, (T), 20: 15576
magnetohydrodynamic, in solar wind, 20: 37387
mathematical analysis of, in solids, 17: 18911 (UCRL-7271)
measurement, development of equipment and methods for, 16: 18029(R) (EURAEC-225)
measurement from shock tubes, technique for, (E), 20: 2822 (AWRE-O-60/65)
measurement from 20-ton TNT charge on ground, 18: 34278 (NP-14174 (Vol.1))
measurement in Gnome event, 16: 29065 (VUP-2401)
measurement in tunnels and underground chambers, instrumentation, 17: 2660 (BRL-Memo-1390)
measurement of, transducer evaluation for, 20: 24778 (IDO-17148)
measurement with self-recording gages in Operation Teapot, 16: 3188 (WT-1155)
microwave attenuation by, at Mach 8 to 12, time dependence of attenuation curve for, 18: 16565
microwave attenuation in air, time dependence of, 18: 19227
microwave studies of electrically driven, 17: 36482
microwave studies of electrically driven, in gases, 18: 21448
mitigation of effects by lightweight vermiculite concrete, 17: 5668 (DASA-1263)
model of collisionless, from solar wind interaction with geomagnetic field, (T), 19: 18998
model of ionizing transverse, 18: 19135 (NP-13777)
models for collisionless fronts, (T), 19: 5340
molecule thermal dissociation in, (T), 19: 29010
motion in cold plasma, theory of plane, hydromagnetic, 17: 5517
motion in collision-free plasma in magnetic field, 18: 21386 (NYO-10434)
motion in plasma, 17: 9670 (62-RL-3169E)
motion in steady two-dimensional MHD flow, 18: 20630 (NYO-10436)
motion in tunnels, designs for protection against, 20: 27125 (UCRL-14848-T)
motion in ultrarelativistic fluid, 18: 18780
motion of hydromagnetic ionizing fronts in cylindrical geometry, 18: 35009
motion of non-stationary solid medium with, 16: 19550
motion of solar type II radio wave production from, (T), 20: 4524
motion of, produced by HE explosions, (E), 19: 18569(T) (AWRE-Trans-48)
overpressure measurements, 16: 12813 (WT-1101)
parameters in gases, computer program for calculating, 18: 12765 (LA-2980)
parameters in water near the exploding material, 16: 3585
parameters in water near explosions, 17: 12480
performance for heating magnetically trapped plasma, (T), 19: 23826(T) (UCRL-Trans-1185(L))
photographic examination, design of high-speed camera for, 16: 23852

(UTIA-TN-26)
photography, 16: 2821 (WT-1102)
photography, 16: 11366 (WT-779)
physical effects of, from nuclear explosions, 20: 2078 (BNL-917, pp 1-10)
physical principles of hydrodynamic and hydromagnetic, in controlled thermonuclear fusion, 16: 9532
plasma acceleration and heating by, in electric discharges, 17: 990
plasma acceleration by magnetic, electro-kinetic conversion in, 18: 2975 (AD-283026)
plasma cloud from electromagnetically driven, production and structure of, 18: 19232
plasma density measurement in pressure-driven, (E/T), 20: 22168 (AD-622569)
plasma from hypersonic, electric generator using, 18: 9067 (SC-4960(RR))
plasma precursor ionization in, (E/T), 19: 21471 (IPP-1/24)
plasma production by electromagnetic, 16: 19849
plasma production in air by, 17: 7491
plasma production by electromagnetic, electron density in, 17: 21153
plasma production by hypersonic space vehicle re-entry, for power generation, 18: 32519
plasma production by, microwave measurements of electron density in, (E), 20: 17510 (IPP-3/25)
plasma stability effects, 17: 42134
plasma temperatures behind hypersonic, 16: 12628
population of excited electronic states in, mechanisms of vibrational relaxation for, 16: 19469 (NP-11613)
position register for solid opaque media, 18: 30314 (UCRL-7449)
precursor effect in, microwave study of mechanisms of, 18: 19222
precursor phenomena in, in argon (E), 19: 1057
precursors to pressure-driven, 18: 19221
pressure distribution on front of strong, from electric-discharge shock tube, 20: 11775
pressure effects in chambers resulting from entry through orifices, 16: 12802 (NP-11558)
pressure gages for, design and operation of multidirectional peak, 20: 20914
pressure measurements, preshock, 16: 11365 (WT-777)
pressure measurements in shelters, 17: 29884 (WT-1501)
pressure of, piezoelectric probe for measuring, 17: 36118 (PAN-396/XVIII)
pressure probe for plasma diagnostics, piezoelectric, 20: 42405 (IPP-1/46)
pressure transients from, gage for measuring dynamic, 17: 39371 (AWRE-E-13/63)
processes in magnetohydrodynamics, endothermic and exothermic, 17: 2103
production and effects under water of, by detonation of atomic explosions above water surface, 16: 18725(T) (AEC-tr-5056)
production and observation in plasma, review of Japanese research on, 20: 24530
production and properties in variable-density stars, 16: 16906
production and propagation in explosions of type II supernova, 17: 41698
production and propagation of MHD, 18: 44284 (AD-603951)
production and propagation in hydrogen, (E), 19: 25592
production and propagation in discharge tubes, (E), 20: 20089
production and structure in nearly collisionless plasma, (E), 20: 6501
production by combustion of gases, 17: 4193
production by contraction of linear pinch discharge in helium, current density behind, 18: 19230
production by directed explosions and mechanical impact, 18: 17372(T) (UCRL-Trans-992(L))
production by electric discharge in inert gas, microwave study of, 18: 19228
production by electric and explosive energy, 18: 44134(R) (EURAEC-1101)
production by exploding metallic films, 17: 35260(R) (TID-19135)
production by sparks in gases, 17: 32801
production by time-varying magnetic fields, 16: 33614
production by water decompression in air, one-dimensional analysis of, 20: 16023(R) (IITRI-578P21-16)
production during plasma acceleration, 16: 3764 (LMSD-894830)
production from cavity explosions, 19: 13561(R) (AD-439079)
production from combustion processes, models for, 20: 28689
production from solar corona discharges, effects on cosmic activity, 20: 37486
production in acoustic spark chambers, spark location from analysis of, (T), 20: 21094
production in air from cratering explosions, 18: 36894 (TID-7695 (p.169-80))
production in collapsing cylindrical plasma, 17: 9754
production in cosmic plasma interactions with geomagnetic fields, 16: 3601
production in deuterium–tritium mixtures by accelerated solid particles, attainability of fusion temperatures from, 18: 21418
production in gases, design of shock tube for, 16: 4897 (D1-82-0077)
production in interplanetary medium, by solar flares, (T), 20: 44098
production in inverse pinch devices, 20: 21798
production in linear pinched discharge, 17: 9744
production in magnetohydrodynamic supersonic flow past a wedge, effects of magnetic field on, 17: 41576
production in orthogonal pinch discharge, 17: 9742
production in plasma by triggered spark gaps, 18: 42849
production in plasma expansion, plasma thermalization by, 19: 29412
production in plasma, collisionless, (E), 20: 8215
production in pulsed underwater electric discharge, (T), 20: 28086
production in rarefied plasma in presence of non-isotropic instability, 17: 2376
production in reactor accidents, analysis of, 17: 36897
production in solar plasma interaction with geomagnetic fields, 18: 2723 (IPPJ-12)
production in solar flares, solar proton interactions from, 19: 43026
production in solids, plane-wave explosive system of, 18: 7997 (SC-4967-(RR))
production in T-tube, 18: 13129 (AFOSR-4644)
production of argon plasma by, electron density and temperature during, 18: 19225
production of cylindrical imploding, 19: 44852
production of directed, in electric discharges, 17: 36518
production of imploding spherical, by mirror coil, 18: 26151
production of ionizing switch-on, (T), 20: 25971
production of layer, in low-pressure gas discharges, 19: 1727
production of layer, in low-pressure discharges in neon, 19: 1728
production of layer, in low-pressure gas discharge, 19: 1731
production of magnetoacoustic, in h-f magnetic induction plasma, (E), 20: 28511
production of plane, by exploding foils, 17: 13219
production of surface, by earthquakes and underground explosions, 17: 25444
production of very high-pressure, in metals, 18: 20454 (LADC-5561)
production of, with velocities of Mach 10 to 100, by plasma compression, 17: 9697
production of, electromagnetic, 20: 6158(R) (AD-619999)
production of, electromagnetic, (T), 20: 13637 (IPP-3/28)
profile of collisionless plasma, 16: 3779
profiles in microwave interferometers, determination of longitudinal, 17: 27662
propagation, action, and protection against, from atomic explosion, 16: 9736(T) (JPRS-11811)
propagation along cylindrical electron beams, (T), 19: 20705
propagation and pressure factors of, from nuclear explosions, 16: 17907 (AD-264553)
propagation and structure of magnetohydrodynamic, 17: 2375
propagation and structure of, in electric discharge tubes, (E), 19: 27676
propagation at remote distances from explosion point, 16: 25639
propagation by gas in electromagnetic field, 16: 593(T) (CEA-tr-R-1376)
propagation by nuclear explosion in salt deposit in Salmon event, calculations on, 20: 23323 (UCRL-12326)
propagation from atomic explosions in air, (T), 19: 20675
propagation from Danny Boy underground nuclear test, measurement, (E), 19: 18173 (POR-1809)
propagation from explosions, book, 18: 4331(T) (FTD-TT-63-381)
propagation from explosions in ionosphere, (E), 19: 43224
propagation from high-altitude explosions, 16: 20838
propagation from nuclear explosions, analysis of, 18: 10212 (AFSWC-TDR-63-53)
propagation from nuclear explosions in salt formations, 20: 14663 (UCRL-14463(Rev.1))
propagation from Salmon explosion, 20: 36962
propagation from Salmon explosion, time dependence of, (T), 20: 36963
propagation from tamped and untamped underground nuclear explosions (T), 19: 2473 (UCRL-7916)
propagation from underground nuclear explosions, 18: 23783 (NP-13943(p.209-14))
propagation from underground explosions (T), 19: 643 (DASA-1484)
propagation from underground nuclear explosions, (E/T), 19: 15699
propagation in air, in gravity-wave mode, wind effects, 16: 27769
propagation in air, velocity profiles in laminar boundary layer behind, (E), 19: 18610
propagation in air, charged particle density and temperature in front of, 20: 37880
propagation in argon and xenon, properties of, 19: 41128 (UCRL-12466)
propagation in argon, front curvature in, (E), 19: 44853
propagation in argon plasma, 20: 6478
propagation in argon plasma, microwave reflection technique for,

20: 13936
propagation in argon, electron precursor phenomena in, (T), 20: 15577
propagation in argon plasma, radiation intensity from, (E/T), 20: 22281
propagation in atmosphere from nuclear explosion on Oct. 30, 1961, 16: 5566
propagation in atmosphere, 16: 5107 (SCR-163)
propagation in atmosphere, model for, 16: 20837
propagation in collisionless plasma, 16: 16913
propagation in collisionless plasma, 17: 4192
propagation in collision-free plasma, 18: 9473
propagation in collision-free plasma, (E), 19: 12697
propagation in collisionless plasma, (T), 20: 32652
propagation in compacting plastic medium, 18: 2410(T) (UCRL-Trans-1003(L)
propagation in conical tubes, analysis of, 18: 20647
propagation in conducting gases in magnetic fields, similarity rules for, 18: 28142
propagation in conducting gas in weak magnetic fields (T), 19: 2911
propagation in conducting gases, gradients of flow variables behind, (T), 19: 20664
propagation in continuous media, one-dimensional, (T), 19: 41126 (SCL-DR-65-75)
propagation in conducting incompressible fluids in magnetic fields, (T), 20: 1092
propagation in crushable materials, measurement of, 17: 26127
propagation in crushable solids, 17: 31682(R) (IITRI-A6042-1)
propagation in crushable solids, 18: 3040(R) (IITRI-A6042-2)
propagation in crushable solids, 18: 28935(R) (IITRI-T6042-5)
propagation in crushable solids, 19: 6832(R) (IITRI-578P21-8)
propagation in crushable solids, 19: 6833(R) (IITRI-T6042-7)
propagation in crushable solids, 19: 25640(R) (IITRI-578P21-12)
propagation in degenerate electron plasma, 17: 13653
propagation in deuterium gas, 16: 2308(T) (UCRL-Trans-730(L))
propagation in deuterium plasma, 17: 9731
propagation in di- and monatomic gases, models for, 18: 32945
propagation in double-driver shock tubes, (E), 19: 41162
propagation in ducts of varying cross sections, 18: 2399 (AD-422046 (p.188-93))
propagation in ducts, effects of non-uniformities in piston motion on magnetohydrodynamic, 19: 42932
propagation in ducts and entrance structures of shelters, 20: 39072
propagation in electromagnetic shock tubes, luminous front in, (E), 19: 12683
propagation in electromagnetic shock tube, (T), 20: 21796
propagation in electroneutral media, magnetic deformation and electric structure in wave-front interior during, (T), 20: 21806
propagation in exosphere, Earth's bow shock properties from, 20: 25990
propagation in exponentially decreasing atmospheres, similarity solution, (T), 19: 16260 (UCRL-7980-T)
propagation in exponentially decreasing atmospheres, (T), 20: 15217
propagation in ferroelectric materials, 18: 44154 (SC-DC-64-348)
propagation in fluids, (T), 20: 4707 (UCRL-14318)
propagation in gases in magnetic fields, evolution of trans-Alfvenic, 18: 26122
propagation in gas explosion, numerical solution of unstable one-dimensional flow, 19: 44200(T) (SC-T-65-756)
propagation in gases with discrete velocity distributions, (T), 20: 11779
propagation in gases, properties of ionizing, (T), 20: 17511 (NP-15894)
propagation in gases, ionization from, (T), 20: 22285
propagation in gases, (T), 20: 24191
propagation in gases, front thickness for, (T), 20: 25987
propagation in granite (E/T), 19: 648 (SC-4741(RR))
propagation in ground, elastic half-space solution for, 18: 2397 (AD-422046(p.124-40))
propagation in helium plasma, heating from, (E), 20: 15896
propagation in helium and neon afterglow plasmas, Tonks-Dattner resonance determination of axial, (E), 20: 20044
propagation in high-altitude explosions, geomagnetic field effects from, 18: 3347
propagation in hot rarefied plasma across magnetic field, (T), 20: 26323
propagation in hydrogen, equilibrium attainment after, 16: 21666 (RISÖ-35)
propagation in hydromagnetic fluid, spherical piston, 16: 22712(R) (AFSWC-TDR-62-12(Vol.II)(Chap.2))
propagation in hydromagnetic fluid, spherical piston, 16: 22713(R) (AFSWC-TDR-62-12(Vol.II)(Chap.3))
propagation in hydromagnetic fluid, cylindrical and spherical piston, 16: 22714(R) (AFSWC-TDR-62-12(Vol.II)(Chap.4))
propagation in hydromagnetic fluid and vacuum magnetic field, 16: 22715(R) (AFSWC-TDR-62-12(Vol.II)(Chap.5))
propagation in hydrogen, in magnetically driven shock tubes, (E), 19: 20661 (RLE-TR-428)
propagation in hydrodynamic medium, (T), 19: 26924 (UCRL-12412)
propagation in hydrogen plasma, photoionization and radiational cooling from, (T), 20: 10197(T)
propagation in hydrogen, properties of electromagnetically driven, (T), 20: 21779 (AD-621990)
propagation in hydrogen, equilibrium chemistry of ionizing, (T), 20: 21796
propagation in hydrogen and rare-gas Z-pinch discharge, converging cylinder model for, (E), 20: 24565
propagation in hydrogen, equilibrium conditions for, (T), 20: 28041 (CLM-R-56)
propagation in idealized material and rigid-locking solids, 17: 2081
propagation in ideal gases, analysis of, (E/T), 20: 30169 (UCRL-14198)
propagation in impulse tubes, 18: 32304
propagation in inert solids, review of research on, 20: 7960 (LA-DC-7462)
propagation in infinite homogeneous plasma, 17: 9724
propagation in inhomogeneous media, second-order approximation, 16: 2369
propagation in inhomogeneous gases (T), 19: 1082
propagation in interplanetary space, bistatic-radar measurements of, 20: 31858
propagation in ionized gases, coupling of diffusion and pressure modes, 19: 25071(R) (TID-21667)
propagation in jet propulsion gases, 17: 27538(R) (NP-12767)
propagation in low-density deuterium plasma, 18: 19236
propagation in low-density plasma with strong magnetic field, (T), 19: 27690
propagation in magnetohydrodynamic media, 16: 1149
propagation in magnetic annular shock tube, 16: 25912 (NP-11848)
propagation in magnetic fields, 17: 3612
propagation in magnetohydrodynamics, 18: 1157
propagation in magnetically driven shock tubes, 18: 19231
propagation in magnetic mirrors, effects of, (E), 20: 13921(R) (NP-15703, pp 52-63)
propagation in magnetically driven hydrogen shock tubes, (E), 20: 32615
propagation in MHD shock tubes, (E), 19: 10434
propagation in MHD, computer program for, 20: 36086 (UCRL-14931)
propagation in nonuniform magnetic fields, 20: 6158(R) (AD-619999)
propagation in outer layers of type-II supernova, (T), 19: 20769(T)
propagation in outer stellar layers, (T), 19: 44924(T)
propagation in partially ionized gases, structure of, (E/T), 19: 14133 (NP-14769)
propagation in perpendicular magnetic field, radiative energy flux from one-dimensional plane, (T), 20: 21788
propagation in pinch plasma, (T), 19: 27693
propagation in plasma from hypersonic vehicles, 17: 5430 (AD-276418)
propagation in plasma, 17: 11836 (RADC-TDR-62-186)
propagation in plasmas, magnetic field effects on collisionless, 17: 26687(T)
propagation in plasma, radiation smoothing in, 18: 3005
propagation in plasma, pressure tensor dissipation and isotropization lengths for, 18: 3024
propagation in plasma pinch, compression effects of, 18: 21523
propagation in plasma in transverse magnetic fields, analysis of, 18: 26752
propagation in plasma, structure during, 18: 30889 (NP-14082)
propagation in plasma, theory for, 18: 35032
propagation in plasma, velocity of, 18: 44888
propagation in plasma, equations for, (T), 19: 14669 (NP-14787)
propagation in plasma, microwave measurements of, (E), 19: 14692
propagation in plasma, turbulent heating in, 19: 40047
propagation in plasma, heating effects from, 19: 41861 (NP-15255)
propagation in plasma in accelerating tube, splitting of, (E), 19: 41880
propagation in plasma, nonlinear stationary, (T), 19: 41915
propagation in plasma, laser interferometer diagnostics of, 20: 8216
propagation in plasma, microwave interferometry of, (E), 20: 22182 (IPP-3/35)
propagation in plasma, cooperative phenomena in, (T), 20: 24561(T)
propagation in plasma, high-field steady-state, (T), 20: 32604
propagation in plasma, dissipative effects on, (T), 20: 42476
propagation in quasi-neutral two-dimensional plasma, 17: 17377
propagation in quasi-linear flow fields, 17: 24135
propagation in rarefied plasma, 17: 36817
propagation in rarefied plasma, (T), 19: 5273(T) (AEC-tr-6509)
propagation in reactor accidents, computer program for calculating, 20: 1350 (TIM-950)
propagation in red giant stars, 16: 16914
propagation in relativistic magnetohydrodynamics, (T), 20: 19623
propagation in rocks from underground explosions, 17: 19735 (UCRL-Trans-934(L))
propagation in room-temperature hydrogen, ionization from, 18: 36710(R) (AFOSR-64-0301)
propagation in semi-linear flow fields, 17: 24134
propagation in soil and underground structures, 18: 10261 (DASA-1386)

propagation in soils, computer program for nonlinear viscoelastic, 18: 35703 (BRL-1237)
propagation in soils, methods for predicting, 19: 34361(R) (AD-609555)
propagation in solids, blast-wave theory of crater formation by, 17: 39282
propagation in solids, bibliography on, 17: 41554 (NP-13166)
propagation in solids, measurement of front position of, 18: 34357
propagation in solids, research programs on, 19: 32048(R) (NP-15073)
propagation in solid explosives, 19: 42206 (LA-DC-6992)
propagation in solar wind interactions with magnetosphere, (T), 19: 45165
propagation in solar corona, type-II r-f emission from, (T), 20: 29903(T)
propagation in solids, profiles for, (T), 20: 41513(R) (UCRL-14744, pp 19-36)
propagation in stars, 17: 39833
propagation in stars, radiation effects in theory of, 19: 37431(T) (FTD-TT-65-82)
propagation in stellar explosions, 17: 13036
propagation in steel, 18: 4243(R) (EURAEC-613)
propagation in stellar atmospheres, effects of gravitational property changes on, 18: 18540
propagation in T tube, blast-wave theory of flow behind front in, 18: 19234
propagation in theta-pinch plasma, 18: 22971
propagation in thermal plasmas, density and temperature behind, (T), 19: 40051
propagation in theta-pinch plasma, analysis using Fokker–Planck method, (T), 20: 30560 (LA-DC-7282)
propagation in theta-pinch hydrogen plasma, oscillatory, (E/T), 20: 34745
propagation in tubes with precursor arc, 18: 28143
propagation in various construction materials following rapid loading, 16: 12209 (AFSWC-TR-61-31(II))
propagation in viscoelastic bars, 16: 13706 (TID-15198)
propagation in water in liquid driver column of shock tube, 16: 13735
propagation, nonequilibrium phenomena, 16: 9528(T) (FTD-TT-61-196)
propagation of acoustic and elastic, in cylindrical media from point source, (T), 19: 30418 (VESIAC-6796VU)
propagation of atomic-explosion, in hydraulic conduits, (E/T), 19: 11382
propagation of collisionless, in low-density plasma, (E), 19: 5362
propagation of cylindrical, in dissipating media, 17: 9059
propagation of cylindrical, in fluid containing uniform transverse magnetic field, 17: 24108
propagation of cylindrical, in linear pinch discharge, 18: 3017
propagation of electromagnetic, in gyromagnetic media, 18: 10645
propagation of electromagnetically driven, 18: 26795
propagation of electromagnetic, in dielectric medium, (T), 19: 28916 (IPPJ-31)
propagation of electromagnetic, in nonlinear transmission lines, (T), 19: 37229
propagation of electromagnetically driven, in transverse magnetic fields, (T), 20: 7962
propagation of elliptically polarized monochromatic MHD, (T), 19: 6412
propagation of finite-amplitude, along magnetic field in plasma, (T), 19: 31354
propagation of, from underground thermonuclear explosion, long-range, 17: 31801 (PNE-202F)
propagation of hydromagnetic, evolutionary effects in, 17: 9052
propagation of hydromagnetic, from high-altitude explosions, 18: 40434
propagation of hydromagnetic, in inhomogeneous magnetic field, (T), 19: 12693
propagation of hydromagnetic, in magnetosphere, (T), 19: 19008
propagation of hydromagnetic, in gases in arbitrarily oriented magnetic fields, (T), 20: 30177
propagation of, in electrogasdynamics, pseudosimilar and self-similar solutions for, 16: 32496 (USCEC-83-215)
propagation of longitudinal, along plasma column, 17: 2384
propagation of magnetohydrodynamic switch-on, in hydrogen, 18: 7422
propagation of magnetohydrodynamic, conditions for, 18: 10245
propagation of magnetogasdynamic viscous, in hypersonic flows, 18: 30936
propagation of magnetic, in plasma, 19: 19264(R) (UCRL-12028(p.81-120))
propagation of MHD, in cold and preheated gas, 18: 11338
propagation of MHD, in transverse magnetic field, 18: 14599
propagation of MHD, in plasma, 18: 35006
propagation of MHD, 18: 44288 (NP-14347)
propagation of MHD, ionizing effects in (E/T), 19: 3395 (AD-606894)
propagation of MHD, in gases, 19: 27689
propagation of MHD, from explosions, (T), 19: 27692
propagation of MHD, in argon–oxygen mixtures, (E), 19: 26939
propagation of MHD, in argon–oxygen mixtures, (E), 20: 32217 (N-65-33713)
propagation of normal ionizing, in electromagnetic fields, 18: 44288 (NP-14347)
propagation of precursor, from TNT detonation at ground level, 20: 18923 (N-65-22654)
propagation of pulsed electromagnetic, in nonlinear medium, (T), 19: 12702
propagation of rarefaction, in plasma, (T), 19: 10433
propagation of spherical, in stars, (T), 20: 31871
propagation of strong ionizing, in hydrogen, (E/T), 19: 11829 (NP-14674)
propagation of successive, in gases, 16: 2606(T) (SCL-T-377)
propagation of weak adiabatic, in magnetic field in plasma, (T), 19: 27678
propagation of, gas velocity behind, 18: 40058
propagation parameters of MHD ionizing, in a conducting media, 19: 39267 (NP-15157)
propagation paths for weak hydromagnetic, calculated, 18: 32684
propagation, physical nature, 16: 2312
propagation through ionized gas, effects of magnetic fields, 16: 11064 (AD-259452)
propagation through rocks, 16: 29189 (UCRL-13039)
propagation through gases, 18: 24235
propagation velocity from magnetodynamic pulses, 16: 27771
propagations in heterogeneous atmosphere, 17: 12478
properties, 17: 16776 (GAMD-2288)
properties at high pressures, theory of, 18: 21728 (UCRL-7307-T)
properties from high-altitude explosions, 16: 20839
properties in collisionless regions of stellar coronae, 16: 16912
properties in gases, 17: 37873
properties in MHD plasma flow, 20: 32231
properties in relativistic, anisotropic, magnetohydrodynamic, 17: 28066
properties of, around expanding spheres in ideal fluids, 17: 19585(R) (STL-6112)
properties of, Burnett approach to solution of Boltzmann equation for calculating, 17: 24089
properties of collisionless, in annular shock tubes, 17: 9789
properties of collision-free hydromagnetic, in interplanetary space, (E/T), 20: 31891
properties of electromagnetic generated, interferometric measurements of, (E), 20: 13636 (IPP-3/24)
properties of magnetohydrodynamic, 16: 9530(T) (JPRS-11725)
properties of magnetogasdynamic, in gases of variable conductivity, 16: 21178
properties of MGD steady-state, dissipative model for, 20: 34352
properties of oblique, in steady, two-dimensional, hydromagnetic flow, 16: 29960
properties of plane perpendicular magnetogasdynamic, in fully ionized perfect gas, 18: 26693 (RISO-76)
properties of, produced by magnetic piston plasma accelerator, 17: 29659 (SSD-TDR-63-72)
properties of second standing, in magnetosheath, 20: 21821
properties of strong cylindrical, 17: 6844
properties of, effects of dissociation, equilibrium, and ionization on, (E), 19: 6386 (NP-14546)
properties of, produced by condenser discharge in gas tube, 18: 20629 (NP-13850)
protection against, response spectra of isolation systems of underground fallout shelters for, 20: 23342 (AD-627516)
proton acceleration and scattering by hydromagnetic, in solar corona, (T), 19: 25145
pulse calculation from, slide rule for, 20: 32219 (SCL-DC-66-2)
radiation emission from, near earth and in interplanetary gas, (E), 19: 10177
radiation from, air ionization by, 17: 25919
radiation mechanism, ultrarelativistic, 16: 23181(T) (FTD-TT-61-2)
radiations behind, in air and nitrogen, 17: 32705 (BSD-TDR-63-102)
radioinduced, external to quartz discharge tubes, 18: 40679
ranges of, from nuclear explosion Gnome, 16: 12804 (PNE-110P)
Rankine-Hugoniot relations in dense high-temperature gas, 18: 44285 (AFCRL-63-898)
reaction effects of, review of Soviet research on, 19: 32786 (AD-610054)
reactions with air, electron recombination with nitrogen oxide ions in, 18: 42184
reactions with gases, Mach stems in, 18: 26137
reactions with gases, plasma production in, (T), 19: 8510
reactions with geomagnetic fields, effects of high-altitude explosion induced, 18: 3347
reactions with hydrogen, Stark profiles of Lyman-α and -β lines in, 18: 36102
reactions with liquid argon, compression in, (E/T), 20: 30170 (UCRL-14251)
reactions with nitrogen gas, spectral excitation in, 18: 32493
reactions with styrofoam, analysis of, (E/T), 20: 3324(R) (IITRI-578P21-13)

recording of, coaxial electric discharge pins for, 18: 33862
reflection against end plate in high-explosive tubes, 18: 34332
reflection by walls, 17: 41656
reflection from rigid walls, analysis of, 18: 26123
reflection from walls, pressure effects, 16: 7990
reflection in argon and helium thermal plasmas, (T), 20: 6512
reflection in em shock tube, (E), 20: 30697
reflection of electromagnetically driven, properties of plasmas produced by, 18: 17137
relaxation behind, in gases, 17: 20786
relaxation of gas mixture behind, entropy variations in, 16: 882
review, lecture notes, 16: 4895 (D1-82-0024)
role in thermonuclear research, 16: 17190
scattering by inhomogeneous regions, 16: 9367
scattering by prolate spheroids, 16: 8017
scattering of hydromagnetic, on rigid wall, (T), 20: 11796
seeding of inert-gas, effects on electric conductivity from, (E/T), 19: 35526 (NRC-7884)
separation from hot gas in shock tubes, 19: 7673
shape in shock tubes, (E/T), 19: 6800
shapes in magnetic annular tubes, 16: 18241
shapes in magnetic annular tubes, model for, 16: 18242
shield for, balsa wood as reactor blast, (E), 19: 38092 (IITRI-S78P21-9)
shock strength vs. area variations in channels containing monatomic conducting fluids, 17: 32742
space-charge separation in magnetohydrodynamic, 16: 29943
spectra from strong, uv, 17: 13643
spectra of ground shock produced by nuclear detonations, 16: 2837 (WT-1487)
spectra of helium in, emission, 17: 31613
spectral analysis, to control shock uniformity in shock testing, 16: 8975 (SCR-267)
spectrum model for atmospheric, 16: 16580
splitting of non-evolutional magnetohydrodynamic, 16: 12626
stability, 17: 36483
stability and growth of small ripples in plane, existence of configuration for forward-facing shock, contact discontinuity, and backward-facing rarefaction, 17: 36484
stability and structure of, in stellar atmosphere, (T), 19: 8062
stability and structure of trans-Alfvénic, in gases of finite conductivity, 19: 23180
stability and structure in plasma, 19: 45422
stability and structure in interplanetary space, (T), 20: 19326 (N-65-23194)
stability in MGD flow past wedge, (T), 20: 19631
stability of MHD, in conducting fluids, 18: 20649
stability of planar hydrodynamic, 16: 22721(R) (AFSWC-TDR-62-12 (Vol.II)(Chap.11))
stability of step, through fluids, 17: 5127
stability of step, interpretation of criterion for, 18: 20624 (LADC-5814)
stress tensor in structure from, calculation of, 17: 20128(T) (UCRL-Trans-936(L))
structure, 16: 12271
structure, 16: 21662 (AFSWC-TDR-62-42)
structure across magnetic field in plasma, 16: 3586
structure in argon, thickness of, 18: 28144
structure in argon plasma, uhf diagnostics for, 20: 46898
structure in atomic hydrogen in internal relaxation region, (T), 19: 39280
structure in dense plasma at high temperature, 16: 12640
structure in dilute plasma, 18: 26697(T) (AEC-tr-5589(p.554-64))
structure in discrete-velocity gas, 18: 34325
structure in electromagnetic shock tubes, (E), 19: 37983
structure in finite plasma, one-dimensional, (T), 20: 12234
structure in fully ionized plasma, (T), 19: 41928
structure in gases, 18: 26786
structure in ionized hydrogen with radiative processes (T), 19: 1718 (NP-14442)
structure in ionized gases with anisotropic viscosity, (T), 19: 11836
structure in luminescent hydrogen plasma, (E), 20: 8200
structure in magnetohydrodynamics, 16: 21206
structure in magnetohydrodynamics, effects of electron inertia on, 18: 26149
structure in monatomic gases, 16: 18279
structure in monatomic gases, 17: 20795
structure in neutral gases and plasma, (T), 19: 39984
structure in nonlinear transmission lines, (T), 19: 37230
structure in partially ionized gas, 17: 34582
structure in partially ionized gases, 19: 37225
structure in partially ionized gases, (T), 20: 7968(T)
structure in partially ionized plasma, Navier-Stokes model for steady plane, (T), 20: 10182
structure in plasma, multi-component theory, 16: 3762 (AFOSR-1618)
structure in plasma, 16: 14166
structure in plasma, mathematical analysis of, 17: 988
structure in plasma, effects of magnetic fields on, 17: 5434 (DCAS-TDR-62-12)
structure in plasma, breakdown of bimodal distribution of molecular velocities in, 17: 36777
structure in plasma, 18: 26740
structure in plasma in magnetic field, 18: 28808
structure in plasma in magnetic fields, model for, 19: 37905 (AD-609942)
structure in plasma, (T), 20: 12227
structure in plasma, radiation smoothing of, 20: 21775 (AD-620835)
structure in plasma flow past bodies in magnetic field, (E), 20: 22251
structure in rarefied plasma, 17: 40182
structure in rarefied gases, conference on, 20: 28091
structure in relativistic fluid dynamics, (T), 20: 2844
structure in slightly ionized gas, Hall current effects on, (T), 20: 25967
structure of, 18: 28094(R) (TID-20607)
structure of Alfvén, (T), 20: 44414
structure of collision free, 16: 15716 (AFOSR-2266)
structure of collisionless MHD, in magnetospheric plasma, (T), 19: 29132 (NYO-1480-12)
structure of collisionless, in magnetized hydrogen plasma, (E), 20: 4977
structure of cylindrical, plasma magnetic compression experiment for study of, 18: 36709 (AFCRL-64-293)
structure of electromagnetically produced, 18: 30935
structure of, in rarefied plasma, 17: 26735
structure of ionizing, 16: 19850
structure of magnetohydrodynamic, in dense media, 17: 6901
structure of, magnetohydrodynamic theory of, 17: 26243
structure of magnetohydrodynamic, in ionized hydrogen, 17: 39707 (AD-414622)
structure of magnetospheric, determination of, (T), 19: 27348
structure of MHD, effects of electron temperature and Hall currents on, 20: 30191
structure of plane, in plasma, 18: 34998
structure of radiative, in hydrogen, (T), 20: 7965
structure of radiative, (E/T), 20: 32670
structure of radiative hydrogen, Navier-Stokes equation for, 20: 32241
structure of self-ionizing electric discharge-driven, in magnetic field, 18: 19224
structure of slow-ionizing, 18: 14606
structure of slow, in two-fluid system with dissipation, 18: 24226
structure of strong plane, solution of Boltzmann equations by two-fluid model, 16: 16852
structure of strong collision-free, in plasma in magnetic field, (T), 19: 37931 (N64-27248)
structure of thermal radiation-resisted, with vibrational nonequilibrium, (T), 19: 20680
structure of weak, in plasma, 16: 32516
structure of, book on, 19: 41161
structure of, in collisionless plasma, 18: 42162(R) (TID-20963)
structure of, in two-fluid system without dissipation, 18: 22952
structure of, kinetic theory solutions for, 18: 26138
temperature measurement in shocked copper, 18: 3404 (LADC-5731)
theory of electromagnetically driven, 16: 29958
theory of, in magnetohydrodynamics, 17: 9699
theory of MHD ionizing, 19: 18566 (NP-14858)
theory of strong converging, in plasma, 17: 9753
thermal excitation of powdered solids by, analysis of spectra from, 17: 33820
thermodynamics of, in gases, 18: 24303
transient loading of blunt cylinders by, numerical calculations for, 19: 18092
transition region in collisionless plasma, fluid dynamic equations for, 18: 19235
transitions in chemically reacting gases and plasmas, 18: 15390
transonic flow around bodies, analysis of, (T), 20: 6160 (NP-15604)
transport in ideal fluids, jump conditions for, 20: 11889
use for rarefied deuterium plasma containment, 20: 26319
use for recombination in hydrogen–oxygen mixtures, 20: 31216 (LA-DC-7659)
use for superheating gas in MHD generator, 19: 12144
use for superheating gas in MHD generators, (T), 20: 39686
use in crushing refractory materials, 18: 32100 (AERE-M-1261)
use in determining ductile-brittle temperatures in small steel samples, 18: 44134(R) (EURAEC-1101)
use in high-pressure physics, 19: 39274(T) (JPRS-30799)
use in reactor fuel element sheathing, 19: 34670(P)
use of strong collisionless, in deuterium plasma heating, (E), 20: 26329
uses for measuring ductility of steels, 18: 35987(R) (EURAEC-1019)
uses in cleaning high-temperature filter media, 16: 29235 (TID-7627 (p.349-71))
uses of axially imploding, for heating cylindrical plasma, (E), 19: 47845

velocity and planarity of magnetically driven, 17: 19501
velocity in plasma, microwave measurements of, 18: 9460 (NP-13530)
velocity in plasma, measurement of, (E), 19: 23855
velocity of, electric contactor pins for measuring, 19: 9458
viscosity effects in radiation-structured, (T), 19: 11821 (AD-609106)
Short-Lived Fission Products
see Fission Products (Short-Lived)
Showers
see Cascade Showers
SIALIC ACID
biochemical reactions of rat erythrocyte, effects of bacterial α-amylase on, 20: 42714 (UCRL-16246, pp 119-25)
effects of, on surface charge of animal cells, 17: 38706 (UCRL-10898)
radiation effects on blood content of, in rabbits, 17: 33739
Sicklemia
see Anemia
Sickness
see Radiation Sickness
Siderophilin
see Transferrin
Siemens Reactor (MZFR)
see MZFR (Siemens Reactor)
SIERRA NEVADA MOUNTAINS
granite age estimation in California, by argon–potassium method, 19: 28564
rubidium-87–strontium-87 relations in, 18: 3981(R) (NYO-10517(p.17-22))
strontium-86/-87 ratios in granitic rocks in, of Calif., 19: 28543
Sieves
see Screens
Sight
see Vision
Sigma Hyperons
see Hyperons (Σ)
SIGMA PILES
(A constant and reproducible thermal-neutron source consisting of a RaBe neutron source surrounded by enough moderator to thermalize the neutrons; used for making absolute cross section and flux measurements.)
design in combination with subcritical reactors, 16: 6911 (TID-7619 (p.89-108))
graphite, neutron flux distribution in cavity region of, 16: 33986 (NASA-TN-D-1460)
standardization of Kansas State, 16: 24761 (TID-15667)
Sigma Reactors
see Sigma Piles
Sigmion
see Radiation Detection Instruments (Ion Current Type)
SILANE
alkyl-, yields of, from radiolysis of silicon hydrides in presence of ethylene, 19: 44066
alkyl, yields in radiolysis of liquid tetramethylsilane, 20: 18729(R) (NYO-2007-9)
alkylchloro-, radioinduced chlorination of, mechanism of, 19: 24580
allyl-, radiation effects on polymerization of, 16: 23747
allyl-, radioinduced polymerization of, 18: 317
allyl-, radioinduced polymerization with acrylonitrile and styrene, 18: 317
allylhydro-, polymerization and copolymerization of, catalytic, and radio-induced, 16: 25459
aryl, properties of, for high-temperature hydraulic fluid and lubricant uses, 16: 10511 (DC-58-7-45)
aryloxytrimethyl-, solvolysis of, in methane, mechanism of, 16: 30930(R) (NYO-2669)
chloro-, radiation chlorination of, 18: 37221
chloromethyl-, molecular structure, 16: 14729
chloroorganic, preparation of carbon-14-labeled, 18: 43551
chloropropyl-, radioinduced formation of, calculation of basic parameters for, 20: 3993
decomposition of, silent electric discharge, radiolytic, and thermal, 17: 25690(R) (NYO-10472)
decomposition, radiolytic and thermal, 16: 14771(R) (NYO-9863)
diallyl-, radioinduced polymerization of, gamma, 19: 7579
diallyl-, radioinduced polymerization of, kinetics of x, 20: 25163
dimethyldichloro-, radioinduced chlorination of, 18: 306
germyl- and methyl-, yields in mercury sensitized photolysis of germane and silane systems, 20: 18729(R) (NYO-2007-9)
germyl-, mass spectra and preparation of, 20: 3863(R) (IS-1200(Sect. C))
heat of formation of SiH_4, Si_2H_6, and Si_3H_8, 17: 27322 (UCRL-7301-T)
hydrogen bonding in, effects of substitutions on, 17: 8110
ion-molecule reactions in, 20: 20725(R) (NYO-3570-2)
ionization by x rays at high energies, spectra of, 18: 41506(R) (ML-TDR-64-169)
mass spectra, 19: 9046(R) (IS-900(Sect.C))
methoxy-, microwave spectra of, 20: 31221(R) (UCRL-16658, pp 73-87)
methyltriallyl-, radioinduced polymerization of, 19: 11189
methyltrichloro, pyrolysis to silicon carbide for refractory metal coatings, 20: 37189
methyltrivinyl-, frequency sweep double resonance spectra of, 17: 6076
neutron scattering cross sections at 4 to 11 A, 17: 31077(R) (CU(PNPL)-228)
phenylmethyldichloro-, radioinduced chlorination of, 18: 306
phenyltriallyl-, radioinduced polymerization of, 19: 11189
physical and thermodynamic properties, 16: 26644(R) (NP-11755)
preparation and properties, 17: 25690(R) (NYO-10472)
preparation, decomposition, and effects of electric discharge on, 16: 8667(R) (NYO-9862)
preparation of, for use as radiation targets, 17: 5369
preparation of silicate polymers, 16: 20350(R) (AGC-0423-01-3)
properties for use in radioinduced synthesis of semiconductor materials, 16: 27034 (NYO-9864)
properties, improvement of physical by addition of vinyl groups, 16: 20350(R) (AGC-0423-01-3)
radiation effects at 250°C, 16: 14770(R) (NYO-9861)
radiation effects on, neutron, 19: 45679(R) (NYO-1859-11)
radiation effects on, in krypton at 4.2°K, ESR of free radicals from gamma, 20: 40968
radioinduced in phosphine and phosphine–silane, recoil silicon atom reactions in, 20: 43315
radioinduced polymerization of vinyl triethoxy-, 16: 19274
radioinduced reactions with alkenes, gamma, 17: 1551
radiolysis, effects of acetylene, carbon dioxide, and water on hydrogen yield, 16: 20478
radiolysis of, yields in gamma, 20: 20725(R) (NYO-3570-2)
separation of deuterated, gas chromatographic, 18: 39383
separation of silicon isotopes from mono-, by thermal diffusion, 17: 41324
spectra of methyl, infrared, 16: 20428
spectra of methyl trideutero-, infrared, 16: 20428
tetramethyl-, radiolysis of liquid, mechanisms and yields in, 20: 18729(R) (NYO-2007-9)
tetramethyl-, radiolysis of solid, yields and mechanisms in, 20: 36883
thermal-diffusion separation of silicon isotopes in mono-, 17: 29238
trimethyl-, ionization of, by electron impact, 16: 17708(R) (TID-14812)
vinyltriethoxy-, radioinduced polymerization of, 19: 18006
viscosity, effects of crosslinking agents, 16: 20350(R) (AGC-0423-01-3)
GeH_4–SiH_4, preparation of volatile hydrides by mercury sensitized photolysis of, 20: 18729(R) (NYO-2007-9)
iodomethane–SiH_4, preparation of volatile hydrides by mercury sensitized photolysis of, 20: 18729(R) (NYO-2007-9)
methyl-, distillation of, for separation of silicon isotopes, 17: 22073
PH_3–SiH_4, radiation effects on di- and monosilane production in, recoil silicon atom reactions in neutron, 20: 43315
SbH_3–Si_2H_6, heat of explosion, 17: 27322 (UCRL-7301-T)
SILANE, DIMETHYL-
spectra of, effects of deuterium on infrared, 19: 11119
SILANE, ETHYNYL-
microwave spectra and structure of, isotope effects on, 20: 3977
spectra of deuterated and normal, infrared, 18: 10125
SILANE, TETRAPHENYL-
effects on scintillator quenching in benzene, 19: 46362
radiolysis of, in benzene, 19: 46362
SILANE, TRIETHOXYVINYL-
radioinduced polymerization of, at low temperatures, 20: 1893(R) (AD-618228)
SILENT BUTTE QUADRANGLE (NEV.)
geologic map of, 18: 41639 (TEI-850)
Silica
see Silicon Oxides
Silicate Glass
see Glass
SILICATE ROCKS
see also Rocks
analysis for beryllium, development of spectrographic technique for, 16: 5587
analysis for cerium, lanthanum, neodymium, scandium, and yttrium, 16: 25287
analysis for cerium, hafnium, thorium, and zirconium by ion exchange and spectrography, 19: 17805
analysis for cesium by flame photometry, 18: 33500
analysis for cesium and rubidium by ion exchange and activation methods, 20: 43133
analysis for germanium in G-1 and W-1, activation, 20: 35426
analysis for gold, activation, 17: 10573
analysis for indium and thallium, quantitative spectrographic, 16: 18839
analysis for lanthanum, samarium, scandium, and yttrium, activation,

18: 39128
analysis for light-weight elements, x-ray fluorescence spectrographic, 16: 30353
analysis for molybdenum, tantalum, tin, and tungsten, activation, 16: 1712
analysis for niobium, radiometric-spectrophotometric, 19: 43943
analysis for rare earths, activation, 20: 2056
analysis for sodium in diabase, neutron activation, 16: 5278
analysis for sodium, flame photometric, 19: 46191
analysis for strontium, emission-spectrographic, 16: 17608
analysis for tin traces, activation, 18: 21963
analysis of alumino-, for potassium and sodium by fast-neutron activation, 20: 33172(T) (AEC-tr-6639, pp 64-6)
analysis of, neutron activation, 18: 5514
analysis of, methods for, 20: 16337 (RMO-3001(Rev.1)(Suppl.))
analysis of, quantometric and spectrographic, 18: 19910
lithium isotope abundance in, ratio to meteorites, 17: 23524
neutron activation of, from underground nuclear explosions (T), 19: 679 (HNS-1229-54)
neutron diffusion parameters in, determination of, using pulsed source, 20: 14772
petrogenesis of, in Sierra Nevada and Yosemite National Park, relation of deuterium–hydrogen ratio to, 17: 12461
separation of transuranic elements from, flowsheet for chemical, 17: 24750(R) (UCRL-10624)
sorptive properties of pyroclastic, for fission products, 17: 35940 (UJV-951/63)
sorptive properties for cesium and strontium from synthetic river water, 17: 35710 (UJV-528)
sorptive properties of pyroclastic, for decontamination of waste solutions, 19: 24444
strontium isotopic composition of sials, evidence for separation from continental basement from, 17: 25460

SILICATES
(See also silicates of specific elements.)
see also Aluminum Silicates
see also Calcium Silicates
see also Ethyl Silicates
see also Fluosilicates
see also Iron Silicates
see also Lithium Silicates
see also Magnesium Silicates
see also Potassium Silicates
see also Rare Earth Silicates
see also Silicate Rocks
see also Sodium Aluminum Silicates
see also Sodium Silicates
see also Thorium Silicates
see also Uranium Silicates
see also Zinc Silicates
see also Zirconium Silicates
analysis for alkali metals, flame photometric, 16: 32939
analysis for beryllium by fluorometric method, 17: 35641
analysis for cesium and rubidium, flame photometric and radiochemical, 18: 35460
analysis for germanium, quantitative spectrographic, 16: 18839
analysis for gold by neutron activation methods, 20: 26785
analysis for hafnium, thorium, titanium, and zirconium, simultaneously, spectrographic, 18: 19912
analysis for impurities, activation, 20: 26782
analysis for light-weight elements, x-ray fluorescence spectrographic, 16: 30353
analysis for metals, spectrographic, 19: 13266
analysis for moisture, development of cadmium probe for, 16: 22504
analysis for oxygen isotopes using bromine pentafluoride, 17: 30481
analysis for thorium, 16: 398(T) (CEA-tr-A-954)
analysis for zirconium in eudialyte using p-iodoamygdalic acid, gravimetric, 18: 17749
charged-particle track etching in crystalline, 17: 4999
content in Atlantic Ocean, measurements on, 20: 28878 (NYO-1918-138)
content in Atlantic Ocean, measurements on, 20: 28877 (NYO-1918-124)
content in Mediterranean Sea, effects of season, temperature, and Nile River flooding on, 20: 43508(R) (NP-16179)
content in Sargasso Sea, annual and seasonal variations in, 18: 21711 (NYO-3140-1B)
crystal growth of tri- and tetravalent, from oxide melt, 18: 44046(R) (ORNL-3670(p.6-10))
decontamination by removal of iron-59 activity, evaluation of wetting agents for, 16: 25660(T) (JPRS-13691(p.8-12))
determination in cements and cement raw materials by radiometric titration, 17: 40711 (TID-7655(p.291-301))
diffusion of radioisotopes in melted, 19: 37085
dissolution by acids in sealed tubes, 19: 17781(R) (ORNL-3750)
effect of, on reactor effluent radionuclides, 20: 45215 (BNWL-282)
effects of, on reduction of plutonium(IV) by uranium(IV), 20: 35597
effects on corrosion of aluminum by high-purity water at 100°C, 17: 18706
effects on strontium-89 transport in bean and pea plants, 20: 26625
effects on structure and properties of sintered alumina bodies, 19: 32740(T) (NP-tr-1239)
emissivity of mixture with carbon black to 2000°F, 16: 30801(R) (PWA-1878)
emissivity with carbon black at 200 to 1800°F, total, 16: 30802(R) (PWA-1966)
fixation of fission products in melted, 17: 10226
formation of extremely small holes in, using fission fragments, 17: 25991
fusion in geological environments, 18: 31048(R) (COO-689-42)
heats of formation of, equation for estimation and correlation of, 20: 35482 (UCRL-16865)
immiscibility in melted, statistical model for, 19: 23071
isotopic exchange of oxygen between carbon dioxide and, effects of water on rates of, 17: 25179
model for prediction of oxidation equilibria, 16: 14378(R) (NYO-2302)
oxygen isotopic exchange between vitreous or crystallized, and water enriched in oxygen-18, 17: 23836
production of contracting gaseous spheres, (T), 20: 19345
radiation effects on organic, cosmic, 17: 32693
radiation effects on thermal control coatings of, in nuclear spacecraft, 18: 20603
radiation effects on coatings of, for spacecraft, 20: 2428 (NASA-SP-55, pp 365-79)
radioactive waste fixation in poly-, 20: 45226
radioinduced luminescence of, proton, (E), 20: 28623
radioisotope fixation in fused, safety precautions for, 18: 15661
radiolysis of aqueous solutions of, at 77°K, yields of hydrogen from gamma, 20: 18748
role in origin of life on earth, 18: 35268 (UR-656)
sorptive properties for cesium and strontium, 17: 32045(R) (TID-19184)
sorptive properties for cesium and strontium from synthetic river water, 17: 35710 (UJV-528)
surface phenomena in melts of, 18: 32078
technology of, properties of metals and their compounds for use in, 18: 7250
thermoelectric properties, 18: 818(R) (NP-13266)
Al–B–silicate–Na, preparation as phosphor for neutron detection, 19: 15927
Al–Li–Mg–silicate, preparation as phosphor for neutron detection, 19: 15927

SILICIC ACIDS
additive effects on densification of thorium oxide–uranium oxide pellets, 16: 7874 (ANL-6375)
immunological properties of, in guinea pigs, 19: 15000
phase transformations, effect of pressure and irradiation on solid-solid, (E), 20: 40306
radiation effects on phase transformations in, under high pressure, 20: 33968
radiation resistance of diesters of, 19: 24561
tungsto-, isopiestic studies of aqueous solutions of, 16: 32976

SILICIDES
see also Cerium Silicides
see also Cesium Silicides
see also Chromium Silicides
see also Dysprosium Silicides
see also Europium Silicides
see also Gadolinium Silicides
see also Hafnium Silicides
see also Iron Silicides
see also Lanthanum Silicides
see also Magnesium Silicides
see also Molybdenum Silicides
see also Neodymium Silicides
see also Niobium Silicides
see also Osmium Silicides
see also Plutonium Silicides
see also Praseodymium Silicides
see also Rare Earth Silicides
see also Rhenium Silicides
see also Ruthenium Silicides
see also Scandium Silicides
see also Strontium Silicides
see also Tantalum Silicides
see also Thorium Silicides
see also Titanium Silicides
see also Tungsten Silicides
see also Uranium Silicides
see also Vanadium Silicides

see also Yttrium Silicides
see also Zirconium Silicides
book: *Hard Materials*, in German, 18: 7261
book: *High-Temperature Materials*. No. 1, *Materials Index*, 18: 24075
book: *Silicides and Their Use in Engineering*, 16: 16341(T) (FTD-TT-61-409)
coating of molybdenum and tungsten by, studies of oxidation protection provided by, 19: 7848(R) (ASD-TDR-63-753(Pt.II))
coatings on tungsten, evaluation of, 18: 14440
crystal structure of, 17: 23872(R) (TID-18626)
crystal structure of three-component, 19: 9152
data tabulations on, 18: 32079
deformation and fracture of, 17: 4886(R) (AD-275610)
deposition of coatings of, on metals by electrolysis in fused bath, 16: 18010(P)
deposition on C-129Y niobium alloy, 19: 11667 (D2-20282-1)
deposition on D-14 niobium alloy, 18: 34052 (RTD-TDR-63-4063)
deposition on metals, 19: 11711
deposition on molybdenum and niobium, 18: 34209
deposition on niobium alloys B-66 and D-43, 18: 14373(R) (NP-13498)
deposition on niobium alloys B-66, FS-85, and X-110, 18: 14353(R) (AD-408310)
deposition on niobium alloys as oxidation-resistant coatings, fluidized-bed process for, 20: 43881
deposition on tantalum alloys by pack cementation, 18: 30105(R) (AD-429028)
development of coatings of, for niobium–titanium–vanadium alloys, 17: 30938(R) (NP-12971)
development of coatings of, for titanium-base alloys, 16: 29341 (NP-11990)
development of coatings of, for niobium–titanium–vanadium alloys, 17: 6562(R) (ARF-B-6001-1)
development of coatings of, for tantalum base alloys, additive effects of aluminum, boron, manganese, and vanadium on, 17: 23945(R) (ASD-TDR-63-232)
development of coatings of, for niobium–titanium–vanadium alloys, 16: 19334(R) (ARF-2227-5)
development, requirements, and uses for aerospace components, 16: 10425 (ASD-TR-61-322(p.679-709))
developments in high-temperature, 16: 27641(T) (FTD-TT-62-503)
diffusion of coatings of, in molybdenum-titanium alloy sheet at 2500°C, 18: 39824 (NASA-TN-D-2039)
effects of coatings of, on mechanical properties of niobium–titanium–vanadium alloys, 19: 15996(R) (IITRI-B6019-4)
effects of coatings of, on niobium alloys B-66 and X-110, 17: 39525(R) (AD-416459)
effects of coatings of, on tensile behavior of molybdenum and niobium alloys, 20: 27549
emittance properties of oxidation-protective coatings of di-, on refractory metals, 19: 13869(R) (ASD-TDR-63-269)
evaporation rate and vapor pressure of, 17: 21691
fabrication method for, 20: 9479(P)
fabrication of refractory metal, 18: 7263
failures in coatings of, characteristics of low-temperature, 16: 30808 (UCRL-6937)
heats of formation of metallic, 16: 19266
metallography of types for use above 2500°C, 16: 30803 (TID-11432)
preparation and properties of refractory, review, 17: 14863(T) (JPRS-17446)
preparation and properties of refractory metal, 17: 14864(T) (JPRS-17750)
preparation of pseudo, 17: 18668(R) (AFOSR-2647)
preparation of three-component, 19: 9152
preparation of, crucible-free, 18: 12112
preparation, properties, and uses of refractory metal, 16: 25768(T) (NASA-TT-F-102)
preparation, properties, and uses of, review on, 16: 27640(T) (FTD-TT-62-430)
production and properties of, German book on, 18: 7261
production, properties, and uses of refractory, 19: 47020(T) (AEC-tr-6616)
properties and structure correlations of, review of, 17: 30987(T) (AEC-tr-5873)
properties and uses of rare-earth, 17: 23999
properties as coatings for B-66 and D-43 alloys, 18: 20523(R) (NP-13811)
properties as coating for refractory materials, 18: 30190
properties as coatings for B-66, D-36, and TZM alloys, 18: 30118(R) (RTD-TDR-63-4006(Pt.I))
properties as coating for refractory metals, 20: 4418
properties for high-temperature uses, effects of preparation and fabrication methods on, 20: 7511
properties of coatings of, on vanadium-base alloys at high temperatures, 17: 12610(R) (ARF-B6001-2)
properties of coatings of, for protection of refractory metals, 20: 33825
properties of high-melting, 16: 25835
properties of high-temperature energy-storage, survey of thermophysical and transport, 19: 35002 (TID-7687(Suppl.))
properties of oxidation-resistant coatings of, on niobium-base alloys, 19: 26801(R) (AD-607530)
properties of refractory, review, 17: 3522
properties of, for high-temperature coatings, 20: 37192
protective effects on B-66 and D-43 niobium alloys, 18: 24068(R) (NP-13955)
protective effects of coatings of, against oxidation of molybdenum-titanium alloy sheet at 2500°C, 18: 39825 (NASA-TN-D-2040)
protective effects of coatings of, against oxidation of niobium–vanadium alloys at 2000 to 2400°F, 16: 27587 (ARF-2227-6)
protective effects of coatings of, on niobium alloys at high temperatures, 17: 12585 (AD-277775)
reactions of refractories coated with, with combustion gas species in launch pad abort environments, 20: 19192 (SC-DR-65-1918)
reactions with combustion gas species in launch pad abort environments, 20: 39312 (SC-CR-66-2044)
reactions with liquid titanium, 20: 3929
thermoelectric properties, 16: 16708(R) (AD-266128)
thermophysical properties, 16: 2204 (WADC-TR-58-476(Vol.IV)(Rev.))
uses as coatings for corrosion protection of niobium alloys, 19: 11682

SILICON
absorption of infrared radiation by semiconducting, (E), 20: 30735(R) (TID-22970, pp 331-73)
abundance in peculiar magnetic stars, 17: 5178
abundance in primary cosmic radiation, 17: 22403 (AD-282243)
abundance in solar photosphere, 18: 32347
abundance in solar corona, (T), 20: 31865
abundance in stars, 17: 5178
abundance in 3 Centauri A, 16: 4659
abundance variations in A, Ap, and B stars, 18: 24274
addition of trace-amounts to chromium–nickel steel, method for, 20: 41418(R) (GEAP-5150)
additive effects on oxidation of $NbAl_3$ at 760°C, 16: 27590(R) (DRI-2043)
additive effects on corrosion of chromium–molybdenum steel by carbon dioxide, 16: 29344(T) (AEC-tr-5303)
additive effects on corrosion of aluminum–iron–nickel alloys by water, 16: 30739 (ANL-FGF-298)
additive effects on delta-prime phase of plutonium, 17: 3535
additive effects on aluminum–niobium alloy oxidation, 17: 4902(R) (DRI-2061)
additive effects on aluminum–niobium–titanium alloy oxidation, 17: 4903(R) (DRI-2075)
additive effects on nitric acid corrosion of chromium–nickel steel, 17: 14774(T) (AEC-tr-5646)
additive effects on hardness of uranium alloys, 17: 14737(R) (NMI-7258)
additive effects on beryllium–zirconium intermetallic compounds, 17: 14725(R) (BBC-114)
additive effects on mechanical properties of vanadium, 17: 25771 (ASD-TDR-62-667)
additive effects on metallography of uranium, 17: 29327 (TID-18998)
additive effects on resistance ratio of beryllium crystals, 17: 30950(R) (NMI-2117)
additive effects on ignition temperature of plutonium in air and oxygen, 17: 36860(R) (ANL-6648)
additive effects on uranium, effects of quenching temperature on, 17: 39627
additive effects on ductility and electric conductivity of hardened steel, 17: 39545(T,R) (EURAEC-599)
additive effects on post irradiation annealing effects on density changes in molybdenum–uranium alloys, 17: 39571
additive effects on beryllium crystals, 17: 41353(R) (NMI-2120)
additive effects on grain-refinement and alpha to beta transformation in uranium, 17: 41468
additive effects on corrosion of zirconium by steam, 18: 7134 (AERE-R-4458)
additive effects on radioinduced swelling of uranium–molybdenum alloys, 18: 8870 (NAA-SR-6262)
additive effects on oxidation resistance of aluminum–niobium–titanium alloys, 18: 8749(R) (DRI-2134)
additive effects on uranium crystal structure, 18: 25269(R) (NLCO-905)
additive effects on niobium oxidation, 18: 25936
additive effects on electric conductivity, hardness, and structure of niobium, 18: 25999
additive effects on corrosion of zirconium alloys by steam, 18: 26824(R) (ANL-6885)
additive effects on mechanical and oxidation properties of zirconium beryllides at high temperatures, 18: 27946 (BBC-120)

additive effects on composition and mechanical properties of magnesium–neodymium alloys, 18: 28000
alpha elastic scattering at 24.7 Mev, relative cross sections for, 18: 34902
alpha elastic scattering by, distorted-wave model in, (E/T), 20: 1238
alpha reactions (α,n) with, neutron yields from, 17: 33017
alpha reactions (α,n) with, neutron yields from, 17: 33018
alpha reactions (α,2α) at 0.915 Bev, clusters in, 17: 26593
alpha reactions at 8.78 Mev, electron-hole pair generation energy in, 17: 25837
alpha reactions, neutron yields from, 16: 33803
alpha reactions with, electron-hole pair production in, 19: 2630
alpha scattering at 25 Mev by, differential cross sections for elastic (E), 19: 1234 (PAN-347)
alpha scattering at 28 Mev, distorted-wave and optical model analysis of, (T), 19: 29294
analysis by neutron activation, model for error analysis in, 20: 33162(T) (AEC-tr-6639, pp 18-21)
analysis for aluminum by neutron activation, 20: 17822
analysis for antimony, substoichiometric activation, 18: 39123
analysis for argon, activation, 20: 16335(R) (NBS-TN-276)
analysis for arsenic and copper, activation, 18: 13676
analysis for arsenic traces, substoichiometric activation, 18: 39122
analysis for boron, 16: 30344
analysis for boron, neutron-reaction, 18: 15993
analysis for boron by neutron capture, 18: 43427
analysis for boron by neutron capture, 18: 43428
analysis for boron by deuteron or proton activation, 20: 18582
analysis for boron by neutron activation, 20: 33160(T) (AEC-tr-6639, pp 1-12)
analysis for carbon and oxygen, electron-probe, 18: 17744
analysis for contaminants, activation, 19: 2240
analysis for deposited boron films, activation, 16: 20346
analysis for impurities, methods of spectrochemical, 16: 22038
analysis for impurities, activation, 18: 10010
analysis for impurities, activation, 18: 33502
analysis for impurities by neutron activation methods, 19: 22126
analysis for impurities by activation methods, 19: 24451
analysis for impurities by radioactivation and ion-exchange chromatography, 19: 46228
analysis for lithium, activation, 20: 20560 (EUR-2753.f)
analysis for manganese, activation, 18: 6773
analysis for oxygen, alpha activation, 17: 38947
analysis for oxygen, activation, 20: 2531 (AD-618304)
analysis for sodium by gamma spectrometry, 18: 15981
analysis for traces of gold by neutron activation methods, 19: 40437
analysis for trace amounts of copper by activation methods, 19: 43973
analysis for trace amounts of gallium, activation, 20: 16396
analysis of high-purity, activation, 16: 22022
annealing of ion-bombarded, effects on impurity concentrations, (E), 20: 40345
annealing of, kinetics of complex defect, 20: 43968
anodic oxide film capacitance on, effects of proton space charge on, 19: 13365
avalanche discharges under particle irradiation, resolution, 16: 19454
background count in surface-barrier, 18: 22331 (CLOR/IBJ-II-22)
barrier layer depth in n-i-p detectors of, 20: 43742
bibliography on, Defense Metals Information Center selected accessions, January 1963, 17: 14739 (NP-12525)
bombardment by positive ions for producing junctions, 17: 22311
bonding of neodymium oxides to, 19: 13871(R) (BMI-1691(Del.))
boron ion reactions with n-type, implantation doping from, 18: 33921
boron ion reactions with n-type, electric conductivity of inversion layers formed from, 20: 26375(T)
boron-ion reactions at 10 to 80 kev, production of electric junctions by, (E), 20: 20123
boron-lithium pairing energy in, (E), 19: 18708
bremsstrahlung from single-crystal, spectra of, (E), 20: 13345(R) (NP-15772)
bremsstrahlung reactions (y,n) at 15 to 38 Mev, displacement effects in, 18: 7329
bremsstrahlung reaction cross sections in crystals of, 16: 11033
bremsstrahlung reactions (y,π^0) at 166 Mev, angular distributions from, (E), 20: 4898
bremsstrahlung reactions (y,p) at 32 Mev, proton energy spectra from, (E), 20: 32394
carrier interaction and nuclear magnetic relaxation in, (T), 19: 34729
cascade production in p-n, particle counting by, 20: 5793
cesium-ion reactions at 1 to 20 kev, channeling effects and penetration in, 20: 20124
characteristics as particle detectors, 16: 17851
characteristics of npp$^+$, as charged particle detector, 16: 16546
charge collection time of detectors of lithium-compensated, 20: 43703
charge collection efficiency of surface-barrier detectors of, 20: 43705
charged particle detection using, 18: 41828
charged particle ranges in, nomographs, 16: 29541
charged-particle energy-loss spectra in, effects of orientation on, 19: 6182 (BNL-8633)
charged-particle ionization loss in, density effects on, (T), 20: 28642
charged-particle scattering by crystals of, blocking effects in emergence of, (E), 19: 33336
chlorination of, kinetics, 19: 42454 (BM-RI-6649)
coating with cesium, 16: 19456(R) (AD-263112)
coating with molybdenum by vacuum evaporation using electron bombardment, 19: 36394
coating with neodymium and promethium compounds, 18: 34034(R) (BMI-1672(Del.))
coating with neodymium trifluoride, 19: 13871(R) (BMI-1691(Del.))
coating with promethium, 18: 40970(R) (BMI-1674(Del.))
construction and performance review, 17: 1754
content and distribution in acid igneous rocks of Africa, 18: 37358
content in distilled beryllium, calculation and determination of, 19: 22104 (UCRL-12253)
content in fallout from Chinese atomic test, Oct. 1964, 20: 39110
content in high-purity beryllium, 19: 13216
content in high-purity depleted uranium metal, 19: 24481 (GAT-T-1141)
content in high-velocity A stars, 18: 36135
content in SAP, 19: 22993 (RISO-96)
content in siliceous black shale, 17: 39272
contents in meteorites, 18: 34398
corrosion by aluminum–silicon and water of coatings of, on uranium, 19: 40949 (ISC-640)
corrosion by mercury at 600 to 1000°F, 18: 27913
corrosion of crystals of, volume effect by, 16: 25722(T) (UCRL-Trans-830)
corrosion resistance to mercury at 900°F, 20: 2264
corrosive effects on Zircaloy-2 in steam and water at 750 and 680°F, 16: 10463
corrosive effects on refractories, at 1600 to 2200°K, 17: 9113
cosmic-ray reactions with, in stony meteorites, production of helium-3 and neon-21 by, 18: 20204
crystal defect formation thresholds in, 18: 30219
crystal lattice parameters, 17: 4489 (GAT-T-1051)
crystal lattice vibrations in, having diamond structure, 16: 31581 (AECL-1573)
crystal structure of epitaxially deposited, origin of stacking faults in, 17: 18807
crystal structure of, electron paramagnetic resonance studies of lattice vacancies in, 17: 35774
crystal structure of, neutron diffraction studies of, 18: 14519
crystal structure from neutron diffraction, 18: 37674 (A/CONF.28/P/488)
crystal structure of, x-ray-diffraction study of, 18: 44035(R) (HW-82651(p.3.1-59))
crystal structure powder diffraction patterns, 19: 17795
crystal structure of, electron diffraction and microscopy methods for studying, 20: 31715(R) (UCRL-16658, pp 105-20)
crystals of, for neutron detection, 17: 12575(P)
current carrier lifetimes in lithium-compensated, 19: 41964 (JINR-P-2201)
current in high-resistivity semiconductors of n-type, reverse, 20: 41300
current leakage and noise in lithium-drifted detectors of, geometric control of, 19: 46754 (BNL-9535)
defects in p-i-n detectors of, determination of, 20: 11103 (JINR-P-2489)
defects in solar cells of, 19: 43997(R) (UCRL-11887)
defects in, change in configuration of point, due to stress, 19: 22988(R) (NYO-2811-23)
density and lattice constant of crystals of, effects of doping materials on, 16: 15126(R) (NP-11584)
deposition of coatings of, on refractory metals, 17: 4964
deposition on beryllia of single-crystal, chemical vapor, 20: 21249
deposition on fuel rods for corrosion protection, method for, 20: 39350(P)
deposition on molybdenum, protective effects of electrolytic, 19: 22908
deposition on molybdenum and tantalum, process for, 19: 47073
deposition on niobium–zirconium alloy by fluidized bed method, 18: 25896(R) (PF-63-3)
deposition on refractory metals by fluidized-bed process, 20: 29630
deposition on sintered molybdenum powder for oxidation protection, 20: 37204
deposition on tantalum alloys by pack cementation, 18: 30105(R) (AD-429028)
deposition on uranium by diffusion from molten magnesium bath, 19: 40949 (ISC-640)
deposition on vanadium-base alloys for oxidation protection, 19: 20459(R) (IITRI-B6019-6)
description of lithium-compensated detectors of, 20: 31605
design and performance of detectors of, for charged particle identification,

20: 13076 (UR-875-117)
design and performance of p-n, for solar cells, 17: 30642
design and performance of n-p-p, for fast neutron dosimetry, 17: 32411
design and performance of lithium-drifted and p-i-n, for gamma radiation, 19: 13738 (UCRL-13106)
design and uses of lithium-drifted detectors of, 20: 7359 (EUR-2580.e)
design of, for photovoltaic power generation in space, 17: 2634
design of high-voltage lithium-drifted detectors of, 20: 46051 (UCRL-16718)
design of lithium-drifted detector of, 20: 11170(P)
detection limit and sorption characteristics of, use of hollow cathode tube for study of, 17: 24080
determination, activation, 16: 2967(R) (TID-14310)
determination as impurity in and volatilization from tungsten, semi-quantitative spectrographic, 16: 4131 (BM-RI-5903)
determination as impurity in fused uranium dioxide, 18: 602 (DP-819)
determination as trace impurity in uranium, 18: 29591
determination by activation using 14-Mev neutrons, 18: 9966 (CEA-2358)
determination by activation analysis, mobile neutron generator for, 18: 36565
determination by activation methods, 19: 19796
determination by activation analysis, interference of (n,p), (n,α) to (n,γ) reactions in, (E), 19: 29318
determination by activation methods using automated equipment, 20: 1765
determination by bremsstrahlung-activation gamma spectra, 20: 22960
determination by charged-particle reactions at 2 Mev, 20: 43097
determination by fast neutron activation, 17: 4479
determination by spectrochemical methods, voltage-fluctuation patterns in, 19: 40416
determination by thermal-neutron activation methods, sensitivity for, 19: 9071
determination by x-ray spectrometry using electron-beam excitation, 17: 15908
determination by x-ray fluorescence analysis, 19: 22154
determination in aluminum–silicon systems, x-ray fluorescence, 16: 22039
determination in aluminum alloys by fast neutron activation, 16: 24574
determination in artificial graphite, 18: 9584
determination in aluminum alloys by activation, 19: 46157(R) (MLM-1254)
determination in aluminum ingots, x-ray fluorescence, 20: 8828 (K-1638)
determination in alumina and graphite, interferences in activation, 20: 16360
determination in aluminum by x-ray spectrography using direct electron excitation, 20: 26755
determination in americium and plutonium by spark-source mass spectrography, 20: 40816 (RFP-699)
determination in beryl ores, gravimetric, 16: 12954 (PG-Report-267)
determination in beryllium, 16: 26912
determination in beryllium oxide, spectrophotometric, 18: 3694
determination in barium–boron oxide–lanthanum–silicon–thorium optical glass, titrimetric, 18: 12000
determination in beryllium by x-ray fluorescence, 18: 27291 (Y-DA-590)
determination in boron, x-ray-fluorescence, 18: 29564(R) (NBL-210 (p.41-7))
determination in beryllium oxide, device for quantitative, 19: 11007
determination in beryllium by activation, 19: 24415
determination in bauxites by neutron activation methods, 19: 36277
determination in boron by activation methods, 20: 3879(R) (MLM-1266)
determination in beryllium oxide, spectrographic comparison of standards on, 20: 6998 (AAEC/TM-294)
determination in boron, activation, 20: 18568(R) (NBL-230)
determination in beryllium, x-ray-fluorescence, 20: 35401 (Y-1542)
determination in bauxite, activation, 20: 40812 (ORO-2980-14)
determination in cast iron by fast neutron activation, 16: 24573
determination in coal by nuclear techniques, 17: 31985 (CONF-124-1)
determination in calcium–silicon systems, method for, 18: 1555
determination in coal, activation, 18: 13614 (CONF-313-2)
determination in coal by activation and fast-neutron-scattering methods, 18: 29579
determination in cerium, erbium, and lutetium, mass spectrographic, 19: 2232
determination in coal by activation and neutron scattering, 19: 5777(R) (TID-20080)
determination in cement raw materials by x-ray emission method using alpha and x-ray sources, 20: 23568
determination in coal by neutron activation, 20: 33249
determination in carbon–silicon–uranium systems, spectrographic, 20: 35391 (CEA-R-2966)
determination in coal using neutron activation, system for continuous on-line, 20: 36769
determination in coal by activation, on-line, 20: 39025 (ORO-2980-12)
determination in earth formations by neutron-gamma well logging, device, 16: 17906(P)
determination in europium oxide, spectrographic, 17: 2931
determination in earth formations, well logging method for, 19: 15772
determination in epitaxial layers by neutron activation methods, 19: 17825
determination in fallout particles, x-ray micro-, 17: 36055
determination in ferro-niobium, gravimetric, 19: 28242
determination in gallium arsenides by neutron activation, 16: 25293
determination in gallium arsenide, activation, 17: 32004
determination in geological samples, activation, 19: 36243(R) (X64-17610)
determination in graphite and basalts by neutron activation methods, 20: 29140
determination in highly radioactive fallout particles, x-ray microscopic, 18: 23794
determination in high-purity tantalum by spectrography using d-c arc method, 20: 20608
determination in industrial solutions, quantometric and spectrographic, 18: 19910
determination in iron, activation, 18: 20425
determination in iron and steel by activation analysis using 14-Mev neutrons, 19: 43965
determination in iron, activation, 20: 7006 (KN-65-140(R))
determination in igneous and metamorphic apatites, spectrographic, 20: 26787
determination in lanthanum oxide, spectrographic, 20: 22895
determination in meteorites, activation, 17: 33851
determination in Magnox alloys, spectrochemical, 17: 40734
determination in Magnox alloys, spectrographic, 18: 3682
determination in magnesium, spectrochemical, 18: 11967(R) (MCW-1482 (p.37-46))
determination in molybdenum and its compounds, spectrographic, 18: 17766
determination in magnesium oxide, spectrographic, 19: 283 (AERE-R-4420)
determination in meteorites, activation, 19: 7349
determination in molybdenum and uranium silicides, 19: 10996
determination in minerals by neutron activation, 19: 30424
determination in molybdenum and tungsten, spectrographic, 19: 30143
determination in Magnox alloys, spectrochemical, 19: 42414 (JEN-146-DQ/I-47)
determination in meteorites, fast-neutron activation, 19: 43927 (CONF-650405-16)
determination in meteorites, activation, 20: 22875 (ORO-2670-10)
determination in niobium, spectrographic, 16: 1721
determination in niobium by radioactivation analysis, 16: 23633 (TID-7629(p.239-44))
determination in niobium and its alloys, 16: 25294
determination in nuclear graphite, activation, 19: 7337
determination in niobium or niobium oxide by d-c arc excitation, photometric, 19: 26268
determination in niobium or niobium oxide by fusion and d-c arc excitation, photometric, 19: 26269
determination in niobium–silicon systems, spectrophotometric, 19: 46171 (KAPL-M-6492)
determination in ore, activation, 16: 689
determination in ocean-bottom cores by activation analysis, 17: 15886 (TID-18125)
determination in ocean-bottom core samples by activation analysis, engineering drawings of equipment for, 17: 35667
determination in plutonium, spectrographic, 16: 14616(R) (NBL-177)
determination in plutonium, spectrographic, 17: 12182(R) (NBL-188)
determination in plutonium materials, gravimetric, 19: 291 (LA-3134)
determination in powdered samples by spectrochemical methods, 19: 22120
determination in plutonium fluorides and peroxides, review on spectrographic, 20: 14464 (RFP-599)
determination in petroleum, activation, 20: 29139
determination in plutonium by carrier distillation methods, spectrographic, 20: 40814 (RFP-664)
determination in presence of iron, use of lithium-drifted germanium detector for, 20: 43081 (ORO-2980-13)
determination in powder samples by spectrographic methods, semi-quantitative, 20: 43104
determination in rare earth oxides, spectrographic method for, 16: 20327
determination in reactor-grade uranium oxide, activation, 19: 5827
determination in reactor coolant water, 19: 26229 (INR-590/VIII)
determination in rocks, activation, 20: 20646
determination in stratospheric aerosols, 16: 25609 (AFCRL-62-299)
determination in stainless steel, x-ray spectrographic, 17: 21611 (EUR-203.f)
determination in siliceous rocks, activation, 18: 5514
determination in subsurface strata of borehole, neutron activation, 18: 12373(P)

determination in silicate rocks, quantometric and spectrographic, 18: 19910
determination in solids by spark source mass spectrometry, quantitative, 19: 13247
determination in sodium uranate, spectrochemical, 19: 15367
determination in SAP powders by different laboratories, statistics on, 19: 19750 (EUR-2286.f)
determination in stony meteorites by activation, 19: 26250
determination in silicates, activation, 20: 26782
determination in sputum of tubercular and silicotic patients by activation methods, 20: 36542
determination in sintered and zone refined boron-10, spectrographic, 20: 43090(R) (TID-23342)
determination in SAP, methods for, 20: 45574 (EUR-3064.f)
determination in thorium dioxide, spectrophotometric, 17: 12182(R) (NBL-188)
determination in tantalum by d-c arc method, spectrographic, 18: 19894
determination in thorium by silicomolybdate blue method, 18: 35468
determination in thorium compounds, spectrophotometric, 18: 39055 (AEET/ANAL/30)
determination in tungstic hydride, spectrographic, 19: 30144
determination in trace amounts in aluminum by x-ray spectrography, 19: 38571
determination in uranium, spectrophotometric, 16: 8673 (CNEN-97)
determination in uranium compounds, spectrophotometric, 16: 32935
determination in uranium, colorimetric, 17: 7968
determination in uranium(IV-VI) oxide by carrier distillation excitation, effects of graphite electrode grade on, 17: 10538 (TID-16295)
determination in uranium-233-labeled uranium dioxide, spectrographic, 18: 9980
determination in uranium, methods for, 18: 9991
determination in uranium oxide by carrier-distillation spectrography, tests of electrodes for, 19: 13202(R) (NLCO-940(p.6.1-4))
determination in uranium and its compounds and alloys, methods for, 19: 19823
determination in uranium compounds, absorptiometric, 19: 24406 (PG-Report-632)
determination in uranium silicide, spectrochemical, 19: 32059(R) (IDO-14655)
determination in uranium tetrafluoride, spectrographic, 20: 14473
determination in uranium silicides using electron microprobe, 20: 14442(R) (MCW-1493, pp 5-13)
determination in uranium by carrier distillation, spectrographic, 20: 18563 (EUR-2647.f)
determination in uranium silicides, method for, 20: 20557 (AERE-R-5129)
determination in uranium trioxide by emission spectrography, 20: 40802 (HW-65402(Rev.1))
determination in uranium(IV-VI) oxides, effects of graphite electrode grade on carrier-distillation spectroscopic, 20: 40807 (NLCO-976)
determination in vanadium, chemico-spectrographic, 18: 13708
determination in water, silver-spark spectrographic, 17: 1381 (IDO-14591)
determination in water produced in nuclear reactors for marine propulsion, methods for, 17: 33789 (EUR-224.i)
determination in zirconium chloride, nitrate, and sulfate by silicomolybdic blue method, 17: 38951
determination in zirconium diboride, 18: 19882
determination of, in plutonium, spectrographic, 17: 10548
determination of, in silicon–uranium systems, 17: 15892
determination of, in residues by iron flux method, spectrographic, 17: 19942 (PG-Report-157)
determination of, in human lung tissue, activation, 17: 21631
determination of trace amounts in rare earth compounds, spectrographic, 16: 28869 (JEN-107-DQ/I-33)
determination of traces in beryllium, photometric, 17: 19963
determination of traces of, in plutonium, spectrophotometric, 19: 26230 (LA-3247)
determination of traces of, in uranium using electron microprobe, 20: 225 (CONF-650810-2)
determination of trace amounts of, in uranium dioxide, 20: 14494
determination of trace amounts of, in beryllium by spectrography, 20: 16352
determination of trace amounts of, by reactor neutron activation methods, 20: 26760
determination of, by alpha scattering methods, 20: 22964
determination of, in iron, equipment used in activation methods for, 20: 40848
determination simultaneously with oxygen in meteorites and rocks, activation, 18: 11984
development for particle discrimination by time-of-flight methods, 18: 33932
development for semiconductor detectors, 19: 11513
development of cerium-containing, for shielding uses, 17: 2462(R) (BNL-731(p.47-52))
development of coatings of, for tantalum alloy and metal protection, 16: 24148(R) (ASD-TR-61-676)
development of contoured p-n, 18: 41773(R) (NYO-3246-1)
development of contoured p-n, 18: 41774(R) (NYO-3246-2)
development of dE/dx surface-barrier detectors of, 19: 30568
development of detector telescopes of, 19: 11526
development of device containing plastic scintillator and diodes of, for measurement of absorbed dose from high energy electrons, 20: 40746(R) (NYO-3510-2)
development of dosimeters of, for fast neutrons, 20: 11094(R) (COO-1226-10)
development of fast-response, for alpha particles, 19: 11519
development of lithium-drifted detectors of, 18: 41847
development of lithium-drifted detectors of, 19: 22700 (UCRL-11946)
development of lithium-drifted detectors of, for whole-body dosimetry, 20: 33626(R) (N-65-32043)
development of lithium-drifted, for gamma and x dosimeters, 17: 31058
development of lithium-drifted, 18: 14592(R) (PR-P-60)
development of lithium-drifted detectors of, 19: 11515
development of lithium-compensated diode, 19: 11517
development of n–p detectors for nuclear spectroscopy, 16: 1961
development of n-p, for solar cells, 17: 35226
development of nuclear-compensated, 18: 33920
development of oxide-passivated p-n, for particle detection, 18: 39672
development of proton recoil telescope of, for neutron flux and spectra measurements, 19: 11533
development progress, 16: 10759
dielectric properties of, energy band and electronic structure calculations of, 18: 39231
diffusion and reactions in niobium, 17: 34460
diffusion coefficients in, method for determining self-, 20: 27537
diffusion from coating into niobium, phase and structure studies, 16: 533(T) (NP-tr-789)
diffusion in air at 5000°K, 16: 15312(T)
diffusion in chromium, 20: 23741
diffusion in couples with aluminum, uranium, and vanadium, 19: 30731 (EUR-1819.e(p.37-48))
diffusion in gamma–cerium, electro-, 19: 34722
diffusion in gamma-cerium, gamma-uranium, and epsilon-plutonium, electro-, 20: 23734
diffusion in gold, methods for measuring, 20: 23733
diffusion of arsenic, boron, gallium, and phosphorus in, 18: 11540(T) (AEC-tr-6322)
diffusion of helium in, by ion bombardment and neutron irradiation, 18: 31476
diffusion of helium in, 19: 19934
diffusion of lithium ions in p-type, 19: 44001 (ZFK-PHA-12, pp 40-9)
diffusion of lithium in p-type, electrophotographic determination of, 19: 46997 (JINR-P-2282)
diffusion of oxygen in, 19: 23114
diffusion of phosphorus in films of, composition of surface layers and solubility limits during, 19: 6327
diffusion of rare gases in crystals of, mechanism, 17: 8953 (UCRL-10466)
dislocations in, use of white x radiation for spectra of, 18: 34186
donor ground state energies in, corrections to shallow, 17: 36479
doping of crystals of, by ion bombardment to produce solid-state detectors, 16: 19132
doping of, using ion implantation techniques, 20: 35863 (ORNL-TM-1495)
drifting of, automatic apparatus for lithium-, 18: 20344 (UCRL-11261)
edge emission in electron-bombarded crystals of, 16: 5777 (NP-11201)
effect of coatings of, on ductile-to-brittle transition of niobium–titanium–vanadium alloys, 19: 32692(R) (AD-426040)
effect on mechanical properties of zone-refined beryllium, 19: 34686(R) (NMI-1266)
effects of additions of, to sintering properties of beryllium powders, 20: 41428 (SCL-DC-66-57)
effects of coatings of, on silver alloy brazing of beryllium to niobium–1 zirconium alloy, 19: 44606 (PWAC-483)
effects of content of, on stress-corrosion of chromium–iron–nickel-base alloys by boiling magnesium chloride, 20: 23599 (COO-1319-36)
effects of, on chromium-iron-manganese-nickel alloys, 16: 30822
effects of, on surface oxidation of niobium, 17: 8746
effects of traces of, on corrosion of chromium–nickel steel, 20: 41418(R) (GEAP-5150)
effects of, on activation determination of aluminum in ores, 20: 10781
effects of, on oxidation of niobium alloys, 17: 22122
effects on age hardening in vanadium–niobium–tantalum and vanadium–niobium–titanium alloys, 20: 31709(R) (IITRI-B6042-5)
effects on aging and tensile properties of lithium–magnesium alloys, 18: 30211

effects on aging of Haynes 25 Alloy, 19: 42850 (NASA-TN-D-2989)
effects on allotropic transformation temperature of uranium, 19: 13993(R) (NLCO-940(p.7.1-4))
effects on aluminum corrosion, 17: 1881
effects on aluminum–niobium oxidation by air, 16: 24174 (TID-16032)
effects on beryllium crystals, 18: 24066(R) (NMI-2126)
effects on beta phase stability in plutonium, 16: 19352 (HW-SA-2560)
effects on cesium ion and neutral emission from hot porous tungsten, 19: 39164 (N64-22193)
effects on chromium steel, 16: 3503
effects on compactibility and compressibility of beryllium powder, 20: 25533
effects on corrosion of aluminum–nickel alloys by water at 230 and 265°C, 16: 22544 (KR-19)
effects on corrosion of chromium–molybdenum steel by carbon dioxide, 16: 22556
effects on corrosion resistance of molybdenum, niobium, tungsten, 16: 25721(T) (FTD-TT-61-31(p.60-9))
effects on corrosion of aluminum, 17: 18707
effects on corrosion of aluminum–nickel alloys by water, 17: 21387(R) (KR-42)
effects on corrosion of Zircaloy-2 at high temperatures, 17: 27751 (WAPD-T-1567)
effects on corrosion resistance of beryllium, 19: 22913(P)
effects on corrosion of austenitic stainless steels by nitric acid–potassium dichromate solutions, 19: 36977 (APED-4670)
effects on corrosion and hydrogen absorption characteristics of Zircaloy-4 and nickel-free Zircaloy-2, 20: 25490 (WAPD-TM-544)
effects on corrosion resistance of Hastelloy C, 16: 22636
effects on creep and thermal cycling resistance of uranium, 18: 42104(P)
effects on deformation of uranium, 19: 16206(P)
effects on deformation of zone-refined beryllium, 19: 18460(R) (NMI-1265)
effects on deformation properties of beryllium single crystals, 20: 5844
effects on determination of phosphorus in uranium by isotope dilution methods, 20: 8865
effects on determination of chromium in ores by neutron activation analysis, 20: 36750
effects on dislocation properties in iron, 19: 16070 (EURAEC-1075)
effects on dissolution of aluminum by nitric acid, 17: 23431 (IDO-14606)
effects on dissolution of aluminum-base fuels by nitric acid, 20: 27036(R) (IDO-14661, pp 1-44)
effects on ductility of pure beryllium, 18: 41933 (TID-11295(3rd Ed.))
effects on ductility of fissium–uranium–zirconium alloys, 19: 47004 (NMI-4997, pp 45-54)
effects on ductility of low-alloy steel, 20: 27481(R) (EURAEC-1419 and App.)
effects on electronic structure of bcc alloys of 3d-transition metals, 18: 27949 (COO-1198-165)
effects on fabrication of uranium, 19: 11711
effects on fabrication and mechanical properties of niobium–tantalum–titanium–vanadium alloy sheet, 19: 20552(R) (IITRI-B6021-6)
effects on fracture mechanisms in beryllium single crystals, 20: 23714
effects on grain size in beta heat-treated uranium, 16: 261(R) (MCW-1465)
effects on growth of beryllium oxide crystals, 17: 30511 (NAA-SR-8235)
effects on hardness properties of Nitinol alloy, 20: 2310 (AD-618681)
effects on hardness of beta-quenched uranium, 17: 11097(R) (NMI-7257)
effects on high-temperature properties of uranium alloys, 16: 2246
effects on hot hardness and microstructure of aluminum–iron–uranium alloy, 20: 5848
effects on hot workability of Type 304 stainless steel containing boron, 16: 2144 (ANL-6393)
effects on hot-cracking susceptibility of Monel, 19: 30751 (WERL-8844-8)
effects on hot-ductility of beryllium, 19: 7897 (CEA-R-2445)
effects on hot-working properties of electron-beam-melted molybdenum, 20: 23720
effects on impact strength of weld metal of arc welding electrode, 19: 14051
effects on internal friction of molybdenum and tungsten, 20: 27508
effects on isotopic exchange between cyclohexane and deuterium, 20: 1838
effects on magnetic moments of iron–nickel alloys, neutron-diffraction analysis of, 18: 27990
effects on mechanical properties of aluminum, 17: 18707
effects on mechanical properties of beryllium crystals, 18: 24134(R) (NMI-1257)
effects on mechanical properties of uranium, 19: 7940
effects on mechanical properties of niobium, 19: 11734
effects on mechanical properties of austenitic and austeno-ferritic stainless steels, 19: 42803(R) (EURAEC-1397)
effects on microstructure of uranium–zirconium alloys, 18: 22485 (MCW-1483)
effects on network structure in uranium, 19: 47060
effects on oxidation resistance of beryllides, 17: 20450(R) (BBC-116)
effects on oxidation resistance of graphite, 18: 24087 (WADD-TR-61-72(Vol.XXX))
effects on oxidation resistance and strength of chromium–magnesia composites, 19: 41022(R) (NP-15292)
effects on oxidation resistance of beryllium–niobium and beryllium–zirconium alloys, 20: 5844
effects on oxidation of aluminum–niobium alloys, 16: 10456(R) (TID-14956)
effects on phase transformations in steel, 18: 24152(T,R) (EURAEC-1001)
effects on phase transformations in gallium–plutonium alloy and plutonium, differential thermal analysis of, 20: 41452 (MLM-1172)
effects on phosphorus determination by neutron activation methods, 19: 19828
effects on point defects in iron, 19: 47094(T) (ORNL-tr-668)
effects on preparation of uranium carbide by carbothermic reduction of oxide, 20: 33841 (NAA-SR-10624)
effects on pressure sintering of beryllium powder, 20: 25534
effects on properties of uranium carbide dispersions in chromium or iron, 18: 42106(P)
effects on properties of Zircaloy-2, 18: 44031 (BM-RI-6536)
effects on properties of boron steel, 20: 39426
effects on properties of magnesium-base alloys for fuel-element cladding, 20: 39443(P)
effects on quench-induced texture of alpha-uranium, 19: 30739 (MCW-1491)
effects on radioinduced swelling of molybdenum–uranium alloy, 18: 41933 (TID-11295(3rd Ed.))
effects on radioinduced swelling of clad uranium fuel tubes in pressurized heavy-water reactor, 19: 37163 (CONF-650904-3)
effects on radioinduced cavitational swelling of uranium, 19: 37164 (CONF-650904-4)
effects on radioinduced swelling in uranium irradiated at 400 to 500°C, 20: 31666
effects on radioinduced swelling in uranium, 20: 37302
effects on reduction of niobium alloys, 17: 32492
effects on rolling properties of uranium, 18: 44098(R) (NLCO-920 (p.37-45))
effects on rolling properties of uranium, 20: 5866
effects on sinterability of beryllium powder, 18: 41994(P)
effects on sintering and densification of beryllium oxide powders of, 19: 24962
effects on sintering of beryllia powder, 20: 35857 (AAEC-TM-311)
effects on spalling of niobium at high temperatures, 18: 20474 (TID-12794)
effects on stability of magnesium–uranium–zinc systems, 18: 17921(R) (ANL-6725(p.31-88))
effects on stainless steel corrosion by nitric acid–potassium dichromate, 19: 40947(R) (EURAEC-1403)
effects on stainless steel corrosion by magnesium chloride, 19: 42803(R) (EURAEC-1397)
effects on stainless steel oxidation by steam, 20: 9421(R) (EURAEC-1486)
effects on tensile properties of vanadium-base alloys, 20: 21333(R) (IITRI-B6042-4)
effects on thermal expansion of niobium, 18: 22516
effects on thermoelectric properties of MCC 50, 19: 12129(R) (ASD-TDR-62-896(Pt.II))
effects on uranium crystal structure, 18: 43889(R) (NLCO-920(p.19-24))
effects on uranium alloys, 16: 33477(R) (NMI-7253)
effects on vanadium alloys, 16: 6746
effects on vanadium alloys at 1800°F, 16: 6747
effects on Zircaloy-2 corrosion and hydrogen pickup in steam and water, 18: 16440 (WAPD-283)
effects on zirconium corrosion by hydrochloric acid at 150 to 250°C, 16: 13533
efficiency of *p-n* junctions of, in x-ray measurements, 20: 29540
efficiency of p-n, in semiconductor detectors, 19: 26665 (NP-14875)
electric conductivity and electron flux in, 16: 30901(R) (GACD-3178)
electric conductivity of, equipment for measuring, 18: 14492
electric conductivity of deposited coatings of, 17: 25690(R) (NYO-10472)
electric conductivity and Hall coefficient of electron-bombarded n-type crystals of, 16: 10651
electric currents in surface barrier detectors of, reverse, 19: 11514
electric field strength relations for surface-barrier detectors of, 18: 33954
electric potential of oxide-passivated high-resistivity, calculations of surface, 19: 34691 (UCRL-11508)
electric properties of cesium-treated, 16: 19462(R) (AD-268422)
electric properties of, analysis using NMR methods, 18: 44827

electric properties of, p–n transition in, (E), 19: 23954 (JINR-P-2002)
electric properties of paramagnetic defect in electron-irradiated p-type, 20: 42549
electric properties of, effects of light on, 19: 3015 (AWRE-O-57/64)
electric properties of diffused, effects of processes and treatments on, 19: 46727 (UCRL-16197)
electric quadrupole and magnetic dipole transitions for isoelectronic sequence of, 20: 4553
electrodiffusion in solid bismuth, 19: 32677 (BNWL-67)
electron attenuation in semiconducting, energy losses and spectra in, 18: 28148
electron attenuation and diffraction by crystals of, 17: 620
electron backscattering at 1 Mev, angular distribution and energy spectra of, 20: 27301
electron bombardment of crystals of, reverse current enhancement in, 17: 18564
electron-electron scattering in quasi-intrinsic, 17: 31201
electron emission from surface of, energy of room temperature, 17: 9038
electron emission from electrodes of semiconducting, 18: 20152
electron emission by single crystals of, after electron bombardment, 19: 47263
electron energy loss in, angular dependence of intensities on, 16: 19524
electron energy loss in, angular dependence of characteristic, 16: 19545
electron energy loss in thin solid foils of, calculation of, 18: 8943
electron energy losses in, continuous, (T), 20: 24626(T)
electron energy losses at 50 kev in, spectra of, (E), 20: 32732
electron energy loss and scattering at 100 to 400 kev in single crystal foils of, near radiation damage threshold, (E), 20: 42536
electron extinction in crystals of, distance for, 18: 5918
electron inelastic scattering by, temperature-dependent cross section for, (E), 20: 9677
electron momentum distribution in, positron annihilation method for determining, 20: 37736 (COO-1297-7)
electron pair production in screened nuclear field in, (T), 19: 43280
electron paramagnetic resonance of electron-irradiated p-type, 20: 42549
electron range-energy relations in, 16: 33582 (NRL-5828)
electron ranges in, 18: 32247
electron ranges in, at 0 to 500 kev, 19: 9727 (ARL-64-151)
electron reactions at 150 Mev, polarization in, (E), 19: 16852(R) (NP-14647)
electron reactions of 720 Mev, bremsstrahlung production by, (E), 19: 25167
electron reactions with crystals of, at 575 Mev, bremsstrahlung spectra of, 16: 13800
electron reactions with single crystals at 15 Mev, coherent bremsstrahlung radiation from, (E), 20: 45020
electron reactions with, electron-hole pair generation in, 19: 2630
electron reactions with detectors of p-n, internal pulse amplification in, 18: 33959
electron scattering in single crystals of, at 575 Mev, enhancement of soft component of bremsstrahlung from, 18: 721
electron scattering by, effects of angle of incidence and energy on inelastic, 19: 16406(T)
electron scattering by, bremsstrahlung-production cross sections for, (E), 19: 18682 (NASA-TN-D-2659)
electron scattering at 80 kev, transmission Kikuchi lines in, (E), 19: 27071
electron spectra of, in electric fields, (E), 19: 23953(R) (AD-606407)
electron spin resonance in neutron-irradiated, 17: 596
electron transmission through, energy characteristics of, 18: 14747(T)
electron transmission through thin foils of, plasmon excitation in, (E), 20: 15951
electron-hole pair production in lithium-compensated, temperature dependence of energy for, (E), 20: 45028
electron-nuclear double resonance in phosphorus-doped, packet-shifting, 18: 41437
electronic properties of single-crystal, effects of ion-bombardment on, 20: 17151
electroplating of p-type, with phosphorus-31, 18: 34005(R) (ORNL-TM-879)
emissivity, 17: 31009
energy levels, 17: 41873 (WASH-1044)
energy levels of ionic, Hartree-Fock wave functions for, (T), 20: 25716 (AD-631601)
energy resolution of n-p, for nuclear particles, 18: 20395
europium sulfide epitaxial growth on crystals of, 19: 11079
evaluation for use as charged-particle detectors, 16: 29116 (UCRL-9052)
evaluation of coatings of, for high-temperature protection of vanadium alloys, 16: 2168(R) (ARF-2227-2)
evaporation from titanium, vanadium, and zirconium, 18: 14398
explosibility of powders of, 19: 36698 (BM-RI-6516)
fabrication and testing as p-type semiconductor detectors, 18: 23984
fabrication for gamma-transient detectors, 19: 11499 (UCRL-13128)
fabrication for nuclear spectroscopy, 20: 32373(R) (COO-1530-1)
fabrication into monolithic random pulse generators, (E), 19: 19436 (SC-DC-64-1154)
fabrication into semiconductor device, 19: 32600(P)
fabrication of detectors of p-type, 20: 41363(P)
fabrication of diffused and lithium-drifted detectors of, 19: 20328(R) (UCRL-11828(p.225-6))
fabrication of junctions of, using ion implantation, 20: 21098
fabrication of lithium-drifted detectors of, 19: 42720 (UCRL-16190)
fabrication of lithium-drifted radiation detectors of, techniques for, 20: 7450
fabrication of lithium-drifted surface-barrier detectors of, 20: 19079
fabrication of lithium-doped diodes of, 20: 19106(R) (N-65-19886)
fabrication of lithium-drifted p-i-n, 20: 1580(P)
fabrication of p-n, by alpha irradiation of silicon, 17: 14921
fabrication of P-N (E/T), 19: 776 (NP-14332)
fabrication of semiconductors of, by neutron transmutation doping, 18: 37662 (BNL-874(p.10-11))
fabrication of shallow diffused diodes of, 20: 46050 (UCRL-14651)
fabrication, ore processing, properties, and uses of, 18: 35949
fabrication, testing, properties, and uses of surface-barrier detectors of, 20: 19078
Fermi-levels in, 16: 24158 (K-1526)
finishing and polishing wafers of, techniques for, 18: 17977(R) (ORNL-TM-793)
fission fragment detection in surface barriers of, multiplication in pulse height response to, 18: 33915
fission-fragment damage in, (E), 19: 39245
fluorescence yields in proportional and scintillation detectors, 18: 3796
fluorination at high temperatures, kinetics of, 18: 27354(R) (ASD-TDR-62-204(Pt.III))
free carrier absorption in n-type, effects of metallic precipitates on, 16: 29485 (TID-16383)
gamma absorption by crystals of, coherence effects in, 17: 19100
gamma attenuation coefficients at 0.03 to 10 Mev, 19: 35569
gamma attenuation coefficients at 0.01 to 100 Mev, 20: 36350
gamma linear polarization by crystals of, 17: 4004
gamma-ray spectra of, in boreholes, 17: 40996
gamma reactions (γ,n) from threshold to 80 Mev, cross sections for, 18: 11209 (LNF-63/47(p.194-8))
gamma reactions (γ,n) at 12 to 30 Mev, cross sections for, (E), 19: 25542
gamma reactions (γ,d) and (γ,p) at 30 to 90 Mev, 16: 24835
gamma reactions (γ,n) at 0 to 80 Mev, 17: 40095
gamma resonance scattering, pulse-height spectra, 16: 8225
gamma spectra from 14-Mev neutron activation of, determination by, 19: 26241
gamma spectrum for, thermal neutron capture, 17: 38063(R) (IITRI-1193-26)
hardness of crystals of, 16: 10728
Hartree-Fock potential of neutral atoms of, analytical expressions for, 18: 16656
heat of combustion, 16: 1652(T) (AEC-tr-4862)
helium and hydrogen ion attenuation at 0.1 to 500 Mev, tables for, 20: 41619 (CEA-R-3042)
helium ion channeling reactions at 209 ev, thermochemical properties for, (T), 19: 39395
helium ion energy-range relations in, 18: 14726 (UCRL-10647)
helium-3 reactions with, production of short-lived radioisotopes in, 17: 26633
helium-4 scattering by, anomalous energy loss in, 20: 7422
illumination effects on Kikuchi pattern of wedge of single-crystal, 18: 32160
impregnation of graphite with, *in vacuo*, 17: 32554
infrared absorption in electron- and neutron-bombarded crystals of, 16: 10652
ion bombardment of n-type, production of p-type surface layers in, (E), 19: 23179
ion energies from spark sources using, 19: 7778
ion exchange with hydrogen and sodium, elution dynamics of, 18: 27459
ion ranges in, heavy, 17: 41521(R) (AD-419705)
ion reactions with crystals of, doping mechanisms in, 18: 22137
ion-pairing in lithium-drifted, 18: 33922
ionization by collisions with nitrogen and oxygen molecules, 18: 755
ionization equilibria in sun, (T), 20: 19338
iron magnetic resonance in, electric and magnetic field effects, 16: 15443
iron-57 Mössbauer spectra in iron diffused in *n*- and *p*-type, 17: 13263
iron-57 Moessbauer spectra in n- and p-type, 16: 29545
iron-57 Mössbauer spectra in, 20: 30766
isochromatic bremsstrahlung of, structure of, 17: 22295
isotopic ratios in tektites, 18: 32340
krypton ion adsorption and retention, in electric discharge, 16: 29516
krypton-85 ion reactions with, during glow discharge, 17: 16870

lithium-ion drift in p-type monocrystals of, (E), 20: 21337 (JINR-P-2598)
magneto-resistance of gamma-irradiated n-type crystals of, 16: 10653
meson (μ^+) depolarization in, (E), 19: 12167 (NEVIS-124)
meson (π^-) capture below 140 Mev, gamma spectra from, (E), 20: 42314
meson (π) and proton energy loss distributions in, (E), 20: 7418
meson (π) energy losses in, measurement at 50 to 365 Mev, (E), 20: 7411
meson (μ) capture, Fermi interactions in, 16: 15590
meson (μ^-) capture by, x-ray spectra from, 17: 26578
meson (μ^-) magnetic moment in mesic, 16: 13865 (NEVIS-101)
meson (μ^-) reactions, polarization retention measurements, 16: 8230
meson(μ^-) capture by, multiplicity distributions of neutrons emitted in, 18: 40516 (UCRL-11243)
minority-carrier diffusion lengths in, 17: 8963
molecular constants and thermodynamic functions of, triatomic, (T), 20: 29921
neutron absorption by, measurements for $E_0 \leq 30$ Mev, 20: 24575 (LNF-66/7)
neutron absorption cross section in pitchblende, thermal, 20: 37994
neutron capture by, average level widths of compound nucleus from, (E), 20: 32424
neutron capture cross sections, 16: 26509
neutron capture in, transmutation doping and defect formation by, 18: 30278
neutron cross section, corrections, 16: 24796 (UNC-5002)
neutron cross sections at 1.44 ev (E), 19: 3288
neutron cross sections from 0.037 ev to 18 Mev, tables of, 20: 44661 (UNC-5139)
neutron diffraction properties of, 20: 26396(R) (IDO-17140)
neutron dispersion relations for modes in highly doped crystals of, 17: 25859(R) (PR-P-56(p.35-42))
neutron elastic and inelastic scattering at 2.45 to 5.80 Mev, (E/T), 20: 10103
neutron elastic scattering at 1.95 Mev, polarization in, 18: 30816
neutron elastic scattering by, differential cross section for, (E), 19: 5238
neutron elastic scattering at 3.5 to 4.8 Mev, differential cross sections for, (E/T), 19: 14564
neutron elastic scattering at 0.8 Mev, angular distributions of, (T), 19: 37884
neutron elastic scattering at 0.8 Mev, cross sections for, (T), 20: 15770
neutron elastic scattering at 0.57 to 2.28 Mev, cross sections for, (E/T), 20: 30345 (EUR-2798.e)
neutron elastic scattering 0.57 to 2.28 Mev, differential cross sections for, (E), 20: 40069(R) (EANDC(E)-66(U)
neutron elastic scattering at 7.5 Mev, angular distribution for, (E), 20: 46588 (LA-DC-7853)
neutron elastic scattering at 3.2 Mev, (E/T), 20: 46644
neutron inelastic scattering at 14 Mev, 18: 41831
neutron inelastic scattering at 14 Mev, collective-state excitation by, (E/T), 19: 23697
neutron inelastic scattering at 14.1 Mev, gamma yields from, (E), 19: 35417
neutron photoproduction cross section, 18: 2921
neutron radiative capture cross sections at 30 and 65 kev, 18: 34274(R) (NIRS-2(p.3-15))
neutron reactions at 0.1 to 100 Mev, total cross sections for, 16: 11021
neutron reactions (n,p) at 14 Mev, angular distributions and spectra from, 16: 11028
neutron reactions at high energies, table of radioisotopes produced in, 17: 794 (CERN-62-22)
neutron reactions (n,γ) at high and low energies, gamma spectra for, 17: 26419(R) (ARF-1193-23)
neutron reactions with, production of short-lived radioisotopes in, 17: 26633
neutron reactions with, 17: 41238 (AD-289566)
neutron reactions with, use for study of neutron-induced reactions, 17: 41994
neutron reactions (n,α) at 13.6 to 15 Mev, cross sections for, 18: 16971
neutron reactions with, in semiconductor detectors, 18: 24599 (NP-13930 (p.26-38))
neutron reactions at 5 to 9 Mev, semiconductor detector studies of cross sections for, 18: 24600 (NP-13930(p.39-40))
neutron reactions with, gamma radiation from, 18: 30735(R) (TID-20657)
neutron reactions (n,γ) with semiconducting, phosphorus-31 production in thermal, 18: 33920
neutron reactions at 4 to 5 Mev, compound-nucleus level widths from, 18: 36645
neutron reactions with, calculations of cross sections for, 18: 42673
neutron reactions (n,γ) with, gamma spectra from fast, 18: 44807
neutron reactions (n,γ) with, phosphorus production in thermal, 19: 11205
neutron reactions with, ionization produced by recoil atoms in, 19: 26911
neutron reactions (n,α), (n,np) and (n,p) at 14 Mev, ionization energy of reaction products from, 19: 29236 (GA-6136)
neutron reactions (n,α) and (n,p) in diodes, neutron spectrum measurements by, 19: 28661
neutron reactions (n,n'γ) at 0 to 14 Mev, energy absorption in, 19: 39769 (SC-DC-65-1544)
neutron reactions (n,n'γ) at 3.0 to 4.5 Mev, gamma angular distributions from, (E/T), 19: 47589(R) (TID-22012, 53-66)
neutron reactions (n,α) and (n,p) in, recoil ionization defects from, (E), 20: 13989
neutron reactions (n,n'γ) at 14 Mev, elemental analysis by, 20: 27170 (UCRL-14654-T)
neutron scattering at 200 to 700 kev, differential cross sections and polarization in, 16: 23117
neutron scattering at 3.4 to 4.6 Mev, angular distributions, 16: 26507
neutron scattering at 3.1 Mev, cross sections, 16: 29743
neutron scattering at 90 kev, angular distributions and cross sections for, 16: 33800
neutron scattering, 17: 41873 (WASH-1044)
neutron scattering by, differential cross section and polarization for, 17: 41528(R) (ANL-6720(p.16-28))
neutron scattering at 2.45 to 5.80 Mev, energy spectra of, (E), 19: 19095 (WASH-1053)
neutron scattering in crystalline, oscillatory signal interference effects on thermal, 19: 19076
neutron scattering at 0.56 Mev, polarization effects on, (T), 19: 19108
neutron scattering at 2.45 to 5.80 Mev, (E/T), 19: 23620
neutron scattering by crystals of, phonon dispersion relations for, 16: 7173
neutron scattering by, cross sections for free and coherent, 20: 15682
neutron scattering by, Debye-Waller factor for, 20: 24791 (IKF-16)
neutron scattering at 7.5 Mev, time spectrum at 135°, (E), 20: 46588 (LA-DC-7853)
neutron separation energy, (E), 20: 24329(R) (ANL-7108, pp 1-4)
neutron spin-orbit interactions in crystals of, 17: 20963
neutron total cross sections at 2.8 to 5.2 Mev, 18: 6210
neutron total cross section at 0.5 to 1.2 Mev, effective, 18: 11195(R) (EANDC(E)-49(L))
neutron total cross section from 0.5 to 1.2 Mev, (E), 19: 19116
neutron total cross sections at 6.3 to 9.1 Mev, (E), 19: 35378(R) (EANDC(E)-57(U))
neutron total cross sections at high energies, fluctuations in, 20: 38173
neutron total cross section from 5.0 to 8.5 Mev, fluctuations in, (E), 20: 44743
neutron tracks in crystals of, analysis of fast, 17: 11272
neutron transmission in crystalline, 18: 42579 (BLG-260)
neutron transmutation reactions in, 17: 14944(R) (NYO-10088)
nitrogen nucleus reactions at 27.5 Mev, 17: 7252
noise characteristics of, as planar bipolar transistor, (E/T), 19: 36766 (TID-21939)
noise limit for p-type detectors, theoretical, 16: 30600 (UCRL-9529)
nuclear dynamic polarization of phosphorus-doped, 18: 34334
nuclear magnetic resonance in, ultrasonic determination of, 17: 16779 (ISS-62/17)
nuclear polarization by hot electrons, 18: 37780(T)
nuclear resonance fluorescence in, (E), 19: 41828
nucleophilic displacements on, mechanism of, 16: 14378(R) (NYO-2302)
optical absorption coefficients for, monochromatic, 16: 4155 (GA-2528 (Vol.III))
order in calcium boron silicates, 18: 25366
oscillations in, electron beam-induced, 18: 10399
oxidation in oxygen plasma, (E), 20: 5740 (TID-22407)
oxidation of coatings of, on niobium alloys, 16: 32085
oxidation testing of coatings of, on vanadium alloys at 2000 to 2400°F, 17: 35997(R) (IITRE-B6001-5)
oxidation tests on coatings of, on vanadium alloys, 16: 6706(R) (ARF-2227-3)
oxidation, tracer studies of mechanism of, 19: 9098 (UCRL-7631-T)
parameters for n-p-n, 18: 3424 (TID-19705)
particle simulators for detectors of, fast infrared emitting diodes as, 18: 41860
partition coefficients and reciprocal ionic radii, 17: 27562 (INSJ-54)
performance and production for particle detection, 18: 5637 (PAN-444/1s,II,IX)
performance as alpha spectrometer, 16: 23840 (CEA-2138)
performance as alpha detector, 17: 4840
performance as dE/dx particle detectors, 18: 30069
performance as detector for high-energy bromine and iodine ions, (E), 19: 36814(R) (ORNL-3778(p.125-7))
performance as fast-neutron dosimeter, 20: 21095
performance as fast neutron spectrometer, 16: 27263 (TID-16326)
performance as fast-neutron and gamma-ray detectors, 18: 20413
performance as i-r modulators, (E/T), 19: 38914 (SC-DC-65-1332)
performance as neutron threshold detector in presence of x rays,

20: 41333
performance as radiation detectors, 18: 6163 (NP-13349)
performance as surface-barrier detector, pulse rise-time for, 18: 23983
performance as x-ray spectrometer, 17: 6458
performance for alpha, beta, and gamma dosimetry, (E), 20: 7406
performance for alpha particles, effects of dead layer on, 19: 18310
performance for gamma and neutron dosimetry, 20: 29518 (BNWL-SA-27)
performance for low-background counting of alpha and beta particles, 20: 31540
performance for measuring beta spectra from strontium-90–yttrium-90, 20: 29520 (CLOR-45/D)
performance for time calibration of fast photomultipliers, (E), 19: 22690 (EUR-2247.e)
performance in alpha spectrometers, 19: 11530
performance in alpha spectrometers, 18: 18192
performance in betavoltaic batteries, 20: 11546 (SC-RR-65-671)
performance in beta spectrometers, 18: 12470
performance in E(dE/dx) detectors for particle discrimination, 20: 33643
performance in fission fragment measurements, surface effects in, 20: 7438
performance in heavy ion detectors, energy dispersion and pulse height defect in, (T), 20: 11138
performance in high-resistivity surface-barrier detectors, 18: 30008
performance in high-resolution nuclear spectroscopy, 16: 7716
performance in random-time pulse generation, 18: 29936
performance in recoil-analyzing detectors, 18: 18222
performance in semiconductor detectors, in vacuum, 17: 16896
performance in semiconductor detectors, (T), 20: 19063
performance in solar cells, (E), 19: 43030 (PIC-SOL-209/5.1(Vol.II))
performance in surface-barrier radiation detectors, 18: 20354
performance of coatings of, on Pebble Bed Reactor fuel, 16: 9663 (NYO-9064)
performance of crystals of, as radiation detector, response to fission fragments and heavy ions in, 17: 26459(R) (ORNL-3425(p.130-3))
performance of detectors of, in beta spectrometers, 19: 15898
performance of detectors of, for alpha dosimetry, 20: 5721 (CLOR/IBJ-II-37/D)
performance of detectors of, for total neutron cross section measurements, 20: 13101
performance of detectors of, for energy measurements on californium-252 fission fragments, 20: 19070
performance of high resistivity surface barrier detectors of, 19: 18307
performance of junctions of, in beta spectrometers, 20: 23457 (CEA-R-2839)
performance of layers of, in radiation telescopes, 19: 42711 (JINR-P-2262)
performance of lithium-drifted, for radiation detection, 18: 20355
performance of lithium-drifted, for low-energy gamma detection, 18: 20373
performance of lithium-drifted, in semiconductor detectors, 18: 27790(R) (ORNL-3578(p.46-59))
performance of lithium fluoride sandwiches of, in neutron spectrometers, 19: 11531
performance of lithium-drifted, in internal conversion coefficient spectrometers, 19: 11577
performance of lithium-drifted, for radiation detection in thermal-vacuum environment, (E), 19: 40902
performance of lithium-drifted, in gamma spectrometers, 19: 42706 (AERE-M-1602)
performance of lithium-drifted, for detection and identification of particles, (E), 19: 44517
performance of lithium-drifted, for alpha and proton detection, 19: 46770 (UCRL-16354)
performance of lithium-drifted, as surface-barrier detectors, 20: 5767
performance of lithium-drifted semiconductors of, for gamma spectroscopy, 20: 13067 (JUL-308-RB)
performance of lithium-drifted p-i-n junction of, in beta dosimetry, 20: 14886
performance of lithium-drifted diodes of, as radiation detectors, 20: 21064
performance of lithium-drifted detectors of, for electrons, 20: 27301
performance of lithium-drifted p-i-n, as photon counter, 16: 22317(R) (AD-269972)
performance of lithium-drifted, as electron detectors, 18: 12443(R) (AD-413449)
performance of lithium-drifted, as light pulse detector, 18: 14213 (JINR-P-1526)
performance of lithium-drifted *p-i-n*, as radiation detector, 18: 14278
performance of lithium-drifted p-i-n, for gamma and x rays, 18: 23967
performance of lithium-drifted p-i-n, as gamma pair spectrometers, 18: 33912
performance of lithium-doped, for high-energy particles, 19: 11528
performance of multiple barrier, in semiconductor detectors, 19: 11518
performance of n-type, in beta spectroscopy below 4.2°K, 18: 2076
performance of nuclear-compensated detectors of, 19: 36807 (CEA-R-2722)
performance of p-n, in logarithmic amplifiers, 17: 32349
performance of p-i-n junction detectors of, 20: 31537
performance of p-n, for fast neutron dosimetry, 20: 25374 (AD-631742)
performance of p-n junctions of, for particle detection, 20: 31498 (AD-632527)
performance of p-n, for solar protons, 18: 14707
performance of p-n, in particle detectors, 19: 7803
performance of pelletized, for control of radiant heat transfer in nuclear rockets, (E), 19: 24148 (NASA-CR-210)
performance of redrift-treated lithium-drifted detectors of, 20: 41311
performance of semiconductor detectors of, for spectrometric analysis of beta source mixtures, 19: 32111
performance of semiconductor detectors of, for neutron spectrometry, (E), 20: 4997(R) (EUR-2494.d)
performance of semiconductors of, for hydrogen and nitrogen ion detection, 20: 17253(R) (ORNL-3908, pp 90-9)
performance of solar cells of, for detection of electron bursts from plasma, 20: 15916
performance of surface barrier detectors of, for fission fragments, 19: 26700
performance of surface-barrier p-type, for alpha particles, 19: 42757
performance of surface-barrier, as 10 to 200 kev particle detector, 20: 11115
performance of surface-barrier detectors of, 20: 11124(T)
performance of surface-barrier, as radiation detectors, 18: 6161 (NP-13346)
performance of surface barrier, for fission fragments, 19: 11524
performance of telescope detectors of, for charge and energy spectrometry of cosmic particles, 20: 37575
phosphorus ion reactions with single crystals of, doping effect in, (E), 20: 12280
phosphorus ion reactions with p-type, for production of solar cells, 20: 15302(T)
phosphorus-ion reactions at 10 to 80 kev, production of electric junctions by, (E), 20: 20123
phosphorus-31 electron spin relaxation time in, carrier concentration effects on, 19: 9134
photoconductivity in neutron-irradiated p-type, kinetics, 16: 18096
photocurrent production in transistors of, anomalous, (E/T), 20: 31612 (SC-DC-66-1415)
photoeffects in surface-barrier diodes, 16: 8924
photoelectron emission from cesium-treated, 16: 19456(R) (AD-263112)
photoelectron emission yields at 2 to 6 ev from cesiated surfaces of, spectral analysis of, 19: 39406
photon absorption coefficients and mean opacities, 16: 4153 (GA-2528 (Vol.I))
photon absorption constants for, 18: 24356 (ANL-6802(p.64-5))
photon reactions with Coulomb field of, pair production total cross sections for high-energy, (T), 20: 17754
photon scattering, resonant, 16: 2334
photoproton production at 24 Mev, 16: 2534
piezoelectric properties for use in high-temperature strain gages, 17: 39370 (ARL-63-147)
plastic deformation in, by diffusion of phosphorus, 18: 39938
positron annihilation in single crystals of, electron-positron wave functions from, 18: 40281
potassium ion reactions with crystals of, secondary emission properties from, 17: 24160(T)
potassium-ion reactions at 1 to 20 kev, channeling effects and penetration in, 20: 20124
preparation and performance of lithium-drifted surface-barrier detectors of, 18: 23982
preparation and performance of lithium-drifted, for radiation detectors, 19: 6187
preparation and properties for surface-barrier detectors, 18: 29999
preparation and properties as photocell, 18: 37520(T) (AEC-tr-6398(p.355-61))
preparation and properties of shallowly diffused junctions of, 20: 21099
preparation and use for particle detection, 17: 8597 (TID-15552)
preparation for detectors with wide sensitivity range, 19: 44470 (ZFK-PHA-12, pp 25-9)
preparation for isotopic targets, 20: 696(R) (ORNL-3829)
preparation for particle detectors, 19: 9488 (PPAD-529-E)
preparation for radiation damage studies, 18: 16528 (SC-DC-64-346)
preparation of, by diffusion of aluminum into silicon carbide crystals, 17: 8882(R) (EURAEC-306)
preparation of cesium-doped, 17: 39476
preparation of crystals of, effects of copper, gold, and iron impurities on, 19: 22126
preparation of, design of apparatus and method for, 17: 20408(P)

preparation of, design of apparatus and method for, 17: 20409(P)
preparation of, for charged particle spectroscopy, 17: 366(T) (AEC-tr-5369)
preparation of lithium-drifted, 20: 11097
preparation of p-n, for nuclear particle detection, 16: 5526
preparation of p-i-n junctions of, using lithium drifting, 20: 31537
preparation of p-i-n detectors of, by lithium ion drift, (E), 20: 43741
preparation of p-n, by implantation of cesium and sodium ions, (E), 20: 46953
preparation of p-n, method for, 19: 33708(P)
preparation of p-n, by lithium diffusion, 19: 44000 (ZFK-PHA-12, pp 33-9)
preparation of p-n, by phosphorus diffusion, 19: 43999 (ZFK-PHA-12, pp 7-9)
preparation of self-supporting films of, (E), 19: 44650
preparation of, separation of metal from reaction products in, 17: 20410(P)
preparation of targets of, by reductive evaporation, 19: 19139
preparation of, use of vacuum techniques in, 17: 23885
preparation of, phosphorus diffusion method for, 18: 22341 (PAN-484/II)
preparation processes for high-purity, radiochemical analysis, 16: 16075
production by ion implantation doping, 18: 33921
production in h-f electrodeless plasmatron, 20: 17959
production of, by sintering at 470 to 1150°C, mechanism and technique for, 17: 32497
production of high-resistivity, with neutron-induced phosphorus impurities, 19: 11205
production of nuclear compensated, from thermal neutron irradiation of p-type, 20: 27257 (AWRE-O-24/66)
production of nuclear compensated, by thermal neutron bombardment, 20: 27257 (AWRE-O-24/66)
production of p-n junctions by ion bombardment, 17: 10773 (ASD-TDR-62-428)
properties and use of diodes of, for radiation detection, 20: 11126
properties and use of semiconductor detectors of, for electron and gamma spectroscopy, 20: 39232
properties as alpha detector, 18: 2019 (CLOR-I-B-IBJ-18)
properties as fast neutron spectrometer, 17: 34884 (TID-19047)
properties as gamma dosimeter, 18: 2068
properties as high-energy meson and proton spectrometer, 18: 20410
properties as neutron detector, 16: 27358
properties as neutron detector, 17: 1757
properties as particle detectors, time-response, 18: 24023
properties as radiation detectors, review, 18: 14225 (UCRL-11302)
properties as radiation detectors, 18: 31963
properties as semiconductor detector, 18: 20376
properties as surface-barrier detector, 16: 27359
properties as surface-barrier detector, 18: 18193
properties as x-ray fluorescence analyzer, 18: 12022
properties for nuclear batteries, 18: 9068 (SC-DC-3530)
properties for nuclear batteries, 18: 9068 (SC-DC-3530)
properties for thermal neutron detector, 17: 25599 (PAN-377/1-B,IX)
properties for use in radiation dosimeters, 17: 18587(R) (AD-283836)
properties in conduction counters, 16: 27357
properties in fast neutron spectrometer, 18: 18177 (TID-20418)
properties in in-pile gamma dosimetry, 18: 31934
properties in neutron detectors, 18: 8918(R) (PR-P-59(p.21-36))
properties in solar cells, review, 17: 1714
properties of crystals of, as surface barrier detector of alpha particles and protons, 17: 376
properties of p-n, for radiation detection, 19: 32566
properties of pressure transducers of, (E), 20: 5216 (SC-TM-65-457)
properties of rare earth doped, electric and optical, 20: 20122
properties of semiconductor detectors of, 18: 20377
properties of semiconducting, thermal cycling effects on, 20: 30785
properties of semiconductor detectors of, 20: 39230
properties of shallow junctions of, produced by ion implantation, (E), 20: 46953
properties of single-crystal, as gamma or charged particle detector, 20: 4259(P)
protective effects of coatings of, against oxidation of niobium, tantalum, and its alloys, 17: 22109(R) (ASD-TDR-63-160)
proton channeling in crystals of, at 2.1 Mev, 18: 33917
proton elastic scattering at 30 to 50 Mev, models for, 20: 15730(R) (RHEL/R-112, pp 67-98)
proton energy losses in single crystals of, axial and planar effects in, (E), 20: 1334
proton energy-loss spectra in monocrystalline (E), 19: 1078
proton elastic scattering at 17.8 Mev, polarization in, (E/T), 19: 14599
proton range-energy relations in, 16: 33582 (NRL-5828)
proton ranges in, 18: 32247
proton ranges in, at 0 to 500 kev, 19: 9727 (ARL-64-151)
proton reactions (p,γ) with, effects of crystal orientation on yields from, 18: 42727
proton reactions at 150 Mev, gamma spectra from, 16: 31088
proton reactions at 130 to 400 Mev, production cross sections for isotopes in, 17: 28943(R) (TID-18961)
proton reactions at 97 Mev, delayed emission in, 18: 6189
proton reactions at 130 to 400 Mev, isotope formation cross sections for, 18: 22881
proton reactions at 8 to 13 Mev, gamma and neutron yields in, 18: 44775
proton reactions at 0.5 to 3 Mev, formation cross sections for nuclides from, 18: 43601(R) (TID-21007)
proton reactions at 0.05 to 2.9 Bev, induced activity data and cross sections for spallation, (E/T), 20: 32549
proton reactions (p,p'), phosphorus-29* levels from, 16: 24795 (TID-15331)
proton reactions with, rare gas and tritium production cross sections for, 18: 15189 (CERN-64-12)
proton reactions with, production of delayed proton emitters in, (E), 19: 14546
proton scattering by, anomalous energy loss in, 20: 7422
proton scattering by single crystals of, particle blocking effects in, (E), 20: 23873(R) (ANL-7108, pp 37-41)
proton scattering at 29 and 49 Mev, asymmetries in elastic and inelastic, (E), 20: 32440
proton transmission at 5 Mev, direction and energy distributions from, (E), 19: 41788
pulse amplification in p-n, internal, (E), 19: 28660
pulse preamplifiers for detectors of, transistorized, 19: 11523
pulse rise time in detectors of, electron mobility effects on, 19: 20359
purification, vacuum techniques for, 16: 12046
quantum effects in, at very low temperatures, 16: 29565
radiation absorption by, x, (E), 19: 28674
radiation and temperature effects on n-p and p-n, in solar cells, 19: 9550
radiation attenuation by, critical energies and units for, 17: 38420
radiation damage and annealing in crystalline, Hall effect measurements of, 18: 16534
radiation damage and annealing of carrier lifetime in, 18: 22537
radiation damage and annealing in, 18: 22541
radiation damage at low temperatures in degenerate, 20: 22346
radiation damage by beta particles at 77°K, x-ray study of interstitial defects, 16: 29459
radiation damage detection by field effect, (T), 19: 39252
radiation damage effects on detection performance of p-n, alpha, 18: 30255
radiation damage effects in lithium-drifted p-i-n, alpha, fast neutron, and proton, 18: 33913
radiation damage effects in lithium-drifted p-i-n, gamma, 18: 33914
radiation damage in, gamma and thermal neutron, 16: 33532
radiation damage in, proton, 17: 34490 (NP-13032)
radiation damage in p-type, effects of impurities on, 17: 36351 (TID-17503)
radiation damage in, energy levels of defect centers induced by electron and proton, 17: 39673 (NP-13137)
radiation damage in uniform avalanche diodes of, neutron, 18: 16528 (SC-DC-64-346)
radiation damage in, 18: 32247
radiation damage in, energy dependence of proton, 18: 36057
radiation damage in solar cells, proton, 19: 14112
radiation damage in field-effect transistors, contribution of neutron spectra to, 19: 13819
radiation damage in solar-cell, effects of doping impurities on, 19: 18538 (NASA-TN-D-2711)
radiation damage in transistors, short-term annealing of neutron, 19: 30595 (GA-6008)
radiation damage in semiconductors of, comparison of gamma and neutron, 19: 32615 (NAA-SR-10856)
radiation damage in, effects of aluminum and boron on electron, 19: 34593 (NP-15090)
radiation damage in solar-cell, 4-Mev alpha, 19: 42772 (UCRL-16061)
radiation damage in, calculations of proton, 19: 44747 (NP-15463)
radiation damage in semiconducting crystals of, correlation of neutron and proton, 17: 32678
radiation damage in, electron and neutron, 20: 908
radiation damage in diodes of, neutron, 20: 7460
radiation damage in p-type, transient electron, 20: 13128(R) (NP-15835(Suppl.))
radiation damage in solar cells of, proton, 20: 19095 (N-65-16347)
radiation damage in, effects of impurities on electron, 20: 19102(R) (N-65-19693)
radiation damage in, energy dependence of electron, 20: 19105 (N-65-19870)
radiation damage in space environment, electron and proton, 20: 21165
radiation damage in solar cells of, alpha particle and proton, 20: 27364 (NASA-TN-D-3427)

radiation damage in transistors of, energy dependence of fission-neutron and gamma, 20: 29579 (NAA-SR-11887)
radiation damage in solar cells of, electron and proton, 20: 33734
radiation damage in solar cells of, thermal annealing of, 20: 35808 (N-66-18378)
radiation damage in reactors, use as a measurement of neutron spectra, 17: 11594 (SCTM-205-62(53))
radiation damage in, single collision neutron, 18: 34248
radiation damage on carrier lifetime in, containing copper and iron, annealing of, 17: 20525
radiation damage of solar cells of, electron and proton, 18: 12726 (NASA-TN-D-2098)
radiation damage to crystals of, at 40- and 440-Mev, proton, 17: 18365 (TID-7652(p.220-9))
radiation damage to, 17: 18362 (TID-7652(p.118-35))
radiation damage, neutron spectrum normalization for, 19: 34747 (NAA-SR-10612)
radiation defect annealing in, mechanisms, 16: 22676
radiation-defect annealing in, 17: 27928(T)
radiation defect in n- and p-type crystals of, energy spectra of gamma, 17: 22256
radiation defects in lithium-doped, electron, 17: 27927(T)
radiation defects in crystals of, electron paramagnetic resonance study of, 16: 13653
radiation defects in crystals of, deep levels of, 17: 6767(T)
radiation deflection on, critical angles of, 17: 12704
radiation detection in p-n, pulse enhancement in, 18: 10418
radiation effects on introduction of trapping levels in, 16: 6817(R) (ORNL-3213(p.57-80))
radiation effects of thermal neutrons, radiation doping, 16: 16056
radiation effects on electrical and optical properties, 16: 24234 (ARL-62-343)
radiation effects on electron spin resonance, recombination, and trapping in, 17: 2004(R) (NP-12180)
radiation effects on defect energy levels in p-, electron, 17: 2035(T)
radiation effects on, in photovoltaic cells, 17: 4995
radiation effects on, proton, 17: 8891
radiation effects on solar cells of, in Van Allen belts, 17: 16884
radiation effects of electrons on carrier lifetime in, 17: 16736(R) (GA-3872)
radiation effects on, 0.01- to 1.8-Bev proton, 17: 16758
radiation effects on, 17: 20511(R) (GACD-3223)
radiation effects on diffusion in, mechanism of annihilation of point defects at 800 to 1200°C, 17: 34514
radiation effects on, neutron, 17: 36355
radiation effects on, by ion bombardment in a glow discharge, 17: 37741
radiation effects on, effects of illumination and temperature on, 17: 39681
radiation effects on thermal conductivity at 80 and 399°K, fast neutron, 17: 39684
radiation effects on thermal conductivity of, fast-neutron, 17: 41505
radiation effects on acceptor levels in n-type float-zone, 17: 41509
radiation effects on properties of, 18: 2318
radiation effects on thermal conductivity of, fast-neutron, 18: 2319
radiation effects on properties of, proton, 18: 2320
radiation effects on luminescence of, electron, 18: 4303(R) (NP-13321)
radiation effects in phosphorus-doped crystals of, electron and gamma, 18: 7323
radiation effects on electric properties of, proton, 18: 7334
radiation effects on circuits containing transistors of, environmental, 18: 7014
radiation effects on transistors of, in lunar excursion module, 18: 7015
radiation effects on transistors of, 18: 7016
radiation effects on, electron, 18: 7287(R) (GA-4797)
radiation effects on photoconductivity spectra of n-type, electron, 18: 8895(T)
radiation effects on solar cells of, electron and proton, 18: 10596
radiation effects on, in surface-barrier detectors, 18: 20357
radiation effects on, comparison of proton and neutron, 18: 22527(R) (NASA-CR-40)
radiation effects on, in planar transistors, 18: 22535 (SC-TM-64-69)
radiation effects at 40 and 440 Mev on transistors of, proton, 18: 26091
radiation effects on solar cells, effects of impurities on electron and proton, 18: 28058
radiation effects on, electron, 18: 30235(R) (N64-20726)
radiation effects on, electron and proton, 18: 30236(R) (NASA-CR-62)
radiation effects on, 18: 30276
radiation effects on holes in, electron and neutron, 18: 32231 (SC-R-64-193)
radiation effects on, energy dependence of neutron, 18: 32234 (SC-R-64-196)
radiation effects on defects in, 18: 34216 (NASA-TN-D-2364)
radiation effects on carrier lifetime in, effects of dosage and impurities on, 18: 34228
radiation effects on thermoelectric properties of, 18: 34237
radiation effects on oxygen-doped, infrared absorption bands in electron, 18: 34239
radiation effects on carrier lifetimes in, electron and x-ray, 18: 36038(R) (AD-433623)
radiation effects on surface barrier diodes of, gamma, 18: 37773
radiation effects on n-type, orientation dependence of, 18: 37781(T)
radiation effects on, review on, 18: 37787
radiation effects on x-ray diffraction by, fast-neutron, 18: 39992 (EUR-1643.e(p.231-45))
radiation effects on electrical characteristics by defect production, 16: 5754 (CEA-1892)
radiation effects on gallium diffusion in phosphorus-doped, 16: 13652
radiation effects on carrier life-times and mobilities, proton, 16: 12175 (CERN-62-5)
radiation effects of electrons and protons, 16: 19439 (REIC-23)
radiation effects of protons at 20.5 to 740 Mev, 16: 21093 (NP-11655)
radiation effects on general purpose and microwave diodes of, neutron, 16: 27692 (ASD-TDR-62-12)
radiation effects, 16: 32612(R) (NP-12046)
radiation effects on, electron, 16: 33535
radiation effects on electric properties of, gamma, 16: 33539
radiation effects, 17: 2011 (USNRDL-TR-577)
radiation effects on Zener, neutron, 17: 3553
radiation effects on, permanent and transient, 17: 3556
radiation effects on p-n solar-cell, electron and proton, 17: 9116
radiation effects on electrical characteristics and photocurrent, 17: 8882(R) (EURAEC-306)
radiation effects on photovoltaic cells of, cosmic-proton, 17: 8908
radiation effects, 17: 11263 (NP-12361)
radiation effects on, in space, 17: 16885
radiation effects on power output of, cosmic protons, 17: 18367 (TID-7652(p.243-59))
radiation effects on nonequilibrium-carrier lifetime in, neutron, 17: 27929(T)
radiation effects on, neutron, 17: 32680
radiation effects on surface of gas-encapsulated n-p-n, 17: 34520
radiation effects on n-p cells of, electron and proton, 18: 2305
radiation effects on, neutron-proton equivalence, 18: 2306
radiation effects on p-i-n, neutron, 18: 2321
radiation effects on, review on, 18: 2303
radiation effects on, 18: 7016
radiation effects on n-p-n, gamma and neutron, 18: 12412 (AFCRL-63-753)
radiation effects on surface-barrier, proton, 18: 14212 (JINR-P-1516)
radiation effects on diode, gamma and neutron, 18: 24937 (APEX-917)
radiation effects on electric properties of p-n, electron and proton, 18: 28080
radiation effects on, 18: 30031
radiation effects on electric properties of, 18: 32254
radiation effects on capacitance and collection efficiency and time in p-i-n, 18: 32257
radiation effects of, alpha, 18: 32061(R) (UCRL-11317(p.198-203))
radiation effects on webbed dendritic solar cell, electron, 18: 36041 (APL-TDR-64-20)
radiation effects on reverse-biased, 18: 40029
radiation effects on n/p and p/n solar cell, in space, 19: 4543
radiation effects on, neutron, 19: 7769(R) (NYO-3124-1)
radiation effects on, hardening against, 19: 9547
radiation effects on multiplication values in p-n, neutron, 19: 9549
radiation effects on, surface-effect response curves for, 19: 11608
radiation effects on n and p, 19: 18545
radiation effects on p-n, gamma, 19: 20627
radiation effects on, gamma, 19: 23164(R) (SU-SEL-64-103)
radiation effects on, 19: 22810(R) (AD-422160)
radiation effects on n-p and p-n, at 2 Mev, 19: 22813
radiation effects on silicon dioxide-passivated, 19: 22814
radiation effects on photoelectric properties of p-n, neutron, (E), 19: 26715
radiation effects on defect charge state of semiconductor, 19: 41974
radiation effects on electric properties of, 18: 39995 (GA-3087)
radiation effects on electric properties of zone-refined, neutron, 18: 40005 (ONR-16(Vol.1)(p.246-62))
radiation effects on solar cells of Relay I and Relay II, 18: 40036
radiation effects on injection of A centers in single crystals of, 18: 44263
radiation effects on absorption spectra in near infrared region, electron and neutron, 18: 44264
radiation effects on, energy dependence of electron, 18: 44277
radiation effects on polycrystalline solar cells of, electron, 18: 44278
radiation effects on electric properties of, gamma and neutron, 19: 1003(R) (ORNL-3676(p.112-21))

radiation effects on conduction-band energy levels in, gamma, 19: 1012
radiation effects on, bremsstrahlung and fast-neutron, 19: 2864
radiation effects on design tradeoffs in transistors of, fast neutron, 19: 4541
radiation effects on, proton, 19: 7826
radiation effects on crystal structure, 6.5-Mev proton, 19: 9746
radiation effects on performance in semiconductor detectors, 19: 11610
radiation effects on, neutron, 19: 13813 (WL-TDR-64-97)
radiation effects on field-effect transistors at extreme temperatures, 19: 13815
radiation effects on diodes, 19: 13817
radiation effects on performance of high-frequency transistors, fast-neutron, 19: 15938
radiation effects on transistors of, cosmic, 19: 18348
radiation effects on surface of transistors of, gamma, 19: 23127 (R64MCD500)
radiation effects on A-center in, spectra of recombination, 19: 23135
radiation effects on, infrared defect absorption bands in electron, 19: 23137
radiation effects on silicon dioxide-passivated, 19: 22814
radiation effects on gain of n-p-n planar transistors, neutron, 19: 24884 (SC-TM-261-63(14))
radiation effects on p-type, levels in gamma, 19: 26892
radiation effects on breakdown and response of transistors of, neutron, 19: 28696 (AD-607561)
radiation effects on gain of transistors, gamma, 19: 30593(R) (AD-608959)
radiation effects on spectra of point defects in, neutron, 19: 33513 (AD-611194)
radiation effects on diffusion of impurities in, 19: 32048(R) (NP-15073)
radiation effects on infrared absorption spectra of oriented single-crystal zone-refined, 19: 32617(R) (NP-15091)
radiation effects on photoconductivity spectra of zone-refined, electron, 19: 32617(R) (NP-15091)
radiation effects on electric properties of, electron, 19: 32617(R) (NP-15091)
radiation effects on infrared absorption spectra of, fast-neutron, 19: 32773 (AD-611145)
radiation effects on defect introduction rates in, energy dependence of electron, 19: 34593 (NP-15090)
radiation effects on power degradation of, energy dependence of proton, 19: 34593 (NP-15090)
radiation effects on recombination in, gamma, (E), 19: 40085
radiation effects on, electron-hole pair production in high-energy particle, (T), 19: 39250
radiation effects on crystal structure of, microplasm studies of, 19: 39254
radiation effects on conductivity of n-type, electron and neutron, 19: 40935 (SC-DC-65-1247)
radiation effects on diodes of, alpha, 19: 40937 (UCRL-11958)
radiation effects on efficiency of solar cells of, electron, 19: 40931 (AD-609424)
radiation effects on photoconductivity in semiconductors of, electron, 19: 40933(R) (NP-15300)
radiation effects on photoconductivity in semiconductors of, electron, 19: 40934(R) (NP-15301)
radiation effects on thermally stimulated conductivity of, neutron, (E), 19: 41985
radiation effects on ultrapure crystals of, electron, 19: 41998(T)
radiation effects on gate field-effect transistors insulated by, electron, (E), 19: 44549
radiation effects on semiconductors of, 19: 47076 (AD-612090)
radiation effects on, electron, (E), 19: 47092(R) (TID-22141)
radiation effects on annealing, conductivity, and Hall coefficient of n-type crystals of, at 5, 15, and 45 Mev, 17: 37606
radiation effects on crystals of, 17: 34554(R) (ORNL-3480(p.79-94))
radiation effects on gallium diffusion in phosphorus-doped crystals of, 16: 13652
radiation effects on infrared absorption and photoconductivity in p-type crystals of, neutron, 16: 13671
radiation effects on infrared absorption spectra of crystals of, helium ion and proton, 17: 37579
radiation effects on infrared absorption bands in crystals of, fast neutron, 16: 25866
radiation effects on semiconductor applications of crystals of, 16: 15980
radiation effects on phonon absorption bands in crystals of, neutron, 16: 22699
radiation effects on defect distributions in crystals of, electron, 17: 598(T)
radiation effects on defect spectra in n- and p-type crystals of, electron, 17: 2034(T)
radiation effects on crystals of, permanent and transient, 17: 3555
radiation effects on infrared absorption spectra of n- and p-type crystals of, neutron, 17: 5010(T)
radiation effects on crystals of, proton, 17: 6759
radiation effects on crystals of, proton, 17: 12719 (N62-12598)
radiation effects on crystals of, proton, 17: 27891 (JINR-P-1247)
radiation effects on electric conductivity of crystals of, electron, 17: 22218(R) (GA-4164)
radiation effects on electric conductivity, Hall coefficient, and Hall mobility of zone-refined p-type crystals of, 17: 29379 (NRL-5930)
radiation effects on crystals of, annealing of gamma, 17: 29969
radiation effects on crystals of, electron and gamma, 17: 30128
radiation effects on crystals of, at 1 Mev, electron, 17: 34488 (NP-13014)
radiation effects on crystals of, review, 17: 34513
radiation effects on crystals of, protective effects of glass coatings against, 17: 34526
radiation effects on structure of crystals of, electron-paramagnetic-resonance studies of, 17: 37286
radiation effects on phosphorus-doped crystals of, illumination and temperature dependence of gamma, 17: 27898
radiation effects on p-type crystals of, lithium-ion, 16: 27721
radiation effects on lithium-doped single crystals of, electron, 17: 2033(T)
radiation effects on crystal structure of, mechanism of beta, 20: 2426 (LA-3387)
radiation effects on, 20: 2481
radiation effects on close-pair defects at 0 to 90°K, 20: 2482
radiation effects on thermal conductivity of monocrystals of, at 80 to 300°K, 20: 2487
radiation effects on, proton, 20: 2489
radiation effects on, EPR studies of, 20: 2490
radiation effects on n-type and p-type, 20: 2496
radiation effects on semiconducting, 20: 2497
radiation effects on diffusion of impurities in, 20: 2508
radiation effects on, anisotropy of displacement energy for, 20: 2515
radiation effects on, high-energy electron and proton, 20: 2517
radiation effects on, high-energy electron, 20: 2518
radiation effects on electric properties of, annealing during fabrication of p-n junctions of fast-neutron, 20: 2440
radiation effects on transistors of, (E), 20: 4261 (AD-623078)
radiation effects on gain degradation in transistors of, effects of operating conditions on, 20: 4267
radiation effects on diodes of, fast-neutron, 20: 4999(R) (ORNL-2599)
radiation effects on thermal conductivity of single crystals of, electron, (E), 20: 5919
radiation effects on surface state density of MOS structures of, γ, 20: 7463
radiation effects on thermal conductivity of monocrystalline, neutron, 20: 7648
radiation effects on, 20: 9023
radiation effects on n-p-n gain degradation, neutron, (E/T), 20: 9302 (RLDP-65-13)
radiation effects on spacecraft solar cells of, 20: 9303
radiation effects on rectifier, fast neutron, 20: 9306
radiation effects on electric properties of oxide-covered, ionizing, 20: 7647
radiation effects on p-i-n junctions of, electron, gamma, and x, 20: 11173 (D2-84071-1)
radiation effects on transistors of, electron and gamma, 20: 11182
radiation effects on x-ray diffraction by crystalline, alpha, 20: 12281
radiation effects on photoconductivity of, electron, (E), 20: 11351(R) (NP-15611, pp 48-89)
radiation effects on atomic displacements in, by protons at 30 Mev to 1 Bev, 20: 11356
radiation effects on p-type, Hall effect measurement of gamma, 20: 11360
radiation effects on, neutron, 20: 14920 (TID-22664)
radiation effects on electric properties of conductivity-modulated p-i-n diodes of, 20: 16912
radiation effects on defects in solar cells of, effects of impurities on electron and proton, 20: 17125 (NASA-CR-404)
radiation effects on single-crystal, alpha and beta, (E/T), 20: 19273(E) (BNL-929, pp 3-43)
radiation effects on, effects of impurities on, 20: 19106(R) (N-65-19886)
radiation effects on photovoltaic parameters of solar cells of, proton, 20: 19106(R) (N-65-19886)
radiation effects on electric properties of MOS structures of, 20: 19113
radiation effects on impurity diffusion in, electron and proton, 20: 21147(R) (AD-621049)
radiation effects on electric properties of, neutron, 20: 21150 (HMI-B-45)
radiation effects on defect introduction rate in n-type, energy dependence of electron, 20: 21154(R) (N-65-23290)
radiation effects on MOS FET transistor of, annealing of gamma, 20: 21159
radiation effects on transistors of, prediction of transient, 20: 21166
radiation effects on recombination centers in, gamma, 20: 21439

radiation effects on lithium-drifted p-i-n, 20: 2510
radiation effects on p-n, charge and field dependence of, 20: 2511
radiation effects on n-p-n, neutron, 20: 2184(R) (AD-614618)
radiation effects on n-p-n, neutron, 20: 2185(R) (AD-618194)
radiation effects on, for semiconductors, 20: 2413 (AD-618688)
radiation effects on, neutron, 20: 7464
radiation effects on, surface effects in, 20: 23517(R) (AD-625533)
radiation effects on high-gain low-current transistors of, electron, 20: 23518 (AD-627605)
radiation effects on MOS capacitors of, electron, 20: 23523
radiation effects on surface of semiconductors of, gamma, 20: 25447(R) (N-66-15448)
radiation effects on n- and p-type, ESR spectral studies on, 20: 25618(R) (N-65-33506)
radiation effects on transistors of, effects of annealing on gamma and neutron, 20: 27619
radiation effects on electric properties of transistors of, 20: 27366
radiation effects on chlorine and phosphorus diffusion in, neutron, (E), 20: 28612
radiation effects on planar transistors of, gamma, 20: 29577 (CEA-R-2959)
radiation effects on, transient annealing from neutron, 20: 31613 (SC-DC-66-1443)
radiation effects on lithium-doped, electron, 20: 31614
radiation effects on single-crystal solar cells of, proton, 20: 31616
radiation effects on near infrared absorption spectra of, fast-neutron, 20: 34837(T)
radiation effects on high resistivity n and p type, donor production from gamma and thermal neutron, 20: 35806 (CEA-R-2918)
radiation effects on MOS transistors of, positive charge distribution in dielectric layer from x, (E), 20: 37130
radiation effects on insulated-gate FET transistors on substrate of, photocurrent contribution to drain current from, 20: 37132
radiation effects on, transient annealing from neutron, 20: 37129 (SC-DC-66-1820)
radiation effects on, 1-Mev electron, (E), 20: 39458 (NP-16225)
radiation effects on short-circuit current of, proton, (E), 20: 40299
radiation effects at 293°K on n-type, neutron and gamma, (E), 20: 40303
radiation effects on, oxygen ion, (E), 20: 40314
radiation effects on infrared absorption spectrum of, neutron, (E), 20: 40340
radiation effects on defects in crystals of, fast neutron, (E), 20: 42567(T)
radiation effects on single crystals of, electron, 20: 44998
radiation effects on, channeling pattern formation in ion, 20: 45022
radiation effects on phosphorus-doped, fast neutron, 20: 43986 (AD-637937)
radiation effects on, electron, 20: 46598(R) (RPI-328-68)
radiation effects on structure and photoelectric properties of, annealing of electrons, 20: 45719
radiation effects, gamma, 19: 39269(R) (SU-SEL-64-133)
radiation ionization, 16: 6799
radiation noise in detectors of, measurement of, 20: 693 (NP-15172)
radiation resistance of p-type base silicon solar cells, 16: 3556
radiation response of power transistors of, effects of design on, (E/T), 20: 21148(R) (AD-630835)
radiation response of power transistors of, effects of design on, (E/T), 20: 21149(R) (AD-630836)
radiation transient effects on, pulsed, 17: 2045
radiochemistry, 16: 5369 (NAS-NS-3049)
radioinduced annealing and Frenkel defects in crystals of, interactions of gold, nickel, and oxygen with, 17: 37610
radioinduced base current in transistors of, neutron, 19: 40936 (SC-R-65-912)
radioinduced color centers in, ENDOR and EPR in electron, 18: 22153
radioinduced current in diodes of, theory of fast neutron, 17: 39686
radioinduced damage in n- and p-type, transient electron, (E), 20: 11176(R) (NP-15835)
radioinduced damage in, energy and orientation dependence of electron, 20: 11364
radioinduced damage effects on carrier lifetime in p-type, gamma, (E), 20: 14922
radioinduced damage in solar cells of p-type, temperature dependence of electron, 20: 19115
radioinduced damage in semiconductors of, gain degradation from, 20: 21169
radioinduced damage in integrated circuits, gamma and neutron, 20: 35811
radioinduced damage in p-type, photoconductivity spectrum from electron, 20: 41379
radioinduced damage in n- and p-type, electron, 20: 45018
radioinduced defect introduction rates in n- and p-type, in the vicinity of the radiation damage threshold, 17: 5015
radioinduced defects in, electron paramagnetic resonance spectra of, 17: 31038
radioinduced defects in n-type, distribution with depth, 17: 37585
radioinduced defects in lithium-doped, 18: 5823
radioinduced defects in impurity-doped crystals of, energy levels of electron, 18: 26089(T)
radioinduced defect formation rate in, oxygen effects on neutron A-center, (E), 19: 11801(T)
radioinduced defects in, review on, 19: 11811
radioinduced defects in, effects of lithium impurity on, 19: 16240(T)
radioinduced defects in, EPR studies of divacancy in electron, 19: 18549
radioinduced defects in p-type, gamma, (E), 19: 30836
radioinduced defects in, anisotropy of electron, 19: 34761
radioinduced defects in n and p-type, electron, 19: 34765
radioinduced defects in n- and p-type crystals of, spectra of fast electron and neutron, 17: 37608
radioinduced defects in lithium-activated crystals of, fast electron, 17: 37609
radioinduced defects in n-type crystals of, effects of annealing on, 17: 37611
radioinduced defects in, 20: 904
radioinduced defects in, structural properties of, 20: 2486
radioinduced defects in, effects of doping with lithium on, 20: 2491
radioinduced defects in, annealing of, 20: 2506
radioinduced defects in, 20: 2516
radioinduced defects in, annealing and drift mobility of, 20: 2507
radioinduced defects in, electron, (E), 20: 4508(R) (RPI-328-40)
radioinduced defects in, annealing of electron, 20: 5920
radioinduced defect formation in electron-injected p-type, gamma, 20: 7637
radioinduced defects in, infrared absorption bands of electron, 20: 11347(R) (NP-15611, pp 5-18)
radioinduced defects in, energy dependence of electron, 20: 14925
radioinduced defects in, interaction between lithium and electron, 20: 19102(R) (N-65-19693)
radioinduced defects in, types of, 20: 19104(R) (N-64-19867)
radioinduced defect in, energy dependence and properties of electron, 20: 19106(R) (N-65-19886)
radioinduced defects in phosphorus-doped, electron, 20: 19108(R) (N-65-21459)
radioinduced defects in, introduction rate of electron, 20: 19110(R) (N-65-21762)
radioinduced defects in solar cells of p-type, annealing of electron, 20: 19114
radioinduced defects in, radiative recombination of gamma, 20: 25627(T)
radioinduced defects in, depth distribution of 300-kev-electron, 20: 31791
radioinduced defect clusters in n-type, fast-neutron, (E), 20: 31792
radioinduced defect levels in, annealing characteristics of, 20: 33727 (N-66-10647)
radioinduced defects in single-crystal, 20: 35932 (LA-3501)
radioinduced defects in n- and p-type, annealing of neutron, 20: 40334(T)
radioinduced defects in p-type, energy levels of neutron, 20: 46950
radioinduced diffusion in crystals of, 17: 37612
radioinduced dimensional changes in crystals of, at about 50 and 115°K, electron, 16: 10645
radioinduced divacancy in, electron, 16: 244
radioinduced divacancies and vacancies in, electron, 19: 18550
radioinduced doping in, neutron, 18: 18156
radioinduced doping for p-n, neutron, 18: 18156
radioinduced E centers in arsenic-, antimony-, and bismuth-doped, annealing of gamma and electron, (E), 20: 22323
radioinduced effects at energies below 300 kev in n-type, electron, 20: 45001
radioinduced electron-cavity pair formation in p-n layers of crystals of, 17: 27932
radioinduced electron-hole pairs in n-type, formation energy for alpha, 20: 2362
radioinduced infrared absorption spectra from defects formed in, 17: 35775
radioinduced infrared absorption bands in oxygen-doped, low-temperature electron, (E), 20: 24595
radioinduced infrared defect absorption bands in, annealing of electron, 20: 33726 (N-65-32169)
radioinduced ionization of, in semiconductor-detector diodes, 17: 37256
radioinduced ionization of, temperature effects on energy of, x, 20: 46959(T)
radioinduced isotopic exchange of hydroxyl ions on colloidal, with deuterium, 20: 29276
radioinduced lattice displacements in, calculation of production rate of proton, 17: 14906
radioinduced length changes in n-type, proton, 20: 25621

radioinduced modifications in crystals of, by 50- to 100-kev electron bombardment, 16: 15258
radioinduced near-infrared absorption bands in, electron and neutron, 19: 11228(T)
radioinduced noise in detectors of, electromagnetic, (E), 20: 14923
radioinduced oxygen-defect complexes in, infrared absorption spectra of electron and neutron, (E), 20: 13998
radioinduced paramagnetic centers in electron-irradiated, 17: 20529
radioinduced production of helium and hydrogen in, neutron, 19: 26901
radioinduced regeneration effects in p-n junction, in isolated circuits, 20: 21168
radioinduced resistance fluctuations in transistors of, carrier removal effects on electron, (E/T), 20: 2188
radioinduced spin-1 centers in, fast neutron, 17: 39694
radioinduced surface damage in transistors of, electron, 20: 7465
radioinduced surface degradation in MOS transistors of, gamma, 20: 9305
radioinduced surface damage in, gamma, 20: 21172
radioinduced transmutation doping, 19: 13439
reactions of diffused impurities in, 20: 29709(R) (TID-22970, pp 65-119)
reactions of recoil, with gaseous phosphine and phosphine–silane mixtures, production of silanes by, 20: 43315
reactions with alkaline earth fluorides in gaseous phase, 18: 27356 (CONF-74-27)
reactions with carbon–uranium tetrafluoride mixtures, 16: 2685(R) (TID-13814)
reactions with crucibles of refractory compounds with boron, carbon, and nitrogen at 400 to 1500°C, 19: 37112
reactions with fast neutrons, helium and hydrogen production in type 347 stainless steel in, 20: 7490(R) (BMI-1745, Sect.A)
reactions with hafnium or zirconium oxides for reduction to metal, 19: 5889
reactions with hafnium oxide in electron-beam furnace, 19: 34661
reactions with lanthanum and lanthanum oxides to prepare lanthanum silicides, 19: 38613
reactions with magnesium to 645°C, 19: 22997 (TRG-Report-842)
reactions with Magnox alloy, 19: 22997 (TRG-Report-842)
reactions with metals in vacuum, temperature effects in, 18: 37626
reactions with organic matrix materials in ice-water system, 18: 15722 (TID-20332)
reactions with plutonium oxide during sintering, 17: 14209 (LA-2828)
reactions with plutonia at high temperatures, 19: 39125(R) (BNWL-91)
reactions with sodium beryllate solutions, 17: 16002
reactions with strontia at 1200°C, 19: 38593(T) (ORNL-tr-674)
reactions with uranium oxide during sintering, 17: 14209 (LA-2828)
reactions with uranium tetrafluoride, 17: 32182(R) (GTR-17)
reactions with uranium to 650°C, 19: 22997 (TRG-Report-842)
reactions with uranium(IV) oxide, floating-zone, 20: 8951
reactions with volatile fission products, fixation in, 19: 25781(P)
recombination and trapping in normal and irradiated crystals of, 17: 11383
recombination time in, method for measurement of, during radiation, 17: 18870
research progress on, 17: 41521(R) (AD-419705)
response of fission chambers of, to channeled argon-40 and iodine-127 ions, 20: 41324
response of lithium-drifted, for beta and gamma radiation, 20: 31519
response of lithium-drifted p-i-n, to alpha and beta particles, 18: 33916
response of lithium-compensated, to gamma rays at low temperatures, 19: 11529
response of semiconductor fission detectors of, to argon-40 and iodine-127 ions, (E), 20: 39470(R) (ORNL-3924)
response to electrons, transient, 18: 33919
response to gamma rays, Monte Carlo calculation of characteristics of, 20: 43701
response to heavy ions, 18: 14207 (CONF-354-4)
semiconducting properties, 18: 30218
sensitivity of semiconductor detectors of, to pulsed x radiation, 19: 6205
separation from antimony by solvent extraction using cupferron, 18: 39123
separation from arsenic by solvent extraction using diethyldithiocarbamate, 18: 39122
separation from graphite above 1750°C in inert gases, 19: 38762
separation from niobium by electrolysis, 18: 35926 (BM-RI-6506)
separation from phosphorus, 19: 15332(R) (BNL-841(p.52-62))
separation from reactor fuels by dissolution and sand filtration, 20: 43426 (ORNL-TM-1650)
separation from sea water by sorption on ferric hydroxide gel, 18: 37083
separation from titanium, vanadium, and zirconium by zone melting, 18: 8456
separation from uranium ore concentrates by fusion with ammonium bifluoride, 18: 1483(R) (ANL-6687(p.27-85))
separation from uranium yellow cake by carbonate leaching, 19: 18082(P)
separation frum uranium ore concentrates, methods development for, 17: 36860(R) (ANL-6648)
silicon-29 magnetic resonance in crystals of, theory of double, 17: 33929
Slater-Condon parameters of, determined from spectral data, 17: 31118
solubility in aluminum-uranium alloy at 950°C, 17: 25775(R) (NMI-7246)
solubility in beta phase of cobalt–niobium alloys, 18: 34145
solubility in liquid zinc, 20: 22966 (ANL-7083)
solubility in lithium at 482 to 1010°C, 16: 6718 (NEPA-1465)
solubility in $ZrBe_{13}$ and Zr_2Be_{17} at 70 to 2500°F, 18: 27946(R) (BBC-120)
solvent properties for nickel, determination by neutron activation, 17: 8828
solvent properties for nickel, determination of, 17: 30151
solvent properties for sodium at 800°C, 19: 39204
sorption from nitric acid by ion exchange paper, 19: 24435
spark patterns produced by grinding of, 18: 19493(T) (SC-T-64147)
specifications for n-p-n, 18: 3416 (TID-19697)
specifications for diffused mesa switching, Illinois Univ., 18: 3417 (TID-19698)
specifications for miniature switching, Illinois Univ., 18: 3418 (TID-19699)
spectra of atomic, in plasma jets, (E), 19: 41287
spectra of, correlation of dissociation energies and excitation potentials in flame, 17: 14234
spectra of fast-neutron-irradiated, infrared absorption, 19: 32773 (AD-611145)
spectra of, in aluminum–iron alloys and iron–silicon systems, 17: 30516 (TID-19080)
spectra of, K x-ray, 17: 30484
spectra of minerals, effects of temperature on infrared, 17: 33880
spectra of oxygen-doped, effects of fast neutrons and 2-Mev electrons on, (E), 20: 40302
spectra of phosphorus-doped, vibration, (E), 19: 14079
spectra of point defects in, absorption, 18: 2254
spectra of point defects in, absorption, 19: 33513 (AD-611194)
spectra of, effects of lithium and lithium oxide donor impurities on infrared, 19: 42499
spectra of, wavelengths of Lyman lines in, 20: 25731
spin-orbit coupling effects in, 16: 3530 (ANL-6463)
sputtering anisotropy of single crystals of, 18: 28124
sputtering at 50 to 600 ev by rare gas ions, 17: 8931(R) (NP-12389)
sputtering by argon ions, full-plane threshold energies for, 17: 37743
sputtering by helium ions at 600 ev, yield curves for, 17: 25870(R) (X62-11400)
sputtering by noble-gas ions at 100 to 600 ev, yields from, 16: 22753
sputtering of crystals of, by argon ions at 1 to 5 kev, yields from, 17: 5089
sputtering of crystals of, by cations to 800 ev, atom spatial distributions from, 16: 22758
supercoductivity under high pressure, (E), 19: 39701
superconductivity under high pressure, (E), 20: 40039
surface contamination of, use of radioisotopes for detection of, 18: 20420
surface contouring of radiation detectors of diffused junction, 20: 46044(R) (NYO-3246-6)
surface effects in lithium-drifted, 18: 20326 (BNL-7853)
surface field stability in p-n, 18: 2078
surface layer removal by vibratory polishing, 20: 7504
surface properties in semiconductors, 20: 29569
surface texture, determination of pole figures by reflection method, 16: 21017 (AE-68)
temperature effects in, 16: 27360
thermal capacity of, at 100 to 1100°C, 17: 4445 (IS-500(Sect.C))
thermal conductivity at 300 to 1400°K, 19: 9767(R) (IS-900(Sect.P))
thermal cycling effects on surface barrier diodes of, 20: 30785
thermal energy storage in, in solar-thermionic power supplies, 17: 9113
thermal expansion, 19: 1053(R) (PR-P-62)
thermal expansion coefficient of crystals of, at low temperatures, 16: 2302 (TID-14230)
thermal properties of, Kapitza resistance, 17: 18826
thermionic work function of, effects of sorbed sodium on, 19: 41124(R) (NP-15108)
thermodynamics of, Debye-Waller factors for, 17: 39768
use as diffusion barrier between aluminum clad and uranium fuel, 18: 13264
use as high-speed switches, 16: 25581 (UCRL-6012-T(Rev.1))
use as surface barrier detector with guard ring, 18: 16314
use as target and detector for (n,α) reactions at 14.55 Mev, 18: 38069 (NP-14111)
use for neutron monitoring at 14 Mev, 16: 5539
use in corrosion-resistance treatment of metals, 19: 36989(P)
use in detectors for energetic electron and proton measurements from rockets, 20: 7386
use in determining absolute scale of x-ray wavelengths, 18: 34340
use in fast-neutron spectrometers, 18: 18206

use in gamma detection and measurement (E/T), 19: 776 (NP-14332)
use in gamma dosimetry, 16: 17924
use in lithium compensated focal plane detectors, for beta spectrometers, 20: 41326
use in neutron detection, 18: 41762 (CEA-R-2491)
use in photovoltaic cells, 20: 15305
use in promethium-147 nuclear battery, 18: 27827
use in radiation-resistant magnetic amplifiers, 16: 15987
use in scintillation counters, 16: 695
use in vacuum encapsulated lithium-drift telescope detectors, 20: 41376
use of diodes of, for neutron diffraction analysis, 20: 43730
use of lithium-drifted p-i-n, for radiation detection, 17: 41309
use of p-n, in solar cell x-ray detector, 17: 22025
use of p-n junction as dosimeter, 17: 20372
use of p-type, in transmission counters for nuclear particle detection, 17: 6440 (UCRL-10030)
use of photodiodes of, for uv radiation detector, 18: 37539
use of semiconductors of, for wide-range gamma dosimetry, 20: 19015 (AD-629511)
use of surface-barrier, in fast neutron spectrometry, (E), 19: 20334
uses, 18: 23902
rock samples from, age determination of, 19: 22567(R) (NYO-1669-10)
vacuum effects on, in radiation detectors, 17: 3373 (ARL-62-416)
vapor pressure, 20: 331
vaporization by electron bombardment, 19: 34660
vaporization coefficients of single crystal, 19: 46956 (NP-15514(Vol.1))
x-ray absorption in, cross sections for, 18: 32779
x-ray absorption spectra of K shell in gaseous silicon chlorides; (E), 20: 19389
x-ray diffraction by boron-doped, 18: 39992 (EUR-1643.e(p.231-45))
x-ray diffraction by single crystals of, Pendelloesung fringes in, (E/T), 19: 39287
x-ray diffraction by, effects of fast neutrons and impurities on, (E), 20: 24612
x-ray emission spectra of, L and K, (E), 20: 41350
x-ray reflection from orders in crystals of, half-widths of, 17: 31007
x-ray reflections from, relative intensities of higher order, 19: 26627 (CALT-221-7)
x-ray scattering by single crystals of, diffuse bands in, 18: 16551 (TID-20364)
x-ray scattering by single-crystal, small-angle, 18: 20555
x-ray scattering by crystals of, anti-Stokes and Stokes modified lines in, 18: 35242 (CALT-221-2)
x-ray total cross sections at 15 to 30 Mev, (E), 19: 12573
x-ray transmission in perfect crystals of, abnormal aspects of, 17: 6063
x-ray transmission by imperfect crystals of, 17: 6064
xenon ion reactions with, sputtering in, 17: 39709 (ARL-63-125)
xenon-125 ion ranges in monocrystalline, 18: 28097
xenon-125 ranges at 20 to 80 kev, 18: 20812

SILICON ALCOHOLATES

tert-butyl, infrared spectra of, 18: 1720

Silicon Alloys

see Silicon Systems

SILICON BORIDES

deposition and oxidation of coatings of, on graphite, 19: 6270(R) (WADD-TR-61-72(Vol.XXXIV))
inflammability of powdered, at 180 to 1100°C, 18: 44211
production of compounds, in vaporization of boron-carbon-silicon systems, 16: 9144 (WADD-TR-60-782(Pt.III))

SILICON BRONZE

analysis for molybdenum and tin using 8-quinolinol, spectrophotometric, 16: 16314
corrosion by simulated N-reactor secondary water, 17: 37480 (HW-76358)

SILICON CARBIDES

see also Carborundum

analysis by beta spectroscopy, qualitative and quantitative, 18: 25303
analysis by neutron activation, 20: 33167(T) (AEC-tr-6639, pp 42-5)
analysis for antimony, arsenic, copper, phosphorus, and zinc, activation, 17: 38964
analysis for carbon using electron microprobe, 19: 43966
analysis for impurities, 16: 22530 (ARF-3133-23)
analysis of quantitative micro-, 19: 30076 (EUR-1819.e(p.15-23))
argon ion sputtering, atom ejection patterns in, 16: 2203(R) (TID-14257)
bibliography on production and properties of, 17: 25709 (TRG-Inf.-Ser.-295)
bonding of coatings of, using aluminum phosphate, 18: 5737(R) (PWA-2255)
bonding to platinum and tungsten, alloys for, 18: 27791(R) (WCAP-2596)
bonding to titanium with graphite spacer, 18: 37649 (A/CONF.28/P/432)
bonding to titanium, 19: 20505 (JAERI-1071)
bonding to tungsten, 18: 2035(R) (WCAP-2403)
carbon-13 magnetic resonance in crystals of, theory of double, 17: 33929
chemical stabilities and thermodynamic properties, 16: 19266
coating of, effects of, on oxidation resistance of graphite, 20: 29773
coating with uranium, 18: 27791(R) (WCAP-2596)
collapse of long hollow cylinder of, surrounded by a concentric cylinder of uranium, 17: 4958
combustion in fluorine, 18: 1485(R) (ANL-6687(p.153-66))
combustion in fluorine, calorimetry of, 18: 43440(R) (ANL-6800(p.305-25))
combustion in fluorine, kinetics of, 19: 15408(R) (ANL-6900(p.221-31))
combustion with fluorine, data on, 20: 5523(R) (ANL-6925, pp 175-85)
comminution of, effects of impact strength, microhardness, shear modulus, and thermal expansion on, 18: 44220(T)
compatibility with urania, 20: 11224
compatibility with cesium vapor at 1800°C, 20: 31669
corrosion by magnesium halide–zinc halide fluxes at high temperatures, 19: 17176(R) (ANL-6965(p.1-41))
corrosion by plasma jets, 19: 9627
corrosion of beryllia-coated, by fused alloy–salt mixtures, 18: 36751 (ANL-6912)
creep at room temperature to 2730°F, 16: 7879 (DC-58-7-146)
crystal defects in, electron microscopy of, 19: 31456
decomposition of, crystal structure of graphite formed in, 19: 39185
deformation properties, 20: 886
deformation properties and hardness of, at high temperatures, 20: 33920
deposition from tetrachloride, 18: 41933 (TID-11295(3rd Ed.))
deposition method for, thermochemical, 19: 44640 (ORNL-P-1446-1)
deposition of coatings of, on refractory bodies, method for, 17: 16628(P)
deposition of, from vapor, 18: 44101(R) (ORNL-3670(p.67-76))
deposition on uranium dicarbide particles in fluidized bed, 20: 9469
development for neutron detectors, 16: 25573(R) (WCAP-1989)
development for neutron detectors, 17: 22005 (EURAEC-587)
development of coatings of, 18: 4257(R) (PWA-2279)
development of, for use in neutron counter diodes, 16: 33162(R) (WCAP-2053)
development of junctions of, for neutron counting, 16: 22333(R) (WCAP-1874)
development of junctions of, for neutron counting, 16: 22334(R) (WCAP-1929)
development of junction-gate type field-effect transistors of, 20: 12276 (NYO-3405-4)
diffusion of aluminum in, 18: 27791(R) (WCAP-2596)
dissolution of, for fuel element reprocessing, 19: 11286
doping of, using ion implantation techniques, 20: 35863 (ORNL-TM-1495)
effects of coatings of, on thermal radiation properties of molybdenum, 16: 32039(R) (PWA-1863)
effects on thermoelectric properties of MCC 50, 19: 12129(R) (ASD-TDR-62-896(Pt.II))
elastic properties and strength of boron-doped crystals of, 17: 25777(R) (NP-12874)
electric conduction theory with two trap levels in crystals of, 16: 337(R) (NP-10868)
electric potential of diodes of, 20: 29709(R) (TID-22970, pp 65-119)
electric properties of irradiated crystals of, effects of pulse annealing on, 16: 33513 (EURAEC-403)
emissivity, 17: 31009
emissivity at 600 to 1800°F, 16: 32118 (NASA-TN-D-998)
emissivity of, measurements of, 17: 16787(R) (PWA-2163)
energy levels in crystals of, multiple, 16: 33010
enthalpy and specific heat at high temperatures, 19: 2852
enthalpy of formation of, 20: 31213(R) (ANL-7175, pp 119-58)
fabrication into high-temperature neutron detectors, 18: 2035(R) (WCAP-2403)
fabrication into high-temperature neutron detectors, 18: 18179(R) (WCAP-2562)
fabrication of ceramic bodies of, 18: 12602 (Y-1450)
fabrication of core retainer plates of, 16: 22531 (DC-60-1-51)
fabrication of thin-walled articles, 17: 16628(P)
fission fragment recoil in, expansion induced by, 19: 18547
friction between surfaces of, at high temperatures in vacuum, argon, helium, and nitrogen atmospheres, 19: 28826
glaze for coating of, on graphite, 20: 29696(P)
Hall and resistivity measurements at 300 to 1000°K, 16: 5489 (EURAEC-161)
hardness and surface friction of, effects of temperature on, 20: 29771
hardness of crystals of, 16: 10728
hardness of, effects of temperature on, 17: 36316
heat flux in coatings of, for use at 40 atm pressure, 19: 25723(R) (GA-5036)
heat of formation of, development of methods for determining, 18: 17770(R) (ANL-6725(p.191-200))
heat of formation of, development of method for determining, 18: 43440(R) (ANL-6800(p.305-25))
heat of formation, 19: 32118(R) (ANL-7020(p.165-74))
interactions with gas flow in MHD generators, 20: 41738

light reactions with, electrons, ions, and neutral atoms from laser-induced, 17: 18923
mechanical properties of single crystals, 16: 30795 (NP-12049)
mechanical properties of crystals of, 16: 22334(R) (WCAP-1929)
melting temperature, evaluation for space technology, 18: 16521
mercury ion sputtering, atom ejection patterns in, 16: 2203(R) (TID-14257)
neon ion sputtering, atom ejection patterns in, 16: 2203(R) (TID-14257)
oxidation of coatings of, on graphite, 19: 6270(R) (WADD-TR-61-72 (Vol.XXXIV))
oxidation resistance at high temperatures, effects of metal additives on, 19: 36993(P)
performance as barriers in thermionic diodes, 18: 28309
performance as graphite coating under irradiation, oxidation, and thermal cycling conditions, 20: 43825 (BNWL-242)
performance as semiconductor neutron detector, (E), 19: 18256(R) (EURAEC-1215)
performance as surface-barrier neutron detectors, 18: 22347(T,R) (EURAEC-1008)
performance for in-pile flux mapping, 19: 36824 (WCAP-5482)
performance in nuclear particle detectors at high temperatures, 18: 33918
performance of coatings of, on Pebble Bed Reactor fuel, 16: 9663 (NYO-9064)
performance of oxynitride-bonded crucibles of, for flux-metal systems, 19: 32279(R) (ANL-7020(p.3-99))
performance of semiconductor diodes of, for alpha and fission fragment detection and measurement, 20: 46073
performance of uranium-235-coated semiconductor diodes of, for reactor neutron detection and measurement, 20: 46073
permeability to combustion gas and hydrogen at high temperatures, 18: 44491(R) (AD-601111)
physical properties, effects of impurity contents, 16: 22530 (ARF-3133-23)
piezoelectric properties for use in high-temperature strain gages, 17: 39370 (ARL-63-147)
preparation and fabrication by thermochemical deposition, 19: 7462
preparation and properties of, for neutron surface barrier detectors, 18: 489(R) (EURAEC-287)
preparation and properties for protective coatings on molybdenum and tungsten, 20: 37189
preparation and testing of pure and boron- and aluminum nitride-containing crystals of, 16: 4452(R) (NP-11144)
preparation of coatings of, on elemental carbon, 17: 8773(P)
preparation of crystals of, 16: 22333(R) (WCAP-1874)
preparation of, for use in neutron detectors, 17: 358(R) (EURAEC-51)
preparation of pyrolytic, symposium on, 20: 37179
preparation of very pure, 19: 4608(P)
preparation, properties, and aerospace applications, 19: 37142
pressing, equipment and techniques for hot, 16: 5699
pressing high density, apparatus for hot, 16: 19267
production of compounds, in vaporization of boron-carbon-silicon systems, 16: 9144 (WADD-TR-60-782(Pt.III))
production of crystals of, 17: 14653(R) (WCAP-2175)
properties as barrier shell for thermionic energy converters, (E), 20: 4359(R) (AD-618923)
properties as magnetohydrodynamic electrodes, 18: 7458 (PWA-2125)
properties as reactor fuel element cladding, 19: 25723(R) (GA-5036)
properties for aerospace applications, 19: 37143
properties for skull reclamation process crucibles, 20: 5594(R) (ANL-6925, pp 21-106)
properties of, dispersion velocity dependence on mechanical and thermal, 17: 27873
properties of extruded and vapor-deposited, 19: 24079(R) (GA-5487)
properties of, at 2000°C, for use in thermionic converters, 20: 29729
radiation and thermal effects on lattice expansion in, 17: 436
radiation damage, annealing, 16: 22333(R) (WCAP-1874)
radiation effects on lattice parameters, 16: 576(T) (AEC-tr-4697)
radiation effects on p-n junctions of, 16: 16524(R) (EURAEC-185)
radiation effects, 16: 19072(R) (EURAEC-246)
radiation effects on junctions, 16: 20751
radiation effects on curvature of, fission-fragment, 17: 23864(R) (BMI-1619(Del.))
radiation effects on diodes of, 17: 32404(R) (WCAP-2274)
radiation effects on, fission-fragment, 18: 2352
radiation effects on luminescence of, gamma and neutron, 18: 16122
radiation effects on mechanical properties of, 18: 16526 (NP-13663)
radiation effects on p-n junctions of, 18: 42082(T)
radiation effects on, 19: 6213(R) (EURAEC-1113)
radiation effects on performance in semiconductor detectors, 19: 11610
radiation effects on p-n junctions of, electron, fast neutron, and proton, 19: 16244
radiation effects on detectors of, neutron, 19: 34592(R) (EURAEC-1384)
radiation effects on, temperature dependence of, 19: 44759
radiation effects on crystals of, 16: 16524(R) (EURAEC-185)
radiation effects on crystals of, at 100 to 500°C, 16: 17816(R) (EURAEC-107)
radiation effects on Hall coefficients and resistivity of crystals of, 17: 8882(R) (EURAEC-306)
radiation effects on curvature of poly and single crystals of, fission-fragment, 17: 23864(R) (BMI-1619(Del.))
radiation effects on electric properties of n-type and p-type, 20: 2503
radiation effects on semiconducting properties, 20: 2504
radiation effects on coatings of, fast-neutron and fission fragment, 20: 9596
radiation effects on transistors of, neutron, 20: 12276 (NYO-3405-4)
radiation spectra of electron-excited crystals of, (E), 20: 42565(T)
radioinduced conductivity and n-p effect in, x, (E), 20: 15967
radioinduced stresses in, from fission fragment bombardment, 17: 27888 (BMI-1635)
radioinduced swelling of, fission fragment, 20: 11227
rare-gas bombardment of, mass-spectrometric analysis of particles from, 17: 38971
reactions with barium, potassium, and sodium chlorides, 20: 26816 (HW-72369)
reactions with cesium vapor at high temperatures, 19: 9628
reactions with fluorine, thermodynamics of, 20: 20650(R) (ANL-7055, pp 167-76)
reactions with uranium dioxide to 1925°C, 19: 22997 (TRG-Report-842)
reactions with uranium carbides, 20: 9555
sintering of, symposium on, 20: 37179
spectra of nitrogen impurities in crystals of, photoluminescence, 16: 33009
spectral emittance at 800 to 5000°F, 16: 18939
sputtering by argon ions at 2 kev, 19: 31456
sputtering by argon ions at 75 to 600 ev, yields from, (E), 20: 31914
sputtering by noble-gas ions at 10 to 600 ev, yields, 16: 19564
strength characteristics of cermets containing, 16: 2211(T) (DEG-Inf.-Ser.-176)
strength characteristics of heat resistant cermets containing, 17: 18680(T) (FTD-TT-62-1473(p.12-24))
strength, effects of heating method on durable, 16: 3507
surface friction of, symposium on, 20: 37179
testing core retainer plates, 16: 22531 (DC-60-1-51)
thermal capacity at 30 to 800°C, 17: 4523
thermal conductivities at 300 to 1000°C, 16: 19393
thermal expansion at temperatures up to 2000°C, 17: 12688
thermal properties of cermets containing, 17: 18681(T) (FTD-TT-62-1473 (p.25-30))
thermal stress properties of coatings, 19: 25723(R) (GA-5036)
thickness of coatings of, for use at 40 atm pressure, 19: 25723(R) (GA-5036)
use as coating and matrix for uranium carbide spheroids, 20: 31706(P)
use as intermediate layer for coating fuel particles, 19: 26888
use in neutron detectors at high temperatures, 17: 34300
use in refractory fuel material, 18: 34071(P)
use of uranium-235-coated, in neutron detectors, 17: 37420(R) (WCAP-2382)
uses in cold electron ion gage, 17: 14943(R) (NYO-9812)
wear characteristics, 16: 30518
x-ray intensities of one-dimensional disordered crystals of, 18: 6575(T) (AI-Trans-20)
B_4C–SiC, analysis by x-ray diffraction, 17: 1383 (KAPL-M-FHG-1)
B_4C–SiC, corrosion by water at 680°C, 18: 16427 (WAPD-244)
B_4C–SiC, fabrication, 18: 16427 (WAPD-244)
B_4C–SiC, phase equilibria in, 17: 21668 (KAPL-2216)
B_4C–SiC, radioinduced release of helium from, 16: 10623 (WAPD-255)
Cr_3C_2–SiC, oxidation tests at 1400 and 1500°C, 19: 9624 (SCNC-270)
Cr_3C_2–SiC–TiC, oxidation tests at 1400 and 1500°C, 19: 9624 (SCNC-270)
Cr_3C_2–SiC–ZrC, oxidation tests at 1400°C, 19: 9624 (SCNC-270)
C–SiC, coating on nuclear fuel particles, method for, 20: 25557(P)
C–SiC–UC_2, inter-diffusion in, electron beam analysis of, 18: 39058 (EUR-1643.e(p.275-300))
graphite–SiC, preparation, 16: 33374(R) (NP-12083)
graphite–SiC, production of high thermal resistance, 17: 32554
graphite–SiC, properties as magnetohydrodynamic electrodes, 18: 7458 (PWA-2125)
graphite–SiC, thermal conductivities of, at 300 to 1000°C, 16: 19393
graphite–SiC, thermal shock resistance, 16: 24176 (WADD-TR-60-749 (Pt.II))
$MoSi_2$–SiC, oxidation tests at 1400 and 1500°C, 19: 9624 (SCNC-270)
$MoSi_2$–SiC–TiC, oxidation tests at 1400 to 1650°C, 19: 9624 (SCNC-270)
$MoSi_2$–SiC–ZrC, oxidation tests at 1400 and 1500°C, 19: 9624 (SCNC-270)

NbC–SiC, oxidation tests at 1400 and 1500°C, 19: 9624 (SCNC-270)
NbC–SiC–TiC, oxidation tests at 1400 and 1500°C, 19: 9624 (SCNC-270)
NbC–SiC–ZrC, oxidation tests at 1400°C, 19: 9624 (SCNC-270)
SiC–SiO_2, emissivity of aluminum- and stainless steel-bonded at 300 to 1450°F, 16: 14358(R) (PWA-2043)
SiC–SiO_2, endurance of aluminum phosphate-bonded coating of, 17: 6675(R) (PWA-2128)
SiC–SiO_2, endurance tests of coatings of, 18: 5737(R) (PWA-2255)
SiC–SiO_2, total hemispherical emittance at high temperatures, 17: 6731
SiC–TaC, oxidation tests at 1400 to 1650°C, 19: 9624 (SCNC-270)
SiC–TaC–TiC, oxidation tests at 1400 and 1500°C, 19: 9624 (SCNC-270)
SiC–TaC–ZrC, oxidation tests at 1400°C, 19: 9624 (SCNC-270)
SiC–TiC, oxidation tests at 1400 and 1500°C, 19: 9624 (SCNC-270)
SiC–TiC–VC, oxidation tests at 1400 and 1500°C, 19: 9624 (SCNC-270)
SiC–TiC–ZrC, oxidation tests at 1400 and 1500°C, 19: 9624 (SCNC-270)
SiC–UC, development of dispersion, 18: 37606 (A/CONF.28/P/152)
SiC–UC, fabrication of fuel elements of, process for, 20: 5873(P)
SiC–UC, performance in gas-cooled reactors, 18: 21659
SiC–UO_2, fabrication of fuel particles of, 20: 21297(T) (NP-tr-1371)
SiC–VC, oxidation tests at 1400 and 1500°C, 19: 9624 (SCNC-270)
SiC–VC–ZrC, oxidation tests at 1400°C, 19: 9624 (SCNC-270)
SiC–ZrC, oxidation tests at 1400 and 1500°C, 19: 9624 (SCNC-270)
Si–SiC, corrosion of, by molten sodium, 16: 28646(R) (ORNL-2247 (Pts.1-5))
Si–SiC, performance of, as coating on Pebble Bed Reactor fuel, 16: 9663 (NYO-9064)

SILICON CHLORIDES
analysis for boron, 16: 30345
properties, 20: 29623(R) (TID-22970, pp 121-256)
radiation effects on aerosols of, x, 20: 4015
radioinduced electron spin resonance spectra in, 19: 9787
radiolysis of, in presence of vinyl monomers, 17: 18130
radiolysis of $SiCl_4$, radical production during gamma, 20: 45760
reactions of, with molybdenum in hydrogen, 17: 21681
reactions with uranium hexafluoride, 20: 36803
reactions with zirconium oxide films, 16: 9141(R) (NMI-2101)
silicon K-absorption spectrum in gaseous, (E), 20: 19389
BCl_3–H–$SiCl_4$, reaction with boron–molybdenum–silicon systems, 18: 34146

SILICON COMPOUNDS
analysis for impurities by radioactivation and ion-exchange chromatography, 19: 46228
diffusion of silicon in, method for determining, 20: 27537

SILICON COUPLES
Ag/Si, properties of, as semiconductor alpha-particle detector, 16: 7708
Al/Cr/Si/U, diffusion in, with chromium and silicon as diffusion barriers, 20: 23741
Al/SiO_2/Si, radiation effects on capacitors of, electron, 19: 26713
Al/Si/U/V, multiphase diffusion studies in, 19: 30731 (EUR-1819.e (p.37-48))
Au/Si, properties of, as semiconductor alpha-particle detector, 16: 27270(T) (FTD-TT-62-863)

SILICON FLUORIDES
see also Manganese Silicon Fluorides
chemical effects on plutonium in uranium(VI) fluoride mixtures, 18: 43706(R) (ANL-6800(p.197-296))
determination in anhydrons hydrofluoric acid, iodometric, 16: 17589 (PG-Report-292)
electron spin resonance studies of gamma-irradiated, at 4 and 77°K, 16: 5239
enthalpy of formation and lattice energies of, Madelung constants for, 20: 26352
heat of formation, determination by fluorine bomb calorimetry, 16: 7518 (ANL-6472)
heat of formation, 16: 12649(R) (ANL-6485)
heat of formation, 16: 20299(R) (ANL-6477(p.155-67))
heat of formation, 17: 8005 (TID-15554)
heat of formation, 17: 7655(R) (ANL-6600)
heat of formation of gaseous, 18: 27356 (CONF-74-27)
heat of formation, 19: 17177(R) (ANL-6965(p.42-83))
ionization of, by inelastically scattered electrons, 16: 32173 (NP-12052)
meson (K) capture in crystals of, cobalt-58 gamma emission for dealignment and ionic couplings in, 17: 26581
nuclear magnetic resonance spectra of, collision-narrowing theory of, 19: 38629
properties of, for use in gas-cooled reactors, 17: 25076(R) (ORNL-3417 (p.170-5))
radioinduced reactions with benzenes, 17: 29936
reactions with beryllium aluminum silicate, structural evidence, 16: 1782
reactions with fluorine and xenon, formation of xenon hexafluorosilicate by, 18: 17822
spectra of diatomic, in plasma jets, (E), 19: 41287
spectra of, silicon-29 isotope effects on nuclear magnetic resonance, 18: 3745
spectra, Raman, 17: 25236
stability of, radiation and thermal effects on, 17: 10516 (ORNL-TM-475)
thermodynamic properties, 16: 5780(R) (TID-14461)
thermodynamic properties of, from 15°K to triple point, 17: 6056 (WRU-202)
thermodynamic properties, 17: 25108
use as scavengers for radioactive particles, 16: 19184 (TID-15305)
vapor pressure of liquid, up to critical point, 18: 3722 (UCRL-7167)
vapor pressure up to critical point, 18: 41374 (UCRL-7167(Rev.I))
methane–SiF_4, radiolysis yields in, 19: 46324(R) (AGN-8132)

SILICON HALIDES
production process for, 20: 33315(P)

SILICON HYDRIDES
see also Silane
decomposition of, mercury-photosensitized, 18: 12142(R) (NYO-7988)
electron drift velocities in deuterated and normal, at low energy, 19: 46393
mass spectra of volatile, 17: 6791 (IS-424)
mass spectral studies, 16: 9282 (IS-386)
radioinduced free radicals of, in krypton, 20: 36909
radiolysis of monosilane, mechanism of electron, 19: 17956(R) (NYO-2007-8)
radiolysis of, addition to ethylene of fragments from, 19: 44066
reactions with olefins, telomerization, 18: 9796(T) (SC-T-64-41)
spectra of, calculation of bond energy and heat of formation from mass, 17: 14255
spectra of, kinetic energy of appearance potentials in mass, 17: 14254
spectra of normal and deuterated, infrared, 16: 27018
spectra of normal and deuterated, frequency shifts from gas to crystal, 16: 27019
stability of, radiation and thermal effects on, 17: 10516 (ORNL-TM-475)
synthesis of, procedure for, 20: 31218(R) (UCRL-16658, pp 1-9)
vibrational relaxation times in, effects of deuteron substitution on, 17: 12286
yields in gamma radiolysis of silane, 20: 20725(R) (NYO-3570-2)

SILICON IODIDES
reactions with hafnium and zirconium chlorides, 16: 30407

SILICON IONS
effects on formation of single-crystal beryllium oxide, 20: 36814
electron inelastic scattering cross section, (T), 19: 9902
energy levels and wave functions for, (T), 19: 16370 (UCRL-7943-T)
energy levels of, (T), 20: 11450 (UCRL-7842-T)
production in high-frequency source, 17: 23725
reactions with hydrogen atoms in interstellar space, cooling in, 18: 42272
Slater-Condon parameters of, determined from spectral data, 17: 31118
spectra in Scylla plasma, x-ray, 17: 13639
spectral line broadening in, Stark nonhydrogen, 18: 28877
spectral line intensities of lithium-like, 18: 17185
spectral locations and widths in plasma, 18: 21409(T)
sputtering ratio for polycrystalline copper, 16: 9114
temperature of stellarator, Doppler effect, 16: 7211

SILICON ISOTOPES
effects on microwave spectra and structure of ethynylsilane, 20: 3977
gamma reactions on, cross sections for, 19: 12496
neutron reactions (n,α) and (n,p), use for fast neutron spectroscopy, 17: 23766
neutron reactions, 18: 11195(R) (EANDC(E)-49(L))
nuclear energy levels and properties, survey, 16: 18483
proton decay, 18: 18876 (KFK-185)
separation and preparation of targets at ORNL calutron, 20: 19153
separation by isotopic exchange, 19: 18369
separation by thermal diffusion in monosilane, 17: 29238
separation of, process data on electromagnetic, 18: 2128(R) (ORNL-TM-658)
separation of stable, in calutrons, 18: 34005(R) (ORNL-TM-879)
separation of, preparation of silicon sulfides for electromagnetic, 20: 41400 (ORNL-3301(Suppl.1))

SILICON ISOTOPES Si-25
beta decay of, delayed proton emission in, 18: 40523
beta decay of, delayed proton spectra from, 20: 28269 (BNL-10196)
beta decay of, log ft values for superallowed transitions in, (E), 20: 24407
decay of, aluminum-25 levels from beta-delayed proton, (E), 20: 32505
decay of, delayed proton emission in, (E), 19: 14546
decay of, delayed proton emission in, (E), 19: 47613
decay of, log ft values for, (T), 19: 21379
decay scheme, 18: 6189
half life, (E), 20: 32505
production and properties of, (E), 19: 14546
proton-emission decay of, spectrum of, (E), 19: 21297

SILICON ISOTOPES Si-26
beta decay, 18: 32776

beta decay energies, 16: 7061
beta decay of, branching ratios and half life of, 18: 2911
beta decay of, branching ratios, energies, and half lives, 19: 47603
energy levels of, from helium-3 reactions (He-3,n) with magnesium-24, (E), 19: 45355
mass, (E), 19: 31320
neutron reactions (n,p) at 0 to 20 Mev, cross sections for, 20: 19810 (EUR-119.e(Vol.2))
preparation and decay, 17: 26633

SILICON ISOTOPES Si-27

beta decay of, model for relative period of, 17: 29632
energy levels, 16: 28091 (UCRL-6756)
energy levels, (E), 20: 38053
energy levels and gamma spectra, 16: 31088
energy levels from aluminum-27 (p,n) reactions at 30 and 50 Mev, (E), 20: 6361
gamma spectra, 20: 44634(R) (IDO-17188)
half life, (E), 19: 14595
proton reactions (p,n) at 6.0 to 7.5 Mev, absolute cross sections and angular distributions for, (E/T), 20: 17775

SILICON ISOTOPES Si-28

alpha elastic and inelastic scattering at 22.5 Mev, differential cross sections for, 17: 33101
alpha elastic scattering at 3 Mev, yield curves for, 17: 26433(R) (ORNL-3425(p.17-18))
alpha elastic scattering at 6 to 17 Mev, excitation functions and angular distributions of, 18: 1084
alpha elastic scattering at large angles, energy dependence of, 18: 42754
alpha elastic scattering at 28.5 Mev, optical potentials in, (E/T), 20: 4859
alpha fission of, cross sections for symmetric, 17: 5369
alpha inelastic scattering by, angular correlations in, 18: 16928 (ANL-6848(p.153-8))
alpha inelastic scattering at 28.5 Mev, excited core model of, (E/T), 19: 19175
alpha inelastic scattering at 28.4 Mev, collective enhancement of 3- state in, (T), 20: 22107
alpha reactions (α,p) with, 18: 18961
alpha reactions (α,p) at 18.35 Mev, differential cross sections for, 18: 24687
alpha reactions (α,γ) with, 18: 34924
alpha reactions (α,γ) at 1.6 to 3.2 Mev, angular correlations and distributions from (E), 19: 1677
alpha reactions ($\alpha,\alpha'\gamma$) at 22.5 Mev, angular correlations in (E/T), 19: 3305
alpha reactions (α,γ) with, distributions from, (E), 19: 14517 (CONF-640301(p.109-42))
alpha reactions (α,α') at 22.5 Mev, alpha-gamma angular correlations in, 19: 21457
alpha reactions (α,γ) at 3.2 to 4.3 Mev, energy levels from, (E), 20: 11994
alpha reactions (α,d) at 42 to 53 Mev, deuteron energy spectra from, (E), 20: 12061
alpha reactions (α,d) at 42 to 53 Mev, energy spectra from, (E), 20: 24358(R) (UCRL-16580, pp 1-93)
alpha reactions (α,p) at 19 Mev, distributions from, 17: 876
alpha reactions (α,p) at 14 Mev, proton angular distributions, 17: 11612 (AFOSR-2975)
alpha reactions (α,n), threshold of, 17: 11715
alpha reactions, (α,γ), resonance in, 17: 16916
alpha reactions (α,p) at 16–26 Mev, mechanisms in, 17: 38303
alpha scattering at 24.8 Mev, excitation of 6.27-Mev (3^+) level by, 18: 19076
alpha scattering at 6 to 19 Mev, analysis of, 18: 24712
alpha scattering at 28.5 Mev by, cross sections for elastic and inelastic, (E), 19: 23642
alpha scattering at 28.5 Mev, (E), 19: 31262
alpha scattering at 16.2 and 27 Mev, production of unnatural-parity state from, (E), 20: 26175
alpha scattering by, differential cross sections of fourth excited state, 17: 9589
bremsstrahlung reactions (γ,p) at 24 Mev, cross sections for, 17: 17155
bremsstrahlung reactions (γ,n) with, excitation of E1 states in, 18: 19086
bremsstrahlung reactions (γ,p) at 15 to 30 Mev, energy distribution of protons from, 18: 21325
bremsstrahlung reactions (γp) with, proton energy distribution in, (E), 19: 39938
bremsstrahlung reactions (γ,α) and (γ,p) at 16.2 to 23.2 Mev, cross sections for, (E), 19: 43289
bremsstrahlung reactions (γ,p) at 25.5 Mev, energy spectra from, (E), 19: 47699
decay of resonance levels in, branching ratios for, 18: 28656
decay scheme of, branching ratios for, 17: 34913
decay schemes of excited states, 16: 11000
description using Hartree-Fock approximation with density-dependent two-nucleon interaction, (T), 20: 44785
deuteron and proton inelastic scattering by, levels from, (T), 19: 14489 (ANL-6878(p.143-73))
deuteron elastic and inelastic scattering at 10.9–11.8 Mev, angular distributions for, 17: 34914
deuteron elastic scattering at 11.5 Mev, angular distribution, 16: 5869
deuteron inelastic scattering at 13.6 Mev, angular distributions, 16: 23140
deuteron inelastic scattering at 13.6 Mev, differential cross sections for, 17: 38259
deuteron radiative capture by, 17: 11634(R) (TID-17696)
deuteron reactions (d,p), measurement of Q_0 values for, 16: 11038
deuteron reactions (d,p) at 15 Mev, angular dependence of proton polarization in, 16: 21597
deuteron reactions (d,p) at 15 Mev, effects of spin-orbit distortion, 16: 26284
deuteron reactions (d,α) at 5.5 to 7.5 Mev, angular distributions and cross sections for, 16: 26309
deuteron reactions (d,α) at 5.5 to 7.5 Mev, analysis, 16: 31081
deuteron reactions (d,p) of, polarization of protons from, 16: 32176(R) (PR-P-53)
deuteron reactions (d,p) at 15 Mev, proton polarization in, 17: 837
deuteron reactions (d,p) at 13.8 Mev, proton polarization from, 17: 7286
deuteron reactions (d,p) with strong absorption, 17: 21055
deuteron reactions (d,p) at 13.6 Mev, angular distributions from, 17: 24414
deuteron reactions (d,p) at 15 Mev, distorted-wave predictions for proton polarization from, 17: 26429(R) (ORNL-3425(p.5-8))
deuteron reactions (d,n) and (d,p) with, energy level reduced widths in sharp resonance region of, 17: 31535
deuteron reactions (d,p) with, cross sections and energy levels of, 17: 33066
deuteron reactions (d,p), proton polarization from, 17: 36716
deuteron reactions (d,p) at 7.5 Mev, silicon-29 energy level parameters from, 17: 38240
deuteron reactions (d,p) at 15 Mev, effect of optical parameter variations on angular distributions and polarizations in, 17: 38251
deuteron reactions (d,p) with, polarization in s-wave capture, 17: 38254
deuteron reactions (d,p) with, gamma angular correlations in direct, 17: 38258
deuteron reactions (d,p) with, compound nucleus formation effects in, 17: 38222
deuteron reactions (d,n) with, angular distribution for, 17: 41873 (WASH-1044)
deuteron reactions (d,p) with, distorted-wave calculations of angular distributions from, 17: 26588
deuteron reactions (d,p) at 10 Mev, polarization and stripping in, 18: 4619
deuteron reactions (d,p) with, stripping model for, 18: 6162 (NP-13348)
deuteron reactions (d,p) at 10 Mev, polarization in, 18: 9393
deuteron reactions (d,p) on, distributions from polarized, 18: 10703
deuteron reactions (d,n) at 3 and 4.4 Mev, emission spectra of, 18: 12453 (CONF-340-15)
deuteron reactions (d,p) at 15 Mev, polarization angular distributions from, 18: 13104
deuteron reactions (d,p) with, distributions from polarized, 18: 16617
deuteron reactions (d,n) with, angular distributions and cross sections for, 18: 24611 (NP-13930(p.132-3))
deuteron reactions (d,p) at 22 Mev, angular distribution asymmetries in, 18: 30341 (CEA-R-2366)
deuteron reactions (d,p) at 2 to 3 Mev, mechanisms for, 18: 32841
deuteron reactions (d,p) at 21 Mev, proton polarization from, (E), 19: 6636 (NASA-TR-R-218)
deuteron reactions (d,p) with, Born approximation for, (E/T), 19: 8399 (NP-14543)
deuteron reactions (d,p) with, spins of states from, (E), 19: 14495 (ANL-6878(p.279-301))
deuteron reactions (d,n), at 7.0 Mev, (E), 19: 14765(R) (ANL-6977)
deuteron reactions (d,p) with, target core excitation in, (T), 19: 21433
deuteron reactions (d,p) at 10 Mev, cross sections for, 19: 33302
deuteron reactions (d,p) with, silicon-29 level widths from, (E), 19: 35457
deuteron reactions (d,p) at 2 to 3 Mev, angular distributions and total cross sections for, (E), 19: 43398
deuteron reactions (d,n) at 4 and 5 Mev, angular distributions for, (E/T), 19: 43278 (NP-15358)
deuteron reactions (d,p) at 1.7 to 3.7 Mev, cross sections for, (E), 20: 1244
deuteron reactions (d,α) at 11.45 to 12.10 Mev, (E), 20: 6369

deuteron reactions (d,α) at 5.5 to 6.7 Mev, (E), 20: 8154
deuteron reactions (d,n) at 7.0 to 10.0 Mev, (E), 20: 19805(R) (ANL-7110, pp 1-28)
deuteron reactions (d,p), silicon-29 levels from, (E), 20: 19846
deuteron reactions (d,p) with, gamma angular correlations from, (E), 20: 30360 (WASH-1068)
deuteron reactions (d,p) at 11 and 13 Mev, angular-momentum effects on angular distribution from, (E), 20: 32512
deuteron reactions (d,pγ) at 4 to 6 Mev, angular correlations of, (E/T), 20: 38086
deuteron reactions (d,p) with, differential cross section for, (T), 20: 42387
deuteron reactions (d,α) at 6.98 to 9.86 Mev, isospin selection rule in, (E), 20: 44841
deuteron reactions (d,α), 20: 46580(R) (BMwF-FBK-66-05)
deuteron scattering by, angular distributions from, 18: 17021
deuteron scattering at 12.8 Mev, angular distributions for, 18: 36599
deuteron scattering at 22 Mev, angular distribution of polarized, (E), 19: 33303
electron inelastic scattering at 40 to 70 Mev, M1 transitions following, 18: 24675
electron inelastic scattering at 55 Mev, cross sections for, 18: 32781
electron inelastic scattering by, excitation of giant resonance levels in, (T), 19: 6673
electron inelastic scattering by, effects of surface oscillations on form factors for, (T), 19: 6716
electron inelastic scattering at 153 and 223 Mev/c, giant-dipole-resonance excitation in, (E), 19: 31224 (LAL-1133)
electron scattering shape parameters, 16: 11007
electron scattering by, 19: 46643(R) (LAL-1136)
energy level lifetimes, from resonance scattering of bremsstrahlung, 16: 26275
energy level lifetimes, (E), 20: 17651(R) (AD-612192)
energy level octupole transitions in, from proton reactions (p,γ) with aluminum-27 at 1.119 Mev, 19: 33310
energy level parities and spins, 18: 18908
energy level spacings, 16: 6018
energy level transitions in, internal-pair formation coefficient for 12.33-Mev, (E), 20: 13843
energy levels, 17: 7262
energy levels, 17: 19253
energy levels, 17: 40098
energy levels, 17: 41964
energy levels, 18: 26661
energy levels, 18: 34822
energy levels, 19: 3268
energy levels, 19: 3266
energy levels, (E), 19: 41828
energy levels, 18: 24625 (WASH-1046)
energy levels and nuclear structure of, collective model for, 17: 36400 (NP-13020(p.96-100))
energy levels and gamma spectra of, (E), 19: 14516 (CONF-640301 (p.80-108))
energy levels at 12 to 13 Mev, 17: 5321 (BRL-Memo-1392)
energy levels from proton reactions in aluminum-27, 16: 8199
energy levels from oxygen-16 reactions (O-16,α) with oxygen-16, (E), 20: 28304
energy levels from proton scattering by aluminum-27 at 3.5 to 11.3 Mev, width of, (E), 20: 30415
energy levels from magnesium-25 (α,nγ) reactions, branching ratios and lifetimes of, (E), 20: 34678
energy levels in, model of proton-hole coupling to, (T), 20: 12052
energy levels near 15 Mev, (E), 20: 9959(R) (AEET-214)
energy levels of, excitation energies, parities, and spins of, 18: 9389
energy levels of, parity and spin for, 17: 28324
energy levels of, parity and spin for 12.54-Mev resonance, 17: 28328
energy levels of, properties of 6.88-Mev doublet, 17: 29603
energy levels of, parity and spin of resonance, 17: 33045
energy levels of, spins and parities of excited, 17: 10240(R) (NP-12208)
energy levels of, spin assignments for, 17: 33012
energy levels of, width of 2^+ 1.77 Mev, 17: 40033
energy levels of, structure of giant dipole resonance for ground and first-excited, 18: 19050
energy levels of, shell model calculations for, 18: 32782
energy levels of, shell model calculations for, 18: 32783
energy levels of, anomalous ordering of, 18: 36651
energy levels of, gamma correlations in de-excitation of, 18: 42644 (NP-14329)
energy levels of, resonance parameters for, 18: 42698
energy levels of, statistical tensor analysis of odd-parity, (E/T), 19: 10275
energy levels of, lifetime of 6.880-Mev, 19: 23363(R) (NP-14954)
energy levels of, from proton reactions (p,γ) with aluminum-27, 19: 23804
energy levels of, 0^+, (T), 19: 25548
energy levels of, lifetime of 6.88 Mev, (E), 19: 35479
energy levels of, decay of 7.80-Mev, (E), 19: 35501
energy levels of, parity and spin of excited, 19: 35421
energy levels of, parity and spin of, (E/T), 19: 37589(R) (TID-22012, pp 53-66)
energy levels of, random phase approximation for excited, 19: 47652
energy levels of, parity and spin of, (E), 20: 5928(R) (PR-P-66)
energy levels of, alpha-particle models for, 20: 26159
energy levels of, electromagnetic properties of giant dipole resonances in s-d, 20: 26165
energy levels of, Hartree-Fock calculations for, 20: 34564
energy-level positions and transitions in, calculations using particle-hole model, (T), 20: 42199
energy-level transitions from electron inelastic scattering at 30 to 56 Mev, (E), 20: 46796
excitation of giant dipole resonance in, (T), 19: 14520 (CONF-640301 (p.182-218))
gamma reaction, cross section fluctuations in, 18: 11195(R) (EANDC(E)-49(L))
gamma reactions (γ,p) up to 21 Mev, cross sections for, 18: 34901
gamma reactions (γ,α) and (γ,p) at 17.5 to 22.3 Mev, 18: 40569
gamma reactions (γ,α) and (γ,p) at 13 to 20 Mev, 18: 42723
gamma reactions (γ,p) with, cross sections, (E/T), 19: 14528 (LAL-1120)
gamma reactions (γ,α) with, spectra for, (E), 19: 16879
gamma reactions (γ,α) and (γ,p) in surface barrier detectors, pulse height defect for, 19: 30561
gamma reactions (γ,p) at 17.64 Mev, cross section for, (E), 19: 35378(R) (EANDC(E)-57(U))
gamma reactions (γ,α) at 17.64 Mev, cross section for, (E), 19: 35378(R) (EANDC(E)-57(U))
gamma reactions (γ,α) and (γ,p) at 17.4 to 22.3 Mev, cross sections for, (E), 19: 45310
gamma reactions (γ,p) with, cross sections and spectra for, (E), 20: 46782
gamma reactions (γ,n), thresholds, 16: 4870
gamma reactions (γ,n) and (γ,p) at 10 to 27 Mev, cross sections, 16: 23057
gamma reactions (γ,p) at 17.6 Mev, cross section fluctuations in, 17: 15301
gamma reactions (γ,n) with, cross sections for, 17: 40091
gamma reactions (γ,n) with, cross section for, 18: 2856
gamma resonance scattering by, level lifetimes from, (E), 20: 28334
gamma transitions in, (E), 19: 19112
helium-3 reactions (He-3,n) with, Q-value for, (E), 19: 31320
helium-3 reactions (He-3,n) at 5.5 Mev, sulfur-30 levels from, (E), 19: 45355
helium-3 reactions (He-3,d) at 24.4 Mev, momentum spectra from, (E), 20: 13345(R) (NP-15772)
helium-3 reactions (He-3,p) at 12 Mev, Q value for, 20: 16331 (GA-6568)
helium-3 reactions (He-3,t) at 37.8 to 40.1 Mev, phosphorus-28 levels and mass from, (E), 20: 32473
meson (μ^-) capture by protons in, rate of, 20: 38166
neutron elastic and inelastic scattering at 14.1 Mev, 18: 26600
neutron elastic and inelastic scattering at 2.45 to 5.80 Mev, cross sections for, (E), 20: 15811
neutron elastic scattering cross sections for, optical model calculations of, 18: 32726 (AERE-R-4649)
neutron inelastic scattering at 14.2 Mev, core excitation model for, (E/T), 19: 37854
neutron inelastic scattering at 14 Mev, (E), 19: 43373
neutron inelastic scattering at 3 to 4.5 Mev, angular distributions and energy levels from, (E/T), 19: 47638
neutron inelastic scattering at 2.8 Mev, gamma spectra from, (E), 20: 8085 (USNRDL-TR-916)
neutron inelastic scattering at 7.5 Mev, gamma spectra from, (E), 20: 46588 (LA-DC-7853)
neutron inelastic scattering at 4.0, 6.0, and 7.5 Mev, gamma angular distribution from, (E), 20: 46588 (LA-DC-7853)
neutron inelastic scattering at 7.5 Mev, differential cross sections for, (E), 20: 46588 (LA-DC-7853)
neutron reactions (n,α) at 14.6 Mev, 16: 17076
neutron reactions (n,α) at 13.5 to 14.7 Mev, cross-section oscillations in, 16: 21413
neutron reactions (n,α) at 14 Mev, 16: 23130
neutron reactions (n,α) at 14.6 Mev, alpha spectra from, 16: 24846
neutron reactions (n,α) at 6.8 to 18 Mev, spectra from, 16: 25589
neutron reactions (n,p) and (n,α) at high energies, spectra from, 16: 26306
neutron reactions (n,α) and (n,d) at 14 Mev, spectra from, 16: 26297
neutron reactions (n,α) at 12.5 to 18.5 Mev cross sections, 16: 31081
neutron reactions (n,np) and (n,pγ) at 14 Mev, cross sections for,

17: 2242 (TID-16949)
neutron reactions (n,p) at 14.8 Mev, cross sections and product half lives for, 17: 2242 (TID-16949)
neutron reactions (n,α) at 12.15 to 18.4 Mev, Ericson fluctuations in, 17: 9556
neutron reactions (n,α) and (n,p) at 14 Mev, spectra from, 17: 9567
neutron reactions (n,p), proton angular distribution from, 17: 9566
neutron reactions (n,α) at 13.4 and 13.8 Mev, energy spectrum, 17: 17145
neutron reactions (n,α) and (n,p) on, excitation functions, 17: 19295
neutron reactions (n,p) at 14 Mev, distorted-wave Born approximation with exchange interaction, 17: 24497
neutron reactions (n,α) with, intensity fluctuations in excitation functions for, 17: 28295
neutron reactions (n,α) and (n,p) at 6 to 9 Mev, fluctuations in cross sections for, 17: 29613
neutron reactions at 4.6 to 8.5 Mev, 17: 34884 (TID-19047)
neutron reactions (n,p) at 14 Mev, 17: 36410 (NP-13020(p.169-73))
neutron reactions (n,α) and (n,p) at 1.0–5.5 Mev, cross sections and energy spectra for, 17: 38302
neutron reactions (n,α) at 12.15–18.4 Mev, cross section fluctuations in, 17: 38221
neutron reactions (n,p) at 12.5 to 21.0 Mev with, cross sections for, 17: 40049
neutron reactions (n,α) with, alpha spectra from, 18: 6161 (NP-13346)
neutron reactions (n,α) with, spectra from, 18: 6163 (NP-13349)
neutron reactions (n,p) at 14 Mev, angular distribution calculations using distorted-wave Born approximation, 18: 7750
neutron reactions (n,p) at 14 Mev, analysis of direct, 18: 9358
neutron reactions at 12.5 to 21 Mev, cross sections for, 18: 16970
neutron reactions (n,α) at 14 Mev, nuclear shell effects in cross sections for, 18: 18977
neutron reactions (n,p) at 14.1 Mev, exchange effects and finite range in, 18: 18998
neutron reactions (n,xγ) at 14.8 Mev, cross section and gamma spectrum for, 18: 30736(R) (TID-20658)
neutron reactions (n,n' γ) at 3.0 to 4.35 Mev, angular distributions from, 18: 30736(R) (TID-20658)
neutron reactions (n,α) at 14.55 Mev, cross sections for, 18: 38069 (NP-14111)
neutron reactions (n,p) with, angular distributions from, (E), 19: 11526
neutron reactions (n,α) and (n,p) at 5.2 to 9.0 Mev, cross sections for, (E), 19: 12511
neutron reactions (n,α) with, spectra for, (E), 19: 16879
neutron reactions (n,α) at 14.8 Mev, angular distributions from, (E), 19: 21318
neutron reactions (n,p), thermal, 19: 22801
neutron reactions (n,α), (n,d), and (n,p) at 14 Mev, (E), 19: 23782
neutron reactions (n,p) at 14.8 Mev, cross sections for, (E), 19: 27516
neutron reactions (n,p), cross sections for, 19: 29228(R) (AEET/NP/10)
neutron reactions ($n,p_{0,1}$) at 5.2 to 7.2 Mev, cross sections for, (E), 19: 35378(R) (EANDC(E)-57(U))
neutron reactions (n,α_0) at 5.2 to 7.2 Mev, cross sections for, (E), 19: 35378(R) (EANDC(E)-57(U))
neutron reactions (n,α) and (n,p) at 13.5 to 14.4 Mev, cross section for, (E), 20: 1163
neutron reactions (n,α) at 14.8 Mev, direct interaction models for, (T), 20: 12002
neutron reactions (n,p) at 14.8 Mev, cross sections for, (E), 20: 12133
neutron reactions (n,α) at 14.8 Mev, angular distributions from, (E/T), 20: 12030
neutron reactions (n,α) and (n,p) at 13.95 Mev, recoil ionization defects from, (E), 20: 13989
neutron reactions (n,2n) at 12 to 18 Mev, cross sections for, (E), 20: 15863
neutron reactions (n,p) with, sensitivity of, for activation analysis, 20: 16332 (GA-6691)
neutron reactions (n,p) at 9.1 to 21 Mev, angular distributions from, (E/T), 20: 19813 (IKF-14)
neutron reactions (n,γ), silicon-29 levels from, (E), 20: 19846
neutron reactions with, use for fast neutron spectroscopy, 20: 27290
neutron reactions (n,p) at 14.8 Mev, cross sections for, (E), 20: 30394
neutron reactions (n,α) and (n,p) at 13.95 and 14.6 Mev, angular and energy distributions from, (E), 20: 32431
neutron reactions (n,n'γ) near 4 Mev, gamma production cross sections for, (E/T), 20: 34515 (CONF-660303-34)
neutron reactions (n,α) at 12 to 23 Mev, (E), 20: 38036
neutron reactions (n,α) with, DWBA analysis of, (T), 20: 42391
neutron reactions, Q values for, 19: 44450(R) (IBK-120a)
neutron scattering at 200 to 700 kev, differential cross sections and polarization in, 16: 23117
neutron scattering at 14 Mev, differential cross sections for (E/T), 19: 3298
neutron scattering at 14 Mev by, cross sections for, (E/T), 19: 21441
neutron threshold reactions with, cross sections for, 17: 36653 (EUR-119.e)
nuclear excitation by 180° electron scattering, 17: 5388
nuclear properties in shell model, 20: 15730 (RHEL/R-112, pp 67-98)
nuclear resonance fluorescence in, 18: 42779
nuclear surface oscillations in, calculation of, 17: 40019
nucleon binding energies and single-particle levels for, (T), 19: 43340
nucleon charge-independent pairing in nondegenerate $2s_{1/2}$ and $1d_{5/2}$ shells of, 20: 24453
nucleon inelastic scattering, core excitation model for, (E/T), 19: 37854
nucleon spatial correlations in, 19: 19152
photon reactions (γ,α) and (γ,p) at 17.62 Mev, fluctuations in, (E/T), 19: 8433
photon reactions at 16 to 60 Mev, cross sections for, (E), 20: 42523(R) (IS-1500(Sect.P))
production in alpha reactions (α,t) with aluminum-27 at 28.6 Mev, level population in, (E), 20: 19876
properties of, Hartree-Fock calculations of, (T), 20: 24323 (AD-624314)
proton elastic scattering at 40 Mev, cross sections for, (E/T), 20: 30353(R) (ORNL-3940, pp 1-61)
proton inelastic scattering at low energies, reaction mechanisms for, 16: 21393
proton inelastic scattering by, angular correlations for, 18: 7780
proton inelastic scattering by, excited states from, 18: 17042
proton inelastic scattering at 17.5 Mev, (E), 20: 1192
proton inelastic scattering at 155 Mev, cross sections and energy levels from, (E), 20: 6354
proton inelastic scattering at 40 Mev, polarization asymmetry in, (E), 20: 24440
proton inelastic scattering at 3.09 Mev, recoil-nuclei slowing down from, (E), 20: 28334
proton inelastic scattering at 40 Mev, cross sections for, (E/T), 20: 30353(R) (ORNL-3940, pp 1-61)
proton inelastic scattering, energy levels from, (T), 19: 14489 (ANL-6878(p.143-73))
proton reactions (p,2p) at 185 Mev, 18: 26567
proton reactions (p,γ) at 1.3 to 3.2 Mev, 18: 26593
proton reactions (p,γ) at 4.0 to 12.5 Mev, angular distributions and resonances in, (E), 19: 19095 (WASH-1053)
proton reactions (p,2p) at 460 Mev, (E/T), 20: 11948 (AD-624318)
proton reactions (p,2p) at 140 Mev, energy spectra and angular correlation distributions from, (E), 20: 17741
proton reactions (p,γ) at 0.3 to 2.1 Mev, resonance strengths for, (E), 20: 42182
proton reactions (p,γ) with, phosphorus-29 energy levels from, (E), 20: 44790
proton reactions (p,n) with, phosphorus-28 mass from threshold energy for, (E), 20: 44812
proton reactions at 150 Mev, gamma spectra from, 16: 31088
proton reactions at 150, 340, and 660 Mev, cascade theory for, (T), 19: 41811(T)
proton reactions (p,p'), phosphorus-29* levels from, 16: 24795 (TID-15331)
proton reactions (p,γ), at 500 to 1900 kev resonances for, 16: 32432
proton reactions (p,p'γ) with, energy levels from, 17: 40033
proton scattering at 367 kev, energy level reduced widths in sharp resonance region of, 17: 31535
proton scattering at 29 Mev, 18: 14590(R) (NIRL/R/60)
proton scattering at high-energies, spin-flip, 18: 38125
proton scattering at 30 and 50 Mev, polarization angular distributions from, (E), 19: 28962(R) (NIRL/R/81)
proton scattering at 30.3 Mev, differential cross sections for, (E), 20: 6339
reactions in stars, statistical equilibrium for, 20: 21492
receiver materials testing for beam accelerated, 18: 27812(R) (ORNL-TM-415)
spectra, isotope shifts in atomic, 16: 27784
spectral shift relative to silicon-30, 16: 12476
triton reactions (t,p) at 10 Mev, angular distributions from, 18: 19021
triton reactions (t,p) with, properties of, (T), 20: 11972 (NP-15716)

SILICON ISOTOPES Si-29

alpha reactions (α,n) at 3.7 to 5 Mev, cross section fluctuations, 16: 24845
deuteron reaction (d,α) at 5.5 to 5.8 Mev, mechanism of, (E), 20: 8142
deuteron reactions (d,p), spins and parities of certain states, 16: 4837
deuteron reactions (d,p), proton distributions from, 16: 12544
deuteron reactions (d,p) on, energy levels from, 17: 19370
deuteron reactions (d,p) at 13.6 Mev, angular distributions from, 17: 24414
deuteron reactions (d,p)Si^{29} with, angular distributions of, 17: 36685
deuteron reactions (d,p) with, stripping model for, 18: 6162 (NP-13348)
deuteron reactions (d,p) with, proton polarization from, 18: 16994
electron anisotropic hyperfine interactions with, shallow donor, 20: 6001

energy level density parameters from sulfur-32 (n,α) reactions, (E/T), 20: 10010
energy level lifetimes, from resonance scattering of bremsstrahlung, 16: 26275
energy level resonances in, 16: 23117
energy level spacings, 16: 6018
energy level transitions from silicon-28 (d,p) reactions, angular correlations for, (E), 20: 30360 (WASH-1068)
energy levels, 18: 44788
energy levels at 1.28 and 2.05 Mev, (E/T), 20: 38086
energy levels from deuteron beam reactions with light nuclei, 16: 11040
energy levels from deuteron reactions (d,p) on silicon-28 at 2 to 3 Mev, 19: 43398
energy levels of, angular momentum, reduced widths, and spin assignments for, 17: 38240
energy levels of, shell model calculations for, 18: 32782
energy levels of, shell model calculations for, 18: 32783
energy levels of, models for collective, (T), 19: 14518 (CONF-640301 (p.143-64))
energy levels of, E1 transition widths of, (E), 19: 23703
energy levels of, spin of, (E/T), 19: 23754
energy levels of, width of 6.379-Mev in, (E), 19: 35457
energy levels of, g-factor and lifetime of, (E), 20: 19846
gamma reactions (γ,N$\pi^{\pm}$) with, polarization of nucleons from, 18: 19009
gamma reactions (γ,n), thresholds, 16: 4870
gamma reactions (γ,p) at 10 to 27 Mev, cross sections, 16: 23057
gamma reactions (γ,π^-), cross sections for, 17: 6975
gamma reactions (γ,π^-) with, nuclear polarization in, 18: 6208
helium-3 reactions (He-3,d), Q value for, 20: 16331 (GA-6568)
lifetime of first excited state of, 18: 15319
magnetic moments and M1 transition probabilities in $2s_{1/2}$ $1d_{1/2}$ shell, (T), 19: 47641
magnetic resonance in silicon crystals, theory of double, 17: 33929
neutron compound inelastic scattering at 3 Mev, angular correlation functions for, 18: 9402
neutron cross sections of, 17: 40046
neutron reactions (n,α) at 14 Mev, 16: 8184
neutron reactions (n,α) at 14 Mev, 16: 23130
neutron reactions (n,α) at 14 Mev, spectra from, 16: 26297
neutron reactions (n,p) and (n,α) at high energies, spectra from, 16: 26306
neutron reactions (n,2p) at 14.8 Mev, cross section limit, product half life, and Q values for, 17: 2242 (TID-16949)
neutron reactions (n,p) at 14.8 Mev, separation energies for, 17: 2242 (TID-16949)
neutron reactions (n,αγ), (n,αn), (n,2n) (n,pγ), and (n,pn) at 14.8 Mev, cross sections for, 17: 2242 (TID-16949)
neutron reactions (n,α), energy levels of magnesium-26 from, 17: 15275
neutron reactions (n,α) at 13.4 and 13.8 Mev, energy spectrum, 17: 17145
neutron reactions (n,α) and (n,p) on, excitation functions, 17: 19295
neutron reactions (n,α), cross section of, 17: 23766
neutron reactions (n,α) at 6 to 9 Mev, fluctuations in cross sections for, 17: 29613
neutron reactions (d,p) with, cross sections and energy levels of, 17: 33066
neutron reactions at 4.6 to 8.5 Mev, 17: 34884 (TID-19047)
neutron reactions (n,2p) at 14.7 Mev, cross-section limits for, 17: 36707
neutron reactions (n,α) at 1.0–5.5 Mev, cross sections and energy spectra for, 17: 38302
neutron reactions (n,α) at 2.2 to 3.8 Mev, cross section for, 17: 38061 (AE-115)
neutron reactions (n,2p) at 14.8 Mev, cross-section limits for, 18: 1077
neutron reactions (n,α) with, alpha spectra from, 18: 6161 (NP-13346)
neutron reactions (n,α) with, spectra from, 18: 6163 (NP-13349)
neutron reactions (n,α) at 2.2 to 3.8 Mev, cross sections for, 18: 7731
neutron reactions (n,α) with, nuclear properties from, 18: 16995
neutron reactions (n,α) at 14 Mev, nuclear shell effects in cross sections for, 18: 18977
neutron reactions (n,α) at 5.2 to 9.0 Mev, cross sections for, (E), 19: 12511
neutron reactions (n,α) at 13 to 15 Mev, mechanisms for, (E), 19: 14537 (PAN-540/I)
neutron reactions (n,α) at 14.37 to 14.57 Mev, (E), 19: 14559
neutron reactions (n,α) at 13.6 to 15.6 Mev, excitation function for, 19: 45290 (ZFK-PHA-12, pp 110-12)
neutron reactions (n,α) at 13.4 to 15.0 Mev, excitation function for, (E), 20: 15800
neutron reactions (n,α) at 12 to 23 Mev, (E), 20: 38036
neutron reactions, Q values for, 19: 44450(R) (IBK-120a)
neutron total cross sections at 3–5 Mev, fast, 17: 28287
nuclear magnetic resonance in silicon, effects of nonmetal–metal transitions on, 18: 44827
nuclear magnetic resonance, 19: 14162
nuclear polarization in, dynamic methods for, 17: 13592
performance in nuclear gyroscopes, (T), 19: 20279 (RTD-TDR-63-4001)
preparation as radiation target material, 18: 27811(R) (ORNL-TM-198)
preparation as radiation target material, methods development for, 18: 27815(R) (ORNL-TM-718)
production in alpha reactions (α,d) with aluminum-27 at 28.6 Mev, level population in, (E), 20: 19876
production in aluminum-27 (d,α) and (d,p) compound-nucleus reactions at 1.4 to 2.3 Mev, 18: 36641
proton elastic scattering at 1200 to 2200 kev, 19: 3265
proton reactions (p,γ) at 1.4 Mev, gamma transitions in, 18: 17059
proton reactions (p,γ) at 1.420 to 2.160 Mev, levels from, (E), 19: 27552
proton reactions (p,γ) with phosphorus-30 energy levels from, (E), 20: 38062
proton reactions (p,γ) at 0.3 to 2.1 Mev, resonance strengths for, (E), 20: 42182
proton reactions (p,γ) at 1330 kev, 16: 7134
proton reactions (p,γ) below 1 Mev, parity and spin, 16: 12513
proton reactions (p,γ) at 1.3 to 1.5 Mev, resonances at 1375 and 1500 kev, 16: 17145
proton reactions (p,d), polarization effects in, 17: 2238 (NIRL/R/16 (p.51-2))
proton reactions (p,γ), study of 1308-kev resonance in, 17: 26496
proton reactions (p,γ) with, angular distributions for, 17: 31397 (CONF-46-29)
reactions of, calculation of angular distributions in stripping, 17: 13498
separation by distillation of methylsilane, 17: 22073
separation from monosilane by thermal diffusion, 17: 41324
spectra of isotopic shifts with fluorine, nuclear magnetic resonance, 18: 3745
spin-orbit interactions, 18: 18942
triton reactions (t,p) at 10 Mev, angular distributions from, 18: 19021
triton reactions (t,n), analysis by direct knock-out reaction model, (T), 20: 8162
triton reactions (t,p) at 10 Mev, DWBA analysis of angular distributions for, (E/T), 20: 28326

SILICON ISOTOPES Si-30

alpha reactions (α,γ) at 2.1 to 3.3 Mev, resonances in, 18: 19055
alpha reactions (α,γ) at 1.6 to 3.2 Mev, angular correlations and distributions from (E), 19: 1677
alpha reactions (α,γ) with, distributions from, (E), 19: 14517 (CONF-640301(p.109-42))
alpha reactions (α,γ) at 3.25 to 4.25 Mev, resonance energy levels in, (E), 19: 43315
alpha reactions (α,γ) at 3.2 to 4.3 Mev, energy levels from, (E), 20: 11994
bremsstrahlung reactions (γ,2p) at 51.4 Mev, magnesium-28 yields from, (E), 20: 12094
deuteron reactions (d,p), cross sections, 16: 12553
deuteron reactions (d,p) at 6.6 Mev, angular distributions from, 18: 2974
deuteron reactions (d,p) with, stripping model for, 18: 6162 (NP-13348)
deuteron reactions (d,γ) with, 18: 7697(R) (TID-19931)
deuteron reactions (d,p) at 2 to 3 Mev, mechanisms for, 18: 32841
deuteron reactions (d,n) with, (E), 19: 21376
deuteron reactions (d,γ) at 5.3 to 14.1 Mev, cross sections for, 19: 25476(R) (TID-21525)
deuteron reactions (d,p) at 2 to 3 Mev, angular distributions and total cross sections for, (E), 19: 43398
deuteron reactions (d,n) at 4 and 5 Mev, phosphorus-31 isobaric analog and negative parity states from, (E), 20: 10049
deuteron reactions (d,γ), cross sections for phosphorus-32 production by, 20: 16508(R) (NYO-2771-13)
deuteron reactions (d,α) at 6.5 and 6.7 Mev, angular distributions from, (E), 20: 19971
deuteron reactions (d,p) at 1.5 to 2.5 Mev, excitation functions and cross sections for, 20: 26121
deuteron reactions (d,p) at 10 Mev, differential cross section for, 20: 40065(R) (BMwF-FB-K-66-01)
deuteron reactions (d,p), 20: 46580(R) (BMwF-FBK-66-05)
electromagnetic transition probabilities from weak-coupling unified model for, 17: 11661
energy level spin, 3.77-Mev, 18: 22894
energy levels, 16: 31108
energy levels, 17: 7104 (NP-12330(p.119-21))
energy levels, 17: 19370
energy levels, 18: 19021
energy levels, (E), 19: 16900
energy levels at 8.149 and 8.571 Mev, 16: 12544
energy levels excited by (α,p) reactions on aluminum-27, 16: 21417
energy levels from deuteron beam reactions with light nuclei, 16: 11040
energy levels from alpha reactions (α,p) with aluminum-27 at 1.0 to 3.3 Mev, resonance, (E), 19: 47672
energy levels of, spin assignments for, 17: 33012

energy levels of, shell model calculations for, 18: 32782
energy levels of, shell model calculations for, 18: 32783
energy levels of, shell model calculations of, (E/T), 19: 14512 (CONF-640301(p.1-12))
gamma reactions (γ,n) thresholds, 16: 4870
gamma reactions (γ,p) at 10 to 27 Mev, cross sections, 16: 23057
gamma transitions in, low-level, 18: 22894
helium-3 reactions (He-3,d), 20: 46580(R) (BMwF-FBK-66-05)
mass, (E), 19: 31320
neutron capture cross section at 14.7 Mev, (E), 20: 46614
neutron reactions (n,p) at 14 Mev, cross section for, 18: 4607
neutron reactions (n,α) at 14.8 Mev, cross sections for, (E), 19: 27516
neutron reactions, Q values for, 19: 44450(R) (IBK-120a)
nuclear surface oscillations in, calculation of, 17: 40019
nucleon charge-independent pairing in nondegenerate $2s_{1/2}$ and $1d_{5/2}$ shells of, 20: 24453
proton differential elastic scattering cross section at 1 to 2 Mev, (E), 20: 38105
proton elastic scattering at 1 to 3.65 Mev, 17: 9604
proton reactions (p,γ) at 1.00 to 1.53 Mev, angular correlations for, 18: 17080
proton reactions (p,γ) at 3.0 to 3.6 Mev, polarization in, 18: 19115
proton reactions (p,γ) at 1.5 to 3.0 Mev, resonances in, 18: 22863 (AD-417228)
proton reactions (p,γ) at 2 Mev, polarization in gamma spectra from, 18: 24662
proton reactions (p,γ), phosphorus-31 spin-parity from, 18: 26635
proton reactions (p,γ) at 1.0 to 1.55 Mev, energy levels from, 19: 1678
proton reactions (p,γ) at 1.0 to 1.5 Mev, phosphorus-31 levels from, (E), 20: 26172
proton reactions (p,γ) at 0.3 to 2.0 Mev, phosphorus-31 levels from, (E), 20: 28433
proton reactions (p,γ) at 1.53 to 2.00 Mev, phosphorus-31 resonance levels from, (E), 20: 28432
proton reactions (p,γ) at 0.3 to 2.1 Mev, resonance strengths for, (E), 20: 42182
proton reactions (p,γ), gamma rays from, 16: 4814
proton reactions (p,2p) and (p,3p), excitation functions for, 16: 33892
proton reactions (p,xp) at 100 to 400 Mev, cross sections for, 17: 5323 (NYO-8921)
proton reactions (p,γ), polarization of gamma rays from, 17: 7278
proton reactions (p,α) at 1177–1509 kev, phosphorus-31 excited states from, 17: 28321
proton reactions (p,γ) with, phosphorus-31 energy-level studies from, 17: 38166
separation by distillation of methylsilane, 17: 22073
separation by thermal diffusion, 16: 450 (NP-10908)
separation from monosilane by thermal diffusion, 17: 41324
spectra, isotope shifts in atomic, 16: 27784
spectral shifts relative to silicon-28, 16: 12476
triton reactions (t,p) with, silicon-32 production in, (E), 20: 34557
triton reactions (t,p), production of silicon-32, 16: 15667
triton reactions (t,p) with, production of silicon-32 in, 17: 11738
vibrations in, collective, 17: 11661

SILICON ISOTOPES Si-31

beta decay of, relations between beta and gamma moments in, 18: 18975
beta decay of, shell model calculations of ft values in, (T), 20: 6393
content in reactor effluent water, effects of sodium silicate addition on, 18: 36752 (HW-75782)
determination in rats after neutron activation, 18: 38730
energy level spacings, 16: 6018
energy levels, 18: 19021
energy levels from deuteron beam reactions with light nuclei, 16: 11040
energy levels from deuteron reactions (d,p) on silicon-30 at 2 to 3 Mev, (E), 19: 43398
energy levels of, shell model calculations for, 18: 32782
energy levels of, shell model calculations for, 18: 32783
gamma dose constants for, 20: 46617
gamma spectra, 17: 34966
incorporation in organic compounds by recoil techniques, 19: 32241
magnetic moments and M1 transition probabilities in $2s_{1/2}$ $1d_{1/2}$ shell, (T), 19: 47641
neutron activation of, dose measurement by, 18: 23890 (SCPRI(S)-92)
neutron reactions (n,γ) with, cross section for, (E), 20: 34557
nuclear surface excitations, 18: 2974
preparation and separation by recoil method, 16: 2103(T) (UCRL-Trans-552(L))
production by neutron reactions (n,γ), 18: 37592
production in atmosphere by neutron activation of airborne dust, inhalation hazard from, 19: 26589
production in proton reaction on heavy nuclei at 660 Mev, 16: 29864

SILICON ISOTOPES Si-32

beta decay of, shell model calculations of ft values in, (T), 20: 6393
beta spectrum, 18: 26586
beta spectrum, 18: 20023 (TID-20510)
content and production in exosphere, 19: 14120
content in marine samples, 17: 30739
content in rain water in India, 17: 30739
content in sea water at various depths, 18: 39488 (NP-14127)
energy levels of, alpha-particle models for, 20: 26159
gamma reactions (γ,n) at 26.5 Mev, photoneutron spectra, 17: 33032
half life, 17: 11738
neutron reactions (n,p), cross sections for fast, 17: 12722 (TID-17839)
production by silicon-30(t,p) reactions, 16: 15667
production by triton reactions (t,p) with silicon-30, 17: 11738
production in atmosphere by cosmic rays and fallout pattern of, 20: 33520
production in iron by 730-Mev protons, cross sections for, 18: 17049
production in triton reactions (t,p) with silicon-30, (E), 20: 34557
tracer use in gross atmospheric circulation, 19: 16247
use as tracer in physical and chemical processes in upper layers of the Earth, atmosphere, hydrosphere, and lithosphere, 20: 33520
use for dating ground waters, 20: 31432

SILICON NITRIDES

crystal structure and properties in iron alloys, 19: 22230
deformation properties and hardness of, at high temperatures, 20: 33920
development as high-temperature radome material, 18: 34054 (UCRL-7795)
emissivity at 600 to 1800°F, 16: 32118 (NASA-TN-D-998)
mechanical properties and structure of whiskers of, 19: 4646 (AWRE-O-70/64)
preparation and properties for use at 1200°C, 16: 25795
properties and possible uses at high temperatures, 19: 41081
properties and structure, relation between, 16: 19261
reactions with barium, potassium, and sodium chlorides, 20: 26816 (HW-72369)
reactions with basalt, copper matte, slags, and molten salts, 20: 14989
reactions with molten metals at 400 to 1500°C, 19: 37112
spectra of molecular, electronic, 19: 34148 (UCRL-11979)
strength of powdered, at 20 to 2800°C, 18: 39984
surface friction of, symposium on, 20: 37179
thermal properties to 5000°F, 16: 18938
thermal properties, 16: 22597 (WADD-TR-60-924)
thermal properties of, at 500 to 5000°F, 17: 16636 (ASD-TDR-62-765)
thermophysical properties, 16: 3506
thermophysical properties, 18: 34054 (UCRL-7795)
Be_3N_2–Si_3N_4, phase studies, 16: 19264

SILICON OXIDES

abundance correlation with strontium isotope in Hawaiian lava, 18: 3991(R) (NYO-10517(p.99-103))
activation energy of slip-cast fused, 17: 8814(R) (TID-17530)
addition effects on radiation resistance of nitrile elastomers, 16: 30903 (HW-66977)
additive effects on properties of beryllium oxides, 16: 2732 (GA-2262)
additive effects on sinterability of plutonium(IV) oxide–uranium(IV) oxide mixtures, 17: 36253(R) (NUMEC-P-59)
additive effects on neutron-irradiation effects on graphite, 17: 36349(R) (SCC-18)
additive effects on mechanical properties of aluminum, 17: 37551
additive effects on zirconium oxide compacts, 18: 2261
additive effects on radioinduced reactions of isobutane and olefins, 18: 13836(R) (NYO-10025)
additive effects on fabrication and properties of tungsten, 18: 20443(R) (AD-416199)
analysis for acidic hydrogen and water in colloidal, isotopic dilution, 20: 45595
analysis for aluminum, spectrophotometric, 17: 32028
analysis for barium, calcium, and strontium in irradiated, activation, 20: 20636
analysis for impurities by radioactivation and ion-exchange chromatography, 19: 46228
analysis for impurities, activation, 20: 20632
analysis for impurities, activation, 20: 20634
analysis for impurities, activation, 20: 20635
analysis for microimpurities by neutron activation and ion exchange chromatography, 20: 33166(T) (AEC-tr-6639, pp 36-41)
analysis for oxygen by inert gas fusion method, 18: 21955 (CONF-117-42)
analysis for oxygen by activation using helium-3 ions, detection limits and sensitivity of, 20: 20565 (ORNL-P-1216)
analysis for rare earths, emission spectrographic, 20: 12810
analysis for rhenium, activation, 16: 1711
analysis for sodium by gamma spectrometry, 18: 15981
analysis for sodium, MOS and radiochemical, 20: 36744
analysis for trace elements, ion exchange chromatography and activation, 17: 19979
analysis for trace impurities, mass spectrometric, 19: 26226 (CEA-R-2721)

analysis for water, sensitivity of neutron moisture probe for, 16: 698
analysis, ion exchange chromatography in activation, 16: 6377
analysis of colloidal, for sodium by neutron activation, 17: 4482
analytical use for decontamination of aqueous solutions, 20: 1742 (INR-636/XIII/J)
analytical use in determination of strontium in soil, 19: 26243
beta backscattering, 16: 9409
buffer effects of, in spectrochemical analysis of niobium–tantalum mixtures, 17: 15899
casting fused, slip, 17: 3387(R) (TID-17322)
casting of fiber-reinforced fused, process development for slip-, 20: 15058(R) (SC-DC-66-1130)
catalytic activity for decomposing nitrous oxide, 17: 41333(R) (ANL-6677)
catalytic effects on radioinduced polymerization of styrene, 18: 12219
catalytic effects on radioinduced isomerization of 2-butene, 18: 23667
catalytic effects on radiolysis of carbon dioxide, 19: 2400
catalytic effects on radioinduced oxidation of hydrocarbons, 19: 4215
catalytic properties of silica gel for hydrogen-deuterium exchange, effects of aluminum impurity and gamma rays on, 18: 5276
chemical nature of surface of, effects on physicomechanical properties of rubber, 17: 40879
coalescence of agate with water drops, rate measurements, 19: 28471(R) (TID-21855)
coating and impregnating of fused, with alumina and silica, 16: 15123 (NP-11319)
coating of, effects of, on oxidation resistance of graphite, 20: 29773
compatibility with bromine–lead–lead bromide systems at 900°C, 20: 1559 (BNL-9573)
compressive strength of slip-cast fused, 17: 8814(R) (TID-17530)
content in Amazon River, effects on biology, chemistry, and hydrography of Atlantic Ocean, 20: 28878 (NYO-1918-138)
content in range plants, Miles City, Montana, 1955 to 1960, 19: 45747 (ORNL-TM-1279)
content in thalenites from Japan, 20: 29399
content in zircon from Kyoto Prefecture, Japan, 19: 36296
corrosion by cesium in in-pile thermionic cells, 18: 26259
corrosion by fused alkali halides, 18: 35992(R) (TID-20878)
crystal vibration amplitudes for, mean, 18: 22051
deactivation by scintillation solvents system, 18: 13712
decomposition effects on calcium zirconate at 1350 to 1600°C, 16: 31615
dehydration of xerogel, effects of barium, calcium, and strontium chlorides on thermal, 17: 7945
density and moisture absorption rates of, determination at high temperature, 17: 12626(R) (AD-275787)
density measurement in, using gamma-ray transmission method, 17: 12448
density of powders of, method for determination of bulk, 17: 34462
deposition of coatings of, on fused silica by arc plasma spraying, 16: 15123 (NP-11319)
determination by measurement of x radiation intensity by non-dispersive spectrometry, 17: 38948
determination in beryllium carbide, methods for, 16: 6366 (NEPA-940)
determination in bauxite by neutron activation methods, 19: 36262
determination in cements by x-ray fluorescence, 18: 25275
determination in cement raw mixes, design of spectrometer for, 19: 6170
determination in cements by x-ray emission, 19: 26260
determination in ceramics, glasses, and refractories by coulometric titration, 19: 30099
determination in explosives, methods for, 20: 14470 (UCRL-7873)
determination in minerals and rocks by isotope dilution, 18: 1528
determination in Moldavites by spectrophotometry and x-ray fluorescence, 20: 16711(R) (MIT-1381-13)
determination in potassium silicate and stainless steel, activation, 19: 24611(R) (MLM-1227)
determination in VBWR coolant, 18: 24886(R) (GEAP-4565)
determination in VBWR coolant, 18: 24884(R) (GEAP-4419)
determination of, in reactor cooling water, automatic analyzer for, 16: 31819 (HW-74333)
deuterium exchange between heavy water and hydroxyl groups of silica, 19: 13372
development and properties of heat shield foams of, 16: 29350 (ASD-TR-61-706(Vol.II))
development for removal of pesticides from food extracts, 17: 18333(R) (SAN-1022)
development of coatings of, for thermoelectric elements, 17: 23861(R) (AD-282505)
devitrification of fused, 17: 3387(R) (TID-17322)
dielectric constants, 17: 1941(R) (NP-12214)
dielectric constants and losses, 18: 7214 (NP-13431)
diffusion in sodium disilicate glass, kinetics, 19: 44611 (UCRL-16232)
diffusion of helium in fused, at 25 to 1000°C, effects of tensile stress on, 17: 29329 (UCRL-10755)
diffusion of oxygen ions in vitreous, 16: 7580(R) (RRL-71)
diffusion of phosphorus in films of, composition of surface layers and solubility limits during, 19: 6327
diffusion of water in lattices of spheres of, 17: 33943
diffusion of water in, tritium tracer technique for study of, 18: 10085
dust mixtures of, with molybdenum, titanium, tungsten, and zirconium oxides, effects on lungs in rats of, 16: 27499
effect on radioinduced polymerization of styrenes, 19: 458
effects of additions of, on fast-neutron effects on dimensions and strength of beryllia, 20: 27409(R) (GEMP-58A)
effects of additives of, on modulus of rupture of beryllia, 19: 44599(R) (GEMP-50A)
effects of colloidal, on radiolysis of benzene in aqueous solutions, 20: 20768
effects of, on properties of zirconium oxide-based refractory bricks, 17: 34452
effects on cesium volatilization in radioactive waste processing, 20: 26573
effects on chromium-51 recoil processes in potassium chromate, 19: 13499
effects on counting losses in counting of metal salts by liquid scintillation, 18: 39118
effects on creep properties of uranium dioxide, 19: 14022
effects on crystal growth of zirconium dioxide, 19: 23033
effects on crystal structure of hafnium and zirconium oxides, 19: 26359
effects on fluorescence of uranium in sodium carbonate–sodium fluoride melts, 18: 33506
effects on fritting of beryllium oxide, 18: 22500(T) (UCRL-Trans-1042(L))
effects on gamma radiolysis of aqueous solutions of benzene, 19: 44051 (AE-192)
effects on gamma radiolysis of methanol, catalytic, 20: 18744
effects on homomolecular isotopic exchange of carbon monoxide, catalytic, 19: 26328
effects on ion exchange separation of uranium from sulfate leach liquors on aminated polyvinyl chloride, 20: 25210
effects on isomerization of cyclopropane in presence of deuterium, catalytic, 19: 26369
effects on mouse liver, 18: 41156
effects on oxidation resistance of molybdenum disilicide, 18: 44091
effects on oxidation resistance and strength of chromium–magnesia composites, 19: 41022(R) (NP-15292)
effects on physicomechanical properties of rubbers, 19: 11201
effects on plutonium dioxide–uranium dioxide systems, 18: 34049(R) (NUMEC-P-106)
effects on properties of irradiated latex, 19: 493
effects on properties of irradiated beryllia fuel elements of glasses containing, 19: 32678(R) (GEMP-48A)
effects on radiation behavior of polymers, 18: 24199(T,R) (AEC-tr-6316 (p.359-67))
effects on radioinduced copolymerization, 19: 18000
effects on radioinduced polymerization of diphenylvinylphosphine oxide, 20: 408
effects on radiolysis of propene and 2-methylpropene, 16: 30447(R) (NYO-10024)
effects on rate of polymerization of allyl alcohol, 20: 36880
effects on sintered density of ball-milled uranium dioxide–plutonium dioxide, 18: 27863(R) (NUMEC-2389-1)
effects on sorptive properties of soils for strontium, 19: 46434
effects on stabilization of zirconia by calcium oxides, 20: 867
effects on thermal stability of zirconium oxide, 19: 20585
effects on thermoelectric properties of MCC 40, 19: 12129(R) (ASD-TDR-62-896(Pt.II))
effects on volatilization of cesium from coprecipitate with potassium nickel ferrocyanide, 18: 3728
electric discharge thermal shock effects on, 18: 26806
electric insulating properties of vacuum evaporated films of, 18: 19476 (SC-TM-315-63(14))
electric properties, 18: 26058
electric properties of films of, sandwiched between aluminum and gold, 16: 33497
electron range-energy relations in, 16: 33582 (NRL-5828)
electron spin resonance in irradiated fused, 16: 22176
emissivity at 800 to 5000°K, relation of structure to, 18: 20566
emissivity of, measurements of, 17: 16787(R) (PWA-2163)
emissivity of, comparison of calculated and measured, 19: 6292 (ASD-TDR-62-719(Pt.II))
endurance of coatings of, on space power systems, 16: 25761(R) (PWA-2088)
energy levels of, 20: 6532 (CALT-221-13)
etching by selective radiation, process for photosensitive gas phase, 17: 29277(P)

fabrication and properties of slip-cast fused, 17: 32488(R) (TID-19057)
fabrication and properties of slip-cast fused, 18: 10451(R) (TID-20026)
fabrication for radome use, 16: 24132(R) (NP-11713)
fabrication of fused, 17: 4931 (NP-12306)
fabrication of fused, by slip casting, 17: 27807(R) (TID-18891)
firing of slip-cast fused, 17: 8814(R) (TID-17530)
fission fragment recoil in, expansion induced by, 19: 18547
formation of films of, by oxygen ion bombardment of silicon, (E), 20: 40314
free energy of formation at 1100°F, 17: 32571(R) (MSAR-63-105)
hardness of crystals of, 16: 10728
heat of formation, determination by fluorine bomb calorimetry, 16: 7518 (ANL-6472)
heat of formation, 16: 12649(R) (ANL-6485)
heat of formation, 16: 20299(R) (ANL-6477(p.155-67))
heat of formation, 17: 7655(R) (ANL-6600)
heat of transformation, 17: 35264(R) (UCRL-10706(p.111-203))
heating of, effects on charge distributions in, 20: 37285
immunological properties of, in guinea pigs, 19: 15000
impregnation with aluminum chlorides, 17: 3461(R) (AD-273895)
ion exchange and sorptive properties of silica gel, literature survey, 19: 15670 (KFK-233)
ion exchange properties of, in nitrate melts, 17: 27500
ion exchange properties for cations, 19: 7328
light scattering by neutron-irradiated vitreous, 17: 4952
machining characteristics, 17: 34358(R) (ASD-TDR-63-581)
mechanical properties of fiber-reinforced slip-cast fused, 20: 15058(R) (SC-DC-66-1130)
mechanical properties of composition of phenolic refrasil, 20: 29708
melting temperature, evaluation for space technology, 18: 16521
meson (μ) capture in, 18: 22668 (AD-417241)
mixtures of powders of, with alumina and magnesia, effects of ultrasonic vibrations on pellet fabrication from, 16: 7867 (NYO-10005)
moisture control in agglomeration mixtures of, using neutron probe, 20: 13156
neutron cross sections at 1.44 ev (E), 19: 3288
neutron scattering by, spectra for, (T), 20: 26348 (NP-16010, pp 102-39)
neutron slowing down distributions in dry and water-saturated, 19: 35370(T)
neutron spectra at 14 Mev, 19: 10983(R) (TEES-2671-3)
nuclear magnetic resonance relaxation in water vapor sorbed in, temperature dependence of, 17: 32134
performance as gaseous core reactor tube, 20: 20301 (NP-15906)
performance for thermal energy transfer in gaseous fuel rocket reactors, 19: 40230 (LA-3229, pp 137-47)
performance in crystalline neutron spectrometers, 18: 2095
performance of thin films of, for fast neutron flux measurements, 20: 16851
phase transformations, effect of pressure and irradiation on solid-solid, (E), 20: 40306
physical properties, effects of impregnation with aluminum chloride on, 17: 3461(R) (AD-273895)
physical properties of foam made from slip-cast fused, 18: 22419(R) (TID-20589)
preparation by vapor-phase oxidation of chloride, 19: 5923(P)
preparation of sols of, 19: 24534(P)
preparation, properties, and aerospace applications, 19: 37142
production in h-f electrodeless plasmatron, 20: 17959
properties and structure of colloidal, 17: 6648 (CEA-2129)
properties as fission-recoil detector in amorphous media, 18: 41845
properties as thermal insulation, 19: 25751 (TID-21212)
properties as x-ray fluorescence analyzer, 18: 12022
properties for use in vacuum electrothermics, 19: 11733
properties of colloidal, as desiccant for purifying carbon dioxide, 16: 25299 (AAEC/E-86)
properties of colloidal, as strain gage cement at 1600°F, 16: 25560 (NAMC-ASL-1050(Pt.III))
properties of fused, 17: 3387(R) (TID-17322)
properties of fused, manual on, 19: 2805 (TID-21312)
properties of fused, effects of alumina on, 19: 32048(R) (NP-15073)
properties of fused, as aerospace material, 20: 9537
properties of gel of, for scintillation detector, 19: 13784
properties of heat shield foams of, mechanical and thermal, 16: 29365 (ASD-TR-61-706(Vol.I))
properties of slip-cast, at high temperatures, 17: 18718(R) (TID-18286)
properties under thermal shock conditions, 16: 7919
proton range-energy relations in, 16: 33582 (NRL-5828)
proton reactions with vitreous, at 660 Mev, 17: 41884
radiation damage in crystals of fused, neutron, 18: 8874 (NYO-2937-1)
radiation defect formation in crystals of, 16: 13656
radiation effects on E_1' center concentration and intensity, effects of hydroxyl radical, 16: 6818(R) (ORNL-3213(p.81-90))
radiation effects on optical absorption, 16: 6818(R) (ORNL-3213(p.81-90))
radiation effects on isotope exchange on deuterated colloidal, 16: 22221
radiation effects on slip-cast, fused, fast neutron, 16: 25856
radiation effects on catalytic and sorptive properties of colloidal, review, 16: 31664
radiation effects on surface radicals in colloidal, in ethylene, hydrogen, and oxygen atmospheres, 16: 13664
radiation effects on surface properties of, 17: 3546
radiation effects on colloidal, formation of hydrogen in, 17: 4615(T)
radiation effects on surface properties of gel, 17: 5026
radiation effects on surface reactivity of colloidal, 17: 10509(R) (ORNL-3320(p.30-46))
radiation effects on catalytic activity of, 17: 22227 (TID-18577)
radiation effects on strength of plastics containing, as filler, 17: 30204
radiation effects on sorptive properties of gels of, 17: 33979
radiation effects on vitreous, 17: 34483 (EUR-340.f)
radiation effects on mechanical and physical properties of vitreous, 17: 34521
radiation effects on catalytic properties of colloidal, 17: 39163(P)
radiation effects on coloration and luminescence of, x, 17: 41507
radiation effects on colloidal, spectra of hydrogen atom formation on, 18: 334
radiation effects on sorptive properties of colloidal, gamma, 18: 336
radiation effects on aluminum-doped, bleaching of x, 18: 12742
radiation effects on stress relaxation in, alpha and proton, 18: 14551
radiation effects on sorptive properties of, electron-beam, 18: 16117
radiation effects on low-temperature dielectric relaxation in fused, neutron, 18: 20616
radiation effects on dielectric properties of, neutron, 18: 36059
radiation effects on acidity of colloidal, bremsstrahlung, 18: 35617
radiation effects on sorptive properties of silica gel, gamma, 18: 37196(T) (AEC-tr-6398(p.222-5))
radiation effects on deuterium–hydrogen exchange reactions on colloidal, active centers in, 18: 39308
radiation effects on colloidal, 18: 41557
radiation effects on colloidal, electron paramagnetic resonance studies of, 18: 43701
radiation effects on sorptive properties of colloidal, 18: 43703
radiation effects on surface properties of, studies by infrared spectra of adsorbed molecules, 18: 43628
radiation effects on catalytic reactions of, in formic acid decomposition, 19: 4196(R) (ORNL-3627(p.220-3))
radiation effects on optical transmission properties of synthetic fused, electron, 19: 18537 (NASA-TN-D-2620)
radiation effects on catalytic activity of colloidal, in oxygen isotopic exchange gamma, 19: 26408
radiation effects on catalytic activity in conversion of cyclohexane, 19: 26417
radiation effects on deuterium–hydrogen exchange on surfaces of colloidal, 19: 38626
radiation effects on glass of, annealing of fast neutron, (E), 19: 47108
radiation effects on aerosols of, x, 20: 4015
radiation effects on phase transformations in, neutron, 20: 4462
radiation effects on catalytic activity of colloidal, in deuterium–hydrogen exchange, 20: 8922
radiation effects on structure of, neutron, 20: 17148
radiation effects on gels of, x-ray scattering studies on fast-neutron, 20: 19254 (CONF-650629-3)
radiation effects on contraction and electronic processes in, gamma, 20: 23804
radiation effects on phase transformations in, under high pressure, 20: 33968
radiation effects on charge distributions in, uv and x, 20: 37285
radiation effects on refractive properties of high-purity fused, electron and gamma, 20: 41505
radiation effects on role of, in dealkylation of cumene, 20: 43319
radiation effects on dimensions of fused or glassy, neutron, 20: 46224 (BNL-10560)
radioactive of thin chromatographic layers of, equipment and method for measuring beta, 19: 19792
radioinduced carbonium ion production in colloidal, 16: 22226
radioinduced coloration of fused, thermal annealing of reactor, 19: 47082 (NASA-CR-304)
radioinduced coloration in fused, spectra of thermal annealing effects on fast neutron, 19: 23125 (NP-14958)
radioinduced color centers in colloidal, hydrogen sorption by, 20: 5584
radioinduced color centers in fused, fast neutron, 20: 46224 (BNL-10560)
radioinduced crystallinity in fused, fast neutron, 18: 10599
radioinduced defects in fused, thermal annealing, 17: 8879 (BNL-6053)
radioinduced defects in, use of color center technique for study of annealing and growth of, 18: 42141
radioinduced defects in crystals of, use of color centers for detection and

measurement of, 17: 20509 (BNL-6912)
radioinduced defect formation in high-surface-area, ESR studies of gamma, 20: 27607
radioinduced defects in high-surface-area, ESR studies of effects of adsorbed gases on, 20: 27608
radioinduced dilatations in vitreous, 17: 5016
radioinduced electron spin resonance in, effects of various gases on, 19: 28384
radioinduced electric conductivity in fused, effects of crystalline form and impurity on electron, 20: 17133
radioinduced E_1' centers in fused, relation between ESR, optical absorption, and magnetic susceptibility of, 18: 2489
radioinduced flow and stress relaxation in vitreous, proton, (T), 20: 15971
radioinduced formation of catalytic activity centers in colloidal, 19: 13455
radioinduced graft polymerization of styrene, vinylphosphonic acid dichloranhydride, and vinylpyridine on, 20: 43311
radioinduced hydroxyl bonds and paramagnetic states in, gamma, 18: 22136
radioinduced oxidation of hydrocarbons on, 18: 1725(R) (ORNL-3488 (p.42-54))
radioinduced polarization in, release of space charge in electron, 17: 37584
radioinduced reaction with acrylic acid or styrene for preparation of ion-exchange sorbent, 17: 6140
radioinduced swelling of, fission fragment, 20: 11227
radioinduced volume changes in vitreous, theory of neutron and x, 18: 5834
radiolysis effects on pentane, 16: 3323(T) (AEC-tr-4497(p.162-6))
radiolysis of azoethane adsorbed on, 18: 39316
radiolysis of azoethane adsorbed on, energy transfer in gamma, 20: 23116
radiolysis of colloidal at −195°C, formation of hydrogen atoms in, 16: 17719
radiolysis of colloids of, at 77°K, ESR studies of, 20: 16511
radiolysis of surface silanols on, effects of dose, impurities, and surface area on, 19: 46332(R) (ORNL-3832, pp 50-65)
radiolysis of, gamma, 19: 15565(R) (BNL-841(p.43-51))
rare gas release, 16: 4167
reaction with cerium oxides in hydrogen at high temperatures, 16: 6408
reaction with gadolinium, lanthanum, and neodymium oxides, 16: 6405
reaction with praseodymium oxides, 16: 6406
reaction with uranyl ions on surface of colloidal, mechanism of, 17: 25199
reactions of silica gel with aluminum, thorium, and uranyl ions, surface, 18: 41468
reactions with barium, potassium, and sodium chlorides, 20: 26816 (HW-72369)
reactions with beryllium to 600°C in carbon dioxide and *in vacuo*, 19: 22997 (TRG-Report-842)
reactions with calcium zirconates at 1350 to 1500°C, 16: 10574
reactions with gaseous uranium trioxide, effects of substrate symmetry in, 20: 20649 (AEET-CD-24)
reactions with lanthanum and neodymium oxides in solid state, 20: 36840
reactions with Magnox alloy, 19: 22997 (TRG-Report-842)
reactions with molten AMS 5350 steel and Inconel 713C, 20: 16984
reactions with protactinium oxides, solid-state, 20: 26880
reactions with refractory metals, interfacial, 16: 31595
reactions with samarium oxide *in vacuo*, 20: 26340(R) (AD-631987)
reactions with tantalum in presence of gaseous chloride and iodide at 800 to 1100°C, 18: 17805
reactions with uranium(IV) salts, 19: 15452(T) (ANL-Trans-33(p.228-37))
reactions with uranium to 500°C, 19: 22997 (TRG-Report-842)
reactions with zirconium to 500°C, 19: 22997 (TRG-Report-842)
reactions with zirconium oxides, Gibb's free energy of, 20: 5537
reduction by aluminum dissolved in copper and silver, mechanism of, 17: 14212(R) (NYO-10535)
reduction by calcium and hydrogen in molten salt, 18: 29608 (UCRL-11205)
reduction of, method for, 19: 19139
response of reticulo-endothelial system of dogs to, 20: 8558
scintillation properties of gel, for specific activity measurements, 18: 30007
sealing of fused, to metals, 17: 6676(R) (RADC-TDR-62-401)
separation from liquids in hydrocyclones, 16: 1727 (AAEC/E-65)
separation from rare earth oxides in liquid state, 17: 14287
separation from reactor fuels by dissolution and sand filtration, 20: 43426 (ORNL-TM-1650)
separation from zirconium in zircon, 16: 18998(P)
separation of barium, calcium, and strontium from irradiated, chromatographic method for, 20: 20636
separation of zirconium oxide from, as function of SO_3–ZrO_2 ratio, 17: 32077
sintering of slip-cast, 17: 27807(R) (TID-18891)
slip casting of fused, mechanisms of, 16: 29356(R) (ORO-577)
slip casting of fused, 16: 30022(R) (ORO-578)
solid-phase reactions of, at high pressures, 17: 10503 (NP-12359)
sorbed water on, radiolysis G values for, 20: 8982(R) (ORNL-3830, pp 233-5)
sorption of colloidal, on thorium oxide surfaces, 16: 28923 (TID-16464)
sorption of free radicals formed on highly-dispersive aerosyl by cleavage and ionizing radiation, 16: 5251
sorption of protactinium on colloidal, 19: 32178
sorption of zirconium from TBP solutions by colloidal, 19: 15683
sorption of zirconium-95 on colloidal, effects of phosphoric acid and iron(III) ions on, 19: 28449
sorption of zirconium on colloidal, from nitric acid solution, 19: 30329
sorption on thoria surfaces, 17: 2952 (TID-17364)
sorption on thoria surfaces, infrared and kinetic studies of, 17: 16028
sorption properties for cobalt phenanthroline, 18: 19898
sorptive properties of colloidal, for cesium, potassium, strontium, and rubidium, 16: 27053
sorptive properties of colloidal, for carbon-14-labeled barium carbonate, 16: 13089
sorptive properties for dibutyl phosphate from organic solutions, 17: 23241
sorptive properties of amine-impregnated gels of, for uranium, 17: 28893
sorptive properties for cesium, 17: 36995(R) (TID-19187)
sorptive properties for cesium, 17: 36997(R) (TID-19189)
sorptive properties of colloidal, for protactinium, 17: 10246(R) (ORNL-TM-403)
sorptive properties of colloidal, for protactinium, 17: 39178(R) (ORNL-3452(p.1-25))
sorptive properties for protactinium-233 in fuel processing solutions, 17: 35618(R) (ORNL-TM-545)
sorptive properties of colloidal, for uranium, effects of Arsenazo I on, 18: 13950
sorptive properties for plutonium, uranium, and zirconium, 18: 13971
sorptive properties of colloidal, for fission products, 18: 16144
sorptive properties of gel of, for radon, 18: 19940(T) (SC-T-64-613)
sorptive properties for organic compounds, 18: 25032(T) (SC-T-64-618)
sorptive properties of colloidal, for zirconium from nitric acid solutions, mechanism of, 18: 35509 (UJV-1079/64)
sorptive properties for zirconium in nitric acid in presence of Arsenazo I, EDTA, and oxalic acid, 18: 35536
sorptive properties for zirconium in nitric acid, mechanism of, 18: 35469
sorptive properties of silica gel, 18: 37196(T) (AEC-tr-6398(p.222-5))
sorptive properties of silica gel for cobalt ammines, 18: 37200(T) (AEC-tr-6398(p.362-5))
sorptive properties of cesium, 18: 45155(R) (TID-20980)
sorptive properties for krypton and xenon, 19: 30630(R) (MLM-1245)
sorptive properties of colloids of, for inorganic ions, (E), 19: 30309
sorptive properties of surfaces of, for ions from aqueous solutions, 19: 42200 (COO-1354-5)
sorptive properties for plutonium, acidity effects on, 20: 1849
sorptive properties of colloidal, for protactinium, 20: 9044(R) (ORNL-3830, pp 30-68)
sorptive properties for chloride and potassium ions, effects of pH on, 20: 14651
sorptive properties for protactinium-233 in presence of neutron-irradiated thorium, 20: 25209
specific heat at 500 to 1300°C, measurement of mean, 18: 13779
spectra, Franck-Condon factor arrays for band, 16: 22129
spectra in low frequency region, infrared, 18: 23549
spectra of, amplitudes in vibrational, 17: 35721
spectra of diatomic, in plasma jets, (E), 19: 41287
spectral emittance at 800 to 5000°F, 16: 18939
sputtering by argon at 12 kev, 18: 26806
sputtering by uranium-ion bombardment, measurement of, 20: 46309(T)
stability in gases, 16: 29421
stability of fluorine-containing, 16: 5318(T) (CEA-tr-R-1401)
strength of slip cast fused, effects of firing conditions, 17: 14740 (TID-11295(2nd Ed.))
surface effects on radioinduced alkylation of isobutane and propene, 16: 7578 (NYO-10194)
surface properties of colloidal, effects of adsorption of thorium ions on, 18: 29809
surface tension and viscosity, 17: 4933 (WADD-TR-60-463(Pt.II))
testing for use in shaft seals for potassium space power systems, 20: 2242
thermal conductivity of foams of, for use above 3000°F, 18: 16520
thermal energy storage in, in solar-thermionic power supplies, 17: 9113
thermal-shock effects in tubes of, electric-discharge, 16: 33592
thermal treatment of, deuterium exchange method for determination of internal and surface water liberation by, 18: 1674

thermodynamic properties, 17: 20312 (UCRL-10631)
thermodynamic properties of, tables of, 17: 40777(R) (RAD-SR-63-183)
thorium ion reactions with nitric acid, perchloric acid, and water in pores of gel of, 18: 5279
tumorigenic effects of implants of, in rats, 18: 25053
ultrasonic propagation in deformed fused, 16: 23971 (ANL-6515 (p.121-32))
ultrasonic wave velocity in fused, as function of temperature of, 19: 26804(R) (AD-613350)
use as charge component in refractory materials for glass furnaces, 16: 32131
use as corrosion inhibitor in high-temperature gas-cooled reactors, 20: 14021(P)
use as filler in radiation-cured rubber compounds, 16: 1821
use in ion exchange materials for fission product separation processes, 20: 35177(P)
use in separation of uranium in columns, 19: 9046(R) (IS-900(Sect.C))
use of colloidal as scavengers for radioactive particles, 16: 19184 (TID-15305)
use of colloidal, for drying glove box atmospheres, 16: 5432 (GAMD-1931)
use of colloidal, in thin-layer chromatography, 18: 23155(T) (SC-T-64-611)
use of colloidal, impregnated with cobalt bromide and hydrobromic acid, as moisture indicator, 19: 21783(P)
use of fused, as pyrometer light guide, 16: 11189(R) (APEX-666(Pt.1))
use of kryptonated, for determining water in organic liquids, 20: 18570(R) (NYO-2757-5)
use of, in packing of biological samples for irradiation, 20: 35464
uses for canning reactor fuels, 18: 42977(P)
uses for passivation of silicon junctions, 19: 22814
vaporization of, thermodynamics of, 20: 36841
x ray scattering by amorphous, elimination of Compton components from, 19: 9476 (CONF-640702-3)
yield from quartz sputtering in argon discharge, (E), 19: 41257
Al_2O_3–BaO–CaO–MgO–SiO_2, presintering of compositions in, 19: 20461 (NP-14893)
Al_2O_3–BaO–SiO_2, reactions with zirconium titanates at high temperatures, 16: 5352
Al_2O_3–BeO–SiO_2, radioinduced microcracking of, resistance to fast-neutron, 20: 27585(R) (GEMP-400A, pp 221-62)
Al_2O_3–B_2O_3–SiO_2, phase studies, 16: 9204(R) (NP-11235)
Al_2O_3–B_2O_3–SiO_2, phase studies, 16: 7894(R) (NP-11242)
Al_2O_3–B_2O_3–SiO_2, radiation effects on elastic properties of alkali metal-containing, 19: 7984
Al_2O_3–CaO–SiO_2, absorptive properties for fission products from oxygen, 19: 36649 (AD-614997)
Al_2O_3–CaO–SiO_2, diffusion of fission products in molten, 19: 36649 (AD-614997)
Al_2O_3–CaO–SiO_2, diffusion in, ternary, 19: 43997(R) (UCRL-11889)
Al_2O_3–CaO–SiO_2, reactions with zirconium titanates at high temperatures, 16: 5352
Al_2O_3–CaO–SiO_2, self-diffusion of oxygen in, 16: 13631
Al_2O_3–Cr_2O_3–MgO–SiO_2–TiO_2–ZrO_2, phase diagrams, 20: 8932
Al_2O_3–Cr_2O_3–MgO–SiO_2, preparation for glass seals, 20: 46181(P)
Al_2O_3–Fe_2O_3–MgO–SiO_2, neutron spectra at 14 Mev, 19: 10983(R) (TEES-2671-3)
Al_2O_3–Li_2O–SiO_2, ion exchange properties of synthetic minerals of, 18: 35502 (NYO-2911-1)
Al_2O_3–Li_2O–SiO_2, properties as ion emitter, 18: 22707(R) (AD-420962)
Al_2O_3–MgO–SiO_2, devitrification, 19: 20461 (NP-14893)
Al_2O_3–MgO–SiO_2, spectra of, gamma radiation effects on, 19: 34754
Al_2O_3–MgO–SiO_2, vibratory compaction formation of pellets of, ultrasonic, 16: 7867 (NYO-10005)
Al_2O_3–Nd_2O_3–SiO_2, phase studies, 16: 6433
Al_2O_3–RbO–SiO_2, properties as ion emitter, 18: 22707(R) (AD-420962)
Al_2O_3–SiO_2, analysis of lead fluoride-containing gels of, for fluoride by fast-neutron radioactivation, 20: 40845
Al_2O_3–SiO_2, catalytic effects of platinum-metals-impregnated on hydrogen-oxygen reactions, 18: 27492(R) (GNEC-336)
Al_2O_3–SiO_2, catalytic effects on radiolysis of carbon dioxide, 19: 2400
Al_2O_3–SiO_2, composition and ion exchange properties of, 20: 8836 (TID-22511(Suppl.))
Al_2O_3–SiO_2, effects of dehydration on bound water in, 20: 16413 (CEA-R-2703)
Al_2O_3–SiO_2, effects of irradiated, on reactions of isopropylbenzene, 20: 18768
Al_2O_3–SiO_2, electric properties, 18: 17370(T) (SC-T-64-44)
Al_2O_3–SiO_2, phase studies, 16: 24148(R) (ASD-TR-61-676)
Al_2O_3–SiO_2, preparation of $Al_2O_3 \cdot 10SiO_2$, 17: 36997(R) (TID-19189)
Al_2O_3–SiO_2, preparation, properties, and aerospace applications, 19: 37142
Al_2O_3–SiO_2, preparation and properties of, for use in cesium ion exchange from waste solutions, 20: 10766 (TID-22511)
Al_2O_3–SiO_2, radiation effects on catalytic activity of, 17: 25339
Al_2O_3–SiO_2, radiation effects on cumene reactions on, 18: 43643
Al_2O_3–SiO_2, radiation effects on catalytic reactions of, in formic acid decomposition, 19: 4196(R) (ORNL-3627(p.220-3))
Al_2O_3–SiO_2, radiation effects on activities in acid-catalyzed reactions, 19: 41099
Al_2O_3–SiO_2, radiation effects on color centers and deuterium–hydrogen exchange in catalysts of, gamma, 20: 23117
Al_2O_3–SiO_2, radiation effects on catalytic properties of, gamma, 20: 26955
Al_2O_3–SiO_2, radiation effects on dealkylation of isopropylbenzene on, 20: 26999
Al_2O_3–SiO_2, radioinduced oxidation of hydrocarbons on, 18: 1725(R) (ORNL-3488(p.42-54))
Al_2O_3–SiO_2, radiolysis at –195°C, formation of hydrogen atoms in, 16: 17719
Al_2O_3–SiO_2, reactions with beryllium to 600°C, 19: 22997 (TRG-Report-842)
Al_2O_3–SiO_2, sorptive properties for cesium, 17: 36997(R) (TID-19189)
Al_2O_3–SiO_2, sorptive properties for 2-methylpropane, radioactive exchange studies of, 18: 3803
Al_2O_3–SiO_2, sorptive properties of surfaces of, for ions from aqueous solutions, 19: 42200 (COO-1354-5)
Al_2O_3–SiO_2, sorptive properties of, effects of, on hydrogen yields in beta radiolysis of water, 20: 45714(R) (ORNL-3945, pp 218-20)
Al_2O_3–SiO_2, uses as catalyst in conversion of acetylene to benzene, 20: 18933
Al_2O_3–SiO_2, viscosity, 17: 4933 (WADD-TR-60-463(Pt.II))
Al_2O_3–SiO_2, wetting of tungsten plates by, 20: 23685
Al_2O_3–SiO_2–Na_2O, composition and properties of, 20: 8836 (TID-22511(Suppl.))
Al_2O_3–SiO_2–Na_2O, gamma-ray effects on color centers in, (E), 19: 11800(T)
Al_2O_3–SiO_2–Na_2O, ion exchange properties of, in nitrate melts, 17: 27500
Al_2O_3–SiO_2–Na_2O, ion exchange properties of synthetic minerals of, 18: 35502 (NYO-2911-1)
Al_2O_3–SiO_2–Na_2O, properties for use in separation of cesium from waste solution, 19: 30349(P)
Al_2O_3–SiO_2–UO_2, diffusion of gaseous fission products from, 17: 35115
Al_2O_3–SiO_2–UO_2, xenon-133 diffusion from, 18: 31005
Al_2O_3–SiO_2–Y_2O_3, phase studies and structure of, 18: 43466
Al/SiO_2/Si, radiation effects on capacitors of, electron, 19: 26713
BaO–BeO–SiO_2, preparation, properties, and phase studies, 18: 17843
BaO–B_2O_3–SiO_2, effects of aluminum, lanthanum, and thorium oxides on crystallization of, 20: 15075
BaO–Cs_2O–La_2O_3–Li_2O–SiO_2, electrochemical properties of, effects of added oxides on, 17: 32098
BaO–Gd_2O_3–SiO_2, properties for neutron absorption in reactors, 18: 8824
BaO–La_2O_3–Li_2O–SiO_2, electrochemical properties of glass, 17: 32097
BaO–La_2O_3–SiO_2, properties for neutron absorption in reactors, 18: 8824
BaO–SiO_2, glass formation and structure in, 19: 44015
BaO–SiO_2–ZrO_2, phase studies, 20: 38899
BeO–SiO_2, glass formation and structure in, 19: 44015
B_2O_3–K_2O–SiO_2, radiation effects on elastic properties of, 19: 7984
B_2O_3–Rb_2O–SiO_2, radiation effects on elastic properties of, 19: 7984
B_2O_3–SiO_2, emissivity of aluminum-bonded, at 300 to 900°F, 16: 14358(R) (PWA-2043)
B_2O_3–SiO_2, phase studies, 16: 6722(R) (NP-11233)
B_2O_3–SiO_2, phase studies, 16: 2164 (AD-256389)
B_2O_3–SiO_2, phase studies, 16: 24148(R) (ASD-TR-61-676)
B_2O_3–SiO_2, phase studies on, at 1100 to 1200°C, 16: 8714(R) (NP-11241)
B_2O_3–SiO_2, phase studies on, liquidus diagram from, 16: 9204(R) (NP-11235)
CaO–La_2O_3–SiO_2, phase studies, 17: 6101
CaO–MgO–SiO_2–ZrO_2, properties of, for use as refractory material, 16: 21067
CaO–SiO_2, crystal structure, 19: 38621
CaO–SiO_2, glass formation and structure in, 19: 44015
CaO–SiO_2–Na_2O, diffusion of sodium-22 in solid, residual activity method for self-, 20: 16478
CaO–SiO_2–Na_2O, magnetic susceptibility of, containing iron dispersions, 19: 24989(R) (TID-21673)
CdO–Cs_2O–Li_2O–SiO_2, development and properties of glass as radiation sources, 18: 27814(R) (ORNL-TM-434)
CdO–In_2O_3–SiO_2, properties as control-rod, 19: 11737
CdO–SiO_2, melting point of $CdSiO_3$ and $CdSiO_4$, (E), 19: 17202
CoO–Fe_3O_4–SiO_2, phase studies, 18: 13727(R) (TID-20232)
CoO–MnO–SiO_2, phase studies and thermodynamic properties, 18: 13727(R) (TID-20232)
CoO–MnO–SiO_2, solid solutions in, 19: 13280(R) (TID-21569)
CoO–SiO_2, free energy of formation, 17: 30532

CoO–SiO_2, phase studies, 18: 13727(R) (TID-20232)
CoO–SiO_2, viscosity, 17: 4933 (WADD-TR-60-463(Pt.II))
Cr_2O_3–NiO–SiO_2, endurance of aluminum phosphate-bonded coating of, 17: 6675(R) (PWA-2128)
Cs_2O_3–SiO_2, phase studies, 16: 24148(R) (ASD-TR-61-676)
Cs_2O–La_2O_3–Li_2O–SiO_2, electrode properties of glass, 17: 32096
Cs_2O–PbO–SiO_2, preparation as radiation source material, 18: 27812(R) (ORNL-TM-415)
CsO_2–PbO–SiO_2, preparation and properties, 18: 27813(R) (ORNL-TM-428)
Dy_2O_3–Gd_2O_3–SiO_2, phase studies, 16: 18870
Dy_2O_3–SiO_2, crystal structure of compound formed in, 19: 36375
Er_2O_3–SiO_2–Y_2O_3, phase studies, 16: 22113
Eu_2O_3–K_2O–SiO_2, crystal structure and preparation, 19: 34158
EuO–SiO_2, preparation and crystal structure, 19: 38621
EuO–SiO_2, spectra and crystal structure of, infrared, 19: 38622
FeO–MgO–SiO_2, phase studies and thermodynamic properties, 18: 13727(R) (TID-20232)
FeO–MgO–SiO_2, solid solutions in, 19: 13280(R) (TID-21569)
FeO–MnO–SiO_2, activities at 1150°C, ternary diagram, 19: 13280(R) (TID-21569)
Fe_2O_3–SiO_2, chemical effects of, on radiolysis of propene and 2-methylpropene, 16: 30447(R) (NYO-10024)
Fe_2O_3–SiO_2, surface effects of, on radioinduced alkylation of isobutane and propene, 16: 7578 (NYO-10194)
FeS_2–PbS–SiO_2–ZnS, analysis for lead, x-ray fluorescence, 19: 5825
FeS_2–PbS–SiO_2–ZnS, analysis for lead by gamma-excited x-ray fluorescence, 19: 24477
Gd_2O_3–SiO_2–Na_2O, glass forming temperature of, 20: 4077(R) (IS-1200 (Sect. E))
hexane–SiO_2, radiolysis of, at 77°K, ESR studies of, 20: 16511
hexane–SiO_2, radiolysis of, ESR spectral studies on yields in gamma, 20: 38994(R) (AE-232)
Ho_2O_3–SiO_2, crystal structure of compounds formed in, 19: 36375
La_2O_3–SiO_2, phase studies, 16: 27642(T) (FTD-TT-62-505)
La_2O_3–SiO_2–Yb_2O_3, phase studies, 16: 18871
La_2O_3–Sm_2O_3–SiO_2, phase studies, 16: 18870
Li_2O–SiO_2–ZrO_2, phase studies, 19: 41038
MgO–SiO_2, fabrication and properties of lightweight, 16: 27597 (BM-RI-6025)
MgO–SiO_2, glass formation and structure in, 19: 44015
MgO–SiO_2, preparation, properties, and aerospace applications, 19: 37142
MgO–SiO_2, radiation effects of 1.2-Mev gammas on, at 70 to 400°F, 16: 24244 (TID-15981)
MgO–SiO_2, radiation effects on, fission-fragment, 18: 2352
MgO–SiO_2, radiation effects on forsterite, neutron, 19: 30828(R) (ORNL-3789(p.230-8))
MgO–SiO_2, sorptive properties for cesium, 17: 36997(R) (TID-19189)
MgO–SiO_2, strength of polycrystalline forsterite and steatite, effects of compressive surface layers on, 20: 33860 (AD-634361)
MnO_2–SiO_2, chemical effects of, on radiolysis of propene and 2-methylpropene, 16: 30447(R) (NYO-10024)
MnO_2–SiO_2, phase studies, 16: 24148(R) (ASD-TR-61-676)
Na_2O–SiO_2, fixation reactions with purex waste, 19: 17388(R) (HW-84467)
Nb_2O_5–SiO_2, phase diagram, 16: 18054
Nb_2O_5–SiO_2–Na_2O, dielectric properties of glasses in, 17: 12686
Nd_2O_3–SiO_2, phase studies, 19: 9694
$(NH_4)_2CO_3$–$MgCl_2$–SiO_2–$UO_2(NO_3)_2$, reactions in, silicate formation in, 20: 36797
$(NH_4)_2CO_3$–SiO_2–$UO_2(NO_3)_2$, reactions in, silicate formation in, 20: 36797
NiO–SiO_2, sorptive properties for cesium, 17: 36995(R) (TID-19187)
Ni–SiO_2, catalytic effects on isotope exchange between anisole or xylene and deuterium oxide, 17: 27387
PbO–$PbSO_4$–SiO_2, preparation and properties for fixation of waste solutions in, 20: 24809(R) (BNWL-213)
PbO–SiO_2, thermodynamic properties and oxygen pressure in, at 800, 900, 1000, and 1100°C, 19: 46297
PuO_2–SiO_2, preparation and properties of pellets of, 18: 24815(R) (MLM-1184)
PuO_2–SiO_2, preparation and properties of arc-melted glass of, 19: 9603(R) (HW-81601(p.2.1-35))
Sc_2O_3–SiO_2, phase studies and properties of scandium silicates in, 16: 20444
Sc_2O_3–SiO_2, phase studies and structure of, 17: 1993
SiC–SiO_2, emissivity of aluminum- and stainless steel-bonded at 300 to 1450°F, 16: 14358(R) (PWA-2043)
SiC–SiO_2, endurance of aluminum phosphate-bonded coating of, 17: 6675(R) (PWA-2128)
SiC–SiO_2, endurance tests of coatings of, 18: 5737(R) (PWA-2255)
SiC–SiO_2, total hemispherical emittance at high temperatures, 17: 6731
SiO_2–Ag_2SO_4–V_2O_5, radiation effects on catalytic activity of, in oxidation of sulfur dioxide by air, 20: 29291
SiO_2–Na_2O, diffusion of calcium, potassium, and sodium ions in, in melts with calcium, lithium, and potassium oxides, 16: 16048
SiO_2–Na_2O, diffusion of calcium, potassium, and sodium ions in, in melts with calcium, lithium, and potassium oxides, 16: 24038(T) (AEC-tr-5191)
SiO_2–Na_2O–ZnO, absorption in gamma-irradiated, 18: 32202
SiO_2–Na_2O–ZrO_2, phase studies, 20: 13284
SiO_2–SnO_2, sorptive properties for cesium, 17: 36995(R) (TID-19187)
SiO_2–SO_2, properties for use as adsorption refrigeration system, 20: 21174 (SAN-575-12)
SiO_2–spinel, endurance tests of coatings of, 18: 5737(R) (PWA-2255)
SiO_2–SrO, crystal structure, 19: 38621
SiO_2–ThO_2, immiscibility curve for, statistical model for, 19: 23071
SiO_2–ThO_2, liquidus curves and thermodynamic properties, 20: 2326 (IFA-FR-39)
SiO_2–ThO_2, phase studies, 16: 27642(T) (FTD-TT-62-505)
SiO_2–ThO_2, phase studies in hydrogen atmosphere, 20: 23702
SiO_2–ThO_2, processing into 1- to 2-micron-dia spheres, 17: 35850(P)
SiO_2–ThO_2–UO_2, liquidus curves and thermodynamic properties, 20: 2326 (IFA-FR-39)
SiO_2–ThO_2–UO_2, phase studies in hydrogen atmosphere, 20: 23702
SiO_2–UO_2, immiscibility curve for, statistical model for, 19: 23071
SiO_2–UO_2, phase diagram of, 17: 10641
SiO_2–UO_2, phase diagram and crystallization of melts, 17: 14229
SiO_2–UO_2, phase studies, 16: 27642(T) (FTD-TT-62-505)
SiO_2–UO_2, radiation effects on, 16: 29439 (KAPL-1866)
SiO_2–V_2O_5, viscosity, 17: 4933 (WADD-TR-60-463(Pt.II))
SiO_2–V_2O_5–ZrO_2, zircon formation in, 18: 42085
SiO_2–Yb_2O_3, crystal structure of compound formed in, 19: 36375
SiO_2–Yb_2O_3, phase diagram, 16: 6736
SiO_2–YbO, preparation and crystal structure, 19: 38621
SiO_2–YbO, spectra and crystal structure of, infrared, 19: 38622
SiO_2–Y_2O_3, preparation and properties of $Y_2O(SiO_4)$ in, 16: 17689
SiO_2–ZrO_2, ceramic properties, 16: 24210
SiO_2–ZrO_2, ion exchange properties of, in nitrate melts, 17: 27500
SiO_2–ZrO_2, phase transformations in, fluorite, 19: 358(T) (ORNL-tr-201)
SiO_2–ZrO_2, preparation, properties, and aerospace applications, 19: 37142
SiO_2–ZrO_2, use of phosphate-bonded, as mold for casting molybdenum–uranium alloys, 19: 32674 (AD-610003)
Si–SiO_2, electric properties of interfaces in, 19: 46727 (UCRL-16197)
Sm_2O_3–SiO_2, phase diagram, 16: 6736
SmO–SiO_2, preparation and crystal structure, 19: 38621
Sm_2O_3–SiO_2, preparation, properties, and structure of $Sm_4(SiO_4)_3$ in, 20: 36784(R) (AD-636054)
SmO–SiO_2, spectra and crystal structure of, infrared, 19: 38622

SILICON STEEL

heat treatments at 900°C, austenizing effects on PM 24, 20: 43891 (EURAEC-1686)
magnetic properties of flat-rolled, variation with processing techniques, 20: 17009 (CONF-650922, pp 287-96)
mechanical properties, effects of tempering at 525 to 950°F on, 16: 520 (DMIC-Memo-132)
radiation effects on hardening in mild, effects of dose and temperature on neutron, 19: 37186
radiation effects on fatigue of A212B, neutron, 20: 39406 (WAPD-T-1864)
stresses after magnetic losses and plastic elongation in, 16: 9214(R) (TID-14810)
C–Cr–Mn–Mo–Ni–Si, strength and toughness of dynamically strain-aged, 20: 7584 (UCRL-16363)
C–Cr–Mn–Mo–Ni–Si–V, strength and toughness of dynamically strain-aged, 20: 7584 (UCRL-16363)
Cr–Mn–Si, corrosion by mercury and sodium amalgam at 200 to 500°C, 18: 18312(T) (CEA-tr-A-1455)
C–Si, reactions with beryllium to 600°C in carbon dioxide, 19: 22997 (TRG-Report-842)
C–Si, specification for A212 Grade B plate specimens for irradiation testing, 17: 41343 (HW-74938)
Mn–Si, radiation effects on plastic deformation of, 17: 32684
Mn–Si, review on radiation effects on crystal lattice of, 18: 14565

SILICON SULFIDES

preparation and evaluation for electromagnetic separation of silicon isotopes, 20: 41400 (ORNL-3301(Suppl.1))

SILICON SYSTEMS

fabrication of refractory composite, method for, 19: 28794(P)
formation and structure of $R(Me,X)_2$ type compounds in, 19: 30767
preparation of fine-grained alpha-phase, 19: 24930(P)
properties for aerospace applications, handbook, 19: 14063
structure of intermetallic compounds with transition metals, x-ray, and micro-, 16: 14701(T) (DC-59-3-176)

Al–Be–Cu–Si, elastic properties and microstructure of sintered, 19: 26870
Al–Be–Si, phase studies, 16: 29417
Al–Be–Si, phase studies on liquidization, 17: 39576
Al–Bi–Pu–Si, phase studies and properties of, bibliographic study of, 16: 32115 (KFK-105)
Al–Ce–Si, phase analysis and structure, 17: 36327
Al–C–Fe–Si–U, radioinduced swelling in, effects of pressure on reactor, 20: 745(R) (BNWL-120, pp 3.1-22)
Al–C–Mo–Ni–Si–U–Zr, preparation and fabrication as refractory fuel material, 18: 34071(P)
Al–Cr–Fe–Mn–Mo–Ni–Si, machining characteristics, 17: 14778(R) (ASD-TR-7-532a(IX))
Al–Cr–Fe–Si–U, properties for reactor fuel, 19: 6300(R) (NMI-7292)
Al–Cr–Fe–Si–U, radioinduced swelling in, resistance to, 19: 47103
Al–Cr–Fe–Si–U, thermal expansion rates for, 20: 33880 (NLCO-946, pp 103-6)
Al–Cr–Mo–Si, phase studies, 18: 12704
Al–Cr–Ni–Si, fabrication methods effects on thermoelectric properties of, 17: 30824
Al–Cr–Si, coating processes for cementation on refractory metals, 18: 34091
Al–Cr–Si, coatings for niobium and niobium alloys, development of oxidation-protection, 20: 7514 (DC-60-4-179)
Al–Cr–Si, crystal structure and phase studies on, 18: 12704
Al–Cr–Si, development and testing of, on molybdenum, 16: 2174(R) (ER-11462-2)
Al–Cr–Si, development of oxidation-resistant, for molybdenum, 16: 6705 (AD-261006)
Al–Cr–Si, optical properties of, at high temperatures, emittance and reflectance, 16: 12236 (WADD-TR-60-370)
Al–Cr–Si, properties as protective coatings on niobium alloys, 19: 7876(R) (ML-TDR-64-71)
Al–Cr–Si, properties of, for use as protective coating on niobium and its alloys, 20: 29651
Al–Cr–Si, protective effects as coating on molybdenum and molybdenum–titanium alloy, 19: 47061
Al–Cr–Si–Ti–V, properties of aged, 20: 4360(R) (AD-619399)
Al–Cu–Fe–Mn–Ni–Si–Ti, corrosion by molten fluoride mixture at 650°C, 17: 34345 (BMI-X-247)
Al–Cu–Si, dissolution in nitric acid, effects of mercuric nitrate catalyst on, 18: 31658(R) (IDO-14635)
Al–Fe–Mg–Ni–Si–Ti–Zr, coating with aluminum–nickel layers by chemical deposition, 19: 39143(P)
Al–Fe–Mg–Ni–Si, corrosion by water and steam, 20: 763 (BNWL-125)
Al–Fe–Mg–Ni–Si, performance as fuel element cladding, 20: 8439(R) (KR-97)
Al–Fe–Mg–Si, corrosion by water and steam, 20: 763 (BNWL-125)
Al–Fe–Mo–Si–U, radioinduced swelling in, resistance to, 19: 47103
Al–Fe–Mo–Si–U, thermal expansion rates for, 20: 33880 (NLCO-946, pp 103-6)
Al–Fe–Ni–Si, corrosion by water and steam, 20: 763 (BNWL-125)
Al–Fe–Ni–Si, fabrication methods effects on thermoelectric properties of, 17: 30824
Al–Fe–Si, radioinduced swelling of, factors affecting, 19: 34745(R) (HW-84384(p.8.1-5))
Al–Fe–Si–U, casting procedures for NPR billets, 19: 42824(R) (NLCO-955, pp 5.1-16)
Al–Fe–Si–U, effects of forming method on mechanical properties and microstructure of, 19: 30800
Al–Fe–Si–U, fabrication of rods and tubes by rolling, 18: 25940 (BMI-X-294)
Al–Fe–Si–U, hardening by heat treatment, 19: 4653 (NMI-7097-1(Del.))
Al–Fe–Si–U, hot hardness and microstructure of, effects of heat treatments on, 19: 40958
Al–Fe–Si–U, properties for reactor fuel, 19: 6300(R) (NMI-7292)
Al–Fe–Si–U, properties of, effects of chromium and molybdenum on high-temperature, 19: 40958
Al–Fe–Si–U, radioinduced swelling of, pressure inhibition of, 19: 34741(R) (BNWL-79(p.3.1-22))
Al–Fe–Si–U, radioinduced swelling in, resistance to, 19: 47103
Al–Fe–Si–U, radioinduced swelling of, effects of pressure on, 20: 9567(R) (BNWL-166, pp 3.24-9)
Al–Fe–Si–U, radioinduced swelling of, factors affecting, 20: 27570(R) (BNWL-207, pp 3.17-35)
Al–Hf–Si, phase diagram at 1200°C, 17: 22196
Al–Hf–Si, phase studies, 17: 18733 (AD-278041L)
Al–Hf–Si, phase studies, 19: 14060
Al–Hf–Si, structure of phases in, 18: 18388
Al–Li–Si, preparation and sorptive properties, 17: 19712 (TID-7644 (p.201-10))
Al–Mg–Ni–Si, fatigue properties of IFA-3 aluminum-base, 20: 7566 (KR-99)
Al–Mg–Ni–Si, fatigue properties at 250 to 350°C, low-cycle, 20: 13308
Al–Mg–Ni–Si, properties for use as fuel element canning material, 17: 14735 (KR-31)
Al–Mg–Si, additive effects of beryllium on, 17: 39561
Al–Mg–Si, aging and quenching characteristics of, electron transmission microscopy studies of, 16: 24194
Al–Mg–Si, dispersion hardening of, effect of pre-aging on, 16: 10598
Al–Mg–Si, effect of homogenization on, 17: 12701
Al–Mg–Si, effects of magnesium silicide particles on creep deformation and grain-size stability of, 18: 42061
Al–Mg–Si, fabrication of cylinders of Anticorodal, using magnetic fields, 20: 19199 (RT/EL-(65)9)
Al–Mg–Si, hardening behavior of, effects of annealing and quenching conditions on, 17: 22182
Al–Mg–Si, mechanical properties and part strength of, effects of beryllium of, 19: 4702
Al–Mg–Si, origin and development of cup and cone defects in, at room temperature, 18: 27933
Al–Mn–Ni–Si, air and helium effects on voltage drifts in thermocouples of, 17: 30829
Al–Mn–Ni–Si, behavior of Alumel thermocouple wire in carbon dioxide–carbon monoxide, 19: 22664 (ORNL-P-1070)
Al–Mn–Ni–Si, magnetic field effects on thermocouple wires of, 17: 30828
Al–Mn–Ni–Si, neutron-induced composition changes in, 17: 30826
Al–Mn–Ni–Si, radiation effects on thermoelectric properties, 18: 32237
Al–Mn–Ni–Si, reactions with beryllium to 600°C in carbon dioxide and *in vacuo*, 19: 22997 (TRG-Report-842)
Al–Mn–Ni–Si, reactions with Magnox alloy to 550°C in argon and carbon dioxide, 19: 22997 (TRG-Report-842)
Al–Mn–Si, phase studies, 19: 14060
Al–Mo–Si, crystal structure and phase studies on, 18: 12704
Al–Mo–Si, oxidation kinetics at 800 to 1200°C, 20: 7530
Al–Mo–Si–U, deformation resistance of, at high temperatures, 19: 16206(P)
Al–NaF–Si–Sn, development for use as vanadium alloy coating, 18: 39819(R) (IITRI-B6019-5)
Al–Nb–Si, crystal structure and phase studies, 18: 12704
Al–Nb–Si–Sn, development for use as vanadium alloy coating, 18: 39819(R) (IITRI-B6019-5)
Al–Nb–Si–Ti, oxidation by air at 760 to 1360°C, 17: 27780(R) (DRI-2104)
Al–Ni–Pu–Si, radiation effects on Zircaloy-clad, 20: 46143(R) (HW-66081)
Al–Ni–Si, corrosion by water at 315°C, alloying effects of magnesium and zinc on, 17: 37005(R) (KR-49)
Al–Ni–Si, corrosion behavior and mechanical properties in high-temperature water, 18: 25931
Al–Ni–Si, corrosion by ultra-pure water at 25, 50, and 100°C, 18: 32093
Al–Ni–Si, corrosion resistance of sintered, 19: 11682
Al_2O_3–Si, fluidization, 18: 18294(R) (NP-13758)
Al_2O_3–Si–NaF, properties as coating for D-43 and TZM alloys, 20: 37276
Al–Pt–Si, crystallographic parameters, 17: 18822
Al–Pu–Si, phase studies and properties of, bibliographic study of, 16: 32115 (KFK-105)
Al–Pu–Si, preparation of corrosion-resistant, 17: 36219(P)
Al–Pu–Si, preparation and corrosion resistance, 18: 41493(P)
Al–Pu–Si, preparation and properties as reactor fuel, 19: 37150(P)
Al–Pu–Si, radiation effects on clad, 16: 30075 (HW-70158(Pt.I))
Al–Pu–Si, radiation stability, neutron, 16: 24640
Al–Si, activation analysis for phosphorus in hypereutectic, 17: 5994
Al–Si, analysis for silicon, x-ray fluorescence, 16: 22039
Al–Si, annealing of eutectic, metallographic study, 16: 9165 (HW-69401)
Al–Si, annealing neutron-irradiated, 17: 39693
Al–Si, annealing and growth of films of, 20: 15030 (ANL-7102)
Al–Si, corrosion properties and fabrication for cladding, 17: 11120
Al–Si, corrosion by heavy water, 18: 37637 (A/CONF.28/P/591)
Al–Si, corrosion by aluminum–silicon and water of coatings of, on uranium, 19: 40949 (ISC-640)
Al–Si, crack fracture, 17: 36303 (TID-17914)
Al–Si, crack initiation, elastic moduli, and temperature stresses in, 18: 18353(R) (TID-20389)
Al–Si, crystal structure of eutectic, effects of phosphorus on, 20: 31716(R) (UCRL-16658, pp 121-32)
Al–Si, deposition on niobium alloys for high-temperature protection, diffusion, 16: 2120 (ASD-TR-61-66(Pt.I))
Al–Si, development and testing of, on molybdenum, 16: 2174(R) (ER-11462-2)
Al–Si, development of, for tantalum alloy and metal protection, 16: 24148(R) (ASD-TR-61-676)
Al–Si, development of oxidation-resistant, for molybdenum, 16: 6705 (AD-216006)

Al–Si, diffusion of coatings of, in uranium core, electron microprobe analysis of, 17: 28779(R) (MCW-1480)
Al–Si, dispersion in graphite, optimum pressure and temperature for liquid, 20: 39355 (EUR-2988.f)
Al–Si, dissolution in nitric acid, effects of mercuric nitrate catalyst on, 18: 31658(R) (IDO-14635)
Al–Si, ductility of two-phase, effects of composition and particle size on, 20: 15055(R) (NYO-2394-19)
Al–Si, effects of thermal cycling on stability of, 18: 16492
Al–Si, electric conductivity and phase diagram, 16: 15213
Al–Si, explosibility of powders of, 19: 36698 (BM-RI-6516)
Al–Si, filler effects on fusion welding of beryllium, 18: 14449
Al–Si, fracture initiation in, cracking of silicon particles in, 19: 965 (TID-21218)
Al–Si, grain boundary diffusion, 16: 19427
Al–Si, ion energies from spark sources using, 19: 7778
Al–Si, mechanical properties of, precipitation effects on, 17: 29332(T) (AEC-tr-5879)
Al–Si, microstructure of, electron microscopic studies using ultramicrotome, 18: 7206 (GAT-T-1121)
Al–Si, microstructure model of, 20: 41454 (NYO-2394-22)
Al–Si, optical properties of, at high temperatures, emittance and reflectance, 16: 12236 (WADD-TR-60-370)
Al–Si, properties of, for use as protective coating on niobium and its alloys, 20: 29651
Al–Si, properties of intermetallic compounds in, tabulation of, 20: 43972
Al–Si, radiation effects on, recovery from neutron-induced, 20: 905
Al–Si, reactions with uranium, metallographic and microautoradiographic study of, 19: 46951 (NMI-4996, pp 19-26)
Al–Si, sample preparation for electron transmission studies, 20: 15055(R) (NYO-2394-19)
Al–Si, use in bonding aluminum sheaths to uranium fuel elements, 20: 802(P)
Al–Si, work-softening of, effects of second phase on, 17: 24002
Al–Si–Sn, development of, as oxidation-resistant coating for tantalum alloys, 16: 24163(R) (NP-11711)
Al–Si–Sn, development for use as vanadium alloy coating, 18: 39819(R) (IITRI-B6019-5)
Al–Si–Ti, crystallographic parameters, 17: 18822
Al–Si–Ti, phase diagram at 1200°C, 17: 22196
Al–Si–Ti, phase studies, 17: 18733 (AD-278041L)
Al–Si–Ti, phase studies, 19: 14060
Al–Si–U, burnup in reactors, 18: 15603 (BNL-6730)
Al–Si–U, diffusion in, 17: 29255 (ZFK-WF-13)
Al–Si–U, extrusion of irradiation specimens, 16: 11233(R) (NMI-7242)
Al–Si–U, fabrication of tubular, 16: 12747(R) (NMI-7244)
Al–Si–U, fabrication by casting and splat cooling, 18: 24066(R) (NMI-2126)
Al–Si–U, fabrication and properties of hot-pressed and splat-cooled, 18: 24067(R) (NMI-2127)
Al–Si–U, fabrication and properties of splatcooled SLIS, 18: 35938(R) (NMI-2129)
Al–Si–U, grain structure after gamma treatment, 17: 23957(R) (NMI-7247)
Al–Si–U, hardening by heat treatment, 19: 4653 (NMI-7097-1(Del.))
Al–Si–U, hardness and rollability of, 17: 12697
Al–Si–U, hardness of splat-cooled, at 600°C, 18: 24066(R) (NMI-2126)
Al–Si–U, hardness to 500°C, 17: 25775(R) (NMI-7246)
Al–Si–U, hot hardness and microstructure of, effects of heat treatments on, 19: 40958
Al–Si–U, mechanical properties of, hot hardness behavior of, 16: 30085(R) (NMI-7249)
Al–Si–U, mechanical properties and structure, 17: 11096(R) (NMI-7256)
Al–Si–U, phase studies of UAl_4–U_3Si_2 system in, 16: 10599
Al–Si–U, phase studies of uranium-rich region, 16: 24217
Al–Si–U, phase studies, 17: 39621
Al–Si–U, preparation and properties of splat-cooled SLIS, 19: 32683(R) (NMI-1262)
Al–Si–U, properties of splat-cooled, 20: 11224
Al–Si–U, radiation effects, 16: 12748(R) (NMI-7245)
Al–Si–U, radiation effects on structure of dispersion-type fuel elements of, 19: 47084 (NMI-4997, pp 124-33)
Al–Si–U, radiation effects on clarification and coalescence time during processing of, in organic solvents, 20: 29333 (RT-CHI-(65)33)
Al–Si–U, radioinduced swelling in, resistance to, 19: 47103
Al–Si–U, reactions with aluminum at 600°C, 20: 19178(R) (IDO-17154)
Al–Si–V, crystal structure and phase studies, 18: 12704
Al–Si–V, superconductivity of solid solutions in, 20: 17043
Al–Si–Zr, crystallographic parameters, 17: 18822
Al–Si–Zr, phase diagram at 1200°C, 17: 22196
Al–Si–Zr, phase studies, 17: 6729
Al–Si–Zr, phase studies, 17: 18733 (AD-278041L)
Al–Si–Zr, phase studies, 19: 14060
Al–Si–Zr, structure of phases in, 18: 18388
Au–Si, electron transfer in dilute, 17: 37189
Au–Si, phases and structure of, effects of liquid quenching on, 19: 45696 (CALT-221-12)
Au–Si, preparation by simultaneous sputtering, 17: 4892
B–C–Fe–Ni–Si, corrosion of, by water in pressurized water reactors, 16: 7855
B–C–Si, thermophysical properties, 16: 3506
B–C–Si, vaporization of, detection of molecular species produced in, 16: 9144 (WADD-TR-60-782(Pt.III))
B–Co–Ni–Si, corrosion by liquid sodium at 700 and 1200°F, 20: 9422 (NAA-SR-11326)
B–Cr–Fe–Ni–Si, galling tests of Colmonoy 5 and 6 for HTGR valve seats, 19: 11304 (GAMD-3058)
B–Cr–Fe–Si, properties as anti-oxidation coatings for niobium alloys, 17: 14802(R) (AD-278727)
B–Cr–Ni–Si, corrosion by liquid sodium at 700 and 1200°F, 20: 9422 (NAA-SR-11326)
B–Cr–Si, properties as protective coatings on niobium-base alloys, 19: 7876(R) (ML-TDR-64-71)
B–Fe–Ni–Si, corrosion by liquid sodium at 700 and 1200°F, 20: 9422 (NAA-SR-11326)
B–Mo–Si, diffusion reactions in boron chloride–hydrogen–silicon chloride, 18: 34146
B–Ni–Si, brazing alloy for tungsten carbide–cobalt cermet to TZM molybdenum alloy, 20: 4307(R) (ORNL-3870, pp 238-42)
B–Ni–Si, corrosion by liquid sodium at 700 and 1200°F, 20: 9422 (NAA-SR-11326)
B–O–Si, phase studies, 16: 2164 (AD-256389)
B–O–Si, phase studies at 1300°C, 16: 8714(R) (NP-11241)
B–Si, analysis, chemical, 16: 23599 (ARL-180)
B–Si, development of, for tantalum alloy and metal protection, 16: 24148(R) (ASD-TR-61-676)
B–Si, phase studies on, at high pressures, 16: 13508(R) (AD-262812)
B–Si, properties as reactor control material, 17: 3904
B–Si–Zr, crystal structure of compound range ZrB_2–$ZrSi_2$ in, 16: 4175
B–graphite–Si–Ti, properties for aerospace applications, 19: 37144
Ba–B_2O_3–La–Si–Th, titrimetric analysis, 18: 12000
Be–C–Si, phase diagrams, 20: 27541
Be–Hf–Si, crystal structure of HfBeSi and $HfBe_2$–$HfSi_2$, 16: 4175
Be–Mo–Si, compounds in, properties of, for use in aerospace technology, 20: 29770
Be–Mo–Si, properties for high-temperature applications, 17: 543 (WADD-TR-60-889(Pt.II))
Be–Nb–Si, properties for high-temperature applications, 17: 543 (WADD-TR-60-889(Pt.II))
Be–Si, corrosion resistance, 19: 22913(P)
Be–Si, deposition on beryllium, fused-slurry, 19: 13914 (CONF-729-4)
Be–Si, structure, effects of ultra-rapid quenching on, 17: 14812(R) (ASD-TDR-62-181)
Be–Si–Ta, properties for high-temperature applications, 17: 543 (WADD-TR-60-889(Pt.II))
Be–Si–V, superconductivity of solid solutions in, 20: 17043
Be–Si–W, properties for high-temperature applications, 17: 543 (WADD-TR-60-889(Pt.II))
Be–Si–Zr, crystal structure of $ZrBe_2$–$ZrSi_2$, 16: 4175
Be–Si–Zr, properties for high-temperature applications, 17: 543 (WADD-TR-60-889(Pt.II))
Bi–Si, phase studies, 19: 37072
C–Cr–Fe–Mn–Mo–Si–Ti, corrosion of 5 Croloy Ti by steam and chloride salt at high temperatures, 18: 4161 (GEAP-4351)
C–Cr–Fe–Mn–Mo–Si, corrosion of Croloy 1¼ and 5Si by liquid bismuth alloys, 18: 4193 (BNL-811)
C–Cr–Fe–Mn–Mo–Si, corrosion of Croloy 1¼ by liquid lead alloys, 18: 4193 (BNL-811)
C–Cr–Fe–Mn–Si, radiation effects on thermal decomposition of, 18: 30259
C–Cr–Mn–Si, galling tests of Aircolite for HTGR valve seats, 19: 11304 (GAMD-3058)
C–Cr–Si, crystal structure and phase studies on, 18: 10561
C–Fe–Si, crystal structure and phase studies on, 18: 10561
C–Fe–Si, explosibility of powders of, 19: 36698 (BM-RI-6516)
C–Fe–Si, relaxation phenomena in, magnetic studies of, 18: 30203
C–Ir–Si, stability of solid phases, 16: 20394
C–Mn–Ni–Si, use for braze bonding stainless steel cans to stainless steel–uranium dioxide cermets, 19: 4635
C–Mn–P–Si–S, crack growth testing of, 20: 28694(R) (GEAP-4964)
C–Mn–Si, crystal structure and phase studies on, 18: 10561
C–Mo–Si, superconducting transition temperature of $Mo_{4.8}Si_3C_{0.6}$, 20: 17607
C–Mo–Si, phase studies of $Mo_{4.8}Si_3C_{0.6}$ in, 20: 7587
C–Os–Si, stability of solid phases in, 16: 20394
C–Pd–Si, stability of solid phases in, 16: 20394

C–Pt–Si, stability of solid phases in, 16: 20394
C–Re–Si, crystal structure and phase studies on, 18: 10561
C–Re–Si, stability of solid phases in, 16: 20394
C–Rh–Si, stability of solid phases in, 16: 20394
C–Ru–Si, stability of solid phases in, 16: 20394
C–Si, effects on fabrication and tensile properties of niobium–tantalum–titanium–vanadium alloys, 19: 32719(R) (AD-609727)
C–Si, phase studies at high pressures, 16: 13508(R) (AD-262812)
C–Si–U, analysis for silicon, spectrographic, 20: 35391 (CEA-R-2966)
C–Si–U, phase studies, 20: 9555
C–Si–U, phase studies of, at room temperature, 20: 39413
C–Si–U, structure of $U_3C_5Si_2$ phase in, 19: 25003
C–Si–V, crystal structure and phase studies on, 18: 10561
Ca–Si, analysis for calcium, cerium, iron, rare earths, and silicon, 18: 1555
Ce–Ni–Si, formation of compounds with AlB_2 type structure in, 19: 30767
Ce–Si, magnetic properties of compounds in, 19: 37082
Ce–Si–Th, phase studies and structure of, 20: 35918
Ce–Si–U, phase studies and structure of, 20: 35918
Co–Fe–Si, Mössbauer effect in, 20: 40300
Co–Hf–Si, crystal structure of compounds in, 20: 23726
Co–Mg–Si, thermal capacity at 1.5 to 4°K, 20: 27494(R) (NYO-3454-6)
Co–Mo–Si, oxidation, strength, and ductility at high temperatures, 20: 25611(P)
Co–Nb–Si, crystal structure of ternary compounds in, 19: 23096
Co–Nb–Si, crystal structure of compounds in, 19: 41069
Co–Pd–Si, metastable amorphous ferromagnetic phases in, 19: 33687 (CALT-221-10)
Co–Re–Si, phase studies and crystal structure, 18: 22077
Co–Sc–Si, crystal structure, G phases in, 17: 14876
Co–Si–Th, crystal structure of compound in, 19: 20568
Co–Si–U, melting point, 16: 6104(R) (LAMS-2647)
Co–Si–U, phase studies of, eutectic temperature and composition from, 16: 17297(R) (LAMS-2681)
Co–Si–U, phase studies and crystal structures, 19: 18503
Cr–Co–Fe–Mn–Ni–Si–W, bonding of, controlling factors in diffusion, 19: 24964
Cr–Cu–Fe–Mn–Ni–Si, corrosion of Incoloy 800 by superheated steam, 18: 21668(R) (GEMP-274)
Cr–Cu–Fe–Mn–Ni–Si, corrosion of Incoloy 800 by superheated steam containing chloride, 18: 30129 (GEAP-4450)
Cr–Cu–Fe–Mn–Ni–Si, corrosion of Incoloy 800 by superheated steam, 18: 30130 (GEAP-4495)
Cr–Cu–Fe–Mn–Ni–Si, fabrication of Incoloy 800 tubes for use as fuel cladding, 18: 32101 (GEAP-4557)
Cr–Cu–Fe–Mn–Ni–Si, performance of Incoloy 800 as fuel cladding for supercritical-water reactors, 18: 35691(R) (WCAP-3374-1)
Cr–Cu–Fe–Mn–Ni–Si, properties of Incoloy 800 as fuel sheaths in nuclear superheat reactors, 18: 44033 (GEAP-4633)
Cr–Cu–Fe–Mn–Ni–Si, strain cycle tests of Incoloy 800 tubes, 18: 39813 (GEAP-4462)
Cr–Fe–Mn–Mo–Ni–Si, corrosion and metallurgical changes in, caused by steam at 1200 to 1500°F, 16: 24126
Cr–Fe–Mn–Mo–Si, corrosion of Sicromo by cesium, 17: 30944
Cr–Fe–Ni–Si, corrosion cracking in, mechanisms of stress-, 20: 16968 (COO-1319-33)
Cr–Fe–Ni–Si, fabrication methods effects on thermoelectric properties of, 17: 30824
Cr–Mn–Ni–Si, mechanical properties of, effects of steam at 1050°F on, 18: 4795(R) (GEAP-3924)
Cr–Mo–Si, corrosion by mercury at 600 to 1000°F, 18: 27913
Cr–Mo–Si, deposition of coatings of, on and evaluation for FS-85 alloy in air to 2600°F, 17: 36188(R) (AD-289857)
Cr–Mo–Si, deposition on niobium alloys B-66 and D-43, 18: 14373(R) (NP-13498)
Cr–Mo–Si, deposition on niobium alloys B-66, FS-85, and X-110, 18: 14353(R) (AD-408310)
Cr–Mo–Si, oxidation resistance properties as coatings for niobium alloys, 17: 16633(R) (AD-296341)
Cr–Mo–Si, phase studies and thermal properties, 19: 26861
Cr–Mo–Si, properties as anti-oxidation coatings for niobium alloys, 17: 14802(R) (AD-278727)
Cr–Mo–Si, properties as coating for B-66 and D-43 alloys, 18: 20523(R) (NP-13811)
Cr–Mo–Si, properties of, for use as protective coating on niobium and its alloys, 20: 29651
Cr–Ni–Si, corrosion by liquid sodium at 700 and 1200°F, 20: 9422 (NAA-SR-11326)
Cr–Ni–Si, fabrication methods effects on thermoelectric properties of, 17: 30824
Cr–Ni–Si, use for brazing Inconel in reactor environments, 17: 36272
Cr–Rh–Si, phase study of Cr_3O-type structures in, 19: 44702 (TID-22200)
Cr–Si, barrier effects on diffusion in aluminum–uranium alloys, 19: 42871
Cr–Si, development of, for tantalum alloy and metal protection, 16: 24148(R) (ASD-TR-61-676)
Cr–Si, electronic structure of compounds in, 19: 16177
Cr–Si, preparation, properties, and uses of, review on, 16: 27640(T) (FTD-TT-62-430)
Cr–Si–Sn, phase study of Cr_3O-type structures in, 19: 44702 (TID-22200)
Cr–Si–Th, crystal structure of compound in, 19: 20568
Cr–Si–Ti, coating processes for cementation on refractory metals, 18: 34091
Cr–Si–Ti, coatings of, for niobium alloys, 17: 6510 (ASD-TDR-62-934)
Cr–Si–Ti, deposition of, on niobium, process development for, 16: 15125 (NP-11483)
Cr–Si–Ti, deposition of coatings of, on and evaluation for FS-85 alloy in air to 2600°F, 17: 36188(R) (AD-289857)
Cr–Si–Ti, deposition of, on niobium alloys for protection at high temperature, diffusion, 16: 2120 (ASD-TR-61-66(Pt.I))
Cr–Si–Ti, deposition on niobium alloys B-66 and D-43, 18: 14373(R) (NP-13498)
Cr–Si–Ti, deposition on niobium alloys B-66, FS-85, and X-110, 18: 14353(R) (AD-408310)
Cr–Si–Ti, deposition on B-66 and D-36 alloys for high-temperature oxidation protection, 18: 30118(R) (RTD-TDR-63-4006(Pt.I))
Cr–Si–Ti, deposition and performance as oxidation-resistant coating for niobium alloys, 20: 43827 (GTR-19)
Cr–Si–Ti, development of protective coatings of, for niobium alloys, 18: 30127 (ASD-TDR-62-934(Pt.II))
Cr–Si–Ti, effects of coatings of, on niobium alloys B-66 and X-110, 17: 39525(R) (AD-416459)
Cr–Si–Ti, heat treatment of coating of, on niobium alloy bolt and nut, 18: 35978 (AD-431856)
Cr–Si–Ti, oxidation resistance properties as coating for niobium alloys, 17: 16633(R) (AD-296341)
Cr–Si–Ti, phase studies, 18: 549(R) (NP-13241)
Cr–Si–Ti, properties as anti-oxidation coatings for niobium alloys, 17: 14802(R) (AD-278727)
Cr–Si–Ti, properties for coating niobium alloys, 18: 7274
Cr–Si–Ti, properties as coating for B-66 and D-43 alloys, 18: 20523(R) (NP-13811)
Cr–Si–Ti, properties of, for use as protective coating on niobium and its alloys, 20: 29651
Cr–Si–Ti, protective effects on B-66 and D-43 niobium alloys, 18: 24068(R) (NP-13955)
Cr–Si–U, phase studies and crystal structures of compounds in, 19: 18503
Cr–Si–U, preparation and crystal structure of compounds in, 19: 19871
Cr–Si–U, thermal expansion rates for, 20: 33880 (NLCO-946, pp 103-6)
Cr–Si–U–Zr, fatigue tests on compression and tension of, 18: 36021
Cr–Si–W, phase studies, 17: 18733 (AD-278041L)
Cr–Si–W, properties of, for use as protective coating on niobium and its alloys, 20: 29651
Cs–Si, crystal structure, 18: 30216
Cu–Mg–Si, electronic specific heats at 1.5 to 4°K, 19: 30743(R) (NYO-3454-1)
Cu–Ni–Si, corrosion of, by acid, 16: 12057
Cu–Ni–Si, use for braze bonding stainless steel cans to stainless steel–uranium dioxide cermets, 19: 4635
Cu–Si, annealing twins in, nature of, 18: 7216(R) (TID-19872)
Cu–Si, deposition on molybdenum for oxidation protection, 20: 11236
Cu–Si, effects on wetting of graphite at high temperatures, 20: 29764
Cu–Si, internal friction studies of, 19: 25623(R) (TID-21682)
Cu–Si, radiation effects on diffusion-controlled reactions in, 16: 33567
Cu–Si, stacking faults in crystals of, (E/T), 20: 13971 (AD-625834)
Cu–Si–Th, crystal structure of compound in, 19: 20568
Dy–Si, phase studies, 16: 17967(R) (USBM-U-887)
Dy–Si, physical properties, (E), 19: 16188
Er–Si, physical properties, (E), 19: 16188
Fe–Mo–Ni–Si, corrosion of, by lithium fluoride–sodium fluoride–zirconium fluoride systems at 500°C, 16: 4502 (TID-13691)
Fe–Nb–Si, effects of carbon content on properties and reduction of, 17: 32492
Fe–Ni–Ru–Si–W, properties at 1400 to 2000°F, 17: 14808(R) (ARF-2158-24)
Fe–Ni–Si, fabrication methods effects on thermoelectric properties of, 17: 30824
Fe–Ni–Si, neutron scattering by, cross sections for magnetic, 18: 27990
Fe–Pd–Si, metastable amorphous ferromagnetic phases in, 19: 33687 (CALT-221-10)
Fe–Re–Si, phase studies and crystal structure, 18: 22077
Fe–Si, brittle fracture in, relation between twinning and, 19: 26815 (EURAEC-1195)
Fe–Si, comparison of activation and vacuum fusion methods for analysis

for oxygen in, 18: 43419
Fe–Si, corrosion of, review, 19: 7868
Fe–Si, creep at high temperatures, 20: 31714(R) (UCRL-16658, pp 99-103)
Fe–Si, crystal properties of, thermal effects on, 16: 4550 (WADD-TR-60-893)
Fe–Si, crystal structure, 17: 30985(R) (TID-19070)
Fe–Si, dislocation arrangements in, effects on twinning on, 18: 32131 (ASD-TDR-63-360(Pt.II))
Fe–Si, dislocation mobility in crystals of, 18: 34122(R) (GA-4900)
Fe–Si, dislocation structure of annealed and deformed, 19: 26882(R) (EURAEC-1343)
Fe–Si, elastic properties of iron-base single-crystal, 20: 41412(R) (IS-1500(Sect. M))
Fe–Si, electronic structure of, 17: 31001
Fe–Si, flow stress at room temperature, relations with strain, 18: 18413(R) (EURAEC-975)
Fe–Si, magnetic properties, 17: 10240(R) (NP-12208)
Fe–Si, magnetic properties at 400 to 700°C, 18: 8892
Fe–Si, magnetic structure of, studies by neutron scattering, 17: 34465
Fe–Si, magnetic structure from polarized neutron diffraction, 18: 37710
Fe–Si, mechanical and thermophysical properties of Cubex and AMS5210, at 80 to 1400°F, 18: 41928(R) (NASA-CR-54089)
Fe–Si, mechanical properties of, 19: 34675(R) (EURAEC-1394)
Fe–Si, Mossbauer effect in, 17: 29627
Fe–Si, neutron diffraction by, 20: 10231
Fe–Si, neutron radiation effects on, 18: 32255
Fe–Si, phase transformations in, hydrostatic pressure effects on, 16: 4550 (WADD-TR-60-893)
Fe–Si, phase transition behavior of, impulsive loading effects on, 17: 16649 (LADC-5396)
Fe–Si, plastic deformation of, effects of atomic order on, 20: 4297(R) (IS-1200(Sect.M))
Fe–Si, properties of Cubex for use in space electric power systems, 20: 4379 (NASA-CR-54091)
Fe–Si, radiation effects on diffusion-controlled reactions in, 17: 31055
Fe–Si, radiation effects on magnetic relaxation in, fast neutron, 17: 37784
Fe–Si, radiation effects on magnetic properties of, neutron, 18: 8892
Fe–Si, radiation effects of neutrons on ductile-brittle transitions in, 18: 36045(R) (EURAEC-1100)
Fe–Si, radiation effects on magnetic properties of, fast-neutron, 20: 27566 (AERE-R-5194)
Fe–Si, resistivity at 77 to 1325°K with quenching, 19: 1004(R) (ORNL-3676(p.125-56))
Fe–Si, spectroscopy, 17: 30516 (TID-19080)
Fe–Si, stress of, dislocation mobility in, 17: 27783(R) (GA-4227)
Fe–Si, thermodynamic properties, 20: 23014
Fe–Si–Th, crystal structure of compound in, 19: 20568
Fe–Si–U, crystal structure of intermetallic phase U_3Fe_4Si in, 19: 6338
Fe–Si–U, crystal structure of U_2Fe_3Si, 20: 5848
Fe–Si–U, hardening by heat treatment, 19: 4653 (NMI-7097-1(Del.))
Fe–Si–U, melting point, 16: 6104(R) (LAMS-2647)
Fe–Si–U, particle size distribution in, effects of heat treatments on, 18: 32042(R) (HW-81269(p.3.1-38))
Fe–Si–U, phase studies, 16: 32880(R) (MCW-1475)
Fe–Si–U, phase studies of, eutectic temperature and composition in, 16: 17297(R) (LAMS-2681)
Fe–Si–U, phase studies, 17: 27858
Fe–Si–U, phase studies, 18: 39866
Fe–Si–U, phase studies, 19: 4651(R) (MCW-1484(p.9-13))
Fe–Si–U, precipitation of second-phase particles in, metallographic techniques for quantitative studies of, 18: 32045 (HW-SA-3579)
Fe–Si–U, precipitation of second-phase particles in, quantitative metallography of, 19: 30643 (BNWL-30)
Fe–Si–U, preferred orientation of, relations of, to electric conductivity, 19: 4652(R) (MCW-1484(p.15-31))
Fe–Si–U, preparation and crystal structure of compounds in, 19: 19871
Fe–Si–U, radioinduced swelling of, effects of temperature on, 18: 44035(R) (HW-82651(p.3.1-59))
Fe–Si–U, radioinduced swelling in, 19: 23124(R) (HW-83298(p.8.1-4))
Fe–Si–U, radioinduced swelling of, factors affecting, 19: 30648(R) (HW-84573(p.3.1-74))
Fe–Si–U, radioinduced swelling in, resistance to, 19: 47103
Fe–Si–U, radioinduced swelling of, effects of pressure on, 20: 9567(R) (BNWL-166, pp 3.24-9)
Fe–Si–U, radioinduced swelling of, factors affecting, 20: 27570(R) (BNWL-207, pp 3.17-35)
Fe–Si–V, crystal structure of D-phase, (E/T), 20: 30734(R) (TID-22970, pp 1-63)
Fe–Si–V, magnetic hyperfine field and electric quadrupole coupling in, (E), 20: 28657
Fe–Si–W, development and properties, 16: 3483(T) (JPRS-8937(p.43-81))
fissium–Si–U, fabrication of reactor fuel, 17: 41418(P)
Gd–Si, phase studies, 16: 17967(R) (USBM-U-887)
Gd–Si, physical properties, (E), 19: 16188
Ge–Mg–Si, radiation effects on electric properties of $Mg_2Ge_{0.8}Si_{0.2}$, 20: 2502
Ge–Nb–Si, structure and thermoelectric properties, 17: 23987
Ge–Si, mechanical properties of cast and hot-pressed, 19: 7907 (NAA-SR-Memo-10457)
Ge–Si, performance in thermoelectric cells, 17: 34336
Ge–Si, performance of power generating thermocouple of, 17: 36280(R) (AD-291456)
Ge–Si, performance in modular thermoelectric cells, 18: 36225(R) (AD-600365)
Ge–Si, preparation for radiation detectors, 20: 2182(P)
Ge–Si, properties for thermocouples, 19: 39430(R) (AD-426092)
Ge–Si, superconductivity of, 18: 15103
Ge–Si, thermoelectric properties, 20: 40451
Ge–Si, use in thermoelectric converters for space power systems, 19: 45664
Ge–Si–Ta, structure and thermoelectric properties, 17: 23987
Ge–Si–Th, crystal structure and phase studies on, 18: 12707
Ge–Si–Th, phase studies on, 18: 7234
Ge–Si–U, structure and thermoelectric properties, 17: 29352
Ge–Si–V, superconductivity of solid solutions in, 20: 17043
graphite–Si, properties for aerospace applications, 19: 37144
Hf–Fe–Si, crystal structure of compounds in, 20: 23726
Ir–Si, heats of formation, 16: 20394
Ir–Si, properties for thermoelectric power generation, 17: 36280(R) (AD-291456)
K–Si, crystal structure, 18: 30216
Li–Mg–Si, fabrication and properties of cast, 20: 15007 (NP-15881)
Mg–Ni–Si, corrosion by steam and water at high temperatures, 19: 30669(R) (HW-84573(p.5.1-22))
Mg–Si, corrosion by steam and water at high temperatures, 19: 30669(R) (HW-84573(p.5.1-22))
Mn–Si, development of, for tantalum alloy and metal protection, 16: 24148(R) (ASD-TR-61-676)
Mg–Si, electric conductivity, Hall coefficients and mobility, and Seebeck coefficients at 7 to 1000°K of p- and n-type Mg_2Si single, 16: 25799 (IS-362)
Mn–Si, thermal expansion coefficients of, x-ray diffraction studies of, 16: 33489 (ASD-TR-61-676)
Mn–Si–Th, crystal structure of compound in, 19: 20568
Mn–Si–Ti, phase studies, 19: 14060
Mn–Si–U, eutectic temperature and composition in, 16: 17297(R) (LAMS-2681)
Mn–Si–U, melting point, 16: 6104(R) (LAMS-2647)
Mn–Si–U, phase studies and crystal structures of compounds in, 19: 18503
Mn–Si–U, preparation and crystal structure of compounds in, 19: 19871
Mo–Nb–Si, phase diagram and properties of, 20: 23683
Mo–Nb–Si, phase studies and properties of, 19: 39194
Mo–Si, diffusion reactions at 1250°C, 18: 26001
Mo–Si, effects of Nb_3Sn on crystal structure of Mo_5Si in, 18: 12705
Mo–Si, effects on wetting of graphite at high temperatures, 20: 29764
Mo–Si, electronic structure of compounds in, 19: 16177
Mo–Si, heats of dissociation, 17: 4933 (WADD-TR-60-463(Pt.II))
Mo–Si, oxidation of, at 1000 to 1725°C, kinetics of, 16: 27588 (ASD-TDR-62-203(Pt-1))
Mo–Si, preparation, properties, and uses of, review on, 16: 27640(T) (FTD-TT-62-430)
Mo–Si–U, fission effects on, reduction of swelling in, 18: 24996(R) (NAA-SR-8888(Sect.VI))
Mo–Si–U, hot hardness and microstructure, 19: 32734 (NMI-7075)
Mo–Si–U, hot hardness and microstructure of, effects of quenching temperature on, 20: 31666
Mo–Si–U, preparation and crystal structure of compounds in, 19: 19871
Mo–Si–U, structure of $U_4Mo_5Si_3$, 18: 12716
Mo–Si–U, thermal expansion rates for, 20: 33880 (NLCO-946, pp 103-6)
Mo–Si–V, phase studies and properties, 16: 30849
Mo–Si–W, deposition on D-14 niobium alloy, 18: 34052 (RTD-TDR-63-4063)
Mo–Si–W, phase studies, 17: 18733 (AD-278041L)
NaF–Si, properties as pack-coating material for high-temperature oxidation protection of vanadium alloys, 17: 35997(R) (IITRE-B6001-5)
Nb–Pu–Si, phase diagram, 17: 14740 (TID-11295(2nd Ed.))
Nb–Pu–Si, properties as reactor fuel, 17: 8763
Nb–Rh–Si, phase study of Cr_3O-type structures in, 19: 44702 (TID-22200)
Nb–Si, analysis for silicon, spectrophotometric, 19: 46171 (KAPL-M-6492)
Nb–Si, electric and mechanical properties, 18: 24158
Nb–Si, mechanical properties, 19: 11734
Nb–Si, mechanical properties of, effects of composition on,

20: 11288(T) (AD-622477)
Nb–Si, oxidation kinetics, 19: 28757(T) (FTD-TT-64-1154)
Nb–Si, preparation, properties, and uses of, review on, 16: 27640(T) (FTD-TT-62-430)
Nb–Si, preparation and structure of Nb_5Si, 17: 18782
Nb–Si, preparation of superconducting, empiricism for, 18: 14518
Nb–Si–Sn, superconducting properties of Nb_5SnSi, 17: 27861
Nb–Si–V, phase studies, 18: 42088
Nb–Si–W, phase studies on, 18: 14505
Nb–Si–W, phase studies and microstructure, 18: 42091
Nb–Si–W, preparation and properties of, 18: 14505
Nb–Si–W, properties and structure of, 17: 16710
Ni–Pd–Si, metastable amorphous ferromagnetic phases in, 19: 33687 (CALT-221-10)
Ni–rare earth–Si, crystal structure of $R_3Ni_6Si_2$ compounds in, 20: 31253
Ni–Re–Si, phase studies and crystal structure, 18: 22077
Ni–Sc–Si, crystal structure, G phases in, 17: 14876
Ni–Si, corrosion by steam and water at high temperatures, 19: 30669(R) (HW-84573(p.5.1-22))
Ni–Si, fabrication methods effects on thermoelectric properties of, 17: 30824
Ni–Si, phase studies, 16: 22595 (TID-15971)
Ni–Si–Th, crystal structure of compound in, 19: 20568
Ni–Si–Ti, phase studies, 18: 549(R) (NP-13241)
Ni–Si–U, melting point, 16: 6104(R) (LAMS-2647)
O–Si–Ti–W–Zr, development of, for protection of tungsten against oxidation at high temperatures, 17: 14837(R) (NP-12595)
O–Si–Ti–W–Zr, development for high-temperature oxidation protection of tungsten, 18: 565(R) (NP-13243)
O–Si–Ti–W–Zr, development for high-temperature oxidation protection of tungsten, 18: 24086(R) (NP-13898)
O–Si–Ti–W–Zr, oxidation resistance of, testing as tungsten coating, 17: 6519(R) (NP-12293)
O–Si–W, development for high-temperature oxidation protection of tungsten, 18: 565(R) (NP-13243)
O–Si–W, development for high-temperature oxidation protection of tungsten, 18: 24086(R) (NP-13898)
Pd–Si, heats of formation, 16: 20394
Pd–Si, metastable phases from very rapid cooling of molten, 18: 30169 (CALT-221-1)
Pd–Si, phase studies, 18: 44132 (CALT-221-4)
Pt–Si, heats of formation, 16: 20394
Pu–Si, crystal structure of Pu_3Si_2, 18: 13354(R) (BMI-1657(Del.))
Pu–Si, crystal structure of Pu_3Si_2, 18: 37689
Pu–Si, density and phases of plutonium-base, 20: 46144(R) (HW-67765)
Pu–Si, ignition temperatures in air and oxygen, 17: 35079(R) (ANL-6749)
Pu–Si, phase diagram, 19: 7905 (LADC-6199)
Pu–Si, phase studies and properties of, bibliographic study of, 16: 32115 (KFK-105)
Pu–Si, phase studies, 17: 28565(R) (LAMS-2915)
Pu–Si, phase studies, 18: 17351(R) (BMI-1659(Del.))
Pu–Si, physical properties of intermetallic compounds in, 20: 7554 (BNWL-SA-385)
Pu–Si, preparation and phase studies, 16: 17966(R) (BMI-1541(Del.))
Pu–Si, preparation, 17: 16568
Pu–Si, structure, 17: 3536
Pu–Si–Ti, density and phases of plutonium-base, 20: 46144(R) (HW-67765)
Rb–Si, crystal structure, 18: 30216
Rh–Si, heats of formation, 16: 20394
Rh–Si–V, phase study of Cr_3O-type structures in, 19: 44702 (TID-22200)
Sc–Si, crystal structure of AB type compound in, 19: 37063
Sc–Si, crystal structure, 18: 13795
Sc–Si, preparation and crystal structure, 19: 28835
Si–Ag, performance as oxidation-resistant coating for niobium alloys, 20: 43827 (GTR-19)
Si–Ag, phases and structure of, effects of liquid quenching on, 19: 45696 (CALT-221-12)
Si–Na, crystal structure, 18: 30216
Si–SiC, corrosion of, by molten sodium, 16: 28646(R) (ORNL-2247(Pts.1-5))
Si–SiC, performance of, as coating on Pebble Bed Reactor fuel, 16: 9663 (NYO-9064)
Si–SiO_2, electric properties of interfaces in, 19: 46727 (UCRL-16197)
Si–Sn–V, phase study of Cr_3O-type structures in, 19: 44702 (TID-22200)
Si–Sn–V, superconductivity of solid solutions in, 20: 17043
Si–stainless steel, corrosion by steam at 650°C, 19: 44616(R) (ANL-7000, pp 122-37)
Si–Ta, properties as high-temperature brazing alloys, 17: 25688(R) (GEMP-177A)
Si–Ta–Ti–V, phase studies, 18: 549(R) (NP-13241)
Si–Ta–V, phase studies on intermetallic compounds in, 20: 17075
Si–Tc, crystal structure and phase studies, 18: 25970(R) (ANL-6868 (p.303-25))
Si–Tc, crystal structure of $TcSi_2$ in, 19: 47055
Si–Tc, phase studies, 19: 7928
Si–Tc, phase studies, 19: 44678(R) (ANL-7000, pp 186-200)
Si–Th, crystal structure and phase studies on, 18: 12707
Si–Th, phase transformations in, 18: 37701
Si–Th, preparation, properties, and uses of, review on, 16: 27640(T) (FTD-TT-62-430)
Si–Th, properties of, for use as thermal breeder fuels, 16: 12651 (BMI-1568)
Si–Th–U, corrosion and oxidation, 16: 24630
Si–Th–U, properties of, for use as thermal breeder fuels, 16: 12651 (BMI-1568)
Si–Ti, combustibility temperature of, 19: 37093
Si–Ti, development of, for tantalum alloy and metal protection, 16: 24148(R) (ASD-TR-61-676)
Si–Ti, preparation, properties, and uses of, review on, 16: 27640(T) (FTD-TT-62-430)
Si–TiN, physical properties, 17: 3902
Si–Ti–V, aging characteristics and phase studies, 16: 6746
Si–Ti–W, oxidation kinetics, 19: 28757(T) (FTD-TT-64-1154)
Si–Ti–W–Zr, properties as protective coatings for tungsten at high temperatures, 19: 13888 (ML-TDR-64-227)
Si–Ti–Zr, tensile properties at room temperature, 18: 18380
Si–U, analysis of, for silicon, 17: 15892
Si–U, bibliography on use of, as fuel, 16: 15201 (VDIT-53)
Si–U, evaluation of tubes of, for irradiation testing, 16: 7865 (NMI-7204)
Si–U, extrusion of, for irradiation specimens, 16: 11233(R) (NMI-7242)
Si–U, extrusion of, for irradiation testing, 16: 30086(R) (NMI-7250)
Si–U, extrusion into rods from alpha phase, (E), 19: 22923 (NMI-7004)
Si–U, fabrication and properties, 16: 25735(R) (NMI-7251)
Si–U, grain structure after beta treatment, 17: 23957(R) (NMI-7247)
Si–U, hardening by heat treatment, 19: 4653 (NMI-7097-1(Del.))
Si–U, hardness at 20 to 600°C, 17: 23957(R) (NMI-7247)
Si–U, hot hardness and microstructure of, effects of heat treatments on, 19: 40958
Si–U, mechanical properties of, at high temperatures, 16: 30086(R) (NMI-7250)
Si–U, mechanical properties and phase studies, 17: 39625
Si–U, metallographic tests on arc melted, 20: 29775
Si–U, phase studies, 17: 29255 (ZFK-WF-13)
Si–U, phase studies, 17: 39620
Si–U, phase studies, 17: 39623
Si–U, phase studies, 17: 39624
Si–U, phase studies and temperature effects on, 17: 41466
Si–U, phase studies at 500 to 1200°C in uranium-rich, 18: 44141 (MCW-1486)
Si–U, phase studies, 19: 40958
Si–U, phase studies, 20: 8951
Si–U, phase transformation (β–α'), 17: 39626
Si–U, phase transformation in, mechanisms for beta-to-alpha, 20: 27519
Si–U, preparation of tubular, for HWCTR test irradiation, 16: 30085(R) (NMI-7249)
Si–U, preparation, properties, and uses of, review on, 16: 27640(T) (FTD-TT-62-430)
Si–U, processing of tubular, for HWCTR irradiation screening tests, 16: 30087(R) (NMI-7252)
Si–U, quench-rate effects on texture of, 19: 30739 (MCW-1491)
Si–U, radioinduced swelling in, resistance to, 19: 47103
Si–U, sintering by hot pressing, reaction, 16: 24136
Si–U, spectrographic analysis for aluminum, 18: 35451 (PG-Report-390)
Si–U, thermodynamic properties, 16: 15215
Si–U, thermodynamic properties of, 18: 44224
Si–U–Zr, phase studies of uranium-rich, 16: 2257
Si–V, barrier effects on diffusion in aluminum–uranium alloys, 19: 42871
Si–V, critical field limits at superconducting temperatures, 17: 3635
Si–V, development of, for tantalum alloy and metal protection, 16: 24148(R) (ASD-TR-61-676)
Si–V, fabrication, properties, testing, and uses of superconducting, 19: 16110
Si–V, magnetic flux distributions in superconductors of, (E), 19: 10194
Si–V, magnetic properties of superconducting, effects of temperature on critical field, 16: 15467
Si–V, magnetic properties of superconducting, 18: 9262(R) (NP-13492)
Si–V, negative surface energy model of superconductivity of, 17: 9040
Si–V, preparation, properties, and uses of, review on, 16: 27640(T) (FTD-TT-62-430)
Si–V, preparation and properties of thin-film hard superconducting, 18: 28501
Si–V, pressure effects on superconductivity of, 18: 15078
Si–V, properties of superconducting, 18: 6127
Si–V, radiation effects on superconducting properties of, fast-neutron,

18: 10583
Si–V, radiation effects on superconductivity of, neutron, 18: 34683(R) (NP-14136)
Si–V, strong phonon effects in superconductors of, 18: 40449
Si–V, superconductivity, 16: 16830
Si–V, superconductivity of, isotope effects on, 17: 34617
Si–V, superconductivity, 17: 41604
Si–V, superconducting transition temperature of V_3Si, effects of stresses on (E), 19: 1496
Si–V, superconductivity of fused, 20: 15123
Si–W, dissociation pressures, 17: 4933 (WADD-TR-60-463(Pt.II))
Si–W, impact, oxidation, and shock resistance, 16: 5720(R) (NP-11178)
Si–W, oxidation kinetics, 19: 28757(T) (FTD-TT-64-1154)
Si–W, phase diagram, 20: 11296
Si–W, properties of, for tungsten oxidation protection, effects of additives on, 16: 10537(R) (NP-11387)
Si–W, properties for high-temperature applications, 17: 543 (WADD-TR-60-889(Pt.II))
Si–W, properties as protective coatings for tungsten at high temperatures, 19: 13888 (ML-TDR-64-227)
(Si–W)–Ti–Zr, development for high-temperature oxidation protection of tungsten, 17: 14837(R) (NP-12595)
Si–Y, crystal structure, 18: 13795
Si–Zr, atomic number effects correction in electron probe microanalysis of, 17: 27268
Si–Zr, combustibility temperature of, 19: 37093
Si–Zr, combustion diagram of, 18: 39935
Si–Zr, phase studies, 19: 14060
Si–Zr, preparation, 16: 20980(T,R) (EURAEC-26)
Si–Zr, preparation, properties, and uses of, review on, 16: 27640(T) (FTD-TT-62-430)
Sm–Si, physical properties, (E), 19: 16188

SILICON, TETRAMETHYL-
ionization by electron impact, 16: 17708(R) (TID-14812)
nuclear magnetic resonance spectra, effects of temperature on chemical shifts from methane, 16: 1758
radiolysis of gaseous, mechanism of x, 19: 17956(R) (NYO-2007-8)

SILICONE POLYMERS
see also Silicone Rubbers
dimethyl-, preparation for embedding in human body, 20: 33395(P)
dimethyl-, radiation effects on mechanical properties of, gamma, 20: 25622
neutron scattering by, thermal, 17: 36669 (WASH-1042)
preparation, 19: 30295(P)
preparation of nitrile-containing, 19: 32204(P)
radiation chemistry of, electron spin resonance studies of, 18: 27591
radiation effects on properties of coatings, 17: 36362
radiation effects on stabilities of, electron, 18: 39313
radiation effects on, 19: 32244(P)
radiation effects on electric and physical properties of, gamma and neutron, 20: 11344 (N65-35361)
radiation effects on, role of LET in gamma and helium-4/lithium-7, 20: 20764
radiation effects on, light-scattering and viscosity measurements of gamma, 20: 20765
radiation effects on, with high phenyl content, gamma, 20: 25622
radiation effects on, in air and vacuum at 38 to 121°C, 20: 26969
radiation effects on viscoelastic properties of filled and unfilled, gamma, 20: 26971
radiation effects on, in various gaseous atmospheres, gamma, 20: 40974
radioinduced chlorosulfonylation of, 17: 28996
radioinduced crosslinking, protective effects of sulfur against, 16: 20507
radioinduced cross linking, 19: 30295(P)
radioinduced introduction of Si-H groups into, 16: 27106(P)
radioinduced polymerization of solid, epitaxy in, 18: 25502(T) (AEC-tr-6372(p.323-30))
radioinduced polymerization of, activation energy and kinetics of, 18: 25503(T) (AEC-tr-6372(p.331-47))
synthesis of radiation-resistant, 16: 3055(P)
trifluoropropyl-, radiation effects on mechanical properties of, gamma, 20: 25622
phosphors–tritiated silicone polymers, preparation of luminous compositions from, 20: 20787(P)

SILICONE RUBBERS
see also Silicone Polymers
compressive creep and stress relaxation of foams of, 18: 42023 (UCRL-7988)
diffusion of radon and tritium through films of, 18: 16550 (TID-7688 (p.64-7))
electric properties of unfilled and filled, data sheets on, 18: 12631 (DS-127)
neutron scattering at 4 to 11 Å, 18: 34752(R) (CU(PNPL)-234)
permeability to carbon dioxide–hydrogen mixtures, 20: 29362
preparation of radiation-resistant, 16: 16303(P)
preparation of radioisotope-containing, 17: 39520(P)
preparation with improved radiation resistance, 16: 16444(P)
properties of, effects of low temperature on, 20: 4417
radiation and temperature effects on O-ring pressure seals, 16: 15245 (DC-59-10-15)
radiation effects at high temperatures, 16: 10614 (DC-60-3-244)
radiation effects on engineering properties, 16: 25843 (NARF-62-5T)
radiation effects on dielectric properties of, gamma, 16: 29450
radiation effects on pseudo-equilibrium stress-strain and tensile strength of, 16: 32151 (NARF-62-9T)
radiation effects on compression-set behavior of, 17: 36347(R) (NARF-62-18P)
radiation effects on electric insulators of, gamma and neutron, 18: 12412 (AFCRL-63-753)
radiation effects on, gamma and neutron, 18: 24937 (APEX-917)
radiation effects on Silastic 7-170 and SE 550, hardening against, 19: 9547
radiation effects on, gamma and neutron absorption doses in, 19: 15578
radiation effects on viscoelastic properties of, gamma, 20: 29313
radioinduced chlorination, 16: 23759
radioinduced vulcanization, 16: 27616(P)
radioinduced vulcanization of, effects of *m*-phenylene di- and *N*-phenyl-maleimides on, 17: 32167
radioinduced vulcanization, 17: 40878
radioinduced vulcanization of hetero-, properties of products produced by, 18: 8886
radiovulcanization, advantages of, 16: 25684
radiovulcanization of, economics and sources for, 19: 1016
specifications for sealant applications, 19: 18399 (TID-21513)
thermal stability of radiovulcanizates, 16: 8782
use in metallographic replication, 19: 46932 (NMI-4999, pp 60-8)
use in replication of irradiated samples, 19: 47091 (NMI-4999, pp 69-77)
use with powdered lead in flexible shielding materials, 20: 25338(P)

SILICONES
curing of, by irradiation, 17: 6769(P)
effects on radioinduced changes in dielectric properties of mica paper, 20: 1897 (NASA-TN-D-3032)
molecular weights of polysiloxanes from intrinsic viscosity measurements, 18: 36889 (SC-DR-64-978)
neutron attenuation by, with polymer-chip additives, 17: 41375(P)
neutron scattering at 4 to 11 A by polymethyl siloxane, 18: 34752(R) (CU(PNPL)-234)
performance of DC-705, in glass diffusion pumps, 19: 32414(R) (WERL-2823-18)
performance of DC-705, in glass diffusion pumps, 20: 39098(R) (WERL-2823-21)
preparation and conductive properties of silver-impregnated adhesive, 18: 45173(R) (MLM-1203)
preparation and properties as adhesive materials, 18: 29145(R) (MLM-1185)
preparation and properties of phenylchlorophenyl siloxane at 20 to 100°C, 19: 32202(P)
preparation and properties of methylphenyl siloxane as gaskets, seals, and electric insulators, 19: 32205(P)
preparation and uses of trifluoromethylphenyl siloxane, 19: 32245(P)
preparation of cyclosiloxanes, 19: 32244(P)
preparation of methylvinyl siloxane, effects of curing catalysts in, 19: 32206(P)
preparation of phenyl siloxane, 19: 32242(P)
preparation of phenylvinyl siloxane, 19: 32203(P)
properties as adhesives, 18: 45175(R) (MLM-1209)
properties as adhesives, 18: 45174(R) (MLM-1204)
properties of DC 269 and RTV 615 as curing matrices for flexible conductive adhesives, 18: 45174(R) (MLM-1204)
protective effects against radiation in dimethylsiloxane polymers, 17: 21759
radiation chlorination of, 18: 37221
radiation effects on physical properties, gamma, 16: 30902 (HW-61923)
radiation effects on, 16: 32150 (NARF-62-8T)
radiation effects on dimethyl-diphenyl siloxane copolymer, temperature dependence of crosslinking of, 17: 20069
radiation effects on compression-set behavior of elastomeric, 17: 29378 (NARF-63-2T)
radiation effects on, cosmic, 17: 32693
radiation effects on electric properties of, for use as dielectric fluids, 18: 656 (NARF-63-7T)
radiation effects on electric properties of fluid, relations with temperature, 18: 11512(R) (NARF-63-9p)
radiation effects on thermal control coatings of, in nuclear spacecraft, 18: 20603
radiation effects on tensile strength of, 18: 27594
radiation effects on electric conductivity and ion mobility, x, 18: 27498

radiation effects on dynamic modulus properties of, 18: 41538
radiation effects on insulation life of, combined gamma and thermal, 19: 4723
radiation effects on electrically insulating, 19: 24584
radiation effects on coatings of, for spacecraft, 20: 2428 (NASA-SP-55, pp 365-79)
radiation effects on dielectric and mechanical properties of, combined effects of low-temperature, vacuum, and gamma and neutron, 20: 21152 (N-65-22353)
radiation effects on stabilities of arylmethyl, 18: 39313
radiation effects on, materials selection for, 17: 37566(R) (FZK-142)
radiation effects on viscosity of solutions of dimethyl siloxane, 18: 29722(T,R) (AEC-tr-6231(p.212-19))
radiation effects on crosslinking rate of vulcanized dimethyl siloxane (RTV-11) at 100 to 325°F, 19: 9188
radiation resistance, 19: 24561
radiation resistance, high-temperature flexibility, and thermal stability of phenyl siloxane, 19: 32242(P)
radiation resistance of trifluoromethylphenyl siloxane, 19: 32245(P)
radioinduced addition to textiles, for waterproofing, 20: 4033
radioinduced bulk photovoltaic effect in, in contact with metals, 18: 18443
radioinduced chlorination of polydimethyl-, and polyphenyldimethyl-, at 0°C, 17: 10715
radioinduced chlorination of dimethyl, gamma, 18: 29725(T,R) (AEC-tr-6231(p.230-2))
radioinduced crosslinking of methyl siloxane, effects on NMR spectra, 17: 32682
radioinduced free radical formation in polydimethyl siloxane, 18: 41548
radioinduced grafting on cotton cloth, 19: 9197
radioinduced graft polymerization on leather, 20: 25179(P)
radioinduced oxidation, gas evolution and peroxide formation in, 16: 30456
radioinduced oxidation of dimethyl siloxane, 18: 29727(T,R) (AEC-tr-6231(p.239-44))
radioinduced polymerization of hexamethylcyclosiloxane with α-trioxymethylene, 19: 11199
radioinduced polymerization of hexamethylcyclotrisiloxane in solid phase, 20: 1903
radioinduced polymerization on sodium chloride and stainless steel surfaces, electron, 20: 7176
radioinduced polymerization of hexamethylcyclotrisiloxane, kinetics of gamma, 20: 35564
radioinduced polymerization of, 1-octamethylcyclotetrasiloxane, 18: 39329
radioinduced polymerization of hexamethylcyclotrisiloxane with gaseous ethylene, 19: 15565(R) (BNL-841(p.43-51))
radiolysis of octamethylcyclotetrasiloxane, effects of dose, dose rate, scavengers, and temperature, 16: 22224
radiolysis of, gamma, 20: 25162
synthesis of iodine-131-labeled, 18: 10123
use as sealants for electrical cables and conduits, 19: 11306 (HW-65182RD)
vibrational frequencies of deuterated, 16: 14747
vinyl-, radioinduced polymerization of, gamma, 20: 25162
air–silicone fluids, theory of two-phase annular flows of, 18: 25657(R) (NYO-3114-1)
silicone–TiO_2, radiation effects on, kryptonate method for determining uv, 20: 18570(R) (NYO-2757-5)
silicone–TBP, solvent properties for ions from molten nitrate at 150°C, 19: 19833 (CEA-R-2628)

SILICOÖRGANIC COMPOUNDS
see also Silane
chemical nature of surface of, effects on physicomechanical properties of rubber, 17: 40879
exchange of surface hydroxyl groups in aerosol, 16: 1793
luminescence quenching effects on diphenylanthracene and p-tetraphenyl in benzene and cyclohexane solutions, 17: 4564
polarizability of liquid tetrachloride, corrections for zero-field many-body, 17: 4526
preparation by irradiation of hydrocarbons and silicon chlorides and fluorides, 16: 26990
preparation of deuterium-labeled trimethylsilanol, 19: 5901
preparation of polymeric, 18: 8036(T) (SC-T-533)
preparation of saturated fluorocarbon, with high solvent resistance, 17: 39093(P)
quenching effects on polyvinyltoluene scintillators, 18: 12197
radiation effects on reactions between organosilicon hydrides and vinyl silicon compounds, 17: 16068
radiation effects on, EPR study of, 20: 4012
radiation effects on, EPR study of electron, 20: 36883
radioinduced chlorination using gamma radiation, 20: 23081(T) (AEC-tr-6466/1, pp 187-90)
radioinduced grafting on cotton cloth, 19: 9197
radiolysis of, EPR studies of yields of stabilized charges in low-temperature, 20: 40962
studies of 5-trimethylsilylnorbornenes, 18: 9775(R) (TID-19992)

Silicotungstic Acid
see Heteropoly Acids

SILK
deuterium-hydrogen exchange of fibroin between heavy and light water and, 18: 23470
identification of Japanese, activation analysis and gamma spectra, 18: 35907(R) (NCSC-2477-2)
radioinduced polymerization with acrylonitrile, methyl methacrylate, and styrene, 18: 319

SILKWORMS
effects of temperature on radioinduced sterility in male, 20: 42930
genetic studies of, 20: 26655(R) (NP-15975)
oxygen-18 uptake by tyrosine in, from atmosphere, 19: 48
radiation effects on oxygen uptake by, effects of temperature on post-, 17: 17816
radiation effects on number of blood cells in larvae of, 17: 30221
radiation effects on activities of digestive enzymes in, 19: 8889
radiation effects on, genetic, 19: 21862(R) (NP-14937(p.93-116))
radiation effects on eggs of *Bombyx mori L.*, 19: 24302
radiation effects in, lethal, 19: 43787
radiation effects in, genetic, 19: 43787
radiation effects in, genetic, 19: 43784
radiation effects on gonial cells in, mutagenic fission neutron and gamma, 19: 45883
radiation effects on, frequency of mutagenic β and γ, 20: 12692
radiation effects on spermatogonia of, x, 20: 22614(R) (NIRS-4, pp 28-34)
radiation effects on sperm of, genetic, RBE of fast neutron and γ, 20: 38626
radiation effects on chromosomes in spermatocytes of, uv, 20: 42895
radiation effects, genetic, 19: 21915
radiation effects, genetic, 19: 21916
radiation killing of cocoons, 17: 12525
radioinduced mutations in germ cells of, effects of sex on gamma, 18: 11839
radioinduced mutations of, 19: 43786
radioinduced sterility in, relation of spermatogenesis to, 19: 8865
radiomimetic substances in, genetic and lethal effects of, 19: 43787
radiosensitivity of spermatogonia in larvae of, 19: 43783
radiosensitivity of eggs of *Bombyx mori*, 19: 45904
radiosensitivity of eggs of, 20: 72
radiosterilization effects on spermatogenesis of, 19: 10859

Siloxanes
see Silicones

SILTS
accumulation rates of marine, thorium-230/thorium method for determination, 16: 16583
age determination using thorium-230 to thorium-232 ratio, 16: 4383
age estimation and paleography of, in New Jersey Triassic Basin, 20: 18924(R) (NYO-1669-11)
age estimation in ocean sediments by protactinium-231/thorium-230 ratio, 17: 40990 (TID-19555)
age estimation in ocean sediments by ionium and protactinium methods, 19: 7702 (NYO-8925)
age estimation of ocean, by thorium-230 to protactinium-231 ratio, 19: 13638
age estimation of, from protactinium-231 deposition rates, 20: 18926 (NYO-3450-1, pp 29-40)
age of, Black Sea and Indigirka River, USSR, 19: 46621
analysis for alpha and beta activity in Hartbeespoort Dam, South Africa, 19: 11459
analysis for antimony, activation, 20: 43080 (ORO-2670-15)
analysis for bromine in deep-sea, activation, 20: 40811 (ORO-2670-13)
analysis for calcium, magnesium, and strontium, 20: 12540(R) (NYO-2882-8)
analysis for carbon-14 in Black Sea, use for age determination of Holocene, 17: 40994
analysis for fission products in White Oak Creek drainage basin, 16: 2058(R) (ORNL-3189(p.6-13))
analysis for hafnium and zirconium, neutron activation, 17: 31986 (TID-19179)
analysis for isoprenoid alkanes, methods for, 20: 16633 (UCRL-16605)
analysis for plutonium-239, radiochemical, 19: 11000
analysis for protactinium, method for, 18: 35485
analysis for radium, thorium-230, and uranium, methods for, 18: 6766
analysis for rare-earth and yttrium abundance, activation, 16: 20841
analysis for rare earths, thorium, and uranium by ion exchange, review on, 20: 3888 (TID-22402)
analysis for scandium, activation, 20: 22886
analysis for trace elements, spectroscopic, 19: 36315

analysis for uranium by extraction-luminescence, 16: 28904
analysis for uranium, fluorometric, 19: 30085(R) (TID-21853)
analysis for uranium by ion exchange separation and fluorimetry, 19: 46223
analysis in surface waters, activation, 20: 1739(R) (GA-4297)
analysis of Clinch River, radiochemical, 17: 2810 (ORNL-3370)
analysis of Clinch River bottom, for radioactive materials, 20: 8479(R) (ORNL-3849, pp 1-42)
analysis of Clinch River, for radionuclide distribution, 20: 45223
analysis of Columbia River, 17: 10850(R) (HW-73337(p.77-157))
analysis of Columbia River effluent, for sediment type and radioactivity of, 18: 12338 (TID-20200)
analysis of deep ocean cores for strontium, magnesium, and manganese in fossil foraminiferal carbonates, 16: 29187 (TID-16359)
analysis of deep-sea, for cosmogenic nuclei, (E), 19: 4358
analysis of marine, for gamma-emitters, 17: 15530
analysis of ocean-bottom by activation analysis, engineering drawings of equipment for, 17: 35667
analysis of river, activation, 20: 14439(R) (GA-5556)
analysis, spectrochemical, 16: 4379
beryllium-10 content of sea, 17: 30739
beta activity measurement from, 17: 5972 (PG-Report-403)
binding mechanisms in, 20: 25282 (RLO-1750-4)
boron content in fresh and salt water, 17: 3175
carbon-12/-13 ratios in, 20: 45917
cerium-144 content in Ligurian Sea, 19: 30412
cesium transport by, in estuaries and streams, 18: 35726
cesium-137 content in, of White Oak Lake, Tenn., 20: 10449
cesium-137 distribution and fixation in, of lacustrine origin, 19: 46681
chemical composition of, in Bay of Roquebrune, 20: 36553
cobalt-58 distribution in, in flowing and non-flowing systems, 20: 6716
cobalt-58 uptake and release by aquatic, in ecological environment, 20: 24834 (TID-22878)
concentration in rivers and streams, design of radiometric gage for monitoring, 20: 27229 (NYO-2983-1)
content in rivers and streams, x-ray attenuation gage for measuring, 18: 16195 (TID-7689(p.142))
content in rivers and streams, radioisotope technique for monitoring, 20: 23280
content of manganese-54 and zinc-65 in Columbia River, 20: 40523(R) (RLO-1750-8(Vol.1))
content of suspended sediment in river waters, radiometric instrument for measuring, 20: 37057
content of trace elements in ocean, effects of removal, supply, and transport mechanisms on, 20: 18892 (NYO-3450-1, pp 41-89)
cosmogenic nuclides in deep ocean sediments, search for, 19: 13621 (BNL-7881)
density and concentration of, equipment for measuring, 20: 41156
density and moisture content of ocean-bottom, measurement of, by gamma scattering, 20: 23527 (CONF-651206)
density in lakes and streams, uses of radioisotopes in measuring, 19: 13830
density measurement in ocean bottoms, radiometric meter for *in situ*, 19: 6147 (ORO-622)
density measurements of, using gamma sources, instrument for, 20: 37150
density of deep-sea, nuclear probe for *in situ* measurements of, 20: 551
density of ocean-bottom, equipment for measurement by gamma scattering, 19: 20419
density of, measurement by attenuation of transmitted gamma rays, 19: 17838
desorption of iodine from, effects of temperature on, 20: 8479(R) (ORNL-3849, pp 1-42)
desorption of radioiodine from, by air and water, 20: 600 (ORNL-P-1581)
determination in surface waters, radiological gage for, (E), 19: 29133(R) (NYO-10221)
distribution and radionuclide sorption of, in river-estuary systems, 20: 39121
distribution of radioisotopes in, 18: 1342(T) (JPRS-21816)
distribution of radioactive, from Columbia River, 20: 27154
distribution of, with sorbed radioisotopes in San Francisco Bay, 17: 40527 (TID-7664(p.149-59))
distributions in fresh-water systems, heterogeneous equilibria in, 17: 40522 (TID-7664(p.61-70))
drift measurement on Portugal seacoasts, tracer study, 16: 24005
drift measurements in, using tracer techniques, 20: 33541
exchange capacity and mineralogy of fluvial, 17: 40523 (TID-7664 (p.71-90))
fission product sorption by, 18: 1899 (TID-19559)
fixation capacities, 20: 43544
fluorine content, 18: 25686
formation of marine, fission product accumulation coefficients during, 18: 21780(T) (JPRS-24227)
gamma emission in, use of *in situ* probe for measuring, 19: 26267
geochemistry of deep-sea, trace element studies on, 20: 18892 (NYO-3450-1, pp 41-89)
geochemistry of marine, 18: 39479 (TID-21074)
geologic dating of, using potassium–argon method, 20: 16711(R) (MIT-1381-13)
geologic provenance of sea, use of strontium-87/-86 ratio to determine, 20: 45928
gold content of deep-sea, 19: 23242
hafnium content of deep-sea, neutron activation measurement of, 18: 32339
ion exchange capacity and mineral composition of, in Guadalupe River, 20: 24832 (TID-22872)
ion exchange properties of alluvial, underlying MTR holding pond, 17: 19709 (TID-7644(p.151-75))
iridium content of deep-sea, 19: 23242
iron/manganese distribution in marine, 20: 18895 (NYO-3450-1, pp 217-76)
leaching river, for removal of radium-226, 17: 5653
leaching river, for removal of radium-226, 18: 22177
lead isotope in pelagic, occurrence and significance, 16: 17894
lead isotopic composition in, from Baltic and Canadian Shield regions, 20: 18894 (NYO-3450-1, pp 169-84)
lead isotopic composition in, from Pacific Ocean near Japan Trench, 20: 25298
lead isotopic ratios in ocean-bottom, 19: 15758
manganese content, 17: 33602
manganese content of open-ocean, mechanism of deposition of, 20: 12540(R) (NYO-2882-8)
manganese content of deep-sea, activation analysis and thorium-230 dating of, 20: 12976
marine, deposition rates of, 18: 22244 (CONF-498-2)
measurement in rivers and streams, radioisotopic methods for, 20: 23527 (CONF-651206)
mineralogy and physical properties of, from vicinity of Brookhaven National Lab., Upton, N. Y., 18: 1909
monitoring for radioactivity by analysis of biological materials, 16: 9003
monitoring of, design of gage for, 20: 43561
motion of river bed, tracer study, 19: 18178(T) (OTS-64-11459/2 (p.31-8))
motion of, tracer studies of, 20: 548
movement and origin of Australian, tracer study of, 19: 7695
movement in alluvial rivers, tracer techniques for measuring, 18: 1918
movement in ebb channel, Firth of Forth, tracer study on, 20: 11022 (AERE-R-5080)
movement in Oxcars spoil ground, Firth of Forth, use of scandium-46 for, 20: 4166 (AERE-R-4980)
movement of coastal, tracer studies of, 19: 13830
phosphorus content, 18: 25686
phosphorus-32 adsorption on, in salt-marsh ecosystems, 20: 40573
platinum content in deep-sea, 19: 23242
praseodymium-144 content in Ligurian Sea, 19: 30412
promethium-147 content in Ligurian Sea, 19: 30412
protactinium-231 content in ocean, 19: 13638
radioactive contamination of, near uranium mines, 20: 45974
radioactivity determinations in Czechoslovakian, beta, 19: 32477
radioactivity in Escaut River, Belgium, control of, 20: 22515(T) (ORNL-tr-965)
radioactivity in, continuous sampling for, 20: 43523
radioactivity levels of lake, factors affecting variations in, 20: 7265
radioactivity measurements in, of Columbia River and Pacific Ocean, 20: 25282 (RLO-1750-4)
radioactivity of Atlantic Ocean, fallout, 19: 44253(R) (NYO-2174-36)
radioactivity of Columbia River, 18: 20219
radioactivity of Colorado River, 19: 18163
radioactivity of coastal marine, 20: 22536(R) (TID-22837)
radioactivity of Columbia River estuary, 20: 45890(R) (RLO-1750-8 (Vol.2)(Paper 2))
radioactivity of Hokutolite hot spring deposit, 18: 1902
radioactivity of Hokutolite, ratio of thorium and uranium decay series in, 18: 41654
radioactivity of littoral sediments of Ligurian Sea (E), 19: 2534
radioactivity of Ligurian Sea coast, 19: 24723
radioactivity of Pacific Ocean, as indicator of interplanetary proton flux, 20: 23918
radioactivity of, from Mediterranean Sea, 1960 to 1963, 18: 15759(R) (TID-20366)
radioactivity of, from Adriatic and Ligurian Seas, 19: 15757(R) (TID-21521)
radioactivity of, in White Oak Lake from waste disposal, 19: 26591
radioactivity of, from Clinch River system, 20: 45216 (ORNL-3721)
radioisotope accumulation by organic, in ocean, 20: 41146
radioisotope content of, in Columbia River, 19: 20(R) (HW-81746(p.3.86-94))

radioisotope content in, in Columbia River, effects of particle size on, 19: 621(R) (HW-81746(p.3.81-3))
radioisotope content of, mollusk uptake of, 19: 1996
radioisotope distribution in streams on, 17: 40536 (TID-7664(p.327-52))
radioisotope distribution in, 19: 22545
radioisotope scavenging by marine, 17: 33561
radioisotope sorption and release by, in Guadalupe River drainage basin, 17: 40525 (TID-7664(p.113-25))
radioisotope sorption and release by, 17: 40526 (TID-7664(p.127-48))
radioisotope sorption by marine, 20: 32883
radioisotope transport by, 20: 43544
radioisotopes diffusion in interstitial water of ocean, 20: 45910
radioisotopes in, chemical properties of, 20: 33502
radiological monitoring, 17: 29151
radionuclide content in, 19: 3885
radionuclide distribution in, from coastal and offshore waters of Oregon and Washington, 19: 27910 (UWFL-86)
radionuclide distribution in, from nuclear plant wastes, 20: 38742
radium content, 18: 25686
radium, radon, and uranium contents of, in Black Sea and Lake Techirghiol, 20: 10512
rare earth content in, variation in, 17: 25435
rare earth distribution in, 20: 20877
rare earths content in marine, 17: 30719
reactions with organic matrix materials in ice-water system, 18: 15722 (TID-20332)
rhodium-106 migration and fixation in, 18: 17345
ruthenium-106 migration and fixation in, 18: 17345
ruthenium-106 sorption by, 20: 10855
sedimentation measurement in Bombay Harbor, tracer study, 16: 24002
separation of alkaline earths, rare earths, thorium, and uranium from, by ion exchange, 20: 14469(R) (TID-22650)
silicon-32 content in sea sediments, 17: 30739
sorption of fission products by river, 19: 8740(R) (IAEA-R-37-5)
sorption of radionuclides by Columbia River, 19: 15784(R) (HW-83614)
sorptive properties for fission products, 16: 14371
sorptive properties of marine, for radioisotopes, 17: 37021(T) (JPRS-20795(p.1-6))
sorptive properties for cesium and strontium, effects of aluminum and iron hydroxides and potassium on, 18: 17344
sorptive properties for fission products in rivers, 18: 35238 (STI/DOC/10/28(p.9-20))
sorptive properties for radionuclides in Columbia River, 18: 35761 (HW-79279)
sorptive properties for zinc in rivers, 18: 38711 (NYO-10544)
sorptive properties for cesium-137, 18: 36928(T) (JPRS-26056(p.1-8))
sorptive properties for zinc, effects of soft clams and tubificid worms on, 18: 45176 (NYO-10544(Rev.))
sorptive properties for nitrosylruthenium in scale-model aquatic ecosystem, 19: 21 (ORO-620)
sorptive properties for radioisotopes, 19: 21825
sorptive properties of terrigenous, for radioisotopes, 19: 42600(R) (NP-15342)
sorptive properties for cesium-137 and strontium-89 in Guadalupe River, 20: 24832 (TID-22872)
sorptive properties of, for ruthenium chlorides and nitrosyls in aquatic environment, 20: 26606 (TID-22870)
sorptive properties for cerium-144 in surface waters, 20: 33501
sorptive properties for radioruthenium in different solutions, 20: 40890
strontium transport by, in estuaries and streams, 18: 35726
strontium-86/-87 ratio of deep-sea, 20: 45928
strontium-90 content in, 1965, 19: 45748(R) (TID-22193)
studies of uranium-bearing, mineralogical, petrographical, and paleobotanical, 19: 26568 (NYO-10361)
study in southeastern Chukchi Sea, 19: 25802 (PNE-458)
survey of bottom sediments of Bogue Sound area, North Carolina, 17: 31817(R) (TID-19122)
tantalum content in deep-sea, 19: 14207
thorium content, 18: 25686
thorium content in Ligurian Sea, 19: 30412
thorium isotope abundances in ocean, 20: 29412
thorium separation from, method for chemical, 19: 46190
thorium-230 content of ocean, 19: 13638
thorium-230 to thorium-232 ratios in, from Caribbean Sea, 20: 25297
tracer studies on, computer program for processing data from, 20: 16632 (AAEC/TM-303)
transport by tides in Solway Firth, 19: 10662 (PG-Report-605)
transport in Irish Sea, mechanism for, 20: 45889 (PG-Report-587)
transport in watercourses, tracer studies, 16: 16070
uptake and release of cesium-137 and strontium-85 by aquatic, 20: 24833 (TID-22877)
uranium content in Japanese sediments, 16: 20844
uranium content in Japan, 17: 14499
uranium content in, in water of Lake Issyk-Kul, USSR, 19: 38855
uranium content in, 18: 25686
uranium content of, in Black Sea and Mediterranean Sea, 19: 22585
uranium isotope abundances in, 20: 29412
uranium occurrences in, abnormal, 20: 7291
zinc-65 distribution in, in flowing and non-flowing aqueous systems, 20: 6715
zinc-65 sorption on Columbia River, 20: 45261(R) (RLO-1750-8(Vol.2), (Paper 1))
zinc-65 uptake and release by, in aqueous environment, 20: 26608 (TID-22876)
zirconium contents in deep-sea, neutron activation measurements of, 18: 32339

SILVER

abrasion of, friction, wear, and work-hardening during, 18: 18363
abundance in solar atmosphere, 16: 29599 (AFOSR-3024)
activity coefficient of plutonium in liquid, estimated, 20: 43819
agglomeration and condensation of vaporized, after quenching, 18: 36837(R) (IITRI-C6007-12)
alloying effects on radiation effects on copper at low temperatures, 17: 37614
alloying effects on corrosion resistance of zirconium in carbon dioxide, 18: 12576 (GEAP-4089(Vol.I)(Paper 3))
alloying effects on composition and mechanical properties of magnesium–neodymium alloys, 18: 28000
alpha elastic scattering at 24.7 Mev, relative cross sections for, 18: 34902
alpha elastic scattering at 18.7 to 40 Mev, optical model for, 19: 14605
alpha particle energy loss and straggling in foils of, 20: 44144
alpha reactions (α,n) at 12 to 18 Mev (E/T), 19: 3362
alpha reactions (α,n) at 17 Mev, level density parameters from, (E), 20: 38115
alpha reactions (α,p) at 30 Mev, angular distributions from, 17: 5339
alpha reactions (α,α') at 48 Mev with, alpha energy spectra and angular distributions from, 17: 20996 (UCRL-9898)
alpha reactions (α,p) at 52 Mev, K-x ray production cross sections for, 17: 38220
alpha scattering at 25 Mev by, differential cross sections for elastic (E), 19: 1234 (PAN-347)
alpha scattering at 28 Mev, distorted-wave and optical model analysis of, (T), 19: 29294
alpha scattering at 28.4 Mev, angular distributions from, (E), 20: 22047
analysis and determination, 20: 14500
analysis for copper and gold, activation, 19: 28271
analysis for gold, iridium, palladium, and platinum, activation techniques for, 16: 3326(T) (AEC-tr-4497(p.179-88))
analysis for hydrogen, nitrogen, and oxygen, vacuum fusion, 18: 33491
analysis for impurities by activation methods, 19: 19796
analysis for microimpurities in solid, spectrographic, 17: 27308
analysis of, self-shielding effects in neutron activation, 18: 31387
annealing of cold-worked, 17: 35264(R) (UCRL-10706(p.111-203))
annealing spectra of irradiated, 16: 29441 (TID-16378)
argon ion large-angle scattering, 18: 16667
argon ion sputtering at 160 to 200 ev, angular distributions from, 19: 41259
atomic displacements from electron bombardment of crystals of, at 0.5 to 1.3 Mev, 16: 13651
atomic potentials and separations in, 18: 42071
atomic weight of natural, 16: 11943
behavior in fused lithium chloride–potassium chloride eutectic, chromatographic and electrophoretic, 18: 43479
beryllium-9 reactions at 85 Mev, beryllium-8 production mechanism in, 17: 22658
beta absorption and backscattering by, 19: 30127
beta absorption by, 18: 14609
beta absorption, effects of atomic weight on, 18: 26812(T) (AEC-tr-6372(p.11-15))
beta scattering by, measurement of saturated backscattering from, 18: 35057
beta transmission through, backscattering from, 18: 26813(T) (AEC-tr-6372(p.17-28))
boiling, use in Grover heat pipe for high heat transfer, 19: 24667 (LA-3211)
brazing to beryllium, 17: 25683 (ASD-TDR-62-509(Vol.II))
bremsstrahlung dissociation at 250 to 1150 Mev, 16: 7101
bremsstrahlung reactions (γ,p) at 24 Mev, direct photoeffect and evaporation contributions in, 17: 38209
bremsstrahlung reactions (γ,K⁺) at 1054 Mev, yields from, 18: 13109
bremsstrahlung reactions (γ,α) with, spectra and yields for, (E), 19: 23668
bremsstrahlung reactions (γ,t) at 37 Mev, yields in, (E), 19: 47596(R) (TID-22141, pp 94-7)
bremsstrahlung reactions (γ,t) at 31.2 to 55.7 Mev, yields from, (E),

20: 10086
bremsstrahlung reactions (γ,α) at 32.5 Mev, alpha spectra and yields in, (E), 20: 26231
bromination of hydrosol of, development of highly sensitive nuclear emulsions by, 18: 33962
bromine ion slowing down in, at 10 to 100 Mev, (E), 19: 37457(R) (ORNL-3778(p.123-5))
carbon ion reactions at 9.7 Mev, charge-exchange cross sections and ionization from, (E), 20: 17724
carbon-12 scattering at 9.7 Mev, charge distributions in, (E), 20: 7724
catalytic effects on cerium sulfate autoreduction in sulfuric acid solutions, 18: 12086
catalytic effects on deuterium oxide exchange reactions with *p*-xylene, 18: 13822
catalytic effects on decomposition of deuterated formic acid, 19: 2369
catalytic effects on dissolution of ceramics, 20: 9088(P)
cesium ion reactions on, negative-ion yields from, 17: 5087
characteristics as radiation target, incorporated into nuclear emulsion, 16: 16967 (NP-11592(Vol.I)(p.307-25))
charged particle reactions with, cross sections for, 17: 34886 (UCRL-10783)
charged-particle reactions with, dE/dx and range-energy graphs for, 20: 46601 (UCRL-2426(Vol.2)(1966 Rev.))
charged-particle reactions with, range-momentum and dP/dx graphs for, 20: 46342 (UCRL-2426(Vol.4)(1966 Ed.))
chlorine ion energy losses in, at 2 to 40 Mev, (E), 19: 6461
coating foils of, with bismuth-212, lead-212, or polonium-212, 20: 9034
coating of beryllium with, 17: 4919(P)
coating with beryllium, electrolytic, 20: 40864 (BMwF-FBK-66-10)
coating with technetium-99 by electrodeposition from pertechnetate solution, 19: 26350
colloidal solutions of, effects on DNA synthesis in peripheral blood cells in rabbits, 17: 10291
compatibility with lead telluride, 16: 24161 (NAA-SR-Memo-7172)
compressibility at high pressures, 17: 3494 (UCRL-6696-T)
compression textures in, 18: 44145(R) (ORNL-3670(p.11-16))
content and distribution in beef heart, 19: 45753 (AE-191)
content in African pitchblende, estimation of induced fission vs spontaneous fission from, 20: 37994
content in Canyon Diablo meteorite, isotopic composition of, (E), 20: 31861
content in human heart, neutron activation determination of, 18: 33457 (AE-146)
content in meteorites, 20: 42064
content in organs and tissues of humans outside continental U. S., 19: 21831
content in Pacific sector of Antarctic Ocean, 19: 42634(R) (YALE-2912-10)
content in river waters, 17: 30687
content in snow, use of, as tracer in studying atmospheric precipitation phenomena, 20: 27144 (BNWL-SA-650)
content in solar atmosphere, (E), 19: 39345
content in teeth after use in dental restorations, 20: 27
content in Van Arkel-refined zirconium, comparison with Knoll-refined, 17: 33819
corrosion by acids and chloride salts in chemical plants, 16: 20983
corrosion by liquid bismuth, 19: 23355(R) (BNL-867(p.1-117))
corrosion of, review, 19: 7868
corrosion resistance to mercury at 900°F, 20: 2264
corrosive effects on tantalum–tungsten alloys at 1900°C, 19: 21690(R) (LA-3244)
cosmic-ray spallation of, yield curves for, 18: 15244
critical constants and temperature range of liquid, 17: 6711
crystal lattice parameter change at 0 to 500 kilobars in x-ray piston cell, 18: 8621
crystal structure of equilibrium concentrations and properties of vacancies in, 17: 35782
crystal structure of, effects of hydrostatic pressure on vacancies in, 17: 35785
crystal structure from argon-ion bombardment ejection patterns, 18: 28130
crystal structure changes in thermal expansion, Bradburn Fürth equation of state for calculating, 18: 30206
crystal structure of, electron diffraction and microscopy methods for studying, 20: 31715(R) (UCRL-16658, pp 105-20)
crystal structure of evaporated films of, x-ray studies of, 20: 35892 (NYO-3347-1)
crystallization with thionalid, tracer study of, 16: 12961 (USNRDL-TR-551)
decomposition voltage potential in fluorides at 500°C, 19: 17781(R) (ORNL-3750)
defect clusters in irradiated crystals of, 16: 13649
deformation, quenching and radioinduced point defects in, stages for recovery of, 17: 37617
deformation, stored energy increase and release after, 16: 25821
deposition of fission products on, factors affecting, 19: 36960(R) (ORNL-3807, pp 80-142)
deposition on copper tubes, method for, 18: 17977(R) (ORNL-TM-793)
deposition on copper-plated beryllium–copper alloy by electrolytic methods, 18: 22460 (RFP-366)
deposition on pyrolytic graphite for use as analytical standard, electro-, 20: 5503
deposition on solid electrodes by voltammetry, 19: 37010
deposition on thallium, effects of, on properties as beta source at 300 to 500°C, 20: 43400
deposition on uranium, techniques for electrolytic, 17: 34387
deposition on vanadium-base alloys for oxidation protection, 19: 20459(R) (IITRI-B6019-6)
deposition on beryllium, electrolytic, 18: 39846
desorption energy on molybdenum and nickel, tracer study, 17: 36474
desorption of iodide ions from, tracer studies of effects of electric fields, pressure, and temperature on, 20: 43250
determination, activation, 16: 2967(R) (TID-14310)
determination as impurity in and volatilization from tungsten, semi-quantitative spectrographic, 16: 4131 (BM-RI-5903)
determination as impurity in tetrabutylammonium hydroxide, 16: 17600
determination as trace in standard rocks G-1 and W-1, spectrographic, 16: 20831
determination as trace impurity in uranium, 18: 29591
determination by activation with bremsstrahlung, 16: 22027
determination by activation and isotope dilution, substoichiometric, 18: 21997
determination by calculation of weight from activities and neutron fluxes measured after irradiation, 18: 27297
determination by charged-particle reactions at 2 Mev, 20: 43097
determination by neutron activation, 20: 35390 (CEA-R-2965)
determination by spectroscopy using high-frequency plasma flames, 18: 10020
determination by spectrochemical methods, voltage-fluctuation patterns in, 19: 40416
determination by thermal-neutron activation methods, sensitivity for, 19: 9071
determination by titration using hydrochloric acid, end-point determination by beta reflection in, 19: 19787
determination by x-ray absorption analysis, evaluation of gamma-emitter activity in, 20: 14498
determination in aluminum as trace impurity, activation, 17: 10546
determination in aqueous solutions, fabrication of pyrolytic graphite electrode for, 17: 40723
determination in aqueous solutions by isotope exchange reaction, 18: 23430
determination in biological materials, activation, 16: 23403
determination in bismuth metal, activation, 16: 28895
determination in biological materials by ion exchange and gamma spectrometry, 18: 13660
determination in bismuth, activation, 18: 13682
determination in biological materials, activation, 18: 33464 (NASA-CR-52997)
determination in bismuth by γ,γ-coincidence counting, activation, 19: 46193
determination in biological materials by neutron activation analysis, 20: 7046
determination in biological materials, use of automated gamma spectrometers in activation, 20: 38843
determination in cadmium-containing materials by activation analysis, 17: 15912
determination in chromium oxide-silver oxide, intensity ratio technique for x-ray spectrometric, 18: 15972
determination in cadmium compounds, activation, 18: 43408
determination in copper by activation, 19: 40422
determination in copper samples by radioisotope dilution, 20: 16335(R) (NBS-TN-276)
determination in conductive tissue of beef heart, activation, 20: 31176
determination in copper coins by neutron activation methods, 20: 40800 (CNAEM-35)
determination in diabase and granite by spark source mass spectrography, 19: 11406
determination in europium oxide, spectrographic, 17: 2931
determination in erbium, mass spectrographic, 19: 2232
determination in film emulsions by x-ray fluorescence, use of gamma-excited x-ray sources for, 19: 15376
determination in gold targets, activation, 16: 22020
determination in germanium dioxide and lead, activation, 17: 35660
determination in galena, colorimetric, 18: 31048(R) (COO-689-42)
determination in ground water, emission spectrographic, 18: 43790(R) (TID-21137)
determination in gold and palladium by neutron activation techniques,

20: 26789
determination in human teeth, gamma spectrometric, 16: 8671 (AE-61)
determination in high-purity quartz and organic filter media, activation, 19: 7347
determination in human tooth enamel, gamma spectrometric, 19: 17794
determination in human heart tissue, activation, 20: 31175
determination in iron and nickel base alloys, spectrographic, 16: 11539
determination in irradiated film dose meters, optical density evaluation by, 19: 9506
determination in lead, activation, 18: 5232
determination in lead, nondestructive activation, 19: 5834
determination in meteorites, 17: 25445
determination in mass spectrometer at 10^{-8} gram, 18: 39057 (CONF-520-1)
determination in minerals by neutron activation, 19: 30424
determination in minerals, spectrochemical, 19: 39265(R) (IA-1021)
determination in minerals by activation, 19: 39265(R) (IA-1021)
determination in minerals and ores, activation, 20: 20574
determination in nickel steel and electro-etch residues, activation, 17: 5984
determination in nucleic acids, activation, 18: 19892
determination in old Roman copper coins, 19: 13198 (CNAEM-21(Pt.1))
determination in potassium nitrate–sodium nitrate systems, voltammetric, 17: 15853(R) (ORNL-3397(p.24-6))
determination in pharmaceutical preparations by beta backscattering, 18: 182
determination in pharmaceuticals, method for, 18: 5217
determination in pure uranium compounds by solvent extraction using dithizone, 18: 33509
determination in paint by activation, age estimation of white lead by, 19: 11035
determination in powdered samples by spectrochemical methods, 19: 22120
determination in platinum by neutron activation, 20: 3863(R) (IS-1200 (Sect. C))
determination in plutonium by carrier distillation methods, spectrographic, 20: 40814 (RFP-664)
determination in powder samples by spectrographic methods, semi-quantitative, 20: 43104
determination in quartz and filter media by neutron activation and radiochemical methods, 18: 39073
determination in rare earth oxides, spectrographic method for, 16: 20327
determination in reactor-grade uranium dioxide, activation, 19: 5827
determination in rocks from resonance and thermal neutron capture cross sections, 20: 22962
determination in sea water using thionalid, 16: 12961 (USNRDL-TR-551)
determination in small solid samples by mass spectroscopy, design of ion source for, 18: 23406 (CONF-512-4)
determination in silicon, activation, 18: 33502
determination in surface waters by activation analysis, 18: 37072 (A/CONF.28/P/854)
determination in sea water, activation, 18: 43790(R) (TID-21137)
determination in sandy rocks, activation, 19: 2239
determination in solids by spark source mass spectrometry, quantitative, 19: 13247
determination in sea water by neutron activation methods, 19: 22574
determination in sea water by quantitative solvent extraction and spectrography, 19: 28253
determination in solutions by atomic absorption, 20: 14457(R) (ORNL-3889, pp 36-39)
determination in silicon dioxide, activation, 20: 20634
determination in silicates, activation, 20: 26782
determination in solutions by neutron activation, 20: 33179(T) (AEC-tr-6639, pp 92-6)
determination in seawater, activation, 20: 40834
determination in thorium compounds using dithizone, method for, 18: 1560
determination in thorium nitrate and oxide, photometric, 18: 1561
determination in tantalum by anion exchange in hydrofluoric–nitric acid mixtures, 18: 35455
determination in tantalum by activation, 19: 24416
determination in tin and zinc by isotopic dilution and activation methods, 19: 28231
determination in teeth, gamma spectrometric method using neutron activation for, 19: 30090
determination in thumbnail clippings, activation, 20: 14439(R) (GA-5556)
determination in uranium, photometric, 18: 1539
determination in uranium-233-labeled uranium dioxide, spectrographic, 18: 9980
determination in uranium tetrafluoride, spectrographic, 20: 14473
determination in vanadium, chemico-spectrographic, 18: 13708
determination in white lead for age determination of paintings, activation, 19: 5820
determination in x-ray films by x-ray absorption, 19: 32078
determination in zirconium by activation, 19: 24418
determination of, in uranium by anodic stripping coulometry, 17: 19977
determination of, ionization methods for mass-spectrometric, 17: 38975
determination of microgram concentration, radiometric, 16: 4144
determination of photolytic, in irradiated photographic emulsions by neutron activation, 20: 35450
determination of, radiometric, 17: 5952 (IA-772)
determination of trace amounts in rare earth compounds, spectrographic, 16: 28869 (JEN-107-DQ/I-33)
determination of traces, activation, 17: 21648
determination of traces of, using oxycellulose, 17: 35656
determination of trace amounts of, by substoichiometric radioisotopic dilution analysis, 20: 1786
determination of trace amounts of, in beryllium by spectrography, 20: 16352
determination of trace amounts of, by reactor neutron activation methods, 20: 26760
determination of traces of, in palladium by neutron activation methods, 20: 26798
determination of, optimum sample position in activation, 18: 19906
determination of, silver-109 neutron resonance activation integral for, (E), 20: 10789
determination of, use of azo dyes in spectrophotometric, 20: 22925
determination of, by alpha scattering methods, 20: 22964
determination of, by neutron activation methods, 20: 29078(R) (AD-633252)
determination of, in high-purity lead by neutron activation analysis, 20: 35412
determination of, using isoöctylthioglycolate, 20: 40796(R) (IS-1500 (Sect.C))
determination of, in rainwater from silver iodide-seeded clouds in Australia, 20: 40838
determination of, in rainwater, ion-exchange separation in, 20: 40839
determination of, in ores, equipment used in activation methods for, 20: 40848
determination of, by automatic beta back-scattering radiometric tritration, 20: 45577
determination, solvent extraction sampling technique for activation, 17: 33818
deuteron attenuation by films of, at 1.5 to 4.5 Mev, 16: 15668
deuteron disintegration in nuclear fields, (E), 20: 46786
deuteron elastic scattering at 11.8 Mev, angular distributions, 16: 3637
deuteron elastic scattering at 11.8 Mev, optical model analysis of, 17: 38192
deuteron elastic scattering at 26 Mev, angular distributions from, 18: 28634
deuteron elastic scattering at 15 Mev, strong absorption model analysis of, 18: 42708
deuteron elastic scattering at 25.3 Mev, optical model analysis of, (E/T), 20: 3053
deuteron elastic scattering at 27.5 Mev, angular distribution for, (E/T), 20: 3057
deuteron reactions (d,α) at 15 Mev, cross sections and energy distributions for, 16: 11020
deuteron reactions (d,α) at 24-Mev with, alpha energy spectra and angular distribution from, 17: 20996 (UCRL-9898)
deuteron reactions (d,n) at 26 Mev, neutron flux and spectra for, 18: 30037
deuteron scattering at 11.8 Mev, 17: 31539
deuteron scattering at 26.5 Mev, total cross sections for, (E), 19: 5164
diffusion and electric mobility in bismuth, 17: 31798(R) (BNL-782 (p.60-91))
diffusion and precipitation of rare gases in, 16: 30852
diffusion and solubility in germanium at 700 to 930°C, tracer study, 16: 16057
diffusion coefficient for, self-, 17: 14745(T) (AEC-tr-5663)
diffusion in beryllium at 656 to 900°C, 20: 37250
diffusion in bismuth at 400 to 542°C, 19: 36949(R) (BNL-900(p.121-97))
diffusion in disordered and ordered beta brass, 16: 4578
diffusion in gold, formation of porosity during, 18: 10544 (UCRL-10383)
diffusion in graphite, 18: 2275
diffusion in graphite, 18: 39911 (UCRL-7324)
diffusion in graphite, 19: 26832
diffusion in liquid silver, 18: 32147 (TID-20758)
diffusion in lithium chloride potassium chloride and cesium and sodium nitrates, 18: 12087
diffusion in moving grain boundaries in copper at 725°C, 16: 16046
diffusion in pyrolytic graphite, 20: 5846
diffusion in silver–zinc alloy, 18: 9773 (TID-19979)
diffusion in silver, effects of torsion strain on, 19: 27852 (NYO-10722)
diffusion in tungsten, effects of, 19: 2783
diffusion in, effects of pressure on rate of self-, 20: 23740
diffusion into SAP, study using electron microprobe, 19: 30077 (EUR-1819.e(p.27-36))

diffusion of antimony and ruthenium in, thermal, 18: 44151(R) (ORNL-3670(p.129-31))
diffusion of antimony and indium in, effects of pressure on, 20: 23740
diffusion of antimony and ruthenium in, 19: 4658 (ORNL-3710)
diffusion of cobalt, iron, and nickel in, at 600 to 850°C, 17: 20457 (NYO-9438)
diffusion of cobalt, iron, and nickel in, at 600 to 850°C, 17: 19998
diffusion of cobalt and iron in, 17: 30152
diffusion of heterovalent solutes in liquid, 18: 32147 (TID-20758)
diffusion of hydrogen in, studies of, by d(d,p)T reaction, 17: 17289
diffusion of iron in crystals of, isotope effects on, 16: 16047
diffusion of lead in, effects of alpha bombardment on, 18: 44151(R) (ORNL-3670(p.129-31))
diffusion of oxygen in, pressure and temperature dependence of, 17: 27821
diffusion of palladium in, 18: 25969(R) (ANL-6868(p.287-302))
diffusion of palladium in, 19: 11682
diffusion of rare gases in, 16: 5736
diffusion of rare earths in crystals of, 17: 19997
diffusion of xenon in, 19: 16088
diffusion of, in alpha- and beta-zirconium, tracer studies of, 20: 43974
diffusion on surfaces of crystalline, self-, 19: 6302 (NYO-2994-3)
diffusion rate in sintered aluminum, 18: 5225
disappearance rates for mesons (μ^-) in, Z-law analysis of, 16: 2305(R) (UCRL-9704)
dislocation damping in crystals of, 17: 35264(R) (UCRL-10706(p.111-203))
dislocation dissociation in crystals of, 18: 2238
dissociation energy of gaseous and heat of vaporization of solid, correlation of, 17: 6095
dissolution in silver halides, thermodynamic studies of, 20: 24971(R) (BNL-954, pp 50-83)
dissolution in tin at 700°C, heat of, 20: 23012
distribution between phases in molten boron oxide–sodium chloride–sodium oxide at 830°C, 20: 7201
distribution coefficient between aqueous solution and substituted anilines, 16: 2967(R) (TID-14310)
distribution coefficient between fused bismuth and fused salt eutectic, 17: 21683
distribution in sea water, effects of depth on, 20: 18892 (NYO-3450-1, pp 41-89)
distribution of, between nitric acid and ion-exchange resin, synergistic effects of thorium on, 17: 15948 (LA-2836)
distributions in sea water, geographical and vertical, 19: 22574
effect on determination of copper in bismuth by neutron activation methods, 19: 43941
effect on the dissolution of ceramics containing beryllium oxide, catalytic, 20: 2252(P)
effects as coating on light and refractory metals and their alloys, 19: 4605
effects as infiltrant on properties of graphite containing carbides and metals, 20: 29764
effects of films of, on superconducting transition temperature of tin, 17: 5139
effects of, on recovery of copper from radiation effects below 60°K, 16: 33543
effects of, on shielding properties of lead, 17: 33256
effects on copper oxidation, 20: 4320(R) (ORNL-3870, pp 70-4)
effects on corrosion resistance of beryllium, 19: 22913(P)
effects on determination of copper in high-purity metals by activation methods, 19: 43973
effects on determination of iridium in ores by neutron activation analysis, 20: 36751
effects on diffusion of niobium, 17: 23876(R) (USBM-U-1031)
effects on ductility of iodide chromium, 18: 32189
effects on evaporation of tungsten oxides from tungsten surfaces, 20: 33820(TID-23122)
effects on fluorescence of uranium in sodium carbonate–sodium fluoride melts, 18: 33506
effects on fracture mechanisms in beryllium single crystals, 20: 23714
effects on fusion welding of beryllium, 16: 5692 (WADD-TR-60-917)
effects on fusion welding of beryllium, 18: 14449
effects on gamma radiolysis of crystalline potassium nitrate, 18: 1747
effects on gas absorption by thorium-containing getter, 17: 16620(P)
effects on gastrointestinal absorption of copper-64 in rats, 20: 16182
effects on grain boundary of copper at 200 to 1000°C, 20: 2348 (UCRL-16051)
effects on homomolecular isotopic exchange of carbon monoxide, catalytic, 19: 26328
effects on hydrochloric acid cleavage of organotin compounds in methanol–water, 20: 6687(R) (NYO-3453-1)
effects on luminescence of alkali halides, 19: 22313
effects on luminescence of copper-activated zinc sulfide phosphor, 17: 11228(T)
effects on nuclear electric quadrupole resonance in copper, 17: 18825
effects on oxidation of graphite, 19: 22911
effects on radiation resistance of potassium-aluminoborate glass, 18: 24813(R) (ANL-6880(p.49-67))
effects on sorptive properties of iron oxide for iodine-131, 20: 36800
effects on strength of sintered tungsten and tungsten carbide compacts, 19: 23092
effects on stress corrosion of aluminum–copper–magnesium–zinc alloys, 18: 25946(T) (RSIC-177)
effects on superconductivity of niobium–tin alloys, (E), 19: 41609
effects on superconducting energy gap in aluminum, (E), 20: 15658
effects on surface tension of copper, 16: 7901(T) (AEC-tr-4980)
efficiency drift of foil of, in secondary electron monitor for linear accelerator at 15 Mev, 18: 24253
electric conductivity, effects of magnetic fields up to 400 kgauss, 16: 15451
electric conductivity at 1.2°K, effects of magnetic fields on, 19: 27735(R) (NAA-SR-10850)
electric conductivity of liquid, 20: 41476
electric conductivity of whiskers of, under alpha irradiation, 17: 16762
electric mobility in molten bismuth, 18: 4160(R) (BNL-799(p.74-100))
electric mobility in bismuth, 18: 12627(R) (BNL-823(p.66-93))
electric mobility in molten bismuth, 19: 15991(R) (BNL-841(p.63-101))
electrochemical potentials, tracer studies, 16: 3348(T) (AEC-tr-4497 (p.389-99))
electrode properties for reactions of oxygen and hydrogen peroxide in alkaline solution, 19: 36338(R) (NP–15160)
electrode properties of single-crystal, 20: 22871(R) (MIT-905-52, pp 42-73)
electrodiffusion in solid bismuth, 19: 32677 (BNWL-67)
electromagnetic wave reactions with foils of, plasma radiation from, (E), 20: 6548
electromagnetic wave propagation in, helicon, (E), 20: 44993 (NYO-2150-19)
electromigration of, 18: 40994(R) (TID-21052)
electron and positron disintegration, 18: 24625 (WASH-1046)
electron and positron reactions at 100 to 400 kev, excitation cross sections for K ionization in, 20: 15257
electron backscattering and transmission, 16: 944
electron backscattering at 1 to 3.5 Mev, 16: 12344
electron backscattering and transmission at 1–2 Mev, 19: 29442
electron backscattering coefficients for, empirical equations of, 19: 37794 (NASA-TN-D-2909)
electron beam backscattering by, calorimetric measurement of energy of, 19: 12072
electron beam energy loss in, 18: 10786
electron bombardment of, emission spectra from, 18: 18562
electron bombardment of films of, products from, 18: 24319
electron diffraction scattering by thin foils of, analyzing system for, 18: 20670
electron diffusion depths at 20 kev in, 18: 8923
electron diffusion in slabs of, differential energy spectra and number transmission for, (T), 20: 15936
electron emission by, photographic effects of secondary, 17: 24102
electron emission from, after high-energy molecular bombardment, 18: 18564
electron emission from foils of, laser-induced, (E), 19: 20814
electron energy loss at 1 Mev in very thin layers, 16: 12383
electron energy loss in, effect of contaminants, 16: 19488
electron energy loss, angular dependence of characteristic, 16: 19545
electron energy loss in films of, 18: 36107
electron energy losses in foils of, (E), 19: 4850
electron energy loss in thin films of, (E), 19: 8113
electron energy loss in thin foils of, (E/T), 19: 44961
electron energy losses in, characteristic, (T), 20: 5015
electron inelastic scattering, energy distribution, 17: 13595(T)
electron inelastic scattering by thin films of, theory for, 17: 5281(T)
electron mean free paths in, energetic, 17: 9045
electron paramagnetic resonance of free atoms of, in solid solutions of silver salts, (E), 20: 15975(T)
electron penetration at 1 to 10 kev, 16: 18368
electron plasma losses at 3.6 ev in foils of, foil-thickness and temperature dependence of, (E), 20: 38400
electron-positron annihilation cross section for, third-order Coulomb wave function for single-quantum, 18: 2641
electron ranges in films of, at 5 to 30 kev, (E), 19: 6392
electron reactions at 40 kev, photon emission from, 17: 39308(R) (ORNL-3492(p.134-43))
electron reactions with foils of, light emission in, 18: 16649 (ORNL-3485)
electron reactions with, characteristic x radiation from, (T), 19: 14242
electron reactions up to 10 Mev, cross sections for atomic displacements in, (T), 19: 28992 (ORNL-3813)

electron reactions at 70 Mev with thin foils of, secondary emission from, 19: 37463
electron reactions with foils of, bremsstrahlung and photon emission in, 19: 42929 (ORNL-TM-1105)
electron reactions with crystals of, determination of interatomic potentials in, (T), 19: 47882 (RISO-103)
electron reactions with films of, emission spectra from, 17: 32669 (ORNL-3450)
electron reactions at 2.5 to 4.0 Mev, bremsstrahlung spectra from, (E), 20: 6432
electron reactions with thin foils of, transition radiation from, (E), 20: 15968
electron reactions at 6 to 60 kev, transient radiation from, (E), 20: 15268
electron reactions at 6 to 23 kev, optical transition radiation from, 20: 21518
electron reactions at 40 to 80 kev with thick foils of, radiation emission from, (E), 20: 32708
electron reactions at 18 Mev, anomalous secondary electron emission from, 20: 44117
electron scattering at 0.8 and 1.5 Mev, energy-loss spectra, 16: 8136
electron scattering by, energy-loss spectra from, 17: 14982
electron scattering at 60 to 100 kev, layer-thickness dependence of, 17: 26241
electron scattering at 1 Mev, angular dependence of bremsstrahlung energy loss in, 17: 29635
electron scattering by cesium-coated, parameters for 0.05 to 5.0 ev, 18: 10834
electron scattering by, energy loss mechanisms in relativistic, 18: 34258(R) (AD-417250)
electron scattering in evaporated thin films of, multiple, 18: 37844
electron scattering by foils of, surface loss effects on angular distributions in, 18: 38176
electron scattering by, electromagnetic spectra from, 18: 44442
electron scattering by foils of, depolarization in, (E/T), 19: 10276
electron scattering at 0.6 to 1.8 Mev, backscatter and secondary emission in, (E), 19: 29441 (NASA-TN-D-2782)
electron scattering by films of, background intensities in, 17: 2071
electron scattering by thin films of, intensity distribution of elastic and inelastic, 17: 18988
electron scattering by foils of, at 10 kev, 17: 24141
electron scattering by films of, differential cross sections for multiple, (E), 20: 4485
electron scattering by, surface plasmon excitation radiation from, (E), 20: 5017
electron scattering at 1 to 10 Mev by thick targets of, energy spectra of retrofugal flux from, (E), 20: 19395
electron scattering in thin foils of, angular distributions of 100-kev, 20: 35999 (SGAE-PH-40/1966)
electron scattering at 3.5 to 14.1 Mev on, backscattering from, (E), 20: 44115
electron scattering at 3.2 to 14.1 Mev, backscattering energy distributions from, (E), 20: 44116
electron secondary emission in argon ion bombardment, 16: 6845
electron secondary emission coefficient, 16: 12276
electron secondary emission from thin foils of, (E), 20: 13103
electron spectra from, j-j coupling for L Auger, 20: 15237 (CONF-233(Vol.3), pp 371-97)
electron spin resonance in colloidal solutions and films of, (E), 20: 17981
electron transition radiation intensity from, 16: 27916(T) (AEC-tr-5234)
electron transmission by thin layers of, effects of temperature on, 18: 42198
electron transmission by layers of, temperature dependence of, (E/T), 19: 12073
electron transmission in foils of, low-energy, 19: 41969 (ORNL-TM-1153)
electron transmission through films of, energy loss dependence on layer thickness in, 17: 29399(T) (AEC-tr-5876)
electron transport in, Monte Carlo method for, 18: 28010
electron-induced transition radiation and bremsstrahlung from foils of, grazing-incidence, 20: 44111 (ORNL-TM-1571)
energy level transitions in, Coster-Kronig, (T), 20: 15238 (CONF-233 (Vol.3), pp 398-418)
energy level widths for, K, (T), 20: 15239 (CONF-233(Vol.3), pp 419-39)
energy levels and quantum states in atoms of, method for calculating, 19: 9901
energy levels of, from Thomas-Fermi-Dirac potential, (T), 20: 15267
exchange between sodium nitrate (liquid) and zeolite, 17: 33767 (IA-810)
exploding wire phenomena in, use for shock excitation of parallel oscillating circuits, (E), 19: 23191
explosion of wire, time-to-burst, 17: 13203
explosion of wires of, in nitrogen, x-ray analysis of aerosol composition and size produced by, 18: 41381
fabrication by ultrasonic hot pressing, 16: 10484 (NYO-10007)
fabrication of beryllium-fiber-reinforced, 18: 41925(R) (IITRI-B241-8)
Fermi surface electric and thermal conductivities near 0°K, 16: 22787
Fermi surface of, magnetoacoustic measurements on, 18: 13007(R) (NP-13592)
fission fragment ranges in, 20: 3982(R) (AGN-8156)
fission of, by protons at 600 Mev, 17: 7086 (NP-12319)
fission product stopping in, ionization of inner electron shells, 16: 13834
fluorescence yields in proportional and scintillation detectors, 18: 3796
fracture under impulsive loading, 16: 25759 (NP-11890)
friction coefficient with nitrided titanium-base alloy *in vacuo*, 20: 7571 (NAA-SR-9644)
gamma attenuation coefficient of, temperature dependence of cobalt-60, (E), 19: 5391
gamma dose rates in tube of, from neutron capture, (E/T), 19: 38022
gamma elastic scattering cross sections to 1.33 Mev, (E/T), 19: 45327
gamma elastic scattering at 280 and 662 kev, Z dependence of cross section for, (E), 20: 22060
gamma reactions (γ,γ') with, method for measuring cross sections, 18: 24637
gamma reactions (γ,n) with, neutron angular distribution from, 18: 34935
gamma reactions at 6.13 Mev, electron pair production cross sections for, (E), 19: 39787 (SGAE-PH-19/1965)
gamma reactions at 145, 280, and 320 kev, cross sections for electron production in, (T), 19: 47329
gamma reactions at 320 kev, absolute photoelectric cross sections for, (E), 20: 11496
gamma reactions at 6.13 Mev, pair-production cross sections for, (E), 20: 37746
gamma reactions (γ,p), cross sections for, 17: 21030
gamma reactions (γ,n) at 9 to 17 Mev, equipment and method of measuring yields from, 18: 1076
gamma reactions on, effects of E1 resonances on, 16: 33906
gamma scattering at 7 and 17 Mev, Delbruck, 17: 11745
gamma scattering at 662 kev, Rayleigh, 18: 26292
gamma scattering at 411 kev, cross sections at 60 to 150°, 19: 1174
gamma spectra from neutron capture by, 16: 8162(R) (ARF-1193-6)
gamma spectra from 14-Mev neutron activation of, determination by, 19: 26241
gold-197 Mössbauer isomer shift and residual electric conductivity in, (E), 19: 10346
growth of films of, sputtering, 18: 24074
heat of solution in liquid silver–tin alloy and tin at 828°K, 18: 30164(R) (AD-429007)
heat transfer to boiling helium, 17: 37342
helium and hydrogen ion attenuation at 0.1 to 500 Mev, tables for, 20: 41619 (CEA-R-3042)
helium evolution after bombardment with helium ions, 18: 28103
helium ion energy-range relations in, 18: 14726 (UCRL-10647)
helium ion range-energy relations in, (E), 19: 9888 (NAS-NRC-PUB-1133(p.17-37))
helium ion reactions at 320 to 880 Mev, formation of magnesium-28 and sodium-24 in, 17: 31525
helium ion reactions, ejection of magnesium-28 and sodium-24 from, 16: 2498 (UCRL-9683)
helium ion scattering by, Auger electron emission from, (T), 19: 41270
helium-4 energy-range relations to 2 Mev, 16: 8003
helium-3 reactions (He-3,n) at 19 to 25 Mev, angular distributions and cross sections for, (E), 20: 22132
hydrogen atom and ion reactions at 10 to 40 kev, secondary electron emission from, (E), 20: 31533
hydrogen ion range-energy relations in, (E), 19: 9888 (NAS-NRC-PUB-1133(p.17-37))
hydrogen ion reactions at 260 kev, uv radiation emission in, 18: 20781
hyperon (Λ) binding energy and decay, 18: 15184 (CERN-64-1(p.113-16))
incorporation by hydrothermally synthesized galena, effects of recrystallization temperature on, 18: 43828
internal friction in cold-worked, 16: 29397
iodine deposition on, from vapor phase, 20: 215 (CONF-650407, pp 142-77)
iodine deposition on wires of, properties of, 20: 13261(R) (ORNL-3885, pp 87-149)
iodine deposition on, in turbulent helium flow stream at 400 to 500°F, 20: 28687 (ORNL-TM-1386)
iodine deposition on surfaces of, 20: 35893(R) (ORNL-3951, pp 84-134)
iodine ion slowing-down in, at 10 to 100 Mev, (E), 19: 37457(R) (ORNL-3778(p.123-5))
ion elastic scattering by, nuclear radius and surface-thickness analysis from, (E/T), 19: 33251 (UCRL-11781)
ion emission from foils of, laser-induced, (E), 19: 20814
ion exchange between sodium zeolite and silver-sodium nitrate melts, 18: 9752 (IA-900)
ion exchange in concentrated hydrochloric and perchloric acids, dis-

tribution coefficients for, 18: 17759
ion exchange paper chromatography of, 18: 17785
ion exchange with aluminum and sodium on Dowex 50W resin, rate of, 17: 32053
ion range-energy relations in, (E), 19: 9893 (NAS-NRC-PUB-1133(p.173-86))
ion ranges at 10 to 100 Mev, bromine and iodine, 20: 41647
ion ranges in, determination from collection experiments, 17: 6820
ion reactions with foils of, sticking factors of rare gas, 19: 34610
ion reactions with emulsion nuclei of, recoil range-momentum relation for, (E), 19: 39883
ion scattering on, energy loss in boron and nitrogen, (E/T), 20: 9668
ionization of, by thermal methods after complex formation, 17: 38975
ionization on rhenium surfaces, (E), 19: 27733
ionization on rhenium and tungsten, effects of condensed layers and residual gases on, 19: 47222(T) (ORNL-tr-679)
iron-57 Mössbauer effect in, localized magnetic moments from, 19: 18511
iron-57 Mössbauer spectra in, 20: 30766
isotopic abundance ratios in terrestrial, 16: 7762
laser beam reactions on surfaces of, momentum transfer by giant-pulsed, (E), 20: 31810
levitation of molten, electromagnetic, 17: 11092 (NAA-SR-Memo-615)
light absorption by, mechanism of photographic sensitivity from, (T), 20: 11121
light scattering by bound electrons in, second-harmonic generation and Raman effects in, (T), 20: 12245
Lilienfeld emission from, 18: 10796
lithium reactions at 20 to 60 kev, secondary electron emission from, (E), 20: 19363
lubricating effects of films of, on cermet friction at high temperatures, 16: 5708 (ASD-TR-61-301)
magnetoplasma resonance in, 17: 16841
magnetoresistance at 1.2°K, 19: 12865(R) (NAA-SR-10501)
manganese-54 orientation in, gamma-ray anisotropy from, (E), 20: 22097
mechanical properties of internally oxidized, 20: 3639 (UCRL-11194)
melting point of, correlation with energy of motion of monovacancies, 18: 26037
melting temperature of, equations for calculating, 18: 25990
meson (K^-) capture by, electron emission in, 18: 11260
meson (K^-) capture by, hyperfragment production in, (E), 19: 10020 (UCRL-11328(Rev.1))
meson (K^-) reactions at 1.3 and 1.5 Bev/c, lithium-8 production in, 18: 36653
meson (K^-) reactions at 1.5 to 3 Bev/c, light charged particle emission in, (E), 19: 47651
meson (μ^-) capture at 149 Mev/c, x-ray spectra from, (E), 19: 5168
meson (μ^-) capture by, probability for, (T), 20: 28456
meson (π^-) reactions at 7.5 Bev, fragment production in, 18: 11280
meson (π^-) reactions at 17 Bev in nuclear emulsions, (T), 20: 38060
meson (π^-) reactions in nuclear emulsions at 1.7 Bev/c, proton spectra from, 20: 46932(R) (ORNL-3973(Vol.2), pp 71-84)
meson (π) reactions at 17.5 Bev, helium isotope production in, 18: 38102
meson (π) reactions with, fast secondaries from (E), 19: 1672
meson and nucleon reactions with, in emulsions, 18: 40614
meson (K^-) capture, star properties from, 16: 12357
meson (μ) capture, Fermi interactions in, 16: 15590
meson (μ) capture in, neutron emission from, 16: 18474
meson (μ) scattering, x-ray emission in, 16: 19705
meson (μ^-) capture and decay in, electron spectra, 16: 4725
meson (μ^-) capture in, neutron and nuclear properties from, 17: 39981 (UCRL-10516)
meson (μ^-) decay in mesic, skin dependence, 16: 974
meson (μ^-) elastic scattering cross sections, 16: 7117
meson (π^-) capture by, single charged particle emission in, 17: 11679
meson (π^-) reactions with emulsion, angular distribution of relativistic particles from 16-Bev, 17: 26462 (PAN-367/VI)
meson(K^-) reactions at 1.3 and 1.5 Bev/c, 18: 40547
meson(μ^-) capture by, multiplicity distributions of neutrons emitted in, 18: 40516 (UCRL-11243)
meson(π) reactions at 17 Bev/c, 18: 40551
molecular-beam scattering by single crystals of, spatial distributions in, (E), 20: 44121
Mössbauer effect of gold-197 in, relation between chemical shift and electronegativity in, 20: 7055 (UCRL-16436)
motion of particulate, on graphite surfaces, 18: 27872
negative ion emission, after positive ion bombardment, 18: 28121
neon-20 range-energy relations in, at 0.4 to 6 Mev, 16: 8003
neon-20 reactions in emulsion with, models for, 18: 17010
neon-20 reactions at 200 Mev, mechanisms of, 18: 24732
neon-20 reactions at 200 Mev, in emulsions, (E), 20: 40083
neutron absorption and total cross sections for, at 24 kev, 18: 4531 (EANDC-33U(p.41-3))
neutron absorption by strips of, in reactor control systems, 18: 28943
neutron absorption by, cross sections for thermal, 19: 33350
neutron absorption properties of, burnup effects on, (E), 19: 40163
neutron absorption cross sections at 24 kev, (E), 19: 45230
neutron absorption integrals for, infinite-dilution, (E), 20: 6558(R) (ANL-7115, pp 42-67)
neutron absorption cross section in pitchblende, thermal, 20: 37994
neutron activation in photographic emulsions, dose to emulsions from, 17: 18620
neutron activation in spherical samples of, self-shielding effects in, 18: 6764
neutron activation of, shielding effects during thermal, 18: 6184(T) (SC-T-523)
neutron capture by, gamma spectra from fast, 17: 13513
neutron capture by, use of lead spectrometer for studying, 18: 24608 (NP-13930(p.110-11))
neutron capture by, 18: 40630
neutron capture cross sections, 16: 14084
neutron capture cross sections, 16: 26509
neutron capture cross sections, 17: 2222 (JINR-P-1010)
neutron capture cross sections at 30 kev, 17: 26521
neutron capture cross section at 24 Mev, 17: 33005 (ORNL-TM-636)
neutron capture cross sections, 17: 41873 (WASH-1044)
neutron capture cross section at 0.1 to 50 kev, measurement of, 18: 8659
neutron capture cross section of, energy dependence of radiative (E/T), 19: 3391
neutron capture cross sections at 0.025 to 20 kev, (E), 19: 35378(R) (EANDC(E)-57(U))
neutron capture cross section measurement at 80 to 200 kev, errors in using boron monitors for, (E), 20: 30352 (NASA-TR-R-240)
neutron capture cross section discrepancies for, explanation by boron (n,α) cross sections in flux monitoring, 20: 44611 (CONF-660303, pp 486-501)
neutron capture gamma spectra, 16: 19745(R) (ARF-1193-9)
neutron capture resonance integrals, (E), 20: 40146
neutron cross sections, 16: 33199
neutron cross sections at 1.44 ev (E), 19: 3288
neutron cross sections of, shell effects on thermal, (E), 19: 47618
neutron detection from (n,γ) reactions in, resolution study of photographic image method for thermal, 17: 37430
neutron elastic and inelastic scattering by, fast, (E/T), 20: 19805(R) (ANL-7110, pp 1-28)
neutron elastic scattering at 0.65 Mev, angular distributions for, 18: 17089
neutron elastic scattering at 5.0 Mev, angular distribution, 18: 26668
neutron elastic scattering cross sections of natural, 18: 35060(R) (ANL-6904)
neutron elastic scattering at 0.3 to 1.5 Mev, differential cross sections for (E), 19: 3381
neutron elastic scattering at 3.3 Mev, asymmetry in polarized, (E/T), 19: 10343
neutron elastic scattering at 0.3 to 1.5 Mev, angular distributions from, (E), 19: 19095 (WASH-1053)
neutron elastic scattering at 0.2 to 1.5 Mev, cross sections for, 19: 31462(R) (ANL-7028)
neutron elastic scattering at 1 Mev, differential cross sections for, (E/T), 20: 9981 (WASH-1064)
neutron elastic scattering at 5 Mev, angular distributions from, (E), 20: 46794
neutron elastic scattering at 3.2 Mev, (E/T), 20: 46644
neutron inelastic scattering at 14 Mev, level density and nuclear temperature for fast, 17: 31492
neutron inelastic scattering at 4.0 to 6.5 Mev, energy spectra, 18: 26668
neutron inelastic scattering at 3.5 to 8.5 Mev, energy dependence of level density parameters from, (E), 20: 13827
neutron inelastic scattering at 5.8 and 7.5 Mev, gamma spectra from thermal, (E), 20: 22069
neutron radiative capture cross sections, 16: 14059
neutron radiative capture cross sections, 17: 4037
neutron radiative capture cross sections for, measurement of, 17: 15253(R) (GA-3874)
neutron radiative capture cross section at 18 to 300 kev, fast, 17: 21009
neutron radiative capture cross sections at 30 and 65 kev, 18: 34274(R) (NIRS-2(p.3-15))
neutron reactions (n,t), cross section, 16: 7048
neutron reactions ($n,n'\gamma$), cross-section analysis, 16: 8237
neutron reactions at 0.1 to 100 Mev, total cross sections for, 16: 11021
neutron reactions at thermal energies, cross sections, 16: 10961 (TID-14868)
neutron reactions (n,np) and ($n,p\gamma$) at 14 Mev, cross sections for, 17: 2242 (TID-16949)
neutron reactions (n,t), cross sections for, 17: 2242 (TID-16949)
neutron reactions (n,t) with, cross sections for, 17: 9619
neutron reactions with, effects of burn-up on thermal absorption cross

sections for, 17: 15214 (GEAP-4017)
neutron reactions (n,t) on, cross sections for, 17: 31434
neutron reactions at 385 Mev, spallation phenomena in, 18: 2853
neutron reactions with, evaporation effects in, 18: 30751
neutron reactions (n,γ) at epithermal to 30 kev, energy dependence in, 18: 38075(T) (AEC-tr-6398(p.70-80))
neutron reactions (n,γ) with, effective cross sections for, (E), 19: 16958
neutron reactions (n,α) at 14 Mev, angular and energy distributions from, (E), 19: 29279
neutron reactions (n,2n) with, fission-averaged cross sections, 19: 29319
neutron reactions (n,nγ) at 0.3 to 2.6 Mev, excitation cross sections for, (E/T), 19: 31284
neutron reactions (n,n′γ) with, cross section for, 19: 45263 (JAERI-1078)
neutron reactions (n,α) in nuclear emulsions at 18.3 Mev, angular distributions and energy spectra from, (E), 20: 26209
neutron resonance absorption integrals for, epithermal (E/T), 19: 1547 (CEA-R-2486)
neutron resonance integrals, 20: 32781
neutron scattering at 1 Mev, 16: 3662
neutron scattering angular distribution, 16: 12419 (ANL-5567(Rev.))
neutron scattering by, measurement of polarization in, 17: 2243(R) (TID-17083)
neutron scattering at 14 Mev, nuclear temperature after excitation by, 18: 15235
neutron scattering at 3 to 650 kev, cross sections, phase shifts, and strength functions for, (E), 19: 10319
neutron scattering by, angular distribution in, 19: 31252
neutron scattering at 0.3 to 1.5 Mev, differential cross sections for, (E), 20: 13829
neutron self-shielding effect in activation, formula for measuring, 16: 16415
neutron thermal, self-shielding effects in activation, 18: 33488
neutron total cross sections at 0.0001 to 0.1 ev, 16: 18430
neutron total cross section of, fast, 17: 20982 (HW-SA-2875)
neutron total cross sections at 10 to 100 kev, 18: 4525 (BNL-7349)
neutron total cross sections at 0.1 to 4 kev, (E), 19: 12572
neutron total cross sections of, measurement using neutron velocity spectrometer, (E), 19: 19095 (WASH-1053)
neutron transmission in, 19: 15926
nitrogen ion ranges at 0.4 and 2.5 Mev, (E), 19: 41269
nitrogen-14 energy-range relations at 0.4 to 6 Mev, 16: 8003
nitrogen-14 reactions with emulsion, recoil range-energy ratio for, (E), 19: 43360
nuclear levels in, spacing distributions and correlations for, 18: 2955
nucleation on tungsten, field-emission microscopy of, 18: 26054
nucleon reactions at high energies, secondary nucleon yields from, (E/T), 19: 21242 (NP-14837)
nucleon scattering at 2.8 and 6.8 Mev, angular distributions from, 18: 38080(T) (AEC-tr-6398(p.120-5))
optical constants of evaporated films of, at 2500 to 3700 Å, 19: 26923 (TID-21850)
optical constants, alloying effects of cadmium on, 18: 28090 (IS-863)
optical emission of irradiated films of, 16: 25847 (ORNL-3114)
optical properties of bulk and vacuum-evaporated, 19: 7539(R) (ORNL-3697(p.131-43))
optical properties of crystals of, effects of argon-ion bombardment and vacuum annealing on, 17: 18767 (TID-16688)
oxidation from rotating platinum electrode, determination of oxidizing agents by, 19: 30093
oxidation of, determination of free energy states in, 17: 34400 (CONF-155-1)
oxidizing properties of divalent, 16: 14378(R) (NYO-2302)
oxygen exchange and sorption by, mass-spectrometric analysis of mechanisms, 17: 40825
oxygen ion energy losses in, at 2 to 40 Mev, (E), 19: 6461
oxygen pumping at surface of, 19: 32413(R) (WERL-2823-17)
oxygen-16 reactions at 167 Mev, charged-particle yields in, 17: 28252 (UCRL-10693)
oxygen-16 reactions at 167 Mev, charged-particle emission in, 18: 34780 (UCRL-11349)
oxygen-16 reactions at 167 Mev, particle spectra from, (E/T), 19: 10336
oxygen-18 exchange reactions on films of, kinetics of, 20: 18808
particle waves and phonon fission in crystals of, 18: 27874
performance as electrodes, tracer study of diffusion and evaporation, 18: 37476(T) (AEC-tr-6398(p.232-45))
performance in ultraviolet polarization, (E), 20: 7659(R) (ORNL-3849, pp 101-50)
photoactivation of natural, excitation levels in nuclear, (E), 20: 19865
photoelectric and optical properties of films of, in extreme ultraviolet, (E), 20: 44995 (ORNL-TM-1392)
photoelectron distribution from cesium-137 gammas, 16: 4635
photoelectron distribution from, cesium-137 gamma, 17: 6833
photoelectron emission of films of, excited by soft x rays, effective depth for, 18: 5875(T)
photoelectron production cross section of, for 662-kev gamma radiation, (E), 19: 4835
photoelectron production by 145-kev gamma rays, cross section for, (E), 19: 4836
photoelectron production by 145-, 280-, and 320-kev gamma rays, cross sections for, (T), 19: 47329
photofission at 300 to 1000 Mev, cross sections for, 18: 24655
photon excited plasma from, (E), 20: 46886
photon reactions with, proton angular distributions and yields at >8 Mev, 17: 28265
photovoltaic properties of coatings of, on anodized zirconium electrodes, (E), 19: 36768 (TID-21971)
plasma energy of, (E), 19: 30781
plastic behavior of whiskers of, under alpha irradiation, 17: 16762
plutonium determination on plates of, by alpha counting, 20: 36736
polarization of nuclei of, in iron and nickel, 18: 31361(R) (UCRL-11213 (p.87-138))
polarography of, in acetone solution, 17: 14253
positron lifetime in, 16: 3626
potassium ion bombardment at 20 kev, penetration, deceleration, and range-energy relations in, 19: 23266
potentials of single-crystal, face, 19: 36220(R) (MIT-2098-142)
precipitation from nitric acid solutions using sodium borohydride, 18: 13358(R) (MLM-1151)
precipitation using dimethylbenzenearsonic acid, 19: 9136
precipitation using trichlorobenzenearsonic acid, 19: 9137
precipitation with copper diethyldithiocarbaminate, 17: 4475
preparation and structure of films of, evaporated on rock salt crystals, 17: 29333(T) (NP-tr-1032)
preparation from nitrate, photolytic and radiolytic, 18: 1725(R) (ORNL-3488(p.42-54))
preparation of crystals of, by Bridgman technique in graphite crucibles, 16: 6813(R) (ORNL-3213(p.44))
preparation of microporous films of, 17: 29311(P)
preparation of photoelectric strip-converters of, for use in beta spectroscopy, 19: 18311
preparation of porous membranes of, for ultrafiltration, 18: 19934 (NP-13874)
preparation of single-crystal, 18: 12042(R) (TID-20114)
preparation of thin layers of, for use as cyclotron irradiation target, 19: 28966
preparation of thin layers of, using evaporation by levitation heating, 20: 25521 (AERE-R-5097, Paper 23)
production of colloidal, by photon irradiation of silver bromides, 16: 25867
properties as reactor control material, 16: 32120 (TID-16597)
properties for use as high-altitude tracer, 19: 4404 (TLW-1092)
properties of beryllium-fiber-reinforced, 18: 41925(R) (IITRI-B241-8)
properties of, effects of impurities on, 17: 41442
properties of, electrical and thermal, 17: 25381 (ASD-TDR-62-118)
properties of, for use as cathode in electrolytic separation of deuterium, 17: 22074
properties of Inconel- and type 321 stainless steel-clad wires of, at 80 to 1600°F, 18: 41928(R) (NASA-CR-54089)
properties of liquid, 16: 19370 (TIM-65)
properties of, research program on, 20: 1562(R) (NYO-2684-39)
properties, theory of infrared and optical, 16: 25758 (NP-11675)
protective effects against nucleic acid decomposition by nuclease, 18: 25085 (SGAE-BL-5/1964)
proton attenuation at 1 to 1000 Mev, 17: 18909 (TID-18436)
proton attenuation at 28.7 Mev in, 17: 37861
proton attenuation by films of, at 1.5 to 4.5 Mev, 16: 15668
proton elastic and inelastic scattering at 6.8 Mev, 17: 24414
proton elastic scattering at 57 Mev, angular distributions and polarizations, 16: 23056
proton elastic scattering at 9–22 Mev, optical-model analysis of, 17: 28316
proton elastic scattering at 17.8 Mev, polarization of, (E), 20: 32439
proton fission at 9 Bev, multiple production of fragments, 16: 1073
proton fission at 1 to 3 Bev, alpha and fission-fragment emission, 16: 18515
proton fission at 9 Bev, charge spectra from, 16: 26329
proton fission at 600 Mev, cross sections for, 16: 33865
proton fission at 140 Mev, cross sections, relative yields and mass distribution from, 17: 16053(R) (TID-18261(p.49-60))
proton fission at 19 Bev, lithium-8 from, 17: 33081
proton fission at 140 Mev, relative yields of nuclides in, 18: 13839(R) (TID-20201)
proton fission at 60 to 140 Mev, formation cross sections of products from, 19: 22282(R) (NYO-1930-40)
proton nonelastic scattering cross sections at 10 Mev, 17: 13581
proton range-energy relations in, multiple-scattering effects on, (E/T),

19: 9891 (NAS-NRC-PUB-1133(p.69-98))
proton reaction at 120 and 660 Mev, 17: 17149
proton reactions (p,n) with, isobaric states from, 18: 14590(R) (NIRL/R/60)
proton reactions (p,n) at 30 and 50 Mev, isobaric-state excitation in, (E/T), 20: 6361
proton reactions (p,n) at 30 to 50 Mev, distributions from, 20: 15729(R) (RHEL/R-112, pp 37-66)
proton reactions (p,d) at 57 Mev, energy spectra from, (E), 20: 17725
proton reactions at 77 to 133 Mev, cross sections for elastic, 16: 12480
proton reactions at 0.1 to 0.5 Mev, characteristic x-ray yields from, 16: 33633
proton reactions at 540 Mev, cross section for production of rare gases from, 17: 19255
proton reactions at 320 to 880 Mev, formation of magnesium-28 and sodium-24 in, 17: 31525
proton reactions at 2 and 9 Bev, emission of short-range fragments in, 18: 11279
proton reactions at 260 kev, uv radiation emission in, 18: 20781
proton reactions at 660 Mev, angular distribution of fragments from spallation, 18: 21229
proton reactions at 2.9 Bev, ranges of recoil products from, 18: 26648
proton reactions at 2 to 9 Bev, fragment angular correlations for, 18: 34940
proton reactions at 9 and 24 Bev, lithium-8 production in, 18: 36653
proton reactions at 19.5 Bev, helium isotope production in, 18: 38102
proton reactions at 9 and 25 Bev, 18: 40547
proton reactions at 24 Bev/c, 18: 40551
proton reactions at 600 Mev, distributions from spallation (E/T), 19: 3257
proton reactions at 157 Mev, nucleon clustering from, (E), 19: 41831
proton reactions at 2 Bev, lithium-8 production in, (E), 20: 6409
proton reactions at 3 Bev, fission and fragmentation products from, (E), 20: 5756
proton reactions at 1.84 Bev, sodium-24 energy spectra and yield in, (T), 20: 12067
proton reactions at 13.8 Bev/c in emulsions, intranuclear cascades from, (E), 20: 28397
proton reactions at 0.05 to 2.9 Bev, induced activity data and cross sections for spallation, (E/T), 20: 32549
proton reactions at 600 Mev, cross sections for meson ($\pi^{\pm}$) production in, 20: 38186
proton reactions at 200 and 400 Mev, formation cross section and half life of silver-101 yields in, 20: 42179
proton reactions in emulsions at 25 Bev/c, lithium-8 fragment recoil from, (E), 20: 17748
proton reactions (p,n) at 42 to 150 Mev, cross sections, 16: 23096
proton reactions (p,α), (p,d), (p,p), and (p,t) at 57 Mev, 16: 29774 (JAERI-1020(p.194-200))
proton reactions (p,n) on, spectra from, 17: 17226
proton reactions (p,n) with, time-of-flight neutron spectrum from, 17: 20994 (UCRL-7233)
proton reactions (p,d) at 57 Mev, neutron binding energies in, 17: 38229
proton reactions (p,α) at 30, 43, and 56.3 Mev, angular distributions and energy spectra from, 17: 40039
proton reactions with emulsion, boron-8 and lithium-8 emission frequency in 9 and 24 Bev, 17: 26464 (PAN-397/VI)
proton reactions with, rare gas and tritium production cross sections for, 18: 15189 (CERN-64-12)
proton reactions with monocrystals, electron and ion emission in, 18: 42295(R) (ANL-6879(p.114-29))
proton reactions with, fast secondaries from (E), 19: 1672
proton reactions with, phosphorus-32 and -33 production in, (E), 20: 12034
proton reactions with, ejection of magnesium-28 and sodium-24 in, 16: 2498 (UCRL-9683)
proton scattering by, neutron, prong, and proton spectra and distributions for, 17: 22564 (ORNL-3383)
proton scattering at 9.4–22.2 Mev, local optical potentials for, 17: 38185
proton scattering at 1.5 Mev, x-ray emission from, 18: 14664
proton scattering at 9.4 Mev, polarization in, (E), 20: 8129
proton scattering at 28 Mev, cross sections for elastic, (E/T), 20: 10094
proton slowing down in, (T), 19: 17023
proton spallation of, yield curve for, 18: 15244
proton spallation at 660 Mev, 18: 21230
proton spallation at 660 Mev, angular distribution of fragments from, 18: 44753
proton spallation at 340 Mev, production of neutron-deficient isotopes in, 20: 24376
proton symmetric fission reactions at 60 to 140 Mev, (E/T), 19: 37799 (NYO-1930-43)
proton total cross sections at 8.5 to 11 Mev, (E), 19: 43323
proton total reaction cross sections, 18: 18987
proton transmission in foils of, low-energy, (E), 19: 41969 (ORNL-TM-1153)
purification of, radiochemical method for, 20: 8838 (UCRL-14258)
quenching in liquid nitrogen, production and movement of vacancies in, 17: 1925 (CEA-2116)
radiation annealing effects at 4.5°K, 18: 14562
radiation annealing of Frenkel defects in, statistical model for, 18: 32252
radiation attenuation by, critical energies and units for, 17: 38420
radiation damage, 16: 29460
radiation damage, cross section for atomic displacement by electrons at 0.5 to 3 Mev, 16: 564 (61-GC-166)
radiation damage from fast neutrons at 4.5°K, effects of defect concentration on annealing of, 18: 14561
radiation damage in, production and recovery of electron-induced, 16: 27719
radiation dosimetry device made of phosphate glass activated with, 18: 14268
radiation effects on temperature of, electron, 16: 33388
radiation effects on pure, reactor-neutron, 17: 5001
radiation effects on electric resistance of, 17: 6732 (62-GC-207)
radiation effects of neutrons on colloidal, gamma-recoil products from, 17: 8190
radiation effects, 17: 8877 (AFCRL-62-316)
radiation effects of deuterons on, annealing below 60°K, 17: 18884
radiation effects on self-diffusion-controlled reactions in, 17: 31055
radiation effects on plastic deformation of, 17: 32684
radiation effects of radium on colloidal, 17: 35458(T) (AEC-tr-5947)
radiation effects on, mechanisms for annealing and producing, 18: 2322
radiation effects on diffusion of lead in, alpha, 18: 4172(R) (ORNL-3470 (p.67-74))
radiation effects on, Stage III annealing of 10-Mev proton, 18: 5833
radiation effects on, at low temperatures, saturation phenomena in defect production by neutron, 18: 16531(T) (AI-Trans-38)
radiation effects on crystalline, 18: 26069(R) (ANL-6868(p.373-417))
radiation effects on indium-111 gamma angular correlations in, 18: 26085
radiation effects on, bibliography, 18: 40009 (UCRL-7810)
radiation effects on defect distributions in, cascade theory of, 19: 9749
radiation effects on fixation of, by Kupffer liver cells, 19: 17638
radiation effects on electric resistivity at 4°K, fast neutron, 19: 44739(R) (ANL-7000, pp 233-77)
radiation effects on, lattice atom displacement probabilities in deuteron and neutron, (T), 19: 47104
radiation effects on electrochemical properties of electrodes of, in oxygen fuel cell, 17: 1720
radiation effects on thin films of, neutron, 16: 22680
radiation effects on films of, light emission, 17: 2787(R) (ORNL-3347 (p.73-100))
radiation effects on lead diffusion in, alpha, 20: 4385(R) (ORNL-3870, pp 15-19)
radiation effects on battery electrodes of, gamma-, 20: 17115(R) (AI-65-264)
radiation effects on electrodes of, gamma, 20: 33944(R) (N-65-34010)
radiation effects on absorption spectra of, x, 20: 34092
radiation effects at cryotemperatures on, recovery rates of electron, 20: 44022
radiation effects on valence of, in glasses, gamma, (E), 20: 44012
radiation from electron-bombarded foils of, temperature and thickness in transition, 18: 26224
radiochemistry, review, 16: 206 (NAS-NS-3047)
radioinduced coloring and luminescence, of potassium chloride-doped with, x, (E), 19: 27717
radioinduced diffusion of lead and silver in, alpha, (E/T), 20: 44002
radioinduced oxidation of films of, gamma and neutron, 16: 27702
radioinduced oxidation of films of, 16: 27096
radioinduced point defects in, 16: 33553
radioinduced recombination luminescence of sodium chloride phosphors doped with, x, (E/T), 19: 27722
radioinduced resistivity changes in thin layers of, silver ion, (E), 20: 44004
radioluminescence of alkali halides activated with, temperature effects on electron, (E), 19: 27718
radioluminescence of alkali halide crystals doped with, electron and photon, 19: 27714
radon-222 ranges in, determination using alpha spectral analysis, 19: 35513
range of energetic atoms of, in silver, Monte Carlo calculations of, 17: 14968
range of energetic atoms in solids, Monte Carlo calculations, 18: 28111
rare-gas ion reactions at 1 to 10 kev, secondary-electron emission in, (E), 19: 39404
reactions of atomic, spectral line broadening in, 18: 32485
reactions with aluminum to 500°C *in vacuo*, 19: 22997 (TRG-Report-842)

reactions with benzenearsonic acid and its derivatives in acid media, precipitation, 17: 12198
reactions with beryllium, copper, stainless steel, and niobium alloys to 760°C *in vacuo*, 19: 44606 (PWAC-483)
reactions with beryllium to 600°C *in vacuo*, 19: 22997 (TRG-Report-842)
reactions with carbon dioxide, 16: 2993 (NP-10967)
reactions with dilituric acid, thermolysis of salt formed by, 18: 35467
reactions with magnesium to 450°C, 19: 22997 (TRG-Report-842)
reactions with Magnox alloy to 450°C in argon, 19: 22997 (TRG-Report-842)
reactions with permanganate ions during pulse-radiolysis of solutions, 20: 10914
reactions with potassium hydroxide (liquid) and sodium hydroxide, 16: 179
reactions with sodium in liquid ammonia, intermetallic phase production in, 18: 23149(T) (ANL-Trans-8)
reactions with sodium, high-temperature, 20: 15033(R) (ANL-7152, pp 87-96)
reactivity effects on ZR-2 assembly, 18: 38335
reduction of tungsten trioxide of, 16: 22072(T) (AEC-tr-5125)
removal of brazing flux of, from metals, descaling solution for, 20: 21238 (NP-15928)
selective attack on, by argon ions, study of pseudo-periods, 18: 28122
self-diffusion in, surface kinetics of, 17: 19460(R) (TID-16980)
self-diffusion of, effects of oxygen on, 17: 8711(R) (TID-17556)
separation as ferrocyanide on filter paper by precipitation chromatography, 17: 40932
separation by ion exchange on thallous phosphotungstate, 16: 25485
separation by reversed-phase chromatography and solvent extraction using tri-*n*-octylphosphine sulfide, 19: 19753 (IS-T-3)
separation by solvent extraction of diethyldithiocarbamate, radiochemical, 17: 19964
separation from acid solutions by solvent extraction using N,N′,N″-trihexylphosphorothioic triamide, 19: 17781(R) (ORNL-3750)
separation from acid chlorides by solvent extraction using amines, 19: 28443(R) (ORNL-3785)
separation from alkaline solution by extraction with trioctylamine, 16: 273
separation from aqueous solutions by solvent extraction using tri-*n*-butylphosphine sulfide, 17: 10754
separation from berkelium by solvent extraction, 19: 22112
separation from bismuth, cadmium, copper, lead, and zinc by anion exchange, 16: 16463
separation from cadmium by electrolytic methods, 17: 15912
separation from cadmium and rhodium by solvent extraction, 17: 28945 (USNRDL-TR-648)
separation from cadmium, indium, and tin by filtration through copper powder bed, 19: 32284 (USNRDL-TR-844)
separation from chromium, manganese, nickel, and rare earths by ion exchange chromatography, 20: 20634
separation from copper, lead, and zinc by solvent extraction using tri-*n*-octylphosphine sulfide, 19: 19753 (IS-T-3)
separation from electrolytes by ion exchange, 19: 36463(R) (TID-22060)
separation from fission products by solvent extraction using TBP and TOPO, 17: 243
separation from fission products, 19: 2425
separation from hydrochloric acid solutions by solvent extraction using 2-ethylhexanol, 19: 36252
separation from indium and rhodium by carrier precipitation, 17: 2242 (TID-16949)
separation from mercury and thallium, electrochromatographic, 16: 5273
separation from metal ionic mixtures, electrochromatographic, 17: 10753
separation from mixtures by cation exchange chromatography, 20: 40847
separation from monovalent ions by ion exchange using thallous phosphotungstate, 16: 11698(R) (TID-15020(p.57-60))
separation from nitric acid solutions by solvent extraction using tridodecylamine in toluene, 19: 5991(R) (MITNE-54)
separation from nitric acid solutions by solvent extraction using tridodecylamine in toluene, 19: 5990(R) (MITNE-50)
separation from nitric acid solutions, ion exchange selectivity scales for, 19: 9257
separation from nitric acid by solvent extraction using tri-*n*-octylphosphine sulfide, 20: 244
separation from other metals by ion exchange chromatography in tartrate medium, tracer studies of, 19: 7627
separation from other metals by ion exchange, 19: 15692
separation from other elements by partition chromatography, 20: 4054
separation from other inorganic ions by paper chromatography, 20: 12939
separation from other elements by ion exchange using triisooctylamine, 20: 43439
separation from palladium, 20: 46624
separation from perchloric acid solutions by ion exchange materials, 20: 20823
separation from plutonium by ion exchange in nitric acid, 18: 22170 (LA-3040)
separation from rare earths by ion exchange in isopropyl alcohol, 18: 20104
separation from solutions by sorption on fluorinated surfaces of glass and quartz, 19: 32310
separation from uranyl ions by solvent extraction using dithizone, 18: 29582
separation from uranium by chromatography on cellulose columns, tracer studies of, 19: 40687
separation from zinc in aqueous solution by solvent extraction using dithizone–chloroform, 19: 26471
separation of trace amounts of, from alkali metals, alkaline earths, and rare earths, 20: 1958
separation of, from thallium by ion-exchange chromatography, 20: 36935
separation of, from zinc, in hydrochloric acid solutions by ion-exchange chromatography, 20: 45809
shock wave interactions with, thermodynamic parameters from mirror-image approximation for particle velocity and pressure in, 17: 37676
sintering mechanism study, 19: 18398(R) (RPI-2408-1)
sintering of loose powder of, kinetics of low-temperature, 18: 15721 (TID-20331)
sintering of loose powder of, near 300°C, 19: 20465 (TID-20344)
sintering of, studies on, 20: 16992(R) (RPI-2408-4)
solubility in liquid sodium, effects of free energy gradient on, 18: 22488 (NAA-SR-8381)
solubility in liquid zinc, 20: 22966 (ANL-7083)
solubility in mercury, 17: 28906
solubility in silver chloride, 19: 36216(R) (BNL-900(p.29-72))
solvent properties for plutonium, 16: 25474 (IS-470)
solvent properties for holmium, solid, 17: 36297 (IS-594)
sorption by arsenic, cadmium, lead, and zinc sulfides, 18: 1614(R) (ORNL-3488(p.65-90))
sorption by zeolite from molten nitrate, 18: 12255 (IA-864)
sorption from hydrochloric acid by cellulose and resin paper ion exchangers, 18: 16139
sorption from nitric acid by ion exchange paper, 19: 24435
sorption of americium-241 and protactinium-233 by, from water–ethanol solutions, 18: 23724
sorption on anion exchange papers in hydrobromic and hydrochloric acids and lithium chloride, 18: 25374
sorption on water-handling surfaces, 18: 45176 (NYO-10544(Rev.))
sorptive properties for iodine, 16: 29230 (TID-7627(p.242-62))
sorptive properties for iodine, 16: 29234 (TID-7627(p.327-48))
sorptive properties for iodine, 17: 14197 (AERE-R-4114)
sorptive properties for low concentrations of iodine, 17: 18171 (AERE-R-4219)
sorptive properties for promethium, cerium, zirconium, niobium, tritium, and sulfate ions, tracer study of, 17: 35693 (NP-12983)
sorptive properties for oxygen, 19: 36338(R) (NP–15160)
sorptive properties of surfaces of, for iodine in high-temperature helium loop, 19: 40397 (ORNL-TM-1134)
sorptive properties for deuterium and hydrogen at low temperatures, 19: 42879
sorptive properties of particles of, for radioiodine, 20: 216 (CONF-650407, pp 242-75)
sorptive properties for oxygen, isotopic exchange studies of, 20: 7084
sorptive properties for oxygen, kinetics of, 20: 18808
sorptive properties for cadmium and mercury, 16: 26009
spalling of, stress effects on time-dependent, 18: 30182
specific heat at 2 to 4°K, 19: 34689 (TID-20986)
spectra in reaction zone of acetylene air flame, excitation of atomic, 17: 27371(T)
spectra, isotopic shift in I and II, 16: 19541
spectra of low-energy x rays from target, effects of electrons in 80 to 180A region, 16: 23032
spectra of, isotope shift in, (E), 19: 35512
spectra of, time evolution of lines in emission, 20: 7062
spectra of, x-ray L-absorption and -emission, 18: 34412
spectra of, x-ray L-emission, 18: 34410
sputtering at 50 to 600 ev by rare gas ions, 17: 8931(R) (NP-12389)
sputtering by argon ions, full-plane threshold energies for, 17: 37743
sputtering by argon at 40 to 80 kev, angular and energy distribution from, 18: 20783
sputtering by argon at 30 to 170 kev, yields from, 18: 22673
sputtering by argon ions, effects of impact angle on angular distribution of atoms from, 19: 25153
sputtering by argon ions at 30 to 170 kev, (E), 19: 44937(R) (TID-22140)
sputtering by argon ions at 1 to 7 kev, (E/T), 20: 13414 (JUL-304-RW)
sputtering by cesium at 2–5 kv, 17: 21830
sputtering by deuterons, 18: 42295(R) (ANL-6879(p.114-29))
sputtering by helium ions at 600 ev, yield curves for, 17: 25870(R) (X62-11400)

sputtering by helium, krypton, neon, and xenon ions at 3 to 7 kev, tracer study of, 18: 751
sputtering by hydrogen and deuterium ions at 9.25 kv, coefficients of, 16: 32185
sputtering by hydrogen ions, yields from, 18: 8926
sputtering by ions at 45 kev, thermal spikes in, (E), 19: 20838
sputtering by molecules in upper atmosphere, (E), 19: 25149
sputtering by noble-gas ions at 100 to 600 ev, yields from, 16: 22753
sputtering by protons at 2 and 300 Mev, (E), 20: 13414 (JUL-304-RW)
sputtering by rare gas ions at 3 to 7 kev, 18: 37853
sputtering of crystals of, by argon ions at 1 to 10 kev, effects of crystalline orientation on, 17: 41598
sputtering of films of, by krypton ions, 16: 27806
sputtering of, by deuterons, helium ions, and protons at 0.1 to 4.0 Mev, (E), 20: 31905
sputtering ratios at 10 to 65 kev for cations, 16: 9116
sputtering yields for noble-gas ions, 16: 22748
stacking-fault energy, 18: 20550
stopping power for lead-208 alpha recoil nuclei, (E), 20: 37470
structure of liquid, x-ray diffraction studies of, 18: 14475 (TID-20304)
sublimation of monocrystalline, angular distributions from, 19: 41259
superconducting energy gap of films of, proximity effects of lead films on induced, 20: 19754
superconducting energy gap in binary films with tin, (E), 20: 34425
superconducting films of, edge-effect suppression in, 18: 26482
superconducting properties, 17: 19
superconducting transition temperature in, 16: 15334
superconducting transition temperature of tin laminates with, 20: 44567
superconductivity, 18: 24179
superconductivity of, 20: 40047
surface tension, 16: 7901(T) (AEC-tr-4980)
surface tension, 16: 1772
surface tension of liquid, relation to critical temperature and surface energy, 16: 25351
surface tension of, measurement by pendant drop method, 19: 47065
thermal conductivity of liquid, estimation of, 20: 41477
thermodynamic properties at high pressures and temperatures, 19: 40459 (NP-15324)
thickness as coating on copper, beta-x-ray fluorescence analysis of, 18: 27322
thickness measurement by alpha energy degradation, 20: 3982(R) (AGN-8156)
thickness uniformity of commercial films of, 17: 11104 (TID-16252)
tin-119 Mössbauer effect in, 20: 12315
tracer applications survey, 16: 1359
twinning at 4.2, 77, and 300°K, 16: 6810(R) (ORNL-3213(p.15-23))
use as electrodes in ionization chamber for neutron flux monitoring, 20: 43680
use as filter for radiographic inspection of steel, 19: 44209(R) (EURAEC-1422)
use for braze bonding stainless steel cans to stainless steel–uranium dioxide cermets, 19: 4635
use for coating insulators in fission chambers, 16: 5483 (DC-55-11-112)
use for neutron flux measurements, multi-velocity corrections in, 20: 29539
use in bonding aluminum and aluminum alloys, 17: 41402(P)
use in brazing and diffusion bonding beryllium to stainless steel, 19: 30691 (N64-28460)
use in G-M counters with activable cathodes, for measurement of fast neutron fluxes, 20: 43729
use in neutron flux detector utilizing calorimetric conversion, 18: 14290(P)
use in thermocouples, 17: 21993
use of radioactive, for infection foci studies, 16: 1391
use of stable, as tracer in biology experiments, with neutron activation of samples, and radiometric analysis, 18: 33175 (BNL-7772)
vacancy annihilation and precipitation in, clustered, 18: 7244
vapor pressure at 1150 and 1250°C, 17: 37519(T) (AEC-tr-5983)
vapor pressure measurements at 1403 to 1601°K, 17: 29330(R) (UNC-5056)
vaporization coefficients of single crystal, 19: 46956 (NP-15514(Vol.1))
vaporization losses from liquid droplets of, during re-entry ablation, 19: 27813 (SC-RR-65-138)
vaporization studies, 18: 27815(R) (ORNL-TM-718)
viscosity of liquid, 19: 44701(R) (TID-22144)
viscosity of liquid, based on atomic parameters, 20: 20656 (UCRL-11930)
viscosity of, relation of atomic mobility to, 17: 4945
wetting behavior of liquid, on solid beryllium, effects of atmosphere and temperature on, 17: 27795 (ORNL-3438)
wetting behavior of liquid, on solid beryllium, 17: 33323(R) (ORNL-3445 (p.199-217))
wetting behavior of liquid, on solid beryllium, 18: 28035
work function, effects on minimum sparking potential in hydrogen, 16: 19608
x-radiation production efficiency, 16: 8137
x-ray emission at 80 to 180Å, 16: 8129
x-ray emission by, yield of L-shell, 18: 7732
x-ray emission of absolute intensity of Kα, 17: 25973
x-ray spectra of, using promethium-147 beta source, 17: 27280
x-ray emission by, yields of L-shell, 18: 28253
x-ray mass absorption coefficients at 7 to 17 A, (E), 19: 6394
x-ray spectra of, precision redetermination of wavelength of $K\alpha_1$ line in, 18: 34341
x-ray total cross sections at 15 to 30 Mev, (E), 19: 12573
x-ray yields from, L-shell, 18: 40573
x-ray-diffraction analysis of liquid, 18: 10542(R) (TID-20065)
xenon-133 ranges and retention at 1–150 kev, energy and flux dependence of, 17: 28002
yields from gamma radiolysis of aqueous silver perchlorate solutions, 20: 26962
zirconium dioxide electric conductivity on electrodes of, 20: 7589

SILVER ACETATES

oxidative effects on uranium acetate in liquid ammonia, 20: 26839
oxidizing effects on uranium compounds in ammonia, 17: 175

SILVER ACETYLIDES

Ag_2C_2–$AgNO_3$, qualification tests on spray-deposited and light-initiated explosives of, 20: 10814 (SCL-DC-65-96)

SILVER ALLOYS

as bearing material for steam and water, 17: 3427(R) (NP-12233)
book: *Neutron Absorber Materials for Reactor Control*, 16: 23288
crystal symmetry patterns of, Kikuchi analysis of, 20: 31715(R) (UCRL-16658, pp 105-20)
development of, for brazing uses, 17: 14786 (KR-33)
effects of beryllium additions on, 20: 37275
electric field gradients in dilute, effects of electron rearrangement and lattice distortion on, 17: 35777
electrode properties for oxygen reduction in hydroxide solutions, 19: 36338(R) (NP–15160)
performance of Silflake 850 for temperature sensor joining to copper, 19: 5528 (NAA-SR-Memo-10211)
properties of, research program on, 20: 1562(R) (NYO-2684-39)
soldering to beryllium, 18: 10511
superconductivity of metastable intermetallic compounds in, 18: 24142 (TID-20617)
superconductivity, 18: 24179
use as reactor control rod materials, 16: 5749(P)
Ag–Na, phase studies, 20: 25474(R) (BNL-954, pp 122-67)
Ag–Re, radiation effects on solid-film lubricants of, 19: 23121
Ag–Sn, atomic distribution in molten, x-ray diffraction study of, 19: 11729 (YALE-2560-5)
Ag–Sn, chemical shift and electronegativity of tin-119 in, 20: 7055 (UCRL-16436)
Ag–Sn, heat of solution at 425°C, 19: 44678(R) (ANL-7000, pp 186-200)
Ag–Sn, properties and structure, 16: 15198(R) (TID-15390)
Ag–Sn, solute distribution and thermal curves of solidification of, 17: 20500
Ag–Sn, specific heats at 2 to 4°K of, 19: 34689 (TID-20986)
Ag–Sn, thermodynamic properties, 18: 30164(R) (AD-429007)
Ag–Sn, tin-119 Mössbauer effect in, 19: 11761
Ag–Sn, x-ray-diffraction analysis of liquid, 18: 10542(R) (TID-20065)
Ag–Sr, crystal structure of AB_2-type compound in, 20: 24589(R) (NYO-3560-3)
Ag–Sr, sample preparation, metallographic, 20: 27418
Ag–Ta, fabrication and properties of impregnated, 18: 4270
Ag–Ta, preparation and properties of impregnated, 17: 32495
Ag–Tb, crystal structure, 17: 16658 (TID-18197)
Ag–Tb, crystal structure studies, 19: 44678(R) (ANL-7000, pp 186-200)
Ag–Tb, electric conductivity, 20: 25583
Ag–Tb, magnetic properties of intermetallic compound with CsCl structure in, 19: 2814
Ag–Tb, magnetic structure, 18: 39954
Ag–Tb–Y, crystallography, 20: 4391(R) (ORNL-3870, pp 75-82)
Ag–Th, phase studies, 16: 30877
Ag–Th, phase studies, 19: 14044
Ag–Th, phase studies, 20: 11224
Ag–Th, superconducting properties, 16: 22631
Ag–Ti, mechanical properties of intermetallic compounds in, effects of composition and structure on, 17: 541 (WADD-TR-60-184(Pt.III))
Ag–Ti–Zr, tensile properties at room temperature, 18: 18380
Ag–Tm, crystal structure, 17: 16658 (TID-18197)
Ag–Tm, crystal structure studies, 19: 44678(R) (ANL-7000, pp 186-200)
Ag–Tm, electric conductivity, 20: 25583
Ag–Tm, magnetic properties of intermetallic compound with CsCl structure in, 19: 2814
Ag–U, composition of splatcooled, 18: 8726(R) (NMI-2123(p.47-51))
Ag–U, fabrication of SLIS, 18: 5735(R) (NMI-2122)

Ag–U, thermodynamic properties of, 18: 44224
Ag–W, corrosion by carbon dioxide at 2250°C, 17: 34328(R) (NP-12991)
Ag–W, corrosion by carbon dioxide at 2250°C, 19: 46956 (NP-15514 (Vol.1))
Ag–W, fabrication and properties of impregnated, 18: 4270
Ag–W, fabrication of rocket motor nozzle of, 20: 29685
Ag–W, preparation and properties of infiltrated, 19: 20559 (NP-14892)
Ag–W, properties of, effects of processing conditions on, 20: 25540
Ag–W, sintering in presence of liquid phase, kinetics of, 20: 2286
Ag–Y, crystal structure studies, 19: 44678(R) (ANL-7000, pp 186-200)
Ag–Y, crystal structure of intermetallic compound YAg_2 in, 20: 15102
Ag–Y, electric conductivity, 20: 25583
Ag–Y, phase diagrams, 19: 7941
Ag–Zn, crystal structure studies, 19: 44678(R) (ANL-7000, pp 186-200)
Ag–Zn, diffusion in, activation energies for, 17: 35264(R) (UCRL-10706(p.111-203))
Ag–Zn, diffusion activation energies in dilute solid solutions of, relation with Zener relaxation activation energy, 18: 9773 (TID-19979)
Ag–Zn, heat of formation and phase studies, 16: 10502 (AROD-2287.15)
Ag–Zn, phase studies, 16: 551
Ag–Zn, properties and structure, 16: 15198(R) (TID-15390)
Ag–Zn, radiation effects on diffusion-controlled reactions in, 17: 31055
Ag–Zn, relaxation studies of vacancy annealing in solid solutions of, 18: 15723(R) (TID-20334)
Ag–Zn, relaxation studies of vacancy annealing in solid solutions of, 19: 22988(R) (NYO-2811-23)
Ag–Zn, solute distribution and thermal curves of solidification of, 17: 20500
Ag–Zn, Zener relaxation distribution parameter, 16: 12230 (TID-15085)
Ag–Zr, density of electronic states in, 18: 4247(R) (ORNL-3470(p.20-6))
Ag–Zr, thermal capacity at 1.2 to 4.5°K, 17: 30966 (CONF-22-15)
Al–Ag, annealing neutron-irradiated, 17: 39693
Al–Ag, creep in hexagonal intermediate phase, 17: 35264(R) (UCRL-10706(p.111-203))
Al–Ag, deformation of, yield drop in, 18: 44145(R) (ORNL-3670 (p.11-16))
Al–Ag, diffusion and precipitation of silver in thin foils of, 17: 22167 (UCRL-10198)
Al–Ag, diffusion in, activation energies for, 17: 35264(R) (UCRL-10706(p.111-203))
Al–Ag, dislocation reactions in intermetallic precipitates of, 17: 6687
Al–Ag, dislocation etch pits in hexagonal crystals of, 18: 33200 (UCRL-10871)
Al–Ag, electric conductivity and phase diagram, 16: 15213
Al–Ag, electron plasma oscillations in, 19: 9702
Al–Ag, fabrication and properties of compacted, 18: 41925(R) (IITRI-B241-8)
Al–Ag, Guinier-Preston zones in, x-ray and electron microscopic studies of size of, 19: 39172(T) (ORNL-tr-633)
Al–Ag, mechanical properties, 16: 17993(R) (ARF-2212-4)
Al–Ag, metastable miscibility gap from integrated small-angle x ray scattering, 19: 38028 (ORNL-P-1396)
Al–Ag, ordering of intermetallic compound Ag_3Al, 19: 1949 (UCRL-11928)
Al–Ag, precipitate structure, 17: 14868
Al–Ag, preparation by levitation melting, 20: 25521 (AERE-R-5097, Paper 23)
Al–Ag, properties and structure, 16: 15198(R) (TID-15390)
Al–Ag, radiation effects on, mechanisms of recovery from electron, 19: 27735(R) (NAA-SR-10850)
Al–Ag, radiation effects on, annealing electron, 19: 40286(R) (NAA-SR-11200)
Al–Ag, segregation processes, 16: 10595
Al–Ag, slip in intermediate hexagonal phase of, mechanism of prismatic, 18: 33202 (UCRL-10917)
Al–Ag, strain hardening of, x-ray studies of segregation zones in, 19: 39174(T) (ORNL-tr-635)
Al–Ag, structure of thin films of, prepared by fusion method, 17: 12683
Al–Ag, tensile properties of, effects of beryllium particle dispersions on, 16: 21019(R) (ARF-2212-5)
Al–Ag, use for neutron dosimetry, 20: 21025 (AERE-R-5122)
Al–Ag, use of as matrix for preparation of beryllium composites, 16: 33443(R) (ARF-2212-6)
Al–Ag, yield strength of intermetallic, temperature effects on, 17: 6685 (UCRL-9992)
Al–Be–Ge–Ag, fabrication and properties of compacted, 18: 41925(R) (IITRI-B241-8)
Al–Cd–In–Ag–Sn, use of, for reactor control rods, 17: 10040(P)
Al–Ge–Ag, fabrication and properties of compacted, 18: 41925(R) (IITRI-B241-8)
Al–Mn–Ag, ferromagnetism, 16: 22638
Al–Mn–Ag, phase studies, 16: 22637
Au–Ag, analysis of, by electron backscattering, 16: 19282
Au–Ag, atomic number effects correction in electron probe microanalysis of, 17: 27268
Au–Ag, correlation of Mossbauer isomer shift and residual electric resistivity in, 18: 44291 (ORNL-P-400)
Au–Ag, deformation by explosive loading and torsion at 4 to 300°K, annealing effects on, 17: 29328(R) (TID-19007)
Au–Ag, diffusion in, effects of composition and vacancy flux on self-, 20: 23738
Au–Ag, electric conductivity and Mossbauer shifts of gold in, 18: 26534(R) (ORNL-3582(p.16-17))
Au–Ag, electron energy losses from plasma oscillations in, (E), 19: 30781
Au–Ag, electron transfer in dilute, 17: 37189
Au–Ag, Mössbauer isomer shift correlation with residual electrical resistance of, 17: 26453(R) (ORNL-3425(p.103-11))
Au–Ag, thermodynamic properties of, 19: 32048(R) (NP-15073)
Au–Ag, tin-119 Mössbauer effect in, 19: 11761
Au–Ag, Zener relaxation in, effects of concentration on, 17: 35783
Au–Ag–Sn, solute interactions in dilute, (E/T), 20: 2349 (UCRL-16320)
Au–Ag–Zn, disorder and reflectivity of beta phase, 17: 23965(R) (TID-18632)
Au–Pu–Ag–U, phase studies and properties of, bibliographic study of, 16: 32115 (KFK-105)
Be–Ag, fabrication and properties of compacted, 18: 41925(R) (IITRI-B241-8)
Be–Ag, phase studies, 16: 2180 (NMI-1252)
Be–Ag, phase studies, 19: 14076
Be–Ag, preparation of beryllium-base, for precision instruments, 20: 39374(P)
Be–Ag, radiation effects at 80°K on, resistivity recovery from proton, 20: 21445
Bi–Ag, coprecipitation of radioactive tracers in, 17: 6683 (UCRL-6452 (Pt.II))
Bi–Ag, diagnostic use of thermocouples of, for plasmoid diffusion, (E), 19: 6771
Bi–Ag, electric conductivity, 18: 12627(R) (BNL-823(p.66-93))
Bi–Ag, electric conductivity at 300 to 540°C, 19: 15991(R) (BNL-841 (p.63-101))
Bi–Ag, superconductivity, 20: 44554
Ca–Ag, crystal structure of AB_2-type compound in, 20: 24589(R) (NYO-3560-3)
Ca–Ag, structural characteristics, 16: 7913
Cd–Ag, crystal structure of, effect of high pressure on, (E), 20: 13316
Cd–Ag, deformation of silver-rich, effects of, on electric conductivity and mechanical properties, 20: 33870(R) (MIT-1002-1)
Cd–Ag, diffusion in, activation energies for, 17: 35264(R) (UCRL-10706(p.111-203))
Cd–Ag, fabrication of control rods of clad, 16: 12074
Cd–Ag, fabrication of steel-clad control rods of, 20: 9475(P)
Cd–Ag, heats of formation of silver-rich, 20: 33870(R) (MIT-1002-1)
Cd–Ag, mechanical properties of internally oxidized, 20: 3639 (UCRL-11194)
Cd–Ag, optical properties, 19: 9767(R) (IS-900(Sect.P))
Cd–Ag, radiation effects on diffusion-controlled reactions in, 17: 31055
Cd–Ag, tensile properties of, testing, (E), 19: 20554 (LA-3161)
Cd–Ag–Zn, phase studies, 16: 22634
Cd–Cu–Ag, analysis for cadmium, x-ray fluorescence spectrometric, 19: 34105 (LA-3305)
Cd–Eu–Ag, preparation for reactor control rods, 17: 29273(P)
Cd–Gd–Ag, magnetic properties of intermetallic compounds of, conduction-electron concentration effects on, (E), 20: 24657
Cd–In–Ag, coating with nickel, 18: 39846
Cd–In–Ag, corrosion by boric acid–potassium hydroxide solutions, 18: 30133 (WCAP-3737)
Cd–In–Ag, corrosion by aqueous solutions, galvanic, 18: 41959 (WCAP-1844)
Cd–In–Ag, corrosion by borated water at 600°F, 20: 5846
Cd–In–Ag, design calculations for control rod clusters of, 19: 35627 (WCAP-3269-38)
Cd–In–Ag, development of, for use in SM-type reactor alternate absorbers, 16: 28520 (APAE-116)
Cd–In–Ag, extrusion, properties, and structure of control rods of, 18: 5755
Cd–In–Ag, fabrication of stainless steel-clad control rods of, 16: 12074
Cd–In–Ag, fabrication, performance, and properties for control rod use, 18: 32031 (A/CONF.28/P/253)
Cd–In–Ag, fabrication of steel-clad control rods of, 20: 9475(P)
Cd–In–Ag, fabrication of reactor control rods of, 20: 21317(P)
Cd–In–Ag, mechanical properties of, for use as reactor control rod material, 16: 3932(P)
Cd–In–Ag, neutron absorption properties of bare and nickel-plated, 16: 25796
Cd–In–Ag, properties of, as reactor control material, 16: 32120

(TID-16597)
Cd–In–Ag, properties as control rod material, effects of palladium, platinum, and tin on, 19: 18402 (WCAP-3269-29)
Cd–In–Ag, properties for use in control rods in reactors, review of, 19: 22885
Cd–In–Ag, properties as control rod material, effects of palladium, platinum, and tin additions on, 20: 5850
Cd–In–Ag, radiation effects on nickel-plated, 17: 41333(R) (ANL-6677)
Cd–In–Ag, radiation effects on mechanical properties of, 18: 18306
Cd–In–Ag, radiation effects on microstructure, 18: 26897(R) (ANL-6868 (p.175-87))
Cd–In–Ag, radiation effects on dimensions and mechanical properties of, 19: 40197(R) (WCAP-3718)
Cd–In–Ag, radiation effects on dimensions and mechanical properties of, 19: 40198(R) (WCAP-3721)
Cd–In–Ag, radiation effects on plated, 19: 44736 (ANL-6883)
Cd–In–Ag, radiation effects on mechanical properties of, thermal-neutron, 20: 31668
Cd–In–Ag, radiation effects on silver-base, in-reactor, 20: 39461 (WCAP-6074)
Cd–In–Ag, reactivity worth of rod clusters of (E/T), 19: 3572
Cd–In–Ag, reactivity worths of cruciform rods of, (E), 19: 12767 (ACNP-64568)
Cd–In–Ag, reactivity worths of rods of, in critical and exponential assemblies, (E), 19: 17200
Cd–In–Ag, reactivity worths in uranium–Zircaloy-2, 19: 40196(R) (WCAP-3269-6)
Cd–In–Ag, reactivity worths of, 19: 40197(R) (WCAP-3718)
Cd–In–Ag, reactivity effects of cruciform rods of, in large PWR, 19: 45533 (WCAP-3269-33)
Cd–In–Ag, reactivity worths of rod clusters of, (E/T), 19: 45535 (WCAP-3269-47)
Cd–In–Ag, reactivity worths in water-moderated uranium oxide cores, 20: 20210 (WCAP-3269-39)
Cd–In–Ag, reactivity worths of arrays of tubes filled with, 20: 40381
Cd–In–Ag, reactor criticality effects of rods of, 18: 3069
Cd–In–Ag, thermal stability, (E), 19: 5490(R) (WCAP-3269-2)
Cd–In–Ag–Sn, corrosion by aqueous solutions, galvanic, 18: 41959 (WCAP-1844)
Cd–In–Ag–Sn, radiation effects on dimensions and mechanical properties of, 19: 40197(R) (WCAP-3718)
Cd–In–Ag–Sn, radiation effects on dimensions and mechanical properties of, 19: 40198(R) (WCAP-3721)
Ce–Ag, magnetic properties of intermetallic compound with CsCl structure in, 19: 2814
Cr–Ag, ductility of liquid-phase sintered, 19: 37140
Cs–Ag, radiation effects on photoelectric sensitivity of phototubes of, 18: 28055
Cu–Ag, annealing of neutron-irradiated, effects of impurities on, 16: 29458 (AERE-R-3843)
Cu–Ag, annealing twins in, nature of, 18: 7216(R) (TID-19872)
Cu–Ag, annealing of, sulfur diffusion during, 18: 37686(T) (AEC-tr-6398(p.322-7))
Cu–Ag, brazing of graphite to, 17: 32547
Cu–Ag, brazing of, to graphite, 16: 19322
Cu–Ag, clustered vacancy annihilation and precipitation in, 18: 7244
Cu–Ag, diffusion in, activation energies for, 17: 35264(R) (UCRL-10706(p.111-203))
Cu–Ag, ductility of, effects of liquid cesium on, 18: 14354(R) (ARF-B215-12)
Cu–Ag, metallurgical bonding to titanium by extrusion, 18: 27937
Cu–Ag, metastable phases from plasma-jet spraying, 18: 37625
Cu–Ag, transformation kinetics of metastable solid solutions in, 18: 40972 (CALT-221-3)
Cu–Ag, use as brazing alloys for refractory metals, 18: 7956(R) (GA-3992(Pt.I))
Cu–Au–Ag, disorder and reflectivity of beta phase, 17: 23965(R) (TID-18632)
Cu–Au–Ag, restoration in deformed, 17: 10240(R) (NP-12208)
Cu–Au–Ag, thermodynamics of, 17: 8815(R) (TID-17546)
Cu–Au–Ag, thermodynamic properties of, 19: 25622 (NYO-2722-1)
Cu–Pd–Ag, use for braze bonding stainless steel cans to stainless steel–uranium dioxide cermets, 19: 46535
Dy–Ag, crystal structure studies, 19: 44678(R) (ANL-7000, pp 186-200)
Dy–Ag, electric conductivity, 20: 25583
Dy–Ag, magnetic properties of intermetallic compound with CsCl structure in, 19: 2814
Dy–Ag, paramagnetic susceptibility of, (E), 20: 8062(R) (COO-720-058)
Er–Ag, crystal structure of intermetallic phases in, 19: 37068
Er–Ag, crystal structure studies, 19: 44678(R) (ANL-7000, pp 186-200)
Er–Ag, electric conductivity, 20: 25583
Er–Ag, electron paramagnetic resonance in, non-S-state, (E), 20: 31764
Er–Ag, magnetic properties of intermetallic compound with CsCl structure in, 19: 2814
Er–Ag, paramagnetic susceptibility of, (E), 20: 8062(R) (COO-720-058)
Eu–Ag, phase studies, 20: 11327
Eu–Ag, preparation for reactor control rods, 17: 29273(P)
Eu–Ag, sample preparation, metallographic, 20: 27418
Eu–In–Ag, preparation for reactor control rods, 17: 29273(P)
Fe–Ag, properties of composite-type, 20: 29624(R) (TID-22970, pp 257-329)
Ga–Ag, superconductivity of, (E), 19: 47531
Gd–Ag, crystal structure of equi-atomic compound of, 19: 28818
Gd–Ag, crystal structure studies, 19: 44678(R) (ANL-7000, pp 186-200)
Gd–Ag, electric conductivity of, 18: 30196
Gd–Ag, electric conductivity at low temperatures in magnetic fields, 20: 9530
Gd–Ag, magnetic properties of intermetallic compound with CsCl structure in, 19: 2814
Gd–Ag, magnetic properties of, 20: 29752
Gd–Ag, thermal capacity of dilute, at low temperatures, (E), 20: 31762
Gd–Ag–Zn, magnetic properties of intermetallic compounds of, conduction-electron concentration effects on, (E), 20: 24657
Gd–Au–Ag, magnetic properties of, 20: 29752
Gd–Hg, electric conductivity, 20: 25583
Gd–In–Ag, magnetic properties of, 20: 29752
Ge–Ag, diffusion in, activation energies for, 17: 35264(R) (UCRL-10706(p.111-203))
Ge–Ag, metastable phases from very rapid cooling of molten, 18: 30169 (CALT-221-1)
Ge–Ag, metastable phase from plasma-jet spraying, 18: 37625
Hg–Ag, superconducting transistion in gamma phase, 18: 22830
Hg–Ag, uses as electrode in oscillographic determination of rare earths, 20: 38811
Ho–Ag, crystal structure, 17: 16658 (TID-18197)
Ho–Ag, crystal structure of intermetallic phases in, 19: 37068
Ho–Ag, crystal structure studies, 19: 44678(R) (ANL-7000, pp 186-200)
Ho–Ag, electric conductivity at low temperatures in magnetic fields, 20: 9530
Ho–Ag, electric conductivity, 20: 25583
Ho–Ag, formation of intermetallic compound and eutectic in, 17: 36297 (IS-594)
Ho–Ag, magnetic properties of intermetallic compound with CsCl structure in, 19: 2814
Ho–Ag, phase studies, 18: 1489(R) (IS-700(Sect.C))
Ho–Ag, phase studies, 20: 31749
In–Ag, crystal structure of, effect of high pressure on, (E), 20: 13316
In–Ag, diffusion in, activation energies for, 17: 35264(R) (UCRL-10706(p.111-203))
In–Ag, fabrication of steel-clad control rods of, 20: 9475(P)
In–Ag, oxidation of, kinetics, mechanism, and microstructure of internal, 20: 23619
In–Ag, properties as control rod material, 18: 38275 (A/CONF.28/P/354)
In–Ag, stacking-fault energies in, methods of determining, 20: 31713(R) (UCRL-16658, pp 93-8)
In–Ag, superconducting properties, 16: 22631
In–Ag, tin-119 Mössbauer effect in, 19: 11761
In–Ag–Sn, solute interactions in dilute, (E/T), 20: 2349 (UCRL-16320)
In–Ag–Tb, crystallography, 20: 4391(R) (ORNL-3870, pp 75-82)
La–Ag, superconductivity, 20: 26022 (CALT-221-15)
La–Ag, superconductivity of, effects of pressure on, 20: 42101
La–Ag, vaporization of, mass spectrometric studies of, 20: 3957
La–Ag–Tb, crystallography, 20: 4391(R) (ORNL-3870, pp 75-82)
Li–Ag, diffusion of tritium in irradiated, 19: 22975(R) (EURAEC-1314)
Li–Ag, diffusion of tritium in, 20: 2317 (EURAEC-1830)
Li–Ag, diffusion of tritium in, 20: 7613
Li–Ag, meson (μ^-) capture by, relation to Fermi-Teller Z Law, 17: 2246 (UCRL-10429)
Li–Ag, meson (μ^-) capture by, relation to Fermi-Teller Z-law, 18: 9109
Li–Ag, radiation effects on helium diffusion in LiAg, 18: 36050(T,R) (EURAEC-1006)
Li–Ag, radiation effects at 80°K on, resistivity recovery from proton, 20: 21445
Li–Ag, stacking fault probabilities in, 17: 20447 (AD-286443)
Li–Ag, thermal conductivity, 20: 5181(R) (ORNL-3029)
Lu–Ag, crystal structure studies, 19: 44678(R) (ANL-7000, pp 186-200)
Mg–Ag, annealing behavior of internally oxidized, at low temperatures, 17: 34418 (UCRL-10816)
Mg–Ag, annealing of cold-worked, effects of internal oxidation on, 17: 35264(R) (UCRL-10706(p.111-203))
Mg–Ag, annealing of deformed AgMg, 19: 39168(R) (TID-22015)
Mg–Ag, crystal structure of, effect of high pressure on, (E), 20: 13316
Mg–Ag, crystal structure of silver-rich, disorder-order transformations of, 20: 33870(R) (MIT-1002-1)
Mg–Ag, deformation of single crystals of, at 77 to 300°K, 19: 43997(R) (UCRL-11889)

Mg–Ag, deformation of silver-rich, effects of, on electric conductivity and tensile properties, 20: 33870(R) (MIT-1002-1)
Mg–Ag, deformation of intermetallic compound in, effects of annealing on, 20: 33870(R) (MIT-1002-1)
Mg–Ag, entropy of formation of AgMg ordered phase, (T), 20: 2349 (UCRL-16320)
Mg–Ag, heat of formation at 0°C, 17: 29328(R) (TID-19007)
Mg–Ag, heats of formation of silver-rich solid solutions, 19: 39168(R) (TID-22015)
Mg–Ag, heats of formation of silver-rich, 20: 33870(R) (MIT-1002-1)
Mg–Ag, lithium reactions at 20 to 60 kev, secondary electron emission from, (E), 20: 19363
Mg–Ag, mechanical properties of intermetallic compounds in, effects of composition and structure on, 17: 541 (WADD-TR-60-184(Pt.III))
Mg–Ag, mechanical properties of internally oxidized, 20: 3639 (UCRL-11194)
Mg–Ag, oxidation, 17: 3569 (ASD-TDR-62-707)
Mg–Ag, performance as dynodes, effects of cesium on, 18: 23865
Mg–Ag, performance as photomultiplier dynodes, 18: 35841(R) (TID-20422)
Mg–Ag, performance as photomultiplier dynodes, 18: 35844(R) (TID-20425)
Mg–Ag, performance as dynodes in high-speed photomultipliers, (E), 19: 15875(R) (TID-21213)
Mg–Ag, photosensitivity of, 20: 17984
Mg–Ag, properties of, effects of physical parameters on, 16: 5724 (WADD-TR-60-184(Pt.II))
Mg–Ag, self-diffusion of silver-110 in, 18: 26051
Mg–Ag, slip in AgMg at low temperature, mechanism of, 18: 33201 (UCRL-10916)
Mg–Ag, solvent properties of, for chromium–uranium alloy fuels, 16: 16464
Mg–Ag, stoichiometry and temperature effects on pest degradation in AgMg in, 18: 42055
Mg–Ag, use of, in separation of thorium and uranium, 16: 8810 (NAA-SR-6666)
Mn–Ag, thermal capacity below 1°K, 20: 29791
Mn–Pd–Ag, use for braze bonding stainless steel cans to stainless steel–uranium dioxide cermets, 19: 4635
Nb–Ag, fabrication and properties of impregnated, 18: 4270
Nb–Ag, preparation and properties of impregnated, 17: 32495
Nd–Ag, electric conductivity at low temperatures in magnetic fields, 20: 9530
Nd–Ag, electric conductivity, 20: 25583
Nd–Ag, magnetic properties of intermetallic compound with CsCl structure in, 19: 2814
Ni–Ag, deposition on beryllium, 19: 13914 (CONF-729-4)
Ni–Ag, production of, by sintering at 470 to 1150°C, 17: 32497
Pb–Ag, diffusion in, activation energies for, 17: 35264(R) (UCRL-10706(p.111-203))
Pb–Ag, heat of formation of liquid, 19: 43997(R) (UCRL-11889)
Pb–Ag, solute distribution and thermal curves of solidification of, 17: 20500
Pb–Ag, thermodynamic properties of, 20: 5223 (UCRL-16303)
Pb–Ag, thermodynamic properties, 20: 31717(R) (UCRL-16658, pp 143-9)
Pb–Ag–Sn, mechanical properties of, at cryogenic temperatures, 17: 8874
Pd–Ag, catalytic properties for benzene hydrogenation, 19: 17417(R) (NYO-3217-1)
Pd–Ag, corrosion by boiling hydrochloric acid, 18: 32089 (TID-20777 (p.25-32))
Pd–Ag, diffusion in, activation energies for, 17: 35264(R) (UCRL-10706(p.111-203))
Pd–Ag, diffusion of deuterium and hydrogen in, 20: 43934
Pd–Ag, diffusion of deuterium and hydrogen in, effects of pressure and temperature on, 20: 43935
Pd–Ag, electric conductivity and Hall constant of, 17: 580
Pd–Ag, electric properties of cold-worked, effects of annealing on, 18: 11526 (TID-20051)
Pd–Ag, electric properties of, effects of cold working on, 18: 11527 (TID-20057)
Pd–Ag, film-lubricating effects of, on cermet friction at high temperatures, 16: 5708 (ASD-TR-61-301)
Pd–Ag, heat of formation and phase studies, 16: 10502 (AROD-2287.15)
Pd–Ag, lubricity for journal bearings, 17: 25382 (ASD-TR-61-705)
Pd–Ag, magnetic susceptibility and resistivity changes accompanying plastic deformation of, 16: 7896 (TID-14631)
Pd–Ag, properties as diffusion element for hydrogen isotope separation, 19: 11654(P)
Pd–Ag, sorptive properties for rare gases, 18: 41679(R) (NYO-841-1)
Pd–Ag, thermodynamic properties, 19: 44678(R) (ANL-7000, pp 186-200)
Pd–Ag, tin-119 Mössbauer effect in, 19: 11761
Pd–Ag, use in deuterium–hydrogen separation by diffusion and electrolysis, 20: 31256
Pd–Ag–Tb, crystallography, 20: 4391(R) (ORNL-3870, pp 75-82)
Pd–Ag–U, hydrogen diffusion through, 19: 28464(P)
Pr–Ag, magnetic properties of intermetallic compound with CsCl structure in, 19: 2814
Pu–Ag, phase studies and properties of, bibliographic study of, 16: 32115 (KFK-105)
Pu–Ag, preparation and properties, 17: 16556
Pu–Ag, structure of intermetallic compounds in, 17: 3536
Pu–Ag, thermodynamic properties of, 18: 44224
Pu–Ag–U, phase studies and properties of, bibliographic study of, 16: 32115 (KFK-105)
rare earth–Ag, crystal structure of equiatomic intermetallic compounds of, 20: 21399
rare earth–Ag, electric conductivity of CsCl-type phases in, 19: 41005 (CALT-221-11)
rare earth–Ag, magnetic properties and structure, 20: 4448
rare earth–Ag, preparation from amalgams by heating, 20: 19185
Rh–Ag–Ti, superconductivity, 18: 21112
Sb–Ag, crystal structure of, effect of high pressure on, (E), 20: 13316
Sb–Ag, diffusion in, activation energies for, 17: 35264(R) (UCRL-10706(p.111-203))
Sc–Ag, crystal structure, 17: 41333(R) (ANL-6677)
Sc–Ag, crystal structure studies, 19: 44678(R) (ANL-7000, pp 186-200)
Sc–Ag, structure of intermetallic compound ScAg in, 17: 1988
Sm–Ag, crystal structure, 17: 16658 (TID-18197)
Sm–Ag, crystal structure of intermetallic compounds AgSm and Ag_5Sm in, 20: 4447
Sm–Ag, magnetic properties of intermetallic compound with CsCl structure in, 19: 2814
Sm–Ag, phase diagrams, 19: 7941

SILVER BROMATES

solubility in water and water-d_2, thermodynamics of, 17: 28882
solubility in water and water-d_2, electrolyte effects on, 17: 28884
thermal decomposition of, search for perbromate in, 19: 36402

SILVER BROMIDES

charged particle reactions with electrons in, in emulsion, 18: 23908
charged-particle reactions in emulsions, latent image formation in, 19: 44387 (CERN-65-4(Vol.II), pp III-10)
electron energy band structure of crystals of, calculation by augmented plane wave method, 19: 14229(R) (AD-607917)
formation in molten potassium nitrate at 403 to 500°C, association constants, 16: 17652
hardness of crystals of, 16: 10728
heat of solution in liquid nitrates, 17: 28869
ion conductivity of crystals of, pressure coefficient of, 18: 9791(T) (AI-Trans-28)
ion energies from spark sources using, 19: 7778
luminescence and photoconductivity at low temperatures, 19: 10679 (NYO-2471-5)
meson (K^-) capture in emulsion, Auger electron spectra from, 17: 26568
optical properties, 20: 36359(R) (TID-22992)
performance in nuclear emulsions, impurity effects on, 19: 44392 (CERN-65-4(Vol.II), pp II44-9)
photochemical behavior of illuminated crystals of, with divalent impurities, 16: 19527
preparation for nuclear emulsions, 19: 44396 (CERN-65-4(Vol.II), pp III1-4)
proton reactions at 1 to 2 Bev, alpha evaporation in, 18: 30811
proton reactions at 150, 340, and 660 Mev, cascade theory for, (T), 19: 41811(T)
radiation effects, photon, 16: 25867
radiation effects on spectra of doped crystals, 19: 9211
radioinduced ESR in, gamma, light, and uv, (E), 20: 17981
radioinduced luminescence and photoconductivity of, x- and uv-, 19: 42917
reactions in fused salts, formation constants of complex ions, 16: 4128
reactions with triethanolamine in emulsions, 18: 23552
reduction by electron bombardment, 17: 25333
sensitivity of crystals of, in ionographic emulsions, 18: 20336 (NP-13851)
sensitivity of emulsion microcrystals of, for electrons, 20: 37122
sensitivity of nuclear emulsion of, effects of gold on high-intensity reciprocity law in, 19: 30174
solubility in aqueous alkali metal halide solutions, 17: 25325
spectra of crystals of, modification of optical absorption, by dissolved divalent impurities, 16: 19526
structure of crystals of, latent image study of, 16: 23967 (ANL-6515 (p.81-6))
thermodynamic properties in *N,N*-dimethylformamide and *N*-methylformamide solutions, 20: 3924 (TID-22366)
AgBr–AgCl, phase diagrams, 20: 36787 (YALE-2723(Vol.1))

AgBr–NaBi, phase diagrams, 20: 36787 (YALE-2723(Vol.1))
AgBr–NaBr, phase diagrams, 20: 36787 (YALE-2723(Vol.1))
AgBr–TlBr, phase diagrams, 20: 36787 (YALE-2723(Vol.1))
$CdBr_2$–AgBr, ion conductivity of anomalous mixed crystals of, pressure coefficient of, 18: 9791(T) (AI-Trans-28)
$CdBr_2$–AgBr, phase diagrams, 20: 36787 (YALE-2723(Vol.1))
CuBr–AgBr, phase diagrams, 20: 36787 (YALE-2723(Vol.1))
KBr–AgBr, phase diagrams, 20: 36787 (YALE-2723(Vol.1))
KI–AgBr, phase diagrams, 20: 36787 (YALE-2723(Vol.1))
LiBr–AgBr, phase diagrams, 20: 36787 (YALE-2723(Vol.1))
RbBr–AgBr, phase diagrams, 20: 36787 (YALE-2723(Vol.1))

SILVER CARBONATES

disintegration, effects of cadmium carbonate on radiation and thermal, 16: 3052
radiolysis of, effects of cadmium impurities on, 18: 337
reactions with cesium zinc ferrocyanide, 16: 10116(P)
structural properties, 17: 14210 (NBS-MON-25(Sect.1))
thermal decomposition of irradiated, effects of cadmium impurities on, 18: 337

SILVER CHLORATES

spectra of liquid, infrared reflection, 16: 18889

SILVER CHLORIDES

analysis for chloride ions, radiometric, 19: 10986
charged particle tracks in large crystals of, delineation of, 16: 25546 (AFOSR-3030)
charged particle tracks in, delineation of, 17: 15053 (NASA-TN-D-1547)
charged-particle tracks in, determination of, 19: 44386 (CERN-65-4 (Vol.II), pp 121-5)
chlorine-36 exchange between crystals of, rate of, 20: 12869
chlorine-36 exchange between crystals and solutions, 20: 14572
cobalt-57 Mössbauer emission spectra in, quadrupole splitting in, (E), 20: 22340
complexing and solubility in potassium nitrate–sodium nitrate solutions, 16: 3012
compressibility up to 30,000 kg/cm², 19: 4663(T) (UCRL-Trans-1087(L))
crystal dislocations, 19: 34480
defects in, production and properties of point, 20: 20365
diffusion of silver ions in pure crystals of, tracer study, 19: 15409 (COO-1197-12)
diffusion of sodium ions in crystals of, mechanism for, (E), 20: 15966
effects on thermal conductivity of sodium chloride, 19: 25783 (COO-1198-238)
efficiency as sequestering agent for iodine-131, acidity, concentration, and temperature effects on, 19: 15378
electric conductivity of thin film in aqueous silver electrolytes, 18: 16005(R) (TID-20354)
electric conductivity of pure crystals of, 19: 15409 (COO-1197-12)
electric conductivity of crystalline, 20: 3863(R) (IS-1200(Sect. C))
electrochemical properties of, interface of, in aqueous solutions, 20: 8486 (NYO-3228-5)
electron energy band structure of crystals of, calculation by augmented plane wave method, 19: 14229(R) (AD-607917)
electron trapping in crystals of, 18: 34280(R) (NYO-2680-1)
electronic processes in surface layers of, 17: 606 (TID-17018)
electronic properties of, design of device for determining, 17: 6792(R) (ISS 62/14)
ferric ion ESR spectrum in, 19: 10671 (COO-1198-228)
fission recoil tracks in, observation of, 17: 5082
fluorescence of doped and pure, blue-green emission band shift in, 17: 32161
hardness of crystalline, 16: 10728
heat of formation, 16: 108
heat of solution in liquid nitrates, 17: 28869
interface in aqueous solutions, properties and structure of, 20: 9498(R) (NYO-3228-6)
ion exchange properties of silica gel containing, for iodine-131, 18: 22128(T) (NP-tr-1138)
iron ESR spectra in, 20: 22311(R) (AD-622068)
luminescence and photoconductivity at low temperatures, 19: 10679 (NYO-2471-5)
luminescence in, production by x irradiation, 16: 13734
luminescence intensity dependence on intensity of excitation, 16: 22143
properties as nuclear disintegration detector, 17: 7261
radioinduced luminescence in, 17: 10712
morphology of interface between liquid and solid, 18: 16005(R) (TID-20354)
photoconductivity and radioinduced luminescence in, x, (E), 19: 32759
point defects, 16: 22731 (TID-16132)
polarography in mixture of potassium and sodium chlorides, 16: 2954
preparation of kryptonated, by diffusion, 20: 18570(R) (NYO-2757-5)
pressure gradient in, between anvils, 17: 35263(R) (UCRL-10706 (p.1-110))
properties as spectroscopic carrier, 16: 32938
properties of, effects of impurities on, 18: 1489(R) (IS-700(Sect.C))
radiation effects, 17: 11129
radiation effects on crystal structure of, mechanism of beta, 20: 2426 (LA-3387)
radioinduced decoration of crystals of, 18: 36040 (AFOSR-J1553)
radioinduced defect formation in, thermal annealing of uv and x, 20: 32731
radioinduced defects in single-crystal, 20: 35932 (LA-3501)
radioinduced electronic processes in surface layers of, effects of oxygen on, 19: 35867 (NYO-2471-2)
radioinduced ESR in, gamma, light, and uv, (E), 20: 17981
radioinduced luminescence and photoconductivity of, x- and uv-, 19: 42917
reactions in fused salts, formation constants of complex ions, 16: 4128
reactions with cesium, 18: 31699
reduction by niobium in fused halides, 18: 16032
silver-110m exchange between crystals and solutions, 20: 14572
solubility in water, tracer studies of effects of chloride ions on, 18: 41339
solvent properties for silver, 19: 36216(R) (BNL-900(p.29-72))
sorptive properties of carrier solutions of, for radioiodine, 19: 5759 (NP-14263)
spectra of, emission technique for study of infrared, 18: 3744
thermal conductivity of crystalline, 19: 9046(R) (IS-900(Sect.C))
thermal expansion at 100 to 300°K, 16: 13697 (NP-11338)
thermochemical properties of, 20: 40922
thermodynamic formation constants in molten potassium nitrate at 385°C, 16: 17650
use as ion exchanger, in determination of iodine-131 in milk, urine, and water, 20: 35404
use for detecting charged particles, 20: 21060
use in particle track detectors, 19: 13746
use in thin-film memory cells, 18: 27849 (SC-TM-282-63(74))
use of large single crystals of, in charged particle detection, 19: 44378 (CERN-65-4(Vol.I), pp 1-15)
use to detect cosmic particles and nuclear processes, 16: 23931
valence band structure, 17: 6053 (TID-17447)
vapor pressures at high temperatures, 17: 28058
Ag–AgCl, electrode potentials in methanol at 25 to 45°C, 18: 4918(R) (TID-19727)
Ag–AgCl, free energy of solution of, 19: 11103
AgBr–AgCl, phase diagrams, 20: 36787 (YALE-2723(Vol.1))
AgCl–AgF, use as carrier for distillation analysis of uranium oxides, 18: 9984
AgCl–AgI, phase diagrams, 20: 36787 (YALE-2723(Vol.1))
AgCl–NaCl, heat of mixing of, effects of composition and temperature on, 20: 23011
AgCl–NaCl, phase diagrams, 20: 36787 (YALE-2723(Vol.1))
AgCl–NaCl, thermostimulated electron emission from crystallophosphor of, 19: 25170(T)
AgCl–TlCl, phase diagrams, 20: 36787 (YALE-2723(Vol.1))
$CaCl_2$–AgCl, phase diagrams, 20: 36787 (YALE-2723(Vol.1))
$CdCl_2$–AgCl, phase diagrams, 20: 36787 (YALE-2723(Vol.1))
CsCl–AgCl, phase diagrams, 20: 36787 (YALE-2723(Vol.1))
CuCl–AgCl, phase diagrams, 20: 36787 (YALE-2723(Vol.1))
HgI_2–AgCl, phase diagrams, 20: 36787 (YALE-2723(Vol.1))
$InCl_3$–AgCl, phase diagram, 16: 2931(T) (AEC-tr-4870)
$InCl_3$–AgCl, phase diagrams, 20: 36787 (YALE-2723(Vol.1))
KCl–AgCl, phase diagrams, 20: 36787 (YALE-2723(Vol.1))
LiCl–AgCl, phase diagrams, 20: 36787 (YALE-2723(Vol.1))
$MgCl_2$–AgCl, phase diagrams, 20: 36787 (YALE-2723(Vol.1))
$PbCl_2$–AgCl, phase diagrams, 20: 36787 (YALE-2723(Vol.1))
RbCl–AgCl, phase diagrams, 20: 36787 (YALE-2723(Vol.1))

SILVER CHROMATES

chloride exchange, 16: 22018
precipitation of astatine with, from oxidizing solutions, 19: 32303

SILVER COMPLEXES

chlorophyllin, radiosensitivity effects in mice, gamma, 20: 1692
with α, β, γ, δ-tetraphenylporphines, retentions in Szilard-Chalmers (n,γ) recoil reactions in, 19: 40612
with azo dyes, composition of, radiometric and spectrophotometric studies of, 20: 22925
with carbamic acid, synthesis, 16: 6425
with cyclooctatetraene, chemical properties, 17: 40427(R) (NYO-10063(p.1-6))
with dialkyl phosphoric acids, preparation and properties, 18: 25429
with diethyldithiophosphate, solvent extraction from mineral acids using carbon tetrachloride, 16: 28926(T) (AEC-tr-5202)
with dipyridyl-o-phenanthroline and pyridine, electron paramagnetic resonance of divalent, 16: 3005
with mercaptosuccinic acid and 2,3-dimercaptosuccinic acid, formation and properties of, 18: 8394 (TID-20013)
with *N*-(2-pyridylmethyl)iminodiacetic acid, stability of, 17: 15993

with nitrates, properties, 18: 1489(R) (IS-700(Sect.C))
with olefins, stability of, deuterium isotope effects on, 19: 26310
with oxalate, electrochemical studies of, 17: 20051
with rhodanine, stability of, 20: 23008
with tetraphenylporphine in dioxane, gamma radiolysis of, 20: 36889
with thiodibenzoylmethane, stability of, 20: 20693
with uranium fluorides, crystal structure, 19: 28304
yields of, from gamma-irradiated silver salt solutions at 77°K, 20: 12895

SILVER COMPOUNDS
detonation of azide, properties of gases from, 16: 18113 (NP-11463 (Pt.3)(p.357-63))
electron paramagnetic resonance of divalent, in acid solutions, 16: 3005
radiation effects on, comparison with free radical reactions, 18: 27501
thermolysis of diliturate, 19: 19824

SILVER CYANAMIDES
radiation damage to crystal lattices of, fission fragment, 17: 34506
radioinduced decomposition, 18: 17913
thermal decomposition, 18: 17913

SILVER DEUTERIDES
emission spectrum at 3100 to 3900 Å for silver-107 and -109 labeled, 16: 25331
spectra, effects of rotation-vibration interactions on molecular, 16: 31622

Silver Dichromates
see Silver Chromates

SILVER DYSPROSIUM SULFIDES
crystal structure, 20: 29158

SILVER ERBIUM SULFIDES
crystal structure, 20: 29158

SILVER FLUOBORATES
solubility in hydrofluoric acid, 16: 2948

SILVER FLUORIDES
reactions of hydrofluoric acid solutions of, with protactinium oxide, preparation of $AgPaF_6$ by, 20: 45673
reactions with uranium pentafluoride, crystal structure of products from, 19: 28304
AgCl–AgF, use as carrier for distillation analysis of uranium oxides, 18: 9984
AgF–D_2O, radioinduced free silver atoms in solid solutions of, EPR of x, (E), 20: 15975(T)
AgF–H_2O, radioinduced free silver atoms in solid solutions of, EPR of x, (E), 20: 15975(T)
AgF–ZnF_2, phase diagrams, 20: 36787 (YALE-2723(Vol.1))
ethanol–AgF, radioinduced free silver atoms in solid solutions of, EPR of x, (E), 20: 15975(T)
methanol–AgF, radioinduced free silver atoms in solid solutions of, EPR of x, (E), 20: 15975(T)

SILVER FLUORUTHENATES
preparation and structural chemistry of, 17: 41761

SILVER GADOLINIUM SULFIDES
crystal structure, 20: 29158

SILVER GLASS
cleaning technique for dosimeters of, 20: 5742(R) (UCRL-14351)
radioinduced coloration in phosphate, gamma, 16: 21099
radioinduced fluorescence of, ultraviolet, 19: 2413
use in personnel monitoring dosimeter, 18: 4103

SILVER HALIDES
crystal growth and structure, 19: 45474 (CERN-65-4(Vol.II), pp III21-30)
crystal structure of, research on imperfections in, 20: 28607(R) (NYO-2471-21)
electron-phonon interactions in crystals of, non-equilibrium, 18: 14657
ion bombardment effects on, in photographic emulsions, 19: 9463
magnetoresistance, 16: 10664 (AFOSR-2040)
performance as nuclear emulsions, 18: 20414
performance in nuclear emulsions, 19: 44393 (CERN-65-4(Vol.II), pp II50-63)
radiation monitoring using emulsions of, 17: 6487(P)
sensitivity of grain centers of, 18: 35633
solubility in aqueous solutions, 16: 23706
solvent properties for silver, 20: 24971(R) (BNL-954, pp 50-83)
space charge calculations, (E/T), 20: 4476(R) (IS-1200(Sect.P))
use in x-ray film, shortage of supply for, 20: 26720

SILVER HOLMIUM SULFIDES
crystal structure, 20: 29158

SILVER HYDRIDES
see also Silver Deuterides
emission spectrum, 16: 25331
spectra, effects of rotation-vibration interactions on molecular, 16: 31622
spectra of normal and deuterated, in far ultraviolet, 20: 25040

SILVER IODATES
chloride exchange, 16: 22017
precipitation of astatine with, from oxidizing solutions, 19: 32303
solubility in water, effects of silver-110 labeling on, 17: 28787
$AgIO_3$–AgI–$AgNO_3$, phase diagram, 17: 23305 (TID-16914)
$AgIO_3$–AgI–$AgNO_3$, phase studies, 18: 1633

SILVER IODIDES
corrosive effects of solid and vaporized, on Inconel at 400°C in helium, 18: 30985(R) (GA-4786)
deposition of injected iodine-131-labeled, in capillaries, 19: 21843
diffusion of iodine-131 in irradiated, 20: 26929
efficiency as sequestering agent for iodine-131, acidity, concentration, and temperature effects on, 19: 15378
electrokinetic potential and ion exchange of precipitates of, effects of barium, lanthanum, and thorium on, 18: 8346
exchange reactions with iodoacetic acid in aqueous nitric acid solutions, 19: 11296
formation in molten potassium nitrate at 402°C, association constants, 16: 17652
hardness of crystalline, 16: 10728
injections in rabbits, therapeutic elimination of radioactive, 19: 14989
iodine-131 exchange with methyl iodide, effects of surface structure on, 20: 5544
iodine-131 exchange with iodine ions, effects of cobalt and uranyl nitrates on, 20: 16432
iodine-131 exchange between, and potassium iodide, kinetics of, 20: 16460
ion association of, in molten alkali nitrate solutions, 17: 30504 (CONF-14-20)
ion conductivity of crystals of, pressure coefficient of, 18: 9791(T) (AI-Trans-28)
labeling with iodine-131 and aerosol preparation, 19: 20027
labeling with iodine-131 by isotope exchange, 20: 26929
oxidizing effects on uranium compounds in ammonia, 17: 175
phase transitions at high pressure, 16: 22795
preparation of beta sources of, method for, 20: 10935 (USNRDL-TR-948)
preparation of colloidal, 17: 3026(R) (TID-17250)
preparation of kryptonated, by diffusion, 20: 18570(R) (NYO-2757-5)
reactions with organic matrix materials in ice-water system, 18: 15722 (TID-20332)
silver-110 exchange between, and silver nitrate, kinetics of, 20: 16460
solubility in aqueous alkali metal halide solutions, 17: 25325
sorptive properties for thorium ions, tracer studies, 16: 103
sorptive properties of carrier solutions of, for radioiodine, 19: 5759 (NP-14263)
sorptive properties for lanthanum and neodymium cations, effects of acidity on, 19: 13331
sorptive properties for thorium ions, effects of acidity on, 19: 13332
sorptive properties for cobalt, europium, and sodium ions, tracer studies on, 20: 20683
stability, 19: 36960(R) (ORNL-3807, pp 80-142)
stability of, thermal, 20: 4185(R) (ORNL-3843, pp 169-234)
structure of, Madelung constant and repulsion factor calculations for, 19: 43471 (NAA-SR-11150)
thermodynamic properties in *N,N*-dimethylformamide and *N*-methylformamide solutions, 20: 3924 (TID-22366)
uses of smoke of, for meteorological studies of waste gas diffusion, 19: 14117
AgBr–AgI, phase diagrams, 20: 36787 (YALE-2723(Vol.1))
AgCl–AgI, phase diagrams, 20: 36787 (YALE-2723(Vol.1))
AgI–NaI, phase diagrams, 20: 36787 (YALE-2723(Vol.1))
$AgIO_3$–AgI–$AgNO_3$, phase diagram, 17: 23305 (TID-16914)
$AgIO_3$–AgI–$AgNO_3$, phase studies, 18: 1633
CuI–AgI, phase diagrams, 20: 36787 (YALE-2723(Vol.1))
KI–AgI, phase diagrams, 20: 36787 (YALE-2723(Vol.1))
LiI–AgI, phase diagrams, 20: 36787 (YALE-2723(Vol.1))
PbI_2–AgI, ion conductivity of anomalous mixed crystals of, pressure coefficient of, 18: 9791(T) (AI-Trans-28)
PbI_2–AgI, phase diagrams, 20: 36787 (YALE-2723(Vol.1))
RbI–AgI, phase diagrams, 20: 36787 (YALE-2723(Vol.1))

SILVER IONS
angular distributions of sublimed and sputtered, from silver monocrystals, 19: 41259
antishielding factors for, perturbed wave functions for, 17: 37644 (BNL-6681)
association with bromide and chloride ions in molten nitrates, 19: 34142(R) (NYO-2873-7)
association with chloride in liquid cesium, lithium, and potassium nitrate mixtures, constants for, 18: 19975
association with iodide ion in molten alkali nitrates, constant for, 17: 28829(R) (TID-18959)
catalytic effects on reactions of hydrogen peroxide with uranium(VI) ions, 16: 111
catalytic properties of, for use in cerium(IV) oxidimetry, 17: 176
complex formation by, optimum conditions for, 19: 13374
diffusion in fused potassium chloride, 18: 35992(R) (TID-20878)

diffusion in molten silver nitrate–sodium nitrate, 19: 31646 (TID-20866)
diffusion in pure silver chloride crystals, tracer study, 19: 15409 (COO-1197-12)
effect on optical bleaching of F center in potassium chloride crystals (E/T), 19: 2386
effects of irradiation by, on resistivity of thin silver layers, (E), 20: 44004
effects on far-infrared spectrum of potassium iodide, 19: 17405 (CONF-651-83)
electromotive force measurement in potassium nitrate–sodium nitrate systems, 16: 108
electron paramagnetic resonance spectra of, in irradiated frozen silver nitrate and silver sulfate solutions, 20: 33376
electron scattering by, anomalous transmission effects in, 17: 620
electron trapping efficiency of, in gamma-irradiated sulfate glasses, 20: 33378
electronic wave functions for nuclear magnetic moment perturbations, tables of, 17: 36374 (BNL-6491)
energies in high-speed plasma beams in vacuum arcs, 18: 40708
energy transfer to rare earth ions in compounds, (E), 19: 17936
exchange for sodium ions in sodium nitrate occluded zeolites, 17: 35253(R) (IA-775)
fluorescence of silver chloride crystals doped with, blue-green emission band shift in, 17: 32161
nuclear hexadecapole coupling in, second-order quadrupole effect in, 16: 29559 (BNL-6038)
photoionization cross sections for, 17: 647
photoluminescence of neutralized, use in dosimeters, 20: 16837
production of, source for, 19: 9457
quadrupole antishielding factor of, 17: 22607
radioinduced reduction of, in irradiated aqueous sulfate glasses at 77°K, 20: 33378
radioinduced reduction to atomic state in glasses, gamma, (E), 20: 44012
radiolysis of aqueous solutions of, pulse, 19: 38728
radiolysis of, aqueous solutions of, 20: 10922
radioprotective effects in mice, 18: 13567
range-energy relations in aluminum, (E), 19: 9893 (NAS-NRC-PUB-1133 (p.173-86))
reactions with gases and solids below 1 Mev, range determinations, 16: 10954 (EFINS-61-68)
reactions with hydrated electrons, pulse radiolysis studies of, 19: 17913
separation by ion exchange on thallous phosphotungstate, 16: 25485
separation by thin-layer ionophoresis, 18: 10185
sorption by diallyl phosphate and polystyrene methylenephosphonic acid resins, 16: 13051
sorption by hydrous thorium hydroxide, temperature effects on, 19: 11110
sorption by polymers, 17: 14354
sorption from perchloric acid solutions by cellulose and acid resin sulfonic acid exchangers, 18: 35473
toxicity of, in mouse, determination by LD_{50} on thirtieth day of, 17: 17719
voltammetric properties of, on glassy carbon electrode, 19: 13217

SILVER ISOTOPES
abundance in Canyon Diablo meteorite, 20: 39102
abundance of, mass spectrographic determination of, 18: 8298
content in iron meteorites, 16: 20829
content in meteorites, 17: 25468
decay of isomeric, energy and half life for, (E), 19: 10329
determination in radiation sources, extraction radiometric titration method for, 20: 20567 (UJV-1418/65)
deuteron reactions at 15 Mev, isomeric states from, (E), 20: 15856
diffusion in beryllium, tracer studies on, 20: 15037 (CEA-R-2621)
energy levels, interactions, nuclear moments, and transitions in, 17: 24381 (AD-403411)
gamma reactions on, cross sections for, 19: 12496
gamma spectra, 16: 3671(R) (TID-14241)
isomeric transitions of E_3 type, 16: 31066 (NP-11746)
masses of stable, 19: 10358
neon-20 reactions on, neutrons from, 17: 9593
neutron reactions with, calculations of cadmium buildup in, (T), 19: 33246 (KAPL-M-6455)
precipitation in bismuth alloys, 17: 6683 (UCRL-6452(Pt.II))
preparation of foils of, by rolling, 20: 25519 (AERE-R-5097, Paper 21)
proton reactions at 9 Bev, lithium-8 from, 17: 19376
proton reactions on, cadmium-109 yields from, 17: 8153
separation from uranium-238 fission products, 18: 13887
separation of, Aston band effects on mass-spectrometric, 18: 18267
separation of, efficiency of molecular beam chopper unit for, 18: 39783
spectra of, shifts in x-ray, 18: 17064(T)

SILVER ISOTOPES Ag-100
production in 340-Mev proton spallation of silver, 20: 24376

SILVER ISOTOPES Ag-101
half life and formation cross section of, from proton reactions on indium and silver at 200 and 400 Mev, 20: 42179
production in 340-Mev proton spallation of silver, 20: 24376

SILVER ISOTOPES Ag-102
decay, (E), 20: 8166
decay of, beta and gamma radiation from, 18: 15314
half life, 20: 24376

SILVER ISOTOPES Ag-103
decay, (E), 20: 46242(R) (TID-23239)
decay scheme, 16: 29849
energy levels, decay schemes and half lives, 16: 28049

SILVER ISOTOPES Ag-104
beta decay of, transitions to vibrational levels in, 18: 36625
beta emission from, hindrance phenomena in, 16: 23073
decay of isomeric, (E), 20: 46242(R) (TID-23239)
gamma emission by isomeric, 20: 24376
hyperfine structure in iron and nickel, 18: 16954 (UCRL-11143)
polarization in iron and nickel, (E), 19: 16995

SILVER ISOTOPES Ag-105
decay scheme, 17: 33028
decay scheme, 18: 13120
decay schemes, 16: 7033
decay schemes, electron K-capture, 16: 26295
energy levels from cadmium-105 decay, (E), 20: 34653
energy levels of, effects of collective vibrational motion on anomalous coupling, (T), 20: 28420
gamma spectra, (E), 20: 14845 (AD-620434)
gamma spectra, 18: 24585(R) (IDO-16969)
hyperfine structure, 17: 11706
nuclear magnetic moment, 17: 11706
separation from rhodium, rapid carrier-free method for, 16: 8785
uptake by brain tumors, 18: 1471

SILVER ISOTOPES Ag-106
beta decay half life (E), 19: 3295
beta decay of, transitions to vibrational levels in, 18: 36625
beta emission from, hindrance phenomena in, 16: 23073
conversion electron spectrum of metastable, 18: 34817
decay of, palladium-106 energy levels from, 17: 26594
energy level densities in, effects of spin on, 16: 33853
gamma spectra, 18: 24585(R) (IDO-16969)
gamma spectra, (E), 19: 16840(R) (IDO-17050)
uptake by brain tumors, 18: 1471

SILVER ISOTOPES Ag-107
abundance ratio to palladium-107, relation to solar-system age, 16: 16901
abundance ratio with silver-109 in natural silver, 16: 11943
activity of isomeric, induced in food radiopreservation, 20: 33744
alpha excitation of, reorientation effect in, (E), 19: 25475(R) (ORNL-TM-1044)
alpha reactions (α,n) with, isomer ratios from, 18: 30815
alpha reactions (α,2n) at 28 Mev, indium-109 gamma transitions from, (E), 19: 39861
alpha reactions (α,2n) at 22 Mev, isomer production in, (E), 19: 41802(T)
alpha reactions (α,2n) with, indium-109 levels from, (E), 20: 28472
alpha reactions (α,n), isomeric cross section for formation of indium-110, 16: 2477 (ANL-6405)
alpha reactions (α,n), indium-110 production from, 16: 21381
alpha reactions (α,α2n), cross sections for, 16: 33814
alpha reactions (α,kn) and (α,αkn) on, k = 1 to 3, 17: 19294
alpha reactions with, excitation functions for, (T), 20: 32373(R) (COO-1530-1)
bremsstrahlung reactions at 0.8 Mev, excitation of isomeric states in, 18: 2945
carbon-12 reactions with, angular momentum effects in, 17: 36657 (JINR-P-1347)
carbon-12 scattering, 17: 22558 (JINR-P-1244)
carbon-12 elastic scattering at 124.5 Mev (E/T), 19: 3364
carbon-12 reactions (C-12,N-13) with, angular distributions from, (E), 20: 42153 (JINR-E-2824)
carbon-12 reactions at 70 to 130 Mev, cross sections for, 19: 1554 (JINR-P-1745)
content in meteorites, 18: 10755
decay in compound-nucleus reactions, angular momentum effects in, 18: 28645
decay schemes, 16: 17125
deuteron elastic scattering at 12 Mev, 18: 38109
deuteron elastic scattering at 13.6 Mev, angular distributions from, 18: 40632
deuteron elastic scattering at 15 Mev, optical model for, 19: 14604
deuteron scattering at 12 Mev, distributions from, (E), 19: 10260 (UCRL-7670)
disintegration by electrons and positrons, cross sections for, (E), 19: 37861
energy level quantum numbers and transitions, (E), 20: 44782
energy level strength functions for, 16: 26518

energy level transitions in, retardations in l-allowed M1, (T), 19: 21323
energy levels, 16: 5988
energy levels and gamma spectra, 16: 26280
energy levels of, detection of isomeric, 17: 29953
energy levels of, resonant excitation of isomeric, 17: 34889(T) (AEC-tr-5968)
energy levels of, effects of collective vibrational motion on anomalous coupling, (T), 20: 28420
gamma dose constants for metastable, 20: 46617
gamma inelastic scattering at 6 to 26 Mev, cross sections for, 18: 6258
gamma reactions (γ,n), yield ratios, 16: 19820
gamma reactions (γ,n) to 23 Mev, neutron yields from, 16: 26357
gamma reactions (γ,n) on, nuclear excited states from, 16: 33853
gamma reactions (γ,n) with, energy-range relation for recoiling atoms from, 17: 31053
hyperfine structure $^2D_{5/2}$ and $^4F_{9/2}$ states of, 20: 44141
meson (μ^-) capture by proton pairs in, (E/T), 19: 41753
meson (μ) capture at 4.76 Mev, neutron emission in, 16: 18486
neutron activation cross sections at 24 kev, (E), 19: 16935
neutron capture at thermal energies, beta emission asymmetries from polarized, 16: 23086
neutron capture cross sections at 1 to 30 kev, 18: 4534 (EANDC-33U(p.114-35))
neutron capture resonance distinction by spin, 16: 14056
neutron capture resonances in silver due to, assignment of, 17: 15253(R) (GA-3874)
neutron reactions (n,2n) at 14.8 Mev, cross sections for, 16: 7072
neutron reactions (n,2n), excitation functions for, 16: 21352 (NP-11667)
neutron reactions (n,2n), (n,pγ), and (n,pn) at 14.8 Mev, cross sections for, 17: 2242 (TID-16949)
neutron reactions [(n,αn) + (n,nα)] at 14.8 Mev, cross section limit, product half life, and Q value for, 17: 2242 (TID-16949)
neutron reactions [(n,αn) + (n,nα)], separation energies for, 17: 2242 (TID-16949)
neutron reactions (n,αγ) and (n,αn) at 14.8 Mev, cross sections for, 17: 2242 (TID-16949)
neutron reactions (n,γγ), measurement of γγ coincidences in, 17: 7285
neutron reactions (n,2n) at 14.1 Mev, cross sections for, 17: 15299
neutron reactions (n,2n) at 12 to 19.6 Mev, cross sections, 17: 19344
neutron reactions (n,2n) at 14 Mev, cross sections for, 17: 26547
neutron reactions (n,α) and (n,nα) at 14.8 Mev, differential cross sections, energy spectra, and level density parameters for, 17: 26606
neutron reactions (n,2n) at 14 Mev, measurement of cross sections for, 17: 34903
neutron reactions (n,nα) at 14.7 Mev, upper limit for cross section of, 17: 36707
neutron reactions (n,nα) at 14.8 Mev, maximum cross-section limits for, 18: 1077
neutron reactions (n,γ) with, 88-kev transition in thermal, 18: 7782
neutron reactions (n,2n) at 14 Mev, shell effects in, (T), 19: 12536
neutron reactions (n,γ), cross section for, 19: 26718 (ORNL-3802)
neutron reactions (n,γ), gamma spectra in 16.6-ev resonance of, 19: 39781 (JAERI-1073)
neutron reactions (n,α) with, total cross sections for, 20: 8078(R) (NYO-1082-2)
neutron reactions (n,α) at 12 to 23 Mev, (E), 20: 38036
neutron reactions (n,2n) at 13.56 to 14.7 Mev, excitation functions for, (E), 20: 46614
neutron resonance capture, 16: 5996
neutron resonance cross sections of, determination of, by boron absorption technique, 16: 28036 (TID-16059)
nitrogen-14 reactions at 70 to 130 Mev, cross sections for, 19: 1554 (JINR-P-1745)
nucleon probability density in, (T), 19: 27579
oxygen-16 excitation of, reorientation effect in, (E), 19: 25475(R) (ORNL-TM-1044)
oxygen-16 reactions at 70 to 130 Mev with, cross sections for, 19: 1554 (JINR-P-1745)
photoactivation of isomeric, cross sections for, 18: 7705
photoactivation of, excitation levels in, (E), 20: 19865
photon scattering at 4 to 24 Mev, cross sections for inelastic, 16: 21641
photoreactions (γ,n) on, cross sections for, (E), 19: 10356
preparation of thin layers of, for use as cyclotron irradiation target, 19: 28966
production in compound-nucleus reactions, level densities from, 18: 26645
proton reactions (p,2n) at 12 to 14 Mev, conversion electrons from, 18: 40561
proton reactions (p,α) with, cadmium-108 level widths from, (E/T), 20: 30360 (WASH-1068)
proton reactions (p,2nγ) at 12 Mev, cadmium-106 energy-level transitions from, (E), 20: 46684
proton reactions at 57 Mev on, proton distributions from, 17: 7197
proton reactions at 0.25 to 5 Bev, fragment production in, (T), 19: 43365
proton reactions (p,γ) in stars, 16: 12308
proton reactions (p,n) at 5 to 10.5 Mev, cross sections, 16: 31106
proton scattering at 13 Mev, differential cross sections for elastic and inelastic, (E), 20: 39470(R) (ORNL-3924)
radioinduced transmutation of, in single-crystal alloys, 18: 17909
radioinduced transmutation effects in, 19: 11682
reactions with carbon-12, compound nucleus formation cross sections for, 17: 17118 (JINR-P-1162)
separation from cadmium-107 parent by condensation on metal surface, 17: 33973(T) (AEC-tr-5962)
separation from palladium, rapid carrier-free method for, 16: 8785

SILVER ISOTOPES Ag-108

beta decay asymmetry, 16: 23086
beta decay half life (E), 19: 3295
beta decay of polarized, produced by capture of polarized neutrons, 18: 21201 (KR-64(Sect.XXVIII))
beta decay of, transitions to vibrational levels in, 18: 36625
beta emission from, hindrance phenomena in, 16: 23073
decay branching ratios and maximum positron energy, 17: 9599
decay of isomeric, (E), 20: 17786
decay of metastable, effects on silver-110 half-life measurements, 16: 8198
decay of metastable, isomeric (E), 19: 1607
decay of, electron capture, (E), 19: 12611
decay of, experimental determination of half life for, 18: 30949 (NYO-9077)
decay of, gamma transitions in, (E), 19: 8414
deuteron reactions (d,p) at 13.6 Mev, proton spectra from, 16: 26356
energy level of, low-lying, (E), 20: 38135
energy levels, 17: 7285
energy levels, 20: 46803
energy levels from isomer decay, (E), 20: 17786
Fermi gas coefficient and nuclear temperature, 18: 998 (AD-299005)
gamma dose constants for, 20: 46617
gamma emission by, 18: 8313
gamma spectra, 16: 4751 (JAERI-4019)
gamma spectra, 16: 32418
gamma spectra, 17: 34966
half life of, measurement, 19: 798
magnetic moment and spin of, measurement of, 18: 17068
neutron elastic scattering at 1.509 Mev, polarization in, 17: 31410 (TID-19051)
nucleon scattering at 14 to 17 Mev, optical model analysis of, (T), 19: 23700
partial widths of excited states, 16: 5996
proton reactions (p,n) at 30 and 50 Mev with, excitation of isobaric states in, 17: 41926

SILVER ISOTOPES Ag-109

abundance ratio with silver-107 in natural silver, 16: 11943
activity of isomeric, induced in food radiopreservation, 20: 33744
alpha excitation of, reorientation effects in, (E), 19: 25475(R) (ORNL-TM-1044)
alpha reactions (α,3n) with, isomer ratios from, 18: 30815
alpha reactions (α,n) at 12 to 18 Mev (E/T), 19: 3362
alpha reactions (α,n), (α,2n), and (α,3n) at 10 to 40 Mev, excitation functions for, (E), 19: 27524
alpha reactions (α,3n), indium-110 production from, 16: 21381
alpha reactions (α,n) and (α,2n) on, excitation functions for, 16: 33900
bremsstrahlung reactions at 0.8 Mev, excitation of isomeric states in, 18: 2945
carbon-12 reactions (C-12,N-13) with, angular distributions from, (E), 20: 42153 (JINR-E-2824)
content in meteorites, 18: 10755
decay of isomeric, 88-kev transition in, 18: 7782
decay of, transition rates for, (E), 19: 23780
decay schemes, 16: 17125
deuteron elastic scattering at 12 Mev, 18: 38109
deuteron elastic scattering at 13.6 Mev, angular distributions from, 18: 40632
deuteron scattering at 12 Mev, distributions from, (E), 19: 10260 (UCRL-7670)
electron conversion coefficients for, 88-kev, (E), 19: 43337
energy level strength functions for, 16: 26518
energy level transitions in, retardations in l-allowed M1, (T), 19: 21323
energy level transitions in, gamma spectra from, (E), 20: 4476(R) (IS-1200(Sect.P))
energy level transitions from cadmium-109 decay, conversion coefficients for, (E), 20: 36231
energy levels, 16: 5988
energy levels from calcium-112 (p,α) reactions, (E), 20: 46242(R) (TID-23239)
energy levels of, detection of isomeric, 17: 29953

energy levels of, effects of collective vibrational motion on anomalous coupling, (T), 20: 28420
gamma dose constants for, 20: 46617
gamma spectra, 17: 34966
gamma transition energy of isomeric, (E), 20: 1174
half life of isomeric, (E), 20: 44712
hyperfine structure $^2D_{5/2}$ and $^4F_{9/2}$ states of, 20: 44141
internal conversion coefficients of, (E), 19: 6660
isomeric transitions in, K-shell conversion coefficient ratios for, 20: 34680
meson (μ) capture at 4.76 Mev, neutron emission in, 16: 18486
neutron activation cross section at 24 kev, (E), 20: 12135
neutron capture at thermal energies, beta emission asymmetries from polarized, 16: 23086
neutron capture by, resonance integral of, (T), 20: 10789
neutron capture by, polarization of silver-110 from, (E), 20: 12098
neutron capture cross sections at 1 to 30 kev, 18: 4534 (EANDC-33U(p.114-35))
neutron capture resonance distinction by spin, 16: 14056
neutron capture resonances in silver due to, assignment of, 17: 15253(R) (GA-3874)
neutron cross sections at 0.414 ev to 10 Mev, 16: 9427 (GA-2451 (Vol.III))
neutron reactions (n,2n) at 14.8 Mev, cross sections for, 16: 7072
neutron reactions (n,p) at 14 Mev, electron conversion spectra, 16: 10249
neutron reactions (n,γ) at fission energies, 16: 18429
neutron reactions (n,p) at 7.0 to 19.8 Mev, cross sections for, 16: 19782
neutron reactions (n,2n), (n,pγ), and (n,pn) at 14.8 Mev, cross sections for, 17: 2242 (TID-16949)
neutron reactions [(n,αn) + (n,nα)] at 14.8 Mev, cross section limit, product half life, and Q value for, 17: 2242 (TID-16949)
neutron reactions (n,α) at 14.8 Mev, cross sections for, 17: 2242 (TID-16949)
neutron reactions (n,$\alpha\gamma$) and (n,αn) at 14.8 Mev, cross sections for, 17: 2242 (TID-16949)
neutron reactions [(n,αn) + (n,nα)], separation energies for, 17: 2242 (TID-16949)
neutron reactions (n,2n) at 14 Mev, cross sections for, 17: 26547
neutron reactions (n,nα) at 14.7 Mev, upper limit for cross section of, 17: 36707
neutron reactions (n,nα) at 14.8 Mev, maximum cross-section limits for, 18: 1077
neutron reactions (n,γ) with, lifetimes of excited states produced by, 18: 6259
neutron reactions (n,γ) with, 88-kev transition in thermal, 18: 7782
neutron reactions (n,γ) with, gamma energy measurements at 660 kev in, 18: 24637
neutron reactions (n,γ) with, gamma spectra from, 18: 28600
neutron reactions (n,2n) at 14 Mev, shell effects in, (T), 19: 12536
neutron reactions (n,γ), cross section for, 19: 26718 (ORNL-3802)
neutron reactions (n,γ), activation cross section for, (E), 19: 35378(R) (EANDC(E)-57(U))
neutron reactions (n,γ), gamma spectra in 5.2-ev resonance of, 19: 39781 (JAERI-1073)
neutron reactions (n,γ) with, Westcott factor for, (E), 20: 46627
neutron resonance capture, 16: 5996
neutron resonance cross sections of, determination of, by boron absorption technique, 16: 28036 (TID-16059)
neutron transmission at 30 ev to 20 kev, resonance parameters for, (E), 20: 12072
nuclear moment and spin of isomeric, (E), 20: 12073
oxygen-16 excitation of, reorientation effect in, (E), 19: 25475(R) (ORNL-TM-1044)
performance as epithermal neutron index monitor, for long irradiations, 19: 42707 (AERE-R-4866)
photoactivation of isomeric, cross sections for, 18: 7705
photoactivation of, excitation levels in, (E), 20: 19865
photoreactions (y,n) on, cross sections for, (E), 19: 10356
preparation as gamma source by electrolytic precipitation, 17: 23728
proton reactions (p,2n) at 12 to 14 Mev, conversion electrons from, 18: 40561
proton reactions (p,n) at 370 Mev, nuclear-structure effects in, (E/T), 20: 1213
proton reactions (p,2nγ) at 14.3 Mev, gamma transitions from, (E), 20: 36166 (INSJ-98)
proton reactions (p,n) at 3.0 to 5.8 Mev, strength functions for, (E), 20: 39470(R) (ORNL-3924)
proton reactions (p,2nγ) at 12 Mev, cadmium-108 energy-level transitions from, (E), 20: 46684
proton reactions at 57 Mev on, proton distributions from, 17: 7197
proton reactions (p,γ) in stars, 16: 12308
proton reactions (p,n) at 5 to 10.5 Mev, cross sections, 16: 31106
proton reactions with, nucleon cascades from, 18: 16974
use as epithermal flux monitor, 16: 19066 (CRDC-1083)

SILVER ISOTOPES Ag-110

beta decay asymmetry, 16: 23086
beta decay of polarized, produced by capture of polarized neutrons, 18: 21201 (KR-64(Sect.XXVIII))
beta decay of, circular polarization of gamma radiation following, 18: 21309
beta decay of, Coulomb matrix elements and impurity coefficients in, 18: 28665
beta decay of, gamma-gamma directional correlations in, (E), 19: 5243
beta decay of, transitions to vibrational levels in, 18: 36625
beta emission from, hindrance phenomena in, 16: 23073
beta-gamma circular polarization correlation, 16: 11045
book: *Isobaric Nuclei with Mass Number A = 110*, 18: 2960
content in coastal and oceanic crustacea, fish, and mollusks, 19: 30410
content in marine organisms, 1963 and 1964, 20: 23303
content in polonium process waste stream, 18: 13358(R) (MLM-1151)
content in stratospheric and tropospheric samples in Project Star Dust, 1963, 20: 16727(R) (HASL-168)
content in stratospheric and tropospheric samples in Project Star Dust, 1964, 20: 16728(R) (HASL-169)
content of isomeric, in lead shielding of scintillation detectors, 20: 33708
decay, 18: 17051
decay and hyperfine structure in iron and nickel, 18: 16954 (UCRL-11143)
decay of, branching ratios in, 17: 38146
decay of, correction factors for, 17: 24384 (AERE-R-4237)
decay of isomer, beta, 17: 17251
decay of isomeric, spectra of, 18: 11234
decay of isomeric, internal conversion spectrum from, 18: 24738
decay of isomers, positron emission in, 17: 9578
decay of metastable, beta and gamma spectra from, 16: 21380
decay of metastable, 18: 9752 (IA-900)
decay of metastable, isomeric (E), 19: 1607
decay of metastable, multipolarity of 116-kev isomeric (E), 19: 1608
decay of metastable, conversion electron-K x-ray coincidence in, 19: 9771(R) (PR-P-63)
decay of, electron capture, (E), 19: 12611
decay, positron spectra from, 16: 6599
decay scheme, 18: 42777
decay schemes, 16: 21380
determination in aqueous solutions by scintillation counting, 18: 29580
determination in atmospheric and precipitation samples, methods for radiochemical, 20: 14430 (AD-620219)
determination in antique gold coins by activation and gamma spectrometry, 20: 40829
determination in decay mixtures, computer program for, 19: 32110
determination of internal, by radiochemical urine analysis, 18: 33519
determination of, gamma spectrometric, 19: 32545 (CEA-R-2461)
deuteron reactions (d,p) at 13.6 Mev, proton spectra from, 16: 26356
diffusion in magnesium, 17: 22200(T)
diffusion in magnesium–silver alloys, self-, 18: 26051
diffusion in zinc single crystals, anisotropic, 16: 6753
energy level transitions in isomeric, 18: 40528
energy levels between ground and metastable states, detection of, 18: 42672
energy levels from silver-109 (n,γ) reactions, 18: 28600
energy levels of, lifetimes of, 18: 6259
energy measurements for β-transitions to cadmium-110, 17: 35253(R) (IA-775)
exchange between silver chloride crystals and solutions, 20: 14572
exchange between silver iodide and silver nitrate, kinetics of, 20: 16460
gamma dose constants for, 20: 46617
gamma emission by, 18: 8313
gamma emission from metastable, 20: 6436
gamma spectra, 16: 4751 (JAERI-4019)
gamma spectra, 17: 34966
gamma spectra, 18: 1050
gamma spectra of, multipolarities of, 18: 2403(R) (PR-P-58)
gamma-gamma coincidence spectra of, 18: 24637
half life, 16: 26213 (AE-78)
half life, 17: 5352
half life, 18: 33943
half-life measurements in metastable, 16: 8198
incorporation in proteins, method for, 19: 29836
incorporation in silver iodide aerosols, 19: 20027
internal conversion spectrum, 17: 40054
isomeric-pair production by neutron activation, yield ratios of, 17: 7248
measurement in atmosphere, 20: 8980(R) (BNWL-36, pp 3.1-122)
metabolism by amphibian larvae, 19: 21826
metabolism by rats, 18: 43180(R) (LA-3132-MS(p.93-9))
migration and retention in lithosphere at NRTS, Idaho, 18: 17349

migration to rat brain tissue, activation analysis of, 19: 10983(R) (TEES-2671-3)
neutron capture cross section of metastable, 17: 33026
neutron reactions at 7.8 to 64 kev, activation cross sections for, (E), 20: 40069(R) (EANDC(E)-66(U))
nuclear magnetic moment, (E), 19: 16995
nuclear moment and spin of metastable, EPR determination of, (E/T), 20: 24358(R) (UCRL-16580, pp 1-93)
partial widths of excited states, 16: 5996
polarization in iron and nickel, (E), 19: 16995
polarization of, from neutron capture by silver-109, (E), 20: 12098
positron spectrum, 16: 33834
preparation of carrier-free amalgams of, 18: 5207 (SC-DC-3503)
production using Rossendorf Reactor in East Germany, 19: 20436
sensitivity for activation analysis using beta-gamma-gamma sum-coincidence gamma spectrometer, 20: 16335(R) (NBS-TN-276)
separation from fission products by amalgam exchange, radiochemical, 18: 16148
separation from waste solutions by alluvial silts, 17: 19709 (TID-7644 (p.151-75))
solvent distribution between mercury and aqueous mercurous perchlorate, 18: 31483
sorption by guinea pig skin, disappearance measurements of, 20: 32910
sorption of carrier-free, from aqueous solutions on Pyrex, 17: 23384 (SCR-593)
sorption of carrier-free, from various solutions on glass, 16: 5657 (TID-14423)
sorption of colloidal, from solutions, 18: 5207 (SC-DC-3503)
tissue distribution in fish, 17: 12114
tracer use for measurement of sand and silt drift on Portugal seacoasts, 16: 24005
tracer use for silver diffusion in beryllium, 20: 37250
tumor induction in monkeys by, 17: 35465
uptake by soil, effects of natural extracts from plants and trees on, 19: 53
use as indicator in titrations, 16: 22024
use as tracer in studying sand movement in river, 19: 2676 (CONF-188-2)
use in control of blast furnace lining wear, 18: 6914 (NP-13436)
use in determining residence time of solids in tanks, 20: 46105 (BM-RI-6855)
use in microcoulometer, 18: 10437
use in radio-release method for tracing stream flows, 19: 34326 (TID-21881)
uses in complexometric titrations for radiometric end point detection, 19: 9067
uses in fingerprint detection by autoradiography, 18: 30071(T)
uses in radio release determination of vanadium in aqueous solutions, 19: 4069
uses of isomer of, in silver iodate, as indicator in EDTA back-titration, 20: 26769

SILVER ISOTOPES Ag-111

beta decay of, angular correlations in, 18: 17018
beta decay of, cadmium-111 level structure from, (E), 20: 22083
beta decay scheme, 18: 42683
content in atmosphere after Chinese atmospheric tests, 20: 23344 (AEET-240)
content in fallout and precipation near Leningrad, 20: 16704
content in rain water, Fayetteville, Arkansas, Oct. 1964, 20: 16663 (TID-21470)
decay of, correction factors for, 17: 24384 (AERE-R-4237)
decay schemes, 16: 17125
deposition in solution, kinetics of anodic, 19: 17921
determination by chloride precipitation and counting, 16: 18809 (AERE-AM-89)
determination in mixed fission products, 16: 2988
determination of, gamma spectrometric, 19: 32545 (CEA-R-2461)
distribution and volatility in air-burst debris, 20: 9184 (USNRDL-TR-933)
distribution from nuclear excavation in basalt, 20: 613
distribution in lymphatic vessels of dogs and rabbits, 19: 35921
effects on cambium cells and macrocytes in patients, 20: 38769
energy levels, 20: 6402
energy levels, (E), 20: 12145
energy levels and gamma spectra, (E), 20: 9960(R) (AEET-228)
energy levels of, effects of collective vibrational motion on anomalous coupling, (T), 20: 28420
energy of, from 23-Mev deuteron fission of uranium-238, 17: 11646 (UCRL-10193)
gamma dose constants for, 20: 46617
incorporation in proteins, method for, 19: 29836
preparation of carrier-free, from neutron-irradiated palladium, 20: 41023
preparation of colloidal, for use in radiotherapy, 18: 39023(T) (AEC-tr-6390(p.540-4))
production in helium ion fission of uranium-235 and -238, cross sections for, 17: 17126 (TID-18165)
production of carrier-free, electrolytic, 16: 24083
ranges of thermal-fission, in aluminum, (E/T), 20: 24351(R) (MIT-905-52, pp 1-41)
release from pyrolytic carbon-coated fuel particles, 19: 39228 (BMI-1734)
separation and purification for medical use, 18: 37581 (A/CONF.28/P/457)
separation from fission products by precipitation as chloride, 18: 5427
separation from irradiated palladium by crystallization and electrodeposition, 19: 9275
separation from neutron-irradiated palladium by solvent extraction, 19: 15571(R) (TID-21385)
separation of carrier-free, from neutron-irradiated palladium, 16: 5383
uptake by aquatic insects, coefficient of accumulation for, 19: 25857
uptake by brain tumors, 18: 1471
uptake by dogs, effects on skin homografts, 18: 19605
uptake by lymph nodes, carcinoma therapy using, 18: 21939
use in preparation of sources for radiotherapy, 18: 29536
use in radiotherapy, 20: 42796
yield in epi-cadmium neutron fission of plutonium-239, (E), 19: 27585
yield in proton fission of uranium-238 at 150 Mev, kinetic energy and range of, 19: 27498
yields from helium ion-induced fission of lead-207 at 41.1 to 26.3 Mev, 20: 37996
yields from neutron fission of plutonium-239, uranium-235, and uranium-238, 16: 1037(T) (AEC-tr-4696)
yields from photofission of uranium by 650-Mev bremsstrahlung, 20: 22040
yields from thorium-232 fission, (E), 20: 17860
yields in neutron fission of uranium at 14.7 Mev, 18: 44835
yields in neutron fission of natural thorium at 14.7 Mev, 18: 44836
yields in proton fission of uranium-238 at 150 Mev, excitation energy and momentum transfer of, 19: 27499
yields in proton fission of uranium-238 at 7.1, 9.4, and 12.0 Mev, 20: 37995
yields in thermal neutron fission of plutonium-239, 19: 16873

SILVER ISOTOPES Ag-112

beta decay scheme for, 17: 2287
distribution and volatility in air-burst debris, 20: 9184 (USNRDL-TR-933)
gamma spectra, 18: 32850
hyperfine structure and nuclear spin of, 18: 13101
neutron reactions (n,α) at 14 Mev, nuclear shell effects in cross sections for, 18: 18977
nuclear magnetic moment and spin of, 16: 31074 (UCRL-10334)
ranges and recoil properties from proton fission of uranium-238, 16: 11695(R) (TID-15020(p.37-41))
ranges from fission of plutonium-239, radiochemical determination of, 20: 34525 (KFK-401)
yield in proton fission of uranium-238 at 150 Mev, kinetic energy and range of, 19: 27498
yields from alpha and deuteron fission of uranium-233, 16: 24351
yields in neutron fission of natural thorium at 14.7 Mev, 18: 44836
yields in proton fission of uranium-238 at 150 Mev, excitation energy and momentum transfer of, 19: 27499
yields in proton fission of uranium at 170 Mev, 20: 42177
yields in uranium-235 fission, (E), 19: 5569(R) (MIT-2098-64)

SILVER ISOTOPES Ag-113

energy levels of, effects of collective vibrational motion on anomalous coupling, (T), 20: 28420
hyperfine structure and nuclear spin of, 18: 13101
nuclear magnetic moment and spin of, 16: 31074 (UCRL-10334)
production in helium ion fission of uranium-235 and -238, cross sections for, 17: 17126 (TID-18165)
ranges from fission of plutonium-239, radiochemical determination of, 20: 34525 (KFK-401)
yields from helium ion-induced fission of lead-207 at 41.1 to 26.3 Mev, 20: 37996
yields in epi-cadmium and thermal neutron fission of plutonium-239, (E), 19: 27585
yields in helium-ion fission of lead-206, 18: 2844 (TID-19654)
yields in neutron fission of uranium at 14.7 Mev, 18: 44835
yields in neutron fission of natural thorium at 14.7 Mev, 18: 44836
yields in proton fission of uranium-238 at 7.1, 9.4, and 12.0 Mev, 20: 37995

SILVER ISOTOPES Ag-115

beta decay scheme of, 19: 1628
decay and half life of, spectra of, 18: 4620
decay of, 16: 30930(R) (NYO-2669)
decay, (E), 19: 5569(R) (MIT-2098-64)
tissue distribution in fish, 17: 12114
yields in neutron fission of uranium at 14.7 Mev, 18: 44835

SILVER ISOTOPES Ag-116
decay and half life of, spectra of, 18: 4620
SILVER ISOTOPES Ag-117
decay and half life of, spectra of, 18: 4620
SILVER METAPHOSPHATES
$Al(PO_3)_3$–$LiPO_3$–$AgPO_3$, radio-photoluminescence polarization of glasses of, 19: 40588
SILVER NITRATES
compressibility at 0 to 10,000 atm, 20: 10272(R) (NAA-SR-9339)
effects on gamma-induced polymerization of acrylonitrile in dimethylformamide, 18: 23595(T,R) (AEC-tr-6316(p.145-51))
electric conductivity of fused, in cells with fritted glass disks, 18: 6565(R) (TID-19853)
electroosmosis in concentrated aqueous solutions of, 19: 14912(R) (NYO-1938-2)
formation quotients in silver bromate solutions, 17: 28884
heat of solution of silver bromide and chloride in liquid, 17: 28869
incorporation in filter papers for radioiodine sampling, 20: 16756
ion exchange and sorption on glass surfaces, 20: 16469
ion exchange with sodium porcelain, 18: 17802
melting properties at 0 to 10,000 atm, 17: 28825 (NAA-SR-8422)
oxidizing effects on uranium compounds in ammonia, 17: 175
radiation damage to, annealing of, 17: 29001
radiation effects on aqueous, electron, 18: 37213(T) (AEC-tr-6398(p.481-5))
radiation effects on, at 77°K, electron spin resonance studies of, 19: 34225
radiation effects at 77°K on, ESR studies of x, 20: 29310
radiolysis of frozen solutions of, EPR spectra of free radicals from gamma, 20: 33376
radiolysis of, mechanism of, 17: 3043
radiolysis of, alpha, gamma, and optical, 18: 23687
reactions of complexed, in alcohol and nitric acid, 19: 9046(R) (IS-900(Sect.C))
reactions of, with gaseous iodine, 16: 31585 (TID-16807)
reactions of, with iodine vapor, phase equilibria in, 17: 23305 (TID-16914)
reactions with benzyl and *p*-nitrobenzyl bromides, carbon-14 isotope effects in, 18: 3787
reactions with iodine in off-gases, thermodynamics, 19: 7354 (HW-38311(Rev.))
reactions with metals in nonaqueous solvents, 16: 5311(R) (TID-14361)
reactions with uranium hydrides in heavy water, 18: 41398
reduction to silver, photolytic and radiolytic, 18: 1725(R) (ORNL-3488(p.42-54))
separation by reversed-phase partition chromatography using organophosphorus compounds, 18: 25614
silver-110 exchange between, and silver iodide, kinetics of, 20: 16460
sorption by glass surfaces, 20: 18846
sorption in guinea pigs, percutaneous tracer study, 19: 12927
sorption of liquid, in Linde Molecular Sieve 4A, 17: 33767 (IA-810)
spectra in tri-n-octylphosphine oxide solutions, infrared, 18: 10075
spectrum at low temperatures, infrared, 16: 33002
thermal conductivity and viscosity at 214 to 318°C, 17: 8008(R) (TID-17673)
use as thermal neutron monitor, 18: 23896
acetonitrile–$AgNO_3$, electric conductivity and viscosity of, 18: 25000 (RPI-1999-3)
acetonitrile–$AgNO_3$, structure of solutions of, 20: 1565(R) (RPI-1999-6)
Ag–$AgNO_3$, cation exchange in molten, 20: 2520(R) (IA-920)
Ag_2C_2–$AgNO_3$, qualification tests on spray-deposited and light-initiated explosives of, 20: 10814 (SCL-DC-65-96)
$AgIO_3$–AgI–$AgNO_3$, phase diagram, 17: 23305 (TID-16914)
$AgIO_3$–AgI–$AgNO_3$, phase studies, 18: 1633
$AgNO_3$–D_2O, radioinduced free silver atoms in solid solutions of, EPR of x, (E), 20: 15975(T)
$AgNO_3$–H_2O, radioinduced free silver atoms in solid solutions of, EPR of x, (E), 20: 15975(T)
$AgNO_3$–$NaNO_3$, cation exchange between Linde Molecular Sieve 4A zeolite and liquid, 18: 43443 (IA-968)
$AgNO_3$–$NaNO_3$, chronopotentiometric study of friction coefficients in molten, 19: 31646 (TID-20866)
$AgNO_3$–$NaNO_3$, electrochemical and thermochemical properties of fused, 20: 10804 (EUR-2466.e, pp 9-19)
$AgNO_3$–$NaNO_3$, thermodynamics of molten, 19: 2273 (IA-941)
benzonitrile–$AgNO_3$, electric conductivity and viscosity of, 18: 25000 (RPI-1999-3)
benzonitrile–$AgNO_3$, structure of solutions of, 20: 1565(R) (RPI-1999-6)
$CsNO_3$–$AgNO_3$, diffusion and transport processes in molten, on ceramic oxides, 20: 40866 (EUR-2954.e)
ethanol–$AgNO_3$, radioinduced free silver atoms in solid solutions of, EPR of x, (E), 20: 15975(T)
KNO_3–$AgNO_3$, electrochemical and thermochemical properties of fused, 20: 10804 (EUR-2466.e, pp 9-19)
KNO_3–$AgNO_3$, spectra of fused, infrared, 17: 37175 (URS-74)
$LiNO_3$–$AgNO_3$, cation exchange in fused, 19: 26917(R) (IA-984)
$LiNO_3$–$AgNO_3$, electrochemical and thermochemical properties of fused, 20: 10804 (EUR-2466.e, pp 9-19)
methanol–$AgNO_3$, radioinduced free silver atoms in solid solutions of, EPR of x, (E), 20: 15975(T)
NH_3–$AgNO_3$, for oxidation of saccharides on paper chromatograms, 17: 33825
$RbNO_3$–$AgNO_3$, electrochemical and thermochemical properties of fused, 20: 10804 (EUR-2466.e, pp 9-19)
SILVER NITRITES
radiation effects on rate of thermal decomposition of, x, 20: 41000
SILVER OXALATES
electrochemical studies of, 17: 20051
photolysis of, effects of cadmium and lead ions on, 20: 5583
photolysis of, EPR studies of uv, 20: 25135
radiation decomposition at 126°C, 16: 13667
radioinduced paramagnetic centers in, gamma and uv, 20: 25135
radiolysis, effects of cadmium, 16: 30463
radiolysis of, effects of cadmium impurities on, 18: 337
radiolysis of, effects of cadmium and lead ions on, 20: 5583
radiolysis of, EPR studies of gamma, 20: 25135
thermal decomposition, effects of cadmium and irradiation, 16: 30463
thermal decomposition of irradiated, effects of cadmium impurities on, 18: 337
Ag–$Ag_2C_2O_4$, radiation effects on catalytic activity of, in decomposition of hydrogen peroxide, 19: 26389
Ag–silver oxalate, gamma radiation effects on catalytic activity of, 20: 16523
SILVER OXIDES
analysis for oxygen-18, mass spectrometric, 20: 8852
catalytic effects on isotopic exchange reactions between chlorobenzene and labeled sodium chloride, 18: 35568
determination in swimming pool reactor coolant, activation and chemical, 20: 38800 (PAEC(C)RE-652)
effects on mice, 19: 43831
free energy of formation, (E), 19: 17202
free energy states of, on silver, 17: 34400 (CONF-155-1)
radiation effects on films of, on glass, 16: 21108
radiation effects on thermal decomposition of, 19: 11813
spectra in low frequency region, infrared, 18: 23549
spectra of, in 300 to 1000 mμ region, reflectance, 17: 15970
structural properties of monovalent, 17: 14210 (NBS-MON-25(Sect.1))
structure of, from radioinduced oxidation of silver, 16: 27096
Ag_2O–ZrO_2, crystal structure and phase studies, 17: 37503(R) (AD-290693)
Cr_2O_3–Ag_2O, intensity ratio technique for x-ray spectrometric analysis for chromium and silver in, 18: 15972
SILVER PERCHLORATES
effects on electron exchange reactions between thallium and uranium in methanol–water solutions, 18: 27418
radiolysis of aqueous solutions of, silver yields from gamma, 20: 26962
$AgClO_4$–D_2O, radioinduced free silver atoms in solid solutions of, EPR of x, (E), 20: 15975(T)
$AgClO_4$–H_2O, radioinduced free silver atoms in solid solutions of, EPR of x, (E), 20: 15975(T)
ethanol–$AgClO_4$, radioinduced free silver atoms in solid solutions of, EPR of x, (E), 20: 15975(T)
methanol–$AgClO_4$, radioinduced free silver atoms in solid solutions of, EPR of x, (E), 20: 15975(T)
SILVER PERIODATES
proton spin-lattice relaxation time in ferroelectric phase, 16: 4610(R) (NP-11058)
SILVER PERMANGANATES
radiation effects on thermal decomposition of, 17: 14342
radiation effects on, x-ray diffraction studies on, 18: 44247
radiation effects on thermal decomposition of, 19: 11813
SILVER PERXENATES
spectra of, infrared absorption, 17: 35680 (CONF-126-18)
SILVER PHOSPHATES
performance of glasses of, in luminescent dosimeters, 20: 9291
polarography in lithium and lithium sodium metaphosphates at 750 and 730°C, 18: 1516
use in radiation dosimeters, 19: 13807(P)
Ag–$AgPO_3$, development and testing as standard electrode for emf studies in alkali metaphosphates, 20: 5529(R) (SC-DC-65-1706)
SILVER PROTACTINIUM FLUORIDES
preparation and properties of $AgPaF_6$, 20: 45673
Silver Ruthenium Fluorides
see Silver Fluoruthenates

SILVER SALTS
protective effects against iodine-131 toxicity in animals, 17: 6005
radiolysis of, at 77°K, yields of silver complexes from, 20: 12895
SILVER SAMARIUM SULFIDES
crystal structure, 20: 29158
SILVER SELENIDES
radiation effects on electric and thermal properties of, electron, 18: 2315
SILVER SULFATES
radiolysis of frozen solutions of, EPR spectra of free radicals from gamma, 20: 33376
solubility in deuterated sulfuric acid solutions at 25 to 225°C, 17: 28868
solubility in deuteriosulfuric acid and heavy water, 18: 1614(R) (ORNL-3488(p.65-90))
solubility in electrolytic solutions of nitrates and sulfates, 17: 2989
solubility in potassium sulfate electrolyte mixtures, 17: 10511(R) (ORNL-3320(p.56-82))
solubility products at 25°C, 19: 15571(R) (TID-21385)
thermodynamic properties of aqueous, to 275°C, 16: 18873
use as contrast agent in electron microscopy of graft polymers, 18: 12169
$Ag–Ag_2SO_4$, emf measurements vs $Hg–HgSO_4$ in all-metal cell, 19: 36340 (ORNL-P-814)
$Ag_2SO_4–D_2O$, radioinduced free silver atoms in solid solutions of, EPR of x, (E), 20: 15975(T)
$Ag_2SO_4–H_2O$, radioinduced free silver atoms in solid solutions of, EPR of x, (E), 20: 15975(T)
ethanol–Ag_2SO_4, radioinduced free silver atoms in solid solutions of, EPR of x, (E), 20: 15975(T)
methanol–Ag_2SO_4, radioinduced free silver atoms in solid solutions of, EPR of x, (E), 20: 15975(T)
$SiO_2–Ag_2SO_4–V_2O_5$, radiation effects on catalytic activity of, in oxidation of sulfur dioxide by air, 20: 29291
SILVER SULFIDES
thermal conductivity, 16: 9211(R) (TID-14561)
thermal conductivity, 17: 8010(R) (TID-17767)
$Ag_2S–Tb_2S_3$, crystal structure, 20: 26829
$Ce_2S_3–Ag_2S$, crystal structure, 20: 26829
$Dy_2S_3–Ag_2S$, crystal structure, 20: 26829
$Gd_2S_3–Ag_2S$, crystal structure, 20: 26829
$La_2S_3–Ag_2S$, crystal structure, 20: 26829
$Nd_2S_3–Ag_2S$, crystal structure, 20: 26829
$Pr_2S_3–Ag_2S$, crystal structure, 20: 26829
$Sm_2S_3–Ag_2S$, crystal structure, 20: 26829
SILVER SYSTEMS
Ag–AgCl, electrode potentials in methanol at 25 to 45°C, 18: 4918(R) (TID-19727)
Ag–AgCl, free energy of solution of, 19: 11103
$Ag–Ag_2C_2O_4$, radiation effects on catalytic activity of, in decomposition of hydrogen peroxide, 19: 26389
$Ag–AgNO_3$, cation exchange in molten, 20: 2520(R) (IA-920)
$Ag–AgPO_3$, development and testing as standard electrode for emf studies in alkali metaphosphates, 20: 5529(R) (SC-DC-65-1706)
$Ag–Ag_2SO_4$, emf measurements vs $Hg–HgSO_4$ in all-metal cell, 19: 36340 (ORNL-P-814)
Ag–NaCl, radioinduced color centers in, x, 20: 38396
Ag–silver oxalate, gamma radiation effects on catalytic activity of, 20: 16523
Ag–TaC, production and properties of skeletal carbide composites of, 19: 46941 (NP-15514(Vol.3))
Ag–Te, crystal structure, metastable, 16: 13586 (TID-14981)
Ag–Te, metastable phases from very rapid cooling of molten, 18: 30169 (CALT-221-1)
$Ag–Y–Y_2O_3$, preparation and semiconducting properties of, 19: 22965 (AL-TDR-64-239)
$Al_2O_3–Ag$, preparation of wires of, with oxide homogeneously dispersed, 20: 16992(R) (RPI-2408-4)
$Al_2O_3–Ag$, preparation and properties of alumina-base cermets of, 20: 37209
$Al_2O_3–Pd–Ag$, preparation and properties of alumina-base cermets of, 20: 37209
As–O–Ag, crystal structure powder diffraction pattern of phases in, 19: 17795
B–Co–Ag, crystal structure, 20: 14532
Bi–Ag–S, crystal structure powder diffraction patterns of phases in, 19: 17795
B–Ni–Ag, crystal structure, 20: 14532
Br–Cl–Ag, crystal structure powder diffraction patterns of phases in, 19: 17795
Ca–Ag–NaCl, radioinduced color centers in, x, 20: 38396
$CaWO_4–Ag$, ion energies from spark sources using, 19: 7778
Cu–Ag–TaC, production of cermets of, 20: 2261(R) (UCRI-326)
$Gd–Gd_2O_3–Ag$, preparation and semiconducting properties of, 19: 22965 (AL-TDR-64-239)
In–Ag–Te, superconductivity in, 18: 32699
Kr–Ag, structure of solid solutions of, 19: 5841 (CEA-R-2528)
$Mg–MgCl_2–Ag$, thermodynamic properties, 18: 3671(R) (BNL-799 (p.26-54))
MgO–Ag, annealing effects on structure of dispersion-hardened, 20: 2325 (HW-SA-3767)
Mg–O–Ag, internal friction in, 17: 35264(R) (UCRL-10706(p.111-203))
MgO–Ag, structure of deformed, 20: 2324 (HW-SA-3765)
MgO–Ag, studies of surfaces of, 19: 36338(R) (NP–15160)
MgO–Pd–Ag, preparation and properties of magnesia-base cermets of, 20: 37209
$NbS_3–Ag$, crystal structure of $Ag_{0.7}NbS_3$, 17: 23310
Pb–Ag, superconducting properties of coated wires of, 18: 15118
$Pd–Ag–ZrO_2$, preparation and properties of zirconia-base cermets of, 20: 37209
Sb–Ag–Te, properties for thermoelectric power generation, 17: 36280(R) (AD-291456)
Sb–Ag–Te, thermoelectric properties, 16: 16708(R) (AD-266128)
Sb–Ge–Ag–Te, power generation by thermocouples of, 17: 36280(R) (AD-291456)
Si–Ag, performance as oxidation-resistant coating for niobium alloys, 20: 43827 (GTR-19)
Si–Ag, phases and structure of, effects of liquid quenching on, 19: 45696 (CALT-221-12)
SILVER TERBIUM SULFIDES
crystal structure, 20: 29158
SILVER THIOCYANATES
radiation damage to crystal lattices of, fission fragment, 17: 34506
radiation effects on aqueous solutions of, x, 18: 37206(T) (AEC-tr-6398(p.408-11))
SILVER THULIUM SULFIDES
crystal structure, 20: 29158
SILVER TUNGSTATES
reduction by carbon monoxide, isotherms for, 16: 22072(T) (AEC-tr-5125)
SILVER URANATES
preparation and properties, 18: 20012
SILVER URANIUM FLUORIDES
crystal structure of, containing pentavalent uranium, 19: 25004
SILVER VANADATES
preparation of kryptonates of, by diffusion, 20: 18570(R) (NYO-2757-5)
SILVER YTTERBIUM SULFIDES
crystal structure, 20: 29158
SILVER YTTRIUM SULFIDES
crystal structure, 20: 29158
SIMEA Reactor
see Latina Power Reactor
Simpson Audio Detector
see Radiation Detection Instruments (Audio Pulse Type)
Simpson Methane Flow Chamber
see Proportional Detectors
Simpson Methane Flow Scaler
see Scalers
Simulators
see Reactor Simulators
SINGAPORE
fall-out monitoring, 1960 to 1961, 16: 394 (AERE-R-3766)
SINGLE CRYSTALS
analysis by neutron diffraction, accurate intensity measurements in, 18: 41380
analysis of pure, equipment and procedures for, 20: 29141
bibliography, 20: 11276 (PAEC(A)IN-657)
book: *Single Crystal Diffractometry*, 20: 46962
charged-particle reactions with, stopping power for, 20: 39595
charged-particle scattering by, particle blocking effects in, (E), 20: 23873(R) (ANL-7108, pp 37-41)
conference on films of, Blue Bell, Penn., May 13 to 15, 1963, 19: 37145
cutting of, methods for precise, 17: 30804
cutting of, acid saw for, 19: 31634 (NYO-3029-2)
defects in lithium-doped cobaltous oxide, at 900 to 1200°C, analysis of, 20: 41458(R) (TID-23268)
deformation in, resolution of stresses in, 20: 11331
deformation of alpha-phase zirconium alloy, effects of preferred orientation on, 20: 37226
density determination by hydrostatic weighing, 17: 1941(R) (NP-12214)
development for mixing infrared and visible laser output, 19: 39269(R) (SU-SEL-64-133)
diffusion in, measurement of volume, 18: 23522
diffusion of iron and nickel in magnesia, 20: 31719(R) (UCRL-16658, pp 155-69)
diffusion of xenon from uranium nitride, tracer study of, 20: 43981
dislocation reactions and hardening in body-centered cubic, 20: 43923
dislocations in dimolybdenum carbide, effects of structure and annealing on, 20: 37247

elastic properties of iron-base, in aluminum–iron alloys, 20: 41412(R) (IS-1500(Sect. M))
elastic properties of iron-base, in iron–silicon systems, 20: 41412(R) (IS-1500(Sect. M))
electrochemical studies of silver, 20: 22871(R) (MIT-905-52, pp 42-73)
electron scattering by, "monochromatic" bremsstrahlung from, 17: 20890
electron spin resonance spectra of oriented radicals in irradiated, 18: 33630
gamma circular polarization by birefringent, 17: 9255
gamma nuclear-resonant scattering in, 18: 26657
grown by pulling from melt, impurity striations in non-rotated antimony–indium, 20: 1573 (TID-22314)
growth by sputtering, 16: 17991(P)
growth by Verneuil method, 20: 3919(R) (ORNL-3870, pp 3-6)
growth for preparation of isotopic targets, 20: 696(R) (ORNL-3829)
growth in arc-image furnace, 17: 27515
growth of, bibliography on epitaxial, 17: 41355 (NP-13168)
growth of highly perfect fluoride, for use in lasers, 17: 37744
growth of metallic, electron-beam floating-zone melting furnace for, 18: 8739
growth rate of, effect of vertical temperature gradient on controlled, 20: 41064(R) (IS-1500(Sect.E))
hydride orientation in zirconium, effects of stress on, 20: 37269
internal friction of magnesium, effects of lithium on, 20: 33883 (NYO-2471-19)
ion reactions at high energy, secondary electron emission in, (E), 20: 23874(R) (ANL-7108, pp 43-56)
ion scattering by, energy distribution in, (E), 19: 39297
lattice dynamics of one-dimensional, with free ends, (T), 19: 40079 (NP-15114)
lattice parameters of, x-ray diffractometer determination of, 17: 39016 (AAEC/TM-211)
neutron attenuation by phonons in, (T), 20: 38371
neutron-diffraction analysis of, correction for secondary extinction effects in, 17: 784 (AERE-R-3692)
neutron-diffraction analysis of, at elevated temperatures, 17: 12545
neutron diffractometry of, equipment for high-pressure, 20: 43473(T)
neutron reflection by, theory, (T), 19: 8379 (UCRL-7611(Rev.I))
neutron scattering in, measurement of one-phonon, 19: 46753 (AERE-R-4895)
neutron transmission through, interference phenomena in, 20: 36360 (ZFK-RN-32)
nuclear quadrupole resonance in, energy levels and line intensities from, (T), 20: 3284
nuclear quadrupole spin-lattice relaxation for I = 5/2 in, 20: 24447
nuclear spin resonance lines in, energy levels and relative intensities of, 17: 24072(T) (JPRS-19316(p.162-76))
optical properties of lithium niobate, 20: 43950
orientation in tungsten, effects on ductile-brittle transitions, 20: 39397 (NASA-TM-X-1252)
orientation of, computer program for determining, 18: 4326 (LA-2974)
plastic deformation and work hardening of f.c.c., 17: 35767
preparation, 20: 41412(R) (IS-1500(Sect. M))
preparation and properties of garnet, 17: 3369 (AD-276084)
preparation from melt by pulling technique in protective atmosphere, 17: 1941(R) (NP-12214)
preparation in metals by electron-beam zone melting, 18: 22463(T) (JPRS-22336(p.6-9))
preparation of, 20: 41064(R) (IS-1500(Sect.E))
preparation of bismuth and gadolinium, 20: 4077(R) (IS-1200(Sect. E))
preparation of high-melting, equipment for, 20: 4077(R) (IS-1200(Sect. E))
preparation of high-purity inorganic, 20: 40874 (ORNL-RMIC-5)
preparation of lithium fluoride, methods for, 20: 22857(R) (ORNL-3913, pp 111-32)
preparation of molybdenum, by floating-zone methods, 20: 33859(R) (AD-634128)
preparation of rare earth, methods for, (E/T), 20: 30735(R) (TID-22970, pp 331-73)
preparation of refractory, 16: 22114
preparation of salt, procedure for, 20: 35484(T) (UCRL-Trans-10027)
preparation of spherical, refractory, (E), 19: 40991
preparation of thin films, by cathodic sputtering, 18: 28113
preparation of urania, 20: 17158(R) (ORNL-3900, pp 82-149)
production methods for, 20: 43910(R) (TID-23269)
production of delta-plutonium, methods for, 20: 41453(R) (NUMEC-3428-21)
production of refractory, method and apparatus for, 19: 4609(P)
properties of system of Fermi-Dirac particles, 16: 11856 (NP-11386)
properties of, dielectric and optical, 20: 29709(R) (TID-22970, pp 65-119)
pyroelectric properties of, for use as radiation detectors, 19: 30540
radiation effects on, electron resonance study of, at 20 to 300°K, 20: 10876
radiation effects from excited electrons in, fission-fragment, (T), 20: 26368
radiation scattering by ionic, effects of charged defects on, 16: 22919
radioinduced transmutations in, 18: 17909
slip mechanisms in, of hexagonal close-packed phases, 18: 44156 (UCRL-11418)
sputtering by ions, (T), 19: 14262(T)
sputtering by ions, energy dependence of, (T), 19: 41271(T)
sputtering by ions, mechanism of, 20: 42553
sputtering yields from, effects of collision focusing on, 18: 32368
strength of niobium–tantalum alloy, 20: 37215
structure analysis of, computer program for intensity data processing in, 18: 22409 (LA-3043)
structure calculations, computer program for least-squares, 19: 31445 (LA-3259)
structure of, design of x-ray camera for study of, 17: 8531 (PAN-333/I-B)
x-ray diffraction and transmission by, intensity distributions in, (T), 19: 32789
x-ray scattering by, broad diffuse bands from electron-lattice resonance in, 18: 16551 (TID-20364)
Sintered Aluminum Products
see SAP

SINTERING

book: *Fundamental Phenomena in the Material Sciences*. Vol. 1, 19: 37147
book: *Strength of Sintered Materials and Alloys at Room and High Temperatures*, 17: 34468
by volume diffusion, review of, 18: 39852 (AAEC/E-121)
caking in, use of radioisotopes for control of, 16: 33384
cyclic, effects on porosity of metal powders, 18: 18337
development and evaluation of techniques of, for electronic tube seal fabrication, 17: 23906(R) (RADC-TDR-63-43)
development of processes in, review of, 17: 11090 (IS-460)
effects on density, porosity, and thermal stability of pure beryllium and uranium oxide powders, 20: 25537
effects on materials, methods for determining, 20: 13319
equation for one-mechanism diffusion, 20: 15009 (TID-22491)
equipment and conditions for, of borides, nitrides, and silicides, 17: 22142
equipment and methods for metal-tube, 18: 5759(P)
kinetics of, measurement from powder compact shrinkage, 17: 421(R) (TID-17007)
kinetics of, effects of temperature on, 20: 41064(R) (IS-1500(Sect.E))
kinetics of, in the presence of liquid phase, 20: 2286
mass transport mechanisms in, effects of externally applied forces on, 17: 18719(R) (TID-18324)
material transport in, study of mechanisms of, 18: 44107 (ORNL-P-427)
material transport mechanism in, studies, 19: 20465 (TID-20344)
mechanism of materials transport during, studies of, 19: 18398(R) (RPI-2408-1)
mechanisms, 18: 6550(R) (GTR-20)
mechanisms in, electric resistance measurements to determine, 16: 13517 (TID-15139)
mechanisms in oxide, 18: 4217(T) (AEC-tr-6159)
mechanisms in, research on, 20: 29623(R) (TID-22970, pp 121-256)
mechanisms of, in crystalline powders, 17: 32542(T) (UCRL-Trans-953(L))
mechanisms of, in hydrogen and steam, 18: 20489
mechanisms of, use of resonant frequency determinations in following, 20: 7535 (IS-T-48)
methods for low temperature, 16: 30755 (UNC-3006)
methods for, of fluids and solids, 20: 25532
methods of low-temperature, 17: 12626(R) (AD-275787)
moisture content of materials for, method of measurement using neutrons, 18: 18299
mold material development, 16: 13169 (CNLM-1730)
of oxides, review of lattice defects in, 17: 16534
of oxides, studies, 20: 43813(R) (COO-1122-3)
process development for semicontinuous pressure, 20: 46160(R) (AD-638453)
process for cermet powders, 20: 33842 (NASA-TN-D-3511)
process for metal oxide powder, 19: 40995(P)
process for preparing porous metals by, 19: 11715(P)
process for urania fuel fabrication, 20: 35861 (KR-89, pp 181-96)
process for urania, oxidizing effects of impurities on, 20: 39390 (CEA-R-3003)
process kinetics and theoretical analysis of techniques, 16: 24116
processes for, 17: 41419(P)
radiation effects on, of refractory materials, 17: 4899
relation to thermal conductivity, 18: 39853 (AAEC/TM-245)
review of theories of, 19: 6261 (RISO-89)
shrinkage in, non-uniform, 17: 32582
shrinkage in, equation for isothermal, 20: 33931

shrinkage in, method for evaluation, 19: 13902 (TID-21624)
studies on, 20: 16992(R) (RPI-2408-4)
theory of solid-state, 16: 25698 (NP-11636)
theory of solid-state, 17: 14748(T) (AERE-Trans-899)
topology of, 18: 32060(R) (TID-20826)
two-particle model for, size sensitivity of, 17: 1839
vacancy diffusion along grain boundaries during, 16: 10485(R) (SEP-259)

SIOUX FALLS POWER REACTOR
(Northern States Power Company)
bibliography on, 17: 31734 (TID-3556(Rev.2))
butterfly valve cavitation tests for, 17: 22845 (ACNP-62004)
components, fabrication specifications and inspection program, 16: 28517 (ACNP-6121)
construction and design features, (E), 19: 40217
construction and operation status, 19: 5487 (SAN-8003(p.1-12))
containment leak rate tests, 20: 14143 (PAPP-6401)
control of, development of burnable poisons for, 17: 24671 (ACNP-63003)
control rod design and testing for, 17: 17531 (ACNP-63001)
control rod design for, 18: 33093 (ACNP-64014)
control rod drive for, design and evaluation of, 18: 3160 (ACNP-63018)
control rod drive for, design of prototype, (E), 19: 40135
control rods, design, 16: 18679
control rods of, burnup limits for, 18: 9632 (ACNP-63006)
coolant chemistry control for, 17: 38468 (TID-7674(p.19-21))
coolant chemistry in, 19: 4197 (SAN-8003(p.90-133))
coolant recirculation system for, analysis of, 18: 9633 (ACNP-63026)
core flooding, pressurization, and temperature coefficients, 20: 16059 (ACNP-65600)
criticality measurements and predictions of, 19: 29669
criticality studies, (E), 19: 5488 (SAN-8003(p.163-89))
criticality studies of boiler core, 19: 45557(R) (ACNP-65557)
criticality studies, (E), 20: 5107(R) (ACNP-66589)
criticality tests on boiler slab core loading, 19: 38165(R) (ACNP-65531)
description, 17: 5611
design and development, 16: 24962(R) (ACNP-62005)
design and development of, review, (E), 19: 43546
design and operation of, data on, 17: 42367
design description, 16: 19997 (TID-8538)
design of clustered-pin superheater lattice experiments for use in, 17: 24672 (ACNP-63005)
design of, hydraulic and thermal analyses of, 17: 1102 (ACNP-62017)
development, 16: 33990 (TID-7634)
development, 17: 22846(R) (ACNP-62035)
development, 18: 33083 (A/CONF.28/P/215)
development, 20: 36458 (BNL-10309)
development and operation, Jan.–Mar. 1964, 18: 33094(R) (ACNP-64024)
development, Apr.–June 1963, 18: 1225(R) (ACNP-63027)
development, April through June 1961, 16: 2727(R) (ACNP-6119)
development, April to June 1962, 17: 7595(R) (ACNP-62018)
development, January through March, 1962, 16: 28518(R) (ACNP-62012)
development, July–Sept. 1963, 18: 9634(R) (ACNP-63034)
development, July through September 1961, 16: 14272(R) (ACNP-6123)
development of internal components for, 17: 35128 (ACNP-62031)
development of, Jan.-Mar. 1963, 17: 29777(R) (ACNP-63016)
development of steam separator for, 16: 30049 (ACNP-62006)
development of, technical progress, July to September 1962, 17: 17529(R) (ACNP-62034)
development of, survey, 19: 29697
development status, 16: 7295 (TID-7617)
development status, 17: 38490 (TID-7674(p.67-8))
development, Oct.–Dec. 1963, 18: 15514(R) (ACNP-64005)
dynamic and steady-state characteristic simulation on analog computer, 16: 11183 (ACNP-62001)
dynamics of, simulator studies on, 18: 21628 (ACNP-63033)
fuel element boxes, stress and deflection of boiler, 16: 23309 (ACNP-62010)
fuel element development for superheater core, 17: 21238 (TID-7658 (p.82-9))
fuel element fabrication and testing for superheater core, 17: 38473 (TID-7674(p.34-6))
fuel element fabrication for, collapse-clad, 18: 26914 (ACNP-63031)
fuel element handling and transfer systems for, (E), 19: 10528 (ACNP-64015)
fuel element processing for, 18: 31658(R) (IDO-14635)
fuel element testing for, heat transfer loop for, 17: 42324 (ACNP-63017)
fuel element thermal shock testing, superheater, 19: 27772 (ACNP-64010)
fuel element welding, process for end closure, 17: 36922 (ACNP-63023)
fuel elements, computer program for analysis of heat transfer and steam flow in, 16: 7824 (ACNP-6118)
fuel elements for, pressure drop and void fractions in simulated boiler, 17: 22781 (ACNP-63002)
fuel elements for, performance of aluminum-clad uranium dioxide, 18: 15513 (ACNP-64004)
fuel elements for, design of boiler, (E), 19: 17262 (ACNP-64016)
fuel elements for, neutronic characteristics of clustered-pin superheater, (E), 19: 38166 (ACNP-65533)
fuel rod vibration testing for, 18: 30980 (ACNP-64011)
heat transfer studies for, 17: 10812
instrumentation for superheater core, 17: 21245 (TID-7658(p.115-19))
neutron flux distribution in superheater cells of, 16: 32568 (ACNP-62020)
neutron flux mapping in borated core of, (E/T), 20: 30874 (ACNP-65612)
neutron flux peaking in, comparison of calculated and experimental values 16: 744
nozzle galling test, 16: 11182 (ACNP-6108)
nuclear design of, experimental analysis of, (E), 19: 10529 (ACNP-64601)
operation and safeguards of, regulatory actions relative to, 19: 12795
operation and testing program, 20: 26501
operation, March–Dec., 1964, 19: 45593(R) (TID-22168)
pressure vessel closure testing, 17: 2573 (ACNP-62002)
pressure vessel structural design, 16: 15888(R) (ACNP-6115)
recirculation pump development and testing, 17: 4293 (ACNP-6114(Rev.))
safeguards analyses, Part II, 16: 24961 (ACNP-5905)
shielding for, design of, 16: 32567 (ACNP-62016)
shutdown heat transfer in superheat fuel elements, 16: 9604 (ACNP-6124)
startup analysis, 18: 19344 (ACNP-64006)
startup organization and program for preoperational testing of, 17: 28521 (ACNP-6112(Rev.1))
superheater fuel element for, corrosion tests of, 19: 16010 (ACNP-62024)
superheater heat transfer and pressure drop testing, 17: 28522 (ACNP-62030)
testing of, summary of single-rod burnout heat flux experiments, 17: 11977 (ACNP-62028)
testing, program and organization for preoperational and initial startup, 16: 26582 (ACNP-6112)

630A Critical Assembly
see Maritime Nuclear Steam Generator

Sizewell Power Reactors
see Calder Hall Reactors

SKELETON
see also Bones
abnormalities in, of offspring of irradiated mice, 17: 7841
aging of, autoradiography of, 19: 21817(R) (BNL-867(p.119-50))
aging, growth, and repair of, autoradiographic studies on, 20: 18185(R) (BNL-929, pp 126-47)
analysis for cesium-137, stable strontium, and radium-226, 18: 41644(R) (HASL-149)
analysis for natural strontium in beagle, 17: 38641(R) (UCD-108(p.75-89))
analysis for plutonium-239 by whole-body gamma ray counting, 16: 21907(R) (COO-225(p.76-83))
analysis for thorium-232, thorium-228, and radium-228 in, after injection of Thorotrast, 17: 2802 (TID-17200)
beta radioactivity of, of newborn children in Erevan, USSR, 1960, 18: 27053
bone mineral content in human lumbar vertebrae, effects of age and sex on, 20: 45280(R) (COO-119-234, pp 191-210)
book: *Radiation Injuries to Bone Structure*, 18: 29379
calcium content of, effects of age on, 19: 8752
calcium content of rat, effects of parathormone injection on, 17: 38709
calcium deposition in selected bones of, 16: 21888
calcium uptake by beagle, 17: 38638(R) (UCID-108(p.45-51))
calcium-strontium discrimination in rabbit, 20: 16178
calcium-45 deposition in cow and goat, 16: 8505
calcium-45 retention in rat, effects of diet on, 20: 12594(R) (NP-15679)
calcium-45 retention in rat, effects of diet on, 20: 12595(R) (NP-15680)
calcium-45 retention in rat, effects of diet on, 20: 12598(R) (NP-15683)
calcium-45 uptake by rat, effects of stable strontium on, 17: 31831(T) (JPRS-19626)
calcium-45 uptake by miniature pig, effects of age on, 18: 19539
calcium-45 urinary excretion from, effects of chemical agents on, of intact and parathyroidectomized rats, 16: 7401
calcium-47 clearance from dog, 18: 17451
calcium-47 retention in rat, effects of diet on, 20: 12596(R) (NP-15681)
calcium-47 retention in rat, effects of diet on, 20: 12597(R) (NP-15682)
calcium-47 uptake by, in normal and rachitic rats, 17: 15591
cerium-144 content in rat, after intratracheal administration, 19: 40313
cerium-144 deposition in sheep, 16: 9907
cerium-144 mobilization in, effects of DTPA on, 17: 12109(T)
cerium-144 uptake by dog, 19: 3862
cesium-137 deposition in sheep, 16: 9907

cesium-137 uptake and distribution in rat, 19: 21835
clearance of cerium-144-labeled cerium chloride and fluoride from, 17: 1242(R) (TID-17178)
development of, effects of aminoacetonitrile on, 19: 19471(R) (ANL-6938(p.162-78))
effects of radiation sickness on joints, 16: 23524
effects of radium-226 on bone and joint changes in human, long-term, 19: 17470
effects of vitamins A and D deficiency on growth and maturation of rat, 20: 16148 (NYO-2779-9)
europium-152 uptake by rat, effects of DTPA and EDTA on, 19: 27920
fluorine-18 distribution in living, positron camera determination of, 19: 31708(R) (UCRL-11833(p.100-11))
gallium-68 distribution in rat, 19: 26161(R) (ORINS-49(p.79-97))
gold-198 distribution in synovia and tissues of, in mice, 17: 19759
growth and development of beagle, effects of continuous ingestion of strontium-90, 16: 25153(R) (UCD-106)
growth of, autoradiography of, 19: 21817(R) (BNL-867(p.119-50))
histidine uptake and distribution in cells, 16: 14401
lead-210 content following administration of radium-226, 17: 12130 (TID-17819)
lead-210 mobilization in, effects of DTPA on, 17: 12109(T)
marrow distribution in rat, tracer study, 17: 23005
metabolism of, methods of investigating overall, 20: 5237(R) (UR-668, pp 55-109)
metabolism of, tracer studies in man during health and disease, 20: 3664(R) (TID-22324)
mineral changes in, use of iodine-125 in x-ray unit for measuring, 20: 3803 (ORNL-IIC-5, pp 257-76)
mineral content in, x-ray transmission measurement of, 20: 3886 (ORNL-IIC-5, pp 290-4)
mineral content of human vertebrae, effects on crushing strength, 20: 45247(R) (COO-119-234, pp 211-26)
mineralization dynamics of, in fetal chickens, 20: 40558
phosphorus content of, effects of age on, 19: 8752
phosphorus-32 uptake by, of man, 18: 21786
phosphorus-32 urinary excretion from, effects of chemical agents in intact and parathyroidectomized rats, 16: 7401
plutonium content in dog, 16: 26719
plutonium-239 deposition in dogs, long-term study, 17: 10329
plutonium-239 content in lobster, 20: 18227
plutonium-239 inhaled in deposition, 16: 8504
plutonium-239 removal from rat, effectiveness of complexants in, 19: 6975
plutonium-239 removal from rat, effects of pentacinium inhalation on, 19: 17475
praseodymium-144 uptake by dog, 19: 3862
promethium-147 metabolism in mouse, effects of [(carboxymethylimino)-bis(ethylenenitrilo)]tetraacetic acid on, 20: 35235
protein synthesis in mouse, tracer study, 19: 2001 (BNL-8471)
radiation damage to, from bone-seeking isotopes, 18: 13511
radiation dose from deposited radium-226 in, of man, 19: 21814(R) (ANL-6839(p.18-39))
radiation dose from strontium isotopes to human, 20: 43605
radiation dose to dog, from ingested strontium-90, 19: 43726(R) (UCD-472-112, pp 120-5)
radiation dose to human, time variation of strontium-90, 20: 5429
radiation dose to dog, after chronic enteral administration of strontium-90, β, 20: 16266
radiation dose to human, from strontium-90 content in river water, 20: 30943(R) (ORNL-TM-1465)
radiation effects on fracture healing, 16: 21913 (NP-11750)
radiation effects on growth and development, chronic, low-level exposure, 17: 17751(R) (AD-283327)
radiation effects of phosphorus-32 injections *in utero* on development of, in rat fetuses, 17: 19816
radiation effects on cytochromoxidase and succinic dehydrogenase activity in rabbit, fractionated gamma and x-ray, 17: 31979
radiation effects on, from hemangioma radiotherapy, 17: 38678
radiation effects on developing limb, in chick embryos, 18: 9834 (TID-20063)
radiation effects on growth of, in rabbits, 18: 21837
radiation effects on growth of rat, acute and long-term, 19: 8809
radiation effects on development of, in prenatally exposed cattle, sheep, and swine, 19: 15096
radiation effects on ATP content in rat, 19: 17626
radiation effects on mouse, *in utero* gamma and x-ray, 19: 17646
radiation effects on acid and alkaline phosphatase and esterase activity in muscle of guinea pig, 19: 19574
radiation effects on development of fish embryo, x, 19: 31670(R) (NIRS-3(p.19-56))
radiation effects on, 19: 33802
radiation effects on dog, ingested strontium-90, 19: 43882 (UCD-472-112, pp 50-8)
radiation effects on calcium deposition in mouse, effects of age on, 19: 21975
radiation effects on development of, in mouse embryos, x, 20: 5395
radiation effects on development of axial, in salamanders, x, 20: 5312
radiation effects on development of, in mouse embryos, x, 20: 5316
radiation effects on development of, in mouse embryos, x, 20: 5326
radiation effects on development of, in mouse embryos, x, 20: 5327
radiation effects on development of, in mouse embryos, x, 20: 5337
radiation effects on development of, in mouse embryos, x, 20: 6891
radiation effects on calcium uptake by rat, tracer study of x, 20: 10587
radiation effects on developing, in rat fetuses, x, 20: 10616
radiation effects on growth of rat, β, 20: 16267
radiation effects on carbohydrate-phosphate metabolism in muscles in animal, γ, 20: 32956
radiation effects on aminotransferase activities in muscle in rat, neutron, 20: 36601
radiation effects on, from treatment of pelvic tumors, 20: 38767
radiation effects on, in mice irradiated *in utero*, 20: 40649
radiation effects on metabolism in epiphysis and metaphysis of rat, x, 20: 42785
radiation effects on, of progeny from female mice irradiated prior to mating, 20: 45399
radiation effects on, pathological, 16: 21913 (NP-11750)
radiation injuries, relation of radiation dose, 16: 31441
radiation injuries of, after hemangiomata therapy, 18: 17500
radiation injuries of vertebrae column, after radiotherapy during childhood, 20: 1702
radiation injuries of, in children treated for hemangiomas by radium, 20: 38787
radiation injury of, after radiotherapy, 19: 34021
radioinduced anomalies in chick embryos, 17: 19850
radioinduced anomalies in fetal, 19: 19533
radioinduced anomalies of, in cattle, sheep, and swine exposed *in utero*, 20: 14337
radioinduced deformities in human, following radiotherapy for skin hemangiomas, gamma and x, 20: 22636
radioinduced dominant mutation effects on mouse, frequency of, 19: 24290
radioinduced injuries of, review of, 17: 35562
radioinduced malformations in fetal mouse, 19: 21927
radioinduced scoliosis and bony changes, after radiotherapy of Wilms's tumor and neuroblastoma, 16: 32813
radioinduced scoliosis and bony changes, after radiotherapy of Wilms's tumor, 16: 32814
radioinduced variations in mouse, 19: 7091
radioinduced vertebral malformations in mouse fetus, 19: 21928
radioisotope scanning of, 19: 17754
radioisotope scanning of, using strontium-85, 19: 42396
radionuclide effects on, of beagles, 17: 19887
radiosensitivity of developing, 19: 7109
radiosensitivity of developing, in children, 19: 10883
radiosensitivity of, 19: 12970
radiotherapy effects on offspring deformities of, 18: 11784
radium distribution and retention in, 17: 10309 (TID-17644)
radium-226 and -228 burdens on human, relation of biological response and internal dose effects from, 19: 25900
radium-226 content in human fetal, 19: 20216
radium-226 distribution in swine, 18: 29299
radium-238 distribution in, after Thorotrast injections, 17: 10351
sarcomas of, in beagles fed strontium-90, 17: 38646(R) (UCD-108(p.150-9))
scandium-47 and calcium-47 metabolism in rats, 20: 40545
strontium biological half life in human, 18: 13436
strontium content of rat, effects of parathormone injection on, 17: 38709
strontium deposition, effects of diet and age, tracer study, 16: 17419
strontium deposition in selected bones of, 16: 21888
strontium movement in human, 17: 5712
strontium removal, effectiveness of chemical compounds, 17: 21428(T) (JPRS-18936)
strontium saturation in mammalian, 16: 20108
strontium-85 deposition, effects of chelates and isotopic dilution, 16: 12868
strontium-89 elimination, effect of rickets on, 16: 11415
strontium-90 levels in human, factors affecting, 16: 19204
strontium-90 sorption by, in mice, rats, and rabbits, 17: 13956
strontium-90 uptake by, in embryos in pregnant cows, 16: 26716
strontium-85 clearance from dog, 18: 17451
strontium-85 retention by female rat, effects of chelating agents on, 20: 12596(R) (NP-15681)
strontium-85 retention in rat, effects of diet on, 20: 12595(R) (NP-15680)
strontium-85 retention in rat, effects of diet on, 20: 12596(R) (NP-15681)
strontium-85 retention in rat effects of diet on, 20: 12597(R) (NP-15682)

strontium-85 retention in rat, effects of diet on, 20: 12598(R) (NP-15683)
strontium-85 retention in rat, effects of diet on, 20: 12594(R) (NP-15679)
strontium-85 uptake by human axial, 19: 9035
strontium-85 uptake and retention by rat, effects of calcium-activated barium sulfate on, 19: 17466
strontium-85 uptake by, in normal and rachitic rats, 17: 15591
strontium-89 deposition in cow and goat, 16: 8505
strontium-89 removal from, effects on dietary phosphorus and magnesium on, 19: 21845
strontium-89 uptake by mice, effects of hexametaphosphate on, 19: 2019
strontium-90 content of human, 1963, 18: 18041(R) (HASL-144)
strontium-90 content in human, calculation of, 18: 23224
strontium-90 content in human, determined by accumulation in teeth, 18: 31110
strontium-90 content of rat, effects of contaminated diet on, 19: 29881
strontium-90 content in human, in Germany, 19: 38876 (NP-14927)
strontium-90 content in rat, after chronic oral administration, effects of age, 19: 40323
strontium-90 content of dog, after chronic ingestion, effects of age, 19: 40324
strontium-90 content in dog, after chronic ingestion, 19: 40325
strontium-90 content of dog, after chronic ingestion, 19: 40327
strontium-90 content in swine, after chronic ingestion, 19: 40328
strontium-90 content of cattle, effects of age, 19: 40330
strontium-90 content in, of sheep fetus after intravenous or oral administration to mother, 19: 40331
strontium-90 content and distribution in monkey, after intravenous and oral administration, 20: 28896
strontium-90 content of, effects on content in dog hair, 20: 30972 (TID-22027)
strontium-90 deposition in developing, effects of calcium on, 18: 11609
strontium-90 deposition kinetics in, of man, 18: 20235 (NP-13868)
strontium-90 deposition in sheep, 16: 9907
strontium-90 distribution in selected bones, 16: 21888
strontium-90 metabolism in human, effects of age, 19: 21848
strontium-90 metabolism in rabbit, effects of dietary calcium and inflammation on, 19: 40343
strontium-90 metabolism in calf, after ingestion by mother or self, effects of age on, 19: 40329
strontium-90 metabolism in dog, rabbit, and rat, effects of magnesium sulfate on, 19: 42254
strontium-90 metabolism in dog, 19: 43679(R) (UCD-472-112, pp 109-19)
strontium-90 uptake by mammalian, effects of diet on, 18: 19533
strontium-90 uptake and distribution in rat, effects of calcium-rich diet on, 19: 21836
strontium-90 uptake and distribution by dog, after oral ingestion, 19: 25880
strontium-90 uptake by rat, effects of calcium and phosphorus content of diet on, 20: 10549
strontium-90 uptake by beagle, 17: 38638(R) (UCD-108(p.45-51))
strontium-90 uptake by rat, effects of stable strontium on, 17: 31831(T) (JPRS-19626)
strontium-90 uptake by miniature pig, age effects on, 18: 19539
sulfur-35 uptake and retention by chick, effects of diet and vitamin B_{12} on, 17: 21446
thorium content in rat, after inhalation, 20: 28897
thorium distribution in rat, after single inhalation of thorium chloride and citrate aerosols, 17: 23042
thorium-232 and -228 distribution in, injection of Thorotrast, 17: 10351
thorium-232 content in human, 20: 30989
tracer studies of, properties of plutonium-237 for, 20: 18221
transuranic element absorption by, 18: 11586
tumor development in, after inhalation of uranium fission products by dogs, 16: 30245
uptake and excretion of radioisotopes by, effects of sodium phosphates on, 16: 32706
uptake of cerium-144 and yttrium-91 by rat, effects of DTPA complexes in removal of, 19: 26256
uptake of chelating reagents, tracer study of, 19: 26917(R) (IA-984)
yttrium-91 uptake and elimination by guinea pig, effects of diethylenetriaminepentaacetic acid on, 19: 3864

Skidoo
see Critical Assemblies

SKIN
see also Radiodermatitis
absorption of tritium oxide through, 20: 41185 (AECL-2594)
actinium-227 uptake by melanin, 18: 3451(R) (COO-228(p.133-9))
allergic reaction to chemically induced dermatitis in guinea pigs, 18: 38854
allergy of, beryllium bronze induced, 18: 34
analysis for arsenic, activation, 20: 8827(R) (GA-6152)
analysis for estrogen in, of broilers fed 3,4-dianisyl-2-*t*-3-hexene, use of tritium for, 17: 27050
analysis for iron, design of x-ray microprobe analyzer for, 17: 12220
analysis for uranium, 17: 33512
analysis of epidermis for enzymes, 16: 12882(R) (TID-14882)
analysis of epidermis for desoxyribonucleic acid using indole reaction, 17: 24827(R) (ACRH-18(p.105-13))
analysis of rattlesnake, neutron activation, 20: 18618
analysis of tattoo marks for metals, activation, 16: 32924
anatomy and physiology of, 18: 25038 (AHSB(RP)R-39(p.1-10))
barium-133 uptake by melanin of, 18: 3851(R) (COO-228(p.133-9))
beryllium nitrate effects on guinea pigs, injected, 17: 15598
beta absorption by, protective effects of adrenaline and tannin in rats against, 17: 15553
beta absorption by toad, from strontium-90/yttrium-90, 19: 12915
beta dosimetry of, using field-type instruments, 20: 41274 (ORNL-TM-1581)
blood flow through dog, krypton-85 measurement of, 18: 25070
cadmium-109 uptake and distribution in, in mice, 18: 3457
calcium-45 distribution in rat, effects of age on, 18: 33
calcium-45 exchange between blood and, in hyperparathyroid and normal rats, 19: 6953
calcium-47 uptake by rat, 20: 40557
carcinoma induced by radioactive fall-out, 16: 6328
carcinoma of, depth and dose homogeneity in radiotherapy of, 17: 35356
cesium-137 contamination of, 19: 690 (JAERI-1059)
cesium-137 contamination of rat, subsequent transcutaneous sorption, 20: 45292
cesium-137 uptake by rat, after exposure to chloride and nitrate aerosol solutions, 19: 3858
chlorine-36 sorption by burned and normal, 20: 14255
chromium-51 absorption by guinea pig, 19: 21847
chromium-51 uptake through excised human and guinea pig, as sodium chromate, 20: 35202
chromium-51 uptake through guinea pig, as sodium chromate, 20: 35209
cobalt-58 uptake through excised human and guinea pig, as cobalt chloride, 20: 35202
contamination by carbon-14-labeled chloroacetic acid, 19: 42374
contamination by plutonium, method for treatment of, 20: 20943 (RFP-453)
contamination by radioactive materials, recommendation for physician in removal of, 19: 19494
contamination of pig, by phosphorus-32, strontium-90, and yttrium-90, 18: 4953
contamination of, by antimony-125, polonium-210, promethium-147, sulfur-35, thallium-204, effects of acidity of soiling solution on, 20: 43010
contamination with plutonium, excretion following, 17: 37044
cutaneous reactions of, to radiotherapy of female genital cancer, 20: 40679
decontamination from yttrium-91 and plutonium-239 using ultrasonic energy, 16: 3994 (HW-51938)
decontamination of cesium-137 on, 19: 690 (JAERI-1059)
decontamination of radioactivity on, 19: 22636
decontamination of, chemicals and processes for, 17: 29146
decontamination of, review of methods for, 18: 25233
decontamination of, 18: 33812
decontamination of, methods for, 19: 24807
decontamination of, film method for, 20: 25337
dermatitis due to calcium and sodium uranyl carbonate sensitization, 18: 4977
dermatitis induced on fingers of radium and strontium-90 workers, 17: 17914
dermatitis induced by luminous paint, 17: 17915
dermitis induced by allergy to uranium salts, 16: 28683
deuterium movement through dog, 18: 4991
deuterium oxide effects on potential and resistance of isolated frog, 18: 31107
disease induction by light-induced reactions of photodynamic compounds, 18: 26983 (NYO-2734-1)
diseases induced on guinea pig, protective effects of x radiation against, 17: 21502
diseases of, effects on radium therapy of uterine carcinoma, 20: 45532
dose calculations for radiotherapy of, source distances from, 20: 38750
edema induced by injected cystamine in rats, 17: 1344
effects of dose-time factors on radiotherapy of rat, 20: 40764
effects of inflammation on uptake of gold-198 colloids, 17: 5679
effects of injected plutonium, in swine, 16: 25122(R) (HW-72500 (p.50-1))
effects of injected plutonium-239 in swine, 17: 13920 (HW-SA-2626)
effects of intradermal injections of rare earth chlorides on, of guinea pigs, 18: 1360
effects of irradiation by beta particles prior to application of 7,12-

dimethylbenzanthracene on, 20: 28973
effects of layers of, on sorption of electromagnetic energy in man, 20: 45439
effects of radiation sickness on blood vessels and temperature, 16: 23518
effects of radiodermatitis on content of cobalt, copper, nickel, and zinc in human and rabbit, 20: 45309
effects of radiotherapy of breasts on, 16: 1509
effects of radium-224 on diseases of, 20: 43046
effects of solvents and stable rare earths on rabbit, toxic, 20: 25(R) (TID-22294)
effects of synthetic polyinosinic acid on vascular permeability of guinea pig, 19: 31664(R) (ACRH-23(p.110-17))
effects of trauma on enzyme activity in guinea pig, 19: 33789(R) (NYO-3445-3)
effects of ultraviolet-irradiated linolenic acid extract on mouse, 19: 38366
effects of ultraviolet radiation and thiol compounds on histidase in guinea pig, 20: 32947
effects of various histamine liberators on calcification produced by various metals in rat, 20: 36557
effects of working in uranium mines on, 17: 41167
fallout absorption through rat, 18: 29232
fallout and radiation effects on recurrence of Brocq's disease, 17: 23105
fallout relation to neurodermatitis, 18: 5163
gamma absorption by, formula for dosimetry of, 19: 28591
heparin content of rat, effects of cortisone and x radiation on, 17: 37076
herpes zoster incidence associated with irradiated neoplasms, 16: 28724
histology of, 18: 33224
homografts in mice, effects of bacterial infection on, 18: 19511
immune response to transplanted tumors in mouse, following x-radiation cure of previously transplanted tumors, 20: 40643
induction of contact dermatitis, ulcers and granulomata from beryllium contact of, 20: 42752
infection of, in irradiated rabbits, effectiveness of antibiotic therapy for, 18: 23315
infections in rabbit, effects of leukopenia on, 20: 5315
iodine-131 absorption by, effects of stable iodine on, 18: 3608
iodine-131 absorption by swine, 20: 10518(R) (BNWL-122, pp 55-8)
iodine-131 absorption by normal, burned, and wounded, 18: 11557(R) (AD-412416)
iodine-131 content in, of man and rats, 18: 23207(T) (JPRS-24704 (p.6-11))
iodine-131 uptake by, in animals and chickens, 18: 33251
iodine-131 uptake by thyroid transplants in rabbit, 19: 31722
ionization reactions with electromagnetic radiation, 17: 31871
iron-59 uptake by mouse, from bath water, 20: 28892
keratinization in epidermis, role of nucleic acid splitting enzymes, 16: 8534(R) (ACRH-16(p.141-50))
lesions on military personnel from beta exposure, factors influencing, 16: 17930
light effects on inflammation and pigmentation, 16: 18796
magnesium-28 uptake by magnesium-deficient rat, 19: 27933
manganese-52 uptake by mouse, 18: 17452
melanomas in hamster, pathology of, 19: 45906
mercury-203 uptake by rat, after repeated vapor inhalation, 19: 3860
mercury-203 uptake through excised human and guinea pig, as mercuric chloride, 20: 35202
metabolism in, of man, 19: 29848 (ACRH-103(p.62-75))
metabolism of hydroxyproline and proline in collagen of rat, isotopic dilution method for studying, 20: 36562
mitosis in mouse, effects of strain on induced, 17: 28755
morphology of ultrastructure of human, 20: 8678
particle adhesion to, mechanisms of, 20: 7316(R) (ORNL-3849, pp 215-29)
perfusion of, on dogs, method for, 17: 24826(R) (ACRH-18(p.101-4))
permeability, effects of internally deposited radioisotopes on, 16: 59
permeability to phosphorus-32 and calcium-45 in rabbits, effects of electric stimulation on, 18: 43197
permeability to radioactive contaminants, 18: 25056 (AHSB(RP)R-39 (p.79-86))
phosphorus-32 uptake by subcutaneous, 16: 25164
phosphorus-32 transport velocity from, effects of grid and sieve irradiation, 16: 1568
phosphorus-32 uptake by tumors of, 19: 5607
phosphorus-32 uptake and excretion by chicken, 19: 8765
photosensitivity of, relation to uv sensitivity, 20: 3767
photosensitivity of, effects of furocoumarins on, 20: 18466
plutonium-239 effects in swine after intradermal injection, 18: 41077(R) (HW-80500(p.120-2))
plutonium-239 sorption through rabbit, 20: 16183
preservation by freezing, 16: 30218(R) (TID-16537)
protection against ultraviolet light and x radiation, 16: 18801
protection during sieve irradiation, 16: 6352
protection from radiation by percental opening in sieve irradiation, 17: 5898
radiation burn healing, polysaccharide content in, 16: 4120
radiation dosage measurements for, from particulate contamination, radioautographic, 16: 30188 (HW-SA-2617)
radiation dose calculation for arc therapy, gamma and x-ray, 19: 10960
radiation dose calculation from external contamination, evaluation of methods for beta and gamma, 19: 44328
radiation dose from radiologic examinations for congenital heart disease, 16: 20890
radiation dose measurements using phantom, method for, 17: 35528
radiation dose received by, from contamination with beta and gamma emitters, 18: 1465
radiation dose to, via slit-shaped field, effects on rabbit brain of, 17: 38757
radiation dose to, magnetic field method for reducing therapeutic, 18: 39018
radiation dose to, in arc therapy, 19: 22062
radiation dose to, method for estimation of beta, 19: 22618
radiation dose to, during diagnostic radiography, 20: 1704
radiation dose to, during extraoral radiography, 20: 14412
radiation dose to, methods for measuring radiographically induced, 20: 18505
radiation dose to, during diagnostic radiography, x, 20: 22845
radiation doses to, in gynecological examination, 20: 40770
radiation dosimetry, 18: 25083 (AHSB(RP)R-39(p.44-68))
radiation dosimetry for, exit-surface correction factors for, 18: 11930
radiation dosimetry in, from external exposure, 18: 25082 (AHSB(RP)R-39(p.31-43))
radiation effect on rabbit, uv and x, 18: 27078
radiation effects on glucose and water level, 16: 40
radiation effects on collagen deposition, effects of *L*-triiodothyronine, 16: 1642
radiation effects on keloid formation on, 16: 1563
radiation effects, beta, 16: 2077
radiation effects, effects of phospholipids in ultraviolet, 16: 14542
radiation effects on collagen and hydroxyproline content, 16: 5206
radiation effects on synthesis of glycogen, 16: 6345
radiation effects on pH, 16: 8605
radiation effects on epidermis, biochemical and enzymatic, 16: 12882(R) (TID-14882)
radiation effects on electrolyte permeability, 16: 16301
radiation effects, delayed and indirect heavy ion and millibeam, 16: 16190
radiation effects in exposed workers, 16: 17939
radiation effects on wheal resorption time, 16: 20145
radiation effects on chemically induced eczema, 16: 20163
radiation effects on liquid diffusion in animal, during hibernation, 16: 20213
radiation effects, dependence on dose fractionation and time, 16: 20224
radiation effects on elasticity, 16: 21921
radiation effects on, 16: 23444
radiation effects on photoceptors in frogs, 16: 23444
radiation effects on mast cells in rats, ultrasoft x, 16: 25206
radiation effects on, therapeutic effects of blood serum injections on, 16: 26873
radiation effects on immune reactions, 16: 28785
radiation effects on photoceptors in frogs, 16: 30224(T) (FTD-TT-62-501 (p.17-23))
radiation effects on antigenicity and tumorogenesis, high-level-dose, 16: 30218(R) (TID-16537)
radiation effects on, effects of dose fractionation on fast electron, 16: 31503
radiation effects on frog, 16: 31419
radiation effects of small daily x-ray doses, in guinea pigs, 16: 32775
radiation effects of beta particles on biochemistry of epidermis of guinea pigs, 16: 32779
radiation effects combined with actinomycin D on, on man and mice, 17: 28741
radiation effects combined with microwaves on, of guinea pigs, 17: 21545
radiation effects from fallout on, of cattle, 17: 17805
radiation effects from treatment of carcinoma and benign conditions, cosmetic factors, 17: 1268
radiation effects of fractionated beta- and x-ray doses on, in rat tails, 17: 24999
radiation effects on, 17: 25030
radiation effects on, air cooling during therapeutic, 17: 13890
radiation effects on, appearances of radiobiotropism in, 17: 15757
radiation effects on absorption of iodine-131-labeled sodium iodide by rat, 17: 31957
radiation effects on basal cell carcinomas in, therapeutic, 17: 17801

radiation effects on collagen fraction in rat, 17: 1329
radiation effects on collagen fraction in, 17: 1330
radiation effects on, case study of beta, 17: 13904
radiation effects on conductivity of rabbit, 17: 27089
radiation effects on cell renewal system in epithelium of, 17: 35443 (BNL-6500)
radiation effects on, compared with effects of chemical carcinogens, 17: 40638
radiation effects on desoxyribonucleic acid synthesis and mitosis in mouse, tracer study, 17: 59
radiation effects on diffusion in guinea pig, effects of induced hibernation on, 17: 24908
radiation effects on fatty acid composition of lipids, 17: 5825
radiation effects on guinea pig, protective effects of cortisone against, 17: 5915
radiation effects on glycogen metabolism in, of dogs, 17: 17852
radiation effects on guinea pig, protective effects of serotonin and related compounds against, 17: 21504
radiation effects on histologic structure of hair follicles in castrated mice, 17: 1249
radiation effects on human, energy dependence of x, 17: 37109
radiation effects on immune response of rabbit, 17: 28744
radiation effects on mitosis in rat, 17: 15694
radiation effects on metastases in, in breast cancer therapy, 17: 17898
radiation effects on mouse, elongate microbeam, 17: 23154
radiation effects on mast cells and eosinophils of, in rats, 17: 30433
radiation effects on pig, fractionated and single fast neutron and x-ray, 17: 12146
radiation effects on, protection against electron-beam, 17: 14070
radiation effects on phosphorus-32 uptake by DNA and RNA in rat, 17: 15694
radiation effects on rabbit, effects of spatial fractionation on sieve, 17: 4424
radiation effects on receptor apparatus of, in man, 17: 5851
radiation effects on rat, fast neutron and x-ray relative biological effectiveness for, 17: 12145
radiation effects on, reduced oxygen enhancement effect in fast neutron and x-ray, 17: 12147
radiation effects on staphylococci injections on rabbit, 17: 21520
radiation effects on, therapeutic, 17: 17927
radiation effects on tritium content in mouse, 17: 27181
radiation effects on tyrosinase activity of, in mouse and rat, gamma, 17: 37095
radiation effects on, television-tube gamma, 17: 39326
radiation effects, protective effects of serotonin, 17: 2879
radiation effects on mouse, proton, 18: 1372 (BNL-7359)
radiation effects on thermal conductivity of, uv and x, 18: 3561
radiation effects on long-term aging of, on mice, 18: 3574
radiation effects on, from cesium-137 therapy, 18: 3637
radiation effects on, from therapy of malignant tumors of mammary glands, ovaries, and uterus, 18: 3644
radiation effects on guinea pig melanocytes in, x, 18: 5053
radiation effects on human, ultraviolet, 18: 5110
radiation effects on permeability of rabbit, gamma, 18: 5129(T)
radiation effects on regeneration of burns of epithelium of, in rats, 18: 8121(T) (JPRS-22556(p.1-13))
radiation effects on abdominal, in rats, 18: 8122(T) (JPRS-22556 (p.14-26))
radiation effects on disulfide and sulfhydryl groups in rat, single-exposure uv, 18: 8166
radiation effects on dermis, epidermis, scales, and serum proteins of human, uv, 18: 8168
radiation effects on, after pretreatment with carcinogen and tumor enhancer, 18: 8186
radiation effects on, ultraviolet, 18: 8195(R) (AD-402191)
radiation effects on metabolism in rat, 18: 11741
radiation effects on cells, 18: 11825
radiation effects on mouse, protective effects of cysteamine against x, 18: 11861
radiation effects on neurons in dog, polonium-210 and strontium-90, 18: 13463(T) (JPRS-23559(Del.)(p.36-42))
radiation effects on erythema on rat tails, fractionated fast electron, 18: 13552
radiation effects on sensitivity of, in guinea pigs, 18: 15825
radiation effects on mouse, of heavy charged particles, 18: 15827
radiation effects on temperature of dog and monkey, dose relation to, 18: 17544
radiation effects on permeability of cattle and rat, x, 18: 17646
radiation effects on homografts of dog, from bismuth-206 and silver-111, 18: 19605
radiation effects on mitosis in malignant and nonmalignant hyperplasia of mouse, 18: 19704
radiation effects on, in accidental exposure, 18: 19706
radiation effects on, in telegammatherapy using cesium-137, 18: 19716
radiation effects on rat, protective effects of cystamine and cysteamine against, x, 18: 19784
radiation effects on, comparison of gamma and x, 18: 21945
radiation effects on homograft survival in rat, beta, 18: 25112
radiation effects on homograft survival in rat, x, 18: 25114
radiation effects on rabbit, fluid flow method for detection of, 18: 25134
radiation effects on, 18: 25146
radiation effects on rabbit, beta and x, 18: 29470
radiation effects on oxygen uptake by human, uv and x, 18: 29269
radiation effects on polarization resistance of, x, 18: 29282
radiation effects on tanning of mouse, ultraviolet, 18: 31174
radiation effects on homografts of, in thymectomized mice, 18: 31234
radiation effects on content of trace elements in, 18: 33285(T) (JPRS-25502)
radiation effects on mouse immunity to carcinomas of, x, 18: 35357
radiation effects on ascorbic acid and glutathione content in guinea pig, beta, 18: 38871
radiation effects on, pathophysiological, 18: 38983
radiation effects on stainability of cells in rat, x, 18: 41135
radiation effects on, treatment of, 18: 41245
radiation effects on enzymatic and biochemical reactions in guinea pig epidermis, 18: 43223(R) (NYO-1727-1)
radiation effects on nucleic acid and protein synthesis in epidermis of guinea pigs, uv, 19: 123
radiation effects on acid and alkaline phosphatase activity in guinea pig, 19: 130
radiation effects on human, fallout, 19: 177
radiation effects on plasma volume and vascular permeability in rabbit, x, 19: 2142
radiation effects on guinea pig, 19: 2114
radiation effects on, epilation-dose, 19: 2124
radiation effects on, treatment of, 19: 3989
radiation effects of hemangioma therapy on, 19: 4029
radiation effects on DNAase in guinea pig, beta, 19: 5700
radiation effects on rat, ultraviolet, 19: 7190
radiation effects on enzyme activity in guinea pig, 19: 8882
radiation effects on guinea pig, chronic, 19: 8891
radiation effects on human, following breast radiotherapy, beta and x, 19: 8901
radiation effects on human, ultracellular, beta and x, 19: 8902
radiation effects on blood flow in human, telangiectasis development as repair sign in, 19: 10827
radiation effects on glycogen and mucopolysaccharides in guinea pig, x, 19: 10835
radiation effects on rat, protective effects of 8-methoxypsoralen against beta and x, 19: 15225
radiation effects on, role of enzymes in depletion and restoration of, 19: 21941
radiation effects on pig, fractionated, 19: 21888
radiation effects on sulfhydryl content in rat, ultraviolet, 19: 21929
radiation effects on mouse, ultraviolet, 19: 21930
radiation effects on acanthosis in guinea pig, quality effects on, 19: 24285
radiation effects on ulceration of healing rat, 19: 26007
radiation effects on collagen/hexosamine ratio in, use as aging index in Hiroshima bomb survivors, 19: 25926
radiation effects on viability of grafts of, 19: 28105
radiation effects with Scarlet Red on planocellular metaphasia of sebaceous glands in rabbit, 19: 28085
radiation effects on metabolism in frog, 19: 29901(R) (RLO-1754-1)
radiation effects on phosphorus-32 metabolism in frog and rat, uv, 19: 31883
radiation effects on human, Nyasaland background, 19: 31823
radiation effects on enzyme activity in guinea pig, 19: 33789(R) (NYO-3445-3)
radiation effects on cobalt, copper, nickel, and zinc contents in rabbit, 19: 33910
radiation effects on absorptive properties of frog, 19: 33791
radiation effects on wheal resorption time in, mechanism for uv and x, 19: 33812
radiation effects on, of guinea pigs, 19: 35990
radiation effects on blood flow in human, uv, 19: 36032
radiation effects on patch tests on guinea pig and human, uv, 19: 36033
radiation effects on monkey, beta, 19: 42258 (LA-3365)
radiation effects in, ultraviolet, 19: 43764
radiation effects on mouse and rabbit, recovery processes in, 19: 45987
radiation effects on mouse, effects of dose-fractionation on electron, 19: 45885
radiation effects on granular and transitional cell layers in human, 19: 45913
radiation effects in, toxic effects of ultraviolet, 20: 74
radiation effects on sulfhydryl content of rat, uv, 20: 93

radiation effects on free radical properties of melanin in, uv, 20: 1684
radiation effects on, cosmic, 20: 3731
radiation effects on herpes zoster inflammations in, x, 20: 3836
radiation effects on, gamma and x, 20: 3847
radiation effects on ratio of soluble to insoluble collagen in hamster, x, 20: 5330
radiation effects on melanin content in human, uv, 20: 6840
radiation effects on metabolism in human, uv, 20: 8678
radiation effects on tadpole tail, effects of starvation during irradiation on x, 20: 10676
radiation effects on guinea pig and rabbit, mechanism for x, 20: 12623
radiation effects on transplanted Yoshida sarcoma cells in rat, tracer study, 20: 16188
radiation effects on pigments in human and guinea pig, uv, 20: 16261
radiation effects on rat, continuous and pulsed electron, 20: 16269
radiation effects on rabbit, sieve-controlled x, 20: 18357
radiation effects on swine, ionizing, 20: 18185(R) (BNL-929, pp 126-47)
radiation effects on, following radium therapy of cervical cancer combined with telecobalt or x rays, 20: 18309
radiation effects on nitrogen content in mouse, effects of bone marrow transplants on x, 20: 20407 (ORNL-P-1118)
radiation effects on melanin patterns in human, solar, 20: 20458
radiation effects on mouse, x, 20: 20475
radiation effects on, of urethan-treated mice, x, 20: 20476
radiation effects on vascular permeability of guinea pig, β, 20: 22729
radiation effects on pigmentation of, uv, 20: 22721
radiation effects on cholesterol and glucose contents of rat, uv, 20: 26689
radiation effects on cellular permeability in onion, x, 20: 28900
radiation effects on mast cells in mouse, uv, 20: 28937
radiation effects on wound healing in rat, effects of hormones on γ, 20: 31061
radiation effects on, variations with anatomic location and time of uv, 20: 32971
radiation effects on pigment mosaics in human, cellular survival curve test for, 20: 32981
radiation effects on tadpole, in aqueous carbon-14-labeled acrylamide solutions, 20: 32986
radiation effects on animal, pathology of, 20: 33063
radiation effects on epilation of mouse, protective effects of blood serum against, 20: 33081
radiation effects on properties of tanned animal, gamma, 20: 35820
radiation effects on human, after therapy of hemangioma, 20: 35381
radiation effects on skin pigments as used in study of melanin affinity for chloroquine, uv, 20: 36564
radiation effects on collagen in kangaroo and mouse, uv, 20: 36595
radiation effects on DNase in guinea pig, 20: 38591(R) (NYO-3445-7)
radiation effects on mouse, biological, 20: 38627
radiation effects on microflora of, 20: 38644
radiation effects on human, solar, review of, 20: 40696
radiation effects on carcinogenesis induced by dimethylbenzanthracene in mouse, beta and x, 20: 42969
radiation effects on guinea pig, protective effects of cysteamine against, 20: 42990
radiation effects on mouse, comparison of electron, neutron, and x, 20: 45426
radiation effects on capillaries in, of hands, 20: 45435
radiation effects on precipitation of collagen in, uv, 17: 30325
radiation effects on, boron-10 (n,α), 18: 8099 (BNL-7541)
radiation effects on, 18: 25081 (AHSB(RP)R-39(p.21-9))
radiation effects on mammalian, heavy-particles cosmic, 17: 10363(R) (TID-17676)
radiation effects on phospholipids in mouse, uv, 17: 37074
radiation effects on melanin synthesis in mouse, uv, 18: 5017
radiation effects on severity of contact dermatitis, 17: 2843
radiation effects on tubercular lupus, 17: 10441
radiation effects on light dermatosis, 19: 12990
radiation field size factor determinations, 16: 4085
radiation hazards to, during radiodiagnosis of lung diseases, 19: 46110
radiation hazards to human and mouse, uv, 20: 32970
radiation injuries, protective effects of hyaluronidase against, 16: 8596
radiation injuries to, from therapy of neoplasms in early childhood, 17: 4400
radiation injuries of, treatment, 17: 27104
radiation injuries to, treatment of, 17: 30395
radiation injuries of, in mice, effects of continued hair plucking on, 17: 40653
radiation injuries of, protective effects of carotene–chlorophyll paste against, 18: 6686
radiation injuries to, histocytological study and therapy of, 18: 17543
radiation injuries of rabbit, protective effects of esculin against, 18: 23372
radiation injuries from particulate nuclear rocket reactor fuel, 18: 31789 (NUS-167)
radiation injuries of, relation of, to carcinoma, 18: 31238
radiation injuries of mouse, protective effects of 2,3-dimercaptosuccinic acid against, 18: 31271
radiation injuries of, in rats, 18: 33340
radiation injuries and regeneration of, of rats, 18: 38970
radiation injuries to, of hands in medical profession, 19: 224
radiation injuries of thoracic, after radiotherapy of breast cancer, 19: 4027
radiation injuries on rabbit, survival of autotransplants on burn wounds over, 19: 8926
radiation injuries of capillaries of, rapid identification of, 19: 24286
radiation injuries to, on hands of medical personnel and physicians, 19: 24321
radiation injuries of rat, pathology of, 19: 45957
radiation injuries of, thermal, 19: 45818 (TDCK-33500)
radiation injuries of, protective effects of chloroquine against, in guinea pigs, 19: 46019
radiation injuries of, protection effects of triprolidine for ultraviolet, 20: 132
radiation injuries of swine, pathology, 20: 1609 (BNL-9477)
radiation injuries of, protective effects of sulfur and glutathione against γ, 20: 10702
radiation injuries of guinea pig, pathology of β, 20: 38591(R) (NYO-3445-7)
radiation injury, 18: 25214 (AHSB(RP)R-39(p.87-93))
radiation injury of human, therapeutic effects of peloidin on, 19: 2173
radiation of human, herpes zoster induction by, x, 18: 17685
radiation penetration and sorption by, 17: 24998
radiation protection of, in radiotherapy using barium, bismuth, lead and zinc pastes, 18: 19832
radiation reaction, detection with dye reagents, 16: 1569
radiation reaction, effects of materials affecting dynamics of reactive inflammation, 16: 8625
radiation reactions on, in electron bean therapy, 19: 26193
radiation sorption by psoriatic parakeratotic stratum corneum, 17: 5689
radiation tolerance in human, methods for increasing, 18: 29468
radiation tolerance limits of, convergent pendulum, 19: 140
radiation use on, legal aspects, 18: 31327
radiation used with cortisone on, effects on homografts in rabbits of, x, 18: 19613(T)
radio-epidermolysis repair, 16: 11485
radioactive contamination of rabbit, by phosphorus-32, strontium-90, and yttrium-90, 18: 12392
radioactive contamination of, maximum permissible levels for, 19: 24796
radioactive contamination of, action levels in medical treatment of, 19: 46008
radioactive contamination of, tolerance standards for, 19: 44311
radioactive contamination of pig, using solutions of radioisotopes, 20: 40
radioactive contamination of, 20: 39151
radioactive decontamination, 18: 25213 (AHSB(RP)R-39(p.69-77))
radiodermatitis and necrosis, review on, 17: 17936
radiodermatitis in rabbit, effects on zinc content of, 18: 38908
radiodiagnosis of, 19: 31949
radioinduced burns on rabbit, effects of auto- and homografts on, 17: 17865
radioinduced burns of, from x-ray therapy, 17: 35489
radioinduced burns of, treatment of x, 18: 35340
radioinduced cancer on human, prevention and treatment of, 19: 17631
radioinduced cancers of, after radiotherapy of benign tumors, 19: 32027
radioinduced cancer of, 19: 45945
radioinduced cancer in man, x, 17: 33674
radioinduced carcinoma after therapeutic exposure in infancy, 16: 16236
radioinduced carcinoma on, after therapy for hemangioma, 17: 27130
radioinduced carcinoma of, histopathology of x, 17: 35513
radioinduced carcinomas in, treatment of uv and x, 18: 38980
radioinduced carcinoma of, after radium therapy, 20: 38788
radioinduced changes after radiotherapy of Wilms's tumor, 16: 32814
radioinduced changes in urocanic acid in epidermis using ultraviolet light, 17: 28767
radioinduced chromosomal aberrations in cultures of human, x, 18: 19563
radioinduced chromosomal aberrations in human, 18: 31141
radioinduced complications in, following facial radiotherapy, alpha, beta, and gamma, 20: 22652
radioinduced dermatitis of, effects on collagen content of skin, 19: 28208
radioinduced dermatitis on rabbit ears, reactions of boron-10 and thermal neutron, 17: 10475
radioinduced development of melanotic tumors on, x, 17: 28722
radioinduced enzymatic changes, 16: 5208
radioinduced epilation in guinea pigs, 17: 1281
radioinduced epilation in guinea pigs, 17: 1282
radioinduced epilation of mouse, protective effects of macromolecules against x, 17: 35472

radioinduced epilation of mouse, protective effects of heparinized mouse serum against x, 20: 24915
radioinduced epilation, x, 18: 38844
radioinduced erythema, effects of dose fractionation, 17: 15661
radioinduced erythema of, from ultraviolet flashes, 18: 29369
radioinduced erythema and pigmentation of, reaction mechanisms for ultraviolet, 19: 35969
radioinduced erythema of mouse, effects of histamine and histidine on uv, 20: 6798
radioinduced erythema in human, differences in 250- and 300-nm uv, 20: 22722
radioinduced erythema of, sensitizing effects of topical drugs on uv, 20: 22781
radioinduced erythema and pigmentation of, effects of intermittent exposure on uv, 17: 35572
radioinduced erythema and pigmentation of, effects of intermittent exposure on uv, 17: 35570
radioinduced erythema, protective effects of Delial against, 17: 30393
radioinduced, follow-up studies of occupational radium and x-ray, 17: 17916
radioinduced hemolysis of erythrocytes in patient with protoporphyrinemia, 19: 28033
radioinduced hyperpigmentation in skin induced by, 17: 1280
radioinduced inflammation of, 18: 11770
radioinduced inflammation of, gamma or x, 19: 32023
radioinduced *Lupus erythematosus* in human, uv, 20: 14309
radioinduced melanization in goldfish, effects of adrenocorticotropic hormone, 17: 12167
radioinduced necrosis in, 17: 37135
radioinduced necrosis, treatment of, 18: 29385
radioinduced pigmentation of, synergistic effects of dimethylchlortetracycline on, 19: 12971
radioinduced sarcomas on human, from therapy of lupus vulgaris, 19: 15066
radioinduced sarcomas on guinea pig, 19: 15066
radioinduced, surgical treatment of x, 17: 35378
radioinduced tumors, mechanisms of formation, 16: 11464(R) (TID-15118)
radioinduced tumors, 16: 5201(T)
radioinduced tumors, 16: 28770
radioinduced tumors of, histology of, 17: 15806
radioinduced tumor of, 20 years after exposure, 17: 40589
radioinduced tumors of, in rats, 18: 11652(R) (TID-20122)
radioinduced tumors of, ultraviolet, 18: 27127
radioinduced ulcers, pathogenesis of, 16: 11478
radioinduced ulcers, pathogenesis of, 16: 20132(T) (JPRS-13644)
radioinduced ulcers on, surgical treatment of, 17: 17663
radioinduced ulcers on, in x-ray therapy of skin carcinomas, 18: 19714
radioinduced ulcers on, treatment of, 19: 195
radioinduced variation in interstitial mucopolysaccharides, effects of hibernation on, 16: 11484
radioinduced wounds on, blood vessel regeneration during healing of, 18: 11752
radioiodine decontamination of, use of lugol solution for, 19: 13096
radioisotope sorption by rat, 20: 14253
radioisotope sorption by guinea pig, disappearance measurement for, 20: 32910
radionecrosis in rat, recovery from x, 20: 22638
radiosensitivity, 17: 5813
radiosensitivity, 19: 8905
radiosensitivity, age factor in, 16: 7431
radiosensitivity, effects of actinomycin D on, 16: 8496
radiosensitivity, effects of actinomycin D on, 16: 8497
radiosensitivity effects of aloe juice, 16: 11493
radiosensitivity, effects of lowering temperature from 50 to 55°F, 16: 8613
radiosensitivity, effect of consecutive irradiations at different sites, 16: 18773
radiosensitivity, effects of oxygen tension, 16: 23466
radiosensitivity, effects of cooling during radiotherapy, 16: 28822
radiosensitivity, effects of lowering temperature of irradiation field on skin sparing, 17: 1341
radiosensitivity, effects of dose fractionation, 17: 15662
radiosensitivity of enzyme activity, 16: 12918
radiosensitivity of blood vessels, connective tissues, epidermis, hair bulbs, and sebaceous glands, 16: 8598
radiosensitivity of, effects of previous exposure on, in rats, 18: 9915
radiosensitivity of mouse, 18: 25081 (AHSB(RP)R-39(p.21-9))
radiosensitivity of mouse, effects of anoxia on, 18: 33408
radiosensitivity of, of rabbit ears, 18: 36956(R) (UCRL-11387(p.127-39))
radiosensitivity of, in rats, 18: 38971
radiosensitivity of, of ruminants, 18: 38993 (HW-SA-3693)
radiosensitivity of, 19: 15243
radiosensitivity of, 19: 17714
radiosensitivity of human, 19: 19605
radiosensitivity of rat, to ultraviolet radiation, effects of methoxypsoralen on, 19: 21929
radiosensitivity of, 19: 30039
radiosensitivity of, 19: 29968
radiosensitivity of rabbit, 19: 31816
radiosensitivity of rat head, 19: 36097
radiosensitivity of, effects of anabolic steroid ointment on, 19: 38468
radiosensitivity of rabbit, effects of 5-fluorouracil on, 19: 40394
radiosensitivity of human, 19: 43819
radiosensitivity of human, 19: 46085
radiosensitivity of, of nipple and flank of guinea pigs, 19: 45869
radiosensitivity of human, ultraviolet, 19: 45907
radiosensitivity of, thermal, 20: 614
radiosensitivity of, effects of drugs on uv, 20: 73
radiosensitivity of, effects of oxygen pressure on, β, 20: 3727
radiosensitivity of human, 20: 6846
radiosensitivity of, effects of dose fractionation on γ and x, 20: 6827
radiosensitivity of, effects of content of sulfhydryl radicals on γ, 20: 10702
radiosensitivity of, γ, 20: 16323
radiosensitivity of, effects of temperature on, 20: 18454
radiosensitivity of, neutron and x, 20: 18548
radiosensitivity of rat, β and x, 20: 22745
radiosensitivity of guinea pig, effects of chemical radioprotective compounds on x, 20: 22793
radiosensitivity of, in air and in hyperbaric oxygen, 20: 40721
radiosensitivity of mouse, effects of cysteine and cysteamine on, 20: 42998(R) (EUR-2992.f)
radiosensitivity to thermal neutrons and heavy particles from $B^{10}(n,\gamma)Li^7$ reaction, 16: 26841 (BNL-5197)
radiosensitivity, effect of dose fractionation on, 18: 25192
radiotherapy combined with steroid treatment of allergic dermatitis of, 17: 1244
radiotherapy, dosage determination of phosphorus-32 contact, 16: 4099
radiotherapy effects on growth in man, 16: 5140
radiotherapy effects of electrons at 10 to 40 Mev, 16: 5144
radiotherapy effects on, effects of acupuncture and Chinese drugs on, 16: 28677(T) (JPRS-14829(p.574-83))
radiotherapy effects on, 17: 37124
radiotherapy for, effects on hair, 17: 38791
radiotherapy of, 19: 30039
radiotherapy of acne vulgaris of, x, 18: 25235
radiotherapy of carcinomas of, using contact irradiation and oxygen infiltration, 18: 41284
radiotherapy of cancers of, 19: 28164
radiotherapy of cancer of, effectiveness of cobalt-60 medium depth apparatus for, 19: 36157
radiotherapy of carcinomas of, 20: 1718
radiotherapy of carcinomas of, 20: 6928
radiotherapy of, concept of precalculated dose distributions in, 16: 26693
radiotherapy of cutaneous epitheliomas, 16: 20092
radiotherapy of diseases in human, gonadal dose from x, 20: 5445
radiotherapy of diseases of, beta, 20: 29072
radiotherapy of, dose measurement in, 17: 38649
radiotherapy of, effectiveness of, 17: 16347
radiotherapy of, evaluation of, 17: 35364
radiotherapy of, gonadal dose from, 17: 38657
radiotherapy of hemangiomas, design of soft x-ray tube for, 17: 26991
radiotherapy of hemangiomas of, in infants, 20: 1719
radiotherapy of hemangiomas of, effects on skeleton of children of gamma and x, 20: 22636
radiotherapy of hemangiomas, contra-indications, 19: 38511
radiotherapy of human, effects on offspring of chromosomal aberrations following, 20: 5351
radiotherapy of lichen planus, 19: 28145
radiotherapy of lupus erythematosus, ultraviolet, 19: 28179
radiotherapy of, production of skin cancer by, 17: 16347
radiotherapy of rabbit, biological effects and dosimetry of electron contamination of gamma beam in cesium-137, 19: 7234
radiotherapy of, time-dose-area model for cancer, 18: 1476
radiotherapy of tumors of, dosage determination for, 17: 27009
radiotherapy of tumors of, glycogen behavior after x, 18: 36977
radiotherapy of tumors of, dose absorption calculation for soft x-ray, 19: 17736
radiotherapy of tumors of, leukemogenic effects of gamma, 19: 29950
radiotherapy of tumors of, 19: 31948
radiotherapy of tumors of, 20: 6975
radiotherapy of tumors of, β, 20: 16325
radiotherapy of tumors of, β, 20: 18528
radiotherapy of tumors of facial, absorbed dose in brain from x, 20: 38765
radiotherapy of, using strontium-90, 17: 30315
radiotherapy of, beta *vs.* x, 18: 29469

radiotherapy of, beta sources for, 19: 34004
radiotherapy of, carcinogenic effects of, 18: 29388
radiotherapy of, cancer induction by, 18: 31202
radiotherapy of, dose charts for, 19: 7240
radiotherapy of, dosimetry for, 19: 36202
radiotherapy of, evaluation of, 19: 17714
radiotherapy of, effects on aminopeptidase activity in urine, 19: 30017
radiotherapy of, histological changes from, 18: 29470
radiotherapy of, inflammation resulting from, 19: 15267
radiotherapy of, leukemia and tumor induction by, 18: 29408
radiotherapy of, late pathological effects, 19: 31988
radiotherapy of, response of mycosis fungoides to, combined colchicine therapy, 20: 40763
radiotherapy of, using combined orthovoltage x radiation and cobalt-60, dose curves for, 20: 38792
radiotherapy of, use of krypton-85 beta sources for, 19: 10969
radiotherapy of, using beta applicator, 19: 36158
radiotherapy of, x, 17: 2842
radiotherapy using electrons, reaction at energies up to 32 Mev, 16: 14397
radiotherapy using electron beams, 17: 31824
radiotherapy using radium-224, hazards from, 17: 27608
radiotherapy using strontium-90 and yttrium-90, 19: 34005
radiotherapy with ultraviolet or x radiation, reticulocyte increases in peripheral blood in, 18: 19712
radiotherapy with phosphorus-32, 19: 15322
radiovaccination by combined treatment of x radiation with injection of dinitrophenol, methylene blue, and aminothiazole, 16: 18737
radiovaccination effects in, characteristics of, 17: 28724
radiovaccination from repeated exposures on same area, 17: 12151
radium-224 and -226 uptake by melanin of, 18: 3851(R) (COO-228 (p.133-9))
radon-222 diffusion through rat, as affected by temperature and uv-irradiation, 20: 42790
reactions during acute radiation syndrome, 19: 31828
reactions on, from radiotherapy of cancer of bladder, 17: 21552
regeneration of burns, effects of radiation sickness, 16: 32745(T) (JPRS-15018(p.98-106))
removal of thallium-204 from, effectiveness of solutions for, 16: 20895
simulant for determining thermal effects, 16: 12810 (WT-772)
sodium-22 sorption by burned and normal, 20: 14255
sorption of cadmium chloride, cobalt chloride, silver nitrate, and zinc chloride by guinea pig, tracer study, 19: 12927
sorption of labeled tributyl phosphate by rabbit, design of interchangeable collimator for measurement of, 17: 21404
sorption of strontium-85 and strontium-89 by, protective effects of fatty acid gels, 19: 21997
sorption routes in, percutaneous, 18: 33224
sorptive properties for sodium-24, effects of calcium chloride and salt bath concentration on, 16: 4027
sorptive state of fat in, monitoring of expired radioactive carbon dioxide for determination of, 17: 21434
spectrum of deep layers, infrared and ultraviolet absorption, 16: 18746
spreading effect in irradiation, India ink study, 16: 14578
strontium-85 absorption by normal, burned, and wounded, 18: 11557(R) (AD-412416)
strontium-85 uptake by melanin of, 18: 3851(R) (COO-228(p.133-9))
strontium-90 sorption by animal, effects of cleansing agents on, 20: 35674
strontium-90 uptake by rabbit, effects of detergent treatment on, 20: 29461
sulfur content in human, estimation of, 20: 30982
sunlight effects on thickness of negroid and white, 18: 8167
temperature at various distances from thermonuclear explosions, 17: 13962 (ASD-TR-61-510)
therapy of hemangiomas using frozen carbon dioxide or surgery, 19: 38511
thermal injuries, 16: 1297 (AD-256030)
thermal radiation protection, by fabrics, 16: 11980 (WT-770)
thermal transitions in collagen, effects of deuterium, 16: 26674
thorium-228 uptake by melanin of, 18: 3851(R) (COO-228(p.133-9))
treatment of reactions on, after radiotherapy, 19: 202
tritiated water sorption by burned and normal, 20: 14255
tritium contamination of, by contact with metal, 18: 37447 (USNRDL-TR-761)
tritium uptake by, from contaminated surfaces, 20: 45271(R) (AERE-PR-HPM-9, pp 26-31)
tumor incidence in mice receiving 9,10-dimethyl-1,2-benzanthracene and gamma or x irradiation, 16: 17492
tumors, radiosensitivity in rats, 17: 1274
ulcers of, in patients undergoing radiotherapy, 17: 35477
ulcers of, healing effects of menthyl pantothenate ointment on, 19: 198
ultrasonic decontamination of rat, contaminated with radioisotopes, 20: 42811
uptake of dissolved substances by, quantitative measurement of, 19: 14966
use of guinea pig, as test system for radioprotective compounds, 20: 18485
use of myographic signals for control functions, study of feasibility of, 19: 46459 (CONF-640508, pp 100-57)
wounds of, mechanism of repair, 17: 28601
yttrium-90 uptake by melanin of, 18: 3851(R) (COO-228(p.133-9))

SKIN GRAFTING
see also Tissue Transplants
clearance determination in, tracer studies of, 18: 27277
effect of graft-host reaction to, on wound healing in mice, 18: 8119 (USNRDL-TR-683)
effects of cell-free spleen extracts on immune reactions of man to, 20: 45483
effects of exposure of grafts to ultraviolet radiation on viability, 18: 25113
effects of extracorporeal irradiation on, 19: 29962
effects of extracorporeal γ irradiation of blood and lymph on rejection of, in calves, 20: 20485
effects of extracorporeal irradiation of blood or lymph on graft take, 20: 40744 (BNL-10403)
effects of local irradiation on take of autologous transplants, 16: 17454
effects of surgery on graft survival, 19: 13156
effects of thymectomy on graft survival and immune response to, in dogs, 19: 3976
effects of thymus gland on take of homografts in irradiated mice, 18: 113
effects of urethane and sublethal x irradiation on take of, in mice, 16: 11487
effects of 6-purinethiol on rat, 20: 10506
effects on mitotic response of thymus-derived cells in irradiated mice, 20: 35339
for scald burns on rabbits during radiation sickness, 17: 106
genetic factors affecting take in mice, 17: 15585
homograft response to, in irradiated adult mice, effects of thymus on, 17: 40662 (USNRDL-TR-661)
homograft survival in lethally irradiated mice, 16: 11492
homograft tolerance in long-lived radiation chimeras, effects of lymphoid cell injections on, 16: 2901
immune reactions and radiation effects on graft survival, 16: 14403
immune reactions, effects of irradiation, 16: 17549
immune reactions, effects of irradiation and injection of donor-type spleen cells in mice, 17: 96
immune reactions inducing tolerance, in mice, 17: 28775
immune reactions in mouse radiation chimeras to, 19: 17504
immune reactions in mouse radiation chimeras to, 19: 17505
immune reactions induced by, in mice, 19: 33807
immune reactions of mice to, 19: 29883 (ACRH-103(p.1-27))
immune reactions to, in allogenic mouse radiation chimeras, 18: 17411 (USNRDL-TR-709)
immune reactions to, in mice, 18: 29177
immune reactions to, after temporary chimerism in irradiated rats, 18: 33387
immune reactions to, in mouse radiation chimeras, 20: 6883
immune reactions to, in mice, 20: 10632
immune response of mouse radiation chimeras, effects of gamma-globulin type on, 19: 21943
immunological reactions in mice, 17: 15758
in allogenetic radiation chimeras, 17: 25036
methods for, in radiodermatitis of fingers, 19: 31909
protein distribution after, tracer studies of, in mice, 18: 29177
radiation effects on take in rabbits, 16: 20276
radiation effects on take in mice, 16: 20267
radiation effects on survival of homologous, in rats, 16: 32820
radiation effects in rabbits, role of antibodies in, 17: 10425
radiation effects on tolerance to, in mice, 17: 15760
radiation effects on take in mice, effects of antisera, 17: 19810 (USNRDL-TR-625)
radiation effects on response to allogenic and xenogenic, in mice, 17: 21468 (USNRDL-TR-628)
radiation effects on tolerance to, in mice with and without urethan, 17: 24993
radiation effects on immune response, in mice, 17: 24899 (USNRDL-TR-636)
radiation effects on mouse chimeras tested by, 17: 33675
radiation effects on response to, in mice, 17: 33749
radiation effects on immune reactions to, in mice, 18: 115
radiation effects on survival of auto- and homo-, on rabbit ears, 18: 5028
radiation effects on mouse, effects of prior newborn liver injection on x, 18: 31237
radiation effects on acceptance of grafts, in rabbits, effects of post-irradiation time on, 18: 33386
radiation effects on graft acceptance in mice, effects of injected spleen

and lymph node cells on, 18: 33388
radiation effects on mouse tolerance to, x, 18: 43293
radiation effects on, in twin cattle, 19: 3836(R) (ORO-625(p.70-85))
radiation effects on graft survival and immune response to, in dogs, 19: 3976
radiation effects on graft survival in mice, effects of 6-mercaptopurine and 5-bromodeoxyuridine on, 19: 8909
radiation effects on take in dogs of, 19: 8781(R) (AD-422394)
radiation effects on graft take in mice, 19: 8838
radiation effects on graft survival, 19: 13156
radiation effects on survival of rabbit, protective effects of lysozyme against, 19: 17671
radiation effects on reactions of burn wounds to, in rabbits, 19: 21905
radiation effects on take of allogenic grafts in mice, 19: 26027
radiation effects on immune reactions to, in mice, 19: 28093
radiation effects on take of autografts, 19: 28105
radiation effects on immunological tolerance to, in parabiotic mice, x, 19: 28006
radiation effects on immune reactions of mice to, 19: 28032
radiation effects on immune reactions to, in rabbits and rats, 19: 29942
radiation effects on survival of grafts for, in rabbits, 19: 29944
radiation effects on, between cattle twins, 19: 29980
radiation effects combined with splenectomy and thymectomy on, in mice, 19: 29982
radiation effects combined with spleen cells and thymus grafts on, in mice, 19: 29983
radiation effects combined with bone marrow and thymectomy on, in mice, 19: 29984
radiation effects on immunological tolerance to, after cell transfer in mice, 19: 29985
radiation effects on immune reactions to, gamma, 19: 31834
radiation effects on immune reactions to homografts, 19: 36037
radiation effects with spleen cell transplants on tolerance to, in adult and newborn mice, 19: 38376
radiation effects on immune reactions to, in thymectomized mice, 20: 5408 (USNRDL-TR-920)
radiation effects on graft take in rats, x, 20: 5335
radiation effects on survival of rabbit, effects of 6-purinethiol on, x, 20: 8719
radiation effects combined with 6-purinethiol on rat, x, 20: 10506
radiation effects on response of mice to allogenic, effects of isogenic grafts on, 20: 12656
radiation effects on rabbit, 20: 20477
radiation effects on immune reactions to, in mice, 20: 22741
radiation effects on survival in mice, x, 20: 24930
radiation effects on response of thymectomized chickens to, 20: 29014
radiation effects on immune reactions to, in allogeneic mouse chimeras, 20: 45473
radio-epidermolysis repairs through early, 16: 11485
radioinduced tolerance in rat fetuses to maternal, 18: 41121
radiosensitivity of response to allogenic and xenogenic, in rats, 17: 15646 (USNRDL-TR-619)
radiosensitivity of response to allogenic, in mice sensitized with Freund's adjuvant and spleen cells, 19: 8928
radiosensitivity of immunologically competent cells involved in, 20: 45357 (EUR-3060.f)
reaction of radioinduced mouse mutants to, 18: 6621(R) (UCSF-23)
reactions to, effects of extracorporeal irradiation of blood and lymph on, 20: 6926 (BNL-9726)
rejection by radiation chimeras, 16: 16178 (USNRDL-TR-553)
survival in cattle, effects of extracorporeally irradiated blood and lymph on, 20: 8617 (BNL-9801)
survival in irradiated mice receiving spleen cell injections, effects of A-methopterin on, 16: 26874
survival in mice, effects of large doses of subcellular fractions on, 20: 24930
survival of auto-, on burns of rabbits with radiation injuries, 19: 8926
survival of rat graft in lethally irradiated mice restored using fetal liver, 16: 8626
survival on burns of irradiated rabbits, 17: 17865
takes in rabbits, effects of whole-body irradiation and injections of hematopoietic tissues on, 16: 8661
technique for repair of radioinduced skin lesions, 19: 30021
technique for repair of radioinduced skin lesions, 19: 30022
therapeutic effects in radioinduced mouse chimeras, 17: 4432
tolerance to CBA, in C3H, 18: 1367
tolerance to, in mice, acquired by transfer of tolerant state, 17: 19769
tolerance to, in hybrid x-irradiated mice given skin from parents, 20: 40651
use for repair of radiation injuries, 20: 3724

SKIN LESIONS

chemically-induced dermatitis, 19: 13069
fallout-induced, 19: 15212
pathology of, induced by plutonium-238, plutonium-239, or neptunium-239 in swine, 17: 35312(R) (HW-76000(p.149-55))
pathology of radioinduced, ultraviolet, 20: 74
pathology of radioinduced, 20: 3724
radiation effects on healing of, effects of single or fractionated doses in rats, 18: 43248
radiation effects on survival of rats with, 19: 7148
radiation effects on wheal resorption, ultraviolet, 19: 28146
radiation effects on wheal resorption, x, 19: 28146
radiation effects on cholinesterase and tyrosinase activity in, uv, 19: 43809
radiation effects on healing of mouse, effects of radioprotective compounds on x, 20: 6878
radiation effects on occurrence of herpes zoster on human, therapeutic, 20: 35380
radioinduced acute, therapy using pancreas extract, 17: 10490
radioinduced by close-in fallout, protection against, 19: 34397 (BNL-9188)
radioinduced by therapy for retinoblastoma, 17: 23198
radioinduced by therapy, 18: 38842
radioinduced during therapy, surgical repair of, 19: 46085
radioinduced erythema in radiotherapy patients, effects of hydroxyurea on, 19: 5729
radioinduced erythemic, uv, 20: 14310
radioinduced erythemal, theory for uv, 20: 24928
radioinduced, follow-up studies of occupational radium and x-ray, 17: 17916
radioinduced human, use of fresh blood autofibrin films for treatment of, 19: 19642
radioinduced in guinea pigs, pathology of, 19: 45869
radioinduced in guinea pigs, effects of, on amino acids and enzymes, 19: 45887
radioinduced in man, differences in caudal and cranial erythemic electron, 19: 33995
radioinduced in man, dose determinations for erythemal uv, 19: 45881
radioinduced in man, design and performance of remission photometer for measuring erythemic, 20: 21011
radioinduced in man, surgical closure of, 20: 22774
radioinduced in man from accidental or intentional exposure, 20: 183
radioinduced in medical personnel, 19: 3981
radioinduced in mice, x, 20: 20475
radioinduced in mice and rats, role of adipose tissue in repair of x, 20: 28946
radioinduced in rabbits by x radiation, 17: 35477
radioinduced in rats, effects of Padutin treatment on, 19: 24367 (EUR-2151.f)
radioinduced, morphology of surgical treatment of, 16: 20278
radioinduced on hands by occupational exposure, surgical treatment of, 17: 21475
radioinduced on man, surgical treatment of, 17: 21479
radioinduced on mice, healing effects of triglyceride ointment on, 17: 21585
radioinduced, pathology and treatment, 17: 10494
radioinduced, pathology, 17: 28758
radioinduced, pathology, 17: 33745
radioinduced rat, regeneration process in, 18: 11792
radioinduced, therapeutic effectiveness of ointments containing steroids and antibiotics, 16: 20155
radioinduced, treatment using blood factor, Actihemyl, 16: 14602
radioinduced ulcers, etiology, pathology, and therapy of, 19: 38513
radioinduced, after radiotherapy of benign tumor, 19: 31988
radioinduced, in guinea pigs, effects of treatment with cigerol and linol, 18: 33413
radioinduced, phosphorus-32 and radium, 20: 24916
radioinduced, surgical repair of, 19: 30021
radioinduced, surgical repair of, 19: 30022
radioinduced, therapeutic effects of locally applied cortisone on, 18: 41262
radioinduced, treatment with salve, 19: 3993
radioinduced, treatment of, 20: 10658
radiotherapy of, 19: 31948
radiotherapy of, 20: 8791
radiotherapy of benign, x, 20: 3812
radiotherapy of carcinoma of nose, 19: 28144
radiotherapy of carcinomas of eyelid, 19: 46052
radiotherapy of facial, choroido-retinal damage following, 20: 14297
radiotherapy of hemangioma, safety measures for, 20: 14418
radiotherapy of malignant, 18: 11677
radiotherapy of metastatic, arising from internal neoplasms, 20: 43039
radiotherapy of reticuloses, clinical and practical aspects of, 19: 31952
radiotherapy of warts, 19: 233
radiotherapy of, comparison of gamma and x ray sources for, 20: 171
radiotherapy of, design of gamma applicator for, 20: 177

radiotherapy of, electron-beam, 18: 11933
radiotherapy of, laser, 20: 40776
radiotherapy of, with phosphorus-32, 19: 15287
radiotherapy using beta source, dosimetry, 19: 43880 (NP-15270)
repair of radioinduced, in rats, effects of desoxyribonucleic acid content on, 18: 9915
role of cholesterol metabolism in psoriasis, 19: 31661(R) (ACRH-23 (p.62-9))
therapy of radioinduced, using Padutin, 20: 45356 (EUR-2752.e)
treatment of radioinduced, 19: 25940

SKLODOWSKITES
spatial group determination in, application of Collin's method, 17: 21907
structure, 17: 21908

SKULL MOUNTAIN QUADRANGLE (NEV.)
geologic map of, 17: 4731

SL-1 Reactors
see Army Reactors (SL-1)

SLAGS
analysis for niobium and tantalum by ion exchange, 16: 16312
analysis for niobium and tantalum, fluorescence spectrometric, 17: 32007
analysis for uranium, radiometric, 16: 18824
analysis of, for niobium and tantalum, x-ray spectrum, 17: 15900
dissolution, design of continuous dissolver for, 16: 4219 (HW-68630)
dissolution of plutonium-bearing, 16: 11781 (HW-69415)
dissolution of plutonium, equipment for, 18: 35651
dissolution of plutonium, dissolver performance for, 19: 44111 (BNWL-121)
radioactivity measurements on building block, 16: 20871 (PAN-269/1-A)
separation of scandium from blast-furnace, 19: 20081
separation of uranium from phosphate, 16: 27115(P)
separation of uranium from fluoride, 17: 29022(P)
use of blast-furnace, for purification of radioactive wastes, 18: 40965
use of molten, as heat-exchange medium for MHD generator system, 20: 12971(P)
uses of high-density, from lead smelting, in concretes for radiation shielding, 19: 18508

SLEEP REACTOR
(Swedish Low Energy Experimental Pile.)
description, 17: 22887
fuel rod neutron resonance absorption, 16: 24759 (AE-77)
instrumentation of, spectrometers for, 18: 11479 (ANL-6797(p.183-92))
neutron spectra in central channel of, resonance integrals for, 18: 6454
neutron spectra in, foil-activation measurement of, 19: 3771 (AE-155)

SLICK ROCK DISTRICT (COLO.)
geologic map, 16: 3255
uranium equilibrium and migration in sandstone deposits in, 19: 24742
uranium isotopic fractionation in sandstone of, 19: 20187

SLUG CANNING
see also Radiation Target Cans
burst detection equipment arrangement, 16: 3230(P)
end plug fastening by constricting grove in, apparatus for, 18: 41999(P)
hydrostatic methods of, 18: 42001(P)
methods development for reactor materials, 18: 14446
methods development for reactor materials, 18: 32119
methods development for reactor materials, 18: 41987
sealing pyrolytic graphite sheaths for, 18: 42005(P)
techniques for, 18: 12619(P)
techniques for, development of, 17: 11130

SLUG CANS
see also Radiation Target Cans
corrosion by steam, 18: 30143
corrosion of, during underwater storage, 17: 16598
design for improved stability, 19: 24059(P)
design for increased strength, 19: 24060(P)
design for metal oxide slugs, 16: 17253(P)
design for rigidity, 16: 15879(P)
design of composite aluminum–aluminum oxide, 19: 44661(P)
design of end closure, 17: 2566(P)
design of finned, 19: 29600(P)
design of finned, 19: 29603(P)
design with helical fins, 19: 29601(P)
design with herring-bone casing, 16: 4997
development for gas-cooled graphite-moderated reactors, 18: 15496(T) (AEC-tr-6329)
development of Magnox, 18: 37614 (A/CONF.28/P/560)
development of stainless steel, 18: 26946
development of, effects of environment on, 18: 26096
fabrication of aluminum, for uranium fuel, 19: 16037
fabrication with fins, 16: 15873(P)
filling with helium, prevention of air leaks during, 16: 15880(P)
heat exchanger design for, 18: 8470(P)
materials for, evaluation of magnesium-0.5 to 1.0 wt% zirconium alloy for, 19: 20610(P)
radiation damage in, detection limits of, 17: 5007
removal device for, 18: 12274(P)
sealing of sintered oxidized aluminum, beryllium, or magnesium, method for, 17: 42260(P)
spacer design for, 19: 42074(P)
testing of thin-walled, under pressure, 16: 27416
wall thickness measurement, radiometric gage for, 16: 27525
welding method for, 19: 24972(P)

SLUG ELEMENTS
see also Long Cartridges
see also Reactor Breeding Elements
see also Reactor Fuel Elements
see also Slugs
canning apparatus for, design of, 20: 5029(P)
cladding removal device for, 19: 26497(P)
design, 18: 11421(P)
extrusion of hollow, technique for, 17: 36242 (BRB-73)
extrusion of I&E, by high-energy-rate process, 17: 1892 (BRB-61)
fabrication of, design of cave for, 19: 46509 (UCRL-12497-T)
failure detection equipment arrangement, 16: 3230(P)
failure detection in reactors, description of French fission product detector for, 16: 8324
failure in reactors, principles of detection systems, 16: 8323
failure in reactors, design of detection system for, 17: 28515(P)
failure of, system for detecting, 18: 9679
failure of, coolant monitoring system for detecting, 20: 10315(P)
fission products from natural uranium, neutron absorption cross section for, 17: 20055 (CRRP-1133)
handling device for, 18: 6444(P)
radiation effects statistics, 16: 27693 (HW-72322)
thermal stresses in, analysis of, 16: 34127 (NAA-SR-Memo-7456)

SLUGS
analysis for aluminum and thorium in aluminum-coated thorium, titritmetric, 20: 43071 (IDO-14679, pp 75-191)
bonding of uranium slug to aluminum can, 17: 16625(P)
corrosion pitting of uranium, environmental effects on, 20: 25486 (NLCO-957)
critical mass studies on aluminum–uranium-235, 20: 46994 (ORNL-3272)
dejacketing of SRE Core I, 16: 14690(R) (ORNL-TM-121)
extrusion of I&E, development of combined alpha phase extrusion-beta phase quench technique for DYNAPAK, 17: 36242 (BRB-73)
fabrication of hollow by DYNAPAK extrusion, 17: 1891 (BRB-58)
neutron resonance absorption by, 16: 29730
preparation of fissure-free plutonium, method for, 17: 41411(P)
processing of radioactive, engineering drawings of cave for, 19: 22437
properties of powder metallurgy improved impact extrusions of aluminum as, 17: 11177
testing of, nondestructive method for, 20: 14711
thermal cycling, 16: 9657(R) (NAA-SR-1109)

SLURREX
see Boiling Reactor Experiments

SLURRIES
see also Bismuth Alloy Slurries
see also Hanford Waste Slurries
see also Homogeneous Reactors
see also Oxide Slurries
see also Reactor Slurries
see also Sodium Alloy Slurries
see also Suspensions
see also Thorium Alloy Slurries
see also Thorium Slurries
see also Uranium Alloy Slurries
see also Uranium Slurries
abrasiveness of, radiometric measurement, 19: 2689
analysis of waste, for solids, 19: 17781(R) (ORNL-3750)
concentration in pipe lines, radiometric densitometer for measuring spatial, 20: 13049
dehydration of radioactive, effects of polymers on, 20: 45218(T) (KFK-tr-201)
density monitoring during processing, radioactivity gages for, 18: 2124
density of coal and rock, radiometric measurement of, 19: 24897
density of, radiometric measurements of, 19: 24898
drying apparatus for, 19: 38800(P)
fission recoil energy deposition in, calculation, 17: 25897
flow of, heat transfer in two-phase, 18: 20171 (TID-7694(p.18-23))
flow through pipes, Bingham viscosity and yield stress for, 20: 10998
handling and filtration of radioactive, 20: 14210
heat and mass transfer in, 17: 6232
heat transfer from coal, in closed-cycle gas turbines, 20: 33429(R) (TID-23117)
heat transfer of, in water fluidized system, 18: 3957 (TID-19477)
injection of radioactive, in cement, 18: 17346
lift coefficients of spherical particles moving in still fluid in tube,

18: 12764 (IS-615)
particle size distribution in fuel, radiometric measurements of, 20: 7598
settling in, radiation gage for measuring, 19: 24836(P)
stabilization of aluminum powder, using bentonite strengtheners and phosphate salt stabilizers, 18: 18294(R) (NP-13758)
zeta potential of molybdenum disilicide, 18: 18294(R) (NP-13758)
Slurry Reactor
see Homogeneous Reactor Experiment
SM-1 Reactors
see Army Reactors (SM-1)
SM-2 Reactors
see Army Reactors (SM-2)
Small Submarine Reactor
see Submarine Reactors (SIC)
SMOKE GENERATORS
see also Aerosol Generators
see also Smokes
see also Stack Disposal
use in evaluation of recyclings and transit times of ventilation systems, 18: 43874
Smoke Ring
see Pinch Devices
SMOKES
chimney plume rise, formula for predicting, 18: 13384(T) (AEC-tr-6330)
control of inhaled cigarette, in dogs during iron-59 exposure experiments, instrument for, 19: 43668 (HW-SA-3618)
detection of, comparison of ionization and photoelectric methods for, 19: 44355
detection of, development of photometer for, 20: 37168(R) (BMI-1771)
detection of, photometer design for, 20: 37169(R) (BMI-1774)
diffusion at ambient temperature from chimney, 16: 23991(T) (AWRE-Trans-34)
diffusion from stacks, uses of silver iodide for studying, 19: 14117
diffusion from stacks, wind tunnel scale model experiments on, 19: 44764 (BNL-914, pp 14-17)
diffusion of, equipment for scale-model experiments on, 19: 20656(R) (ANL-6938(p.257-73))
diffusion of, floating instantaneous-source type, (T), 19: 47111(T) (UCRL-Trans-1229(L))
effects of admixtures of, on current intensity in ionization chamber, 19: 44355
effects of chronic exposure to cigarette, on pulmonary clearance in dogs, 20: 3655 (BNWL-SA-224)
flow around buildings, 20: 562 (CONF-650407, pp 455-9)
iodide scavenging by rain and snow from Hanford stock gases, measurement of, 20: 41188(R) (BNWL-235-1)
polonium-210 absorption in lungs from cigarette, 20: 24947
polonium-210 content in mainstream cigarette, 19: 36132
polonium-210 content of tobacco, 19: 40805 (NRS-30)
polonium-210 content of cigarette, 20: 158
polonium-210 content in tobacco, 20: 8572
polonium-210 content in cigarette, uptake and distribution in lung tissues of, 20: 14798
polonium-210 content in tobacco, 20: 16264
polonium-210 content in tobacco, 20: 37030
polonium-210 content in tobacco, effects on lung content of cigarette smokers, 20: 40531 (A/AC.82/G/L-1045(Rev.1))
polonium-210 content in tobacco, 20: 45506
polonium-210 in cigarette, 20: 18965
radiation effects on pyrolytic products of, from irradiated cigarettes, 20: 3984 (ORO-633)
rise from stacks, formulas for, 19: 20653(R) (ANL-6938(p.209-41))
sorptive properties for radioiodine, 20: 216 (CPNF-650407, pp 242-75)
suction into chimney slipstreams at high wind speeds, deflector for preventing, 19: 2483
suction into chimney slipstreams at high wind speeds, device for preventing, 19: 6134
use as screens against thermal effects of nuclear weapons, 18: 427 (AD-412733)
use in evaluation of atmospheric diffusion, 16: 11974(R) (JAERI-5003 (p.251-5))
SNAILS
analysis for trace amounts of sodium, radiochemical, 18: 19841 (CONF-187-112)
beta activity of, in Italy, 1962, 18: 18040 (BIO/03/63)
calcium deposition in shells of fresh water, tracer study of, 19: 35923
calcium fixation by shells of fresh water, 18: 4974
calcium uptake and accumulation by, 19: 6933(R) (ORNL-3697(p.95-104))
calcium uptake by aquatic, role of ionic diffusion in, 20: 30991
excretion of foreign particles by, tracer study in Bullia, 19: 43695
iron-59 uptake and distribution in, 17: 17714
labeling of, use of cobalt-60 for, 17: 21406
metabolism of manganese and strontium by, 19: 10731(R) (NP-14669)
phosphorus-32 uptake by, from *E. coli* in stream ecosystems, 20: 40529
physiology of, trace element, 20: 45312
radiation effects on development of eggs of *Australorbis glabratus*, 18: 38835
radiation effects on development of *Australorbis glabratus* exposed as eggs, 18: 38836
radiation effects on population kinetics of, effects of age on x, 19: 2138
radiation effects on population kinetics of, x, 19: 2139
radiation effects on spleen cells of *Molge vulgaris*, in tissue culture, 19: 43826
radiation effects on, gamma, 20: 12545(R) (PAEC(A)AR651)
radiation effects on, y, 20: 31116
radiation experiments on, single-hit curves, 20: 40515
radioactivity of Lake Maggiore, 1961, 19: 10731(R) (NP-14669)
radioactivity of Lake Maggiore, 1952 to 1961, 19: 11391(R) (NP-14658)
radioisotope uptake by, in Clinch River, 17: 39306(R) (ORNL-3492 (p.107-15))
radionuclide uptake from water in pond, 18: 25079
radiosensitivity of, effects of age on, 18: 19698
radium-226 accumulation by *Lymnaea stagnalis*, 17: 13944
rubidium-86 uptake and distribution in, 17: 17714
shell analysis for strontium-90 due to fall-out in Hungary, 16: 8510
sodium-22 uptake and distribution in, 17: 17714
strontium deposition in shells of, 20: 6711(R) (ORNL-3849, pp 43-100)
strontium deposition in shells of fresh-water, tracer studies of, 19: 35923
strontium fixation by shells of fresh water, 18: 4974
strontium uptake accumulation by, 19: 6933(R) (ORNL-3697(p.95-104))
strontium-85 uptake and distribution in, 17: 17714
strontium-90 metabolism by, 19: 11391(R) (NP-14658)
toxic effects of copper, cadmium, and zinc in *Australorbis glabratus*, 18: 19489(R) (TID-20469)
zinc metabolism, tracer study, 17: 24865
SNAP Reactors
see Systems for Nuclear Auxiliary Power (SNAP)
SNAPPER OPERATION
see also Tumbler Operation
effects on ionosphere, 17: 2666 (WT-547)
effects on radio propagation, 17: 2666 (WT-547)
shock waves in, effect of topography on, 17: 6276 (WT-502)
SNARE (Sandia)
see Critical Assemblies
SNOW
accumulation at South Pole, radioactive measurements on rate of, 18: 37379
accumulation at South Pole, oxygen and hydrogen isotope variations in, 19: 26563
age estimation of polar, by polonium-210 counting, 20: 27151
analysis for cesium-137, strontium-89, and strontium-90 by electrodialysis and gamma spectroscopy, 19: 19809
analysis for fission products from fallout, gamma spectroscopic, 17: 30762
analysis for tritium in New Zealand, 1956 to 1960, 16: 16078
analysis of Antarctic, for tritium, 1960 and 1961, 17: 28614
beta activity in water from, nuclear explosion dating by measurement of gross, 19: 22606
cerium-144 to cesium-137 abundance ratio in, Bucharest, Romania, Winter 1963/1964, 20: 27163
cesium-137 content in Antarctic, 1939-61, 19: 11400
dating of, by deuterium content, 18: 36071
decontamination under cold-weather and thawing conditions, 18: 31754 (NDL-TR-58(Pt.I))
decontamination under cold-weather and thawing conditions, 18: 31755 (NDL-TR-58(Pt.II))
density measurements on, use of radioactive sources for, 17: 36017
density profile measurement in, using nuclear techniques, 20: 39130
density profiles of, tracer techniques for developing, 19: 13830
deposition of fallout by, meteorological aspects of, 17: 37349 (NSEC-98)
deposition of iodine and water vapors from air to, 19: 1031 (CRL-86)
detection of thin film of, on surfaces, radiometric device for, 20: 25372(P)
deuterium content of Antarctic deposits, 17: 29141
effects on fallout, 20: 14746
effects on removal of radioiodine vapor from atmosphere, washout coefficients for, 20: 27190 (BNWL-SA-155)
evaporation of, surface-to-air concentration gradients in analysis of, 20: 41150 (AECL-2576)
fallout accumulation in antarctic, 17: 41008
fallout altitude distribution in, 17: 3244
fallout concentration by, 17: 33547
fallout contributions of, to natural background, 18: 10290
fallout monitoring in, at end of 1959-60 winter season, 17: 1664

fallout monitoring in, collected in Bucharest, Dec. 24, 1962, to Jan. 6, 1963, 18: 12348
fallout monitoring in Switzerland, 1956 to 1961, 18: 20218
fission product contents in, on Balkan Mountains from fallout, 19: 15800
gamma activity and spectra from fallout in, 20: 25283
hydrologic studies of, tracer studies of, 17: 3656
iodine-131 content in, relation of lower atmospheric contamination to, 18: 41663
lead content in, 17: 32274
lead content in Greenland, role of industrial lead pollutants in, 20: 18944 (NYO-3450-1, pp 213-15)
lead content in polar, analysis of, 20: 45915(R) (CALT-427-14)
lead isotopes in, in Los Angeles basin, California, effects of automobile exhausts on, 19: 11453
lead isotopic composition in, 17: 32274
lead-210 content of Antarctic, effects of solar activity on, 19: 16341
measurement of, by radiological telemetering, 18: 31848
nitrogen content in, at South Pole, 19: 18138
oxygen isotope content in, annual layer identification by seasonal variation in, 17: 30699
oxygen isotope ratio in, from Antarctica, 17: 18306
oxygen-16 and -18 content in, on Alpine glaciers, 20: 33517
oxygen-16 and -18 content in firn layer of summer 1957–1958 at South Pole, 20: 33518
oxygen-16 to oxygen-18 ratio in St. Elias Mountain, Canada, 20: 39123
oxygen-16/oxygen-18 ratio in Antarctic, 19: 611
properties of, measurement with radioactive sources, 17: 34139
radioactivity from cerium-144 and cesium-137 in Bucharest, 19: 36654
radioactivity in Antarctic, 18: 35749
radioactivity in Japan in 1962, 18: 10287
radioactivity in Nagaoka City, Japan, 1963, 19: 11435
radioactivity in Nagaoka City, Japan, in 1964, 19: 32438
radioactivity in, at Nagaoka City, Japan, 1965, 20: 31411
radioactivity of Alpine glacier, dating from, 20: 14740
radioactivity of Indiana, determination of gamma, 20: 11020
radioactivity of, from barium-140 and zirconium-95 content in Germany, 1961 to 1963, 20: 16766
radioinduced heating of, gamma and neutron, 18: 7930 (NP-13424)
radiotracer exchange between air and, 19: 32785 (AECL-2232)
stratigraphy in drilling at Antarctica, oxygen isotope, 19: 26564
strontium-90 content in Antarctic, 1939–1961, 19: 11400
sulfur isotopic composition, 16: 5569
thickness measurements using radioisotopes, 16: 27528
trace materials in, use of, for studying atmospheric precipitation processes, 20: 27144 (BNWL-SA-650)
tritium content in, in France since November 1958, 17: 29144
tritium content of Antarctic, 18: 12353
tritium content of, Moscow, Dec. 1961 to Dec. 1963, 20: 29409
tritium measurement in, after enrichment by thermal diffusion, 19: 46613
washout coefficients for stack disposal of iodine-131 vapor, 20: 37033
water content at Lysa Hora, performance of radiometric gage for measuring, 18: 18151
water content in, use of natural radioactivity in determining, 20: 43559
water content of, radiometric measurement of, 17: 347
water content of, review of radiometric gages for determination of, 19: 2582
water content of, gamma counting of, Fichtelberg, Germany, 20: 550
water content of, gamma-transmission measurement of, 20: 23527 (CONF-651206)
water deposits in, gamma spectroscopic determination of, 20: 549

SNSE Reactor
see Argonaut Reactor

SOAP SOLUTIONS
rupture of bubbles in, by alpha particles, 17: 37257
use as flotation agent in waste processing, 20: 10447

SOAPS
preparation and properties of heavy metallic, 20: 35931

Soapstone
see Steatites

Soda Ash
see Sodium Carbonates

SODALITES
diffusion of sodium ions in, tracer and conductivity studies of, 19: 12869(R) (NYO-1154-1)

SODIUM
see also Alkali Metals
abundance in solar atmosphere, 16: 29599 (AFOSR-3024)
abundance in solar atmosphere, Stark broadening effect on determination of, (T), 20: 27706
alpha reactions (α,n) with, neutron yields from, 17: 33017
alpha reactions (α,n) with, neutron yields from, 17: 33018
analysis and sampling of, procedures for, 17: 7563(R) (PRDC-TR-59)
analysis for boron, spectrophotometric, 17: 17971 (PG-Report-415)
analysis for carbon, 16: 16690 (TID-7626(Pt.I)(p.146-9))
analysis for carbon, 17: 5948 (AWRE-O-62/62)
analysis for carbon, method for, 17: 27244(T) (AEC-tr-6839)
analysis for carbon, isotope-dilution, 18: 1587
analysis for carbon traces, 18: 9968 (CEA-2370)
analysis for carbon traces, gravimetric, 18: 13624 (LA-3035)
analysis for carbon in primary cooling system of HNPF, 18: 21637 (NAA-SR-Memo-8214)
analysis for carbon, difficulties in methods for, 18: 27891 (NASA-SP-41(p.61-5))
analysis for carbon and oxygen, 18: 33678(R) (ANL-6875)
analysis for carbon by isotope dilution mass spectrometry, 18: 33477
analysis for carbon and oxygen, 18: 36751 (ANL-6912)
analysis for carbon by dry oxidation, 18: 43359(R) (ANL-6800(p.43-196))
analysis for carbon, USAEC round-robin programs on, 19: 2210 (GEAP-4602)
analysis for carbon, in mass transfer loop, 19: 5770 (GEAP-4540)
analysis for carbon, combustion-chromatographic method for, 19: 9055 (APDA-164)
analysis for carbonate carbon, 19: 15340 (APDA-166)
analysis for carbon and oxygen, methods for, 19: 15662(R) (ANL-6900 (p.45-142))
analysis for carbon at ppm level, 19: 26239
analysis for carbon, hydrogen, and oxygen impurities, development of methods for, 19: 30079 (MSAR-65-58)
analysis for carbon and oxygen, 19: 32279(R) (ANL-7020(p.3-99))
analysis for carbon, corrections for, 19: 40112(R) (ANL-7046(p.36-66))
analysis for carbon and oxygen, methods for, 20: 5594(R) (ANL-6925, pp 21-106)
analysis for carbon, distillation method for, 20: 22878 (TRG-Report-1185)
analysis for carbon by combustion, 20: 31213(R) (ANL-7175, pp 119-58)
analysis for carbon, method for, 20: 42619(R) (ANL-7245, pp 1-28)
analysis for carbon, methods for, 20: 46963(R) (ANL-7132)
analysis for elemental carbon, isotope dilution mass spectrometry method for, 17: 27317 (NAA-SR-7918)
analysis for hydrogen by isotope dilution, 17: 40726
analysis for hydrogen traces, gravimetric, 18: 17725 (LA-3049)
analysis for hydrogen, 18: 31375(T) (AEC-tr-6438)
analysis for hydrogen and oxygen, rapid amalgamation method for, 19: 300 (ORNL-P-539)
analysis for hydrogen at 1 ppm and up, 19: 13228
analysis for hydrogen in loop, by diffusion gasometry, 20: 12767 (GEAP-4833)
analysis for hydrogen by vacuum distillation and gas chromatography, 20: 35388 (APDA-183)
analysis for impurities, performance tests of instruments for, 18: 5216(R) (TID-19818)
analysis for impurities in Fermi reactor, 18: 7931(R) (PRDC-TR-74)
analysis for impurities in sodium technology loop, contamination meter for, 18: 17973 (APDA-163)
analysis for impurities, gamma activation, 19: 7339
analysis for impurities, design of resistivity meter for, (E), 19: 13204 (SAN-8002(p.265-75))
analysis for impurities by spark source mass spectrography, 19: 19830
analysis for impurities in, methods for, 19: 34672 (BMI-X-10129)
analysis for impurities, development of methods for, 19: 40409(R) (MSAR-65-95)
analysis for impurities, evaluation of methods for, 20: 3880(R) (MSAR-65-150)
analysis for impurities, coolant loop in-line instruments for, 20: 10322 (CONF-650620, pp 255-70)
analysis for impurities, techniques for, 20: 10322 (CONF-650620, pp 255-70)
analysis for impurities, instrumentation performance for, 20: 8816(R) (APDA-178, pp 30-42)
analysis for impurities in loop transfer, methods for, 20: 12766 (GEAP-4178)
analysis for impurities using mass spectrometry, solvent extraction, and surface tension, 20: 14445(R) (MSAR-66-10)
analysis for impurities, methods of, 20: 22520(R) (NAA-SR-11805)
analysis for impurities, development of techniques for, 20: 38797(R) (MSAR-66-150)
analysis for impurities, methods for, 20: 46966(R) (NAA-SR-12010)
analysis for nitrogen, volumetric, 17: 27232 (LA-2892)
analysis for oxide in liquid, apparatus for, 17: 16409(P)
analysis for oxides, by electric potential measurement, 19: 40409(R) (MSAR-65-95)
analysis for oxygen by amalgamation with mercury, 16: 12952 (PAN-256/VIII)
analysis for oxygen, 16: 16689 (TID-7626(Pt.I)(p.143-5))
analysis for oxygen, methods determination, 16: 16688 (TID-7626 (Pt.I)(p.141-2))

analysis for oxygen, gasometric and gravimetric, 16: 18822
analysis for oxygen, 16: 28560 (TID-7623(p.161-7))
analysis for oxygen traces, 17: 7967
analysis for oxygen in liquid, design of meter for continuous, 17: 12531(R) (UNC-5000)
analysis for oxygen in liquid, electrochemical, 17: 12532(R) (UNC-5010)
analysis for oxygen in liquid, meter for continuous, 17: 12533(R) (UNC-5032)
analysis for oxygen, 17: 15878(R) (NDA-2154-5)
analysis for oxygen, continuous electrochemical analyzer for, 17: 15889(R) (UNC-5050)
analysis for oxygen by isotopic dilution techniques, 18: 4160(R) (BNL-799(p.74-100))
analysis for oxygen, method of sampling for, 18: 13612 (CEA-2369)
analysis for oxygen, activation, 18: 17769(R) (ANL-6725(p.99-111))
analysis for oxygen, amalgamation method for, 18: 19919
analysis for oxygen in test loop, 18: 35060(R) (ANL-6904)
analysis for oxygen, activation, 18: 44925(R) (ANL-6923(p.14-45))
analysis for oxygen, activation, 18: 43359(R) (ANL-6800(p.43-196))
analysis for oxygen, design of electrochemical cell for continuous, (E), 19: 13205 (SAN-800(p.276-85))
analysis for oxygen by activation, 19: 17176(R) (ANL-6965(p.1-41))
analysis for oxygen, 19: 15332(R) (BNL-841(p.52-62))
analysis for oxygen, activation, 19: 35613(R) (LA-3316)
analysis for oxygen, 19: 38539 (APDA-168)
analysis for oxygen, monitoring instruments for, 19: 42807(T) (PG-Inf.Ser.-10)
analysis for oxygen traces, 19: 43932 (LA-3343)
analysis for oxygen, use of mercury method for, 17: 27245(T) (AEC-tr-5840)
analysis for oxygen, engineering drawings of sodium sampler design for, 20: 1799
analysis for oxygen, operating manual for gas analyzer for, 20: 3889 (UNC-5113)
analysis for oxygen, methods for, 20: 8447 (PWAC-491)
analysis for oxygen, instrument for, 20: 8825 (CONF-650620, pp 271-5)
analysis for oxygen, amalgamation method for, 20: 14432 (ANL-7123)
analysis for oxygen by distillation and titration, 20: 16349
analysis for oxygen, device for interference reduction and sensitivity improvement in activation, 20: 43075 (LA-DC-7931)
analysis of Fermi reactor coolant, for carbon and carbonates, 17: 4253(R) (PRDC-TR-58)
analysis of high-purity, 20: 35841(R) (NAA-SR-11900)
analysis of liquid, for oxygen, 17: 27731 (NASA-TM-X-884)
analysis of liquid, for oxygen using continuous electrochemical analyzer, 16: 30602(R) (UNC-5028)
analysis of liquid, for hydrogen, spectrographic method, 16: 7686 (NAA-SR-5732)
analysis of liquid, for oxide by automatic measurement of plugging temperature, 18: 13646(T) (AEC-tr-6353)
analysis of liquid, for sodium oxide, 18: 21698(R) (ANL-6860)
analysis of liquid, for impurities, development of methods for, 18: 23411(R) (TID-20614)
analysis of liquid, for carbon, 19: 4590 (MSAR-61-42)
analysis of liquid, for hydrogen and oxygen, 19: 17850 (CEA-R-2583)
analysis of liquid, for oxygen, electrolytic method for continuous, 19: 22153
analysis of liquid, for carbon, 20: 10272(R) (NAA-SR-9339)
analysis of liquid, for oxygen, methods for, 20: 33222
analysis of liquid, for carbon, 20: 43135
analysis of reactor-coolant, for absorbed impurities, 19: 6827(R) (ANL-6944(p.13-52))
analysis of, for metallic and oxygen impurities by emission spectrography, 20: 43083 (R-66SD3012)
analysis of, use of activation methods for, 18: 29577
atomic excited states of, lifetimes of, 18: 22692
atomic vibration frequency distribution functions for, sampling method calculation for normal mode, 18: 18571
bearing material use in liquid, 17: 3379(R) (BMI-1596(Del.))
behavior in amine solutions, model for prediction of, 18: 8365
behavior in fused lithium chloride–potassium chloride eutectic, chromatographic and electrophoretic, 18: 43479
bibliography on liquid, 20: 27415 (TRG-Inf.Ser.-312)
bibliography on technology of liquid, 18: 929 (NP-14434)
boiling and condensing of, heat transfer coefficients in nucleate, 17: 20153 (BNL-756(p.97-113))
boiling and condensation of, studies on, 19: 582 (NASA-CR-54050)
boiling burnout and heat transfer in liquid, test of, 20: 47034
boiling burnout heat flux, 19: 24673 (NP-14953)
boiling heat transfer, pool, 16: 27189(R) (AD-270678)
boiling heat transfer by, development of equipment and methods for studying, 17: 20169 (BNL-756(p.380-5))
boiling heat transfer studies, 17: 35988 (NAA-SR-7909)
boiling heat transfer studies, 18: 28919(R) (NAA-SR-9090)
boiling heat transfer of, apparatus for studies of effects of surface conditions on, 19: 4313 (ORNL-3605(Vol.1)(p.263-85))
boiling heat transfer in, nucleate, 19: 4322 (ORNL-3605(Vol.2) (p.86-109))
boiling heat transfer by, 19: 18126
boiling heat transfer in, 20: 5627
boiling heat transfer and critical heat flux for, in forced convection, 20: 10990 (NAA-SR-11586)
boiling in forced-convection flow, 20: 33472
boiling initiation in, superheat requirements for nucleate, 19: 11366
boiling instabilities in liquid, nucleate, 19: 46551
boiling of, equipment for studies of pool, 17: 20155 (BNL-756(p.126-30))
boiling of liquid, acoustic noise production in nucleate, 17: 32251 (TRG-Report-549)
boiling of, analysis of low-vapor forced-convection, 18: 31725(R) (SAN-409-5)
boiling of, calculation of liquid superheat due to surface conditions in nucleate, 20: 25263
boiling of, effects of surface conditions on nucleate, 19: 46549
boiling of, forced-convection and pool, 19: 4320 (ORNL-3605(Vol.2) (p.24-46))
boiling of, superheat in, 20: 482 (ORNL-P-1659)
boiling of, vapor volume fractions in, 18: 20170 (TID-7694(p.11-17))
boiling on heating surface at free convection, (E/T), 20: 14693(T) (AD-625791)
boiling studies, Argonne program, 19: 32361 (CONF-640507(p.125-37))
boiling, analysis of liquid superheat for nucleate, 19: 13576 (ANL-6980)
boiling, research program on heat flux of film, 18: 37347(R) (TID-20942)
bonding interactions and thermodynamic properties of, 17: 22258 (IS-409)
burning and fission product release rates from, 18: 28919(R) (NAA-SR-9090)
canning for neutron scattering experiments, method for, 19: 20503 (EUR-2242.e)
carbon content of SRE, carburization potential of, 17: 17597 (NAA-SR-Memo-7804)
carbon mass transfer from graphite into liquid, 19: 32279(R) (ANL-7020(p.3-99))
carbon mass transport by liquid, 18: 2187
carburization of 304 stainless steel in liquid, 16: 16682 (TID-7626(Pt.I) (p.92-100))
cavitation damage in liquid, research program on, 18: 34075 (NASA-CR-54071)
cavitation damage in liquid, research program on, 19: 30670(R) (NASA-CR-54332)
cavitation damage in liquid, 20: 2243
cavitation effects of liquid, on five alloys to 1500°F, 20: 46154 20: 46154 (NASA-CR-72035)
cesium-137 removal from, performance of graphite for, 20: 8390(R) (LA-3431)
chemical properties, 20: 35841(R) (NAA-SR-11900)
chemical states of carbon, nitrogen, and oxygen in, 19: 39157 (CNLM-6337)
circulation system for liquid construction and operation of, 16: 20576
collisions of atoms of, with rare gas atoms and hydrogen and nitrogen molecules, ionization in, (E), 20: 2639
combustion in nitrogen and oxygen, properties of aerosols from, 20: 35668 (LA-3491)
combustion in reactors, properties of, 20: 45047 (NAA-SR-12041)
combustion of liquid, fission product release in (E), 19: 2429
combustion of reactor coolant, fission product release in, 19: 40286(R) (NAA-SR-11200)
combustion of reactor coolant, fission-product release in, 20: 22520(R) (NAA-SR-11805)
combustion of reactor coolant, fission product release in, 20: 46966(R) (NAA-SR-12010)
combustion of, dispersion of iodine and oxide particles from, 18: 35247(R) (NAA-SR-9700)
combustion of, facility for studying, 20: 10272(R) (NAA-SR-9339)
combustion of, particle and iodine release from, 19: 40803 (NAA-SR-Memo-9719)
combustion of, properties of aerosols produced in, 20: 37022 (LA-DC-6942)
combustion of, studies of variables and fission product release in, 20: 558 (CONF-650407, pp 94-117)
compatibility of liquid, with metals, 18: 7125(R) (LAMS-3021)
compatibility of liquid, with stainless steel–uranium carbide, 16: 823
compatibility with molybdenum alloys used as fuel cladding material, 16: 24145 (ANL-6268)
compatibility with plutonium nitride at 600°C, 17: 26944(R) (BMI-1630 (Del.))
compatibility with niobium and vanadium alloys at 650°C, 17: 41333(R) (ANL-6677)

compatibility with plutonium nitrides, 18: 24988(R) (BMI-1665(Del.))
compatibility with niobium–zirconium alloys at high temperatures, 20: 2236
compatibility with nonnuclear materials in Fermi reactor, 20: 9377 (CONF-650620, pp 85-104)
compatibility with EBR-II heat transfer system components, 20: 9416 (CONF-650620, pp 127-32)
compatibility with components of SRE heat transfer system, 20: 9415 (CONF-650620, pp 105-26)
compatibility with urania and plutonia–urania fuels, 20: 33795
components development, conference on, 20: 9376 (CONF-650620)
compressibility and thermal capacity of liquid, (E), 20: 9120(R) (APDA-178, pp 50-63)
condensation of saturated vapor in nozzles, theory, 17: 8345
condensation of vapors of, irreversible, 18: 34323
condensation of, use of electromagnetic field for control of laminar film, 19: 11365
conductivity of liquid, Lorentz number from electric and thermal, (E), 20: 9509
containment of boiling, development of loops for, 18: 12627(R) (BNL-823 (p.66-93))
contamination by hydride, response of instruments to, 18: 10345(R) (TID-20126)
content and distribution patterns of, in natural waters of Umra, Rajasthan, 17: 29098
content and distribution in acid igneous rocks of Africa, 18: 37358
content in atmosphere and on beaches, effects of weather on, 20: 4148 (AD-623515)
content in calf intestine, effects of diet on, 20: 32908(R) (ORO-648, pp 71-90)
content in cellular fluids, 17: 5694
content in diet, effects on retention of cesium-137, 17: 31836
content in distilled beryllium, calculation and determination of, 19: 22104 (UCRL-12253)
content in frogs, comparison of chemical and neutron activation analysis, 20: 46030(R) (AERE-PR-HPM-9, pp 6-17)
content in ground water in National Reactor Testing Station, Idaho, 18: 18037
content in high-velocity A stars, 18: 36135
content in human erythrocytes after irradiation, 16: 9807
content in lambs and pigs, 17: 30268
content in mammalian cells, effects of cell cycle stage on, 20: 18204(R) (LA-3432, pp 130-77)
content in meteoritic chondrules, (E), 19: 28536
content in mouse urine, radiosensitivity prediction by, 18: 33321
content in Phaseolus, effects of rare earths on, 20: 18237
content in pulmonary tissue relative to beryllium, 17: 28647
content in sea urchin egg and ionic transport across egg membrane, 17: 33503
content in sea urchin eggs, 18: 21801
content in Van Arkel-refined zirconium, comparison with Knoll-refined, 17: 33819
content in Victorian australites, 16: 2029
contents in meteorites, 18: 34398
contents in meteoritic and terrestrial matter, 19: 37428(R) (N64-32896)
corrosion and mass transfer of low-alloy and stainless steels in flowing, 20: 9414 (CONF-650620, pp 18-35)
corrosion and mass transfer of low-alloy and stainless steels in flowing liquid, 20: 39345 (GEAP-4831)
corrosion resistance to mercury at 900°F, 20: 2264
corrosive and mass transfer effects on stainless steels, 16: 28558 (TID-7623(p.135-48))
corrosive and structural effects on chromium steel and stainless steel at high temperatures, 17: 1874(R) (MSAR-62-109)
corrosive and structural effects on chromium-molybdenum carbon steel and type 316 stainless steel at 1100 and 1200°F, 17: 32571(R) (MSAR-63-105)
corrosive and structural effects on Armco Iron, chromium–molybdenum carbon steel, and types 304 and 316 stainless steel at 1200°F, 18: 8755(R) (MSAR-63-174)
corrosive effects on loop construction materials at 1870°F, 16: 16678 (TID-7626(Pt.I)(p.42-62))
corrosive effects on stainless steel at 1050 to 1600°F, 16: 16692 (TIM-490)
corrosive effects on niobium–uranium and niobium–uranium–zirconium alloys at 1600 and 1800°C, 16: 17966(R) (BMI-1541(Del.))
corrosive effects on niobium–zirconium alloys at 1500 to 2400°F, 16: 16677 (TID-7626(Pt.I)(p.23-34))
corrosive effects on austenitic and ferro-perlitic steels at 600 and 700°C, 16: 22561
corrosive effects on niobium–zirconium alloys at 2200°F, 16: 20042(R) (BNL-696)
corrosive effects on steel, carbon mass transfer, 16: 22160
corrosive effects on containment alloys and metals at high temperatures, review, 16: 25714 (DMIC-169)
corrosive effects on metal components, design of loop for studying, 16: 29089(T) (AEC-tr-5310)
corrosive effects on ceramic materials at 500 and 750°C, static, 16: 29340 (KAPL-M-LRM-2)
corrosive effects of liquid, on reactor materials, 16: 32087
corrosive effects on steel, 16: 33436(T) (AEC-tr-5408)
corrosive effects on austenitic and ferro-perlitic steels at 600 and 700°C, 16: 33437(T) (AEC-tr-5409)
corrosive effects on Hastelloy X-stainless steel loop, 16: 15147 (TIM-573)
corrosive effects on beryllium, stainless steel, and zirconium in Sodium Reactor Experiment, 16: 1191 (NAA-SR-5363)
corrosive effects of, on nitrided steel at 80 to 750°F, 16: 4450(R) (BMI-1546(Del.))
corrosive effects on carbon steels and refractory metals at 600 to 1400°F, 17: 2464(R) (BNL-731(p.59-94))
corrosive effects of liquid, on beryllium, 17: 7565(R) (PWAC-161)
corrosive effects of liquid, on reactor materials, 17: 7606(R) (ORNL-1515)
corrosive effects on beryllium oxide, 17: 7606(R) (ORNL-1515)
corrosive effects on metals at 1000 to 1600°F, 17: 11129
corrosive effects on steel at 1200°F, 17: 18750(R) (MSAR-59-133)
corrosive effects on niobium–zirconium alloys at 1400 to 2400°F, 17: 19726 (BNL-759(p.54-77))
corrosive effects on stainless steel, 17: 25733
corrosive effects on chromium–nickel and nickel steels at 1000°C, 17: 27756
corrosive effects on chromium–molybdenum steel and stainless steel at 1100 to 1200°F, 17: 29252(R) (MSAR-63-91)
corrosive effects on steels at 1000 to 1300°F, 17: 29280 (GEAP-3726)
corrosive effects on chromium–molybdenum steel and type 316 stainless steel at 1100 and 1200°F, 17: 29281(R) (MSAR-63-57)
corrosive effects, 17: 31798(R) (BNL-782(p.60-91))
corrosive effects on niobium–titanium–vanadium alloy at 650°C, 17: 35078(R) (ANL-6739)
corrosive effects on niobium alloys at 650°C, 17: 36861(R) (ANL-6764)
corrosive effects on structural materials, 17: 36873 (LADC-5783)
corrosive effects of flowing, on niobium alloys, 17: 37001(R) (ANL-6780)
corrosive effects on steels, test run data on, 17: 37479 (GEAP-4181)
corrosive effects on tantalum, 17: 40342(R) (LAMS-2973)
corrosive effects on mechanical properties of ferritic steel and stainless steel at 1200°F, 17: 39538(R) (MSAR-63-125)
corrosive effects on austenitic and ferritic steels at 1100 and 1200°F, 18: 564(R) (MSAR-63-142)
corrosive effects of liquid, 18: 3298(R) (ORNL-2221(Pts.1-5)(Del.))
corrosive effects of flowing, on niobium alloys, 18: 3038(R) (ANL-6801)
corrosive effects of liquid, on steels and tantalum, 18: 2186
corrosive effects on steels and zirconium, 18: 2187
corrosive effects on chromium–molybdenum alloy steels at high temperatures, 18: 4167 (NAA-SR-7544)
corrosive effects on molybdenum, niobium, niobium–zirconium alloy, and tantalum at 760 to 1315°C, 18: 4160(R) (BNL-799(p.74-100))
corrosive effects on stainless steel and steel, 18: 4195 (GEAP-4182)
corrosive effects on steels at high temperatures, test facilities for, 18: 4197 (MSAR-63-161)
corrosive effects on chromium–molybdenum carbon steel at 1100°F, 18: 4201(R) (TID-19756)
corrosive effects on steel, test loops for studies of, 18: 7137 (GEAP-3725)
corrosive effects on type 347 stainless steel under magnetostriction cavitation conditions, 18: 7931(R) (PRDC-TR-74)
corrosive effects of liquid, on reactor materials, 18: 8760
corrosive effects on mechanical properties of chromium–molybdenum steel and type 316 stainless steel at high temperatures, 18: 10472(R) (MSAR-64-6)
corrosive effects on stainless steel and steels, test run data on, 18: 12575 (GEAP-3726(Vol.3))
corrosive effects on mechanical properties of chromium–molybdenum steel and stainless steel, 18: 12582(R) (MSAR-64-14)
corrosive effects on austenitic stainless steels, 18: 12583(T) (AEC-tr-6328)
corrosive effects on Type-304 stainless steel, 18: 14379 (TID-7676(p.25-37))
corrosive effects of liquid, on steels, 18: 14417
corrosive effects on reactor materials, 18: 15563
corrosive effects on type 316 stainless steel, 18: 15566
corrosive effects of cold- and hot-trapped, on tantalum, 18: 15567
corrosive effects on reactor materials, 18: 15568
corrosive effects on niobium alloys at 650°C, 18: 15663(R) (ANL-6808)

corrosive effects on stainless steel clad-ceramic fuels, 18: 14532(R) (CEND-190)
corrosive effects of liquid, on plutonium nitride, 18: 17351(R) (BMI-1659(Del.))
corrosive effects on reactor fuel cladding materials at 540 and 650°C, effects of carbon and oxygen content on, 18: 19456(R) (ANL-6840)
corrosive effects of liquid, technical progress review on, 18: 18307
corrosive effects on mechanical properties of type 316 stainless steel at 1200°F, 18: 18314 (MSAR-64-18)
corrosive effects on chromium-molybdenum steel at 1100°F, effects of carbon and oxygen on, 18: 18315(R) (MSAR-64-30)
corrosive effects on type 316 stainless steel at 1200°F, effects of carbon and oxygen on, 18: 18315(R) (MSAR-64-30)
corrosive effects on niobium and vandium alloys, 18: 21698(R) (ANL-6860)
corrosive effects on AISI 316 SS, Hastelloy C, Incoloy, molybdenum, and Timken 16-25-6 at 1200°F, 18: 20472 (NAA-SR-Memo-9340)
corrosive effects on metals, 18: 25937
corrosive effects on refractory alloys at 650°C, 18: 26893(R) (ANL-6868 (p.11-108))
corrosive effects of liquid, effects of carbon on, 18: 27891 (NASA-SP-41(p.61-5))
corrosive effects of liquid, downstream effect in, 18: 27897 (NASA-SP-41 (p.91-5))
corrosive effects on stainless steel and chromium–molybdenum steel at high temperatures, 18: 30131(R) (MSAR-64-65)
corrosive effects of liquid, on reactor materials, 18: 32072
corrosive effects of liquid, review of, 18: 32082 (A/CONF.28/P/244)
corrosive effects on stainless steel and other iron alloys, mechanism of, 18: 32084 (GEAP-4313)
corrosive effects of flowing, on chromium steel, chromium–molybdenum steel, and stainless steel, 18: 34073(R) (GEAP-4438)
corrosive effects on steels at high temperatures, 18: 35956(R) (MSAR-64-93)
corrosive effects on compatibility of uranium carbide fuels with cladding materials, 18: 35957 (NAA-SR-7502)
corrosive effects on mechanical properties of chromium–molybdenum steel at 1100°F in air and helium, 18: 35988 (MSAR-64-81)
corrosive effects on steels, development of loop and techniques for studying, 18: 35955(R) (MSAR-60-34)
corrosive effects on titanium–vanadium alloys, 18: 36751 (ANL-6912)
corrosive effects on aluminum–iron alloys, 18: 37604 (A/CONF.28/P/71)
corrosive effects on reactor materials, 18: 37634 (A/CONF.28/P/343)
corrosive effects on low-alloy steel, 18: 38467 (A/CONF.28/P/537)
corrosive effects of boiling, on niobium–zirconium alloy, 18: 41933 (TID-11295(3rd Ed.))
corrosive effects on reactor materials, 18: 41947
corrosive effects on zirconium at high temperatures, 18: 44926(R) (ANL-6923(p.46-78))
corrosive effects on titanium–vanadium alloys at 650°C, 18: 44925(R) (ANL-6923(p.14-45))
corrosive effects on mechanical properties of chromium-molybdenum steel and type 316 stainless steels at 1200°F, 19: 928(R) (MSAR-64-112)
corrosive effects on Croloy 2¼ steel to 1200°F, 19: 565(R) (BAW-1280-15)
corrosive effects on Croloy 2¼ steel to 1200°F, 19: 566(R) (BAW-1280-16)
corrosive effects on Croloy 2¼ steel at 1250°F, 19: 568(R) (TID-20894)
corrosive effects on steels at 1200°F, 19: 4590(R) (MSAR-61-42)
corrosive effects on steel at 1200°F, 19: 4591(R) (MSAR-61-105)
corrosive effects on steel at 1200°F, 19: 4592(R) (MSAR-61-114)
corrosive effects on Croloy 2¼ and type 316 stainless steel, design stress curves for minimizing, 19: 4613 (BW-67-3)
corrosive effects on steels at 1200°F, research program on, 19: 4618(R) (MSAR-61-60)
corrosive effects on steels at 1200°F, 19: 4619(R) (MSAR-61-67)
corrosive effects on steels at 1200°F, equipment for studies of, 19: 4620(R) (MSAR-61-100)
corrosive effects on mechanical properties of chromium–molybdenum steel and type 316 stainless steel at 1100 and 1200°F, 19: 4621(R) (MSAR-62-142)
corrosive effects on mechanical properties of chromium–molybdenum steel and type 316 stainless steel at 1100 and 1200°F, 19: 4622(R) (MSAR-62-159)
corrosive effects on mechanical properties of chromium–molybdenum steel and type 316 stainless steel at 1100 and 1200°F, 19: 4623(R) (MSAR-63-6)
corrosive effects on steels at 1200°F, 19: 4624(R) (MSAR-63-75)
corrosive effects on reactor fuel alloy at 1000°F, 19: 4625 (NDA-14-22)
corrosive effects on steels at 450, 600, and 750°C, 19: 4629
corrosive effects on stainless steel and steels, test run data on, 19: 7866 (GEAP-4437)
corrosive effects on mechanical properties of type 304 and 316 stainless steel, 19: 11692(R) (MSAR-64-144)
corrosive effects on alloys, facility for studying, (E), 19: 13916 (SAN-8002(p.189-209))
corrosive effects of calcium-gettered, on zirconium alloys at 650°C, 19: 14765(R) (ANL-6977)
corrosive effects on reactor components and materials, facility for determining, (E), 19: 13599 (SAN-8002(p.151-75))
corrosive effects on Croloy 2¼ and type 316 stainless steel components in model steam generator, 19: 15712(R) (BAW-1280-18)
corrosive effects on titanium–vanadium alloys at 650°C, 19: 17176(R) (ANL-6965(p.1-41))
corrosive effects on materials in steam generator, 19: 20107(R) (BAW-1280-22)
corrosive effects on cerium–cobalt–plutonium alloys at 650°C, 19: 21690(R) (LA-3244)
corrosive effects on stainless steels, literature survey, 19: 20472 (IDO-14651)
corrosive effects on plutonium nitrides, 19: 22864(R) (BMI-1704(Del.))
corrosive effects on steel in loop tests, 19: 22894 (GEAP-4183)
corrosive effects on mechanical properties of chromium-molybdenum steel and type 316 stainless steel, 19: 22896(R) (MSAR-65-47)
corrosive effects on titanium–vanadium alloys at 650°C, 19: 23991(R) (ANL-7003)
corrosive effects on zirconium, 19: 23991(R) (ANL-7003)
corrosive effects of boiling on refractory metal alloys, 19: 22890 (BNL-9018)
corrosive effects on stainless steel at 600 to 1300°C, 19: 27735(R) (NAA-SR-10850)
corrosive effects on titanium–vanadium alloys at 650°C, 19: 29468(R) (ANL-7017)
corrosive effects on zirconium at 540°C, 19: 29468(R) (ANL-7017)
corrosive effects on refractory metals at 1260°C, 19: 28764
corrosive effects on refractory alloys at high temperatures, 19: 31462(R) (ANL-7028)
corrosive effects on titanium–vanadium alloys at 650°C, effects of oxygen on, 19: 35604(R) (ANL-7045(p.1-23))
corrosive effects on chromium–titanium–vanadium alloys, effects of oxygen on, 19: 35604(R) (ANL-7045(p.1-23))
corrosive effects on niobium–titanium–vanadium alloys at 650°C, effects of oxygen on, 19: 35604(R) (ANL-7045(p.1-23))
corrosive effects on molybdenum–titanium–vanadium alloys at 650°C, effects of oxygen on, 19: 35604(R) (ANL-7045(p.1-23))
corrosive effects on tantalum–titanium–vanadium alloys at 650°C, effects of oxygen on, 19: 35604(R) (ANL-7045(p.1-23))
corrosive effects on metals, 19: 34643
corrosive effects on refractory alloys at high temperatures, 19: 36949(R) (BNL-900(p.121-97))
corrosive effects on titanium–vanadium alloys at 650°C, 19: 40177(R) (ANL-7046(p.1-35))
corrosive effects on zirconium at 540°C, 19: 40112(R) (ANL-7046 (p.36-66))
corrosive effects of vaporous, on zirconium, 19: 40113(R) (ANL-7071)
corrosive effects on type 316 stainless steel, effects of carbon and oxygen on, 19: 40969(R) (MSAR-65-96)
corrosive effects on zirconium at 540°C of oxygenated, effects of polarizing current on, 19: 44616(R) (ANL-7000, pp 122-37)
corrosive effects of oxygen-contaminated, on titanium–vanadium alloys, 19: 44587(R) (ANL-7000, pp 3-63)
corrosive effects on type 316 stainless steel at 1000°F, 20: 769(R) (NASA-CR-54459)
corrosive effects on titanium–vanadium alloys, 20: 3320(R) (ANL-7082, pp 1-28)
corrosive effects on metals, dependence on polarization, 20: 3321(R) (ANL-7082, pp 29-53)
corrosive effects on niobium–zirconium alloy at high temperatures, 20: 2268
corrosive effects of flowing, on type-316 stainless steel at high temperatures, 20: 2274
corrosive effects on metals, loop geometry effects on, 20: 2295
corrosive effects on austenitic and ferritic steel, in pumped systems, 20: 2296
corrosive effects on stainless steel and other structural materials, review on, 20: 4318 (CNLM-5359)
corrosive effects on binary vanadium alloys, 20: 6601(R) (ANL-7115, pp 1-41)
corrosive effects on vanadium–20 titanium alloy at 650°C, 20: 5846
corrosive effects on stainless steel, effects of corrosion loop location on, 20: 5846
corrosive effects on chromium–titanium–vanadium alloy, effects of chromium content on, 20: 5851
corrosive effects on mechanical properties of austenitic stainless steel, 20: 8394(R) (NAA-SR-11450, Sect.2)

corrosive effects on Croloy 2¼ and type 316 stainless steel, 20: 9418 (CONF-650620, pp 204-31)
corrosive effects of liquid, on nickel-base brazing alloys at 700 and 1200°F, 20: 9422 (NAA-SR-11326)
corrosive effects on niobium–1 zirconium alloy at 2000°F, 20: 9423(R) (NASA-CR-54735)
corrosive effects on steels at 1000 to 1200°F of flowing, equation for, 20: 11227
corrosive effects of oxygen-contaminated, on refractory alloys, (E), 20: 14007(R) (ANL-7122, pp 1-41)
corrosive effects on aluminum–titanium–vanadium alloys, 20: 16060(R) (ANL-7152, pp 1-49)
corrosive effects on mechanical properties of type 304 stainless steel at 1200°F, 20: 14981(R) (MSAR-66-09)
corrosive effects on chromium–molybdenum steel and type 316 stainless steel, 20: 14979 (GEAP-4835)
corrosive effects on type 316 stainless steel at 1100 and 1200°C, mechanisms of, 20: 16970 (GEAP-4832)
corrosive effects on Croloy 2¼ steel, 20: 16599(R) (BAW-1280-34)
corrosive effects on alloy steels, 20: 23601(R) (GEAP-4837)
corrosive effects on titanium–vanadium alloys at 650°C, 20: 26394(R) (ANL-7193)
corrosive effects on niobium–zirconium alloys at high temperatures, 20: 25474(R) (BNL-954, pp 122-67)
corrosive effects on titanium carbides and tungsten carbides at 1205°C, 20: 25474(R) (BNL-954, pp 122-67)
corrosive effects on reactor materials at high temperatures, effects of carbon on, 20: 31213(R) (ANL-7175, pp 119-58)
corrosive effects on vanadium–titanium alloys at 650°C, effects of oxygen content on, 20: 31669
corrosive effects of liquid, on stainless steels and vanadium-based alloys, 20: 33822
corrosive effects on heat-resisting alloys at 1315 to 2200°C, 20: 25474(R) (BNL-954, pp 122-67)
corrosive effects on chromium–titanium–vanadium alloys at 650°C, 20: 36391(R) (ANL-7219, pp 1-27)
corrosive effects on titanium–vanadium alloys at 550 to 750°C, 20: 45106(R) (ANL-7249)
corrosive effects of liquid on steels in loops, statistical analysis of data on, 20: 43826 (GEAP-4830)
corrosive effects on vanadium-base alloys at 650°C, 20: 43809 (BNL-50003)
corrosive effects on stainless steel 304, 20: 45106(R) (ANL-7249)
corrosive effects of liquid on five alloys to 1500°F, 20: 46154 (NASA-CR-72035)
creep, activation quantities for, 16: 18040 (TID-15209)
critical flow of liquid, model calculations, 19: 11346 (COO-926-33)
critical temperature and densities of liquid and vaporous, 20: 12815 (ANL-7025)
crystal dynamics, frequency-wave vector, 17: 575
crystal lattice dynamic properties, (T), 19: 16120
crystal lattice dynamics, neutron spectrometric studies of, 16: 32107 (AECL-1571)
crystal lattice vibrations in, model for, 18: 28005
crystal lattice vibrations in, (T), 19: 14078
crystal lattice vibrations in, frequency distribution of, 17: 25808
crystal vacancy concentration in, 18: 22514
crystal vacancy concentration in, equilibrium, 19: 982
crystallization with thionalid, tracer study of, 16: 12961 (USNRDL-TR-551)
cyclotron resonance with helicon waves in, Doppler-shifted, 18: 22571
defects in, measurement of equilibrium concentrations of point, 19: 22988(R) (NYO-2811-23)
density and thermodynamic properties of, 20: 20802(R) (ANL-7055, pp 21-98)
density as a function of temperature to 2000°F, 19: 32724(R) (AFML-TR-65-99)
density of cooling liquid, effects on reactivity in fast dilute reactors of, 16: 21711 (AEEW-M-225)
density of vapors of, use of interferometric and optical pumping techniques in measuring, 17: 32047 (TID-19198)
density of, at critical temperature, radiometric techniques for measuring critical, 20: 29742
design of high-temperature pressure transducer for molten systems at 100 to 400°C, 16: 30584 (LA-2727)
desorption and diffusion from metals, activation energies for, 16: 19568
detection limit and sorption characteristics of, use of hollow cathode tube for study of, 17: 24080
determination, activation, 16: 2967(R) (TID-14310)
determination as impurity in and volatilization from tungsten, semi-quantitative spectrographic, 16: 4131 (BM-RI-5903)
determination as impurity in natural fluorites by activation methods, 19: 17835
determination by activation analysis, interference of (n,p), (n,α) to (n,γ) reactions in, (E), 19: 29318
determination by calculation of weight from activities and neutron fluxes measured after irradiation, 18: 27297
determination by charged-particle reactions at 2 Mev, 20: 43097
determination by flame photometry, 19: 44122
determination by flame photometry, 20: 4053
determination by radiocomplexometric back titration using silver-110-labeled silver iodate, 19: 9067
determination by spectroscopy using high-frequency plasma flames, 18: 10020
determination by spectrochemical methods, voltage-fluctuation patterns in, 19: 40416
determination by thermal-neutron activation methods, sensitivity for, 19: 9071
determination by x-ray fluorescence analysis, 19: 22154
determination in aluminum, activation, 17: 39013
determination in artificial graphite, 18: 9584
determination in aluminum and magnesium, effects of threshold reactions on activation, 19: 4085
determination in alumina, flame photometric, 19: 26233 (PG-Report-628)
determination in alum, alumina, and gelatin by neutron activation, 19: 26262
determination in aluminum by flame photometry, 19: 46207
determination in automobile lubricants, activation, 20: 14439(R) (GA-5556)
determination in automobile tire rubber, activation, 20: 14439(R) (GA-5556)
determination in automobile paint, activation, 20: 14439(R) (GA-5556)
determination in asbestos using ion exchange, activation, 20: 16336(R) (NYO-10175)
determination in aluminosilicate rocks by fast-neutron activation, 20: 33172(T) (AEC-tr-6639, pp 64-6)
determination in americium and plutonium by spark-source mass spectrography, 20: 40816 (RFP-699)
determination in aluminum and aluminum alloys by activation methods, 20: 43155
determination in beryllium flake and powder by carrier distillation, spectrographic, 16: 4136 (PG-Report-58(2nd Ed.))
determination in beryllium, flame photometric, 16: 25274 (Y-1394)
determination in biological materials, neutron-activation, 16: 12985
determination in blood serum, flame photometric method, 17: 17706 (PG-Report-424)
determination in beryllium, activation, 17: 25123
determination in blood, lake water, and urine, thermal neutron activation, 18: 5220
determination in bismuth, activation, 18: 13682
determination in biphenyl and diphenylmethane, activation, 19: 2241
determination in biologic material, activation analysis method for, 19: 9075
determination in biological tissues, activation, 19: 15333 (AE-168)
determination in biological fluids, activation, 19: 17817
determination in beryllium by activation, 19: 24415
determination in biological materials, neutron activation, 19: 46165 (CEA-R-2837)
determination in beef heart, neutron activation, 19: 45753 (AE-191)
determination in beryllium oxide, spectrographic comparison of standards on, 20: 6998 (AAEC/TM-294)
determination in biological materials, activation, 20: 22928
determination in bones, neutron activation and autoradiographic, 20: 22565
determination in boron by neutron activation, 20: 33173(T) (AEC-tr-6639, pp 67-9)
determination in biological materials, radiochemical separation methods for activation, 20: 38842
determination in blood serum, activation, 20: 38851
determination in biological materials, use of automated gamma spectrometers in activation, 20: 38843
determination in chicken by neutron activation, 16: 20337
determination in carbon, activation, 17: 17987
determination in clays, rocks, and sands, activation, 18: 43401
determination in cerium and erbium, mass spectrographic, 19: 2232
determination in cottonseed, activation, 19: 19771(R) (TEES-2671-4 (Chap.9))
determination in copper by activation, 19: 40422
determination in carbonate, phosphate, silicate, and uranium rocks, flame photometric, 19: 46191
determination in commercial plastics, activation, 20: 14439(R) (GA-5556)
determination in cigarette tobacco, activation, 20: 14439(R) (GA-5556)
determination in conductive tissue of beef heart, activation, 20: 31176
determination in drugs, activation, 19: 4081
determination in drugs, hair, oils, river silts, soils, and tobacco, activation, 20: 1739(R) (GA-4297)

determination in europium oxide, spectrographic, 17: 2931
determination in europium, thulium, and ytterbium, atomic absorption spectrophotometric, 17: 40727
determination in enamel of teeth, neutron activation, 19: 38562
determination in filter papers by neutron activation methods, 19: 19786
determination in graphite by x-ray spectrography, 19: 38571
determination in greases and soils, activation, 20: 1728(R) (GA-4041)
determination in glass samples, activation, 20: 14439(R) (GA-5556)
determination in graphite by x-ray spectrography using direct electron excitation, 20: 26755
determination in high-purity aluminum by proton irradiation and mass spectrometry, 16: 4145
determination in human teeth, gamma spectrometric, 16: 8671 (AE-61)
determination in human mandibular articular disc by gamma spectrometry and neutron activation, 17: 28811
determination in human whole blood, activation, 17: 40739
determination in hair by activation methods for identification of individuals, 19: 17824
determination in heavy fuel oils by neutron-activated analysis, 19: 38550
determination in hair and paint in criminal cases, activation, 20: 8827(R) (GA-6152)
determination in hair samples in criminal cases, activation, 20: 14439(R) (GA-5556)
determination in human heart tissue, activation, 20: 31175
determination in lead, activation, 18: 13677
determination in man, tracer study, 16: 14416
determination in meteorites and terrestrial rocks, activation, 17: 33851
determination in molybdenum and its compounds, spectrographic, 18: 17766
determination in marble samples from Aegean Islands, Greece, and Turkey, activation, 19: 5830
determination in meteorites, activation, 19: 7349
determination in minerals by neutron activation, 19: 30424
determination in mineral and natural waters, flame photometric, 20: 38798 (NIJS-R-465)
determination in mosaic virus and nucleic acids in tobacco plants, activation, 20: 38846
determination in niobium by radioactivation analysis, 16: 23633 (TID-7629(p.239-44))
determination in natural diamonds, activation, 17: 31995
determination in nucleic acids, activation, 18: 19892
determination in niobium and tantalum by activation, 19: 24416
determination in nuclear grade uranium, flame photometric, 19: 42418 (NIJS-R-448)
determination in nuclear grade uranium by flame photometry, 20: 26811
determination in ocean-bottom cores by activation analysis, 17: 15886 (TID-18125)
determination in ocean-bottom core samples by activation analysis, engineering drawings of equipment for, 17: 35667
determination in oils and silts in water, activation, 20: 14439(R) (GA-5556)
determination in organic compounds containing sulfur, spectroscopic, 20: 26776
determination in polyphenyls by activation analysis, 17: 38945
determination in pure aluminum, activation, 19: 19775(R) (UCRL-11828(p.197-9))
determination in powdered samples by spectrochemical methods, 19: 22120
determination in polycarbonates by neutron activation, 19: 36263
determination in plutonium fluorides and peroxides, review on spectrographic, 20: 14464 (RFP-599)
determination in paper samples in criminal cases, activation, 20: 14439(R) (GA-5556)
determination in potassium halogenides, activation, 20: 20560 (EUR-2753.f)
determination in polyethylene by activation analysis, 20: 33168(T) (AEC-tr-6639, pp 46-9)
determination in powder samples by spectrographic methods, semi-quantitative, 20: 43104
determination in quartz, activation, 18: 33494
determination in quartz crystals from Providencia area, Zacatecas, Mexico, activation, 20: 18631 (NYO-2266-1)
determination in rare earth oxides, spectrographic method for, 16: 20327
determination in rare earths at 1 to 1000 ppm level, 17: 1377 (BM-RI-6097)
determination in rocks, activation, 18: 39516(T) (AEC-tr-6390(p.355-64))
determination in rocks and soils in Norway, activation, 19: 308
determination in rice whiskey, activation, 20: 14439(R) (GA-5556)
determination in silicate minerals and rocks, neutron activation, 16: 5278
determination in salt solutions by spectrophotometric titration using 1,3-dimethylvioluric acid, 16: 12968
determination in silicate rocks, x-ray fluorescence spectrographic, 16: 30353
determination in silicates, flame photometric, 16: 32939
determination in silica-alumina gels by neutron activation, 17: 4482
determination in sea-urchin eggs, activation, 17: 30117
determination in sodium tungsten bronze, activation, 17: 31994
determination in siliceous rocks, activation, 18: 5514
determination in silicon and silicon oxides by gamma spectrometry, 18: 15981
determination in silicon, activation, 18: 33502
determination in surface waters by activation analysis, 18: 37072 (A/CONF.28/P/854)
determination in silicon, activation, 19: 2240
determination in sea water, activation, 19: 10983(R) (TEES-2671-3)
determination in sea urchin eggs, activation, 19: 32103
determination in selenium by neutron activation methods, 20: 1769
determination in soils, activation, 20: 14439(R) (GA-5556)
determination in silicon dioxide, activation, 20: 20633
determination in sulfide ores by neutron activation methods, 20: 26759
determination in silicates, activation, 20: 26782
determination in silicon by neutron activation, model for error analysis in, 20: 33162(T) (AEC-tr-6639, pp 18-21)
determination in silicon oxides, MOS and radiochemical, 20: 36744
determination in sintered and zone refined boron-10, spectrographic, 20: 43090(R) (TID-23342)
determination in telluric acid, neutron-activation, 16: 7487(T) (JPRS-10874)
determination in terphenyls and plastics, neutron activation, 17: 23273
determination in terphenyls, activation, 17: 28813
determination in tissue, after neutron activation, 17: 31813 (AERE-R-4309)
determination in tungsten activation, 18: 3701
determination in tissue samples, activation, 18: 21980
determination in tantalum by anion exchange in hydrofluoric–nitric acid mixtures, 18: 35455
determination in terphenyls, use of computers in activation, 19: 7335
determination in tungstic hydride, spectrographic, 19: 30144
determination in tungsten bronze, spectrographic, 20: 3863(R) (IS-1200 (Sect. C))
determination in thumbnail clippings, activation, 20: 14439(R) (GA-5556)
determination in tin oxide, activation, 20: 20577
determination in uranium tetrafluoride, spectrographic, 16: 11515 (PG-Report-59)
determination in uranyl nitrates by flame photometric analysis, 16: 11774(R) (NLCO-685)
determination in uranium compounds, spectroscopic, 16: 20525(R) (MCW-1472)
determination in uranium concentrates and ores, gravimetric, 16: 130 (PG-Report-3)
determination in uranium and its compounds, flame photometric, 18: 13701
determination in uranium trioxide by emission spectrography, 20: 40802 (HW-65402(Rev.1))
determination in water, silver-spark spectrographic, 17: 1381 (IDO-14591)
determination in water produced in nuclear reactors for marine propulsion, methods for, 17: 33789 (EUR-224.i)
determination in wood in criminal cases, activation, 20: 14439(R) (GA-5556)
determination in zirconium by activation, 19: 24418
determination of, in complex matrices, activation, 17: 19940 (IA-799)
determination of traces, flame photometric, 16: 134(T) (CEA-tr-X-400)
determination of trace amounts in rare earth compounds, spectrographic, 16: 28869 (JEN-107-DQ/I-33)
determination of trace amounts of, in biological materials, radiochemical, 18: 19841 (CONF-187-112)
determination of trace amounts of, in snails, radiochemical, 18: 19841 (CONF-187-112)
determination of trace amounts in uranium compounds, activation, 20: 1784
determination of trace amounts of, in uranium dioxide, 20: 14494
determination of trace amounts of, by reactor neutron activation methods, 20: 26760
determination of traces of, in crude oils, by nondestructive activation analysis, 20: 33196
determination of, by alpha scattering methods, 20: 22964
determination of, in carbazole by neutron activation methods, 20: 43116
determination of, in standard rocks by neutron activation and gamma spectrometric methods, 20: 45587
determination of, in water by neutron activation analysis using freezing, 20: 45602
determination, use of photoneutron counting in activation, 19: 36322
determination, use of pulsed neutrons in activation, 19: 36323
development and testing of regenerative lead–sodium bimetallic emf cells, (E), 20: 14179(R) (ANL-7122, pp 70-81)

diffusion along dislocations in lithium fluoride crystals, 17: 37594
diffusion coefficient and lifetime in electric arc-plasma, 16: 15312(T)
diffusion in agar gels, self-, 20: 25099
diffusion in dilute aqueous solutions of, 17: 21706
diffusion in mixed solutions of heparin sodium salt and cesium chloride, tracer studies of, 20: 8928
diffusion in molten sodium nitrate, coefficient of, 20: 38871(R) (NYO-1769-54)
diffusion in oxide melts, 16: 16048
diffusion in oxide melts, 16: 24038(T) (AEC-tr-5191)
diffusion into liquid sodium chloride, temperature effects on, 18: 31492
diffusion near 238°K to 3500 atm, self, 16: 15220
diffusion of atoms of, in arc discharge, (E), 19: 21555
diffusion of carbon in liquid, 16: 32951 (NAA-SR-Memo-7497)
diffusion of fission products from melted irradiated uranium in liquid, 17: 31684 (NAA-SR-Memo-8247)
diffusion of fission products in, from uranium carbide, 18: 13233(R) (BNL-823(p.1-19))
diffusion of fission products into, from irradiated cerium–cobalt–plutonium alloys, 20: 5848
diffusion of fission products from high-temperature, factor affecting, 20: 40357 (NAA-SR-11766)
diffusion of iodine in, at 900 to 1400°F, 18: 25326 (NAA-SR-Memo-9383)
diffusion of liquid, neutron scattering studies of, 16: 24271 (AERE-R-4043)
diffusion of lithium-6 and -7 in, isotope effect in, 20: 3305(T)
diffusion of nickel in, to molybdenum surface, 18: 27893 (NASA-SP-41 (p.73-4))
diffusion through cellophane membrane, coefficients of, 20: 43239
diffusion through zinc phosphate membranes, 16: 28857
dilatometry in argon and helium, 19: 22988(R) (NYO-2811-23)
dislocation on {110} planes in bcc, dissociation of, 20: 33918
dislocations in primary slip systems of crystals of, dynamic behavior of, 17: 37526
dissolution from uranium carbide fuels using butyl cellosolve and butyl bromide, 19: 11278
dissolution of stainless steel-clad, in nitric acid, electrolytic, 17: 4295(R) (DP-740)
dissolution of stainless steel-clad, in nitric acid, electrolytic, 17: 32192(R) (DP-839)
distribution among cellular fractions of dog kidney, 20: 35224
distribution between aqueous waste and CSREX solvent, 17: 35244 (HW-SA-2982)
distribution coefficient between immiscible phases in aluminum chloride–lithium chloride–potassium chloride system at 625°C, 17: 35616 (HW-SA-2804)
distribution in D2EHPA-aqueous system, tracer studies of, 17: 40713 (TID-7655(p.312-20))
distribution in liquid cerium–cobalt–plutonium fuel irradiated in contact with sodium, 19: 16219 (LA-DC-6753)
distribution in microcline and quartz sand, 17: 2643 (UCRL-13048)
distribution in soils at Eurochemic site in Belgium, 16: 34144(T,R) (EURAEC-275)
effects as carrier in precipitation of sodium-22 with potassium perchlorate, 20: 35423
effects in cesium-vapor ion propulsion engines, 18: 29825(R) (NP-14044)
effects of carbon-contaminated, on austenitic stainless steel, 20: 2244
effects of films of, on work function of pyrographite, 18: 30166(R) (AD-439716)
effects of high-carbon and -oxygen, on mechanical properties of type 316 stainless steel at 1200°F, 19: 18457(R) (MSAR-65-38)
effects of high-carbon, on mechanical properties of type 316 stainless steel, at 1200°F, 20: 11235 (MSAE-65-194)
effects of high-carbon liquid, on types 304 and 316 stainless steels, 20: 33817 (MSAR-66-119)
effects of high-oxygen, on 304 stainless steel creep-rupture properties, 20: 43809 (BNL-50003)
effects of high-temperature, on instruments and mechanical devices, 20: 46966(R) (NAA-SR-12010)
effects of liquid, on design and materials of mechanical parts, 17: 3378(R) (BMI-1583(Del.))
effects of liquid, on friction and wear of sliding surfaces, 17: 14727(R) (BMI-1600(Del.))
effects of liquid, on creep and fatigue properties of chromium–molybdenum steel and type 316 stainless steel, 18: 8754 (MSAR-63-168)
effects of liquid, on physical properties of steels, (E), 19: 13998 (SAN-8002(p.210-30))
effects of liquid, on stainless steel, 18: 1245 (LADC-5936)
effects of molten, on chromium–molybdenum and stainless steels, 17: 14768(R) (MSAR-63-33)
effects of oxygen-contaminated, on mechanical properties of type 316 stainless steel at 1200°F, 20: 29704 (MSAR-66-78)
effects of sorbed, on germanium crystal electron reflection, 19: 41124(R) (NP-15108)
effects of sorbed, on germanium and silicon work function, 19: 41124(R) (NP-15108)
effects of various salts of, on growth of Clostridium in fish, 20: 9313 (CONF-651024, pp 3-6)
effects of, on enzyme activity in erythrocyte membranes, 18: 29342
effects on air ionization in space vehicle hypersonic re-entry flights, 19: 41121 (N64-30658)
effects on carbon content of austenitic stainless steels, 19: 26768(R) (MSAR-65-62)
effects on ceramic reactor fuels, 19: 20458 (GEAP-4283)
effects on cesium fuel for ion engines, 18: 20626(R) (NP-13800)
effects on cesium ionization, impurity, 18: 35491(R) (ASD-TDR-63-476(Pt.II))
effects on cesium-137 uptake by pea and wheat plants, 19: 51
effects on cesium-137 content in peas and wheat, 19: 14982
effects on chlorine determination in paper pulp by activation methods, 20: 8854
effects on chromium–molybdenum and stainless steel at 1200°F, 17: 18756(R) (MSAR-63-47)
effects on conversion of radioactive wastes to glass-like solids for disposal, 20: 42690(P)
effects on creep-rupture properties of chromium–molybdenum carbon steel and type 316 stainless steel at 1100 and 1200°F, 17: 34406(R) (MSAR-63-117)
effects on creep rate of type 316 stainless steel at 1200°F, 20: 11227
effects on Croloy 2¼ and type 316 stainless steel, 19: 7676(R) (BAW-1280-20)
effects on crystal structure of barium and strontium tantalates, 19: 13308
effects on defective ceramic fuel elements, internal vapor-pressure, 19: 1872 (CONF-446-41)
effects on design stress for Croloy 2¼ and type 316 stainless steel, 20: 5851
effects on determination of copper by neutron activation methods, 18: 43436
effects on determination of lithium in uranium by flame photometry, 20: 25014
effects on determination of gold in ores by neutron activation, 20: 33171(T) (AEC-tr-6639, pp 60-3)
effects on determination of silver in solutions by activation analysis, 20: 33179(T) (AEC-tr-6639, pp 92-6)
effects on determination of chromium in ores by neutron activation analysis, 20: 36750
effects on dimensions of graphite combined with effects of fast neutrons, 20: 9570 (CONF-650620, pp 47-84)
effects on distribution of strontium-90 in water-bearing strata by ground waters, 19: 46602
effects on electron spin resonance of boronated graphite, (E), 20: 44008
effects on ESR spectra of polycrystalline graphite, 20: 23785
effects on fatigue behavior of large stainless steel bellows at 1200°F, 18: 39404 (NAA-SR-9762)
effects on flame photometry of cesium, 19: 7368
effects on friction and wear properties of molybdenum–tungsten–chromium alloys, 20: 7588
effects on friction and wear of sliding surfaces, 17: 35251(R) (BMI-1632(Del.))
effects on Inconel centrifugal pump impellers during operation at 1050 to 1400°F, 17: 39228
effects on lubricating properties of fused fluoride coatings on chromium–nickel alloy, 18: 33695 (NASA-TN-D-2348)
effects on mechanical properties of Cr–Mo and stainless steels, 17: 3425(R) (MSAR-62-126)
effects on mechanical properties of chromium–molybdenum steel and type 316 stainless steel, 18: 22445(R) (MSAR-64-45)
effects on mechanical properties of chromium–molybdenum steel and types 304 and 316 stainless steel at 1200°F, 19: 6298(R) (MSAR-64-126)
effects on mechanical properties of stainless steels at 1200°F, 19: 11726(R) (MSAR-65-05)
effects on mechanical properties of stainless steels at 1200°F, 19: 18456(R) (MSAR-65-28)
effects on mechanical properties of Croloy 2¼ at 1100°F, 20: 5846
effects on mechanical properties of chromium–molybdenum steel, 20: 11227
effects on mechanical properties of austenitic and ferritic stainless steel at high temperatures, 20: 25567(R) (MSAR-66-71)
effects on mechanical properties of steels at 1100°F, 20: 43897 (MSAR-66-174)
effects on neutron-induced dimension changes in graphite, 20: 31667
effects on nitrogen-14 hyperfine coupling constants in EPR spectra of chloronitrobenzene, 18: 16068
effects on physical properties of stainless steel at 1200°F, 17: 18754(R)

(MSAR-62-77)
effects on physical properties of stainless steel at 1200°F, 17: 18755(R) (MSAR-62-92)
effects on physical properties of stainless steel at 1200°F, 17: 18751(R) (MSAR-62-33)
effects on physical properties of stainless steel at 1200°F, 17: 18752(R) (MSAR-62-41)
effects on physical properties of stainless steel at 1200°F, 17: 18753(R) (MSAR-62-50)
effects on physical properties of stainless steel at 1200°F, 18: 7149(R) (MSAR-62-12)
effects on physical properties of type 316 stainless steel at 1200°F, 18: 32144(R) (MSAR-64-75)
effects on physical properties on Armco iron, chromium-molybdenum steel, and stainless steel at 1200°F, 19: 901(R) (MSAR-64-102)
effects on physical properties of graphite at high temperatures, 20: 8394(R) (NAA-SR-11450, Sect.2)
effects on potassium chloride absorption center properties, 16: 2338
effects on properties of chromium steel and stainless steel at 1200°F, 17: 533(R) (MSAR-61-29)
effects on properties of Purex Waste-2 melts, 20: 24809(R) (BNWL-213)
effects on radiochemical determination of strontium in animal or vegetable samples, 20: 22906
effects on radioinduced reactions between stainless steel and uranium silicides, 19: 42805 (NAA-SR-10621)
effects on radioinduced polymerization of solid 3,3-*bis*-chloromethyl-oxetane, 18: 33651
effects on reactor components, Large Component Test Loop heat transfer system for studying, 18: 21570 (NAA-SR-Memo-8217)
effects on reactor materials at high temperatures, 20: 20183
effects on reactor materials, 20: 35841(R) (NAA-SR-11900)
effects on reactor structural materials, 20: 46995
effects on rupture of type 316 stainless steel of high-carbon or -oxygen, 20: 2258(R) (MSAR-65-149)
effects on separation of uranium from sulfate solutions by solvent extraction using trioctylamine, 18: 27627
effects on sintering and densification of beryllium oxide powders of, 19: 24962
effects on solubility of uranium in bismuth, 16: 25815 (BNL-5156)
effects on stainless steel bellows, at 1200°F, 20: 10375(R) (NAA-SR-11650, Sect. 2)
effects on strength of steels, 16: 25720(T) (FTD-TT-61-31(p.41-59))
effects on strontium-85 uptake by freshwater fish, 19: 8757
effects on uptake of strontium-90 by barley and pea plants, 18: 33241
effects on x-irradiation coloration of lithium fluoride crystals, 16: 13661
elastic vibrations in, pressure dependence, 16: 4526 (D1-82-0103)
electric conductivity at 98 to 853°C, 16: 32953 (PWAC-376)
electric conductivity at 2 to 300°K, effects of pressure on, 17: 3528
electric conductivity of, instrumentation for determining, 17: 21978 (TID-18545)
electric conductivity at 100 to 1000°C, 17: 25258
electric conductivity of, instrumentation for measuring, 17: 30800(R) (TID-18997)
electric conductivity of, instrumentation for measuring, 17: 30801(R) (TID-19017)
electric conductivity of, method for increasing impurity-type, 17: 32843(P)
electric conductivity of, effects of pressure and temperature on, 17: 37849
electric conductivity effects on flames, 18: 12791
electric conductivity of liquid, effects of specific volume on, 18: 12671
electric conductivity at temperatures up to 853°C, 18: 14455 (CNLM-4094)
electric conductivity and Hall constant of liquid, in pseudopotential, 18: 22494 (TID-19959(Rev.))
electric conductivity of liquid and solid, (T), 19: 7953
electric conductivity of liquid, temperature dependence of, 19: 16079 (TID-21647)
electric conductivity and thermal conductivity of liquid, to 2000°F, 19: 16203
electric conductivity and thermoelectric power of liquid, (T), 19: 23052
electric conductivity to 2000°F, 19: 32724(R) (AFML-TR-65-99)
electric conductivity at 100 to 1000°C, 20: 17026 (RT/ING-(65)17)
electric conductivity of liquid, effect of alkali impurities on, 20: 23728
electric conductivity of liquid, 20: 41476
electric dipole moments of, ratio of atomic to electron, 20: 39598
electric discharge in, spectra of high-pressure vapor, 18: 28172
electric mobility in amalgams, 18: 546 (IP-488)
electrode potentials in tetrahydrofuran solution of sodium perchlorate, 18: 19837(R) (MIT-905-1)
electromigration in, Soret effect, 19: 42459(R) (RPI-1044-7)
electron affinities and ionization potentials, 17: 20741
electron bombardment of, emission spectra from, 18: 18562
electron collision, calculated attenuation factor for, 17: 14970
electron elastic scattering cross sections at low energies, 18: 24298 (N64-13373)
electron elastic scattering by, cross sections for, 18: 32381
electron elastic scattering at 0.1 to 2.0 ev, cross sections for, (T), 19: 20842
electron emission effects on germanium, 17: 41553(R) (NP-13160)
electron energy levels of, g factors for, 18: 40146
electron energy loss spectra at 0.8 and 1.5 Mev, 16: 12273
electron exchange energy of gaseous, in periodic potential, 17: 26715
electron excitation cross sections of transitions of, (T), 19: 8090
electron Fermi surface of, positron annihilation studies of, 19: 12102
electron gases in, spin-paramagnetic properties of, 17: 18974
electron inelastic reactions at near-resonance conditions, transitions in, 18: 9011
electron interactions with atomic, electron exchange in, 20: 39582(T) (AERE-Trans-1053)
electron mass shift in interactions with phonons in crystals of, 17: 23996
electron pair production in screened nuclear field in, (T), 19: 43280
electron paramagnetic relaxation effects in ammonia–potassium solutions, 16: 3008
electron paramagnetic resonance of dispersion in mineral oil, 16: 18121(R) (RADC-TN-61-199)
electron reactions on atomic and ionic, excitation cross sections for, 16: 15306(T)
electron reactions with, ionization cross sections for, (E), 19: 12081
electron reactions with, excitation function for metastable autoionizing state in, (E), 19: 14230(R) (AD-608160)
electron reactions with, cross sections for inelastic, (T), 19: 25178
electron reactions with, ionization cross sections for, (T), 20: 19400
electron reactions with atomic ionization in, (T), 19: 34887
electron scattering at 1 to 10 ev, total cross sections for, 17: 669
electron scattering by, cross sections for, 18: 9022
electron scattering by, ESR frequency shifts in, 18: 22682
electron scattering by, 18: 40167
electron scattering by atoms of, theory for low energies, 18: 42301
electron scattering at 0.003 to 25.0 ev, exchange effects and polarization in, (T), 19: 41286
electron scattering by atomic, cross sections for, (T), 20: 17286
electron spectra of, Auger, (E), 20: 25745
electron spin resonance spectra of atoms in matrices of argon, krypton, and xenon at liquid helium temperatures, 16: 5246
electron spin resonance saturation in, paramagnetic susceptibility from, 17: 41620
electron structure of liquid and solid, from photon angular correlations in positron annihilation, 17: 39760
electron structure, 18: 20548
electron total collision cross section, 16: 19757(T) (AD-265707)
electron transitions in, x-ray emission in double, 18: 18579
electron transmission through foils of, plasma oscillations from, (E), 20: 15955
electronic polarizabilities of, 16: 29575 (BNL-6003)
electronic resonance frequency shift induced by nuclear polarization in, (E), 19: 10375
electronic structure, 17: 32659
electronic structure and nuclear spin of, irradiation studies of, (E), 19: 10375
electronic wave functions for dipole perturbations of atomic, tables of, 17: 36374 (BNL-6491)
energy band calculations for, 16: 30960
energy gap spectrum of, electron correlation effects on, 17: 34636
energy levels of ionic, Hartree-Fock wave functions for, (T), 20: 25716 (AD-631601)
energy levels of ionized, forbidden transitions in, 20: 37432
energy levels of, Zeeman quenching of metastable autoionizing, (E), 19: 14230(R) (AD-608160)
energy levels of, collision-induced mixing in first excited, (E/T), 19: 30945 (TID-21817)
equilibrium and standard free energy constants for, in methanol and methanol-water solvents, 18: 8362
erosive effects on type 316 stainless steel at 400 and 1000°F, 19: 30670(R) (NASA-CR-54332)
erosive effects on Cb-132, Stellite 6-B, type 316 stainless steel, T-222, and TZM alloys, 20: 769(R) (NASA-CR-54459)
erosive effects on metals, 20: 5861
evaporation of sodium iodide from, mechanisms of, 20: 40357 (NAA-SR-11766)
exchange in cells, tracer study of, 17: 7723
exchange in chelating ion resin, self-, 18: 19972
exchange reactions with calcium, magnesium, and potassium on ion exchange resin, equilibrium constant for, 17: 27038
exchange reactions between amalgam and aqueous hydroxide, separation factors for, 18: 2127(R) (ORNL-3488(p.21-41))
exchange with cesium and strontium on montmorillonites, 20: 27042

excited states concentration in low-energy plasma ions of, 17: 35260(R) (TID-19135)
excretion in feces and urine in colostomized pullets, 19: 43693
excretion in man, effects of dietary potassium levels, 17: 5713
excretion in sweat, tracer study, 17: 15700
explosion of contained, method for measuring pressure-time history of, 17: 20126 (NOLTR-62-45)
explosions in, pressure produced by contained, 20: 38459 (ANL-7120, pp 720-33)
expulsion into air, equipment and method for study of, 20: 38500 (ANL-7120, pp 868-72)
extinguishment of fires of, 17: 30753(R) (MSAR-63-19)
Fermi surface electric and thermal conductivities at 90°K, 16: 22787
Fermi surface of, magnetoacoustic measurements on, 18: 13007(R) (NP-13592)
Fermi surface of, from positron annihilation data, (E), 20: 20169
fire protection systems for, carbon dioxide, 20: 9180 (ORNL-TM-1309)
fires in, model of reactor, 19: 27735(R) (NAA-SR-10850)
fission product distribution in reactor, 19: 27735(R) (NAA-SR-10850)
fission product release from liquid, 17: 35083 (CONF-39-66)
fission product retention by reactor coolant, 18: 11383 (NAA-SR-9163)
fission product retention by, at 900 to 1500°F, 18: 37064 (NAA-SR-Memo-8712)
fission product release from uranium dioxide particles dispersed in, 19: 2729 (RT/CHI(64)-8)
fission product retention by, 19: 10675(R) (NAA-SR-9999)
fission product retention by, 19: 12865(R) (NAA-SR-10501)
fission product retention by, out-of-pile and in-pile studies at high temperatures, 19: 19344 (NAA-SR-9287)
fission product retention by liquid, 19: 27735(R) (NAA-SR-10850)
fission product retention in reactor-coolant, 19: 40286(R) (NAA-SR-11200)
fission product release in fires of, 19: 12865(R) (NAA-SR-10501)
fission product retention and plating in liquid, studies, 20: 557 (CONF-650407, pp 73-93)
fission product retention by coolants of, 20: 8316(R) (NAA-SR-11450, Sect.7)
fission product release from burning, atmospheric contamination from, 20: 8316(R) (NAA-SR-11450, Sect.7)
fission product release in fires of coolant, 20: 8395(R) (NAA-SR-11450, Sect.3)
fission product retention by boiling, 20: 10272(R) (NAA-SR-9339)
fission product retention in coolants of, 20: 10275(R) (NAA-SR-11650, Sect. 5)
fission product retention and behavior in reactor coolants of, 20: 46966(R) (NAA-SR-12010)
fission product release during in-reactor fires, 18: 24891(R) (NAA-SR-8888(Sect.I))
fission-product retention by, 18: 24816(R) (NAA-SR-8888(Sect.IV))
fission-product retention by, in vented-fuel reactors, 20: 38477 (ANL-7120, pp 855-61)
flow and heat transfer under boiling and condensing conditions, two-phase, 18: 18000(R) (NP-13751(Vol.I))
flow and heat transfer under boiling and condensing conditions, 18: 18001(R) (NP-13751(Vol.II))
flow and heat transfer at 2100°F, 19: 14765(R) (ANL-6977)
flow control of liquid, for heat transfer regulation in reactors, 16: 24952 (TID-15913)
flow controller evaluation for, at temperatures up to 1200°F, 18: 5465 (NAA-SR-7534)
flow facility for magneto-fluid-dynamic research, 16: 13220
flow from upper plenum of 200-Mw(e) SGR, hydraulic analysis of, 18: 21639 (NAA-SR-Memo-9241)
flow in reactor cooling systems, studies of two-phase, 19: 12865(R) (NAA-SR-10501)
flow in reactor cooling systems, sonic velocities in two-phase, 20: 6559(R) (ANL-7115, pp 77-83)
flow in reactor cooling systems, pressure drop in two-phase, 20: 46966(R) (NAA-SR-12010)
flow in rectangular duct, magnetohydrodynamic, (E), 20: 39706
flow of liquid, calculation of two-phase critical, 18: 6921 (ANL-6779)
flow of liquid, system design for monitoring, 17: 8336
flow of liquid, design of in-pile controller for, (E), 19: 40135
flow of liquid, facility for two-phase, 19: 23991(R) (ANL-7003)
flow of liquid, loop experiments on two-phase adiabatic, 20: 29374(R) (ANL-7190, pp 156-66)
flow of liquid, mixing tee design and performance for, 18: 21567 (NAA-SR-Memo-7485)
flow of two-phase, parameters of, 19: 4327 (ORNL-3605(Vol.2)(p.270-92))
flow of vaporized, in supersonic nozzles, 17: 37641(R) (AD-290819)
flow of, calculation of void coefficient for two-phase, 19: 31462(R) (ANL-7028)
flow, permanent magnet coupling for controller, 16: 25569 (TID-15915)
flow through steam generators, distributor for, 19: 31474 (BAW-1280-23)
flow through steam generators, distributor for, 19: 31475 (BAW-1280-24)
flowmeter for, suitability of E-core flux-distortion type, 17: 27655 (NAA-SR-Memo-6117)
flowmeters for, calibration of magnetic, 20: 4077(R) (IS-1200(Sect. E))
flowmeters for, calibration of magnetic, 20: 41064(R) (IS-1500(Sect.E))
fluid flow and heat transfer in toroidal channel, effects of magnetic field, 16: 30559 (UCRL-9574)
friction and surface damage between pairs of materials immersed in liquid, 16: 22506
friction behavior of oxidized Hastelloy B and C in liquid, at 600 to 1200°F, 18: 7985(R) (BMI-1650(Del.))
friction of sliding surfaces in molten, 16: 28642(R) (BMI-1581(Del.))
friction of sliding Hastelloy B, Hastelloy C, and nickel in liquid, at temperatures up to 650°C, 17: 40423(R) (BMI-1639(Del.))
fume removal from fires of, by glass fabric filters, 16: 12660 (TID-14979)
galvanomagnetic properties, 16: 2353
gamma attenuation, 17: 21318 (NAA-SR-Memo-3556 and Add.)
gamma attenuation coefficient of, temperature dependence of cobalt-60, (E), 19: 5391
gamma attenuation coefficients at 0.03 to 10 Mev, 19: 35569
gamma attenuation coefficients at 0.01 to 100 Mev, 20: 36350
gamma reactions (γ,n) from threshold to 80 Mev, cross sections for, 18: 11209 (LNF-63/47(p.194-8))
gamma reactions (γ,p) at 2 to 10 Mev, cross sections of, 17: 5343
gamma reactions (γ,n) at 0 to 80 Mev, 17: 40095
gamma spectra from 14-Mev neutron activation of, determination by, 19: 26241
gas phase over carbon-containing liquid, chromatographic studies of, 18: 39051 (NAA-SR-8448)
gyromagnetic ratio of rare-gas trapped, shifts in, 18: 9016
Hall coefficient and low-frequency magneto-plasma resonances in, at 4°K, 16: 29566
handling and purification of, for use in corrosion test loop, 20: 21293 (R-66SD3007)
handling of liquid, 20: 4330(T) (ORNL-tr-854)
handling, physical properties, and reactions, 16: 4404 (TRG-Report-25)
Hartree-Fock potential of neutral atoms of, analytical expressions for, 18: 16656
heat capacity at low temperatures, 16: 6724 (UCRL-9880)
heat exchanger for use with water and, 19: 36628(P)
heat of adsorption on tungsten, 16: 26009
heat of adsorption by tungsten substrates, atom-metal theories on, 19: 34139 (N64-27740)
heat of adsorption by tungsten, atom-atom interaction theory on, 19: 34140 (N64-27741)
heat of vaporization and vapor pressure of, 20: 43884 (AGN-8191(Vol.1))
heat transfer and pressure drop in 2-phase forced-convection flow, 19: 27735(R) (NAA-SR-10850)
heat transfer and fluid flow studies in convection loop, 19: 36607 (INR-588/IX/R)
heat transfer at high heat fluxes, 20: 2008(R) (AD-622825)
heat transfer by boiling, 18: 44926(R) (ANL-6923(p.46-78))
heat transfer by bubble boiling of, effects of pressure on, 19: 24682
heat transfer by boiling, burnout heat flux in, 20: 2023
heat transfer by liquid, design and operation of loop for studying, 16: 29090(T) (AEC-tr-5330)
heat transfer by liquid, 18: 18282 (BNL-844)
heat transfer by liquid, design of test installation for study of, 18: 25661
heat transfer by, in turbulent flow, 20: 12483
heat transfer by, at 900°K, in tubes, 20: 12488
heat transfer characteristics of liquid, measurement of boiling, burnout, and void fractions, 20: 10272(R) (NAA-SR-9339)
heat transfer coefficients of condensing, 17: 20163 (BNL-756(p.276-85))
heat transfer coefficients, 20: 10368 (CONF-650620, pp 143-55)
heat transfer, design and operation of loop for, 16: 11834
heat transfer from boiling, 16: 16689 (TID-7626(Pt.I)(p.143-5))
heat transfer from liquid, to potassium-sodium alloy (liquid), 16: 17780 (TIM-5)
heat transfer from staggered tube bundle in transversal stream of liquid, 16: 33137
heat transfer from boiling, 16: 13207 (NAA-SR-6769)
heat transfer from, in nucleate boiling tests, 17: 18268 (NAA-SR-Memo-8279)
heat transfer from flowing, to stainless-steel tube, 17: 32253
heat transfer from spray of hot liquid, to vertical plate, 19: 4325 (ORNL-3605(Vol.2)(p.235-49))
heat transfer in boiling, 20: 8395(R) (NAA-SR-11450, Sect.3)
heat transfer in liquid, burnout problems in, 18: 20193
heat transfer in reactors, study using water as stand-in, 19: 17178(R) (ANL-6965(p.91-8))
heat transfer in two-phase, 18: 24891(R) (NAA-SR-8888(Sect.I))
heat transfer of boiling, forced- and natural-circulation, 18: 20160(R)

(AD-423679)
heat transfer of boiling, forced- and natural-circulation, 18: 20166(R) (NP-13810)
heat transfer of boiling, effect of surface conditions on, (E), 20: 2017(R) (TID-22312)
heat transfer of boiling, 20: 46963(R) (ANL-7132)
heat transfer of liquid, 17: 282(T) (FTD-TT-61-395(p.121-34))
heat transfer of liquid, to tubes under steady and turbulent flow conditions, 17: 1615
heat transfer of longitudinally flowing, between rod bunches, 18: 33744
heat transfer of liquid, in tubes, 18: 35693
heat transfer of liquid, under forced-convection flow conditions, 19: 10675(R) (NAA-SR-9999)
heat transfer properties of liquid, design of test loop for studying, 16: 29089(T) (AEC-tr-5310)
heat transfer properties of boiling, 20: 27101 (ANL-7100, pp 549-71)
heat transfer research on, 17: 27535 (BNL-801)
heat transfer to liquid, in flow through a copper pipe, effects of oxygen on, 17: 21885
heat transfer to liquid, pool- and forced-convection boiling in, (E), 19: 4308 (NAA-SR-9477)
heat transfer to liquid, flowing in-line through closely packed rod bundles, (T), 20: 35629
heat transfer to, effects of surface conditions on nucleate pool boiling, 19: 18114 (MIT-3357-1)
heat transfer under boiling and condensing conditions, 17: 11098(R) (NP-12433)
heat transfer under boiling and condensing conditions, 17: 29070(R) (NP-12934)
heat transfer under incipient boiling conditions, laboratory experiments on, 18: 43759 (TID-7697(p.4.9.1-3))
heat transport efficiency in steam generators, 17: 5627
heater design for, electron-bombardment, 18: 20132 (NAA-SR-Memo-8289)
heater operation in event of leak, 19: 4273 (NAA-SR-Memo-10250)
helium and hydrogen ion attenuation at 0.1 to 500 Mev, tables for, 20: 41619 (CEA-R-3042)
helium–3 scattering at 26–33 Mev, cross sections for elastic, 17: 21090
hydrogen content in, effects on embrittlement of tantalum, 20: 42682 (LA-3508)
hydrogen reactions at −195°C, 16: 112
hydromagnetic wave propagation and resonances in liquid, 18: 44299
hyperfine spectra in x-irradiated beryl crystals, 20: 15982(T)
hyperfine structure, 16: 21129(R) (NP-11640)
imperfections in, study of point, 17: 14847 (TID-16526)
impurities in, instrumentation development for determining, 20: 14024(R) (APDA-182)
impurities in, magnetic effects of, 19: 40409(R) (MSAR-65-95)
in gastric mucosa, effects on electric potential, 17: 15645 (USNRDL-TR-608)
interatomic forces in, 17: 36427 (NP-13020(p.318-39))
intracellular components and exchange reactions in muscle, tracer study, 16: 14441
iodine-131 partition in liquid, measurement of liquid/vapor phases of, 20: 45944(R) (AERE-PR-HPM-9, pp 1-6)
ion-core states in, effects of crystal field on, 16: 25884 (D1-82-0171)
ion exchange behavior on Dowex-50W resin, 17: 40781 (UCRL-10595)
ion exchange equilibria in system with cesium, 16: 20457
ion exchange equilibria with, rate of cesium movement in chromatographic, 16: 20458
ion exchange equilibria in ternary cation systems, tracer study of, 18: 22024
ion exchange in concentrated hydrochloric and perchloric acids, distribution coefficients for, 18: 17759
ion exchange in ethylenediamine-Dowex-50 systems, 19: 865(R) (ORNL-3679(p.23-38))
ion exchange of, on sulfurized styrene polymers, thermodynamics of, 17: 21795
ion exchange on clinoptilolite, 17: 19704 (TID-7644(p.13-28))
ion exchange on clinoptilolite, 17: 19707 (TID-7644(p.83-114))
ion exchange on minerals, 20: 38858 (BNWL-235-3, pp 23-51)
ion exchange on montmorillonites, thermodynamics of, 17: 19704 (TID-7644(p.13-28))
ion exchange on phosphate glass electrode, 18: 3780
ion exchange on zirconium-base and clay-mineral ion exchangers, 17: 25364
ion exchange properties on zirconyl oxalates, 20: 18840
ion exchange with cesium on clinoptilolite, 16: 17673
ion exchange with soil, tracer study, 16: 32710
ion exchange with silver and zinc on Dowex 50W resin, rate of, 17: 32053
ion exchange with barium and cesium on montmorillonite, thermodynamics of, 17: 37299
ion exchange with cesium on calcined montmorillonite, 17: 40943
ion exchange with calcium and silicon, elution dynamics of, 18: 27459
ion exchange with cerium in chernozem containing 4% humus, tracer studies of, 18: 39171(T) (AEC-tr-6390(p.451-9))
ion exchange with alkali metal uranates, 18: 219
ion oscillatory potentials in liquid, (T), 19: 4695
ion pairing interactions in, (T), 20: 17008 (CEA-R-2820)
ionic mobilities in lithium, potassium, and sodium nitrate systems, 18: 1645
ionic nucleation for vaporized, 17: 37641(R) (AD-290819)
ionization by electron bombardment, 16: 29573 (UCRL-6806)
ionization by hot tungsten, efficiency of surface, 19: 44938 (UCRL-14117)
ionization lifetime, effects of electric field, 17: 10197 (NASA-TN-D-1563)
ionization on iridium, efficiency of, 19: 19262(R) (UCRL-12028(p.51-66))
ionization on rhenium, platinum–tungsten, and tungsten surfaces, 19: 16261 (UCRL-11606)
isotope exchange with alkali metal uranates, 18: 219
leaching using ammonia (liquid), 16: 22047 (GEAP-4006)
level indicator for liquid, 20: 30875(R) (ANL-7190, pp 143-55)
level monitor for liquid, engineering drawings for, 17: 39403
Lilienfeld emission from, 18: 10796
liquid, analysis for contaminants, emission spectrographic, 20: 41420(R) (MSAR-66-149)
liquid, corrosive effects on stainless steel at high temperatures, 20: 41420(R) (MSAR-66-149)
loop contamination by hydride, response of instruments to, 17: 35963(R) (TID-19364)
lubrication effects on sliding surfaces of 2¼ Croloy and Stellite-6, 16: 17966(R) (BMI-1541(Del.))
magnetic moment of diatomic, rotational, 17: 25959
magnetic moments of molecular, rotational, 18: 40147
magnetic properties of, de Haas–van Alphen effect in, 18: 39955
magnetic properties of excited, effects on polarization of resonance radiation, 19: 6462(T)
magnetic spin susceptibility, 16: 16713 (AROD-431:44)
magnetic susceptibility of molecules of, method for calculation of, 17: 31109
magnetoplasma resonance in, satellites in, 17: 36490
magnetoplasma resonance in, Doppler shifted cyclotron absorption of, 17; 39753
mass transfer in system of liquid, with stainless steel, 17: 6575(R) (TID-17384)
mass transfer in system of liquid, with stainless steel, 17: 6576(R) (TID-17386)
mass transfer of carbon between alloys in liquid, mechanism of, 17: 12622
materials compatibility with, for nuclear uses, (E/T), 19: 14775 (SAN-8002)
measurement of level, wetting, and bubbles in liquid, apparatus for, 18: 33827 (EUR-1823.d)
melting temperature of, equations for calculating, 18: 25990
meson (π^+) double charge exchange on, 18; 38141
meson (μ) capture, Fermi interactions in, 16: 15590
metabolism by erythrocytes in patients with cardiac insufficiency, 16: 20101
metabolism in bone, tracer study, 16: 31438
metabolism in endocrine disorders, tracer study, 17: 1216
metabolism in greasewood and hopsage trees, 18: 41044(R) (HW-80500 (p.226-9))
metabolism in man, tracer studies using sodium-22 and whole-body counter, 16: 16156
metabolism in man, tracer study, 17: 23068
metabolism in man, tracer study, 18: 38754
metabolism in mouse gastrointestinal tract, protective effects of AET against, 19: 7198
metabolism in patients with essential hypertension, 16: 1454
metabolism in rats, effects of diuretic agents on, 17: 18486
monitoring for hydrogen of liquid, design of apparatus for continuous, 16: 20320 (NAA-SR-6986)
monitoring in reactor coolants, engineering drawings of system for, 18: 16288
neutron absorption cross sections, 16: 18429
neutron absorption cross section, thermal, (E), 19: 31244 (ZfK-RN-23)
neutron absorption by, measurements for $E_0 \leq 30$ Mev, 20: 24575 (LNF-66/7)
neutron absorption cross section in pitchblende, thermal, 20: 37994
neutron activation in phantoms, fast, 17: 5736
neutron activation of, measurement of neutron flux density by, 17: 25601 (PAN-408/1X)
neutron activation cross sections of, thermal, 17: 26466 (PAN-407/1X)
neutron activation of body, use of, for exposure measurements, 20: 7315(R) (ORNL-3849, pp 151-82)
neutron attenuation by, fast, 18: 42612

neutron capture at 10 to 135 kev, cross sections for, (E), 20: 17718
neutron capture cross sections at 10 to 140 kev, (E), 19: 35378(R) (EANDC(E)-57(U))
neutron capture cross sections at 0 to 700 kev, (E), 20: 46599(R) (RPI-328-68, pp 1-62)
neutron coherent scattering by liquid, thermal, (T), 19: 12473
neutron cross sections, library of 40-group BPG and spectral "B" codes, 16: 12422 (BAW-158)
neutron cross sections, corrections, 16: 24796 (UNC-5002)
neutron cross sections for, fast, 17: 28245 (KFK-120)
neutron cross sections for, at 0.001 to 0.05 ev, 18: 22884
neutron cross sections at 4.2 to 6.2 Mev, measurement of total (E), 19: 3318
neutron cross sections at 1 to 4 Mev, optical model analysis of, (T), 19: 14504 (BNL-904)
neutron cross sections, 19: 14828(R) (GEAP-4723)
neutron cross sections for, from 0.414 ev to 5.5 Mev, 19: 45244 (AEEW-M-472)
neutron cross sections for, 20: 14062 (JUL-214-RG)
neutron cross sections and shielding coefficients for, 20: 22383(T) (AEC-tr-6693)
neutron cross sections at 1 ev to 40 kev, (T), 20: 24335 (BNL-10085)
neutron diffraction by, structure studies using slow, 19: 23971
neutron elastic and inelastic scattering by, fast, 20: 19805(R) (ANL-7110, pp 1-28)
neutron elastic scattering anisotropy in, 18: 15137 (NAA-SR-Memo-9020)
neutron elastic scattering at 0.3 Mev, angular distributions for, 18: 17090
neutron elastic scattering at 0.3 to 1.5 Mev, cross sections for, 19: 31462(R) (ANL-7028)
neutron elastic scattering at 0.8 Mev, angular distributions of, (T), 19: 37884
neutron elastic scattering at 0.8 Mev, cross sections for, (T), 20: 15770
neutron fluxes in, transport theory calculations for, 17: 39952(T) (AEC-tr-6057)
neutron inelastic scattering at 14 Mev, 16: 3686
neutron inelastic scattering at 80 to 198°C, cold, 16: 32378
neutron inelastic scattering by, 17: 4041
neutron inelastic scattering by, 17: 22271 (MMPP-NPC-1-4)
neutron inelastic scattering by liquid, cross sections for thermal, 18: 22860
neutron inelastic scattering by liquid, first-moment calculations of, 18: 40474 (IDO-16977(p.23-43))
neutron inelastic scattering by liquid, (E), 19: 31217 (IDO-17042(p.11-47))
neutron inelastic scattering at 14.1 Mev, gamma yields from, (E), 19: 35417
neutron inelastic scattering at 14.1 Mev, spectra for, (E), 20: 28268 (FEI-30)
neutron interaction threshold values for fission spectrum, 16: 7036
neutron microscopic cross sections for, 17: 41866 (NAA-SR-Memo-8904)
neutron radiative capture cross sections at 30 and 65 kev, 18: 34274(R) (NIRS-2(p.3-15))
neutron reactions at high energies, table of radioisotopes produced in, 17: 794 (CERN-62-22)
neutron reactions with, activation cross sections for thermal, 18: 15302
neutron reactions at 1 ev to 40 kev, cross sections for, (T), 20: 13753 (BNL-961)
neutron reactions (n,n'γ) at 14 Mev, elemental analysis by, 20: 27170 (UCRL-14654-T)
neutron reactions at 14.7 Mev, gamma emission in, (E), 20: 42146 (AD-638014)
neutron removal cross sections for, effective fast, 16: 24797 (WADC-TR-58-266)
neutron resonance Doppler coefficient for, 16: 33973 (ANL-6601)
neutron resonance scattering by, 18: 21698(R) (ANL-6860)
neutron resonance absorption measurements for, 20: 30358(R) (RPI-328-56, pp 1-48)
neutron scattering angular distribution, 16: 12419 (ANL-5567(Rev.))
neutron scattering resonance cross sections for, fast, 16: 24387
neutron scattering at 2.5 Mev, inelastic cross sections, 16: 29741
neutron scattering at 0.026 to 0.10 ev, 17: 4330(R) (IDO-16781)
neutron scattering from liquid, at 0.025 to 0.1 ev and 23 to 200°C, 17: 4333(R) (IDO-16805(p.7-35))
neutron scattering by liquid, at 110°C, 17: 4976
neutron scattering by liquid, energy transfer in thermal, 17: 17183
neutron scattering by liquid, 17: 22967(R) (IDO-16857)
neutron scattering by liquid, differential cross sections for thermal, 17: 36669 (WASH-1042)
neutron scattering at 0.25 to 2.2 Mev, differential cross section and polarization for, 17: 41873 (WASH-1044)
neutron scattering at 0.2 to 2.2 Mev, polarization in, 17: 41528(R) (ANL-6720(p.16-28))
neutron scattering by, cross section and polarization for, 18: 7677 (CONF-340-6)
neutron scattering in, energy transfer in, 18: 24625 (WASH-1046)
neutron scattering cross sections at 0.5 to 0.8 Mev, 18: 26571
neutron scattering at 0.2 to 2.2 Mev, 18: 38116
neutron scattering by liquid, dynamics of, (E), 19: 45235
neutron scattering by liquid, review on, (E), 20: 19799
neutron scattering by liquid, spectra for, (T), 20: 26348 (NP-16010, pp 102-39)
neutron scattering by, Monte Carlo solutions for multiple, 20: 26062 (CEA-R-2971)
neutron slowing-down in, fission, 17: 41845(T) (AEC-tr-6092)
neutron spectra in cylinder of, fast, (E), 19: 33232
neutron total cross sections at 28.4 Mev, 16: 5969
neutron total cross sections at 3 to 15 Mev, 16: 27732(R) (HW-73116 (p.51-63))
neutron total cross section, 17: 15272
neutron total cross section of, fast, 17: 20982 (HW-SA-2875)
neutron total cross sections at 0.9 to 2.1 Mev, 18: 2890
neutron total cross sections at 2.8 to 5.2 Mev, 18: 6210
neutron total cross section of, 18: 11195(R) (EANDC(E)-49(L))
neutron total cross sections at 2 to 10 Mev, 18: 16973
neutron total cross sections at 8.58 to 11.59 Mev, 18: 24591(R) (LMSC-4-50-62-1)
neutron total cross sections at 28 Mev, 18: 44711
neutron total cross section of, fast, (E), 20: 19805(R) (ANL-7110, pp 1-28)
neutron total cross section from 5.0 to 8.5 Mev, fluctuations in, (E), 20: 44743
nuclear ferromagnetic state in, stability of, 18: 5868
nuclear magnetic resonance of liquid, 20: 7744
nuclear magnetic resonance spin-lattice relaxation in sodium chlorides, effects of magnetic field on, (E), 20: 34866
[illegible]ear polarization of, Overhauser effect in, 17: 38167
[illegible] quadrupole resonance, 17: 10592 (IS-520)
nuclear spin of, Overhauser polarization of, 17: 41944
nuclear spin temperature in, (E), 19: 25451
optical orientation of atomic, effects of spin-exchange collisions on, 16: 6864
oxygen content in liquid, methods for controlling, 20: 1534(R) (LA-3370)
oxygen pickup from stainless steel containers, 19: 40177(R) (ANL-7046(p.1-35))
oxygen species dissolved in liquid, 16: 22159
particle waves and phonon fission in crystals of, 18: 27874
partition coefficients and reciprocal ionic radii, 17: 27562 (INSJ-54)
performance as coolant in direct-contact cores, 18: 19334
performance as coolant containing suspended fuels, 18: 23051(P)
performance as coolant in 1000-Mwe fast breeder reactors, (E/T), 19: 10532 (COO-279)
performance as heater for steam generators, 19: 13577(R) (BAW-1280-21)
performance as reactor coolant, evaluation of, 18: 20192
performance as reactor coolant, reliability of, 18: 20194
performance as superconducting magnet, 19: 31335(R) (UCRL-12303)
performance as working fluid in MHD cell, (T), 19: 4875
performance in cryogenic magnet coils, 20: 9888 (CONF-650512, pp 152-5)
performance in electrohydrodynamic cells for space uses, 17: 9122
performance in heat transfer capillary structures, 18: 22228
performance in thermionic cells, 18: 18617 (CONF-458-2)
performance of liquid, as working fluid in 1000-Mw(t) steam generators, 19: 13582 (SAN-8002(p.231-57))
performance of pure vapors of, in magnetohydrodynamic cells, 17: 32817
phonon dispersion curve and interatomic potential of, (T), 19: 14077
phonon dispersion curves for bcc, (T), 19: 16128
photoionization cross sections for, 17: 647
photoionization of, cross sections for, 17: 10681(R) (TID-17743)
photon absorption cross sections for vapors of, at 1000 to 2400 Å, 18: 34443
photon reactions with Coulomb field of, pair production total cross sections for high-energy, (T), 20: 17754
photovoltaic properties of coatings of, on anodized zirconium electrodes, (E), 19: 36768 (TID-21971)
physical properties of liquid, review, 18: 20516 (EUR-599.d)
physical properties of liquid, 19: 28821
physical properties at boiling point to 1300°C, 19: 34643
pinch instabilities in solid, self-, 17: 37469
plasma of, production of low-temperature fully ionized quiescent, 18: 9528
plasma seeded with, electric and microwave properties of, 17: 40155 (ARL-63-159)
polarization of, time evolution of dynamic nuclear enhancement, (E/T), 19: 8463
polarization vectors in crystals of, neutron scattering analysis of, 16: 32170 (AECL-1572)

polarography of, in acetone solution, 17: 14253
positron annihilation in, angular correlations from, (E), 19: 41285
positron annihilation in, temperature effects in, (E/T), 20: 20167
positron annihilation in, lifetimes and two-gamma correlations from, (E/T), 20: 34255
positron annihilation in, calculation of probability of, 20: 36058
positron annihilation in, angular correlation of photons from, (E), 20: 37784
positron annihilation with core electrons in, momentum distributions for, (T), 20: 37821
positron effective mass in, (T), 20: 37815
positron lifetime in, (T), 19: 14360
positron lifetimes in, 16: 3199
positron lifetimes in, 16: 9364
positron mass in, band effective, 20: 41853
positron thermalization in, (E), 20: 11660
precipitation with cerium--cadmium intermetallic compounds from liquid cadmium, 18: 34192
preparation for coolant loop studies, 20: 22520(R) (NAA-SR-11805)
preparation of crystals of, 19: 22988(R) (NYO-2811-23)
preparation of pure, by fusion electrolysis, 18: 22090(P)
preparation of purified, 20: 22520(R) (NAA-SR-11805)
preparation of ultrapure, 20: 46966(R) (NAA-SR-12010)
pressure pulses in locally heated channels of, 19: 39090(R) (ANL-7046 (p.78-82))
pressure-volume characteristics at low temperatures, 17: 14936 (IS-623)
properties and uses of liquid, review of, 19: 6353
properties as conductor in high-field d-c cryogenic magnet coils, 16: 15403
properties as reactor coolants, 16: 28545 (TID-7623(p.2-8))
properties as reactor coolant, 18: 6412(R) (GEAP-3888)
properties as reactor coolant, 18: 19283
properties as reactor working fluid, 18: 35198 (NAA-SR-8617(Vol.I))
properties as reactor coolant, technological review of, 20: 12330 (TID-8541, pp 321-425)
properties as working fluid in Rankine power cycle, 20: 41398
properties at high temperatures, 17: 14839(R) (NRL-5904)
properties at high temperatures, 18: 608(R) (NRL-5988)
properties for coolant in reactor using fused plutonium as fuel, 18: 44997(P)
properties for heat pipe uses, preparations for measurement of, 20: 41438(R) (AGN-8187)
properties for reduction of zirconium tetrachloride, 16: 12087 (BM-RI-5933)
properties for use in aircraft reactor PWAR-6, 16: 15901 (FXM-2210)
properties in cryogenic magnet coils, 16: 31881
properties of, Coulomb correlation effects on, 17: 31226
properties of forced convection boiling, at low pressure, 20: 27094 (ANL-7100, pp 189-94)
properties of liquid, 16: 19370 (TIM-65)
properties of liquid, as reactor coolant, 16: 23830 (BNL-5377)
properties of liquid, for space applications, handbook of, 16: 5088 (WADD-TR-61-96)
properties of liquid, for use as space electric-power systems, 17: 39246
properties of liquid, at the boiling point to 1300°C, 17: 34402 (EUR-357.d)
properties of vaporized, as magnetohydrodynamic generator working fluid, 17: 25862 (R62SD94)
properties of, effects of low temperature on, 20: 4417
protective effects against nucleic acid decomposition by nuclease, 18: 25085 (SGAE-BL-5/1964)
proton inelastic cross sections at 10 to 50 Mev, (E), 19: 30567
proton reactions at 150 Mev, gamma spectra from, 16: 31088
proton reactions at 97 Mev, delayed emission in, 18: 6189
proton reactions at 2.2 Bev, beryllium-12 production in, (E), 19: 19184
proton reactions (p,pn) at 20 to 150 Mev, excitation functions for, 16: 28042
proton reactions with, production of delayed proton emitters in, (E), 19: 14546
proton reactions with atoms of, production of highly excited hydrogen atoms by charge-exchange, (E), 20: 11471(T)
proton reactions with, ionization cross sections for, (T), 20: 19400
proton reactions with atomic, ionization in, (T), 19: 34887
proton scattering by, excitation cross sections for, 16: 28156
pump design for liquid, 17: 16176 (NAA-SR-Memo-7955)
pump development for liquid, 18: 20131 (NAA-SR-Memo-2368(Rev.))
pump for, design of induction, 20: 4077(R) (IS-1200(Sect. E))
pump for, induction, 20: 41064(R) (IS-1500(Sect.E))
pumping in 1 to 1.5 kMw(e) reactors, pumps for, (E), 19: 13570 (SAN-8002(p.258-64))
pumping of liquid, electromagnetic pumps for, 18: 12293(R) (N63-15259)
pumping systems for liquid, 16: 32598(P)
pumps for, development of, 19: 9281(R) (IS-900(Sect.E))
purification, 18: 33678(R) (ANL-6875)
purification, 19: 32279(R) (ANL-7020(p.3-99))
purification, 20: 35841(R) (NAA-SR-11900)
purification and handling of, for use in corrosion loop, 20: 43083 (R-66SD3012)
purification by cold trapping, 16: 28538 (NAA-SR-6801)
purification by distillation, 17: 35965 (UCRL-7401)
purification by distillation, 18: 19456(R) (ANL-6840)
purification by in-line methods, design and operation of loop for, 19: 44162(R) (APDA-174, pp 33-55)
purification by vacuum distillation, 16: 4453(T) (DEG-Inf-Ser-87)
purification from oxygen, equipment for, 19: 42807(T) (PG-Inf.Ser.-10)
purification in circulation loops, reaction-product, 20: 1960
purification methods for, 20: 31213(R) (ANL-7175, pp 119-58)
purification of liquid, cermet filtration method for, 17: 18682(T) (FTD-TT-62-1473(p.31-7))
purification of loop-flow, in-line methods for, 20: 28691(R) (APDA-185)
purification of reactor coolant, design and operation of equipment for, 17: 17436
purification of reactor-coolant, development of methods for, 19: 10675(R) (NAA-SR-9999)
purification of, development of methods for, 20: 5594(R) (ANL-6925, pp 21-106)
purification of, development of methods for, 20: 42619(R) (ANL-7245, pp 1-28)
purification of, for use as liquid-metal coolant, 19: 22984(R) (NASA-CR-54167)
purity control recommendations for liquid, 17: 265 (APAE-112(Vol.IV))
purity in liquid-metal-cooled reactors, methods for controlling, 19: 34672 (BMI-X-10129)
purity of reactor, monitoring and maintaining, 19: 12865(R) (NAA-SR-10501)
quantum defect for ^2S state, 17: 20736
radiation absorption by gaseous, 18: 1113 (ARL-63-151(p.322-35))
radiation attenuation by, critical energies and units for, 17: 38420
radiation attenuation properties of vaporous, effects on radiation heat transfer properties of arc and plasma systems of, 20: 28479 (AD-631469)
radiation effect on rat intestinal, 19: 31908
radiation effects and isochronal annealing data at 4°K, 16: 6810(R) (ORNL-3213(p.15-23))
radiation effects of neutrons on electric conductivity at low temperatures, 16: 16789
radiation effects on secretion by parotid gland, 17: 1293
radiation effects on exchange of, through cell membranes, 17: 1264
radiation effects on urinary excretion of, x, 17: 10463
radiation effects, 17: 11129
radiation effects on excretion in saliva, 17: 15719
radiation effects on metabolism of, 17: 33696
radiation effects on urinary excretion of, in rats, 17: 35608
radiation effects on mouse excretion of, x, 17: 40584
radiation effects on rat excretion of, x, 18: 9875
radiation effects on tumor metabolism of, 18: 9904
radiation effects on gastrointestinal absorption of, in rats and dogs, 18: 11654 (USNRDL-TR-693)
radiation effects on rabbit and rat metabolism of, 18: 11790
radiation effects on transport of, in dog kidney, 18: 13440(R) (AD-401681)
radiation effects on transport in rat blood cells, gamma, 18: 13508
radiation effects on content of, in rat serum and urine, x, 18: 15842
radiation effects on transport of, in erythrocytes, 18: 29342
radiation effects on metabolism of, by fish, 18: 33272(R) (NIRS-2(p.31-42))
radiation effects on transport of, in dogs and monkeys, transcapillary, 18: 36951(R) (TID-20979)
radiation effects on metabolism of, in salivary glands of rats, 18: 43247
radiation effects on excretion of, by fish, 18: 43280
radiation effects on goldfish metabolism of, gamma, 19: 105
radiation effects on transport of mouse spleen, x, 19: 13070
radiation effects on physiology of content of, in developing guinea pig brain, 19: 19534
radiation effects on rat metabolism of, protective effects of mercaptamine against x, 19: 33792
radiation effects on flux in erythrocytes of, 19: 33856
radiation effects on content of, in blood of dogs, 19: 33869
radiation effects on rat intestinal metabolism of, protective effects of AET and cysteamine against, 19: 46027
radiation effects on content in dog blood, β and γ, 20: 5381
radiation effects on content of, in monkey erythrocytes and plasma, 20: 6765
radiation effects on content of, in blood of rabbits, α, 20: 6870
radiation effects on urinary excretion in mice, fractionated x, 20: 6889
radiation effects on erythrocyte uptake of, factors affecting γ, 20: 8610

radiation effects on content in muscle, γ and x, 20: 18293 (NP-14898)
radiation effects on content in animal cell nuclei, x, 20: 20422
radiation effects on content of, in milk after mammary gland exposure in cattle and goats, gamma and x, 20: 22594
radiative lifetime of $^2P-^2S$ transition of gaseous, 19: 43997(R) (UCRL-11889)
radiative lifetime of excited electronic states in, 20: 31219(R) (UCRL-16658, pp 11-20)
radioactivity of reactor-coolant, 19: 27735(R) (NAA-SR-10850)
radiochemistry, 16: 14767 (NAS-NS-3055)
radioinduced excretion of, by fish, lethal effects of, 18: 29330
radioinduced formation in sodium chloride by 50-kev electrons, 20: 20781
radioinduced heating in tanks of liquid, 17: 21318 (NAA-SR-Memo-3556 and Add.)
radioinduced production of helium and hydrogen in, neutron, 19: 26901
radiolysis of hexane in presence of, yields in, 19: 46324(R) (AGN-8132)
radiosensitivity effects on plants, 19: 42369
radiosensitivity effects on mitosis in rat bone marrow cells, x, 20: 18326
rare gas reactions with, ionization cross sections for excited, (T), 20: 31917
ratio to potassium in mouse urine, prediction of x-radiation response by, 20: 14266
reaction with water, loop for testing small leak, 20: 10285(R) (APDA-178, pp 18-29)
reactions of carbon with nitrogen in liquid, cyanide formation in, 20: 7094
reactions of carbon-rich, with low-alloy and stainless steels, 20: 9413 (CONF-650620, pp 1-17)
reactions of gaseous, with graphite, kinetics of, 16: 18894
reactions of gaseous, with mercury vapor, luminescence from, 18: 767
reactions of gaseous, with rare earth chlorides, thermodynamics of, 20: 43222
reactions of liquid, with steam, effects on steam generators, 17: 21223 (NAA-SR-8140)
reactions of liquid, with hydrogen at 150 to 250°C and 150 Torr, 17: 41451
reactions of liquid, with carbon monoxide, 18: 26824(R) (ANL-6885)
reactions of liquid, with gases, 19: 32279(R) (ANL-7020(p.3-99))
reactions of liquid, with molybdenum, tungsten, and uranium oxides, 19: 44021
reactions of liquid, with reactor materials at high temperatures, 20: 38499 (ANL-7120, pp 839-47)
reactions of oxygen-rich, with low-alloy and stainless steels, 20: 9413 (CONF-650620, pp 1-17)
reactions of vaporous, with glasses, pyrolytic graphite, and refractories at 940°C, 16: 25318 (RAD-TM-60-44)
reactions with air and water, studies on, 18: 19283
reactions with air, pressures and temperatures of, 19: 35604(R) (ANL-7045(p.1-23))
reactions with air in reactors, model for processes in, (T), 20: 10851
reactions with air, calculations on, · 20: 20925(R) (ANL-7055, pp 177-212)
reactions with air, shock production from combustion, 20: 28689
reactions with air at high temperatures, · 20: 31440(R) (ANL-7175, pp 159-83)
reactions with alkali metal atoms, van der Waals potentials for, (E), 19: 27107
reactions with alkali metal atoms and hydrogen atoms, spin-exchange, (T), 19: 43011
reactions with allyl compounds in solvents, 19: 5932 (TID-21381)
reactions with anthracene and tetrahydrofuran, reducing, 19: 36451(R) (BNL-900(p.73-104))
reactions with austenitic stainless steel, 16: 4451 (NAA-SR-6386)
reactions with benzophenone, spin distributions in, 17: 4535
reactions with breeder-reactor materials, (E), 19: 35800
reactions with carbon, effects on metal corrosion, · 20: 20802(R) (ANL-7055, pp 21-98)
reactions with cerium–cobalt–plutonium alloys at high temperatures, 20: 33771 (LA-3495)
reactions with cladding materials at high temperatures, 19: 39090(R) (ANL-7046(p.78-82))
reactions with coolant cover gas impurities, 19: 17176(R) (ANL-6965 (p.1-41))
reactions with defective uranium dioxide fuel elements, 17: 3897
reactions with EBR-II Mark-I fuel at 800 to 1004°C, 19: 31530(R) (ANL-7010(p.77-177))
reactions with fast reactor materials, research plans for, 20: 6552(R) (ANL-6925, pp 187-233)
reactions with fission products, 20: 24971(R) (BNL-954, pp 50-83)
reactions with gases, spin relaxation cross sections for, 18: 30418
reactions with graphite, 18: 24907 (ORNL-TM-870)
reactions with hydrogen, sodium hydroxide, and pyrex glass, 19: 17850 (CEA-R-2583)
reactions with hydrogen, light modulation in spin-exchange, (E), 19: 41262
reactions with inert cover gas impurities, 20: 5594(R) (ANL-6925, pp 21-106)
reactions with iodine released from uranium and uranium carbide, 20: 5878 (BNL-9667)
reactions with metals at high temperatures, 20: 15033(R) (ANL-7152, pp 87-96)
reactions with metals at high temperatures, · 20: 20925(R) (ANL-7055, pp 177-212)
reactions with other elements in liquid ammonia, saline compound and intermetallic phase production in, 18: 23149(T) (ANL-Trans-8)
reactions with oxygen, concentration effects on, 19: 32048(R) (NP-15073)
reactions with piaselenol in tetrahydrofuran, 19: 15332(R) (BNL-841 (p.52-62))
reactions with plutonium and plutonium alloys, aerosol characteristics in burning, 19: 28327
reactions with plutonia–urania at 750°C, effects of fuel stoichiometry on, 20: 29618(R) (GEAP-4982)
reactions with quaternary ammonium salts in liquid ammonia, 19: 5933 (TID-21391)
reactions with rare gases in atomic beams, cross sections for, (E/T), 19: 9942
reactions with reactor materials at high temperatures, · 20: 31440(R) (ANL-7175, pp 159-83)
reactions with sea water, use as hydrogen generator for recovering deeply submerged objects, 20: 1567 (SC-RR-65-380)
reactions with sodium carbonate, 19: 35608(R) (APDA-170)
reactions with stainless steel balls at high temperatures, 20: 26459(R) (BNL-954, pp 1-15)
reactions with tantalum at high temperatures, 20: 33771 (LA-3495)
reactions with uranium hexafluoride in conversion to metal, 17: 18164
reactions with uranium carbide at 125 to 250°C, 19: 37202(R) (BNL-900 (p.1-28))
reactions with water in Sodium Reactor Experiment pipe gallery, hazards analysis of, 18: 24894 (NAA-SR-Memo-7743)
reactions with water, thermodynamics of, 18: 33528 (NP-14080)
reactions with water owing to small leaks in steam generators, 18: 35663(R) (TID-20936)
reactions with water in boiler, engineering analysis, 19: 7676(R) (BAW-1280-20)
reactions with water, thermodynamic calculations of, 19: 9107
reactions with water, analysis of, 19: 13577(R) (BAW-1280-21)
reactions with water in steam generators, studies of problems produced by, 19: 20107(R) (BAW-1280-22)
reactions with water, literature review on, 19: 28284 (APDA-167)
reactions with water, effects on design of superheaters, 19: 31474 (BAW-1280-23)
reactions with water, effects on design of superheaters, 19: 31475 (BAW-1280-24)
reactions with water in reactors, testing of, 19: 35608(R) (APDA-170)
reactions with water in steam generators, 19: 38803(R) (BAW-1280-26)
reactions with water, test loop for, 19: 44161(R) (APDA-174, pp 25-32)
reactions with water in prototype boiler, analysis, 19: 46529 (APDA-175)
reactions with water, analysis of, 19: 46530(R) (BAW-1280-27)
reactions with water in boilers, engineering analysis of, 19: 46531(R) (BAW-1280-28)
reactions with water, effects on design of steam generators, 20: 4100 (BW-67-2(a))
reactions with water in pipes, 20: 9417 (CONF-650620, pp 156-65)
reactions with water, research program on, 20: 9419 (CONF-650620, pp 232-43)
reactions with water, test facility for studying, 20: 10290 (CONF-650620, pp 244-54)
reactions with water in steam generators, 20: 12386 (APDA-176)
reactions with water in sodium-heated steam generators, 20: 12391 (BAW-1280-28(Vol.3))
reactions with water, loop development for analyzing, 20: 14024(R) (APDA-182)
reactions with water in steam generators, 20: 14149(T,R) (ORNL-tr-900)
reactions with water, 20: 28691(R) (APDA-185)
reactions with zirconium, mechanisms of oxidation, 19: 9125
reactions with zirconium chlorides in fused salts, 19: 22950
reactivity coefficients in large fast reactors, 16: 26545
reactivity coefficients of voids in, in reactors, 18: 24813(R) (ANL-6880(p.49-67))
reactivity coefficient in fast oxide reactors, 20: 46995
reactivity effects of, as fast-ceramic-reactor coolant, 18: 35146(R) (GEAP-4601)
reactivity void coefficients of liquid, (E), 19: 14765(R) (ANL-6977)
reactivity void coefficients in fast reactors, 20: 38418 (ANL-7120, pp 413-20)

reactivity void coefficients of, calculation of, 20: 38419 (ANL-7120, pp 421-2)
reactivity void coefficients of, in ZPR-6, 20: 38426 (ANL-7120, pp 598-602)
reactivity worths in fast reactor, 16: 931 (ANL-6338)
reactor criticality effects, 16: 24407
reactor criticality effects of voids in, 18: 11407
reactor criticality effects, 18: 15562
reactor criticality effects, 18: 30963
reactor criticality effects in SRE Core II, 18: 35149 (NAA-SR-9509)
reactor criticality effects of voids in, fast (T), 19: 3541
reactor criticality effects of voids of, in fast assemblies (E/T), 19: 3543
reactor criticality effects of voids in, 19: 14828(R) (GEAP-4723)
reactor criticality effects of, void coefficients for, 19: 40158 (UNC-5123)
reactor criticality effects per atom, (E), 19: 42077 (ANL-7014)
reactor criticality effects on plutonium–thorium and plutonium–uranium fueled fast reactors, 20: 5068
reactor criticality effects of voids in, 20: 8388 (IA-1057)
reactor criticality effects of voids in, fast, 20: 10274(R) (NAA-SR-11605, Sect. 1)
reactor criticality effects in large fast reactors, (T), 20: 10332(T) (EURFNR-12F)
reduction of zirconium tetrachloride using, preparation of zirconium by, 17: 16615
removal from clothing of personnel, comparison of deluge and multi-spray showers for, 18: 4020 (NAA-SR-Memo-2068)
research programs on liquid, in France and Great Britain, 17: 27731 (NASA-TM-X-884)
retention by clays, 19: 36300
multi-spray showers for, 18: 4020 (NAA-SR-Memo-2068)
sample preparation for Second Round Carbon-in-Sodium Analysis program, 18: 37065 (NAA-SR-Memo-9294(Rev.))
sampling from circuit for impurity analysis, device for, 18: 11975(T) (AEC-tr-6304)
sampling liquid, methods for, 19: 40112(R) (ANL-7046(p.36-66))
sampling of atmospheric, device for, 20: 4148 (AD-623515)
sampling of cold-trapped, method for, 20: 41420(R) (MSAR-66-149)
sampling of, in the Fermi cooling system, 17: 1049(R) (PRDC-TR-57)
sampling of liquid, in flow through circuit, 18: 13612 (CEA-2369)
scattering by mercury beams at 7 to 500 ev, cross sections for, 20: 39599
separation by electrophoresis on zirconium phosphate paper, 17: 4467
separation by reversed-phase chromatography on D2EHPA treated paper, 18: 16141
separation by solvent extraction using di(2-ethylhexyl)phosphoric acid, 19: 4250(R) (ORNL-3627(p.177-208))
separation from alkali metal salts by chromatography, 17: 12368(T) (UCRL-Trans-895(L))
separation from barium, calcium, and strontium by solvent extraction using di-2-ethylhexyl phosphoric acid, 17: 3073(R) (TID-17265)
separation from barium, calcium, and strontium by solvent extraction using bis(2-ethylhexyl)-phosphoric acid, 17: 25358(R) (SRO-70)
separation from barium, calcium, and strontium by solvent extraction using D2EHPA, 18: 5418 (SRO-56)
separation from barium, cesium, and uranium by ion exchange, 19: 44091
separation from biological material, 18: 1822
separation from biological samples by ion exchange, 20: 45312
separation from cadmium by coprecipitation with cadmium–cerium alloy, 16: 16464
separation from calcium and strontium by ion exchange on zeolites, tracer studies of equilibria in, 19: 528(R) (HW-81746(p.4.15-23))
separation from carbonaceous matter by centrifugation, 19: 23991(R) (ANL-7003)
separation from carbon by filtration, 19: 29468(R) (ANL-7017)
separation from carbon, methods development for, 19: 31462(R) (ANL-7028)
separation from calcium by residue adsorption, 19: 36555
separation from calcium, magnesium, potassium, and strontium by ion exchange, 19: 44122
separation from cerium by ion exchange on chernozem, 16: 20460
separation from cesium by solvent extraction using nitrobenzene, mechanism of, 17: 6194
separation from cesium by ion exchange on clinoptilolite, effects of heat treatment on, 17: 8238 (HW-75296)
separation from cerium by ion exchange, 18: 8445(R) (HW-78388 (p.4.1-15))
separation from cesium and potassium by ion exchange on zeolites, tracer studies of, 19: 527(R) (HW-81746(p.4.5-11))
separation from cesium, potassium, and rubidium by ion exchange on zirconium phosphate, 20: 22863 (CEA-R-2835)
separation from chloride solutions by ion exchange, 20: 4053
separation from cobalt and manganese by electrophoretic focusing, 18: 35466
separation from electrolytes by ion exchange, 19: 36463(R) (TID-22060)
separation from fused salts by ion exchange, tracer studies of, 20: 10958
separation from hydrochloric acid solutions by solvent extraction using 2-ethylhexanol, 19: 36252
separation from in-pile-loop atmosphere at 1200°F, vapor trap for, 19: 28482
separation from irradiated magnesium, methods for, 20: 43550(R) (NYO-844-67)
separation from lithium by amalgam exchange, 17: 4635
separation from lithium by ion exchange chromatography, 18: 21975
separation from lithium fluoride by zone refining, 18: 22019(R) (ORNL-3591(p.231-40))
separation from lithium by ion exchange on moving bed, 19: 11275
separation from lithium by ion exchange, 19: 15571(R) (TID-21385)
separation from manganese by electrophoretic focusing, 18: 35466
separation from magnesium cyclotron targets by solvent extraction using ethanol, 19: 40686
separation from muscle, 17: 30268
separation from nitric acid by solvent extraction using di(2-ethylhexyl)-phosphoric acid, 17: 3070(R) (ORNL-TM-265)
separation from nitrate solutions by solvent extraction using bis(2-ethylhexyl)-phosphoric acid, mechanism of, 17: 25362
separation from nitric or sulfuric acid solutions, ion exchange selectivity scales for, 19: 9257
separation from nitrate solutions by solvent extraction using HDEHP, equilibria and mechanism of, 19: 24440
separation from nitrate solutions by solvent extraction using bis(2-ethylhexyl) phosphate, 20: 45795(R) (ORNL-3945, pp 176-88)
separation from other metals in pyridine hydrochloride by ion exchange, 17: 10747 (TID-15923)
separation from other inorganic ions by paper chromatography, 20: 12939
separation from polystyrene and *p*-toluene sulfonates by ion exchange, 19: 36463(R) (TID-22060)
separation from rhenium by anion exchange chromatography, 19: 24433
separation from rock solutions, 20: 45916(R) (MIT-1381-12)
separation from solutions of ammonium and cesium chlorides by ion exchange on clinoptilolite, tracer studies of equilibria in, 19: 13542
separation from solutions by ion exchange on clays, effects of heat treatment on, 19: 30342
separation from strontium by ion exchange, 19: 22443(P)
separation from uranium ore concentrates, 18: 5431(P)
separation of barium, calcium, and strontium from irradiated, by chromatography, 20: 20636
separation of cesium-137 from liquid, by gettering, 20: 33427
separation of oxygen from liquid, evaluation of hot-trap material for, 18: 1245 (LADC-5936)
separation of radioactive, from activation samples, 19: 19768(R) (TEES-2671-4(Chap.6))
separation of trace elements from, by precipitation ion exchange, 20: 1958
sodium ion reactions at 0.9 to 2.4 kev, charge exchange in, 18: 28265
soil content of, effects on strontium-85 uptake by plants, 20: 10534(R) (BNWL-122, pp 168-9)
soil content of, effects on calcium-45 uptake by plants, 20: 10534(R) (BNWL-122, pp 168-9)
soil content of, effects on cesium-137 uptake by plants, 20: 10534(R) (BNWL-122, pp 168-9)
solubility in ethylenediamine, 18: 8364
solubility in fused sodium halides, 19: 24064(R) (ANL-6997)
solubility in fused halide salts, 20: 6024(R) (ANL-6925(p.235-47))
solubility in liquid zinc, 20: 22966 (ANL-7083)
solubility in molten sodium chloride–sodium fluoride–sodium iodide eutectic, 19: 32924(R) (ANL-7020(p.198-225))
solubility in silicon crystals at 800°C, 19: 39204
solubility in sodium fluoride, 16: 13063
solubility in sodium bromide–sodium hydroxide–sodium iodide mixture, mechanism of, 18: 4275
solubility of hydrogen in liquid, at 250 to 330°C, 19: 17889
solvent partition in tributyl phosphate–hydrochloric acid or –nitric acid systems, 18: 33685
solvent properties for niobium and zirconium at 1470 to 2507°F, 16: 30365(R) (NRL-5844)
solvent properties of liquid, for oxygen, 16: 32956(T) (AEC-tr-5412)
solvent properties of molten, for carbon, 17: 14768(R) (MSAR-63-33)
solvent properties for argon at 200°C, 17: 37001(R) (ANL-6780)
solvent properties for chromium, iron, and nickel at 600°C, 18: 14401 (BNL-7553)
solvent properties for oxygen at 300°C, 18: 14401 (BNL-7553)
solvent properties for iron, catalytic effects of oxygen on, 18: 14401 (BNL-7553)
solvent properties of liquid, for carbon, 18: 17769(R) (ANL-6725(p.99-111))
solvent properties of liquid, for metals, effects of free energy gradient on, 18: 22488 (NAA-SR-8381)

solvent properties of liquid, for carbon, 18: 26824(R) (ANL-6885)
solvent properties for fission products at 900 to 1400°C, 18: 27450
solvent properties for hydrogen, apparatus for studying, 18: 27470
solvent properties for hydrogen at 400 to 1200°F, 18: 32144(R) (MSAR-64-75)
solvent properties for rare gases, 18: 33678(R) (ANL-6875)
solvent properties of liquid, for argon, 18: 43359(R) (ANL-6800(p.43-196))
solvent properties of liquid, for krypton, 19: 15662(R) (ANL-6900(p.45-142))
solvent properties for cerium–cobalt–plutonium alloys at 475 to 650°C, 19: 35613(R) (LA-3316)
solvent properties for carbon, 20: 5594(R) (ANL-6925, pp 21-106)
solvent properties for niobium–1 zirconium at 800 to 1380°C, 20: 5846
solvent properties of liquid, for oxygen, 20: 9390
solvent properties for oxygen at 110 to 550°C, equation for, 20: 31669
sorption and ionization on tungsten, effects of surface nonuniformity on, 17: 14221(T) (AEC-tr-5668)
sorption by ammonium molybdo-, tin, titanium, and zirconium phosphates, comparison of, 20: 45795(R) (ORNL-3945, pp 176-88)
sorption by barley roots, effects of uranium(IV) oxides on, 20: 16174(R) (RLO-1547-3)
sorption by calcium and potassium zeolites, selectivity coefficients for, 18: 23480
sorption by chabazite in lithium, potassium, and sodium nitrates, 20: 16340 (USNRDL-TR-970)
sorption by clinoptilolite, Linde 4AXW, AW-13X, AW-400, AW-500, and Norton Zeolon, thermodynamic properties of, 18: 4886(R) (HW-79140)
sorption by Dowex 50W X8 in presence of cesium and rubidium, 17: 8020
sorption by Dowex 50W X8 from acidic alcohol solutions in presence of cesium, ternary equilibria, 17: 8021
sorption by Dowex 50 X8 in ammonia, effects of anions on, 18: 19837(R) (MIT-905-1)
sorption by gamma-alumina and inorganic ion exchange materials from fused salts, 19: 38771
sorption by mineral ion exchangers from fused sodium nitrate, 18: 39169 (USNRDL-TR-754)
sorption by nuclear sulfonic acid resin, 17: 28855
sorption by peat, 19: 11261 (NP-14668)
sorption by phosphoric acid resins, effects of acidity on selectivity coefficients for, 18: 23481
sorption by tungsten under migration equilibrium conditions, 19: 22226(T)
sorption by Type X zeolite in presence of cerium, strontium, and yttrium, equilibrium in, 19: 22416
sorption by uranyl phosphate at 30 to 1020°C, 19: 24442
sorption by zirconium oxides, effects of previous hydrogen adsorption on, 17: 4500(T) (AEC-tr-5529)
sorption by zirconium phosphate gel, 19: 9256
sorption of liquid, by graphite at 500 to 900°F, 17: 8709 (NP-12487)
sorption on ceric phosphate ion exchanger, 19: 15661 (AFCRL-64-1018)
sorption on quartz, measurements by ion-exchange membrane electrodes, 18: 25327 (RT/GEO(64)-1)
sorptive properties of liquid, for iodine at 500 and 1000°F, 16: 33006
sorptive properties of liquid, for hydrogen, 20: 8816(R) (APDA-178, pp 30-42)
sound absorption in liquid, magnetically induced, 18: 26131
sound attenuation by liquid, measuring methods for, 19: 44342(R) (APDA-174, pp 67-70)
sound-wave attenuation by, use in liquid scanning, 19: 35608(R) (APDA-170)
specific heat and vibrational spectra, (T), 19: 11863
specific heat of crystals of, 16: 15222
specific volume at 1577 to 2491°F, (E), 20: 43946
specifications for reactor, 18: 15563
spectra at high pressures, ESR, 18: 28269
spectra at high temperatures, pressure effects on emission, 16: 16819
spectra, electron collision study of excitation functions, 16: 22145
spectra in acetylene–air flame, effects of aluminum, uranium, and vanadium on, 18: 13701
spectra in ammonia, ESR, 18: 22042
spectra in ethylenediamine, absorption, 18: 8363
spectra in rare gas matrices, optical absorption, (E/T), 19: 7477
spectra in reaction zone of acetylene air flame, excitation of atomic, 17: 27371(T)
spectra in solar chromospheric spicules, absorption, 16: 29604
spectra of, from electron excitation, 18: 759
spectra of, K x-ray, 17: 30484
spectra of vapors of, absorption, 19: 30844 (ARL-65-53)
spectra of, wavelengths of Lyman lines in, 20: 25731
spectral line intensities in airglow, variations of, (E), 19: 18986
spectrum in molten lithium fluoride–potassium fluoride–sodium fluoride eutectic, 19: 9096 (ORNL-P-403)
spectrum of, vibrational, 17: 7132 (NP-12330(p.399-406))
spin densities and wave functions in liquid ammonia, (E), 19: 6451
spin-relaxation time of optically oriented vapor of, effects of spin-exchange collisions in buffer gas, 17: 39771
strength at room temperature, shear and tensile, 16: 22589 (KAPL-M-EEB-6)
substitution in calcium tungstates, theory of coupled, 18: 10089
superconducting transition temperature in, 16: 15334
superconductivity of, 20: 40047
surface tension of liquid, relation to critical temperature and surface energy, 16: 25351
surface tension of, effects of oxygen on, 20: 3880(R) (MSAR-65-150)
technology for fast reactors, 20: 12419(T,R) (EURFNR-1F)
technology for fast reactors, 20: 42577(R) (ANL-7230)
technology of liquid, review, 17: 16535
technology of liquid, developments in, 18: 20464
technology of liquid, review on, 20: 4330(T) (ORNL-tr-854)
temperature distribution in heated, in irradiation capsule, 18: 45128 (TID-7697(p.4.8.1-4))
temperature in MHD cell, (E), 20: 2673
thermal capacity at 0.4 to 30°K, 18: 6118
thermal capacity of lattice, 17: 8063
thermal capacity of liquid, 19: 25033
thermal capacity of liquid, corresponding states correlation of configurational, 20: 20657 (UCRL-11931)
thermal conductivity of liquid, 16: 2220
thermal conductivity at high temperatures, 18: 14455 (CNLM-4094)
thermal conductivity of, at 90 to 850°C, 20: 2370
thermal conductivity of, dependence of, on oxide concentration, 20: 5901
thermal conductivity of vaporous, at 750°C, 20: 20651(R) (CU-2660-26)
thermal conductivity of liquid, estimation of, 20: 41477
thermal conductivity, 16: 16713 (AROD-431-44)
thermal contact resistance of liquid, with stainless steel, measurement of, 16: 10444
thermal contact resistance of stainless steel to liquid, 19: 16186
thermal properties of liquid, 17: 3426(R) (NP-12189)
thermal properties of liquid, determination in loops, 18: 6932
thermal properties of solidified wastes of, 20: 12517(R) (BNWL-170)
thermal properties of liquid and vaporous, 20: 39028
thermodynamic and transport properties of liquid, 16: 18932
thermodynamic properties at 298 to 10000°K, 16: 22736(T) (FTD-TT-62-415)
thermodynamic properties and equilibrium composition of gaseous, at 400 to 10,000°K, 18: 607 (NOLTR-62-170)
thermodynamic properties of vaporous, 19: 20116(R) (SAN-409-12)
thermodynamic properties of vapors of, (T), 19: 18509
thermodynamic properties of, at high temperatures, 20: 1815 (NRL-6241)
thermodynamic properties of vaporous, potential energy curves and second virial coefficients for determining, (T), 20: 8878 (CONF-650559-9)
thermodynamic properties of liquid, Prandtl number at 0 to 700°C for, 20: 31724
thermodynamic properties of, research on liquid and vaporous, 20: 41439(R) (AGN-8198)
thermodynamic properties at boiling point to 2550°F, (E), 20: 43944
thermodynamics of liquid, niobium loop for, 20: 43879
thermoelectric potentials at 25 to 900°C, 19: 4656 (ORNL-3605(Vol.1) (p.116-38))
thermoelectric power up to 3000 atm, and at room temperature, 16: 9240
thermoelectric properties of liquid, 17: 1979
thermoelectric properties, 20: 25474(R) (BNL-954, pp 122-67)
thermophysical properties of liquid, 16: 16741
thermophysical properties at high temperatures, 18: 42018(R) (NRL-6128)
tracer applications survey, 16: 1359
transport across erythrocyte membranes, tracer study, 20: 22564
transport in hamster intestine, effects of heavy water and water on active and passive, 20: 18212
transport mechanisms in rat stomach, 18: 19521 (USNRDL-TR-716)
trisbenzoyl-, luminescence in, 16: 14739
ultrasonic attenuation in, properties of, 20: 8322 (APDA-179)
ultrasonic attenuation in liquid, measurement of, (E), 20: 9120(R) (APDA-178, pp 50-63)
ultrasonic attenuation in liquid, transducer measurement of, 20: 10286 (APDA-180)
ultrasonic inspection of, transducer development for, 20: 14024(R) (APDA-182)
uptake and loss in relation to active mechanism for sodium extrusion in Scenedesmus cells, 20: 30994
uptake by barley seedlings, effects of greasewood forest soil on, 20: 12575
uptake by eye lenses with radioinduced cataracts, 18: 15816(T) (CEA-tr-R-1635)
uptake by plants, mechanism of, 20: 8583
uptake by yeast cells, effects of acidity on, 19: 8762
use as reactor coolant, review on, 18: 26829

use as reactor fuel element filling, 17: 22837(P)
use for determining charged-particle concentration in plasma from quadratic Stark effect, (T), 20: 24568
use in reduction of yttrium fluorides, 16: 2992 (IS-374)
uses for bonding stainless steel to uranium carbide, eddy-current evaluation of, 19: 20531
vacancy concentrations in, measurement of equilibrium, 18: 15723(R) (TID-20334)
vapor pressure, 17: 30536
vapor pressure of, determination of, by spectra photometric measurement of resonance line absorption, 16: 29483 (R60SD330)
vapor pressure of, correspondence with cesium, mercury, potassium, and rubidium, 18: 16035
vapor pressure to 25 atm, 19: 33704
vapor pressures at 2540°F, saturation, (E), 20: 43945
vapor trail along rocket trajectory, camera technique for determining space coordinates of, 18: 29153 (SC-TM-64-527)
vaporization in helium flow, 16: 33122 (NAA-SR-Memo-7393)
vaporization in reactor coolant channels, 20: 20201(R) (ANL-7110, pp 311-401)
vaporization of, testing equipment design for measurement of, 19: 10540(R) (GEAP-4594)
vaporization phenomena, 16: 33126 (UNC-5021)
viscosity of liquid, from melting to critical points, 19: 18518
viscosity of liquid, kinematic, 19: 44701(R) (TID-22144)
viscosity of liquid, based on atomic parameters, 20: 20656 (UCRL-11930)
viscosity of, relation of atomic mobility to, 17: 4945
void coefficient measurements in ZPR-VI, 18: 35060(R) (ANL-6904)
volatility during calcination of sulfate-deficient Purex waste, effects of aluminum on, 18: 19448(R) (ORNL-TM-757)
wave function for valence electron of, one-body model of, 20: 25729
wave propagation in plasma of, 18: 13168
wear of bearing materials in liquid, at temperatures up to 500°C, 16: 29080
wear of carburized steel ball on iron in liquid, at 400 to 1200°F, 17: 26944(R) (BMI-1630(Del.))
wetting chromium, molybdenum, and tungsten surfaces by liquid, effects of time and temperature on, 19: 17897
wetting cobalt, iron, and nickel by liquid, effects of barium and calcium additions to liquid and of oxide films, 16: 25782
wetting of niobium-zirconium alloys, effects of temperature on, 20: 37168(R) (BMI-1771)
wetting of uranium nitride by liquid, use of, in preparation of pastes, 20: 20802(R) (ANL-7055, pp 21-98)
wetting of uranium nitride, temperature effects on, 20: 37168(R) (BMI-1771)
wetting properties for ceramic fuels, 20: 5594(R) (ANL-6925, pp 21-106)
x-ray spectra of, plasmon satellites in, 17: 13424
x-ray total cross sections at 15 to 30 Mev, (E), 19: 12573

SODIUM ACETATES
see also Acetic Acid, Fluoro-, Sodium Salts
dissociation constant of alpha-deuterated-, potentiometric and spectrophotometric determination of, 17: 15990
effects on cesium-137 desorption from soils, 20: 30943(R) (ORNL-TM-1465)
effects on pH of dialyzed zirconyl chloride, 17: 35718
effects on yields in radiolysis of nitrous oxide aqueous solutions, 18: 31601
effects on yields in radiolysis of deuterated sodium formate aqueous solutions containing nitrous oxide, 18: 31602
magnetic resonance of irradiated, 19: 9206
neutron reactions at 0.03 to 0.5 ev, total cross sections for, (E), 19: 25483
nuclear magnetic resonance spectra of long-range coupling between carbon-13 and protons in, 16: 17661
radiation effects on hydrogen abstraction from deuterated, isotope effects in, 19: 4216
radiolysis of aqueous solutions of, 18: 31563 (AD-429919)
radiosensitivity effects on pea seeds, 17: 38881
reactions with sodium hydroxide to prepare methane, 19: 46319
scavenging effects on electron and hydrogen yields in irradiated aqueous solutions, 17: 4602
scavenging effects on hydrogen yield in radiolysis of aqueous solutions, 17: 37265
separation from uranyl bis(dibenzoylmethane) by solvent extraction into chloroform, 16: 11792
transfer between heavy and light water, ionic hydration in, 17: 6096
polyethylene–sodium acetate, determination of fractional composition by x-ray beam attenuation measurements, 20: 3885 (ORNL-IIC-5, pp 277-89)

SODIUM ACETYLIDES
crystal structure, 17: 6692(T) (AEC-tr-5486)

SODIUM ACID CARBONATES
corrosive effects with radiation on metals, 16: 17976(R) (EURAEC-94)
corrosive effects on alloy steels, 16: 22558
corrosive effects on stainless steel, 17: 16594(T,R) (EURAEC-29)
decontamination effects of, with ultrasonics on rat skin contaminated with ^{131}I, ^{32}P, or ^{90}Sr, 20: 42811
effects on reduction of niobium oxide using carbon, 20: 16483
properties in decontamination of cotton fibers contaminated by uranyl nitrate, 19: 26599
radiolysis in ice, electron and hydrogen atom production in gamma, 17: 34026
radiolysis of deaerated aqueous solutions of, pulsed-electron, 20: 10913
radiolysis of frozen aqueous solutions of, ESR spectral studies on radical reactions in, 20: 40994
reaction with uranyl carbonate complexes, 18: 25428
reactions with uranyl carbonate complexes, 16: 4211(T) (JPRS-11292)
solvent properties of solutions of, for radium and uranium, 18: 23711
$NaHCO_3$–NaCl, corrosive effects on stainless steel types 304, 316, and 410, 17: 502(T,R) (EURAEC-293)
$NaHCO_3$–NaCl, corrosive effects on chromium–nickel steel at 20°C, 17: 25727(T) (EURAEC-676)
$NaHCO_3$–NaCl, corrosive effects on chromium and chromium–nickel steels, 17: 25726(T) (EURAEC-675)
$NaHCO_3$–NaCl, corrosive effects on stainless steel, 18: 8734(T,R) (EURAEC-735)
$NaHCO_3$–NaCl, protection and rupture potential effects on steels at 40 and 80°C, 17: 25728(T) (EURAEC-677)
$NaHCO_3$–$UO_2(ClO_4)_2$, potentiometric and refractometric studies of reactions in, 17: 39080

SODIUM ACID FLUORIDES
bonding of hydrogen in, diffraction and spectral data on nature of, 18: 3751
crystal structure, 18: 1489(R) (IS-700(Sect.C))
crystal structure, 18: 5252 (IS-678)
molecular motions, neutron scattering studies of low-frequency, 17: 39019 (BNL-6722)
properties for use as fusing agent for decomposition of thorium ore, 20: 333
radioinduced trapped-hole centers in, electron, 19: 13424(R) (NYO-2047-30)
symmetry of ionic, 18: 1599 (BNL-7373)

SODIUM ACID PHOSPHATES
analysis of phosphorus-32-labeled, for radiochemical impurities, chromatographic, 18: 167 (PAN-392/XIII)
corrosive effects on stainless steel, 18: 7148(R) (HW-78962(p.5.13-23))
effects on reactions of hydroxyl radicals with iodide ions in pulse radiolysis, 19: 26444
production of phosphorus-32-labeled aerosols of, design and performance of generator for, 20: 20924 (AEET-232)
radiation effects on, effects of annealing on neutron, 17: 23419
radiolysis in ice, electron and hydrogen atom production in gamma, 17: 34026
reactions with uranyl salts in solution, 19: 15457(T) (ANL-Trans-33 (p.280-9))
use of solutions of, as coolant for machining uranium in presence of chloride traces, 19: 18432 (Y-1475)

SODIUM ACID PHOSPHITES
radiolysis of, thermal annealing of phosphorus-32 formed in, 18: 5367
radiolysis of, effects of pH on gamma, 20: 14600
radiolysis of, in sodium nitrate solutions, effects of pH on yields from, 20: 14601

SODIUM ACID SULFATES
corrosive effects on reactor cooling systems, evaluation of, 19: 36984
effects on nitrogen-15 exchange between nitric acid and nitric oxide, 20: 9363(R) (NYO-755-2, Paper 3)
radiolysis in ice, electron and hydrogen atom production in gamma, 17: 34026
$KHSO_4$–$NaHSO_4$, electrochemical study of molten eutectic of, 19: 13272 (CEA-R-2567)

SODIUM ACID SULFITES
reactions with iodine compounds, 19: 40402 (BMI-X-10137)

SODIUM ALCOHOLATES
radiation effects on, ESR spectra following, 18: 37240
rate effects on methanolysis of sodium borohydride, 16: 13043

SODIUM ALLOY SLURRIES
Na–U, hydrodynamic, mechanical, and metallurgical behavior, 16: 2163 (AAEC/E-70)
Na–U, loop design and operation for, 16: 1875 (AAEC/E-69)

SODIUM ALLOYS
density measurement of, equipment for, 20: 25474(R) (BNL-954, pp 122-67)
phase equilibria and free energy relations in liquid, 18: 22488 (NAA-SR-8381)
Ag–Na, phase studies, 20: 25474(R) (BNL-954, pp 122-67)

Au–Na, solubility in sodium halide melts, 20: 40796(R) (IS-1500(Sect.C))
Ba–Na, phase equilibria in, 17: 23964(R) (TID-18619)
Ba–Na, phase studies, 16: 13010(R) (TID-15150)
Ba–Na, phase studies, 18: 27970 (TID-20637)
Bi–Na, corrosive effects of molten, on low-carbon steel, 19: 32924(R) (ANL-7020(p.198-225))
Bi–Na, corrosive effects on carbon steel and stainless steel, 20: 2275
Bi–Na, corrosive effects on stainless steel at high temperatures, 20: 31959(R) (ANL-7175, pp 184-211)
Bi–Na, equilibria in regenerative cells, liquid-vapor, (E), 20: 21566(R) (ANL-7055, pp 213-29)
Bi–Na, properties and vapor pressures of, effects of composition and temperature on, 20: 31959(R) (ANL-7175, pp 184-211)
Bi–Na, reactions of Na_3Bi with molten lithium chloride and sodium iodide, 19: 32924(R) (ANL-7020(p.198-225))
Bi–Na, solubility of intermetallic, in halides, 19: 17359(R) (ANL-6965 (p.84-90))
Bi–Na, solubility of Na_3Bi in molten sodium chloride–sodium fluoride–sodium iodide eutectic, 19: 32924(R) (ANL-7020(p.198-225))
Bi–Na, solubility of intermetallic compound in, in fused halide salts, 20: 6024(R) (ANL-6925(p.235-47))
Bi–Na, solubility in sodium halide mixtures, (E), 20: 21566(R) (ANL-7055, pp 213-29)
Bi–Na, solubility in sodium halide melts, 20: 40796(R) (IS-1500(Sect.C))
Bi–Na, thermodynamic properties, 20: 31959(R) (ANL-7175, pp 184-211)
Bi–Na, vaporization of, mass spectrometric study of, 19: 16445(R) (ANL-6900(p.304-29))
Bi–Na, vaporization in regenerative cell, 19: 32924(R) (ANL-7020 (p.198-225))
Cd–Na, phase studies, 20: 25474(R) (BNL-954, pp 122-67)
Cd–Na, properties of, chemical and physical, 20: 38856 (BNL-10372)
Cs–K–Na, electric conductivity and thermal conductivity of liquid, to 2000°F, 19: 16203
Cs–K–Na, preparation and use for power production, 19: 47936(P)
Cs–Na, enthalpy of mixing at 111°C, 18: 8832
Cs–Na, thermoelectric power at low temperatures, (T), 19: 9705
Ge–Na, crystal structure, 18: 30216
Hg–Na, corrosive effects on steels, 18: 18312(T) (CEA-tr-A-1455)
Hg–Na, effects of liquid, on ductility of copper–beryllium alloy, 17: 36220 (AD-287255)
Hg–Na, electric mobility of sodium in liquid, 18: 546 (IP-488)
Hg–Na, nuclear magnetic resonance in, 18: 42036
Hg–Na, solvent properties for rare earths, 17: 40939
K–Na, activity of hydrogen in, effects of lithium additions on, 20: 9425 (ORNL-3898)
K–Na, analysis for hydrogen and oxygen, 19: 300 (ORNL-P-539)
K–Na, analysis for oxygen, 20: 1799
K–Na, analysis for oxygen, methods for, 20: 8447 (PWAC-491)
K–Na, analysis of liquid, for oxygen, 17: 27731 (NASA-TM-X-884)
K–Na, analysis of liquid, for oxide by automatic measurement of plugging temperature, 18: 13646(T) (AEC-tr-6353)
K–Na, atomic structure of, x-ray- and neutron-diffraction studies of, 20: 15080
K–Na, bibliography on, 20: 27415 (TRG-Inf.Ser.-312)
K–Na, bibliography on technology of liquid, 18: 929 (NP-14434)
K–Na, chemistry and impurity analysis of reactor-coolant, 18: 21661
K–Na, chemistry in experimental SNAP-8 reactor, 20: 3564
K–Na, circulation in MHD ducts, (E), 20: 39716
K–Na, combustion fume removal by glass fabric filters, 16: 12660 (TID-14979)
K–Na, compatibility with aluminum and uranium nitride at high temperatures, 18: 643 (BMI-1638)
K–Na, compatibility with bearing materials for SNAP-50/SPUR coolant pumps, 20: 10419 (PWAC-468)
K–Na, compatibility with urania and plutonia–urania fuels, 20: 33795
K–Na, compressibility of liquid, at 100°C, 16: 29406
K–Na, corrosive effects of liquid, on Hastelloy X and Inconel loops, 16: 15146 (PWAC-203)
K–Na, corrosive effects of liquid, on Hastelloy X and stainless steel at 1100 to 1500°F, 16: 16691 (TIM-435)
K–Na, corrosive effects of liquid, on Hastelloy and Haynes 25 alloy at 1200 to 1500°F, 16: 16681 (TID-7626(Pt.I)(p.87-91))
K–Na, corrosive effects of liquid, on reactor materials, 16: 32087
K–Na, corrosive effects of liquid, on stainless steel tubes, 16: 13538
K–Na, corrosive effects of liquid, on stainless steel tubes, 16: 27594
K–Na, corrosive effects on reactor materials, 17: 7565(R) (PWAC-161)
K–Na, corrosive effects on beryllium oxide, 17: 7606(R) (ORNL-1515)
K–Na, corrosive effects on uranium mononitride at 260 and 480°C, 17: 30906 (BMI-1633)
K–Na, corrosive effects on UBe_{13}–$ZrBe_{13}$, 17: 34329(R) (TID-14146)
K–Na, corrosive effects of liquid, 18: 3298(R) (ORNL-2221(Pts.1-5) (Del.))
K–Na, corrosive effects of liquid, on reactor materials, 18: 8760
K–Na, corrosive effects on uranium nitrides at 500°C, 18: 32035(R) (BMI-X-10073)
K–Na, corrosive effects on reactor materials, 18: 37634 (A/CONF.28/P/343)
K–Na, corrosive effects on uranium nitride, 19: 885 (BMI-1692)
K–Na, corrosive effects on brazing alloys, 19: 6486(R) (GEST-2037)
K–Na, corrosive effects on stainless steels, literature survey, 19: 20472 (IDO-14651)
K–Na, corrosive effects on structural alloys, research program on, 19: 20477(R) (ORNL-3604)
K–Na, corrosive effects on structural alloys at high temperatures, loop experiments, 19: 20478(R) (ORNL-3618)
K–Na, corrosive effects on structural alloys at high temperatures, loop experiments, 19: 20479(R) (ORNL-3671)
K–Na, corrosive effects on structural alloys at high temperatures, mass transfer in, 19: 20480(R) (ORNL-3730)
K–Na, corrosive and mass transfer effects on stainless steel, 19: 22897 (TIM-655)
K–Na, corrosive effects on reactor materials, 19: 24939(R) (ORNL-3784)
K–Na, corrosive effects on reactor coolant loop materials, 19: 28755(R) (ORNL-3823)
K–Na, corrosive effects on niobium–zirconium alloy in stainless steel loop at 1250°F, 19: 34640 (CNLM-6246)
K–Na, corrosive effects on metals, 19: 34643
K–Na, corrosive effects on niobium–zirconium alloy at 1250°F, effects of carbon, nitrogen and oxygen on, 19: 44626 (TIM-896)
K–Na, corrosive effects on reactor cooling system materials, 20: 773(R) (ORNL-3859)
K–Na, corrosive effects on boron carbide–stainless steel at 1000°F, 20: 776 (TIM-822)
K–Na, corrosive effects on niobium–zirconium alloy and type 316 stainless steel, 20: 2273
K–Na, corrosive effects on niobium and niobium–zirconium alloy, 20: 5181(R) (ORNL-3029)
K–Na, corrosive effects on stainless steel and other structural materials, review on, 20: 4318 (CNLM-5359)
K–Na, corrosive effects on niobium–1 zirconium and type 316 stainless steel, 20: 4323(R) (ORNL-3870, pp 308-11)
K–Na, corrosive effects on Croloy 9M, INOR-8, and types 316 and 347 stainless steel, 20: 5851
K–Na, corrosive effects on SNAP-8 system materials, effects of temperature and velocity on, 20: 9425 (ORNL-3898)
K–Na, corrosive effects on types 316 and 347 stainless steel, 20: 9425 (ORNL-3898)
K–Na, corrosive effects on Hastelloy N, effects of oxygen on, 20: 9425 (ORNL-3898)
K–Na, corrosive effects on Croloy 9M, INOR-8, and type 347 stainless steel, 20: 4322(R) (ORNL-3870, pp 305-7)
K–Na, decontamination device for liquid, 16: 13345
K–Na, determination of, in air, 16: 18646(R) (ORNL-2247(Pts.1-5))
K–Na, determination of, in air, 16: 28647(R) (ORNL-2340(Pts.1-5))
K–Na, diffusion of hydrogen in liquid, 18: 23061(R) (ORNL-3591 (p.217-22))
K–Na, distillation, 17: 7606(R) (ORNL-1515)
K–Na, effects as drying agent on radioinduced polymerization of styrene, 19: 24560
K–Na, effects of hydrogen-containing, on niobium, 16: 25402
K–Na, effects of molten, on elastomers, 18: 3298(R) (ORNL-2221 (Pts.1-5)(Del.))
K–Na, effects of impurities on operation of heat transfer system of, 18: 17310
K–Na, effects on electric conductivity of argon and nitrogen plasma, (E), 19: 10380 (AEDC-TDR-64-119)
K–Na, effects on hydrogen diffusion through stainless steel, 19: 30154(R) (ORNL-3789(p.308-17))
K–Na, effects on mechanical properties of Croloy 9M from decarburization by, 20: 9425 (ORNL-3898)
K–Na, effects on hydrogen diffusion through type 316 stainless steel, 20: 9425 (ORNL-3898)
K–Na, effects on properties of chromium–molybdenum steels, 20: 16972(R) (NASA-CR-54719)
K–Na, electric conductivity at temperatures up to 855°C, 18: 14455 (CNLM-4094)
K–Na, electric conductivity and thermal conductivity of liquid, to 2000°F, 19: 16203
K–Na, electric conductivity to 2000°F of eutectic, 19: 32724(R) (AFML-TR-65-99)
K–Na, enthalpy of mixing at 111°C, 18: 8832
K–Na, erosive effects on stainless steel, 20: 39023 (NAA-SR-11952)
K–Na, facility for studying fires of, 20: 10272(R) (NAA-SR-9339)
K–Na, fire prevention by handling in cellosolve-kerosene system with

liquid nitrogen fire extinguisher, 16: 27160 (HW-74194)
K–Na, flexibility and stress analysis of piping system for, in nuclear powered airplane, 19: 22509 (PWAC-123)
K–Na, handling and purification for SNAP 10A, 19: 3725 (NAA-SR-Memo-10169)
K–Na, handling of irradiated capsules containing, 16: 27160 (HW-74194)
K–Na, handling of liquid, 16: 29128
K–Na, handling, physical properties, and reactions of liquid, 16: 4404 (TRG-Report-25)
K–Na, heat transfer from molten sodium to liquid, 16: 17780 (TIM-5)
K–Na, heat transfer properties in space power systems, 17: 8337
K–Na, heat transfer of liquid, 17: 19723 (BNL-759(p.14-38))
K–Na, heat transfer of, in circular tubes, 17: 30668
K–Na, heat transfer properties, 17: 35222 (PWA-2240)
K–Na, heat transfer to, flowing in-line through 19-rod bundle, 18: 3671(R) (BNL-799(p.26-54))
K–Na, heat transfer to copper pipes, 18: 16173 (NP-13656)
K–Na, heat transfer properties of, in flow in circular tubes, 19: 34699
K–Na, heat transfer in flow through rod-bundles, 19: 36216(R) (BNL-900(p.29-72))
K–Na, heat transfer during vertical upflow of, 19: 46528 (ANL-7038)
K–Na, heat transfer to, flowing through bundle of circular rods, 19: 46553
K–Na, heat transfer in vertical tubes at low Peclet number, 20: 27111(T) (BNL-tr-6)
K–Na, hydride precipitation in, 19: 20478(R) (ORNL-3618)
K–Na, hydrogen solubility in, 19: 28326
K–Na, hydromagnetic wave propagation in liquid, in waveguides, (E/T), 19: 4758
K–Na, instructions for transfer of liquid, to forced convection in-pile loop, 17: 24617 (CNLM-1192)
K–Na, lubricating properties of liquid, 18: 594(R) (ASD-TDR-63-134)
K–Na, magnetic field interactions with surface waves on, 17: 16784 (NASA-TR-R-161)
K–Na, Nusselt numbers for liquid, 19: 11355
K–Na, performance of thermionic diodes with liquid collectors of, 17: 27988
K–Na, performance in Canberra homopolar generator liquid metal jet system, 18: 8620
K–Na, performance as fast reactor coolant, 18: 29040(R) (GEAP-4480)
K–Na, performance in MHD cell with and without gas phase, 19: 1207 (ANL-6870)
K–Na, performance in SNAP-8 power conversion system, 19: 19410(R) (NASA-CR-54219)
K–Na, performance as lubricant for rotor bearings, 19: 32333 (NYO-3363-1)
K–Na, performance in MHD cells, 19: 48053(R) (ANL-7090, pp 55-68)
K–Na, performance in d-c MHD cells, 20: 27790
K–Na, phase studies, 20: 41455(R) (NYO-2731-7)
K–Na, physical and thermal properties of liquid, at the boiling point to 1300°C, 17: 34402 (EUR-357.d)
K–Na, physical and thermodynamic properties of, 20: 35110 (CNLM-5584(Vol.3))
K–Na, physical properties of liquid, review, 18: 20516 (EUR-599.d)
K–Na, physical properties of liquid, 19: 28821
K–Na, physical properties at boiling point to 1300°C, 19: 34643
K–Na, pressure losses for 1600°F operation in in-pile loop, 16: 13213 (TIM-483(Suppl.1))
K–Na, properties of, for space applications, handbook on, 16: 5088 (WADD-TR-61-96)
K–Na, properties of liquid, 16: 19370 (TIM-65)
K–Na, properties of liquid, as reactor coolants, 16: 23830 (BNL-5377)
K–Na, properties of liquid, as reactor coolants, 16: 28545 (TID-7623 (p.2-8))
K–Na, properties of liquid, for use in aircraft reactor PWAR-6 design, 16: 15901 (FXM-2210)
K–Na, properties for use as space electric-power systems, 17: 39246
K–Na, properties as reactor working fluid, 18: 35198 (NAA-SR-8617 (Vol.I))
K–Na, properties and uses of liquid, 19: 6353
K–Na, pumping of liquid, electromagnetic pumps for, 18: 12293(R) (N63-15259)
K–Na, pumping of, development of thermoelectric pumps for, (E), 19: 20096 (NAA-SR-Memo-10729)
K–Na, pumps for liquid, minimum-weight calculations for, 19: 29033 (NAA-SR-Memo-10784)
K–Na, pumps for liquid, 20: 35114 (CONF-651026, pp 186-200)
K–Na, purification by cold-trapping, 18: 21657
K–Na, purification by solvent extraction using naphthalene–tetrahydrofuran, 19: 40409(R) (MSAR-65-95)
K–Na, reactions with water, 17: 2939 (HW-67717)
K–Na, research programs on liquid, in France and Great Britain, 17: 27731 (NASA-TM-X-884)
K–Na, sampling from engineering test rigs for oxide analysis, 17: 33802 (TIM-711)
K–Na, separation of hydrogen from liquid, by addition of lithium, 20: 25107(P)
K–Na, solubility of hydrogen in liquid, 19: 28755(R) (ORNL-3823)
K–Na, solvent properties for hydrogen, apparatus for measurement of, 19: 20477(R) (ORNL-3604)
K–Na, solvent properties for hydrogen at 1100°F, 19: 20479(R) (ORNL-3671)
K–Na, solvent properties for hydrogen at 752 to 1300°F, 19: 20480(R) (ORNL-3730)
K–Na, solvent properties for hydrogen as functions of temperature and pressure, 19: 24939(R) (ORNL-3784)
K–Na, solvent properties for calcium at 500 to 800°F, 19: 26282 (CONF-650411-4)
K–Na, solvent properties for hydrogen, 20: 9425 (ORNL-3898)
K–Na, solvent properties for calcium, 20: 33863 (CNLM-6335)
K–Na, theory of molten, 19: 28744
K–Na, thermal conductivity of liquid, 16: 25535
K–Na, thermal properties of, effects on reactor transients, 18: 35146(R) (GEAP-4601)
K–Na, thermocouple response time in liquid, 19: 22659 (EUR-2281.f)
K–Na, thermodynamic properties, 19: 15662(R) (ANL-6900(p.45-142))
K–Na, thermodynamic properties at 414°K, 19: 32279(R) (ANL-7020 (p.3-99))
K–Na, thermodynamic properties of liquid, 20: 5594(R) (ANL-6925, pp 21-106)
K–Na, thermodynamic properties, 20: 20802(R) (ANL-7055, pp 21-98)
K–Na, thermodynamic properties, 20: 31213(R) (ANL-7175, pp 119-58)
K–Na, thermodynamic properties of liquid, Prandtl number at 0 to 700°C for, 20: 31724
K–Na, thermoelectric properties of liquid, 17: 1979
K–Na, thermoelectric power at low temperatures, (T), 19: 9705
K–Na, thermophysical properties of, 20: 8447 (PWAC-491)
K–Na, uranium testing in, capsule fabrication for, 20: 33940 (DP-MS-66-1)
K–Na, use as reactor fuel element filling, 17: 22837(P)
K–Na, use in condensers for space power plants, 19: 9331 (PWA-2320 (Vol.I))
K–Na, use in MHD generators with two-phase flow, 20: 41728
K–Na, use in MHD conversion systems, 20: 41733
K–Na, vapor pressure of, 17: 4947
K–Na, vapor pressure, 17: 36861(R) (ANL-6764)
K–Na, vapor pressures and activities of sodium and potassium in, 18: 20569
K–Na, vapor pressure of eutectic, to 1935°F, 19: 32724(R) (AFML-TR-65-99)
K–Na, viscosity and wetting of uranium dioxide slurries by, 17: 22784(R) (ARF-3124-1)
K–Na, viscosity of, at −10 to 148.9°C, 20: 5908
Li–K–Na, solvent properties for hydrogen as function of lithium content, 19: 24939(R) (ORNL-3784)
Li–Na, density and miscibility of liquid, 20: 41455(R) (NYO-2731-7)
Li–Na, performance as coolant in liquid metal cooled reactors, 19: 37202(R) (BNL-900(p.1-28))
Na–Sn, solubility in sodium halide melts, 20: 40796(R) (IS-1500(Sect.C))
Na–Sr, phase equilibria in, 17: 23964(R) (TID-18619)
Na–Sr, phase studies, 16: 13010(R) (TID-15150)
Na–Sr, phase studies, 18: 25984 (TID-20639)
Na–Tl, crystal structure of Na_2Tl in, 20: 33868 (IS-T-82)
Na–Tl, crystal structure of intermetallic compounds, 20: 41412(R) (IS-1500(Sect. M))
Na–Tl, nuclear magnetic resonance, 17: 18785
Na–Tl, solubility in sodium halide melts, 20: 40796(R) (IS-1500(Sect.C))
Na–U, properties for breeder blankets, 19: 35608(R) (APDA-170)
Na–Zr, phase studies, 20: 35924
Pb–Na, corrosive effects on Inconel and stainless steel, 17: 7606(R) (ORNL-1515)
Pb–Na, corrosive effects on stainless steel at high temperatures, 20: 31959(R) (ANL-7175, pp 184-211)
Pb–Na, crystal structure of intermetallic compounds in, 18: 30216
Pb–Na, preparation of kryptonates of, by diffusion, 20: 18570(R) (NYO-2757-5)
Pb–Na, properties as reducing agent for multivalent cations in acid solutions, 19: 17867
Pb–Na, properties at high temperatures, 20: 31959(R) (ANL-7175, pp 184-211)
Pb–Na, solidification and structure of, effects of high cooling rate on, 19: 9673(T) (SC-T-64-2011)
Pb–Na, solubility in sodium halide melts, 20: 40796(R) (IS-1500(Sect.C))
Pu–Na, phase studies and properties of, bibliographic study of, 16: 32115 (KFK-105)
Rb–Na, enthalpy of mixing at 111°C, 18: 8832
Rb–Na, thermoelectric power at low temperatures, (T), 19: 9705

Sb–Cs–K–Na, photosensitivity of, 20: 17984
Sb–Na, electric conductivity of Na_3Sb, temperature dependence of, 19: 41124(R) (NP-15108)
Sb–Na, photoemissive properties of, 17: 41553(R) (NP-13160)
Sb–Na, properties of Na_3Sb bulk and films, 18: 30166(R) (AD-439716)
Sb–Na, solubility in sodium halide melts, 20: 40796(R) (IS-1500(Sect.C))
Sodium Aluminum Fluorides
see Sodium Fluoaluminates
SODIUM ALUMINUM HYDRIDES
free energy and heat of formation, 17: 37183
preparation, 17: 25188
SODIUM ALUMINUM SILICATES
see also Albites
cesium-137 release from Decalso gel at 1350 to 1500°C, 16: 14684 (HW-69274)
glasses of, electric conductivity measurements of the densification of, 19: 24989(R) (TID-21673)
preparation, 17: 19712 (TID-7644(p.201-10))
solid-phase reactions of, at high pressures, 17: 10503 (NP-12359)
sorptive properties of zeolites A and X for benzene, n-hexane and hexene at 260 to 482°C, 16: 17667
sorptive properties of Decalso, for cesium, 20: 16578
spectra of water molecules in, low frequency motions in neutron, 18: 22045
SODIUM ALUMINUM TETRAETHYL
synthesis, 17: 25187
SODIUM AMERICIUM FLUORIDES
crystal structure of $Na_7Am_6F_{31}$, 20: 38898
SODIUM AMIDES
dimerization of triphenylcyclopropene by, in liquid ammonia, 17: 39084
SODIUM ARSENATES
arsenic-75 NQR in, 16: 16360
effectiveness in prevention of polonium poisoning, 16: 6313(T) (JPRS-11322(p.406-21))
effects on strontium-85 elution from mouse bones, 19: 43706
effects on 4-aminobutyric acid content of brain in dogs, 19: 45979
evaluation for brain-blood barrier uses, 16: 22 (IA-668)
radioinduced radicals in disodium hydrogen arsenate, ESR of x, 18: 22148
solvent properties for nucleic acid in *Escherichia coli*, 19: 29923
toxic effects of, protective effects of thiazolidinecarboxylic acid derivatives against, in mice and rats, 18: 17670
SODIUM ASTATIDES
entropy and thermal capacity at 0 to 300°K, 20: 1859
SODIUM AZIDES
analytical use in the spectrophotometric determination of uranium, 16: 12975
effects on action-potentials of x-irradiated nerve fibers, 18: 23277
effects on phosphate and rubidium uptake by isolated cells of bean seedlings and tobacco leaves, 20: 14217 (COO-888-43)
effects on radiomimetic effects of nitrosoamides on herb seeds, 19: 43870
nitrogen production and trapping in x-irradiated, at low temperatures, 16: 5250
photolysis and spectra, ultraviolet, 16: 2348
protective effects against radiation damage to plant cells, 18: 23374
radiation effects on photoelectric properties of, 17: 27468
radiation effects on paramagnetic resonance of trapped nitrogen atoms in, 17: 35885
radiation stability of, gamma, 19: 15593
radioinduced crystallite overgrowth on, 16: 33411
radioinduced defects in, ESR spectral studies on, 20: 15942 (NYO-2150-11)
radioinduced formation of N_3^- defects in, studies of x, 20: 40966
radioinduced nitrogen free radicals in, EPR spectra of x, 20: 13970 (AD-611432, pp 135-47)
radiosensitivity effects on DNA, γ, 20: 8732
reactions with nitrogen-13 recoil atoms and thermal decomposition of, activities of yields in, 18: 33663
therapeutic effects of, against radiation injuries in mice, 18: 5135(R) (NP-13281(p.45-56))
Sodium Benzoate
see Benzoic Acid, Sodium Salts
Sodium Beryllium Fluorides
see Sodium Fluoberyllates
SODIUM BERYLLIUM PHOSPHATES
crystal structure, 16: 20442
Sodium Bicarbonates
see Sodium Acid Carbonates
SODIUM BISMUTHATES
oxidative effects on aqueous uranium(IV), 16: 11602
SODIUM BORATE GLASS
electron reactions in, proportional counter for x ray emission at small angles in, 17: 37438
radiation effects in, electron paramagnetic resonance study of, 17: 22253
radioinduced optical absorption in, effects of structure on, 17: 2044
structure, nuclear quadrupole studies, 16: 27643
thermoluminescence of magnesium-, nickel-, and uranium-oxide-seeded, 16: 13060
SODIUM BORATES
see also Borax
see also Sodium Tetraborates
effects on polarization of steel and uranium, 19: 7914
effects on polarization of steel–uranium couples in aqueous solutions, 19: 9619 (AMRA-TR-64-33)
effects on production of malonaldehyde in gamma radiolysis of galactose, 20: 35540
ion exchange with potassium chloride at 830°C, tracer study, 19: 34150 (USNRDL-TR-847)
molecular structure in vapor, 16: 27026
partition between vapor and liquid phases in boiling-water reactors, 18: 19380
radiation effects on optical absorption in, x, 18: 10154
solvent properties of melts of, for rare earths, 20: 26846
spectra in vapor, infrared, 17: 15945 (AROD-006.8)
spectra of, infrared, 17: 18048
use for neutron capture therapy of brain tumors in man, 17: 10282
vaporization phenomena of, mass-spectrometric study of, 17: 15944 (AROD-006.7)
B_2O_3–$NaBO_2$–NaCl, immiscibility diagram of liquid, 18: 40996 (USNRDL-TR-752)
B_2O_3–$NaBO_2$–NaBr, immiscibility diagram of liquid, 18: 40996 (USNRDL-TR-752)
B_2O_3–$NaBO_2$–NaI, immiscibility diagram of liquid, 18: 40996 (USNRDL-TR-752)
SODIUM BORIDES
LaB_6–NaB_6, production and properties, 19: 23016(T) (JPRS-28849 (p.238-43))
SODIUM BOROHYDRIDES
analytical uses for precipitation of heavy-metal ions, 18: 13358(R) (MLM-1151)
analytical uses of, for precipitation of heavy metals from nitric acid solutions, 17: 21389(R) (MLM-1145)
hydrolysis in aqueous solution, salt and solvent isotope effects on, 16: 13041
hydrolysis in aqueous tetramethylamine, geometry of activated complex formed in, 16: 13042
hydrolysis in water-d_2, catalytic effects of cobalt, palladium, and platinum on, 18: 13753
hydrolysis of, deuterium isotope effects on, 20: 306
polarography of, 17: 174
reactions with methanol, effects of sodium carbonate and methoxide on, 16: 13043
reducing effects on heavy metal cations, 17: 17625(R) (MLM-1144)
solvolysis of, deuterium isotope effect in, 19: 5917
use in synthesis of tritium-labeled digoxin, 20: 42722
uses for activation of catalysts for hydrogen isotope exchange, 19: 7428
SODIUM BROMATES
bromine-79 double nuclear magnetic resonance transitions in, 18: 9406
neutron reactions bromine-79 (n,γ) and bromine-79 (n,2n) in, distribution of labeled bromine in, 19: 18042
photolysis of gamma-irradiated and normal, kinetics of, 20: 29248 (BNL-9672)
radiation effects on thermal decomposition, 17: 18102 (BNL-6257)
radiation effects on ESR in, electron and gamma, 18: 29772
radiolysis of crystalline, yields of bromate decomposition and bromide ion in, 18: 43639
radiolysis of, gamma, neutron, and lithium-6 fission product recoil, 20: 36899
radiolysis yields, 16: 10073
reactions with uranium and neptunium in molten lithium nitrate–sodium nitrate, 20: 7073
thermal decomposition kinetics, 18: 40971 (BNL-7683)
thermal decomposition of, search for perbromate in, 19: 36402
thermodynamic properties of crystalline, at 25°C, 16: 18875
SODIUM BROMIDES
activity and osmotic coefficients in heavy water at 25°C, 20: 16488
activity coefficients in dilute alkali halide–cadmium nitrate solutions at 240 and 300°C, 16: 17651
activity coefficients of highly concentrated aqueous, 20: 2520(R) (IA-920)
analysis for chloride and iodide ions by bremsstrahlung-activation methods, 20: 29112
beta absorption and backscattering by, calculation of elemental stopping powers from, 19: 30127

Born repulsive potential in crystals of, 17: 2062 (TID-17185)
bromine-79 and -81 NMR spectra in, effects of bromine on, 20: 14573
bromine-79 chemical shift, E2 coupling, and spin-lattice relaxation in, 18: 12094
cohesive energy of crystals of, Born analysis for, 17: 32084
corrosive effects on titanium alloys at 650°F, 19: 44621 (CONF-651006-1)
crystal lattice energy of, relation of self energy of gaseous ions to, 18: 16017
crystal structure lattice dynamics of, eigenvalues and eigenvectors for, 20: 33262 (UCRL-14822)
crystal vibrations in impure, localized modes for determination of frequencies of, 18: 12103
diffusion of bromine in, coefficient determination for, 19: 11109
effects on prevention and reduction of generalized and local reactions in human radiotherapy, 19: 13109
effects on self-diffusion of water at 23°C, 19: 32159
effects on thermal conductivity of sodium chloride, 19: 25783 (COO-1198-238)
electron energy loss spectra at 0.8 and 1.5 Mev, 16: 12275
electron energy loss spectra in, 19: 16404
electron reactions with vacuum-cleaved surfaces of, electron emission in, (E), 19: 23287
electron-positron annihilation in, 18: 28345
europium sulfide epitaxial growth on crystals of, 19: 11079
hardness of crystals of, 16: 10728
heat of solution in liquid nitrates, 17: 28869
intercrystalline energies in binary systems, 16: 7558
nuclear quadrupole coupling constants in crystals of, 16: 24654
photoemission yields at 10 to 21 ev, (E), 19: 11861
positron annihilation in, three-quantum, (E), 19: 10066
preparation of single-crystal, 20: 35484(T) (UCRL-Trans-10027)
radiation effects on luminescence centers in silver-activated, x, 19: 41977
radiation effects on phosphorescence of, influence of F-band illumination on x, 19: 40570
radiation effects on absorption and luminescence spectra of nickel-, silver-, or tin-activated, 19: 47884(T) (IS-Trans-18)
radiation effects on crystal structure of, mechanism of beta, 20: 2426 (LA-3387)
radiation effects on electric conductivity of, (E), 20: 2434(R) (TID-22242)
radiation effects on mechanical properties of, 20: 26975
radioinduced bleaching of, neutron, 19: 11227(T)
radioinduced color centers in single crystals of, annealing of, (E), 19: 17974
radioinduced color centers and luminescence in silver-activated, 19: 34254
radioinduced defects in single-crystal, 20: 35932 (LA-3501)
reactions in dioxane–water solutions, nuclear magnetic resonance spectra of, 17: 40800
reactions with praseodymium bromide, 19: 40469
reduction by high-frequency hydrogen discharge to hydrogen halide and metal, 19: 39180
reduction by high-frequency discharges in helium, hydrogen, and nitrogen, role of electrons in, 19: 39181
samarium spectra in crystals of, at low temperatures, 18: 25406(T)
sodium-23 magnetic shielding in crystals of, 17: 21696
sorptive properties of, for cadmium-115, indium, mercury, and zinc-65, 17: 15992
spectra of crystals of, F-center positions in, 17: 27377
spectra of, microwave rotational, 16: 29560
spectra of U centers in, infrared absorption, 19: 35587(T) (ANL-Trans-206)
spectral characteristics of silver-activated crystals of, 16: 10742
thermal capacity at 10 to 300°K, 16: 32226
thermodynamic properties in *N*-methylformamide solutions, 20: 3924 (TID-22366)
thermodynamic properties in anhydrous *N*-methylformamide solutions, 20: 3925 (TID-22366, App. B)
thermodynamics of, in anhydrous *N,N*-dimethylformamide and *N*-methylformamide at 25°C, 20: 3926 (TID-22374)
vibrational frequencies in crystals of, 16: 32221
AgBr–NaBr, phase diagrams, 20: 36787 (YALE-2723(Vol.1))
$AlBr_3$–NaBr, impedance of polarized platinum micro-electrodes in, 16: 2232
$BaBr_2$–NaBr, phase diagrams, 20: 36787 (YALE-2723(Vol.1))
$Ba(NO_3)_2$–NaBr, phase studies, 17: 32112
B_2O_3–$NaBO_3$–NaBr, immiscibility diagram of liquid, 18: 40996 (USNRDL-TR-752)
$CaBr_2$–NaBr, phase diagrams, 20: 36787 (YALE-2723(Vol.1))
$CdBr_2$–NaBr, phase diagrams, 20: 36787 (YALE-2723(Vol.1))
CsBr–NaBr, phase diagrams, 20: 36788 (YALE-2723(Vol.2))
$ErBr_3$–NaBr, complex formation in, 20: 12871
KBr–NaBr, heat of mixing of, effects of composition and temperature on, 20: 23011
KBr–NaBr, phase diagrams, 20: 36788 (YALE-2723(Vol.2))
KBr–NaBr, solvent properties for niobium, 18: 16032
KCl–NaBr, microstructure and phase studies, 18: 18372
KF–NaBr, microstructure and phase studies, 18: 18372
LiBr–NaBr, phase diagrams, 20: 36788 (YALE-2723(Vol.2))
LiBr–NaBr, phase studies, 17: 1505
LiCl–NaBr, microstructure and phase studies, 18: 18372
LiF–NaBr, microstructure and phase studies, 18: 18372
$MgBr_2$–NaBr, phase diagrams, 20: 36788 (YALE-2723(Vol.2))
NaBr–H_2SO_4, radioinduced absorption spectra in, at 77°K, 20: 16534
NaBr–NaCl, heat of mixing of, effects of composition and temperature on, 20: 23011
NaBr–NaCl, microstructure and phase studies, 18: 18372
NaBr–NaCl, phase diagrams, 20: 36788 (YALE-2723(Vol.2))
NaBr–NaCl, radioinduced F-bands in, effects of Schottky defects on, 20: 14605
NaBr–NaF, microstructure and phase studies, 18: 18372
NaBr–NaF, phase diagrams, 20: 36788 (YALE-2723(Vol.2))
NaBr–NaI, phase diagrams, 20: 36788 (YALE-2723(Vol.2))
NaBr–NaOH–NaI, solvent properties for metallic sodium, 18: 4275
NaBr–NaOH, thermal conductivity at low temperatures, 19: 31629 (COO-1198-239)
NaBr–$SrBr_2$, phase diagrams, 20: 36788 (YALE-2723(Vol.2))
NaBr–TlBr, phase diagrams, 20: 36788 (YALE-2723(Vol.2))
$NdBr_3$–NaBr, complex formation in, refractometric studies of, 19: 46254
$PbBr_2$–NaBr, phase diagrams, 20: 36788 (YALE-2723(Vol.2))
RbBr–NaBr, phase diagrams, 20: 36788 (YALE-2723(Vol.2))

Sodium Bromoacetates
see Acetic Acid, Bromo-, Sodium Salts

SODIUM BRONZE
Na–W, analysis for sodium, activation, 17: 31994
Na–W, heat capacity and thermodynamics at 15 to 300°K, 18: 16030
Na–W, nuclear magnetic resonance, 16: 10568
Na–W, nuclear magnetic resonance of tungsten-183 in, 16: 29552
Na–W, positron annihilation in, (E/T), 19: 41158
Na–W, spin-lattice relaxation time of sodium-23 in, 16: 29552

SODIUM CARBONATES
analysis for carbon dioxide, microdiffusion, 16: 25291
analysis for oxygen-18, mass spectrometric, 20: 8852
analysis for rare earth oxides in natron, activation, 20: 1731 (BNL-9614)
analysis for uranium(VI) by u-v absorption, 20: 16354
beta backscattering, 16: 9409
carbon exchange with potassium cyanide, 16: 23558
content of, in sediments of Bay of Roquebrune, 20: 36553
corrosive effects on chrome and nickel steels, effects of chlorine and oxidants, 17: 12616
development for SEFOR core materials, 20: 38531 (GEAP-5133)
effects of volatilization of cesium from coprecipitate with potassium nickel ferrocyanide, 18: 3728
effects on carbothermal reduction of uranium oxides, 20: 23030
effects on corrosion of niobium and tantalum at 21 and 98°C, 19: 22900
effects on densification of thorium oxide–uranium oxide pellets, 16: 7874 (ANL-6375)
effects on radiation peroxidation of kerosene, 16: 8775
effects on radiolysis of aqueous polyvinyl alcohol solutions, 19: 2387
effects on reactions of hydroxyl radicals with iodide ions in pulse radiolysis, 19: 26444
effects on reduction of uranium(VI) oxide by carbon monoxide, 18: 27430
effects on renal excretion of calcium-45 and strontium-90 in dog, 16: 1447
effects on strontium-85 elution from mouse bones, 19: 43706
oxidation-reduction effects in carbon-uranium systems, 16: 17755
performance as sensitizer for nuclear emulsions, 19: 44406 (CERN-65-4(Vol.II), pp IV41-5)
precipitation of uranium from solutions of, 18: 27325
precipitation of uranium(VI) with, in presence of alkaline earth chlorides, 19: 19870
preparation of thin films of, by molecular plating, 20: 25027 (AERE-R-5097, Paper 17)
radiolysis of aqueous solutions of, at various pH's, 20: 35549
radiolysis of frozen aqueous solutions of, ESR spectral studies on radical reactions in, 20: 40994
rate effects on methanolysis of sodium borohydride, 16: 13043
reaction with cerium, neodymium, and samarium oxides, 16: 18917
reaction with uranium(VI) oxides, 17: 4622
reaction with uranyl carbonate complexes, 18: 25428
reactions of carbon-14-labeled, with lactic acid, apparatus for production of labeled carbon dioxide in air stream, 20: 35218
reactions with rare earth oxides, properties and structure of compounds formed in, 19: 46241(R) (TID-22207, Paper A)

reactions with sodium, 19: 35608(R) (APDA-170)
reactions with thorium oxalates, 17: 1474
reactions with uranyl carbonate complexes, 16: 4211(T) (JPRS-11292)
reactions with uranyl nitrates, 16: 30410
reactions with uranium dioxide, 18: 41463
reactions with uranium oxides, formation of uranates in, 19: 15424(T) (ANL-Trans-33(p.34-43))
reactions with yttrium fluorides at 550 to 700°C, 20: 29223
scavenging effects on electron and hydrogen yields in irradiated aqueous solutions, 17: 4602
scavenging effects on hydrogen yield in radiolysis of aqueous solutions, 17: 37265
solubility in water at 25°, 16: 185
solvent properties of solutions of, for corundum, pressure effects on, 17: 28874
solvent properties of aqueous solutions of, for radium and uranium, 18: 16133
solvent properties for highly radioactive fallout particles, 18: 23795
solvent properties in paper chromatographic separation of inorganic cations, 18: 39388
sorptive properties for silver-110m, 17: 23384 (SCR-593)
spectra of americium(VI) in, 17: 14257
spectra of hydrated electron in, effects of nitrous oxide on, 17: 1436
thermal decomposition of, differential thermal and x-ray diffraction analysis of, 17: 4495 (TID-13772)
use in slow-spray leaching of low-grade uranium ores, 19: 28460(P)
use in uranium stripping from trioctylamine extracts, 18: 5426
$BaCl_2$–Na_2CO_3–$UO_2(NO_3)_2$, uranium precipitation in, mechanism of, 20: 38928
$CaCl_2$–Na_2CO_3–$UO_2(NO_3)_2$, uranium precipitation in, mechanism of, 20: 38928
Li_2CO_3–K_2CO_3–Na_2CO_3, heat transfer to uranium from molten, 17: 10805 (Y-1410)
Li_2CO_3–K_2CO_3–Na_2CO_3, phase diagram, 19: 10567(R) (ORNL-3708 (p.304-20))
$MgCl_2$–Na_2CO_3–$UO_2(NO_3)_2$, uranium precipitation in, mechanism of, 20: 38928
Na_2CO_3–D_2O, phase diagram of, 20: 38994(R) (AE-232)
Na_2CO_3–H_2O, phase diagram of, 20: 38994(R) (AE-232)
Na_2CO_3–H_2O, radiolysis of oxygenated solutions of, 20: 14614
Na_2CO_3–NaCl, corrosive effects of, on stainless steel, 17: 22114(T,R) (EURAEC-557)
Na_2CO_3–$NaNO_3$, use for processing molybdenum- and niobium-containing irradiated fuels by oxidation, 20: 18834
Na_2CO_3–NaOH, descaling effects on steam oxidized iron- and nickel-base alloys, 18: 22441 (HW-79048)
Na_2CO_3–Na_2SO_4, thermodynamic consistency tests of phase equilibrium of, 19: 42958
Na_2CO_3–$SrCl_2$, precipitation of uranium from uranyl nitrate solutions by, 19: 26299
Na_2CO_3–$SrCl_2$–$UO_2(NO_3)_2$, uranium precipitation in, mechanism of, 20: 38928
Na_2CO_3–$UO_2(NO_3)_2$, criticality of aqueous solutions of, 20: 5666 (TID-21995)
$NaHCO_3$–NaCl, protection and rupture potential effects on steels at 40 and 80°C, 17: 25728(T) (EURAEC-677)
Na_2CO_3–$UO_2(ClO_4)_2$, potentiometric and refractometric studies of reactions in, 17: 39080

SODIUM CHLORATES

annealing neutron-irradiated, thermal, 16: 25444
chlorine-34, -36, and -38 oxidation states in irradiated, 16: 25443
chlorine-35 nuclear quadrupole coupling in, Stark effects in, 18: 34301
chlorine-35 spin echo and NQR in monocrystalline, 20: 3144
labeling with chlorine-38 by neutron activation, 19: 17982
liquid-vapor equilibrium of aqueous, at 25°C, 19: 5569(R) (MIT-2098-64)
protective effects of, against radiation inactivation of taka-amylase, 17: 15592
radiation damage, linearity of gamma, 19: 31448(R) (RPI-3030-3)
radiation effects on nuclear quadrupole resonance in, 17: 36450(R) (TID-19275)
radiation effects on nuclear magnetic resonance of sodium-23 in single crystals of, 18: 28095(R) (TID-20669)
radiation effects on ESR in, electron and gamma, 18: 29772
radiation effects on color centers in single crystals of, 20: 7143
radiation effects on internal stress and NQR frequency shift in, gamma, 20: 10239
radiation effects on, 20: 20365
radiation effects on chlorine-35 NQR in, gamma and x, 20: 20118
radioinduced color center formation in, 17: 37834
radioinduced color center formation in, thermal bleaching of, 20: 12900
radioinduced color centers in, paramagnetism of x, (E), 20: 15961
radioinduced defects in, electron paramagnetic resonance study of x, 19: 24568(T)
radiolysis, effects of annealing, 16: 20506
radiolysis of, comparison of chloride yields and post-irradiation annealing behavior for alpha and gamma, 17: 40874
radiolysis of, effects of annealing on yields from, 18: 1725(R) (ORNL-3488(p.42-54))
radiolysis of, ESR spectra of gamma, 19: 24559
radiolysis of, thermal effects of alpha particles in, 19: 429(R) (ORNL-3679(p.39-48))
reduction for preparation of chlorine dioxide, 17: 14227(T) (DEG-Inf/Ser.146)
sodium-23 NMR in, quadrupole splitting of, 18: 23464
sodium-23 NMR in, population inversion of, 18: 27436
spectra of chlorine-35 at 4.2 to 54°K in, pure quadrupole resonance, 18: 775
spectra of liquid, infrared reflection, 16: 18889
spin lattice relaxation time of chlorine-35 between quadrupole resonance levels in, 16: 6004

SODIUM CHLORIDES

activity and osmotic coefficients in heavy water at 25°C, 20: 16488
activity coefficients in methanol–water mixture at 25°C, rule for calculation, 16: 16375
activity coefficients for, in mixtures with hydrochloric acid, 17: 30513 (ORNL-3471)
activity coefficients in aqueous and organic-water solvents, 18: 1615(R) (ORNL-3488(p.123-8))
activity coefficients in hydrochloric acid–sodium chloride solutions, 18: 1614(R) (ORNL-3488(p.65-90))
activity coefficients of ions in solutions of, effects of surface potential on, 18: 6799(T) (AEC-tr-6244)
activity coefficients in glycol, glycol acetates, glycerol, and glycerol acetates, 19: 348(R) (ORNL-3679(p.117-26))
activity coefficients in polymethacrylic acid, 19: 36463(R) (TID-22060)
analysis for bromine, activation, 18: 21990
analysis for cesium, spectrometric, 17: 10565
analysis for chlorine-38 and sodium-24, calculation method for, 18: 20069
analysis for iodide ions by bremsstrahlung-activation methods, 20: 29112
analysis for pH and volatile matter, method outline, 16: 9952 (PG-Report-299)
analysis for water, sensitivity of neutron moisture probe for, 16: 698
analysis of single crystals of, activation, 20: 12805
analysis of, method for evaluation of random errors in activation, 20: 36734
analytical use for separation of molybdenum-99 from technetium-99m sorbed on aluminum oxide, 20: 38997 (NIJS-R-483)
atomic exchange of chlorine between chlorine gas and, 19: 2344
beryllium growth textures on, 20: 3306(T)
beta absorption and backscattering by, calculation of elemental stopping powers from, 19: 30127
beta reflection by aqueous solutions of, effects of density on, 18: 29589
beta scattering by, measurement of saturated backscattering from, 18: 35057
Born repulsive energy in crystals of, determination of, from thermodynamic data, 17: 3609
Born repulsive potential in crystals of, 17: 2062 (TID-17185)
chlorine isotope separation in aqueous solutions of, by ion mobility, 19: 22858
chlorine release from gamma-irradiated, 18: 6537(R) (ORNL-TM-603)
chlorine-36 oxidation states in neutron-irradiated, 16: 25443
chlorine-35 chemical shift, E2 coupling, and spin-lattice relaxation in, 18: 12094
chlorine-35 NMR in, dislocations from, 19: 17939
chlorine-35 spin-lattice and spin-spin relaxation times in, at high temperatures, 18: 5293
cleavage energy of crystals of, effects of color center density and testing environment, 18: 25973 (ASD-TDR-63-605(Pt.II))
cohesive energy of crystals of, Born analysis for, 17: 32084
color centers and recombination luminescence of copper- and nickel-doped, 19: 27715
color centers in crystals of, multiplicative approximation of F', (T), 19: 31450 (IS-Trans-14)
color centers in thallium-doped, equipment for measuring relaxation of, 20: 30754
color centers in, zero-phonon transitions of, 18: 793
color centers in, ENDOR of, (T), 19: 19920
color centers in, spectra of, 19: 23972
color centers in, wave functions for F, (T), 20: 17977(R) (NYO-2047-36, App.2)
complex formation in aqueous solutions with thorium(IV) chlorides, methods of detection, 16: 25358
compressibility at high pressures, 17: 3494 (UCRL-6696-T)
contamination rate of crystals of, from electron beams, reduction of, 16: 16841

content in blood plasma of irradiated fish, effects of salinity of environment on, 20: 42885
content in Mediterranean Sea, effects of season, temperature, and Nile River flooding on, 20: 43508(R) (NP-16179)
corrosion by iodine pentafluoride, infrared studies, 16: 9155 (TID-14852)
corrosive effects on 1Cr18Ni9T stainless steel, 16: 488(T) (AEC-tr-4683)
corrosive effects on alloys and metals in chemical plants, 16: 20983
corrosive effects on high-strength alloys and steels under static stress, 16: 25717(R) (NP-11948)
corrosive effects on stainless steels under stress, mechanism of, 16: 30733 (ARF-2181-12)
corrosive effects of, on engineering metals, 17: 22123
corrosive effects on iron at 25 to 70°C, 18: 1615(R) (ORNL-3488 (p.123-8))
corrosive effects of solutions of, on stainless steels, effects of tensile pull on breakdown and protection voltages in, 18: 14411(T) (EURAEC-928)
corrosive effects on austenitic stainless steel, effects of surface grinding on, 18: 20470 (CONF-492-1)
corrosive effects on zinc, tracer studies on, 18: 25927
corrosive effects of 3% solutions of, on copper–nickel alloys at 80°C, 18: 32089 (TID-20777(p.25-32))
corrosive effects of solutions of, on magnesium alloys, 19: 6271(T) (JPRS-27451)
corrosive effects on structural materials, 19: 12859
corrosive effects on austenitic stainless steel, 19: 22893 (DP-957)
corrosive effects on chromium–iron–nickel alloys at 600°F, 19: 30667(R) (COO-1319-24)
corrosive effects on aluminum, 19: 30673(R) (ORNL-3789(p.293-305))
corrosive effects on titanium at 100 to 200°C, 19: 30673(R) (ORNL-3789(p.293-305))
corrosive effects on types 5454 and 6061 aluminum alloys at 150°C, electrochemical, 19: 39117 (ORNL-P-1430)
corrosive effects on titanium alloys at 100 and 200°C, electrochemical, 19: 39117 (ORNL-P-1430)
corrosive effects on chromium–iron–nickel alloys, 19: 40967(R) (COO-1319-27)
corrosive effects on titanium alloys at 650°F, 19: 44621 (CONF-651006-1)
corrosive effects on molybdenum and vanadium, stress-, 20: 2254 (BM-RI-6680)
corrosive effects on type 304 stainless steel at 90°C, 20: 5846
corrosive effects on type 304 stainless steel, factors controlling, 20: 5851
corrosive effects on molybdenum and tungsten at 35, 60, and 100°C, 20: 11230 (BM-RI-6715)
corrosive effects on molybdenum and tungsten coupled with aluminum, copper, or magnesium, galvanic, 20: 11230 (BM-RI-6715)
corrosive effects on magnesium and its alloys, electrochemistry of pitting, 20: 11231 (CEA-R-2815)
corrosive effects of aqueous, on aluminum alloys and titanium, 20: 22857(R) (ORNL-3913, pp 111-32)
corrosive effects on high-purity stainless steels, effects of steel composition on stress-, 20: 27482(R) (EURAEC-1453)
corrosive effects on austenitic and austeno-ferritic stainless steels, stress-, 20: 29639(R) (EURAEC-1578)
corrosive effects on titanium-base alloys, 20: 33858(R) (AD-634094)
corrosive effects of aqueous solutions of, on stainless steel, 20: 35852(T) (AEC-tr-6738)
corrosive effects of aqueous, on stainless steel at 650°F, 20: 41418(R) (GEAP-5150)
corrosive effects on rhenium at 25 and 100°C, 20: 21275
critical state of aqueous solutions of, 19: 17863(T) (AI-Trans-76)
crystal lattice constants of, effects of pressure on, 20: 34816 (IDO-17170)
crystal lattice energy of, relation of self energy of gaseous ions to, 18: 16017
crystal lattice energy, 18: 22555(T) (AI-Trans-43)
crystal lattice local-mode resonance of hydrogen-doped, Mössbauer effect analog with, (E/T), 20: 24610
crystal lattice vibrations of, eigenvectors for, 18: 21726 (TID-20487)
crystal structure stability from many-body interactions in, 18: 10648
crystal structure powder diffraction patterns, 19: 17795
crystal structure, 19: 23355(R) (BNL-867(p.1-117))
crystal structure lattice dynamics of, eigenvalues and eigenvectors for, 20: 33262 (UCRL-14822)
crystal vibrations in impure, localized modes for determination of frequencies of, 18: 12103
defect motion in, activation energies for, 18: 34280(R) (NYO-2680-1)
deformation of rock salt, at high temperature and pressure, 19: 42198
deformation properties, 20: 886
density of aqueous, precise measurement of, 19: 347(R) (ORNL-3679 (p.60-83))
determination as impurity in cesium and rubidium chlorides, flame photometric, 16: 7495
determination in sodium hydroxide solutions by beta backscattering, 18: 37096
dielectric breakdown of crystals of, temperature for, 17: 20682
diffusion coefficient and mobility of F centers in crystals of, 17: 1423(T) (SCL-T-438)
diffusion during stable and unstable flow, 19: 5896
diffusion in glycerol at 32°C, tracer study of, 18: 15998 (TID-7688 (p.52-63))
diffusion in molten, effects of temperature on self-, 19: 26338
diffusion in pure, from electric conductivity and radiotracer measurements, 19: 17408 (COO-1197-9)
diffusion of cesium, potassium, rubidium, and sodium into liquid, temperature effects on, 18: 31492
diffusion of cobalt-60 and nickel-63 in crystals of, coefficients for, 18: 39224
diffusion of lead in molten, 16: 30388
diffusion of sodium-24-labeled, through arachnoidal membrane, 18: 43206
diffusion of sodium-22-labeled, in two-compartment system, 19: 44025
diffusion of sodium-22 and -24 in crystals of, isotope effects on, 17: 617
diffusion of sulfur-35 from irradiated, 20: 25134
diffusion of zinc in pure and zinc-doped, 18: 25969(R) (ANL-6868 (p.287-302))
dislocation pinning in crystals of, 16: 12190
dissociation of thin films of, by low-energy electron bombardment, 17: 20537 (ASD-TDR-63-175)
dissolution and contact melting of irradiated crystals of, 16: 5772
ductility of <100>, <110>, and <111> crystals of, 16: 1275(R) (NP-10832)
effects of excess ingestion of, on induction of hypertension in man and rats, genetic control of, 18: 21702 (BNL-7971)
effects of ingestion of excess, on hypertension in rats and man, 18: 15668 (BNL-7787)
effects of ingestion of, on induction of hypertension in rats, 18: 36875 (BNL-7318)
effects on ammonia yield in radiolysis of cystine, 17: 32158
effects on analysis of uranium oxide for trace elements by emission spectrography, 17: 21634
effects on cation movements in bentonites, 18: 38775(R) (ORO-624)
effects on chemical corrosion of metals, 16: 17976(R) (EURAEC-94)
effects on corrosion behavior of steel, 16: 13531(R) (EURAEC-30)
effects on dissociation of boric acid in solution, 18: 31376(T) (UCRL-Trans-1053(L))
effects on DNA-histone linkages in irradiated deoxyribonucleohistone solutions, 20: 40586
effects on Drosophila, mutagenic, 19: 28011
effects on efficiency of actinide and lanthanide separations by ion exchange chromatography, 20: 20822
effects on electron exchange reactions between thallium and uranium in methanol–water solutions, 18: 27418
effects on formation of corrosion-resistant films on titanium and zirconium oxides, 18: 20481
effects on heterometric determination of vanadium, 19: 36289
effects on homomolecular isotopic exchange of carbon monoxide, catalytic, 19: 26328
effects on hypertension in man and rats, review on, 20: 10451 (BNL-8671)
effects on iodine-131 excretion by calves, 20: 18223
effects on irradiated rats, 20: 45322(R) (UCLA-12-595, pp 6-28)
effects on non-metallic structural materials for solvent containers, 20: 26816 (HW-72369)
effects on pH of dialyzed zirconyl chloride, 17: 35718
effects on potentiation of radiation effects on bacteria, 19: 33893
effects on radiation damage to thymocyte nuclei, 17: 35506
effects on radiation effects on ionic permeability of rooster erythrocytes, 19: 19577
effects on radiation stability of thiamine hydrochloride, 20: 4018
effects on radioinduced inactivation of β-amylase, synergistic, 19: 17558
effects on radioinduced changes in proteins, 20: 49
effects on radioinactivation of microorganisms, 17: 30027
effects on radiopreserved seafood, 20: 29583(R) (TID-22515)
effects on self-diffusion of water at 23°C, 19: 32159
effects on solvent extraction of cobalt acetylacetonate using isopropyl alcohol, 20: 7211
effects on solvent extraction of uranyl acetylacetonate using chloroform, 20: 7211
effects on sorption of dyes by labeled barium sulfate, 18: 39305
effects on spectra and vaporization of minerals in a-c arc, tracer studies, 16: 30393
effects on stress corrosion cracking in chromium–iron–nickel alloys, 20: 11233(R) (COO-1319-32)
effects on strontium-85 elution from mouse bones, 19: 43706
effects on vapor pressure of saturated heavy and light water solutions,

20: 38994(R) (AE-232)
effects on wholesomeness of radiation processed meat, 20: 700 (AD-621921)
effects on yields in radiolysis of D-sorbitol, 19: 5961
elastic properties of deposits in Project Cowboy tests, 16: 23804 (RM-3105-AEC)
electric conductivity of polycrystalline, effects of pressure on, 18: 8018 (TID-19897)
electric conductivity of pure and zinc-doped monocrystalline, 18: 25969(R) (ANL-6868(p.287-302))
electric conductivity in light and heavy water at 25°C, 20: 14540
electric potential induced by plastic deformation of crystals of, 17: 2098
electrolysis of zirconium tetrafluoride in, anode effect in, 16: 17970
electron bombardment, 17: 3569 (ASD-TDR-62-707)
electron bombardment at 100 to 600 ev, multiple emissions from, 18: 34450
electron emission zone thickness and yield for, photoemission spectra of secondary, 17: 39792(T)
electron emission from crystals of, effects of positive-ion bombardment on exo-, 17: 6831
electron energy loss spectra at 0.8 and 1.5 Mev, 16: 12275
electron energy loss spectra in, 19: 16404
electron Hall mobility in, 18: 39233
electron interactions in, exciton production in, (E), 19: 35590
electron multiplication in, (E), 19: 18528
electron pair annihilation in, effects of crystal orientation on photon angular distributions from, (E/T), 20: 25793
electron reactions with, ion desorption in, 17: 41553(R) (NP-13160)
electron reactions with vacuum-cleaved surfaces of, electron emission in, (E), 19: 23287
electron reactions of crystals of, at 0.2 to 12 ev, 17: 35789
electron scattering by crystals of, Kikuchi line intensities in, 16: 12252
electron spin resonance spectra of nitrogen centers in nitrate-doped crystals, 18: 31530
electron transmission through films of, excitons and plasma oscillations in, (E), 20: 15953
electron transmission in thin films of, energy losses and color centers from, (E), 20: 30776
electron-nuclear double resonance studies of crystals of, 16: 21194
energy levels of F-band in, spin-orbit splitting in first excited, (T), 19: 8093
equation of state of, dynamic, (E), 19: 30848(R) (UCRL-12473(p.31-63))
europium ion spectra in, absorption and fluorescence, 18: 13759
europium sulfide epitaxial growth on crystals of, 19: 11079
evaporation mechanisms, 20: 32684(R) (UCRL-16658, pp 21-38)
exchange in linear transfer system, interfusion effect in, 19: 2324
exciton states in crystals of, relaxation of, (T), 19: 43474
film growth on, evaporated cobalt, 20: 10469 (COO-1198-229)
fluorescence and absorption spectra of praseodymium in single crystals of, 20: 20663
formation of particulate, in nuclear explosions over sea areas, 19: 24719
grain-boundary sliding in crystals of, 16: 30791 (NRC-182)
growth of crystals of, effects of micro-impurities on, 16: 9296(T) (CEA-tr-R-1419)
growth of crystals of, orientation phenomena in, 16: 32908(T) (AEC-tr-5392)
H centers in, energy calculations for, 18: 34280(R) (NYO-2680-1)
hardness of crystals of, 16: 10728
harmonics of crystalline, electric field effects on ultrasonic, 19: 32048(R) (NP-15073)
heat of solution in liquid nitrates, 17: 28869
heat of solution in heavy and light water, (E), 20: 1825
Hugoniot equations of state of rock salt, 17: 1634 (UCRL-13004)
hydrolysis of uranyl ion in, equilibria in, 18: 13735
hydrolysis of uranyl ion in, complexes in, 18: 13734
impurity-vacancy pairs in crystals of, stress-induced reorientation of, 18: 19485 (TID-20430)
intercrystalline energies in binary systems, 16: 7558
iodination processes, tracer studies, 16: 26962 (PAN-282/XVI)
ion association and hydration in aqueous solutions of, x-ray diffraction studies on, 20: 14228 (TID-22527)
ion reactions at low energies, secondary electron emission from argon and helium, (E), 20: 9675(T)
ion reactions at 40 kev, lattice disorders from krypton and xenon, (E), 20: 27597
ion reactions at 40 to 2000 ev, electron emission from argon and helium, (E), 20: 31912
ion self-diffusion mobilities in, determination from tracer transfer rate coefficients, 20: 425
ionic binding of sodium in, determination from tracer transfer rate coefficients, 20: 327
ionic conductivity, contribution of cubic term, 16: 12181(R) (TID-15041)
ionic conductivity in plastically deformed crystals of, measurements of excess, 16: 25316 (NP-11921)
ionic transport coefficients for, at 25°C, 20: 38909
isotopic exchange reactions of chlorine-36-labeled, with chlorobenzene, 18: 35568
labeling with sodium-24 and aerosol preparation, 19: 20027
light absorption and refractive index at fusion, 19: 11115
liquid-vapor equilibrium of aqueous, at 25°C, 19: 5569(R) (MIT-2098-64)
luminescence centers in tin-activated crystals of, effects of plastic deformation and radiation on structure of, 17: 26001
luminescence from dissolution in water of irradiated, quenching effects of oxygen on, 17: 10612
luminescence in cadmium- and cobalt-activated crystals of, 17: 12817
luminescence in dissolution of irradiated, in thallium chloride solution, (E), 19: 5963
luminescence of rare earths in crystalline, 19: 11010
luminescence of thallium-activated, photon multiplication in, 19: 34186(T)
luminescence of x-irradiated crystals of, 16: 13733
luminescence of x-irradiated crystals of, 17: 5112
luminescence of, effects of electric field on, 19: 15514(T)
luminescence patterns from mechanical de-excitation of beta-irradiated, 20: 10240(T)
luminescence spectra of europium-activated crystals of, 17: 16862
mass transport in vapor phase between disks of, tracer studies of, 18: 22058
mechanical properties of solidified, determination using shock loading, 19: 4348 (IITRI-A6040-1)
melting of, volume change in, 20: 25572(R) (NASA-CR-67221)
metal films on crystals of, deposition and structure of, 17: 29333(T) (NP-tr-1032)
migration in sand columns wetted by water, 16: 6517 (IA-687)
molal volume and salt-induced structure transitions of aqueous, 19: 46237(R) (ORNL-3832, pp 76-99)
Mössbauer effect in iron ions in cobalt chloride precipitated in crystals of, 17: 31199
Mössbauer effect in iron ions in crystals of, vacancy-impurity associated state of, 17: 31200
neutron diffraction pattern of crystals of, 17: 20318
neutron double Bragg scattering by single crystals of, angular distributions in, 16: 26211
neutron reactions at 0.025 ev, gamma spectra from, 16: 18437
neutron reactions at 0.025 ev, gamma spectra from, 16: 29791(T) (AEC-tr-5221)
neutron reflectivity by crystals of, 16: 20637 (JAERI-1030(Suppl.))
neutron removal cross sections for, effective fast, 16: 24797 (WADC-TR-58-266)
neutron scattering by crystals of, structure factors for cold, 17: 27392(T)
neutron scattering by radioinduced defects in single crystals of, cold, 20: 26365(T)
neutron spin-orbit interactions in crystals of, 17: 20963
neutron total cross sections of, temperature effects of magnetic order on, 18: 36034
neutron transmission through, 405-ev resonance for chlorine-35 from, (E), 19: 43271 (JINR-P-2198)
nuclear explosion effects on, at Gnome site measured by acoustical methods, 18: 39523
nuclear quadrupole coupling constants in crystals of, 16: 24654
nuclear spin diffusion in, interruptions in, 17: 4531
optical properties of alpha color centers in crystals of, 17: 35788
osmotic coefficients as function of concentration at high temperatures, 16: 14735
osmotic coefficient at 140°C, 17: 40805
osmotic coefficients of aqueous, at 165°C, 19: 30151(R) (ORNL-3789 (p.139-63))
penetration of glass fiber filters by aerosols of, effects of particle size on, 18: 41949
penetration of plastically deformed crystals of, by water, 18: 4919 (TID-19729)
performance in crystalline neutron spectrometers, 18: 2095
performance of crystals of, as neutron monochromators, 19: 6184 (IDO-17022)
permeability measurements of rock salt, 16: 3252
phase studies, 20: 35841(R) (NAA-SR-11900)
phase studies of systems with molybdates and tungstates, 16: 17623(T) (AEC-tr-4456(p.225-30))
phase transformations in, under shock compression, (E), 19: 30848(R) (UCRL-12473(p.31-63))
photoelectric current in x-irradiated crystals of, effects of F-center concentration on, 17: 2068(T) (SCL-T-441)
photoelectric effect in crystals of, at 20 to 500°C, 16: 21142(T) (CEA-tr-A-1087)

photoelectron emission in, numerical analysis, 17: 22380
photoemission yields at 10 to 21 ev, (E), 19: 11861
photoluminescence of activated and pure 200- to 300-mμ and x-ray, (E), 19: 27723
photon scattering to 14 ev, electron excitation in, (E), 19: 27716
physical properties and occurrence of deposits of, bibliography on, 18: 31041 (KFK-205)
polarography in mixture of lithium and potassium chlorides, 16: 2953
positron annihilation in, three-quantum, (E), 19: 10066
positron diffusion in, anomalous lifetime components in, 18: 7486
positron lifetime in crystals of, 17: 31180
potassium ion reactions with crystals of, secondary emission properties from, 17: 24169(T)
precipitation of crystals of, with lead and strontium, tracer studies of, 16: 3338(T) (AEC-tr-4497(p.279-87))
preparation and properties of evaporated films of, 19: 13378
preparation of clean, thin single-crystal films of, method for, 17: 37629
preparation of curved crystals of, dies and lapping techniques for, 18: 17977(R) (ORNL-TM-793)
preparation of single-crystal, 20: 35484(T) (UCRL-Trans-10027)
pressure effects on halite, detection by irradiation, 19: 5972
production of aerosols of, design of spinning-disk generator for, 19: 4287
production of sodium-24-labeled aerosols of, design and performance of generator for, 20: 20924 (AEET-232)
properties as x-ray fluorescence analyzers, 18: 12022
properties of solutions of, in dimethyl sulfoxide, 20: 293 (UCRL-16330)
properties of thallium-activated, in radiation dosimetry, 19: 30557
protection against radioinduced inactivation in bacteriophage lambda phase using, 20: 33078
protective effects of, against radiation inactivation of taka-amylase, 17: 15592
protective effects of physiological solutions of, against radiation, 17: 15846
proton relaxation times in aqueous solutions of, 18: 23559
radiation and thermal effects on, 18: 13631(R) (ORNL-3537(p.30-46))
radiation damage by beta particles at 77°K, x-ray study of interstitial defects, 16: 29459
radiation effects on thermal expansion, 16: 7949
radiation effects on heat of solution and stored energy, calorimetric measurements, 16: 13644 (TID-15043)
radiation effects on susceptibility to, in rats, 16: 17494
radiation effects on thermoluminescence and magnetic properties, 16: 19455
radiation effects on aerosols of, 17: 3026(R) (TID-17250)
radiation effects on dielectric changes and thermoluminescence, 17: 18153
radiation effects, measurement of stored energy in, 17: 18886
radiation effects on plastic deformation of single crystals of, gamma, 18: 7281 (BNL-7502)
radiation effects on crystalline, 18: 10579(R) (TID-20064)
radiation effects on nuclear magnetic resonance of sodium-23 in, 18: 13845
radiation effects on thermoluminescence of single crystals of, kinetics of alpha, 18: 13864
radiation effects on, low-temperature x, 18: 16106
radiation effects on electric conductivity of, effects of impurities on x, 18: 20588
radiation effects on crystalline, 40-Mev alpha, 18: 26071 (NASA-TN-D-2329)
radiation effects on dislocation distribution and microhardness of, 18: 26082
radiation effects on absorption spectra of, optical and thermal bleaching of, 18: 27587
radiation effects on dislocation distribution and microhardness of etched faces of, 18: 40031(T)
radiation effects on, temperature dependence of critical resolved shear stress in gamma, 18: 43651
radiation effects on, 19: 5972
radiation effects on thermoluminescent kinetics, 19: 7560
radiation effects on F centers in crystalline, x on and R centers on, 19: 11214(T)
radiation effects on, 19: 12859
radiation effects on crystalline, 19: 14091(R) (TID-21625)
radiation effects on, chemistry of sulfur-35 production in neutron, 19: 13504
radiation effects on, alpha, (E), 19: 15605
radiation effects on dislocation nucleation and motion stress, 19: 17985
radiation effects on luminescence of copper-doped, 19: 19964
radiation effects on thermal properties of crystals and solid solutions of, gamma and neutron, 19: 19986
radiation effects on stored energy in, gamma, 19: 19987
radiation effects on luminescence of poly-activated, 19: 22313
radiation effects on thermoelectric charge displacement in, 19: 22328
radiation effects on electric conductivity of divalent-cation-doped, x, (E), 19: 26386
radiation effects on color centers and photostimulated emission spectra, 19: 34243
radiation effects on thermal de-excitation processes in nickel-activated, 19: 41101(T)
radiation effects on F centers and photostimulated emission in, x, (E), 19: 41980
radiation effects on luminescence of europium-activated, visible and x, 19: 40567
radiation effects on photoluminescence of, x, 19: 40569
radiation effects on phosphorescence of, influence of F-band illumination on x, 19: 40570
radiation effects on luminescence of nickel-activated, electric-field pre-exposure in x, 19: 40571
radiation effects on electroluminescence of, x, 19: 40572
radiation effects on luminescence centers in silver-activated, x, 19: 41977
radiation effects on structure of, electron microscopy of gamma, 19: 42914
radiation effects on absorption and luminescence spectra of nickel-, silver-, or tin-activated, 19: 47884(T) (IS-Trans-18)
radiation effects on crystals of, 16: 9264(R) (TID-14001)
radiation effects on dielectric breakdown in crystals of, uv, 16: 29465
radiation effects on crystals of, 17: 2008(R) (TID-17027)
radiation effects on color centers and thermal bleaching of crystals of, 17: 3559
radiation effects on crystals of, 17: 14899(R) (TID-17935)
radiation effects on dimensional stability of crystals of, at room temperature, 17: 5018
radiation effects on structure of crystals of, x-ray, 17: 2031(T)
radiation effects on coefficient of linear expansion of crystals of, 17: 14367(T)
radiation effects on hardness of crystals of, 17: 14919
radiation effects on crystals of, electron, 17: 24017
radiation effects on dislocations in crystals of, x-ray, 17: 25908
radiation effects on physical properties of crystals of, gamma, 17: 29967
radiation effects on density change and F-center formation in crystals of, x, 17: 34031
radiation effects on crystals of, at low temperatures, 17: 37623
radiation effects on bleaching of F centers in crystals of, at low temperatures, 17: 37626
radiation effects on crystal structure of, mechanism of beta, 20: 2426 (LA-3387)
radiation effects on ultrasonic attenuation in, effects of frequency and temperature on, 20: 10230 (NYO-2471-11)
radiation effects on cleavage crack propagation in single-crystal, 20: 16513
radiation effects on sodium formation in, 50-kev-electron, 20: 20781
radiation effects on absorption spectra of, x, 20: 21424 (N-65-23332)
radiation effects on thermoluminescence in silver-doped, electron, 20: 26378(T)
radiation effects on mechanical properties of, 20: 26975
radiation effects on, color centers in ionic, effect of F centers from gamma and neutron, 20: 30739
radiation effects on color-center destruction and recombination luminescence in silver-doped, x, 20: 32693
radiation effects on color-center destruction and recombination luminescence in silver–calcium-activated, x, 20: 32694
radiation effects on optical absorption spectra of crystals of, gamma and neutron, (E), 20: 34834
radiation effects on coloration and d-c conductivity in pure and doped, x, (E), 20: 38373
radiation effects on silver-doped, model for de-excitation curves of x, 20: 42561
radiation effects on microhardness and dislocation mobility of, x, (E), 20: 45005
radiation interstitial and vacancy formations in crystals of, x-ray, 16: 13658
radioinduced anion vacancies in crystals of, effect of bleaching irradiation on concentration of, 16: 10647
radioinduced bleaching of, neutron, 19: 11227(T)
radioinduced chlorine formation in, 17: 39298(R) (ORNL-3492(p.19-37))
radioinduced color center formation in, 17: 18147
radioinduced color-center formation and emission spectra, 17: 25960
radioinduced coloration and volume expansion in, 18: 20598
radioinduced color center in, Zeeman effect in, 18: 33644
radioinduced color centers in calcium-doped crystals of, polarized absorption study of, 19: 17409 (COO-1197-10)
radioinduced color centers in single crystals of, annealing of, (E), 19: 17974
radioinduced color center formation in, 19: 34239
radioinduced color center formation and annealing in, 19: 34241

radioinduced color center formation and photostimulated emission spectra, 19: 34242
radioinduced color center formation in unactivated and thallium-activated, 19: 34250
radioinduced color center formation and luminescence of silver-activated, 19: 34251
radioinduced color centers and luminescence in silver-activated, 19: 34254
radioinduced coloration in gamma-irradiated, x, (E), 19: 40105
radioinduced coloration level in, gamma- and x, 19: 42550
radioinduced coloration in crystals of, effect of manganese concentration on, 16: 13661
radioinduced color centers in crystals of, growth and thermal bleaching of, 16: 13675
radioinduced color center formation in crystals of, effects of deformation on, 17: 22362
radioinduced color center formation in crystals of, at 10 to 325°K, effects of deformation on, 16: 18249
radioinduced color centers in crystals of, electronic and ionic processes in, 17: 25334
radioinduced color center formation in crystals of, effects of high pressure at low temperatures on, 17: 25341
radioinduced color centers in thallium-doped, photon and thermal, (E), 20: 30754
radioinduced crystallite overgrowth on crystals of, 16: 33411
radioinduced defects in, use of color center technique for detection and measurement of, 18: 42141
radioinduced defects in crystals of, use of color centers for detection and measurement of, 17: 20509 (BNL-6912)
radioinduced defects in crystals of, x, (E), 20: 13973(R) (NYO-3033-1)
radioinduced defects in single-crystal, 20: 35932 (LA-3501)
radioinduced dislocations in, x, 18: 12773
radioinduced dislocations and point defects in, relation between, 18: 37779
radioinduced dislocation pinning in crystals of, 17: 35768
radioinduced F and M color centers in, x, 20: 32691
radioinduced F centers in, electron and x, 18: 10601
radioinduced F center formation in crystalline, x, 18: 36067
radioinduced F centers in pure and calcium-doped, gamma, 20: 44996
radioinduced F-centers in, kinetics of x, 19: 22379(T)
radioinduced F-center formation in, effects of temperature on, 19: 34252
radioinduced F-center formation in, temperature dependence of x, 20: 32724(T)
radioinduced F-center coloration in, gamma, 20: 24855
radioinduced formation of chlorine in, 18: 19448(R) (ORNL-TM-757)
radioinduced formation of color centers in crystals of, effects of x-ray intensity on, 17: 36491
radioinduced hardening in, temperature dependence of flow stress in y, 20: 6538
radioinduced heating of crystals of, proton, 17: 36358
radioinduced luminescence at 4 to 80°K, x, 18: 33648
radioinduced luminescence mechanisms in, x, 19: 2388
radioinduced luminescence of indium- and thallium-activated, electron and photon, (E), 19: 27721
radioinduced luminescence of single crystals of, effects of pressure on x-ray, 19: 30274(T)
radioinduced luminescence in, de-excitation of light sums from x, 19: 46379(T)
radioinduced luminescence of crystals of, 16: 25914 (NP-11920)
radioinduced luminescence of silver-activated single crystals of, x, 20: 26388
radioinduced M centers in crystals of, oscillator strength of, 17: 37625
radioinduced N centers in, symmetry of, 20: 20159
radioinduced plastic flow in, x, 19: 40594
radioinduced polymerization of silicone oil on, electron, 20: 7176
radioinduced production of F centers in crystals of, effects of x-ray intensity on, 16: 29009
radioinduced recombination luminescence in silver-activated crystals of, mechanisms for, 18: 296(T)
radioinduced recombination luminescence of silver-activated, x, (E/T), 19: 27722
radioinduced Schottky disorder and lattice relaxation in single crystals of, x, (E), 20: 32712
radioinduced sulfur-35 production in, thermal-neutron, 20: 25134
radioluminescence of activated, temperature effects on electron, (E), 19: 27718
radioluminescence and optical flash in nickel-activated phosphors of, x, (E), 19: 27719
radiolysis of aqueous solutions of, pulse, 19: 7566
radiolysis of azoethane adsorbed on, energy transfer in gamma, 20: 23116
radiolysis of, separation of products from, using iron hydroxide, 17: 23452
radiolysis of, chlorine production from gamma, 19: 8675(R) (ORNL-3697 (p.19-31))
radiolysis of, mechanism of gamma, 18: 16119
radiosensitivity effects on red cell membranes, 17: 15787
radiosensitivity effects on pea seeds, 17: 38881
radiosensitivity effect on barley seeds, 18: 33409
radiosensitivity effects on *Clostridium botulinum* spores, 18: 43299
radiosensitivity effects on Clostridium spores, y, 20: 6834
reactions in dioxane–water solutions, nuclear magnetic resonance spectra of, 17: 40800
reactions of fused, with chromium fluoride or lanthanum oxide, 20: 10821
reactions on zirconyl phosphate membrane electrodes, 18: 27460
reactions with cerium chlorides, 17: 31795(R) (BNL-782(p.18-43))
reactions with chlorine, electronic defects in exchange, 19: 13378
reactions with erbium, europium, and holmium chlorides, thermogravimetric study of, 20: 8944
reactions with niobium oxychlorides, 17: 1503
reactions with niobium oxychloride, enthalpies of formation of double compounds in, 17: 4550
reactions with niobium oxychlorides, 18: 22070
reactions with plutonium(III) chlorides and chlorine gas, formation of plutonium(IV) ions by, 16: 16367
reactions with rare earth chlorides, analysis of, 16: 14753
reactions with strontium chloride, kinetics of exchange, 18: 4886(R) (HW-79140)
reactions with uranium(IV-VI) oxide at high temperatures, 19: 15429(T) (ANL-Trans-33(p.70-4))
reactions with yttrium chloride, 19: 7502
recoil chemistry of sulfur-35 in neutron-irradiated, evidence for neutral species in, 19: 9166 (COO-32-106)
reduction by high-frequency hydrogen discharge to hydrogen halide and metal, 19: 39180
reduction by high-frequency discharges in helium, hydrogen, and nitrogen, role of electrons in, 19: 39181
RNA distribution between quaternary ammonium chlorides and solutions of, 19: 31704(R) (ORNL-3768(p.157-63))
scintillation properties at low temperatures, 16: 20707
self-diffusion effects of, on water at 25°C, 17: 10613
self-diffusion of ions in liquid, coefficients of, 17: 4513
separation from cerium, 18: 5435(P)
separation from water by hyperfiltration through cellulose acetate and ion exchange filters, 18: 1615(R) (ORNL-3488(p.123-8)
shock wave effects on, 16: 22051 (ORNL-TM-256)
slip mechanisms of rock salt, 20: 29624(R) (TID-22970, pp 257-329)
slip systems in crystals of, independent, 17: 23361
sodium-23 magnetic shielding in crystals of, 17: 21696
sodium-23 NMR in, deformation effects on, 19: 7481
sodium-23 NMR in, dislocations from, 19: 17939
sodium-23 NMR spin-lattice relaxation in, effects of magnetic field on, (E), 20: 34866
sodium-23 nuclear magnetic relaxation in crystals of, below 900°K, 16: 18253
sodium-23 polarization in, containing molecular chloride ions, (E), 19: 43497
sodium-23 spin-lattice and spin-spin relaxation times in, at high temperatures, 18: 5293
sodium-24 beta spectra in, 19: 31237 (SGAE-PH-13/1964)
solubility in saturated water mixtures of glycol, glycerol, and their acetates, 18: 13717 (CONF-415-2)
solvent effects on irradiated polyvinyl alcohol acetalized with glyoxylic acid, 16: 18951
solvent properties for cesium calcium ferrocyanide, 16: 11679
solvent properties for beryllium, 16: 16373
solvent properties for rare earths, 17: 12373
solvent properties of aqueous solutions of, for radium and uranium, 18: 16133
solvent properties of aqueous solutions of, for calcium sulfates, 18: 22018(R) (ORNL-3591(p.205-12))
solvent properties in paper chromatographic separation of inorganic cations, 18: 39388
solvent properties of aqueous solutions of, for cerium chlorides, 18: 43524
solvent properties for zinc chloride, 19: 44677(R) (ANL-7000, pp 183-5)
sorption by zirconium oxide from dilute aqueous solutions, 18: 6819
sorption of labeled, by chlorinated polyvinyl-chloride filters, 19: 20228
sorptive properties for aluminum, 16: 26009
spectra in, optical absorption, 18: 25408
spectra of color centers in bleached and irradiated tin-activated, electron and hole trapping in, 18: 12243
spectra of compressed, absorption, 20: 24357(R) (UCRL-14538)
spectra of, effects of temperature on, 17: 39070
spectra of F-centers in crystals of, 17: 27377
spectra of labeled, molecular beam, 17: 4554

spectra of lead- and thallium-activated, pressure effects on absorption and emission, 18: 37130
spectra of M and R centers in F band region of colored crystals of, 17: 8902
spectra of nuclei near impurities in, detection of quadrupole, 18: 14630
spectra of suspensions of, in thin polyethylene films, infrared transmission, 19: 19917
spectra of thin films of, calculation of infrared, 17: 631
spectra of trivalent samarium ions in, luminescence, 18: 30423(T)
spectra of U centers in, infrared absorption, 19: 35587(T) (ANL-Trans-206)
spectra of uranium(IV) chloride in, 17: 14261
spectra of ytterbium in, absorption, 19: 11010
sputtering by argon ions at 2 to 10 kev, yields from, (E), 19: 23271
sputtering by argon ions at 2 to 4 kev, surface topography of, (E), 19: 30944 (NIJS-R-433)
stored energy in x-irradiated crystals of, measurement of, 17: 595
superconducting properties of cubic, empirical correlations for, 18: 34684 (UCRL-11368)
surface energy of crystals of, 17: 37505 (ASD-TDR-63-605(Pt.I))
surface tension at 1100 to 1365°K, 17: 28828(R) (TID-18951)
thermal capacity at 10 to 300°K, 16: 32226
thermal conductivity of rock salt, 18: 20530 (UCRL-6894(Rev.II))
thermal conductivity, effects of impurity ions on, 19: 25783 (COO-1198-238)
thermal expansion at low temperatures, 19: 42507
thermal expansion of crystals of, at low temperatures, 16: 2302 (TID-14230)
thermal expansion of crystals of, at 100 to 300°K, 16: 13697 (NP-11338)
thermal glow curve of crystals of, origin of first peak in, 17: 30602(T)
thermal stability, 18: 19448(R) (ORNL-TM-757)
thermodynamic and transport properties of liquid, 16: 18932
thermodynamic properties in *N,N*-dimethylformamide and *N*-methylformamide solutions, 20: 3924 (TID-22366)
thermodynamic properties in anhydrous *N*-methylformamide solutions, 20: 3925 (TID-22366, App. B)
thermodynamic properties of, in heavy water, 20: 10847
thermodynamics of titanium in liquid, oxygen equilibrium potential diagram for, 16: 20426
thermodynamics of, in anhydrous *N*-methylformamide at 25°C, 20: 3926 (TID-22374)
thermoluminescence after x irradiation of single crystals of, effects of illumination on, 18: 2453
thermoluminescence of irradiated crystals of, effects of hydrostatic pressure on, at low temperatures, 17: 8015 (UCRL-10497)
thermoluminescence from x-ray excitation of crystals of, dependence of, on gas pressure and sample size, 17: 25288
thermoluminescent spectra of crystals of, irradiated by alpha particles, effects of hydroxide ions on, 17: 18859 (NASA-TN-D-1662)
transfer between heavy and light water, ionic hydration in, 17: 6096
transfer from heavy water to water, free energy and entropy of, 20: 16488
transfer in heavy and light water solutions in membrane potentials, free energy of, 17: 2986
transference and solvation phenomena in ethanol and water, 16: 2944
transition of single-crystal to polycrystal, mechanisms of, 19: 32048(R) (NP-15073)
ultrasonic velocity changes in deformed crystals of, effects of dislocation pinning on, 17: 35768
ultrasonic wave attenuation and diffraction in crystals of, 16: 15126(R) (NP-11584)
use in chlorination of columbite and ilmenite for separation of constituents, 16: 13065
use in testing high-efficiency air-conditioning filters, 18: 14005 (TID-7677(p.553-71))
use of crystals of, as neutron monochromators, 16: 18454
use of molten, in separation of fission products from irradiated thorium and uranium oxides, 20: 43454
use of sodium-22-labeled, for study of sternal marrow circulation, 19: 5618
vacancies produced by fast neutrons in gamma-irradiated crystals of, 17: 11377
vacancy production in ionized crystals of, theory of halogen injection in, 17: 34516
vapor pressure effects on zirconium chloride at 300 to 525°K, 18: 13752
vibrational frequencies in crystals of, 16: 32220
vibrational frequencies in crystals of, 16: 32221
viscosity effects on polyacrylamide radiation dosimeters, 18: 12474
volumetric properties in molten systems with potassium and sodium chlorides and iodides, 16: 539
wave functions of F centers in, (T), 19: 17953 (COO-1197-11)
x-ray-diffraction properties above 10 Å, 18: 2097
x-ray diffraction analysis at 5.898 kev, 20: 40294
x-ray scattering by crystals of, effects of anharmonic vibration on Debye-Waller factor for diffuse, (T), 19: 25630
x-ray scattering cross sections, 18: 20035
AgCl–NaCl, heat of mixing of, effects of composition and temperature on, 20: 23011
AgCl–NaCl, phase diagrams, 20: 36787 (YALE-2723(Vol.1))
AgCl–NaCl, thermostimulated electron emission from crystallophosphor of, 19: 25170(T)
Ag–NaCl, radioinduced color centers in, x, 20: 38396
$AlCl_3$–Bi–NaCl, spectra of reaction products of, absorption, 20: 3921(R) (ORNL-3870, pp 56-60)
$AlCl_3$–NaCl, density equations for molten, 20: 3921(R) (ORNL-3870, pp 56-60)
$AlCl_3$–NaCl, phase diagrams, 20: 36787 (YALE-2723(Vol.1))
$AlCl_3$–NaCl, stability of zirconium dichloride in, 20: 1822(T) (ANL-Trans-233)
Al–Mg–$MgCl_2$–KCl–NaCl, corrosive effects on steels and tantalum at 500 to 800°C, (E), 20: 14007(R) (ANL-7122, pp 1-41)
$BaCl_2$–CaF_2–NaCl, phase studies, 17: 23376
$BaCl_2$–LiCl–NaCl, phase studies, 17: 32120
$BaCl_2$–NaCl–H_2O, activity coefficient determination by ultracentrifugation, 19: 46237(R) (ORNL-3832, pp 76-99)
$BaCl_2$–NaCl, effects on non-metallic structural materials for solvent containers, 20: 26816 (HW-72369)
$BaCl_2$–NaCl, phase diagrams, 20: 36787 (YALE-2723(Vol.1))
$BaCl_2$–NaCl, reactions with refractory metal borides, carbides, nitrides, and oxides, 20: 14989
$BaCl_2$–NaCl, stability of zirconium dichloride in, 20: 1822(T) (ANL-Trans-233)
$BaCl_2$–NaCl, testing for use in viscous protection of high-temperature dies, 17: 11081(R) (ASD-TR-7-886(Vol.VII))
$BaCl_2$–NaCl, thermodynamic properties, 18: 11958(R) (BNL-823(p.20-47))
BaF_2–CaF_2–KCl–NaCl, phase diagram, 17: 3005
$BeCl_2$–NaCl, electrochemistry of fused, activity coefficients in, 19: 30700
$BeCl_2$–NaCl, phase diagrams, 20: 36787 (YALE-2723(Vol.1))
$BeCl_2$–NaCl, vapor pressure at 400°C, 17: 12294
Bi–NaCl–$ZnCl_2$, spectra of reaction products of, absorption, 20: 3921(R) (ORNL-3870, pp 56-60)
B_2O_3–$NaBO_2$–NaCl, immiscibility diagram of liquid, 18: 40996 (USNRDL-TR-752)
B_2O_3–NaCl, radioinduced defects in, ESR spectra of gamma, 20: 19256(R) (NYO-2024-9)
B_2O_3–NaCl–Na_2O, distribution of cesium and rubidium in immiscible phases of, 17: 1566 (USNRDL-TR-588)
B_2O_3–NaCl–Na_2O, distribution of solutes between phases in, at 830°C, 18: 33534 (USNRDL-TR-760)
B_2O_3–NaCl–Na_2O, distribution of alkali metals, alkaline earths, and rare earths between phases in, at 830°C, 20: 7201
Ca–Ag–NaCl, radioinduced color centers in, x, 20: 38396
$CaCl_2$–NaCl, phase diagrams, 20: 36787 (YALE-2723(Vol.1))
$CaCl_2$–NaCl–$ThCl_4$, phase studies of thorium chloride–eutectic mixtures, 19: 2280(T) (IS-Trans-7)
$CaCl_2$–NaCl, reactions with refractory metal borides, carbides, nitrides, and oxides, 20: 14989
$CaCl_2$–NaCl, solvent properties for niobium, 18: 16032
$CaCl_2$–NaCl, stability of zirconium dichloride in, 20: 1822(T) (ANL-Trans-233)
$CaCl_2$–NaCl, thermodynamic properties at 820°C, 18: 3671(R) (BNL-799(p.26-54))
$CaSO_4$–NaCl, thermodynamic properties of aqueous, 20: 22857(R) (ORNL-3913, pp 111-32)
$CdCl_2$–CsCl–NaCl, phase diagram, 17: 3003
$CdCl_2$–NaCl, phase diagrams, 20: 36787 (YALE-2723(Vol.1))
$CdCl_2$–NaCl, radioinduced color center formation and impurity distribution, 18: 5862(T)
Cd–LiCl–Mg–$MgCl_2$–NaCl–U–Zn, corrosive effects on reactor materials, 18: 36751 (ANL-6912)
Cd–Mg–$MgCl_2$–Pu–KCl–NaCl, corrosive effects on SS 304, 18: 36751 (ANL-6912)
$CeCl_3$–NaCl–H_2O, chemical and physical properties, 20: 8945
$CeCl_3$–NaCl–$SnCl_2$, phase studies and structure, 17: 18085
$CeCl_3$–NaCl, thermodynamic properties of fused, 17: 7992 (BNL-6589)
CsCl–NaCl, phase diagrams, 20: 36788 (YALE-2723(Vol.2))
$CuCl_2$–NaCl, radiation effects on absorption spectra of, x, 20: 7172
Cu–$MgCl_2$–KCl–NaCl, corrosive effects on ferrous alloys, 20: 31314(R) (ANL-7175, pp 1-41)
Cu–Mg–$MgCl_2$–KCl–NaCl–U, chemical compatibility with vitreous carbon containers at 800°C, (E), 20: 14007(R) (ANL-7122, pp 1-41)
$DyCl_3$–NaCl, phase studies on, 19: 30202
$ErCl_3$–NaCl, complex formation in, 20: 12871
$GdCl_3$–NaCl, phase studies on, 19: 30202
HCl–NaCl, thermodynamic properties of, 19: 46237(R) (ORNL-3832,

pp 76-99)
$HgCl_2$–NaCl, phase diagrams, 20: 36788 (YALE-2723(Vol.2))
$IaCl_3$–NaCl, phase diagram, 16: 2931(T) (AEC-tr-4870)
$InCl_3$–NaCl, phase diagrams, 20: 36788 (YALE-2723(Vol.2))
KBr–NaCl, microstructure and phase studies, 18: 18372
KBr–NaCl, phase diagrams, 20: 36788 (YALE-2723(Vol.2))
KCl–K_2ZrF_6–NaCl, decomposition potentials in electrolysis of, 19: 19850(T) (NP-tr-1230)
KCl–K_2ZrF_6–NaCl–Na_2ZrF_6, phase studies, 19: 406
KCl–NaCl, corrosive effects of fused, on stainless steel at 800°, 16: 19422
KCl–NaCl, corrosive effects on metals at 700, 800, and 900°C, 18: 24089
KCl–NaCl, corrosive effects on zirconium, 20: 5855(T) (JPRS-32341, pp 24-31)
KCl–NaCl, diffusion of lead in molten, 16: 30388
KCl–NaCl, diffusion coefficients of uranium (III), (IV), and (VI) ions in molten, 19: 32127(T) (NP-tr-1236(p.7-11))
KCl–NaCl, dissolution of zirconium in fused mixtures of, 18: 31517
KCl–NaCl, effects of molten, on reaction of uranium dioxide with chlorine, 20: 5547
KCl–NaCl, effects on non-metallic structural materials for solvent containers, 20: 26816 (HW-72369)
KCl–NaCl, electric double layer capacity of metals in, 17: 8092
KCl–NaCl, electrode potentials of thorium tetrachloride in, 18: 27371
KCl–NaCl–UCl_4, electrolysis of molten, cathode polarization in, 19: 32128(T) (NP-tr-1236(p.12-20))
KCl–NaCl–UO_2Cl_2, electrolysis of molten, cathode polarization in, 19: 32128(T) (NP-tr-1236(p.12-20))
KCl–NaCl–UCl_3, electrolysis of molten, cathode polarization in, 19: 32128(T) (NP-tr-1236(p.12-20))
KCl–NaCl–UO_2Cl_2, equilibrium potentials of uranium dioxide electrodes at 670 to 900°C in molten, 19: 32126(T) (NP-tr-1236(p.1-6))
KCl–NaCl, interface phenomena with liquid lead, 18: 34050(R) (ORNL-3626(p.59-164))
KCl–NaCl, ion exchange with sodium porcelain, 18: 17802
KCl–NaCl, microstructure and phase studies, 18: 18372
KCl–NaCl–$NbCl_4$, phase diagram and structure of, 17: 1489
KCl–NaCl–UCl_3, phase diagram, 19: 10567(R) (ORNL-3708(p.304-20))
KCl–NaCl, phase diagrams, 20: 36788 (YALE-2723(Vol.2))
KCl–NaCl–$ThCl_4$, phase studies of thorium chloride–eutectic mixtures, 19: 2280(T) (IS-Trans-7)
KCl–NaCl–YCl_3, phase studies on, 20: 1872
KCl–NaCl, polarization of uranium and uranyl chlorides on molybdenum and platinum electrodes in, 18: 22065
KCl–NaCl, polarization of molybdenum during electrolysis in fused, 20: 14562
KCl–NaCl, polarography in fused, 16: 2954
KCl–NaCl, reactions of ammonia with uranium tetrachloride in molten, precipitation of uranium nitrides by, 20: 18698
KCl–NaCl, solvent properties for niobium, 18: 16032
KCl–NaCl, stability of zirconium dichloride in, 20: 1822(T) (ANL-Trans-233)
KCl–NaCl–$ZrCl_4$, stability of zirconium dichloride in, 20: 1822(T) (ANL-Trans-233)
KCl–NaCl, thermodynamic properties of fused, 17: 7992 (BNL-6589)
KCl–NaCl, use of fused, in attempts to prepare uranium sulfide, 19: 38574 (ANL-7008)
KCl–NaCl–UF_4, uses in electrolytic processing of irradiated uranium fuels, 19: 46448
KCl–NaCl, zirconium equilibrium potentials in molten equimolar, 16: 5360(T)
KCl–$PrCl_3$–NaCl, phase diagram, 17: 3002
KCl–$SmCl_3$–NaCl, phase studies, 19: 40517
KCl–SmCl–NaCl, phase studies, 19: 40517
KF–NaCl, microstructure and phase studies, 18: 18372
$LaCl_3$–NaCl, compound formation in saturated vapor of, at 1100 to 1350°C, 20: 29227
LiBr–NaCl, microstructure and phase studies, 18: 18372
LiCl–KCl–NaCl, phase studies, 17: 1506
LiCl–KCl–NaCl–$ThCl_4$, phase studies of thorium chloride–eutectic mixtures, 19: 2280(T) (IS-Trans-7)
LiCl–$MgCl_2$–NaCl, effects on corrosion of ferrous alloys by cadmium–magnesium–uranium–zinc at 600 and 650°C, 19: 32279(R) (ANL-7020(p.3-99))
LiCl–$MgCl_2$–NaCl, liquidus lines at 450 to 600°C, 18: 35060(R) (ANL-6904)
LiCl–$MgCl_2$–NaCl, liquidus temperatures, 19: 32279(R) (ANL-7020 (p.3-99))
LiCl–$MgCl_2$–NaCl, melting points of, effects of composition on, 20: 5594(R) (ANL-6925, pp 21-106)
LiCl–$MgCl_2$–NaCl, phase studies on, 18: 24813(R) (ANL-6880 (p.49-67))
LiCl–$MgCl_2$–NaCl, phase studies, 19: 15662(R) (ANL-6900(p.45-142))
LiCl–Mg–$MgCl_2$–NaCl–Zn, corrosive effects on reactor materials, 18: 36751 (ANL-6912)
LiCl–NaCl, effects of molten, on reaction of uranium dioxide with chlorine, 20: 5547
LiCl–NaCl, phase diagrams, 20: 36788 (YALE-2723(Vol.2))
LiCl–NaCl, phase studies, 17: 1505
LiF–NaCl, microstructure and phase studies, 18: 18372
LiH–NaCl, electric and thermodynamic properties, 19: 16445(R) (ANL-6900(p.304-29))
LiH–NaCl, phase diagram, 18: 35060(R) (ANL-6904)
LiH–NaCl, phase studies, 19: 16445(R) (ANL-6900(p.304-29))
LiH–NaCl, phase studies, 20: 10832
LiH–NaCl, thermodynamic properties, 19: 32924(R) (ANL-7020(p.198-225))
$MgCl_2$–KCl–NaCl, corrosive effects with cadmium alloys, on stainless steel, 20: 20802(R) (ANL-7055, pp 21-98)
$MgCl_2$–KCl–NaCl, distribution of rare earths, plutonium, and uranium between magnesium alloys and, 19: 32279(R) (ANL-7020(p.3-99))
$MgCl_2$–KCl–NaCl, electrolysis of uranyl chloride in, preparation of uranium dioxide by, 18: 2206
$MgCl_2$–KCl–NaCl–UO_2Cl_2, electrolysis of molten, at 500 to 600°C, 20: 43266(P)
$MgCl_2$–KCl–NaCl, exchange of barium ions between potassium hexatitanate and molten, 19: 32279(R) (ANL-7020(p.3-99))
$MgCl_2$–KCl–NaCl, exchange of plutonium in liquid systems with magnesium–zinc alloys, thermodynamics of, 20: 43819
$MgCl_2$–KCl–NaCl, rate processes in packed column during bismuth extraction from, 17: 27492 (BNL-791)
$MgCl_2$–KCl–NaCl, separation of rare earths from, by extraction using aluminum–magnesium alloys, 19: 17176(R) (ANL-6965(p.1-41))
$MgCl_2$–KCl–NaCl, separation of rare earth fission products from, by extraction using magnesium alloys, 20: 3865 (ANL-7064)
$MgCl_2$–KCl–NaCl, solvent properties for cerium and uranium from bismuth–magnesium alloy at 500°C, 17: 10581 (BNL-639)
$MgCl_2$–KCl–NaCl, solvent properties for praseodymium, 18: 24952(R) (ANL-6880(p.6-48))
$MgCl_2$–KCl–NaCl, solvent properties for lanthanum, plutonium, and praseodymium, 20: 5594(R) (ANL-6925, pp 21-106)
$MgCl_2$–KCl–NaCl, solvent properties for uranium, 20: 5594(R) (ANL-6925, pp 21-106)
$MgCl_2$–KCl–NaCl, solvent properties of liquid, for praseodymium, 20: 20802(R) (ANL-7055, pp 21-98)
$MgCl_2$–KCl–NaCl, use as bath in electrolytic production of uranium dioxide crystals, 19: 34199(P)
$MgCl_2$–NaCl, corrosive effects on stainless steels, effects of pH on, 19: 42803(R) (EURAEC-1397)
$MgCl_2$–NaCl, corrosive effects on titanium-base alloys at 550 to 600°F, stress-, 20: 11227
$MgCl_2$–NaCl, phase diagrams, 20: 36788 (YALE-2723(Vol.2))
$MgCl_2$–NaCl, solvent properties for niobium, 18: 16032
$MgCl_2$–NaCl, stability of zirconium dichloride in, 20: 1822(T) (ANL-Trans-233)
$MgCl_2$–NaCl, thermodynamic properties of fused, 16: 20042(R) (BNL-696)
$MgCl_2$–NaCl, thermodynamic properties of fused, 17: 7992 (BNL-6589)
$MnCl_2$–NaCl, radioinduced color center formation and impurity distribution, 18: 5862(T)
NaBr–NaCl, heat of mixing of, effects of composition and temperature on, 20: 23011
NaBr–NaCl, microstructure and phase studies, 18: 18372
NaBr–NaCl, phase diagrams, 20: 36788 (YALE-2723(Vol.2))
NaBr–NaCl, radioinduced F-bands in, effects of Schottky defects on, 20: 14605
NaCl–H_2O, spectra of, molar extinction coefficients for infrared-absorption, 20: 25092
NaCl–H_2SO_4, radioinduced absorption spectra in, at 77°K, 20: 16534
NaCl–K_2NbF_7–ZrF_4, production of niobium–zirconium alloys by electrolysis of, 18: 16431
NaCl–$NaClO_4$, osmotic pressure, 18: 19837(R) (MIT-905-1)
NaCl–NaF–NaI, density of, temperature effects on, (E), 20: 21566(R) (ANL-7055, pp 213-29)
NaCl–NaF, microstructure and phase studies, 18: 18372
NaCl–NaF–NaI, properties in bismuth–sodium emf cells, 19: 17359(R) (ANL-6965(p.84-90))
NaCl–NaF–NaI, solvent properties for bismuth and sodium, 19: 24064(R) (ANL-6997)
NaCl–NaF–NaI, solvent properties for sodium and Na_3Bi intermetallic compound, 19: 32924(R) (ANL-7020(p.198-225))
NaCl–NaF–NaI, solvent properties for bismuth–sodium alloys and sodium, 20: 6024(R) (ANL-6925(p.235-47))
NaCl–NaF–NaI, solvent properties for bismuth–sodium alloys, (E), 20: 21566(R) (ANL-7055, pp 213-29)
NaCl–NaOH, thermal conductivity at low temperatures, 19: 31629

(COO-1198-239)
NaCl–$SrCl_2$, performance in fusion-electrolytic preparation of sodium at 565°C, 18: 22090(P)
NaCl–$SrCl_2$, scattering of visible light by, images from, 18: 10642
NaCl–$SrCl_2$, thermodynamic properties, 18: 11958(R) (BNL-823(p.20-47))
NaCl–$TaCl_5$, phase studies, 18: 41456
NaCl–$ThCl_4$, phase diagram, 19: 2280(T) (IS-Trans-7)
NaCl–UCl_4, petrology, 17: 7606(R) (ORNL-1515)
NaCl–UCl_4, thermodynamic properties of, 18: 31510
NaCl–UF_4, phase studies, 18: 45002(R) (LA-3163-MS)
NaCl–UF_4, uranium production by electrolysis of, 20: 12876(P)
NaCl–UF_3–UF_4, phase studies, 18: 45002(R) (LA-3163-MS)
NaCl–UO_2, fission product recoil ranges in, 20: 37997
NaCl–YCl_3, phase diagrams, 18: 13792
NaCl–$ZnCl_2$, diffusion and ionic conductivity in, 19: 44677(R) (ANL-7000, pp 183-5)
NaCl–$ZrCl_4$, phase studies, 18: 3298(R) (ORNL-2221(Pts.1-5)(Del.))
Na_2CO_3–NaCl, corrosive effects of, on stainless steel, 17: 22114(T,R) (EURAEC-557)
$NaHCO_3$–NaCl, corrosive effects on stainless steel types 304, 316, and 410, 17: 502(T,R) (EURAEC-293)
$NaHCO_3$–NaCl, corrosive effects on chromium and chromium–nickel steels, 17: 25626(T) (EURAEC-675)
$NaHCO_3$–NaCl, corrosive effects on chromium–nickel steel at 20°C, 17: 25727(T) (EURAEC-676)
$NaHCO_3$–NaCl, corrosive effects on stainless steel, 18: 8734(T,R) (EURAEC-735)
$NaHCO_3$–NaCl, protection and rupture potential effects on steels at 40 and 80°C, 17: 25728(T) (EURAEC-677)
Na–NaCl, free energy of solution of, 19: 11103
$NbCl_5$–KCl–NaCl, phase studies, 16: 30431
$NbCl_5$–NaCl, phase studies, 16: 30431
$NbCl_5$–NaCl–$TaCl_5$, phase studies, 17: 25251
$NdCl_3$–NaCl, complex formation in, refractometric studies of, 19: 46254
$NiCl_2$–NaCl, spectra of nickel(II) in melts of, absorption, 20: 3921(R) (ORNL-3870, pp 56-60)
Ni–NaCl, thermostimulated electron emission from crystallophosphor of, 19: 25170(T)
$PbCl_2$–NaCl, radiation effects on absorption spectra of, x, 20: 7172
$PbCl_2$–NaCl, radioinduced color center formation and impurity distribution, 18: 5862(T)
$PuCl_3$–KCl–NaCl, phase diagram, predicted, 18: 22010(R) (ORNL-3591 (p.3-15))
$PuCl_3$–KCl–NaCl, phase diagram, 19: 10567(R) (ORNL-3708(p.304-20))
$PuCl_3$–KCl–NaCl, phase studies and properties as reactor fuels, 18: 34050(R) (ORNL-3626(p.59-164))
$PuCl_3$–KCl–NaCl–UCl_3, use as reactor fuel, 18: 19358 (ANL-6792 (p.553-70))
RbCl–NaCl, heat of mixing of, effects of composition and temperature on, 20: 23011
RbCl–NaCl, ion exchange with sodium porcelain, 18: 17802
$ScCl_3$–NaCl, phase diagrams, 18: 17796
$SmCl_3$–NaCl, phase diagrams, 18: 43523

SODIUM CHLORITES
annealing neutron-irradiated, thermal, 16: 25444
oxidative effects on iodine-131 solutions, 17: 10682
oxidative effects on tritium-labeled aldoses, kinetic isotope effects in, 18: 25459
oxidative effects on carbon-14- and tritium-labeled glucose, kinetic isotope effects in, 18: 25459
oxidizing effects on stainless steel types 304, 316, and 410, 17: 502(T,R) (EURAEC-293)
properties for use as labeled clathrates in determination of gases, 18: 17866(R) (NYO-2766)
protective effects of, against radiation inactivation of taka-amylase, 17: 15592
radiation effects on, in aqueous solutions, 19: 13482

Sodium Chloroacetates
see Acetic Acid, Chloro-, Sodium Salts

SODIUM CHLOROIRIDATES
radiation and thermal annealing effects on iridium-192 recoils in, 19: 13493
radiation effects on, neutron, 18: 43632
reactions with iridium-192 recoil ions, chemical behavior of labeled compound yields in, 18: 33662
recoil chemistry of iridium-192 in neutron-irradiated, 19: 13422 (JUL-181-RC)
recoil processes in neutron irradiated, products from, 19: 42572
thermal annealing of chemical radiation damage in solid, 17: 34515

SODIUM, (N-CHLORO-p-TOLUENESULFONAMIDO)-
use as oxidizing agent in preparation of insulin-iodine-131, 17: 34013
use in radioiodination of tissue-soluble proteins in rabbits and rats, 20: 43274

SODIUM CHLOROURANATES
formation in reactions of sodium chloride with uranium(IV-VI) oxide, 19: 15429(T) (ANL-Trans-33(p.70-4))

SODIUM CHROMATES
analysis for oxygen-18, mass spectrometric, 20: 8852
analysis of, for trivalent chromium-51 using thin-layer chromatography and scintillation counting, 20: 43114
corrosion inhibition by, stainless-steel, 18: 20477
corrosion inhibiting effects on carbon steel, 19: 21714 (RL-REA-592)
determination in brine solutions, volumetric, 16: 1704 (PG-Report-246)
effects on dissolution of plutonium dioxide pellets in nitric acid, 19: 20050 (ORNL-3695)
heat of solution and thermodynamic properties of, in sodium nitrate, 18: 5283
nuclear magnetic resonance of oxygen-17 in, 17: 3645
oxidation states of chromium-51 bearing, method for determining, 19: 31696
oxygen-18 exchange between gaseous oxygen and, mechanism and rate of, 20: 422
preparation and tracer uses of chromium-51-labeled, 19: 14955 (CEA-R-2585)
preparation, properties, and radioactivity of chromium-51-labeled, 17: 21412
properties of fused hydrates of, for use in electrophoresis of uranyl compounds, 19: 42602
radiation effects on impurity-doped, effect of lattice defects on annealing processes for thermal neutron, 18: 3857
radiation effects on corrosion inhibition action on iron and steel, 19: 28414
reactions in dioxane–water solutions, nuclear magnetic resonance spectra of, 17: 40800
uptake of chromium-51-labeled, by clams, 20: 40575
use in radio-release method for tracing stream flows, 19: 34326 (TID-21881)
yields from radiolysis of sodium chromite, 20: 33357

SODIUM CHROMITES
radioinduced oxidation of, at various oxygen pressures, gamma, 20: 33357

SODIUM CITRATES
effectiveness in removal of radioisotopes from body, 19: 43700
effects of, on strontium-89 and -90 distribution in rats, 17: 12107
effects of, on strontium-89 binding by bones in guinea pigs, 17: 12108
effects of, on excretion of strontium-90 from mice, 20: 32922
effects on pH of dialyzed zirconyl chloride, 17: 35718
effects on polarization of steel and uranium, 19: 7914
effects on polarization of steel–uranium couples in aqueous solutions, 19: 9619 (AMRA-TR-64-33)
effects on radioinduced degradation of DNA in *E. coli*, 20: 31144
effects on renal excretion of calcium-45 and strontium-90 in dog, 16: 1447
effects on strontium-85 elution from mouse bones, 19: 43706
effects on strontium-90 excretion by mice, 20: 8561
properties for use as decontaminating solution, 18: 31822
protective effects with aminoalkylphosphinic acids against beryllium poisoning in mice and rats, 19: 12924
radioinduced peroxides in, effects of oxygen atmosphere on gamma, 20: 23107
radiolysis of pentadeuterate and -hydrate of, ESR spectra of, 19: 42543
radiosensitivity effects on DNA in bacteria, 16: 26815
separation from uranyl bis(dibenzoylmethane) by solvent extraction into chloroform, 16: 11792

SODIUM COMPLEXES
formation in liquid ammonia, electron structure of, 17: 18016(T) (UCRL-Trans-903(L))
octafluoroprotactinate, properties of, 19: 15509
tetranitritonitrosohydroxyruthenate, crystal structure of, neutron diffraction studies of, 19: 15503
with benzoylacetone, luminescence in, 16: 14739
with bis(2-ethylhexyl) phosphate, reactions with TBP, 20: 9049(R) (ORNL-3830, pp 193-221)
with cerium octatungstates, preparation and physico-chemical properties of, 19: 13369
with diacetamide, properties and spectra of, 20: 8494 (TID-22449)
with malate, evidence for, 16: 32999
with malic acid, formation constant of, 17: 28788
with *N*-(2-pyridylmethyl)iminodiacetic acid, stability of, 17: 15993
with thorium and pyrogallol, preparation, 19: 28240
with trisbenzoylacetonate and trisbenzoylmethide chelates, luminescence, 16: 14739
with uranyl acetate in aqueous solution, spectra of, 17: 6081

SODIUM COMPOUNDS
allyl sulfonates, effects on electrodeposition of nickel, tracer studies of, 18: 10099

boiling of aqueous solutions, hydrodynamic model for nucleate pool, 16: 20605
catalytic effects on radioinduced polymerization of isobutene, 18: 12220
ion pair associations in ethylenediamine, 16: 5407(R) (TID-14329)
luminescence characteristics of cyanoplatinate(II), 17: 14352
organic, radiolysis yields in, 19: 46324(R) (AGN-8132)
solubility and thermolysis of diliturate, 19: 19824
sorption of tridecylate, on rare earth minerals, tracer studies of oxygen effects, 16: 27655
thermolysis curves for diliturates, 18: 27305
with molybdenum and tungsten bronzes, preparation, properties, and structure of, 20: 43213

SODIUM CURIUM FLUORIDES
crystal structure of $Na_7Cm_6F_{31}$, 20: 38898

SODIUM CYANAMIDE
radioinduced color centers in, 18: 8420
thermal decomposition, 18: 17913

SODIUM CYANIDES
corrosive effects with radiation on metals, 16: 17976(R) (EURAEC-94)
effects on radioinduced permeability of erythrocytes, 20: 5342
preparation of carbon-14-labeled, 17: 10517 (PAN-336/XIII)
protective effects against radiation damage, reaction mechanisms, 16: 26855
protective effects against radiation injuries in mice, 17: 23086(R) (NP-12760(p.92-102))
protective effects against radiation damage in mice and rats, 17: 28677 (TID-17148)
radiation effects on, at 300°K, ESR studies of gamma, 20: 43350
radiosensitivity effects on mice and rats, 16: 31391(R) (ANL-6535 (p.55-7))
reactions with hydrocyanic acid, separation of carbon-13 by, 16: 12839

SODIUM DECYL SULFATES
micelle formation and hydrophobic bonding of, in heavy water, 20: 18687

SODIUM DEUTERIDES
see also Sodium Hydrides

Sodium Dichromates
see Sodium Chromates

Sodium Diethyldithiocarbamates
see Carbamic Acid, Diethyldithio-, Sodium Salts

SODIUM DITHIONITES
protective effects against x rays in dormant seeds, 18: 21923
protective effects against radioinduced injuries and mutations in rice seed, 19: 26121
spectra of irradiated, ESR, (E), 19: 17972

Sodium Diuranates
see Sodium Uranates

SODIUM DODECYL SULFATES
effects of, on binding of beryllium by bovine serum albumin, 17: 30261
effects on deuterium–hydrogen exchange in chicken heart lactic dehydrogenase, 19: 17462
effects on radiosensitivity of free DNA and mouse thymus deoxyribonucleoprotein, 19: 146
micelle formation and hydrophobic bonding of, in heavy water, 20: 18687
solvent properties for cerium, cobalt, and promethium sorbed on charcoal powders, 20: 5675
sorptive properties of surface layer for recoil bismuth ions, 16: 23585
use for washing radioactively contaminated surfaces, 20: 5675
Antarox DM-970–sodium hexametaphosphate–sodium dodecyl sulfate–$NaNO_3$–sulfosalicylic acid, efficiency of, as radioactivity decontamination solution for cotton protective clothing, 20: 29477

SODIUM DODECYL SULFONATES
use as foaming agent in treatment of wastes, 16: 7328(R) (TID-14472)

SODIUM ETHOXIDE
radiation effects on, ESR spectra following, 18: 37240
reactions with 1-bromo-2-phenylpropane, effects of deuterium and tritium on rate of, 18: 10138
reactions with 2-phenylethyltrimethylammonium iodide, deuterium isotope effects on, 19: 19947

SODIUM EUROPIUM SULFIDES
EuS–$NaEuS_2$, magnetic exchange interactions in, effects of dilution and lattice changes on, 19: 38068

SODIUM EUROPIUM TUNGSTATES
terbium ion excitation and relaxation in, 17: 39057

SODIUM FERROCYANIDES
iron-57 Mössbauer spectra from, (E), 20: 3296
iron-57 Mössbauer effect in, (E), 20: 9977 (TID-22403)
reactions with zirconyl chlorides in acid solutions, 16: 18913

SODIUM FLUOALUMINATES
see also Cryolites
Na_3AlF_6–WO_3, tungsten oxide single crystal growth in molten, 20: 43257

SODIUM FLUOBERYLLATES
spectra of, vibration, 17: 40796
$NaBeF_3$–$NaPO_3$, phase diagrams of, 20: 14557
Na_2BeF_4–NaF–Na_2ZrF_6, phase studies, 19: 7487

SODIUM FLUORIDE COMPLEXES
with hydrogen fluoride and uranium fluorides, formation of, 18: 207 (ORNL-3497)
with molybdenum, tungsten, and uranium hexafluorides, preparation and dissociation pressures of, 19: 2292
with molybdenum, tungsten, and uranium hexafluorides, preparation, 20: 22987
with molybdenum, tungsten, and uranium hexafluorides, dissociation pressures of, 18: 43362 (ORNL-P-321)
with rare earth fluorides, crystal structure, 18: 22010(R) (ORNL-3591 (p.3-15))
with rare earth fluorides, phase studies, 18: 23441 (CONF-405-40)

SODIUM FLUORIDES
see also Lithium Sodium Zirconium Fluorides
see also Potassium Sodium Thorium Fluorides
see also Sodium Yttrium Fluorides
analysis for molecular fluorine, chromatographic, 18: 174
analytical use for thorium determination by titration, 19: 43970
beta absorption and backscattering by, calculation of elemental stopping powers from, 19: 30127
Born repulsive potential in crystals of, 17: 2062 (TID-17185)
cohesive energy of crystals of, Born analysis for, 17: 32084
color centers in irradiated, F_2^+, 20: 45029
color centers in, zero-phonon transitions of, 18: 793
color centers in, hyperfine structure of V_k, 19: 2326
color centers in, ENDOR spectra of, (E), 19: 14230(R) (AD-608160)
crystal lattice energy of, relation of self energy of gaseous ions to, 18: 16017
crystal structure lattice dynamics of, eigenvalues and eigenvectors for, 20: 33262 (UCRL-14822)
crystal vibrations in impure, localized modes for determination of frequencies of, 18: 12103
dipole moment, quadrupole coupling, and spin rotation interaction constants, 18: 31361(R) (UCRL-11213(p.87-138))
ductility and yield points of crystalline, effects of impurities on, 19: 45679(R) (NYO-1859-11)
effectiveness in removal of radioisotopes from body, 19: 43700
effects on electric conductivity of uranium dioxide, 18: 39894 (EURAEC-1110)
effects on formation of cerium chromite in reactions between cerium oxide and chromium trifluoride, 20: 35489
effects on melting points of aluminum fluoride–potassium fluoride–zirconium fluoride mixtures, 20: 9045(R) (ORNL-3830, pp 69-96)
effects on radioinduced degradation of DNA in *E. coli*, 20: 31144
effects on strontium-85 elution from mouse bones, 19: 43706
effects on thermal conductivity of sodium chloride, 19: 25783 (COO-1198-238)
electron energy loss spectra at 0.8 and 1.5 Mev, 16: 12275
electron energy loss spectra in, 19: 16404
electron energy losses in thin films of, (E), 19: 30869
electron penetration depths at 1 to 30 kev, 18: 44476
electron-nuclear double resonance and electron paramagnetic resonance spectra of crystals of, F-center structure from, 17: 27376
electron-positron annihilation in, 18: 28345
fluorine replacement by chlorine in, 16: 26992
fluorine-19 NMR in crystals of, 16: 29579
fluorine-19 NMR in, deformation effects on, 19: 7481
fluorine-19 nuclear magnetic relaxation in crystals of, below 900°K, 16: 18253
freezing point depressions by tetravalent fluoride solutes, 17: 6088
freezing point depressions in, effects of cadmium and transition metal difluorides on, 17: 37213
freezing point depressions of, effects of trivalent fluorides on, 18: 5284
freezing point of, effects of trifluorides on, 17: 25062(R) (ORNL-3417 (p.41-50))
growth of crystals of, orientation phenomena in, 16: 32908(T) (AEC-tr-5392)
growth of crystals of, preferred orientation in, 16: 33486(T) (AEC-tr-5391)
growth of thin vapor-deposited layers of, 16: 32909(T) (AEC-tr-5393)
hardness of crystals of, 16: 10728
heat of solution in heavy and light water, (E), 20: 1825
hyperfine structure of, Stark- and Zeeman-effect splitting of, 19: 23785
intercrystalline energies in binary systems, 16: 7558
ion penetration depths at 1 to 30 kev, 18: 44476
ion range-energy relations for, (T), 19: 30967
ionization cross sections and partial pressure in systems with zirconium fluorides, 18: 31533
iron ion lifetime in, 20: 26350 (STI-DOC-10/50)
iron-57 Mössbauer effect in, 19: 26393

light absorption and refractive index at fusion, 19: 11115
luminescence centers in uranium(VI)-activated crystals of, piezospectroscopic study of, 17: 34030(T)
mechanical properties of single-crystal, effects of uranium additions on, 20: 13277
melting of, volume change in, 20: 25572(R) (NASA-CR-67221)
melting point, 16: 6411
molecular properties of, beam electric resonance studies of, 19: 19848(R) (UCRL-11828(p.193-7))
nuclear quadrupole coupling constants in crystals of, 16: 24654
optical properties of alpha color centers in crystals of, 17: 35788
paramagnetism of M-center in crystals of, 17: 169
performance in solar thermal storage system, (E), 19: 12150
phase studies with rare earth fluorides, 19: 30149(R) (ORNL-3789(p.3-35))
phonon scattering by *F* centers in crystalline, thermal conductivity measurements of, 18: 2448
photoemission yields at 10 to 21 ev, (E), 19: 11861
positron annihilation in, three-quantum, (E), 19: 10066
positron annihilation in crystals of, theory of, 17: 17301
potassium ion reactions with crystals of, secondary emission properties from, 17: 24160(T)
properties of molten, for use as reactor fuel, 20: 4376 (JUL-268-RG)
proton relaxation times in aqueous solutions of, 18: 23559
radiation effects on, containing iron group impurities, 16: 7539
radiation effects of neutrons on, nuclear magnetic resonance studies of, 17: 16111
radiation effects on absorption spectra of, x-, 18: 41542
radiation effects on, containing nickel ion, 19: 457
radiation effects on crystals of, at 3×10^{20} nvt, 16: 13645(R) (TID-15230)
radiation effects on mechanical properties of, 20: 26975
radioinduced color centers in crystals of, temperature dependence of x, 18: 20039 (COO-1044-14)
radioinduced color centers in lithium-doped, hyperfine structure of, (E/T), 19: 33524
radioinduced color center formation in crystals of, 20: 1908
radioinduced color centers in, at 80 and 200°K, 20: 20106 (COO-1044-23)
radioinduced color centers in, zero-phonon lines of, electron and neutron, (E), 20: 45035
radioinduced defects in, ESR of, (E/T), 20: 17975(R) (NYO-2047-36)
radioinduced F-center absorption spectra of, effects of temperature on, 20: 12892
radioinduced luminescence of M-centers in crystals of, (E), 19: 32167
radioinduced M′ and R′ centers in, zero-phonon transitions in electron and x, 20: 34854
radioinduced N band in, x, (E), 20: 34838
radioinduced point defects in crystals of, mechanism of, 17: 37622
radiolysis of azoethane adsorbed on, energy transfer in gamma, 20: 23116
reactions of fused, with chromium fluoride or lanthanum oxide, 20: 10821
reactions with beryllium aluminum silicate, structural evidence, 16: 1782
reactions with hafnium fluorides in aqueous solution, 17: 35831
reactions with niobium and zirconium in organophosphorus solvents, 19: 13532(R) (ORNL-TM-1020)
reactions with sodium hydride, 16: 8713 (NEPA-1841)
reactions with uranium sulfate and tetrafluoride in aqueous solutions, 17: 1472
reactions with uranium pentafluoride, complexing in, 17: 8040
reactions with uranium hexafluoride at 80 to 200°C, kinetics and thermometry of, 19: 17876
reactions with uranium(VI) fluoride in inert *n*-perfluoroheptane, 20: 8904
reactions with xenon oxyfluorides, 20: 14523
reduction by high-frequency hydrogen discharge to hydrogen halide and metal, 19: 39180
reduction by high-frequency discharges in helium, hydrogen, and nitrogen, role of electrons in, 19: 39181
scintillation properties at low temperatures, 16: 20707
separation from uranyl bis(dibenzoylmethane) by solvent extraction into chloroform, 16: 11792
sodium-23 magnetic shielding in crystals of, 17: 21696
sodium-23 NMR in, deformation effects on, 19: 7481
sodium-23 nuclear magnetic relaxation in crystals of, below 900°K, 16: 18253
solvent properties for sodium, 16: 13063
solvent properties for plutonium tetrafluoride, 16: 16392
solvent properties of molten, for hafnium, titanium, and zirconium oxides at 1000 to 1200°C, 17: 8016(T) (AEC-tr-5601)
sorption of chromium fluoride from uranium hexafluoride stream on pellets, 19: 32283(R) (ORNL-TM-1103)
sorption of uranium(VI) fluoride by, 16: 14617(R) (ORNL-TM-136)
sorptive properties for uranium hexafluoride, 17: 39179(R) (ORNL-3452 (p.26-50))
sorptive properties for gaseous uranium hexafluoride, kinetics, 17: 40684(R) (ORNL-TM-608)
sorptive properties for uranium hexafluoride, mechanism of, 18: 1616 (ORNL-3494)
sorptive properties for uranium hexafluoride from gas stream, mechanism of, 18: 41372 (ORNL-P-281)
sorptive properties for uranium hexafluoride, 18: 41303(R) (ORNL-TM-642)
sorptive properties for uranium hexafluoride, studies of sorption-desorption cycles in, 18: 43362 (ORNL-P-321)
sorptive properties for uranium hexafluoride, 19: 4247(R) (ORNL-3627 (p.29-72))
sorptive properties for uranium (VI) fluoride, 19: 4256(R) (ORNL-TM-886)
sorptive properties for uranium hexafluoride, 19: 11264(R) (ORNL-TM-937)
sorptive properties for uranium hexafluoride from gaseous streams, study of parameters in, 19: 18052(R) (ORNL-TM-1027)
sorptive properties of porous, for plutonium hexafluoride, 19: 22445(P)
sorptive properties for plutonium hexafluoride, 19: 32280(R) (ANL-7020(p.100-49))
sorptive properties for uranium hexafluoride, 20: 7189(R) (EURAEC-1339)
sorptive properties for uranium hexafluoride, 20: 7192(R) (K-1649)
sorptive properties for uranium hexafluoride, 20: 9045(R) (ORNL-3830, pp 69-96)
sorptive properties for uranium hexafluoride, 20: 12925(R) (EURAEC-1446)
sorptive properties for volatile fission-product halides, 20: 12925(R) (EURAEC-1446)
sorptive properties for uranium hexafluoride, 20: 18824(R) (EURAEC-1536)
sorptive properties for chromium fluorides, 20: 20808(R) (ORNL-3916)
sorptive properties of solid, for volatile fluorides in uranium hexafluoride, 20: 27038 (K-1666)
sorptive properties of, for hydrogen fluoride and uranium hexafluoride, 20: 33413(R) (K-1669)
sorptive properties for plutonium hexafluoride, 20: 45789(R) (ORNL-3945, pp 48-71)
sorptive properties for uranium hexafluoride in presence of bromine fluorides, 20: 45789(R) (ORNL-3945, pp 48-71)
spectra in, optical absorption, 18: 25408
spectra of F-centers in crystals of, 17: 27377
spectra of, infrared, 17: 28878
spectra of uranium-activated, relaxation luminescence, 17: 5125(T)
spectra of uranium-activated, polarization effects on luminescence, 18: 31502(T)
spectroscopy of molecular beams of, millimeter-wave, (E), 19: 27089
spectroscopy of, measurement of rotational transitions in, 20: 1876
spectrum of ionic crystals of, absorption band, 17: 12592(R) (TID-17912 (p.1-7))
structure of thin vapor-deposited layers of, 16: 32909(T) (AEC-tr-5393)
tests of pellets of, for uranium hexafluoride sorption from gas stream, 19: 24613(R) (ORNL-TM-1092)
thermal capacity at 20 to 250°K, 16: 32226
thermodynamic properties of liquid and solid systems of, 16: 26960 (ORNL-1956)
thermodynamic properties in *N,N*-dimethylformamide and *N*-methylformamide solutions, 20: 3924 (TID-22366)
transfer between heavy and light water, ionic hydration in, 17: 6096
use in fluorine-18 metabolism studies, 20: 40554
use in separation of fission products from irradiated uranium dioxide, 16: 11780 (EURAEC-165)
use of fluorine-18-labeled, for biomedical studies in dogs and man, 20: 27032
vibrational frequencies in crystals of, 16: 32221
wave functions of F centers in, (T), 19: 17953 (COO-1197-11)
AlF_3–LiF–NaF, phase diagram of, 18: 35503 (ORNL-3594)
AlF_3–NaF, phase diagrams, 20: 22856(R) (ORNL-3913, pp 1-51)
AlF_3–NaF, phase diagrams, 20: 36787 (YALE-2723(Vol.1))
Al–NaF–Si–Sn, development for use as vanadium alloy coating, 18: 39819(R) (IITRI-B6019-5)
Al_2O_3–Si–NaF, properties as coating for D-43 and TZM alloys, 20: 37276
AmF_3–NaF, phase studies, 19: 30149(R) (ORNL-3789(p.3-35))
$BaCl_2$–$CaCl_2$–CaF_2–NaF, phase studies, 17: 23376
BaF_2–NaF, phase diagrams, 20: 36787 (YALE-2723(Vol.1))
BeF_2–KF–NaF, viscosity, 16: 26961 (ORNL-2278)
BeF_2–LiF–NaF, corrosive effects of liquid, on nickel-base alloys, 16: 20974 (BMI-X-198)
BeF_2–LiF–NaF–ZrF_4, corrosive effects on nickel alloys at 500°C, 17: 29279 (BMI-X-227)
BeF_2–LiF–NaF–ZrF_4, corrosive effects on nickel alloys and Zircaloy-2 at 500°C, 17: 36222 (BMI-X-253)
BeF_2–LiF–NaF, phase diagram, 18: 39385

BeF_2–LiF–NaF, properties of liquid, as reactor coolant, 16: 23830 (BNL-5377)
BeF_2–LiF–NaF, solvent properties for reactor fuels, 18: 39385
BeF_2–LiF–NaF, viscosity, 16: 26961 (ORNL-2278)
BeF_2–LiF–NaF–UF_4, viscosity, 16: 26961 (ORNL-2278)
BeF_2–NaF, phase diagram, 16: 17638(T) (AEC-tr-4459(p.181-90))
BeF_2–NaF, phase diagram, 19: 10564(R) (ORNL-3708(p.214-51))
BeF_2–NaF, phase diagrams, 20: 36787 (YALE-2723(Vol.1))
BeF_2–NaF, properties of liquid, as reactor coolant, 16: 23830 (BNL-5377)
BeF_2–NaF, use in molten-salt reactor, 20: 14129 (JUL-315-RG)
BeF_2–NaF, viscosity, 16: 26961 (ORNL-2278)
BeF_2–NaF–ThF_4, phase equilibria, 18: 33582
BeF_2–NaF–UF_4, phase diagram, 17: 27336
BeF_2–NaF–ZrF_4, phase studies, 16: 17554(R) (ORNL-3262(p.3-18))
BeF_2–RbF–NaF–UF_4, phase studies, 18: 3298(R) (ORNL-2221(Pts.1-5)(Del.))
BiF_3–NaF, crystal structure, 19: 30149(R) (ORNL-3789(p.3-35))
BiF_3–NaF, phase studies, 19: 30149(R) (ORNL-3789(p.3-35))
BkF_3–NaF, phase studies, 19: 30149(R) (ORNL-3789(p.3-35))
B_2O_3–LiF–K_2ZrF_6–NaF, electrolysis of, 18: 37159
CaF_2–CeF_3–NaF, crystal structure and solubility, 18: 3774
CaF_2–NaF, lubricating properties of fused coatings of, in air, hydrogen, liquid sodium, and vacuum, 18: 33695 (NASA-TN-D-2348)
CaF_2–NaF, phase diagrams, 20: 36787 (YALE-2723(Vol.1))
CaF_2–NaF–YF_3, crystal structure and solubility, 18: 3774
$CdCl_2$–NaF, phase diagrams, 20: 36787 (YALE-2723(Vol.1))
CeF_3–NaF, density and molar volume of, 43165 (BM-RI-6836)
CeF_3–NaF, phase diagrams at 300 to 1300°C, 20: 33278
CeF_3–NaF, phase studies, 16: 2939
CeF_3–NaF, phase studies, 19: 30149(R) (ORNL-3789(p.3-35))
CfF_3–NaF, phase studies, 19: 30149(R) (ORNL-3789(p.3-35))
citric acid–NaF, solvent properties for zirconium, 18: 13970
CmF_3–NaF, phase studies, 19: 30149(R) (ORNL-3789(p.3-35))
CrF_3–NaF, phase diagrams, 20: 9045(R) (ORNL-3830, pp 69-96)
CsF–NaF, phase diagrams, 20: 36788 (YALE-2723(Vol.2))
DyF_3–NaF, phase diagrams at 300 to 1300°C, 20: 33278
DyF_3–NaF, phase studies, 19: 30149(R) (ORNL-3789(p.3-35))
ErF_3–NaF, phase diagrams at 300 to 1300°C, 20: 33278
ErF_3–NaF, phase studies, 19: 30149(R) (ORNL-3789(p.3-35))
EuF_3–NaF, phase diagrams at 300 to 1300°C, 20: 33278
EuF_3–NaF, phase studies, 19: 30149(R) (ORNL-3789(p.3-35))
F–LiF–NaF–ZrF_4, corrosive effects on nickel fluorinator and nickel alloys at 500°C, 19: 18051 (ORNL-3623)
GdF_3–NaF, phase diagrams at 300 to 1300°C, 20: 33278
GdF_3–NaF, phase studies, 19: 30149(R) (ORNL-3789(p.3-35))
HF–LiF–NaF–ZrF_4, corrosive effects on INOR-8, effects of cathodic protection on, 19: 920 (BMI-X-312)
HF–LiF–NaF–ZrF_4, corrosive effects on INOR-8 at 650°C, effects of inert gas sparge on, 19: 16012 (BMI-X-329)
HF–LiF–NaF–ZrF_4, corrosive effects on INOR-8 hydrofluorinator at 500 to 650°C, 19: 18051 (ORNL-3623)
HoF_3–NaF, phase diagrams at 300 to 1300°C, 20: 33278
HoF_3–NaF, phase studies, 19: 30149(R) (ORNL-3789(p.3-35))
KBr–NaF, microstructure and phase studies, 18: 18372
KCl–NaF, microstructure and phase studies, 18: 18372
KF–NaF, anodic overvoltages of nickel electrodes in molten eutectic, 20: 284 (EUR-804.e)
KF–NaF, density and molar volume of, 20: 43165 (BM-RI-6836)
KF–NaF, phase diagrams, 20: 36788 (YALE-2723(Vol.2))
KF–NaF, reactions with cerium, neodymium and samarium oxides at 900 to 1100°C, 17: 32111
KF–NaF–ThF_4, crystal structure, 19: 30149(R) (ORNL-3789(p.3-35))
KF–NaF–ThF_4, phase diagram, 19: 10567(R) (ORNL-3708(p.304-20))
KF–NaF–ThF_4, phase studies and properties as reactor blankets, 18: 34050(R) (ORNL-3626(p.59-164))
KF–NaF–ThF_4, phase studies, 19: 30149(R) (ORNL-3789(p.3-35))
KF–NaF–UF_4, crystal structure, 19: 30149(R) (ORNL-3789(p.3-35))
KF–NaF–UF_4, separation of uranium from, by boron trifluoride treatment, 16: 8809 (NAA-SR-269)
KF–NaF–UF_4, viscosity, 16: 26961 (ORNL-2278)
KF–NaF–ZrF_4, phase diagram of, liquidus surface in, 18: 16008(T) (ORNL-tr-31)
KF–NaF–ZrF_4, phase studies and structure, 18: 27453
KF–NaF–ZrF_4, spectra of, emission technique for study of, 18: 3744
KF–NaF–ZrF_4, viscosity, 16: 26961 (ORNL-2278)
KF–ScF_3–NaF, phase studies, 19: 40512
LaF_3–KF–NaF, phase studies, 20: 8939
LaF_3–NaF, density and molar volume of, 43165 (BM-RI-6836)
LaF_3–NaF, phase diagrams at 300 to 1300°C, 20: 33278
LaF_3–NaF, phase studies, 19: 30149(R) (ORNL-3789(p.3-35))
LaF_3–NaF, phase studies, 20: 8939
LiBr–NaF, microstructure and phase studies, 18: 18372
LiCl–NaF, microstructure and phase studies, 18: 18372
LiF–KF–NaF, analysis for nickel, voltammetric, 18: 29585
LiF–KF–NaF, analysis for nickel by voltammetry, 19: 17781(R) (ORNL-3750)
LiF–KF–NaF, analysis of molten, for iron, uranium, and zirconium, 18: 13630(R) (ORNL-3537(p.23-30))
LiF–KF–NaF, anodic overvoltages of nickel electrodes in molten eutectic, 20: 284 (EUR-804.e)
LiF–KF–NaF, chronopotentiometry and voltammetry of iron in liquid, 18: 19966
LiF–KF–NaF, coordination of nickel ions in, 18: 12077
LiF–KF–NaF–UF_4, corrosive effects of, on Inconel, 16: 32174(R) (ORNL-1339)
LiF–KF–NaF–UF_4, corrosive effects on nickel-base alloys, 16: 32080 (ORNL-TM-328)
LiF–KF–NaF, design of windowless cell for spectrophotometry of, 18: 8294
LiF–KF–NaF, electrochemistry of hydrated and oxygenated melts, 18: 39156 (EUR-1643.e(p.327-45))
LiF–KF–NaF, electrochemical reduction of iron and nickel ions in liquid, 18: 43445 (ORNL-P-324)
LiF–KF–NaF, electrode reactions of hydrogen and oxygen in molten, 19: 36330 (EUR–2249.e)
LiF–KF–NaF, electrodeposition of tantalum from, potassium tantalum fluoride in, 19: 36395
LiF–KF–NaF, heat transfer of liquid, at 500 to 900°C, radiant, 16: 19054
LiF–KF–NaF, phase diagram, 19: 10564(R) (ORNL-3708(p.214-51))
LiF–KF–NaF–UF_4, preparation, 18: 3298(R) (ORNL-2221(Pts.1-5)(Del.))
LiF–KF–NaF, properties of liquid, as reactor coolant, 16: 23830 (BNL-5377)
LiF–KF–NaF, reactions in molten eutectic, spectrophotometric studies of redox, 19: 9096 (ORNL-P-403)
LiF–KF–NaF, reactions of liquid, with active metals, 19: 23163(R) (ORNL-3650(p.111-86))
LiF–KF–NaF, solvent properties of, for argon, helium, neon, and xenon, 16: 18877
LiF–KF–NaF, spectra of cobalt ions in, absorption, 20: 14453(R) (ORNL-3889, pp 12-14)
LiF–KF–NaF–UF_4, spectrophotometric analysis for iron using thiocyanate, 17: 25117 (ORNL-TM-472)
LiF–KF–NaF–UF_4, viscosity, 16: 26961 (ORNL-2278)
LiF–KF–NaF, viscosity, 16: 26961 (ORNL-2278)
LiF–KF–NaF, voltammetry of iron at 470 to 545°C in liquid, 18: 226
LiF–NaF, corrosive effects of liquid, on alumina at 900°C, 16: 17565(R) (ORNL-3262(p.107-9))
LiF–NaF, density and molar volume of, 20: 43165 (BM-RI-6836)
LiF–NaF, effects on coated-particle fuels at 800 to 1000°C, 19: 20463 (ORNL-TM-431)
LiF–NaF, enthalpies of mixing at 1278°K, 19: 280(R) (ORNL-3679 (p.94-116))
LiF–NaF, microstructure and phase studies, 18: 18372
LiF–NaF, mixing enthalpies of molten, molar, 19: 46161(R) (ORNL-3832, pp 116-50)
LiF–NaF, phase diagrams, 20: 36788 (YALE-2723(Vol.2))
LiF–NaF, phase studies, 16: 17554(R) (ORNL-3262(p.3-18))
LiF–NaF, viscosity of liquid, 16: 26961 (ORNL-2278)
LiF–NaF–ThF_4, crystal structure, 19: 30149(R) (ORNL-3789(p.3-35))
LiF–NaF–ThF_4, phase diagram, 20: 8399(R) (ORNL-3872)
LiF–NaF–ThF_4, phase studies, 19: 30149(R) (ORNL-3789(p.3-35))
LiF–NaF–UF_4–ZrF_4, corrosive effects of, on nickel fluorinator in conjunction with fluorine, 16: 10455 (ORNL-3253)
LiF–NaF–UF_4–ZrF_4, fluorination, determination of half times for uranium removal in, 17: 37292(R) (ORNL-TM-586)
LiF–NaF–UF_4–ZrF_4, viscosity, 16: 26961 (ORNL-2278)
LiF–NaF–ZrF_4, corrosive effects of, on nickel, 16: 4450(R) (BMI-1546 (Del.))
LiF–NaF–ZrF_4, corrosive effects of, on HyMu-80 at 500°C, 16: 4502 (TID-13691)
LiF–NaF–ZrF_4, corrosive effects of, on INOR-8 hydrofluorinator in conjunction with hydrofluoric acid, 16: 10455 (ORNL-3253)
LiF–NaF–ZrF_4, corrosive effects of liquid, on nickel and nickel alloys, 17: 6571 (ORNL-TM-411)
LiF–NaF–ZrF_4, corrosive effects on nickel-base alloys at 650°C, 17: 34345 (BMI-X-247)
LiF–NaF–ZrF_4, corrosive effects of molten, on nickel alloys at 500 to 650°C, 17: 35251(R) (BMI-1632(Del.))
LiF–NaF–ZrF_4, corrosive effects on construction materials under hydrofluorination conditions, 17: 40423(R) (BMI-1639(Del.))
LiF–NaF–ZrF_4, corrosive effects on HyMu 80 and INOR-8 at 500°C in presence of fluorine and hydrofluoric acid, 18: 10468 (BMI-X-269)
LiF–NaF–ZrF_4, corrosive effects on INOR-8 and HyMu-80 at 650°C during hydrofluorination of stainless steel and Zircaloy-2, 18: 30128 (BMI-X-288)

LiF–NaF–ZrF_4, corrosive effects on HyMu-80 and INOR-8 under hydrofluorination conditions, 18: 34034(R) (BMI-1672(Del.))
LiF–NaF–ZrF_4, corrosive effects on INOR-8 at 650°C, 18: 40970(R) (BMI-1674(Del.))
LiF–NaF–ZrF_4, corrosive effects on HyMu 80 and INOR-8 under fluorination and hydrofluorination conditions, 19: 2744 (BMI-X-315)
LiF–NaF–ZrF_4, corrosive effects on Inor-8 under hydrofluorination conditions, 19: 2716(R) (BMI-1681(Del.))
LiF–NaF–ZrF_4, corrosive effects on INOR-8, effects of argon on, 19: 13871(R) (BMI-1691(Del.))
LiF–NaF–ZrF_4, crystallography and phase studies on, 19: 37101
LiF–NaF–ZrF_4, density and surface tension of liquid, 19: 5875
LiF–NaF–ZrF_4, phase diagram, 18: 22010(R) (ORNL-3591(p.3-15))
LiF–NaF–ZrF_4, phase diagram, 18: 39385
LiF–NaF–ZrF, separation of plutonium hexafluoride from, by volatilization, 17: 39179(R) (ORNL-3452(p.26-50))
LiF–NaF–ZrF_4, separation of uranium hexafluoride from, by continuous fluorination, 20: 45790(R) (ORNL-3945, pp 72-8)
LiF–NaF–ZrF_4, solvent properties for reactor fuels, 18: 39385
LiF–NaF–ZrF_4, viscosity, 16: 26961 (ORNL-2278)
$Li_4P_2O_7$–$K_4P_2O_7$–NaF, phase diagram, 17: 3004
LuF_3–NaF, phase diagrams, 20: 22856(R) (ORNL-3913, pp 1-51)
LuF_3–NaF, phase diagrams at 300 to 1300°C, 20: 33278
LuF_3–NaF, phase studies, 19: 30149(R) (ORNL-3789(p.3-35))
MgF_2–NaF, phase diagrams, 20: 36788 (YALE-2723(Vol.2))
Na_2BeF_4–NaF–Na_2ZrF_6, phase studies, 19: 7487
NaBr–NaF, microstructure and phase studies, 18: 18372
NaBr–NaF, phase diagrams, 20: 36788 (YALE-2723(Vol.2))
NaCl–NaF–NaI, density of, temperature effects on, (E), 20: 21566(R) (ANL-7055, pp 213-29)
NaCl–NaF, microstructure and phase studies, 18: 18372
NaCl–NaF–NaI, properties in bismuth–sodium emf cells, 19: 17359(R) (ANL-6965(p.84-90))
NaCl–NaF–NaI, solvent properties for bismuth and sodium, 19: 24064(R) (ANL-6997)
NaCl–NaF–NaI, solvent properties for sodium and Na_3Bi intermetallic compound, 19: 32924(R) (ANL-7020(p.198-225))
NaCl–NaF–NaI, solvent properties for bismuth–sodium alloys and sodium, 20: 6024(R) (ANL-6925(p.235-47))
NaCl–NaF–NaI, solvent properties for bismuth–sodium alloys, (E), 20: 21566(R) (ANL-7055, pp 213-29)
NaF–NaI, phase diagrams, 20: 36788 (YALE-2723(Vol.2))
NaF–$Na_2U_2O_7$, crystal structure and intergrowth mechanisms, 17: 40820
NaF–Si, properties as pack-coating material for high-temperature oxidation protection of vanadium alloys, 17: 35997(R) (IITRE-B6001-5)
NaF–SrF_2, phase diagrams, 20: 36788 (YALE-2723(Vol.2))
NaF–TbF_3, phase diagrams at 300 to 1300°C, 20: 33278
NaF–TbF_3, phase studies, 19: 30149(R) (ORNL-3789(p.3-35))
NaF–ThF_4, crystal structure, 19: 30149(R) (ORNL-3789(p.3-35))
NaF–ThF_4, density and molar volume of, 20: 43165 (BM-RI-6836)
NaF–ThF_4, electric conductivity and density of liquid, up to 1000°C, 18: 35492 (BM-RI-6500)
NaF–ThF_4–UF_4, phase equilibria in, 17: 11216
NaF–ThF_4–UF_4, phase studies, 16: 17554(R) (ORNL-3262(p.3-18))
NaF–ThF_4–UF_4, phase studies, 17: 14214 (ORNL-3304)
NaF–TmF_3, phase diagrams at 300 to 1300°C, 20: 33278
NaF–TmF_3, phase studies, 19: 30149(R) (ORNL-3789(p.3-35))
NaF–UF_3, compound formation in, 20: 26848
NaF–UF_5, crystal structure, 19: 30149(R) (ORNL-3789(p.3-35))
NaF–UF_4, crystal structure, 19: 30149(R) (ORNL-3789(p.3-35))
NaF–UF_4, decomposition of, thermobalance study of, 19: 20258 (JAERI-1070)
NaF–UF_4, density and molar volume of, 20: 43165 (BM-RI-6836)
NaF–UF_4, electric conductivity and density of liquid, up to 1000°C, 18: 35492 (BM-RI-6500)
NaF–UF_3, phase studies, 19: 30149(R) (ORNL-3789(p.3-35))
NaF–UF_4, viscosity, 16: 26961 (ORNL-2278)
NaF–UF_4–ZrF_4, corrosive effects on Inconel, effects of thermal cycling on, 18: 29147 (NASA-SP-41(p.273-303))
NaF–UF_4–ZrF_4, fluorination and volatilization of, for uranium separation, 16: 13167(P)
NaF–UF_4–ZrF_4, level measurement of fused, by Inconel level indicators, 16: 31823 (ORNL-TM-331)
NaF–UF_4–ZrF_4, phase diagram, 19: 10564(R) (ORNL-3708(p.214-51))
NaF–UF_4–ZrF_4, phase studies, 17: 7606(R) (ORNL-1515)
NaF–UF_4–ZrF_4, phase studies, 18: 3298(R) (ORNL-2221(Pts.1-5)(Del.))
NaF–UF_4–ZrF_4, separation of uranium from, by boron trifluoride treatment, 16: 8809 (NAA-SR-269)
NaF–UF_4–ZrF_4, solvent properties of liquid, for rare earth fluorides, 16: 23595
NaF–UF_4–ZrF_4, thermal capacity at 550 to 850°C, 17: 7606(R) (ORNL-1515)
NaF–UF_4–ZrF_4, vapor pressures, 18: 3298(R) (ORNL-2221(Pts.1-5)(Del.))
NaF–UF_4–ZrF_4, viscosity, 16: 26961 (ORNL-2278)
NaF–$UO_3(OH)_2$, crystal structure and intergrowth mechanisms, 17: 40820
NaF–YbF_3, phase diagrams at 300 to 1300°C, 20: 33278
NaF–YbF_3, phase studies, 19: 30149(R) (ORNL-3789(p.3-35))
NaF–YF_3, density and molar volume of, 20: 43165 (BM-RI-6836)
NaF–YF_3, phase diagrams at 300 to 1300°C, 20: 33278
NaF–YF_3, phase equilibria in, 17: 39045
NaF–YF_3, phase studies, 16: 17554(R) (ORNL-3262(p.3-18))
NaF–YF_3, phase studies, 17: 25060(R) (ORNL-3417(p.3-16))
NaF–YF_3, phase studies of order-disorder effects and solid solutions, 17: 30506 (CONF-20-21)
NaF–ZnF_2, phase diagrams, 20: 36788 (YALE-2723(Vol.2))
NaF–ZrF_4, ionization cross sections and partial vapor pressures, 17: 33891
NaF–ZrF_4, phase diagram, 19: 10564(R) (ORNL-3708(p.214-51))
NaF–ZrF_4, solvent properties of, for argon, helium, neon, and xenon, 16: 18877
NaF–ZrF_4, thermodynamic properties, mass spectrometric studies of, 18: 31533
NaF–ZrF_4, vapor pressures, 18: 3298(R) (ORNL-2221(Pts.1-5)(Del.))
NaF–ZrF_4, viscosity of, 16: 26961 (ORNL-2278)
NdF_3–NaF, phase diagrams at 300 to 1300°C, 20: 33278
NdF_3–NaF, phase studies, 19: 30149(R) (ORNL-3789(p.3-35))
NpF_3–NaF, phase studies, 19: 30149(R) (ORNL-3789(p.3-35))
PaF_3–NaF, phase studies, 19: 30149(R) (ORNL-3789(p.3-35))
PbF_2–NaF, phase diagrams, 20: 36788 (YALE-2723(Vol.2))
PmF_3–NaF, phase diagrams at 300 to 1300°C, 20: 33278
PmF_3–NaF, phase studies, 19: 30149(R) (ORNL-3789(p.3-35))
PrF_3–NaF, phase diagrams at 300 to 1300°C, 20: 33278
PrF_3–NaF, phase studies, 19: 30149(R) (ORNL-3789(p.3-35))
PuF_3–NaF, phase studies, 16: 2939
PuF_3–NaF, phase studies, 19: 30149(R) (ORNL-3789(p.3-35))
rare earth fluorides–NaF, variations in composition of complex compounds of, 20: 22856(R) (ORNL-3931, pp 1-51)
RbF–NaF, phase diagrams, 20: 36788 (YALE-2723(Vol.2))
RbF–NaF–UF_4, phase studies, 18: 3298(R) (ORNL-2221(Pts.1-5)(Del.))
RbF–NaF–UF_3–ZrF_4, viscosity, 16: 26961 (ORNL-2278)
RbF–NaF–UF_4–ZrF_4, viscosity, 16: 26961 (ORNL-2278)
ScF_3–NaF, crystal structure of Na_3ScF_6 and $NaScF_4$ in, 20: 22856(R) (ORNL-3913, pp 1-51)
ScF_3–NaF, phase diagram, 18: 37126
ScF_3–NaF, phase diagrams, 20: 22856(R) (ORNL-3913, pp 1-51)
ScF_3–NaF, phase studies, 19: 30149(R) (ORNL-3789(p.3-35))
ScF_3–NaF, preparation and properties of Na_3ScF_6, 19: 40512
SmF_3–NaF, phase diagrams at 300 to 1300°C, 20: 33278
SmF_3–NaF, phase studies, 19: 30149(R) (ORNL-3789(p.3-35))

SODIUM FLUOSILICATES
crystal structure, 19: 3815 (UCRL-11130)
reactions with beryllium aluminum silicate, structural evidence, 16: 1782
reactions with beryl, 17: 28821 (AERE-R-4182)
reactions with dysprosium, gadolinium, and yttrium chlorides, precipitation in, 20: 1870
reactions with scandium in hydrochloric acid solutions, 20: 14566
stability in dry and moist heated air, 16: 13040
methane–Na_2SiF_6, radiolysis yields in, 19: 46324(R) (AGN-8132)

SODIUM FLUOTANTALATES
preparation and structural chemistry of, 17: 41761

SODIUM FLUOURANATES
spectra of, absorption, 18: 22033
structure, 19: 15423(T) (ANL-Trans-33(p.24-33))

SODIUM FLUOZIRCONATES
crystal structure, 19: 22169
precipitation from dissolved reactor fuels, flowsheet for, 17: 8266
reactions with zirconium oxide in fused systems, 18: 10201
stability in dry and moist heated air, 16: 13040
KCl–K_2ZrF_6–NaCl–Na_2ZrF_6, phase studies, 19: 406
Na_2BeF_4–NaF–Na_2ZrF_6, phase studies, 19: 7487

SODIUM FORMATES
catalytic effects on radiation peroxidation of kerosene, 16: 8775
complex with uranium(IV) oxyformate, 18: 13747
decomposition induced by ultrasound, hydrogen yields in, 18: 27525
effects on pH of dialyzed zirconyl chloride, 17: 35718
effects on radiolysis of aqueous solutions of cytosine, 19: 34227
effects on reactions of hydroxyl radicals with iodide ions in pulse radiolysis, 19: 26444
effects on self-irradiation decomposition of tritium-labeled organic compounds, 20: 16533
effects on uv photolysis of aqueous methanol solutions, 18: 43634
effects on yields in radiolysis of nitrous oxide aqueous solutions, 18: 31601
precipitation of fluorides and zirconium from fuel dissolver solutions using, 16: 23782 (IDO-14582)

radiation effects on, properties as chemical dosimeter, 17: 40862
radiation effects on hydrogen abstraction from deuterated, isotope effects in, 19: 4216
radiation effects on, electron spin resonance of free radicals from, 19: 9238
radiation effects on aqueous solutions of, carbon dioxide yields in, 19: 33738(R) (N64-22756)
radiation effects of recoils from thermal neutron-boron-10 reactions on deuterated, 19: 36514
radiolysis, CO_2^- electron absorption spectra in gamma, 16: 16430
radiolysis, effects of thermal annealing on yields, 16: 11745
radiolysis in heavy and light water, hydrogen yields from, 19: 5960
radiolysis of aqueous solutions, isotope effects of water-d_2 on, 16: 33030
radiolysis of aqueous solutions of, 18: 31563 (AD-429919)
radiolysis of aqueous solutions of deuterated, effects of nitrous oxide and organic solutes on yields in, 18: 31602
radiolysis of deaerated aqueous solutions of, pulsed-electron, 20: 10913
radiolysis of deuterated, effects of nitrous oxide environment on, 18: 10139(R) (AD-403358)
radiolysis of frozen aqueous solutions of, ESR spectral studies on radical reactions in, 20: 40994
radiolysis of, effects of bicarbonate and nitrous oxide on, 18: 10139(R) (AD-403358)
radiolysis, spectra of CO_2^- radical in, 16: 16435
scavenging effects on electron and hydrogen yields in irradiated aqueous solutions, 17: 4602
scavenging effects on hydrogen yield in radiolysis of aqueous solutions, 17: 37265
solvent properties for fluorine, uranium, and zirconium, 18: 12276(P)
sonolysis in water, hydrogen isotope effects in, 18: 12067
spectra of carbon-14-labeled, infrared, 19: 5938
use in simultaneous precipitation of fluoride and zirconium from dissolver solutions, 18: 33690(P)
use of carbon-14-labeled, in Gulliver program, 19: 33739(R) (N64-22793)

SODIUM GADOLINATES
magnetic properties and structure of, 18: 25397

SODIUM GADOLINIUM TUNGSTATES
energy exchange from neodymium to ytterbium ions in calibo glass, (E), 19: 29463

SODIUM GALLATES
effect on nucleic acid content in organs of healthy and irradiated rats, 17: 24900(T) (JPRS-19355)
effects of, on radiation sickness in dogs, 18: 29393(T)
mutagenic effects on *Vicia faba*, 18: 11591
protective effects of, against radiation injuries in dogs, 18: 29393(T)
protective effects against x radiation in mice, 18: 31133(T) (JPRS-25274)
protective effects against radiation injuries in dogs, 18: 43325
radiosensitivity effects in mice, x, 18: 38978
use for prophylaxis and therapy of radiation sickness in mice and rats, 20: 38728

SODIUM GRAPHITE REACTORS
see also Hallam Power Reactor
see also Sodium Reactor Experiment
calandria core creep acceleration temperatures, (T), 20: 10377 (NAA-SR-Memo-11433)
calandria core development for 1000-Mw(e), 20: 8394(R) (NAA-SR-11450, Sect.2)
calandria core for large, development of, 19: 40286(R) (NAA-SR-11200)
calandria core maintenance tools for, development of remote, 20: 12405 (NAA-SR-Memo-11576)
calandria core of large, development, 19: 12865(R) (NAA-SR-10501)
calandria remote maintenance tool development, 20: 26466 (NAA-SR-11202)
calandria vessel peripheral hanger tests, 20: 6618 (NAA-SR-Memo-11415)
calandria vessel stayed head study, 20: 6616 (NAA-SR-Memo-11324)
control rod development for LSGR, 19: 40126 (NAA-SR-11327)
control rod development for, dry and wet, 20: 8394(R) (NAA-SR-11450, Sect.2)
control rods for, 19: 10775(R) (NAA-SR-9999)
coolant flow in large, hydraulic testing of, (E), 19: 36609 (NAA-SR-11123)
coolant removal from upper plenum of 200-Mw(e), hydraulics of, 18: 21639 (NAA-SR-Memo-9241)
core hydraulic and thermal analyses for 1000-Mw(e) alternate fuel, 18: 21616 (NAA-SR-Memo-9569)
core optimization of 1000-Mw(e), 19: 5479 (NAA-SR-9501)
critical experiments for advanced, 19: 27735(R) (NAA-SR-10850)
criticality studies in uranium monocarbide lattices of, (E), 20: 6586 (NAA-SR-Memo-11313)
criticality studies, 20: 8397(R) (NAA-SR-11450, Sect.5)
criticality studies on two-region, (E), 19: 25686 (NAA-SR-Memo-9977)
design and development of 1000-Mw(e), 19: 40286(R) (NAA-SR-11200)
design and economics of 200-Mw(e), 17: 31722 (CONF-51-4)
design and evaluation of large, 19: 27735(R) (NAA-SR-10850)
design and evaluation of 200-Mw(e) prototype, 19: 42094 (NAA-SR-11314)
design of 200-Mwe prototype, 19: 12865(R) (NAA-SR-10501)
development and operation, 1964, 19: 10675(R) (NAA-SR-9999)
development of components and fuels for, 18: 24891(R) (NAA-SR-8888(Sect.I))
development of 200- and 1000-Mwe, (E), 19: 10548 (NAA-SR-9213(Vol.I))
development review, 20: 1513
economics of advanced-converter, (T), 19: 10552 (ORNL-3686)
economics of 1000-Mw(e), (E), 19: 8637 (NAA-SR-9213(Suppl.))
economics of 1000-Mw(e) power, (E), 19: 8637 (NAA-SR-9213(Suppl.))
economics of 1000-Mw(e) sodium-graphite power, (E), 19: 8637 (NAA-SR-9213(Suppl.))
exponential experiments for advanced, (E), 19: 21692 (NAA-SR-Memo-9976)
exponential experiments for advanced sodium-graphite power, (E), 19: 21692 (NAA-SR-Memo-9976)
fuel channel variable orifice design for Advanced Sodium Cooled Reactor, 18: 21568 (NAA-SR-Memo-8079)
fuel element design and fabrication for, 18: 35968 (NAA-SR-9988)
fuel element development for 1000-Mw(e), 20: 8394(R) (NAA-SR-11450, Sect.2)
fuel element development for Advanced Sodium Cooled Reactor, 18: 21614 (NAA-SR-Memo-8017)
fuel element grapple and hold-down-latch development for, 18: 21638 (NAA-SR-Memo-8266)
fuel element irradiation testing for LSGR, 20: 45113 (NAA-SR-11440)
fuel handling system for, development of, 19: 10675(R) (NAA-SR-9999)
heat transfer system for large, buckling test apparatus for, 20: 8329 (NAA-SR-11423)
lattice parameters versus pitch for ASCR closed lattices, 15-group diffusion study of, 18: 21600 (NAA-SR-Memo-9489)
material bucklings of ASCR, 18: 21599 (NAA-SR-Memo-9382)
neutron transport in lattices of, multigroup calculation methods for, (T), 19: 17279 (NAA-SR-10531)
reactivity temperature transients in 200-Mw(e) operation and accidents, analysis of, 20: 6620 (NAA-SR-Memo-11458)
review and survey of power, 18: 35161 (TID-8540(p.71-129))
safety analysis and siting of, 19: 17329
shutdown procedures, 19: 35766 (NAA-SR-Memo-11041)
steam cycles of, optimization of 350- to 400-Mw(e), 20: 1514
steam cycle optimization for large sodium-graphite power plants, 18: 40840 (NAA-SR-9488)
tube joints in calandria cores of large, equipment for cutting and re-welding bottom of process, 19: 40125 (NAA-SR-9821)
tubes for, design and testing of, 19: 41019 (NAA-SR-11323)
tubes of, moderator dimensional stability effects on, 20: 6619 (NAA-SR-Memo-11416)
vibration analysis of fuel element and process channel for large, 18: 21615 (NAA-SR-Memo-9164)

SODIUM HAFNATES
preparation, structure, and thermal stability, 16: 30413

SODIUM HAFNIUM SILICATES
crystal structure, 19: 19916(T)

SODIUM HALIDES
effects on oxidation of uranium dioxide, 18: 19943
lattice properties of, 17: 28844
physical properties, 16: 32216
physicochemical properties, 16: 12801(R) (IA-685)
properties of systems with cesium halides, 16: 5348
radiation effects on luminescence of doped, at 90 and 295°K, 19: 45488
sodium-23 nuclear relaxation time in crystals of, 17: 16018
solvent properties for intermetallic sodium compounds, 20: 40796(R) (IS-1500(Sect.C))

SODIUM HEXADECYL SULFATES
specific conductance and surface tension, 16: 17881(R) (MITS-47)

SODIUM HYDRIDES
see also Sodium Deuterides
dissociation properties, 16: 8713 (NEPA-1841)
electron-nuclear double resonance studies, 16: 21194
potential-energy curve of excited state of, 17: 29416
radiation effects on catalytic activity in hydrogen-deuterium exchange, 17: 18125
radiolysis at 4.2°K, hydrogen nonproduction in gamma, 16: 7600
reactions with calcium hydride and sodium fluoride, 16: 8713 (NEPA-1841)
separation from sodium in circulation loops, 20: 1960
solubility in liquid sodium, effects of free energy gradient on, 18: 22488

(NAA-SR-8381)
NaH–NaOH, dissociation properties, 16: 8713 (NEPA-1841)
NaH–NaOH, dissociation properties, 16: 20388
NaH–NaOH, phase studies, 17: 25253
Na–NaH–NaOH, corrosive effects on Croloy 2¼, 20: 4317 (BAW-1280-30)
Na–NaH–NaOH, corrosive effects on Croloy 2¼ steel, 20: 16599(R) (BAW-1280-34)
Sodium Hydrosulfites
see Sodium Dithionites
SODIUM HYDROXIDES
analysis for deuterium by decomposition and gas chromatography, 20: 35441
analysis for iodine in solutions of, colorimetric, 20: 43071 (IDO-14679, pp 75-191)
analysis of solutions of, by beta particle backscattering, 18: 37096
analytical use in titration of aqueous boric acid, 18: 23412 (UCRL-7756)
catalytic properties for activation of molecular hydrogen, 17: 38917
corrosive effects on stainless steels under stress, mechanism of, 16: 30733 (ARF-2181-12)
corrosive effects on nickel, 17: 7606(R) (ORNL-1515)
corrosive effects on niobium and vanadium, effects of acidity and current density on anodic, 18: 25929
corrosive effects on uranium nitride at 300°C, 18: 32035(R) (BMI-X-10073)
corrosive effects on Croloy 2¼ steel to 1200°F, 19: 565(R) (BAW-1280-15)
corrosive effects on Croloy 2¼ steel to 1200°F, 19: 566(R) (BAW-1280-16)
corrosive effects of aqueous solutions of, on Croloy 2¼, 19: 4303(R) (BAW-1280-17)
corrosive effects on Croloy 2¼ steel, 19: 13582 (SAN-8002(p.231-57))
corrosive effects on metals, anodic, 19: 28420(R) (NP-14825)
corrosive effects on Croloy, testing methods for, 19: 31474 (BAW-1280-23)
corrosive effects on Croloy, testing methods for, 19: 31475 (BAW-1280-24)
corrosive effects of solutions of, on Croloy 2¼ at 0 to 900°F, 19: 38803(R) (BAW-1280-26)
corrosive effects on titanium alloys at 650°F, 19: 44621 (CONF-651006-1)
corrosive effects on Croloy 2¼ steel, 19: 46478(R) (BAW-1280-25)
corrosive effects of aqueous solutions of, on Croloy 2¼ at high temperatures, 19: 46530(R) (BAW-1280-27)
corrosive effects on molybdenum and vanadium, stress-, 20: 2254 (BM-RI-6680)
corrosive effects of aqueous solutions of, on Croloy 2¼, 20: 4317 (BAW-1280-30)
corrosive effects on Croloy, 20: 4100 (BW-67-2(a))
corrosive effects of aqueous solutions of, on type-304 stainless steel, 20: 7526
corrosive effects on molybdenum, tungsten, and vanadium at 35 and 60°C, 20: 11230 (BM-RI-6715)
corrosive effects on vanadium-base alloys at low temperatures, 20: 11230 (BM-RI-6715)
corrosive effects on molybdenum and tungsten coupled with aluminum, copper, or magnesium, galvanic, 20: 11230 (BM-RI-6715)
corrosive effects on magnesium and its alloys, electrochemistry of pitting, 20: 11231 (CEA-R-2815)
corrosive effects on Croloy 2¼ steel, 20: 16599(R) (BAW-1280-34)
determination in fuel descaling make-up solutions, 19: 32059(R) (IDO-14655)
deuterium and hydrogen isotopic fractionation between equilibrium vapor phase and aqueous solutions of, 18: 35550
deuterium exchange with hydrogen in phenylphosphonous acid in, 17: 40839
dissolution of aluminum by, 18: 40813 (NP-10417)
effects on corrosion of niobium and tantalum at 21 and 98°C, 19: 22900
effects on electron spin resonance spectra of trapped electrons in irradiated ice, 19: 22314
effects on electron yields from radiolysis of frozen solutions, 19: 36513
effects on fission tracks in glasses, 20: 5713 (AD-623384)
effects on isomeric transitions in chemical separation of tellurium isomers, 18: 39095
effects on mutarotations of β-D-fructose and α-D-glucose, 20: 36577
effects on photoreduction of 4-benzoylphenyltrimethylammonium chloride, 20: 7129(R) (NYO-2499-17)
effects on properties of quartz, 19: 22279
effects on radioinduced viscosity changes in aqueous solutions of polyvinyl alcohol, 18: 29740(T,R) (AEC-tr-6231(p.339-41))
effects on radioinduced reduction of potassium manganate, 19: 26398
effects on radioinduced oxidation of cumene, 20: 18727 (JAERI-1100)
effects on radiolysis of water, 19: 505
effects on radiolysis of aqueous polyvinyl alcohol solutions, 19: 2387
effects on self-diffusion of water at 23°C, 19: 32159
effects on uranium sorption by platinized carbon, 20: 16581
electrolytic effects on sedimentation rate of uranium (IV–VI) oxide suspensions, 16: 23699
flocculation effects on thorium oxide slurries, 16: 26956 (JAERI-1033)
magnetic relaxation of trapped electrons in frozen, 20: 26923(R) (COO-1528-5)
neutron scattering by lattice of, spectra from inelastic, 18: 39154 (EUR-1643.e(p.174-80))
performance as sensitizer for nuclear emulsions, 19: 44406 (CERN-65-4(Vol.II), pp IV41-5)
polarography of, using teflon dropping mercury electrode, 17: 5987
production from lime and salt, using ion exchange, 19: 15693
properties of liquid, as reactor coolant, 16: 23830 (BNL-5377)
radiation chemistry of glasses of, at 77 to 150°K, ESR studies of gamma and ultraviolet, 20: 45730
radiation effects on reactions with uranium monocarbide, in-pile, 19: 7948
radiation effects on oxygenated aqueous solutions of, polarographic studies of 10-Mev pulsed electron, 20: 33337 (RISO-114)
radiation effects on normal and deuterated at 77°K, gamma, 20: 36871
radiation effects on frozen aqueous solutions of, EPR spectra of gamma, 20: 43290 (COO-1528-7)
radiolysis of aqueous solution with sodium sulfite, hydrogen yield in, 16: 23716 (PAN-290/ChR)
radiolysis of frozen solutions of, at 77°K, electron trapping in, 19: 17997
radiolysis of manganese oxides in, mechanisms and yields in, 18: 10144
radiolysis of terephthalic acid solutions of, 14-Mev neutron, 18: 22351
radiolysis of, hydrated electron absorption spectrum and reaction constants for, 18: 23691
radiolysis of, yields of hydrogen and oxygen from gamma, 20: 33356
reactions of liquid, with noble metals and oxides, 16: 179
reactions with cerium salts, 16: 5350
reactions with coconut oil, tracer study of, 20: 12545(R) (PAEC(A)AR651)
reactions with lanthanum salts, 16: 5351
reactions with liquid sodium, 19: 17850 (CEA-R-2583)
reactions with lutetium chlorides, 17: 1492
reactions with oxygen and sodium sulfite, radioinduced free radicals in, 16: 5262
reactions with potassium zirconium fluorides in aqueous solutions, 16: 5340
reactions with sodium acetate to prepare methane, 19: 46319
reactions with sulfuric acid, heats of, 17: 27323 (UCRL-7325-T)
reactions with thorium chloride, effects of pH on, 19: 11111
reactions with thorium carbide at 40 and 80°C, 19: 34163
reactions with uranyl salts, 16: 20368(T) (AEC-tr-4457(p.98-107))
reactions with uranyl nitrate, conductometric studies, 17: 15999
reactions with uranyl nitrate solutions, 18: 33063 (NP-14078)
reactions with uranyl nitrate in aqueous solution, formation of compounds in, 19: 15433(T) (ANL-Trans-33(p.89-100))
reactions with yttrium chlorides, preparation of yttrium hydroxides by, 20: 26873
reactions with zirconium nitrate, oxychloride, and sulfate, 16: 13045
separation of francium from, by solvent extraction using 4-*sec*-butyl-2-α-methylbenzylphenol, 20: 5601
separation of technetium-99 from, by solvent extraction using pyridine, 17: 39113
solvent properties for yttrium hydroxides, 16: 123
solvent properties for beryllium, 16: 33061 (AAEC/E-93)
solvent properties of solutions of, for corundum, pressure effects on, 17: 28874
solvent properties for aluminum in recirculation dissolver, 18: 1794 (NP-13270)
solvent properties for reactor fuel materials, 18: 31658(R) (IDO-14635)
solvent properties in paper chromatographic separation of inorganic cations, 18: 39388
solvent properties for uranium under anodic polarization conditions, 19: 13533 (RPI-Z714-4)
solvent properties for aluminum casing on uranium spent fuel element, 19: 41086(P)
solvent properties for SAP, 19: 40655 (RT/CHI(65)-1)
solvent properties for aluminum, 20: 4048(R) (NP-15406)
spectra of deuterated, in heavy water, infrared, 18: 31532
spectra of structure of water in, near-infrared, 17: 40803
thermal conductivity at 650 to 1000°F, 17: 7606(R) (ORNL-1515)
thermal properties for use as reactor coolant, 16: 7293 (NEPA-1476)
tributyl phosphate solubility in, 18: 17719
use as scrubber material for ruthenium tetroxide, 18: 34006(R) (ORNL-TM-889)
use in fine control of suspension reactors, 19: 38114(P)
use in removing residual energy from irradiated cellulosic materials, 20: 46126(P)
use in uranium recovery from scrap uranium tetrafluoride, 16: 1857

(MCW-1466)
viscosity at 340 to 448°C, 17: 7606(R) (ORNL-1515)
CaO–NaOH, sorptive properties of soda lime for fluorine and hydrofluoric acid, thermobalance study, 19: 20258 (JAERI-1070)
$KMnO_4$–NaOH, corrosive effects on corroded type-304 stainless steel, 19: 2756
KOH–NaOH, radiation effects on electron binding in frozen aqueous solutions of, 17: 8172
KOH–NaOH, solvent properties for beryllium oxide, 20: 8897
KOH–NaOH, use of, in preparation of potassium sodium niobates and tantalates, 16: 2940
LiOH–NaOH, spectra of fused, infrared, 17: 37175 (URS-74)
NaBr–NaOH–NaI, solvent properties for metallic sodium, 18: 4275
NaBr–NaOH, thermal conductivity at low temperatures, 19: 31629 (COO-1198-239)
NaCl–NaOH, thermal conductivity at low temperatures, 19: 31629 (COO-1198-239)
Na_2CO_3–NaOH, descaling effects on steam oxidized iron- and nickel-base alloys, 18: 22441 (HW-79048)
NaH–NaOH, dissociation properties, 16: 8713 (NEPA-1841)
NaH–NaOH, phase studies and thermal stability, 16: 20388
NaH–NaOH, phase studies, 17: 25253
Na–NaH–NaOH, corrosive effects on Croloy 2¼, 20: 4317 (BAW-1280-30)
Na–NaH–NaOH, corrosive effects on Croloy 2¼ steel, 20: 16599(R) (BAW-1280-34)
Na–NaOH, corrosive effects on Croloy 2¼, 19: 4303(R) (BAW-1280-17)
Na–NaOH, corrosive effects on Croloy 2¼ at 900°F, 19: 7676(R) (BAW-1280-20)
Na–NaOH, corrosive effects on Croloy 2¼, 20: 4317 (BAW-1280-30)
Na–NaOH, corrosive effects on Croloy 2¼ steel, 20: 16599(R) (BAW-1280-34)
NaOH–H_2O, radiolysis of oxygenated systems of, 20: 14614
NaOH–$NaNO_3$, solvent properties for irradiated aluminum–plutonium alloys, 18: 22167 (DP-874)
NaOH–$NaNO_3$, use for processing molybdenum- and niobium-containing irradiated fuels by oxidation, 20: 18834
NaOH–Na_3PO_4–Na_2WO_4, electrolytic etching and polishing of rhenium–tungsten alloys in, 18: 27931
NaOH–terephthalic acid, radiation effects on hydroxyterephthalic acid production in, 19: 834
O–NaOH–Na_2SO_3–H_2O, radiolysis of, hydrogen yield in, 16: 23716 (PAN-290/ChR)

SODIUM HYPOCHLORITES
corrosive effects on molybdenum, tungsten, and vanadium at 35 and 60°C, 20: 11230 (BW-RI-6715)
protective effects of, against radiation inactivation of taka-amylase, 17: 15592
removal from salt-cycle scrubber by hydrogen peroxide, 18: 27278(R) (HW-79280(p.4.1-28))
H_2O_2–NaOCl, chemiluminescence at 3000 to 7500 A, 18: 25371

SODIUM HYPOPHOSPHITES
reactions with phosphorus-32 recoil atoms, labeling positions in, 19: 42567
reactions with uranyl nitrate in solution, effects of uv radiation on, 19: 15459(T) (ANL-Trans-33(p.293-8))

SODIUM IODATES
iodine-131 beta decay in, properties of xenon oxide compounds formed by, 20: 38984
properties of, for half life experiments, 17: 29578
tellurium-125 Mössbauer effect in, (E), 20: 20148

SODIUM IODIDES
absorption band in thallium-activated crystals of, oscillator strength of 4.23-ev, 20: 26389
activity and osmotic coefficients in heavy water at 25°C, 20: 16488
activity coefficients in dilute alkali halide–cadmium nitrate solutions at 240 and 300°C, 16: 17651
analysis for rubidium in rubidium-doped, thalliated crystals of, using sodium tetraphenylboron, 17: 5989
analysis of iodine-125- or iodine-131-labeled, for impurities by paper chromatography, 20: 5515
analysis of iodine-131-labeled, by paper chromatography, 20: 16372
angular correlation attenuation coefficients for photopeaks measured by crystals of, 17: 32427
bibliography on uses in scintillation counting and spectrometry, 16: 4315 (ANL-6446)
bibliography on uses of crystals of, in scintillation counting and spectrometry, 16: 4315 (ANL-6446)
Born repulsive potential in crystals of, 17: 2062 (TID-17185)
calibration of crystals of, for gamma detection, 18: 7697(R) (TID-19931)
characteristics of thallium-activated crystals of, for whole-body counter, 16: 8950
coating for crystals of, reflective, 17: 6491(P)
cohesive energy of crystals of, Born analysis for, 17: 32084
corrosive effects on austenitic stainless steel, 19: 22893 (DP-957)
corrosive effects on titanium alloys at 650°F, 19: 44621 (CONF-651006-1)
counting efficiencies of thallium-activated crystals of, 17: 34261
crystal lattice dynamics of, 18: 14729
crystal lattice energy of, relation of self energy of gaseous ions to, 18: 16017
crystal lattice vibrations of lithium- and potassium-doped, 19: 14229(R) (AD-607917)
crystal lattice vibrations in, 17: 31181
crystal structure lattice dynamics of, eigenvalues and eigenvectors for, 20: 33262 (UCRL-14822)
crystal vibrations in impure, localized modes for determination of frequencies of, 18: 12103
cutting, mounting, and performance of crystals of, for use in gamma and x-ray spectrometers of 15 to 100 kev, 16: 3224
decomposition of stored solutions containing iodine-131, 17: 5693
development for well counters, 19: 29506(R) (GEAP-4845)
development of crystals of, for scintillation detector collimator system for gamma detection, 16: 27274
diffusion of iodine-131-labeled, through arachnoidal membrane, 18: 43206
effects on iodine-131 uptake by thyroid of children, 18: 8087
effects on NMR spectra of formamide, 20: 40805(R) (MLM-1325, pp 63-70)
effects on radioinduced changes in proteins, 20: 49
effects on self-diffusion of water at 23°C, 19: 32159
effects on thermal conductivity of sodium chloride, 19: 25783 (COO-1198-238)
efficiencies in cylindrical scintillation gamma detectors, table of, (T), 20: 29562
efficiency and peak-to-peak ratio for scintillation detectors of, absolute, 20: 41307
efficiency and resolution of thin crystal, in scintillation detector, 20: 18562(R) (EUR-2640.e)
efficiency for detecting gamma rays, 19: 44515
efficiency of crystals of, machine program for calculating, 16: 13278 (DC-57-10-63)
efficiency of crystals of, in scintillation detectors, 20: 11127
efficiency of thallium-activated, for protons, 18: 7050(R) (ORNL-3499 (Vol.II)(p.93-4))
efficiency of thallium-activated crystals of, gamma, 18: 25865
efficiency of thallium-activated scintillators, 19: 6926
efficiency of thallium-doped scintillators of, for x-ray detection, 20: 16836
electric breakdown strength of crystals of, 17: 35698 (TID-17035)
electric discharges in gaseous, in presence of argon or mercury, (E), 19: 6786
electron energy loss spectra at 0.8 and 1.5 Mev, 16: 12275
electron-positron annihilation in, 18: 28345
energy resolution of thallium-activated, device for measuring, 18: 30047
energy resolution of thallium-activated phosphors of crystals of, effects of various factors on, 16: 15340
energy resolution and pulse-height coefficients of thallium-activated, temperature dependence of, 20: 23476
etching of single crystals of thallium-activated, (E), 19: 22225(T)
evaluation of large thallium-activated crystals of, for measurement of radioisotopes in environmental samples, 16: 9055
evaporation from sodium, mechanisms of, 20: 40357 (NAA-SR-11766)
exchange reactions with ethyl, methyl, and propyl iodides in ethanol and methanol, 19: 11296
gamma absorption by, effective atomic numbers for, 19: 40069
gamma attenuation coefficients of thallium-activated crystals of, finite solid-angle corrections for, 17: 23778
gamma attenuation coefficients at 0.01 to 100 Mev, 20: 36350
gamma detection efficiencies of annular and well type crystals of, at 0.1 to 6 Mev, 17: 37419 (TID-17630)
gamma detection using thallium-activated crystals of, angular resolution correction in, (E), 19: 34492
gamma energy absorption at 122 kev to 2.62 Mev in thallium-activated, peak-total ratios for, 20: 19075
gamma photofractions for well-type scintillation crystals of, 20: 19076
gamma photopeak efficiencies of thallium-activated crystals of, for various geometries, 18: 18231
gamma reactions with thallium-activated, photo fractions for, 18: 29978 (KFK-188)
gamma reactions with thallium-activated crystals of, electron pair production cross sections for, (E), 19: 21294
gamma reactions with thallium-activated, absolute light yield from, 19: 42729
gamma reactions with crystals of, tables of efficiencies and photofractions for, 17: 4062 (TID-14059)
gamma response of thallium-activated crystals of, nonproportional, 19: 821
gamma spectra response of crystals of, computer analysis of, 16: 1030

(UCRL-9748)
gamma-ray attenuation factors for angular correlation and angular distribution measurements of crystals of, 16: 19135
gamma-ray detection using crystals of, 18: 22345(R) (UCRL-11184(p.86-90))
gamma-ray efficiencies of well-type thallium-activated crystals of, 17: 36150 (IS-606)
hardness of crystals of, 16: 10728
heat of solution in anhydrous ethylenediamine, 16: 5407(R) (TID-14329)
heat treatment effects on thallium-activated scintillators of, 18: 39649
injection into myocardium, tracer measurement of coronary blood flow by, 17: 28612
interaction of iodine-131-labeled, with iron oxide aerosols, 18: 12388 (UR-636)
intercrystalline energies in binary systems, 16: 7558
iodine-127 bonding in crystals of, quadrupole coupling effects on covalent, 16: 18275
iodine-127 chemical shift, E2 coupling, and spin-lattice relaxation in, 18: 12094
iodine-127 NMR spectra in, effects of iodine on, 20: 14573
iodine-127 nuclear quadrupole relaxation in, 18: 17812
iodine-129 gamma emission in crystals of, Debye-Waller factor and second order Doppler shift for, (T), 20: 20150
iodine-129 Mössbauer effect in crystals of, Debye-Waller factor for, (T), 20: 8297
ion association and hydration in aqueous solutions of, x-ray diffraction studies on, 20: 14228 (TID-22527)
ion self-diffusion in liquid, coefficients of, 17: 4513
ionization on rhenium, platinum–tungsten, and tungsten surfaces, 19: 16261 (UCRL-11606)
isotope exchange with organic iodides, electrochemical determinations of kinetics in, 18: 25424
light intensity from pure crystals of, dependence on absolute temperature, (T), 20: 22317
luminescence efficiencies of thallium-activated, gamma, 18: 20076
luminescence of thallium-activated, time pattern of, 17: 3590
luminescence of thallium-activated crystals of, 17: 21767
luminescence response to monoenergetic gamma radiation, (T), 19: 30520 (IDO-17017)
luminescence under combined gamma and neutron radiation, 18: 18219
luminescence yields of, absolute gamma, 19: 40593(T)
magnetic moment of molecular, rotational, (E), 20: 11484
metabolism in cattle, 18: 38775(R) (ORO-624)
metabolism of iodine-131-labeled, by monkey respiratory tract and thyroid, 19: 45776
metabolism of iodine-125-labeled, in lactating cows, 19: 45781
Mössbauer fractions and specific heats of diatomic lattices of, 19: 28321
neutron inelastic scattering by crystals of, 17: 4041
neutron scattering by crystals of, structure factors for cold, 17: 27392(T)
nuclear quadrupole coupling constants in crystals of, 16: 24654
nuclear spin diffusion in crystals of, interruptions in, 17: 4531
performance as counter on satellite, background activity induced by trapped protons in, (E), 19: 23524
performance in gamma spectrometry, 18: 34755 (IDO-16880-1)
performance in scintillation gamma spectrometers, 18: 20331 (KR-64 (Sect.X))
performance in scintillation camera for radiodiagnosis, 20: 25389 (UCRL-16724)
performance of crystals of, as gamma detectors for whole-body counters, 16: 16143
performance of crystal scintillation counters of, for gamma detection, 20: 19090
performance of detectors of, voltage-to-peak ratios for zero-thickness sources, 20: 41312
performance of radiation counters for whole-body counting, 20: 31443 (CONF-650673-1)
performance of scintillating for ground contamination isopleths, 20: 7358(R) (EGG-1183-2057)
performance of scintillation detectors of, for underwater use, 20: 31499 (AD-633752)
performance of thallium-activated, in gamma spectrometers, 18: 30015
performance of thallium-activated, for gamma detection, 19: 20358
performance of thallium-activated, for gamma detection, 19: 34557
performance of thallium-activated crystals of, for gamma ray detection, 17: 34858
performance of thallium-activated, for gamma spectroscopy, 20: 13067 (JUL-308-RB)
performance of thallium-activated, in gamma spectrometers, 20: 13098
photo-efficiency of thallium-activated crystals of, for uncollimated gamma rays, 17: 22013
photoemission yields at 10 to 21 ev, (E), 19: 11861
photofraction of cylindrical thallium-activated crystals of, for 0.32- to 2.76-Mev gamma radiation, 17: 32415
photoluminescence of indium- and thallium-activated, effects of excitation wavelength, temperature, and time on, 18: 12242
photon scattering to 14 ev, electron excitation in, (E), 19: 27716
photopeak efficiencies of thallium-activated crystals of, 17: 34262
physical properties of activated crystals of, 17: 22029
positron annihilation in, three-quantum, (E), 19: 10066
preparation and properties of thallium-activated crystals of, 17: 7121 (NP-12330(p.214-19))
preparation for use in x-ray diffraction studies, sealing process for, 20: 41328
preparation of carrier-free and high-specific-activity iodine-131-labeled, electrochemical method for, 20: 45778
properties as fast neutron detector, 18: 12456 (EIR-59)
properties of crystals of, as neutron detectors, 16: 14079
properties of crystals of, in luminescence chamber for scattering analysis, 16: 31918
protective effects against radiation damage in crop plants, 19: 43877
proton losses in crystals of, corrections for, (E), 19: 30567
pulse amplitude resolution in thallium-activated crystals of, 17: 10964
purification of iodine-131-labeled, by electrophoresis and chromatography, 20: 12918
purification of iodine-131-labeled, by paper chromatography, 20: 16372
purity of iodine-131-labeled, thin-layer chromatography tests for, 19: 30120
purity of radioactive, techniques for determination of, 17: 35651
quadrupole effects in, nuclear magnetic resonance study of, 19: 20620(R) (NYO-2024-8)
radiation background of scintillation spectrometer of, cosmic, 20: 11132
radiation effects on absorption of iodine-131-labeled, by rat skin, 17: 31957
radiation effects on thallium-activated crystals of, at 10^4 to 10^8 r, 18: 18201
radiation effects on scintillation properties of thallium-activated crystals of, 19: 24566(T)
radiation effects on luminescence and scintillation behavior of thallium-activated, x, (E), 19: 27725
radiation effects on crystal structure of, mechanism of beta, 20: 2426 (LA-3387)
radiation effects on thermoluminescence and trapping centers of thallium-activated, 20: 7160(T)
radiation effects on mechanical properties of, 20: 26975
radiation effects on thallium-activated, x, (T), 20: 41344
radiation effects on, effects of partial absorption on beta, 20: 40504(R) (ORNL-3922, pp 146-60)
radiation from thallium-activated crystals of, containing beta emitters, (E), 19: 34517
radioinduced bleaching of, neutron, 19: 11227(T)
radioinduced color centers in single crystals of, annealing of, (E), 19: 17974
radioinduced defects in single-crystal, 20: 35932 (LA-3501)
radioinduced light emission from thallium-doped packed crystal of, angular dependence of intensity from gamma, (E), 20: 23502
radioinduced luminescence of thallium-activated crystals of, effects of temperature on, 19: 11204
radioinduced luminescence of thallium-activated, effects of plastic deformation on, 19: 15625(T)
radioinduced luminescence of thallium-activated crystals of, x, (E), 19: 40908(T)
radioinduced luminescence spectra of thallium-activated crystal phosphors of, thermal and x, 19: 40568
radioinduced luminescence in nonactivated, origin of, 20: 8287 (ORNL-P-1701)
radioinduced luminescence of thallium-activated, spectral composition of, 20: 14611(T)
radioinduced luminescence of thallium-activated, excitation mechanism in x, 20: 17991(T)
radioinduced photoluminescence spectra of thallium-activated, x, (E), 20: 6537
radioisotope absolute standardization using, method for, 18: 1742
radioluminescence efficiency of thallium-activated, temperature dependence of α and x, 19: 9209
reactions in dioxane–water solutions, nuclear magnetic resonance spectra of, 17: 40800
reactions with dodecane and sodium bisulfide, 19: 40402 (BMI-X-10137)
reactions with Na_3Bi intermetallic compound, 19: 32924(R) (ANL-7020 (p.198-225))
reduction by high-frequency hydrogen discharge to hydrogen halide and metal, 19: 39180
reduction by high-frequency discharges in helium, hydrogen, and nitrogen, role of electrons in, 19: 39181
resolution of crystals of, in scintiscanners, 19: 42740
resolution response of crystals of thallium-activated, for electrons,

20: 43704
resolving power of thallium-activated crystals of, for beta particles, 19: 42750
resolving power of thallium-activated crystals of, mounting method for enhancement of, 17: 1769
response of crystals of, to gamma radiation, effects of nonproportional, 16: 11890
response of crystals of, to gamma radiation, 20: 5181(R) (ORNL-3029)
response of crystals of, to photons, 20: 4299(R) (ORNL-2711)
response of partially shielded crystals of, to gamma radiation, 16: 13305 (USNRDL-TR-543)
response of thallium-activated, to gamma radiation, 18: 43974
response of thallium-activated, to electron pairs and gamma radiation, 19: 823
response of thallium-activated crystals of, to gamma radiation in precipitates, (T), 19: 22540
response of thallium-activated crystals of, gamma, 16: 14083
response of thallium-activated phosphors of crystals of, to gamma radiation, effect of thermal treatment on, 16: 15342
response of thallium-activated crystals of, to diffracted x rays, 16: 19503
response of thallium-activated crystals of, to x rays and low-energy gamma rays, 16: 23879
response of thallium-activated crystals of, nonproportional, 16: 27354
response of thallium-activated crystals of, to low-energy charged particles, 17: 9055
response of thallium-activated crystals of, to K and L absorption boundary x rays, 17: 8643
response of thallium-activated crystals of, to high-energy electrons, 17: 20368
response of thallium-activated crystals of, to gamma radiation, 17: 22967(R) (IDO-16857)
response of thallium-activated crystals of, effects of, on single-crystal summing spectra, 17: 25891
response of thallium-activated crystals of, to x and γ rays, 17: 25310
response of thallium-activated crystals of, to heavy particles, effects of delta rays on, 16: 23880
response of thallium-activated, to electrons, 20: 5181(R) (ORNL-3029)
response to electrons at 0.6 to 1 Mev, 18: 33902
response to 150-Mev protons, ionization curves from, 20: 14891
samarium spectra in crystals of, at low temperatures, 18: 25406(T)
scintillation efficiencies of thallium-activated crystals, to gamma rays, 18: 18230
scintillation efficiencies of, for 0.3- to 1.5-Mev photons, 19: 6180 (AAEC/TM-268)
scintillation efficiency of tallium-activated, for gamma detection, computer program for calculating, 19: 11582
scintillation efficiencies of crystals of, for gamma radiation, 19: 39009
scintillation efficiency of thallium-activated crystals of, to gamma rays and electrons, 16: 20713
scintillation efficiency of thallium-activated, effect of temperature on, 20: 11118
scintillation in, energy dependence of gamma, 18: 2034 (UCRL-10986)
scintillation intensity of thallium-activated crystals of, measurement of time dependence of, by delayed-coincidence method, 16: 368
scintillation mechanisms in pure and thallium-doped, 18: 29797
scintillation of, thallium dimer in, 18: 22679
scintillation performance of thallium-activated crystals of, 16: 2967(R) (TID-14310)
scintillation performance of thallium-doped, activator concentration effects on, 20: 16850
scintillation processes in crystals of, 18: 33636
scintillation processes in thallium-activated, 18: 33636
scintillation process in, energy transfer and role of thallium dimers in, 20: 28608 (NYO-3408-5)
scintillation properties at low temperatures, 16: 20707
scintillation properties of thallium-activated crystals of, for counting aqueous cylindrical gamma sources, 19: 6193
scintillation properties of thallium-activated crystals of, 16: 33205
scintillation properties of thallium-activated crystals of, 17: 21768
scintillation properties of americium-241-doped thallium-activated crystals of, 20: 33664
scintillation properties of monocrystals of, impurity effects on, 20: 41347
scintillation resolving time of thallium-activated, 18: 23979
scintillation resolution of thallium-activated crystals of, effects of dislocations on, 16: 23882
scintillation response and stopping power for electrons and positrons in thallium-activated, 19: 15914
scintillation response of thallium-activated crystals of, to heavy ions, 16: 3847(R) (ORNL-3193(p.74-8))
scintillation response of crystals of, to alphas and protons, 16: 23883
scintillation responses of thallium-doped crystals of, to gamma radiation, 17: 14351
scintillation response of thallium-doped, to 5- to 1000-kev electrons, (E), 20: 12899
scintillation response to electrons and x rays, 20: 25373 (AD-631709)
scintillation yields for $2 < Z < 20$ ions, linear relation for, 20: 21084
sensitivity and origin of background of crystals of, used as gamma detectors in whole-body counters, 16: 16135
sensitivity to gamma rays, (T), 19: 13765
separation from spent fuel elements by extraction into nitrobenzene, 18: 6895
separation of iodine-131-labeled, from labeled Hippuran, 20: 45774
sodium-23 magnetic shielding in crystals of, 17: 21696
sodium-23 nuclear quadrupole relaxation in, 18: 17812
sorptive properties of, for cadmium-115, indium, mercury, and zinc-65, 17: 15992
spectra from thallium-activated, low-temperature, 20: 37441(T)
spectra of crystals of, effects of temperature and thallium concentration on absorption, 17: 21769
spectra of F-centers in crystals of, 17: 27377
spectra of fused, ultraviolet absorption, 17: 2461(R) (BNL-731(p.18-46))
spectra of, microwave rotational, 16: 29560
spectra of thallium-activated, pressure effects on absorption and emission, 18: 37130
spectral effects on infrared absorption of liquid ammonia–sodium systems, 16: 18856 (UCRL-10062)
stabilization system for detectors of, design of, 20: 7358(R) (EGG-1183-2057)
subcutaneous resorption in rat, effects of lethal x-radiation exposure, 17: 40665
thallium dimer properties in scintillation process of, 20: 28609(R) (NYO-3408-6)
thermal capacity at 5 to 260°K, 16: 32226
thermal expansion at low temperatures, 19: 42507
thermodynamic properties of, in heavy water, 20: 10847
thermodynamics of, in anhydrous *N,N*-dimethylformamide and *N*-methylformamide at 25°C, 20: 3926 (TID-22374)
time resolution of scintillators of, for gamma rays, 19: 26699
time resolution of scintillation detectors using thallium-activated, 20: 23456(R) (ANL-7108, pp 5-16)
time resolution of scintillation counters using thallium-activated, 20: 33662
tracer uses of iodine-131-labeled, for edema, 18: 33231(R) (NIRS-2 (p.49-56))
use for calibration of radioisotopes emitting gamma rays in coincidence, 19: 32276
use for standardization of radioisotopes with complex decay schemes, 19: 15654
use for thermal neutron flux measurements, 17: 4825
use in anti-Compton mantle of lithium-drifted germanium gamma spectrometers, 20: 27300
use in gamma coincidence counters, 20: 41295
use in gamma spectrometric measurements of radioisotopes, 19: 32545 (CEA-R-2461)
use in nanosecond x-ray scintillation detectors, 20: 41325
use of crystals of, for absolute standardization of beta emitters, 18: 7069
use of crystals of, in gamma spectroscopy, methods for decoding complex response in, 16: 14924 (TIM-637)
use of iodine-131-labeled, for tumor localization in man and rats, 17: 26992
use of thallium-activated, in measuring scandium-47 in samples containing calcium-47, 19: 7612
use of thallium-activated crystals of, for high-energy gamma detection, 19: 11568
use of thallium-activated, for standardization of gamma sources, 19: 13754
use of thallium-activated, in scintillation-type well logging device, 20: 29445(P)
use of thallium-activated crystals of, for detection of high energy gamma radiation, 20: 35746 (IEA-108)
use of well-type thallium-activated crystals of, for detection of gamma radiation from uranium-235 fission products, (E/T), 19: 40891
vibrational frequencies of crystals of, 16: 32221
volumetric properties in molten systems with potassium and sodium chlorides and iodides, 16: 539
x-ray scattering by crystals of, effects of anharmonic vibration on Debye-Waller factor for diffuse, (T), 19: 25630
AgI–NaI, phase diagrams, 20: 36787 (YALE-2723(Vol.1))
B_2O_3–$NaBO_2$–NaI, immiscibility diagram of liquid, 18: 40996 (USNRDL-TR-752)
B_2O_3–NaI, radioinduced defects in, ESR spectra of gamma, 20: 19256(R) (NYO-2024-9)
CdI_2–NaI, phase diagrams, 20: 36788 (YALE-2723(Vol.2))
KI–NaI, phase diagrams, 20: 36788 (YALE-2723(Vol.2))

methanol–NaI, properties for oxide particle suspension in centrifuges, 20: 36933
MgI_2–NaI, phase diagrams, 20: 36788 (YALE-2723(Vol.2))
NaBr–NaI, phase diagrams, 20: 36788 (YALE-2723(Vol.2))
NaBr–NaOH–NaI, solvent properties for metallic sodium, 18: 4275
NaCl–NaF–NaI, density of, temperature effects on, (E), 20: 21566(R) (ANL-7055, pp 213-29)
NaCl–NaF–NaI, properties in bismuth–sodium emf cells, 19: 17359(R) (ANL-6965(p.84-90))
NaCl–NaF–NaI, solvent properties for bismuth and sodium, 19: 24064(R) (ANL-6997)
NaCl–NaF–NaI, solvent properties for sodium and Na_3Bi intermediate compound, 19: 32924(R) (ANL-7020(p.198-225))
NaCl–NaF–NaI, solvent properties for bismuth–sodium alloys and sodium, 20: 6024(R) (ANL-6925(p.235-47))
NaCl–NaF–NaI, solvent properties for bismuth–sodium alloys, (E), 20: 21566(R) (ANL-7055, pp 213-29)
NaF–NaI, phase diagrams, 20: 36788 (YALE-2723(Vol.2))
NaI–H_2SO_4, radioinduced absorption spectra in, at 77°K, 20: 16534
PbI_2–NaI, phase diagrams, 20: 36788 (YALE-2723(Vol.2))

SODIUM IONS

binding in polyelectrolyte solutions, determination from tracer transfer rate coefficients, 20: 327
conductance in bentonites, relation between heavy water diffusion activation energies and exchangeable, 16: 13075
content in growing yeast cells, 20: 5251(R) (UR-668, pp 123-49)
content in Matsesta mineral water, 19: 655
desorption from tungsten surfaces, mass spectrometric study of, 20: 31907
detection and measurement of, scintillation detector for, 18: 5662
determination in perchloric acid solutions by Donnan membrane equilibrium, 18: 43403
diffusion in bentonite clay-water pastes, self-, 16: 20425
diffusion in bentonite–water systems, relation of activity to, 20: 33260(R) (ORO-648, pp 103-22)
diffusion in chabazites, self-, 17: 20029
diffusion in molten rubidium chloride and iodide, coefficients of, 17: 4513
diffusion in pure sodium chloride, 19: 17408 (COO-1197-9)
diffusion in silver chloride crystals, mechanism for, (E), 20: 15966
diffusion in sodalite, tracer and conductivity studies of, 19: 12869(R) (NYO-1154-1)
dissociation of fast negative, in rare gases, (T), 20: 29947
distribution between phases in boron oxide–sodium chloride–sodium oxide system at 830°C, 18: 33534 (USNRDL-TR-760)
distribution coefficient in zone melting of lithium fluoride, 19: 34144 (ORNL-3658)
effects of interlayer of, on cesium sorption by montmorillonite, 20: 12873
effects on adsorption of europium on barium sulfates, 19: 32306
effects on carbon dioxide radical (CO_2^-) ESR, 20: 20161
effects on electron spin resonance spectra of irradiated silicate glasses, 20: 42538
effects on far-infrared spectrum of potassium iodide, 19: 17405 (CONF-651-83)
effects on formation of single-crystal beryllium oxide, 20: 36814
effects on heated tantalum targets, secondary-ion distribution from, 17: 18912(T) (FTD-TT-62-1719)
effects on hydrogen yields in radiolysis of 2-propanol in water, 18: 13885
effects on oyster myocardium, 19: 14942
effects on radioinduced goldfish melanophores, 19: 189
effects on shift of laser emission of europium benzoylacetonate, (E), 19: 6455
effects on sorption of nitrogen, oxygen, and rare gases on zeolite for gas chromatographic separations, 18: 41328
effects on sorption of cesium-137 and rubidium-86 on tungsten ferrocyanide, 19: 15679
effects on sorptive properties of rhyodacite tuff for radioisotopes, 19: 48085
efflux from rat liver slices, relation to pyridine nucleotides, 20: 42758
efflux from rat liver slices, effects of potassium ion, glycosides, and antibiotics, 20: 42759
electron affinities of, relativistic and nonrelativistic, 17: 27996
electron configuration for, analytical solutions, 16: 10724
electron reactions below threshold to 1 kev, cross sections for single ionization in, (E), 20: 11490
electron scattering by, anomalous transmission effects in, 17: 620
emission by aluminosilicate emitters, mass-analysis of, 18: 30166(R) (AD-439716)
energy levels and wave functions for, (T), 19: 16370 (UCRL-7943-T)
energy levels and transition probabilities for, (T), 19: 18677 (ANL-6959)
energy levels of, (T), 20: 11450 (UCRL-7842-T)
energy loss in gases and solids, 16: 12295
enthalpy of formation in aqueous solutions, 19: 22167(T) (UCRL-Trans-1099(L))
entropy and heat of formation in aqueous solution, equation for calculation of, 18: 22066
exchange in lithium chloride resin systems, 16: 6414
exchange on Dowex 50 resins in ethylenediamine, 19: 13531 (ORNL-P-902)
exchange on iron hydroxide, 19: 13525 (KFK-216)
exchange on natural and synthetic exchangers, 16: 20356 (JÜL-32-RC)
exchange reactions in Dowex 50 and ethylenediamine–thiocyanate solutions, 18: 2127(R) (ORNL-3488(p.21-41))
exchange with barium on zeolite, thermodynamics of, 20: 18629(R) (NP-15353)
exchange with calcium ions, theory of sorption dynamics of, 18: 27463
exchange with hydrogen on thorium oxide and zirconium phosphate, kinetics, 16: 13050
exchange with potassium ions in solid potassium hexatitanate, 16: 13008(R) (TID-15006)
exchange with precipitated uranates in solution, 19: 15437(T) (ANL-Trans-33(p.127-41))
hydration numbers, 17: 30544
implantation in silicon, p-n junction production by, (E), 20: 46953
impurity effects on color centers in germanium-doped quartz, spectra of, 17: 35883
migration in fused sodium nitrate, isotope effect in, 20: 29185
mobility in clays, model for predicting rates of, 20: 25086
mobility in sodium vapor, 17: 8975
motion in air, density measurements from, 18: 37487(T) (NASA-TT-F-141(p.132-42))
orientation of water molecules in field of, 18: 5285
penetration in aluminum single crystals, channeling in, 18: 28098
production of plasma of, on hot rhenium plates, 17: 3613
radiation effects on diffusion of, in animal cells, 17: 30021
radiation effects on human erythrocytes flux of, x, 18: 15873
radiation effects on Carassius melanophore response to, x, 19: 31670(R) (NIRS-3(p.19-56))
radiolysis of aqueous solutions of, pulse, 19: 38728
radioprotective effects in mice, 18: 13567
range-energy relations in aluminum, (E), 19: 9893 (NAS-NRC-PUB-1133 (p.173-86))
ranges in aluminum, 17: 24139
reactions of monovalent, with dinonylnaphthalenesulfonic acid, effects of diluent on, 20: 43447
reactions with atoms and ions at 0.4 to 2 kev, radiation emission from, 18: 36145
reactions with cesium, rubidium, and sodium at 0.9 to 2.4 kev, charge exchange in, 18: 28265
reactions with gases at low energy, double charge exchange in, (E), 20: 27763
reactions with gas atoms and molecules at 1 to 30 kev, charge-exchange cross sections for, (E), 20: 34112
reactions with nitrogen at 0.4 to 2 kev, charge exchange and excitation in, 18: 32449
reactions with rare gases, energy losses in, 16: 4880
reactions with rare gases at 30 kev, energy distributions in, 17: 34649
reactions with tantalum and tungsten, temperature effects in sputtering, 19: 27102
scattering by molybdenum at 0.4 to 4 kev, secondary electron emission in, (E), 19: 14236(T) (ORNL-tr-467)
separation from alkali metal ions and mercury, silver and thallium, electrochromatographic, 16: 5273
separation from aluminum, calcium, and magnesium by ion exchange, 16: 17768
separation from aqueous solutions by ion exchange using silica gel, 19: 7328
separation from cesium by nitrobenzene, 17: 21720
separation from cesium ions by sorption on uranyl hydrophosphate, 19: 10978 (UJV-1193/64)
separation from spent fuel elements by extraction into nitrobenzene, 18: 6895
Slater-Condon parameters of, determined from spectral data, 17: 31118
slowing down in argon, deuterium, neon, and hydrogen at 50 kev, 18: 32288
solubility in heavy and light water at 25°C, activity coefficients of, 18: 19837(R) (MIT-905-1)
solvent extraction from molten nitrate by liquid silicone–TBP at 150°C, 19: 19833 (CEA-R-2628)
sorption of Amberlite, effects of anions on, 19: 46899(R) (ORNL-3832 pp 33-49)
sorption by cotton cloth, acidity effects on, 18: 35515
sorption by diallyl phosphate and polystyrene methylenephosphonic acid resins, 16: 13051
sorption by Dowex-5 in hydrobromic, hydrochloric, hydriodic, and perchloric acids, 16: 11607

sorption by silver iodide, tracer studies on, 20: 20683
sorption by uranyl hydrogen phosphate, 18: 43482
sorption from aqueous solutions by peat, 20: 7002 (INR-609/XIX/D)
sorption on tungsten, calculated heat of, 18: 37798 (NASA-TN-D-2460)
sorption on zirconyl phosphate ion exchange resins, 16: 10021
sorption on zirconium phosphates, tracer studies of, 19: 32293
spectra in Scylla plasma, x-ray, 17: 13639
sputtering ratio for polycrystalline copper, 16: 9114
toxicity of, in mouse, determination by LD_{50} on thirtieth day of, 17: 17719
transference numbers in pure liquid sodium nitrate, 17: 27345
uptake by barley roots, uranyl effects on selective inhibition in, 20: 20402
uptake by cheatgrass in greasewood forests, 20: 12575
van der Waals radii of, relation of hydration energy to, 18: 16016

SODIUM ISOTOPES
beta spectra, (E), 20: 35741 (CEA-R-2950)
distributions from proton reactions with aluminum at 660 Mev, angular and energy, 18: 7714
gamma reactions on, cross sections for, 19: 12496
nuclear energy levels and properties, survey, 16: 18483
preparation, determination, and properties of radioactive, 16: 1349
production by neutron reactions (n,γ) at 15 Mev, 17: 30159
production in helium ion and proton reactions with niobium at 240 to 880 Mev, cross sections for, 18: 42745
proton decay, 18: 18876 (KFK-185)
separation by amalgam exchange, calculation of coefficients for, 19: 18373
separation by ion exchange methods, coefficients for, 19: 11643
spectra of excited, 16: 13177(R) (NP-11413)

SODIUM ISOTOPES Na-20
alpha decay of, semiclassical approximation for, 17: 31415
alpha decay of, isobaric spin nonconservation in, 18: 38117
alpha decay spectra of, 19: 35615(R) (NP-15037)
energy in isobaric multiplets (T), 19: 3368
energy levels and mass for, 19: 12557
energy levels and mass of, measurement from neon-20(He-3,t) reaction, (E/T), 20: 24358(R) (UCRL-16580, pp 1-93)
mass, (E), 19: 19205
mass of, determination from Q values, (T), 20: 19273(R) (BNL-929, pp 3-43)

SODIUM ISOTOPES Na-21
beta decay of, model for relative period of, 17: 29632
beta-decay branching ratios in, 18: 26565
energy level deexcitation and spin, of 3.56-Mev, 18: 22878
energy level spacings, 16: 6018
energy levels, 16: 7097
energy levels and gamma spectra, 16: 31088
energy levels from neon-20(d,n) reactions, 16: 12458
energy levels from deuteron reactions (d,n) in neon, 17: 7170
energy levels from $Ne^{20}(d,n\gamma)$ reaction, 17: 19254
energy levels from neon-20 (p,γ) reactions at 1.17 Mev, (E), 19: 41838
energy levels of, measurement of first excited, 17: 7171
energy levels of, parity and spin of, 18: 19108
energy levels of, excited, 18: 32736 (NP-14092)
energy levels of, models for collective, (T), 19: 14518 (CONF-640301 (p.143-64))
energy levels of, collective representation of low-lying, (T), 19: 41757
energy levels, (E), 19: 5174
gamma de-excitation angular correlations and branching ratios, (E/T), 20: 34642
handling, 17: 21095
magnetic moment, spin, and hyperfine structure of 23-sec, (E), 19: 16970
nuclear density distributions of, from neon-20 (p,γ) reactions at 0.25–1.25 Mev, 17: 31473
nuclear structure of, rotation-vibration model for, 20: 6441
polarization of, measurement by optical pumping, 17: 21095
production, 17: 21095
production in nitrogen-14 reactions on carbon-12, cross sections for, (E), 19: 47667
proton emission from, intensity of delayed, (E), 20: 24407

SODIUM ISOTOPES Na-22
activity isolation in mixtures, inverse matrix method for, 18: 12176
activity of sources of, coincidence method for standardizing, 19: 34257 (NP-15101)
activity of sources of, γ-γ coincidence method for standardizing, 20: 33399
activity of, method for determining gamma, 20: 9196
beta decay, beta-gamma circular-polarization correlation parameters in, 16: 15683
beta decay, beta gamma circular polarization anisotropy in, 16: 28034 (PUC-1962-71)
beta decay matrix elements for, 18: 42724
beta decay of, high-energy gamma detection in, 17: 30885
beta decay of, angular correlations in, 18: 34752(R) (CU(PNPL)-234)
beta decay of, backward diffusion in aluminum from, (E), 20: 9982(T) (MLM-1285(tr))
beta decay of, beta–gamma directional correlation in, (E), 20: 3054
beta decay of, β-γ directional correlations in, (E), 20: 10089
beta decay of, circular polarization of gamma radiation following, 18: 21309
beta decay of, corrections for foil absorption in 4π counting of, (E), 19: 26654 (EUR-2248.e)
beta decay of, direct-interaction ionization probability for, (T), 20: 19934
beta decay of, energy of positron group from, (E), 20: 16867
beta decay of, higher order effects in allowed transitions in, (E), 19: 33325
beta decay of, ratio of electron capture to positron emission in, 18: 21245
beta decay of, spin dependence of Rayleigh scattering from, (E), 20: 3082
beta decay of, with electron pair formation in neon-22, (E), 20: 40134
beta decay, spectra of low-energy electrons accompanying, 16: 19801
beta emission, pseudoscalar interactions in, 16: 23116
beta polarization from, (E), 19: 16943
beta spectra corrections, 16: 12465
beta spectra measurements by solid-state detectors, 17: 32421
beta transitions in, comparative half lives of $\Delta I = 3$, (T), 20: 4874
beta transitions in, higher-order effects in allowed, (E), 20: 17678 (COO-1420-113)
binding of ionic, in polyelectrolyte solutions, 20: 327
calibration for radiodiagrams, 18: 34274(R) (NIRS-2(p.3-15))
calibration of, by sum peak method using sodium iodide crystal, 19: 32276
content and production in exosphere, 19: 14120
content in air samples collected at Richland, Wash., 1962, 1963, and 1964, 19: 2541
content in atmosphere, 1962 and 1963, 18: 43819
content in atmosphere, 1962 and 1963, 19: 22535 (HW-SA-3487)
content in atmosphere, 19: 46603
content in atmosphere, 1962 through mid-1964, 20: 8980(R) (BNWL-36, pp 3.1-122)
content in Bogou iron meteorite, 20: 16674
content in Canadian biota, 20: 4161
content in caribou and reindeer meat, 19: 44289 (HW-SA-3750)
content in Eskimo urine, 19: 44289 (HW-SA-3750)
content in fallout, food, and man, 20: 8980(R) (BNWL-36, pp 3.1-122)
content in food and man, study by coincidence gamma spectra, 18: 43372 (HW-SA-3680)
content in food and man, 20: 9166(R) (BNWL-36, pp 2.1-58)
content in food chain, ratio to fallout of, 20: 16678
content in food, 1962 and 1963, 19: 22535 (HW-SA-3487)
content in ground level air and precipitation, 18: 37865
content in Italian milk, 20: 20950
content in man, relation of content in milk and food to, 19: 20225
content in man, 1962 and 1963, 19: 22535 (HW-SA-3487)
content in Pribram meteorite, cosmic ray exposure flux from, (E), 20: 7688
content in rain water at Leghorn, Italy, 20: 18907
content in rain water, 1962-1964, 20: 43546
content in rainwater at Ispra during 1963 and 1964, 19: 34373
content in stone meteorites, gamma spectrometric study of, 18: 2515
content in stratospheric and tropospheric samples in Project Star Dust, 1963, 20: 16727(R) (HASL-168)
content in stratospheric and tropospheric samples in Project Star Dust, 1964, 20: 16728(R) (HASL-169)
content in urine, effects of diet on, 18: 43799 (HW-SA-3688)
content on air filters at Hanford, methods of gamma spectrometry for monitoring, 19: 620(R) (HW-81746(p.3.51-5))
contents in air in Hanford Works Area, 19: 13626 (HW-SA-3742)
contents in biological materials and rain water, 19: 13626 (HW-SA-3742)
decay in sun, 1.28-Mev gamma flux from, (T), 20: 27695
decay of, ratio of electron capture to positron emission in, 18: 2886
decay of, branching ratios for electron-capture, (E), 20: 19831 (NP-15912)
decay of, K-capture to positron ratios for, (E), 20: 15711 (CONF-233 (Vol. 2), pp 345-58)
decay of, positron polarization in, 18: 16552(R) (UCRL-11132)
decay of, shape of allowed positron spectrum in, 19: 3393
decay scheme, 18: 38097
decay scheme of, calibration of, 19: 33349
decay scheme of, removal of fictitious cascades from, 18: 21251
determination in aged actinium fluoride, 18: 29146(R) (MLM-1192)
determination in aqueous solutions by scintillation counting, 18: 29580
determination in atmospheric and precipitation samples, methods for radiochemical, 20: 14430 (AD-620219)

determination in aqueous solutions by precipitation with potassium perchlorate and counting, effects of quantity of sodium carrier on, 20: 35423
determination in Bruderheim chondrite, 16: 917
determination in meteorites, γ–γ coincidence, 16: 6887
determination in man, whole-body counting, 16: 16158
determination in man, whole-body counting, 16: 16155
determination in meteorites, 17: 12452 (LA-2765)
determination in milk, radiochemical, 19: 42433
determination in presence of iodine-131 using single-channel amplitude analyzer, 20: 22920
determination in stone meteorites, radiometric, 17: 10839
determination in urine, gamma spectrometric, 19: 32 (HW-SA-3641)
determination simultaneously with iodine-131 using single-channel amplitude analyzer, 19: 30121
diffusion coefficient in fused potassium nitrate–lithium nitrate, 18: 13741
diffusion in potassium chloride and sodium chloride, isotope effects on, 17: 617
diffusion in soda–alumina–silica glass, tracer study of, 20: 25062
diffusion in sodium nitrates, apparatus for measuring, 18: 29661
diffusion in sodium oxide–calcium oxide–silicon oxide systems, residual activity method for self-, 20: 16478
diffusion in sodium nitrates, effects of pressure on, 20: 38872(R) (NYO-1769-68)
diffusion of, current velocity measurement of natural waters by *in situ*, 18: 1906
diffusion of ionic, through squid axon membrane, 18: 29
effects of phototaxic behavior in Euglena, 20: 24889
effects on sodium ion diffusion in silver chloride, (E), 20: 15966
effects on sodium electromigration in fused sodium nitrate, 20: 29185
electron capture positron decay branching ratio of, exchange effects on Fierz interference term in, 18: 18902
electron pair production cross section near threshold, (E), 19: 21252(R) (UCRL-11828(p.35-8))
energy level population in (α,d) reactions, 18: 34779 (UCRL-11341)
energy level spectrum of, SU(3) method for shell model for, 19: 17030
energy levels, 18: 34821
energy levels, (E), 20: 12061
energy levels (E), 19: 1612
energy levels and gamma spectra, 16: 31088
energy levels and gamma spectra of, 19: 1589
energy levels from neon-22 (d,n) reactions, 16: 12458
energy levels from helium-3 reactions (He-3,$p\gamma$) with neon-20 at 5.35 Mev, (E), 20: 30400
energy levels of, from magnesium-24 (d,α) and sodium-23 (He^3,α) reactions, 18: 17055
energy levels of, $(d_{5/2})^1$ and $(f_{7/2})^1$, 18: 16933 (ANL-6848(p.182-7))
energy levels of, collective model for delayed gamma transitions of, 18: 28610
energy levels of, unified model wave function for low-lying rotational, (T), 20: 15814
energy levels of, wave functions in shell model for, 20: 28371
exchange between molten salts and sodalite, 19: 12869(R) (NYO-1154-1)
exchange in linear transfer system, interfusion effect in, 19: 2324
exchange in sodium chloride solutions, rate coefficients for, 20: 425
excretion of, effects of radiotherapy on fecal and urinary, 17: 21445
gamma dose constants for, 20: 46617
gamma emission by, methods of measuring, 20: 8870
gamma spectra, 16: 5518
gamma spectra, 16: 11883
gamma spectra, 16: 19081
gamma spectra, 17: 34967
gamma spectra, (E), 19: 14563
gamma spectra of, effects of nonlinear response of NaI(Tl) on single-crystal summing, 17: 25891
gamma spectra of, dependence of shape on measuring conditions of scintillation, 18: 18232
gamma spectra of, least-squares analysis of, 18: 33926
gamma spectrum of, 17: 22008 (LADC-5609)
gamma transition at 1274.6 kev, (E), 20: 3043
gamma transitions in, design of spectrometer for study of angular correlations of, 18: 2044
half life, 16: 2541
half life, 20: 16331 (GA-6568)
half life, 20: 8076 (NP-15663)
half life in patients with essential hypertension, biological, 16: 1454
half life measurements from 440-Mev proton reactions with stone meteorites, 17: 28943(R) (TID-18961)
measurement of activity in human body from diagnosis by whole-body counting, 19: 15284
metabolism by marine fish and invertebrates, 20: 26549(R) (NP-15915)
metabolism by monkeys, comparison with iodine-131, 18: 43179(R) (LA-3132-MS(p.84-92))
metabolism in tropical marine organisms, 16: 5132 (TID-14420)
mobility of ionic, in aqueous solutions of potassium nitrate at 25°C, 18: 23467
neutron cross sections, 17: 34278
neutron reactions (n,γ) with, cross sections for thermal, 18: 7777
nuclear structure of, configuration mixing and independent particle motion in, (T), 20: 12128
nucleon charge-independent pairing in nondegenerate $2s_{1/2}$ and $1d_{5/2}$ shells of, 20: 24453
nucleon clustering in, theory of, 18: 32851
nucleon interactions in, effects on 0°($T = 1$) levels, 18: 19092
photoproduction in linear accelerator at 20 Mev, 17: 30161
placental permeability studies using, review of, 18: 1345
positron decay of, measurement of polarization in, 18: 4610
positron emission, half life, and production of, 18: 5179 (TID-7673 (p.371-87))
positron spectra, 16: 1062
positron spectra, 17: 32424
positron spectra, 18: 42777
positron spectra, 18: 34783(T) (ORNL-tr-235)
positron spectra, 19: 6639 (TID-21387)
positron spectra of, shape of intense, 19: 15571(R) (TID-21385)
positron spectrum measurement, 17: 8634
preparation by irradiation of magnesium in cyclotron, 19: 40686
preparation of, from irradiated magnesium, 17: 15284
production and separation of, method for, 17: 10676 (NP-12231)
production by high-energy protons on elements $12 \leq Z \leq 50$, 19: 37835(R) (TID-22024)
production by proton reaction in aluminum at 29.7 to 50.6 Mev, cross sections for, 18: 18957
production in (α,n) reactions, 19: 33252(T) (ORNL-tr-627)
production in aluminum-27 (p,3p3n) reactions, cross sections for, 17: 11663
production in aluminum-27 (p,3p,3n) reaction at 155 Mev, cross section, 16: 13971
production in atmosphere, 19: 46603
production in chondrites by cosmic radiation, 18: 12365
production in cyclotrons, yields, 16: 12590
production in helium-ion reactions with aluminum-27, 16: 33814
production in neutron fission of uranium (IV) fluoride, 17: 33030
production in nitrogen-14 reactions on oxygen-16, cross sections for, (E), 19: 47667
production in proton reactions on magnesium, yields from, 17: 8153
production in proton reactions with magnesium and silicon at 130 to 400 Mev, cross sections for, 17: 28943(R) (TID-18961)
production in proton reactions with aluminum at 100 and 450 Mev, 17: 28943(R) (TID-18961)
production in proton reactions with magnesium and silicon at 130 to 400 Mev, cross sections for, 18: 22881
production in proton spallation on light elements at 29 Bev, 18: 28701
production in proton reactions (p,αpn) with aluminum-27 at 28.2 to 55.1 Mev, (E), 19: 27528
production in proton spallation of aluminum at 28 Bev, cross sections, 16: 29842 (BNL-6034)
production in proton reactions on aluminum-27 at 40 to 150 Mev, 17: 2274
production in Van Allen proton reactions, 16: 9761(R) (UCRL-9897 (p.131-3))
production in 20-Mev linear electron accelerator, purity and yield in, 19: 32836
production of, by 16-Mev cyclotron in Yugoslavia, 17: 17321
production of carrier-free, in ORNL cyclotron, 19: 22851 (ORNL-TM-1047 (p.72-6))
proton elastic and inelastic scattering, 17: 2313
radiation effects on efflux of, in isolated rat nerves, 19: 26087
scintillation spectra, relation to source thickness, 16: 4630
scintillator quenching by, 18: 20352
separation from cyclotron targets, 19: 40637(T) (ORNL-tr-625)
separation from deuteron-irradiated magnesium targets, 19: 44100
separation from sodium hydroxide amalgams, 17: 10508(R) (ORNL-3320(p.22-9))
sorption by burned and normal skin, 20: 14255
sorption by guinea pig skin, disappearance measurements of, 20: 32910
sorption in dogs, blood analysis determination of, 18: 4980
sorption in wounds, 18: 29218
sorption through burns and wounds in rats, 18: 29232
spectra of, design of 4π scintillation positron spectrometer for, 18: 4125
standards of, for diagnostic and therapeutic use, 17: 21744
tracer use in blood flow determination in human skin, 19: 36032
tracer use in gross atmospheric circulation, 19: 16247
tracer use in study of ion exchange between sodium borate and potassium chloride at 830°C, 19: 34150 (USNRDL-TR-847)
tracer uses for atmospheric-circulation studies, 17: 18302

transfer rate across isolated pericardium, 16: 31456
transport in hamster intestine, effects of heavy water and water on active and passive, 20: 18212
uptake and distribution of, in snail, 17: 17714
uptake and distribution of, in organs and tissues in mice and rabbits, kinetics of, 17: 21429
uptake and distribution in rats with renal function block and thyroidectomy, 19: 14981
uptake and transfer by oat seedlings, 19: 11535
uptake by cell nuclei in Chironomus salivary glands, 20: 24850
uptake by fresh and coagulated tissues of teeth, 20: 35217
uptake by lenses of galactose-fed rats, 20: 30978
uptake by species in reservoir, 19: 35926
uptake by strophanthin-treated rabbit erythrocytes, membrane permeability study of, 18: 17417
uptake of, by rabbit eye lens in culture, 20: 5256
use as gamma source in well logging, 20: 41165
use as tracer in studies of sodium metabolism in bone, 16: 31438
use as tracer, for skeletal metabolism studies, 20: 3664(R) (TID-22324)
use in hematology and radiodiagnosis, 18: 17695
use in measuring human sodium uptake, 18: 38754
use in radiodiagnosis, techniques for, 18: 29503
use in tracer studies in biology, 19: 58
uses of, diagnostic, 19: 24391
yields in proton spallation of copper at 24 Bev, 16: 24859

SODIUM ISOTOPES Na-23

alpha differential scattering cross sections at 18.4 Mev, 18: 40583
alpha reactions (α,p) at 3.6–5.3 Mev, gamma energy spectra and excitation function from, 18: 7704
alpha reactions (α,γ) with, distributions from, (E), 19: 14517 (CONF-640301(p.109-42))
alpha reactions (α,p) at 1.0 to 3.3 Mev, proton emission in, (E), 19: 14618
alpha reactions (α,p) at 19 Mev, distributions from, 17: 876
alpha reactions (α,p) at 22 Mev, angular distributions from, 17: 28288
alpha scattering at 18 Mev, (E), 20: 12099
alpha scattering at 18 Mev, cross sections for, (T), 20: 22134
content in urine after γ-radiotherapy, 17: 33696
deuteron reactions (d,p) at 9 Mev, proton angular distributions, 16: 3715
deuteron reactions (d,α) and (d,p), measurement of Q_0 values for, 16: 11038
deuteron reactions (d,p) and (d,t), excitation functions for, 16: 33888
deuteron reactions (d,p) at 7.8 Mev, 17: 33055
deuteron reactions (d,p) on, at 7.8 Mev, 17: 38164
deuteron reactions (d,n) at 2.5–3.0 Mev, angular distributions and energy level excitation in, 17: 38231
deuteron reactions (d,p) at 1.51 Mev, angular distributions and excited levels in, 18: 26659
deuteron reactions (d,α) at 9.3 Mev, 2I + 1 rule in, (E/T), 19: 23754
deuteron reactions (d,α) at 2.0 to 2.5 Mev, differential cross sections of, (E), 19: 39835
deuteron reactions (d,α) at 9.3 Mev, differential cross sections for, (E), 19: 41684
deuteron reactions (d,α) at 4.9 to 5.5 Mev, neon-21 excited states from, (E), 19: 47633
deuteron reactions (d,p) at 1.0 to 2.5 Mev, (E), 20: 1185
deuteron reactions (d,p) at 1.5 Mev, neutron-capture angular momenta for levels from, (E/T), 20: 22150
deuteron reactions (d,p) at 400 to 700 kev, total cross section for, (E), 20: 34538
diffusion in molten sodium nitrate at constant volume, 20: 38872(R) (NYO-1769-68)
electron energy level crossing effects in, (T), 19: 25152
electron g_J factor for, (E), 20: 36008
electron inelastic scattering at 58.5 Mev, 4.431-Mev excited state from, (E), 19: 43292
electron magnetic elastic scattering at 41.5 Mev, 17: 7222
electron reactions with, polarization of spectral line radiation by, (E), 19: 44956
electron scattering by, study of nuclear magnetic transitions by inelastic, 17: 19078
electron scattering by, 18: 9344
electron-spin-resonance spectra in rare-gas matrices at 4.2°K, 16: 23702
energy level at 4.431 Mev, properties of, 18: 42736
energy level at 440 kev, mean lifetime and width, 17: 5386
energy level distributions, (T), 19: 45313
energy level lifetimes, from resonance scattering of bremsstrahlung, 16: 26275
energy level of, 7.1-Mev (E), 19: 3344
energy level schemes, intrinsic states in, 16: 21407
energy level spacings, 16: 6018
energy level transitions in, 17: 11660
energy levels, 16: 23063
energy levels, 17: 2313
energy levels, 18: 19042
energy levels, 18: 19033
energy levels, 18: 34832
energy levels, 19: 23363(R) (NP-14954)
energy levels and gamma spectra of, 18: 17001
energy levels from proton reactions (p,α) with magnesium-26 at 9.90 Mev, 16: 26310
energy levels from deuteron reactions (d,n) in neon, 17: 7170
energy levels from neon-22 (p,γ) reactions at 1.28 to 1.86 Mev, (E), 19: 41838
energy levels from proton reactions (p,γ) with neon-22, (E), 20: 26113
energy levels from proton reactions (p,αγ) with magnesium-26 at 9.3 to 10.5 Mev, (E), 20: 32509
energy levels from magnesium-26 (p,αγ) reactions, gamma multipole mixing ratios and spins for, (E), 20: 32567
energy levels, ground state, 16: 6864
energy levels in, 16: 21498
energy levels of, spin of, 18: 13068
energy levels of, suitability of collective model for predicting excited, 18: 21327
energy levels of, excited, 18: 32736 (NP-14092)
energy levels of, models for collective, (T), 19: 14518 (CONF-640301 (p.143-64))
energy levels of, parity and spin of, (E), 19: 27530
energy levels of, collective representation of low-lying, (T), 19: 41757
energy levels of, low-lying J = ½, (T), 20: 44754
excited state of, mean life of first, 17: 24462
fallout of cosmic-ray-produced, 16: 16585
fluorine isotope reactions (F^{19},F^{18}) up to 43 Mev, 16: 21428
gamma de-excitation angular correlations and branching ratios, (E/T), 20: 34642
gamma reactions (γ,p) with, cross sections, (E/T), 19: 14528 (LAL-1120)
gamma reactions (γ,n) with, cross section for, 18: 2856
gamma resonance scattering by, level lifetimes from, (E), 20: 28334
gamma transitions from neon-22 (p,γ) reactions at 1.278 Mev, (E), 19: 41837
gyromagnetic ratio for, in $^2S_{1/2}$ ground state, (E), 20: 28415
helium-3 elastic scattering by, optical model analysis of, 18: 40638
helium-3 reactions (He^3,α), sodium-22 energy levels from, 18: 17055
helium-3 reactions (He-3,α) at 12 Mev, Q value for, 20: 16331 (GA-6568)
hyperfine structure of, Stark- and Zeeman-effect splitting of, 19: 23785
hyperfine structure of, crossing of Zeeman levels in, (T), 20: 9664(T)
hyperfine structure of $3^2P_{1/2}$ state of, in strong magnetic field, 20: 34107
hyperfine structure of $3^2P_{1/2}$ states of, (E), 20: 34108
ion reactions with, neutron-transfer mechanisms in, (E), 19: 37823(R) (ORNL-3800(p.1-49))
magnetic resonance in Rochelle salt, second order quadrupole shifts of, 17: 33930
magnetic shielding in alkali-halide crystals, 17: 21696
neutrino pair emission from excited states of, 19: 43366
neutron activation cross sections, 17: 10139
neutron capture by, total cross section for thermal, 17: 38024(T) (AEC-tr-5734(p.109-12))
neutron capture cross section at 14.7 Mev, (E), 20: 46614
neutron cross sections and nuclear data for, 18: 7680 (KFK-120(Pt.III))
neutron excitation cross section up to 4 Mev, 18: 32805
neutron inelastic scattering cross sections to 3.97 Mev by, 16: 26508
neutron inelastic scattering by, direct processes in fast, (T), 19: 43310
neutron inelastic scattering at 5.0 Mev, Q values for, (E), 20: 30360 (WASH-1068)
neutron radiative capture cross section from 1.0 to 19.5 Mev, (E), 20: 42332
neutron reaction (n,α) at 12.6 to 18.7 Mev, cross sections for, (E), 20: 40069(R) (EANDC(E)-66(U))
neutron reactions (n,2n) at 12.5 to 21 Mev, cross sections, 16: 5968
neutron reactions (n,γ) at fission energies, 16: 18429
neutron reactions (n,α) at 14 Mev, angular and energy distributions from, 16: 26245
neutron reactions (n,α) at 14 Mev, absolute cross sections, 16: 28083
neutron reactions at 14 Mev on, alpha distributions from, 17: 13511
neutron reactions (n,α) and (n,p) at 14.6 Mev, ratio of cross sections for, 17: 21034
neutron reactions (n,p) at 14 Mev, 17: 36410 (NP-13020(p.169-73))
neutron reactions (n,α), (n,γ), (n,2n), and (n,p) at 14.6 Mev with, cross sections for, 17: 40027
neutron reactions at 0.01 to 14 Mev, data compilation for, 18: 13039 (AEEW-R-254)
neutron reactions (n,γ) with, activation cross sections for short-lived isomers in, 18: 15219

neutron reactions with, cross sections at 13 to 21 Mev, 18: 16969
neutron reactions (n,α) at 14 Mev, 18: 17057
neutron reactions (n,γ), cross sections for, 18: 16947 (NP-13661)
neutron reactions (n,γ) with, spectra from resonant, 18: 26542(R) (ORNL-3582(p.71-5))
neutron reactions (n,n'γ) at 1.0 and 4.0 Mev, cross sections and spectra for, 18: 30736(R) (TID-20658)
neutron reactions (n,α) with, angular distribution for, 18: 34876
neutron reactions (n,α) at 14 Mev, direct-interaction model for, 18: 34769 (NP-14085)
neutron reactions (n,2n) at 12.5 to 16.5 Mev, cross sections for, (E), 19: 6666
neutron reactions (n,α), (n,2n), and (n,p) at 12 to 21 Mev, cross sections for, (E/T), 19: 10287
neutron reactions (n,2n) with, cross sections for, (E), 19: 5230
neutron reactions (n,2n) at 14 Mev, shell effects in, (T), 19: 12536
neutron reactions (n,p) at 14.8 Mev, cross sections for, (E), 19: 27516
neutron reactions (n,p), cross sections for, 19: 29228(R) (AEET/NP/10)
neutron reactions (n,2n) with, fission-averaged cross sections, 19: 29319
neutron reactions with, cross sections for fast, (E), 19: 33279
neutron reactions (n,2n) at 12.6 to 16.6 Mev, cross sections for, (E), 19: 35378(R) (EANDC(E)-57(U))
neutron reactions (n,d) at 14 Mev, angular distributions from, (E/T), 19: 47644
neutron reactions (n,p) at 14.8 Mev, cross sections for, (E), 20: 12133
neutron reactions (n,α) and (n,p) at 4 to 14 Mev, cross sections for, (E/T), 20: 13773 (IKF-13)
neutron reactions (n,p) with, sensitivity of, for activation analysis, 20: 16332 (GA-6691)
neutron reactions (n,2n) at 10 to 20 Mev, cross sections for, 20: 19810 (EUR-119.e(Vol.2))
neutron reactions (n,p) at 0 to 20 Mev, cross sections for, 20: 19810 (EUR-119.e(Vol.2))
neutron reactions (n,γ) with, cross sections for, (E), 20: 30360 (WASH-1068)
neutron reactions (n,p) at 14.8 Mev, cross sections for, (E), 20: 30394
neutron reactions (n,α),(n,αn') and (n,n'α) at 12.6 to 18.7 Mev, cross sections for, (E), 20: 32540
neutron reactions (n,p) at 14.8 Mev, cross sections for, (E), 20: 36212
neutron reactions (n,p) at 14.7 Mev, cross section for, (E), 20: 46614
neutron resonance integral, 17: 11979(R) (DP-805)
neutron resonance integrals and self-shielding factors for detector foils of, 17: 17106 (DP-817)
neutron scattering cross sections at 1.5 Mev, multiple scatter corrections by Monte Carlo, 16: 9454
neutron scattering at 0.5 to 4 Mev, cross sections for, 16: 23064
neutron scattering at 0.4 to 1.2 Mev, cross sections for, 18: 9331
neutron scattering at 0 to 4 Mev, nuclear model calculations of, 18: 24597 (NP-13930(p.15))
neutron scattering at 0.3 to 1.5 Mev, cross sections for, (E), 20: 34644
neutron threshold reactions with, cross sections for, 17: 36653 (EUR-119.e)
neutron total cross section at 900–2000 kev, 18: 11195(R) (EANDC(E)-49(L))
nitrogen ion scattering at 11 Mev, Coulomb excitation in, 18: 38128
nitrogen reactions (N^{14},α) with, 17: 24053(R) (ORNL-3432)
nitrogen-ion scattering at 16.2 and 17.7 Mev, gamma polarization from, (E), 20: 15759
nitrogen-14 reactions (N-14,α) at 27 Mev, angular momentum effects in, 18: 24726
nitrogen-14 reaction (N-14,O-15) at 27.5 Mev, excitation functions for, 18: 28573(R) (ORNL-3630(p.1-17))
nitrogen-14 reactions (N-14,p2n) with, excitation functions for, 18: 28573(R) (ORNL-3630(p.1-17))
nitrogen-14 reactions (N-14,α) with, quantum mechanical spin-cutoff parameters for, 18: 28573(R) (ORNL-3630(p.1-17))
nitrogen-14 reactions at 27 Mev, angular-momentum effects in, compound-nucleus, (E), 19: 12590
nuclear electric dipole moment of, 18: 30418
nuclear magnetic resonance in tungsten bronze, 16: 10568
nuclear magnetic relaxation in crystals below 900°K, 16: 18253
nuclear magnetic resonance, Knight shifts, 17: 635
nuclear magnetic resonance spectra of, in electrolyte solutions, 17: 27365
nuclear magnetic resonance at 30 to 120°C, 17: 34957
nuclear magnetic resonance in crystals, 17: 41569(T) (JPRS-21326 (p.69-80))
nuclear magnetic relaxation in sodium chloride at high temperatures, 18: 5293
nuclear magnetic resonance spectra in sodium bromide, chloride, and iodide, gradient-elastic tensor from quadrupole broadening in, 18: 16562
nuclear magnetic resonance in sodium chlorates, quadrupole splitting of, 18: 23464
nuclear magnetic resonance in sodium chlorides and fluorides, deformation effects on, 19: 7481
nuclear magnetic resonance of, chemical shifting by paramagnetic ions, 18: 25425
nuclear magnetic resonance in irradiated sodium chlorate single crystals, 18: 28095(R) (TID-20669)
nuclear magnetic resonance in sodium chlorates, population inversion of, 18: 27436
nuclear magnetic resonance in sodium tungstates, relaxation of, 18: 42194
nuclear magnetic resonance, Knight shifts, 18: 42036
nuclear magnetic resonance in sodium chloride crystals, dislocations from, 19: 17939
nuclear polarization in, dynamic methods for, 17: 13592
nuclear quadrupole coupling tensors in natrolite, 16: 14727
nuclear quadrupole coupling constants in alkali halide crystals, 16: 24654
nuclear quadrupole coupling in borates, 17: 7127 (NP-12330(p.295-301))
nuclear quadrupole coupling constants in sodium nitrite, temperature dependence of, 17: 10646
nuclear quadrupole interactions with impurity nuclei in sodium chloride, detection of spectra from, 18: 14630
nuclear quadrupole relaxation in sodium iodides, 18: 17812
nuclear quadrupole coupling in Rochelle salt, temperature dependence, 18: 28095(R) (TID-20669)
nuclear relaxation time in sodium halide crystals, 17: 16018
nuclear spin flop-in transitions, 17: 11299(R) (ANL-6612)
nuclear spin resonance, 17: 41967
nuclear spin temperatures at lattice temperatures of 10^{-6} °K in, NMR technique for, 18: 9283
nuclear structure of, rotation-vibration model for, 20: 6441
performance as solar neutrino detector, 20: 37793
performance in nuclear gyroscopes, (T), 19: 20279 (RTD-TDR-63-4001)
polarization in sodium chloride containing molecular chloride ions, (E), 19: 43497
production in atmosphere by cosmic radiation, 16: 16585
production in proton reactions (p,3p2n) with aluminum-27 at 155 Mev, cross section for, 17: 29621
properties of, for use as threshold detector in in-pile loops, 20: 26924(R) (MIT-334-48)
proton inelastic scattering by, resonance effects in Coulomb excitation from, 18: 2879
proton inelastic scattering by, excited states from, 18: 17071
proton inelastic scattering at 155 Mev, cross sections and energy levels from, (E), 20: 6354
proton inelastic scattering at 1.77 to 2.80 Mev, recoil-nuclei slowing down from, (E), 20: 28334
proton reactions (p,α) at 200 to 850 kev, resonances in, 18: 11263
proton reactions (p,γ) at 250 kev, angular distributions from, 18: 11275
proton reactions (p,γ) at 3.8 to 11.6 Mev, 18: 18949
proton reactions (p,γ) with, cross sections, 18: 34752(R) (CU(PNPL)-234)
proton reactions (p,pγ) at 828 to 1100 kev, excitation and resonances in, 18: 34836
proton reactions (p,γ), (p,αγ), and (p,p'γ) at 860 to 1470 kev, 18: 44824
proton reactions (p,pn) at 30 to 155 Mev (E/T), 19: 3313
proton reactions (p,α) at 1.416 Mev, resonance levels in, (E), 19: 5240
proton reactions (p,α) with, differential cross sections for, 19: 11525
proton reactions (p,α) with, cross section fluctuations in, (E), 19: 14499 (ANL-6878(p.457-77))
proton reactions (p,α) at 7.5 Mev with, cross sections for, (E), 19: 23643
proton reactions (p,p'γ), interference effect in excitation, (T), 19: 27457
proton reactions (p,γ) at 300 to 750 kev, gamma branching in, (E/T), 20: 6295 (NP-15647)
proton reactions (p,p'γ) at 1281 and 1456 kev, gamma angular distribution from, 20: 15846
proton reactions (p,t) at 39.8 Mev, (E), 20: 36176(R) (TID-22971, pp 41-140)
proton reactions (p,2p) at 155 Mev, proton energy spectra from, (E), 20: 42360
proton reactions (p,γ) at 0.3 to 2.1 Mev, resonance strengths for, (E), 20: 42182
proton reactions (p,αγ) with, parity of resonances in, (E), 20: 46707
proton reactions at 150 Mev, gamma spectra from, 16: 31088
proton reactions (p,pn), excitation functions, 16: 5963
proton reactions (p,γ) at 0.58 to 1.42 Mev, gamma emission, 16: 9458
proton reactions (p,α) at 6.9 to 7.3 Mev, angular distributions, 16: 10997
proton reactions (p,γ) at 300 to 750 kev, resonance effects, 16: 12486
proton reactions (p,p'γ), cross sections, 16: 19798
proton reactions (p,pn) at 20 to 155 Mev, excitation functions for, 16: 21484

proton reactions (p,γ) at 10 to 27 Mev, cross sections, 16: 23057
proton reactions (p,α) on, Q-values for, 17: 2291
proton reactions (p,γ) at 300–800 kev, parity and spin assignments for, 17: 24447
proton reactions (p,α) at 100 to 450 kev, 17: 31519
proton reactions (p,γ) Mg^{24} at 0.877 Mev, 17: 34906
proton reactions (p,α) at 3–12 Mev, angular distributions and excitation curves for, 17: 34916
proton reactions (p,2p) at 180 Mev, proton binding energies in, 17: 38229
proton reactions (p,p'γ) at 850 to 910 kev, interference between Coulomb excitation and inelastic scattering in, 17: 40065
proton reactions (p,α) at 1.5 to 6.0 Mev, threshold measurements on, 18: 6200
proton scattering by, 18: 7696(R) (ORNL-TM-761)
proton scattering at high-energies, spin-flip, 18: 38125
radiation effects on nuclear magnetic resonance of, in sodium chloride, 18: 13845
reactions with hydrogen gas at 10 to 50 kev, stopping powers from, 18: 32453
recoil energy and charge spectra from beta decay of neon-23, 16: 22996(R) (ORNL-3268(p.62-5))
recoil energy spectrum at 100 to 500 ev from beta decay of neon-23, 18: 2919
scattering by carbon, electronic stopping cross sections in, 17: 37670
separation from sodium hydroxide analgams, 17: 10508(R) (ORNL-3320(p.22-9))
spectra in alkali metal–ammonia solutions, Knight shifts and relaxation times in, 19: 7386
spectra of, effects of hydrogen, nitrogen, and rare gases on density shifts in hyperfine structure of, 19: 30951
spin-lattice relaxation time in sodium tungsten bronze, 16: 29552
superfluidity effects in, 18: 2951
thermal activation of bare and cadmium-clad foils of, 17: 36347(R) (NARF-62-18P)
triton reactions (t,p) at 5.89 to 5.96 Mev, energy levels from, 16: 17092
x-ray spectra of μ- and π-mesic atoms of, (E), 20: 34103

SODIUM ISOTOPES Na-24
accumulation in aquatic insects, 17: 5702 (HW-SA-2848)
activity determination by 4π beta-gamma coincidence method, corrections for, 19: 20385
activity in HNPF reactor systems, specific, 19: 38179 (NAA-SR-Memo-3830)
activity of, method for determining gamma, 20: 9196
activity suppression by boron-10, 19: 32058(R) (GA-5978)
angular distributions in gold-197 and uranium-238 (Na-20, Na-24) reactions at 130 Mev, (T), 19: 12539
atmospheric contamination with, in medical facilities, 18: 5156
atmospheric contamination with, in nuclear medical facility, 18: 5158
attenuation by tungsten single crystals at 0.25 to 160 kev, 18: 44457
behavior in sewage waste disposal, 17: 36061
beta activity of, design of 4π beta plastic scintillator for measurement of, 17: 6459
beta decay, 18: 21306
beta decay, beta-gamma circular-polarization correlation parameters in, 16: 15683
beta decay of, conserved vector current theory for, 17: 26556
beta decay of, β-γ circular polarization correlation from, (E), 20: 30542
beta decay of, charge dependence of nuclear forces in ΔT = ±1, 18: 19024
beta decay of, circular polarization of gamma radiation following, 18: 21309
beta decay of, Coulomb matrix elements and impurity coefficients in, 18: 28665
beta decay of, Fermi matrix element for, 18: 44781
beta decay of, Fermi matrix elements for, (T), 19: 35389 (KFK-313)
beta decay of, Fermi matrix element for, (T), 20: 19898
beta decay of, meson exchange effects in gamma circular polarization following, 18: 21269
beta decay strength of, coincidence method for determining, 18: 38177
beta spectra, (E), 19: 34609
beta spectra, small order form factor, 16: 31064 (IS-252)
beta spectra, source thickness effect in, 19: 31237 (SGAE-PH-13/1964)
beta spectrum, measurement of, 17: 38096
calibration of, by sum peak method using sodium iodide crystal, 19: 32276
clearance from human gastrocnemius muscle, 19: 8770
content and properties of, in food, 19: 18218
content in atmosphere, 1962 and 1963, 18: 43819
content in exhaust air from Canada-India Reactor, 19: 17356 (AEET/HP/TM-11)
content in Hanford personnel, 18: 36920 (HW-82409)
content in Hanford reactor effluent, 19: 685(R) (HW-81746(p.3.33-6))
content in Hanford reactor coolant, estimation of aluminum component corrosion from, 19: 925(R) (HW-81746(p.3.44-9))
content in man, calibration of shadow-shield whole-body counter for determining, 19: 27(R) (HW-81746(p.2.16-18))
content in personnel at Hanford, summary of whole-body counter results for 1960, 18: 35760 (HW-67245(Rev.))
content in PNPF coolant, monitoring standardization for determining, 20: 6615 (NAA-SR-10888(Rev.))
content in rain samples, 20: 8980(R) (BNWL-36, pp 3.1-122)
content in rain water, study by coincidence gamma spectra, 18: 43372 (HW-SA-3680)
content in rain water, 20: 43546
content in reactor effluent water, effects of sodium silicate addition on, 18: 36752 (HW-75782)
content in reactor effluent, effect of SiO_2 on, 20: 45215 (BNWL-282)
contents in biological materials and rain water, 19: 13626 (HW-SA-3742)
counting of, liquid-scintillation, 19: 10722
decay, beta-gamma circular-polarization correlation and isospin conservation in, 16: 21616
decay of, calibration of ionization chamber for particles from, 19: 6194
decay, polarization of electrons in beta, 16: 21614
decay schemes, determination methods, 16: 10667 (DC-60-1-106)
detection in body, calibration of whole-body monitor for, 18: 29875 (AEEW-M-334)
detection in gastrointestinal tract from drinking water, continuous monitoring system for, 20: 27191 (BNWL-SA-212)
detection in man, instrument sensitivity for, 18: 14196 (AEEW-M-335)
determination by photoneutron emission, 17: 35253(R) (IA-775)
determination in air, blood, urine, and water, radiochemical procedures for, 18: 13642 (SC-4783(RR))
determination in aluminum by beta counting, self-absorption coefficients for, 18: 13669
determination in atmospheric aerosols by activation analysis, 18: 29566(R) (NP-14096(p.17-22))
determination in aqueous solutions by Cherenkov counting, 19: 42581
determination in aqueous solutions by detection of Cherenkov radiation, 19: 46215
determination in blood by gamma spectrometry, 17: 5968 (PG-Report-385)
determination in copra and desiccated-coconut oils, activation, 20: 14463 (PAEC(D)CH-652)
determination in calcium-47, chromatographic, 20: 38827
determination in heavy-water moderator by sequential analysis, 18: 27287 (DP-886)
determination in IRL Reactor pool by gamma spectrometry, 17: 40702 (TID-7655(p.107-18))
determination in man, whole-body counting after neutron activation, 19: 22137
determination in neutron-irradiated clays and soils, 20: 43607
determination in organic reactor coolant, 18: 21553 (NAA-SR-Memo-7771)
determination in presence of bromine-82 and potassium-42 in serum and urine, 18: 9998
determination in phantoms, whole-body counter for, 18: 14260
determination in river water, activation, 17: 30185
determination in rain water, 18: 6205
determination in swimming pool reactor coolant, activation and chemical, 20: 38800 (PAEC(C)RE-652)
determination in urine, gamma spectrometric, 19: 32 (HW-SA-3641)
determination of, in man, whole-body counting, 18: 2021(R) (HW-77609 (Sect.2))
determination of levels in man after accidental neutron exposure, 17: 5775 (TID-14529)
determination of physicochemical state of, in liquid media by paper electrophoresis and radioactivity recording, 18: 33590
determination of, efficiency of Cherenkov counting methods for, 20: 31184
diffusion in potassium chloride and sodium chloride, isotope effects on, 17: 617
diffusion of ionic, through squid axon membrane, 18: 29
diffusion of sodium chloride-incorporated, through arachnoid membrane, 18: 43206
disappearance from uterus during normal and toxemic pregnancy, 16: 20116
dispersion of, caused by fire, 19: 40830 (SC-RR-65-98, pp 719-22)
distribution in soils exposed to nuclear detonations, 16: 12814 (WT-1117)
dosimetry for diagnostic and therapeutic use of, 19: 10930(T) (JPRS-27527)
dosimetry in animals using hematological changes, 20: 14314
dosimetry of, equation for internal, 20: 18955
effects on animals, physicological, 18: 41195
effects on blood and hematopoietic system, 20: 28982
effects on catecholamine metabolism in rats, 20: 28939

effects on conditioned reflexes of dogs, 20: 29009
effects on dog kidneys, 19: 3955
effects on dog nervous activity, 18: 38924
effects on gastric secretion in dogs, effects of food type stimuli on, 18: 11600
effects on rats, long-term, 18: 5133(T)
effects on reticulocytes in blood of rats, 16: 30287
effects on sodium ion diffusion in silver chloride, (E), 20: 15966
effects on stomach gland activity in dogs, 19: 3956
effects on vascularization of healing wounds in animals, 16: 1436
electron pair production cross section near threshold, (E), 19: 21252(R) (UCRL-11828(p.35-8))
elimination from body, methods for, 17: 1183
energy level densities in, effects of spin on, 16: 33853
energy level spacings, 16: 6018
energy levels, 18: 26659
energy levels and gamma spectra, 16: 26254
energy levels at low excitation in, rotational band assignments for, 18: 19031
energy levels at 630 to 860 kev, 16: 3724
energy levels from deuteron beam reactions with light nuclei, 16: 11040
energy levels from sodium-23 (d,p) reactions, neutron-capture angular momenta for, (E), 20: 22150
energy levels from magnesium-26 (p,He-3) reactions, isobaric analogue, (E), 20: 44758
energy levels of, thermal neutron activation cross sections of isomeric, 17: 38024(T) (AEC-tr-5734(p.109-12))
energy levels of, unified model wave function for low-lying rotational, (T), 20: 15814
energy levels up to 7 Mev, 17: 33055
energy spectra and yields in proton reactions with copper, silver, and bismuth at 1.84 Bev, (T), 20: 12067
exchange between alkali metal ions and precipitated uranates in solution, 19: 15437(T) (ANL-Trans-33(p.127-41))
fluoride contamination with, method for preventing fluorine-18-labeled, 19: 33764
gamma angular correlations for, 18: 30772
gamma dose constants for, 20: 46617
gamma dose level from, in IRT-2000, 20: 36532
gamma dose rate from, design of slide-rule calculator for, 17: 39316 (RCC-R-165)
gamma specific emission coefficient, 17: 6431 (CEA-2036)
gamma spectra, 16: 18467
gamma spectra, 16: 20628 (ANL-6499)
gamma spectra, 17: 16438
gamma spectra, 17: 34966
gamma spectra, 20: 44634(R) (IDO-17188)
gamma spectra and half lives of millisecond isomeric, (E), 20: 28431
gamma spectra of, effects of nonlinear response of NaI(Tl) on single-crystal summing, 17: 25891
gamma spectra of, high-energy, 16: 28074
gamma spectra of, computer program for determination of, 19: 18387
gamma spectrum, 18: 18174 (BRL-1230)
half life, 16: 2541
half life, 17: 11628 (TID-15849)
half life measurements from 440-Mev proton reactions with stone meteorites, 17: 28943(R) (TID-18961)
half life, biological, 16: 1498(T) (JPRS-10469)
hyperfine structure and magnetic moments of, (E/T), 20: 19273(R) (BNL-929, pp 3-43)
incorporation in sodium chloride aerosols, 19: 20027
leakage from radioisotope packages after fire tests, 19: 40831 (SC-RR-65-98, pp 723-31)
mass difference between, and aluminum-24, analysis of, 18: 44781
measurement of steam-water specific gravity in boiler, 17: 6378
metabolism in mercaptamine-treated rats used to study sodium balance, 19: 33792
mobility of ionic, in aqueous solutions of potassium nitrate at 25°C, 18: 23467
movement of, within an ice-covered lake, 18: 10270
neutron activation of, in burros and phantoms, 16: 28998
neutron activation in bone samples, 16: 31438
neutron reaction (n,p), resonance doublet configurations from, 16: 29781 (JINR-P-999)
neutron reactions (n,α) at 14 Mev, nuclear shell effects in cross sections for, 18: 18977
neutron reactions with, gamma radiation from, 18: 30735(R) (TID-20657)
neutron separation energy, (E), 20: 24329(R) (ANL-7108, pp 1-4)
nuclear magnetic moment and hyperfine structure, (E), 20: 46740
nuclear structure, 17: 38164
nuclear structure, 18: 19031
penetration of nerve cord in cockroach, 16: 16117
permeability of dog renal tubules to, 18: 29228
permeability of mammary gland to, 16: 5142
positron spectra of, effects of backscattering on, 18: 7076
preparation and properties of, for use as neutron sources, 18: 16379
preparation for magnetic beta spectrometers, 19: 34609
preparation for medical uses, 17: 7713
production and use of, 17: 6171
production at PRR, methods for, 20: 12545(R) (PAEC(A)AR651)
production by high-energy protons on elements $12 \leq Z \leq 50$, 19: 37835(R) (TID-22024)
production by neutron reactions (n,α) and (n,p), 17: 30165
production by neutron irradiation of aluminum oxide and magnesium carbonate, 18: 32000(T) (ORNL-tr-230)
production by neutron irradiation of magnesium oxide, 18: 31999(T) (ORNL-tr-191)
production by neutron reactions (n,α) and (n,p) reactions with aluminum-27 and magnesium-24, 19: 2701
production by neutron irradiation of aluminum foil and magnesium carbonate, 19: 15610
production by proton reaction in aluminum at 29.7 to 50.6 Mev, cross sections for, 18: 18957
production cross sections for, target mass dependence of, 17: 28247(R) (TID-18788)
production in aluminum-27(n,α) and magnesium-24(n,p) reactions in JRR-1, 16: 17730
production in aluminum-27 (p,3pn) reactions, cross sections for, 17: 11663
production in aluminum-27(n,α) reactions, forward-backward asymmetry of, 17: 19336
production in aluminum-27 (n,α) reactions, 18: 24592 (NP-13913)
production in asbestos cement by neutron irradiation, quality control by, 20: 21204
production in atmosphere by neutron activation of airborne dust, inhalation hazard from, 19: 26589
production in carbon-12 reactions with aluminum-27 at 3.0 to 126.0 Mev, 16: 9460
production in cosmic radiation reactions with argon, 18: 6205
production in helium ion and proton reactions with copper, gold, silver, and uranium, 16: 2498 (UCRL-9683)
production in helium-ion reactions with aluminum-27 and magnesium-25, 16: 33814
production in helium ion and proton reactions with copper, gold, silver, and uranium at 320 to 880 Mev, 17: 31525
production in nitrogen-14 reactions with aluminum-27 at 8.0 to 147.0 Mev, 16: 9460
production in nitrogen-14 reactions on carbon-12, cross sections for, (E), 19: 47667
production in oxygen-16 reactions with aluminum-27 at 8.0 to 168.0 Mev, 16: 9460
production in proton reaction on heavy nuclei at 660 Mev, 16: 29864
production in proton reactions with magnesium and silicon at 130 to 400 Mev, cross sections for, 17: 28943(R) (TID-18961)
production in proton reactions with iron at 1 Bev, cross sections for, 17: 28943(R) (TID-18961)
production in proton reactions with simulated stone meteorites at 1 Bev, 17: 28943(R) (TID-18961)
production in proton reactions with aluminum at 100 and 450 Mev, 17: 28943(R) (TID-18961)
production in proton reactions with iron at 450 Mev, 17: 28943(R) (TID-18961)
production in proton fragmentation of bismuth at 2.9 Bev, 18: 15284
production in proton reactions with magnesium and silicon at 130 to 400 Mev, cross sections for, 18: 22881
production in proton reactions with silver at 2.9 Bev, range studies of, 18: 26648
production in proton spallation of chlorine, copper, and vanadium, energy spectra of, 19: 8453
production in proton reactions on magnesium, 19: 37835(R) (TID-22024)
production in proton spallation of aluminum at 28 Bev, cross sections, 16: 29842 (BNL-6034)
production in proton reactions for, cross sections, 17: 17149
production in proton reactions on aluminum-27 at 40 to 150 Mev, 17: 2274
production in reactor by neutron reactions (n,α), 17: 24508
production in reactors, 17: 29943
production in reactors, 17: 29945
production in tissues by neutron activation, 18: 38729
production in Van Allen proton reactions, 16: 9761(R) (UCRL-9897 (p.131-3))
production of carrier-free, 18: 12523 (SGAE-1963/3B)
production of carrier-free, by neutron irradiation of magnesium, 18: 43675
production of ground-state and isomeric, in carbon-12 (N-14,2p) reactions at 20 to 65 Mev, (E), 19: 29242 (JINR-E-2012)
production of high-specific-activity, by irradiation of aluminum and dissolution in acid, 19: 11649

production of isomeric, in neutron activation of aluminum and magnesium at 14.3 Mev, (E), 20: 19809 (CEA-R-2900)
production of short-lived isomer of, by thermal neutron reactions (n,γ), cross sections for, 18: 15219
production of, facility for, 18: 38550 (A/CONF.28/P/816)
production of, method for, 19: 11647
production using Rossendorf Reactor in East Germany, 19: 20436
proton inelastic scattering by, dispersion formulas for, 17: 34906
radiation effects on passage of, in central nervous system in rats, 17: 28746
radiation effects from small doses of, used in radiodiagnosis, 18: 38896
radiation effects from injected, on metabolism of electrolytes and nitrogen in dogs, 20: 5381
radioinduced in asbestos cement products by neutrons, tracer use of, 20: 16920 (SGAE-IB/IA-7/1965)
radiotherapy of cancer using, 18: 29485
range distributions in amorphous oxides at 0.5 to 160 kev, 18: 36588
range in aluminum at 1 to 100 kev, 17: 36675
ranges in aluminum, interatomic potential from, (T), 19: 20837
recoil and range in aluminum during high-energy proton bombardment, 17: 7230
recoil in neutron reactions (n,α) with aluminum-27 at 14.8 Mev, ranges for, 18: 2859
recoil range in aluminum from neutron reactions (n,α) with aluminum-27, 17: 41910
recoil range of, from (n,α) and (n,p) reactions with aluminum-27, 18: 44765
resorption by rabbit muscles, 17: 30266
sensitivity for activation analysis using beta-gamma-gamma sum-coincidence gamma spectrometer, 20: 16335(R) (NBS-TN-276)
separation by electromagnetic methods for use as radiation source, 19: 4570 (SGAE-PH-6/1964)
separation from aluminum-27 reaction products by vaporization, 19: 24601(P)
separation from neutron-irradiated biological materials, use of Szilard-Chalmers effect in, 20: 18583
separation from neutron-activated biological samples, 20: 45312
separation from potassium-42, electrophoretic, 18: 33590
separation of ionic, at submicromolar concentrations by paper electrophoresis, 16: 17710
separation using ion exchange, 19: 2424
sorption by Columbia River particulate material, 18: 35761 (HW-79279)
sorption by skin, effects of calcium chloride and salt bath concentration on, 16: 4027
sorption from reactor effluent by particles in Columbia River, 19: 215(R) (HW-81746(p.3.81))
sorption on porous carbon electrodes, spectra of ion movement in chromatographic, 19: 36271
sorption rate in rabbit muscle with ligated vena femoralis, 18: 9830
standards of, for diagnostic and therapeutic use, 17: 21744
toxicology of, in rabbits, 18: 4995(T)
tracer applications in industry, 17: 6372
tracer use in flow-rate and leak measurements, 17: 6376
tracer use in measurements of arterial blood circulation, 19: 10973
tracer use in subterranean water flow measurements, 17: 6377
tracer uses in biology, 18: 36915
tracer uses in studies of blood circulation in muscles, 18: 38755
transfer from blood to bile in guinea pigs, 17: 33528
transport of, in lakes in Wisconsin, 17: 4715
uptake by infected regions in guinea pigs, 17: 35433
uptake from tooth cavities in dogs, 20: 45303
use as beta source for therapy, 20: 8799
use as tracer for measuring Columbia River flow times, 20: 20916
use as tracer in pulp and paper research, 17: 32328
use for determining efficiency of water treatment plants, 19: 2671
use for determining action of diuretics in swine, 20: 12613
use for flow measurement of rivers, 18: 1912
use for measurement of dilution and flow of rivers, 18: 1933
use in clinical diagnosis with ORINS linear scanner, 16: 7704
use in detection of irrigation water storage leaks, 17: 6371
use in measurement of myometrial blood flow during pregnancy, 20: 38747
use in measurements of sodium ion efflux from rat liver slices, 20: 42758
use in measuring efficiency of absolute filters, 18: 6974 (RISO-66)
use in medical diagnostics, 19: 46136
use in placental permeability studies, review of, 18: 1345
use in radiodiagnosis, review on, 19: 38505
use in studies of sodium ion efflux from rat liver slices, 20: 42759
use in study of calcium uranate precipitation from solution, 19: 15448(T) (ANL-Trans-33(p.203-12))
use in studying mixing process in artificial coal production, 19: 24888
use in testing high-efficiency filters, 19: 44281 (AEET-202)
use in tracer studies of mass transport of sodium chloride in vapor phase, 18: 22058
use in tracer studies in biology, 19: 58
use in water to study flow and soil absorption, 17: 25533
use of body activity as measure of neutron dose, 16: 33196
uses as gamma source for detection of flaws in steel foils and plates, 20: 29390
uses for tracing movement of beach sediments, 19: 13830
yields from high-energy proton reactions, 20: 18556(R) (BNL-929, pp 66-82)
yields in proton spallation of copper at 24 Bev, 16: 24859

SODIUM ISOTOPES Na-25
energy levels, 16: 17092
energy levels, 16: 21627
gamma dose constants for, 20: 46617

SODIUM ISOTOPES Na-26
preparation and decay, 17: 26633

SODIUM LACTATES
effects on pH of dialyzed zirconyl chloride, 17: 35718
use in cation exchange of rare earths and yttrium, 19: 24432

SODIUM LANTHANUM NITRATES
formation, 19: 7363

SODIUM LANTHANUM SULFATES
solubility and metathesis, in nitric acid, 19: 46428(R) (ORNL-3847)

SODIUM MANGANESE FLUORIDES
magnetic structure, 18: 35493 (BNL-7278)

Sodium Metaborates
see Sodium Borates

Sodium Metatantalates
see Sodium Tantalates

SODIUM METHOXIDE
radiation effects on, ESR spectra following, 18: 37240
reactions with *p*-nitrobenzyl chloride, mechanism of, 19: 32048(R) (NP-15073)
reactions with 2,2-diphenylethyl benzenesulfonate, effects of deuterium and tritium on, 20: 38912
methanol–sodium methoxide, perfluorocarbanion formation in deuterium–hydrogen exchange in monohydrofluorocarbons in, 18: 25451

SODIUM MOLYBDATES
analysis for oxygen-18, mass spectrometric, 20: 8852
analytical use in titrimetric determination of cerium, 18: 25287
analytical use in amperometric determination of zirconium, 18: 39137
analytical use in conductometric determination of yttrium, 20: 35433
effects on hydrolysis of lactose in oxygen-18-labeled water, catalytic, 19: 30177
heat of solution and thermodynamic properties of, in sodium nitrate, 18: 5283
hydrolysis of, acidity measurements, equilibrium ultracentrifugation, and Raman spectra of aggregates in, 18: 22035
molecular condensation in reactions with nitric acid, conductometric studies of, 17: 10611(T) (UCRL-Trans-894(L))
oxygen isotopic exchange in melts of, at 700 to 955°C, 19: 40506
oxygen-17 NMR in, 17: 3645
oxygen-18 exchange between gaseous oxygen and, mechanism and rate of, 20: 422
photosensitivity of, effects of titanium dioxide on, 20: 10837
production, properties, and structure of, 19: 44021
radioinduced molybdenum pentavalent ion formation in, ESR study of gamma, 20: 25153
reaction of, with thorium for quantitative precipitation of thorium molybdate, 17: 27457
solvent partition in aqueous nitric and perchloric acids, 18: 10191
spectra of crystalline, infrared and Raman, 18: 1613(R) (ORNL-3488 (p.18-20))
spectra of, infrared and Raman, 18: 29641
structural properties, 17: 14210 (NBS-MON-25(Sect.1))
uses in titrimetric determination of thorium, 20: 29092
$H_4Fe(CN)_6$–Na_2MoO_4, ion exchange properties for cesium-137 and strontium-90, 20: 3871 (EUR-2497.e)
$LaMoO_4$–$NaMoO_4$, preparation and properties of monocrystalline, as laser material, 20: 7064
$NaMoO_4$–$TbMoO_4$, preparation and properties of monocrystalline, as laser material, 20: 7064
$NdMoO_4$–$NaMoO_4$, preparation and properties of monocrystalline, as laser material, 20: 7064
$PrMoO_4$–$NaMoO_4$, preparation and properties of monocrystalline, as laser material, 20: 7064

SODIUM NEODYMIUM FLUORIDES
crystal structure, 19: 30167
crystal structure, 19: 30149(R) (ORNL-3789(p.3-35))
crystal structure, 20: 17158(R) (ORNL-3900, pp 82-149)

SODIUM NEODYMIUM TUNGSTATES
spectra of, diffuse reflectance, 18: 13689

SODIUM NEPTUNIUM FLUORIDES

crystal structure of $Na_7Np_6F_{31}$, 20: 38898
SODIUM NIOBATES
see also Potassium Sodium Niobates
crystal structure of, at 0 to 900°C, 17: 23862(R) (AD-286036)
crystal structure, 19: 37059
electric properties of pure and vanadium-doped, up to 150 kv/cm, 16: 22745
occurrence of mineral, in Colorado, 17: 1646
phase transformations in, x-ray study of, 18: 6826(T)
polarization of, spontaneous, 17: 8024
reactions with hydrogen peroxide at 0°C, 16: 30391
structure at high temperatures, 19: 7843(R) (AD-420637)
$LiNbO_3$–$NaNbO_3$, phase studies and electric properties, 16: 23687
$NaNbO_3$–$NaTaO_3$, phase relations in solid state, 17: 18060
$NaNbO_3$–$NaTaO_3$, phase studies, 18: 24162
$NaNbO_3$–$Sr(NbO_3)_2$, phase studies and electric properties, 16: 23687
SODIUM NITRATES
analysis for trace elements by activation methods, isotopic ion exchange in, 20: 33193
analytical use for ion exchange separation of americium, curium, and rare earths, 20: 18562(R) (EUR-2640.e)
association constants in molten, 17: 28829(R) (TID-18959)
association of silver ions with bromide and chloride ions in molten, 19: 34142(R) (NYO-2873-7)
beta reactions with, Cherenkov radiation detection in, 20: 5792
cation exchange of thallium nitrate mixtures with, with zeolites, 17: 35253(R) (IA-775)
corrosion inhibiting effects on carbon steel, 19: 21714 (RL-REA-592)
corrosive effects with radiation on metals, 16: 17976(R) (EURAEC-94)
corrosive effects on high-strength alloys and steels under static stress, 16: 25717(R) (NP-11948)
corrosive effects on zinc, tracer studies on, 18: 25927
crystallization from melts, fission product uptake and separation in directional, 19: 40683
decomposition by deuterium and helium ions at 2 to 16 kev, 17: 28984
diffusion and electric mobility of ions in, tracer study on, 20: 16414 (CEA-R-2806)
diffusion of alkaline earth ions in fused, tracer studies of, 20: 25085
diffusion of cesium and sodium in, coefficients of, 20: 38871(R) (NYO-1769-54)
diffusion of cesium-134 and sodium-23 in molten, at constant volume, 20: 38872(R) (NYO-1769-68)
diffusion of silver in, coefficient and heat of, 18: 12087
diffusion of sodium-22 in, apparatus for measuring, 18: 29661
diffusion of sodium-22 in, effects of pressure on, 20: 38872(R) (NYO-1769-68)
effects of fused, on efficiency of mineral ion exchangers, 20: 10958
effects on dissolution of plutonium dioxide and uranium dioxide pellets in nitric acid, 19: 20050 (ORNL-3695)
effects on methemoglobinemia formation in irradiated and non-irradiated rabbits, 19: 26021
effects on nitrogen-15 exchange between nitric acid and nitric oxide, 20: 9363(R) (NYO-755-2, Paper 3)
effects on nitrogen-15 concentration by nitric acid–nitric oxide exchange, 20: 31639(R) (NYO-755-1, pp 77-129)
effects on nitrogen-15 exchange between nitric acid and nitric oxide, 18: 2132(R) (TID-19592(Sect.IV))
effects on oxygen balance in bone marrow and brain of rabbits, 18: 19801
effects on pH of dialyzed zirconyl chloride, 17: 35718
effects on plutonium analysis, 16: 125 (CEA-1977)
effects on preparation of iodine-131-labeled hippuran, 20: 43403
effects on radiolysis of aqueous sodium hydroxide glasses at 77 to 150°K, 20: 45730
effects on radiosterilization of hams, 16: 4005 (NP-11113)
effects on solvent extraction of cobalt acetylacetonate using isopropyl alcohol, 20: 7211
effects on sorption of dyes by labeled barium sulfate, 18: 39305
effects on sorptive properties of ammonium phosphotungstate for fission products, 17: 34062
effects on wholesomeness of radiation processed meat, 20: 700 (AD-621921)
effects on yields in radiolysis of nitrous oxide aqueous solutions, 18: 31601
effects on yields in radiolysis of deuterated sodium formate aqueous solutions containing nitrous oxide, 18: 31602
electric conductivity of fused, d-c measurements of, 18: 13719 (IS-667)
electric conductivity of molten, direct current measurement of, 18: 26018
electrodeionization in resin packed beds, 18: 21999 (AERE-R-4517)
electron paramagnetic resonance of electron-irradiated, 17: 28953
electron spin resonance of irradiated, (E), 19: 5888
elution of calcium from cation resin, 16: 2978
heat of solution in anhydrous ethylenediamine, 16: 5407(R) (TID-14329)
heat of solution of sodium bromide and chloride in liquid, 17: 28869
ion exchange distribution of alkali and alkaline earth metals between chabazite and fused, 20: 16340 (USNRDL-TR-970)
ion transference numbers in liquid, 17: 27345
melting points and volumes of fusion at 0 to 10,000 atm, 19: 19884
mercury chloride extraction from solutions of, by polyphenyls, 17: 35253(R) (IA-775)
occlusion on sodium zeolite, 16: 12801(R) (IA-685)
pH measurement in, comparison of glass- and quinhydrone-electrodes for, 19: 28443(R) (ORNL-3785)
physicochemical properties, 16: 12801(R) (IA-685)
polymerization effects on tetravalent plutonium in acid media, 17: 27319 (ORNL-TM-585)
potentials of nickel electrode in, 16: 25322 (TID-16292)
properties in chemical radiation dosimetry, 19: 39042
protective effects against reticulo-endothelial function decrease in irradiated mice, 16: 14547
protective effects of, against radiation injuries in mice, 18: 23356(R) (NP-13918(p.99-106))
protective effects against radiation in mouse intestine, 18: 31304
protective effects against radiation lethality in mice, oxygen effects on, 19: 24376
radiation damage in crystals of, electron spin resonance of, 17: 35253(R) (IA-775)
radiation damage to, annealing of, 17: 29001
radiation decomposition of crystals of, 16: 13668
radiation effects on thermodynamics of, 16: 33032
radiation effects on electron spin resonance spectra of single crystals of, 18: 13863
radiation effects on dislocation boundaries in single crystals of, 18: 13883
radiation effects on, 18: 20080
radiation effects on, electron spin resonance studies of, 19: 9239
radiation effects on, electron paramagnetic resonance spectra of trapped nitrogen dioxide radicals from, 19: 15590
radioinduced decomposition of, review on, 18: 43604
radioinduced nitrate ions in, ESR and hfs of x, (E), 20: 15965
radioinduced paramagnetic centers in, 20: 3988
radioinduced radical formation in, annealing of, 17: 27422 (TID-17105)
radiolysis, effects of intensity on, 16: 16425
radiolysis of aqueous solutions of, kinetics and recombination of radicals in, 17: 25336
radiolysis of aqueous solutions of, mechanisms in, 17: 35872 (UJV-952)
radiolysis of aqueous solutions of, direct effect in, 17: 37262
radiolysis of aqueous, primary reducing species in, 18: 1725(R) (ORNL-3488(p.42-54))
radiolysis of aqueous solutions of, 18: 31563 (AD-429919)
radiolysis of aqueous solutions of, 19: 32222
radiolysis of aqueous solutions of, ESR spectral studies on radicals in gamma, 20: 43310
radiolysis of concentrated aqueous solutions of, 18: 13850
radiolysis of concentrated aqueous solutions of, mechanism of, 18: 17869 (UJV-976/63)
radiolysis of concentrated aqueous solutions of, 19: 501
radiolysis of crystals of, gamma, 19: 432 (TID-21236)
radiolysis of crystals of, effects of linear energy transfer on alpha, gamma, and x, 16: 17737
radiolysis of crystals of, lattice compressibility relation in, 16: 25453
radiolysis of frozen solutions of, electron paramagnetic resonance studies of free radicals induced in electron, 18: 17885
radiolysis of frozen aqueous, EPR study of products from electron, 18: 37214(T) (AEC-tr-6398(p.486-94))
radiolysis of frozen solutions of, formation of nitrogen dioxide in, 18: 43638
radiolysis of frozen, at 77°K, yields of nitrite ion from gamma, 20: 38950
radiolysis of, mechanism of, 17: 3043
radiolysis of silver-activated, optical properties of fragments produced by, 19: 2384
radiolysis of, at 77, 300, and 400°K, effects of pressure on, 20: 10891
radiolysis of, effects of methanol and nitrite radicals on yields from pulse, 20: 43321
radiosensitivity effects of, in mice, 17: 37067(T) (JPRS-20964)
radiosensitivity effects on *Clostridium botulinum* spores, 18: 43299
radiosensitivity effects on *E. coli*, 19: 26059
reactions in dioxane–water solutions, nuclear magnetic resonance spectra of, 17: 40800
reactions with Linde 4A zeolite, formation of occlusion compounds in, 17: 35253(R) (IA-775)
reactions with niobium and zirconium in organophosphorus solvents, 19: 13532(R) (ORNL-TM-1020)
reactions with TBP, thermal effects on, 17: 10510(R) (ORNL-3320 (p.47-55))
reactions with uranium(IV-VI) oxide, 19: 15431(T) (ANL-Trans-33

(p.77-8))
reduction to ammonia using hydrochloric acid solutions, nitrogen isotope effects in, 18: 2127(R) (ORNL-3488(p.21-41))
reduction to ammonia using sodium hydroxide solutions, nitrogen isotope effects in, 18: 2127(R) (ORNL-3488(p.21-41))
salting-out properties in uranyl nitrate extraction from aqueous solutions, 17: 10770
scavenging effects on hydrogen yield in radiolysis of aqueous solutions, 17: 37265
separation from nitric acid by solvent extraction using trilaurylamine, 16: 23791 (TID-16139)
sodium ion electromigration in fused, isotope effect in, 20: 29185
solubility in Clanex feeds, 20: 9047(R) (ORNL-3830, pp 157-73)
solvent effects on catalytic decomposition of bromate, 17: 2982
solvent properties of liquid, for barium and strontium nitrates, heats of solution, 16: 32998
solvent properties for uranyl nitrate, 17: 3007
solvent properties in paper chromatographic separation of inorganic cations, 18: 39388
solvent properties for calcium sulfate at 125 to 350°C, aqueous, 19: 30673(R) (ORNL-3789(p.293-305))
solvent properties for lanthanum dibutyl phosphate, 19: 22238
solvent properties of aqueous, for calcium hydroxides, 20: 23602(R) (ORNL-3913, pp 53-73)
sorption of alkali and alkaline earth metals from fused, by mineral ion exchangers, 18: 39169 (USNRDL-TR-754)
sorption of liquid, in Linde Molecular Sieve 4A, 17: 33767 (IA-810)
spectra of, emission technique for study of infrared, 18: 3744
spectra of liquid, ultraviolet absorption, 18: 11958(R) (BNL-823(p.20-47))
spectra of structure of water in, near-infrared, 17: 40803
spectra of, laser excitation of Raman, 20: 38872(R) (NYO-1769-68)
spectra, infrared, 16: 14748
spectrum at low temperatures, infrared, 16: 33002
thermodynamic properties of crystals of, 18: 6574(T) (AI-Trans-17)
transfer between heavy and light water, ionic hydration in, 17: 6096
transport number of cation in fused, 17: 6080
use for processing irradiated fuels containing molybdenum and niobium by oxidation, 20: 18834
use in Purex waste processing, 18: 27278(R) (HW-79280(p.4.1-28))
x-ray scattering cross sections, 18: 20035
$AgNO_3$–$NaNO_3$, cation exchange between Linde Molecular Sieve 4A zeolite and liquid, 18: 43443 (IA-968)
$AgNO_3$–$NaNO_3$, chronopotentiometric study of friction coefficients in molten, 19: 31646 (TID-20866)
$AgNO_3$–$NaNO_3$, electrochemical and thermochemical properties of fused, 20: 10804 (EUR-2466.e, pp 9-19)
$AgNO_3$–$NaNO_3$, thermodynamics of molten, 19: 2273 (IA-941)
$Al(NO_3)_3$–HNO_3–$NaNO_3$, separation of americium-243 and curium-244 from, using TBP, 20: 5495 (DP-972)
Antarox DM-970–sodium hexametaphosphate–sodium dodecyl sulfate–$NaNO_3$–sulfosalicylic acid, efficiency of, as radioactivity decontamination solution for cotton protective clothing, 20: 29477
$BaBr_2$–$NaNO_3$, phase studies, 17: 32112
$Ca(NO_3)_2$–$NaNO_3$–H_2O, solubility at 10, 20, and 30°C, 18: 1698
$CaNO_3$–$NaNO_3$, diffusion and transport processes in molten, on ceramic oxides, 20: 40866 (EUR-2954.e)
H_3BO_3–$NaNO_3$, thermal decomposition of, 17: 30582(R) (IDO-14611)
kerosene–$NaNO_3$–TBP–$UO_2(NO_3)_2$, flow properties of, in stacked-clone contactor, 20: 45798(R) (ORNL-3945, pp 230-2)
KNO_3–$NaNO_3$, complexing reactions of cobalt(II) and nickel(II) with halide ions in fused, 18: 8335 (TID-19998)
KNO_3–$NaNO_3$–$NaNO_2$, corrosive effects on Zircaloy-2 and zirconium at 400 to 600°C, 17: 25724 (TID-18773)
KNO_3–$NaNO_3$, density of, 17: 37186
KNO_3–$NaNO_3$, diffusion and electric mobility of ions in, 20: 16414 (CEA-R-2806)
KNO_3–$NaNO_3$, diffusion of alkaline earth ions in fused, tracer studies of, 20: 25085
KNO_3–$NaNO_3$, dissociation of nitrate ion in fused, 18: 200 (IS-618)
KNO_3–$NaNO_3$–$NaNO_2$, effects of fused, on Zircaloy-2 and zirconium, 20: 25506
KNO_3–$NaNO_3$, electric conductivity and density of fused eutectic, effects of added salts on, 18: 8334 (TID-19997)
KNO_3–$NaNO_3$, electric conductivity of fused, d-c measurements of, 18: 13719 (IS-667)
KNO_3–$NaNO_3$, electric conductivity of molten, 18: 26018
KNO_3–$NaNO_3$, electric conductivity of fused, effects of added salts on, 19: 26290 (NYO-2780-1)
KNO_3–$NaNO_3$, electromotive force measurements of silver and chlorine ions in, 16: 108
KNO_3–$NaNO_3$, impedance of polarized platinum micro-electrodes in, 16: 2232
KNO_3–$NaNO_3$, ion transfer in fused, 20: 10805 (EUR-2466.e, pp 21-30)
KNO_3–$NaNO_3$, mobilities of like charge ions in, 18: 1645
KNO_3–$NaNO_3$, nitrate ion decomposition by pyrosulfate ions in fused, 18: 8323 (IS-742)
KNO_3–$NaNO_3$, polarographic behavior of water in molten, at 350°C, 19: 17859 (TID-21511)
KNO_3–$NaNO_3$, polarography of oxygen and hydroxyl ions in molten, 20: 285 (EUR-2496.e)
KNO_3–$NaNO_3$, properties of cobalt(II) ions in, effects of bromides, chlorides, and fluorides on, 17: 10605(R) (TID-17816)
KNO_3–$NaNO_3$, purification from nitrites and water by nitrogen-dioxide bubbling, 20: 10272(R) (NAA-SR-9339)
KNO_3–$NaNO_3$, solvent properties of, for silver chloride at 280°C, 16: 3012
KNO_3–$NaNO_3$, stability of transition-metal cyanides in molten, 19: 32122(R) (NYO-2747-3)
KNO_2–$NaNO_3$, use in preparation of aluminum–nickel coatings, 19: 39143(P)
$LiClO_4$–KNO_3–$NaNO_3$, density at 230 to 400°C, 19: 4134
$LiClO_4$–$NdNO_3$–KNO_3–$NaNO_3$, density at 230 to 400°C, 19: 4134
$LiNO_3$–KNO_3–$NaNO_3$, distribution of ions between liquid–TBP and molten, at 150°C, 19: 19833 (CEA-R-2628)
$LiNO_3$–KNO_3–$NaNO_3$, electric conductivity at 134 to 384°C, 18: 26020
$LiNO_3$–KNO_3–$NaNO_3$, mobilities of like charge ions in, 18: 1645
$LiNO_3$–KNO_3–$NaNO_3$, polarography of cations in liquid, oscillographic, 19: 2271 (EUR-1908.e)
$LiNO_3$–KNO_3–$NaNO_3$, polarography of oxygen and hydroxyl ions in molten, oscillographic, 20: 285 (EUR-2496.e)
$LiNO_3$–$NaNO_3$, diffusion and electric mobility of ions in, 20: 16414 (CEA-R-2806)
$LiNO_3$–$NaNO_3$, electric conductivity of, 17: 14222(T) (AEC-tr-5676)
$LiNO_3$–$NaNO_3$, electric conductivity of fused, d-c measurements of, 18: 13719 (IS-667)
$LiNO_3$–$NaNO_3$, electric conductivity of molten, 18: 26018
$LiNO_3$–$NaNO_3$, isotope separation by countercurrent electromigration in liquid, 17: 23829
$LiNO_3$–$NaNO_3$, reactions of neptunium and uranium with sodium bromate in molten, 20: 7073
$LiNO_3$–$NaNO_3$, solvent properties for water vapor, 20: 1812 (EUR-2495.e)
$LiNO_3$–$NaNO_3$, spectra of fused, infrared, 17: 37175 (URS-74)
methanol–$NaNO_3$, radiolysis of oxygen-saturated, 18: 12147(R) (RRL-127)
methanol–$NaNO_3$, radiolysis of aerated, deaerated, and oxygenated aqueous, 18: 22117(R) (RRL-133)
methanol–$NaNO_3$, radiolysis of aqueous solutions of, 18: 43641
Na_2CO_3–$NaNO_3$, use for processing molybdenum- and niobium-containing irradiated fuels by oxidation, 20: 18834
$NaNO_3$–$NaNO_2$, radiation effects on equilibrium in, 18: 12165
$NaNO_3$–$TlNO_3$, diffusion and transport processes in molten, on ceramic oxides, 20: 40866 (EUR-2954.e)
$NaNO_3$–$UO_2(NO_3)_2$, chemical properties of aqueous solutions of, isopiestic studies of, 19: 392
$NaNO_3$–$UO_2(NO_3)_2$, properties of complexes in aqueous solutions of, physicochemical, 19: 17916
NaOH–$NaNO_3$, solvent properties for irradiated aluminum–plutonium alloys, 18: 22167 (DP-874)
NaOH–$NaNO_3$, use for processing molybdenum- and niobium-containing irradiated fuels by oxidation, 20: 18834
$NdNO_3$–KNO_3–$NaNO_3$, density at 230 to 400°C, 19: 4134
$RbNO_3$–$NaNO_3$, density of, 17: 37186
Sodium Nitrilotriacetates
see Acetic Acid, Nitrilotri-, Sodium Salts

SODIUM NITRITES

effect on cathodic corrosion of stainless steel in nitric acid, 19: 36983
effects on dissolution of uranium dioxide pellets in nitric acid, 19: 20050 (ORNL-3695)
effects on mutation induction in *Schizosaccharomyces pombe*, comparison of radioinduced mutations with, 19: 26035
effects on radiolysis of aqueous sodium hydroxide glasses at 77 to 150°K, 20: 45730
effects on TBP-Amsco extraction of niobium, ruthenium, and zirconium, 19: 13532(R) (ORNL-TM-1020)
effects on yields in radiolysis of nitrous oxide aqueous solutions, 18: 31601
effects on yields in radiolysis of deuterated sodium formate aqueous solutions containing nitrous oxide, 18: 31602
nitrogen-15 NMR in, chemical shifts in, 18: 23530
phase transformations in, 17: 37811
protective effects against x rays in mice, 16: 14460(R) (NP-11359 (p.76-80))
protective effects against radiation injuries and nitrogen mustard in *E. coli*, 16: 16297
protective effects of, against radiation inactivation of taka-amylase,

17: 15592
protective effects against radiation injuries in mice, 19: 8955(R) (NP-14448(p.108-15))
protective effects against radioinduced inactivation of β-amylase, 19: 17558
radiation effects on single crystals of, gamma, 18: 29771
radiation effects on visible absorption spectra of nitrogen dioxide in, 19: 2412
radiation effects on corrosion inhibition action on iron and steel, 19: 28414
radiation effects on aqueous solutions of, for inhibition of steel corrosion by water, 20: 23606 (UJV-1453/65)
radiolysis at room temperature, paramagnetic species from gamma, (E), 19: 24563
radiolysis of aqueous solutions of, containing mercuric salts, 17: 35888
radiolysis of aqueous solutions of, 18: 31563 (AD-429919)
radiolysis of frozen solutions of, electron paramagnetic resonance studies of free radicals induced in electron, 18: 17885
radiolysis of frozen solutions of, at 77°K, electron spin resonance studies of, 19: 17996
radiolysis of frozen aqueous solutions of, ESR spectral studies on, 20: 43309
radioprotective activity in *E. coli*, method of determining, 17: 35409
radiosensitivity effects in spleen, 16: 4001(R) (NP-11020(p.78-81))
radiosensitivity effects of, effects of tissue oxygen on, 16: 30229
radiosensitivity effects on *Clostridium botulinum* spores, 18: 43299
radiosensitivity effects on *E. coli*, 19: 26059
reactions with ruthenium, chromatography studies, 16: 4171
reduction to ammonia using sodium hydroxide solutions, nitrogen isotope effects in, 18: 2127(R) (ORNL-3488(p.21-41))
sodium-23 nuclear quadrupole coupling in, temperature effects on, 17: 10646
spectra of gamma-irradiated single-crystal, infrared absorption, 18: 16100
therapeutic effects of, against radiation injuries in mice, 18: 5135(R) (NP-13281(p.45-56))
transport number of cation in fused, 17: 6080
use with α-naphthol for precipitation of uranium from homogeneous solution, 19: 13302
KNO_3–$NaNO_3$–$NaNO_2$, corrosive effects on Zircaloy-2 and zirconium at 400 to 600°C, 17: 25724 (TID-18773)
KNO_3–$NaNO_3$–$NaNO_2$, effects of fused, on Zircaloy-2 and zirconium, 20: 25506
KNO_3–$NaNO_2$, use in preparation of aluminum–nickel coatings, 19: 39143(P)
$NaNO_2$–H_2SO_4, in oxidation of iodides to molecular iodine, 20: 39103(R) (BNWL-235-3, pp 51-69)
$NaNO_3$–$NaNO_2$, radiation effects on equilibrium in, 18: 12165

SODIUM NITROPRUSSIDE
properties as absorber in iron-57 Mössbauer studies, 20: 22158
properties as standard for iron-57 Mössbauer studies, 20: 20684
properties for use as standard for Mössbauer spectroscopy, 20: 16335(R) (NBS-TN-276)
radiation effects on EPR spectra of, electron, 20: 7156
radiation effects on crystals of, ESR studies of pairwise trapping from gamma, 20: 29280
radiolysis of powdered, ESR of trapped electrons in, 19: 2385

SODIUM OXALATES
see also Sodium Thorium Oxalates
analytical uses in determination of cerium, 19: 15395
effects on pH of dialyzed zirconyl chloride, 17: 35718
radiation effects on oxidation by mercuric chloride, gamma, 19: 32219
radiolysis, spectra of CO_2^- radical in, 16: 16435
reactions with ammonium and uranyl oxalates, 17: 3006
separation from uranyl bis(dibenzoylmethane) by solvent extraction into chloroform, 16: 11792
spectra, infrared, 16: 32982

SODIUM OXALATOHAFNATES
tetrakis-, crystal structure of trihydrates of, 17: 8102

SODIUM OXALATOZIRCONATES
crystal and molecular structure of, stereoisomerism in, 17: 18031
tetrakis-, crystal structure of trihydrates of, 17: 8102

SODIUM OXIDES
analysis for cesium, potassium, rubidium, and sodium, activation, 20: 20633
analysis for hydrogen, gas chromatographic, 19: 24064(R) (ANL-6997)
content in nickelveyite uranium mineral, 19: 40799
content in thalenites from Japan, 20: 29399
corrosive effects on aluminum alloys, kryptonate method for determining, 20: 18570(R) (NYO-2757-5)
determination in clay, acetic acid leachates, sand, and silt, spectrochemical, 16: 4379
determination in liquid sodium, 18: 21698(R) (ANL-6860)
determination in Moldavites by mass spectrometry and x-ray fluorescence, 20: 16711(R) (MIT-1381-13)
determination in silicate rocks, x-ray fluorescence spectrographic, 16: 30353
determination in sodium by electric potential measurement, 19: 40409(R) (MSAR-65-95)
determination in sodium loop, instrumentation performance for, 20: 8816(R) (APDA-178, pp 30-42)
determination in sodium-cooled-reactor cooling systems, (E), 20: 14008(R) (ANL-7122, pp 42-69)
diffusion in sodium disilicate glass, kinetics, 19: 44611 (UCRL-16232)
dispersion from sodium fires, 19: 27735(R) (NAA-SR-10850)
distribution of aerosols of, from sodium fires, 19: 12865(R) (NAA-SR-10501)
effects on elastic properties of irradiated aluminum oxide–boron oxide–silicon oxide glasses, 19: 7984
effects on homomolecular isotopic exchange of carbon monoxide, catalytic, 19: 26328
effects on ion-exchange properties of aluminum silicates, 20: 43449
effects on thermal conductivity of sodium, 20: 5901
formation of, free energy of, 18: 14401 (BNL-7553)
free energy of formation at 1100°F, 17: 32571(R) (MSAR-63-105)
growth of scheelite single-crystal $Na_{0.5}Dy_{0.5}TeO_4$, $Na_{0.5}Pr_{0.5}MoO_4$, and $Na_{0.5}Tm_{0.5}MoO_4$, 19: 26304
impurities in, equipment for control of, 20: 3321(R) (ANL-7082, pp 29-53)
magnetic susceptibility of, at 63°K to room temperature, (E), 20: 42169(R) (UCRL-14744, pp 1-18)
particle size distribution of, in liquid sodium combustion (E), 19: 2429
phase equilibria in systems with boric and thorium oxides, 16: 32106(R) (AD-271937)
preparation, 20: 14511(R) (ORNL-3889, pp 71-3)
production and dispersion in fires, 19: 40286(R) (NAA-SR-11200)
reactions with americium oxide, properties of ternary oxides formed in, 19: 28286 (KFK-280)
reactions with molybdenum at 400°C, 17: 35251(R) (BMI-1632(Del.))
reactions with protactinium oxides, solid-state, 20: 26880
reactions with ytterbium oxide in presence of nitric acid, 19: 42514
release during sodium reactor coolant fires, 19: 10675(R) (NAA-SR-9999)
separation from sodium in circulation loops, 20: 1960
solubility in liquid sodium, effects of free energy gradient on, 18: 22488 (NAA-SR-8381)
thermal properties, 19: 47010(R) (ORNL-3832, pp 107-50)
Al_2O_3–SiO_2–Na_2O, composition and properties of, 20: 8836 (TID-22511(Suppl.))
Al_2O_3–SiO_2–Na_2O, gamma-ray effects on color centers in, (E), 19: 11800(T)
Al_2O_3–SiO_2–Na_2O, ion exchange properties of, in nitrate melts, 17: 27500
Al_2O_3–SiO_2–Na_2O, ion exchange properties of synthetic minerals of, 18: 35502 (NYO-2911-1)
Al_2O_3–SiO_2–Na_2O, properties for use in separation of cesium from waste solution, 19: 30349(P)
AmO_2–Na_2O, crystal structure, preparation, and properties, 19: 32746
AmO_2–Na_2O, crystal structure, preparation, and properties, 19: 32747
BaO–Na_2O–Tc_2O_7, compound formation in solid state reactions in, 20: 7050 (KFK-341)
BaO–O–Na_2O–Tc_2O_7, compound formation in, 20: 31244
BeO–Na_2O, effects of calcium, silicon, and strontium in, 17: 16002
B_2O_3–CeO_2–Na_2O, phase studies at 690 to 1100°C, 20: 26846
B_2O_3–Eu_2O_3–Na_2O, spectra at liquid nitrogen temperature and room temperature, absorption and emission, 20: 36813
B_2O_3–NaCl–Na_2O, distribution of cesium and rubidium in immiscible phases of, 17: 1566 (USNRDL-TR-588)
B_2O_3–NaCl–Na_2O, distribution of solutes between phases in, at 830°C, 18: 33534 (USNRDL-TR-760)
B_2O_3–NaCl–Na_2O, distribution of alkali metals, alkaline earths, and rare earths between phases in, at 830°C, 20: 7201
B_2O_3–Na_2O, entropy of vitrification of, 16: 25325 (USNRDL-TR-566)
B_2O_3–Na_2O, radiation effects on ESR spectra of, 18: 26079
B_2O_3–Na_2O–UO_3, glass formation and properties in, 17: 35848
B_2O_3–Nd_2O_3–Na_2O, phase studies at 690 to 1100°C, 20: 26846
CaO–Na_2O–Tc_2O_7, compound formation in solid state reactions in, 20: 7050 (KFK-341)
CaO–SiO_2–Na_2O, diffusion of sodium-22 in solid, residual activity method for self-, 20: 16478
CaO–SiO_2–Na_2O, magnetic susceptibility of, containing iron dispersions, 19: 24989(R) (TID-21673)
Gd_2O_3–MoO_3–Na_2O, crystal growth in, composition diagrams for, 19: 17902
Gd_2O_3–SiO_2–Na_2O, glass forming temperature of, 20: 4077(R) (IS-1200 (Sect. E))
Na_2O–SiO_2, fixation reactions with Purex waste, 19: 17388(R) (HW-84467)

Na_2O–SrO–Tc_2O_7, compound formation in solid state reactions in, 20: 7050 (KFK-341)
Na_2O–Ta_2O_5, crystal structure of phases in, 19: 37059
Na_2O–UO_3, crystal structure, preparation, and properties, 19: 32746
Nb_2O_5–Na_2O, crystal structure of phases in, 19: 37059
Nb_2O_5–SiO_2–Na_2O, dielectric properties of glasses in, 17: 12686
NpO_2–Na_2O, crystal structure, preparation, and properties, 19: 32746
NpO_2–Na_2O, crystal structure, preparation, and properties, 19: 32747
NpO_2–O–Na_2O, crystal structure and thermal stability of phases in, 18: 27358 (KFK-196)
NpO_2–O–Na_2O, lattice constants and thermal stability, 18: 36036
O–Na_2O–SrO–Tc_2O_7, compound formation in, 20: 31244
O–Na_2O–UO_3, lattice constants and thermal stability, 18: 36036
O–PuO_2–Na_2O, crystal structure and thermal stability of phases in, 18: 27358 (KFK-196)
O–PuO_2–Na_2O, lattice constants and thermal stability, 18: 36036
Pa_2O_5–Na_2O, crystal structure, preparation, and properties, 19: 32747
P_2O_5–Na_2O–UO_3, phase studies, 16: 15188(R) (NP-11412)
PuO_2–Na_2O, crystal structure, preparation, and properties, 19: 32746
PuO_2–Na_2O, crystal structure, preparation, and properties, 19: 32747
SiO_2–Na_2O, diffusion of calcium, potassium, and sodium ions in, in melts with calcium, lithium, and potassium oxides, 16: 16048
SiO_2–Na_2O, diffusion of calcium, potassium, and sodium ions in, in melts with calcium, lithium, and potassium oxides, 16: 24038(T) (AEC-tr-5191)
SiO_2–Na_2O–ZnO, absorption in gamma-irradiated, 18: 32202
SiO_2–Na_2O–ZrO_2, phase studies, 20: 13284
Sodium Pentachlorophenolate
see Sodium, (Pentachlorophenoxy)-
SODIUM, (PENTACHLOROPHENOXY)-
penetration in wood, radioactivation determination of factors affecting selective, 20: 29161
SODIUM PERBORATES
magnetic properties, 20: 1571(R) (TID-22186)
SODIUM PERCHLORATES
annealing neutron-irradiated, thermal, 16: 25444
aqua ions in, half-wave potential shift of, 18: 21712(R) (NYO-10065)
chlorine-38 oxidation states in neutron-irradiated, 16: 25443
corrosive effects on zirconium, 20: 31687
DNA extraction from phage using, 19: 31683(R) (UCRL-11833(p.26-8))
effects on electron exchange reactions between thallium and uranium in methanol–water solutions, 18: 27418
effects on iodine-131 uptake by thyroid gland, 17: 27048
effects on nitrogen-15 exchange between nitric acid and nitric oxide, 20: 9363(R) (NYO-755-2, Paper 3)
effects on solvent extraction of cobalt acetylacetonate using isopropyl alcohol, 20: 7211
hydrolysis of thorium by, mechanism and products at 0, 25, and 95°C, 19: 30151(R) (ORNL-3789(p.139-63))
hydrolysis of uranyl ion in, complexes in, 18: 13734
hydrolysis of uranyl ion in, equilibria in, 18: 13737
labeling with chlorine-38 by neutron activation, 19: 17982
labeling with chlorine-36, 19: 20028
protective effects of, against radiation inactivation of taka-amylase, 17: 15592
radiation effects on frozen deuterated and normal aqueous solutions of, EPR studies on gamma, 20: 45721
radioinduced decomposition, 19: 13453
radioinduced decomposition of, mechanism for, 19: 13454
radiolysis of frozen solutions of, ESR studies of decomposition of radicals from gamma, 20: 40960
radiolysis of, mechanism and products of, 18: 3860
reactions in dioxane–water solutions, nuclear magnetic resonance spectra of, 17: 40800
separation from uranyl bis(dibenzoylmethane) by solvent extraction into chloroform, 16: 11792
solvent properties of solutions of, for zirconium hydroxide, 20: 36789
spectra of structure of water in, near-infrared, 17: 40803
sulfur-35 and -38 activity in irradiated, chemical fate, 16: 11757
$Ca(ClO_4)_2$–$NaClO_4$, phase studies, 17: 21714
$Cu(ClO_4)_2$–$NaClO_4$, osmotic pressure, 18: 19837(R) (MIT-905-1)
NaCl–$NaClO_4$, osmotic pressure, 18: 19837(R) (MIT-905-1)
4-methyl-2-pentanol–$NaClO_4$, hydrolysis of vanadium in, 18: 27415
SODIUM PERIODATES
iodine-127 and -129 Mössbauer isomer shifts in, (E), 20: 20139
SODIUM PERMANGANATES
radiation effects on thermal decomposition of, 19: 11813
use in determination of cesium-137, 20: 35406
SODIUM PEROXIDE
sintering with plutonium dioxide, 20: 16350
Sodium Peroxyborates
see Sodium Perborates
SODIUM PERPROTACTINATES
formation of insoluble, 20: 38890
SODIUM PERRHENATES
heat of solution and thermodynamic properties of, in sodium nitrate, 18: 5283
Sodium Peruranates
see Sodium Uranates
SODIUM PERXENATES
analytical uses in determination of americium, 19: 15361
crystal structure of hydrated, 18: 5332
crystal structure of octahydrate of, 18: 41395
crystal structure of hexahydrate of, 18: 41396
crystal structure, 19: 23355(R) (BNL-867(p.1-117))
hexahydrate of, identification of, by crystal structure, 17: 40818
Mössbauer effect in xenon-129 in, 18: 5340
preparation and properties, 18: 1604 (CONF-126-19)
preparation and properties of, 18: 25357
preparation and structure of hexahydrate of, 18: 31361(R) (UCRL-11213 (p.87-138))
reactions with water, intermediates in, 19: 34162
reduction in alkaline solutions at dropping mercury electrodes, 18: 43505
spectra of, infrared absorption, 17: 35680 (CONF-126-18)
uses in spectrophotometric determination of manganese, 20: 16351
xenon ion reactions and valences in aqueous, 17: 35679 (CONF-126-11)
SODIUM PHENYL PHOSPHATES
radiation effects on hydrolysis by exposure to alkali phosphatase, 19: 26439
SODIUM PHOSPHATES
see also Sodium Uranyl Phosphates
aerosols of, effects on deposition and retention of inhaled cerium-144 particles in mice, 18: 29371
analytical use in determination of gadolinium, 18: 33481
analytical use of trimeta-, for luminescent determination of uranium in solution, 16: 14674
chelate formation effects of hexameta-, on cobalt-60 distribution in rat, 16: 12873
complexes with uranium, separation from rare earths by ion exchange, 20: 1762
corrosive effects on high-strength alloys and steels under static stress, 16: 25717(R) (NP-11948)
corrosive effects of aqueous solutions of, on stressed AISI 304 stainless steel at 275°C, 18: 14407(R) (HW-79766(p.5.1-16))
corrosive effects of mono-, on stainless steel, 18: 27856(R) (HW-79280 (p.9.1-4))
crystallization effects on strontium sulfate, 16: 10025
diffusion of phosphorus-32-labeled, through arachnoidal membrane, 18: 43206
effectiveness in removal of radioisotopes from body, 19: 43700
effects on amino acid and protein restoration in irradiated guinea pigs, rabbits, and rats, 18: 9911
effects on corrosion of niobium and tantalum at 21 and 98°C, 19: 22900
effects on incorporated radioisotopes, 16: 32706
effects on radiolysis of aqueous polyvinyl alcohol solutions, 19: 2387
effects on radiosterilization of hams, 16: 4005 (NP-11113)
electron spin resonance of irradiated and of phosphorus-32-labeled, 19: 9181
"hideout" at solid-liquid boundary layer, 17: 8378
luminescence of uranium(VI)-activated, 18: 1700
preparation and use of hypo-, for separation of cerium and thorium, 17: 21701
preparation of phosphorus-32 labeled soluble, 17: 28973
production from monazites by electromagnetic separation and decomposition, 20: 23220
protective effects against radiation damage in HeLa cells, 19: 17678
radiation annealing of, effects of hydrogen content on, 18: 35597
radiation effects on cadmium- and nickel-activated, spectra of ion formation in uv and x-ray, 19: 25060
radiation effects on pure and sodium sulfate-doped, ESR studies of gamma, 20: 36870
radioinduced formation of complex polyphosphates in, 20: 12902
radioinduced luminescence in, 20: 23186(P)
radioinduced polymerization by neutrons, 16: 10066
radiolysis in ice, electron and hydrogen atom production in gamma, 17: 34026
radiolysis of, hydrogen yields in, 18: 33645
reactions of trivalent, with hafnium in solution, 17: 28861
reactions with atomic hydrogen and polarons radioinduced in ice, 18: 13858
reactions with cerium sulfates, 17: 8039
reactions with cerium, neodymium, and samarium oxides, spectra of compounds formed in, 19: 38668
reactions with phosphorus-32 recoil atoms, labeling positions in, 19: 42567
reactions with rare earths and transition metals, 20: 5529(R) (SC-DC-

65-1706)
reactions with trivalent rare earths to form complexes, 19: 17880
reactions with uranyl nitrates in aqueous solutions, 17: 25171
reactions with uranyl nitrate, formation of uranyl triphosphate in, 17: 40809
reactions with yttrium chlorides, 19: 38619
solubility in benzene, 17: 10740(R) (ORNL-TM-181)
sorption by aluminum oxides from water, 20: 10438(R) (ORNL-3830, pp 96-139)
spectra of americium(VI) in, 17: 14257
spectra of, in 300 to 1000 mμ region, reflectance, 17: 15970
stability of phosphorus-32-labeled polymeta-, chromatographic study, 16: 16414
Szilard-Chalmers reactions in neutron-irradiated, distribution of phosphorus-32 in products of, 18: 43617
use of, in paper electrophoresis of americium-241, cesium-134, curium-246, europium-152, promethium-147, and zirconium-95, 20: 43451
Antarox DM-970–sodium hexametaphosphate–sodium dodecyl sulfate–$NaNO_3$–sulfosalicylic acid, efficiency of, as radioactivity decontamination solution for cotton protective clothing, 20: 29477
KPO_3–$NaPO_3$, reference electrode for emf studies in, 20: 5529(R) (SC-DC-65-1706)
$LiPO_3$–$NaPO_3$, polarography of metal oxides at 730°C in, 18: 1516
Li_2SO_4–$NaPO_3$, molar volume and surface tension of fused, 18: 32177
$NaBeF_3$–$NaPO_3$, phase diagrams of, 20: 14557
NaOH–Na_3PO_4–Na_2WO_4, electrolytic etching and polishing of rhenium–tungsten alloys in, 18: 27931
$NaPO_3$–Na_2SO_4, molar volume and surface tension of fused, 18: 32177
$Na_3P_3O_{10}$–Na_2SO_4, polarographic analysis for uranium(IV), 17: 5990
$NaPO_3$–UO_2SO_4, molar volume and surface tension of fused, 18: 32177
$NaPO_3$–WO_3, tungsten oxide single crystal growth in molten, 20: 43257
Rb_2SO_4–$NaPO_3$, molar volume and surface tension of fused, 18: 32177
SODIUM PHTHALOCYANINES
Szilard-Chalmers reaction on gamma-irradiated, 17: 28999
SODIUM PLUTONIUM FLUORIDES
crystal structure of $Na_7Pu_6F_{31}$, 20: 38898
SODIUM PLUTONYL ACETATES
metabolism in rats, 19: 40317
Sodium Polyphosphates
see Sodium Phosphates
Sodium Potassium Niobates
see Potassium Sodium Niobates
Sodium Potassium Tantalates
see Potassium Sodium Tantalates
Sodium Potassium Tartrates
see Potassium Sodium Tartrates
SODIUM PRASEODYMIUM CHLORIDES
properties, 19: 40469
Sodium Propionates
see Propionic Acid, Sodium Salts
SODIUM PROTACTINIUM FLUORIDES
preparation and crystal structure of $NaPaF_6$, 20: 25055
preparation and properties of, 20: 18681
preparation and properties of Na_3PaF_8, 20: 22994
SODIUM PYROPHOSPHATES
effects on incorporated radioisotopes, 16: 32706
effects on sedimentation rate of uranium (VI-VI) oxide suspensions, 16: 23699
labeling with phosphorus-32, 20: 8956
protective effects against lethal effects of x rays, 16: 4069
radiolysis of, thermal annealing of phosphorus-32 formed in, 18: 5367
reactions with cadmium nitrates, 16: 30415
reactions with gadolinium chlorides, 18: 41448
reactions with uranyl nitrate, 20: 16472
KF–$Na_4P_2O_7$, phase studies, 17: 32114
Li_4F_4–$K_4P_2O_7$–$Na_4P_2O_7$, phase studies, 17: 25254
$Li_4P_2O_7$–K_4F_4–$Na_4P_2O_7$, phase studies, 17: 25254
SODIUM RARE-EARTH SELENIDES
crystal structure, 19: 36356
SODIUM RARE-EARTH SULFATES
analysis for rare earths, spectrochemical, 18: 1527
crystal structure, 19: 7501
SODIUM RARE-EARTH SULFIDES
crystal structure, 19: 19862
SODIUM RARE-EARTH TUNGSTATES
fluorescence of europium in, effects of rare earth ion substitution on, 16: 18196
fluorescence properties of europium in crystals of, 17: 34655
SODIUM REACTOR EXPERIMENT
compatibility of sodium with components in heat transfer system of, 20: 9415 (CONF-650620, pp 105-26)
component development for, 20: 10375(R) (NAA-SR-11650, Sect. 2)
components and test facilities for, design, 19: 35635
components of, operation effects on, 19: 40286(R) (NAA-SR-11200)
control element heat transfer parameter study for SRE-PEP third core, 18: 15449 (NAA-SR-Memo-9281)
control of, development of safety-rod drop-time test system for use in, 18: 6491 (NAA-SR-7880)
control rod absorber assembly thermal analysis, 17: 29719 (NAA-SR-Memo-8529)
control rod calibrations for thorium-uranium fuel, 16: 26597 (NAA-SR-6585)
control rod heating calculations for 525-Mw(e) SGR, 18: 15450 (NAA-SR-Memo-9336)
control rod performance, 18: 21571 (NAA-SR-Memo-9003)
control rod shielding requirements, 16: 14305 (NAA-SR-Memo-2188)
control system for, integrated power demand, 16: 2767
coolant eddy-current brake design, 16: 14839 (NAA-SR-Memo-6753)
coolant pump design and performance, 18: 21571 (NAA-SR-Memo-9003)
coolant purification for, hot- and cold-trap performance for, 18: 21571 (NAA-SR-Memo-9003)
coolant purification in, carbon and fission-product retention in cold traps for, 19: 43575
coolant radioactivity in, effects of impurities on, 20: 40357 (NAA-SR-11766)
coolant system rupture in ESCR, hazards analysis, 16: 5028 (NAA-SR-Memo-4823)
coolant system rupture analysis, 16: 5028 (NAA-SR-Memo-4823)
cooling system activity transfer and corrosion, 16: 1191 (NAA-SR-5363)
cooling system, modification to allow 30-Mwt operation, 16: 28539 (NAA-SR-Memo-7294)
cooling system of, performance of components of primary, 19: 42096 (NAA-SR-11396)
cooling system of, evaluation of long-term operation of, 19: 43572
cooling system replacement, 19: 43560
core design, calandria-type, 16: 9593(P)
core design for, (E), 19: 17241
Core II dynamics, model of, 17: 40343 (NAA-SR-8431)
core II nuclear parameters, calculation of, 18: 36806 (NAA-SR-9430)
core II performance in, 18: 21571 (NAA-SR-Memo-9003)
Core II physics tests, 18: 40841 (NAA-SR-9510)
Core III and fuel element design modifications and performance for development of ASCR, 17: 42347 (NAA-SR-Memo-8734)
core III nuclear analysis for, 18: 20455 (NAA-SR-Memo-9406)
Core III test element fabrication, 19: 12865(R) (NAA-SR-10501)
core normalcy, development of techniques for continuous monitoring, 16: 793
core replacement, 19: 43559
core-2 flow and power ramp stability tests on, 16: 26223 (NAA-SR-7250)
core-2 start-up problems and operation, 16: 7304
decontamination, 16: 12840
design and development, 16: 9657(R) (NAA-SR-1109)
design and operations of, 18: 33074 (A/CONF.28/P/206)
design and operations of, 20: 10272(R) (NAA-SR-9339)
design and operations of, 20: 46966(R) (NAA-SR-12010)
design description and operation, 16: 28551 (TID-7623(p.63-72))
design modifications for increased power generation, 16: 11276
design, development, and operation, 19: 27735(R) (NAA-SR-10850)
development and operation of, 17: 4243(R) (NAA-SR-7400(Sect.I))
development and operation, July–Sept. 1963, 18: 28919(R) (NAA-SR-9090)
development and operation, 1964, 19: 10675(R) (NAA-SR-9999)
development and operation, 20: 22520(R) (NAA-SR-11805)
development for power expansion, 19: 40286(R) (NAA-SR-11200)
experimental facilities of, analysis of long-term operation of, 20: 8397(R) (NAA-SR-11450, Sect.5)
fission product contamination distribution in, 16: 12740 (NAA-SR-6890)
fuel cladding failure monitor for, (E), 19: 8575 (NAA-SR-6463)
fuel clusters from, chemical and mechanical processing of, 16: 32883(R) (ORNL-3314(p.1-39))
fuel dejacketing, 16: 10102(R) (ORNL-TM-65)
fuel dejacketing studies, 16: 14817(R) (ORNL-TM-112)
fuel element decanning for, performance of mechanical equipment for, 17: 3715
fuel element dejacketing, 16: 7615(R) (ORNL-TM-35)
fuel element dejacketing studies, 17: 10743(R) (ORNL-TM-457)
fuel element design and performance, review, 16: 16669
fuel element design and performance, 18: 21571 (NAA-SR-Memo-9003)
fuel element design for, spring-loaded bowable core II prototype, (E), 19: 5480 (NAA-SR-10152)
fuel element disassembly for, fire protection system for, 20: 9180 (ORNL-TM-1309)
fuel element radiation damage, 16: 822
fuel element stabilization, method for prevention of thermal bowing, 16: 19990 (NAA-SR-6879)
fuel element temperature oscillations in Core II, 18: 29072

fuel element temperature distributions in core II, (E), 19: 14835 (NAA-SR-10153)
fuel element temperature oscillations in core 2, (T), 19: 29644 (NAA-SR-10154)
fuel element thermal performance in core III, 18: 21556 (NAA-SR-Memo-9431)
fuel element transient thermal behavior in, 16: 28442
fuel elements for, hydraulic testing of 9-rod assembly for 3rd core, 17: 28443 (NAA-SR-Memo-8406)
fuel handling, dose rates from shielding of machine for, 16: 24948 (NAA-SR-Memo-7212)
fuel handling equipment design, 17: 13779 (NAA-SR-5599)
fuel handling machine for core III, design of, 19: 29645 (NAA-SR-10817)
fuel processing, 16: 17617(R) (ORNL-TM-122)
fuel processing for Core II, 18: 24891(R) (NAA-SR-8888(Sect.I))
fuel rod bowing, 16: 24536
fuel rod bowing in operation, 17: 12017
fuel rod bowing in, detection and elimination of, 17: 13680 (NAA-SR-7705)
fuel rods, effects of bowing on reactor stability, 16: 21722 (NAA-SR-6878)
fuel-element temperature oscillations in, during startup, (E), 19: 8639 (NAA-SR-10151)
fuel-element temperature oscillations in core II of, 19: 29660
gallery gas of, hazards of freon in, 17: 19625 (NAA-SR-Memo-8041)
hazards analysis of sodium-water reaction in pipe gallery, 18: 24894 (NAA-SR-Memo-7743)
heat transfer in Core III of, 17: 19674 (NAA-SR-7925)
heat transfer protection system for, operation and testing of, 20: 12406 (NAA-SR-Memo-11648)
heat transfer system demolition in Power Expansion Program, 19: 45579 (NAA-SR-11414)
hydraulic design of SRE-PEP core III variable orifice, 18: 21572 (NAA-SR-Memo-9253)
kinetics and safety of, (E/T), 19: 17247
loading of, photography and viewing apparatus for fuel and moderator, 18: 23059 (NAA-SR-6387)
loading with thorium-uranium fuel, 16: 12324 (NAA-SR-6608)
maintenance, 16: 15938
materials selection for, problems in, 18: 15568
moderator and reflector elements for, design and performance of Zircaloy-2-clad, 20: 12404 (NAA-SR-11160)
moderator can rupture in, analysis of graphite transport into sodium from, 18: 32951 (NAA-SR-Memo-7497)
moderator elements for, reliability testing of, 20: 6621 (NAA-SR-Memo-11556)
moderator heat transfer analysis in SRE-PEP third core, 18: 15448 (NAA-SR-Memo-9183)
moderator sampling after irradiation, drilling method for, 19: 14836 (NAA-SR-10721)
modification of, review of procedures, 20: 40429
neutron diffusion in, 16: 34070 (NAA-SR-Memo-7415)
neutron flux distributions and leakage currents for, 16: 4975 (NAA-SR-Memo-865(Rev.))
noise and oscillation tests, comparison, 17: 26808
nuclear materials handling and shipping, 20: 8393(R) (NAA-SR-11450, Sect.1)
operating experience, 16: 633
operation, 16: 31297
operation, 18: 35247(R) (NAA-SR-9700)
operation and power expansion modifications of, 19: 12865(R) (NAA-SR-10501)
operation and power expansion modifications of, 20: 8393(R) (NAA-SR-11450, Sect. 1)
operation data for development of sodium graphite reactors, 16: 31290
operation during 1963, 18: 24891(R) (NAA-SR-8888(Sect.I))
operation, experience, survey of, 16: 5038
operation of, carburizing potential relation to temperature limitations for, 17: 17597 (NAA-SR-Memo-7804)
operation of Core II, period spikes in, 18: 40843 (NAA-SR-Memo-9523)
operation of sodium systems of, exposure history, 19: 10550 (NAA-SR-Memo-10593)
operation of, design modifications and tests for, 20: 35841(R) (NAA-SR-11900)
operation, July–Sept. 1965, 20: 10375(R) (NAA-SR-11650, Sect. 2)
performance upgrading to 30 Mwt, modifications for, (E), 19: 21732 (NAA-SR-10379)
physics experiments in, 20: 1356
power levels in, methods of flattening, 17: 4300 (NAA-SR-6403)
power ramp analysis using analog computer, 18: 27845 (NAA-SR-7929)
prompt power coefficient analysis, 16: 778
prompt power coefficient for, 17: 5588
radioisotope production in, economic and technical feasibility of, 19: 28723
reactivity calculations and measurements for, 18: 11444 (TID-7672(p.123-56))
reactivity changes in, Monte Carlo calculations on, 18: 7922 (CONF-360-7)
reactivity, effects of fuel movement in Core III on, 17: 19622 (NAA-SR-Memo-7879)
reactivity, isothermal temperature coefficients for thorium–uranium fuel, 16: 4973 (NAA-SR-6357)
reactivity monitoring for, on-line "meter" for core II, 19: 5481 (NAA-SR-10186)
reactivity of, calculational method for surveillance of, (E), 19: 5544 (NAA-SR-10010)
reactivity of, computer program for surveillance of, 19: 5482 (NAA-SR-Memo-7936)
recovery of damaged core, operation description, 16: 4974 (NAA-SR-6359)
safeguards analysis for, Core III, 18: 40846 (NAA-SR-Memo-9741)
safety analysis for, with fast-flux test section in center of core, (T), 20: 6676 (NAA-SR-11234)
safety rod drop-time measurement, timing system for, 19: 3490
shutdown of, identification of real and spurious scrams in, 17: 28442 (NAA-SR-Memo-6688)
sodium reactivity worth in Core II, 18: 35149 (NAA-SR-9509)
steam generator design and performance, 17: 25414 (TID-18072)
transfer function for Core 2, oscillator measurement of, 18: 30947 (NAA-SR-7264)
use as fast-flux fuel irradiation facility, 19: 3682
viewing equipment for core of, design of, 19: 35762 (NAA-SR-10006)
waste disposal system, operation, 16: 7334
waste materials handling and shipping, 20: 8393(R) (NAA-SR-11450, Sect.1)

SODIUM RHENATES
oxygen-17 NMR in, 17: 3645

Sodium Rhodizonates
see Rhodizonic Acid, Sodium Salts

SODIUM SALICYLATES
analytical use in titrimetric determination of beryllium, 17: 6011
effectiveness in removal of radioisotopes from body, 19: 43700
effects on strontium-85 body burdens in mice and rats, 20: 18229
effects on thyroidal release of iodine-131 in thyrotoxicosis patients, 19: 3868
radiation effects on luminosity of aqueous solutions, 18: 23580 (PAN-488/XVII)
radioinduced luminescence of, duration of α, β, uv, and x, 18: 8427(T)
radiosensitivity effects on DNA, γ, 20: 8732
radiosterilization, 18: 13558
reactions with neodymium chlorides in aqueous solutions, preparation of neodymium salicylate by, 20: 26895
therapeutic effects in radiation sickness, 16: 9931
use as milk preservative for radioactivity monitoring, 19: 26593
sodium salicylate–$Th(NO_3)_4$, properties, 17: 25249

SODIUM SALTS
(See also salts of specific organic acids under the name of the parent acid)
analysis for potassium by atomic absorption, 19: 26242
effects on excretion of strontium isotopes by mice, 20: 8564
effects on growth of *Clostridium botulinum* Type E in sea foods, 20: 41384(R) (TID-22833)
preparation of sodalite, 16: 13008(R) (TID-15006)

SODIUM SAMARIUM BROMIDES
preparation, 20: 29204

SODIUM SAMARIUM CHLORIDES
preparation, 20: 29204

SODIUM SAMARIUM FERROCYANIDES
preparation and properties, 19: 22246
thermal decomposition, 19: 22247

SODIUM SELENATES
radioinduced luminescence in, 20: 23186(P)
reduction of, effects of selenium-76 and selenium-82 in, 20: 18642

SODIUM SELENITES
dielectric properties of partially deuterated single crystals of, dependence on deuterium concentration, (E), 20: 1333
ferroelectric properties of, hydrogen isotope effects in, 19: 36418(T)
heat of solution, 20: 38900
heat of solution, 20: 38901
proton spin lattice relaxation time in irradiated, dose and temperature dependence of, (E), 19: 45477 (NIJS-R-444)
radiation effects on ferroelectric properties of $NaH_3(SeO_3)_2$, gamma, 19: 26884 (NIJS-R-442)
radiation effects on electron spin resonance spectra of $NaH_3(SeO_3)_2$ and $NaD_3(SeO_3)_2$, gamma, 19: 26378 (NIJS-R-439)
radiation effects on single-crystal $NaH_3(SeO_3)_2$, effects of deuterium on

EPR spectra from gamma, 20: 40972
radioinduced luminescence in, 20: 23186(P)
radioinduced paramagnetic centers in, ESR spectra of, 19: 46390
radioinduced paramagnetic centers in, ESR spectra from alpha, beta, gamma, and neutron, (E), 20: 15972
reduction of, effects of selenium-76 and selenium-82 in, 20: 18642

SODIUM SILICATE GLASS
dielectric properties, effects of niobia on, 17: 12686
diffusion of iron in, 17: 35264(R) (UCRL-10706(p.111-203))
diffusion of iron into, at 900 to 1050°C, 18: 10545 (UCRL-1116)
diffusion of iron oxides in di-, kinetics, 19: 44611 (UCRL-16232)
diffusion of iron into di-, 19: 43997(R) (UCRL-11889)
diffusion of iron oxide in, 20: 31719(R) (UCRL-16658, pp 155-69)
preparation and devitrification properties of fuel- and neutron absorbent-bearing, 20: 13209 (ANL-7062)
preparation and properties containing uranium, 16: 11645
radiation effects on electric conductivity of, 17: 24020
radiation effects on electric conductivity of, fast neutron, 19: 18543
radiation effects on magnetoresistance of, gamma, 20: 24628(T)
radioinduced color centers, inhibition by cerium, 16: 32159
radioinduced color centers in, effects of melting conditions on, 19: 7985
radioinduced coloration of impurity-doped, electron, 19: 13460
radioinduced color centers in, effects of cerium on kinetics of, 19: 42912
radioinduced color centers in, gamma, (E/T), 20: 9588(T)
radioinduced optical absorption in, effects of structure on, 17: 2044
radioinduced optical absorption centers in, γ, 18: 32202
resistance to caustic soda, effects of lanthanum and zirconium on, 18: 32201
structure of, containing plutonium(IV) oxide, x-ray-diffraction study of, 19: 16075 (MLM-1163(p.P-1-10))

SODIUM SILICATES
corrosion inhibiting effects on carbon steel, 19: 21714 (RL-REA-592)
crystallization and melting kinetics of, 20: 29623(R) (TID-22970, pp 121-256)
effect of, on reactor effluent radionuclides, 20: 45215 (BNWL-282)
effects on radionuclide contents in reactor effluent water, 18: 36752 (HW-75782)
heat transfer effects of coatings on solids, boiling, 16: 13217
reaction with lanthanum sulfate, preparation of lanthanum silicates by, 18: 25433
reactions with lanthanum sulfate, preparation of lanthanum silicate by, 19: 40518
reactions with phenylmethyl dichlorosilane for preparation of silicate silane polymers, 16: 20350(R) (AGC-0423-01-3)
reactions with uranium(IV) salts, 19: 15452(T) (ANL-Trans-33(p.228-37))
reactions with uranium(IV-VI) oxide in presence of oxygen, formation of uranates in, 19: 15453(T) (ANL-Trans-33(p.238-44))
scintillation properties in liquid helium, 18: 25849
thermal properties, 16: 11504(T) (NP-tr-837)
graphite–MoS_2–Na_2SiO_3–H_2O, radiation effects on properties as solid-film lubricants, 17: 36347(R) (NARF-62-18P)
graphite–MoS_2–Na_2SiO_3, radiation effects on solid-film lubricants of, 19: 23121
graphite–MoS_2–$NaSiO_3$, radiation effects on lubricant wear properties of solid films, 19: 44095

SODIUM SPACE
determination, radioisotope dilution method, 19: 15006
effects of AET on, in rats, 20: 18458
measurement in man of, tracer method, 19: 34058
measurement in man, tracer study, 20: 6993
measurement of, tracer method, 19: 43898
radiation effects, 16: 4057
radiation effects on shift in rat, x, 18: 38866

SODIUM STANNATES
Mossbauer effect on tin-119 isomers in, 17: 21086

SODIUM STEARATES
catalytic effects on radiation peroxidation of kerosene, 16: 8775

Sodium Succinates
see Succinic Acid, Sodium Salts

SODIUM SULFATES
see also Sodium Acid Sulfates
see also Sodium Dodecyl Sulfates
see also Sodium Thiosulfates
additive effects on gamma-induced polymerization of acrylonitrile in aqueous solution, 18: 29716(T,R) (AEC-tr-6231(p.175-85))
analysis of, for sulfur-35, combustion method for, 20: 36721
catalytic activity, effects of sulfur-35 and x radiation, 16: 227
catalytic activity of, effects of sulfur-35 labeling on, 18: 12188
catalytic properties for cyclohexanol dehydration, radiation effects, 16: 27099
chlorine-34 oxidation states in proton-irradiated, 16: 25443
corrosive effects on 1Cr18Ni9T stainless steel, 16: 488(T) (AEC-tr-4683)
corrosive effects on steel, 16: 12059
corrosive effects on high-strength alloys and steels under static stress, 16: 25717(R) (NP-11948)
corrosive effects of, on engineering metals, 17: 22123
corrosive effects on zinc, tracer studies on, 18: 25927
crystallization from simulated glass melter condensate, 20: 40476(R) (BNWL-267)
distribution of sulfur-35-labeled, in growing pigeon feathers, 20: 45317
effects of sulfur-35-labeled, on skeletal growth in rats, 20: 16267
effects of, on excretion of strontium-90 from mice, 20: 32922
effects on cerium reactions with oxalic acid in sulfuric acid media, 18: 33537
effects on distortion in development of nuclear emulsions, 19: 40884
effects on electron exchange reactions between thallium and uranium in methanol–water solutions, 18: 27418
effects on ESR spectra of irradiated sodium polyphosphates, 20: 36870
effects on gamma-induced polymerization of acrylonitrile in aqueous solution, 18: 29716(T,R) (AEC-tr-6231(p.175-85))
effects on nitrogen-15 exchange between nitric acid and nitric oxide, 20: 9363(R) (NYO-755-2, Paper 3)
effects on pH of dialyzed zirconyl chloride, 17: 35718
effects on phenol formation by radioinduced oxidation of benzene, 18: 17876
effects on polymerization of acrylonitrile in aqueous solution, 16: 30455
effects on solubilities of alkaline earth sulfates in water, 19: 30156 (ORNL-tr-649)
effects on solvent extraction of cobalt acetylacetonate using isopropyl alcohol, 20: 7211
effects on solvent extraction of uranyl acetylacetonate using chloroform, 20: 7211
effects on strontium-85 uptake by rats, 19: 6959
effects on strontium-85 metabolism in rats, 19: 33743
effects on strontium-85 elution from mouse bones, 19: 43706
effects on strontium-90 excretion by mice, 20: 8563
effects on strontium-85 excretion by rats, 20: 26612
effects on uv photolysis of aqueous methanol solutions, 18: 43634
effects on yields in radiolysis of nitrous oxide aqueous solutions, 18: 31601
heat of solution and thermodynamic properties of, in sodium nitrate, 18: 5283
heat of transformation, 17: 35264(R) (UCRL-10706(p.111-203))
hydrolysis of uranyl ion in, complexes in, 18: 13734
metabolism of sulfur-35-labeled, in rat aorta, 20: 8590
neutron reactions (n,p) with sulfur-32 in, thermal annealing of recoil effects in, 18: 299
osmotic coefficients as function of concentration at high temperatures, 16: 14735
osmotic coefficient at 140°C, 17: 40805
osmotic coefficients of aqueous, at 165°C, 19: 30151(R) (ORNL-3789 (p.139-63))
osmotic properties at 152°C, 18: 22014(R) (ORNL-3591(p.84-101))
oxygen isotopic exchange in melts of, at 700 to 955°C, 19: 40506
oxygen-18 exchange with oxygen, 17: 39130
physicochemical properties, 16: 12801(R) (IA-685)
polarography in lithium and lithium sodium metaphosphates at 750 and 730°C, 18: 1516
preparation of sulfur-35-labeled, 16: 22230
properties as decontaminant for water cooled reactors, 16: 20984
protective effects against radiation damage in crop plants, 19: 43877
radiation effects on phase transformations in, 17: 16066
radiation effects on, hydrogen peroxide yields in (E), 19: 456
radiation effects on catalytic activity, 19: 5969
radiation effects on uptake of sulfur-35-labeled, by rat liver, 20: 10542
radiation effects on metabolism of sulfur-35-labeled, in rat liver, x, 20: 20410
radiation effects on oxygenated aqueous solutions of, polarographic studies of 10-Mev pulsed electron, 20: 33337 (RISO-114)
radioinduced phosphorus in, oxidation states of, 20: 33341
radiolysis in ice, electron and hydrogen atom production in gamma, 17: 34026
radiolysis of alkaline and neutral solutions of, effects of air and oxygen on, 19: 461
radiolysis of anhydrous and hydrated, gamma, 20: 36903
radiolysis of aqueous solutions of, temperature effects on hydrogen peroxide yield in, 19: 13470
radiolysis of deaerated aqueous solutions of, cation polarization and hydrogen peroxide formation in gamma, 20: 18782
radiosensitivity effects on *E. coli*, 16: 28853
reaction with cerium, neodymium, and samarium oxides, 16: 18917
reactions in dioxane–water solutions, nuclear magnetic resonance spectra of, 17: 40800
reactions with alkaline earth and rare earth elements, thorium, and uranium, precipitation, 17: 10621
reactions with spodumene at 700 to 1000°C, 16: 9998

reactions with uranium(IV-VI) oxide, 19: 15430(T) (ANL-Trans-33 (p.75-6))
reactions with zirconium oxychloride, 16: 5334
separation from barren carbonate leach liquor in uranium recovery from ore, 16: 17757(P)
separation of fission products from glass melter condensate of, method for, 20: 24809(R) (BNWL-213)
solvent properties for beryllium oxide in beryllium aluminum silicates, 16: 11801
solvent properties for boron in mixture with hydrogen peroxide, 16: 28909
solvent properties for highly radioactive fallout particles, 18: 23795
solvent properties in paper chromatographic separation of inorganic cations, 18: 39388
sulfur valence in, beta spectroscopy for, 18: 25303
sulfur-35 exchange with sulfur trioxide, radiation effects, 16: 27099
thermodynamic properties, 17: 20312 (UCRL-10631)
benzene–didecylamine–Na_2SO_4–H_2SO_4–H_2O, solvent properties for uranyl sulfate, interface and transferring species in, 20: 43424 (ORNL-P-2359)
$Ce_2(SO_4)_3$–Na_2SO_4, thermal stability, 19: 40511
$Gd_2(SO_4)_3$–Na_2SO_4, thermal stability, 19: 40511
$La_2(SO_4)_3$–Na_2SO_4, thermal stability, 19: 40511
$MgSO_4$–Na_2SO_4, catalytic effects on conversion of cyclohexanol to cyclohexene, effects of impurities on, 17: 39191(R) (ORNL-3452 (p.210))
$MgSO_4$–Na_2SO_4, effects of sulfur-35 on exchange reactions in, 20: 10936(T) (CEA-tr-A-1855)
$MgSO_4$–Na_2SO_4, radiation effects on catalytic dehydration of cyclohexanol in vapor phase, 17: 12742
$MgSO_4$–$NaSO_4$, radiation effects on catalytic dehydration of cyclohexanol by, 17: 37263
$MgSO_4$–$NaSO_4$, specific surface of radioactive catalysts of, 18: 41308(T) (ORNL-tr-259)
$MgSO_4$–Na_2SO_4, surface area and radioactivity of sulfur-35-labeled, 19: 20013
Na_2CO_3–Na_2SO_4, thermodynamic consistency tests of phase equilibrium of, 19: 42958
$NaPO_3$–Na_2SO_4, molar volume and surface tension of fused, 18: 32177
$Na_3P_3O_{10}$–Na_2SO_4, polarographic analysis for uranium(IV), 17: 5990
Na_2SO_4–SO_3, effects of sulfur-35 on exchange reactions in, 20: 10936(T) (CEA-tr-A-1855)
Na_2SO_4–UO_2SO_4, phase diagrams and thermal analysis of, 20: 45697
$Nd_2(SO_4)_3$–Na_2SO_4, thermal stability, 19: 40511
O–Na_2SO_4, effects of sulfur-35 on exchange reactions in, 20: 10936(T) (CEA-tr-A-1855)
$Pr_2(SO_4)_3$–Na_2SO_4, thermal stability, 19: 40511
$Sm_2(SO_4)_3$–Na_2SO_4, thermal stability, 19: 40511

SODIUM SULFIDES

corrosive effects on 1Cr18Ni9T stainless steel, 16: 488(T) (AEC-tr-4683)
effects of, on activity of hydrogen dehydrogenase, exchange reactions and kinetics of, 17: 19793
effects of, on excretion of strontium-90 from mice, 20: 32922
effects on bactericidal activity in irradiated *p*-bromophenol, 19: 46007
effects on bactericidal activity of irradiated *p*-bromophenol, 19: 45834
effects on radioinduced degradation of DNA in *E. coli*, 20: 31144
neutron reactions (n,p) with sulfur-32 in, thermal annealing of recoil effects in, 18: 299
preparation of thin films of, by molecular plating, 20: 25027 (AERE-R-5097, Paper 17)
protective effects against radioinduced oxidation of iron(II), 16: 27085
protective effects against radiation injuries in mice, 18: 11844(R) (NP-13555(p.64-83))
protective effects on amidol photographic developer, 18: 23554
radiation effects on oxygenated aqueous solutions of, polarographic studies of 10-Mev pulsed electron, 20: 33337 (RISO-114)
radioinduced oxidation in aqueous solutions, 16: 7579 (PAN-259/CHR)
radiolysis of aqueous solution with sodium hydroxide, hydrogen yield in, 16: 23716 (PAN-290/ChR)
radiosensitivity effects in mice, x, 20: 14393
reactions with oxygen and sodium hydroxide, radioinduced free radicals in, 16: 5262
spectra of oxygen-18-labeled, infrared, 17: 25198
sulfur exchange with sulfur dioxide, 16: 23574
sulfur valence in, beta spectroscopy for, 18: 25303
therapeutic effects on radioinduced leukopenia, 16: 2916
therapeutic effects on radiation injuries in hematopoietic system, 16: 14594
therapeutic effects in radiation sickness, 17: 5927
therapeutic effects on radiation injuries in mice, 17: 33485(R) (NP-13010 (p.49-54))
therapeutic effects of, against radiation injuries in mice, 18: 5136(R) (NP-13281(p.57-69))
therapeutic effects against radiation sickness in dogs, 18: 8225
use in therapy radiation sickness in rats, condition of maxillodental system during, 19: 8976
use of sulfur-35-labeled, for thiamine hydrochloride determination, 20: 7040
use to remove oxygen from HWCTR cooling water, 19: 11668(R) (DP-945)
O–NaOH–Na_2SO_3–H_2O, radiolysis of, hydrogen yield in, 16: 23716 (PAN-290/ChR)

SODIUM SYSTEMS

Al–B–silicate–Na, preparation as phosphor for neutron detection, 19: 15927
Ar–Na, excitation transfer in first excited states of sodium, cross sections for collision-induced, (E), 20: 11499
C–Na, carburization effects on type 304 stainless steel, 19: 44624 (NAA-SR-Memo-4387)
Ca–H–Na, phase equilibrium studies in clinoptilolite, 17: 31681(R) (HW-76559)
He–Na, excitation transfer in first excited states of sodium, cross sections for collision-induced, (E), 20: 11499
H–K–Na, phase studies, 19: 30154(R) (ORNL-3789(p.308-17))
H–Li–K–Na, phase studies, 19: 28755(R) (ORNL-3823)
H–Li–K–Na, phase studies, 19: 30154(R) (ORNL-3789(p.308-17))
H–O–Na, studies of, 19: 17850 (CEA-R-2583)
K–Na–UO_2, performance as reactor fuel slurries, 18: 32215 (A/CONF.28/P/241)
K–Na–UO_2, studies of slurry as potential fuel, 17: 11077 (ANL-6644)
Kr–Na, excitation transfer in first excited states of sodium, cross sections for collision-induced, (E), 20: 11499
Mn–Na–Te, thermoelectric properties at high temperatures, 17: 29854(R) (MND-2584-4)
Mo–O–Na, equilibrium distribution of oxygen in, at 500 to 800°C, 18: 4253(R) (ORNL-3470(p.63-6))
Na–H_2O, reaction thermodynamics, 16: 12843
Na–NaCl, free energy of solution of, 19: 11103
Na–NaH–NaOH, corrosive effects on Croloy 2¼, 20: 4317 (BAW-1280-30)
Na–NaH–NaOH, corrosive effects on Croloy 2¼ steel, 20: 16599(R) (BAW-1280-34)
Na–NaOH, corrosive effects on Croloy 2¼, 19: 4303(R) (BAW-1280-17)
Na–NaOH, corrosive effects on Croloy 2¼ at 900°F, 19: 7676(R) (BAW-1280-20)
Na–NaOH, corrosive effects on Croloy 2¼, 20: 4317 (BAW-1280-30)
Na–NaOH, corrosive effects on Croloy 2¼ steel, 20: 16599(R) (BAW-1280-34)
Na–UC, corrosive effects on stainless steel, 19: 40113(R) (ANL-7071)
Na–UC, properties for paste blanket-fuel, 20: 28691(R) (APDA-185)
Na–UC, testing of breeding blanket slurries of, (E), 20: 10366(R) (APDA-178, pp 10-17)
Na–UN, corrosive effects on stainless steel, 19: 40113(R) (ANL-7071)
Na–UN, preparation of pastes of, 19: 29468(R) (ANL-7017)
Na–UN, preparation of paste of, for use as blanket fuel, 19: 32279(R) (ANL-7020(p.3-99))
Na–UN, properties for use as reactor blanket material, 19: 6828(R) (ANL-6944(p.53-76))
Na–UO_2, corrosive effects on stainless steel, 19: 40113(R) (ANL-7071)
Na–WO_3, superconductivity of sodium tungsten bronzes, (E), 19: 8351
Na–WO_3, superconductivity of bronze, (E), 19: 23568
Na–Xe, excitation transfer in first excited states of sodium, cross sections for collision-induced, (E), 20: 11499
Nb–O–Na, equilibrium distribution of oxygen in, at 500 to 800°C, 18: 4253(R) (ORNL-3470(p.63-6))
Ne–Na, excitation transfer in first excited states of sodium, cross sections for collision-induced, (E), 20: 11499
NH_3–Na, electron-nuclear double resonance studies of solutions of, 18: 26154
NH_3–Na, heat of solution and volumes of, 18: 31429 (UCRL-7265-T)
NH_3–Na, reactions of, with ethanol, mechanism of, 16: 32985
NH_3–Na, spectra of liquid, effects of temperature on infrared, 16: 18856 (UCRL-10062)
NH_3–Na, spectra of sodium-23 Knight shifts and relaxation times in, 19: 7386
NH_3–Na–Sn, preparation and structure of saltlike compound $Na_xSn_y \cdot xNH_3$, 18: 31058(T) (ANL-Trans-34)

NH_3–Pb–Na, preparation and structure of saltlike compound $Na_4Pb_9 \cdot xNH_3$, 18: 31058(T) (ANL-Trans-34)
O–K–Na, effects of oxygen content on corrosive effects of, 19: 24939(R) (ORNL-3784)
O–Na–Ta, equilibrium distribution of oxygen in, at 500 to 800°C, 18: 4253(R) (ORNL-3470(p.63-6))
O–Na–U, phase studies at 600 to 1000°C, 19: 23031
O–Na–U, phase studies at 600 to 1000°C, 20: 31666
O–Na–W, equilibrium distribution of oxygen in, at 500 to 800°C, 18: 4253(R) (ORNL-3470(p.63-6))
O–Na–Zr, equilibrium distribution of oxygen in, at 500 to 800°C, 18: 4253(R) (ORNL-3470(p.63-6))
Sb–Cs–K–Na–Te, photosensitivity of, 20: 17984
Si–Na, crystal structure, 18: 30216

SODIUM TANTALATES
see also Potassium Sodium Tantalates
crystal structure, 19: 37059
$NaNbO_3$–$NaTaO_3$, phase relations in solid state, 17: 18060
$NaNbO_3$–$NaTaO_3$, phase studies, 18: 24162

SODIUM TARTRATES
see also Potassium Sodium Tartrates
effects on pH of dialyzed zirconyl chloride, 17: 35718
separation from uranyl bis(dibenzoylmethane) by solvent extraction into chloroform, 16: 11792

SODIUM TECHNETATES
oxygen-17 NMR in, 17: 3645
preparation, properties, and structure of, 19: 24510

SODIUM TELLURATES
Mössbauer absorption spectrum, 17: 25167 (UCRL-7045)
radiolysis in aqueous solutions with nitrous oxide, yields in, 20: 393
tellurium-125 Mössbauer effect in, (E), 20: 20148
tellurium-127 from labeled, effects of thermal annealing on, 18: 41539

Sodium Test Facility
see Heat Transfer Systems

SODIUM TETRABORATES
see also Borax
corrosive effects on structural materials, 20: 16976
nuclear magnetic resonance in deuterated, (E), 19: 15547
preparation from boron samples for isotopic analysis, procedure for, 19: 30081(R) (NBL-216)
radiation effects on catalytic effects of, on para- to orthohydrogen conversion at 77°K, 20: 23790
$CaSO_4$–$Na_2B_4O_7$, preparation and properties for fixation of waste solutions in, 20: 24809(R) (BNWL-213)
$PbSO_4$–$Na_2B_4O_7$, preparation and properties for fixation of waste solutions in, 20: 24809(R) (BNWL-213)

SODIUM TETRAFLUOROBORATES
viscosity at 436 to 466°C, 20: 22856(R) (ORNL-3913, pp 1-51)

SODIUM TETRAMETHOXYBORATES
formation in methanolysis of sodium borohydride, effects of sodium carbonate and methoxide on, 16: 13043

SODIUM TETRAPHENYLBORATES
protective effects against cesium-137 uptake by rat intestine, 19: 8767
solvent properties for cesium, 19: 46441
sorption of cesium from aqueous solutions of, by glass, polyethylene, and Teflon, 20: 40915
use in determination of rubidium, 17: 5989

SODIUM TETRATHIONATES
radiation effects on, ESR studies of, 19: 24551
radiation effects on, at 77°K, EPR studies of, 20: 8990
radiolysis of dihydrate of, tracer studies of mechanism of, 20: 9005

SODIUM THIOCYANATES
sulfur-35 exchange between, and 4-chlorobenzhydryl thiocyanate, 20: 29237
KCN–NaSCN, reactions with organic compounds, 19: 32048(R) (NP-15073)

SODIUM THIOSULFATES
complexes with cysteine, protective effects of, against radiation injuries in mice, 19: 46006
complexes with uranyl ions, preparation and thermodynamic properties of, 17: 38927
decomposition and oxidation, 16: 23574
decontamination effects of, with ultrasonics on rat skin contaminated with ^{131}I, ^{32}P, or ^{90}Sr, 20: 42811
effects on permeation of rubidium-86 in x-irradiated isolated frog heart, 20: 3794
effects on strontium-85 elution from mouse bones, 19: 43706
nuclear spin resonance lines in, energy levels and relative intensities of, 17: 24072(T) (JPRS-19316(p.162-76))
preparation of sulfur-35-labeled, 18: 8417
properties in dosimeter film processing, 19: 15807
properties of aqueous, for sorption of aerosol iodine, 18: 41679(R) (NYO-841-1)
protective effects against x radiation in animal cells, 17: 15769
protective effects of, against epilation in mice produced by x radiation, 17: 35472
protective effects of, against radiation injuries in aortic wall, 17: 40644
protective effects against radiation injuries in mice, reaction mechanisms of, 19: 10899
radiation effects on alkaline solutions, 16: 28987
radiation effects on electron magnetic resonance in, gamma, 17: 32166
radiation effects on electron spin resonance spectra of, 17: 32746
radiation effects on single crystals of, ESR spectra of free radicals in, 20: 374
radioinduced electron paramagnetic resonance signals in hydrated, 19: 9233
radiolysis of sulfur-35-labeled, scintillation counting of radioactive hydrogen sulfide from, 19: 17818
radiolysis of, ESR spectra of free radicals induced by, 19: 34222
radiolysis of, tracer studies of mechanisms in, 19: 17970
radiosensitivity effects in bacteria, 17: 35509
radiosensitivity effects on cattle and rat skin permeability, x, 18: 17646
radiosensitivity effects on blood vessels in rabbit heart, x, 20: 18456
spectra of gamma-irradiated single crystals of, electron spin resonance, 18: 5387
sulfur valence in, beta spectroscopy for, 18: 25303
sulfur-35 exchange with sulfide, kinetics of, 18: 39200

SODIUM THORIUM CARBONATES
formation and stability, 17: 1474

SODIUM THORIUM HYDROXIDE PHOSPHATES
preparation and properties of, 20: 29160

SODIUM THORIUM OXALATES
formation and stability, 17: 1474

SODIUM THORIUM PHOSPHATES
preparation and crystal structure, 20: 8902
preparation and properties of, 20: 29160

SODIUM THORIUM SULFATES
preparation and properties, 20: 8941
preparation and properties of, 20: 29218

SODIUM TITANIUM CHLORIDES
magnetic susceptibility, effects of temperature on, 16: 20423

Sodium Trifluoroacetates
see Acetic Acid, Trifluoro-, Sodium Salts

SODIUM TUNGSTATES
see also Sodium Europium Tungstates
see also Sodium Neodymium Tungstates
analysis for oxygen-18, mass spectrometric, 20: 8852
analytical use for titration of gadolinium in presence of bromocresol purple and methyl red mixed indicators, 18: 33510
analytical use in determination of neodymium, 18: 21964
analytical use in determination of lanthanum by amperometric titration, 19: 42428
effects on hydrolysis of lactose in oxygen-18-labeled water, catalytic, 19: 30177
effects on spectrofluorometric determination of rare earths, 20: 12787
electric conductivity, 18: 2401(R) (IS-700(Sect.P))
electrical properties, 17: 6658 (IS-433)
electron spin resonance in, (E/T), 20: 4476(R) (IS-1200(Sect.P))
enthalpies at 80 to 300°C, 20: 4297(R) (IS-1200(Sect.M))
enthalpy of, at 50 to 260°C, 20: 41412(R) (IS-1500(Sect. M))
fluorescence of lanthanide ions in, effects of pH, concentration, temperature, and time on, 20: 43210
fluorescence of trivalent lanthanide ions in, 20: 43211
hydrolysis, 19: 347(R) (ORNL-3679(p.60-83))
oxygen isotopic exchange in melts of, at 700 to 955°C, 19: 40506
oxygen-18 exchange with gaseous oxygen near 750°C, 16: 7534
oxygen-17 NMR in, 17: 3645
oxygen-18 exchange between gaseous oxygen and, mechanism and rate of, 20: 422
photosensitivity of, effects of titanium dioxide on, 20: 10837
polarography in lithium and lithium sodium metaphosphates at 750 and 730°C, 18: 1516
production, properties, and structure of, 19: 44021
properties of, electronic, (E/T), 20: 4476(R) (IS-1200(Sect.P))
properties, electric and thermal, 19: 9767(R) (IS-900(Sect.P))
radiation effects on phase transformations in, 17: 16066
sodium-23 NMR in, relaxation of, 18: 42194
spectra of crystalline, infrared and Raman, 18: 1613(R) (ORNL-3488 (p.18-20))
spectra of, infrared and Raman, 18: 29641
spectra of, Raman, 19: 347(R) (ORNL-3679(p.60-83))
structural properties, 17: 14210 (NBS-MON-25(Sect.1))
thermal capacity, (E), 20: 4476(R) (IS-1200(Sect.P))
thermal capacity at 10 to 300°K, 18: 2401(R) (IS-700(Sect.P))
thermodynamic properties at low temperatures, 19: 9046(R) (IS-900 (Sect.C))
tungsten-185 exchange in aqueous system of meta- and ortho-,

20: 12822 (IS-T-68)
uses in amperometric titration of thorium, 20: 26781
uses in determination of rare earths, 20: 18608
uses in determination of thorium by conductometric titration, 20: 20592
$H_4Fe(CN)_6$–Na_2WO_4, ion exchange properties for cesium-137 and strontium-90, 20: 3871 (EUR-2497.e)
$H_4Fe(CN)_6$–Na_2WO_4, preparation and ion exchange properties of, 20: 7083
$Na_6(H_2W_{12}O_{40})$–Na_2WO_4, isotopic exchange in, 20: 3863(R) (IS-1200 (Sect. C))
NaOH–Na_3PO_4–Na_2WO_4, electrolytic etching and polishing of rhenium–tungsten alloys in, 18: 27931
Na_2WO_4–WO_3, density and electric conductivity of molten, 19: 24528
Na_2WO_4–WO_3, electric conductivity and density of molten, 18: 31471
$Nd_2(WO_4)_3$–Na_2WO_4, phase diagrams, 20: 37241
O–$Na_2W_2O_{11}$, activation energy of oxygen-16 and -18 exchange at 400 to 750°C in, 18: 27456

SODIUM TUNGSTOCERATES
preparation and physicochemical properties, 20: 43253

SODIUM URANATES
see also Sodium Fluouranates
analysis of, use of quantometer in, 19: 15367
burnup and fission product removal, design of loop for studying, 16: 34002(T) (AEC-tr-5309)
composition and structure of, precipitated from solutions of sodium hydroxide and uranyl nitrate, 19: 15434(T) (ANL-Trans-33(p.101-9))
conversion into fluorides, 16: 18980(P)
crystal structure and uranyl bond lengths from infrared spectra, 19: 23957
formation and composition of, by reactions of sodium carbonate with uranium oxides, 19: 15424(T) (ANL-Trans-33(p.34-43))
formation by reaction of silicate with uranium oxide in presence of oxygen, 19: 15453(T) (ANL-Trans-33(p.238-44))
formation in aqueous media, 16: 20385
formation in reactions of sodium chloride with uranium(IV-VI) oxide, 19: 15429(T) (ANL-Trans-33(p.70-4))
formation in reaction of sodium sulfate with uranium(IV-VI) oxide, 19: 15430(T) (ANL-Trans-33(p.75-6))
formation in reaction of sodium nitrate with uranium(IV-VI) oxide, 19: 15431(T) (ANL-Trans-33(p.77-8))
heat of formation of mono-, 19: 15442(T) (ANL-Trans-33(p.170-2))
hydrolysis and decomposition in dilute solutions, physicochemical studies, 16: 17637(T) (AEC-tr-4459(p.113-27))
hydrolysis of mono-, 19: 15435(T) (ANL-Trans-33(p.110-13))
ion exchange between alkali metal ions and precipitated, in solution, 19: 15437(T) (ANL-Trans-33(p.127-41))
ion exchange with cerium, lithium, potassium, and rubidium, 18: 219
isotope exchange with cesium, lithium, potassium, and rubidium, 18: 219
isotopic exchange reactions with oxygen-18, activation energies for, 19: 24593
isotopic exchange between gaseous oxygen and, 19: 30190
isotopic exchange between alkali metal ions and precipitated, in solution, 19: 15437(T) (ANL-Trans-33(p.127-41))
precipitation, conductometric studies, 17: 15999
precipitation of poly-, from aqueous solutions, 19: 15432(T) (ANL-Trans-33(p.79-88))
preparation and properties, 18: 17827
preparation and properties, 19: 42462
preparation from carbonate leach liquor at Eldorado Beaverlodge Mill, 20: 25212
processing for vanadium separation, 19: 18085(P)
purification from vanadium and other impurities, 16: 17704(P)
radiation hazards from use of, as coloring agent for artificial teeth, 19: 38473 (NP-14923)
reactions with hydrogen above 600°C to prepare uranium dioxide, 19: 17906
reduction by hydrogen, 19: 15440(T) (ANL-Trans-33(p.153-64))
spectra and structure, 18: 25388
structural properties for uranyl bonding, 17: 15959 (TID-18140)
structure of di-, 19: 15423(T) (ANL-Trans-33(p.24-33))
structure of mono-, 19: 15421(T) (ANL-Trans-33(p.4-16))
structure of mono-, 19: 15422(T) (ANL-Trans-33(p.17-23))
thermal capacity of mono-, at 390 to 916°C, 19: 15443(T) (ANL-Trans-33 (p.173-5))
thermal stability of mono-, 19: 15438(T) (ANL-Trans-33(p.142-7))
thermal stability of poly-, 19: 15438(T) (ANL-Trans-33(p.148-52))
$CaUO_4$–$Na_2U_2O_7$, structure and properties, 17: 21605
NaF–$Na_2U_2O_7$, crystal structure and intergrowth mechanisms, 17: 40820

SODIUM URANIUM(IV) FLUORIDES
fluorination, preparation of trisodium uranium(V) fluoride by, 16: 25328(T) (AEC-tr-5205)
preparation, electrochemical, 17: 1370
production from uranyl nitrate by dry method, pilot plant for, 16: 20530

SODIUM URANIUM (V) FLUORIDES
preparation and properties, 17: 35690 (LADC-5861)
preparation and structure, 16: 25328(T) (AEC-tr-5205)
preparation, crystal structure, and properties, 19: 26300

SODIUM URANIUM(VI) FLUORIDES
preparation and properties, 17: 12228 (TID-16242)
preparation of single crystals, 20: 8904

SODIUM URANIUM PHOSPHATES
preparation and crystal structure, 20: 8902

SODIUM URANYL ACETATES
Cotton effect in optically active crystals of, temperature dependence of, 20: 34853
electro-optic effect in, (E), 20: 10243
exciton rotatory dispersion of single crystals of, 20: 34852
infrared absorption spectrum of monocrystalline, at room temperature, 20: 43285
luminescence of crystals of, circular, 19: 19921
luminescence spectra of single crystals of, polarization of, 20: 25097
optical activity of crystalline, dispersion of circular dichroism in, 19: 24519(T)
optical properties of crystalline, 19: 24518
radioinduced luminescence in crystals of, laser beam, 19: 20010
spectra at 4 and 20°K absorption, 16: 22147
spectra of single crystals, circular dichroism and optical activity effects, 16: 19516(T)

SODIUM URANYL CARBONATES
dermatitis-induction by, 18: 4977
formation of complex dicarbonate, 16: 1658
reactions with ammonium uranyl compounds, 16: 118
stability constants, 16: 30410

SODIUM URANYL OXALATES
crystal structure and dielectric polarization of hydrated, 18: 41457

SODIUM URANYL PHOSPHATES
precipitation from solutions of sodium hydrophosphate and uranyl salts, 19: 15457(T) (ANL-Trans-33(p.280-9))
solubility in phosphoric acid, products of, 19: 24443
solubility of, tracer studies of, 18: 23545

SODIUM URANYL VANADATES
behavior in solutions, 19: 15462(T) (ANL-Trans-33(p.315-22))

SODIUM VANADATES
analytical use in amperometric determination of uranyl ions, 20: 255
oxygen-17 NMR in, 17: 3645
reactions with thorium salts, electrometric study of, 20: 36822
reactions with uranyl nitrate in solution, formation of uranyl vanadate in, 19: 15461(T) (ANL-Trans-33(p.305-14))
reactions with uranyl nitrate, 20: 12796
stoichiometry of, activation determination of, 18: 8293
use in radio-release method for tracing stream flows, 19: 34326 (TID-21881)

SODIUM VANADYL VANADATES
thermoelectric properties of liquid, 17: 6633 (AD-274831)

SODIUM XENATES
effects on mice, metabolic and toxicologic, 18: 4993
Mössbauer effect in, 17: 32089
preparation and properties, 19: 38624

SODIUM YTTERBIUM BROMIDES
formation and stability of, in aqueous solutions, 19: 30182

SODIUM YTTERBIUM CHLORIDES
formation and stability of, in aqueous solutions, 19: 30182

SODIUM YTTERBIUM OXIDES
preparation and properties, 19: 42514
preparation, properties, and structure of, 19: 46241(R) (TID-22207, Paper A)

SODIUM YTTRIUM FLUORIDES
crystal structure, 17: 25060(R) (ORNL-3417(p.3-16))
crystal structure and preparation, 17: 33888
crystal structure, 19: 30149(R) (ORNL-3789(p.3-35))

SODIUM ZIRCONATES
preparation and uses, 19: 38647
preparation, structure, and thermal stability, 16: 30413
production from zirconium ores, 16: 14763(P)

SODIUM ZIRCONIUM FLUORIDES
crystal structure, 20: 22856(R) (ORNL-3913, pp 1-51)
structure, 17: 25173

SODIUM ZIRCONIUM SILICATES
crystal structure, 19: 19916(T)
preparation, 17: 30564(P)
preparation and properties, 16: 120
preparation and properties of $Na_2ZrSi_2O_7$, 20: 43220

SOIL MECHANICS
use to determine soil behavior during projectile penetration, 20: 45240 (SC-RR-66-376)

see also Silts
see also Soil Mechanics
acid leaching of strontium from, 20: 8552(R) (TID-22443, pp 1-33)
age estimation of loess from Russian Steppe by carbon-14 method, 18: 25685
age of humus podzols, carbon-14 determination of, 18: 20223
agricultural properties of, tracer studies of effects of phosphorus compounds on, 19: 5599
alpha activity in, equipment for measuring, 20: 6694(R) (MIT-952-2)
alpha radioactivity, 18: 35382
amelioration of, use of gamma and neutron sources in studies of, 17: 12484
analysis and mapping of White Oak Creek watershed, 19: 6932(R) (ORNL-3697(p.85-94))
analysis by neutron activation, 20: 7041
analysis for antimony-125 from fallout, radiochemical, 18: 23431
analysis for beryllium at high explosive assembly test facility, 16: 2067
analysis for beta radioactivity at JAERI from 1956 to 1960, 16: 11965(R) (JAERI-5003(p.177-81))
analysis for beta activity, cesium-137, and strontium-90, radiochemical procedures for, 18: 13642 (SC-4783(RR))
analysis for calcium, strontium, and strontium-90 in soil-vegetation covers, flame spectrometric, 18: 39112
analysis for calcium, flame spectrometric, 19: 35890(T)
analysis for carbon-14 in fossil, use for age determination of Holocene, 17: 40994
analysis for cerium-144 and strontium-90 by solvent extraction and counting, 17: 21624
analysis for cerium-144, cesium-137, and strontium-90, radiochemical, 18: 8287(T) (AEC-tr-6049(p.47-74))
analysis for cerium-144, 18: 25265 (HASL-143)
analysis for cesium-137, radiochemical, 17: 33784 (DP-831(p.21-37))
analysis for cesium-137, rapid method for, 19: 19805
analysis for cesium-134, cobalt-60, and europium-152 and -154 after nuclear detonation, gamma spectroscopic, 19: 19829
analysis for cesium-137, radiochemical method for, 19: 28232
analysis for cesium-137 and strontium-90, method for, 20: 40853
analysis for cobalt, review of methods for, 17: 38943
analysis for copper, activation, 18: 21986
analysis for copper, neutron activation, 19: 30400(R) (ANL-6971(p.83-8))
analysis for dysprosium and scandium, activation and spectrometric, 16: 2975
analysis for elements in Norway, activation, 19: 308
analysis for exchangeable calcium and strontium using ammonium acetate, 20: 22948
analysis for fall-out fission products, 16: 6643 (DASA-1300(Vol.4))
analysis for fallout, 1963 and 1964, gamma spectrometric, 19: 30400(R) (ANL-6971(p.83-8))
analysis for fission products, gamma spectroscopic, 18: 1942 (CEA-2231)
analysis for iodine, 17: 7963(T) (CEA-tr-A-1179)
analysis for micronutrient elements, activation, 18: 21994
analysis for moisture by neutron scattering, 17: 1414
analysis for moisture using radiation, comparison of methods for, 18: 425
analysis for moisture, neutron method for, 18: 5505
analysis for moisture, neutron moderation method for, 18: 19905
analysis for moisture content, design of instrument using neutron source for, 18: 27821
analysis for moisture using neutron probe, 18: 29929 (NP-13993)
analysis for moisture, neutron monitor for, 18: 35808 (HW-82009)
analysis for moisture using neutron moderation, 18: 39565 (COO-712-73)
analysis for moisture by gamma scattering measurements, effects of soil density on, 18: 39106
analysis for moisture by neutron probing, 20: 31435
analysis for moisture using neutron scattering, 20: 41115(P)
analysis for plutonium and uranium traces, 18: 31372 (NDL-SP-7)
analysis for plutonium-239, radiochemical, 19: 11000
analysis for plutonium, radiochemical, 20: 8980(R) (BNWL-36, pp 3.1-122)
analysis for potassium, thorium, and uranium, spectrometric, 16: 9011
analysis for potassium, radiometric, 17: 40756
analysis for potassium, thorium, and uranium, gamma spectrometric techniques for, 18: 35888
analysis for potassium, activation, 19: 30113
analysis for potassium by gamma spectrometry, 19: 30123
analysis for radioactivity from fall-out, 16: 6644 (DASA-1300(Vol.5))
analysis for radioactive contamination, 17: 12516
analysis for radioactivity in France, 18: 16204(R) (SCPRI(RM)-XII-1963)
analysis for radionuclides by gamma spectrometry, 18: 35740
analysis for radioisotopes in sectioned cores of, autoradiographic, 19: 32106
analysis for radioisotopes, 20: 45264(R) (UCLA-12-595, pp 72-89)
analysis for radium-226, radiochemical, 17: 10531 (ANL-6637(p.97-9))
analysis for radon and thoron in gases, 16: 28701(R) (TID-16349)
analysis for radon using beta activity of daughter products, 18: 12018
analysis for rare earths by activation and focusing chromatography, 17: 30219
analysis for scandium, activation, 20: 22886
analysis for strontium-90, 16: 6381
analysis for strontium isotopes, 16: 18818 (TID-15415)
analysis for strontium, atomic-absorption spectrophotometric, 16: 26913
analysis for strontium, barium, calcium, and trace elements, 18: 3447 (NYO-10581)
analysis for strontium-90, method for, 18: 39089
analysis for strontium-89 and -90, radiochemical, 19: 19739 (AERE-AM-101)
analysis for strontium by emission spectrography, 19: 26243
analysis for strontium-90, flame spectrometric, 19: 35890(T)
analysis for strontium-90, samples collected in 1962, 17: 27592(R) (HASL-138)
analysis for thorium by barium sulfate precipitation, fluorometric, 18: 11988
analysis for total radioactivity, 18: 8285(T) (AEC-tr-6049(p.11-21))
analysis for total beta activity and potassium, 18: 41349
analysis for trace elements, isotope dilution, 20: 6726 (STI/DOC/10/48)
analysis for trace elements, neutron activation, 20: 6726 (STI/DOC/10/48)
analysis for tritiated water, liquid scintillation counting method for, 18: 23419
analysis for uranium by anion exchange, chromatographic, 16: 18845
analysis for uranium alpha activity by precipitation, 16: 23596 (AERE-R-3499)
analysis for uranium by extraction-luminescence, 16: 28904
analysis for uranium by alpha counting, 17: 1374 (AERE-AM-85)
analysis for uranium, radiochemical procedure for, 19: 30081(R) (NBL-216)
analysis for uranium by alpha measurement and chemical methods, 19: 36298
analysis for uranium using Arsenazo III, photometric, 20: 36774
analysis for water by neutron thermalization, 16: 11998 (NP-11380)
analysis for water by neutron scattering, 18: 41600
analysis for water, neutron radiometric, 19: 7720
analysis for water content, theory of neutronic method for, 19: 26234 (RISO-97)
analysis in bore hole, design of gamma-gamma probe for, 18: 27717
analysis in crime detection, activation, 20: 1738(R) (GA-4041)
analysis in crime detection, activation, 20: 1739(R) (GA-4297)
analysis in crime detection, activation, 20: 1736(R) (GA-3491)
analysis in criminal cases, activation, 20: 14439(R) (GA-5556)
analysis of, activation, 16: 31547 (ORNL-TM-363)
analysis of, for radioactive materials in Germany, 16: 32721
analysis of Formosan, for strontium-90, 17: 29984
analysis of, neutron-activation methods for, 17: 30036
analysis of residual, spectrochemical, 16: 4379
analysis of suspensions of, for carbon-14, liquid scintillation counting, 18: 29599
analysis of, activation, 18: 12006
analysis of, by neutron activation methods, 20: 35419
analysis of, for water content, by neutron scattering, 20: 39141
analysis of, laboratory methods for, 18: 29567 (TID-20640)
analysis of, neutron activation, 20: 31434
analysis of, oxygen-isotope, 18: 33787
analysis of, use of radioisotopes in, 18: 31992
analysis of, use of paper chromatography in, 20: 35389 (CEA-R-2791)
analysis, neutron activation, 19: 36291
antimony-125 content, 18: 19516
beryllium sorption in, effects of acidity on, 19: 45802
beta activity in, leachable, 20: 25286
beta activity of, in Italy, 1962, 18: 18040 (BIO/03/63)
beta activity of, effects of, on free air ionization near air-ground interface, 20: 27196 (HASL-170)
bibliography on tracer methods for moisture measurements in, 18: 24044 (NP-13931)
blast effects of underground nuclear explosions on, 18: 23783 (NP-13943(p.209-14))
book: *Natural Radioactivity of Plants and Soils*, 20: 29437
book: *Radioactive Fallout, Soils, Plants, Foods, Man*, 19: 26619
book: *Radioactivity of Soils and Methods of Measurement*, 20: 41139
burial of contaminated, tracer techniques for studying, 18: 39718 (CONF-646-1)
calcium and strontium-90 availability to plants from, effects of contact time and mineral type on, 20: 8584
calcium content of, effects on radiostrontium uptake by plants, 20: 18303

calcium content of Egyptian, 16: 4020 (A/AC.82/G/L.665)
calcium exchange with plants, tracer study, 17: 27046
calcium separation from, using potassium ferrocyanide, 18: 27631
calcium sorption by plowed, 18: 16217
calcium uptake by plants from, 19: 54
calcium-to-strontium ratio in, effects of morphological form on, 20: 43534
calcium-45 content of, effects of stable calcium on, 18: 43797
calcium-45 uptake by plants from, effects of sodium content on, 20: 10534(R) (BNWL-122, pp 168-9)
carbon dioxide fixation by nitrifying bacteria in, 19: 35941
carbon dioxide isotopic composition in, effects on carbon-13 variations in secondary calcites, 19: 38854
carbon-14 content in humus, relation of river mollusks content to, 18: 12341
cation exchange capacity in colloidal, tracer study, 17: 25135
cation migration into, during radioactive waste disposal, physicochemical equilibria in, 17: 29869(T) (EURAEC-417)
cerium-144 content in samples collected in 1963, 18: 18041(R) (HASL-144)
cerium-144 diffusion in, 18: 35722
cerium, iron, and manganese uptake by colloids of, 20: 19
cesium displacement and sorption by, effects of salt solutions on, 17: 39072
cesium distribution in, effects of quantity on, 19: 42241 (CEA-R-2708)
cesium separation from vermiculite, ion-exchange process for, 19: 26360
cesium sorption from natural waters, Cape Thompson, Alaska, 18: 25688 (TID-20638)
cesium uptake by barley from, 19: 42241 (CEA-R-2708)
cesium uptake by plants from, effects of chemical composition on, 20: 18208(R) (TID-22715)
cesium-134 distribution in, effect of moisture on, 17: 1230 (ORNL-3328)
cesium-137 content in, 1960 correlation with rainfall in United Kingdom, 16: 27417 (AERE-R-4018)
cesium-137 content in Colorado, 20: 12984
cesium-137 content in, of Cache la Poudre, Colorado, 20: 16723 (COO-1156-11)
cesium-137 content in, in Japan, 20: 16169
cesium-137 content in Chicago, Ill., 1965, 20: 43512(R) (ANL-7135, pp 315-27)
cesium-137 content in, in Japan, 1960 and 1961, 20: 43518(T) (NSJ-tr-54)
cesium-137 content at Nevada Test Site farm, 19: 43662(R) (UCLA-12-565, pp 97-128)
cesium-137 content in, near nuclear power plants in England, 18: 6775
cesium-137 content of, methods for decreasing, 19: 18209
cesium-137 deposition in, effects of weathering on, 18: 10285
cesium-137 desorption from, effects of sodium acetate on, 20: 30943(R) (ORNL-TM-1465)
cesium-137 downward movement in, during leaching with deionized water, 17: 32979
cesium-137 in, contamination of food chain by, 18: 16239
cesium-137 in, uptake by plants, 20: 16678
cesium-137 migration in Czech, 19: 5559 (UJV-1107/64)
cesium-137 sorption by, successive desorption method for calculating, 20: 20618
cesium-137 sorption by plowed, 18: 16217
cesium-137 transfer from, to dairy cattle feeds, 20: 37038
cesium-137 transport in, effects of vegetation, 19: 32420 (ORNL-P-1239)
cesium-137 uptake by, effects of ammonium, potassium, and rubidium ions on, 19: 27946
cesium-137 uptake by plants from, effects of sodium content on, 20: 10534(R) (BNWL-122, pp 168-9)
cesium-137 uptake by forest, 20: 20879 (BNWL-SA-530)
cesium-137 uptake from, effects of nitrogen, potassium, and phosphorus levels, 17: 2893
cesium-137 uptake from, by wheat, 18: 15761
cesium-144 distribution in, in Moscow region, 19: 22549
characteristics of Hanford Area, Wash., 20: 24818 (BNWL-243)
chemical properties of, in White Oak Lake bed, 17: 4369 (ORO-585)
chemical properties of Costa Rican, effects of recent volcanic ash and fertilizers on, 19: 35865(R) (NYO-2043-108(p.49-69))
chemical properties of, thin section technique for studies of, 20: 8537(R) (TID-22443, pp 83-99)
chemical properties of recent volcanic ash, 20: 42850(R) (NYO-2043-130)
chemical properties of recent volcanic ash, 20: 45248(R) (NYO-2043-129)
chemical reactions with fission products, 17: 31816(R) (ORO-605)
chemistry of, tracer studies, 20: 20389 (STI-PUB-108)
compaction of, effects on rubidium-86 and strontium-89 diffusion, 20: 18816
composition and ion exchange properties of, 20: 8979(R) (BNWL-36)
composition, effects on uptake of fission products by plants, 16: 20885
composition, effects on uptake of fission products by plants, 16: 20886
composition of Hanford, 20: 8817(R) (BNWL-36, pp 4.1-77)
composition of, effect on radon gas in air, 20: 39114
conference on soil-underground protective structure interaction, Univ. of Arizona, Tucson, Ariz., June 8 to 11, 1964, 19: 13607
contamination by buried glass-fixed fission products, at Chalk River, 18: 33165 (ERI-6)
contamination by fission products, 16: 5152
contamination by fallout, 18: 12358
contamination by fallout fission, 19: 18192 (EUR-2107.f)
contamination by iodine isotopes from nuclear explosions, 17: 6322 (UCLA-499)
contamination, detection by tree analysis, 16: 23406 (CEA-2131)
contamination measurements in King, Ontario, Oct. 1958 to July 1961, 16: 13375
contamination, method for assessing, 16: 19153 (A/AC.82/G/L.709)
content in dredged mixture, use of gamma sources for measurement of, 17: 30177
copper distribution in, 20: 7041
copper fractionation in neutron-activated, 20: 31325
cosmic meson (μ) energy losses in, below 100 Tev, (T), 19: 41296
crater formation by high explosives in alluvium, model for, (T), 19: 28535
decomposition of carbon-14-labeled acetate in, carbon dioxide evolution and oxygen uptake during, 18: 39301
decontamination of, measures for, 17: 36041
decontamination under cold-weather and thawing conditions, 18: 31755 (NDL-TR-58(Pt.II))
deformation by cylindrical projectiles, 18: 25001(R) (SC-DC-64-459)
density and moisture of, calibration of neutron-gamma probe for, 20: 16374
density and moisture content determinations using radiometric gages, conference on, 20: 29504
density and moisture content of, radiometric methods for determining, 20: 29505
density and moisture content determinations for, efficiencies of radiometric devices for, 20: 29506
density and moisture content in, performance of radiometric gages for determining, 20: 29507
density and moisture content of, radiometric surface gages for determining, 20: 29508
density and moisture content of, gamma and neutron well logging equipment for, 20: 33537
density determination of, by gamma attenuation method, 17: 30090
density determinations for, gamma-scattering-meter errors in, 20: 14837
density determination using gamma sources, devices for, 18: 5506
density measurements, design analysis of gamma-scattering meter for, 16: 13300 (TID-14178)
density measurements of, using gamma scattering method, 17: 27301
density measurement for detection of underground nuclear explosions, 18: 12410 (AD-406377)
density measurements on, by gamma scattering, 19: 22830
density measurements using gamma-scatter gages, composition effects in, (E), 19: 28567
density measurements by gamma scattering, 19: 40755
density measurement of, using gamma back-scattering, gage response in, 20: 37020
density measurements on, in climatology program, 18: 14577(R) (ANL-6769(p.230-9))
density of, neutron attenuation measurement of bulk, 17: 30729
density of, apparatus for measurement of, 18: 25775(P)
density of, bibliography on nuclear methods for measuring, 16: 23982 (AERE-Bib-140)
density of, design of radiometric equipment for measuring, 20: 623 (NP-15529)
density of, radiation back-scattering methods for measuring, 20: 29594
density of, radiometric devices for measurement of, 19: 13656
density of, tracer studies, 19: 18181
density of, use of radioisotopes in determining, 20: 43762
density of, use of gamma attenuation in measuring, 17: 34131
density of, use of radioisotopes in determining, 18: 25699(T) (OTS-63-11008(p.15-21))
density of, use of radioisotopes in determining, 18: 27824
density of, use of radioisotopes in determining, 18: 39719 (RT/GEO(64)-10)
density of, use of nuclear gage in determining, 19: 9447 (NP-14610)
diethylstilbestrol decomposition in, tracer study, 19: 11155
diffusion coefficients in loam, effects of compaction on rubidium-86 and strontium-89, 20: 18816
diffusion of cesium-137 and strontium-90 in, 17: 30034
diffusion of gamma emitters from waste disposal sites in, 19: 1944(R) (HW-81746(p.4.32-6))

diffusion of ground water in heterogeneous, in-place measurement of, 19: 604(R) (HW-81746(p.4.47-9))
diffusion of ground water in, stream functions for, 19: 605(R) (HW-81746 (p.4.50-3))
diffusion of liquid wastes through partially saturated, measurement of parameters for, 19: 1945(R) (HW-81746(p.4.39-42))
diffusion of polonium-216 and radon-220 from surfaces of, 20: 43543
diffusion of radon from, effects of meteorological conditions on, 20: 5646
diffusion of tritiated water in, method for measurement of, 17: 39281
diffusion of water through partially saturated, equations for determining, 19: 602(R) (HW-81746(p.4.37-9))
diffusion of water in partially saturated, equations for relating parameters in, 19: 603(R) (HW-81746(p.4.42-7))
distribution of radioactive elements in USSR, 18: 37360 (A/CONF.28/P/385)
dynamic behavior of, radiographic techniques for studying, 18: 2395 (AD-422046(p.86-91))
dynamic tests of clay, one-dimensional and triaxial, 19: 9285 (RTD-TDR-63-3116)
dynamics of, radiographic techniques for study of, 17: 12450 (AFSWC-TDR-62-44)
ecology of desert, 16: 25148(R) (HW-72500(p.161-4))
effect of potassium content of, on uptake of fission products by plants, 17: 35322(R) (HW-76000(p.208-10))
effects of acidity of, on cesium-137 content in peas and wheat, 19: 14982
effects of beryllium on, 19: 43662(R) (UCLA-12-565, pp 97-128)
effects of calcium and strontium levels on uptake of strontium-90 by clover, 16: 7400
effects of colloids in, on uptake of cerium, iron, and manganese by corn, 20: 22547 (TID-21702)
effects of fertility levels of, on uptake of calcium, magnesium, phosphorus, strontium, and zinc by corn plants, 20: 40735 (NYO-2744-37)
effects of greasewood forest, on sodium uptake by growing plants, 20: 12575
effects of irrigating, on cesium-137 and strontium-90 uptake by rice, 20: 40574
effects of temperature of, on uptake of strontium-90, cesium-137, and zirconium-95 by corn plants, 16: 17431
effects of, on radiosensitivity of tobacco mutations, 20: 40613 (N-66-18147)
effects on cesium, cobalt, and strontium uptake by plants, 17: 17749
effects on cesium uptake by barley, 19: 42241 (CEA-R-2708)
effects on cesium-137 uptake by ryegrass, 19: 10763
effects on cesium-137 uptake by buckwheat plants, 19: 35898
effects on fallout uptake by plants, 20: 43596
effects on fission product entry into food chain, 20: 33260(R) (ORO-648, pp 103-22)
effects on iodine-131 uptake by sagebrush, 20: 28883
effects on strontium-90 content of alfalfa and grass in West Slovakia, USSR, 19: 45750
effects on strontium-90 uptake by agricultural plants, 20: 3679
effects on strontium-90 uptake by plants, 20: 6745
element content of, in New Jersey, 19: 25834
enzyme reactions in, 19: 11155
equation of state of Nevada alluvium, 17: 3149 (LAMS-2760)
erosion of, radioisotopes in studies of, 17: 27583
evolution of carbon-14-labeled carbon dioxide by, 19: 33738(R) (N64-22756)
fallout contamination of, ecological effects, 19: 19504 (RM-2801-PR)
fallout content in Japanese, effects of soil particle size on, 20: 39112
fallout content of U. S., 1962 and 1963, 19: 629 (TID-7696(p.101-10))
fallout content of, 1962 to 1964, 19: 9370 (NP-14556(p.11-80))
fallout distribution in Japanese, 20: 14751
fallout fission product transfer in, 18: 3446 (NAS-NRC-Pub-1092)
fallout fission product contamination of, in Europe and South America, 18: 31753 (CLOR-26)
fallout levels in Italian, 1961, 17: 27591 (EUR-223.i)
fallout migration in, 19: 15756 (NP-14814)
fallout migration into, effects of alternate freezing and thawing on, 19: 42636 (AD-609645)
fallout monitoring in Japan, 17: 18308
fallout monitoring in Tokyo, 1961, 17: 36082
fallout monitoring in Switzerland, 1956 to 1961, 18: 20218
fallout monitoring in Canada, 1964, 18: 31788 (NP-14052)
fallout monitoring in, Canada, March 1966, 20: 33556 (NP-16124)
fallout penetration, 17: 1232
fallout uptake by, in England, 18: 20208 (AERE-R-4415)
fertility of, use of chemical and tracer techniques in studies of, 19: 10723
fission product behavior in, 16: 10346
fission product behavior in, 17: 40541
fission product behavior in, 17: 1177(R) (HW-70050(p.143-219))
fission product contamination of, by fallout from radiological warfare, 18: 19515 (NP-13796)
fission product contamination of, by underground thermonuclear explosions, 18: 27702 (PNE-239F)
fission product contamination of, effects of farming practices on, 18: 43871
fission product contents in, on Balkan Mountains from fallout, 19: 15800
fission product contamination of, effects on seeds of grain plants, 19: 19508(T) (JPRS-28977)
fission product contents in, (E), 19: 36662
fission product distribution in, survey of, 19: 3834
fission product distribution in, 19: 21811(R) (UCLA-12-541(p.101-30))
fission product distribution in, Buenos Aires, Argentina, 20: 8538
fission product fixation by, 19: 24760
fission product leaching in, 18: 27702 (PNE-239F)
fission product migration in, 16: 11342(R) (EURAEC-83)
fission product migration in, 16: 26636(R) (EURAEC-84)
fission product migration in, 17: 1159 (HW-SA-2744)
fission product motion in, effects of chelating agents on, 19: 38329 (TID-20471)
fission product percolation in, effects of physiochemical characteristics, 16: 25050 (TID-7628(p.198-210))
fission product separation from, radiochemical methods for, 18: 22185
fission product transport through, 17: 10820 (BNL-6554)
fission product transport in, tracer study, 20: 18188(R) (ORO-635)
fission product transport in, effects of chelating agents on, 20: 18211(R) (UCLA-12-576, pp 88-111)
fission product uptake by plants, 16: 2874 (UCLA-485)
fission product uptake by plants from, 18: 15735(R) (ARCRL-10)
fission product uptake from, 18: 33239
fission products transfer to wheat plants from contaminated, 17: 38725
flow in, multidimensional partially saturated, 17: 6256 (HW-SA-2854)
flow of water in, evaluation of equations for, 18: 45155(R) (TID-20980)
fluid flow and seepage in, 17: 14474 (HW-SA-2890)
fluid flow in, computer program for multidimensional partially-saturated steady, 17: 40999
fluid flow in heterogeneous partially saturated, computer program for calculating, 18: 26975 (HW-72335(Pt.2))
fungi from Nevada Test Site, characteristics and taxonomy, 19: 35880
fusion at impact sites as possible origin of tektites, 16: 15008
gamma absorption by, mass coefficients for, 18: 25700
gamma activity in, leachable, 20: 25286
gamma attenuation, 16: 4943 (NP-11129)
gamma dosimetry in, methods for, 20: 16687
gamma scattering by, effects of mineral and moisture content on volume weight determination by, 19: 26566
gamma spectra of neutron-irradiated, changes of, 20: 43607
gamma spectra of samples of, from Nevada Proving Grounds, 17: 37014(R) (NYO-9505(p.95-111))
geochemical properties, effects on retention of radionuclides, 16: 25052 (TID-7628(p.214-36))
geohydrologic features affecting waste disposal, measurement, 16: 25042 (TID-7628(p.77-98))
geologic dating of podzols in southern Canadian tundra using radiocarbon, 19: 7721
ground water velocity in, device for measuring, 20: 20875 (EUR-2481.f)
heat flux measurements on, in climatology program, 18: 14577(R) (ANL-6769(p.230-9))
heating by radioactive material leaking from waste storage tanks, 18: 26976 (HW-80848)
heating of, using coolant from power reactors, 20: 32843
herbicide distribution in, 18: 15735(R) (ARCRL-10)
humus formation on forest floor, role of microörganisms in breakdown of leaf litter, 19: 1960 (ORNL-P-517)
humidity of, tracer studies of, 19: 18181
humus formation on forest floor, role of microörganisms in breakdown of leaf litter, 19: 1961 (ORNL-P-586)
hydraulic properties of porous, tracer studies of, 19: 18185
impact effects on footing-soil system, failure modes in, 18: 10260 (AD-428283)
infiltration velocity of desert alluvium, effects of Sedan and Scooter explosions on, 17: 34066 (PNE-221F)
inspection for buried objects, using x-ray backscatter, 18: 23782 (NP-13943(p.117-27))
interactions with underground shelters, effects on shelter design, 20: 39070
interfaces with water, scintillation detector for locating, 20: 19092
iodine sorption from natural waters, Cape Thompson, Alaska, 18: 25688 (TID-20638)
iodine-131 contamination of, after stack release, 19: 624 (IDO-12035)
iodine-131 deposition and retention on, effects of moisture and temperature on, 20: 10717(R) (BNWL-122, pp 166-7)
iodine-131 retention by clays and organic matter of, 19: 14924 (TID-21588)

ion content variability studies, 20: 40532(R) (COO-1097-17)
ion diffusion in, tracer technique for determining, 19: 5897
ion equilibria in, 16: 34144(T,R) (EURAEC-275)
ion exchange and sorptive properties for cesium, effects of calcium and potassium chlorides on, 17: 39071
ion exchange capacity measurement, radiotracer method for, 19: 9094 (CEA-R-2543)
ion exchange processes, effects of moisture content, tracer study, 16: 32710
ion exchange processes in, 20: 6726 (STI/DOC/10/48)
ion exchange properties for waste processing, 18: 33164 (CONF-179-S)
ion exchange properties of, isotope studies, 20: 218(R) (STI/DOC/10/42, pp 1-22)
ion exchange properties for anions, 20: 8817(R) (BNWL-36, pp 4.1-77)
ionic migration in, tracer study, 20: 6726 (STI/DOC/10/48)
irrigation control in, neutron probes for, 20: 633
isotope transport in, by runoff water, 18: 35724
isotopic analysis of, at low altitudes, gamma spectrometric, 16: 3248
isotopic exchange with soil solution, and plants, kinetics, 16: 32712
isotopic exchange in soil-solution systems, 17: 15581
isotopic exchange in suspensions of, method for continuous recording of, 20: 36793
layer profiles in, radioisotopes in study of, 17: 27583
manganese content, 17: 33602
meson (μ) absorption at 10^{10} to 10^{12} ev, energy transfer in cosmic, (T), 20: 23953
microorganism detection in Martian, radiobiochemical probe for, 16: 34135
microorganisms in, effects of atomic explosions on, 20: 45962 (RM-4827-TAB)
mineral cycling in mesophytic forest, tracer study, 16: 25150(R) (TID-15963)
moisture content at Neotoma Valley, Ohio, ecological effects in forest environment, 19: 6900 (TID-21354)
moisture content and surface density of compacted, radiometric methods for measuring, 20: 29581 (AD-633785)
moisture content determination by neutron scattering, cadmium standards for probes for, 19: 38869
moisture content determination in, cost comparison of neutron-moderation and gravimetric methods of, 20: 43094
moisture content determinations, uses of radioisotopes in, 18: 25699(T) (OTS-63-11008(p.15-21))
moisture content in, calibration of neutron probe for, 17: 35400
moisture content in, use of radioisotopes for measurement of, 17: 35401
moisture content in, neutron scattering measurement of, 17: 35402
moisture content in, use of neutron probe on lysimeters and small watersheds, 17: 35403
moisture content in, gamma attenuation measurement of, 19: 17837
moisture content in, determination by neutron thermalization, 20: 544
moisture content in organic, neutron method for measuring, 20: 14756
moisture content, measured with neutron probe, 16: 9424
moisture content of, effects of plant cover on, 17: 35328(R) (HW-76000(p.232-8))
moisture content of, device for measurement of, 17: 41011
moisture content of, neutron scattering method for measuring, 19: 11405
moisture content of, effects of greasewood shrub canopy on, 19: 24202 (HW-SA-3511)
moisture content of, neutron probe measurement, 20: 20915
moisture content of, use of neutron meters in measuring, 20: 39131
moisture content of, neutron hygrometer for measurement of, 20: 43558
moisture content of, measurement using radioisotopes, 18: 29719 (RT/GEO(64)-10)
moisture content of, radiometric devices for measurement of, 19: 13656
moisture content of, radioisotopes in studies of, 17: 27583
moisture content prediction for top layer of, for induced activity prediction system, 18: 16206 (USNRDL-TR-662)
moisture content, variance in neutron-scattering determination of, 18: 10004
moisture content, radioisotope studies of, 20: 548
moisture determination, neutron scattering method, 17: 25136
moisture determination in, neutron moderation method for, 17: 30090
moisture determination in, by neutron moisture meter, 17: 30091
moisture determination in, by neutron energy losses, effects of chlorine, iron, and potassium on, 20: 19118
moisture determination using nuclear gages, 19: 9447 (NP-14610)
moisture determinations using fast-neutron sondes, 16: 13411 (NP-11381)
moisture measurements using neutron probe, 16: 5291
moisture measurements of, effect of borehole diameter on calibration of neutron probe for, 18: 5523
moisture measurement in, neutron probe for, 18: 5541(P)
moisture measurements in boreholes, neutron methods for, 18: 5524
moisture measurements in, performance of neutron-scattering probes for, 18: 27774
moisture measurement in, by activation analysis, 20: 9167(R) (BNWL-36, pp 5.1-102)
moisture measurements using neutron well logging, effects of iron and potassium content on, 20: 33539
moisture measurement in, bibliography of nuclear methods for, 16: 23982 (AERE-Bib-140)
moisture measurements using radioisotopes, 18: 27824
moisture measurements on, in climatology program, 18: 14577(R) (ANL-6759(p.230-9))
moisture measurement using thermal neutrons design and calibration of apparatus for, 16: 16620
moisture meters for, composition and density effects on neutron, 20: 14771
moisture movement in, field tracer method for, 18: 4007 (DPSPU-63-30-29)
moisture probes, calibration of neutron, 16: 5545
moisture probes, efficiency and sensitivity of neutron, 17: 38953
monitoring for alpha activity, 16: 364
monitoring for radioactivity at Julich Nuclear Research Institute, Germany, 17: 307 (JUL-55-ST)
monitoring for radioactivity at Argonne, 1960 and 1961, 17: 36023(R) (ANL-6736)
monitoring for radioactivity in German Federal Republic, Jan.-March 1961, 19: 18227
motion following explosions in sandy, 18: 2728(T) (UCRL-Trans-995(L))
motion in Gnome explosion, 17: 35962 (PNE-108F)
motion of subsurface inclusions in, from surface blast, 19: 24692 (NP-15009)
motion of, from underground explosions, analysis of, 16: 413
movement of calcium-45 and strontium-89 in, effects of calcium and strontium acetates on, 20: 32925
movement of chemicals in, survey of, 18: 6549 (CONF-349-1)
movement of pollutants through, transport analysis of, 20: 27192 (BNWL-SA-671)
movement of radioactive wastes through, methods of tracking, 16: 32619 (HW-SA-2707)
neutron absorption by elements in, 17: 30091
neutron activation by atomic explosion, 16: 12814 (WT-1117)
neutron activation of, gamma dose curves from, (T), 19: 46589 (UCRL-14332)
neutron albedos on, hydrogen content dependence of, 18: 19257 (BRL-1224)
neutron attenuation in, 16: 4943 (NP-11129)
neutron capture fractions for, at numbers and energy emitted by fission weapons, 20: 45885 (AD-639446)
neutron distribution from air-burst atomic explosions, effects of moisture, 16: 2817 (USNRDL-TR-530)
neutron distributions in strata of, in well logging, 19: 34389(T)
neutron flux distribution around point source of fast neutrons, thermal, (T), 20: 40058
neutron reactions with, effect on measured gamma dose, 16: 7769 (NDL-TR-18)
neutron reflection by, fast, 18: 2827
neutron reflection by, albedo for fast, 18: 15146 (RRA-M31)
neutron reflection by surfaces of, absorbed dose in air from, (T), 20: 6528
neutron transmission in, at 0.5 to 14 Mev, 17: 9478 (BRL-1174)
neutron transport and reflection by, at Nevada Test Site, 17: 24599 (BRL-1190)
neutron transport in, Monte Carlo calculations of fast, 17: 34843
nitrogen-15 content in, 19: 6089
nutrient distribution in, tracer studies, 20: 3710(R) (EUR-2493.e)
nutrient movement in, activation determination of, 19: 31696
nutrient properties, tracer study, 16: 32715
nutrient transport in, tracer studies on, 20: 33540
nutrient uptake by plants from, effects of osmotic water pressure, 19: 10772
of Rongelap Atoll, Marshall Islands, study, 19: 9363 (TID-21432)
particle deposition from atmosphere on, tracer studies using copper-64 on, 19: 20658
permeability, 18: 3388(R) (HW-77609(Sect.4))
permeability and flow saturation of, calculation as function of capillary pressure, 19: 9361 (HW-SA-3753)
permeability by moisture, effects of treatment with bentonites, 16: 25066 (TID-7628(p.462-8))
permeability of, computational scheme for in-place measurement of, 17: 6790 (HW-SA-2405)
permeability of, equipment and method for measuring, 16: 34144(T,R) (EURAEC-275)
phosphate absorption by barley plants from clay, effects of method of fertilizer application on, 19: 35940
phosphate reserves of assimilable, tracer study, 19: 24243(T) (JPRS-29457)
phosphorus availability in Brazilian cerrado, tracer studies of effects of

limestone on, 18: 37061 (A/CONF.28/P/850)
phosphorus content of, uses of chemical, ion-exchange, and tracer techniques to determine, 19: 10723
phosphorus exchange tracer study, 16: 32711
phosphorus-32 uptake by maize roots from, effects of placement on, 17: 38724
physical properties, 17: 5666 (AD-274294)
physical properties of, tracer studies of changes in, 19: 18182
physical properties of, 20: 6726 (STI/DOC/10/48)
physical properties of, thin section technique for studies of, 20: 8537(R) (TID-22443, pp 83-99)
physical properties of, radiometric probe for determining, 20: 14773
plant relations to, in arid regions, 18: 23168(R) (STI/DOC/10/25(p.99-111))
plutonium percolation in, 16: 25054 (TID-7628(p.248-81))
polonium-210 content in, 20: 16189
polonium-210 content in, used for tobacco cultivation, 19: 4424
porosity of alluvium at Nevada Test Site, measurement using density logs, 17: 25432 (TID-18690)
porosity of ground-water aquifers, tracer technique for, 19: 22576
potassium sorption and release from, use of potassium-40 and -42 for determining, 18: 37397
potassium, thorium, and uranium contents of, gamma spectrometric measurements of, 20: 43542
preparation of cesium-137-labeled forest floor, 20: 6711(R) (ORNL-3849, pp 43-100)
preparation of samples of, for environmental radiation surveillance, 20: 42733
projectile penetration in, 20: 45240 (SC-RR-66-376)
properties as water fallout filter, 19: 15754 (NP-14781)
properties for liquid waste flow in, 20: 8821(R) (BNWL-36, pp 4.1-77)
properties of alluvium in Nevada Test Site, geology and physical, 17: 36010 (PNE-234P)
properties of Belgian, for retention of radioelements, 17: 27602(T) (EURAEC-416)
properties of, effects on plant uptake of calcium-45 and strontium-90, 18: 29192 (TID-20781)
properties of, effects on plant absorption of cesium-137 and strontium-89, 19: 12911 (NP-14752)
properties of, effects on plant absorption of cesium-137 and strontium-89, 19: 12912 (NP-14761)
properties of, effects on enrichment of forage vegetation by cesium-137 and strontium-90, 20: 3665(T) (CEA-tr-X-619)
properties of, effects of, on plant uptake of radioisotopes, 20: 18174(R) (NP-15771)
properties of, tracer studies of, 18: 43996
radiation dose rate from natural radioactivity in, 18: 29871
radiation effects on availability of inorganic ions in, 16: 16176 (NP-11578)
radiation effects on number of microorganisms in samples, 17: 1298
radiation effects on physical properties of sand and sandy loam, gamma and neutron, 17: 12099
radiation effects on properties and microorganisms, 17: 30334
radiation effects on nitrogen and phosphorus content in, 17: 39143
radiation effects on, electron and gamma, 18: 23171
radiation effects on, for subsequent plant growth, 18: 23318
radiation effects on fertility of, 18: 29363
radiation effects on survival of fungi in, gamma, 18: 29285
radiation effects on microorganisms in, gamma, 18: 38899
radiation effects on composition, 19: 5964
radiation effects on fertility of, gamma, 19: 25995
radiation effects on amino acids in, gamma, 19: 45941
radiation effects on moisture content of, in forests, 20: 3653 (BNL-8466)
radiation effects on, gamma, 20: 40637(R) (ORO-2754-7)
radiation monitoring at Ames, Jan.-June 1965, 19: 44302 (TID-22173)
radiation monitoring in German, 1965, 20: 4164
radiation monitoring in California, 20: 38735(R) (NYO-1704-13)
radiation shielding of underground vegetative plant parts by, 17: 33573
radiation uses in studies of, 19: 1999
radioactive contamination, 16: 10343
radioactive contamination of, relation to plant contamination, 18: 3622
radioactive contamination of, monitoring in EURATOM member states, 19: 2537
radioactive contamination of, Federal Republic of Germany, 1955 to 1962, 19: 24788
radioactive contamination of, effects on plant ecology, 19: 38331
radioactive contamination of, movement patterns in, 19: 40274
radioactive contamination of, effects on foods, 20: 14243(R) (TID-22626)
radioactive contamination in Japan, 1961–64, 20: 43615
radioactive particle deposition on pasture, rate of, 20: 16160 (UCRL-14739(Pt.2))
radioactive sludge injection into, methods for, 18: 17346
radioactive solution placement in soils, development of probe for, 16: 20850
radioactive solution injection into, noncontaminating probe for, 19: 36685
radioactive waste disposal in, hydrodynamics of, 20: 32883
radioactive waste retention hydrologic factors affecting, 16: 25041 (TID-7628(p.67-76))
radioactivity content in, in Italy Jan.–June 1962, 17: 36024 (BIO/26/62)
radioactivity control in, methods for, 18: 12393
radioactivity content and distributions in USSR, 19: 30415
radioactivity content of, from fallout in West Germany, 20: 40570
radioactivity content of, from fallout in West Germany, 20: 43626
radioactivity distribution in, techniques for measuring alpha, 16: 9010
radioactivity distribution and effects in, 18: 9817
radioactivity distribution in Kansas, cesium-137 and strontium-90, 19: 20657(R) (DASA-1309)
radioactivity distribution in, after plowing under radioactive dust, methods of determining, 19: 20182
radioactivity due to fallout in, 18: 18044
radioactivity due to radium and uranium in, effects on spermatogenesis in field mice living on, 20: 5387
radioactivity from fall-out in 1958–1959, spectra of, 16: 27434
radioactivity from natural sources, 19: 13122(T) (JPRS-27535)
radioactivity from carbon-14-acetate decomposition, 19: 21824
radioactivity from cesium-137 and strontium-90 in Faeroe Islands, 1964, 20: 7320 (RISO-108)
radioactivity from cesium-137 and strontium-90 in Greenland, 1964, 20: 7321 (RISO-109)
radioactivity in Brazilian, 20: 45259 (NYO-2577-3)
radioactivity in, from fall-out in Japan, 16: 26688(T) (AEC-tr-4642)
radioactivity in German, 1965, 20: 23412
radioactivity in German, 1965, 20: 23413
radioactivity in Ontario, under pine trees, 18: 6955
radioactivity in Spain, 18: 35754
radioactivity in vicinity of AERE, cesium-137 and strontium-90, 20: 14784(R) (AERE-R-5015)
radioactivity in West German Republic, 19: 38904
radioactivity in 1958, 1959, and 1960 at Ispra, 16: 4983 (NP-10731 (p.129-44))
radioactivity in, decay of neutron-induced, 19: 21811(R) (UCLA-12-541 (p.101-30))
radioactivity in, effects on growth of corn seedlings in, β, 20: 5305
radioactivity in, of EURATOM countries, 1964, 20: 13000(R) (EUR-2520.i)
radioactivity in, 1963 to 1965, 20: 18980
radioactivity in, of watershed of Boulder City, Colo., 20: 20379 (COO-1191-10)
radioactivity in, from natural sources, pulse-height spectra measurements of, 20: 33519
radioactivity induced by neutron sources in, calculations, 19: 32422 (UCRL-12407)
radioactivity induced in, by Operation Bren, 19: 47569 (CEX-62-50)
radioactivity induced in, by underground explosions, 19: 46473 (UCRL-14249)
radioactivity induced in, decay characteristics of neutron, 20: 12582
radioactivity induced in, neutron, 20: 18211(R) (UCLA-12-576, pp 88-111)
radioactivity induced in, neutron, 20: 43607
radioactivity measurements in New Zealand, 20: 40521(R) (NP-16270)
radioactivity monitoring in West German Republic, July–Sept. 1964, 19: 15816
radioactivity monitoring in Italy, 19: 42637 (BIO/32/63)
radioactivity monitoring in Netherlands, 1963, 20: 39118
radioactivity of Arctic, effects of natural radioactivity on, 18: 25055 (NP-13985)
radioactivity of Brazilian, 19: 36708 (NYO-3273-5)
radioactivity of British, 20: 35651
radioactivity of Canadian, June 1965, 19: 44251 (NP-15519, pp 23-51)
radioactivity of European, 1962, 20: 23392
radioactivity of German, 1962, 19: 38858
radioactivity of, hazards of natural, 17: 6341
radioactivity of, hazards from fallout, 17: 41074
radioactivity of Hartsells loam in Tennessee, 18: 35723
radioactivity of, in USSR, 17: 1663(T) (JPRS-15920(42-6))
radioactivity of Italian, network for monitoring, 19: 30467
radioactivity of Indiana, determination of gamma, 20: 11019
radioactivity of, measurements in Federal Republic of Germany, January to March 1962, 17: 15624
radioactivity of, measurements in Federal Republic of Germany, April to June 1962, 17: 15625
radioactivity of, measurements of gamma, 17: 32264 (UCRL-10636)
radioactivity of, measurements of natural and artificial, in Indiana, 18: 8563
radioactivity of, Sharpsburg, Washington Co., Maryland, 17: 41135

radioactivity of, standardization of gamma detectors for measuring, 18: 8561
radioactivity of U. S., natural, 19: 629 (TID-7696(p.101-10))
radioactivity of USSR, 1958, 17: 6288
radioactivity of world-wide samples, 1963 and 1964, 18: 41644(R) (HASL-149)
radioactivity of West German, monitoring for, 19: 15819
radioactivity of, in Germany, 3rd quarter 1962, 18: 12357
radioactivity of, in Federal Republic of Germany, 4th quarter, 1962 18: 11898
radioactivity of, methods for estimation of natural, 18: 14076
radioactivity of, in Federal Republic of Germany, 3rd quarter 1962, 18: 14091
radioactivity of, methods for measurement of natural, 18: 18043(T) (JPRS-23912)
radioactivity of, in Brazil, 18: 41649 (TID-20955)
radioactivity of, in Peru, 19: 15794
radioactivity of, in Lima, Peru, 19: 15795
radioactivity of, in Austria, 1963, 19: 38860
radioactivity of, effects on incidence of stomach cancer in population of region, 20: 4197
radioactivity of, bibliography on natural, 20: 5668 (WASH-1061)
radioactivity of, in India, Nov. 1963, 20: 7294 (AEET/HP/Environ/4)
radioactivity of, hazards to human organs from, 20: 7324(T) (CEA-tr-R-1350)
radiocontamination, autoradiographic determination, 16: 6628
radioelement migration in, tracer studies, 18: 38685 (A/CONF.28/P/774)
radioinduced sterilization, 18: 31059
radioisotope accumulation by, gamma spectrometric determination of, 19: 3833
radioisotope behavior in, 19: 31685
radioisotope concentrations in, maximum permissible, 18: 25733
radioisotope contents of, methods of controlling, 19: 2536
radioisotope contents of, from Chariot site environment, 19: 25796 (PNE-445)
radioisotope contents of, from Chariot site environment, 19: 25799(R) (PNE-448)
radioisotope contents of, from Chariot site environment, 19: 25797 (PNE-446)
radioisotope content of, in Ispra environs, Italy, 1965, 20: 33553 (EUR-2965.e)
radioisotope dispersion and fixation in, role of ground water in, 19: 2538
radioisotope dispersion and movement in, mechanisms of, 20: 20875 (EUR-2481.f)
radioisotope distributions in, from irrigation water containing radioactive wastes, 19: 10666
radioisotope distribution in, model for, 20: 16168
radioisotope fixation in, effects of fertilization on, 19: 3832
radioisotope fixation and transfer to vegetation by, 17: 24795
radioisotope injection into probe for rapid, 19: 38870
radioisotope injection into, use of agar-solidified solutions, 20: 8557
radioisotope ion exchange in, 18: 17342
radioisotope migration and retention in, conference on, 18: 17336
radioisotope migration in, 16: 18703 (CRER-1077)
radioisotope movement in, around buried wastes, 17: 24733 (DPSPU-63-30-2)
radioisotope movement in, 18: 422
radioisotope movement in, geologic and hydrologic studies on, 18: 16207
radioisotope movement in, method for study of, 18: 16216
radioisotope movement in, Belgian studies on, 18: 17341
radioisotope movement in, physicochemical reactions of, 18: 16208
radioisotope movement in, Belgian studies on, 19: 10659(R) (EURAEC-703)
radioisotope movement through, effects of chelates and water on, 19: 36661
radioisotope movement in, 20: 30943(R) (ORNL-TM-1465)
radioisotope permeability and retention in, device for measuring, 18: 16215
radioisotope removal from, by barley and by extracting solutions, tungsten-185, plutonium-239, and lead-210, 20: 22538
radioisotope solubility in, effects on plant uptake, 20: 12608
radioisotopes in, factors affecting biological importance of, 20: 12915
radiological monitoring at Indian Point Power Reactor, 18: 8530
radiological monitoring of large areas for plutonium-239 resulting from non-nuclear detonation of nuclear weapons, 19: 22641
radionuclide solubility in activated, 20: 25286
radiosensitivity effects on Azotobacter of, gamma, 19: 28018
radiosensitivity effects on conifer-hardwood forests, fast-neutron, 20: 12672
radiosensitivity of bacteria in, 18: 41215
radioisotope uptake by, 18: 35239
radiosterilization, effects on respiration, 16: 26683
radiosterilization of, effects of, on bacteria, enzymes, and plant growth in, 17: 23196
radiosterilization of, enzymatic and microbial activity in, 18: 120
radiosterilization, 18: 15885
radiosterilization of, gamma, 19: 11155
radiosterilized, growth of microorganisms in, 18: 15885
radium uptake by plants from, 19: 54
radium-226 content in, Bombay and Kerala, India, 20: 16747
radium-226 content in, used for tobacco cultivation, 19: 4424
radium-226 uptake by vegetables and cereals from, 20: 42792
radon content of, effects of meteorological factors, soil moisture, and underground nuclear explosions on, 17: 37013(R) (NYO-9505(p.87-94))
radon content of gases from, effects of Antler and Chena underground explosion on, 19: 6096 (NP-14511)
radon emission from, in European USSR and Kazakhstan, 20: 16691
radon spectra from, 20: 22853(R) (ANL-7060)
radon-220 and radon-222 content in surface, effects of underground nuclear explosions on, 17: 36008 (EGG-B-2516)
radon-220 content in, 19: 13639
radon-222 contents and flux at surface, effects of atmospheric variables on, 18: 35737
radon-222 diffusion in, coefficients for, 19: 13639
radon-222 diffusion into atmosphere from, 19: 36664
rain water percolation through, 19: 44235 (DPSPU-64-30-23)
rare earth behavior in, 17: 1177(R) (HW-70050(p.143-219))
rare earth, thorium, and yttrium contents in Tomsk region, 20: 2065
reactions with cesium-137 and potassium-40, effects of stable cesium and potassium, 17: 1233
reactions with cesium, 18: 8064(T) (JPRS-22656)
reactions with fission product elements, 19: 4049(R) (ORO-625(p.93-102))
reactions with rare earths, 16: 25052 (TID-7628(p.214-36))
reflectance properties of, effects of underground nuclear explosions on, 18: 1319 (NP-13300)
removal from contaminated lawns, development and testing of procedure for, 20: 23343 (AD-631529)
resistance to horizontal loading, lateral-plate bearing tests on mechanics of, 19: 46465 (AD-613991)
rhodium-106 migration and fixation in, 18: 17345
rubidium uptake by, effects of type and moisture content of, 17: 36015
rubidium-86 absorption and diffusion in, 18: 16199
rubidium-86 uptake by, factors affecting, 18: 23227
rubidium-86 uptake by maize roots from, effects of placement on, 17: 38724
ruthenium content of, in White Oak Lake bed, 17: 39275
ruthenium-106 migration and fixation in, 18: 17345
ruthenium-106 sorption by, 20: 10855
sampling of alluvial, for waste disposal, 17: 21373 (IDO-12027)
sampling of, and preparation for radiochemical analysis, 18: 8519(T) (AEC-tr-6049(p.1-10))
sampling of, in New Zealand, 17: 5750(R) (DXRL-F6)
sampling to assess radioactive contamination from fall-out, 16: 10353
scavenging of fission products from water by, 17: 30765
seepage of liquid wastes in, 17: 36993(R) (TID-19164)
seepage of liquid wastes in, 17: 36994(R) (TID-19186)
seepage of liquid wastes in, 17: 36995(R) (TID-19187)
seepage of liquid wastes in, 17: 36996(R) (TID-19188)
seepage of liquid wastes in, 17: 36997(R) (TID-19189)
seismic wave attenuation in geologic discontinuity, acceleration, stresses, and velocity in, 19: 46580 (AD-613287)
shielding properties of, in high-energy accelerators, 17: 5057
shielding properties, 19: 11423(R) (UCRL-12004)
shock wave behavior in clayey, 16: 3584
sodium-22 in, uptake by plants, 20: 16678
sorption of alkaline earths and rare earths by chernozem, tracer studies of, 18: 39171(T) (AEC-tr-6390(p.451-9))
sorption of cesium, iodine, and strontium by, from Cape Thompson, Alaska area, 20: 31426 (PNE-481, pp 1121-39)
sorption of cobalt-60 on peat, 19: 22412
sorption of radiocerium by chernozem, 16: 20460
sorption of radioisotopes by, 17: 33409
sorption of sulfates, tracer study, 16: 32713
sorptive effects of humus on uptake of fission products by cereals, peas, and vetch, 16: 14451
sorptive effects of composition and humus, on uptake of fission products by oats and peas, 16: 14452
sorptive properties as waste disposal medium, 16: 8(T) (AEC-tr-4142 (p.33-42))
sorptive properties, 16: 7330(T) (CEA-tr-R-1427)
sorptive properties for fission products, 16: 16026(T) (CEA-tr-A-1106)
sorptive properties for radioisotopes, 16: 25048 (TID-7628(p.179-86))
sorptive properties of humus for uranium(IV) and (VI), 16: 25364
sorptive properties for strontium-90, 16: 27013

sorptive properties for cerium, 16: 27014
sorptive properties for rare earths, 16: 28973
sorptive properties for strontium-90, 16: 31628
sorptive properties for strontium, 17: 19710 (TID-7644(p.177-86))
sorptive properties for radioisotopes, 17: 41088
sorptive properties for cesium-134, effects of acidity on, 18: 22251
sorptive properties for waste solutions, 18: 24980(T,R) (EURAEC-300)
sorptive properties for cesium, 18: 27620(R) (TID-20662)
sorptive properties for chromium and cobalt from solutions, 18: 35235 (IDO-12036)
sorptive properties for cesium from solutions, 19: 36543(R) (TID-21955)
sorptive properties for strontium, effects of aluminum oxides, calcium carbonates, and silicon oxides on, 19: 46434
sorptive properties for cesium, review of selective, 20: 1555
sorptive properties for cesium-137, 20: 8479(R) (ORNL-3849, pp 1-42)
sorptive properties for radioisotopes, 20: 12545(R) (PAEC(A)AR651)
sorptive properties for cesium and strontium, effects of aluminum oxide and iron oxide on, 20: 14652
sorptive properties for cesium-137, 20: 20696
sorptive properties for cesium, 20: 22541(T)
sorptive properties of turfy-meadow, for yttrium, effects of iron on, 20: 28881
sorptive properties for ions, tracer studies of, 20: 32883
sorptive properties of, for cesium and strontium, 20: 33260(R) (ORO-648, pp 103-22)
sorptive properties for radioisotopes, effects of disodium salt of EDTA on, 20: 35227
sorptive properties for radioruthenium in different solutions, 20: 40890
sorptive properties for cerium and yttrium, effects of acidity and concentration on, 20: 40914
sorptive properties for strontium-90 effect of soaking on, 20: 45907
sorptive properties for cesium at Saclay, 16: 20826
stabilization, evaluation of materials, 16: 12812 (WT-781)
stable strontium, strontium-90, and calcium mobilities in turf-podzolic and black earth, 20: 40520 (NP-16261)
sterilization of, using gamma radiation, methyl bromide, and steam, 18: 35908
sterilization with methyl bromide, effects on uptake of iodine-131 by pine trees, 17: 15735
stress propagation in, apparatus for studying, 18: 683 (DASA-1266-2)
stress propagation in, methods for predicting, 19: 34361(R) (AD-609555)
stress wave propagation in, effects of inelasticity and viscosity on, 18: 2396 (AD-422046(p.107-23))
strontium and strontium-90 content of, in Egypt, 16: 4020 (A/AC.82/G/L.665)
strontium applications to agricultural, effects on strontium-90 uptake by clover and rye grass, 20: 20381
strontium content of, effects on strontium content of vegetables, 17: 17746
strontium content at Warsaw, 18: 33778
strontium content of, plant uptake of radiostrontium and, 18: 38733
strontium content of, effects of crop rotation and mulch on, tracer study, 20: 8552(R) (TID-22443, pp 1-33)
strontium distribution in, effects of various conditions on, 19: 19474(T) (CEA-tr-A-1616)
strontium distribution in, effects of organic compounds on, tracer study, 20: 8553(R) (TID-22443, pp 34-54)
strontium exchange in Alaskan, factors affecting, 18: 33777
strontium fixation by calcium carbonates in, 18: 29231
strontium isotope uptake from, effects of mineral fertilizers, 17: 15613
strontium precipitation from calcareous, calcium carbonate method for, 18: 33594
strontium separation from, using potassium ferrocyanide, 18: 27631
strontium sorption from natural waters, Cape Thompson, Alaska, 18: 25688 (TID-20638)
strontium transport, 18: 43170(R) (EUR-1882.e(p.31-6))
strontium transport in, effects of organic compounds on, 20: 35239
strontium uptake by plants from, effects of freezing on, 20: 8552(R) (TID-22443, pp 1-33)
strontium uptake by trees from, effects of calcium content and acidity on, 20: 8554(R) (TID-22443, pp 100-11)
strontium uptake by edible plants from, effects of calcium content on, 20: 40537(R) (TID-23052)
strontium-85 fixation in, 16: 32682
strontium-90 concentration in, of Palermo in November and December 1961, 17: 13958
strontium-90 contamination and analysis in Poland, 16: 3253
strontium-90 content in, 1959, 16: 429 (TID-13945)
strontium-90 content, 1960 and 1961, 16: 6645(R) (HASL-117)
strontium-90 content in Germany, 1958–61, 16: 11941
strontium-90 content in East Germany, 16: 21892
strontium-90 content in world-wide samples of, in 1960–1961, 17: 3166 (TID-17090)
strontium-90 contents in, in Germany, 1961, 17: 30284
strontium-90 content in, 1956 to 1961, 18: 8524(T) (AEC-tr-6049 (p.225-32))
strontium-90 deposition in, from rainfall, Clallam County, Washington, 1957–60, 16: 19171
strontium-90 deposition in Polish, effects of calcium content and acidity on, 17: 14471 (CLOR-12)
strontium-90 deposition in, from fallout in Italy, 1962, 18: 6952
strontium-90 distribution in, data tabulation, 16: 14448 (NYO-9934)
strontium-90 equilibrium parameters in the presence of other ions, 16: 9012
strontium-90 migration, vertical, 16: 10333
strontium-90 migration in, 18: 8524(T) (AEC-tr-6049(p.225-32))
strontium-90 movement on surface, 16: 22452 (TID-7632(p.299-305))
strontium-90 redistribution in small cultivated watersheds, 17: 39278
strontium-90 retention, factors affecting, 17: 2782 (BLG-103)
strontium-85 extraction from, method for, 18: 14143
strontium-85 uptake by plants from, effects of sodium content on, 20: 10534(R) (BNWL-122, pp 168-9)
strontium-89 and -90 content in, around nuclear power plants in England, 18: 6775
strontium-89 and strontium-90 uptake by, age effects on, 18: 18045
strontium-89 contamination of, retention and loss of, 19: 38332
strontium-89 diffusion in, effects of electric field on, 20: 11053
strontium-90 content in, in New York City area to 1961, 18: 10280
strontium-90 content of, in German Democratic Republic, 1962, 18: 15909
strontium-90 content in, in USSR, 18: 27030
strontium-90 content in Western Slovakia, 18: 33776
strontium-90 content in, Zagreb, 1962 and 1963, 18: 39089
strontium-90 content in, Australia, 1962, 18: 39493
strontium-90 content of Canadian, 1963, 19: 9368 (NP-14459)
strontium-90 content in Canadian, 1958 to 1963, 19: 9379
strontium-90 content of, effects on contamination of vegetables, 19: 11394
strontium-90 content in Soviet Union, 1959-60, 19: 24706
strontium-90 content in arid-region, 19: 26549
strontium-90 content in New Zealand, 19: 35892 (NP-15082)
strontium-90 content in German, 19: 38876 (NP-14927)
strontium-90 content of, in German Democratic Republic, 1963, 19: 46610
strontium-90 content in Venezuelan, 20: 9143
strontium-90 content in, effects on plant content of, 20: 14236
strontium-90 content in, effects of depth on, 20: 20882(R) (HASL-171)
strontium-90 content above and on surfaces of, 20: 31421
strontium-90 content in Australian, 1964, 20: 33566
strontium-90 content of, Neotoma Valley, Ohio, 1958 through 1964, 20: 36548 (TID-23036)
strontium-90 content in, in Japan, 1960 and 1961, 20: 43518(T) (NSJ-tr-54)
strontium-90 content in, and subsequent uptake by milk, 20: 45886 (NP-16262)
strontium-90 content in East German, 20: 45893
strontium-90 content in Icelandic, 1958 to 1964, 20: 45908
strontium-90 content of German Democratic Republic, 1963 and 1964, 20: 45964 (SZS-7/66)
strontium-90 content of, effects of stable strontium on, 18: 43797
strontium-90 content in, methods for decreasing, 19: 18209
strontium-90 diffusion in, effects of calcium on, 20: 12523
strontium-90 diffusion in, effects of soil composition on, 20: 18232
strontium-90 diffusion in, effects of properties on, 20: 38918(T)
strontium-90 distributions in, 19: 22548
strontium-90 distribution in, in Moscow region, 19: 22549
strontium-90 downward movement in, during leaching with deionized water, 17: 32979
strontium-90 in, contamination of food chains by, 18: 16239
strontium-90 migration in Czech, 19: 5559 (UJV-1107/64)
strontium-90 movement through, 19: 2542
strontium-90 movement in, 20: 39117(T)
strontium-90 reactions with organic matter in, 18: 27698
strontium-90 retention by, effects of potassium phosphates on, 19: 4127
strontium-90 retention by, effects of chemical treatments on, 20: 20875 (EUR-2481.f)
strontium-90 separation from, 20: 20882(R) (HASL-171)
strontium-90 sorption by ploughed, 18: 16217
strontium-90 transfer to oats, effects of content of stable strontium, potassium phosphate, and lime, 19: 19475(T) (JPRS-27940(p.10-17))
strontium-90 uptake, adsorption, and leaching by, effects of potassium and lime on, 18: 17457
strontium-90 uptake by oat plants from, effects of soil type and fertilizer program on, 19: 40310
strontium-90 uptake by plants from, effects of phosphate content on, 19: 45774
strontium-90 uptake by plants from, effects of minerals on, 20: 26613
strontium-90 uptake by plants from, effects of calcium content and

mechanical properties on, 20: 30985
strontium-90 uptake by wheat from, 18: 15761
study methods for, following atomic explosions, 20: 45952 (HI-647-RR)
sulfate exchange and sorption by loss-retentive, 16: 23539
tantalum content, 19: 14207
temperature cycle harmonic analysis, 16: 2871(R) (ANL-6398(p.110-29))
temperature data at 1 cm, multiple regression analysis, 16: 30187(R) (ANL-6474(p.82-92))
temperature distribution in, following nuclear explosion, 19: 13563
temperature of, effects of neutron meter access tubes on, 18: 16201
temperature regime in, effects of meteorological parameters, 16: 10272 (ANL-6470)
temperatures in Ogotoruk Valley, Alaska, variation of, 18: 29868
temperatures of, around radioactive waste tank leaks, 20: 35172 (BNWL-181)
thermal diffusivities, 16: 2871(R) (ANL-6398(p.110-29))
thermal radiation reflectivity, 16: 23854 (WT-543)
thorium and uranium isotope distribution in, age estimation from, 20: 39144
thorium distribution in, effects of soil formation processes on, 20: 23333
thorium isotopic ratios in, in Molodova, Ukraine, 17: 21917
thoron content in gases from, effects of Antler and Chena underground explosions on, 19: 6096 (NP-14511)
tracer studies, 17: 33541
trafficability estimation by gamma spectroscopy, 20: 43542
translocation of strontium and calcium, 20: 40524(R) (TID-23271)
transport of pollutants through, relation of fluid flow in porous media to, 20: 27193 (BNWL-SA-678)
types of, in Neotoma Valley, Ohio, 19: 6897 (TID-21332)
uptake of DDT by carrots from, tracer study, 19: 33719(R) (SAN-536-10)
uptake of radioisotopes by, effects of natural extracts from plants and trees on, 19: 53
uranium content in, effects on content in man, 19: 19490
uranium isotope ratio in, in Molodova, Ukraine, 17: 21917
use of nuclear explosions in studies on, bibliography on, 20: 18855 (CEA-Bib-66)
use of radioisotopes in organic matter studies, 20: 42795
uses for purification of radioactive sewer waters, 19: 22412
washing from cloth, neutron activation methods of measuring, 18: 8317
waste disposal in injection in, hydrodynamics of, 20: 18163(R) (NP-15859)
waste disposal in, economics and hazards of, 20: 28852 (IDO-12052)
waste movement through, from seepage pits, 16: 28634 (CRER-1089)
waste solution dispersion in, tracer study, 20: 42687
waste transport by ground water in, analysis, 19: 40268 (BNWL-63)
waste transport in, effects of ground water on, 20: 8817(R) (BNWL-36, pp 4.1-77)
waste transport in, 20: 8979(R) (BNWL-36)
water content in, volume of influence of neutron probe for determining, 19: 36678
water content in, effects of bulk density and hydrogen form on calibration of meter for measuring, 19: 38948
water content in, neutronic method for determining, 20: 632
water content measured by gamma ray absorption, 17: 8508
water content of, neutron hygrometer for measuring, 18: 12424
water flow in, 20: 8979(R) (BNWL-36)
water flow in, application of diffusion theory to, 17: 39280
water flow in heterogeneous and homogeneous, mathematical analysis, 16: 25045 (TID-7628(p.130-44))
water flow in, use of gamma attenuation in measuring, 17: 34131
water uptake by, tracer technique for measuring, 18: 24045
wave propagation in, computer program for nonlinear viscoelastic, 18: 35703 (BRL-1237)
weight of, radiometric determination of, 18: 22245
zinc deficiency in, effects of, on plant growth, 17: 40498(R) (TID-19389(App.C))

SOL-GEL PROCESS

development of, for spherical UO_2–ThO_2 particle preparation, 20: 40391
flowsheets for, 20: 39006
for production of dense thoria, 20: 43850 (CONF-660524-15)
preparation of thoria–urania-233 fuel by, 20: 45094(R) (BAW-3460-2)

SOLAR BATTERIES

behavior of, theoretical investigation of graded-base, 17: 8930(R) (NP-12356)
bibliography on, 18: 1833 (AD-249100)
bibliography on radiation effects, 16: 5762 (NP-11193)
book: *Energy Conversion*, 18: 12866
characteristics for space vehicle electric power system, 16: 18700
characteristics of gallium arsenide, 17: 1716
collector calibration for, 17: 9131
conference, 20: 21581
conference, 20: 21582
conference, 20: 21583
defects in silicon cells, 19: 43997(R) (UCRL-11889)
description of, for uses in space vehicles, 16: 28633
description of, for International Ionospheric Satellite, 17: 9127
design analysis of, for space power, (T), 19: 18745
design analysis of lithium fluoride, 20: 9698 (NASA-CR-54752)
design and characteristics, 16: 25080 (ASD-TR-61-11(Vol.I))
design and development of thermoelectric, 16: 34122 (ASD-TR-61-315)
design and development for thermionic power systems, 17: 24726 (ASD-TDR-62-877)
design and performance of radiation-resistant, 17: 9116
design and performance of thermionic, (E), 19: 16449(R) (TRW-ER-5632)
design and reliability, 17: 9105
design and testing of high-temperature thermionic, 18: 40214 (APL-TDR-64-92)
design, fabrication, and testing of thermionic, for space uses, 17: 9126
design for communication satellites in Van Allen belt, 16: 34132
design of Brayton cycle, with heat storage system, (E), 19: 12150
design of converter for, 19: 39443(P)
design of, for a lunar mobile surface vehicle, 17: 4348 (61SPC3)
design of, for Telstar power system, 17: 9118
design of front-wall cadmium sulfide photovoltaic, 17: 9109
design of inexpensive, 16: 30542(P)
design of thermionic, for electrical power source of Mars spacecraft, 17: 8924 (JPL-TR-32-171)
development, 17: 4354 (ASD-TR-61-242)
development, 18: 20879
development, 18: 20880
development, 19: 8134
development, 20: 15305
development, 18: 30475(R) (AFCRL-63-940)
development, 18: 24356 (ANL-6802(p.64-5))
development, 20: 19420 (N-65-25271)
development and feasibility of radiation-resistant, 16: 13639(R) (EOS-2080-ML-1)
development and testing of thermionic, 18: 16744(R) (TRW-ER-5802)
development and testing of thermoelectric, 18: 26251(R) (AD-437280)
development and testing of Sunflower, (E), 19: 9311 (NASA-CR-54174)
development and testing thin-film, (E), 19: 43030 (PIC-SOL-209/5.1 (Vol.II))
development for manned space stations, 19: 10009
development for Manned Orbital Research Laboratory power generation, 20: 31387
development for space, 17: 10203
development for space vehicle power, 17: 42412
development for space vehicles, 18: 5973 (AD-423714)
development for space power systems, status of, 18: 34001
development for space power, 20: 29977 (N-65-32716)
development for use in photovoltaic power generator, 16: 14360 (WADD-TR-60-849)
development for use with thermoelectric cells, for space, (E), 19: 16444(R) (AFAPL-TR-64-135)
development of cesium-vapor thermionic, for space uses, 17: 9117
development of condenser-subcooler for Sunflower, (E), 19: 9310 (NASA-CR-54013)
development of direct energy converters, 16: 17813(R) (AD-263107)
development of drift-field radiation-resistant, 20: 36015 (N-66-18407)
development of epitaxial structures for silicon, (E/T), 20: 30724 (NASA-CR-461)
development of flat-plate thermoelectric, 17: 11300 (ASD-TDR-62-214)
development of graded-base radiation-resistant, 17: 6795(R) (NP-12317)
development of graded-base radiation-resistant, 17: 24046(R) (NP-12791)
development of metal–semiconductor, 16: 16518 (ASD-TR-61-564)
development of multi-kilowatt, for space stations, 19: 10006
development of n-p and thin-film, 17: 35226
development of photovoltaic and thermoelectric, 18: 24353 (ANL-6802(p.24-5))
development of radiation-resistant, 16: 12214(R) (EOS-2080-ML-2)
development of radiation-resistant, feasibility studies, 16: 15270 (NP-11488)
development of radiation-resistant cell, 17: 10777(R) (NP-12474)
development of radiation-resistant, 20: 16910 (N-65-18448)
development of radiation-resistant, 20: 19101(R) (N-65-19687)
development of Rankine-cycle Sunflower system, 17: 9133
development of regenerative system using nitrosyl chloride, 16: 16480 (WADD-TR-60-821(Pt.II))
development of solar cell dosimeter, 16: 17815 (BNL-721)
development of solar-thermionic, 20: 15294 (CONF-640921, pp 9-45)
development of Sunflower, 18: 24085(R) (NASA-CR-54053)
development of thermionic, for space uses, 17: 9130
development of thermionic, for generation of 500 watts in orbital flight, 17: 12752(R) (ASD-TDR-62-94)
development of thermionic, 17: 34540(R) (NP-13058)

development of thermoelectric, for space uses, 18: 24351(R) (AD-427285)
development of thermionic, 18: 30494 (TID-7687(p.294-320))
development of thermoelectrostatic, using thin dielectric films, (E), 19: 10005
development of thermoelectric, with thermal storage system, (E), 19: 10007
development of thermionic, 20: 19421 (N-65-25406)
development of 15-kw turboelectric, 17: 9110
development of 30 kw, 19: 10010
development of, NASA Semiannual Report to Congress, Jan. 1 to June 30, 1964, 19: 19453
development of, reasons for, 18: 14777 (CONF-414-2)
development progress, 16: 10759
development, with liquid metal heated thermionic converters, 19: 10011
developments in radiation-resistant, 16: 32615
efficiency in high-flux-level regions, 17: 9115
efficiency of photovoltaic, effects of p-layer resistance on, 17: 25885
electric properties of, effects of light on, 19: 3015 (AWRE-O-57/64)
electron energy deposition in shielded, 18: 7842(R) (ORNL-3499 (Vol.II)(p.12-13))
energy conversion in, review, 19: 41319
evaluation for space power system application, 16: 7324 (D2-5523)
evaluation for sun mission, 20: 41124
fabrication by ion implantation, 17: 20323
fabrication of p-n junction, using ion implantation technique, 20: 20125
illumination intensity effects on, using silicon p-n junctions, 17: 24034(R) (ARF-1214-TR-2)
instrumentation for thermionic, 20: 19419 (N-65-24874)
minority-carrier diffusion lengths in silicon, 17: 8963
operation and response of solar energy converters, 17: 6552
performance as power source for ion thrustors for spacecraft, (T), 19: 26521 (APL-TDR-64-52(Vol.II))
performance as space-vehicle power supplies, 17: 9111
performance estimation for thermionic, 19: 12151
performance for electric-power and life-support systems on spacecraft, (E/T), 20: 5820 (NASA-CR-316)
performance for space applications, 20: 723 (NP-15531)
performance in artificial radiation belt, 17: 14426
performance in space, prediction of, 17: 9104
performance in space systems, power-matching regulators for, 17: 34073
performance of high-resistivity silicon photodiodes, 17: 4646
performance of silicon photoelectric cells as, 16: 8917(T) (FTD-TT-61-56)
performance of silicon, for detection of electron bursts from plasma, 20: 15916
performance of thermoelectric, for space uses, 17: 9128
performance of thermoelectric, for space uses, 17: 9132
performance of thermionic, 19: 10012
performance of, review, 18: 22712
performance with electrohydrodynamic cells for space uses, 17: 9122
performance with hydrogen for spacecraft propulsion, (E/T), 19: 17346 (NASA-CR-59366)
production of silicon, by phosphorus-ion bombardment, 20: 15302(T)
properties, 16: 27741 (NP-11716)
properties evaluation for use outside earth's atmosphere, 16: 25029 (AD-269180)
properties of n-p silicon, as gamma-ray dose rate meter, 18: 4080 (BNL-7310)
properties of silicon, review, 17: 1714
properties of, comparison with isotope cells, 20: 39306 (DP-1066(Vol.1), pp V.17-25)
protection against radiation during Cosmos 41 flight, 20: 39171(T)
radiation and temperature effects on silicon junction, 19: 9550
radiation damage by protons, 17: 31047
radiation damage by electrons in gallium arsenide and silicon, energy dependence of, 17: 39672 (NP-13133)
radiation damage in gallium arsenide and silicon cells, proton, 19: 14112
radiation damage in silicon, effects of doping impurities on, 19: 18538 (NASA-TN-D-2711)
radiation damage in Van Allen Radiation Belt, proton, (T), 19: 19336
radiation damage in silicon, 4-Mev alpha, 19: 42772 (UCRL-16061)
radiation damage in, electron and proton, 20: 16910 (N-65-18448)
radiation damage in Van Allen belts, 20: 34353(R) (N-65-34401)
radiation damage in silicon, electron and proton, 20: 33734
radiation damage in silicon, thermal annealing of, 20: 35808 (N-66-18378)
radiation damage of protons to gallium arsenide and silicon, 17: 39670 (NP-13155)
radiation damage of silicon cells in, electron and proton, 18: 12726 (NASA-TN-D-2098)
radiation damage of, development of detectors for determining, 20: 34353(R) (N-65-34401)
radiation damage to, 17: 18362 (TID-7652(p.118-35))
radiation damage to, by 96-Mev protons, 17: 34489 (NP-13031)
radiation damage to silicon, 17: 39668(R) (N62-11316)
radiation damage to silicon, 17: 41495(R) (N62-11325)
radiation effects on performance, 16: 6544 (ONR-9(Vol.I)(p.143-55))
radiation effects of protons in space at 3 to 13 Mev, 16: 18084 (LMSD-703735-1)
radiation effects, 16: 19439 (REIC-23)
radiation effects on silicon, 16: 21092(R) (GACD-3001)
radiation effects of protons at 20.5 to 740 Mev on silicon, 16: 21093 (NP-11655)
radiation effects, 16: 32612(R) (NP-12046)
radiation effects on, in space, 17: 1715
radiation effects on semiconductor, permanent and transient, 17: 3556
radiation effects, 17: 11263 (NP-12361)
radiation effects on silicon, in Van Allen belts, 17: 16884
radiation effects on silicon, 17: 16736(R) (GA-3872)
radiation effects on power output of, cosmic protons, 17: 18367 (TID-7652(p.243-59))
radiation effects on silicon, 17: 20511(R) (GACD-3223)
radiation effects on operation of, using silicon p-n junctions, 17: 24034(R) (ARF-1214-TR-2)
radiation effects on, 1-Mev electron, 17: 34488 (NP-13014)
radiation effects on, in artificial Van Allen belt, 17: 34665
radiation effects on gallium arsenide and silicon, 17: 36347(R) (NARF-62-18P)
radiation effects on, in space, handbook on, 17: 39671 (NASA-SP-3003)
radiation effects on, use of quartz in shielding from, 17: 42404
radiation effects on, electron, 17: 41521(R) (AD-419705)
radiation effects on, 18: 658 (REIC-32)
radiation effects on silicon, neutron-proton equivalence, 18: 2306
radiation effects on n-on-p and p-on-n types at 1 Mev, 18: 5820
radiation effects on, 18: 7016
radiation effects on, power output degradation in Van Allen belts, 18: 10358
radiation effects on gallium arsenide and silicon, electron and proton, 18: 10596
radiation effects on, Van Allen, 18: 12753
radiation effects on silicon, effects of impurities on electron and proton, 18: 28058
radiation effects on, 18: 32247
radiation effects on silicon, energy dependence of neutron, 18: 32234 (SC-R-64-196)
radiation effects on webbed dendritic silicon, electron, 18: 36041 (APL-TDR-64-20)
radiation effects on gallium arsenide and silicon, on Relay I and Relay II, 18: 40036
radiation effects on cadmium sulfide, electron and proton, 18: 40037
radiation effects on polycrystalline silicon, 18: 44278
radiation effects on gallium arsenide and silicon, in space, 19: 4543
radiation effects on gallium arsenide and silicon, proton, 19: 7826
radiation effects on silicon, permanent, (E), 19: 15941
radiation effects on satellite, in Van Allen belts, 19: 23511
radiation effects on satellite-carried, 19: 23512
radiation effects on n-p and p-n, at 2 Mev, 19: 22813
radiation effects on lithium-drifted silicon p-i-n diodes, (E), 19: 28702
radiation effects on n-p silicon, electron, (E), 19: 32619
radiation effects on gain of, Q-factor technique for neutron, 19: 36865 (FZK-224)
radiation effects on, in space environment, 19: 39059
radiation effects on efficiency of silicon, electron, 19: 40931 (AD-609424)
radiation effects on, in space vehicles, 19: 46875
radiation effects on concentrator coatings for, alpha and proton, 20: 7655
radiation effects on silicon, in space vehicles, 20: 9303
radiation effects on satellite, from artificial radiation belt, (E), 20: 13131
radiation effects on n-p and p-n, annealing of proton, 20: 14919(R) (N65-20653)
radiation effects on defects in silicon, effects of impurities on electron and proton, 20: 17125 (NASA-CR-404)
radiation effects on junctions, proton, 20: 16907(R) (N-65-17517)
radiation effects on gallium arsenide and silicon, proton, 20: 19095 (N-65-16347)
radiation effects on silicon, electron, 20: 19105 (N-65-19870)
radiation effects on gallium arsenide and silicon, proton, 20: 19106(R) (N-65-19886)
radiation effects at 10 to 90°C, electron, 20: 21161
radiation effects on silicon solar cells, proton, 20: 23516 (AD-625440)
radiation effects on selenium and silicon cells, electron, 20: 23762(R) (AD-624884)
radiation effects on partially shielded cells, proton, 20: 27368
radiation effects on thin-film cadmium sulfide and single-crystal silicon,

proton, 20: 31616
radiation effects on drift-field, proton, 20: 33729(R) (N-66-12189)
radiation effects on silicon, transient annealing from neutron, 20: 37129 (SC-DC-66-1820)
radiation effects on silicon, 1-Mev electron, (E), 20: 39458 (NP-16225)
radiation effects on gallium arsenide and silicon, proton, 20: 40299
radiation protection for Explorer XVI, 17: 37638
radiation resistance of p-type base silicon solar cells, 16: 3556
radiation resistance of modified phosphorus-diffused cells, 16: 10758
radiation resistance of lithium-doped silicon, 20: 31614
radioinduced damage in p-type silicon, temperature dependence of electron, 20: 19115
radioinduced damage in n- and p-type silicon, electron, 20: 45018
radioinduced defects in p-type silicon, annealing of electron, 20: 19114
reflector characteristics for, summary, 17: 9121
shielding in Advanced Orbiting Solar Observatory, (T), 19: 25618
status, 19: 27135
studies by Explorer XII, data summary, 16: 20851
survey of photovoltaic, photoemissive, thermoelectric and thermionic, for spacecraft power systems, 17: 1723
survey of space, 18: 9721
temperature control in operation of, 17: 4355 (ASD-TR-61-689)
temperature effects on operation of, using silicon p-n junctions, 17: 24034(R) (ARF-1214-TR-2)
testing, 18: 33703
testing facility and methods for, 17: 9114
testing of thermionic, for space uses, 17: 9134
thermal energy storage in, materials for, 17: 34075
use as power supplies for space vehicles, 17: 1722
use as radiation detectors, 17: 3684
use for extraction of water from rocks, comparison of nuclear power with, 19: 34360 (AD-608225)
use in space vehicles, 17: 13856
use of silicon cell in cobalt-60 source assay unit, 19: 36802 (BNL-923)
use of silicon, in radiation dosimetry, 17: 27696
use of silicon n-p junction, for measuring x rays, 19: 7794
use of silicon solar cell to measure intense radiation, 16: 13359
uses in electric propulsion systems for space, 20: 31382
uses of radioinduced deterioration of, for neutron dosimetry, 20: 6679 (NP-15645)
uses of silicon, as integrating gamma dosimeters, (E), 19: 18254 (BNL-902)

SOLAR FLARES

activity of chromospheric, effects on light elements on, 18: 18544
alpha and proton energy spectra from, 20: 5969
alpha beams from, dosimetric evaluation of, (T), 19: 30909 (AD-611323)
alpha emission, detection and measurement, 16: 8083
alpha flux from, 18: 34389
alpha fluxes from, computer program for calculating, 20: 32674 (NP-15697(Vol.3))
analyses of July 1961, 18: 44403
analysis for proton flux, 16: 1275(R) (NP-10832)
analysis of cosmic-ray burst of May 4, 1960, 18: 30453(T) (NASA-TT-F-127(p.235-66))
analysis of high-energy, 16: 27892
analysis of July 1961 event for hydrogen isotopes, 18: 34382 (NP-14141)
analysis of type II and III radio bursts, 16: 24656 (ML-879)
analysis of, on July 16, 1959, 18: 44373
area of, center-limb effect of, 18: 24272 (NP-13804)
association with type III radio bursts, (T), 19: 4809
atmospheric density variations during, 18: 7615
bibliography, 17: 27937 (AID-62-155)
biological effects of radiation from, in space flight, (E), 19: 29946
book: *Solar Flares*, 19: 18676
bremsstrahlung bursts from "explosive", 18: 44395
characteristics of type IV radio bursts from, 17: 12910
characteristics of type IV bursts from, 17: 12913
characteristics of type IV bursts from, 17: 12914
charged particles from, connection with type III absorption in the ionosphere, 17: 13187(R)
charged-particle acceleration in, 18: 44410
charged-particle energy and rigidity spectra in polar regions from, (E), 20: 11855
chromospheric, cosmic-ray intensity dependence on location of, 16: 10779
chromospheric striation obscured by, 16: 26046 (AFCRL-834)
classification, 18: 44375
classification of, optical, 18: 18594 (NP-13684)
conference on November 1960, 17: 22405 (AFCRL-62-441)
conference on physics of, 18: 44371
configuration of proton-emitting, (T), 20: 37346
contribution to radiation dose in space vehicles, 17: 5646
corona, acoustic waves, electron density, magnetic fields, and effects on troposphere, 16: 27418 (NP-11961)
coronal condensations and loop prominences in, 19: 25124
corpuscular radiation from, optical evidence for, 17: 12920
correlation of x-ray bursts and type III radiobursts in, 18: 7397
correlation with cosmic intensity increases, 17: 12949
cosmic electron production, on September 3, 1960, 16: 3604
cosmic neutron intensity changes associated with, 17: 12925
cosmic nuclei intensity during, 17: 19027(T)
cosmic particle emission from, 18: 44396
cosmic-particle observations Sept. 1960, 17: 3940
cosmic particles from, motion in geomagnetic fields, (T), 19: 18720 (CRGP-1208)
cosmic-proton propagation from, above 1 Bev, 17: 698
cosmic proton spectra from, 16: 29620
cosmic radiation emission during Y phase of, (T), 19: 9848
cosmic radiation from, space-travel hazard from, 17: 18358 (TID-7652 (p.12-32))
cosmic radiation from September 3, 1960, time variation of, 17: 20817
cosmic radiation from chromospheric, asymmetry in (E/T), 19: 2959
cosmic radiation intensity increases associated with, 17: 12926
cosmic radiation intensity changes associated with, 17: 12935
cosmic radiation intensity during July 1961, 17: 20818
cosmic radiation intensity from, changes in, 17: 24248
cosmic radiation in, origin of, 18: 20723
cosmic radiation variations with, 17: 19011 (AFCRL-63-242)
cosmic ray composition, energy spectra, and time variations in fourteen, 16: 16186
cosmic ray effect, new methods of analysis, 16: 10782
cosmic-ray energy spectrum during, 17: 12946
cosmic-ray fluxes and spectra from, for nuclei with $Z \geq 6$, 16: 29618
cosmic-ray increases associated with, 17: 12912
cosmic-ray increase associated with Nov. 1960, 17: 12931
cosmic-ray intensity effects of, in auroral zones, 16: 29526
cosmic ray intensity effects of, 17: 11455
cosmic-ray intensity from, during polar absorption events, 17: 12929
cosmic ray intensity increase during Dec. 1957, 18: 28273 (AFCRL-63-855)
cosmic ray observations on May 4 and Nov. 12 and 15, 1960, anisotropies, 16: 10783
cosmic ray observations at sea level, interplanetary magnetic-field deductions from, 16: 10784
cosmic ray occurrence from geomagnetic storm correlations, 16: 9337 (NASA-TN-D-1010)
cosmic-ray spectra and geomagnetic storms from, 16: 29619
cosmic ray spectra from, 17: 16927
cosmic ray variation effects, 16: 8042 (NP-11232(p.136-48))
cosmic-shower production on Nov. 10 to 20, 1960, 16: 15508
cosmic-ray multiply charged nuclei from July 18, 1961, 20: 39564
cosmic-ray variations during, measurement of, 18: 36178(R) (AFOSR-424)
data compilation for 1954–1964, 20: 37886
data during geomagnetic storm for Sept. 1963, 20: 28138
data for April 1965, 19: 45178
data for fourth quarter, 1964, 19: 47468
data for Jan. to July 1965, 20: 28137
data for second quarter of 1962, 17: 8996
data for second quarter 1965, 20: 21830
data from IGY and IGC, catalog of, 18: 42522
data on, 17: 20212
data on, 17: 34676
data on March 1964, 18: 34391
data on recent, 17: 37896
density of plasma of, 17: 5187
descriptions of, during 1962 and April 1964, 18: 40430
detection and measurement in Feb. 1958, 16: 18204
detection and measurement on April 15, 1963, ionospheric absorption from, 17: 39830
detection and measurement of, from nearby stars, (E), 19: 41203 (AD-600154)
detection of particle streams from, using high-frequency radio waves, 18: 26247
detection of proton events, Apollo system for, 18: 30066
detection of solar-produced heavy nuclei ($Z \geq 6$) during Nov. 1960, 18: 7446
detection of, frequency and observing-time patterns in, (E), 20: 2575
detection of, radio method for, 18: 24284
detection of, radio method for, 19: 20759
deuteron production in, (E), 19: 2954
development of class 3+, 17: 19024
distribution of chromospheric, correlation with Forbush decreases, (E/T), 20: 23971
distributions in solar longitude, 18: 40182
disturbances propagating from, model for, 20: 46273 (AD-640661)
duration of, 16: 26631 (RM-2825-PR)

effect on ionization of nocturnal ionospheric D region, 20: 19662
effect on nucleon component of cosmic radiation, 17: 3943
effect on outer Van Allen zone, 17: 5184
effect on oxygen-1 line intensity in airglow, 18: 44672
effects from July 1959, 16: 15514
effects in E and D ionosphere layers, 18: 24283
effects in lower ionosphere, vlf-wave, 18: 32683
effects of chromospheric, on cosmic-ray hard component, (E), 19: 12051(T)
effects of chromospheric, on ionosphere, (E), 19: 34850(T)
effects of chromospheric, on polar-cap-region anomalous absorption, 20: 30225
effects of, in the ionosphere, 16: 32250 (RAD-SR-62-19)
effects of July occurrences on cosmic radiation at high latitudes, 16: 911
effects of, review of geophysical, 17: 32871
effects of simulated, on space vehicle shielding, 17: 11902 (ORNL-3317)
effects of sunspot activity on geomagnetic activity on earth, 18: 42520
effects of sunspot-region, geomagnetic, 19: 12419
effects of, and seasons on critical F2-layer frequencies, 20: 39959(T)
effects on absorption-time profiles of polar-cap absorption, 18: 18598
effects on Arctic communications, 18: 16841
effects on carbon-14 content of atmosphere, 20: 23573
effects on charged particle distribution in radiation belts, (T), 19: 21137
effects on cosmic radiation intensity in New Hampshire, 16: 910
effects on cosmic radiation and geomagnetic storms, 17: 12932
effects on cosmic nucleon intensity, 17: 12934
effects on cosmic nucleon attenuation by air, 17: 12978
effects on cosmic radiation variations, 18: 12842(T) (NP-tr-1090)
effects on cosmic radiation in May 1959, 18: 30446(T) (NASA-TT-F-127(p.89-131))
effects on cosmic neutron intensity, 18: 30451(T) (NASA-TT-F-127 (p.213-22))
effects on cosmic neutron intensity, 19: 20878(T)
effects on cosmic ray intensity, 20: 7757(T) (NASA-TT-F-91, pp 158-63)
effects on cosmic ray intensity, 20: 7759
effects on cosmic ray energy and intensity, (E), 20: 37537
effects on cosmic-ray intensity, 18: 30454(T) (NASA-TT-F-127(p.267-73))
effects on cosmic-ray intensity variations in 27-day cycle, 18: 30457(T) (NASA-TT-F-127(p.312-14))
effects on cosmic-ray primary-secondary coupling coefficients, 18: 34472(T) (NASA-TT-F-126(p.273-9))
effects on cosmic-ray intensity, sudden commencements correlated with, 20: 44419
effects on critical frequencies of ionosphere, 20: 39965(T)
effects on directional distribution of cosmic mesons, 20: 44422
effects on Drosophila in magnetic field, 16: 31409
effects on earth's rotational period, 18: 7638
effects on electron density profiles over India, 18: 11071
effects on electron density of ionosphere, 19: 25431
effects on electron density in ionospheric D-region, (E), 19: 27322
effects on electron and proton distributions in outer radiation belts, (E), 19: 41312
effects on electron density in ionospheric F2 region, 20: 19663
effects on etiology of multiple sclerosis, 20: 40639
effects on flux density in outer belt, 17: 12901
effects on Forbush decreases, 17: 12950
effects on Forbush decreases, 17: 12982
effects on galactic cosmic particle intensity, 18: 44481 (EFINS-63-68)
effects on geomagnetic activity, 17: 22974
effects on geomagnetic field, data for 1962, 17: 28113
effects on geomagnetic and ionospheric conditions, 18: 16842
effects on geomagnetic field, 18: 44399
effects on geomagnetic field, 18: 44401
effects on geomagnetic fields, 19: 30912
effects on geomagnetic fields and cosmic-ray intensity, (E/T), 19: 32915
effects on geomagnetic storm sudden commencements in equatorial electrojet region, (E), 19: 35257
effects on geomagnetic disturbances, (T), 19: 45163
effects on geomagnetic variations, 19: 47480
effects on geomagnetic fields, (T), 20: 1101
effects on geomagnetic storm sudden commencements, (T), 20: 1107
effects on geomagnetic storm development and ionospheric disturbances, 20: 30230
effects on geomagnetic sudden commencements, 20: 44466
effects on hard and neutron components of cosmic radiation (T), 19: 3009
effects on hydrogen Lyman-alpha spectra, 18: 44378
effects on intensity of cosmic radiation, measurements in space flights, 16: 33668
effects on intensity of cosmic electrons near earth, 17: 13006
effects on intensity of cosmic radiation, (E), 20: 17313(T)
effects on interplanetary gas, 17: 12984
effects on interplanetary magnetic fields, (E), 20: 4527
effects on ionospheric cosmic-noise absorption and enhancements, similarity of, 17: 32857
effects on ionospheric radio communications, 18: 16823
effects on ionospheric D- and E-regions, 18: 16832
effects on ionospheric radio wave propagation, 18: 16844
effects on ionosphere, 18: 32679 (AD-428169)
effects on ionospheric vlf propagation, 18: 44644 (UAG-R-154)
effects on ionospheric F2 layer, 18: 44653
effects on ionosphere (E), 19: 3167
effects on ionospheric D-region, (E), 19: 23527
effects on ionospheric F2 region, 19: 39675
effects on ionospheric RF transmission, 19: 39682
effects on ionospheric sudden disturbances, 19: 41573 (RPU-S19)
effects on ionospheric D region, v-l-f propagation for determining, 20: 15604
effects on ionospheric D-region electron production and recombination rates, (E/T), 20: 28115
effects on ionosphere, sudden enhancements of atmospherics from, 20: 34372
effects on latitudinal distribution of atmospheric ozone, 17: 29483
effects on lead-210 content in neve from Antarctica, 19: 16341
effects on long vlf propagation paths, in 1961, 19: 37710 (NBS-TN-210)
effects on, low-energy cosmic nucleon intensities, 17: 12924
effects on manned space flight, computer analyses of, 18: 35048 (AMRL-TDR-64-11)
effects on manned military space vehicles, (T), 20: 2656 (NASA-SP-71, pp 265-86)
effects on materials in space vehicles, 20: 4312
effects on metals and plastics, tolerance limits for, 17: 22241
effects on neutron and proton dosages to man in supersonic flight in upper atmosphere, 18: 30399
effects on occurrence of ionospheric E_s, statistical analysis for 1953 to 59, 18: 11070
effects on outer Van Allen belt, 17: 3941
effects on particulate radiation environment inside the magnetosphere, 19: 23946
effects on polar cap absorption events, 17: 12940
effects on polar cap radio wave absorption, 17: 41668 (UAG-R-129)
effects on polar cap absorption, 18: 36415(T)
effects on polar cap on mass, (E/T), 19: 20763
effects on polar cap absorption and Forbush decreases, asymmetries in, (T), 19: 37716
effects on propagation of atmospherics, (T), 20: 28119
effects on radio communications, conference on, 18: 16822
effects on radio wave absorption in ionospheric D-region, 18: 16834
effects on radio wave propagation at oblique incidence, 18: 16840
effects on radio wave absorption in ionosphere, polar blackouts in, 18: 16826
effects on radio-wave propagation in ionosphere, (E), 20: 24205
effects on rats, lethal, 17: 18373 (TID-7652(p.375-92))
effects on relaxation time of ionosphere, 20: 32267
effects on reproduction of *Drosophila melanogaster*, in magnetic fields, (E), 19: 15136
effects on solar and geophysical phenomena, 20: 42047
effects on solar magnetic field, 17: 28109
effects on solar magnetic field, 20: 39557
effects on solar magnetic field, 20: 39558
effects on solar proton flux, 17: 12994
effects on solar wind, 19: 18668
effects on space flights, 20: 30222(T) (NASA-TT-F-389, pp 758-63)
effects on space-vehicle flight-control, 18: 37473 (ASD-TDR-63-75)
effects on sudden frequency deviations in ionosphere, 20: 32268
effects on terrestrial events, (E), 20: 2855
effects on transarctic h-f radio wave propagation, 18: 16831
effects on tropospheric pressure variations, (E), 20: 30237(T)
effects on troposphere, (T), 20: 34394(T)
effects on upper atmosphere variations, 17: 5170
effects on upper atmospheric air density, 18: 7612
effects on upper atmosphere, (E), 20: 24208 (AD-626167)
effects on uv spectra of sun, 18: 44377
effects on vhf radio wave ionospheric propagation at low latitudes, 18: 16839
effects on vlf radio wave propagation in ionosphere, 18: 16830
electromagnetic radiation from, continuum, 17: 9153
electromagnetic radiation from, mechanism for, 20: 23852
electromagnetic wave emission with continuous spectra during, 20: 2580
electron acceleration in, radio noise from, 17: 3950
electron density of large, time variation of, (E), 19: 9851
electron emission and propagation from, (E), 20: 31869
electron emission from, pre-sudden commencement effects from, 19: 35288
electron flux in atmosphere following, 16: 19669

electron precipitation during geomagnetic storms, 17: 3944
electron production from, 20: 19412
electron temperature and spectra in, (T), 19: 9846
emission from, uv- and x-radiation, 19: 16362
emission of particles and x rays by, measurement and theory, 18: 16641
emission of particles in, effects on atmospheric circulation of, (T), 19: 16741
emission of protons from, review, 17: 34697
emission of radio and corpuscular radiation in July 1961, 17: 5181
emission of type-IV r-f, effects of medium on, (T), 20: 25710(T)
emission of, effects of subsurface magnetic fields on, 18: 42254 (TID-21105)
emission spectra in, curves of growth for, (T), 19: 12042
emissions from, Lyman alpha and x-ray, 16: 21232
emissions from, models for microwave and x-ray, 19: 44931
emissions from, OSO I observations of microwave and x-ray, 18: 44388
emissions from, OSO I observations of microwave and x-ray, 18: 44389
emissions from, theory of radio and x ray, 18: 44405
energy of, 17: 13181(T)
energy of, 16: 26631 (RM-2825-PR)
energy release in, mechanism for, 17: 26263
energy release mechanisms for, considering standing hydromagnetic waves, (T), 19: 23824 (NP-14890)
energy spectrum, 16: 32644(R) (UCRL-10211(p.16-42))
excitation of type II and III radio bursts from, 17: 12919
fine structure of Forbush decreases accompanying, 17: 12945
flash phase of, physical phenomenon in, (E), 19: 47188 (ADD-613636)
Forbush decreases and questionable geomagnetic disturbances, 20: 44420
Forbush decreases, intensity recovery from, 20: 44421
formation and properties of, model for, (T), 19: 47188 (AD-613636)
frequency drift and time profile of 200 Mc type III, and electron temperature of corona, 17: 34686
frequency of, 16: 26631 (RM-2825-PR)
gamma emission by, (E/T), 19: 9852
gamma emission from, mechanism for, (T), 19: 44916(T)
gamma emission from sodium-22 decay in chromospheric, 20: 27695
gamma emission in, mechanism of, 19: 41289
gamma production in chromospheric, from radiating electrons, 18: 4394(T)
gamma production in, analysis of, 20: 44093
gamma radiation from, upper limits of high-energy, 17: 22407
generation by varying solar magnetic fields, 17: 13273(T)
geomagnetic disturbances and plages, relation between, 17: 13183(T)
geomagnetic effects of, 17: 31249
geomagnetic effects of, location of ionospheric current system causing, 18: 7597
geomagnetic storm production by, dynamical theory of, 16: 27893
geomagnetic storm production by, 16: 27894
geomagnetic sudden-commencement production by, 16: 29531
geotectonic effects from, indirect, 18: 24528
geotectonic movements from, 18: 11050
hazards at supersonic transport altitudes, 20: 40525
hazards of, 17: 18359 (TID-7652(p.86-7))
hazards of, evaluation of, (T), 20: 5966 (AD-618905)
hazards of, in manned space flights, 20: 29058
hazards to man of, during space flight, 19: 31803(T) (UCRL-Trans-1225)
hazards to man of, during space flight, 19: 31810
heliographic position of, asymmetric effects on geomagnetic fields, 19: 33119(T) (AD-611031)
helium abundance and energy in Nov. 12, 1960, 17: 5193
helium nuclei from, energy and flux of, 17: 24220
helium production following, in satellite materials, 16: 19519
hydrogen abundance and energy in Nov. 12, 1960, 17: 5193
hydrogen ion emission in, negative, 20: 34036
hydrogen nuclei from, energy and flux of, 17: 24220
hydrogen production in, isotopic abundances for (E), 19: 2940
incidence of, comparison with magnetic transients, 17: 3922
intensity increases of cosmic nuclei associated with, 17: 12936
intensity of particle flux of Sept. 3, 1960, 17: 12939
intensity of, statistical relation to sunspots, 17: 39826
ion content in, rare-gas, 20: 44104
ionization from, altitude of, 16: 19647
ionization in D region by, v-l-f phase observations of, 17: 37908
ionization in F2 region, decay of, 17: 6933
ionosphere F2 layer ionization increases from, 16: 15492
ionospheric disturbances at high latitudes following large, space-time distribution of, 18: 11047
ionospheric effects, 16: 21233
ionospheric effects of Sept. 1961, phase observations on, 17: 5101
ionospheric effects in F2 region, 18: 16643
ionospheric effects, 18: 16644
ionospheric effects of, 18: 16733
ionospheric effects of, 18: 40178
ionospheric ionization produced by, observation of, (E/T), 19: 4823
loop formation following, mass balance for, 18: 44381
loop prominences in, 18: 44380
lunar luminescence excitation by, 18: 10758
magnetic cloud ejection during, effects on cosmic and geomagnetic storms, 16: 24667
magnetic disturbances during, relation of auroral displays to, 20: 37887
magnetic disturbances during, relation of auroral displays to, 20: 37888
magnetic effects on, 18: 44383
magnetic energy dissipation during, 18: 44409
magnetic energy storage and release in, 18: 44386
magnetic field and sunspot configurations during, 17: 13181(T)
magnetic field annihilation and reconnection in, 17: 32859
magnetic field behavior during, 18: 44384
magnetic field energy dissipation by finite conductivity instability in, 18: 44413
magnetic field observations at, 18: 44385
magnetic field of, 18: 10730
magnetic field stability near, 18: 44414
magnetic flux topological variations in, (T), 20: 32656
measurement of, indices for, 18: 28209
measurements and nature, 16: 19660
measurements during Nov. 1960, 16: 24306
measurements from Explorer VI and Pioneer V with proportional counter telescope, 16: 20526 (AD-269307)
measurements in July 1959 and Nov. 1960, 16: 15517
measurements of type III and III*, photometric and positional, 17: 32875
mechanism and spectral properties of, 19: 16363
mechanism for, 17: 31247
mechanisms of, nonthermal, 18: 44395
microwave emission in, (E), 19: 37443
model, 18: 30396
model, (T), 20: 15214
model for high-energy phase of, 20: 44086
model of, for use in radiobiological studies, 18: 31228
models for, (T), 19: 4805
neutron emission in, (T), 20: 9634 (D1-82-0484)
neutron flux following, search for solar, 20: 44452
neutron flux variation with, atmospheric, 18: 9047 (D1-82-0257)
neutron monitor survey during, coupling functions for, 18: 7447
neutron production in, (T), 19: 44902
neutrons in, detection of protons from decay of, 20: 21495
nuclear reactions in, Discoverer-17 studies of, 18: 44400
nuclear reactions in, gamma and neutron production in, 18: 44416
nuclei from, energy and flux spectra of heavy, 17: 24220
nuclei in Nov. 12, 1960, abundance and energy of heavy, 17: 5193
observations of, in 1963, 18: 42293
observations on May 4, 1960, analysis of (E), 19: 3010
occurrence during geomagnetic storms, (E), 19: 5076
occurrence of, design of alarm systems for, 18: 7013
occurrence of limb, radio event correlations with, (E), 20: 25713
occurrence of, magnetic field destruction by, 17: 3910(T) (FTD-TT-62-99)
occurrence of, prediction of, 17: 19015
occurrence of proton-emitting, 1966-1968, 20: 25693
occurrence of type-IV radio, correlation with cosmic-ray intensity, 19: 25195
occurrence of type IV radio, during 1956-1963, 20: 23846
occurrence of, alarm system for detecting, 18: 10752
occurrence of, association with type II bursts, 20: 25714
occurrence of, association of sunspot magnetic fields, cosmic rays, and radio bursts with, 20: 44102
occurrence of, correlations with sunspot acceleration, 19: 23239
occurrence of, correlation with pre-existing calcium network, (E), 20: 2578
occurrence of, correlation with sporadic decameter-range r-f emission, (E), 20: 25711(T)
occurrence of, correlation with aurorae, 20: 39956
occurrence of, cosmic radiation intensity variations during, 19: 23329
occurrence of, mechanism for, (T), 20: 27712
occurrence of, methods for predicting, 20: 5967(R) (AD-619740)
occurrence of, radiation emission from, 20: 46469(T)
occurrence of, regularities in, 18: 28207
occurrence of, relation to noise bursts and short-wave fadeouts, 18: 10738
occurrence of, relation to radio emission, 18: 28279
occurrence of, short-wave fadeout from, (T), 19: 4818
occurrence of, 1957-58 and 1960-63, autocorrelation of, 19: 32865
occurrences from 1957 to 1961, correlations with geomagnetic storms, 19: 12043
occurrences of active dark filaments and type III bursts in coincidence, 18: 5905
occurrences of chromospheric, data for 1963, 19: 23240

occurrences of, research on, 19: 32852(R) (AD-608730)
optical characteristics of radio wave-emitting, 18: 44374
origin of, evaluation of magnetohydrodynamic vortices as, 17: 692
origin of, discharge theory of, 18: 44412
origin of, hydromagnetic instability as, 18: 44411
origin of, plasma cloud and shock wave effect on, 20: 44471
particle acceleration mechanism in, 19: 14222
particle acceleration in, intensities at earth from, 20: 23849
particle acceleration from filaments, model for, 18: 44915
particle distribution in, 18: 4412 (ASD-TDR-62-606)
particle emission in, 17: 12996
particle emission from, 18: 7390
particle emission from, propagation of, 18: 7392
particle emission from, effects of interplanetary magnetic fields on, 18: 7443
particle emission from, properties of, 18: 36152
particle emission from, 18: 44407
particle emission from, at high energies (E/T), 19: 2952
particle emission from, 19: 14204
particle emission by, (T), 20: 23851
particle flux and radiation dose rate from, 16: 20241
particle flux in Sept. 28, 1961, 17: 6921
particle generation in, relation to type-IV bursts, 18: 44397
particle precipitations from, in the geomagnetic field, energy spectrum and behavior of, 17: 12872
particle production in, model for high-energy, 17: 18361 (TID-7652(p.96-117))
particles from, diffusion model for propagation of, 20: 11428(T)
photometry of eruptive phenomena in, 19: 41234
photon emission from, ionospheric effects from, 18: 28465
physical conditions in, 17: 15043
physics, 16: 9343
plasma ejection in, 17: 12981
polar-cap absorption event production by, 16: 27895
polar cap absorption relation to, 17: 36561 (UAG-R-127(Pt.I))
prediction for space flight, 17: 5164
prediction for space flight, 17: 35332 (NP-13060(p.301-38))
prediction of, 18: 7383
prediction of, 20: 5966 (AD-618905)
prediction of, review, 17: 28124
prediction of, statistical method for, 17: 18360 (TID-7652(p.88-95))
prediction of, observations and theory of, 20: 34004 (AD-627686, pp 25-38)
prediction of, statistical method for, 19: 25121
prediction techalque for proton, long-range, 20: 31879
prediction using perceptrons, 20: 19324 (N-65-21300)
production by skin effect in twisted magnetic fields, (T), 19: 9840
production of, effects of plasma instabilities on, 17: 33166
production of helium-3 and tritium by, in atmosphere, 16: 33300
production of mechanisms for, 18: 7830
production of type-IV, theory of, 19: 1148
production of, angular momentum exchange between planet and sun as mechanism for, 20: 41610
production of, solar wind concept of, 18: 44417
propagation of disturbances from, through interplanetary space, 16: 30996
properties, 16: 15517
properties, 19: 30912
properties, (E/T), 20: 9639
properties and localization of chromospheric, 19: 47191(T) (NASA-TT-F-250)
properties and terrestrial effects of, 17: 7678
properties and theory of, 19: 14204
properties of, 18: 32355
properties of, (T), 20: 11438
properties of chromospheric limb, (T), 20: 29905(T)
properties of class 3, correlation between optical and radio, (T), 20: 2582
properties of corpuscular streams from chromospheric, 20: 25692
properties of four related, on Sept. 1957, (E), 20: 37347
properties of heavy nuclei from, 17: 12937
properties of limb, (E), 20: 25713
properties of proton-emitting, 18: 28220
properties of Sept. 26, 1963, (E), 19: 16354
properties of sympathetic, 20: 9651
properties of weak chromospheric, 19: 47190(T) (NASA-TT-F-248)
properties of, associated with dark filaments and radio bursts, (T), 19: 4799
properties of, data for Sept. 1963, 19: 41603
properties of, relation to loop prominences, 18: 42269
properties of, review (E/T), 19: 2945
properties of, review of, (E/T), 19: 6437
properties of, spectrophotometric studies of, 18: 24269 (NP-13801)
properties of, spectral analysis for determining, 20: 17230
properties of, sunspot cycle relation to, 20: 39563
properties of, with associated cosmic-ray event, (E), 19: 4798
protection of man against, in space flights, 18: 12390
proton acceleration from, at 3 to 20 Mev, (E), 19: 20766
proton beams from, dosimetric evaluation of, (T), 19: 30909 (AD-611323)
proton distributions from, models for, 18: 28295
proton distributions from, in space, 20: 15191 (N65-20996)
proton distribution from, diffusion effects in, (T), 20: 17228 (N-65-18275)
proton dose from, in tissue behind slab shields, (T), 20: 35350
proton dose in space vehicle from, calculation, 19: 17173
proton doses and spectra of, 18: 44482
proton doses from, calculation of, (T), 20: 2658 (NASA-SP-71, pp 527-33)
proton doses from, properties of, 20: 37915
proton ejection in, 17: 12981
proton emission and energies, 16: 20239
proton emission, detection and measurement, 16: 8083
proton emission, flux at terrestrial polar regions, 16: 5847
proton emission from, 17: 12928
proton emission from, prediction of, 17: 25964
proton emission from May 12, 1959, 17: 27596 (NP-12905)
proton emission from, 17: 35332 (NP-13060(p.301-38))
proton emission from, intensity of, 18: 5964
proton emission from, space vehicle shielding for, 18: 9558 (ORNL-3520)
proton emission from, longitude distribution of, 19: 25123
proton emission from, correlation of satellite and ground-based observations of, (E), 20: 19351
proton emission from, flight time and PCA effects of, 20: 34037
proton emission from, design of r-f warning system for, 20: 34009 (N-66-16405)
proton emission from, pre-sudden commencement effects from, 19: 35288
proton emission in, 18: 6716
proton emission in, diffusive model for, 18: 30389
proton emission in (E), 19: 3005
proton energy and intensity in, 17: 12942
proton flux at 1.5 Mev in magnetosphere, geomagnetic cutoff of, 18: 14766
proton flux from, 19: 16326 (REIC-37)
proton fluxes from, 17: 34713
proton fluxes from, correlations with cosmic noise absorption and geomagnetic and interplanetary fields, (E), 20: 11852
proton fluxes from, computer program for calculating, 20: 32674 (NP-15697(Vol.3))
proton fluxes in, of July 1961, 17: 6920
proton hazards during space flight, 16: 29210 (NASA-TN-D-1383)
proton injection into radiation belts, 17: 12899
proton injection into auroral zone, July 1961, 18: 7444
proton intensities during Nov. 1960, 17: 12941
proton intensity during Nov. 1960, 17: 12943
proton intensity during, on Sept. 28, 1961, 18: 7441
proton intensity from, 18: 28287
proton intensity in, time dependence of, 17: 12944
proton measurements during Sept. 3, 1960, 17: 12938
proton production in active regions of, 17: 12927
proton propagation from, 18: 44402
proton propagation and spectra from, 19: 25122
proton propagation from, in interplanetary magnetic field, (T), 20: 39575
proton radiation from, total rem dose for, 17: 18374 (TID-7652(p.393-401))
proton relative biological effectiveness from, 19: 33704
protons from, aluminum shielding attenuation of, 18: 7844(R) (ORNL-3499(Vol.II)(p.25-6))
protons from, depth doses and energy distributions of, 17: 18371 (TID-7652(p.309-42))
protons from, measurement of, 17: 12788(R) (ORNL-3360(p.225-9))
protons from, activation of space vehicles by, (T), 19: 29023
protons from, diffusion in interplanetary space of, 20: 5970
protons from, effects on spacecraft, 18: 28904
protons from, effects on manned space missions, (T), 19: 20873 (D2-11608)
protons in, protection of astronauts against, 19: 30009
protons of, secondary, gamma dose in shielding from, (T), 19: 25547
radiation burst emission during, r-f and x, (T), 20: 27704
radiation density and dosage from type 3+, 17: 25966
radiation dose absorbed in astronaut from, evaluation, 19: 38014 (N64-29363)
radiation dose from, in atmosphere of polar regions at 36,000 and 70,000 feet, 18: 31834
radiation dose from, calculations of, 16: 26631 (RM-2825-PR)
radiation dose measurements for, 18: 31228
radiation dose to crew and passengers during supersonic flight from, 20: 14797
radiation doses to spacecraft from, proton, 16: 30992
radiation effects on spacecraft personnel, (T), 20: 2655 (NASA-SP-71,

pp 85-96)
radiation effects of simulated, on mice, gamma, 20: 18443
radiation emission from November 12 and 15, 1960 events, 16: 2390
radiation emission from July 10, 1959 event, 16: 2391
radiation emission from, geophysical effects of, 18: 28212
radiation emission from, geophysical effects of, 18: 28464
radiation emission from, 18: 22653
radiation emission from, 18: 32358
radiation emission from, intensities of higher harmonics in cyclotron, 19: 23247
radiation emission during, Forbush decreases from, 19: 25240
radiation emission from, corpuscular and electromagnetic, 20: 11438
radiation emission from, 20: 29875(T) (NASA-TT-F-389, pp 732-9)
radiation exposure to astronauts from, recommended allowable, 17: 27605
radiation from, 17: 36548 (NASA-TR-R-169)
radiation from, 18: 4415
radiation from, low-rigidity, 17: 28130
radiation from sunspot covering, type IV, 17: 24222
radiation from, contribution of characteristic x rays to, (T), 19: 47197
radiation from, continuum electromagnetic, 20: 13409
radiation from, monitoring in stratosphere, 18: 37037
radiation from, properties of corpuscular, 18: 44401
radiation hazards from, during space flight, 16: 20245
radiation hazards, 17: 2815 (AD-275605)
radiation hazards, 17: 2816 (AD-276049)
radiation hazards evaluation, 18: 29877 (D2-90469)
radiation hazards to manned space vehicles from, calculations, 19: 35563
radiation hazards to astronauts, 19: 45890
radiation hazards for space flight, protection against, (T), 20: 15192 (N65-21000)
radiation hazards to astronauts from, 20: 36627
radiation hazards to astronauts from, 20: 38603(T) (AD-629422)
radiation hazards in supersonic jet aircraft, calculations using Monte Carlo method, 20: 46932(R) (ORNL-3973(Vol.2), pp 71-84)
radiation intensity increases from, on August 20, 1960, detection by second Sputnik, 17: 34702
radiation spectrum during, (E), 19: 20756
radiation types and levels in, 19: 11608
radiative energy loss of material from, 20: 25687
radio burst height and motion in, 17: 12915
radio burst source and size in, 17: 12916
radio bursts from, features from type IV, 17: 12909
radio bursts from, relations of types II and IV to optical phenomena and geomagnetic activity, 18: 11097
radio emission during, 18: 44391
radio emission during, 19: 16364
radio emission from, 17: 12922
radio emission from, 18: 8977
radio emission from, type-IV, 18: 44393
radio emission from, type IV, (T), 19: 34854
radio emission from, corpuscular and proton cloud as source of, 19: 35319
radio emission from, pre-absorption events in bursts of type-IV, (E), 20: 21500
radio emission in, type III, 18: 44394
radio emission on Sept. 28, 1961, by class 3, characteristics of, 17: 41695
radio waves from, sudden frequency deviations in, 17: 24223
radio-wave emission after, particle cloud as source for, (T), 19: 9850
radioactivity induced in Discoverer 17 by solar protons, 17: 5098
radiofrequency radiation from filaments, model for, 18: 44915
radiowave emission in, theory of type-III, 18: 44916
radiowave emission in, theory of type-III, 18: 44406
radiowave emission from, 18: 44407
radiowave emission during, Sept. 28, 1961, 19: 28979
relation to changes in sunspot areas, 18: 7382
relation to cosmic-ray intensity, 16: 5846
relation to cosmic nuclear-component intensity, 16: 12319(T)
relation to geomagnetic storms, 18: 7637
relation to loop prominence occurrence, 18: 26193
relation to polar cap absorption time variations, 17: 36562 (UAG-R-127 (Pt.II))
relation to solar radio bursts, 17: 24211
relation to solar wind velocity, 18: 30391
relation to subsequent noise storms at 169 Mc, 18: 44392
relations to auroral and ionospheric disturbances, 17: 5047(T) (AD-275256)
relations with geomagnetic disturbances, 18: 44641(R) (AFCRL-64-275)
review (E/T), 19: 1146
review, 18: 14755 (AD-401660)
riometer observations of PCA events, 17: 12930
shielding against, 18: 26815
shielding against alpha particles and protons from, (T), 20: 3251 (NASA-SP-71, pp 507-12)
shielding from, in lunar spacecraft design, 17: 5528
shielding manned space vehicles against, (T), 20: 3245 (NASA-SP-71, pp 407-14)
shielding of manned space vehicles from, 17: 16877
shielding proton component of, 18: 3035
shielding space vehicle personnel from, using superconducting-magnet dynamic shielding, (T), 20: 3241 (NASA-SP-71, pp 199-209)
shock wave production in interplanetary medium by, (T), 20: 44098
solar type radio burst from flare star, 18: 16638
source, 18: 30397
spectra, 18: 24271 (NP-13803)
spectra of α particles and protons from, 17: 19018
spectra of Hα line in 3+, 17: 3916
spectra of photons from, at 500 to 1000 Mc, 17: 19003
spectra of radio bursts, electromagnetic- and plasma-wave, 16: 29924
spectra of x rays from, 18: 16645
spectra of, analysis of optical, 20: 34070
spectra of, asymmetry and broadening in emission lines, 18: 44379
spectra of, Stark broadening of high Balmer lines in, 18: 44382
spectral analysis of, 20: 17230
spectral broadening in prominences and, Balmer-line, (E), 19: 9854
spectral effects on solar electromagnetic emission, 16: 30991
spectral line width in, H_α, (E), 19: 9855
spectral variations during, measurements and models for, 17: 19004
spectrography of, 18: 44376
statistics, 18: 24270 (NP-13802)
structure, 18: 44372
structure model of, 17: 12918
structure of nimbus of, (T), 19: 41228
structure of plasma cloud of, internal, 17: 12979
structure of, experimental observations of, 18: 44404
structure of, from gamma spectra, 19: 32879
sunspot variations over one solar cycle, effects on cosmic nucleus intensities, 18: 42342
tabulation of sunspot numbers for 1963 and January 1964, 18: 26453
terrestial effects on outer radiation belt intensities, 17: 2150(T)
terrestrial effects of, polar-cap absorption events, 17: 14504
theory of strong explosions in, 17: 13286(T)
theory of, as point explosions in nonhomogeneous atmosphere, 20: 25712(T)
theory of, magnetic energy storage and dissipation in, 18: 44410
theory of, review of, 20: 19325 (N-65-22651)
thermal dissipation from material in, magnetic field effects on, (T), 20: 25688
triton production in, (E), 19: 2954
ultraviolet radiation from, properties of, 18: 28210
x radiation from, at 8 to 20 Å, 17: 26259
x radiation from, theory of inverse Compton effect as cause of, 18: 22661
x radiation from, inverse-Compton-effect mechanism for, (E/T), 19: 4807
x-ray burst from event on Sept. 28, 1961, 16: 21238 (NP-11658)
x-ray burst of September 28, 1961, 17: 5091
x-ray bursts, relation to radio bursts, 16: 5848
x-ray emission from, 16: 895
x ray emission from, study of, 17: 13291(T)
x-ray emission from, during sunspot maximum conditions, 18: 5910
x-ray emission in ionosphere, 16: 894
x-ray-spectrometric study of, on March 13, 1962, by Orbiting Solar Observatory, 18: 7396
x-ray bursts from, analysis of 20- to 100-kev, (E), 19: 43019 (NASA-TN-D-2798, pp 163-8)
x-ray emission and charge-particle flux at 10^3 km, 19: 34917
x-ray emission during, Sept. 28, 1961, 19: 28979
x-ray emission from, intensity of, 18: 10731
x-ray emission from, variability of spectra of, 18: 28216
x-ray emission from energetic, 18: 44387
x-ray emission from, 18: 44390
x-ray emission from, 18: 44407
x-ray emission from, (T), 19: 20890
x-ray emission from proton-emitting, (E/T), 19: 25135(T)
x-ray emission from, 19: 32856
x-ray emission from, (E/T), 19: 32857
x-ray emission from, behind solar disk, (T), 19: 44894(T) (AD-424481)
x-ray emission from, processes involved in, (E), 20: 34073
x-ray emission in, (T), 19: 14218(T)
x-ray emission in, radio astronomy study of, 18: 32337(T) (AD-428086)
x-ray emission in, (E), 19: 4814
x-ray enhancements during, correlated with microwave bursts, 20: 44101
x-ray flux from, variations in, 18: 28219
x-ray spectra from, 20: 37360

SOLAR FURNACES
design characteristics of station steam boilers, 16: 4277(T) (AEC-tr-4496)

uses of, conference on, 19: 25085

SOLAR POWER

see also Solar Furnaces

bibliography on, 16: 32237 (SB-418(Suppl.1))
bibliography on conversion optics, 16: 12237(T) (AEC-tr-4471(Add.))
book: *Solar Energy Resources of the Georgian SSR*, 16: 15285(T) (NP-tr-873)
conversion systems, control of Rankine cycle, 17: 21370 (NP-12688)
development and economics of, for communications satellites, 20: 29608
development status for manned orbital space stations, 18: 39419
generation of, cone- and column-concentrator for, 17: 36534
generation problems of space vehicles, 16: 5091
production of, collector system for, 17: 9100
production of, inflatable turboelectric generator for, 17: 30643
production of, space environmental effects on semiconductor p-n junctions for, 17: 30642
production, photovoltaic cell optimization for, 16: 18145 (ASD-TR-61-11(Vol.II))
system design for lunar vehicle, 20: 45870
system for Orbiting Astronomical Observatory, 17: 37322
thermoelectric generator system design and testing, 17: 7642(R) (AD-276092)
transmission of, development of thermal radiation focusing guide for, 17: 3573(R) (NP-12206)
uses of, bibliography on, 16: 1296 (SB-418)
uses of, conference on, 19: 25085

SOLAR RADIATION

see also Actinic Radiations

absorption and emission by space vehicle metals, effects of hydrogen ion sputtering on ratio of, 18: 8904
absorption and photoionization cross sections of nitrogen and oxygen for (E), 19: 3156
absorption by atmosphere and ionosphere, 19: 39363
absorption of L_α, in earth's upper atmosphere, (E) 20: 6211
absorption of solar wind by interplanetary gases, nonadiabatic expansion for, 20: 19352
absorptivity measurements on, equipment for, 18: 39420
acceleration and propagation at high energy, (T), 19: 25206
acceleration and space distributions of high-energy particulate, 19: 16434
acceleration of corpuscular, in electromagnetic fields, (T), 20: 955
acceleration of proton, at 3 to 20 Mev, (E), 19: 20766
acceleration of protons, by hydromagnetic shock waves, (T), 19: 41230
acceleration of, mechanism for, (T), 20: 27712
acceleration of, mechanism for, (T), 20: 28133
analysis for neutrinos, problems in, 18: 24295
anisotropy in, as viewed from terrestrial frame of reference, 18: 9048
argon ionization by, in upper atmosphere, 18: 28462
association of solar wind with geomagnetic disturbance, 19: 42988
association of type III, with flares, (T), 19: 4809
atmosphere earth balance, fall and summer, 19: 9757
auroral and geomagnetic storm production by solar streams, 16: 29504
bibliography on, 18: 1833 (AD-249100)
bibliography on solar wind, 20: 35985 (NASA-SP-7026)
book: *Atmospheric Radiation. I. Theoretical Basis*, 19: 21156
book: *Cosmic Rays, Solar Particles and Space Research*, 18: 20821
book: *Interplanetary Dynamical Processes*, 18: 5911
book: *Solar Flares*, 19: 18676
book: *Solar Plasma, Geomagnetism, and Aurora*, 18: 42549
boundary of solar wind with magnetosphere, model for broad disordered transition region in, 18: 18798
boundary of solar wind with magnetosphere, 20: 17249
boundary with closed magnetopause, 19: 23538
bursts of x-ray, short intensity increases of heavy cosmic nuclei accompanying, 20: 29965
capture of ionic, using aluminum foils, 20: 44697
characteristics of chromospheric flares, 16: 27418 (NP-11961)
charge composition of, energetic-particle, 18: 44398
charge distribution of corpuscular, system for determining, 20: 17307 (CONF-651001-34)
charged-particle penetration into magnetosphere, (T), 20: 42069
classification and frequency of solar radio storms, (E/T), 19: 9847
collimator design and assembly for, 20: 24350(P)
composition of solar wind, method for determining, 19: 27123
composition of solar wind, 20: 11437
composition of, in relation to PCA events, 20: 23915
conference on, 20: 15234
conference on solar wind, 20: 31880
conversion to electricity in dielectric films, 18: 11513 (NP-13539)
corpuscle stream reaction with geomagnetic field, 16: 24657 (R62SD30)
corpuscular, absorption at high geomagnetic latitudes, 17: 13275(T)
corpuscular streams in space, determination from IGY data, 18: 7449
corpuscular streams of, atmospheric disturbances from type M, 18: 9259(T)
cosmic primary energy spectrum during maximum, 17: 16932
cosmic ray adiabatic deceleration by solar wind, (T), 20: 27781
cosmic ray friction effects on solar wind, model for, 20: 37372
cosmic-ray intensity effects of, in auroral zones, 16: 29526
cosmic-ray modulation by solar wind, (E), 19: 27121
description of type IV r-f, 17: 32877
detection and measurement of 10- to 400-Å, 17: 13320
detection and measurement of, instruments for, 18: 2563
detection and measurement of x-ray and Lyman-alpha, on August 19 and 20, 1960, 18: 7398
detection and measurement of, at 1,900,000 km from the earth, 18: 7391
detection and measurement of x-ray spectra in, satellite instrumentation for, 18: 7088
detection and measurement using cadmium sulfide crystals, 18: 10803 (LNF-63/54(p.28))
detection and measurement of x, below 20 Å, 18: 16640
detection and measurement at Scott Base, New Zealand, during IGY 1957 to 58, 18: 18602
detection and measurement of uv and x, use of thermoluminescent phosphor for, 18: 18229(T)
detection and measurement in stratosphere following large solar flares, 18: 37037
detection and measurement of, in field, 19: 6899 (TID-21353)
detection and measurement of, at Neotoma Valley, Ohio, 19: 6899 (TID-21353)
detection and measurement of, by Mariner 2 solar plasma instrument, 19: 28634 (N64-20603)
detection and measurement of x, satellite system for, 19: 28655
detection and measurement of x, photographic emulsions for, 19: 30549
detection and measurement of neutrinos, (E), 19: 32908 (BNL-9119)
detection and measurement of x-ray, photographic films for, 19: 32864
detection and measurement of x, satellite instrumentation for, 19: 34922
detection and measurement of x, using rockets and satellites, (E), 19: 43020
detection and measurement of x, instruments for, 20: 16904
detection and measurement of x, design of spectrometer for, 20: 27272
detection and measurement of x, fabrication and operation of ionization chamber for, 20: 31511 (N-66-16936)
detection and measurement in stratosphere, flare of class 3+ generated, 20: 46469(T)
detection and properties of solar wind (E/T), 19: 2949
detection of heavy nuclei in, during Nov. 1960, 18: 7446
detection of neutrino component of, possibility of, 18: 44341 (BNL-8217)
detection of neutrino, by gallium-71 (ν,e-) reactions, (T), 20: 11537
detection of neutrino, by capture in chlorine-37, (T), 20: 37366
detection of particle streams in, using high-frequency radio waves, 18: 26247
detection of proton, time distributions of terrestrial, (E), 20: 15233
detection of, using h-f radio waves, 17: 41677
detection of x rays in, design of electronic equipment for, 17: 34249
detection of, methods for, 19: 14222
deuterium abundance in, system for determining, 20: 17307 (CONF-651001-34)
deuterium abundance in solar wind, design and testing of detector for measuring, 20: 23474
diagnostics of, plasma probe for, 18: 18611
diffusion coefficient of protons of, energy dependence of, (T), 19: 12109
diffusion in interplanetary space, model for anisotropic, 20: 9645
diffusion of flare, in interplanetary space, 20: 5970
diffusion of, radial magnetic field in, 18: 24330
distributions in space, 17: 7676
disturbances in solar wind, detectability of, (T), 19: 9860
doses in low-shielding space systems, 20: 16300
dosimetric evaluation of alpha and proton, 19: 30909 (AD-611323)
dosimetry of protons in space, 18: 6716
dosimetry of, during space flight, 20: 18943 (N-65-21724)
dynamics of solar wind, 18: 30382
dynamics of solar wind, (T), 20: 41617
economic aspects as energy source, 18: 40216
effect of solar wind on magnetic field of moon, 20: 21502
effects in upper atmosphere of Jupiter, (T), 19: 17238
effects of alpha particles on ionospheric radio wave absorption, 18: 26445
effects of asymmetric solar wind on cosmic rays, 18: 30458(T) (NASA-TT-F-127(p.315-20))
effects of corpuscular, on F region of ionosphere, 18: 7595
effects of corpuscular, on the atmosphere, 18: 13006
effects of corpuscular, on outer atmosphere, 18: 24526
effects of corpuscular streams on SC geomagnetic storms, 18: 24518
effects of corpuscular, on magnetosphere, 18: 28495
effects of corpuscular stream of, on cosmic-ray variations, 18: 30448(T) (NASA-TT-F-127(p.151-98))

effects of corpuscular streams of, on cosmic-ray variations, 18: 30450(T) (NASA-TT-F-127(p.208-12))
effects of corpuscular, on magnetosphere, 18: 44646
effects of corpuscular, on geomagnetic storms, 18: 44651
effects of corpuscular, on geomagnetic sudden impulses, 18: 44664
effects of corpuscular stream, on energy of geomagnetic storms, (T), 19: 21135(T)
effects of corpuscular and electromagnetic, on earth's atmosphere, 19: 25134
effects of corpuscular, on cosmic radiation anisotropy near earth, 20: 7754(T) (NASA-TT-F-91, pp 121-6)
effects of corpuscular-beam eclipse on geomagnetic micropulsations, (E), 20: 15618
effects of corpuscular, on radio-wave absorption in ionosphere, 20: 23917
effects of corpuscular and electromagnetic, terrestrial, 19: 25134
effects of electromagnetic, on ionospheric behavior and composition, 19: 16751
effects of electromagnetic, on geomagnetic fields, 19: 30912
effects of extreme uv, on atmospheric density and temperature variations, (E), 20: 9866
effects of flare-associated, 18: 28464
effects of interplanetary magnetic fields on low-energy, 18: 7443
effects of interplanetary magnetic field on solar wind, 18: 18545
effects of M-region, on geomagnetic pulsations, 19: 47454
effects of magnetic fields of corpuscular, on cosmic ray diurnal variations, 20: 7755(T) (NASA-TT-F-91, pp 127-50)
effects of nonflare x, in ionospheric D region, 18: 42537
effects of particle streams on atmospheric disturbances, 19: 47495
effects of polar cap absorption from, on 12-Mc radio wave propagation in ionosphere, 18: 16827
effects of proton solar wind on photometric properties of Mercury, 20: 34023
effects of proton, on D layer of ionosphere, 18: 16642
effects of protons on n-p and p-n solar cells, annealing of, 20: 14919(R) (N65-20653)
effects of solar wind on geomagnetic field, 18: 18796
effects of solar wind on geomagnetic field, spherical harmonic expansion of, 18: 18797
effects of solar wind on magnetosphere (E), 19: 3152
effects of solar wind on magnetospheric boundary, (T), 19: 6431
effects of solar wind on magnetospheric stability, (T), 19: 18977
effects of solar wind discontinuity on magnetospheric boundary, (T), 19: 21148
effects of solar wind on geomagnetic fields, (T), 19: 31166
effects of solar wind on rotating magnetosphere, (T), 19: 31156
effects of solar wind on cosmic-ray intensity, (T), 19: 34901(T)
effects of solar wind on ionosphere, (T), 19: 39676
effects of solar wind on M-region geomagnetic storms, 19: 37714
effects of solar wind, on magnetospheric boundary, (T), 20: 11838
effects of solar wind, on long-period geomagnetic pulsation polarization, (T), 20: 15615
effects of solar wind on plasma in geomagnetic tail, 20: 21828
effects of solar wind on geomagnetic activity, 20: 24220
effects of solar wind on Van Allen belts, 20: 30204(T) (NASA-TT-F-389, pp 375-86)
effects of solar wind on type-1 comet tails, (T), 20: 31898
effects of solar wind, on angular momentum of Sun, 20: 34024
effects of solar wind on charged-particle motion in geomagnetic fields, 20: 34360 (N-66-17230)
effects of solar wind on cosmic ray intensity variations, (T), 20: 37517
effects of sunrise uv, on ionospheric E and F layers, 19: 33118(T) (AD-611029)
effects of u-v, on atmospheric temperature (E), 19: 3153
effects of uv and x, on ionosphere, 19: 37432
effects of uv, on electron temperature in F-region of ionosphere, (E), 19: 43227
effects of xenon-simulated, on plant leaves, 20: 18391
effect of 3000 Mc, on sudden ionospheric disturbances, (T), 19: 10170
effects of, combined with uv radiation on Xanthium leaves, 20: 18391
effects on Arctic h-f propagation, 18: 16825
effects on atmospheric density and temperature, 18: 28463
effects on atmospheric density and temperature, 18: 44665
effects on atmospheric polar cap absorption of cosmic radio waves (E), 19: 2992
effects on atmosphere, (T), 19: 42978
effects on atmosphere and lithosphere, 20: 46489
effects on auroral glow emission, 18: 36423
effects on auroras, 18: 24524
effects on biological materials, review on, 19: 36069
effects on boundary and distortion of geomagnetic field, 18: 15034
effects on chlorophyll a and net production rates in Columbia River algae, 20: 20382 (BNWL-SA-623)
effects on comet structure, 20: 37386(T)
effects on coronal rotation, 20: 44073
effects on cosmic radiation during IGY, 16: 30997
effects on cosmic radiation intensity, 17: 24256(T)
effects on cosmic radiation intensity variations near earth, 20: 7750(T) (NASA-TT-F-91, pp 64-81)
effects on critical frequencies and ionization of ionosphere, (E), 19: 31139
effects on diurnal cosmic-ray variations, 18: 30463(T) (NASA-TT-F-127(p.383-6))
effects on early evolution of life, 19: 28548
effects on earth atmosphere, ionization, 20: 9858
effects on earth's rotational period, 18: 7638
effects on electric components of lunar excursion module, 18: 7015
effects on electron production rate in ionosphere, (E/T), 19: 41598
effects on electron distribution in Van Allen belts, 20: 32260
effects on element abundances in solar corona and photosphere, (T), 20: 15222
effects on fallout distribution in atmosphere, 18: 42146
effects on Forbush decreases, (E), 19: 41305
effects on formation of ionospheric D region, calculations for determining, 20: 46452 (AD-630094)
effects on gastric transit in laparotomized and vagotomized rats, 20: 20414
effects on geomagnetic fields, steady-state, 16: 29532
effects on geomagnetic fields, during magnetic storms, 17: 32864
effects on geomagnetic activity, 18: 15032
effects on geomagnetic activity, 18: 24531
effects on geomagnetic storms, 18: 28225
effects on geomagnetic storms, 18: 28460
effects on geomagnetic fields, 18: 42527
effects on geomagnetic field, 18: 44399
effects on geomagnetic storm sudden commencements, 19: 35288
effects on geomagnetic storms, 19: 39673
effects on geomagnetic storms, (E), 19: 41602
effects on human skin, review of, 20: 40696
effects on ionization of F_2-region of ionosphere, (E), 19: 33120
effects on ionization variations in E_1, F_1, and F_2 layers, 20: 6187
effects on ionospheric critical frequencies in equatorial transition region, 17: 24115
effects on ionosphere, 18: 28212
effects on ionosphere, 18: 28220
effects on ionosphere, 18: 32679 (AD-428169)
effects on ionospheric D and E layers, (E/T), 19: 12403(T)
effects on ionosphere, abstracts on, 19: 14420 (ATD-P-64-51)
effects on ionospheric sudden disturbances, 19: 41573 (RPU-S19)
effects on ionosphere, 19: 47496
effects on isotropy of galactic cosmic rays, (E/T), 19: 4866
effects on lower ionospheric ionization, (E), 20: 4737
effects on lunar atmosphere density, 18: 18546
effects on lunar surface, 18: 34392
effects on *Lupus erythematosus*, 20: 14309
effects on magnetic disturbances at Earth surface, during sudden commencements, (T), 19: 45163
effects on manned space flight, 18: 12793
effects on manned space flight, computer analyses of, 18: 35048 (AMRL-TDR-64-11)
effects on neutron and proton dosages to man in supersonic flight in upper atmosphere, 18: 30399
effects on Nuclear Test Detection Satellites, simulation testing of, 20: 29440
effects on outer magnetospheric field lines and plasma, (T), 19: 45162
effects on PCA events, 18: 28466
effects on physical properties of earth's upper atmosphere, 16: 27862
effects on polar-glow aurora, 18: 44658
effects on pressure distribution in lower atmosphere, (E), 19: 20780(T)
effects on reflectance of paint systems for space vehicles, 18: 26097
effects on reflectance and thermal emittance of spacecraft thermal-control coatings, 20: 7653
effects on riometer measurements of alpha particle, (T), 20: 46455 (AD-630183)
effects on rocks and rock powders, simulation of, 19: 44896
effects on semiannual variation of geomagnetic activity, 16: 22839
effects on skin, treatment of carcinogenic, 18: 38980
effects on sudden impulse pairs in magnetic storms, 19: 39681
effects on threshold for magnetospheric transition-region plasma instability, (T), 19: 47460
effects on troposphere, (T), 20: 34394(T)
effects on Van Allen belts, 18: 11093
effects on melanin patterns in man, 20: 20458
electromagnetic energy flow in solar wind, Poynting vector for, (T), 19: 25118
electromagnetic properties of corpuscular streams of, 18: 30454(T) (NASA-TT-F-127(p.267-73))

electron and ion density in solar wind-magnetosphere region, 20: 39978
electron components of, 18: 4417
electron detection and measurement in, (E), 20: 31886
electron production by x-, during solar flares, 19: 47480
element abundances in solar wind, (T), 20: 17236
emission and propagation of energetic, that excites polar-cap blackouts, 16: 24305
emission and properties, 17: 36548 (NASA-TR-R-169)
emission beyond Balmer limit, continuous, 17: 13276(T)
emission during class 3+ flares, 17: 19024
emission during flares, 18: 8977
emission during flare events, 18: 22653
emission during flares, 18: 44390
emission during flares of, (T), 20: 23851
emission during solar flares, 20: 29875(T) (NASA-TT-F-389, pp 732-9)
emission during Y phase of solar flares, (T), 19: 9848
emission from flares, 18: 44396
emission from flares, flight time and PCA effects of, 20: 34037
emission from M-regions, 18: 28213
emission from noise-storm centers at 169 Mc, 18: 44392
emission from solar flares, relation to radio bursts, 17: 41695
emission from solar flares, correlation of type III radiobursts and high-energy x radiation in, 18: 7397
emission in conjunction with polar-cap absorption events, 16: 27895
emission mechanisms, 18: 7390
emission mechanisms for x, during flares, (E/T), 19: 4807
emission of cm and dm radio, correlation with sunspot area, 18: 44391
emission of coronal r-f, in continuous spectrum, 20: 29904(T)
emission of corpuscular, from coronal expansion, 17: 34696
emission of corpuscular and wave, periodic, 18: 6097
emission of corpuscular, on descending branch of activity cycle, 19: 44921(T)
emission of corpuscular, coronal line intensity as index of, 20: 25709(T)
emission of electromagnetic, mechanisms for flare, 20: 23852
emission of, frequency and magnitude of, 17: 25965
emission of gamma, during solar flare, (E/T), 19: 9852
emission of gamma, from flares, (T), 19: 44916(T)
emission of low-energy, relation to type IV radio outbursts, 17: 28121
emission of microwave and x, OSO I observations of, 18: 44388
emission of microwave and x, OSO I observations of, 18: 44389
emission of neutron, 20: 23857
emission of noise bursts, relation to flares and short-wave fadeouts, 18: 10738
emission of particulate, from flares and prominences, 19: 12041
emission of particulate, intensities at earth from flare, 20: 23849
emission of, prediction of, 17: 25964
emission of, properties of, chromospheric eruptions associated with, 18: 5909
emission of protons in, review, 17: 34697
emission of proton, cosmic-ray increases from, 18: 5952
emission of proton, intensity of flare, 18: 5964
emission of proton and r-f, relations between, (E/T), 19: 4817
emission of proton, radio emission as criterion for warning of, (E), 19: 8053
emission of protons, longitude distribution of, 19: 25123
emission of proton, hydromagnetic model for, 19: 25144
emission of protons, correlation of satellite and ground-based observations of, (E), 20: 19351
emission of proton, design of r-f warning system for, 20: 34009 (N-66-16405)
emission of r-f, frequency drift of type III, 17: 32855
emission of r-f, from active regions, 17: 41705(T)
emission of r-f, high-resolution study of 3–21 cm, 17: 28110
emission of r-f, properties of peaks in type I, 17: 41703(T)
emission of r-f and x, during flare, 19: 28979
emission of r-f and proton, correlation of, 20: 23907 (N-66-15620)
emission of r-f and x, during solar flares, (T), 20: 27704
emission of r-f, during geomagnetic storms, 19: 5076
emission of r-f, from type II outburst, (T), 19: 41229
emission of r-f, from type III and IV outbursts, 20: 27692
emission of r-f, in meter wavelength range, 19: 44920(T)
emission of radio-wave, correlations with geomagnetic storms from 1957 to 1961, 19: 12043
emission of thermal x-ray, during quiet periods, (T), 20: 27703
emission of type III, high-resolution studies at 11.4-m wavelength, 17: 24221
emission of type IV, from flares covering sunspots, 17: 24222
emission of type IV, relation to inverse phase of cosmic radiation intensity, 17: 34704
emission of type IV, relation to diurnal variation of cosmic radiation intensity, 17: 34705
emission of type II r-f, mechanism for, 18: 18554(T)
emission of type-IV radio bursts, correlations with inverse-phase cosmic-ray intensity variations, 19: 25221
emission of uv, from activity centers, 18: 28215
emission of x, at 8 to 20 Å, 17: 26259
emission of x, during flare and non-flare sunspot maximum conditions, 18: 5910
emission of x rays during flares, 18: 44387
emission of x-ray, discrimination from nuclear-detonation x rays, 20: 15603
emission of x-ray, processes involved in, (E), 20: 34073
emission of x-ray, correlated with microwave bursts during solar flares, 20: 44101
emission of x, during flare and quiet periods, 18: 16645
emission of x, during flare and quiet periods, (T), 19: 14218(T)
emission of x, from solar flares, 19: 34917
emission of x, from corona, 19: 41209(T) (N64-22932)
emission of x, measurement and theory, 18: 16641
emission of 40-kev electron, (E), 20: 5971
emission of 9.4-kMc type-IV, from activity centers, 18: 44393
emission of, duration of, (T), 20: 27698(T)
emission of, mechanisms for, 18: 32355
emission time and angular width of corpuscular streams, 18: 30443(T) (NASA-TT-F-127(p.48-51))
energy, 16: 20231
energy and intensity of, (E), 19: 32857
energy and intensity spectra of neutron, above 1 Mev, (T), 19: 44902
energy and intensity spectra of neutron, near earth, (E/T), 19: 44903
energy and mass spectra of, 18: 7448
energy density of, relation to cosmic ray intensity, 19: 37442
energy density variations in solar wind, geomagnetic effects of, (T), 19: 29137
energy of gamma, spectra of, 19: 32879
energy spectra, 19: 32852(R) (AD-608730)
energy spectra and intensity time dependence of proton, in stratosphere, (E), 20: 37536
energy spectra of proton, 18: 14707
energy spectra of x, below 60 Å, (E), 19: 39333
energy spectra of alpha and proton, from flares, 20: 5969
energy spectra of neutrino, (T), 20: 9646
energy spectra of helium ion and proton, in co-rotation with sun, 20: 37371
entry into geomagnetic fields, mechanisms for anomalous, 17: 37923
events of July 1961, models for, 18: 30465
extension of the solar wind into space, 18: 5911
field of, capture of small absorbing particles by, 17: 6914
flight time of cosmic and proton, to earth, 19: 23332
flow of plasma, around moon, (T), 19: 4813
flow properties of solar wind, compositional, anisotropic, and nonradial, (E), 20: 34049
fluctuations in, during 1962 and April 1964, 18: 40430
flux and rigidity spectra of alpha and proton, (T), 19: 41232
flux at magnetospheric boundary, 18: 15026
flux in interplanetary space, 19: 39364
flux intensity of, correlation with geomagnetic K_p index, (E), 20: 9859
flux measurements in, (E), 19: 6436
flux of coronal, at 10Å (T), 19: 1158(T)
flux of gamma, (E), 20: 34042
flux of neutrino, models for, 18: 42259
flux of neutron, at 20 to 160 Mev, (E), 20: 37375
flux of nuclei ($Z \geq 3$) in, (E), 20: 37567
flux of photon, variation with depth in photosphere, (T), 19: 39342
flux of plasma, correlations with geomagnetic disturbances, (E), 19: 41580
flux of proton at conjugate stations, correlation with PCA, 19: 35266
flux of proton, at 0.6 to 100 Mev, anisotropy and fluctuations in, (E), 20: 34045
flux of proton, correlation with geomagnetic and solar phenomena, 20: 23905 (AD-627416)
flux of proton, from flares, 19: 16326 (REIC-37)
flux of proton, near earth, 19: 1469
flux of protons, from flares, 20: 23858
flux of solar wind beyond 1 a.u., method for calculating, 20: 19352
flux of x, (E), 19: 41231
flux of x, at 44 to 60 Å, 18: 44354
flux of x, correlation of ionospheric parameters with, 19: 35306
flux of x, variations in, 18: 28219
flux of, anisotropic, (E), 20: 34130
flux of, diffusion mechanism of diurnal variations of, (E/T), 19: 20875
frequency harmonic structure and band splitting of type II r-f, (T), 20: 4524
frequency spectra of r-f, bremsstrahlung and synchrotron mechanisms in, 18: 18553(T)
frequency spectrum of slowly varying component of r-f, 20: 29908

generalization and extension of the basic solar wind model, 18: 5911
geomagnetic activity dependence on solar plasma velocity, (E/T), 19: 19013
geomagnetic cavity in solar wind, neutral point of, (T), 20: 37895
geomagnetic effects of relativistic solar flares, (E), 19: 10168
geomagnetic field compression by, 17: 16282
geomagnetic field penetration by, 18: 18594 (NP-13684)
geomagnetic-field disturbances by, Stormer's theory for, 19: 12393
geomagnetic-field distortion by solar wind, effects on cosmic-neutron asymptotic cones of acceptance, (T), 19: 16421
geophysical effects of proton component of, 18: 34388
hazards for manned spacecraft based on model environment, estimates of proton, 18: 39560
hazards in space flight to moon, review of, 19: 27058
hazards of, in space flight, 20: 10719(T) (NASA-TT-F-353, pp 3-20)
hazards to aircraft passengers in high-altitude supersonic flight from, 20: 31468
heating effects of ultraviolet, on ionospheric electrons, 17: 28115
heating effects on earth's upper atmosphere of corpuscular, 16: 29528
heating of solar wind by conduction, 18: 7380
heating of thermosphere by, 18: 7613
heating of upper atmosphere by electromagnetic and corpuscular, 18: 7610
heating of wind, conductive, (T), 19: 34842
hydrodynamic model of solar wind, 18: 5911
hydrogen atom flux in plasma (T), 19: 1153
hydrogen in, interactions with Venus atmosphere, (T), 19: 9871
injection into magnetosphere, mechanism for, 18: 18830
intensities above sea level, spectral, 17: 27201
intensities at high terrestrial latitudes, temporal variations of, 17: 24243
intensities in satellite environment, review, 16: 32252 (NASA-TN-D-1360)
intensities in satellite environment, review, 16: 32253 (NASA-TN-D-1361)
intensities of proton at high terrestrial latitudes, 17: 24244
intensity at Earth, effects of solar activity on zone of incidence from, 20: 23850
intensity in ionosphere during solar eclipse, 18: 10816
intensity increases in, before sudden commencements, 17: 19017
intensity modulation in interplanetary space, (T), 20: 37542
intensity of, during November 12–23, 1960, 17: 13296 (N62-11289)
intensity of extreme ultraviolet, (T), 19: 47210
intensity of flare-produced proton, 18: 28287
intensity of flare-associated, during Sept. 1963, 20: 11429(T)
intensity of ionizing, during total solar eclipse, 19: 35244
intensity of low-energy protons in space, (E), 20: 17318
intensity of neutrino, using capture in chlorine-37, (E), 19: 30968 (BNL-9093)
intensity of proton, 29.5-day cycle in, 18: 42334
intensity of solar wind, correlations with cosmic ray 27-day intensity modulation, (E), 20: 37528
intensity of x rays, satellite measurements, 17: 15065(T)
intensity of x-ray, (E), 19: 23246
intensity of, cosmic-ray secular variation with, 18: 24331
intensity of, Mariner IV data on, 20: 37341 (N-66-17354)
intensity variations of low-rigidity neutrons at sea level and top of atmosphere, 16: 27869
intensity variations of nuclei and protons in, diffusion model for, 17: 32885
intensity variations during solar maximum and minimum, crossed-telescope observations of, 18: 30459(T) (NASA-TT-F-127(p.321-45))
intensity variations of, review of, 19: 25198
intensity variations during solar flare, (E), 19: 34815(T)
intensity variations of, correlation of ground-based and satellite measurements of, 20: 19327 (N-65-27406)
intensity variations of solar wind with phase of solar activity cycle, 20: 28139(T)
intensity variations of x, 20: 29874(T) (NASA-TT-F-389, pp 714-31)
interaction between magnetosphere and solar plasma, 18: 44670
interaction of solar plasma with geo-shock-wave, Forbush decreases from, 18: 28201 (NP-13988)
interaction of solar wind with magnetohydrodynamic wake of moon, (E/T), 19: 16343
interaction of solar wind with geomagnetic fields, 19: 16749
interaction of solar wind with magnetosphere, frictional, (T), 19: 23529
interaction of solar wind with magnetosphere, (E), 19: 29399
interaction of solar wind with magnetosphere, 20: 1098
interaction of solar plasma with magnetosphere, (T), 20: 15593
interaction of solar wind with magnetosphere, magnetic field perturbation from simulated, (E), 20: 17546
interaction of solar wind with magnetosphere, effect of earths's rotation on, (T), 20: 24209 (N-65-33285)
interaction of solar wind with magnetosphere, (T), 20: 24224
interaction of solar wind with comets, 20: 31896
interaction of solar wind with magnetosphere, simulation of, 20: 32284
interaction of solar wind with earth, moon, and planets, bibliography on, 20: 35985 (NASA-SP-7026)
interaction of solar wind with magnetosphere, proton velocity distributions in, (T), 20: 36116
interaction of solar with lunar surface, 20: 44035
interaction of solar wind with magnetosphere, boundary, tail, and ring current effects on, (T), 20: 46493
interaction with geomagnetic field, 17: 6913
interaction with magnetic fields of comets, (T), 19: 14220(T)
interaction with solar magnetic field, (T), 20: 37349
interaction with solar magnetic field, (T), 20: 39573
interactions and properties of solar wind (T), 19: 2950
interactions in earth's magnetosphere, geomagnetic storm sudden commencements from, 18: 7603
interactions in ionosphere, effects on electron density profiles, 18: 4418
interactions in solar atmosphere, ion production in, 18: 4389(T)
interactions of corpuscular, with geomagnetic field, (T), 19: 12387
interactions of corpuscular, with geomagnetic field, (T), 20: 44439
interactions of solar wind with galactic magnetic field, theoretical study of interface in, 18: 19246
interactions of solar wind with magnetosphere, storm production by frictional, 18: 18824
interactions of solar wind with comets, 18: 36151
interactions of solar wind with geomagnetic field, (E), 19: 5338
interactions of solar wind with magnetosphere, geomagnetic cavity from, (T), 19: 21146
interactions of solar wind with comet tails, (T), 19: 23235 (SC-RR-64-967)
interactions of solar wind with geomagnetic fields, 19: 33153
interactions of solar wind with geomagnetic fields, (T), 19: 43018(R) (AD-609216)
interactions of solar wind with magnetopause, (T), 20: 15620
interactions of solar corpuscular stream with geomagnetic fields, (T), 20: 17547(T)
interactions of solar plasma with geomagnetic fields, (E), 20: 17551
interactions of solar wind with planets, (T), 20: 17232
interactions of solar wind with magnetosphere, 20: 30210(T) (NASA-TT-F-389, pp 499-517)
interactions of solar wind with comets, MHD aspects of, (T), 20: 31897
interactions of solar wind with magnetosphere, fluid dynamics of, (T), 20: 32275
interactions of solar wind with magnetosphere, particle aspects of, (T), 20: 32276
interactions of solar wind with magnetosphere, shock wave from, (E/T), 20: 32281
interactions of solar wind with geomagnetic fields, (E), 20: 32286
interactions of solar wind with moon, effects of interplanetary magnetic fields on, 20: 34006 (N-66-10681)
interactions of solar wind with magnetosphere, models of, 20: 34076
interactions of solar wind with geomagnetic field, 20: 44460
interactions of weak corpuscular, with upper atmosphere, ulf radiation from, 18: 11035
interactions of, with cosmic radiation and geomagnetic fields, 17: 20814 (AFCRL-62-442)
interactions with geomagnetic fields, investigation of, 17: 11449 (ML-975)
interactions with geomagnetic fields, theory, 17: 15050
interactions with Martian atmosphere, biological implications of neutron production in, 17: 32881
interactions with comets, interplanetary plasma probing by, 17: 41667 (NASA-TN-D-1901)
interactions with earth's magnetic field, 17: 40430(R) (NYO-10063(p.52-60))
interactions with geomagnetic fields, 18: 2723 (IPPJ-12)
interactions with geomagnetic fields, simulation of, 18: 2731
interactions with cometary atmospheres, plasma envelope collapse and r-f emission in, 18: 4393(T)
interactions with geomagnetic field, oscillations in cavity produced by, 18: 11041
interactions with ionospheric plasma, irregularities from, 18: 11068
interactions with geomagnetic fields, model for, 18: 15017 (N63-17339)
interactions with geomagnetic cavity in magnetosphere, 18: 15036
interactions with geomagnetic field, experimental simulation of, 18: 15407
interactions with magnetosphere, 18: 16629 (AD-430410)
interactions with magnetosphere, hydromagnetic coupling in, 18: 18831
interactions with geomagnetic fields, 18: 20722
interactions with atmospheres of comets, 18: 24282
interactions with magnetosphere, energy transfer in, 18: 28494

interactions with plasma, 18: 34984
interactions with geomagnetic fields, boundary region in, 18: 34675
interactions with geomagnetic fields, sudden-commencement storms from, 18: 40432
interactions with geomagnetic fields, boundary determinations in, 18: 42550
interactions with geomagnetic fields (E/T), 19: 3172
interactions with earth's magnetic field, 19: 5569(R) (MIT-2098-64)
interactions with geomagnetic field, model for, (E), 19: 10181
interactions with magnetosphere, geomagnetic storms from, 19: 25435
interactions with extraterrestrial dust as argon source in atmosphere, 19: 33156
interactions with geomagnetic fields, (T), 19: 45164
interactions with magnetosphere, MHD shock propagation from, (T), 19: 45165
interactions with interplanetary magnetic fields, 20: 4529
interactions with cometary tails, 20: 31874
interactions with moon, lunar magnetosphere from, (T), 20: 31899
interactions with geomagnetic field, boundary layers in, 20: 46925
interface with geomagnetic field, stability of, 17: 5173
interface with geomagnetic field, 17: 5174
interplanetary dust grain perturbation by, 18: 24279
interpretation and observation of, 18: 18594 (NP-13684)
ionization of D layer of atmosphere by x, at 2 to 60 Å, 16: 29626
ionospheric effects of gamma and x, 18: 16848
ionospheric effects of sunspots, 1953 to 1960, 18: 16851
ionospheric heating by extreme ultraviolet, 17: 37907
luminescence induced on moon by proton component, 18: 28281
magnetic field effects on, interplanetary, (E/T), 19: 8060
magnetic field polarity of solar wind stream, variations in, 20: 31860
magnetic field structure in corpuscular streams of, force-free, (T), 20: 23855
magnetic fields in wind, (E), 20: 15215
magnetic fields of corpuscular streams of, structure of, (E/T), 19: 12048(T)
magnetic fields of streams of, effects on field of moon, 20: 19328 (NP-15939)
magnetohydrodynamic discontinuities in solar wind, 20: 37387
magnetosphere interface with, hydromagnetic stability of, 18: 30390
measurement in polar cap regions using absorption events, (E), 20: 11863
measurement of flare-produced 20- to 100-kev x, (E), 19: 43019 (NASA-TN-D-2798, pp 163-8)
measurement of ionizing, in auroral zone from balloon flights, 20: 46451(R) (AD-628761)
measurement of r-f, indices for, 18: 28209
measurement of x-ray flux below 10 A by Russian geophysical rockets and sputniks, 18: 7450
measurement of 1.6 cm, 17: 22282(T) (JPRS-18823)
measurement of, in forest ecosystem, 19: 12906 (TID-21357)
measurement of, Mariner IV instrumentation for, 20: 37341 (N-66-17354)
measurement of, use of satellites for, 19: 9833
measurement using solar-thermionic flight test vehicle, 20: 35983 (N-66-17619)
measurements during Nov. 1960, 16: 24306
measurements in Antarctic, 18: 42279
measurements of fluxes of corpuscular, (E), 19: 6436
measurements on radio, 18: 10727 (NP-13550)
measurements on short-wave, survey of, 18: 10726 (NP-13522)
measurements on solar wind in space, 18: 42292
mechanisms of r-f and x, 18: 5908
microwave, determination of coronal electron density from, 17: 13280(T)
model for solar wind, exospheric, (T), 20: 17236
model for solar wind, boundary perturbations and stability of, 20: 41586
model of solar wind, inviscid, (T), 19: 44904
model of solar wind, two-fluid, 20: 19349
model of solar wind, viscous, (T), 20: 37350
modulation of cosmic protons and helium nuclei by, (T), 20: 41670
modulation of galactic cosmic radiation by solar wind, (T), 19: 32917
monitoring of, instruments for, 17: 16471
motion and position of r-f type II sources of, comparison with type III, 17: 31248
motion in magnetosphere, diamagnetic ring current, (T), 19: 33146
motion of energetic charged particulate, in interplanetary space, (T), 19: 16429
neutrino flux and elastic scattering, limits on, 18: 20713
neutrino flux and elastic scattering in, upper limit on, 19: 37452
neutron detection in, 19: 47279
neutron emission near solar minimum, search for, (E), 20: 44452
nuclear composition and rigidity spectra, 18: 24326
nucleon lifetimes in, 19: 37452
origin, 18: 20827
origin and evolution of, 17: 13332(T)
origin of quasistationary corpuscular streams of, hypotheses for, 20: 7696(T)
origin of solar wind, (T), 20: 31893
particle abundances in (E), 19: 2953
particle acceleration and properties in, heavy, 19: 18732
particle content in solar wind, 20: 34008 (N-66-12966)
particle-wave interactions in solar wind, fluid models for, 20: 41615
penetration of charge particles into magnetosphere, processes in, 20: 30205(T) (NASA-TT-F-389, pp 386-425)
penetration of solar wind into geomagnetic field, (T), 19: 12422
penetration of solar wind, in magnetosphere, (T), 20: 24227
plasma flow in solar wind, correlation to lunar eclipse brightness, 20: 41604
plasma structure in M-region storms, (E/T), 19: 19014
polar cap absorption by ionizing effect of, analysis by corrected geomagnetic coordinates, (E), 20: 44472
precipitation in polar cap regions, vlf phase recording network for determining, 20: 11856
prediction technique for proton, long-range, 20: 31879
pressure drop before geomagnetic storms, 18: 30665
production and propagation of, review of, 19: 14222
production in high-energy events and behavior in planetary space, 16: 27892
production of corpuscular, hypotheses for, 16: 29615
production of decimeter radio bursts, detection of, 17: 24214
production of Forbush decreases by solar winds, 16: 29621
production of gamma, by radiating electrons, 18: 4394(T)
production of neutrino, in helium-3 ($p,e^+\nu$) reactions, 19: 32869
production of protons in flares, 18: 44397
production of proton, by hydromagnetic shocks, 19: 43026
production of solar wind, (T), 19: 28981
production of, cosmic radiation increase due to flare, 18: 20723
production of, mechanisms of, 19: 32856
production of, processes for, 18: 32358
propagation, 16: 19643
propagation and spectra of protons from flares, 18: 44402
propagation and spectra of protons from flares, 19: 25122
propagation in interplanetary space following solar flares, 16: 30996
propagation in interplanetary space, (T), 19: 20757
propagation in space, dynamics of, 18: 44398
propagation of corpuscular, in interplanetary space, (T), 20: 19327 (N-65-27406)
propagation of energetic, 18: 5911
propagation of intense r-f, into night hemisphere, (E), 20: 23860
propagation of, measured by Explorer VII, 18: 7392
propagation of particles from flare, diffusion model for, 20: 11428(T)
propagation of proton, interplanetary magnetic field effects on, 19: 41228
propagation of proton, anisotropic, (E), 20: 34058
propagation of proton, review of, 20: 37493
propagation of r-f and x, correlation of, 18: 4395
propagation of r-f, during flare events, (T), 19: 4799
propagation of solar particles in interplanetary space, diffusion model for, (T), 19: 32911
propagation of solar particles in interplanetary space, (E/T), 19: 32915
propagation of, processes for, 18: 32358
propagation through interplanetary space, 18: 28212
properties, 17: 16939
properties and structure of corpuscular, with force-free magnetic fields, 18: 7393
properties and terrestrial effects of, 17: 7678
properties of, 20: 16745
properties of corpuscular and r-f, 18: 28211
properties of corpuscular, 18: 30671
properties of corpuscular, from geomagnetic disturbances, (E), 19: 12050(T)
properties of corpuscular streams, (E), 19: 21155(T)
properties of corpuscular streams from chromospheric flares, 20: 25692
properties of high-energy corpuscular (E/T), 19: 2952
properties of high energy fluxes of, in space, 19: 14222
properties of high-energy corpuscular, review of, 20: 23869
properties of M-region of corpuscular, 18: 28213
properties of particulate, review on, 20: 9649
properties of plasma, in interplanetary space, 18: 28214
properties of positive-ion component of solar wind, (E), 20: 44078
properties of r-f, 20: 21506
properties of r-f, during eclipse, 19: 34856
properties of r-f, data for Sept. 1963, 19: 41603
properties of solar wind, 18: 20717
properties of solar wind near Venus, (E), 19: 23245
properties of solar wind, hydrodynamic model for, (T), 19: 25125
properties of solar wind, review of, 20: 7990
properties of solar wind, (E), 20: 11438
properties of solar wind, review of, 20: 15232
properties of solar wind, models for, (T), 20: 15190 (AD-620407)

properties of solar wind, 20: 21496
properties of solar wind, (E), 20: 31881
properties of solar wind, (E/T), 20: 31889
properties of solar wind, and geomagnetic interactions, 20: 44069 (IPPJ-44(J))
properties of type IV, 18: 10751
properties of type IV r-f, (T), 19: 34854
properties of type III radio bursts in solar corona, (E), 19: 41218
properties of uv, 18: 28210
properties of, conference on, 19: 37510
properties of, determination by cosmic ray intensity variations due to changes in interplanetary electromagnetic states, 18: 24345
properties of, from solar corona and solar flares, 20: 13409
properties of, review, 18: 12827
properties of, review of, 18: 36152
properties of, review (E/T), 19: 2945
properties of, review of, (E/T), 19: 6437
properties of, review, 20: 2653 (NASA-SP-71, pp 19-29)
properties of, review of, 20: 19645 (NASA-SP-97)
proton flux variations in, periodic, (E), 20: 31885
proton temperature in solar wind, measurement of, (T), 20: 19350
protons in, carbon-14 production in atmosphere by neutrons from, 18: 20817
radiality of corpuscular, from plages, 17: 13331(T)
radiation effects on drift-field, protons, 20: 33730(R) (N-66-12193)
radio-absorption effects in ionosphere, 17: 13295 (AFOSR-4548)
radio emission from 1953 to 1963, 19: 41217
radio emission in corona, determination of stream velocities by, 19: 47189(T) (N64-31082)
radio emissions, review of, 19: 16364
radio-frequency, noncoherent mechanisms of sporadic, 17: 13329(T)
radio-frequency, relation to flare importances, 17: 24211
radio-frequency, study of, 17: 13289(T)
radio-frequency, 5-year catalog of type II and type IV, 17: 16912
radio noise storms, classification of, 19: 9853
radio-wave emission from corpuscular and proton cloud of, after solar flare, (T), 19: 9850
reactions in Cytherean and Martian atmospheres, ionization in, (T), 19: 16357
reactions in ionospheric D region, ionization from, (E/T), 19: 12385 (AFCRL-63-747)
reactions in polar ionosphere, ionization enhancement from, 18: 6094
reactions in terrestrial atmosphere, fluorescence from photon, 17: 32873
reactions of, nuclear synthesis in, 20: 17234
reactions with atoms in lunar dust, 20: 7695
reactions with cesium atoms, ionization from, (T), 20: 11549
reactions with geomagnetic cavity, bow shock stand-off distance in, (T), 19: 6438
reactions with ionosphere, heating from, 18: 28481
reactions with lunar surface, effects of, 18: 5906
reactions with magnetosphere, neutral-point expansion of, 18: 22810
reactions with magnetosphere, simulation of, (E), 19: 5056
reactions with magnetosphere and moon, (E/T), 19: 8060
reactions with magnetosphere, shock structure from, (T), 19: 29132 (NYO-1480-12)
reactions with meteorites, gas production from, 20: 5976
reactions with molecules in comets, ionization from, 18: 8998(T)
relation to cosmic radiation intensity variations, 18: 20814 (AD-434540)
relation to cosmic radiation and geomagnetic index, 18: 30391
relation to short-wave fadeouts, 18: 10738
relation to solar activity, 18: 2722 (AID-Report-P-63-28)
research on neutrino, using isotopic composition of solar material, 20: 37369
research programs of U. S. Army on, 1962 summary, 17: 33413(R) (NP-12967)
research progress on, 18: 21712(R) (NYO-10065)
review, 19: 14203
review, 18: 14755 (AD-401660)
review of uv and x, from different solar regions, 19: 16362
riometer observation on plasma, multifrequency, (T), 19: 4823
rocket research program of U.S. IGY-IGC, third compilation, 18: 16580
role in origin of life, 19: 45721 (UCRL-14254)
separation from geomagnetic field, solutions for boundary shape in presence of ring current for, 17: 31246 (NASA-TR-R-177)
separation from geomagnetic field, shape of boundary of, 18: 15035
shielding against proton, aluminum, 19: 30009
shielding against proton, analysis of, 20: 34781 (N-66-16495)
shielding protons, 18: 13178 (ORNL-3549)
shielding space vehicles against, 17: 22769
shock boundary in solar wind, 19: 47211
shock wave production in wind, effects on geomagnetic storms, (T), 20: 4744
shock-wave excitation of oscillations in plasma, 18: 30873 (AFCRL-63-577)
short wave, apparatus for study of, 17: 12540
short wave, investigation of, 17: 13328
simulation, 18: 33703
simulation of, beam divergence effects in, (T), 19: 18104
solar wind effects on diurnal cosmic-ray variations, 16: 26059
solar wind hydrodynamics, 16: 3597
solar-wind simulation for Pioneer space vehicle, using plasma sources, 20: 31877
spectra at 10 to 400 A from solar flares, x-ray, 18: 7396
spectra during flares, measurements and models for, 17: 19004
spectra of electromagnetic, 16: 20232
spectra of electromagnetic, 16: 30991
spectra of flare-produced photons, at 500 to 1000 Mc, 17: 19003
spectra of flare-produced α particles and protons, 17: 19018
spectra of ions of lithium I sequence in, ultraviolet, 18: 7395
spectra of iron in, uv, (E), 19: 12637(R) (LA-3202-MS)
spectra of iron ions in, simulation in Scylla I, (E), 19: 32854(R) (LA-3320(p.100-3))
spectra of, line energies and intensities in low wavelength, 17: 26257
spectra of, profile of calcium II K_{321} in, 18: 4390(T)
spectra of protons, exponential rigidity form for, 18: 10812
spectra of protons, r-f, and x, associated with flares, 18: 28220
spectra of r-f, data compilation for 1959, 18: 7371
spectra of radio-frequency, 17: 13292(T)
spectra of u-v and x, 20: 29873 (NASA-SP-100)
spectra of ultraviolet and x, 17: 24227
spectra of uv and x, 18: 10731
spectra of vacuum u-v, 19: 45396 (LA-DC-7120)
spectra of x, anomalies in, 18: 28218
spectra of x, during subflare activity, 18: 28217
spectra of x, variability of, 18: 28216
spectra of, data on microwave, uv, and x-ray, 19: 20785
spectra of, search for quarks in far uv, (E), 20: 46375
spectra of, solar flare effects on lines of, 18: 44379
spectra of, ultraviolet, 18: 44641(R) (AFCRL-64-275)
spectral variations during solar flares, hydrogen Lyman-alpha, 18: 44378
spectral width of, effective H, (E/T), 19: 9845
spectrometer for 1 to 10 Å, 18: 487 (AFCRL-62-1105)
spectroscopy of neutrino, (T), 19: 8058
spectrum during solar burst, (E), 19: 20756
spectrum of flare-produced, 18: 21094
spectrum of radio-frequency, 17: 13283(T)
spectrum of 4 to 14 Å, (E), 19: 4814
spectrum of, absolute intensities of xvs, 19: 32855
sputtering of bodies in earth orbit by, material loss from, 17: 41694
stability of corpuscular streams of, Cherenkov and synchrotron, 18: 44347
stability of corpuscular streams of, (E), 19: 12049(T)
stability of magnetosphere-solar wind interface, (T), 19: 9861
structure of corpuscular streams, 18: 36412(T)
structure of fast streams of, correlation with geomagnetic storm, (T), 20: 4745
structure of solar wind, models for, 20: 31890
structure of solar wind, determination using radio astronomy, 20: 31888
sunspot effects on temperature of ionospheric F region, (T), 19: 10166
survey of interplanetary electromagnetic, 17: 34701
temperature and velocity of solar plasma (E/T), 19: 2958
temperature at 4 mm, brightness, 18: 26192
terrestrial accretion from, 16: 15009
theory of neutrinos in, 18: 14907
theory of solar wind, 19: 2955
theory of solar wind, review on, 20: 9648
time characteristics of radio and x-ray emission, study of, 17: 13291(T)
trajectories of proton, in geomagnetic field, (T), 20: 44461
transmission to the troposphere, 16: 27418 (NP-11961)
transport properties of, in interplanetary space, 17: 2143
use in waste evaporation, 20: 10437(R) (NP-15662)
use in waste evaporation, 20: 18164(R) (NP-15874)
use of hydrogen, for space power and propulsion system, design study of, 19: 34998 (N64-26578)
Van Allen outer belt deformation by, 17: 24246
variation of 10.7-cm and extreme u-v, over solar cycle, 19: 37444
variations in, factors affecting, 20: 7748(T) (NASA-TT-F-91)
variations of, density, temperature, and time, 18: 14700 (JPL-TM-33-111)
velocity distributions of protons, in interplanetary space, 18: 28222
velocity of solar wind, nonuniformity of (T), 19: 2957
velocity of solar wind, variation of geomagnetic induces with, (T), 19: 37731
velocity of solar wind, exospheric temperature dependence on, (T), 19: 45179
velocity of solar wind, correlations with solar phenomena, 20: 31882
velocity of solar wind, effects on geomagnetic fields, 20: 34397

velocity of solar wind, correlations with cosmic ray rigidity spectrum, (E), 20: 37533
wave propagation in solar wind, (T), 20: 15216
X agent in, 19: 11232
x-ray emission from solar plasma, (T), 19: 34855
Solar Wind
see Solar Radiation
SOLCOSERYL
antileukopenic effect of, in radio- and chemo-induced leukopenia in rabbits, 18: 17661
radiosensitivity effects on mice and rabbits, 20: 16302
therapeutic use for radiodermatitis, 19: 19633
SOLDERING
see also Brazing
see also Solders
see also Welding
effects on recrystallization in molybdenum, niobium, tantalum, and tungsten, 20: 13267(T) (AD-624909)
equipment for joining components and leads to thin-film circuitry, 19: 5581 (SC-TM-363-63-14)
flux composition for detection under ultraviolet light, 18: 27001(P)
fluxes for aluminum, bibliography on, 18: 14429 (TID-3577)
of materials for use in vacuum systems, 19: 22526
of noble metal alloy wires, 19: 1964 (SC-DR-64-645)
of structural metal components without embrittlement, 17: 20444(P)
process for automatic induction, using infrared radiometer, 19: 21765 (SC-DR-65-74)
processes in, 17: 4917(T)
testing of solderability, review, 19: 40280 (BDX-613-73)
SOLDERS
see also Soldering
analysis for indium, lead, and tin, polarographic, 19: 30629(R) (MLM-1238)
analysis of lead–tin alloy, by radiation absorption, 17: 2915
book: *Metals Reference Book.*, Vol. I and II, 3rd edition, 18: 32080
cold, for joining superconductive materials, 19: 33185(P)
composition and properties, 17: 4917(T)
design of superconducting, optimization of, 20: 16592
mechanical properties of, at cryogenic temperatures, 17: 8874
radiation effects on, 18: 33839 (RTD-TDR-63-4287(Vol.II))
radioactivity of glass, measurement of, 19: 2826
use in sealing metal tubing, 19: 15696 (K-L-6018)
SOLENOIDS
acceleration of superconducting, to hypervelocities, (T), 20: 41554
analysis of axisymmetric, computer programs for, (E/T), 19: 23162 (ORNL-3575)
beam focusing by superconducting, (T), 20: 17197 (CONF-650922, pp 536-40)
cables for superconducting, use of multiwire, 20: 9914
calibration of superconducting, using NMR, 19: 29156 (NYO-2150-4)
characteristics of niobium–zirconium superconducting, 17: 12539
charged particle motion in field of superconducting, 20: 42521
connection of superconducting, with relay switch for electric energy storage, 19: 46475 (AD-612113)
construction of superconducting, at Brookhaven, 18: 16603 (BNL-7534 (p.448))
cooling by thermal conductivity plates, (T), 20: 27239
cooling system for, design of water, 20: 10128 (CONF-650512, pp 177-81)
critical-current degradation, model for, 17: 27944 (NP-12908)
critical current degradation and flux jumping in heat-treated niobium–zirconium, 17: 36469
critical current-field characteristics of short wire samples in superconducting, 17: 37729
critical currents in superconducting, a-c, (E), 19: 25438
critical states of superconducting, (E), 20: 46545
cryostat design for superconducting, with thermal working volume, 20: 32334
current-carrying capacity of niobium–zirconium, 17: 6209
current-carrying capacity of superconductor, 17: 11349
current degradation in niobium–zirconium, 19: 37735(R) (N64-33921)
current degradation in superconducting, (E), 20: 21920
current regulators for superconducting, design of, 19: 38945
degradation effect of superconducting, theory of, 17: 33158(R) (ORNL-3472(p.84-106))
description of model, for magnetic field studies of traveling-wave tubes, 19: 26488 (AD-610579)
description of 100,000-gauss superconducting, 17: 30641
design and fabrication of cryogenic, with integral coolant passages, 20: 17874 (CONF-650922, pp 630-42)
design and operation of superconducting, for generation of homogeneous magnetic fields, 17: 41200
design and operation of, for production of strong magnetic fields, 18: 17972
design and performance of sodium cryogenic, 17: 35965 (UCRL-7401)
design and testing of niobium–tin alloy superconducting, 16: 4610(R) (TID-14435)
design and testing of superconducting, 17: 35260(R) (TID-19135)
design and use in magnetic field production, 16: 2343
design concepts for superconducting, 16: 9510(R) (ORNL-3239(p.79-84))
design concepts for superconducting, 16: 15396
design for measurements at 4.2°K, 20: 24271
design for production of Ioffe fields in plasma regions, 18: 40658 (IPPJ-26)
design for strong fields for adiabatic demagnetization, 20: 4489
design for uniform magnetic field production, 18: 41597(T) (SLAC-Trans-7)
design of air-core, parameters for, 16: 7674 (AFOSR-1525)
design of air-core, computer program for, 20: 45840 (UCRL-70029)
design of eighth-order power optimized, analysis of, (E), 20: 2522 (ORNL-P-1516)
design of, for production of pulsed magnetic fields, 17: 3086 (NIRL/R/19)
design of high-power, with external magnetic circuit, 16: 15411
design of high-field superconducting, 19: 14459(P)
design of high-field d-c, 20: 17158(R) (ORNL-3900, pp 82-149)
design of homogeneous power-optimized, 19: 21486(R) (ORNL-3760 (p.77-93))
design of precooled, for multisecond pulses, 16: 15419
design of superconducting, for 30-kgauss field, 16: 15431
design of superconducting, 16: 27169
design of superconducting, with reduced winding space using Helmholtz coils, 18: 9268
design of superconducting, 19: 23938(P)
design of superconducting, for magnetic field compression, 19: 33184(P)
design of superconducting, for operation at 1°K, 20: 4775 (UCRL-16376)
design of superconducting, for magnetic resonance studies, 20: 9231
design of superconducting, 20: 13667 (JINR-P-2533)
design of superconducting, for NMR spectrometers, 20: 17587 (CONF-650922, pp 517-24)
design of superconducting, for magneto-optical studies, 20: 17588 (CONF-650922, pp 525-9)
design of superconducting, for shielding of space vehicles, 20: 30317
design of symmetrically separated pairs of, with minimum volume, 20: 17180 (CONF-650922, pp 111-25)
design of variable-composition superconducting 70-kOe, 17: 4781
design of water-cooled high-flux, 18: 20129 (ARL-64-29)
design of 300-kgauss, for intermittent operation, 18: 33714
design of 55-kgauss superconducting niobium-zirconium, 16: 15427
design of, determination from specified magnetic fields, (T), 19: 47121 (UCRL-16080)
design optimization, 16: 15404
development for high-temperature valves, 19: 40765(R) (NP-15309)
development of large-volume superconducting, (E), 19: 10189 (RLE-TR-427)
development of superconducting niobium–zirconium, 17: 23712
development of superconducting, for 50-kG magnetic fields, 18: 36520
development of superconducting, 18: 44676 (ORNL-P-488)
development of superconducting, 19: 23594(P)
development of 112 kgauss superconducting, 19: 19058
electric conductivity of, inductive thermometry measurement of, 18: 20282 (HW-SA-3035)
electric conductivity and magnetic inductance of iron core, (E), 19: 18574(T) (ORNL-tr-460(p.61-73))
electric current behavior in, superconducting around breakdown, 18: 9264
electric current degradation in superconducting, flux pinning dependence of, (E), 19: 6608
electric current degradation in superconducting, 20: 26025(R) (N-65-35450)
electric current persistence in superconducting, 17: 11404
electric current sweep circuit for superconducting, 19: 24825
electric current training in superconducting, critical, (E), 19: 10215
electric currents in superconducting, maximum, 17: 36375 (CONF-176-2)
electric eddy current loss and magnetic energy absorbed by cylindrical conducting core in, (T), 19: 18572(T) (ORNL-tr-460(p.20-36))
electric eddy current loss and inductance of, with finite-length core, (E), 19: 18573(T) (ORNL-tr-460(p.37-60))
electric inductance of superconducting, 20: 26032
electric properties of normal region in superconducting niobium–zirconium, 20: 17610
electron beam reactions with, current effects from, (T), 19: 39654
electron scattering by shielded, Aharonov-Bohm effect in, (T), 19: 27315
electron scattering by, Aharonov-Bohm effect for bound states in, (T), 19: 27316

energy storage capacity of superconducting, 18: 15047
energy storage in superconducting, for high-power discharges, 17: 34574
energy storage in superconducting, 18: 15041 (IDA/HQ-63-1412(Vol.I) (p.106-9))
energy storage in superconducting, cryogenic system for, 18: 15042 (IDA/HQ-63-1412(Vol.I)(p.110-11))
fabrication and properties of superconducting, 19: 24958
fabrication of superconductive, from Nb_3Sn, 18: 14445
fabrication of superconducting, from stranded niobium–tin wire, 20: 17593 (CONF-650922, pp 597-603)
fabrication of 59-kgauss superconducting niobium-zirconium, 16: 15428
field energy removal from superconducting, methods for, 18: 34690
flux jumping and degradation in superconducting, 18: 26463
flux jumping and training in superconducting, 18: 26470
magnetic field and inductance of hollow, containing cylindrical conductor, (T), 19: 18571(T) (ORNL-tr-460(p.1-19))
magnetic field distribution in finite helical, 17: 41551 (NASA-TN-D-1993)
magnetic field of short thick cylindrical, inside and outside, 16: 15440
magnetic field of niobium–zirconium superconducting, relation to magnetization of the alloy, 18: 9277
magnetic fields in superconducting, probe for, 19: 9460
magnetic fields in niobium–zirconium superconducting, remanent, 17: 18978
magnetic fields of thick finite-length, axial and radial components of, 17: 25850 (NASA-TR-R-170)
magnetic fields of superconducting niobium–zirconium, 18: 26474
magnetic fields of superconducting, measurement of, using galvanometers and flip coils, 20: 20806(R) (MLM-1274)
magnetization of superconducting, 17: 41592
measurement of neutron polarization by, 17: 9294
neutron depolarization effects in precession magnets of, fast, 19: 21209
particle dynamics in field of tapered, adiabatic approximation for, 17: 11795 (SLAC-4)
performance and protection of superconducting, 19: 25442
performance as magnetic monopoles, 18: 40067
performance for magnetic flux compression, 20: 41091
performance for production of positrons and polarized electrons with Cambridge Synchrotron, 19: 26966 (CEAL-1016)
performance of niobium–tin superconducting, in superfluid helium, (E), 20: 24268
performance of water-cooled, for plasma containment, 18: 21539
plasma acceleration by toroidal, 19: 23937(P)
plasma injection into magnetic fields of, 18: 30932
power losses in superconducting, at low frequencies, 19: 16448(R) (TID-21380(p.85-111))
power supplies, design of low-ripple motor-generator for, 16: 15437
power supply for, design of 104-amp, 20: 20019 (UCRL-14511-T(Rev.1))
preparation of superconducting, 17: 4886(R) (AD-275610)
production of superconducting niobium–tin, for 101-kgauss field, 18: 958
production of 43-kgauss superconducting, from niobium–zirconium alloy, 16: 6564
propagation of normal region in niobium–zirconium superconducting, 20: 42100
properties of large-volume, highly uniform, at ORNL, 20: 44030 (ORNL-P-2492)
properties of superconducting, compensated to sixth order, 18: 20298
properties of superconducting force-free (T), 19: 1479 (NASA-TN-D-2156)
radiation effects on niobium–zirconium, proton, 17: 6756
size effects in superconducting, r-f, (E), 20: 30735(R) (TID-22970, pp 331-73)
stress analysis of cryogenic high-field, 20: 16586 (CONF-650922, pp 723-32)
stresses in multilayer superconducting, (T), 19: 41632
superconducting critical currents in passing through lambda point, a-c, (E), 19: 14438
superconducting, review of materials and causes of current degradation for, 18: 4492
superconducting, distribution of normal region after quenching of, (E), 20: 42103
superconducting, with superconductive shielding at junction, 19: 35346(P)
superconductivity degradation in ribbon-wound niobium stannide, (E), 19: 1515
transition propagation in superconducting, (E/T), 19: 25439
use for producing strong magnetic fields (E), 19: 2897
use for producing high magnetic fields, 19: 37210
use of superconducting, for stabilization of d-c magnetic fields, 17: 18977
use of superconducting niobium-zirconium, with electron microscope, 19: 15841
use of superconducting, in macroparticle acceleration for nuclear fusion, (T), 20: 30717
use of water-cooled, in Mössbauer spectroscopy, 19: 41848

Solid Moderator Reactor
see Aircraft Reactor Critical Experiments

SOLID PROPELLANTS
see also Fluid Propellants
analysis for water, techniques for, 19: 5590 (UCRL-13136)
bibliography on, 18: 11471 (AD-405958)
binder, synthesis of resin for, 16: 258(P)
burning rates and heats of explosions of, effects of irradiated ammonium perchlorate on, 20: 31286
burning rates of, equipment for continuous measurement of, 20: 9131
combustion at ground level, rise of cloud from, 18: 43103 (CONF-647-2)
combustion kinetics, 17: 27538(R) (NP-12767)
combustion of, flame mechanisms in, 17: 3574(R) (NP-12212)
combustion of, effects of additives on rates in, 20: 2668 (AD-615124)
conference on rocket propulsion, Cranfield, England, Jan. 6 to 7, 1961, 16: 5089
conference, Pasadena, Calif., Aug. 28 to Sept. 3, 1960, 16: 14863
curing of, using gamma radiation, 17: 8911(P)
detection of, in the atmosphere by radiometric methods, 16: 32917 (ASD-TR-61-654)
development for space research, 20: 2862
developments and progress of space vehicle, 16: 5098
electric power production using, MHD systems for, 18: 16743 (MHD-646)
exhaust plasma from, microwave attenuation in, 20: 41120
flame mechanisms in, 18: 1094(R) (AD-420576)
flame mechanisms in, 18: 22928(R) (AD-435879)
inspection of, by nondestructive methods, 17: 10184 (AD-275297)
performance of lithium hydride, for nuclear rockets, effects of lithium-6 and -7 on, 17: 12034 (NP-12353)
performance of lithium-6-neutronic, 19: 31461(R) (ANL-7010(p.235-87))
properties of polyoxypropylene glycol, bulk and solution, 16: 1275(R) (NP-10832)
radiation and vacuum effects on burning and mechanical properties of PBAA and polyurethane, 18: 37624(R) (X63-13637)
radiation effects, summary, 16: 16778 (JPL-TR-32-234)
radiation effects on, in outer-space storage, 16: 30894 (ANL-6585)
radiation effects, 17: 16108
radiation effects on mechanical properties of polyurethan, 18: 2295 (JPL-TR-32-518)
radiation effects on burning rates and tensile strengths of composite ammonium perchlorate, electron, 18: 12146 (RAI-314)
radiation effects on burning rates and tensile strengths of, x-, 18: 29756
radiation effects on composite ammonium perchlorate, 19: 7541(R) (RAI-331)
radiation effects on composite ammonium perchlorate, (E), 19: 34215 (AD-612536)
radiation effects on, bibliography on, 20: 4461 (REIC-Memo-28)
radiographic inspection of missile, 16: 5465 (USNRDL-TR-534)
radiographic inspection of, development of scanning detectors for, 17: 10188 (AD-275297(p. 70-4))
radiography with electron linear accelerators, 16: 6622
use in thermionic power supplies, 18: 28317(P)
use of *N,N*-difluoroalkylamines as, 19: 12890(P)

SOLID SOLUTIONS
see also Constitution Diagrams
ammonium ion rotation in, (E), 19: 11136
atomic local arrangements and displacements in, x-ray diffraction techniques for studies of, 19: 31447 (ORNL-P-1240)
clustering of oxygen in niobium–oxygen, measurements of, 20: 37213
clustering of oxygen in niobium–oxygen, mechanism of, 20: 37214
dislocation pairs in fcc, diffraction analysis, 19: 43997(R) (UCRL-11889)
equilibrium order parameters for disordered, quantum theory of, 18: 2701
formation by reactions of metals with refractory materials at high temperatures, 20: 39331(T) (UCRL-Trans-10044)
formation of extensive, effects of electronegativity, 16: 29412
identity with tricalcium phosphate hydrate, structural, 18: 27370
lattice models of, for correction of Vegard's law, 20: 41412(R) (IS-1500 (Sect. M))
magnetic susceptibility and nuclear magnetic resonance in, 18: 26522(R) (ANL-6868(p.326-30))
metallic, methods for prediction of, 17: 16518 (LADC-5380)
neutron scattering in spinel-type, theory of slow, 17: 2218(T)
neutron scattering by impurity atoms in, one-phonon peak in slow, (T), 19: 41991(T)
of alkali halides, theory of formation of sodium chloride type, 17: 20001
particles in, growth and nucleation of precipitate, (E/T), 20: 19273(R) (BNL-929, pp 3-43)
photo- and radioluminescence of, fast electron excitation quenching in, 18: 31561
preparation, 17: 25843(R) (AD-282296)

preparation of phase-stable zirconia, 20: 46153(P)
preparation of single-phase copper-rich, rapid quenching of liquid alloy method for, 17: 18773 (TID-18433)
properties and structures, review, 16: 9245
radiation effects on rate-controlling mechanism for slip in body-centered-cubic, neutron, 20: 43998 (ORNL-3993)
radioinduced free radicals in binary, effects of intermolecular compounds on, 19: 28413
radioinduced spin transfer in crystalline, (E), 20: 43317
scattering of neutrons by unordered, inelastic, (T), 19: 10226
segregation in, calculation of nucleus formation during, 18: 4927(T) (AEC-tr-6158)
short-range-order propagation in binary, 17: 36289 (ASD-TDR-63-567 (Pt.I))
strengthening of, studies of mechanisms of, 19: 13979 (ASD-TDR-63-567(Pt.II))
thermodynamic properties of, models for, (T), 20: 26818 (LA-3481)

SOLID STATE REACTIONS

analysis, thermal, 16: 28878
electric conductivity in, 16: 19366(R) (TID-15228)
material removal from thin films by charged particles, 16: 22754
phase formation in type 316 stainless steel at high temperatures, chi, 20: 41419(R) (GMAD-3643-5)
phase transformations at high pressure and temperature, 19: 2741
proton bridge mechanism for transfer of electric charges and energy in crystals, 20: 34827
radiation effects on, far-infrared, 17: 35260(R) (TID-19135)
research on, at ORNL, 17: 34542(R) (ORNL-3480)
research program summary for M.I.T., 16: 588(R) (NP-10932)
research programs on, summary for Ames Laboratory, 17: 4448 (IS-500 (Sect.P))
research programs on, 17: 12057(R) (BNL-742(p.1-85))
research programs of U. S. Army on, 1962 summary, 17: 33413(R) (NP-12967)
research programs at BNL on, July 1962 to July 1963, 18: 7987(R) (BNL-806(p.3-90))
research programs on, in Israel, 18: 9752 (IA-900)
research programs at Case Inst. of Tech. on, 19: 9766(R) (COO-623-105)
research programs at Risö on, 20: 18174(R) (NP-15771)
research progress, 16: 6805(R) (ORNL-3213)
role of point defects in, 18: 40046 (BNL-7666)
studies for development of ordnance materiel, 16: 6253 (ARGMA-TN-2H1N-30)
studies of, summary of, 16: 30169(R) (ORNL-3313(p.133-78))
topotaxy in, definition of, 18: 36901 (UCRL-10957)

SOLIDS

analysis by irradiation, apparatus for, 16: 26947(P)
analysis by mass spectroscopy, detectors and ion sources for, 16: 30352
analysis by mass spectrometry, use of electron-extraction method in, 17: 33834
analysis by mass spectrography, review on, 18: 14188
analysis by Rutherford scattering, equipment development and theoretical studies, 16: 2095(R) (TID-14226)
analysis by spark-source mass spectrometry, 19: 42411 (CEA-R-2757)
analysis by spark-source mass spectrometry, 20: 31202
analysis for components below 1 ppb, neutron-activation, 18: 27335
analysis for fluorides by automated colorimetry and pyrohydrolysis, 20: 12765 (DP-1004)
analysis for gases by spark source mass spectrography, 19: 19830
analysis for gases, spectral isotopic, (T), 20: 41526
analysis for hydrogen by beta absorption, 20: 16356
analysis for impurities by mass spectrometry, review, 17: 7986
analysis for microimpurities in, spectrographic, 17: 27308
analysis for moisture, microwave apparatus, 16: 8704
analysis for moisture content by neutron moderation, nondestructive, 18: 8303
analysis for nitrogen and oxygen, mass spectrometric, 20: 38831
analysis for trace impurities using mass spectroscopy, 19: 43978
analysis for water by neutron reflection, 18: 6758
analysis, mass spectrometric, 16: 11554
analysis of, by mass spectra obtained with d-c spark in vacuum, 17: 40755
analysis of low-vapor-pressure, by mass spectrography, 20: 31204
analysis of surfaces of, sputtering ion device for mass, 18: 41332
analysis of, by mass spectrometry, review of, 20: 31201
analysis of, design and performance of electron-bombardment ion source for isotopic, 20: 8842
analysis of, neutron spectrometric methods for, 20: 7038
analysis of, sputtering ion source for, 18: 10350
analysis, use of Rutherford scattering in, 16: 25682(R) (TID-16013)
angular momentum tensors for, properties of irreducible, 16: 22766
atom bombardment of binary, with square planar lattice, IBM 7090 program for describing, 17: 16778 (GEMP-192)
atom displacements by fast electrons in, cross sections at threshold to 10 Mev, (T), 19: 28992 (ORNL-3813)
atom dynamics in harmonic, for analysis of Debye-Waller-factor and Mössbauer-thermal-shift measurements, 20: 28660
atom migration and pore motion in, thermodynamics of, 18: 24069 (NP-13957)
atom ranges at 250 ev to 200 kev, theoretical calculations, 16: 6806(R) (ORNL-3213(p.3-8))
atom ranges in, Monte Carlo calculations of energetic, 17: 14968
atom reflection from surfaces of, (T), 19: 42990
atom scattering from, model of, 20: 14227(R) (TID-22419)
atomic collisions in, interatomic shocks resulting from, 16: 27792 (CEA-1954)
atomic motion in, models for bound, 17: 19205 (TID-18432)
atomic motion in, observation of, 19: 25176
atomic vibration frequency distribution functions for, sampling method calculation for normal mode, 18: 18571
atomic vibrations in, study by resonant absorption of slow neutrons, 17: 36433 (NP-13020(p.392-400))
band structure of, gauge invariance of Hartree-Fock approximation for, 19: 23275
behavior in strong electric field, analysis, 17: 13204
beta activity of, detector for low-background, 20: 13102
beta recoil from surfaces of, 16: 26009
beta source diffusion in, method for determining, 19: 4234
bibliography on equipment and methods for measurement of rare gas diffusion in, 18: 684 (EURAEC-420)
bibliography on radiation effects on properties, 16: 2267 (NP-10969)
book: *Effects of Nuclear Radiation on Solids*, 19: 30841
book: *Electron and Ion Processes in Solids*, 20: 43265
book: *Elementary Excitations in Solids*, 19: 23982
book: *Energy Band Theory*, 19: 35602
book: *Fluctuation Phenomena in Solids*, 19: 18623
book: *Group Theory and Solid State Physics*, 19: 11855
book: *Interaction of Radiation with Solids*, Proceedings of International Summer School on Solid-State Physics, Mol, Belgium, August 12 to 31, 1963, 19: 11235
book: *Irradiation Effects in Solids. An Introduction to the Theory*, in German, 19: 37196
book: *Lectures on the Many-Body Problem*, 19: 18596
book: *Low-Temperature Solid State Physics*, 19: 16180
book: *Mechanisms of Solid Friction*, 19: 47075
book: *Nuclear Magnetic Resonance and Relaxation in Solids*, 20: 3316
book: *Photochemistry and Radiation Chemistry of Solid Inorganic Substances*, 20: 35565
book: *Physics of Non-Crystalline Solids*, 19: 40110
book: *Plasma Effects in Solids*, 20: 1346
book: *Radiation Effects on Solids*, 18: 16539
book: *Radiation Effects in Condensed Media*, 18: 43697
book: *Solid State and Low Temperature Physics in the USSR*, 19: 42004
book: *Solid State Physics. XIII.*, 16: 21221
book: *Solid State Physics*, Vol. 16, 19: 14065
book: *Solid State Physics*, Vol. 17, 19: 38036
book: *Solid State Physics*, Vol. 18, 20: 32718
book: *Strength and Structure of Engineering Materials*, 20: 33932
boundary surface processes on, tracer studies, 16: 22168(T) (SCL-T-422)
cascade production in, particle counting by, 20: 5793
catalytic effects of nonmetallic, in presence of radiation, 17: 32178
cavitation damage to, survey of research on, 19: 32695 (CONF-650518)
centroids and inertias for solids of revolution, computer program for, 20: 16154 (Y-1420(Rev.1))
charged particle energy losses in, 18: 16688
charged particle energy losses in, 18: 16544
charged particle tracks in, identification after chemical etching, 19: 39038
charged-particle tracks in, ion-explosion spike mechanism for, 20: 4548
chemical reactivity and radioinduced defects in, review, 16: 10091
chemistry and physics of, bibliography on high-temperature, 20: 5527 (NP-15646)
Cherenkov emission from, shock-initiated, 18: 16767
Cherenkov emission from, shock-initiated, 18: 16768
coalescence and migration of pores in, 18: 26069(R) (ANL-6868(p.373-417))
coding for self-organization, feasibility of, 17: 16506 (SCTM-251-62(24))
color and stoichiometry in, correlation of, 17: 11327 (TID-15759)
color center formation in, by electrons, 17: 18145
compressibility at very high pressures, 16: 15286(T) (UCRL-Trans-794(L))
compressibility measurement in, piston displacement method for, 19: 4663(T) (UCRL-Trans-1087(L))
compressibility of, statistical mechanics derivation of temperature effects on, 17: 18916(T) (UCRL-Trans-928(L))
conference, 20: 12320

conference on condensation and evaporation of, Dayton, Ohio, Sept. 12 to 14, 1962, 19: 13382
conference on inelastic scattering of neutrons in solids and liquids, Vienna, October 11 to 14, 1960, 16: 7145 (STI/PUB/35)
conference on mechanical properties of, for high-temperature uses, 20: 15129
conference on physics and chemistry of solid surfaces, Providence, Rhode Island, June 21 to 26, 1964, 19: 8036
conference on radiation effects, 16: 13647
conference on radiative heat transfer, 17: 8377
conference on reactivity of, in Amsterdam, May 30 to June 4, 1960, 16: 31362
conference on solid state physics, 19: 16300
contacts by, mechanical and thermal properties of, (E/T), 20: 1811 (EUR-2486.e)
crater formation in, blast-wave theory of hypervelocity impact, 17: 39282
crystal structure point defects in, high-pressure studies of, 17: 35784
crystal structure defects in, theory of electron microscopy of, 19: 11129
Debye characteristic temperature determination, 19: 13271 (ASD-TDR-63-881)
defect size measurement by cold neutron scattering, cross section calculation for, 19: 25620 (AERE-R-4853)
defects in, research program on lattice and electronic, 18: 34280(R) (NYO-2680-1)
defects study by electron-nuclear double resonance techniques, 16: 29481(R) (NP-11989)
deformation of crystalline, geometric foundations of continuum mechanics, 16: 4949 (UCRL-9922)
deformation of crystalline, studies of, 16: 30170(R) (ORNL-3313(p.179-208))
deformation of crystalline, 18: 44145(R) (ORNL-3670(p.11-16))
deformation of crystalline, mechanisms of, 19: 23163(R) (ORNL-3650 (p.111-86))
deformation of, review on dislocation dynamics in, 19: 25624 (UCRL-11977)
density fluctuation excitations in many-particle systems of, (T), 19: 18598
density profiles in turbulent flow, (E/T), 20: 16606(R) (TID-22621)
diffraction studies, 16: 21010(R) (AD-264878)
diffusion and coalescence of bubbles in, theory of, 20: 15132 (ANL-7079)
diffusion and thermal defects in, methods for determination of, 18: 7253
diffusion coefficients at various temperatures by continuous process by method of radioactive surfaces, 16: 23704
diffusion coefficient measurement by isotope exchange between gas and phase boundary reaction in, 18: 215(T) (UCRL-Trans-962(L))
diffusion coefficients of, measurement by self-absorption of beta particles in samples of finite thickness, 17: 23589
diffusion in, bibliography on, 18: 617
diffusion in, review of studies on, 19: 11130
diffusion of gases in, successive approximation equations for, 19: 11112
diffusion of gases in, least-square determination of coefficient of, 20: 4377 (NAA-SR-Memo-10741)
diffusion of gases in, computer program for graphic display of coefficients of, 20: 4377 (NAA-SR-Memo-10741)
diffusion of krypton-85 in, 18: 37566(R) (NYO-2757-3)
diffusion of particles in, generalized equations for, (T), 20: 11369
diffusion of radioactive gases in, 16: 11670
diffusion of radioactive inert gases from, tables for computation, 16: 17968(T) (EURAEC-122)
diffusion of rare gases in, measurement, 16: 10528 (HMI-B-19)
diffusion of rare gases in, research program on, 20: 1324(R) (EURAEC-1428)
diffusion of rare gases in, effects of traps on, (T), 20: 2360(T) (ORNL-tr-314)
dislocation interactions in, review of internal friction studies of, 18: 27950 (COO-1198-168)
dislocation kinks in, oscillations of, 20: 30770
dislocation lines in, pinning point distribution near, (T), 19: 23958
dislocation loops in irradiated, elastic interaction energy of, 19: 18531 (AERE-R-4170)
dislocation loops in, review of diffraction analysis of, 19: 25619 (AAEC/TM-283)
dislocation-phonon interactions in, lattice-vibration calculations, 19: 18567 (NYO-2394-14)
dislocations in, origin and multiplication of, 17: 25785 (UCRL-10714)
dispersion relations for electrons and ions in, 19: 2813
distribution constant for, tracer techniques for determining V. G. Khlopin, 16: 3337(T) (AEC-tr-4497(p.270-8))
distribution in gas-solid fluidized beds, 16: 17782
dosimetry using, bibliography on, 20: 11027 (AED-C-21-03)
dynamics of, slow neutron scattering analysis of, 17: 4041
effects as impurities on radiation chemistry processes, 19: 32238
effects on statistical structure of turbulence in fluid flow, (T), 20: 16606(R) (TID-22621)
elastic behavior, effects of plastic deformation, 16: 12034 (TID-15206)
elasticity in, method for measuring third-order, 17: 34552(R) (ORNL-3480(p.65-71))
electromagnetic wave interactions with, electric and thermal effects of, 17: 32674
electron absorption and transmission by, 17: 682(T)
electron and lattice vibration correlations in, in terms of collective motions, 19: 47875 (AD-614136)
electron avalanche formation in, collective energy losses in, (T), 20: 32727(T)
electron band structure of, high-pressure determination of, 20: 14221 (COO-1198-230)
electron beam reactions with, x-ray production in, 20: 36359(R) (TID-22992)
electron behavior in, theory of, 17: 39708 (ARL-62-459)
electron correlations in narrow energy bands in, 18: 5940
electron density of states and propagation in disordered, (T), 19: 18600
electron ejection and trapping in molecular, 17: 16751
electron ejection from, 20: 29499
electron emission after excitation, review on, 17: 6789 (ERDL-1704-RR)
electron emission from, in gas discharges, 18: 26164
electron emission by nonmetallic, thermionic, 18: 30177 (TID-7687 (p.200-13))
electron energy levels, 18: 44290(R) (ORNL-3670(p.54-5))
electron energy level transitions in, (T), 20: 1342
electron energy levels in, 20: 29931(T)
electron energy levels in, pseudo wave functions for, 20: 30773
electron energy loss spectra in, 18: 14728
electron energy losses in, transfer to atoms or molecules, 19: 1029
electron energy losses in, spectrometry of, 19: 1190
electron energy relaxation in, theory of, 17: 6075
electron inelastic scattering, Cherenkov emission from, 16: 29703
electron interactions with, 17: 20537 (ASD-TDR-63-175)
electron interactions in, Fermi liquid theory for, 20: 38403
electron momentum in, 17: 39706(R) (AD-296764)
electron momentum distribution in, determination from annihilation gamma-ray correlations, (T), 19: 23464(T)
electron motion in, with randomly distributed impurities, (T), 20: 44393
electron orbitals in, spin hamiltonian for nonorthogonal, (T), 19: 47254
electron penetration of, (E/T), 19: 12728(T)
electron pins at lattice sites in, magnetic properties of, 17: 525 (AFCRL-922)
electron reactions, cross sections for atomic displacements, 16: 6807(R) (ORNL-3213(p.9))
electron reactions on, distributions of K x rays from, 17: 37871
electron reactions with, excitation of electronic energy levels in, 17: 39309(R) (ORNL-3492(p.143-5))
electron reactions with vacuum-contained, transition radiation from, (E/T), 20: 5008(T) (ORNL-tr-872)
electron relaxation in, theory of, 20: 18016
electron scattering by impurity ions in, anisotropy from, 17: 5282(T)
electron scattering in, theory of, 18: 26212
electron spectra of, in electric fields, (E), 19: 23953(R) (AD-606407)
electron transmission in, (E/T), 20: 7659(R) (ORNL-3849, pp 101-50)
electron transmission in, mean free path of, at 3 ev, 20: 16159(R) (ORNL-3900, pp 150-81)
electron trapping in, photo effects on self, 19: 26917(R) (IA-984)
electron velocity distribution in, 18: 14714(R) (AD-411482)
electronic properties, analysis by cyclotron-resonance methods, 16: 21222
electrons in, self-consistent field theory for, 16: 26015
electrons in, normal-Fermi-liquid theory for, 20: 17993
elementary particle transmission through amorphous, n-state, (T), 19: 45013 (JINR-P-2230)
energy levels in, pseudopotential calculation of, 16: 27820
energy transformations in, method for calorimetric analysis of, 20: 13236 (CEA-R-2797)
enthalpies of surface reactions on, instrumentation for, 20: 16153 (UCRL-16472)
enthalpy of, measurements of, to 2400°C by drop technique, 20: 7114
equation-of-state of, at low temperature, 17: 2941 (IS-359)
equation of state at high pressure, bibliography on, 17: 19929 (UCRL-7160)
equation of state of, temperature-dependent contributions to, 18: 30307 (IS-870)
equation of state of simple, 20: 4476(R) (IS-1200(Sect.P))
equation of state of, properties of, 20: 6533 (NYO-1163-60)
equations of state of, thermal effects on, 19: 9767(R) (IS-900(Sect.P))
evaporation, effects of radioactivity content, 16: 9452
excitations in, review on, 19: 25628
exciton Bose-Einstein excitation in, 16: 24320

fission fragment tracks in, microscopic observations of, 20: 23766 (BNL-9169)
fission-fragment track registration on surfaces of, (E/T), 19: 41138
flow-diverter valve for granular, design of, 20: 22511 (IDO-14666)
fluidization in electrolytes, with crossed electric and magnetic fields, 20: 46442
fracture mechanics of, theory, 19: 9666 (UCRL-11687)
fracture mechanisms in, 17: 433
fracture of, review of time-dependent, 18: 42021 (TID-21107)
fracture stress-grain size relation in brittle, effects of lattice strain on, 18: 8816
free radical determinations at surface of, radiochemical method for, 19: 22130
galvanomagnetic effects in, electron interaction relation to, 16: 24319
gamma absorption, effects of orientation and shape, 16: 5751 (AERE-R-3869)
gamma angular correlation perturbation in, effects of lattice vibrations on, 20: 30762
gamma emission from isomeric nuclei in, (T), 19: 21407
gamma scattering by impurities in, resonance effects, 16: 30982
gamma scattering by, Mössbauer effect in, 17: 9513 (TID-17489)
hardening of crystalline by gas bubbles, semicircular dislocation model for, 16: 16711 (AERE-M-1000)
heat flow in melting, method for calculation, 16: 20610
heat transfer at low temperatures, 19: 33160
heat transfer in crystalline, theoretical analysis of, 17: 8956(T) (UCRL-Trans-832(L))
heat transfer to fluids and gases, thermodynamics of, 16: 10408 (ASD-TR-61-322(p.140-51))
heat transfer to fluidized, from gases, 16: 10147(R) (TID-14825)
heat transfer to fluids in fluidized and packed beds, 18: 35687(R) (COO-774-4)
heat transfer to gases and solids in fluidized and packed beds, 19: 11345(R) (COO-774-5)
heating by electron bombardment, calculation of surface temperature in, 17: 32821
helicon propagation and properties in, (T), 19: 9769 (NYO-2150-3)
high-pressure effects, bibliography and data on, 16: 24115
homogeneity of, x-ray scanning technique for determining, 19: 22514
hydrogen bonding in, lectures on isotope effects on, 20: 30783
hydromagnetic wave propagation in, Alfven and helicon, 18: 42296 (CONF-681-1)
inter-electron coordinates in atomic wavefunctions for, mathematical generalizations of, 18: 30412
interactions in, many-body theory for, 19: 18597
interactions in, morphology of, 20: 5895(R) (TID-22271)
interactions in, quantum-statistical Green-function method for many-body, 19: 23507(T)
interactions of Auger and band electrons in, 19: 6472
ion energy losses in, multicharged, 16: 12295
ion reactions with surfaces of, Auger neutralization in, (E/T), 19: 37219
ion reactions with, studies on, 20: 20121
ion reactions with surfaces of, microbalance for measurement of forces from, 20: 23422 (N-65-33177)
ion reflection from surfaces of, (T), 19: 42990
ion sorption during sputtering, 16: 12280
ion-beam reactions with, diffusion theory for depth distributions from, 20: 20126
ionization energies, 17: 8138(R) (TID-17674)
isotope effects on structural properties, 17: 14291
isotopic diffusion effect in, 20: 3304(T)
krypton-85 absorption by, 18: 12178
krypton-85 absorption by, 18: 12179
laser beam reactions with, plasma production by, 20: 32666
lattice defect mobility in, determination of activation energy using annealing method, 19: 16224(T) (AI-Trans-73)
lattice defects in, diffusion studies of, 19: 45471 (AECL-2309)
lectures on solid state physics, 20: 26345 (NP-16010)
light scattering by, Raman effect in, (T), 19: 27105
light scattering by density fluctuations in, (T), 19: 41971 (UCRL-7968-T)
luminescence, 20: 6551
luminescence in, review of, 18: 16577
magnetic and transport properties, oscillatory effects in high magnetic fields, 16: 15445
magnetic breakdown in, models for, (T), 19: 6383 (NASA-TN-D-2554)
magnetic properties of, theory, 17: 13199
magnetic properties and structure of, 17: 41420(R) (AD-292905)
magnetic properties of, determination by neutron diffraction, 20: 17158(R) (ORNL-3900, pp 82-149)
magnetic properties of, quantum statistical methods for studying, 20: 34864
magnetic resonance of F centers in, model for, 19: 25621(R) (HTRI-1184-16)
magnetic resonance spectrum of F centers in, saturation, 19: 33514(R) (COO-587-17)
magnetic resonance and susceptibilities of two-spin system of magnetic ion-doped, kinetics of exchange-coupled spins in, (T), 20: 26360
magnetic structure of, analytic methods for determining, 19: 9643 (AD-602640)
magnetization measurements using 200-kgauss pulsed magnetic fields, 16: 15456
magneto-optical phenomena in many-electron systems in, perturbation theory for, 19: 40100
mass transfer along temperature gradient in, 19: 38678
mechanical properties of two-phase crystalline, 19: 2741
mechanics of nonlinear, with memory (T), 19: 969 (UCRL-12039)
melting in hot supersonic gas flow, 16: 4287(T) (NP-tr-827(p.27-9))
melting point measurements on, at 800 to 3000°C, 18: 39943
meson (μ^+) stopping in, depolarization and quenching in, (E), 20: 13498
mixing in fluidized-packed beds, particulate movement in, 18: 25658
models for heterogeneous, 18: 16647 (KAPL-M-CHR-7)
moisture measurements in, spin echo spectrometer for, 20: 22867 (INR-619/XV/E)
molecular motions in, review of NMR studies of, 20: 18672
molecular structure of, use of cold neutrons in analysis of, 17: 38916
molecular structure, 20: 6551
Mössbauer dynamics in, 17: 15229
Mössbauer effect in, 17: 41603
Mössbauer effect on impurity nuclei in, 17: 28340
Mössbauer spectra of, nuclear magnetic interaction effects on, (T), 19: 33525
motion in, shock-wave-induced, 16: 19550
neutron diffuse elastic scattering by, diagnostic uses of, (E), 19: 43485
neutron diffusion in, lattice structure effects in, 18: 24577
neutron incoherent inelastic scattering by, 18: 18932
neutron inelastic scattering by, 17: 20967 (STI/PUB/62(Vol.II))
neutron inelastic scattering by, conference on, 19: 45243
neutron inelastic scattering, Cherenkov emission from, 16: 29703
neutron scattering by, conference on, 17: 15228
neutron scattering by, thermal, 17: 36629 (PAN-255)
neutron scattering by, structural research by, 17: 38026(T) (AEC-tr-5734(p.119-39))
neutron scattering by, theoretical study of thermal, 18: 11152
neutron scattering studies of, review, 18: 15312
neutron scattering cross sections of defects in, inclusion of relaxed atoms in calculation of, 18: 42314
neutron scattering by, inelastic, 19: 12468
neutron scattering by, 19: 47889
neutron scattering in, spectra from, (E), 20: 4476(R) (IS-1200(Sect.P))
neutron scattering by, thermal, 20: 8046
neutron scattering in, thermal, (T), 20: 19793
neutron scattering by, molecular motion measurements by, 20: 18674
neutron scattering by, magnetic and thermal property studies from, 20: 34804 (BNL-940, pp 1-7)
neutron spectroscopy of, 20: 32687
neutron thermalization in, 17: 19205 (TID-18432)
neutron thermalization in, approximate models for, 17: 20957 (LA-2834)
neutron thermalization in, Van Hove theory for relaxation times in, 19: 39773
neutron-scattering methods for studies of, low-energy, 20: 34506
nuclear magnetic resonance signals in, shape of, (T), 19: 8422
nuclear magnetic resonance transients in, multiple-phase, (T), 19: 10347
nuclear magnetic resonance measurements in rotating, design of spectrometer for, 20: 28683
nuclear magnetic resonance spin-lattice relaxation in, effects of magnetic field on, (E/T), 20: 34866
nuclear magnetization in, saturation effects of ultrasonics on, 17: 24490
nuclear quadrupole coupling studies in, research program on, 17: 36450(R) (TID-19275)
nuclear quadrupole coupling constants in polycrystalline, determination from nuclear magnetic resonances in, 18: 8351
nuclear quadrupole resonance in, (T), 20: 38019
nuclear relaxation in, lectures on, 20: 30783
nuclear resonances in, design of detector for, 18: 14179
nuclear spin-spin interactions in, NMR theory for, 20: 28618
nuclear spins at lattice sites in, magnetic properties of, 17: 525 (AFCRL-922)
nucleation of precipitates from supersaturated solutions of, review on, 19: 47025(T) (ORNL-tr-637)
nuclei in, internal fields acting on, 17: 13480 (AFOSR-2929)
paramagnetic relaxation in, method of determining, 19: 11046(R) (AROD-2099:22)
particle spin systems in, modified Bloch equations for, 18: 10792
particle spin-spin interactions in, statistical theory of, 18: 30330

performance as working media in nuclear gyroscopes, (T), 19: 20279 (RTD-TDR-63-4001)
perturbation theory for, 16: 31183
perturbations of quadrupole couplings in molecular, physical origins of, 18: 37133
phase studies, hysteresis of contact angles in systems with liquids, 16: 30790(R) (MITS-48)
phase transitions of repulsive lattice gas models, 20: 4708(R) (UCRL-14360, pp 50-73)
phonon-phonon interactions in Bose systems, 17: 11411
phonon scattering in, (T), 18: 26212
photon emission from irradiated, 16: 1941(R) (ORNL-3189(p.140-54))
photon interactions in, properties of, (T), 19: 47332
photon reactions with, magnetic and thermal property studies from, 20: 34804 (BNL-940- pp 1-7)
photon-electron interactions in, "photon-drag" effect in, 18: 21407
photonuclear reactions in, range of recoil atoms from, (E), 20: 30479
physical properties, sonic study, 16: 25547 (AROD-2302.8)
physics of, neutron spectroscopy in, 16: 14043
physics, research program, 16: 2300(R) (TID-14182)
plasma characteristics and occurrence in, 18: 13168
plasma effects in, 19: 21792(R) (ORNL-3650(p.187-219))
plasma instabilities in, (T), 19: 19321
plasma interactions and oscillations in, review on, (T), 19: 18525
plasma waves with mass anisotropy in, amplification of, 20: 22342
pore size distribution in, measurement from nitrogen adsorption data, 17: 1422 (TID-17044)
positron annihilation in, effects of lattice vibrations on, 18: 10571(R) (AD-409118)
positron annihilation in, physics of, 20: 32101
positron lifetimes in, 17: 26384
positron reactions with, review of properties from, 20: 19460
pressure-temperature-volume measurements on, 17: 22268 (IS-409)
properties above 1500°C, review on physical, 18: 37693
properties and structure of non-crystalline, 16: 15199(R) (TID-15403)
properties and use as track detectors, 20: 7375
properties at high temperatures, bibliography on, 20: 43903 (NP-16238)
properties of electro-optical, in logic circuits, 19: 23164(R) (SU-SEL-64-103)
properties of geometric, computer program for calculating, 20: 3633 (SC-TM-64-1686)
properties of magnetic and nonmagnetic, low-temperature, (T), 19: 23590
properties of nonmetallic, research on, (E/T), 19: 38027(R) (ORNL-3841)
properties of, reactor research on, 17: 35189
properties of system of Fermi-Dirac particles, 16: 11856 (NP-11386)
properties of, use of low-power reactors in studying, 17: 35188
properties of, high-pressure Mössbauer studies of, 19: 38025 (COO-1198-266)
properties of, research on, 19: 41967(R) (MIT-QPR-57)
properties of, research on, 19: 41678(R) (PR-P-65)
properties of, theory for, 20: 26053
properties of, ultrasonic determination of, 19: 25071(R) (TID-21667)
properties of, use of Mössbauer effect in study of, 18: 10646
properties under high pressures, measurements using time-of-flight neutron diffractometers, 19: 45476 (IDO-17106)
proton channeling in crystalline, transverse two-dimensional model for, (T), 20: 12279 (UCRL-12311)
quantum cell model for, 19: 15484
quantum theory of, group theory in, 18: 26438
quantum theory review, 16: 15367
radiation chemistry of inorganic, 20: 7131
radiation damage, analysis of annealing processes, 16: 6497
radiation damage by high-energy particles, statistical theory, 16: 24256
radiation damage by neutrons, relations with dosage, 17: 12554 (CEA-2206)
radiation damage, conference summary, 16: 24251
radiation damage in, 17: 8878 (BNL-6051)
radiation damage in, conference on, 18: 30266
radiation damage in, theory for, 18: 30273
radiation damage in, atomic processes in, 18: 30275
radiation damage in, 18: 32247
radiation damage in, diffusionless self-annealing of, 19: 998(R) (ORNL-3676(p.12-23))
radiation damage in, bibliography on Soviet bloc studies of, 19: 14081 (ATD-P-64-50)
radiation damage in, review of theory of, 19: 37174 (ORNL-P-1481)
radiation damage in, lectures on, 20: 30784
radiation damage mechanisms in, 18: 30251
radiation damage tracks in, research on, 19: 39226(R) (AFCRL-65-305)
radiation displacement of atoms in, Auger effects on, 16: 13659
radiation effects on reactions with gases or liquids, 16: 7577 (AERE-M-742)
radiation effects, 16: 12187
radiation effects, energy considerations for neutron, 16: 12186(T) (NP-tr-861)
radiation effects in, studies using 100-kev heavy-ion accelerators, 16: 18092
radiation effects of nuclear radiation and charged particles, 16: 22702
radiation effects, distribution function of displaced atoms, 16: 22816
radiation effects at high energies, 16: 27711
radiation effects, survey, 16: 29464
radiation effects on chemical reactivity of surfaces, review, 16: 31664
radiation effects on, conference on, 16: 33547
radiation effects of nuclear radiation and charged particles, 16: 33525(T) (AEC-tr-5365)
radiation effects of corpuscles on properties, review, 17: 2014
radiation effects on surfaces of, 17: 3545
radiation effects on surfaces of, 17: 3546
radiation effects on crystalline, 17: 4249(R) (NAA-SR-7400(Sect.VII))
radiation effects on, review, 17: 13201
radiation effects on, review, 17: 17645
radiation effects in, correlative collision processes and production of, 17: 22228 (ZFK-WF-15)
radiation effects on, review, 17: 22239
radiation effects on thermal decomposition of, mechanism of, 17: 31035
radiation effects on properties of, neutron, 17: 32694
radiation effects on, conference, 17: 34512
radiation effects on, theoretical consideration of, 17: 36215
radiation effects on magnetic susceptibility of inorganic, 17: 37575(T) (FTD-TT-63-424)
radiation effects on, beta, 17: 39130
radiation effects on absorption and catalytic characteristics of, 17: 39131
radiation effects on, conference on, 18: 2365
radiation effects on, method of describing, 18: 13478
radiation effects on diffusion in, 18: 16543
radiation effects on, atomic collisions in crystals during, 18: 42140
radiation effects on volatility of, sputtering effects of recoil atoms in alpha, 18: 44271
radiation effects on Frenkel-pair densities in, 19: 1020
radiation effects on, electron spin resonance studies of, 19: 366
radiation effects in crystalline, theory of displacement damage, 19: 11815
radiation effects on, theory of, 19: 11236
radiation effects on crystal structure of, reactor irradiation facilities and techniques for studying, 19: 12853
radiation effects on crystal structure of, neutron scattering studies of, 19: 12469
radiation effects on, roles of channeling and range-of-primary in, 19: 11237
radiation effects on reactivity and catalytic activity, 19: 15630
radiation effects thresholds, 19: 16242
radiation effects on, (T), 19: 23157
radiation effects on, annealing of, 19: 30266
radiation effects on, defect structure and saturation from, 19: 41102
radiation effects on, thermal, 20: 2427 (NASA-SP-55)
radiation effects on, analysis of atomic-beam, (T), 20: 7721 (RISO-115)
radiation effects on, review of, 20: 9019
radiation effects on crystal structure and properties of, review of, 20: 15139
radiation effects on, with surface-sorbed gases, 20: 17158(R) (ORNL-3900, pp 82-149)
radiation effects on, research summary, 20: 19273(R) (BNL-929, pp 3-43)
radiation effects on, neutron, 20: 33952
radiation effects on catalytic properties of, 20: 40989
radiation effects on phase transformation points in polymorphic, thermodynamic calculation of, 20: 45034
radiation effects on, review, 20: 46223 (BNL-10543)
radiation effects on diffusion in, fast neutron, 20: 46224 (BNL-10560)
radiation effects on inorganic, review of, 20: 46944
radiation effects on, in space, 17: 34523
radiation emission from nuclei in, energy distributions, 16: 12517
radiation enhanced diffusion in, effects of correlated defects in gamma-, 20: 17131
radiation hardening, 16: 30895 (BNL-5120)
radiation scattering and slowing-down in, 17: 618
radioactivity changes in, in closed liquid-solid system, equipment for continuously measuring, 19: 26456
radioactivity used to determine surface area of, 18: 30079
radiographic studies of, 19: 9348(T) (FTD-MT-63-261)
radioinduced atomic cascades in, integral equation for distribution function of, 20: 36367
radioinduced coloration in, gamma, 16: 21099
radioinduced color centers in, research progress on x, 18: 20627(R) (NP-13815)
radioinduced damage in, step annealing of, 20: 5580
radioinduced decomposition of, review on, 18: 43604

radioinduced defects in, cascade theory for calculation of number of, 17: 12733
radioinduced defects in, fast-neutron, 19: 991 (CEA-R-2510)
radioinduced defects in, scattering law for, 20: 4473
radioinduced defects in, model for change in elastic modulus from, 20: 37296
radioinduced elastic explosions in, laser and neutron beam, (T), 20: 30740
radioinduced faults in, calculation of spatial distribution with rigid sphere approximation of, 17: 14904
radioinduced faults in, review of theories and experimental results on, 17: 18873
radioinduced faults in, review of theoretical and experimental results on, 17: 20521
radioinduced faults in, review of theoretical and experimental results on, 17: 27906
radioinduced free radicals in, ESR studies on, 20: 20729 (PB-181506, pp 85-103)
radioinduced lattice defects in, effects of thermal peaks on, 19: 16227
radioinduced polymerization of monomers in, 20: 9013
radioinduced swelling by gases, theory of, 19: 23130
radioinduced transmutation in, crystal structure effects from, 18: 17909
radiolysis of ionic, 20: 23165
radiolysis of, review of heavy-particle, 18: 13829 (AERE-R-4505)
radiolysis of, review of mechanisms in, 20: 40987
reactions of, performance of plasma bed for chemical, (E), 19: 17151
reactions of, studies of geometric factors in surface, 19: 12882 (TID-21573)
reactions with gases, review of, 18: 8374
reactions with gases, effects of diffusional control on, 18: 13728 (TRG-Report-708)
reactions with gases in fluidized beds, hydrodynamics of, 18: 16135
reactions with gases, role of chemisorption in, 18: 25033(T) (SC-T-64-901)
reactions with gases, apparatus for, 19: 24533(P)
reactions with gases, thermobalance for studying, 19: 24491
reactions with gases, apparatus for continuous two-step, 19: 44042(P)
reactions with gases, potential energy curves for, 20: 40796(R) (IS-1500(Sect.C))
reactions with rare gases, 16: 31720
reactive diffusion characteristics, tracer study, 16: 4426(T) (OTS-61-21970)
reactivity of, conference on, 20: 28684
recoil atoms in, mechanisms of annealing reactions of, 17: 35867 (BNL-7135)
recoil reactions induced by thermal neutrons in, review, 19: 13498
reduced matrix element of an irreducible spherical tensor operator for, derivation of, 20: 1329
representations of systems of dipoles and ions, classical theory, 16: 26019
research, 20: 20114(R) (ORNL-3935)
research at JEEP reactor facility, 20: 20332
research programs in, summaries of USAEC, 18: 9766 (TID-4005 (Pt.1, 7th Ed.))
research programs in, summaries of USAEC, 19: 8713 (TID-4005(Pt.1, 8th Ed.))
response to impulsive pressure-point source in fluid, transient, 18: 2394 (AD-422046(p.1-37))
rotational degrees of freedom in, 19: 1051 (NYO-2391-3)
sampling of, coring techniques and equipment for, 19: 24640 (BNWL-66)
scattering by, law for, 17: 41566(T) (EURAEC-779)
Schroedinger equation for a periodic lattice, solution of, 16: 18251
second sound in, 17: 34604
separation from liquids, engineering drawings of drum filter for continuous, 20: 220
separation of particulate, from gases, 18: 5455(P)
shock front position measurement in, 18: 30314 (UCRL-7449)
shock front position in, method for continuous measurement of, 18: 34357
shock propagation in, profiles for, (T), 20: 41513(R) (UCRL-14744, pp 19-36)
shock wave production in, explosive system for, 18: 7997 (SC-4967-(RR))
shock wave propagation in, rigid-locking, 17: 2081
shock wave propagation in, bibliography, 17: 41554 (NP-13166)
shock wave research on inert, review, 20: 7960 (LA-DC-7462)
sorptive properties of, automatic apparatus for gravimetric measurement of isotherms for, 18: 214(T) (NP-tr-1064)
sorptive properties for gases in ultrahigh vacuum, (T), 19: 17919
sound wave detection and generation in, ultra-high-frequency, 16: 23970 (ANL-6515(p.117-20))
specific heat at low temperatures, 18: 9281
spectra, development of cell for determination of infrared, 16: 22054 (TID-15918)
spectra of molecular, theory of lattice combination bands in, 17: 8057
spectra of, theory of thermal-emission, 17: 31009
spectra of, theory for Raman, 19: 44039
spectral lines in, phonon broadening of, (T), 19: 43500
spin wave scattering in, theory of, 18: 26212
sputtering by ion bombardment, review of, 19: 20819
sputtering by rare-gas ions, tracer studies of angular distribution of yields from, 16: 31729
statistics of assembly of quasiparticles in, (T), 19: 23188
stress distribution in elastic, boundary value problem for, 19: 38029 (SC-RR-65-307)
stress disturbance propagation in elastic deformable, 20: 31331 (UCRL-14616)
stress wave transmission between liquid and visco-elastic Voigt, 16: 6804 (NP-11218)
stress waves in, calculation of, 17: 18911 (UCRL-7271)
stress-relaxation analysis of, creep laws for, (T), 20: 33894
structure of, neutron spectroscopy for determining, 20: 20164
surface area measurement from gas adsorption, computer program for, 19: 2724 (NAA-SR-Memo-10209)
surface area measurements on, using krypton-85, 20: 31353
surface variations of irradiated, photogrammetric techniques for measuring, 20: 9123
surface wave spectrum of monatomic square lattice, effects of impurity layer, 16: 13784
suspension in liquids in tanks by impellers, 19: 36576 (TID-22073)
suspension in liquids by impellers, effects of particle shape on, 19: 36577 (TID-22074)
suspension in liquids by fan turbine impellers, 19: 36578 (TID-22075)
suspensions preparation using glass-water systems, conditions for, 16: 3102(R) (TID-14229)
swelling of, theory of coalescence of gaseous pores in gas-induced, 18: 8820
temperature distribution in, analog computation of, 17: 8319 (ANL-6645)
tensile properties of, review on, 20: 4399 (UCRL-16301)
theory, 19: 39263 (CONF-796)
theory, vacancy interstitial annihilation with interstitial trapping at impurities, 16: 9315
theory, vacancy interstitial annihilation with di-interstitial formation, 16: 9316
thermal analysis of, computer codes for, 19: 24669 (LA-3264)
thermal capacity and conductivity of, flash method of measuring, 17: 11200 (USNRDL-TR-599)
thermal capacity and expansion of, effects of pressure on, 18: 3435(T) (UCRL-Trans-997(L))
thermal capacity and conductivity of, nonlinear estimation method for transient determination of, (T), 20: 27522
thermal conduction in, 17: 21882(T) (NP-tr-997)
thermal conductivity of anisotropic, at high temperatures, 17: 6640 (ASD-TDR-62-608(Pt.I))
thermal conductivity measurement of anisotropic, at high temperatures, 17: 16678
thermal conductivity measurement in irradiated, apparatus and techniques for, 19: 18238 (WAPD-291)
thermal conductivity of, effect of heat transport by radiation on, 20: 22329
thermal decomposition of, application of activated complex theory to, 18: 36900 (UCRL-10791)
thermal diffusion in, using flash-diffusivity technique, 20: 4310(R) (ORNL-P-1699)
thermal expansion coefficient at low temperatures, 16: 2302 (TID-14230)
thermal expansion of, theory for, 18: 44219
thermal properties in space, 17: 34523
thermal radiation properties of, conference on measurement of, 18: 5807
thermionic emission from, effects of band structure on, 17: 11336 (UCRL-6820)
thermodynamic function calculation from dissociation-pressure data, 17: 6108
thermodynamics of interstitial solutions of, with repulsive solute-solute interactions, 17: 39609
thermoelectric properties, 16: 18141(R) (AD-266220)
thermomagnetic wave propagation in, (T), 19: 11849
thickness measurements on, by gamma and x-ray backscattering, 19: 16230
transport equations for electrons in, using "Fermi liquid" theory, 16: 29544
transport of particulate, in fluidized-packed beds, 18: 43706(R) (ANL-6800(p.197-296))
ultrasonic waves in, properties of finite-amplitude, 19: 39268 (ORNL-P-1395)
ultrasound wave propagation in, theory, 18: 45180 (SC-DC-64-1453)
uranyl-ion energy levels in ionic, 18: 29606(R) (RTD-TDR-63-4110)
vacancy introduction into crystalline, at high concentrations, 16: 24309
vapor pressure of porous, measurement by Knudsen effusion method,

17: 27341
vaporization, mechanism study, 16: 19472(R) (RAD-TR-62-19)
wave propagation in, research programs on, 19: 32048(R) (NP-15073)
work-hardening mechanisms in crystalline, 16: 15187 (NAA-SR-6481)
gas–solid, circulator design for suspensions of, 18: 27674
gas–solid, efficiency as working fluid in Brayton cycle, (T), 20: 16606(R) (TID-22621)
gas–solid, flow and heat transfer in turbulent suspensions, 20: 484(R) (TID-22282)
gas–solid, flow in pipes, 20: 41102 (NYO-2930-6)
gas–solid, fluid mechanics and heat transfer in turbulent suspensions of, research program on, 19: 40742(R) (TID-22002)
gas–solid, fluidized bed contacting method for, 19: 12889(P)
gas–solid, phase equilibria in binary, at low temperatures, 16: 32248
liquid–solid, thermodynamic consistency tests for phase equilibrium in, 19: 42958
Solochrome Violet RS
see Benzenesulfonic Acid, 4-Hydroxy-3-(2-Hydroxy-1-Naphthyl)Azo-
SOLUBILITY
calculation of crystalline, 20: 7110
constants for metal oxides and hydroxides in aqueous solutions, review of, 17: 25230
determination of, in two-phase systems, 17: 7996 (MATT-148)
determination of small, radiochemical, 16: 23706
determination of terminal, of gases in metals, high-temperature technique for, 20: 31250
effects of radioisotope tracers on, 17: 28787
effects of, on local tissue dose from strontium-90, 20: 43631
equipment for study of high pressure and temperature, 16: 372
measurements for radioactive materials at high temperatures and pressures, equipment for, 18: 8341
of radioactive aerosols, 19: 26455
radiation effects on polyacrylamide, electron, 20: 18779
SOLUTIONS
acidity of aqueous, control device for, 19: 23163(R) (ORNL-3650(p.111-86))
activities in liquid oxide systems, isopiestic method for determining, 19: 26296 (USNRDL-TR-823)
activity and osmotic coefficients from isopiestic data, computer program for cladding, 19: 5844 (ORNL-3720)
activity profile of radiochromatograph of radioactive, method for analyzing, 20: 20559 (EUR-2626.f)
alkaline, radiation chemistry, 17: 27180
analysis by beta backscattering, equipment for, 20: 26784
analysis by emission spectroscopy, review, 16: 7502
analysis by x-ray fluorescence spectrography, 20: 33148 (EUR-2951.f)
analysis for acetone and 2-butanone in aqueous, by gas chromatography, 20: 18572 (PG-Report-690)
analysis for acidity, titrimetric, 20: 43071 (IDO-14679, pp 75-191)
analysis for complex compounds by partition method, 16: 25368
analysis for elements, design of beta-gamma photometer for, 17: 21629
analysis for fluorides by automated colorimetry and pyrohydrolysis, 20: 12765 (DP-1004)
analysis for plutonium and uranium using gamma absorption, 20: 36767
analysis for radioisotopes by copper-spark spectrography, 16: 16306 (PAN-250/XIII)
analysis for radioisotopes by least-squares resolution of gamma spectra, 20: 36780
analysis for sulfate ions using kryptonated barium carbonates, 20: 18570(R) (NYO-2757-5)
analysis for sulfur in aqueous, activation, 20: 16331 (GA-6568)
analysis for tungsten by gamma absorption, 20: 33186(T) (AEC-tr-6639, pp 126-30)
analysis for uranium, fluorometric, 18: 17745
analysis of aqueous, by beta backscattering, 17: 30115
analysis of aqueous, scintillation radiometric, 18: 8301
analysis of aqueous, for organically bound iodine by neutron activation methods using freezing, 20: 45602
analysis of flowing, polarographic cell for continuous, 18: 3428 (TID-19732)
analysis of fuel-element descaling, methods for, 19: 7274(R) (IDO-14636)
analysis of industrial, quantometric and spectrographic, 18: 19910
analysis of plating, potentiometric, 19: 24611(R) (MLM-1227)
analysis of, technique for spectrographic, 17: 10952
analysis of, use of beta radiation for concentration measurements in, 17: 18111(T) (AEC-tr-5707)
analysis of, x-ray-spectrometric, 17: 40762
book: *The Radiation Chemistry of Water and Aqueous Solutions*, 16: 249
boundary localization between radioactive and inactive, radiometric, 19: 13715
capillary ripple propagation in surfaces of organic acid, 19: 4175 (IS-855)
chemical reactions in, review of fast, 19: 365
chemistry of nonaqueous, coordination model of, 18: 13606 (TID-20241)
composition of scintillation, for measuring tritiated water in soils, 18: 23419
concentration measurements using beta radiation, 16: 13458(T) (AEC-tr-4492(p.254-8))
concentration measurement of, a-c bridge for, 20: 18573 (RISO-120)
concentration of dilute aqueous heat-labile, design of vacuum distillation system for, 18: 23445 (K-1594)
concentrator for, design of, 19: 29826(P)
conference on electronic and atomic structure of metallic solid solutions, 19: 16185
control of pH of unbuffered, apparatus for, 18: 6787 (CONF-202-4)
conversion of radioactive salt, into compact solids, 17: 4620(P)
counting aqueous radioactive, Cherenkov detector for, 19: 23991(R) (ANL-7003)
critical state of aqueous, studies, 19: 17863(T) (AI-Trans-76)
decontamination from phosphorus-32 by ion exchange, 20: 10780
decontamination of aqueous, use of silica gel for, 20: 1742 (INR-636/XIII/J)
density measurements of, using radioisotopes, 19: 24896
density of, radiometric measurements of, 19: 24898
diffusion of radioisotopes in dilute, methods of measuring coefficients for, 19: 396
dispensing of radioactive, for liquid scintillation counting, 19: 30514 (AERE-M-1574)
distillation of, with thermally labile solutes, engineering drawings of vacuum system for, 19: 4165
effect of OH radicals and H atoms on, comparison with x-ray effects, 17: 10717
electric conductivity of aqueous, effects of high pressures and temperatures on, 19: 23163(R) (ORNL-3650(p.111-86))
electric conductivity of acidic aqueous, role of Grotthuss mechanism in, 20: 340
electric conductivity in radiochemical processing plants, instrument for measuring, 20: 12927 (NP-15756)
electrochemical processes in irradiated, 17: 196
electrochemistry of double layer at interface between mercury and aqueous, 18: 8322 (IS-598)
electrokinetic theory, 16: 26970(T) (NP-tr-914)
electron binding in aqueous, model for, 18: 25577
electron exchange in ionic, conductance mechanism in, 20: 8957
electron transfer reactions in, bridging group functions in, 17: 35675 (BNL-6561)
entropies of ions in aqueous, at 25 to 200°C, 19: 7380
evaporation of radioactive, design of apparatus for, 18: 12167
excitation, design of stable plasma jet for, 16: 8691
fluorescence of, energy transport phenomena in, 17: 12812
fluorescence of, relation to absorption and emission energy spectra, 17: 12811
hydrogen atom trapping in frozen gamma-irradiated, effects of oxyanions on, 19: 44054(R) (COO-1365-7)
ion charges in, tracer studies of diffusion coefficients for estimating average, 19: 2285
ion properties in, hard-sphere model for determining, 18: 12069
ion transport in aqueous, isotope effects in, 19: 46898 (HMI-B-44)
ion-solvent interactions in concentrated electrolyte, method for studying, 18: 10035 (CONF-387-1)
ionic solvation in, theory, 19: 36328 (AD-607805)
kinetics and structure of ammonia–metal, 20: 31218(R) (UCRL-16658, pp 1-9)
level control of radioactive, in electronic boiling-down, 17: 4783
luminescence, resonance transfer of excitation energy in, 16: 15280(T) (AEC-tr-5067)
measurement of variations in concentration of, radiometric instrument for, 20: 23431(T) (AEC-tr-6466/1, pp 245-8)
metering radioactive, design of flowmeter for, 20: 39172
mixing during stable and unstable flow, 19: 5896
osmotic coefficients of organic compound, for use as isopiestic reference solutes, 19: 4250(R) (ORNL-3627(p.177-208))
osmotic coefficients and water activities for electrolytes in aqueous, molal, 19: 36331 (IA-1009)
pH adjustments in small volumes of, 18: 1325(R) (UCRL-10934)
phase diagram and thermodynamic properties of isotopic, 17: 23330
phase diagrams of, book, 19: 14061
photo- and radioluminescence of, fast electron excitation quenching in, 18: 31561
photochemical bleaching in frozen aqueous, at 77°K, 19: 7574
photolysis and radiolysis of aqueous, solvated electron conversion into hydrogen atoms in, 17: 8170
polarization of light in mixed, effects of electromagnetic fields and gravity on, 16: 29493(T) (UCRL-Trans-841)
precipitation of metal chelates from homogeneous, review of, 18: 1821

preparation of radioactive standard, of very low volume activity, 17: 25876
properties of aqueous, chemical research on, 19: 23163(R) (ORNL-3650 (p.111-86))
properties of inorganic salts, in dimethyl sulfoxide, 20: 293 (UCRL-16330)
properties of nonaqueous, thermodynamic and transport, 17: 17951(R) (TID-18349)
radiation and hot-atom effects on, bibliography on, 19: 7535 (AD-443451)
radiation chemistry of aqueous, at high intensities, 16: 30479
radiation chemistry of aqueous, effect of acidity on hydrogen yield, 17: 34034
radiation chemistry of aqueous, calorimeters for study of, 18: 20083
radiation chemistry of aqueous, effects of acidity and oxygen on, 18: 25580
radiation chemistry of aqueous, structural model of hydrated electron in, 20: 43322
radiation effects on solutes in dilute, 17: 8504
radiation effects on rabbit reaction to physiological, x, 19: 3959
radiation effects on charge-transfer reactions in frozen acidic, ultraviolet, 19: 22329
radiation effects on buffer, virus inactivation by, 19: 28027
radiation effects on dilute aqueous, review on mechanism and rate of, 20: 390
radiative processes in aqueous, formation of compounds of bound nitrogen by, 20: 25160
radical capture in irradiated aqueous, effects of temperature on, 18: 1487(R) (HW-77609(Sect.3))
radioactive, monitoring equipment for circulating, 20: 38558
radioinduced free radicals, H atoms, and solvated electrons in aqueous frozen, 18: 39344
radioinduced ionization of aqueous, model for radical reaction mechanisms in, 20: 31293
radioinduced oxidation of components of aqueous, chain mechanism for, 19: 508
radioinduced reactive species in, 19: 468
radiolysis of alkaline and neutral aqueous, role of hydrated electrons in, 19: 28396
radiolysis of aqueous, 16: 7579 (PAN-259/CHR)
radiolysis of aqueous, reactions of hydrated electrons in, 17: 39098 (CONF-224-5)
radiolysis of aqueous, model for radical recombination in electron and gamma, 17: 40895
radiolysis of aqueous, diffusion kinetics in, 18: 8408(R) (TID-20006)
radiolysis of aqueous, effects of radical acceptor concentration on yield of molecular products in, 18: 12170
radiolysis of aqueous, gamma, 18: 22155
radiolysis of aqueous, reactivities of hydrated electrons and hydrogen atoms formed in, 18: 31563 (AD-429919)
radiolysis of aqueous, properties of reducing component produced in, 18: 39311
radiolysis of aqueous, interphase phenomena in, 19: 503
radiolysis of aqueous alkaline solutions, 19: 511
radiolysis of aqueous, use in absorption spectroscopy in study of, 20: 63(R) (STI/DOC/10/42, pp 45-55)
radiolysis of aqueous, review on, 20: 7132
radiolysis of aqueous, energy releases in reactions following, 20: 9008
radiolysis of aqueous, reactions of hydrated electron with water in pulse, 20: 10894
radiolysis of aqueous, research progress on, 20: 38939(R) (NYO-2668-13)
radiolysis of concentrated aqueous, 19: 501
radiolysis of dilute inorganic, 18: 20037 (BNL-6978)
radiolysis of, effects of pH on radical yields in, 17: 4614
radiolysis of frozen aqueous, 17: 30606
radiolysis of frozen, formation of solvated electrons in gamma, 19: 40551 (KFK-293)
radiolysis of inorganic and organic, production of transient species in pulse, 20: 26991
radiolysis of neutral, effects of atomic chlorine radicals on, 19: 424(R) (HW-81746(p.3.103-5))
radiolysis of, effects of temperature on radical-capturing reactions in, 19: 425(R) (HW-81746(p.105-7))
radiolysis of, electron spin resonance studies of free radicals formed in, 19: 516
radiolysis of, energy localization in, 18: 10140 (UJV-969/63)
radiolysis of, review of research on pulsed, 19: 365
radiolysis of, spectra of yields in electron, 18: 35593 (UJV-1075/64)
radiolysis, spectrophotometric and polarographic studies of, 18: 37169 (A/CONF.28/P/112)
radiolytic oxidation in aqueous, effects of osmium tetroxide on, 20: 18790
rate constant measurements for reactions of free radicals with solutes in aqueous, 19: 19968
relaxation effects, in aqueous solutions of hydrated metal ions, 16: 180
research program on electrolytic, 19: 34142(R) (NYO-2873-7)
research program on nonaqueous ionic, 20: 1565(R) (RPI-1999-6)
separation of cesium-137 from aqueous, by flotation, 20: 16392
separation of radioactive ions from, method for, 20: 41058(P)
solvent activity in very dilute, test of laws of, 18: 35500 (LA-2997)
sorption of ions at ionized surfaces of, studies using recoil atoms, 18: 5278
sorption of ions from, by alumina, alumina–silica, and silica gel surfaces, 19: 42200 (COO-1354-5)
specific activities of, problems of measurement of low, 17: 202
specific activity of, determination of low, 17: 203
specific gravity of, automated equipment for measuring, engineering drawings of, 20: 16801
spectra of dilute, double-resonance effects and saturation in ESR, (T), 19: 42490
structure of, as applied to charge migration and excitation energy, 19: 411
theory of conformal, use of Morse potential function in second-order, 19: 24488 (TID-21840)
thermal capacities of ions in aqueous, at 25 to 200°C, 19: 7381
thermal conductivity, 19: 28337
thermodynamic properties of aqueous, principle of entropy correspondence for evaluating, 19: 7382
thermodynamics of, theory of Ludwig-Soret effect in, 18: 8488(T) (AEC-tr-6282)
thickening mechanisms, 16: 30790(R) (MITS-48)
transfer, air lift performance at low liquid rates using oversized piping and lateral runs, 16: 1908 (IDO-14561)
transport properties of, research program on, 17: 17953(R) (TID-18448)
transport properties of concentrated electrolyte, 19: 43997(R) (UCRL-11889)
vapor pressure of aqueous, apparatus for measurement of, 17: 33856 (AERE-R-3565(Rev.))
velocity, temperature, and magnetic field strength of dimensionless, 17: 30673
x-ray absorption analysis of, use of beta-excited sources in, 20: 33235

SOLVATION
effects of ionic, on activity functions, 16: 14378(R) (NYO-2302)
in solvent extraction, isopiestic method for determination of, 17: 14387
ionic, isotope effects on, 20: 18643
measurement of level of, by polytherm method, 19: 550
mechanism of selective, in mixed solvents, 20: 2520(R) (IA-920)
of ions, relations with geometric effect at solution-surface interface, 19: 9130
radioinduced electron, in alkali metal hydroxides, 17: 35904
states of *tert*-butyloxonium cations, 20: 23044(R) (MIT-905-52)

SOLVENT EXTRACTION PROCESSES
see also Separation Processes
see also Solvent Partition
amine hydrochloride distribution in aqueous and organic phases of, 19: 5569(R) (MIT-2098-64)
analytical control by gamma monitoring and uranium colorimetry, 16: 1988
analytical control, 16: 4138 (PG-Report-280)
behavior of actinides and fission products in tributyl phosphate and di-2-amyl 2-butylphosphonate, in short-residence contactors, 19: 40645 (CONF-650918-1)
behavior of di-*n*-butyl phosphorothioic acid in, for metal ions, 17: 27408
behavior of dialkyl phosphorodithioic acids in, 17: 27407
behavior of heavy alkylammonium salts in, 20: 24351(R) (MIT-905-52, pp 1-41)
bibliography and review on, 19: 4263
bibliography on solvent extraction systems of cations with organic ligands, 16: 268 (LS-71)
book: *Chemistry of Extraction Processes*, 16: 27131(T) (OTS-61-31210)
book: *Extraction, Theory, Applications, and Apparatus*, 17: 12374
book: *Extraction: Theory, Applications, and Apparatus*, in Russian, 17: 14398
book: *Rare Metal Extraction by Chemical Engineering Techniques*, 18: 13952
book: *Separation of Heavy Metals*, 16: 8822
book: *The Solvent Extraction of Metal Chelates*, 19: 13262
calculations in, review of computer programs for, 19: 24614 (TRG-Report-902)
cascade stagewise conditions for separation of rare earths by TBP, calculation, 18: 20098 (IS-780)
centrifugal contactor for, engineering drawings for multi-stage, 18: 41589
chemistry of metallurgical, inorganic, 18: 3905
coalescence in, mechanisms of and radiation effects on, 19: 4254(R) (ORNL-3627(p.235-46))
coalescence times of streams containing surfactants, design of remotely

operated tester for evaluating, 16: 13140
colloquium. "Extractions in Nuclear Technology," Kowary, Poland, September 1961, 16: 13142
column operating parameters for, tables for calculating, 20: 35581 (ANL-7165)
column performance for uranium–thorium separation using di-*sec*-butylphenylphosphonate, 19: 9252 (ORNL-3732)
concentration changes in Nth vessel of series, nomograph for, 19: 2466 (HW-SA-3261)
contactor development for, using stacked clones, 17: 21594(R) (ORNL-TM-355)
contactor for, development of stacked-clone, 19: 23163(R) (ORNL-3650 (p.111-86))
contactor for, performance of stacked-clone, 20: 9053(R) (ORNL-3830, pp 252-60)
contactor for, performance of stacked-clone, 20: 12928(R) (ORNL-3868)
contactors for spent fuel, development of, 20: 9044(R) (ORNL-3830, pp 30-68)
corrosion of construction materials in reactor fuel reprocessing, 18: 8761
cost estimates for sodium-graphite reactor fuels, 16: 4225 (NAA-SR-Memo-1035)
countercurrent liquid-liquid, with 8-hydroxyquinoline, for determination of trace constituents in sea water, 19: 28253
countercurrent, design of column for fuel processing by, 19: 22446(P)
decomposition of TBP in post-extractive operations, behavior of products from, 18: 6897
decontamination factors in Eurochemic, 18: 39379 (NP-13396)
decontamination factors in Eurochemic flowsheet, tests, 19: 5993 (NP-14447)
degradation of TBP-odorless kerosene solvent in, 18: 6900
description of Windscale, 18: 13955
description of, for reprocessing of thorium fuels, 19: 30324 (ORNL-TM-1139)
description of, for short-lived isotopes, review of, 20: 20826
design for molybdenum in nitric acid solutions, 19: 24632(P)
design for reactor fuel processing, 19: 24633(P)
design for reactor fuels processing using TBP, 19: 38776(P)
design for separating hexavalent uranium from solutions containing beryllium, 20: 9089(P)
design for uranium and/or vanadium in aqueous solutions, 20: 5605(P)
design of amine–ether, for recovery of metal values from aqueous acidic solutions, 20: 12941(P)
design of carbon tetrachloride–TBP, for fuel processing, 18: 37256 (A/CONF.28/P/344)
design of thiocyanate, for beryllium in aqueous solutions, 20: 1974(P)
design using high-voltage electric fields, 19: 28458(P)
development, 16: 7475(R) (ORNL-TM-81)
development, 16: 10102(R) (ORNL-TM-65)
development, 16: 25085 (JAERI-7022)
development, 17: 39185(R) (ORNL-3452(p.168-88))
development, 18: 8454
development, 20: 20365
development, 18: 34007(R) (ORNL-TM-890)
development at Windscale, 18: 37254 (A/CONF.28/P/160)
development at Windscale, 18: 37255 (A/CONF.28/P/161)
development for coextrusion of cerium and thorium by DAMPK and TBP, 18: 37265 (A/CONF.28/P/455)
development for fission products and metals using stearic acid, 17: 21789
development for fission products, 18: 37270 (A/CONF.28/P/512)
development for fuel processing, 19: 23163(R) (ORNL-3650(p.111-86))
development for fuel processing, review, 19: 34283
development for metals using alcohol mixed with compound having higher dielectric constant, 16: 27151(P)
development for plutonium recovery from neutron-bombarded uranium fuel, 16: 13164(P)
development for plutonium and uranium recovery from spent fuels, 20: 4048(R) (NP-15406)
development for plutonium determination in irradiated uranium fuels, 20: 12811
development for processing spent reactor fuels, 17: 10743(R) (ORNL-TM-457)
development for preparation of IMC strontium-90, 18: 5414 (HW-72666)
development for processing irradiated fuels, technical progress review on, 18: 16152
development for processing spent nuclear fuels, (E), 19: 34286
development for processing thorium-bearing fuels, 20: 31326
development for reactor fuels, review, 17: 17451
development for recovery of fissile material from irradiated fuels, 17: 18182 (TID-18299)
development for reactor fuel reprocessing, review of, 17: 21788
development for recovery of uranium from irradiated uranium–zirconium alloy, 17: 34049 (DP-826)
development for recovery of cesium, rare earth, and strontium from radioactive waste solutions, 17: 35244 (HW-SA-2982)
development for reactor fuel processing, 18: 11376
development for reactor fuel processing, 18: 38356 (A/CONF.28/P/65)
development for recovery of fission products from spent fuels, 20: 9050(R) (ORNL-3830, pp 222-7)
development for separation of rare earth nitrates, 16: 87 (IS-335)
development for separation of fission products from hydrochloric acid solutions using triisooctylamine, 17: 30624
development for uranium separation, 17: 1570
development of amine, for rare earths and yttrium, 16: 8803 (BM-RI-5923)
development of amine extraction cycle for plutonium, 16: 21994(R) (ORNL-TM-150)
development of Citriflex head-end, 17: 20102(R) (ORNL-TM-563)
development of Citriflex head-end, for zirconium dissolution, 18: 27618(R) (ORNL-TM-833)
development of countercurrent, using redox reactions in fused salt–liquid metal system, 18: 3878 (IS-660)
development of Eurex process for processing irradiated aluminum–uranium fuels, 17: 23436 (RT/CHI(63)-3)
development of EUREX Process for processing aluminum–uranium alloy, by amine extraction, 19: 11292
development of flowsheets for Kilorod program, 17: 21776(R) (ORNL-TM-410)
development of, for use with Darex, Purex, Thorex, and Zirflex processes, 16: 32883(R) (ORNL-3314(p.1-39))
development of, for recovery of fuel from irradiated materials, 16: 32886(R) (ORNL-3314(p.96-115))
development of, for rare earths in bastnaesites, 17: 142
development of, for irradiated reactor fuels, 17: 8266
development of, for reactor fuel processing, 17: 20123
development of molten metal-salt, for fast breeder reactor fuels, 19: 32279(R) (ANL-7020(p.3-99))
development of packed column, 16: 20305(R) (UCRL-10023)
development of quantitative TBP-petrol, 16: 23653
development of Talspeak process for separating americium and curium from lanthanides, 18: 37297 (ORNL-3559)
development of Talspeak, for extraction of rare earths from actinides, 19: 7263(R) (ORNL-3651)
development of Talspeak, for separation of actinides from rare earths, 19: 28214(R) (ORNL-3739)
development of TALSPEAK, for actinide–lanthanide group separation, 19: 44115 (ORNL-P-1577)
development of Talspeak, for separating actinides from lanthanides, 19: 46428(R) (ORNL-3847)
development of the TBP-Thiocyanate system for separation of thorium from rare earths, 18: 17956
development of, for processing irradiated fuel elements, 20: 36948
development of, for fuel processing, 20: 45815
development review, 16: 23781 (HW-SA-2458)
developments in, for nonferrous metals, review on, 20: 41047
developments in, review of, 18: 20103
developments in, review on, 20: 1741 (IA-1031)
diluent choice for amines, 16: 17764(T) (AEC-tr-5014)
diluent role in, 18: 37286 (A/CONF.28/P/804)
diluents for, stabilization by sulfuric acid, 19: 28443(R) (ORNL-3785)
distribution of elements in systems for, 20: 27037 (JAERI-1106)
distribution of extracted materials in washing portion of, 17: 8256
distribution of solvent molecules around ion, evaluation by thermodynamic theory, 18: 9752 (IA-900)
efficiency, equations for, 17: 18210
efficiency in carrier-free separation of radioisotopes, 18: 22402
efficiency of Primene JM-T–hydrochloric acid systems for, 17: 37302
efficiency of, for 16 metal ions, 19: 13543
equilibria and kinetics of, 19: 4250(R) (ORNL-3627(p.177-208))
equilibrium data for nitric acid and uranium in processing of enriched aluminum–uranium fuels, 18: 3880 (NP-13290)
equipment design and performance, 16: 284
equipment design for, on micro-scale, 18: 25609 (RCC-M-173)
equipment design for, 20: 16582
equipment design for reactor fuel processing by, 20: 18826 (UJV-1441)
equipment development for, 17: 27501
equipment for berkelium, efficiency and hydraulic stability of, 20: 38998(R) (ORNL-3958)
equipment for, development of high-speed stacked-clone contactor, 17: 39195(R) (ORNL-3452(p.221-8))
equipment for fast liquid-liquid, 18: 16146
equipment for, in treating irradiated fuels, 17: 16140 (DP-757)
equipment for transuranium, design of, 20: 45791(R) (ORNL-3945, pp 107-28)
equipment for uniform droplet dispersion in, 20: 1800
equipment for, development of high-speed stacked-clone contactor, 19: 4254(R) (ORNL-3627(p.235-46))
extractant-diluent systems for, 18: 6899

flowsheet for recovery of actinides from spent HTGCR fuels, 19: 42591 (AAEC/E-139)
flowsheet of TBP, for plutonium and uranium at, 18: 13963
flowsheets for, computer calculation of optimum, 17: 29032
flowsheets for tridodecylamine, 18: 13964
flowsheets of Marcoule, 18: 13960
for elements from sulfuric acid solutions using amine–xylene, 19: 4245 (JAERI-1062)
for inorganic ions, data summary on, 17: 23432 (JAERI-1047)
for inorganic species, review, 17: 6179 (IA-740)
for plutonium and uranium from nitric acid solutions using tertiary amines, 17: 29034
for production of pure beryllium oxide, 20: 45823(P)
for rare-earth extraction using Primene JMT, 19: 18072
for recovering actinides from debris formed by nuclear explosion in salt formation, 19: 44156 (DP-956)
for recovering fission products from waste solutions, 18: 6883 (HW-SA-3211)
for salts, effects of ion charge magnitude on, 18: 35482
for separating cerium, cesium, and strontium from acid waste solutions, 19: 5988 (HW-75537)
for separating group IVA, VA, and rare earth elements, 18: 16157(P)
for uranium using kerosene-TBP, engineering drawings of plant for, 18: 13979
head-end techniques for stainless steel, zirconium, and graphite fuel elements, 16: 29051 (ORNL-TM-131)
head-end treatment of aluminum-clad uranium fuel elements, 16: 29052
head-in flowsheet for, shear-leach, 18: 1823
instrumentation for monitoring uranium, design of, 17: 1704 (NLCO-856)
ion charge magnitude effects on, 19: 546
mass transfer mechanism and efficiency of liquid-liquid, 16: 13133
mathematical analysis, 17: 16165
mathematical analysis of, for nitric acid and uranyl nitrate, 17: 18179 (ORNL-TM-358)
mechanism of third-phase formation in liquid-liquid, 18: 39378 (NP-12619)
mechanism of, using dialkylphosphoric acids in, 17: 6197
mechanisms of, mathematical equations for, 19: 4253(R) (ORNL-3627 (p.231-2))
mechanisms of, research on, 20: 17158(R) (ORNL-3900, pp 82-149)
metal complex formation and their role in synergistic effect in, 19: 15680
metal solution and feed preparation, 16: 280
method for plutonium recovery from irradiated fuels using tridodecylamine, 18: 6894
methods for separation of inorganic ions, evaluation of surface-active agents in, 17: 10749 (TID-17746)
model studies using carbon tetrachloride–tributyl phosphate solutions, 17: 24750(R) (UCRL-10624)
operating control of, using an acidity meter, 17: 10972
order of separation and phase diagrams of, method for presenting data on, 19: 2286
organic reagents for, review on mixtures of, 19: 7293
organophosphorus compounds for use in, properties of neutral bifunctional, 20: 38819
partition in, computer analysis of, 18: 39793 (IDO-16977(p.55-72))
patent, 19: 2463(P)
performance and degradation of diluents for TBP and cleanup of degraded solvents, 18: 6898
performance for plutonium in irradiated fuels, 18: 37284 (A/CONF.28/P/787)
performance for separating americium isotopes, curium-242, and plutonium-242, (E), 20: 5823(T) (ORNL-tr-892)
performance for thorium in monazites, 18: 37410 (A/CONF.28/P/521)
performance of Amberlite LA-1 and triisooctylamine for 64 inorganic ions, 16: 3076
performance of kerosene–TBP, for plutonium and uranium purification, 18: 13961
performance of nitric acid–tetrabutyl ethylene and tetrabutyl methylene diphosphonates for metals, 17: 40941
performance of, for separating nitric acid using long-chain amines, effects of nitrates on, 18: 20107
performance, using (tetraphenylarsonium chloride–chloroform)–hydrochloric acid systems, 16: 30501
phase separation in liquid-liquid, use of nickel and nickel arsenide to promote, 19: 36571(P)
plant for uranium fuel, description of laboratory, 16: 13132
plutonium concentration measurement by neutron counting in Plutonium Reclamation Facility, 19: 24608 (HW-75153)
principles of liquid-liquid, chemical and physical, 18: 39088
product distribution calculations, 16: 11805
properties for use in solvent extraction processes, 19: 7629
properties of amine organic phases in, 17: 18175 (HW-SA-2959)
properties of amines for, review of, 18: 356
pulse column control systems in, 18: 17954
pulse columns for countercurrent, at Eurochemic, 20: 16561
purification of degraded solvent systems of, by distillation, 17: 18178 (ORNL-3203)
radiation effects on coalescence rates in, 17: 39195(R) (ORNL-3452 (p.221-8))
radiation effects, 18: 16143
radiation effects on fuel reprocessing, review, 18: 41565 (UJV-945/63)
radiation effects on transplutonium element separation by Clanex, 19: 44115 (ORNL-P-1577)
radiation effects on aromatic diluents and extractants for, gamma, 19: 46430 (ORNL-P-1601)
extraction, 18: 10178 (CEA-2349)
review, 16: 285
review of amine, 18: 13956
review of amine, 18: 13958
review of dibutyl ether, 18: 13956
review of hexone, 16: 283
review of TBP, 16: 282
salting-in and -out in, modified Debye theory for, 18: 9752 (IA-900)
separation of fission products from solvents in, using nascent hydrogen, 17: 39211(P)
separation of fission products from waste solutions by, 20: 27039 (NP-15946)
solvation numbers in, isopiestic method for determination of, 17: 14387
solvent evaluation for fission product extraction, 17: 3072(R) (TID-17264)
solvent evaluation for fission product extraction, 17: 3073(R) (TID-17265)
solvent evaluation for fission product extraction, 18: 5418 (SRO-56)
solvent purification, 18: 1832(P)
solvents for, properties of tertiary phosphine oxides as, 20: 3863(R) (IS-1200(Sect. C))
solvents for, testing of amines as, 19: 4250(R) (ORNL-3627(p.177-208))
solvents for, use of metal dialkyl phosphorodithioate, 19: 17781(R) (ORNL-3750)
stacked clone contactor performance in, 17: 40931(R) (ORNL-TM-613)
study of diluent influence in extraction by tridodecylamine hydrochloride, 19: 20039 (EUR-2246.e)
synergic effects of various systems for plutonium and uranium, 16: 3084
synergistic action in, 19: 30333
Talspeak, for separating actinides from rare earths, 20: 45795(R) (ORNL-3945, pp 176-88)
TBP diluent in, uses of paraffin mixtures for, 18: 25605 (DP-882)
test runs in Kilorod, 17: 39175 (ORNL-TM-673)
test runs of Kilorod system, 17: 39174 (ORNL-TM-671)
tests of flowsheets for separating plutonium, thorium, and uranium from fuel scrap, 19: 40643 (BNWL-57)
tests of Kilorod system, 17: 39173 (ORNL-TM-670)
theory and flowsheets, summary, 16: 281
thermodynamics of, 17: 35618(R) (ORNL-TM-545)
transfer kinetics of amine-uranyl nitrate systems, 18: 39381 (RT/CHI(63)-30)
types of organosphosphorus extractants and their applications to transuranic separations, 18: 352
use for separating rare earths, 19: 2231
use for separation of transplutonium elements, review on, 20: 16402
use in activation analysis, 20: 35457
use in analysis of explosives and explosive simulants, 20: 14470 (UCRL-7873)
use in chemical equilibria studies, 17: 37153
use in determining trace radioiodine compounds, 19: 11015
use in radiochemistry, review of, 18: 20085
use in separation of lanthanides and trivalent actinides, 18: 23699 (CONF-405-37)
use of amides as extractants in, 18: 343 (DP-541)
use of amines and acidic organophosphorus compounds in, review, 19: 20053 (UJV-1202/64)
use of amines as extractants in, 18: 1800 (ORNL-3516)
use of amines for, review of, 19: 318
use of amines in, 18: 5243
use of chelating agent for separating heavy metals from solutions, 17: 25375(P)
use of chelating agent for selectively separating heavy metals from solutions, 17: 25376(P)
use of radioisotopes in, calibration curves, optimum conditions, and sensitivity of determinations in, 20: 245
use with ion exchange for separation of uranium from elements and fission products, 20: 38999 (TID-23229)
used at Marcoule, 17: 39203
uses and types of, survey of, 19: 9265
uses for separating long- and short-lived radioisotopes in wastes, (E),

19: 42197
uses in processing of irradiated fuels, 17: 18196
uses in separation of interfering activities in determination of trace metals by neutron activation, 18: 13652
uses of, for isotope separation, 20: 33760

SOLVENT PARTITION
see also Solvent Extraction Processes
analysis of complex compounds in solutions by, 16: 25368
bibliography and review, 16: 14635
effects of using combinations of extraction agents, 16: 13147
efficiency, component effects on, 16: 13143
equilibria in presence of complexing ions or insoluble compound formation, equations for, 16: 11807
in ion exchange complexing chromatography, equations for, 18: 27464
miscibility gap studies in amine extraction systems, 18: 37275 (A/CONF.28/P/755)
of inorganic species, review of, 17: 18197
of mineral acids between organic extractants and water, theory of, 17: 10767
properties of inorganic ions with Z = 11 to 96, 17: 29959
theoretical analysis, 16: 281
uses in inorganic separations, 16: 9972

SOLVENTS
see also Shellsol
acido-basicity of, general, 19: 40466 (UJV-1209/65)
activity ratios of organic-water, 17: 18009 (TID-18398)
analysis for organic residue from, radioisotopic method for, 19: 38538 (ADR-08-13-63.1)
analysis for uranium content in organic, colorimetric, 17: 33854(P)
analysis for water using krypton-85, 18: 37566(R) (NYO-2757-3)
analysis for water, chromatographic, 20: 31641(R) (NYO-755-1, pp 173-208)
analysis of organic, chemical procedures for, 18: 13642 (SC-4783(RR))
analysis of organic, for water traces using kryptonates, 18: 33450(R) (NYO-2757-4)
association, conductance, and physical properties of organic, tables on, 17: 10504 (NYO-9696)
bubble motion in Varsol, 16: 6535
burning of radioactive, from radiochemical separations processes, 19: 21747 (DP-942)
chemistry of nonaqueous, coordination model of, 18: 13606 (TID-20241)
comparison of, for cleaning metal surfaces, 19: 6008 (RFP-469)
contaminant removal with, 20: 40489 (SC-DC-66-1118)
development of organic, for separating fissionable and source materials, 19: 23163(R) (ORNL-3650(p.111-86))
development of, for cured epoxy resins, 20: 29366(E) (TID-22970, pp 375-91)
dielectric properties, calculations from thermodynamic properties of solvated ions in, 16: 11613
disposal of degraded contaminated, by burning, 19: 21748 (DPSPU-64-30-8B)
effects of organic, on mercury iodide, 19: 39265(R) (IA-1021)
effects of organic, on nitrogen isotope distribution between oxides in gaseous and liquid phases, 20: 16486
effects on chemical kinetics, 19: 4109 (SC-RR-64-1256)
effects on equilibrium on ion exchangers, 19: 11272
effects on gamma-induced graft polymerization of styrene to cotton fabric, 18: 31628
effects on radical reactions in radiolysis of hydrocarbons, 19: 26403
effects on radioinduced graft polymerization of styrene to cellulose acetates, 19: 26412
electrolyte solvation in mixed, ionic free energy of, 20: 2520(R) (IA-920)
evaluation of hydrocarbon diluents for Purex Process, 16: 18984 (DP-671)
evaluation of water-miscible organic, for use in nitric acid–solvent elutriants in anion exchange separation of transplutonic elements, 19: 24603 (ANL-6999)
extraction behavior studies of organic, 18: 27811(R) (ORNL-TM-198)
hydrogen ion reduction in nonaqueous, review of polarographic, 19: 34136 (COO-1148-96)
ion exchange, properties of mixed and non-aqueous, 20: 38818
nuclear polarization of, for measurement of ionic spin-lattice relaxation times, 20: 31221(R) (UCRL-16658, pp 73-87)
polarography of inorganic species in organic, review, 19: 17407 (COO-1148-94)
processing organic, use of electric fields in, 19: 28458(P)
properties and structure of organophosphorus, 20: 3863(R) (IS-1200 (Sect. C))
properties evaluation of organic, for inorganic salts, 17: 6190(T) (AEC-tr-5574)
properties for molybdenum and tungsten, 16: 17769
properties of neutral organophosphorus, 17: 37308
properties of neutral bifunctional organophosphorus compounds for use as, 20: 38819
properties of organic, for metal ions in ion exchange separation processes, 18: 23707(R) (TID-20609)
properties of sulfur-containing organophosphorus, 17: 37309
proton transfer in dipolar aprotic, tracer studies of, 18: 43549
purification for plutonium extraction process by fission product removal in water vapor carry-over, 18: 23698 (CEA-R-2404)
purification of organic, by solvent extraction of hydrocarbons using aqueous solutions of amines, 18: 43731(P)
purification process for, containing trialkyl phosphates, 18: 1832(P)
radiation effects on, in extraction processes, 18: 16143
radiation effects on aromatic diluents for radiochemical processing, gamma, 19: 46430 (ORNL-P-1601)
radiation effects on electric properties of petroleum, bremsstrahlung, 20: 46229 (UCRL-70022)
radiation stability of organic, 17: 14313 (SRIA-101)
radiation stability, 19: 15571(R) (TID-21385)
radioinduced luminescence in mixed, factors affecting minimum, 18: 41525
radiolysis of NEDA and NETA from 180 to 210°C petroleum fraction, effects of naphthalene on, 19: 481
radiolysis of organic, radical captor properties of dinaphthofuranoxyl and DPPH in gamma, 18: 43607
reactions of organic, with burning plutonium, 19: 38879 (RFP-566)
review on, for ion exchange separation of alkaline earths, lanthanides, thorium, and uranium, 20: 14469(R) (TID-22650)
scintillation system for silica deactivation, 18: 13712
separation of fission products from organic, using nascent hydrogen, 17: 39211(P)
solvation properties toward paramagnetic metal ions, nuclear magnetic resonance studies, 16: 22089
solvent properties for plutonium, literature survey on, 17: 32190 (DP-700)
solvent properties of organic, for mercury halides and neodymium nitrates, 18: 9752 (IA-900)
solvent properties of acidic organophosphorus compounds, 18: 37259 (A/CONF.28/P/347)
stability of organic extraction diluents, 19: 4250(R) (ORNL-3627(p.177-208))
synthesis of halogenated fluorinated β-diketones for metal extraction, 16: 16401(P)
system of, for paper chromatography of radioactive intermediary metabolites, 18: 6589
use of amines as, review of, 19: 318
use of paraffins as diluents in Purex Process, 19: 40646 (CONF-650918-2)

SOLVESSO
dipentyl pentylphosphonate–Solvesso-100, analysis for thorium, x-ray spectrometric method for, 19: 42420(R) (NLCO-955, pp 1.1-7)
dipentyl pentylphosphonate–Solvesso-100, analysis for thorium by x-ray spectrometry, 20: 7010 (NLCO-963)
di-*sec*-butyl phenylphosphonate–Solvesso-100, analysis for thorium x-ray spectrometric method for, 19: 42420(R) (NLCO-955, pp 1.1-7)
di-*sec*-butyl phenylphosphonate–Solvesso-100, analysis for thorium by x-ray spectrometry, 20: 7010 (NLCO-963)
Solvesso-100–TBP, analysis for thorium by x-ray spectrometry, 20: 7010 (NLCO-963)
Solvesso 100–trichloroacetic acid, radiation effects on clarification and coalescence time of reactor fuel solutions in nitrated, 20: 29333 (RT-CHI-(65)33)
Solvesso-100–tridodecylamine, solvent properties as extractant in plutonium purification, 19: 28442 (NP-14945)

SOLVOLYSIS
see also Hydrolysis
chlorine isotope effects in, solvent effects, 16: 14378(R) (NYO-2302)
free energy correlations of, thermodynamics of, 19: 32048(R) (NP-15073)
mechanism for benzoyl chloride, 19: 36220(R) (MIT-2098-142)
mechanisms of, isotope effects on, 20: 18643

SONAR EQUIPMENT
see also Sound Generators

SONIC INSPECTION
see also Ultrasonics
beam reflection at solid surface, phase shift in, 18: 27750(R) (HW-79280(p.7.1-22))
critical angle method for studying surfaces, 18: 18014 (HW-79928)
description of systems for, 16: 4365(T) (TG-230-T256)
development, 17: 10187 (AD-275297(p. 51-65))
development of, for welds, 17: 1901(T,R) (EURAEC-375)
development of techniques for detection of defects in Zircaloy tubes, 16: 11927 (HW-70638)
development of, for coating–metal bonds, 18: 39465(R) (IITRI-N213-20)
developments for fuel sheath tubing, 18: 27750(R) (HW-79280(p.7.1-22))
device development for pressure vessel nozzles, 20: 42636(R) (SWRI-1228-4-22)

efficiency for weld defects, 19: 28518(R) (EURABC-1342)
equipment and methods for pressure vessel nozzle welds, 16: 7746
equipment and methods for testing steel welds, 18: 39464(R) (EURAEC-762)
equipment and methods for testing thin-walled tubes, 20: 14713
equipment and techniques of ultrasonic imaging, 17: 30676 (TID-19009)
equipment and techniques of ultrasonic imaging, 18: 25675(R) (ANL-6868 (p.219-28))
equipment design for, for pressure tubes, 18: 40825(R) (CVNA-210)
equipment development for, 18: 8606(R) (HW-78388(p.7.1-10))
equipment for elastic modali determination by, 20: 31708 (ANL-7119)
equipment for, for irradiated fuel rods, 18: 639
equipment for MTR fuel elements, 20: 14195
equipment for pressure-tube, 19: 29627(R) (CVNA-228)
equipment for pressure tube, 19: 45567(R) (CVNA-235)
equipment for sodium-cooled reactors, development of, 20: 8322 (APDA-179)
equipment for sodium, development of, 20: 14024(R) (APDA-182)
equipment for uranium fuel elements, 20: 13318
instrumentation development for materials in liquid sodium media, 20: 9120(R) (APDA-178, pp 50-63)
Lamb waves in, 19: 10715(P)
measurement of grain size in outer annular region of metal bars by, 17: 32263(P)
method for JRR-3 uranium fuel elements, 20: 14194
methods and uses in nuclear industry, 16: 30652
methods development for nondestructive materials testing, 18: 3969(R) (ORNL-3470(p.94-7))
methods for adjacent dissimilar media, critical-angle, 18: 27683 (HW-78321)
methods for irradiated ceramic fuel elements, 19: 39234 (GEAP-4597)
methods for nuclear fuels, 20: 23261
methods for reactor fuel elements, 16: 6619
methods for reactor components, review, 18: 32976 (A/CONF.28/P/245)
methods for reactor materials, 19: 14765(R) (ANL-6977)
methods for reactor components, 20: 14034
methods for reactor fuel elements, 20: 14161
methods for reactor components, 20: 14017 (STI/PUB/105(Vol.2))
methods for stainless steel weld overlay using twin-angle beam search unit, 17: 27761 (TID-18871)
methods for steel welds, 19: 596(R) (EURAEC-1152)
methods for steel-welds, double probe, 19: 32394(R) (EURAEC-1341)
methods for testing steel welds, 18: 39463(R) (EURAEC-663)
methods for thick steel welds, 18: 43771(R) (EURAEC-882)
methods for Zircaloy-2 and -4 tubes, 16: 31955 (HW-72802)
methods of measurement for ceramic coatings, 17: 25425 (WADD-TR-61-91(Pt.III))
methods of ultra-, for sintered beryllium oxide, 20: 11324
methods of, for detection of non-bond in clad structures, 19: 40756
methods of, for Nimrod power plant alternator, 19: 41201
methods of, for nozzle welds in steel pressure vessels, 19: 42025
methods of, for welds in steel pressure vessels, 19: 42024
of brazed joints between heat exchanger tube and tube sheet or header, engineering drawings of equipment for, 18: 27687
of brazed joints between headers and heat exchanger tubes, 19: 23996(R) (ORNL-3650(p.1-110))
of ceramic-metal bonds, 16: 19150(R) (WADD-TR-61-91(Pt.II))
of clad-core bonding in fuel elements, 17: 22927 (TID-7642(p.337-59))
of coating-metal bonds, progress summary, 16: 11925(R) (ARF-6043-23)
of high-temperature materials, 19: 31462(R) (ANL-7028)
of HRT core vessel walls, remote equipment design, 16: 10265 (ORNL-TM-103)
of liquid sodium, 19: 35608(R) (APDA-170)
of molten salt levels, design of sensing probe for, 18: 18136(R) (NYO-2910-2)
of molten salt levels, development of sensing probe for, 18: 31842(R) (NYO-2910-4)
of molten salt levels, design of sensing probe for, 18: 31843(R) (NYO-2910-3)
of NS *Savannah* primary piping for damage, 17: 42340 (BAW-1269)
of pressure vessel steel, procedures for, 19: 22995(R) (SWRI-1243-14(a))
of reactor pressure vessels, equipment and methods for remote, 19: 24090(R) (SWRT-1228-56)
of reactor slurries, for solid particle content, 17: 14602 (NYO-10012)
of small-diameter tubing, engineering drawings of equipment for, 19: 20131
of sodium cooling systems, transducer performance for, 20: 10286 (APDA-180)
of thin wall Zircaloy tubes, 16: 3238 (R61CAP9(Rev.))
of tubing, engineering drawings of mechanical equipment for, 18: 27688
of welded steel plates, equipment for, 17: 6250(P)
of welded steel plates, 17: 39513(T,R) (EURAEC-672)
of welds in steel, 17: 8821(T,R) (EURAEC-450)
of welds in thick wall steel pipe, 17: 6243 (HW-74597)
recording equipment for, evaluation of, 20: 12973(R) (EURAEC-1519)
thin-wall tubing tests using ultrasonic shear waves, 18: 41626 (HW-81957)
transducer masking for elliptical or line beam shapes, 18: 18012 (HW-77465)
transducer testing for ultra-, for fuel element tubes, 18: 31838 (HW-81955)
ultrasonic research and developments at Hanford, 18: 14056 (HW-SA-3307)
ultrasonic wave propagation in nondestructive, 18: 45169 (HW-SA-3697)
use for testing thin Zircaloy tubing for defects, 17: 37003(R) (HW-78118)
use in determination of defect geometry, 16: 8876 (WAL-TR-830.5/3)
use in reactor fuel channels, equipment for, 20: 39175
use of, in determination of elastic constants of graphite, 17: 20455 (HW-75654)
SORA (Fast-Source Pulsed Reactor)
see Research Reactors
SORBIC ACID
potassium salt of, effects of, on storage life of irradiated Dover sole, 20: 9346 (TID-22289)
radiation effects on dimerization and polymerization of crystalline, gamma and uv, 20: 23105
radioinduced solid state polymerization of, kinetics of, 18: 27564
radioinduced solid state polymerization of methyl ester and potassium and sodium salts of, kinetics of, 18: 27564
Sorbitan Monolaurate, Polyoxyethylene Derivative
see Tween 20
SORBITOL
(D-Glucitol)
anhydro-, polyoxyethylene monolaurate, effects on iron-59 uptake in rats, 16: 7390
decomposition of carbon-14-labeled, induced by radiation emitted during storage, 18: 43687
effects on iron-59 absorption in rats, 16: 7390
effects on iron-59 absorption in rats, 18: 1346
inactivity in synthesis of indoleacetic acid from tryptophan, 16: 31403(R) (ANL-6535(p.144-5))
radiolysis of aqueous solutions, effects of oxygen on yields from gamma, 16: 219
radiolysis of aqueous solutions of, mechanism of degradation in gamma, 19: 5961
radiolysis of deaerated solutions, yields from gamma, 16: 220
radiolysis products, 16: 15075
tritium isotope effects on oxidation in *Acetobacter suboxydans*, 16: 17383
tritium position in labeled, 16: 7596
SORBOSE
diacetone, radiation effects on spectra of single crystals of, 17: 40873
effects on iron-59 absorption in rats, 16: 7390
radiation effects on electron spin resonance spectra of single crystals of, 17: 28981
radioinduced free radicals in, gamma, 18: 23651(T,R) (AEC-tr-6316 (p.573-86))
transport in baker's yeast, use of uranyl ion in studies on, 18: 9823
SORPTION
see also Absorption
see also Adsorption
chemi-, bibliography on radiation effects on, 17: 28939 (ORNL-3461)
equipment development for waste processing, 16: 5100(R) (HW-71374)
isotherms of, equipment for automatic gravimetric measurement of, 18: 214(T) (NP-tr-1064)
of gases by charcoal at low temperatures and high vacua, 18: 2777
of strontium on minerals, tracer study, 16: 25049 (TID-7628(p.187-97))
purification of gases by, improvements in, 17: 12306(P)
SOUND
see also Acoustic Waves
see also Noise
see also Phonons
absorbing material for, 19: 35579(P)
absorption and propagation of high-velocity, in liquids, 19: 25071(R) (TID-21667)
absorption by deuterated methane at 26°C, 18: 40052 (TID-21037)
absorption by hydrogen isotopes, rotational relaxation times from, 18: 28261
absorption by liquid helium II, (T), 20: 17611(T)
absorption by metals, 17: 5118
absorption by metals in magnetic field, electrodynamics of, 18: 36507
absorption coefficient in electric and magnetic fields, Weinreich relation for, (T), 19: 14154
absorption, generation, and propagation, 16: 13183(R) (TID-15140)
absorption in current-carrying superconductors, (T), 20: 28229
absorption in helium II, theory of, 17: 6871

absorption in liquid helium II at less than 0.5°K, 16: 29548
absorption in liquid metals, magnetically induced, 18: 26131
absorption in methane-d_2, 19: 8716 (TID-21414)
absorption in paramagnetic materials, design of spectrometer for measuring, 19: 32518
absorption in type II superconductors, theory of, 20: 15663
absorption of, 16: 13183(R) (TID-15140)
absorption of magnetic, in plasma, 17: 29693
amplification by conduction electrons, resonant, 17: 31188
amplification by conduction electrons, magnetic field dependence of, 17: 36492
amplification by conduction electrons with nonspherical energy surfaces, (T), 19: 9791
amplification in semiconductors by drifting electrons, 18: 15711(R) (TID-20256)
amplification of, quantum resonances in, 17: 34591
attenuation by liquid sodium, measurement method for, 19: 44342(R) (APDA-174, pp 67-70)
attenuation coefficient of megacycle second, (E), 19: 41633
attenuation in cylinders of superconducting vanadium, energy gap from u-h-f, 17: 41622
attenuation in tantalum superconductors, energy gap from u-h-f, 17: 41623
attenuation in type II superconductors, (T), 19: 45210
attenuation of u-h-f, in superconducting niobium–zirconium alloys, 17: 39767
attenuation of ultra-, by superconductors, 18: 15711(R) (TID-20256)
correlation of, with heat transfer in boiling, 20: 5628
detection and generation of ultra-high-frequency waves in solids, 16: 23970 (ANL-6515(p.117-20))
detection of h-f, superconducting diodes for, 19: 46739
detection of interaural intensity difference, minimum, 17: 35260(R) (TID-19135)
diagnostic use for neutral gas temperature in plasma column, 18: 38208
effects of resonant field on laminar fluid flow in channels, 17: 8354
effects on controlling grain size of steel ingots and welds, review of, 17: 30947 (DMIC-Memo-166)
effects on electromagnetic wave propagation in plasma, (E), 19: 29408
effects on heat transfer at Reynolds numbers 16,000 to 200,000, 16: 3171 (UCRL-13016)
effects on materials in radiation fields, design of test facility for, 18: 11512(R) (NARF-63-9p)
effects on transforming DNA, inactivating, 20: 12620
effects on tunneling current in superconducting diodes, (E), 19: 21178
emission by Karman vortices, 18: 15711(R) (TID-20256)
emission from Karman vortices, 17: 35260(R) (TID-19135)
emission from Karman vortices, 18: 2404(R) (TID-19651)
emission from nonlinear plasma fluctuations, 18: 42841
emission from traveling striations in glow discharges, mechanism for, 20: 28563
energy transfer in dispersive media, (T), 19: 20688
excitation in weakly ionized plasma, (T), 19: 21561
excitation of zero, in nuclear matter, 18: 24693
human response to, from ultrasonic devices, 18: 21704 (HW-SA-3028)
interactions in many-boson system, excitation spectrum for, 17: 41618
interactions of ultra-, with charged particle beam in piezoelectric crystal, (T), 19: 20672
interactions with electrons, acoustoelectric current from, (T), 19: 14155
measurement using the Mössbauer effect, 17: 3673
observation of ionic waves in arc plasmas, 16: 9506(R) (ORNL-3239 (p.16-46))
physical effects of, description of, 17: 3370 (AD-276381)
power output of monopole source of, 18: 42162(R) (TID-20963)
pressure levels of, produced by ultrasonic devices, 18: 21704 (HW-SA-3028)
production and radiation, 16: 7634(R) (TID-13000)
production by exhaust of KIWI B rocket motor, 20: 26519 (N-66-15495)
production by forced-convection water flow in tubes at supercritical temperatures and pressures, 19: 24677 (WCAP-2056(Pt.IV))
production by modulated high-frequency electric discharge, 18: 42162(R) (TID-20963)
production in steam systems, theory of, 18: 3965
production of, 16: 13183(R) (TID-15140)
production of uhf, in solids, 16: 23970 (ANL-6515(p.117-20))
propagation, 20: 4153(R) (UCRL-14360, pp 73-85)
propagation and scattering by matter near thermodynamic critical point, (T), 19: 11852
propagation from chemical blasts, 20: 43461 (PNE-607F)
propagation in atmosphere, effects of wind on, (T), 19: 16258 (SC-RR-64-1756)
propagation in discharge column of low-pressure plasma, damping in, (E), 19: 17087
propagation in fermion systems, Boltzmann equation for, (T), 19: 10136
propagation in flowing gas–liquid mixtures, velocity of, (E), 19: 13586(T) (WAPD-Trans-15)
propagation in galactic cosmic-ray gas, (T), 20: 25677 (N-66-15458)
propagation in helium-3 (liquid) at 1.4 to 513 psi, 16: 614
propagation in helium-II, fourth sound, 18: 34725
propagation in helium near the critical point, 18: 44686
propagation in helium-3 at low temperatures, (E), 19: 19055
propagation in hydrodynamic medium, (T), 19: 26924 (UCRL-12412)
propagation in inhomogeneous media, forces from, 18: 7582
propagation in low-density plasma, (E), 19: 10447
propagation in magnetic field, wavelength dependence in, 18: 20643
propagation in mixtures of steam and water, speed of, 20: 35614 (AEEW-M-452)
propagation in polyatomic gases, disturbances in, 18: 26135
propagation in rarefied gases, kinetic theory of, 19: 39262 (BNL-8990)
propagation in rarefied gases, kinetic theory of, 20: 19169(R) (BNL-929, pp 106-11)
propagation in solid rods, 16: 23972 (ANL-6515(p.133-61))
propagation in solid-state plasma, (T), 19: 18525
propagation in solid helium-4, shear, 19: 33179
propagation in superfluid helium, equations for, (T), 20: 17640
propagation in superconductors, (T), 20: 42128(T)
propagation in weakly ionized gases, longitudinal, (T), 19: 39293
propagation of field-aligned waves by ionospheric electron streams, 17: 20806
propagation of high-velocity, in liquids, 19: 25071(R) (TID-21667)
propagation of infrasonic, from pulsating auroras in polar atmosphere, 18: 18795
propagation of ionic-wave, in electron-beam plasma, (E), 19: 35514(R) (AD-425796)
propagation of longitudinal waves of, in weakly ionized gas, 18: 7810
propagation of magneto-, in highly conducting plasma, 18: 3014
propagation of third, in superfluid helium films (E), 19: 3185
propagation of ultra-, in plasma, (T), 19: 25571
propagation of, gas kinetic theory for, 18: 40074
propagation over plane boundaries, effects of turbulence on, 17: 13879(R) (TID-17943)
propagation through electrically conducting medium, induced magnetic field from, 18: 9519
radiation effects on seizures induced by x, 18: 69
radiation effects on rat response to, following fetal exposure, 20: 40654
reactions with metals in magnetic fields, nonextremal Fermi-surface orbits from resonances in, 18: 32070
recording devices, performance, 16: 12811 (WT-776)
reflection from a sinusoidal surface, 17: 31073(R) (ANL-6719)
reflection from statistically rough surface, 18: 24516(T) (JPRS-24633)
reflection from statistically uneven surfaces with shadows, 18: 30898(T) (JPRS-25168)
research and development programs at Materials Central, Wright-Patterson AFB, 16: 1292 (WADC-TR-53-373(Suppl.7))
research programs on physical aspects of, 16: 30172(R) (TID-16489)
scattering by an impenetrable sphere, h-f, (T), 19: 41129
scattering by surfaces of arbitrary shape, 16: 21137 (UCRL-6779)
scattering by vortices in liquid helium II (T), 19: 3184
scattering on vapor-liquid helium II boundary, reflection and transformation in, 18: 40461
sorption by manganese sulfate at 25°C, 19: 32048(R) (NP-15073)
sorption in methane, effect of deuteration on, 17: 28923 (TID-18976)
theory of zero, in Boltzmann gases, 19: 1081
transmission in hot cells, development of system for, 17: 25388 (ORNL-TM-565)
transmission, in vicinity of nuclear explosion, 16: 12811 (WT-776)
transport solutions for, coupled with heat flow, 19: 9581 (NYO-1480-5)
use of radioisotopes for generation of, underwater, 20: 25462 (AGN-8135)
velocities in pure metals, 17: 8859
velocity in crystalline helium, (T), 20: 2912
velocity in helium at 0.1 to 1.7°K, 17: 3633
velocity in helium-II at 1.19 to 2.1°K, 17: 5143
velocity in helium (liquid), 17: 20742
velocity in helium-3 and -4 mixtures, 18: 21115
velocity in helium II, (E), 19: 16771
velocity in liquid normal and para hydrogen at 14 to 20.5°K, pressure dependence of, 18: 2766
velocity in liquid helium-3 and -4 down to 1°K, 18: 36453
velocity in many-boson system, 17: 39761
velocity in plasma, ionic, 17: 33153(R) (ORNL-3472(p.24-49))
velocity in plasma, direct measurement of, 17: 35022 (CONF-46-87)
velocity in plasma, 18: 13138(R) (ORNL-3564(p.44-62))
velocity in two-phase sodium flow, 20: 22348
wave distributions in plasma, fluctuating, (T), 19: 29434

SOUND GENERATORS

design for studying liquid–vapor bubble mixtures, 17: 39375 (EURAEC-591)

design of radioisotope-powered, 19: 6227
feasibility of radioisotope-powered underwater, 19: 20405 (MND-3180-1)
radioisotope-powered, development of underwater, 18: 16397 (TID-7689(p.72-6))
Sounding Balloons
see Balloons
Sounding Rockets
see Rockets
Sources
see Radiation Sources
SOUTH AFRICAN RESEARCH REACTOR
control of Safari I, instrumentation for, 18: 21686
SOUTH AMERICA
age measurements on British Guiana dolerite, isotopic method, 17: 23537
beta activity in, Sept. 1961 through August 1965, 20: 7312 (NP-15678)
fallout monitoring in, 18: 31753 (CLOR-26)
fallout monitoring along 80th Meridian (West), 1957 through 1962, 18: 35785
fallout monitoring along 80th Meridian (West), 1963, 18: 35786
fallout monitoring, 1964, 18: 37383
fallout monitoring, 1964, 18: 37384
fallout monitoring, 1963 and 1964, 18: 41644(R) (HASL-149)
fallout monitoring, 1963, 19: 18144(R) (HASL-156)
fallout monitoring, 1965, 20: 29428
radiation monitoring of atmosphere in, 19: 42677
radiation protection programs in, 18: 5150
radioactivity of cattle thyroids in, 18: 35721
SOUTH CAROLINA
aeroradioactivity survey and areal geology of Savannah River Area, 16: 11933 (CEX-58.4.2)
meteorological analyses in Parr, Fairfield County, 20: 14732 (CVNA-172)
SOUTH DAKOTA
(See also headings of the form South Dakota (Fall River Co.))
age of galenas from Black Hills, 16: 29196
ages of uranium minerals in Black Hills, 16: 29197
environmental radiation measurements in, 20: 38735(R) (NYO-1704-13)
fallout monitoring, 1963, 20: 5649(R) (COO-1340-2, pp 54-83)
studies of uranium-bearing lignites from, mineralogical, petrographical, and paleobotanical, 19: 26568 (NYO-10361)
uranium occurrence in southwestern part of Williston Basin, 19: 30434
zoning of mineral deposits in, hydrothermal, 17: 34116 (CONF-123-1)
SOUTH DAKOTA (FALL RIVER CO.)
geologic environment of oxidized uranium deposits in, 16: 29274
Southern California Edison Plant
see San Onfre Power Reactor
SOUTHERN RHODESIA
sulfur-34 content in sulfide deposits in, 19: 36657
SOUTHWEST AFRICA
radioactivity levels in fossil fuels from, 20: 152(R) (NYO-3086-1 Pt.VIII)
SOUTHWEST EXPERIMENTAL FAST OXIDE REACTOR
aspects of international cooperation, 18: 38464 (A/CONF.28/P/533)
construction, design, and testing of, (E), 19: 35811
control element drive mechanisms for, (E), 19: 31613 (WASH-1054 (Pt.I)(p.87-102))
control rod calibration, 20: 46963(R) (ANL-7132)
control systems for, development of, 20: 22496(R) (GEAP-4864)
control systems for, development of, 20: 28830(R) (GEAP-4994)
control systems for, development of, 20: 32860(R) (GEAP-5108)
coolant flow testing for, stability of, 20: 32860(R) (GEAP-5108)
core analysis in ZPR-3, (E), 20: 14007(R) (ANL-7122, pp 1-41)
core design, 20: 28830(R) (GEAP-4994)
core design and fission traverse rates for, 20: 30790(R) (ANL-7204, pp 1-31)
core design criteria for, 20: 32860(R) (GEAP-5108)
core design for, steady-state and transient testing of, 20: 22496(R) (GEAP-4864)
core materials for, description of, 20: 38531 (GEAP-5133)
critical mass of mockup of, in ZPR-III, 20: 36499
criticality calculations for mockup of, in ZPR-3 assembly, 20: 35069
criticality studies, 20: 24734(R) (ANL-7176, pp 1-44)
criticality studies, 20: 26394(R) (ANL-7193)
criticality studies for, 20: 32860(R) (GEAP-5108)
design and development, Mar. 25-June 26, 1964, 19: 10540(R) (GEAP-4594)
design and development, 20: 42629(R) (GEAP-5160)
design of, 16: 11262
development, (T), 20: 10384(T,R) (EURFNR-3F)
development, 20: 5120(R) (GEAP-4799)
development, 19: 24097(T,R) (ORNL-tr-537)
development, 19: 24098(T,R) (ORNL-tr-538)
development and research program, July-Sept. 1964, 20: 22495(R) (GEAP-4742)
development and research program, Feb.-Apr. 1965, 20: 22496(R) (GEAP-4864)
development and research program, Aug.-Oct. 1965, 20: 28830(R) (GEAP-4994)
development and research program, Nov. 1965–Jan. 1966, 20: 32860(R) (GEAP-5108)
development, May 1–July 31, 1965, 20: 36471(R) (GEAP-4934)
fuel alloy development, 19: 2753
fuel cladding transient performance, 20: 28830(R) (GEAP-4994)
fuel compositions in ZPR-III mockup of, 20: 28830(R) (GEAP-4994)
fuel development for, 20: 22496(R) (GEAP-4864)
fuel development for, 20: 28830(R) (GEAP-4994)
fuel development for, 20: 32860(R) (GEAP-5108)
fuel elements for, design of instrumented, 20: 28830(R) (GEAP-4994)
fuel handling procedures for, development of, 20: 28830(R) (GEAP-4994)
fuel handling procedures for, remote, 20: 32860(R) (GEAP-5108)
fuel materials for, description of, 20: 38531 (GEAP-5133)
fuel rod vibrations in, effects of coolant flow on, (E), 20: 18134 (GEAP-4966)
fuel temperature measurement, instrumentation development for, 20: 28830(R) (GEAP-4994)
fuel temperature of, survey of sensors for measuring, 20: 3473 (GEAP-4903)
fuel temperature sensors for, development of, 20: 32860(R) (GEAP-5108)
instrumentation development for, 20: 22496(R) (GEAP-4864)
instrumentation development for, in-pile, 20: 28830(R) (GEAP-4994)
materials selection for, 18: 3257
materials selection for, 18: 15566
neutron capture by uranium-238 in, Doppler effect in, 20: 35068
neutron Doppler measurements in ZPR-3 mockup of, 20: 36391(R) (ANL-7219, pp 1-27)
neutron flux monitoring system for, development of, 20: 32860(R) (GEAP-5108)
neutron physics of mockup of, in ZPR-3 assembly, 20: 35067
reactivity coefficients of, steady state evaluation of, 20: 42631 (KFK-260)
reactivity Doppler coefficient in, prompt supercritical power excursion for determining, 20: 36497(T) (EURFNR-68F)
reactivity effects of Doppler shifts in, 18: 38252 (A/CONF.28/P/644)
reactivity of, 20: 16060(R) (ANL-7152, pp 1-49)
reactivity transients including meltdown, methods for analysis of, 19: 42100 (UNC-5092)
safety hazards analysis for, preliminary, (E), 19: 35848 (NP-15077)
SOVIET UNION
age determination of granites of southwestern Karelia karelides by rubidium–strontium method, 19: 4381
age determination of Pre-Cambrian rocks of Kursk magnetic anomaly by lead–thorium–uranium method, 19: 4390
age estimation of Mginskii marine stratum near Leningrad using carbon-14, 19: 2549
age estimation of Aldanian phlogopites in, 19: 46596
age estimation of upper anthropogenic layer in, 19: 46621
age estimation of materials and relics in, by carbon-14 method, 20: 18931
age estimation of carbonate deposits in, 20: 20887
age of basic rock in Karelia, Kola, and Transbaikal, 17: 3172
age of Saxagan plagiogranites in Krivoi Rog, lead–uranium method estimation of, 19: 26562
ages estimation of upper paleolithic period in region adjoining Dniester River by radiocarbon dating, 17: 16273
antibiotic research in, 19: 6219(T) (JPRS-27558)
atmospheric monitoring for natural radiation, 17: 6286
atmospheric radioactivity, 18: 5483(T) (JPRS-21975(Del.)(p.1-9))
atomic energy program, summary based on publicly available materials, 19: 21762 (RM-2163(RAND))
atomic energy program, 20: 20182(T) (AEC-tr-6700)
beta radioactivity of skeleton of newborn children, 1960, 18: 27053
calcium content in plant residues and soils in, flame spectrometry method for determining, 19: 35890(T)
cerium-144 and strontium-90 distributions in soils of Moscow region, 19: 22549
cerium-144 distribution in soils of Moscow region, 19: 22549
chemical industry in, 16: 6364(T) (JPRS-10613(Pt.II))
contents of thorium and uranium in hydrothermal altered rocks in Kzyl-Ompul, 17: 29102
corrosion research in, observation of, 17: 16592 (TID-17940)
cosmic-ray-monitoring instruments and stations, 16: 889(T) (NP-tr-803)
distribution of radioactive elements in soils in, 18: 37360 (A/CONF.28/P/385)
ecology of, bibliography on, 18: 19487 (TID-20453)
fall-out from 1961 nuclear tests, 16: 9028 (TID-14377)
fallout content in rain water in, 1964, 20: 7270
fallout hazards from 1961 nuclear explosions in, 19: 11393
fallout in atmospheric precipitation in, effects of cloud formation on,

20: 29416
fallout in Vitebsk, 1962–3, 20: 14746
fallout monitoring for tungsten in 1958, 17: 12118
fallout monitoring in Leningrad area of, 1958–60, 17: 16304
fallout monitoring in Crimea, 1960 and 1961, 18: 4031
fallout monitoring at Moscow, 1961–2, 18: 35719
fallout monitoring near Moscow, 1960-1962, 19: 13628 (NP-14718)
fallout monitoring at Moscow in 1961–1962, 19: 15750 (NP-14720)
fallout monitoring, 1961–1962 strontium-90, 19: 28539 (NP-14730)
fallout monitoring, 1963, 19: 44259
fallout monitoring at Vilnius in 1962, 20: 16700
fallout monitoring near Leningrad, 1961–1963, 20: 16701
fallout monitoring of strontium-90 in polar regions of, 20: 16703
fallout monitoring in, 1962, 20: 29406 (NP-14719)
geochemistry and mineralogy of alkali rocks in, 17: 25454
geochemistry of lead-zinc deposits of Klitchkin region, 16: 27451
geochemistry of radioactive elements in soils, 19: 30415
geochronology of Yenisei Mountain Range, 18: 35710
geology of granitic rocks, 16: 25627
ground water age estimation by argon–helium method in Volga region, 19: 36660
hafnium, thorium, uranium, and zirconium contents of zircons from granitoid rocks in middle Dnieper area, 20: 7264
health physics programs in, instrumentation for, 20: 4198
health physics program for medical radiology in, 20: 45997
holocene era in Franz Joseph Land, 16: 9002
isotope and radioisotope production in, 16: 6365(T) (JPRS-10613 (Pt.II)(p.409-40))
isotopic composition of lead ores in Eastern Transbaikal, 19: 44277
mineralogy and geochemistry of rare elements in Cherry Mountains (Urals), 19: 20190
minerals ages in Ural Mountains, alpha-lead, 16: 2032
nuclear power development in, 18: 38431 (A/CONF.28/P/294)
nuclear power development in, 18: 43046
nuclear power development plans, 18: 45042
nuclear power development plans, 19: 1912
nuclear power plant economics in coordinated networks in, 20: 1488
nuclear power production in, 18: 38442 (A/CONF.28/P/316)
nuclear power stations in, economic aspects of, 19: 48014
nuclear research in, literature and organization of, 17: 28589 (EUR-236.e)
nuclear research in, facilities and programs for, 18: 1318
nuclear weapons effects studies, bibliography of, 19: 9762 (AID-P-64-44)
pegmatite age estimation in Biryusa, 19: 20176
plasma and thermonuclear research in, (E/T), 19: 10398 (TID-21189)
radiation and radioisotope uses in, 20: 23530(T) (AEC-tr-6466/1, pp 1-7)
radiation and radioisotope industrial uses in Latvia, 20: 23536(T) (AEC-tr-6466/1, pp 8-12)
radiation chemistry in industry in, 20: 23077(T) (AEC-tr-6466/1, pp 32-8)
radiation detection and protection in, bibliography on, 20: 43666 (AD-623557)
radiation monitoring of Neva River, 16: 2064(T) (AEC-tr-4670)
radiation protection regulations, 17: 10870(T) (JPRS-16995)
radioactive aerosols in atmosphere in, vertical distribution of natural, 18: 10606(T) (AEC-tr-6128(p.92-124))
radioactivity of atmosphere over Lithuania, 1962 to 1964, effects of meteorological conditions on, 20: 23282
radioactivity of clays in oil well sections in Crimea and Eastern Caucasus Foreland, 17: 27572
radioactivity of fish and mollusks from Neman River, 1961, 18: 10279(T) (JPRS-22702(Del.))
radioactivity of grass and weeds in, 19: 28587
radioactivity of surface waters, 16: 22421
radioisotope industrial applications in economic aspects, 19: 13839
radioisotope production in, 18: 37591(T) (AEC-tr-6398(p.34-48))
radioisotope uses in, economics of industrial, 20: 27377
radiological monitoring of air and surface waters of Barents Sea area, 16: 30687(T) (JPRS-14974(p.28-30))
radium-226 content in lagoons and seas in, 20: 18905
radon exhalation from surface of rocks in, 18: 10277(T) (AEC-tr-6128 (p.125-38))
rare earth content of Ural scheelites, 18: 35712
rare earth, thorium, and yttrium contents in soils in Tomsk region, 20: 2065
reactor fuel cycle research in, literature survey, 19: 27767 (ORNL-TM-1133)
reactor safety programs and standards, 20: 30800
research in radiobiology in, 1961, 17: 14048
research in, on production of high magnetic fields, (E/T), 19: 15700 (ATD-P-64-46)
research on cosmic space and upper layers of atmosphere, 18: 5876
research on nuclear weapons effects, review, 19: 32786 (AD-610054)
research on x-radiation effects on nervous system, 20: 22687
research program at Joint Institute for Nuclear Studies, 20: 34160
research reactor development in, 18: 38587 (A/CONF.28/P/296)
rocket and satellite investigations of upper atmosphere and space, bibliography of 1964 publications on, 19: 37200(T) (JPRS-30925)
sanitary protection of environment for radioactive contamination in, evaluation of problems in, 18: 37424 (A/CONF.28/P/379)
scientific research in, translations on organization of, 18: 45197(T) (JPRS-26803)
solar energy resources and applications, book, 16: 15285(T) (NP-tr-873)
stable isotope production and uses in, 20: 16933
strontium-90 content in cattle bones, soil, and grass in, 18: 27030
strontium-90 content of milk in, 1960-1962, 19: 13667 (NP-14696)
strontium-90 content in fresh water basins in, 1961–62, 19: 20160 (NP-14728)
strontium-90 content in soils in, 1959-60, 19: 24706
strontium-90 content in plant residues and soils in, 19: 35890(T)
strontium-90 content in alfalfa and grass in West Slovakia, 19: 45750
strontium-90 content in surface waters in, 1961–1962, 20: 16705
strontium-90 content in drinking water and food in, 20: 41142
sulfur-34 content in sulfides from copper–nickel deposits in, 18: 33767
thermonuclear explosion in, Jan. 15, 1965, 19: 22557
thorium and uranium content in granitoids in Kaib massif, Kazakh, 16: 33292
thorium and uranium deposits in Transbaikal, 17: 3174
thorium and uranium isotopic ratios in peat bog of Kirov District, 18: 31761
thorium and uranium contents in paleozoic granitoids, Eastern Sayan, 19: 15774
thorium and uranium content and magmatic formation behavior in massif, North Kazakhstan, 19: 15775
thorium and uranium occurrence in magmatic rocks of Kuznetsk basin, 19: 36659
thorium and uranium contents of effusive and intrusive formations of northeastern Balkhash foreland, 20: 29418
thorium content and isotopic ratios in ground waters of Kazakhstan, 19: 22542
thorium distribution in nepheline syenites of Lovozero massif, Kola peninsula, 19: 15773
tritium content of rain and snow in Moscow, Dec. 1961 to Dec. 1963, 20: 29409
uranium content in crude oils in Belorussia, 19: 24422
uranium content in basic rocks in Kal Taiga and Patyn in Shoria, 19: 34396
uranium content in traprock formation of Siberian platform, 20: 29419
uranium distribution in rock minerals of Kyzyl-Ompul Mountains, 16: 2031
uses of radiation and radioisotopes in industry in, economic aspects of, 20: 23537(T) (AEC-tr-6466/1, pp 13-25)
virology studies in, 18: 19508(T) (JPRS-23956)
waste disposal standards in, comparison of, with U.S., 20: 12521
welding development in, 17: 32541(T) (FTD-TT-62-1677)

SOVIET UNION (KARELIA)
age determination of granitoids in Sunsk complex of, by rubidium–strontium method, 17: 40995
geology of uraninites in, 16: 22413(T) (CEA-tr-R-1494)

SOVIET UNION (KIRGIZ)
occurrence of copper, molybdenum, and uranium in rocks of Tien Shan Mountains in, 20: 33544

SOVIET UNION (UKRAINE)
radioactivity equilibrium between radium, thorium, and uranium in accessory monazites in, 19: 20189
radioactivity of underground waters in, natural background of, 20: 23289
radioisotope uses in industry in, 18: 44000(T) (JPRS-26803(p.1-3))
radon content in natural waters in Belaya Tserkov district in, 16: 31967
thorium and uranium isotopic composition and ratio in fossil bones, mollusks, natural waters, and soil in, 17: 21917
uranium content in crude oils in, 19: 24422

SOYBEANS
analysis for strontium-90 in United States, 1959-60, 16: 17928
carbon-14 distribution in various stages of ontogenesis, 19: 3867
cesium-137 content in, in Japan, 1963, 20: 45967
effects of enzyme of, combined with x radiation on mortality of mice, 17: 17921
effects of protein from, on growth of chickens, 19: 45761(R) (ORO-631, pp 122-31)
gamma attenuation coefficients for, (E/T), 20: 716
lime-induced iron chlorosis in, 17: 40496(R) (TID-19389(App.A))
phosphatides, effects on bleeding in thrombocytopenic, x-irradiated dogs, 16: 14593
radiation effects on oil extracted from proteins of, relation of odor to, 17: 1690

radiation effects on odor of fried, relation of carbonyl compounds to, 17: 1691
radiation effects on chemical composition of fried curd of, 17: 1688
radiation effects on odor of oil extracts of fried curd crust of, 17: 1689
radiation effects on biological characteristics and chemical composition of kernels, 17: 27071(T) (OTS-62-11755/2(p.99-100))
radiation effects on, gamma, 17: 30033
radiation effects on, thermal neutron vs x, 18: 38848
radiation effects on mitosis in, 19: 96
radiation effects on nitrogen fixation activity in *Rizobium japonicum* in symbiosis with, 19: 12963
radiation effects on nucleic acid metabolism in seeds and seedlings of, 19: 12959 (TID-21460)
radiation effects on plant growth, 19: 33890
radiation effects on roots of, 20: 18198
radiation effects on, genetic, thermal neutron and x, 20: 45388
radioinduced mutations in, γ, 20: 6797(T) (JPRS-33170, pp 240-8)
radioinduced mutations of, use in plant breeding programs, 20: 18419
radioinduced mutations in, thermal-neutron, 20: 45358(R) (NP-16208)
radiosensitivity, 19: 12963
radiosterilization of, effects on mold growth and wholesomeness, 19: 24892
strontium-89 and calcium-45 accumulation, 20: 40532(R) (COO-1097-17)
strontium-90 content in, in Japan, 1963, 20: 45967
strontium-90 uptake by, effects of liming and soil types on, 20: 6745
synthesis of phosphorus-32-labeled phosphatides by, 19: 12918
translocation of phosphorus-32, nitrogen-15, and carbon-14 in seedlings of, 17: 24871

SPACE

antimatter in, 17: 6915(T)
astronomical and geophysical aspects of Soviet research in, 16: 19642
atomic reactions in, 17: 16886
behavior of engineering materials in, 16: 30726
behavior of hydrogen in, 16: 886 (LAMS-2596)
bibliography on, 20: 35985 (NASA-SP-7026)
bibliography on properties and phenomena in, 18: 34383(T) (NASA-TT-F-229)
biological and medical aspects of energies in, 16: 20230
biology of, bibliography on, 18: 4941 (SB-455(Rev.))
biology of, bibliography on, 19: 24268
book: *Advances in Space Research*, 20: 2862
book: *Cosmic Dust*, 18: 20720(T)
book: *Cosmic Rays, Solar Particles and Space Research*, 18: 20821
book: *Cosmical Electrodynamics. Fundamental Principles*, 19: 1163
book: *Handbook of Geophysics and Space Environments*, 20: 25997
book: *Interplanetary Dynamical Processes*, 18: 5911
book: *Nuclear Energy in Space*, 19: 1930
book: *Particles in the Atmosphere and Space*, 20: 32285
book: *Soviet Science of Interstellar Space*, 17: 13265
book: *Space Physics and Radio Astronomy*. (E/T), 19: 2943
book: *Space Physics*. (E/T), 19: 2944
book: *Space Physics*, 19: 34858
book: *Space Physics with Artificial Satellites*, 20: 2863(T)
book: *Space Research, V.*, 19: 35267
book: *Space Science and Technology. Volume 4*, 17: 17610
book: *Space Science*, 18: 32353
book: *Stellar and Interstellar Space Physics*, 20: 34072
charged particle distributions in, development of detectors for, 17: 16895
charged particles and magnetic fields in, 17: 7676
chemical evolution and organic synthesis in primitive planetary environment, (T), 20: 20406 (N-65-27062)
chromospheric activity in, review on, 18: 14712
clouds in interstellar, cyanide molecules in, 18: 36131
communication in outer, x radiation use, 16: 18698 (RADC-TR-61-219)
composition of interstellar, 18: 32354
conference, 16: 17323
conference, 18: 30335
conference on, 18: 5907
conference on effects of space environment on materials, St. Louis, May 7 to 9, 1962, 17: 29261
conference on peaceful uses of, 20: 40486 (NASA-SP-82)
conference on research on, 18: 28468
conference on space research, third international, Washington, May 2 to 8, 1962, 18: 7357
conference on space research, 20: 30195(T) (NASA-TT-F-389)
conference, Rome, May 1959, 16: 14381
contour lines in B, L, at invariant geomagnetic equator, slope of, 17: 34678
cosmic and solar radiation modulation in interplanetary, (T), 20: 37542
cosmic electron spectra in interstellar, from meson (π) decay, (T), 19: 14274 (NASA-CR-148)
cosmic neutron fluxes in, 17: 34273
cosmic noise in, at 18 Mc after Starfish test, enhancement of, 17: 34670
cosmic particle acceleration in, mechanisms for, 18: 9056(T)
cosmic particle scattering by magnetic irregularities in, 18: 22702
cosmic photon production mechanisms in intergalactic, (T), 19: 14275 (NASA-CR-149)
cosmic photons from radio sources in, 18: 36201
cosmic proton interactions and production in interstellar, (T), 19: 12106 (NASA-CR-150)
cosmic proton-nucleus collisions in, radioisotopes from, 17: 9177
cosmic proton reactions with matter in interstellar, secondary proton spectra from, (T), 20: 5973
cosmic radiation distributions and interactions in interplanetary, (T), 19: 29014 (NASA-CR-151)
cosmic radiation effects on meteorites in, 17: 5060
cosmic radiation hazards in, 17: 6305 (BNL-6501)
cosmic radiation hazards in, 18: 16735
cosmic radiation intensity variations in, 16: 26053
cosmic radiation intensity in, 18: 22699
cosmic radiation measurement in, telemetry systems for, 17: 16879
cosmic radiation measurements in, 20: 39627
cosmic-radiation origins in extragalactic and galactic, 16: 32258
cosmic radiation origins in metagalactic, 17: 3953
cosmic radiation properties in galactic and metagalactic, 16: 32259
cosmic radiation production and properties in (E/T), 19: 3003
cosmic ray absorption in ionized gases in interstellar, r-f, (T), 20: 6020
cosmic-ray energy density in intergalactic, 18: 4420(T)
cosmic ray flux in interplanetary, 18: 28287
cosmic-ray intensities in, 17: 24235
cosmic ray intensity in interplanetary, 18: 22703
cosmic ray variations in interplanetary, (E/T), 20: 4522 (CNIE-PE-5)
cosmic-ray distribution in interplanetary, solar, (T), 19: 27114(T)
cosmic-ray intensity gradient and variation in interplanetary, (T), 20: 17312(T)
cosmic-ray propagation in galactic and intergalactic, plasma effects on, (T), 20: 34062(T)
cryogenic simulation, 18: 22844
density of, performance of d-c and r-f resonance electric probes of, (T), 19: 15832
dielectric properties, 18: 11513 (NP-13539)
dimensionality of, in classical and relativistic mechanics, 17: 14987
Dirac monopoles in cosmic, behavior of, 18: 8992
distribution of electrons in outer, determination of, 17: 609(T) (JPRS-15740(p.103-11))
disturbances in, due to fast moving artificial satellites, 17: 16863
dust particles in interplanetary, charged, 20: 37913(T)
effects of interplanetary, on cosmic ray modulation, 20: 37497
effects of radiation conditions on plant growth, 17: 17776(T) (JPRS-18395(p.173-8))
effects on plastics, bibliography on, 17: 2006 (PLASTEC-12)
Einsteinian equations for, description of stationary spherically symmetric solution for, 17: 31142
electrodynamics in, cosmic, 18: 17122(T) (NASA-TT-F-175)
electromagnetic radiation in, survey of, 17: 34701
electromagnetic-signal propagation through, distortion effects, 17: 16890
electromagnetic states of interplanetary, effects of solar winds on, 18: 24345
electromagnetic state changes in interplanetary, cosmic ray intensity variations from, 18: 24345
electron acceleration in interstellar, 17: 2387
electron and proton distributions in, measurements of, 17: 16893
electron bremsstrahlung radiation doses in, computer program for, 19: 40062 (N64-29366)
electron content in cislunar, radar measurements of, (E), 19: 45176
electron content in cislunar region of, effects of coherent density fluctuations on radar determination of, 20: 31857
electron density in interplanetary, limitations of optical methods for measuring, 17: 20810
electron density in intergalactic, 17: 25852(R) (NP-12877)
electron density in, photon flux from model for, 17: 26275
electron density in interplanetary, 18: 22821
electron density in interplanetary, 18: 22822
electron density measurement in, 16: 10774
electron detection and measurement in, system for, 20: 21116
electron distribution in, from neutron decay following bomb explosion, 17: 34669
electron distribution in magnetosphere boundary, Explorer XII observations on, 18: 26246
electron distribution in, measurements of, 17: 16893
electron flux density in interplanetary, (E), 20: 34048
electron spectra measurements by Discoverer 29 and 31, 17: 9171 (UCRL-6902-T)
electrostatic potentials of metallic spheres in interplanetary, 16: 26050
electrostatic screening of bodies in, 16: 18695 (AFOSR-1399)

energetic particles and fields in, physics of, 16: 9343
environment, effects on vehicles and crew in vicinity of earth-moon system, 16: 26627 (ASD-TR-61-201)
environment simulation, use of gaseous and liquid helium in facility for, 17: 28075
environment simulation of, spacecraft testing requirements for, 17: 34085
environment simulation, ultrahigh vacuum systems for, 17: 36465
environment simulation of, for resistance evaluation of electronic equipment, 18: 7018
environment simulation facility for electric propulsion research, 20: 18885 (N-65-23253)
environmental characteristics, 16: 10400 (ASD-TR-61-322(p.1-7))
environmental characteristics of, 17: 2140 (AFCRL-62-270)
environmental effects on glass fabric-reinforced plastic laminates, 16: 5721 (NP-11182)
environmental effects on liquid propellants and their storage systems, bibliography, 16: 21845 (AD-266034)
environmental effects on spacecraft materials, 17: 13869
environmental effects on polymers and nonmetallic materials, 17: 13870
environmental effects on vibration damping materials and techniques, 17: 29262
environmental effects on plastics and elastomers, 17: 29263
environmental effects on fabrication of foamed polyurethane structures, 17: 29264
environmental effects on fluorocarbon plastics, 17: 29265
environmental effects on reinforced plastics, 17: 29266
environmental effects on lubricants, 17: 29270
environmental effects of, evaluation of methods of testing, 17: 29271
environmental effects of, simulation of, 17: 32884 (ABDC-TDR-63-118)
environmental effects on molybdenum disilicide coatings, 17: 36333
environmental effects on Teflon FEP and TFE resins, 18: 12555 (NP-13615)
environmental effects on electronic and mechanical components, literature survey, 18: 30239 (RSIC-151)
environmental effects on materials, 18: 34235
environmental effects on elastomeric and plastic materials, literature survey, 18: 42112 (RSIC-150(Vol.I))
environmental effects on plastics, 18: 42113 (RSIC-150(Vol.I)(App.B))
environmental effects on coatings, 18: 42114 (RSIC-150(Vol.I)(App.C))
environmental effects on structural adhesives, 18: 42115 (RSIC-150 (Vol.I)(App.D))
environmental effects on laminates, 18: 42116 (RSIC-150(Vol.I)(App.F))
environmental effects on plastic potting compounds, 18: 42117 (RSIC-150(Vol.I)(App.G))
environmental effects on seals, O-rings, and gaskets, 18: 42118 (RSIC-150(Vol.I)(App.H))
environmental effects on elastomers, data on, 18: 44239 (RSIC-150 (Vol.I)(App.A))
environmental effects of, on white blood cells, Gemini III experiment design for study of, 19: 8794(R) (ORNL-TM-940)
environmental effects in man, design criteria for man-machine system for studies of, 19: 21812 (AEDC-TDR-63-256)
environmental effects on spacecraft materials and components, 19: 37169 (NP-15115)
environmental properties outside earth's atmosphere, 16: 33522 (REIC-24)
environmental radiation effects on diodes and transistors in, 18: 2383
environmental radiation effects on organic engineering materials, research program on, 19: 9730(R) (FZK-217)
environmental simulation of, for solar absorptivity measurement, 18: 39420
environmental simulation of, extreme high vacuum for, 18: 41630
environmental survey, 19: 44893 (NASA-CR-294)
existence of life in, design of radioisotopic biochemical probe to determine, 16: 18733(R) (NP-11678)
exploration and utilization, 16: 28629
exploration of, development of instrumentation for, 17: 41225
exploration of, results of Soviet, 17: 28594(T) (FTD-TT-62-202)
fields and matter in interplanetary, 17: 7678
fields in, physics of, 16: 9343
galactic and extragalactic astronomy, space techniques, 16: 9335
galaxy distribution in, mathematical analysis of, 20: 34074
gamma and x-ray production in, (T), 19: 27057
gamma production in, experiments for determination of, 17: 28061
gamma radiation flux in, 20: 36095 (CEA-R-2939)
gamma radiation in, measurement and origin of, (E), 19: 8056
gamma radiation measurement in, telemetering system for, 18: 12824
gamma ray intensity in, high-energy, (E/T), 20: 2586
gas cloud formation in interstellar, 18: 22650(T) (JPRS-24435(p.274-304))
gas expansion in intergalactic, relativistic, (T), 20: 37503
gas in galactic, kinetic properties of cosmic-ray, 20: 34127
gas in interstellar, cooling mechanisms for, 18: 42272
gas temperature in intergalactic, 20: 25706(T)
gas temperature in intergalactic, (T), 20: 29879
gases in interplanetary, properties of, 18: 28224
geodesics of space-time surface, gravitational effects on, (T), 19: 47192
geomagnetic-field boundaries in, toward sun, 17: 18301
geomagnetic fields, 16: 20234
geomagnetic fields and magnetism in, 16: 27860(T) (JPRS-13505)
geomagnetic micropulsations in, theory of, 17: 18289 (AFOSR-2764)
helium and hydrogen in interstellar, determination from Lyman-α absorption profile, 17: 34695
helium and hydrogen isotope measurement in, development of counter telescopes for, 19: 39419(R) (ATN-63(9219)-1)
helium in interstellar, determination from Lyman-α absorption profile, 17: 34695
helium isotope measurements in, development of counter telescope for, 19: 39419(R) (ATN-63(9219)-1)
hydrogen atom density in intergalactic, 18: 7374
hydrogen density in intergalactic, limits on ionized, (T), 19: 47196
hydrogen detection in intergalactic space, sensitive method for, (E), 19: 44908
hydrogen distribution in interplanetary, 17: 41690
hydrogen molecule abundance in interstellar, metastable, 18: 10743
hydrogen molecule content in interstellar, 20: 34071
hydrogen molecules in interstellar, para- and ortho-, 17: 3911
hydromagnetic shocks in, collisionless, 18: 34393
hydromagnetic wave propagation in interplanetary, 18: 30379 (NASA-CR-55384(p.313-68))
hydromagnetic wave propagation in (T), 19: 2951
hydromagnetic waves in interplanetary plasma, 20: 35991
hydroxyl radical abundance in interstellar, gas-kinetic exchange reactions for, (T), 20: 19339
interactions of instabilities and waves in, analytic method for, 18: 28862
interplanetary dust grain perturbation in, 18: 24279
ionization fronts in HII region of interstellar, effects of magnetic fields on, 18: 14711
isotropy of, significance of, 16: 28352
light propagation in, Lorentz principle for, 20: 42072
light propagation in, Lorentz principle for, 20: 42073
lubrication in, survey of problems of, 18: 13989
magnetic field effects on solar-injected charged particle propagation and storage in interplanetary, 20: 31884
magnetic field filamentary structure in interplanetary, 20: 34131
magnetic field in, theory and evidence for, 19: 16359
magnetic field inhomogeneities in interplanetary, from propagation of protons from solar flare, (T), 20: 23851
magnetic field origin in, 16: 21234
magnetic field polarity in interplanetary, variations in, 20: 31860
magnetic field structure in interplanetary, (E), 20: 34047
magnetic field structure in interplanetary, review of, 20: 37898
magnetic field-plasma interactions in, 19: 37435
magnetic fields in interplanetary, measurements and properties of, 16: 30993
magnetic fields in interplanetary, model of, 16: 32249 (AFCRL-62-225)
magnetic fields in, review on, 18: 2513(T) (FTD-TT-63-968(p.89-171))
magnetic fields in interplanetary, measurement of, 18: 28225
magnetic fields in interplanetary, properties of, 18: 30671
magnetic fields in, properties of, 18: 32357
magnetic fields in interstellar, properties of, 18: 32354
magnetic fields in, measurement of, 19: 18658
magnetic fields in interplanetary, review of properties of, 20: 7990
magnetic fields in interplanetary, measurements of, (E), 20: 31887
magnetic fields in interplanetary, structure of, 20: 34046
magnetic fields in interstellar, Petschek's mechanism for dissipating, 20: 41595
magnetic structure of galactic and interplanetary, 18: 32504
magnetized clouds in, cosmic-shower production by, 17: 19030
man in, mission of, 17: 18354 (TID-7652(p.vii-xvii))
massive condensation in, theory of, 18: 34394
materials for, techniques and results obtained from study of, 17: 16724
matter accretion by massive objects in interstellar, 18: 42271
matter distribution and motion in intergalactic and interstellar, 20: 23854
meteoroid distributions in interplanetary, 18: 28223
meteoroids and radiation in, 17: 36559
model of interplanetary medium, 17: 5165
model of interplanetary gas, 17: 6909
model of interplanetary medium, 18: 7394
models of cislunar, development for use in design of space flight simulators, 17: 19686(R) (CAL-VG-1403-G-5)
molecular hydrogen abundance in interstellar dust, 16: 2386 (AFOSR-1401)
molecular hydrogen in interstellar, processes for formation of, 17: 39815
molecular hydrogen in interstellar, distribution of, 17: 39816
neutrinos and antineutrinos in, 16: 6938
neutrons in, sources of, 17: 13299 (NASA-TN-D-1696)

nuclear detonation in, emission of Cherenkov electromagnetic radiation from, 19: 31135 (UCRL-7495)
nuclear explosion detection in, by satellite detectors, 19: 774 (LAMS-3074)
nuclear explosions in, satellite detection of (T), 19: 2471 (SC-DC-64-1591)
nuclear reactions in, processes in, 18: 28228
nuclear safety in, outline of standards and evaluation of, 19: 20206 (TID-7698(Pt.I)(p.31-2))
particle distributions in interplanetary, 18: 28223
particulate contents, 16: 20233
photoelectric screening of bodies in, 17: 5166
physics of, discoveries in, 17: 8961
physics, activities at Chalk River, 19: 9771(R) (PR-P-63)
plasma distribution in, 17: 26276
plasma existence and properties in interplanetary, review of, 17: 2365 (TID-17074)
plasma in interplanetary, evidence for, 17: 20809
plasma in, observations on, 18: 24749 (CONF-521-2)
plasma in, properties of, 18: 32357
plasma instability in interstellar, gravitational and magnetic effects on, 20: 42422
plasma interactions with vehicle having electric propulsion device, 17: 31784
plasma interactions with magnetic fields in, (T), 19: 19266(T) (FTD-TT-64-1316(p.948-51))
plasma perturbations in interstellar, fragmentations from, 20: 41593
plasma physics, 20: 44069 (IPPJ-44(J))
plasma probe for interplanetary, 18: 18611
polarization of interstellar, by graphite flakes, 17: 16915
properties at very short distances, (T), 19: 4944
properties between 300 and 22,000 miles, 18: 12996 (RTD-TDR-63-1050)
properties of, conference, 17: 16874
properties of interplanetary, book on, 19: 1162
properties of interplanetary, (E/T), 20: 4522 (CNIE-PE-5)
properties of interstellar, 20: 23866
properties of interplanetary, determination from electromagnetic wave propagation, (T), 20: 28518(T)
properties of, description of instruments for measuring, 19: 2585
properties of, test for isotropy of, 18: 11016
propulsion systems for, nuclear, 17: 33386
proton dosimetry, 16: 13860 (AD-261696)
proton flux in interplanetary, during last 100,000 years, 20: 23918
proton production in, experimental detection of, (T), 19: 4808
proton spectroscopy in, using spark chambers, 18: 39706
radiation and temperature effects on materials in, 17: 34523
radiation damage in silicon devices in, 20: 21165
radiation damage to propellants in, detection of, 16: 30894 (ANL-6585)
radiation distributions in, effects on manned space missions, 20: 2652 (NASA-SP-71, pp 1-4)
radiation dose measurements in, using thermoluminescent dosimeters in recoverable satellites, 17: 41247 (NRL-5938)
radiation doses to tissues from alpha particles and heavy nuclei in solar particle beams in, 20: 37023 (N-65-33865)
radiation dosimetry in, using personnel dosimeters, 20: 45963 (SZS-6/66)
radiation effects on man in, 17: 5868
radiation effects on materials in, 17: 8910
radiation effects in, laboratory for studying, 17: 18364 (TID-7652(p.201-20))
radiation effects in, NASA laboratory for studies of, 17: 32699
radiation effects on telemetry systems in, pulsed, 17: 34522
radiation effects in, evolution of organic compounds by, 17: 38653
radiation effects in, compilation of projects on, 20: 2433 (REIC-Memo-27)
radiation effects in, conference on, 20: 21164
radiation effects on biological materials in, 20: 26711
radiation energy, nature, and fluxes, 17: 17777(T) (JPRS-18395(p.179-202))
radiation environment in *cis*-lunar, 18: 4412 (ASD-TDR-62-606)
radiation environment in, 18: 12757
radiation environment of, 19: 16326 (REIC-37)
radiation environment in, 19: 24268
radiation environment of, 20: 8743 (LA-DC-6827)
radiation environment in, 20: 11181
radiation environment in, review of, 20: 15232
radiation environment in, review on, 20: 17249
radiation environment in, review of effects on electronic components, 20: 16911
radiation environment for space vehicles, 20: 25751 (N-65-35246)
radiation flux in, determination of integral, 18: 2561
radiation hazards in, 18: 141
radiation in, high-energy, 17: 9160
radiation in, measurements and nature of, 16: 19660
radiation in, measurement of solar-flare produced, 18: 4415
radiation measurement from satellites, instruments, 16: 9711 (LMSD-288084)
radiation measurements from Soviet spaceships, 17: 17777(T) (JPRS-18395(p.179-202))
radiation sources and properties, review, 16: 32644(R) (UCRL-10211 (p.16-42))
radiation spectroscopy in, using spark chambers, 18: 27802
radiation transfers in interstellar, (T), 20: 39570
radiations in, shielding from, 17: 15055 (RM-3144-PR)
radiations in, summary of information on, 17: 15052 (AMRL-TDR-62-86)
radio emission in quasi-stellar, 18: 22663
radio sources in extragalactic, declination of, 19: 30926
radio sources in, properties of extended, 18: 26190
radio sources in, neutrino fluxes from, 18: 32346
radio sources in, properties of quasi-stellar, 18: 36127
radio sources in, interplanetary irregularity effects on intensity scintillations of, 19: 1151
radio sources in, spectra of discrete, (E), 20: 7698(T)
radio wave propagation in, book on, 18: 42548
radio wave propagation through ionized gas in intergalactic, dispersion in, (T), 19: 32871
radioisotope applications in explorations of, review, 19: 8731
radionuclide power for, 17: 15517
reactor operation in, electrostatic energy from, (T), 20: 18131
relation to isospace, 16: 3558
remote handling in, evaluation of proposed methods for, 19: 46486 (CONF-640508, pp 233-47)
research in, spectroscopic, 17: 27669
research methods and results in, 16: 15501
research on, 18: 16730(T) (FTD-TT-64-90)
research on cosmic, by Soviets, 18: 5876
research program on, British, 18: 21091
research programs, 16: 14377 (NASA-TN-D-1173)
research programs, 18: 43140(T) (FTD-TT-64-892)
research using rockets and satellites, techniques for, 17: 22955
role of electrostatic forces, 16: 9739
satellite orientation in, determination of, 19: 38957(P)
satellites in, electromagnetic effects near, (T), 19: 39683
shock propagation in interplanetary, collision-free hydromagnetic, (E/T), 20: 31891
shock wave interactions in, effects on geomagnetic storms, 17: 19017
shock waves in interplanetary, production by solar flares, (T), 20: 44098
shock-wave stability and structure in interplanetary, (T), 20: 19326 (N-65-23194)
simulation of conditions in, system for, 18: 29856
simulation of, for ground testing of ion engines, 17: 19685 (AEDC-TDR-62-152)
simulation of, liquid helium and nitrogen supply systems for heat-sink and vacuum, 17: 28078
simulation of, beam divergence effects in, (T), 19: 18104
simulation of, d-c particle accelerator, 18: 29857
simulation of, development of vacuum techniques for, 19: 38842
simulation of, for biological studies, 19: 29893(R) (ANL-6971(p.166-205))
simulation of, problems in nuclear-eryogenic system for reactor testing, 18: 13326
simulation of, vacuum system for, 19: 15743
solar battery degradation in, expression for, 17: 18367 (TID-7652(p.243-59))
solar-battery performance in, testing of, 17: 9114
solar event effects in, review on, 19: 16365
solar-flare disturbance propagation in interplanetary, 16: 30996
solar particle propagation through interplanetary, 18: 28212
solar particles and plasma in interplanetary, 18: 36152
solar plasma in interplanetary, properties of, 18: 28214
solar proton diffusion in interplanetary, model for anisotropic, 20: 9645
solar proton velocity distributions in interplanetary, 18: 28222
solar radiation energy and intensity variations in, 18: 32358
solar radiation propagation in interplanetary, 19: 20757
solar wind, hydrodynamics of, 16: 3597
solar wind in, detection and properties of (E/T), 19: 2949
solar wind velocity in, consequences of nonuniformity, 17: 16913
space environment in, definition of, 20: 11840
spectra of hydroxyl ions in, microwave-emission, (T), 19: 4806
spectra of interstellar, problems in, 18: 8979
spectra of interstellar, 18: 21089
starlight polarization in, 18: 20725
structure of, group theoretical formalism of relativistic quantum theory for, 19: 10127
studies of outer, bibliography of Soviet rocket and satellite, 19: 37200(T) (JPRS-30925)
studies, possible projects for rocket-borne nuclear instruments, 16: 33617

temperatures of, effects on materials, 17: 34523
trajectory calculations for, computer program for generalized, 19: 48096 (SC-DR-65-271)
transport properties of matter in interplanetary, review, 17: 2143
wave propagation in interstellar, cosmic ray damping effects on, (T), 20: 29959
x-ray production in interplanetary, (T), 19: 34855
x-ray production in, (T), 19: 27057
x-ray scattering by grains in interstellar, small-angle, 19: 30919
x-ray sources in, 18: 26200
x-ray sources in, Galactic Radio Spur Association with Scorpio, 19: 1152
x-ray sources in, properties of Scorpius, (E), 20: 29882
x-ray sources in, in direction of north galactic pole, 20: 44095

Space Charge
see Electric Arcs

SPACE FLIGHT
see also Astronautics
air ionization in hypersonic re-entry, effects of cesium and sodium-contaminated cone materials on, 19: 41121 (N64-30658)
analysis of logistic vehicle for lunar, using nuclear-electric propulsion, 18: 35210
analysis of lunar, 19: 34857
analysis of straight-line flight to Mars, 16: 17326
bibliographies on biological effects of, 19: 8786 (NASA-SP-7011(02))
bibliography, December 1961, 16: 9719 (NP-11321)
bibliography on, 19: 42231 (NASA-SP-7011(11))
bibliography on biological aspects of space environmental conditions, 18: 4943 (SB-521)
bibliography on biology of, 18: 6587 (NP-13406)
bibliography on biological aspects, 19: 21787 (NASA-SP-7001(08))
bibliography on economic and legal aspects of, 17: 21390 (NP-12729)
bibliography on effects on polymeric materials, 16: 5722 (NP-11194)
bibliography on legal and economic questions of atomic energy, rocket technology, and space travel, 18: 4908 (NP-13324)
bibliography on legal and economic questions on, 18: 29148 (NP-13994)
bibliography on nuclear, 20: 35128 (NP-16129)
bibliography on propulsion and power units, 16: 12783 (CNLM-2370-3 (Pt.I))
bibliography with abstracts, Nov. 1961, 16: 6243 (NP-11176)
biological aspects of space environmental conditions, 19: 24268
biological effects of radiation in, in animal cells, 16: 32723 (AF-SAM-62-67)
biological effects of radiation in, 17: 16341
biological effects on microorganisms and tissue cultures, 17: 17774(T) (JPRS-18395(p.148-55))
biological effects on plant seeds and fungus spores, 17: 17775(T) (JPRS-18395(p.161-72))
biological effects of radiations encountered during, 17: 35276(T) (FTD-MT-62-78)
biological effects of, bibliography on, 18: 35261 (NASA-SP-7011)
biological effects on plants and animals, preparation for studies of, 19: 2074(R) (ORNL-3700(p.98-100))
biological effects of, 19: 8786 (NASA-SP-7011(02))
biological effects of cosmic radiation in, (E), 19: 29946
biological effects in man of, 19: 42232(T) (ANL-Trans-209)
biological effects in man, bibliography on, 19: 43718 (NASA-SP-7011(12))
biological effects in man, bibliography on, 19: 43719 (NASA-SP-7011(13))
biological effects of, bibliography on, 19: 21790 (NP-14982)
biological experiment design of Gemini III mission, 19: 8794(R) (ORNL-TM-940)
book: *Advances in Space Technology*, 18: 20673
book: *Astronautical Engineering and Science from Peenemunde to Planetary Space, Honoring the Fiftieth Birthday of Wernher von Braun*, 18: 18493
book: *Dynamics of Manned Lifting Planetary Entry*, 17: 33438
book: *Electromagnetic Aspects of Hypersonic Flight*, 20: 7991
book: *Geophysics and Space Data Bulletin No. 3*, 19: 47447 (AD-612083)
book: *Ion Propulsion for Space Flight*, 19: 7672
book: *Physiological Problems in Space Exploration*, 18: 21757
book: *Power Systems for Space Flight*, 18: 22578
book: *Problems in Cosmic Biology*, 17: 27196
book: *Problems of Radiation Safety of Cosmic Flights*, 19: 36088
book: *Problems of Radiation Safety in Space Flights. Physical and Biological Studies with High-Energy Protons*, 20: 10604(T) (NASA-TT-F-353)
book: *Problems of Space Biology*, 17: 17769(T) (JPRS-18395)
book: *Radiation Safety in Cosmic Flights*, 20: 23417
book: *Space Propulsion*, 20: 7249
conference, 17: 18353 (TID-7652)
conference, 19: 13611
conference on aeronautical sciences, 20: 14729
conference on business opportunities in nuclear, 17: 19695
conference on environmental sciences in, Los Angeles, Apr. 17, 18, and 19, 1963, 18: 12792
conference on environmental aspects of, 20: 24828
conference on materials in space technology, London, Nov. 22, 1961, 18: 44081
conference on propulsion, Pasadena, Calif., Aug. 24 to 26, 1960, 16: 5090
conference on simulation in space technology, 19: 38784
control equipment for, radiation effects on, 17: 30795(R) (AD-258338)
control systems for, radiation effects on, 19: 849(R) (FDL-TDR-64-30)
control systems, research program on radiation effects on, 18: 29920(R) (IBM-63-521-21)
cosmic radiation effects on manned, 16: 13843 (AD-262399)
cosmic radiation effects on astronauts, 18: 43238
cosmic radiation effects on manned, 20: 2652 (NASA-SP-71, pp 1-4)
cosmic radiation effects on manned military, (T), 20: 2656 (NASA-SP-71, pp 265-86)
data analysis and display for SNAP-10A tests, computer program for, 18: 38563 (NAA-SR-Memo-9440)
detection of living organisms during, instrument for, 20: 18187(R) (N-65-16497)
development of manned exploratory, 20: 4525
development of structural materials applicable to, requirements for, 16: 10401 (ASD-TR-61-322(p.8-24))
effects of acceleration, vibration, weightlessness, and cosmic radiation in, 17: 17773(T) (JPRS-18395(p.136-47))
effects of acceleration, radiation, and vibration during, 19: 38358 (AD-612660)
effects of cosmic ray particles on body tissues, 20: 41187 (BNL-9468)
effects of drugs on biological stress in astronauts during, 20: 6915
effects of electrical, gravitational, and magnetic fields encountered during, on development and growth of plants, laboratory study on, 20: 42703(R) (ANL-7136, pp 302-14)
effects of heavy cosmic-ray particles encountered during, on corn seeds, 18: 3474 (BNL-6857)
effects of, on immune reactions in dogs, 17: 35278(T) (FTD-MT-62-78 (p.250-62))
effects of, on man, 17: 27115
effects of radiation and zero-gravity on leukocyte chromosome aberration induction, 20: 40635(R) (ORNL-TM-1550)
effects of radiation, vibration, and weightlessness in, 17: 17771(T) (JPRS-18395(p.104-22))
effects of simulated, on biocompatibility of Neurospora, 20: 40508 (ORNL-3922, pp 196-9)
effects of weightlessness on growth of wheat seedlings during, preliminary study, 19: 43717 (NASA-CR-303)
effects of, on genetics of seeds of pine and wheat, 20: 42912
effects on animals, (E), 19: 29841
effects on animals, physiological, 20: 22623(T) (UCRL-Trans-1232)
effects on auditory organs, 18: 41194
effects on biological indexes in Drosophila, 17: 27200
effects on biological materials, 20: 18363
effects on biological systems, 20: 32894 (AD-627686, pp 435-52)
effects on chromosomes of peas and wheat, 18: 1327(T) (FTD-TT-63-968(p.332-41))
effects on chromosomal rearrangements in Tradescantia, 18: 5042
effects on chromosomal aberrations in *Tradescantia paludosa*, 19: 15068
effects on chromosome aberrations in roots of higher plants, Vostok-5 and -6 results on, 20: 42909
effects on Drosophila, genetic, 17: 17771(T) (JPRS-18395(p.104-22))
effects on Drosophila, genetic, 17: 35279(T) (FTD-MT-62-78(p.303-24))
effects on Drosophila, genetic, 17: 35283(T) (FTD-MT-62-78(p.350-8))
effects on gamete lethality in Drosophila, causes, 18: 38860
effects on Habrobracon sperm, 19: 43721(R) (ORNL-TM-1217)
effects on hematopoietic organs in mice, 17: 27198
effects on human leukocytes, equipment for testing, 20: 12642 (Y-IA-17)
effects on man, 18: 13392
effects on man, 20: 16231 (UCRL-16377)
effects on man, bibliography on biological, 20: 56 (NASA-SP-7011(15))
effects on man, medical and physiological, 20: 32893 (AD-627686, pp 357-84)
effects on microspores of *Tradescantia*, 20: 28971
effects on mouse brains, 18: 5056
effects on mouse genetics, 20: 42986
effects on mutations of *Drosophila melanogaster*, 17: 33678
effects on mutations in Drosophila, 17: 35280(T) (FTD-MT-62-78(p.324-(p.324-9))
effects on mutations in fungi and higher plants, 17: 35281(T) (FTD-MT-62-78(p.329-44))
effects on phage production, radiosensitivity, and viability of *Escherichia*

coli cultures, · 20: 42912
effects on physical reactivity of organisms, (E), 19: 3898(T) (FTD-TT-64-1077(p.234-46))
effects on plants and seeds, 18: 1326(T) (FTD-TT-63-968(p.326-31))
effects on plants, genetic, 17: 35282(T) (FTD-MT-62-78(p.344-9))
effects on seeds, genetic, 20: 1649
effects on serotonin content of blood, 17: 35284(T) (FTD-MT-62-78 (p.358-69))
effects on serotonin content in animal blood, 19: 15095
effects on *Tradescantia paludosa* microspores, 18: 43265
effects on Tradescantia, 18: 43265
effects on wheat seeds and plants grown from them, 20: 31058
electric power for manned orbital space station, use of SNAP-2 for, 17: 24724 (AI-7950)
electric power requirements for, 19: 28472
electric, nuclear power sources for, 18: 13320
electron spectrometers for use in Gemini Project, 20: 21116
electronic equipment for, radiation vulnerability of, 20: 31619
electronics for, conference on, 18: 8042
energy and free flight time for elliptical trajectories in, minimum, (T), 19: 14920 (SC-TM-64-1708)
energy dissipation in tissues during, 20: 18290(R) (N-65-16483)
energy requirements for manned Jupiter-capture missions, 17: 7664
environment estimates, 16: 2792 (P-1335(RAND))
environment models for simulators, 17: 19686(R) (CAL-VG-1403-G-5)
environmental control and power in, biochemical fuel cells for, 17: 5663
environmental effects on vehicle structural materials, propulsion and re-entry, 18: 1840
environmental effects on vehicle structural materials, problems in, 19: 30832
environmental hazards in vicinity of earth-moon system, 16: 26627 (ASD-TR-61-201)
environmental problems of man in, conference on, 19: 45746
exposure to space radiation during, 20: 41219
feasibility of interstellar, 17: 17603 (JPL-TR-32-233)
feasibility of nuclear-propelled manned interplanetary landing mission, 20: 36999
fission product decay in SNAPSHOT I, 20: 12466 (NAA-SR-11642)
gas storage in, supercritical cryogenic systems for, 17: 9123
hazards from cosmic radiation during, 17: 35277(T) (FTD-MT-62-78 (p.37-148))
hazards from cosmic particles to, 17: 37017 (BNL-6621)
hazards from solar flares, predictions of, 17: 5164
hazards in, evaluation by assessing function of vestibular apparatus, 20: 45413
human engineering for, 19: 25820 (AD-608798)
human stresses in, methods for improving tolerance to, 19: 43842
instrumentation for, fabrication and testing of, 19: 32543(R) (AD-609255)
instrumentation in, shielding requirements for, 18: 10358
interaction experiment for Gemini-3, 20: 40508(R) (ORNL-3922, pp 196-9)
ion engines for, automatic control systems for, 18: 33698
launch abort environment studies, review, 19: 24749 (SC-RR-64-1651)
launchings, thermal energy measurement in extreme environments from aborted, 19: 11310(R) (SC-DC-64-1433)
legal aspects of future, 16: 5099
magnetic field effects, 16: 20234
magnetic-field interaction with dipole for propulsion in, (T), 19: 9790
magnetohydrodynamic propulsion, review of developments, 16: 6247
magnetohydrodynamics in theory of, 18: 2993
maneuvers in, energy requirements for, (E/T), 19: 17346 (NASA-CR-59366)
manned interstellar, feasibility of relativistic, 17: 26959
manned lunar missions, use of nuclear rocket engines in, 16: 3975 (NP-11035)
medical problems in, 18: 25045
meteorite encounter, psychological aspects of, 16: 20233
meteoroid penetration data from Explorer XVI, 18: 741
mission analysis for nuclear propulsion, 16: 6242 (LAMS-2632)
mission analysis for solar-heated hydrogen propulsion system, 19: 20137 (NASA-CR-59332)
mission analysis for nuclear rocket, Earth-Mars, 19: 29750 (NP-14985)
mission analysis for modular nuclear-rocket systems, Earth—Mars, 19: 32409
mission analysis for manned Mars landing using electric propulsion, 20: 9127 (NASA-TN-D-3194)
mission capabilities of electric propulsion for, 17: 32223
mission concept for manned Earth-Mars, with electric propulsion, 17: 21849
mission parameters for Martian round-trip, using dual electric-nuclear engine, 17: 28575
mission parameters for Jupiter orbit, using electric propulsion, 17: 32221
mission parameters for Mars, moon, and Venus, using nuclear propulsion, 18: 9722
mission parameters for planetary, using nuclear propulsion, 18: 11477
mission parameters for MGD propulsion system, lunar, 18: 10631
mission parameters for solar probe, 18: 33135
mission profile for manned Mars, using nuclear electric and rocket propulsion, 20: 12492
mission requirements for unmanned scientific probes, 17: 38573(R) (63SD760)
mission studies, development of manned orbiting research laboratory for, 19: 17341(R) (NAA-SR-10496)
missions analysis for unmanned fly-by and orbit, 19: 32401 (65SD4296)
nuclear auxiliary power unit for lunar exploration, 16: 15954
nuclear-power applications in, 16: 15950
nuclear power for, survey of Project Rover, 17: 26923
nuclear power supplies for, impact effects studies in safety assessment of, 18: 14114 (SC-DR-316-63)
nuclear power uses in, radiation safety problems for, 16: 15949
nuclear propulsion, hearings before Eighty-seventh Congress, 16: 8437
nuclear rocket applications in, 17: 29862
nuclear rocket applications in, projected mission requirements for, 19: 12814
nuclear rockets for, performance of, 19: 32408
nuclear rockets for manned, shielding mass requirements for, · 20: 8448
nuclear rockets in, 18: 35214
nuclear safety in, 18: 6513 (CONF-311-8)
nuclear systems for, development program for, 19: 1932
nuclear systems for, mission integration of, 19: 45661
nucleonics in, bibliography on, 19: 17440
orbits around Mars and Venus, trajectory parameters of entry and escape from, 19: 45649 (N64-32637)
payload and velocity determinations of nuclear rocket propulsion requirements for manned Mars spacecraft, 18: 4843
personnel protection against G forces, servo-restraint system for, 19: 46485 (CONF-640508, pp 210-23)
phantom for use in, design of dose-equated plastic, 20: 31455
plasma propulsion, 16: 28271
power conversion systems for, survey of, 19: 27131 (IRD-64-36(Pt.3))
power plants for electric-power and life-support systems in manned space stations, (E/T), 20: 5820 (NASA-CR-316)
power plants for, use of liquid metals as working fluids in, 18: 15602
power plants for, development of thermoelectromagnetic pumps for Rankine-cycle, (E), 20: 1988 (NAA-SR-11198)
power plants for, review of types of, 20: 41514(T) (AI-Trans-209)
power requirements, 16: 10399 (ASD-TR-61-322)
power requirements for unmanned, nuclear-electric, 19: 3713 (64SD892)
power sources for, safety problems in, 18: 31781 (A/CONF.28/P/286)
power sources for, atomic and electrical energy, 19: 12815
power supplies for, economic and technical problems in development of, 18: 13323
power system for Apollo mission, SNAP-27, 20: 33756
power systems, evaluation of solar batteries for, 16: 7324 (D2-5523)
power systems for, thermodynamic characteristics of Brayton-cycle, 17: 37344
power systems for, properties of liquid metals for electric, 17: 39246
power systems for, waste-heat radiators for, 20: 3556
power systems for, lectures on, 20: 29977 (N-65-32716)
preparation of Habrobracon and Neurospora packages for 1966 biosatellite, 20: 6783(R) (ORNL-3853, pp 105-10)
programs development for Ranger, Mariner A, and Mariner B, 16: 11335(R) (NP-11344)
programs of NATO countries, 16: 5097
propulsion by nuclear energy, survey of development, 16: 31339
propulsion, developments and progress, 16: 5098
propulsion development for planetary exploration, comparison of electric and nuclear, 19: 11388
propulsion development for, 19: 40222 (LA-3229, pp 10-47)
propulsion for, electric, 17: 37320
propulsion for, capabilities of solid-core heat-exchanger nuclear rocket, (T), 19: 10627
propulsion for, nuclear, 18: 31024
propulsion in, conference on, Chicago, Nov. 1961, 16: 18727
propulsion in, conference on nuclear, 17: 38438 (TID-7653(Pt.I))
propulsion in, ion acceleration device for, 19: 15738(P)
propulsion in, using electric thrusters and steam power plants, 20: 5639
propulsion of unmanned missions by nuclear stages, 17: 4362
propulsion requirements for electric systems, 16: 14363
propulsion requirements for interplanetary, 17: 7645
propulsion requirements and techniques for orbit launching, 17: 26922 (NASA-TN-D-1570)
propulsion requirements for Jupiter and Mars orbital, electric, 17: 32210
propulsion requirements for Mars mission, nuclear, 17: 42403 (LADC-5961)
propulsion requirements for unmanned scientific planetary missions,

18: 6510(R) (63SD886)
propulsion requirements for unmanned scientific planetary missions, 18: 35197(R) (64SD700)
propulsion requirements for interplanetary, interstellar, and lunar, 16: 1278 (UCRL-6570)
propulsion, review of dynamic engine development for, 17: 2630
propulsion system flight-testing for, ion, 17: 2638
propulsion system for, design of electric, 19: 22521
propulsion systems for, electric, 17: 8285
propulsion systems for Mars and Venus mission, parameters for electric, 17: 32222
propulsion systems for Mars missions, comparison of chemical, electrical, and nuclear upper-stage, 17: 33384
propulsion systems for, survey of, 17: 33387
propulsion systems for, effects of environment on, 17: 37323
propulsion systems for, electric, 18: 10208
propulsion systems for extended, electric, 19: 22524
propulsion systems for, review of cryogenic, heat transfer problems in, 19: 36634 (LA-DC-7224)
propulsion systems for, photonic, 19: 38837
propulsion systems for, development of electric, 19: 40768
propulsion systems for, survey on nuclear, 19: 42632
propulsion systems for, performance of plasma-jet, 20: 500
propulsion systems for, performance analysis of nuclear-electric, 16: 9710 (JPL-TR-32-159)
proton exposure during, evaluation of, 18: 22274 (N64-13186)
radiation damage to microelectronic equipment in, proton, 18: 30295
radiation dosage in, measurements of, 17: 23560(T)
radiation dose distributions in, 19: 30010
radiation dose estimates for Apollo, 20: 18190(R) (UCRL-16613)
radiation dose estimations for, 20: 32962 (AD-627686, pp 423-33)
radiation dose from solar particle storms to shielded astronauts, 16: 14366
radiation dose to astronauts in, computer codes for evaluation of absorbed, 19: 38014 (N64-29363)
radiation doses during manned, to Mars, 18: 28296
radiation doses during manned, to moon, 19: 27058
radiation doses from inner and outer radiation belts during manned, 20: 2663
radiation doses in, from bremsstrahlung and electrons in Van Allen radiation belts, 17: 18387 (TID-7652(p.760-72))
radiation doses in Vostok-3 and -4, 18: 10323
radiation doses to Gagarin and Titov in, 17: 34703
radiation doses to astronauts during ninth Mercury-Atlas mission, 20: 18942 (N-65-17115)
radiation doses to crews of space vehicles in, tolerable, 20: 24945(T) (N-65-35524)
radiation dosimeter for Apollo, 20: 25382(R) (N-65-36441)
radiation dosimetry in, role of time factor in, 16: 16188
radiation dosimetry of body tissues during manned, 17: 14086
radiation dosimetry instruments for tissue-equivalent plastic manikins, 17: 25585 (AFSWC-TDR-63-19)
radiation dosimetry during, effects of shielding on, 20: 18943 (N-65-21724)
radiation dosimetry during, using botanical materials, 20: 18964
radiation dosimetry in, detector for, 20: 33724(P)
radiation effects studies, 16: 10418 (ASD-TR-61-322(p.532-8))
radiation effects on materials in, 17: 8910
radiation effects of, on chromosomes and mutations in Drosophila, 17: 21549
radiation effects on electrical connectors and encapsulants for reactors in, 17: 37636
radiation effects during, high-energy, 18: 21902
radiation effects on man in, 18: 27082
radiation effects on control systems for, 18: 37473 (ASD-TDR-63-75)
radiation effects on astronauts during, predictions of, 19: 25907(R) (ORINS-49(p.127-31))
radiation effects on growth of wheat seedlings during, preliminary study, 19: 43717 (NASA-CR-303)
radiation effects on biological systems during, 20: 122
radiation effects on white blood cells of man during, 20: 5297 (ORNL-P-1734)
radiation effects on plants during, uv, 20: 18365
radiation effects on mice in simulated, gamma, 20: 18443
radiation effects on hematopoietic system of man during, 20: 31029 (BNL-10221)
radiation effects on phage induction and viability in *E. coli* during, cosmic, 20: 42910
radiation effects on phage induction and viability in β-mercaptopropylamine-treated *E. coli* during, cosmic, 20: 42911
radiation effects on man during, cosmic, 17: 22957
radiation environment of manned, 18: 12793
radiation environment during Apollo mission, 19: 21992
radiation environment for 230-day Earth-to-Mars, evaluation of, 20: 7655
radiation exposure in supersonic transports, 16: 29210 (NASA-TN-D-1383)
radiation exposure during, computational procedure for, 17: 18386 (TID-7652(p.739-59))
radiation exposure to astronauts from solar flares, recommended allowable, 17: 27605
radiation hazards, 16: 3598 (AD-257272)
radiation hazards in, relation to actinic spectrum time variations, 16: 8085
radiation hazards, analysis of Sputnik V data on, 16: 13848
radiation hazards for man, 16: 20242
radiation hazards in, electromagnetic, 16: 20244
radiation hazards, 16: 20245
radiation hazards from particles heavier than carbon, 16: 20246
radiation hazards from nuclear power plants, 16: 29265
radiation hazards, 16: 32644(R) (UCRL-10211(p.16-42))
radiation hazards, 17: 2815 (AD-275605)
radiation hazards, 17: 2816 (AD-276049)
radiation hazards in, 17: 14557
radiation hazards in, method for predicting human response to, 17: 17917
radiation hazards from protons, 17: 27596 (NP-12905)
radiation hazards, 17: 27197
radiation hazards from proton-induced radioactivity in inner radiation belt, 17: 28686(R) (UCRL-10683(p.1-14))
radiation hazards, 17: 35332 (NP-13060(p.301-38))
radiation hazards, 17: 39337
radiation hazards, 17: 41712 (RM-3043-PR)
radiation hazards from protons in, 18: 9932 (AD-402259)
radiation hazards in, 18: 21829(T) (FTD-TT-64-33)
radiation hazards from protons during, 18: 27067(R) (ORNL-3601 (p.110-15))
radiation hazards of human, 18: 29908
radiation hazards during, 18: 31824
radiation hazards in, 18: 31834
radiation hazards of, 18: 31228
radiation hazards during, 18: 33354
radiation hazards in, computer analyses of, 18: 35048 (AMRL-TDR-64-11)
radiation hazards of, 18: 38994
radiation hazards for manned, model environment for estimates of solar proton, 18: 39560
radiation hazards in, 18: 41677 (MTP-AERO-64-4)
radiation hazards during, cosmic, 18: 43841
radiation hazards assessment, 18: 43230(R) (ORNL-TM-924)
radiation hazards of, 19: 2184 (LA-DC-6681)
radiation hazards during, protective effects of hypoxia against, 19: 3995
radiation hazards in, statistical calculations of, 19: 7218
radiation hazards during, 19: 7742
radiation hazards in, 19: 14430
radiation hazards in, physiological foundations of, 19: 18198
radiation hazards in, review on use of protective drugs in, 19: 30001
radiation hazards to man in, biological effects of, 19: 46001
radiation hazards, 19: 45890
radiation hazards to man in, 20: 10719(T) (NASA-TT-F-353, pp 3-20)
radiation hazards from solar proton events, 20: 15191 (N65-20996)
radiation hazards from solar flares, protection against, (T), 20: 15192 (N65-21000)
radiation hazards during, 20: 16745
radiation hazards of, 20: 30222(T) (NASA-TT-F-389, pp 758-63)
radiation hazards in manned, method of evaluating, 20: 29058
radiation hazards from Lunar and Martian, tabulation of, 20: 32674 (NP-15697(Vol.3))
radiation hazards in, proton, 20: 31095
radiation hazards to astronauts from highly ionizing radiation, 20: 36627
radiation-induced activity in biological specimens in second Soviet, 17: 7845
radiation monitoring system for, development of, 18: 496
radiation monitoring on Project Mercury, 18: 43835
radiation problems in, biological and medical aspects, 16: 23432
radiation protection, 17: 17777(T) (JPRS-18395(p.179-202))
radiation protection problems for man in, 18: 12390
radiation protection of eyes during, 18: 25044
radiation protection measures for, 18: 33815
radiation protection in, electron bremsstrahlung, 19: 30008
radiation protection in, solar-flare proton, 19: 30009
radiation protection during long-duration, 19: 31803(T) (UCRL-Trans-1225)
radiation protection during, 19: 31810
radiation protection of astronauts during, 20: 38603(T) (AD-629422)
radiation protection during Voskhod I and Voskhod II, 20: 44990
radiation safety, 17: 17770(T) (JPRS-18395(p.9-25))
radiation safety criteria for manned, design and operational, 20: 8743

(LA-DC-6827)
radiation shielding in, 17: 19696
radiation tolerance criteria for man in, 16: 20882
radiation zone surveys in Russian, 16: 33667
radiobiological aspects of manned, exposure limits for, 17: 25969
radiobiological problems in Soviet, 18: 29303
radiobiological problems encountered in, 18: 37035(T)
radiobiology problems in, 19: 46000
radiological monitoring of missile test ranges, 18: 8556 (SC-DC-3553 (p.255-8))
re-entry burnup enhancement of hydrided uranium–zirconium fuel alloys, 18: 9619 (SC-DC-3553(p.295-327))
re-entry burnup of fueled-graphite particles, 18: 9620 (SC-DC-3553(p.329-50))
re-entry hazards from nuclear engine materials, source term program analysis of, 18: 8557 (SC-DC-3553(p.351-60))
re-entry, magnetohydrodynamic application of air during, 16: 18570
re-entry problems in, aerothermodynamic effects on, 17: 24728 (MND-P-2953)
re-entry safety hazards evaluation for SNAP-2 and -10A, 17: 38575 (NAA-SR-8303)
re-entry trajectories into gravitational field avoiding radiation belts, 16: 8082
re-entry burnup of reactor core materials, 18: 33130(R) (SC-DC-64-1061)
re-entry test of SNAP unit, RFD-2, 19: 24903 (SC-RR-65-45)
reentry analyses, 16: 28629
reentry simulation, design concepts for ARGMA 8000-kw plasma facility for, 16: 25499 (ARGMA-TN-2H5N)
rendezvous of Mariner II with Venus, 17: 28577
report of NASA activities to Congress, 17: 1157
report of NASA activities to Congress on, July-Dec. 1963, 19: 6884(R) (NP-14462)
research developments, summary, 16: 6244 (NP-11177)
research program at Oak Ridge National Laboratory, 1961 to 1963, 18: 13448(R) (ORNL-TM-720)
research programs on, NASA Semiannual Report to Congress, Jan. 1 to June 30, 1964, 19: 19453
rocket reactor power levels for unmanned travel to Mars, 16: 9712 (NASA-TN-D-474)
safety aspects of nuclear rocket operation, research program on, 19: 3726(R) (NUS-179)
safety hazards in manned, from solar flares, (T), 19: 20873 (D2-11608)
safety, health and nuclear technology, 16: 4411
safety problems of nuclear origin in, 17: 22949 (LADC-5765)
shielding for, design of minimum-weight, 17: 18388 (TID-7652(p.773-93))
shielding for, ionization loss and Monte Carlo calculations for, 17: 18383 (TID-7652(p.682-97))
shielding of, bibliography on, 20: 13965 (ORNL-RSIC-11)
shielding requirements for minimum exposure in, 16: 24013 (NASA-TN-D-1267)
shielding requirements for manned, 17: 16877
shielding requirements for, 17: 18382 (TID-7652(p.662-81))
simulation of, design of chamber for, 17: 3853
simulation of, facilities for, 17: 3854
simulation of ion engine performance in, 18: 34261 (AEDC-TDR-64-127)
solar event warning system for Apollo, 18: 30066
Soviet experimental results, bibliography, 16: 12790 (TID-15207)
Soviet experimental results on cosmic space and upper layers of atmosphere, 18: 5876
space and planetary environments, 17: 2140 (AFCRL-62-270)
technology of, conference, 17: 7674
thermal protection of materials in, use of mass transfer cooling for, 16: 3477 (WADD-TR-59-366(Pt.III))
thrust vector determination by differential comparison with unthrusted orbit, 16: 6251
use of reactors in, 19: 43591
use of simulated, for testing Habrobracon, 20: 40508(R) (ORNL-3922, pp 196-9)
uses for analyzing space phenomena, conference, 17: 16874
Van Allen proton time-integrated flux for low-acceleration trajectories, 18: 20816
vehicle motion in earth-moon-sun system, equations for, (T), 19: 14208

SPACE MEDICINE
bibliography, 19: 21790 (NP-14982)
bibliography on, 18: 4942 (SB-519)
bibliography on, 18: 6587 (NP-13406)
bibliography on, 18: 35261 (NASA-SP-7011)
bibliography on, 19: 21787 (NASA-SP-7011(08))
bibliography on, 19: 42231 (NASA-SP-7011(11))
bibliography on, 19: 43718 (NASA-SP-7011(12))
bibliography on, 19: 43719 (NASA-SP-7011(13))
bibliography on, 20: 56 (NASA-SP-7011(15))
bibliography on, 20: 20369 (NASA-SP-7011(22))
biological significance of supersonic transport radiation environment, 20: 40525
book: *Problems of Space Biology*, 17: 17769(T) (JPRS-18395)
cybernetics in, problems of, 17: 22956
effects of space environment on physiological functions of 5 USSR astronauts during flights of one orbit to 2 days, 19: 42232(T) (ANL-Trans-209)
environmental problems of man in space, conference on, 19: 45746
for astronauts, 19: 25820 (AD-608798)
hazards of space flight, 17: 17769(T) (JPRS-18395)
lectures on, 17: 35331 (NP-13060)
method for predicting human response to ionizing radiation, 17: 17917
proton tissue dose distribution, 16: 6256 (ONR-9(Vol.2)(p.420-32))
radiation dose relative biological effectiveness studies in, 18: 21897
radiation dose studies, 19: 24268
radiation doses from solar flares, proton, 16: 30992
radiation effects on astronauts during Apollo mission, 19: 21992
research programs on, NASA Semiannual Report to Congress, Jan. 1 to June 30, 1964, 19: 19453
review of recent developments in, 19: 31810
survey, 17: 20273
survey of space biology problems, 16: 12859
use of drugs in, review on, 19: 30001

SPACE POWER UNIT REACTOR
(AiResearch Mfg. Co.)
bearing tests for liquid metal pumps in, 19: 40703 (TIM-916)
boiler development for SNAP-50/SPUR, 20: 3554
boiler two-phase flow stability in SNAP-50/SPUR, simulation study of, 19: 4302 (APL-TDR-64-117)
design and development, 16: 30094(R) (SY-5396-R1)
design of generator and loop components for, 17: 30939(R) (SY-5396-R4)
development, 17: 7610(R) (SY-5396-R2)
development, 17: 12036(R) (SY-5396-R3)
development, 17: 26100
development, 17: 35218 (CONF-39-52)
development, 18: 29103(R) (APS-5071-R)
development, 19: 29732(R) (APS-5152-R2)
development, Apr.–June 1963, 17: 35223(R) (SY-5396-R5)
development, July-Sept. 1963, 18: 6516 (SY-5396-R6)
development of SNAP-50/SPUR for lunar bases and space propulsion, 20: 3553
frequency converter design for, 19: 29731(R) (APS-5152-R1(Suppl.1))
mission capabilities of SNAP-50/SPUR electric propulsion, (T), 19: 8660 (PWAC-447)
pump bearing development for, 19: 46458 (CNLM-6342)
radiator design and fabrication study, 18: 23095
test facility for, evaluation of, (E), 19: 31591 (CNLM-5983)
testing, 18: 24945
turbogenerator for, bearing analysis for, 18: 1281 (ASD-TDR-63-833)
turbogenerator liquid-potassium bearing tests, 18: 21666 (APL-TDR-64-27)

Space Travelers
see Astronauts

SPACE VEHICLES
see also Rockets
see also Satellites
ablation and heating of cylindrical and spherical re-entry bodies, methods for predicting, 19: 46537 (SC-RR-65-187)
aerodynamics of Saturn VN, 19: 44137 (N64-24017)
altitude control and orbit adjustment, 1-kev plasmajet thrusters for, 17: 17629
altitude reference system for, roll stabilized gyro, 20: 9129 (SC-R-65-1023)
analysis of ion-propelled, for satellite and probe missions, 17: 15513 (N62-11131)
analysis of lunar, using nuclear-electric propulsion, 18: 35210
assembly of beryllium alloy components for methods of, 20: 43859 (NASA-TM-X-53453(Vol.6))
atmospheric ionization by, effects on high-speed flight, 16: 29945
attitude control during interplanetary missions, evaluation of electric engines for, 17: 31777
beryllium fabrication and testing for use in Gemini, 19: 13975
beryllium uses in, 20: 23714
bibliography on electrically propelled, 16: 29480 (NP-11967)
bibliography on nuclear energy for, 16: 23345 (NP-11732)
bibliography on power for, 17: 4349 (AD-273676)
bibliography on power for, 17: 4350 (AD-273677)
bibliography on power for, 17: 4351 (AD-273678)
blast effects on, explosive simulation of nuclear, 18: 31687 (LADC-6458)
book: *Advances in Space Technology*, 18: 20673
book: *Astronautical Engineering and Science from Peenemunde to Planetary Space, Honoring the Fiftieth Birthday of Wernher von Braun*, 18: 18493

book: *Materials Science Research*, Vol. 2, 19: 37135
book: *Nuklearna Propulzija* (Nuclear Propulsion), 18: 4839
book: *Space Materials Handbook*, 20: 4312
carbon dioxide sensor for Gemini, 20: 37064
ceramic coatings for use in, flame-sprayed, 18: 16521
charged particle distribution around, (E/T), 19: 23189
coatings for components, development of high-temperature-resistant, 16: 15203 (WCLT-TM-59-104)
communications system concept for nuclear-powered interplanetary, 17: 21372
compatibility tests of Agena, with SNAP-10A FSEM-3, 19: 31597 (NAA-SR-11129)
component coating of, review of processes for, 17: 41383 (DMIC-Memo-172)
components for, heat treatment methods for beryllium alloy, 20: 43858 (NASA-TM-X-53453(Vol.5))
components of, cleaning and surface preparation for fabrication of beryllium alloy, 20: 43857 (NASA-TM-X-53453(Vol.4))
components of, forming methods for beryllium alloy, 20: 43856 (NASA-TM-X-53453(Vol.2))
condenser design and development, 16: 14354 (NASA-TN-D-1188)
conference, 17: 18353 (TID-7652)
conference, 19: 13611
conference on, 18: 11507 (AD-427700)
conference on aeronautical sciences, 20: 14729
conference on simulation in space technology, 19: 38784
construction materials for, thermal radiation properties of, 16: 32039(R) (PWA-1863)
construction of, use of beryllium in, 17: 32485 (MAB-193-M)
control and computer systems for, development of radiation-resistant, 17: 39687
control and guidance of ion-propelled, 16: 2787 (JPL-TR-32-166)
control of flight of, magnetohydrodynamic, (T), 19: 10421
control of, ion engine systems for, 18: 33699
control of, radioisotope thruster for altitude, 19: 42631
control system design for operation in nuclear radiation environment, 18: 11472 (ASD-TDR-62-424(Vol.1))
control systems for, review of pneumatic, 17: 26926
control systems for, radiation effects on, 19: 849(R) (FDL-TDR-64-30)
cosmic proton doses to, from solar activity, 18: 28904
cosmic proton dosimetry in, using silicon detector arrays, (E), 20: 2133 (NASA-SP-71, pp 245-50)
cosmic ray research using Mars-1 and Luna-4, 18: 42331(T) (FTD-TT-64-892(p.202-16))
damage by micrometeoroid impact (E/T), 19: 2947
description of, with nuclear propulsion, 17: 10210
design and development of Navigator, 18: 6510(R) (63SD886)
design and development of thermionic- and turboelectric-powered, 18: 35197(R) (64SD700)
design and operations criteria for manned, 19: 24268
design and operation of manned, environmental and radiobiology parameters in, 19: 26583
design and performance of Scout for SNAP-10A re-entry flight demonstration No. 1, 18: 31021 (SC-RR-64-511)
design, effects of space environment, 16: 26627 (ASD-TR-61-201)
design for Apollo mission, 19: 21992
design for maintenance of orbiting satellites, 19: 2488
design for manned Earth-Mars mission, 17: 21849
design for manned Mars mission, 20: 12492
design of altimetric system for, 19: 46749(P)
design of lunar excursion module, environmental effects on, 19: 36594
design of manned nuclear, 17: 17613
design of manned Van-Allen-belt, for heat, micrometeoroid, and radiation protection, (T), 19: 11315
design of mission-support components for (E), 19: 2919
design of nuclear for planetary landing missions, 16: 26628 (JPL-TR-32-231)
design of nuclear-electric, parametric approach for, 18: 9711 (63SD235)
design of nuclear thermoelectric powered, computer program for, 20: 6660 (NAA-SR-Memo-11514)
design of nuclear-electric, 18: 23091
design of nuclear-electric, for high-energy missions, 19: 44228
design of probe for detecting life on Mars, 17: 2633
design of solar probe, 18: 33135
design of unmanned nuclear, 16: 32611 (JPL-TR-32-281)
design of, for comfort of astronauts, 19: 25820 (AD-608798)
design of, influence of radiation on, 19: 44550
design parameters and performance of orbit-launched nuclear, 17: 26922 (NASA-TN-D-1570)
development, 16: 11335(R) (NP-11344)
development for unmanned scientific probes, 17: 38573(R) (63SD760)
development in West Germany, review, 18: 45070
development, landing, and propulsion of, review, 17: 17610
development of drive coupling for use in, 17: 5642(R) (NP-12270)
development of folded-flow reactor for, 17: 2583 (NP-12087)
development of manned orbiting station with SNAP-8 power plant (E/T), 19: 3712 (64SD647)
development of manned orbiting research laboratory, 19: 17341(R) (NAA-SR-10496)
development of Mariner, Ranger, and Voyager, 16: 11336(R) (NP-11385)
development of nuclear-electric-propelled unmanned, for Jupiter trip, 16: 34130
development of nuclear-powered, 17: 10206
development of nuclear propulsion for, 17: 22954 (TID-18558)
development of nuclear-powered, 17: 42402 (HW-SA-3205)
development of radiation-resistant flight control systems for, 17: 36336(R) (AD-295101)
development of radiation-resistant flight control systems for, 17: 36984(R) (AD-295100)
development of Ranger and Mariner A, 16: 3976(R) (NP-11109)
development of single-stage nuclear, 17: 12038
development of working fluids, 16: 10410 (ASD-TR-61-322(p.339-55))
development of, conference on, 20: 7717
development of, NASA Semiannual Report to Congress, Jan. 1 to June 30, 1964, 19: 19453
development of, review of programs for (E), 19: 2918
dynamic analysis of Sampler for Aerospace Nuclear Debris flight, 19: 44142 (SC-RR-65-286)
effects of meteoric particles, radiation, and space vacuum on, estimates of magnitude and nature of, 20: 2036 (AD-618030)
electric circuits of, design of switchgear for, 20: 20986(R) (N-65-29823)
electric energy for, development of radionuclide batteries to provide, 18: 5980
electric generating and propulsion system integration in, procedure for analysis and optimization of, 17: 24723(R) (AD-282752)
electric generator for, thermal analysis of superconducting, 17: 25381 (ASD-TDR-62-118)
electric power for, development of isotopic generators for, 20: 16115
electric power generation in, using closed Brayton cycle, 19: 44205
electric power requirements of, 19: 28472
electric power systems for, characteristics, 16: 18700
electric power systems for, review of, 18: 2576
electric power system for manned orbital, 18: 33719
electric power systems for, electrostatic, 18: 33720
electric power systems for, using mercury cycle, 18: 36846
electric propelled, capabilities and requirements for, 19: 32401 (65SD4296)
electric propulsion, power generation for, 16: 14355(R) (NP-11415)
electric propulsion of, design of powerplants for, 17: 13857
electric systems for, survey of advanced, 17: 3852
electromagnetic wave scattering by, in atmospheric plasma, (T), 19: 23820 (AD-606290)
electron bremsstrahlung radiation doses in, computer program for, 19: 40062 (N64-29366)
electron dose calculations for, models for, (T), 19: 23947
electron dosimetry for, (T), 20: 15936
electron reactions with Apollo wall sections, bremsstrahlung dose rates and spectra from, 20: 1306 (NASA-TM-X-1140)
electron shielding for, (E), 20: 42520
electronic equipment for, model for resistance evaluation of, 18: 7018
electronic equipment packaging for, 19: 2528
electronic equipment of, internal contamination of heated and irradiated components by microbes, 20: 18993 (N-65-24356)
electrostatic potential of spherical metallic, in interplanetary space, 16: 26050
electrostatic propulsion of, colloid engines for, 17: 4361
energy conversion and balance in manned, 16: 20237
energy requirements for manned Jupiter-capture missions, 17: 7664
entry into planetary atmospheres, acceleration measurements in, (T), 19: 41123 (NASA-TR-R-225)
entry of, dynamics of planetary, 17: 33438
environment considerations for thermal protective coatings, 16: 10414 (ASD-TR-61-322(p.436-55))
environmental control and power in, biochemical fuel cells for, 17: 5663
environmental effects of micrometeorites and radiation on, 16: 30916
environmental effects on, meteoroids and radiation, 17: 36559
environmental testing of, for SNAP-10A safety flight, 18: 23085 (SC-DR-285-63)
environmental testing of, laboratory and equipment for, 19: 4280 (NAA-SR-Memo-9438)
equipment design and materials considerations, 16: 2790 (NP-10947)
equipment for analysis of lunar surface, 20: 21003
equipment in Soviet, for analysis of cosmic-ray intensity, 19: 2650
experiments for solar-thermionic flight test, analysis of secondary, 20: 35983 (N-66-17619)
fabrication of beryllium structures for, 20: 46165 (NASA-TM-X-

53453(Vol.3))
flight demonstration (RFD-1) for SNAP 10A, 19: 1927 (SC-RR-64-502)
flight operations and missions for nuclear rockets, 19: 24157
flight-control systems for, design of radiation-resistant, 18: 37473 (ASD-TDR-63-75)
fuel leak detection using tracer, 17: 8556
fuel-tank radiation shielding, 16: 1269 (AD-256894)
fusion propulsion system requirements for interstellar probe, 17: 31759 (JPL-TR-32-397)
gamma spectrometer for Ranger, 16: 33193
gas storage in, supercritical cryogenic systems for, 17: 9123
guidance theory, 16: 26644(R) (NP-11755)
gyroscopes for, development of radiation-resistant control moment, 18: 7017
handling of, equipment for remote, 19: 46500 (CONF-641120, pp 67-70)
hazards to biological systems from atmospheric reentry and burnup of nuclear rocket reactors and power supplies for, 20: 42740 (LA-DC-7764)
hazards to man from use of radioisotopes in, 20: 46003
heat radiation to Agena mockup from SNAP-10A NPU, 18: 40930 (NAA-SR-Memo-9337)
heat transfer fluids for, 17: 34102
heat-shield ablation, instrumentation for measurement of, 20: 16778 (NASA-TN-D-3329)
heat-shield sublimation and ablation, use of radioisotopes in measuring, 20: 720
instrument design problems, review, 16: 34134
instrumentation and materials development, 16: 12789(R) (NP-11384)
instrumentation design requirements, 16: 25588
instrumentation design for, use of radiation in flight-control, 18: 31836 (ASD-TDR-63-697)
instrumentation for radiation measurements, calibration of, 17: 8586 (APGC-TDR-62-27)
instrumentation for, design of inverted magnetron-type mass spectrometer for analysis of planetary atmospheres, 17: 30837
instrumentation for exploratory, development, 17: 41225
instrumentation for SNAP-10A, shielding for (E/T), 19: 3722 (NAA-SR-9647)
instrumentation for, 19: 2585
instrumentation for cosmic ray intensity measurements, 20: 4252(T) (FTD-TT-64-1228)
instrumentation for Mariner IV, operation and sensitivity of, 20: 37341 (N-66-17354)
instrumentation of, redundant pulse-height discriminator for, 18: 16284
instrumentation of Mariner C, for detection and measurement of cosmic radiation, 20: 16822 (N-65-19927)
instrumentation of Mariner C, for trapped particle detection, 20: 19034(R) (N-65-27827)
instrumentation on Mariner A, for plasma measurements, 19: 34896 (N64-27821)
instruments for, 18: 20412
interactions of electrically propelled, with plasma in space, 17: 31784
interactions with ionized media, 20: 17537 (JPLAI/LS-641)
ion engines and power conditioning for, 19: 22521
ion engines for, 18: 33704
ion engines for space, accelerator grid erosion in electron-bombardment, (E/T), 19: 6014
ion engines for, effects of secondary electron emission in, 20: 16624 (N-65-17749)
ion engines for, flight testing of, 20: 16625 (N-65-19272)
ion engines for, power supplies for, 20: 18883 (N-65-21432)
ion engines for, power-conditioning systems for, 20: 31357
ion engines for, power conditioning for contact-ionization, 20: 31360
ion engines for, status of, 18: 37307
ion-engine systems for, development of lightweight, 20: 31364
launch information tabulation to Feb. 1962, 18: 20673
life support in, role of carbon monoxide in, 20: 28880
lifting surfaces for re-entry of, properties of infiltrated tungsten for, 20: 37188
lubricant development, 16: 10411 (ASD-TR-61-322(p.356-81))
lubrication problems in, 17: 6548
lubrication requirements for, review of, 18: 367 (AEDC-TDR-63-154)
lubrication techniques for power equipment in, developments in, 16: 10412 (ASD-TR-61-322(p.382-90))
magnetohydrodynamic generator for, for re-entry, 17: 33441
maintenance of nuclear powered, 18: 4845
maintenance of orbiting, design concept of remotely operated service module for, 19: 6039
maintenance of orbiting, remotely operated manipulator system for, 19: 46487 (CONF-640508, pp 248-303)
materials and structures for, 16: 19397
materials and structures for, conference on, 20: 877
materials development, 16: 6245 (NP-11181)
materials development for, powder metallurgy techniques in, 17: 1864
materials development for, 19: 37142
materials development for, 19: 37143
materials development for, 19: 37144
materials for, cryotemperature, radiation, and vacuum effects on, 18: 652(R) (FZK-163)
materials for, effects of radiation and cryotemperatures on mechanical properties of, 17: 37567(R) (FZK-161-2(Vol.II))
materials for ion propulsion systems, 17: 6544
materials for, performance under simulated space conditions, 17: 27506 (NP-12906)
materials for, properties of graphite, 16: 30825
materials for, properties of polymeric, 16: 30827
materials for, review on, 17: 4985
materials for, review of research on beryllium and beryllium compounds as, 17: 18742(R) (DCAS-TDR-62-62)
materials for, survey, 16: 30826
materials for, techniques and results obtained from study of, 17: 16724
materials for, evaluation of beryllium, titanium, and zirconium as, 20: 7503
materials for, evaluation of, 20: 15129
materials for, fabrication and properties of, 20: 29680
materials for, high-energy radiation effects on, 18: 44275
materials for, preparation of ceramic and metallic foam, 19: 37141
materials for, properties of glass as, 20: 7512
materials for, radiation effects on, 18: 44274
materials for, review of environmental effects on, 20: 7649
materials for, testing of, 20: 23794
materials of, radioinduced heating in nuclear propelled, 16: 32117 (NARF-62-12T)
materials testing for, 18: 10578 (NP-13539(Paper 8))
materials testing for nuclear-powered, 18: 34247
materials testing, 20: 11520
materials used in, performance and selection of, 20: 16944 (NASA-SP-3025)
metals for process equipment in, review on, 17: 39556
meteoroid bombardment effects on, simulation of, 18: 20707
methods for beryllium fabrication, 20: 46165 (NASA-TM-X-53453(Vol.3))
mission analysis for, using electric propulsion systems, 19: 6018
mission parameters for nuclear orbit launch, thrust and weight analysis of interplanetary, 17: 35234
mission performance evaluation, 18: 21674 (NASA-TN-D-2157)
motion analysis of probes, 16: 1275(R) (NP-10832)
motion in earth-moon-sun system, equations for, (T), 19: 14208
motion in interplanetary space and ionosphere, electromagnetic effects from, (T), 19: 39683
motion in Newtonian force field, (T), 19: 34857
motion under influence of earth-moon system, 19: 41205 (N64-31725)
neutron activation of structural materials in, (T), 19: 45461 (N64-25922)
neutron dose rates in, 18: 802 (AFCRL-63-214)
neutron doses in, from cosmic proton reactions in shielding, 18: 28538
neutron dosimetry in, spectrometers for, 18: 31936
nose cone aerodynamic properties, blunt and sharp, 19: 19439 (SC-R-64-1311)
nuclear equipment for determinations of elemental constituents of lunar surface, 16: 11339 (UCRL-5916)
nuclear power plants for, development, 16: 20236
nuclear power plants, effects of space radiation on, 16: 24547
nuclear power plants for, performance comparison of gas-cycle, 17: 31778
nuclear power systems for, review of, 18: 3303
nuclear power uses in, heat rejection problems for, 17: 16230(R) (PWA-16230)
nuclear-powered, development for, 16: 15943
nuclear-powered, development of heat rejection systems for, 17: 28574(R) (PWA-2197)
nuclear-powered, flight testing of SNAP-8 propulsion system for 70-kw(e), 16: 5079 (JPL-TR-32-190)
nuclear-powered, materials testing for, 18: 651(R) (FZK-147)
nuclear-powered, upper atmosphere re-entry study, 16: 16010 (MND-P-2699(Vol.II))
nuclear propulsion system fuel fate on re-entry, methods for determining, 16: 14352 (MND-P-2699(Vol.I))
nuclear rocket propulsion for manned Mars mission, 18: 4843
nuclear rocket system for Saturn V, modular, 19: 32409
nuclear rockets for manned, shielding mass requirements for, 20: 8448
nuclear safety hazards during launch and re-entry, 18: 9716 (SC-DC-3553(p.103-27))
nuclear systems in, evaluation of shadow shielding for, 16: 15993
nuclear-powered, contamination of stratosphere by, 18: 37367 (CONF-337-45)
nuclear-powered, design of beryllium-reflected thermoelectric reactor for, (E), 19: 5538(P)

nuclear-powered, development, 19: 33704
nuclear-powered, materials problems for, 18: 10464
nuclear-powered, use of thermionic elements in, 18: 20837
orbits of, determination of, 18: 2409(T) (FTD-TT-63-968)
particle and field investigations using U. S., 18: 21090
particle reactions with metal surfaces of, (E/T), 19: 25149
payload optimization for power-limited, 17: 21848
performance as solar-proton shielding, for manned missions, (T), 19: 20873 (D2-11608)
performance of arc-plasmajet thrustors, 16: 1276 (PLR-90)
performance of nuclear, instrumentation requirements for evaluation, 16: 11331 (JPL-TR-32-160)
performance of nuclear-electric, using SNAP-50, 18: 35211
performance of, book on, 20: 7249
performance parameters for interplanetary nuclear, 19: 45649 (N64-32637)
plasma engine for, steady-state operation of coaxial pulsed two-stage, 20: 31365
plasma engines for, propellant injection devices for, 20: 31363
plasma-jet engines for, performance of repetitively pulsed two-stage, 20: 23270 (N-66-16038)
plasma-jet engines for, performance of, 20: 25273 (N-65-15226)
plasma-jet engines for, development of coaxial, 20: 25275 (N-65-33367)
plastics applications for, in future, 17: 4365
power, analysis of nuclear turbo-generator cycle using reacting gas, 16: 11330 (ERR-SD-135)
power and propulsion systems, review of Kiwi, Rover, and SNAP, 16: 21857
power conversion systems for, recuperated Brayton cycle for, 17: 34103
power for, potential of nuclear energy for, 17: 10185 (AD-275297 (p. 15-17))
power for, reactor shield design for producing, 17: 12039
power generation during re-entry, performance of magnetohydrodynamic channel, 16: 31148
power generation in, analysis on nuclear, 20: 35130(T) (N-66-14377)
power generation problems, 16: 5091
power generator using hypersonic shock plasma around, 18: 9067 (SC-4960(RR))
power generators for, hypersonic plasma, 18: 32519
power generators for, hypersonic plasma thermionic, 20: 9701
power generators for, hypersonic plasma thermionic, (E/T), 20: 46322 (SC-RR-66-358)
power plant coolant requirements for, reactor, 19: 1923 (ANL-6857)
power plant design for, TRIKT-50, 20: 12482
power plant development, review of design and material problems in, 16: 10420 (ASD-TR-61-322(p.589-601))
power plant development for, 16: 17327
power plant for, torque production by SNAP-10A, (T), 20: 1528 (NAA-SR-11207)
power plant integration in Navigator, 17: 38573(R) (63SD760)
power plant pump development for, 19: 38781(R) (N64-25903)
power plants for, development of radiators for, 17: 4358(R) (PWA-2100)
power plants for, design and development of advanced solar thermionic, 17: 24726 (ASD-TDR-62-877)
power plants for, description of nuclear-electrogenerator, 17: 33391
power plants for, design of Brayton-cycle nuclear, 17: 35233
power plants for, development of nuclear-thermionic, 18: 7956(R) (GA-3992(Pt.I))
power plants for, feasibility of nuclear-thermionic, 17: 24725 (ASD-TDR-62-827)
power plants for, feasibility of nuclear-thermionic, 17: 42401(R) (AD-296862)
power plants for, ground-based safety analysis of nuclear, 18: 1955 (SC-DC-3248)
power plants for, integration studies on, 18: 4831 (ASD-TDR-63-428 (Pt.I))
power plants for, integration studies on, 18: 4832(ASD-TDR-63-428 (Pt.II))
power plants for Manned Orbiting Research Laboratory, SNAP-8, 19: 21720 (NAA-SR-10318)
power plants for manned orbiting stations, development of nuclear, (E), 19: 29730 (64SD-913)
power plants for manned, efficiency of thermally integrated electric-power/life-support, (E/T), 20: 5820 (NASA-CR-316)
power plants for unmanned, performance of SNAP-8 for, 17: 33392
power plants for, feasibility of nuclear-thermionic, 18: 12852(R) (AD-409570)
power plants for, distribution and generation subsystems in, 18: 24942
power plants for, development of nuclear- and solar-thermoelectric, 18: 24351(R) (AD-427285)
power plants for, development of thermionic, 18: 24370(R) (PWA-2337)
power plants for, development of thermoelectric, 18: 26251(R) (AD-437280)
power plants for, description of radioisotope, 18: 27830
power plants for, development of heat transfer systems for, 18: 29844(R) (SAN-409-1)
power plants for, development of nuclear-thermionic, 18: 35929(R) (GA-4769(Pt.I))
power plants for, development of MHD, 18: 40219
power plants for, design of 2.5- to 10-Mw(e) thermionic reactor, 19: 3728 (PWA-2319)
power plants for, startup of nuclear Rankine-cycle, 19: 3729 (PWA-2342)
power plants for, repairable nuclear (T), 19: 3743
power plants for, mission capabilities of SNAP-50/SPUR, (T), 19: 8660 (PWAC-447)
power plants for, condenser development for Sunflower solar, (E), 19: 9310 (NASA-CR-54013)
power plants for, development of Sunflower solar, (E), 19: 9311 (NASA-CR-54174)
power plants for, performance of fast beryllium-reflected cermet, (T), 19: 14876 (HW-78756)
power plants for, development of superconducting, (E), 19: 13566(R) (AD-421061)
power plants for, development of thermoelectric, (E), 19: 16444(R) (AFAPL-TR-64-135)
power plants for, re-entry burnup of nuclear, (E/T), 19: 17350 (RTD-TDR-63-3002)
power plants for, safety of reactor, 19: 19412
power plants for, development of pumps for mercury Rankine-cycle, 19: 20096 (NAA-SR-Memo-10729)
power plants for, description of multi-kwe nuclear-thermoelectric, (E/T), 19: 29771
power plants for, design of nuclear-reactor, (E/T), 19: 31590 (AI-Memo-7585(Rev.2))
power plants for, development of nuclear, (E), 19: 35840
power plants for, development, (E/T), 19: 38836 (NASA-SP-79)
power plants for, analysis of radiators for nuclear, (T), 19: 40731 (AD-609969)
power plants for, performance of nuclear-thermionic, 19: 45648 (GA-6478)
power plants for, analysis of nuclear Brayton-cycle, 19: 48048 (GE-65SD4251)
power plants for, design studies of, 20: 4299(R) (ORNL-2711)
power plants for, parameters of fast thermionic-reactor, 20: 12483
power plants for, review of nuclear, 20: 12484
power plants for, temperature distribution in fast thermionic reactor, 20: 12486
power plants for, weight of radiators for steam-cycle, 20: 14688 (N65-20692)
power plants for, development of uranium carbide–zirconium carbide fuels for thermionic, 20: 14959(R) (N65-20797)
power plants for, development of uranium carbide–zirconium carbide fuel for thermionic, 20: 14960(R) (N65-20798)
power plants for, development of uranium carbide–zirconium carbide fuel for, 20: 14961(R) (N65-20801)
power plants for, development of thermionic, 20: 14962(R) (N65-20803)
power plants for, performance of nuclear-thermionic, 20: 25463 (N-65-34908)
power plants for, transient kinetics of nuclear-thermionic, 20: 35143
power plants for, review of types of, 20: 41514(T) (AI-Trans-209)
power plants, Joule cycle development for, 16: 17322
power plants of, destruction of nuclear, during re-entry, (E), 19: 8661 (SC-RR-64-516)
power plants, performance of nuclear-electric, 16: 9709 (JPL-TR-32-158)
power plants, performance of nuclear-thermionic and -turbogenerator, 16: 28626
power plants, revolving-belt radiators for heat rejection from, 16: 28625
power plants, shielding design optimization, 16: 14365
power plants using electrochemical reaction of liquid mercury and potassium, nuclear, 20: 22485
power requirements, survey, 16: 10423 (ASD-TR-61-322(p.636-50))
power requirements, power sources, and conversion systems for, 17: 13856
power sources, fission electric cell evaluation for, 16: 19465 (JPL-TR-32-101)
power sources for, design of 200-w conduction-cooled reactor for, 17: 35216 (ANL-6694)
power sources for large payloads, 20: 36998
power sources for, review of radioisotopes as, 19: 13842 (HW-SA-3416)
power sources for, radiation effects on silicon solar-cell, 20: 9303
power sources for, safety aspects of nuclear, 20: 18949 (SC-DC-66-1369)
power sources for, radioisotope and reactor, 20: 30926
power sources for, use of isotopic, 20: 41397
power supplies and propulsion systems for, review on electric, 19: 34348
power supplies, characteristics of radioisotope-fueled thermoelectric,

16: 20033
power supplies for, 16: 26598 (NAA-SR-7144)
power supplies for nuclear instruments in, 16: 33099
power supplies for, use of solar cell systems, 17: 1722
power supplies for, design of silicon photovoltaic-cell, 17: 2634
power supplies for, development of nuclear, 17: 2635
power supplies for, design of solar photovoltaic, 17: 9109
power supplies for, development of solar turboelectric, 17: 9110
power supplies for, performance of superconducting magnet, 17: 9112
power supplies for, performance of solar-thermionic, 17: 9113
power supplies for, testing of solar-cell, 17: 9114
power supplies for inner-solar-system, solar-cell, 17: 9115
power supplies for, development of cesium solar-thermionic, 17: 9117
power supplies for, development of electrostatic, 17: 9119
power supplies for, oblique-field electrostatic, 17: 9120
power supplies for, colloidal electrohydrodynamic, 17: 9122
power supplies for, performance of magnetohydrodynamic, 17: 9124
power supplies for, performance of photovoltaic, 17: 9125
power supplies for, design and testing of solar-thermionic, 17: 9126
power supplies for, solar reflectors for thermionic, 17: 9129
power supplies for, thermionic vapor-filled cavity, 17: 9130
power supplies for, calibration of solar collectors for, 17: 9131
power supplies for, performance of solar-thermoelectric, 17: 9132
power supplies for, testing of solar-thermionic, 17: 9134
power supplies for, heat exchangers for nuclear, 17: 8103
power supplies for, requirements through 1976, 17: 7680
power supplies for, development of, 17: 10203
power supplies for, development of nuclear, 17: 10213
power supplies for, performance of liquid alkali metals in, 17: 8337
power supplies for, radiation effects on photovoltaic, 17: 8908
power supplies for Mars flight, design of solar-energy thermionic, 17: 8924 (JPL-TR-32-171)
power supplies for, development of Sunflower Rankine-cycle, 17: 9133
power supplies for, design of nuclear-photovoltaic, 17: 18215(R) (ASD-TDR-63-244)
power supplies for, optimization of radiation-cooled converter for nuclear-thermionic, 17: 24079
power supplies for, design of electric, 17: 29857(R) (NP-12888(Vol.1))
power supplies for, design of components for electric, 17: 29858(R) (NP-12888(Vol.2))
power supplies for, design of electric, 17: 29859(R) (NP-12888(Vol.3))
power supplies for, design of electric, 17: 29860(R) (NP-12888(Vol.4))
power supplies for, entropy production and performance of magnetohydrodynamic, 17: 32824
power supplies for, evaluation of, 17: 34072
power supplies for, system parameter effects on weight of, 17: 34086
power supplies for, development of dynamic energy conversion, 17: 35229
power supplies for, in-radiator positioning of nuclear-thermionic, 17: 35230
power supplies for, potential of 1-Mw nuclear thermomechanical, 17: 35231
power supplies for, nuclear-magnetogasdynamic, 17: 42411
power supplies for, development of solar thermionic, 17: 42412
power supplies for, performance of perforated ion engine emitters for, 17: 41577
power supplies for, development of isotope-fueled, 17: 41607
power supplies for, bibliography on, 18: 1833 (AD-249100)
power supplies for, use of nuclear thermionic systems for, 18: 4427
power supplies for, design of nuclear-thermoelectric, 18: 7964
power supplies for, design and performance of lithium-cooled uranium carbide-fueled 300-kw(e) advanced reactor for, 18: 9716 (SC-DC-3553 (p.103-27))
power supplies for, factors affecting, 18: 13321
power supplies for, problems in development of, 18: 13322
power supplies for, properties of Brayton-cycle, 18: 21679
power supplies for mobile lunar exploration, selection of, 18: 22579
power supplies for, launch-testing of Rankine-cycle, 18: 22581
power supplies for, development of reactor-heated thermionic, 18: 22716
power supplies for manned, selection of, 18: 28314
power supplies for manned station, design of SNAP-2, 18: 33136
power supplies for, development status of, 18: 39419
power supplies for, design analysis of solar thermionic, (T), 19: 18745
power supplies for, radioisotope and reactor, 19: 28714 (SC-DC-65-1131)
power supplies for, magnetohydrodynamic generators for, 19: 39442
power supplies for, design of fission-electric cell reactor, 20: 1468 (JPL-TR-32-741)
power supplies for, liquid metal MHD cell, 20: 4573
power supplies for, design of Brayton cycle cavity receiver for solar, 20: 9698 (NASA-CR-54752)
power supplies for, use of radioisotope, 20: 11188 (BLG-330)
power supplies for, properties of, 20: 12476(T) (AD-622352)
power supplies for, thermionic reactors for, 20: 12478
power supplies for, instrumentation for solar-thermionic, 20: 19419 (N-65-24874)
power supplies for, ancillary equipment for solar-thermionic, 20: 19420 (N-65-25271)
power supplies for, development of solar-thermionic, 20: 19421 (N-65-25406)
power supplies for, performance of 1-Mw superconducting, 20: 19424 (NASA-TN-D-3345)
power supplies for, conference on, 20: 21582
power supplies for, evaluation of Rankine and Brayton cycles for, 20: 40452
power supplies for, evaluation of Brayton and Rankine cycles for, 20: 41398
power supplies for manned space stations, Brayton and Rankine, 20: 41679 (NASA-CR-543)
power supplies of, design of radiative heat exchangers for, 17: 2636
power supplies of, performance of solar-thermoelectric, 17: 9128
power supplies, performance of magnetohydrodynamic, 16: 21151
power supplies, review, 16: 33088
power supplies, estimated performance of solar-thermionic, 19: 12151
power supply for Surveyor, design of radioisotope-fueled, 16: 34124 (MND-2570)
power supply for Sunblazer, design of radioisotope-fueled, 20: 23571 (AD-624684)
power supply for, development of thin film solar cell, 19: 10010
power supply for, design of hydride-moderated thermionic reactor, 20: 12479
power supply for, radiator design for, 20: 12480
power supply for, thermionic reactor concept for, 20: 27794
power supply limitations and requirements for, 17: 10212
power-supply performance in, 17: 9111
power supply systems for, development of nuclear, 17: 31768
power supply systems for, evaluation of emergency, 18: 31995
power system design for, 17: 4348 (61SPC3)
power system design for, computer-programmed parameter study of nuclear, 18: 33129 (NP-14062)
power systems development for manned, 18: 29107 (NAA-SR-9715)
power systems, effects of weightlessness on, 16: 21852
power systems for, description of chemical, nuclear, and solar, 16: 28633
power systems for, 17: 19694
power systems for, development of radiation-resistant pneumatic, 17: 23460(R) (GD/C-63-068)
power systems for, development of radioisotope-fueled thermoelectric generator for, 17: 29853(R) (MND-1123)
power systems for, development of radioisotope-fueled thermoelectric generator for, 17: 29855(R) (MND-P-3008)
power systems for, development of radioisotope-fueled thermoelectric generator for, 17: 29856(R) (MND-P-3009)
power systems for, development of radioisotope-fueled thermoelectric generator as, 17: 31760(R) (MND-P-1175)
power systems for, development of radioisotope-fueled thermoelectric generator as, 17: 31761(R) (MND-P-3001)
power systems for, development of radioisotope-fueled thermoelectric generator as, 17: 31762(R) (MND-P-3002)
power systems for, development of radioisotope-fueled thermoelectric generators as, 17: 31763(R) (MND-P-3003)
power systems for, development of radioisotope-fueled thermoelectric generator for, 17: 31764(R) (MND-P-3004)
power systems for, development of radiation-resistant pneumatic, 17: 32208(R) (GDC-63-140)
power systems for, development of closed-Brayton-cycle, 17: 36987 (SY-5394-R(Vol.I))
power systems for, development of advanced-Brayton-cycle, 17: 36988 (SY-5394-R(Vol.II))
power systems for, thermodynamic performance of magnetohydrodynamic, 17: 38577 (R62SD83)
power systems for, development of out-of-core nuclear thermionic generators for, 18: 810(R) (63SD862)
power systems for, review of nuclear thermionic, 18: 2580
power systems for, possibilities of magnetohydrodynamic generators for, 18: 4426
power systems for, development of large turbo-nuclear, 18: 4840
power systems for, auxiliary, 18: 5973 (AD-423714)
power systems for, review of, 18: 8941
power systems for manned, comparison of, 19: 10009
power systems for logistic, selection criteria for, 19: 10013
power systems for manned, adoption of nuclear, (E), 19: 10633
power systems for use on lunar surface, status of radioisotope-fueled, 20: 19132 (N-65-24571)
power systems for earth-orbiting laboratory, radioisotope, 20: 33753
power systems for, materials development for, 18: 34046(R) (NASA-CR-54041)
power systems for, radiator area characteristics of out-of-pile thermionic, 18: 36229 (NASA-TN-D-2429)

power systems for, using thin dielectric film thermoelectrostatic generation, (E), 19: 10005
power systems for, solar cell, 19: 10006
power systems for, development of solar thermoelectric, (E), 19: 10007
power systems for, fuel cell, (T), 19: 10008
power systems for, development of liquid metal heated solar thermionic, 19: 10011
power systems for, evaluation of radioisotope, 19: 9564
power systems for, heat storage in solar Brayton cycle, (E), 19: 12150
power systems for, flight performance of SNAP-10A, 20: 1530
power systems for, bearing materials for Rankine-cycle, 20: 3555
power systems for, design study of fission-electric cell-reactor, 20: 3577
power systems for, ceramic-refractory metal seals for, 20: 2292
power systems for, fabrication of beryllium radiators for, 20: 2293
power systems for, design problems of, 20: 4999(R) (ORNL-2599)
power systems for, heat transfer pipes performance for, (T), 20: 11542 (EUR-2534.e)
power systems for, re-entry ablation of strontium-90 fuel capsules for, 20: 11189 (MND-3062-25)
power systems for, use of gas-cooled reactors in thermionic, 20: 16110 (AD-620650)
power systems for, using Rankine cycle, 20: 16111 (N65-16315)
power systems for, performance of thermionic, (T), 20: 15292 (AD-620511)
power systems for, testing of carbide cathodes for thermionic, 20: 15046(R) (N65-15820)
power systems for, electrodeless MHD cell, 20: 19423 (N-65-27044)
power systems for, development of electric switchgear for nuclear, 20: 18851(R) (N-65-26627)
power systems for, use of fuel cells with radioisotope-fueled, 20: 19418 (N-65-22973)
power systems for, conference on, 20: 21097
power systems for, development of electric switchgear for nuclear, 20: 25225(R) (N-65-35969)
power systems for, development of electrical switchgear for nuclear-electric, 20: 25278(R) (N-66-15788)
power systems for, development of radioisotope-fueled, 20: 27391
power systems for, hazards reduction techniques for isotope-fueled, 20: 33755
power systems for, development of nuclear, 20: 47058
power systems for, development of nuclear, 20: 47096
power systems of, evaluation of nuclear, 17: 4359 (TID-17306)
power systems, parametric study of electric, 16: 26629(R) (NP-11728)
power systems, reliability limitations of electronic components in, 16: 15975
power systems, review, 17: 12035 (NP-12492)
power transmission in, design of thermal radiation guides for, 16: 29479(R) (NP-11935)
power units for, disposal of nuclear auxiliary, at re-entry, 17: 16310 (AFSWC-TDR-62-83)
power utilization concepts, 17: 12033 (ASD-TDR-62-591)
power-generating systems for unmanned, nuclear-electric, 19: 3713 (64SD892)
prelaunch operations of nuclear, meteorological studies of, 18: 8908 (SC-DC-3553(p.209-18))
pressure vessel for, design of membrane double wall interconnected, 19: 29827(P)
propellant feed systems for ion engines in, 18: 23754 (NASA-CR-51)
propellant flow through meteoroid punctures in, 17: 41661
propellant gage for, use of krypton-85 in, 20: 721
propellant pumping in, design of pumps for, 18: 1856
propellant systems of, foams and plastic films for insulation of cryogenic, 17: 28090
propellant tanks of, insulation of liquid-hydrogen, 17: 28086
propellant tanks of, external insulation for liquid-hydrogen, 17: 28087
propellant tanks of, compressible external insulation for liquid-hydrogen, 17: 28088
propellant tanks of, internal insulation for liquid-hydrogen, 17: 28089
propellant temperature rise in, theoretical effects of heating on, 19: 13597
propulsion and power generation, 16: 2794
propulsion, book, 16: 28629
propulsion by Alfvén wave generation, (T), 19: 15737
propulsion by arc-jet thrustors, review, 19: 32404 (NASA-TN-D-2868)
propulsion by arcjets, feasibility, 16: 21854
propulsion by coherent x-rays, (T), 20: 36997
propulsion by contained nuclear explosions, 16: 17328
propulsion by controlled fusion, research on, 18: 4666
propulsion by crossed-field magneto-aerodynamic devices, 18: 41599
propulsion by electric devices, study, 16: 16008 (JPL-TM-33-42)
propulsion by electrostatic generators, feasibility, 16: 21855
propulsion by electrothermal thrustors, 17: 13858
propulsion by electromagnetic thrustors, 17: 13859
propulsion by electrostatic thrustors, 17: 13860
propulsion by electric-arc accelerators, 17: 15010
propulsion by electron-bombardment ion rocket, evaluation of, 18: 4349
propulsion by electrostatic thrustors, problems from molecular flow patterns and space-charge flow in, 18: 18499
propulsion by electric spraying of liquids, 19: 7657
propulsion by fluid- and solid-core reactors, 16: 28631
propulsion by fusion power, conceptual design of system for, 18: 4667
propulsion by ion systems, 16: 17324
propulsion by neutral plasma, accelerator for continuous operation, 18: 18500
propulsion by nuclear rocket, 16: 17325
propulsion by plasma guns, design problems in, 17: 32225
propulsion by pulsed-pinch plasma systems, 17: 15015
propulsion by pulsed plasma rail accelerator, 18: 41592
propulsion by radioisotope electrogenerators and thermonuclear devices, 17: 13861
propulsion by radioisotope-heated thrusters, POODLE program for, 19: 20428 (TID-7698(Pt.I)(p.257-76))
propulsion by rockets, (T), 19: 34350
propulsion by thermonuclear fusion, feasibility of, 18: 34973 (ASD-TDR-63-696)
propulsion, critical evaluation of nuclear, 16: 15932
propulsion, developments and progress, 16: 5098
propulsion, development of electric systems for, 16: 31336(R) (NP-12011)
propulsion, electromagnetic pinch effect to accelerate ionized gases for, 16: 17320 (PPL-116)
propulsion, evaluation of thermionic diode system for conversion of reactor heat for, 16: 9716 (NASA-TN-D-1110)
propulsion, exhaust velocity for plasma, 16: 14362
propulsion for, bibliography on ion, 18: 6909 (AD-406690)
propulsion for earth-lunar cargo transfer, economics of electric, 19: 44232
propulsion for lunar exploration, electric, 17: 19692
propulsion, hydrogen propellant storage in unmanned nuclear Mars vehicles, 16: 9713 (NASA-TN-D-587)
propulsion in manned Mars missions, nuclear-electric, 20: 45871
propulsion, nuclear systems using magnetohydrodynamic generators, 16: 28624
propulsion of, behavior of nuclear systems for, 16: 28630
propulsion of, by SNAP systems, feasibility of, 16: 30150 (NAA-SR-7085)
propulsion of, characteristics of ion sources for, 17: 6900
propulsion of, computer analysis of ion systems for, 17: 4364
propulsion of, conference on nuclear, 17: 38438 (TID-7653(Pt.I))
propulsion of, design and theory of ion gun for, 17: 29657(R) (ML-1038)
propulsion of, development of electric power systems for, 17: 10199(R) (NP-12323)
propulsion of, development of plasma acceleration devices for, 17: 31578 (SSD-TDR-63-120)
propulsion of, development of electric systems for, 17: 41640
propulsion of, electrostatic system design for, 17: 5645
propulsion of, feasibility of nuclear systems for, 17: 13850
propulsion of, impulsive magnetohydrodynamic devices for, 18: 4353
propulsion of manned, development of nuclear, 18: 33133
propulsion of, nuclear, 17: 3835
propulsion of, nuclear systems for, 17: 10214
propulsion of, nuclear requirements for Mars mission, 17: 42403 (LADC-5961)
propulsion of, performance of a-c and d-c arc-jet systems for, 17: 7649
propulsion of, performance of crossed-field plasma accelerators for, 17: 7647
propulsion of, performance of plasma reactors for, 17: 10201
propulsion of, performance of thermonuclear systems for, 17: 16891
propulsion of, performance of cerium-144 electrostatic system for, 17: 33390
propulsion of, potentials of cerium-144 electrostatic, 17: 42405
propulsion of, power supplies for electric, 17: 10215
propulsion of, radioisotope systems for, 17: 17611
propulsion of, status and trends in, 17: 22958
propulsion of, study of ion guns for, 17: 17605(R) (N62-11311)
propulsion of, using nuclear energy, 16: 28627
propulsion of, analysis of cavity reactor for, 18: 13327
propulsion of, analysis of ion thrustors for, (T), 19: 26521 (APL-TDR-64-52(Vol.II))
propulsion of, annular magnetic Hall current generator for, 19: 6021
propulsion of, bibliography on electric, 19: 2467 (JPLAI-LS-587)
propulsion of, by neutral atom ejection from solids, 18: 14753
propulsion of, by accelerating ions from exploding wires, 20: 45872(P)
propulsion of, cavity nuclear reactors for, 19: 48046 (AD-613998)
propulsion of, characteristics of ion engines for, (E), 19: 11384 (D2-20646)
propulsion of, cold-plasma induction system for, 20: 2041
propulsion of, cryogenic fuels for, 18: 15122

propulsion of, cryogenic nuclear disruption process for, (T), 19: 36637 (NP-15148)
propulsion of, design of electrohydrodynamic colloid system for, 18: 18495
propulsion of, design of gamma-radioisotope thrustor for, (E), 19: 28715
propulsion of, design of plasma engine for, 20: 20874(P)
propulsion of, design of ion engine for, 20: 39095(P)
propulsion of, development of cesium ion engines for, 18: 17968 (NP-13769)
propulsion of, development of electric systems for, 18: 18494
propulsion of, development of ion engines for, 18: 23740(R) (NP-13899)
propulsion of, development of electric, 18: 37314
propulsion of, development of ion engines for, 19: 4743(R) (NP-14444)
propulsion of, development and efficiency of plasma-jet engine for, 20: 497(R) (AD-612175)
propulsion of, development of 0.015-lb-thrust ion-beam engines for, (E), 20: 498 (NASA-CR-54136)
propulsion of, development of ion engines for, 20: 11006(R) (NP-15824)
propulsion of, electrothermal, 18: 13995 (ATN-64(9227)-3)
propulsion of, electrothermal, 19: 6908
propulsion of, energy conversion problems in electric, 18: 24358 (ANL-6802(p.89-99))
propulsion of, fabrication and testing of ion engines for electric, 19: 34343 (N64-22453)
propulsion of, feasibility of solar power electric, 20: 31382
propulsion of, ion engine for, 19: 6907
propulsion of, ion engine development for, 20: 12975
propulsion of, materials testing facility for electrical, 20: 41122
propulsion of, optimization of propellant consumption in nuclear-rocket, (T), 19: 25748 (LA-DC-6837)
propulsion of, performance of cesium-vapor ion engines for, 18: 29825(R) (NP-14044)
propulsion of, performance of electron-bombardment, ion engines for, 19: 6013
propulsion of, performance of ion thrustors for, (E/T), 19: 11385 (NASA-TN-D-2635)
propulsion of, performance of plasma-jet engines for, 20: 500
propulsion of, performance of electron-bombardment thrustor systems for, 20: 5637
propulsion of, plasma properties in, by plasma engines, 18: 29925(R) (MDL-Q3)
propulsion of, plasma-jet design for, 19: 6016
propulsion of, power control in ion, 19: 6015
propulsion of, properties of fast and thermal thermionic reactors for, 20: 12478
propulsion of, pulsed coaxial plasma gun as thrustor for, (E/T), 19: 36636 (N64-29222)
propulsion of, reactivity of gaseous-core reactors for, (T), 19: 14875 (GNE/Phys/64-16)
propulsion of, regeneratively cooled plasma-jet engine for, 19: 6909
propulsion of, space-charge neutralization in ion engines for, 19: 6478
propulsion of, status of thermionic, 18: 30484 (TID-7687(p.10-20))
propulsion of, status of arc-jet, 18: 33705
propulsion of, survey of requirements and prospects of nuclear reactors for, 18: 21678
propulsion of, thermodynamics of Brayton cycles for, (T), 19: 10625
propulsion of, using nuclear explosions, 19: 28527
propulsion, performance of magnetohydrodynamic devices for, 16: 28632
propulsion requirements for planetary and interplanetary missions, 17: 31776
propulsion, review of nuclear systems for, 16: 18701
propulsion, review of developments in electric, 16: 21853
propulsion stage design, influences of nuclear engine on, 17: 17612
propulsion, status of electric, 16: 16007 (AFCRL-357)
propulsion system optimization for interplanetary, 16: 15990
propulsion system for, using radioisotope sources, 18: 27829
propulsion system for manned, electrothermal arc-jet, 18: 33706
propulsion system for, status of high-specific-impulse, plasma-jet, 19: 6019
propulsion system for, using resistance-heated gas flow, 19: 6906
propulsion system for, development of mercury-fueled ion engine, 20: 18884(R) (N-65-22975)
propulsion system for, use of oxide-coated brush cathodes in electron-bombardment ion engine, 20: 18886 (N-65-25549)
propulsion systems, performance analysis of thermionic converters for use in, 16: 3962 (AD-258108)
propulsion systems, radiations in, 16: 23432
propulsion systems for, flight testing of ion, 17: 2638
propulsion systems for, ion-beam-neutralizer performance in, 17: 7646
propulsion systems for deep-space missions, 17: 6543
propulsion systems for, materials for plasma, 17: 6545
propulsion systems for, closed-loop dynamics of nuclear, 17: 12037
propulsion systems for, research on, 17: 16195
propulsion systems for, review of low-thrust, 17: 22959
propulsion systems for, descriptions of advanced, 17: 22972
propulsion systems for, eccentricity and inclination changes effected by low-thrust, 17: 32218
propulsion systems for, Jupiter orbit parameters for electric, 17: 32221
propulsion systems for Mars and Venus mission, parameters for electric, 17: 32222
propulsion systems for, using superconducting magnets, 17: 32224
propulsion systems for, design of fusion, 17: 35235
propulsion systems for, theoretical performance of electrostatic thrustors of, 17: 38576 (NASA-TR-R-174)
propulsion systems for, optimization of electric, 17: 37319
propulsion systems for manned, electric, 18: 1839
propulsion systems for nuclear electric and rocket, 18: 7959 (NP-13478)
propulsion systems for, Douglas research on, 18: 9714 (NP-13468)
propulsion systems for, survey of nuclear and solar, 18: 9721
propulsion systems for, performance of nuclear, 18: 9722
propulsion systems for, MGD, 18: 10631
propulsion systems for, effects of propellant stream velocity distribution on performance of power-limited, 18: 20639
propulsion systems development for, facility for, 18: 27646
propulsion systems for, status of electrostatic, 18: 29815
propulsion systems for, performance of, 18: 29817
propulsion systems for, arcjet, 18: 29816
propulsion systems for, nuclear, 18: 31025
propulsion systems for, nuclear power sources for electrical, 18: 31027
propulsion systems for, d-c-to-d-c converters for electric, 18: 34497(R) (NP-12888(Vol.5))
propulsion systems for, status of electric, 18: 33702
propulsion systems for, development status of nuclear, 18: 35216
propulsion systems for, thermionic plasma, 18: 35664
propulsion systems for, test facility for nuclear-electric, 18: 39418
propulsion systems for, design of electrostatic, 18: 40083
propulsion systems for, steam-powered electric, 19: 3714 (ASTRA-G-41.3)
propulsion systems for, research and development of electric, 19: 9319
propulsion systems for, development of nuclear, 19: 15734
propulsion systems for, electric, 19: 15735
propulsion systems for, development of nuclear-electric, 19: 15736
propulsion systems for, performance of nuclear and solar, (E/T), 19: 17346 (NASA-CR-59366)
propulsion systems for, mission analysis for solar-heated hydrogen, 19: 20137 (NASA-CR-59332)
propulsion systems for, development of electrostatic, (T), 19: 22518 (NASA-TN-D-2172)
propulsion systems for, electric, 19: 22524
propulsion systems for, thrust optimization for nuclear, (T), 19: 24145 (AD-606336)
propulsion systems for, testing SERT I electric in, (E), 19: 26522 (NASA-TN-D-2718)
propulsion systems for, development of electric, 19: 28526 (P-2881-1 (RAND))
propulsion systems for, using radioisotope sources, 19: 28528
propulsion systems for, status of nuclear-electric, 19: 28529
propulsion systems for, mission performance of nuclear-electric, (T), 19: 28530
propulsion systems for, EHD, fusion, and MHD, 19: 28531
propulsion systems for, electric development of SNAP-50, 19: 32402(R) (N64-18173)
propulsion systems for, performance of electrostatic, (T), 19: 34341 (AD-613047)
propulsion systems for, review on, 19: 34347
propulsion systems for, optimization of nuclear, (T), 19: 34353
propulsion systems for, nuclear-electro-generator for, 19: 34356(P)
propulsion systems for, electric, 19: 40771
propulsion systems for, materials for gas-heating nuclear-reactor, (E/T), 19: 43588 (UCRL-14148-T)
propulsion systems for, development of electrothermal, 19: 44220 (N64-31011)
propulsion systems for, effects of coherent radiation on stability of electron-beam, (T), 20: 499 (NP-15541)
propulsion systems for, design and performance of radioisotope, 20: 5634
propulsion systems for, manned Mars landing mission using electric, 20: 9127 (NASA-TN-D-3194)
propulsion systems for, propellant valve development for, 20: 11007(R) (NP-15831)
propulsion systems for, mission performance of nuclear-electric, 20: 14724(65SD5322-A)
propulsion systems for, charged colloid sources for electrostatic, 20: 14725 (N65-15876)
propulsion systems for, testing of plasma-jet, 20: 14726 (NASA-CR-54746)
propulsion systems for, mission performance of electric, 20: 16628

propulsion systems for, facility for testing electric, 20: 18885 (N-65-23253)
propulsion system for SERT I, thrust measurement of ion, 20: 23271 (NASA-TN-D-3407)
propulsion systems for, optimal combination of, (T), 20: 23272(T) (TG-230-T464)
propulsion systems for, environmental aspects of nuclear, 20: 23273
propulsion systems for, design and performance of nuclear-rocket, 20: 25276 (N-65-35350)
propulsion systems for, design and performance of nuclear-rocket, 20: 25277 (N-65-35410)
propulsion systems for, feasibility and reliability of electric, 20: 27138
propulsion systems for, development and performance of surface ionization, 20: 27139
propulsion systems for, ion and electromagnetic review of, 20: 29394
propulsion systems for, reliability of electric, 20: 31359
propulsion systems using radioisotopes for propellant heating, 20: 31361
propulsion systems for stability control and station keeping, description of, 20: 31387
propulsion using Alfven waves, (T), 19: 37728
protection against meteorites for interplanetary missions, 17: 31782
proton activation of, solar-flare, (T), 19: 29023
proton depth dose in, formula for, 18: 42871
proton dose in, shielding code system for calculation of, (T), 19: 17173
proton dose rates in shielded, formulas for, (T), 20: 34795
proton dose rates in, 18: 802 (AFCRL-63-214)
proton shielding, calculations, 16: 3886(R) (ORNL-3193(p.325-9))
proton shielding of Apollo Command Module, effectiveness measurement using gamma radiation, 20: 24579
pumps for, development of electromagnetic, 18: 12293(R) (N63-15259)
pyrolytic materials for reentry, 17: 6550
radar echo area of, effect of plasma slab on, 18: 36705 (AFCRL-63-943)
radiation and cryotemperature effects on non-metallic materials for, 17: 34518
radiation and temperature effects on materials in, 17: 34523
radiation damage and doses in Van Allen Radiation Belt, proton, (T), 19: 19336
radiation damage in, annealing of, 18: 12758
radiation detection systems of Soviet, 16: 27281
radiation detection equipment for, four-decade count-rate meter, 19: 13737 (UCRL-7688)
radiation-detector designs for, 17: 16892
radiation detectors on, performance of nuclear-emulsion, 18: 23955
radiation detectors for, development methods for nuclear-emulsion, 18: 23956
radiation distributions and effects in SNAPSHOT, 20: 14175 (TID-22418)
radiation dosage determinations in, calculation principles, 16: 21844 (AD-263476)
radiation dosage in space, computer program for, 16: 29612 (NARF-62-11T)
radiation dose from electron transmission through shield of, computer program for, 19: 38016 (N64-29368)
radiation dose in Apollo, sector analysis of shielding against, 19: 38015 (N64-29365)
radiation dose measurements at 200 to 400 km, 1960–1963, 19: 700
radiation dose rates from structure activation in, 17: 39007
radiation dose rates in, computer program for calculating proton, 19: 36124 (N64-29369)
radiation doses from solar flares, proton, 16: 30992
radiation doses from solar-flare protons in, calculations of, (T), 20: 2658 (NASA-SP-71, pp 527-33)
radiation doses from solar-flare heavy nuclei, 20: 16300
radiation doses in, from neutrons scattered from power supply, 16: 28622
radiation doses in, evaluation of, 17: 5646
radiation doses in, shielding geometry effects on, 18: 15420 (N63-19990)
radiation doses in manned, during missions to Mars, 18: 28296
radiation doses inside (E/T), 19: 2190
radiation doses in, computer programs for calculating, 20: 15930 (NP-15697(Vol.2))
radiation doses in, during ninth Mercury-Atlas mission, 20: 18942 (N-65-17115)
radiation doses to, effects of anisotropy of geomagnetically trapped particles on, 19: 23341
radiation doses to crews of, tolerable, 20: 24945(T) (N-65-35524)
radiation dosimetry in, 20: 39158
radiation effects on flight control systems, 16: 15979
radiation effects on control and guidance systems, 16: 15985
radiation effects on materials of, 17: 8910
radiation effects of Van-Allen neutrons and protons on, 17: 16876
radiation effects on electronic components in, 17: 18574
radiation effects on materials of, tolerance limits for, 17: [illegible]
radiation effects on, NASA laboratory for studies of, 17: 32699
radiation effects on telemetry systems in, pulsed, 17: 34522
radiation effects on semiconductor devices in, proton, 17: 34524
radiation effects on flight control systems of, research program on, 17: 36985(R) (AD-295102)
radiation effects on dielectrics in, under high-temperature space environs, 17: 39704
radiation effects on electronic components of lunar excursion, estimate of, 18: 7015
radiation effects on electronic systems of, 18: 7016
radiation effects on digital computer circuitry in, pulsed, 18: 8894
radiation effects on electronic systems, components, and materials of, bibliography on, 18: 12717 (AD-296358)
radiation effects on components and materials for, 18: 12757
radiation effects on electronics of nuclear, 18: 20304
radiation effects on paint systems for thermal control in, 18: 26097
radiation effects on telemetry electronics of, 18: 33838 (RTD-TDR-63-4287(Vol.I))
radiation effects on components and materials for, 18: 44249
radiation effects on materials for, 18: 44250
radiation effects on materials for, 19: 6360(R) (FZK-188-2)
radiation effects on semiconductor electronic components in, cosmic, 19: 18348
radiation effects on materials and components of, testing for charged-particle, 19: 37169 (NP-15115)
radiation effects on, simulation of, 19: 39059
radiation effects on components of, review of, 19: 46875
radiation effects of solar flares on personnel in, (T), 20: 2655 (NASA-SP-71, pp 85-96)
radiation effects on thermal control coatings for, 20: 2428 (NASA-SP-55, pp 365-79)
radiation effects on manned military, cosmic, (T), 20: 2656 (NASA-SP-71, pp 265-86)
radiation effects on occupants of high-altitude aircraft, cosmic, (T), 20: 2657 (NASA-SP-71, pp 287-99)
radiation effects on optical properties of thermal-control coatings on, electron, proton, and uv, 20: 7654
radiation effects on properties of thermal-control coatings on, alpha and proton, 20: 7655
radiation effects on reflectance and thermal emittance of thermal-control coatings on, solar-wind, 20: 7653
radiation effects on hydraulic systems for, 20: 11181
radiation effects on optical properties of temperature-control coatings of, electron, 20: 19259
radiation effects on electric system of, proton, 20: 23520 (N-65-11073)
radiation environment of interior, 16: 20235
radiation environments for *cis*-lunar, 18: 4412 (ASD-TDR-62-606)
radiation environment from trapped particles, 20: 2849
radiation environment, 20: 25751 (N-65-35246)
radiation field from antennas of re-entry, conical-sheath plasma interactions with, (T), 19: 29397 (SSD-TDR-64-184)
radiation flux in Van Allen belts, proton, 20: 32244 (N-66-13126)
radiation flux on, computer code for, 17: 35236
radiation heating effects on materials for, 18: 11512(R) (NARF-63-9p)
radiation heating in, 19: 23149
radiation protection of astronauts in Apollo Command/Service Module, (T), 20: 3244 (NASA-SP-71, pp 365-75)
radiation protection for cosmonauts of Voskhod I and Voskhod II, 20: 44990
radiation shield for aft bulkhead on Centaur, fabrication of, 20: 36349 (N-66-18473)
radiation shielding in, 18: 20240
radiation studies using Mariner II, 17: 9160
radiation-resistant polymeric materials development for, 19: 28372
radiator design for nuclear-electric, 18: 23779
radiator for, analysis of finned beryllium as, 18: 23094
radiator materials for, 18: 24138(R) (PWA-2206(Vol.I))
radiator materials for, 18: 24139(R) (PWA-2206(Vol.II))
radiator materials for, 18: 24140(R) (PWA-2206(Vol.III))
radiator materials for, 18: 27968(R) (PWA-2309)
radiator weight for, 18: 6929
radiators for, materials selection for, 17: 33393
radiators for nuclear powerplants in, coatings for, 20: 43816(R) (PWA-2877)
radio communication from, through plasma sheath, 17: 33440
radioactivity induced due to Van Allen belts, 16: 9761(R) (UCRL-9897 (p.131-3))
radiofrequency blackout on reentry of atmosphere, 16: 28620 (NP-11924)
radioinduced changes in solar radiation absorptance to emittance ratios of surfaces of, hydrogen ion, 18: 8904
radioinduced heating in, 17: 3839
radioisotope power-generating system for manned space laboratory, 19: 44571

radiometric equipment on second Soviet, 16: 13326
re-entry of nuclear, safety hazards, 18: 4836 (SC-DC-3249)
re-entry of, self-powered magnetohydrodynamic control for, 17: 9081
re-entry ablation and sublimation of heat shield of, measurement using radioisotopes, 20: 20860
re-entry behavior of zirconium hydride-uranium fuel elements in, (E), 19: 10628
re-entry burnup studies of reactor fuel elements, 18: 24933 (AFSWC-TDR-63-51)
re-entry flight demonstration No. 1, SNAP-10A/Scout, 18: 31021 (SC-RR-64-511)
re-entry flight demonstration testing of SNAP 10A, 18: 36839 (NAA-SR-9479)
re-entry flight demonstration (RFD-2) for SNAP reactors, optical instrumentation for, 18: 36843 (SC-RR-64-968)
re-entry flight demonstration-1 for SNAP-10A, disassembly analysis for (E/T), 19: 3730 (SC-RR-64-515)
re-entry flight demonstration test for, (E), 19: 5531 (SC-RR-64-517)
re-entry flight test (RFD-2), stability analysis of, 19: 34344 (SC-RR-65-129)
re-entry heating of, sharp-cone study of aerodynamic, 19: 5585 (SCL-TM-64-87)
re-entry heating rates for, methods for calculating, (T), 20: 12467 (NAA-SR-11704)
re-entry interactions of nuclear particulate fuel with biological specimens, 18: 31789 (NUS-167)
re-entry of nuclear, safety hazards in, 18: 29108 (SC-DC-64-855)
re-entry of nuclear-powered, enhancement of fuel burnup during, (E), 19: 17351 (RTD-TDR-63-3054)
re-entry of, ablation testing of materials for, (E), 19: 47117(R) (SC-DC-65-1698)
re-entry of, ablation phenomena in, 20: 9091(R) (SC-DC-65-1893)
re-entry of, air ionization in hypersonic, (T), 19: 41121 (N64-30658)
re-entry of, conference on plasma sheath effects on, 20: 7991
re-entry of, MHD control and use of dissipated energy from, 19: 35000 (NP-15086)
re-entry of, model for dynamic response analysis of, 18: 43122 (SCL-DR-64-64)
re-entry of, plasma jet for simulating, 19: 46477 (ARL-65-121)
re-entry of, self-powered MHD control for (T), 19: 1224
re-entry simulation for, production of arc-heated gas for, 18: 13171
re-entry surfaces of, development of metal-reinforced refractory ceramic coatings for, 19: 9608 (ML-TDR-64-81)
re-entry to Earths atmosphere, development of refractory metal coatings for use in, 18: 34209
re-entry trajectories for, computer programs for calculating, 20: 16113 (SC-RR-66-22)
reactor operation in, charge build-up in, (T), 20: 38529
reactor shielding for, design of lithium hydride tungsten, 18: 21676 (SSD-TDR-63-217)
reactors for, reliability of, 19: 25753
reentry heating of, zirconium hydride ablation in, 20: 33884(R) (SC-CR-66-2029)
reentry of Apollo-type, nonequilibrium ionization phenomena in plasma sheath from, (T), 20: 44861 (NASA-CR-596)
reentry of, thermionic power generation from, 20: 31961 (SC-DC-66-1115)
reentry plasma sheath of, signal diffraction effects in, 20: 42438
refractory metals for thermal protection in, status of, 18: 34062
requirements for, for asteroid capture, 17: 19693
response to impulsive mechanical and thermal loadings, (T), 20: 24683
safety considerations for RIFT Project, 18: 9717 (SC-DC-3553 (p.131-43))
safety in launching of first two, problems in, 18: 6985
safety of nuclear-powered, 17: 10209
safety of nuclear powered, 18: 3305
safety of nuclear-powered, conference on, 18: 8551 (SC-DC-3553)
safety of nuclear power systems in, 19: 10632
safety of nuclear, (E/T), 19: 10656
safety philosophy of NASA for aerospace nuclear systems, 18: 8554 (SC-DC-3553(p.33-7))
safety philosophy of USAF for nuclear systems, 18: 8555 (SC-DC-3553 (p.47-51))
safety program for radioisotope and reactor systems in, review of, 17: 23569
shield ablation measuring system for, feasibility of radioisotope, 20: 36353
shield design for Apollo, 18: 3034
shield requirements for Apollo, 18: 3033
shielding, 16: 14203 (NARF-62-1T)
shielding, 16: 26631 (RM-2825-PR)
shielding, 18: 7844(R) (ORNL-3499(Vol.II)(p.25-6))
shielding, 18: 19258 (ORNL-3583)
shielding against electromagnetic radiation, 16: 20244
shielding against solar-flare protons, 18: 28295
shielding against cosmic protons, minimum-weight shields for, 18: 28906
shielding against cosmic protons, general-geometry code for, 18: 28907
shielding against charged particles, system for (T), 19: 3457
shielding against electrons, calculations for (T), 19: 3460
shielding against electrons, magnetic dipole and mass, (E/T), 19: 8560
shielding against cosmic protons, analysis of, 19: 27058
shielding against cosmic electrons, materials for, (E), 19: 29459
shielding against protons at 200 to 250 Mev, 19: 31443
shielding against electrons in artificial radiation belt using superconducting magnets, (T), 19: 31424
shielding against charged particles, superconducting magnet system for, 19: 42615
shielding against protons, design of spherical minimum-mass configurations for, (T), 20: 3242 (NASA-SP-71, pp 225-8)
shielding against protons, spherical configurations for, (T), 20: 3243 (NASA-SP-71, pp 229-34)
shielding against solar-flare alpha particles and protons, (T), 20: 3251 (NASA-SP-71, pp 507-12)
shielding against cosmic alpha particles and protons, tabulations for, 20: 12265 (NP-15697(Vol.I))
shielding against charged particles using dipole magnetic fields, simulation of, 20: 24578
shielding by selective orientation in anisotropic cosmic-particle fluxes, (T), 20: 3249 (NASA-SP-71, pp 473-6)
shielding calculations for, 17: 2416 (UCRL-10439)
shielding calculations for, 20: 17965
shielding design, 16: 24910
shielding design criteria for earth satellites, 19: 23946
shielding design for, optimization theory for proton, 18: 24805 (UNC-5049)
shielding design for, solar-proton, 18: 26815
shielding design for manned, radiation, (T), 19: 10455
shielding design for manned, using superconducting coils, 20: 30317
shielding effectiveness of, gamma attenuation measurements of, 18: 16231 (TID-7689(p.76-80))
shielding, evaluation of methods for, 17: 15376 (N62-11035)
shielding for, combination of active and passive, 17: 18390 (TID-7652(p.819-28))
shielding for, computer program for magnetic field, 17: 18389 (TID-7652(p.808-18))
shielding for, design of minimum-weight, 17: 18388 (TID-7652(p.773-93))
shielding for, electrostatic, 17: 17395
shielding for, feasibility of electromagnetic, 17: 31633 (ASD-TDR-63-194)
shielding for, ionization loss and Monte Carlo calculations for, 17: 18383 (TID-7652(p.682-97))
shielding for manned, active, 17: 4212
shielding for manned, effective residual dose concept for, 19: 45470
shielding for manned, performance of copper as, (T), 20: 3240 (NASA-SP-71, pp 183-8)
shielding for manned, mass calculations for, (T), 20: 3245 (NASA-SP-71, pp 407-14)
shielding for manned, (T), 20: 5673
shielding for nuclear-powered, utilizing radiation scattering, 18: 13183(P)
shielding for, analysis of electrostatic, 18: 24807
shielding for, design of magnetic, 20: 40291
shielding for, electron, 19: 23951
shielding for, performance of superconducting-magnet dynamic, (T), 20: 3241 (NASA-SP-71, pp 199-209)
shielding for, solar-proton, 18: 13178 (ORNL-3549)
shielding from cosmic particles by magnetic-field shields, 16: 15432
shielding from cosmic protons, synthesis theory for, 18: 28905
shielding from cosmic protons, computer analysis of, 18: 40745
shielding from cosmic radiation, 20: 23417
shielding from primary cosmic protons in 100-Mev range, (T), 19: 14536 (ORNL-P-848)
shielding from solar flares and Van-Allen protons, 17: 16877
shielding in proton environment, minimum-weight shield synthesis technique for spherical (T), 19: 1817 (UNC-5086)
shielding lunar, for optimized protection against environmental hazards 17: 5528
shielding manned, 17: 22769
shielding of Apollo, gamma probe technique for evaluating, 19: 23949
shielding of, bremsstrahlung dose behind idealized, 17: 12789(R) (ORNL-3360(p.231-5))
shielding of, electron-induced bremsstrahlung behind idealized, 17: 12790(R) (ORNL-3360(p.236-8))
shielding of, for solar flare protons, 18: 9558 (ORNL-3520)
shielding of isotopic power sources for, for payload protection, 18: 11362
shielding of manned, 16: 33659 (NASA-TN-D-1474)

shielding of manned, 16: 33959 (FZK-144)
shielding of manned, 18: 19265
shielding of manned, computer analyses of, 18: 35048 (AMRL-TDR-64-11)
shielding of manned, operating in near-earth environment, computer analysis of, 19: 22651
shielding of manned, calculations for, 19: 35563
shielding of manned, 19: 40063 (NP-15125)
shielding of manned, nuclear-propelled, 20: 20093 (N-65-22849)
shielding of, material requirements for, 17: 26741 (ORNL-TM-552)
shielding of, minimum structural mass for magnetic, 17: 28410
shielding of, prospects of active electrostatic and magnetic, 17: 10200 (NP-12371)
shielding of, radiation from solar proton reactions in, 17: 3811
shielding of reactors in, weight optimization for shadow, 18: 32978 (GA-5128)
shielding of, bibliography on, 20: 20098 (ORNL-RSIC-12(Vol.I))
shielding of, computer programs for calculations on, 19: 41954 (NP-15338)
shielding of, electromagnetic, 18: 13010
shielding of, electromagnetic, 19: 41952(R) (N64-31552)
shielding of, magnetic, 18: 26107 (ERR-FW-210)
shielding of, problems in, 18: 26816
shielding of, problems in, 19: 40072
shielding of, straightahead approximations for proton, 19: 17159(R) (ORNL-3714(Vol.II)(p.97-118))
shielding of, theory of magnetic, 18: 42867 (MTP-RP-64-1)
shielding of, validity of straightahead approximation in, (T), 19: 17161 (ORNL-P-786)
shielding offered by re-entry vehicles, proton, 17: 2629
shielding on, evaluation of effectiveness of, 18: 28903
shielding parameters for, 18: 31824
shielding requirements, 16: 14351(R) (LNP-NR-140)
shielding requirements, 16: 20241
shielding requirements for, 17: 18382 (TID-7652(p.662-81))
shielding requirements for nuclear-powered, 17: 35333 (NP-13060 (p.339-64))
shielding requirements for manned orbiting, (T), 19: 23944
shielding studies, 17: 11902 (ORNL-3317)
shielding studies for Apollo, instrumentation for, 17: 14607(R) (ORNL-3378(p.1-17))
shielding with magnetic fields, 20: 40292
simulators for, outer-space environment models for use with, 17: 19686(R) (CAL-VG-1403-G-5)
solar reflector characteristics for, 17: 9121
solar-wind simulation for Pioneer, using plasma sources, 20: 31877
space environmental effects on materials used in, 17: 13869
space environmental effects on polymers and nonmetallic materials used in, 17: 13870
space environmental testing of nuclear-powered, 18: 10262
sphere reentry of, slot antenna performance during, 20: 23425 (SC-R-65-992)
stress analysis of pressurized multicell shell structure for, 18: 25633 (ERR-AN-336)
structural materials for, development of high-temperature, 18: 1840
structural materials for, problems in selection of, 19: 30832
structural materials for, symposium on, 20: 9537
structures for, fabrication of beryllium, 19: 16045
structures for, radioinduced memory of polyethylene for self-erecting, 18: 12728 (RAI-308)
switchgear development for, 18: 33828(R) (NASA-CR-54059)
temperature-control engineering of nuclear-electric ion-propelled, 16: 25031 (JPL-TR-32-232)
test of re-entry, during simulated overpressure blast, 20: 462 (SC-DC-65-1554)
testing hulls for, in hypersonic flow of dissociated and ionized hydrogen, 19: 20124
testing of radiator-condenser structure R/C 6, vibration, 18: 43740 (NAA-SR-Memo-9963)
testing of SNAP-10A/Agena power system, 20: 22477
testing of, space environment simulation requirements for, 17: 34085
testing of, conference on, 20: 24828
testing of, for nuclear test detection, 18: 33703
testing RFD-2 re-entry vehicle, (E), 19: 21763 (SC-DR-64-1741)
testing SNAP 10A, environmental, 18: 38564 (SC-DC-3409)
thermal control surfaces in, 17: 6549
thermal protection of lifting re-entry, 17: 13849
thermal protective system for, materials for, 18: 32199
thermal radiation from shock layers of, in re-entry, 17: 15539
thermionic cell using plasma flow around, performance of, (E/T), 19: 4880
thermoelectric generator for, design and performance of static nuclear-powered, 17: 29861
tracking, development of facilities for, 16: 11335(R) (NP-11344)
trajectories along Van Allen radiation belts, calculation of time-integrated proton and electron fluxes for, 19: 37491 (N64-29364)
trajectories of, determination of, for interplanetary travel, 16: 26644(R) (NP-11755)
transportation of nuclear propulsion stages, ground, 18: 4844
use in high-latitude studies, 20: 11842
use of alpha sources in low-thrust, 18: 17324
use of beryllium in, nonstructural and structural, 18: 34141
use of nuclear powered, for transport, 16: 32613 (NP-12074)
use of polyvinyl chloride for coatings on, 20: 384
use of refractory materials for, 19: 44735
uses of radioisotopes in operation of life-support systems in, 20: 21174 (SAN-575-12)
vibration testing of re-entry flight demonstration vehicle for SNAP-10A, 19: 18132 (SC-TM-65-31)
vibrations in flight, system for analysis of, 18: 16280 (SC-TM-328-62(72))
weight of, reduction of inert, 19: 36644
welding of alloys and metals for, electron beam, 18: 34092
wind tunnel force testing of RFD-2 nozzle configuration, 18: 33187 (SC-DC-64-1016)
wind tunnel tests of tangent ogive shape at Mach 2.0, 19: 8709 (SC-TM-64-1281)
wind tunnel tests of RFD-2 re-entry, 19: 8710 (SC-TM-64-1288)

SPAIN
beneficiation of copper–uranium minerals, 16: 405
civilian defense organization in, 19: 28590
electric power production and distribution in, 20: 4081
fallout monitoring in air and rain water in Madrid, April 1964, 19: 636
fallout monitoring at Valencia, 1962–1963, 19: 30405
fallout monitoring at Moncloa Station, Madrid, 1964, 19: 46597
fallout monitoring at Moncloa Station, 1959 to 1965, 20: 9141
fallout monitoring in Valencia, 1964, 20: 29408
granites in northwestern, ages of, 20: 41153
heavy water production at Sabinanigo, pilot-plant for, 19: 26740
nuclear power development plans, 18: 45042
nuclear power development plans, 19: 1912
nuclear power development in, 19: 48011
nuclear power development in, 20: 40441
nuclear power plant development and utilization in, 20: 1576
nuclear power use in, for electricity production, 20: 40442
power grid in, role of nuclear power in, 18: 38521 (A/CONF.28/P/863)
radiation dosimetry practices in, 18: 16268
radiation processing of food in, review of, 20: 31628
radioactivity of biological materials near Andujar uranium installation, 20: 43001
radioactivity surveys, environmental, 18: 35754
radioisotope production in, 19: 20432(T) (ORNL-tr-295)
radioisotope production and uses in, 1964, 20: 14926
radioisotope uses in, economics of industrial, 20: 27377
uranium deposits, genetic-structural relations in, 16: 22402 (JEN-101-SIG/I-1)
uranium production and uses in, in 1964, 19: 39105
uranium resources in, 20: 28868
waste processing pilot plant at Junta de Energia Nuclear, 20: 26567

SPALLATION
(Specific reactions may be found under headings for participating nuclei and particles and in some cases also under particles produced.)
see also Rupture
see also Thermal Rupture
alpha emission in, 17: 11663
angular correlations in proton, 18: 21229
angular correlation analysis for, 18: 21230
cross sections at very high energies, 16: 28092
effect of atmospheric gas, on radium content in rain water, 20: 43529
measurement of near-surface, in Salmon experiment, 20: 43462 (UCRL-13225)
mechanisms for 600-Mev proton-induced (E/T), 19: 3257
of mercury, use in accelerator radiation monitoring, 20: 41276 (UCRL-16769)
research program at Naples, 16: 25900 (LNF-62/37(p.115-17))

SPALLATION PRODUCTS
see also Fission Products
angular distributions of, in emulsions irradiated by 660-Mev protons, 18: 44753
charge distributions from complex nuclei, 17: 28253 (UCRL-10741)
distributions in nuclear emulsion (E/T), 19: 3257
polarization of nucleons from deuteron spallation in nuclear electromagnetic fields, (T), 20: 26201
production cross section in proton reactions with nuclei at 660 Mev, (E), 20: 28470

SPANISH REACTORS (DON)
coolant research program for, 16: 25312 (JEN-90-DQ/1-24)

description of, 18: 38482 (A/CONF.28/P/601)
description of Spanish DON Project, 18: 38482 (A/CONF.28/P/601)
design concepts, 20: 8420
design of heavy-water-moderated organic-cooled pilot plant for, 16: 32588
design of prototypic, 20: 5162
development objectives and problems, 20: 26494
fuel element fabrication for exponential experiment in, welding techniques for, 20: 12401 (JEN-156-DMe/113)
fuel handling machine for, power cell design for, 20: 45163
fuel handling system for, hook mechanism design and testing, 20: 45162

SPANISH REACTORS (JEN-1)
accident analysis, maximum credible, 16: 22485
containment structure leak testing, 20: 12332
control system, 18: 1300 (JEN-118-DF/I-35)
control system, 18: 15629
corrosion and fission product determination in water of, 18: 31037
design and operation, 18: 3325 (TID-7663(p.145-60))
design and performance, 16: 26617 (JEN-97-DF/I-30)
fuel elements for, design of pilot plant for reprocessing, 20: 4066
neutron flux determinations, fast, 16: 11323
neutron flux distribution in, automatic sample changer for activation measurements of, 19: 10655
neutron flux measurement by manganese detectors, 16: 11324
neutron flux measurements in beam holes, 16: 30139 (JEN-103-DF/I-31)
neutron flux monitoring for use in activation analysis, preparation of materials for, 19: 7285
radiation monitoring equipment for, 20: 1538
use for activation analysis, experimental facilities and methods for, 18: 15631
use for production of radioisotopes from fission products, 18: 15632
use for radioisotope production, 18: 15630
uses for neutron physics research and radioisotope production, 20: 20320
uses of, 17: 10156
water deionization in, 19: 45678 (JEN-149-DQ/I-50)

SPARK CHAMBERS
array design, 16: 20680
cameras for, ten msec deadtime, 19: 9531
cascade particle detection in, efficiency for, 18: 33966
characteristics and operation of, review of present state of development, 18: 31956
characteristics and uses in cosmic-ray physics, review of, 20: 23480
characteristics of, 17: 1753
characteristics of wire-plate corona, for alpha particles, 17: 1761
characteristics of, 17: 18634
characteristics of neon–alcohol chamber, 17: 27697
characteristics of parallel-plate and triggered multi-wire, 17: 32442
characteristics of multiplate, with different gas fillings, 18: 5629 (JINR-P-1416)
charged particle ionization power in, 19: 20339
charged-particle momentum measurements in two-electrode, errors in, 19: 36858
charged-particle momenta in, determination of, (T), 20: 27259 (CERN-66-17)
charged-particle scattering in, Molière theory for multiple, 20: 43744
clearing time in magnetic field, 17: 3311 (PPAD-454E)
conference on, 18: 31869 (CERN-64-30)
construction and design of, for large magnetic-field systems, 17: 336 (TID-16859)
cosmic ray data from, analysis of, 19: 13863(R) (TID-21413)
current splitting in divided-electrode, 20: 37109
data analysis for, flying-spot digitizer for, 18: 5620 (CERN-63-34 (p.161-9))
data analysis for, computer use for, 20: 31508(R) (COO-1018-1075)
data analysis of, track centering system for flying spot digitizers for, 20: 41263 (CERN-66-23)
data analysis systems for, review, 17: 23694
data analysis system for, automatic, 18: 5622 (CERN-63-34(p.185-9))
data analysis system for, flying-spot digitizer on-line with IBM 7090 for automatic, 18: 23998
data analysis system for, automatic, 18: 41825
data analysis system for, design of CHLOE, (E), 19: 46793
data analysis, trace following device for, 17: 23700
data analysis, computer program for, 18: 23872 (BNL-833)
data collection and reduction system, automatic, 16: 8948
data extraction from, photoelectric digitalized method for, 20: 27302
data extraction systems for, spatial resolution of, 18: 33924
data handler for on-line computer for AGS experiments, 18: 30338 (BNL-7921)
data handling for wire, magnetostrictive delay-line readout for, 19: 787 (UCRL-11620)
data handling for wire, digital readout circuits for (E), 19: 2600 (BNL-8519)
data handling for triggered wire, ferrite-core matrix geometry for, 19: 4451 (CERN-64-44)
data handling for, film preselector system for, 18: 39611 (BNL-876)
data handling for, design of reader for photographic film for, 18: 41757 (BNL-877)
data handling for, digital system for, 18: 41759 (BNL-8327)
data handling system using television cameras, 18: 18234
data handling system for Brookhaven AGS, 18: 35833 (BNL-852)
data handling systems for, 18: 41769 (JINR-E-1806)
data handling systems for, computer, 19: 36913
data processing for scattering experiment in sonic, 18: 24000
data processing systems for, 18: 5623 (CERN-63-34(p.191-200))
data processing system for, 18: 5627 (CERN-63-34(p.259-63))
data processing system for, 19: 42710 (JINR-P-2223)
data readout systems for, magnetostrictive and piezoelectric, 20: 23465 (UCRL-16536)
data readout system of magnetostrictive, electronic system for, 20: 25387 (PPAD-583D)
data readout system for magnetostrictive, design of, 20: 25388 (UCRL-16539)
data readouts for, development of magnetostrictive, 20: 46054 (UCRL-17121)
delay time between particle passage and spark in, reduction in, 16: 23910 (BNL-6101)
description of, containing integral discharge capacitor, 17: 39440
description of digitized wire, using printed-circuit techniques, 18: 31879 (CERN-64-30(p.111-16))
description of digitized, (E), 19: 34624
description of frame-type and pen-box-type, with interelectrode gap of 1 cm, 20: 43724
description of, used as particle detector, 17: 12562
description of, for Minnesota Linear Accelerator and Van de Graaff Laboratory, 20: 35763(R) (TID-22971, pp 141-83)
design, 17: 40433(R) (NYO-10063(p.71-89))
design, 18: 30053
design, 19: 5569(R) (MIT-2098-64)
design and development, 20: 20365
design and efficiency of, 17: 8604(T) (DEG-Inf-Ser-285)
design and efficiency, 18: 483
design and improvements, 16: 22381
design and operation of neon-filled 50-plate, 16: 10190 (PPAD-419F)
design and operation mechanisms of, 18: 39660
design and operation of self-triggering, 19: 11556
design and operation of neon-filled, 19: 40886
design and performance of helium-filled, 16: 2001
design and performance of multiple-wire, 16: 5542
design and performance of multiple-wire, 16: 7709
design and performance of open-air alpha detectors, 16: 10211
design and performance in particle-interaction measurements at high energies, 16: 10213
design and performance of plane-parallel, 16: 11902
design and performance, 16: 20729
design and performance, 16: 20730
design and performance of cylindrical, 16: 20731
design and performance for rare modes of meson decay, 16: 20732
design and performance of radiation-image type, 16: 20733
design and performance of plane-parallel, 16: 25575(T) (AEC-tr-5239)
design and performance of argon-filled pulse-triggered, 16: 27319
design and performance as beam position indicators and pulse counters, 16: 27363
design and performance for detecting meson (μ^-) conversion to electrons, 16: 27365
design and performance of thin-foil, 16: 31940
design and performance of parallel-plate, 16: 31941
design and performance of, with large magnetic fields, 17: 1749 (TID-16860)
design and performance of dielectrode, with large discharge intervals, 17: 20377
design and performance of digitized, 17: 23655
design and performance of modular, 17: 23657
design and performance of neon-filled, 18: 2093
design and performance for proton polarization measurements, 18: 8655
design and performance of large-gap, 18: 30067
design and performance of, 18: 39661
design and performance of single-gap, 19: 7784 (LNF-64/46)
design and performance of, review of, 19: 11591
design and performance of lumped delay line, 19: 20372
design and performance, 19: 22785
design and performance of isotropic discharge, for relativistic charged particles, 19: 34544
design and performance of, for detection of secondary mesons, 17: 23661
design and performance of CERN neutrino, 17: 23664
design and performance of triggered-liquid, 17: 23709

design and performance of discharge chamber, 17: 27705
design and performance of, for secondary meson (π) detection, 17: 30875
design and performance for high-energy cosmic particles, 17: 41297
design and performance of, with stereo track photography, 17: 41302
design and performance of air-shower, 20: 13345(R) (NP-15772)
design and performance, for gamma cameras, 20: 21082
design and performance, 20: 27285
design and performance of crossed-wire, for beta- and gamma-emitting nuclides distribution determination, 20: 33710
design and performance of, review on, 20: 37043
design and performance of gas-filled image intensifier, for gamma and x rays from radioisotopes in human organs, 20: 41299
design and performance of low temperature, using helium and neon gas, 20: 41329
design and performance of pressurized discharge, at 33 kg/cm² and room temperature, 20: 41294
design and performance on on-line wire spectrometer, for 5- to 30-Bev/c particles, 20: 41297
design and performance for cosmic gamma radiation, 20: 43734
design for automatic data retrieval, 18: 43960
design for charged-particle detection, 16: 6577
design for charged particles, 18: 37546
design for cosmic particle interactions above 100 Bev, 20: 5724 (CONF-640919, pp II13-23)
design for cosmic-radiation spectrometers, 18: 27802
design for cosmic-proton spectroscopy, 18: 39706
design for detecting neutrinos, 16: 31923
design for detecting double beta decay of calcium-48, 20: 22010(R) (NYO-72-28)
design for determining neutron diffraction patterns, 16: 6538 (IFA-FN-21)
design for high-energy particles, 20: 9289
design for image intensifiers, 17: 8635
design for magnetic spectrographs, 18: 18209
design for magnetic particle track spectrometry, 18: 41840
design for measuring neutron spatial distributions, 16: 14977(P)
design for observation of multiple particles, (E), 19: 34489
design modification of Rosenblum-type, 18: 8679
design of air-filled, for cosmic particle detector, 18: 18240
design of carbon-plate, for polarization experiments, 17: 24275 (UCRL-10629)
design of corona-type, for fission-fragment detection, 19: 10335
design of cosmic-ray, for interactions at 300 Bev, 20: 5725 (CONF-640919, pp II27-30)
design of curved acoustic, 17: 20347 (ISS-63/26)
design of curved acoustic, 18: 43933 (ISS-64/26)
design of cylindrical spark chamber, 16: 19127
design of digitized, 17: 3327
design of digitized, for automatic measurement of particle interactions, 19: 39450 (BNL-9232)
design of digitized, for detection and measurement of cosmic gamma radiation, 20: 21121
design of electronic, with data recording on magnetic tape, 16: 23909
design of face-view, for recording successive particles, 16: 31942 (BNL-5031)
design of five-chamber, 18: 31967
design of flash-tube detectors, 20: 7401
design of, for cosmic-ray detection, 17: 34242
design of, for detection of neutrons, 17: 16484(P)
design of, for 3 Bev accelerator storage ring, 17: 21116 (SLAC-5(p.133-64))
design of high-pressure helium- or hydrogen-filled, (E), 19: 44502
design of image intensifier for, 17: 8527 (JINR-P-1063)
design of isotropic, 20: 16860(T)
design of large-area multiwire, 18: 39697
design of large, surrounded by magnetic fields, (E), 19: 46796
design of large, with metal mesh electrodes, 18: 20370
design of magnetic-field, 17: 23658
design of magnetic, for CERN neutrino experiment, 18: 12450 (CERN-63-37(p.131-43))
design of microwave discharge, 16: 31938
design of microwave discharge chambers, (E), 20: 7412
design of multi-wire, for handling many particles, 19: 822
design of multiple-wire, for alpha detection, 17: 41285
design of neutrino, 18: 26166 (BNL-837(p.170-89))
design of one-dimensional multiwire, 18: 8649(R) (TID-19940(p.77-118))
design of scintillation-detector, for electrons, with discrimination against mesons (π), 19: 44522
design of self-triggering, 18: 35883
design of self-triggering projection discharge, for fast neutrons, 19: 30564
design of short dead-time corona streamer, for measuring alpha particles and neutrons, 16: 13340
design of single-gap, for spark location by sonic waves, 16: 341 (NYO-9540)
design of spark-chamber hodoscope, 16: 1936 (CERN-61-25)
design of well-type, for determination of alpha activity in beryllium–polonium neutron sources, 18: 4124
design of wide-gap track, (E), 19: 46779
design of wire, with external acoustic transducers, 20: 2132 (JINR-P-2368)
design of 3π, for high-energy gamma detection, 19: 832
design using incomplete spark discharge for observation of particle tracks, 18: 22368
design using magnetostrictive effect, (E), 19: 46783
design with acoustic spark location, 20: 43725
design with photographic recording for detection and measurement of cosmic gamma radiation, 20: 21122
design with vidicon readout for detection and measurement of cosmic gamma radiation, 20: 21119
detection characteristics of planar-cathode, 16: 6562
determination of spark positions in, using delay-line electrodes, 16: 27306
development, 18: 10386
development, 18: 14270
development, 18: 33923
development, 18: 33965
development, 19: 46820
development, 20: 33651
development, 19: 46643(R) (LAL-1136)
development, 18: 21712(R) (NYO-10065)
development and future uses of, review of, 17: 4140 (BNL-6512(p.128-33))
development and operation, 18: 862(R) (TID-19590)
development and performance of streamer, 20: 5739 (SLAC-PUB-140)
development and performance of automatic retrieval, 20: 11093(R) (COO-614-34, Sect. IIA)
development and properties of, review on, 19: 24866
development and testing, 17: 40431(R) (NYO-10063(p.61-2))
development and uses, review, 17: 23650
development and uses of, review, 19: 771 (JINR-P-1810)
development and uses of wire, (E), 19: 46804
development for capture-to-fission ratio measurements, 19: 46766(R) (TID-22141, pp 67-79)
development for cosmic showers, 19: 13788
development for gamma-ray astronomy, 19: 36220(R) (MIT-2098-142)
development for high energy physics, future, 18: 7028 (BNL-7393)
development for high-energy particle detection, 20: 649 (BNL-9543)
development for high-energy physics, 20: 39241
development for measurement of neutron flux at reactor startup, 16: 22325 (DP-523)
development for particle detection, 19: 13746
development for polarization analysis in photoproduction, 17: 37661(R) (TID-19415)
development for relativistic charged particles, 18: 23874 (JINR-P-1619)
development for tracing particle tracks, 19: 32048(R) (NP-15073)
development for uranium-233, 19: 23209(R) (RPI-328-20)
development in USSR, 16: 25567 (NP-11947)
development of acoustic, 18: 2585(R) (ISS-63/37)
development of computer-integrated, 19: 18383(R) (TID-21595)
development of computer-integrated, 19: 26747(R) (COO-614-23)
development of corona discharge, for thermal neutrons, 18: 16328
development of current, for use as multichannel ladder counter with magnetic spectrometers, 20: 27308
development of digitized sonic, for counter hodoscope and on-line computer, 18: 29971 (BNL-7894)
development of digitized discharge planes for, 18: 31880 (CERN-64-30 (p.117-22))
development of digitized, for on-line computer data analysis, 19: 13863(R) (TID-21413)
development of digitized, 20: 46037 (BNL-10576)
development of, for particle-track labeling in bubble chambers, 16: 31814 (BNL-6242)
development of integrated wire, for on-line operation with a computer, 18: 31882 (CERN-64-30(p.129-31))
development of isotropic monogap, pulsed with damped oscillations, 20: 16886
development of magnetostrictive wire, 20: 33619 (COO-1545-5)
development of multi-wire, with ferrite memory cores, 18: 20371
development of r-f pulsed-electric-field, gas-filled, 16: 33200
development of, review of, 17: 41300
development of self-triggering medical, 18: 23976
development of sonic, 17: 23654
development of sonic-chamber, and scanning equipment, 17: 32915 (TID-7668(Sect. VII))
development of wire-chamber with on-line computer, 18: 25779 (CONF-

182-15)
development of wire, for inelastic electron-proton scattering, 18: 31881 (CERN-64-30(p.123-8))
development of wire, 20: 25781(R) (COO-1195-56)
development of, with ferrite core memories, 17: 16427 (PPAD-461E)
development of, for imaging of γ radioisotope distribution patterns, 20: 6997
development of, for high-energy particle measurement, 20: 27273
development of, review of, 19: 13747
development of, review on, 19: 18333
development of, review of, 20: 33634 (UCRL-16542)
development review, 16: 31915
development status, 16: 20641 (NP-11616)
development using magnetic field for high resolution, 16: 31824 (PPAD-455 E)
development with magnetic core readout, 19: 11569
developments in, for track imaging, 17: 22051
discharge along particle tracks in, 16: 31939
discharge channels along tracks in, 17: 23662
discharge characteristics of, effects of gas admixtures on, 18: 14210 (JINR-P-1498)
discharge conditions along path of ionizing particle in, evaluation, 16: 20638 (JINR-D-870)
discharge planes for, design and operation of, (E), 19: 46784
drift velocities in spark fields, method for measuring, 19: 2613
efficiency calculations for, 19: 22719
efficiency for cosmic showers, 18: 8684
efficiency for cosmic particles, 19: 20378
efficiency for electron shower detection, 17: 23653
efficiency of large-gap neon-filled, at 600 mm Hg, 20: 37088
efficiency of spark formation in neon, effects of voltage rise time on, 18: 14219 (TID-20246)
efficiency of, calculation of, 20: 31558
efficiency of, effects of electron attachment on, 18: 18197
efficiency, spark scatter, and spark width in, pressure dependence of, 17: 25603 (PPAD-485-F)
electric characteristics of Rosenblum, effects of circuitry on, 17: 41284
electric currents and discharges in divided-electrode, (E), 20: 7403
electric field propagation between plates of, 18: 29979 (LNF-64/11)
electrical characteristics of sphere-plane type, 16: 20738
electrodes for, development of, 18: 14211 (JINR-P-1499)
electrodes for, development of, 19: 22749
electrodes of, electrostatic field around, (T), 20: 4241 (JINR-P-2364)
electromagnetic showers in multiplate, lateral structure of, 20: 27958
electron showers in lead-plate, 17: 3335
electrophotography for, 18: 31899 (CERN-64-30(p.341-4))
elementary particles in, method for determining properties of, 19: 44490(T) (BNL-tr-1)
engineering drawings for pulse line, 19: 6208
equipment for ΣΛ parity experiment, engineering drawings, 17: 22528
events in, on-line flying-spot digitizer analysis of, 18: 5619 (CERN-63-34(p.141-59))
events in, system for analysis of, 18: 5621 (CERN-63-34(p.171-83))
fabrication of, 19: 32554(T) (UCRL-Trans-1193)
feasibility of liquid-helium, 17: 8949 (TID-17787)
film scanning systems for, development of, 20: 13163(R) (ANL-7129)
foils for, stretching device for aluminum, 20: 43724
gases in, equipment for purifying, 18: 39666
gases in, filling and purification system for, 20: 43724
illumination of, design of remote light source with light-pipes for, 19: 34471 (CERN-65-13)
image intensifiers for, design and performance of, 20: 21020 (AD-621069)
image transformer for, design of electron-optical, 17: 41274
instrumentation for, used as hodoscopes, 17: 38609 (CU(PNPL)-227 (p.172-3))
interaction vertices in analysis with, geometrical optimization of, (T), 19: 11563
ionization density measurements in microwave discharge chambers, (E), 20: 7413
ionization discrimination properties of helium, argon, and helium-argon, 20: 9286
ionization effects from hyperon(Λ^0) decay, 16: 23908
ionization power measurements on mesons (π^+) and protons in, 18: 41796
logic system for magnetic, electronic, 19: 30517 (CERN-65-21)
magnet model for 2-meter, development of, 20: 19041 (SLAC-57)
magnetic field effects on spark mixing in, (E), 20: 7371(T) (BNL-tr-17)
magnets for, design using tape-wound coils, 20: 16809 (CONF-650922, pp 253-61)
mechanism and theory of corona, 17: 14657
memory cell period in, 18: 24473
memory time in, 18: 18176 (NP-13716)
memory time of large-gap neon-filled, 19: 18317
meson (π) ionization power in, fluctuations in measurements of, 19: 18315
microphone operation in sonic, for charge-exchange experiments, 18: 31889 (CERN-64-30(p.191-202))
microphones for acoustic, design of, 18: 35876
momentum measurements on single charged particles with, 17: 24255
neon recovery from, system for, 19: 28633 (MIT-2098-51)
neutrino events in, analysis of, 18: 12895 (CERN-63-37(p.163-77))
neutrino interactions in, at high energies, 20: 34146 (CU-1932-256)
operating characteristics in discharge regime, 17: 1758
operating characteristics of wide-gap, 20: 27294
operating mechanisms and performance of, review of, 19: 18275
operation above about 2 kv, corona effects, 16: 11892
operation and performance with magnetic tape recording system, 19: 36855
operation and performance of wide-gap track, (E), 19: 46781
operation in air, 18: 41813
operation in magnetic fields, 16: 27361
operation in magnetic fields, 18: 16327
operation mechanism of corona-less, with inhomogeneous electric fields, 16: 27312
operation of corrugated-plate, for alpha and neutron detection, 20: 11120
operation of filament–plate, in air, 18: 18213
operation of isotropic, performance in avalanche and streamer modes of, 20: 25381 (CERN-66-14)
operation of parallel, efficiency of, 17: 11048
operation of sonic, for elastic deuteron scattering on carbon, 18: 31885 (CERN-64-30(p.147-55))
operation of sonic, for proton-proton elastic scattering at 26 Bev, 18: 31886 (CERN-64-30(p.157-69))
operation of sonic, for small-angle proton-proton elastic scattering, 18: 31888 (CERN-64-30(p.183-90))
operation of sonic, electronic data handling requirements for, 18: 31890 (CERN-64-30(p.211-19))
operation of spherical- and wire-anode, 18: 37511 (NP-14116)
operation of wide-gap, design and performance of Marx high-voltage pulse generator for, 20: 41330
operation of wire-electrode, with programmed discharges, 19: 28670
operation of wire, automatic data processing in, 18: 31896 (CERN-64-30 (p.287-98))
operation of, mechanisms for, 18: 23968
operation of, modes of, (E), 19: 13761
operation of, with secondary discharge, 18: 31883 (CERN-64-30 (p.133-9))
operation of, with isolated electrodes, 19: 34545
operation on-line into computer, 18: 8709(R) (TID-19993)
optical system for, design of, 17: 337 (TID-16861)
optical system for use with standard magnet and, 17: 23659
particle ionization ability measurements in, 18: 24473
particle kinematics in, use of multiple scattering and secondary sparks in determining, 20: 31570
particle ranges and tracks in thick-plate (E), 19: 773 (LAL-1114)
particle track analysis in, automatic digital device for, 17: 20552 (CERN-62-37(p.73-80))
particle track analysis in, using flying-spot devices, (E), 19: 38976 (CERN-65-11(p. 57-69))
particle track analysis in, using flying-spot devices, (E), 19: 38977 (CERN-65-11(p.71-9))
particle track analysis in photographs from, flying-spot systems for, (E), 19: 46787
particle track analysis in, system for, 19: 46789
particle track analysis in photographs from, (E), 19: 46790
particle track analysis in, review of systems for, (E), 19: 46791
particle track analysis in, use of AROMA code for, (E), 19: 46794
particle track analysis in photographs from, use of graph theory for, (T), 19: 46795
particle track analysis in photographs from, on-line computer system for, (E), 19: 46811
particle track analysis in, using raster-scan methods on photographs, (E), 19: 46786
particle track brilliance in, effects of ionizing power on, 17: 34250
particle track brightness in, photomultiplier and galvanometer for measuring, 20: 31582
particle track coordinates in wire, magnetostrictive readout for, 19: 15904
particle track coordinate measurements in, television method for, 19: 26661 (JINR-P-2057)
particle track coordinates in, electrophotographic device for evaluating, 20: 21037 (JINR-P-2594)
particle track coordinates in, geometric reconstruction procedure for, 20: 43711
particle track identification in, use of relative ionization in, 17: 23652
particle track location accuracy in triggered, 16: 20684

particle track location in multi-wire, accuracy of, 17: 32443
particle track luminosities in large gap, 19: 15910
particle track measuring in, semiautomatic scanning device for, 20: 2130 (JINR-P-2340)
particle track photographic techniques for, 18: 35834 (BNL-7282)
particle track photography in, geometric distortion effects on, (T), 20: 7364 (JINR-P-2420)
particle track processing, automatic device for, 17: 20553 (CERN-62-37(p.83-92))
particle track recording on x-ray film, 19: 20368
particle track registration at all angles in, (E), 19: 34512
particle track registration and data extraction in, 20: 39210 (JINR-P-2745)
particle track scanning system for, programmed automatic spot, 20: 13106
particle tracks in two-electrode, in a magnetic field, 18: 8668
particle tracks in lead-plate, analysis of, 18: 23973
particle tracks in, magnetic tapes for recording, 19: 18321
particle tracks in, filmless digitizing of location of, 19: 20354
particle tracks in, spark pairing correction to, (T), 19: 34507
particle tracks in, oblique, 19: 42743
particle tracks in wide-gap, errors in, (E), 19: 44514
particle tracks in, device for automatic analysis of, 19: 44496
particle tracks in wire electrode, resolution of ambiguities in, (E/T), 20: 650(R) (COO-614-37, Sect. 2C)
particle tracks in, method for improvement of, 20: 7385
particle tracks in, flying spot digitizers for analysis of, 20: 16840
particle tracks in, pulse-pattern generator for analysis of, 20: 16881
particle trajectories in, accuracy of determining, 18: 30042
particle trajectories in, spark deviations from, 18: 30043
particle trajectory determination in wide-gap, 19: 4509
particle trajectories in, spark localization for, 19: 9510
particle trajectories in, methods for analyzing, 19: 15903
particle trajectory location in, accuracy of, (T), 20: 29527 (ITEF-341)
particle trajectories in, factors influencing discharge development along, 20: 41304
particle-track localization efficiency of, for different triggering modes, 20: 21048
performance as ladder counter for particle momentum analysis, 20: 653 (LAL-1143)
performance for alpha particle trajectories, 19: 28625 (AROD-3816.1)
performance for alpha particle detection and tracing, 20: 35728 (AD-635209)
performance for analyzing extensive air showers, 18: 2559
performance for analysis and location of neutrino interactions in emulsions, 20: 6052
performance for decay $\mu \rightarrow e + \gamma$ and $\mu \rightarrow 3e$, 17: 41275
performance for determination of amplitude of elastic p-p scattering, 19: 31089
performance for determining electron drift velocity variations in gases, 19: 47116 (BNL-9443)
performance for detection of electron showers at 0.5 to 8 Bev, 19: 47354
performance for discriminating electrons and pions, (E), 19: 46782
performance for electron shower measurements, 18: 2048
performance for electron spectroscopy from meson (μ) decay, 19: 46785
performance for electron momentum measurements, 20: 39207 (ISS-66/18)
performance for fission fragment detection in alpha background, 17: 32403 (UCRL-7169)
performance for multiple particle detection, 20: 11114 (UR-875-66)
performance for neutrino-nucleon interactions, 18: 12448 (CERN-63-37(p.43-75))
performance for particle detection, comparison with photographic emulsions, 18: 23906
performance for recording meson (π^+)-proton interactions at 180°, 20: 16815 (JINR-P-2506)
performance for spatial reproduction of charged particle tracks, 17: 41262
performance in CERN neutrino experiment, 18: 12452 (CERN-63-37 (p.215-17))
performance in determining particle entrance coordinates for emulsion chambers, 17: 23679
performance in high-energy reaction measurements, 16: 27362
performance in high-intensity pulsed magnetic fields, 17: 12569
performance in high pulsed magnetic fields, 17: 23714
performance in high-energy gamma detection, 20: 9287
performance in magnetic field, 18: 8685
performance in system with nuclear emulsions for determining point of incidence of particles, 20: 31569
performance in x or gamma cameras, 19: 17756
performance of acoustic, for determining track positions, 17: 4829
performance of air-gap, for multiple-track detection, 17: 23759
performance of air, with dielectric, 18: 39693
performance of argon filled, 17: 22042
performance of argon-filled, 18: 16337
performance of arrays of, for measuring particle momenta, (E), 20: 5730 (JINR-E-2366)
performance of Cherenkov-counter triggered, for detecting meson (π^0)-decay photons, 20: 11099 (JINR-P-2436)
performance of circular, using automatic current-method analysis, (E), 19: 44498
performance of circular, with electric localization, 20: 5735 (LYCEN-6523)
performance of controlled-discharge, (E), 19: 39028
performance of corrugated-plate, in neutron detection and measurement, 20: 16894
performance of helium- and neon-filled streamer, 20: 37110
performance of high-pressure helium-filled streamer, 19: 7805
performance of high-pressure helium-filled streamer, 20: 39245
performance of methane-filled, 16: 23867
performance of microwave, 20: 31534
performance of multiple wire-cavity, for fast neutrons, 19: 15892
performance of multiple-wire, (E), 20: 7416
performance of multiple-wire, for divergent alpha particles and neutrons, 20: 41317
performance of neon- and argon-filled, with large electrode intervals, 16: 22384
performance of single wire-plate, for alpha particles, 20: 9270
performance of sonic, for proton interactions, 19: 15911
performance of sonic, for proton detection at 20 Bev, (E), 19: 46800
performance of symmetric wire, for track coordinate determination, 20: 2129 (JINR-P-2312)
performance of two-electrode, with large discharge gaps, 18: 39694
performance of wide-gap, (E), 19: 13798
performance of wide-gap, for detecting vertex events, (E), 19: 44507
performance of wide-gap, for track analysis, (E), 19: 46780
performance of, effects of filler gas on, 19: 13787
performance of, effects of background loading on, 20: 27262 (JINR-P-2661)
performance of, filled with neon and neon mixtures, 19: 22750
performance of, with foil and massive electrodes, 19: 2625
performance of, with series feed of gaps, 19: 28630 (JINR-P-1937)
performance on track regime, 18: 39692
performance using sonic spark location principle, 17: 23742 (NYO-10261)
performance using vidicon techniques for charged particle counting, 20: 37114
performance with avalanche and primary-ionization triggering, (E), 19: 40898
performance with on-line computers for analyzing nuclear events, (E), 19: 46806
photograph scanner for, automatic, 18: 30028
photograph scanning system for, performance of cathode-ray tube, 20: 11104 (LNF-65/33)
photoregistration device for, design of, 17: 30878
plate fabrication, 16: 13353
power supplies for, parallel and series, 20: 31571
power supply for streamer, performance of high-voltage, (E/T), 20: 11142
processing of data from, computer program for, 17: 39428
properties and uses, 18: 39641
properties and uses, review, 19: 39019
properties of, 20: 33705
properties of air-filled, 19: 2615
properties of, for strong interaction physics, 17: 21115 (SLAC-5(p.90-132))
properties of neon flash tubes, 16: 10248
properties of photographic-film data acquisition systems for, 18: 31905 (CERN-64-30(p.367-9))
proton ionization power in, fluctuations in measurement of, 19: 18315
proton ionizing power in helium- and neon-filled, measurement of, (E), 20: 2128 (JINR-E-2324)
proton ionizing power in, measurement of, 20: 43691
pulse generator for relativistic, 18: 23843
pulse generators for, design of, 18: 41862
pulse generators for, thyratron, 19: 42752
pulse generators with short signal delay for, 19: 42753
pulse modulators for, design and operation of, 17: 30857 (UCRL-10887)
pulse observation on oscilloscope, design of input stage connector for, 18: 8682
pulser design for, 20: 39270
pulser for, for air-borne experiments, 18: 25828 (TID-20646)
radiation effects of beta particles on performance for alpha counting, 18: 41791
resolution of, developments for three-dimensional, 18: 31901 (CERN-64-30(p.351-6))
response capacity of, to alpha particles and neutrons, 17: 20356
response of wide-gap, during time of sensitivity to previous spark, (E), 19: 44518
review, 16: 23907

review, 17: 34247
review, 18: 23971
review, 18: 33967
review, 19: 830
review of two-electrode, in magnetic field, 19: 11592
scanner development for proton polarization measurements using 1.3-Bev electron synchrotron, vidicon, 18: 31878 (CERN-64-30(p.105-9))
scanner for, automatic digitization of events by vidicon, 18: 31875 (CERN-64-30(p.65-79))
scanner for, operation of discrete vidicon, 18: 31874 (CERN-64-30 (p.57-63))
scanners for, description of vidicon, at Univ. of Chicago, 18: 31876 (CERN-64-30(p.81-93))
scanning, closed-circuit television operation in, 16: 27364
scanning of, direct-view vidicon system for, 18: 14222 (UCRL-11146)
scanning photographs of, cathode ray tube device for, 17: 23699
scanning system for, design of, 17: 29192 (BNL-7048)
scanning systems for, automatic, 17: 38607 (CU(PNPL)-227(p.167-70))
selective photography in, decision-making method for, 18: 7057 (TID-19841)
sensitive time of, effects of gas mixtures on, 17: 23651
sensitive time of wide-gap, method for determining, 20: 27304
sensitive volume of wire-plate type, 16: 7698
shower efficiency in, 18: 39693
signal spread in wire plate, 17: 3346
spark accuracy relative to particle trajectory in, 18: 39693
spark alignment in, 18: 14211 (JINR-P-1499)
spark channel formation in air gap, 19: 47146
spark detection in sonic, equipment for, 19: 36808 (CERN-65-19)
spark discharge emergence in large gap, conditions of, 19: 18316
spark displacement in, determination of, (E), 19: 20344
spark displacement in magnetic fields, 19: 22748
spark displacement in magnetic fields, (E/T), 20: 2131 (JINR-P-2344)
spark formation along particle track in, 17: 11038
spark formation in, streamer theory for, 18: 12451 (CERN-63-37(p.145-62))
spark formation in large-gap, mechanisms of, (E/T), 19: 13739(T) (UCRL-Trans-1171)
spark localization in wire, magnetostrictive, 18: 31897 (CERN-64-30 (p.325-31))
spark localization in, using magnetostrictive electrodes, 19: 4507
spark localization in, design of field lens for, 20: 19020 (CALT-68-30)
spark localization and recording in, method of, 20: 27296
spark location in acoustic, from shock wave analysis, (T), 20: 21094
spark position determination in, method for, 18: 8664
spark position in, acoustic detection of, 18: 7339 (ISS-63/40)
spark position in sonic, data recording systems for, 18: 31903 (CERN-64-30(p.363-5))
spark position in sonic, mathematical location of, 18: 31887 (CERN-64-30(p.171-82))
spark position in sonic, buffer store system for, 19: 36931
spark position in sonic, analog computer and display system for, 19: 36936
spark position in, determination from distribution of currents from electrode, 18: 31898 (CERN-64-30(p.333-40))
spark position in, automatic recorder for, 18: 39645
spark position recording using magnetic tape, 18: 31900 (CERN-64-30 (p.345-9))
spark positions in, review of acoustic and Vidicon techniques for direct digitized readout of, 19: 30533 (UCRL-16087)
spark positions in multiwire, memory and readout system for, 19: 34521
spark rectifying point in, location of, 19: 22749
spark spatial accuracy in, 18: 33924
spark-gap-trigger amplifiers for, design of, 19: 9493 (UCRL-11517)
sparking efficiency and threshold voltage, 20: 37105
status, 19: 36857
technology of, 18: 20378
track analysis for, flying-spot systems for, (E), 19: 36812 (MIT-2098-155)
track analysis from, using flying-spot system, (E), 19: 38972 (CERN-65-11(p.7-13))
track analysis in, using flying-spot devices, (E), 19: 38973 (CERN-65-11(p.15-23))
track analysis in, using flying-spot devices, (E), 19: 38974 (CERN-65-11(p.25-33))
track data processing for, LINK and PAIR computer programs for CDC-3600 spark-image, 18: 31895 (CERN-64-30(p.265-78))
track identification in wire, using on-line computer, 18: 31894 (CERN-64-30(p.261-3))
track measurement in accuracy of, 17: 29200 (LNF-63/33)
track photographs from, automatic scanner for, 19: 34562
track photographs from, electroluminescent panels as pulsed fiducial marks for, 20: 21090
track pictures from, particle kinematics from, (T), 20: 11100 (JINR-P-2467)
track reconstruction in transparent-electrode, rectilinear, 19: 30516 (CERN-65-15)
track recording on magnetic tape, 20: 27297
transducer for sonic, 18: 39636
triggering circuits for, electronic, 18: 10395
triggering circuit development for, 18: 25827 (NAS-NRC-Pub-1184 (p.325-30))
triggering circuit for, design of, (E), 19: 4461 (LNF-64/39)
triggering of sonic, solid-state units for, 18: 23999
triggering systems for, design of fast, 17: 4856
triode for, development of nanosecond, 17: 41272
use as pulse generator for testing fast coincidence circuits, 16: 5534
use at electron accelerators, 20: 15187
use for detecting sub-nuclear particles in the ZGS, 18: 16326
use for detection in photon interactions, 19: 39041
use for mixed fields of ionizing radiation, 19: 20373
use for particle track location in emulsions, 19: 44445 (CERN-65-4 (Vol.II), pp X74-83)
use in antineutrino experiments, 20: 21607 (CERN-65-32, pp 161-8)
use in CERN "missing-mass spectrometer," 18: 31873 (CERN-64-30 (p.49-56))
use in cosmic gamma flux studies, (E), 19: 44970
use in determining lower limit for intermediate boson, mass, 20: 21596 (CERN-65-32, pp 11-24)
use in elastic scattering experiments at high energy, 18: 20897 (CERN-64-6(p.31-48))
use in elementary particle physics, 18: 42377(R) (TID-21014)
use in gamma radiodiagnosis, 20: 5461
use in high-energy physics, 17: 23660
use in high-energy physics, techniques for, 17: 23663
use in high-energy nuclear physics, 19: 26678
use in high-energy physics, 19: 46834
use in identifying high-energy particle tracks in bubble chambers, 17: 12553 (BNL-746)
use in magnetic fields, 16: 374
use in meson (π) production studies, (E), 19: 13799
use in meson (π) interaction studies, 17: 23656
use in meson(μ) decay spectrum measurements with on-line computer, 18: 31872 (CERN-64-30(p.41-8))
use in momentum measurements on cosmic charged particles, 20: 27347
use in neutrino detection, 20: 21030 (CERN-65-32, pp 223-4)
use in neutrino experiments at CERN using deuterium targets, 19: 39612
use in neutron spectrometers, 16: 14978(P)
use in proton synchrotron experiments, 18: 20401
use in satellites for gamma measurements, 18: 31877 (CERN-64-30 (p.95-104))
use in spectrometer for cosmic protons, 20: 21120
use of coaxial symmetrical flow, for carbon dioxide and thermal neutrons, 18: 20348
use of digitized, in elastic scattering studies with on-line computer, 19: 22862
use of ferrite core memories for recording spark locations in wire, 17: 14678
use of high-resistance electrodes in, for high efficiency in many-particle detection, 17: 32417
use of sonic, for beam momentum measurements, 18: 31892 (CERN-64-30 (p.229-36))
use of sonic, in study of reaction $\pi^- + p \rightarrow f^0 + n$, 18: 31893 (CERN-64-30(p.251-60))
use of sonic, with pair spectrometer, 18: 31891 (CERN-64-30(p.221-7))
use with emulsions for cosmic radiation studies, 18: 39695
use with nuclear emulsions for cosmic radiation detection, 18: 39674
uses for beam experiments, design of event-gate module for, (E), 20: 7399
uses of sonic, for analyzing proton scattering below 20 mrad, 20: 5720 (CERN-65-33)
vidicon data acquisition systems for, 18: 31902 (CERN-64-30(p.361-3))
vidicon design for, (E), 19: 46788
vidicon scanner for automatic digitization of, 18: 31918 (UCRL-11209 (Rev.))
voltage generators for, design of, 18: 30048
voltage pulser for, design and performance of compact low-inductance, 20: 41293
wire arrays in, properties of, 18: 31904 (CERN-64-30(p.365-7))
x-ray production from discharges in, 20: 43714

SPARK SHADOWGRAPH PHOTOGRAPHY
analysis in, design of measuring projector for, 16: 31832 (UCRL-10251)
light source design for, 18: 21717 (SC-R-64-119)
use in plasma diagnostics, 20: 8254

Sparking
see Electric Arcs

SPARTEINE SULFATE

preparation of tritium-labeled, 20: 35571
SPATA
see Cystine, (p-Sulfamoylphenyl)arsylene-
Special Power Excursion Reactor Tests (SPERT)
see Reactor Safety Experiments
SPECIAL PURPOSE POWER PLANT REACTOR
critical facility shielding, 16: 9551 (NAA-SR-Memo-1891)
Specific Gravity
see Density
SPECIFIC HEAT
see also Thermal Capacity
anharmonic contributions to, 16: 21185
anharmonic deviations at intermediate temperatures, 17: 37648 (LADC-5748)
calculation for material at 0.3 to 4.2°K, computer program for, 16: 15099 (ANL-6497)
determination at low temperatures, design of helium-3 cryostat for, 16: 32949 (ANL-6594)
determination at low temperatures, use of helium-3 temperature scale for, 17: 15952 (LADC-5711)
determination at 16 to 100°K, apparatus for, 16: 1792
determination in-pile, method and equipment for, 20: 33605 (UCRL-14766)
electron interaction effects on, in metals, 17: 571
measurement as fuaction of pressure, method for, 19: 43997(R) (UCRL-11889)
measurement at low temperatures, method for, 20: 13693
measurement at 0.4 to 4.2°K, helium-3 cryostat for, 19: 33162
measurement by pulse heating, circuit diagram for, 20: 4388(R) (ORNL-3870, pp 44-9)
measurement from 250 to 1000°C, calorimeter for, 20: 37278
measurement in electrical conductors, pulse heating calorimetric method for, 19: 40700 (ORNL-TM-1187)
measurement in electrical conductors, pulse heating calorimetric technique for, 20: 827 (ORNL-P-1670)
measurement in gases and solids at low temperatures, 18: 9281
measurement in metals, methods for, (E), 20: 30734(R) (TID-22970, pp 1-63)
measurement of, down to 0.3°K using helium-3, 18: 9284
measurement of, of paramagnetic salts down to 0.03°K, apparatus for, 18: 9288
of degenerate electron gas, 18: 30902
of many-boson gas, 17: 31170
of refractory materials at 30 to 800°C, 17: 4523
of 47 technical solids at 1 to 300°K, tables, 16: 6803 (NBS-Mon-21)
temperature effects on, in spin systems in magnetic fields, 19: 1172
SPECTER RANGE NW QUADRANGLE (NEV.)
geologic map of, 17: 4725
SPECTRA
see also Alpha Spectra
see also Beta Spectra
see also Cosmic-Ray Spectra
see also Emission Spectra
see also Gamma Spectra
see also Infrared Spectra
see also Light Spectra
see also Meson Spectra
see also Neutron Spectra
see also Nuclear Spectra
see also Photon Spectra
see also Positron Spectra
see also Proton Spectra
see also Ultraviolet Spectra
see also X-ray Spectra
analysis of, concepts in statistical, 17: 39452 (BNL-7215)
analysis of helium star, 18: 16630
analysis of, method for pulse-height, 18: 3706(P)
analysis of multicomponent time-dependent, from decay of radionuclides, 17: 20981 (HW-75806)
analysis of overlapped, computer programs for, 20: 8834(R) (ORNL-3830, pp 236-47)
analysis of shock-excited, from powdered solids, 17: 33820
atlas of cometary, 18: 22648 (AFCRC-TR-56-267)
atomic, determination of Slater-Condon parameters from, 17: 31118
atomic, effects of Coulomb interactions on energy distribution of terms and line arrays in, 17: 6798 (RM-2947-AEC)
bibliography and review of vibrational, of molten salts, 17: 32041 (ORNL-3413)
book: *Nuclear Magnetic Resonance and Electron Spin Resonance Spectra. Index for 1958–1963*, 20: 30510
book: *Solid State Physics. XIII.*, 16: 21221
book: *Spectroscopic Properties of Rare Earths*, 19: 17940
book: *Statistical Theories of Spectra*, 19: 35507
book: *Statistical Theories of Spectra: Fluctuations*, 19: 37202(R) (BNL-900(p.1-28))
calculation of ESR, computer programs for, 20: 27718 (AD-632523)
calculation of invariant mass, produced by mesons (K^-) in emulsions at 40 to 100 Mev, (T), 19: 26917(R) (IA-984)
calculations by asymptotic self-consistency method, 16: 13882
collective effects in atomic, 18: 30404 (TID-20760)
coupling constants in NMR, perturbation theory for extreme, (T), 19: 44945
data from multichannel analyzers, determination of parameters from grouped samples of, 17: 1770
detection and measurement of, using iterative unfolding method (T), 19: 20316 (ANL-6984)
determination by gas model, propagation of approximation errors in, 17: 8947 (TID-15543)
distortion of pulse-height, by pile-up effect, (T), 20: 27634
Doppler shift in, monochromator wavelength modulator for detection of, 17: 25548 (MATT-162)
Doppler shift of, method for detecting, 18: 16343
electric field effects on, theory, 18: 40170
energy level expectation value fluctuations in unitary ensemble for, 17: 40112
energy shift of, gravitational, (T), 19: 18669
energy shift of, zero-point and Lamb, 20: 31908
fragmentation patterns for molecules, correlation of vibrational isotope shifts with, 19: 4139
gravitational effects on, line displacements in, 20: 21843
gravity effects on stellar, 18: 14705
hyperfine structure splitting and isotope shift, 16: 32406(T) (NP-tr-916)
hyperfine structure and isotope shifts in, determination by interferometric method, 17: 21101
isotope effects in optical, 17: 36434 (NP-13020(p.401-10))
isotope shift in heavy-element, 17: 39023 (NP-13125)
isotope shifts in, theory of, 17: 36711
isotopic shift in, computation of, 18: 5863(T)
isotopic shifts in, 17: 27396
line broadening and shifts in, pressure, 17: 25945
line broadening by Doppler effects in, integral tables for calculating, (T), 19: 15983 (TID-21304)
line broadening in, quantum mechanical theory of, 16: 19629
line broadening in, determination of charged particle concentration in low pressure discharge by, 18: 16659(T)
line broadening of Balmer, for high quantum number, 18: 8949
line identification in, computer program for, 17: 36387 (MATT-90)
line intensities for seventy elements between 2000 and 9000 A, tables, 16: 16337 (NBS-MON-32(Pt.II))
line shapes in ESR, 18: 31474
line width analyses in ESR, assignment of hyperfine splittings by, 18: 31473
line width of atomic, time evolution of density operator for, (T), 19: 39386
line widths in, calculation by Green's functions, 17: 11358
lines of, collision broadening of, 18: 18575
lines of, pressure broadening of, (T), 20: 21519
magnetic field effects on Doppler shift of stellar, 18: 24289
measurement of, errors due to apparatus in, 18: 18143
nuclear and relativistic effects in atomic, 17: 26610
of f^n systems, matrix elements of rhombic potentials for fine-structure analysis of, 19: 15506
optical phenomena in atomic, 17: 20789(T)
properties of atomic, statistical, 18: 2953
properties of nebular recombination, 18: 16631
properties of nebular recombination, 18: 16632
properties of nebular recombination, 18: 16633
properties of, statistical, 17: 27938 (BNL-6396)
properties of stellar, from atmosphere models, 18: 40104
recording of, effects of channel width on accuracy of, 18: 5578
red shift in, deBroglie photon aging theory for, 20: 25694
reproducibility, effects of fluctuations in inflow and excitation conditions, 16: 23205
resolution corrections in digitized statistical, response matrices for, 20: 27628
statistical analysis of radiation detector energy, 18: 29972 (CEA-2396)
structure of, of disordered systems, 18: 30428
theory of absorption and broadband emission, Einstein relations for (T), 19: 1076
theory of coronal, proton excitation lines in, 18: 16635
theory of magnetic multiple resonance, 18: 42307
theory of rotation, 17: 18929
transitions in atomic and molecular, radiationless, 17: 24175
unfolding of measured distributions in, 19: 28732 (ORNL-3743)
vibrational, of inorganic compounds, 17: 40780(R) (TID-19487)
SPECTRAL SHIFT CONTROL REACTOR

characteristics and economic aspects, 16: 18684
criticality and reactivity of, 18: 3169 (BAW-1274)
criticality studies with Savannah fuel charge, 16: 30017 (KR-21)
criticality studies and small lattice experiments, 16: 33977(R) (BAW-1259)
criticality studies of enriched lattices moderated by heavy water–water mixtures, 17: 7627(R) (BAW-1262)
criticality studies and small lattice experiments in, 17: 24712(R) (BAW-1266)
criticality studies with Small Lattice Experiment, 17: 42400
description and economics, 17: 33349
description of 450-Mw(e) plant, 17: 13790
design analysis, 17: 28456 (TID-7650(p.172-93))
design and characteristics, 17: 7580
design and economic aspects, 16: 18651 (BAW-1241)
design and economic aspects of, for electric power production, 17: 24691
development, 16: 1232(R) (BAW-1221)
development, 17: 2601
development, 18: 33078 (A/CONF.28/P/210)
development of, 16: 30006(R) (BAW-1250)
economics of advanced-converter power, (T), 19: 10552 (ORNL-3686)
exponential measurements at high temperatures, 16: 17228 (BAW-1233)
fuel criticality studies, 16: 11190(R) (BAW-1240)
fuel-cycle analysis of, physics model for, 18: 3194 (TID-7665(p.40-56))
fuel lattice nuclear properties, hazards evaluation of experiment for measuring, 16: 23257 (BAW-1248)
fuel management in, 18: 3195 (TID-7665(p.82-7))
fuel preparation for, economics of sol-gel method of, 20: 33846 (ORNL-TM-1109(Rev.))
hazards evaluation, 16: 20863 (BAW-1215(& Suppl.1))
kinetics, 18: 4786 (BAW-1273)
neutron physics, 17: 29706(R) (BAW-1271)
operation of, economics and technical aspects of, 19: 38186 (ORNL-TM-1145)
performance, 18: 7902
physics, age measurements, 16: 6096 (BAW-1234)
physics experiments to demonstrate principle, 16: 17227 (BAW-1230 (Pt.I))
reactivity loss compensation in, circuit for coolant purification and re-injection for, 18: 42910(P)

SPECTROGRAM COMPARATORS

see also Densitometers
description of automatic measuring and recording system for, 19: 20288(R) (UCRL-11828(p.232-3))
design and performance of automatic, 18: 41714 (LA-3100)
design for obtaining photometric profile, 19: 6148 (RT/GEO(64)-13)
design of automatic, high-resolution, 17: 25547 (LADC-5192)

SPECTROMETERS

see also Alpha Spectrometers
see also Beta Spectrometers
see also Cosmic-Ray Spectrometers
see also Gamma Spectrometers
see also Infrared Spectrometers
see also Mass Spectrometers
see also Microwave Spectrometers
see also Neutron Spectrometers
see also Proton Spectrometers
see also Quantometers
see also Radiofrequency Spectrometers
see also X-Ray Spectrometers
aberrations in magnetic, equations for second- and third-order, 18: 5581
aberrations of asymmetrical Czerny-Turner, 19: 22662 (LA-3201)
absorption cell design for alkali metal vapors at high temperatures, 19: 30844 (ARL-65-53)
amplifiers and multipliers for, with semiconductor detectors, (E/T), 19: 34552
amplitude discriminator designed around monovibrator for, 19: 30576
analysis and design of, for fission product flight time measurements, 17: 36117 (ORNL-3486)
background monitor phototube for, 20: 33197
beam aberrations in quadrupole charged-particle (T), 19: 770 (INSJ-78)
beam analysis and optics in double-focusing "n½", 20: 14822(R) (RHEL/R-112, pp 99-128)
beta-gamma and beta-electron angular correlation operation of multichannel, 16: 6585
book: *Nuclear Pulse Spectrometry*, 16: 7731
burner for atomic absorption, design and performance of long-path oxy-acetylene, 20: 10761 (IS-T-69)
calibration and tests for transmission measurements on alkali metal vapors, 19: 30844 (ARL-65-53)
calibration of grazing-incidence grating-type, at 44 Å, 19: 16372
calibration of multichannel, method for, 18: 16331
calibration of Purdue broad-range magnetic, 20: 27260 (COO-1420-123)
charged particle focusing in, using azimuth-dependent magnetic fields, (T), 19: 34510
charged particle trajectories in magnetic, Fermat principle for, (T), 20: 16821 (LAL-1151)
charged-particle intensity distribution in line focus of, wave optics of, 18: 20407
collimator system for, design of 250-slit, two-section type, 16: 1018(R) (AFOSR-1396)
compensating circuits for 1.3-Bev double-focusing 180°, 19: 772 (LAL-1104)
components design for double-focusing magnetic "n½", 20: 14822(R) (RHEL/R-112, pp 99-128)
conference on photographic and spectroscopic optics, 20: 21458
construction and properties of focusing parabola, 17: 1729
construction and performance of thin-semiconductor pulse, 17: 4852
construction of spherical-condenser charged-particle, 19: 4506
control system for multiple, development of computerized, 20: 18988(R) (BNL-929, pp 58-66)
cosmic-particle contributions to background of low-level scintillation, 18: 4081 (CONF-16-15)
data analysis from, using multichannel analyzer with routing system, (E), 20: 5769
data processing from, using numerical adapted filters, (E), 19: 40906
deflecting and dispersion properties of electrostatic prism, for charged-particle beam analysis, (T), 20: 14868
description of Australian, 16: 4604 (ANU/P-235)
description of electrostatic deflection, for ionospheric particles, 20: 11158
description of internal-source scintillation, 17: 41287
description of low-energy electron impact, for determination of electronic energy levels, 17: 8054
description of optical-maser-homodyne, 18: 30298(R) (AD-439695)
description of, for electron paramagnetic resonance below 1°K, 19: 22666
descriptions of, for analytical studies of nuclear reactions, 18: 2007
design and applications of particle, using semiconductor detectors, 18: 20330 (CEA-2388)
design and characteristics of, for measuring nuclear magnetic resonance in liquids, 18: 18142
design and construction of recording, for ferromagnetic resonance measurements, 17: 41197
design and fabrication of nuclear magnetic resonance, 16: 16525 (NP-11497)
design and operation of ultrasonic cw, for electron spin-phonon interactions in solids, 16: 23950
design and operation of fast coincidence single-channel, 16: 29115 (TID-16345)
design and operation of magnetic, employing spark chambers, 16: 33158 (UCRL-10250)
design and operation of quantometer for analysis of nuclear materials, 17: 27270
design and operation of orthogonal dispersion, for missing mass spectra, 19: 36821 (UCRL-11995)
design and operation of spark, for high-energy particles, 20: 9289
design and performance of semiconductor, for charged particles, 17: 366(T) (AEC-tr-5369)
design and performance of direct-reading photoelectric, 17: 10953
design and performance of constant-velocity-drive, for study of the Mössbauer effect, 17: 17954(R) (TID-18450)
design and performance of, review, 17: 41226
design and performance of Cherenkov, for electron and photon energy 18: 2094
design and performance of silicon semiconductor for charged particles, 18: 23962
design and performance of electron-impact excitation, 18: 28243
design and performance of Schmidt spectrograph for plasma diagnostics, 19: 12642 (SSD-TDR-64-170)
design and performance, 19: 13695
design and performance of double-focusing, 19: 28962(R) (NIRL/R/81)
design and performance of electron time-of-flight, 20: 7659(R) (ORNL-3849, pp 101-50)
design and performance of ENDOR, 20: 32525
design and performance of high-resolution magnetic, with large solid angle, 20: 33623 (MIT-2098-167)
design and performance of electronic digital, for experimental nuclear physics, 20: 37128
design and performance of simultaneous alpha and beta, using cesium iodide, 20: 39217
design and performance of on-line wire spark chamber, for 5- to 30-Bev/c particles, 20: 41297
design and properties of interferential, 17: 34245

design and testing of, for molecular beam velocity selection, 17: 25579
design and use of, in helium-6 energy level studies, 16: 32395 (LADC-5388)
design and use of electron impact, for measuring energies of excited electronic states of molecules, 17: 25266
design and use of magnetic, review on, 20: 14841
design calculations for ionization, 20: 14892
design for determination of uranium isotopes, 17: 10971
design for determining elements in gases, 18: 37107(P)
design for isotopic analysis of uranium, 18: 12432(P)
design for neutral particle energy analysis, 18: 13136(R) (ORNL-3564 (p.14-27))
design for neutron absorption cross sections, 19: 19095 (WASH-1053)
design for NMR studies, 19: 9767(R) (IS-900(Sect.P))
design, for nuclear polarizability measurement, 16: 4773
design for polygonal magnetic analysis of angular distributions from nuclear reactions, 16: 33207
design for production of narrow Balmer lines in atomic hydrogen (E), 19: 1176
design for recording spectrum variations with time, 16: 20578(P)
design for studies of plasma discharges, 16: 21684
design modification for isotopic shift studies, 20: 20662
design of automatic mass, for isotopic analysis of lithium, 16: 17826 (Y-1385)
design of bipolar-transistor preamplifiers for scintillation, 19: 42714(R) (ORNL-3782, pp 11-19)
design of broad-range-type, for use with cyclotron, 16: 6036 (NYO-9683)
design of broad-band, for atmospheric gases, 18: 44643(R) (SSD-TDR-63-77)
design of broad-range system for magnetic, using nuclear emulsions, 20: 41306
design of charged particle, 20: 39502
design of crossed-field, for plasma ions, 19: 6186 (JUL-200-PP)
design of Digitron time-interval, 18: 34752(R) (CU(PNPL)-234)
design of double-focusing magnetic, (T), 19: 26711
design of double-focusing magnetic, for electron scattering studies, 20: 16808 (CONF-650922, pp 154-63)
design of echelle grating, for determination of isotopic abundance of uranium, 17: 10970
design of electron paramagnetic resonance, with combined frequency and magnetic field modulation, 18: 25762
design of electron spin resonance, 19: 32515
design of electron-gamma, for conversion-electron angular correlations, 20: 23427(R) (UCRL-16580, pp 219-50)
design of emission, for nitrogen determination in argon, 16: 16570(P)
design of Fabry-Perot, for isotopic analysis, 16: 22011
design of Fabry-Perot, for isotopic analyses, 17: 10969
design of, for high transmission, dispersion, and resolution, 17: 25660(P)
design of frequency-swept nuclear magnetic resonance, for all nuclei, 17: 18578
design of grazing-incidence, for photographic and photoelectric recording, 19: 20348
design of HDIX, for neutron-diffraction studies of crystals and powders, engineering drawings for, 17: 27674
design of high aperture ratio, 20: 31481(T) (AERE-Trans-1050)
design of high-resolution magnetic, for ORIC, 20: 31822 (ORNL-P-2260)
design of hyperfrequency, for study of irradiated single crystals at 20 to 300°K, 20: 10876
design of image-forming slitless, for cosmic and solar x rays, 20: 27272
design of interferometric, for measuring gas temperature, 18: 25764(P)
design of ion cyclotron resonance, 19: 18245
design of magnetic, with focusing lens, 17: 18649(P)
design of magnetic stereo-type, for analysis of heavy nucleons from nuclear reactions, 17: 24776
design of magnetic lens, for beta-gamma correlation studies, 18: 18884 (TID-20390)
design of magnetic track, with spark chambers, 18: 41840
design of magnetic-lens, for e-e and e-γ correlations, 18: 42772
design of magnetic, for electrons, 19: 9508
design of magnetic, for charged-particle nuclear reactions, (E/T), 19: 11538
design of magnetic, for high energy particle detection, 19: 22720
design of magnetic, for particle analysis, 19: 22765
design of magnets for strong focusing pair, 16: 6031 (DESY-A2.82)
design of multi-dimensional selector with magnetic memory, 16: 20774
design of multichannel, 17: 11049
design of multichannel, for measurements on geomagnetically trapped charged particles, 19: 24870
design of multichannel, for measuring geomagnetically trapped particles, 19: 28656
design of multichannel charged-particle, 20: 13118(P)
design of multichannel charged-particle, with delay means to sequentially record detector signals, 20: 25442(P)
design of multiple-gap magnetic, for charged particles, 17: 14637
design of multislit photoelectric grating, for nebula electron density determination, 19: 9867
design of nuclear magnetic resonance, using modulation, 17: 6421
design of nuclear magnetic resonance, for spin decoupling experiments, 17: 18579
design of nuclear-quadrupole-resonance Zeeman, 17: 26249
design of photoelectric double-beam, for 2000 to 20,000 Å, 20: 25390
design of $\pi\sqrt{2}$, 18: 21313
design of portable, for radiological monitoring, 20: 31601
design of scanning collimated, for measuring particle energy spectra in DCX-2, (E), 20: 3178 (ORNL-P-1513)
design of solid-state, for charged-particle studies in aurorae, 18: 20364
design of spark-chamber, for cosmic radiation, 18: 27802
design of spin echo, for moisture measurements in solids, 20: 22867 (INR-619/XV/E)
design of split-pole magnetic, 20: 33624 (MIT-2098-168)
design of sum-coincidence, 18: 24604 (NP-13930(p.54-5))
design of thin-window gas targets for, 16: 7727
design of time-resolving, for operation at 500 to 2500 A, 16: 11921(P)
design of two-crystal, for proton energies in inner Van Allen belt, 18: 2747
design of two-beam optical, 19: 26632 (INP-317)
design of vacuum-grating, for electron probe microanalysis of light elements, 18: 15986
design of velocity selector for subthermal charged particles, 17: 6466
design of velocity, for Mössbauer effect, 18: 10417
design of velocity, for Bevatron beams, (E), 19: 20326 (UCRL-11787)
design of, beam transport optics for, (T), 20: 5944 (SLAC-PUB-132)
design of, combined with analyzer for biology studies, 20: 31525
design of, for simultaneous determination of heavy and light elements, 19: 6170
designs of Compton, 16: 8930
detectors for magnetic, design of, 18: 18209
detectors in multi-unit arrays for, gaps between, 20: 41315
development, 18: 14592(R) (PR-P-60)
development, 18: 24625 (WASH-1046)
development and performance, 19: 26922(R) (PR-P-64)
development at Uppsala Univ., 18: 30709(R) (AFOSR-4867)
development for determination of uranium-235, 16: 23616 (TID-7629 (p.22-30))
development for determination of fuel element burnup, 17: 7976
development for fission fragment times of flight, 19: 30563
development for neutron-charged particle reactions, 17: 31797(R) (BNL-782(p.51-9))
development for plasma studies, 19: 44357
development for sputtering yield measurements, 20: 43660
development of automated for analyses of beryllium on filter paper discs, 16: 23614 (TID-7629(p.1-15))
development of current spark chamber as multichannel ladder counter for, 20: 27308
development of, for measurement of temperature in transparent plasma, 17: 9672 (AFOSR-1100)
development of, for Apollo shielding studies, 17: 14607(R) (ORNL-3378(p.1-17))
development of high-transmission bent-crystal, 17: 17627(R) (NYO-2304)
development of high-transmission bent-crystal, 18: 19837(R) (MIT-905-1)
development of liquid scintillation, for carbon-14 and tritium detection, 18: 34274(R) (NIRS-2(p.3-15))
development of magnetic, for measuring angular distributions from nuclear reactions, 17: 24775
development of magnetic short-lens, with scintillation counter as detector, 18: 39640
development of magnetic-particle, with field alterations, 20: 29558
development of scintillation, for charged particles, 19: 15894
development of thin radiator telescope for particle energy distributions, 19: 18303
development of time-of-flight, for fission fragments, 19: 32580
direct reading attachment for emission, development of, 20: 22876 (RFP-644)
dispersion and stigmatism of magnetic, (T), 19: 11562
electron electrostatic acceleration in long magnetic, 20: 25396
electron source for time-of-flight, 19: 32531(P)
energy calibration and focusing properties of 120° double-focusing magnetic, (T), 19: 4525
evaluation for clinical use, 20: 40734(R) (NYO-901-54, pp 24-5)
excitation chambers for, design for radioactive samples, 19: 17781(R) (ORNL-3750)
focusing of magnetic, using position finding detector, 20: 5745(T) (NP-tr-1302)
focusing properties of field of form $r^{-1} \sin^{-1} \theta$ in, 17: 6414
focusing properties of magnetic, 18: 5580

focusing scheme for magnetic, for heavy particles, 17: 41283
induction and intensity, design and characteristics instrument for control of, 17: 14634
irradiation of wet biological systems using ESR, 18: 20293
line profile measurement with dual-grating, nonuniform, 19: 15915
liquid scintillation, carbon-14 and hydrogen-3 measurement in color-quenched, 19: 31672(R) (NIRS-3(p.65-77))
liquid scintillation, circuitry for automatic, 20: 43749(P)
magnet and timing controls for Compton, 17: 6438 (TID-15530)
magnet pole face computation for focusing, ideal, 17: 14632
magnetic field aberrations in charged-particle, 19: 20365
magnetic field boundaries in wedge-type, 18: 12420 (SLAC-24)
magnetic field distribution for charged-particle, 17: 14631
magnetic field measurement and stabilization in, devices for, 19: 44352 (UJV-1339/65)
magnetic field stabilization in EPR, 19: 32519
magnets for, pole shaping for strong- and weak-focusing, 17: 32791
metering devices for, characteristics, 16: 22386
noise modification for electron spin resonance, 18: 1487(R) (HW-77609(Sect.3))
operation of magnetic, sensitive to weak transverse static fields, (E/T), 20: 4255
performance in clinical counting, 19: 7221 (ORNL-P-750)
performance in determining intensity of overlapping spectral lines, errors in, 18: 18143
performance of combination time-of-flight proton-recoil, 19: 39265(R) (IA-1021)
performance of gallium arsenide detector, for charged particles, 20: 41313
performance of gamma scintillation, for environmental monitoring, (E), 19: 22692 (HASL-150)
performance of magnetic, for meson (K°) decays, 20: 16814 (ITEF-386)
performance of neutral-particle energy analyzing, 19: 21481(R) (ORNL-3760(p.10-22))
performance of scintillation, for charged-particle mass discrimination, 19: 9518
performance of semi-circular magnetic, 16: 17848
performance of spark chamber ladder counter for particle momentum analysis, 20: 653 (LAL-1143)
performance of surface-barrier, for alpha particles, 19: 9515
performance of surface-barrier magnetic, for alpha particles and deutrons, 20: 27286
performance of, with hybrid preamplifier, 20: 41298
performance using sideband technique in variable-frequency NMR, 17: 3274 (UCRL-9791)
performance with semiconductor detectors, 16: 4349
pole-piece-surface calculations in magnetic, 16: 5538
position and quality of images in, effects of stray magnetic fields on, 16: 29119(T) (AEC-tr-5282)
properties for nuclear research, 19: 13804
properties of, for nuclear research, 17: 41305
properties of magnetic, with inclined-plane pole faces, 16: 7719
properties of magnetic, matrix method for calculating, 16: 30624
properties of magnetic, with field variation, 20: 21036 (JINR-P-2573)
properties of single-crystal magnetic, for relativistic particles, (E/T), 20: 31563
properties of, magnetic and optical, 19: 13724 (LAL-1118)
pulse amplifiers for, with current input, 19: 24849
pulse-height analyzer for time-of-flight, design of 512-channel, 20: 13097
pulse-height spectra of scintillation, analysis of, 18: 33925
readout for, design of comparative, 19: 32534(P)
recording system for uv, design of photoelectric, 20: 41267 (MPI-PAE-P1-30/66)
resolution of magnetic, effects of field inhomogeneities on, (T), 20: 13091
resolution of, effects of multichannel analyzer channel width on, 20: 39204 (INR-694/III/PL)
resolving power and solid angle of single-lens, 17: 10895 (KFK-113)
review of magnetic, for charged-particle nuclear reactions, 18: 14284
scanning device for ISP-51, mirror, 19: 32521
scattering chambers, design and construction, 16: 367
scintillation detectors for magnetic, performance of, 20: 41289
screening measures for liquid scintillation-type, effectiveness of, 18: 35855
sensitivity of electron paramagnetic resonance, (E), 19: 32510
setup and performance of 22-foot concave-grating, 19: 15821 (AEET/Spec./2)
shutters for, design of 1.5- to 3000-μsec, (E), 20: 2125 (CEA-R-2816)
signal-to-noise ratio enhancement in, by continuous averaging, 16: 31829 (UCRL-6727-T)
slit function corrections for, 17: 4771 (NP-12236)
spectrum stabilization circuits for pulse-height, (E), 20: 7420
stabilization of scintillation, photomultiplier-gain, 19: 34542
stabilization of scintillation, digital system for, 20: 46041 (FEI-37)
stabilization system for, development of digital pulse-height analyzer, 20: 41269(R) (ORNL-3875, pp 4-12)
stabilization system for scintillation and semiconductor, self-contained, 20: 43712
sweep marker design, 16: 19128
testing optical, 18: 24300(R) (NP-13953)
transmission of $\sqrt{2}\pi$, 17: 32727(R) (PR-P-57(p.69-85))
use in biology, 20: 9167(R) (BNWL-36, pp 5.1-102)
use of crystal, for determination of rare gas thermal neutron absorption and scattering cross sections, 17: 5319
use of goniometer with high-temperature x-ray diffractometers, 16: 23837 (ARL-62-315)
use of magnetic, as spectrograph, 18: 43907
use of magnetic, for beta-decay measurements, 19: 26694
use of nuclear magnetic resonance, to control chemical and distillation processes, 16: 26951(P)
use of permanent magnet, with x rays for electron spectroscopy in chemical analysis, 20: 26776
use of summing coincidence, and total absorption, for measuring gamma-emitting nuclides, 20: 43022
use with activation detector for criticality accident dosimetry, 19: 44537
use with Swedish research reactors, 18: 11479 (ANL-6797(p.183-92))
uses in electron-beam analysis of metals, 18: 22429(T) (TRG-Inf-Ser-382)
uses in physics research, 20: 18174(R) (NP-15771)

SPECTROPHOTOMETERS
burner design for, engineering drawings of acetylene–oxygen, 20: 1798
data readout system for, engineering drawings for, 20: 14901
description of atomic absorption, for determination of cadmium traces, 18: 31366 (CRDC-1193)
design and performance for determining electron density in transient plasma, 20: 10155
design for glove boxes, 20: 4048(R) (NP-15406)
design for measurements on fluids during gamma irradiation, 16: 14960
design modification for continuous recording of titration of fluoride ion, 18: 13628(R) (ORNL-3537(p.1-17))
design of atomic absorption, 18: 16281
design of cell assembly for, 17: 10511(R) (ORNL-3320(p.56-82))
design of continuous-recording, 19: 9437 (BNL-8703)
design of flame, 18: 13628(R) (ORNL-3537(p.1-17))
design of high-sensitivity rapid-response, 17: 17652(R) (UCRL-10634)
design of high-temperature, high-pressure, 17: 39192(R) (ORNL-3452 (p.211-15))
design of high-pressure high-temperature, 19: 4105(R) (ORNL-3627 (p.224-30))
design of low-temperature liquid i-r absorption cell, (E), 19: 37205(R) (ORNL-3778)
design of windowless, for use with corrosive liquids, 18: 8294
development, 17: 15854(R) (ORNL-3397(p.26-38))
development for plasma diagnostics, 20: 26251(R) (NASA-CR-67221, pp 2.2-5)
development high-resolution, single-beam flame type using commercial components, 16: 23617 (TID-7629(p.31-41))
development of direct-reading, 17: 15851(R) (ORNL-3397(p.1-16))
development of high-pressure-temperature, 20: 8834(R) (ORNL-3830, pp 236-47)
development of x-ray, for simultaneous analysis of several elements, 18: 37537
development of, for studies on uranium and transuranium elements in aqueous solutions at high temperature, 20: 45629(R) (ORNL-3945, pp 221-7)
digital data output and miniature circulating-loop systems for, 17: 39192(R) (ORNL-3452(p.211-15))
engineering drawings of electronic circuitry of Bausch and Lomb, 19: 748
furnace design for, 19: 34448
operation of plasma-emission, 19: 5569(R) (MIT-2098-64)
performance of atomic absorption, in potassium determination, 19: 26242
performance of high-temperature, in analysis of fused salts, 19: 17781(R) (ORNL-3750)
performance of Hilger Uvispek, 18: 12411 (AEET/Anal./18)
phosphoroscope design and performance for SF-4, 19: 32522
polarization effects in infrared grating, 19: 44345 (LA-DC-6719)
safety circuit for, flame, 19: 17781(R) (ORNL-3750)
use in determining ozone content of uv radiation rooms, 20: 43011
wave length scale calibration using neodymium and samarium chlorides, 16: 31534

SPECTROPHOTOMETRY
see also Colorimetry
absorption measurements in liquid samples during irradiation, factors influencing, 18: 269 (PAN-431/XVII)

atomic absorption methods of, for determination of trace elements in molybdenum and tungsten, 20: 43154
book: *Advances in Catalysis and Related Subjects*, 18: 33453
book: *Atomic-Absorption Spectrophotometry*, 16: 25297
cell design for low-temperature studies of radioinduced color centers in alkali metal halide crystals, 18: 20622 (COO-1044-16)
conference on photographic and spectroscopic optics, 20: 21458
data analysis for, computer program for, 18: 13631(R) (ORNL-3537 (p.30-46))
data reduction to reaction rate constants, computer program for, 20: 7053 (RFP-629)
determination of residual activity of irradiated dehydrogenase, 20: 42816
development for liquid fluoride analysis, 19: 23163(R) (ORNL-3650 (p.111-86))
development of deuterated high-temperature solvents for, 17: 10511(R) (ORNL-3320(p.56-82))
development of flame, 16: 22028
development of high-temperature, 16: 32897(R) (ORNL-3314(p.187-90))
effects of sample conditions and properties on line intensity, 17: 35617(R) (NYO-10329)
equipment for, development of logarithmic converter and integrater as, 17: 3266 (TID-14150)
equipment for radioactive-solution, 20: 12813(P)
equipment for studies of redox reactions in molten fluoride salts, 19: 9096 (ORNL-P-403)
flame, method for determining calcium, strontium, and strontium-90 by, 19: 35890(T)
method for calculating equilibrium constants of complexes, 18: 31422 (HW-SA-3505)
method for studying radiosensitivity effects of dimethyl sulfoxide on catalase, 19: 33970
methods and reagents for spectrophotofluorimetry, 20: 29083(R) (UCRL-14767)
methods of, for ultra-pure substances, review of, 20: 45590
micro-, method for determining DNA content in rat megakaryocytes, 19: 31677(R) (ORNL-3768(p.119-30))
of fused salts, effects of temperature on isosbestic points in, 17: 2984
of lanthanides in fused salts, review, 16: 1701 (IA-631)
of metal-ammonia solutions at low temperatures, 17: 2957 (UCRL-9887)
of molten salt systems, 18: 13630(R) (ORNL-3537(p.23-30))
of samples over wide pressure and temperature ranges, equipment and methods for, 19: 347(R) (ORNL-3679(p.60-83))
oxyacetylene burner for atomic absorption, design of laminar-flow, 20: 29083(R) (UCRL-14767)
use for determination of formation constants and classification of complexes, 19: 26365
use in solar flare observations, 18: 24269 (NP-13801)
use of atomic-absorption, in isotope analysis, 17: 40717 (TID-7655 (p.390-9))
uses in determination of hydrated electrons in gamma-irradiated solutions, 19: 5959
uses of atomic absorption, 20: 31167(R) (ANL-7175, pp 217-25)

SPECTROSCOPY

see also Beta Spectroscopy
see also Gamma Spectroscopy
see also Infrared Spectroscopy
see also Mass Spectrography
see also Microwave Spectroscopy
see also Neutron Spectroscopy
see also Ultraviolet Spectroscopy
see also X-Ray Spectroscopy
accuracy of, effects of standard preparation on, 19: 40434
analysis of pure metals, review, 16: 9940 (BM-IC-8039)
analysis of radioactive solutions using copper-spark method, 17: 123
analysis of reactor substances for traces, review, 17: 126
analysis of reactor materials by, review of methods for, 19: 5809
analysis of refractory samples, predistillation in, 17: 124
analysis of trace impurities by optical emission, review, 19: 43929 (IS-1237)
analysis using carrier distillation technique, use of mechanical packer in, 19: 19743 (CEA-R-2619)
analytical use for nonmetals, using high-current low-voltage sparks, 19: 30087(T) (IS-Trans-15)
analytical uses of, at Arco Chemical Plant, 16: 30327(R) (IDO-14588)
analytical uses of, manual on, 20: 33155 (PG-Report-177(Rev.))
apparatus and process for, of small amounts of elements in a gas, 17: 4487(P)
apparatus for flash filament desorption, 19: 9046(R) (IS-900(Sect.C))
apparatus for the preliminary evaporation of trace impurities from samples, 17: 10951
apparatus for vaporization-concentration method of spectrochemical analysis, 18: 35490
application of Wigner coefficients for SU, group to, 17: 11928
atomic distributions in electric arc discharges in, 19: 30108
atomic, data handling and analysis system for, 19: 5885
atomic, matrices for electrostatic interactions of dnsp configurations in, 19: 34893
background from superposed pulses in nuclear, device for reducing, 17: 32441
bibliography and review on emission, 16: 14642
bibliography and review on atomic absorption, 16: 14643
bibliography and review on absorption, 16: 14646
bibliography and review on Raman, 16: 14648
bibliography on high-temperature, 19: 17857 (NP-14810)
bibliography on high-temperature, 19: 26289 (NP-15042)
bibliography on high-temperature, 19: 43993 (NP-15379)
bibliography on microwave, 17: 14124 (UCRL-10404)
bibliography on, in high-temperature chemistry of condensed phases and gases, 20: 18630 (NP-15896)
book: *Advances in Spectroscopy. II.*, 16: 14681
book: *Applied Spectrometry of Ionizing Radiation*, 19: 13804
book: *Coincidence Tables for Atomic Spectroscopy*, in German, 19: 26278
book: *Developments in Applied Spectroscopy*, 19: 38572
book: *Electronics in Nuclear Radiation Spectrometry*, 17: 41305
book: *Emission Spectral Analysis of Nuclear Materials*, 16: 5297
book: *Fused Salts*, 19: 7513
book: *High Resolution Nuclear Magnetic Resonance Spectroscopy, Vol. I*, 20: 41255
book: *Interactions of Nonequilibrium Radiation with Materials*, 20: 23903
book: *Introduction to the Theory of Atomic Spectra*, 18: 18593
book: *Methods of Experimental Physics. III.*, 16: 19551
book: *Nuclear Pulse Spectrometry*, 16: 7731
book: *Plasma Spectroscopy*, 18: 40730
book: *Selected Topics in Nuclear Spectroscopy*, 18: 36688
book: *Spectral Analysis of Pure Metals and Alloys*, 17: 1413
book: *Spectroscopy*, 17: 6023
book: *The Encyclopedia of X Rays and Gamma Rays*, 18: 8043
book: *Topics in Radiofrequency Spectroscopy*, 17: 8093
bremsstrahlung fluorescence, methods of, 18: 29586
conference on, 17: 25274
conference on, 20: 27637
conference on applied, Chicago, May 15-18, 1961, 17: 2927
conference on applications, equipment, and techniques in, 18: 20676
conference on nuclear, 19: 16885
conference on photographic and spectroscopic optics, 20: 21458
conference on physics problems in, 18: 32283
conference on spectral line shape and molecular interactions, summary, 16: 2296 (K-1495)
conference on, Eighth International, Lucerne, Switzerland, Sept. 14 to 18, 1959, 18: 27316
coordinate grids for plates in, 17: 41296
copper-spark method in, 17: 15934
cosmic-particle contributions to background of low-level scintillation, 18: 4081 (CONF-16-15)
data acquisition systems for nuclear, computer uses for, 20: 6307 (UCRL-16439)
density measurement in emission, errors of, 19: 13700 (BNL-7830)
description of optical pumping method, 16: 22780
description of plasma burner for flame, 17: 28803(T) (AEC-tr-5867)
design concept of spectrochemical source, 16: 20304 (CRL-73)
design of alternating-magnetic-field generators for nuclear-quadrupole-resonance, 17: 4794
design of flash photolysis apparatus with short discharge time, 19: 719 (CEA-R-2462)
determination of elements by atomic, bibliography on, 20: 20563 (NP-15918)
determination of isotopic abundances, 17: 10969
determination of trace elements in powders by, 16: 32921 (PAN-312/VIII)
determination of trace contaminants in metals by, 17: 30476
development, 17: 496(R) (KAPL-2000-19)
development and uses of scintillation, in nondestructive testing, 16: 31956 (HW-SA-2728)
development for monitoring fissiochemical reactions, 20: 3982(R) (AGN-8156)
development of atomic-absorption, review of, 17: 40715 (TID-7655(p.333-78))
development of emission, for analytical uses, 20: 3863(R) (IS-1200 (Sect. C))
development of, for use in analytical chemistry, 17: 4445 (IS-500(Sect.C))
development of high-resolution, for isotope analyses and Zeeman effect studies, 16: 26901 (NYO-10058)
development of high-energy, using activation detectors, (E/T), 20: 29521 (CONF-651109, pp 213-23)
development of impulse, 16: 19083

development of level crossing, 16: 29481(R) (NP-11989)
development of magnetic, 17: 1941(R) (NP-12214)
development of microwave and radiofrequency, 17: 10514(R) (ORNL-3320(p.104-25))
development of microwave and r-f, 19: 23163(R) (ORNL-3650(p.111-86))
development of nuclear, with energy resolution of a part per million, (E), 19: 35476
development of plasma, 17: 40427(R) (NYO-10063(p.1-6))
development of semiquantitative visual, 20: 14457(R) (ORNL-3889, pp 36-39)
developments and techniques of atomic absorption, in analytical chemistry, 16: 9973
developments in absorption, review of, 18: 19860
developments in atomic and autoionized beam, 20: 7722
developments in emission, review of, 18: 19863
developments in, for use in analytical chemistry, 16: 9974
developments of, at Idaho Chemical Processing Plant, 17: 27231(R) (IDO-14605)
diagnostic use for plasma temperature measurements, 18: 32911
diagnostic use for arc plasma, local emission coefficients for, (T), 19: 12792
diagnostic use for plasma arc tunnel flows, (E/T), 19: 14658 (ASD-TDR-63-98)
diagnostic use for hydrogen plasma, parameters for, 19: 19236 (IPP-1/23)
diagnostic use for discharge plasma, 19: 23844
diagnostic use for plasma electron density measurements, 19: 31322 (AD-610631)
diagnostic use for plasma property studies, 19: 39960(R) (N64-33202)
diagnostic use in MPD cells, 18: 32521
Dirac and Pauli theory in, first order perturbation calculus formulas for transition between, 17: 34576
distillation of trace impurities, effects of spectroscopic carriers on, 16: 32938
drift-correcting computer subroutine for nuclear, 19: 11660
electric arc voltage fluctuations in, 19: 40416
electric discharge effects on plutonium spectra in hollow cathodes, 19: 11011(T)
electro-optical parameters from infrared band intensities of isotopic molecules, 19: 25169(T)
electrodes in emission, use of pyrolytic graphite plate, 19: 13267
electron shell order in ionized atoms, 18: 20758
electron spin resonance spectra, theoretically calculated multicomponent symmetrical, 18: 8948(T)
emission of solutions, review, 16: 7502
emission spectra sensitivity for, 19: 30128
emission, element detection sensitivities using oxyacetylene flame in, 19: 42413 (IS-T-26)
equipment for atomic-absorption, 17: 40716 (TID-7655(p.379-89))
equipment for, design of rotating-mirror camera for time resolution of spectra in region from 2000 to 7000 A, 17: 1701 (JUL-53-PP)
equipment for proton, 17: 18377 (TID-7652(p.523-94))
evaporation methods in, 17: 33835
flame, correlation of dissociation energies and excitation energies of oxyhydrogen, 17: 14234
focusing in homogeneous sector magnetic field, theory, 16: 19137
Hartree-Fock wave functions and oscillator strengths for $Z = 3$ to 10 isoelectronic sequence, 18: 7412
review of Hungarian research in, 16: 25091
instrument operation and service manual for scintillation and semiconductor, 16: 23846 (ORNL-TM-137)
instrumentation development for nuclear, 16: 11859(R) (ORNL-3191 (p.1-18))
instrumentation development for micro-, 17: 8219(R) (MCW-1479)
intensity of Stokes lines in gases, 18: 7344
lectures on nuclear, 17: 4107
light sources for atomic absorption, performance of spectral continua as, 20: 3863(R) (IS-1200(Sect. C))
limits of self-absorption, 17: 27294(T)
line broadening by Doppler effects in, integral tables for calculating, (T), 19: 15983 (TID-21304)
line broadening of Balmer series for high quantum number, 18: 8949
line intensities of plasma at 3000 to 50,000°K in, effects of gas-vapor compositions on, 18: 10021
measurement of short spin-lattice relaxation times by solvent nuclear polarization, 20: 31221(R) (UCRL-16658, pp 73-87)
measurements of molten materials, development of thermostatically controlled oven for, 17: 35253(R) (IA-775)
method for broad emission line, 17: 3288
method for contaminant determination, 19: 34134(P)
method for obtaining comparable photographs of an oscilloscope display in analysis by the gray-wedge technique in, 17: 32464(P)
method for optical atomic, accelerator, 19: 32903
method of, for plasma temperature determination, 17: 24558 (ARL-62-460)
method suitable for both powders and solutions, 17: 10952
methods for isotope detection, 17: 12276(T)
methods for optical atomic, accelerator, 18: 28254
methods for plasma-jet, 20: 17901
methods for spectroscopic averaging, 20: 46710
methods for spectroscopic averaging, combinatorial, (T), 20: 46711
methods for transient species, 19: 26452
methods of atomic absorption, development and uses of, 18: 43438
methods of copper-spark, 17: 40707 (TID-7655(p.193-211))
methods of molecular, 17: 12203
methods of, for semiquantitative simultaneous determination of 30 elements in powder samples, 20: 43104
methods using gallium oxide, 19: 19774 (UCRL-7962)
methods using high-frequency plasma flames, 18: 10020
modification of Rydberg-Klein-Rees method for obtaining potential curves for doublet states, 16: 13700 (NP-11429)
nuclear alignment using heavy-ion reactions, 20: 34603
nuclear, application of fast-slow coincidence circuit with time to pulse-height converter to, 17: 11033
nuclear emulsion track counting method for optical, 20: 25395
nuclear, high-speed digital computer techniques in, 17: 24513
nuclear inequality for unfolding continuous energy spectra in, 17: 26199
nuclear magnetic resonance, principles and uses of, 18: 12002
nuclear magnetic resonance, review on long-range H^1–H^1 spin-spin coupling in, 18: 24234
nuclear magnetic resonance, in superconducting magnetic fields, 18: 43920
nuclear, operation and performance of gold-doped silicon detector for high resolution, 16: 7716
nuclear shell model uses in, (T), 20: 9974 (PUC-937-171)
nuclear, use in reactor technology, review of, 17: 26198
nuclear, uses for direct reactions, 20: 8086 (ZFK-TPH-15)
nuclear, uses of polarized neutrons in, 18: 12929
nuclear, Wiener filtering for low noise level of amplifiers in, 18: 10396
numerical, for solving time-dependent Schroedinger equation, 19: 39642
of electron and nuclear spin resonances, 16: 17552 (AD-263735)
of electron energy losses in solids, 19: 1190
of ionic media, 16: 30170(R) (ORNL-3313(p.179-208))
of minerals and ores, review, 16: 28911
of radioisotopes, engineering drawings of controlled atmosphere chamber for, 18: 17983
optical maser heterodyning techniques in, development of, 17: 14926(R) (AD-296893)
performance of internal-source scintillation, 17: 41287
performance of, using sifted powders, 17: 14142 (PAN-370/VIII)
plasma diagnostics by, dense, 17: 42038 (ARL-63-105)
plasma diagnostics using image intensifiers and interference, 18: 19198
plasma diagnostics in, 18: 28754 (AD-415622)
plasma structure diagnostics by bremsstrahlung and line radiation, 18: 1095(R) (AFCRL-62-184)
proton magnetic resonance, use of deuterated organisms in, 20: 16165
pulse amplitude distributions in, Kotel'nikov's theorem for relating energy to, 19: 31080
pulse-height spectra in, pile-up-effect distortion of, (T), 20: 27634
quantum defect method in, proof of, 16: 22784(T)
radioisotope uses in analysis by, 16: 3330(T) (AEC-tr-4497(p.206-14))
reduced matrix element of an irreducible spherical tensor operator for, derivation of, 20: 1329
research on nuclear, (T), 20: 4475(R) (ANL-7081, pp 95-119)
research program in nuclear, Hungarian, 19: 16913
research programs on nuclear, at Marie Curie Sklodowska University, Poland, 18: 21989
research programs at Uppsala University on, 18: 30709(R) (AFOSR-4867)
research progress in, 20: 40796(R) (IS-1500(Sect.C))
review of atomic emission, 19: 28296
review of atomic, from *Optika i Spektroskopiya* (U.S.S.R.), 18: 778
review of fluorescence, 18: 39053(T) (AERE-Trans-1005)
review of nuclear applications of emission, 19: 13233
review of nuclear, 20: 46803
review of shock-tube, 18: 28168
review on atomic- and molecular-beam, 19: 23311
sample preparation for determination of boron in reactor graphite, 16: 9965
semiconductor detectors for nuclear, lectures on, 19: 44466 (UCRL-16231)
sensitivity of arc plasma, 19: 28268
sensitivity of emission, extension for trace elements, 18: 5242
solar, 17: 26257
source design for Raman, high-intensity electrodeless, 17: 12542
source design for emission, plasma-discharge sputtering, 20: 8877(P)
source development for uranium isotope measurements by emission, 18: 33459 (CEA-R-2428)

source for emission, use of graphite cloth as excitation, 19: 32116(P)
source for, design of plasma-jet, 20: 10798(P)
spark excitation processes in, time resolution of, 18: 3433(T) (AEC-tr-6130)
spectral profiles in, determination from correlation measurements, 19: 16275
spectrum expander for semiconductor-detector, charge-compensation, 19: 13769
spectrum mapping equipment and methods, 16: 16011 (R62SD28)
spectrum stabilization circuits for pulse-height, (E), 20: 7420
techniques of high-resolution, for study of uranium spectrum, 19: 18236 (LA-3182)
terminology in nuclear, 18: 39643
theory of atomic beam optical double resonance, 19: 39369 (NP-15140)
theory of atomic, use of annihilation and creation operators in, 20: 22859(R) (UCRL-16580, pp 149-205)
theory of nuclear, group, 18: 2958
theory of optical, 19: 25081
theory of resonance optical rotation, 18: 10990
theory of resonance broadening of spectral lines by atom-atom impacts, (T), 20: 2620
theory of wing broadening of hydrogen Lyman α line by electrons and ions in a plasma, (T), 20: 3217
transformation matrices for atomic, 20: 2604
use for determination of trace elements, book, 17: 25158
use for nondestructive determination of burnup in nuclear fuels, 20: 11004
use for plasma diagnostics with spatial resolution, 18: 19189
use for plasma electron temperature measurements, 20: 24517
use for plasma thermodynamics study, 18: 38226
use in determining trace elements in uranium, 19: 11037
use in diagnostics of arc plasma, (E), 20: 20010(R) (N-65-23211)
use in plasma diagnostics, 18: 42799 (SCTM-93-63(71)(p.44-54))
use in plasma diagnostics, 20: 8257
use in plasma diagnostics, line broadening in, (T), 20: 8258
use in plasma diagnostics, (T), 20: 8259
use in plasma ion temperature measurement, 20: 34769
use in radiation chemistry and radiobiology, review on, 19: 838
use in study of beryllium content in lung tissue, 17: 28647
use in study of charged particle beam interactions with plasma, (T), 20: 10196(T)
use in study of oxide structures, 16: 19366(R) (TID-15228)
use of angular correlations measurements in nuclear, 16: 21351 (NP-11651)
use of combined electric-dipole and magnetic-dipole EPR, for studies on gaseous atom-molecule reactions, 19: 11108
use of copper-spark method in analysis of radioactive solutions, 16: 16306 (PAN-250/XIII)
use of electrodeless discharge lamps in atomic, 17: 36466
use of fluorescent x rays produced by beta particles for, 17: 5982(T) (CEA-tr-X-461)
use of lasers for cancer, advantages of, 20: 40776
use of optical, for isotopic analysis, 17: 17979
use of optical, in isotopic analysis, 18: 13611 (CEA-2301)
use of porous cups in, 17: 30468 (CONF-48-1)
use of spark-emission, for chemical analysis, 18: 1571
use of spectral data in determination of anharmonic potential energy constants for molecules, 20: 31949
use of time-resolved optical, in determining thermodynamic state of plasmas produced in electromagnetic shock tubes, 18: 40685
use of Van de Graaff accelerators in optical, 18: 8969
use of Zeeman, for plasma diagnostics, 17: 15035
uses for analysis of induction-coupled plasmas and aerosols, 20: 7005 (IS-T-51)
uses in measurement of electron density and temperature in hollow pinch, 19: 6727 (IPP-1/16)
uses in plasma diagnostics, 17: 15342 (AD-275762)
uses in semi-quantitative analysis of powdered samples, 19: 22120
uses in studies on gaseous reactions at high temperatures, bibliography on, 20: 7051 (NP-15643)
uses of atomic absorption, analytical, 19: 46166 (DP-980)
uses of nuclear magnetic resonance, in organic chemistry, 17: 18101
uses of Zeeman, for measurement of time-varying magnetic fields, (E), 19: 20257 (IPP-1/19)
wavelength measurements with concave grating spectrograph, 17: 33884
Zeeman effect in magnetic field, 17: 28034(T)

SPERM

see also Spermatogenesis
effects of deuterium oxide on helical stability of DNA in salmon, 20: 35204
effects of ingested deuterium oxide on mouse, 20: 10550
effects of irradiated, on embryonic lethality in mouse progeny, 19: 42303
effects of maturity of, on radioinduced mutation frequency in male Drosophila, 19: 38390
effects of temperature on irradiated silkworm, 20: 42930
glycine metabolism in, tracer study, 17: 30254
mitosis in, of mealy bug, 18: 65
phosphorus-32 metabolism in cock, 19: 35925
radiation effects on mature, in *Drosophila virilis*, 16: 9869
radiation effects on Drosophila, gamma and neutron, 16: 28817
radiation effects on alkaline phosphatase, DNA, and RNA contents of rabbit, 16: 30291
radiation effects on mouse, x-, 16: 31487
radiation effects on Drosophila, effects of nitric oxide, oxygen, and temperature on, 17: 7885
radiation effects on chromosomes, 17: 15637(R) (TID-18135)
radiation effects on nucleic acid content, vitality, and fecundating ability, 17: 15689
radiation effects on planaria, 17: 17810
radiation effects on salmon, protective effects of cysteamine against, 17: 23233
radiation effects on fertilization of normal eggs by *Fundulus heteroclitus*, 17: 23107
radiation effects on mutation frequency in *Drosophila*, effects of cyanide and dose rate on, 17: 24901
radiation effects on, relative proton and x, 17: 30365
radiation effects on, mathematical model for mutation and killing of cells in, 17: 38822
radiation effects on Drosophila, gametic genotype effects on x, 18: 3567
radiation effects on insemination and retention of, in *Drosophila melanogaster*, 18: 9859
radiation effects on ploidy of mouse, x, 18: 11663
radiation effects on Drosophila, effects of storage techniques on x, 18: 13490
radiation effects on production of, in dogs, x, 18: 15892
radiation effects on trypsin digestion of desoxyribonucleoproteins in *Misgurnus fossilis*, 18: 17574
radiation effects on genetic response of Drosophila, neutron and x, 18: 19647
radiation effects on human, after accidental exposure, 18: 19648
radiation effects on chicken, effects on fertility and hatchability, 18: 19664
radiation effects on metabolism in bull, gamma, 18: 23297
radiation effects on metabolism of, gamma, 18: 23334
radiation effects on sea urchin, 18: 23339
radiation effects on count of, in guinea pigs, 18: 25191
radiation effects on number and morphology of, in bulls, 18: 25185
radiation effects on Drosophila, genetic, 18: 35344
radiation effects on developing, in grasshoppers, 18: 35302(R) (AD-438540)
radiation effects on production of bull, 18: 38775(R) (ORO-624)
radiation effects on production of rabbit, gamma, 18: 38775(R) (ORO-624)
radiation effects on developing rat, protective effects of olive oil against, 18: 38775(R) (ORO-624)
radiation effects on mutagenesis in mouse, protective effects of AET against x, 18: 38987
radiation effects on production in swine, 18: 38775(R) (ORO-624)
radiation effects on desoxyribonucleic acid in, effects of oxygen on, 18: 41164
radiation effects on activity of rat, 19: 68(R) (AD-600960)
radiation effects on mouse, whole-body, 19: 168
radiation effects on *Misgurnus fossilis* L., effects of dose on, 19: 2102
radiation effects on rat, fast neutron and gamma, 19: 10833
radiation effects on guinea pig production of, x, 19: 10875
radiation effects on frog, 19: 12978
radiation effects on mutability of female and male *Drosophila melanogaster* mature, 19: 15085
radiation effects on lethal mutation induction in mature animal, RBE of fast neutron, gamma, proton, and x-ray, 19: 17607
radiation effects on viability of bovine, gamma, 19: 17544
radiation effects on, 19: 21792(R) (ORNL-3650(p.187-219))
radiation effects with tretamine on induction of dominant lethal mutations in screw-worm fly, 19: 24289
radiation effects on structure of Y chromosomes in *Drosophila hydei*, 19: 24298
radiation effects on reduced spindle fiber birefringence in *Nephrotoma suturalis*, uv, 19: 25967
radiation effects on Drosophila, protective effects of nitrogen against x, 19: 29960
radiation effects on electrophoretic mobility of rabbit, 19: 31879
radiation effects on development of grasshopper, 19: 33813
radiation effects on Habrobracon, gamma, 19: 43721(R) (ORNL-TM-1217)
radiation effects on Drosophila, mutagenic gamma, 19: 43724(R) (TID-22160)
radiation effects on Drosophila spermatocytes, from incorporated tritium-labeled thymidine or uridine, β, 20: 1657

radiation effects on bull production of, fractionated-dose whole-body x, 20: 14336
radiation effects on Drosophila, combined with acceleration, 20: 14343
radiation effects on Drosophila, combined with vibration, 20: 14343
radiation effects on maturation of human, x, 20: 22617(R) (RLO-1780-1)
radiation effects on bovine epididymal, x, 20: 29013
radiation effects on human, from gonadal exposure, 20: 31034(R) (RLO-1780-7)
radiation effects on human, after gonadal exposure, 20: 31035(R) (RLO-1780-8)
radiation effects on Drosophila, in succeeding generations after oocyte exposure, gamma, 20: 36625
radiation effects on silkworm, genetic, RBE of fast neutrons and γ, 20: 38626
radiation effects on morphology and viability of bull, x, 20: 40610(R) (COO-895-9)
radiation effects on morphology and motility of bull, in suspensions, γ, 20: 42950
radiation effects on morphology and numbers in rats, x, 20: 42961
radiation injuries in, repair of premutational uv and x, 20: 31040
radiation injuries in frogs, and subsequent effects on embryos, 20: 45256
radiation injury and recovery in *Drosophila*, 16: 7456
radioinduced changes in X and Y chromosomes at four-strand stage in, in Drosophila, 17: 28737
radioinduced chromosome breakage in, in Drosophila, 17: 10403
radioinduced cleavage delay in *Arbacia punctulata*, recovery from, 17: 5895
radioinduced dominant lethal mutations in mouse, 19: 38394
radioinduced dominant lethals in mouse, effects of dose on x, 20: 18351
radioinduced dominant lethality in, of olive fruit fly, 20: 40674
radioinduced genetic damage to, control by storage, 18: 17490
radioinduced genetic damage to, postirradiation modification of, 19: 8943
radioinduced lethal factors in mouse, effects of mercaptoethylamine on, 17: 7855
radioinduced mutations at specific loci in Drosophila, 16: 28747(R) (TID-16429)
radioinduced mutations at specific loci in Drosophila, 16: 28748(R) (TID-16430)
radioinduced mutations in Drosophila, dose-frequency response of, 18: 9860
radioinduced mutations in mouse, effects of dose rate and fractionation on, 18: 11837
radioinduced mutations in Drosophila, effects of fractionation and intensity on gamma, 18: 11838
radioinduced mutations in silkworm, effects of sex on gamma, 18: 11839
radioinduced mutations in Drosophila, effects of chloramphenicol, dinitrophenol, nitrogen, oxygen, and ribonuclease on, 18: 11887
radioinduced mutations in Drosophila, gamma, 19: 15131
radioinduced mutations in mouse x, 19: 15132
radioinduced mutations in Drosophila, x, 20: 5301(R) (UR-668, pp 1-54)
radioinduced mutations in male *D. melanogaster*, effects of age on, 20: 12636 (TID-21459)
radioinduced mutations in Drosophila, x, 20: 18336
radioinduced mutations in Drosophila, effects of dose on x, 20: 24893
radioinduced mutation frequency in Drosophila, protective effects of 2,4-dinitrophenol against gamma, 20: 33079
radioinduced translocations in mouse, 19: 38396
radiosensitivity, 17: 27090
radiosensitivity, effects of oxygen and recovery mechanisms in Drosophila, 17: 7840
radiosensitivity in Drosophila, effects of developmental stage, 16: 25192
radiosensitivity in Drosophila, 17: 1238(R) (TID-17002)
radiosensitivity, in Drosophila, 17: 28709
radiosensitivity in *Drosophila melanogaster*, 18: 9856
radiosensitivity of loach, 16: 30301
radiosensitivity of Drosophila, 17: 1236(R) (TID-17000)
radiosensitivity of Drosophila, 17: 1237(R) (TID-17001)
radiosensitivity of Drosophila, 17: 1239(R) (TID-17003)
radiosensitivity of spermatogonia in mice, relation of cell cycle stage to, 17: 4415
radiosensitivity of spermatogonia, gamma and x-ray, 17: 40579
radiosensitivity of Drosophila, 18: 5117
radiosensitivity of, in mice and monkeys, 18: 6672
radiosensitivity of, in mice and monkeys, 18: 6673
radiosensitivity of, conference on, 18: 11828
radiosensitivity of Drosophila, cytological evaluation of, 18: 11841
radiosensitivity of Drosophila, 18: 29296
radiosensitivity of Drosophila, 18: 29297
radiosensitivity of chicken, 19: 7087
radiosensitivity of Drosophila, 19: 10840
radiosensitivity of Drosophila, 19: 10841
radiosensitivity of Drosophila, 19: 10842
radiosensitivity of Drosophila, effects of nitrogen, 19: 25981
radiosensitivity of planaria, 19: 35971
radiosensitivity of Drosophila, 19: 45949
radiosensitivity of screw-worm fly, 19: 45950
radiosensitivity of mouse, effects of genotype on, 20: 3711(R) (NYO-3314-2)
radiosensitivity of mouse, effects of streptomycin on, 20: 14404
radiosensitivity of human, tracer study on, 20: 31035(R) (RLO-1780-8)
reparative effects of DNA from various organs on, after x-irradiation, 20: 40723
selenium-75 metabolism in cock, 19: 35925
storage of Drosophila, mutagenic effects of, 18: 33273(R) (NIRS-2(p.42-8))
temperature effects on brood pattern of x-irradiated Drosophila, 18: 23279

SPERMATOGENESIS
see also Gonads
cesium-137 effects on rat, 17: 15704
desoxyribonucleic acid synthesis during, tracer study, 17: 5720
effects of estrogenic hormones on rat, comparison of, with radiation effects, 18: 23332
effects of strontium-90 injection on, in mice, 17: 33713
effects of temperature on irradiated germ cells during, in male silkworms, 20: 42930
effects of uv-irradiation during silkworm, on chromosomes, 20: 42895
helium effects on Drosophila, 20: 38596(R) (SAN-590-1)
maintenance, patterns, and radiosensitivity of, in insects, 20: 14224 (TID-21562)
meiosis duration in monkeys, 16: 8575
mutagenic effects of formaldehyde food and x rays in, of Drosophila, 17: 31892
radiation and streptonigrin effects on *Drosophila melanogaster*, 19: 31889
radiation effects of spermatozoa exposure on induction of paternal sex chromosome losses, 16: 9867
radiation effects and polysaccharide reactions, 16: 21939
radiation effects in rat and mouse, whole-body exposure, 17: 1269
radiation effects on, in male mice and rats, 17: 7854
radiation effects in mice, long-term gamma, 17: 7856
radiation effects in mice, chronic gamma exposure, 17: 10361 (TID-15852)
radiation effects on differentiation and induction of, in grasshoppers, 17: 14040
radiation effects on, in mice, 17: 21472
radiation effects on mouse, effects of head and trunk shielding on, 17: 30329
radiation effects on, from ingested strontium-90 in dogs, 17: 31929
radiation effects on occurrence frequencies of mutations in, 17: 31936
radiation effects on chromosomal rearrangement in, in monkeys, 17: 31950
radiation effects on mink, x, 18: 83
radiation effects on mouse chromosomes in, 18: 3571
radiation effects on chromosome aberrations in, in monkeys, 18: 5108
radiation effects on Drosophila, 18: 8157
radiation effects on mouse, x, 18: 11734
radiation effects on cytochemistry of Stenobothrus, x, 18: 19615
radiation effects on, x, 18: 23324
radiation effects on rat, comparison of electron, with effects of estrogenic hormones, 18: 23332
radiation effects on Drosophila, x, 18: 27112
radiation effects on, in mice, 18: 27007(R) (ORNL-3601(p.83-91))
radiation effects on insect, x, 18: 29338
radiation effects on, in man, design of irradiation facility for study of neutron, 18: 29245 (TID-20783)
radiation effects on Drosophila X chromosome during, gamma, 18: 33378
radiation effects on, in Drosophila, 18: 35302(R) (AD-438540)
radiation effects on monkey, x, 18: 36999
radiation effects on spermatocytes and spermatogonia in *Macaca mulatta*, 18: 43290
radiation effects on mouse, protective effects of AET against, 19: 206
radiation effects on, in sterilized silkworms, 19: 8865
radiation effects on silkworm, relation to sterility of, 19: 10831
radiation effects on bovine, 19: 17572
radiation effects on Sitophilus, sterilization, 19: 30602
radiation effects on, in mice, 19: 29968
radiation effects on, in grasshoppers, 19: 33813
radiation effects on, in male gypsy moths, 19: 36030
radiation effects on mouse, x, 20: 65(R) (TID-22174)
radiation effects on, in field mice living on radioactive soils, 20: 5387
radiation effects on dog, x, 20: 5301(R) (UR-668, pp 1-54)
radiation effects on early stages of, in adult *D. melanogaster* males, 20: 12637 (TID-21466)
radiation effects on Drosophila, mutagenic, 20: 16229(R) (NYO-1472-1)

radiation effects on mitotic delay in, of *Drosophila melanogaster*, 20: 18354
radiation effects on Drosophila, x, 20: 18310
radiation effects on, in lizards, 20: 20444(R) (TID-22820)
radiation effects on mouse, effects of age at irradiation of x, 20: 20499
radiation effects on human, x, 20: 22617(R) (RLO-1780-1)
radiation effects on Drosophila, protective effects of arginine against gamma, 20: 22780
radiation effects on Drosophila, effects of temperature on x, 20: 22662
radiation effects on mouse, x, 20: 24934
radiation effects on rate and timing of, in man, 20: 31034(R) (RLO-1780-7)
radiation effects on monkey, γ and x, 20: 31117
radiation effects from polonium-210 on mouse testes, 20: 31063
radiation effects on frequency of chromosome breaks in *D. melanogaster* at different stages of, x, 20: 32995
radiation effects in *Drosophila melanogaster*, x, 20: 38607
radiation effects on human, x, 20: 40627(R) (ORNL-3922, pp 84-8)
radiation effects on bull, x, 20: 40610(R) (COO-895-9)
radiation effects on rat, following exposure at birth, x, 20: 40682
radiation effects on germ cell ultrastructure during rat, following exposure at birth, x, 20: 40683
radiation effects on mouse, γ and x, 20: 42942
radiation effects on rat, x, 20: 42961
radiation induced mutational rate, in *Drosophila melanogaster*, 17: 31894
radiation injuries, recovery mechanisms, 16: 7454
radioinduced and spontaneous translocations in immature and mature germ cells in Drosophila, 17: 12138
radioinduced mutations in Drosophila, effects of dose on x, 20: 24893
radioinduced mutations in mice during, frequency of x, 20: 40627(R) (ORNL-3922, pp 84-8)
radiosensitivity and recovery of Drosophila, role of oxygen in determining, 19: 38463
radiosensitivity in Drosophila, 16: 25192
radiosensitivity in rainbow trout, 16: 25213
radiosensitivity in sex-linked lethal recessives of *Drosophila melanogaster*, effects of air, nitrogen, and oxygen on, 16: 28763 (RT/BIO (62)45)
radiosensitivity in Drosophila, 17: 74
radiosensitivity in Drosophila, 17: 1236(R) (TID-17000)
radiosensitivity in Drosophila, 17: 1237(R) (TID-17001)
radiosensitivity in Drosophila, 17: 1238(R) (TID-17002)
radiosensitivity in Drosophila, 17: 1239(R) (TID-17003)
radiosensitivity in female and male chick embryos, 17: 10375
radiosensitivity in mice, 17: 15637(R) (TID-18135)
radiosensitivity, in Drosophila, 17: 28683(R) (TID-19003)
radiosensitivity of, in *Drosophila melanogaster* at different stages, 17: 17841
radiosensitivity of cells during, 17: 25026
radiosensitivity of *Drosophila melanogaster*, 17: 35455(R) (TID-19302)
radiosensitivity of stages of, in Habrobracon eggs, x, 18: 3568
radiosensitivity of oocytes in *Drosophila melanogaster*, changes in, 18: 11829
radiosensitivity of Drosophila, gamma, 18: 13489
radiosensitivity of, in mice, 18: 17588
radiosensitivity of various stages in rat, 18: 23331
radiosensitivity of various stages of, in Drosophila, 18: 41183
radiosensitivity of, in cattle, 19: 3892(R) (ORO-625(p.28-37))
radiosensitivity of, in swine, 19: 8875
radiosensitivity of Drosophila, protracted dose effects on, 19: 10823
radiosensitivity of Drosophila, 19: 10840
radiosensitivity of Drosophila, 19: 10841
radiosensitivity of rat, fast neutron and gamma, 19: 10833
radiosensitivity of, in mice, 19: 28076
radiosensitivity of, in Drosophila, 19: 28103
radiosensitivity of, in domestic animals, 19: 45813(R) (ORO-631, pp 36-44)
radiosensitivity of, 20: 12686
radiosterilization effects on, in silkworms, 19: 10859
rate in man, tracer study of, 18: 23176
timing of, in Drosophila, 20: 6778(R) (ORNL-3853, pp 62-5)
timing of, in man, 20: 22617(R) (RLO-1780-1)
Spermine
see 1,4-Butanediamine, N,N′-bis(3-Aminopropyl)-
SPERT (Special Power Excursion Reactor Tests.)
see Reactor Safety Experiments
SPHALERITES
deuterium content of fluid inclusions in, from Mexico, 20: 16634
formation during ore deposition in Providencia area, Zacatecas, Mexico, geology of, 20: 18631 (NYO-2266-1)
precipitation with cadmium ions from aqueous solutions, 20: 18631 (NYO-2266-1)
structure, 16: 16804 (AFOSR-2300)
sulfur isotope distribution in, from Broken Hill South, New South Wales, 16: 17890
SPHERES
see also Reactor Fuel Spheres
acceleration of shell, analysis of steady-state, 18: 36905 (UCRL-13063)
analysis of filament-wound, with polar opening, 19: 40698 (ACF-9)
attachment to nozzles, stress analysis of, 20: 35600(R) (ORNL-3951, pp 164-8)
behavior in magnetic field of gravitating, 16: 18116 (NP-11463(Pt.3) (p.447-55))
bonding of hollow metal, 16: 3481 (WAL-TR-375/1)
buckling of hollow, 18: 37306 (TID-20950)
burst strength of thin-walled, 17: 39225
charged, distribution of charged particles near moving, 16: 9293 (USCEC-83-210)
coating with metals, 16: 3481 (WAL-TR-375/1)
collapse of large-mass gaseous, gravitational, 20: 25681
compaction by vibration, theory of, 18: 19456(R) (ANL-6840)
contraction of gravitating, 18: 40114
contraction of helium-hydrogen, physical conditions in, (T), 20: 19345
cooling of heat-generating solid, temperature distributions in, 20: 41106
creep in thin-shell, effects of temperature on primary, 19: 18088
critical dimensions of graphite–uranium–water, 18: 807 (LAMS-2955)
criticality of interacting arrays of, model for, (T), 20: 16034
criticality of plutonium nitrate, 19: 25245(R) (HW-84369(p.45-51))
criticality of stainless steel, containing plutonium nitrates, 17: 31081(R) (HW-77311(p.40-7))
criticality of, Boltzmann solutions for, 18: 38334 (TID-20933)
criticality studies on arrays of, 18: 42921 (K-DP-46)
criticality studies on inhomogeneously loaded, (T), 19: 29024
criticality studies of plutonium nitrate, 20: 29471
defects in, elastic effects for double-force, 19: 38024 (BNL-8322)
density distributions of particles of, use of log-normal function for calculating mass and number, 20: 9181 (SC-TM-65-397)
design and testing of prestressed concrete shell, for containing explosions, 18: 8462 (LA-2901)
diffusion of binary gas mixtures from, thermal, 17: 173
diffusion of gases from, tables of coefficients of, 17: 39712 (BNL-6764)
diffusion of water in lattices of silica, 17: 33943
distribution function for classical system of hard, radial, 17: 25949
drag loading from blast waves in Operation Teapot, 16: 2828 (WT-1114)
ejection from conducting fluid in magnetic field, 17: 24170
elastic formation of hollow, differential equation for, 17: 23467
electric breakdown between planes and, in vacuum, 18: 20138
electromagnetic field propagation into, 17: 24054 (SCR-623)
electromagnetic forces on, in conducting liquids in magnetic fields, 19: 1058
electromagnetic levitational forces on conducting, potential-well description of, (T), 19: 6403
electromagnetic wave scattering by, (T), 19: 47299(R) (AD-614046)
electron thermionic emission from charged metallic, 16: 2329
electrostatic potential of metallic, in interplanetary space, 16: 26050
equipartition state in fluid, instability of, 18: 36139
expansion of charged dust, after relativistic collapse, (T), 20: 25699(T)
extraction from a large stock, design of apparatus for, 17: 30649(P)
fabrication of micro-metallic, method for, 20: 35880(P)
fabrication of monocrystalline, from refractory materials, (E), 19: 40991
fabrication of small ceramic, device for, 17: 1905
flow and mass diffusion in beds of, 18: 14032(R) (ORNL-3523(p.414-42))
flow through non-ionized gas, drag in, 17: 29071 (NYO-10427)
fluid flow around oscillating, MHD of, (T), 20: 6161 (NP-15630)
fluid flow behind, MHD effects in (E/T), 19: 3016 (BSD-TDR-64-107)
fluid flow past fixed, in presence of magnetic field, 16: 5473
fluidization, uniform, 16: 22308(T) (NP-tr-896)
fracture mechanics and stability of, review on, 20: 13248 (GEAP-4678)
friction factors in fluid flow through cylindrical bed of, effects of Reynolds number on, 17: 25416 (TID-18717)
gamma absorption in, 17: 35449 (TID-17870)
gamma attenuation from, 17: 42154 (PWAC-397)
gamma transmission through shielding, Monte Carlo calculations for, 18: 35052
gamma-ray attenuation in, heat production in, (T), 19: 31431
gas flow around, stationary monatomic, 16: 22709 (AD-271032)
graphite diffusion and flow of gas in packed beds of, 19: 36612(R) (ORNL-3807, pp 189-217)
gravitational collapse of charged dust, relativistic model for, (T), 20: 2879
gravitational collapse of rotating, (T), 20: 34412
heat and mass transfer measurements in beds of, 17: 33326(R) (ORNL-3445(p.298-328))
heat flow in two-layer composite, 17: 1619
heat transfer around, in forced convection, 19: 18126
heat transfer between gas and, with free and forced convection, 17: 8351

heat transfer in beds of oriented, 16: 1909 (NYO-7809)
heat transfer of, with uniform energy generation, 17: 38454 (TID-7653 (Pt.I)(p.126-73))
heat transfer to contiguous spherical shells from, computer program for temperature transients in, 18: 42881 (LA-3115-MS)
heat transfer to flowing liquid metal, 19: 13578 (BNL-7664-R)
heat transfer to water flow, forced-convection, 16: 17807
heating by air, equations for free-flight, 19: 30653(R) (TID-21723)
hydrostatic equations for gaseous, in general relativity, (T), 20: 15211
hydrostatic support by isotropic pressure, (T), 19: 6581
hypersonic gas flow, wake pressure, 16: 1275(R) (NP-10832)
impact effects on hollow, research program on, 20: 463(R) (SC-DC-65-1634)
impact testing of hollow, 18: 20195(R) (SC-DC-64-383)
impact testing of hollow, development of equipment and methods for, 18: 29813(R) (SC-DC-64-1034)
impact testing of hollow, development of equipment and methods for, 19: 557(R) (SC-DC-64-1509)
impact testing of hollow, equipment and methods for, 19: 26482(R) (SC-DC-65-1305)
interactions of hard, Monte Carlo calculations of, (T), 19: 8007 (NYO-1480-3)
joining to cylinders, stress-magnitude predictions for, 20: 457(R) (BMI-X-276)
joining to cylindrical surfaces, stress analysis for, (T), 19: 22457 (ORNL-3755)
lift coefficients of, moving in still fluid in tubes, 18: 12764 (IS-615)
machining and measurement of, to submicron tolerances, 20: 46146 (Y-KE-204(Rev.))
magnetic field effects on superconducting, force calculations for, (T), 20: 26023 (JPL-TR-32-806)
magnetohydrodynamic flow about uniformly magnetized, first-order, 17: 3104 (AD-275462)
magnetohydrodynamic flow around magnetized, 18: 40049 (NP-14232)
magnetohydrodynamic drag on oscillating, in conducting fluid, (T), 20: 30179
material requirements for reinforced Maxwell bodies, (T), 20: 12944
mixing theory of systems of rigid, 16: 19466 (LA-2667)
motion in fluids and ionized gases, 19: 41114 (AD-617258)
motion in high-temperature air, electron-ion recombination in wake of hypervelocity, 17: 41662
motion in MHD fluid, oscillatory, 18: 30309 (NP-14087)
motion in smooth rotating drums, 19: 40982 (ORNL-3819)
motion in viscous liquid at large Reynolds number, 16: 6535
motion of conducting and non-conducting, through conducting fluid in transverse magnetic field, 17: 32784
motion of conducting, in inhomogeneous magnetic fields, (T), 19: 37236
motion of graphite, through stainless steel pipes, 18: 28937(R) (ORNL-3578(p.100-21))
motion of non-conducting through conducting fluid in presence of magnetic field, 16: 30706 (AROD-407:59)
motion of non-conducting, through conducting fluid in transverse magnetic field, 17: 32783
movement of soda-lime glass, on glass wall of wind tunnel, 19: 7210(R) (ORNL-3697(p.213-22))
neutron absorption by randomly distributed, computer analysis of, 17: 12583 (WAPD-TM-352)
neutron absorption by, shell transmission theory for, 18: 4536 (EANDC-33U(p.161-3))
neutron buckling and decay in uranyl nitrate, prompt, 18: 6140(R) (ORNL-3499(Vol.I)(p.57-8))
neutron buckling of partially-filled, method for determining full-body equivalents for, 18: 22705(R) (HW-80020(p.38-48))
neutron collision probabilities in, with arbitrary radial source distribution, 17: 3750
neutron decay in lead, P_n analysis of fast, 18: 7664 (TID-19909)
neutron diffusion in, computer program for multigroup adjoint (T), 19: 1522 (IA-936)
neutron diffusion in, computer program for, 19: 14461 (AEEW-M-469)
neutron distribution in, point source transport solution for position and velocity dependent, 17: 9492
neutron flux distributions in air- and boron trifluoride-filled, 18: 34731 (NASA-CR-54110)
neutron flux in pulsed, variational calculation of, 18: 7659 (CONF-187-27)
neutron flux in small, time dependence of, 18: 2813
neutron multiplication in bare uranium-235, 18: 5972(R) (ORNL-3499 (Vol.I)(p.77-81))
neutron multiplication in aqueous uranyl fluoride and nitrate, 18: 6141(R) (ORNL-3499(Vol.I)(p.68))
neutron self-shielding effect in metallic, 16: 16415
neutron spectra in graphite-lead, fast, (E/T), 19: 29546
neutron transport in one-dimensional, Green's functions for one-velocity, 18: 44722
neutron transport in, discrete ordinates angular quadrature of equations for, (T), 19: 14465 (LA-3186)
neutron transport in finite, spherical harmonic method for Milne analog in, 19: 19068
neutron transport in, j_N analysis of, 20: 16022 (EUR-2627.e)
oscillations in pulsing gravitating, nonradial resonance-type, 20: 28572
packing, 18: 26893(R) (ANL-6868(p.11-108))
packing configuration of, computer analysis of, 20: 26533(R) (BNL-954, pp 16-49)
packing in cylindrical vessels, computer analysis of, 20: 41063 (BNL-997)
packing in rhombohedron at maximum density, calculations for, 17: 11088 (HW-73057)
plastic deformation of dynamic- and static-loaded, 18: 7865(R) (TID-19871)
plastic deformation of dynamic- and static-loaded, 18: 32980(R) (IITRI-8262-6)
positions in packed beds, methods of determining, 19: 37202(R) (BNL-900(p.1-28))
positions in packed beds, methods of determining, 20: 26459(R) (BNL-954, pp 1-15)
pressure pulse propagation in fluid, 18: 18794
production of accurate ceramic, grinding device for, 17: 36276(P)
propagation in gaseous, spherical, (T), 20: 31871
proton depth dose measurements in large lucite, 18: 4946(R) (UCRL-11033(p.19-28))
proton depth-dose measurements in tissue-equivalent, 20: 1620 (UCRL-16154)
proton dose measurements in tissue, 19: 9492 (UCRL-10980(Rev.))
radiation absorption by, in spherical arrangement, cross section for high-energy, 17: 20861
radiation absorption by rigid, Monte Carlo study of density and transparency distributions in, 18: 6409
radiation absorption in, (T), 19: 17164
radiation attenuation by opaque, high-energy, 17: 20860
radiation dose on surface above a spherical, symmetrically radiating solid, 17: 24162
radiation dose rates from source, computer program for, 18: 43159 (ORNL-TM-803)
radiation doses from, computer program for (T), 19: 1813 (ORNL-TM-817)
radiation dosimetry of homogeneous, 17: 33446(R) (ANL-6723(p.16-27))
radiation dosimetry in, electron, 20: 4204
radiation effects on strength of hollow, 17: 6754(T) (FTD-TT-62-719)
radiation field diffraction on, 18: 24516(T) (JPRS-24633)
radiation field of gamma-emitting, 19: 23380
radiation transport in, formulation of, (T), 20: 1303 (AD-614250)
radioactive sources in the form of, dose-rate measurements for, 17: 37033
radioactivity measurements on, 16: 10259
reactions in three-body systems of, phase-space domains for, (T), 19: 8027
reactions with plasma, density and momentum measurements from, 18: 30924
ring current interactions with conducting, 18: 26770
rotation, differential, 16: 6851
rotation in conducting viscous fluid in magnetic fields, 18: 20664
scattering patterns of conductivity, in microwave region, 16: 943
sound wave scattering by impenetrable, h-f, (T), 19: 41129
stability of gaseous, in magnetic field, (T), 20: 25701
stability of gravitationally bound, of perfect fluid, (T), 19: 41563
stability of polytropic stellar, relativistic, (T), 19: 44925(T)
stability of relativistic fluid, 18: 40066
stress analysis of static-loaded, with rigidly reinforced opening, 19: 1825(R) (IITRI-578P22-11)
stress analysis of thick-concrete hollow, steady-state, 20: 27123
stresses analysis of steel, 20: 43491 (ORNL-P-2472)
structural analysis for reactor containment, (E/T), 19: 8574 (IITRI-578P22-9)
structure factors for, calculation of, 17: 37951
superconductivity of hollow, magnetic field effects on, 17: 32809
support by tension wires, analysis, 19: 36579 (UCRL-13160(Pt.1))
support by tension wires in cylindrical shell, model studies, 19: 36581 (UCRL-13160(Pt.3))
suspension of superconducting, in magnetic fields, 18: 30677
temperature distribution in gamma-active, (T), 19: 42191 (AEET/HP/TH-20)
temperature solution for, with distributed source and variable surface heat transfer, 19: 4301 (AAEC/E-128)
testing of, design of high-pressure gas tunnel for hydrodynamic and thermodynamic, 19: 22492
thermal shock resistance, 16: 24176 (WADD-TR-60-749(Pt.II))
thermoelastic stresses in, with nonuniform heat generation and variable

surface heat transfer coefficient, 19: 28467 (AAEC/TM-285)
transient effects of magnetic field penetration into superconducting, 17: 16816
use of ceramic, for studies of gastrointestinal transit of manganese-54 or uranium carbide particles, 20: 42740 (LA-DC-7764)
uses of small solid, as heat-transfer control elements in nuclear rockets, (E), 19: 24148 (NASA-CR-210)
vibrations of concentric shells, thermally induced, 18: 27634 (UCRL-7402)
void fraction in bed of randomly packed, 19: 18118 (PAN-519/IX)
Spherical Cavity Reactor
see Rocket Reactors
SPHEROIDS
equilibrium of uniformly rotating, general relativity effects on, (T), 20: 15627
heat transfer to fluid, in two-phase flow, 17: 14456 (TID-17889)
irradiation of, equipment for, 17: 6224(P)
production of, equipment and method for, 18: 5762(P)
shock wave scattering by prolate, 16: 8017
SPHINGOMYELIN
radioinduced in beef, chemical analysis of, 19: 46878 (NP-15455)
Spiderwort
see Tradescantia
Spin
see Nuclear Spin
SPINAL CORD
mercury-203 uptake by rat, after repeated vapor inhalation, 19: 3860
radiation effects on reflex activity of rabbit, 16: 1480(T) (JPRS-10170 (p.178-97))
radiation effects on chick embryo, 16: 6323
radiation effects on ventral root potentials in cats, 16: 16261
radiation effects on neuronal activity in cats, 16: 16262
radiation effects in white mice, 16: 16285
radiation effects on neurons in, 16: 23502
radiation effects of repeated low dose and single high dose, 16: 23482
radiation effects in neonatal rats, 16: 26788
radiation effects on reflex activity, role of hypothalamus in, 16: 30299
radiation effects on synaptic activity, 17: 23172
radiation effects on nucleoproteides of ganglia from, 17: 35499
radiation effects on neonatal rat, x, 17: 35521
radiation effects on histology of, in neonatal rats, 17: 35522
radiation effects on hypertensive rat, x, 17: 38811
radiation effects on rat, neurological changes from, x, 18: 17528
radiation effects on medullar vessels in rabbits, 18: 17563
radiation effects on rat, proton, 18: 31140
radiation effects on ascorbic acid content of dog, 18: 31219
radiation effects on Nissl granules in rat, 18: 33349
radiation effects on, diagnosis of, 18: 38830
radiation effects on ganglia in rat, proton, 18: 38916
radiation effects on cell nuclei in rat, proton, 18: 38917
radiation effects on cells of rat, proton, 18: 38918
radiation effects on, x, 18: 41161
radiation effects on, 18: 41162
radiation effects on, following respiratory tract tumor therapy, 19: 237
radiation effects on rat, x, 19: 3920
radiation effects on synaptic activities in cat, 19: 26088
radiation effects on convulsions in aging and newborn rat, whole-body, 19: 26089
radiation effects on blood in human, after hypophyseal radium therapy, 19: 29949
radiation effects on, in rat embryos, 19: 33834
radiation effects on reflex arc of, whole-body gamma, 19: 38358 (AD-612660)
radiation effects of chorioallantoid grafted, on marrow production in chickens, 19: 43761
radiation effects on development in salamanders of, x, 20: 5312
radiation effects on rat, x, 20: 6826
radiation effects on rodent, pathological manifestations of, 20: 24908
radiation effects on innervation system on meninges of dog, 20: 42881
radiation effects on rat, following neonatal exposure, proton, 20: 14299
radiation injuries of, pathology of, in mice, 17: 40545 (BNL-7284)
radiation injuries of, resulting from radiotherapy of tumors, 18: 38829
radiation injuries of ganglia of, in rats, 18: 38781
radiation injuries of ganglia of, in rats, 18: 38920
radiation injuries of dog, pathology and recovery of, 18: 38954
radiation injuries of, in rats, 19: 2061 (BNL-8451)
radiation injuries of, induced by radiotherapy of lung carcinoma, 20: 100
radiation injuries of, induced by therapy, 20: 18406
radiation injury after radiotherapy, 17: 95
radiation injury in supervoltage therapy, x, 20: 20545
radiation injury of, during radiotherapy, 19: 151
radiodiagnosis of tumors of, properties of radioisotopes for, 19: 7242
radiodiagnosis of neurological syndromes in, by myeloscintigraphy after administration of iodine-131, 19: 19720
radiodiagnosis using Thorotrast, nervous system injuries from, 18: 19659
radioinduced cordotomy, using strontium-90 needle, 19: 30013 (ACRH-103(p.104-20))
radioinduced injuries to, mechanisms involved in, 20: 45440
radioinduced myelitis in human, x, 20: 3771
radioinduced myelopathy in dog, Thorotrast, 20: 20455
radioinduced tumors of, in rabbits, 19: 33937
radiosensitivity, 16: 6303(T) (JPRS-11322(p.227-47))
radiosensitivity, 16: 32768
radiosensitivity of, in dogs and rabbits, x, 17: 33628
radiosensitivity of, in rats, 18: 6622 (USNRDL-TR-682)
radiosensitivity of, in man, 19: 31953
radiosensitivity of, in man, 20: 16251
radiosensitivity of, tolerance curves for, 20: 45441
radiotherapy for pain in, beta, 18: 17691
radiotherapy of tumors in, effects on central nervous system, 19: 36055
shielding of, during radiotherapy of spinal tumors, 20: 6976
strontium uptake by lesions, in man, 16: 20081
SPINELS
dislocation and slip mechanisms in, 19: 32048(R) (NP-15073)
effects on oxidation resistance and strength of chromium–magnesia composites, 19: 41022(R) (NP-15292)
emissivity of coatings of nickel-chrome, at 800 to 1800°F, 18: 4257(R) (PWA-2279)
emittance of nickel-chrome, at 300 to 2200°F, hemispherical, 18: 5737(R) (PWA-2255)
fabrication and properties of lightweight chrome, 16: 27597 (BM-RI-6025)
formation by solid-state reactions of aluminum and cobalt oxides, tracer study of mechanism of, 19: 43998 (UCRL-12396)
paramagnetic resonance of trivalent chromium, ions in, 17: 1990
preparation and properties of, symposium on, 20: 37179
preparation of magnesium and manganese rare earth selenides, (E), 19: 13297
properties as induction furnace coil lining material, petrographic analysis of, 18: 43381(R) (NLCO-920(p.25-9))
properties of chromium-doped, 20: 29709(R) (TID-22970, pp 65-119)
properties of cobalt manganese oxide, 17: 12232(R) (TID-17828)
radioinduced blistering of, ion, (E), 20: 29816
radioinduced cavities and exfoliation in, helium-ion and proton, 18: 2313
reactions with graphite, mechanism for, 17: 27344
sintering characteristics of, 19: 20461 (NP-14893)
strength of polycrystalline, effects of compressive surface layers on, 20: 33860 (AD-634361)
thermal conductivity of, for use above 3000°F, 18: 16520
thermal properties, 18: 7201 (ASD-TDR-63-597)
thermal properties to melting point, 20: 878
vaporization of, to 2300°C, 20: 13265(T) (AD-623208)
SiO_2–spinel, endurance tests of coatings of, 18: 5737(R) (PWA-2255)
SPINNER COLUMNS
development of, for foam separation uses, 16: 32905(R) (ORNL-TM-292))
SPIRO[2.4]HEPTA-4,6-DIENE
spectra of molecular fragmentation in, design of pulsed ion source for, 19: 15474
SPIRO[3,3]HEPTANE, 2,6-DIOXA-
radioinduced polymerization of, mass spectra of primary processes in, 18: 27563
radioinduced solid state polymerization of, 18: 27555
SPIRO[5.5]UNDECANE, 1,5,7,11-TETRATHIA-
preparation by reaction of trimethylene trithiocarbonate and 2,2′-iminodiethanol, 17: 27412
SPLEEN
analysis for alpha activity in normal human, spectroscopic, 16: 17433
analysis for copper, magnesium, phosphorus, and zinc, neutron activation, 19: 13206 (SGAE-BL-13/1964)
analysis for phosphorus-32 in mouse and rabbit, by deuteron activation and radioautography, 17: 21620
analysis for trace elements in human, of subjects from outside continental U. S., 19: 21831
analysis of, for thorium dioxide in cancerous, microradiography technique for, 17: 21623
analysis of tissues from, for carbon-14, combustion procedure in liquid scintillation counting for, 20: 20570
analysis of, for carbon-14 and tritium by scintillation counting, combustion method for, 20: 36721
antibody formation in, reaction mechanisms, 16: 16196
antibody production by cells of, cultured *in vivo* in irradiated mice, 19: 3905
antibody production by cells of, quantitative antigen effects on, 19: 31676(R) (ORNL-3768(p.112-18))
antibody response in cells of, variations in kinetic indices of, 19: 31676(R) (ORNL-3768(p.112-18))
antibody synthesis in rabbit, during radiation sickness, 18: 41178

antigenicity of cell-free extracts of human, 20: 45483
calcium-45 distribution in rat, effects of age on, 18: 33
calcium-45 deposition in cow and goat, 16: 8505
carbon-14 uptake by ribose in rat purines and pyrimidines in, 19: 3841
cell injections from rat, mouse tolerance to, 18: 1367
cell injections in irradiated mice, F_1 hybrid anti-parent immunological reaction in, 16: 12857
cell renewal in lymphatic nodules of, in rats, 18: 36863 (BNL-7167)
cell transplantation in irradiated mice, repopulation during serial, 17: 23130
cerium-144 uptake by dog, 19: 3862
cerium-144 uptake, distribution, and excretion by rat, 19: 17471
cesium-134 and rubidium-86 uptake by dog, 17: 35428
cesium-137 effects in mice, 16: 1537
cesium-137 content in human, 19: 25895
cesium-137 effects on mouse, protective effects of chemicals against, 18: 17647
cesium-137 uptake by rat, 18: 17442
cesium-137 uptake by rat, cesium chloride and steroid effects on, 18: 17443
cesium-137 uptake by rat, after exposure to chloride and nitrate aerosol solutions, 19: 3858
chlorine-36-labeled 6-chlorocoumarin distribution in rabbit, 18: 12026
chromium-51 binding by cells of, *in vitro*, 19: 10750
clearance of cerium-144-labeled cerium chloride and fluoride from, 17: 1242(R) (TID-17178)
colinesterase activity in rabbit, effects of immunization on, 19: 19609
colony formation and weight used as methods for assaying immunity to marrow transplants in mice, 20: 5372
content of RNA in mouse, effects of immune reactions on, 20: 6780(R) (ORNL-3853, pp 93-7)
delineation of, by scanning after the injection of damaged chromium-51-labeled erythrocytes, 18: 5183 (TID-7673(p.468-83))
depiction of, by radioisotope scanning, 19: 17747
deposition of inhaled plutonium-239 particles in, 16: 8504
desoxyribonuclease activity, effects of whole-body irradiation, 16: 11405
diseases, diagnosis with aid of contrast radiography and radioisotope scanning, 16: 25101
distribution of radioprotective mercaptoalkylguanidines in, 16: 1631
DNA and RNA synthesis in mouse, effects of estradiol on, 20: 40577
effectiveness of injections of parental cells of, in treatment of radiation injuries, 16: 26838
effects of ACTH and radiation on phosphorus-32 distribution in, in rats, 18: 6690
effects of cell-free extract, on recovery of bone marrow from radiation injury, 17: 27073
effects of cell injection or surgery of, on rat liver regeneration after x irradiation, 18: 38981
effects of cell injections of, combined with radiation on graft tolerance in mice, 19: 29983
effects of cell transplants of, on radiation midlethal dose killing effect in mice, 20: 33074
effects of cell transplants of, on diphtheria immunity in irradiated guinea pigs, 20: 35344
effects of cells of, on radiosensitivity of allogenic skin graft response in mice, 19: 8928
effects of cosmic radiation, vibration, acceleration, and weightlessness, 17: 17772(T) (JPRS-18395(p.123-35))
effects of cysteine and β-mercaptoethylamine on sorptive properties of irradiated tissues in, 16: 30258
effects of cytochrome C on oxidative phosphorylation in mitochondria isolated from, of irradiated animals, 20: 45500
effects of E 39 and x radiation on cell respiration, 16: 1507
effects of extracts of, on radiation recovery of bone marrow cells, 17: 33623
effects of injected cells of, on liver morphology and function in irradiated mice, 16: 26823
effects of injected cells of, combined with radiation on blood system and organs in mice, 19: 8833
effects of injected cells of, on radioinduced chimeras in mice, 20: 22789
effects of injected suspensions on effects of radiotherapy of lymphosarcoma in dogs, 20: 45551
effects of irradiated cells of, on immune response in mice, 19: 17538
effects of labeled cell injection into irradiated mice, 17: 30399
effects of lethal irradiation in rats, protective effects of desoxyribonucleic acid, 16: 20283
effects of methionine sulfoximine on, in rats, 17: 17712
effects of methyl palmitate on lipids in mouse, 20: 14241 (TID-21437)
effects of nitrogen mustard on morphology and physiology of rat, 18: 15822
effects of orally administered polonium-210 on rat, pathologic, 19: 2148
effects of oxytetracycline on productive follicles of whole-body-irradiated chickens, 16: 9878
effects of polonium-210 on rat, after single intravenous doses, histologic, 19: 2145
effects of polonium-210 on rat, after multiple intravenous doses, pathologic, 19: 2147
effects of radioprotective drugs on damage induced by alkylating agents, 20: 40664
effects of removal of, on survival after irradiation, 17: 25038
effects of removal of, on whole-body radiation effects on mice, 19: 8906
effects of removal of, on radiation response of hematopoietic system of dogs, 20: 29029
effects of removal on effects of radiotherapy of lymphosarcoma in dogs, 20: 45551
effects of shielding of, on proliferation of erythropoietin-responsive erythrocytes in irradiated mice, 20: 45479
effects of splenectomy on radiosensitivity of mice, 18: 41198
effects of splenectomy combined with radiation on skin homotransplantation in mice, 19: 29982
effects of strontium-90 injections in albino rat parents on offspring, 16: 4062
effects of sulfur-35 on, in mice and rats, 17: 35515
effects of surgical removal on mouse thrombocytosis, 18: 11745
effects of surgical removal of, on life span of irradiated mice, 18: 17556
effects of surgical removal of, on recovery of dogs from radiation injuries, 19: 22008
effects of surgical removal of, on immune reactions in mice, 19: 24301
effects of surgical removal of, on radiosensitivity of bone marrow cells in rats, 20: 24881
effects of surgical removal in Thorotrast patients, 20: 45503
effects of Thorotrast on, pathological, 20: 5355
effects of transfers from irradiated donors on antibody response to antigen in rats, 16: 26857
effects of x irradiation of, on peripheral blood picture of healthy rats, 16: 8577
effects on bone marrow metabolism, tracer study in rats, 18: 29422
effects on bone marrow function, 19: 31967
effects on colony-forming units in mouse radiation chimeras, 19: 17679
effects on granulocyte release from bone marrow, 19: 29945
effects on immunological tolerance to skin homografts in mice, 17: 96
effects on leukocyte release, tracer study in rats, 18: 29422
effects on phosphorus-32 uptake by rat bone marrow, 18: 17603
effects on radiation resistance of animals, 17: 15754
effects on radioinduced changes in amino acid metabolism by mice, 18: 27233
effects on radioinduced tumor development in rats, 19: 15220
effects with radiation on polyvalent tolerance in adult and newborn mice, 19: 38376
enzymatic activity, toxic effects of radioprotective agents, 16: 14456(R) (NP-11359(p.1-15))
enzyme activity, effects of antimetabolites and cytotoxic and radiomimetic agents on, 16: 3998(R) (NP-11020(p.26-37))
enzyme activity, effects of whole-body irradiation, 16: 14573
erythropoiesis in rabbit, stimulation by erythropoietin, 19: 10868
erythropoiesis in mouse, effects of erythropoietin, 19: 31699(R) (ACRH-23(p.21-32))
erythropoietic activity of, in lethally irradiated mice injected with bone marrow, 20: 18295(R) (UCLA-12-576, pp 27-56)
extracts, effectiveness in treatment of radiation sickness, 16: 6358
extracts of γ-irradiated, effects on nitrogen metabolism in frog liver, 20: 18207 (NIJS-R-473)
extracts, protective effects against lethal whole-body irradiation in guinea pigs, 16: 9924
extracts, protective effects against radiation injuries, 16: 14501
fractionation by isopycnic separation and zonal centrifugation, 18: 35678(R) (ORNL-3656)
function tests using mercury-197-labeled hydroxypropane, 20: 35362
glycoprotein content in, of mouse and rat radiation chimeras with secondary disease after bone marrow grafting, 20: 45487
gold-198 distribution in, after intracardiac injections in rats, 17: 15607
gold-198 incorporation by, 17: 33501
gold-198 colloid metabolism in, 20: 3822
gold-198 uptake by rat, 19: 12938
grafting of cells of mouse, effects on runt disease development, 18: 38718
growth of bone marrow transplants in dog, 20: 3652
growth of injected peritoneal cells in, in lethally irradiated mice, 17: 7805 (USNRDL-TR-597)
growth of injected cells of, in irradiated mice, 18: 27003(R) (ORNL-3601(p.27-46))
hematopoietic cell clones produced in, of irradiated mice, 19: 10898(R) (TID-21613)
hematopoietic stem cell reproduction in, in irradiated mice, 19: 7118
histology, effects of extracorporeal irradiation of blood, 17: 15639(R) (TID-18194)
homogenates of sheep, protective factor for radioinduced mouse leukemia

in, 18: 27222
homogenates, protective effects of transfusions of, against radiation injuries in guinea pigs, 18: 25230
homograft reactions, 17: 5762(R) (AD-276039)
hyaline deposits in, of mouse radiation chimeras, 19: 10797
immune reaction to injected cells of, in irradiated rats, 19: 42339
immune reactions in, of mouse radiation chimeras, 17: 7850
immune reactions in, of mice, effects of age on, 18: 27065(R) (ORNL-3601(p.98-104))
immune reactions in mouse, 18: 27209(R) (ORNL-3601(p.116-27))
immune reactions in cultures of heterologous radiation chimeras, 20: 5397
immune reactions in rat, role of microsomes in, 20: 6721(R) (ORNL-3853, pp 161-9)
immune reactions in, of mice, 20: 6883
immune reactions of mice to injected homogenates of, 18: 43116 (ORNL-P-274)
immune reactions to tissue transplants of, 19: 13068
immune reactions to injected cells of, in rabbits, 19: 17447
immune reactions to transplants of, in mice, 19: 25885
immune reactions to injected cells of, in mice, 19: 27967
inhibitory effects on tumor growth in irradiated mice of homologous cells from, 18: 43307
injection of cells of, into neonatal mice, effects on immune response to skin grafts, 17: 28775
injuries to cell nuclei in mouse, from x rays in combination with acceleration or vibrations, 20: 42986
iodine-125, -131, and -132 uptake by child, dose levels for, 19: 8779
iodine-131 uptake and distribution in rat, from labeled atabrine, 19: 14988
iron-59 uptake in rats, 16: 7390
iron-59 uptake by mouse, determination of marrow transplant efficiency using, 18: 31090
iron-59 uptake by mouse, use in assessing radiosensitivity of marrow cells, 20: 40634 (ORNL-P-2312)
isolation of radiation-mortality reducing factor, 17: 14108
isolation of radioprotective factor from, 17: 30238
lymph cells in mouse, effects of antibody production on morphology of, 20: 40632(R) (ORNL-3922, pp 175-91)
lymphocyte proliferation, effects of whole-body irradiation, 16: 14511
lymphoid regeneration in mouse, effects of thymus on, 20: 42984
lysosome reactions in rat, 19: 6945(R) (ANL-6906(p.113-17))
lysosome studies on mouse, after treatment with mixed bacterial toxins and anthramycin, 20: 40736
magnesium-28 uptake by magnesium-deficient rat, 19: 27933
mercury-203 uptake by rat, after repeated vapor inhalation, 19: 3860
mouse hybrid, transplanted cells inducing tolerance in parental mouse strain, 20: 40651
nitrophenylbenzamine content in rat, 19: 46011
nucleic acid metabolism in irradiated rat, effects of injected DNA on, 17: 13929
oxygen consumption by mouse, relation of, to radiosensitivity, 20: 22712
oxygen content of, effects of chemicals on, 17: 2892
oxygen levels, effects of sodium nitrite on, 16: 4001(R) (NP-11020 (p.78-81))
oxygen tension of mouse, effects of cysteamine, cyanide, and high-pressure oxygen on, 19: 43869
phosphatase activity in, after injection of hematopoietic tissue in irradiated mice, 17: 27111
phosphatase activity in, effects of transplanted hematopoietic tissues on, in mice, 17: 35314(R) (HW-76000(p.161-6))
phosphatase release from rat, 18: 43243
phosphorus-32 effects on lymphocytes in, in rabbits, 16: 4050
phosphorus-32 uptake into deoxyribonucleic acid, effects of iodoacetic acid on x-irradiated rats, 16: 4068
phosphorus-32 uptake by phospholipids in, in irradiated and normal mice, 17: 4419
phosphorus-32 uptake and excretion by chicken, 19: 8765
photoscanning of, after injection of labeled colloidal albumin, 18: 19813 (CONF-164-11)
plutonium content in dog, 16: 26719
plutonium distribution among chemical forms in, 17: 30275
plutonium-239 removal from mouse, using calcium salt and pentaethyl ester of carboxymethyliminobis(ethylenenitrilo)tetraacetic acid, 18: 23369
plutonium-239 removal from rat, effectiveness of complexants in, 19: 6975
polonium-210 content in rat, after intraperitoneal administration, 19: 2055
polonium-210 distribution and metabolism by dog, man, mouse, rabbit, and rat, comparison of, 19: 2052
polonium-210 uptake and distribution by rat, effects of physicochemical state on, 19: 2040
polonium-210 uptake by rat, after single gavage or intravenous dose, 19: 2043
polonium-210 uptake and distribution by cat, 19: 2044
polonium-210 uptake and distribution by rat, long-term, 19: 2045
polonium-210 uptake and distribution by rat, comparison of multiple and single dose effects on, 19: 2046
polonium-210 uptake and distribution by cat and rat, effects of administration route on, 19: 2047
polonium-210 uptake and distribution by rat, after intratracheal administration, 19: 2048
polonium-210 uptake and distribution by rat, after inhalation, 19: 2050
polonium-210 uptake and distribution by rat, after inhalation by nose exposure, 19: 2051
polonium-210 uptake and distribution by rabbit, after intratracheal administration, 19: 2053
polonium-210 uptake, distribution, and removal in rabbit, after colloidal intratracheal administration, 19: 2049
praseodymium-144 uptake by dog, 19: 3862
preparation of tritium-labeled mouse, 20: 26593
primary immune response of germinal centers of, in mice, 18: 24998 (ORNL-3595)
proliferation of, by transplanted marrow cells in irradiated mice, 18: 25189
promethium-147 distribution in mouse, after intraperitoneal and intravenous injection, 20: 35236
protective effects against radiation in mice, 16: 20160
protective effects of cells against radiation in mice, 16: 20263
protective effects of, in injected fetal cells against radiation injuries in mice, 17: 5810
protective effects of foreign cells of, on blood and tissue changes in lethally irradiated mice, 17: 10434
protective effects of extracts of, against radiation injuries in hematopoietic system in guinea pigs, 17: 10369
protective effects of extracts of, against radiation injuries in hematopoietic system in guinea pigs, 17: 10370
protective effects of transplants, in radiation injury, 17: 14100
protective effects of injections or removal of, against whole-body irradiation in mice, 17: 15811
protective effects of, with bone marrow cells against lethal radiation in mice, 17: 15814
protective effects of, against lethal radiation in dogs, technique for preparation of suspensions for, 17: 15845
protective effects of dialyzed and whole homogenates of, against lethal radiation in mice, 17: 15812
protective effects of shielded implants of, against radiation injuries in mice, 17: 17785
protective effects of removal of, against radiation damage to erythropoiesis in rabbits, 17: 21559
protective effects of homotransplants of, against radiation injuries in dogs, 17: 25049
protective effects of shielding of, against radiation injuries in dogs, 17: 25049
protective effects of transplants of, against radiation injuries in mice, 17: 38893
protective effects of aqueous extract of, against radiation injuries, 18: 8205
protective effects of tissue transplants of, against radiosensitivity of mice, 18: 17658
protective effects of removal of, on decreases in iron uptake by erythrocytes in irradiated mice, tracer studies of, 18: 29423
protective effects of cloned cells of, against radiation damage in mice, 19: 8979
protective effects of transplants of, against radiation effects on protein metabolism in rabbits, 19: 15116
protective effects of extracts of, against radiation effects on oxidative phosphorylation in rat mitochondria, 19: 17673
protective effects of transplants of, against midlethal radiation effects on, 19: 17675
protective effects of transplants of, against radiation injuries in dogs, 19: 24371
protective effects against radiation damage in mice, cell number required for, 19: 26135
protective effects of, against radiation injuries in rats, 19: 33961
protective effects of injected tissues of, against radiation injuries in mice, 19: 36100(R) (NP-15170)
protective effects of immunological unresponsiveness induction against radiation effects in mice, 19: 38454
protective effects of injected tissues of, against radiation injuries in rats, 19: 46023
protective effects of desoxyribonucleic acid extracts from homologous, against radiation injuries in rats, 20: 136
radiation and vaccination effects on mouse, x, 18: 19740
radiation damage of lymphoid centers, effects of thymus on recovery from, 17: 15752
radiation dose effects on weight and activity, 20: 42957

radiation dose to cat, human, and rat, from iodine-131 incorporated in Tolpovidone, 19: 14987
radiation dose to, from injected thorotrast, 19: 15292
radiation effects on DNA, in rats protected by cystamine, 16: 56
radiation effects on serotonin level in rat, 16: 73
radiation effects, in guinea pigs injected with bone marrow, 16: 1628
radiation effects on DNA structure, 16: 1472(T) (JPRS-10170(p.24-37))
radiation effects with and without europium nitrate and nitric acid, 16: 4004(R) (NP-11020(p.105-16))
radiation effects on quantity of porphyrin bodies, in guinea pigs, 16: 4082
radiation effects, high-level whole-body, 16: 7461
radiation effects on blood vessels in, fractional whole-body, 16: 8592
radiation effects on desoxyribonucleic acids prepared from, 16: 9840(R) (TID-14992)
radiation effects on nucleic acid phosphate, and phospholipid content in rat, 16: 14552
radiation effects on phosphorus metabolism in rat, 16: 14530
radiation effects on adenosine triphosphatase activity, protective effects of chemicals, 16: 14457(R) (NP-11359(p.16-27))
radiation effects on distribution and specific activity of enzymes in fractions of rat, whole-body, 16: 17491
radiation effects on DNA synthesis in rat, 16: 17510
radiation effects on antibody formation by cells in mice, 16: 20274
radiation effects, relation to bone marrow radiation damage, 16: 20262
radiation effects on nucleoproteins in, 16: 23468
radiation effects on DNA and RNA in, gamma and x, 16: 25208
radiation effects on nucleic acid metabolism in mouse, gamma and x, 16: 25212
radiation effects on nucleic acid metabolism in mouse, protective effects of AET and MEA against, 16: 25255
radiation effects on mouse, fractionated and protracted fast neutron, 16: 26656(R) (NP-11966(p.1-26))
radiation effects on enzyme activities in rat, protective effects of chemicals against, 16: 26659(R) (NP-11966(p.43-54))
radiation effects on dehydrogenase activity in, in rats, 16: 26661(R) (NP-11966(p.65-78))
radiation effects on hematopoiesis in embryonic, 16: 26790
radiation effects on blood system in, in rabbits, 16: 26864
radiation effects on functional activity, 16: 28759
radiation effects on oxidative phosphorylation uncoupling in rabbit and rat, whole-body gamma and x, 16: 28774
radiation effects on antibody synthesis, 16: 28784
radiation effects on, protection against, 16: 28851
radiation effects combined with antigen on plasma cell reactions in, in rabbits, 17: 17860
radiation effects combined with microwaves on, of guinea pigs, 17: 21545
radiation effects of 14-Mev neutrons, comparison with other tissues, 17: 2860
radiation effects on activity of proteolytic enzymes in mouse, 17: 33631
radiation effects on adenosine triphosphatase activity in rat, 17: 37144
radiation effects on antigenic properties, 17: 64
radiation effects on antibody production in rabbit, protective effects of antigen against, 17: 21526
radiation effects on ascorbic acid content of, x, 17: 37096
radiation effects on bacteria infiltration into, in dogs, 17: 4433
radiation effects on capacity of, to destroy endotoxins in rats, 17: 33709
radiation effects on cell elements in mouse, 17: 23131
radiation effects on cells of, in tissue culture, 17: 31946
radiation effects on chromium-51 uptake by mouse, protective effects of serotonin against, 17: 14021
radiation effects on desoxyribonucleic acid, whole-body exposure, 17: 15636(R) (TID-18061)
radiation effects on desoxyribonucleoprotein in, in mice, 17: 15706
radiation effects on development of amyloidosis in mouse, injected with casein, 17: 25046
radiation effects on desoxyribonucleotide concentration in, whole-body, 17: 28727
radiation effects on DNase activity and nucleic acid content in, in chick embryos, 17: 14014
radiation effects on DNA synthesis in mouse, 17: 28728
radiation effects on DNA, nucleoproteins, and RNA content in, in chicken, 17: 31955
radiation effects on enzyme activity in rat, protective effects of chemicals against, 17: 19875
radiation effects on enzyme content, whole-body exposure, 17: 24966
radiation effects on enzyme activity, x, 17: 30355
radiation effects on, from localized abdominal irradiation of mice, 17: 12123 (BNL-6586)
radiation effects on histopathology of, in rats following brain exposure, 17: 7904(T)
radiation effects on histochemistry of, in mice, 17: 30383
radiation effects on histamine levels of guinea pig, x, 17: 38776
radiation effects on iron-59 uptake by mouse, 17: 30386
radiation effects on methionine synthesis in rabbit, 17: 15843
radiation effects on mouse, fractionated and single dose, 17: 19911
radiation effects on mouse, cosmic, 17: 27198
radiation effects on nitrogen excretion, protective effects of histamine and cysteamine, 17: 23159
radiation effects on nucleic acid content in, in guinea pigs, 17: 14101
radiation effects on oxidative phosphorylation in rat, protective effects of cystamine against, 17: 14099
radiation effects on rat, pre-exposed to low doses, 17: 27137
radiation effects on rabbit, thorotrast, 17: 38824
radiation effects on respiration in rat, formula for analysis of dose dependence in, 17: 23177
radiation effects on reactivity of sulfhydryl groups in, 17: 35500
radiation effects on stability of desoxyribonucleoprotein and desoxyribonucleic acid in, of rats, 17: 40605
radiation effects on tritiated thymidine uptake by rat, effects of erythropoietin on, 17: 19853
radiation effects on ultraviolet fluorescence in nuclei and mitochondria of rat, x, 17: 37093
radiation effects on zinc-65 content of mouse, x, 17: 33725
radiation effects repair processes in mouse, fractionated, 17: 23156
radiation effects on coenzyme A content of mouse, 17: 38837
radiation effects on lymphoid tissue of rats, whole-body, 17: 30431
radiation effects on DNA polymerase content in rat, x, 18: 82
radiation effects on bactericidal activity of fixed phagocytes in, effects of injected ribonucleic acid in mice on, 18: 109
radiation effects on proliferative capacity and immunologic activity of cells of, in mice, 18: 114
radiation effects on formation of oxidation products in lipids in rat, 18: 3522
radiation effects on cytology and hematopoiesis in rat, single and divided radiation dose, 18: 3556
radiation effects on cell morphology and weight of, in mice, 18: 3493 (TID-18352)
radiation effects on, from cerebral arteriography with thorium(IV) oxides, 18: 3581
radiation effects on acceptance of injected, in mice, 18: 6625
radiation effects on 5-hydroxytryptamine content in, 18: 6631
radiation effects on nucleic acid content in guinea-pig, 18: 8220
radiation effects on desoxyribonuclease activity of mitochondria and extracts of, from rats, 18: 8124(T) (JPRS-22613(Del.))(p.12-28))
radiation effects on, production of antimitotic factor in x, 18: 8172
radiation effects on oxidative phosphorylation in, of rats, 18: 8200(T)
radiation effects on desoxyribonucleic acid content of, in mice, 18: 11759
radiation effects on cells, 18: 11815
radiation effects on DNA and RNA content in rat, biochemical indexes of chronic low-dose gamma, 18: 13515
radiation effects on morphology and physiology of rat, 18: 15822
radiation effects on rat, early, 18: 15863
radiation effects on enzyme activity and phosphate metabolism in mitochondria of rat, 18: 17467(R) (ANL-6790(p.145-9))
radiation effects on lysosomes of rat, 18: 17633(R) (ANL-6790(p.150-5))
radiation effects on cells of mouse, analysis of clones from, 18: 17635(R) (TID-20443)
radiation effects on rat, protective effects of iodoacetic acid against, 18: 17664
radiation effects on DNA in rat, 18: 19682
radiation effects on iron-59 uptake by mouse, x, 18: 19594
radiation effects on phosphonucleoside content of rat, 18: 19702
radiation effects on extracellular space in, 18: 19718
radiation effects on mouse mortality, effects of age on cells from, on, 18: 19727
radiation effects on leukocyte glycogen content in mouse, when used with antigens, x, 18: 19741
radiation effects on proteolysis in mouse, x, 18: 19744
radiation effects on mouse, protective effects of homologous cells against, 18: 19767
radiation effects on histology and saline-soluble DNA content in mouse, 18: 23257
radiation effects on mercamine metabolism in, 18: 23304
radiation effects on DNA level in lymphocytes of, in rats, 18: 25137
radiation effects on response to virus infection of, in mice, 18: 25223
radiation effects on desoxyribonucleic acid of rat, 18: 25084 (NYO-2568-1)
radiation effects on desoxyribonucleic acid synthesis in mouse, *in vitro*, 18: 25186
radiation effects on adenosine triphosphate content, 18: 27088
radiation effects on mouse cell transplant from, x, 18: 27120
radiation effects on iron-59 uptake by rabbit, dynamics of, 18: 27141
radiation effects on nucleic acid content in, of rats and mice, 18: 27192
radiation effects on DNA synthesis in mouse, gamma, 18: 27130

radiation effects on erythropoiesis after irradiation of rabbit, 18: 29359
radiation effects on, in the presence of Endoxan or Trenimon, 18: 29365
radiation effects on, effects on immune response, 18: 29381
radiation effects on mouse, Friend's disease development from, 18: 29284
radiation effects on DNA synthesis in antigen stimulated cell cultures of rabbit, 18: 29325
radiation effects on bacterial immunity of mouse, 18: 31181
radiation effects on amino acid decarboxylase activity in, 18: 31195
radiation effects on lymphocyte ultrastructure in rat, x, 18: 31210
radiation effects on lipid, nucleic acid, and protein synthesis in rat, 18: 33382
radiation effects on enzyme activity in rat, 18: 35371
radiation effects on mouse, protective effects of drugs against x, 18: 36966
radiation effects on erythropoiesis in, 18: 36982
radiation effects on antibody production by transplanted, gamma, 18: 37001
radiation effects on amino acid content of mouse, 18: 37004
radiation effects on human, Thorotrast, 18: 38846
radiation effects on mouse, after cell injection, x, 18: 38863
radiation effects on selenium-75 metabolism in chick, gamma, 18: 38882
radiation effects on lymphocyte reduction in, beta, 18: 38902
radiation effects on cell morphology of, from colloidal gold-198 in tumor-bearing rats, 18: 41184
radiation effects on mouse, gamma, 18: 41201
radiation effects on, significance of, 18: 41240
radiation effects on desoxyribonucleic acid synthesis in mouse, after repeated exposures, 18: 41169
radiation effects on oxidative properties of mouse, effects of β-amino-ethyl sulfate on, 18: 41167
radiation effects on oxidative phosphorylation in rat, gamma, 18: 43244
radiation effects on dehydrogenase activity in rat, 18: 43286
radiation effects on deoxyribonuclease activity in, 18: 43289
radiation effects on colony-forming cells among colonies of, in mice, 19: 120
radiation effects on, Thorotrast, 19: 139
radiation effects on stem cell release by mouse, effects of thigh-shielding on, 19: 2129
radiation effects on reticulo-endothelium of rat, gamma, 19: 3951
radiation effects on soluble albumins in rabbit, x, 19: 3968
radiation effects on hematopoietic tissue in mouse, 19: 5648
radiation effects on desoxyribonuclease content in rats, 19: 5659
radiation effects on fine structure of mouse, gamma and x-ray, 19: 7170
radiation effects on cholesterol content of rat, 19: 8885
radiation effects on chicken, internal phosphorus-32, 19: 8887
radiation effects on hydrogen bond rupture in DNA in rat, 19: 8916
radiation effects on DNA and ribonuclease contents and thymidine uptake by rat, after head exposure, 19: 10851
radiation effects on acid deoxyribonuclease activity in mouse, 19: 10895
radiation effects on weight of mouse, proton, 19: 13041
radiation effects on desoxyribonuclease content of mouse, 19: 13059
radiation effects on endogenous respiration in mouse, x, 19: 13070
radiation effects on anaerobic glycolysis in mouse, x, 19: 13070
radiation effects on electrolyte transport in mouse, x, 19: 13070
radiation effects on immune responses of, in thymectomized mice, 19: 15217
radiation effects on reticulocytes in area of rabbit, abscopal, 19: 15056
radiation effects on DNA synthesis in mouse, effects of antigen injection on, 19: 15102
radiation effects on relative pool size of potentially competent cells in nonprimed and primed cells of, 19: 15103
radiation effects on growth and senescence of primary antibody-forming potential in mouse, 19: 15104
radiation effects on chromium, manganese, and nickel content in dog, 19: 17537
radiation effects on antibody formation in cells of, in recipient mice, 19: 17546
radiation effects on oxygen tension in mouse, 19: 17564
radiation effects on ATP content in rat, 19: 17626
radiation effects with and without chemotherapy on function and morphology of rat, 19: 17644
radiation effects on reduced glutathione behavior in rat, 19: 17650
radiation effects on peroxide decay in DNA in rat, 19: 19541
radiation effects on uptake of sulfur-35-labeled methionine by proteins in rabbit, 19: 19604
radiation effects on host-cell interactions in mice with grafts of, 19: 19615
radiation effects on amyloidosis in hyaline deposits in mouse, after liver and marrow injections, 19: 19650
radiation effects on electrical conductivity of rat, 19: 21867(T) (JPRS-28782(p.42-6))
radiation effects on activity of ATPase in mitochondria in rat, 19: 21869
radiation effects on response of mice to injected cells of, 19: 21943
radiation effects on acid deoxyribonuclease activity in mouse, whole-body, 19: 24345
radiation effects on cholesterol metabolism in rat, 19: 26017
radiation effects on nucleic acid content in rabbit, 19: 26032
radiation effects on nucleic acid content in rat, 19: 26032
radiation effects on nuclear ATP synthesis in mouse and rat, x, 19: 26062
radiation effects on histology of mouse, protective effects of bone marrow grafts against, 19: 26145
radiation effects on rabbit, effects on bone marrow hematopoietic activity, 19: 25991
radiation effects on immune reactions of embryonic chick, x, 19: 29837
radiation effects on electric properties of, in rats, 19: 29905(T) (JPRS-29112(p.19-25))
radiation effects on deoxyribopolynucleotides in animal, x, 19: 29933
radiation effects on DNA synthesis in rat, x, 19: 29934
radiation effects on hematopoiesis in mouse, x, 19: 29935
radiation effects on secondary antibody-forming potential in mouse, recovery from x, 19: 31676(R) (ORNL-3768(p.112-18))
radiation effects on mouse, effects of injections of bone marrow and spleen cells on, 19: 31918
radiation effects on phosphatase activity in mouse, x, 19: 31870
radiation effects on weight of mouse, x, 19: 31670(R) (NIRS-3(p.19-56))
radiation effects on enzyme activity in rat, 19: 31786(R) (NP-15072 (p.29-36))
radiation effects on rat, hematologic x, 19: 31820
radiation effects on size of chicken, sub-lethal, 19: 33913
radiation effects on ovarian transplant in rat, 19: 33925
radiation effects on immunity to homotransplants of, 19: 33930
radiation effects on immune reactions to transplants of, in mice, 19: 36029
radiation effects on DNA ribonuclease in, x, 19: 39265(R) (IA-1021)
radiation effects on serum proteins in mouse, following rat chimera transplant, 19: 38404
radiation effects on morphology of rat, fast neutron, 19: 38444
radiation effects on adenosine triphosphatase activity in rat, effects of various drugs on, 19: 43860(R) (NP-15310, pp 14-25)
radiation effects on cell migration in blood stream of rats after antigen stimulation, 19: 43822
radiation effects on cells of *Molge vulgaris*, in tissue culture, 19: 43826
radiation effects on phosphatase content of, in rats, 19: 43739
radiation effects on weight in mice of, genetic factors, 19: 45956
radiation effects on antibody production by transferred cells of, in mice, 19: 45986
radiation effects on immune reactions to grafts of parental, in rats, 20: 86
radiation effects on mouse, histopathological gamma, 20: 105
radiation effects on thiol content in rat, whole-body, 20: 108
radiation effects on immune reactions to injected cells of, in rats, 20: 1632
radiation effects on exteriorized rat, x, 20: 3775
radiation effects on exteriorized rabbit, x, 20: 3775
radiation effects on oxidative phosphorylation in nuclei from rat, 20: 5341
radiation effects on DNA from rat, x, 20: 6762
radiation effects on cell repopulation in, tracer study of γ, 20: 6812
radiation effects on antibody formation by cells of mouse, 20: 6780(R) (ORNL-3853, pp 93-7)
radiation effects on activity of proteinases from rat, γ, 20: 8609
radiation effects on growth of bone marrow transplants in mouse, neutron and x, 20: 8710
radiation effects on human, after Thorotrast carotidography, 20: 10680
radiation effects on biochemical properties of homogenates of mouse, γ, 20: 10577
radiation effects on lactic- and malic-acid dehydrogenases in extracts of rat, x, 20: 10583
radiation effects on desoxyribonucleose activity in rat, x, 20: 10622
radiation effects on mouse, model for β, 20: 10640
radiation effects on rat, x, 20: 10598(R) (BNWL-122, pp 107-9)
radiation effects on mouse, cellular x, 20: 12681
radiation effects on enzyme activity in mitochondria of rat, x, 20: 14376
radiation effects on distribution of lymphocytes by cell size in rat, x, 20: 14318
radiation effects on pyridine nucleotidase activity of rat, x, 20: 14362
radiation effects on content of nucleated cells in, of young mice, γ, 20: 14365
radiation effects on iron metabolism in rat, tracer study of γ, 20: 16187
radiation effects on transplanted Yoshida sarcoma cells in rat, tracer study, 20: 16188
radiation effects on catalase activity in rat, 20: 16277
radiation effects on DNA and RNA metabolism in cells of rat, x, 20: 18341
radiation effects on concentration of oxidized and reduced TPN in rat, x,

20: 18343
radiation effects on mouse, γ and proton, 20: 18364
radiation effects on cell reproduction in mouse, survival curve analysis of γ, 20: 18370
radiation effects on dehydrogenase and transaminase activity in mouse, 20: 18280
radiation effects on metabolic activity in rat, x, 20: 20433 (AD-630390)
radiation effects on adenosine triphosphatase activity of rat, 20: 20503(R) (AD-629311, pp 1-14)
radiation effects on colonization of, by transplanted bone marrow cells, fast-neutron and x, 20: 22707
radiation effects on mouse, allograft acceptance following x, 20: 22741
radiation effects on protease activity in mouse, x, 20: 22607
radiation effects on iron-59 uptake by intact and splenectomized mice injected with spleen cells, 20: 22610 (AD-632049)
radiation effects on mouse, cytological x, 20: 22614(R) (NIRS-4, pp 28-34)
radiation effects on rat secondary syndrome following transplantation of rabbit, x, 20: 22637
radiation effects on DNase activity in rat, 20: 31143
radiation effects on DNA synthesis in hamster, effects of temperature on dose-response curve of x, 20: 32945
radiation effects on chick embryo, comparison of *in ovo* and *in vitro* γ, 20: 32984
radiation effects on rat, morphological, x, 20: 33059
radiation effects on weight of mouse, neutron and x, 20: 33068
radiation effects on granulocyte distribution in rat, whole-body x, 20: 32930
radiation effects on DNA activity in rat, effects of cysteine on whole-body x, 20: 35249
radiation effects on DNA and RNA contents of, in rats, effects of monoethanolamine on x, 20: 35326
radiation effects on hematopoietic response in guinea pig, effects of unilateral limb shielding on gamma, 20: 36611
radiation effects on histology of rat, during immune response, local x, 20: 36637
radiation effects on homografts of, in dogs by lymphatic ablation, 20: 36641
radiation effects on colony formation by injected bone marrow cells in mouse, 20: 38708(R) (IAEA-3173-5)
radiation effects on DNA and RNA synthesis in marrow-protected mice, effects of estradiol on x, 20: 40577
radiation effects on cells of, incubated with phytochemagglutinin, x, 20: 40588
radiation effects on uptake of sulfur-35-labeled mycobacterial vaccine by microsomes and mitochondria in rat, x, 20: 42907
radiation effects on cells of, in mice injected with 5-methoxytryptamine and cystamine, 20: 42938
radiation effects on, in mice centrifuged prior to gamma or proton exposure, 20: 42985
radiation effects on rat, protective effects of barbamyl and serotonin on γ, 20: 43008
radiation effects on mouse, whole-body x, 20: 45434
radiation effects on mouse, effects of cytostatic drugs on, 20: 45494
radiation effects on cholinesterase activity in rabbit, 19: 19609
radiation effects on folic acid activation in rat, x, 16: 1552
radiation injuries, protective effects of pantothenic acid against, 16: 4122
radiation injuries, histology, 16: 28797
radiation injuries in, effects of spleen extract injections in guinea pigs on, 17: 10369
radiation injuries, 17: 21517
radiation injuries, protective effects of citrin-unithiol compounds against, 18: 1451
radiation injuries of, resulting from injected Thorotrast, 18: 38828
radiation injuries from Thorotrast in, 19: 24266
radiation injuries, protective effects of *p*-aminopropiophenone, 19: 31902(R) (NP-15072(p.82-7))
radiation injuries, protective effects of aminoethylisothiuronium, dimethylsulfoxide, and *p*-aminopropiophenone, 19: 31901(R) (NP-15072 (p.71-81))
radiation injuries and recovery of, in rats, 19: 36010
radiation injuries of enzyme systems in rat, protective effects of glycine against, 19: 38467
radiation injuries in mouse, fast-neutron, gamma, or combined fast-neutron and gamma, 20: 45417
radiation injury on rat, effects of fractionated doses on regeneration of x, 20: 40702
radiation protective effect of shielding, 17: 30424
radiation protective effect of extracts of, in mice, 17: 33758
radiation scanning of, using technetium-99m, 18: 15913 (TID-7689(p.1-11))
radioactive contamination of human, from fallout, 17: 16346
radiodiagnosis in, using iodine-131-labeled albumin, 18: 21936
radiodiagnosis in, preparation and properties of mercury-197-labeled 1-mercuri-2-hydroxypropane for, 19: 15306
radiodiagnosis in, by photoscanning using iodine-131-labeled human serum albumin, 19: 19710
radiodiagnosis of diseases of, bibliography on, 18: 3631 (AED-C-10-01)
radiodiagnosis of lesions in, 18: 5183 (TID-7673(p.468-83))
radiodiagnosis of diseases of, by uptake measurements of radioactive colloids, 19: 10968
radiodiagnosis of hemolytic anemia by photoscanning of, using heat-treated chromium-51-labeled erythrocytes, 19: 19725
radiodiagnosis of defects and tumors of, by scintiscanning using chromium-51, 19: 19726
radiodiagnosis of function of, by scintiscanning using chromium-51, 19: 19727
radiodiagnosis of diseases of, 19: 22019(R) (UCLA-12-541(p.51-91))
radiodiagnosis of diseases of, using chromium-51 and external counting, 19: 30062
radiodiagnosis of diseases of, 19: 34053
radiodiagnosis of diseases of, 19: 43886
radiodiagnosis of diseases of, using mercury-197- and -203-labeled organic compounds, 20: 26733
radiodiagnosis of, diseases of, biological aspects in choice of scanning agents for, 18: 6737
radiodiagnosis of, using mercury-197 scintigraphy, 20: 6946
radiodiagnostic use of technetium-99 in, feasibility of, 19: 34072
radiography of, use of colloidal technetium-99m in, 20: 29065
radioinduced change in antigenic properties, 17: 63
radioinduced changes in, effects of chemical compounds on, 17: 13970(R) (NP-12484(p.26-34))
radioinduced chromosomal aberrations in mouse, x, 19: 45911
radioinduced lesions in human, Thorotrast, 20: 22635
radioinduced modifications of the adenine-nucleotide content in, 16: 8624
radioinduced mononucleated giant erythropoietic cells in fragments from, mechanism for x, 20: 18325
radioinduced nodule formation in mouse, 19: 43682(R) (UCLA-12-565, pp 33-57)
radioinduced nucleoprotein loss in cell nuclei of, in first four hours after x irradiation, 17: 27157
radioinduced peroxide formation in lipids of rat, electron and x, 19: 25959
radioinduced splenomegaly in mouse, effects of graft-versus-host reaction on x, 20: 24887
radioinduced tumors of, from thorotrast angiography, 17: 35462
radioinduced weight variations, effects of cysteamine on, 16: 11500
radioisotope distribution in, phantom studies of, 19: 17747
radioisotope scanning of, pharmaceuticals for, 19: 5741
radioisotope scanning of, 19: 13140
radioisotope scanning techniques for, 20: 43051
radioisotope uptake by, effects of sodium phosphates on, 16: 32706
radiosensitivity, 16: 12924
radiosensitivity, 16: 17459(T)
radiosensitivity, 16: 21871
radiosensitivity, 16: 21899(R) (AFSWP-920)
radiosensitivity, 16: 26824
radiosensitivity, 19: 7024
radiosensitivity, effects on uptake and distribution of phosphorus-32 16: 4055
radiosensitivity effects of, whole-body, 17: 90
radiosensitivity effects of removal of, 18: 31285
radiosensitivity effects of transplants of mouse parental, 18: 33320
radiosensitivity effects of oxygen tension of mouse, 19: 21995(R) (NP-14779(p.64-9))
radiosensitivity effects in guinea pigs and rats of transplants of bovine, x, 19: 24372
radiosensitivity effects in mice, 19: 31918
radiosensitivity effects of phospholipid extracts of, in mice, 20: 10704
radiosensitivity effects of marrow transplants into mouse, 20: 10713
radiosensitivity effects of homogenates from mouse, x, 20: 18433
radiosensitivity effects of tissue extracts of, on mouse tumor, 20: 18460
radiosensitivity effects of extracts of calf, 20: 18493
radiosensitivity effects of lyophilized extracts of calf, in rat, 20: 18497
radiosensitivity effects of sheep, on leukemia in mice, 20: 22738
radiosensitivity effects of injected, in mice, 20: 31127
radiosensitivity effects of extract and removal of, on nitrogen metabolism in frog liver, 20: 35307
radiosensitivity in rats, erythropoietic recovery by bone marrow treatment, 16: 32848
radiosensitivity in leukemic patients, 17: 17882
radiosensitivity of agglutinin-forming and homograft-rejecting capacities of cells, 16: 32784
radiosensitivity of respiration and phosphorylation of mitochondria, 17: 1246

radiosensitivity of desoxyribonucleic acid synthesis in lymphocytes, 17: 5830
radiosensitivity of hematopoiesis in, of rats, mice, and guinea pigs, 18: 107
radiosensitivity of DNA in mouse, 18: 11703
radiosensitivity of hematopoietic tissues in, of rats and mice, 18: 27192
radiosensitivity of cells of, in mice, 19: 13012
radiosensitivity of hemopoietic colony-forming cells of, before and after transplantation in mice, 19: 17601
radiosensitivity of, in rats, 19: 22078
radiosensitivity of, in rats, 19: 28056
radiosensitivity of mouse, effects of β-mercaptoethylamine on, 20: 20511
radiosensitivity of mouse, effects of bacterial toxins on, 20: 20512
radiosensitivity of rat, effects of thioacetamide on x, 20: 38694
radiotherapy of, for enlargement and leukemia, 17: 38660
radiotherapy of mouse, synergistic effects of Mitomycin C and Endoxan in, 20: 31131
radiotherapy of, in leukemia, 20: 40720
radium-228 biological half life in, 18: 34274(R) (NIRS-2(p.3-15))
radium-228 determination in, alpha spectrometric, 18: 17699
reactions of cells of, with humoral H-2 antibodies in irradiated and normal embryonic and newborn mice, 17: 21519
recolonization of, in x-irradiated mice following lymphoid or myeloid transplants, 20: 40727
regulation of blood cell populations in mice by stem cell compartment of, following strontium-89-induced damage to bone marrow, 20: 45424
removal, effects of time before irradiation on radiation syndrome, 16: 6362
removal of damaged erythrocytes by, 18: 5183 (TID-7673(p.468-83))
removal of rat, therapeutic effects of post-irradiation, 18: 33415
reparative effects of DNA from, on sperm of x-irradiated rat, 20: 40723
repopulation of, by transplanted bone-marrow in irradiated mice, 18: 11757
response to injected bone marrow in irradiated mice, 16: 11435(R) (ANL-6464(p.22-3))
reticular cells in mouse, role in erythropoiesis and lymphocytopoiesis, 20: 12681
scanning technique for, 18: 35434
scintigraphy of, using mercury-197-labeled bromomercurihydroxypropane, 20: 22817
scintillation scanning of, methods for, 19: 5752
scintillation scanning of, methods of preparing labeled erythrocytes for, 19: 42584
shielding during irradiation, effects on antibody response to antigens, 16: 26858
shielding, effects of, on irradiated thymic lymphocytes, 20: 142
splenectomy effects on recovery from radiation injuries, 16: 8622
strontium-89 deposition in cow and goat, 16: 8505
strontium-90 content of dog, at various times after injection, 20: 8545(R) (COO-119-239, pp 81-7)
strontium-90 retention in mouse, after intraperitoneal or subcutaneous injection, 20: 18225
sulfhydryl content in mouse, effects of cysteamine, cyanide, and high-pressure oxygen on, 19: 43869
sulfhydryl content in, of radioresistant mice, 20: 14351
sulfur-35-labeled mercapto group uptake by mouse, 18: 43312
surgical removal of, radiosensitivity effects in mice of, 17: 35471
surgical removal of mouse, effects on reticulo-endothelial function, 20: 14374
surgical removal of mouse, radiosensitivity effects on fetuses, 20: 18436
temperature of, effects of radon on, 16: 11476
therapeutic effect of removal, on irradiated rats, 16: 4072
therapeutic effects of transplants from irradiated donors against radiation in mice, 16: 32842
therapeutic effects of injected cells of, factors in, 17: 14106
therapeutic effects of homogenates of, on tumors, 19: 10963
therapeutic use of cell grafts from, in radiotherapy recovery, 17: 35370
thorium dioxide uptake in rabbit, colloidal, 16: 25162
thorium dioxide uptake by rat, 18: 31103
thorium-228 decay in beagle, metabolism of bismuth-212, lead-212, and radium-224 from, 19: 45798
tissue proteins of rat, effects of radioprotective sulfur compounds on, 18: 31303
toxic effects of uranyl nitrate on rat, 19: 14980
trace element content in rat, effects of x radiation and nitrogen mustard on, 17: 40547(R) (NYO-10569)
transfer of cells of, in mice, 19: 13012
transplantation in dogs, 19: 19521
transplantation in dogs and man, 19: 19522
transplantation in irradiated mice, protection from killing effect of, 19: 19651
transplantation of fresh and preserved, in treatment of radiation sickness in rabbits, 17: 5926
transplantation of, in *in vivo* cultures, models for study of immune reactions in, 17: 13915
transplantation of, immune reactions to, 18: 27019(R) (TID-20719)
transplants in γ-irradiated mice, effects of methotrexate on, 20: 29035
transplants, effects on recovery of irradiated dogs, 19: 4002
tritium uptake from thymidine by proteins in mouse, 20: 35216
tumor localization by scintillation scanning utilizing closed circuit television, 16: 8498
tumorigenic effects of dried cell injections of mouse, 18: 36938
uptake and distribution of thorium dioxide in mouse, rabbit, and rat, 20: 35223
uptake of phosphorus-32-labeled Endoxan and thio-TEPA by rat, 20: 45315
use in assaying viable cells in transplanted lymphoma suspensions, 18: 19671
use of extract as radiation protection factor, 20: 40658
use of iodine-131-labeled colloidal albumin as scanning agent, 20: 40777
weight norms for human, use in establishing standards for radiation dosimetry, 20: 20374
weight of mouse, effects of growth of infused bone marrow cells on, 20: 6775(R) (ORNL-3853, pp 36-49)
yttrium-90 content of monkey, after intravenous injection, 17: 38729
yttrium-90 distribution in mouse, after intratumoral injection, 17: 30213
yttrium-90 localization in rabbits, injected, 17: 21405
yttrium-91 metabolism by mouse, effects of hexametaphosphate on, 19: 3865
yttrium-91 uptake and elimination by guinea pig, effects of diethylene-triaminepentaacetic acid on, 19: 3864
yttrium-91 uptake, distribution, and excretion by rat, 19: 17471
zinc-65 metabolism in rabbit, 18: 43190
zinc-65 uptake and retention by rat, 18: 36933
zinc-65 uptake and distribution in human, 19: 17480
zinc-65 uptake and distribution in normal and tumorous, in man, 19: 43699
zinc-65 uptake by chicken, dietary effects on, 19: 14962
zinc-65 uptake by rat, effects of dietary copper, molybdenum, and zinc on, 19: 35915

Splices
see Cables

SPODUMENES
see also Lithium Aluminum Silicates
processing, evaluation of methods for, 17: 220
reaction with sodium sulfate at 700 to 1000°C, 16: 9998

SPONGES
radiation effects on cells in, beta, 19: 24353
strontium ion effects on cellular aggregation in, 18: 29207

SPONTANEOUS FISSION
alpha particle emission in ternary, mechanisms for, 18: 40606
energy release in, (T), 20: 17862
fragment excitation energies and threshold in, 16: 26361
fragments from, shell influence on, 17: 32723(R) (PR-P-57(p.5-20))
half life of, from superfluid model, (T), 20: 4876
in nuclei with $Z \geq 98$, 17: 5326 (UCRL-10474)
lifetimes of heavy-element, (T), 20: 22043
occurrence in heavy nuclides (A = 255), 16: 18510
regularity in, 19: 45271 (JINR-P-2265)
review, 20: 19992
systematics of, in heavy even-even nuclei, 18: 40604
theory review, (T), 19: 6711

SPORES
bacterial, heat activation of, 19: 32640
cytology and control mechanisms for formation of, by *Bacillus cereus* and *B. subtilis*, 20: 1582(R) (NYO-2038-2)
desoxyribonucleic acid synthesis during germination of *Bacillus subtilis*, effects of chloramphenicol on, 19: 33727
effects of space flight on Tradescantia micro-, 18: 43265
genesis of fungal, reaction mechanisms in, 20: 12695
growth of *Clostridium botulinum*, Type E, 18: 36877 (CONF-639-1)
growth of *Clostridium botulinum*, Type E, 18: 36879 (CONF-640-1)
growth of *Clostridium botulinum* Type E, 18: 36878 (CONF-639-2)
growth of *Clostridium botulinum*, 19: 15014 (CONF-641002(p.82-7))
nucleic acid biosynthesis during development of *Bacillus subtilis*, tracer studies of, 18: 43185 (ORNL-P-422)
photoproducts induced in bacterial, by uv, 20: 16159(R) (ORNL-3900, pp 150-81)
physiology of *Clostridium botulinum*, 19: 29885(R) (AD-611359)
production of dry, of *Bacillus megaterium*, 18: 27014(R) (ORNL-3601(p.216-21))
radiation effects on *Rhizopus stolonifer*, protective effects of germination inhibition against, 18: 23288

radiation effects on *Rhizopus stolonifer*, protective effects of oxygen against, 18: 23288
radiation effects in bacterial, protective effects of glycerol against, 18: 31279
radiation effects on germination and growth of *B. subtilis*, 18: 33292
radiation effects on *Pyrenochaeta terrestris*, 18: 38881
radiation effects on bacterial, mechanisms for x, 19: 181
radiation effects on *Clostridium botulinum*, in canned pork, 19: 3925
radiation effects on *Clostridium botulinum*, 19: 15957 (CONF-641002 (p.77-81))
radiation effects on germination of *Bacillus subtilis*, 19: 15042
radiation effects on fungal, 19: 19558
radiation effects on fungal, 19: 19559
radiation effects on survival of Clostridium, 19: 27963
radiation effects on *Clostridium botulinum*, 19: 29885(R) (AD-611359)
radiation effects on photoproducts in *B. megaterium*, uv, 19: 31796(R) (ORNL-3768(p.187-94))
radiation effects on *Bacillus megaterium*, labeled with tritiated thymidine, 19: 36072
radiation effects on growth of *Cl. botulinum* Type E in fish, 19: 42779(R) (TID-22126)
radiation effects on oxygen concentrations in Neurospora conidial, x, 19: 42365
radiation effects on Neurospora conidial, protective effects of endogenous anoxia and MEA against x, 19: 42365
radiation effects on formation of, by yeast, 20: 1664
radiation effects on, genetic, 20: 1622 (WT-820)
radiation effects on germination of *Funaria hygrometrica*, 20: 3781
radiation effects on Clostridium, effects of sodium chloride on γ, 20: 6834
radiation effects on *Trichophyton terrestre*, uv, 20: 6888
radiation effects on fungal, on fruits, 20: 9320 (CONF-651024, pp 34-8)
radiation effects on fungal, on strawberries, γ, 20: 9323 (CONF-651024, pp 49-52)
radiation effects on development of *Clostridium botulinum*, in shrimp, 20: 9328 (CONF-651024, pp 78-80)
radiation effects on development of *Clostridium botulinum* type F, γ, 20: 9329 (CONF-651024, pp 81-4)
radiation effects on growth of *Clostridium botulinum*, in fish filets, γ, 20: 9337 (CONF-651024, pp 107-10)
radiation effects on bacterial, review, 20: 14389
radiation effects on *Bacillus cereus*, x, 20: 18344
radiation effects on *Bacillus megaterium*, effects of hydrogen sulfide and nitric oxide on, 20: 18434
radiation effects on germination of Actinomyces, 20: 24935
radiation effects on fern, effects of moisture on γ, 20: 32969(R) (ORO-648, pp 123-58)
radiation effects on dipicolinic acid content in *Bacillus cereus*, x, 20: 35240
radiation effects on germination of *Ustilago avenae*, x, 20: 38672
radiation effects on differentiating bacterial, repair of uv, 20: 40504(R) (ORNL-3922, pp 146-60)
radiation effects on induction and liberation of phages by Actinomyces, effects of ultrasonic vibration on uv, 20: 45407
radioinduced free radical formation in, 19: 27969
radioinduced free radicals in *B. subtilis*, γ, 20: 22601
radioinduced inactivation of bacterial, gamma, 18: 29253
radioinduced inactivation of *Clostridium botulinum*, factors affecting dose required for, 20: 40601
radioinduced thymine dimers in bacterial, 19: 2077(R) (ORNL-3700 (p.180-6))
radioresistance of *Bacillus subtilis*, 19: 3890(R) (NYO-3103-1)
radioresistance of *Aureobasidium pullulans*, 19: 13009
radiosensitivity of bacterial, 18: 33278 (STI/DOC/10/28(p.39-66))
radiosensitivity of desoxyribonucleic acid in *B. subtilis*, effects of 5-bromodeoxyuridine on, 18: 33402
radiosensitivity of bacterial, effects of freezing and postirradiation heating on gamma, 18: 33996
radiosensitivity of *Clostridium botulinum*, effects of chemicals on, 18: 43299
radiosensitivity of *Clostridium botulinum*, in canned meat, effects of chemical additives on, 19: 5636
radiosensitivity of, of citrus fruit-decay fungi, 19: 5691
radiosensitivity of *Bacillus cereus*, 19: 8844
radiosensitivity of *Clostridium botulinum*, 19: 12950 (COO-1095-3)
radiosensitivity of colony-forming ability in *B. subtilis*, effects of heat treatments on gamma, 19: 13108
radiosensitivity of DNA transforming ability in *B. subtilis*, effects of heat treatments on gamma, 19: 13108
radiosensitivity of *Clostridium botulinum*, 19: 15014 (CONF-641002 (p.82-7))
radiosensitivity of *B. subtilis* and *S. faecium*, effects of dried media on, 19: 15036
radiosensitivity of *Clostridium perfringens* type A spores, 19: 24270
radiosensitivity of *Clostridium botulinum* Type E, 19: 26734
radiosensitivity of Clostridium, 19: 26735
radiosensitivity of, effects of nitric oxide or water on, 19: 29886(R) (ANL-6971(p.29-46))
radiosensitivity of *Bacillus subtilis*, genetic factors, 19: 33851
radiosensitivity of *Clostridium botulinum*, effects of temperature, 19: 36875
radiosensitivity of *Cl. botulinum* Type E, 19: 42778(R) (TID-22001)
radiosensitivity of Clostridium, effects of pH and phosphate solutions on, 19: 43865
radiosensitivity of *Bacillus subtilis*, 19: 43793
radiosensitivity of *Bacillus subtilis*, effects of germination on uv, 19: 45848
radiosensitivity of pathological, 19: 46890
radiosensitivity of *Clostridium perfringens* Type A, gamma, 20: 1679
radiosensitivity of *Clostridium botulinum* type E, effects of food additives and temperature on, 20: 9340 (CONF-651024, pp 117-23)
radiosensitivity of cell stages in Chlamydomonas, effects of repair mechanisms on uv, 20: 12687
radiosensitivity of *Cl. botulinum*, in canned chopped ham, 20: 13134 (AD-625252)
radiosensitivity of *B. cereus*, mechanism for, 20: 14263
radiosensitivity of Clostridium, γ, 20: 18340
radiosensitivity of, effects of chemicals on, 20: 37144
radiosensitivity of *Clostridium botulinum* type E, γ, 20: 40699
radiosensitivity of *Clostridium botulinum*, type E, 20: 43775
radiosensitivity of fungi, effects of chemical radiosensitizers on γ, 20: 43784
repair of x-radioinduced chromosome aberrations in Tradescantia micro-, 20: 42977(R) (ORO-2669-2)
use as radiation dosimeter during space flight, 20: 18964

Spot Tests
see Colorimetry

SPPP
see Special Purpose Power Plant Reactor

SPRAY COLUMNS
heights of transfer unit calculations for countercurrent foam-liquid, 16: 33070(R) (ORNL-TM-297)

Spraying
see Metal Spraying

SPRAYS
droplet evaporation in high temperature convective environments, properties of, (T), 20: 14692 (UCRL-16656)
effects of urethan foam, on air leaks in buildings, 20: 41200 (ORNL-TM-1551)
heat transfer and pressure drop in steam–water, 18: 14025 (EURAEC-153)
instability of preformed charged liquid drops injected into an accelerating field, 18: 18501
powder feeder for ultrafine particles, development of arc, 20: 4298 (LA-DC-7275)
use in reactor containment decontamination, 19: 24781

SPRF
see Sandia Pulsed Reactor

SPRF-II
see Sandia Pulsed Reactor-II

SPRINGS
(See also materials used for springs; for springs of water, see Ground Waters.)
deformation of Inconel X, under constant load at 900°F, 16: 7881 (DC-59-1-242)
design for suspending and supplying electricity to holding magnets for reactor control rods, 19: 1829(P)
development of mechanism with constant negative spring rate, 18: 9763 (SC-TM-293-63(13))
development of pneumatic, for vibration damping and isolation, (T), 20: 3613 (CONF-651016-1)
effects of loads on pre-stressed Inconel-X, at 1000°F, 16: 6710 (DC-58-6-150)
radiation effects on creep of graphite, 16: 25870
radioactivity of Euganean, 18: 43807
response of linear damped lumped spring-mass systems, transfer function formalism for transient, 19: 45710 (SC-TM-64-1772)
response of two coupled mass spring systems with dampers, tables and graphs, 16: 589 (SCR-408)

SPRUCE PINE DISTRICT (N. C.)
ages of uranium minerals, 16: 29197

SPUR
see Space Power Unit Reactor

SPUTTERING
(See also specific materials sputtered and inducing particles)
analytical use of, accuracy of quantitative, 18: 41332

anisotropy in single crystals, 18: 28124
at low ion energies, review, 18: 28119
atom ejection in low-energy, of single crystals of bcc metals, 17: 37467
atomic collisions focusing in bcc crystals, (E), 20: 9676(T)
bibliography, 16: 2299 (NP-10971)
book: *Atomic and Ionic Impact Phenomena on Metal Surface*, 19: 35601
by deuterons in the Rutherford collision region, 16: 21183
cathode erosion by, in high-pressure discharges, 17: 24086
conference on ionic bombardment theory and applications, Bellevue, France, Dec. 4 to 8, 1962, 18: 40169(T)
control of, in regenerative collector target, 20: 41122
design of system for measuring, inside electron microscopes, 16: 27806
design of system for simultaneous multicomponent, 17: 4892
design of system for multilayer simultaneous deposition of uniform-resistance films by, 18: 7354
development for film growth and nucleation in glow discharge environment, 17: 36464
development, survey of activities at various laboratories, 16: 13638(R) (ARF-1188-1)
ejection patterns for semiconductor, (E), 20: 40305
energy chain effects in, 18: 28118
energy distribution of sputtered particles in, 18: 14625
energy of atoms in, calorimetric measurement of average, 17: 11374
equipment and methods for studies of, 16: 32185
equipment for studying, design and testing of, 20: 5981(R) (AD-620002)
equipment for, design of high-vacuum, 18: 33875(P)
equipment for, design and performance of, 19: 38930
film preparation by, review of, 18: 2177
film production by cathodic, chamber design for thin, 16: 16433
focusing in, 17: 9022
growth of, vs. evaporation in metal films, (E), 20: 39587
ion sorption by solids during, 16: 12280
ion sources for, design and performance of duoplasmatron, 20: 35612
mass analysis of neutral particles and ions from metal targets, 17: 37746
mass spectrometric study of, 18: 42298 (ORNL-P-193)
mechanism for metals, 18: 18296 (ZFK-WF-6)
mechanism of, effects of incident ion angle, 17: 11318 (NP-12357)
mechanism of single-crystal, 20: 42553
mechanisms in accelerator tubes (E), 19: 2924 (LA-DC-6540)
mechanisms of, 18: 4360
mechanisms of reactive, 18: 8950
mechanisms of, by rare gas ion, 18: 20745
methods of, for dielectrics, 16: 33607
micromachining by, through mask of contamination, 19: 39136
model for calculations of, 20: 19407
of metals by argon ions, full-plane threshold energies for, 17: 37743
of solids, review, 17: 6813(T) (NP-tr-930)
patterns of, method for examining, 18: 8942
production of thin single crystals by cathodic, 18: 28113
properties of, review of, 19: 20819
rates of, in glow discharges, effects of current on, 16: 19563
research progress, review, 16: 21115 (AD-267458(Pt.I))
research progress, 20: 19359(R) (N-65-24388)
research using mass spectrometry, 20: 4215(R) (ANL-7081, pp 134-49)
secondary emission mechanism in, 20: 46298
study by field emission microscopy, techniques of, 20: 32742
surface phenomena connected with, in aluminum and copper targets, 18: 28104
surface re-emission law in free molecule flow, 18: 40152
theory, 19: 25175
theory for focused-collision effects at high energies, 16: 19562
threshold effects in mechanical collision theory, 16: 22749
use for analysis of solids, 18: 10350
use for space propulsion, 18: 14753
use in epitaxial growth of gold and silver films, 18: 24074
use in neutral beam detection, 18: 2457
use in surface preparation for plating, 20: 14670 (SC-R-65-997)
use of asymmetric a-c, for obtaining high-purity superconducting films, 18: 2752
use of cathodic, in uranium cleaning, 20: 33261 (RFP-674)
velocity distribution of sputtered atoms, measurement, 17: 20330
yield measurements by electron microscopy, 16: 22748
yields at low bombarding energies, 16: 21116 (AD-267458(Pt.V))
yields crossover in single-crystal copper, (E), 20: 39589
yields from collector systems for ion engines, 18: 41590 (AEDC-TDR-64-105)
yields from high-energy, mass spectrometric study of, (E/T), 20: 31905
yields from hydrogen ion, on metals, 18: 8926
yields from low-energy, resonance absorption and emission spectroscopy of, (E), 19: 4837
yields from monocrystal, effect of collision focusing on, 18: 32368
yields from, scanning spectrometer for, 20: 43660
yields of noble-gas ion, of nuclei with $4 \leq Z \leq 92$ at 100 to 600 ev, 16: 22753

SQUALENE
biosynthesis from farnesyl pyrophosphate, tracer studies of stereochemistry of hydrogen transfer in, 18: 43553
metabolic effects, 17: 16360(R) (NP-12597)
radiolysis, 18: 1727 (RTD-TDR-63-4133)
radiolysis at –196 to 350°C, yields, 18: 25551
radiolysis effects on, electron and gamma, 18: 31578
radiolysis of, mechanism and yields in, 18: 5390
radiolysis of, product yields in, 18: 274 (USNRDL-TR-671)

Squash
see Magnetic Mirror Machines

Squawker-Blinker
see Rate Meters

SQUID
radioinduced browning, effects of sugar, 16: 24071

SQUIRRELS
ecology of *Citellus parryi*, Cape Thompson area, Alaska, 19: 25786 (PNE-421)
effects of nematode infection on central nervous system of ground, 20: 42835(R) (ANL-7136, pp 63-80)
hematology of White Oak Lake area, 19: 6931(R) (ORNL-3697(p.65-84))
labeling with calcium-45 for population studies, 20: 12583
liver regeneration in, effects of hibernation on, 17: 7655(R) (ANL-6600)
radiation effects on catecholamine content in tissues in hibernating, 17: 35504
radiation effects on immune reactions during hibernation of *Citellus tridecemlineatus*, 19: 7013(R) (ANL-6906(p.23-6))
radiation effects on glucose absorption by intestines in active and hibernating, 19: 45841
radiation effects on ground, gamma and x, 20: 18291(R) (N-65-17058)
radiation effects on hibernating ground, effects of temperature on γ and x, 20: 42835(R) (ANL-7136, pp 63-80)
radiosensitivity of *Citellus tridecemlineatus*, effects of hibernation on, 19: 29892(R) (ANL-6971(p.143-58))
sodium-22 content in muscles of Canadian, 20: 4161

SRE
see Sodium Reactor Experiment

SS Materials Accounting
see SF Materials Accounting

SSCR
see Spectral Shift Control Reactor

STABILIZATION
see also Passivation

STABLE ISOTOPES
(See also specific stable isotopes.)
abundance, 17: 32709 (IFA/SN/17)
abundance ratios in Earth's mantle, 20: 32245(T) (NSJ-tr-48)
analysis and separation of mixtures of, review on methods for, 20: 26745 (IFA-IS-34)
atomic masses of, from Z = 44 to 54, table of, 18: 1057
atomic masses of, of Z = 32 to 42, table of, 18: 1056
availability of, index for, 18: 12500
bibliography on electromagnetically-enriched, 17: 17628 (ORNL-3266)
book: *Stable Isotopes. Catalog for Stable Isotopes, Compounds, and Products with Enriched Stable Isotopes*, 20: 16933
catalog of, Atomic Energy of Canada Ltd., 20: 32891
catalog, ORNL, 17: 26961
characteristics of available, 17: 26962
conference on, 17: 2671
conference on, German Academy of Sciences, Oct. 28 to Nov. 2, 1963, Leipzig, 20: 19120
content in tissues, radioisotope dose estimation from, 20: 6719(R) (ORNL-3849, pp 183-213)
contents in meteorites, 18: 34400
detection and measurement, 16: 1351
determination by mass spectroscopy, 19: 2245
determination by spectroscopical analysis, 17: 7980
determination in gaseous substances, effects of gas-flow conditions on accuracy of mass spectrometric, 18: 1997
enrichment and use, 20: 28864(R) (NP-15976)
enrichment in columns, kinetics of, 17: 2674
equilibrium abundances, 16: 12306
inventory of, research pools for, 19: 22821 (ORNL-TM-1047(p.87-92))
neutron capture cross sections, thermal, 17: 32709 (IFA/SN/17)
obtention, application, and analysis of, 17: 2672
physiological effects of, bibliographic study, 17: 2714
preparation as radiation target materials, methods development for, 18: 27815(R) (ORNL-TM-718)
preparation from fission products, 18: 18265
procurement of, procedures for, 19: 22820 (ORNL-TM-1047(p.83-6))
production and uses in German Democratic Republic, 18: 39784
production in Spain, 20: 11191 (JEN-150-DQ/I-51)

production of, survey of methods for, 20: 46135
production, separation, and use, 16: 212(T) (CEA-tr-R-1361)
properties of, as a probe for liquid- and solid-state investigations, 18: 5884
sales inventory and distribution, 18: 27811(R) (ORNL-TM-198)
separation by chemical and ion-exchange methods, 17: 23814
separation by electromagnetic processes, 19: 22818(R) (ORNL-3650 (p.221-38))
separation by ion exchange, 17: 23811
separation by thermal diffusion methods, 18: 32006
separation from other uranium isotopes, 19: 2699
separation of, 17: 2673
separation of, review of methods for, 18: 4146
separation of, economics of cascade, 20: 4284(T) (CEA-tr-X-617)
separation of, electromagnetic and photochemical methods for, 19: 4577
separation of, irreversible processes for, 19: 4576
separation of, principles and methods for, 19: 867
separation of, review of irreversible processes for, 18: 32007
separation of, reversible processes for, 19: 4574
separation of, theory of irreversible processes for, 19: 4575
tracer uses, 18: 27338
use in biological studies, developments in, 20: 45302
use in catalysis research, 17: 41186
use in chemistry, geology, and physics, 20: 41380(T) (IFA-IS-36)
use in human metabolic studies, 20: 45318
use of, with activation analysis for *in vivo* diagnosis, 20: 26729
uses in agriculture, industry, medicine and research, bibliography, 16: 19216 (TID-4563(3rd Rev.))
uses in biology, bibliography on, 18: 3444
uses in physical chemistry, 17: 10643
uses in research, selected translations from Russian on, 18: 25868(T) (OTS-63-11008)
uses in studying reaction mechanisms of organic compounds, 20: 348
uses of, review, 18: 14293

STACK DISPOSAL

see also Meteorology
see also Radiation
see also Smoke Generators
see also Smokes
activity levels at Elk River Power Reactor, 20: 1547 (CEND-512)
air pollution by, Russian studies of, 19: 14116(T) (JPRS-28343)
air pollution evaluation, factors in, 18: 40042 (HW-SA-3685)
analysis of iodine and xenon radioisotopes in, 18: 27789(R) (ORNL-3578(p.37-45))
at Belgian Research Centre, Mol, meteorological aspects, 17: 2645
atmospheric contamination from, 19: 24713
atmospheric contamination from, method for determining, 20: 27198 (JAERI-1101)
atmospheric diffusion formula for, 16: 25079
atmospheric dispersion studies of releases near ground level, correlation with meteorological predictions, 18: 4017 (HW-SA-3176)
atmospheric dispersion of radioactive pollutants, 18: 37419 (A/CONF.28/P/27)
atmospheric pollution by, study by activation analysis, 17: 3663
beta monitoring in, equipment for, 20: 25399
by atomic energy industries, effects of, on contamination of biosphere, 17: 37056(T) (FTD-TT-63-664)
chimney device for preventing suction of smoke into slipstream at high wind speeds, 19: 6134
contamination from, at NRTS waste processing facility, 20: 45219
contamination of ground-level air by, 18: 33801 (HW-80204)
deflector to prevent suction of smoke into chimney slipstreams at high wind speeds, 19: 2483
deposition and washout calculations for, 17: 39268 (ORO-599)
design and performance of meteorologically operated facility at Enrico Fermi Atomic Power Plant, 18: 11501
diffusion in, wind tunnel scale model experiments on, 19: 44764 (BNL-914, pp 14-17)
diffusion of airborne effluents near buildings, 19: 661 (AECL-2043)
diffusion of atmospheric effluents, equations for predicting, 20: 23334 (AAEC-TM-307)
diffusion of atmospheric effluents at Mol, Belgium, 20: 23346 (BLG-365(Vol.1))
diffusion of gaseous waste from stacks in Tokai-mura, Japan, 18: 16226 (NP-13687)
diffusion studies using silver iodide, 19: 14117
dilution of long- and short-term emissions in Eurochemic, estimates of minimum, 20: 18162 (NP-15754)
dispersion of wind-borne particles from, methods for estimation of, 18: 28081 (AHSB(RP)-R-42)
effectiveness of, in control of air pollution by industry, 17: 36004 (BNL-784)
effects on radioactivity of atmosphere in Hanford area, 19: 38874 (BNWL-SA-53)
effluent diffusion in, in vicinity of Mol, Belgium, 20: 27187 (BLG-365(Vol.2))
environs monitoring at Reactor Centrum Nederland Research Establishment, Petten, 18: 37439 (CONF-337-7)
equipment and monitoring, 16: 28636 (ORNL-TM-282)
facilities at Marcoule, chimney baffle model studies, 16: 4367 (CEA-2004)
filters for iodine separation in, 19: 29805(P)
from radiochemical building, wind tunnel model tests on flow, 18: 22545 (AEEW-R-227)
from reactor buildings, 19: 6880
gas composition estimation, 17: 4329 (HW-71251)
gas diffusion in atmosphere, laws of turbulent, 19: 4405(T) (ANL-Trans-126)
gas effluent monitoring system for, 18: 6988
gas-handling system for, design of, 20: 11050
ground radioactivity from, calculation of maximum concentration of, 18: 37449(T) (ANL-Trans-76)
hazards of, sampling evaluation of, 18: 44280 (LA-DC-6106)
inhalation dose distributions from, 17: 41082
iodide scavenging by rain and snow from Hanford stack gases, measurements, 20: 41188(R) (BNWL-235-1)
iodine-131 hazards from, 20: 46001
iodine-131 levels from, at BNL, 20: 43608
iodine-131 monitoring of, for efficiency of activated charcoal, 20: 4179 (LA-3363)
iodine-131 release rates in reactor, 19: 8644
measurement of wastes vented by Russian VVR-S reactor, 1959 to 63, 18: 23111
monitor design for detection and measurement of argon-41, 16: 11969(R) (JAERI-5003(p.191-5))
monitor for activity buildup on filters in, 19: 760 (DP-908)
monitoring, 20: 518
monitoring at Brookhaven Hot Laboratory complex, 20: 45948 (BNL-10527)
monitoring at CRNL site, 20: 33503 (AECL-2575)
monitoring at ERR site, 20: 1452 (ACNP-63628)
monitoring at ORNL, equipment and procedures for, 16: 29226 (TID-7627 (p.168-86))
monitoring at SM-1, sampling program for, 19: 28573 (AP-Note-439)
monitoring, by measurement of argon-41 in effluent gas, 17: 25129
monitoring for beta activity in, design of detector for, 17: 11017
monitoring for radioactivity in, 20: 14811
monitoring in beryllium production plants, 20: 43629
monitoring in, engineering drawings of equipment for, 20: 28858
monitoring of argon-41 effluent from Brookhaven Reactor, 19: 46640 (BNL-915)
monitoring of environs for effectiveness of, 17: 39283 (AHSB(RP)R-26)
monitoring of, for iodine-131, cesium-137, and uranium fission products, 18: 3388(R) (HW-77609(Sect.4))
monitoring of, use of photographic film detectors for, 17: 36163
monitoring system for, large-volume continuous, 18: 3058
of gases from glass fixation of fission products, 17: 10237
of iodine-131, design of filter, 17: 3204 (CEA-2164)
of iodine-131, monitoring, 17: 32284 (DPSPU-63-30-26B)
of iodine-131, contamination of milk after accidental release, 18: 43873
of iodine-131, effects of amount and meteorological conditions on metabolism by man, 19: 624 (IDO-12035)
of iodine-131, environmental contamination by acute release from, 19: 22014 (HW-SA-3338)
of iodine-131, survey at selected AEC sites, 18: 37443 (ORNL-NSIC-3)
of iodine-131, vegetation contamination by, 18: 41645(R) (HW-80500 (p.177-80))
of radioactive effluent gases at Hanford Works, 17: 4367 (HW-SA-2629)
of radioactive effluent gases, equipment for, 19: 15820
of radioactive gases, equipment development for, 17: 36037(R) (TID-19365)
of radioactive gases, monitoring for iodine-131, 18: 37389
of radioactive gases, determination of chimney height for, 18: 39555
permissible discharge rates for reactor operation, 16: 11961(R) (JAERI-5003(p.134-46))
plume rise behavior in scale-model tests, 19: 20656(R) (ANL-6938(p.257-73))
plume rise formulas for, 19: 20653(R) (ANL-6938(p.209-41))
plume rise from stack, graphs for estimating, 18: 16235(T) (AEC-tr-6365)
plume rise in, effects of engineering and meteorological factors on, 19: 11818
processing methods in, fog spray and foam, 20: 1550 (RL-SA-50)
radiation monitoring at Bettis Lab., 1966, 20: 43586 (PNRO-DEV-136)
radioactive contamination of atmosphere from fossil-fuel plants, 20: 152(R) (NYO-3086-1 Pt.VIII)
radioactive effluent gases from Los Alamos Water Boiler, 18: 4887

(LAMS-2937)
radioactive particle removal, 16: 19014 (ORNL-310)
radioactivity from, calculation of maximum ground level concentration, 17: 42414 (GAT-R-327)
radioactivity monitoring in, sensitivity of equipment for, 18: 14125 (TID-7677(p.317-30))
radioactivity released in, at KEMA Suspension Test Reactor, 18: 4856
radiochemical analysis of, method for, 20: 8980(R) (BNWL-36, pp 3.1-122)
radioiodine monitoring in Purex Process, efficiency of, 17: 35239 (DPSPU-63-30-4B)
release of tritiated water vapor from, 17: 34140
removal of radioactive gases and aerosols, 16: 18709(T) (JPRS-12637)
removal of radioiodine, 16: 11342(R) (EURAEC-83)
removal of radioiodine, 16: 17332(R) (EURAEC-25)
removal of radioiodine, 16: 26636(R) (EURAEC-84)
research program on, USAEC, 18: 39529 (CONF-337-5)
sampling uranium in vapor, efficiency of traverse-type stack probe for, 16: 4328 (Y-1372)
scrub tower design for removal of halogen-acid off-gases, 17: 5648
standards for release of cesium-137 and strontium-90 by, derivation of, 20: 45504
system development for, 20: 47085
washout coefficients for iodine-131 vapor, rain and snow, 20: 37033
wind effects on, 19: 18555

STAINING

density of uranyl formate, negative, for macromolecular viruses, 20: 22533
methods for biological electron microscopy, 20: 5250(R) (UR-668, pp 110-16)
of cell nucleoli, 16: 17363
of cells from cancer patients with acridine orange, effects of radiotherapy on, 19: 38488
of chick embryo sections, procedure for avoiding background graining in, 17: 13913
of nucleoproteins, chromatin affinity for lead hydroxide and uranyl acetate in, 17: 21436
radiation effects on rat skin cell, x, 18: 41135
radiation effects on response of mycobacteria to, 20: 16195
removal from stripping-film radioautographs, procedure for, 17: 26988

STAINLESS STEEL

abrasive for, preparation of alumina–zirconia, 19: 32690(P)
adherence of calcium titanate coatings to AISI-310, 19: 18465(R) (PWA-2518)
adhesives for, development, 16: 2192 (NP-10986)
aging characteristics of, 20: 36477 (KR-89, pp 197-237)
analysis and fabrication of, 17: 16594(T,R) (EURAEC-29)
analysis for arsenic and manganese, activation, 20: 16338 (RT/CHI-(65)36)
analysis for boron using curcumin, 17: 25118 (PG-Report-251)
analysis for boron, 18: 8271 (KAPL-M-SLJ-10)
analysis for boron, emission spectrographic, 19: 7274(R) (IDO-14636)
analysis for boron by neutron cross section measurements, 20: 29117
analysis for carbon, gasometric, 18: 11973 (PG-Report-540)
analysis for carbon, nonaqueous titrimetric, 20: 8837 (UCRL-12201)
analysis for carbon by combustion method, 20: 26740 (AERE-R-5192)
analysis for carbon, titrimetric, 20: 43067(R) (IDO-14679, pp 6-46)
analysis for cerium, photometric, 20: 16380
analysis for chromium, x-ray fluorescence, 16: 31550(T) (CEA-tr-X-436)
analysis for chromium, iron, and nickel, electron microprobe, 19: 38536 (ACF-6)
analysis for chromium and molybdenum, use of beta source in x-ray spectral methods for, 20: 22961
analysis for cobalt, radiochemical, 16: 14669
analysis for cobalt and silicon, x-ray spectrographic, 17: 21611 (EUR-203.f)
analysis for cobalt, activation, 19: 2222
analysis for elements, spark-source mass spectrographic, 19: 34114 (WAPD-T-1662)
analysis for hafnium or zirconium using catechol violet, colorimetric, 19: 19780
analysis for impurities by spark source mass spectrography, 19: 19830
analysis for manganese, radiochemical, 19: 7274(R) (IDO-14636)
analysis for martensite, method for, 19: 40947(R) (EURAEC-1403)
analysis for niobium and tantalum simultaneously, activation, 18: 1519
analysis for nitrogen, method for, 19: 38537 (ACF-7)
analysis for oxygen, fast-neutron activation, 16: 26914
analysis for oxygen, activation, 18: 19886
analysis for oxygen by activation, isotope dilution, and vacuum fusion methods, 19: 43947
analysis for oxygen, activation, 20: 16331 (GA-6568)
analysis for rare earths by spectrochemical methods, 17: 497(R) (KAPL-2000-19(p.I.1-I.28))
analysis for silicon, activation, 19: 24611(R) (MLM-1227)
analysis for strontium, method for radiochemical, 20: 43069(R) (IDO-14679, pp 51-9)
analysis for tantalum, spectrophotometric, 16: 16313
analysis for uranium, 16: 5263 (APEX-169)
analysis for uranium, 16: 5264 (APEX-170)
analysis for uranium dioxide content in compacts of, spectrometric, 18: 6777
analysis of activated corrosion products for radiomanganese, 16: 31559
analysis of corrosion products, outline of methods, 17: 14173
analysis of coupons of, for fission products, 20: 43072(R) (IDO-14679, pp 193-229)
analysis of, for carbon, nitrogen, and oxygen, 17: 22114(T,R) (EURAEC-557)
analysis of, for tungsten by solvent extraction using 8-quinolinol, 17: 19952
analysis of irradiated, by group separation and gamma spectrometry, 18: 41325
analysis of microspheres, activation, 17: 27253
analysis of microspheres of, activation, 17: 26208
analysis of neutron-irradiated, for radionuclides, 17: 15858(R) (ORNL-3397(p.17-112))
analysis of oxidized, for cobalt and manganese, neutron activation, 16: 12668 (WAPD-BT-24(p.89-98))
analysis of sodium-carburized, for carbon, 19: 12865(R) (NAA-SR-10501)
analysis of solutions of, for boron, spectrochemical, 19: 32059(R) (IDO-14655)
analysis of, corrections for interelement effects in x-ray spectrochemical, 20: 22957
annealing of irradiated type 347 pressure tube, simulated in-reactor, 18: 37759 (BMI-1683)
arc initiation by toroidal discharge on, effects of contamination on, 18: 7802
bibliography on, DMIC selected accessions, Sept. 1962, 17: 419 (NP-12170)
bonding by gas pressure, 17: 15532(R) (BMI-1607(Del.))
bonding, development of brazing alloy for, 16: 2181(R) (NP-10933)
bonding, development of heat-resistant adhesives, 16: 10538 (NP-11400)
bonding of coating of, to uranium dioxide platelets, gas-pressure techniques for, 17: 508 (BMI-1597)
bonding of, pressure, 17: 29294 (BMI-1637)
bonding of, stability of adhesives for, 17: 11175
bonding of, to Zircaloy, effects of surface preparation on, 16: 28642(R) (BMI-1581(Del.))
bonding of, to Zircaloy-2 by various techniques, 16: 32092 (BMI-1594)
bonding of type 304, to Zircaloy-2, diffusion, 20: 13222
bonding of type 316, to chromium–molybdenum steel and niobium, 17: 36200(R) (NP-13033)
bonding of types 316, 321, and 347, to refractory metals and alloys, process development for explosive, 20: 21295(R) (WANL-PR-(EE)-002)
bonding of 316, to graphite, brazing techniques for, 20: 2294
bonding of, controlling factors in diffusion, 19: 24964
bonding to aluminum, 18: 39411(R) (APCI-541103)
bonding to aluminum and Zircaloy, explosive, 19: 26780 (AECL-2209)
bonding to aluminum, extrusion and hot-press, 19: 26781 (AECL-2241)
bonding to aluminum, method for diffusionless, 20: 46179(P)
bonding to beryllium, 19: 11711
bonding to carbon steel pressure vessels, testing of, 20: 16617
bonding to copper and niobium alloys, 17: 1897(R) (NP-12144)
bonding to iron–nickel alloys, 16: 30744 (CVNA-44)
bonding to lead shielding, effects on mechanical properties, 17: 34383
bonding to metals by extrusion, 18: 27937
bonding to refractory metals and alloys of types 321 and 347, explosive, 20: 11243(R) (WANL-PR(EE)-001)
bonding to Scotchlite SPR704 reflective material, 19: 40917
bonding to UO_2–stainless steel cermet, 19: 4642(P)
bonding to uranium carbide by sodium, eddy-current inspection of, 19: 20531
bonding to uranium carbide and iron–uranium carbide cermets, 20: 9468
bonding to Zircaloy-2 by indentation, 16: 2149 (OEL-MET-3306)
bonding to Zircaloy by tandem extrusion, 16: 13548 (NMI-7216)
bonding to zircaloy, 16: 24149(R) (BMI-X-204)
bonding to Zircaloy-2 by explosive joining, friction bonding, and modified roll forming, 16: 15154(R) (BMI-X-193)
bonding to Zircaloy-2, 19: 10541(R) (GEAP-4703)
bonding to zirconium by hot coextrusion in iron jacket, 18: 41997(P)
bonding with beryllium and beryllium-transport alloys, diffusion, 16: 6704
boron deposition on rods of, electrolytic, (E), 19: 16044
boron distribution in, activation determination of, 17: 21627
boron-10 content in modified 304, vacuum control, 16: 2125
boron-10 content in modified 304, vacuum control, 16: 2126
boronization of, procedure for, 20: 11260
braze bonding to stainless steel–uranium dioxide cermets, 19: 4635

brazed joints, nondestructive testing of, 19: 13935 (ANL-6924) (ORNL-2834)
brazing alloys for, corrosion in pressurized water at 565°F, 16: 16675
brazing and welding properties, review, 16: 10424 (ASD-TR-61-322 (p.661-76))
brazing and welding of type 316, 17: 7606(R) (ORNL-1515)
brazing, effects of argon-hydrogen atmosphere, 16: 13569 (CNLM-1729)
brazing of, evaluation of alloys for, 17: 21231 (TID-7658(p.48-56))
brazing of type 347, to copper, 18: 18332 (NAA-SR-Memo-9435)
brazing of type 347, in joining flanges to sintered filters for use at 1300°F, 20: 786 (ORNL-TM-1252)
brazing of type 406, 17: 41333(R) (ANL-6677)
brazing stainless steel-clad copper fins to tubes of, technique for, 20: 4307(R) (ORNL-3870, pp 238-42)
brazing to beryllium, vacuum, 16: 22572
brazing to beryllium, vacuum furnace, 16: 29357 (UCRL-6391)
brazing to copper for boiler fabrication, 16: 2150 (ORNL-TM-40)
brazing to copper, microprobe study of joint, 18: 2199 (NAA-SR-Memo-9088)
brazing to Zircaloy-2, 17: 4889(T,R) (EURAEC-322)
brazing to Zircaloy-2, 18: 14361(R) (EURAEC-254)
brazing type 316, to beryllium using silver, 19: 44606 (PWAC-483)
brazing Zircaloy-2 to 304, eutectic, 16: 9179
bremsstrahlung production by electrons at 5 to 20 kev, 16: 329 (CLM-R-11)
brittle fracture at cryogenic temperatures, 17: 22181
buckling of tubes of, effects of lateral external pressure on creep and instantaneous, 17: 11192 (ORNL-3299)
burnout in rod bundles of, effects of spacing on, 20: 33453 (DP-1013)
burst and collapse pressures of tubes of AISI 304 L, 19: 46986 (KR-96)
bursting of cladding tubes of, in loss-of-coolant accident in boiling and pressurized water reactors, 17: 32620
calcination of compacts of, in sulfur at 150°C, 17: 19697 (DP-713)
calcination of nitrated, phase transformations in, 17: 15524 (IDO-14601)
carbide precipitation in type 316, by sodium at 1100°F, 19: 7676(R) (BAW-1280-20)
carbon behavior in, effects of uranium on, 18: 18402
carbon content of austenitic, effects of high temperature sodium on, 19: 26768(R) (MSAR-65-62)
carbon content of, effects of liquid metal loop conditions on, 20: 41419(R) (GMAD-3643-5)
carbon monoxide desorption from type 304, 19: 32413(R) (WERL-2823-17)
carbon reactions in, effects of uranium on, 19: 30801
carburization as cladding for uranium carbide fuel, method of preventing, 20: 7547(P)
carburization by graphite at low pressure, 17: 14828 (NAA-SR-Memo-7832)
carburization by uranium carbide, 17: 14740 (TID-11295(2nd Ed.))
carburization in carbon dioxide at high temperatures, 18: 41933 (TID-11295(3rd Ed.))
carburization in Hallam Power reactor core, control program for, 19: 3696
carburization in high-carbon sodium, effects of stress on, 20: 33817 (MSAR-66-119)
carburization in sodium, 16: 4451 (NAA-SR-6386)
carburization in sodium at 1000 to 1600°F, 16: 16682 (TID-7626 (Pt.I)(p.92-100))
carburization of, by uranium carbide, 17: 23902 (NAA-SR-6246)
carburization of type 304, by flowing carbon dioxide, 17: 14740 (TID-11295(2nd Ed.))
carburization of type 304, by uranium carbide, 18: 10537 (NAA-SR-Memo-9015)
carburization of types 304 and 316, in sodium saturated with carbon at 1200°F, 18: 24084(R) (MSAR-64-51)
carburization of types 304 and 316, 18: 32144(R) (MSAR-64-75)
carburization of type 304 and 316, by carbon-saturated sodium at 1200°F, 19: 901(R) (MSAR-64-102)
carburization of type 304 by carbon–sodium, effects on mechanical properties, 19: 44624 (NAA-SR-Memo-4387)
carburization of types 304 and 316, by carbon-rich sodium at 1200°F, 20: 9413 (CONF-650620, pp 1-17)
carburization of types 304 and 316, by high-carbon sodium at 1200°F, 20: 11235 (MSAE-65-194)
carburization of, theory for strain-enhanced, 19: 32682 (MSAR-65-89)
carburization reactions with carbon monoxide-carbon dioxide atmosphere, 16: 28372(R) (ORNL-3302(p.46-56))
carburization surveillance of HNPF core materials, 18: 21637 (NAA-SR-Memo-8214)
casting and powder-metallurgy forming of precipitation-hardenable, 20: 35865 (RSIC-491)
cavitation by liquid sodium, 18: 34075 (NASA-CR-54071)
cavitation damage in mercury and water, 18: 3955 (NP-13319)
cavitation damage in mercury flow of type 302, tracer study of, 18: 8483 (NP-13517)
cavitation damage of stressed, in mercury, 19: 2725 (NP-14437)
cavitation damage of 304-L, 316, and 410, correlation with mechanical properties, 19: 2714 (AD-606050)
cavitation damage in mercury and water, 19: 9623 (NP-14632)
cavitation damage of types 304 and 316, in bismuth–lead alloy at 500°F, 19: 24938 (NP-15024)
cavitation damage of types 304 and 316, in bismuth–lead alloy at 500 and 1500°F, 20: 771 (NP-15558)
cavitation damage to 316, in liquid sodium, 20: 2243
cavitation damage in liquid, at high temperatures, 20: 33835
cavitation damage of type 316, in liquid sodium to 1500°F, 20: 46154 (NASA-CR-72035)
cavitation damage in type 302, 17: 4971
cavitation damage, tracer study, 19: 585 (NP-14441)
cavitation of types 304 and 316 in bismuth–lead alloy at 500 and 1500°F, ultrasonic-induced, 19: 39116 (NP-15263)
cesium deposition on, 20: 22411(R) (GA-6113)
chemical reactions with liquid potassium at high temperatures, carbides and phases from, 20: 41419(R) (GMAD-3643-5)
chlorination of, corrosion and reaction rates in processing by, 18: 39386
cladding thickness on reactor fuel elements, use of x ray for determination of, 18: 6939
cladding tubes of, with beryllium, 19: 30691 (N64-28460)
coating by neptunium and plutonium by electrolytic deposition, 20: 21287 (AE-217)
coating by zirconium from vapor of iodides, 17: 32507
coating heavy-gage low-alloy steel with, process for weld, 19: 36998(R) (EURAEC-1296)
coating of, by plasma-arc spraying, 17: 32545
coating of plates of, with thorium, uranium, neptunium, and plutonium by electrodeposition, 19: 32059(R) (IDO-14655)
coating of type 316, with Solaramic 5210-2c glass, 18: 24085(R) (NASA-CR-54053)
coating of, for reactor fuel elements, high-temperature properties of, 17: 7571 (TID-17402)
coating on, thermal conductivity and emissivity of ceramic, 19: 23076
coating with actinides, target preparation by, 20: 43396
coating with aluminum oxide by flame spraying, 16: 16641 (ARL-59)
coating with americium or uranium by electrolysis, 20: 27009
coating with boron and cadmium, 16: 7519 (CRCE-1039)
coating with cesium and rubidium by deposition from carbon dioxide, 17: 32061
coating with neptunium, method for quantitative electrolytic, 20: 45675
coating with neptunium-239 and plutonium-239, method for, 19: 36361
coating with rare earths, electrolytic, 20: 5867
coating with thorium by electrolysis, 16: 20963
coating with tungsten and zirconium oxide by flame spraying, 16: 4455
coating with uranium dioxide by spraying, 16: 3814(R) (ATL-A-121)
coating with zirconium, effects of iodine circulation rate, pressure, and temperature on, 17: 39555
cobalt-57 incorporation in, for Mössbauer studies, 18: 22561
collapse characteristics of tubes of types 304 and 347, studies of instantaneous- and creep-, 18: 16159 (ORNL-3555)
collapse pressures of tubular, length-diameter relations of, 18: 16422(R) (CEND-204)
combustion behavior, 16: 10508 (DC-55-5-17)
compatibility and encapsulation with neodymium, promethium, and samarium oxides, 20: 11267 (BNWL-SA-488)
compatibility of AISI 304, with lead telluride at 600 to 700°C, 17: 23927 (WCAP-1703)
compatibility of AISI 304 and 430, with bismuth germanium telluride and lead telluride at 500 to 700°C, 17: 23971 (WCAP-1868)
compatibility of AISI 302, with calcium at 650°C, 17: 37003(R) (HW-78118)
compatibility of molten type 304, with uranium dioxide at 1600°C, 18: 2161(R) (HW-76302)
compatibility of type 304 with uranium alloys, 17: 41333(R) (ANL-6677)
compatibility of type 304, with uranium nitrides at high temperatures, 18: 542(R) (BMI-X-10061)
compatibility of type 316, with plutonium carbide–uranium carbide, 18: 8729 (UNC-5074)
compatibility of types 304 and 430, with boron carbide at 750 to 1300°F, 18: 14371 (NAA-SR-8702)
compatibility of type 304, with fissium–plutonium–uranium alloys at 600 and 650°C, 18: 15663(R) (ANL-6808)
compatibility of type 316, with plutonium carbide–uranium carbide systems at 1500°F, 18: 16426(R) (UNC-5068)
compatibility of type 321, with thorium and uranium borides and carbides, 18: 20450(R) (BMI-1661(Del.))
compatibility of type 304, with fissium–uranium alloys, fissium–

plutonium–uranium alloys, and uranium to 1200°C, 18: 26893(R) (ANL-6868(p.11-108))
compatibility of type 304, with plutonium nitride–uranium nitride pellets at 1000°C, 18: 30113(R) (HW-76304(p.2.1-43))
compatibility of type 304, with uranium nitrides at 1000 to 1350°C, 18: 32037(R) (BMI-X-10092)
compatibility of type 316 with plutonium carbide–uranium carbide, 19: 24923(R) (UNC-5081)
compatibility of type 316, in sodium-heated boiler containing Croloy 2¼, 19: 44133(R) (BAW-1280-21)
compatibility of type 304, with plutonium-uranium carbides, 20: 6600(R) (ANL-7105, pp 1-35)
compatibility of type 316, with niobium–1 zirconium in 650°C sodium, 20: 7518 (PWAC-501)
compatibility of type-347, with beryllium at 500 to 650°C in vacuum, 20: 8925
compatibility of type 304, with plutonium and uranium carbides, 20: 30790(R) (ANL-7204, pp 1-31)
compatibility of type 316L, with plutonium carbide–uranium carbide up to 900°C, 20: 31675
compatibility of type 304, with plutonium–uranium–zirconium alloy to 800°C, 20: 31666
compatibility of 304, with plutonium–uranium–zirconium alloys, 20: 2229
compatibility of 304, with plutonium–thorium–uranium alloys, 20: 2230
compatibility of 316, with cadmium sulfate, 20: 38447 (WCAP-2867)
compatibility with uranium carbide in sodium (liquid), 16: 823
compatibility with boron carbide, 17: 18759 (NAA-SR-Memo-8055)
compatibility with urania and uranium, 17: 29255 (ZFK-WF-13)
compatibility with graphite, 17: 33324(R) (ORNL-3445(p.218-50))
compatibility with zirconium carbide, 17: 41364(T,R) (EURAEC-562)
compatibility with plutonium dioxide–uranium dioxide pellets at 1000°C, 17: 41358(R) (NUMEC-P-105)
compatibility with uranium carbide and uranium carbide–uranium sulfide at 1150°C, 17: 40422(R) (ANL-6784)
compatibility with uranium nitrides at 1200 to 1350°C, 18: 32035(R) (BMI-X-10073)
compatibility with zirconium carbide at 600°C, 18: 32064(T,R) (EURAEC-1064)
compatibility with beryllium–thorium–uranium alloy at 1500°F, 18: 34032(R) (BMI-1668(Del.))
compatibility with beryllium–thorium–uranium alloys and carbon–thorium–uranium systems, 18: 34034(R) (BMI-1672(Del.))
compatibility with lead telluride at 600 to 700°C, 17: 23927 (WCAP-1703)
compatibility with uranium nitride at 1300°C, 18: 34035(R) (BMI-X-10053)
compatibility with beryllium–thorium–uranium alloy, 18: 34033(R) (BMI-1669(Del.))
compatibility with uranium carbide fuels in sodium, 18: 35957 (NAA-SR-7502)
compatibility with uranium and uranium carbides, 18: 40827 (EUR-1830.e(Pt.II))
compatibility with liquid lead, 18: 40827 (EUR-1830.e(Pt.II))
compatibility with arc-melted europium oxide and molybdate at 1150°C, 18: 44053(R) (ORNL-3670(p.166-72))
compatibility with fuel materials, 18: 44053(R) (ORNL-3670(p.166-72))
compatibility with uranium nitride, 19: 2717(R) (BMI-X-10100)
compatibility with zirconium carbide at 600°C, 19: 7853(R) (EURAEC-1173)
compatibility with boron carbide, 19: 11681
compatibility with zirconium carbides at high temperatures, 19: 13874(R) (EURAEC-1179)
compatibility with hypostoichiometric plutonium mononitride at 820°C of type 304, 20: 7493(R) (BMI-1748(Del.))
compatibility with hypostoichiometric uranium carbides, 20: 8394(R) (NAA-SR-11450, Sect. 2)
compatibility with uranium carbide and uranium carbide–10 uranium sulfide at 1150°C of type 304, 20: 9556
compatibility with plutonium–uranium carbides at 590 and 820°C of type 316, 20: 9437
compatibility with indium at 1300°F of types 316 and 410, 20: 11215(R) (NASA-CR-54718)
compatibility with urania, 20: 11224
compatibility with boron carbide of types 304 and 430, 20: 11226
compatibility with water in reactor environment, 20: 14996
compatibility with plutonium carbide–uranium carbide and uranium carbide, 20: 26740 (AERE-R-5192)
compatibility with uranium monocarbides, additive effects on, 20: 33784
compatibility with mixed carbide fast breeder reactor fuels, 20: 38466 (ANL-7120, pp 301-13)
compatibility with mixed-carbide fast reactor fuels, 20: 38467 (ANL-7120, pp 314-27)
composition of commercial type 304, 19: 39152(R) (BMI-X-10132)
composition of $M_{23}C_6$ type carbides in, 16: 19378(T) (AEC-tr-5059)
contamination and decontamination of, in water-cooled reactors, 18: 19267 (DP-829)
contamination and decontamination in uranium–zirconium processing equipment, 18: 23705 (ORNL-TM-837)
contamination by radionuclides in water-cooled reactors, 16: 21717 (DP-682)
cooling of tubular, data on required air mass velocity, 16: 8348 (DC-56-12-29)
corrosion, 16: 11774(R) (NLCO-685)
corrosion, 16: 27589 (BM-RI-5990)
corrosion, 17: 6572 (OTS-61-31480)
corrosion, 18: 22451
corrosion and mass transfer of type 316, by sodium at 1000 to 1300°F, 17: 29280 (GEAP-3726)
corrosion and mass transfer in potassium-sodium alloy loop, 19: 22897 (TIM-655)
corrosion and mass transfer of type 316, in flowing sodium, 20: 9414 (CONF-650620, pp 18-35)
corrosion and mass transfer of type 316, in flowing sodium, 20: 39345 (GEAP-4831)
corrosion and mechanical properties of types 304, 347, and 422 as gas turbine material, 16: 32114 (IDO-28591)
corrosion and mechanical properties of, effects of carbon, sulfur, and uranium on, 19: 30801
corrosion and mechanical properties of, effects of nitrogen and uranium on, 19: 30804
corrosion and metallurgical changes by steam at 1200 to 1500°F, 16: 24126
corrosion and radiation effects on cladding samples of, 17: 19631(R) (ORNL-3416)
corrosion at high temperature, admixture effects on, 16: 13536
corrosion at 25 and 250°C in oxygen and water, microgravimetric measurement of, 17: 16585(R) (EURAEC-569)
corrosion by acetic, citric, formic, and lactic acids, 17: 25734
corrosion by acid, 16: 12057
corrosion by acidic nitrate waste solutions, 17: 39490 (ORNL-3474)
corrosion by acidic solutions, effects of molybdenum and uranium on, 20: 4325 (TB-58)
corrosion by acids and chloride salts in chemical plants, 16: 20983
corrosion by air and steam at 1100 to 1500°F, scale formation, 16: 24125
corrosion by air at 1750°F after 10,000 hours, 17: 41379
corrosion by air, helium, and sodium at high temperatures, 18: 30131(R) (MSAR-64-65)
corrosion by air, helium, and liquid sodium, 18: 35956(R) (MSAR-64-93)
corrosion by air, carbon oxides, hydrogen sulfide, and sulfur dioxide to 1200°C, 18: 39844
corrosion by anisole–boron trifluoride, evaluation of, 20: 19135(R) (K-C-718)
corrosion by aqueous thoria-urania slurries, in-pile tests, 16: 10621 (ORNL-3222)
corrosion by aqueous hydrogen sulfide, 17: 8717
corrosion by aqueous solutions, review, 18: 32081 (A/CONF.28/P/243)
corrosion by aqueous solutions, galvanic, 18: 41959 (WCAP-1844)
corrosion by aqueous chlorides, 19: 29651(R) (WCAP-3269-3)
corrosion by aqueous chemical shim solutions at 600°F, 19: 40198(R) (WCAP-3721)
corrosion by aqueous solutions of sodium chloride at temperatures up to 100°C, 20: 35852(T) (AEC-tr-6738)
corrosion by aqueous iron chloride, effects of carbon, manganese, and silicon traces on, 20: 41418(R) (GEAP-5150)
corrosion by argon–nitrogen at 900°C, 19: 32279(R) (ANL-7020(p.3-99))
corrosion by bicarbonate solutions, effects of chloride and oxidants, 16: 22558
corrosion by bicarbonate solutions, effects of chloride and electrode voltage on, 18: 14405 (EURAEC-142)
corrosion by bismuth–tin alloy, effects of flow rate and temperature on, 19: 44616(R) (ANL-7000, pp 122-37)
corrosion by bismuth-sodium alloy, 20: 2275
corrosion by bismuth and tin, 20: 2275
corrosion by bismuth at 850°C, 20: 6024(R) (ANL-6925(p.235-47))
corrosion by bismuth and tin at 700 to 1000°C, 20: 46963(R) (ANL-7132)
corrosion by boiling nitric acid–stainless steel solution, 16: 1854(R) (IDO-14553)
corrosion by boiling nitric acid and sulfuric acid solutions, 17: 39494
corrosion by boiling magnesium chloride, 18: 4761(R) (GEAP-4383)
corrosion by boiling magnesium chloride, 18: 4796(R) (GEAP-4153)
corrosion by boiling acid–fluoride systems, 18: 39841 (HW-80658)
corrosion by boiling simulated Darex waste, 18: 43091(R) (ORNL-TM-830)
corrosion by boiling dichromate–nitric acid, effects of steel composition on, 20: 767(R) (GEAP-4915)
corrosion by boiling potassium, effects on mechanical properties, 20: 5181(R) (ORNL-3029)
corrosion by boiling nitrates in radioactive waste, 20: 5856

corrosion by boiling water reactor coolants, effects of ammonia on suppression of, 20: 26920 (AECL-2562)
corrosion by borated water at 600°F, 20: 5846
corrosion by boric acid, (E), 19: 5490(R) (WCAP-3269-2)
corrosion by boron-containing solutions, 20: 16976
corrosion by cadmium–magnesium–uranium–zinc/chloride flux at 600 and 650°C, 19: 32279(R) (ANL-7020(p.3-99))
corrosion by cadmium–magnesium–uranium–zinc alloys with chloride flux at 600 to 650°C, 20: 5594(R) (ANL-6925, pp 21-106)
corrosion by calcined Redox wastes, 18: 45148(R) (HW-83320)
corrosion by carbon dioxide and water, 16: 32083(T) (CEA-tr-A-1148)
corrosion by carbon dioxide at 600 to 700°C, 17: 25740
corrosion by carbon dioxide, 17: 40341(R) (GNEC-141(Del.))
corrosion by carbon dioxide at 650 to 800°C, 18: 26096
corrosion by carbon dioxide at 500 to 700°C and 60 atm, 18: 37630 (A/CONF.28/P/63)
corrosion by carbon dioxide at 1100 to 1800°F, 19: 20487
corrosion by carbon dioxide, helium, nitrogen, and steam, 20: 9408 (BNWL-154)
corrosion by ceramic uranium–sodium pastes, 19: 40113(R) (ANL-7071)
corrosion by cesium at 1600 to 2500°F, 16: 16684 (TID-7626(Pt.I) (p.109-10))
corrosion by cesium, 17: 21835
corrosion by cesium at 1600°F, role of oxygen in, 18: 16447
corrosion by cesium at 750°C, 18: 20873
corrosion by cesium at 400°C, 20: 4337
corrosion by cesium at 400°C of types 17-4PH, 17-7PH, and AM 350, 20: 11227
corrosion by chemical cleaning, evaluation of, 19: 36984
corrosion by chemical shim solutions at 600°C, 19: 45601(R) (WCAP-3750)
corrosion by chlorides in heat exchangers, 17: 3422 (DP-694)
corrosion by chlorides at high temperatures, 18: 4795(R) (GEAP-3924)
corrosion by chlorides, 19: 3711
corrosion by chlorides, stress, 19: 45601(R) (WCAP-3750)
corrosion by chlorine trifluoride–urania reaction-gas mixtures, 20: 12925(R) (EURAEC-1446)
corrosion by chromium ions in hot nitric acid solution, effects of carbon black and sulfur on, 19: 18418(P)
corrosion by coal gasification products at high temperatures, 19: 42127(R) (TID-22009)
corrosion by copper sulfate, nitric acid, and sulfuric acid, potentiokinetic studies on, 17: 25729(T) (EURAEC-678)
corrosion by copper chloride at high temperatures, 18: 4796(R) (GEAP-4153)
corrosion by copper–magnesium chloride system at 600 to 800°C, 20: 31314(R) (ANL-7175, pp 1-41)
corrosion by Darex waste at 900°C, 19: 30671(R) (ORNL-3789(p.122-5))
corrosion by decontaminating solutions, 16: 20984
corrosion by decontaminating solution, 16: 24496
corrosion by decontaminating solutions, 19: 2756
corrosion by flowing sodium at 1000 to 1200°F of type 316, equation for, 20: 11227
corrosion by flowing water at pH 5 and 100°C, dynamic, 20: 43833 (ORNL-TM-1030)
corrosion by fluorine–oxygen atmosphere in fluidized alumina bed, 18: 3671(R) (BNL-799(p.26-54))
corrosion by fluoride volatility process environment, 19: 32280(R) (ANL-7020(p.100-49))
corrosion by fluorides and nitric acid, effects of welds on, 20: 27036(R) (IDO-14661, pp 1-44)
corrosion by FTW-65 Purex waste, 19: 31617(R) (ORNL-TM-1081)
corrosion by fuel storage-basin water, electrochemical, 20: 28853(R) (IDO-14661, pp 45-82)
corrosion by fused salts at 650°C, 19: 35604(R) (ANL-7045(p.1-23))
corrosion by gas–oil, hydrogenated terphenyl, and monoisopropylbiphenyl at 330 to 400°C, 20: 25492(T) (AECL-2330, pp 196-217)
corrosion by gaseous and liquid cesium, 17: 30944
corrosion by gases, liquid metals, and water, (E), 19: 4670
corrosion by heavy water in HWCTR, 19: 11668(R) (DP-945)
corrosion by helium, 17: 3423 (GA-2998)
corrosion by high-level radioactive waste, 17: 14767 (IDO-14600)
corrosion by high-pressure water at 260 and 280°C, 19: 16022
corrosion by hydrofluoric-nitric acid mixtures, effects of aluminum nitrate on, 16: 24120 (HW-73211)
corrosion by hydrofluoric acid–nitric acid, 17: 10246(R) (ORNL-TM-403)
corrosion by hydrofluoric-nitric acid, effects of boron-10 on, 17: 32517 (RFP-307)
corrosion by hydrofluoric acid fuel-dissolver solutions, 18: 17929(R) (IDO-14616)
corrosion by hydrochloric acid in fluidized beds, 19: 15663(R) (ANL-6900(p.143-202))
corrosion by hydrofluoric acid–nitric acid solutions, effects of aluminum, iron, and thorium ions on, 20: 14982(R) (NLCO-970, pp 6.1-4)
corrosion by impure Santowax, 17: 23891 (NAA-SR-7755)
corrosion by in-pile OMRE coolant, effects on properties, 18: 35937 (NAA-SR-9796)
corrosion by inhibited molten lead, 19: 32655(R) (MND-P-3005)
corrosion by iodine vapor, 16: 6216 (GAMD-1330)
corrosion by liquid lead and mercury, 17: 31761(R) (MND-P-3001)
corrosion by liquid lead and mercury, 17: 31762(R) (MND-P-3002)
corrosion by liquid sodium, 17: 36873 (LADC-5783)
corrosion by liquid metals, review of, 18: 32082 (A/CONF.28/P/244)
corrosion by liquid sodium, mechanism of, 18: 32084 (GEAP-4313)
corrosion by liquid bismuth and lead, 19: 4630
corrosion by liquid potassium, 19: 23996(R) (ORNL-3650(p.1-110))
corrosion by liquid potassium, sodium, and potassium–sodium alloy, 19: 34643
corrosion by liquid metals, 20: 31959(R) (ANL-7175, pp 184-211)
corrosion by liquid sodium, 18: 12583(T) (AEC-tr-6328)
corrosion by liquid sodium, 20: 33822
corrosion by lithium at 1500 to 1900°F, 17: 6570 (ORNL-2674)
corrosion by lithium at 1500°F of austenitic, 19: 36980 (PWAC-355)
corrosion by lithium at 1100 to 1600°F of type 316, 19: 36980 (PWAC-355)
corrosion by lithium chloride–potassium chloride, effects of electrolytic heating and frozen wall on, 20: 27431 (HW-72572)
corrosion by magnesium chloride of austenitic and austeno-ferritic, 19: 42803(R) (EURAEC-1397)
corrosion by mercury, 17: 31763(R) (MND-P-3003)
corrosion by mercury at high temperatures, 18: 7152
corrosion by mercury and sodium amalgam at 200 to 500°C, 18: 18312(T) (CEA-tr-A-1455)
corrosion by mercury at 600 to 1000°F, 18: 27913
corrosion by mercury at 350 to 1350°F, 19: 32657(R) (MND-P-3007)
corrosion by mercury vapor at 1250°C of type 316, 20: 11214(R) (NASA-CR-54717)
corrosion by molten salt, 17: 12064(R) (NLCO-865(p.37-42))
corrosion by molten cadmium–magnesium–zinc alloy at 500, 750, and 850°C, 20: 2265
corrosion by molten cadmium–magnesium alloys at 750°C, 20: 2265
corrosion by nitric acid solutions, effects of formaldehyde, nitrogen oxides, and process solutions on, 16: 266(R) (DP-626)
corrosion by nitric acid solutions, 16: 17759 (DP-647)
corrosion by nitric vapors at 375°C, 16: 33071(T,R) (EURAEC-337)
corrosion by nitric acid, 17: 40389
corrosion by nitric acid containing chloride ion, 18: 4202
corrosion by nitric acid containing dissolved chromium, 18: 8454
corrosion by nitric acid, 18: 16152
corrosion by nitric acid–potassium dichromate solutions of austenitic, 19: 36977 (APED-4670)
corrosion by nitric acid–potassium dichromate, effects of silicon on, 19: 40947(R) (EURAEC-1403)
corrosion by nitric acid, effects of Mn, Ce, and Cr additions on, 16: 13534
corrosion by nitrogen and sodium, development of loops and techniques for studying, 18: 35955(R) (MSAR-60-34)
corrosion by oxides from Saxton steam generator, chemical analysis of, (E), 20: 10382(R) (WCAP-3269-13)
corrosion by oxygenated steam at 600°C, 18: 3038(R) (ANL-6801)
corrosion by oxygenated steam, 18: 14400 (ACNP-64001)
corrosion by potassium–sodium alloys (liquid), 16: 13538
corrosion by potassium–sodium alloys (liquid) at 1100 to 1500°F, 16: 16691 (TIM-435)
corrosion by potassium bicarbonate, radiation effects, 16: 27591(R) (EURAEC-284)
corrosion by potassium–sodium alloy and sodium, literature survey, 19: 20472 (IDO-14651)
corrosion by potassium–sodium alloy of types 316 and 347, 19: 28755(R) (ORNL-3823)
corrosion by potassium at 870°C, type 316, 19: 30674 (ORNL-3790)
corrosion by potassium–sodium alloys and sodium, review on, 20: 4318 (CNLM-5359)
corrosion by potassium–sodium at 1425°F of types 316 and 347, effects of oxygen on, 20: 5851
corrosion by potassium–sodium of types 316 and 347, 20: 9425 (ORNL-3898)
corrosion by Purex waste, 17: 10246(R) (ORNL-TM-403)
corrosion by radioactive waste solutions, 19: 12859
corrosion by reactor coolant, 16: 491(T) (CEA-tr-A-979)
corrosion by reactor coolant-shim solutions, 19: 29651(R) (WCAP-3269-3)
corrosion by rubidium at 1800°F, 16: 14834 (AGN-8034)
corrosion by simulated boiling-water reactor environment at 546°F, 16: 33439

corrosion by sodium in Sodium Reactor Experiment, 16: 1191 (NAA-SR-5363)
corrosion by sodium (liquid), 16: 15147 (TIM-573)
corrosion by sodium at 1050 to 1600°F, 16: 16692 (TIM-490)
corrosion by sodium bicarbonate solutions, 16: 17978(R) (EURAEC-175)
corrosion by sodium, 16: 28558 (TID-7623(p.135-48))
corrosion by sodium at high temperatures, 17: 1874(R) (MSAR-62-109)
corrosion by sodium, effects of oxygen on, 17: 25733
corrosion by sodium (liquid), 18: 2186
corrosion by sodium (liquid), 18: 2187
corrosion by sodium bicarbonate–sodium chloride solutions, 18: 8734(T,R) (EURAEC-735)
corrosion by sodium at 1200°F, 18: 20472 (NAA-SR-Memo-9340)
corrosion by sodium chloride in presence of moisture, 19: 12859
corrosion by sodium at high temperatures, effects on mechanical properties, 19: 22896(R) (MSAR-65-47)
corrosion by sodium at 600 to 1300°C, 19: 27735(R) (NAA-SR-10850)
corrosion by sodium of type 316, effects of carbon and oxygen on, 19: 40969(R) (MSAR-65-96)
corrosion by sodium, statistics of weight change in loop, 19: 22894 (GEAP-4183)
corrosion by sodium, effects of corrosion loop location on, 20: 5846
corrosion by sodium at 1000 to 1250°F of type 316, 20: 9418 (CONF-650620, pp 204-31)
corrosion by sodium in loops of type 316, statistical analysis of data on, 20: 43826 (GEAP-4830)
corrosion by steam at 546°F, 16: 15145 (NP-11552)
corrosion by steam–water mixtures at 245 to 287°C at flows of 266 to 553 g/cm² sec, 16: 7853 (EURAEC-151)
corrosion by steam at 1100 to 1500°F, effects on heat-transfer properties of tubes, 16: 24127
corrosion by steam at 3000 psi, 17: 13678(R) (HW-75914)
corrosion by steam at 650°C and 600 psi, 17: 15385(R) (ANL-6683)
corrosion by steam and water at 100 to 600°C, 17: 23894
corrosion by steam at 275°C, effects of manganese dioxide, potassium permanganate, and sodium hydroxide on, 17: 27730(R) (HW-77052)
corrosion by steam at 800 to 1300°C, 18: 2185
corrosion by steam and water in reactor environment, 18: 34076 (TID-8540(p.213-330))
corrosion by steam and water at high temperatures, effects of surface treatment on, 17: 34350
corrosion by steam–water spray, 17: 35093(R) (EURAEC-622)
corrosion by steam and water at high temperatures, 17: 39493(T,R) (EURAEC-757)
corrosion by steam at 1300°C, hydrogen evolution in, 17: 40422(R) (ANL-6784)
corrosion by steam at high temperatures, 18: 4796(R) (GEAP-4153)
corrosion by steam at 400°C, 18: 8734(T,R) (EURAEC-735)
corrosion by steam–water mixtures, 18: 20182 (TID-7694(p.108-49))
corrosion by steam, 18: 30143
corrosion by steam and water in reactor environment, 18: 34076 (TID-8540(p.213-330))
corrosion by steam and water, 18: 37635 (A/CONF.28/P/445)
corrosion by steam at 600 and 650°C, 18: 41933 (TID-11295(3rd Ed.))
corrosion by steam at high temperatures, 18: 45022(R) (GNEC-327)
corrosion by steam–water sprays, 19: 1875(R) (EURAEC-1011)
corrosion by steam and water at high temperatures, 19: 7865(R) (EURAEC-1237)
corrosion by steam at high temperatures, 19: 38178(R) (GEAP-4790)
corrosion by steam of type-300 series, at 800 to 1410°F with heat transfer, 19: 39115 (GEAP-4760)
corrosion by steam of types 304 and 406, at 1050 and 1150°F, isothermal, 19: 39115 (GEAP-4760)
corrosion by steam at 1050°F of type 304, effects of surface preparation on, 19: 39115 (GEAP-4760)
corrosion by steam at 750°C of types 304, 316, 321, 347, and 406, 19: 44616(R) (ANL-7000, pp 122-37)
corrosion by steam under nuclear superheat reactor conditions, 19: 45572(R) (GEAP-4755)
corrosion by steam at high temperature, 19: 45572(R) (GEAP-4755)
corrosion by steam at 400°C and water at 300°C, effects of surface treatments on, 20: 5846
corrosion by steam at 2000°F of type 304, 20: 5851
corrosion by steam of type 304, effects of heating rate on, 20: 9378(R) (GEMP-54A)
corrosion by steam at melting point of type 304, 20: 27430(R) (GEMP-400A, pp 203-20)
corrosion by Sulfex solutions and Zirflex solutions, 17: 2461(R) (BNL-731(p.18-46))
corrosion by sulfuric acid solutions, 16: 17977(R) (EURAEC-141)
corrosion by sulfuric acid and sodium bicarbonate solutions, 17: 16594(T,R) (EURAEC-29)
corrosion by sulfuric acid solution, review on, 17: 25730(T) (EURAEC-679)
corrosion by superheated steam, 17: 21226 (TID-7658(p.1-14))
corrosion by superheated steam, effects of oxygen and surface treatment on, 17: 21227 (TID-7658(p.14-16))
corrosion by superheated steam, 17: 21228 (TID-7658(p.16-20))
corrosion by superheated steam, cycle tests of, 17: 21229 (TID-7658 (p.20-6))
corrosion by superheated steam, 17: 21230 (TID-7658(p.27-47))
corrosion by superheated steam and water, 17: 21231 (TID-7658(p.48-56))
corrosion by superheated steam, 17: 19720 (ANL-6698)
corrosion by superheated steam, 18: 21668(R) (GEMP-274)
corrosion by superheated steam containing chloride, 18: 30129 (GEAP-4450)
corrosion by superheated steam, effects of surface preparation on, 18: 41962
corrosion by supercritical water, (E), 19: 14851(R) (WCAP-2703)
corrosion by superheated steam, effects of hydrogen and oxygen on intergranular, 19: 22891(R) (CEND-525)
corrosion by terphenyls, 16: 22551
corrosion by terphenyls at 400 to 450°C, 17: 37478 (EUR-379.e)
corrosion by terphenyls, chlorine evolution in, 19: 20469 (EUR-2279.e)
corrosion by terphenyls, 16: 22551
corrosion by titanium sponge, 18: 17921(R) (ANL-6725(p.31-88))
corrosion by titanium sponge at 900°C, 18: 33678(R) (ANL-6875)
corrosion by ultrasonic-induced cavitation in liquid metals, 19: 28767
corrosion by uranium hexafluoride up to 1000°C, 18: 20469 (CEA-2385)
corrosion by uranyl sulfate solutions, 16: 17563(R) (ORNL-3262 (p.90-8))
corrosion by water at high temperatures in reactors, 16: 2141
corrosion by water at high temperatures, 16: 3415
corrosion by water and steam at 300 and 400°C, effects of surface treatment on, 18: 25922(T) (EURAEC-1038)
corrosion by 1200° sodium, 17: 18750(R) (MSAR-59-133)
corrosion cracking in dilute sodium chloride, effects of surface grinding on, 18: 20470 (CONF-492-1)
corrosion cracking in high-temperature water, 18: 32095
corrosion in terphenyl at 450°C, 18: 40827 (EUR-1830-e(Pt.II))
corrosion of Carpenter-20 electrodes, in electrolytic dissolution of stainless steel- and zirconium-matrix fuels, 16: 16464
corrosion of, effects of Teflon on, 17: 24639 (WAPD-BT-28(p.53-9))
corrosion of type 310, by air and nitrogen–oxygen atmospheres at 1750 and 1850°F, 17: 25723 (IDO-28605)
corrosion of type 20/25 chromium–nickel, by steam and water at high temperatures, effects of surface states on, 18: 44085(R) (EURAEC-1122)
corrosion of types 302, 303, 304, 304L, 316, and 347, by pressurized water at 500 to 600°F, 17: 29282 (ORNL-TM-539)
corrosion of type 410, by steam and water at high temperatures, effects of surface states on, 18: 44085(R) (EURAEC-1122)
corrosion of types 430, 442, and 446, by pressurized water at 500 to 600°F, 17: 29282 (ORNL-TM-539)
corrosion by uranyl sulfate solution at 280°C, in-pile, 17: 27750 (ORNL-3099)
corrosion by uranyl sulfate solutions at 235 and 250°C, in-pile loop experiments on, 17: 34348 (ORNL-3131)
corrosion by uranyl solutions containing nitric or phosphoric acid at 95°C for 3 years, 18: 39842 (LA-3101)
corrosion by uranyl nitrates and uranyl phosphates, 20: 5846
corrosion by waste melts, 19: 22405(R) (HW-83298(p.4.1-25))
corrosion by waste calciner off-gas, 19: 38285(R) (BNWL-76)
corrosion by water, tracer techniques for measurement of cavitation and erosion, 16: 692
corrosion by water at 100 atm. and 310°C, effects of electropolishing, 16: 490(T) (AEC-tr-4698)
corrosion by water, electrochemical, 16: 12055
corrosion by water, 16: 13532 (MND-E-2727)
corrosion by water at critical parameters, electrochemistry, 16: 22562
corrosion by water at critical parameters, electrochemical, 16: 33435(T) (AEC-tr-5405)
corrosion by water at 600°F, radiation effects on, 17: 1131 (YAEC-182 (Pt.I))
corrosion by water in simulated boiling-water reactor operation, 17: 30936 (GEAP-4020)
corrosion by water in HFIR, 18: 22013(R) (ORNL-3591(p.70-6))
corrosion by water, oxide film tenacity and release of retained film radioactivity in, 18: 24082 (HW-79811)
corrosion by water under Advanced Test Reactor conditions, 18: 34074 (IDO-24460)
corrosion by water containing chlorides, 19: 2754
corrosion by water or water vapor in radiation environment, 19: 7870
corrosion by water at 25 and 360°C, 19: 16019
corrosion by water, evaluation of scanning electron microscope and spinning-source mass spectrograph microprobe for studying,

19: 22665 (WERL-1114-1)
corrosion by water and steam at high temperatures, dynamic and static studies of, 19: 24936(R) (EURAEC-1308)
corrosion by water at 100°C, 19: 30671(R) (ORNL-3789(p.122-5))
corrosion by water and steam at high temperatures, effects of surface treatment on, 19: 34644
corrosion by water at 515°F, 20: 5134(R) (WCAP-3269-12)
corrosion by water in Saxton and Yankee Reactors, 20: 8429
corrosion by water in reactor environment, method for testing, 20: 7526
corrosion by water at high temperatures, 20: 20183
corrosion by water under in-pile conditions, 20: 35839 (KR-89, pp 112-30)
corrosion by water, gamma radiation effects on, 20: 37182
corrosion by water, effects of dissolved impurities on, 20: 41418(R) (GEAP-5150)
corrosion by wet steam, 18: 6913 (NP-13409)
corrosion by zinc vapor at 900°C, 19: 26778
corrosion by zirconium fluoride at 350 to 830°C, 16: 33438
corrosion cracking by distilled water, and solutions of sodium sulfate, nitric acid, sodium hydroxide, and sodium chloride, 16: 489(T) (AEC-tr-4684)
corrosion cracking of precipitation-hardening, 17: 32531
corrosion cracking in dilute chloride solutions, effects of acidity on, 18: 20471 (CONF-492-2)
corrosion cracking in uranyl sulfate solutions containing copper sulfate and sulfuric acid, 18: 20477
corrosion cracking of welded, electrochemical study of, 18: 44086 (KAPL-M-6172)
corrosion cracking in, effects of chloride ion on, 19: 2755
corrosion cracking in austenitic, effects of corrosion media on type of, 20: 767(R) (GEAP-4915)
corrosion cracking in austenitic, factors affecting intergranular, 20: 767(R) (GEAP-4915)
corrosion cracking in sodium at 1000°F of type 316, stress, 20: 769(R) (NASA-CR-54459)
corrosion cracking by magnesium chloride of austenitic and austeno-ferritic, stress-, 20: 2256(R) (EURAEC-1449)
corrosion cracking by sodium chloride of type 304, factors controlling stress-, 20: 5851
corrosion cracking by magnesium chloride of series 200, 300, and 400, stress-, 20: 9408 (BNWL-154)
corrosion cracking of austenitic, role of dislocations in stress-, 20: 35847 (DP-1008)
corrosion cracks in tubes of type 304, from PWR 1B Steam Generator, stress-, 20: 7490(R) (BMI-1745, Sect.A)
corrosion failure in calcium, lithium, and magnesium chlorides, stress, 20: 4328 (WCAP-3269-50)
corrosion in decontamination of pressurized-water reactors, 19: 2746 (HW-SA-2333(Rev.))
corrosion in fused sodium chloride–potassium chloride, effects of diffusion, 16: 19422
corrosion in HWCTR, 19: 38262 (DP-964)
corrosion in hydrochloric acid medium, chemical and electrochemical, 16: 19289
corrosion in monosodium phosphate, 18: 27856(R) (HW-79280(p.9.1-4))
corrosion in nitric acid, effect of hexavalent chromium on intergranular, 16: 19423
corrosion in nitric acid, effects of uranyl nitrate and sodium nitrate on cathodic, 19: 36983
corrosion in PM-1 Reactor control rod drive system pressure thimble, 18: 24890 (MND-M-3088 & Add.1)
corrosion in reactors, 19: 20488
corrosion in SGHWR environment, 20: 36479 (KR-89, pp 265-89)
corrosion in SM-1 reactor vessel studs, effects of heat treatment and stress, 16: 14275 (APAE-110)
corrosion in sodium diuranate calciners, 20: 25212
corrosion in solvent extraction processes for reactor fuels, 18: 8761
corrosion in steam generator of pressurized water reactor, 16: 7856
corrosion in waste fixation in glass, 19: 33676 (ORNL-3640)
corrosion in water-cooled reactors, problems of, 18: 16445
corrosion loss in reactor circuit, measurement using eddy-current sensing device, 18: 41958 (UJV-924/63)
corrosion mass transfer in potassium of types 316 and 321, to niobium–zirconium alloy, 19: 9622(R) (NASA-CR-54200)
corrosion of AISI 304,, by simulated N-reactor secondary water, 17: 37480 (HW-76358)
corrosion of, alloying effects of uranium on, 18: 2180 (NP-13261(p.207-34))
corrosion of aluminum-modified type 304, by steam at 650°C, 18: 19456(R) (ANL-8640)
corrosion of austenitic, in reactor systems, 18: 18326
corrosion of austenitic, use of radiation sources in measuring, 18: 30160
corrosion of austenitic, in steam-water mixtures in reactor environment, 19: 24997
corrosion of austenitic, by water, stress-, 19: 46959
corrosion of austenitic and austeno-ferritic, by chloride solutions, stress-, 20: 29639(R) (EURAEC-1578)
corrosion of, bibliography on, 17: 16593 (VDIT-5a)
corrosion of, by aqueous sodium bicarbonate, effects of chlorides on, 16: 29345(T,R) (EURAEC-228)
corrosion of, by Darex and Zirflex solutions, 16: 32883(R) (ORNL-3314 (p.1-39))
corrosion of, by electrolytic dissolver solutions, 16: 30495(R) (IDO-14589)
corrosion of, by fluoride-bearing fuel-processing wastes, 16: 30495(R) (IDO-14589)
corrosion of, by hydrochloric acid and sodium carbonate solutions, 17: 22114(T,R) (EURAEC-557)
corrosion of, by mercury, 16: 29336(R) (AGC-0584-04-3)
corrosion of, by steam-water mixtures, 16: 34082(T,R) (EURAEC-40)
corrosion of, by steam at 650°C, effects of surface preparation on, 17: 1870 (ANL-FGF-381)
corrosion of, by steam and water at 350°C, 17: 1876 (TID-17220(Pt.1))
corrosion of, by steam–water spray, 17: 11941(R) (EURAEC-475)
corrosion of, by steam at 1050°F, 17: 16587 (GEAP-4165)
corrosion of, by steam-water spray, 17: 17406(R) (EURAEC-519)
corrosion of, by superheated steam, 16: 30717(R) (ANL-6516)
corrosion of, by Sulfex and Zirflex solutions, 16: 33064 (BNL-752)
corrosion of Carpenter 20, type 304L, and type 309SCb, in simulated chloride volatility process waste solutions at 25 and 50°C, 17: 35618(R) (ORNL-TM-545)
corrosion of Carpenter 20 and type 304L, effects of oxidation-dissolution cycles in graphite fuels on, 17: 35618(R) (ORNL-TM-545)
corrosion of Carpenter 20SCb, by solutions produced in head-end processes for fuel, 19: 20481 (ORNL-3787)
corrosion of Carpenter-20, by hydrofluoric acid dissolver solutions, 20: 33411 (IDO-14674)
corrosion of chrome-plated, by water in ETR, 18: 15673(R) (IDO-16932)
corrosion of chrome-plated, by water at 515°F, 20: 5134(R) (WCAP-3269-12)
corrosion of commercial and pure 18/10, by hydrochloric acid and nitric acid-potassium bichromate solutions, 18: 18320(T,R) (EURAEC-976)
corrosion of high-purity and industrial 18-10, by steam–water and boiling nitric acid with hexavalent chromium, 19: 11690(R) (EURAEC-1213)
corrosion of high-purity, by chloride solutions, effects of composition on stress-, 20: 27482(R) (EURAEC-1453)
corrosion of, in high-temperature water and steam, surface state effects on, 17: 16595(T,R) (EURAEC-552)
corrosion of irradiated and unirradiated, by borated water at 600°F, effects of boron additions, 17: 1872 (BMI-B&W-653)
corrosion of niobium-containing, by carbon dioxide–carbon monoxide, 18: 37631 (A/CONF.28/P/157)
corrosion of pure 18/8, by hydrochloric acid, 17: 11115(T,R) (EURAEC-482)
corrosion of series 300 and 400, by zinc vapor at 900°C, 17: 36860(R) (ANL-6648)
corrosion of stressed, in monosodium phosphate solutions, 18: 7148(R) (HW-78962(p.5.13-23))
corrosion of stressed AISI 304, by sodium phosphate solutions at 275°C, 18: 14407(R) (HW-79766(p.5.1-16))
corrosion of tubes in liquid-liquid heat exchangers, 16: 9153 (MND-E-2681)
corrosion of tubes by liquid potassium–sodium alloy, 16: 27594
corrosion of tubes of type 304, by steam–water at 2000°F, 19: 7862 (APED-4413)
corrosion of type 1Cr18Ni9T in distilled water, sodium sulfate, sodium sulfite, nitric acid, hydrochloric acid, sulfuric acid, sodium hydroxide, and sodium chloride solutions at temperatures to 300°C and pressure of 87 atmospheres, 16: 488(T) (AEC-tr-4683)
corrosion of type 304L and 309 SCb, by Sulfex and Zirflex process solutions, 16: 33064 (BNL-752)
corrosion of type 309SCb by nitric acid–hydrofluoric acid, ammonium fluoride, and ammonium fluoride–ammonium nitrate solutions, 16: 16464
corrosion of type 304 by polyphenyls at 330 to 400°C, 16: 22547
corrosion of type 304 by wet steam, 16: 22554
corrosion of type 304 under superheat reactor conditions, effects of chlorides and stress on, 16: 29339 (GEAP-4025)
corrosion of type 304, in simulated superheat reactor environment, 16: 30734 (GEAP-3779)
corrosion of type 304-L, by Purex waste acid, 16: 30735 (HW-73378)
corrosion of type 304, by superheated steam, 17: 3900
corrosion of type 304 by molten uranium and uranium–fissium alloy, penetration rates at 1100 to 1350°C, 17: 3430
corrosion of type 310, by cesium at high temperatures, design of capsules for testing, 17: 3426(R) (NP-12189)
corrosion of type 304, by lead (liquid) at high temperatures, 17: 7606(R)

(ORNL-1515)
corrosion of type 302, by steam at 1000°F, 17: 23890(R) (BMI-X-10040)
corrosion of type 304L, in Purex FTW, 17: 26932(R) (ORNL-TM-516)
corrosion of type 316, by air, helium, and sodium at 1200°F, 17: 29281(R) (MSAR-63-57)
corrosion of type 304, by water at 354°C, 17: 34330(R) (USBM-U-1057)
corrosion of type 304L, by simulated 1965 FTW solutions, 17: 35618(R) (ORNL-TM-545)
corrosion of type 316 by sodium, test run data on, 17: 37479 (GEAP-4181)
corrosion of type 300 series under simulated superheat reactor conditions, 17: 39487 (GEAP-4310)
corrosion of type 304, by steam at 400°C and water at 300°C, 17: 39491(T,R) (EURAEC-704)
corrosion of type 304, by reactor superheated steam, 17: 40270 (GEAP-4240)
corrosion of type 316, by sodium at 1200°F, 18: 564(R) (MSAR-63-142)
corrosion of type 304, by water at 354°C, 18: 2174(R) (USBM-U-1082)
corrosion of type 304, by liquid bismuth alloys, 18: 4193 (BNL-811)
corrosion of type 316, by liquid sodium in test loop, 18: 4195 (GEAP-4182)
corrosion of type 304L, by salts and wastes at high temperatures, 18: 6537(R) (ORNL-TM-603)
corrosion of type 347, by sodium under magnetostriction cavitation conditions, 18: 7931(R) (PRDC-TR-74)
corrosion of type 304, by terphenyl, 18: 11366 (BNL-7650)
corrosion of type 316, by sodium at high temperatures, 18: 10472(R) (MSAR-64-6)
corrosion of type 304, by steam at 300 and 400°C and water at 300°C, 18: 10475(T,R) (EURAEC-864)
corrosion of type 316, by flowing sodium, test run data on, 18: 12575 (GEAP-3726(Vol.3))
corrosion of type 304, in calcium, lithium, and magnesium chlorides, 18: 14415
corrosion of type 304, by steam and water to 500°C, 18: 16442(T,R) (EURAEC-960)
corrosion of type 304, by SM-1 reactor coolant, 18: 19342 (ACNP-62842)
corrosion of type 304L, by refluxing FTW-65 waste solutions, 18: 19448(R) (ORNL-TM-757)
corrosion of type 316, by oxygen-contaminated and carbon-saturated sodium at 1200°F, 18: 18315(R) (MSAR-64-30)
corrosion of type 316, by lithium, lithium halide–lithium hydride systems, and lithium hydrides at 1000 to 1650°F, 18: 24085(R) (NASA-CR-54053)
corrosion of type 347, by lithium hydrides at 1165 to 1600°F, 18: 24085(R) (NASA-CR-54053)
corrosion of type 304, by sodium at 650°C, 18: 26893(R) (ANL-6868(p.11-108))
corrosion of type 347, by uranyl sulfate solutions, hydrodynamic aspects of, 18: 29147 (NASA-SP-41(p.273-303))
corrosion of type 304, by high-temperature steam and water, 18: 30135(T,R) (EURAEC-1047)
corrosion of Type 316, by flowing sodium, 18: 34073(R) (GEAP-4438)
corrosion of type 304, by nitric acid, 18: 37620 (ANL-6703(p.536-65))
corrosion of Type 304, by water at 300°C, 18: 39849
corrosion of type 405, by fused halide salts and oxygen at high temperatures, 18: 44930(R) (ANL-6936(p.17-38))
corrosion of type 304 ELC and 304L, by magnesium fluoride slag digestion slurry at 100 to 135°F, 18: 43712(R) (NLCO-920(p.63-70))
corrosion of type 304, by steam and water at high temperatures, effects of surface states on, 18: 44085(R) (EURAEC-1122)
corrosion of type 304, by heavy water (E), 19: 3643 (HPR-35(Vol.II) (Sect.10))
corrosion of type 304 clad, in fuel elements irradiated at 1500°F in helium, 19: 2726 (ORNL-3684)
corrosion of type 304, in heavy water-cooled reactors, Savannah River Plant experience with, 19: 4614 (CONF-654-23)
corrosion of type 310, by helium-heated coal gases, 19: 8650(R) (TID-21288)
corrosion of type 316, by flowing sodium, test run data on, 19: 7866 (GEAP-4437)
corrosion of type 304, by steam containing oxygen, 19: 7262(R) (CEND-508)
corrosion of type 316, by sodium at 1100°F, carbide precipitation in, 19: 15712(R) (BAW-1280-18)
corrosion of type 316, in sodium-heated steam generator after 4000 hr, 19: 20107(R) (BAW-1280-22)
corrosion of type 310 by Purex waste–colemanite melt at 900°C, 19: 25775(R) (HW-84603(p.8-31))
corrosion of type 304, by molten bismuth, static, 19: 32924(R) (ANL-7020(p.198-225))
corrosion of type 316, by boiling potassium, 19: 34640 (CNLM-6246)
corrosion of type 430, by metal chlorides at high temperatures, 19: 40113(R) (ANL-7071)
corrosion of type 318, by lithium fluoride in cyclic high-temperature environment, 20: 4326 (TRW-ER-6561)
corrosion of type 316, by potassium at 870°C, 20: 4307(R) (ORNL-3870, pp 238-42)
corrosion of type 304, by fused fluoride salts, 20: 4308(R) (ORNL-3870, pp 243-60)
corrosion of type 410, by lead at 1215°F, 20: 4308(R) (ORNL-3870, pp 243-60)
corrosion of type 347, by potassium–sodium, effects of hydrogen and oxygen on, 20: 4322(R) (ORNL-3870, pp 305-7)
corrosion of type 316, by potassium–sodium eutectic, 20: 4323(R) (ORNL-3870, pp 308-11)
corrosion of type 304, by sodium chloride at 90°C, effects of pH on stress-, 20: 5846
corrosion of type 304 and 405, by aluminum–magnesium–magnesium chloride–potassium chloride–sodium chloride systems at 500 to 800°C, 20: 14007(R) (ANL-7122, pp 1-41)
corrosion of type 304, by water at 300°C, effects of flow rate and surface treatment on, 20: 14978 (EURAEC-1546)
corrosion of type 316, by sodium at 1200°F, 20: 14979 (GEAP-4835)
corrosion of type 304, effects on nitrogen content on stress-, 20: 16969(R) (EURAEC-1579)
corrosion of type 316, by sodium at 1100 and 1200°C, mechanisms of, 20: 16970 (GEAP-4832)
corrosion of type 304, by bismuth–tin alloy at 200 to 1100°C, kinetics of hydrodynamic, 20: 21260 (ANL-6985)
corrosion of type 405, by cadmium alloy–fused chloride mixtures at high temperatures, 20: 20802(R) (ANL-7055, pp 21-98)
corrosion of type 405, by liquid plutonium and uranium alloys, 20: 20802(R) (ANL-7055, pp 21-98)
corrosion of type 316, by sodium, 20: 23601(R) (GEAP-4839)
corrosion of type 410, by lead at 1210°F, 20: 23603 (ORNL-TM-1437)
corrosion of type 304, by iron chloride solutions at 275°C, electrochemical studies of, 20: 25616(R) (GEAP-5085)
corrosion of type 304, by steam at 1000 to 1250°C, kinetics of, 20: 27409(R) (GEMP-58A)
corrosion of type 304, by boric acid at 600°F, 20: 31669
corrosion of type 316, by liquid potassium at high temperatures, 20: 41419(R) (GMAD-3643-5)
corrosion of type 304, in air and sodium, 20: 45106(R) (ANL-7249)
corrosion of type-304, by liquid sodium, 18: 14379 (TID-7676(p.25-37))
corrosion of type-304, in superheated steam, 19: 4197 (SAN-8003 ((p.90-133))
corrosion of type-304, in VBWR, stress-assisted intergranular, 20: 7525
corrosion of type-304, by chromic acid, copper chlorides, iron chlorides, and sodium hydroxides, 20: 7526
corrosion of types 347 and 446 by lead at 1000 to 1500°F, 16: 6516 (APEX-166)
corrosion of types 304, 316, and 410, by sodium bicarbonate-sodium chloride solutions, 17: 502(T,R) (EURAEC-293)
corrosion of types 304, 304L, and 309SCb by boiling nitric acid, effect of reductants on, 17: 4295(R) (DP-740)
corrosion of types 304 and 430, by lead–sodium alloys at high temperatures, 17: 7606(R) (ORNL-1515)
corrosion of types 304 and 406, by steam at 650°C, 17: 26750(R) (ANL-6717)
corrosion of types 304, 304L, and 316L, by oxygenated steam, 17: 29777(R) (ACNP-63016)
corrosion of types 17-4PH, 410, 420, 431, and 440C, by pressurized water at 500 to 600°F, 17: 29282 (ORNL-TM-539)
corrosion of types 304 and 406, by steam at 650°C, 17: 36861(R) (ANL-6764)
corrosion of types 304, 310, 316, 347, and 406, by superheated steam, 17: 38465 (TID-7674(p.11-16))
corrosion of types 17–4 PH, 304L, 406, 430, and 446, by oxygenated steam at 500°C and 3000 psi, 17: 38466 (TID-7674(p.16))
corrosion of types 304 and 406, by oxygenated-superheated steam, 17: 38463 (TID-7674(p.8-10))
corrosion of types 304, 304L, 316, and 316L, by oxygenated-saturated and superheated steam, 17: 38462 (TID-7674(p.4-8))
corrosion of types 304, 316, 321, 347, and 406, by superheated steam, 17: 41333(R) (ANL-6677)
corrosion of types 304 and 406, by ferric chloride and superheated steam, 18: 1241(R) (GEAP-4332)
corrosion of types 17-4 PH 304, 316, 406, 430, 446, and PDRL-102, by superheated steam at 1020 and 1350°F, 18: 7957(R) (GEMP-257)
corrosion of types 304 and 347, by steam containing chloride, 18: 7928 (GNEC-257)
corrosion of types 304 and 316, by sodium saturated with carbon at 1200°F, 18: 8755(R) (MSAR-63-174)
corrosion of types 304, 316, 321, and 410, electrochemical, 18: 14404(R)

(EURAEC-95)
corrosion of types 304, 316, and 410, in salt solutions, effects of tensile pull on breakdown and protection voltages in, 18: 14411(T) (EURAEC-928)
corrosion of types 304 and 347, by flowing helium containing water vapor, effects of sodium chloride contamination on, 18: 15493(R) (ORNL-3523(p.193-226))
corrosion of types 304, 406, 430, and 446, by steam at 540 and 650°C, 18: 25919(R) (ANL-6868(p.190-200))
corrosion of types 405 and 406, by oxygenated steam at 650°C, effects of aluminum, titanium, and yttrium additions on, 18: 26894(R) (ANL-6868(p.109-16))
corrosion of types 17-4PH, 304L, 316L, 406, 430, and 446, by superheated steam at 550°C, 18: 32139(R) (HW-81269(p.5.1-23))
corrosion of types 304, 316, 347, and 406, by superheated steam, 18: 44931(R) (ANL-6936(p.39-72))
corrosion of types 304 and 406, in VBWR coolant water, 18: 45020(R) (GEAP-4619)
corrosion of types 304 and 316, by sodium with high carbon content at 1200°F, 19: 6298(R) (MSAR-64-126)
corrosion of types 316 and 347, by potassium–sodium alloy, research program on, 19: 20477(R) (ORNL-3604)
corrosion of types 347 and 316, by potassium–sodium alloy at high temperatures, loop experiments, 19: 20479(R) (ORNL-3671)
corrosion of types 316 and 347, by potassium–sodium alloy at high temperatures, mass transfer in, 19: 20480(R) (ORNL-3730)
corrosion of types 316 and 347 by potassium–sodium alloy at high temperatures, carbon mass transfer in, 19: 20478(R) (ORNL-3618)
corrosion of types 316 and 347, by liquid sodium–potassium in test loop, 19: 24939(R) (ORNL-3784)
corrosion of types 304 and 410 by boric acid and boric acid–lithium hydroxide, 19: 42816 (WCAP-3725)
corrosion of types 416 and 430F, by aqueous mineral acid solutions, effects of uranium on, 20: 14983 (NP-15875)
corrosion of types 304 and 316, by argon–nitrogen mixtures at 900°C, 20: 20802(R) (ANL-7055, pp 21-98)
corrosion of types 304 and 403, in Saxton steam generator, 20: 30884(R) (WCAP-3269-16)
corrosion of types 304 and 410, by mercury at 593 to 703°C, 20: 29646
corrosion of types 304, 316, and 17-4 PH, by heavy water at 315°C, 20: 31669
corrosion of types 316, 321, 347, and 19-9DL, by lithium hydride at 900, 1200, and 1400°F, 20: 31669
corrosion of types AISI 304 and 410, by steam and water at high pressures and temperatures, 20: 33815(R) (EURAEC-1625)
corrosion of types 304 and 316, by high-carbon sodium, effects of stress on phase transformations in, 20: 33817 (MSAR-66-119)
corrosion of types 309S, 310, and 446, by boiling hydrofluoric acid–nitric acid solutions, 20: 37169(R) (BMI-1774)
corrosion of uncoupled and coupled, by water, 19: 28756 (ORNL-TM-1029)
corrosion of, use of radioisotopes for study of, 17: 33822
corrosion of, used to clad reactor pressure vessels, 18: 2235(T) (CEA-tr-X-487)
corrosion of welded fuel elements of, 17: 3418 (APAE-Memo-248)
corrosion of welded, by fixed wastes at 200 to 500°C, 18: 19448(R) (ORNL-TM-757)
corrosion of Zircaloy-2 bonds of, by ammoniated water at 600°F, 17: 499(R) (KAPL-2000-19(p.III.1-III.9))
corrosion of 17-4 PH, 304, 308, 309, 309L, 316, 403, 410, and 440C, by boric acid–potassium hydroxide solutions, 18: 30133 (WCAP-3737)
corrosion of 18-8, intergranular, 16: 19290
corrosion of 18-8, causes and mechanisms of intercrystalline, 16: 22545
corrosion of 18-8 Ti, by boiling nitric acid after thermal treatment near the solidus, 16: 27665
corrosion of 18/8, 18/10, and type 304, by hydrochloric acid solutions, 18: 18317(T,R) (EURAEC-631)
corrosion of 18/8, 18/10, and type 304, by ferric chloride, magnesium chloride, and steam, 18: 18318(T,R) (EURAEC-836)
corrosion of 20Cb, effects of increased nickel content in intergranular, 20: 29643
corrosion of 300-series, in in-pile high-purity boiling water, 20: 18089 (NAA-SR-Memo-10178)
corrosion of 304 and 347, by stresses and aqueous solutions, 18: 24125(R) (CEND-3256-209)
corrosion of 304 and 405, by fused alloy–salt mixtures, 18: 36751 (ANL-6912)
corrosion of 304, 316, 321, 347, and 406, by steam, 18: 26824(R) (ANL-6885)
corrosion of 304, in boiling water reactors, 18: 27910
corrosion of 304, 316, 321, 347, and 406, by steam, 18: 36751 (ANL-6912)
corrosion of 304L, by boiling nitric acid, 17: 8266
corrosion of 304L, by nitric acid, 18: 39843 (NP-9807)
corrosion of 309SCb, in dissolution of zirconium alloy fuels, conditions for minimizing, 18: 35639 (DP-872)
corrosion of 310, by steam and water at 800 to 1500°F, 20: 3471(R) (GEAP-4861)
corrosion of 316 and 347, by liquid potassium–sodium in test loops, 20: 773(R) (ORNL-3859)
corrosion of 316, by sodium, (E), 19: 13916 (SAN-8002(p.189-209))
corrosion of 316, by potassium–sodium system, 20: 2273
corrosion of 316, by flowing sodium at high temperatures, 20: 2274
corrosion of 316, in pumped sodium systems, 20: 2296
corrosion of, by fused cadmium chloride-base salts at 650°C, 20: 31314(R) (ANL-7175, pp 1-41)
corrosion of, effects on uses in reactors, 20: 46148
corrosion of, effects on uses in reactors, 20: 46149
corrosion-product deposition on, in pressurized water reactors, 16: 1183 (AECL-1265(Paper 7))
corrosion product release and deposition rates, in boric acid solutions at high temperatures, 19: 13918 (WCAP-5368)
corrosion products in reactor cooling systems, reactivity induced in, 16: 31210 (HW-SA-2508)
corrosion products of, analysis of, 17: 14771 (TID-16092)
corrosion products of, sorptive properties for boric acid from solutions, out-of-pile and in-pile studies of, 18: 27905 (WCAP-3730)
corrosion products films on, composition of, 19: 40961
corrosion properties of, effects of metal purity on, 20: 11227
corrosion resistance of type 430, effects of molybdenum or uranium alloying additions on, 20: 16975 (NP-15900)
corrosion studies, 16: 6802(R) (KR-12)
corrosion studies of, technical progress review, 17: 11129
corrosion studies, 18: 14396
corrosion studies on, technical progress review on, 18: 18307
corrosion studies, 19: 931 (TID-21221(p.87-109))
coupling of, with carbon steel in water, galvanic effects of, 17: 22116(T) (EURAEC-573)
coupling to aluminum in HFIR, 18: 22013(R) (ORNL-3591(p.70-6))
crack growth in, mechanisms of fatigue, 20: 46981(R) (GEAP-5147)
crack growth rate tests for type 304, 20: 28695(R) (GEAP-5082)
crack susceptibility of, effects of processing on, 19: 32048(R) (NP-15073)
cracking of type 304, in reactor fuel element cladding, mechanism of, 20: 23597 (COO-1319-30)
cracking of 304 cladding, on reactor vessels, 20: 3321(R) (ANL-7082, pp 29-53)
cracking under simulated reactor conditions, 19: 2754
creep acceleration temperatures of type 304, (T), 20: 10377 (NAA-SR-Memo-11433)
creep and fatigue properties of type 316, effects of air, helium, and sodium on, 18: 8754 (MSAR-63-168)
creep and stress rupture properties of type 304, effects of annealing, cold working, and pre-straining on, 18: 4254(R) (ORNL-3470(p.89-93))
creep and stress rupture of 304 and 316, effects of grain size and temperature on, 19: 40286(R) (NAA-SR-11200)
creep at 500°C, in-reactor tests of, 18: 44036(R) (HW-82651(p.4.1-49))
creep at 500°C, in-reactor tests of, 19: 23124(R) (HW-83298(p.8.1-4))
creep behavior of type 304 austenitic, effects of oxygen on high temperature, 19: 30746 (ORNL-TM-1124)
creep buckling and collapse properties of tubes of type 304, 19: 41019 (NAA-SR-11323)
creep collapse of fuel element cans of, 20: 9389
creep in argon–oxygen environment at 815°C of type 304, effects of oxygen content on, 20: 11227
creep of type 304L in lithium, biaxial, 18: 34030 (APL-TDR-64-73)
creep of 304, in-reactor testing of, 19: 34745(R) (HW-84384(p.8.1-5))
creep properties at 500 to 600°C of type 304, in-reactor, 20: 5851
creep properties in liquid lithium, 19: 11682
creep properties of type 304, effects of environment on, 16: 30797 (ORNL-2972)
creep properties of AM-350, at 800°F, 19: 32733 (NAA-SR-11047)
creep rate in air, helium, and sodium at 1200°F of type 316, 20: 11227
creep-rupture properties of thin-wall tubes of type 316, 17: 16682
creep-rupture properties of type 316, effects of air, helium, and sodium at 1200°F on, 17: 34406(R) (MSAR-63-117)
creep-rupture properties of type 316, effects of air, helium, and sodium at 1200°F on, 18: 32144(R) (MSAR-64-75)
creep-rupture properties of type 316, effects of vacuum evaporation on, 18: 44049(R) (ORNL-3670(p.77-111))
creep-rupture properties of austenitic, effects of variations in chemical composition on, 20: 33877 (NAA-SR-Memo-11788)
creep-rupture properties of 304, in 1200°F high-oxygen sodium, 20: 43809 (BNL-50003)
crystal structure effects on iron-57 Mössbauer spectra in, 16: 18245
crystal structure of, effects of heating on, 17: 558
crystal structure and mechanical properties of, prepared from high-purity

metals, 18: 24151(T) (EURAEC-986)
crystal structure of type 304, dilatometric effects of nitrogen on, 20: 41449(R) (EURAEC-1676)
crystal structure and properties of, effects of heating on, 17: 559
cutting and sealing pipes, development of die for, 16: 4250 (ORNL-TM-8)
decontamination, 16: 12840
decontamination by removal of iron-59 activity, evaluation of wetting agents for, 16: 25660(T) (JPRS-13691(p.8-12))
decontamination by oxalate–peroxide solutions, 17: 33318(R) (ORNL-3445(p.30-6))
decontamination by oxalate–peroxide solutions, 17: 33322(R) (ORNL-3445(p.138-98))
decontamination by oxalate–peroxide solutions, 18: 15532(R) (ORNL-3523(p.40-58))
decontamination by electrolytic polishing, 19: 4409
decontamination, effects of temperature, 16: 23779 (DC-61-6-5)
decontamination effects on intergranularly attacked areas in type 304, 19: 20471 (HW-SA-3628)
decontamination of, evaluation of oxalate–peroxide solution for, 17: 8247(R) (ORNL-3308)
decontamination of type 304, 17: 11959 (TID-15779)
decontamination of, using phosphoric acid, 17: 31676 (DP-793)
decontamination of, using hot oxalic acid solutions containing fluoride and hydrogen peroxide, 17: 39197(R) (ORNL-3452(p.232-3))
decontamination of, electrolytic, 18: 9741 (CEA-2353)
decontamination of, comparison of solutions for, 18: 35127(R) (GEAP-3771-13)
decontamination of, solutions for, 19: 696 (UJV-1114/64)
decontamination of, using acid oxalate–peroxide solutions, 19: 4046(R) (ORNL-3627(p.247-8))
decontamination of, in heavy water system of RA reactor, 20: 23389
decontamination process, 16: 2957(P)
decontamination procedures, 18: 39814 (GEAP-4532)
decontamination research, 19: 9047 (ORNL-P-718)
deformation of, as fuel element cladding, 19: 39220
degasification of type 304, by electron bombardment, 20: 915 (ORNL-TM-1166)
deposition of coating of, on molybdenum, niobium, and tantalum, 17: 22147
deposition of protactinium on, method for quantitative electro-, 19: 24961
deposition of, on thick carbon steel, arc process development for, 16: 29360(T,R) (EURAEC-272)
deposition on heavy gage steels by welding, development of methods for, 20: 16991(R) (EURAEC-1557)
deposition on low alloy steel by welding, development of methods for, 20: 16990(R) (EURAEC-1556)
deposition on steel, methods development for, 19: 20504(R) (EURAEC-1228)
deposition on thick steel plates, 19: 40979(R) (EURAEC-1351)
deposition on thick 1.2 MD07 A and Soudotenax 56 steel plates by welding, 20: 5862(R) (EURAEC-1481)
descaling of steam-oxidized by sodium carbonate–sodium hydroxide solution, 18: 22441 (HW-79048)
design stress curves for type 316, for extended service in sodium environment, 19: 4613 (BW-67-3)
design stress for type 316, in sodium environment, 20: 5851
desorption of actinides from, 18: 16376(R) (MLM-1157)
desorption of gases in ultravacuum, pulsed thermal, 17: 18933
desorption of gases from, flash-filament technique in ultra-high vacuum for, 16: 31723
desorption of organic monolayers from, use of low-energy ions in, 16: 19464 (ARL-62-305)
deuterium ion reactions with 304 at 40 kev, sputtering from, 20: 39581(R) (ORNL-3989, pp 134)
deuteron bombardment at 2 Mev, distribution from, 16: 23964 (ANL-23964 (ANL-6515(p.9-27))
development and properties of type 416, as thermoelectric material, 17: 23861(R) (AD-282505)
development and properties for fuel-element cladding, review, 16: 16661
development and properties of high-strength high-temperature corrosion-resistant AFC-77, 18: 20446 (ASD-TDR-63-766)
development as reactor material, 18: 44075
development for Rapsodie pressure vessel, 19: 2718 (CEA-TP-1593)
development of corrosion-resistant, 18: 12581 (HW-78186)
development of precipitation hardening, 19: 24965
development of type 347, for uranium-dioxide fuel element cladding, 17: 14746(T,R) (AEC-tr-5667)
development of, for ball bearings, 20: 29366(R) (TID-22970, pp 375-91)
diffusion and permeation of deuterium and hydrogen in S110, oxygen effects on, 19: 46991 (AWRE-O-47/65)
diffusion in chromium–molybdenum steel, niobium, and niobium–zirconium alloy, 17: 36200(R) (NP-13033)
diffusion in, effects of crystal deformation on, 16: 25831
diffusion in uranium carbide at 820°C, 16: 6686(R) (NDA-2162-5)
diffusion into copper at 900°C of type V2A, 20: 5850
diffusion of carbon into type 316, from Croloy 9M in composite tubing, 20: 19189 (N-65-21161)
diffusion of carbon in, from ferritic steel, 17: 33323(R) (ORNL-3445 (p.199-217))
diffusion of deuterium and hydrogen in type 316, 19: 28755(R) (ORNL-3823)
diffusion of fissium–uranium alloy through, 18: 19393
diffusion of fission products in 304, mechanisms of, 19: 39152(R) (BMI-X-10132)
diffusion of fission products in 304, 20: 2389
diffusion of fission products in irradiated type 304, at 600 to 1200°C, 20: 21232 (BMI-1763)
diffusion of hydrogen in, effects of glass and oxide coatings, 16: 2179 (NAA-SR-6109)
diffusion of hydrogen in, at high temperatures, 16: 8713 (NEPA-1841)
diffusion of hydrogen ions through, 19: 18478
diffusion of hydrogen in type 316, at 1000 to 1300°F, 19: 20479(R) (ORNL-3671)
diffusion of hydrogen in type 316, at 1100 to 1300°F, 19: 20480(R) (ORNL-3730)
diffusion of hydrogen in type 316, in presence or absence of liquid sodium–potassium, 19: 24939(R) (ORNL-3784)
diffusion of hydrogen in, effects of potassium–sodium alloy on, 19: 30154(R) (ORNL-3789(p.308-17))
diffusion of hydrogen through type 316, effects of potassium–sodium on, 20: 9425 (ORNL-3898)
diffusion of hydrogen through coatings on, effects of base metal-coating reactions on, 20: 14987
diffusion of hydrogen in type AISI 304L, at high pressures and temperatures, 20: 33815(R) (EURAEC-1625)
diffusion of type 304, into fissium–uranium alloy at 550 to 700°C, 18: 32129 (ANL-6816)
diffusion of xenon in coating of, 16: 29368 (BNL-5113)
diffusion penetration of types 347 and 430 by plutonium-uranium alloys, 16: 28555 (TID-7623(p.105-21))
diffusion with plutonium–thorium–uranium at 650°C, 19: 17177(R) (ANL-6965(p.42-83))
dimensional stability, effects of thermal cycling, 16: 29884(R) (Y-795)
dislocation arrangement in type 304, effects of strain and temperature on, 19: 16020
dislocation etch pits in 18-8, metallographic technique for detecting and observing, 16: 29401
dislocation in neutron-irradiated and quenched, 16: 16790
dissolution, 16: 16464
dissolution by electrolysis, 16: 18985(R) (DP-720)
dissolution by gaseous hydrogen fluoride–nitrogen–oxygen, 19: 31462(R) (ANL-7028)
dissolution by hydrofluorination in fused-salt fluorides, 18: 39385
dissolution by hydrofluoric acid and fluoride salts in volatility separation processes, 19: 4247(R) (ORNL-3627(p.29-72))
dissolution by nitric acid–sulfuric acid in stainless steel vessels, 19: 11301(P)
dissolution in ARCO process, 16: 1855(R) (IDO-14560)
dissolution in bismuth–tin eutectics, 18: 44926(R) (ANL-6923(p.46-78))
dissolution in nitric acid, 16: 266(R) (DP-626)
dissolution in nitric acid solutions, effects of chromium ion on electrolytic, 16: 18652(R) (DP-706)
dissolution in nitrate solutions, electrolytic, 16: 23783 (IDO-14584)
dissolution in nitric acid, electrolytic, 17: 20097(R) (DP-824)
dissolution in nitric acid solutions, electrolytic, 17: 32192(R) (DP-839)
dissolution in nitric acid, evaluation of electromagnetic dissolver for, 17: 33769 (ORNL-TM-598)
dissolution in nitric acid solutions, electrolytic, 18: 31658(R) (IDO-14635)
dissolution in nitric acid, effects of magnetic fields on electrolytic, 19: 4254(R) (ORNL-3627(p.235-46))
dissolution in Sulfex process, 17: 23434 (ORNL-3404)
dissolution methods, 16: 1855(R) (IDO-14560)
dissolution of cladding on reactor fuel elements, electrolytic, 16: 10118(P)
dissolution of coating of, on uranium dioxide fuels, 17: 35951(P)
dissolution of, in aqua regia, off-gas composition from, 16: 30368 (TID-11021)
dissolution of irradiated, equipment and methods for, 18: 25610 (SGAE-CH-4/1964)
dissolution of potassium–sodium eutectic in hydrofluoric acid, 16: 14817(R) (ORNL-TM-112)
dissolution of type 304 in nitric acid, electrolytic, 16: 1854(R) (IDO-14553)

dissolution of type 347, by hydrofluoric acid in fluoride melt at 650°C, 18: 30128 (BMI-X-288)
dissolution of, electrolytic, 18: 20115
dissolution of, media for, 18: 26903
dissolution of, operation of pilot plant for electrolytic, 20: 36949
drilling of precipitation-hardening, 17: 6615
ductility and grain growth, 18: 39916(T,R) (EURAEC-1119)
ductility and rupture strength of types 304 and 316, 20: 22520(R) (NAA-SR-11805)
ductility and tensile properties of irradiated type 304, effects of heat treatments on, 18: 44050(R) (ORNL-3670(p.116-21))
ductility of austenitic, effects of cerium, lanthanum, and yttrium alloying additions on, 20: 31669
ductility of types 302 and 430, effects of liquid cesium on, 18: 14354(R) (ARF-B215-12)
ductility of, at −269°C, 20: 21416
ductility of, effects of pre-irradiation heat treatment on, 20: 7644
economics of, as power reactor fuel cladding, 19: 17264 (AD-422953)
effects of carbon-contaminated sodium on austenitic, 20: 2244
effects of contact with, on corrosion of Magnox alloys, 19: 11694
effects of decontaminating and descaling solution on metal loss on, 20: 21238 (NP-15928)
effects of dissolved, on Inconel, stainless steel, and titanium corrosion by nitric acid, 16: 1854(R) (IDO-14553)
effects of low-cobalt, on cobalt-60 activity in coolant of pressurized water reactors, 19: 45495 (WAPD-T-1653)
effects of platinized, on hydrogen-oxygen reactions, 18: 27492(R) (GNEC-336)
effects of reactor environment on, review of, 17: 25830 (HW-SA-3000)
effects of reflectors of, on prompt neutron decay in uranium cylinders, (E), 20: 36440
effects of sodium on mechanical properties of austenitic and ferritic, at high temperatures, 20: 25567(R) (MSAR-66-71)
effects of type 302B, on molybdenum–plutonium dioxide compacts, 18: 547 (LAMS-2898)
effects on critical cylinder diameters of hydrogen moderated uranium compounds, 19: 18736 (K-1629)
effects on plutonium precipitation from cadmium–magnesium–zinc solution at 600°C, 19: 32279(R) (ANL-7020(p.3-99))
effects on reactions of bromine pentafluoride with uranium, 20: 20803(R) (ANL-7055, pp 99-162)
effects on stability of magnesium–uranium–zinc systems, 18: 17921(R) (ANL-6725(p.31-88))
effects on steel corrosion by water, 19: 29808(R) (KR-94)
elastic properties of pipes of, at high temperatures, 18: 34175
elastic properties of, as fuel sheathing pipes for pressurized water reactors, 20: 23719
electric breakdown between plane-sphere electrode geometry of, in vacuum, 18: 20138
electric breakdown between electrodes of, minimum energy for, (E), 20: 46908
electric conductivity of solenoids of, inductive thermometry measurement of, 18: 20282 (HW-SA-3035)
electric conductivity of type 446, effects of temperature on, 19: 9281(R) (IS-900(Sect. E))
electric conductivity of 304, effects of carbon on, 19: 40409(R) (MSAR-65-95)
electrochemical attack of phases in, selective, 19: 10709(T) (EURAEC-1186)
electrochemical machining of, effects of friction, surface finish, and tool erosion on, 17: 34386
electrochemical properties in sulfuric acid, 18: 8734(T,R) (EURAEC-735)
electrodes of, electric discharge effects on, arcing in, 18: 26806
electromagnetic wave absorption and electron reactions on, elastic wave generation in, 17: 37732
electron beam reactions with, physical aspects of penetrations from, 20: 40347
electron bombardment of, ion desorption spectrum from, (E), 19: 9941
electron emission from, after high-energy molecular bombardment, 18: 18564
electron emission from foils of, laser-induced, (E), 19: 20814
electron emission from cesiated and vacuum surfaces of 304, (E), 19: 41284
electron reactions at 70 Mev with type 320, secondary emission from, 19: 37403
electron scattering by cesium-coated, parameters for 0.05 to 5.0 ev, 18: 10834
electron secondary emission from thin foils of, (E), 20: 13103
electroplating with uranium, 18: 29611
embrittlement by precipitations, literature survey of, 18: 5783 (TRG-Report-564)
emissivity of coated 310, in vacuum, 18: 24138(R) (PWA-2206(Vol.I))
emissivity of coated 310, in vacuum, 18: 24139(R) (PWA-2206(Vol.II))
emissivity of coated 310, in vacuum, 18: 24140(R) (PWA-2206(Vol.III))
emissivity of ReKide-C-coated at 300 to 1450°C, 16: 14358(R) (PWA-2043)
emissivity of titanate coatings on type 310, 20: 15057(R) (PWA-2750)
emissivity of titanate-coated, at high temperatures, 20: 43816(R) (PWA-2877)
emissivity of type 316, commercial coating for improving, 20: 4307(R) (ORNL-3870, pp 238-42)
emittance at 600 to 950°K, procedure for measurement of, 18: 5808
emittance of AISI-310, at 1000 to 2000°F, hemispherical, 18: 5737(R) (PWA-2255)
emittance of type 316, total hemispherical, 18: 44049(R) (ORNL-3670 (p.77-111))
emittance properties of titanate coatings on AISI-310, 19: 18465(R) (PWA-2518)
erosion by liquid potassium–sodium alloy, 20: 39023 (NAA-SR-11952)
erosion by mercury vapor at 640°F of type 347, 410, 17-4PH, and PH15-7Mo, 20: 11214(R) (NASA-CR-54717)
erosion by sodium at 400, 1000, and 1500°F of type 316, 20: 769(R) (NASA-CR-54459)
erosion of rotating disks of type 316, by water, 19: 44625 (TIM-894)
erosion of type 316 austenitic, by sodium at 400 and 1000°F, 19: 30670(R) (NASA-CR-54332)
erosion of types 304 and 316, by mercury, water, and bismuth–lead alloy, cavitation, 20: 29640 (NP-16048)
erosion of 316, by liquid sodium, 20: 5861
erosion rate of type 302, 17: 4971
etching by ion bombardment, 18: 2284(T)
evaluation for use in Pathfinder boiler fuel-element nozzle, galling tests, 16: 11182 (ACNP-6107)
evaluation of ACI# CD_4M Cu, as male connector material in fuel reprocessing, 19: 44607 (RL-SEP-508)
evaluation of cold-worked, for fuel clad in Connecticut Yankee reactor, 19: 27784 (UNC-5095)
evaporation in high vacuum, 18: 44049(R) (ORNL-3670(p.77-111))
evaporation of types 304, 316, and 446 in high vacuum at temperatures up to 980°C, 19: 4595 (ORNL-3677)
evaporation rate measurements for type 316, at 1400 to 1800°C and 5×10^{-7} to 5×10^{-9} torr, 18: 4255(R) (ORNL-3470(p.98-125))
explosibility of powders of, 19: 36698 (BM-RI-6516)
extruding type 403, for end fittings in reactors, 17: 34380
extrusion of PH 15–7 Mo, into T-sections, 19: 7874(R) (ASD-TDR-7-911(V))
extrusion of type 304 austenitic, Dynapak, 19: 30686(R) (AD-608945)
fabrication, 16: 7889 (NP-11196(p.16-20))
fabrication and properties of 18/8, 18/10, and type 304, 18: 18317(T,R) (EURAEC-631)
fabrication and properties of pure 18/10, 18: 18320(T,R) (EURAEC-976)
fabrication and properties of type 406, 18: 26894(R) (ANL-6868(p.109-16))
fabrication and properties of types 304 and 347, for stress corrosion cracking tests, 20: 4370 (CEND-3256-250)
fabrication and testing of thick, for use in reactor containers, 17: 1959(T,R) (EURAEC-279)
fabrication and testing for reactor uses, 20: 37174
fabrication as forged fuel chambers for Canadian nuclear power, 17: 33333
fabrication by explosive forming of Types 301 and 302, 16: 2151 (WAL-624.5/1)
fabrication by magnetic-pulse forming, 20: 40490 (Y-1483)
fabrication for corrosive radioactive service, specifications for, 17: 34370 (TID-19154)
fabrication for reactor fuel tubes, 18: 40858 (NP-14272)
fabrication for reactor fuel tubes containing uranium dioxide pellets, 19: 39147(P)
fabrication for use in reactors, 19: 37008
fabrication into heat exchanger tubes, 17: 522
fabrication into tubes, 19: 33628
fabrication of control rods of, for EGCR, 20: 21292 (ORNL-3932)
fabrication of cylinders of, using magnetic fields, 20: 19199 (RT/EL-(65)9)
fabrication of, development of methods for, 17: 21232 (TID-7658(p.56))
fabrication of dispersion fuel elements from, 16: 4450(R) (BMI-1546 (Del.))
fabrication of fuel cans of, for AGR, 19: 39134
fabrication of fuel element tubes of types 304, 304L, 310, 316, 347, and 348, 18: 1241(R) (GEAP-4332)
fabrication of high-quality tubing of, 17: 16603 (ANL-FGF-409)
fabrication of PH15-7Mo, by extrusion, 18: 18329(R) (ASD-TDR-7-945 (IV))
fabrication of reactor components of, by electron beam and TIG welding, 18: 14447
fabrication of reactor fuel cans, 18: 557

fabrication of type 304, 18: 27812(R) (ORNL-TM-415)
fabrication of type 304 tubes, material degradation in, 18: 37620 (ANL-6703(p.536-65))
fabrication of type-406, as superheater fuel cladding, 19: 4597 (SAN-8003(p.13-89))
fabrication of type 304, for pellet fuel rods, 18: 28999 (GEAP-4407)
fabrication of ultra-thin foils of, technique for, 18: 2207
fabrication of ultra-thin foils of, 19: 13959
fabrication of uranium dioxide canned tubes of, 17: 41406(P)
fabrication of uranium dioxide canned tubes of, 17: 41409(P)
fabrication, properties, and testing of 17-7 PH, 16: 5693 (XDC-59-1-173)
fabrication properties of semiaustenitic precipitation-hardenable, survey, 16: 15173 (DMIC-164)
fabrication, performance, and properties, as fuel cladding material, 18: 32033 (A/CONF.28/P/255)
fabrication, Savannah River Plant manual on, 19: 9632 (DP-860(Vol.II))
failure of fuel rod cladding of, in BWR at critical heat flux, 19: 24057
failure of seamless tubes of type 304, 18: 37620 (ANL-6703(p.536-65))
fatigue behavior of large bellows of type 304, in sodium at 1200°F, 18: 39404 (NAA-SR-9762)
fatigue burst testing of reactor fuel tubes of type 304, 20: 36391(R) (ANL-7219, pp 1-27)
fatigue detection in, methods for, 19: 36749(R) (HW-84609(p.7.1-17))
fatigue detection before crack initiation using ultrasonic techniques, 20: 5867
fatigue in sodium at 1000 and 1500°F of type 316, high-frequency, 20: 769(R) (NASA-CR-54459)
fatigue of AM 350, energy criterion for, (T), 20: 27521
fatigue of, at low strain cycles, 17: 1944 (TID-16455)
fatigue of type 304, at high temperatures, 18: 7129(R) (ORNL-3529 (p.71-143))
fatigue of type 304, at 800°C, plastic, 20: 2320(R) (GEMP-52A, pp 23-5)
fatigue of type 304, crack growth testing of, 20: 28694(R) (GEAP-4964)
fatigue properties of type 316 at 1500°F, effects of environment, 16: 526 (NRL-5666)
fatigue properties of type 347, 19: 24670 (NAA-SR-9827)
fatigue properties of welded joints between A105 carbon steel and, 19: 34658(R) (SWRI-1228-64)
fatigue strength of weldments of, to type A105 carbon steel, 20: 39404 (SWRI-1228-4-20)
fatigue testing of type 316 in liquid sodium at 1000 and 1500°F, high-frequency, 20: 46154 (NASA-CR-72035)
fatigue tests of type 316 in air and helium at 1200°F, 19: 4591(R) (MSAR-61-105)
fatigue tests of type 316, in air, 19: 4592(R) (MSAR-61-114)
fatigue tests of type 403 and 304-L, 19: 7889(R) (ATL-A-143)
fatigue tests of type 304, in air and high-oxygen sodium at 1200°F, 19: 11726(R) (MSAR-65-05)
fatigue tests of type 304, in air and sodium at 1200°F, 19: 18456(R) (MSAR-65-28)
fatigue properties at 816°C of type 304, plastic, 20: 27486(R) (GEMP-400A, pp 185-201)
fission product deposition on, from flowing helium, 18: 3066
fission product deposition on, in turbulent air streams, 18: 3067
fission product deposition on, from gas streams, 18: 7926(R) (GA-3307)
fission product deposition from helium stream on walls of, effects of distance and time on, 19: 24746 (ORNL-P-1182)
fission product deposition on, method for determining, 20: 7573 (ORNL-TM-1330)
fission product deposition on, from air–steam mixtures, 20: 20940(R) (ORNL-3915)
fission product plateout on type 405, from helium system, 16: 29369 (GA-1934)
flow of paste of, in sodium loop, 20: 3460
fracture by fragments of runaway reactors, 16: 12844
fracture mechanism at 1100°C, 16: 3501
fracture strength measurement at room temperature, method for, 20: 41444(R) (COO-1477-5)
fracture toughness, 17: 16640 (DMIC-Memo-164)
friction and wear measurements on 17-4 PH, in pressurized water environment, 19: 22462 (WAPD-288)
galling of, testing of coatings for protection against, 18: 20134(R) (ORNL-TM-792)
galling tests of type 308, for HTGR valve seats, 19: 11304 (GAMD-3058)
gamma absorption at 14.4 Mev, Mössbauer effect in, 18: 22923
gamma dose rates in tube of, from neutron capture, (E/T), 19: 38022
gamma emission from thermal neutron activation of types 304 and 347, 17: 27889 (EUR-103.f)
gamma heating in DFR, (E), 19: 42117
gamma reactions in, secondary gammas from, 16: 716
gamma resonance absorption in type 310, 16: 26225 (NP-11913)
gamma transmission in slabs of, (E), 19: 14728 (APEX-581)
gas contents of atomized powder compacts of PH 15–7 Mo, 19: 7874(R) (ASD-TDR-7-911(V))
gas desorption from surface of type 304, by electron bombardment, 19: 9359 (ORNL-P-818)
grinding of austenitic, effects of variables, 17: 6625
hardening of PH15-7 Mo, at 500 to 800°F, 18: 39904 (NAA-SR-Memo-9905)
hardness of type 310, effects of exposure to air at 1200 to 1400°F on, 20: 31669
heat conductance of contact interference with aluminum during transient heating, 19: 30379 (UCRL-14227-T)
heat flux and thickness of coatings of, for use at 40 atm pressure, 19: 25723(R) (GA-5036)
heat transfer across contacting surfaces of, 18: 33735 (MIT-2079-2)
heat transfer and pressure drop in eccentric tubes, 16: 25526 (NYO-9649)
heat transfer and recombination of hydrogen atoms on, 17: 21888
heat transfer from, by nucleate boiling, 18: 23761 (AEEW-R-180)
heat transfer from fuel cans of, to boiling water, 18: 29006(T) (EURAEC-1009)
heat transfer in irradiation capsules at 0 to 600°C, 16: 1905 (CNI-92)
heat transfer properties of fins of, 17: 8372
heat transfer to, by flowing sodium, 17: 32253
heat treatment of type 347, effects of composition on, 20: 29616(R) (BMI-1738)
helium penetration through the walls of tubes of, 17: 39226
hemispherical emittance values at 100 to 500°C for types 310 and 316, total, 18: 4255(R) (ORNL-3470(p.98-125))
high-strength, bibliography on, 17: 6521 (NP-12417)
hot shortness of type 347, effects of titanium and zirconium on, 17: 32628
hydrogen atom reactions at 10 to 40 kev, secondary electron emission from, 20: 31533
hydrogen ion bombardment of, production of free protons in, 18: 30413
hydrogen ion sputtering on, analysis of, 20: 44131
hydrogenation of type 304, effects on ductility, 20: 41418(R) (GEAP-5150)
impact analysis of, tracer techniques for, 18: 10251
impact strength of type 316, relation to carbon content, 19: 6298(R) (MSAR-64-126)
impact testing of, high-velocity, 20: 33490 (CONF-651026, pp 737-68)
impurity release in B-1 stellarator plasma, (E), 19: 10392(R) (MATT-Q-21)
inclusions, autoradiographic methods for studying, 16: 16052
inspection of thin-walled reactor grade tubing of, procedure for, 18: 14057
inspection of tubular, sonic, 18: 4795(R) (GEAP-3924)
internal friction of type 304, at 80 to 423°F, 19: 40968(R) (EURAEC-1424)
iodine deposition on, factors affecting, 19: 22461(R) (ORNL-3776 (p.57-70))
iodine deposition on, from vapor phase, 20: 215 (CONF-650407, pp 142-77)
iodine deposition on surfaces of type 316, 20: 35893(R) (ORNL-3951, pp 84-134)
iodine deposition on wires of, properties of, 20: 13261(R) (ORNL-3885, pp 87-149)
iodine deposition on, in turbulent helium flow stream at 400 to 500°F, 20: 28687 (ORNL-TM-1386)
iodine-131 deposition and transport on, model for, (E/T), 20: 21785 (ORNL-TM-1330(Rev.))
ion emission from heated surfaces of type 303, below 1000°K, (E), 19: 23181
ion emission from foils of, laser-induced, (E), 19: 20814
ion emission from cesiated and vacuum surfaces of type 304, (E), 19: 41284
ion reactions with stellarator walls of, re-emission rates for helium and hydrogen, (E), 20: 17922
iron-57 gamma emission in, s-electron density from isomer shifts in spectra of, 17: 37777
iron-57 Mössbauer spectra in, at −150 to +150°C, 17: 13230
iron-57 Mössbauer spectra in, temperature effects on, 17: 13231
iron-57 Mössbauer spectra in, at 20 to 850°C, 17: 13232
iron-57 Mössbauer-scattering spectra in, 17: 13252
iron-57 K-conversion Mössbauer spectrum in, (E), 20: 19847
iron-57 Mössbauer effect in, (E), 19: 6395
iron-57 Mössbauer effect in, temperature dependence of, (T), 19: 10309
iron-57 Mössbauer effect in 201, 301, 316, and AM 355, (E), 19: 21338
iron-57 Mössbauer effect in, (E), 20: 12296
iron-57 Mössbauer effect in, self-absorption effects on, (E), 20: 17990
joining, development of adhesives for, 16: 3397(R) (NP-10984)
joining of carbon steel and stainless steel to, parameters for friction, 20: 31670
joining of sheet, to Zircaloy tubes, by rolling techniques, 17: 510 (CWAED-54)

joining of tubular, to Zircaloy, 16: 29313 (DP-723)
joining of Type 304L tubes to Zircaloy-2 tubes by hot tandem extrusion, 19: 24948 (GEAP-4756)
joining of type 316, to T-111 alloy, 20: 43830(R) (NASA-CR-72029)
joining plates containing boron-10 by resistance foil-seam welding process, 16: 3423 (KAPL-M-SAT-7)
joining to beryllium, development of brazing method for, 18: 20134(R) (ORNL-TM-792)
joining to SAP, by hot pressing, 19: 24089(R) (SRO-114)
joining to Zircaloy-2, development, 16: 4450(R) (BMI-1546(Del.))
joining to Zircaloy-2 by hard-soldering, 16: 16649(R) (EURAEC-194 (App.6))
joining to Zircaloy, 16: 32105
joining to Zircaloy-2, explosive, 18: 2208
joining to Zircaloy-2, 18: 11432(R) (DP-875)
joining to Zircaloy by tandem extrusion, 19: 2734
joining to Zircaloy by tandem extrusion, 19: 13970
joining to Zircaloy-2 by diffusion, 19: 16028 (CEA-R-2634)
joining to zirconium or zirconium alloy tubes, method for, 19: 37018(P)
light emission from, at 50°C in 0.25 to 27 μ wavelength region, 17: 15953 (NASA-TN-D-1523)
light reactions with, electrons, ions, and neutral atoms from laser-induced, 17: 18923
machining specifications for flat, notched tensile specimens of type 348, 17: 14782 (HW-73759)
machining type 403, for end fittings in reactors, 17: 34380
magnetic susceptibility of type 18-8, 16: 25882 (ASD-TR-61-630)
martensite transformation in, 17: 29315 (CERN-63-11)
mass transfer by lithium at 1100 to 1600°F, 16: 10462
mass transfer by sodium, 18: 15566
mass transfer by sodium, 18: 15568
mass transfer from type 316 and 321 to niobium–1% zirconium alloy in liquid potassium, research program on, 19: 20474(R) (NASA-CR-54281)
mass transfer in system of, with liquid sodium, 17: 6575(R) (TID-17384)
mass transfer in system of, with liquid sodium, 17: 6576(R) (TID-17386)
mass transfer of carbon and nitrogen from 316, to niobium–zirconium alloy in liquid potassium, 20: 2239
mass transfer to niobium–zirconium alloy from types 316 and 321, in liquid potassium at 1400°F, 19: 40970(R) (NASA-CR-54390)
mechanical properties at 800°C, 16: 13620
mechanical properties of type 304, effects of various gases at high temperatures, 16: 22644
mechanical properties of type 304, effects of argon, carbon dioxide, and oxygen to 1700°F on, 16: 32081 (ORNL-TM-339)
mechanical properties at cryogenic temperatures, 16: 27622(R) (AD-271176)
mechanical properties of, effects of carbon dioxide, 16: 30167 (ORNL-3313(p.19-64))
mechanical properties, 17: 3379(R) (BMI-1596(Del.))
mechanical properties of, effects of sodium (liquid) on, 17: 3425(R) (MSAR-62-126)
mechanical properties, 17: 11129
mechanical properties at high temperatures, 17: 12664 (GEAP-4060)
mechanical properties of irradiated type 347, effects of 1000 and 1800°F annealing on, 17: 16733 (BMI-1621)
mechanical properties at 70 to 2000°F, 17: 18758 (NAA-SR-Memo-8052)
mechanical properties of, combined effects of irradiation and cryogenic temperatures on, 17: 22181
mechanical properties of type 316, at 1100 to 1200°F, effects of air, helium, and sodium on, 17: 29252(R) (MSAR-63-91)
mechanical properties of Type 316, effects of 1200°F sodium on, 17: 39538(R) (MSAR-63-125)
mechanical properties, alloying effects of rare earths on, 17: 39583
mechanical properties of type 304, 18: 2174(R) (USBM-U-1082)
mechanical properties of, used to clad reactor pressure vessels, 18: 2235(T) (CEA-tr-X-487)
mechanical properties, 18: 8734(T,R) (EURAEC-735)
mechanical properties of type 316, effects of sodium and contaminants on, 18: 12582(R) (MSAR-64-14)
mechanical properties of type 316, effects of air, helium, and sodium at 1200°F on, 18: 18314 (MSAR-64-18)
mechanical properties of type 316, effects of sodium and contaminants on, 18: 22445(R) (MSAR-64-45)
mechanical properties of 347, for reactor fuel tubes, 18: 24854(R) (CEND-2863-211)
mechanical properties at high pressures and temperatures, 18: 25972 (ASD-TDR-63-90(Vol.II))
mechanical properties of type 304 at high temperatures, effects of hydrogen on, 18: 27966 (ORNL-3600)
mechanical properties of 347, for use in fuel tubes, 18: 45001(R) (CEND-2863-217)
mechanical properties, 18: 45022(R) (GNEC-327)
mechanical properties of type 316, effects of air, helium, and sodium at 1200°F on, 19: 928(R) (MSAR-64-112)
mechanical properties of, effects of cold-work and temperature on, 19: 2871
mechanical properties of, effects of mercury cavitation under stress on, 19: 2725 (NP-14437)
mechanical properties of type 316, effects of 1200°F sodium on, 19: 4621(R) (MSAR-62-142)
mechanical properties of Type 316, effects of 1200°F sodium on, 19: 4622(R) (MSAR-62-159)
mechanical properties of Type 316, effects of 1200°F sodium on, 19: 4623(R) (MSAR-63-6)
mechanical properties of type 316, effects of air, helium, and sodium at 1200°F on, 19: 6298(R) (MSAR-64-126)
mechanical properties and microstructure of type 304, effects of cold work, neutrons, and temperature on, 19: 7847 (APED-4542)
mechanical properties of type 304 and 316, effects of air, helium, and sodium at 1200°F on, 19: 11692(R) (MSAR-64-144)
mechanical properties of type 316, effects of high-carbon- and oxygen-sodium at 1200°F, 19: 11726(R) (MSAR-65-05)
mechanical properties of annealed and cold-worked tubular, at 300°C, 19: 14767(R) (KR-86)
mechanical properties of type 316, effects of sodium at 1200°F on, 19: 18456(R) (MSAR-65-28)
mechanical properties of type 316, effects of high-carbon and -oxygen sodium at 1200°F on, 19: 18457(R) (MSAR-65-38)
mechanical properties of austenitic, 19: 24997
mechanical properties of austenitic, effects of pressure and temperature on, 19: 40286(R) (NAA-SR-11200)
mechanical properties of 347, effects of heat treatments on, 19: 39091(R) (BMI-1723(Del.))
mechanical properties and microstructure of high purity, 19: 40947(R) (EURAEC-1403)
mechanical properties of 347 and 348, effects of heat treatments on, 19: 42801(R) (BMI-1721(Del.))
mechanical properties of austenitic and austeno-ferritic, effects of silicon additions on, 19: 42803(R) (EURAEC-1397)
mechanical properties at 75 to 1200°F, effects of heat treatment on, 19: 46913(R) (BMI-1733(Del.))
mechanical properties at cryogenic temperatures, 19: 47013 (PB-171809(Rev.)(Suppl.2))
mechanical properties of 316, effects of lithium on, 20: 4299(R) (ORNL-2711)
mechanical properties at high temperatures under stress, thermodynamic method for evaluating, 20: 5913(R) (EURAEC-1488)
mechanical properties of high-purity, effects of carbon content and tempering on, 20: 9421(R) (EURAEC-1486)
mechanical properties of type 316, effects of high-carbon sodium on, at 1200°F, 20: 11235 (MSAE-65-194)
mechanical properties of type 304, effects of high-carbon sodium at 1200°F on, 20: 14981(R) (MSAR-66-09)
mechanical properties of type 304, effects of high-oxygen sodium at 1200°F on, 20: 14981(R) (MSAR-66-09)
mechanical properties of Swedish pressure vessel, 20: 21228 (AE-221)
mechanical properties of austenitic and austeno-ferritic, effects of test temperature on, 20: 2256(R) (EURAEC-1449)
mechanical properties of high-purity, effects of composition on, 20: 27482(R) (EURAEC-1453)
mechanical properties of type 316, effects of oxygen-contaminated sodium on, at 1200°F, 20: 29704 (MSAR-66-78)
mechanical properties of type 304 and type 316, testing of, 20: 35841(R) (NAA-SR-11900)
mechanical properties of, corrosive effects of contaminated high-temperature liquid sodium on, 20: 41420(R) (MSAR-66-149)
mechanical properties of type 304, at 1200°F in air and helium, 20: 41420(R) (MSAR-66-149)
mechanical properties of type 316, corrosive effects of air and liquid potassium at high temperatures on, 20: 41419(R) (GMAD-3643-5)
mechanical properties of type 316, effects of air, helium, and sodium at 1100°F on, 20: 43897 (MSAR-66-174)
mechanical properties of austenitic, effects of thermomechanical treatments on, 20: 43916 (UCRL-16922)
mechanical properties of austenitic, effects of temperature on, 19: 23119 (BNWL-1)
mechanical properties at cryogenic temperatures, relations with microstructure, 16: 27622(R) (AD-271176)
mechanical properties at high pressures and temperatures, 18: 25972 (ASD-TDR-63-90(Vol.II))
microstructure of high-purity, of 18/8 type, 16: 16739
microstructure of types 316 and 316L, effects of heat treatments at 650°C on, 20: 27499(T) (ORNL-tr-961)
milling, 17: 6612

mist removal from air streams by screen of, 19: 28577(R) (UCRL-12378)
Mössbauer effect, effects of magnetic fields, 16: 16828
Mössbauer effect in, 18: 9441
neutron capture by, gamma spectra from thermal, (E), 19: 5545 (ORNL-3609)
neutron cross sections, library of 40-group BPG and spectral "B" codes, 16: 12422 (BAW-158)
neutron cross sections for 304, 20: 4829 (GEMP-173(Suppl.1))
neutron flux distribution in slabs, emergent gamma flux from, 16: 31177 (NARF-62-6T)
neutron propagation in slabs of, in contact with uranium slabs, (E), 19: 12454 (EUR-1637.f)
neutron reactions in types 304 and 316, yields of helium and hydrogen produced by fast, 19: 44746 (NAA-SR-Memo-10626)
neutron reactions with type 347, helium and hydrogen production in fast, 20: 7490(R) (BMI-1745, Sect.A)
neutron reactions with 17-7 PH, 321, and 403 types, activation response of, 20: 28591 (DC-59-3-90)
neutron reactions, production of secondary gamma rays in, 16: 716
neutron resonance integrals, 19: 12865(R) (NAA-SR-10501)
neutron scattering angular distribution, 16: 12419 (ANL-5567(Rev.))
neutron shielding efficiency of, measurement of, 18: 15425 (UNC-5072)
neutron spectra in, measurement of, (E), 19: 37770
neutron transmission in slabs of, (E), 19: 14728 (APEX-581)
nitridation of, parameters effecting integrity of coatings obtained by, 17: 1049(R) (PRDC-TR-57)
nitridation of type 308, by ammonia–hydrogen at 1000°F, 20: 27428(R) (EURAEC-1630)
nitriding experiments on type 304 wires, 19: 16015 (EURAEC-1322)
nitrogen reactions in, effects of uranium on, 19: 30804
nuclear properties of, for use in reactor cores, 17: 4106
optical properties at high temperatures, emittance and reflectance, 16: 12236 (WADD-TR-60-370)
outgassing behavior, 16: 18019 (AEDC-TDR-62-19)
outgassing measurements on, 16: 31718
outgassing of type 304 by electrons in storage rings, 18: 32313 (LNF-64/19)
oxidation by air at 980°C, 18: 2174(R) (USBM-U-1082)
oxidation by carbon di- and monoxide systems, 17: 21342
oxidation by carbon dioxide–carbon monoxide mixtures, 20: 21383
oxidation by high-temperature steam, use of electron-beam microprobe to study, 19: 17774 (GEAP-4490)
oxidation by steam of type 304, effects of surface work-hardening on, 20: 765(R) (EURAEC-1387)
oxidation by steam at 500°C of type 304, effects of surface finishing on, 20: 766(R) (EURAEC-1445)
oxidation by steam, effects of purity and silicon content on, 20: 9421(R) (EURAEC-1486)
oxidation by water of type 304, effects of surface finish on, 20: 765(R) (EURAEC-1387)
oxidation by water of type 410, effects of surface finish on, 20: 766(R) (EURAEC-1445)
oxidation by water of type 304, effects of flow rate on, 20: 766(R) (EURAEC-1445)
oxidation in agitated bed of alumina containing metal fluorides, 18: 11958(R) (BNL-823(p.20-47))
oxidation in nitric acid, electrolytic, 16: 17759 (DP-647)
oxidation of chromized 446, at 1900 to 2200°F, 16: 10451 (DC-60-6-125)
oxidation of cladding of, by steam in TREAT transient experiments, 19: 38132 (ORNL-P-1287)
oxidation of nitrided type 304, by EGCR coolant conditions, 17: 33319(R) (ORNL-3445(p.37-62))
oxidation of nitrided type 304, 18: 4764(R) (ORNL-3470(p.129-56))
oxidation of type-316, in CANEL applications, catastrophic, 16: 15148 (TIM-645)
oxidation of type 310, by nitrogen–oxygen at 1750°F, 17: 28528(R) (IDO-28607)
oxidation of type-405, by air at 600°C, 20: 5594(R) (ANL-6925, pp 21-106)
oxidation of types 304 and 316, by oxygen-rich sodium at 1200°F of types, 20: 9413 (CONF-650620, pp 1-17)
oxidation of types 304, 321, and 410 by steam at 400 to 600°C, effects of surface work-hardening on, 20: 14977(R) (EURAEC-1500)
oxidation of, effects of fluoride on, 19: 15331(R) (BNL-841(p.18-42))
oxidation resistance of type 405, at 650°C, 19: 32279(R) (ANL-7020 (p.3-99))
passivation, 18: 2183(T,R) (EURAEC-285)
passivation by surface exchange of chromate ions with aqueous ions, 19: 930(R) (ORNL-3679(p.84-7))
passivation of 18/8, 18/10, and type 304, by air and nitric acid, 18: 18318(T,R) (EURAEC-836)
passivation of 18/8 and 18/10, analysis by coulometry, 18: 32063(T,R) (EURAEC-1060)
passivation of, galvanostatic studies of effects of crystal structure on, 19: 22905
passivation using nitric acid for use with ferrosulfate radiation dosimetry method, 18: 12469
penetration of Type 304, by liquid uranium–fissium alloy, 17: 26118
penetration rates of type 304, by hydrofluoric acid–oxygen in fluid bed at 550°C, 19: 32280(R) (ANL-7020(p.100-49))
performance as anodes for high-voltage vacuum discharge, (E), 19: 9303 (CERN-64-50)
performance as boiling-reactor fuel cladding, 18: 29069
performance as cladding for ceramic and cermet fuels, (E), 19: 40172
performance as cladding on EBR-II Mark I fuel pins, (E), 20: 14009(R) (ANL-7122, pp 82-90)
performance as fuel cladding in supercritical-water reactors, 18: 35691(R) (WCAP-3374-1)
performance as fuel coatings in PWR, 19: 34632
performance as fuel element cladding in large PWR, 20: 12418(R) (WCAP-3739)
performance as fuel cladding under coolant-loss conditions, 20: 20221
performance as fuel jacket material for fast reactors, 20: 38465 (ANL-7120, pp 289-300)
performance as fuel cladding in water-cooled power reactors, 18: 38279 (A/CONF.28/P/593)
performance as waste container material in skull reclamation processes, 17: 14116(R) (ANL-6596(p.29-118))
performance in EBWR pressure vessel, 20: 10365 (ANL-7117)
performance in nuclear superheated steam environments, 18: 4161 (GEAP-4351)
performance in Sodium Test Facility, 18: 15567
performance of centrifugally cast, in SPERT III primary piping, 17: 34324 (IDO-16887)
performance of coating of, on reactor fuel rods, 17: 35166
performance of low-manganese, for ionization chamber construction, 20: 5716 (AEEW-M-470)
performance of sensitized type 304, as fuel cladding for pressurized-water reactors, 20: 33792
performance of type 304, in ultrasonic liquid-metal level indicators, 20: 13031(R) (NYO-2910-13)
performance of type 316, as cladding for plutonium–uranium fuel alloys, (E), 20: 14007(R) (ANL-7122, pp 1-41)
performance of type 304, as cladding for alloy and carbide fuels, (E), 20: 14007(R) (ANL-7122, pp 1-41)
performance of type 304, in accelerating electrodes in cesium-contact ion thrustors, 20: 31383
performance of type 304, in pellet fuel rods, 18: 28999 (GEAP-4407)
performance of 17-4 PH, in LAMPRE, 18: 15567
performance of 304, as fuel cladding in fast reactors, 18: 24952(R) (ANL-6880(p.6-48))
performance of 304, 310, and 406, in nuclear-superheater environment, 18: 24886(R) (GEAP-4565)
performance of 304, 316, 347, and 406, in nuclear superheater environment, 18: 24884(R) (GEAP-4419)
performance of 304, as PWR fuel cladding, 18: 29018
performance of 304, 310, 348, and 406, in nuclear-superheater environment, 19: 10541(R) (GEAP-4703)
performance of 304 and 310, as EVESR fuel cladding, (E), 19: 10538 (GEAP-4425)
performance of 304, in measuring carbon in sodium, 19: 40409(R) (MSAR-65-95)
performance of 316 and 20/25 niobium-, as fuel cladding in nuclear superheat environment, 19: 28860
performance of 406, as cladding for superheater fuel elements, 18: 28025
phase studies of martensite in, analysis by magnetic moments, 18: 32063(T,R) (EURAEC-1060)
phase transformation studies during calcination of nitrates of, 17: 30582(R) (IDO-14611)
physical properties of, effects of sodium at 1200°F on, 17: 533(R) (MSAR-61-29)
physical properties of, effects of sodium at 1100 to 1200°F on, 17: 534(R) (MSAR-62-23)
physical properties of, effects of annealing at 425 to 525°C on, 17: 563
physical properties of, effects of 1200°F sodium on, 17: 18755(R) (MSAR-62-92)
physical properties of, effects of high-temperature sodium on, 17: 18756(R) (MSAR-63-47)
physical properties of, effects of 1200°F sodium on, 17: 18751(R) (MSAR-62-33)
physical properties of, effects of 1200°F sodium on, 17: 18752(R) (MSAR-62-41)
physical properties of, effects of 1200°F sodium on, 17: 18753(R) (MSAR-62-50)
physical properties of, effects of 1200°F sodium on, 17: 18754(R) (MSAR-62-77)

physical properties of type 316, effects of air, helium, and sodium at 70 and 1200°F on, 17: 32571(R) (MSAR-63-105)
physical properties of, effects of liquid sodium on, 18: 1245 (LADC-5936)
physical properties of type 304, effects of annealing on, 18: 32043(R) (HW-81269(p.4.1-64))
physical properties of type 316, effects of air, helium, and sodium containing carbon and oxygen at 1200°F on, 19: 901(R) (MSAR-64-102)
physical properties of type 316, effects of 1200°F sodium on, 19: 4624(R) (MSAR-63-75)
physical properties of 316, in air, helium, and sodium, (E), 19: 13998 (SAN-8002(p.210-30))
physical properties at 650°C of type 304 and 316, 19: 27773 (ANL-6939)
physical properties of, equipment and methods for measuring, 20: 14719
physical properties of, effects of 1200°F sodium on, 18: 7149(R) (MSAR-62-12)
physical properties of, effects of 1200°F sodium on, 18: 7149(R) (MSAR-62-12)
pipes of, measurement of motion of graphite spheres through, 18: 28937(R) (ORNL-3578(p.100-21))
plasma accelerator electrodes of, mass losses by pulsed, (E), 19: 17082
plasticity and structure of, effects of cerium on, 19: 23022(T) (JPRS-28849(p.310-18))
plasticity of, effects of cerium on, 19: 23018(T) (JPRS-28849(p.279-85))
plating, 17: 8758(T,R) (EURAEC-458)
polishing of, effect on mechanical properties of electrolytic, 19: 28776 (DMIC-213)
precipitation of chromium and niobium carbides at grain boundaries in, 16: 33422
precipitation of niobium carbide in, effect of heat treatment on, 16: 33423
preparation and properties of cold compacted and sintered type 302B, 18: 547 (LAMS-2898)
preparation of coating of, for large-thickness steels, 17: 22135(T,R) (EURAEC-564)
preparation of foamed, for aerospace uses, 19: 37141
preparation of iron-57-enriched, for neutron flux measurements, 18: 2128(R) (ORNL-TM-658)
preparation of low-cobalt, 17: 12606(P)
pressing on fuel elements for cladding, by reactor internal pressure, 20: 46178(P)
processing claddings of, on spent uranium fuel elements, 19: 28452
production facilities, list of European, 16: 10452 (EURAEC-31)
production of, by sintering at 470 to 1150°C, mechanism and technique for, 17: 32497
properties, 18: 15565
properties and performance as fuel cladding for Marviken superheater elements, 19: 28770
properties and structure of type 304, 19: 28870(R) (BMI-X-10121)
properties as claddings for uranium carbide fuels, 17: 16650 (NAA-SR-7696)
properties as cladding and structural materials in reactors, 18: 32072
properties as cladding and structural material in reactors, 18: 41947
properties as fast reactor material, 18: 15566
properties as fuel element cladding, 18: 13260
properties as fuel element cladding, 18: 15563
properties as high-temperature reactor structural material, 19: 4597 (SAN-8003(p.13-89))
properties as neutron reflector in fast-breeder reactors, 18: 4700
properties as nuclear poison, 16: 7795
properties as reactor pressure vessel material, 18: 3240
properties as reflector in fast reactor, 18: 4746
properties as superheat fuel cladding, 19: 4597 (SAN-8003(p.13-89))
properties as water-reactor fuel cladding, corrosion-resistance and mechanical strength, 18: 37610 (A/CONF.28/P/419)
properties at −400 to 100°F, 18: 42020 (PB-171809(Rev.))
properties at high temperature, effects of cold work, 16: 27622(R) (AD-271176)
properties at low temperatures, 18: 22493(R) (PB-171809-6)
properties for application to 1200°F, 16: 10403 (ASD-TR-61-322 (p.40-54))
properties for containers of liquefied plutonium alloys with molten salts, 20: 5594(R) (ANL-6925, pp 21-106)
properties for fuel cladding for water-cooled reactors, 20: 35839 (KR-89, pp 112-30)
properties for fuel cladding for steam-cooled reactors, 20: 35840 (KR-89, pp 131-52)
properties for liquid-metal fast breeder reactor, 18: 29039 (GEAP-4418 (Vol.II))
properties for pressure vessels, 16: 19384
properties for structural use in gas-cooled reactors, 16: 19993 (NYO-9793)
properties for use in process tubes for nuclear superheat reactors, 16: 31254 (GEAP-3784)
properties for use in filtering carbon from sodium, 17: 18220 (NAA-SR-8239)
properties for use in cermet filters for purification of sodium (liquid), 17: 18682(T) (FTD-TT-62-1473(p.31-7))
properties for use as canning materials for fuel elements, 18: 39981
properties for use in process equipment, manual on, 19: 887 (DP-860 (Vol.I))
properties for use in reactors, 19: 4670
properties for use in reactors, 19: 6366
properties for use as fuel element sheaths, 19: 4708(P)
properties for use as fuel cladding material, 19: 11679
properties for use as matrix for burnable reactor poisons, 19: 11681
properties for use as reactor material, 19: 13907
properties for use in ultrahigh vacuum systems, (E), 19: 30760
properties for use as fuel cladding material in reactors, 19: 39206
properties for use in exchange column for boron isotope separations using anisole–boron trifluoride, 20: 25467 (K-1653)
properties in carbon monoxide and dioxide at high temperatures, 16: 30731(P)
properties in high-temperature argon-nitrogen, 19: 14765(R) (ANL-6977)
properties in liquid-metal fast flux reactor, 19: 34672 (BMI-X-10129)
properties in reactor fuel cans, 18: 557
properties of, alloying effects of uranium on, 18: 2229 (NP-13261(p.136-83))
properties of, as cladding for reactor fuel elements, 17: 8820 (XDCL-60-8-40)
properties of austenitic, at −400 to 100°F, 19: 26803(R) (AD-611165)
properties of austenitic, 20: 13186 (TRG-Report-840)
properties of austenitic, 20: 22502(R) (NAA-SR-11805)
properties of austenitic, for Rapsodie pressure vessel, 20: 42652(T) (EURFNR-92F)
properties of bimetal tubes for niobium or niobium–1 zirconium alloy and type 316, 20: 11214(R) (NASA-CR-54717)
properties of bonded joints with Zircaloy, 17: 13672(R) (DP-815)
properties of boron-loaded, as nuclear poison, 17: 232 (RFP-265)
properties of boron-alloyed, for nuclear reactors, 18: 27983
properties of boron-containing, 16: 3516(P)
properties of Carpenter-20, for use in hydrofluoric acid fuel dissolvers, 17: 8242 (IDO-14594)
properties of coating of series 300, for fuel cladding, 17: 12665 (GEAP-4095)
properties of compacts of, as reactor core material, 16: 25762 (SCNC-264)
properties of flame-sprayed coatings of, for use in space technology, 18: 16521
properties of, for reactor pressure vessels, 18: 3256
properties of low-manganese, as reactor material, 18: 8838
properties of powders of, as thermal insulation, 19: 25751 (TID-21212)
properties of precipitation-hardening, in water-cooled reactors, 16: 7859
properties of, rare earth alloying effects on, 17: 39584
properties of, research programs on thermal-stress-fatigue, 16: 30719(R) (ATL-A-130)
properties of type 304, as reactor material, 16: 18050
properties of types 304 and 347, as reactor control material, 16: 32120 (TID-16597)
properties of type 304, effects of rolling and swaging on, 17: 14781 (GEAP-3997)
properties of type 410, for reactor pressure vessels, 17: 23912 (TID-7620(Pt.I)(p.95-116))
properties of types 304, 310, and 347, as fuel element cladding materials, 17: 36927(R) (GEAP-4075)
properties of types 304, 310, 316, 347, and 406, as fuel element cladding materials, 17: 36928(R) (GEAP-4126)
properties of types 304, 310, 316, 347, and 406, as fuel element cladding materials, 17: 36929(R) (GEAP-4243)
properties of type 347, as cladding for reactor fuel elements, 18: 6412(R) (GEAP-3888)
properties of type 347, for gas-cooled reactor uses, 19: 2716(R) (BMI-1681(Del.))
properties of types 304 and 316, for fuel cladding, 19: 12865(R) (NAA-SR-10501)
properties of type 347 for reactor uses, 19: 22865(R) (BMI-1711(Del.))
properties of type 347, for gas cooled reactor uses, 19: 30642(R) (BMI-1707(Del.))
properties of type 310, as weld-filler metal, 20: 11214(R) (NASA-CR-54717)
properties of types 310 and 316, effects of rare earth alloying additions on, 20: 17078
properties of types 304 and 348, mechanical and physical, 20: 33861 (BAW-237)
properties of type 316, effects of molten sodium on mechanical and physical, 17: 14768(R) (MSAR-63-33)
properties of welded sheaths, sheets, and tubes of, 18: 7172
properties of, effects of rare earths on corrosion and mechanical,

19: 22878(T) (JPRS-28849(p.286-91))
properties of, effects of low temperature on, 20: 4417
properties of, effects of sodium coolant on, 20: 46995
properties of, effects of temperature on mechanical and physical, 17: 16760
properties of, flow and fracture, 19: 7972
properties of, for use as fuel cladding, 20: 21383
properties of, review of methods of improving, 19: 18523
proton reactions at 660 Mev, 17: 41884
proton reactions in, production of cobalt-57 by cosmic, 17: 3938
puncture resistance of type 304L, effects of temperature on, 20: 43492 (ORNL-TM-1312(Vol.2))
radiation absorption by surface of, exposed to plasma radiation, (E), 19: 10443
radiation absorption at 80°K by, thermal, 19: 26885 (NIRL-R-83)
radiation damage in 410, 16: 21086 (AECL-1484)
radiation damage to, in use for encapsulating radiation sources, 18: 12139(R) (BNL-823(p.48-56))
radiation effects on mechanical properties, bibliography, 16: 5756 (DP-579)
radiation effects on stress-rupture strength, tube burst tests, 16: 6823(R) (ORNL-3213(p.124-33))
radiation effects on friction and wear properties of type 304, 16: 10604 (APEX-671)
radiation effects on reactions with water at high temperatures, 16: 11575 (ANL-6250)
radiation effects at −423°F, 16: 13640 (ERR-AN-085)
radiation effects, 16: 14375(R) (BMI-1557(Del.))
radiation effects on corrosion by chemicals, 16: 17976(R) (EURAEC-94)
radiation effects, 16: 17977(R) (EURAEC-141)
radiation effects, 16: 17978(R) (EURAEC-175)
radiation effects on corrosion by uranyl sulfate at 280°C, 16: 17982 (ORNL-2962)
radiation effects on tensile properties of borided, 16: 22648 (DC-60-2-726)
radiation effects on electrochemical properties, 16: 22678
radiation effects on relaxation of elastic stresses in bent plates of, neutron, 16: 22704
radiation effects on torsional stresses in, 16: 24236 (DP-669)
radiation effects on mechanical properties, 16: 24239 (HW-SA-2547)
radiation effects, 16: 28379(R) (ORNL-3302(p.232-79))
radiation effects at cryogenic temperatures, 16: 27622(R) (AD-271176)
radiation effects on relaxation of elastic stresses in, neutron, 16: 27699(T) (AEC-tr-5257)
radiation effects on type 304, effects of boron content on, 16: 30910 (TID-12047)
radiation effects on mechanical properties, 16: 33519 (ORNL-TM-337)
radiation effects on properties, review, 16: 33546
radiation effects on mechanical properties, fast neutron, 16: 572 (REIC-20)
radiation effects on mechanical properties, 17: 591
radiation effects on boron-containing type 304, 17: 2000 (BMI-B&W-654)
radiation effects on corrosion by water, 17: 2018
radiation effects on corrosion of, by high-temperature steam and water, 17: 1877 (TID-17220(Pt.2))
radiation effects on corrosion by indium–gallium alloy (liquid), 17: 2013
radiation effects on mechanical and tensile properties, 17: 3378(R) (BMI-1583(Del.))
radiation effects on type 347, 17: 3379(R) (BMI-1596(Del.))
radiation effects on creep, 17: 7553(R) (HW-74761(p.9.1-37))
radiation effects on mechanical properties of type 347, at 1150 to 1700°F, 17: 7606(R) (ORNL-1515)
radiation effects on type 347, 17: 6511(R) (BMI-1593(Del.))
radiation effects on tensile properties of type 347, 17: 12712 (BMI-1609)
radiation effects on tensile properties of type 304, 17: 12715 (GEAP-3983)
radiation effects on corrosion of, in-reactor, 17: 13678(R) (HW-75914)
radiation effects on mechanical properties of type 347, 17: 14740 (TID-11295(2nd Ed.))
radiation effects on type 347, 17: 14727(R) (BMI-1600(Del.))
radiation effects on mechanical properties of, 17: 21230 (TID-7658 (p.27-47))
radiation effects on AISI 316, 17: 27730(R) (HW-77052)
radiation effects on mechanical properties at high temperatures of Type 347, 17: 26163
radiation effects on tensile properties at cryogenic temperature, neutron, 17: 28102
radiation effects on mechanical properties of AISI 348 and 304, 17: 27730(R) (HW-77052)
radiation effects on Type 347, 17: 22966(R) (BMI-1614(Del.))
radiation effects on, in nine year's use as gamma source capsule, 17: 30783 (ORNL-TM-584)
radiation effects on impact strength of 17-4 PH and 304, neutron, 17: 31066
radiation effects on mechanical properties of 347, neutron, 17: 31067
radiation effects on rupture-stress properties of 304, neutron, 17: 31068
radiation effects on corrosion, mechanical, physical and thermal properties of, 17: 32679
radiation effects on stress-rupture properties of, 17: 34557(R) (ORNL-3480(p.117-42))
radiation effects on pitting of 316L, in chloride solutions, 17: 39481(R) (EURAEC-611)
radiation effects on corrosion of, 17: 39485(R) (EURAEC-738)
radiation effects on mechanical properties and structure of, neutron, 17: 39683
radiation effects on corrosion of, by oxygen and water vapor, 17: 39482(R) (EURAEC-616)
radiation effects on mechanical properties of, critical factors in interpretation of, 17: 41515
radiation effects on passivation of types 304 and 410, 18: 2183(T,R) (EURAEC-285)
radiation effects on corrosion of type 304, 18: 2356
radiation effects on tensile properties of type 304, at 343°C, 18: 4761(R) (GEAP-4383)
radiation effects on tandem-extruded joints between Zircaloy-2 and, neutron, 18: 7284 (DP-859)
radiation effects on AISI-406, 18: 7292(R) (HW-77954(p.4.1-12))
radiation effects on mechanical properties of, 18: 7294(R) (HW-77954(p.4.19-77))
radiation effects on mechanical properties of, 18: 7302(R) (HW-78962 (p.4.50-126))
radiation effects on type 347, 18: 7985(R) (BMI-1650(Del.))
radiation effects on mechanical properties of, 18: 7955(R) (HW-78962 (p.6.20-4))
radiation effects on mechanical properties, 18: 8866(R) (HW-78388 (p.8.1-7))
radiation effects on mechanical properties of type 347, neutron, 18: 13354(R) (BMI-1657(Del.))
radiation effects on electrochemical corrosion of type 316L, by air- and nitrogen-saturated solutions, 18: 14406(R) (EURAEC-852)
radiation effects on tensile properties of, neutron, 18: 14537(R) (HW-79766(p.4.1-76))
radiation effects on fracture properties of AISI 348, 18: 14537(R) (HW-79766(p.4.1-76))
radiation effects on fracture strain and strain rate of chromium–nickel–niobium-stabilized, 18: 15493(R) (ORNL-3523(p.193-226))
radiation effects on mechanical properties of Type 347, 18: 17351(R) (BMI-1659(Del.))
radiation effects on tensile properties of, 18: 18307
radiation effects on tensile properties of pressure tube of type 347, effects of annealing on fast neutron, 18: 20450(R) (BMI-1661(Del.))
radiation effects on corrosion of, by oxygen and water vapor, 18: 22524 (EURAEC-874)
radiation effects on mechanical properties of austenitic, 18: 24192 (HW-SA-3221)
radiation effects on mechanical properties, neutron, 18: 28043(R) (HW-79280(p.8.1-6))
radiation effects on 304 and 347 at low temperatures, 18: 28048 (NP-13980)
radiation effects on embrittlement of, at high temperature, effects of heat treatment on, 18: 28061
radiation effects on tensile properties of, fast-neutron, 18: 28079
radiation effects on types 304 and 347, fast-neutron, 18: 30238(R) (NP-14102)
radiation effects on mechanical properties of type 347 pressure tubes, effects of high temperature on fast neutron, 18: 28052 (WAPD-T-1574)
radiation effects on engineering properties of, review, 18: 32216 (A/CONF.28/P/242)
radiation effects on mechanical properties of niobium-stabilized austenitic, neutron, 18: 34218 (ORNL-TM-881)
radiation effects on pitting of type 304, by potassium bicarbonate–potassium chloride electrolyte saturated with nitrogen at 25°C, 18: 37639(R) (EURAEC-1130)
radiation effects on mechanical properties of type 347, fast neutron, 18: 40028
radiation effects on mechanical properties of, 18: 40970(R) (BMI-1674(Del.))
radiation effects on, in presence of chemical impurities, 18: 40970(R) (BMI-1674(Del.))
radiation effects on austentic, neutron, 18: 41933 (TID-11295(3rd Ed.))
radiation effects on types 304, 310, 348, and 406, 18: 45020(R) (GEAP-4619)
radiation effects on mechanical properties of AISI 406, 18: 44036(R) (HW-82651(p.4.1-49))
radiation effects on mechanical properties of austenitic, 18: 44036(R) (HW-82651(p.4.1-49))

radiation effects on mechanical properties of, neutron, 18: 44050(R) (ORNL-3670(p.116-21))
radiation effects on stress-rupture properties of niobium-stabilized chromium–nickel, neutron, 18: 44054(R) (ORNL-3670(p.174-200))
radiation effects on structure of, neutron, 19: 997(R) (NYO-2994-1)
radiation effects on type-304 (E), 19: 3687
radiation effects on ductility of pressure tubes of, in-pile, 19: 2870
radiation effects on type-304, neutron, 19: 2871
radiation effects on types 304 and 347, neutron, 19: 2872
radiation effects on tensile elongation of types 304, 316, 347, and 406, at high temperatures, neutrons, 19: 2880
radiation effects on types 304VM, 310VM, and 348, in superheated steams, 19: 2881
radiation effects on mechanical properties of type 347, fast neutron, 19: 2716(R) (BMI-1681(Del.))
radiation effects on catalytic reactions of, in formic acid decomposition, 19: 4196(R) (ORNL-3627(p.220-3))
radiation effects on, (E), 19: 4670
radiation effects on types A-286 and 310, fast-neutron, 19: 6364(R) (NP-14443)
radiation effects on mechanical properties, phase changes, and structure, 19: 6366
radiation effects on mechanical properties and microstructure of type 304, neutron, 19: 7847 (APED-4542)
radiation effects on, in use as fuel matrix, 19: 11679
radiation effects on stress-rupture properties of A-286, 19: 11682
radiation effects, 19: 14084(R) (HW-81984(p.8.1-3))
radiation effects on tensile properties of type 347, fast neutron, 19: 13871(R) (BMI-1691(Del.))
radiation effects on tensile properties of types A-286, AM350, and 440C, at 30°R, 19: 14086(R) (N65-13446)
radiation effects on creep of type 304, at 500 to 600°C, 19: 16212(R) (HW-84281(p.4.6-7))
radiation effects on nil ductility temperature of A212B, neutron, 19: 18259 (HW-SA-3541)
radiation effects on mechanical properties of type 347, 19: 18420(R) (BMI-1694(Del.))
radiation effects on mechanical properties of type 347, fast-neutron, 19: 22864(R) (BMI-1704(Del.))
radiation effects on type 347, neutron, 19: 22865(R) (BMI-1711(Del.))
radiation effects on AISI 304 and 348, 19: 22895(R) (HW-83298(p.9.1-3))
radiation effects on fuel rod cladding of, in-pile, 19: 24123
radiation effects on tensile properties of types A-353 and 17-7PH at 30°R, 19: 25048(R) (NP-14889)
radiation effects on tensile properties of type T-450 at 30°R, 19: 25048(R) (NP-14889)
radiation effects on fuel rod jackets of, 19: 26876 (ANL-6750)
radiation effects on mechanical properties of 304 and 316, 19: 27735(R) (NAA-SR-10850)
radiation effects on type 304, fission-fragment, 19: 28870(R) (BMI-X-10121)
radiation effects on mechanical properties of 304, 310, and 347, neutron, 19: 29675
radiation effects on mechanical properties of, neutron, 19: 28906
radiation effects on, fast neutron, 19: 30642(R) (BMI-1707(Del.))
radiation effects on, fast neutron, 19: 30649(R) (HW-84573(p.4.1-31))
radiation effects on fuel-cladding, 19: 32777 (ORNL-3504)
radiation effects on microhardness and microstructure of type 304, fast-neutron, 19: 33603(R) (GEAP-4816)
radiation effects on high-temperature ductility of niobium-stabilized austenitic, thermal-neutron, 19: 32774 (AE-186)
radiation effects on mechanical properties of type 304, at 550°C and 30,000 psi, fast neutron, 19: 34742(R) (BNWL-79(p.4.1-30))
radiation effects on tensile properties of, as function of exposure and test temperature, fast neutron, 19: 34743 (GEAP-4754)
radiation effects on embrittlement of, neutron, 19: 34756
radiation effects on mechanical properties of 304, 347, and 17-7 PH, (E), 19: 35622
radiation effects on creep of, in reactor, 19: 37167(R) (HW-84609 (p.8.1-7))
radiation effects on diffusion of hydrogen in, gamma, 19: 37170(R) (ORNL-3807, pp 249-76)
radiation effects on mechanical properties of, 19: 37170(R) (ORNL-3807, pp 249-76)
radiation effects on, gamma, 19: 36451(R) (BNL-900(p.73-104))
radiation effects on 304, neutron, 19: 40286(R) (NAA-SR-11200)
radiation effects on 347, neutron, 19: 39091(R) (BMI-1723(Del.))
radiation effects on ductility of type 304, fast neutron, 19: 39236 (WCAP-3269-36)
radiation effects on mechanical properties of type 304, fission-fragment and neutron, 19: 39229(R) (BMI-X-10134)
radiation effects on stress-strain properties of type 304, neutron, 19: 40961
radiation effects on mechanical properties of austenitic chrome nickel, neutron, 19: 41093(T) (FTD-TT-65-125)
radiation effects on, neutron, 19: 42801(R) (BMI-1721(Del.))
radiation effects on fuel clad of, under superheat conditions, 19: 42903 (GEAP-4775)
radiation effects on Type 304 cladding, high-temperature neutron, 19: 42905 (NAA-SR-11134)
radiation effects on, in-reactor, 19: 45669(R) (APDA-174, pp 61-6)
radiation effects on constant-stress-rate rupture properties of niobium-stabilized, neutron, 19: 44750 (ORNL-TM-1216)
radiation effects on tensile properties of type 304, fast and thermal neutron, 19: 44743 (GEAP-3634)
radiation effects on 347, neutron, 19: 46912(R) (BMI-1727(Del.))
radiation effects on 347, fast neutron, 19: 46913(R) (BMI-1733(Del.))
radiation effects on stress corrosion of, in magnesium chloride, 19: 47079 (AERE-R-5014)
radiation effects on, neutron, 19: 7996
radiation effects on creep in type 304, neutron, 20: 889(R) (BNWL-120, pp 4.1-59)
radiation effects on ductility of types 304 and 348, fast neutron, 20: 889(R) (BNWL-120, pp 4.1-59)
radiation effects on embrittlement of type 304, effects of boron on, 20: 898
radiation effects on type 304, electron and uv, 20: 910
radiation effects at cryogenic temperatures, 20: 2459
radiation effects on bursting pressure and fatigue life of pressure tubes of, neutron, 20: 2435 (WAPD-T-1720)
radiation effects on mechanical properties of, at high temperatures, 20: 2430 (ORNL-P-1713)
radiation effects on mechanical properties of types 304 and 347, at 25 to 850°C, 20: 2477
radiation effects on stress-rupture properties of 304, 20: 5181(R) (ORNL-3029)
radiation effects on in-pile corrosion of, by aqueous solutions, 20: 5852(R) (EURAEC-1522)
radiation effects on mechanical properties of, thermodynamic method for evaluating, 20: 5913(R) (EURAEC-1488)
radiation effects on corrosion of types 304 and 347, by Santowax OM at 500 to 700°F, fast-neutron, 20: 5846
radiation effects on mechanical properties of type 347, irradiated at 80 to 1500°F, fast-neutron, 20: 5846
radiation effects on ductility of types 304 and 348, effects of irradiation temperature on, 20: 5851
radiation effects on mechanical properties of austenitic, 20: 8394(R) (NAA-SR-11450, Sect.2)
radiation effects on mechanical properties of type 304, fast-neutron and fission-fragment, 20: 7628(R) (BMI-X-10146)
radiation effects on austenitic, in Fermi Fast Breeder Reactor, 20: 8434
radiation effects on mechanical properties and microstructure of type-348, in Yankee Reactor, 20: 7642
radiation effects on mechanical properties and microstructure of type-304, neutron, 20: 7643
radiation effects on ductility of type-304, following cold working or solution annealing, 20: 7644
radiation effects on creep at 550°C of type 304, in-reactor, 20: 9568(R) (BNWL-166, pp 4.1-7)
radiation effects on tensile properties of type 410, fast-neutron, 20: 9576(R) (ORNL-3878)
radiation effects on permeability of type 205, 20: 9618
radiation effects on stress-rupture of 20/25/Nb-stabilized, combined heat treatment and in-reactor, 20: 11227
radiation effects on corrosion susceptibility and tensile properties of type 304, reactor, 20: 13325(R) (GEAP-4968)
radiation effects on mechanical properties of austenitic, neutron, 20: 13333
radiation effects on corrosion resistance of type 304L, gamma, 20: 17118(R) (EURAEC-1564)
radiation effects on fuel cladding of type 304, reactor, 20: 17120 (GEAP-4916)
radiation effects on ductility of, role of helium bubbles in, 20: 17141
radiation effects on austenitic, neutron, 20: 21383
radiation effects on strain fatigue of austenitic, neutron, 20: 21426 (N-65-24714)
radiation effects on tensile properties of type 347, fast-neutron, 20: 23582(R) (BMI-1765)
radiation effects on tensile properties of AM350 and AISI 440c, at 30°R, 20: 23772(R) (N-65-13446)
radiation effects on corrosion of type 304, by nitric acid–potassium dichromate, γ, 20: 25616(R) (GEAP-5085)
radiation effects on thermoelectric properties of, γ, 20: 25616(R) (GEAP-5085)
radiation effects from fission fragments on mechanical properties and strain of, 20: 27567 (BMI-1766)

radiation effects on fuel claddings of, 20: 28733(R) (GEAP-4919)
radiation effects on mechanical properties of AISI 304, 316-L, and 348, neutron, 20: 27573(R) (BNWL-207, pp 4.8-31)
radiation effects on carbide fuel cladding of type 316, neutron, 20: 27593(R) (UNC-5134(Vol.2))
radiation effects on tensile properties of types 304, 310, and 347, irradiated at 30°R, fast-neutron, 20: 27589(R) (NASA-CR-54881)
radiation effects on tensile properties of AISI 440C, AM-350, and 17-7 PH, irradiated at 30°R, fast-neutron, 20: 27589(R) (NASA-CR-54881)
radiation effects on stress-rupture properties of type 304L, 20: 30790(R) (ANL-7204, pp 1-31)
radiation effects on type 304, cladding on urania fuel elements, thermal-neutron, 20: 29806 (ORNL-TM-1511)
radiation effects on mechanical properties of, in-reactor, 20: 31785 (ORNL-P-2162)
radiation effects on ductility of type 304, effects of carbon content on fast- and thermal-neutron, 20: 31669
radiation effects on fuel element cladding of, in-pile, 20: 33867 (GEAP-4849)
radiation effects on type 316L and type 17-4 PH, fast neutron, 20: 33960
radiation effects on rupture strength of type 304, fast neutron, 20: 33961
radiation effects on mechanical properties of type 347, neutron, 20: 35834(R) (BMI-1767)
radiation effects on tensile properties by helium doping and boron-10 transmutation, 20: 35841(R) (NAA-SR-11900)
radiation effects on mechanical properties of, in-pile, 20: 35839 (KR-89, pp 112-307)
radiation effects on austenitic, 20: 37174
radiation effects on type 347, neutron, 20: 37168(R) (BMI-1771)
radiation effects on type 347, neutron, 20: 37169(R) (BMI-1774)
radiation effects on tensile properties of niobium-stabilized, in-reactor, 20: 37284
radiation effects on mechanical properties of types 17-4PH, AM-350, A-236, 405, and 406, neutron, 20: 37286
radiation effects on fuel cladding of type 304, 20: 42626(R) (GEAP-4951)
radiation effects on corrosion by iron chloride, 20: 41418(R) (GEAP-5150)
radiation effects on type 304, neutron, 20: 45106(R) (ANL-7249)
radiation effects on mechanical properties of type 304, 20: 43999 (ORNL-TM-1544)
radiation effects on formation of intergranular voids and cracks at 650 to 850°C in austenitic, thermal-neutron, 20: 44016
radiation effects on types 304 and 308, in-reactor, 20: 44027
radiation effects on ductility of type 316, alpha and neutron, 20: 44015
radiation effects on martensite content of 304 and 348, annealing and cold work relations in, neutron, 20: 46225 (BNWL-238)
radiation effects on, neutron, 20: 46148
radiation effects on, neutron, 20: 46149
radiation effects at cryotemperatures on tensile and shear properties of, 20: 46539
radiation effects on A302B and A350 LF-1, criteria for evaluating, neutron, 20: 46228 (NRL-6415)
radiation effects on, review on, 17: 25830 (HW-SA-3000)
radiation effects on mechanical and physical properties of, 17: 16760
radiation effects on mechanical properties of austenitic, 19: 23119 (BNWL-1)
radiation effects on boron-10-containing austenitic, 16: 32156 (WAPD-262)
radiation effects on boron-10 enriched, 16: 12666 (WAPD-BT-24 (p.65-84))
radiation effects of fission fragment bombardment, 16: 33407
radiation effects on impact strength of A-286, neutron, 17: 31066
radiation effects on mechanical properties of, neutron, 18: 8868 (HW-SA-3268)
radiation effects on mechanical properties, 18: 16525 (NP-13657)
radiation effects on mechanical properties, neutron, 18: 37739 (A/CONF.28/P/162)
radiation effects of fission fragment bombardment, 16: 33407
radiation effects on boron-10-enriched, 16: 12666 (WAPD-BT-24 (p.65-84))
radiation effects on mechanical properties, neutron, 18: 37739 (A/CONF.28/P/162)
radiation embrittlement of type-304, at high temperatures, 19: 28885
radiation embrittlement of, effects of grain size on neutron, 20: 13335
radiation embrittlement of austenitic, thermal-neutron, 20: 15141
radioactive contamination build-up on, from dilute solutions of plutonium, 19: 2747 (NP-14343(Discussion, Session II))
radioactivity induced in, in JRR-1 cooling loops, 16: 11957(R) (JAERI-5003(p.112-14))
radioactivity induced in, spectra of, 18: 6462(R) (ORNL-3499(Vol.I) (p.93-7))
radiography of boron in 304, using neutrons, (E), 20: 3471(R) (GEAP-4861)
radiography of circumferential welds in small-diameter tubes of, x-ray generator for, 20: 7242 (LA-DC-6977)
radiography of thin section, techniques for low-voltage, 16: 23980
radiography, techniques for low-voltage, 16: 10264 (ORNL-3252)
radioinduced cracking in type 347, fast-neutron, 20: 29618(R) (GEAP-4982)
radioinduced creep in neutron-irradiated, transient, 17: 34505
radioinduced defect clusters in, 16: 13649
radioinduced embrittlement of type 304, effects of boron on neutron, 20: 4460(R) (ORNL-3870, pp 140-5)
radioinduced embrittlement of, effects of grain size on neutron, 20: 4460(R) (ORNL-3870, pp 140-5)
radioinduced embrittlement of types 304 and 304L, at 650 to 842°C, neutron, 20: 4460(R) (ORNL-3870, pp 140-5)
radioinduced embrittlement of type 304, effects of grain boundary carbides on neutron, 20: 4460(R) (ORNL-3870, pp 140-5)
radioinduced embrittlement of type 304, effects of titanium additions on neutron, 20: 4460(R) (ORNL-3870, pp 140-5)
radioinduced embrittlement of austenitic, mechanisms for neutron, 20: 25623
radioinduced embrittlement of pressure vessels of 17-4PH, neutron, 20: 27610
radioinduced embrittlement in austenitic, neutron, 20: 31801
radioinduced embrittlement in type 304, effects of boron additions on fast-neutron, 20: 31669
radioinduced embrittlement in type 304, effects of titanium additions on fast- and thermal-neutron, 20: 31669
radioinduced embrittlement of, at 700 to 900°C, neutron, 20: 33946 (ORNL-TM-1516)
radioinduced heating of, gamma, 18: 10346(R) (X64-11113)
radioinduced lattice defects in, electron microscopic observations of, 19: 11812
radioinduced polymerization of silicone oil on, electron, 20: 7176
radioinduced production of helium and hydrogen in, neutron, 19: 26901
radioinduced reactions with U_3Si_2, effects of sodium on neutron, 19: 42805 (NAA-SR-10621)
radioinduced reactions with urania, 20: 1465(R) (GEAP-4894)
radioinduced strain relaxation in, 17: 454
reaction of 304, with sodium, high-temperature, 20: 15033(R) (ANL-7152, pp 87-96)
reactions of clad of type 304, with steam at 1500°C and 15 psig, 19: 32447(R) (ANL-7020(p.175-97))
reactions of type 316, with water at 315°C and 1500 psi, 17: 36860(R) (ANL-6648)
reactions of type 316, with water at 1000 to 4000°C, 17: 40421(R) (ANL-6766)
reactions of type 302, with water under simulated nuclear incident conditions, 18: 1486(R) (ANL-6687(p.167-87))
reactions of type 304, with carbon dioxide at high temperatures, 18: 44050(R) (ORNL-3670(p.116-21))
reactions of type 316, with plutonium carbide–uranium carbide at 760°C, 19: 24992(R) (UNC-5094)
reactions of type 316, with boron carbide in potassium–sodium alloy at 1000°F, 20: 776 (TIM-822)
reactions of type 316L, with plutonium carbide–uranium carbide, 20: 9438
reactions of type 304, with steam at 1400°C, 20: 14009(R) (ANL-7122, pp 82-90)
reactions of type 316L, with plutonia, 20: 14965(R) (NUMEC-3524-12)
reactions of type 304, with uranium nitride at 1000 to 1350°C, 20: 19187 (BMI-1760)
reactions of type 300 series; with combustion gas species in launch pad abort environments, 20: 19192 (SC-DR-65-1918)
reactions of type 304, with uranium monocarbide at 820°C, 20: 27416(R) (UNC-5134(Vol.1))
reactions of type 316, with plutonium uranium carbide at 820°C, 20: 27416(R) (UNC-5134(Vol.1))
reactions of type 304, with plutonium–thorium–uranium alloy, 20: 31666
reactions of type 304, with steam at 900 to 1500°C, 20: 31669
reactions of type 316, with sodium in steam generators, 20: 33803
reactions of, with water at high temperatures, 16: 28641(R) (ANL-6543)
reactions of, with graphite at 540 to 705°C, 16: 33376 (ORNL-TM-338)
reactions of, with uranium dioxide at high temperatures, 16: 33375 (NYO-10469)
reactions with beryllium to 600°C in argon, carbon dioxide, and *in vacuo*, 19: 22997 (TRG-Report-842)
reactions with carbon dioxide, 16: 2993 (NP-10967)
reactions with carbon dioxide, 19: 23996(R) (ORNL-3650(p.1-110))
reactions with chlorine trifluoride and hydrofluoric acid, 20: 18824(R) (EURAEC-1536)
reactions with combustion gas species in launch pad abort environments, 20: 39312 (SC-CR-2044)

reactions with europium molybdate, 20: 4305(R) (ORNL-3870, pp 187-90)
reactions with fission-product iodine, surface, 19: 25051(R) (ORNL-3731(p.111-51))
reactions with fissium–uranium at 1100 to 1250° in TREAT, 19: 31530(R) (ANL-7010(p.77-177))
reactions with fissium–plutonium–uranium alloys at 750°C of type 304, 19: 44587(R) (ANL-7000, pp 3-63)
reactions with helium in low concentrations of carbon dioxide and monoxide, 16: 29342 (ORNL-TM-293)
reactions with hydrofluoric acid–oxygen mixtures, 20: 5595(R) (ANL-6925, pp 107-64)
reactions with hydrochloric acid in air-fluidized beds, 20: 5595(R) (ANL-6925, pp 107-64)
reactions with hydrofluoric acid–oxygen mixtures at high temperatures, 20: 18824(R) (EURAEC-1536)
reactions with magnesium to 500°C *in vacuo*, 19: 22997 (TRG-Report-842)
reactions with Magnox alloy to 500°C in argon, 19: 22997 (TRG-Report-842)
reactions with metals at 540 to 760°C *in vacuo* by type 316, 19: 44606 (PWAC-483)
reactions with metals to 1550°C in different atmospheres, 19: 22997 (TRG-Report-842)
reactions with molybdenum–plutonium–uranium alloys, 16: 4484
reactions with nitrogen at 900°C, 19: 24064(R) (ANL-6997)
reactions with oxygen, equilibrium oxygen pressures produced in, 20: 277 (AERE-R-4942)
reactions with phosphorus and sulfur compounds in oils up to 700°C, 16: 16054
reactions with plutonium oxide during sintering, 17: 14209 (LA-2828)
reactions with plutonium carbide at 1000°C, 17: 14740 (TID-11295 (2nd Ed.))
reactions with plutonium nitride, 18: 34032(R) (BMI-1668(Del.))
reactions with plutonium–uranium fuels at high temperatures, 19: 40177(R) (ANL-7046(p.1-35))
reactions with plutonium–thorium–uranium alloys at 650°C, 19: 44674(R) (ANL-7000, pp 69-83)
reactions with plutonium–uranium–zirconium alloys at high temperatures, 20: 3320(R) (ANL-7082, pp 1-28)
reactions with plutonium nitride and uranium nitride at high temperatures, 20: 37169(R) (BMI-1774)
reactions with radioiodine, surface, 19: 22162(R) (ORNL-3776(p.17-22))
reactions with sodium at high temperatures, 19: 39090(R) (ANL-7046 (p.78-82))
reactions with sodium at high temperatures, 20: 20925(R) (ANL-7055, pp 177-212)
reactions with sodium at high temperatures, ¼-inch ball tests of, 20: 26459(R) (BNL-954, pp 1-15)
reactions with sodium at high temperatures, 20: 31440(R) (ANL-7175, pp 159-83)
reactions with steam, reactor safety studies of, 18: 33678(R) (ANL-6875)
reactions with steam at 1100 to 1400°C, effects of pressure on, 19: 17174(R) (ANL-6900(p.232-303))
reactions with steam and water at high temperatures, 20: 4183(R) (ORNL-3843, pp 2-70)
reactions with steam during LOFT meltdown, 20: 26394(R) (ANL-7193)
reactions with steam at 1400 to 1500°C, hydrogen evolution from, 20: 31440(R) (ANL-7175, pp 159-83)
reactions with thoria-urania slurries during 2200-hr Low Intensity Reactor Test, 16: 17568(R) (ORNL-3262(p.114-22))
reactions with uranium di- and monocarbides and nitride at 1000°C, 16: 30829
reactions with uranium oxide during sintering, 17: 14209 (LA-2828)
reactions with uranium monocarbide at 1000 to 2400°C, 18: 8795 (HW-72031)
reactions with uranium to 700°C *in vacuo*, compatibility of, 19: 22997 (TRG-Report-842)
reactions with uranium carbide at high temperatures, 19: 27735(R) (NAA-SR-10850)
reactions with urania at 1530°C, 19: 22989(R) (ORNL-3776(p.37-40))
reactions with uranium mononitride at high temperatures, 20: 37168(R) (BMI-1771)
reactions with water, thermodynamics, 16: 12843
reactions with water, exploding wire study, 17: 9107
reactions with water at 25 to 200°C, 17: 14119(R) (ANL-6596(p.175-200))
reactions with water at high temperatures, 17: 17447
reactions with water, energy release from, 18: 245
reactions with water at high temperatures, research summary on, 19: 13671(R) (WASH-1052)
reactions with water at high temperatures during core meltdown, (E/T), 19: 47960(T) (ORNL-tr-694)
reactions with water during reactor accidents, 20: 16019(R) (BMI-X-10154)
reactivity effects as reflector on beryllium-oxide-moderated uranium-235-fueled subcritical systems, 16: 18622 (UCRL-6729)
reactivity worth calculation of, 20: 6279(R) (AI-65-225)
reactivity worth in fuel-element handling casks, 20: 35151 (ORNL-TM-1488)
reactivity worths of rods of, in critical and exponential assemblies, (E), 19: 17200
reactivity worths of type 304, 19: 38178(R) (GEAP-4790)
reactor criticality effects, 18: 15562
reactor criticality effects, 18: 30963
reactor tubes of, graphite dimensional stability effects on, 20: 6619 (NAA-SR-Memo-11416)
reduction of oxide films on type 304, effects of surface treatment on coulometric, 20: 17118(R) (EURAEC-1564)
reflector savings coefficient with plutonium nitrates, 16: 18158(R) (HW-72586(p.54-65))
removal from ceramic pellets, device for, 18: 17977(R) (ORNL-TM-793)
removal from fuel elements by sulfex process, 20: 4048(R) (NP-15406)
removal from fuel elements using hydrofluoric acid–oxygen solutions, 20: 20808(R) (ORNL-3916)
removal from fuel elements using atomized hydrochloric acid, 20: 41060(P)
removal from reactor fuel elements, method for, 19: 2462(P)
removal from uranium dioxide, fluid-bed fluoride volatility process for, 20: 12923 (ANL-6898)
removal of coating of, from oxide fuel elements, development of chemical process for, 16: 29032(R) (BNL-749)
removal of coating of, from uranium in skull reclamation process, 17: 1359(R) (ANL-6569)
removal of iodine and cesium from, using heat, 19: 4046(R) (ORNL-3627(p.247-8))
removal of oxides from, descaling solution for, 20: 21238 (NP-15928)
response of cylinders of 304 and 304L, to explosive loads, 20: 18019(R) (IDO-17146)
review of status and future potential of, for defense, 18: 8718 (DMIC-Memo-183)
rupture mechanisms of type 304, determination by time-to-rupture tests, 20: 41445(R) (EURAEC-1622)
rupture of claddings of, at high temperatures, 18: 2274
rupture of type 304 tubular, at 550°C, effects of stress on, 19: 14765(R) (ANL-6977)
rupture of type 304, effects of carburization on stress, 19: 44623 (NAA-SR-10487)
rupture of type 316, effects of high-carbon or -oxygen sodium at 1200°F on, 20: 2258(R) (MSAR-65-149)
rupture properties of niobium-stabilized austenitic, effects of heat treatments on, 20: 4306(R) (ORNL-3870, pp 194-213)
rupture strength of type 316 in helium at 1300 and 1500°F, 17: 4980
sealing thermocouple sheath of, into Magnox end cap, 19: 2770
separation from thoria–urania system by leaching, 19: 11264(R) (ORNL-TM-937)
separation from uranium dioxide by fluorination–oxidation volatility, 18: 3671(R) (BNL-799(p.26-54))
separation from uranium dioxide by fluid-bed fluorination reactions, 18: 19456(R) (ANL-6840)
separation from uranium, 17: 21805(P)
separation of chromium, iron, and nickel from, by mercury cathode electrolysis, 16: 1854(R) (IDO-14553)
separation of chromium, iron, and nickel from, by electrolysis, 16: 12794 (IDO-14570)
separation of structural constituents, method, 16: 4558
separation of uranium dioxide from, by fluid-bed oxidation, 17: 35078(R) (ANL-6739)
separation of uranium dioxide from, by fluid-bed oxidation and fluorination-oxidation methods, 17: 35079(R) (ANL-6749)
separation of uranium dioxide from, by fluid-bed oxidation and oxidation-fluorination reactions, 17: 36861(R) (ANL-6764)
separation of uranium from enriched fuel of, continuous electrolytic process for, 20: 7191 (IDO-14643)
shot peening AISI 410 for protection against stress corrosion cracking, 16: 7854
sigma phase in austenitic, metallographic identification of, 19: 32723 (AECL-2234)
sintering, 16: 21078
sintering with dispersed plutonium dioxide–uranium dioxide systems, 17: 1832
soldering to zirconium alloys, method for, 17: 20444(P)
solvent properties for nitrogen at 1000°F, effects of ammonia–hydrogen ratio on, 19: 40968(R) (EURAEC-1424)
sorption of bound water from passive films on tracer studies of, 19: 34183
sorption of cesium by, 19: 36960(R) (ORNL-3807, pp 80-142)
sorption on radioiodine on tubes of 304, in sampling systems, 18: 35773(R) (UCRL-7811)
sorptive properties for radioisotopes in boiling-water reactor,

16: 20303(R) (ANL-6477(p.224-30))
sorptive properties for promethium-147, surface, 17: 11244
sorptive properties for promethium, cerium, zirconium, niobium, tritium, and sulfate ions, tracer study of, 17: 35693 (NP-12983)
sorptive properties for iodine, 18: 22112(R) (ORNL-3591(p.185-90))
sorptive properties for young fission products from solutions, 18: 33448 (IDO-14644)
sorptive properties for radioisotopes, precision of drop method measurements of, 19: 7493
sorptive properties for iodine-131 released from irradiated fuel, 19: 34409 (ORNL-P-1324)
sorptive properties of surfaces of, for iodine in high-temperature helium loop, 19: 40397 (ORNL-TM-1134)
sorptive properties for fission-product iodine from various environments, 20: 574 (CONF-650407, pp 730-46)
sorptive properties for cesium, 20: 4185(R) (ORNL-3843, pp 169-234)
sorptive properties for ionic radioisotopes in aqueous solutions, effects of acidity on, 20: 7003 (INR-634/V/C)
sorptive properties for radioisotopes, effects of pH on, 20: 25073
sorptive properties for oxygen, 20: 28742(R) (GA-6418)
sorptive properties for fission products from lithium hydroxide solution, 19: 32059(R) (IDO-14655)
specification for types 304 and 348 plate, sheet, and strip, 17: 41348 (HW-75477)
specification guides at HAPO for, 18: 3922 (TID-15245(Rev.))
specification guides at HAPO for, 18: 3923 (TID-15246(Vol.I)(Rev.))
specifications for tubing of, 17: 14417 (HW-68067(Rev.1))
specifications of types 304, 304L, 310, 316, 347, and 348 for use in fuel element tubes, 18: 1241(R) (GEAP-4332)
sputtering at 50 to 600 ev by rare gas ions, 17: 8931(R) (NP-12389)
sputtering by argon ions at 1 to 5 kev, yields from, 17: 5089
sputtering by cesium ions, (E/T), 19: 6477
sputtering by deuterium and krypton ions at 5 to 30 kev, coefficients of, 17: 25979
sputtering by deuterons at 30 kev, yields from, 20: 17892(R) (ORNL-3908, pp 149-53)
sputtering by uranium-ion bombardment, measurement of, 20: 46309(T)
sputtering with electric arc, characteristic stages, 16: 20968
stability of, effects of thermal cycling on, 18: 16492
steam reactions with uranium dioxide coated with type 304, 19: 28771
strain cycle tests of tubes of Type 304, 18: 39813 (GEAP-4462)
strain cycling fatigue, 19: 28809 (AP-Note-418)
strain effects on type 304, effects of environment on plastic, 19: 45572(R) (GEAP-4755)
strain fatigue limit of Type 304, biaxial, 20: 12418(R) (WCAP-3739)
strain measurements at 2000°F by optical methods, 17: 18745 (HE-150-204)
strain rates, 16: 9172(R) (NP-11351)
strain testing of type-304, for sodium-cooled reactors, 18: 24891(R) (NAA-SR-8888(Sect.I))
strength, effects of severe stress and thermal histories, 16: 21023 (ASD-TR-61-194)
strength of type-309 sheet, 16: 7239 (DC-52-25-70)
strengthening mechanisms in austenitic and ferritic, 20: 817 (CONF-710)
stress analysis of type 316 for use in sodium-heated boiler (E/T), 19: 1871 (BW-67-2(Vol.2))
stress-corrosion cracking of high-strength, review, 16: 2133 (DMIC-158)
stress-corrosion cracking of 17-4 PH, 16: 2178 (HW-68608)
stress-corrosion cracking, abstracts of reports on, 16: 20978 (DP-683)
stress-corrosion cracking of 17-4 PH, in lithium hydroxide solution at 464°F, 16: 33429 (DP-779)
stress-corrosion cracking and fracture of type 4340 and H-11, 17: 1940 (NP-12197)
stress-corrosion cracking of austenitic, in reactors, review of, 17: 23571
stress-corrosion cracking of austenitic, effects of water environment on, 17: 32529
stress-corrosion cracking by potassium permanganate-sodium hydroxide solutions, 17: 37003(R) (HW-78118)
stress-corrosion cracking of austenitic and type 347, in water, 17: 41380
stress-corrosion cracking in chloride solutions, tracer study of, 18: 4194 (CONF-329-1)
stress corrosion cracking of type 304, mechanism of, 19: 921(R) (DP-907)
stress corrosion cracking of austenitic, in lithium, magnesium, nickel, and sodium chlorides, 19: 22893 (DP-957)
stress corrosion cracking of austenitic, by wetted thermal insulation, 19: 46949 (CONF-650905-2)
stress-corrosion cracking of types 304, 308, 309, 310, and 316, by boiler water at 500°F and sea water at 550°F, 17: 27749 (KAPL-M-CC-3)
stress-corrosion cracking susceptibility of, effects of structure on, 17: 36206 (UCRL-10712)
stress-corrosion cracking of sensitized and nonsensitized, 18: 8748(R) (CEND-198)
stress-corrosion embrittlement of type 304, in magnesium chloride, 17: 3419
stress corrosion in aqueous and non-aqueous media, mechanism of, 16: 30733 (ARF-2181-12)
stress corrosion in magnesium chloride, 18: 39839(R) (EURAEC-1116)
stress corrosion in magnesium chloride, 19: 26766(R) (EURAEC-1309)
stress corrosion of Type 304, chloride-induced, 17: 1875 (TID-16888)
stress corrosion of type 410, effects of untempered martensite, 17: 3432
stress corrosion of, effects of fabrication, 17: 15391(R) (GEAP-4155)
stress corrosion of, review of principal factors affecting, 17: 18702(T) (CEA-tr-R-1639)
stress corrosion of type 304, in simulated superheat reactor environment, 17: 22112 (GEAP-4165A)
stress corrosion of Type 304, by heavy water, 17: 32516 (DPSPU-62-30-26)
stress corrosion of commercial and pure 18/10, in magnesium chloride, 18: 32063(T,R) (EURAEC-1060)
stress corrosion of 19-9DL alloy by lithium hydride, 18: 32083 (APEX-674)
stress corrosion of Type 316L, by superheated steam, 19: 16010 (ACNP-62024)
stress corrosion of austenitic, effects of nitrogen content on, 19: 24937(R) (EURAEC-1346)
stress corrosion of type 304, by steam containing chloride and oxygen, 19: 28213 (CEND-529)
stress corrosion of, effects of nitrogen on, 19: 893(R) (EURAEC-1216)
stress corrosion of, research program on effects of nitrogen content on, 19: 16015 (EURAEC-1322)
stress of, failure behavior in hoop, 19: 11682
stress-relieving, 17: 23923 (TID-7620(Pt.I)(p.225-42))
stress-relieving cast, 17: 23924 (TID-7620(Pt.I)(p.243-50))
stress rupture at 1250°F of type 304, effects of carbon, nitrogen, phosphorus, and sulfur on, 19: 32733 (NAA-SR-11047)
stress-rupture in-pile testing, 17: 5040(R) (ORNL-3364(p.125-50))
stress-rupture of types-454, 458, and 304, 16: 28554 (TID-7623(p.97-104))
stress rupture of tubular, 16: 30167 (ORNL-3313(p.19-64))
stress rupture of tubular, at 550°C in argon, 19: 29468(R) (ANL-7017)
stress-rupture properties of type-304 tubing of, at 1100 to 2200°F, 17: 25780 (ORNL-TM-535)
stress rupture testing of niobium-stabilized, 18: 30116(R) (ORNL-3619(p.123-46))
stress-corrosion cracking of sensitized and nonsensitized, 18: 14402(R) (CEND-202)
stress-corrosion cracking of type 304, by steam at 530°F, 18: 35497(R) (GNEC-354)
stress-corrosion cracking of type 304, mechanism of chloride-induced, 19: 2745 (CONF-778-3)
stress-corrosion cracking by chloride, surface treatment effects on inhibition of, 19: 16023
stress-corrosion cracking in magnesium chloride, effects of purity on, 19: 40947(R) (EURAEC-1403)
stress-corrosion cracking in chloride solution, 18: 27904 (ORNL-TM-14)
stress-corrosion of type 304, in magnesium chloride at 142°C, 19: 16020
stress-hydrogen cracking of Type 410, 20: 772 (NYO-3257-1)
stress-rupture at 1250°F, type 304, 20: 31669
stress-rupture of 304, effects of carburization on, 19: 40286(R) (NAA-SR-11200)
stress-rupture properties of niobium-stabilized austenitic, in-reactor, 18: 34218 (ORNL-TM-881)
stress-rupture properties in high temperature sodium environment, 20: 8394(R) (NAA-SR-11450, Sect.2)
stress-rupture properties of type 304, 19: 10675(R) (NAA-SR-9999)
stress-rupture tests of EGCR fuel clad tubes of type 304, 19: 11673 (ORNL-TM-1004)
structural modifications in 18-8 Ti, after thermal treatment near the solidus, 16: 27665
structure of pure 18/8, 17: 11115(T,R) (EURAEC-482)
sulfur behavior in, effects of uranium on, 18: 18402
sulfur reactions in, effects of uranium on, 19: 30801
surface friction in sodium environments, 17: 6511(R) (BMI-1593(Del.))
surface friction of clean, in sodium (liquid), 17: 2080
surface temperature of, kryptonate method for determining, 20: 18570(R) (NYO-2757-5)
temperature gradients in irradiation specimens of, measuring methods for, 17: 12720 (NP-12501)
tensile fatigue of type 305, 17: 6663 (MATT-154)
tensile properties of 304 ELC tubing, 16: 3466 (SCDR-38-61)
tensile properties of type 304 at low temperatures, 16: 6789(R) (NP-11236)
tensile properties, tube-burst testing for evaluation, 16: 28379(R) (ORNL-3302(p.232-79))
tensile properties of, radiation and temperature effects on, 16: 28642(R)

(BMI-1581(Del.))
tensile properties, 17: 6661 (JPL-TR-32-222)
tensile properties, 17: 11937(R) (ARF-4132-16)
tensile properties of specimens from clad isostatic pressed fuel rods, 17: 13676(R) (GEAP-4049)
tensile properties of types A-286, 353, 304, 310, and 347, at 30 and 540°R, 17: 25776(R) (NP-12812)
tensile properties of type-304, 17: 34330(R) (USBM-U-1057)
tensile properties of type 304, at 1500 to 2000°F, 17: 35104 (NAA-SR-Memo-3034)
tensile properties of, summary of fracture tests of, 18: 601 (DMIC-Memo-174)
tensile properties of vacuum-melted tubular, 18: 4796(R) (GEAP-4153)
tensile properties of type 304, 18: 7865(R) (TID-19871)
tensile properties of annealed and cold-worked tubular, at 20°C, 18: 21706(R) (KR-66)
tensile properties at 20 and 400°C of irradiated pressure tubes of type 347, after postirradiation annealing, 18: 24988(R) (BMI-1665(Del.))
tensile properties of 17-7PH and 440C, evaluation, 18: 30238(R) (NP-14102)
tensile properties of types A-286 and 310, 19: 6364(R) (NP-14443)
tensile properties of 17-7PH, A286, and 347, testing, (E), 19: 20554 (LA-3161)
tensile properties of AM-350, at 75, 800, and 900°F, 19: 32733 (NAA-SR-11047)
tensile properties of, testing of, 19: 35763(R) (NAA-SR-10743)
tensile properties of type 406, on aging at 1000 and 2000°F in steam, 19: 39156(R) (CEND-532)
tensile properties of type 302, effects of exposure to cesium at 650°C on, 20: 11227
tensile properties of type 304, effects of nitrogen content on, 20: 27428(R) (EURAEC-1630)
tensile properties of type 310, at 1300°F, effects of heat treatments on, 20: 29618(R) (GEAP-4982)
tensile properties of types 321 and 347, effects of heated lithium hydride on, 19: 22983 (NAA-SR-Memo-10885)
tensile testing of tubes of, 18: 38255(R) (KR-72)
testing cladding of, nondestructive methods for, 20: 14711
testing collapse pressure of tubes of, 18: 7202(R) (CEND-199)
testing for advanced BONUS core, 18: 29043 (GNEC-345)
testing for EGCR fuel elements, 17: 2502
testing for use in reactor containment, 19: 5397(R) (TID-21056)
testing fuel cladding of, loss-of-coolant, 18: 38363 (A/CONF.28/P/438)
testing in boss seals at 3000 psig and −65 to 600°F, 16: 10514 (DC-60-2-112)
testing of boron-10-containing poison plates for Shippingport PWR, 19: 14845 (WAPD-BT-31(p.1-17))
testing of cladding tubes of, automatic device for ultrasonic, 20: 14717
testing of coatings of, for reactor fuel pins, 18: 39811 (EUR-1608.f)
testing of, for use in fuel element roll and swage cladding, 17: 13676(R) (GEAP-4049)
testing of fuel claddings of, economics of nondestructive, 20: 14032
testing of fuel cladding of, eddy current, 20: 14033
testing of low-cobalt type 304 tubing, for use as fuel cladding, 19: 9601 (GEAP-3470)
testing of, nondestructive, 18: 9636 (ANL-6632)
testing of thin cladding tubes of, ultrasonic, 19: 15992 (CEA-R-2577)
testing of thin-wall tubing of, ultrasonic, 18: 35699 (HW-81956)
testing of tubes of, nondestructive, 18: 3038(R) (ANL-6801)
testing of type 316, for sodium superheater steam generators, 19: 31474 (BAW-1280-23)
testing of type 316, for sodium superheater steam generators, 19: 31475 (BAW-1280-24)
testing of 316, for use in liquid-metal turbine blades and nozzles, 20: 2240
testing of, engineering drawings of phase-sensitive eddy-current concentrator for, 19: 20132
testing tapered tubes of type 316, nondestructive, 18: 4255(R) (ORNL-3470(p.98-125))
testing type 304, as cladding for plutonia–urania fuel, 20: 28767 (WCAP-3385-53)
testing type-304, structural defect, 19: 4597 (SAN-8003(p.13-89))
testing, mechanical and thermal, 18: 27856(R) (HW-79280(p.9.1-4))
tests of tubes of AISI 304 L, collapse, 19: 29808(R) (KR-94)
texture of, cold-worked at low temperatures, 16: 27646
thermal conductance of interfaces with uranium dioxide, 17: 27546
thermal conductivity, 17: 6673 (ORNL-2065)
thermal conductivity of contacts of, 17: 14841 (NYO-9458)
thermal conductivity across contacting surfaces of, 17: 22276 (NYO-9459)
thermal conductivity and diffusivity of, 19: 17177(R) (ANL-6965(p.42-83))
thermal conductivity of AISI-316, Wiedemann-Franz-Lorenz law for, 19: 26827
thermal conductivity of powders of, 17: 27368
thermal conductivity of, measurement at high temperatures, 20: 41479
thermal contact resistance with liquid sodium, measurement, 16: 10444
thermal contact resistance to liquid sodium, 19: 16186
thermal cycling effects on welds of, 18: 16422(R) (CEND-204)
thermal cycling of type-310 and type-347, cracks from, 20: 35864 (RFP-741)
thermal decomposition of simulated, 17: 4492 (IDO-14597)
thermal expansion at room temperature to 1000°C, 16: 4476
thermal expansion of fuel materials of, during fast burst accident, 20: 6602 (BNWL-SA-346)
thermal fatigue testing of, for use as denitrator pot material, 18: 39810 (DP-901)
thermal properties at high temperatures, 16: 4551 (WADD-TR-60-904)
thermal properties of type-304, 16: 22597 (WADD-TR-60-924)
thermal properties of, data compilation, 17: 8801 (DMIC-177(Vol.2))
thermal properties, 18: 7202(R) (CEND-199)
thermal properties of 347, effects on reactor transients, 18: 35146(R) (GEAP-4601)
thermal radiation properties of surface-oxidized, 16: 32039(R) (PWA-1863)
thermal radiation properties of, effects of various coatings on, 16: 32039(R) (PWA-1863)
thermal radiation properties of A 286, 17: 542 (WADD-TR-60-370 (Pt.II))
thermal radiation spectral emittance of chromate on, 17: 41563 (WADD-TR-60-370(Pt.III))
thermal radiative properties, 17: 6650 (DMIC-177(Vol.I))
thermal response and microstructure of type 310, at 1400°F, 19: 39158 (GEAP-4751)
thermal strain measurements in tubes of type 304, during transient heating by plasma, 19: 34692 (UCRL-13147(Pt.2))
thermal stress analysis, 16: 5460 (HW-71668)
thermal-stress and strain-cycling fatigue, 17: 20449(R) (ATL-A-134)
thermal stress behavior of, 17: 527(R) (ATL-A-131)
thermal-stress-fatigue testing of types 304 and 304-L, 17: 20448(R) (ATL-A-133)
thermal-stress-fatigue properties of type 304, 17: 27775(R) (ATL-T-135)
thermal-stress-fatigue properties of types 304L and 403, 18: 596(R) (ATL-A-139)
thermal stress fatigue tests of types 304, 304-L, and 403, 19: 13980(R) (ATL-A-144)
thermal stress fatigue of types 304, 304L, and 403, 20: 11227
thermal-stress-fatigue testing of types 304 and 304-L, 17: 32566(R) (ATL-A-137)
thermal stress properties of coatings, 19: 24076(R) (GA-4966)
thermal stress properties of coatings, 19: 25723(R) (GA-5036)
thermal stresses and fatigue, 17: 30963 (ATL-A-136)
thermal-stress fatigue properties of types 304 and 304-L, 18: 42011 (ATL-A-141)
thermal-stress-fatigue properties of type 403, 18: 10521(R) (ATL-A-140)
thermal-stress-fatigue properties of type 403, 18: 22474(R) (ATL-A-142)
thermoelectric emission and work function of, in cesium vapor, (E), 19: 6447
thermoelectric potentials at 25 to 900°C, 19: 4656 (ORNL-3605(Vol.1) (p.116-38))
thickness of sheered plates of, design of beta gage for determination of, 17: 30169
transfer of carbon and nitrogen to niobium–zirconium alloy in potassium, 20: 2270
type 310, effect of sigma phase on mechanical properties of, 19: 32723 (AECL-2234)
uranium fission rate attenuation by, 18: 6411(R) (ANL-6706)
use as cathode in electrolytic reduction of uranyl and plutonium(IV) ions, 19: 42474
use as cover for reactor fuel plates, 16: 28476(P)
use as fuel in gas-cooled reactors, comparison of cermet with stainless-steel-clad rods, 16: 5058
use as fuel-element cladding for boiling-water reactors, 20: 30903
use as lining for Zircaloy-2 cladding for fuel rods, 18: 22456 (GEAP-4555)
use for fission product deposition studies, recommendations for, 20: 5665 (ORNL-TM-1304)
use in G-M counters with activable cathodes, for measurement of fast neutron fluxes, 20: 43729
use in nozzles for high-temperature thermometry in gases, 19: 20277 (ORNL-P-1068)
use in reactor control rod cladding, 20: 21317(P)
use in reactor coolant assemblies, end shielding, and moderator vessel, 17: 34379
use in reactor fuel cans, 18: 26946
use in reactor pressure vessels, review on, 18: 44076
use of type 347, in gas-cooled reactors, 18: 34034(R) (BMI-1672(Del.))

use of 1100°-aged 17-4 pH, in control rod drive assemblies in Indian Point Power Reactor, 18: 40853 (NP-14250)
uses in fuel element end caps to reduce creep, 18: 42102(P)
vaporization of types 304, 316, and 446, at 760 to 980°C, rates of, 18: 28038
vibration of wires of type 321, effects of length on, 18: 16376(R) (MLM-1157)
wear and corrosion testing as journal bearing material, 20: 43823 (AECL-2566)
wear effects on SAP in fretting corrosion, 20: 43843
wear in borated and lithiated water, 19: 45601(R) (WCAP-3750)
wear in carbon dioxide at high temperatures, 16: 29079
wear performance of, comparison with Inconel, 16: 34000 (WAPD-BT-26 (p.71-90))
wear properties of plasma-arc-deposited coatings of, 20: 21319 (AD-621064)
wear testing of 17-4 PH and 304, for Army PM reactor use, 19: 31545 (MND-2706-13)
weld behavior, highly restrained partial penetration, 16: 6699 (WAPD-TM-290)
weld post heating by electron beams, 17: 25764
welding, 18: 8715(R) (CEND-186)
welding, 16: 2154
welding at 100 to 150 kv, electron beam equipment and techniques for, 16: 19272
welding by argon-arc method, uses of carbon dioxide in, 19: 20534
welding by friction, 17: 1908
welding by solid-state methods, 19: 22937
welding by ultrasonic techniques, 16: 2145 (CEND-80)
welding characteristics of types 304, 309, 314, 321, and 403, 16: 4510 (DMIC-Memo-140)
welding closure of waste storage containers of, remote, 18: 14424 (HW-79522)
welding, development of tungsten-arc techniques, 16: 6693 (NAA-SR-Memo-5887)
welding electrodes for type 347, 16: 3428 (NYO-9725)
welding, feasibility of ultrasonic, 16: 19308 (PWAC-165)
welding fission product containers of, remote, 17: 15522 (HW-73933)
welding, for canning reactor fuel elements, 16: 33463
welding for mildly corrosive nonradioactive service, specifications for, 17: 32540 (TID-19161)
welding for nuclear reactor plants, safety requirements for, 20: 11259
welding for sealing fission-product waste containers, remote methods for, 18: 6536 (HW-79393)
welding inside chromium–molybdenum–nickel steel pressure vessel, 18: 27926
welding of austenitic, control standards, radiographic techniques and specifications for, 20: 800
welding of cladding tape of, to steel, 20: 43852 (EURAEC-1685)
welding of closure joint in reactor vessels of Type 316, tests of, 19: 20509 (NAA-SR-Memo-10633)
welding of, equipment and properties for electron-beam, 17: 34378
welding of, evaluation of electron-beam, 16: 31763
welding of, for gas-loop development, 17: 27730(R) (HW-77052)
welding of fuel element spacer to, projection, 20: 12377(R) (CEND-2863-236)
welding of pipes and plates of, Hanford procedures for, 19: 20523 (TID-20625(Vol.III)(Rev.I))
welding of pipes and plates of, Hanford procedures for, 19: 20522 (TID-20625(Vol.II)(Rev.I))
welding of reactor process tubes of, study of erosion during electric, 18: 37664 (NAA-SR-Memo-9221)
welding of, requirements and techniques for high-integrity, 16: 33451 (HW-SA-2702)
welding of sheaths of, equipment, parameters, and techniques for resistance-seam, 17: 32549
welding of, specifications for radiographic testing of, 17: 34375 (TID-19159)
welding of tube sheets of, to Zircaloy-2 tubes, 20: 15019
welding of tubular, to wire spacers, 18: 5750(R) (CEND-157)
welding of type 304, power-force programmed ultrasonic, 18: 12594 (AD-427997)
welding of type 304, use of power-force programming in ultrasonic, 19: 13933(R) (AD-422935)
welding of type 316, to Inconel, 17: 29293 (APAE-123)
welding of type 316, to Hastelloy X-280 using Hastelloy alloys as filler metal, 19: 34627(R) (BNWL-79(p.6.1-20))
welding of type 347, to vanadium, 17: 23864(R) (BMI-1619(Del.))
welding of type 410, to Zircaloy-2, explosive, 18: 4222
welding of types 304 and 321, automatic inert gas tungsten arc, 20: 11246
welding of, characteristics of electron beam, 18: 34112
welding of, Hanford guide to procedures and specifications for, 18: 24103 (TID-20625(Vol.II))
welding of, Hanford guide to procedures, specifications, and qualification test records for, 18: 24104 (TID-20625(Vol.III))
welding of, techniques for cold, 19: 34357 (N64-24831)
welding of, to assemble or seal plutonium-containing fuel elements, 18: 24100 (HW-SA-3146)
welding parameters for type 304, electron-beam, 20: 5867
welding properties, 16: 10486 (TID-14971)
welding properties of fuel cans of type 304, effects of vibratory-compacting of powders on, 20: 13177(R) (EURAEC-1504)
welding reactor tubes of, equipment and techniques for TIG, 18: 14438
welding, segregation of phosphorus and sulfur, 16: 16052
welding sheaths, sheets, and tubes of, techniques for, 18: 7172
welding specifications for heat exchangers, 17: 34371 (TID-19155)
welding specifications, 17: 34372 (TID-19156)
welding specifications for types 304L, 308L, and 316L, fusion, 17: 34373 (TID-19157)
welding specifications, 17: 34374 (TID-19158)
welding specifications for types 304L, 308L, and 316L, fusion, 17: 34376 (TID-19160)
welding specifications for structural quality welds for mildly corrosive nonradioactive service, 20: 29662 (HWS-8242(Rev.5))
welding specifications for process quality welds for mildly corrosive radioactive service, 20: 29661 (HWS-3241(Rev.4))
welding thermal cycles, 17: 8768
welding to austenitic, 17: 23921 (TID-7620(Pt.I)(p.209-16))
welding to boron and carbon steel, 17: 8766
welding to boron-alloy steel, 17: 23914 (TID-7620(Pt.I)(p.126-43))
welding to boron stainless steel, evaluation of, 20: 35872
welding to ceramics, graphite, and metals in SNAP reactor environment at 700 to 1300°F, self-, 20: 7570 (NAA-SR-9643)
welding to chromium–molybdenum steel, 19: 4592(R) (MSAR-61-114)
welding to Croloy 9M, 19: 20475(R) (ORNL-3538)
welding to ferritic, 17: 23921 (TID-7620(Pt.I)(p.209-16))
welding to Hastelloy X and Inconel, 20: 3472(R) (GEAP-4891)
welding to Inconel, engineering drawings of portable welder for, 18: 44121
welding to INOR-8 of type 347, strength testing of joints in, 18: 4174(R) (ORNL-3470(p.157-72))
welding to molybdenum, explosive techniques for, 16: 3419 (ASD-TR-61-124)
welding to molybdenum and niobium, 20: 21309
welding to plutonium-containing fuel elements for reactors use, method for arc, 18: 44120
welding to Zircaloy-2, 17: 11084(R) (EURAEC-388)
welding to 9 chromium–1 molybdenum steel of type 316, weld-filler metal for, 20: 11214(R) (NASA-CR-54717)
welding tubes of, techniques for, 18: 7173
welding type 304, to AISI 4130 steel, dilution in, 19: 6285
welding type 316, 16: 33120 (APAE-122)
welding, ultrasonic, 16: 4515 (NP-11054)
welding 308L, weld metal for, 17: 23917 (TID-7620(Pt.I)(p.160-7))
welds in, sonic inspection using twin-angle beam technique, 17: 27761 (TID-18871)
welds of austenitic, to superalloys, mechanical properties, 17: 39501 (HW-78574)
wetting by bismuth–lead eutectics, 20: 4077(R) (IS-1200(Sect. E))
wetting by hydrogen, contact angle for, 17: 28083
wetting by lead–bismuth eutectics, 20: 41064(R) (IS-1500(Sect.E))
wetting of types 310, 410, and 430, by bismuth–lead eutectic, 20: 7564 (IS-T-56)
x-ray absorption coefficients at 40 to 130 kev, 17: 12600
x-ray attenuation coefficients, 17: 14740 (TID-11295(2nd Ed.))
x-ray attenuation in types 304 and 307, measurement of, 20: 29707 (ORNL-TM-1457)
Al–stainless steel, corrosion by oxygenated steam at 650°C, 17: 40422(R) (ANL-6784)
Al–stainless steel, corrosion by steam at 650°C, 19: 44616(R) (ANL-7000, pp 122-37)
Al–stainless steel–U, neutron transport in cells of, (E), 19: 17367(T) (CEA-tr-X-552)
B_4C–stainless steel, fabrication and performance as reactor control elements, (E), 19: 17201
Be–stainless steel, vacuum-pressure braze cladding of, 18: 7177
B–stainless steel, burnup of control rods of, 18: 9632 (ACNP-63006)
B–stainless steel, corrosion by boronated water at 600°F, 19: 39110
B–stainless steel, ductility of, effects of ultrasound on, 20: 37221
B–stainless steel, extrusion of fuel cladding of, 19: 39110
B–stainless steel, fabrication of control rods of, for Sioux Falls Power Reactor, 18: 33093 (ACNP-64014)
B–stainless steel, fabrication, performance, and properties for control rod use, 18: 32031 (A/CONF.28/P/253)
B–stainless steel, gamma and neutron transmission in slabs of, (E),

19: 14728 (APEX-581)
B–stainless steel, mechanical properties of, effects of boron content on, 19: 39110
B–stainless steels, mechanical properties of irradiated fuel cladding of, 20: 17121 (GEAP-4918)
B–stainless steel, performance as reactor poison, 18: 28943
B–stainless steel, performance as fuel element cladding, 19: 3689
B–stainless steel, properties as control rod material, 19: 2734
B–stainless steel, radiation effects on mechanical properties of, fast and thermal neutron, 19: 39110
B–stainless steel, radiation effects on corrosion resistance of, fast and thermal neutron, 19: 39110
B–stainless steel, radiation effects on poison elements of, in-pile, 20: 16089(R) (WAPD-MRP-114)
B–stainless steel, radiation effects on corrosion resistance of modified austenitic, neutron, 20: 17118(R) (EURAEC-1564)
B-stainless steel, reactivity worths of cruciform rods of, (E), 19: 12767 (ACNP-64568)
B–stainless steel, weld joint design for tubes of, 19: 39110
Ce–stainless steel, corrosion by steam at 650°C, 19: 44616(R) (ANL-7000, pp 122-37)
C–Pb–stainless steel, fabrication and properties for radioactive fuel element shipping containers, 18: 14139
Cr–Ni–stainless steel 304, corrosion in Saxton steam generator, 20: 30884(R) (WCAP-3269-16)
Cr–Ni–stainless steel, strain fatigue limits of, biaxial, 20: 12418(R) (WCAP-3739)
C–stainless steel-304, ductility at high temperatures, 20: 28751(R) (GEAP-5125)
Cu–Mo–stainless steel, vacuum pressure braze cladding of, 18: 7177
Dy_2O_3–stainless steel, radiation effects on, 19: 15991(R) (BNL-841 (p.63-101))
Eu_2O_3–stainless steel, corrosion of, by water, 17: 17446
Eu_2O_3–stainless steel 304L–TiO_2, corrosion by water at high temperatures, 20: 31678 (HIT-3583-24)
Eu_2O_3–stainless steel, development of, as flux suppressors for Army Reactors (SM-1), 16: 28541(R) (ORNL-2703)
Eu_2O_3–stainless steel, fabrication of, for control rods, 16: 28541(R) (ORNL-2703)
Eu_2O_3–stainless steel, properties of, as reactor control material, 16: 32120 (TID-16597)
Eu_2O_3–stainless steel, properties of cermets of, 17: 6664 (MND-M-2346)
Eu_2O_3–stainless steel, radiation effects on stainless-steel-clad, 18: 4177(R) (ORNL-3470(p.221-6))
Eu_2O_3–stainless steel, radiation effects on control rods of, reactor, 20: 17129 (ORNL-TM-1407)
Gd_2O_3–stainless steel, properties of, as reactor control material, 16: 32120 (TID-16597)
Gd–stainless steel, corrosion by water at 354°C, 17: 34330(R) (USBM-U-1057)
Gd–stainless steel, corrosion by water at 354°C, 18: 2174(R) (USBM-U-1082)
Gd–stainless steel, fabrication and tensile properties, 17: 34330(R) (USBM-U-1057)
Gd–stainless steel, fabrication and mechanical properties, 18: 2174(R) (USBM-U-1082)
Gd–stainless steel, fabrication and phase studies on, (E), 19: 16189
Gd–stainless steel, oxidation by air at 980°C, 18: 2174(R) (USBM-U-1082)
Gd-stainless steel, phase diagram, 17: 14740 (TID-11295(2nd Ed.))
Gd–stainless steel, phase relations and properties, 19: 32675 (BM-RI-6636)
Gd–stainless steel, phase studies at 500 to 1500°C, 17: 34330(R) (USBM-U-1057)
Gd–stainless steel, tensile properties at high temperatures, 18: 14384(R) (USBM-U-1091)
graphite–stainless steel, heat transfer from colloidal gas suspensions of, 19: 42127(R) (TID-22009)
Nb–stainless steel-Zr, compatibility studies, 20: 8447 (PWAC-491)
Nb–stainless steel, creep and oxidation properties of, 17: 30927
N–stainless steel, flow of suspensions of, in process-heat reactor systems, 19: 17333(R) (TID-21596)
PuO_2–stainless steel–UO_2, analysis of cermets of, for plutonium, 20: 222 (AERE-R-4975)
PuO_2–stainless steel, development for fast power reactors, 18: 19353 (ANL-6792(p.315-28))
PuO_2–stainless steel, fabrication, 19: 22921(R) (HW-81603(p.6.1-11))
PuO_2–stainless steel–UO_2, fabrication of cermets of, 19: 22915 (AERE-M-1314)
PuO_2–stainless steel, fabrication into pins, 19: 39125(R) (BNWL-91)
Pu_2O_3–stainless steel, fabrication and postirradiation examination of cermets of, 20: 7498 (BNWL-SA-415)
PuO_2–stainless steel, fabrication and postirradiation examination of cermets of, 20: 7498 (BNWL-SA-415)
PuO_2–stainless steel, fabrication of dispersion fuels of, process for, 20: 31666
PuO_2–stainless steel, performance as fast-reactor driver fuel, (E), 20: 5192 (BNWL-SA-251)
PuO_2–stainless steel, performance as FTR fuel, 20: 42676 (BNWL-281)
PuO_2–stainless steel, preparation and properties of sintered type 302B, 18: 547 (LAMS-2898)
PuO_2–stainless steel, preparation by pneumatic impaction, 18: 8721(R) (HW-78388(p.5.1-22))
PuO_2–stainless steel, preparation of compacts of, 18: 12547(R) (HW-76303(p.3.1-37))
PuO_2–stainless steel, preparation and properties of pneumatically impacted, 18: 29001(R) (HW-79280(p.5.1-25))
PuO_2–stainless steel, preparation and stability of pneumatic impacted, 19: 9603(R) (HW-81601(p.2.1-35))
PuO_2–stainless steel, preparation and properties of, 19: 22869(R) (HW-83298(p.5.1-38))
PuO_2–stainless steel–UO_2, radiation effects on, in-pile, (E), 20: 5192 (BNWL-SA-251)
PuO_2–stainless steel, radiation effects on, in-pile, (E), 20: 5192 (BNWL-SA-251)
PuO_2–stainless steel, radiation effects on microstructure of cermets of, reactor, 20: 7532(R) (BNWL-150, pp 5.1-33)
PuO_2–stainless steel, radiation effects on, effects of sample density on, 20: 31666
PuO_2–stainless steel, thermal expansion at 25 to 1290°C, 20: 27474(R) (BNWL-198, pp 1.1-22)
Si–stainless steel, corrosion by steam at 650°C, 19: 44616(R) (ANL-7000, pp 122-37)
stainless steel–UO_2, analysis of, for enriched uranium by x-ray fluorescence, 17: 12182(R) (NBL-188)
stainless steel–UO_2, burnup testing, 18: 19392
stainless steel–ZrC, compatibility with uranium carbide–zirconium carbide, 18: 24072(T,R) (EURAEC-934)
stainless steel–UO_2, development and testing as dispersion fuel material, 18: 4178(R) (ORNL-3470(p.227-31))
stainless steel–UO_2, electrolytic dissolution of, 18: 20115
stainless steel–U, electrolytic dissolution using nitric acid, 20: 27036(R) (IDO-14661, pp 1-44)
stainless steel–UO_2, extrusion of billets of, methods for, 20: 43848(R) (BNWL-269, pp 5.1-36)
stainless steel–UO_2, fabrication by extrusion and sintering, 17: 1856
stainless steel–UO_2, fabrication of dispersions, 17: 14790 (ORNL-TM-446)
stainless steel–UO_2, fabrication into wires and testing, 17: 22130 (SEP-232)
stainless steel–V, fabrication of tubular, 18: 15663(R) (ANL-6808)
stainless steel–UO_2, fabrication and properties of cylindrical and tubular fuel elements of compacts of, 17: 33276
stainless steel–UO_2, fabrication by roll bonding of, clad with stainless steel, 20: 5866
stainless steel–UO_2, fabrication and postirradiation examination of cermets of, 20: 7498 (BNWL-SA-415)
stainless steel–UO_2, fabrication by roll bonding, 20: 11260
stainless steel–ZrB_2, fabrication of dispersions of, process development for, 20: 19177(R) (BMI-1757)
stainless steel–UO_2, fabrication of fuel plates from, 20: 37168(R) (BMI-1771)
stainless steel–UO_2, fabrication by extrusion and sintering for disperse fuel elements, 16: 27607(T) (AERE-Trans-883)
stainless steel–UO_2, fabrication and properties of, 16: 29335
stainless steel–UO_2, fission-induced failure model for, 20: 39459 (TRG-Report-1278)
stainless steel–UO_2, inspection of irradiated OMRE fuel elements of, 20: 10272(R) (NAA-SR-9339)
stainless steel–UO_2, mechanical properties, 17: 41434 (ORNL-TM-665)
stainless steel–UO_2, mechanical properties of, 16: 30167 (ORNL-3313(p.19-64))
stainless steel–UO_2, mechanical properties as reactor core material, 16: 25762 (SCNC-264)
stainless steel–UO_2, performance of fuel elements of, 17: 27863
stainless steel–U, performance of highly enriched plates of, as reactor fuels with natural-urania pins, (E), 19: 33575 (AP-Note-444)
stainless steel–UO_2, bonding of cermet of, to stainless steel cladding, 19: 4642(P)
stainless steel–UO_2, braze bonding to stainless steel cans, 19: 4635
stainless steel–UO_2, dissolution of irradiated, development of methods for, 19: 7274(R) (IDO-14636)
stainless steel–UO_2, dissolution using hydrochloric–hydrofluoric–nitric acid mixtures, 19: 36217(R) (IDO-14656)
stainless steel–UO_2, fabrication of stainless steel clad, 19: 14806(R) (HW-81984(p.5.1-55))

stainless steel–UO_2, fabrication by rolling, 19: 18421(R) (BMI-1697 (Del.))
stainless steel–UO_2, fabrication by rolling, 19: 18420(R) (BMI-1694 (Del.))
stainless steel–UO_2, fabrication, 19: 22921(R) (HW-81603(p.6.1-11))
stainless steel–UO_2, fabrication into pins, 19: 39125(R) (BNWL-91)
stainless steel–UO_2, fabrication of fuel elements of, 19: 40958
stainless steel–UO_2, fabrication into reactor fuel elements, (E), 19: 40172
stainless steel–UO_2, melting point, 19: 22989(R) (ORNL-3776(p.37-40))
stainless steel–UO_2, melting point, 19: 31478(R) (ORNL-3789 (p.251-62))
stainless steel–UO_2, performance as fuels for Army PM reactors, (E), 19: 31545 (MND-2706-13)
stainless steel–UO_2, preparation of fuel plates of, 20: 5843
stainless steel–UO_2, preparation of dispersions of, 20: 5848
stainless steel–UO_2, processing by fluoride volatility, 19: 23991(R) (ANL-7003)
stainless steel–U, processing method for VBWR fuel elements of, 20: 9043 (IDO-14658)
stainless steel–UO_2, processing by fluorination for uranium recovery, 20: 20803(R) (ANL-7055, pp 99-162)
stainless steel–UO_2, processing by fluid-bed fluoride volatility, 20: 20801 (ANL-6830)
stainless steel–U, processing for uranium recovery by solvent extraction, 20: 27036(R) (IDO-14661, pp 1-44)
stainless steel–UO_2, fabrication of dispersion fuel plates of, 20: 23582(R) (BMI-1765)
stainless steel–UO_2, fabrication and radiation effects on pellets of, 20: 26459(R) (BNL-954, pp 1-15)
stainless steel–UO_2, fabrication for AARR fuel, 20: 30787(R) (ANL-7190, pp 11-14)
stainless steel–UO_2, properties of, mechanical and thermal, 19: 14033
stainless steel–UO_2, properties as fuel plates, 19: 30642(R) (BMI-1707(Del.))
stainless steel–UO_2, properties as reactor fuel, 16: 24477
stainless steel–UO_2, radiation effects on matrix swelling of, to 700°F, 18: 4177(R) (ORNL-3470(p.221-6))
stainless steel–UO_2, radiation effects on plates of dispersions of, (E), 19: 4717 (ORNL-3709)
stainless steel–UO_2, radiation stability, 19: 11792
stainless steel–UO_2, radiation effects on, 19: 40958
stainless steel–UO_2, radiation effects on, in-pile, (E), 20: 5192 (BNWL-SA-251)
stainless steel–UO_2, radiation effects on, in-reactor, 20: 46222 (BNL-10521)
stainless steel–UO_2, radiation effects on, 16: 9655 (MND-M-2583)
stainless steel–UO_2, radiation effects on, 16: 584
stainless steel–UO_2, sintering of, 20: 14965(R) (NUMEC-3524-12)
stainless steel–UO_2, testing in Spert I, 19: 20616 (IDO-17011)
stainless steel–Y, corrosion by steam at 650°C, 19: 44616(R) (ANL-7000, pp 122-37)
stainless steel–Zr, corrosion by steam at 650°C, 19: 44616(R) (ANL-7000, pp 122-37)
stainless steel–UO_2, thermal cycling between 50 and 800°C, 20: 5848
stainless steel–UO_2, thermal expansion of fuel plates of, 16: 30834
stainless steel–UO_2, thermal testing of compacts of, 18: 12547(R) (HW-76303(p.3.1-37))

STAINLESS STEEL COUPLES

see also Steel Couples
Al/stainless steel, contact thermal conductance of, 20: 31712 (UCRL-14227(Rev.1))
Al/stainless steel, corrosion, 17: 16584(R) (EURAEC-550)
Al/stainless steel, corrosion of, growth and initiation of pitting in, 16: 24121 (KR-18)
Be/stainless steel, brazing and diffusion bonding with silver, 19: 30691 (N64-28460)
ceramics/stainless steel, contact thermal conductivity of, 20: 31712 (UCRL-14227(Rev.1))
Cu/Nb/stainless steel, diffusion in bimetallic tubing of, with iron diffusion barrier, inter-, 20: 11215(R) (NASA-CR-54718)
Cu/stainless steel, diffusion characteristics of, 19: 917
Fe/Nb/stainless steel, diffusion in bimetallic tubing of, with iron diffusion barrier, inter-, 20: 11215(R) (NASA-CR-54718)
Fe/Nb/stainless steel/V, diffusion in bimetallic tubing of, with iron and vanadium diffusion barriers, inter-, 20: 11215(R) (NASA-CR-54718)
Fe/Nb–Zr/stainless steel, diffusion in bimetallic tubing of, with iron diffusion barrier, inter-, 20: 11215(R) (NASA-CR-54718)
Fe/Nb–Zr/stainless steel/V, diffusion in bimetallic tubing of, with iron and vanadium diffusion barriers, inter-, 20: 11215(R) (NASA-CR-54718)
Fe/stainless steel/Ta, diffusion in bimetallic tubing of, with iron diffusion barrier, inter-, 20: 11215(R) (NASA-CR-54718)
Fe/stainless steel/Ta/V, diffusion in bimetallic tubing of, with iron and vanadium diffusion barriers, inter-, 20: 11215(R) (NASA-CR-54718)
Mg/stainless steel, corrosion pitting by chloride ions, 20: 11231 (CEA-R-2815)
Mo/Ni/Nb/stainless steel, diffusion in bimetallic tubing of, with molybdenum and nickel diffusion barriers, inter-, 20: 11215(R) (NASA-CR-54718)
Mo/Ni/Nb–Zr/stainless steel, diffusion in bimetallic tubing of, with molybdenum and nickel diffusion barriers, inter-, 20: 11215(R) (NASA-CR-54718)
Mo/Ni/stainless steel/Ta, diffusion in bimetallic tubing of, with molybdenum and nickel diffusion barriers, inter-, 20: 11215(R) (NASA-CR-54718)
Nb/stainless steel, diffusion in bimetallic tubing of, inter-, 20: 11215(R) (NASA-CR-54718)
Nb/stainless steel, properties of duplex tubing for mercury Rankine boilers, 20: 9495 (NAA-SR-11191)
Nb–Zr/stainless steel, diffusion in, 17: 34413 (TID-19109)
Nb–Zr/stainless steel, diffusion in bimetallic tubing of, inter-, 20: 11215(R) (NASA-CR-54718)
stainless steel/Ta, diffusion in bimetallic tubing of, inter-, 20: 11215(R) (NASA-CR-54718)
stainless steel/Sn/Zr, roll-form bonding of, 16: 17966(R) (BMI-1541 (Del.))

STANDARD ELECTRODES

development and performance for electrochemical studies on metals in molten alkali metaphosphates, 20: 5529(R) (SC-DC-65-1706)
isotopic effects in reactions on, equation for determining stoichiometric number of rate-determining step in, 18: 25400
potential of, isotope exchange effects on, 16: 26971
reactions on nickel, mechanism of isotopic exchange in, 18: 227

Standard Reactors

see Sigma Piles

STANDARDS

see also Radiation Protection
see also Safety
calibration for metrology, effects of temperature variations on, 19: 15698(T) (UCRL-Trans-1145(L))
calibration in large defense plant, 19: 17392 (BDX-613-43)
calibration of cobalt-60, for thermal neutron dosimetry, 17: 41242 (EUR-422.e)
calibration of cobalt-60 sources, 19: 28421 (NP-15052)
calibration of graphite-block, for thermal neutrons, 20: 45060
calibration of isotopic, 19: 35378(R) (EANDC(E)-57(U))
calibration of tritiated toluene radioactivity, 19: 15651
compilation of U. S. nuclear, 1964 ASA, 20: 12559
construction and calibration of photoneutron, 18: 2784
convention on minimum international, regarding civil liability for nuclear damage, 19: 7758
definition of ionizing-radiation, 19: 18215
description of resistance, temperature, and voltage, 18: 27755(R) (ORNL-3578(p.78-95))
description of, for calibrating beta-particle counters, 18: 43948
design and performance of, for uranium hexafluoride pressure gages in micron region, 20: 41252
design code of ASME for unfired pressure vessels, 19: 22448 (CONF-650409-1)
development for radioisotopes in Australia, 20: 16746
development for reactor safety, 16: 22476
development of atomic frequency, using optical pumping in gas cells, 16: 27765
development of nuclear, 20: 45987
development of radiation protection, by AEC, 19: 2557
development program for laboratory, 20: 25345 (SC-DC-66-1491)
establishment of, for glove box evaluation and testing, 20: 18947 (RFP-343)
Euratom Bureau for Nuclear Measurements, activities of, 19: 20088
evaluation of contamination, 20: 45973
for atomic weights and nuclidic masses, 16: 18805
for by-product regulation, AEC-state cooperation in, 18: 25715
for cleaning nuclear reactor component systems, 19: 35629
for construction of boilers and pressure vessels, 19: 45507
for estimating recrystallization, inclusions, and stringers in uranium, 18: 34047 (NLCO-910)
for film badges, British, 18: 37469
for food radiopreservation, preparation of food additive petition for, 18: 21819 (TID-7684(p.79-80))
for iodine-131, British, 17: 36070
for iodine-131 exposure, 18: 43816
for medical and occupational radiation exposure, 18: 29433
for medical use of radiation, 18: 29894
for medical use of radiations, 18: 29905
for packaging of radioactive materials for transport, 19: 40810 (SC-RR-65-98, pp 32-44)

for personnel working with ionizing radiations in Yugoslavia, 19: 46654(T) (JPRS-31993)
for radiation and radioactivity, 19: 2558
for radiation exposure, EURATOM, 18: 39538
for radiation protection and radiodiagnosis, governmental, 18: 21941
for radiation protection in Canada, 18: 29887
for radiation protection of Canadian personnel, 18: 29888
for radiation protection, 18: 39543
for radiation protection in industry, 19: 712
for radioactive contamination of surfaces, 19: 44311
for radioactive material use, role of the state in, 18: 22300
for radioactive materials shipping, legal, 18: 35797
for radioactivity measurement, international comparison of, 17: 30081
for radioactivity measurement, international agreement on, 20: 27219
for radioisotope distribution and procurement in Australia, 18: 29161
for radioisotope regulation in France, 18: 43867
for radium control, 18: 22305
for rating grain size of beta heat-treated uranium fuel cores, 18: 32048 (NLCO-909)
for reactor safety, 17: 7557 (HW-SA-2507)
for shipping radioactive materials, 19: 714
for solution calorimetry, 17: 27323 (UCRL-7325-T)
for sulfur isotopic analyses, 17: 20229
for sulfur isotopic analyses in New Zealand, recalibration of meteorite, 17: 20231
for tungsten sheet quality, recommended, 18: 22235 (MAB-196-M)
for water radioactivity, 17: 27613
for x-ray equipment inspection, 18: 41264
for x-ray laboratories in Poland, 18: 43330
frequency comparison between hydrogen maser and cesium beam tube, (E), 19: 13711
frequency comparison between hydrogen maser and Swiss cesium beam standard, (E), 19: 13712
geochemical, analysis for bromine by neutron activation, 19: 13235
heat treatment, for fabricating heavy-wall reactor vessels, 20: 33909
in activation analysis, National Bureau of Standards facilities and techniques for developing, 19: 40450
isotopic compositions of 16 uranium isotope, by National Bureau of Standards, 20: 10795
isotopic evaluation of NBS Secondary Generative Uranium, 18: 21958 (KY-456)
legal, for handling radioactive materials, 18: 39557
mass comparison for radium, (E), 19: 14158
materials management policies of AEC, nuclear, 20: 33549 (CONF-660308, pp 131-42)
materials management licensing policies of AEC, plutonium, 20: 33550 (CONF-660308, pp 143-8)
materials testing methods in, for welds, 20: 25268 (ORNL-P-2107)
measurement of electrical quantities, comparative, (E), 19: 4276
measurements of nuclear, Euratom bureau for, 20: 26591
nuclear, fifth meeting of European-American Nuclear Data Committee on, 17: 39970 (EANDC-28(L))
of length using krypton-86 gamma wavelength, 16: 18210
of neutron flux density, 17: 9069
of radiation exposure at Oak Ridge, Tenn. and Paducah, Ky., 17: 23548 (KY-400)
of radioactivity, model format for certificate of, 18: 1989
preparation and calibration of radium, 20: 1941
preparation at EURATOM CBNM, 19: 3226
preparation for mass spectrometric analysis, 19: 36217(R) (IDO-14656)
preparation for neutron activation analysis, 18: 9989
preparation for radioisotopes, 20: 23208
preparation of beta-source, 20: 9041(P)
preparation of biological-material, for intercomparison of elementary analyses, 20: 35466
preparation of isotopic, 19: 35378(R) EANDC(E)-57(U))
preparation of radioactive solutions as, with very low volume activity, 17: 25876
preparation of uranium-235 isotopic, by blending of oxides, 16: 9355 (DEG-Report-248)
preparation of, in Czechoslovakia, 20: 39279
purity of high-purity uranium, 19: 17780 (KY-481)
radiation liability insurance, in industry and medicine, 18: 35798
radiation protection, Federal Radiation Council views on, 19: 9431
radiation protection, philosophical influences on, 19: 9432
radiation protection, for EGCR, 20: 7299 (EGCR-4(Suppl.1))
radiation quantities and units, 17: 27625
radiation safety, in manned space flight, 20: 8743 (LA-DC-6827)
radioactive source, weighing techniques for, 19: 11546
radioactivity, availability and use of, 18: 9797
radioactivity, data requirements for, 19: 36720
radioisotope, equipment and methods for, 20: 7185 (AEET-224)
radiopharmaceutical, U. S. Food and Drug Administration policy on, 20: 26716
radiopharmaceutical, government responsibilities in maintaining, 20: 26717
recommendations of ICRU for evaluation methods for radiological equipment and materials, 18: 16279 (NP-13746)
safety, for radiation protection, 17: 14573
safety regulations for radioactive materials, lecture, 17: 14552
specification for confinement seals in Hanford buildings 105-N and 109-N, 19: 11326 (HWS-6574(Rev.1))
specification for gantry and trolley for fuel handling cask, 19: 20099 (TID-21644)
specification for plutonium dioxide–uranium dioxide particles for fuel use, 19: 34679 (HW-84512RD)
specification guides for architectural and civil engineering at HAPO, 18: 3921 (TID-15244(Rev.))
specification guides for chemical, mechanical, sanitary, and steam engineering at HAPO, 18: 3922 (TID-15245(Rev.))
specification guides for chemical, civil, electrical, and mechanical engineering at HAPO, 18: 3923 (TID-15246(Vol.I)(Rev.))
specification guides for equipment and procedures, instrumentation, and structural engineering at HAPO, 18: 3924 (TID-15246(Vol.II)(Rev.))
specification guides for civil, electrical, mechanical, and structural engineering at HAPO, 18: 3925 (TID-19753)
specification guides for engineering at HAPO, index for, 18: 3926 (TID-19755)
specification guides for protective clothing at HAPO, 18: 4026 (TID-19754)
specification guides for instrumentation and instruments at HAPO, 18: 4059 (TID-19752)
specification guides for welding at HAPO, 18: 4215 (TID-15247(Rev.))
specifications for fabrication of stainless steel for corrosive radioactive service, 17: 34370 (TID-19154)
specifications for piping and pressure vessels, fabrication and materials, 18: 10258
specifications for fabrication of fuel elements for Plutonium Recycle Test Reactor Mark I-M, 18: 16452 (HW-79290)
specifications for fuel element fabrication for Plutonium Recycle Test Reactor, 18: 16453 (HW-79291)
specifications for fabrication of PIN gamma-transient detectors, 19: 11499 (UCRL-13128)
specifications for gages and parts on engineering drawings, (E), 19: 12876 (SC-TM-64-669)
specifications for iodine-131, for thyroidal uptake measurements, 20: 16315
sulfur isotopic abundances in standard meteorites, 17: 20230
tabulation of international and national nuclear, 20: 35180 (ORNL-NSIC-18)
tabulation of U. S. nuclear, 20: 25322 (ORNL-NSIC-11)
techniques for proportional counting of nickel-63 and sulfur-35, 18: 31866 (AWRE-O-26/64)
uranium contents of international, 20: 43563
uranium isotope mass spectrometer performance in analysis of, 19: 30081(R) (NBL-216)
use of internal, in liquid scintillation counting, dispenser for, 20: 16834
use of monomolecular films as beta sources, 20: 16143 (AD-620276)
x-ray dose definition and measurement, 18: 29322

STANFORD LINEAR ACCELERATOR

alignment techniques, 19: 37265
beam current monitors for, evaluation of, 18: 10698 (SLAC-25(Pt.I) (p.30-62))
beam deflection and transport system for, pulsed bending magnet for, (E), 19: 4774 (SLAC-PUB-53)
beam deflection and transport systems for, (E), 19: 14178 (SLAC-29)
beam dumps and collimators for, design of water-cooled, 19: 37375
beam focusing of, misalignment and quadrupole errors of multiplet lens combinations for sector, 17: 26646 (SLAC-15)
beam inflection system for, 19: 37371
beam injector design and testing for, 19: 37364
beam intensities from, estimates of secondary, 17: 21115 (SLAC-5(p.90-132))
beam interactions with laser beam, monochromatic gamma beam production in, (E/T), 20: 936 (SLAC-41)
beam interactions in storage ring of, angular distributions from electron, (E), 20: 21588 (AD-623658)
beam position and charge monitoring circuits for, design and performance of, 20: 41544 (SLAC-63)
beam position monitoring electronics for, design and performance of, 19: 37374
beam position monitor for, 20: 39506
beam production and transport at, 18: 10699 (SLAC-25(Pt.I)(p.63-87))
beam profile monitor for, design and performance of, 20: 41562
beam separation by traveling-wave r-f structures, 18: 18528

beam separators in, traveling-wave, 19: 11969
beam stoppers for, materials for, 18: 7841(R) (ORNL-3499(Vol.II) (p.9-11))
beam storage ring for, antiproton and meson (μ) trapping by, 20: 2547 (UR-375-98)
beam switching magnets for, high repetition rate pulsers for, 19: 37320
beam switching system for, 19: 39327
beam switchyard instrumentation for, 19: 37386
beam testing for, water activation in, 20: 25658 (SLAC-TN-66-4)
beam tests with sectors 1 and 2, 20: 7677 (SLAC-50)
beam transport magnets for, calibration of, 20: 17206 (CONF-650922, pp 823-34)
beam transport optics and experimental areas for, 19: 11959
beam transport systems for, magnetic design measurements for, (E/T), 19: 4775 (SLAC-PUB-57)
beam transport systems for, radiation effects on, 19: 37372
beams of, technique for mass analysis of, 17: 21119 (SLAC-5(p.222-36))
construction of, status of, 19: 26986 (MURA-714(p.131-43))
controls and instrumentation for, 19: 37270
coupler asymmetry and stray magnetic fields in, tolerances on, 18: 8957 (SLAC-20)
description, 18: 36115
description, (E), 19: 14179 (SLAC-PUB-52)
design and development, 16: 15705(R) (TID-15350)
design and development of, status report on, 17: 7320 (BNL-6511 (p.128-61))
design and development, Apr.–June 1964, 19: 11866(R) (SLAC-32)
design and development, July–Sept. 1964, 19: 25099(R) (SLAC-34)
design and development history and research uses of, 20: 31824 (SLAC-62)
design and experimental program for, 20: 29862
design and fabrication of accelerating structure, 17: 17316 (SLAC-7)
design and uses, 17: 34083
development, 16: 2565(R) (TID-14180)
development, 17: 17317(R) (SLAC-8)
development, 17: 29643(R) (SLAC-16)
development, 17: 42015(R) (SLAC-18)
development, 18: 8958(R) (SLAC-23)
development, 16: 28185 (TID-7636(p.79-118))
development, 18: 22593(R) (SLAC-27)
development, 19: 41170 (SLAC-42)
development, 20: 5943(R) (SLAC-48)
development, 20: 13366(R) (SLAC-53)
development and construction, 17: 889(R) (SLAC-1)
development status, 19: 11924
development, Jan. 1–Mar. 31, 1964, 18: 34372(R) (SLAC-30)
development, Jan. 1–Mar. 31, 1966, 20: 39497(R) (SLAC-65)
development, Jan.-March 1965, 20: 937(R) (SLAC-45)
development, Oct.–Dec. 1965, 20: 25656(R) (SLAC-59)
developments, 17: 35000(R) (SLAC-10)
drift tube design, 20: 39503
electron–proton interactions in, kinematics of, 18: 10880 (SLAC-25(Pt.I) (p.125-33))
electron-proton scattering experiments with, spectrometer for, 18: 10700 (SLAC-25(Pt.I)(p.149-59))
experimental program of, 18: 10696 (SLAC-25(Pt.I))
experiments at, arrangement for meson (μ)-proton elastic scattering, 17: 21118 (SLAC-5(p.193-221))
experiments for, on secondary particle interactions with protons, 17: 21114 (SLAC-5(p.79-89))
focusing system for two-mile, misalignment and quadrupole error effects in, 17: 19419 (SLAC-11)
hydrogen bubble chamber for, design and use of, 17: 21113 (SLAC-5 (p.40-78))
instrumentation of 3-Bev storage ring, 17: 21116 (SLAC-5(p.133-64))
klystron amplifier tube for, development of, 17: 39381(R) (TID-19482)
klystron tubes for, assembly and performance of, 18: 2500(R) (TID-19422)
klystrons for, assembly procedures and components for, 18: 2501(R) (TID-19422(Suppl.II))
magnet coil insulation for, charged-particle effects on, 19: 32830 (SLAC-40)
magnet design for, 18: 36111 (SLAC-28)
magnet pulser for, beam switching, 19: 27025 (SLAC-36)
magnetic field measurement techniques for, 19: 34813 (SLAC-39)
magnetic field measurement and spectroscopy for quadrupole magnet for, 19: 37313
magnetic field measurements in strong-focusing lenses of, (E/T), 20: 13365 (SLAC-39(Rev.))
magnetic fields in, EMR measurements of pulsed, 18: 22315 (SLAC-26)
magnets for, electric and magnetic properties of quadrupole, 20: 19304 (SLAC-55)
magnets for, magnetic centers of quadrupole, 20: 39503
meson (π) fluxes at, estimates of, 18: 10697 (SLAC-25(Pt.I)(p.1-18))
microwave networks for, accurate phase length measurements for, 20: 35965 (SLAC-PUB-181)
operation of, 20: 29864
photon beam from, 17: 21109 (SLAC-5(p.1-19))
positron production at 300 Mev, 16: 12579 (HEPL-249)
power supplies for, development of klystron (E), 19: 2927 (SLAC-PUB-56)
power supplies for, development of klystron, 19: 37274
power supplies for, design of c-w, 20: 19290 (CALT-68-64)
power supplies for, performance of hydrogen thyratron, 20: 31825 (SLAC-PUB-192)
power supply for, development of klystron, 18: 44321 (SLAC-PUB-48)
power supply for, microwave window testing for klystrons for, 18: 44322 (SLAC-PUB-49)
power supply for, window materials design and properties for klystron, 19: 37279
power supply for, performance of klystron, 20: 7677 (SLAC-50)
radiation effects on magnet insulation in, 19: 37350
radiation hazards, 20: 29849 (CONF-651109, pp 442-58)
scattering experiment with, 180° electron-proton, 18: 10701 (SLAC-25 (Pt.I)(p.160-6))
sector focusing in two-mile, optical properties of quadrupole multiplets for, 17: 19421 (SLAC-14)
shielding against d-c magnetic fields, development of, 18: 30940
shielding design calculations for, 17: 9646 (ORNL-3289)
shielding for, meson-nucleon cascade calculations for transverse, 17: 15322 (ORNL-3365)
shielding for, nucleon-meson cascade calculations of transverse, 17: 19418 (ORNL-3412)
shielding for, transverse radiation, 17: 17318 (SLAC-9)
shielding for, performance of transverse, (T), 19: 18751 (ORNL-3734)
shielding requirements, computer analysis, 16: 3888(R) (ORNL-3193 (p.339-41))
shielding system for, magnetic, 19: 37381
storage ring design, 20: 27680
storage ring for, advantages and design of 10-Bev, 17: 21117 (SLAC-5 (p.165-92))
storage ring for 10-Bev mesons(μ), 19: 37326
storage rings for development of 500 Mev, 19: 37396
storage rings for, vertical instabilities in electron, 18: 16595 (BNL-7534(p.375-8))
thermionic diode housing for, 20: 39506
trigger-system design for subsystems switching in, 19: 30888 (SLAC-35)
use of, 17: 21108 (SLAC-5)
vacuum couplings and valves for, 19: 37351
vacuum system for, design of, 19: 37352
vacuum system of, in-line oil trap for, 19: 37358
vacuum valve for, development of stainless steel, 19: 37359
waveguide network for, phase adjustment of high-power, 19: 37269

STANNATES
see also Barium Stannates
see also Calcium Stannates
see also Lead Stannates
see also Sodium Stannates
see also Strontium Stannates
see also Tin Compounds
gamma emission by tin-119 in ammonium chloro, isomer energy shifts, 16: 12545
radiolysis of aqueous solutions of, at 77°K, yields of hydrogen from gamma, 20: 18748

STAR
see Shield Test Air Reactor

Star Production
see Photographic Film Detectors

Starfish
see Echinoderms

Starfish Burst
see Dominic Operation

STARCHES
analysis for trace elements, activation, 19: 24400 (KR-91)
effects of irradiated, in inhibiting lead corrosion in water, 19: 11806
hydrogen isotope exchange in, 16: 461
labeling with tritium, 19: 44102
metabolism in sapwood of *Populus deltoides*, 19: 17463
preparation of carbon-14-labeled, by photosynthesis, 16: 18908
radiation effects on solutions, 16: 15047(R) (TID-15389)
radiation effects on potato, 16: 22237
radiation effects, 16: 23750
radiation effects on, in rice, 16: 27520
radiation effects on, electron-, gamma-, neutron-, and x-, 16: 31669
radiation effects on 2.5% solution of, 17: 16087
radiation effects on corrosive properties, gamma, 18: 8426
radiation effects on color of iodoacetic acid mixture and use as chemical

dosimeter, 18: 19751
radiation effects on flour, gamma, 18: 25139
radiation effects on structure of potato, 18: 35605
radiation effects on properties of, as adhesive and dyeing mordant, 20: 20767
radiation effects on, GPR studies of gamma, 20: 23098
radiation effects on acidity of corn and potato, effects of gases and vacuum on gamma, 20: 33367
radiation effects on, in maize, 20: 35250
radiation effects on potato, effects of water content on gamma, 20: 36599
radiation effects on concentration of, in potato tubers, x, 20: 38690
radiation effects on wheat flour, gamma, 20: 40599
radiation effects on alpha and beta amylases in corn and potato, gamma, 20: 42798 (NP-16224)
radiation effects on content in cotton pollen, gamma, 20: 42896
radiation effects on hydrolysis of, in barley endosperms, γ, 20: 45422
radioinduced free radicals in, gamma, 18: 23651(T,R) (AEC-tr-6316 (p.573-86))
radioinduced free radicals in, reactions with sulfur dioxide, 18: 29747(T,R) (AEC-tr-6231(p.439-50))
radiolysis, 17: 208
radiolysis of potato, effects of water content on gamma, 20: 20737
radiolysis of solid, yields in, 18: 310
radiolysis of solutions of, gamma, 17: 1550
sorptive properties for organic compounds, 18: 25032(T) (SC-T-64-618)
therapeutic effects of, on radiation sickness in rats, 18: 5139(T) (JPRS-22123)

STARK EFFECT
electron impact effects on line broadening, 16: 13687 (CEA-2070)
hydrogen line strengths in, numerical tables for $n \leq 25$, 18: 32360 (AWRE-O-17/64)
in plasma microfield, 19: 1740
in research on light and matter, 19: 23321
in spectral lines of plasma, 17: 21128 (AFOSR-TN-60-779)
measurement in nitrogen plasma, ion line shifts, 19: 39952 (AFCRL-65-348)
on hyperfine structure of potassium fluoride, 18: 20762
radial field distribution measurement in Penning discharge by, 17: 16804
theory of, produced by charged particles near emitters, 18: 40170
use for measuring electric field strength in plasma, 18: 17188
use for plasma electron concentration measurements, (E), 19: 5327(T)
use in high-frequency field strength measurements in plasma, 16: 23204
use in measuring molecular dipole moments, 20: 3958
variation of matrix elements of hydrogen atom dipole in uniform external electric field, (T), 19: 4825 (CEA-R-2544)

STARS
see also Nebulas
see also Sun
absorption coefficients and opacities for, (T), 20: 7707
abundance analysis of supergiant in large Magellanic Cloud, 19: 14212
abundances of elements in 3 Centauri A, 16: 4659
abundances of elements in, 16: 29599 (AFOSR-3024)
adiabatic invariants of, in galactic field, (T), 20: 14950(R) (COO-614-41)
age determination and evolution, (T), 20: 7715
age determination of A, B, and F, 20: 37417
ages of clusters of, common origin determination of, 18: 16639
analysis of superdense, 19: 12059
analysis of Taurus A, radiometric, 17: 35260(R) (TID-19135)
angular momentum transfer between ejected particles and binary, 17: 39820
angular size of x-ray source Sco X-1, 20: 34029
antineutrino production in neutron, by neutron-neutron interaction, (T), 19: 37448
associations of, review of O and T, 19: 20794
atmosphere and plasma winds of, (T), 19: 20783
atmosphere layer of, oscillations in hot-corona-surrounded nonadiabatic, (T), 19: 37438
atmosphere model computation methods for, 16: 18288
atmospheres of cool, continuous absorption of helium negative ions in, (T), 19: 25130
atmospheres of, ionization-equilibrium equation of state for, 17: 3917
atmospheres of metallic-line, models for, (T), 19: 18654
atmospheres of neutron, x-ray spectra of, (T), 20: 2568
atmospheres of O and B, properties of, (E/T), 19: 4786
atmospheres of, absorption coefficient in non-gray model for, 18: 36143
atmospheres of, asymptotic value of optical thickness of, 18: 42278
atmospheres of, effects of helium hydride ion in model, (T), 19: 41240
atmospheres of, evaporative and hydrodynamic models for, 20: 39556
atmospheres of, fluxes and line intensities from models for, 18: 40104
atmospheres of, line intensities in models for, (T), 19: 18651
atmospheres of, limb-darkening predictions in, 20: 34022
atmospheres of, radiative transfer in spherically symmetric, (T), 19: 32860
atmospheres of, shock-wave propagation in, 18: 18540
atmospheres of, shock-wave structure and stability in, (T), 19: 8062
atmospheric parameters for Kappa paroris, 17: 34683
atmospheric phenomena in, periodic, 18: 36134
atmospheric turbulence in nearly stable, 16: 16904
atomic reactions in atmospheres, 17: 16886
baryon conservation in superdense, (T), 19: 4810
beryllium abundance in F- and G-type dwarf, lithium/beryllium value from, (E), 20: 19330
beta decay in interiors, 16: 22831
beta decay in interiors of, exclusion principle inhibition of, 17: 39818
beta decay in, photon-induced, (T), 20: 31878
beta decay of interior nuclei, 16: 3802
beta decay of isotopes within, effects of exclusion principle on, 17: 39818
binding energies of starlike condensates of 10^3 to 10^9 solar masses in general relativity, 18: 7378
binding energy of magnetoturbulent supermassive, upper limit of, 20: 34011
bolometric-correction and effective-temperature scale for, 17: 37905
book: *Astrophysics and Space Science*, 19: 20782
book: *Dynamics of Stellar Systems*, 19: 39329(T)
book: *Gravitational Theory and Gravitational Collapse*, 19: 34859
book: *Quasi-Stellar Sources and Gravitational Collapse*, 19: 23254
book: *Star Evolution*, 19: 20786
book: *Stellar and Interstellar Space Physics*, 20: 34072
book: *Stellar and Solar Magnetic Fields*, 19: 44932
book: *Stellar Interiors*, Vol. 6, 18: 32352
book: *Stellar Structure*, 20: 7704
brightness and color of Cassiopeia (SA19), 19: 30916
carbon ion continuous absorption in, 19: 1149
carbon negative ion continuous absorption in, free-free, 20: 31864
carbon-nitrogen-oxygen cycle, rate of proton reactions (p,α) with oxygen-17 at 490 to 1580 kev, 16: 8227
carbon-12, neon-20, and oxygen-16 abundances in giant, (T), 20: 25698
carbon-13 content in, indicator for, 20: 25686
carbon, nitrogen, and oxygen abundances in, (T), 19: 25128
charged-particle acceleration in magnetic fields of, processes for, 18: 32354
charged-particle acceleration in supernova, bremsstrahlung absorption by electrons for, (T), 20: 25708(T)
chromospheres of, electron distribution functions in, (T), 19: 32862
chromospheres of, properties of, 20: 21504
chromospheric properties and rotation of main-sequence, (E), 20: 29883
collapse in clusters or galaxies, accelerated processes in, 18: 32342
collapse in expanding universe, gravitational, (T), 20: 32306
collapse mechanisms, 18: 14706
collapse of, (T), 20: 39555
collapse of high-temperature, model with neutrino surface intensity and energy loss for gravitational, 20: 41612
collapse of magnetic, gravitational, (T), 19: 4822
collapse of massive, 18: 7379
collapse of neutron and presupernova, 19: 34835 (N64-22572)
collapse of, boundary conditions for gravitational, 19: 43228
collapse of, energy-momentum tensor for, 18: 24291
collapse of, exterior metric for, (T), 20: 15228
collapse of, flux resistance to gravitational, 19: 18951
collapse of, gravitational, (T), 19: 14210
collapse of, gravitational, 20: 25681
collapse of, hydrodynamic calculations of general-relativistic, (T), 20: 11434
collapse of, Kerr solution of Einstein equations for, (T), 20: 11435
collapse of, neutrino emission during, 20: 46280
collapse of, observation of high-energy neutrinos emitted during, 20: 46280
collapse of, oscillatory motion of, 20: 44106
collapse of, relativistic neutrino transport theory for gravitational, 20: 32296
composition and evaluation of, 19: 8054
composition of Crab Nebula, neutron-star hypothesis for, (E/T), 19: 29013 (MIT-2098-123)
composition of HD 26 and HD 201626, 18: 30383
composition of high-velocity A, 18: 36135
composition of SCO-X1, electron-cloud hypothesis for, (E/T), 19: 29013 (MIT-2098-123)
Compton scattering in quasars, importance of inverse, 20: 46289
configuration of hyperons, 16: 22828
configurations of, Fermi-Dirac functions for computation of, 17: 39825
content of nitrogen-14 to carbon-12 in surface of, during helium burning, (T), 19: 9843
contraction of helium-hydrogen, physical conditions in, (T), 20: 19345

contraction of proto-, (T), 19: 30933
contraction of, energy release in gravitational, (T), 19: 20768(T)
contraction of, properties of, 20: 37396
convections zones in atmospheres of, 16: 22822
convective envelope depth in lower main sequence, lithium depletion effects on, (T), 19: 39336
convective stability in massive, effects of hydrogen burning on, 20: 34012
cooling and detectability of neutron, 20: 37355
cooling of neutron, by Urca process, 19: 9870
cooling of neutron, composite equations of state with nuclear forces for, (T), 19: 39355
cooling of neutron, effects of neutrino emission on, (T), 20: 15201
cooling of neutron, (T), 20: 34075
core motion in, overshooting in convective, (T), 20: 15208
corona dynamics of, subsonic and supersonic solutions for, (T), 19: 34841
corona of, density and temperature of, 18: 8996(T)
corona spectral lines of, proton excitation of, 18: 16635
coronal expansion of, equations for, 18: 36140
coronas and winds of, dynamical properties of, 18: 10739
coronas and winds of, dynamical properties of, 18: 10740
coronas of, particle collisions in, 17: 41696
cosmic particle production and acceleration by supernova, 18: 44489(T)
cosmic ray origin in supernova, (T), 20: 37498
cosmic x-ray sources in Sagittarius and Scorpio, positions of three, (E), 19: 44968
cosmic-ray emission from radio source, 20: 37490
cosmic-ray production in supernovae, 19: 20903
cyclotron radiation emission at optical energies, 18: 42264
declination of extragalactic radio sources, (E), 19: 30926
density and mass for equilibrium state of, relativity theory for, 20: 7700
density distribution in circumstellar envelopes formed by rotational ejection, (T), 19: 9836
density of white dwarf and type-I supernovae, 19: 20800
detection and identification of quasars, (E/T), 19: 18667
detection of, in Lyman-α wavelength region, 17: 34695
detection of neutron-core, 17: 24210
detection of radio-source, hidden by moon, 20: 19348
detection of x-ray source, at 20 to 200 kev, (E), 20: 21490
deuterium abundance in galaxy, upper limit, 16: 27864
deuterium abundance in, upper limits for, (E), 20: 15197
deuterium content in magnetic, 19: 25127
development of associations of, theory of, 18: 34394
diameter of quasi-stellar radio sources, (T), 19: 9869
diffraction patterns of radio-, equatorial irregularities in, 17: 24219
distances and luminosities of quasars, 20: 29896
distribution of Cepheid, in large population-I-component galaxies, (T), 20: 19334
distribution of quasi-stellar radio sources in steady state cosmology, 20: 29897
distribution of x-ray source, supernova correlations with, 20: 21497
dynamic evolution in globular clusters (T), 19: 1138(R) (AFCRL-64-572(B1-19))
dynamics analysis of, 19: 26747(R) (COO-614-23)
dynamics of atmospheres and outer layers of intrinsic variable, 16: 16905
dynamics of dense photon, 20: 37357
dynamics of spherical systems of, models for, 17: 41686
effects of quasi-stellar-radiosource, on universe models, (T), 20: 19354
effects on nonconstant scattering opacity on massive, initially composed
ejection of quasars from peculiar galaxies, ratio of blue-red shifts, 20: 44085
electroacoustic wave propagation in interior of, screening in, (T), 20: 34742
electromagnetic radiation from antineutrino–neutrino super-, (T), 19: 16472 (JINR-P-1933)
electromagnetic waves from radio, intensity variations of, (E), 19: 23328 (AFCRL-64-743)
electron capture in interior of, 18: 10748
electron capture processes at high temperatures, energy losses in, (T), 19: 16348
electron Compton scattering in semidegenerate region of, opacity from, (T), 20: 15209
electron degeneracy in, pair production effects on, (T), 20: 15229
electron density and temperature in upper atmosphere of, distributions of (T), 19: 1156(T)
electron density in chromospheres of, 18: 28231(T)
electron density in gaseous nebulae, monochromators and spectrometers for determination of, 19: 9867
electron emission density from Hercules A, 3C433, and 3C295, 17: 25852(R) (NP-12877)
electron pair annihilation in, neutrino spectra from, 18: 30393
electron pressure ratio to gas pressure in atmospheres of, 19: 47187 (AD-612182)
electron-ion recombination in coronal plasma of, coefficients for, (T), 19: 34847
electrostatic potential distribution around, from stellar winds, (T), 20: 41617
element abundance in 53 Tauri, 18: 10742
element abundance analysis of HD 101065, 20: 25703
element abundance determination in CH, 20: 37424
element abundance differences among population I, 20: 37425
element abundance in peculiar A, 20: 37426
element abundances in high-velocity A, 16: 16896
element abundances in, neutrino emission effects on, 16: 22826
element abundances and origins in red giants, 17: 15045
element abundances in G dwarfs, ratio to hydrogen, 17: 24199
element abundances in ζ Herculis and G dwarfs, 17: 32852
element abundances in red giant, theory for, 18: 16634
element abundances in K-giant, 18: 34385
element abundances in, (T), 19: 20762
element abundances in barium, 19: 37446
element abundances in, 19: 47187 (AD-612182)
element abundances in, effects of beta-decay and neutron capture rates on, 20: 13410
element abundances in, determination of, 20: 37422
element formation in giant stars, heavy, 17: 3913
element formation mechanisms in, (T), 19: 41235
element production in, review of processes for, 20: 15231
element synthesis in, review, 17: 17650
element synthesis in supernova, alpha and proton reaction rates for $20 \leq A \leq 40$, 17: 34693
element synthesis in, 17: 36557
element synthesis and destruction in types A and B, (T), 20: 2565
element synthesis in, theory of fast neutron capture cross sections in, 20: 34669
element transport in, from neutron capture, 20: 37423
elements in, ionization equilibrium equation for, 17: 28112
emission effects on age estimation of old clusters, stellar-wind, (T), 19: 9842
emission lines of carbon in hydrogen ionization regions of, forbidden, 17: 6903
emission sources for radio galaxies, theory of, 18: 16636
energy from quasars, quark model for, 20: 44094
energy from radio-source and quasi-stellar, effects on matter creation, (T), 20: 23864
energy generation in, neutrino role in, 18: 44341 (BNL-8217)
energy generation in convective cores of, (T), 20: 9635
energy losses of neutron, by gravitational radiation, (T), 19: 37689
energy of neutron, correlation with light curves of type-I supernova, (T), 20: 2584
energy of quasi-stellar radio sources, 19: 39359
energy of white dwarf models of, total, 17: 32858
energy origin, review of hypotheses, 16: 6885
energy output of quasi-, (T), 19: 37557
energy production in, (T), 19: 16342
energy production in quasi-stellar radio sources, (T), 19: 30934
energy production for radio-source, cosmological theory for, 20: 23865
energy release from massive, gravitational effects on, 18: 7379
energy source for quasi-, (T), 19: 23250
energy source for quasi-stellar radio-source, monopole gravitational field as, 20: 19714
energy sources for quasistellar, subnuclear processes as, (T), 20: 21498
energy sources in, 19: 2942
energy sources in quasi-stellar radio sources, expansion as, (T), 19: 34837
energy spectra of neutron, at absolute zero temperature, (T), 20: 4531
energy spectra of nonthermal radio, effect of electron distribution function on, (T), 20: 11427
energy transfer from point explosion in, 18: 44365(T)
energy transfer in, collective effects on radiative, (T), 19: 37451
energy transport in hydrogen ionization zone of giant, 17: 6904
energy transport in, boundary of convective, (T), 20: 954
energy transport in, by turbulent convection, 20: 37394
envelopes and interiors of, calculations of, 17: 24198
envelopes of nova, dynamics of, 17: 13287(T)
equation of state for interior of, numerical evaluation of, (T), 20: 15213
equations of motion for, numerical integration of n-body problem for clusters, 18: 30381(T) (UCRL-Trans-1069(L)(Pt.2))
equilibrium of large superdense, gas of heavy particles in, (T), 19: 42979
evolution, (T), 20: 21512
evolution and nucleogenesis, 16: 18114 (NP-11463(Pt.3)(p.419-29))
evolution and populations of, 19: 32878
evolution and properties of, 17: 24197

evolution and properties of relativistic cosmic objects, (T), 19: 18674
evolution and properties, (T), 19: 44928(T)
evolution and radiation mechanism of neutron, from supernova, 20: 29900
evolution and rotation of, in Hertzsprung gap, 20: 34017
evolution and stability of spherical, in hydrostatic equilibrium, (T), 19: 20801
evolution and structure of medium-mass, (T), 19: 4791
evolution and structure of helium, numerical models of, 20: 958
evolution and structure of helium, (T), 20: 15195
evolution and structure of, analytical models for, 20: 37391
evolution, effects of radiation pressures on dust flow through ambient gases, 16: 27859 (CRSR-119)
evolution from gravitational contraction to nuclear burning, 19: 30920
evolution from hydrogen to helium burning, 17: 3915
evolution from main sequence through core-helium burning, (T), 20: 15207
evolution of, (T), 19: 20784
evolution of, (T), 19: 27055
evolution of binary, 20: 37429
evolution of binary, 20: 46277
evolution of central, in planetary nebulae, 17: 32849
evolution of close binary systems of, review of, (E/T), 19: 20803
evolution of, effects of neutrino processes on late stages of, 17: 32850
evolution of Eta Carinae, 19: 20796
evolution of extended radio sources, (T), 20: 15200
evolution of helium, internal, (T), 20: 15202
evolution of helium, of intermediate mass, (T), 20: 44105
evolution of homogeneous spherical gas of proto-, 20: 34005 (CNIE-PT-4)
evolution of hydrogen ion region in, (T), 20: 15199
evolution of massive, from hydrogen exhaustion to onset of carbon burning, 16: 29601
evolution of massive, carbon production in, 18: 34386
evolution of massive, helium burning in, (T), 19: 47202
evolution of massive, (T), 20: 34067(T)
evolution of medium-mass, processes in early, (T), 20: 2567
evolution of non-hydrogenic population-I, 17: 13269
evolution of O-type hydrogen-burning, 18: 7376
evolution of O-type gravitational contraction and hydrogen exhaustion in, 18: 42262
evolution of O, during helium burning, (T), 20: 15218
evolution of one solar mass, 20: 37401
evolution of Population II, 16: 16915
evolution of population II, carbon core growth and shell helium flashes in, (T), 20: 15227
evolution of Population II, 20: 34015
evolution of population II red giants, 20: 41587
evolution of pre-main-sequence, initial condition effects on, (T), 20: 29884
evolution of protostar to quasistatic equilibrium, dynamical and thermal, (T), 20: 13408
evolution of quasars, probability of, (T), 19: 44922(T)
evolution of quasars, gravitation theory for, 19: 47209
evolution of rotating nonmagnetic, pre-main-sequence, (T), 20: 15219
evolution of rotating proto-, 20: 31872
evolution of seven solar mass, 20: 37405
evolution of small-mass, in pre-main-sequence stages, 18: 7386
evolution of supernova, 19: 34835 (N64-22572)
evolution of three solar mass, 20: 37402
evolution of type II supernovas, neutrino emission and mass loss in, 18: 7377
evolution of, advanced stages in, 20: 37404
evolution of, axial rotations in, 20: 41584(T) (UCRL-Trans-10040)
evolution of, beryllium and deuterium depletion in pre-main-sequence, 20: 27688
evolution of, calculation of main-sequence, 20: 37400
evolution of, calculations on pre-main-sequence, 20: 39574
evolution of, computer program for solution of time-dependent equations in, 19: 41210(T) (N64-25282)
evolution of, contraction and magnetic activity in, (T), 19: 20793
evolution of, contraction phase of, 20: 37397
evolution of, from main sequence through core helium burning, (T), 20: 19335
evolution of, from main sequence through core helium burning, (T), 20: 19334
evolution of, from main sequence through core helium burning, (T), 20: 19336
evolution of, from system of gravitationally interacting point-mass particles, 20: 26010(T)
evolution of, initial carbon-nitrogen-oxygen abundances for, 19: 30921
evolution of, model envelopes for superadiabatic layers in, (T), 20: 15196
evolution of, neutrino emission in, 18: 18551(T)
evolution of, neutrino density in, 18: 24273
evolution of, neutrino-pair processes in, (T), 19: 44927(T)
evolution of, nucleosynthesis in, 20: 37392
evolution of, observational approach to, 19: 20788
evolution of, relation to galactic evolution, 19: 20797
evolution of, review of theories of, 19: 20787
evolution of, role of magnetic activity in, 20: 37399
evolution of, schematic pre-main-sequence, 20: 37398
evolution of, silicon-28 statistical equilibrium for, 20: 21492
evolution of, survey on, 20: 37367
evolution of, theory of final stage of, 18: 14706
evolution of, theory for, 18: 32354
evolution of, theory of, 18: 42290
evolution of, through development phases and end state, (T), 19: 47201
evolution of, time sequences for, 18: 10747
evolution of, two-body motion in, 18: 18555(T)
evolution of, with helium-rich cores, 19: 20798
evolution processes in, (T), 20: 7706
evolution studies of supernovae, equations of state for, 16: 5836 (UCRL-6465)
evolutionary hydrogen-burning in, termination via beryllium-7-proton reactions, 20: 44076
evolutionary theories for, extension to advanced phases of nuclear burning, 18: 8990
evolutionary time scales for late carbon-burning phases of, with neutrino emission, 17: 24201
evolutionary tracks of massive main-sequence, (T), 19: 37440
excitation of atoms and ions by electron impact, 17: 6905
existence of collapsed, in binaries, (T), 20: 29889
expansion of radio-emitting, relativistic control, (T), 20: 44083
expansion of, after relativistic collapse, (T), 20: 25699(T)
expansion of, moment of inertia variations in, 20: 37384(T)
explosion in galaxies, 19: 32873
explosion of supernova, into interstellar magnetic field, (T), 20: 2569
explosion of supernova, into interstellar magnetic field, (T), 20: 2570
explosion of type II supernova, properties of, 20: 37407
explosions in, mechanism of, 17: 13036
explosions in supernovae, dynamics of, 17: 13037
explosions in, neutrino mechanism of type II supernova, (T), 19: 14200 (UCRL-12191)
explosions of, dynamic analysis of, 16: 32251
explosions of supernovae, 17: 13044
explosions of supernova, multiple bounce theory for cold plasma bubble in, (T), 19: 39344
explosions of supernovas, gravitational energy source in, (T), 20: 25680
explosions of supernova, effects of, on carbon-14 content in growth rings of trees, 20: 25310
explosions of, from cosmic-ray interactions at 10^{80} ev, 19: 20758
explosions of, hydrodynamic properties of supernova, (T), 20: 11425 (UCRL-7777)
fermion interactions in superdense, attractive, (T), 19: 25138
flare activity in M dwarf, mechanisms for, (T), 20: 25702
flare activity in, theory for, 18: 32343
flare activity of nearby, 19: 41203 (AD-600154)
fluid rotation in, variational principle for hydrostatic equilibrium of relativistic, (T), 20: 5974
formation and energy generation of, (T), 19: 28985
formation in elliptical galaxies as radio sources, 16: 21235
formation in expanding universe, 17: 9161
formation in rotating magnetic clouds, (T), 20: 39568
formation of, (T), 20: 31873
formation of, 20: 41585(T) (UCRL-Trans-10041)
formation of clusters of, in space, 17: 13039
formation of, initial stage, 17: 6916
formation of neutron, electromagnetic wave emission during, 18: 44353
formation of, opacity of diffuse cosmic matter in early stages of, 18: 7375
formation of quasi-stellar radio sources, spherical galaxies in process of, 18: 26196
formation of quasi-stellar, mechanisms for, 18: 36129
formation of rare light elements in stellar surfaces, 16: 4661
formation of white-dwarf, mass loss in, 19: 39337
formation of young clusters of, rates for, 20: 34013
formation of, rates of, (T), 19: 18661
formation of, role of neutrinos in, 18: 40111
formation of, statistical model for, (T), 20: 2574
formation of, theory for, 18: 22651(T) (JPRS-24435(p.309-15))
formation of, thermal instability role in, 20: 41601
formation rates of, two-color diagram for, (T), 20: 19347
galactic magnetic field, cosmic radiation and radio emissivity in open model of, 16: 15482
gamma absorption in quasars, high-energy, 20: 44084
gamma emission from, directional detector for measuring, 19: 15905

gamma emission from quasar 3C286, low-energy, (E), 19: 39357
gamma emission from supernova remnants, 19: 44930
gamma flux from magnetic variables and quasi-stellar sources, 19: 32859
gamma flux from, upper limits for, (E), 20: 34042
gamma fluxes from radio-, limits to, 18: 30394
gamma fluxes from quasistellar radio sources, (E), 19: 34898
gamma radiation from, measuring instrument for, 19: 26917(R) (IA-984)
gas circulation in, meridian, (T), 20: 7713
gas clouds in dense clusters of, quasar model for, (T), 19: 47199
gas flow in binary systems of, (T), 19: 16332
gas flow in, boundary conditions at nonstationary ionization front in, (T), 20: 2572
gas flow in, model for nonstationary ionization fronts for, (T), 20: 2571
gravitational collapse of energetically exhausted, 16: 18535
gravitational collapse of quasi-, 18: 8989
gravitational collapse of super-, 18: 18754
gravitational collapse of massive, radiation from, 18: 20715
gravitational collapse of, theory for, 18: 42255
gravitational collapse of, relativistic equations for, 18: 42286
gravitational collapse, 18: 42287
gravitational collapse of rotating, 19: 27056
gravitational collapse of, dynamics of cylindrical electromagnetic universe for, 19: 28978 (ORNL-3758)
gravitational collapse of, theories on, 19: 32867
gravitational collapse of, hydrodynamic calculations of, 19: 37430 (UCRL-14242)
gravitational collapse of, Schwarzschild metric and energy release in, 19: 37679
gravitational collapse of, scalar wave interactions with Schwarzschild metric in, 20: 957
gravitational collapse of, (T), 20: 15230
gravitational collapse of, relativistic MHD theory for, 20: 28153
gravitational collapse of, in general relativity theory, 20: 34034
gravitational collapse in quasar nuclei, oscillatory, 20: 34055
gravitational collapse of rotating radio sources, (T), 20: 34412
gravitational collapse of quasars, irreversibility of, 20: 44082
gravitational field of rotating superdense, 20: 25707(T)
gravitational instabilities of inhomogeneous cosmic gases (T), 19: 1147
gravitational radiation from binary systems of, (T), 19: 41206 (N64-33291)
gravitational radiation from novas, quasars, and supernovas, (T), 20: 2877(T)
gravitational radiation emission by, (T), 20: 2884
gravitational radiation emission from double, spectral density function for, 20: 26011(T)
helium burning in, effects of carbon-12 excited states on, 17: 19006
helium burning in massive, equilibrium models for, 18: 42261
helium burning in degenerate cores of, model for onset of, 20: 31866
helium burning processes in, 17: 19002
helium-burning reactions in, mechanisms for, 17: 9159
helium-composed, equilibrium models for pure, 17: 24216
helium content of, 19: 47193
helium flash in, (T), 19: 16355
helium ionization in, 18: 22658
helium-3 and light elements on surfaces of, origin of, 17: 13038
helium-3 existence in 3 Centauri A, 16: 4658
helium-burning in semi-degenerate, equilibrium models for, 18: 42260
hydrodynamic analysis of large supernovae, 18: 4413 (UCRL-7551)
hydrogen content in clusters of, ionized and neutral, 18: 12822
hydrogen content in Cygnus X, ionized and neutral, 18: 12823
hydrogen, properties of, effects of small fraction of carbon-12 on, 17: 41672
hydromagnetic properties, 16: 16638
hydromagnetic stability of atmospheres of, (T), 19: 10160 (NASA-TN-D-2218)
hydromagnetic waves in gases of, dispersion relation for small-amplitude, 17: 24224
hydromagnetic wave propagation in supernova, equations for, (T), 20: 15198
hydrostatic equations for degenerate and neutron, in general relativity, (T), 20: 15211
hyperon, equation for density of, 16: 22829
identification of quasi-stellar radio sources, (E), 19: 16338
identification of quasi-stellar radio sources, 20: 19340
identification of extragalactic radio-source, 20: 31853
identification of x-ray source Sco X-3, as supernova remnant, 20: 34051
identification of quasars, 20: 44090
implosion of, behavior of radiation from, (T), 19: 4792
intensity variations of quasistellar sources, 20: 34026
interactions in neutron, effects of strong, 20: 44074
interactions under gravitation, computation methods for n-body, 19: 37441
internal structure of massive, 16: 12307
ionization equilibrium in, pressure, 18: 10749
ionization equilibrium in atmosphere of, enhancement of, (T), 19: 44914(T)
ionization fronts in, stability of, 18: 36132
isotopic abundances of carbon, nitrogen, and oxygen in, effects of helium and hydrogen burning on, (T), 19: 41242
kinetics in galactic force field, 18: 22660
kinetics of systems of, irreversibility in, 18: 36138
lead abundance in, mechanism for, (T), 20: 29887
light curve of Nova Herculis 1934, comparison with lightning current, (T), 20: 38260
light emission from variable, pulsation theory of, 18: 10737
light from, gravitational lenses for increasing intensity of, 18: 8985
light from, relation of galactic arm to polarization of, 17: 13041
light from, interstellar polarization of, 18: 20725
light output from 3C 273 supernova, 18: 5904
lithium abundance in types F0 to G5 giant, (T), 20: 25685
lithium content in carbon, (E/T), 19: 4802
lithium content in F and G giants, from convective mixing, (E/T), 19: 6435
lithium content of magnetic and normal, (E), 19: 16337
lithium depletion during pre-main-sequence contraction, (T), 20: 2566
lithium depletion in main-sequence, 20: 37421
lithium isotope ratios in dwarf, 18: 42265
lithium isotope ratio in Hyades F, (E/T), 20: 2577
luminosity fluctuations of, interval for time dilation of, 20: 25689
luminosity in gravitational collapse, (T), 19: 42987(T)
luminosity of, gravitational, (T), 19: 16361
luminosity of, gravitational effects of neutrino and photon, (T), 19: 44910
luminosity of, neutrino and photon, (T), 19: 44927(T)
magnesium content in atmospheres of O and B, (T), 19: 4785
magnetic field of collapsing, 20: 41602
magnetic field properties, 16: 2385
magnetic fields in planetary nebulae, plasma streaming in, (T), 19: 12044
magnetic fields in photosphere of, random microscopic, 19: 30922
magnetic fields in, review of theories on, 19: 34834 (N64-21684)
magnetic fields in quasars, 20: 31868
magnetic fields of, magnetohydrodynamic explanation of existence of, 17: 26255
magnetic fields of, magnetohydrodynamic explanation of existence of, 17: 26256
magnetic fields of, origin of, 18: 22650(T) (JPRS-24435(p.274-304))
magnetic fields of collapsing, 18: 37833
magnetic fields of neutron, 19: 18670
magnetic fields of, production of radio waves by turbulent, 19: 25133
magnetic fields of, relativistic effects on, 19: 42982
magnetic fields of polytropic, equilibrium, (T), 20: 19343
magnetic fields of, (E/T), 20: 41616
magnetic fields, theory of thermal generation, 16: 2387 (ML-837)
magnetic-field effect on structure of, (T), 19: 20802
magnetism of, test for dynamo theory of, 17: 25449
magnetoacoustic wave emission by, 18: 44364(T)
magnetohydrodynamic phenomena in atmospheres of, 18: 18533 (AFCRL-63-674)
magnetostatic models for rotating, conducting, spherical, and liquid, 16: 15483
mass and radius of visible quasars, limits on, 20: 21501
mass determination of hot isothermal white dwarfs, critical, (T), 20: 37383(T)
mass ejection modes in binary, effects on orbital period, 17: 39819
mass loss by steady-state gas outflow, 16: 16907
mass loss by steady-state gas outflow, 16: 16908
mass loss from, 18: 10732
mass loss from highly evolved, (T), 20: 34050
mass loss from red giants, 20: 37415
mass loss from spherical systems of, distribution function for rates of, 18: 4385
mass loss from T Tauri, (T), 19: 9837
mass loss from T Tauri, 20: 37414
mass loss in close binary systems of, period changes from, 18: 44345
mass loss in T Tauri, 19: 9881
mass of quasi-stellar objects, 20: 29888
mass transfer in close binary systems of, orbital variations from, 18: 44346
mass-luminosity relation for, 20: 37427
masses of, equilibrium configurations and densities of, 17: 13282(T)
matter phase states in high-density, 18: 7384
metal abundance and synthesis in halo red giant HD 122563, spectral analysis of, 19: 28982
metal abundance in Population II halo, 18: 8983
metal abundances in, two-color diagram for, (T), 20: 19347
metal index of, effects of chemical composition on, 18: 36136
model for globular-cluster formation, quasars as prototypes in, (T), 19: 39356

model for helium-abundant, massive homogeneous, 17: 26262
model for homogeneous, of moderate mass, (T), 19: 16331
model for neutron, effects of nuclear forces on, 20: 37356
model for superstars and galactic evolution, scintillation, 20: 37358
model of quasi-stellar radio sources, (T), 19: 42985(T)
model of quasi-stellar radio source CTA 102, (T), 19: 47198
model of quasi-stellar radio sources, 20: 44087
models for carbon-burning, neutrino energy-loss effects on, (T), 20: 15194
models for main-sequence and subdwarf, (T), 20: 7708
models for mass of vanishing convective core, (T), 19: 39334
models for massive, 17: 41672
models for massive hot, in general relativity, 20: 19333
models for pulsational instability of cepheid, (T), 19: 20799
models for, baryonic, (T), 19: 16330
models for, dynamical stability of neutron, 18: 26199
models of helium, self-excited oscillations in stellar-envelope, 20: 34020
models of helium, self-excited oscillations in stellar-envelope, 20: 34021
models of massive, in homologous gravitational contraction, (T), 19: 42976
models of very massive, many-body forces and multi-baryon concept for, (T), 20: 9643
models of zero-temperature, 16: 4657
models of, numerical calculations for, 19: 20790
molecular condensation and equilibria in atmosphere of, (T), 19: 39352
molecule temperatures in atmosphere of carbon, (T), 20: 23845
motion of gravitating gaseous masses in magnetic fields in (T), 19: 1161
motion of, relativity equations for, 18: 44363(T)
motion within galaxy, field equation solutions for determining, 18: 36125
multiple nucleon pair formation and supernovae explosions, 16: 22827
nature of strong radio sources, 17: 15049
nebula of 3C-273, (T), 19: 20767(T)
nebular variables and nebulosities, 19: 20795
nebulosity of radio source Cassiopeia A, models for, 20: 27707
neon-20 production in supernova, 17: 16916
neutretto emission from, processes for, 18: 2517
neutrino and nuclear processes in, (T), 20: 4534
neutrino atmospheres of, 18: 42253 (JINR-E-1752)
neutrino detection and measurement for interior analysis of, 18: 18548
neutrino emission from, 16: 4732
neutrino emission by supernova, 16: 5837
neutrino emission in, theory, 16: 24659
neutrino emission by, energy loss by, 17: 15046
neutrino emission in, possible mechanism for, 17: 20940
neutrino emission from massive, collapse of central region by, 18: 7379
neutrino emission by, theory for, 18: 14703 (NP-13704)
neutrino emission from stars under gravitational collapse, 18: 37834
neutrino emission from, mass loss from, 18: 44343
neutrino emission by, mechanisms for, 18: 44344
neutrino emission from plasma of, (T), 19: 4790
neutrino emission, 19: 12055
neutrino emission from neutron, (T), 19: 18671
neutrino emission from, neutral current effects in, (T), 19: 20772(T)
neutrino emission in late stages of evolution of massive, (T), 19: 37447
neutrino emission from, (T), 19: 39361
neutrino emission from, energy balance in universe by, (T), 20: 2587
neutrino emission from, mechanism of, 20: 13519
neutrino emission from Tau A, 20: 27693
neutrino emission in later stages of evolution of massive, 20: 35984 (N-66-18361)
neutrino emission from collapsing, methods for observing, 20: 37379
neutrino emission from neutron, properties of, 20: 37355
neutrino energy losses from vibrating neutron, 20: 41605
neutrino interactions and production in, review on, 19: 25139
neutrino motion in superdense, (T), 20: 41596
neutrino pair emission by stellar plasma, 17: 11446
neutrino pair emission by excited nuclei in, 18: 34932
neutrino pair production in, processes for, 17: 41708
neutrino processes in, 18: 14706
neutrino processes and pair production in massive, (T), 19: 14201
neutrino processes in pre-supernova evolution, 20: 37406
neutrino production in massive helium, 18: 36150
neutrino production in gravitational field of, (T), 19: 4821
neutrino-cooling and observability of neutron, (T), 20: 4532
neutrino-pair emission from plasma in, (T), 20: 7692
neutron capture for slow nucleosynthesis in red giant, 19: 12604
neutron capture in, integrated flux distributions for, 20: 29887
neutron capture processes in, 17: 9158
neutron capture processes in, element synthesis by, 17: 32883
neutron production in, 18: 17055
neutron reactions in, nucleosynthesis from, 20: 34674
neutron, corona and wind production by vibrating, 19: 37499
neutron, cosmic ray production by vibrating, 19: 37499
neutron, oscillation periods in, 19: 32866
nova envelope luminescence by shock wave interaction, 17: 20811
novae, as possible sources of cosmic rays, 17: 13334(T)
nuclear abundances in, 18: 26187 (BNL-837(p.193-233))
nuclear beta decay in interiors of, photon-induced, (T), 20: 4530
nuclear reaction rates in solid-like, (T), 19: 16350
nuclear reaction rates in white-dwarf, (T), 20: 34075
nuclear reactions in, theory on origin of elements by, 18: 22652
nuclear reactions in, theory for origin of elements, 18: 22667
nuclear reactions in, theory for, 19: 39805
nuclear reactions in, rates of nonresonant, (T), 20: 15221
nuclear reactions in, temperature dependence of rates of p-p-cycle, (T), 20: 23847
nuclear reactions on surface of, effects on electromagnetic activity, 20: 37399
nuclear reactions in interiors of, at (5 to 30) $\times 10^8$ °K, (T), 20: 37377
nuclear synthesis in, proton-rich, 16: 12308
nuclear synthesis in, by fast-neutron capture, 17: 32869
nuclear-reaction rate in white dwarf, density and temperature dependence of, (T), 19: 25143
nucleosynthesis abundance calculations for, mass law dependence on, 20: 44070 (LA-DC-7885)
nucleosynthesis in, observed abundance anomalies indicating, 19: 20792
nucleosynthesis in γ Pavonis and ζ^1 Reticuli, element underabundance in, (T), 20: 19337
nucleosynthesis in, cross sections for, 20: 24350 (LA-DC-7774)
observation of solar type radio burst from flare, 18: 16638
observation of 3C48, performance of photographic emulsion for, 20: 34027
opacities of, radiation transport processes for calculations of, 19: 28977 (LADC-6429)
opacity in atmospheres of, 17: 3920
opacity of, relativistic Rosseland, (T), 20: 25679
optical and radio magnitudes of quasars, correlation with red shift, 20: 34054
optical positions for radio sources, 20: 34010
origin of binary, fission theory for, 20: 15219
origin of carbon, and second helium flash, 20: 44100
origin of matter in steady-state universe, quasars as, 20: 37361
origin of planetary nebulae from fast novae, (T), 19: 9849
origin of quasi-stellar objects, (T), 20: 29877
origin of, theory of, 17: 19007
oscillations of neutron, (T), 19: 39358
oscillations of, radiative effects in radial, (T), 19: 27061
outbursts of nova, cause of, 17: 13293(T)
particle configurations from supernovae, relativistic, 16: 26048
particle ejection from L_1 in binary RW Tauri, trajectories in, (T), 19: 9856
particle statistics at high temperatures, 19: 16349
particle velocities in 3C273, anomalous, (T), 19: 28984
photometry of B-type, 20: 37418
photon density from intergalactic, (T), 20: 37374
photon emission from, gravity effects on, 18: 14705
photon emission from gravitationally intense, (T), 20: 25700
photon emission from quasars, limits of, 20: 44947
photon flux from, limits for high energy, (E), 20: 37547
photon production in local radiosources, search for 10-Tev, (E), 20: 23967
photosphere boundary conditions for, method for integration downward from, (T), 20: 2581
photospheric convection and granulation, 16: 16909
plasma phenomena in supernova, 18: 4661(T)
polarization in dynamical systems of, 20: 35829(R) (COO-614-45)
position measurements on quasistellar, optical and radio data on, 20: 34025
position of quasi-stellar radio sources, optical, (E), 19: 16339
positional correlations of nearby, 19: 20439(R) (COO-614-31)
positron-capture processes as a possible source of the p elements in, (T), 19: 34838
processes in interior of, atomic and nuclear theory of physical, 17: 20812
properties and occurrence frequencies of supernova, (T), 20: 7711
properties determined by electron-positron pairs at high temperatures, 16: 10772
properties of baryon (T), 19: 1155(T)
properties of central region of collapsing, with spherical symmetry and pressure gradient, 20: 41613
properties of extremely red, in 0.68 to 0.92 and 2.01 to 2.41 μ range, (E), 19: 39347
properties of field horizontal branch and RR Lyrae, 20: 37419
properties of galactic, 18: 10734
properties of helium shell-burning, equilibrium, 20: 34016

properties of horizontal branch, color-magnitude diagrams for, 20: 34014
properties of horizontal-branch, hydrogen-burning models for, 20: 39566
properties of hyperon and neutron, 16: 9333(T) (FTD-TT-61-314)
properties of magnetic, (T), 20: 7712
properties of massive hydrogen, effects of scattering opacity variations on, (T), 19: 4803
properties of nova and supernova, (T), 20: 7710
properties of quasi-stellar radio sources, 18: 30398
properties of quasi-stellar galaxies, (E/T), 19: 34845
properties of quasi-stellar radio-source, review of, 20: 19353
properties of quasistellar objects, 20: 25705(T)
properties of quasi-stellar objects, models for, 20: 29876
properties of quasi-stellar objects and radio sources, 20: 37370
properties of quasi-stellar radio sources, optical, 20: 37382(T)
properties of quasars, (T), 20: 41608
properties of radio, 18: 44369(T)
properties of Scorpius x-ray source, (E), 20: 29882
properties of super-, 18: 37833
properties of superdense neutron, at absolute zero, (T), 19: 16351
properties of ultraviolet quasi-stellar radio sources, (E), 19: 39349
properties of white-dwarf, (T), 20: 7709
properties of x-ray source, 20: 29900
properties of, book on, 20: 11436
properties of, neutrino probe for determining, (T), 20: 9646
properties of, research using nuclear-explosion-produced plasma for, 20: 23238
properties of, review of, (T), 20: 4533
properties of, survey on, 20: 37367
proton reactions of CNO bi-cycle in, 17: 3914
proton–proton chain in, termination by deuterium- and helium-3-burning reactions, 18: 18537
proton–proton chain in, termination at high densities, 18: 18538
proton-proton interaction in white dwarfs, (T), 19: 20771(T)
pulsation of envelopes of RR Lyrae and Cepheid type, 18: 20716
pulsations from, excitation and growth of, 20: 37412
pulsations from, normal modes of radial, 20: 41588
pulsations from, normal modes of radial, 20: 41589
pulsations from, properties of, 20: 37413
pulsations of, Roche model for radial adiabatic, 18: 36126
quark production in quasars, (T), 20: 17411
quasi-, radio sources, expansion as an energy source in, (T), 19: 34837
quasi-stellar radio sources identification, 20: 44088
radiation absorption by negative hydrogen ions in atmospheres of, coefficients for, 18: 36142
radiation absorption in, (T), 19: 41211
radiation density at surface of, (T), 20: 7691
radiation diffusion and hydrodynamics in, method for calculating, 20: 34019
radiation emission by two-body systems of, corpuscular, 18: 18555(T)
radiation emission by, 19: 14203
radiation emission by galaxies, bremsstrahlung and synchrotron x-, (T), 19: 20765
radiation emission and propagation from quasi-stellar radio sources, (T), 20: 17242
radiation from dipole magnetic fields in, model for synchrotron, 17: 24200
radiation from neutron, cosmic x, 18: 30386
radiation from newly formed, hydrogen ionization by, (T), 20: 2562(R) (AD-614715)
radiation from 3C-273 at 0.35 to 1.1 μ, photoelectric measurement of, 20: 46281
radiation from, Schwarzschild metric for, 19: 39273(R) (UCRL-12204, pp 60-5)
radiation pressure in interior of, (T), 19: 39335
radiation scattering in outer layers of, transfer equation for isotropic, 18: 42277
radiation scattering in outer layers of, transfer equation for isotropic, 18: 42276
radiations from collapsing and anticollapsing, 20: 41597
radiations from, origin of microwave background, 20: 37362
radiative energy loss of flare-ejected material from, 20: 25687
radiative transfer in atmospheres of, book on, 17: 26264(T)
radiative-acoustic waves in gaseous, 19: 41219
radio brightness contours of 3C273, (E), 19: 41226
radio brightness distributions of, spectra of spatial frequencies of, (T), 19: 6434
radio emission from supernova, relation to galactic arm, 17: 13041
radio emission from Sagittarius-A, interstellar neutral hydrogen absorption of, 17: 41701(T)
radio emission from flare, (T), 19: 42984(T)
radio emission from, comparison with Jupiter radio emission, 20: 21510
radio emission from Crab nebula source, quasi-stellar, and supernova-remnant, coherent plasma mechanism for, 20: 29880
radio emission from 3C-48 quasar, intensity fluctuations of, 20: 41598
radio emission of quasars and supernova remnants, coherent plasma mechanism for, (T), 20: 27701
radio emission sources, identification of, 17: 32847
radio signal amplitude variation indices from varied angular-diameter, ionospheric low-latitude irregularity determination from, (T), 20: 24386
radio spectra of 3C343, (E), 19: 34846
radio spectra of 3C273 A and B, strength of, 20: 29898
radio structure of IC 443 supernova remnant, (E/T), 19: 4788
radio wave emission by, 18: 34395
radio wave emission from Taurus A at 25 to 55 cm, (E), 19: 9873(T)
radio wave intensity variations of quasars, magnetic bremsstrahlung contributions to, (T), 20: 13407
radio wave spectrum of Cygnus A, theory for, 18: 28229(T)
radioactivity in type I supernova, (T), 19: 39338
reactions in interior of supernova, synthesis of iron-group elements by rapid, 17: 39835
reactions in peculiar magnetic, surface, 17: 5178
relaxation time in clusters, 20: 35829(R) (COO-614-45)
review (E/T), 19: 1140
review of nuclear astrophysics, 19: 20791
rotation effects on parameters of superdense, model for, (T), 20: 9640(T)
rotation effects on electromagnetic activity, 20: 37399
rotation of neutron, 20: 37363
shock propagation in exponentially decreasing atmospheres of, (T), 20: 15217
shock propagation in polytrope-5, model for spherical, 20: 31871
shock structure in, radiative, (E/T), 20: 32670
shock-wave effects in variable-density, 16: 16906
shock-wave generation and propagation in explosion of type II supernova, 17: 41698
shock-wave propagation in, equations and models for, 17: 39833
shock wave propagation from, particle acceleration in, (T), 19: 20770(T)
shock wave propagation in, radiation effects in theory of, 19: 37431(T) (FTD-TT-65-82)
shock wave propagation in outer layers of, (T), 19: 44924(T)
shock waves in coronal collisionless region, 16: 16912
size of superdense Fermi gas, (T), 19: 25138
sodium-23(p,α)neon-20 reaction rate in, at (5 to 10)$\times 10^8$ °K, 17: 31519
spectra and location of x-ray sources, (E), 20: 15220
spectra from quasars, properties of, 20: 44072
spectra of binary pygmy Lp 101-15/16, (E), 20: 34061
spectra of carbon-12 and -13 in, 18: 740
spectra of Cassiopeia α, 18: 15711(R) (TID-20256)
spectra of distant quasi-stellar objects, mechanisms for absorption, (T), 20: 29890
spectra of early-type, high hydrogen lines in, 17: 26260
spectra of, electromagnetic emission, 17: 7677
spectra of extremely red, (E), 19: 39348
spectra of helium, analysis of, 18: 16630
spectra of high-energy particles in supernovas, 18: 14769
spectra of, information obtained from, 17: 21209
spectra of interstellar medium, problems in, 18: 8979
spectra of late-type, Hα as discriminant of luminosity in, 18: 36137
spectra of main-sequence B, comparison of calculated and observed continuous, 18: 20714
spectra of neutral hydrogen in Virgo cluster, 17: 39831
spectra of nonthermal radio-sources, 20: 29878
spectra of peculiar A, oxygen abundance anomaly in, 17: 3912
spectra of quasars, interpretation of line, 20: 34053
spectra of quasars, red shift in, 20: 46290
spectra of quasistellar sources, 20: 34028
spectra of, recombination coefficient for helium and hydrogen lines in emission, 18: 8996(T)
spectra of rotating gravitational Zeeman effect in, 19: 34851(T)
spectra of Sp^3-configuration coronal ions in, ultraviolet, (T), 19: 9877(T)
spectra of T Tauri, uv excess in, 20: 37420
spectra of 3 Centauri A, element abundances from ultraviolet, 17: 32851
spectra of 56 Arietis, three-color photometry, 16: 29600 (TID-16442)
spectra of, associated with radio source MSH 14-121, 19: 30923
spectra of, gravitational energy shift of, (T), 19: 18669
spectra of, magnetic field effects on Doppler shift of, 18: 24289
spectra of, photon energy loss mechanism for red shift of, (T), 19: 14205
spectra of, saturation effects on absorption, (T), 19: 18660
spectra of, source-function equality in multiplier, (T), 19: 9834
spectra of, source-function equality in multiplet, (T), 19: 9841
spectra shift from quasars, red, 20: 44103
spectra shift of quasars, evolutionary aspects from, 20: 44092
spectra variations with temperature, 18: 21089
spectral energy distribution near Balmer limit for nonstable, 18: 44370(T)
spectral intensities of, (E), 19: 42977
spectral line widths for, with hydrogen ion absorption, 18: 30392
spectral red-shift of, photon energy loss mechanism for, (T), 19: 4811

spectrophotometry of η Carinae, photoelectric, 20: 23863
spectrophotometry of quasars, photoelectric, 20: 44071
spectrum of, effects of synchrotron radiation of relativistic electrons on, 17: 13271(T)
spectrum of quasi-stellar radio source 3C 273, (E), 19: 16340
spectrum of 3C9, for intergalactic molecular hydrogen extinction, (E), 20: 37353
stability, (T), 20: 7714
stability and wave propagation in corona and wind of, (T), 20: 15216
stability in magnetic field, gravitational, (T), 20: 25701
stability of Cepheid, models for, 20: 37411
stability of helium, vibrational, (T), 19: 42975
stability of magnetoturbulent massive, relativistic, (T), 20: 2579
stability of massive, in general relativity, 18: 42274
stability of polytropic spheres for, relativistic, (T), 19: 44925(T)
stability of rotating massive, in general relativity, 20: 23861
stability of self-gravitating and radiating gaseous, virial theorem for, 19: 28976 (D1-82-0366)
stability of supermassive, effects of magnetoturbulent energy on, 19: 47200
stability of supermassive, general relativistic, (T), 20: 25704
stability of supermassive, effects of rotation on, 20: 27689
stability of very massive, effect of rotation on gravitational, (T), 19: 39354
stability of white dwarfs, relativistic effects on dynamic, 20: 27686
stability of, adiabatic exponent for helium-iron transition and pair creation for, (T), 20: 2588
stability of, dynamic and hydrostatic, 18: 14706
stability of, general relativity for nonradial and radial, (T), 20: 15210
stability of, neutrino-emission and nuclear-equilibrium effects on dynamic, (T), 19: 37439
stellar winds from, 18: 5911
structure analysis, 16: 18115 (NP-11463(Pt.3)(p.431-46))
structure and properties of, 19: 8064
structure of low-mass, models for, 17: 28108
structure of massive highly relativistic, internal, (T), 20: 25678
structure of neutron and white-dwarf, static, 19: 34835 (N64-22572)
structure of quasi-stellar radio sources, (T), 19: 30930
structure of quasi-stellar radio source 3C 273 B, 20: 9642
structure of superdense, (T), 19: 30936
structure of very dense, baryon configurations in, 16: 30990
structure of, degenerate electron gas, 18: 44849 (AFCRL-64-528)
structure of, effects of chemical composition on, 18: 36136
structure of, integration of equations of, 18: 42263
structure of, integration of equations for, 20: 44099
structure of, photon absorption and opacity calculations for determining, 20: 37393
structure of, review of models for, 19: 20789
superconductivity in, at 10^8 to 10^9 °K, 18: 18549
superfluidity of neutron, (T), 19: 14226
supernova, disturbances in interstellar medium surrounding, 17: 13288(T)
supernova processes in, neutron stars as remnants of, 17: 32880
supernova production processes, 18: 14706
supernova spectra comparison with californium, 16: 9334
supernovae as cosmic ray sources, 16: 6897
supernovae, influence of cosmic rays on magnetic fields and filament formation in shells of, 17: 13330(T)
synchrotron radiation spectra from radiosources, 20: 46278
temperature distributions in partially degenerate helium cores in, neutrino loss effects on, (T), 19: 41237
temperature of white dwarfs, cooling of, 20: 37408
temperature structure of model atmospheres of, (T), 19: 9835
temperature structure of atmospheric model calculations of, 20: 2564
theory of formation and detection of neutron stars, 18: 14706
theory of neutrino, 18: 28208
theory of neutron-hyperon, 18: 22664
theory of neutron, for celestial x-ray sources, 18: 32344
theory of neutron, as x-ray sources, 18: 42257
theory of novae and novalike, 18: 10733
theory of novas and quasi-, 20: 17243
theory of quasars, 19: 30931
theory of quasistellar radio sources, review of developments, 19: 32867
theory of supernova, 19: 44909
thermal conductivity in cores of degenerate, internal magnetic field effects on, (T), 19: 37436
thermal dissipation of flare-ejected material from, magnetic field effects on, 20: 25688
thermodynamic properties, (T), 19: 39339
thermodynamic properties of matter, (T), 20: 34065(T)
thermonuclear energy release in polytropes, effects of rapid rotation on, (T), 19: 34839
thermonuclear reactions in helium-less, heavy nuclei from, 17: 19009
thermonuclear reactions at low energies in giant, 17: 36406 (NP-13020(p.145-9))
thermonuclear reactions in pulsing, effective density and temperature exponents for 3α, (T), 20: 21491
tides in closed binary, properties of, 20: 46276
tin isotope abundances in giant stars and supernovae, 16: 22782
transition from hydrogen to helium burning in, 16: 29607
transuranic element synthesis in, 20: 40144
velocity dispersion of gaseous nebulae and supergiant, 18: 22657
velocity distributions of G dwarfs, metal deficiency dependent, 17: 24199
velocity fields in atmospheres, 16: 16910
wave propagation in supernova remnant plasma, cosmic ray damping effects on, (T), 20: 29959
winds from, hydrodynamic model of, (T), 19: 25125
x radiation from, 17: 36550
x-radiation synchrotron emission from electron belts of magnetic neutron, (T), 19: 42980
x-ray emission at 0.2 to 20 kev, rocket detection of, 19: 39332
x-ray emission by neutron, 18: 20711
x-ray emission by Crab Nebula, 18: 42294
x-ray emission by neutron, effects of nuclear forces on, 19: 32866
x-ray emission from neutron, 18: 18547
x-ray emission from supernova, 18: 42258
x-ray emission from remnants of supernova, mechanism for, (T), 19: 4801
x-ray emission from, optical focusing systems for, 19: 14224
x-ray emission from neutron, with magnetosphere, (T), 19: 18664
x-ray emission from neutron, 19: 32858
x-ray emission from corona of, 19: 32858
x-ray emission from, (T), 19: 44923(T)
x-ray emission from flare, 20: 34129
x-ray emission from neutron, (T), 20: 17240
x-ray emission from Sco X-1, 20: 34030
x-ray emission from, review and analysis of, 20: 17248
x-ray emission from supernovae, effects of early radiation field and high-energy electrons on, 20: 21499
x-ray emission, spectra of, 18: 10741
x-ray production in supernova remnants, 18: 30377 (CONF-320-5)
x-ray source in Scorpius, electron cloud theory for, 18: 18534 (CONF-455-1)
x-ray source, spectra of 20- to 58-kev, (E), 20: 37376
of pure hydrogen, 19: 4803
electromagnetic waves from very dense, 18: 44353
element abundances in Kappa Pavonis, 17: 34683
element distribution in magnetic, cause of anomalous, 16: 19651
gravities of F-type, 16: 22821
helium burning in red giant, 18: 20727
helium burning in, 18: 36147
hydrogen abundance, molecular, 16: 2386 (AFOSR-1401)
hydrogen burning in red giant, 18: 20727
hydrogen burning in, 18: 36147
interiors of, revised solar model with solar neutrino spectrum for analysis of, 18: 18548
magnesium abundance variations in A, Ap, and B, 18: 24274
magnesium abundance in atmospheres of O and B, (T), 19: 4785
neutron photoproduction on protons in, implications in stellar evolution, 17: 39834
processes in, research on atomic and plasma, 19: 32853(R) (AD-610847)
pulsation calculation for, 18: 20716
silicon abundance variations in A, Ap, and B, 18: 24274
solar radiation from, 16: 32253 (NASA-TN-D-1361)
spectra of helium white dwarf, (T), 19: 9878(T)
spectral absorption in, (T), 19: 18652
spectral absorption in, (T), 19: 18653
stability of white-dwarf, mass limit in, 18: 30385
stability of, effects of second helium ionization on, 17: 39821
temperature of white dwarfs and type-I supernovae, review of, 19: 20800
temperatures of F-type, 16: 22821
temperatures of helium white dwarfs, (T), 19: 9878(T)
thermal radiation from, 16: 32253 (NASA-TN-D-1361)
two-body motion of, with corpuscular radiation emission, 18: 18555(T)
x-ray emission by neutron, 18: 42257
x-ray spectra near Galactic center and in Scorpius, (E), 19: 44967
x-ray spectra of Cyg XR-1, Tau XR-1, and Sco XR-1, 20: 29901
x-ray spectra of Scorpius (SCO-XR-1), (E), 20: 2585

Static Eliminators
see Radioactive Static Eliminators

Statistical Analysis
see Statistics

Statistical Mechanics
see Mechanics

STATISTICS
see also Biometry

see also Mathematics
see also Particle Statistics
see also Sampling
see also Stochastic Methods
accuracy in intensity-correlation and particle-counting experiments, quantum-mechanical analysis of, 19: 45151
analysis of biological data, 16: 11436(R) (ANL-6464(p.24-31))
analysis of count data in radiochemistry, background problems in, 19: 34256 (BNWL-SA-10)
analysis of data on trace elements in U. S. subjects, 20: 6719(R) (ORNL-3849, pp 183-213)
analysis of data with errors in more than one variable, multiple least-squares, 17: 8965
analysis of economics of nuclear cavities, 20: 39014(R) (TID-23184)
analysis of effects of variables on fissiochemical reactions, 19: 40547(R) (AGN-8137(Vol.I))
analysis of gamma spectra by modified weighted least squares, 18: 1959(R) (TID-19669)
analysis of Gaussian distributions, development of graph paper for, 16: 13506
analysis of isotope distributions in tissues, 17: 24856
analysis of multi-factor tables in, 17: 4381
analysis of neutron resonance parameters, 18: 2954
analysis of nonindependent random pulse-trains by, 16: 33621
analysis of population mortality data, Monte Carlo, 20: 42698(R) (ANL-7136, pp 80-94)
analysis of punch card records of film dosimeter data for radiation exposure trends, 19: 20241
analysis of radiation injury repair in mice, 17: 23232
analysis of radioactivity of surface waters in Poland, 1958 to 1962, 19: 15799
analysis of spectra, 17: 39452 (BNL-7215)
analysis of survey of radioinduced cancer, 18: 31206
analytic solution of the Percus-Yevick equation, 18: 21029
angular momentum statistical tensors, properties, 16: 22766
apparatus functions for low-accuracy measurements, unfolding of, (T), 20: 13038
approaches to equilibrium in dense classical fluids, 16: 13789
atomic models in, quantum corrections to Thomas-Fermi-Dirac, (T), 19: 30942 (LA-3268)
binomial sampling in, tables for, 20: 16150 (ORNL-2909)
Boltzmann equation for binary gas mixtures, use of kinetic model in, 17: 39723 (R63SD76)
Boltzmann's equation, derivation of, 18: 24507
book: *Ergodic Theories*, 16: 27852
book: *Fundamental Problems in Statistical Mechanics*, 16: 20949
book: *Handbook of Statistical Tables*, 16: 27557
book: *Lectures on the Many-Body Problem*, 17: 17060
book: *Physics in the Soviet Union*, 16: 14218
book: *Quantum Theory of Many-Particle Systems*, 16: 21223
book: *Statistical Inference for Markov Processes*, 16: 9330
book: *Statistical Mechanics of Charged Particles*, 18: 22804
book: *Statistical Theories of Spectra*, 19: 35507
book: *Studies in Statistical Mechanics*. I., 16: 15356
book: *The Theory of Branching Processes*, 18: 32298
Bose systems in quantum, degenerate (T), 19: 1407 (NP-14400)
boson interactions in quantum, Green functions for, 18: 18761
Calabro Kappa Square statistic, tables, 18: 39798 (UCRL-7920)
canonical commutation relations of non-relativistic Bose gas, 17: 2456
central force problems in, 20: 4488
chance coincidences in fast-slow coincidence systems, 18: 8663
classical, of a system of particles, 17: 26300
cluster analysis method, 18: 2 (TID-19599)
cluster expansion methods in quantum, 19: 14407(T) (UCRL-Trans-1090(L))
cluster formulation of the exact equation for the evolution of a classical many-body system, 17: 38422
cluster-star equations in, generating functionals for inversion of, 19: 39084
cluster-star equations in, Möbius formula for inversion of, 19: 39083
coincident-event correlation counting, (T), 19: 11548
commutation relations between field variables, trilinear, 18: 5841(R) (AROD-2800.12)
comparisons of soil and foliar analysis by, 18: 3447 (NYO-10581)
compatibility of probability theory and quantum mechanics, 18: 14978
compound decision problems, asymptotic solutions to, 18: 19455 (ANL-6820)
compound distributions, parameter estimation for, 19: 9575 (HW-SA-3762)
computer analysis of genetic data on human population, 19: 42653 (AECL-2222)
computer program for generation of normally distributed random numbers, 18: 5725 (ORNL-TM-737)
computer program for calculations in, 19: 18381 (KAPL-M-6436)
computer program for pulse-height analysis for radionuclide assay data, 20: 11202(R) (NYO-3136-2, App. 1)
computer program using maximum likelihood method for IBM-709 and -7090, 16: 19241 (UCRL-10153)
conference on use of vital and health, for genetic and radiation studies, 17: 12088
correlation functions in classical statistical mechanics, (T), 20: 1082 (COO-720-053)
correlation methods, application to measurement of high antireactivities of sub-critical reactors, 18: 19316
correlations and spacing distributions for nuclear levels, 18: 2955
cost estimates and control in construction projects, computer system, 16: 15106 (HW-SA-2444)
counting, effect of long decay chains, 17: 25594(R) (ANL-6646(p.78-91))
criteria for differential cross section measurements with minimum uncertainty, (T), 19: 47601
criteria for medical examination of blood picture of personnel, evaluation of, 18: 8577
data analysis using, computer program for, 19: 32669(R) (UCRL-11833 (p.154-7))
data reduction methods for physics, 16: 2114 (NRL-5667)
definition of normal product and Wick's theorem in, 18: 44636
derivation of fluctuation compressibility theorem and its application to the pairing model of superconductors, 17: 11398
detection threshold and limit of electron microprobe analysis, 19: 30077 (EUR-1819.e(p.27-36))
determination of radioactive material rate count, 16: 28422 (WAPD-BT-25(p.95-102))
determination of track densities in bubble chambers and emulsions, 16: 19509
development of two sequential two-sample grouped rank tests for use with screening experiments, 16: 26734 (NP-11847)
distributed lag demand functions, 19: 26747(R) (COO-614-23)
distribution functions in classical fluids, approximations of pair, 16: 26445
distribution functions in dense classical fluids, evolution, 16: 13788
distribution functions in dense classical fluids, evolution, 16: 13790
distribution functions for many-body systems in, 18: 44445
distribution functions in astronomy, 19: 26747(R) (COO-614-23)
distribution law for random variables, using composition law for elementary measures, (T), 19: 20440 (EUR-2251.i)
distribution of events at output of system with variable dead-time, time, (T), 19: 15883
distribution of stochastic fields, 16: 24882 (ARL-250)
distribution theory development and solutions, 18: 4155 (HMI-B-30)
distributions of radioactivity rates, 17: 29990
dynamics of certain spherical charge distributions, 20: 41517
dynamics of condensed systems in quantum (T), 19: 1460
effects on efficiencies of radiation detection instruments, 19: 797
effects on measurements of radioactivity, 19: 4466 (PAN-525/VIII)
electromagnetic random processes in quantum, (T), 19: 27290(T) (JPRS-29075(p.48-55))
electron-gas partition function, 16: 8281
energy calculations for dense charged Bose gases, ground-state, 16: 33639
energy eigenvalues in quantum, calculation by Green's functions, 17: 11357
energy-level distributions in complex nuclei in, 17: 2451
energy levels of matter in quantum, 17: 15295
equations in, Markovian master equations from Liouville, 19: 25080
error derivation from, in pulse counting, 18: 43959
error determination in one-parameter systems, 19: 42225 (UCRL-12050)
error propagation in resolution corrections, (T), 20: 13040
errors in distribution measurements from pile-up effects, 18: 41913
errors in measurement of nuclear radiation pulses, 17: 16449
errors in measuring and calculating normalized nuclear counting rates, 19: 2712
errors in transfer function measurements on noisy reactor systems, (T), 19: 19367
errors in variable normalized counting rates, 20: 33703
estimation of counting rates with background corrections, 18: 8641 (HW-76279)
estimation of fixed length confidence interval, 18: 3412 (TID-18403)
estimation of nuclear plant design data, 16: 14330
estimators in biases and covariances of maximum likelihood, 19: 36900 (K-1633)
evaluation of hemograms of nuclear power plant personnel, 18: 8580
evaluation of measurements, 17: 8383 (TID-17656)
evaluation of, for radioisotope tracer studies, 19: 31758
evolution of isolated systems, entropy in, (T), 19: 42954
evolution of many-body systems in quantum, 17: 14996
fermion systems, maximum entropy calculations for, 16: 13787
fluctuations in Monte Carlo intranuclear cascade calculations, 18: 13056

(ORNL-TM-771)
formalism for Brownian motion, (T), 19: 14160
formalism for counting correlations in boson beams, 18: 37989
formalism for degenerate Bose systems, quantum, 20: 46527
formalism for detector performance for radioactive preparations, 19: 15879
formalism for electromagnetic fields and spin, 18: 40395
formalism for energy level density for medium and heavy nuclei, 19: 41655 (BNL-934)
formalism for ideal gas thermal capacity, 18: 36389
formalism for irreversible processes with minimum entropy production, (T), 19: 34790
formalism for method of effective counts for combining experimental results, 19: 18605
formalism for molecule pair distribution in gases, 20: 7959 (ANL-7063)
formalism for neutron gas approach to equilibrium, (T), 19: 16830
formalism for nonequilibrium gas kinetics, 18: 40072
formalism for nuclear particle counting and pulse spectrometry, generating functions in, 18: 33964
formalism for optical radiation coherence, (T), 19: 18952
formalism for particle mixtures with type-dependent intermolecular potentials, (T), 19: 41130
formalism for plasma kinetics, Dyson equation technique in, 18: 26753
formalism for plasmas, 20: 46890
formalism for propagation modes of thermal and coherent radiation mixtures, 19: 25407
formalism for quantum systems of hard lines, 18: 42477
formalism for real gases and plasma, 19: 31342
formalism for scaled pulses, (T), 20: 14890
formalism for spin-spin interactions in solids, 18: 30330
formalism for thermodynamic adiabatic processes, 18: 28153
formalism for velocity-dependent potentials in many-body interactions (T), 19: 3050
formalism of para-, for elementary particles, (T), 19: 5002
formalism of quantum, for optical rotation, 20: 37927
formulation in mechanics using occupational numbers, 16: 3559
formulation of quantum statistical mechanics, using Green's functions, 19: 16262 (UCRL-12158)
functional integrals in, 17: 17066
gas condensation in, theory for classical, 18: 28147
gaseous fluctuations and turbulence in, 17: 2101
Gaussian distribution curves in, superposition of, 18: 44018 (ISS-64/6)
Gaussian random functions as a tool in mechanics, 17: 31233
grand partition functions at non-zero temperatures, 16: 2661
Green's function in many-body, 17: 17069
higher-order spacing distributions for a class of unitary ensembles, 18: 24679
ideogram for measurements, properties of, 18: 535 (JINR-P-1346)
in correlation of radon content in air to weather conditions, 16: 2869(R) (ANL-6398(p.86-95))
information theory for nonequilibrium, 18: 42496
information theory in quantum statistical mechanics, 19: 18943
interacting systems in, description of weakly, strongly, or completely correlated, 17: 16799
interactions of correlated subsystems in, irreversible processes in, 18: 4334
interactions of correlated subsystems in, time-dependent distributions in, 18: 4333
irreversible processes in many-body systems in quantum, 17: 18955
iterative process for sample analysis, 20: 42698(R) (ANL-7136, pp 80-94)
kinetics of matter, effects on scattering parameters, 16: 26440
lattice gas properties, dependence on mesh size, 18: 40053 (UCRL-7572-T)
lectures on least squares theory and maximum likelihood, 18: 22407 (CERN-64-18)
lectures on statistical physics, 18: 22582
linear estimation of chemical mixtures, 19: 19769(R) (TEES-2671-4 (Chap.7))
linear velocity-gradient term in time-dependent pair distribution function, 17: 31655
linked-cluster theorem and unitarity, 18: 41912
Liouville equation in, reversibility of, 18: 36104
Liouville theorem of statistical mechanics, general forms of, 20: 5830 (CERN-65-38)
Liouville's equation for relativistic dynamics, 16: 14207 (ARL-236)
machining procedures for, 20: 43864 (Y-1550)
magnetic fields in nonrotating, upper-main-sequence, structure of poloidal, weak, (T), 20: 27705
magnetic resonances in quantum, 17: 19172
many-body systems in, approach to equilibrium, 18: 22583
master-equation derivations in, for quantum systems, 17: 2449
maximum in ideogram of Gaussian distribution, 18: 10446 (JINR-P-1460)
maximum likelihood method for analysis of data with $x^m dx$ distribution, 20: 23811
measurement of kernels of nonlinear systems by crosscorrelation with Gaussian non-white inputs, 16: 4610(R) (TID-14435)
measurement points in intensity function with unknown parameters, optimum number of, 18: 22360
mechanics and partition theory of numbers, 16: 18108 (NP-11463(Pt.2) (p.275-88))
mechanics, functional averaging method in classical, 17: 9001
mechanics of classical and quantum systems in, 17: 2447
mechanics of equally likely quantum systems in, 18: 22803
mechanics of one-dimensional systems with Coulomb forces, 16: 32203 (MATT-108)
method for analyzing interactions in microbial populations, 20: 6706
method for selecting tests, 18: 30093 (EUR-1824.i)
method for study of delayed triple nuclear cascades, 20: 40160
methods for estimating design data, 16: 7642
methods for quality control of environmental radioassay, 19: 36716
methods in neutron physics, 17: 17471
methods in, for plant dynamics analysis, 20: 18878
methods of bias detection and estimation, 18: 533 (HW-SA-3173)
methods of, for nuclear materials management, 20: 35181 (SRIA-115P49-1)
minimum systematic variance method for evaluating the most probable values of two parameters, 17: 8699 (NP-12396)
model for angular momentum conservation for abnormal rotation of hydroxyl radical split from water, 18: 16024
model for estimation of defect frequency in extrusion, rolling, and welding of steel pipes, 18: 22457 (HW-76573)
model for nuclear reaction emission, 16: 12505
model for nuclear level partial radiation widths, 17: 41536(R) (ANL-6767)
models for, multiple minima in least squares solutions of, 17: 23846 (LADC-5484)
multivariate regression analysis of sex ratio among offspring from irradiated women, 20: 10657
neutrino emission from, (T), 20: 7706
nuclear spin relation to, 16: 3621
of counters in cascade connection, (T), 19: 15884
of counting data, 20: 33629 (NAS-NS-3109)
of counting losses in activation analysis, 19: 19766(R) (TEES-2671-4(Chap.3))
of double isotope liquid scintillation counting by internal standard technique, 18: 19872
of electron current fluctuations in Townsend discharges, (T), 19: 21551
of electron multiplier tubes, (T), 19: 6201
of electron-photon gas, 17: 26247
of electrons in screening constant model of complex atoms, 18: 20731 (RM-3803-AEC)
of emulsion scanning, 18: 33892
of fluctuating quantities measurements, analysis of accuracy in, 17: 330 (CLM-R-22)
of geochemical processes in formation of magmatic rocks, 19: 650
of irreversible processes in polymer solutions, 17: 18100
of multicomponent charged particle systems, quantum, (T), 19: 16692
of nuclear level intervals and widths, 18: 24598 (NP-13930(p.17-25))
of number and size of particles in materials, 17: 29256(T) (AEC-tr-5833)
of open systems in contact with thermal reservoirs, 17: 663
of photomultiplier output signals, (E), 19: 22672
of solar flares, 18: 24270 (NP-13802)
of spin resonance saturation, 17: 3631
of thermodynamic equilibrium, 17: 41578
of thermodynamics, lectures on, 17: 8943 (NP-12450)
on dosage in radiation exposure to man, 17: 12092
on industrial accidents, effects of tendency to report minor injuries on, 18: 15691 (ORNL-3563)
on uranium reserves, 20: 39101
operations on quantum and random fields in, similarities of, 19: 1450
output distributions of counting systems, 19: 820
output of counter cascades, 19: 2612
para-, for free particles, 17: 24269 (NYO-10241)
parameters in, power-series expansion for, 20: 17527
partition function in quantum, estimations of, 17: 9003
performance of Weibull, in studies of strength of brittle materials, (T), 19: 24991 (UCRL-12405)
perturbation representation diagrams in quantum, elimination of, 18: 18775
perturbation theory for many-body systems in quantum, 17: 18919
population trends for critical branching processes, 16: 12015 (RM-2869-PR)
potential distribution method in, 18: 8934
prediction analysis of exponential functions, 20: 2217
probabilities in, description of nomograph for approximating, (T),

19: 13862 (SC-R-64-1348)
probability distribution for classical fluids, 16: 5805
probability distribution analyzer having electrostatic storage, design and performance, 16: 14937
probability distributions of avalanche electrons in proportional counters, 18: 39677
probability distributions of observations in physical experiments, 19: 28734 (RISÖ-88)
probability equations for system behavior in reliability technology, 18: 40992 (SC-R-64-198)
probability of chance coincidences from target bombardment with variable beam, 18: 31945
procedures for process start and control, 18: 33189 (SC-R-64-148)
processing random field hypotheses, 19: 23164(R) (SU-SEL-64-103)
programming and variational principles of classical and statistical mechanics, dynamic, 16: 24295
properties of atomic and nuclear spectra, conference on, 18: 2953
properties of Bardeen–Cooper–Schrieffer distribution, 18: 26491
properties of transport equations subject to diffusivity equations, 16: 3550
quantum, evolution to equilibrium for a simple model, 17: 33231
quantum, for negative-energy bosons and fermions, 17: 16998
quantum many-body systems in, models for equilibrium, 16: 22768
quantum many-body systems in, models for nonequilibrium, 16: 22769
quantum many-body problem in, (T), 19: 39263 (CONF-796)
quantum mechanical derivation of generalized Boltzmann equation, 20: 42082
quantum, models for non-equilibrium finite systems, 16: 4946 (AFOSR-1138)
quantum operators in, relation to measurable quantities, 17: 13172
quantum properties of gases obeying "intermediate", 17: 633
quantum properties of systems of interacting particles in, 17: 2083
quantum properties of systems of interacting particles in, 17: 13447
quantum, review, 16: 15366
quantum theory for free space using, 16: 24920
quantum theory for non-equilibrium in chemically reactive fluids, 18: 6813
quantum theory of relaxation in isolated spin systems, 19: 21121
quantum, transport and Wigner functions for fluids, 16: 15359
quantum-mechanical extension of Lebowitz-Penrose theorem on van der Waals theory, 20: 42081
queueing theory in particle counting, 18: 25890
radiation damage theory, for high-energy particles on crystalline solids, 16: 24256
radiation transport in, spectral theory for stationary operator for, 20: 17658
random distribution function for branching process, convergence of, 18: 20892 (AD-434059)
random number generation for Monte Carlo, methods of, 18: 2144 (IDO-16921)
random number generation, method for, 18: 16411 (CERN-64-13(Vol.I) (p.173-6))
random number generator for ZRA-1 computer, 20: 7484 (ZFK-TPH-14)
random variable autocorrelation in, from independent random numbers, 18: 36874 (BNL-7299)
random walk in, solutions for three-dimensional, 18: 15717 (TID-20325)
random walk with partially reflecting barrier, one-dimensional, (T), 19: 30855
random-matrix theory in, eigenvalue distributions from ensembles in (T), 19: 1054 (PUC-1964-153)
random-walk processes in, analysis using invariant imbedding, (T), 19: 20660 (P-1113(RAND))
randomness test for multi-phase structures, 17: 12231 (TID-17814)
reactor stability as stochastic process with feedback, 20: 34917
reciprocity relation for strongly coupled systems, validity of Onsager's, 17: 39757
reconstruction of analog signals from nonuniformly spaced samples, 19: 44809 (SC-DR-65-291)
recording of, on somatic effects of radiation in man, 17: 12090
regression methods applied in estimating fallout from a nuclear detonation, 17: 6306 (CDRP-182-105)
regression model adequacy in radionuclide assay, test for, 20: 11203(R) (NYO-3136-2, App. 2)
relation to nuclear spin in electromagnetic fields, 16: 12346
relation to nuclear spin in relativistic quantum field theory, 16: 12375
research, 20: 21224 (ORNL-3919)
research programs at ORNL, 1963, 19: 21792(R) (ORNL-3650(p.187-219))
research programs at ORNL, 1964, 19: 22859(R) (ORNL-3766)
research programs on, 1964 Army Dept. summary, 19: 32048(R) (NP-10573)
research progress at ORNL, 18: 14347(R) (ORNL-3567)
resolution of Fokker-Planck equation using Campbell theorems, 17: 20674
response relations in, minimum bias designs for exponential, (T), 20: 13167 (ORNL-3873)
Spearman's footrule, examination of, 17: 12451 (CDRP-182-114)
specific heat of spin systems at negative and positive absolute temperatures, 19: 1172
spectral line widths in quantum, calculation by Green's functions, 17: 11358
spin temperature formalism in quantum, (T), 20: 2864 (COO-1198-300)
stationary-state solutions to Boltzmann equation, 17: 32766
statistical behavior of linear systems, 17: 6891
stochastic Markovian processes, variation principle in, 16: 22527
symplectic ensemble in, multichannel reduced-width amplitude distribution for, 18: 4480
tabulations of Calabro kappa-square reliability values, 19: 9583 (UCRL-7920(Rev.I))
techniques used in studying zirconium alloy steam service, 18: 8750 (GEAP-4453)
test for presence of preferred orientation in aggregates of crystallites, 18: 25269(R) (NLCO-905)
theory for adaptive pattern recognition, 19: 13863(R) (TID-21413)
theory for distributions of energy levels of complex systems, 16: 32415
theory for distribution of energy levels of complex systems, 17: 20396
theory for electromagnetic fields, phase-space distribution function in, 20: 11880
theory for energy levels of complex systems, 17: 28282
theory for fission dynamics, 18: 36672
theory for magnetic spin relaxation, 19: 16288
theory for many-body systems, pair correlation function diagrams in, 19: 1079
theory for many-body systems, properties of pseudo-markovian collision operator in, 19: 1080
theory for multivariable systems, pseudo-random binary sequences in, 19: 39078
theory for nuclear reaction cross sections, 18: 32837
theory for relaxation in isolated spin systems, 18: 35561
theory for reliability, 19: 26915(R) (AD-609133)
theory for variance in background and optimum counting times in mass spectrometry, 18: 19878
theory of broadening of spectral lines in plasma, generalization of, 18: 21405
theory of eigenvalues of random matrices, 17: 28283
theory of Fermi liquids, with both long- and short-range forces, 16: 33624
theory of Fermi liquids, with both long- and short-range forces, 16: 33625
theory of Fermi-Thomas, corrections, 17: 9006
theory of irreversible processes in, 16: 32206
theory of linear transport coefficients in, 19: 9589
theory of many-particle systems, 19: 30867
theory of relaxation in isolated spin systems, quantum, 18: 16046
thermal conductivity of Fermi gases, 16: 32228
thermodynamic Green's functions in statistical mechanics, (T), 19: 11826 (KFKI-64-2)
three-body scattering operator in nonequilibrium, 17: 38423
tolerance factors, tables of one-sided normal, 19: 35873 (TID-21021)
tolerance limits, 16: 27547 (KAPL-M-GLB-8)
transport in, equivalence of Boltzmann and Navier-Stokes equations for, (T), 19: 11830 (NYO-1480-7)
transport properties of matter in, theory, 17: 6818
unfolding of measured distributions in, 19: 28732 (ORNL-3743)
use for analysis of pulse-height distribution data from gamma scintillation counting, 20: 11201(R) (NYO-3136-2)
use for estimating probability of light bulb failure, 20: 11205(R) (NYO-3136-2, App. 4)
use for indirect measurements of power spectral densities, 18: 4742 (LADC-5845)
use for interpretation of high-energy nuclear excitation functions, (T), 19: 31222 (LA-3266)
use for nuclear-decay distributions, 20: 19851
use for radiation detector performance, 20: 19851
use in analysis of reactor hot channel and hot spot calculations, 16: 18616(R) (EURAEC-191)
use in analysis of nonstationary vibrations in missiles, 18: 4910 (SC-DC-2049)
use in analysis of measured distributions, 19: 15981(R) (ORNL-3714 (Vol.I)(p.70-7))
use in analysis of data on leukemia incidence in populations, 20: 5471
use in analysis of pulse-height distribution from scintillation counting of mixed radionuclides, 20: 11204(R) (NYO-3136-2, App. 3)
use in analysis of radiation injury recovery, 20: 42829 (AD-635167)
use in analysis of late effects of radiation from atomic explosions, 17: 6332
use in analysis of cell population kinetics, 17: 2783 (BNL-6362)

use in analysis of radiation effects on tumor incidence in Hiroshima and Nagasaki, 17: 6333
use in analysis of energy spectra, 18: 29972 (CEA-2396)
use in counting weak radiation sources, 20: 27333
use in determination of dose-modification factors, 18: 27247
use in environmental radiation monitoring, 19: 7751
use in environs monitoring program, 16: 13397
use in examination of records and inventories for nuclear materials management, 18: 2145 (IDO-16925(p.67-75))
use in fallout distribution studies, 20: 7335
use in formulation of rational thermodynamics, 16: 18110 (NP-11463 (Pt.2)(p.313-23))
use in health physics, 17: 10869 (Y-KB-7)
use in measurement of system transfer functions, 17: 11947 (HW-SA-2558)
use in pathogenetic studies on radiation injuries, 19: 8881
use in radiation monitoring, survey of, 18: 4022 (NP-13312)
use in radiobiology, 16: 26774
use in SS materials accounting, 16: 3267 (TID-7615(p.7-13))
use in studies of etiology of malignant neoplasms in human populations, 20: 5307
use in studies of radiation effects on life span of dogs, 18: 25094(R) (UCD-472-109(p.173-7))
use in studies on properties and structure of beryllium oxide, 20: 23657 (UCRL-14759)
use in theory of compound nuclear reactions, 17: 41892
use in treatment of hot channel factors for compact reactors, 17: 31730 (NAA-SR-8468)
use of error, for radiation detector time determination, 20: 19053
use of error, for scintillation detector performance, 20: 19054
use of Gaussian function in, 18: 30646
use of generating functions in, to solve combinatorial problems, 16: 9304
use of Henry straight line in gamma spectra analysis, 17: 41856 (CEA-2296)
use of log normal distribution in radiation protection work, 19: 26156 (AERE-R-4736)
use of Poisson, in nuclear measurements, 19: 25491
use of probability theory in reactor core design, 17: 29709 (GEAP-3819)
use of quantum, in plasma spectral line shapes analyses, 18: 36721 (RTD-TDR-63-3130)
use of, in radiobiological research, 18: 25172
uses for analysis of dead-time effects on counter efficiency, 18: 33899
uses for analysis of nuclear-data measurements, 18: 37472 (A/CONF.28/P/633)
uses for controlling scanning efficiency in nuclear emulsion, 18: 23944
uses in communications theory, 18: 28094(R) (TID-20607)
uses in communication theory, 19: 39270(R) (TID-21894)
uses in evaluation of radiation protection procedures, 17: 41051
uses in high-energy physics, 18: 16408 (CERN-64-13(Vol.I)(p.1-86))
uses in physics, 16: 15108 (JINR-R-292)
uses in processing and transmission of information, 19: 39270(R) (TID-21894)
uses in seismological nuclear-blast detection, (T), 19: 18172 (NP-14809)
uses in stochastic neutron-transport theory, 19: 29189
value prediction for unobservable random variables, 20: 19169(R) (BNL-929, pp 106-11)
Weibull's modulus for brittle materials, method for obtaining, 19: 3814 (UCRL-7527)
wind fluctuation, for prediction of atmospheric particle diffusion, 16: 5614

Statitrons
see Electrostatic Generators

STEAM
see also Water Vapor
acoustic properties of, in pipes, 18: 3965
aerosol behavior in condensing, 18: 35260(R) (AERE-PR/HPM-5)
analysis for iodine, methods for, 19: 22458(R) (ORNL-3776(p.23-37))
analysis of superheated, for gases, instrument for automatic, 17: 40705 (TID-7655(p.147-175))
analysis of superheated, for gases, design of gas chromatograph for, 18: 23407 (DP-880)
behavior as fog-flow coolant, 17: 11965 (UNC-5008-I)
bubbling through liquids, hydrodynamics, 16: 4277(T) (AEC-tr-4496)
burnout and heat transfer in once-through superheating of, 18: 27667
burnout heat flux in tubes, effects of diameter and pressure on, 17: 30664(R) (TID-19089)
burns by, theory of retinal, 17: 35360
chloride deposition from, onto superheater fuel clad materials, tracer studies of, 18: 8751 (GNEC-295)
compression in surge tanks, pressure transients from, 18: 27671
condensation by water in reactor accidents, 16: 14258
condensation embryos in expanding streams of, 18: 37855
condensation in nozzles, 17: 8345
condensation in pool water, performance of pressure suppression containment system in, 19: 47927
condensation in tubes, flow stability in, 19: 2514 (PWA-2315)
condensation on horizontal rotating cylinder, heat transfer in, 17: 23493
condensation system for, in reactor failure, 19: 33649(P)
contamination of superheated, in boiling reactors, 18: 4805
control of, in turbines, 17: 4686(P)
corrosion effects on beryllium at 325 and 500°C, 18: 4192 (AERE-R-4422)
corrosive and erosive properties of flowing wet, design of loop for studying, 16: 5666 (EURAEC-98)
corrosive effects on zirconium and zirconium alloys at 500°C, hydrogen uptake, 16: 485 (AERE-R-3768)
corrosive effects on zirconium and zirconium alloys, bibliography, 16: 4504 (VDIT-7.1)
corrosive effects on zirconium alloys, 16: 7857
corrosive effects on Zircaloy-2 at 750°F, effects of impurities on, 16: 10463
corrosive effects on zirconium alloys, 16: 11274
corrosive effects on Zircaloy-2, 16: 12050 (HW-71771)
corrosive effects on aluminum and aluminum alloys, 16: 22548
corrosive effects of flowing wet, on 304 stainless steel and Zircaloy-2, 16: 22554
corrosive effects on stainless steel tubes at 1100 to 1500°F and 2 kpsi, 16: 24125
corrosive effects on tubing alloys at 1200 to 1500°F, 16: 24126
corrosive effects on stainless steel tubes, effects on heat-transfer properties, 16: 24127
corrosive effects at 1000 to 1300°F on niobium-base alloys, additive optimization, 16: 25695(R) (BMI-X-188)
corrosive effects of superheated, on stainless steel and Zircaloy-2 process tubes, 16: 31254 (GEAP-3784)
corrosive effects on Zircaloy-2 and -4 at high temperatures, 16: 33433 (WAPD-TM-307)
corrosive effects on steels at 546°F, 16: 33439
corrosive effects on $CaO-UO_2-ZrO_2$ and CeO_2-UO_2 systems at 625°C, 16: 33511(R) (CEND-162)
corrosive effects of, on stainless steel at 650°C, 17: 1870 (ANL-FGF-381)
corrosive effects of superheated, on type 304 stainless steel, 17: 3900
corrosive effects on nickel-plated steel, 17: 13878(R) (KR-36)
corrosive effects on zirconium alloys, 17: 14740 (TID-11295(2nd Ed.))
corrosive effects on aluminum, 17: 18698 (JAERI-1035)
corrosive effects on metals, inhibition using boric acid, 17: 20428(P)
corrosive effects of superheated, on stainless steel, 17: 21226 (TID-7658(p.1-14))
corrosive effects of superheated, on stainless steel, effects of oxygen and surface treatment on, 17: 21227 (TID-7658(p.14-16))
corrosive effects of superheated, on stainless steel, 17: 21228 (TID-7658(p.16-20))
corrosive effects of superheated, on Hastelloy X, Incoloy, Inconel, and stainless steel, 17: 21229 (TID-7658(p.20-6))
corrosive effects of superheated, on nickel alloys and stainless steel, 17: 21230 (TID-7658(p.27-47))
corrosive effects of superheated, on stainless steel, 17: 21231 (TID-7658(p.48-56))
corrosive effects on niobium-base alloys at 540°C, 17: 36221 (BMI-1636)
corrosive effects on reactor materials, 17: 37001(R) (ANL-6780)
corrosive effects on Zircaloy-2, effects of carbon content on, 17: 37465 (WAPD-T-1508)
corrosive effects of superheated, on niobium–zirconium and Zircaloy-2, 17: 39470(T,R) (EURAEC-619)
corrosive effects on niobium–tin–zirconium and Zircaloy-2, 17: 39472(T,R) (EURAEC-668)
corrosive effects on alloys at 650°C, 17: 40422(R) (ANL-6784)
corrosive effects on Zircaloy-2, effects of dissolved oxygen on, 18: 567
corrosive effects on stainless steel at 800 to 1300°F, 18: 2185
corrosive effects on copper–zirconium alloys, 18: 2191
corrosive effects of superheated, on Zircaloy-2, 18: 2193
corrosive effects on niobium alloys at 1000°F, 18: 2184
corrosive effects of nuclear superheated, on alloys at 1050°F, 18: 4161 (GEAP-4351)
corrosive effects on zirconium alloys at temperatures up to 500°C, test facility for, 18: 4196 (GEAP-4393)
corrosive effects of wet, on stainless steel and Zircaloy-2, 18: 6913 (NP-13409)
corrosive effects on zirconium alloys, 18: 7134 (AERE-R-4458)
corrosive effects on niobium–zirconium alloy, 18: 7135 (AERE-R-4459)
corrosive effects on iron and nickel alloys at 3000 psi and 550°C, 18: 7143(R) (HW-77954(p.5.20-3))
corrosive effects on Zircaloy-2, 18: 7147(R) (HW-78962(p.5.1-12))
corrosive effects of chloride-containing, on Inconel and stainless steels, 18: 7928 (GNEC-257)

corrosive effects on stainless steel at 400°C, 18: 8734(T,R) (EURAEC-735)
corrosive effects on Zircaloy-2 and -3 at 750°F and 1500 psi, 18: 10452 (TID-20058)
corrosive effects on Zircaloy-2 and -4 at 400°C, hydrogen pickup in, 18: 10471 (HW-67437)
corrosive effects on zirconium, 18: 10476(T) (JPRS-22697(p.8-26))
corrosive effects on Zircaloy-2 at 750°F, 18: 12558 (ORNL-TM-739)
corrosive effects on niobium–tin–zirconium alloy, 18: 12574 (APED-4364)
corrosive effects of oxygenated, on stainless steel, 18: 14400 (ACNP-64001)
corrosive effects on niobium–tin–zirconium alloy, 18: 14545(T,R) (EURAEC-863)
corrosive effects on niobium–tin–zirconium alloy, 18: 14358(R) (EURAEC-135)
corrosive effects on niobium–tin–zirconium alloy, 18: 14360(R) (EURAEC-199)
corrosive effects on fueled and unfueled graphite spheres, 18: 15492(R) (ORNL-3523(p.127-92))
corrosive effects on graphite at 1000 to 1800°K and 450 psig, test facility for, 18: 15532(R) (ORNL-3523(p.40-58))
corrosive effects on Zircaloy-2, additive effects of nitrogen, oxygen, and silicon on, 18: 16440 (WAPD-283)
corrosive effects on chromium–nickel alloy and other alloys, 18: 21668(R) (GEMP-274)
corrosive effects on zirconium alloys under neutron irradiation, 18: 22152
corrosive effects on Zircaloy-2 at 750°F, 18: 27884 (KAPL-2000-21 (p.VI.1-4))
corrosive effects on chromium–niobium alloy at 750 to 900°F, 18: 27861 (KAPL-2000-21(p.VII.1-5))
corrosive effects on niobium–tin–zirconium alloy at 400°C, 18: 30110 (EUR-86.d)
corrosive effects of superheated chloride-containing, on stainless steels and high-nickel alloys, 18: 30129 (GEAP-4450)
corrosive effects of superheated, on Incoloy 800, 18: 30130 (GEAP-4495)
corrosive effects on fuel cladding, 18: 30143
corrosive effects on reactor materials, 18: 36817
corrosive effects on scratched Zircaloy-2 cladding of NPR fuel element, 18: 37640 (HW-75359)
corrosive effects on reactor materials, 18: 37635 (A/CONF.28/P/445)
corrosive effects on zirconium alloys, 18: 39847
corrosive effects on alloys and stainless steels, 18: 41933 (TID-11295 (3rd Ed.))
corrosive effects on chromium–titanium–vanadium alloy at 540°C, 18: 41933 (TID-11295(3rd Ed.))
corrosive effects on zirconium-base alloys, 18: 41933 (TID-11295(3rd Ed.))
corrosive effects on niobium–tin–zirconium alloy at 750 to 900°F, 18: 41957 (KAPL-3018)
corrosive effects on aluminum and its alloys at high temperatures in reactors, survey, 19: 922 (HW-69876)
corrosive effects on consolidated Zircaloy-2 powder at 750°F, effects of nitrogen and oxygen on, 19: 927 (KAPL-3060)
corrosive effects on superheater materials, 19: 4197 (SAN-8003(p.90-133))
corrosive effects on Zircaloy-2 and -4 tubing at 400°C, 19: 4587 (GEAP-4739)
corrosive effects of superheated, on fuel cladding, 19: 4615(R) (EURAEC-1115)
corrosive effects on sintered aluminum–iron–nickel compacts at 450°C, 19: 4607(P)
corrosive effects on steels at high temperatures, 19: 7865(R) (EURAEC-1237)
corrosive effects on type 304 stainless steel, 19: 7262(R) (CEND-508)
corrosive effects on chromium–niobium–titanium–vanadium alloy, 19: 9620 (BMI-1700)
corrosive effects on zirconium alloys, 19: 14765(R) (ANL-6977)
corrosive effects on iron and nickel alloys, effects of pressure and oxygen on, 19: 13883(R) (HW-81984(p.9.1-6))
corrosive effects on Zircaloy-2 and zirconium–niobium–tin alloy at 400°C, in-pile, 19: 16208(R) (EURAEC-1249)
corrosive effects of superheated, on superheater fuel element, 19: 16010 (ACNP-62024)
corrosive effects of superheated, on nickel and stainless steel, 19: 16010 (ACNP-62024)
corrosive effects on nuclear structural materials, review, 19: 16013 (CEA-R-2600)
corrosive effects on chromium–iron–nickel alloys at high temperatures, 19: 17774 (GEAP-4490)
corrosive effects on aluminum-chromium-iron-yttrium alloys, 19: 18390(R) (GEMP-43A)
corrosive effects on cadmium-indium-silver alloys, effects of added metals on, 19: 18402 (WCAP-3269-29)
corrosive effects on zirconium and its alloys at 500°C and 1000 psi in presence of boric acid, 19: 20492
corrosive effects on Incoloy and Inconel, 19: 24098(T,R) (ORNL-tr-538)
corrosive effects on Zircaloy-2 and -4, 19: 22870(R) (HW-83601)
corrosive effects on steels at high temperatures, 19: 24936(R) (EURAEC-1308)
corrosive effects on zirconium alloys, 19: 24982(R) (EURAEC-1270)
corrosive effects on ceria–urania and urania–zirconia, 19: 25044(R) (CEND-2936-222)
corrosive effects of chloride- and oxygen-containing, on stressed type 304 stainless steel, 19: 28213 (CEND-529)
corrosive effects at 400 and 450°C on niobium–zirconium alloys with alloy additions, 19: 30668(R) (EURAEC-1274)
corrosive effects on Zircaloy-2, effects of irradiation and treatments on, 19: 30650(R) (ORNL-3789(p.126-38))
corrosive effects on zirconium alloys at 400°C, 19: 30681
corrosive effects on Zircaloy-2, effects of structure on, 19: 30682
corrosive effects at 400°C on nickel–zirconium-base alloys with aluminum, tin, and titanium additions, 19: 32696(R) (EURAEC-783)
corrosive effects at 400°C on vanadium–zirconium-base alloys with aluminum, tin, and titanium additions, 19: 32696(R) (EURAEC-783)
corrosive effects on metals, inhibition by boric acid, 19: 32701(P)
corrosive effects on reactor cooling system materials at high temperatures, 19: 38178(R) (GEAP-4790)
corrosive effects of superheated, on Incoloy-800, 19: 36986
corrosive effects of superheated, on fuel cladding materials, 19: 36987
corrosive effects on Hastelloy-X, heat transfer and isothermal, 19: 39115 (GEAP-4860)
corrosive effects on stainless steel, heat transfer and isothermal, 19: 39115 (GEAP-4760)
corrosive effects on Incoloy-800 and Inconel-600, effects of surface preparation on, 19: 39115 (GEAP-4760)
corrosive effects on type 304 stainless steel, effects of surface preparation on, 19: 39115 (GEAP-4760)
corrosive effects on Inconel-600 and -625, heat transfer and isothermal, 19: 39115 (GEAP-4760)
corrosive effects on Incoloy-800 and -825, heat transfer and isothermal, 19: 39115 (GEAP-4760)
corrosive effects on aluminum–chromium–iron–yttrium alloy at 500 to 1300°C, 19: 40961
corrosive effects on iron–nickel–zirconium alloy, effects of alloy microstructure on, 19: 44616(R) (ANL-7000, pp 122-37)
corrosive effects on copper–zirconium and nickel–zirconium alloys at 540°C, 19: 44616(R) (ANL-7000, pp 122-37)
corrosive effects on zirconium-based alloys, effects of pressure on, 19: 44616(R) (ANL-7000, pp 122-37)
corrosive effects on stainless steel at 650°C, effects of alloy additions on, 19: 44616(R) (ANL-7000, pp 122-37)
corrosive effects on Incoloy 800, effects of aluminum additions on, 19: 44616(R) (ANL-7000, pp 122-37)
corrosive effects at 750°C on Inconel 600, 625, and X750, 19: 44616(R) (ANL-7000, pp 122-37)
corrosive effects at 750°C on types 304, 316, 321, 347, and 406 stainless steels, 19: 44616(R) (ANL-7000, pp 122-37)
corrosive effects on materials for reactor cooling systems, 19: 45572(R) (GEAP-4755)
corrosive effects on carbon steel, 19: 44627
corrosive effects on niobium–zirconium alloys, 19: 44629
corrosive effects on aluminum–chromium–iron–yttrium alloys at 730°C, 19: 44598(R) (GEMP-49A)
corrosive effects on iron-based 1041 alloy, effects of preoxidation and strain on, 19: 44598(R) (GEMP-49A)
corrosive effects at 750°C on Incoloy 800, Rene 41, and Nichrome V, 19: 44616(R) (ANL-7000, pp 122-37))
corrosive effects on high-silicon aluminum alloys, 20: 763 (BNWL-125)
corrosive effects on type 304 stainless steel, effects of surface finish on, 20: 766(R) (EURAEC-1445)
corrosive effects on type 304 stainless steel, effects of surface work-hardening on, 20: 765(R) (EURAEC-1387)
corrosive effects on aluminum–chromium–iron–yttrium alloy, effects of pre-oxidation and strain on, 20: 2223(R) (GEMP-51A)
corrosive effects on niobium–tin–zirconium alloys, effects of alloy additions on, 20: 2255(R) (EURAEC-1323)
corrosive effects on Zircaloy-4, effects of air introduction on, 20: 2257(R) (GEMP-57A, pp 47-52)
corrosive effects on low-alloy and stainless steels, effects of surface treatments on, 20: 5846
corrosive effects on Incoloy 800 at 705°C, 20: 5846
corrosive effects on Zircaloy-2 powders at 750°F, effects of nitrogen and oxygen additions on, 20: 5851
corrosive effects on type 304 stainless steel and Zircaloy-2 at 2000°F, 20: 5851
corrosive effects on Zircaloy-2, effects of heat treatments on, 20: 5846

corrosive effects on Zircaloy-2 and Zircaloy-4 at 1200 to 1600°C, 20: 9378(R) (GEMP-54A)
corrosive effects of type 304 stainless steel, effects of heating rate on, 20: 9378(R) (GEMP-54A)
corrosive effects on iron- and nickel-base alloys, 20: 9408 (BNWL-154)
corrosive effects of flowing, on rhenium at 850 to 1700°C, 20: 9429
corrosive effects of flowing, on tungsten at 1000 to 1700°C, 20: 9430
corrosive effects on uranium monocarbide and uranium monocarbide–10 iron at 300 to 1000°C, 20: 9434
corrosive effects on zirconium-base alloys, effects of nitrogen impurity content on, 20: 14980(R) (GEAP-5065)
corrosive effects on zirconium-base alloys, effects of metallurgical processing variables on, 20: 14980(R) (GEAP-5065)
corrosive effects on welded joints of niobium–zirconium alloys, 20: 19195
corrosive effects on zirconium at 500°C, effects of surface contamination on, 20: 21268
corrosive effects on type 304 stainless steel at 1000 to 1250°C, kinetics of, 20: 27409(R) (GEMP-58A)
corrosive effects on iron–chromium–aluminum–yttrium alloys, effects of chromium content on, 20: 27411(R) (GEMP-400A, pp 135-63)
corrosive effects on Incoloy-800 and Inconel-625, 20: 28750(R) (GEAP-5061)
corrosive effects on Incoloy-800 and Inconel-625, 20: 28751(R) (GEAP-5125)
corrosive effects on Zircaloy-2 and -4 at 1200 and 1400°C, 20: 27430(R) (GEMP-400A, pp 203-20)
corrosive effects on type 304 stainless steel at melting point, 20: 27430(R) (GEMP-400A, pp 203-20)
corrosive effects on nickel-coated aluminum fuel plates, 20: 30794(R) (IDO-17147, pp 1-12)
corrosive effects on zirconium–chromium–iron alloy, effects of fabrication process and nitride content on, 20: 29660(R) (GEAP-4960)
corrosive effects on niobium–tin–zirconium alloys, composition of oxide film formed by, 20: 31669
corrosive effects on carbon steels, stainless steels, and Zircaloy-2 at high pressures and temperatures, 20: 33815(R) (EURAEC-1625)
corrosive effects of superheated, on Inconel 625, 20: 33829
corrosive effects of superheated, on Inconel 625, 20: 33830
corrosive effects on chromium–iron–zirconium alloys at 300 to 500°C, 20: 39356(R) (GEAP-5134)
corrosive effects on copper–molybdenum–zirconium alloys, effects of heat treatments on, 20: 39347 (NP-16239)
decomposition on metals, thermal, 18: 26824(R) (ANL-6885)
decomposition on metals, thermal, 19: 17174(R) (ANL-6900(p.232-303))
density determinations in low-pressure turbines by beta absorption, 18: 39772
density in boilers, radiometric measurement of, 18: 14305
density of steam–water mixtures in fuel elements, measurement with radiometric gage, 17: 3277
deuterium exchange with hydrogen, heat recovery, 16: 2106(P)
deuterium exchange with hydrogen in presence of fissionable material for production of heavy water, 20: 1884(P)
diffusion from commercial graphite at 1000°C, 17: 4986
diffusion in water for fog-cooled reactor, equipment for, 18: 42961(P)
dryer design for, performance of mechanical, 17: 3895
drying and superheating of, in boiling reactors, 17: 10036(P)
effects of superheated, on zirconium alloys, evaluation of, 18: 18284 (CONF-187-36)
effects on chromium–iron–zirconium alloy at 300, 400, and 500°C, 20: 31677(R) (GEAP-4840)
effects on dehydration and thermal decomposition of uranyl nitrate hydrates, 19: 32152
effects on fission-product iodine, 19: 36216(R) (BNL-900(p.29-72))
effects on fission product release from melted stainless-steel clad uranium dioxide fuel elements, 20: 559 (CONF-650407, pp 276-91)
effects on niobium–yttrium–zirconium alloy at 400-500°C, 20: 2276(P)
effects on separation of iodine vapor from air streams by adsorption on charcoal, 18: 23386 (CONF-12-3)
effects on soils, sterilization, 20: 40637(R) (ORO-2754-7)
effects on tensile properties of Inconel, Incoloy, and Hastelloy-X alloys of, at 1050 and 1100°F, 19: 32732 (GEAP-4745)
effects on Zircaloy-2 at 350, 400, and 450°C, 20: 25499
effects on Zircaloy, 20: 25500
effects on Zircaloy-4 reactions with urania during dynamic heating to 1750°C, 20: 27409(R) (GEMP-58A)
effects on zirconium alloys, 20: 25504
embrittlement of Zircaloy-4 during dynamic heating, 20: 2257(R) (GEMP-52A, pp 47-52)
entrainment by downcomers in natural circulation, 16: 832
entrainment in axial separators in reactors, calculation of, 18: 40747 (APED-4564)
entrapment in circulating boiling systems, reduction of, 17: 18259 (ANL-6674)
exit quality in boiling water reactor channels, evaluation of system for control of, 17: 1609 (TID-17091)
filtration of radioactive, filter system for, 17: 36878 (TID-17548)
fission product release into condensing, from molten fuel elements, 19: 44285 (BNWL-SA-29)
flow in irregular annular gaps, turbulent, 16: 8879(T) (AEC-tr-4960)
flow of superheated, past fuel cylinders, 19: 18106 (AECL-2225)
flow rate of, measurement by total-sample method, 18: 35697
generator for, forced-flow once-through, 20: 30821(P)
handling in nuclear power plants, 17: 4755(P)
heat conductivity of deuterated and normal, at 100 to 500°C, 17: 32076
heat transfer and pressure drop of superheated, in a thin annulus, 16: 27230
heat transfer and pressure drop of superheated, in thin annulus, 17: 28522 (ACNP-62030)
heat transfer by superheated, 17: 34095 (GEAP-4258)
heat transfer coefficients for, 20: 12341
heat transfer from bubble surface in turbulent subcooled water stream, 16: 13215
heat transfer from tube wall to superheated, effects of turbulence promoters on, 19: 9327 (GEAP-4749)
heat transfer in condensation of high-pressure, in pipes, local coefficients of, 18: 29846(T) (AEC-tr-6431)
heat transfer in stainless steel tubes, 17: 1613
heat transfer in subcooled, for high system pressures and hot surface charges, (T), 19: 46544
heat transfer properties of superheated, 17: 289
heat transfer properties at sub- and supercritical pressures, 18: 11451(R) (WCAP-2525)
heat transfer properties in rod bundles with turbulence promoters, (E), 20: 3471(R) (GEAP-4861)
heat transfer to, in supercritical pressure region, design of loop for studying, 17: 21253 (TID-7658(p.156-7))
heat transfer to superheated, from annular assemblies, 17: 21252 (TID-7658(p.153-5))
heat transfer to superheated, at high pressure, 17: 38476 (TID-7674 (p.46-8))
heat transfer to superheated, forced-convection (E), 19: 2515 (WCAP-2056(Pt.III))
heat transfer to supercritical, (E), 19: 4329 (SAN-8003(p.134-62))
heat transfer to superheated, in cylindrical tubes, 20: 7232 (WCAP-5480)
heat transfer to wet, from bilaterally and internally cooled fuel elements, 16: 27199(T) (EURAEC-45)
iodine release from irradiated uranium and its oxide into, chemical states of, 19: 28361 (BNL-9174)
iodine transfer with water, 18: 39178
isotopic exchange with tritium, rate of, 19: 30462
liquid entrainment by, 16: 17803(T) (TIL/T-5028)
mass transfer in systems with water, performance of cocurrent distillation contacting device for, 17: 18233
monitoring of, from fission products, 20: 16825 (ORNL-TM-1442)
neutron scattering by, 17: 38026(T) (AEC-tr-5734(p.119-39))
nitrogen-16 distribution between water and, in boiling reactors, 20: 6638
oxidation of Zircaloy-2 by, effects of pressure on, 17: 36234
oxidative effect on aluminum at 800 to 1400°C, 19: 32697
oxidative effects on aluminum–uranium alloy at 930 to 1400°C, 19: 32697
oxidative effects on aluminum–chromium–iron–yttrium alloys, 19: 36952(R) (GEMP-47A, pp 13-26)
oxidative effects on fueled and unfueled graphite spheres at 800 to 1000°C, 20: 27433 (ORNL-P-1416)
oxidizing effects on zirconium and zirconium alloys, 18: 12589
performance as coolant for 1000-Mw(e) fast breeder reactor, 20: 22452
physical properties of, at high pressure and temperature, 20: 43173 (NAA-SR-Memo-12006)
preparation of superheated, from reactor coolant, equipment and process for, 18: 45071(P)
pressure control system for, in EBR-2, 20: 12438
pressure drop in condensing flow of, method for calculating static, 20: 1814 (NAA-SR-63333)
production in power plants, review on, 19: 22498(T)
production in pressurized water reactors without heat exchanger, 20: 20285(P)
production in reactor cores, method for, 19: 33651(P)
production in reactors with tubular fuel assembly, method for, 20: 24771(P)
production of low-temperature, using nuclear energy, 19: 25745
production of superheated, system for, 19: 24687(P)
properties as reactor coolant, 16: 12693
properties as reactor coolant, 16: 23830 (BNL-5377)
properties for use as reactor coolant, 18: 31002
properties of, for use as reactor coolants, 17: 5579 (NDA-2132-5)
properties of heavy water, at saturation, calculation of, 19: 28295

properties of wet, as reactor coolant, 16: 3942 (NDA-2132-6)
quality control at exit in boiling reactors, device for automatic, 19: 33591 (CONF-640507(p.209-12))
quality control in boiling reactors, development of automatic device for, 18: 12313 (CONF-187-72)
quality estimation in pipes by x ray scattering, 16: 25551 (CRRP-1086)
quality of boiling reactor, automatic control of, 18: 3228
quality of, monitor design for determining, 17: 3894
radiation effects on reactions with pyrolytic-carbon at 1000 to 1400°C, neutron, 20: 23600 (GA-7005)
radioactivity deposition from nuclearly superheated, in VBWR, 17: 35096 (GEAP-4141)
radiolytic gases in, research program on catalytic recombination of, 19: 24396(R) (GNEC-320)
radiolytic hydrogen yield in loop, 17: 40266(R) (EURAEC-728)
reactions in plutonium and uranium tetrafluorides, 20: 4046(R) (EURAEC-1340)
reactions of flowing, with molybdenum at 1100 to 1700°C, 19: 26774
reactions with aluminum at 1200 to 1600°C, 17: 36860(R) (ANL-6648)
reactions with aluminum–uranium alloys at 1200 to 1600°C, 18: 23817(R) (ANL-6880(p.72-8))
reactions with aluminum and its alloys, 18: 35060(R) (ANL-6904)
reactions with aluminum and its alloys at 800 to 1300°C, 19: 11682
reactions with aluminum and aluminum alloys at 1200 to 1600°C, 19: 17174(R) (ANL-6900(p.232-303))
reactions with aluminum at high pressures and temperatures, 20: 20925(R) (ANL-7055, pp 177-212)
reactions with aluminum, stainless steel, and urania at high temperatures, 20: 31440(R) (ANL-7175, pp 159-83)
reactions with carbon at 900 to 1300°C, kinetic study of, 17: 1418 (NP-12185)
reactions with clad urania fuels, 20: 2221(R) (ANL-7082, pp 62-73)
reactions with cladding materials and urania at high temperatures, 20: 6552(R) (ANL-6925, pp 187-233)
reactions with fuel materials, 19: 11679
reactions with fuel cladding in TREAT transient experiments, 19: 38132 (ORNL-P-1287)
reactions with graphite at 800 to 1200°C, 16: 17573(R) (ORNL-3262 (p.144-5))
reactions with graphite and fueled graphite spheres, 18: 22017(R) (ORNL-3591(p.124-7))
reactions with graphite, catalytic effects of barium, cesium, and strontium on, 18: 25321 (GA-5215)
reactions with graphite in EGCR, facility for, 18: 29055 (ORNL-TM-856)
reactions with graphite at 1200 to 1600°F and 30 to 300 psig, 19: 19391 (ORNL-TM-984)
reactions with graphite, 19: 23996(R) (ORNL-3650(p.1-110))
reactions with graphite at 1300 to 1600°F, 19: 25727(R) (ORNL-3731 (p.252-71))
reactions with graphite in EGCR, (E), 19: 29682
reactions with graphite at 800 to 1000°C, effects of burnoff on, 19: 30672(R) (ORNL-3789(p.202-7))
reactions with graphite at 1350 to 1600°F, 19: 38183(R) (ORNL-3807, pp 238-48)
reactions with graphite, 20: 11225
reactions with graphite at 1300 to 1600°F, 20: 19191 (ORNL-TM-1430)
reactions with graphite at high temperatures, 20: 28742(R) (GA-6418)
reactions with graphite, high-temperature, 20: 36490(R) (ORNL-3951, pp 192-3)
reactions with hydrogen and uranium hexafluoride to prepare uranium dioxide, 19: 32180(P)
reactions with iodine released from uranium and uranium carbide, 20: 5878 (BNL-9667)
reactions with iron at 950 to 1400°C, kinetics of, 20: 31669
reactions with liquid aluminum, kinetics of, 17: 26115
reactions with liquid aluminum at 1200 to 1750°C, 18: 2216 (CONF-39-105)
reactions with liquid urania in TREAT, 20: 4183(R) (ORNL-3843, pp 2-70)
reactions with metals, reactor safety studies of, 18: 33678(R) (ANL-6875)
reactions with metals at high temperatures, 19: 28771
reactions with molybdenum and uranium at high temperatures, 18: 44922(R) (ANL-6800(p.326-402))
reactions with molybdenum, niobium, and tantalum, 20: 31669
reactions with nitrided steel at 1050°F, 19: 38183(R) (ORNL-3807, pp 238-48)
reactions with outgassed graphite at 1000°C, effects of mullite on, 19: 26348
reactions with plutonium at 200 to 500°C, use in safe oxidation of scrap and skulls, 20: 43854 (HW-66431)
reactions with pyrolytic carbon at 700 to 1100°C, 17: 25074(R) (ORNL-3417(p.157-62))
reactions with pyrolytic-carbon-coated thorium uranium dicarbide fuel particles at 1000 to 1400°C, 20: 23600 (GA-7005)
reactions with reactor components, during transients, 18: 36751 (ANL-6912)
reactions with refractory metals at temperatures up to 1700°C, kinetics of, 19: 32447 (ANL-7020(p.175-97))
reactions with refractory metals at high temperatures, 20: 6552(R) (ANL-6925, pp 187-233)
reactions with rhenium and tungsten to 1700°C, 20: 31669
reactions with stainless steel-clad urania, 19: 14765(R) (ANL-6977)
reactions with stainless steel- and Zircaloy-2-clad uranium dioxide pellets at 1500°C and 15 psig, 19: 32447(R) (ANL-7020(p.175-97))
reactions with stainless steel, effects of purity and silicon content on, 20: 9421(R) (EURAEC-1486)
reactions with stainless steels at 400 to 600°C, effects of surface work-hardening on, 20: 14977(R) (EURAEC-1500)
reactions with stainless steel during LOFT meltdown, 20: 26394(R) (ANL-7193)
reactions with type 304 stainless steel at 1400°C, 20: 14009(R) (ANL-7122, pp 82-90)
reactions with type 304 stainless steel and Zircaloy-2 at 900 to 1500°C, 20: 31669
reactions with uranium, isothermal studies of, 17: 1359(R) (ANL-6569)
reactions with uranium hexafluoride in fluidized bed, 19: 5927(P)
reactions with uranium carbide at 1000 to 1200°C, 19: 13299
reactions with uranium dioxides, effects on oxygen/uranium ratio of, 20: 6559(R) (ANL-7115, pp 77-83)
reactions with uranium at 600 to 1600°C, 20: 5843
reactions with uranium carbide in defective fuel elements, oxidation, (E/T), 20: 12380
reactions with uranium nitride and uranium carbide oxides at 200 to 1000°C, 20: 29645
reactions with uranium and aluminum–uranium alloys at 400 to 1600°C, kinetics of isothermal, 20: 29188
reactions with uranium dioxide at 1500°C, 20: 33787
reactions with uranium hexafluoride to prepare uranium dioxide, 20: 37205
reactions with zirconium in reactor core meltdown, 19: 29651(R) (WCAP-3269-3)
reactions with Zircaloy-2 in simulated reactor loss-of-coolant accident, 19: 45496 (WCAP-3269-30)
reactions with zirconium in loss-of-coolant reactor accident calculations, 20: 582 (CONF-650407, pp 938-69)
reactions with Zircaloy-4 during dynamic heating, 20: 27430(R) (GEMP-400A, pp 203-20)
reactions with Zircaloy at high temperature, 20: 33806
recombination of hydrogen and oxygen in, studies of catalytic, 19: 28213 (CEND-529)
sampling of reactor, instrumentation for, 20: 1466(R) (HPR-63)
separation, determination of carryunder at Moss Landing facility, 16: 17800 (GEAP-3562)
separation from saturated water mixtures, separator design, 16: 11814 (GEAP-3787)
separation from water in boiling reactors, centrifugal, 16: 14874 (EURAEC-148)
separation from water, design of baffle separators for, 17: 13785
separation from water, research programs on, 17: 14414(R) (ACNP-62033)
separation from water by gravity, carry-under studies, 17: 16240
separation from water, loop for testing equipment for, 17: 21249 (TID-7658(p.134-8))
separation from water, in reactor, development of radial vane separator for, 17: 21250 (TID-7658(p.139-45))
separation from water, development of centrifugal separators for, 17: 23457(R) (ACNP-63013)
separation from water, development of centrifugal separators for, 17: 32206(R) (ACNP-63021)
separation from water using full circle radial vane separator, 17: 38476 (TID-7674(p.46-8))
separation from water, development of centrifugal separators for, 17: 38477 (TID-7674(p.48))
separation from water, development of centrifugal separators for, 17: 40954(R) (ACNP-63028)
separation from water in boiling water reactor, methods for, 18: 11463
separation from water, development of centrifugal separators for, 18: 10205(R) (ACNP-63035)
separation from water, development of centrifugal separators for, 18: 20128(R) (ACNP-64021)
separation from water, development of centrifugal separators for, 18: 33693(R) (ACNP-64026)
separation from water, development of centrifugal separators for, 19: 555(R) (ACNP-64028)
separation from water, development of radial-vane separator for,

19: 6026(R) (GEAP-4728)
separation from water, development of equipment for, 19: 9299(R) (ACNP-64030)
separation from water, development of radial vane separator for, 19: 26490(R) (GEAP-4847)
separation from water in boiling reactors, separator for, 19: 27795
separation from water in high pressure loop, void fraction, 19: 28490 (ACNP-65002)
separation from water, methods development for, 19: 32344(R) (ACNP-65001)
separation from water, development of devices for, 19: 38801(R) (ACNP-65004)
separation from water, development of separators for, 19: 44131 (ACNP-65003)
separation from water, design of device for, 20: 2024(P)
separation from water, performance of radial-vane separator for, 20: 18864 (GEAP-4935)
separation from water, radial vane separator development for, 20: 28696(R) (GEAP-5084)
separation from water, performance of radial vane separator for, 20: 39019(R) (GEAP-5149)
separation in superheaters, mechanism of, 18: 4796(R) (GEAP-4153)
separation of iodine from, at 120 to 275°C, 18: 3890
separation requirements for large superheater reactors, 16: 24969 (CEND-116)
separator design for boiling reactor, 20: 35100(P)
simulation of superheated, for neutron moderation studies, 20: 20216
soil sterilization by, 18: 35908
superheaters for, review of developments in, 19: 48012
superheating for nuclear power plant, 19: 45630(P)
superheating of, design modification of generator for, 18: 17993(P)
superheating of, integral boiler reactor design for, 20: 30913(P)
superheating of, reactor design for, 19: 17331(P)
thermal capacity during phase transition in supercritical region, 16: 15291
thermal capacity of, in supercritical state, 18: 12055
thermal conductivity in flow through duct, 16: 13240
thermal conductivity characteristics in flow, in annulus, 16: 13238
thermal conductivity of heavy-water, 17: 23366
transport properties, 16: 18933
tritium exchange with hydrogen, 18: 10081
use in operating submarine engines, design study, 16: 23798 (AD-269390)
use in Rankine power systems for manned space stations, 19: 10009
use of high-temperature, for gasification of coal, 17: 42354(R) (TID-19443)
use of high-temperature, for gasification of coal, 17: 42355(R) (TID-19475)
use with detergent for decontamination, 16: 10326
velocity in water in Halden boiling test loop, 19: 27779 (HPR-52)
void fraction measurements in, ultrasonic instruments for, 18: 35809(R) (NYO-10559)
void fractions in, ultrasonic instruments for measuring, 18: 35810(R) (NYO-10610)
volume fractions in flowing and non-flowing two-phase mixtures, 19: 22502
volume in heated channel in open-loop operation, dilatation technique for measuring, 19: 30386
water content in boiler, use of radioisotopes for determining, 19: 20418
wetness of turbine exhaust, reduction of, 18: 25660
air–H–steam, fission-product behavior in, during in-pile uranium-dioxide melting, (E), 19: 29596
air–steam, fission product removal by steam suppression system, 20: 576 (CONF-650407, pp 776-804)
air–steam, fission-product behavior in, during in-pile uranium-dioxide melting, (E), 19: 29596
air–steam, iodine sorption from, by charcoal, 20: 4086(R) (ORNL-3843, pp 137-67)
air–steam, separation of volatile iodides from, by activated charcoal, 19: 22163(R) (ORNL-3776(p.43-6))
H–steam, reactions with uranium hexafluoride in fluidized bed, 19: 13270 (ANL-6902)
NH_3–steam, radiolysis in in-pile loops, 17: 39094 (AECL-1800)
steam–H_2O, boiling burnout in vertical tubes, empirical correlation for, 20: 12968
steam–H_2O, bubble- and slug-flow effects on volume fraction of, 20: 23257
steam–H_2O, burnout in flows with axially nonuniform heat flux, (E), 20: 14696
steam–H_2O, calculation of steam volume fractions in boiling, 17: 14466
steam–H_2O, corrosive effects on Zircaloy-2, 20: 6566(R) (EURAEC-1382)
steam–H_2O, critical flow, (T), 20: 20: 488
steam–H_2O, critical heat flux in forced flow, 18: 31723 (NP-14072)
steam–H_2O, density in boiler, use of radioisotope for measuring, 20: 9348
steam–H_2O, flow in radial-vane separators, 20: 39019(R) (GEAP-5149)
steam–H_2O, flow in vertical tubes, 20: 18869(R) (NYO-3114-10)
steam–H_2O, flow patterns of, two-phase, 17: 7613(R) (UNC-5042)
steam–H_2O, flow void fractions in, 17: 3111 (NASA-TN-D-1440)
steam–H_2O, heat flux dryout in internally heated annuli, (E), 20: 4099 (AECL-2332)
steam–H_2O, heat transfer in mixtures of, 20: 27108(R) (GEAP-5146)
steam–H_2O, heat transfer in, bibliography on, 20: 35617 (AERE-Bib-150)
steam–H_2O, heat transfer in circular pipes, 20: 43477 (CONF-661102-1)
steam–H_2O, heat transfer and pressure drop for flow in round vertical tubes, 20: 5623 (EURAEC-1325)
steam–H_2O, heat transfer and hydrodynamics in mixtures of, 20: 6566(R) (EURAEC-1382)
steam–H_2O, mixing methods for, development of, 17: 1115(R) (EURAEC-48)
steam–H_2O, momentum flux measurement by impulse method for flow of, 20: 5624 (MIT-3496-1)
steam–H_2O, phase and velocity distribution in vertical upflow in round tubes, (E), 20: 7227 (EURAEC-1283)
steam–H_2O, phase velocity distribution for flowing systems of, 20: 18874
steam–H_2O, power-to-void transfer functions in BWR, (E/T), 20: 8344 (ANL-7041)
steam–H_2O, pressure drop in natural-circulation single-component flow at low pressures, 20: 2021
steam–H_2O, research program on mixing and separation, 17: 15389(R) (EURAEC-46)
steam–H_2O, research programs on separation of, 17: 14414(R) (ACNP-62033)
steam–water, critical flow tests for, 17: 1148 (HW-69488)
steam–H_2O, separator design for, 17: 42389(P)
steam-H_2O, separator testing for, 20: 35033
steam–H_2O, separator development for, radial-vane, 20: 10291(R) (GEAP-4967)
steam–H_2O, sound propagation in, speed of, 20: 35614 (AEEW-M-452)
steam–H_2O, specific gravity in boilers, 17: 6378
steam–H_2O, void fraction measurement using acoustic methods, 20: 20187 (EURAEC-1361)
steam–water, analysis of boiling convection channel flows of, (E), 19: 46538(R) (TID-22148)
steam–water, analytical model for critical flow of, (T), 19: 36620
steam–water, behavior of, in low-pressure critical discharge from constant area pipes, 16: 8870 (HW-68934(Rev.))
steam–water, behavior of, under fog flow conditions, droplet diffusion model for predicting, 16: 19991(R) (NDA-2169-2)
steam–water, boiling burnout, review, 19: 2518
steam–water, boiling heat transfer in upward flow in tubes, CAN-2-experimental data on, 19: 6069 (EURAEC-1084)
steam–water, boiling in coiled tubes, departure from nucleate, 18: 37348 (TID-20983)
steam–water, burnout and pressure drops in flow of, in round tubes, 16: 23816 (EURAEC-42)
steam–water, burnout heat flux and flow dynamics in, 16: 13237
steam–water, burnout heat flux in annulus, 18: 33730 (AERE-R-4352)
steam–water, burnout heat fluxes in forced flow of, 18: 37330 (A/CONF.28/P/327a)
steam–water, burnout in annular flow, effects of test section geometry on, 19: 9323 (AERE-R-3961)
steam–water, corrosive effects of, on stainless steel and Zircaloy-2 at 245 to 287°C at flows of 266 to 553 g/cm²/sec, 16: 7853 (EURAEC-151)
steam–water, corrosive effects on Zircaloy-2, 18: 8476(R) (EURAEC-830)
steam–water, corrosive effects on Zircaloy-2 tubes, 18: 37636 (A/CONF.28/P/574)
steam–water, corrosive effects on stainless steel and Zircaloy-2 claddings at 2000°F, 19: 7862 (APED-4413)
steam–water, corrosive effects on high-purity and industrial 18-10 stainless steels, 19: 11690(R) (EURAEC-1213)
steam–water, corrosive effects on stainless steel, 19: 24997
steam–water, corrosive effects on chromium-nickel and stainless steels, 19: 34644
steam–water, critical discharge from pipe elbows and tees, 19: 22475 (BNWL-34)
steam–water, critical flow through short tubes, 17: 37332 (HW-77594)
steam–water, critical flow from pipe at high upstream pressures, 18: 29838 (HW-80535)
steam–water, critical flow through short pipes, choking in, 19: 32377 (CONF-640507(p.479-81))
steam–water, critical flow in blowdown of tanks, analysis, 19: 38083

(WAPD-T-1791)
steam–water, critical heat load in tubes, effects of tube diameter on, 18: 8489(T) (AEC-tr-6287)
steam–water, critical heat fluxes for flow of, in circular channels at 100 to 180 atm, 18: 22224(T) (AEC-tr-6393)
steam–water, critical heat flux in forced-convective high-quality flow in tubes and roughened annuli, 19: 13574 (AECL-2109)
steam–water, critical heat flux and film thickness in, 19: 30369 (APPE-24)
steam–water, critical mass velocity in, comparison of results with homogeneous- and separated-flow models, 16: 31792 (HW-65739)
steam–water, density of, use of neutron source for measurement of, 16: 13273 (AERE-EL/M-97)
steam–water, design of separator device for, 16: 11814 (GEAP-3787)
steam–water, development for use as reactor coolant, 17: 40267(R) (EURAEC-750)
steam–water, discharge of critical, from pipes, 16: 835
steam–water, effect of pipe and entrance properties on flow rates of, 20: 41107
steam–water, effects of flow rate and pressure on burnout heat fluxes in cylindrical tubes, 18: 14043
steam–water-d_s, electric conductivity of, impedance void meter for (E), 19: 3641 (HPR-35(Vol.I)(Sect.9))
steam–water, expansion of very low quality steam through nozzles, 16: 14882 (UCRL-6152)
steam–water, expansion process through de Laval nozzle, models for, 16: 14883 (UCRL-6230)
steam–water, film boiling in heated tubes, 18: 6928(T) (AEC-tr-6252)
steam–water, flow and heat transfer properties, 19: 588 (TID-21221 (p.7-86))
steam–water, flow and heat transfer in experimental loops, 19: 11348(R) (EURAEC-1219)
steam–water, flow during metastable conditions, critical, 18: 1849(R) (TID-19493(Sect.3))
steam–water, flow in BWR, (T), 19: 42624
steam–water, flow in forced-circulation boiler tubes, review, 19: 26507
steam–water, flow in riser channel, true steam content in natural, 18: 27660(T) (AEC-tr-6402)
steam–water, flow in vertical tubes, pressure drops in, 18: 20164 (EURAEC-1004)
steam–water, flow of, adiabatic two-phase, 16: 17804
steam–water, flow of, holdup vapor fractions in two-phase countercurrent, 18: 8482 (KAPL-2295)
steam–water, flow of, in elbows, pressure drop in, 16: 19046 (HW-SA-2564)
steam–water, flow of, in overexpanded nozzles, shock effects in, 16: 7663 (UCRL-6676)
steam–water, flow of, in pipes, analyses of, 16: 4277(T) (AEC-tr-4496)
steam–water, flow of, slip ratios at high void fractions, 18: 1848(R) (TID-19493(Sect.2))
steam–water, flow of, through aperture, 16: 20615
steam–water, flow of, analysis using turbine flowmeters (E/T), 19: 22478 (CONF-640607(Vol.II)(Paper D-6))
steam–water, flow parameter correlation in annular flow of, 19: 15718(R) (NYO-3114-5)
steam–water, flow past fuel cylinders, vibrations in axial, 19: 18106 (AECL-2225)
steam–water, flow pressure drop across thick plate restrictions in, 18: 25665
steam–water, flow through apertures, 17: 35990(R) (TID-19326)
steam–water, flow with liquid entrainment in circular pipes, (T), 20: 28056
steam–water, fluid flow and heat transfer in high-pressure, 16: 18624
steam–water, fluid flow in simulated, 16: 8869 (EURAEC-150)
steam–water, fluid flow and heat transfer properties in circular tubes, 19: 1875(R) (EURAEC-1011)
steam–water heat transfer by, 16: 14327
steam–water, heat transfer by, design of facility for studies on, 16: 8867 (EURAEC-41)
steam–water, heat transfer by, in round tubes, 16: 25530(T) (EURAEC-42)
steam–water, heat transfer properties, 16: 2690(T) (TT-985)
steam–water, heat transfer properties, 16: 26603(T,R) (EURAEC-36)
steam–water, heat transfer properties, 16: 26604(T,R) (EURAEC-38)
steam–water, heat transfer properties, 16: 34082(T,R) (EURAEC-40)
steam–water, heat transfer by, 17: 21872 (CISE-R-62)
steam–water, heat transfer of, in round vertical tubes, 17: 32244 (EURAEC-637)
steam–water, heat transfer to, flowing in round vertical tubes with non-uniform axial power distribution, 17: 32245 (EURAEC-671)
steam–water, heat transfer by, 17: 34092(R) (EURAEC-299)
steam–water, heat transfer, 18: 8476(R) (EURAEC-830)
steam–water, heat transfer experiments on, equipment for, 18: 8478 (EURAEC-862)
steam–water, heat transfer and pressure drop in sprays of, 18: 14025 (EURAEC-153)
steam–water, heat transfer to, flowing in heated tube, 18: 16171 (EURAEC-929)
steam–water, heat transfer in flows through pipes, 18: 24910(R) (SRO-101)
steam–water, heat transfer properties in circular tubes, 18: 28932(R) (EURAEC-1013)
steam–water, heat transfer crisis in, 18: 29853
steam–water, heat transfer from fuel assembly to, 18: 37324 (A/CONF.28/P/16)
steam–water, heat transfer parameters of channel flows of, 19: 590
steam–water, heat transfer crisis in forced convection, review of experimental studies of, 19: 15715 (EURAEC-1085)
steam–water, heat transfer crisis in, 19: 18123
steam–water, heat transfer, from rod cluster type fuel elements to, 19: 22473 (AERE-R-3960)
steam–water, instabilities in two-phase flow of, 17: 34088 (AERE-M-1105)
steam–water, interfaces of, detection using ultrasonic instruments, (E), 19: 24013 (CONF-640607(Vol.I)(Paper A-14))
steam–water, kinetics of mixing and separation, 16: 17799(R) (EURAEC-209)
steam–water, liquid film breakdown in annular two-phase flow, 19: 28509
steam–water, moisture separation in, 16: 1921
steam–water, performance in reactor spray cooling, 18: 17999(R) (EURAEC-923)
steam–water, phase composition in heated pipes, 18: 12320
steam–water, pressure drop in vertical heated and unheated annuli for forced convective flow, 16: 25519 (AERE-R-3808)
steam–water, pressure drop in forced boiling flow, 18: 33745
steam–water, pressure drop in two-phase flow of, 19: 32376 (CONF-640507(p.459-78))
steam–water, pressure drop in two-phase flow through piping components, 19: 32378 (CONF-640507(p.483-7))
steam–water, pressure gradients in critical flow of, theory for predicting, 17: 39247
steam–water, pressure pulsations in heat transfer by, 20: 43478(R) (EURAEC-1620)
steam–water, properties of, for use as reactor coolant, 16: 3398(R) (EURAEC-332)
steam–water, properties as reactor coolant, 19: 25672(P)
steam–water, separation of water entrainment from, efficiency of screens for, 16: 26470 (KAPL-2000-18)
steam–water, separator development for, (E), 19: 4330 (SAN-8003 (p.190-9))
steam–water, slip ratio of, at 212°F, 20: 43482 (ORNL-TM-1519)
steam–water, slug-annular flow regime, transition at high pressures, 18: 17997 (ANL-6796)
steam–water, sound velocity in two-phase flows of, (E), 19: 13586(T) (WAPD-Trans-15)
steam–water, steam volume fractions in flowing and static (E), 19: 3579
steam–water, theoretical model for predicting maximum flow rate of, 18: 41623
steam–water, thermal conductivity of, during evaporation in horizontal tubes, 16: 13227
steam–water, thermal conductivity characteristics of, flowing in annulus, 16: 13238
steam–water, two-phase critical flow model, use in calculations for liquid metal systems, 18: 6921 (ANL-6779)
steam–water, two-phase critical flow rates, comparison of calculated and observed, 18: 8480 (GEAP-4395)
steam–water, two-phase critical flow in annuli, 17: 16239
steam-water, two-phase expansion through convergent-divergent nozzle, 18: 25662
steam–water, two-phase flow through apertures, 18: 27652 (COO-926-31)
steam–water, two-phase pressure drop in piping components, 18: 35689 (HW-80970(Rev.1))
steam–water, two-phase flow at 600 to 1400 psia in pipes and channels, pressure drop, 18: 41614 (GEAP-4616)
steam–water, two-phase pressure drop across contractions and expansions, 18: 41615 (GEAP-4622)
steam–water, two-phase flow of, heat transfer and hydrodynamic studies, 19: 32358 (CONF-640507(p.79-87))
steam–water, two-phase vessel blowdown from pipes, theory, 19: 38802 (APED-4827)
steam–water, two-phase flow at 1200 psig, orifice and venturi measurements of, 19: 46526 (AECL-2273)
steam–water, vapor volume fractions in vertical flow in duct, 19: 11344(R) (ACNP-64029)
steam–water, vaporization of, during flow, growing-bubble model for,

16: 16504(R) (TID-15429)
steam–water, velocity of rising steam in, 16: 24510
steam–water, void fraction measurements in, by gamma attenuation techniques, 17: 32241(R) (ACNP-63020)
steam–water, void fractions in, instruments for measuring, (E), 19: 24071 (CONF-640607(Vol.II)(Paper D-8))
steam–water, void fraction measurement by x-ray attenuation in two-phase flow of, 19: 40745
Steam-cooled Reactors
see Water Cooled Reactors
STEAM ENGINEERING
book: *Thermal Power Engineering for Nuclear Installations*, 16: 26605(T) (FTD-TT-61-241)
cycle optimization for large sodium-graphite nuclear power plants, 18: 40840 (NAA-SR-9488)
cycle optimization for large sodium-cooled nuclear power plants, 19: 5489 (TID-21292)
cycle optimization for 350 to 400-Mw(e) sodium graphite reactors, 20: 1514
design and development of radial-vane steam separators, 17: 31729 (GEAP-4272)
design and development of radial-vane steam separators, 19: 6026(R) (GEAP-4728)
design and development of radial vane steam separator, 19: 45574(R) (GEAP-4914)
development of mercury-steam binary cycles for sodium-cooled power reactors, feasibility of, 17: 31737 (WCAP-1832)
dual-pressure steam cycle analysis, 17: 29038 (DEG-Report-201)
forced convection boiling studies, 16: 13211 (TID-14632)
potassium-steam binary vapor cycle for molten-salt nuclear power plant, 18: 40869 (ORNL-3584)
separation device development for integral boiler-superheater nuclear reactor, 16: 4238 (CEND-136)
specification guides at HAPO for, 18: 3922 (TID-15245(Rev.))
specification guides at HAPO for, 18: 3923 (TID-15246(Vol.I)(Rev.))
steam-cycle performance, influence on nuclear power costs, 17: 33356
testing of gravity steam separators, 16: 3938 (CEND-127)
thermal cycle for gas-cooled reactors, 16: 15941
translation of *Heat Power Engineering, Part I*, USSR, 1959, 16: 4277(T) (AEC-tr-4496)
void distribution measurements in vertical two-phase flow using gamma beam, equipment for, 17: 30660(R) (GEAP-4275)
Steam Engines
see External Combustion Engines
STEAM GENERATING HEAVY WATER MODERATED REACTOR
description, 18: 19391
description, 20: 5163
design, 20: 5142
design and development, 19: 40205
design and development, 20: 45173
design and development of 100-Mw(e), 18: 38412 (A/CONF.28/P/129)
design and development of 100-Mw(e), 18: 38418 (A/CONF.28/P/143)
development, 20: 26479
development of 100-Mw(e), at Winfrith, 18: 31011
fuel burnup in, plutonium, 19: 45578 (JAERI-1080)
fuel cycle for, analysis of, 20: 45180
fuel elements for, design and development of, 20: 36479 (KR-89, pp 265-89)
fuel management in, 19: 29656
fuel management in, 20: 10409
pressure vessel fabrication for, 19: 33636
safety of, computer model for studying, 19: 40214
Steam Generators
see Boilers
STEAM POWER PLANTS
accidents in, arrangement for preventing pressure buildup in steam-releasing, 17: 28550(P)
book: *The Principles of Power Generation*, 19: 22498(T)
coolant systems in, failures in, 18: 11466
defense of coal-fired, against nuclear attack, comparison with nuclear plants, 17: 7656 (BNL-6080)
design and cost of fossil-fueled, forecast of trends in, 17: 32214
design and performance of 15,000-hp compact, 16: 20558 (AD-269397)
design for indirect reactor steam generators, 18: 26951(P)
design of liquid metal-heated, fossil fuel-fired, 17: 5627
design of marine, 17: 30656(P)
design of superheated, 17: 31746(P)
design of superheated, 19: 24687(P)
design using liquid-metal cooled reactor, 20: 42657(P)
development of compact military, 19: 11368
development of thermionic-converter toppers for turbines, for increased efficiency, 18: 14795
dynamic analysis of recirculation loop in, for study of water level control, 19: 34328 (WCAP-3269-10)
economics of combined desalination–electric-power-producing, (E), 19: 10551 (NYO-3316-1)
economics of fossil-fuel, of 300–1500 Mw, 20: 45242 (TID-22978(Rev.))
economics of, in sea water desalination plants, 20: 22461
efficiency and economy of, development of, 17: 5628
efficiency of, combined with MHD generator, 19: 12138
failures in piping systems, review of service, 17: 23568
feasibility for lunar base operation, 19: 3611 (ASTRA-G-39.2)
materials development for, 18: 26946
nozzle design for superheated, 17: 31747(P)
operation of, using fossil or nuclear fuel, 17: 19664(P)
operation with nuclear plants, economics of integrated, 20: 35092
performance compared to nuclear power plants, 18: 19388
performance with electric thrusters for space propulsion, 20: 5639
pipe weld inspection at New Zealand geothermal, using gamma radiography, 19: 597
proposal for, as addition to NPR, 17: 10123
thermal efficiency of, compared with magnetohydrodynamic generators, 17: 9082
transmissions for, hydrokinetic, 16: 22282 (AD-269395)
use in electric propulsion systems for space, 19: 3714 (ASTRA-G-41.3)
welding in, 16: 2154
STEARATES
(Salts of stearic acid)
see also Aluminum Sterates
see also Barium Stearates
see also Calcium Stearates
see also Cesium Stearates
see also Lead Stearates
see also Rubidium Stearates
see also Sodium Stearates
hydrogenation, 16: 28670(R) (UCLA-507)
use as coating in aluminum bonding, 18: 19503(P)
uses in preparation of multilayer membrane electrodes, 18: 5275
stearate–stearic acid, labeling with calcium-45, barium-140, and lanthanum-140, 20: 43238
stearate–stearic acid, reactions with barium, calcium, and lanthanum ions, effects of pH on, 20: 43238
STEARIC ACID
chromatography of tritiated, use of windowless gas-flow counter for detecting weak beta activity in, 18: 35862
desorption from metal surfaces by low-energy ions, 16: 19464 (ARL-62-305)
determination in commercial coconut oils, gas chromatographic, 20: 14463 (PAEC(D)CH-652)
effects on iodination of bovine serum albumin, 18: 11596
etching of lithium fluoride crystals by, adsorption-locking and Rebinder effect in, 16: 20437
labeling with carbon-14, 20: 8977
metabolism, tracer study, 16: 28670(R) (UCLA-507)
preparation of tritiated, by uv-induced exchange, 16: 1819
properties of monolayers of, on water and heavy water at 15, 25, and 37°C, 20: 26886
protective effects against uranium corrosion by moist air, 19: 30655(R) (UCRL-13094)
radiation effects on aerosols of, 17: 3026(R) (TID-17250)
radiation effects on discoloration of, effects of amino acids on, 17: 14341
radiation effects on uptake of, by lipids in human bone marrow, 18: 19552(R) (NYO-2769-1)
radioinduced emanation from, holdup time of, (E), 20: 6298(R) (PPAD-2137-566)
radioinduced inclusions in compound with urea, 16: 3047
radiolysis of aqueous solutions of, mechanism of oxidation in, 19: 13477
radiolysis of, formation of carbonyls by gamma and ultraviolet, 17: 21748
reactions with oxalyl chloride to prepare acyl chloride, 19: 32197
separation from lauric and myristic acids by reversed-phase chromatography using polymerized cellulose, 18: 16145
solvent properties for metals and fission products, 17: 21789
sorption by copper, gold, and iron films from hexadecane solution, 17: 6078
spectra of carbon-14-labeled, infrared, 19: 5938
use as grinding aid in producing very fine uranium carbide particles, 19: 20513(R) (NCSC-2981-3)
use of carbon-14-labeled, for surface area measurements of powders, 16: 5380
stearate–stearic acid, labeling with calcium-45, barium-140, and lanthanum-140, 20: 43238
stearate–stearic acid, reactions with barium, calcium, and lanthanum ions, effects of pH on, 20: 43238
stearic acid–TBP–H_2O, effect of hydrogen bonding on uranium distribution in, 20: 18845

STEARIC ACID, ETHYL ESTER
protective effects against lethal irradiation in mice, 17: 27156
protective effects of injected, against radiation injuries in mice, 18: 25217
STEARIC ACID, METHYL ESTER
chromatography of labeled, tritium isotope effects in, 19: 13242
labeling with tritium, 20: 23002
protective effects of, against radiation injury in gonads of male mice, 16: 20285
radiolysis and storage of tritium-labeled, self-, 20: 1938 (EUR-2452.e)
radiolysis of clathrates containing tritium-labeled, self-, 19: 46359
radiolysis of tritium-labeled, by self-irradiation during storage, 18: 43693
radiolysis of tritium-labeled, self-, 19: 46360
separation of labeled, tritium–carbon-14 isotope effects in chromatographic, 20: 43394
spectra of carbon-14-labeled, infrared, 19: 5938
STEARIC ACID, VINYL ESTER
crystal structure, 17: 3027(R) (TID-17273)
radioinduced polymerization of single crystals of, 19: 36476
structure, 18: 272(R) (TID-19484)
STEARIC ACID, VINYL ESTER POLYMERS
crystal structure, 19: 36476
preparation of, by irradiation of crystalline vinyl stearate, 16: 31365
radioinduced crosslinking with polyvinyl chloride, 16: 1820
structure, 18: 272(R) (TID-19484)
STEATITES
development and properties as construction material, 19: 16039
electric properties, 18: 26058
frictional properties, 17: 8818 (UCRL-13052)
radiation effects on thermal properties, 18: 22529(R) (ORNL-3591 (p.147-55))
radiation effects on, neutron, 19: 30828(R) (ORNL-3789(p.230-8))
STEEL
see also Aluminum Steel
see also Austenite
see also Boron Steel
see also Carbon Steel
see also Chromium Steel
see also Cobalt Steel
see also Manganese Steel
see also Martensites
see also Molybdenum Steel
see also Nickel Steel
see also Niobium Steel
see also Silicon Steel
see also Stainless Steel
see also Titanium Steel
see also Tungsten Steel
see also Uranium Steel
see also Vanadium Steel
acoustic properties of 4340, 18: 31842(R) (NYO-2910-4)
adhesion to ethylene propylene rubber, 16: 16707(R) (AD-265319)
aging, 17: 3466 (ASD-TR-61-351)
aluminum distribution in, tracer studies of, 18: 14297(T) (NP-tr-1109)
analysis by x-ray fluorescence, 18: 25275
analysis by x-ray fluorescence using promethium-147/aluminum source, 20: 3883 (ORNL-IIC-5, pp 154-81)
analysis for alloying elements, polarographic, 17: 28797 (AEET/ANAL/8)
analysis for aluminum, spectrophotometric, 17: 32028
analysis for aluminum, computer use for activation, 20: 16335(R) (NBS-TN-276)
analysis for arsenic, cobalt, and manganese, neutron activation, 16: 20330
analysis for arsenic in lead-free, spectrographic, 16: 23597 (AERE-R-3974)
analysis for arsenic, cerium, and lanthanum, use of radioisotopes for, 17: 33822
analysis for boron traces, isotopic dilution, 16: 18826
analysis for boron using neutron activation depression by boron-10, 19: 5776 (SGAE-IB/IA-5/1964)
analysis for boron using predispersive spectrometer, spectrographic, 20: 22864 (CEA-R-2914)
analysis for boron, spectrographic, 20: 33158 (Y-1543)
analysis for boron, carbon, nitrogen, and oxygen, x-ray spectrochemical method for, 20: 43161
analysis for carbon, activation, 17: 35663
analysis for carbon traces, method for, 18: 17732(T) (CEA-tr-X-537)
analysis for carbon using activation methods, 19: 7316
analysis for carbon by measuring prompt gammas following deuteron bombardment, 19: 34116
analysis for carbon by gamma spectroscopy, 20: 3894
analysis for carbon, activation, 20: 16331 (GA-6568)
analysis for cerium, 17: 25141
analysis for cerium, lanthanum, neodymium, and praseodymium, spectrophotometric, 17: 25142
analysis for cerium, nephelometric, 18: 37103
analysis for cerium by anion exchange separation and titration, 19: 7282
analysis for cerium by potentiometric titration, 19: 13237
analysis for cerium, photometric, 20: 16380
analysis for chromium, molybdenum, niobium, and tungsten, rapid method for, 19: 17844
analysis for cobalt, activation, 18: 13676
analysis for cobalt by activation methods, 19: 19784
analysis for cobalt by x-ray spectrography using direct electron excitation, 20: 26755
analysis for cobalt, effects of ions on gravimetric, 20: 43145
analysis for copper, activation, 19: 10985(T) (AEC-tr-6227/3(p.193-200))
analysis for impurities, spectrographic, 20: 3863(R) (IS-1200(Sect. C))
analysis for impurities, activation, 20: 22940
analysis for lanthanum, activation, 17: 25519(T) (AEC-tr-5824)
analysis for lead and molybdenum by x-ray fluorescence methods, 20: 20642
analysis for molybdenum and tin using 8-quinolinol, spectrophotometric, 16: 16314
analysis for molybdenum by extraction using 6,7-dihydroxy-2,4-diphenylbenzopyrylium chloride, photometric, 16: 1717
analysis for molybdenum and tungsten, x-ray spectrochemical, 17: 5997
analysis for molybdenum, activation, 18: 8265 (AE-128)
analysis for niobium, chromatographic, 16: 12801(R) (IA-685)
analysis for niobium, spectrophotometric, 16: 16315
analysis for niobium, spectrophotometric, 18: 35479
analysis for niobium and tantalum by neutron activation, 19: 24420
analysis for niobium by neutron activation, 19: 43942
analysis for nitrogen, design of modified Kjeldahl apparatus for, 16: 8682 (TID-11411)
analysis for nitrogen and oxygen, 18: 1489(R) (IS-700(Sect.C))
analysis for nitrogen and oxygen, development of methods for, 19: 9046(R) (IS-900(Sect.C))
analysis for nitrogen and oxygen by d-c carbon-arc, gas chromatographic technique, 19: 9069
analysis for nitrogen by vacuum extraction and fusion, review on, 19: 22109
analysis for nitrogen, 19: 22230
analysis for nitrogen by isotope dilution method, comparison with vacuum fusion method, 19: 26246
analysis for oxygen, fast-neutron activation, 16: 26914
analysis for oxygen, activation, 17: 36209
analysis for oxygen, activation, 18: 25304
analysis for oxygen, design of equipment for activation, 18: 29595
analysis for oxygen, activation, 19: 7311
analysis for oxygen by isotope dilution, comparison with vacuum fusion method, 19: 26245
analysis for oxygen using 14-Mev neutrons, nondestructive method for, 19: 30103
analysis for oxygen by isotope dilution method, 19: 43946
analysis for oxygen, comparison of activation and vacuum fusion methods for, 20: 8831 (NP-15634)
analysis for oxygen, activation, 20: 10771
analysis for oxygen, comparison of hot-extraction and activation, 20: 16400
analysis for oxygen, activation, 20: 16357
analysis for oxygen by neutron activation methods, 20: 26774
analysis for oxygen, activation, 20: 29138
analysis for oxygen by neutron activation, 20: 33154 (NLCO-979)
analysis for oxygen by activation methods, 20: 35460
analysis for oxygen, instrument for neutron activation methods of, 20: 43160
analysis for radioisotopes in mass transfer samples, methods for, 20: 12766 (GEAP-4178)
analysis for rare earths and yttrium in cast, spectrophotometric, 16: 17602
analysis for rare earths, 19: 40445
analysis for rare earth inclusions, procedure for, 20: 41415
analysis for silicon by activation methods using 14-Mev neutrons, 19: 43965
analysis for thorium using Arsenazo III, spectrophotometric, 19: 15393
analysis for tin traces, activation, 18: 21963
analysis for titanium, photometric, 16: 22040
analysis for trace amounts of cobalt by x-ray spectrography, 19: 38571
analysis for tungsten by isotope dilution, 16: 11562
analysis for tungsten, activation, 17: 12209
analysis for tungsten, x-ray fluorescence, 19: 5825
analysis for tungsten, radiometric, 19: 7333
analysis for tungsten by gamma-excited x-ray fluorescence, 19: 24477
analysis for tungsten by backscattering of beta particles, 19: 28234

analysis for uranium, radiometric, 16: 12951 (NP-11585)
analysis for uranium, methods for, 16: 23604 (NP-11873)
analysis for uranium by ion exchange-photometric method, 17: 2906 (WAL-TR-823/3)
analysis for uranium, summary of methods for, 18: 1503 (NP-13261 (p.259-96))
analysis for uranium, using anion exchange separation, 19: 7620(R) (TID-21411)
analysis for uranium, photometric, 19: 17813
analysis for vanadium, thermal neutron activation, 17: 35647
analysis for yttrium by solution spectrographic method, 20: 266
analysis for zirconium, photometric, 17: 35653
analysis for zirconium using p-iodoamygdalic acid, gravimetric, 18: 17749
analysis for zirconium using arsenazo III, photometric, 18: 27343
analysis for zirconium, photometric, 19: 17812
analysis of, chemical and spectrographic, 17: 1392(T) (CEA-tr-X-457)
analysis of high-alloy, for cerium, photometric, 20: 43143
analysis of irradiated, for activation products, by ion-exchange separation and gamma spectrometry, 19: 46195
analysis of old Damascus sword for trace elements, activation, 19: 15346 (IS-1105)
analysis of rods of, for oxygen, by neutron-activation and vacuum-fusion techniques, 20: 29088
analysis of segregation in, use of beta sources for, 16: 30350
analysis of, for cerium and vanadium, differential amperometric, 20: 33246
analysis of, for oxygen, equipment used in activation methods for, 20: 40848
analysis of, use of activation methods for, 18: 29577
analysis of, use of cerium-141 and sulfur-35 for macroradiographic and radiometric, 19: 22833
analysis of, using radioisotope portable analyzer, 20: 20642
annealing effects on SOUDOMETAL-56, 17: 14750(T,R) (EURAEC-459)
annealing effects on radioinduced embrittlement of, 20: 25474(R) (BNL-954, pp 122-67)
annealing of ingots of, electron beam for strip, 17: 32822
annealing of, use of Mössbauer effect in studying, 18: 10256
attenuation of secondaries produced in proton reactions with beryllium at 10 and 19.2 Bev/c, (E), 19: 14739
autoradiography to distinguish carbides from matrix, 16: 15045 (NYO-9858)
bend tests on 100mm-thick types A, 11A, 13C, 15A, 21A, 23A, 27A, and 32A, 17: 39509(T,R) (EURAEC-615)
bibliography, 16: 19248 (NP-11628)
bibliography on, Defense Metals Information Center selected accessions, January 1963, 17: 14739 (NP-12525)
bibliography on, DMIC selected accessions, Sept. 1962, 17: 419 (NP-12170)
bibliography on, DMIC accessions, May 1963, 17: 29246 (AD-407822)
bibliography on maraging, 19: 16004 (UCRL-12223)
bonding to lead, methods for, 18: 32953
bonding to tantalum–tungsten alloy by explosive techniques, 19: 11711
bonding to Zircaloy by extrusion, 16: 9169 (NMI-4771)
bonding to Zircaloy-2, hot-swaging method for diffusion, 20: 27456
book: *Applications of Radioactive Isotopes in Steel Ingot Structure Studies*, 17: 41185
book: *Machining Difficult Alloys*, 17: 6608
book: *Radiation Effects on Toughness of Ferritic Steels for Reactor Vessels*, 18: 40035
boridizing for reactor reactivity control during down-time, 19: 34639(R) (BNWL-79(p.5.1-11))
braze cladding titanium and zirconium on, technique for vacuum-pressure, 18: 7177
brazed joints, nondestructive testing of, 19: 13935 (ANL-6924)
brazing and welding properties, review, 16: 10424 (ASD-TR-61-322 (p.661-76))
brazing of, to beryllium, 17: 3441 (ERR-FW-043)
brazing, plating, ultrasonic testing, and welding of, used for reactor components, 17: 33260
brittle failure in welded joints in, effects of symmetry on, 20: 9441(R) (EURAEC-1352)
brittle fracture, 16: 3491
brittle fracture, bibliography, 16: 10530 (HW-71794)
brittle fracture, equipment and method for testing, 16: 8980
brittle fracture of, tests for estimating crack propagation transition temperature of, 17: 22203
brittle fracture of mild, effects of residual stresses on, 19: 32048(R) (NP-15073)
brittle fracture propagation in, 18: 4243(R) (EURAEC-613)
brittle fracture propagation in, running, 18: 16470(R) (EURAEC-913)
brittle fracture propagation in pressure vessel, 18: 37678 (A/CONF.28/P/727)
brittle fracture propagation in pressure vessel, 18: 44134(R) (EURAEC-1101)
brittle fracture properties of, bend test to measure effects of welding on, 20: 11240(R) (EURAEC-1520)
brittle fracture properties of, effects of weld distribution and size on, 20: 11240(R) (EURAEC-1520)
brittle fractures in, review of, 17: 37520(T) (TRG-Inf-Ser-88)
brittle transition temperature determination for, 17: 8803(R) (EURAEC-398)
brittle-ductile transition measurement in, stress wave attenuation method for, 19: 9656(R) (EURAEC-1284)
brittleness, effects of crystalline fracture, 16: 531(T) (DEG-Inf-Ser-107)
brittleness in, during time-to-rupture tests, theory of notch-, 20: 25563 (EURAEC-1350)
broaching of high-strength, tool design for, 17: 6621
broaching of type 4340, 17: 6622
carbon content of mild, effects of radiation and strain aging on, 17: 27909
carbon content optimization in heat-treated, method for, 18: 43135 (TID-21143)
carbon deposition on mild, from gases, 20: 28742(R) (GA-6418)
carbon deposition on, mechanism of, 20: 45114(R) (NP-16272)
carburization of, effects of impurities on vacuum, 20: 41412(R) (IS-1500 (Sect. M))
casting, 17: 4910(R) (MAB-139-M(C7))
casting of, for study of brittleness, 17: 547(T,R) (EURAEC-340)
casting of, radiometric level control in continuous, 20: 43761
casting of, use of gamma radiation in control of, 17: 326
cathodic protection of submerged and underground, use of depleted uranium for, 17: 36191 (BM-RI-6285)
caustic embrittlement of, in boiler plates, 18: 23148(T) (AEC-tr-6389)
cavitation by bismuth, lead, and mercury, 16: 13537
cavitation by bismuth, lead, and mercury, 16: 33434(T) (AEC-tr-5382)
cavitation damage of 1020 mild, correlation with mechanical properties, 19: 2714 (AD-606050)
cesium ion deposition on, under oxidizing conditions, 18: 5747
chloride ion deposition on, under oxidizing conditions, 18: 5747
cladding very thick, with stainless steel, 19: 40979(R) (EURAEC-1351)
cladding with stainless steel of heavy-gage, study of welding method for, 20: 43852 (EURAEC-1685)
classification of, for use in nuclear industry, 20: 33895
coating by plasma-sprayed tungsten, fusion-bonding of, 20: 11242 (UCRL-12153)
coating heavy-gage low-alloy, process for stainless steel weld, 19: 36998(R) (EURAEC-1296)
coating of plate, with stainless steel, 16: 26654 (ACCESS-134)
coating of, specifications for use of vinyl materials in, 17: 22100 (TID-18523)
coating thickness of tin on sheets of, x-ray-fluorescence method for measuring, 19: 28743
coating thickness of gold on, use of proton beam scattering for measuring, 20: 21246
coating with cadmium by sputtering, 17: 25747 (SCDR-82-63)
coating with carbide for protection against liquid metal corrosion, 16: 13526(P)
coating with carbon from carbon monoxide, 20: 31670
coating with ceramics, radiometric method for measuring thickness, 16: 503(T) (CEA-tr-R-1394)
coating with chromium containing ceramic dispersions, electrolytic, 20: 21286 (AD-621920)
coating with epoxy resin in NASA Research Reactor, 16: 14257
coating with lead, method for, 18: 32952
coating with nickel–phosphorus system, for corrosion protection, 17: 12613
coating with stainless steel, methods development for, 19: 20504(R) (EURAEC-1228)
coating with stainless steel by welding, development of methods for, 20: 16990(R) (EURAEC-1556)
coating with stainless steel by welding, development of methods for, 20: 16991(R) (EURAEC-1557)
coating with tin, tracer studies of mechanisms in, 16: 13438(T) (AEC-tr-4492(p.135-9))
coating with uranium oxide by electrolysis, effects of electrolyte on, 20: 18691
coating with zirconium oxide by flame spraying, 16: 4455
coating with zirconium, effects of iodine circulation rate, pressure, and temperature on, 17: 39555
cobalt content in, for reactor uses, 18: 26034
compatibility of AISI 4130, with boron carbide at 750 to 1300°F, 18: 14371 (NAA-SR-8702)
compatibility of coatings of, with plutonium, thorium, and uranium, 17: 8843
composition of austenitic, for improved service in reactor structures, 18: 18309(P)

compressibility of SAE 1010, design of dies for testing, 17: 23462(R) (NYO-10588)
conference on wide, close-tolerance steel sheets, Pacific Palisades, June 27 and 28, 1961, 16: 4507 (ASD-TR-61-7-787a)
cooling transformation characteristics of A302B, 20: 833 (WERL-8844-5)
corrosion, 16: 27589 (BM-RI-5990)
corrosion, 17: 6572 (OTS-61-31480)
corrosion, 18: 22451
corrosion behavior of weldments, 16: 7892 (NP-11196(p.85-8))
corrosion behavior of rust-proof, effects of sodium chloride, 16: 13531(R) (EURAEC-30)
corrosion by acid solutions, effects of uranium addition, 16: 5669 (NP-11171)
corrosion by acids and chloride salts in chemical plants, 16: 20983
corrosion by air, carbon oxides, hydrogen sulfide, and sulfur dioxide to 1200°C, 18: 39844
corrosion by alkali metals, 18: 37634 (A/CONF.28/P/343)
corrosion by ammoniated and pure water at 230 and 315°C, 18: 21706(R) (KR-66)
corrosion by aqueous hydrogen sulfide, 17: 8717
corrosion by aqueous solutions, review, 18: 32081 (A/CONF.28/P/243)
corrosion by bicarbonate solutions, effects of chloride and oxidants, 16: 22558
corrosion by biphenyl vapor, 18: 12314 (IDO-11006)
corrosion by bismuth (liquid), thermoelectric potential effect on, 17: 3421 (BNL-5574)
corrosion by bismuth–lead eutectic, 17: 4906
corrosion by bismuth and tin at 700 to 1000°C, 20: 46963(R) (ANL-7132)
corrosion by boiling water, 18: 37638 (A/CONF.28/P/592)
corrosion by carbon dioxide at 0 to 15 atm and 450 to 500°C, 16: 20986
corrosion by carbon dioxide under pressure, properties of surface films formed during, 17: 29288
corrosion by carbon dioxide, 17: 40341(R) (GNEC-141(Del.))
corrosion by carbon dioxide–carbon monoxide, 18: 37631 (A/CONF.28/P/157)
corrosion by carbon dioxide at 1100 to 1800°F, 19: 20487
corrosion by carbon dioxide at high temperatures, 20: 33821
corrosion by cesium at 400°C, 20: 4337
corrosion by decontaminating solution, stress, 20: 21238 (NP-15928)
corrosion by flowing water at 230°C, 17: 21387(R) (KR-42)
corrosion by gas–oil, hydrogenated terphenyl, and monoisopropylbiphenyl at 330 to 400°C, 20: 25492(T) (AECL-2330, pp 196-217)
corrosion by gases in atmosphere, 16: 12058
corrosion by heavy water, 19: 43603
corrosion by heavy water in Savannah River Components Test Reactor, 20: 29654
corrosion by helium containing oxygen, 17: 38431(R) (GA-2372)
corrosion by impure Santowax, 17: 23891 (NAA-SR-7755)
corrosion by in-pile OMRE coolant, effects on properties, 18: 35937 (NAA-SR-9796)
corrosion by liquid sodium, carbon mass transfer, 16: 22160
corrosion by liquid alkali metals, 17: 6557
corrosion by liquid bismuth alloys, 18: 4193 (BNL-811)
corrosion by liquid sodium, effects of chromium, niobium, oxygen, and titanium on, 18: 14417
corrosion by liquid sodium at 450, 600, and 750°C, effects of composition on, 19: 4629
corrosion by lithium hydroxide at 316°C, 16: 4618(R) (NP-11098(p.47-52))
corrosion by mercury, measurement using tracer techniques, 18: 27336
corrosion by nitric vapors at 375°C, 16: 33071(T,R) (EURAEC-337)
corrosion by polyphenyls at 330 to 400°C, 16: 22547
corrosion by salt spray, measurement of, by x-ray induction method, 20: 19196
corrosion by sea water and water in evaporator environments, review, 20: 43834 (ORNL-TM-1612)
corrosion by simulated boiling-water reactor environment at 546°F, 16: 33439
corrosion by sodium (liquid), carbon mass transfer in, 16: 33436(T) (AEC-tr-5408)
corrosion by sodium at high temperatures, test facilities for, 18: 4197 (MSAR-63-161)
corrosion by sodium, test loops for studies of, 18: 7137 (GEAP-3725)
corrosion by sodium, effects of carbon on, 18: 27891 (NASA-SP-41 (p.61-5))
corrosion by sodium at high temperatures, effects on mechanical properties, 19: 22896(R) (MSAR-65-47)
corrosion by soft water, use of irradiated corn starch for prevention of, 19: 935(P)
corrosion by steam and water, 19: 14767(R) (KR-86)
corrosion by steam at 400°C and water at 300°C, effects of surface treatments on, 20: 5846
corrosion by terphenyls, 16: 22551
corrosion by terphenyl, 18: 13233(R) (BNL-823(p.1-19))
corrosion by uranyl sulfate solutions at 235 and 250°C, in-pile loop experiments on, 17: 34348 (ORNL-3131)
corrosion by vapor and water at high temperatures, 17: 11134 (EURAEC-474)
corrosion by water, corrosion product formation and release, 16: 4490 (AECL-1265(Paper 5))
corrosion by water, effects of chlorine ions and oxygen on stress, 16: 10459(T) (NSF-62-35(2))
corrosion by water at critical parameters, electrochemistry, 16: 22562
corrosion by water at critical parameters, electrochemical, 16: 33435(T) (AEC-tr-5405)
corrosion by water and steam at 300 and 400°C, effects of surface treatment on, 18: 25922(T) (EURAEC-1038)
corrosion by water, effects of pretreatments on, 19: 3806(R) (KR-79)
corrosion by water and steam at high temperatures, dynamic and static studies of, 19: 24936(R) (EURAEC-1308)
corrosion by water at high temperatures, studies, 19: 29808(R) (KR-94)
corrosion by water, radiation effects on aqueous sodium nitrite solutions for inhibition of, 20: 23606(UJV-1453/65)
corrosion cracking of high-strength, 17: 32531
corrosion cracking of, metallographic explanations of stress, 19: 13928
corrosion, effects of surface saturation with aluminum or chromium, 16: 25721(T) (FTD-TT-61-31(p.60-9))
corrosion in HWCTR, 19: 38262 (DP-964)
corrosion in oxygen-containing aqueous media, 17: 16599
corrosion in reactors, 19: 20488
corrosion in water-cooled reactors, 18: 11373
corrosion in water-cooled reactors, problems of, 18: 16445
corrosion, intensiostatic and potentiostatic methods for study of, 16: 19288(T) (HW-tr-36)
corrosion of AISI type 1020, by copper–magnesium chloride system at 600 to 800°C, 20: 31314(R) (ANL-7175, pp 1-41)
corrosion of, alloying effects of uranium on, 18: 2180 (NP-13261(p.207-34))
corrosion of ASTM-A 285 C mild, by terphenyls, 18: 11366 (BNL-7650)
corrosion of austenitic and ferro-perlitic, by liquid sodium at 600 and 700°C, 16: 22561
corrosion of austenitic and ferro-perlitic, by liquid sodium at 600 and 700°C, 16: 33437(T) (AEC-tr-5409)
corrosion of austenitic and ferritic, in pumped sodium systems, 20: 2296
corrosion of austenitic and ferritic, by trichloroethylene, tracer studies of, 20: 29655
corrosion of boilerplate, by steam and water at high temperatures, 19: 7865(R) (EURAEC-1237)
corrosion of, by ammonium and sodium chlorides and sulfates, 17: 22123
corrosion of, by ionized air, 16: 31267 (NP-11754(Vol.I)(Sect.II))
corrosion of, by water, 17: 5656(R) (KR-29)
corrosion of Creusot 1.2 MD07 boilerplate, by steam at 400°C and water at 300°C, 17: 39491(T,R) (EURAEC-704)
corrosion of Creusot 1.2 MD07 boilerplate, by steam at 300 and 400°C and water at 300°C, 18: 10475(T,R) (EURAEC-864)
corrosion of Creusot 1.2 MD07 boilerplate, by steam and water at 300°C, 18: 16442(T,R) (EURAEC-960)
corrosion of ferritic, by sodium (liquid), 18: 2187
corrosion of ferritic, review of aqueous, 19: 16013 (CEA-R-2600)
corrosion of low-alloy 12XM by water, 16: 2138(T) (SCL-T-376)
corrosion of mild, by boiling water, effects of hydrogen and oxygen on, 17: 22113 (KR-39)
corrosion of mild, in HWCTR, 18: 13331 (DP-801)
corrosion of mild, in Heavy Water Components Test Reactor, 19: 16014 (CONF-446-81)
corrosion of mild, by Purex waste solutions, 20: 40476(R) (BNWL-267)
corrosion of nickel-plated, by water and steam, 17: 13878(R) (KR-36)
corrosion of reactor pressure-vessels, 18: 8737
corrosion of soft and low-alloyed, by water at 25 and 360°C, 19: 16019
corrosion of type 410, by liquid bismuth at 600°C, concentrations of chromium and iron in bismuth during, 18: 27886 (NASA-SP-41(p.21-6))
corrosion of 1020, by molten bismuth, static, 19: 32924(R) (ANL-7020 (p.198-225))
corrosion of 12 KhM and 40 by sodium chloride, sulfate, and sulfite, 16: 487(T) (AEC-tr-4666)
corrosion of, beta backscattering for evaluation of, 19: 2751
corrosion of, inhibition effects of pertechnetate ion on, 18: 18323
corrosion of, review, 19: 7868
corrosion-product deposition on, in pressurized water reactors, 16: 1183 (AECL-1265(Paper 7))
corrosion protection, tracer studies of reactions of oil additives with metal, 16: 13427(T) (AEC-tr-4492(p.76-81))
corrosion protection by additives in oils, design of apparatus for studying with tracer techniques, 16: 13431(T) (AEC-tr-4492(p.96-8))
corrosion resistance in acid medium, 17: 16597

cosmic ray reactions with, argon, manganese, and tritium from, 17: 37922
crack arrest tests on reactor pressure vessel, 16: 8978
crack detection by gamma defectoscopy, 16: 19152
crack failure in cylindrical vessels of, effects of pressure and temperature on, 18: 18017
crack fracture, 17: 36303 (TID-17914)
crack growth rate tests for type A-212, 20: 28695(R) (GEAP-5082)
crack initiation in A302B, study of methods for, 19: 904 (SWRI-1228-31)
crack propagation and strength in high-performance, 16: 19335 (ASD-TR-61-207)
crack-propagation resistance, 18: 5769 (AD-290278)
crack propagation in D2 tool, in air, argon, and vacuum, 20: 27576(R) (BNWL-207, pp 4.44-55)
crack propagation in A 302-B, mechanisms of, 20: 35896 (TID-23138)
crack testing of, (E), 19: 22974(R) (EURAEC-1275)
cracking in welded plates, 17: 39508(T,R) (EURAEC-614)
cracking in welded, effects of deposited-metal phase transformation temperatures on, 18: 39858(R) (EURAEC-1117)
creep of, thermodynamics of, 18: 22481(R) (EURAEC-964)
creep properties of Unimach 2 at high temperatures, 16: 3446 (ASD-TR-61-216)
creep rupture and fatigue evaluation of H-11 tool, 18: 29103(R) (APS-5071-R)
creep-rupture properties, 17: 39531(R) (EURAEC-689)
creep rupture properties of welded HT70, in pressure vessels at 500 to 1350°C, 20: 4446
crystal structure, development of micro-furnace for analysis, 17: 340(T,R) (EURAEC-342)
crystal structure of, effects of reactions with high-temperature compressed gas streams, 17: 561
crystal structure and strength of, effects of carbon pairs on, 18: 32150(R) (UCRL-11317(p.150-8))
crystal structure and stress relief of thick-plate, 20: 41450(R) (EURAEC-1684)
crystal structures of ausformed, 20: 31715(R) (UCRL-16658, pp 105-20)
crystallography of martensitic, 18: 20537(T,R) (EURAEC-977)
decarburization effects on properties of ultrahigh-strength, 16: 24152 (DMIC-Memo-154)
decontamination by ultrasonic methods, 17: 15519 (CEA-2209)
decontamination from strontium-90 by detergents, 19: 4421
decontamination from iodine-131, phosphorus-32, and sulfur-35, effects of detergents on, 19: 4422
decontamination from cobalt-60, effects of surface finish on, 19: 4423
decontamination of radioisotope-contaminated, electrolytic surface, 18: 35946
decontamination of, ultrasonic, 20: 16767
decontamination using oxalate--peroxide solutions, surface, 19: 23996(R) (ORNL-3650(p.1-10))
deformation, 17: 3466 (ASD-TR-61-351)
deformation behavior of, effects of interstitial atom-dislocstion interactions on, 17: 25827
deoxidation by rare earths, 19: 22166(T) (JPRS-28849(p.272-8))
deoxidation by rare earth metals, 20: 7529
deposition of stainless steel cladding on 1.2 MD07 A and Soudotenax 56, by welding, 20: 5862(R) (EURAEC-1481)
deposition on aluminum- or zirconium-jacketed fuel elements, 18: 41481(P)
deposition on silver alloy reactor control rods, 20: 9475(P)
design of low-alloy, for reactor pressure vessels, 20: 39444(P)
development and properties for use in reactors, 17: 22106
development and uses of ultra-high-strength, 19: 25039
development as reactor material, 18: 44075
development for reactor pressure vessels, 16: 4539 (NP-11151)
development of ductile high-strength, review, 18: 44158 (UCRL-11588)
development of high-yield-strength ductile, 19: 43997(R) (UCRL-11889)
development of low-alloy ferritic, for high-temperature sodium systems, 20: 9417 (CONF-650620, pp 156-65)
development of low-alloy, for pressure vessels, 20: 21417(P)
development of new, at I. P. Bardin Institute, USSR, 16: 3497
development of plates of, for nuclear power plants, 19: 38196(T) (NSJ-37)
development of radiation-resistant, with rare earth content, 18: 12573(P)
development of ultrahigh-strength, by nucleation of precipitates, 17: 35264(R) (UCRL-10706(p.111-203))
developments in high-temperature, 16: 27641(T) (FTD-TT-62-503)
diffusion of carbon from ferritic, to austenitic stainless steel, 17: 33323(R) (ORNL-3445(p.199-217))
diffusion of chromium in, effects of carbon content, 16: 24199
diffusion of gold at 950 to 1370°C in, use as tracer in wear measurements, 19: 32753
diffusion of helium through tubes of, 18: 39920
diffusion of hydrogen in proton-irradiated mild, at room temperature, 16: 22783
diffusion of hydrogen in, method for measurement of parameters of, 17: 1966
diffusion of hydrogen in, 18: 28034
dislocation networks in, method of analysis, 16: 19348(R) (EURAEC-239)
dissolution of reactor fuel element casings, process, 16: 27150(P)
drilling of high-strength, 17: 6615
ductile-brittle transition temperature determination, research program, 17: 11187(R) (EURAEC-447)
ductile-brittle transition temperature measurement of, research program on, 17: 39533(R) (EURAEC-727)
ductile-brittle transition temperature measurement in, 18: 4243(R) (EURAEC-613)
ductile-brittle transition temperature measurement of, 18: 8793(R) (EURAEC-827)
ductile-brittle transition temperature determination, 18: 16470(R) (EURAEC-913)
ductile-brittle transition temperatures of, measurement of, 18: 35987(R) (EURAEC-1019)
ductile-brittle transition temperature measurement in pressure vessel, 19: 11724(R) (EURAEC-1217)
ductility and gamma grain growth of austenitic, 18: 39916(T,R) (EURAEC-1119)
ductility behavior of 4-inch plate of A302-B, Charpy-V notch, 20: 43997(R) (NRL-Memo-1663)
ductility of A-212 Grade B, nondestructive methods for determining transition temperature in, 17: 34111(R) (SWRI-1296-6-2)
ductility of austenitic, effects of liquation on hot, 17: 20477
ductility of A302 B, 18: 20528(R) (SWRI-1228-18)
ductility of A302B, Ducol W30, and Soudotenax 56, plastic fatigue, 19: 32731(R) (EURAEC-1349)
ductility of A52, A302, Ducol W30, and Soudotenax 56, plastic fatigue, 19: 9654(R) (EURAEC-1102)
ductility of, effects of plastic strain on, 17: 11171(T,R) (EURAEC-330)
ductility of, effects of metallic additives on, 17: 14862(T) (EURAEC-515)
ductility of, evaluation of cadmium plating systems for decreasing effects of hydrogen on, 17: 20454 (D3-4657)
ductility of hardened and tempered low-carbon martensitic, effects of boron, carbon, nickel, and titanium additions on, 17: 39547(T,R) (EURAEC-636)
ductility of hardened and tempered low-carbon martensitic, effects of alloying elements and impurities on, 17: 39546(T,R) (EURAEC-600 (Pt.3))
ductility of hardened, tempered, and embrittled low-carbon martensitic, effects of alloying elements and impurities on, 17: 39549(T,R) (EURAEC-698)
ductility of mild, effects of strain rate and specimen dimensions on, 20: 28866 (UCRL-14619)
ductility of pressure vessel, nondestructive testing of transition temperature in, 18: 10250(R) (SWRI-1296-6-8)
ductility of pressure-vessel effects of fatigue on, 20: 41446(R) (EURAEC-1624)
ductility of SOUDOTENAX-56, annealing effects on, 17: 12634(T,R) (EURAEC-378)
ductility of SOUDOTENAX-56, 17: 14750(T,R) (EURAEC-459)
ductility of, testing of small samples for, 17: 291(R) (EURAEC-308)
ductility of types A, C, 10A, 10B, 13C, 17A, 17C, 21A, 23A, and 27A, 18: 10503(T,R) (EURAEC-813)
ductility of uranium-bearing, 19: 7980(R) (NRL-Memo-1468)
ductility of welded joints in, development equipment and test procedures for determining, 17: 547(T,R) (EURAEC-340)
ductility of welded joints in, parameter study, 17: 12636(T,R) (EURAEC-501)
ductility of welded joints in, parameter study of, 17: 39506(T,R) (EURAEC-539)
ductility of welded, effects of weld composition and fabrication techniques on, 18: 39856(R) (EURAEC-1021)
ductility of welded, effects of hot work-hardening on, 18: 39863(T,R) (EURAEC-1118)
ductility of 1045, pressure effects on, 19: 46983 (AD-612159)
ductility of 13C, 17C, and 27A, 18: 10501(T,R) (EURAEC-787)
ductility of, at −269°C, 20: 21416
ductility of, effects on hydrogen on, 18: 24153(T,R) (EURAEC-1002)
ductility of, effects of rare earths on, 19: 37089
ductility, review of reversible temper brittleness, 17: 548(T,R) (EURAEC-341)
ductility transition temperature of, methods for measuring shift in, 17: 23496(R) (EURAEC-652)
ductility transition temperature of hardened, alloying effects of additives and impurities on, 17: 39545(T,R) (EURAEC-599)
ductility transition temperature of, nondestructive methods of measuring nil, 18: 410 (SWRI-1296-6-5)

durability of case-hardened, tracer studies, 16: 13416(T) (AEC-tr-4492) (p.6-15)
dynamic yield behavior of explosively loaded, 17: 4949
effects of abdominal shielding of, on survival of irradiated rats, 20: 18441
effects of decontaminating and descaling solution on metal loss on, 20: 21238 (NP-15928)
effects on fission ratio measurements in fast reactors, 16: 4958 (ANL-6468)
effects on plutonium precipitation from cadmium–magnesium–zinc solution at 600°C, 19: 32279(R) (ANL-7020(p.3-99))
elastic moduli of 4340, at 0 to 1600°F from ultrasonic measurements, 18: 20196 (UCRL-7326)
electric conductivity of hardened, alloying effects of additives and impurities on, 17: 39545(T,R) (EURAEC-599)
electrochemical properties of IX18H9T in aqueous solutions, 16: 1891(T) (SCL-T-372)
electrochemical properties of radioactive, 20: 31231
electrode potentials of irradiated Armco and low-carbon, in distilled water and in aqueous solutions of various inhibitors, 17: 8835
embrittlement and permeation of SAE 4130, by deuterium and hydrogen, 17: 32521
embrittlement by deuterium and hydrogen, effects of gas content on SAE 4130, 17: 32522
embrittlement by hydrogen of high-strength, effects of uranium on, 19: 6299 (NAEC-AML-1759)
embrittlement by plastic fatigue of Ducol W30 and Soudotenax 56, 20: 15039 (EURAEC-1475)
embrittlement in, hardness measurements for detection of, 20: 860
embrittlement of hydrogenated, solute-induced, 20: 5846
embrittlement of low-alloy, by plastic fatigue, 20: 7560 (EURAEC-1461)
embrittlement of pressure vessels of, by plastic fatigue, 20: 5881(R) (EURAEC-1441)
embrittlement of reactor-vessel, studies, 19: 966 (TID-21221(p.111-54))
embrittlement of reactor pressure vessel, plastic fatigue, 20: 29701(R) (EURAEC-1547)
enameling of sheet, causes of fish-scale defects in, 18: 9793(T) (Al-Trans-30)
engineering properties of Mar-Strained, 17: 6639 (ASD-TDR-62-230)
erosion by mercury vapor at 640°F of Dynacut tool, 20: 11214(R) (NASA-CR-54717)
expansion and quenchability tests of Super Elso, 19: 9600(R) (EURAEC-1209)
extrusion by hydrostatic methods, 19: 18436
extrusion by hydrostatic methods, 19: 44651
extrusion of complex shapes of 4340, using ceramic dies, 19: 9636(R) (NMI-9700-24)
extrusion of, development of dies for, 17: 4911(R) (NMI-9700.3)
extrusion of, fabrication of intermetallic die for, 17: 23905(R) (NMI-9700.9)
extrusion of mild, pressures and flow behavior in, 19: 24944 (AAEC/E-132)
extrusion of, evaluation of liners for, 18: 18328(R) (ASD-TDR-7-945(III))
extrusion, rolling, and welding of, estimation of defect frequency in, 18: 22457 (HW-76573)
fabrication and mechanical properties of A105-II and A302-B, 18: 20457(R) (SWRI-1228-19)
fabrication and properties of, research program for studying, 18: 18286(R) (EURAEC-966)
fabrication and properties of extruded and forged, 18: 20447(R) (ASD-TR-7-797(IX))
fabrication and properties of extruded, review, 19: 881(R) (AD-600363)
fabrication by explosive forming of AM355 PH and 4340 low alloy, 16: 2151 (WAL-624.5/1)
fabrication for use in reactors, 19: 37008
fabrication method for reactor, 17: 12648(P)
fabrication of high-strength, effects of variables on dimensional factors, 16: 5682 (DMIC-163)
fabrication of laminated shields for low-level gamma-counting facilities from, 16: 33318 (TID-16825)
fabrication of SAE 4340, by extrusion, 18: 18329(R) (ASD-TDR-7-945 (IV))
fabrication of shielding materials of, 20: 2301(P)
fabrication of tube shells of AISI 1018, by extrusion, 18: 4255(R) (ORNL-3470(p.98-125))
fabrication of tubes of, by sink and stretch reduction, 19: 30692 (NLCO-923)
fabrication of vertical-rib sandwich panels of maraging, by roll-welding, 20: 25509(R) (AD-632831)
fabrication of, welding techniques in, 17: 16611(T,R) (EURAEC-551)
fabrication specifications for boilers and pressure vessels, ASME code for, 18: 19287
failure by low-cycle plastic fatigue of pressure vessel, nondestructive testing techniques for, 20: 5894 (SWRI-1228-3-3)
failure mechanisms in, in reactor pressure vessels, 20: 2402
failure of pressure vessel, study of delayed, 20: 889(R) (BNWL-120, pp 4.1-59)
failure of pressure vessels of, (E), 20: 33911
fatigue and strain of low-carbon-alloy, in creep range, 18: 28021
fatigue at low endurance, during strain and stress, 16: 13615
fatigue crack growth in high-strength, methods of determining, 20: 33858(R) (AD-634094)
fatigue crack propagation in A302B, 18: 10541(R) (TID-20059)
fatigue detection before crack initiation using ultrasonic techniques, 20: 5867
fatigue effects in, 17: 38552(R) (SWRI-5-1348-7-1)
fatigue embrittlement of, studies of, 19: 18454(R) (EURAEC-1276)
fatigue endurance limit of C-1118, from cyclic tensile tests, 18: 39898 (IS-929)
fatigue of A-212, 304-L, and 4340, eddy current detection of, 19: 34425(R) (HW-84384(p.7.1-27))
fatigue of pressure vessel, 18: 6936(R) (TID-19919)
fatigue of structural, in-pile testing, 17: 17623(R) (IDO-16827)
fatigue properties of A302 B, with stressing at ambient temperature and stress relieving, 18: 20528(R) (SWRI-1228-18)
fatigue properties of A105 and A302, 18: 35154(R) (SWRI-1228-28)
fatigue properties of A105-II, A212-B, and A302-B, 19: 12735(R) (SWRI-1228-42)
fatigue strength for uses in pressure vessels, effects of weld defects on, 18: 25680 (TID-20648)
fatigue strength of pressure-vessel, 17: 25424 (TID-18710)
fatigue strength of wrought, effects of cracks and notches on, 18: 18346 (HW-74884)
fatigue strength of A302B, effects of weld defects on, 18: 41627(R) (TID-21011)
fatigue strength of A302B, 19: 905 (SWRI-1228-37)
fatigue strength of A201 and A302, effects of cyclic pressure on, 19: 24988(R) (SWRI-1228-51)
fatigue strength of A212B, effects of size on, 19: 24988(R) (SWRI-1228-51)
fatigue strength of pressure-vessel, cyclic testing of, 19: 26821(R) (SWRI-1228-57)
fatigue strength of pressure-vessel, cyclic testing of, 19: 34688(R) (SWRI-1228-61)
fatigue strength of A302B, effects of weld defects on, 19: 45503(R) (SWRI-1228-69)
fatigue strength of pressure-vessel, 20: 45862(R) (SWRI-1228P1-28)
fatigue tests of A302-B plate at 550°F, in-reactor low-cycle, 19: 34748 (NRL-Memo-1596)
fatigue tests of strained and stress-relieved A302 Grade B, 19: 13900(R) (SWRI-1228-54)
fatigue tests on pressure vessel, 20: 13255 (KAPL-3108)
fatigue under strain-controlled low-cycle conditions, 16: 16767
fission product deposition on, factors affecting, 19: 36960(R) (ORNL-3807, pp 80-142)
flaw detection by radiography, 16: 12042
flaws in, use of gamma radiation for detecting, 17: 25521
flaws in, uses of gamma sources for detection of, 20: 29390
fractography of A302B plate and welded, 19: 905 (SWRI-1228-37)
fracture initiation in, mechanisms of, 20: 29623(R) (TID-22970, pp 121-256)
fracture mechanics in pressure vessel, 19: 26808 (AHSB(S)R-81)
fracture mechanics in, in reactor pressure vessels, 20: 2401
fracture mechanisms in, 17: 433
fracture modes in surfaces of Hy 80, 110, and 150, electron microscopy of, 20: 9485 (AD-623567)
fracture of, biaxial brittle, 17: 6245 (NP-12374)
fracture of pressure-vessel, 17: 34394 (AHSB(S)R-46)
fracture of thick plates of, apparatus for testing brittle, 18: 18019
fracture of, method for testing biaxial brittle, 19: 34340
fracture propagation in, 17: 11187(R) (EURAEC-447)
fracture strength of A302B, effects of strain rate on, 19: 9657 (HW-SA-3770)
fracture surfaces of, analysis by electron microscopy, 17: 11185 (D1-82-0169)
fracture testing, 17: 34113 (TRG-Report-576)
fracture tests of high-strength, 19: 20462(R) (NRL-6258)
fracture toughness of A302-B, 18: 44138 (KAPL-3031)
fracture toughness of A302B, plane-strain, 19: 9669 (WERL-8844-3)
fracture toughness of A302-B, 19: 24984 (KAPL-3088)
fracture toughness of pressure vessel, test procedure development for measuring, 19: 42845(R) (COO-1477-1)
fracture toughness of pressure vessel, development of method for measuring, 20: 7241(R) (COO-1477-2)
fracture toughness of biaxial brittle fracture specimen of, effects of loading geometry on, 20: 10486 (WAPD-TM-554)

fracture toughness of low-strength, moderate-toughness, method for testing, 20: 23661 (WERL-8844-11)
fracture toughness of cold-rolled, 20: 28695(R) (GEAP-5082)
fracture toughness tests on type A-302B, of various sizes, 20: 27479 (CONF-660406-1)
fracture toughness of reactor pressure vessel, development of test procedures for, 20: 29700(R) (COO-1477-4)
fracture toughness of A302B, data summary, 20: 46186 (GEAP-5014)
fracture toughness of turbine/generator rotor, data summary, 20: 46186 (GEAP-5014)
fracture under impulsive loading, 16: 25759 (NP-11890)
friction and wear of carburized, ball against Armco iron flat at 70 to 1200°F, 17: 25685(R) (BMI-1624(Del.))
friction coefficients of nitrided, in sodium at 80 to 750°C, 16: 4450(R) (BMI-1546(Del.))
friction coefficient with uranium, 17: 18740 (BMI-X-226)
gamma absorption by, 16: 24223
gamma attenuation in vertical slab, geometry and barrier attenuation, 16: 24603
gamma attenuation by slabs of, 17: 4210 (DASA-1318)
gamma attenuation, 17: 21318 (NAA-SR-Memo-3556 and Add.)
gamma attenuation by, air-scattered, 19: 29439 (CEX-63.3)
gamma attenuation factors for, (E), 20: 20094 (NP-15926)
gamma attenuation in, tables of equivalent thickness of, 20: 44989
gamma attenuation in, 17: 1042 (JUL-54-RE)
gamma backscatter spectra from, 17: 34735 (PAEC(D)PH635)
gamma backscattering from semi-infinite slabs of, differential dose rates for, (E), 19: 43465
gamma contamination from ruthenium-103 in sheets for use in shielding, 18: 43801(R) (LA-3132-MS(p.145-52))
gamma dose albedos for, differential, 20: 3270
gamma dose attenuation in ducts in, variation with energy, (E/T), 20: 34798
gamma dose buildup on slabs of, 18: 3037
gamma dose buildup factors for, 20: 10228
gamma dose buildup factors for, 20: 15933(T) (ORNL-tr-1060)
gamma dose rates from activation of, induced by nuclear explosion in air, 19: 36705 (NP-15146)
gamma penetration in slabs of (E/T), 19: 3455 (USNRDL-TR-730)
gamma scattering by parallel slabs of, 18: 28909
gamma scattering by cylinders of, evaluation of functions for (E/T), 19: 3466
gamma shielding properties of slabs of, 18: 19259 (USNRDL-TR-707)
gamma streaming in pipes of, 19: 35573
gamma transmission through pipe walls of, thickness dependence of, (T), 20: 1320
gamma transmission through pipes of, Monte Carlo calculation of, 20: 16114
gamma transmission in slabs of, (E), 19: 14728 (APEX-581)
grain growth during welding of austenitic, effects of temperature and time on, 17: 39514(T,R) (EURAEC-699)
grain growth in austenitic, effects of alloying elements, temperature, and time on, 17: 41437(T,R) (EURAEC-598)
grain growth in mild, effects of niobium carbide on, 19: 985
grain size control in ingots and welds, effects of sonic vibrations on, review of, 17: 30947 (DMIC-Memo-166)
grain size in cast, titanium effects on control of, 19: 46980 (AD-611800)
grain size in, effects of zirconium and its carbides, nitrides, and oxides on austenitic, 17: 32627
hardening by shot-peening, 16: 3434
hardening of austenitic, 16: 6751
hardening of, effects of alloying additions on, 18: 16509
hardness and structure of quenched, 16: 21069
hardness, effect of boron addition, 16: 2249
hardness of deformed and thermal cycled martensitic, 18: 32150(R) (UCRL-11317(p.150-8))
heat flux on submerged, during boiling of organic coolants, 20: 12965
heat production in electrically heated tube of, calculation of, 19: 22480 (EUR-2182.e)
heat transfer with aluminum and steel in surface contact, equation for calculating, 18: 41620
heat treatment for restoring types C and 17A, embrittled by strain at 300°C, 17: 39509(T,R) (EURAEC-615)
heat treatment of G13L, 16: 10442
heat treatment of, effect of temperature variations on, 20: 43456(T) (ORNL-tr-1348)
heat treatment temperature analysis by x-ray diffraction, 17: 292 (HW-74643)
high-strength, bibliography on, 17: 6521 (NP-12417)
homogeneity of thick plate of Super Elso, 19: 7900(R) (EURAEC-1192)
hydrogen embrittlement in pressure vessels of, in pressurized-water reactors, 18: 5796
impact properties of weld heat-affected A212 B, 18: 20529 (TID-20463)
impact shock testing of irradiated SM-1 pressure vessel, 17: 19630(R) (ORNL-3386)
impact strength of thick, effects of heat treatments on, 19: 41007(R) (EURAEC-1400)
impregnation with beryllium, diffusion, 20: 27455
inclusions, autoradiographic methods for studying, 16: 16052
inclusions in, effects of rare earths on nonmetallic, 19: 22877(T) (JPRS-28849(p.264-71))
inclusions, tracer techniques for identifying nonmetallic, 16: 12043
inspection of pressure-vessel, using electric and sonic methods, 19: 22995(R) (SWRI-1243-14(a))
inspection of rolled sheet, magnetic and sonic, 16: 29358(T,R) (EURAEC-244)
inspection of, ultrasonic, 20: 29389
internal friction evolution in, quenched after thermal treatment at 720°C, 17: 18800
interstitial atom-dislocation effects in, 17: 3466 (ASD-TR-61-351)
iodine deposition on, factors affecting, 19: 22461(R) (ORNL-3776(p.57-70))
iodine deposition on, from vapor phase, 20: 215 (CONF-650407, pp 142-77)
iodine deposition on, in turbulent helium flow stream at 400 to 500°F, 20: 28687 (ORNL-TM-1386)
iodine-131 deposition and transport on, model for, (E/T), 20: 21785 (ORNL-TM-1330(Rev.))
ion energies from spark sources using, 19: 7778
joint with Zircaloy-2, evaluation of expanded, 17: 8806 (HW-75135)
ladle-treating and production of medium-carbon, alloying effects of rare earth metals and oxides on, 16: 7840 (BM-RI-5895)
lead distribution in austenitic, effects of cerium additions on, 19: 23019(T) (JPRS-28849(p.292-6))
machining, 17: 3439(R) (ASD-TR-7-532a(VIII))
machining characteristics of high-strength 4130, 4330, and 4340, 17: 6609
machining characteristics, 17: 34358(R) (ASD-TDR-63-581)
machining procedures for, 20: 43864 (Y-1550)
magnetic potential drop in, 17: 38337 (CERN-63-19(p.190-2))
magnetic properties of flat-rolled, variation with composition and processing techniques, 20: 17009
magnetic properties for use in gradient magnets, determination of, 20: 17010 (CONF-650922, pp 297-304)
mass transfer by friction, tracer studies, 16: 13419(T) (AEC-tr-4492 (p.28-34))
mass transfer during rolling friction, tracer studies, 16: 13421(T) (AEC-tr-4492(p.37-9))
mass transfer in liquid bismuth, 17: 12617
mechanical properties of AISI type 502 at room temperature to 1500°F, 16: 2195 (ORNL-TM-39)
mechanical properties of austenitic, effect of deformation temperature, 16: 6752
mechanical properties deterioration by friction in cogwheels of coal-mining machines, tracer studies, 16: 13428(T) (AEC-tr-4492(p.82-7))
mechanical properties, effects of niobium content, 16: 16737
mechanical properties of pressure vessel, radiation effects, 16: 26654 (ACCESS-134)
mechanical properties of high-strength, 17: 6651 (DMIC-178)
mechanical properties for pressure vessels, 17: 8716(T,R) (EURAEC-498)
mechanical properties of SAE 4340, effects of potassium at 1000°F, 17: 12036(R) (SY-5396-R3)
mechanical properties of reactor pressure vessel, effects of stress relieving treatments on, 17: 12681
mechanical properties of USS T-1, for pressure vessels, 17: 14792(R) (TID-17930)
mechanical properties of reactor, effects of post-irradiation heat treatment on, 17: 16752
mechanical properties of A-302B, 17: 37569(R) (GA-4287)
mechanical properties of, effect of lanthanum on, 17: 39578
mechanical properties of, effects of cerium on, 17: 39579
mechanical properties of welded joints in high-tensile, effects of additives and processing on, 18: 2237(T,R) (EURAEC-729)
mechanical properties of ML-12, effects of rare earths on, 18: 2257
mechanical properties of tungsten carbide-containing, effects of alloying method used on, 18: 14450(T)
mechanical properties of types 13C, 15A, 17C, 21A, 23A, 27A, and 37A, 18: 16458(T,R) (EURAEC-811)
mechanical properties of embrittled, quenched, and tempered, 18: 16485(T,R) (EURAEC-829)
mechanical properties of, effects of uranium on, 18: 18281 (BM-RI-6403)
mechanical properties of, statistical evaluation of time-to-rupture tests of, 18: 22481(R) (EURAEC-964)
mechanical properties of two high-strength, 18: 33199 (UCRL-10811)

mechanical properties of types 13C, 17C, 23A, 23C, 27A, 33A, and 37A, 18: 34089(T,R) (EURAEC-915)
mechanical properties of strain-hardened, 18: 43137 (UCRL-10981)
mechanical properties of types A, B, C, 17A, 17C, 23C, 33A, 37A, and 47A, 19: 9633(R) (EURAEC-1106)
mechanical properties of A-201, A-302, and T-1, for pressure vessels, 19: 13999(R) (SWRI-1228-43)
mechanical properties for use in reactor pressure vessels, (T), 19: 17192
mechanical properties of AISI A212B and A302B-A, 19: 22995(R) (SWRI-1243-14(a))
mechanical properties of electrochemically machined, 19: 28776 (DMIC-213)
mechanical properties of heat-resisting cast, effect of uranium on, 19: 30802
mechanical properties of low-alloy, high-strength, effects of uranium on, 19: 30803
mechanical properties and structure of, effects of uranium on, 19: 32764
mechanical properties of A302B, effects of heat treatment and prestrain on, 19: 34677 (GA-6454)
mechanical properties at cryogenic temperatures, 19: 47013 (PB-171809(Rev.)(Suppl.2))
mechanical properties of electron-beam-melted, 19: 46972
mechanical properties of plates of Acier AMMO, effects of specimen location on, 20: 21331(R) (EURAEC-1569)
mechanical properties of high-strength, effects of processing on, 20: 33858(R) (AD-634094)
mechanical properties of, effects of cryogenic temperatures on, 17: 6542
metallographic studies of Sputnik 4 fragment, 17: 37470
metallurgical bonding to stainless steel by extrusion, 18: 27937
metallurgical bonding to zirconium alloys by extrusion, 18: 27937
microstructural studies of strengthening in ausformed, 19: 18468 (UCRL-11861)
microstructure of weld heat-affected A212 B, 18: 20529 (TID-20463)
microstructure of A302B, 20: 833 (WERL-8844-5)
milling of high-strength, 17: 6612
Mössbauer effect in, plastic deformation effects in, 18: 25903(T)
neutron absorption properties in control rods, 16: 30040
neutron absorption by inserts of, in uranyl nitrate critical assemblies, (E), 20: 14091
neutron attenuation by slabs of, 17: 11900 (NARF-62-16T)
neutron attenuation by, from 14-Mev source, 18: 19821
neutron attenuation in, 17: 1042 (JUL-54-RE)
neutron capture in, gamma dose from, 19: 17182
neutron cross sections, 18: 30963
neutron diffusion in blocks of, 18: 26521
neutron scattering by cylindrical, fast, (E/T), 19: 17157(R) (ORNL-3714(Vol.I)(p.43-67))
neutron scattering from cylinders of, Monte Carlo calculations for fast, (E), 19: 35349 (ORNL-TM-1156)
neutron scattering by cylinders of, fast, (E/T), 20: 3265
neutron scattering by cylinders of, spectra from fast, (E/T), 20: 38007
neutron transmission by, at 0.2 to 10 Mev, 18: 28547
neutron transmission in slabs of, (E), 19: 14728 (APEX-581)
niobium carbide precipitation in austenitic creep-resisting, 18: 37726
nitridation conditions and nitride layer depth, 16: 10441
nitridation of, in caustic embrittlement of boiler plates, 18: 23148(T) (AEC-tr-6389)
notch toughness of maraging, metallographic study of, 19: 20541 (AD-604868)
notch-brittleness during time-to-rupture tests, theory, 19: 47081 (EURAEC-1432)
optical properties at high temperatures, emittance and reflectance, 16: 12236 (WADD-TR-60-370)
oxidation at 800 to 1200°C, effects on arsenic content in, 17: 25519(T) (AEC-tr-5824)
oxidation by carbon dioxide at 25 atm. and 350 to 600°C, 16: 22535(T) (AEC-tr-5195)
oxidation by water of Creusot 1.2 MD 07 boilerplate, effects of flow rate on, 20: 765(R) (EURAEC-1387)
oxidation in gas-cooled reactors, 18: 11372
particle size and lattice distortion of crystalline, effects of cold pressing on, 17: 18780(T) (TRG-Inf-Ser-107)
passivation of, ion exchange of chromate ions on surface with aqueous ions, 18: 2181(R) (ORNL-3488(p.91-5))
penetration of plates of, by projectiles from runaway reactor, 18: 3042 (SRIA-113)
performance as NERVA II shield, 20: 35129 (WANL-TME-1153)
performance in reactor pressure vessels, 18: 7255
performance in reactor pressure circuits, 18: 38271 (A/CONF.28/P/144)
performance of A 302 B, in very thick pressure vessels, 18: 40772
performance of A302B and HY-100, for reactor pressure vessels, 18: 28944
performance of high-speed tool, in end milling of U-500 alloy, 17: 6614
performance of 1018, as melting-point temperature sensors up to 6000°F, (E), 19: 30489 (SC-DC-65-1237)
performance of 302B, as reactor pressure vessel, 18: 28948
permeability of, to helium and hydrogen, bibliography on, 17: 37492(R) (SCL-B-107)
phase transformations during heat treatment, structural mechanism, 16: 15218
phase transformations in, apparatus for determination of temperature of austenite decomposition, 17: 1960(T,R) (EURAEC-343)
phase transformation of low carbon austenite 18-10 to martensite during cold working at very low temperatures, 17: 16531
phase transformations in, method for determining temperature of ductile-brittle, 17: 16644(R) (EURAEC-561)
phase transformation point variation for, effects of alloying elements and impurities on, 17: 41438(T,R) (EURAEC-799)
phase transformations in low-alloy, effects of additives on, 18: 24152(T,R) (EURAEC-1001)
phase transformations in, analysis of martensitic, 18: 24994(R) (MND-2531-1)
physical properties of, effects of 1200°F sodium on, 19: 4590(R) (MSAR-61-42)
physical properties of, effects of 1200°F sodium on, 19: 4591(R) (MSAR-61-105)
physical properties of, effects of 1200°F sodium on, 19: 4592(R) (MSAR-61-114)
physical properties of, effects of 1200°F sodium on, 19: 4618(R) (MSAR-61-60)
physical properties of, effects of 1200°F sodium on, 19: 4619(R) (MSAR-61-67)
physical properties of, equipment for studies of effects of 1200°F sodium on, 19: 4620(R) (MSAR-61-100)
plastic deformation of ferritic lamellar-pearlite, identification of kink bands in, 20: 835(T) (AERE-Trans-1035)
plastic fatigue of A302, Ducol W, and Soudotenax, effects on fragility, 18: 30180(T,R) (EURAEC-1017)
plastic fatigue of A302, Ducol W, and Soudotenax, relation to ductility, 19: 11723(R) (EURAEC-1207)
plastic strain of SOUDOTENAX-56, 17: 12634(T,R) (EURAEC-378)
plasticity and relaxation strength, 16: 30835
plasticity of, effects of cerium on, 19: 23018(T) (JPRS-28849(p.279-85))
plating of, evaluation of, 17: 6534(T,R) (EURAEC-329)
plating of, evaluation of stainless, 17: 6537(T,R) (EURAEC-377)
plating of, with stainless steel, metallographic aspects of, 17: 22135(T,R) (EURAEC-564)
plating with gold from electroless bath, 18: 35507(R) (UCRL-13070)
polarization of, effects of sodium borate and sodium citrate on, 19: 7914
polishing by electrolytic methods, 18: 24107(T) (SC-T-64-903)
polymorphism in, overdriving effects on dynamics of, 19: 20555 (LA-3215)
preferred orientation in rolled electrical, determination of, 18: 36033
preparation and properties of ultrahigh-strength, 16: 15174 (DMIC-Memo-149)
preparation and properties of non-aging low-carbon electrochemical, 16: 24198
preparation of, damage to industry for, from nuclear explosions, 18: 22269 (AD-419518)
pressure strength of vessels of, factors affecting, 18: 18018
pressure wave diffraction by shell of, in elastic medium, 17: 1581 (NP-12181)
production and fabrication for use in reactors, industrial problems created by, 18: 14389
production and properties of high-strength martensitic, by cyclic transformation of austenite, 20: 754 (UCRL-16121)
production by open-hearth process, use of radioisotopes for studying, 20: 14939
production by vacuum metallurgy, 16: 20967
production of, by sintering at 470 to 1150°C, mechanism and technique for, 17: 32497
production of cold-rolled tape, use of radioisotopes for controlling technology in, 16: 13472(T) (AEC-tr-4492(p.311-16))
production of, neutron activation analysis in, 17: 33849
production of shielding doors, 17: 7504
properties, alloying effects of uranium, 16: 9206 (NP-11340)
properties and structure of high-purity, effects of lead and rare earths on, 20: 9506(T) (ORNL-tr-922)
properties and uses of specialty, review of, 19: 25040
properties as boiler materials at high temperatures, review of, 18: 554(T) (TRG-Inf-Ser-330)
properties as cladding and structural materials in reactors, 18: 32072
properties as cladding and structural material in reactors, 18: 41947
properties as fast-neutron shield, experiment for, 18: 30949 (NYO-9077)
properties as magnet material, 20: 41097
properties as reactor material, 20: 1312
properties as reactor containment material, 20: 30815

properties as structural materials in gas-cooled graphite-moderated reactors, 18: 558
properties at −400 to 100°F, 18: 42020 (PB-171809(Rev.))
properties at low temperatures, 18: 22493(R) (PB-171809-6)
properties, effects of helium atmosphere, 16: 6212(R) (GA-1532)
properties for aerospace uses, 19: 47068
properties for application to 1200°F, 16: 10403 (ASD-TR-61-322 (p.40-54))
properties for British nuclear power plants, 16: 13619
properties for cryogenic applications, 19: 23070
properties for fuel element canning, 18: 42034
properties for use in reactor pressure vessels, survey, 16: 24215
properties for use as reactor pressure vessels, 18: 34097
properties for use as shielding for ship reactor, 19: 3770
properties for use as fuel-element cladding, 19: 22884
properties for use in reactor construction, 19: 22885
properties of acid open hearth, effects of rare earths on, 19: 23017(T) (JPRS-28849(p.250-63))
properties of alloy, alloying effects of uranium on, 18: 2229 (NP-13261 (p.136-83))
properties of ASTM A-212, for EGCR pressure vessel, 19: 25054(R) (ORNL-3731(p.272-89))
properties of austenitic, for use as fuel cladding, 20: 21383
properties of, book on impurity effects on, 17: 27881
properties of ceramic-coated, for use as liner for extrusion billet container, 18: 18328(R) (ASD-TDR-7-945(III))
properties of, for use as cathode in electrolytic separation of deuterium, 17: 22074
properties of low-alloy, for pressure vessels, 16: 26497 (TID-16138)
properties of low-carbon martensitic, 18: 10546(T,R) (EURAEC-432)
properties of low-alloy, effects of uranium on isothermal transformation and hardenability, 18: 39888 (BM-RI-6515)
properties of low-alloy, effects of temperature on mechanical and physical, 17: 16760
properties of pressure-vessel, 18: 38274 (A/CONF.28/P/331)
properties of radiation-sensitive and insensitive A302B, 20: 2437 (WERL-8844-6)
properties of reactor, summary of, 20: 13186 (TRG-Report-840)
properties of skin and heart of Super Elso, 20: 818 (EURAEC-1348)
properties of type 1020, for containers of liquefied plutonium alloys with molten salts, 20: 5594(R) (ANL-6925, pp 21-106)
properties of welded sheaths, sheets, and tubes of, 18: 7172
properties of welded, 18: 10501(T,R) (EURAEC-787)
properties of welded, 18: 10503(T,R) (EURAEC-813)
properties of welded, 18: 16458(T,R) (EURAEC-811)
properties of welded, 18: 34089(T,R) (EURAEC-915)
properties of welded, 19: 9633(R) (EURAEC-1106)
properties of welded, 19: 32703(R) (EURAEC-1297)
properties of welded joints in thick plates of 1.2 MD07, 20: 11239(R) (EURAEC-1468)
properties of 17-4 PH type for use in army reactors SM-1 and PM-2, 16: 9618 (APAE-97)
properties of, alloying effects of uranium on, 18: 28013
properties of, alloying effects of lanthanum on, 19: 37128
properties of, effects of cerium and lanthanum on, 18: 14526
properties of, effects of uranium on, 18: 18401
properties of, effects of substructure on mechanical and tensile, 20: 4372(R) (GA-6724)
properties of, effects of additions and impurities on, 20: 46194(T) (AD-634697)
properties of, strain softening effects on, 20: 2311 (AD-618925)
properties of, used for reactor pressure vessel, 20: 11286 (UJV-1405/65)
properties testing for use in Elk River Reactor pressure vessel, 20: 42636(R) (SWRI-1228-4-22)
properties under shock loading, 17: 11937(R) (ARF-4132-16)
property requirements for nuclear power projects, fulfillment of, 18: 18376
proton attenuation in, 10- and 19.2-Bev/c, (E), 19: 14738
proton beam reactions at 10 Bev, nuclear shower production in, (E/T), 19: 17160(R) (ORNL-3714(Vol.II)(p.119-33))
proton beam scattering by, nucleon-meson cascades from, 20: 27683
proton cascade reactions at 10 and 19.2 Bev/c, shielding properties in, (E), 19: 14735
proton reactions at 19.2 Bev/c, nuclear cascade distribution in, (E), 19: 14736
proton reactions at 10 Bev/c, nuclear cascade distributions in, (E), 19: 14737
proton reactions at 10 and 20 Bev/c, Monte Carlo method for meson-nucleon cascades in, 19: 14740
proton reactions at 1 and 3 Bev, meson-nucleon cascade in, (E/T), 20: 10222 (ORNL-3852)
proton reactions with nuclei in, at 10 and 20 Bev/c, (T), 19: 45317
proton shielding by, shower production in 9-Bev/c, 18: 7843(R) (ORNL-3499(Vol.II)(p.14-22))
puncture-resistance of hot-rolled type ASTM A245 grade A, effects of temperature on, 20: 43492 (ORNL-TM-1312(Vol.2))
radiation absorbed dose rates in, calorimetric measurement of reactor, 19: 45467
radiation damage by neutrons, spectral dependence, 16: 24638
radiation damage in ferritic, neutron spectral effects on, 18: 10581 (WAPD-T-1622(Rev.))
radiation damage to, correction for effects of neutron spectra on, 16: 27694 (ORNL-TM-299)
radiation effects on properties, 16: 579
radiation effects on magnetic properties of SA 212B, 16: 628
radiation effects, gamma and neutron, 16: 2717
radiation effects on properties, for pressure vessels, 16: 2274
radiation effects on ductile-brittle transition, development of apparatus and techniques for studying, 16: 5758(R) (EURAEC-93)
radiation effects, 16: 7890 (NP-11196(p.34-41))
radiation effects on notch ductility, 16: 9263 (NRL-5731)
radiation effects of fast neutrons, review of experimental results, 16: 10629
radiation effects on strain-aged pressure vessel, 16: 10640
radiation effects on friction and wear properties of M2 tool, 16: 10604 (APEX-671)
radiation effects at 500°F, 16: 12649(R) (ANL-6485)
radiation effects on brittle-fracture properties, 16: 13642 (ORNL-TM-132)
radiation effects of fast neutrons, review of experimental results, 16: 15251
radiation effects, review of experimental results on fast neutron, 16: 6792
radiation effects on corrosion by chemicals, 16: 17976(R) (EURAEC-94)
radiation effects on pressure vessel, 16: 18081(R) (EURAEC-180)
radiation effects on properties of MSt3b and MSt3u, neutron, 16: 19449
radiation effects on brittle-ductile transition in En2, neutron, 16: 21068
radiation effects on pressure vessel, 16: 21090(R) (EURAEC-140)
radiation effects on atmospheric corrosion, 16: 21098
radiation effects on mechanical properties of mild, 16: 21100
radiation effects on electrochemical properties, 16: 22678
radiation effects on shielding properties, neutron, 16: 23245 (NDL-TR-19)
radiation effects on heat strength of low-carbon, 16: 25859
radiation effects on notch ductility of A212-B, 16: 29468
radiation effects on, in reactor pressure vessels, 16: 30915
radiation effects on mechanical properties of, 16: 32144(R) (EURAEC-370)
radiation effects on, 16: 32145 (FZM-1943)
radiation effects on stress properties of, 16: 33514(R) (GA-3410)
radiation effects on mechanical properties, fast neutron, 16: 572 (REIC-20)
radiation effects on mechanical properties, neutron, 16: 4585 (DP-581)
radiation effects, 17: 6735 (AE-90)
radiation effects on, 17: 35078(R) (ANL-6739)
radiation effects on brittle fracture and strain aging in, 17: 462
radiation effects on brittle-rupture properties of, survey of, 17: 16743 (TID-17682)
radiation effects on Charpy impact properties of ASTM A 302 grade B, neutron, 17: 31061
radiation effects on Charpy impact properties of A-302B, 17: 37569(R) (GA-4287)
radiation effects on corrosion, mechanical, physical and thermal properties of, 17: 32679
radiation effects on ductility, 17: 14740 (TID-11295(2nd Ed.))
radiation effects on ductility transition temperature of pressure-vessel, 17: 37574 (WAPD-T-1570)
radiation effects on ductile-brittle transition in pressure vessel, research program on, 17: 39663(R) (EURAEC-673)
radiation effects on ductile-brittle transition of pressure vessel, 17: 41492(R) (EURAEC-758)
radiation effects on embrittlement and hardening in ferritic, neutron, 17: 31059
radiation effects on free carbon in mild, 17: 27909
radiation effects on impact and tensile properties of low-alloy and unalloyed basic, 17: 36359
radiation effects on, in-pile, 17: 14909
radiation effects on, in different reactor spectra, 17: 26169
radiation effects on, in SL-1 pressure vessel, comparison with other steels, 17: 26171
radiation effects on mechanical properties of, neutron, 17: 465
radiation effects on mechanical properties, 17: 11129
radiation effects on mechanical properties and structure of, neutron, 17: 39683
radiation effects on mechanical properties of, critical factors in interpretation of, 17: 41515

radiation effects on, neutron, 17: 38552(R) (SWRI-5-1348-7-1)
radiation effects on notch ductility of, 17: 23918 (TID-7620(Pt.I) (p.168-90))
radiation effects on pressure-vessel, review, 17: 13728
radiation effects on pressure-vessel, anomalous embrittling in, 17: 26172
radiation effects on properties of precipitation-hardening, neutron, 17: 31054
radiation effects on properties of construction, for reactor pressure vessels, 17: 41513
radiation effects on stresses in, 17: 5040(R) (ORNL-3364(p.125-50))
radiation effects on strength of surface layer of, electron beam, 17: 20520
radiation effects on strength of, electron, 17: 27905
radiation effects on, surveillance tests on, 17: 31062
radiation effects on tensile properties, 17: 14891(R) (GA-3882)
radiation effects on tensile properties of, effects of temperature on, 17: 29384
radiation effects on tensile properties of A-302B, neutron, 17: 37570(R) (GA-4484)
radiation effects on U-8, 17: 16541
radiation effects on brittle fracture properties, neutron, 17: 2037
radiation effects on, neutron, 17: 18851 (ASD-TDR-62-530)
radiation effects on nil ductility transition temperature of, nondestructive methods of measuring, 18: 410 (SWRI-1296-6-5)
radiation effects on brittle-ductile transition of, correlation of neutron, 18: 644 (CONF-39-99)
radiation effects on tensile-test samples of, in EL-3, 18: 650 (EURAEC-390)
radiation effects on passivation of boiler plate, 18: 2183(T,R) (EURAEC-285)
radiation effects on mechanical properties, 18: 4160(R) (BNL-799 (p.74-100))
radiation effects on tubes of, subjected to multiaxial stress, 18: 5815(R) (GA-4742)
radiation effects on ductile-brittle transition in pressure vessel, neutron, 18: 7307 (NRL-5984)
radiation effects on ductile-brittle transition in, neutron, 18: 8863(R) (EURAEC-817)
radiation effects on tensile properties of high-strength, effects of irradiation temperature on fast neutron, 18: 8877(T) (EURAEC-816)
radiation effects on pressure-vessel, fast neutron, 18: 8905
radiation effects on structure of, effects of temperature on electron beam, 18: 10587
radiation effects on electrochemical properties of boilerplate CSX, in nitrogen-saturated potassium hydroxide, 18: 10470(R) (EURAEC-812)
radiation effects on ductile-brittle transition in pressure vessel, 18: 12722(R) (EURAEC-542)
radiation effects on SA2128, 18: 15426(R) (ANL-6810)
radiation effects on mechanical properties, 18: 16525 (NP-13657)
radiation effects on mechanical properties of, 18: 16526 (NP-13663)
radiation effects on structural properties of, neutron, 18: 16527(R) (NRL-Memo-1393)
radiation effects on pressure-vessel, 18: 18413(R) (EURAEC-975)
radiation effects on, 18: 18307
radiation effects on dimensional stability of hardened, neutron, 18: 20584 (SC-R-64-120)
radiation effects on creep of, 18: 22481(R) (EURAEC-964)
radiation effects on stressed tubes of A302B, neutron, 18: 24190(R) (GA-5037)
radiation effects on microstructure of pressure vessel-grade, fast neutron, 18: 26092
radiation effects on tensile properties of, neutron, 18: 26096
radiation effects on electrochemical behavior, 18: 25553
radiation effects on pressure vessel, neutron, 18: 26925 (GEAP-4423)
radiation effects on ductile-brittle transition in pressure-vessel, neutron, 18: 28040(R) (EURAEC-1022)
radiation effects of fast neutrons on, additive effects of nitrogen on, 18: 28041(R) (EURAEC-1046)
radiation effects on physical properties of 212B, 18: 28072
radiation effects on corrosion of, in HWCTR, 18: 28073
radiation effects on brittleness of A212B and modified Hy 80, neutron, 18: 30229 (BNL-8015)
radiation effects on mechanical properties of A-302B, neutron, 18: 30234(R) (GA-5259)
radiation effects on brittleness of, neutron, 18: 30253
radiation effects on brittleness of, neutron, 18: 30258
radiation effects on A-286, fast-neutron, 18: 30111(R) (GEMP-35A)
radiation effects on engineering properties of, review, 18: 32216 (A/CONF.28/P/242)
radiation effects on pressure-vessel, research program on fast-neutron, 18: 34219 (RCN-26)
radiation effects on stressed tubes of A302B, neutron, 18: 36046(R) (GA-5495)
radiation effects on nil-ductility transitions in A212B and A302B, 18: 36048(R) (SWRI-1243-14)
radiation effects on brittleness of ferrite-pearlite, neutron, 18: 37745 (A/CONF.28/P/339)
radiation effects on stress-rupture strength of austenitic, reactor, 18: 37746 (A/CONF.28/P/339a)
radiation effects on embrittlement of pressure-vessel, neutron, 18: 37749 (A/CONF.28/P/420)
radiation effects on, effects of carbon, nitrogen, and titanium on fast-neutron, 18: 37763(R) (EURAEC-1103)
radiation effects on, review on, 18: 37786
radiation effects on fatigue properties of A302-B, 18: 40003 (NRL-6127)
radiation effects on pressure-vessel, neutron, 18: 40004 (NRL-Memo-1502)
radiation effects on nil-ductility transition temperature of, fast neutron, 18: 40008 (SWRI-1228-30)
radiation effects on, neutron, 18: 40020
radiation effects on type 1018, 18: 43114(R) (NP-14236)
radiation effects on surface structure of, 18: 44251
radiation effects on notch ductility of A212B and A302B, effects of postirradiation annealing on, 19: 996(R) (NRL-Memo-1351)
radiation effects on mechanical properties, fast- and thermal-neutron, 19: 1004(R) (ORNL-3676(p.125-56))
radiation effects on, neutron, 19: 4719(T) (AEC-tr-6227/2(p.63-72))
radiation effects on elongation, stress, and work hardening in low-alloy and mild, 19: 4726
radiation effects on ductile-brittle transition in pressure-vessel, research program on, 19: 7975(R) (EURAEC-1218)
radiation effects on mechanical properties of stressed A-302B, neutron, 19: 7977(R) (GA-5636)
radiation effects on physical properties of A212B, A301B, A302B, A350-LF3, and Hy-80, 19: 7980(R) (NRL-Memo-1468)
radiation effects on mechanical properties of A-302B, effects of multiaxial stresses on neutron, 19: 9731 (GA-5273)
radiation effects on ductility of, research on neutron, 19: 9735(R) (NRL-Memo-1424)
radiation effects on rupture properties of, 19: 11777(R) (EURAEC-1243)
radiation effects on notch ductility of A212-B and A353, neutron, 19: 11781(R) (NRL-Memo-1556)
radiation effects on notch ductility of A302-B steel, neutron, 19: 11781(R) (NRL-Memo-1556)
radiation effects on notch ductility of A302-B, fast-neutron, 19: 11780 (NRL-6179)
radiation effects on yield stress of mild, annealing of, 19: 11789
radiation effects on stressed, equipment for testing, 19: 11378(P)
radiation effects on brittleness, 19: 11682
radiation effects on ductile-brittle transition temperature of, correlation of neutron, 19: 16222 (WAPD-TM-471)
radiation effects on mechanical properties of, research program on effects of carbon and nitrogen on fast-neutron, 19: 18534(R) (EURAEC-1318)
radiation effects on reactor pressure vessel, surveillance program for, 19: 21607 (APED-4773)
radiation effects on mechanical properties of AISI A212B and A302B-A, 19: 22995(R) (SWRI-1243-14(a))
radiation effects on, use of equivalent dose and temperature concepts in, 19: 25055 (TRG-Report-511)
radiation effects on pressure-vessel, 19: 25054(R) (ORNL-3731(p.272-89))
radiation effects on protective action of corrosion inhibitors on, 19: 28414
radiation effects on fatigue properties of A302-B plate at 550°F, neutron, 19: 34748 (NRL-Memo-1596)
radiation effects on, evaluation for fast-reactor uses, (E/T), 19: 35634
radiation effects on EGCR-types of, 19: 37170(R) (ORNL-3807 pp 249-76)
radiation effects on hardening in mild, effects of dose and temperature on neutron, 19: 37186
radiation effects on type 4340, 19: 40112(R) (ANL-7046(p.36-66))
radiation effects on, research program on effects of nitrogen on fast neutron, 19: 44741 (EURAEC-1383)
radiation effects on, research program on effects of nitrogen on fast-neutron, 19: 44742(R) (EURAEC-1430)
radiation effects on pressure vessel, 20: 1352(T,R) (JPRS-31526)
radiation effects on stressed, device for investigating in-pile, 20: 1385(P)
radiation effects on reactor structures of, 20: 2408(P) (AD-614899)
radiation effects on A302B, annealing effects on, 20: 2455
radiation effects on, neutron, 20: 2474
radiation effects on, in pressure vessels, 20: 2479
radiation effects on mechanical properties of, 20: 2409(R) (AD-617319)
radiation effects on hardening and embrittlement of bcc, 20: 2472
radiation effects on nil ductility temperature and stress wave attenuation of, methods for determining, 20: 4457(R) (EURAEC-1474)

radiation effects on austenitic and ferritic, fission-fragment, 20: 4469
radiation effects on mechanical properties of low-alloy, fast-neutron, 20: 5921
radiation effects on wear resistance of, fast-neutron, 20: 15140
radiation effects on atomic arrangement in, 20: 18046(R) (ORNL-3900, pp 2-81)
radiation effects on pressure vessels of low-alloy, fast-neutron, 20: 21228 (AE-221)
radiation effects on lower yield point of ferritic, computer calculation of neutron, 20: 27584(R) (GEMP-400A, pp 169-84)
radiation effects on ferritic, neutron, 20: 27596
radiation effects on embrittlement of, method for comparing neutron, 20: 27611
radiation effects on low-temperature brittleness of, 20: 30815
radiation effects on embrittlement of reactor structural, neutron, 20: 29825
radiation effects on mechanical properties of low-alloy pressure vessel, fast-neutron, 20: 31796
radiation effects on types Hy-80, A212B, A302B, and A336, neutron, 20: 37286
radiation effects on antifriction and strength properties of No. 45, neutron, 20: 41498
radiation effects on embrittlement of pressure-vessel, neutron, 20: 41494(R) (EURAEC-1617)
radiation effects on, method for comparison of neutron, 20: 41504
radiation effects on notch ductility of, neutron spectral effects in, 20: 43997(R) (NRL-Memo-1663)
radiation effects on mechanical properties of ASTM A302B, neutron, 20: 46237
radiation effects on mechanical properties of A302B pressure vessel, neutron, comparison of U. S. and Japanese, 20: 46236
radiation effects on mechanical and physical properties of low-alloy, 17: 16760
radiation effects, neutron, 19: 7992
radiation embrittlement and hardening in, neutron dose rate and spectrum effects on, 17: 31064
radiation embrittlement of pressure-vessel, relief by annealing, 19: 4716(R) (NRL-Memo-1534)
radiation embrittlement of Soudotenax and T-1, neutron, 20: 17117 (EURAEC-1558)
radiation embrittlement of A350-LF1, annealing effects on neutron, 20: 43997(R) (NRL-Memo-1663)
radiation stability of reactor pressure vessel, stress effects on, 19: 20631
radioactivity, natural, 16: 11956(R) (JAERI-5003(p.107-11))
radiography of defects, causes of image blurring in, 16: 13490(T) (AEC-tr-4492(p.393-8))
radiography of thin, ytterbium-169, 18: 20425
radiography of thick plates of, electron linear accelerator for, 20: 21477
radiography of, using cobalt-60 and electron linear accelerator, 17: 34433
radiography of welds in pipes of, x-ray, 17: 292 (HW-74643)
radiography of, thermal neutron, 18: 43776
radiography of, using cesium-137 and cobalt-60, 19: 32395
radiography of, using isotopes, 20: 39286 (DP-1066(Vol.1), pp IV.43-5)
radiography using electron linear accelerators, 16: 6622
radiography using cold neutrons, 20: 16616
radioinduced embrittlement of pressure-vessel, neutron, 18: 41933 (TID-11295(3rd Ed.))
radioinduced embrittlement of pressure-vessel, neutron, 19: 2859 (NRL-6160)
radioinduced embrittlement of pressure-vessel, review of 1964 Geneva papers on, 19: 24779
radioinduced embrittlement of A353, A336, and T-1, neutron, 20: 27610
radioinduced embrittlement of, remotely controlled equipment for evaluating, 20: 41113
radioinduced embrittlement, measurements using stress wave attenuation, 20: 43993(R) (EURA EC-1691)
radioinduced embrittlement and recovery in ferritic, neutron, 20: 44019
radioinduced gamma activity of, neutron, 19: 37178
radioinduced heating in research reactors, 16: 940(T) (AEC-tr-4763)
radioinduced heating rates, 16: 9431 (NARF-61-38T)
radioinduced heating of 4130, effects on strength of, 17: 3840
radioinduced nitriding of, 17: 29896
radioinduced relaxation of stresses in, 18: 42120(T) (AEC-tr-6474)
reactions of molten AMS 5350, with alumina, fused silica, zircon, and zirconia, 20: 16984
reactions of nitrided, with steam at 1050°F, 19: 38183(T) (ORNL-3807, pp 238-48)
reactions with aluminum to 300°C in helium and hydrogen, 19: 22997 (TRG-Report-842)
reactions with beryllium to 600°C in carbon dioxide and *in vacuo*, 19: 22997 (TRG-Report-842)
reactions with carbon dioxide to 450°C, 19: 22997 (TRG-Report-842)
reactions with chlorine-36-labeled trichloroethylene, hydrochloric acid formation in, 18: 35637
reactions with liquid sodium in reactors, (E), 19: 35800
reactions with liquid sodium at high temperatures, 20: 38499 (ANL-7120, pp 839-47)
reactions with Magnox alloy to 700°C in air, argon, and carbon dioxide, 19: 22997 (TRG-Report-842)
reactions with oxygen, equilibrium oxygen pressures produced in, 20: 277 (AERE-R-4942)
reactions with phosphorus and sulfur compounds in oils up to 700°C, 16: 16054
reactions with radioiodine, surface, 19: 22162(R) (ORNL-3776(p.17-22))
reactions with sodium at high temperatures, 19: 39090(R) (ANL-7046 (p.78-82))
reactions with sodium at high temperatures, 20: 20925(R) (ANL-7055, pp 177-212)
reactions with water at high temperatures, survey of mechanism, 17: 16601
reactivity effects as reflector on beryllium-oxide-moderated uranium-235-fueled subcritical systems, 16: 18622 (UCRL-6729)
reactivity worth of control rods of, 18: 44975
reactor criticality effects, (E), 19: 42077 (ANL-7014)
refining by electron beam melting, 18: 27875
review of status and future potential of, for defense, 18: 8718 (DMIC-Memo-183)
rupture properties of large welded specimens of HT 70, 18: 8855
segregation of phosphorus and sulfur in, autoradiographic study, 18: 30121(T) (NP-tr-1150)
separation of alkaline earths, rare earths, thorium, and uranium from, by ion exchange, 20: 14469(R) (TID-22650)
separation of cerium from high-alloy, by precipitation using hydrofluoric acid, 18: 33504
separation of molybdenum from, by reversed-phase chromatography using hydrochloric and sulfuric acids, 18: 25280
separation of niobium and tantalum from, radiochemical evaluation of extraction process for, 17: 236
separation of oxygen and sulfur from, by compound formation with uranium at 1600°C, 20: 20692
shear properties in by-pass valve rocker arm driver, 16: 19344 (DC-59-12-117)
shielding attenuation factors for, radioisotope and fission-product, 18: 22984 (NYO-10721)
shielding properties, 16: 33318 (TID-16825)
shielding properties for mesons (μ), 18: 26165 (BNL-837(p.91-113))
shielding properties of, testing of, 18: 32948(R) (EUR-534.d(Pt.I))
shielding properties, 19: 11423(R) (UCRL-12004)
solidification of industrial ingots of, tracer study of convection currents in, 17: 25519(T) (AEC-tr-5824)
solvent properties for nitrogen, review on, 19: 22109
sorption of radiocesium and radioiodine on, 19: 30301(R) (ORNL-3789 (p.277-86))
sorptive properties for iodine-131 released from irradiated fuel, 19: 34409 (ORNL-P-1324)
sorptive properties for tritium, effects of texture on, 19: 47018 (USNRDL-TR-890)
spalling of, stress effects on time-dependent, 18: 30182
specification for type 355 plate, sheet, and strip for irradiation testing, 17: 41347 (HW-75208)
sputtering by mercury ions, yield from spheres of, 17: 25870(R) (X62-11400)
stability of prestressed-concrete pressure vessel liners of, 20: 24682
strain aging of conventional and ausform H-11, at 300 to 900°F, 19: 16081 (UCRL-11569)
strain aging of conventional and ausform H-11, 19: 43997(R) (UCRL-11889)
strain aging of conventional and ausform H-11, up to 900°F, 20: 43915 (UCRL-16761)
strain cycling fatigue, 19: 28809 (AP-Note-418)
strength at brittle rupture of, for pressure vessel construction, 19: 26829
strength, effects of sodium, 16: 25720(T) (FTD-TT-61-31(p.41-59))
strength, effects of high-temperature thermomechanical treatment, 16: 30819
strength of ausformed, 19: 43997(R) (UCRL-11889)
strength of, effects on pressure vessel design, 16: 31705
strength of H-11, notch, 19: 32048(R) (NP-15073)
strength of pearlitic and spheroidized, analysis of, 20: 41454 (NYO-2394-22)
strength of reactor containment shells of, 20: 30813
strength of, effects of ausforming, strain aging, and vacuum melting on, 19: 25039
strength requirements of pressure vessel, 20: 30894
strengthening by ausform process, 18: 43137 (UCRL-10981)
strengthening by deformation and hardening, 16: 13522
strengthening mechanisms in austenitic and ferritic, 20: 817 (CONF-710)

strengthening of ausformed, mechanism of, 18: 44157 (UCRL-11520)
strengthening of, review of methods for, 19: 18473(T) (JPRS-28859)
stress analysis of mild, 18: 24824(R) (TID-20613)
stress analysis of ultra-high-strength, x-ray methods for, 19: 22515
stress-corrosion cracking of high-strength, in synthetic environment, 16: 25717(R) (NP-11948)
stress corrosion susceptibility of, effects of purity on, 17: 18701(T) (AEC-tr-5724)
stress fatigue in pressure vessels, method of predicting, 18: 24130 (D2-22437)
stress measurement in stainless steel-clad plate, residual, 16: 22539
stress-relieving, 17: 23925 (TID-7620(Pt.I)(p.251-7))
stress resistance to alternating thermal stresses, 16: 22643
stress rupture properties of stainless-clad, at 500 and 600°C, 18: 10567
stress-corrosion of mild, effects of aging, aluminum content, and heat treatment on, 18: 24088(T) (AEC-tr-6394)
stress-relaxation at 650°C of low-alloy, effects of prior deformation on, 20: 29702(R) (EURAEC-1616)
stress-strain distribution in lap-jointed thin shells of, 18: 18355 (UCRL-7304)
stresses in, feasibility of infrared detection of, 17: 27508 (SCTM-59-63(25))
stresses in heavy weldments of, measurement of residual, 19: 42819 (DF65SL-205)
stresses in, plates clad with stainless steel, 17: 6586
structural properties and uses in reactors, survey, 16: 16036
structural properties, 18: 8737
structure and properties of construction, effects of rare earths on, 19: 23020(T) (JPRS-28849(p.297-302))
structure of case-hardened, x-ray analysis, 16: 13416(T) (AEC-tr-4492 (p.6-15))
structure of nitrided zones in, 16: 24182(T) (AEC-tr-5203)
structure of rolled, neutron diffraction analysis of, 18: 2115
sulfur distributions in mild, used for welding, 17: 29892
surface changes in, probe for determination during heat treatments, 20: 46204
surface density of plating materials of, by gamma backscatter, 18: 41753
surface tension of Armco, effects of cerium and lanthanum on, 17: 32598
tensile properties, 16: 22586 (DMIC-Memo-150)
tensile properties of, apparatus for studying effects of hydrogen on, 17: 1961(T,R) (EURAEC-344)
tensile properties of low-alloy, 17: 6661 (JPL-TR-32-222)
tensile properties, 17: 14890(R) (GA-3724)
tensile properties of, effects of cycle loading on, 17: 18746 (HW-75484)
tensile properties of type 4340, 17: 36987 (SY-5394-R(Vol.I))
tensile properties of, normalized vs. quenched and tempered, 18: 4279
tensile properties of ASTM A53-B and A335-22, 18: 7865(R) (TID-19871)
tensile properties of AM 350, evaluation, 18: 30238(R) (NP-14102)
tensile properties of welded joints of, containing defects, 20: 9441(R) (EURAEC-1352)
tensile properties of low-alloy strain-aged, 20: 31716(R) (UCRL-16658, pp 121-32)
tensile strength of soft, 20: 4365 (AES-3)
tensile strength of flawed wide plates of, 20: 33912
testing for oxide inclusion, neutron irradiation method for nondestructive, 19: 11379(P)
testing for shrinkage pipes in, using industrial betatron, 17: 36002
testing in SNAP radiator-condenser, 19: 24146 (NAA-SR-Memo-10704)
testing of, as reinforcements in blast-resistant concrete structures, 17: 30632 (AD-408447)
testing of pipes of, design of gammascope for, 19: 28519
testing of plates for Japanese reactor pressure vessel, 18: 19382
testing of pressure vessel, fatigue, 19: 24090(R) (SWRI-1228-56)
testing of thick welded, ultrasonic, 18: 43771(R) (EURAEC-882)
testing of, use of cesium-137 in non-destructive, 17: 10817
testing of welded, radiographic and ultrasonic, 18: 39463(R) (EURAEC-663)
testing of welded, radiographic and ultrasonic, 18: 39464(R) (EURAEC-762)
testing of welded, radiographic, 19: 595(R) (EURAEC-1151)
testing of welded, ultrasonic, 19: 596(R) (EURAEC-1152)
testing of, properties of gamma sources for, 18: 27686
testing of, use of iridium-192 in radiographic, 20: 36994
testing pressure-vessel, nondestructive methods for, 20: 14709
tests of high-strength, correlation of Charpy, 19: 20462(R) (NRL-6258)
tests of tunnel liners used in Hardhat shot, static, 18: 37305 (RTD-TDR-63-3041(Vol.IV))
thermal conductivity of, evaluation of cut bar method for measuring, 19: 41029
thermal cycling, 16: 25085 (JAERI-7022)
thermal expansion, x-ray studies, 17: 16667
thermal neutron flux distributions in, 17: 4026 (TID-14073)
thermal stress, 16: 20811(P)
thermal stress analysis, 16: 5460 (HW-71668)
thermal-stress-fatigue properties of ASTM A302B, 18: 596(R) (ATL-A-139)
thermal stress fatigue tests of A302-B, 19: 13980(R) (ATL-A-144)
thermal-stress-fatigue properties of ASTM A302B, 18: 10521(R) (ATL-A-140)
thermal-stress-fatigue properties of A302B and A387D, 18: 22474(R) (ATL-A-142)
thermomechanical treatment of ball-bearing, 16: 13523
thermomechanical treatment, effects on cutting strength and ductility of cutting, 16: 13524
thickness control for use in thin-walled parts, use of radioisotopes in, 16: 13487(T) (AEC-tr-4492(p.379-84))
thickness control by use of gammascopy, 16: 13488(T) (AEC-tr-4492 (p.385-9))
thickness gaging by radiation, 16: 12042
thickness measurements, development of apparatus utilizing radiation for, 16: 13462(T) (AEC-tr-4492(p.274))
thickness of in-place sheets of, radiometric methods of measuring, 20: 29581 (AD-633785)
thickness of plates of, use of gamma rays for measuring, 20: 23569
thickness of, use of radioisotopes for measuring, 20: 23560
tin coating thicknesses on, measurement by gamma excitation of x-ray fluorescence, 18: 24046 (PAN-485/I-A)
ultrasonic inspection of welds in thick wall pipe of, 17: 6243 (HW-74597)
ultrasonic propagation in deformed type C1018, 16: 23971 (ANL-6515(p.121-32))
ultrasonic testing of butt-welded, equipment for, 17: 6250(P)
ultrasonic wave attenuation and diffraction, 16: 15126(R) (NP-11584)
uranium in, method for recovery and segregation of, 19: 4672
uranium oxide and sulfide distributions in molten, 19: 16134
use for gas-cooled reactor pressure vessels, review of British practices for, 18: 8737
use for power reactor pressure vessels, review of, 18: 15515 (CEA-Bib-39)
use for reactor containment, 20: 28701
use in containment of water-cooled power reactors, 20: 12447
use in coolant-flow rotameters for water-cooled reactors, 16: 27393(P)
use of ferritic, in reactor pressure vessels, 18: 44076
use of low-carbon corrosion-resistant, for lining reactor housing, 20: 26415(P)
use of strands of, in reactor biological shield for accident containment, 20: 12346
use of uranium in, depleted, 17: 3385 (TID-8212)
uses in pressure vessels for light-water power reactors, 19: 27786
uses of high-strength, for rocket-motor cases, 17: 6651 (DMIC-178)
wear against SAP and steels, 20: 15998 (EUR-2117.n)
wear and corrosion testing as journal bearing material, 20: 43823 (AECL-2566)
wear in carbon dioxide at high temperatures, 16: 29079
wear in liquid sodium at temperatures up to 500°C, 16: 29080
wear of carburized, against iron in argon and sodium at temperatures up to 1200°F, 17: 26944(R) (BMI-1630(Del.))
weld bead deposition and properties on sheet specimens of, 18: 14435(T,R) (EURAEC-907)
weld cracking in plates of, 18: 8781(T,R) (EURAEC-881)
weld cracking in, review of theories, effects, causes, and control of, 18: 25941 (DMIC-197)
weld embrittlement in, effects of high temperature on, 19: 23090
weld parameters of B-66 and TZM, effects of InFab atmosphere on, 18: 16450(R) (AD-431672)
weld post heating by electron beams, 17: 25764
weld testing in, development of radiographic and ultrasonic, 18: 12563(T) (EURAEC-192)
welded joints in thick, effects of filler metal and flux on, 19: 41007(R) (EURAEC-1400)
welded joints in very thick plates of, research program on, 19: 42820(R) (EURAEC-1252)
welding AISI 4130, to type 304 stainless steel, dilution in, 19: 6285
welding and notch impact strength of joints of ASTM 302B, 19: 13940(R) (EURAEC-1242)
welding and weldment-inspection techniques for, 18: 30158(T,R) (EURAEC-1036)
welding by ascending vertical process, residual stresses from, 19: 13939(R) (EURAEC-1097)
welding by electro-key method, 16: 18004(R) (EURAEC-219)
welding by electroslag process, residual stresses from rising vertical, 17: 39510(T,R) (EURAEC-617)
welding by electroslag process, residual stresses from rising vertical, 18: 10500(T,R) (EURAEC-739)
welding by explosive methods, 19: 11711
welding by friction, 17: 1908

welding characteristics of types 8740, 8630, and A-286, 16: 4510 (DMIC-Memo-140)
welding high-strength low-alloy, development of filler materials and procedures for, 20: 5867
welding high-tensile-strength, materials for, 19: 26796
welding high-tensile-strength, materials and procedures for, 19: 26797
welding mild, to boron steel, evaluation of, 20: 35872
welding, non-destructive seam testing of, 16: 29352(R) (EURAEC-304)
welding of Am-355, ultrasonic, 16: 19295 (ASD-TR-7-888(1))
welding of Creusot 1.2 MD07, 18: 39857(R) (EURAEC-1107)
welding of, electroslag vertical, 17: 6602(T,R) (EURAEC-392)
welding of, electroslag technique for, 17: 22136(T,R) (EURAEC-585)
welding of, electron-beam, 18: 4220
welding of, for reactor use, 17: 18720(T,R) (EURAEC-470)
welding of high-strength, ductility of joints in, 17: 11113(T,R) (EURAEC-430)
welding of high-strength, electrodes for, 17: 23932
welding of low-alloy, on site, 17: 524(P)
welding of pressure-vessel, by arc techniques, 17: 41391(T,R) (EURAEC-771)
welding of pressure-vessel, gas-arc, 20: 43851(R) (EURAEC-1671)
welding of reactor, effects of flux and rod compositions on, 16: 29359(T,R) (EURAEC-251)
welding of reactor, by electro-slag processes, 17: 1902(T,R) (EURAEC-397)
welding of reactor, techniques for, 17: 16616
welding of reactor, research program on electroslag, 17: 39511(T,R) (EURAEC-659)
welding of reactor, by electroslag techniques, 17: 41389(T,R) (EURAEC-763)
welding of reactor, by electroslag techniques, 18: 10504(T,R) (EURAEC-849)
welding of reactor, by electroslag techniques, 18: 20488(T,R) (EURAEC-970)
welding of, testing equipment for simulating, 17: 39507(T,R) (EURAEC-601)
welding of, thermal cycling calculations for, 18: 8776(T,R) (EURAEC-433)
welding of thick, 17: 22137(T,R) (EURAEC-586)
welding of thick, 17: 39509(T,R) (EURAEC-615)
welding of thick, 18: 10501(T,R) (EURAEC-787)
welding of thick, 18: 10503(T,R) (EURAEC-813)
welding of thick, 18: 16458(T,R) (EURAEC-811)
welding of thick, 18: 34089(T,R) (EURAEC-915)
welding of thick, 19: 9633(R) (EURAEC-1106)
welding of thick ASTM A302B, by electroslag techniques, 18: 25945(T,R) (EURAEC-1039)
welding of thick, by submerged-arc techniques, 17: 39513(T,R) (EURAEC-672)
welding of thick, development, 17: 8759(T) (EURAEC-486)
welding of thick plates and rings of, in pressure vessel fabrication, 19: 11702(T) (ORNL-tr-406)
welding of thick plates of, process development for, 20: 9442(R) (EURAEC-1518)
welding of thick plates of, process development for, 20: 9443(R) (EURAEC-1473)
welding of thick plates of, process development for, 20: 25523(R) (EURAEC-1277)
welding of thick, by submerged-arc techniques, 18: 10505(T,R) (EURAEC-853)
welding of thick, by submerged-arc techniques, 18: 16459(T,R) (EURAEC-962)
welding of thick, measurement of thermal cycle during, 19: 24947(R) (EURAEC-1280)
welding of, to thermocouples, stresses generated by electrogas, 17: 22133(T,R) (EURAEC-532)
welding of types A, C, 13C, 23A, and 27A, transformation zones in, 18: 10501(T,R) (EURAEC-787)
welding of types 13C and 23A, transformation zones in, 17: 39509(T,R) (EURAEC-615)
welding of very thick components of, 16: 26654 (ACCESS-134)
welding of very thick, development, 16: 29361(T,R) (EURAEC-273)
welding of very thick, research program on, 19: 18426(R) (EURAEC-1227)
welding of very thick plates of, process development for, 20: 23621(R) (EURAEC-1548)
welding of, use of gamma radiation in control of, 17: 326
welding plates of, for use in high vacuum test rig, 18: 7169
welding, quality control by irradiation method, 16: 13485(T) (AEC-tr-4492(p.369-73))
welding reactor vessels of, metallurgical processes in submerged-arc, 18: 44114
welding sheaths, sheets, and tubes of, techniques for, 18: 7172
welding technology for BH-51, 20: 8433
welding thick, 19: 32703(R) (EURAEC-1297)
welding thick ASTM A302B, 15-GKhNF, 15-GSKhMFR, 16-GNM, and 22K, by electroslag techniques, 19: 9634(R) (EURAEC-1166)
welding thick high-tension, in reactors, 19: 22948
welding thick pieces of, development of processes for, 18: 39862(T,R) (EURAEC-1007)
welding thick plates of, process development for, 20: 7534(R) (EURAEC-1208)
welding thick, electroslag, 19: 11703(T) (ORNL-tr-407)
welding to ceramics, graphite, and metals in SNAP reactor environment at 700 to 1300°F, self-, 20: 7570 (NAA-SR-9643)
welding to steel, explosive techniques for, 16: 3419 (ASD-TR-61-124)
welding tubes of, techniques for, 18: 7173
welding type St-37, electro-slag, 16: 33460(T,R) (EURAEC-315)
welding, ultrasonic, 16: 4515 (NP-11054)
welds between austenitic and ferritic, effects of sodium at 1200°F on, 17: 533(R) (MSAR-61-29)
welds, creep rupture and galling tests, 16: 6213(R) (GA-1738)
welds in, sonic inspection using twin-angle beam technique, 17: 27761 (TID-18871)
welds in thick plates of, betatron detector with scintillation counters for inspection of, 20: 19233
welds in, measurement of residual stresses in, 20: 25524 (EURAEC-1562)
welds in, methods for ultrasonic inspection of, 19: 42025
welds in, radiographic and ultrasonic methods for inspecting, 19: 42024
welds of heavy-gage, research programs on strength of, 20: 41410(R) (EURAEC-1612)
welds of high-tensile, preparation for research on strength of, 20: 41448(R) (EURAEC-1670)
x-ray absorption data for, 17: 32610
x-ray absorption by, 16: 24223
Al–steel, use in radiator-condenser, (E), 19: 5523 (NAA-SR-Memo-9866)
Gd–steel, fabrication and phase studies on, (E), 19: 16189
graphite–steel, use as multilayer neutron shield, 18: 42869 (UJV-1032/64)
LiH–steels, performance as NERVA II shield, 20: 35129 (WANL-TME-1153)
polythene–steel, neutron transmission at 0.2 to 10 Mev, 18: 28547

STEEL COUPLES

steel/U, polarization in aqueous solutions, effects of sodium borate and citrate on, 19: 9619 (AMRA-TR-64-33)

STEEL COUPLES

see also Stainless Steel Couples

STELLARATORS

see also Matterhorn Project
see also Thermonuclear Reactors
bibliography, 17: 28361 (NP-12921)
blankets for, research on, (T), 19: 10392(R) (MATT-Q-21)
charged particle motion in, with magnetic rotational transform, 17: 31595
charged-particle motion in, disturbances in, 19: 19273
design, 16: 3797(P)
design improvements, 16: 6068(P)
development, 16: 2584(R) (MATT-Q-15)
development, 17: 960 (NP-12171)
development, 20: 36295
electrostatic and magnetic field calculation for, (T), 20: 26246 (LA-3416)
injector for injecting atoms or molecular ions into plasma, 16: 31175(P)
injector for, plasma diffusion in Q-1 (E/T), 19: 1704 (MATT-291)
instrumentation for, development of, 17: 9676(R) (MATT-Q-19)
kink instabilities in, (T), 19: 10392(R) (MATT-Q-21)
magnet designs and magnetic fields in Figure-8 and Model C, 16: 15472
magnetic field configuration for, (T), 19: 6801
magnetic field force lines in, from vortex currents flowing over the surface of a torus, 17: 29679
magnetic field force lines in, effects of small perturbations on, 18: 26790
magnetic field lines of force rotational transform in, 18: 32942
magnetic field parameters, 16: 6053
magnetic field perturbations in, 16: 32502 (GA-2925)
magnetic field rotational transforms, 16: 7216
magnetic field structure in, helical, 16: 28299
magnetic fields of, disturbances of helical, (T), 19: 5374
magnetic fields with helical symmetry in, (E), 19: 25568
magnetic lines in, crimping and toroid effects on, (T), 19: 5373
magnetic region enclosed by separata, 16: 6054
magnetic surfaces in Etude, effects of transverse magnetic fields on, 18: 17178
magnetic surfaces and plasma containment in helical field of, (T), 19: 31351

magnetic surfaces in L-1, with double helical field, 20: 22298
operation of Q-1 and Q-3, 17: 9676(R) (MATT-Q-19)
parameters and properties, status, 16: 9540
plasma confinement in, high-temperature, 17: 22765(P)
plasma containment geometries in, 18: 36743
plasma containment in, force line angles in, (E), 19: 6768
plasma containment by rotation in, 19: 21593(P)
plasma containment in, (T), 19: 31417
plasma containment by, instabilities in, (T), 20: 1260 (MATT-370)
plasma containment in, 20: 36303
plasma currents during enhanced diffusion, 16: 23227
plasma diffusion across magnetic field in, 18: 3003
plasma diffusion across magnetic fields in, mechanisms for enhanced, (T), 19: 19240 (IPP-2/31)
plasma diffusion measurements, 17: 9727
plasma drift instabilities in, 17: 5499
plasma equilibrium in toroidal magnetic axis, 20: 42424
plasma heating device, 16: 4939(P)
plasma heating in, 17: 21199(P)
plasma heating in alpha, effects of electron-ion interactions on, (E), 19: 5369
plasma hydromagnetic kink instabilities in, zero-pressure, (E/T), 19: 12672
plasma injection, 16: 15753
plasma injection and confinement in multipolar helical-field, 20: 30657
plasma injection into L-1, 20: 44874(T) (MATT-Trans-36)
plasma instabilities in, 17: 7448
plasma ion-wave instabilities, effect of charge exchange on critical current for start of, 16: 14164
plasma loss in Etude, effects of plasma noise on, 17: 9676(R) (MATT-Q-19)
plasma loss rates in minimum-B, alkali, (E/T), 20: 30656
plasma losses in magnetic field of, quiescent thermal, (E/T), 19: 37929 (MPI-PA-29/64)
plasma magnetic compression heating in, 17: 17326 (MATT-133)
plasma motion in region of magnetic surfaces bounded by separatrix in, (T), 19: 23834(T) (AEC-tr-6527(p.367-72))
plasma of S-1, interactions of runaway electrons and, (E), 20: 3186
plasma oscillations in, excitation and thermalization of, (E), 20: 24544(T)
plasma particle losses in, 18: 17228
plasma probe system for, design and performance of, 17: 36751 (MATT-139)
plasma production by magnetic pumping in, 18: 17156
plasma stability during ohmic heating in, 16: 7209
plasma stability in, current convective, 16: 14178
plasma stability in, interchange, 17: 28389
plasma stability in helical, 18: 11310
plasma stability in negative V″, pressure effects of, (T), 20: 30561 (MATT-415)
plasma stability in negative V, 20: 38243
plasma stability theory for, 20: 28494(R) (MATT-Q-22, pp 215-319)
plasma temperature in, Doppler effect, 16: 7211
radiation monitoring equipment for, 19: 43415 (MATT-347)
runaway electrons from, model of, (E), 19: 10392(R) (MATT-Q-21)
stability of, effect of finite ion gyration radius on, 17: 11788 (MATT-119)
stability of negative V″, theory of, 20: 28494(R) (MATT-Q-22, pp 215-319)

STELLARATORS (A-2)
development, 16: 29905(R) (MATT-Q-18)
ion reactions with stainless steel wall of, re-emission rates for helium and hydrogen, (E), 20: 17922
plasma density fluctuations in, (E), 19: 5331
plasma density variations in, azimuthal, (E), 20: 13915 (MATT-402)
stability of, analysis of hydromagnetic, (E/T), 20: 28493(R) (MATT-Q-22, pp 113-214)

STELLARATORS (B)
plasma heating in, diffusion coefficient during, 16: 2584(R) (MATT-Q-15)

STELLARATORS (B-1)
development, 16: 29905(R) (MATT-Q-18)
electric field characteristics and plasma losses in, 17: 19456 (NP-12651)
ion wave excitation in, 16: 9500(R) (MATT-Q-17)
tank walls of, impurity ion release by, (E), 19: 10392(R) (MATT-Q-21)

STELLARATORS (B-3)
development, 16: 29905(R) (MATT-Q-18)
development and operation, 17: 9676(R) (MATT-Q-19)
electron temperature and plasma density, probe studies, 16: 9500(R) (MATT-Q-17)
plasma containment times, 16: 23228
plasma diffusion and properties in, 17: 33145 (MATT-157)
plasma diffusion losses during ohmic heating, 16: 23226
plasma heating in, (E), 19: 10392(R) (MATT-Q-21)
plasma production and heating in, (E), 19: 45398 (MATT-332)
plasma rotation in, effects of radial electric fields on, (E/T), 20: 28493(R) (MATT-Q-22, pp 113-214)
stability regions in, magnetic axis form effects on, 17: 42044 (CEA-2319)

STELLARATORS (B-65)
development and operation, 17: 9676(R) (MATT-Q-19)
ion gage development for, 16: 2585(R) (MATT-Q-16)
ion wave existence in, 16: 2584(R) (MATT-Q-15)

STELLARATORS (B-66)
development, 16: 29905(R) (MATT-Q-18)
development and operation, 17: 9676(R) (MATT-Q-19)
ion cyclotron wave propagation in, 16: 2584(R) (MATT-Q-15)
ion cyclotron wave polarization vector rotation direction in, 16: 2585(R) (MATT-Q-16)
ion energy distribution in, 17: 19456 (NP-12651)
plasma pressure in, axial variation model of, 20: 28493(R) (MATT-Q-22, pp 113-214)
wave propagation in, 16: 9500(R) (MATT-Q-17)

STELLARATORS (C)
characteristics, 16: 2763
charged particle energy distributions in, (E), 19: 23924
cooling system for, design and operation of, 20: 12173 (MATT-315)
data recording and display system for, development of semi-automatic, 20: 30573
data recording system for, (E/T), 20: 28495(R) (MATT-Q-22, pp 321-85)
design and development, 20: 28492(R) (MATT-Q-22, pp 1-111)
development, 16: 29905(R) (MATT-Q-18)
development, 17: 19456 (NP-12651)
development, 18: 2981(R) (MATT-Q-20)
development and operation, 16: 2585(R) (MATT-Q-16)
development and operation, 17: 9676(R) (MATT-Q-19)
development and use in research, (E/T), 19: 10392(R) (MATT-Q-21)
development of, review of, 20: 3196
development status of, 20: 20365
discharges in, impurity radiation power losses in, 17: 31575 (MATT-194)
discharges in, source of neutral atoms and molecules in, 17: 28348 (MATT-161)
discharges in, light emission by helium and hydrogen during, 19: 27608 (MATT-305)
discharges in, temperatures of neutral atoms in, (E), 20: 44911
Doppler broadening in, effects on stability, (E/T), 19: 10392(R) (MATT-Q-21)
electric discharges in, light emission by hydrogen during, (E), 20: 12171 (MATT-270)
electric discharges in, particle-loss rates for, (E), 20: 12239
electric discharges in, recombination rate of doubly ionized helium in, 20: 30600
electron runaway in, 17: 21135 (MATT-164)
electron temperatures in, 18: 21378 (MATT-251)
gas injection into vacuum system of, fast-acting valve for, 18: 15331 (MATT-225)
ion cyclotron wave production in deuterium-hydrogen plasma in, optimum, (E/T), 20: 4984
ion gage filament testing for, 18: 22323
magnetic field determination of, confining, 20: 10120 (CONF-650512, pp 100-4)
magnetic flux path adjustment by coil tilting, 16: 15401
magnetic pumping system of, design of power supply for, 20: 10132 (CONF-650512, pp 213-20)
microwave propagation in plasma in, (E/T), 19: 19298
neutral helium in, temperature of, (E), 19: 10392(R) (MATT-Q-21)
ohmic heating in, hydrogen loss and return in, 18: 2981(R) (MATT-Q-20)
operation, 16: 2584(R) (MATT-Q-15)
oxygen ion concentrations, 18: 21378 (MATT-251)
plasma behavior in, effects of helical field on, 17: 42119
plasma containment times, 16: 23228
plasma containment and power balance in, 18: 7815
plasma containment in, 19: 37914 (IPP-2/36(p.71-82))
plasma containment in, (T), 19: 45397 (MATT-282)
plasma electron heating in, from ion cyclotron waves, 20: 46873
plasma equilibrium in, current-carrying toroidal, 17: 28393
plasma excitation and ionization in, neon ion, 20: 38250
plasma fluctuations and control of pumpout in, (T), 20: 38266
plasma heating by radiofrequency techniques, 16: 1125
plasma heating in, high-Q capacitor development for, 20: 10131 (CONF-650512, pp 201-12)
plasma heating in, models of ion cyclotron resonance, 20: 28492(R) (MATT-Q-22, pp 1-111)
plasma heating in, by ion cyclotron resonance, 20: 30577
plasma hydromagnetic kink instabilities in, zero-pressure, (E/T), 19: 12672
plasma impurity level in, 16: 9500(R) (MATT-Q-17)
plasma ion heating in, using ion-cyclotron-resonance, (E), 19: 47832

plasma losses from heating in, (E), 20: 4942 (MATT-372)
plasma particle losses and power balances in, (E), 19: 47854
plasma pressure and temperature in, perpendicular, (E), 19: 21511
plasma properties in, transverse magnetic field effects on, 20: 46880
plasma stability in, toroidal, (E), 20: 38268
plasma temperature measurement in, Doppler method of, 18: 17170
plasma temperature in, (E), 19: 14708
plasmas in, studies of, 17: 19456 (NP-12651)
power balance in helium discharges in, 19: 37927 (MATT-268)
power supplies for, arc damage in grid wires of, 20: 46818 (MATT-383)
radiation and power balance in, impurity, 18: 21377 (MATT-247)
seal for, production of bakeable ceramic-to-metal, 18: 10495 (MATT-228)
spark gap switch for ringing circuit of, behavior of, 17: 31567 (CONF-24-11)
symmetrization of, 18: 9487
vacuum system for, problems in construction, 16: 31715

Stellite
see Cobalt Alloys

STERILITY
effects of iodine-131 thyroidectomy on rat, 19: 35992
effects of radiomimetic agents on mouse, 18: 23177
effects of temperature on radioinduced, in male silkworms, 20: 42930
radiation effects on, in workers in Japan, 16: 25214
radiation effects on, of male mice after embryonic exposure, 16: 28756(T) (JPRS-14833)
radiation effects on mouse, cause of, 17: 19910
radiation effects on *Rhodnius prolixus*, x, 18: 3519
radiation effects on male mice, pre- and post-natal, 18: 11665
radiation effects on mouse, x, 18: 15893
radiation effects on codling moth, gamma, 18: 21852
radiation effects on cotton moth, 18: 23283
radiation effects on mouse, gamma, 18: 23326
radiation effects of ultraviolet radiation on, in *Drosophila melanogaster*, 18: 29271
radiation effects on cow, 18: 38775(R) (ORO-624)
radiation effects on, in premature female mice, 19: 8816
radioinduced in Anopheles, gamma, 18: 19654
radioinduced in Drosophila, relation of X-autosomal translocations to, 20: 42709(R) (TID-23233)
radioinduced in human males after accidental exposure, 18: 19648
radioinduced in insects, gamma, 18: 22199 (TID-7684(p.55-7))
radioinduced in insects, effects of air and carbon dioxide on, gamma, 18: 23276
radioinduced in jute, gamma, 20: 40681
radioinduced in Khapra beetle pupae, gamma, 18: 31250
radioinduced in male dogs, x, 18: 15892
radioinduced in Mexican fruit flies, effects of dose on gamma, 20: 3745
radioinduced in mice, protection against, using serotonin, 18: 19711
radioinduced in mice, x, 18: 23325
radioinduced in miners, 18: 29429
radioinduced in mice, effects of oocyte destruction on, 19: 31791(R) (ORNL-3768(p.89-93))
radioinduced in mice following fetal and suckling exposure, gamma, 19: 33796
radioinduced in mice, x, 20: 65(R) (TID-22174)
radioinduced in mosquitoes, gamma, 16: 26843
radioinduced in silkworms, 19: 10831
radiotherapy of, x, 20: 45546

STERILIZATION
see also Radiosterilization
goals and standards for, 20: 14234
methods for, of radioactive pharmaceuticals, 20: 27020
of microorganisms, bibliography, 17: 31765 (N63-16122)
of sewage by heat and radiation from a reactor, 17: 23542 (AD-286432)
of surgical materials, conference on, 17: 4760
radiation effects on, of codling moths, gamma, 18: 21852
radioinduced in Drosophila males, effects of X chromosome translocations on, x, 19: 31789(R) (ORNL-3768(p.58-63))
radioinduced in male rats, gamma, 19: 36026
radioinduced in medical preparations, gamma, 18: 21862
techniques for virus isolation by zonal centrifugation, 20: 7(R) (ORNL-3883)
testing of radiopharmaceuticals, 20: 27023

STEROIDS
biogenesis and metabolism in elderly men, tracer study on, 20: 38547(R) (NYO-918-15)
calcium-47 distribution and kinetics in dogs as affected by, 18: 15795
chromatography of acetylated, deuterium and hydrogen isotope effects in gas-liquid, 19: 19893
complications induced by, after radiotherapy, 18: 9954
determination in body fluids and tissues, 19: 29854(R) (TID-21859)
determination in body fluids and tissues, radiometric methods for, 20: 22932
determination in urine using paper chromatography, 20: 38547(R) (NYO-918-15)
determination of, tracer techniques for, 17: 18503
deuterium incorporation in, 20: 20799
effectiveness in treatment of allergic dermatitis, 17: 1244
effects of anabolic, on calcium-47 and strontium-85 retention in rats, 19: 19476
effects of, on growth of tumor cells in culture, 20: 5296(R) (NP-15585)
effects on calcium metabolism in dogs, 18: 6601
effects on calcium-47 metabolism in osteoporosis patients, 19: 6997
effects on cesium-134 metabolism in rat muscle, 19: 31733
effects on development of female fish, 20: 16263
effects on enzyme activity in liver of irradiated rats, 18: 23241(R) (NP-13918(p.13-27))
effects on enzyme synthesis in rat liver, 18: 35315(R) (NP-14210 (p.14-24))
effects on excretion of iodine in guinea pigs, effects of sex and dose size, 17: 13947
effects on excretion of taurine and sulfate by rats, 18: 25006 (TID-18927)
effects on excretion of strontium isotopes by mice, 20: 8564
effects on fluoride ion uptake by bones, 17: 35253(R) (IA-775)
effects on immune reactions to bone marrow grafts in mice, 19: 33728
effects on joint inflammations in rats, 19: 31669(R) (ACRH-23(p.170-74))
effects on manganese metabolism, 16: 5136
effects on nucleic acid synthesis in rats, 18: 27011(R) (ORNL-3601 (p.188-206))
effects on phosphorus metabolism in normal and castrated rats, 18: 36
effects on radiosensitivity of enzyme systems in rat liver, 18: 23352(R) (NP-13918(p.28-41))
effects on radiosensitivity of enzyme systems in rat liver, 19: 8787(R) (NP-14448(p.1-12))
effects on radiosensitivity of enzyme systems in rat liver, 19: 8788(R) (NP-14448(p.13-20))
effects on ribonucleic acid synthesis in rats, 19: 2008(R) (ORNL-3700 (p.157-72))
effects on strontium metabolism in man, 19: 45805
effects on sulfur metabolism in rats, 19: 5625
effects on survival of lethally irradiated rats, 18: 5141(T) (JPRS-22180(Excerpt))
effects on survival of lethally irradiated rats, 18: 5141(T) (JPRS-22180(Excerpt))
excretion of adrenal, effects of ingestion of radon-containing water on, 20: 8577
fever-production by, 18: 15755
formaldehydogenic, urinary levels of, effects of hypothalamic lesions, liver injury, and radiation on rat, 17: 23099
hemolytic effects of, on erythrocytes, 19: 14943
hydroxycortico-, radiotherapy effects on excretion of, gamma and x, 17: 35586
identification of, using radiochemical paper electrophoresis of the hydrazones of, 20: 29132
labeling of keto, with tritium, by adsorption chromatography, 19: 32194
labeling pregnenolone and progesterone with carbon-14 and tritium, 19: 32254
labeling with tritium, review of methods for, 18: 43590
mass spectra of fragmentation in 1- and 4-keto, 18: 12135
metabolism in animals, tracer studies, 19: 31749
metabolism in Cushing's disease, effects of adrenalectomy and radio-induced pituitary ablation on, 19: 26163
metabolism in man, tracer studies, 16: 28743(R) (NYO-10152)
metabolism of hormones, radioisotope studies, 16: 1382
metabolism of, in man, 19: 29854(R) (TID-21859)
oxidation by dichlorodicyanoquinone, isotope effects, 19: 4182
pharmacological effects of, 19: 29848 (ACRH-103(p.62-75))
photochemical rearrangement of 3,20-diethylenedioxy-11-oxo-C-nor-5α-pregnane, formation of aldehyde in uv, 18: 33634
physiological effects on mitochondria, 17: 7798(R) (TID-17544)
physiological effects in man, 19: 31667(R) (ACRH-23(p.143-57))
preparation and uses of sulfur-35- and tritium-labeled, 20: 38547(R) (NYO-918-15)
preparation of carbon-14 and tritium labeled, 19: 29854(R) (TID-21859)
preparation of poly-deuterated analogs of 5 α-androstan-11-one, 17: 30569
preparation of tritium-labeled, 18: 31079
preparation of tritium-labeled, method for, 19: 20025
preparation of tritium-labeled estriol-3-glucosiduronate by guinea pig liver homogenate, 20: 31312
protective effects of dexamethasone against radioinduced leukopenia, 16: 20269
protective effects of prednisolone against radioinduced injury to ureter, 17: 5820

radiation chemistry of estrone in acetic acid, x, 20: 5274
radiation effects on conjugation by liver and kidney, tracer study, 17: 24888(R) (COO-227(p.151-69))
radiation effects on excretion of, in urine, 19: 8911
radiation effects on synthesis by testes, 19: 10783(R) (COO-119-231 (p.76-84))
radiation effects on mouse, protective effects of heparin against, 20: 10705
radiation effects on content in blood of burros, neutron, 20: 18296(R) (UCLA-12-576, pp 57-60)
radiation effects on content in guinea pigs, x, 20: 28975
radiation effects on excretion and production of, as guinea pig urine, 20: 38547(R) (NYO-918-15)
radioinduced decomposition of tritiated cortexolone, effects of molecular structure on, 20: 14578 (EUR-2435.f)
radiolysis of high-specific-activity tritium-labeled, by self-irradiation, 18: 43691
radiosensitivity effects on enzyme metabolism in liver of young rats, 16: 26660(R) (NP-11966(p.55-64))
radiosensitivity effects of methandrostenolone on rats, 20: 14402
radiosensitivity effects of methandrostandiol, in mice and rats, 20: 18477
separation by gas–liquid chromatography, 19: 22143
separation of, from phosphors, chromatographic, 17: 14380
spectra of hydrogen transfer reactions in poly-deuterated analogs of 5 α-androstan-11-one, 17: 30569
structure elucidation by isotope labeling and mass spectrometry, 19: 7534
structure of, analysis by field ion mass spectrometry, 20: 31199
synthesis, 19: 8952(R) (AD-601838)
synthesis by adrenal cortex tissue, 16: 17387
synthesis of corticosteroids in placental tissues, 16: 17386
synthesis of tritium-labeled, 16: 17385
synthesis of tritiated, 18: 10116 (EUR-412.f)
therapeutic effects of ointments, in radioinduced skin lesions, 16: 20155
therapeutic use of, in malignant lymph diseases, 18: 13390(R) (ORINS-43)
transformation of, by testicular tissue in rats, effects of localized head irradiation on, 18: 29240(R) (COO-119-229(p.80-92))
tritium-labeling of digitogenin, 18: 27491
use for therapy of bone marrow failure induced by anemia or leukemia, 20: 3793
17-hydroxycortico, excretion in carcinoma patients injected with ACTH, 17: 35410
19-norandrostenolone phenylpropionate, radioprotective effects of, in rat testes, 17: 35461
3-oxo-4,5-oxido-, photochemical rearrangement of, 18: 33635

STEROIDS, 17-KETO-
determination in urine using paper chromatography, 20: 38547(R) (NYO-918-15)
deuterium uptake by C-19 angular methyl group in, 18: 22106
excretion in irradiated cervical carcinoma, 18: 33287
excretion of tritium-labeled, after injection of labeled testosterone, 20: 18230
excretion of, after radiotherapy of female genital carcinoma, 19: 22067
labeling with tritium, distribution and orientation of label in, 20: 23064
radiation effects on urinary excretion, whole-body exposure, 16: 20209
radiation effects on blood plasma content of, in dogs, 18: 6698
radiation effects on monkey secretion of, 18: 38867
radiation effects on adolescent excretion of, after *in utero* atomic explosion exposure, 19: 3941
radiation effects on human urinary, 19: 5714
radiation effects on content of, in blood plasma, 19: 7144
radiation effects on content of, in rat urine, 19: 38443
radiation effects on, following tumor therapy, 20: 16209
radiation effects on, in man, 20: 31035(R) (RLO-1780-8)
radiation effects on content in dog blood, x, 20: 38684
radiotherapy effects on urinary excretion of, 17: 35585
radiotherapy effects on excretion of, gamma and x, 17: 35586
use in determining radiation response, 20: 16209

STEROLS
see also Bile Acids
see also Cholesterol
see also Estrogens
see also Gonadal Hormones
see also Testosterone
see also Vitamin D
labeling of desmosterol and lanosterol with carbon-14, 20: 16548
metabolism in rat liver homogenates, tracer study, 20: 42737(R) (ANL-7136, pp 231-42)
metabolism of, in insects, tracer studies of, 18: 6595(R) (TID-19836)
metabolism of, tracer studies, 19: 29849(R) (ANL-6971(p.1-28))
radiation effects, 16: 27519
radiation effects on synthesis in rats of, x, 20: 38638
radiation effects on yeast, x, 20: 45415
separation of double-labeled, isotope fractionation in adsorption chromatographic, 18: 43391
synthesis of dehydrostigmasterol in plants, mechanisms of, 19: 31760

STIBINE, TRIMETHYL-
decomposition in ion source of mass spectrometer, mechanism of, 20: 14584(R) (TID-22444)

STIBINE, TRIPHENYL-
effects on G-values in radioinduced polymerization of triethylene glycol dimethacrylate, 17: 37254 (TID-19381)
effects on radioinduced polymerization of triethylene glycol dimethacrylate, 18: 31569 (TID-20812)
effects on scintillation quenching in benzene, 19: 46362
inhibiting effects on radioinduced and thermally induced polymerization of monomers, 16: 30448 (TID-15961)
radiation effects on, from neutrons and high-energy recoils, 19: 22361
radiation effects on liquid and solid, chemical effects of energetic recoil atoms created by neutron, 19: 42568
radiolysis of, in benzene, 19: 46362

STIBINES
see also Antimony Hydrides
heat of explosion, 17: 27322 (UCRL-7301-T)
heat of formation, 17: 27322 (UCRL-7301-T)
preparation by flash electrolysis, for separation of antimony from fission product mixtures, 19: 18058
radioinduced free radicals of, in krypton, 20: 36909
spectra of, absorption, 18: 22027
SbH_3–$B_{10}H_{14}$, heat of explosion, 17: 27322 (UCRL-7301-T)
SbH_3–Ge_2H_6, heat of explosion, 17: 27322 (UCRL-7301-T)
SbH_3–Si_2H_6, heat of explosion, 17: 27322 (UCRL-7301-T)

STIBONIUM COMPOUNDS
hexapyridinyl- bromide, crystal structure, 20: 35474 (IS-T-89)

Stilbazogall I
see 2,2'-Stilbenedisulfonic Acid, 4,4'-Bis[(2,3,4-Trihydroxyphenyl)azo]-

Stilbazogall II
see 2,2'-Stilbenedisulfonic Acid, 4,4'-Bis[(6-Carboxy-2,3,4-trihydroxyphenyl)azo]-

STILBENE
alpha excitation of, pulse-height ratios for, 18: 20408
effects on gamma radiation effects on aliphatic or aromatic ketones, ESR studies on, 20: 43313
effects on radioinduced decomposition of Santowax-OM1, 20: 20708 (AEET-213)
effects on yields from gamma radiolysis of 2-methyltetrahydrofuran, 19: 28406
efficiency as neutron counter, 18: 7072
efficiency as neutron counter, 19: 24848
electron excitation of, pulse-height ratios for, 18: 20408
exchange reactions with deuterium oxide, mechanism of platinum-catalyzed, 16: 16344
fluorescence decay time in, 16: 29507
fluorescence mechanisms in crystals of, particle separation by, 16: 6990
isomerization of, by triplet molecules and free radicals from gamma radiolysis of benzene and cyclohexane, 20: 40961
luminescence decay in, from 3 to 200 nsec, 17: 14349
luminescence, decay of slow component of, 17: 32426
luminescence decay rate in, slow-component of, (E), 19: 34475 (INR-604/XIX/D)
luminescence of, discrimination of alpha-, deuteron-, and proton-produced, 18: 16324
performance as phosphor in neutron time-of-flight detectors, 19: 11542
performance for gamma detection and measurement in high neutron flux, 20: 31602
performance for neutron flux measurements at 14-Mev, 19: 28628 (EUR-1815.e(Rev.)(p.246-53))
performance in Compton scintillation gamma spectrometer, 18: 5656
performance in neutron spectrometers, 20: 13063 (JAERI-1092)
performance in scintillation detectors for fast neutrons, 19: 22798
performance in scintillation detectors, effects of high voltage on, 19: 34482
phosphorescence of, circuit for discriminating gamma and 14.85-Mev neutron, 17: 23618
phosphorescent pulse distribution for 1- to 15-Mev neutrons, 16: 3669 (TID-13075)
photofluorescence decay times, in nanosecond region, 16: 4357
photoluminescence decay of crystals of, to 250 nsec, 16: 27834
polarographic behavior at dropping mercury electrodes, 16: 95 (TID-14097)
properties as neutron dosimeter, 17: 22002 (AERE-R-4244)
properties as particle discriminator, effects of particle energy and temperature on, 18: 4098

properties in fast neutron spectrometers, 19: 30574
properties of crystals of, as fast neutron spectrometer, 17: 41120
radiation effects on *trans-cis* isomerization of, in methanol solutions, 20: 14579(R) (NYO-2383-15)
radiation effects on diffusion of triplet excitons in, 20: 38957
radioinduced isomerization of, in methanol solutions, effects of additives on gamma, 20: 29287
radioinduced isomerization of, values for gamma and x, 20: 33334 (NYO-3242-13)
radioinduced isomerization of, in benzene and cyclohexane, 20: 35554
radioinduced isomerization of, in benzene, gamma, 20: 38948
radioinduced polarization of fluorescence from, 18: 25594
radioinduced scintillation of crystals of, effects of temperature on, 17: 29018
radiolysis of *cis-* and *trans-*, spectra of yields in, 19: 46345
radiolysis of, effects of naphthalene, phenanthrene, and triphenylene on isomerization in, 20: 18735
radiolysis of, in cyclohexane and benzene, 20: 40961
response to charged particles, 18: 41824
scintillation anisotropy in, from fast neutrons, 17: 14350
scintillation decay time of, 19: 24864
scintillation decay of, at 0 to 100 nsec, (E), 20: 7157
scintillation intensity in crystals of, measurement of time dependence by delayed-coincidence method, 16: 368
scintillation intensity in crystals of, time dependence of, (T), 20: 14615
scintillation pulse-shape discrimination in, circuit for determining, 20: 16839
scintillation response of crystalline, to alpha particles, gamma rays, and fast neutrons, 17: 34869
scintillation response of crystalline, slow component in, 18: 29674
scintillation response of, particle discrimination from, (E/T), 19: 4458 (ISS-64/23)
scintillation response of, time-dependent, 20: 16813 (INR-653/IA/D)
spectra of, and of partially deuterated harmonic vibrational wave numbers in, 16: 23705
use in neutron scintillation counters, 20: 31532
use of crystals of, in neutron spectrometers, 17: 36143 (AERE-R-4269)
use of radiopolymerized in gas-liquid chromatography, 19: 24469
bibenzyl–stilbene, spectra of naphthacene impurities in crystals of, 16: 30985

STILBENE, 4,4'-DIPHENYL-
radiation effects on carbon tetrachloride polycrystalline solutions of, spectra of resonance charge transfer in, 20: 18752
radioinduced fluorescence of, in naphthalene, 20: 3994
scintillation properties in liquid helium, 18: 25849

STILBENE, α,α'-DIMETHYL-
radioinduced isomerization of, in benzene, gamma, 20: 38948

STILBENE, α-METHYL-
radioinduced isomerization of, in benzene, gamma, 20: 38948

4,4'-STILBENEDIOL, α,α'-DIETHYL-
decomposition in soil of, tracer study, 19: 11155
distribution in man of carbon-14-labeled, 19: 45797
effects of, combined with surgery and radiation on prostate carcinomas, 20: 8765
effects on hemorrhagic diathesis in rats fed irradiated beef, 17: 28610
protective effects against radiation sickness in mice, 17: 30457
protective effects against radiation sickness in hamsters, 17: 30458
protective effects against radiation injuries in hamsters, 18: 17671
protective effects against radiation damage in mouse and rat tumors, 19: 7180
radiosensitivity effects, 17: 30424
radiosensitivity effects, 18: 19799
radiosensitivity effects in rats, 20: 10709
reaction of normal and malignant tissues to, 17: 31939
uptake by cattle liver of carbon-14-labeled, 19: 45797

2,2'-STILBENEDISULFONIC ACID

2,2'-STILBENEDISULFONIC ACID, 4,4'-BIS[(6-CARBOXY-2,3,4-TRIHYDROXYPHENYL)AZO]-
analytic use for zirconium determination, 19: 40441
analytical uses in determination of zirconium, 19: 30138

2,2'-STILBENEDISULFONIC ACID, 4,4'-BIS(1,8-DIHYDROXY-3,6-DISULFO-2-NAPHTHYL)AZO-
analytical uses for determination of scandium, 20: 7037

2,2'-STILBENEDISULFONIC ACID, 4,4'-BIS[(2,3,4-TRIHYDROXY-PHENYL)AZO]-
analytic use for zirconium determination, 19: 40441

STILBENES
cis-trans isomerization, mechanism of thermal, photochemical and radio-induced, 19: 13402 (KFK-244)
effects on radiolysis of cyclohexane, role of electron affinities in, 20: 35561
isomerization of, in irradiated benzene, 20: 43360
radiation effects on carbon tetrachloride polycrystalline solutions of, spectra of resonance charge transfer in, 20: 18752

Stilbestrol, Diethyl-
see *4,4'-Stilbenediol, α,α'-Diethyl-*

Stills
see *Distillation Apparatus*

STIRRING APPARATUS
see also Mixing
design for feed-sampling tank, engineering drawings for, 20: 342
design of low-speed agitator for Redox Process, 17: 3065 (HW-52755)
design of magnetic, for closed diffusion cell, 18: 31695 (TID-19277)
design of magnetic, for diffusion cells, engineering drawings for, 20: 221
development for skull reclamation process, 20: 5594(R) (ANL-6925, pp 21-106)
development of magnetic, for multiphase sealed liquids, 16: 19071 (DP-704)
performance in turbine mixers, methods of measurement, 16: 302(T) (AEC-tr-4846)

STOCHASTIC METHODS
see also Mathematics
see also Monte Carlo Method
calculation of neutron slowing down in infinite homogeneous moderator by, 16: 18411
field theory, S-matrix in, 17: 13394
for anisotropic diffusion of neutrons, 16: 31061
for measurement of dynamic nuclear reactor parameters, 16: 775
models for distribution of radioactive material in compartmental biological systems, 19: 28126 (ORNL-3809)
models for distribution of radioactive materials in compartmental biological systems, 20: 18427 (ORNL-3920)
models for neutron multiplication in reactors, 18: 35070 (TID-7679 (p.29-59))
operators in linear, properties and use of, 17: 14722
reactor kinetics model with xenon feedback effects, (T), 19: 33611 (WAPD-T-1684)
reduction of Cartesian tensors for spin-one systems, 16: 17961 (NYO-10031)
reversing, backward Monte Carlo method for, 16: 9138 (UCRL-6649)
sequent correlations in evolutionary stochastic point processes and application to cascade theories, 18: 36283
series analysis, generalization of Schuster test for autocorrelated, 16: 3390(T) (SCL-T-388)
stability of multiplicative, with linear feedback, 19: 17438 (WAPD-T-1479)
statistics in, master equations for Markov processes in, 19: 25080
theoretical-numerical basis of the stochastic number theory, 18: 21734(T) (ORNL-tr-42)
theory application to physical problems and relation to quantum mechanisms, 16: 18105 (NP-11463(Pt.2)(p.239-53))
theory of sand movements in rivers, 19: 13618 (NP-14667)
use for analysis of inhomogeneous materials performance, 17: 3354 (KAPL-M-CHR-6)
use for analysis of heterogeneous material, 18: 16647 (KAPL-M-CHR-7)
use for indirect measurements of power spectral densities, 18: 4742 (LADC-5845)
use in deriving Hamiltonians for finite many-body systems, 16: 4946 (AFOSR-1138)
use in lattice model concept of neutron transport, 20: 9956
use in model of interacting field, 17: 38425
use in reactor theory, bibliography on, 20: 26426 (IFA-FR-47)
use of positive semi-groups in Markow's, 17: 20392 (JUL-101-PP)

STOCKDALE QUADRANGLE (TEXAS)
geologic map, 16: 2040

STOMACH
see also Gastrointestinal Tract
analysis of content of, for jack rabbits, 17: 35406 (TID-17965)
autoradiographic diagnosis of carcinomas of, 19: 13182
autoradiography of malignancy in, 20: 24958
bioelectrogenic mechanisms in rat, ionic relation of, 18: 19521 (USNRDL-TR-716)
calcium-45 distribution in rat, effects of age on, 18: 33
cancer etiology in, 20: 4197
cancer of, use of *in vivo* radioautography for diagnosis of, 17: 28622
carcinoma diagnosis in, tracer methods for, 19: 15319
cesium-137 content in bull, fallout, 19: 20215
chloride exchange in mucosa of, in frogs, tracer study, 19: 35937
electric potential in mucosa of, effects of sodium on, 17: 15645 (USNRDL-TR-608)
fatty acid absorption in frog, tracer study, 19: 35938
gastric ulcer in swine, effects of paternal irradiations on, 20: 45362(R) (TID-23311)
grafts of whole organ, effects of gamma radiation on acid secretion, 17: 14039

hyalinization of, in non-irradiated patients, 20: 8515
incidence of cancer of, among Japanese surviving atomic disasters, 20: 42697 (ABCC-18-65)
intragastric beta irradiation, effectiveness in treatment of peptic ulcers and gastric neoplasms, 17: 10367 (TID-17727)
iodine-131 content in, after intravenous injection for myocardial infarction detection, 17: 5685
iodine-131 deposition in, gonad exposure from, 16: 25668
iodine-131 uptake and distribution in rat, from labeled atabrine, 19: 14988
iodine-131 uptake by fetal, effects of age on, 20: 5259
iodine-131 uptake by, 20: 31160
mercury-203 uptake by rat, after repeated vapor inhalation, 19: 3860
photoscanning of, after injection of labeled colloidal albumin, 18: 19813 (CONF-164-11)
polonium-210 uptake and distribution by cat, 19: 2044
polonium-210 uptake and distribution by rat, after inhalation by nose exposure, 19: 2051
radiation effects on gastric retention, whole-body, 16: 12898
radiation effects, protective effects of desoxyribonucleic acid against whole-body, 16: 12925
radiation effects on closure of hole in gastric wall using homotransplant, 16: 4114(T) (JPRS-10882)
radiation effects on chromium-51 uptake by mouse, protective effects of serotonin against, 17: 14021
radiation effects on nervous elements of, in rats, 17: 30432
radiation effects on morphology and secretory function of, 18: 122(T)
radiation effects on gastric secretion in dogs after feeding, whole-body, 18: 5106
radiation effects on nervous response of rabbit, 18: 17586
radiation effects on food passage time in, in rats, 18: 25172
radiation effects on gastric juices secretion by, in dogs, 18: 38960
radiation effects on bioelectric activity in isolated rat, x, 19: 2141
radiation effects on bioelectric activity in rat, factors affecting x, 19: 2140
radiation effects on gland activity in dog, sodium-24, 19: 3956
radiation effects on human, x, 19: 5715
radiation effects on histidine decarboxylase activity in rat, 19: 17604
radiation effects on ATP content in rat, 19: 17626
radiation effects on cancers of, preoperative, 19: 25989
radiation effects on ultrastructure of gastric fundus glands in mouse, 20: 111
radiation effects on absorption of fatty acids in, x, 20: 3754
radiation effects on gastric juice secretion in dog, x, 20: 5384
radiation effects on carcinostatic properties of tumor extracts from, x, 20: 12625
radiation effects on glucose diffusion in rat, uv, 20: 20414
radiation effects on metabolic activity in rat, x, 20: 20433 (AD-630390)
radiation effects on physiological changes in, of patients given dexphenmetrazine or phenmetrazine, 20: 33110
radiation effects on emptying in rat, part-body x, 20: 36628
radiation effects on gastric secretion in dog, 18: 5105
radiation injuries of, after radiotherapy of extragastric cancers, 19: 34008
radiodiagnosis of carcinomas of, using iodine-131 scintigraphy, 20: 22846
radiography of, effects of mass diagnostic, 17: 8445
radioinduced ulcers of, after γ radiotherapy of lumbar lymph nodes, 20: 43019
radiotherapy of cancer of, case report, 19: 15308
radiotherapy of cancer in, irradiation area in, 19: 22061
radiotherapy of cancer of, effects on appetite and body weight, 19: 21952
radiotherapy of cancer of, effects on blood and hepatic function, 19: 21953
radiotherapy of carcinomas of, use of lead grating for x, 20: 38763
radiotherapy of cancers of, 20: 38772
radiotherapy of human, effects of glycerol-guaiacol-ether on gastric changes after, 18: 9923
removal of part of, effects on iron absorption, 18: 29223
secretions in dog, effects of chemicals on, 18: 5105
secretory function, effects of peroral administration of radon water on, 16: 16209
sodium-24 effects on secretion in dog, effects of food type stimuli on, 18: 11600
sorptive capacity of dogs, effects of centimeter band radio waves on, 17: 10315
strontium-90 content in bull, from fallout, 19: 20215
temperature determinations in human, radiological telemetering system for, 20: 22801(T) (JPRS-34501)
therapeutic elimination of injected radioactive silver iodide particles from rabbit, 19: 14989
therapy of functional and inflammatory diseases of, using radon baths, 16: 2908
transit time of ceramic spheres containing manganese-54 or uranium carbide particles in, of animals and man, 20: 42740 (LA-DC-7764)
tumor and ulcer localization in, by photoscanning after administration of iodine-131-labeled iodide, 19: 19717
tumors in, probe design for detecting, 19: 42741
uptake of iodine-131-labeled iodide, 19: 10756
weight norms for human, use in establishing standards for radiation dosimetry, 20: 20374
zinc-65 metabolism in rabbit, 18: 43190

Storage
see Handling and Storage

STORAGE BATTERIES
see also Alkaline Batteries
anode polymorphism in, lead oxide, 20: 35719
characteristics of nickel- and silver-cadmium, for space vehicle electric power systems, 16: 18700
description of, for International Ionospheric Satellite, 17: 9127
design of nickel–cadmium, for Telstar power system, 17: 9118
development for space power systems, status of, 18: 34001
development of rechargeable cadmium–nickel, for space systems, 17: 35226
membrane separation for, fabrication process for, 20: 25177(P)
performance as emergency power systems for space vehicles, 18: 31995
performance in space systems, power-matching regulators for, 17: 34073
survey of, for automobile operation using nuclear energy, 19: 2465 (BNL-7447)
testing output of telemetry-system, (E), 19: 20280 (SCL-DR-64-128)

Storage Rings
see Accelerators

Storage Tubes
see Memory Devices

STPR
see Shield Test Pool Reactor

Straight Tube Aircraft Reactor (STAR)
see Aircraft Reactors

STRAIN GAGES
see also Extensometers
attachment of, using flame-spraying process, 19: 46723 (RFP-641)
calibration to 700°F, 16: 14852 (UCRL-6720)
cements for high-temperature, tests of, 19: 46715 (EUR-2473.f)
cements for 1600°F, 16: 25560 (NAMC-ASL-1050(Pt.III))
ceramic binders for electric, 16: 22592(R) (NAMC-ASL-1050(Pt.V))
circuitry of, and recording equipment for, 17: 6405 (SCTM-364-61(73))
data reduction and reading errors, 16: 19015 (SCTM-362-61(73))
design and evaluation of 3-dimensional, 17: 10783 (TID-17773)
design and performance for Project Dribble, 20: 12990 (NVO-1312-1 (Vol.2))
design for fuel pin warpage measurements, 20: 5703
design for measuring radial thermal strains in tubes during transient heating by plasma, 19: 34692 (UCRL-13147(Pt.2))
design for reactor fuel channel gaps, 20: 39175
design for studying strain anisotropy in Zircaloy-2 tubing, 20: 4304(R) (ORNL-3870, pp 171-83)
design of aging tester, 17: 30962(R) (ASD-TDR-63-238)
design of diameter, for high-temperature biaxial stress testing, 18: 14370 (KAPL-M-JOS-2)
design of semiconductor, analysis for, (E), 20: 5216 (SC-TM-65-457)
development and testing of aluminum–chromium–iron, for use at 1600°F, 16: 25559 (NAMC-ASL-1050(Pt.II))
development and testing of high-temperature, 20: 22520(R) (NAA-SR-11805)
development for SRE evaluation, 20: 10375(R) (NAA-SR-11650, Sect. 2)
development for use at 1600°F, 16: 13293 (NAMC-ASL-1050(Pt.I))
development of high-temperature, radiation-resistant, 20: 11070
development of high-temperature, 20: 35841(R) (NAA-SR-11900)
development of high-temperature, 20: 46966(R) (NAA-SR-12010)
development of optical, for measurements of specimens at 2000°F, 17: 18745 (HE-150-204)
development, preparation of high-temperature bonding materials curable at low temperatures, 16: 22591(R) (NAMC-ASL-1050(Pt.IV))
error analysis of two-component balance in, 18: 25002 (SC-TM-64-8)
failures in, detection and diagnosis of, 20: 22523 (UCRL-14602)
installation and use in tests of EGCR pressure vessel tests, 17: 28482 (TID-18888)
materials development for high-temperature, 17: 39370 (ARL-63-147)
performance at high temperature, 17: 36124 (UCRL-7276)
performance evaluation of unbonded, for use as pressure transducers, 17: 4795
performance for magneto-caloric measurements, 17: 25867 (TID-18768)
performance, for measuring effects of atomic explosions, 16: 11356 (WT-1)
performance for measuring transient forces from chemical explosions, 20: 24778 (IDO-17148)
performance of, in a radiation environment, evaluation of, 17: 18508(R) (AFSWC-TDR-62-63)

performance on Spert I oxide-core fuel-pin cladding, (E), 19: 30483 (IDO-17042(p.48-63))
position for stress measurements on 30-Mw steam generator prototype for sodium cooled reactor systems, 20: 8326 (COO-1213-27)
pulsing of, at low power for measurements in plastics, 16: 33157 (UCRL-7071)
radiation effects on lead wire insulation, 16: 15247 (NRL-5674)
radiation effects on, transient neutron, 17: 26081
radiation effects on performance of, transient nuclear, 18: 8608 (IDO-16914)
radiation effects on NERVA, cryogenic, 19: 3718 (FZK-184-1)
radiation effects on, 19: 2668
radiation effects on, 19: 14868 (FZK-170-4)
radiation effects on, 19: 14871 (FZK-170-7)
radiation effects on, fast-neutron, 19: 13812 (FZK-184-3)
radiation effects on, transient, 19: 39055 (GA-6266)
radiation effects on operation of, gamma and neutron, (E), 20: 14170 (EGG-1183-2019)
radiation stability of in-pile resistance, 20: 29578 (EUR-2649.e)
radioinduced electric transients in circuits of, reactor, 19: 4547
response to dynamic pressure surges of 400 to 5000 psi, (E), 19: 30483 (IDO-17042(p.48-63))
testing by mechanical shock and transient radiation, 17: 35254(R) (IDO-16898)
testing for measuring strains in reactor pressure vessel, 17: 346
testing in Spert, 17: 17623(R) (IDO-16827)
testing sodium, 16: 33151 (NAA-SR-Memo-7598)
use as pressure transducer in vacuum fusion analysis, 18: 29917 (CONF-546-1)
use in fuel assembly testing, in PWR, 19: 48000(R) (WCAP-3738)
use in materials testing and stress analysis of pressure vessels, 20: 18880 (Y-RD-5)
use in pressure measurements on reactor fuel elements, 20: 11174(R) (IDO-17112, pp 81-91)
use in stress measurements in threaded closure of pressure vessel, 19: 4284 (Y-1471)
uses in reactors, (E), 19: 22658 (CONF-640607(Vol.II)(Paper E-1))
uses of electrical-resistance, bibliography on, 17: 23610 (SCTM-365-61(73))

STRAINERS

see also Filters
description for sampling organic drift material in streams, 19: 14908 (HW-SA-3385)

STRANGE PARTICLES

(Particles of strangeness $S \neq 0$)
see also Hyperons
see also Mesons (K)
bibliography on, 18: 24214 (AED-C-23-01)
book: *Fundamental Particles*, 19: 21072
book: *Strange Particles*, 17: 34818
correlations of, in meson (π^-)-nucleon collisions, 17: 9360
coupling constants and vertex functions for composite, 16: 9389
decay, 16: 18101 (NP-11463(Pt.2)(p.195-211))
decay, 17: 20567 (UCRL-10022(p.42-5))
decay, 18: 44520 (NEVIS-125)
decay branching ratios and modes, lifetimes, and spin, 16: 10931
decay mode and evidence, with mass higher than meson (K), 16: 8056 (NP-11232(p.259-65))
decay of, existence of $\Delta S = -\Delta Q$ in, 17: 6996
decay of, forbidden multimeson configurations in, 17: 16952 (JINR-P-1161)
decay of, selection rule $|\Delta I| = \frac{1}{2}$ in nonleptonic, 17: 773
decay of, selection rules in, 17: 39886
decay of, branching ratios and rates of, (T), 19: 21045
decay of, Cabibbo's theory of leptonic, 18: 10957
decay of, $\Delta I = \frac{1}{2}$ selection rule in nonleptonic, 18: 37941
decay of, diagrams for, 19: 14398
decay of, isospin structure of, 18: 44573
decay of, leptonic, (E/T), 19: 25359
decay of, nonleptonic, (T), 20: 6035 (CERN-64-13(Vol.4), pp 1-49)
decay of, selection rules in, (T), 19: 12317
decay of, selection rules in nonleptonic, (T), 20: 6085
decay of, spurion in nonleptonic, 18: 44576
decay of, spurion model for selection rules in nonleptonic, 20: 13607
decay of, SU_3-invariance violation in leptonic, (T), 19: 6540
decay of, SU(3) models for leptonic, 19: 12163 (JINR-P-1829)
decay of, theory for, 18: 40348
decay of, transformation properties of nonleptonic, 18: 10959
decay of, unitary symmetry scheme for leptonic, 20: 13466
decay of, up-down asymmetries in, 18: 36350
decays of, model for $\Delta S/\Delta Q = -1$, 17: 9278
decays of, selection rules for non-leptonic, 18: 4429 (CONF-231-3)
decays of, $\Delta I = \frac{1}{2}$ and $\Delta S = \Delta Q$ rules in weak, 18: 28424
decays of, $\Delta T = \frac{1}{2}$ rule for nonleptonic (T), 19: 3064
decays of, rates of leptonic, (T), 19: 33054
deviations from doublet symmetry, 16: 9390
Feynman diagrams majorization for, 16: 19721
form factors, 18: 40314
formation from (K, π, K^-) and (N, Y, Ξ) triplets above 10 Bev, 16: 10902
global symmetry resonances, 16: 9387
interactions and properties, research programs, 16: 18124(R) (UCRL-10113)
interactions and symmetry properties, 16: 10920
interactions at high energies, hyperon and nucleon magnetic moments from, 16: 24739
interactions, characteristics of strong, 16: 18102 (NP-11463(Pt.2)(p.213-22))
interactions, classification summary, 16: 17002 (NP-11592(Vol.II)(p.141-9))
interactions, effects of Pais doublets on weak, 16: 2655
interactions of, analysis of leptonic currents in weak, 17: 9245
interactions of, application of Mandelstam representation to problems connected with, 17: 22431 (NP-12591(Pt.II))
interactions of, formal theory for, 17: 17079
interactions of, methods for testing the CPT theorem of weak, 17: 13432
interactions of, model for current conservation of weak, 17: 20894
interactions of, parity conservation in strong, 17: 29609
interactions of, review of properties of strong, 17: 5054
interactions of, resonances in, 17: 24186
interactions of, selection rules for strangeness nonzero systems imposed by the symmetrical Sakata model, 16: 27920
interactions of, structure of strangeness-violating nonleptonic weak, 17: 9246
interactions of $Y_{\frac{3}{2}}^{*}$ with K*, 18: 7520
interactions of, coupling constants for, (T), 19: 31039
interactions of, weak, (T), 19: 4894 (JINR-P-1789)
interactions of, weak, (T), 20: 4634
interactions of, weak, (T), 20: 6035 (CERN-64-13(Vol.4), pp 1-49)
interactions, Universal-Fermi-type scheme, 16: 3643
interactions with mesons (π), 16: 22935
interactions with nucleons in nuclei, 18: 7520
interpretation of Y_1^* from p–Λ interactions, 16: 18347
isobars of, empirical mass relations involving, 17: 36606
lepton decay constants, 16: 22956
leptonic decay, validity of $\Delta S = \Delta Q$ selection rule, 16: 7020 (TID-14474)
leptonic decays, 16: 10812 (CERN-61-30)
model for, mass relations for meson (π)-nucleon interaction, 17: 20904
model of, spurion, 17: 9450
parastatistics of, 17: 17001
parities of, 16: 17003 (NP-11592(Vol.II)(p.151-75))
parities of, method for determining, 17: 36573 (JINR-E-1271)
parity determination of, from total cross sections for interactions of spin-½ particles, 18: 6045
parity of, determination using polarized protons, (E), 19: 16656
photoproduction near the threshold, 17: 7051
photoproduction on nucleons, 17: 19107
photoproduction on protons, resonances in, (T), 19: 4936
production and properties, 16: 18100 (NP-11463(Pt.2)(p.187-94))
production and properties of, 17: 11556
production as Kπ resonant state in meson (π^-)-proton interactions at 726 Mev, 17: 34766
production as Kπ resonant state in meson (K^-)-proton interactions at 725 Mev, 17: 34767
production by electrons and photons in Regge pole hypothesis, asymptotic behaviors in, 18: 32528 (IFA-HE-53)
production by high-energy neutrinos, (E), 19: 29042 (CERN-65-12)
production by meson (π^-)-proton interaction at 16 and 24 Bev, 16: 16937 (NP-11592(Vol.I)(p.93-100))
production by meson (π^-)-proton interactions at 10 Bev/c, 17: 9361
production by meson (π^-)-proton interactions, associated, 17: 19131
production from meson (K) and (π) interactions with hyperons (Σ), isotopic relations for, 17: 28172
production in antinucleon annihilation and meson (π)-nucleon interactions, 17: 32920
production in antiproton-proton and proton-proton interactions at high momenta, 18: 42365 (JINR-E-1790)
production in bremsstrahlung-proton interactions at 0.5 to 4.8 Bev (E), 19: 1233 (MIT-2098-79)
production in CERN neutrino experiment, 18: 40375
production in electron–nucleon interactions, 18: 10928
production in electron-nucleon interactions, (T), 19: 32958
production in elementary-particle interactions at high energies, 18: 34509 (NP-14086)
production in gamma-proton interactions at 0.5 to 4.8 Bev, (E), 19: 4976
production in meson (π^-)-proton interactions at 1.6 Bev/c, 16: 16978 (NP-11592(Vol.I)(p.375-83))

production in meson (π)-nucleon interactions, model for, 16: 33737
production in meson (π^-)-proton interactions, resonances in, 17: 9370
production in meson (π^-)-proton interactions, 17: 13452
production in meson (π^-) reactions on xenon nuclei, 17: 28339
production in meson (π^-)-proton interactions at 1170 Mev/c, 17: 34739 (UCRL-10838)
production in meson(π^+)-proton interactions at 2.08 Bev/c, 17: 36583 (TID-19342)
production in meson (π^+)-nucleon collisions, correlations in, 17: 41765
production in meson (π^+)-proton interactions, 17: 41737 (CONF-46-102)
production in meson (π^-)-proton interactions at 1.7 Bev/c, 18: 862(R) (TID-19590)
production in meson (π^-)-proton interactions, 18: 14810 (JINR-P-1506)
production in meson (π^-)-nucleon interactions at 6.1 to 18.1 Bev/c, 18: 16776
production in meson (π^-)-proton interactions at 10 Bev/c, 18: 40294
production in meson(π^+)-proton interactions, 18: 44511 (BNL-8311)
production in meson (π^-)-proton interactions at 10 Bev (E/T), 19: 1403
production in meson (π^-)-proton interactions at 3 Bev/c, (E/T), 19: 10084
production in meson (π^-)-proton interactions at 3 Bev, 19: 14393
production in meson ($\pi^\pm$) interactions at 1170 Mev/c, (E), 19: 25265(R) (UCRL-11776)
production in meson (π^-)-proton interactions at 2.7 Bev/c, (E), 19: 37524 (COO-1428-12)
production in meson (π^-)-proton interactions at 2.77 Bev/c, 18: 18702
production in meson (π^+)- and (π^-)-proton interactions at 4 Bev/c, cross sections for, (E), 20: 32029
production in meson (π^+) interactions with protons at 8 Bev/c, cross sections for, (E), 20: 37770
production in meson (π^-)-neutron interactions at 3.5 Bev/c, cross sections for, (E), 20: 39842
production in neutrino reactions on nuclei and nucleons, cross sections, 16: 27965
production in neutron-proton collisions, 17: 13386
production in nucleon-nucleon collisions, upper limit for, 18: 40358
production in proton-meson interactions, 16: 10918
production in proton interactions, 16: 10877
production in proton interactions at 2 Bev, 16: 15570
production in proton reactions with nuclei, 16: 26089 (NP-11832)
production in proton-proton interactions at 25 Bev/c, 18: 44540
production in proton-proton interactions at 8 Bev/c, (E), 20: 25781(R) (COO-1195-56)
production in showers, transverse momentum distributions, 16: 986
production of neutral, in proton–proton interactions, 18: 42447
production of resonance states of, 18: 14946
production of Y_1^* resonance in meson($\bar{K}$)–nucleon interactions at low energies, 17: 36605
production of Y_1^* in meson (K^-)-proton interactions at 1.15 Bev/c, 16: 17042
production of Z^- baryon, 18: 4452
production of, selection rule in higher symmetries for, (T), 19: 4971
production of, singularities in triangle diagrams for, 19: 1266
properties of new, 17: 5233
properties of resonance, 18: 28425
properties of, review of, 18: 4447
properties of Y^* from hyperon (Λ)–proton interactions, 16: 18352
properties of, Heisenberg's nonlinear theory for, 20: 13554
properties, quantum field theory for, 16: 10928
reactions with nuclei, 18: 15290
resonance states of, review, 18: 10892
resonances of, 18: 42368 (JINR-E-1804)
resonances of isobaric, research status, 16: 17004 (NP-11592(Vol.II) (p.177-89))
resonances, theoretical models, 16: 17005 (NP-11592(Vol.II)(p.191-204))
resonant states of meson (π^-)-proton reaction-induced, 16: 32302 (UCRL-10286)
resonant states of, 17: 7014
search for single-strange mesons, 16: 5876
spin states (Y_1^*), 16: 6976
spin-statistics connection for, 17: 29539
theory, 16: 4720
theory, 16: 16947 (NP-11592(Vol.I)(p.163-8))
theory of interactions, review, 16: 1178
theory of, review on, 18: 7492
theory of, spurion (T), 19: 1378
theory of, spurion, 19: 31038
uses in research on complex nuclei, 17: 36641 (CERN-63-28(p.1-36))

STRATIGRAPHY
measurement in basalt sequence beneath Hanford area, 20: 39099(R) (BNWL-235-3, pp 1-23)
measurement of strata shrinkage, cobalt-60 method for, 20: 11024
radioactive-waste-disposal studies in, (E), 19: 35858
settling-rate measurements at Nigata City, Japan, using cobalt-60 depth markers, 17: 40993
sulfur isotope abundance in basic sills, 17: 23523

STRATOSPHERE
accumulation for, review of recent accomplishments in data, 18: 2730
aerosol composition in, 16: 25609 (AFCRL-62-299)
air circulation in, 16: 4374 (TID-13093)
air sampling equipment, balloon-borne, 16: 27420(R) (TID-16015)
air transfer to troposphere from, tracer study of, 20: 23314
analysis for bomb-produced beryllium-7 and strontium-89, 17: 32759
analysis for fallout, 1963 and 1964, gamma spectrometric, 19: 30400(R) (ANL-6971(p.83-8))
behavior and properties of, possible effects of rocket programs, 17: 2142 (GCA(10-S)-61-68(Del.))
beryllium-7 content of, in 1961 and 1962, (E), 19: 5061
beryllium-7 content in, from Soviet nuclear tests, 16: 13401
carbon-14 content of, total and fallout, 1953 to 1964, 19: 20155 (HASL-159)
carbon-14 in, over southern England, 1956-60, 16: 13384
cerium-144 residence time, factors affecting, 16: 22447 (TID-7632(p.223-41))
charged-particle content in, (E), 20: 44463
charged-particle density in, measurement of, 19: 29150
circulation in, tracer study, 18: 10617
circulation in, tracer study of, (E), 19: 4739
circulation in, tracer studies of gross, 19: 16247
circulation patterns in, 18: 31053(R) (TID-20764)
contamination of aircraft by, 16: 15015 (AFSWC-TN-59-29)
cosmic and solar radiation intensity in, (E), 20: 37536
cosmic particle density and ionization in, 16: 900
cosmic particle density in, 17: 26276
cosmic radiation density in, radio probe for measuring, 19: 20346
cosmic radiation intensity measurements, 16: 10799
cosmic radiation in, secular variation of, 18: 24331
cosmic ray flux in, 18: 28287
cosmic ray intensity fluctuations in, 18: 32503
cosmic ray intensity in, (E), 19: 20876(T)
cosmic ray intensity variations during geomagnetic storms, (E), 19: 20877(T)
cosmic-ray intensity variations in, cyclic, (E), 20: 37532
cosmic-ray intensity in, temperature dependence of, (E), 20: 37591
cosmic-ray dosimetry, 17: 5765 (AFCRL-62-244)
cosmic-ray flux variation in, height dependence of, (E), 20: 37552
cosmic-ray intensity increases in, associated with short-period pulsations of geomagnetic field, 18: 30452(T) (NASA-TT-F-127(p.223-34))
cosmic-ray intensity in, latitudinal measurements of, 18: 40176
cosmic-ray intensity in, relation to solar activity, (E), 19: 12052(T)
cosmic-ray intensity in, latitude dependence of, (E), 19: 20892
cosmic-ray intensity and spectra in, secular variations of, (E), 19: 25207
cosmic-ray variations in, detection of 27-day, 18: 30455(T) (NASA-TT-F-127(p.274-80))
dispersion of radioactive aerosols in, 20: 16643
eddy fluxes and biennial oscillations in, 20: 4150 (MIT-2241-7)
electron density measurements, 18: 11026 (BRL-1187)
energy cycle in lower, 18: 11028 (TID-20111)
energy generation through radiative processes in, (E), 19: 18969 (TID-21471)
fallout concentrations in north polar, 1962, 16: 33301
fallout contamination of, methods of monitoring, 18: 37367 (CONF-337-45)
fallout contamination of airplanes in, 19: 30463
fallout content and transport in, 20: 16698
fallout content in, after test ban treaty of August 5, 1963, 18: 14083
fallout content in, residence time of, 19: 40789
fallout content in polar, 1963, 19: 44260
fallout content of, radiation hazards to passengers and ground crews of jet planes from, 19: 9408
fallout content of, meridional mixing of, 19: 15760
fallout content of, review on, 20: 23313
fallout distribution in, mathematical model, 17: 8389(R) (NYO-10392)
fallout distribution in, 18: 8522(T) (AEC-tr-6049(p.161-201))
fallout exchange with troposphere, Springfield study of, 19: 26913 (AD-607980)
fallout holdup and deposition from, development of Star Dust model of, 19: 14114(R) (DASA-1305)
fallout in northern, 1963-64, 19: 40785 (TID-21224)
fallout in, deposition and distribution of, 20: 16697
fallout mixing and transport in, model of, 17: 36006(R) (DASA-1303)
fallout mixing and transport in, model of, 17: 36007(R) (DASA-1304)
fallout monitoring, 1961, 17: 3162 (TID-16988(Paper 5))
fallout monitoring in, 17: 41027(R) (NYO-9678)
fallout monitoring, 1962 to 1964, 19: 9370 (NP-14556(p.11-80))
fallout monitoring, 19: 20162(R) (NYO-3276-9)

fallout monitoring, in Star Dust Project, 19: 20657(R) (DASA-1309)
fallout monitoring in Star Dust Project, 1963, 20: 16727(R) (HASL-168)
fallout monitoring in Project Star Dust, 1964, 20: 16728(R) (HASL-169)
fallout monitoring, 1957 to 1960, 16: 6639 (DASA-1300(Vol.1))
fallout monitoring, 1957 to 1960, 16: 6640 (DASA-1300(Vol.2A))
fallout monitoring, 1957 to 1960, 16: 6641 (DASA-1300(Vol.2B))
fallout monitoring, 1957 to 1960, 16: 6642 (DASA-1300(Vol.3))
fallout particle size and vertical distribution, 16: 22443 (TID-7632 (p.170-87))
fallout residence time in, 18: 35716 (IA-888)
fallout residence time in, analysis for 1958–1961, 17: 23527
fallout sampling in, design of equipment for, 18: 27701(R) (NYO-2363-1)
fallout sampling in, equipment for, 19: 14115(R) (NYO-2363-2)
fallout strontium-90 deposition from, effects of meteorological activity on, 20: 23285 (HNS-58)
fallout studies using seasonal model, 20: 45888(R) (NYO-3654-1)
fallout transport mechanisms in, 18: 23799
fallout transport from, to troposphere, 18: 37381
fallout transport and mixing in, 19: 9367 (IAEA-R-1)
fallout transport from, by intense convective storms, 19: 22560
fallout transport in, meteorological factors in, 20: 523
fallout transport from, 20: 5649(R) (COO-1340-2, pp 54-83)
fallout transport from, effects of cyclonic activity in, 20: 5650(R) (COO-1340-2, pp 84-109)
fallout transport from northern to southern hemisphere in 1961 and 62, 20: 14749
fission product distributions in, from atomic weapons tests, 18: 4039
fission product transport, meteorological, seasonal, and latitudinal factors, 16: 22446 (TID-7632(p.210-22))
fission products in, fate and physical properties of, 19: 15762
fission-product monitoring by balloon filters, 1965, 20: 41131(R) (HASL-172)
gamma spectra measurement in, design of spectrometer circuitry for, 17: 14650 (TID-16186)
general circulation in lower, based on analysis of vertical and horizontal motions, 16: 22445 (TID-7632(p.204-9))
isobaric height conditions and wind temperature in, during IGY, 20: 4151 (MIT-2241-14)
mass transport to troposphere, 17: 4699
mass variations in, relation to fission product concentration in surface air, 18: 7337
meridional circulation in, during International Geophysical Year, 17: 6274 (TID-17467)
meteorological data on, 18: 37367 (CONF-337-45)
meteorological processes influencing transfer of fission products to troposphere, 16: 4417
mixing and transfer processes, 16: 6642 (DASA-1300(Vol.3))
models and processes of lower, (T), 19: 41570 (CONF-765-11)
monitoring, 17: 16320(R) (NYO-9675)
monitoring, development and testing of particle collectors, 16: 29188(R) (TID-16498)
monitoring for radiation from large solar flares, 18: 37037
monitoring of fallout in, 17: 36006(R) (DASA-1303)
monitoring of fallout in, 17: 36007(R) (DASA-1304)
nuclear bomb debris transport in, 16: 8990 (IA-670)
ozone and water vapor distribution in, review on, 20: 23279
ozone transport and exchange, meteorological, seasonal, and latitudinal factors, 16: 22446 (TID-7632(p.210-22))
particle flux in, increases of ionizing, (E), 20: 37907
particle transport, tracer study, 16: 16584
particulates, interaction between radioactive and non-radioactive, 16: 22439 (TID-7632(p.98-119))
radioactive aerosols in, half life of, 20: 11014
radioactive aerosol distribution in, meteorological factors affecting, 20: 23309
radioactive nuclide distribution in, 16: 6642 (DASA-1300(Vol.3))
radioactivity, 17: 18291(R) (NYO-9677)
radioactivity in, artificial, 18: 21082
radioactivity in, 1960–1963, carbon-14 and strontium-90, 20: 23314
radioactivity transport to troposphere, 17: 4699
radioisotope content in, production mechanisms for, 18: 21080
radioisotope distributions in, 18: 35715(R) (DASA-1307)
radioisotope levels in, 17: 5751(R) (HASL-132)
radioisotope monitoring in, using aircraft and balloons, 18: 30297(R) (NYO-10498)
radionuclide activities in air filter samples collected in 1961 and 1962 during Project Star Dust, 19: 9755 (HASL-153)
sampling, design of electrostatic precipitator for, 17: 16319(R) (NYO-9674)
sampling equipment for, balloon borne, 17: 18291(R) (NYO-9677)
sampling equipment for, design of balloon-borne direct-flow filter, 18: 43752
sampling in, electrostatic precipitator development for, 19: 44801(R) (NYO-2363-3)
sampling of, for radioisotopes, 17: 6271(R) (NYO-10464)
sampling of, design and development of air ejector particle sampler for, 19: 720(R) (COO-401-105)
sound velocity in middle, calculation from nuclear explosion recordings, 18: 2748
strontium isotope distribution in, Australian and U. S. data, 16: 24012(R) (HASL-127)
strontium-90 residence time, 16: 22424
strontium-90 retention time in, 18: 5550
strontium-90 storage in, during nuclear moratorium, 18: 2391
strontium-89 and -90 content in, from Chinese nuclear test, 20: 27155
strontium-89 content, from Soviet nuclear tests, 16: 13401
strontium-90 content in, 1963 to 1966, 20: 41131(R) (HASL-172)
strontium-90 residence time in, factors influencing, 16: 22447 (TID-7632(p.223-41))
strontium-90 transfer to troposphere from, mechanisms of, 20: 23314
studies of equatorial, balloon flights over Hyderabad, India, 17: 39269 (TID-19483)
temperature and wind structure of, review of mechanisms for, 20: 33505
temperature maxima in middle, from nuclear explosion recordings, (T), 18: 2748
temperature profiles and energy transport in lower, models for meridional, 19: 31133 (MIT-2241-4)
transport processes in, eddy-flux, 19: 30842 (MIT-2241-3)
tritium content in water in, origin of, 16: 7763
tritium deposition from, in rain water in Asia and Europe, 17: 34124
tritium in, over southern England, 1956-60, 16: 13384
water content measurements in, problems of automatic frost-point hygrometers for, 19: 44339 (AD-608503)
water vapor distribution in, review on, 20: 23279
water vapor in, over southern England, 1956 to 1960, 16: 13384
water vapor measurements in, alpha radiation hygrometer for, 19: 32501 (AD-608498)
wind profiles determined from sodium cloud drifts at twilight, 16: 30663(R) (TID-16336)
wind structure of, review of mechanisms for, 20: 33505
wind temperature and isobaric height conditions during IGY, 18: 20619 (TID-20511)

Streamer Chambers
see Spark Chambers

STREPTOMYCES
carbon-14-labeled actinomycin biosynthesis in, from labeled amino acids, 18: 43572
radiation effects on, protection against, 17: 38770
radiation effects on, background, 18: 19560
radiation effects on antibiotic formation by, 18: 38803
radiation effects on antibiotic formation by, 18: 38804
radiation effects on cellular ultrastructure in spores of, electron, 19: 26065
radioinduced mutations in, uv and x, 18: 17486
radioprotective agent assay with, method for, 18: 127
radiosensitivity effects of enzyme extracts of, in *E. coli* and Streptomyces, 17: 38770
ultraviolet induced mutations, 17: 30376
use in biosynthesis of tritium-labeled actinomycins, 20: 36545

STREPTOMYCIN
analysis, activation, 16: 26939
chemical structure, 16: 8568(T)
effects of radiation sickness on permeability of blood-brain barrier to, 18: 41256
effects of, mutagenic, 17: 19912
effects on autoinfection in mice during radiation sickness, 18: 90
effects on cancer cells in mice, mutagenic, 17: 2793
effects on immunogenicity, survival, and virulence of leptospira in guinea pigs, 19: 42342
effects on inhibition of recovery in lethally irradiated *Rhizopus stolonifer*, 19: 17596
effects on manifestations of acute radiation sickness, 16: 17532(T) (FTD-TT-62-144)
effects on metabolism in paramecium, 19: 2068(R) (ORNL-3700(p.34-57))
effects on mutations in Russian broad bean (*Vicia faba*), 16: 30288
effects on permutational damage induced in Paramecium by triethylene melamine, 20: 5417
effects on protein synthesis in tubercle bacilli, tracer study, 20: 6755
effects on radiation injuries, reaction mechanisms, 16: 8568(T)
effects on radiation effects on human tissue cultures, 20: 31121
effects on radioinduced mutations in *Drosophila melanogaster*, 18: 11886
effects on *Staphylococcus albus*, 18: 13454 (TID-20223)
effects on viability of *E. coli*, 20: 20457
effects on viral replication in lysogenic systems, 20: 22771
effects with x radiation on mutation frequency in Chlorella, 20: 32993

protective effects against radiation damage to onion bulbs, 16: 11474
protective effects against radiation sickness in monkeys, 16: 26875
protective effects of, against radiation, 17: 15846
protective effects against radiation damage to yeast, 17: 28731
protective effects against radiation injury to chromosomes of reproductive cells in mice, 18: 23359(T) (JPRS-24593(p.120-5))
protective effects against small radiation doses in human cells, 18: 36946 (A/CONF.28/P/386)
protective effects against whole-body radiation effects on mouse chromosomes, 19: 196
protective effects against radiation injuries in mice, 19: 4000
protective effects against radiation effects on dogs, 19: 7156
protective effects against radiation damage to chromosomes in human tissue culture cells, threshold for, 19: 17685
protective effects against 19-norandrostenolone effects on acute radiation disease in rats, 19: 19624
protective effects against radiation injuries in rats, 19: 21999
protective effects against mortality from *Pseudomonas aeruginosa* in irradiated mice, 19: 36121
radiation effects on blood components of rabbits treated with, x, 19: 3971
radiation effects on resistance of *Staphylococcus aureus* strain 209P to, 19: 15059
radiation effects on distribution of, in organisms, 19: 21898
radiation effects on inhibition of bacteriophage multiplication in *Staphylococcus albus*, ultraviolet, 19: 36091
radiation effects on sensitivity of blue-green algae to, 19: 35966
radiation inactivation of resistance markers in bacteria, 16: 14485
radiosensitivity effects on permutational damage in Paramecium, x, 20: 5417
radiosensitivity effects combined with marrow transplants in mice, y, 20: 8738
radiosensitivity effects on mouse sperm, 20: 14404
radiosensitivity effects in *Staphylococcus aureus*, y, 20: 14313
radiosensitivity effects on yield of temperature-sensitive mutations in Paramecium, x, 20: 18349
radiosterilization of, effects on properties, 16: 8470(T) (JPRS-12194)
resistance of bacteria treated with irradiated DNA to, 16: 72
resistance of irradiated desoxyribonucleic acid to, 17: 40567
therapeutic effects against acute intestinal radiation death in rat, 16: 17543
therapeutic effects of, on radiation sickness in rats, 18: 5139(T) (JPRS-22123)
use in acute radiation sickness therapy, 20: 8739

Stress, Biological
see Biological Stress

STRESS ANALYSIS
see also Mechanics
around holes in thick plates loaded in uniaxial tension, 19: 31461(R) (ANL-7010(p.235-87))
bending and stretching in coupled circular plates, 19: 7655
bending of circular plates under a uniform load on a concentric circle, 18: 43739 (ANL-6905)
beta sources for use in, kryptonate, 20: 43765
book: *Post-Buckling Behavior of Cylindrical Shells*, 18: 29814(T) (NASA-TT-F-90)
book: *Strength and Structure of Engineering Materials*, 20: 33932
book: *Thermal Stress Techniques in the Nuclear Industry*, 19: 47922 (TID-22119)
buckling and creep buckling of spherical shells under uniform external pressure, 18: 37306 (TID-20950)
by infrared spectroscopy, feasibility of, 17: 27508 (SCTM-59-63(25))
calculation for growth of concentric cylinders, computer program for, 20: 7634 (WAPD-TM-514)
calculation of axisymmetric and plane elasticity problems for, computer program for, 20: 20862 (WAPD-TM-555)
calculation of residual stresses in stainless steel-clad steel plate, 16: 22539
collapse pressure for cylindrical-spherical pressure vessels, 20: 465
comparison of approximate formulas for burst strength of finite cylinders, 17: 26130
computer FORTRAN II programs CTAC and MODE for forces and deflections in linear elastic structures, 16: 6520 (WAPD-TM-259)
computer program for, 17: 16173 (KAPL-M-JVM-4)
computer program for, 18: 1882 (KAPL-2292)
computer program for, 18: 13987 (WAPD-TM-398)
computer program for axisymmetric thin shells of revolution, 19: 44219 (ACF-8)
computer program for bodies of revolution, 19: 21609 (GAMD-5001 (Rev.2))
computer program for solving thermoelastic problems, 19: 11309 (ORNL-3624)
computer program for, of composite bodies of revolution, 20: 5033 (GA-6588)
computer program for composite tubes, 20: 39394 (GEMP-415)
computer use in, 17: 13705
constitutive equations for nonlinear solids in, multiple-time argument material functions with memory in, 19: 969 (UCRL-12039)
cylindrical shell deformation under static pressure loadings, 17: 39227
deflections and stresses in perforated beams during bending, 16: 16477 (TIM-390)
deflections and stresses of thin spherical shells during bending, measurement and theory of, 17: 16664 (UCRL-13064)
deformation of annular rings by external pressures, 16: 8842(T) (IG-Inf.-Ser.-45)
deformation of elastic circular plates on elastic foundation, 18: 27635
determination of materials behavior from true stress-strain relations, 16: 20806 (NAA-SR-6376)
determination of plastic pressure-deformation in pressure vessel of anisotropic material, theory for, 16: 21735
determination of strain hardening in compound cylinders, theory for, 16: 20965
determination of transient stress distribution in rods, effects of rapid internal heat generation on, 17: 16260 (HE-150-210)
dislocation concepts of plastic wave propagation, 17: 11198 (UCRL-10498)
dynamic stress concentrations in elastic plate with rigid circular inclusion, 16: 10132 (NP-11405)
edge rotation and deflection of a cone for several loading conditions, 17: 39217 (NAA-SR-Memo-8582)
effects of nozzles in spherical pressure vessels, 20: 1364
effects of plastic elongation on residual, 16: 9214(R) (TID-14810)
equations for deflection and stress in boiler fuel element boxes in Pathfinder Reactor, 16: 23309 (ACNP-62010)
equipment and methods for steam generator prototype, 20: 8326 (COO-1213-27)
equipment for, construction and calibration of, 19: 22985(R) (NP-14951)
facility design for brittle materials, 16: 12109(R) (ORO-518)
finite element, of axisymmetric composite structures, 19: 40165 (GA-6303)
for channel walls in turbulent fluid flow, 20: 45857
for hexagonal cylinders and rings under uniform internal pressure, 16: 14873 (DC-61-4-55)
for junctions of cylindrical and spherical surfaces, (T), 19: 22457 (ORNL-3755)
formulas for, of thick-wall cylinders, 20: 4076 (HIC-1-1564-3(Vol.2))
fundamental principles of experimental, 17: 13713
in fabrication of reactor pressure vessels, 17: 29303
in materials with delayed yielding, wave propagation, 16: 3400(T) (UCRL-Trans-729)
in plates welded by ascending-vertical method, 19: 13939(R) (EURAEC-1097)
in reactor engineering, mechanical and thermal, 18: 38259
in reactor materials, 17: 7532(R) (ARF-K6018-3)
in sheets welded by vertical ascending method, 18: 35973(T,R) (EURAEC-1023)
inelastic continuum theory of dilatating aggregate materials, 19: 18087 (WAPD-TM-421)
inertial load on a plate under blast loading, 18: 17359 (SCL-TM-64-34)
instrumentation and techniques, 16: 13173 (DC-59-2-149)
lectures on, at Bettis Reactor Engineering School, 17: 19587 (WAPD-TM-300)
limiting load-bearing capacity of reinforced concrete plates, 18: 5441 (JUL-128-RG)
matrix progression method for complex structures, 17: 13707
method for stress calculation in magnet coils, 20: 46243(T) (AERE-Trans-1056)
methods for solving plane stress problems in elasticity, 19: 31650 (UCRL-7186-T(Rev.1))
methods for, using models, 20: 33431(T) (ORNL-tr-1229)
methods in, 17: 11937(R) (ARF-4132-16)
methods of, evaluation of, 17: 24640 (WAPD-BT-28(p.61-75))
of air blast loading of spherical reinforced concrete domes, 20: 2035 (AD-615017)
of alloys and steels, 17: 39531(R) (EURAEC-689)
of annular fuel elements, (T), 19: 17259
of attachment region of hemispherical shells with radially attached nozzles, (E), 19: 44144 (TID-22134)
of axisymmetric intersecting shells of revolution, 19: 36582
of axisymmetric redundant structures, equations for, 19: 13606
of axisymmetric thin shells, computer program for, 17: 6507
of axisymmetric thin shells of revolution, computer program for, 19: 1948 (ACF-2)
of axisymmetric thin shells subjected to pressure and high temperatures, 19: 9282 (LAMS-3083)
of beams and fuel elements, 17: 26867 (ORNL-TM-557)
of bellows, 19: 4272 (NAA-SR-4527)

of bolted closures, computer program for, 19: 44145 (TID-22138)
of bolted joints, 18: 13982 (KAPL-M-6100)
of cascade spherical pressure vessels, 19: 38170 (AFOSR-65-0315)
of cavities in rock under dynamic loading from nuclear explosions, 19: 7962 (DASA-1357(App.G)(Vol.IV))
of ceramic seals, 18: 44041 (MATT-293)
of circular divider plate during hydraulic pressure surge transients, 16: 320 (WAPD-BT-23(p.17-26))
of composite tubes under load and temperature gradient, 19: 4269 (GEMP-288)
of concentric-ring fuel elements, 18: 33059 (DC-60-1-60)
of concrete pressure-vessel ceiling model (E), 19: 3624 (GAMD-5049 (Rev.))
of concrete pressure vessels for 1000-Mwe power reactors, (T), 19: 29637 (GAMD-5277)
of concrete primary shields for reactors, 19: 29478
of conical, cylindrical, and spherical shells, 20: 4999(R) (ORNL-2599)
of containment structures from internal dynamic and static loading, 20: 14028 (IITRI-578P22-14)
of core support grid plates for FARET, 19: 17357 (ANL-6778)
of crushable reactor shielding, computer programs for, 19: 6832(R) (IITRI-578P21-8)
of crushable reactor shielding, computer programs for, 19: 6833(R) (IITRI-T6042-7)
of cryogenic high-field solenoids, 20: 16586 (CONF-650922, pp 723-32)
of cylinder under opposite axial line loads, 16: 7656 (DC-58-3-147)
of cylindrical bar, effect of lateral inertia on propagation of plastic strain in, 18: 35658 (LAMS-3081)
of cylindrical cavity with impinging shock wave, 18: 30313 (RTD-TDR-63-3021)
of cylindrical hole in semi-infinite elastic bodies, (T), 20: 12943 (ANL-7097)
of cylindrical pressure vessel with ellipsoidal head and short head-to-cylinder transition section, 16: 16478 (TIM-408)
of cylindrical shells, computer program for, 16: 30514 (KAPL-M-EC-20)
of cylindrical shell clamped along oblique contour, 18: 21733(T) (ORNL-tr-19)
of deep underground shelters, 18: 1884 (AD-422046(p.55-85))
of dynamically loaded cylindrical shell, 19: 10691 (SCL-DR-64-113)
of elastic disturbance propagation in deformable solids, 20: 31331 (UCRL-14616)
of elastic plane body, boundary value problem for, 19: 38029 (SC-RR-65-307)
of fast reactor fuel cladding, 20: 10274(R) (NAA-SR-11605, Sect. 1)
of filament-wound shell structures, 18: 26115 (SCL-TM-64-53)
of flat perforated plates with triangular and rectangular hole patterns, 18: 4926 (WAPD-T-1559)
of fuel cans under thermal cycling and internal pressure, 18: 41934 (TRG-Report-790)
of fuel rod cladding in NS *Savannah* Core II, 19: 10613 (GEAP-3339)
of heat exchangers for sodium-cooled reactors, 20: 5131(R) (UNC-5135)
of hemispherical lightweight cellular core with flexible support shell, 18: 8021 (UCRL-7473)
of hemispherical pressure vessel with single radially attached nozzle, computer program for, 20: 459 (ORNL-3817)
of hexagonal box under internal pressure, 17: 39218 (NAA-SR-Memo-8670)
of hexagonal reactor tubes, 20: 39384 (BNWL-263)
of holes in covers of pressure vessels subjected to internal pressure, 18: 31741
of hollow circumferentially notched round bars, intensity factors for, 20: 43912 (UCRL-14859)
of hollow hexagons subjected to external pressure, 16: 9192 (DC-59-4-27)
of hyperbolic notches in flat plates, 19: 36583
of impact effects on spherical shells, (T), 20: 26589(R) (SC-CR-66-2025)
of irradiated fuel element, 18: 26906
of isothermally heated uranium, relaxation curves for, 20: 43936
of long, thick, uniformly curved plates, 19: 20130
of loosely coupled tube sheets, 19: 6020
of mechanical strength of dispersion fuel elements, 18: 7907(T) (EURAEC-709)
of mechanical structures, computer program for, 20: 29367 (TRG-Report-1089)
of metallic fuel elements, 18: 32038 (DC-60-2-285)
of metals, 17: 39534(R) (EURAEC-791)
of metals, radiation effects on, 18: 14535(R) (EURAEC-878)
of nonlinear buckling of elastic rectangular plates, 18: 15674 (IMM-NYU-316)
of normally intersecting cylindrical shells, 20: 466
of nozzle-to-spherical shell attachments, 20: 35600(R) (ORNL-3951, pp 164-8)
of nuclear reactor pressure vessel, 17: 33252
of octagonal-shaped rotating disk, mathematical elastic solution to, 18: 36898 (UCRL-7186)
of parabolic graphite beams, 18: 12557 (ORNL-TM-722)
of perforated cylindrical shell subjected to boundary and surface forces, 18: 18453 (IMM-NYU-320)
of perforated plates in bending, comparison with experiment, 19: 6010 (TID-21356)
of perforated plates subjected to equal biaxial stress, 19: 46557 (NP-15459)
of piping in reactor primary cooling systems, 19: 38176 (GEAP-4578)
of piping in reactor primary cooling systems, 20: 46981(R) (GEAP-5147)
of piping systems, computer program for, 18: 35657 (LA-2929)
of plates, drive system for determining, 20: 18879 (AWRE-O-21/66)
of plexiglass model of thick-walled vessel, comparison of experimental and numerical, 19: 22503 (GAMD-5503)
of polycrystalline material using x rays, 17: 30989(T) (TRG-Inf.-Ser.-310)
of porous materials rapidly compressed by explosives, 17: 295
of potassium–sodium alloy piping system for nuclear powered airplane, 19: 22509 (PWAC-123)
of pressure vessels, 17: 18224 (WAPD-T-1510)
of pressure vessels, 18: 6936(R) (TID-19919)
of pressure vessel nozzles in bending fatigue, 19: 13999(R) (SWRI-1228-43)
of prestressed concrete structures by finite element method, computer program for, 19: 20086 (GAMD-5926)
of primary creep rates in thin-walled pressure tubing, 16: 3453 (HW-60611)
of projectiles penetrating reactor containment during meltdown, 20: 32744 (SRIA-1)
of pyrolytic-carbon coatings for fuel particles, model for, 20: 2235
of radioisotope transport containers, from internal pressures, 20: 14667 (ORNL-TM-1312(Vol.1))
of reactor coolant pipes, 20: 28694(R) (GEAP-4964)
of reactor cooling system piping, computer code for, 20: 12338(R) (GEAP-4911)
of reactor fuel elements, numerical methods for, 16: 30044
of reactor fuel element end caps, 18: 29003 (HW-SA-3104)
of reactor fuel plate cladding, 20: 3453
of reactor pressure vessel, 18: 6418 (GAMD-3470)
of reactor pressure vessel, 18: 6419 (GAMD-3470(App.I))
of reactor shielding materials, 18: 36759 (IITRI-578P21-6)
of reactor vessels, computer techniques for, 16: 30043
of reinforced circular and rectangular flat plates, (T), 20: 7240 (ANL-7039)
of reinforced cylindrical shells, 20: 33432
of reinforced openings in pressure vessels, 17: 25394
of reinforced penetrations in prestressed concrete pressure vessels, 19: 29480
of rod drawing, 17: 39500 (GA-3683)
of rotating disks, (T), 20: 467
of salt columns in salt mines, 20: 45217 (ORNL-P-2126)
of shallow anisotropic plastic shells, 19: 28473
of shallow spherical shells, 19: 21620
of shear pins under single shear conditions, 19: 6007 (KAPL-M-6422)
of shells and plates, 17: 13706
of shells of revolution, computer program for, 16: 26470 (KAPL-2000-18)
of shock-induced spall fractures, 17: 18768 (TID-16706)
of short cylinders with arbitrary edge loading, (T), 19: 17343 (NAA-SR-Memo-10293)
of SNAP-10A piping system, 19: 31598 (NAA-SR-Memo-9817)
of SNAP-2 reactor-vessel top head, 19: 31600 (NAA-SR-Memo-10695)
of sodium-heated steam generator, 20: 12390 (BAW-1280-28(Vol.2))
of spherical pressure vessel with single radial nozzle, 20: 43491 (ORNL-P-2472)
of spherical steam generator, photoelastic, 18: 10218 (NAA-SR-8515)
of square box with internal pressure, 17: 35958 (NAA-SR-Memo-7470)
of stacked cylinder matrices, 16: 7843 (DC-60-8-94)
of statically indeterminate structures, 17: 13704
of supporting grids of perpendicular beams, 18: 13984 (ORNL-3535)
of tape-wound magnet coils, (T), 20: 1264 (NBS-8843)
of thick-walled concrete pressure vessel, 19: 28469 (GAMD-6027)
of time factor in spherical shell subjected to internal pressure, 19: 13559(T) (RISLEY-Trans-280)
of tube sheets, 17: 256 (WAPD-DLE-320)
of tube subjected to axial load and internal pressure, 17: 37569(R) (GA-4287)
of tube subjected to biaxial and uniaxial loads, 18: 30234(R) (GA-5259)
of two parallel plates connected by numerous tubes, 18: 40769
of two-dimensional bodies, computer program for plane, 19: 24641 (GAMD-5239)
of U-tube type heat exchangers, computer program for, 19: 32385

(KAPL-M-6459)
of viscoelastic media subjected to thermal variations, 19: 29479
of wave-propagated disturbances in elastic-plastic cylinders, 20: 30954 (UCRL-14617)
of welded materials, 17: 11172(T,R) (EURAEC-391)
of welding deposits, 17: 1900(T,R) (EURAEC-331)
of welding deposits from rising vertical electroslag processes, 17: 39510(T,R) (EURAEC-617)
of welding deposits from rising vertical electroslag processes, 18: 10500(T,R) (EURAEC-739)
of Zircaloy fuel-element containers for NS *Savannah*, 17: 34411 (ORNL-TM-483)
of 37-tube modular steam generator head, experimental, 18: 10230 (NAA-SR-8514)
of 4000-psi steel pressure vessel fracture, 17: 1940 (NP-12197)
photoelastic nondestructive methods for experimental, 20: 2026 (UCRL-13188)
photoelastic, of reactor pressure vessels, 20: 32751
photoelastic, of stresses around nozzles of reactor pressure vessels, 19: 31482
plastic deformation during thermal cycling of attached elements, 18: 28024
pressure-deflection relation for clamped circular plate in the plastic range, 18: 44064 (WAPD-282)
radiographic studies of, 19: 9348(T) (FTD-MT-63-261)
ratcheting growth of element under parabolic thermal cycling, 19: 2739
shear force and stress distributions in transversely impacted beams, determination using spark cinematography, 16: 4364(T) (SCL-T-390)
strain determination using moire fringe technique, 20: 1574 (UCRL-13156)
strength of thin-walled cylinders subjected to dynamic internal pressures, 17: 26129
strength of thin-walled cylinders subjected to dynamic internal pressures, 17: 40955 (CONF-39-100)
stress concentrations in nozzle rings of pressure vessels, 20: 1365
stress-wave propagation in an elastic-plastic compatible medium, 17: 26128
stress-strain distribution in lap-jointed thin shells, 18: 18355 (UCRL-7304)
stress-strain relationships of polycrystalline graphite under compression up to fracture, 19: 39186
techniques for, photostress and photoelastic, 16: 21026 (DC-59-6-224 and Add.)
testing equipment for, design and adjustments of Ford plane strain and Siebel conical dies for, 17: 23462(R) (NYO-10588)
thermal, for plates and shells, 17: 13708
thermoelastic, of epitrochoidal cylindrical reactor fuel elements, 20: 35882 (AAEC-TM-312)
thermoviscoelastic, approximate method for, 20: 31334
use of piezoelectric crystals for, 16: 20808 (PNE-105P)
uses for measuring ductility of steels, 18: 35987(R) (EURAEC-1019)
von Karman equations for bending of rectangular plates, iterative solutions of, 18: 28089 (IMM-NYU-322)
wave transmission between liquid and visco-elastic Voigt solid, 16: 6804 (NP-11218)
x-ray methods of, for ultra-high-strength materials, 19: 22515

STRESS CORROSION

abstracts of reports on, 16: 20978 (DP-683)
crack formation in, circulating autoclave for studying, 20: 33814 (COO-1319-40)
crack initiation in, role of chloride in, 19: 4197 (SAN-8003(p.90-133))
cracking and fracture of 4000-psi steel pressure vessels, mechanisms of, 17: 1940 (NP-12197)
design of potassium refluxing capsule for study of refractory metal, 20: 13191(R) (NASA-CR-54476)
effects of nitrogen on type 304 stainless steel, 20: 41449(R) (EURAEC-1676)
in nonferrous alloys and steel, mechanisms, 17: 18701(T) (AEC-tr-5724)
mechanisms and examples of, in reactor systems, 18: 18326
mechanisms of transgranular cracking due to, 20: 779
metallographic conditions for, review of, 19: 13928
of austenitic alloys, effects of structure on, 17: 36206 (UCRL-10712)
of reactor metals and alloys, mechanisms, 16: 12056
protection against, by protective corrosion films, 16: 12053(T) (AEC-tr-5007)
research on, equipment and sample preparation for, 19: 24932(R) (COO-1319-12)
review of fuel-element-cladding, 18: 34076 (TID-8540(p.213-330))
shot peening for protection against, 16: 7854
stacking fault energy in, 18: 22448 (UCRL-10890)
symposia on, New York, March 11–15, 1963, 20: 21276

STRIPED HILLS QUADRANGLE (NEV.)

geologic map of, 17: 4723

Strong Focusing

see Alternating-Gradient Focusing

STRONTIUM

see also Alkaline Earth Metals

absorption by barley, genotype effect on rate of, 20: 36575
absorption by gills of fish, tracer study, 20: 8576
abundance and isotopic compositions of, in brines under Salton Sea area, California, 20: 29414
abundance in Earth, theoretical method for determining, 19: 15771
abundance in Grenville, Canada, rocks, 18: 3985(R) (NYO-10517 (p.43-9))
abundance in Massachusetts Dedham granites, 18: 3987(R) (NYO-10517(p.53-4))
abundance in northern Appalachian granitic and volcanic rocks, 18: 3989(R) (NYO-10517(p.65-84))
abundance in Quebec igneous rocks, 18: 3992(R) (NYO-10517(p.105-10))
abundance in rocks, least squares analysis of, 18: 3999(R) (NYO-10517(p.129-31))
abundance in rocks, determination of rock origin from, 19: 46607
abundance in solar atmosphere, 16: 29599 (AFOSR-3024)
abundance in solar system, (T), 19: 6433
abundance in stony meteorites, 18: 4382(R) (NYO-10517(p.7-15))
abundance in sun, (E), 20: 17237
abundance in tektites, variation of, 18: 3983(R) (NYO-10517(p.27-38))
abundance in 3 Centauri A, upper limit, 16: 4659
abundance relation to rubidium in Sierra Nevada plutonic intrusives, 18: 3981(R) (NYO-10517(p.17-22))
accumulation in corn, genetic analysis of, 19: 41
accumulation of, in corn, genetic control of, 18: 8016(R) (TID-19851)
acid leaching from soils, 20: 8552(R) (TID-22443, pp 1-33)
age determinations in pegmatite deposits in Camughera-Moncucco, Italy, 18: 420
age estimations in minerals and volcanic rocks, 16: 14997(R) (NYO-3942)
analysis for scandium after solvent extraction using diantipyrilmethane, 18: 13702
analytical chemistry review, 16: 32944
atomic excited states of, lifetimes of, 18: 22692
atomic structure of, correlation effects in, 18: 7427
atomic structure, random-phase approximations for calculation of, 17: 8954 (UCRL-10510)
Auger spectrum, 17: 16810
bibliography on metabolism in animals and man, 17: 5747
binding by serum proteins, 16: 20111
calcification inhibition in rats fed, 18: 23
chelation of, development of agents for, 18: 8393(R) (TID-19989)
color centers in potassium chloride induced by, electron-nuclear double resonance study of Z_1, 19: 31627 (COO-1198-192)
composition of, in carbonatite, 17: 12469
concentration by marine organisms, 17: 12112
concentration using cation exchange with alkali metal- and alkyl ammonium phosphomolybdates, 16: 18898
contamination in mineral analyses using laboratory glassware, 18: 19888
contamination of goat milk by, mechanism of, 19: 8759
content and distribution in chicken eggs, effects of dietary strontium and calcium on, 20: 40569
content and ratio of strontium-87 to -86 in oceanic tholeiitic basalt, 20: 4145
content and strontium-chlorinity relation in Sargasso Sea water, 19: 614
content in acid igneous rocks of Africa, 18: 37358
content in African pitchblende, estimation of induced fission vs spontaneous fission from, 20: 37994
content in algae, fish, and snails in Clinch River, 19: 6933(R) (ORNL-3697(p.95-104))
content in alkali igneous rocks, 16: 31970
content in Ammonoosuc volcanics and Monson gneiss in New England, age estimations from, 20: 16711(R) (MIT-1381-13)
content in Australian granite, age estimation from, 20: 45883
content in blood and bone, metabolic effects on, 18: 38752
content in blood serum and bones in rats, mechanism of parathyroid hormone effects on, 17: 10264
content in blood serum on fetal and maternal side of placenta at birth, discrimination in, 18: 1359
content in bone and diet, relation between, 16: 11413
content in bone ash from female sheep and fetuses, 16: 17430 (A/AC.82/G/L.756)
content in bones, effects of age, 19: 33750
content in brain in Huntington's chorea, 18: 4976
content in calcites in Providencia area, Zacatecas, Mexico, 20: 18631 (NYO-2266-1)
content in calcite crystals from lead–zinc deposits, 20: 18631 (NYO-2266-1)
content in chondrites and chondrules, age estimation from, 20: 529

content in clams in Clinch and Tennessee Rivers, 16: 23410 (ORNL-TM-270)
content in deep crustal material, 18: 23801
content in diet in representative U. S. cities, 1962, 18: 1982
content in diet, effects on strontium-85 metabolism in rats, 19: 5613
content in diet, effects on metabolism of strontium-89, 16: 28714
content in diet, effects on deposition of strontium-89 and calcium-45 in bones, 17: 23061
content in egg yolks after administration to hens, 18: 13439
content in excreta and tissues in breast-fed babies, 19: 31719
content in fallout in Bratislava, Czechoslovakia, 1962-1963, 19: 18214
content in fetal body fluids, 17: 5731
content in foods, 19: 26574 (CEA-R-2707)
content in granites, quartzites, and slate in Massachusetts, age estimation from, 20: 16711(R) (MIT-1381-13)
content in Great Lakes and Hudson Bay, geochemistry of, 20: 16711(R) (MIT-1381-13)
content in Heemskirk granites, 20: 33521
content in helium d-c arc plasma, pressure dependence of, 18: 1138(T)
content in herbage, milk, plant-base, and soil in nuclear power plant environments in England, 18: 6775
content in high-velocity A stars, 18: 36135
content in human bones, foods, soil, and water in Egypt, 16: 4020 (A/AC.82/G/L.665)
content in human bones and diet, 16: 23370 (AERE-R-4035)
content in human brain, relation to Huntington's chorea, 17: 35419
content in human blood, bone, and soft tissue, 20: 22853(R) (ANL-7060)
content in human bone, 17: 5751(R) (HASL-132)
content in human skeleton, 17: 39287(R) (HASL-140)
content in human skeletons, 18: 41644(R) (HASL-149)
content in igneous rocks of Assynt and Scourie areas, Scotland, age estimations from, 19: 6115
content in Indian vegetables, 18: 25067
content in Jardine-Crevasse Mountain area, Montana, age estimation from, 20: 16711(R) (MIT-1381-13)
content in man, 19: 13122(T) (JPRS-27535)
content in man, spectrographic method for determining, 19: 40309(R) (NP-15180)
content in marine organisms, 19: 31696
content in marine aragonite oolites and sea water, 20: 18631 (NYO-2266-1)
content in milk and milk products, 16: 33331
content in milk and milk products, effects of processing on, 17: 17711(T) (JPRS-18492(p.26-33))
content in Mytilus shell, ecological effects on, 19: 26251
content in open-ocean silts, 20: 12540(R) (NYO-2882-8)
content in organs and tissues of humans outside continental U. S., 19: 21831
content in Pacific skeletal aragonites, 18: 33259
content in *Pisum sativum*, effects of calcium/strontium ratio on, 19: 25874
content in plankton, ecology studies, 16: 11388(R) (TID-14994)
content in rabbit skeleton, 20: 16178
content in rat blood serum and bone, effects of parathormone on, 17: 38709
content in rat diet, effects on calcium-47 and strontium-85 metabolism, 20: 14251
content in rat kidney mitochondria, effects of vitamin D on, 20: 8559
content in red-colored Paleozoic deposits in Northern Tien Shan, 20: 14780(T) (AEC-tr-6579)
content in river waters, 17: 30687
content in rock on Mid-Atlantic Ridge, 18: 39504
content in sea water, human contamination by, 19: 40309(R) (NP-15180)
content in sea water from Indian Ocean, uptake by marine organisms, 20: 40572
content in skeletal carbonates of marine organisms, 20: 24851
content in soil at Warsaw, 18: 33778
content in soil, effects of, on content in vegetables, 17: 17746
content in soil, effects on strontium-90 accumulation in oats, 19: 19475(T) (JPRS-27940(p.10-17))
content in soils and vegetation in New Jersey, 19: 25834
content in soils, effects of crop rotation on, tracer study, 20: 8552(R) (TID-22443, pp 1-33)
content in Spanish rock, 20: 41153
content in stone meteorites, 16: 31969
content in subterranean Bulgarian salt water, 19: 38851
content in tektites, relation to origin, 16: 9007
content in tektites in Moldavia, age estimation from, 20: 16711(R) (MIT-1381-13)
content in tissues of young and aged dogs, 20: 40540(R) (UCD-472-113, pp 17-56)
content in Triassic reef in Austrian Alps, theory of recrystallization mechanism from, 20: 18631 (NYO-2266-1)
content in 1000- to 2000-year-old clam shells, 20: 6711(R) (ORNL-3849, pp 43-100)
content of, in components of Canadian diet, 17: 15587 (CRER-1068)
content ratio to rubidium in geological materials, differentiation of Earth's mantle by studying, 20: 16711(R) (MIT-1381-13)
crystal structure above 35 kbar, 17: 39553
crystal structure of, pressure-induced f-c-c to b-c-c transformation in, 19: 7922
crystallization with thionalid, tracer study of, 16: 12961 (USNRDL-TR-551)
decorporation from rat skeleton, effects of strontium disodium chelate of 2,2'-bis[di(carboxymethyl)amino]diethyl ether, 16: 20060
depletion from calves by hemodialysis, tracer study of, 19: 43673 (TID-22147)
deposition in bone, factors affecting, 16: 19204
deposition in bones of 30- to 630-day-old white rats, 16: 9913
deposition in bone, effects of fluoride content, tracer study, 17: 31841
deposition in clam shells, morphology and, 19: 2059
deposition in snail shells, 20: 6711(R) (ORNL-3849, pp 43-100)
deposition of, in egg yolk after feeding to hens, 17: 21451
deposition of, in egg shell after feeding to hens, 17: 21452
desorption from tungsten, kinetics of thermal, 19: 7405
determination as trace in standard rocks G-1 and W-1, spectrographic, 16: 20831
determination by chromatography and flame spectrophotometry, 17: 14178
determination by charged-particle reactions at 2 Mev, 20: 43097
determination by flame photometry using d-c plasma jets, 19: 43924 (AERE-R-4990)
determination by flame photometry, 19: 44122
determination by flame photometry, 20: 4053
determination by potentiometric titrations, 18: 1489(R) (IS-700(Sect.C))
determination by precipitation as diliturate, 19: 19824
determination by spectroscopy using high-frequency plasma flames, 18: 10020
determination by spectroscopy using plasma jet, 20: 14492
determination by thermal-neutron activation methods, sensitivity for, 19: 9071
determination by x-ray fluorescence after paper electrophoretic separation, 17: 1406
determination by x-ray fluorescence analysis, 19: 15398
determination by 14-Mev neutron activation, 19: 26241
determination in alkali feldspars and micas by emission spectrography, 18: 13651
determination in air filters and surface fallout, 20: 25001
determination in aqueous solutions, polarographic, 20: 33220
determination in bones, 16: 22457 (TID-7632(p.376-80))
determination in biological materials and soil extracts, atomic-absorption spectrophotometric, 16: 26913
determination in bone, neutron-activation, 16: 4146
determination in blood and urine after ingestion, tracer study, 17: 13946
determination in bones, excreta, food, and water, flame photometric, 18: 11983
determination in biological samples, soils, and waters, flame spectrophotometric, 18: 15957 (RT/PROT(63)-13)
determination in barium chromate by x-ray emission spectroscopy, 18: 31380
determination in biological materials by atomic absorption methods, ion-exchange separation of phosphate for, 19: 7286
determination in biological tissues, activation, 19: 15333 (AE-168)
determination in bone, method using flame photometry and ion exchange for, 19: 38345
determination in bone, radiochromatographic method for, 20: 8824 (CONF-727, pp 174-8)
determination in bone ash, spectrographic, 20: 10774
determination in biological and geological samples by x-ray fluorescence methods, 20: 16345
determination in bone, ion exchange-photometric, 20: 22872(R) (NIRS-4, pp 12-17)
determination in biological materials and food by ion exchange chromatography, 20: 35447
determination in clay, acetic acid leachates, sand, and silt, spectrochemical, 16: 4379
determination in calcareous materials, flame spectrophotometric, 16: 17595
determination in calcium, polarographic, 16: 18828
determination in carbonatites, spectrographic, 17: 27228 (EUR-32.f)
determination in coal ash, spectrophotometric, 17: 38934
determination in clay by x-ray emission spectrometry, 17: 38954
determination in corn leaves, method for, 18: 39067
determination in carbon dioxide and oxygen atmospheres, spectrographic, 19: 2226
determination in calcareous media by flame photometry, 20: 29363

determination in diabase W-1 and granite G-1, spectrographic, 16: 17895
determination in diet, 16: 22457 (TID-7632(p.376-80))
determination in dog food and beagle skeletons, 17: 38641(R) (UCD-108(p.75-89))
determination in drinking and rain water, 20: 7021
determination in dust samples by microchemical methods and autoradiography, 20: 14472
determination in egg yolks, flame photometric, 18: 13439
determination in environmental media using neutron activation, 19: 36250
determination in enamel of teeth, neutron activation, 19: 38562
determination in environmental samples, 20: 40809 (NP-16235)
determination in fossil foraminiferal carbonates from deep ocean cores, 16: 29187 (TID-16359)
determination in food and bone by x-ray fluorescence, 19: 22113
determination in fission products, 20: 33191
determination in fission product solutions, method for, 20: 40803 (KFK-387)
determination in granite, x-ray fluorescence, 18: 6769
determination in human teeth, gamma spectrometric, 16: 8671 (AE-61)
determination in human mandibular articular disc by gamma spectrometry and neutron activation, 17: 28811
determination in hydroxyapatites, diffraction, 17: 35418
determination in human whole blood, activation, 17: 40739
determination in irradiated silica, activation, 20: 20636
determination in irradiated fuel effluents, methods for, 20: 22862 (CEA-R-2553)
determination in igneous and metamorphic apatites, spectrographic, 20: 26787
determination in leaves, micro-, 18: 25067
determination in lanthanum oxide, spectrographic, 20: 22895
determination in milk by gel filtration, 16: 23654
determination in minerals and rocks, flame photometric, 16: 400(T) (CEA-tr-R-1382)
determination in milk and water by x-ray fluorescence, 17: 38962
determination in minerals, chromatographic and flame spectrophotometric, 17: 40745
determination in molybdenum and its compounds, spectrographic, 18: 17766
determination in metals and alloys by mass spectrography using isotope dilution, 19: 15405
determination in minerals by neutron activation, 19: 30424
determination in Moldavites by mass spectrometry and x-ray fluorescence, 20: 16711(R) (MIT-1381-13)
determination in milk, activation, 20: 25003
determination in mineral and natural waters, flame photometric, 20: 38798 (NIJS-R-465)
determination in natural waters, tracer studies of ion adsorption on glass and plastic surfaces in, 19: 30097
determination in nuclear grade uranium, flame photometric, 19: 42418 (NIJS-R-448)
determination in nuclear grade uranium by flame photometry, 20: 26811
determination in ores, x-ray-fluorescence, 16: 9967
determination in open basins, spectrophotometric, 18: 27328
determination in presence of barium and calcium, scheme for, 16: 146
determination in presence of alkaline earth metals by paper chromatography and flame spectrophotometry, 16: 11549
determination in presence of barium and calcium by indirect derivatographic method, 16: 22035
determination in plutonium, flame photometric, 18: 8772(R) (NUMEC-P-104)
determination in potassium chloride and iodide crystals, activation, 18: 17737
determination in plant materials, chromatographic, 18: 27329
determination in powdered samples by spectrochemical methods, 19: 22120
determination in presence of calcium, 19: 26467(R) (TID-21796)
determination in plant residues and soils, flame spectrometry method for, 19: 35890(T)
determination in plutonium fluorides and peroxides, review on spectrographic, 20: 14464 (RFP-597)
determination in presence of barium and calcium by ring oven techniques, 20: 16388
determination in plankton in presence of calcium, spectrophotometric, 20: 26809
determination in powder samples by spectrographic methods, semi-quantitative, 20: 43104
determination in recent carbonate sediments of northern Florida Keys area, 16: 27456
determination in rare earths at 1 to 1000 ppm level, 17: 1377 (BM-RI-6097)
determination in rat femurs, neutron activation, 17: 30005
determination in rocks, 17: 30495
determination in rocks, comparison of mass and x-ray spectrometric, 18: 3678(R) (NYO-10517(p.135-41))
determination in reactor waters, spectrochemical, 20: 256
determination in rocks by x-ray spectrography, 20: 16711(R) (MIT-1381-13)
determination in solutions of fission products, development of radio-electrochromatographic method for, 16: 3347(T) (AEC-tr-4497(p.382-8))
determination in silicate materials, emission-spectrographic, 16: 17608
determination in strontium-90 recovery samples, methods for, 16: 23601 (HW-69677)
determination in sea water, isotope dilution, 18: 1547
determination in soils and vegetation, spectrographic, 18: 3447 (NYO-10581)
determination in sea water, spectrophotometric, 18: 29574
determination in soil-vegetation covers, flame spectrometric, 18: 39112
determination in sea water, x-ray-fluorescence, 18: 43790(R) (TID-21137)
determination in silicates, spectrographic, 19: 13266
determination in sea water by neutron activation methods, 19: 22574
determination in soil by emission spectrography, 19: 26243
determination in sea water and silts, spectroscopic, 19: 36315
determination in sea water, flame photometric, 20: 22871(R) (MIT-905-52, (pp 42-73)
determination in seawater, activation, 20: 25007
determination in silicates, activation, 20: 26782
determination in seawater, activation, 20: 40834
determination in stainless steel, method for radiochemical, 20: 43069(R) (IDO-14679, pp 51-9)
determination in tap-water, x-ray fluorescence spectrometric, 17: 10553
determination in tissue, after neutron activation, 17: 31813 (AERE-R-4309)
determination in tantalum by anion exchange in hydrofluoric–nitric acid mixtures, 18: 35455
determination in urine and water by counting after adsorption on phosphate gel mats, 16: 12953 (PAN-268/X)
determination in urine in presence of calcium, 17: 23284
determination in uranium, spectrographic, 18: 35444 (HW-77694)
determination in water, silver-spark spectrographic, 17: 1381 (IDO-14591)
determination in water, measurement techniques for, 18: 1976
determination in water and biological material, flame spectrophotometric, 19: 5766 (AE-163)
determination in water, spectrochemical, 19: 39265(R) (IA-1021)
determination, micro-coulometric, 16: 25285
determination of, elimination of phosphate interference in flame photometric, 17: 7955 (IA-770)
determination of effects of beam filters on x-ray fluorescence, 19: 30069 (AAEC/TM-289)
determination of, in sea water, spectrometric, 17: 17990
determination of, in residues by iron flux method, spectrographic, 17: 19942 (PG-Report-157)
determination of, in proportion to calcium in human bones and teeth, photometric, 17: 23271
determination of, radiometric, 17: 5952 (IA-772)
determination of radioactive, by precipitation and counting, 17: 35626 (AERE-AM-3)
determination of ratio of calcium to, in human bone and tooth ashes, flame photometric, 18: 1495 (AERE-AM-96)
determination of ratio to calcium in powder samples, x-ray-fluorescence, 18: 19849 (PG-Report-583)
determination of radioactive, radiochemical, 18: 37075 (AERE-AM-99)
determination of stable, in food, bones, and milk of beagles, 17: 38640(R) (UCD-108(p.66-74))
determination of traces of, using oxycellulose, 17: 35656
determination of trace amounts of, by reactor neutron activation methods, 20: 26760
determination of trace amounts of, using dimethylsulfonazo DAL, photometric, 20: 33221
determination of traces of, in biological materials, activation, 20: 38837
determination of, x-ray-fluorescence, 18: 6761
determination of, uses of radioactive tracers in, 18: 15962 (TID-7689(p.81-5))
determination of, radiometric titration, 18: 27311
determination of, submicrogram radiochromatographic, 19: 313
determination of, in presence of calcium, 19: 46197
determination of, in presence of calcium, x-ray fluorescent, 20: 232(R) (NYO-901-37, pp 80-4)
determination of, using Arsenazo III, photometric, 20: 36778
determination of, evaluation of titrimetric EDTA method with visual indicator end points for, 20: 43067(R) (IDO-14679, pp 6-46)
determination, turbidimetric method for, 17: 30499
determination using cerium perchlorate, titrimetric, 18: 186
determination using cyclohexanediaminetetraacetic acid, potentiometric, 18: 33507
determination using disodium tetrahydroxyquinone paper, colorimetric, 19: 7291

deuteron reactions, yttrium-86 isomer production in, 16: 17115
deuteron scattering at 11.8 Mev, 17: 31539
dietary availability from milk, tracer study, 16: 20899
diffusion from ceramic wastes, effects of volatilization on, 20: 18156 (BNWL-SA-453)
diffusion from in-pile-destroyed fuel elements, 18: 22530(R) (ORNL-3591(p.175-81))
diffusion from irradiated uranium, effects of burnup and irradiation level on, 16: 25841 (HW-72321)
diffusion from irradiated cerium–cobalt–plutonium alloy to sodium at 550°C, 20: 5848
diffusion from liquid urania in containment mockup experiments, 20: 4184(R) (ORNL-3843, pp 71-135)
diffusion from sodium at high temperatures, factors affecting, 20: 40357 (NAA-SR-11766)
diffusion from strontium carbonate, effects of air and temperature, 16: 16336 (HW-69692)
diffusion in aqueous solutions, tracer techniques for measurement of self-, 19: 398
diffusion in biotites at low temperatures, 16: 13379
diffusion in reactor-grade graphite, 20: 23735
diffusion in synthetic zeolites, tracer studies of kinetics of self-, 20: 18686
diffusion in uranium dioxide single crystals, 19: 5904
diffusion in uranium, 19: 16062 (CEA-R-2446)
diffusion of, in glass, activation energy and coefficient of, 17: 10642
diffusion, colloid formation, and electric charge in dilute solutions, tracer studies of, 19: 2285
dissociation energy of gaseous and heat of vaporization of solid, correlation of, 17: 6095
distribution among cellular fractions of dog kidney, 20: 35224
distribution between phases in molten boron oxide–sodium chloride–sodium oxide at 830°C, 20: 7201
distribution coefficient between fused bismuth and fused salt eutectic, 17: 21683
distribution coefficient between immiscible phases in aluminum chloride–lithium chloride–potassium chloride system at 625°C, 17: 35616 (HW-SA-2804)
distribution in blood plasma, 18: 11608
distribution in bones and tissues in man, 19: 6948(R) (ORNL-3697(p.178-92))
distribution in deep-sea silts and sea water, 20: 18892 (NYO-3450-1, pp 41-89)
distribution in gypsum and anhydrite forms of calcium sulfate, from 0 to 80°C, tracer studies of, 20: 43534
distribution in liquid lead-zinc alloy, 16: 11187(R) (ANL-6509)
distribution in microcline and quartz sand, 17: 2643 (UCRL-13048)
distribution in mixtures, radiometric analysis of, 17: 14282
distribution in minerals under controlled conditions, 18: 3996(R) (NYO-10517(p.123-4))
distribution in ores from Providencia, Mexico, 16: 25319 (TID-16128)
distribution in Pisum, factors affecting, 19: 24254
distribution in sea water, 18: 43790(R) (TID-21137)
distribution in soil, effects of various conditions on, 19: 19474(T) (CEA-tr-A-1616)
distribution in soil, effects of organic compounds on, tracer study, 20: 8553(R) (TID-22443, pp 34-54)
distribution in subterranean Bulgarian salt water, 19: 38851
distribution in White Oak Creek, 16: 12795(R) (ORNL-TM-133)
distribution of foliar-applied, in corn and soybean plants, tracer study, 17: 15590(R) (TID-18161)
distribution of, with cesium, plutonium, and uranium between lead and zinc at 702 to 760°C, 16: 28641(R) (ANL-6543)
distributions in electric arc discharges, image-spectrogram studies of, 19: 30108
effects of carrier, on strontium-89 deposition in chick bone, 18: 13427
effects of dietary, on parathyroid function in rats, 19: 12917
effects of dietary, on calcium-45 and strontium-85 retention by rat skeleton, 20: 12594(R) (NP-15679)
effects of dietary, on calcium-45 and strontium-85 retention by rat skeleton, 20: 12595(R) (NP-15680)
effects of Huntington's chorea on brain quantities of, 18: 29235
effects of impurity of, on radioinduced F centers in potassium chloride crystals, (E), 20: 15980(T)
effects of inherited radiogenic, on shale age determination, 18: 3988(R) (NYO-10517(p.55-64))
effects of injected, on mineralization of dentin in rat teeth, 18: 15792
effects of injected, on incisor dentin, 18: 29312
effects of soil levels on plant uptake of strontium-90, 16: 7400
effects of stable, on calcium-45 and strontium-90 content of clays and soils, 18: 43797
effects of stable, on non-metabolic strontium-89 uptake and deposition in tops of bean plants, 19: 43703
effects of, with calcium on manganese sorption by barley roots, 20: 16174(R) (RLO-1547-3)
effects on adenosine triphosphatase formation in wheat roots, 20: 30992
effects on adrenal medullary secretion in cats, 19: 35917
effects on barium and strontium retention in rats of dietary, 20: 38566
effects on cardiac contractility and membrane resting potentials, 17: 1205
effects on cardiac contraction, 17: 5686
effects on cartilage growth in rats, 20: 16181
effects on cellular aggregation in sponges, 18: 29207
effects on contraction of smooth muscles of rabbit aorta, 19: 25851
effects on contraction of heart, 20: 22551
effects on corrosion resistance of beryllium, 19: 22913(P)
effects on corrosion of graphite by water vapor, 20: 31667
effects on crystal structure of bone, 20: 232(R) (NYO-901-37, pp 80-4)
effects on determination of cesium by flame photometry, 16: 4133 (IA-607)
effects on determination of lithium in uranium by flame photometry, 20: 25014
effects on distribution of strontium-90 in water-bearing strata by ground waters, 19: 46602
effects on electric conductivity of flames, 18: 12791
effects on electric properties of lead titanate–lead zirconate solid solutions, 19: 30799
effects on F centers in x-irradiated potassium chloride crystals, 19: 24567(T)
effects on F-centers and electric conductivity of irradiated potassium chloride crystals, 18: 31584
effects on F-centers radioinduced in potassium bromide by proton beam at 6 Mev, 20: 23788
effects on ferroelectric properties of lead titanate–zirconate, 19: 1965 (SC-TM-64-670)
effects on flame photometry of calcium, 19: 7368
effects on grain size of aluminum–magnesium alloy and magnesium, 18: 39947
effects on growth and nitrogen fixation in Nostoc, 18: 33237
effects on histology of rats on calcium-deficient diet, 17: 27018
effects on hyperparathyroidism induced by calcium-deficient diet, 16: 32662
effects on inotropic action of fluoride in rat ventricle, 20: 36567
effects on lead titanate–zirconate ceramics at 4 to 77°K, 16: 13605
effects on muscle contraction, 19: 33725
effects on properties of dentin, in rat teeth, 19: 43687
effects on proton-induced vacancies in potassium bromide doped with, (E), 20: 15977(T)
effects on radioinduced color centers in potassium chlorides, (E), 20: 45041(T)
effects on rat incisor dentin, tracer study using sulfur-35, 18: 29202
effects on rat liver mitochondria, physiological, 19: 43688
effects on reconstitution of blastocyst formation in rabbits, 19: 25864
effects on separation of uranium from chloride solutions by solvent extraction using trioctylamine, 18: 27626
effects on spectrophotometric determination of thorium, 19: 24408
effects on steam–graphite reaction, 18: 25321 (GA-5215)
effects on strontium-85 excretion by man, 17: 28633
effects on strontium-90 uptake by oats, 18: 23206(T) (JPRS-24290 (p.43-7))
effects on strontium-90 metabolism in mammals, 19: 38335 (NP-14926)
effects on strontium-90 uptake by plants from soils, 19: 40310
effects on strontium-85 and strontium-89 excretion by goats, 20: 40568
effects on uptake of calcium-45 and strontium-90 in rat skeleton, 17: 31831(T) (JPRS-19626)
effects on x-irradiation coloration of potassium chloride crystals, 16: 13661
electric conductivity of, effects of temperature and pressure on, 17: 36494
electron band structure of, from absolute reflectance measurements, (E), 19: 35594
electron binding energies of, measurements for, 17: 18924
electron binding energies of, K- and L-shell, 20: 46603 (UCRL-16798)
electron energy levels of, lifetime of $^1P_1$, 18: 22695
electron secondary emission, 17: 25978
electron-impact ionization, cross sections for, 19: 31335(R) (UCRL-12303)
elimination of deposited, from man, effects of therapy on, 19: 13097
elution from ion exchange materials, effects of temperature on, 17: 19707 (TID-7644(p.83-114))
energy level transitions in, Coster-Kronig, (T), 20: 15238 (CONF-233 (Vol.3), pp 398-418)
energy level widths for, K, (T), 20: 15239 (CONF-233(Vol.3), pp 419-39)
energy levels of, lifetimes of excited, 17: 8928(R) (NP-12325)
equilibrium and standard free energy constants for, in methanol and methanol-water solvents, 18: 8362

evolution in earth mantle, reconstruction of, 18: 3997(R) (NYO-10517 (p.125-6))
exchange in Alaskan soil, factors affecting, 18: 33777
exchange with cesium and sodium on montmorillonites, 20: 27042
excretion and metabolism in man, review, 20: 8542 (CONF-727, pp 85-101)
excretion and metabolism of, use in dosimetry, 20: 20398
excretion and plasma concentration in man, comparison, 16: 1449
excretion and tubular reabsorption of, 18: 11620
excretion by fish, renal, 20: 23374(R) (NIRS-4, pp 81-7)
excretion by gill in fish, 17: 12113
excretion by man, 19: 6948(R) (ORNL-3697(p.178-92))
excretion by rat kidneys, theory and experiments on, 17: 21426
excretion by rat kidneys, effects of tetracyclines on, 20: 32928
excretion by rats, urinary, 19: 21821
excretion from body of experimental animals, technique for, 16: 30194
excretion in rats, effects of pyridoxine on, 20: 16176
excretion in urine, development of chelating agents for enhancing, 16: 5130 (TID-14373)
excretion in urine, tracer study, 17: 10310(R) (TID-17789)
excretion of urinary, 19: 29879
excretion of, effects of chelates on urinary, 20: 18209 (TID-22717)
excretion of, in urine of fish, tracer study, 20: 6741
extraction from Radgendorf clay, 16: 23351
fixation by clay minerals, 17: 1164
fixation by soil calcium carbonates, 18: 29231
fixation in basalt in waste processing, 20: 24814
fixation of, by shells of fresh water snails, 18: 4974
fixation on calcite, minerals, and rocks, 16: 16019 (CEA-2114)
fixation on ion exchange beds in storage containers, 18: 9742 (HW-SA-3233)
fluorescence yields in proportional and scintillation detectors, 18: 3796
geochemistry and mineralogy of, in Cherry Mountains (Urals), USSR, book, 19: 20190
geochemistry of marine, 18: 41640
half life in human skeleton, biological, 18: 13436
heat of sublimation and vapor pressure of, 18: 16517
hemodialysis in cattle, 18: 38775(R) (ORO-624)
incorporation and removal from animals, mechanisms for, 18: 27051
incorporation in calcium fluoride and phosphate precipitates, 18: 19949
influx rate across trout gills, tracer study, 16: 25116(R) (HW-72500 (p.23-5))
infusion of, in man, calcium tolerance test compared with effects of, 17: 21430
intestinal absorption of, tracer study in rats, 20: 3669
ion density and temperature in ionized, spectroscopic determination of, (E), 19: 41883
ion exchange behavior in hydrochloric acid–organic solvent media, 18: 39124
ion exchange by glauconite, acidity effects on, 18: 39259
ion exchange in concentrated hydrochloric and perchloric acids, distribution coefficients of, 18: 17759
ion exchange in soils, 18: 17342
ion exchange on Bio-chelex 100, activation energy and diffusion coefficients for, 18: 1641
ion exchange on calcium carbonate–sand mixtures, 17: 19711 (TID-7644(p.187-99))
ion exchange on minerals, 20: 38858 (BNWL-235-3, pp 23-51)
ion exchange on phosphate glass electrode, 18: 3780
ion exchange on zirconium-base and clay-mineral ion exchangers, 17: 25364
ion exchange reactions with hydrogen on ferrocyanide molybdate, kinetics of, 20: 18564 (EUR-2748.e)
ionic mobilities in lithium, potassium, and sodium nitrate systems, 18: 1645
ionization of, Auger effect in, 18: 16698
ionization on tungsten single crystals, surface atomic beam, 17: 37758
isotopic composition in surface water from North Atlantic Ocean, 19: 22541
isotopic composition in, mass discrimination in spectrometric measurements on, 20: 40821
leaching from leaves, effects on plant nutrition, 19: 8777
light resonant absorption by ionized, ion density and temperature determination from, (E), 19: 41883
localization of, in plant tissue by autohistoradiographical methods, 20: 26617
melting point, 18: 25984 (TID-20639)
melting temperature of, equations for calculating, 18: 25990
metabolism, 19: 63
metabolism, 19: 45729(R) (NYO-910-23, pp 1-111)
metabolism by animals and plants, 19: 25870
metabolism by dogs, 16: 32639(R) (TID-16459)
metabolism by dogs, 16: 32689(R) (TID-16458)
metabolism by fresh-water snails and fixation in shell, tracer studies of, 19: 35923
metabolism by maize, effects of genotype, environment, and nitrogen fertilization on, 19: 33740(R) (NYO-2744-26)
metabolism by marine organisms, tracer study of, 17: 30281(R) (TID-19104)
metabolism by mitochondria from rat liver and kidney, effects of added calcium or strontium, tracer study, 17: 1225
metabolism by plankton, 17: 14540(R) (TID-18021)
metabolism by plants, tracer study of, 18: 38774(R) (EUR-1881.e)
metabolism by plants, effects of soil conditions on, 19: 19474(T) (CEA-tr-A-1616)
metabolism by plants, effects of calcium content of nutrient solution on, 19: 25836 (EUR-487.f(Vol.I))
metabolism by plants, replacement of calcium by, tracer study, 17: 28653
metabolism by plants, effects of culture method and calcium on, 19: 25837 (EUR-487.f(Vol.II))
metabolism by rats, effects of diet on, 18: 33805(R) (NIRS-2(p.57-67))
metabolism by snails, 19: 10731(R) (NP-14669)
metabolism by *Tetrahymena pyriformis*, effects of drugs on, 19: 31735
metabolism in Acantharia, tracer study, 20: 12591(R) (EUR-2475.f)
metabolism in animals, tracer study, 17: 23028
metabolism in animals, effects of dietary phosphates on, 20: 8(R) (STI/DOC/10/42, pp 23-43)
metabolism in animals, techniques for studying, 20: 32926
metabolism in beef cattle, 18: 38775(R) (ORO-624)
metabolism in bone, effects of diet and age, tracer study, 16: 17419
metabolism in bone, tracer study, 16: 20064
metabolism in bones in rats, 16: 20118
metabolism in bones in rats, 16: 32694(T) (AEC-tr-5418)
metabolism in bone, 17: 1212
metabolism in bones of animals, 18: 1348
metabolism in bone in child, effects of rickets on, 18: 38760
metabolism in bones, triple tracer method for measuring simultaneously with calcium and phosphorus, 19: 31780
metabolism in bones, effects of age on, 19: 44250 (NP-15269)
metabolism in bone of rats, effects of pyridoxal on, 20: 14246
metabolism in bones, compartmental analysis, 20: 20400
metabolism in bone, effects of dietary protein levels, 17: 5745
metabolism in cancer patients during radiotherapy, 17: 40502
metabolism in children and adolescents, 20: 28889
metabolism in corn, genetic control of, 18: 3454(R) (TID-19786)
metabolism in corn plants, genetic control of, 18: 6596(R) (TID-19842)
metabolism in deer and sheep, tracer study of, 20: 12609
metabolism in domestic animals, tracer study, 17: 31816(R) (ORO-605)
metabolism in fetal and newborn rats, tracer study, 19: 19473 (UR-661)
metabolism in fish, tracer study, 16: 11951 (HW-72107)
metabolism in human fetuses, 19: 43701
metabolism in mammals, 18: 6976(R) (TID-19893)
metabolism in man, tracer study, 16: 28670(R) (UCLA-507)
metabolism in man, computer study, 17: 23032 (BNL-6208)
metabolism in man, tracer study, 17: 27049
metabolism in man, relation to calcium metabolism, tracer study, 17: 30262
metabolism in man, 18: 25073
metabolism in man, 20: 18185(R) (BNL-929, pp 126-47)
metabolism in man, 20: 28890
metabolism in man, effects of steroid hormones on, 19: 45805
metabolism in mitochondria, 19: 31725
metabolism in newborn man and rat, 19: 29865
metabolism in nursing puppies, effects of calcium content of diet on, 19: 43676(R) (UCD-472-112, pp 80-5)
metabolism in *Pisum sativum*, tracer study, 20: 12605
metabolism in plants, tracer study, 19: 27916
metabolism in rats, tracer study, 17: 27029
metabolism in rats, 19: 19500 (NP-14907)
metabolism in rats, 19: 21821
metabolism in rats, effects of calcium, phosphorus, or strontium content in diet, tracer study, 20: 38566
metabolism in skeleton of man, tracer study, 17: 10293 (BNL-6108)
metabolism in wheat seedlings, 20: 38548(R) (ORO-2410-1)
metabolism of, 19: 29879
metabolism of, by corn plants, effects of environment on, 18: 3453 (TID-19757)
metabolism of, effects of calcium on, 17: 35426
metabolism of, effects of dietary phosphorus levels on, in rats, 17: 38714
metabolism of, in fish, 18: 4975
metabolism of, in mice, effects of dietary levels of phosphorus on, 17: 38715
metabolism of, kinetics of, 17: 25042
metabolism of radioactive, 16: 14449(R) (TID-14780)
metabolism of, in mice and rats, effects of age and diet on, 20: 35237

metabolism of, review, 19: 66
migration in aquifers, laboratory studies of, 17: 39270 (UCRL-13074)
migration in soils and ground-table water, 18: 38685 (A/CONF.28/P/774)
migration in turf-podzolic and black earth soil, 20: 40520 (NP-16261)
movement in ground water at Savannah River Plant, 17: 4700
movement in ground waters, correlation with distribution coefficient, 18: 8516 (HNS-1229-21)
movement in human skeleton, 17: 5712
movement through soils, 18: 43170(R) (EUR-1882.e(p.31-6))
neutron absorption cross sections, 16: 18429
neutron absorption cross sections at 24 kev, (E), 19: 45230
neutron absorption cross section in pitchblende, thermal, 20: 37994
neutron capture cross sections, 16: 26509
neutron elastic scattering at 3.3 Mev, asymmetry in polarized, (E/T), 19: 10343
neutron elastic scattering at 1 Mev, differential cross sections for, (E/T), 20: 9981 (WASH-1064)
neutron elastic scattering at 3.2 Mev, (E/T), 20: 46644
neutron interaction threshold values for fission spectrum, 16: 7036
neutron radiative capture cross sections at 30 and 65 kev, 18: 34274(R) (NIRS-2(p.3-15))
neutron reactions at 3.7 Mev, cross-section measurements, 16: 8224
neutron reactions (n,γ) at low energies, gamma spectra for, 17: 26419(R) (ARF-1193-23)
neutron scattering at 1 Mev, 16: 3662
neutron scattering at 2.5 Mev, inelastic cross sections, 16: 29741
neutron scattering by, measurement of polarization in, 17: 2243(R) (TID-17083)
neutron scattering at 0.4 to 1.2 Mev, cross sections for, 18: 9331
neutron total cross section of, fast, 17: 20982 (HW-SA-2875)
nitridation kinetics, 16: 2139
oxidation kinetics, 16: 2139
partition coefficients and reciprocal ionic radii, 17: 27562 (INSJ-54)
phase diagrams of crystalline, at high pressures, 18: 623
phase transformations, 18: 25984 (TID-20639)
placental transfer of, in pregnant rats, 18: 1364
precipitation as complex with cesium, lead, or rubidium chlorides from melt, 18: 23540
precipitation by iron hydroxides, 16: 27509
precipitation in calcareous soils by calcium carbonates, 18: 33594
precipitation of, from solutions, use of dilituric acid in, 17: 16055(R) (TID-18261(p.71-2))
precipitation on semi-burned dolomite by aqueous solution, 16: 22070(T) (AEC-tr-4460(p.269-73))
precipitation using dimethylbenzenearsonic acid, 19: 9136
precipitation with sodium chloride crystals, tracer studies, 16: 3338(T) (AEC-tr-4497(p.279-87))
precipitation with aragonites and calcites at 90 to 100°C, 17: 30515 (TID-19012)
precipitation with cerium–cadmium intermetallic compounds from liquid cadmium, 18: 34192
precipitation with ferric hydroxide, tracer studies of, 18: 39172(T) (AEC-tr-6390(p.460-5))
precipitation with aragonite and calcite, 16: 25319 (TID-16128)
preparation by reduction of barium salt using catalytic nascent hydrogen, 19: 46253(T) (ORNL-tr-803)
production by decomposition of strontia by silicon, 19: 38593(T) (ORNL-tr-674)
production from sulfide by electrolysis and vacuum distillation, 18: 13804(P)
production in fission of uranium-235, yields, 16: 6438(R) (TID-14466)
properties of, for use in silicate technology, 18: 7250
proton reactions (p,n) at 18.5 Mev, angular distributions of quasielastic, 18: 40587
proton reactions with neutral ground state of, formation of excited hydrogen atoms in, (T), 20: 41634
purification by hydroxide precipitation, 19: 24604 (BNWL-46)
purification by vacuum distillation, 18: 25984 (TID-20639)
purification of, radiochemical method for, 20: 8838 (UCRL-14258)
quantum defect for ^3S state, 17: 20736
radiation effects on electric conductivity of alkali halides doped with, x, (E), 19: 26386
radiation effects on metabolism of, in adult dog bones, electron, 20: 6896
radiochemistry, 17: 210
radiosensitivity effects on plants, 19: 42369
ranges of recoil, in sodium chloride–uranium dioxide mixtures, 20: 37997
ratio to calcium, effects on absorption and growth in *Pisum sativum* of, 18: 31094
reactions with ammonium nitrate and oxalate and potassium and sodium sulfates, precipitation, 17: 10621
reactions with autoprothrombin C, complexing in, 19: 32190
reactions with clays, exchange, 19: 46239(R) (ORO-631, pp 132-41)
reactions with flavone derivatives, precipitate formation in, 19: 13373
reactions with sodium beryllate solutions, 17: 16002
reactions with sorbent minerals, tracer study, 16: 25049 (TID-7628 (p.187-97))
reactions, with gelatin, potentiometric studies on binding, 18: 41423
removal from bone by chelating agents, 16: 31455
retention by clays, 19: 36300
retention by mice, effects of thyroid hormones on, 20: 22853(R) (ANL-7060)
retention in bones, effects of chelating agents, 16: 28699 (TID-7639)
retention of dietary, in human infants, 17: 23063
saturation of mammalian skeleton with, 16: 20108
scattering on beryllium–copper alloy at 5 kev, secondary electrons from, 20: 41620 (NIJS-R-471)
separation by amalgam exchange technique, 17: 34038
separation by amalgam exchange, 17: 34051 (TID-18898)
separation by anion exchange in acetic acid–nitric acid medium, 18: 16131
separation by anion exchange in acid-organic solvent media, 18: 23707(R) (TID-20609)
separation by anion exchange in mixed aqueous and non-aqueous systems, 19: 2243
separation by complex formation with pectins, 16: 3286(T) (JPRS-9706(p.50-5))
separation by electrophoresis on zirconium phosphate paper, 17: 4467
separation by electrodialysis using ion exchange membranes, 18: 31653 (COO-770-12)
separation by ion exchange, 17: 14154(T) (CEA-tr-X-485)
separation by ion exchange on vermiculite, 18: 19450(T) (CEA-tr-A-1462)
separation by reversed-phase chromatography on D2EHPA treated paper, 18: 16141
separation by reversed-phase chromatography using paper treated with di-(2-ethylhexyl) orthophosphoric acid, 18: 39096
separation by solvent extraction, 16: 14824
separation by solvent extraction using organic solvents, 16: 18989
separation by solvent extraction using di(2-ethylhexyl) phosphoric acid, effects of diluents and synergistic agents on, 18: 1799(R) (ORNL-3496)
separation by solvent extraction using di(2-ethylhexyl)phosphoric acid, 19: 4250(R) (ORNL-3627(p.177-208))
separation by solvent extraction from salt solutions, synergistic effects of bis(2-ethylhexyl) phosphate on, 20: 9049(R) (ORNL-3830, pp 193-221)
separation from acid solutions by solvent extraction, 18: 43724
separation from acid waste solutions, solvent extraction process for, 19: 5988 (HW-75537)
separation from acid waste solutions by ion exchange, 19: 7613 (BLG-267)
separation from alkaline earth elements, aluminum, and iron by cation exchange, 18: 17959
separation from alkali metals by ion exchange using vanadium ferrocyanide, 20: 12932
separation from alumina calcine by leaching with dilute nitric acid or distilled water, 20: 40478 (IN-1011)
separation from aqueous solutions by foam, 16: 14819(R) (RAI-100)
separation from aqueous wastes containing sodium salts by ion exchange, properties of zeolites for, 17: 8240 (HW-SA-2364)
separation from aqueous solutions by solvent extraction using oxine, 18: 17937 (PAEC(D)CH-638)
separation from aqueous waste solutions by solvent extraction followed by ion exchange, 18: 45160(P)
separation from aqueous solutions by countercurrent sorption, 19: 6879 (UJV-1108/64)
separation from aqueous solutions, properties of tuff cation exchanger for, 19: 38768
separation from aqueous solutions by ions exchange on ferrocyanide tungstate, 20: 7083
separation from aqueous solutions by solvent extraction using bis(2-ethylhexyl) phosphate, 20: 9049(R) (ORNL-3830, pp 193-221)
separation from aqueous solutions by solvent extraction using monoalkyl ester of phosphoric acid, 20: 29365(P)
separation from ashes of beef bones, milk, and fish, 20: 40858
separation from barium by solvent extraction, 16: 31678 (IS-363)
separation from barium, calcium, and magnesium by paper electrophoresis, 17: 21786
separation from barium and calcium using complexone III, 17: 30494
separation from barium in rain water, method for, 18: 3903
separation from barium, calcium, and magnesium by cation exchange, 18: 17958
separation from barium by exchange between amalgam and solution, 18: 23734
separation from barium and calcium in plant materials, chromatographic,

18: 27329
separation from barium by chromate precipitation, evaluation of methods for, 18: 31380
separation from barium by paper electrochromatography, 18: 41573
separation from barium, calcium, and thorium, paper chromatographic, 19: 4238
separation from barium by complex formation with 2-phenyl-4,5,6,7-tetrahydroindazol-3-one-5,5-dicarboxylic acid, 19: 26472
separation from barium and cesium by ion exchange on granulated zirconyl phosphate, 20: 41055
separation from barium by cation exchange using DTPA and HEDTA as eluants, 20: 41040 (ORNL-TM-1342)
separation from barium, calcium, and cesium by ion exchange using heated Dowex column, 20: 43436
separation from beryllium using arsonic acids, 16: 8685(T) (AWRE/TRANS/25)
separation from berkelium by solvent extraction, 19: 22112
separation from brines containing calcium, 16: 14764(P)
separation from calcium, chromatographic, 16: 174
separation from calcium on chelating resin, 16: 11699(R) (TID-15020 (p.61-4))
separation from calcium, 16: 11584(T) (CEA-tr-R-1421)
separation from cadmium by coprecipitation with cadmium–cerium alloy, 16: 16464
separation from calcium by selective precipitation of strontium sulfate, 16: 31590(T) (CEA-tr-A-1135)
separation from calcium by solvent extraction using sodium rhodizonate, 16: 12991
separation from calcium by paper chromatography, 17: 14172
separation from calcium by ion exchange using EDTA, 17: 34057
separation from calcium in milk by liquid ion exchange, 18: 1514
separation from calcium using butyl Cellosolve, 18: 1804(T) (CEA-tr-X-494)
separation from calcium and magnesium by anion exchange, 18: 16132
separation from calcium by continuous electrophoresis, 18: 23721
separation from calcium in soils using potassium ferrocyanide, radiochemical, 18: 27631
separation from calcium by solvent extraction, effects of sodium concentration in organic feed on, 18: 34007(R) (ORNL-TM-890)
separation from calcium, 18: 37390
separation from calcium and magnesium by reversed-phase partition chromatography, 18: 39078
separation from calcium by ion exchange using EDTA, 18: 41567(T) (ORNL-tr-175)
separation from calcium and sodium by ion exchange on zeolites, tracer studies of equilibria in, 19: 528(R) (HW-81746(p.4.15-23))
separation from calcium by solvent extraction using di(2-ethylhexyl) phosphoric acid, 19: 4251(R) (ORNL-3627(p.209-15))
separation from calcium and magnesium by ion exchange, 19: 9046(R) (IS-900(Sect.C))
separation from calcium and magnesium by ion exchange on zirconium molybdate crystals, 19: 13218
separation from calcium by ion exchange, 19: 18061
separation from calcium by desorption, 19: 24611(R) (MLM-1227)
separation from calcium by residue adsorption, 19: 36555
separation from calcium using pyridine-2,6-dicarboxylic acid resins, chromatographic, 19: 40674
separation from calcium, magnesium, potassium, and sodium by ion exchange, 19: 44122
separation from calcium by precipitation as sulfate, 20: 9071
separation from calcium in milk, 20: 20938 (NP-15921)
separation from calcium by exchange in amalgam–solution system, 20: 20829
separation from calcium by nitrate solubility in 1-butanol, 20: 24980 (SZS-2(1966))
separation from calcium and magnesium by ion exchange, 20: 29363
separation from cerium by anion exchange, 16: 126 (HW-69737)
separation from cesium by foam techniques, 16: 1649(R) (ORNL-TM-1)
separation from cesium by ion exchange on zirconium phosphate, 16: 7617(T) (CEA-tr-X-336)
separation from cesium by sorption by, ammonium phosphotungstate, 16: 13049
separation from cerium, cesium, and yttrium by paper chromatography using iron(III) hydroxide, 17: 21782
separation from cerium by ion exchange, 18: 8445(R) (HW-78388 (p.4.1-15))
separation from cesium by electrodialysis, 19: 30319 (COO-770-11)
separation from cesium by ion exchange on zinc ferrocyanide, 20: 7198
separation from cesium by electrodialysis, 20: 18842
separation from cesium by ion exchange on cellulose phosphate, 20: 31324
separation from cesium by sorption by vermiculite, effects of EDTA and pH on, 20: 43130
separation from chloride solutions by solvent extraction using amines, 18: 1799(R) (ORNL-3496)
separation from chloride solutions by ion exchange, 20: 4053
separation from condensate wastes containing ammonia by cation exchange, 16: 26638 (HW-71627)
separation from contaminated solutions by coprecipitation with barium sulfate, 20: 18579 (UJV-1489)
separation from dilute solutions by precipitation with calcium oxalate using dimethyl oxalate, 20: 29154
separation from fission product mixtures, ion exchange, 17: 244
separation from fission product solutions by nitrate precipitation, 18: 11499 (AERE-R-4493)
separation from fission products by solvent extraction using D2EHPA, 18: 16147
separation from fission products by sorption on ferric hydroxide, 18: 20102 (UJV-850/63)
separation from fission products in air samples by paper chromatography, 19: 317
separation from fission product waste by solvent extraction, demonstration of Csrex process for, 19: 5557 (HW-81091)
separation from fission products by ion exchange, equipment for, 19: 36593
separation from fission products, review on method for, 20: 14436 (BNWL-SA-504)
separation from grass, milk, and water by amalgam exchange, 17: 6132(R) (TID-17272)
separation from graphite above 1750°C in inert gases, 19: 38762
separation from hydrochloric acid solutions by solvent extraction using 2-ethylhexanol, 19: 36252
separation from irradiated fuel by solvent extraction, economics of, 19: 44121
separation from irradiated silica and sodium by chromatography, 20: 20636
separation from IWW Purex waste, 17: 10246(R) (ORNL-TM-403)
separation from liquid wastes by ion exchange using zeolite taff, 19: 44123
separation from lithium beryllium fluorides by solvent extraction using bismuth–lithium alloys, 20: 45790(R) (ORNL-3945, pp 72-8)
separation from low-level waste by foam separation columns, effects of pH and calcium and sodium ion concentrations, 16: 22269(R) (TID-15919)
separation from low-level waste, using foam column, 19: 30322 (ORNL-3527)
separation from low-level waste water, 20: 1549 (ORNL-3811)
separation from mineral acid by solvent extraction using phosphonic and phosphoric acid esters, 16: 31680
separation from milk, cation exchange method for, 17: 8469
separation from milk, 20: 1975(P)
separation from milk by ion exchange process, 20: 45826(P)
separation from nitric acid solutions by adsorption, 16: 1854(R) (IDO-14553)
separation from nitrate solutions by solvent extraction using di(2-ethylhexyl)phosphoric acid, 17: 17949(R) (ORNL-TM-449)
separation from nitrate solutions by solvent extraction using di(2-ethylhexyl)-phosphoric acid, mechanism of, 17: 25362
separation from nitric-acid solutions by solvent extraction using amides, 17: 39185(R) (ORNL-3452(p.168-88))
separation from nitric acid solutions, ion exchange selectivity scales for, 19: 9257
separation from nitrate solutions by solvent extraction using HDEHP, equilibria and mechanism of, 19: 24440
separation from other fission products by sorption on silica gel, 18: 16144
separation from other fission products by paper electrochromatography, 18: 41575
separation from other fission products by solvent extraction, 19: 18075
separation from other alkaline earths and rare earths, 19: 19789
separation from other metals by reversed-phase chromatography, 19: 30331
separation from other metals by partition chromatography of chloride solutions, tracer studies of, 19: 32288
separation from other fission products by solvent extraction using benzene–oxine solutions, 19: 46440
separation from other inorganic ions by paper chromatography, 20: 12939
separation from other metals by extraction chromatography using TOPO, tracer studies of, 20: 27054
separation from other fission products by ion exchange, 20: 35587 (IEA-101)
separation from other fission products and uranium by chromatography using ion-exchange paper, 20: 35440
separation from oxalic acid solution by solvent extraction using triisooctylamine, 19: 22409
separation from perchloric acid solutions by solvent extraction using bis(di-*n*-hexylphosphinyl)methane, 18: 9970 (IS-777)

separation from perchloric acid solutions by ion exchange materials, 20: 20823
separation from perchlorate solutions by solvent extraction using bis-(2-ethylhexyl) phosphate, 20: 45795(R) (ORNL-3945, pp 176-88)
separation from products of fission-fragment-induced radiolysis, 20: 40951 (RPI-321-6)
separation from Purex waste solution by ion exchange, 16: 1649(R) (ORNL-TM-1)
separation from Purex wastes, 16: 8439 (ORNL-3204)
separation from Purex wastes by carrier-precipitation process, 16: 17333 (HW-69534)
separation from Purex waste, 16: 30492 (HW-SA-1939)
separation from Purex Process wastes by solvent extraction, 17: 3070(R) (ORNL-TM-265)
separation from Purex solution by solvent extraction using amines, 17: 3070(R) (ORNL-TM-265)
separation from Purex Process wastes by solvent extraction, 17: 4625 (HW-SA-2767)
separation from Purex 1WW waste by solvent extraction using di(2-ethylhexyl)phosphoric acid, 17: 17949(R) (ORNL-TM-449)
separation from Purex feed by solvent extraction using D2EAPA, 17: 39186(R) (ORNL-3452(p.189-94))
separation from Purex waste ruthenium extraction phase using D2EHPA, 18: 16377(R) (ORNL-TM-515)
separation from Purex waste by solvent extraction using D2EHPA, 18: 17935(R) (ORNL-TM-532)
separation from Purex Process wastes by precipitation, 18: 22168 (DP-877)
separation from Purex wastes by ion exchange, 18: 25606 (ORNL-3585)
separation from Purex acid waste by solvent extraction using D2EHPA, 18: 29136 (HW-79762(Pt.2))
separation from Purex waste by solvent extraction, 18: 31655 (HW-79762 (Pt.1))
separation from Purex wastes by solvent extraction using di(2-ethylhexyl)phosphoric acid, 19: 4251(R) (ORNL-3627(p.209-15))
separation from Purex wastes by solvent extraction using carboxylic acids, 19: 4251(R) (ORNL-3627(p.209-15))
separation from Purex wastes, improved sulfate precipitation process for, 19: 5987 (HW-74036)
separation from Purex waste by lead sulfate carrier precipitation, 19: 24198
separation from Purex waste solutions by solvent extraction, flowsheet for, 20: 45796(R) (ORNL-3945, pp 195-8)
separation from Purex wastes by ion exchange, 18: 27279(R) (HW-80284 (p.A.1-23))
separation from rare earths by ion exchange in isopropyl alcohol, 18: 20104
separation from radioactive waste water by ferric hydroxide flocculation, 18: 24981
separation from rare earths by ion exchange chromatography, 20: 18827
separation from radioactive waste solutions, 20: 38538
separation from reprocessing effluents by ion exchange in acid medium, 18: 37281 (A/CONF.28/P/772)
separation from rubidium by isotope dilution, 16: 20332
separation from rubidium, cesium, and yttrium by chromatography, 18: 31669
separation from rubidium by sorption by strontium carbonate, 20: 27057
separation from salt solution by ion exchange using basic lead sulfate, 18: 25262(P)
separation from salts by solvent extraction using 8-mercaptoquinoline in chloroform, 20: 10759 (INP-427/C)
separation from sea water, method for shipboard, 20: 7256(R) (TID-22411, App.A)
separation from sewage water by sorption on multiclone dust from gasification of coke, 20: 18170
separation from seawater by sorption on ferric hydroxide ion exchange material, 20: 22923
separation from simulated waste by ion exchange, 17: 19705 (TID-7644 (p.29-45))
separation from solutions by carrier precipitation, 16: 16467(P)
separation from solutions in foam column, 16: 17617(R) (ORNL-TM-122)
separation from solutions by ion exchange, 16: 26467(R) (HW-73100)
separation from solutions using foam methods, effects of calcium, 16: 29039(R) (RAI-101)
separation from solutions by foam distillation, 16: 30510(P)
separation from sodium by solvent extraction using di-2-ethylhexyl phosphoric acid, 17: 3073(R) (TID-17265)
separation from sodium by solvent extraction using bis(2-ethylhexyl)-phosphoric acid, 17: 25358(R) (SRO-70)
separation from solutions by solvent extraction using hydroxamic acid, 17: 39185(R) (ORNL-3452(p.168-88))
separation from sodium by solvent extraction using D2EHPA, 18: 5418 (SRO-56)
separation from soil, radiochemical methods for, 18: 22185
separation from solutions by ion exchange on earth materials, 18: 33164 (CONF-179-5)
separation from solutions by solvent extraction using di-(2-ethylhexyl) phosphoric acid, effects of pH on, 19: 537
separation from solutions by solvent extraction, review of methods for, 19: 13543
separation from solutions of fission products by ion exchange, 19: 22443(P)
separation from solutions by ion exchange on clays, effects of heat treatment on, 19: 30342
separation from solutions of irradiated uranium-235 by precipitation, 19: 36217(R) (IDO-14656)
separation from soils using ammonium acetate, 20: 22948
separation from stored Purex waste by lead sulfate carrier precipitation, 19: 20035 (BNWL-4)
separation from sulfate-containing waste solutions, 20: 5210(P)
separation from synthetic Purex sludge by precipitation, 18: 45148(R) (HW-83320)
separation from thorium by ion exchange, 16: 30435
separation from trivalent rare earths by cation exchange, 17: 10734 (IS-508)
separation from uranium by ion exchange and elution with ascorbic acid, 18: 25611(T) (AEC-tr-6227/1(p.1-8))
separation from urine, chromatographic, 19: 519 (TID-7696(p.53-63))
separation from uranium by ion exchange, 19: 9259
separation from uranium by ion exchange on stannic phosphate, 19: 18060
separation from uranium and plutonium by solvent extraction, 19: 32286
separation from uranium by chromatography on cellulose columns, tracer studies of, 19: 40687
separation from uranium by reversed-phase partition chromatography, 20: 10784
separation from uranium by combined ion exchange-solvent extraction using nitric acid--tetrahydrofuran solutions, 20: 20811
separation from waste products, effects of calcium and pH, 16: 7328(R) (TID-14472)
separation from waste solutions by sorption by zeolites, 16: 5100(R) (HW-71374)
separation from waste solutions, effects of calcium, pH, and sodium, 17: 12366(R) (RAI-104)
separation from wastes by ion exchange, 17: 19708 (TID-7644(p.115-50))
separation from waste solutions, testing of minerals for, 17: 26932(R) (ORNL-TM-516)
separation from waste solutions by combined iron-phosphate coagulation and foam process, 17: 28584(R) (RAI-113)
separation from waste solutions by combined sodium carbonate-hydroxide precipitation and foam process, 17: 28584(R) (RAI-113)
separation from waste solutions by flotation, 17: 35240 (EUR-262.e)
separation from wastes by solvent extraction, 17: 35244 (HW-SA-2982)
separation from waste solutions by ion exchange on alumina or vermiculite, 17: 36999
separation from waste water by ferric hydroxide flocculation, 17: 42426
separation from waste solutions by ion exchange, 18: 6548(P)
separation from water, method for, 18: 33484
separation from waste solutions by sorption on coagulated slurry of natural adsorbent, 18: 43092 (UJV-973/63)
separation from waste solutions by sorption on precipitated aluminum and iron oxides, 19: 5560 (UJV-1112/64)
separation from water and snow by electrodialysis, 19: 19809
separation from water by foam, 19: 23996(R) (ORNL-3650(p.1-110))
separation from waste water, methods for, 19: 40276
separation from waste solutions using countercurrent liquid-foam columns, 20: 12526
separation from water by ion exchange using bentonite and gypsum, 20: 29348
separation from water by precipitation, kinetics of, 20: 31318 (BMwF-FBK-65-04)
separation from water, effects of stirring speed and cation-anion resin ratio on, 20: 35595
separation from water by foaming, 20: 36934
separation from waste solutions, 20: 42689
separation from water by flocculation, precipitation, and filtration, 20: 45999
separation from yttrium by thin-layer chromatography, 18: 17949
separation from yttrium by sorption on gelatin foam, 18: 23735
separation from yttrium by paper electrophoresis, 19: 36285
separation from yttrium by ion exchange, 19: 38774
separation from yttrium, chromatographic, 19: 44120
separation from yttrium by ion exchange, 19: 46196
separation from yttrium by chromatographic methods, 19: 46436
separation from yttrium by paper electrophoresis, 20: 29336
separation from yttrium by paper chromatography, effects of calcium on,

20: 29349
separation from yttrium by ion exchange, 20: 43430
separation in foam-liquid columns, 16: 14690(R) (ORNL-TM-121)
separation of fission product, radiochemical, 16: 24564
separation of, from fission products by solvent extraction, 16: 32887(R) (ORNL-3314(p.116-25))
separation of, from Purex waste by ion exchange, 16: 32887(R) (ORNL-3314(p.116-25))
separation of, from calcium, chromatographic, 17: 21781
separation of, properties of foaming agents for, 16: 27125(R) (TID-16397)
separation of, properties of foaming agents for, 16: 27126(R) (TID-16398)
separation of, radiochemical procedure for, 17: 6132(R) (TID-17272)
separation of radio-, from Clinch River water using treatment plant, 20: 592 (K-C-785)
separation of silver from, by cation exchange chromatography, 20: 40847
separation of thorium from, by precipitation using fluoboric acid, 18: 5425
separation of trace elements from, by precipitation ion exchange, 20: 1958
separation of yttrium-90 from, by ion exchange, 19: 7626
separation of, from mixed fission products by solvent extraction using bis(2-ethylhexyl) phosphate, 20: 33191
separation of, from rubidium and yttrium by precipitation with iron hydroxide, 20: 33422
separation of, from thallium by ion-exchange chromatography, 20: 36935
separation using α-hydroxyisobutyric acid, chromatographic, 18: 16142
Slater-Condon parameters of, determined from spectral data, 17: 31118
solubility behavior in the aluminum nitrate freeze-melt process, 18: 17930(R) (IDO-14625)
solubility in bismuth at 300 to 700°C, 16: 24216
solubility in liquid zinc, 20: 22966 (ANL-7083)
solubility in zinc at 428 to 727°C, 17: 14116(R) (ANL-6596(p.29-118))
solubility of, in bones, 18: 33240
solvent extraction from Purex wastes, flowsheet for, 17: 10740(R) (ORNL-TM-181)
solvent extraction from Purex FTW, flowsheet development for, 17: 17615(R) (HW-76262)
solvent extraction by acidic organophosphorus compounds, mechanisms of, 17: 37303
solvent partition in D2EHPA–hydrochloric acid, 18: 16147
solvent partition between liquid lead and zinc, 18: 31495
solvent partition in tributyl phosphate–hydrochloric acid or –nitric acid systems, 18: 33685
sorption and dispersion in citrus trees, 17: 35253(R) (IA-775)
sorption and excretion in breast-fed babies, effects of phosphates on, 18: 29219
sorption and mobility in beans and tomatoes, (E), 19: 10755
sorption by aluminum oxides and silicates, 17: 32045(R) (TID-19184)
sorption by alumina, clay minerals, and Conasauga shale, 18: 43091(R) (ORNL-TM-830)
sorption by alumina, clays, and shale, 19: 7617(R) (ORNL-3697(p.49-53))
sorption by aluminum oxide–silicon dioxide ion exchangers, 20: 8836 (TID-22511(Suppl.))
sorption by ammonium phosphomolybdates, mechanism of, 18: 25378
sorption by ammonium molybdo-, tin, titanium, and zirconium phosphates, comparison of, 20: 45795(R) (ORNL-3945, pp 176-88)
sorption by arsenates, hydrous oxides, and silicates, 18: 45155(R) (TID-20980)
sorption by barium sulfates, 18: 29883 (UJV-936/63)
sorption by barium sulfate, 18: 43448 (UJV-1113/64)
sorption by barium sulfate–calcium sulfate systems, 20: 18835
sorption by bismuth iodates, 20: 43448
sorption by bone, tracer studies, 16: 31429
sorption by bones and intestines in rats, dietary effects on discrimination in, 17: 35425
sorption by calcined bentonite, 18: 12099
sorption by calcium-activated barium sulfate, 20: 22973 (UJV-956/63)
sorption by clay materials, effects of calcium and sodium on, 17: 19713 (TID-7644(p.211-25))
sorption by clay minerals, effects of aluminum and iron oxides on, 18: 17344
sorption by clay minerals and soils, 20: 33260(R) (ORO-648, pp 103-22)
sorption by clays at pH 0 to 14, 18: 39391
sorption by clays and sands in radioactive decontamination, 19: 36560
sorption by clinoptilolite, Linde 4AXW, AW-13X, AW-400, AW-500, and Norton Zeolon, thermodynamic properties of, 18: 4886(R) (HW-79140)
sorption by Egyptian clays and soils, 18: 37288 (A/CONF.28/P/813)
sorption by ferric silicate, 17: 32046(R) (TID-19185)
sorption by glass and polyethylene, 20: 23211
sorption by hydrous ferric oxide and limonite, 17: 36993(R) (TID-19164)
sorption by hydrous ferric oxide, 17: 36995(R) (TID-19187)
sorption by hydrous ferric oxide, 17: 36997(R) (TID-19189)
sorption by hydroxide-treated kaolin, 16: 33005
sorption by intestine, effects of parathyroid removal, tracer study in rats, 16: 4024
sorption by intestine in rats, effects of calcium and magnesium on, 18: 8082
sorption by intestine, tracer study, 16: 6282
sorption by intestine, effects of alkaline earths and pH on, 16: 23398 (HW-SA-2519)
sorption by ion exchange materials, 18: 1614(R) (ORNL-3488(p.65-90))
sorption by ion exchange on titanium oxide, 20: 39002
sorption by iron hydroxide and manganese dioxide, 16: 11735
sorption by Linde AW-4A, AW-13X, AW-400, and AW-500, 17: 38578(R) (HW-78188)
sorption by Linde 4A zeolite, effects of flow, particle size, and temperature on, 17: 17615(R) (HW-76262)
sorption by Linde AW-4A, 18: 4886(R) (HW-79140)
sorption by maize, effects of aluminum and calcium content in substrate, 17: 7751(R) (TID-17552)
sorption by minerals in permeable formations, 17: 39296(R) (ORNL-3492(p.3-12))
sorption by peat, 19: 11261 (NP-14668)
sorption by plants and animals, 17: 19746 (TID-18468(p.311-52))
sorption by plants, through roots and leaves, tracer study of maize, 18: 31088
sorption by potassium-treated vermiculites, 18: 6537(R) (ORNL-TM-603)
sorption by silica gel, 16: 27053
sorption by sodium-based zeolites, 19: 25777(R) (HW-84603(p.37-49))
sorption by soils, 17: 1177(R) (HW-70050(p.143-219))
sorption by soils and clay minerals, effects of aluminum oxide and iron oxide on, 20: 14652
sorption by strontium carbonate, 20: 27057
sorption by tungsten, migration in, 18: 22038
sorption by Type X zeolite in presence of cerium and sodium, equilibrium in, 19: 22416
sorption by uranyl phosphate at 30 to 1020°C, 19: 24442
sorption by zeolites, effects of competing cations on mass action coefficients in, 17: 35683 (HW-SA-2837)
sorption by zeolites in waste processing, 18: 15656 (HW-SA-3333)
sorption by zeolite, 18: 27279(R) (HW-80284(p.4.1-23))
sorption by zeolites from multicomponent systems, 19: 2272 (HW-SA-3199)
sorption by zirconyl phosphate, temperature effects on, 17: 23345
sorption by zirconium phosphate gel, 19: 9256
sorption by zirconium silicate phosphate gel, 20: 38994(R) (AE-232)
sorption from aqueous solutions by pyroclastic rocks, 17: 35940 (UJV-951/63)
sorption from aqueous solutions by soils, 19: 46434
sorption from calcium sulfate solution by barium sulfate, 19: 36275
sorption from gastrointestinal tract in rat, tracer study, 16: 17416
sorption from intestine in rachitic chicks, effects of vitamin D on, 18: 11618
sorption from natural waters by earth materials, Cape Thompson, Alaska, 18: 25688 (TID-20638)
sorption from Purex-type waste by clays, feldspars, limestone, sands, and shales, 16: 11343 (ORNL-TM-127)
sorption from seawater by manganese dioxide, 20: 24973 (AD-632528)
sorption from solutions by aluminosilicates, 19: 4257 (UJV-1106/64)
sorption from solutions by tuffs, 19: 48081 (RT/PROT(65)19)
sorption from synthetic river water by silicate minerals and rocks, 17: 35710 (UJV-528)
sorption from waste solutions by minerals, 16: 2801(R) (ORNL-3189 (p.27-42))
sorption from waste solutions by soils and minerals, 17: 2785(R) (ORNL-3347(p.1-46))
sorption from water by clay minerals, 16: 2808(R) (ORNL-TM-15)
sorption of, by clay, effect of pH on, 16: 20075
sorption of, effects of lactose on, in rats, 18: 11619
sorption on Albanian clays, 17: 2647
sorption on crandallite, 17: 20226
sorption on iron(III) hydroxide, effects of hydrogen and phosphate ions on, 19: 28448
sorption on soil from Cape Thompson, Alaska area, 20: 31425 (PNE-481, pp 1121-39)
sorption on terrigenous sediments and Pacific red clay, 19: 42600(R) (NP-15342)
sorption on tungsten ferrocyanide, tracer studies of, 19: 40679
sorption on Victorian brown coal, 16: 25033 (AAEC/TM138)
sorption on zeolites, calculation of loadings for multication systems, 17: 40770 (HW-78461)
sorption, retention, and urinary excretion of, in bottle- and breast-fed babies, 17: 5730
sorptive by minerals, 17: 39301(R) (ORNL-3492(p.52-70))

sorptive discrimination from calcium in newt renal tubules, 19: 31672(R) (NIRS-3(p.65-77))
spark patterns produced by grinding of, 18: 19493(T) (SC-T-64-47)
spectra and optical maser action of samarium-doped, 16: 27827
spectra in reaction zone of acetylene air flame, excitation of atomic, 17: 27371(T)
spectra, lifetime of first excited resonance state, 16: 29481(R) (NP-11989)
spectra of, low energy neutron-capture gamma, 17: 15943(R) (ARF-1193-20)
spectra of, effects of calcium, potassium, and rubidium on flame photometric, 19: 7368
spectra of, in hydrogen flames, effects of nitrogen and oxygen on, 20: 35487
spectra, oscillator strengths in absorption, 16: 15315(T)
spectral line oscillator strengths, 16: 18224(T)
substitution for calcium in hydroxyapatite, extent of, 17: 35418
substitution for calcium in maize, 18: 21784
synthesis in halo red giant star HD 122563, spectral analysis of, 19: 28982
toxic effects in animals and plants, 19: 25870
toxic effects in dogs, 16: 32689(R) (TID-16458)
toxic effects in dogs, 16: 32639(R) (TID-16459)
toxic effects in swine, 16: 18752
toxicology of radioactive, 18: 11613
transfer across biological membranes, 18: 11615
transfer across biological membranes, 18: 11617
transport across intestinal membranes, tracer study, 20: 14243(R) (TID-22626)
transport by stream and estuarine sediments, 18: 35726
transport in mammary gland, 18: 11621
transport in root of *Zea mays*, 20: 45270 (AD-639836)
transport in soils, effects of organic compounds on, 20: 35239
uptake and retention by bones, effects of magnesium on, 18: 41063
uptake and transport in Rainbow Trout gill, relation with calcium in, 19: 17468
uptake by algae, effects of calcium content of water, 16: 12874
uptake by apatite synthetic crystals, 17: 29095
uptake by aquatic gastropods, 17: 35416
uptake by banana leaf disks, effects of light on, 18: 15798
uptake by body organs and skeleton, effects of sodium phosphates on, 16: 32706
uptake by bone tissue, mechanism of, 20: 30973
uptake by brown trout, 18: 16243
uptake by *Chlorella pyrenoidosa* in continuous culture, 18: 35299
uptake by corn plants, effects of soil fertility on, 20: 40735 (NYO-2744-37)
uptake by crops and factors affecting translocation in soil, 20: 40524(R) (TID-23271)
uptake by edible plants, effects of calcium content of soil and plant species, tracer study, 20: 40537(R) (TID-23052)
uptake by fish from diet and water, tracer study, 16: 11951 (HW-72107)
uptake by fish gills, comparison with calcium, 18: 33805(R) (NIRS-2 (p.57-67))
uptake by freshwater mollusks, mechanisms of, 19: 6971
uptake by glass, coated glass, and polyethylene from neutral solutions, 16: 18806
uptake by grass, 18: 38733
uptake by humans, therapy for, 18: 1461
uptake by lobsters, comparison with calcium and cesium, 16: 8490
uptake by man from cereals and milk, relative, 16: 14453
uptake by oats, effects of osmotic pressure on, 18: 43170(R) (EUR-1882.e(p.31-6))
uptake by plankton fauna Acantari, 18: 17447
uptake by plants, effects of soil colloids on, 17: 17749
uptake by plants, effects of calcium content of nutrients on, 18: 8(R) (TID-19498)
uptake by plants, effects of chemicals and rain water on, 20: 8538
uptake by plants, effects of soil freezing on, 20: 8552(R) (TID-22443, pp 1-33)
uptake by plants, effects of calcium on, 20: 20360(R) (PRNC-73)
uptake by plants, effects of organic compounds on, 20: 35239
uptake by rat liver mitochondria, effects on respiration, 19: 14972
uptake by recently molted crayfish, model for, 17: 13941
uptake by rice, effects of irrigation on, 20: 40574
uptake by roots of *Zea mays*, 17: 15610
uptake by spinal cord lesions in man, 16: 20081
uptake by *Streptococcus lactis*, ratio to calcium, 16: 14437
uptake by trees, effects of calcium content and acidity of soil on, 20: 8554(R) (TID-22443, pp 100-11)
uptake by woody plants, regularities in, 19: 6964
uptake from water by trout, 17: 21441
uptake, metabolism, and excretion, tracer studies, 16: 1386
uptake of, by rat liver mitochondria, tracer study of, 17: 35303(R) (HW-76000(p.95-7))
uptake, excretion, and retention by infants on normal diet, 19: 25901
use as inner standard in activation analysis of organic compounds for nitrogen, 20: 33165(T) (AEC-tr-6639, pp 32-5)
use as tracer, survey, 16: 1359
use in diet to control radiotoxicity of strontium-90, 20: 45497
use in estimating alfalfa root activity, 19: 25875
use in x-ray filters, 20: 5692
vapor pressure at 400 to 600°C, tracer study of, 17: 32050(T) (AEC-tr-5911)
vapor pressure at 2000°K, 17: 40388
vaporization from graphite powder, thermodynamics of, 20: 28742(R) (GA-6418)
work function of films of, effects of base metals on, 16: 9231

STRONTIUM ACETATES
effects on strontium-89 movement in soils and on uptake by barley, 20: 32925

STRONTIUM ALLOYS
Ag–Sr, crystal structure of AB_2-type compound in, 20: 24589(R) (NYO-3560-3)
Ag–Sr, sample preparation, metallographic, 20: 27418
Be–Sr, analysis of intermetallic compound $SrBe_{13}$ in, to confirm formula, 19: 28266
Be–Sr, corrosion resistance, 19: 22913(P)
Be–Sr, properties and structure of intermetallic compound $SrBe_{13}$ in, 18: 39962(T)
Cd–Sr, phase studies, 20: 11327
Cd–Sr, sample preparation, metallographic, 20: 27418
Ga–Sr, preparation and properties of MX_4-type compounds in, 18: 37723
Hg–Sr, properties of intermetallic compounds in, 19: 37081
In–Sr, preparation and properties of MX_4-type compounds in, 18: 37723
In–Sr, sample preparation, metallographic, 20: 27418
Li–Sr, crystal structure, 16: 12233 (TID-15217)
Li–Sr, crystal structure of Sr_5Li_{23}, 19: 26825(T) (FTD-TT-64-1145)
Li–Sr, phase diagram, 16: 13587 (TID-15218)
Li–Sr, phase studies, 16: 13010(R) (TID-15150)
Li–Sr, structure of intermetallic compounds in, 17: 23964(R) (TID-18619)
Mg–Sr, crystal structure of Sr_8Mg_{17} in, 17: 29334
Mg–Sr, crystal structures of intermetallic compounds of, 20: 41455(R) (NYO-2731-7)
Mg–Sr, elastic constants of, relation to cohesion and stability of intermetallic phases, 18: 44228
Mg–Sr, phase studies, 16: 13010(R) (TID-15150)
Mg–Sr, properties of intermetallic compounds in, 19: 39177
Mg–Sr, structure of intermetallic compounds in, 17: 23964(R) (TID-18619)
Na–Sr, phase equilibria in, 17: 23964(R) (TID-18619)
Na–Sr, phase studies, 16: 13010(R) (TID-15150)
Na–Sr, phase studies, 18: 25984 (TID-20639)
Ni–Sr, phase studies, 20: 4442
Sr–Sn, thermoelectric properties of intermetallic compound Sr_5Sn in, 16: 18017(R) (AD-266019)
Sr–Tl, preparation and properties of MX_4-type compounds in, 18: 37723
Sr–Zn, crystal structure of $SrZn_5$ in, 18: 8814
Sr–Zn, crystal structure of AB_2-type compound in, 20: 24589(R) (NYO-3560-3)
Sr–Zn, intermetallic compound with $CeCu_2$-type structure in, 20: 21352 (TID-21745)

STRONTIUM ALUMINATES
development for luminescent coating on erythemal mercury-vapor lamps, 17: 29478(P)
preparation of single crystals, 16: 22114

STRONTIUM ANTIMONATES
crystallography of, with perovskite-like structure, 19: 25014

STRONTIUM AZIDES
enthalpy of formation, 19: 7361(T) (AERE-Trans-1011)
properties at 77 and 298°K, optical and photoelectric, 17: 29013
radiation effects on thermal decomposition, pre-, 19: 22356

Strontium Barium Oxides
see Barium Strontium Oxides

Strontium Beryllium Oxides
see Beryllium Strontium Oxides

STRONTIUM BORATES
fluorescent properties of terbium-activated, 19: 15515
luminescence of copper- and copper-lead-activated, 16: 25975
preparation of hydrated, 18: 12036 (NOLC-585)
spectra of, infrared, 17: 18048

STRONTIUM BORIDES
electric conductivity, 17: 2131
electric properties, 17: 11306 (IS-473)
electric resistance, 19: 6356
electron structure and physical properties of crystals of, 17: 27875
evaporation rate and vapor pressure at 1100 to 2000°C, 16: 2208(T)

(AEC-tr-4865)
physical properties of SrB_4, 16: 12154
preparation and properties of SrB_6, 16: 6758
preparation, properties, and uses, 17: 2959(T) (AEC-tr-5264)
thermal conductivity, 17: 28843

STRONTIUM BROMATES
radiolysis of anhydrous, 18: 1725(R) (ORNL-3488(p.42-54))
radiolysis of, gamma, 20: 23115
radiolysis of, gamma, neutron, and lithium-6 fission product recoil, 20: 36899
thermal decomposition of, search for perbromate in, 19: 36402

STRONTIUM BROMIDES
binding energy of gaseous, 16: 28964
crystal lattice energy of, relation of self energy of gaseous ions to, 18: 16017
crystal structure, 18: 5286
dissociation energy of gaseous, 18: 32153(R) (UCRL-11317(p.176-97))
electric dipole moments and geometry of, 17: 40801
enthalpy and lattice energies of, calculation of, 19: 17901
heats of fusion and transition, 17: 28870
properties of, physical and thermodynamic, 20: 7049 (IS-T-50)
thermodynamic properties at 60 to 1200°K, 16: 14683 (BM-RI-5967)
vapor pressure enthalpies and equations for, 20: 41412(R) (IS-1500 (Sect. M))
vaporization of, 17: 2956 (UCRL-9840)
$BaBr_2$–$SrBr_2$, phase diagrams, 20: 36787 (YALE-2723(Vol.1))
KBr–$SrBr_2$, phase diagrams, 20: 36788 (YALE-2723(Vol.2))
LiBr–$SrBr_2$, phase diagrams, 20: 36788 (YALE-2723(Vol.2))
NaBr–$SrBr_2$, phase diagrams, 20: 36788 (YALE-2723(Vol.2))
$SrBr_2$–SrI_2, phase diagrams, 20: 36788 (YALE-2723(Vol.2))

Strontium Calcium Titanates
see Calcium Strontium Titanates

STRONTIUM CARBIDES
crystal structure, 17: 6692(T) (AEC-tr-5486)
lattice energy of, calculation of Madelung, 19: 28866
preparation and properties of di-, 20: 810 (AERE-R-5011)
vaporization of, 20: 810 (AERE-R-5011)

STRONTIUM CARBONATES
analysis for rare earths, activation, 20: 24351(R) (MIT-905-52, pp 1-41)
calcium ion coprecipitation with, 17: 2950 (TID-17253)
decomposition at high pressures up to 400 atmospheres, 17: 12262
deposition of injected strontium-85-labeled, in capillaries, 19: 21843
effects on densification of thorium oxide–uranium oxide pellets, 16: 7874 (ANL-6375)
effects on sinterability of plutonium(IV) oxides, 17: 36253(R) (NUMEC-P-59)
ion exchange equilibrium on surfaces of ionic crystals, 19: 42517
ion exchange properties for barium, calcium, and strontium on surface of, tracer study of, 18: 43504
precipitation for shipment, performance of filter cask insert for, 16: 8833 (HW-69781)
precipitation for shipment, testing of filter cask for, 16: 8834 (HW-72295)
production of pure, from brines containing calcium, 16: 14764(P)
radiation effects on structure of, fast neutron, 18: 34241
radiation effects on phase transformations in, neutron, 20: 35946
reactions with hafnium oxide, solid-state, 16: 5355
reactions with lithium fluoride at high temperatures, product solubilities, 19: 11140(P)
reactions with rare earth oxides, ternary oxide formation in, 19: 46242(R) (TID-22207, Paper B)
reactions with rare earth oxides, ionic field strengths as criteria for compound formation in, 19: 46246(R) (TID-22207, Paper F)
reactions with titania to produce strontium titanates, 17: 29854(R) (MND-2584-4)
release of strontium, effects of air and temperature, 16: 16336 (HW-69692)
release of strontium from, effects of air and temperature, 16: 16336 (HW-69692)
sorptive properties for strontium, 20: 27057
spectrum at low temperatures, infrared, 16: 33002
strontium isotope ratio, 18: 3993(R) (NYO-10517(p.111))
thermoluminescence properties of, for use as radiation dosimeter, 20: 36913
$SrCO_3$–SrO, equilibria at high pressures, 17: 12262

STRONTIUM CERIUM FLUORIDES
preparation, properties, and structure of, 20: 40867 (KFK-385)

STRONTIUM CHLORATES
radioinduced defects in, electron paramagnetic resonance study of x, 19: 24568(T)

STRONTIUM CHLORIDES
binding energy of gaseous, 16: 28964
crystal dynamics of hexahydrate of, neutron spectrometric studies of, 19: 9095 (JINR-P-1904)
crystal lattice energy of, relation of self energy of gaseous ions to, 18: 16017
crystal structure disorders in, 20: 45701
crystallization in heavy and light water mixtures, fractionation of hydrogen isotopes by, 19: 13329
dehydration effects on silica xerogel, thermal, 17: 7945
dielectric losses in, temperature dependence of, 19: 19851(T) (ORNL-tr-491)
diffusion coefficients of, tracer technique for measurement of, 17: 4549
diffusion in molten, effects of temperature on self-, 19: 26338
diffusion in, self-, 20: 38871(R) (NYO-1769-54)
diffusion of water in, coefficients of, 20: 1865
dissociation energy of gaseous, 18: 32153(R) (UCRL-11317(p.176-97))
effects on cation movements in bentonites, 18: 38775(R) (ORO-624)
effects on dissociation of boric acid in solution, 18: 31376(T) (UCRL-Trans-1053(L))
effects on strontium-85 elution from mouse bones, 19: 43706
electric conductance in water, effects of transference number on equivalent, 16: 3010
electric dipole moments and geometry of, 17: 40801
electric properties of, effects of lattice energy and temperature on, 19: 21601(T) (ORNL-tr-490)
electrolytic properties in mixtures with magnesium chlorides, 18: 5275
enthalpy and lattice energies of, calculation of, 19: 17901
entropy and heat content of, at 298 to 1200°K, 17: 37184
fluorescence properties of samarium doped, 17: 34655
hardness of crystalline divalent, 16: 10728
heats of fusion and transition, 17: 28870
ion mobilities in liquid, 16: 157 (IS-344)
ionic properties, 17: 30517 (TID-19102)
light reflection from, far-infrared vibration mode from, (E), 20: 15958
manganese EPR in, spectra of, 18: 13780(T)
precipitation of uranium(VI) with, in presence of sodium carbonate, 19: 19870
properties of solutions of, in dimethyl sulfoxide, 20: 293 (UCRL-16330)
protective effects of aqueous solutions of, against radiation in barley seedlings, 18: 23368
radioinduced coloration in, spectra of, 18: 33643
radioinduced V_k center in single crystals of, x, 20: 40319
reactions with calcium and sodium chlorides, kinetics of exchange, 18: 4886(R) (HW-79140)
reactions with europium and lead chlorides, 17: 23371
reactions with pectins, 16: 3286(T) (JPRS-9706(p.50-5))
reduction by calcium carbide, 19: 46251(T) (ORNL-tr-673)
reduction of rare earth-activated, by solid-state electrolysis, 18: 43469
separation from salts by extraction chromatography using organic phosphorus compounds, 20: 10759 (INP-427/C)
Soret coefficients and transport heats at 25°C, 16: 11666
sorption by glass, tracer studies of kinetics of, 20: 43251
sublimation and vaporization of, 19: 36386
thermodynamic properties at 0 to 300°K, 18: 197 (BM-RI-6316)
thermodynamic properties at 298 to 1200°K, 18: 2231(R) (ORNL-3488 (p.96-101))
transitions of divalent samarium in, selection rules for, 17: 18064
uptake by man, 20: 20466
use as column packing for gas chromatography of polyphenyls, 18: 17931 (IDO-16912)
use as flux in preparation of rare-earth-activated strontium sulfide crystals, 16: 15314(T)
vaporization of, 17: 2956 (UCRL-9840)
$BaCl_2$–$SrCl_2$, phase diagrams, 20: 36787 (YALE-2723(Vol.1))
$CaCl_2$–$SrCl_2$, phase diagrams, 20: 36787 (YALE-2723(Vol.1))
$CaCl_2$–$SrCl_2$, sorption by antimony and arsenic sulfide sols, 19: 11073
$CdCl_2$–$SrCl_2$, phase diagrams, 20: 36787 (YALE-2723(Vol.1))
CsCl–$SrCl_2$, phase diagrams, 20: 36788 (YALE-2723(Vol.2))
HCl–$SrCl_2$, electric conductivity of aqueous solutions of, effects of pressure on, 19: 5870
KCl–$SrCl_2$, free energy of formation of K_2SrCl_4 and KSr_2Cl_5 at 450 and 550°C, 19: 38575 (BNL-9343)
KCl–$SrCl_2$, phase diagrams, 20: 36788 (YALE-2723(Vol.2))
KCl–$SrCl_2$, thermodynamic properties at 750°C, 20: 24971(R) (BNL-954, pp 50-83)
KCl–$SrCl_2$, vapor pressure, 18: 25435
LiCl–$SrCl_2$, phase diagrams, 20: 36788 (YALE-2723(Vol.2))
$MgCl_2$–$SrCl_2$, phase diagrams, 20: 36788 (YALE-2723(Vol.2))
NaCl–$SrCl_2$, performance in fusion-electrolytic preparation of sodium at 565°C, 18: 22090(P)
NaCl–$SrCl_2$, scattering of visible light by, images from, 18: 10642
NaCl–$SrCl_2$, thermodynamic properties, 18: 11958(R) (BNL-823(p.20-47))
Na_2CO_3–$SrCl_2$, precipitation of uranium from uranyl nitrate solutions by, 19: 26299
Na_2CO_3–$SrCl_2$–$UO_2(NO_3)_2$, uranium precipitation in, mechanism of,

20: 38928
$PbCl_2$–$SrCl_2$, phase diagrams, 20: 36788 (YALE-2723(Vol.2))
$PuCl_3$–$SrCl_2$, phase studies, 16: 6419
RbCl–$SrCl_2$, phase diagrams, 20: 36788 (YALE-2723(Vol.2))
$SrCl_2$–SrF_2, phase diagrams, 20: 36788 (YALE-2723(Vol.2))
$SrCl_2$–TlCl, phase diagrams, 20: 36788 (YALE-2723(Vol.2))
$SrCl_2$–$ZnCl_2$, phase diagrams, 20: 36788 (YALE-2723(Vol.2))
Sr–$SrCl_2$, electric conductivity of molten, 16: 32194
Sr–$SrCl_2$, free energy of solution of, 19: 11103

STRONTIUM CHROMATES
crystal structure, 16: 5319

STRONTIUM CHROMIUM LANTHANUM OXIDES
crystal structure, 20: 12865

STRONTIUM CITRATES
effects on excretion of strontium isotopes by mice, 20: 8564
preparation and equilibrium constant of complex, 16: 13046

STRONTIUM COBALT LANTHANUM OXIDES
crystal structure, 20: 12865

STRONTIUM COBALT LANTHANUM TITANIUM OXIDES
crystal structure, 20: 12865

STRONTIUM COMPLEXES
formation and properties of α-picoline–thiocyanate, 17: 27332
formation of, 18: 6711
stability constants of, determination of, by metal distribution between aqueous phase and ion exchanger, 20: 16481
stability of, equations for, 20: 8934
with [(1,2-dimethylethylene)dinitrilo]- and (propylenedinitrilo)-tetraacetic acids, stability of, 20: 12594(R) (NP-15679)
with (1,2-cyclopentylenedinitrilo)tetraacetic acid, stability of, 20: 12595(R) (NP-15680)
with adenosine triphosphate, stability constants, 16: 7556
with adenosinephosphoric acids, stability constants, 16: 28948
with aminoacetone-*N*,*N*-diacetic acid, dissociation and stability constants of, 18: 19946
with arsenazo III, formation mechanism of, 17: 6007
with bis(2-ethylhexyl) phosphate, reactions with TBP, 20: 9049(R) (ORNL-3830, pp 193-221)
with complexones, stability, 16: 11791(T) (AWRE/TRANS/27)
with condensed phosphates, stability constants, 17: 2962
with cupferron, thermal dissociation, 19: 7366
with diacetamide, properties and spectra of, 20: 8494 (TID-22449)
with dicarboxymethylethylenediaminobismethylphosphinic acid, stability and dissociation constants, 19: 22237
with EDTA, effects on leaching of cesium from vermiculities, 20: 43130
with EDTA, migration in electrodialysis cell, 19: 20052 (ORNL-TM-1035)
with ethylenediaminetetraacetato-yttrium acid, stability constants, 17: 21730
with fatty acids, formation of, 16: 8668(T) (AWRE/Trans/26)
with mercaptosuccinic acid and 2,3-dimercaptosuccinic acid, formation and properties of, 18: 8394 (TID-20013)
with *N*-(2-pyridylmethyl)iminodiacetic acid, stability of, 17: 15993
with organic acids, composition and stability constants, 16: 18916
with phosphates, ion-exchange study of nature and stability, 16: 16399
with phosphates, stability constants of, 16: 28944
with polyaminocarboxylic acids, stability of, 17: 40840
with tetracycline, stability, 17: 23052
with 1,2-(diaminocyclopentane)tetraacetic acid, stability, 16: 30416
with 2-methyl-4,6-heptanedione, stability constants of, 19: 11056(T) (AEC-tr-6227/3(p.183-92))
with 2-phenyl-4,5,6,7-tetrahydroindazol-3-one-5,5-dicarboxylic acid, stability of, 19: 26472
with 2,6-pyridinedicarboxylic acid, ion exchange properties of, 20: 18685
with 8-quinolinol, stability at high temperatures, 16: 10009

STRONTIUM COMPOUNDS
crystal structure and homogeneity ranges of, with rare earth selenides, sulfides, and tellurides, 19: 37052
crystallography of, with perovskite-like structure, 19: 25014
distribution in acid igneous rocks of Africa, 18: 37358
effects on congenital skeletal anomalies in rats, 18: 17448
electric conductivity of m-benzenedisulfonate in water, 17: 14268
electric conductivity in nonaqueous solvents, 18: 41472
luminescence characteristics of cyanoplatinate(II), 17: 14352
preparation and crystal structure of scandates, 19: 13364
properties of organic, review of chemical and physical, 16: 28969
thermolysis of diliturate, 19: 19824

STRONTIUM DEUTERIDES
absorption bands, rotational analysis of uv, (E), 20: 40331
spectra of, rotational analysis of uv-absorption, 18: 18465

Strontium Diuranates
see Strontium Uranates

STRONTIUM FERRATES
magnetic properties of modified, 17: 37699
Mössbauer effect, 16: 13777
Mössbauer effect in, 19: 7516
preparation and properties of, 20: 38859 (CEA-R-2895)
separation processes for, 20: 38859 (CEA-R-2895)
$SrFeO_3$–$SrTiO_3$, effects of tetravalent iron content on electric and magnetic properties of, 17: 23983

STRONTIUM FERRITES
heats of formation and thermodynamics of, 18: 27365

STRONTIUM FLUOBERYLLATES
dissociation pressure, 17: 21602

STRONTIUM FLUORIDES
see also Rubidium Strontium Fluorides
absorption bands of colored and uncolored crystals of, models for, 16: 16857
binding energy of gaseous, 16: 28964
cerium ion spectra in crystals of, trivalent, 17: 33928(T)
charge compensation and paramagnetic resonance of tetravalent uranium in, 17: 656
charge compensation by fluoride ions in rare earth-doped, 20: 2520(R) (IA-920)
cohesive and surface energies of crystals of, 16: 16386
coloring of crystals of, under imposed voltage, moving striations in additive, 16: 16860
crystal lattice energy of, relation of self energy of gaseous ions to, 18: 16017
crystal structure disorders in, 20: 45701
dielectric losses in, frequency and temperature dependences of, 19: 19851(T) (ORNL-tr-491)
diffusion of manganese in, electron spin resonance studies, 16: 11653
disprosium ESR in, at –268°C, 19: 23164(R) (SU-SEL-64-103)
dissociation energy of gaseous, 18: 32153(R) (UCRL-11317(p.176-97))
dysprosium EPR in crystals of, 20: 10264
dysprosium ion energy levels in cubic hosts of, 19: 15519
dysprosium ion luminescence spectra in, 18: 6802
elastic properties at 4.2 to 300°K, 19: 2328
electric dipole moments and geometry of, 17: 40801
electric properties of, effects of lattice energy and temperature on, 19: 21601(T) (ORNL-tr-490)
energy levels of neodymium-doped, ground-state splitting in, (T), 19: 9898(T) (JPRS-27372(p.32-5))
enthalpy and lattice energies of, calculation of, 19: 17901
erbium ion absorption and emission spectra in, 18: 8428(T)
europium absorption and luminescence spectra in, 17: 4547(T)
europium EPR in crystals of, 18: 9020(T)
europium EPR in crystals of, cubic field splitting of spectra of, 17: 39063
europium ion ESR in, 19: 7511
europium ion fluorescence spectra in, energy level transitions for, (E), 19: 42997
europium ion spectra in, absorption and fluorescence, 18: 13759
fluorescence of praseodymium-doped, as infrared quantum counters, 18: 2070
fluorescent properties of neodymium and thulium trivalent ions in crystals of, 17: 37177
gadolinium EPR in crystals of, effects of hydrolysis and thermal treatment on, 17: 20037
gadolinium EPR in crystals of, cubic field splitting of spectra of, 17: 39063
gadolinium ion EPR in, 18: 2417
gadolinium ion ESR in, 19: 7511
growth of highly perfect single crystals of, for use in lasers, 17: 37744
hardness of crystalline divalent, 16: 10728
heat of reaction of, with aluminum, 17: 35800
heat of sublimation of, Langmuir studies of, 19: 26342
heat of sublimation and vapor pressure of, 20: 26874
holmium ion absorption and emission spectra in, 18: 8428(T)
hydrogen-atom ESR spectra in interstitial sites in, 19: 2330
infrared attenuation and reflection by crystals of, 16: 33012
infrared quantum counter action in erbium-doped, 18: 17907
ion localized vibrations in, spectra of deuterium and hydrogen, 20: 15969
laser action and absorption and luminescence spectra of trivalent gadolinium in crystals of, 17: 20028(T)
laser action threshold in uranium-doped crystals of, scattering extinction coefficient for, 17: 22305
luminescence centers in rare earth-activated, 19: 41978
luminescence properties of manganese-activated, correlation to electron spin resonance spectra, 18: 2487
luminescence spectra of rare earth ions in, 19: 19854
manganese ion ESR in, 19: 7511
neodymium ion luminescence in, at 4.2, 77, and 300°K, 19: 34185(T)
preparation of crystals of, by Czochralski method, 16: 1754
radiation effects on absorption spectra of crystals of, at 2000 to 8000 Å, gamma, 16: 14799(T)

radioinduced color center formation in yttrium-doped crystals of, 17: 18146
radioinduced color center formation in yttrium-doped crystals of, 17: 22251
radioinduced Moiré patterns in crystals of, 17: 31031
radioinduced reduction of trivalent neodymium ion in, in presence of dysprosium, erbium, gadolinium, holmium, or thulium, gamma, 20: 26982(T)
reduction by calcium carbide, 19: 46251(T) (ORNL-tr-673)
samarium fluorescence in crystals of, vibronic spectra of, 18: 10094
samarium ion transitions in, selection rules for, 17: 18064
samarium ions absorption and luminescence spectra in, 16: 27803(T)
samarium spectra in, Zeeman effect for f-d transitions in, (E/T), 19: 4145(T)
solubility in double fluorides of neptunium, plutonium, thorium, and uranium, 20: 40867 (KFK-385)
sorptive properties for plutonium hexafluoride, 20: 45789(R) (ORNL-3945, pp 48-71)
spectra of divalent-samarium-containing crystals of, Zeeman effect in absorption and luminescence, 17: 16011(T)
spectra of divalent-samarium-containing crystals of, deformation splitting of lines in, 17: 16012(T)
spectra of uranium-activated, relaxation luminescence, 17: 5125(T)
surface energy of {110} face of crystals of, calculation of, 17: 32749
terbium ion, luminescence in, spectra, 18: 6802
thermodynamic properties of, use of mass spectrometer in studying, 17: 25269
thermodynamic properties at 0 to 300°K, 18: 197 (BM-RI-6316)
thermodynamic properties of gaseous, mass spectrometric studies of, 18: 27356 (CONF-74-Z7)
thermoluminescence of rare earth-activated, capture levels and recombination nature of, 18: 31503(T)
thulium ion fluorescence in, two-step excitation of, (E), 20: 28613
thulium ions EPR in, spectra, 19: 26917(R) (IA-984)
uranium ion EPR in, 18: 2472
uranium(IV) in crystals of, paramagnetic resonance and optical spectra of, 16: 30399
vaporization of, 17: 2956 (UCRL-9840)
ytterbium absorption and luminescence spectra in, 17: 4547(T)
BaF_2–SrF_2, phase diagrams, 20: 36787 (YALE-2723(Vol.1))
BeF_2–SrF_2, phase diagrams, 20: 36787 (YALE-2723(Vol.1))
CaF_2–LiF–SrF_2, phase studies, 16: 198
CaF_2–SrF_2, phase diagrams, 20: 36787 (YALE-2723(Vol.1))
CaF_2–SrF_2, properties of samarium-doped crystalline, chemical and optical, 19: 9128
CeF_3–SrF_2, solubility studies on, 20: 40867 (KFK-385)
KF–SrF_2, phase diagrams, 20: 36788 (YALE-2723(Vol.2))
LiF–K_3AlF_6–SrF_2, phase diagram of, 18: 35503 (ORNL-3594)
LiF–SrF_2, phase diagrams, 20: 36788 (YALE-2723(Vol.2))
LiF–SrF_2, solvent properties for uranium dioxide at 1150°C, 19: 11050 (MCW-1490)
NaF–SrF_2, phase diagrams, 20: 36788 (YALE-2723(Vol.2))
$SrCl_2$–SrF_2, phase diagrams, 20: 36788 (YALE-2723(Vol.2))
SrF_2–YF_3, phase studies, 19: 38615

STRONTIUM FLUOSILICATES
stability in dry and moist heated air, 16: 13040

STRONTIUM GALLIUM LANTHANUM OXIDES
crystal structure, 20: 12865

STRONTIUM GERMANATES
crystal structure and symmetry, as model for *α* wollastonite, 16: 20441
structure, 17: 20043(T)

STRONTIUM HAFNATES
effects on phase transitions of lead hafnate, 16: 23688
growth of small single crystals of, 19: 47008(R) (NP-15429)
structure, 19: 37040(R) (NP-15118)
$PbHfO_3$–$SrHfO_3$, dielectric properties, 17: 30531

STRONTIUM HYDRIDES
absorption bands, rotational analysis of uv, (E), 20: 40331
dissociation properties, 16: 8713 (NEPA-1841)
phase studies, 19: 9604(R) (IS-900(Sect.M))
preparation and properties as reactor moderator material, 18: 32074
spectra of deuterated and natural, 2927 and 2928 Å bands in, 17: 28892
spectra of deuterated, analysis of emission, 18: 1653
spectra of, rotational analysis of uv-absorption, 18: 18465
LiH–SrH_2, phase studies, 19: 19881
LiH–SrH_2, ternary perovskite phases in, 18: 22036
Sr–SrH_2, phase studies, 17: 40771 (IS-613)
Sr–SrH_2, phase studies, 18: 2163(R) (IS-700(Sect.M))

STRONTIUM HYDROXIDES
bond energy of SrOH, 20: 294(T) (UCRL-Trans-1239(L))
crystal structure of hydrated, from neutron diffraction, 18: 37143
crystal structure of hydrates of, 20: 20694
neutron scattering by lattice of, spectra from inelastic, 18: 39154 (EUR-1643.e(p.174-80))
reactions with uranyl nitrate in solution, formation of compounds in, 19: 15447(T) (ANL-Trans-33(p.194-202))
thermal capacity at 570 to 900°C, 17: 7606(R) (ORNL-1515)
$Be(OH)_2$–$Sr(OH)_2$, preparation and properties of, 20: 10836
H_3PO_4–$Sr(OH)_2$, precipitate formation in, phase transformations in, 20: 20690

STRONTIUM IODATES
preparation of hydrated, 18: 12036 (NOLC-585)

STRONTIUM IODIDES
binding energy of gaseous, 16: 28964
crystal lattice energy of, relation of self energy of gaseous ions to, 18: 16017
dissociation energy of gaseous, 18: 32153(R) (UCRL-11317(p.176-97))
electric dipole moments and geometry of, 17: 40801
enthalpy and lattice energies of, calculation of, 19: 17901
heat of fusion, 17: 28870
properties of, physical and thermodynamic, 20: 7049 (IS-T-50)
thermal decomposition at 90 to 980°C, 19: 15493
vapor pressure enthalpies and equations for, 20: 41412(R) (IS-1500 (Sect. M))
vaporization of, 17: 2956 (UCRL-9840)
$BaBr_2$–SrI_2, phase diagrams, 20: 36787 (YALE-2723(Vol.1))
BaI_2–SrI_2, phase diagrams, 20: 36787 (YALE-2723(Vol.1))
$SrBr_2$–SrI_2, phase diagrams, 20: 36788 (YALE-2723(Vol.2))

STRONTIUM IONS
activity coefficient function in perchlorate solutions, 18: 10035 (CONF-387-1)
complex formation by, optimum conditions for, 19: 13374
determination in perchloric acid solutions by Donnan membrane equilibrium, 18: 43403
diffusion coefficients in chabazites, relationship between self- and exchange-, 17: 20030
diffusion in bentonite clay-water pastes, self-, 16: 20425
diffusion in chabazites, self-, 17: 20029
displacement in soils by beryllium, 19: 45802
distribution between phases in boron oxide–sodium chloride–sodium oxide system at 830°C, 18: 33534 (USNRDL-TR-760)
effects on cardiac activity, 17: 38722
effects on electrolytic precipitation of cerium oxide, 19: 34223
effects on nitrate ion yields from radiolysis of potassium nitrate, 20: 43329
effects on oyster myocardium, 19: 14942
effects on radioinduced color center formation in potassium chloride crystals, 19: 46371
entropy and heat of formation in aqueous solution, equation for calculation of, 18: 22066
exchange between solution and ionic crystals, 16: 23575
exchange equilibria with cerium, cesium, and hydrogen ions, 19: 5914
exchange on alkaline earth sulfate surfaces, equilibrium in, 18: 41442
exchange on natural and synthetic exchangers, 16: 20356 (JÜL-32-RC)
exchange with hydrogen ions on ferric hydroxide, 16: 27057
exchange with hydrogen ions on manganic hydroxide, 16: 27058
hydration numbers, 17: 30544
hydrolysis of divalent, 16: 3028
ion exchange on surface of alkaline earth carbonates, tracer study of, 18: 43504
mobility in clays, model for predicting rates of, 20: 25086
precipitation with calcite and aragonite from aqueous solutions at 150°C, 18: 6795 (TID-19901)
precipitation with aragonite and calcite at 90 to 100°C, 18: 39482
precipitation with aragonite and calcite from aqueous solutions, 20: 18631 (NYO-2266-1)
precipitation with aragonite, 17: 2950 (TID-17253)
production of artificial clouds of, in upper atmosphere, (E), 19: 16744
radiation effects on ionic thermoconductivity of potassium chloride doped with, x, 18: 31620
radioprotective effects in mice, 18: 13567
separation by thin-layer ionophoresis, 18: 10185
separation from solutions by foam, 18: 17939 (TID-20461)
solvent extraction from molten nitrate by liquid silicone–TBP at 150°C, 19: 19833 (CEA-R-2628)
sorption by aminodiacetate resin Dowex A-1, 20: 16358
sorption by cotton cloth, acidity effects on, 18: 35515
sorption by diallyl phosphate and polystyrene methylenephosphonic acid resins, 16: 13051
sorption by Dowex-5 in hydrobromic, hydrochloric, hydriodic, and perchloric acids, 16: 11607
sorption by manganese dioxide, effects of ethyl alcohol on, 16: 31629
sorption by polymers, 17: 14354
sorption by zirconyl phosphate ion exchange resins, 16: 10021
sorption from aqueous solutions by peat, 20: 7002 (INR-609/XIX/D)
sorption of divalent, by phosphorus-containing ion exchangers, from

acetic acid–sodium acetate solutions, 20: 35593
sorption on zirconium phosphates, tracer studies of, 19: 32293
spectra of, with o-semiquinones, electron spin resonance, 18: 39190
thermodynamic properties of aqueous, 19: 46282
toxicity of, in mouse, determination by LD_{50} on thirtieth day of, 17: 17719
uptake by rat liver mitochondria, mechanism and requirements of, 19: 14970
uptake by rat liver mitochondria, calcium competition in ATP- and respiration-supported systems, 19: 14971
uptake by rat liver mitochondria, 20: 24842
use for exchange in clay mineral studies, comparison with calcium and magnesium, 18: 16200
van der Waals radii of, relation of hydration energy to, 18: 16016

STRONTIUM IRON LANTHANUM OXIDES
crystal structure, 20: 12865

STRONTIUM IRON NIOBATES
preparation, phase transition, and structure, 16: 11664

STRONTIUM IRON TANTALATES
phase transition, 19: 20591
phase transition at 250°C, 17: 2117(T)
preparation and structure, 16: 11664

STRONTIUM ISOTOPES
abundance correlation with silica in Hawaiian lava, 18: 3991(R) (NYO-10517(p.99-103))
abundance in carbonate and carbonatite rocks, 18: 3986(R) (NYO-10517(p.51-2))
abundance in carbonatites, 18: 14068
abundance in Grenville, Canada, rocks, 18: 3985(R) (NYO-10517 (p.43-9))
abundance in igneous rock, 18: 4000(R) (NYO-10517(p.133-4))
abundance in North American Precambrian Shield rocks, 17: 20210
abundance in northern Atlantic Ocean, 18: 3984(R) (NYO-10517 (p.39-42))
abundance in rocks in Roskruge range, Pima County, Arizona, 19: 44236 (TID-22086)
abundance in rocks from Réunion Island, 19: 46584
abundance in stony meteorites, 18: 4382(R) (NYO-10517(p.7-15))
abundance in tektites, variation of, 18: 3983(R) (NYO-10517(p.27-38))
abundance ratios in rocks and rock derivates, effects of magmatic differentiation on, 19: 46600
abundances in stone meteorites, 16: 31969
accumulation of, in acantharia, 17: 30285
composition in limestone, carbonatites, and strontium minerals, 17: 25446
composition in strontium, mass discrimination in spectrometric measurements on, 20: 40821
content in animals and plants exposed to fallout from underground explosion, 19: 32421 (PNE-237F)
content in man, permissible, 17: 27165
content in minerals, variation of, 16: 14997(R) (NYO-3942)
content in rocks from Indian Ocean islands, 19: 40791
content in vein type mineral deposits, 18: 3979(R) (NYO-10517)
contents in calcites, significance in carbonatite genesis, 19: 42648
determination in biological materials, 17: 27165
determination in environmental samples, radiochemical, 17: 32282 (AECL-1745)
determination in foods and agricultural products, 16: 10353
determination in food and milk, 18: 39059 (NP-14260)
determination in metamorphosed Precambrian igneous rocks, 18: 43795
determination in radioactive solutions, radiochemical, 16: 9947 (PG-Report-282)
determination, radiochemical, 16: 18818 (TID-15415)
deuteron inelastic scattering by, distributions from, 17: 9546
diffusion from irradiated uranium oxidized in air, helium, and steam, 16: 9047
effects on life span and disease incidence in mice, 20: 45359 (ORNL-P-2407)
energy levels, interactions, nuclear moments, and transitions in, 17: 24381 (AD-403411)
energy levels of, theory of low-lying vibrational, 17: 5365
enrichment by ion migration in molten halides, 16: 464
exchange between ions on surface of strontium sulfate crystals, activation energy for, 20: 26881
exchange on surface of ionic crystals, 17: 23373
exchange, transfer unit heights in foam-liquid column for, 16: 14617(R) (ORNL-TM-136)
fixation by muds, 20: 43544
fractionation in bomb debris, 19: 7327
gamma reactions on, cross sections for, 19: 12496
hazards of, in animal foodstuff, review, 17: 310
isomeric transitions, M_4-type, 16: 22985 (NP-11747)
isomeric transitions of E_3 type, 16: 31066 (NP-11746)
isotopic mixing constants of, volume, (T), 20: 19970
levels in human diet, 18: 17395
metabolism by algae and fish, 17: 23033 (DPSPU-63-30-3)
metabolism by cattle, sheep, and swine, 19: 3835(R) (ORO-625(p.64-9))
metabolism in man and dogs, power function for biological model, 17: 25587(R) (ANL-6646(p.5-29))
metabolism of radioactive, method for exact localization in, 18: 4989
migration and sorption in soil, 17: 33409
neutron capture, 18: 7696(R) (ORNL-TM-761)
neutron capture, 18: 24625 (WASH-1046)
nuclear masses and binding energies, 16: 1066
occurrence of, in meteorites, minerals, and rocks; bibliography on, 17: 6270(R) (NYO-10325)
passage through food chains into human diet, 16: 10342
percolation in soil, effects of physicochemical characteristics of soil, 16: 25050 (TID-7628(p.198-210))
preparation and properties, 17: 210
preparation, determination, and properties of radioactive, 16: 1349
preparation of accelerator targets of, 19: 38658
production in plutonium-239 fission, 18: 38085(T) (AEC-tr-6398(p.288-95))
purification of electromagnetically separated, 20: 37163
radiation hazards from, in fallout, 19: 11390 (AWRE-T-57/58)
redistribution during metamorphism in Panamint Range, California, 18: 33793
removal from animals, effectiveness of chelating agents for, 18: 14 (EUR-368.d)
separation by amalgam exchange, calculation of coefficients for, 19: 18373
separation by isotopic exchange, 19: 18369
separation by sorption on charcoal, 19: 28455(P)
separation, contamination in electromagnetic, 16: 9101
separation, electromagnetic, 16: 9107
separation from biological and dust samples, 19: 10999
separation from fission products by cation exchange, 16: 8805 (HW-70998)
separation from impurities by amalgam exchange, 16: 2967(R) (TID-14310)
separation from milk, ion exchange method, 16: 10352
separation from milk, by ion exchange, 17: 27223(P)
separation from milk, ion exchange, 19: 34415
separation from reservoir water by filtration–ion exchange, 20: 40484
separation of radioactive, from sulfuric acid solutions, 17: 18169 (AERE-AM-92)
separation of, performance of separator for, 20: 16928(R) (INSJ-92)
sorption by natural minerals, 17: 7653(R) (ORNL-TM-396)
toxic effects in dogs, 17: 10294(R) (COO-226)
uptake by bacteria, 16: 26705
uptake from soils by plants, effect of mineral fertilizers, 17: 15613
use in age estimation of rocks, 17: 4706
use in geological dating, method and equipment for, 20: 43500(R) (COO-689-60)
use in geological dating, method for, 20: 43501(R) (COO-689-60, App.A-1)
use in geological dating, method for, 20: 43502(R) (COO-689-60, App.A-2)
use of strontium-87/strontium-86 in geological dating, 20: 43503(R) (COO-689-60, App.A-3)
uses as tracer for calcium, 17: 2875
variation in Canadian rocks, 20: 45916(R) (MIT-1381-12)
yields from thermal-neutron fission of thorium-229, 20: 28303
yields in thorium-232 helium-ion fission, 17: 22567 (UCRL-10673)

STRONTIUM ISOTOPES Sr-80
determination in environmental samples, 20: 40809 (NP-16235)

STRONTIUM ISOTOPES Sr-82
decay gamma spectrum, 17: 4078
decay scheme, 16: 24812

STRONTIUM ISOTOPES Sr-83
beta decay scheme and gamma spectra, 18: 21354
decay schemes and energy levels, 16: 7052
gamma decay, 17: 26507
gamma spectra, (E), 19: 16840(R) (IDO-17050)
half life, 18: 13082
production in proton reactions with silver at 2.9 Bev, range studies of, 18: 26648

STRONTIUM ISOTOPES Sr-84
abundance ratio to strontium-88, discrimination factor in mass spectrometric determination, 16: 5513
determination of, in biological materials, activation, 17: 19957
deuteron elastic scattering at 13.6 Mev, angular distributions for, 18: 34942
deuteron elastic scattering at 13.6 Mev, angular distributions from, 18: 40632
energy levels and gamma spectra, 16: 31184
neutron capture by, isomeric cross section ratios for, (E), 20: 22052
neutron cross sections of, from 2.5 to 25,000 ev, (E), 19: 27458
neutron reactions (n,2n) at 14.8 Mev, cross sections for, 16: 7072

neutron reactions at 14.6 Mev, mechanisms and shell effects, 16: 12487
neutron reactions (n,2n) at 14 Mev, shell effects in, (T), 19: 12536
nitrogen ion reactions at 44 and 52 Mev, Coulomb excitation in, 18: 7718
production in stars, 16: 12308
proton reactions (p,2n) at 39 Mev, production of yttrium-83 by, 18: 13082

STRONTIUM ISOTOPES Sr-85

availability to man of, from flour and milk, 19: 36733
binding of, by blood serum proteins, 20: 3697
binding with plasma proteins in patients with bone metastases, 20: 20404
body burdens in mice and rats, effects of sodium salicylate on, 20: 18229
bremsstrahlung efficiencies in mammals, effects of size on whole-body, 18: 29196(R) (COO-119-229(p.170-85))
clearance from dog skeleton, 18: 17451
clearance rates in dog plasma, 16: 1447
content in blood and bone of rats, age and sex dependence of, 17: 10347
content in blood of dogs after intravenous injection, 19: 6898 (TID-21339)
content in human feces and urine, estimation of strontium-90 ingestion or inhalation by, 19: 25883
content in human saliva, 19: 17479
content in human urine following intravenous injection, method for estimating strontium-90 burdens using, 20: 32
content in water, maximum permissible, 17: 39311(R) (ORNL-3492 (p.157-75))
decay and half life, 17: 17298
decay of, fluorescent yield of rubidium L-shell from electron capture, 18: 7732
decay of strontium titanate-incorporated, in marine environments, 20: 43592 (USNRDL-TR-1042)
decay of, local energy deposition due to electron-capture and internal conversion, 20: 18958
decay scheme and half life, 16: 29829
deposition in mouse embryos, autoradiographic determination, 19: 14953 (BNL-7859)
detection and measurement of injected, in man, whole-body counting, 18: 5642 (TID-7673(p.236-49))
detection and measurement in man of, whole-body, 20: 5426
detection of deposited, in man by radiometric analysis of excreta, 19: 30460
determination in blood serum ultrafiltrates, 16: 25115(R) (HW-72500 (p.19-22))
determination in decontaminated waste water, gamma spectrometric, 18: 43385 (ORNL-P-447)
determination in dilute waste solutions by computer resolution of gamma spectra, 19: 9063 (ORNL-3744)
determination in excreta, radiochemical, 19: 43671 (PG-Report-662)
determination in man, whole-body counting, 16: 16159
determination in man, whole-body counting, 16: 16161
determination in man, whole-body counting, 16: 16162
determination in man by whole-body counting, 16: 19172(R) (AD-266007)
determination in milk, method for total, 18: 1514
determination in presence of strontium-89 and -90, radiometric, 19: 17820
determination in rats, whole-body counting, 19: 43671 (PG-Report-662)
determination in radioisotope mixtures using simultaneous equations, gamma spectrometric, 20: 40837
determination in tissues, radiochemical, 19: 43671 (PG-Report-662)
determination of, with calcium-45 in whole algae cells, liquid scintillation spectrometric, 20: 36747
determination simultaneously with calcium-45 by oxalate precipitation, 19: 24463
diagnostic and therapeutic use, review of various aspects for, 18: 17693
diagnostic use for skeletal diseases, 19: 31965
diagnostic use for bone lesions, 19: 46133
diagnostic use for bone metastases, 19: 45729(R) (NYO-910-23, pp 1-111)
diagnostic use for bone lesions, 19: 45757(R) (NYO-910-23, pp 183-92)
diagnostic use in bone scanning, 18: 17703
diagnostic use in photoscanning bone metastases, 19: 5745
diagnostic use of, in localization of metastatic bone tumors, 19: 34067
diagnostic uses in studies on calcium metabolism in bones, 17: 7708
diagnostic uses of, 19: 24391
diffusion from simulated solid wastes, 20: 12517(R) (BNWL-170)
diffusion in sandstone, 19: 8673(R) (ORNL-3697(p.3-10))
dispersion and movement in soils, mechanism of, 20: 20875 (EUR-2481.f)
dispersion in aqueous vermiculite, effects of chemicals on, 20: 8479(R) (ORNL-3849, pp 1-42)
distribution between phases of centrifugally fractionated milk, 18: 17952
distribution in body, two-crystal counter for determining, 19: 30580
distribution in bones and teeth of rats, 19: 33742
distribution in Purex HW solutions, effects of acidity on, 17: 35618(R) (ORNL-TM-545)
distribution in shallow fresh-water ponds, 17: 40521 (TID-7664(p.43-60))
distribution in skeleton of, in patients with bone tumors, whole-body counting of nanocurie activities, 18: 27244
distribution of tracer dose in man, whole-body counting of, 18: 33233(R) (NYO-910-9)
dosimetry of, in nuclear medicine, 20: 26713
effect of chelating agents on retention in mammals, 16: 29327 (KFK-76)
effects on calcium-45 or -47 activity after intravenous injection, 19: 6999
energy from, determination of total, 19: 38878 (ORNL-P-1405)
energy level densities in, effects of spin on, 16: 33853
energy levels, 18: 13048 (JINR-P-1510)
energy levels and gamma spectra, 16: 32425
energy levels from yttrium-85 decay, parity and spin of, (E), 20: 17670 (AD-629576)
energy levels from yttrium-85 decay, (E), 20: 26186
exchange between ions on surface of strontium sulfate crystals, 20: 26881
exchange between strontium sulfate crystals, rate of, 20: 12869
exchange between strontium sulfate crystals and solutions, 20: 14572
excretion by goats, effects of dietary calcium and strontium on, 20: 40568
excretion by isopods under field and laboratory conditions, 20: 12610
excretion by kidneys of dogs, 20: 30
excretion by man, effects of calcium, chelates, and strontium on fecal and urinary, 17: 28633
excretion by man relative to blood, 16: 28717
excretion by man, effects of high dietary content of phosphorus on, 19: 57
excretion by mice, agents affecting, 17: 38707
excretion by mice, rabbits, and rats, 19: 21828
excretion by normal man, 17: 24855
excretion by rats, effects of tetracycline, 17: 19766
excretion by rats, fecal to urinary ratio of, 20: 22542 (BNWL-SA-625)
excretion by rats, effects of sulfates of barium and sodium on, 20: 26612
excretion in man, effects of treatment using ammonium chloride and calcium, 16: 6283
excretion in man, effects of calcium salts of bis-2-aminoethyl ether tetraacetate and gluconate on, 16: 9828
excretion in man, effects of ammonium chloride and calcium, 17: 1213
excretion in man, urinary, 17: 1217
excretion in rat feces and urine, effects of dietary phosphorus on, 20: 12594(R) (NP-15679)
excretion in urine of dogs in presence of calcium-45, 18: 8092
excretion of, in patient with multiple myeloma treated with androgens and corticosteroids, 17: 21438
excretion of injected, effects of drugs on, 17: 30079
excretion of, effects of various chemicals in mice, 20: 8564
excretion of, effects of chemical agents on, 18: 31102
excretion rates in dog, renal, 16: 1447
exposure to, maximum permissible occupational, 18: 15907
gamma dose constants for, 20: 46617
gamma spectra, 17: 34966
gamma spectra, (E), 20: 28462
gamma spectrum, 18: 18174 (BRL-1230)
gamma spectrum of, 17: 22008 (LADC-5609)
half life, 20: 8076 (NP-15663)
localization of injected, in patients with bone disease, whole-body counting, 18: 5173 (TID-7673(p.205-73))
metabolism, 18: 35260(R) (AERE-PR/HPM-5)
metabolism and retention by rats, effects of dietary phosphorus on, 20: 12600(R) (NP-15685)
metabolism by cows, goats, and hogs, 20: 12588(R) (AD-626320)
metabolism by embryonic chick bone, effects of parathyroid hormone on, 17: 13933
metabolism by fresh-water plants, 19: 35939
metabolism by rats, scintillation-counter measurements of whole-body retention in, 18: 43175(R) (LA-3132-MS(p.42-8))
metabolism by rats, effects of carbonates, magnesium oxide, and phosphates on, 20: 12606
metabolism by rats, effects of dietary strontium on, 20: 14251
metabolism, effects of chelating agents and isotopic dilution, 16: 12868
metabolism, effects of age, in miniature swine, 16: 25113(R) (HW-72500(p.13-14))
metabolism in bone tumor metastases, 16: 28725
metabolism in bones of rats treated with testosterone, 17: 10348
metabolism in bones, compartmental analysis, 20: 20400
metabolism in bones in man, 20: 26636
metabolism in dogs, effects of age on, 19: 2039
metabolism in dogs, effects of age on, 19: 10766
metabolism in fish, 20: 32914
metabolism in gastrointestinal tract, effect of dietary calcium and hormones on, 20: 8578
metabolism in gastrointestinal tract, method for determining, 20: 8578
metabolism in human bone, 18: 21
metabolism in laying hens, 18: 38761
metabolism in live mice, design of radiation detectors for measuring, 20: 36556
metabolism in man, 16: 32639(R) (TID-16459)
metabolism in man, 17: 5670(R) (LAMS-2780(p.17-84))

metabolism in man, 19: 22019(R) (UCLA-12-541(p.51-91))
metabolism in man, 19: 29848 (ACRH-103(p.62-75))
metabolism in mice, effects of tetracycline treatment, 17: 5670(R) (LAMS-2780(p.17-84))
metabolism in mice, effects of environmental temperature on, 18: 15770(R) (LAMS-3034(p.65-72))
metabolism in mice and rats, effects of age on, 19: 2038
metabolism in mice, rabbits, and rats, 19: 21828
metabolism in miniature swine, effects of administration as titanate or chloride on, 18: 23200 (HW-SA-3350)
metabolism in rats, effects of glucose, lactose, and lysine on, 18: 11559(R) (TID-19977)
metabolism in rats, effects of calcium and strontium dietary contents and age on, 19: 5613
metabolism in rats, effects of citrate on, 19: 24748(R) (PG-Report-647)
metabolism in rats, effects of sulfates on, 19: 33743
metabolism in rats, 19: 43671 (PG-Report-662)
metabolism in rats, effects of dietary phosphorus on, 20: 12596(R) (NP-15681)
metabolism in rats, techniques for studying, 20: 32926
metabolism of bone-fixed, dietary factors, 16: 28721 (BNL-5859)
metabolism of, in wrist in disuse osteoporosis in man, kinetics of, 17: 12081
metabolism of ingested, in man, 19: 15747 (ACRH-102)
motion in soil, effects of chelating agents on, 19: 38329 (TID-20471)
movement across ileal segments in rats, effects of alginic acid on, 19: 31737
movement in soils, 20: 30943(R) (ORNL-TM-1465)
movement of, in human body, 17: 17718
photosynthesis and uptake of, in freshwater plankton, effects of light on, 20: 36568
placental transfer in mice, 20: 14244
plasma and renal clearance in man, 20: 18226
precipitation from urine as oxalate and phosphate, 17: 10276
production method for, 17: 10676 (NP-12231)
production of carrier-free, in ORNL cyclotron, 19: 22851 (ORNL-TM-1047 (p.72-6))
production of isomeric and ground-state, from strontium-84 neutron capture, (E), 20: 22052
production using ORNL 86-in. cyclotron, 20: 2212
properties of chelated, as ground-water tracer, 19: 13657
radiation effects on metabolism in rats, 17: 5670(R) (LAMS-2780(p.17-84))
radiation effects on rat intestinal sorption of, x, 20: 22600
radiation effects on metabolism of, following pituitary irradiation, alpha, 20: 42744(R) (UCRL-16246, pp 19-35)
removal from bone *in vitro*, 18: 1349
removal from milk by contacting with bone preparations in absorption column, 18: 6976(R) (TID-19893)
removal from milk by electrodialysis, 18: 12257 (NP-13620)
removal from milk, ion-exchange resins for, 18: 13925
removal from milk, ion exchange method for, 18: 17952
removal from rat bones, effectiveness of chelating agents and other compounds for, 19: 43700
removal from rat body by high strontium diets, 20: 38566
removal from rats, effects of chelating agents on, 20: 12598(R) (NP-15683)
removal of bone-deposited, effects of chelating agents and salts on, 19: 43706
retention by bone, effects of chemical agents on, 18: 31102
retention by clays, 19: 36300
retention by dogs, calculation by two-compartment model having age variables, 19: 6949(R) (ORNL-3697(p.193-8))
retention by lichen, 20: 23283 (BNWL-SA-556)
retention by man, 17: 24858
retention by rat skeleton, effects of phosphorus and strontium in diet on, 20: 12595(R) (NP-15680)
retention by rat skeleton labeled *in utero*, effects of dietary calcium and phosphate on, 20: 12599(R) (NP-15684)
retention by rat skeleton, effects of dietary phosphorus and strontium on, 20: 12594(R) (NP-15679)
retention by rat, effects of dietary phosphorus on, 20: 12597(R) (NP-15682)
retention by rats, effects of calcium and phosphate in diet on, 20: 12598(R) (NP-15683)
retention by skeleton in female rats, effects of chelating agents on, 20: 12596(R) (NP-15681)
retention in human bones, 18: 13416 (CONF-355-4)
retention in man, measured by whole-body counting, 16: 26710 (BNL-5805)
retention in skeletons, effects of tetracycline on, 17: 13942
retention in swine, 20: 42739(R) (COO-1339-3)
retention of dietary, by rabbits, 17: 17742
retention of, in mice and rats, effects of tetracycline on, 18: 23220
secretion in human saliva, 19: 17479
separation from milk, ion exchange method for, 16: 17935
separation from milk, ion-exchange, 18: 3895
separation from milk, effects of acidification on, 18: 39539
separation from milk, ion exchange, 19: 11396
separation from milk, ion exchange, 19: 11397
separation from milk, 19: 26467(R) (TID-21796)
separation from milk, ion-exchange, 19: 34371
separation from milk using calcium phosphate precipitation method, 20: 16382
separation from milk using tricalcium phosphate, effects of, on milk composition, 20: 33580
separation from sea water by sorption by metal sulfide-ion exchange resins, 20: 29345
separation from soil, method for, 18: 14143
separation from sodium sulfate glass melter condensate, method for, 20: 24809(R) (BNWL-213)
separation from water using U. S. Army equipment, 19: 36717
separation method for, 17: 10676 (NP-12231)
separation of, from milk, by ion-exchange, pilot plant for, 17: 18423
separation of, from americium-241, radiochemical, 17: 19954
separation using mixed oxide scavenger, 20: 40476(R) (BNWL-267)
sorption and distribution in chicks, effects of vitamin D, 17: 23024
sorption by intestine in rats, 16: 25114(R) (HW-72500(p.15-18))
sorption by skin, protective effects of fatty acid gels, 19: 21997
sorption by various soils, temperature effects on, 17: 19710 (TID-7644 (p.177-86))
sorption from sea water on ferric hydroxide resin, 19: 32787(R) (NIRS-3(1-17))
sorption in dogs, gastrointestinal, 19: 43677(R) (UCD-472-112, pp 86-96)
sorption of, by kidneys in dog and man, calcium discrimination in, 17: 19760
sorption of, by small intestine in rat from liquid and solid food, 17: 13938
sorption of dietary, by rabbits, 17: 17742
sorption of, effects of calcium phosphate on, 17: 37047
sorption of, effects of carrier on biological, 19: 6999
sorption on zeolites, effects of heat on, 18: 1312 (HW-77830)
sorption reactions of, on minerals, 20: 41178 (AD-635547)
sorption through burns and wounds in rats, 18: 29232
sorption through normal, burned, and wounded skin, 18: 11557(R) (AD-412416)
tracer applications in studies of bone metabolism, 16: 31428
tracer solution preparations, 16: 14997(R) (NYO-3942)
tracer use for scanning of skeleton, 19: 42396
tracer use in bone fracture healing study, 18: 4951
tracer use in bone metabolism studies, 19: 34045
tracer use in strontium–calcium metabolic relation, 17: 35426
tracer use of, for measuring long-term calcium metabolism in human bones, 20: 42764
tracer uses in studies on calcium metabolism, 18: 38737
transfer from fetus to mother, 16: 8486 (UCLA-498)
transfer from strontium titanate to sea water, 18: 31363 (USNRDL-TR-745)
transfer in rat lacrimal and salivary glands, effects of acetylcholine on, 19: 8747
translocation of, from leaves of bean and corn plants, 19: 5623
transport in dogwood trees, 20: 8534(R) (ORNL-P-1820)
transport in isolated corn root segments, 20: 45269 (AD-639699)
transport in model river, factors affecting, 20: 24833 (TID-22877)
transport in soils by runoff water, 18: 35724
uptake and distribution of, in snail, 17: 17714
uptake and exchange in bones of dogs, 20: 40684
uptake and excretion of intravenously administered, 18: 11585
uptake and release by plankton, plants, and sediments in aquatic system, 20: 24833 (TID-22877)
uptake and retention by rat skeleton, effects of calcium-activated barium sulfate on, 19: 17466
uptake and retention in rats, effects of cortisone and anabolic steroids on, 19: 19476
uptake and retention by man, whole-body, 19: 35893(R) (NYO-3234-1)
uptake and retention by leaves, effects of relative humidity and temperature on, 20: 30996
uptake and specific activity in rat plasma and urine, 19: 31736
uptake and turnover in bone, pathological effects on, 19: 7006
uptake by algae in settling ponds, 20: 24815
uptake by aortic wall of rats, 20: 14252
uptake by axial skeleton in man, 19: 9035
uptake by barley seedlings, effects of greasewood forest soil on, 20: 12575
uptake by biological organisms in fresh-water pond, 18: 25079
uptake by bone metastases from breast cancer, 17: 27019
uptake by bone tumors, 20: 6731

uptake by bone, parathyroid hormone removal of, 18: 33231(R) (NIRS-2(p.49-56))
uptake by bone, use in diagnosing bone cancer, 20: 18513
uptake by bones and human body following oral administration, 20: 42762
uptake by cancellous bones in rats, 20: 6736
uptake by fractured human bones, 20: 40542
uptake by freshwater fish, effects of calcium, magnesium, potassium, and sodium on, 19: 8757
uptake by green algae, 18: 38735
uptake by *in vitro* produced melanin, 18: 3451(R) (COO-228(p.133-9))
uptake by man, 20: 20466
uptake by metastatic bone tumors, differential, 18: 15932
uptake by mollusks in lake sediments, 19: 1996
uptake by osteosarcomas, 18: 11578
uptake by plankton crustacea, use of observed ratio equation for predicting, 19: 10777
uptake by plankton, 20: 6711(R) (ORNL-3849, pp 43-100)
uptake by plants and seed of barley, oats, rye, and wheat, 19: 33753
uptake by plants growing in peat-podzolic soils, effects of liming on, 20: 18303
uptake by plasma, 18: 4978
uptake by powdered bone, 18: 28
uptake by rat hair, 20: 1695
uptake by rat liver mitochondria, 19: 25846
uptake by rats, effects of dietary calcium and phosphorus on, 20: 10549
uptake by recently molted crayfish, 17: 13941
uptake by tumorous bones, measurement of, 19: 45757(R) (NYO-910-23, pp 183-92)
uptake from human gastrointestinal tract, effects of sodium alginate on, 20: 16173 (PG-Report-686)
uptake from human gastrointestinal tract, effect of sodium alginate on, 20: 24941
uptake from soil by alfalfa, 16: 32682
uptake in rats, effects of dietary alginate on, 20: 24847
uptake of, by bone lesions in man, *in vivo* counting of, 17: 30211
uptake of, by bones in young rats, effects of fluoridated water on, 17: 27044
uptake of, by skeleton in normal and rachitic rats, 17: 15591
uptake of, from soil by field crops, 17: 35322(R) (HW-76000(p.208-10))
uptake, retention, and excretion by animals, effects of carriers, diet, and non-carriers on, 17: 28630
uptake, retention, and excretion by man, 17: 28631
use as measure of effective bone blood flow in dogs and rabbits, 19: 38340
use as tracer in metabolism studies in deer and sheep, techniques for, 20: 12609
use as tracer in studies on diseases, 19: 35893(R) (NYO-3234-1)
use as tracer, for diagnosis of bone tumors, 20: 3805
use for localization of bone lesions by external counting, 20: 26724
use in bone scanning, 20: 40748
use in bone scanning, value to radiotherapy, 20: 40794
use in bone tumor localization, 19: 19666
use in determining bone formation and resorption rates, 19: 6995
use in diagnosing bone infections, 20: 12735
use in diagnosis of bone diseases, evaluation of, 19: 9035
use in diagnosis of bone tumors by scintillation scanning, 19: 19697
use in localization of metastatic bone lesions, 17: 17876
use in localization of primary and secondary bone tumors in man, 19: 19675
use in maize root transport studies, 20: 45270 (AD-639836)
use in measurement of bone blood flow, 20: 16192
use in radiochemistry and tracer techniques, optimum counting methods for, 18: 33655
use in radiodiagnosis, 18: 25257
use in scintiscanning, review, 20: 22828
use in studies of bone behavior, 16: 1433(R) (TID-14099)
use in studies of bone growth, 20: 8(R) (STI/DOC/10/42, pp 23-43)
use in studying bone turnover in coxarthrosis patients, 19: 7004
use in studying calcium kinetics in hyperparathyroidism, 19: 6994

STRONTIUM ISOTOPES Sr-86

abundance in Connecticut and New Hampshire rocks, 18: 3990(R) (NYO-10517(p.85-95))
abundance in continental soil, 17: 6291
abundance in dunite and serpentinite, 18: 3993(R) (NYO-10517(p.111))
abundance in granites in British Columbia, 18: 3982(R) (NYO-10517 (p.23-5))
abundance in Grenville, Canada, rocks, 18: 3985(R) (NYO-10517 (p.43-9))
abundance in Hawaiian lava, 18: 3991(R) (NYO-10517(p.99-103))
abundance in mafic rocks, initial, 18: 3997(R) (NYO-10517(p.125-6))
abundance in Massachusetts Dedham granites, 18: 3987(R) (NYO-10517(p.53-4))
abundance in meteorite Bjurbole, 18: 4383(R) (NYO-10517(p.119-20))
abundance in northern Atlantic Ocean, 18: 3984(R) (NYO-10517 (p.39-42))
abundance in northern Appalachian granitic and volcanic rocks, 18: 3989(R) (NYO-10517(p.65-84))
abundance in Nova Scotia granitic rocks, 18: 4001(R) (NYO-10517 (p.143-5))
abundance in Quebec igneous rocks, 18: 3992(R) (NYO-10517(p.105-10))
abundance in Sierra Nevada plutonic intrusives, 18: 3981(R) (NYO-10517(p.17-22))
abundance in stony meteorites, 18: 4382(R) (NYO-10517(p.7-15))
abundance in tektites, variation of, 18: 3983(R) (NYO-10517(p.27-38))
abundance in volcanic rocks in western Italy, 18: 3998(R) (NYO-10517(p.127-8))
abundance in volcanic rock in Oahu, 20: 45929
abundance ratio to strontium-87 in limestone and sea water, 16: 22426
abundance ratio to strontium-87 in rocks with different degrees of metamorphosis for age estimation, 19: 36658
abundance ratio to strontium-87 in oceanic and continental basalts, 19: 46607
abundance ratio to rubidium-87 and strontium-87 in glasses from Bosumtwi crater and Ghana and Ivory Coast tektites, 20: 27166
abundance ratios in granite, 20: 33521
content and ratio to other stable strontium isotopes in surface water from North Atlantic Ocean, 19: 22541
content in alkaline Hawaiian basalts, 19: 26546
content in Archean Seas, age estimation from, 20: 16711(R) (MIT-1381-13)
content in Australian Precambrian rock, 20: 41159
content in Bethlehem gneiss, age estimation from, 20: 45916(R) (MIT-1381-12)
content in British Columbian granites, (E), 19: 4383
content in Canadian rock, age estimation from, 20: 45916(R) (MIT-1381-12)
content in carbonate rocks from Keshya and Mkwisi, Zambia, 19: 26547
content in carbonatites and limestones from Ice River, British Columbia, 20: 31406
content in carbonaceous chondrites, age estimation from, 20: 45916(R) (MIT-1381-12)
content in carbonate vein-dikes, age estimation from, 20: 45916(R) (MIT-1381-12)
content in chondrites and chondrules, age estimation from, 20: 529
content in Connecticut pegmatites, age estimation from, 20: 45916(R) (MIT-1381-12)
content in deep crustal material, 18: 23801
content in deep sea sediments, 20: 45928
content in Duluth Gabbro Complex and Endicon Sill, age estimation from, 20: 45916(R) (MIT-1381-12)
content in gangue minerals of hydrothermal deposits, age estimation from, 20: 45916(R) (MIT-1381-12)
content in granites, quartzites, and slate in Massachusetts, age estimation from, 20: 16711(R) (MIT-1381-13)
content in granitic rocks in central Sierra Nevada, California, 19: 28543
content in Great Lakes and Hudson Bay, geochemistry of, 20: 16711(R) (MIT-1381-13)
content in Hawaiian lavas, 18: 20216
content in Hawaiian volcanic rocks, age estimation from, 20: 45916(R) (MIT-1381-12)
content in iron meteorites, 20: 12992
content in Italian volcanic rocks, age estimation from, 20: 45916(R) (MIT-1381-12)
content in Ivory Coast tektites, age estimation from, 20: 45916(R) (MIT-1381-12)
content in metamorphic rocks from Llano Uplift, Texas, age estimation from, 19: 36682
content in meteorites and rocks, primeval, 19: 30426
content in meteorites and rocks, 20: 9157
content in New England volcanic rocks, age estimation from, 20: 45916(R) (MIT-1381-12)
content in Nonesuch Michigan shale, age estimation from, 20: 45916(R) (MIT-1381-12)
content in North Atlantic seawater, 20: 45916(R) (MIT-1381-12)
content in plutonic and metamorphic rocks of New Zealand, 20: 20888
content in ratio with strontium-87 and rubidium-87 in granophyre and tertiary granite from Skye, Scotland, 19: 4365
content in ratio with rubidium-87 in granites of southwestern Karelia karelides, age estimation from, 19: 4382
content in rocks from Indian Ocean islands, 19: 40791
content in rocks in Sweden, 20: 39126
content in rocks, relation of lead isotopic content to, 20: 35645
content in Spanish granites, age estimation from, 20: 41153
content in stony meteorites, age estimation from, 20: 45916(R) (MIT-1381-12)

content in Surinam rocks, age estimations from, 20: 33535
content in Tasmanian dolerites, 19: 32433
content in Tasmanian Heemskirk granite, 20: 9158
content in ultramafic rocks, age estimation from, 20: 45916(R) (MIT-1381-12)
content in volcanic rocks of Hawaii, (E), 19: 20168
content ratio to strontium-87 in sials, evidence for separation from continental basement from, 17: 25460
content ratio to strontium-87 in carbonatites, Ontario, Canada, 19: 44257
content ratio to strontium-87 in carbonate veins and vein-dikes, Idaho, Montana, and Ontario, 20: 12980
content ratio with rubidium-87 and strontium-87 in Grenville Front, Ontario, age estimation from, 19: 4386
deuteron elastic scattering at 13.6 Mev, angular distributions for, 18: 34942
deuteron elastic scattering at 13.6 Mev, angular distributions from, 18: 40632
deuteron reactions (d,n) with, yttrium-87 isomeric pair production in, 17: 19226 (TID-16648)
energy level scheme for yttrium-86 decay-produced, (E/T), 19: 47584(R) (ORNL-3832, pp 1-28)
energy level transitions from rubidium-86 decay, circular polarization of 1084-kev gamma from, (E), 20: 24482
energy level transitions of, K-conversion coefficients, intensities, and multipolarities for, (E), 20: 36229
energy levels and gamma spectra, 16: 12488
energy levels from rubidium-86 decay, (E), 20: 19858
energy levels in, structure of low-lying 2+, 17: 11698
energy levels of, (E/T), 20: 30353(R) (ORNL-3940, pp 1-61)
energy levels of, central and tensor potentials in shell model calculations of, 20: 28360
energy levels of, shell-model potential parameters for low-lying, (T), 20: 38145
energy of first excited state in, 18: 1045
gamma reactions (γ,n) on, nuclear excited states from, 16: 33853
half life of 1.07-Mev excited state, 16: 11886
isotopic ratio with strontium-87 in various samples, double multiplier system for measuring, 18: 14295
neutron cross sections of, from 2.5 to 25,000 ev, (E), 19: 27458
neutron reactions (n,p) at 14 Mev, cross section ratio to strontium-88, 16: 6019
neutron reactions at 14.6 Mev, mechanisms and shell effects, 16: 12487
neutron reactions (n,p) at 7.0 to 19.8 Mev, cross sections for, 16: 19782
neutron reactions (n,p), separation energies for, 17: 2242 (TID-16949)
neutron reactions (n,2n) at 14 Mev, shell effects in, (T), 19: 12536
neutron reactions (n,2n) at 3 Mev above threshold, cross section for, (E), 20: 46614
nitrogen ion reactions at 44 and 52 Mev, Coulomb excitation in, 18: 7718
nucleon interaction potentials in, shell model calculation of, 17: 40031
occurrence in shale formations, 17: 3176
proton reactions (p,n) at 11.2 Mev, cross section for, 17: 40056
redistribution in rocks, effect of temperature and pressure on, 20: 45916(R) (MIT-1381-12)
spike solution calibrations, 16: 14997(R) (NYO-3942)

STRONTIUM ISOTOPES Sr-87
abundance in biotites and muscovites from Blue Ridge and Piedmont, age determinations by, 16: 19165
abundance in Connecticut and New Hampshire rocks, 18: 3990(R) (NYO-10517(p.85-95))
abundance in continental soil, 17: 6291
abundance in dunite and serpentinite, 18: 3993(R) (NYO-10517(p.111))
abundance in granites in British Columbia, 18: 3982(R) (NYO-10517 (p.23-5))
abundance in Grenville, Canada, rocks, 18: 3985(R) (NYO-10517 (p.43-9))
abundance in Hawaiian lava, 18: 3991(R) (NYO-10517(p.99-103))
abundance in mafic rocks, initial, 18: 3997(R) (NYO-10517(p.125-6))
abundance in Massachusetts Dedham granites, 18: 3987(R) (NYO-10517(p.53-4))
abundance in meteorite Bjurbole, 18: 4383(R) (NYO-10517(p.119-20))
abundance in northern Atlantic Ocean, 18: 3984(R) (NYO-10517 (p.39-42))
abundance in northern Appalachian granitic and volcanic rocks, 18: 3989(R) (NYO-10517(p.65-84))
abundance in Nova Scotia granitic rocks, 18: 4001(R) (NYO-10517 (p.143-5))
abundance in Quebec igneous rocks, 18: 3992(R) (NYO-10517(p.105-10))
abundance in Sierra Nevada plutonic intrusives, 18: 3981(R) (NYO-10517(p.17-22))
abundance in stony meteorites, 18: 4382(R) (NYO-10517(p.7-15))
abundance in tektites, variation of, 18: 3983(R) (NYO-10517(p.27-38))
abundance in volcanic rocks in western Italy, 18: 3998(R) (NYO-10517(p.127-8))
abundance in volcanic rock in Oahu, 20: 45929
abundance rate to strontium-86 in rocks with different degrees of metamorphosis for age estimation, 19: 36658
abundance ratio to strontium-86 in limestone and sea water, 16: 22426
abundance ratio to strontium-86 in oceanic and continental basalts, 19: 46607
abundance ratio to strontium-86 in glasses from Bosumtwi crater and Ghana and Ivory Coast tektites, 20: 27166
abundance ratios in granite, 20: 33521
age estimation by rubidium systems with, contact metamorphism effects on biotites, 17: 25457
age estimation by ratio of, to strontium-86, 18: 31748
concentration by A.W.R.E. isotope separator, 19: 34608
content and ratio to other stable strontium isotopes in surface water from North Atlantic Ocean, 19: 22541
content in alkaline Hawaiian basalts, 19: 26546
content in Archean Seas, age estimation from, 20: 16711(R) (MIT-1381-13)
content in Australian Precambrian rock, 20: 41159
content in British Columbian granites, (E), 19: 4383
content in carbonate rocks from Keshya and Mkwisi, Zambia, 19: 26547
content in carbonatites and limestones from Ice River, British Columbia, 20: 31406
content in chondrites and chondrules, age estimation from, 20: 529
content in deep crustal material, 18: 23801
content in deep sea sediments, 20: 45928
content in granites, quartzites, and slate in Massachusetts, age estimation from, 20: 16711(R) (MIT-1381-13)
content in granitic rocks in central Sierra Nevada, California, 19: 28543
content in Great Lakes and Hudson Bay, geochemistry of, 20: 16711(R) (MIT-1381-13)
content in Hawaiian lavas, 18: 20216
content in Hawaiian volcanic rocks, age estimation from, 20: 45916(R) (MIT-1381-12)
content in igneous rocks from Iceland, 19: 42635
content in igneous and metamorphic rocks, Llano Uplift, Texas, 20: 532
content in iron meteorites, 20: 12992
content in lepidolites and pollucites from Elba island, 16: 29192 (RT/GEO(62) 2)
content in metamorphic rocks from Llano Uplift, Texas, age estimation from, 19: 36682
content in meteorites and rocks, primeval, 19: 30426
content in meteorites and rocks, 20: 9157
content in plutonic and metamorphic rocks of New Zealand, 20: 20888
content in ratio with strontium-86 in granophyre and tertiary granite from Skye, Scotland, 19: 4365
content in rocks from Indian Ocean islands, 19: 40791
content in rocks in Sweden, 20: 39126
content in Spanish granites, age estimation from, 20: 41153
content in Surinam rocks, age estimations from, 20: 33535
content in Tasmanian dolerites, 19: 32433
content in Tasmanian Heemskirk granite, 20: 9158
content in tertiary igneous rocks on Isle of Skye, northwest Scotland, 19: 36683
content in volcanic rocks of Hawaii, (E), 19: 20168
content in zircons, age estimation from, 20: 18924(R) (NYO-1669-11)
content ratio to rubidium-87 and strontium-86 in sials, evidence for separation from continental basement from, 17: 25460
content ratio to strontium-86 in carbonatites, Ontario, Canada, 19: 44257
content ratio to strontium-86 in carbonate veins and vein-dikes, Idaho, Montana, and Ontario, 20: 12980
content ratio with strontium-86 in Grenville Front, Ontario, age estimation from, 19: 4386
determination in Antarctic rocks for age estimation, 20: 37015
determination in minerals by spectral isotopic analysis, 17: 34122
determination of isotopic content of, spectral, 17: 2918
deuteron elastic scattering at 13.6 Mev, angular distributions for, 18: 34942
deuteron elastic scattering at 13.6 Mev, angular distributions from, 18: 40632
deuteron reactions (d,2n) with, yttrium-87 isomeric pair production in, 17: 19226 (TID-16648)
diffusion in biotites, 16: 14997(R) (NYO-3942)
dosimetry of metastable, in nuclear medicine, 20: 26713
electric quadrupole moment, 17: 41978
energy from, determination of total, 19: 38878 (ORNL-P-1405)
energy level transitions in isomeric, 389-kev M4, (E), 20: 24358(R) (UCRL-16580, pp 1-93)
energy levels of, detection of isomeric, 17: 29953
energy levels of, structure from isomeric transition in, (T), 20: 19970
gamma dose constants for metastable, 20: 46617
gamma spectra, 17: 34966
gamma transitions in, independent particle model for M4, 19: 17051

helium-3 reactions (He-3,t) at 27.5 Mev, ground- and isomeric-state production in, 18: 18971
internal conversion coefficient, 16: 7066
isotopic ratio with strontium-86 in various samples, 18: 14295
metabolism of metastable, in bones in man, 20: 26636
neutron cross sections of, from 2.5 to 25,000 ev, (E), 19: 27458
neutron reactions at 14.6 Mev, mechanisms and shell effects, 16: 12487
neutron reactions (n,n'), cross sections for, 17: 20988(R) (NYO-10173)
neutron reactions (n,α) at 14 Mev, nuclear shell effects in cross sections for, 18: 18977
neutron reactions (n,γ) at thermal energies, strontium-88 neutron binding energy and energy levels from, (E), 20: 38141
nuclear properties of isomeric, 18: 13626(R) (NYO-10174)
nuclear quadrupole moments, 16: 33908
nuclear quadrupole moment, (E), 20: 3087
occurrence in rocks, use in age estimation, 17: 12462
occurrence in shale formations, 17: 3176
photoactivation of isomeric, cross sections for, 18: 7705
preparation of isomer, 18: 12521(R) (BNL-823(p.57-65))
production, 19: 22818(R) (ORNL-3650(p.221-38))
production facilities for, 19: 36452(R) (BNL-900(p.105-20))
production in geological materials by rubidium-87 decay, 20: 16711(R) (MIT-1381-13)
production of metastable isomeric, by reactor irradiation, (E), 19: 33295
production of 2.8-hr isomer of, for use as gamma source for medical applications, 19: 30306
production of 2.8-hr isomer of, 20: 12917
production of, by yttrium-87 generator, 19: 10951
production of, techniques for, 18: 41892 (BNL-864)
properties and uses of, produced at Brookhaven, 19: 22853 (ORNL-TM-1047(p.113-16))
properties of 2.88-hr isomer of, for use in activation analysis, 17: 20988 (NYO-10173)
proton reactions (p,α) of, Q values for, 18: 27832(R) (ORNL-TM-530(Rev.))
proton reactions (p,α) at 11.2 Mev, cross sections for, 17: 40056
separation of metastable, from yttrium-87, 17: 19725 (BNL-759(p.47-53))
separation of metastable, from yttrium-87, 18: 3672(R) (BNL-799(p.64-73))
separation of 2.8-hr metastable, from yttrium-87 parent by elution, 19: 26718 (ORNL-3802)
transitions of, effect of configuration mixing on M4, (T), 19: 1643
uptake by metastatic bone tumors, 18: 21930
use in age estimation, 19: 13652
use in bone scanning, 18: 17703
use in localization of metastatic bone tumors, 19: 34067
use in photoscanning bone metastases, 19: 5745
use in scintiscanning, review, 20: 22828
yield from glass and plastic generators, 19: 15332(R) (BNL-841(p.52-62))

STRONTIUM ISOTOPES Sr-88

abundance in Grenville, Canada, rocks, 18: 3985(R) (NYO-10517 (p.43-9))
abundance in meteorite Bjurbole, 18: 4383(R) (NYO-10517(p.119-20))
abundance ratio to strontium-84, discrimination factor in mass spectrometric determination, 16: 5513
alpha inelastic scattering at 42 Mev, level structure from, (E), 20: 22138
alpha reactions (α,4nγ) at 48 and 52 Mev, collective levels from, (E), 19: 6671
binding energy from strontium-87 neutron capture, neutron, (E), 20: 38141
content and ratio to other stable strontium isotopes in surface water from North Atlantic Ocean, 19: 22541
conversion coefficients for, K, (E/T), 20: 8080 (ORNL-P-1700)
deuteron (d,p) reactions, proton polarization in, 19: 21447
deuteron elastic scattering at 13.6 Mev, angular distributions for, 18: 34942
deuteron elastic scattering at 13.6 Mev, angular distributions from, 18: 40632
deuteron reactions (d,3n) with, yttrium-87 isomeric pair production in, 17: 19226 (TID-16648)
deuteron reactions (d,p) at 13.6 Mev, angular distributions from, 17: 24414
deuteron reactions (d,p) at 11.1 Mev, energy-level excitation in, 17: 26635
deuteron reactions (d,p) with, cross sections and energy levels of, 17: 33066
deuteron reactions (d,p) with, strontium-89 energy levels from, 18: 15227
deuteron reactions (d,p) with, distorted-wave analysis of, (T), 19: 14486 (ANL-6878(p.23-60))
deuteron reactions (d,p) at 11 Mev, polarization from, (E), 19: 21391
deuteron reactions (d,p) with, spectra from, 19: 21394
deuteron reactions (d,p) at 7 Mev, proton spectra from, (T), 20: 19826 (MIT-2098-229)
electron inelastic scattering by, partial-wave analysis of, 17: 11710
energy level structure, (T), 20: 12146
energy level transitions in, total and K conversion coefficients for, (E), 20: 10065
energy level transitions in, E1 and E3, (T), 20: 36206
energy levels, 18: 36600
energy levels, (E), 19: 17060
energy levels, 19: 29228(R) (AEET/NP/10)
energy levels, (E), 19: 19095 (WASH-1053)
energy levels and gamma spectra, 18: 2962
energy levels from yttrium-88 decay, parity and spin of, (E), 20: 32453
energy levels from strontium-87 neutron capture, (E), 20: 38141
energy levels of, (E), 20: 34530(T) (CONF-660107-46)
energy levels of, search for 0+ state in, 17: 26481
energy levels of, spins and parities of, 18: 21208 (NP-13841)
energy levels of, isobaric analogue, 19: 14640
energy-level lifetime gamma resonance scattering determination of 1.85-Mev, (E/T), 19: 5248
gamma E-2 transitions in, 17: 41965
gamma resonance scattering, (E), 19: 5248
helium-3 reactions (He-3,p) with, isomeric cross section ratios for, (E), 19: 41820
helium-3 reactions (He-3,p) at 14 to 19 Mev, isomer pair production cross sections for, (E), 20: 32430
mass difference from zirconium-90, 17: 17158
neutron capture by, radiation widths of gamma emission from, 19: 47115(R) (ANL-6983)
neutron cross sections of, from 2.5 to 25,000 ev, (E), 19: 27458
neutron reactions (n,n'γ), angular distributions for, 16: 4741(R) (TID-14157)
neutron reactions (n,p) at 14 Mev, cross section ratio to strontium-86, 16: 6019
neutron reactions at 14.6 Mev, mechanisms and shell effects, 16: 12487
neutron reactions (n,n'γ) with, angular distribution of, 18: 2846(R) (TID-19709)
neutron reactions (n,2n) with, cross section for, 18: 11195(R) (EANDC(E)-49(L))
neutron reactions (n,2n) at 12.5 to 19.6 Mev, cross sections for, 18: 24602 (NP-13930(p.43-9))
neutron reactions (n,2n) at 12.6 to 19.6 Mev, excitation functions for, (E), 19: 6669
neutron reactions (n,2n) at 14 Mev, shell effects in, (T), 19: 12536
neutron scattering by, gamma decay of excited levels following, 17: 2243(R) (TID-17083)
nitrogen ion reactions at 44 and 52 Mev, Coulomb excitation in, 18: 7718
nuclear deformations in, oscillator model for, 18: 28731
proton elastic and inelastic scattering at 4.9 to 7.5 Mev, isobaric analog states of strontium-89 in, (E/T), 20: 38076
proton reactions (p,n) and (p,p) at 4 to 5.5 Mev, compound resonances from, 18: 15287
proton reactions (p,αn), Q values for, 18: 27832(R) (ORNL-TM-530(Rev.))
proton reactions (p,n) at 14.2 Mev, angular distributions, Q values, and spectra from, (E), 20: 13345(R) (NP-15772)
proton reactions (p,n) at 4.6 to 5.3 Mev, excitation functions and angular distributions for, (E), 20: 26094 (ORNL-P-2117)
proton reactions (p,n) at 14.2 Mev, Q-values and differential cross sections for, (E/T), 20: 34520 (INSJ-97)
proton reactions (p,γ) with, gamma decay of analog resonances in, (E), 20: 42331
proton reactions (p,n), 16: 4741(R) (TID-14157)
proton reactions (p,γ) in stars, 16: 12308
proton reactions (p,n), thresholds in, 16: 15681
proton reactions (p,n) at 19.2 Mev, isomeric states from, 16: 32441
proton reactions (p,n) at 40 to 150 Mev, excitation functions of, 17: 24426
proton reactions (p,n) at 11.2 Mev, cross section for, 17: 40056
proton scattering by, energy level studies from, (T), 20: 19826 (MIT-2098-229)
yttrium-88 mass difference, 16: 7078

STRONTIUM ISOTOPES Sr-89

accumulation by plants, genetic factors in, 17: 27055
accumulation in barley and wheat grain, effects of genotype and calcium content on, 18: 21789
activity measurements, absolute, 16: 6604
beta decay, internal bremsstrahlung from, 16: 28110
beta decay of, internal bremsstrahlung from, 18: 34837
beta dose determination, 16: 2077
beta dose from spherical particles of, calculational models for, 19: 40635 (NUS-217)
binding of, to bone tissue in guinea pigs, effects of chemical agents on, 17: 12108
contamination of food chain by, from fallout, 18: 39501
contamination of food by, after radiation accident, 19: 46694
content and distribution in suspended matter in seaweed, 20: 612
content in air and rain, up to 1964, 19: 7696 (AERE-R-4687)

content in air, bones, food, soil, and water in Italy, 1962, 18: 18040 (BIO/03/63)
content in alfalfa, bone, cheese, grass, milk, and wine in France, 1958-59, 16: 19194
content in animal bones, fallout, grass, and milk in Italy, Jan.–June 1962, 17: 36024 (BIO/26/62)
content in animal and human organs, effects of calcium on, 17: 24876
content in animals and plants in Sedan fallout field, 19: 43662(R) (UCLA-12-565, pp 97-128)
content in atmosphere, soil, and food in U. S., 1963 to 1965, 20: 18980
content in atmosphere after Chinese atmospheric tests, 20: 23344 (AEET-240)
content in atmosphere, milk, and surface waters near Canadian reactor installations, March 1966, 20: 33556 (NP-16124)
content in atmosphere from underground nuclear explosion, effects of filtering on, 20: 45833 (UCRL-14778)
content in beef roasts, effects of bone on, 16: 17934
content in biosphere and uptake by man, 17: 23564
content in biosphere of, from fallout, 1959 through 1962, 19: 9367 (IAEA-R-1)
content in blood and bone of rats, age and sex dependence of, 17: 10347
content in blood plasma of cows and goats, method for establishing, 18: 19541
content in breast and cow's milk in Canada, 17: 21943
content in Canadian fallout, 10-year dose accumulation from, 18: 13575
content in cow's milk, 18: 23829
content in diet and milk in United Kingdom, 19: 24783
content in diet in U. S., 1961 through 1964, 20: 18920
content in diet, 1964, 19: 22554
content in drinking water in Italy, 19: 42637 (BIO/32/63)
content in environment of Hunterston reactor in Scotland, 18: 8249
content in environment in Greenland in 1963, 19: 6100 (RISÖ-87)
content in environment, 1962 to 1964, 19: 9370 (NP-14556(p.11-80))
content in European milk, 1962, 19: 18143 (EUR-1838.d.f.i.n)
content in fallout in U. S., 18: 43818
content in fallout particles, 20: 2053
content in fallout at 156 world land sites, 1957 to 1965, 20: 16662(R) (HASL-165)
content in fallout and precipitation near Leningrad, 20: 16704
content in fallout from Project Sedan, 20: 25287
content in fallout in Japan, 1965, 20: 31405
content in fallout from USSR nuclear test, Jan. 1965, 20: 39108
content in Finnish milk, 1960 through 1965, 20: 41134 (SFL-A3)
content in food animals, 18: 3618
content in food and milk from EURATOM countries, 1963, 20: 144 (EUR-2460.d,f,i,n)
content in food in U. S., 18: 43818
content in food in Amsterdam, 1960 to 1963, 20: 20949
content in food, protective-action guides for, 20: 45986
content in foods, 20: 9206
content in foodstuffs in United Kingdom, 1961 and 1962, 17: 7785 (ARCRL-8)
content in foodstuffs in Great Britain, 1962, 18: 15735(R) (ARCRL-10)
content in German cheese, Sept. to Nov. 1961, 18: 6984
content in German milk, effects of precipitation on, 20: 11017
content in German rye and wheat, effects of precipitation on, 20: 11017
content in grass, 19: 38332
content in ground-level air along 80th meridian (west) during 1961, 17: 14477 (NRL-5869)
content in herbage, milk, plant-base, and soil in nuclear power plant environments in England, 18: 6775
content in inhaled air, maximum permissible, 17: 6331
content in Lake Huron and Ottawa River, 20: 14738 (NP-15853, pp 21-33)
content in milk after nuclear accident, 20: 18969
content in milk and rain in New Zealand, 17: 4690(R) (DXRL-F5)
content in milk and rain in Fiji Islands, 17: 4690(R) (DXRL-F5)
content in milk and plants before and after Salmon Event, 20: 16743 (VUF-1021)
content in milk, effects of farming practices on, 18: 3624
content in milk from cows on fallout-contaminated pastures, 18: 6973 (NP-13432)
content in milk in Germany, Sept.-Nov. 1961, 17: 34166
content in milk in Iowa, 18: 14138
content in milk in Japan, Nov. 1961 to Oct. 1962, 19: 7707
content in milk in Canada and U. S., 1964, 19: 22557
content in milk in Boston, 19: 28599
content in milk in Italy, 19: 42637 (BIO/32/63)
content in milk in Canada, March 1965, 20: 7305 (NP-15641, pp 9-21)
content in milk in Canada, August 1965, 20: 7310 (NP-15642, pp 20-32)
content in milk in Italy, 1962 and 1963, 20: 9150
content in milk samples collected in U. S. and Canada, 1961 and 1962, 18: 461
content in milk samples from U. S., 1964, 19: 7712
content in milk, Aug. 1964, 19: 22552
content in milk, in Germany, 20: 524
content in milk, 1964, 19: 9368 (NP-14459)
content in organisms and water of Mediterranean Sea, 1962 to 1964, 19: 24721
content in pasteurized milk samples collected in U. S. and Canada, 1963, 18: 12398
content in rain at Fayetteville, Arkansas, 19: 40785 (TID-21224)
content in rain at Tokyo four weeks after Chinese nuclear explosion of May 14, 1965, 20: 5656
content in rain in Fayetteville, Arkansas, 1962 and 1963, 18: 39485 (CONF-337-43)
content in rain water in New Zealand, 17: 5750(R) (DXRL-F6)
content in rain water, Fayetteville, Arkansas, Oct. 1964, 20: 16663 (TID-21470)
content in rain water, Pennsylvania, 1962, 20: 45901
content in rain water and air in Great Britain, 1960 to 1961, 16: 394 (AERE-R-3766)
content in rainwater at Ispra during 1963 and 1964, 19: 34373
content in rivers in Japan from fallout, 18: 1931
content in sintered uranium dioxide pellet, radial distribution of, 20: 4472
content in standard diet in Germany, 19: 44313
content in stratosphere, from Soviet nuclear tests, 16: 13401
content in stratosphere in 1961 and 1962, (E), 19: 5061
content in stratospheric and tropospheric air filter samples collected in 1961 and 1962, 19: 9755 (HASL-153)
content in stratosphere, 19: 20657(R) (DASA-1309)
content in stratospheric and tropospheric samples in Project Star Dust, 1964, 20: 16728(R) (HASL-169)
content in stratospheric and tropospheric samples in Project Star Dust, 1963, 20: 16727(R) (HASL-168)
content in stratosphere and troposphere from Chinese nuclear test, 20: 27155
content in surface waters near Canadian reactors, 20: 7306 (NP-15641, pp 22-9)
content in Swedish food, 1962, 18: 23790 (NP-13828)
content in teen-age diet in U. S., 1963, 18: 37446 (TID-21081)
content in total teen-age diet in U. S., 1963, 19: 9416
content in U. S. milk, 1962, 19: 11450
content in U. S. milk, 1963 and 1964, 19: 18160
content in vegetation in Italy, 1961, 17: 27591 (EUR-223.i)
content in water supplies following nuclear warfare, 19: 42658 (NP-15328)
content in water supplies in Connecticut, 17: 18426
content in water, maximum permissible, 17: 39311(R) (ORNL-3492 (p.157-75))
content in waters near Canadian reactors, April 1965, 20: 41136
content in whole milk and Winnipeg River water in Canada, August 1965, 20: 7311 (NP-15642, pp 33-45)
content in Winnipeg River, 18: 18038 (AECL-1874)
content of, in milk samples collected in U. S., 1963, 17: 41079
content of, in osteosarcoma in dog, 18: 29436(R) (COO-119-229(p.152-69))
content on plants in Sedan fallout field, 20: 7318 (PNE-238F)
contents in fallout at U. S. and world sites, 19: 9365(R) (HASL-155)
cycling of, in a forest ecosystem, 19: 1995(R) (TID-21302)
decay and half life, 16: 29819
decay and half life, 17: 17298
decay of, correction factors for, 17: 24384 (AERE-R-4237)
deposition in chick embryo bones, effects of tetracycline, 17: 19799
deposition in chick bone, effects of calcium and strontium stable carriers on, 18: 13427
deposition in hen eggs, 16: 20109
deposition in Japan, 1957 to 1961, 18: 16214
deposition in precipitation at Westwood, New Jersey, 19: 7701 (NYO-2415-12)
deposition rates and concentration in Pittsburgh precipitation, 17: 18328 (NSEC-89)
deposition, in bone, effects of dietary levels of calcium and strontium, 17: 23061
detection and measurement in fallout from Chinese tests, 20: 25288
determination and sampling procedures for fall-out, 16: 11976 (NYO-9530)
determination in air samples, 16: 6639 (DASA-1300(Vol.1))
determination in air by beta measurement, efficiency of counter for, 19: 20169
determination in algal cells by liquid scintillation, 20: 1603
determination in atmospheric and precipitation samples, methods for radiochemical, 20: 14430 (AD-620219)
determination in animals and plants in presence of calcium-45, strontium-90, and yttrium-90, 20: 25623
determination in atmospheric precipitation, 20: 35448
determination in biological materials, radiochemical, 19: 19739 (AERE-

AM-101)
determination in bones, diet, fallout, milk, plants, urine, and water, methods for, 20: 24980 (SZS-2(1966))
determination in Canadian milk samples, 1963, 18: 12386 (NP-13599)
determination in decay mixtures, computer program for, 19: 32110
determination in environmental samples, 20: 40809 (NP-16235)
determination in French air and rain water, 18: 4036
determination in fresh water basins, radiochemical, 18: 33769 (NP-14091)
determination in food and water, methods for, 18: 35471
determination in food, 18: 35780
determination in foodstuffs in Germany, 1961, 18: 37390
determination in fallout in California, winter, 1961 and 1962, 18: 39498
determination in food, milk, and water, 19: 13232
determination in fallout particles, 19: 17821
determination in food, radiochemical, 19: 24792
determination in food and water, gamma spectrometric, 20: 31180
determination in herbage and milk, method for, 18: 39087
determination in human excreta, estimation of body burden by, 19: 24473
determination in low-activity samples, spectrometric, 18: 43424
determination in mixed fission products, radiochemical, 16: 2988
determination in milk, radiochemical, 17: 21453
determination in milk, radiochemical, 17: 21455
determination in milk after ion exchange separation, 18: 43719
determination in mixture with strontium-90 and yttrium-90 using semiconductor detector, spectrometric, 19: 32111
determination in milk, solid foods, and water, methods for, 20: 16369
determination in natural water reservoirs, rain water, and snow using electrodialysis and gamma spectroscopy, 19: 19809
determination in pitchblende, uranium, and uranyl nitrate, radiochemical, 18: 12025
determination in presence of strontium-85, radiometric, 19: 17820
determination in presence of strontium-90 by paper electrophoresis and beta counting, 19: 36285
determination in presence of strontium-90, beta counting technique for, 20: 31188
determination in reactor effluents, methods for, 17: 35627(R) (AFSWC-TDR-62-146)
determination in rain, radiochemical, 19: 7327
determination in rain water, radiochemical, 19: 30071 (AERE-AM-100)
determination in rainwater, 19: 38852
determination in samples of water, soil, vegetation, and human diet from Greenland, 1962, 18: 6948 (RISO-65)
determination in simulated high-altitude radionuclide samples, radiometric, 19: 13203(R) (NYO-3276-8)
determination in sea water, methods for, 20: 1749 (USNRDL-TR-912)
determination in water, milk, diet, soil, and air samples collected in 1962 and 1963, 18: 6944(R) (HASL-142)
determination in water supplies, chromatographic, 18: 39131
determination in water supplies, 19: 324
determination of bomb-produced, in lower stratosphere, 17: 32759
determination of, in stratosphere, 17: 6271(R) (NYO-10464)
determination of, in biological materials, review of methods for, 17: 23274
determination of, in diets of teenagers and infants throughout U. S., 1962, 18: 1969
determination of microquantities of, precipitated with zinc tetrathiocyanatomercurate(II), 20: 20619
determination of, radiochemical, 18: 8281 (NYO-4700(Rev.))
determination of, radiochemical, 18: 8286(T) (AEC-tr-6049(p.22-46))
determination of, radiochemical, 18: 8288(T) (AEC-tr-6049(p.75-99))
diffusion from irradiated molybdenum–rhenium–tungsten alloy, 19: 44599(R) (GEMP-50A)
diffusion from melted beryllium oxide–uranium dioxide fuel, 17: 26779 (TID-7641(p.148-54))
diffusion from pyrolytic carbon-coated fuel particles, 19: 39228 (BMI-1734)
diffusion from sodium at 900 to 1500°F, 18: 37064 (NAA-SR-Memo-8712)
diffusion in irradiated artificial graphite, 18: 632
diffusion in irradiated Zircaloy-4 at 800°C, 20: 21232 (BMI-1763)
diffusion in soil, effects of electric field on, 20: 11053
diffusion in soil, effects of compaction on, 20: 18816
diffusion of, from irradiated uranium carbide–zirconium carbide, 17: 33272
diffusion of, from impregnated graphite shells of fuel elements, 17: 33273
diffusion of gaseous, from lightly irradiated uranium at 1000 to 2200°C, 17: 35076 (AERE-R-4342)
discrimination from calcium-45 in diet, 16: 8508
dispersion and movement in soils, mechanism of, 20: 20875 (EUR-2481.f)
distribution and volatility in air-burst debris, 20: 9184 (USNRDL-TR-933)
distribution between active manganese dioxide and aqueous solutions, 16: 27015
distribution between core and recombiner of L54 water-boiler reactor, 18: 11492
distribution from nuclear excavation in basalt, 20: 613
distribution in bone tumor sites in mice, 16: 32785
distribution in bone, correlation with bone tumors, 17: 5729
distribution in fallout deposition at world-wide HASL cooperating stations, 16: 24012(R) (HASL-127)
distribution in food, 18: 3605
distribution in food chain, effects of transfer from food to milk of cattle on, 20: 4162
distribution in forest ecosystems after tree inoculation, 20: 12566 (COO-1006-4)
distribution in rats and dogs after inhalation or intratracheal introduction, 17: 40510
distribution in sea water, from waste disposal, 20: 38537
distribution in skeleton of mice and rats, 16: 7395
distribution in soils at Eurochemic site in Belgium, 16: 34144(T,R) (EURAEC-275)
distribution in surface air, hemispheric variations in, 19: 32484
distribution of, in rats, effects of age, diet, and chemical agents on, 17: 12107
dosimetry of, for human fetuses and infants, 20: 43605
effects of injected, on blood picture, 16: 16237
effects of injected, on bone marrow in rats, 17: 30388
effects of injected, on blood picture and blood serum protein content in rats, 19: 33779
effects of injections and transperitoneal administration on digestive organs in mice, 16: 14502
effects of internally deposited, in animals and man, 19: 34945 (NP-15184)
effects of radiation from ingested, on reproduction and development of insects, 17: 76
effects on animal and human organs, 17: 24876
effects on bacteria in sewage processing, 18: 27732
effects on blood and hematopoietic tissue, 20: 28982
effects on bone marrow of mice, splenic mechanism for control of blood cell populations following, 20: 45424
effects on bone, cancerogenic, 16: 7395
effects on determination of strontium-90 in waste solutions, 19: 46196
effects on dogs and rats, 17: 40510
effects on function and structure of pancreas, of injected, 19: 40358(T) (FTD-TT-65-48, pp 577–8)
effects on microflora of sewer water biofilters, 18: 19451(T) (JPRS-23903)
effects on rat bones, tumorigenic, 19: 3917
effects on rat pancreas, 18: 38838
effects on submicroscopic cell structure of bone marrow in rats, 18: 36972
effects on the dairy industry, review of countermeasures for, 18: 3894
electric power production capabilities in nuclear batteries, 18: 825
elimination, effects of magnesium, 16: 9834
elimination from bone, dietary factors, 16: 33316(R) (TID-16769)
elimination from body in laying and non-laying hens, 19: 10770
elimination from rat skeleton, effects of experimental rickets on, 16: 11415
energy levels, 16: 14009
energy levels, 18: 15227
energy levels, determination of neutron, 16: 21495
energy levels of, parity and spin of, (T), 20: 19826 (MIT-2098-229)
energy levels of, analogs in yttrium-89, 20: 38076
energy of, from 23-Mev deuteron fission of uranium-238, 17: 11646 (UCRL-10193)
energy-level density and transitions, (E), 20: 42331
exchange between macrophytic algae and sea water, kinetics of, 20: 45899
excretion by goats, effects of dietary calcium and strontium on, 20: 40568
excretion by organisms, 16: 11420
excretion by rats, 17: 24869
excretion by rats, effects of dietary magnesium, calcium, and phosphorus on, 19: 31757
excretion by ruminants, effects of hydrobiotites on, 18: 11610
excretion of, by rats, effects of cyclohexanediaminotetraacetic acid on, 18: 4998(T)
exposure to, maximum permissible occupational, 18: 15907
fallout levels in United Kingdom, 18: 27706
fallout of, effects of test ban on, 18: 43815
fixation by bone, effects of fluoride, 16: 28722
formulae for assessing body content of, following contamination in adult human males, 20: 42779
genetic control of accumulation in barley and wheat, 20: 40532(R) (COO-1097-17)
global circulation following Chinese nuclear explosion of May 14, 1965,

20: 5656
half life, 20: 8076 (NP-15663)
half life and metabolism of, 20: 38743
half life of, search for isomers in measurements of, 17: 17243
half life of, determination by direct decay, (E), 19: 37847
inhalation in emergency, calculation of acceptable limits for, 16: 9054
leaching from vegetables, 19: 45758 (NYO-2598-24)
measurement in Hungarian rain, from Oct. 1962 to Dec. 1963, 19: 9758
metabolism and body burden of fallout, in man, 1962 to 1964, 19: 9370 (NP-14556(p.11-80))
metabolism by barley seedlings, effects of genotype, 19: 42244 (TID-22106)
metabolism by cattle, effects of diet on, 20: 4162
metabolism by chickens, effects of age and dietary calcium on, 19: 3837(R) (ORO-625(p.86-92))
metabolism by chickens, nutritional and endocrine factors in, 19: 8763
metabolism by dairy cattle, 19: 3836(R) (ORO-625(p.70-85))
metabolism by domestic animals, 19: 24246
metabolism by fresh water algae, fish, and invertebrates, 19: 8740(R) (IAEA-R-37-5)
metabolism by Japanese eel, *Anguilla japonica*, effects of calcium content of environmental water on, 19: 2035
metabolism by marine organisms, 19: 43669(R) (NP-15159)
metabolism by plankton, 18: 35238 (STI/DOC/10/28(p.9-20))
metabolism by plants, 19: 6104
metabolism by plants, 19: 10772
metabolism by rat bones, effects of sodium alginates on, 20: 3671
metabolism by vegetables, 19: 45758 (NYO-2598-24)
metabolism, effects of dietary levels of stable strontium, 16: 28714
metabolism in bones of rats treated with testosterone, 17: 10348
metabolism in bones in chicken embryos, 20: 32909(R) (ORO-648, pp 91-102)
metabolism in chickens, 19: 6973
metabolism in chickens, 19: 45761(R) (ORO-631, pp 122-31)
metabolism in dental caries of rats, 19: 31720
metabolism in domestic animals, 18: 11645(R) (ORO-614)
metabolism in lactating cows, 16: 10347
metabolism in live mice, design of radiation detectors for measuring, 20: 36556
metabolism in mice after liquid aerosol inhalation, effects of hexametaphosphate on, 19: 2019
metabolism in rat bone, effects of dietary algenates on, 19: 21841
metabolism in rats, effects of complexing agents on, 19: 40344
metabolism in rats after oral or intravenous administration, 19: 40321
metabolism in rats after oral administration of mixed uranium fission products, 19: 40322
metabolism in rice plants, 19: 12912 (NP-14761)
metabolism in swine, 18: 38775(R) (ORO-624)
monitoring for, in foods, 17: 17750
monitoring in California fallout in winter 1961 to 62, 18: 10284
monitoring in milk in Canada from fallout, 18: 16229 (NP-13760)
monitoring in River Thames, 17: 35440
movement in Belgian soils, 19: 10659(R) (EURAEC-703)
movement in calcareous soils, 20: 40524(R) (TID-23271)
movement in soils, Belgian studies on, 18: 17341
movement in soils, effects of strontium acetate on, 20: 32925
penetration into intact plants, 17: 2811(R) (TID-17045)
precipitation of, with titanium dioxide hydrate, 17: 14271
preparation of Decalso glass sources of, 18: 34007(R) (ORNL-TM-890)
production in nature by spontaneous fission, 19: 10372
production of carrier-free, by solid solutions, 16: 24084
radiation effects on absorption in swine intestine of, 18: 38775(R) (ORO-624)
radiation effects on swine metabolism of, 19: 5699
radiation effects on metabolism of, in dairy cattle, 19: 43801
radiation effects on metabolism of, in pigs, 20: 32907(R) (ORO-648, pp 62-70)
radiation hazard from atmospheric, calculation of, 20: 31528
radiation hazards from fall-out, through 1961, 16: 30675 (LADC-5370)
radiation hazards to populations from fallout, 18: 27714
radiation hazards of, released by accident, 19: 46696
radiation protection standards for atmospheric, 19: 38877 (NP-15183)
radioactivity and yield from uranium fission, gravimetric method of determining, 18: 27288 (KFK-199)
ranges of thermal-fission, in aluminum, (E/T), 20: 24351(R) (MIT-905-52, pp 1-41)
ranges of uranium-235 fission-recoil, in aluminum, 17: 36651 (EFINS-62-71)
ranges of uranium-238 proton fission-recoil, in aluminum, 17: 36651 (EFINS-62-71)
ratio to strontium-90 in fallout, effects of sampling height on, 19: 7709
removal from mouse skeleton, compounds for, 19: 29999
removal from plant leaves in dry conditions, 17: 33538
removal of skeletally bound, by dietary phosphorus and magnesium, 19: 21845
retention by grass, 19: 38332
secretion in cow and goat milk, 16: 8505
separation by calcium phosphate–humic acid flocculation, 18: 24982
separation from aqueous solutions by countercurrent extraction in foam columns, 19: 18055
separation from aqueous solution by sorption on diatomaceous earth, 20: 12938
separation from calcium-45, selective precipitation, 17: 1544
separation from cerium-144 and cesium-137 by ion exchange on tin phosphate, 18: 13922
separation from dodecylbenzenesulfonate solutions, 17: 10741(R) (ORNL-TM-313)
separation from drinking water using natural sorbents, 19: 24424
separation from fission products solution for radiochemical determination, 19: 19745 (CEA-R-2712)
separation from laboratory radioactive waste waters by contact precipitation, 19: 5564
separation from milk by ion exchange, 19: 7710
separation from milk by electrodialysis, 20: 1972(P)
separation from milk using calcium phosphate precipitation method, 20: 16382
separation from other short-lived uranium fission products, chromatographic, 18: 39393
separation from rain water, use of tracers in filters for, 17: 30184
separation from rain water, method for, 20: 1778
separation from radioisotopes in aqueous solutions by foam chromatography using colloidal manganese dioxide, 20: 20628
separation from reservoir water by phosphate precipitation, 20: 4068
separation from waste solutions by flocculation, 16: 21862
separation from water by chemical precipitation, 18: 20266
separation from waste solutions by Korean acid clay, 19: 24194
separation from waste water by ion exchange on humic acid, 19: 33678
separation from waste solutions by recycle scavenging–precipitation ion exchange process, 20: 10440 (ORNL-3863)
separation from water supplies, using sanitary water-treatment process, 20: 22512 (K-1651)
separation from waste solutions using humic acid column, 20: 36930
separation from waste-water by aerobic treatment, 20: 40483
shipping of, analysis of potential hazards in, 17: 10853 (HW-SA-2518)
sorption and mobility in beans and tomatoes, (E), 19: 10755
sorption and release of, by sediments in Guadalupe River, 20: 24832 (TID-22872)
sorption by calcium phosphate, 16: 28639
sorption by clays, 19: 9367 (IAEA-R-1)
sorption by Dowex 50-X4, glauconites, and montmorillonites, 19: 10659(R) (EURAEC-703)
sorption by glass, plastic, and rubber materials, 19: 5920
sorption by humic acids and peat, 16: 11591
sorption by intestine in rats, 19: 55
sorption by intestine, effects of sodium alginate on, in rats, 19: 3846
sorption by intestine, effects of sodium alginate on, in rats, 19: 3847
sorption by leaves of corn, effects of pH, 16: 28720
sorption by rat intestine, 19: 40
sorption by skin, protective effects of fatty acid gels, 19: 21997
sorption by soil, 17: 27602(T) (EURAEC-416)
sorption of trace amounts of, on aluminum, chrome steel, or paint films, 19: 17920
sorption rat intestine, effects of polysaccharides on, 19: 25884
state of, in blood serum, 18: 6608
stripping from dodecylbenzenesulfonate solution to foam surface, 16: 33070(R) (ORNL-TM-297)
toxic effects in dogs, 16: 11438(R) (ANL-6464(p.38-49))
toxic effects in dogs and man, 16: 28699 (TID-7639)
transfer from contaminated soil to plants, 17: 38725
transfer to cheese and whey from milk, 18: 22299
transport by sediments in streams, lakes, and estuaries, 18: 1899 (TID-19559)
transport in bean and corn plants, effects of chloranilic, malic, oxalic, and tartaric acids on, 20: 26621
transport in bean and pea plants, effects of nitrates, phosphates, and silicates on, 20: 26625
uptake and deposition of non-metabolic, in tops of bean plants, 19: 43703
uptake and distribution in eggs from chickens, 19: 10769
uptake and distribution by bones and eggs of chickens, 19: 12939
uptake and release by watercress, 16: 17434
uptake and retention by apple maggot, 19: 25863
uptake and specific activity in rat plasma and urine, 19: 31736
uptake by abscessed tissues during radiation sickness, 17: 2889
uptake by algae from water, 17: 8400
uptake by algal cells, 20: 1603

uptake by barley and wheat, effects of genotype on, 17: 13896
uptake by barley and wheat, heritability in, 19: 14975
uptake by barley of, from contaminated soils, 20: 5257
uptake by barley plants from soils, effects of strontium acetate on, 20: 32925
uptake by benthos-feeding fish from food and water, 16: 30204
uptake by biosphere, 18: 18092
uptake by bone, effects of sodium alginate on, 19: 6958
uptake by bones of children, fallout contribution to, 18: 37042
uptake by bones, effects of sodium alginate on, 20: 5253
uptake by carp, 18: 5148(T) (JPRS-21989(p.5-10))
uptake by cereal, pea, and vetch crops, effects of humus and lime on, 16: 14451
uptake by desert shrubs, 20: 12572
uptake by eggs and tissues of chickens following intramuscular and oral administration, 18: 38775(R) (ORO-624)
uptake by food plants under field conditions, 17: 40541
uptake by grapefruit trees, 18: 9752 (IA-900)
uptake by grass, milk, and soil, 18: 18045
uptake by intestine, effects of sodium alginate on, 19: 6958
uptake by milk in rabbits and rats, 19: 8766
uptake by plants, 17: 40517 (SA-PR-40(Rev.))
uptake by plants from soil in Japan, 16: 26688(T) (AEC-tr-4642)
uptake by potato roots, foliar leaching and recycling after, 18: 6594 (TID-19810)
uptake by potato tubers after foliar application, 17: 23051
uptake by rat blood and bone, 19: 40
uptake by Rumanian animal foods, 19: 640
uptake from airborne particles by infants, 19: 3855
uptake from soil by crop plants, effects of calcium content of soil on, 18: 19515 (NP-13796)
uptake from soils by plants, 18: 29192 (TID-20781)
uptake in cabbage and potatoes after aerial contamination, 18: 3610
uptake of, by potato tubers after foliar contamination, 17: 33525
uptake through trachea and distribution in bones, liver, and muscles in rabbits, 16: 4026
use in localization of metastatic bone tumors, 19: 34067
use in placental permeability studies, review of, 18: 1345
use in radiochemistry and tracer techniques, optimum counting methods for, 18: 33655
yield in epi-cadmium neutron fission of plutonium-239, (E), 19: 27585
yields from fission neutron of plutonium-239, uranium-235, and uranium-238, 16: 1037(T) (AEC-tr-4696)
yields from neutron fission of thorium-232, 18: 9311 (IS-558)
yields from photofission of uranium by 650-Mev bremsstrahlung, 20: 22040
yields from spontaneous fission of uranium-238, 17: 33109
yields in proton fission of uranium-238 at 7.1, 9.4, and 12.0 Mev, 20: 37995
yields in thermal neutron fission of plutonium-239, 19: 16873

STRONTIUM ISOTOPES Sr-90

see also Sunshine Project

absorption from gastrointestinal tract of rats, effects on anion content of salts on, 20: 8560
absorption from gastrointestinal tract of rats, effects of calcium compounds on, 20: 38569
accumulation by hydrophytes and detritus, effects on decontamination of water in reservoirs, 17: 28644(T) (JPRS-19937(p.29-37))
accumulation by vegetable crops, 19: 21844
accumulation coefficients of, in marine organisms, 18: 21780(T) (JPRS-24227)
accumulation in sea algae, 16: 4023
accumulation in soils near Leningrad, 20: 16702
activity in milk, Potsdam, Germany, 1964, 20: 35680
activity measurements, absolute, 16: 6604
activity measurements in milk in Great Britain, 20: 41186 (ARCRL-15)
activity of mixtures with yttrium-90, external emission from, (E), 19: 22400
availability of fallout, to human populations, 17: 31839
availability to man of, from flour and milk, 19: 36733
availability to plants from soils, effects of contact time and mineral type on, 20: 8584
behavior in food chains, 16: 29264
beta activity of aqueous solutions of, measurement using Cherenkov radiation, 19: 13508
beta activity of, method for measuring relative, 19: 15648 (NP-14698)
beta activity of, method for measuring relative, 19: 15649 (NP-14700)
beta and conversion-electron spectra, 20: 5768
beta angular distribution from thick-layer sources, 16: 10983
beta counting of strontium-90–yttrium-90, corrections for foil absorption in 4π, (E), 19: 26654 (EUR-2248.e)
beta decay of, scintillation performance for, 18: 5398
beta decay of, bremsstrahlung from, (T), 19: 8558 (HW-83784)
beta decay of, bremsstrahlung spectra in, (E), 20: 13761 (CONF-233 (Vol.4), pp 656-68)
beta decay of, internal bremsstrahlung in, 19: 33273
beta decay of, performance of proportional counters for low activity, 19: 30541
beta depth-dose measurement in lucite, 17: 4851
beta dose determination and effects on skin, 16: 2077
beta emission by, scintillation counter for measuring, 20: 14874
beta emission from, determination of end-point energy of, 17: 28183
beta emission from, 18: 45174(R) (MLM-1204)
beta emission of, backscattering from aluminum in 2π geometry, (E), 20: 30369
beta particles from, bremsstrahlung production by, (E), 19: 45284 (TID-22169)
beta polarization from, (E), 20: 28395
beta reactions with, x-ray emission in, (E), 19: 15849
beta sorption from, by toad skin, 19: 12915
beta spectra, 18: 30019
beta spectra from, silicon counters for measuring, 20: 29520 (CLOR-45/D)
beta spectra of, allowed and first-forbidden (E), 19: 3330
beta spectra of, effect of secondary electron emission on, 19: 23312
bibliography on chemical, nuclear, and physical properties and separation processes, 16: 3306 (MND-P-2581-I)
bibliography on properties and separation processes, 16: 5080 (MND-P-2581-III(Pt. I))
biological availability of, in calcined waste solutions, 19: 32467 (IDO-12042)
biological effects, statistical analysis of data, 16: 1564
biological effects from fall-out, survey, 16: 27493
biological effects, 18: 12402
body burden and urinary excretion in man, measurement of, 19: 25902
body burden in man, method for assessment of, 19: 26612
body burden of, maximum permissible, 19: 46634 (AD-423463)
body burdens in man, review of methods for estimating, 20: 32
bone tumors induced in mice by injected, effects of infection on incidence of, 20: 5373
book: *Distribution of Some Radioactive Elements in Animal Organisms*, 16: 2884
bremsstrahlung efficiencies in mammals, effects of size on whole-body, 18: 29196(R) (COO-119-229(p.170-85))
bremsstrahlung excitation by, in thin absorbers, 20: 5000 (ORNL-IIC-5, pp 91-8)
calibration of standard solutions, 17: 10299(R) (COO-226(p.66-70))
chromatography of source of, gas, 18: 27812(R) (ORNL-TM-415)
concentration and distribution in soils, 20: 41139
concentration by fish, 17: 33565
consumption in diet in selected U. S. cities, Nov. and Dec. 1963, 19: 637
containment of, 16: 25651 (HW-71574)
contamination of eggs by, penetration and internal distribution, 20: 40559
contamination of food by, hazards to man from, 17: 12503
contamination of food by, from fallout, 17: 17745
contamination of food chain by, from fallout, 18: 11559(R) (TID-19977)
contamination of food-chains by, protective measures against, 18: 12402
contamination of food by, 1954 to 1964, 18: 31083 (HASL-147)
contamination of food chain by, from fallout, 18: 39501
contamination of food by, 1963 through 1965 (E/T), 19: 695 (TID-21239)
contamination of food chain by, from fallout, 19: 20240
contamination of food by, after radiation accident, 19: 46694
contamination of human diet by, 19: 2186
contamination of pig skin by, 18: 4953
contamination of rabbit skin by, 18: 12392
content above and on surfaces of land and sea, 20: 31421
content and cycling of, in Atlantic Ocean, 1956 to 1960, 17: 33554
content and diffusion in oceans, 20: 43541
content and distributions in soils, 19: 22548
content and distribution in soils of Moscow region, 19: 22549
content and distribution in Chukchi Sea, Alaska, 19: 36655
content and distribution in Clinch and Tennessee Rivers, 19: 42238(R) (ORNL-3721(Suppl.1))
content and distribution of, on surfaces of the Atlantic, Indian, and Pacific Oceans, in 1965, 20: 23301
content and distribution in water and biological materials, Lake Haruna, Japan, 20: 24835
content and distribution in monkey skeletons after intravenous and oral administration, 20: 28896
content and distribution in oceans, 20: 29405 (NP-14694)
content and distribution in Atlantic Ocean and adjoining seas, 1963-64, 20: 43540
content and effects in animal and human organs, effects of calcium on, 17: 24876
content and soluble and insoluble fractions in rain water, USSR, 1964, 20: 7270

content in air and rain water at Los Alamos, 1958 to 1963, 19: 625 (LAMS-2878)
content in air and rain, up to 1964, 19: 7696 (AERE-R-4687)
content in air on Hayes Island, 1960–61, 19: 20157 (NP-14697)
content in air, rain water, grass, sea water, sea plants, animal bone, and human milk in Denmark, 18: 5479 (RISO-63)
content in air, bones, food, soil, and water in Italy, 1962, 18: 18040 (BIO/03/63)
content in air, bones, milk, and rain water collected in Great Britain, 1962, 20: 45909
content in air, fallout, human bone and diet, milk, and rainwater in Japan, 20: 25321 (NP-16036)
content in air, food, soil, and tissues, 1964, 19: 30400(R) (ANL-6971 (p.83-8))
content in air, soil, hay, milk and water in Switzerland, 1963, 20: 43519
content in Alaskan water supplies, 1963, 19: 18164
content in Alaskan Arctic biota, 1959 to 1965, 19: 40780 (BNWL-SA-242)
content in Alaskan deer, 1963 and 1964, 20: 10535(R) (BNWL-122, pp 176-80)
content in Alaskan forage plants, 1963 and 1964, 20: 10535(R) (BNWL-122, pp 176-80)
content in alfalfa, bone, cheese, grass, milk, and wine in France, 1958-59, 16: 19194
content in animal bones, fallout, grass, milk, soil, and water supplies in Italy, Jan.–June 1962, 17: 36024 (BIO/26/62)
content in animal and human bone tissues, 19: 15001
content in animals and vegetation in Northern Alaska from fallout, 17: 27053 (HW-SA-3050)
content in animals and plants of Lapland, 18: 20213
content in animals, drinking water, milk, and plants from nuclear testing, 18: 31760
content in animals and plants in Sedan fallout field, 19: 43662(R) (UCLA-12-565, pp 97-128)
content in animals, birds, bones, foods, grass, rain water, sea water, and soils in Faeroe Islands, 1964, 20: 7320 (RISO-108)
content in animals, diet, plants, rain water, sea water, and soil in Greenland, 1964, 20: 7321 (RISO-109)
content in animals, birds, fish, and plants in region of Cape Thompson, Alaska, 1959 to 1962, 20: 7319 (PNE-480)
content in Antarctic snows, 1939–1961, 19: 11400
content in antlers and bones of Colorado mule deer, 20: 16724 (COO-1156-12)
content in Arctic vegetation, 18: 18047
content in Arctic animals and plants, 18: 36916 (A/CONF.28/P/738)
content in Atlantic Ocean and Black Sea, 16: 26935
content in Atlantic surface waters, 1959–60, 17: 10835
content in Atlantic Ocean surface waters, 1961, 20: 31418
content in atmosphere over Atlantic Ocean, March 8 to July 2, 1961, 17: 31844
content in atmosphere, inventory, 18: 39486 (CONF-337-44)
content in atmosphere, 1954 to 1963, 19: 38861
content in atmosphere, Japan, 1964, 19: 42639 (NP-15278)
content in atmosphere and rain water in Los Alamos, New Mexico, 1963 to 1964, 20: 7301 (LA-3382)
content in atmospheric dust and rain water, 1964–65, 20: 16660 (AERE-R-4997)
content in atmosphere, milk, rain water, water supplies, and wheat in Japan, 1964, 20: 16731 (NP-15883)
content in atmosphere, soil, and food in U. S., 1963 to 1965, 20: 18980
content in atmosphere in Antarctica, 20: 27152
content in atmosphere, milk, and surface waters near Canadian reactor installations, March 1966, 20: 33556 (NP-16124)
content in atmosphere over Spokane, Washington, after Chinese nuclear explosion in May 1965, 20: 33573
content in atmosphere, 1956-60, 18: 8523(T) (AEC-tr-6049(p.202-24))
content in Australian human bones and diet in 1959 and 1960, 16: 7781
content in Australian environment, 1964, 20: 33566
content in average U. S. diet, 1964, 20: 33586
content in Balkan Mountains from fallout, 19: 15800
content in Baltic Sea, 19: 38901
content in Baltic herring, 1965, 20: 41134 (SFL-A3)
content in beef from U.S., 1960 through 1962, 18: 10332
content in biosphere and uptake by man, 17: 23564
content in biosphere of, from fallout, 1959 through 1962, 19: 9367 (IAEA-R-1)
content in biosphere, 1965, 19: 45748(R) (TID-22193)
content in biosphere and man from fallout, 20: 6714
content in biota of Doe Run, Ky., 1959 to 1965, 20: 20884(R) (TID-22815)
content in birds, in Italy, 19: 15763
content in Black Sea, 17: 1631 (A/AC.82/G/L.703)
content in Black Sea surface waters in 1959-1961, 19: 13630 (NP-14796)
content in Black Sea, 1960–1964, 20: 45227
content in blood and urine of Finnish Lapps, 20: 27206(R) (NYO-3446-5)
content in blood and human hair, relation to dietary intake, 20: 45299
content in blood plasma and excretions in humans on low-calcium diet, 18: 1362
content in body after occupational exposure, 16: 5153 (A/AC.82/G/L.654)
content in body and excreta of man from long-term occupational exposure, 19: 26610
content in body and urine of Japanese, 20: 16226 (NP-15891)
content in body, measurements of, in Federal Republic of Germany, January to March 1962, 17: 15624
content in body of watch-dial painters, 16: 27501
content in body, correlation with fallout rate and ground deposition, 19: 11426
content in bone ash from female sheep and fetuses, 16: 17430 (A/AC.82/G/L.756)
content in bone in Great Britain, 1963, 19: 20170
content in bone in Japan, 1961 through 1963, 19: 44266
content in bone of leukemia patients, 17: 33494
content in bone samples collected in Great Britain, 1963, 18: 25735
content in bone samples collected in Poland, 1958 to 1961, 18: 37467
content in bone samples, Great Britain, 1964, 19: 38863
content in bone samples in Australia, 19: 46595
content in bone samples collected in 1964, 20: 33592
content in bone samples in Great Britain, 1965, 20: 39163
content in bone tissue, cabbages, flour, milk, precipitation, and soil of Australia, 1962, 18: 39493
content in bone, in Denmark, 20: 5651 (RISO-107)
content in bone, milk, and soil, 1964, 19: 9368 (NP-14459)
content in bones and milk in Poland, 1959, 16: 6626(T) (GAT-Z-5022)
content in bones and testicular tissues in children and infants in Germany, 1958 to 1960, 16: 11984
content in bones and diet of young children in Argentina, 17: 23038(R) (TID-18649)
content in bones and diet of Argentine children, 19: 20165(R) (TID-21711)
content in bones, food, milk, river water, and tea leaves in Japan, 16: 26688(T) (AEC-tr-4642)
content in bones, food, lake waters, plants, and soil in Italy, 1961, 17: 27591 (EUR-223.i)
content in bones from yearling deer collected between 1950 and 1961, 17: 33548
content in bones in children and fetuses in Denmark, 1961–1962, 18: 12351
content in bones of humans, 17: 8463
content in bones of domestic animals, Japan, 1957 to 1962, 17: 32300
content in bones of cattle, sheep, and swine, species and individual bone differences in, 18: 33240
content in bones of children in Great Britain, 1961 and 1962, 19: 34370
content in bones of adults, effects of diet strontium-90 content on, 19: 45793
content in bones of children in Great Britain, 20: 5415
content in bones of children in U. S., 1965, 20: 16662(R) (HASL-165)
content in bones of children in Argentina sampled in 1965, 20: 39150(R) (NYO-2753-4)
content in bones of yearling deer, 20: 40541(R) (UCD-34P104-3)
content in bones of babies and placenta, 17: 27033
content in bones sampled through 1964, 20: 33594
content in bones sampled in 1965, 20: 41131(R) (HASL-172)
content in bones, effects of age, 19: 33750
content in bones, effects of age on, 19: 38850
content in bones, effects of age on, 19: 44250 (NP-15269)
content in breast and cow's milk in Canada, 17: 21943
content in bulk milk samples in Amsterdam, Holland, 1960-61, 16: 33336
content in cabbage, potatoes, soybeans, and wheat in United States, 1959-60, 16: 17928
content in Canadian wheat, 16: 5148 (CRER-1000)
content in Canadian fallout, 10-year dose accumulation from, 18: 13575
content in Canadian wheat, 1962, 18: 14148
content in Canadian cereal grains, 18: 39537
content in Canadian milk samples, Feb. 1965, 19: 34366 (NP-15079 (p.17-27))
content in Canadian wheat, 1964, 20: 14736 (NP-15853, pp 3-7)
content in Canadian fallout, October 1965, 20: 14737 (NP-15853, pp 8-20)
content in Canadian man and milk, 1960 to 1964, 20: 23390
content in Canadian wheat, 1963, 20: 33588
content in Canadian milk and wheat, 1966, 20: 41198 (NP-16192)
content in Canadian milk, April 1965, 20: 41209
content in caribou, reindeer, and man, effects of diet on, 20: 31442 (BNWL-SA-661)
content in cattle bones, soil, and grass in USSR, 18: 27030
content in central Pacific Ocean, 1961, 20: 31414
content in central Pacific Oacean, 1962 and 1964, 20: 31416

content in cheese and dried milk in Austria, 1960–61, 17: 18432
content in children's teeth, regional variations in, 20: 32913
content in children's teeth, relation of diet and atmospheric radioactivity to, 20: 32913
content in clam shells, 16: 21889
content in clams in Clinch and Tennessee Rivers, 16: 23410 (ORNL-TM-270)
content in clay minerals and soils, effects of stable calcium and strontium on, 18: 43797
content in Clinch and Tennessee Rivers from ORNL, 18: 21697
content in Clinch River, 20-year analysis of, 20: 40479 (ORNL-P-2328)
content in Clinch River from ORNL waste solutions, 20: 45223
content in coastal waters of Japan, 1960 and 1961, 19: 30417
content in Colorado River, 19: 26549
content in Colorado deer, 20: 20384 (COO-1156-13)
content in Columbia River plume, 20: 11023
content in commercial marine animals, effects on radiation levels of food-chain, 19: 17453(T) (JPRS-28560)
content in contaminating solutions, effects on degree of surface contamination, 19: 9422
content in contaminated, whole-body, 20: 46031(R) (AERE-PR-HPM-9, 17-26)
content in cows' and human milk, 1959 to 1961, 20: 13012
content in cow's milk, 18: 23829
content in cow's milk, measure for moderating, 20: 18985
content in cow's milk, effects of diet on, 20: 20882(R) (HASL-171)
content in cyclonic storm precipitation, variations in, 18: 20215
content in deciduous and permanent teeth, 18: 38751
content in deciduous teeth, 18: 43328
content in deciduous teeth from fallout, 19: 42387
content in deciduous teeth, United States, 20: 4160
content in deciduous teeth, 1962, 20: 5655
content in deep waters of the Indian Ocean, 1960 and 1961, 20: 31417
content in deer horns, 18: 39014
content in deer horns, determination of ground contamination from fallout by, 19: 28596
content in detritus from Indian Ocean, 20: 41140
content in diet and bones, 1963, 18: 29869
content in diet and bones of residents of Argentina and Puerto Rico, 18: 41644(R) (HASL-149)
content in diet and environment of Japan, 1963, 19: 9369 (NP-14502)
content in diet and urine of children of Rome, 19: 9372
content in diet and bones of Canadian children, 1962, 19: 9379
content in diet and milk, 1964, 19: 22554
content in diet and milk samples in Israel, 1962 and 1963, 19: 32434
content in diet and excreta in Japan, 19: 38894
content in diet and water sources in Japan, 20: 45887 (NP-16290)
content in diet in Poland, Aug. 1, 1960, through July 31, 1961, 19: 701
content in diet in rural and urban population in Poland, Aug. 1961 to July 1962, 19: 702
content in diet in U. S., 1964, 19: 20154(R) (HASL-158)
content in diet in U. S., 1964, 19: 22562
content in diet in California, 1964, 19: 34413
content in diet in Chicago, New York, and San Francisco, ratio of calcium to, 19: 42677
content in diet in Argentina, 19: 44250 (NP-15269)
content in diet in Japan, 1961 to 1964, 19: 44264
content in diet in U. S., 1960 to 1965, 20: 16662(R) (HASL-165)
content in diet in U. S., 1961 through 1964, 20: 18920
content in diet in Poland, Aug. 1, 1962 to July 31, 1963, 20: 26710
content in diet in California, 20: 31471
content in diet of Rhodesians, 17: 34163
content in diet of residents of selected cities of U. S., 1962 and 1963, 18: 12399
content in diet of human infants, 20: 521(R) (HASL-164)
content in diet of children in Argentina, 1965, 20: 39150(R) (NYO-2750-4)
content in diet of Italian children, 20: 39152
content in diet, milk, and water, 1964, 19: 22552
content in diet, man, milk, and water in United Kingdom, 19: 24783
content in diets and wheat, 1963, 18: 18041(R) (HASL-144)
content in domestic and imported food, 1960, 1961, and 1962, 18: 12400
content in domestic and imported cereals and flour in Finland, 1963 and 1964, 20: 43006
content in Don River basin, Russia, 18: 35776(T) (AEC-tr-6458)
content in dried milk in Czechoslovakia, 1957 to 1963, 19: 18204
content in drinking water in United Kingdom, 1961, 16: 24033
content in drinking water supplies in Great Britain, 1961, 17: 14549
content in drinking water and food in United Arab Republic, 1963, 18: 31750 (A/AC.82/G/L.933)
content in drinking and Weser River water from fallout, 18: 39536
content in drinking water in Great Britain, 1963, 19: 24703 (NP-15013)
content in drinking water in Italy, 19: 42637 (BIO/32/63)
content in drinking water, 17: 15527
content in dust and precipitation, 19: 46632(R) (A/AC.82/G/L.987)
content in Earth's atmosphere and surface, 20: 23291
content in Elbe River, 1961 to 1966, 20: 45225
content in English plants, soil, and water, 18: 20208 (AERE-R-4415)
content in environment of Hunterston reactor in Scotland, 18: 8249
content in environment in Faroes, Denmark, in 1963, 19: 6099 (RISÖ-86)
content in environment in Greenland in 1963, 19: 6100 (RISÖ-87)
content in environment, 1962 to 1964, 19: 9370 (NP-14556(p.11-80))
content in environment of Ispra, Italy, 19: 28546
content in equatorial Pacific and North Atlantic Oceans, 20: 7256(R) (TID-22411, App.A)
content in European milk, 1962, 19: 18143 (EUR-1838.d.f.i.n)
content in experimental dog diet, control of, 19: 43675(R) (UCD-472-112, pp 73-9)
content in fallout and stratospheric storage time for, during nuclear moratorium, 18: 2391
content in fallout and soil in Western Slovakia, 18: 33776
content in fallout, effects of latitude on, 18: 37040
content in fallout in U. S., 18: 43818
content in fallout, food, and rain water in Thailand, 1962 and 1963, 18: 45094(R) (THAI-AEC-2)
content in fallout in Denmark in 1963, 19: 6098 (RISÖ-85)
content in fallout in U. S., 1964, 19: 22562
content in fallout in Western Slovakia, 19: 34367
content in fallout, food, human skeleton, milk, soil, and water in Germany, 19: 38876 (NP-14927)
content in fallout over Australia, 1961 to 1963, 19: 46595
content in fallout particles, 20: 2053
content in fallout, 1964, 20: 11018
content in fallout at 156 world land sites, 1957 to 1965, 20: 16662(R) (HASL-165)
content in fallout and precipitation near Leningrad, 20: 16704
content in fallout, estimation of tritium fallout in southern hemisphere from, 20: 20892
content in fallout in Japan, 1964, 20: 23297
content in fallout, method for measuring previous, 20: 25281 (CEA-R-2930)
content in fallout in Finland, 1962–1965, 20: 26599(R) (NP-16002, Paper 3)
content in fallout in USSR, 1962, 20: 29406 (NP-14719)
content in fallout over Belgium and in Meuse River, 1965, 20: 35644
content in fallout in India, 20: 40572
content in fallout after French nuclear explosion, 17: 6272(R) (ORO-520)
content in fallout, 19: 7748
content in Finnish milk, 1960 through 1965, 20: 41134 (SFL-A3)
content in first bicuspids, relation of, to dietary contamination, 20: 27160
content in fish, food, and surface waters at Ispra, Italy, 1960, 16: 4392 (CNI-95)
content in fish from lake waters in Finland, 1965, 19: 46587(R) (NYO-3446-3)
content in fish in Barents Sea, 19: 24724
content in fish in Clinch River, Tenn. and Lower Three Runs, Savannah River, S. C., 20: 33581
content in fish, effects of water salinity on, 19: 24257
content in flour and milk, 18: 29205
content in fodder and foodstuffs, Zagreb, 1962–63, 18: 39535
content in fodder, grass, and milk in Finland, 1961–62, 19: 7741
content in food, 17: 37026(T) (JPRS-21171(Del.)(p.6-13))
content in food, 17: 5751(R) (HASL-132)
content in food animals, 18: 3618
content in food and man, maximum permissible, 19: 7747
content in food and milk in Czechoslovakia, 19: 18203
content in food and milk in India, 1959 to 1964, 19: 44244 (AEET/AM/40)
content in food and milk from EURATOM countries, 1963, 20: 144 (EUR-2460.d,f,i,n)
content in food chains, 17: 24795
content in food chains in Alaska, 1959 to 1965, 19: 40780 (BNWL-SA-242)
content in food chains in Alaska, 1959 to 1965, 20: 26609
content in food in U. S., 18: 43818
content in food in Austria, 1963, 19: 38860
content in food in Italy, 1962 and 1963, 20: 7277
content in food in Amsterdam, 1960 to 1963, 20: 20949
content in food, method of calculating, 17: 17709(T) (JPRS-18492(p.5-16))
content in food plants in Berlin-Dahlem, 1962, 18: 11889
content in food products, effects of cooking on, 18: 20238(T) (JPRS-24139)
content in food, in Denmark, 20: 5651 (RISO-107)
content in food, Japan, 1964, 19: 42639 (NP-15278)
content in food, protective-action guides for, 20: 45986
content in food, 1963, 18: 31784(R) (HASL-146)

content in foods, 18: 3625
content in foods, 18: 31816
content in foods, 20: 9206
content in foods and in man, 1961, 17: 31846
content in foods and soil in Great Britain, 1964 and 1965, 20: 20926(R) (ARCRL-14)
content in foods from Seoul, Korea, 18: 1977
content in foods in Poland, 1960 and 1961, 18: 39508
content in foods in Australia, 19: 46595
content in foods, 1963-5, 20: 14243(R) (TID-22626)
content in foods, 1962 through 1964, 20: 18915
content in foods, 1962 and 1963, 20: 29433
content in foodstuffs in United Kingdom, 1961 and 1962, 17: 7785 (ARCRL-8)
content in foodstuffs in Great Britain, 1962, 18: 15735(R) (ARCRL-10)
content in fresh water supplies, radiochemical measurement of, 18: 39509
content in fresh water basins in USSR, 1961–62, 19: 20160 (NP-14728)
content in fruits and vegetables, 18: 3621
content in German cheese, Sept. to Nov. 1961, 18: 6984
content in German milk, 1962, 19: 38858
content in German milk, effects of precipitation on, 20: 11017
content in German rye and wheat, effects of precipitation on, 20: 11017
content in grain and grain products, 16: 15037
content in grain and oil-bearing plants, 20: 18906(T)
content in grass and milk samples in Finland, 1959, 16: 9036
content in grass and milk, 1959 to 1962, 19: 45749
content in grass and alfalfa in West Slovakia, USSR, effect of plant calcium on, 19: 45750
content in grass, herbage, milk, and soils in vicinity of AERE, 20: 14784(R) (AERE-R-5015)
content in grazing farm animals, effects of, on human diet, 17: 13960
content in ground-level air along 80th meridian (west) during 1961, 17: 14477 (NRL-5869)
content in ground-level precipitation in storms at Santa Barbara, California and State College, Pennsylvania, 17: 14481(R) (TID-17518)
content in hair, effects of dietary content on, 20: 30972 (TID-22027)
content in hay in Germany, 1953 to 1961, 16: 20128
content in hay in Germany, 1962, 20: 36671
content in herbage, milk, plant-base, and soil in nuclear power plant environments in England, 18: 6775
content in human and animal bone, 1959 and 1960, 17: 1209
content in human and animal foods, 1962 and 1963, 19: 18161
content in human bones, foods, soil, and water in Egypt, 16: 4020 (A/AC.82/G/L.665)
content in human bones in Switzerland, 1960, 16: 9819
content in human bones, effects of age on, 17: 5714
content in human bones in United Kingdom, 17: 14534 (NP-12581)
content in human bones in Poland in 1960 and 1961, 18: 4990
content in human bones, 18: 5151
content in human bones and tissues in Germany, 18: 17432
content in human bone, 1962 and 1963, 19: 7714
content in human bones in Osaka, Japan, 1957–1959, 19: 11426
content in human bones, 1962 and 1963, 19: 21848
content in human bone, 19: 31672(R) (NIRS-3(p.65-77))
content in human bones, collected 1961 to 1965, 19: 42638 (HASL-163)
content in human bones, effects of age on, 19: 42248
content in human bones in United Kingdom, 1964, 20: 7272
content in human bones, effects of age and dose rates on, 20: 6719(R) (ORNL-3849, pp 183-213)
content in human bones in Scotland and United Kingdom, 20: 18922
content in human bones and tissues in Finland, 20: 31142
content in human bones and tissues, 20: 40570
content in human bones and tissues, 20: 43626
content in human bones in Poland, 1962–1964, 20: 45313
content in human diet in Denmark, 1962, 18: 5479 (RISO-63)
content in human diet and in bone samples in Faroe Islands, Denmark, 1962, 18: 5480 (RISO-64)
content in human diet, estimation from excreta analysis, 19: 2018
content in human diet, 19: 24248
content in human diets, assessment of, 16: 10350
content in human hair and diet, relation between, 19: 4368
content in human milk in Toronto, Canada, 16: 9041
content in human placenta, comparison with bone in newborn, 16: 20107
content in human skeleton, 1963, 18: 18041(R) (HASL-144)
content in human skeleton, calculation of, 18: 23224
content in human skeleton determined by accumulation in teeth, 18: 31110
content in human teeth in Great Britain, 19: 33758
content in humans, permissible, 16: 9906
content in Indiana soils, 18: 8563
content in Indo-Antarctic Ocean, 1962, 20: 14749
content in infant diets in representative U. S. cities, 1963, 18: 35792
content in inhaled air, maximum permissible, 17: 6331
content in inland waters in Japan, 17: 21947
content in irrigation water, effects on content in cultivated vegetables, 19: 18140 (CEA-R-2625)
content in Ispra environment, Italy, 1965, 20: 33553 (EUR-2965.e)
content in Israel diet, 19: 26917(R) (IA-984)
content in Italian diet, 18: 39544
content in Japanese daily diet since 1960, 16: 27467 (NP-11941(p.27-9))
content in Japanese waters, 18: 37428 (A/CONF.28/P/849)
content in Japanese diet, hazards of, 19: 7749
content in Japanese diet, 1963, 19: 22626
content in Lake Huron and Ottawa River, 20: 14738 (NP-15853, pp 21-33)
content in Lake Michigan waters and surrounding land areas, 20: 41131(R) (HASL-172)
content in lake waters, equilibrium with yttrium-90, 17: 21940
content in land waters in Japan, 16: 5550 (A/AC.82/G/L.690)
content in Ligurian and Adriatic Seas, 20: 45258(R) (IAEA-2607-12)
content in liquid milk in Canada, Feb. 1966, 20: 27203 (NP-16041, pp 3-13)
content in living persons, whole-body techniques for counting, 20: 35189
content in London rain, 18: 39503
content in luminous paint users, 19: 42676
content in man, 16: 19204
content in man and his environment, 1962, 17: 7773 (NYO-9934(Vol. I))
content in man and his environment, 20: 45886 (NP-16262)
content in man as function of age, model for estimating, (T), 20: 6724 (ORNL-P-1830)
content in man determined from extracted teeth, 20: 45956 (NP-16257)
content in man of, time variation of radiation dose from, 20: 5429
content in man, survey of British population, 1961, 17: 2805
content in man, whole-body, 20: 16303(R) (AD-626384)
content in man, 1965, 19: 34372
content in marine organisms and sea water of Pacific Ocean in vicinity of Japan, 1959 through 1961, 18: 23792 (WP/37)
content in marine animals and plants and water in Baltic Bay of Tvären, 1957 to 1963, 19: 22532 (AE-171)
content in marine organisms in Chukchi Sea, Alaska, 1959 to 1962, 20: 31427 (PNE-481, pp 1141-9)
content in meat diet, plants, and vegetable diet in East Germany, 1961 through 1963, 20: 27222
content in meat supplies from fallout, 19: 30401 (CEA-R-2738)
content in Mexican milk, 1962, 20: 9155
content in milk, 19: 42677
content in milk, 19: 46632(R) (A/AC.82/G/L.987)
content in milk, 20: 596 (NP-15542)
content in milk, 20: 597 (NP-15563)
content in milk, 20: 2046 (BIO/04/64)
content in milk after nuclear accident, 20: 18969
content in milk and soil and deposition rate, 16: 429 (TID-13945)
content in milk and rain in New Zealand, 17: 4690(R) (DXRL-F5)
content in milk and rain in Fiji Islands, 17: 4690(R) (DXRL-F5)
content in milk and milk products, effects of processing on, 17: 17711(T) (JPRS-18492(p.26-33))
content in milk and water samples from U. S., 1963, 18: 12401
content in milk and rain water in New Zealand, 1965, 20: 5664(R) (NP-15639)
content in milk and rain water in Canada, March 1965, 20: 7305 (NP-15641, pp 9-21)
content in milk and water supplies in Hanford, Washington, Jan. to June 1965, 20: 7297 (BNWL-165)
content in milk and rain water in Canada, August 1965, 20: 7310 (NP-15642, pp 20-32)
content in milk and precipitation in Canada, Sept. 1965, 20: 9176 (NP-15763, pp 13-25)
content in milk and surface waters in Canada, Sept. 1965, 20: 9177 (NP-15763, pp 26-38)
content in milk and plants before and after Salmon Event, 20: 16743 (VUF-1021)
content in milk and surface waters in vicinity of Canadian reactors, Feb. 1966, 20: 27204 (NP-16041, pp 14-24)
content in milk and milk products, 20: 29464
content in milk and rain in New Zealand, 1965, 20: 31446(R) (NP-16015)
content in milk and milk products, effects of processing on, 20: 33595
content in milk and milk powder produced in Japan, 1963–64, 20: 43610
content in milk at Potsdam, relation to fallout and rainfall of, 18: 31188
content in milk at Chapelcross, Annan, Scotland, 20: 23407
content in milk, effects of feed and soil levels, 16: 5620
content in milk, effects of farming practices on, 18: 3624
content in milk from fall-out, Canada, Jan.–March 1962, 16: 25616(R) (NP-11914)
content in milk from Holsteins and Jerseys, seasonal variations in,

16: 27503
content in milk from cows on fallout-contaminated pastures, 18: 6973 (NP-13432)
content in milk from fallout in United Kingdom, 18: 22253
content in milk from Oak Ridge environs, 1965, 20: 33557(R) (ORNL-3969)
content in milk in Great Britain, 1961, 16: 19176
content in milk in East Germany, 1960, 16: 19201
content in milk in relation to other foods in Germany, 16: 19202
content in milk in lactating cows, effects of calcium on, 16: 26717
content in milk in Netherlands, 1959 and 1960, 16: 9837
content in milk in United Kingdom, 1960, 17: 6363
content in milk in New Zealand, 17: 5750(R) (DXRL-F6)
content in milk in Great Britain, correlation with deposition rates, 17: 23073
content in milk in Germany, Sept.-Nov. 1961, 17: 34166
content in milk in Italy, 17: 36073
content in milk, infants, and stillborn in Western Germany, 18: 5152
content in milk in Iowa, 18: 14138
content in milk in Italy, 18: 18098
content in milk in England, 18: 20208 (AERE-R-4415)
content in milk in German Federal Republic, Sept. 1961 to Sept. 1962, 18: 19809
content in milk in United Kingdom, 1963, 18: 22308
content in milk in Japan, Nov. 1961 to Oct. 1962, 19: 7707
content in milk in Italy, 1963, 19: 7711
content in milk in New Zealand, July to Sept. 1964, 19: 9371(R) (NP-14618)
content in milk in Ankara, Turkey, Nov. 1961 to Feb. 1964, 19: 11392(R) (NP-14683)
content in milk in New Zealand from fallout, 19: 13682
content in milk in Moscow, Ryazan, and Vologda districts during 1960-1962, 19: 13667 (NP-14696)
content in milk in Potsdam, 1963, 19: 15805
content in milk in Canada, 1964, 19: 20161 (NP-14869)
content in milk in Canada and U. S., 1964, 19: 22557
content in milk in Sweden, 1963, 19: 22558
content in milk in Boston, 19: 28599
content in milk in Canada, 1965, 19: 30440 (NP-15064)
content in milk in Italy, 19: 42637 (BIO/32/63)
content in milk in Japan, 1961 to 1964, 19: 44268
content in milk in Israel, 20: 2520(R) (IA-920)
content in milk in Italy, 1962 and 1963, 20: 9150
content in milk in Canada, Sept. 1965, 20: 9176 (NP-15763, pp 13-25)
content in milk in Calif. 1960 to 1963, 20: 18968
content in milk in cattle, effects of dietary calcium on, 20: 29459
content in milk in U. S., 1962, 20: 29474
content in milk in Norway, 1960 through 1964, 20: 31465
content in milk in Mexico, 1963 to 1965, 20: 40854
content in milk in Bela Horizonte, Brazil, 20: 42999 (NP-15934)
content in milk in Japan, November 1962 to September 1963, 20: 43520
content in milk, mathematical model of effects of transport mechanisms on, 17: 6353
content in milk, measurements at ORNL, 1962, 17: 39294(R) (ORNL-3490)
content in milk of miniature swine, effects of diet, 17: 19796
content in milk of, 17: 36041
content in milk of Brazil, 19: 15786 (NP-14627)
content in milk of, effects of dietary calcium consumed by cows, 19: 40341
content in milk of Mandan-Minot region of North Dakota, 20: 5678
content in milk of East Germany, 1958 and 1959, 20: 7263
content in milk samples, 1958, 1959, and 1960, 16: 19204
content in milk samples from Minnesota, 1959, effects of grass contamination, 17: 10352
content in milk samples collected in U. S. and Canada, 1961 and 1962, 18: 461
content in milk samples from Australia, Europe, India, and U. S., 18: 10282
content in milk samples collected in Germany, 1955 through 1961, 18: 31770
content in milk samples from U. S., 1964, 19: 7712
content in milk samples from Canada and U. S., July 1964, 19: 18159
content in milk sampled in U. S., 1957 to 1963, 19: 22551
content in milk, 1961, 16: 6645(R) (HASL-117)
content in milk, effects of, on radiation dose to children, 18: 25727
content in milk, effects of land fertilization on, 18: 43871
content in milk, effects of atmospheric transport of fallout on, 19: 38857
content in milk, effects of various foodstuffs on, 19: 45772
content in milk, German Federal Republic, 1956 to 1962, 19: 5602
content in milk, Germany, 1962 through 1964, 20: 36674
content in milk, in Germany, 20: 524
content in milk, Italy, 1964, 20: 2047 (EUR-2509.e)
content in milk, Japan, 1964, 19: 42639 (NP-15278)
content in milk, July to December 1964, 20: 45947 (ARCRL-13)
content in milk, long-term predictions of, 20: 23299
content in milk, methods for reducing, 20: 39157
content in milk, rainwater, and soil in New Zealand, 1965, 20: 43581(R) (NP-16245)
content in milk, 1964, 19: 22562
content in milk, 1965 and 1966, 20: 41131(R) (HASL-172)
content in milk, 1958 to 1964, 20: 45886 (NP-16262)
content in Moscow atmosphere, 18: 5483(T) (JPRS-21975(Del.)(p.1-9))
content in muscles and organs in bulls from fallout, 19: 20215
content in natural and processed materials in Australia, 20: 156
content in natural waters, fallout correlations with, 20: 27161
content in New Zealand milk, 19: 35892 (NP-15082)
content in New Zealand rain, 19: 35892 (NP-15082)
content in New Zealand air, 19: 35892 (NP-15082)
content in New Zealand soils, 19: 35892 (NP-15082)
content in New Zealand diet, 19: 35892 (NP-15082)
content in newborn rats, effects of mother's diet on, 18: 17446
content in North Atlantic sea water, 1961, 19: 634(T) (JPRS-25966 (p.42-52))
content in North Pacific Ocean, 19: 36724
content in northern stratosphere, 1962-63, 19: 40785 (TID-21224)
content in Norwegian milk during 1961, 17: 15614 (A/AC.82/G/L.810)
content in ocean fish, effects of content in sea water on, 20: 11054
content in ocean surface waters, 1960 and 1961, 20: 31419
content in ocean water, vertical mixing anomaly from ratio of carbon-14 and cesium-137 to, 17: 25465
content in oceans, 20: 43517(T) (AEC-tr-6798, Paper 2)
content in organisms and water of Mediterranean Sea, 1962 to 1964, 19: 24721
content in Pacific Ocean fish livers, 18: 29208
content in Pacific Ocean surface waters, 1961, 19: 20159 (NP-14726)
content in Pacific Ocean off coasts of California and Japan, 20: 13007(T) (NP-tr-1336)
content in pasteurized milk samples collected in U. S. and Canada, 1963, 18: 12398
content in Pennsylvania precipitation, 18: 1901
content in people in France, 1961–1964, 18: 33429
content in plankton and cuttlefish bone from Mediterranean Sea, 1961 to 1963, 18: 15758(R) (TID-20347)
content in plankton from Mediterranean Sea, 1960 to 1963, 18: 15759(R) (TID-20366)
content in plankton, silts and water of Ligurian and Adriatic Seas, 19: 15757(R) (TID-21521)
content in plankton in Mediterranean, 19: 30452
content in plant tissues, 20: 18906(T)
content in plants and soils of East Germany, 16: 21892
content in plants and soils in Germany, 1961, 17: 30284
content in plants, 1962, 18: 1464
content in plants and soil, methods for decreasing, 19: 18209
content in plants of Bucharest region, (E), 19: 30413
content in plants and soils of German Democratic Republic, 1963, 19: 46610
content in plants and soil of East Germany, 1958 and 1959, 20: 7263
content in plants in East Germany from 1961 to 1963, 20: 43538
content in plants and soils in East Germany, 20: 45893
content in Po Valley rice, effects of crop irrigation on, 20: 12986
content in Polish soils, 16: 3253
content in population of Durango, Colo., and Farmington, N. Mex., 18: 35763 (NP-14161)
content in pork, effect of roasting on, 20: 35215
content in powdered milk in U. S., 1923 to 1961, 19: 24787
content in powdered milk in Uruguay, 1960 and 1962, 19: 26586
content in powdered milk in Japan, 1962 and 1963, 20: 16755
content in precipitation, effects of storm development on, 17: 14478 (NSEC-62)
content in precipitation, grass, milk, potatoes, drinking water, sea water, sheep, sea plants, fish, whales, and birds of Faroe Islands, Denmark, 1962, 18: 5480 (RISO-64)
content in precipitation from convective activity and extratropical cyclones, 19: 1032 (HNS-55)
content in precipitation, Japan, 1964, 19: 42639 (NP-15278)
content in precipitation, meteorological effects on, 17: 3664
content in primary teeth of children, 20: 16763
content in processed materials and rainfall in Australia, 18: 39490 (NRS-17)
content in rabbit diet of, from fallout, 20: 7327
content in rain and snow in Canada, June 1960 to December 1962, 18: 4014 (AECL-1863)
content in rain at Fayetteville, Arkansas, 19: 40785 (TID-21224)
content in rain at Tokyo four weeks after Chinese nuclear explosion of May 14, 1965, 20: 5656

content in rain in Fayetteville, Arkansas, 1962 and 1963, 18: 39485 (CONF-337-43)
content in rain over The Netherlands, from Soviet nuclear tests, 18: 41661
content in rain water, Lower Hutt, New Zealand, 1959 to 1961, 16: 22410 (TID-15817)
content in rain water in New Zealand, 17: 5750(R) (DXRL-F6)
content in rain water from large-scale uplift, 17: 14490
content in rain water in Osaka, Japan, 17: 18295
content in rain water, soil, and vegetables from fallout in Tokyo, 1961, 17: 36082
content in rain water and rivers in Japan, calculation of river run-off from, 18: 4003
content in rain water, relation to physical deformities in infants, 19: 15797
content in rain water, Fayetteville, Arkansas, Oct. 1964, 20: 16663 (TID-21470)
content in rain water in Japan, 1962 and 63, 20: 16671
content in rain water, Pennsylvania, 1962, 20: 45901
content in rain water in Japan, 1964, 20: 45906
content in rain water and air in Great Britain, 1960 to 1961, 16: 394 (AERE-R-3766)
content in rain water, 1956 to 1959, 16: 396 (NS-R-12)
content in rain, effect of altitude on, 20: 45900
content in rainwater at Ispra during 1963 and 1964, 19: 34373
content in rainwater in New Zealand, 20: 35653
content in rat femur during lactation, 16: 11403
content in ratio with cesium-137 in human bones, Moscow, 1961 to 1964, 20: 42741 (NP-16265)
content in rats, effects of calcium-rich diet during lactation on, 18: 23216
content in rice in Japan, 1960, 16: 13406
content in rice in Japan, 1959 and 1962, 19: 44265
content in river water in Japan, 19: 31672(R) (NIRS-3(p.65-77))
content in rivers in Japan from fallout, 18: 1931
content in rivers in Japan from fallout, contribution of meteoric water to, 18: 1932
content in Rongelap foods of, 1963, 19: 8737 (BNL-8657)
content in samples of rain water, milk, and human bone collected in New Zealand, 1963, 18: 20234(R) (NP-13859)
content in sea water, effects on development of fish spawn, 20: 20445(T) (TRG-Inf. Ser.-166)
content in sea water and plankton during 1960 to 1964, relative concentration factors for, 20: 26610
content in sea water, errors in determination of, 20: 31423
content in sediments in White Oak Lake, Oak Ridge, 19: 26591
content in Seveso River, Italy, 20: 33562
content in sintered uranium dioxide pellet, radial distribution of, 20: 4472
content in skeleton, methods for prediction, 16: 22461 (TID-7632 (p.457-76))
content in snow in Bucharest, Dec. 24, 1962, to Jan. 6, 1963, 18: 12348
content in soft tissues of dogs, at various times after injection, 20: 8545(R) (COO-119-239, pp 81-7)
content in soil and plants of German Democratic Republic, 1962, 18: 15909
content in soil and food in United Arab Republic, 1962, 18: 31749 (A/AC.82/G/L.932)
content in soil and food in Palermo in November and December 1961, 17: 13958
content in soil in New York City area to 1961, 18: 10280
content in soil in Zagreb, 1962 and 1963, 18: 39089
content in soil of arid regions, 19: 26549
content in soil of Neotoma Valley, Ohio, 1958 through 1964, 20: 36548 (TID-23036)
content in soil, 1960 and 1961, 16: 6645(R) (HASL-117)
content in soil, effects of stable calcium and strontium on, 19: 21811(R) (UCLA-12-541(p.101-30))
content in soil, effects of depth on, 20: 20882(R) (HASL-171)
content in soil, Japan, 1964, 19: 42639 (NP-15278)
content in soils, 20: 14236
content in soils and plants in German Democratic Republic, 1964, 20: 45964 (SZS-7/66)
content in South China Sea surface waters, November, 1962, 20: 31415
content in soybeans harvested in Japan, 1963, 20: 45967
content in spent power reactor fuels, evaluation of, 20: 14435 (BNWL-SA-503)
content in stratospheric and tropospheric air filter samples collected in 1961 and 1962, 19: 9755 (HASL-153)
content in stratosphere in 1962, 19: 14114(R) (DASA-1305)
content in stratosphere, 19: 20657(R) (DASA-1309)
content in stratospheric and tropospheric samples in Project Star Dust, 1964, 20: 16728(R) (HASL-169)
content in stratospheric and tropospheric samples in Project Star Dust, 1963, 20: 16727(R) (HASL-168)
content in stratosphere and troposphere, 1960–1963, 20: 23314
content in stratosphere and troposphere from Chinese nuclear test, 20: 27155
content in stratosphere, 1963 to 1966, and predictions to 1968, 20: 41131(R) (HASL-172)
content in surface waters of Atlantic Ocean, North Sea, and Baltic Sea, 1961, 18: 22248(T) (JPRS-24281)
content in surface waters of Indian Ocean, 1960 and 1961, 19: 633(T) (JPRS-25966(p.20-27))
content in surface water of Norwegian Sea, 1962 and 1963, 19: 24722
content in surface waters near Canadian reactors, 20: 7306 (NP-15641, pp 22-9)
content in surface air in Antarctica, 1956 to 1963, 20: 9179 (NRL-6341)
content in surface waters in Canada, Sept. 1965, 20: 9177 (NP-15763, pp 26-38)
content in surface layer of atmosphere over Heis Island and Moscow, 20: 16650
content in surface waters in Soviet Union, 1961–1962, 20: 16705
content in surface waters and fallout in Finland, 1961 to 1965, 20: 33510 (SFL-A4)
content in surface waters in U. S., 1965, 20: 33589
content in Swedish food, 1962, 18: 23790 (NP-13828)
content in tea before and after boiling, 17: 41063
content in tea leaves, 20: 9140
content in teen-age diet in U. S., 1963, 18: 37446 (TID-21081)
content in teeth in Great Britain, 19: 15239
content in teeth of children born between 1949 and 1957, 17: 18446
content in teeth of children, determination of body burden from, 18: 39005
content in teeth of Israeli children born 1950 to 1956, 20: 2520(R) (IA-920)
content in teeth, Japan, 1964, 19: 42639 (NP-15278)
content in tissues of small mammals from bed of drained radioactive lake, 16: 17374
content in tobacco in Canada, 19: 34417
content in total diet in United States, 16: 17926
content in total diet composites, 17: 33516
content in total diet samples from Feb. 1963 through May 1964, 18: 43845
content in total teen-age diet in U. S., 1963, 19: 9416
content in Tyrrhenian Sea plankton, 19: 30411
content in U. S. cities, 18: 43865
content in U. S. diet, 1963, 18: 10329
content in U. S. diet, 1963, 18: 35790
content in U. S. diet, 1964, 19: 22555
content in U. S. milk, 1962, 19: 11450
content in U. S. milk, 1963 and 1964, 19: 18160
content in U. S. surface waters, 1964, 19: 18162
content in U. S. wheat and wheat products, 1958 through 1962, 18: 14147
content in upper atmosphere, 19: 14120
content in upper layers of coastal sediments of Ligurian Sea, 20: 526
content in urine in man, effects of diet on, 18: 13823
content in urine of Italian children, 20: 39152
content in urine, methods for determining, 19: 30140
content in vegetables from Italy, 1961, 19: 7708
content in Venezuelan soil, 20: 9143
content in waste water solutions, 16: 1283
content in water supplies in Poland, 1961, 17: 25474 (CLOR-13)
content in water supplies following nuclear warfare, 19: 42658 (NP-15328)
content in water, milk, diet, and human tissues in Japan, 19: 15755 (NP-14797)
content in water, Japan, 1964, 19: 42639 (NP-15278)
content in water, maximum permissible, 17: 39311(R) (ORNL-3492(p.157-75))
content in waters of the southern Pacific Ocean, 1961, 19: 18149(J) (JPRS-28558)
content in waters near Canadian reactors, April 1965, 20: 41136
content in western North Pacific Ocean down to 5,000 m, 16: 5551 (A/AC.82/G/L.697)
content in western North Pacific Ocean, 16: 17901
content in wheat, 17: 5751(R) (HASL-132)
content in wheat and flour, 18: 3619
content in wheat crop, 1962, and in milling products, 17: 39287(R) (EUR-140)
content in wheat flour in France, 1960 to 1962, 20: 45892
content in wheat in United States, 1959, 16: 13405
content in wheat in Idaho and Montana, effects of spring precipitation on, 18: 10286
content in wheat in U. S., 1958 to 1964, 19: 46662
content in wheat in Canada, 1963, 20: 7304 (NP-15641, pp 3-8)
content in wheat plant parts and milling fractions, 18: 35788

content in wheat, 1959, 18: 13403 (HW-SA-2977)
content in wheat, effects of washing with decontaminating solutions on, 20: 29473
content in White Oak Creek drainage basin, 17: 39300(R) (ORNL-3492 (p.51-62))
content in White Oak Creek drainage basin, 19: 6930(R) (ORNL-3697 (p.43-8))
content in whole milk and Winnipeg River water in Canada, August 1956, 20: 7311 (NP-15642, pp 33-45)
content in wild rabbits, use as biological monitor, 17: 33596
content in Winnipeg River, 18: 18038 (AECL-1874)
content in world diet, 1957 through 1961, 17: 8482
content in world soil samples, 1956 to 1961, 18: 8524(T) (AEC-tr-6049 (p.225-32))
content in 1963 U. S. wheat crop, 18: 35787
content in 1964 diet across U. S., 19: 26594
content of fallout, in food, 19: 24791
content of food and milk in Hungary, 18: 29220
content of human bones, 1961 to 1963, 18: 23833
content of, in convective shower precipitation, effects of meteorological conditions on, 17: 39267(R) (HNS-24)
content of, in drinking water supplies in Great Britain, 1962, 17: 36028 (NP-13035)
content of, in "hot zones" in human skeleton, 17: 15606
content of, in human bones from diet, 17: 20262
content of, in Mediterranean plankton, 1961 to 1963, 18: 16(R) (TID-19472)
content of, in milk powder in Japan, 17: 21938
content of, in milk samples collected in U. S., 1963, 17: 41079
content of, in Norway from fallout, 17: 37054 (FFIK-IR-K-253)
content of, in precipitations, meteorological parameters of, 17: 37349 (NSEC-98)
content of, in rain water, 17: 6272(R) (ORO-520)
content of, in teeth of children and adults, 17: 38726
content of ingested, in mammals from waste disposal area, 17: 33551
content of milk, from fallout, 18: 18110
content of, in Australian environment, 1961, 18: 31758
content of, in bones and diet of residents of San Juan, Puerto Rico and New York City, 19: 9376
content of, in fish in Irish Sea, 18: 33248
content of, in grass and milk in West Germany, 1960, 18: 27029
content of, in milk, effects of dietary calcium content on, 18: 11559(R) (TID-19977)
content on surface of earth in 1960–1961, 17: 3166 (TID-17090)
content rain water in Great Britain, 1965, 20: 46030(R) (AERE-PR-HPM-9, pp 6-17)
content ratio to calcium in mouse tissues, 20: 18225
content values for, ICRP recommended changes in maximum permissible, 19: 11439
contents in animals, plants, rain water, and soils from Chariot site environment, 19: 25797 (PNE-446)
contents in atmosphere, food, and soil in Germany, 18: 3629
contents in fallout at U. S. and world sites, 19: 9365(R) (HASL-155)
contents in food, milk, precipitation, and water, world-wide, 19: 34365(R) (HASL-161)
contents in human vertebrae, 1964, 19: 34365(R) (HASL-161)
contents in meats in East Germany from 1961 to 1963, 20: 43538
contents in oceans in 1959 to 1962, Soviet observations on, 18: 37359 (A/CONF.28/P/384)
contents in water in Poland, 1962, 19: 24701 (CLOR-32)
correlation with lead-210 in human bones, 20: 42781
costs and uses, review of future and present, 17: 31681(R) (HW-76559)
countermeasures for, in food chain, 18: 3607
counting efficiency in scintillating gels, (E), 19: 18277
decay modes of fallout, 19: 7748
decay of, correction factors for, 17: 24384 (AERE-R-4237)
deposition and distribution in teeth in dogs, 17: 33523
deposition as carbonate, for use as gamma source, 18: 18202
deposition from atmosphere by precipitation, meteorological influences on, 18: 40041 (CONF-337-42)
deposition from rainfall, Clallam County, Washington, 1957–60, 16: 19171
deposition from stratosphere, time constants for, 18: 5550
deposition from surface and underground nuclear tests, 20: 27162
deposition in Bahamas, comparison of land and oceanic, 20: 7257(R) (TID-22411, App.B)
deposition in body, effects of milk consumption on, 18: 11595
deposition in bone, metabolic pathways, 16: 22434 (TID-7632(p.4-24))
deposition in bones, effects of kinetics of administration, 16: 23441
deposition in Israel during winter of 1961-1962, 17: 35253(R) (IA-775)
deposition in Japan, 1957 to 1961, 18: 16214
deposition in Pacific cyclonic storm, 17: 39266 (HNS-17)
deposition in Polish soil, 17: 14471 (CLOR-12)
deposition in precipitation at Westwood, New Jersey, 19: 7701 (NYO-2415-12)
deposition in precipitation, global, 1965 and 1966, 20: 41131(R) (HASL-172)
deposition in rainstorms in Illinois in July 1962, 20: 23314
deposition in rat teeth, 18: 17438
deposition in rat bone, effects of dietary calcium on, 19: 11426
deposition in rats, effects of polyvinyl pyrrolidone on, 18: 19(T) (JPRS-21511(p.14-19))
deposition in skeleton, effects of tetracycline on, in mice, 18: 35275 (LADC-5996)
deposition in skeleton during growth, effects of calcium on, 18: 11609
deposition in skeleton, dietary factors in, 16: 17419
deposition in skeleton of rats, effects of dietary calcium and phosphorus on, 18: 4970(T) (JPRS-22295(Del.))
deposition in soil from fallout in Italy, 1962, 18: 6952
deposition in Tokyo, 18: 22256
deposition in U. S. in 1964, latitudinal variations in, 18: 41644(R) (HASL-149)
deposition of atmospheric, in Japan, 19: 15764
deposition of coatings of, method for electrolytic, 17: 18729(P)
deposition of fall-out in precipitation, 16: 22451 (TID-7632(p.287-98))
deposition of, from fallout, 17: 7772 (NYO-9533)
deposition of stratospheric, 16: 6643 (DASA-1300(Vol.4))
deposition of, use of molecular plating for quantitative, 20: 41011 (SGAE-CH-34/1966)
deposition on earth from fallout, 1956 to 1961, 18: 8523(T) (AEC-tr-6049(p.202-24))
deposition on earth's surface, 18: 22258
depostion on ground, effects of industrial smog on, 20: 31403
deposition rate of fallout, role of convective storm activity in, 20: 23285 (HNS-58)
deposition rates and concentration in Pittsburgh precipitation, 17: 18328 (NSEC-89)
deposition rates of fallout, in convective shower precipitation, 19: 619(R) (HNS-50)
deposition rates over land and ocean, 20: 25296
deposition with respect to atmospheric release of, calculation of, 20: 2074 (AHSB(RP)M-40)
detection and measurement in urban Chicago atmosphere, 1958–1959, 16: 17885
detection and measurement in solutions, sensitivity of scintillation counters for, 18: 29967 (AERE-R-4638)
detection and measurement of small amounts of, in water, soil, and biological materials, 18: 31919(T) (JPRS-25068(p.1-15))
detection and measurement in solution, use of 4π counter in absolute, 19: 19755 (KFK-252)
detection and measurement on clothing, design of monitor for, 19: 26648 (AECL-2245)
detection and measurement of, using scintillation ion exchange resin, 19: 32098
detection and measurement of, *in vivo*, 20: 7316(R) (ORNL-3849, pp 215-29)
detection in clothing, instrument for, 19: 32544 (AECL-2245)
determination and sampling procedures for fall-out, 16: 11976 (NYO-9530)
determination and vertical diffusion in deep water in western North Pacific, 18: 14080
determination as yttrium hydroxide, effects of other radioisotopes on, 19: 2244
determination by autoradiography using ring-oven method, temperature effects on fading effect in, 20: 251
determination, by β-spectrum analysis, 16: 9958
determination by bremsstrahlung spectrum, method for, 20: 8829(R) (LF-28, pp 13-17)
determination by Kawabata-Held method, 18: 23408 (NVO-162-8)
determination by sorption on glass powder, quantitative, 18: 6767
determination by yttrium-90 precipitation method, 20: 20586
determination, evaluation of injection standards, 16: 5156(R) (COO-224)
determination in air samples in Japan, 16: 420
determination in air samples, 16: 6639 (DASA-1300(Vol.1))
determination in animals and man, radiometric, 16: 10329
determination in air samples collected along 80th meridian, 1959 to 1961, 16: 22444 (TID-7632(p.188-203))
determination in air and rain water samples, 16: 7761
determination in air samples, 17: 14511
determination in ashes, silts, and soils by solvent extraction and counting, 17: 21624
determination in aqueous solutions by chelate extraction and counting, 18: 166 (NP-13232)
determination in ashes and water by ion exchange and counting, 18: 13687
determination in atmosphere, 19: 4375

determination in air by beta measurement, efficiency of counter for, 19: 20169
determination in aerosols, methods and equipment for, 19: 34258 (NP-15102)
determination in aqueous solutions by Cherenkov counting, 19: 42581
determination in atmospheric and precipitation samples, methods for radiochemical, 20: 14430 (AD-620219)
determination in animals and plants in presence of calcium-45, strontium-89, and yttrium-90, 20: 26623
determination in atmospheric precipitation, 20: 35448
determination in biological substrates in presence of calcium-45, 16: 5141
determination in biological materials, 16: 5156(R) (COO-224)
determination in bones of native animals in vicinity of Nevada Proving Grounds, 1958 to 1961, 16: 10309 (UCLA-500)
determination in bones of animals, 16: 11557
determination in bone, milk, and plants, radiometric, 16: 14654
determination in bovine skeleton, 16: 21888
determination in bones, 16: 23402
determination in bone samples collected in Great Britain, 1961, 16: 25168 (NP-11904)
determination in biological materials, radiochemical, 16: 30331 (UWFL-52(Rev.))
determination in bone samples collected in United Kingdom, 1960, 17: 1228
determination in bones of cuttlefish in Adriatic and Ligurian Seas, Nov. 1961 to May 1962, 17: 12120
determination in bone, radiochemical, 17: 14174
determination in bone, samples collected in Norway, 1956 to 1961, 17: 29116 (A/AC.82/G/L.769)
determination in bone samples collected in U. S., 1962 and 1963, 18: 4047
determination in bone samples collected in Great Britain, 1962, 18: 6592 (NP-13454)
determination in bones of fetuses and children, 18: 10000
determination in bone by low-level beta counting, 18: 14233
determination in bone, radiochemical, 18: 23402 (AERE-R-4466)
determination in bone samples, 19: 17770 (CEA-R-2709)
determination in bone ash by solvent extraction and counting of yttrium-90, 19: 17801
determination in biological materials, radiochemical, 19: 19739 (AERE-AM-101)
determination in bones in presence of radioactive contaminants, 19: 19789
determination in biological materials and water supplies, 19: 26543
determination in biological materials, radiochemical, 20: 218(R) (STI/DOC/10/42, pp 1-22)
determination in biological materials, by solvent extraction of yttrium-90 into scintillator solution, 20: 8507(R) (COO-119-233, pp 88-93)
determination in bones, diet, fallout, milk, plants, urine, and water, methods for, 20: 24980 (SZS-2(1966))
determination in bone ash, method for, 20: 43061 (CEA-R-2998)
determination in cesium-137 sulfate, 16: 23631 (TID-7629(p.209-16))
determination in Canadian milk samples, 1963, 18: 12386 (NP-13599)
determination in Clinch and Tennessee River fish, 18: 19448(R) (ORNL-TM-757)
determination in deciduous teeth as an indication of fall-out deposition, 16: 1459
determination in diet, 16: 22458 (TID-7632(p.405-41))
determination in dried milk samples, 16: 22459 (TID-7632(p.415-24))
determination in drinking water, design of equipment for, 18: 6763
determination in diet and excreta of Japanese, 1962 and 1963, 18: 20232 (JAERI-1057)
determination in drinking and river waters and urine by ion exchange, 18: 23421
determination in drinking water using a carrier, triple precipitation, and counting, 18: 25267 (K-1521)
determination in decay mixtures of, computer program for, 19: 32110
determination in drinking water, method for, 20: 3867 (CEA-R-2844)
determination in environmental samples, radiochemical, 18: 8287(T) (AEC-tr-6049(p.47-74))
determination in environmental materials, radiometric, 19: 31696
determination in fecal and urinary excretion, 16: 1430(R) (ORNL-3189 (p.224-7))
determination in foods and milk in United Kingdom, 1960, 16: 5147 (ARCRL-5)
determination in foods consumed in U.S., 1961, 16: 30693
determination in food and milk samples, 1962, 16: 33308(R) (HASL-131)
determination in feces, 17: 17991
determination in food, radiochemical, 17: 27276
determination in French air and rain water, 18: 4036
determination in fallout by ion exchange, 18: 19880
determination in food by solvent extraction using di-(2-ethylhexyl) phosphoric acid and counting, 18: 29584
determination in fresh water basins, radiochemical, 18: 33769 (NP-14091)
determination in food and water, methods for, 18: 35471
determination in food, 18: 35780
determination in foodstuffs in Germany, 1961, 18: 37390
determination in fallout and surface waters, methods for, 18: 39094
determination in fallout in California, winter, 1961 and 1962, 18: 39498
determination in fission products, development of methods for, 19: 7274(R) (IDO-14636)
determination in fallout-contaminated waters by solvent extraction and counting, 19: 11017
determination in food, milk, and water, 19: 13232
determination in fallout particles, 19: 17821
determination in food, radiochemical, 19: 24792
determination in foods, chromatographic, 19: 24430
determination in fallout, methods for, 19: 28420(R) (NP-14825)
determination in food after incineration, 19: 46200
determination in fallout, radiochemical, 20: 22872(R) (NIRS-4, pp 12-17)
determination in food and water, gamma spectrometric, 20: 31180
determination in food by measurement of yttrium-90, slide-rule method for, 20: 35352
determination in food, soil, and surface atmosphere, 20: 40853
determination in grass of Krakow district of Poland, June 1961, 17: 4392
determination in Greenland firn layer, 20: 25285
determination in human urine and waste solutions, 16: 2980
determination in herbage and milk, method for, 18: 39087
determination in human excreta, estimation of body burden by, 19: 24473
determination in hair, method for, 20: 8980(R) (BNWL-36, pp 3.1-122)
determination in irradiated polyphenyls, 16: 7496
determination in low-activity samples, spectrometric, 18: 43424
determination in large volumes of seawater, method for, 19: 44296 (NYO-4700(Rev.)(Suppl.II))
determination in low-activity animal or vegetable samples, radiochemical, 20: 22906
determination in mixed fission products, radiochemical, 16: 2988
determination in milk and rain in New Zealand, 16: 29181 (DXRL-F4)
determination in milk by ion exchange, 16: 28889 (HW-SA-2011)
determination in milk and mixed diet in Great Britain, 1961, 16: 33304(R) (ARCRL-7)
determination in milk samples collected during 1961, 17: 1677
determination in milk and urine, radiochemical, 17: 1176(R) (HW-70050 (p.78-142))
determination in milk, rapid method for, 17: 17977(T) (JPRS-18632)
determination in milk, radiochemical, 17: 21439
determination in milk, radiochemical, 17: 21453
determination in milk, radiochemical, 17: 21455
determination in milk, soil, water, air, diet, and bone, 17: 27592(R) (HASL-138)
determination in milk, 17: 38920 (IEA-60)
determination in milk, method for total, 18: 1514
determination in milk, 18: 3696
determination in milk by ion exchange, 18: 11990
determination in milk, ion exchange, 18: 41343
determination in milk after ion exchange separation, 18: 43719
determination in milk using TTA, 19: 4083
determination in milk, solvent extraction method for, 19: 9077
determination in milk by ion exchange, method for, 19: 32102
determination in mixture with strontium-89 and yttrium using semiconductor detector, spectrometric, 19: 32111
determination in milk, 19: 38556
determination in milk, 19: 38856
determination in mixture with cerium-144, method for, 19: 43962
determination in milk, solid foods, and water, methods for, 20: 16369
determination in milk, 20: 20938 (NP-15921)
determination in milk, 20: 40854
determination in natural waters, 16: 28886
determination in natural water reservoirs, rain water, and snow using electrodialysis and gamma spectroscopy, 19: 19809
determination in presence of calcium and phosphates, 16: 6381
determination in pitchblende, uranium, and uranyl nitrate, radiochemical, 18: 12025
determination in plankton, 19: 4355(R) (TID-21131)
determination in presence of strontium-85, radiometric, 19: 17820
determination in presence of strontium-89 by paper electrophoresis and beta counting, 19: 36285
determination in plant residues and soils, flame spectrometry method for, 19: 35890(T)
determination in precipitation from convective rainstorms, 19: 36651 (COO-1199-6)
determination in presence of yttrium-90 by liquid scintillation spectrometry, 20: 1766
determination in presence of strontium-89, beta counting technique for,

20: 31188
determination in rain water, 16: 10334
determination in rain water, 16: 14996 (NSEC-48)
determination in rain water, 16: 22449 (TID-7632(p.256-70))
determination in river and sea waters in France, 16: 31966
determination in rain water in New Zealand, 16: 9008
determination in rain water by amalgam exchange technique, 17: 34038
determination in reactor effluents, methods for, 17: 35627(R) (AFSWC-TDR-62-146)
determination in rain water, method for, 17: 38952
determination in rainwater, method for, 18: 15958 (SCPRI(S)-81)
determination in rain, milk, and bone, radiochemical, 18: 35472
determination in river waters of U. S., 1959 to 1964, 18: 37386
determination in rain, radiochemical, 19: 7327
determination in rain water, using scintillation gels, (E), 19: 20335
determination in rain water, radiochemical, 19: 30071 (AERE-AM-100)
determination in rainwater, 19: 38852
determination in rain water, method for, 20: 7024
determination in rain water using ion exchange, gamma spectrometric, 20: 36759
determination in rainwater in New Zealand from 1956 to 1959, 20: 43530
determination in sea water, 16: 4132 (CNI-93)
determination in soil samples, 16: 6644 (DASA-1300(Vol.5))
determination in sea water, radiochemical method, 16: 7760
determination in snail shells in Hungary, 16: 8510
determination in stratospheric particles, 16: 22443 (TID-7632(p.170-87))
determination in stratospheric fall-out, 16: 22447 (TID-7632(p.223-41))
determination in stratosphere in Project Star Dust, 16: 23407(R) (DASA-1302)
determination in sea water, method for, 16: 26935
determination in solution using scintillation detector, 17: 6446
determination in samples of water, soil, vegetation, and human diet from Greenland, 1962, 18: 6948 (RISO-65)
determination in soil, vegetation, and water, radiochemical procedures for, 18: 13642 (SC-4783(RR))
determination in samples of milk and rain water collected in Mexico, 1961 to 1963, 18: 27699 (A/AC.82/G/L-931)
determination in stratosphere, 18: 30297(R) (NYO-10498)
determination in soil, method for, 18: 39089
determination in soil-vegetation covers, flame spectrometric, 18: 39112
determination in simulated high-altitude radionuclide samples, radiometric, 19: 13203(R) (NYO-3276-8)
determination in stratospheric fallout, 19: 22544
determination in sectioned soil cores, autoradiographic, 19: 32106
determination in sea water, method for, 19: 36724
determination in sea water, 19: 44253(R) (NYO-2174-36)
determination in sea water, methods for, 20: 1749 (USNRDL-TR-912)
determination in sea water in Genoa, Italy, radiometric, 20: 18592
determination in seawater by precipitation with manganese dioxide, 20: 24973 (AD-632528)
determination in seawater, by coprecipitation with manganese dioxide and counting, 20: 35405
determination in teeth, radiochemical, 17: 28762
determination in upper 10 cm of Formosan soils, 17: 29984
determination in urine, 18: 33518
determination in urine using Cherenkov effect, 19: 46198
determination in urine, 20: 14243(R) (TID-22626)
determination in urine by anion exchange and beta counting, 20: 20583
determination in water by ion exchange, 16: 8684(T) (AERE-Trans-881)
determination in water, radiometric, 16: 22031
determination in water samples, 1962, 16: 33308(R) (HASL-131)
determination in waste water, 17: 380
determination in water, fish, milk, and vegetation at Pembroke, 17: 12493 (CRER-1120)
determination in water, milk, diet, soil, and air samples collected in 1962 and 1963, 18: 6944(R) (HASL-142)
determination in water supply, method for, 18: 10018
determination in water supplies, chromatographic, 18: 39131
determination in water supplies, 19: 324
determination in waste waters, methods for, 19: 19749 (EUR-2118.f)
determination in water, method for rapid control, 19: 24445
determination in water, radiochemical, 20: 1754
determination in water, using Cherenkov effect, 20: 31506 (CEA-R-2915)
determination in water, 20: 40819(T) (CEA-tr-A-1883)
determination in water and milk in Bombay, low-level beta counting method for, 20: 43532
determination of body burden for rats, factors in, 16: 8483 (TID-14845)
determination of body burden by excretion analysis, 16: 8516
determination of beta-emitting, in Korean food, 17: 30032
determination of, in environmental materials, radiochemical procedures for, 16: 20870 (NYO-9934(Vol.III)(Ext.))
determination of, in stratosphere, 17: 6271(R) (NYO-10464)
determination of, in food, soil, and water, 17: 12516
determination of, in biological materials by precipitation using potassium rhodizonate, 17: 19955
determination of, in biological materials, review of methods for, 17: 23274
determination of, in diets of teenagers and infants throughout U. S., 1962, 18: 1969
determination of lifetime accumulation in animals, method of, 17: 30369
determination of long-lived, in fallout in Germany, 1962 and 1963, 19: 4359
determination of physicochemical state of, in liquid media by paper electrophoresis and radioactivity recording, 18: 33590
determination of, radiochemical, 18: 8281 (NYO-4700(Rev.))
determination of, radiochemical, 18: 8286(T) (AEC-tr-6049(p.22-46))
determination of, radiochemical, 18: 8288(T) (AEC-tr-6049(p.75-99))
determination of, in plants and meat and bones of reindeer in Finland, 18: 12347 (PL-86)
determination of, in dog tissues and excreta, 18: 29200 (UCD-472-110)
determination of, in presence of strontium-89, 19: 46196
determination of, efficiency of beta scintillation sandwich counting method for, 20: 5783
determination on filter papers, 19: 42424(R) (NYO-3276-10)
diffusion from strontium titanate heat sources in sea water, (E), 19: 28716
diffusion in basalt, 18: 40962 (UJV-1105/64)
diffusion in basalt, 20: 26552
diffusion in Conasauga shale, 19: 8676(R) (ORNL-3697(p.54-61))
diffusion in fused potassium nitrate–sodium nitrate media, 20: 25085
diffusion in irradiated artificial graphite, 18: 632
diffusion in melted basalt and glass, 19: 37085
diffusion in quartz sand, effects of humic acid on, 20: 23277
diffusion in sands and soils, 16: 27013
diffusion in soil, 18: 14089
diffusion in soil, effects of calcium on, 20: 12523
diffusion in soils, 17: 30034
diffusion in soils, effect of properties on, 20: 38918(T)
diffusion through soil, effects of soil composition on, 20: 18232
diffusion through placenta in rats, 18: 8080(T)
dispersion and transport in soil, 20: 9183 (UCRL-7997)
dispersion in troposphere, global, 20: 33504
dispersion of aerosols of, in stratosphere, 20: 16643
disposal by in-pile activation to stable or short-lived isotopes, (T), 20: 16132 (BNL-8558)
distribution across main thermoclines of Atlantic and Pacific Oceans, model for predicting, 20: 7258(R) (TID-22411, App.C)
distribution and biochemical effects of injected, in liver, 16: 8564(T)
distribution and dosimetry in bones, microscopic, 19: 29880
distribution and levels in the Baltic Sea, 19: 13642
distribution and metabolism in fish organs, age and weight effects on, 19: 35910
distribution and natural carriers of, in sea water, 20: 31422
distribution and retention in tissues, in mice, 16: 21880
distribution and retention in trout, 16: 25117(R) (HW-72500(p.26-9))
distribution and retention of injected, in beagles, 17: 19884
distribution and retention in rat tissues, effects of age, dose, and administration route on, 18: 23243 (UR-642)
distribution and uptake in Japanese rice, 20: 7269
distribution and volatility in air-burst debris, 20: 9184 (USNRDL-TR-933)
distribution between core and recombiner of L54 water-boiler reactor, 18: 11492
distribution from nuclear excavation in basalt, 20: 613
distribution in Atlantic Ocean, from fall-out, 16: 26731
distribution in atmosphere, 18: 42144(T) (AEC-tr-6464)
distribution in atmosphere of Northern Hemisphere, Jan. to April 1963, Star Dust program measurements of, 18: 41642(R) (DASA-1308)
distribution in atmosphere over oceans, dependence of, on meteorological factors, 20: 16699
distribution in Atlantic Ocean, 1957 through 1961, 20: 33526
distribution in biosphere, 19: 25870
distribution in bones in sheep, 17: 5741
distribution in deep sea water near Japan, vertical, 20: 16681
distribution in different levels in Black Sea, 20: 43539
distribution in dog bones, effects of long-term vs. single administration on, 18: 3455(T) (JPRS-21997)
distribution in fallout deposition at world-wide HASL cooperating stations, 16: 24012(R) (HASL-127)
distribution in forest ecology, 16: 4377
distribution in food, 18: 3605
distribution in food chains of, in Arctic regions, 18: 25055 (NP-13985)
distribution in food chain, effects of transfer from food to milk of cattle on, 20: 4162
distribution in man and his environment, data tabulation, 16: 14448 (NYO-

distribution in milk constituents, 17: 36071
distribution in milk products, 18: 23800
distribution in northern Pacific Ocean, 1954–1962, 19: 27838
distribution in non-circulating water basin residues, 19: 30408
distribution in oceans, vertical, 20: 27153
distribution in pumpkin plants after root and foliar contaminations, 19: 2034
distribution in rats and dogs from inhalation, 17: 40510
distribution in rat tissues, 20: 26629
distribution in sea water, from waste disposal, 20: 38537
distribution in sheep bones in Portugal, 20: 22540
distribution in soil, climatic and hydrologic factors, 16: 3239 (AFOSR-1623)
distribution in soil from weapons tests, 17: 16288
distribution in soils in USSR, 18: 37360 (A/CONF.28/P/385)
distribution in soils in Kansas, 19: 20657(R) (DASA-1309)
distribution in soils in USSR, 1959-60, 19: 24706
distribution in strontium titanates, radioautography, 17: 29854(R) (MND-2584-4)
distribution in surface waters, 1956 to 1961, 18: 8525(T) (AEC-tr-6049 (p.233-57))
distribution in surface air, hemispheric variations in, 19: 32484
distribution in surface waters of the Atlantic, Indian, and Pacific Oceans, 1960 and 1961, 20: 31420
distribution in tissues, effects of infection, 17: 19863
distribution in tissues of molting crayfish, 20: 10515(R) (BNWL-122, pp 46-8)
distribution in tissues of animals, 20: 33044
distribution in tissues of guinea pigs, 20: 38662
distribution in tissues of man, 20: 46031(R) (AERE-PR-HPM-9, pp 17-26)
distribution in tumors and metastases in mice, tracer study, 17: 23023
distribution in water-bearing strata, effects of salt content of ground water on, 19: 46602
distribution of fallout, stratospheric, 20: 45888(R) (NYO-3654-1)
distribution of, in rats, effects of age, diet, and chemical agents on, 17: 12107
distribution of, in infant formulas, 17: 29143
distribution of, in whole Norway spruce trees, 17: 37053 (FFIK-IR-K-251)
distribution on ocean surfaces, 20: 43516(T) (AEC-tr-6798, Paper 1)
distributions in oceans, vertical, 17: 32273
distributions in stratosphere, 18: 35715(R) (DASA-1307)
dose distribution in bones, models for, 17: 19906
dose rates from, measurement of surface, 18: 31786 (LADC-4467)
dosimetry in bones, 16: 28700 (TID-12753)
dosimetry in mice after intraperitoneal injection, 20: 18353
dosimetry of beta radiation from deposited, using fluorods, 19: 11602
dosimetry of gamma radiation from deposited, using thermoluminescent detector, 17: 39343
dosimetry of internally deposited beta sources using, 19: 36151
dosimetry of radioapplication of, for eye lesions, 17: 13891
dosimetry of, equation for internal, 20: 18955
dosimetry of, for human fetuses and infants, 20: 43605
dosimetry of, photographic, 19: 26710
effectiveness in treatment of aviation tympanitis, 19: 46038(T) (JPRS-31602, pp 191-7)
effects from fallout on grain quality and yields of crops, 19: 25922
effects in mice, carcinogenic, 20: 22631
effects in rats of, effects of administration rate and dose on, biological, 19: 40336
effects in rats, after chronic low-dose oral administration, biological, 19: 40335
effects of carcinogenic, 18: 29488
effects of chronic exposure to, on hematopoiesis in dogs, 18: 6666
effects of chronic ingestion of, on growth and health of Beagles, 18: 29200 (UCD-472-110)
effects of chronic ingestion of, on kidney function in dogs, 18: 38959
effects of chronic ingestion of, in miniature swine, 18: 41033(R) (HW-80500(p.83-99))
effects of combined yttrium-90 and, on tumorigenesis in rats, 20: 8654
effects of combined cerium-144 or plutonium-239 and, on rats, 20: 10552
effects of continual ingestion during growth period of beagles, 16: 25153(R) (UCD-106)
effects of daily doses on cardiovascular and nervous systems in dogs, 16: 5191
effects of deposited, on mechanical strength of bones, 20: 5289(R) (COO-119-232, pp 88-98)
effects of deposited, on hematopoietic system in dogs, 20: 5290(R) (COO-119-232, pp 165-89)
effects of dietary, on dogs, 17: 38632(R) (UCD-108)
effects of dietary, on dogs, 17: 38646(R) (UCD-108(p.150-9))
effects of dietary, on cholesterol and lipid content of rat blood, 20: 28994

effects of dietary, on miniature swine, 17: 13955
effects of fallout, genetic, 18: 25697
effects of imbedded capsules of, on kidneys of rats, 17: 17812
effects of ingested, on skeleton, 17: 25042
effects of ingested, in domestic animals and man, 17: 35439
effects of ingested, on erythrokinetics in miniature swine, tracer study of, 17: 35301(R) (HW-76000(p.89-92))
effects of ingested, on blood plasma erythropoietin content in miniature swine, 17: 35302(R) (HW-76000(p.93-4))
effects of ingested, on hematological response to massive blood removal in miniature swine, 18: 41087(R) (HW-80500(p.157-61))
effects of ingested, on hematological response to Pseudomonas endotoxin in miniature swine, 18: 41088(R) (HW-80500(p.162-6))
effects of ingested, on antitumor factors in mice, 19: 31813
effects of ingested, on antitumor factor in mice, 19: 31814
effects of ingested, on weight gain in dogs, 19: 43645(R) (UCD-472-112, pp 10-22)
effects of ingested, on blood picture in dogs, 19: 43725(R) (UCD-472-112, pp 44-9)
effects of ingested, on life spans of dogs, 19: 43727(R) (UCD-472-112, pp 126-40)
effects of ingested, on leukocyte values in beagles, 19: 43882 (UCD-472-112, pp 50-8)
effects of ingested, on skeleton of dogs, 19: 43882 (UCD-472-112, pp 50-8)
effects of ingested, in miniature swine, pathological, 20: 10597(R) (BNWL-122, pp 37-45)
effects of ingested, in miniature swine, 17: 35299(R) (HW-76000 (p.66-83))
effects of inhaled, on blood constituents in dogs and rats, 20: 8589(R) (LF-28, pp 209-29)
effects of inhaled, on histology and pathology of rats, 20: 8635(R) (LF-28, pp 164-208)
effects of inhaled, on virus production in feces, nose, and throat of dogs, 20: 8636(R) (LF-28, pp 230-5)
effects of inhaled, on production of bacterial flora in beagles, 20: 8637(R) (LF-28, pp 236-49)
effects of inhaled, on production of spirochetes in mouth and intestines in dogs, 20: 8638(R) (LF-28, pp 250-6)
effects of inhaled, on hematopoietic system in dogs, 20: 8639(R) (LF-28, pp 257-64)
effects of inhaled, on induction of myelogenous leukemia in rats, 20: 8640(R) (LF-28, pp 265-73)
effects of injected, on dogs, 16: 5156(R) (COO-224)
effects of injected, on testicles, 16: 14430
effects of injected, on blood picture, 16: 16237
effects of injected, on mandible of weanling rabbits, 17: 17804
effects of injected, on dogs, 17: 19883
effects of injected, on bone strength in beagles, 17: 19892
effects of injected, on corticosteroid biosynthesis in beagles, 17: 19894
effects of injected, on teeth of rabbits, 17: 19901
effects of injected, on bone marrow and peripheral blood picture of rabbits, 17: 19902
effects of injected, on bone marrow in rats, 17: 30388
effects of injected, on teeth and jaws of rabbits, 17: 37080
effects of injected, on morphology of bone marrow in rats, 18: 17592
effects of injected, on dogs, long-term pathological, 20: 5287(R) (COO-119-232, pp 5-64)
effects of injected, in dogs, pathological, 20: 8626(R) (COO-119-233, pp 5-67)
effects of injected, on blood picture in rats, 20: 8632(R) (LF-28, pp 131-8)
effects of injected, in rats, 20: 22696
effects of injected, on swine bone, 17: 15847
effects of injected, on bone tumors incidence in mice, relation of radiation dose to, 17: 5718
effects of injected, on bones of dogs, 17: 19886
effects of injected, carcinogenic, 17: 25037
effects of injected, in male mice, 17: 14054
effects of injected, on beagles, 17: 19888
effects of injected, on tumor incidence in mice, 16: 23464 (UAC-4763)
effects of injections of, on beagles, 18: 3482(R) (COO-228(p.61-5))
effects of internal deposition in lactating mice on growth of suckling young and mammary glands, 19: 6963
effects of internally deposited in man, biological, 20: 38623
effects of long-term feeding, in miniature swine, 16: 25112(R) (HW-72500(p.1-12))
effects of, on skin, occupational, 17: 17914
effects of radiation from ingested, on spermatogenesis, in dogs, 17: 31929
effects of retained burdens of, on non-skeletal tumor incidence in beagles, 18: 3486(R) (COO-228(p.95-108))

effects of subcutaneously injected, on oral tissues of experimental animals, 20: 42967
effects on acetylcholine content and cholinesterase activity in rat blood, 19: 42308
effects on anaerobic digestion, 17: 36064
effects on animals, carcinogenic, effects of chemical carcinogens on, 20: 10627
effects on animals and man, 20: 18198
effects on antibody formation in guinea pigs, 19: 42316
effects on auditory structures in rabbits, 20: 14316
effects on bacteria, mutagenic, 18: 27121
effects on behavior in dogs after chronic enteral admiaistration, 20: 16266
effects on bio-electrical activity of nerve endings, 17: 30361
effects on blood and hematopoietic tissue, 20: 28982
effects on blood cells in sheep, 16: 9908
effects on blood picture in mice, 20: 18353
effects on blood sugar content, in rats, 18: 27185
effects on bone cancer development in mice, protective effects of zirconium citrate against, 19: 17677
effects on bone marrow by uptake in bones, 20: 29054 (NP-16119)
effects on bone sarcoma incidence, 17: 30367
effects on bone tumor incidence in mice, 18: 6630
effects on bone tumor incidence in mice, 16: 31476 (A/AC.82/G/L.788)
effects on bone tumor incidence in mice, 16: 31477 (A/AC.82/G/L.785)
effects on bone tumors incidence in mice, 16: 31478 (A/AC.82/G/L.790)
effects on bone tumors incidence in mice, relation of radiation dose and dose rate to, 17: 5718
effects on bone tumors incidence in rats, 18: 8139(T)
effects on bones, effects on bone marrow of tumorigenic, 20: 6808
effects on cage reared beagles, 17: 38636(R) (UCD-108(p.27-36))
effects on calcium content and phosphatase activity of blood serum in rats, 18: 27187
effects on central nervous system of mice, effects of chloral and strychnine on, 19: 17578
effects on chick embryos, 18: 38775(R) (ORO-624)
effects on *Chlorella algae*, genetic, 18: 36946 (A/CONF.28/P/386)
effects on cholinesterase activity, 19: 43775
effects on chronic ingestion on reproduction in miniature swine, 17: 5700 (HW-74969)
effects on corneal metabolism in rabbits, 20: 10585
effects on cutaneous angiomas, 20: 18528
effects on DNAase activity in rat urine, 19: 24351
effects on dog sensory nerves, 18: 13463(T) (JPRS-23559(Del.)(p.36-42))
effects on dog skeleton, 20: 16253
effects on dogs, 16: 32705
effects on dogs, 16: 28744 (TID-12163)
effects on euploid cells in human bone marrow, internal, 18: 11715
effects on eyes, 18: 25146
effects on fish embryos, chronic-exposure, 18: 43273
effects on fish spawning, 20: 40527
effects on function and structure of pancreas, of injected, 19: 40358(T) (FTD-TT-65-48, pp 577–8)
effects on gastrointestinal tract during chronic radiation sickness, 20: 10674
effects on glycogen content of liver, in rats, 18: 27185
effects on growth and reproduction in mice, 17: 33633
effects on harvest and grain quality of field crops, 19: 19508(T) (JPRS-28977)
effects on hearts of rat progeny, 19: 33908
effects on hematocrit in rats, 18: 11575 (UR-639)
effects on hematopoietic system in rats, 17: 5822
effects on hematopoietic system in dogs, 19: 24354
effects on hematopoietic system in dogs, 19: 33907
effects on hematopoietic tissues in dogs and swine, acute- and chronic-exposure carcinogenic, 20: 31031 (BNWL-SA-201)
effects on hematopoiesis in rats, 17: 1661(T) (JPRS-15920(p.1-5))
effects on histaminase activity and histamine content in rat blood, 19: 17474
effects on immune response to Leptospira and infectious hepatitis in dogs, 20: 45320 (LF-29)
effects on immunity in pigs, 18: 13518
effects on inactivation and mutation in mycobacterium, 16: 7434
effects on lungs, carcinogenic, 18: 31349
effects on mice after intraperitoneal injection, 20: 18353
effects on mice, biological, of chronic ingestion of, 20: 38551
effects on mice, carcinogenic, 19: 29887(R) (ANL-6971(p.47-58))
effects on mice, genetic, 17: 33713
effects on mice, tumorigenic, 18: 23231(R) (ANL-6823(p.20-43))
effects on mitosis and ploidy in mouse embryos, 18: 41096
effects on mortality, reproduction, and tumor tolerance in mice, 18: 23210
effects on offspring of injected parents, 16: 4062
effects on osteogenic sarcoma development in rat, roentgenography of, 19: 28020
effect on ovarian follicles in mice, 19: 45831
effects on ovaries and reproduction of white rats, 17: 2872
effects on peripheral blood picture, diagnostic significance, 16: 50(T) (AEC-tr-4859)
effects on pituitary gland, 20: 18532
effects on plants, 16: 11472
effects on protein metabolism and tumor development in bones of rats, 19: 7027
effects on quality and yield of grain crops, 19: 35963
effects on rabbits, 17: 14003
effects on radiation dose to human skeleton from content in river water, model for predicting, 20: 30943(R) (ORNL-TM-1465)
effects on rat bones, tumorigenic, 20: 10652
effects on rat bone density and carcinogenesis, variations with mode of administration, 20: 45423
effects on rat pancreas, 18: 38838
effects on rat skeleton, 18: 41124
effects on rats, leukemogenic, 18: 38792
effects on seasonal fluctuations of intestinal flora sensitivity to antibiotics, 16: 16210
effects on serum lactic dehydrogenase levels in beagles, by internal deposition, 20: 112
effects on skeleton, 18: 13511
effects on skin diseases, 17: 30315
effects on strontium-85 elution from mouse bones, 19: 43706
effects on structure of immature rat brain, 19: 86
effects on submicroscopic cell structure of bone marrow in rats, 18: 36972
effects on sulfur-35-labeled sulfate formation in guinea pig eyes, 18: 38810
effects on swine, research program, 16: 7421 (HW-SA-2365)
effects on the dairy industry, review of countermeasures for, 18: 3894
effects on thermal tolerance of fish, 20: 31028 (AECL-2409)
effects on thymidine excretion by rats, 20: 16201
effects on thyroid activity in dogs, 20: 29000
effects on treatment of rickets in rats with vitamin D_2, 19: 19680
effects on tumor development in bones of rats, 19: 7026
effects on tumor development in rat lung, 19: 15049
effects on typhoid bacilli, 19: 33951
effects on wheat, 18: 31171
effects with cesium-137 on survival of rats, 20: 8631(R) (LF-28, pp 128-30)
elimination effectiveness of chemical compounds, 17: 21428(T) (JPRS-18936)
elimination from mice, dietary factors, 17: 5717
elimination of combined cerium-144 or plutonium-239 and, in rats, 20: 10552
elimination of injected, from mice, effects of zirconium citrate on, 18: 35288
energy levels, 18: 28691
equilibrium parameters in soil, in presence of other ions, 16: 9012
evaluation of, for space heat source, 20: 39306 (DP-1066(Vol.1), pp V.17-25)
excretion and skeletal retention, effects of chemical agents on, 18: 31102
excretion by cows in milk, effects of calcium on, 16: 9910
excretion by dogs, urinary and fecal, 17: 38639(R) (UCD-108(p.52-63))
excretion by man during first 22 days after exposure, 17: 2789(R) (ORNL-3347(p.142-54))
excretion by man, effects of intravenous calcium and oral ammonium chloride on urinary, 19: 42252
excretion by mature and young rats, comparison with calcium-45, 20: 45274 (BNWL-SA-825)
excretion by pregnant cows, 16: 26716
excretion by pregnant cows, 16: 9909
excretion by rats, effects of parathyroid extract, citric acid, diet, and lactation, 16: 8484 (TID-14849)
excretion by rats, effects of polyvinyl pyrrolidone on, 18: 19(T) (JPRS-21511(p.14-19))
excretion following occupational exposure, urinary, 16: 5153 (A/AC.82/G/L.654)
excretion from mice, influence of drugs on rate of, 20: 32922
excretion in cow's milk, effects of calcium uptake on, 18: 43170(R) (EUR-1882.e(p.31-6))
excretion in feces and urine in rats, effects of calcium and magnesium on, 16: 27468 (NP-11941(p.30-1))
excretion in mice, effects of aluminum citrate on, 17: 5744
excretion in rats, effects of citrate and salicylate treatments, 20: 37025(R) (PG-Report-705)
excretion in urine and uptake by blood of inhaled, 16: 2071
excretion in urine of man, 17: 23045
excretion in urine in man, relation to strontium-90/calcium ratio in diet,

19: 52
excretion in young adults, 16: 31457
excretion of deposited, effects of EDTA on, in dogs, 20: 5248(R) (COO-119-232, pp 200-2)
excretion of injected, effects of drugs on, 17: 30079
excretion of, by dogs, effects of chronic ingestion on, 18: 29200 (UCD-472-110)
excretion of, by rats, effects of sodium phytate on fecal and urinary, 20: 30977
excretion of, effects of chelating agents in mice, 20: 8561
excretion of, effects of tetracycline, 20: 8562
excretion of, effects of various salts in mice, 20: 8563
excretion of, effects of various chemicals in mice, 20: 8564
exposure to, maximum permissible occupational, 18: 15907
fall-out concentrations in precipitation, meteorological factors, 16: 22448 (TID-7632(p.242-55))
fall-out deposition in temperate zone of northern hemisphere, 16: 5599 (A/AC.82/G/L.696)
fall-out in Fayetteville, Arkansas after 1961 Soviet tests, 16: 31470
fallout in Antarctica, 20: 9145
fallout in Australia, meteorological factors affecting, 20: 523
fallout in Europe, 1954 to 1964, 19: 42645
fallout in New York City, 18: 39505
fallout in New Zealand, July to Sept. 1964, 19: 9371(R) (NP-14618)
fallout in northern hemisphere in 1962-3, 19: 44259
fallout in Pakistan in 1958 to 1962, 19: 6094 (NP-14390)
fallout in USSR during 1961–1962, 19: 28539 (NP-14730)
fallout levels in United Kingdom, 18: 27706
fallout levels in Israel, Oct. 1963 to June 1964, 19: 26917(R) (IA-984)
fallout monitoring near Leningrad in 1961–1963, 20: 16701
fallout monitoring in polar regions of Soviet Union, 20: 16703
fallout of, effects of test ban on, 18: 43815
fallout of, estimation of worldwide, 18: 39505
fallout on Japan, seasonal variations in, 1955 to 1959, 19: 28550
fallout, in Spain, 18: 35754
feeding to beagles, quality control in continuous, 17: 38637(R) (UCD-108(p.37-44))
fixation in skeleton in experimental rickets, 16: 26711
food chain contamination by, effects of plant strontium-90 uptake on, 20: 12607
formulae for assessing body content of, following contamination in adult human males, 20: 42779
fractionation in surface bursts, correlation of data on, 20: 27211 (USNRDL-TR-991)
gamma dose rate from shielded and unshielded, 18: 18621 (ORNL-3576)
gamma emission, 16: 24583
gamma spectra of, least-squares analysis of, 18: 33926
global circulation following Chinese nuclear explosion of May 14, 1965, 20: 5656
global integrals from fall-out, 1958 to 1960, 16: 20905
global levels from fall-out, 1959 to 1961, 16: 22442 (TID-7632(p.149-69))
ground water contamination by, in Shoal Event, hazards from, 20: 16742 (VUF-1014)
half life, (E), 19: 16905
half life, 20: 8076 (NP-15663)
half life and metabolism of, 20: 38743
half life in crappie, biological, 19: 21792(R) (ORNL-3650(p.187-219))
half life of fallout, biological, 19: 7748
half life of inhaled, in man, biological, 19: 35 (TID-7696(p.120-39))
handling and shipping, incorporation in phosphate glass for, 19: 4427(P)
handling of, design testing of shipping casks for, 16: 31985 (HW-SA-2655)
hazards of exposure of children to, 17: 29142
human assimilation and in-body deposition, 16: 24012(R) (HASL-127)
human bones, soft tissues, and standard diet in Germany, 19: 44313
incorporation in beta sources, 20: 25180(R) (BNL-954, pp 84-113)
incorporation in food chain, mechanisms of, 18: 8063(T) (AEC-tr-6049(p.258-70))
incorporation in strontium oxide glass, 18: 39830
incorporation in titanate pellets for thermoelectric generators, 20: 16914(R) (ORNL-3900, pp 182-93)
incorporation into food chain, factors affecting, 16: 5147 (ARCRL-5)
ingestion by Alaskan Eskimos via caribou meat, 1961 through 1965, 20: 23283 (BNWL-SA-556)
inhalation in emergency, calculation of acceptable limits for, 16: 9054
intake by man, maximum permissible constant, 18: 20235 (NP-13868)
intake in food, methods for estimating, 20: 43573 (CONF-765-13)
intake through contaminated water organisms, 16: 5135(T) (CEA-tr-R-1416)
inventory of fallout, world-wide, to 1962, 17: 30761
ion exchange behavior of, on peat and bentonites, 18: 40968
ion exchange on aluminum oxide surface, 20: 33274
leaching from alumina–phosphate glass prepared from calcined alumina waste, 20: 16133 (IDO-14672)
leaching from food plants, 20: 29451(R) (NYO-2598-29)
material balance of, 20: 521(R) (HASL-164)
measurement in fallout, 20: 25288
measurement in Hungarian rain, from Oct. 1962 to Dec. 1963, 19: 9758
measurement in milk samples in New Zealand, 20: 40521(R) (NP-16270)
measurement in rain samples in New Zealand, 20: 40521(R) (NP-16270)
measurement of ingested or inhaled, in man, 19: 25883
measurement of, whole-body counter for, 17: 38642(R) (UCD-108(p.90-122))
metabolism, 18: 23816 (AHSB(S) R-64)
metabolism and body burden of fallout, in man, 1962 to 1964, 19: 9370 (NP-14556(p.11-80))
metabolism and deposition in bone, 16: 32689(R) (TID-16458)
metabolism and retention in man, 18: 25
metabolism and skeletal retention of, effect of age in miniature swine on, 17: 35300(R) (HW-76000(p.84-8))
metabolism and toxic effects of, in avian embryos, 20: 32909(R) (ORO-648, pp 91-102)
metabolism by Acantharia, 19: 24723
metabolism by aquatic organisms, 19: 10719 (AECL-2107)
metabolism by aquatic animals and plants, 19: 11391(R) (NP-14658)
metabolism by cattle, effects of diet on, 20: 4162
metabolism by cattle, effects of dietary calcium on, 20: 8565
metabolism by Chlorella, 18: 41064
metabolism by *Cystoseira barbata* in sea water, 19: 14997
metabolism by domestic animals, 19: 24246
metabolism by fish, 17: 5708(T) (JPRS-15871)
metabolism by five generations of rats in prolonged feeding tests, 18: 41045 (NP-14327)
metabolism by fresh water plants, 18: 35282(T) (AEC-tr-6447)
metabolism by geese, 18: 38774(R) (EUR-1881.e)
metabolism by man, 18: 35290
metabolism by man, 18: 35291
metabolism by man of, 19: 8737 (BNL-8657)
metabolism by man, 19: 45793
metabolism by man, 20: 31142
metabolism by man, 1961 to 1965, 19: 42638 (HASL-163)
metabolism by man, age-dependent models of, 20: 6719(R) (ORNL-3849, pp 183-213)
metabolism by marine plankton, 19: 24242(R) (NP-14901)
metabolism by marine fish and invertebrates, 20: 26549(R) (NP-15915)
metabolism by oat plants, effects of potassium phosphate and calcium hydroxide on, 19: 40310
metabolism by plants and animals, 16: 22460 (TID-7632(p.426-56))
metabolism by plankton, 18: 35238 (STI/DOC/10/28(p.9-20))
metabolism by plants, 19: 6104
metabolism by plankton, 19: 45748(R) (TID-22193)
metabolism by plants, 18: 9821
metabolism by plants, after foliar absorption of, 17: 35437 (TID-17977)
metabolism by plants, 19: 25838 (NP-14903)
metabolism by plants, 19: 45804
metabolism by rats, effects of vitamins A and D on, 18: 41046 (NP-14333)
metabolism by rats, effects of source of ingested, on, 20: 26628
metabolism by ruminants, 18: 38993 (HW-SA-3693)
metabolism by virus, 19: 33782
metabolism in animals and plants of, 19: 25870
metabolism in animals, effects of dietary constituents on, 19: 40342
metabolism in animals and man, 19: 46634 (AD-423463)
metabolism in bones, in man, 17: 5715
metabolism in bones, effects of age, 19: 21848
metabolism in calf skeleton after ingestion by mother or self, effects of age on, 19: 40329
metabolism in dogs after chronic ingestion, 19: 40324
metabolism in dogs after chronic ingestion, 19: 40325
metabolism in dogs and offspring after chronic ingestion, 19: 40327
metabolism in dogs, rabbits, and rats, effects of magnesium sulfate on, 19: 42254
metabolism in dogs, 19: 43679(R) (UCD-472-112, pp 109-19)
metabolism in dogs, effects of age on, 20: 14243(R) (TID-22626)
metabolism in domestic animals, 18: 11645(R) (ORO-614)
metabolism in fetus of cattle after ingestion by the mother, 19: 40330
metabolism in fetus of sheep after intravenous or oral administration to mother, 19: 40331
metabolism in lactating cows, 16: 10347
metabolism in lactating rats, and litters, 19: 10765
metabolism in lactating rats, 20: 35
metabolism in live mice, design of radiation detectors for measuring, 20: 36556
metabolism in mammals, effects of calcium on, 19: 38335 (NP-14926)
metabolism in man, age factors, 17: 115
metabolism in man, 19: 6948(R) (ORNL-3697(p.178-92))
metabolism in man, 19: 24247

metabolism in man, theoretical analysis of, 18: 38738
metabolism in mice after intraperitoneal or subcutaneous injection, 20: 18225
metabolism in milk cows after chronic ingestion, 19: 40332
metabolism in miniature swine, effects of administration as titanate or chloride on, 18: 23200 (HW-SA-3350)
metabolism in oats, effects of soil treatment on, 19: 19475(T) (JPRS-27940(p.10-17))
metabolism in plants, effects of soil on, 19: 24760
metabolism in rabbits, 20: 7327
metabolism in rat bones, effects of vitamin A on, 19: 33774
metabolism in rats, 16: 1481(T) (JPRS-10170(p.198-212))
metabolism in rats, effects of vitamin D_2 on, 18: 27057
metabolism in rats, 19: 2011
metabolism in rats, effects of vitamin D_2 on, 19: 10760
metabolism in rats, 19: 29881
metabolism in rats, effects of vitamin D_3 on, 19: 38347
metabolism in rats after oral or intravenous administration, 19: 40321
metabolism in rats after chronic oral administration, 19: 40323
metabolism in sheep, 19: 45759(R) (ORO-631, pp 77-82)
metabolism in skeleton, effects of dietary calcium and inflammation in rabbits on, 19: 40343
metabolism in swine after chronic ingestion, 19: 40328
metabolism in *Vicia faba*, 16: 31462
metabolism kinetics of, in man, 18: 20235 (NP-13868)
metabolism of, effects of high-calcium diet on, 17: 35421
metabolism of, in bone in young miniature swine, dietary effects on, 17: 13940
metabolism of, by forage plants, effects of soil type and fertilizers on, 20: 3665(T) (CEA-tr-X-619)
metabolism of, in bones of rabbits, 18: 33261
metabolisms in rats after intratracheal administration, 19: 40312
migration in Czech soils, 19: 5559 (UJV-1107/64)
migration in farm and meadow lands, vertical, 16: 10333
migration in soils, 18: 8524(T) (AEC-tr-6049(p.225-32))
migration in soils, contamination of food chains in, 18: 16239
migration in turf-podzolic and black earth soil, 20: 40520 (NP-16261)
migration rate of, in sand, 18: 5475 (UCRL-13010)
mobility of, on paper electrochromatograms, 18: 10159
monitoring airborne, in Japan, Nov. 1961 to March 1962, 19: 2559
monitoring environmental, Mol, 1960, 16: 20813(R) (A/AC.82/G/L.721)
monitoring environmental, Mol, 1960, 16: 20812(R) (A/AC.82/G/L.711)
monitoring for, in foods, 17: 17750
monitoring for, in Ottawa River, 17: 20256
monitoring for, in foods in Austria, 1962, 19: 15804
monitoring in Alaska, 1957 to 1962, 16: 15040
monitoring in Antarctica and between 60°N and 70°S in 1958, 16: 16042
monitoring in atmosphere in Northern and Southern hemispheres, 1958-62, 19: 4407
monitoring in Australia, 1963, 19: 46594
monitoring in California fallout in winter 1961 to 62, 18: 10284
monitoring in Clinch and Tennessee Rivers at Oak Ridge, methods for, 18: 14092
monitoring in food and surface water in Savannah River Plant area, July through Dec. 1965, 20: 27195(R) (DPST-66-30-1)
monitoring in ground-level air, rainwater, and soil in Germany, 1958–61, 16: 11941
monitoring in Iceland, 1958 to 1964, 20: 45908
monitoring in milk in Canada from fallout, 18: 16229 (NP-13760)
monitoring in Nagasaki, Japan, 1959, 18: 14082
monitoring in Ottawa River, program for, 17: 6334
monitoring in River Thames, 17: 35440
monitoring in the Copenhagen area, 17: 12498 (RISO-51)
monitoring of ambient, 18: 14072 (EUR-481.i)
motion in Atlantic Ocean, vertical, 20: 18930
motion in soil, effects of chelating agents on, 19: 38329 (TID-20471)
movement by insects, 19: 21792(R) (ORNL-3650(p.187-219))
movement in Belgian soils, 19: 10659(R) (EURAEC-703)
movement in clay soils, physicochemical reactions in, 18: 16208
movement in Georgian soils, 20: 39117(T)
movement in soils, 20: 30943(R) (ORNL-TM-1465)
movement in soils, method for study of, 18: 16216
movement in soils, Belgian studies on, 18: 17341
movement of, in soil and plants, 18: 1320(R) (NP-13315)
movement on surface of earth by runoff and erosion, 16: 22452 (TID-7632(p.299-305))
movement through soils during leaching with deionized water, 17: 39279
movement through soil, 19: 2542
nuclear deformations in, oscillator model for, 18: 28731
oral administration to fish, force-feeding method for, 17: 40465
pathological effects of injected, in mice, 16: 21953
pathological effects in bones, relation of radiation dose, 16: 31441
pathological effects of injected, in mice, 16: 31479 (A/AC.82/G/L.789)
pathological effects in mice, 16: 32692 (TID-16796)
pathological effects of chronic occupational exposure, 17: 2850
pathological effects in mice, 17: 5907
pathological effects of, ingested in fish, 17: 5701 (HW-SA-2255)
pathological effects in bone in swine, 17: 13919 (HW-SA-2613)
pathological effects of continuous feeding of, on beagles, 17: 19900
pathological effects on dogs, 17: 38645(R) (UCD-108(p.145-9))
pathological effects of, deposited in bones in dogs, 17: 38782
pathological effects of ingested, in rats, 17: 40639
pathological effects of ingested, on liver of dogs, 18: 21781(T) (JPRS-24301(Del.)(p.1-8))
pathological effects of injected, in rat embryos, 18: 23244 (UR-643)
pathological effects of injected, in dogs, 18: 29238(R) (COO-119-229 (p.2-57))
pathological effects in dogs, delayed, 18: 33342
pathological effects on bone, 18: 35266(R) (UCLA-12-529(p.41-7))
pathological effects of chronic ingestion of, in dogs, 18: 38955
pathological effects on gastrointestinal tract of rats, 18: 38973
pathological effects in dog bones, 19: 15148
pathological effects of internally deposited, in animals and man, 19: 35945 (NP-15184)
pathological effects in dogs of injected, 19: 40378
performance as heat source in Ripple I thermionic generator, 19: 46895
performance as space vehicle power supply, 20: 11188 (BLG-330)
performance in Beta-2 nuclear battery, 19: 34606
performance in high-temperature thermoelectric generator for space, 20: 21211 (TID-22350)
performance in portable ultraviolet source, 19: 32654(P)
performance in thermoelectric generators, 20: 723 (NP-15531)
performance in thickness determinations in textile industry, 19: 30613
poisoning by, drug evaluation for emergency treatment of, 19: 40339
precipitation, from highly radioactive waste solutions, 17: 33401
prediction of accumulation in bones in New York City, Poland, and Great Britain, 20: 43619
preparation and incorporation in vitreous enamel for use as beta source, 19: 13832
preparation and properties as radiation source, 18: 27811(R) (ORNL-TM-198)
preparation for use as encapsulated heat sources, engineering drawings of plant for, 18: 27838
preparation for use as radiation source, powder metallurgy methods in, 20: 23009
preparation of carrier-free, by mixed crystal method, 18: 12154
preparation of clean and carrier-free, 20: 43430
preparation of, for use in direct-energy conversion devices, 17: 26245
preparation of reference samples for detector calibration, 18: 30073
preparation of sources of, for direct energy conversion, 19: 26718 (ORNL-3802)
preparation of, for radioecological studies, 20: 28879
preparation of, self-absorption in evaporation method for, 20: 23211
processing into planar beta sources, (E), 19: 40560
processing to encapsulated heat sources, safety evaluation of pilot plant for, 19: 30631 (MND-3137)
production and uses of emitters of, 17: 25344(P)
production at Oak Ridge National Lab., 16: 15081
production in atomic explosions, 20: 23314
production in Canada, 18: 14338
production in copper ores by nuclear explosions, 20: 23236(R) (ORNL-TM-1496)
production in nature by spontaneous fission, 19: 10372
production of carrier-free, by solid solutions, 16: 24084
production of encapsulated sources of, megacurie facility at Hanford for, 20: 45785
properties and useful range in thickness measurements, 16: 2097
properties as heat sources, 16: 16464
properties as heat source for underground uses, 18: 27811(R) (ORNL-TM-198)
properties as heat source, bibliography on nuclear, 20: 33752(R) (N-66-12928)
properties as power source, nuclear and physical, 20: 27389
properties as radioisotope heat source, 18: 9066 (MND-P-2975)
properties for use in argon ionization detector in gas chromatography, 18: 14239
properties for use as heat source in direct conversion devices, 18: 34002
properties of, in energy conversion cells, 17: 12751(R) (ARF-1214-1)
properties of radioapplicators of yttrium-90 and, 20: 18522
properties of, chemical, physical, radiological, and toxicological, 19: 11422 (RSG-A-1)
properties of, in isotopic power sources, 20: 41397
properties of, nuclear and physical, 19: 20402 (TID-7698(Pt.I)(p.17-30))
purification by solvent extraction using bis(2-ethylhexyl) phosphate, 20: 14641 (RL-SA-59)
radiation dose distribution from injected, in rabbits, 17: 19905

radiation dose from insoluble particles of, compared to that from soluble forms, 20: 43631
radiation dose measurements of internally deposited, 16: 17453
radiation dose to mouse gonads from injected, 18: 23185(R) (ANL-6823(p.76-80))
radiation dose to populations from, in fallout, 1963, 18: 31771
radiation dose to dog skeleton from ingested, 19: 43726(R) (UCD-472-112, pp 120-5)
radiation dose to skeleton from, in persons using Clinch River water, 20: 29452 (ORNL-3721(Suppl.3))
radiation dose to bone from, maximum permissible body burden for, 20: 33100
radiation dose to gastrointestinal tract from ingested, calculation of, 20: 43043
radiation effects on nervous system in second generation progenies of dogs exposed to, 16: 28816
radiation effects on tissue distribution in mice, 17: 19848
radiation effects on rat teeth uptake of, x, 18: 19655
radiation effects on Arabidopsis from uptake of, beta, 19: 25936
radiation hazard from atmospheric, in mixture with yttrium-90, 20: 31528
radiation hazards from fall-out, through 1961, 16: 30675 (LADC-5370)
radiation hazards from, in fallout, 17: 39323
radiation hazards from chronic ingestion of, in man, 18: 25073
radiation hazards to populations from fallout, 18: 27714
radiation hazards of fallout, in human food chain, 18: 29227
radiation hazards to industrial workers from luminous paints containing, 18: 37465
radiation hazards to industrial workers from luminous paints containing, 18: 37466
radiation hazards from, in Polish paint industry, 19: 9420
radiation hazards from internally deposited, 19: 15005
radiation hazards of inhalation and ingestion of, by man, 19: 40805 (NRS-30)
radiation hazards from luminous paints containing, 19: 42676
radiation hazards of, released by accident, 19: 46696
radiation injuries from, deposited in bone, 16: 17453
radiation protection standards for atmospheric, 19: 38877 (NP-15183)
radiation sickness induced in rats by injected, 17: 5929
radioactive contamination of water supplies in Connecticut by, from fallout, 17: 18426
radioactive contamination of milk by, from fallout, 17: 17747
radioactivity and yield from uranium fission, gravimetric method of determining, 18: 27288 (KFK-199)
radiochemical analysis, 20: 417(R) (NYO-3086-1 Pt.IX)
radiotoxicity of, control by strontium-rich diet, 20: 45497
ratio to calcium in milk and infants' bones, 18: 15796
ratio to strontium-89 in fallout, effects of sampling height on, 19: 7709
re-entry ablation of molten droplets containing, as space fuel, 19: 4400 (MND-3062-5)
re-entry ablation of fuel capsules of, for space power plants, 20: 11189 (MND-3062-25)
reactions with organic matter in soil, 18: 27698
redistribution in small cultivated watersheds, 17: 39278
release from simulated high-level wastes, 20: 40476(R) (BNWL-267)
release in aircraft fuel pin meltdown, 17: 35117
release to atmosphere from NRTS, 20: 45219
removal from body by chelation, 19: 24238 (AWRE-O-4/65)
removal from bone using chelates and parathyroid hormone, 19: 31671(R) (NIRS-3(p.57-63))
removal from fabrics, using detergents and EDTA, 18: 43864
removal from fabrics using citric acid, detergents, or water, 20: 39161
removal from glass, PVC films, and steel detergents, 19: 4421
removal from ICPP fuel storage basin effluent, 17: 30582(R) (IDO-14611)
removal from leafy vegetables, effectiveness of detergents and water for, 18: 5555
removal from milk, ion-exchange process, 17: 8458
removal from milk, 17: 25302
removal from milk, ion exchange method for, 18: 17952
removal from mouse skeleton compounds for, 19: 29999
removal from rat bone, effects of EDTA and vitamin D on, 18: 31113
removal from rat body by high strontium diets, 20: 38566
removal from raw foods by mechanical processing, 18: 12400
removal from solutions by calcite-phosphate column, 16: 25051 (TID-7628(p.211-13))
removal from surface by chemical reagents, 19: 4419
removal from textiles used for radioprotective clothing, 19: 17834
removal from vegetables by home preparation methods, 19: 11394
removal from wastewater, 18: 18050
removal from water, device for, 18: 16249
removal of, contamination from milk, 17: 27606
removal of, from animals, effects of triethylenetriaminehexaacetic acid on, 17: 15589(R) (TID-18058)
removal of, from rat skin by ultrasonics, 20: 42811
retention by fetal and newborn rats, 20: 5237(R) (UR-668, pp 55-109)
retention by soil, 17: 2782 (BLG-103)
retention by soils, effects of chemical treatments on, 20: 20875 (EUR-2481.f)
retention in beagles, 16: 5156(R) (COO-224)
retention in female rats, effects of lactation on, 18: 30
retention in rats, effects of age and dose on, 20: 5237(R) (UR-668, pp 55-109)
retention of, by mice, effects of phosphorus content of diet on, 17: 38715
retention of dietary, in human infants, 17: 23063
separation and recovery, 16: 8(T) (AEC-tr-4142(p.33-42))
separation by ion exchange, 17: 30074
separation by solvent extraction from irradiated uranium solutions, 17: 8241 (HW-SA-2396)
separation by solvent extraction using butyl phosphate solutions, 18: 6890
separation from aqueous solutions by solvent extraction using TTA, 18: 13930
separation from aqueous solutions, use of silica gel for, 20: 1742 (INR-636/XIII/J)
separation from aqueous solution by sorption on diatomaceous earth, 20: 12938
separation from barium-140 by ion exchange and residue leaching, 19: 13201(R) (MLM-1217)
separation from biologic wastes, ion exchange, 17: 38643(R) (UCD-108(p.123-42))
separation from biological wastes by ion exchange, 19: 45692 (UCD-472-112, pp 141-7))
separation from cesium-137 by ion exchange, 16: 7336
separation from cerium-144 by ion exchange, 17: 240
separation from cerium-144, cesium-137, and zirconium-95 by paper electrophoresis, 18: 1739
separation from cesium-137 and yttrium-90 by ion exchange on allyl phosphate, 19: 11024
separation from cesium-137 and yttrium-90, chromatographic, 19: 26235(T) (CEA-tr-A-1801)
separation from Clinch River sediments, 20: 45216 (ORNL-3721)
separation from fission products by electrophoresis, 16: 6511
separation from fission products by paper electrophoresis, temperature effects, 16: 13100
separation from fission products, 16: 17336
separation from fission products by paper electrophoresis, 16: 33046
separation from fission products by paper electrophoresis, 17: 1403
separation from fission product mixtures by ion exchange, design of semiautomatic device for, 18: 1805
separation from fission products by amalgam exchange, radiochemical, 18: 16148
separation from fission products by thin layer chromatography, 19: 24467
separation from fission products, methods for, 19: 27832(R) (HW-83609)
separation from fission product solutions by oxalic acid precipitation, 20: 20804 (EUR-2754.f)
separation from food and milk, 17: 35441
separation from food and water, 19: 20240
separation from fresh water by ion exchange chromatography, 20: 20627
separation from fuel storage basin effluent by ion exchange, 19: 40651 (IDO-14657)
separation from Hanford wastes for use as heat sources, 18: 33983 (HW-SA-3080(Rev.))
separation from high-level wastes, 17: 33395 (HW-SA-2786)
separation from irradiated fuel by solvent extraction, 18: 37252 (A/CONF.28/P/100)
separation from irradiated uranium by ion exchange chromatography, carrier-free, 19: 38757 (SGAE-CH-17/1965)
separation from irradiated fuels, 20: 25470
separation from irradiated copper ore by leaching and ion exchange, 20: 45570(R) (ORNL-3945, pp 189-94)
separation from low-level process water by ion exchange, 17: 31789 (ORO-603)
separation from low-activity waste by foam treatment, 18: 16129(R) (RAI-116)
separation from low-level waste solutions, ion exchange method for, 20: 47083(R) (ORNL-3945, pp 79-106)
separation from melts by complex formation with cesium, lead, or rubidium chlorides, 18: 23540
separation from milk, ion exchange process, 16: 22279
separation from milk, 16: 27504
separation from milk, method for, 17: 27038
separation from milk, ion exchange, 19: 11396
separation from milk by ion exchange, 19: 34289(P)
separation from milk by moving bed ion exchange columns, 19: 40697(P)
separation from milk by electrodialysis, 20: 1972(P)
separation from milk using calcium phosphate precipitation method, 20: 16382

separation from milk by electrodialysis, pilot plant study of, 20: 12997 (AD-626210)
separation from milk, methods for, 20: 43537
separation from organic waste, 17: 38582
separation from organic waste solutions by ion exchange, 18: 35240
separation from other fission products, large-scale, 18: 31649 (A/CONF.28/P/252)
separation from other fission products by ion exchange, 20: 3871 (EUR-2497.e)
separation from power reactor fuels, economics of, 19: 20036 (BNWL-25)
separation from Purex waste by D2EHPA extraction, 16: 30505
separation from Purex plant solution by solvent extraction using D2EHPA, 18: 5414 (HW-72666)
separation from Purex and Redox process waste by ion exchange, 19: 12859
separation from Purex waste solutions by lead carrier sulfate precipitation, 20: 14641 (RL-SA-59)
separation from rain water, use of tracers in filters for, 17: 30184
separation from rain water, method for, 20: 1778
separation from radioisotopes in aqueous solutions by foam chromatography using colloidal manganese dioxide, 20: 20628
separation from rain water, 20: 37029
separation from reactor gases, trapping system for, 18: 14118 (TID-7677 (p.102-24))
separation from reservoir water by coagulation with aluminum and iron and fast filtration, 20: 4068
separation from sea water, ion exchange, 20: 22872(R) (NIRS-4, pp 12-17)
separation from soil, method for, 20: 20882(R) (HASL-171)
separation from steel surfaces by electrolysis, 18: 35946
separation from storage basin water, 19: 20042(R) (IDO-14646)
separation from uranium fission products using ring oven method, 19: 11021
separation from waste solutions by alluvial silts, 17: 19709 (TID-7644(p.151-75))
separation from waste by Dowex-50W and clinoptilolite, 17: 28581(R) (HW-77299)
separation from waste solutions by ion exchange, 17: 31790 (ORO-604)
separation from waste solutions using clay, lime, phosphates and soda ash, 17: 36998
separation from waste waters by ion exchange, 17: 39180(R) (ORNL-3452(p.51-96))
separation from waste solutions by ion exchange, 18: 5415(R) (IDO-14599)
separation from waste solutions by solvent extraction, 18: 11505(P)
separation from water by chemical precipitation, 18: 20266
separation from waste solutions by foam methods, 19: 12859
separation from waste at Hanford, design of plant for, 19: 13848
separation from wastes in Hanford isotope plant, feasibility study, 19: 20431 (TID-7698(Pt.I)(p.1-16))
separation from wastes at Hanford, 19: 45690 (RL-SA-40)
separation from waste solutions using manganese dioxide, 20: 5206
separation from waste solutions by recycle scavenging–precipitation ion exchange process, 20: 10440 (ORNL-3863)
separation from wastes, engineering drawings of WAFRAX facilities for, 20: 16139
separation from water supplies, using sanitary water-treatment process, 20: 22512 (K-1651)
separation from water using bentonites, gypsum, and superphosphate, 20: 22924
separation from yttrium-90 in carbonate solution by ion exchange, 16: 3077
separation from yttrium-90 using anion exchange resins, 16: 3038(T) (CEA-tr-X-353)
separation from yttrium-90 in carrier-free state, electrochromatographic, 16: 13103
separation from yttrium-90 in aqueous solutions, 16: 2102(T) (CEA-tr-X-403)
separation from yttrium-90, chromatographic, 16: 27078
separation from yttrium-90 using ion exchange resin papers, 16: 11536
separation from yttrium-90 by adsorption on various materials, 17: 2662(R) (MLM-1135)
separation from yttrium-90 by selective adsorption on materials, 17: 7659(R) (MLM-1136)
separation from yttrium-90 by selective sorption on platinum, 17: 7660(R) (MLM-1137)
separation from yttrium-90, chromatographic, 17: 25301
separation from yttrium using diaryl phosphates, 17: 25324
separation from yttrium-90 by sorption, 17: 25295
separation from yttrium-90, use of pyridine in precipitation with ferric hydroxide, 17: 27447
separation from yttrium-90 by solvent extraction using pyridine citrate, 17: 29033
separation from yttrium-90 by amalgam exchange technique, 17: 34038
separation from yttrium-90, carrier-free, 17: 35893
separation from yttrium-90 by solvent extraction using benzene and TTA, 18: 1803(T) (CEA-tr-X-175)
separation from yttrium-90, 18: 13875
separation from yttrium-90 by ion exchange on tin phosphate, 18: 13922
separation from yttrium-90, 18: 23717
separation from yttrium-90 by anion exchange, 18: 41568
separation from yttrium-90 by ion exchange and residue adsorption, 18: 45175(R) (MLM-1209)
separation from yttrium-90, system for, 19: 2706(P)
separation from yttrium-90 using thin-layer chromatography, carrier-free, 19: 5982
separation from yttrium-90 by ion exchange, 19: 36293
separation from yttrium-90 by election process, 20: 2211
separation from yttrium-90 using organic bases as precipitants, 20: 23202
separation from yttrium-90 by ion exchange in DTPA and HEDTA, 20: 25197 (ORNL-3903)
separation in insoluble barium and strontium sulfate columns, 17: 192 (JEN-105-DQ/I-32)
separation of, as oxyquinolate, effects of neodymium, scandium, and thorium on, 18: 1811
separation of, from other fission products in air and rain water, 17: 20203
separation of, from calcium in bones, plants, and water, 17: 19788 (CRER-1134)
separation of, using sulfate columns, 17: 190 (CEA-2166)
separation of yttrium-90 from, by coprecipitation with ferric hydroxide, 18: 22182
separation of, from fission products in nitric acid solutions, chromatographic, 20: 36748
separation on cation exchange resin with scintillating properties and direct counting, 16: 30587 (NYO-9138)
separation using chromatographic paper treated with tri-*n*-octyl phosphate, 17: 35943
shielding of, bremsstrahlung attenuation factors for, 20: 3254
shielding power sources of, 19: 21595 (TID-7698(Pt.I)(p.33-248))
shielding requirements for, 17: 8156
shipment of gross quantities, 16: 31984 (HW-SA-2514)
shipping, 16: 25651 (HW-71574)
shipping, design criteria and hazards evaluation of cask for, 16: 3260 (HW-68081)
shipping, design of casks for, 16: 30695 (HW-SA-2295)
shipping of, analysis of potential hazards in, 17: 10853 (HW-SA-2518)
shipping of, design of cask and protective buffer for, 18: 22273 (HW-68274)
sorption and retention by soils, 16: 25052 (TID-7628(p.214-36))
sorption and retention by rats, effects of radioinduced morbidity on, 16: 31474 (UR-617)
sorption and retention of dietary, by rabbits, 17: 17742
sorption and storage on aluminum silicate zeolites, 20: 14466 (RL-SA-58)
sorption by active manganese dioxide, 17: 30604
sorption by aged horse manure, 20: 31252
sorption by calcite-phosphate columns, extrapolation formula for, 18: 17343
sorption by calcium phosphate, 16: 28639
sorption by calcium-activated barium sulfate, process limiting, 20: 5531 (UJV-1382/65)
sorption by clay and soil, 16: 31628
sorption by clay materials from radioactive solutions, 18: 21696
sorption by clays and soils, 16: 7330(T) (CEA-tr-R-1427)
sorption by clays and sands, 20: 14209 (RT/PHOT(65)29)
sorption by clays and soils, effect of soaking on, 20: 45907
sorption by cultivated plants, 16: 25642 (CEA-2159)
sorption by ferric hydroxide gel, effects of ripening time on, 16: 17725
sorption by ground water and soils, 16: 28634 (CRER-1089)
sorption by humic acids and peat, 16: 11591
sorption by intestine, effects of green tea on, 20: 30987
sorption by ion exchange collectors, 18: 12258 (PAN-453/XIX)
sorption by ion exchange materials from water, 19: 539
sorption by Mytilus, 20: 42770
sorption by newt renal tubules, 18: 17455
sorption by plants, sand, and water, 16: 14371
sorption by plants, role of leaves and roots in, 17: 38732 (NP-13115)
sorption by ploughed soils, 18: 16217
sorption by porous borosilicate glass for use as radiation source, 19: 42785
sorption by pregnant cows, 16: 9909
sorption by skin of animals, effects of cleansing agents on, 20: 35674
sorption by slags, 18: 40965
sorption by sodium aluminosilicate, 16: 25651 (HW-71574)
sorption by soil, 19: 4127

sorption by soils, effects of disodium salt of EDTA on, 20: 35227
sorption by zeolites, 18: 23717
sorption by zeolitic tuff, 19: 12856
sorption from gastrointestinal tracts of rats by sunflower pectins, 16: 3287(T) (JPRS-9706(p.56-62))
sorption from lung, 17: 31835
sorption from radioactive wastes by ion exchange, 20: 14434 (BNWL-180)
sorption from waste solutions, ion exchange, 17: 33408
sorption from waste solutions by pyroclastic rocks, 19: 24444
sorption from waste solutions by aluminum oxide, mechanism of, 20: 16330 (CEA-R-2851)
sorption from waste solutions by clay minerals, 20: 29332 (ORNL-P-1811)
sorption from waste solutions by Yazoo and Zilpha clays, 20: 45221
sorption kinetics, intestinal, 17: 23022
sorption of, by marine silts, 17: 37021(T) (JPRS-20795(p.1-6))
sorption of, by skeleton in mice, rats, and rabbits, 17: 13956
sorption of ingested or inhaled, effects of treatment with barium sulfate, 16: 20077
sorption on coal columns, 18: 38697
sorption on vermiculite from acidic and neutral solutions, 16: 11958(R) (JAERI-5003(p.117-18))
sorption on vermiculite by ion exchange, 17: 25315
standards for atmospheric release of, in milk-producing area, derivation of, 20: 45504
state of, in blood serum, 18: 6608
storage of, method for long-term, 17: 15522 (HW-73933)
storage of wastes of, packaging facilities for, 20: 20348 (RL-SA-60)
stratospheric residence time, 16: 22424
toxic effects in dogs, 16: 11438(R) (ANL-6464(p.38-49))
toxic effects in dogs, 16: 21903(R) (COO-225)
toxic effects in dogs and man, 16: 28699 (TID-7639)
toxic effects in dogs, 19: 10736(R) (COO-119-231(p.6-62))
toxic effects in mice of, effects of strain, 19: 24252
toxic effects in sheep, 17: 15541(R) (ORO-598)
toxic effects in sheep, 19: 45812(R) (ORO-631, pp 1-35)
toxic effects of chronic ingestion of low levels of, in swine, 17: 40482 (HW-SA-3085)
toxic effects of injected, on erythrocytes in rats, 16: 9911
toxic effects of injected, in miniature swine, 16: 25119(R) (HW-72500 (p.36-40))
toxic effects of injections of, on erythrocytes in rats, 16: 26718
toxic effects of injected, in mice, 16: 12870
toxic effects of, in miniature swine, 17: 35288(R) (HW-76000(p.1-10))
toxic effects of, in rat embryos, 18: 11575 (UR-639)
toxic effects of, in luminous paints, 18: 29897
toxic effects on sheep, 19: 3891(R) (ORO-625(p.1-27))
toxicity in avian embryos, 18: 41159
toxicity in dogs, 17: 10295(R) (COO-226(p.3-33))
toxicity in dogs, 20: 40540(R) (UCD-472-113, pp 17-56)
toxicity in dogs, injection charts for studying, 20: 45275(R) (COO-119-234)
toxicity in lambs, 20: 35318
toxicity in rat embryos, 20: 5237(R) (UR-668, pp 55-109)
transfer from contaminated soil to plants, 17: 38725
transfer from mother to fetus, 16: 8486 (UCLA-498)
transfer from mother to offspring in rats after injection during pregnancy, 16: 30200
transfer from mother to progeny in rats, 18: 13432
transfer from placenta to fetus in pregnant rats, discrimination in, 19: 8751(T)
transfer from plants to insects of, through food chain, 17: 33550
transfer of fallout, in soils and plants, 18: 3446 (NAS-NRC-Pub-1092)
transfer through placenta in rats, 18: 35283(T) (JPRS-25464(p.14-21))
transfer to cheese and whey from milk, 18: 22299
transfer to embryos in pregnant cows, 16: 26716
transfer to fetus in cows, 16: 9909
transfer to milk from plasma in sheep, kinetics of, 17: 35304(R) (HW-76000(p.98-108))
translocation from maternal skeleton to progeny during gestation and lactation, 20: 40540(R) (UCD-472-113, pp 17-56)
transport from atmosphere to water supplies, 20: 41141
transport from blood stream into gastrointestinal stream in rats, 20: 36558
transport from stratosphere to ground by intense convective storms, 19: 22560
transport from stratosphere to troposphere, mechanisms of, 20: 23314
transport in soil and plants, 20: 20926(R) (ARCRL-14)
tropospheric residence time of, 17: 6272(R) (ORO-520)
uptake and accumulation by animals and men, permissible levels of, 16: 30689
uptake and accumulation in food plants, effects of soil fertilization on, 19: 3832
uptake and distribution in food chain of, 18: 3449
uptake and distribution in rat bones, effects of calcium-rich diet on, 19: 21836
uptake and distribution in developing roe of Black Sea fish, 19: 25879
uptake and distribution in bones and soft tissues in dogs by oral administration, 19: 25880
uptake and distribution in barley, oats, peas, and wheat, relation to calcium, 20: 42766
uptake and elimination from blood stream in dogs, effects of artificial kidney on, 18: 11599
uptake and excretion of, by dragonfly larvae, 17: 17738(T) (JPRS-18548 (Excerpt))
uptake and excretion from fallout by farm animals, 19: 25886
uptake and release by watercress, 16: 17434
uptake and release by marine animals, kinetics of, 18: 36917 (A/CONF.28/P/811)
uptake and release of, in *Nerita forskali* Recluz in seawater, 20: 218(R) (STI/DOC/10/42, pp 1-22)
uptake and retention by osteosarcomas in mice, 16: 26691
uptake and retention by bone in monkeys, 16: 28660
uptake and retention of by man in United Kingdom, equations for, 20: 42762
uptake and storage by rats, effects on growth of, 18: 38911
uptake as phytate or chloride in sheep and swine, 20: 35215
uptake by agricultural crops, assessment of, 18: 3610
uptake by agricultural plants of, effects of species, soil type, and agronomy practices on, 20: 3679
uptake by alfalfa, oats, timothy, and wheat grown in open and under tents, 19: 25842
uptake by algae, 18: 41054
uptake by algae, effects of calcium and magnesium on, 17: 40531 (TID-7664(p.231-46))
uptake by algae from water, 17: 28661
uptake by algae, effects of EDTA on, 20: 38570
uptake by animals and plants, coefficients of variation for, 19: 1997
uptake by antlers and mandible of deer, 19: 25868
uptake by aquatic insects, coefficient of accumulation for, 19: 25857
uptake by barley and pea plants, effects of calcium, potassium, and sodium on, 18: 33241
uptake by barley pollen grains, mutagenic effects of, 19: 10761
uptake by bean plants, effect of clinoptilolite on, 20: 45264(R) (UCLA-12-595, pp 72-89)
uptake by biosphere, 18: 18092
uptake by bone, effects on tumor incidence, 20: 10628
uptake by bones of children, 18: 29495
uptake by bones of children, fallout contribution to, 18: 37042
uptake by brown trout, 18: 16243
uptake by browsing deer and sheep, food-chain factors affecting, 20: 40541(R) (UCD-34P104-3)
uptake by butter and cheese from milk, 19: 28592
uptake by carp, 18: 5148(T) (JPRS-21989(p.5-10))
uptake by Chironomidae, 18: 36918
uptake by clams, 17: 33566
uptake by clover and rye grass, effects of applications of stable strontium to soil on, 20: 20381
uptake by clover, effects of calcium and strontium amendments, 16: 7400
uptake by corn plants, effects of soil temperature, 16: 17431
uptake by *Cystoseira barbata* from sea water, 19: 14997
uptake by deer and sheep, effects of biological and environmental factors on, 20: 20388 (SAN-34-2)
uptake by deer mandibles, relation of age and sex to, 19: 25869
uptake by dog skeleton after oral administration, 19: 43679(R) (UCD-472-112, pp 109-19)
uptake by Finnish milk, 1960–1963, 18: 22254
uptake by fish roe, 16: 28723
uptake by fish, effects of calcium content in water on, 20: 24836 (AE-224)
uptake by food plants under field conditions, effect of lime on, 17: 7777
uptake by food plants under field conditions, 17: 40541
uptake by foods, 18: 3617
uptake by freshwater clams, 18: 36918
uptake by *Gammarus lacustris*, 17: 15623
uptake by goldfish gills, 16: 20106
uptake by grass, milk, and soil, 18: 18045
uptake by green algae, 18: 38735
uptake by growing rats, effects of vitamins D_3 and A_1 on, 19: 17486
uptake by hair after injection into rats, 17: 15612
uptake by human bone, dependence on age of, 18: 13435
uptake by human bones in United Kingdom, 18: 21802
uptake by human body, 19: 7735(R) (ORNL-3697(p.222-6))
uptake by human bones, effects of calcium uptake on, 20: 5263
uptake by humans and rats, effects of barium sulfate and calcium phosphate on, 17: 28632
uptake by hydrophytes and organic wastes, 18: 3459

uptake by Japanese vegetables from fallout, 18: 33805(R) (NIRS-2 (p.57-67))
uptake by legume and grain plants from soil, 20: 26627
uptake by London babies, 19: 14991
uptake by maize, effects of soil temperature on, 20: 3668
uptake by mammalian skeleton, effects of diet on, 18: 19533
uptake by man, 18: 25693
uptake by man, 18: 37033
uptake by man, factors affecting, 18: 3604
uptake by man following accidental exposure, 20: 9199
uptake by man from diet, absorption coefficient for, 19: 8758
uptake by man of, through drinking water and food chain, 20: 41142
uptake by man, evaluation of body burden in, 19: 46
uptake by man, significance of, 18: 37364 (A/CONF.28/P/769)
uptake by marine organisms, 18: 23212
uptake by marine organisms in Suruga Bay, Japan, 19: 5601 (IAEA-R-19)
uptake by marine organisms, correlation with buildup factor, 20: 18215
uptake by *Melanogrammus aeglefinus* developing spawn, 19: 17483
uptake by milk in United Kingdom, 18: 22252
uptake by oats and peas, effects of humus and soil composition on, 16: 14452
uptake by oats, factors affecting, 18: 23206(T) (JPRS-24290(p.43-7))
uptake by osteosarcomas, 18: 11578
uptake by Pacific Ocean fish, 18: 29892
uptake by pasture grass, effects of calcium content of soil on, 20: 18232
uptake by pigs and sheep compared with calcium, 18: 31104
uptake by pine trees from ground water, 17: 40540
uptake by plankton crustacea, use of observed ratio equation for predicting, 19: 10777
uptake by plant foliage, effects of rainfall on, 18: 458
uptake by plants, 16: 1462
uptake by plants, 16: 10344
uptake by plants, 16: 10345
uptake by plants and soil, 18: 12358
uptake by plants from soil and irrigation water, 18: 33239
uptake by plants growing in peat-podzolic soils, effects of liming on, 20: 18303
uptake by plants in White Oak Lake bed, 16: 2060(R) (ORNL-3189(p.81-104))
uptake by plants in water medium, 19: 35927
uptake by plants in Georgia piedmont, 20: 12985
uptake by plants, effects of liming and soil types on, 20: 6745
uptake by plants, effects of soil minerals on, 20: 26613
uptake by plants, effects of calcium content and mechanical properties of soil on, 20: 30985
uptake by pregnant cows, 16: 26716
uptake by *Prochilodus lineatus* or *Platensis*, 16: 26721(T) (HW-tr-41)
uptake by rabbit bones and plasma, 20: 16178
uptake by rabbit skin, effects of detergent treatment on, 20: 29461
uptake by rainbow trout from diet and water, 16: 28698 (HW-SA-1997)
uptake by rat skeleton, effects of stable strontium on, 17: 31831(T) (JPRS-19626)
uptake by rats, effects of calcium, fat, magnesium, and phosphorus on, 19: 27943
uptake by rats, effects of dietary phosphorus on, 20: 32918
uptake by rice, effects of irrigation on, 20: 40574
uptake by Rumanian animal foods, 19: 640
uptake by salmon and trout eggs from contaminated water, 16: 12878 (PG-Report-288)
uptake by sheep organs, 16: 9907
uptake by skeletons of rats, effects of fluorine on, 16: 11408
uptake by skeleton in miniature pigs, age effects on calcium-45 discrimination in, 18: 19539
uptake by skeleton of growing beagles, ratio with calcium, 17: 38638(R) (UCD-108(p.45-51))
uptake by soil, effects of natural extracts from plants and trees on, 19: 53
uptake by tissues of man following ingestion of contaminated marine animals, 20: 35682
uptake by tree branches, leaves, needles, roots, and stems from soil, 19: 45773
uptake by vegetation in central European area of USSR, May 1963, 19: 35888
uptake by wheat from contaminated soil, 18: 15761
uptake by wheat, effects of variety on, 20: 18970
uptake by white-tailed deer antlers, 18: 31177
uptake, distribution, and excretion by animals, 17: 28637
uptake from airborne particles by infants, 19: 3855
uptake from fallout by humans, 17: 35434
uptake from milk by rats, effects of physico-chemical state on, 20: 18224
uptake from sea water of, by plankton, 17: 33564
uptake from soil by crop plants, effects of calcium content of soil on, 18: 19515 (NP-13796)
uptake from soils by plants, 20: 14236
uptake from soils by plants, 18: 29192 (TID-20781)
uptake from soils by plants, effects of phosphate on, 19: 45774
uptake in fresh water ecological systems, 17: 7781
uptake in relationship to calcium uptake by Austrian population, 1962, 20: 5263
uptake of fallout, by plants, 17: 40517 (SA/PR-40(Rev.))
uptake of, from soil by field crops, 17: 35322(R) (HW-76000(p.208-10))
uptake of, by above-ground plant parts from air, 18: 33235(T) (AEC-tr-6448)
uptake of, by tissues of beagles on chronic ingestion regimen of the radionuclide, 20: 42780
uptake, review of studies of chronic, 17: 10306 (HW-SA-2577)
uptake, adsorption, and leaching by soils, 18: 17457
uptake, excretion, and retention by infants on normal diet, 19: 25901
use as beta source in coal processing, 16: 25414(R) (NYO-10184)
use as beta source for treatment of eye lesions, 19: 30054
use as beta source for treatment of eye lesions, 19: 30018
use as beta source for therapy of hemangiomas in children, 20: 5443
use as beta source for therapy of eye tumors, 20: 6952
use as beta source for therapy of skin lesions, 20: 8791
use as beta source for radiotherapy, 20: 8795
use as beta source for simulation of space radiation, 20: 46102(R) (ORNL-4013)
use as beta source in radiometric measurement of ore pulp flow rates, 20: 46105 (BM-RI-6855)
use as fuel for generator for data telemetry package, 16: 5083 (MND-SR-2615)
use as fuel for thermoelectric generator, 16: 3966(R) (MND-P-2483-2)
use as fuel for thermoelectric generator, 16: 3967(R) (MND-P-2483-3)
use as heat source in SNAP-7 device, radiological hazards of, 20: 39307 (DP-1066(Vol.1), pp V.35-40)
use as heat source in RIPPLE I + II, 20: 39309 (DP-1066(Vol.2), pp III.39-48)
use as heat source for underwater warm-up station, 20: 46102(R) (ORNL-4013)
use as heat source for undersea missions, 20: 45830
use as hydrogenation catalyst, 19: 40553(R) (NYO-2978-34)
use as radiation source in industrial facility, 16: 7810(R) (RAI-200)
use as sealed beta source for radiotherapy, testing of, 19: 36152
use as thermoelectric generator fuel, 16: 34125(R) (MND-P-2483-6)
use as thermoelectric generator fuel in telemetry package, 17: 18898 (MND-SR-2428)
use for bremsstrahlung production in metals, 19: 2672
use for measuring ion exchange capacity of soils, 19: 9094 (CEA-R-2543)
use for mouth tumor therapy, 19: 43912
use for radiotherapy, 20: 16305
use for therapy of skin tumors, 20: 16325
use in beta applicators, 20: 40766
use in beta ionization detector for chromatographic determination of permanent gases, 19: 40415(T) (CEA-tr-R-1839)
use in beta irradiator for high-pressure high-temperature chemical reactions, 20: 355(R) (NYO-2978-42)
use in beta source for ecological studies, 19: 6935 (ORNL-TM-997)
use in beta sources in Soviet Union, survey of, 20: 23544(T) (ARC-tr-6466/1, pp 100-5)
use in dermatology, methods for radiation protection in, 19: 17701
use in dog irradiation, facility design for, 18: 31075
use in evaluation of scrubbing tests on textiles, 19: 24887
use in hemangioma therapy, 20: 10745
use in hydrology, 19: 30425
use in hypophysis destruction, 19: 36198
use in industrial absorption and x-ray fluorescence, 18: 21981
use in luminous paints in watchmaking, 19: 28706
use in neurosurgery, methods for, 19: 34063
use in nuclear batteries, 19: 46897(P)
use in pterygium surgery, 18: 13601
use in pterygium therapy, 18: 11921
use in radiotherapy of cancer, 18: 29485
use in railway signaling systems, 18: 18253
use in skin tumor therapy, 19: 34005
use in space power supply, radiation levels from, 18: 11362
use in therapy of rat rickets, 18: 21934
use in therapy of spinal pain, 18: 17691
use in therapy, applicator needle for, 18: 15912(R) (ACRH-20(p.25-36))
use in thermoelectric converters, 20: 39633 (CEA-R-2788)
use in treatment of hemangioma, 19: 7249
use in whole-body irradiation, design of 24-curie source for, 18: 19819
use in x-ray source, 18: 3657
use in x-ray sources, 20: 36915 (N-66-17678)
use of bremsstrahlung radiation from, for activation determination of beryllium and deuterium, 18: 37081
use of fallout, as metabolic tracer in man, 20: 24837

use of, for removal of static electricity in rubber industry, 17: 21969
use of needles of, for cordotomy, 19: 30013 (ACRH-103(p.104-20))
use of radioapplicators of, for eye tumors, 17: 24840
use with yttrium-90 as beta source for radiation chemistry studies, 16: 7585
use with yttrium-90 as divided beta source in irradiation facility, 20: 23102
used with yttrium-90, bremmsstrahlung efficiency in bone of, 18: 23173
uses, 20: 25470
uses as beta source, industrial, 18: 22388
uses as power source, shielding for, 19: 33704
uses as power source for underwater acoustic beacon, 20: 726
uses as power sources for underwater applications, 20: 29607
uses in direct-conversion power supplies, preparation for, 18: 14334
uses in heat and neutron sources, 18: 27828
uses in Japan, 1950 to 1960, 19: 39060
uses in medicine, 18: 33436
uses in nuclear batteries, (E), 19: 4882(P)
uses of waste, to control termite colonies, 20: 29587
uses of, review on therapeutic, 19: 274
volatility of, in radioactive alumina calcine during high-temperature storage, 20: 14207 (IDO-14670)
volatilization from calcined alumina wastes, 19: 24610(R) (IDO-14638)
volatization loss of, effect of temperature on, 20: 47082 (AEET-250)
waste processing of, by neutron conversion to shorter-lived species, 16: 31341 (BNL-5010)
yields from fission of plutonium-239, uranium-235, and uranium-238, 18: 19516
yields from neutron fission of thorium-232, 18: 9311 (IS-558)
yields from spontaneous fission of uranium-238, 17: 33109
yields from thorium-232 fission, (E), 20: 17860
yields in thermal neutron fission of plutonium-239, 19: 16873
yttrium-90 production from, 17: 3021 (BNL-5454)

STRONTIUM ISOTOPES Sr-91
beta sorption from, as function of atomic number, 17: 28184
determination in fission gases, spectrometric, 16: 25295
determination in heavy-water moderator by sequential analysis, 18: 27287 (DP-886)
half life of, search for isomers in measurements of, 17: 17243
radiation effects on rat intestinal sorption of, x, 20: 22600
radioactivity, 19: 17368
ranges from fission of plutonium-239, radiochemical determination of, 20: 34525 (KFK-401)
release at IRL research reactor, 18: 4880
release to atmosphere in SPERT I destruct, (E), 19: 24172 (IDO-12039)
uptake, distribution and excretion by animals, 17: 28637
yield in proton fission of uranium-238 at 150 Mev, kinetic energy and range of, 19: 27498
yields from helium ion-induced fission of lead-207 at 41.1 to 26.3 Mev, 20: 37996
yields in helium-ion fission of lead-206, 18: 2844 (TID-19654)
yields in neutron-induced and spontaneous fission of uranium-238, 18: 1079
yields in neutron fission of natural thorium at 14.7 Mev, 18: 44836
yields in proton fission of uranium-238 at 150 Mev, excitation energy and momentum transfer of, 19: 27499
yields in proton fission of uranium-238 at 7.1, 9.4, and 12.0 Mev, 20: 37995

STRONTIUM ISOTOPES Sr-92
determination in fission gases, spectrometric, 16: 25295
determination in heavy-water moderator by sequential analysis, 18: 27287 (DP-886)
ranges from fission of plutonium-239, radiochemical determination of, 20: 34525 (KFK-401)
release to atmosphere in SPERT I destruct, (E), 19: 24172 (IDO-12039)
yields from helium ion-induced fission of lead-207 at 41.1 to 26.3 Mev, 20: 37996
yields in neutron-induced and spontaneous fission of uranium-238, 18: 1079

STRONTIUM ISOTOPES Sr-93
beta decay scheme, 16: 31089
beta decay scheme for, 19: 1594
decay of, beta and gamma spectrum in, (E), 19: 17056
decay scheme, 16: 6438(R) (TID-14466)
decay scheme, 19: 29228(R) (AEET/NP/10)
half life, 16: 12468

STRONTIUM ISOTOPES Sr-94
beta decay scheme of, 18: 22920
decay of, beta-gamma spectrum analysis of Q value for, 18: 11191 (ANL-6797(p.455-63))
half life, 20: 30476

STRONTIUM ISOTOPES Sr-95
distribution of intravenously injected, effects of time on, 19: 43883(R) (UCLA-12-565, pp 65-85)
effects on erythropoietic index and iron content in man, 20: 42908
half life, 18: 42778
half life, 20: 30476

STRONTIUM LACTATES
use as contrast media for diagnostic radiography, 18: 25242

STRONTIUM LANTHANUM COBALTATES
magnetic interactions in, direct and superexchange, 17: 37697

STRONTIUM LANTHANUM FERRATES
iron-57 Mössbauer spectra in perovskite series $La_{1-x}Sr_xFeO_3$ ($0 \leq x \leq 1$), (E), 20: 22336

STRONTIUM LANTHANUM MANGANATES(IV)
magnetic interactions in, direct and superexchange, 17: 37697

STRONTIUM LANTHANUM RHODIUM OXIDES
crystal structure, 20: 12865

STRONTIUM MOLYBDATES
distribution coefficients of rare earth niobates in single crystals of, 20: 29746
fluorescence spectra and laser properties of rare earth-activated, niobium-compensated, 19: 36393
gadolinium ion EPR in, 19: 41994(T)
heat of formation, 18: 27461
neodymium(III) optical maser properties at 77°K in, 16: 12251
neodymium ion fluorescent properties in crystals of, 17: 37177
radiation effects on crystal structure of, at 77°K, EPR studies of x, 20: 45759
refractive index of single crystal at 4050 to 7030 Å, 17: 22326
stability of gaseous, 20: 25091
terbium ion excitation and relaxation in, 17: 39057

STRONTIUM NEPTUNIUM FLUORIDES
preparation, properties, and structure of, 20: 40867 (KFK-385)

STRONTIUM NIOBATES
luminescence of, self-activated, 18: 20060
$NaNbO_3$–$Sr(NbO_3)_2$, phase studies and electric properties, 16: 23687
$SrNb_2O_6$–$YbFeO_3$, ferroelectric properties of, 17: 22199(T)

STRONTIUM NITRATES
decontamination, design of radiochemical waste evaporator system for, 16: 14372
decontamination, design of radiochemical waste evaporator system for, 16: 21861
density in mixtures with potassium nitrates, 16: 542
dissolution in liquid alkali nitrates, heats, 16: 32998
ion exchange and sorption on glass surfaces, 20: 16469
purification of commercial, 17: 4558(P)
radioinduced free radicals in, EPR studies of, 20: 18739
radioinduced spin-½ centers in single-crystal, gamma, 18: 23474
reactions of, with dinitrogen tetroxide and spectra of anhydrous, 17: 15995
reactions with pectins, 16: 3286(T) (JPRS-9706(p.50-5))
salting-out properties in uranyl nitrate extraction from aqueous solutions, 17: 10770
solubility in *n*-butyl acetate, 19: 15684
solubility in organic solvents, effects of water on, 17: 6190(T) (AEC-tr-5574)
solvent properties for uranyl nitrate, 17: 3007
sorption by glass surfaces, 20: 18846
spectra, infrared, 16: 14748
spectrum at low temperatures, infrared, 16: 33002
thermodynamic properties at 60 to 1200°K, 16: 14683 (BM-RI-5967)
transfer between heavy and light water, ionic hydration in, 17: 6096
KNO_3–$Sr(NO_3)_2$, association of silver ions with chloride ions in molten, 19: 34142(R) (NYO-2873-7)
$Sr(NO_3)_2$–$UO_2(NO_3)_2$–H_2O, activity coefficients of, at 25°C, 20: 29196
$Sr(NO_3)_2$–$UO_2(NO_3)_2$, complex formation, conductivity, pH, and spectrophotometric studies, 16: 2951

STRONTIUM OXALATES
precipitation with calcium oxalate using dimethyl oxalate, 20: 29154
spectra, infrared, 16: 32982
use as carrier in coprecipitation of microgram amounts of calcium, 18: 31369 (HW-SA-3461)

STRONTIUM OXIDES
see also Barium Strontium Oxides
see also Beryllium Strontium Oxides
beta particle scattering by, bremsstrahlung from, (T), 19: 8558 (HW-83784)
content in Keewatin and Timiskaming volcanic rocks at Kirkland Lake, Ontario, age estimations from, 20: 16711(R) (MIT-1381-13)
content in mckelveyite uranium mineral, 19: 40799
content in volcanic rocks in Lower Cambrian in Canada, age estimation from, 20: 16711(R) (MIT-1381-13)
dielectric losses in, frequency and temperature dependences of, 19: 19851(T) (ORNL-tr-491)
dissociation energy of, mass spectrometric determination of, 18: 23455

(WADD-TR-60-782(Pt.XXII))
dissociation energy of, atomic model for calculation of, 18: 31496
dissociation energies and excitation levels of, 18: 39225
dissociation energy, (E), 19: 8105
dissociation energy of, flame photometric determination of, 19: 42489
effect on allotropic transformations of rare earth sesquioxides, 19: 44731
effects on crystal structure of hafnium and zirconium oxides, 19: 26359
effects on elastic properties of irradiated aluminum oxide–boron oxide–silicon oxide glasses, 19: 7984
effects on plutonium dioxide, 18: 34049(R) (NUMEC-P-106)
effects on reduction of zinc oxide by carbon monoxide, 16: 28943
effects on sintered density of plutonia powders, 19: 40981 (NUMEC-2389-6)
effects on sintering of plutonium dioxide, 18: 27863(R) (NUMEC-2389-1)
electric conductivity at 900 to 1300°C, 17: 172(T)
electric properties of, effects of lattice energy and temperature on, 19: 21601(T) (ORNL-tr-490)
electron charge distribution and electronic states in, 19: 32146
electron paramagnetic resonance of exchange-coupled pairs of doubly ionized europium in, 18: 10676
electronegativity and ion radii of, prediction of phases in binary systems with other oxides from, 19: 23061
erbium EPR in crystals of, 20: 10264
erbium ion paramagnetic resonance in, 19: 4147
europium ion cubic field splitting in, 18: 22061
growth of scheelite single-crystal $Sr_{0.9}Gd_{0.1}MoO_4$ and $Sr_{0.9}Eu_{0.1}MoO_4$, 19: 26304
hardness of crystals of, 16: 10728
lattice energy of, calculation of Madelung, 19: 28866
molecular structure of, microwave and r-f spectra studies of, 19: 32146
performance as coatings on barium electrodes in thermionic cells, 17: 3589
performance as coating for cathodes, 17: 20664
preparation of strontium-90-labeled glass of, radiation hygiene and technology of, 18: 39830
proton reactions at 660 Mev, 18: 23731
radiation effects on films of, on glass, 16: 21108
radiation effects on crystal structure of, 19: 26917(R) (IA-984)
radiation effects on crystalline, 19: 39265(R) (IA-1021)
radioinduced displacements in, electron spin resonance study of, 16: 13657
reactions with aluminum oxides and lanthanum or neodymium oxides at 1400 to 1500°C, 20: 16482
reactions with americium oxide, properties of ternary oxides formed in, 19: 28286 (KFK-280)
reactions with glass, 16: 31376
reactions with lithium fluoride at high temperatures, product solubilities, 19: 11140(P)
reactions with neptunium dioxide, 17: 23359
reactions with silicon at 1200°C, 19: 38593(T) (ORNL-tr-674)
reduction by aluminum carbide, catalytic effects of calcium fluoride on, 19: 46252(T) (ORNL-tr-683)
separation from selenium by partition chromatography on teflon, 18: 23731
sintering effects on cerium oxide, 17: 18836
solubility in vanadium oxide at 685°C, enthalpy for, 20: 7072
spectra, Franck-Condon factor arrays for band, 16: 22129
spectra in low frequency region, infrared, 18: 23549
spectra of europium, gadolinium, and manganese ions in single-crystal, paramagnetic resonance, 18: 37136
spectra of F centers in single crystals of, paramagnetic-resonance, (E), 20: 3087
spectra of rare earth and transition metal ions in, ESR, 19: 26917(R) (IA-984)
spectral emissivity of coatings of, on cathodes, 17: 31124
thermal conductivity of sintered, at 450 to 720°C, 17: 40791
thermionic emission in, shallow donor, 17: 5079
transition metal ion EPR spectra in, 18: 2469
uses in pyrometallurgical processing of irradiated uranium, 19: 32319(P)
uses in refining of irradiated uranium, 19: 30346(P)
vaporization of, thermodynamic data for, 18: 19939 (WADD-TR-60-782 (Pt.XXI))
vaporization of, thermodynamics, 19: 36649 (AD-614997)
$BaO–Fe_2O_3–SrO$, magnetic properties of, 17: 37699
$BaO–Fe_2O_3–SrO$, phase studies on isothermic section at 1100°C, 18: 12659
$BaO–IrO_2–SrO$, crystal structure, 20: 16436
$BaO–RuO_2–SrO$, crystal structure, 20: 16436
BeO–SrO, crystal structure and phase studies, 16: 20381
BeO–SrO, properties as salt bath in melt-refining of fissium alloys, 17: 36860(R) (ANL-6648)
$Bi_2O_3–SrO$, electric conductivity of solid solutions of, 19: 32739(T) (NP-tr-1236(p.92-6))
$B_2O_3–SrO$, emission spectra of cerium- and samarium-activated phosphors of, 19: 40494(T)
$CaO–Fe_2O_3–SrO$, magnetic properties of, 17: 37699
$Ce_2O_3–SrO$, luminescence, 16: 33656
$CeO_2–SrO$, transport numbers in, 19: 32737(T) (NP-tr-1236(p.74-8))
$Dy_2O_3–SrO$, magnetic properties of orthorhombic, 19: 38071
$Dy_2O_3–SrO$, optical properties of compounds formed in, 20: 13278
$Dy_2O_3–SrO$, phase studies, 20: 302
$Er_2O_3–SrO$, optical properties of compounds formed in, 20: 13278
$Er_2O_3–SrO$, phase studies, 20: 302
$Er_2O_3–SrO$, properties of compounds formed by interactions in, 20: 17044
$Eu_2O_3–SrO$, magnetic properties of orthorhombic, 19: 38071
$Eu_2O_3–SrO$, optical properties of compounds formed in, 20: 13278
$Eu_2O_3–SrO$, phase studies, 20: 302
$Eu_2O_3–SrO$, preparation and structure of Eu_2SrO_4, 17: 1428
$Fe_2O_3–PbO–SrO$, magnetic properties of, 17: 37699
$Gd_2O_3–SrO$, magnetic properties of orthorhombic, 19: 38071
$Gd_2O_3–SrO$, optical properties of compounds formed in, 20: 13278
$Gd_2O_3–SrO$, phase studies, 20: 302
$GeO_2–SrO$, glass formation limits in, calculation of upper, 19: 44016
$Ho_2O_3–SrO$, magnetic properties of orthorhombic, 19: 38071
$Ho_2O_3–SrO$, optical properties of compounds formed in, 20: 13278
$Ho_2O_3–SrO$, phase studies, 20: 302
$Ho_2O_3–SrO$, properties of compounds formed by interactions in, 20: 17044
$La_2O_3–SrO$, phase studies, 20: 302
$Li_2O–O–SrO–Tc_2O_7$, compound formation in, 20: 31244
$Li_2O–SrO–Tc_2O_7$, compound formation in solid state reactions in, 20: 7050 (KFK-341)
$Lu_2O_3–SrO$, optical properties of compounds formed in, 20: 13278
$Lu_2O_3–SrO$, phase studies, 20: 302
$Lu_2O_3–SrO$, properties of compounds formed by interactions in, 20: 17044
$Na_2O–SrO–Tc_2O_7$, compound formation in solid state reactions in, 20: 7050 (KFK-341)
$Nd_2O_3–SrO$, phase studies, 20: 302
$O–Na_2O–SrO–Tc_2O_7$, compound formation in, 20: 31244
$O–SrO–Tc_2O_7$, compound formation in, 20: 31244
$Pr_2O_3–SrO$, phase studies, 20: 302
rare earth oxides–SrO, phase studies, 19: 7490
$Sc_2O_3–SrO$, optical properties of compounds formed in, 20: 13278
$Sc_2O_3–SrO$, preparation, phase studies, and properties of, 20: 16898
$SiO_2–SrO$, crystal structure, 19: 38621
$Sm_2O_3–SrO$, optical properties of compounds formed in, 20: 13278
$Sm_2O_3–SrO$, phase studies, 20: 302
$SrCO_3–SrO$, equilibria at high pressures, 17: 12262
$SrO–Tb_2O_3$, magnetic properties of orthorhombic, 19: 38071
$SrO–Tb_2O_3$, optical properties of compounds formed in, 20: 13278
$SrO–Tb_2O_3$, phase studies, 20: 302
$SrO–Tc_2O_7$, compound formation in solid state reactions in, 20: 7050 (KFK-341)
$SrO–TcO_2$, compound formation in solid state reactions in, 20: 7050 (KFK-341)
$SrO–ThO_2$, electric conductivity at 300 to 1000°C, 19: 9715
$SrO–TiO_2$, phase studies, 18: 12660
$SrO–TiO_2–ZrO_2$, phase studies, 17: 1994
$SrO–Tm_2O_3$, optical properties of compounds formed in, 20: 13278
$SrO–Tm_2O_3$, phase studies, 20: 302
$SrO–Tm_2O_3$, properties of compounds formed by interactions in, 20: 17044
$SrO–Yb_2O_3$, optical properties of compounds formed in, 20: 13278
$SrO–Yb_2O_3$, phase studies, 20: 302
$SrO–Yb_2O_3$, properties of compounds formed by interactions in, 20: 17044
$SrO–Y_2O_3$, optical properties of compounds formed in, 20: 13278
$SrO–Y_2O_3$, properties of compounds formed by interactions in, 20: 17044
SrO–ZrO, equilibrium diagram of, 19: 11131
$SrO–ZrO_2$, phase studies on, 20: 23670

STRONTIUM PERCHLORATES
radiation copolymerization of mylar and nylon using, 17: 30047
radioinduced decomposition, 19: 13453
radioinduced decomposition of, mechanism for, 19: 13454
radioinduced graft polymerization of, on cellulose acetate, 17: 30194
radioinduced grafting on polyisobutylene, 16: 29013
radioinduced polymerization in aqueous emulsions, 17: 4596
radiolysis of, mechanism and products of, 18: 3860
reactions with dioxane, structure of addition compound formed in, 17: 4452
thermal properties, 16: 14759

STRONTIUM PERMANGANATES
staining virus with, 19: 35883

STRONTIUM PHOSPHATES
see also Strontium Zirconium Phosphates
analysis, thermal, 16: 28878
crystal structure, 20: 20690
crystal structure of ortho-, 16: 3009

precipitation, 16: 175
preparation and crystal structure of ortho-, 18: 13726 (TID-18650)
preparation and properties of ortho-, 18: 19954
preparation and spectra of indium-activated, 17: 25655
properties of ortho-, 16: 3009
stability constants of, 16: 28944
stability constants, 17: 2962
stability of, 16: 16399
$Ca_3(PO_4)_2$–$Sr_3(PO_4)_2$, phase equilibria and tin-activated luminescence, 16: 3009
$Mg_3(PO_4)_2$–$Sr_3(PO_4)_2$, phase equilibria and tin-activated luminescence in, 16: 3009
$Sr_3(PO_4)_2$–$Zn_3(PO_4)_2$, phase equilibria and tin-activated luminescence, 16: 3009

STRONTIUM PLUTONATES
preparation and crystallography, 19: 24501

STRONTIUM PLUTONIUM FLUORIDES
preparation, properties, and structure of, 20: 40867 (KFK-385)

STRONTIUM SCANDATES
preparation and structure, 18: 16015

STRONTIUM SELENIDES
radioinduced displacements in, electron spin resonance study of, 16: 13657
reactions with rare-earth selenides, compounds from, 19: 372
transition metal ion ESR spectra in, 18: 2469
Ce_2Se_4–Sr_2Se_4, thermoelectric properties, 17: 11296 (AD-278352)

STRONTIUM SILICATES
reactions with lanthanum, neodymium, and yttrium orthosilicates, products from, 17: 1471
$CaSiO_3$–$SrSiO_3$, performance in radioisotopic self-luminous systems, 17: 29964

STRONTIUM SILICIDES
crystal structure, 19: 34154
thermoelectric properties of Sr_2Si, 16: 18017(R) (AD-266019)

STRONTIUM STANNATES
tin-119 gamma resonance absorption in, 16: 32440
tin-119 Mössbauer spectra in, 17: 32107
$BiFeO_3$–$SrSnO_3$, gamma resonance absorption at 23.8 kev in, effects of phase transformations on, 18: 22922

STRONTIUM SULFATES
crystallization, effects of sodium phosphates on, 16: 10025
crystallization of, effects of hexa-, penta-, tetra-, and triphosphates on, 18: 6801
effects on strontium-85 uptake by rats, 19: 6959
effects on strontium-85 metabolism in rats, 19: 33743
exchange of alkaline earth ions on, equilibrium in, 18: 41442
growth in presence of EDTA, spherulitic, 18: 228
hardness of crystalline, 16: 10728
ion exchange equilibrium on surfaces of ionic crystals, 19: 42517
preparation and structure of labeled, 17: 23322
preparation and use of, in fixation of fission products, 17: 190 (CEA-2166)
production of pure, from brines containing calcium, 16: 14764(P)
radiation damage in, electron spin resonance of, 17: 35253(R) (IA-775)
radiation effects on, electron spin resonance studies of gamma and internal sulfur-35 beta, 19: 22304
reactions with clays, solid state formation of feldspars in, 16: 16578
reactions with cristobalite, 17: 15986
reduction by hydrogen, 17: 10246(R) (ORNL-TM-403)
reduction by hydrogen, 18: 33529 (ORNL-3334(Pt.II))
solubility in organic solvents, effects of water on, 17: 6190(T) (AEC-tr-5574)
solubility in sodium sulfate solutions, tracer measurements, 19: 30156 (ORNL-tr-649)
solubility in water, effects of particle size, 16: 23592
solubility of, in aqueous solutions, determination of, 17: 4466
solubility of, in water, determination of, 17: 4466
sorption of orthophosphate ions by ignited, tracer study of, 17: 14248
sorptive properties for fission products, 17: 192 (JEN-105-DQ/I-32)
sorptive properties for phosphorus-32, effects of iron(III) on, 17: 27363
strontium and sulfur isotopic exchange on surfaces of crystals of, activation energy for, 20: 26881
strontium ion exchange with solution, 16: 23575
strontium-85 and sulfur-35 between ions on surface of crystals of, 20: 26881
strontium-85 exchange between crystals of, rate of, 20: 12869
strontium-85 exchange between crystals and solutions, 20: 14572
sulfur-35 exchange between crystals and solutions, 20: 14572
surface energy of, calculation of, 18: 22047
tumorigenic effects of implants of, in rats, 18: 25053

STRONTIUM SULFIDES
see also Strontium Zirconium Sulfides
composition of vaporous, equilibrium, 17: 33905
dissociation energy of, 17: 33906
hardness of crystals of, 16: 10728
luminescence of nickel-activated crystals of, 16: 10694
luminescence properties for gamma dosimetry, infrared-stimulated, 19: 40879 (UCRL-12371)
performance as luminescent dosimeter material, 18: 35773(R) (UCRL-7811)
preparation for luminescence dosimeters, 20: 5742(R) (UCRL-14351)
preparation of europium-, gadolinium-, and samarium-activated crystals of, effects of flux concentration on activator concentration in, 16: 15314(T)
processing of, for strontium production, 18: 13804(P)
properties as gamma detector, 18: 10308(R) (UCRL-7571)
radiation effects on paramagnetic resonance, 16: 12801(R) (IA-685)
radioinduced displacements in, electron spin resonance study of, 16: 13657
reactions with yttrium sulfide, 16: 18864
sublimation of, mass spectrometric study, 19: 43997(R) (UCRL-11889)
transition metal ion ESR spectra in, 18: 2469
trapping levels in activated crystals of, analysis of, by exoelectron emission, 16: 19515(T)
vaporization of, mass spectrometric studies of, 20: 3957
vaporization of, thermodynamic data for, 18: 19939 (WADD-TR-60-782 (Pt.XXI))
BaS–SrS, electronic properties as coatings on cathodes, 18: 30166(R) (AD-439716)
rare earth sulfides–SrS, crystal structure of solid solutions in, 20: 332

STRONTIUM SULFITES
thermal decomposition at 600 to 800°C, effects of duration, gas atmosphere, and temperature on, 18: 9786(T) (AEC-tr-6259)

STRONTIUM SYSTEMS
Ce–Se–Sr, electric properties, 17: 34469
Ce–Sr–Te, electric properties, 17: 34469
rare earths–Sr–S, crystal structure, 19: 13298
rare earths–Se–Sr, crystal structure, 19: 13298
Sr–$SrCl_2$, electric conductivity of molten, 16: 32194
Sr–$SrCl_2$, free energy of solution of, 19: 11103
Sr–SrH_2, phase studies, 17: 40771 (IS-613)
Sr–SrH_2, phase studies, 18: 2163(R) (IS-700(Sect.M))

STRONTIUM TANTALATES
crystal structure of, effects of sodium additions on, 19: 13308
luminescence of, self-activated, 18: 20060
radioinduced phase transformations in, 20: 9006

STRONTIUM TELLURIDES
Ce_2Te_4–Sr_2Te_4, thermoelectric properties, 17: 11296 (AD-278352)

STRONTIUM THIOCYANATES
solubility in water, 16: 23706

STRONTIUM THORIUM FLUORIDES
preparation, properties, and structure of, 20: 40867 (KFK-385)

STRONTIUM TITANATES
see also Bismuth Strontium Titanates
see also Calcium Strontium Titanates
acoustic properties of crystalline, at 4 to −300°K and 10 to 150 mc/sec, 16: 21032 (D1-82-0163)
activity measurements of strontium-90-labeled, 18: 27812(R) (ORNL-TM-415)
beta particle scattering by, bremsstrahlung from, (T), 19: 8558 (HW-83784)
compaction of powders of, by vibration, 18: 39860 (NYO-10216)
contamination of man by strontium-90 labeled, body burden for internal, 19: 26613
crystal dynamics and phase transitions, 18: 19992
crystal lattice dynamics of, temperature dependence of, 17: 5141
crystal lattice vibrations in, frequency wave vector dispersion relations in, 16: 32171 (AECL-1574)
crystal lattice vibrations in, 16: 31635
crystal structure of nonstoichiometric, diffusion of point defects in, 19: 42519
development for semiconductor and thermionic cell applications, 16: 9202(R) (MND-2584-2)
dielectric breakdown of single-crystal, intrinsic, 18: 18469
dielectric constants at 70 to 5000 cm^{-1} in, 16: 24321
dielectric constant and vibration frequencies of, 18: 2404(R) (TID-19651)
dielectric properties, 17: 4960
dielectric properties of monocrystals, 16: 5825
diffusion in, self-, 20: 29623(R) (TID-22970, pp 121-256)
diffusion in, tracer studies of self, 19: 42519
dissolution in sea water, strontium-85 studies of, 18: 31363 (USNRDL-TR-745)
dissolution of irradiated, for analysis, 17: 40722 (TID-7655(p.473-80))
dissolution rates of strontium-90-labeled, in sea water, 19: 32124 (TID-21020)
distribution of strontium-90 in, determination by radioautography,

17: 29854(R) (MND-2584-4)
electric conductivity of, 18: 16045
electron energy bands in, 18: 33586
electron paramagnetic resonance and optical absorption in chromium-, cobalt-, and manganese-doped, 18: 2464
electrostrictive constants of, comparison of experiment and theory, 17: 36488
emissivity, 17: 6675(R) (PWA-2128)
emissivity of flame-sprayed, on stainless steel at 300 to 1800°F, 16: 14358(R) (PWA-2043)
emissivity of, measurements of, 17: 16787(R) (PWA-2163)
emissivity of, comparison of calculated and measured, 19: 6292 (ASD-TDR-62-719(Pt.II))
emittance at high temperatures, total hemispherical, 17: 6731
europium ion spectra in, vibrational, 19: 22258
fabrication by vibratory compaction, 17: 16609(R) (NYO-10214)
fabrication of high-density, for use as radioactive sources, 17: 12632(R) (NYO-10215)
ferroelectric domains and cubic-tetragonal phase transition at low temperatures, 17: 20484
ferroelectric properties at 2.5 to 3000 cm^{-1}, 16: 13796
gadolinium ion EPR in, 16: 29549
impurity ion electron paramagnetic resonance in, pressure and temperature effects on, 18: 9017
iron group EPR spectra in, 18: 2467
iron(III) EPR spectrum in, 18: 25409
metabolism of ingested, in miniature swine, tracer study of, 18: 41034(R) (HW-80500(p.100-1))
microwave absorption above phase transition in pure and doped, 16: 15324
microwave absorption in, 16: 15325
phase studies, 18: 4142 (MND-P-2977)
phase transformations in single crystals of, at 4.2 to 300°K, 18: 8392
phase transition, 19: 20591
phase transition at 110°K, nuclear magnetic resonance study, 17: 12847
piezoelectric properties of reduced, from 4.2 to 296°K, 20: 10250
preparation and properties of crystals of, 17: 1941(R) (NP-12214)
preparation and properties as thermoelectric materials, 17: 29854(R) (MND-2584-4)
preparation and properties of strontium-90-enriched, 18: 4142 (MND-P-2977)
preparation and properties of single crystals of, effects of crystallization temperature on, 20: 41480
preparation by precipitation, 18: 34006(R) (ORNL-TM-889)
preparation by thermal decomposition of titanyl oxalate, 17: 1941(R) (NP-12214)
preparation of dense pellets of, by direct precipitation, 19: 34138 (MND-3062-8)
preparation of monocrystals of, 16: 5825
preparation of strontium-90-bearing pellets of, 20: 16914(R) (ORNL-3900, pp 182-93)
preparation of, method for, 18: 17849(P)
properties as radioisotope heat source, 18: 9066 (MND-P-2975)
radiation effects on electrical properties of monocrystalline, 16: 10633
radiation effects on, split interstitial formation in fast-neutron, 18: 22540
radiation effects on crystal structure and polarization of, fast-neutron 18: 34246
radiation effects on, 19: 11682
radiation effects on single crystals of, neutron, 20: 29826
radioactivity release from strontium-85-labeled, in marine environments, 20: 43592 (USNRDL-TR-1042)
rare earth EPR in, 18: 2466
rare earth EPR in, 18: 2467
rare earth ion spectra in, as crystal field probe, 18: 31459
strontium-90 leach rates from heat sources of, in sea water, (E), 19: 28716
structure defects in single-crystal, migration of point, 19: 42843(R) (COO-359-10)
superconducting critical fields and magnetization of niobium-doped, (E), 20: 37953
superconducting transitions in, 18: 21102
superconducting transition temperature in semiconducting, carrier-concentration effects on, (E/T), 19: 21170
superconductivity of, 19: 42897
superconductivity in, (T), 20: 4781
superconductivity in, 20: 44506
superconductivity in calcium- or barium-doped, 20: 44506
thermal conductivity at low temperatures, electric field dependence of (E/T), 19: 1483 (NYO-2391-5)
thermoelectric properties to 1100°C, 16: 4422(R) (MND-2584)
thermoelectric properties, 16: 9068(R) (MND-2584-3)
use of strontium-90-enriched, in beta irradiator for high-pressure high-temperature chemical reactions, 20: 355(R) (NYO-2978-42)
vibrational structure of, model for, 19: 11769
$BaTiO_3$–$SrTiO_3$, dielectric constant and loss angle, effect of hydrostatic pressure, 16: 10549
$BaTiO_3$–$SrTiO_3$, net-pattern structure in mixed crystals of, 19: 9132
Bi_2O_3·$3TiO_2$–$SrTiO_3$, phase transitions and nonlinear properties of, 17: 23998(T)
$CeTiO_3$–Fe–$SrTiO_3$, electric properties at room temperature to 1000°C, 17: 29854(R) (MND-2584-4)
$CeTiO_3$–Fe–Nd_2O_3–$SrTiO_3$–TiO_2, thermoelectric properties, 17: 29854(R) (MND-2584-4)
$CeTiO_3$–$SrTiO_3$, distribution of cerium-144 in, determination by radio-autography, 17: 29854(R) (MND-2584-4)
Fe–$SrTiO_3$–Y_2O_3–ZrH, electric and thermal properties, 17: 29854(R) (MND-2584-4)
Fe–$SrTiO_3$, preparation and properties as thermoelectric material, 17: 29854(R) (MND-2584-4)
$SrFeO_3$–$SrTiO_3$, effects of tetravalent iron content on electric and magnetic properties of, 17: 23983
$SrTiO_3$–$SrZrO_3$, formation and properties, 17: 1995
$SrTiO_3$–$SrZrO_3$, production and properties, effects of boric acid anhydride on, 17: 25257
$SrTiO_3$–TiO_2–ZrO_2, phase studies on solid solutions of, at 1300°C, 20: 23671

STRONTIUM TUNGSTATES
neodymium ion fluorescent properties in crystals of, 17: 37177
stability of gaseous, 20: 25091
superconductivity of hexagonal bronzes of, 20: 24293
thermionic emission from surfaces of, in vacuum, (E), 20: 17335

STRONTIUM URANATES
composition of, precipitated from solution, 19: 15448(T) (ANL-Trans-33 (p.203-12))
crystal structure of Sr_3UO_6, 20: 19223
preparation and properties of hydrated, 17: 21676
preparation and structure of Sr_2UO_4, 17: 28862
preparation by precipitation and dehydration, 19: 32173
preparation, properties, and spectra of, 20: 40901
structure of anhydrous, formed by calcination of strontium carbonate with uranium peroxide, 19: 15445(T) (ANL-Trans-33(p.180-5))

STRONTIUM URANIUM FLUORIDES
preparation, properties, and structure of, 20: 40867 (KFK-385)

STRONTIUM VANADATES
$SrVO_4$–$ThVO_4$, crystal structure, 19: 15542

STRONTIUM ZIRCONATES
crystal structure, 18: 18276(R) (AD-431996)
dielectric constants of, 18: 42162(R) (TID-20963)
fabrication and properties, 18: 18276(R) (AD-431996)
heat of formation, 18: 17831
mechanical properties of crystalline, effects of temperature on, 19: 2793(R) (AD-607173)
performance as magnetohydrodynamic electric insulation, 18: 12859 (NP-13516)
preparation and physico-technical properties, 16: 5356
preparation and properties of, 18: 24094(R) (AD-436324)
properties and structure of, 19: 11131
properties as magnetohydrodynamic insulation, 18: 7458 (PWA-2125)
properties of, for use at high temperatures, effects of molybdenum on, 17: 34471
properties of, mechanical-thermal, 19: 22985(R) (NP-14951)
properties of, research program on thermal-mechanical, 19: 47008(R) (NP-15429)
stability at high temperatures, 17: 9074
strength properties, effects of calcium zirconate on, 19: 37040(R) (NP-15118)
thermal expansion, 19: 37040(R) (NP-15118)
use as insulators in magnetohydrodynamic power generators, 17: 9073
$CaZrO_3$–$SrZrO_3$, stress-strain characteristics of, 19: 47008(R) (NP-15429)
HfO_2–$SrZrO_3$–W, fabrication and properties of composite coatings of, 19: 32704(R) (IITRI-B237-34)
$PbTiO_3$–$SrZrO_3$, dielectric properties and structure, 16: 18069
$SrTiO_3$–$SrZrO_3$, formation and properties, 17: 1995
$SrTiO_3$–$SrZrO_3$, production and properties, effects of boric acid anhydride on, 17: 25257

STRONTIUM ZIRCONIUM PHOSPHATES
luminescence properties of europium-activated $Sr_2ZrP_2O_9$, 18: 13830 (AFOSR-4647)

STRONTIUM ZIRCONIUM SULFIDES
preparation and structure, 17: 12236

g-Strophanthin
see Ouabain

STRUCTURAL BEAMS
centroids and moment areas of 90° circular beams, 17: 39219 (NAA-SR-Memo-8728)

vibrations in, effects of water on natural frequency of, 20: 4080 (WAPD-TM-535)

STRUCTURAL COLUMNS

analysis of supporting grids of perpendicular beams, 18: 13984 (ORNL-3535)
blast effects on concrete beams reinforced with high-strength deformed bars, 17: 30632 (AD-408447)
buckling problems, computer program for solving, 16: 7827 (DC-58-2-166)
deflections and stresses in perforated beams during bending, 16: 16477 (TIM-390)
design, 17: 40964
design for tank support, 19: 46524(P)
stress analysis of, computer program for, 17: 16173 (KAPL-M-JVM-4)

STRUCTURAL ENGINEERING

analysis of supporting grids of perpendicular beams, 18: 13984 (ORNL-3535)
bibliography on design and construction of nuclear facilities, 17: 8281 (NP-11896)
bibliography on sandwich construction, 16: 1881 (NP-11021)
calculation of stresses, forces, and deflections in linear elastic skeleton structures, computer program for, 18: 39468 (WAPD-TM-417)
continuum aspects of high-strength materials, 18: 37684 (TID-20984)
data for shelter design and construction, 17: 39290 (NAVDOCKS-P-290)
description of NASA space propulsion facility, 19: 7669
design and construction of reactor containment structures, (E/T), 19: 8574 (IITRI-578P22-9)
design of general purpose alpha–gamma hot laboratory, 19: 7670
elastic behavior of shells and plates, 17: 13706
fracture mechanics and stability of materials in, review on, 20: 13248 (GEAP-4678)
linear elastic analysis of statically indeterminate structures, 17: 13704
matrix progression method in, 17: 13707
radioisotope uses in, bibliography on, 18: 10433 (AED-C-01-04)
research programs of U. S. Army on, 1962 summary, 17: 33413(R) (NP-12967)
shear strength of concrete keys, 17: 40956 (DASA-1339)
specification guides at HAPO for, 18: 3921 (TID-15244(Rev.))
specification guides at HAPO for, 18: 3923 (TID-15246(Vol.I)(Rev.))
specification guides at HAPO for, 18: 3924 (TID-15246(Vol.II)(Rev.))
specification guides at HAPO for, 18: 3925 (TID-19753)
statistical methods for estimating design data, 16: 7642
straightening of steel members by heating, 19: 14909 (HW-SA-3414)
use of computers in, 17: 13705
vibration of reactor components, solution of nonlinear, 20: 45061

Structural Materials
see Building Materials

STRUCTURAL PANELS

(See also specific panels, e.g., Plates and Windows.)
see also Plates
see also Windows
blast effects, 16: 12819 (WT-1423)
blast effects measurement, 16: 14991 (WT-724)
blast effects on concrete, 16: 3989 (WT-1130)
blast effects on shelter components, 17: 29880 (WT-801)
blast loading, 16: 2829 (WT-1124)
design of floor slab, footings, end walls, and reinforced concrete arches for shelters, 17: 2656 (AD-274727L)
design of, for entrances for buried shelters, 17: 39291 (NP-13087)
design of laminated, for radiation shielding, 20: 14680(P)
design of sandwich-type, for radiation and fire protection, 20: 14682(P)
development of collision-resisting, for nuclear-powered ships, 18: 23090
evaluation of mineral diffusion board for air flow resistance, particulate removal, and iodine removal, 18: 6975(R) (TID-19850)
fabrication and testing of brazed refractory honeycomb sandwich, 18: 10494 (AD-427700(p.245-80))
for U. S. Army structures, drawings, 16: 11360 (WT-60(Ref.)(Pt.IV))
gamma attenuations by aircraft, 19: 11419 (ORNL-P-745)
gamma shielding properties of, 17: 35067
shielding effects of interior, on dose rates in windowless buildings, 17: 27601 (TO-B-63-6)
shielding properties of a roof slab against fallout, calculation of, 20: 43568 (AD-636787)
time of break measurements, 16: 11356 (WT-1)

STRUCTURES

(See also specific structures, types of structures, and structural members by name.)
see also Underground Structures
air leaks in, effects of urethan spray foam on, 20: 41200 (ORNL-TM-1551)
analysis for protection against fallout, 17: 2734
analysis of dynamic loads with short time histories in, 19: 28524 (UCRL-7794)
analysis of hexagonal box under internal pressure, 17: 39218 (NAA-SR-Memo-8670)
analysis of supporting grids of perpendicular beams, 18: 13984 (ORNL-3535)
bibliography on shielded, 20: 10220 (AED-C-01-11)
blast and thermal effects in Hardtack operation, 16: 19189 (WT-1701)
blast effects, 16: 11358 (WT-29)
blast effects, 16: 12819 (WT-1423)
blast effects from atomic explosions, 16: 12809 (WT-91)
blast effects from Project Gnome, pre-shot and post-shot surveys, 16: 16608 (PNE-127P)
blast effects from Salmon event on residential-type, 20: 4189 (VUF-1030)
blast effects from Salmon event on tall industrial and residential, 20: 4190 (VUF-1031)
blast effects in Greenhouse Operation, 18: 10207 (WT-86)
blast effects in Project Roller Coaster, 19: 7700(R) (NVO-162-17)
blast effects of nuclear airbursts on reinforced, 16: 18720 (WT-1451)
blast effects on concrete cubical, 16: 16574 (WT-721)
blast effects on, from repeated dynamic and static loadings, 17: 25386 (NESCO-P-166-10)
blast effects on German underground, 16: 24020 (WT-1454)
blast effects on industrial-type, 16: 2831 (WT-1129)
blast effects on reinforced concrete, analytical method for, 17: 12392 (DASA-1259)
blast effects on tunnels and underground chambers, 17: 2660 (BRL-Memo-1390)
blast effects on, trajectory analysis of fragments produced by, 20: 3610 (AD-622333)
blast loading, 16: 2829 (WT-1124)
blast loading, effects of shock wave, 17: 29882 (WT-1162)
blast loading instrumentation, 16: 14992 (WT-738)
blast loading of arches and domes, 17: 2659 (AFSWC-TR-61-90)
blast loading of shallow-buried in nuclear explosion, effectiveness of soil in restraining lateral movement, 16: 22289
blast loading of spherical domes of reinforced concrete, stress-strain effects of, 20: 2035 (AD-615017)
blast loading of underground, 16: 17907 (AD-264553)
blast loading of underground reinforced concrete arches, 17: 2656 (AD-274727L)
blast loading of underground, 17: 5666 (AD-274294)
blast loading on horizontal cylindrical shapes, 16: 16481 (WT-722)
blast loading, pressure measurements in Upshot-Knothole Operation, 16: 16482 (WT-740)
blast loading response, 16: 11359 (WT-59)
blast loading studies in Operation Greenhouse, 16: 2818 (WT-85)
block design, 16: 2719(R)
book: *Structures for Nuclear Power*, 18: 24926
burning of Naval buildings due to thermal pulse from nuclear explosion, 18: 29874 (AD-428592)
construction and management of industrial, for use as fall-out shelters, 16: 11988
construction for nuclear medicine, criteria for, 17: 7704
construction of Army, for atomic weapon tests, 16: 12806 (WT-60(REF)Pt.I)
construction of Army, for atomic weapon tests, 16: 12807 (WT-60(REF)Pt.II)
construction of Army, for atomic weapon tests, 16: 12808 (WT-60(REF)Pt.III)
construction of underground shelters, 17: 6324 (USNRDL-TR-582)
construction principles for fallout protection in, 17: 12500 (USNRDL-467)
contamination of roof surfaces by simulated fallout, 17: 20246 (USNRDL-TR-609)
contamination of wooden building by beryllium, at Los Alamos, 18: 29880 (LADC-6219)
damage from ground motion induced by underground nuclear explosions, survey, 19: 561 (UCRL-7964)
debris produced by nuclear blast, analysis, 19: 9287 (URS-639-4)
decontamination, 18: 37440 (NP-14208(Vol.I))
decontamination, 18: 37441 (NP-14208(Vol.II))
decontamination of residences, fallout, 17: 1658 (NDL-TR-33)
decontamination of roofs on, testing of methods for below-freezing conditions, 17: 14531 (NDL-TR-32)
decontamination of radiological, 18: 439 (NP-13126)
decontamination of roofs under cold-weather and thawing conditions, 18: 31754 (NDL-TR-58(Pt.I))
decontamination of roofs under cold-weather and thawing conditions, 18: 31755 (NDL-TR-58(Pt.II))
decontamination of vacated radiation installations, responsibility for, 18: 37455
decontamination of buildings, economics, 19: 6123 (CONF-555-14)
decontamination of roofs by washdown, 19: 6130 (USNRDL-TR-789)
decontamination of, effectiveness of inside and outside, 20: 20923 (AD-626727)
deformation analysis of circular coupled-plate, 20: 46239 (ANL-7145)

design and construction for reactor containment, (E/T), 19: 8574 (IITRI-578P22-9)
design for protection from window-collimated ceiling-scattered fallout radiation, 20: 34801
design for protection of cameras and film, 20: 41223 (EGG-1183-1244)
design of aluminum criticality assembly supporting, 16: 25705 (BNL-4932)
design of barricade, for hazardous pressure systems, 19: 26518 (KAPL-M-6446)
design of beryllium, 17: 3084 (ASD-TR-61-692)
design of dual-use military shelters, 18: 20197 (NAVDOCKS-P-310)
design of low-leakage, for reactor housing, 19: 10675(R) (NAA-SR-9999)
design of metal, to withstand atomic explosion blast, 20: 39053(P)
design of protective, solution of stress wave problems in, 20: 43495(R) (AD-628806)
design of, for livestock protection against fallout in event of nuclear explosion, 19: 18199
development of fibrous, 16: 10426 (ASD-TR-61-322(p.711-37))
diffusion of airborne effluents near buildings, 19: 661 (AECL-2043)
dose rates in windowless, effects of interior partitions on, 17: 27601 (TO-B-63-6)
effects of Salmon explosion on nearby oil and gas facilities, 19: 36589 (VUF-1022)
effects of Shoal explosion on nearby, 19: 1979 (VUF-1015)
evaluation for fallout protection, 20: 7326
evaluation of fallout contamination protection in ventilation systems and water supplies in hospitals, 17: 8466
evaluation of hospitals for fallout protection, 17: 8465
explosion effect on, 20: 39149 (NVO-28)
fabrication of foamed polyurethane, effects of space environment on, 17: 29264
failure modes of impact-loaded footing-soil system, review, 18: 10260 (AD-428283)
fall-out deposition in, 16: 13403
fallout protection afforded by, 17: 31804 (WT-1462)
fallout protection afforded by above-ground and below-ground, 18: 8509 (CEX 59.7b(Part II))
fallout radiation dose rate in blockhouse, window-collimated ceiling-scattered contribution to, 19: 10450 (AD-443549)
fire hazards to occupants of shelters, 18: 31740 (FMRC-15328)
gamma attenuation by roof of concrete blockhouse, 16: 3799 (NDL-TR-6)
gamma attenuation by, 17: 4210 (DASA-1318)
gamma attenuation by concrete blockhouse, 17: 36038 (TO-B-61-34)
gamma attenuation by concrete block, 18: 27690 (NRL-TR-43)
gamma dose distributions in compartmented, from external sources, 20: 3275
gamma dose rate distribution in compartmented steel, 18: 42868 (TO-B-64-1)
gamma dose rate residential, in Norway, 19: 20218
gamma dose rate within, effects of ceiling-scattered rays on, 18: 12387 (TO-B-63-25)
gamma dose rates in concrete, 18: 35055
gamma dose rates in cylindrical and rectangular steel, from fallout, 20: 15931 (TO-B-65-27)
gamma shielding afforded by, model studies, 17: 7497 (DRCL-364)
gamma shielding by concrete blockhouse, 18: 44917 (NUC-E-15)
gamma shielding by, effects of shape on, (T), 19: 29461
gamma shielding by cylindrical steel, floor-barrier reduction factors for, 20: 34800
gamma shielding properties of roofed, 17: 35067
ground motion effects of nuclear detonation on simulated Dribble area building foundations, 19: 562 (VUF-1016)
humidity measurements at sites of, using neutron sources, 17: 15903
incendiary effects from Tumbler shots on frame building, 18: 1889 (WT-510)
joints in filament-wound, 20: 14213 (ACF-15)
leakage from, measurement of rate of, 20: 36978 (NAA-SR-12001)
leakage through cracks and capillaries in reinforced concrete, prediction and control, 18: 21555 (NAA-SR-Memo-9429)
leaks in reinforced-concrete, used as reactor buildings, 18: 28929
materials testing, 16: 11362 (WT-75(Ref.))
missile hazards from underground nuclear explosions, 16: 2819 (WT-338)
neutron flux distribution in multi-legged entranceways in, 17: 26220
nuclear blast effects on, effects of fires on debris produced by, 19: 26519 (URS-639-9)
nuclear blast effects on, calculation of fire resistance to, 20: 16621 (AD-625867)
nuclear weapons effects, 16: 18713 (AFSWC-TN-61-26)
penetration by iodine-131 from atomic cloud, 16: 27502 (AERE-R-3827)
plastic deformation during thermal cycling of attached elements, 18: 28024
plutonium fallout release from explosion within Gravel Gertie structure, 18: 35767 (SC-R-64-127)
pressure buildup in, during blasts, 17: 20128(T) (UCRL-Trans-936(L))
protection against fallout in, engineering method for calculating, 20: 11030 (NBS-MON-76)
protective effects of residential, against external exposure from fallout deposition on ground, 19: 30468
radiation attenuation by residential-type, 16: 30676 (NP-12016)
radiation attenuation by vertical, (E/T), 20: 6516 (AD-617524)
radiation distributions in brick–concrete from cobalt-60 gamma sources, 19: 9407 (SAM-TDR-64-14)
radiation dose rate in multistory windowless, effects of limited strips of contamination on, 17: 26216
radiation dose rates in, from simulated fallout field, effects of interior partitions on, 17: 26217
radiation dose rates from simulated nuclear explosion fallout in multi-story windowless, from limited strips of contamination, 18: 35771 (TO-B-63-76)
radiography of reinforced concrete, 17: 6249
radiological decontamination of, postattack requirements for, 20: 41179 (AD-635821)
radiological decontamination of, postattack, requirements for, 20: 41180 (AD-635822)
radiological decontamination of, postattack requirements for, 20: 41181 (AD-635823)
radiological decontamination of, postattack requirements for, 20: 41182 (AD-635824)
radiological decontamination of, postattack requirements for, 20: 43567 (AD-635820)
response of concrete and steel tubular towers to static and dynamic loads, 20: 39007 (AD-636914)
response of model, to ground motion in SEDAN event, 19: 3810 (PNE-215F)
response spectra of single-degree-of-freedom dynamic, to large air-blast loads from nuclear explosions, 19: 46566 (AD-425747)
seismic effects of underground explosions on, 18: 20127 (UCRL-7773)
shielding analysis of Japanese houses, 19: 7204(R) (ORNL-3697(p.155-9))
shielding characteristics of, used as shelters, 18: 37430 (AD-431995)
shielding for hardened, design of, (T), 20: 3276
shielding properties of multistory, windowless building against fallout, 17: 20245(R) (TO-B-62-58)
shielding properties of concrete, 18: 6404(R) (ORNL-3499(Vol.I)(p.131-6))
shielding properties of Japanese residential, against radiations from atomic explosion, 18: 31783 (CEX-64.3)
shielding properties of, against fallout, 19: 11414 (AD-420472)
shielding properties of Japanese residential, 19: 42655 (CEX-62.11)
shielding properties of, effect of aperture and ceiling-shine on, 20: 43526
shielding properties of, against fallout, calculation of, 20: 43568 (AD-636787)
shock wave diffraction, 16: 14993 (WT-786)
simulants of dynamically loaded, use of models, 17: 5666 (AD-274294)
stress analysis of hemispherical lightweight cellular core with flexible support shell, 18: 8021 (UCRL-7473)
stress analysis of pressurized multicell shell, 18: 25633 (ERR-AN-336)
stress analysis of prestressed concrete, finite element method for, 19: 20086 (GAMD-5926)
stress analysis of, computer program for, 20: 29367 (TRG-Report-1089)
stresses in concrete, sustained-load and temperature effects on steady-state, (T), 20: 25590
stresses in water dam, determination of, 20: 33431(T) (ORNL-tr-1229)
stresses on ceramic materials in, 20: 27533
support for, design of, 17: 9901(P)
tendon configuration in pre-stressed concrete, optimal, 19: 21610 (GAMD-6109)
testing hollow underwater, radiographic method for, 20: 5631(P)
U. S. Army, drawings, 16: 11360 (WT-60(Ref.)(Pt.IV))
vibration, computer program for calculation, 16: 26470 (KAPL-2000-18)
vibration, measurements, 16: 11356 (WT-1)
vulnerability of food-processing plant, to blast and thermal effects of nuclear weapons, 19: 11305 (HRD-63736)

STRYCHNINE
determination in Galen preparations, radiometric, 19: 11012
effects on acceleration tolerance in mice and guinea pigs, 20: 43004
effects on strontium-90 effects on central nervous system in mice, 19: 17578
effects on uranium poisoning in rats, 20: 22555
nitrogen-15 content in, significance of excess, 17: 23043
protective effects against radiation sickness from radium therapy, 16: 5162(T) (JPRS-11242(p.16-24))

STYPHNIC ACID, LEAD SALTS
meson (π^-) capture by, thermal initiation theory of spherical hot spots from, 18: 16026
radiation effects on thermal decomposition, 16: 13105

α-benzyloxy-, free radical-induced rearrangement of, determination of initial and final products of, by isotope dilution, 16: 22093
autoxidation inhibition by 2,6-di-*tert*-butyl-4-methylphenol, 16: 30382 (NRC-6922)
determination in polystyrene and plastic scintillators, radioluminescent, 19: 26274
development of, for gamma scintillation detectors, 17: 181(R) (TID-17019)
dichloro-, radioinduced polymerization with rubber latex, 18: 17920(P)
effect on radioinduced polymerization of methyl acrylate in ethyl chloride, 20: 404
effects as grafts on viscoelastic properties of polyvinyl fluoride, 19: 11203
effects on isomerization of stilbene in gamma radiolysis of benzene and cyclohexane, 20: 40961
effects on polymerization of liquid, ionic mechanism of gamma, 20: 26966
effects on radiation resistance of polyethylene, 19: 22322
effects on radioinduced oxidation of polymethylmethacrylate, 18: 31609
effects on radioinduced degradation of wood fiber, 18: 43705
electronic spectra of, tables, 19: 9156 (IS-450)
graft polymerization on irradiated polyethylene, effect of medium rigidity on termination of trapped polymeric radicals in, 16: 5247
graft polymerization of, on polypropene by pre-irradiation in air at low temperature, 17: 30195
graft polymerization of, on cellulose acetate, ceric ion, preirradiation, and radiation methods for, 17: 31809
grafting to pre-irradiated Teflon, 19: 488
hydration of, mechanism of, 19: 2362
luminescence of, alpha/beta ratio in, 18: 300
meson (π^-) transfer from hydrogen to heavier atoms in, (E), 19: 21281
p-acetamido-, polymerization of, mechanism of, 17: 21747
p-acetamido-, radioinduced polymerization of, crystal structure, 16: 4188(R) (TID-14085)
p-benzamido-, polymerization of, mechanism of, 17: 21747
p-benzamido-, polymerization of, thermally initiated, 17: 3027(R) (TID-17273)
p-nitro-, radioinduced polymerization at low temperatures, 20: 1893(R) (AD-618228)
p,*N*,*N*-dimethylamino-, radioinduced polymerization, 16: 25425
phase equilibria, in polymer-monomer-solvent systems, 16: 445(R) (NYO-9988)
polarographic behavior at dropping mercury electrodes, 16: 95 (TID-14097)
polymerization of deuterated, thermal-induced, 20: 45710
polymerization of, effects of deuterated phenols on, 16: 14711
polymerization of, induced by *tert*-butyl peroxide, 17: 12319
polymerization of, initiated by azobisisobutyronitrile and radiation, 16: 23738
polymerization of, radioinduced ionic, 17: 23410
polymerization on irradiated polybutene-1 sulfone, graft, 19: 36502
polymerization to polyvinyl chloride, catalytic, 20: 23004
polymerization to irradiated polyethylene film, 20: 25147
polymerization to cotton fabrics, catalytic effects of imbibing solutions on, 18: 31511
polymerization with organometallic compounds, 19: 13406(T) (JPRS-28565)
polymerization with pre-irradiated cotton, effects of iron ions, radiation dose, and temperature on, 18: 31624
polymerization with pre-irradiated cotton, effects of solvent on, 18: 31625
production by pyrolysis of ethylbenzene, effects of oxygen on, 19: 27890 (UCRL-16021)
properties of radioinduced graft polymerized polyvinyl alcohol fibers on, 16: 19443
radiation chemistry, 16: 27060
radiation effects on polymers with methyl methacrylate in benzene, effects of oxygen on, 19: 15581
radiation effects on stability of copolymers with divinylbenzene, 19: 9231
radiation effects on, cosmic, 17: 32693
radiation effects on polymerization of emulsions of, gamma, 20: 23212 (AERE-R-3420)
radiation effects on, in poly(vinyl chloride) films at −78 and −196°C, gamma, 20: 26939
radiation effects on emulsion polymerization of, beta, gamma, and x, 18: 1734
radiation effects on polymerization on cotton imbibing catalysts, 18: 31630
radiation grafting with vinyl alcohol polymers, mechanical properties after, 19: 11180
radiation polymerization of, 17: 31796(R) (BNL-782(p.44-50))
radiation polymerization in aqueous suspension, 16: 27073
radiation stability of, mechanisms of, 16: 211(T) (AEC-tr-4470(p.35-9))
radiation- and peroxide-initiated grafting to polyethylene film, 18: 12223
radiochemical grafting on polyvinyl chloride and Teflon films, temperature effects on, 16: 18966
radioinduced copolymerization, anionic and cationic mechanisms of, 16: 209(T) (AEC-tr-4470(p.1-7))
radioinduced copolymerization to methyl methacrylate in ethyl chloride, gamma, 16: 25458
radioinduced copolymerization with methyl methacryalate polymers, 16: 29010
radioinduced copolymerization with formaldehyde, 17: 30139
radioinduced copolymers with ethylene, properties of, 17: 37276
radioinduced curing of, in mixtures with polyesters, electron, 20: 35819
radioinduced emulsion polymerization of, 19: 30236(R) (TID-21683)
radioinduced emulsion polymerization with methyl methacrylate, 17: 40876
radioinduced graft polymerization to polypropylene, 19: 17999
radioinduced graft polymerization on Teflon, diffusion effects in, 19: 22375
radioinduced graft polymerization with ethylene polymers, (E), 19: 26410
radioinduced graft polymerization on cellulose acetate, effect of solvent on, 19: 26412
radioinduced graft polymerization on cellulose, effects of oxygen on, 19: 26420
radioinduced graft polymerization on vinyl chloride polymers, 19: 26422
radioinduced graft polymerization to polyethylene, gamma, 19: 28362 (TID-21885)
radioinduced graft polymerization of, mechanism and spectra of, 19: 36468
radioinduced graft polymerization with polyvinyl chloride, physical properties of products of, 19: 38733
radioinduced graft polymerization of vaporous, with ethylene polymers, 19: 38734
radioinduced grafting to chloroethylene polymers, 19: 38740(P)
radioinduced graft polymerization with polyethylene and polyvinyl chloride, temperature effects on, 19: 44084
radioinduced grafting on polypropylene, 19: 46355
radioinduced graft polymerization on Teflon, gamma, 19: 9183
radioinduced graft polymerization of cotton cellulose onto, 19: 462
radioinduced graft polymerization on amylose, gamma, 19: 9205
radioinduced grafting to polyvinyl fluoride, 19: 11203
radioinduced grafting to vinyl alcohol polymers in methanol solution above 40°C, 19: 11181
radioinduced grafting with methacrylic acid on polyethylene, 19: 13832
radioinduced graft polymerization on ethyl cellulose film, kinetics of, 16: 8780
radioinduced graft polymerization on polyethylene in benzoyl peroxide–dimethylaniline, 16: 11714
radioinduced graft polymerization on polyethylene, effects of slight chlorination on, 16: 22185
radioinduced graft polymerization on polyvinyl alcohol films, effects of ferrous ions on, 16: 22196
radioinduced graft polymerization to nylon, effects of methanol on, 17: 14338
radioinduced graft polymerization to polyethylene, effects of methanol on, 16: 5384
radioinduced graft polymerization in acrylonitrile and methyl acrylate mixture with Teflon, monomer reactivities in, 16: 18963
radioinduced graft polymerization on cellulose in acetic acid, 16: 22189
radioinduced graft polymerization on polyvinyl alcohol films, 16: 22194
radioinduced graft polymerization with polyethylene, 16: 23718(T) (AEC-tr-4321)
radioinduced graft polymerization on cotton cellulose, 16: 23544
radioinduced graft polymerization on cellular acetate, 17: 1548
radioinduced graft polymerization with polymers, effects of methanol on, 17: 4538 (TID-7643(p.233-44))
radioinduced graft polymerization to polypropylene, 17: 4590 (TID-7643(p.345-97))
radioinduced graft polymerization with polyethylene film, composition of, 17: 8179
radioinduced graft polymerization with polyethylene, 17: 8180
radioinduced graft polymerization with cellulose acetate, 17: 8183
radioinduced graft polymerization with polythene, 17: 8154
radioinduced grafting to polyethylene oxide, 17: 18108(R) (TID-18126)
radioinduced grafting of, with nylon 6, 17: 18138
radioinduced grafting of, with polyvinyl alcohol, 17: 18139
radioinduced graft polymerization on wool, 17: 27900
radioinduced graft polymerization on polymethyl methacrylate, 17: 28987
radioinduced graft copolymerization with polypropene, 17: 29913
radioinduced graft copolymerization with cellulose acetate, 17: 29916
radioinduced graft copolymerization with cellulose, 17: 29918
radioinduced graft copolymerization with cellulose fibers, 17: 29939
radioinduced graft copolymerization with polyethylene, 17: 29914
radioinduced graft polymerization of, to polyethylene, preparation of ion exchange membranes from, 17: 30191
radioinduced graft polymerization of, on acrylonitrile–butadiene polymer, 17: 30198

radioinduced graft polymerization of, on nylon 6, properties of product in, 17: 30200
radioinduced graft polymerization of, on polypropene, mechanical properties of product in, 17: 30201
radioinduced graft polymerization of, to polypropene, physical properties of product in, 17: 30202
radioinduced graft polymerization of, to polyethylene, electron spin resonance spectra of, 17: 30203
radioinduced graft polymerization of, to viscose rayon yarn, optimum conditions for, 17: 32676
radioinduced graft polymerization to polyvinyl alcohol, solvent effects on, 17: 33986
radioinduced graft polymerization with polyethylene, 17: 37289
radioinduced graft polymerization on cellulose acetate, 17: 39129
radioinduced graft polymerization on cellulose acetate, 17: 39144
radioinduced graft polymerization of, on polypropene and polytetrafluoroethylene, effects of monomer diffusion on, 17: 30196
radioinduced grafting on wool, effects of methanol and water on, 20: 7154
radioinduced grafting to cellulose, 20: 10873
radioinduced graft polymerization with polyethylene, radical lifetime in gamma, 20: 14624
radioinduced grafting on cellulose fibers, properties of product in, 20: 16507 (INR-671/XVII/C)
radioinduced graft polymerization with polypropylene, properties of product formed by γ, 20: 23127
radioinduced graft polymerization on cellulose, 20: 25176(P)
radioinduced graft polymerization of, on fibrous cotton and nylon, gamma, 20: 35822
radioinduced grafting of, on cellulose theory of, 20: 40979
radioinduced graft polymerization with poly(vinyl chloride), rate of gamma, 20: 40993
radioinduced graft polymerization to polyvinyl chloride in liquid and vapor phases, rate of electron and gamma, 20: 40992
radioinduced graft polymerization on cotton fabric, gamma, 20: 43299
radioinduced graft polymerization on fiber glass, silica gel, and zirconium oxide, preparation of ion exchange material by, 20: 43311
radioinduced graft polymerization on vinyl chloride polymers, gamma, 20: 43372
radioinduced graft polymerization to rayon, effects of chloride additions on, 18: 285
radioinduced graft polymerization to fibrous materials, technique for, 18: 6869
radioinduced graft polymerization reactions with cellulose, yields in, 18: 10176
radioinduced grafting on polyethylene and Teflon, 18: 12222
radioinduced grafting, in mixtures with acrylonitrile, to polyvinyl chloride, 18: 12224
radioinduced grafting, in binary mixtures with acrylonitrile or butadiene, on cellulose or polyvinyl alcohol, 18: 12226
radioinduced grafting on cellulose, effects of water swelling on, 18: 12163
radioinduced graft polymerization with polyethylene, 18: 13902
radioinduced graft copolymerization on cellulose acetate fibers, effects of solvents on gamma, 18: 17880
radioinduced graft polymerization with polyethylene, preparation of acidic cation exchange membranes by, 18: 17904
radioinduced graft copolymerization on cellulose acetate fibers, gamma, 18: 17915
radioinduced graft polymerization on cotton, properties of product formed by, 18: 18252
radioinduced graft polymerization on polyvinyl alcohol, effects of solvents on gamma, 18: 23581(T,R) (AEC-tr-6316(p.66-9))
radioinduced graft polymerization on polyvinyl alcohol, effects of environment on, 18: 23582(T,R) (AEC-tr-6316(p.70-5))
radioinduced graft polymerization on polyvinyl alcohol, gamma, 18: 23583(T,R) (AEC-tr-6316(p.76-8))
radioinduced graft polymerization on polyvinyl alcohol fiber, 18: 23584(T,R) (AEC-tr-6316(p.79-83))
radioinduced graft polymerization on cellulose, gamma, 18: 23585(T,R) (AEC-tr-6316(p.84-8))
radioinduced graft polymerization on preirradiated cellulose, 18: 23586(T,R) (AEC-tr-6316(p.89-94))
radioinduced graft polymerization on preirradiated cellulose, effects of atmosphere on, 18: 23587(T,R) (AEC-tr-6316(p.95-9))
radioinduced graft polymerization on polyethylene and polypropene, gamma, 18: 23589(T,R) (AEC-tr-6316(p.105-13))
radioinduced graft polymerization on polyoxymethylene, 18: 23607(T,R) (AEC-tr-6316(p.223-5))
radioinduced graft polymerization on viscose cellulose, gamma, 18: 23643(T,R) (AEC-tr-6316(p.498-500))
radioinduced graft polymerization on polyethylene terephthalate, gamma, 18: 23657(T,R) (AEC-tr-6316(p.640-9))
radioinduced graft polymerization on cotton and rayon, gamma, 18: 23658(T,R) (AEC-tr-6316(p.650-9))
radioinduced graft polymerization on polypropene, 18: 23624(T,R) (AEC-tr-6316(p.368-80))
radioinduced graft polymerization on casein, 18: 25469 (SRIA-120)
radioinduced graft polymerization on celluloses, solvent effects on, 18: 25474(T) (AEC-tr-6372(p.83-8))
radioinduced graft polymerization on celluloses, effects of chemical treatment, pretreatment, and refining on reactivity of, 18: 25475(T) (AEC-tr-6372(p.89-96))
radioinduced graft polymerization on PVA, heat treatment effects on x-ray scattering in, 18: 25483(T) (AEC-tr-6372(p.141-3))
radioinduced graft polymerization on polypropene, effects of additives and alpha pre-irradiation on, 18: 25506(T) (AEC-tr-6372(p.371-7))
radioinduced graft polymerization on rayon, conditions for, 18: 25534(T) (AEC-tr-6372(p.593-602))
radioinduced graft polymerization to polypropene, effects of additives and alpha pre-irradiation on, 18: 25505(T) (AEC-tr-6372(p.363-9))
radioinduced graft polymerization on viscose rayon, solvent effects on, 18: 25476(T) (AEC-tr-6372(p.97-102))
radioinduced graft polymerization on polypropylene, effects of alpha pre-irradiation on, 18: 27572
radioinduced graft polymerization with capron and ethylene and propene polymers in gaseous phase, 18: 27535
radioinduced graft polymerization on polyethylene at low intensities, 18: 41536
radioinduced graft polymerization onto poly (vinyl alcohol) spun fibers, 18: 27549
radioinduced graft polymerization onto poly (vinyl alcohol) fibers spun from alkali bath, 18: 27550
radioinduced graft polymerization to cellulose pulp, 18: 29697(T,R) (AEC-tr-6231(p.79-90))
radioinduced graft polymerization to polyvinyl alcohol, 18: 29698(T,R) (AEC-tr-6231(p.91-101))
radioinduced graft polymerization to rayon, 18: 29699(T,R) (AEC-tr-6231(p.102-4))
radioinduced graft polymerization to cotton, 18: 29700(T,R) (AEC-tr-6231(p.105-11))
radioinduced graft polymerization to nylon 6 film, 18: 29701(T,R) (AEC-tr-6231(p.112-13))
radioinduced graft polymerization on cellulose fibers, 18: 29720(T,R) (AEC-tr-6231(p.201-4))
radioinduced graft polymerization on chlorinated polyethylene, 18: 29726(T,R) (AEC-tr-6231(p.233-8))
radioinduced graft polymerization to cotton fabric, effects of water content on, 18: 31626
radioinduced graft polymerization to cotton fabric, effects of solvents on gamma, 18: 31628
radioinduced graft polymerization on celluloses, gamma, 18: 31629
radioinduced in 3-methylpentane glasses, effects of carbon tetrachloride on spectra of, 18: 13859
radioinduced ion radical formation in, effects of tetrahydrofuran on, 17: 23395
radioinduced ionic polymerization at −78°C, gamma, 20: 23138
radioinduced ionic polymerization of, kinetics of, 20: 23140
radioinduced ionic polymerization of, in organic solutions at 25°C, 20: 23141
radioinduced ionic polymerization of, kinetic study of gamma, 20: 40978
radioinduced luminescence of, effects of methyl methacrylate on, 20: 4001
radioinduced oxidation at 77°K, electron spin resonance studies of, 19: 475
radioinduced polymerization, gamma, 19: 15565(R) (BNL-841(p.43-51))
radioinduced polymerization with methylmethacrylate, effects of γ-alumina on, 19: 18000
radioinduced polymerization with polyethylene, ESR spectra of products in, 19: 17976
radioinduced polymerization with maleic anhydride, 19: 22349
radioinduced polymerization with polyvinyl chloride, 19: 22307
radioinduced polymerization of, in presence of potassium-sodium alloy drying agent, 19: 24560
radioinduced polymerization with sulfur dioxide, gamma, 19: 24583
radioinduced polymerization with cellulose in wood, 19: 24586
radioinduced polymerization of, effects of electric fields on, 19: 26426
radioinduced polymerization, gamma, 19: 28362 (TID-21885)
radioinduced polymerization with acrylonitrile in wood, gamma, 19: 30234 (ORO-628)
radioinduced polymerization with cellulose, 19: 35615(R) (NP-15037)
radioinduced polymerization at 0 and −78°C, effects of glass powder and zinc oxide powder on, 19: 2380
radioinduced polymerization in methylene dichloride, effects of silicon oxide powder on, 19: 458
radioinduced polymerization of, additive effects on rate of, 19: 13437
radioinduced polymerization of, effects of ethylbenzene and polystyrene

on gamma, 19: 9202
radioinduced polymerization of, in solid mixtures with paraffin oil, mechanism and free radical yields in, 19: 4211
radioinduced polymerization of, ionic mechanism for, 19: 474
radioinduced polymerization of, kinetics of, 19: 2399
radioinduced polymerization with formaldehyde, gamma, 19: 9187
radioinduced polymerization with isobutene at 0 and −78°C, effects of powdered glass and zinc oxide on, 19: 2380
radioinduced polymerization with polyethylene, 19: 454
radioinduced polymerization using krypton-85, 19: 2677 (NYO-2906-1)
radioinduced polymerization in wood, effects of, on properties, 16: 10642
radioinduced polymerization of, effects of degassing on, 16: 202 (AD-256551)
radioinduced polymerization of, effects of variables on, 17: 6175
radioinduced polymerization of, effects of cyclooctatetraene on, 17: 8163
radioinduced polymerization of, at low temperatures, 16: 23740
radioinduced polymerization of, at low temperatures, effects of phase change on, 16: 23741
radioinduced polymerization, effects of irradiation cycle on, 16: 201 (AD-256550)
radioinduced polymerization, effects of degassing and irradiation cycle on, 16: 203 (AD-256552)
radioinduced polymerization, effects of air, degassing, and flame-out on, 16: 204 (AD-256553)
radioinduced polymerization using krypton-85 beta source, 16: 10367 (NYO-2607)
radioinduced polymerization in benzene, helium, and vacuum, 16: 19274
radioinduced polymerization with acrylonitrile, 16: 23739
radioinduced polymerization with acrylonitrile, 16: 23758
radioinduced polymerization with isobutene, 16: 23760
radioinduced polymerization and copolymerization to isobutene in ethyl chloride, gamma, 16: 25457
radioinduced polymerization of, effects of solvents on, 17: 1528 (TID-17219)
radioinduced polymerization of, in solid state, 17: 4578 (TID-7643(p.136-49))
radioinduced polymerization of, effects of water on, 17: 6124 (BNL-5838)
radioinduced polymerization, 17: 19724 (BNL-759(p.39-46))
radioinduced polymerization of, studies of variables in, 17: 23398
radioinduced polymerization with acrylonitrile, 17: 25300
radioinduced polymerization of, in solution, 17: 29908
radioinduced polymerization with maleic acid, phthalic acid, and propylene glycol esters, 17: 32177
radioinduced polymerization of, effects of in-scattering and out-scattering on, 17: 33965 (AD-287561)
radioinduced polymerization with isoprene, tracer technique for determination of monomer reactivity ratios in, 17: 34015
radioinduced polymerization with polypropylene, interferometric studies of, 17: 35880
radioinduced polymerization, 17: 40867
radioinduced polymerization of, mechanism of, 16: 23545
radioinduced polymerization with methyl acrylate in ethyl chloride at −78°C, 20: 404
radioinduced polymerization in ethyl chloride at −78°C, 20: 404
radioinduced polymerization with polyvinyl ester, 20: 1910
radioinduced polymerization at low temperatures, gamma, 20: 1925
radioinduced polymerization with formaldehyde, effects of dichloromethane and ethyl ether on, 20: 1914
radioinduced polymerization with methyl methacrylate, 20: 4001
radioinduced polymerization of, effects of white phosphorus on, 20: 7155
radioinduced polymerization with methyl methacrylate in presence of zinc oxide, 20: 7128(R) (NYO-2206-1)
radioinduced polymerization to polyethylene, 20: 9014
radioinduced polymerization with polyethylene and polyvinylchloride, 20: 14618
radioinduced polymerization with rayon, 20: 16528
radioinduced polymerization of, effects of white phosphorus on gamma, 20: 20736
radioinduced polymerization with isocyanic acid at low temperatures, 20: 20747
radioinduced polymerization of, effects of mineral fillers on gamma, 20: 20778
radioinduced polymerization of, in organic solvents, mechanism and rate of, 20: 23159
radioinduced polymerization of, with trioxane, 20: 23193(P)
radioinduced polymerization to cellulose acetate, 20: 23108
radioinduced polymerization to polyvinyl chloride, gamma, 20: 23121
radioinduced polymerization of, pulsed-electron, 20: 23123
radioinduced polymerization with methyl methacrylate, pulsed-electron, 20: 23123
radioinduced polymerization to cotton, effects of oxygen on gamma, 20: 23137
radioinduced polymerization with isobutene at −78°C, 20: 23139
radioinduced polymerization in dichloromethane at −78°C, 20: 23139
radioinduced polymerization with isobutyl vinyl ether at 25°C, effects of radiation, 20: 23140
radioinduced polymerization with α-methylstyrene, at 25°C, effects of radiation, 20: 23140
radioinduced polymerization of, with acrylonitrile and poly(methyl methacrylate), gamma, 20: 26939
radioinduced polymerization with lignin, gamma, 20: 29288
radioinduced polymerization of, with formaldehyde in bulk and solution, gamma, 20: 40973
radioinduced polymerization on cellulose, 20: 43294
radioinduced polymerization at −78°C, effects of solvents on gamma, 20: 43308
radioinduced polymerization of, effects of ammonia, DPPH, nickel oxide, water, and zinc oxide on gamma, 20: 43338
radioinduced polymerization with α-methylstyrene, effects of ammonia and diethyl ether on, 20: 43338
radioinduced polymerization with isobutyl vinyl ether, effects of ammonia on diethyl ether on, 20: 43338
radioinduced polymerization of, in methylene chloride and toluene solution, effects of moisture and temperature on, 20: 43339
radioinduced polymerization on cotton, 20: 43349
radioinduced polymerization with nylon and natural silk, 18: 319
radioinduced polymerization with allylsilanes, 18: 317
radioinduced polymerization of, at low temperatures in the presence of bromated solvents, 18: 1748
radioinduced polymerization, 18: 3806(R) (BNL-799(p.55-63))
radioinduced polymerization of, effects of water on, 18: 5361 (CONF-117-31)
radioinduced polymerization of, gamma and neutron, 18: 5389
radioinduced polymerization of, effects of zinc oxide on, 18: 10167
radioinduced polymerization in presence of organic additives, yields of free radicals in, 18: 10171
radioinduced polymerization of, effects of LET in, 18: 12198
radioinduced polymerization at −78°C, catalytic effects of silica powders on, 18: 12219
radioinduced polymerization, 18: 12139(R) (BNL-823(p.48-56))
radioinduced polymerization with acrylonitrile and methyl methacrylate, gamma, 18: 12168
radioinduced polymerization with ethylene at 20° C and up to 680 atm, 18: 13900
radioinduced polymerization in wood, 18: 13906
radioinduced polymerization in wood, 18: 17889
radioinduced polymerization with methyl methacrylate on alumina base, gamma, 18: 23594(T,R) (AEC-tr-6316(p.137-44))
radioinduced polymerization with β-propiolactone, 18: 23604(T,R) (AEC-tr-6316(p.190-4))
radioinduced polymerization of, effects of diphenylpicrylhydrazyl on beta, 18: 25486(T) (AEC-tr-6372(p.163-73))
radioinduced polymerization with formaldehyde, kinetics of, 18: 25492(T) (AEC-tr-6372(p.213-22))
radioinduced polymerization of, activation energy and kinetics of, 18: 25503(T) (AEC-tr-6372(p.331-47))
radioinduced polymerization with acrylonitrile, 18: 25535(T) (AEC-tr-6372(p.603-12))
radioinduced polymerization with ethylene, gamma, 18: 29691 (BNL-8056)
radioinduced polymerization, kinetics of electron, 18: 29713(T,R) (AEC-tr-6231(p.159-62))
radioinduced polymerization, solvent effects in gamma, 18: 29715(T,R) (AEC-tr-6231(p.170-4))
radioinduced polymerization with methyl methacrylate, kinetics, 18: 29717(T,R) (AEC-tr-6231(p.186-90))
radioinduced polymerization on cotton fabric, effects of imbibed water and partially grafted polystyrene on, 18: 31627
radioinduced polymerization of, effects of linear energy transfer on, 18: 31638
radioinduced polymerization with formaldehyde, 18: 37178 (BNL-874(p.3-4))
radioinduced polymerization with acrylonitrile at −78°C, gamma, 18: 37216(T) (AEC-tr-6398(p.529-37))
radioinduced polymerization with isobutylene at −78°C, gamma, 18: 37216(T) (AEC-tr-6398(p.529-37))
radioinduced polymerization with methyl methacrylate at −78°C, gamma, 18: 37216(T) (AEC-tr-6398(p.529-37))
radioinduced polymerization with acrylonitrile, dose rate effects on, 18: 39328
radioinduced polymerization of, effects of ion scavengers on, 18: 41513
radioinduced reactions with sulfur dioxides at 30°C, 17: 34021
radioinduced reactions with sulfur dioxide at +30 to −78°C, 17: 34022
radioinduced reactions with greases, preparation of radiation-resistant greases by, 17: 37637
radioinduced reaction with sulfur dioxide at low temperatures,

20: 23188(P)
radioinduced reactions of, for preparation of highly radioresistant greases, 18: 661
radiolysis in cyclohexane, radical ion yields from pulse, 20: 7144
radiolysis of, EPR studies of yields of stabilized charges in low-temperature, 20: 40962
radiolysis of, ESR spectra of free radicals produced by, 19: 17976
radiostability of ion-exchange resins based on, (E), 19: 40129 (ZFK-RN-17(p.114-26))
separation of graft polymer of, with polyethylene from reaction product by fractional precipitation, 17: 8180
spectra in gamma-irradiated organic glasses at −196°C, 17: 6175
spectra of isotope effects in alpha deuterio-, nuclear magnetic resonance, 18: 5287
sulfo-, ion exchange properties of, in neutral and weakly acid range, 18: 23736
trifluoromethyl-, radiation synthesis of, 18: 37181 (BNL-874(p.12-13))
yields in gamma radiolysis of bromophenyl- and bromomethoxyphenyl-ethanes, mechanism of, 17: 39118
acrylic acid–styrene, radioinduced graft polymerization to cotton fabric, properties of products formed in gamma, 20: 40953
acrylic acid–styrene, radioinduced graft polymerization onto poly (vinyl alcohol) fibers, 18: 27547
acrylonitrile–styrene, effects on radiation effects on dynamic mechanical properties of polyvinyl chloride, 20: 25625
acrylonitrile–styrene, product composition in radioinduced graft polymerization with cellulose, 18: 25480(T) (AEC-tr-6372(p.125-7))
acrylonitrile–styrene, radiation effects on *trans*-vinylene groups in, ir spectral studies on gamma, 20: 45715(R) (ORO-2418-1)
acrylonitrile–styrene, radiochemical grafting of, on polyvinyl chloride at 0 to 50°C, 20: 36877
acrylonitrile–styrene, radioinduced graft polymerization on vinyl chloride polymers, 19: 26421
acrylonitrile–styrene, radioinduced graft polymerization with polyethene, 17: 8154
acrylonitrile–styrene, radioinduced graft polymerization of, on acrylonitrile–butadiene polymer, 17: 30198
acrylonitrile–butadiene–styrene, radioinduced graft polymerization of, on polyvinyl alcohol and viscose rayon, 17: 30199
acrylonitrile–styrene, radioinduced graft copolymerization with chloroethylene, 20: 4038
acrylonitrile–styrene, radioinduced graft polymerization onto cellulose, 20: 18799(P)
acrylonitrile–styrene, radioinduced polymerization of, in organic halogen solvents, mechanism of, 20: 23159
acrylonitrile–styrene, radioinduced polymerization of, at −78, 0, and 50°C, effects of dimethylformamide and oil on, 20: 36876
acrylonitrile–styrene, radioinduced grafting on polytetrafluoroethylene, effects of monomer diffusion rate on, 20: 36878
acrylonitrile–butadiene–styrene, radioinduced graft polymerization on cellulose, 18: 27544
acrylonitrile–styrene, radioinduced co- and graft-polymerization onto cellulose, 18: 27545
acrylonitrile–styrene, radioinduced graft polymerization onto poly (vinyl alcohol) fibers, 18: 27547
acrylonitrile–butadiene–styrene, radioinduced graft polymerization onto poly (vinyl alcohol) fibers and powders, 18: 27548
butadiene–styrene, branching viscosities and weights in polymers of, 19: 22278
butadiene–styrene, effects of filler surface chemical nature and radiation on physicomechanical properties of, 17: 40879
butadiene–styrene, filler effects on radiation effects on tensile strength of, 18: 27594
butadiene–styrene, post-irradiation effects on tensile strength of, 18: 27594
butadiene–styrene, radiation effects on reduced branching with and without *N*-phenyl-2-naphthylamine, 19: 22344
butadiene–styrene, radiation effects on intrinsic viscosity with and without *N*-phenyl-2-naphthylamine in, 19: 22342
butadiene–styrene, radiation effects on solubility and swelling with and without *N*-phenyl-2-naphthylamine, 19: 22343
butadiene–styrene, radiation effects on structure of, 17: 27931
butadiene–styrene, radioinduced grafting to cotton or rayon fibers, property changes from, 19: 34221
butadiene–atyrene, radioinduced graft polymerization with cotton or rayon, 20: 363
butadiene–styrene, radioinduced grafting onto cellulose, 20: 18798(P)
butadiene–styrene, radioinduced graft polymerization on celluloses, 18: 25478(T) (AEC-tr-6372(p.109-15))
butadiene–styrene, radioinduced graft polymerization on PVA, 18: 25482(T) (AEC-tr-6372(p.135-40))
butadiene–styrene, radioinduced graft polymerization on polyethylene, 18: 25484(T) (AEC-tr-6372(p.145-57))
butadiene–styrene, radioinduced grafting onto cellulose and regrafting of grafted cellulose, 18: 27546
butadiene–styrene, structural effects in radioinduced graft polymerization on celluloses, 18: 25481(T) (AEC-tr-6372(p.129-34))
butadiene–styrene, technique for radiovulcanization of, 18: 6853
divinylbenzene–styrene, radiation effects on ion-exchange properties of, tracer studies of gamma, 20: 23164
divinylbenzene–styrene, sorptive properties for benzene in resins, 19: 15571(R) (TID-21385)
itaconic anhydride–styrene–vinyl acetate, radioinduced graft polymerization on polypropylene, 18: 27576
maleic anhydride–styrene, properties of polymers in radioinduced graft polymerization of polypropylene to, 18: 27574
maleic anhydride–styrene, radioinduced graft polymerization to polypropylene, 18: 27573
maleic anhydride–styrene, radioinduced polymerization on polypropylene, 18: 27575
maleic anhydride–styrene–vinyl acetate, radioinduced graft polymerization on polypropylene, 18: 27576
methacrylic acid–styrene, radioinduced graft polymerization onto poly (vinyl alcohol), 18: 27547
methyl methacrylate–styrene, radioinduced polymerization of, in organic halogen solvents, mechanism of, 20: 23159
methyl methacrylate–styrene, radioinduced graft polymerization to cotton fabric, properties of products formed in gamma, 20: 40953
methyl methacrylate–styrene, radioinduced graft polymerization onto poly (vinyl alcohol), 18: 27547
polysulfone–styrene, reactions with irradiated polypropene, 18: 25490(T) (AEC-tr-6372(p.197-205))
poly(vinyl acetate)–styrene, radioinduced graft polymerization of, gamma, 20: 45724
styrene–SO_2, radioinduced graft polymerization onto polypropene, 18: 27552
styrene–triphenyltin, response to gamma radiation, (E), 19: 28651
2,4-dimethyl-, radioinduced polymerization of, at low temperatures, 16: 23740
2,4-dimethyl-, radioinduced polymerization of, at low temperatures, effects of phase change on, 16: 23741

STYRENE, DIMETHYL-
radioinduced polymerization with polyethylene or polypropylene to improve dyeability, gamma, 20: 45764(P)

STYRENE, α-METHYL-
effects of water on molecular weight distribution in radioinduced polymerization of, 17: 11285
effects on radioinduced degradation of cellulose acetate, 19: 17998
radiation effects on transient absorption spectra of, pulse, 20: 8986
radioinduced copolymerization and polymerization of, 17: 29938
radioinduced polymerization of, kinetics of, 19: 2399
radioinduced polymerization mechanism in, 19: 26431
radioinduced polymerization with maleic anhydride, 19: 36489
radioinduced polymerization of, gamma, 16: 11739
radioinduced polymerization of, mechanism of, 17: 3030
radioinduced polymerization of, electron density effects on, 17: 20072
radioinduced polymerization with formaldehyde, effects of dichloromethane and ethyl ether on, 20: 1914
radioinduced polymerization of dry, effects of ammonia and trimethylamine on kinetics of gamma, 20: 23170
radioinduced polymerization to cellulose acetate, 20: 23108
radioinduced polymerization in dichloromethane at −78°C, 20: 23139
radioinduced polymerization with styrene, mechanisms of, 20: 23140
radioinduced polymerization with styrene, effects of ammonia and diethyl ether on, 20: 43338
radioinduced polymerization with polyethylene or polypropylene to improve dyeability, gamma, 20: 45764(P)
radioinduced polymerization, 18: 6877(P)
radioinduced polymerization, 18: 20070
radioinduced polymerization with maleic anhydride, 19: 22350
radioinduced polymerization of, anion radical mechanism in, 19: 15619
radioinduced polymerization of, mechanisms of, 19: 30248
radiolysis of, identification of intermediates in polymerization from pulse, 20: 40985
radiolysis of, pulse, 20: 23153

Styrene Oxide
see Benzene, (1,2-Epoxyethyl)-

STYRENE POLYMERS
activity coefficients for univalent electrolyte uptake in sulfonated, effects of crosslinking on, 19: 36463(R) (TID-22060)
aerosols of, particle size distribution in, 20: 5237(R) (UR-668, pp 55-109)
analysis for carbon-14 by liquid scintillation, 16: 16091
analysis for carbon-14 and tritium by combustion and liquid scintillation counting, 20: 16384
analysis for chlorine, activation, 20: 16335(R) (NBS-TN-276)

analysis for styrene by quenching of radioluminescent *p*-terphenyl solutions, 19: 26274
analysis of filters of, for selenium, colorimetric, 20: 43069(R) (IDO-14679, pp 51-9)
beta sorption and glass transition in, effects of temperature on, 17: 11282
coating with graphite for thermal radiation detectors, 19: 30506(P)
diffusion of methyl ethyl ketone in irradiated, 19: 34219
effects on radiation resistance of polyethylene, 19: 22322
effects on radioinduced polymerization of styrene, 19: 9202
electric conductivity during reactor irradiation, device for measurement, 16: 25582
electromotive force in irradiated, kinetics, 16: 4204
electron beam reactions at low energies, space charge buildup from, (E), 20: 22344
electron energy dissipation in, ionization chamber measurements of, 20: 23133
electron energy loss in films of, 17: 15765
electron energy losses and ranges in, 17: 22375
electron energy loss in films of, 18: 36107
electron energy loss in thin films of, (E), 19: 8113
electron inelastic scattering at 20 kev in thin films of, cross sections for, (E), 20: 28640
electron paramagnetic resonance spectra of radicals of, 16: 22134(T)
electron reactions at 20 to 86 Mev, ionization energy losses in, 18: 24702
electron scattering by, excitation of π electrons in, 17: 33997
electron spin resonance spectra in systems with tritium, 16: 25433
explosions in Styrofoam, seismic wave production in, 19: 13561(R) (AD-439079)
filter paper efficiency testing using, 17: 3231 (UCRL-6691)
fission fragment tracks in films of, 18: 2428
fluorescence in polyvinyltoluene containing 1,3,5-triaryl-2-pyrazolines, 16: 13745
fluorescence spectra, relations with molecular weight and styrene monomer content, 16: 21125(R) (ANL-6517)
fluorescence spectra and luminescence quenching in, 19: 7589
free radical produced by hydrogen atom bombardment, formation and reaction rates observed by electron spin resonance, 16: 5245
helium ion stopping cross sections of, 18: 14725 (TID-20303)
ion exchange capacity and structural rigidity, effects on separatory efficiency for rare earths, 16: 20371(T) (AEC-tr-4457(p.187-9))
ion exchange properties of, for separation of plutonium from fission products, iron, and uranium, 17: 21785
ion exchange properties of, for alkali metals, thermodynamics of, 17: 21795
joining of, to polyethylene and teflon, effects of boron-10 and lithium-6 neutron reactions on, 16: 33575
labeling with tritium, 16: 25433
labeling with tritium by gas-exposure method, 17: 32152 (CONF-14-21)
light scattering by aqueous suspension of, 18: 20627(R) (NP-13815)
lithium isotope separation factor in ion exchange in solution of, 18: 20434
luminescence, 16: 31857
luminescence and scintillation properties of 2,5-diaryl-oxazole derivatives in, 17: 11227(T)
luminescence properties of metal-containing, 19: 13406(T) (JPRS-28565)
luminescence spectra, concentration effects on, 16: 15309(T)
meson (K) stopping by emulsions loaded with, 19: 44398 (CERN-65-4 (Vol.II), pp III12-16)
nuclear magnetic resonance spectra of, with polystyrene base, 17: 30551
optical properties, (E), 20: 7659(R) (ORNL-3849, pp 101-50)
osmotic coefficients of sulfonated, effects of concentration on, 19: 36463(R) (TID-22060)
particle ionization losses in polarized layer of, optimum thickness for relativistic, (E), 20: 37435
performance in calorimetric dosimeters for gamma rays and neutrons, 19: 13741
permeability of membranes of, to heavy water, 17: 33890
permeability to carbon dioxide–hydrogen mixtures, 20: 29362
photoconductivity of, effects of gamma intensity on, 17: 8006 (TID-16040)
physical properties of foam, 19: 41000 (ACF-10)
polarization of, by gamma radiation, 18: 28053
positron annihilation on electrons in, lifetimes, 16: 5899
positron lifetimes in, 16: 9364
positron mean life in, temperature dependence of, (E), 19: 10089
positronium formation and annihilation in, effects of temperature on, 20: 9783
preparation for use as cation exchanger, 16: 27008
preparation of filamentary scintillators of, 17: 40844
preparation of graft copolymers with polyolefin, 17: 35861(P)
preparation of lead- and tin-containing, for scintillator uses, 17: 181(R) (TID-17019)
preparation of metal-containing, using phenyl compounds, 19: 7526
preparation of metal-containing, 19: 13406(T) (JPRS-28565)
preparation of thermoplastic, with fire-retardant properties, 17: 35623(P)
preparation of tritium-labeled, by electric discharge, 16: 23551
properties as scintillator for beta detection, 19: 38737
properties of sulfonated, for self exchange of cations in, 18: 43503
properties of surfaces of, effects of sulfuric acid on, 17: 29983
properties of, containing leuko compounds of triphenylmethane dyes as chemical dosimeters, 19: 46369
properties with organic additions for use in gamma dosimetry, 19: 2825
property changes and free radical formation in irradiated, 16: 5249
proton dynamic polarization in, 17: 32779
proton multiple scattering by thin films of, at 75 to 200 kev, (E/T), 19: 41273
proton polarization in neutron-irradiated, 17: 20011
proton polarization and spin relaxation rates in, at low temperatures, (E/T), 20: 3143
proton polarization in, 16: 4776
proton stopping cross sections for, 18: 14725 (TID-20303)
protons polarization in neutron-irradiated, by "solid-effect" method, 16: 27052
pyrolysis products from, chromatographic determination of, 20: 14455(R) (ORNL-3889, pp 25-32)
radiation chemistry, 16: 27060
radiation damage to scintillators, 16: 585
radiation effects on copolymers of α-methyl- and, 16: 3050
radiation effects on photoconductivity at 1.0 to 3.0 × 10^6 rads (H_2O)/min, 16: 5763 (SCR-442)
radiation effects on polymerization processes and rates, 16: 20483
radiation effects on viscosity of α-methyl-, 16: 22186
radiation effects on luminescence, 16: 23761
radiation effects on dynamic properties, 16: 25853(R) (TID-16273)
radiation effects, 16: 27591(R) (EURAEC-284)
radiation effects, 17: 5041(R) (ORNL-3364(p.151-200))
radiation effects on, in carbon tetrachloride solutions, 17: 10709
radiation effects, 17: 12323 (BMI-1610)
radiation effects on phosphors in, 17: 16077
radiation effects on, in nitrate–nitric acid solution, 17: 20514 (IDO-14598)
radiation effects on electric conductivity of, bremsstrahlung, 17: 22257
radiation effects on, 17: 25088(R) (ORNL-3417(p.267-76))
radiation effects on photoconductivity of, 17: 27893 (TID-18843)
radiation effects on photoconductivity decay of, 17: 27895 (TID-18857)
radiation effects of beta particles from tritium decay in labeled, 17: 32152 (CONF-14-21)
radiation effects on electric properties of, gamma, 17: 34498
radiation effects on properties of coatings, 17: 36362
radiation effects on properties of films of copolymers with acrylic acid, 17: 36362
radiation effects on reactions in, alpha and beta, 18: 328
radiation effects on stability of anion exchangers, accelerated electron, 18: 1772
radiation effects on electric insulators of, gamma and neutron, 18: 12412 (AFCRL-63-753)
radiation effects on transient-current decay in insulators of, gamma, 18: 18428
radiation effects, 18: 22113(R) (ORNL-3591(p.223-30))
radiation effects on reactions with chlorine and sulfur dioxide, 18: 25490(T) (AEC-tr-6372(p.197-205))
radiation effects on, ESR spectra of, 18: 25520(T) (AEC-tr-6372(p.481-90))
radiation effects on, hardening against, 19: 9547
radiation effects on, at various molecular weights, 19: 11191
radiation effects on dielectric constant and dissipation factor of, in vacuum, 19: 13444
radiation effects on, comparison of gamma and fast neutron, 19: 17988
radiation effects on thermoelectric charge displacement in, 19: 22328
radiation effects on electric properties, 19: 22390
radiation effects on substituted, 19: 24577
radiation effects on, ESR spectra and free radicals from, 19: 30233(R) (ORNL-3789(p.318-22))
radiation effects on electric conductivity of, gamma, 19: 32779
radiation effects on absorption and desorption processes on, gamma, 19: 34219
radiation effects on, 19: 34247
radiation effects on dielectric properties of, electron, 20: 1897 (NASA-TN-D-3032)
radiation effects on EPR spectra of, 20: 4479(R) (TID-22179, pp 1-83)
radiation effects on mechanical properties and structure of isotactic, 20: 7168
radiation effects on strength of, proton, 20: 10605(T) (NASA-TT-F-

353, pp 21-54)
radiation effects on dielectric constants and paraelectric susceptibility of, 20: 19266
radiation effects on current induction in capacitor of, electron beam, fast neutron, and gamma, 20: 21151 (IBM-66-825-1944)
radiation effects on molecular motion and structure of isotactic, gamma and neutron, 20: 20753
radiation effects on, light-scattering and viscosity measurements of gamma, 20: 20765
radiation effects on dielectric properties of, 20: 21443
radiation effects on, at cryogenic temperatures, 20: 23794
radiation effects on positronium lifetimes in, thermal neutron, (E), 20: 32704
radiation effects on electric properties of, gamma, 20: 33349
radiation effects on photoconductivity processes in, x, 20: 40952 (SC-DC-66-1823)
radiation effects on surface electrification of, gamma, 20: 43337
radiation effects on solutions of, effects of pyrene on, 20: 43355
radiation effects on EPR spectra and thermoluminescence of, 18: 27536
radiation energy deposition in, reactor, 17: 11280
radiation grafting to cellulose, 18: 17900
radiation grafting to cellulose acetate, composition after, 19: 11206
radiation sorption by, surface of, beta, 19: 7993
radioinduced branching in, statistical calculations of viscosity of, 18: 12200
radioinduced chlorination, gamma, 18: 29723(T,R) (AEC-tr-6231 (p.220-4))
radioinduced copolymerization with methyl methacrylate polymers, 16: 29011
radioinduced cross-linking, relative effects of gamma radiation and neutrons, 16: 6820(R) (ORNL-3213(p.92-5))
radioinduced crosslinking, localized neutron, 16: 11772
radioinduced crosslinking and decomposition, polar effects in, 16: 22174
radioinduced crosslinking, localized neutron, 16: 23720(T) (AEC-tr-5144)
radioinduced crosslinking, effects of polyfunctional monomers on, 16: 25418(R) (RAI-306)
radioinduced cross linking in, process for, 17: 40898(P)
radioinduced crosslinking of, effects of allyl acrylate, allyl methacrylate, and diallyl maleate on, 18: 8407 (RAI-329)
radioinduced crosslinking by boron-10 (n,α) reactions, 18: 27611(P)
radioinduced crosslinking and endlinking in, mechanisms of, 18: 31589
radioinduced cross linking of, relation of molecular weight distribution to, 18: 35615
radioinduced crosslinking in, effects of triallyl isocyanurate on, 19: 15594
radioinduced cross-linking with poly(methyl methacrylate) and teflon, localized neutron, 20: 23087(T) (AEC-tr-6466/1, pp 238-41)
radioinduced current oscillations in, extreme vacuum ultraviolet, 19: 44059 (NYO-2949-1)
radioinduced electric conductivity in, 17: 31040
radioinduced electric fields in dielectrics of, electron, 19: 26895
radioinduced formation from α-methylstyrene by electrons, 18: 20070
radioinduced free radicals in, electron spin resonance spectral studies of, 17: 22235
radioinduced free radicals in, effects of pigments on, 18: 24199(T,R) (AEC-tr-6316(p.359-67))
radioinduced free radicals in, reactions with sulfur dioxide, 18: 29747(T,R) (AEC-tr-6231(p.439-50))
radioinduced graft polymerization with acrylonitrile, 16: 228
radioinduced graft polymerization of acrylonitrile on, 16: 23541
radioinduced graft polymerization of, onto cellulose, 17: 20071
radioinduced grafting of, chain-length determination in, 17: 30047
radioinduced graft polymerization of, to cellulose in red pine sapwood, 17: 31807
radioinduced graft polymerization of, to cotton cellulose and rayon, effects of solvent additives and water on, 17: 31808
radioinduced graft polymerization on cellulose acetate, 18: 8418
radioinduced graft polymerization with acrylonitrile, 18: 13890
radioinduced graft polymerization with cotton, thermal stress properties of products in, 18: 20084
radioinduced graft copolymerization with polymethylmethacrylate, 18: 22130
radioinduced grafting to amylose, gamma, 19: 11212
radioinduced grafting to cellulose acetate, molecular weight distribution in, 19: 18019
radioinduced graft polymerization of monomers onto, 18: 20096(P)
radioinduced graft polymerization of acrylonitrile on, 20: 401
radioinduced luminescence in, efficiency of, 18: 23662
radioinduced macroradical formation in, spin density distribution of unpaired electron in, 18: 29782(T)
radioinduced optical absorption bands in, effects of oxygen on bleaching of, 18: 25568
radioinduced photoconductivity, 16: 22653 (TID-16102)
radioinduced photoconductivity of, temperature dependence of transient gamma, 18: 32229 (SC-R-64-191)
radioinduced photoconductivity in, pulsed gamma, 19: 41091 (SC-R-65-943)
radioinduced polymerization effects on glass transition temperature of, 18: 31590
radioinduced polymerization, 18: 37179 (BNL-874(p.5))
radioinduced polymerization crosslinking in, sensitization effects of pyrene on, 18: 43667
radioinduced polymerization of, with methyl methacrylate at −78°C, gamma, 20: 26939
radioinduced polymerization of, with hydrocarbons for radioresistant lubricants, 20: 38973(P)
radioinduced reactions with silica gel, 17: 6140
radioinduced reactions with polymethymethacrylate, 19: 10675(R) (NAA-SR-9999)
radioinduced scintillation output from, alpha, 18: 33638
radioinduced space charge in, by 2-Mev electrons, 19: 44096
radioinduced sulfonation, 18: 29726(T,R) (AEC-tr-6231(p.233-8))
radioinduced thermoluminescence of, effects of *p*-terphenyl on, 18: 27542
radioluminescence efficiency of, molecular weight dependence of, 17: 30585
radiolysis, 16: 23745
radiolysis, 17: 32176
radiolysis, mechanism of resistance to, 16: 23546
radiolysis of copolymer with polymethylmethacrylate, formation of peroxides in, 17: 27475
radiolysis of, electron spin resonance of free radicals produced by, 17: 8168
radiolysis of *p*-substituted, 16: 23742
radiolysis of 1,4-di-[5-phenyloxazolyl-(2)]-benzene in, 17: 29007
radiolysis of, effects of linear energy transfer in, 19: 429(R) (ORNL-3679(p.39-48))
radiolysis of, EPR studies of yields of stabilized charges in low-temperature, 20: 40962
radiosterilization effects on, for use as food packaging material, 19: 21863 (NP-14957)
reactions of deuterated, with deuterium and hydrogen atoms, 19: 10675(R) (NAA-SR-9999)
reactions with deuterium and hydrogen atoms, mechanism and spectra of, 18: 31477
reactions with deuterium, hydrogen, nitrogen and oxygen atoms, spectra from, 19: 27735(R) (NAA-SR-10850)
reactions with muonium, (E), 20: 29247
reactions with polystyryl lithium in benzene solution, 16: 28975(R) (NP-12015)
relative pulse height of plastic scintillators, correlation with electronegativity of p-terphenyls, 16: 7985
scintillation light yield from, 20: 41346
scintillation of, effects of polymerization time on fluorescence spectra of, 18: 13855
scintillation properties of activated, effects of wave shifter concentration on, 17: 7122 (NP-12330(p.220-3))
scintillation properties with POPOP for beta detection, 18: 5398
shielding properties of, 17: 33256
shock impingement studies on styrofoam, (E/T), 20: 3324(R) (IITRI-578P21-13)
solubility in benzene, 19: 24583
sorption of ionic cobalt-60 by, effects of sulfuric acid on, 17: 12239
sorption of x radiation in Grenz-ray region, dosage determination of, 19: 24784
sorptive properties for carrier-free yttrium solutions, effects of surface treatment on, 18: 39247
spectra of arylethylenes, oxazoles, and oxadiazoles in, fluorescence, 19: 24565(T)
thermal degradation of, with divinylbenzene, mechanism of, 20: 38930 (TID-23264)
thermal stability of filters of fibrous, at 105 and 145°C, 20: 43067(R) (IDO-14679, pp 6-46)
thermoluminescence of irradiated, 17: 30134
transformation of carboxylated, copolymers with butadiene and their mixtures with ϵ-caprolactam, 16: 6791(T) (NP-tr-826)
trimethyl-, efficiency as alpha phosphor, 17: 21757
triton energy losses in, 16: 2491 (TID-14145)
triton ranges and stopping cross sections in, 17: 17212
triton scattering and slowing-down by, at 2.7 Mev, 16: 27782
use and properties as membrane filter, 16: 16490(P)
use in gamma scintillation dosimeters, 18: 30050
use in liquid hydrogen targets, 18: 30603
use in preparation of chromatographic resins, 19: 40674
use of aluminized, for optical piping systems, 18: 10419
with acrylonitrile polymers, radiochemical preparation, solubility, and

swelling of, 18: 1749
with acrylonitrile polymers, thermomechanical properties, modulus of elasticity, and deformability of, 18: 1750
with acrylonitrile polymers, radiation effects on, 19: 34247
with butadiene, radiation effects on mechanical properties of, gamma, 20: 20754
with cellulose, radiolysis of, free radical yields in, 20: 10873
with divinylbenzene, properties for use in partition chromatography of uranium and fission products, 19: 30330
with divinylbenzene, radiation stability of sulfonated, 19: 30261
with polyvinyl fluoride, radiation effects on viscoelastic properties at 20 to 170°C, 19: 20001
x-ray scattering by, Smekal-Raman lines in spectra of, 18: 27323
acrylonitrile–polystyrene, radiation effects on polymers of, 20: 43355
methyl methacrylate–polystyrene, radioinduced polymerization effects on transition temperature of, 18: 31590
pentaphene–polystyrene, scintillation properties for gamma rays, 19: 42756
polybutadiene–polystyrene, dose and impurity effects on radioinduced vulcanization of, 19: 36507
polybutadiene–polystyrene, radiation effects on viscoelastic properties of, gamma, 20: 29313
polystyrene–tetraphenylbutadiene, excitation and fluorescence of, 19: 2367
polystyrene–terphenyl, excitation and fluorescence of, 19: 2367
polystyrene–*p*-terphenyl, fluorescence of solid solutions of, 17: 41561 (TID-18167)
polystyrene–tetraphenylbutadiene, fluorescence and transfer efficiency of solid solutions of, 17: 41561 (TID-18167)
polystyrene–rubber, radiation effects on structure of, 17: 27931
poly(vinyl acetate)–polystyrene, tensile properties of grafted and mechanically mixed, comparison of, 20: 45724
PuO_2–polystyrene, critical experiments on compacts of, 18: 36783(R) (HW-81659(p.45-8))
PuO_2–polystyrene, critical experiments on compacts of, (E), 19: 38127(R) (HW-84608(p.77-9))
PuO_2–polystyrene, criticality of, 17: 41731(R) (HW-77871(p.46-53))
PuO_2–polystyrene, criticality measurements on, 18: 11398(R) (HW-79054(p.54-63))
PuO_2–polystyrene, criticality of arrays of, 18: 22850(R) (HW-80020 (p.31-7))
PuO_2–polystyrene, criticality studies on homogeneous configurations of, (E), 19: 16437 (HW-83603)
PuO_2–polystyrene, criticality studies of, (E), 19: 18735 (HW-79572)
PuO_2–polystyrene, criticality experiments on, 19: 42038(R) (BNWL-95, pp 27-35)
PuO_2–polystyrene, criticality studies, (E), 19: 43521
PuO_2–polystyrene, criticality studies on compacts of, 20: 3368 (BNWL-SA-214)
Pu–polystyrene, criticality studies in homogeneous systems, 18: 28990

STYRENESULFONIC ACID, SALTS
diffusion of cesium into, self-, 18: 41404
heats of dilution of cesium, lithium, potassium, and sodium, 19: 347(R) (ORNL-3679(p.60-83))
reactions of sodium, with tetramethylammonium compounds, ion exchange in, 19: 46237(R) (ORNL-3832, pp 76-99)

Subcritical Assemblies
see Exponential Piles

SUBLIMATION
equipment design for uranium hexafluoride purification by, 19: 24535(P)
equipment for, design for microsublimation analysis of fluorinated products, 17: 40691 (CEA-2308)
heat-transfer effects in gas flow, 18: 27676
use of vacuum, for removal of pesticides from food, 18: 43160(R) (SAN-1023)

SUBMARINE ADVANCED REACTOR
design of loop for in-pile fuel element testing, 16: 4960 (APDA-145)

Submarine Boiling Reactor
see Submarine Reactors

SUBMARINE FLEET REACTOR
safety, analysis of possible accidents, 16: 13391 (FXM-3323)

SUBMARINE POWER PLANTS
design and performance of 15,000-hp compact, 16: 20558 (AD-269397)
force and torque variations of 36-cylinder double-acting "steamotor" for, 16: 20556 (AD-269392)
mounting of, external vs internal, 20: 6664
torque converter design and performance for, hydraulic, 16: 22281 (AD-269394)
transmissions for, appraisal of mechanical, 16: 22283 (AD-269400)
transmissions for, hydrokinetic, 16: 22282 (AD-269395)

Submarine Reactor Small
see Submarine Reactors (S1C)

SUBMARINE REACTORS
see also Submarine Advanced Reactor
see also Submarine Fleet Reactor
control and machinery systems maintenance considerations, 16: 24963 (AD-269402)
control system for Czechoslovakian VVR-S, design of automatic, 17: 2483
criticality studies of VVR-M, 17: 42383
design, 18: 29118(P)
design, 20: 16117(P)
design of PWR, with horizontal pressure vessel, 20: 3578(P)
development, 20: 28824
development of British pressurized-water, 17: 5613
development of British pressurized-water, 17: 5614
development of, review of, 18: 35178
economics, 18: 26960
shielding of Russian VVR-M, temperature fields in, 18: 19412
steamotor for, power control of double-acting, 16: 25539 (AD-269391)

SUBMARINE REACTORS (S1C)
environs monitoring for radioactivity, Jan. to June 1962, 18: 1282 (CENRD/HP/62/2)

SUBMARINE REACTORS (S5G)
coolant flow pressure drop in, 16: 23819 (KAPL-M-WAG-1)

SUBMARINES
see also Nuclear Submarines
atmosphere control on nuclear-powered, 20: 20981
atmosphere of, development of, analyzers for, 17: 21393(R) (NRL-5814)
design of Deep Quest, for undersea mineral exploration, 20: 45927
hull model studies on nuclear-powered tanker, 18: 26959 (RTI/ING(63)-4)
power supply for small research, radioisotope-fueled, 20: 4276 (AGN-8128)
propeller drive, design of fluid transmissions for, 16: 23800(R) (AD-269399)
propulsion by steamotor, design study, 16: 23798 (AD-269390)
propulsion, electric motor systems for, 16: 22280 (AD-269388)
propulsion, hydraulic torque converter design and performance for, 16: 22281 (AD-269394)
propulsion, hydrokinetic transmission for, 16: 22282 (AD-269395)
propulsion of, radioisotope power source for, 19: 44572
propulsion of, using cobalt-60 heat source, 20: 43797 (AGN-8163(Vol.3))
propulsion using longitudinal exciting conductors, field configuration for external MHD, 19: 12139
propulsion using radioisotope systems, 20: 11187 (AGN-8138)
radiological instrumentation for Trieste I research, (E), 19: 22703 (USNRDL-TR-805)
speed of, measurement of, using neutron activation of oxygen in water, 20: 25368(P)
taut-line navigation buoys used in the *Thresher* search, 18: 23145 (TID-20535)
testing under high pressures, nuclear excavation of subterranean chamber for, 18: 33709 (SC-TM-64-636)
transmission systems evaluation for steam-powered, 16: 23799 (AD-269398)
transmissions for, appraisal of mechanical, 16: 22283 (AD-269400)

SUBSONIC FLOW
see also Supersonic Flow
see also Transonic Flow
around a thin wing, magnetohydrodynamics of, 17: 39457
research programs on, 1964 Army Dept. summary, 19: 32048(R) (NP-15073)

Succinamic Acid, α-Amino-
see Asparagine

SUCCINAMIC ACID, *N,N*-DIMETHYL-
penetration of carbon-14-labeled, through cuticular membranes, 20: 16146 (COO-888-39)

SUCCINAMIDE
radioinduced free radical formation in, ESR and tracer studies of, 20: 18757

SUCCINAMIDE, N-DIETHYLENE-
radioinduced polymerization in liquid and solid states, 18: 12216

SUCCINATES
determination of carbon-14-labeled, by liquid scintillation counting on paper chromatograms, 20: 14479
effects on iron-59 absorption in rats, 18: 1346
effects on oxygen and strontium uptake by rat liver mitochondria, 19: 14972
effects on phosphate and rubidium uptake by isolated cells of bean seedlings and tobacco leaves, 20: 14217 (COO-888-43)
metabolism by *Staphylococcus aureus* and its radioinduced mutant, 17: 5790(T)
monoheptyldecyltetrapropenyl, preparation of, 19: 17781(R) (ORNL-3750)
radiation effects on oxidation of, in *Vibrio cholerae*, 20: 16198
radiosensitivity effects on DNA, 17: 33726

synthesis from labeled acrylic acid, mechanism of, 16: 31394(R) (ANL-6535(p.90-5))
tritium exchange with water, 16: 23390

SUCCINIC ACID
analysis for carbon, isotope dilution, 18: 1547
benzyl ester, radioinduced de-esterification of, electron dosimetry by, 18: 29770
catalytic effects on oxidation of uranium(IV) by thallium(III) in perchloric acid, 16: 28858
complexes with thorium, formation constants and stability, 17: 21729
complexes with uranium, polarographic behavior of, 18: 41419
complexes with zirconium, 16: 11676
complexing with uranyl ion, bonding and stability constants, 16: 23387 (UR-611)
decomposition of, uranyl sensitized photo-, 17: 10697
derivatives, preparation of calcium uranyl salt, 16: 17628(T) (AEC-tr-4456(p.335-6))
determination by xenon trioxide oxidation, titrimetric, 20: 31196
DL-diamino-, yields in radiolysis of aqueous glycine, 18: 25584
effects on electronic exchange reaction between thallium(I) and (III) in perchloric acid, 17: 24788
effects on rate of reaction between uranium(IV) and thallium(III), 19: 46277
effects on sodium ion efflux from rat liver slices, 20: 42758
ionization constants of substituted, deuterium isotope effects, 18: 27489
N-phenyl-, analytical uses in gravimetric determination of zirconium and thorium, 18: 1570
O,O′-dideutero-, preparation and irradiation of, spectra of free radicals formed by, 16: 11726
oxidation by rat liver tissue, effects of beryllium on, 18: 17435
precipitation of cerium and lanthanum using, 18: 25351
preparation of carbon-14-labeled, 18: 1325(R) (UCRL-10934)
preparation of carbon-14-labeled semialdehyde of, 18: 31551
preparation of tritium-labeled, by charcoal sorption and gas exposure, 16: 17379
production in gamma radiolysis of aqueous fumaric acid, 20: 10875
radiation effects on growth of crystals of, 18: 1730(R) (TID-19668)
radiation effects on single crystal β-, EPR spectra of, 20: 389
radioinduced addition of hydrogen to fumaric acid in single crystals of, 20: 16537
radioinduced electron spin resonance absorption in, 19: 13445
radioinduced electron spin resonance absorption in deuterated, 19: 13445
radioinduced free radicals, 16: 14473(T) (JPRS-12465(p.34-42))
radioinduced free radicals in, 17: 25028
radiolysis of tritium-labeled, ESR spectra of radical yields in self-, 18: 31633
reactions of, with zirconyl chloride, 17: 20014
reactions with aqueous beryllium nitrate solutions, 16: 4126(T) (AAEC/Trans-8)
reactions with hydrochloric acid, heat of, 17: 27323 (UCRL-7325-T)
spectra of irradiated, zero-field electron magnetic resonance, 17: 33899
sulfo-, uses as surface-active agent in preparation of nuclear emulsions, 18: 23495
use of carbon-14-labeled, for preparing labeled marrubiin, 20: 23203
yields from tritium labeling of maleic acid, effects of support on, 19: 42522
succinic acid–urea, radiolysis of, ESR spectra of radicals produced by, 18: 43625

Succinic Acid, Amino-
see Aspartic Acid
Succinic Acid, Cyclohexyl-, Sodium Salt
see Cyclohexanesuccinic Acid, Sodium Salt

SUCCINIC ACID, DIBENZYL ESTERS
isotope effects in autoxidation of deuterated and normal, effects of phenylnaphthylamine on, 20: 45706

SUCCINIC ACID, 2,3-DIMERCAPTO-
chelates with metals, formation and properties of, 18: 8394 (TID-20013)
protective effects of, against radiation injuries in guinea pigs, 18: 31269
protective effects of, against radiation injuries in guinea pigs, effects of isomeric form on, 18: 31270
protective effects of isomer of, against radiation injuries in mice, 18: 31271
radioprotective effects of, on guinea pig exposed to lethal radiation doses, 17: 17839
radiosensitivity effects in guinea pig, DL form, 17: 35487
radiosensitivity effects in guinea pigs, meso form, 17: 35486
radiosensitivity effects in guinea pigs and mice, 20: 18483
toxic effects in dogs, 17: 35413

Succinic Acid, Hydroxy-
see Malic Acid

SUCCINIC ACID, MERCAPTO-
analytical uses in determination of cadmium, 18: 41357
chelates with metals, formation and properties of, 18: 8394 (TID-20013)
complexes with uranium, free energy of formation and spectra of, 18: 19947
protective effects against radiation injuries in guinea pigs, 18: 43305
radioinduced free radicals in, 17: 28963
stability constants of chelate compounds of, with uranyl ion, 16: 17666

Succinic Acid, Methylene-
see Itaconic Acid
Succinic Acid, Oxo-
see Oxalacetic Acid

SUCCINIC ACID, SODIUM SALTS
effects on pH of dialyzed zirconyl chloride, 17: 35718
radiolysis of single crystals of, EPR studies of, 20: 9009
reaction with thorium chloride, conductometric and potentiometric study of, 20: 5555

SUCCINIC ACID, TETRAFLUORO-, SODIUM SALTS
radiolysis of, ESR spectra of free radicals in, 18: 22139

SUCCINIC DEHYDROGENASE
activity in cancerous and normal mouse liver, effects of fatty acid extract from irradiated rabbits on, 16: 25224
activity in hepatomas in rats, effects of chemicals on, 16: 14560
activity in Yoshida sarcoma cells, effects of fatty acid extracts from irradiated rabbits on, 16: 25225
activity of, effects of complete substitution of deuterium for hydrogen on, 17: 23050
radiation effects on activity of, in mouse livers, x, 20: 6852
radiation effects on activity of, in mouse tissue homogenates and skin, uv, 20: 16196
radiation effects on activity in hepatomas in rats, 16: 14560
radiation effects on activity of, in rat brain and cerebellum, 17: 14077
radiation effects on activity of, in liver, nervous system, and skeleton in rabbits, 17: 31979
radiation effects on activity of, in rat liver, 18: 9894
radiosensitivity of, in cows and rats, 17: 7853

SUCCINIC OXIDASE
activity in hepatocyte organelles from Amphiuma, 20: 8573
effects of near-ultraviolet radiation on activity of, in bacteria, 20: 40571
ultraviolet radiation effects on activity of, in *Mycobacterium phlei*, 20: 42810

SUCCINIMIDE, *N*-VINYL-
polymerization with vinyl thioacetate, 18: 35584
radioinduced polymerization of, inhibiting effects of benzoquinone on, 20: 23106
radioinduced polymerization of, in solid state, 19: 5950
radioinduced polymerization of, effects of additives on, 18: 37236
radioinduced polymerization in liquid and solid states, 19: 489
radioinduced polymerization of liquid, 20: 1912
radioinduced solid-state polymerization of, with succinimide, 20: 18776
radioinduced solid-state polymerization of, effects of formed polymer on kinetics of, 19: 42546
radioinduced solid-state polymerization of, with vinylpyrrolidone, 19: 36494
benzoquinone–*N*-vinylsuccinimide, radioinduced solid-state polymerization of, gamma, 20: 23129
phthalic anhydride–*N*-vinylsuccinimide, radioinduced solid-state polymerization of, gamma, 20: 23129

SUCCINIMIDES
radioinduced solid-state polymerization with *N*-vinylsuccinimide, 20: 18776
radiosensitivity effects on *Pseudomonas*, 16: 17509

SUCCINONITRILES
thermodynamic properties of crystalline, 17: 23306 (TID-18635)

SUCROSE
content in irradiated potatoes, 19: 18361
crystal structure from neutron diffraction, 18: 37143
crystal structure of, machine-plotted diagram of, 19: 280(R) (ORNL-3679(p.94-116))
density of solutions of, calculation of, 19: 32187 (K-1635)
density of solutions of, methods for calculating, 18: 11515 (ORNL-3502)
determination in waste solutions, 19: 32059(R) (IDO-14655)
determination of, cerium(IV) oxidimetric, 17: 176
determination of carbon-14-labeled, by liquid scintillation counting on paper chromatograms, 20: 14479
effects on cesium-137 uptake by wheat roots, 19: 50
effects on mitotic cycle in plant cells, 19: 6946 (BNL-7725)
effects on radiation effects on ionic permeability of rooster erythrocytes, 19: 19577
effects on toxicity of praseodymium and samarium nitrates in rats, 16: 26657(R) (NP-11966(p.27-35))
effects on urinary excretion of sodium and potassium after x irradiation, 17: 10463
electron spin resonance spectra of gamma-irradiated single crystals,

16: 10059
inactivity in synthesis of indoleacetic acid from tryptophan, 16: 31403(R) (ANL-6535(p.144-5))
labeling with carbon-14 for use in tracer studies, 19: 7531
polymerase–DNA complex in gradient of, 17: 31832
preparation of carbon-14-labeled, by photosynthesis, 16: 18908
preparation of carbon-14-labeled, apparatus and technique for, 17: 33496
preparation of tritiated, by tritium atom bombardment, 17: 33953 (TID-19259)
properties in damped oscillating manometer, time-dependent, 17: 27654 (LADC-5535)
protective effects against radiation damage to plant cells, 18: 23374
radiation effects on electron paramagnetic spectra, x, 16: 27050
radiation effects on, electron-, gamma-, neutron-, and x-, 16: 31669
radiation effects on, electron spin resonance investigations of gamma, 17: 27454
radiation effects on spectra of single crystals of, 17: 40873
radiation effects on content of, in potatoes, 19: 13834
radiation effects on crystal structure and melting point, 20: 4020
radiation effects on, in aqueous solutions, x, 20: 20748
radiation effects on sorption of, following radiotherapy, 20: 24866
radioinduced free radicals in, gamma, 18: 23651(T,R) (AEC-tr-6316 (p.573-86))
radioinduced luminescence, 17: 40856 (UCRL-10961)
radioinduced radical in single crystals, 16: 29005
radiolysis, 17: 21740
radiolysis in culture media, toxicity of, products from, 20: 8608
radiolysis of solid, yields in, 18: 310
radiolysis of solutions of, gas production in, 17: 6142
radiosensitivity effects on bacterial spores, 18: 35394
radiosensitivity effects on osmosis in Allium epidermal cells, x, 19: 42270
reactions with nitric acid in waste processing, 18: 45174(R) (MLM-1204)
reactions with nitric acid in Purex waste, 18: 19445 (HW-76973(Rev.))
sedimentation in zonal centrifuge, computer program for determining, 18: 11515 (ORNL-3502)
sedimentation of subcellular particles and viruses in, 18: 35678(R) (ORNL-3656)
sedimentation patterns in labeled HeLa cell RNA, 18: 11584
separation from other sugars in photosynthetic chamber by paper chromatography, 20: 43402
structure of, neutron diffraction determination of crystal and molecular, 17: 35807
structure of, neutron diffraction analysis of, crystal and molecular, 18: 1491(R) (ORNL-3488(p.102-22))
structure of, neutron diffraction determination of crystal and molecular, 19: 23163(R) (ORNL-3650(p.111-86))
synthesis in peas by uridine-5-diphosphoglucose transglucosylose, 20: 6766
uptake by sugar pine embryos, tracer study of, 19: 43643(R) (TID-22143)
use in biological zonal centrifuge rotor systems as gradient material, 18: 35678(R) (ORNL-3656)
use in denitration of Purex waste solutions, 17: 35243 (HW-77080)
use in gamma dosimetry to 200 MR, 18: 37448(T) (AEC-tr-6398(p.199-204))
viscosity of aqueous solutions of, calculation of, 18: 35678(R) (ORNL-3656)
viscosity of solutions of, methods for calculating, 18: 11515 (ORNL-3502)
viscosity of solutions of, calculation, 19: 32187 (K-1635)

SUGAR BEETS
effects of seed irradiation on size of leaf tissue nuclei in, 18: 25136
industry, applications of radioisotopes in, 17: 10887
radiation effects on growth and sugar content, protection against, by nitrogen fertilizers, 17: 10442
radiation effects on extracts of cellular structure of leaves of, by seed exposure, 18: 33314
radiation effects on protein and carbohydrate content of, effects of maturity at exposure on, 18: 41186
use of pulp base, as cation exchange material for decontamination of waste water, 16: 20039

SUGAR PHOSPHATES
see also Fructose Phosphates
see also Glucose Phosphates
dephosphorylation by thorium and zirconium ions, 19: 19876
metabolic repair of radioinduced chromosome aberrations in Tradescantia by, 16: 30252
metabolism of hexose and mannitol, in *E. coli*, 20: 6730 (TID-22376)
metabolism of, tracer study of, 18: 35409 (TID-7678(p.107-33))
radiation effects on metabolism of, in human erythrocytes, 19: 22024
reactions with thiamine derivatives during photosynthesis, effects of enzymes on, 18: 17403(R) (UCRL-11046(p.15-20))

SUGARS
(See also the specific sugars.)
see also Carbohydrates
analysis of, behavior of tetra-*O*-acetyl pentopyranoses in chromatographic, 17: 4561(R) (UCRL-10350)
autoradiography of thin layer chromatograms of labeled, method for, 19: 13222
content in blood of irradiated and nonirradiated animals, 18: 27198
content in blood, effects on radiosensitivity of rats, 19: 33966
content in goldfish blood, effects of mammalian ACTH on, 19: 31670(R) (NIRS-3(p.19-56))
crystal structure of natural, mass-spectroscopic studies of, 17: 10557
derivatives of, gas–liquid partition mobilities of pyranose, 17: 4561(R) (UCRL-10350)
distribution in lenses of galactose-fed rats, 20: 30978
effects of maltose and fructose on radiosensitivity of *B. subtilis* spores, 18: 39002
effects on calcination of Purex 1WW solutions, 17: 31681(R) (HW-76559)
effects on denitration of acidic waste solutions, 17: 36991 (HW-75565)
electron spin center formation in carbonized, by oxidation at 700 to 1100°C, 16: 18880
metabolism in mouse brain of, 19: 33760
metabolism in rats of, effects on cataract induction, 19: 33880
moisture content of, in mixtures with sand, neutron gage for determining, 20: 5819
oxidation by *Acetobacter suboxydans*, 16: 26687(R) (UCRL-10156)
preparation of carbon-14-labeled, by use of yeast, 18: 38746
protective effects of, against radiation sickness, review, 17: 14112
radiation effects on 270 mμ absorption coefficient of solutions, 16: 24071
radiation effects on content of, in blood of mice, 17: 30456
radiation effects on rabbit and rat blood content of, biochemical indexes of chronic low-dose gamma, 18: 13515
radiation effects on blood content of, in rats, 18: 27185
radiation effects on metabolism of, in rats, 19: 3895(R) (ORO-625 (p.103-8))
radiation effects on, of egg yolks, 19: 7125
radiation effects on intestinal absorption of, in rats, 19: 33842
radiation effects on sugar beet content of, cysteine effects on, 19: 36118
radiation effects on content in rabbit eyes, 19: 43755
radiation effects on content in pea leaves of, γ, 20: 5280
radiation effects on, in oranges, γ, 20: 31632
radiation effects on content of, in rabbit blood, x, 20: 38686
radiation effects on content of blood, x, 20: 42917
radiation effects on content of, in potatoes, 20: 43773
radiolysis of solutions of, 19: 479
radiolysis, paramagnetic centers produced in, 16: 22171
radiosensitivity effects on catalase, 20: 18449
reactivities of aqueous solutions with radioinduced free radicals, 17: 13966 (HW-SA-2588)
refining of, applications of radioisotopes in, 17: 10887
separation of carbon-14-labeled, in photosynthetic chamber by paper chromatography, 20: 43402
sorptive properties for organic compounds, 18: 25032(T) (SC-T-64-618)
synthesis of carbon-14-labeled, in *Chlorella*, 17: 30016
synthesis of mercaptoamino, 17: 35595(R) (AD-287512)
transport in mammalian cells and tissues, tracer techniques, 16: 1365
use in Purex waste processing, 18: 27278(R) (HW-79280(p.4.1-28))

SULFAMATES
see also Iron Sulfamates
see also Potassium Sulfamates

SULFAMIC ACID
analysis for sulfur by hydrogen reduction, 20: 29083(R) (UCRL-14767)
analytical use as nitrite-destroying reagent in titration of uranium(VI), 16: 8678 (ORNL-TM-113)
chemical effects on ferrous sulfamate at 23 to 55°C, 18: 22004 (DP-871)
corrosive effects on corroded type-304 stainless steel, 19: 2756
properties as decontaminant for water-cooled reactors, 16: 20984
properties of fluoride-bearing aqueous, for etching and pickling zirconium alloys, 20: 39351(P)
solvent properties for plutonium, 16: 25310 (DP-737)
solvent properties for plutonium, 17: 15957 (TID-16387)
solvent properties for magnesium oxide–plutonium dioxide systems, 18: 9646(R) (HW-78388(p.11.1-15))
solvent properties for plutonia powders, 19: 14832(R) (HW-81984 (p.11.1-14))
solvent properties for plutonium, 19: 42520(P)
use in stabilization of plutonium(III) for ion exchange, 16: 13124 (DP-349)
alkali metal bisulfate–sulfamic acid, properties as decontaminating solution for aluminum or zirconium, 20: 41214(P)
ammonium bisulfate–sulfamic acid, properties as decontaminating solution for aluminum or zirconium, 20: 41214(P)

HNO_3–NH_2SO_3H, solvent properties for plutonium, 17: 15957 (TID-16387)
HNO_3–sulfamic acid, solvent properties of, for plutonium, 16: 25310 (DP-737)
sulfamic acid–sulfuric acid, properties as decontaminating solution for aluminum or zirconium, 20: 41214(P)

SULFAMIDES
radiation effects on bacterial volutin induced by, 19: 42280

SULFANILAMIDE
disulfide, protective effects against radioinduced enzyme inactivation, 17: 30303
effects on animal resistance to infections, 19: 7201
effects on uranium elimination from kidneys, 20: 10553
N-2-pyridinyl-, effects on calcium and strontium metabolism by *Tetrahymena pyriformis*, 19: 31735
N-2-thiazolyl-, effects on radiomimetic effects of nitrosoamides on herb seeds, 19: 43870
preparation of tritium-labeled, by charcoal sorption and gas exposure, 16: 17379
protective effects of, on hemagglutinin and infectivity of influenza virus, 17: 15668
radiation effects on metabolism of, in mouse liver, 18: 5002(R) (NP-13281(p.92-103))
radiosensitivity effects on plant seeds, β, 20: 18442

SULFANILIC ACID
analytical use for spectrophotometric determination of cerium, 20: 16398
boric acid–sulfanilic acid, phosphorescence in, 19: 19919

SULFATE COMPLEXES
see also Cerium(III) Sulfate Complexes
see also Cerium(IV) Sulfate Complexes
see also Neptunium(IV) Sulfate Complexes
see also Uranium Sulfate Complexes
see also Uranyl Sulfate Complexes
plutonium, stability constants for, 20: 43244
with americium, europium, lanthanum, and lutetium, equilibrium and stability constants of, 18: 35539
with beryllium, detection of, 17: 2898
with beryllium, ion exchange studies of, 19: 46230 (AAEC/E-136)
with hafnium and zirconium, equilibrium and stability constants of, 18: 27414
with manganese in perchlorate solutions, paramagnetic resonance studies of, 18: 21730 (UCRL-10446)
with neptunium, properties and stability of, 20: 29148
with plutonium(IV), 16: 8744
with protactinium V, stability constants of, 18: 13783
with protactinium, preparation and properties, 19: 17890
with uranium, stability constants of, 18: 23534
with zirconium, stability constants of, 17: 21675
with zirconium, properties, 17: 35825

SULFATE IONS
see also Peroxydisulfate Ions
association with cerous ions, use of cation exchange resins for study of, 18: 1611 (LA-2513)
binding by cuticular membranes from leaves, tracer studies of, 18: 13378 (TID-20186)
determination by precipitation with chromium-51, 18: 39765
determination in aqueous solutions using kryptonated barium carbonate, 20: 18570(R) (NYO-2757-5)
determination in beryllium solutions by cation exchange, 18: 23423
determination of, radiometric, 17: 5952 (IA-772)
determination using barium chromate, spectrophotometric, 16: 30333(T) (AEC-tr-5222)
dissociation constants at 25°C, 19: 15571(R) (TID-21385)
distribution between Dowex 1-X8 and solutions of potassium bicarbonate and carbonate, 18: 25438
effects on copper determination, 20: 36726
effects on corrosion of zirconium alloy by water, 16: 22557
effects on determination of uranium(VI) in presence of uranium(IV), 20: 3903
effects on electron exchange between uranium(IV) and uranium(VI), tracer studies of, 20: 296
effects on isotope exchange between iron(II) and (III), 17: 14262
effects on isotopic exchange between iodide and iodate ions, 20: 43248
effects on nitrate ion yields from radiolysis of potassium nitrate, 20: 43329
effects on oxidation of iron(II) by cerium(IV), catalytic, 19: 26362
effects on polarography of uranium(VI) in acid media, 16: 4182
effects on polarographic determination of uranium, 19: 19797
effects on polarographic determination of thorium, 19: 32077
effects on radioinduced coloring of alkali halide crystals, 18: 39273 (AD-417474)
effects on radiolysis of acetylene, 19: 44082
effects on reactions between uranium(VI) and vanadium(II), 19: 11106
effects on sorption of uranium by ion exchange resins, 20: 29350
effects on spectrophotometric determination of thorium, 19: 24408
effects on thorium and uranium leaching from minerals, 16: 27112
effects on uranyl complexes with tributylphosphine oxide, 20: 40885
effects on valence states of cerium, iron, and uranium ions, 20: 14574
effects on zirconium extraction from nitrate solutions using tributyl phosphate, 20: 27048
electrochemical behavior in lithium chloride–potassium chloride eutectic, 17: 30555
electron spin resonance spectra of, in irradiated aqueous sodium hydroxide glasses at 77 to 150°K, 20: 45730
equilibrium effects on anionic XX resin and uranyl sulfates, 16: 25330
frequency displacements and partial function ratios as function of force constants, 17: 2698
hydration numbers, 17: 30544
precipitation with ferric hydroxide, tracer studies of, 18: 39172(T) (AEC-tr-6390(p.460-5))
radiolysis of aqueous solutions of, pulse, 19: 38728
separation from chloride and phosphate ions by paper chromatography using iron(III) hydroxide, 17: 21782
solvent extraction from molten nitrate by liquid silicone–TBP at 150°C, 19: 19833 (CEA-R-2628)
sorption by platinum, gold, silver, stainless steel, glass, and polyvinyl chloride, tracer study of, 17: 35693 (NP-12983)
sorption on aluminum surfaces, 19: 28427
spectra of, deuterium oxide solvent effects on uv absorption, 18: 43500

SULFATE SPACE
measurement in man, tracer method, 19: 43898

SULFATES
(See also sulfates and acid sulfates of specific elements.)
see also Acid Sulfates
see also Alkali Metal Sulfates
see also Ammonium Sulfates
see also Brucine Sulfate
see also Chondroitin Sulfates
see also Ethyl Sulfates
see also Glycine Sulfates
see also Hexadecyl Sulfates
see also Rare Earth Sulfates
see also Sodium Hexadecyl Sulfates
see also Thiosulfates
see also Uranyl Sulfates
see also Zirconyl Sulfates
analysis for oxygen isotopes, procedure for, 17: 2721
corrosive effects of, on niobium at 300°C, 17: 20426
determination in beryllium oxide, 16: 11526 (UCRL-6639(p.10-15))
determination in beryllium oxide, absorptiometric, 16: 11505 (AERE-AM-86)
determination in geothermal and volcanic waters, 18: 43800 (INS-R-25)
determination in plutonium peroxide and tetrafluoride by infrared spectroscopy, 20: 8850
determination in reactor coolant water, survey of methods for, 18: 1505 (ORNL-TM-724)
determination in scrubber solutions used in Dribble vent gas treatment plant, 19: 46471 (UCRL-14123)
determination in uranium concentrates, photometric, 16: 4208(R) (NLCO-800)
determination in uranium trioxide and uranyl nitrate, gravimetric, 16: 25270 (PG-Report-330)
determination in urine, 17: 17996
determination in water produced in nuclear reactors for marine propulsion, methods for, 17: 33789 (EUR-224.i)
determination of microgram amounts, design of photometric titration equipment, 16: 8683 (TID-14741)
determination of, method for, 17: 28801 (IDO-14316(Suppl.4))
determination of sulfur-35-labeled, in labeled phosphates and pyrophosphates by activation, 18: 23417
determination of, using chromium-51, 17: 23268
distribution of radioactive, in chick stomach, 16: 23401
effects of sulfur-35 on isotope exchange with oxygen and sulfur dioxide, review, 16: 31664
effects on chromium–nickel steel corrosion by sodium acid carbonate-sodium chloride solutions at 20°C, 17: 25727(T) (EURAEC-676)
effects on complexometric titration of zirconium, 18: 41336
effects on corrosion of aluminum by high-purity water at 100°C, 17: 18706
effects on determination of strontium-90 in waste solutions, 19: 46196
effects on disproportionation of uranium(V), 20: 40911
effects on extraction of uranium with TBP-hexane systems, 16: 5405 (MCW-1456)
effects on iron-59 uptake and transport by bean leaf cells and leaves, 20: 14220 (COO-888-48)
effects on phenol yields from radiolysis of benzene, 20: 10878
effects on photometric determination of zirconium, 19: 43972

effects on radioinduced oxidation of iron(II) ions, 16: 13092
effects on spectrophotometric determination of zinc using 1-(2-thiazolylazo)-2-naphthol, 19: 19814
effects on spectrophotometric determination of zirconium, 20: 3895
effects on thermodynamics of uranium solvent extraction by di-2-ethylhexyl phosphoric acid, 18: 12268
effects on thorium dioxide–uranium dioxide fuel particle solubility in fluoride–nitric acid solutions, 20: 18819 (AAEC/E-143)
effects on wheat, genetic, 17: 28713
electrolysis of, formation of ozone in, 17: 2712
exchange by less-retensive soils, 16: 23539
excretion by irradiated and normal rats injected with sulfur-35-labeled cysteine, urinary, 16: 26746
excretion by rats, effects of adrenalectomy on, 18: 25006 (TID-18927)
heat of formation and ionization potentials, 17: 3010
metabolism by mycobacteria, tracer techniques for studying, 19: 31745
metabolism in bacteria, 16: 25151(R) (TID-16073)
metabolism in bone, tracer study, 16: 31439
metabolism in bone fractures during repair, tracer study, 16: 31440
metabolism in cartilage, effects of irradiation, tracer study, 16: 14533
metabolism in liver, tracer study, 17: 10312(T) (AEC-tr-5600)
metabolism of radioactive, in chick stomachs, 16: 23401
metabolism of, in fish, 18: 4975
metabolism of, in Neurospora, tracer study of, 18: 29199(R) (TID-20768)
phase diagrams of, book, 19: 14061
precipitation from waste solutions, 19: 25777(R) (HW-84603(p.37-49))
precipitation from waste solutions in calciner, 20: 8477(R) (BNWL-139)
preparation of carrier-free sulfur-35 labeled-, 18: 12186
properties of waste solutions of, versus sulfate-free samples, 20: 12517(R) (BNWL-170)
radiation effects, measurement of amount and composition of radiation products, 16: 20466 (AERE-R-3409)
radiation effects on metabolism of, in rat brain, 18: 29327
radiation effects on sulfur-35 incorporation by guinea pig eye, strontium-90, 18: 38810
radiation effects on metabolism in rabbit eyes, 19: 12974
radiation effects on uptake by aortic mucopolysaccharides in rabbits, tracer study, 20: 14295
radiolysis of aqueous solutions of, at 77°K, yields of hydrogen from gamma, 20: 18748
reactions with niobium oxides, 16: 122
reduction by bacteria, 18: 4962 (UCRL-10966)
reduction by *Desulfovibrio aestuarii*, 18: 31362(R) (UCRL-11213(p.154-61))
reduction of sulfur-35-labeled, 17: 25098
reduction of, kinetics of bacterial, 20: 23217(R) (UCRL-16580, pp 251-4)
separation from beryllium by solvent extraction using phosphate esters, 16: 25475 (NCL/AE-172)
separation from beryllium fluoride–lithium fluoride systems, 18: 34050(R) (ORNL-3626(p.59-164))
separation from phosphate by thin-layer chromatography, 18: 17949
separation from uranium in anion exchanger desorption, 20: 20827
separation of iron and uranium from, by solvent extraction using bis-(2-ethylhexyl) phosphoric acid, 17: 10766
sorption by leaves, 18: 13377 (TID-20184)
sorption by less-retentive soils, 16: 23539
sorption by soils, tracer study, 16: 32713
sulfur isotopic composition in hypogene, 20: 45921
thermal decomposition of, application of activated complex theory to, 18: 36900 (UCRL-10791)
thermodynamic properties, 18: 17780 (SC-RR-64-67)
uptake by irradiated rabbit cartilage, 16: 32769
use in production of carrier-free phosphorus-32 by irradiation, 16: 7256
uses for selective anodic attack and etching of gamma phases in uranium alloys, 19: 14038
volatility during calcination of sulfate-deficient Purex waste, effects of aluminum on, 18: 19448(R) (ORNL-TM-757)

SULFENIC ACIDS
esters of, chlorinalyses mechanisms of, 19: 417(R) (ORNL-3679 (p.49-59))
methyl ester of *o*-nitro-, crystal structure of, 19: 23355(R) (BNL-867(p.1-117))

SULFEX PROCESS
(Head end process for the dissolution of stainless steel fuels by H_2SO_4.)
construction materials for, corrosion behavior of, 17: 17451
corrosion in, 18: 8454
corrosion of construction materials in, 17: 19724 (BNL-759(p.39-46))
corrosive effects of solutions from, on candidate alloys for centrifuge, 19: 20481 (ORNL-3787)
cost comparison with mechanical shear-leach for processing clad uranium oxide fuels, 16: 16457 (ORNL-3227)
decladding of stainless steel-clad urania fuel specimens in, 17: 23434 (ORNL-3404)
development, 20: 4048(R) (NP-15496)
dissolver vessel materials for, evaluation of, 16: 33064 (BNL-752)
effects of burnup on, 16: 24644
efficiency, hot cell demonstration, 16: 27123 (ORNL-TM-187)
evaluation of, in hot cells, 17: 39178(R) (ORNL-3452(p.1-25))
operation of, hot-cell demonstration of, 17: 26189
performance, hot cell demonstration, 16: 11789 (ORNL-TM-130)
performance with clad plutonia–urania fuels, 20: 9044(R) (ORNL-3830, pp 30-68)

Sulfhydryl Group
see Mercapto Group

SULFIDE, ALLYL-*p*-TOLYL
cleavage by lithium or sodium metal in liquid ammonia, carbon-14 tracer studies of mechanism of, 19: 5931(R) (TID-21368)
cleavage by metals in solvents, 19: 5932 (TID-21381)

Sulfide, 2,2'-Bis[Di(Carboxymethyl)Amino]Diethyl-
see Acetic Acid, Thiobis(Ethylenenitrilo)Tetra-

SULFIDE, DIHEXACOSYL
protective effects against radioinduced viscosity increase in lubricating oils, 18: 3873(P)

SULFIDE, ETHYL PHENYL
electron reactions on, radical ion production from, 18: 6870

SULFIDE, METHYL PHENYL
deuterium exchange, acid-catalyzed, 16: 20306
electron donor properties, 18: 13812 (TID-20249)
electron reactions on, radical ion production from, 18: 6870
spectra of donor sites in Lewis acid adducts of, infrared, 20: 14226 (TID-21586)

SULFIDE IONS
fluorescence of silver chloride crystals doped with, blue-green emission band shift in, 17: 32161
Slater-Condon parameters of, determined from spectral data, 17: 31118
sputtering ratio for polycrystalline copper, 16: 9114

SULFIDES
(See also headings of the form Sulfide, Methyl Phenyl for nonsymmetric organic sulfides)
see also Actinide Sulfides
see also Alkaline Earth Sulfides
see also Butyl Sulfides
see also Carbonyl Sulfide
see also Chromium Sulfides
see also Disulfides
see also Ethyl Sulfides
see also Ethylene Sulfide
see also Methyl Sulfides
see also Phenyl Sulfide
see also Rare Earth Sulfides
see also Zirconyl Sulfides
analysis for sulfur isotopes, 17: 2723
conference on, 18: 37115 (ANL-6856)
conference on compounds of interest in nuclear reactor technology, University of Colorado, Boulder, August 3 to 5, 1964, 19: 7441
crystal structure of intermetallic-phase, 20: 29623(R) (TID-22970, pp 121-256)
crystal structure of three-component, 19: 9152
data tabulations on, 18: 32079
determination in geothermal and volcanic waters, 18: 43800 (INS-R-25)
determination in radiation processes sea foods, chemical, 20: 41384(R) (TID-22833)
determination of, in fluoride mixtures, 16: 34073(R) (ORNL-1294)
dissociation energies of metal, 17: 41534(R) (ANL-6720(p.77-89))
effects as radioprotective agents in mice, relation to chemical structure, 20: 38724
effects on wholesomeness of radiation processed sea foods, 20: 41384(R) (TID-22833)
electric and thermal conductivity of metal, symposium on, 20: 37179
electron beam reactions in, rearrangement in, 20: 23166
genesis of deposits, sulfur isotopic studies, 17: 20228
geological history of adjacent granites, pegmatites, and sulfide ores, 16: 29202
heats of formation of, equation for estimation and correlation of, 20: 35482 (UCRL-16865)
ionization by electron impact, 16: 17708(R) (TID-14812)
ionization potentials of, effects of substitution groups on, 17: 3045
isotopic analysis of, in gold ore deposits of Baleisk region, USSR, 19: 22123
lead isotopic ratios in Sudbury, Ontario, gas source mass spectrometry of, 18: 20203
metabolism in liver, tracer study, 17: 10312(T) (AEC-tr-5600)
phase diagrams of, book, 19: 14061
positron annihilation in, 16: 18882

preparation of actinide, by exothermic reactions, 19: 24538(P)
preparation of compounds of, for testing of radioprotective effects, 19: 15219(R) (NP-14805)
preparation of sulfur-35-labeled organic, 16: 23550
preparation of three-component, 19: 9152
production, properties, and uses of refractory, 19: 47020(T) (AEC-tr-6616)
properties and uses of rare-earth, 17: 23999
properties for aerospace applications, handbook, 19: 14063
radiation effects on organic, cosmic, 17: 32693
radioinduced in fish fillets, determination and separation, 20: 21200
radioinduced oxidation and reduction, 19: 507
radiolysis and synthesis of medium-ring, 18: 303
radiolysis in toluene solutions, energy transfer in, 18: 25548
radiosensitivity effects in *Bacillus cereus*, 18: 11876
reactions with chlorocarbon solvents at high temperatures, 20: 7105
reactions with hafnium salt solutions, 17: 1479
reactions with liquid titanium, 20: 3929
sulfur isotopic composition in hypogene, 20: 45921
sulfur-32/-34 ratio in, use in ore genesis, 20: 45920
sulfur-34 content in, from copper–nickel deposits in Soviet Union, 18: 33767
sulfur-34 content in deposits of, in central Africa, 19: 36657
sulfur-35 exchange between hydrogen sulfide and, 17: 32138
sulfur-35 exchange with thiophene, 20: 3976
synthesis of organic unsaturated, 16: 16451(P)
synthesis of sulfonyl, for testing as radioprotective compounds, 20: 18424
thermodynamic properties, 18: 17780 (SC-RR-64-67)
thermodynamic properties of, 20: 29623(R) (TID-22970, pp 121-256)
thermoelectric properties, 16: 16708(R) (AD-266128)
yield in radiolysis of benzene containing sulfur, 17: 33976

SULFINATES
sodium alkano, synthesis of, 17: 21724(R) (NP-12743)

SULFINIC ACIDS
preparation of compounds of, for testing of radioprotective effects, 19: 15219(R) (NP-14805)
thiol-, radiation effects on, gamma, 19: 13483
yield of cysteine-, in gamma radiolysis of cystine, 16: 1832

SULFITE IONS
effects on luminescence from dissolution of irradiated alkali metal halides, 19: 30239
frequency displacements and partial function ratios as function of force constants, 17: 2698
reactions with sulfur dioxide, separation of sulfur-34 by, 16: 12839

SULFITES
(See also sulfites and acid sulfites of specific elements.)
see also Acid Sulfites
see also Ammonium Uranyl Sulfites
see also Barium Sulfites
see also Calcium Sulfites
see also Hyposulfites
see also Potassium Sulfites
see also Potassium Sulfites
see also Sodium Sulfites
see also Strontium Sulfites
see also Thorium Sulfites
see also Uranyl Sulfites
see also Uranyl Sulfites
determination in scrubber solutions used in Dribble vent gas treatment plant, 19: 46471 (UCRL-14123)
effects on enzymatic activity of irradiated pepsin, 17: 31940
hydro-, protective effects against uv radiation damage in *Chlorella vulgaris*, 19: 17688
performance of resins of, for deoxygenation of water, 18: 27476
radioinduced reactions of bi-, with alpha olefins, 16: 7605(P)
radiolysis of aqueous solutions of, at 77°K, yields of hydrogen from gamma, 20: 18748
uses for selective anodic attack and etching of gamma phases in uranium alloys, 19: 14038

Sulfobromophthalein Sodium
see Bromosulphalein Sodium

SULFONAMIDES
see also Ethenesulfonamide
effects on skin photosensitivity, uv, 20: 73
genetic effects in *Vicia faba* roots, synergistic effects of x and gamma radiation, 19: 21950
radiation effects on bonds with proteins, x, 18: 13847
therapeutic effects in radiation sickness, 16: 9931
use in therapy of acute radiation injury, 20: 45491
5-acetamido-1,3,4-thiadiazole-2-, preparation of labeled, by activation, 17: 10683

SULFONATES
see also Sodium Dodecyl Sulfonates
analytical use of diammonium-5,5′-indigo di-, for determination of zirconium, 16: 16322
diphenylamine-, performance in potassium dichromate titrations, 19: 30081(R) (NBL-216)
effects on plants, review of mutagenic, 20: 16225 (EUR-2715.f)
effects on seeds of *Zea mays*, genetic, 19: 15010 (BNL-7815)
effects on transduction in *Pseudomonas aeruginosa*, 19: 19501(R) (NP-14931)
effects on transduction in *Pseudomonas aeruginosa*, 19: 19502(R) (NP-14932)
effects on wheat, genetic, 17: 28713
exchange of sodium ions with tetramethylammonium, in polystyrene, 19: 46237(R) (ORNL-3832, pp 76-99)
genetic effects on barley seeds, 17: 24810
induction of mutations in barley seeds, 16: 1588
localization of cobalt phthalocyanine tetrasulfonate in mouse tumors, 20: 42840(R) (ANL-7136, pp 164-90)
mutagenic effects in *Vicia faba*, 18: 33303
mutagenic effects, 18: 43218(R) (EUR-1882.e(p.7-26))
mutagenic effects in maize, 19: 19527
nuclear double resonance in potassium nitrosyl-, 16: 31538
peroxylamine di-, zero-field electron magnetic field spectra of, 17: 33899
preparation of compounds of, for testing of radioprotective effects, 19: 15219(R) (NP-14805)
preparation of, for evaluation as radioprotective compound, 19: 24542(R) (NP-14853)
protective effects against radiation injuries in mice, reaction mechanisms, 17: 109
protective effects of, against radiation damage in bovine serum albumin, 17: 28757
protective effects against radiation injuries in *Serratia marcescens*, 19: 33971
protective effects of sodium cysteinethiosulfonate, against radiation injuries of sarcomas in mice, 20: 131
radiation effects on decomposition of, in sewage, 19: 6223
radioinduced degradation of detergent, 20: 4025
radiosensitivity effects on proteins, uv, 20: 22773(R) (AD-621079)
solvent properties for inorganic ions, 17: 10749 (TID-17746)
solvolysis of isopropyl methane- and *p*-toluene-, deuterium isotope effects in water, 16: 164
sorption on hematite, 17: 35617(R) (NYO-10329)
sorption on hematite, isotherms for, 17: 11091(R) (MITS-49)
synthesis of, for testing as radioprotective compound, 18: 8196(R) (AD-425091)
synthesis of, for testing as radioprotective compounds, 19: 28111(R) (NP-15040)
synthesis of, for testing as radioprotective compounds, 20: 18424
thiol-, radiation effects on, gamma, 19: 13483
use of, with hexone in extraction of aluminum, cerium, and iron from Purex solutions, 17: 10739(R) (ORNL-TM-27)

Sulfone, Diphenylene
see Dibenzothiophene, 5,5-Dioxide

SULFONE, ETHYL VINYL
polymerization by catalyst and radiation, 18: 7985(R) (BMI-1650(Del.))
radioinduced copolymerization with β-cyanoethyl acrylate, 18: 20450(R) (BMI-1661(Del.))
radioinduced polymerization, 18: 13354(R) (BMI-1657(Del.))
radioinduced polymerization of, 18: 15664(R) (BMI-1655(Del.))
radioinduced polymerization with β-cyanoethyl acrylate, 18: 17351(R) (BMI-1659(Del.))
radioinduced polymerization, 18: 35924 (BMI-1678)

SULFONE, ETHYL VINYL, POLYMERS
electric properties, 18: 13354(R) (BMI-1657(Del.))
electric properties, 18: 15664(R) (BMI-1655(Del.))
electric properties, 18: 17351(R) (BMI-1659(Del.))

SULFONES
di-, preparation of organic, for evaluation as radioprotective compounds, 19: 24542(R) (NP-14853)
dibenzothiophene, mechanism and properties for graphitization of, 18: 35934 (ML-TDR-64-125(Vol.I))
dichloroethyl, radiosensitivity effects on bacteria, x, 19: 26123
dielectric constants and solvent properties of, for metals, 20: 25120(R) (BNL-954, pp 114-21)
dimethyl-, complexing with nickel(II) ions in melts, 18: 3713(R) (ORNL-3470(p.11-15))
electron beam reactions in, rearrangement in, 20: 23166
free radical reactions in gamma-irradiated alkyl, 16: 5235
neutron activation of, products from, 20: 33336(R) (PRNC-86)
phenyl- and *p*-tolyl 2-octyl-2-d-, deuterium exchange and racemization of, rates of base-catalyzed, 17: 10670
polymerization on irradiated polymers, graft, 19: 36502
polystyrol-, radiochemical preparation of, 17: 34021
polystyrol-, radiochemical preparation of, 17: 34022

protective effects against radiation injury in cells in tissue culture, 17: 10493
radioinduced graft polymerization on solid polymers, 16: 27619(P)
radiolysis, 18: 303
radiolysis of di-p-tolyl, diphenyl, and dibenzthiophene, gamma, 19: 44054(R) (COO-1365-7)
radiolysis of polymers of, ESR spectra of products of gamma, 19: 42553
radiolysis of, ESR spectra of products of gamma, 19: 42553
radiosensitivity effects on plant seeds, β, 20: 18442
polysulfone–styrene, reactions with irradiated polypropene, 18: 25490(T) (AEC-tr-6372(p.197-205))

SULFONIC ACID, ETHYLENE POLYMERS
protective effects against radiation effects on oxidative phosphorylation in rat mitochondria, 19: 17673

SULFONIC ACIDS
see also Methanesulfonic Acids
see also Naphthalenesulfonic Acid, Dinonyl-
see also Naphthalenesulfonic Acids
see also Taurine
see also Toluenesulfonic Acid
β-naphthol-6,8-bi-, analytical uses for gravimetric determination of zirconium, 18: 41323
chloro-, reactions with radioinduced graft polymers of polyethylene and styrene, 18: 17904
cyclopropylmethyl benzene-, synthesis and solvolysis rates of deuterated, 16: 17653
di-potassium 1,2,3,4-tetrahydro-5,8-dihydroxy-1,4-diketonaphthalene-2,6-di-, complexing with thorium, 16: 11642
flavonol-2'-, analytical uses for spectrophotometric determination of zirconium, 18: 19884
flavonol-2'-, analytical use for determination of thorium, 18: 37093
ion exchange properties for chromium, iron, and scandium in acid solutions, 18: 31494
preparation using radiation, technology of, 19: 30253
properties for use as liquid ion exchangers, 19: 15676
properties of, for spectrophotometric determination of scandium, 18: 43425
radiation effects on ion exchange resins of, gaseous evolution in gamma, 20: 18728 (NIJS-R-458)
radiation effects on ion exchange resins of, gamma, 20: 23111
separation from solutions by solvent extraction, effects of ion charge magnitude on, 19: 546
sorptive properties for calcium, magnesium, potassium, and sodium in milk, 17: 28855
sorptive properties of cellulose and resin exchangers of, for metal ions, 18: 35473
thio-, preparation of, for evaluation as radioprotective compounds, 19: 24542(R) (NP-14853)

SULFONIUM COMPOUNDS
decomposition of, isotope effects in, 18: 10120
deuteration of, inverse and normal isotope effects in, 19: 11068
isotope effects on position of proton in E2 transitions in, containing 2-phenylethyl group, 17: 35857
protective effects against radiation injuries in mice, 16: 25253
radiosensitivity of S-adenosyl- and S-methylmethionine, 16: 17738
solubility in heavy and light water at 25°C, activity coefficients of, 18: 19837(R) (MIT-905-1)
solvolysis reactions of halo-, deuterium isotope effects, 16: 28941
sulfur-32/sulfur-34 isotope effects in E2 and SN1-E1 reactions of t-butyldimethylsulfonium iodide in ethanol, 18: 39202
synthesis of S-adenosylmethionine in yeast by enzymes, radiation effects on, 16: 17738
t-butyldimethylsulfonium-α-*t*-fluoroborate, solvolysis in sulfuric acid solutions at 99.2°C, 18: 19837(R) (MIT-905-1)
t-butylmethylphenylsulfonium methylsulfate, preparation and nuclear properties, 18: 19837(R) (MIT-905-1)
2-phenylethyldimethyl-, deuterium exchange with heavy water, 19: 26368

SULFOSALICYLATE COMPLEXES
properties in ion exchange separation of metal cations, 16: 16329
with beryllium, dissociation and stability constants, 16: 4174
with rare earths, composition and formation constants, 19: 40513
with rare earths, preparation and spectra of, 20: 8943
with uranium, composition ratios in, electrophoretic and polarographic studies of, 18: 27375
with uranium, equilibrium and stability of, 18: 25391
with uranyl ions, polarographic properties, 18: 41417

SULFOXIDES
see also Methyl Sulfoxide
aliphatic, solvent properties for mineral acids, 18: 13939
association with phenols, 20: 20360(R) (PRNC-73)
complexes with uranium tetrafluoride, preparation of, 20: 31236
di-*n*-pentyl, solvent properties of, for thorium from hydrochloric acid solution, 18: 1818
dialkyl, solvent properties of, for metals, 20: 45795(R) (ORNL-3945, pp 176-88)
dibenzene, radiation effects on anticorrosive properties of coatings of, 17: 1885
dioctyl-, solvent properties for uranyl chloride and nitrate, 18: 23716
dipentyl-, solvent properties for thorium, 20: 43444
diphenyl-, reactions with niobium and tantalum pentabromides and -chlorides, 18: 25398
electron beam reactions in, rearrangement in, 20: 23166
neutron activation of, products from, 20: 33336(R) (PRNC-86)
preparation and reduction of, 20: 20360(R) (PRNC-73)
protective effects against radiation injuries in mice, 19: 8953(R) (NP-14448(p.36-64))
radiolysis, 18: 303
radiosensitivity effects on *Tribolium confusum* and *T. castaneum*, 20: 10504(R) (BNWL-122, pp 142)
yield of cystine di- in gamma radiolysis of cystine, 16: 1832
dipentyl sulfoxides–TBP, solvent properties for thorium, 20: 43444

SULFUR
abundance in peculiar magnetic stars, 17: 5178
abundance in 3 Centauri A, upper limit, 16: 4659
activation for fast neutron flux measurement, 18: 16356
activation of thick foils of, determination of correction factor for, 18: 37532
addition to butadiene–styrene polymers to increase resistance to irradiation, 19: 37021(P)
alpha reactions (α,n) with, neutron yields from, 17: 33017
analysis by photoneutron emission, 18: 37070 (A/CONF.28/P/825)
analysis for arsenic, neutron activation, 18: 188
analysis for phosphorus-32 by beta counting, self-absorption coefficients for, 18: 13669
analysis for selenium, activation, 17: 15917
beta absorption and backscattering by, 19: 30127
beta stopping powers of, calculation from compound absorption and backscattering, 19: 30127
bremsstrahlung reactions (γ,t) at 37 Mev, yields in, (E), 19: 47596(R) (TID-22141, pp 94-7)
bremsstrahlung reactions (γ,π^0) at 166 Mev, angular distributions from, (E), 20: 4898
bremsstrahlung reactions (γ,n) at threshold to 200 Mev, cross sections for, (E), 20: 22094
bremsstrahlung reactions (γ,p) at 32 Mev, proton energy spectra from, (E), 20: 32394
calibration as neutron-threshold detector, effects of boron-10 shields, 16: 3181 (NDL-TR-9)
chemical bonding in K-x-ray spectra of sulfur compounds, 19: 38588 (UCRL-12496)
chemical properties in lithium chloride-potassium chloride eutectic, 16: 25306 (CEA-2125)
chemistry, inorganic, 16: 8752
colloids, effects on radioinduced changes in aqueous polymer solutions, tracer study, 20: 137
composition of vaporous, equilibrium, 17: 33905
content and structure in meteoritic graphite, 18: 39250
content in African pitchblende, estimation of induced fission vs spontaneous fission from, 20: 37994
content in atmosphere, seasonal variation of, 18: 31764
content in high-purity beryllium, 19: 13216
content in human tissues, estimation of, 20: 30982
content in Mansfield Marine Band, Yorkshire, 18: 27720
content in meteorites, 20: 29893
content in meteorites, 20: 42064
content in siliceous black shale, 17: 39272
contents in meteorites, 18: 34398
cosmic-ray reactions with, in stony meteorites, production of helium-3 and neon-21 by, 18: 20204
crystal structure of orthorhombic, 16: 20380
determination by activation, 19: 26917(R) (IA-984)
determination by charged-particle reactions at 2 Mev, 20: 43097
determination by isotopic dilution, 20: 16362
determination by thermal-neutron activation methods, sensitivity for, 19: 9071
determination by x-ray fluorescence, equipment for, 19: 5826
determination by x-ray fluorescence analysis, 19: 22154
determination in anhydrous hydrofluoric acid, gravimetric, 16: 17589 (PG-Report-292)
determination in algal polysaccharides, neutron activation, 18: 15965
determination in arsenic, activation, 19: 46211
determination in automobile tire rubber, activation, 20: 14439(R) (GA-5556)
determination in aqueous solutions, activation, 20: 16331 (GA-6568)
determination in americium and plutonium by spark-source mass spectrography, 20: 40816 (RFP-699)
determination in beryllium oxide, spectrographic, 16: 1720

determination in beryllium oxide, activation, 16: 14675
determination in beryllium oxide fuels, volumetric, 17: 17974 (UCRL-7204)
determination in beer and paper, activation, 18: 15970
determination in beryllium, niobium, and zirconium and their oxides, luminescent method for, 18: 33513
determination in beryllium, boron, calcium, and sodium, gamma activation, 19: 7339
determination in biological materials, by precipitation using barium-139 and gamma counting, 20: 18609
determination in chicken by neutron activation, 16: 20337
determination in coal, activation, 18: 13614 (CONF-313-2)
determination in coal, heavy oil, and pig iron by combustion, 18: 25302
determination in carbon dioxide, 19: 4063 (PG-Report-623)
determination in coal by activation and neutron scattering, 19: 5777(R) (TID-20080)
determination in carbohydrates by absorption of tritium bremsstrahlung, 19: 22139
determination in copper by activation, 19: 40422
determination in copper, activation, 20: 12793
determination in fission product waste solids by combustion and colorimetry, 20: 38795 (BNWL-265)
determination in graphite, combustion-iodometric titration method, 16: 7484 (Y-1376)
determination in human hair, radiochemical, 16: 23379 (TID-7616 (p.89-97))
determination in heavy oil using iron-55, 17: 1405
determination in heavy oils, x-ray-absorptiometric, 17: 29890
determination in hydrocarbons by bremsstrahlung absorption, 17: 33848
determination in hydrocarbons by radiometric methods, evaluation of radiation sources for, 17: 35642
determination in hydrocarbons by absorption, 18: 21981
determination in hair of accident victims, radiation dosimetry from, 20: 16758
determination in iron, activation, 19: 10980 (EURAEC-1273)
determination in liquid oil products by x-ray absorption, instrument for, 18: 33472(T) (AEC-tr-6399(p.98-114))
determination in lubricating oil, activation, 19: 7340
determination in materials of high neutron absorption cross section by fast-neutron activation, 16: 15070
determination in minerals by neutron activation, 19: 30424
determination in mixture with phosphorus, activation, 20: 18569 (NP-15887)
determination in niobium by radioactivation analysis, 16: 23633 (TID-7629(p.239-44))
determination in nickel steel and electro-etch residues, activation, 17: 5984
determination in nuclear graphite, activation, 19: 7337
determination in naphthalene by x-ray absorption methods, 20: 20615
determination in organic materials by activation analysis, 17: 38946
determination in organic compounds containing sodium, spectroscopic, 20: 26776
determination in organic compounds by hydrogen reduction, 20: 29083(R) (UCRL-14767)
determination in petroleum, x-ray absorption, 16: 7517(P)
determination in polyphenyls, activation, 17: 21625
determination in petroleum by beta absorption analysis, 17: 29160
determination in polyphenyls by activation analysis, 17: 38945
determination in polyphenyls, x-ray-spectrographic, 18: 19844 (ISPRA-455)
determination in petroleum products by radiation absorption, 19: 13214
determination in presence of chlorine and phosphorus by activation methods, 19: 19798
determination in petroleum streams, equipment and method for, 20: 39191(P)
determination in refinery streams, x-ray absorption, 16: 15058
determination in rocks and ores, method for gamma activation, 19: 28277
determination in rare earth sulfides, 20: 16395
determination in solutions, spectrographic, 16: 8672 (AERE-R-3875)
determination in stratospheric aerosols, 16: 25609 (AFCRL-62-299)
determination in solar corona, 18: 40109
determination in solids by spark source mass spectrometry, quantitative, 19: 13247
determination in selenium by activation methods, 19: 19798
determination in steel, activation, 20: 22940
determination in silicates, activation, 20: 26782
determination in sedimentary rocks by neutron activation, 20: 33161(T) (AEC-tr-6639, pp 13-17)
determination in selenium by neutron activation, 20: 35444
determination in thorium and titanium sulfides, combustion, 18: 39140
determination in terphenyls, 19: 2220 (RT/CHI(64)-15)
determination in terphenyl by activation methods, 20: 3873 (EUR-2523.i)
determination in thorium nitrate, methods for, 20: 18568(R) (NBL-230)
determination in terphenyls, 20: 35393 (EUR-2952.i)
determination in uranium and uranium compounds by absorptiometric method, 17: 5966 (PG-Report-364)
determination in uranium trioxide, turbidimetric, 20: 40802 (HW-65402 (Rev.1))
determination in zirconium by activation, 19: 24418
determination of, in petroleum products, radiometric, 16: 32916 (AERE-R-3925)
determination of, in water, activation, 17: 19958
determination of traces of, in uranium compounds, colorimetric, 19: 26228 (GAT-501)
determination of trace amounts of, in iron, activation, 20: 14471
determination of trace amounts of, by reactor neutron activation methods, 20: 26760
determination of, activation method using photoneutron counting for, 19: 5772 (IA-933)
determination of, automatic absorption analyzer for, 19: 17847(P)
determination of, spectrochemical, 19: 30087(T) (IS-Trans-15)
determination of, using Arsenazo III, photometric, 20: 36778
determination of, in carbazole by neutron activation methods, 20: 43116
determination simultaneously with phosphorus in water, activation, 18: 11989
determination simultaneously with zirconium in organic compounds, amperometric, 18: 33514
determination, use of photoneutron counting in activation, 19: 36322
determination, use of pulsed neutrons in activation, 19: 36323
deuteron elastic scattering at 10 to 13 Mev, angular distributions from, 17: 9563
deuteron elastic scattering by, energy dependence and cross section for, 17: 9506 (PAN-202)
deuteron elastic scattering by, energy dependence of angular distributions from, 18: 1052
deuteron reactions (d,p) at 3.2 Mev, 17: 36669 (WASH-1042)
diffusion in CGB graphite at 150°C, 20: 4308(R) (ORNL-3870, pp 243-60)
diffusion in copper and copper alloys during annealing, tracer study of, 18: 37686(T) (AEC-tr-6398(p.322-7))
diffusion in high-melting metals, 19: 2812
diffusion in lead sulfide at 500 to 750°C, mechanism, 18: 37115 (ANL-6856)
diffusion in selenium, radioactive-tracer study of, 18: 37688(T) (AEC-tr-6398(p.334-7))
dissociation energy of S_2, 18: 19939 (WADD-TR-60-782(Pt.XXI))
dissociation of gaseous, mass spectrometric study of, 19: 43997(R) (UCRL-11889)
distribution and retention in bone, 16: 28659
distribution in tissues in mice, tracer study, 16: 28708
distribution of recoil phosphorus-32 and sulfur-35 in neutron-irradiated, 20: 31295
distributions in mild steels, in welds, 17: 29892
effect on stress rupture of type 304 stainless steel at 1250°F, 19: 32733 (NAA-SR-11047)
effects of drinking water containing, on radiosensitivity of mice, 20: 38709
effects of, as filler on tensile strength of irradiated butadiene–styrene elastomers, 18: 27594
effects on alpha and gamma radiolysis of cyclohexane, 20: 40990
effects on corrosion of stainless steel by chromium ions in hot nitric acid, 19: 18418(P)
effects on corrosive properties of biphenyl, 20: 25491(T) (AECL-2330, pp 179-95)
effects on growth of beryllium oxide crystals, 17: 30511 (NAA-SR-8235)
effects on hot workability in stainless steel, effects of uranium on, 18: 18402
effects on hot-cracking susceptibility of Monel, 19: 30751 (WERL-8844-8)
effects on microstructure of uranium, 18: 22485 (MCW-1483)
effects on radioinduced vulcanization of rubber, 19: 498
effects on radioinduced crosslinking of polybutadiene, 19: 22321
effects on radioinduced crosslinking and decomposition of polyethylene, 20: 31279
effects on radiolysis of toluene, 18: 25547
effects on radiolysis of carbon disulfide, 19: 7583
effects on radiopolymerization of acrylonitrile in dimethylformamide, 20: 23172
effects on reaction of alumina with nickel, 20: 35834(R) (BMI-1767)
effects on rubber in presence of radiation, 19: 18364
effects on selenium-75 uptake by sheep blood cells, 18: 3468
effects on stainless steel corrosion with and without uranium additions by aqueous mineral acid solutions, 20: 14983 (NP-15875)
effects on transport of hexavalent uranium by hydrothermal solutions,

17: 35717
effects on yields of ketone and alcohol from γ-irradiated cyclohexane, 20: 33379
electric conductivity, effects of high pressure on, 19: 37047 (UCRL-16075)
electric quadrupole and magnetic dipole transitions for isoelectronic sequence of, (T), 20: 4553
electron pair production in screened nuclear field in, (T), 19: 43280
electron spin resonance spectra of sulfur-35-labeled radical of, radio-induced in 2,4,6-tri-*t*-butylthiophenol, 19: 30241
energy level transitions of μ-mesic atoms of, 2P-1S, (E), 20: 35996 (JINR-P-2735)
energy level widths for, K, (T), 20: 15239 (CONF-233(Vol.3), pp 419-39)
exchange between sulfur gas and sulfur oxides, 16: 23574
exchange of sulfur monochloride, 18: 35579
exchange with sulfur-35 in liquid hydrogen sulfides, effects of acidity on rate of, 20: 27007
excretion and metabolism in man, review, 20: 8542 (CONF-727, pp 85-101)
excretion and metabolism of, use in dosimetry, 20: 20398
fluorescence yields in proportional and scintillation detectors, 18: 3796
gamma attenuation coefficients at 0.03 to 10 Mev, 19: 35569
gamma reactions (γ,n) with, neutron spectra from, 18: 11207 (LNF-63/47(p.182-8))
gamma reactions (γ,n) from threshold to 80 Mev, cross sections for, 18: 11209 (LNF-63/47(p.194-8))
gamma reactions (γ,p), cross sections for, 18: 22897
gamma reactions (γ,n) at 12 to 30 Mev, cross sections for, (E), 19: 25542
gamma reactions (γ,α) at 31 Mev, alpha spectra from, (E), 20: 38037
gamma reactions (γ,d) and (γ,p) at 30 to 90 Mev, 16: 24835
gamma reactions (γ,nt) at 30 to 80 Mev, 16: 24842
gamma reactions (γ,n) at 0 to 80 Mev, 17: 40095
gamma spectrum for, thermal neutron capture, 17: 38063(R) (IITRI-1193-26)
Hartree-Fock potential of neutral atoms of, analytical expressions for, 18: 16656
heating deposits of, *in situ* with radioactive materials, process for, 20: 30950(P)
helium-3 reactions (He-3,2n) at 31.8 Mev, argon-33 production in, (E), 19: 8468
impregnation of calcined alumina with molten, 18: 5415(R) (IDO-14599)
ion exchange in concentrated hydrochloric and perchloric acids, distribution coefficients of, 18: 17759
ionization equilibria in sun, (T), 20: 19338
isotopic analysis of, mass spectrometric, 20: 16379
isotopic composition and origin in volcanoes, 19: 18152
isotopic content in mineralization of Canale Monterano, Italy, 17: 29110
isotopic exchange of, between *p*-iodobenzenesulfonic acid and its anhydride, 17: 21725
isotopic exchange reactions of, use of sulfur-35 for studying, 18: 15999 (TID-7689(p.93-5))
isotopic ratios in uranium sandstone deposits, 19: 22587
labeling with sulfur-35, 20: 12919
maser collision processes in, optical, 18: 32484
meson (μ^-) capture by, x rays from, 18: 19044
meson (μ^-) capture by, angular distributions from, (E), 20: 15720 (JINR-E-2516)
meson (μ^-) capture at high energy, neutron angular distribution from, (E), 20: 46790
meson (μ^+) depolarization in, (E), 19: 12167 (NEVIS-124)
meson (μ^+) depolarization in targets of, (E), 19: 45080
meson (π^-) reactions ($\pi^-,n\gamma$) with, energy spectra from, (E), 19: 21315
meson (π^-) reactions (π^-,γ), energy spectra and yields from, (E), 20: 15794
meson (μ) capture, Fermi interactions in, 16: 15590
meson (μ) scattering, x-ray emission in, 16: 19705
meson (μ^-) capture by, x-ray spectra from, 17: 26578
meson (μ^-) magnetic moment in mesic, 16: 13865 (NEVIS-101)
meson (μ^-) polarization by, 17: 9591
meson (μ^-) reactions, polarization retention measurements, 16: 8230
meson (μ^-) reactions, capture-rate measurements, 16: 8231
meson (μ^+) repolarization in, as a function of external field, 17: 9237
meson reactions($\mu^-,n\nu$) with, angular distributions from, 16: 21426
mesons (μ^-) disappearance rates in, Z-law analysis of, 16: 2305(R) (UCRL-9704)
metabolism by photosynthetic bacteria, 20: 42850(R) (NYO-2043-130)
metabolism by plants, tracer study, 17: 28678(R) (TID-18936)
metabolism in cacao seeds, 20: 42850(R) (NYO-2043-130)
metabolism in lake ecosystem, tracer study, 17: 33598
metabolism in nasal mucosa of rats and guinea pigs, tracer study of, 19: 5626
metabolism in rats, tracer study of, 19: 5625
metabolism of, in lacustrine ecosystem, 18: 6599(R) (TID-19930)
metabolism of, in rats, 18: 3407(R) (NYO-10710)
metabolism of inorganic, in bacteria, 18: 3407(R) (NYO-10710)
metabolism of, in autotropic bacteria, 18: 27011(R) (ORNL-3601 (p.188-206))
metabolism of, in *Rhodospirillum rubrum*, 18: 27016(R) (TID-20708 (p.6-28))
molecular force constants and vibrational assignment of the S_4 molecule, 18: 19463 (LADC-5778)
molecular vibrations, 18: 42295(R) (ANL-6879(p.114-29))
movement in peppermint plant, 16: 23389
neutron absorption cross section in pitchblende, thermal, 20: 37994
neutron activation and photon-producing cross sections, tabulation, 16: 23008 (XDC-60-8-81)
neutron activation, effects of impurities on fast, 17: 30580 (AERE-M-1244)
neutron capture by, average level widths of compound nucleus from, (E), 20: 32424
neutron capture cross sections, 16: 26509
neutron cross sections, 17: 38428 (ANL-6656)
neutron differential scattering cross sections at 14 Mev, 16: 1072
neutron diffraction properties of, 20: 26396(R) (IDO-17140)
neutron elastic and inelastic scattering by, at 14 Mev, 16: 33852
neutron elastic and inelastic scattering, distorted waves approximation in, 17: 38182
neutron elastic and inelastic scattering at 2.45 to 5.80 Mev, (E/T), 20: 10103
neutron elastic scattering at 3.5 to 4.8 Mev, differential cross sections for, (E/T), 19: 14564
neutron flux and spectrum measurements on foils of, 20: 21427(R) (NASA-CR-54904)
neutron inelastic scattering at 14 Mev, excitation cross sections from, 17: 26440(R) (ORNL-3425(p.46-9))
neutron inelastic scattering at 14 Mev, collective-state excitation by, (E/T), 19: 23697
neutron inelastic scattering at 14.1 Mev, gamma yields from, (E), 19: 35417
neutron inelastic scattering at 14.1 Mev, spectra for, (E), 20: 28268 (FEI-30)
neutron photoproduction cross section, 18: 2921
neutron radiative capture cross sections at 30 and 65 kev, 18: 34274(R) (NIRS-2(p.3-15))
neutron reactions at 3.7 Mev, cross-section measurements, 16: 8224
neutron reactions (n,p) at 14 Mev, angular distributions and spectra from, 16: 11028
neutron reactions for production of phosphorus-32, chemical species produced by, 16: 15086
neutron reactions at 3 to 15 Mev, removal cross sections, 16: 29739
neutron reactions at high energies, table of radioisotopes produced in, 17: 794 (CERN-62-22)
neutron reactions (n,γ) at low energies, gamma spectra for, 17: 26419(R) (ARF-1193-23)
neutron reactions with alpha-, preparation of carrier-free phosphorus-32 in, 18: 32002
neutron reactions at 4 to 5 Mev, compound-nucleus level widths from, 18: 36645
neutron reactions with, calculations of cross sections for, 18: 42673
neutron reactions (n,γ) with, gamma spectra from fast, 18: 44807
neutron reactions with, phosphorus-32 production in, 19: 13847
neutron reactions (n,γ) with, polarization from, (E), 19: 23726
neutron reactions at 14 Mev, gamma emission in, (E), 19: 37890
neutron reactions (n,γ) at 0.025 ev, spectra from, 19: 40896
neutron reactions (n,α) and (n,p) with, effects on manganous-sulfate-bath calibration of neutron sources, (E), 20: 8054
neutron reactions with, production of phosphorus-32 in, 20: 35568 (IEA-103)
neutron reactions at 14.7 Mev, gamma emission in, (E), 20: 42146 (AD-638014)
neutron removal cross sections for, effective fast, 16: 24797 (WADC-TR-58-266)
neutron scattering angular distribution, 16: 12419 (ANL-5567(Rev.))
neutron scattering at 3.4 to 4.6 Mev, angular distributions, 16: 26507
neutron scattering at 2.45 to 5.80 Mev, energy spectra of, (E), 19: 19095 (WASH-1053)
neutron scattering at 2.45 to 5.80 Mev, (E/T), 19: 23620
neutron total cross sections at 28.4 Mev, 16: 5969
neutron total cross section, 17: 15272
neutron total cross section of, fast, 17: 20982 (HW-SA-2875)
neutron total cross sections at 2.8 to 5.2 Mev, 18: 6210
neutron total cross section of, effective, 18: 11195(R) (EANDC(E)-49(L))
neutron total cross sections at 0.3 to 2.7 Mev, resonance structure in, 18: 13066
neutron total cross section of, 18: 24625 (WASH-1046)

neutron total cross sections at 28 Mev, 18: 44711
neutron total cross sections at high energies, fluctuations in, 20: 38173
neutron total cross section from 5.0 to 8.5 Mev, fluctuations in, (E), 20: 44743
neutron transport properties at 0.3 to 2.7 Mev, 17: 787(T) (AEC-tr-5413)
nuclear quadrupole resonance, 17: 10592 (IS-520)
origin of Sicilian-type deposits, 16: 22418
oxidation and reduction by bacteria, kinetic isotope effects on, 19: 9112
oxidation of, in irradiated chlorides, 19: 20004
oxidation of, kinetics and mechanisms of, 19: 26382(R) (RPI-321-1)
photon reactions with, neutron production in, 18: 11195(R) (EANDC(E)-49(R))
photon reactions with Coulomb field of, pair production total cross sections for high-energy, (T), 20: 17754
photoproton angular distributions from, 16: 2533
physical properties, effects of high pressure on, 19: 37047 (UCRL-16075)
preparation as radiation target materials, methods development for, 18: 27815(R) (ORNL-TM-718)
preparation of radiation targets and radioactive samples of, by molecular plating, 20: 25027 (AERE-R-5097, Paper 17)
preparation of sulfur-35-labeled, 18: 13762
preparation, properties, and purification of allotropic forms of, below 30°C, 18: 36899 (UCRL-10768)
processing of irradiated, phosphorus-32 separation in solvent dispersion and anion exchange, 20: 9042(P)
properties as organic reactor coolant and moderator stabilizer, 17: 4292(P)
properties as threshold detector for fast neutrons, 17: 20349 (NAA-SR-Memo-4365)
properties as threshold detector, 17: 22003 (CEA-2255)
properties for reducing nitric acid corrosion of stainless steel, 17: 4295(R) (DP-740)
properties for space applications, handbook, 16: 5088 (WADD-TR-61-96)
properties in austenitic stainless steel, effects of uranium on, 19: 30801
properties of liquid, as reactor coolant, 16: 23830 (BNL-5377)
protective effects of colloidal suspensions of, against radioinduced cross-linking of polymers, 16: 20507
protective effects against radiation injuries, 16: 28846
protective effects against radiation in mice, 16: 30305
protective effects against radiation damage in polymers, 17: 5923
protective effects in irradiated dimethylsiloxane polymers, 17: 21759
protective effects of colloidal, against radiation damage in polymers, 17: 27438
protective effects of, against γ radiation injuries of skin, 20: 10702
proton elastic scattering at 17.8 Mev, polarization of, (E), 20: 32439
proton reactions at 150 Mev, gamma spectra from, 16: 31088
proton reactions at 8 to 13 Mev, gamma and neutron yields in, 18: 44775
proton reactions up to 5.7 Mev, gamma emission from, 16: 2535
purification of, radiochemical method for, 20: 8838 (UCRL-14255)
radiation effects on reactions with hydrocarbons, 17: 206
radiation effects on sorption of, by gold, platinum, and tin surfaces, 17: 25831 (PAN-371/V)
radiation effects on electric properties of single-crystal, 18: 7312
radiation effects on rat metabolism of, tracer study of, 18: 13420
radiation effects on electron paramagnetic resonance in rhombic, neutron, 18: 30250
radiation effects on, neutron, 20: 31295
radiation effects on unpaired electron formation on atoms of, in dry proteins, ESR spectral studies on gamma, 20: 35241
radiochemistry, 16: 10049 (NAS-NS-3054)
radioinduced bulk photovoltaic effect in, in contact with metals, 18: 18443
radioinduced production of helium and hydrogen in, neutron, 19: 26901
radioinduced reactions with natural rubber, effects on kinetics of structuration and vulcanizate properties, 16: 8766
radioinduced reactions with natural rubber, 16: 6439(T) (CEA-tr-R-1388)
radioinduced reactions with polyethylene, 19: 499
radioinduced reactions with polyethylene and chlorine, 20: 14621
radiolysis in benzene solution, yields in, 17: 33976
radiolysis in organic solvents, yields in, 18: 27505
radiolysis of monodisperse colloidal, effects on particle size, 19: 38714
radiosensitivity effects on polyphenyls, 16: 25018(R) (IDO-16761(p.1-74))
radiosensitivity effects of, in cyclohexane, 20: 24939
reactions in irradiated proteins, 17: 17895
reactions of S_2 vapor with nitrogen atoms, 19: 10706 (UCRL-11763)
reactions with actinides to form binary compounds, 19: 24538(P)
reactions with beryllium in group VIII transition metal alloys, 20: 37275
reactions with butadiene and isoprene polymers, 16: 23538
reactions with cerium and lanthanum, 17: 8722
reactions with chromium, iron, and niobium alloys in diffusion zones, electron probe microanalysis, 16: 5281
reactions with fast neutrons, helium and hydrogen production in type 347 stainless steel in, 20: 7490(R) (BMI-1745, Sect.A)
reactions with metals up to 700°C, 16: 16054
reactions with oxygen, mass spectrometric study of, 18: 31418 (CEA-R-2398)
reactions with potassium cyanide, kinetic isotope effect in, 20: 35508
reactions with rhodium and zirconium, 20: 3863(R) (IS-1200(Sect. C))
reactions with selenium, tracer studies, 16: 3341(T) (AEC-tr-4497 (p.308-19))
reactions with sodium in liquid ammonia, saline compound production in, 18: 23149(T) (ANL-Trans-8)
reduction of uranium(VI) to uranium(IV), 16: 8710 (GAT-T-961)
removal from vanadium by cerium, 19: 22875(T) (JPRS-28849(p.166-78))
segregation in steels, autoradiographic study, 18: 30121(T) (NP-tr-1150)
segregation in welds in stainless steel, 16: 16052
separation from Dowex-50 resin by solvent extraction using hydrochloric acid and sodium hydroxide solutions, 19: 15571(R) (TID-21385)
separation from liquid iron and steel by compound formation with uranium, 20: 20692
separation from metal fluoride melts, methods for, 19: 30067(R) (ORNL-3789(p.56-98))
separation from other naturally occurring radioactive nuclides and fission products, 19: 15689
separation from phosphorus-32 by solvent extraction, 16: 13123 (BLG-67)
separation from rubidium by ion exchange, 19: 30258
separation from sulfur-33, electromagnetic, (E), 19: 35510
separation from titanium by zone melting, 18: 8456
separation of phosphorus-32 from irradiated, by gas chromatography, 18: 43600 (IA-843)
separation of phosphorus from, by co-precipitation with ferric hydroxide, 20: 41049
Slater-Condon parameters of, determined from spectral data, 17: 31118
solubility in iron, 18: 12003
solubility in molybdenum at 1100°C, 18: 27452
sorption by digestive track of *Nassa reticulata L.*, 16: 7388
sorption by hydrogen-supersaturated iron surfaces, tracer study, 16: 16051
sorption effects on ductile-to-brittle transition in alloyed and unalloyed refractory metals, 16: 25751 (DMIC-Memo-155)
spectra in superconducting copper sulfide, x-ray, 18: 32693(T) (JPRS-25289(p.14-20))
spectra of diatomic sulfur-34 containing, uv rotational, (E/T), 19: 23307
spectra of diatomic, isotope shifts in near infrared bands of, 20: 34098
spectra of, high energy neutron-capture gamma, 17: 15943(R) (ARF-1193-20)
spectra of high-temperature diatomic, in inert matrices, 19: 43997(R) (UCRL-11889)
spectra of highly ionized, inner-shell resonance lines in, 20: 27727
spectra of, infrared, 17: 35263(R) (UCRL-10706(p.1-110))
spectra of, low energy neutron-capture gamma, 17: 15943(R) (ARF-1193-20)
spectra of molecular, in inert gas matrices, u-v absorption, (E), 19: 45480 (UCRL-10771)
spectra of, effects of chemical bonding on x-ray, 20: 291 (UCRL-14379)
spectra of, emission, 18: 22052
spectra of, isolated in inert gas matrices at high temperature, 20: 1818 (UCRL-11976)
structure of, effects of radioactivity on, 17: 37283
sulfur-35 exchange with thiophene, 20: 3976
uptake by *Cladophora fracta*, concentration effects on dynamics of, 19: 25858
use as stabilizer for organic coolants, 16: 14613(R) (IDO-16734)
use as tracer, survey, 16: 1359
use in calcination of radioactive wastes, 17: 19697 (DP-713)
use in preparation of uranium dioxide by reduction of uranyl sulfate, 16: 33060
uses in processing of radioactive wastes, 18: 45159(P)
valence determination by beta spectroscopy, 18: 25303
vapor pressure over iron–sulfur melt at 1580 to 1680°C, 17: 37519(T) (AEC-tr-5983)
vapor pressure variation with composition in molybdenum disulfide at 1100°C, 18: 27452
vaporization, 18: 42295(R) (ANL-6879(p.114-29))
vaporization of allotropic and rhombic, non-equilibrium processes in, 18: 12061
x-ray total cross sections at 15 to 30 Mev, (E), 19: 12573
yields from radiolysis of hydrogen sulfides, 20: 4017
yields from radiolysis of carbon disulfide, 20: 4028
yields in gamma radiolysis of liquid sulfur dioxide, 18: 17896
yields in gamma radiolysis of liquid hydrogen sulfide, effects of 2,2-diphenyl-1-picrylhydrazyl and iodine on, 20: 40997

SULFUR CHLORIDES

analytical use in determination of oxygen in metals and oxides,

16: 14631(T) (UCRL-Trans-801(L))
analytical uses for determination of oxygen in uranium compounds, 18: 27304
chlorine-36 exchange with antimony, tetraethylammonium, and thionyl chlorides in, 18: 17792
effects on radioinduced crosslinking of polyethylene, strength of product in, 19: 15639
labeling with sulfur-35, 20: 25116
preparation and evaluation for electromagnetic separation of sulfur isotopes, 20: 41400 (ORNL-3301(Suppl.1))
reactions of SCl_2 and S_2Cl_2, with ammonia, 18: 31431(R) (UCRL-11317 (p.1-14))
reactions with ammonia, 18: 6797 (UCRL-11081)
reactions with nitrogen atoms, 19: 10706 (UCRL-11763)
reactions with pollucite ores at 550 to 700°C, cesium separation by, 18: 24991 (IS-884)
spectra of, determination of emission, 17: 25108
sulfur isotope exchange with elemental sulfur, 18: 35579
use of mono-, in determination of oxygen in uranium compounds, 18: 27286 (CEA-2367)

SULFUR COMPOUNDS
see also Chemical Warfare Agents
analysis for selenium, activation, 17: 15917
analytical use of sulfonazo for photometric determination of scandium, 16: 31576
analytical uses of organic phosphorus-containing, 19: 46217
biosynthesis of sinigrin, sulfur-35-labeled sodium sulfate incorporation during, 19: 31670(R) (NIRS-3(p.19-56))
chemical structure of ionic complexes of, analysis using Moessbauer spectroscopy, (E), 19: 30238 (WERL-2989-1)
color reactions of acids, 16: 5117(R) (UCRL-9900)
complex formations by, 20: 18449
effects on epoxy polymerization type in organic compounds, 16: 2191(R) (NP-10985)
effects on muscular activity of guinea pig intestine, 19: 46005(T) (JPRS-31933, pp 6-12)
electron spin resonance studies of gamma-irradiated biological, 18: 8439
energy transfer of organic, in radiolysis in toluene solutions, 18: 25548
fluorine magnetic resonance spectra of perfluoroalkyl derivatives of sulfur hexafluoride, 16: 32986
graphitization of heterocyclic, mechanism and properties for, 18: 35934 (ML-TDR-64-125(Vol.I))
ionization by electron impact, 16: 17708(R) (TID-14812)
ionization of 3-methyl-2-thiabutane, 4-thia-1-pentene, and 3,4-dithiahexane by electron impact, 17: 28930
isotopic exchange reactions of, use of sulfur-35 for studying, 18: 15999 (TID-7689(p.93-5))
labeling with carbon-14 and tritium, 19: 31771
magnetic susceptibilities of rare earth, 16: 1681
metabolism by rabbits, tracer study of, 18: 41052
metabolism of labeled, 19: 31771
organic, tracer studies of action in oil for corrosion protection of copper and steel, 16: 13427(T) (AEC-tr-4492(p.76-81))
organic, effects of uv radiation on, 19: 33785(R) (AD-426004)
organic, preparation and reactions of, for biomedical studies, 20: 26903
organic, protective effects against radiation damage in mice, 19: 17689
organic, radiation effects on mixtures of, with amino acids or proteins, ESR spectral studies on, 20: 23126
preparation and properties of labeled, 17: 19801
preparation and properties of organic, 19: 32048(R) (NP-15073)
preparation of fluorine-containing, effects of water on, 20: 1881
preparation of, for testing as radioprotective compounds, 18: 31260(R) (NP-14045)
preparation of, for testing as radioprotective agents, 19: 30219
properties of, for spectrophotometric determination of scandium, 18: 43425
protective effects against x radiation in mice, 16: 14459(R) (NP-11359 (p.35-75))
protective effects against radiation, reaction mechanisms in, 17: 2858
protective effects against radiation injuries in rats, effects of sulfur content on, 17: 31943
protective effects of, against epilation in mice produced by x radiation, 17: 35472
protective effects of, against radiation injuries, 18: 6704
protective effects of cystine, AET, and MEA against radioinduced changes in meat proteins, 18: 11623(R) (AD-407411)
protective effects of disulfides and sulfhydryls against radiation effects on biological systems, mechanism of, 18: 35388
protective effects against radiation injuries in mice, 19: 10903
protective effects against radiation, mechanism of, 19: 13120
protective effects against radiation injuries, reaction mechanisms for, 19: 29997
radiation effects on, in presence of amino acids and proteins, electron spin resonance studies of, 19: 15615
radiation effects on organic, ESR study of electron, 20: 25144
radiation effects on Ascite tumor cells influenced by, x, 18: 17413
radioinduced production in meats, 20: 42973
radioprotective effects of, reaction mechanisms, 20: 5296(R) (NP-15585)
radioprotective effects of water containing, on mice, 20: 45490
radioprotective, evaluation of models for selecting, 20: 38729
radiosensitivity effects of, on animal and plant cells, effects of oxygen on, 17: 23200
radiosensitivity effects in methylene blue, 18: 43310
radiosensitivity effects in animals and plants, 20: 16297(R) (EUR-2548.f)
radiosensitivity effects of, reaction mechanisms for, 20: 18274
reactions of, with atomic nitrogen, 20: 31218(R) (UCRL-16658, pp 1-9)
reactions with metals up to 700°C, 16: 16054
reactions with nitrogen atoms, 19: 43997 (UCRL-11889)
spectra of, chemical bonding in K-x-ray, 19: 38588 (UCRL-12496)
structure of rare earth, 16: 1681
sulfur x-ray spectra in, chemical bonding effects on, 20: 291 (UCRL-14379)
synthesis of sulfur-35-labeled inorganic, review, 17: 8205
synthesis of, for use as radioprotective agents, 19: 46303(R) (NP-15409)

SULFUR DIOXIDES
analysis for oxygen-18, method for, 18: 11987
corrosive effects on steel pipes, 16: 12058
detection and measurement in atmosphere, monitor design for, (E), 19: 44458 (NYO-2767)
determination in air, 16: 15077
determination in anhydrous hydrofluoric acid, iodometric, 16: 17589 (PG-Report-292)
determination in aqueous solutions using krypton-85, 18: 37566(R) (NYO-2757-3)
determination in atmosphere by radio-release method, 19: 9434
determination in air, radioisotopic methods for, 19: 17781(R) (ORNL-3750)
determination in atmosphere, use of radioactive reagent for, 19: 40410 (ORNL-P-494)
determination in atmosphere using radioactive clathrate techniques, 20: 29142
determination in geothermal and volcanic waters, 18: 43800 (INS-R-25)
determination in solution, clathrate method for, 17: 33771 (TID-17223)
determination in superheated steam, design of gas chromatograph for, 18: 23407 (DP-880)
determination in vented gases from underground nuclear explosion, apparatus for, 19: 19776 (UCRL-12169)
determination in waste gases, by absorption of soft gammas, 20: 40828
determination of isotopic molecular weight, 16: 2997(T) (NP-tr-808)
determination of ionized trace, continuous measurement using hydroquinone clathrates, 16: 9954(R) (TID-14811)
determination of, radioluminescent method for, 20: 22952
determination of, use of krypton-85 hydroquinone clathrate in, 20: 35422
determination using kryptonates, 17: 35261(R) (TID-19318)
determination using labeled sodium chlorite-clathrates, effects of moisture on, 18: 17866(R) (NYO-2766)
effects of, on speed of radioinduced crosslinking of polyethylene, 17: 18123
effects of very dilute, on the corrosion of copper and zinc by air, 16: 9157(T) (AEC-tr-5008)
effects on chlorine-36 and sulfur-35 exchange between sulfuryl and thionyl chloride, 19: 24527
effects on electron spin resonance spectrum of free radicals in irradiated polyvinyl chloride, 18: 29746(T,R) (AEC-tr-6231(p.433-8))
effects on electron spin resonance of irradiated silicon oxides, 19: 28384
effects on Geiger-Mueller counter pulse attenuation, 19: 30096
effects on mixtures of molybdenum and vanadium oxides at 650°C, 19: 28823
effects on radioinduced crosslinking of natural rubber, 18: 23637(T,R) (AEC-tr-6316(p.449-55))
effects on radioinduced isomerization of 2-butene, 18: 23666
effects on radioinduced isomerization of 2-butene, 19: 17967
effects on radioinduced carbon dioxide-graphite reactions, (E), 19: 19953 (AERE-R-4201)
effects on solid-state polymerization of *N*-vinylcarbazole, ESR studies of, 20: 23056
effects on solid-state polymerization of *N*-vinylcarbazole, tetraoxane, and trioxane, 20: 23057
electron elastic scattering at 295°K, cross sections, 16: 33844
electron transfer reactions with negative ions, 16: 6471
energy transfer to different vibrations, effects of vibration-translation catalysts on, 16: 3026
force constants of isotopic, 16: 22133(T)
heat of vaporization of, calculation from rigid-sphere equation of state, 18: 224

heat transfer coefficients, nucleate boiling, 19: 7688
isotopic exchange with sulfur isotopes on anion exchanger, 16: 29298
monitoring atmospheric, 16: 11546
neutron reactions (n,γ) on sulfur-34 in, chemical effects in, 17: 23386 (UCRL-10360(Rev.))
oxidation of, in processing of uranium ores, 17: 23428
oxidation of, effects of irradiated vanadium oxide–silicon dioxide–silver sulfate catalyst on, 20: 29291
oxidation to trioxide on platinum catalyst, kinetics, 16: 23584
oxygen-18 exchange, equilibrium constants and partition function ratios for, 16: 18876
oxygen-18 exchange with vanadium pentoxide, 19: 7439
performance as coolant in advanced fast power reactors, 18: 30995(R) (ORNL-3619(p.278-335))
performance as coolants in fast power reactors, 19: 35769 (ORNL-3642)
polymerization in presence of organic monomers on irradiated polymers, graft, 19: 36502
preparation for determination of sulfur-32 ratio with sulfur-34 in ores and rocks, 18: 33501
preparation of, by reaction of sulfur minerals with copper oxide, 17: 25255
radiation effects on reactions of, with hexane, 19: 473
radiation effects on, alpha, 19: 30651(R) (ORNL-3789(p.239-47))
radiation effects on gaseous, alpha, 19: 46332(R) (ORNL-3832, pp 50-65)
radiation effects on evolution of, from sulfonic acid ion exchange resins, 20: 18728 (NIJS-R-458)
radioinduced copolymerization with vinyl acetate at low temperatures, 17: 14339
radioinduced graft polymerization of propene and, on polyethylene, gamma, 18: 23642(T,R) (AEC-tr-6316(p.481-97))
radioinduced inclusions in compound with hydroquinone, 16: 3047
radioinduced ionization of, electron dosimetry by, 18: 29764
radioinduced polymerization of vinyl acetate in liquid, 18: 25537(T) (AEC-tr-6372(p.617-25))
radioinduced polymerization with styrene, gamma, 19: 24583
radioinduced polymerization with ethylene, mechanisms of, 19: 36451(R) (BNL-900(p.73-104))
radioinduced polymerization with vinyl acetate, 20: 18774
radioinduced reactions with styrene at 30°C, 17: 34021
radioinduced reactions with styrene at +30 to –78°C, 17: 34022
radioinduced reactions with chlorine and polyethylene, 18: 22163(P)
radioinduced reactions with acrylamide and methacrylamide monomers and polymers, 18: 23650(T,R) (AEC-tr-6316(p.567-72))
radioinduced reactions with cyclohexane, 18: 29757
radioinduced reactions with chlorine and cyclohexane in carbon tetrachloride, 19: 9172
radioinduced reactions with organic compounds, 19: 22346
radioinduced reactions with unsaturated hydrocarbons, gamma, 19: 36458 (NYO-3334-1)
radioinduced reaction with vinyl monomers at low temperatures, 20: 23188(P)
radiolysis of liquid, yields in gamma, 18: 17896
reactions with carbon-11, mechanisms of, 19: 7417
reactions with free radicals radioinduced in Teflon, electron spin resonance spectra of, 18: 5388
reactions with free radicals from irradiated polytetrafluoroethylene, 18: 8435
reactions with free radicals in irradiated high-molecular compounds, 18: 29747(T,R) (AEC-tr-6231(p.439-50))
reactions with hafnium, niobium, tantalum, titanium, vanadium, and zirconium, 20: 33270
reactions with iodine, energy transfer processes in, 19: 25157
reactions with irradiated ethylene, propene, styrene, and vinyl alcohol polymers and nylon and tetrone, 18: 25490(T) (AEC-tr-6372(p.197-205))
reactions with irradiated polypropene in carbon tetrachloride, 18: 25490(T) (AEC-tr-6372(p.197-205))
reactions with lignin-containing substances to prepare ion exchangers, 19: 22439(P)
reactions with organic compounds and sulfurous acid ions, sulfur isotope fractionation in, 18: 10442
reactions with plutonium and uranium hexafluorides, 20: 445
reactions with sulfite ions, separation of sulfur-34 by, 16: 12839
reactions with sulfur-35, 16: 28982 (UCRL-10360)
reactions with uranium hexafluoride, kinetics of, 20: 3935
review of chemical, radiation, and thermal stability of, 18: 10041 (ORNL-TM-747)
separation from exhaust gases in MHD generator, method for, 20: 29982(P)
sorption by synthetic zeolites, mechanism of, 19: 13330
spectra of oxygen-18-containing, rotational, 18: 25334
spectra of oxygen-18-containing, ground-state rotational, 18: 25335
spectra of oxygen-16 and -18 and sulfur-32, -33, and -34 containing, rotation, (T), 19: 22176
spectra of, rotational, 18: 34292
sulfur exchange between sulfur(VI) solutions and, 20: 7112
sulfur exchange with sulfur gas, sulfites, and sulfates, 16: 23574
sulfur-35 isotopic exchange with sulfuric acid, effects of nitrous oxide on, 19: 26330
thermal capacity of liquid, at boiling point, 18: 19929 (CONF-417-20)
thermodynamic properties, effects of oxygen-18 labeling, 16: 23693
transport properties, 16: 3553
transport properties in pure gaseous and liquid, 16: 18933
use in carbon dioxide reactor cooling streams to inhibit reaction with graphite moderator, 19: 42015(P)
use of liquid, as reactor coolant, 17: 10010(P)
uses of, in production of uranium tetrafluoride by Winlo process, 20: 33257 (NLCO-974)
vapor pressure of liquid, up to critical point, 18: 3722 (UCRL-7167)
vapor pressure up to critical point, 18: 41374 (UCRL-7167(Rev.I))
vapor pressures in isotopic systems of, 17: 23334
vibrational potential function of bent molecules of, third-order, 20: 14559
yields from gamma radiolysis of solid diaryl sulfones, 20: 20760
butadiene–SO_2, radioinduced polymerization of, 18: 37178 (BNL-874(p.3-4))
chlorobutadiene–SO_2, radioinduced polymerization of, 18: 37178 (BNL-874(p.3-4))
H_3PO_4–pyridine–SO_2–H_2O, sulfur-34 exchange in, thermal phase reversal in, 20: 33298
pyridine–SO_2–H_2O, sulfur-34 enrichment in, 19: 18371
SiO_2–SO_2, properties for use as adsorption refrigeration system, 20: 21174 (SAN-575-12)
styrene–SO_2, radioinduced graft polymerization onto polypropene, 18: 27552
2-methyl-1,3-butadiene–SO_2, radioinduced polymerization of, 18: 37178 (BNL-874(p.3-4))

SULFUR FLUORIDES

attachment of gaseous electrons to, 20: 31221(R) (UCRL-16658, pp 73-87)
dielectric breakdown, 18: 32327
effects of seeding by, on supersonic argon plasma stream, 18: 17176
effects on electron density in flame plasma, (E), 19: 40016
effects on hydrogen formation in radiolysis of hydrobromic and hydrochloric acids, 18: 1763
effects on oxygen-18 exchange in carbon dioxide-nitrogen oxide photolysis, 18: 12192
effects on reactions of deuterium and hydrogen with oxygen, 17: 39075
electric arc stability in gaseous, (E), 19: 6404
electric discharge in gaseous, anion production by, 18: 6299 (ASD-TDR-63-858)
electric field strength in, in cascade arcs, (E), 19: 43454
electron attachment coefficients for, measurement by Townsend discharge, 16: 22747
electron attachment reactions of hexa-, rates of, 19: 43997(R) (UCRL-11889)
enthalpy of formation of SF_6, 20: 20650(R) (ANL-7055, pp 167-76)
enthalpy of formation of, 20: 31213(R) (ANL-7175, pp 119-58)
heat of formation of hexa-, 19: 32118(R) (ANL-7020(p.165-74))
hydrogen ion reactions at 10 to 50 kev, equilibrium fractions in, (E), 19: 14243
ionization by alpha particles, impurity and temperature effects on energy of, 18: 18467
ionization by electron bombardment, as negative ion source, 16: 2791 (NP-10980)
ionization by gamma radiation and neutrons, 18: 10346(R) (X64-11113)
ionization cross section for, electron-impact, 19: 38630
ionization cross sections for negative-ion formation, electron-impact, 19: 38631
light scattering by, effects of density and temperature on, 20: 30734(R) (TID-22970, pp 1-63)
meson (μ^+) decay asymmetry in, 16: 10958 (NEVIS-99)
molecular force constants of hexavalent, calculation of, 17: 25174
molecular force constants of SF_6, 20: 26865
molecular structure of, mean-square amplitudes of interatomic distances in hexavalent, 18: 1639
molecular structure of tetra-, 18: 6812
molecular structure of, mean amplitudes of vibration at 0 and 298°K in, 20: 38897
molecule scattering by, cross sections for inelastic, 19: 14265
neutron reactions (n,γ) on sulfur-34 in, chemical effects in, 17: 23386 (UCRL-10360(Rev.))
nuclear magnetic resonance spectra of, collision-narrowing theory of, 19: 38629
oxygen ion reactions at 15 to 50 kev in, equilibrium fractions for, (E), 19: 18687

performance as insulating gas in Van de Graaff accelerators, 19: 37293
plasma quenching by seeding with, argon, 17: 26721
positronium annihilation and formation in, electric field effects, 16: 13683 (AROD-2211.3)
positronium formation in, effects of d-c electric field, 16: 9324
preparation and structure of mono-, 19: 22252
preparation of fluorine-18-labeled, 20: 41020
properties as accelerator insulating gas, 17: 25857(R) (PR-P-56(p.4-18))
properties as Cherenkov counter gas, 17: 18591 (BNL-6889)
properties of, for use in peripheral compressor, 19: 11337
proton spin-lattice relaxation in mixture with hydrogen, 16: 18887
radiation effects on electron energy in ion pair production in, measurement of γ, 20: 31292
radioinduced reactions with benzenes, 17: 29936
radiolysis of, ESR spectra of products of, 20: 38941(R) (RRL-2310-182)
reactions with lead by flash-heating, species formed in, 16: 18902
reactions with sulfur-35, 16: 28982 (UCRL-10360)
reactions with uranium trioxide and uranyl fluorides at 255 to 370°C, 16: 106
reactions with uranium trioxide at 350°C, 18: 41561(R) (EURAEC-884)
reactions with vanadium pentafluoride, 20: 36804
spectra of, determination of emission, 17: 25108
spectra of fluorinated ethyl radicals in, ESR, 20: 25125(R) (RRL-2310-174)
spectra of phosphorus fluoride molecules and radical ion SF_4^+ in irradiated solid SF_6, 20: 25125(R) (RRL-2310-174)
spectra of, sulfur-33 and -34 isotope effects on nuclear magnetic resonance, 18: 3745
spectra, Raman, 17: 25236
stability of, radiation and thermal effects on, 17: 10516 (ORNL-TM-475)
use of SF_6 in fuel reprocessing, 20: 40389
vapor pressure of liquid, up to critical point, 18: 3722 (UCRL-7167)
vapor pressure up to critical point, 18: 41374 (UCRL-7167(Rev.I))
Ar–SF_6, distribution ratio in vortex flow, 20: 20293 (JPL-TR-32-808)
Ar–SF_6, electric conductivity of plasma jet of, 18: 23532
benzene–SF_6, recombination rates for gaseous, 18: 33555
CO–SF_6, diffusion in, 17: 39076
D–SF_6, diffusion in, 17: 39076
NH_3–SF_6, diffusion in, 17: 39076
NO–SF_6, recombination rates for gaseous, 18: 33555
PF_3–SF_6, radiolysis of, ESR spectra of products of, 20: 38941(R) (RRL-2310-182)
SF_6–toluene, radiolysis of, mechanism and yields of products in gamma, 20: 40948(R) (COO-578-3-32)

SULFUR IONS
charge distribution of 10- to 70-Mev stripped, 20: 44136
decomposition, 17: 41534(R) (ANL-6720(p.77-89))
detection in nuclear emulsions and solids, 20: 5755
electron spin resonance of molecular, in alkali halide single crystals, (E/T), 20: 18005
energy levels and wave functions for, (T), 19: 16370 (UCRL-7943-T)
production of, source for, 19: 47157 (AWRE-NR-1/65)
van der Waals radii of, relation of hydration energy to, 18: 16016

SULFUR ISOTOPES
abundance in Australian and New Zealand geological samples, 17: 20232
abundance in galena samples in Finland, 16: 27479
abundance in geothermal and volcanic waters in New Zealand, 18: 43800 (INS-R-25)
abundance in Sicilian sulfur deposits, 16: 22418
abundance ratios in sandstone-type uranium deposits, Gas Hills District, Wyoming, 20: 16670
abundances in meteorite standards, 17: 20230
composition in igneous rocks of Triassic Newark group in eastern United States, 18: 10266
composition in troilite from meteorites, 18: 10266
composition of atmospheric, 16: 5569
conference of biogeochemistry, 17: 20227
content in marine environment, biogeochemical studies on, 20: 18893 (NYO-3450-1, pp 131-48)
content in meteorites, 20: 18909
content in volcanic materials from Australia, New Zealand, and the Pacific, 20: 18909
content ratios in sulfides from gold ore deposits of Baleisk region, USSR, 19: 22123
content ratios in meteorites, variations in, (E), 19: 38847
contents in alunites, anhydrites, pyrites, pyrrhotites, sulfides, and sulfates, 20: 45921
contents in hypogene minerals of volcanic origin in New Zealand, 20: 45921
determination in sulfides, 17: 2723
determination of sulfur-32/sulfur-34 ratio in minerals, 17: 25255
distribution in Abee and Bruderheim meteorites, 16: 416
distribution in galenas and sphalerites from Broken Hill South, New South Wales, 16: 17890
distribution in ore, determination of deposit genesis from, 20: 37011
distribution in preparation and decomposition of melnikovite, 18: 29870
effects on decomposition of thiosulfate, 20: 297
exchange between ions on surface of barium sulfate crystals, activation energy for, 20: 26881
exchange between ions on surface of strontium sulfate crystals, activation energy for, 20: 26881
exchange between sulfur dioxide and sulfur(VI) solutions, 20: 7112
exchange in sulfur compounds, effects of compound structure on rate, 16: 3310(T) (AEC-tr-4497(p.17-29))
fractionation by bacteria, 17: 20233
fractionation by microorganisms, 17: 20234
fractionation of, bacteriogenic, 18: 8098
fractionation of, in Black Sea, 17: 23502
gamma reactions on, cross sections for, 19: 12496
geochemistry in meteorites and sea water, 16: 2028
helium-3 elastic scattering by, optical model for, 17: 5364
incorporation of radioactive, in haloörganic compounds, 19: 44107(P)
metabolism in normal and irradiated mouse embryos, 20: 42765
nuclear energy levels and properties, survey, 16: 18483
nucleon scattering at high energies by, cross sections for, 17: 15280
preparation, determination, and properties of radioactive, 16: 1349
preparation of thin films containing, by molecular plating, 20: 25027 (AERE-R-5097, Paper 17)
radioactive, effects on human erythrocyte diameter and volume from occupational exposure to, 20: 40678
ratios in geothermal and volcanic environment in New Zealand, 20: 45925
separation and preparation of targets at ORNL calutron, 20: 19153
separation by chemical and ion-exchange methods, 17: 23814
separation by distillation and exchange, 19: 13850
separation by electromagnetic methods, 20: 41401(R) (ORNL-4006)
separation by exchange, separation factors for, 16: 12839
separation by exchange between carbon disulfide and xanthates, 16: 15097(P)
separation by ion exchange methods, coefficients for, 19: 11643
separation by isotopic exchange, 19: 18369
separation by thermodiffusion concentration distribution in tubes for, 17: 11059
separation in calutrons, 18: 34005(R) (ORNL-TM-879)
separation of, process data on electromagnetic, 18: 2128(R) (ORNL-TM-658)
separation of stable, in calutrons, 18: 34005(R) (ORNL-TM-879)
separation of, by chemical exchange, 20: 45770
separation of, performance of separator for, 20: 16928(R) (INSJ-92)
separation of, preparation of disulfur dichloride for electromagnetic, 20: 41400 (ORNL-3301(Suppl.1))
sources of atmospheric, 16: 5569
standard measurements, 17: 28615
standards in New Zealand, recalibration of meteorite, 17: 20231
standards, review of primary, 17: 20229
use in studies of genesis of sulfide deposits, 17: 20228
use of stable, in determining origin of sulfides, 20: 41151
variation in nature, 17: 28615

SULFUR ISOTOPES S-29
beta decay of, log ft values for superallowed transitions in, (E), 20: 24407
decay of, log ft values for, (T), 19: 21379
decay scheme, (E), 19: 5205

SULFUR ISOTOPES S-30
beta decay, 18: 32776
beta decay, 20: 44733
beta decay of, branching ratios and half life of, 18: 2911
beta decay of, branching ratios, energies, and half lives, 19: 47603
energy levels of, shell model calculations for, 18: 32782
energy levels of, shell model calculations for, 18: 32783
energy levels of, from helium-3 reactions (He-3,n) with silicon-28, (E), 19: 45355
gamma reactions (γ,d) to 45 Mev, deuteron spectra from, 16: 23068
preparation and decay, 17: 26633

SULFUR ISOTOPES S-31
beta decay of, model for relative period of, 17: 29632
beta spectra, 18: 6280
energy levels, (E), 19: 39827
energy levels, 18: 21210 (PAN-288)
energy levels, (E), 19: 31241(R) (UCRL-12473(p.1-30))
energy levels and gamma spectra, 16: 31088
energy levels from sulfur-32 (He-3,α) reactions, (E), 20: 17780
energy levels of, shell model calculations for, 18: 32782
energy levels of, shell model calculations for, 18: 32783
energy levels of, shell model calculations of, (E/T), 19: 14512 (CONF-640301(p.1-12))

half life, 17: 11715
magnetic moments and M1 transition probabilities in $2s_{1/2}$ $1d_{1/2}$ shell, (T), 19: 47641
yield in (γ,n) reactions in sulfur-32, 17: 5344

SULFUR ISOTOPES S-32

abundance in Mississippi River Valley galenas, 16: 29195
abundance in rocks of Sudbury district, Ontario, 16: 27440
abundance in Utah sulfides, 20: 45920
alpha elastic and inelastic scattering at 12 to 16 Mev, angular distributions for, (E), 20: 46765
alpha elastic scattering at large angles, energy dependence of, 18: 42754
alpha elastic scattering by, DWBA analysis of, (T), 20: 42392
alpha reactions (α,γ) at 2.2 to 3.2 Mev, 18: 21264
alpha reactions (α,d) at 45 to 50 Mev, highly populated levels in, 18: 34779 (UCRL-11341)
alpha reactions (α,γ) at 1.6 to 3.2 Mev, angular correlations and distributions from (E), 19: 1677
alpha reactions (α,γ) with, distributions from, (E), 19: 14517 (CONF-640301(p.109-42))
alpha reactions (α,d) at 42 to 53 Mev, deuteron energy spectra from, (E), 20: 12061
alpha reactions (α,d) at 42 to 53 Mev, energy spectra from, (E), 20: 24358(R) (UCRL-16580, pp 1-93)
alpha reactions (α,n), threshold of, 17: 11715
alpha reactions, (α,γ), resonance in, 17: 16916
alpha reactions (α,p) at 22 Mev, angular distributions from, 17: 28288
alpha reactions with, optical model transmission functions for, (T), 20: 10047
alpha scattering at 18 Mev, cross sections for, (T), 20: 22134
bremsstrahlung reactions (γ,p) at 24 Mev, cross sections for, 17: 17155
bremsstrahlung reactions (γ,n) at 32 Mev, energy spectra for, 17: 38270
bremsstrahlung reactions (γ,n) and (γ,np) at 30 Mev, direct interactions in, 17: 38272
bremsstrahlung reactions (γ,np) at 50 to 300 Mev, (E), 19: 37860
bremsstrahlung reactions (γ,p) at 25.5 Mev, energy spectra from, (E), 19: 47699
content in granites, meteorites, and basic rock strata, 17: 23523
content in meteorites, ratio to sulfur-34, 18: 42281
content ratio with sulfur-34 in Orgueil meteorite, 19: 39351
determination of ratio with sulfur-34 in ores and rocks, 18: 33501
deuteron (d,p) reactions at 1.7 to 3.0 Mev, cross sections for, (E), 20: 30518
deuteron (d,p) reactions at 3.20 Mev, sulfur-33 low-lying levels from, (E), 20: 32565
deuteron elastic and inelastic scattering at 10.0–11.8 Mev, angular distributions for, 17: 34914
deuteron elastic scattering at 11.5 Mev, angular distribution, 16: 5869
deuteron elastic scattering at 2.0 to 2.5 Mev, angular distributions for, (E), 19: 35444
deuteron inelastic scattering by, correlation measurements, 20: 46580(R) (BMwF-FBK-66-05)
deuteron reactions (d,α) at 14.7 Mev, angular distributions from, 16: 28065
deuteron reactions (d,helium-3) at 15 Mev, 17: 4090
deuteron reactions (d,n) with, angular distribution for, 17: 41873 (WASH-1044)
deuteron reactions (d,p) with, distorted-wave calculations of angular distributions from, 17: 26588
deuteron reactions (d,n) at 3 Mev, emission spectra of, 18: 12453 (CONF-340-15)
deuteron reactions (d,He-3) at 12.8 Mev, angular distribution for, 18: 21210 (PAN-288)
deuteron reactions (d,p) at 1 to 2 Mev, 18: 32772
deuteron reactions (d,p) with, cross sections, 18: 34752(R) (CU(PNPL)-234)
deuteron reactions (d,α) at 15 Mev with, cross sections for, (E), 19: 23643
deuteron reactions (d,p) with, sulfur-33 energy levels from, (E), 19: 23815
deuteron reactions (d,α) at 2.0 to 2.5 Mev, angular distributions and excitation functions for, (E), 19: 35444
deuteron reactions (d,p) with, coherent knockout amplitudes in, (T), 19: 47669
deuteron reactions (d,α) at 11.8 and 12.0 Mev, (E), 20: 6369
deuteron reactions (d,p) with, effect of antisymmetrization on distorted wave calculations of, 20: 8161
deuteron reactions (d,p) at 2 to 3 Mev, sulfur-33 levels from, (E), 20: 28389
deuteron reactions (d,p) at 3.20 Mev, sulfur-33 levels from, (E), 20: 30455
deuteron reactions (d,p) at 11 and 13 Mev, angular-momentum effects on angular distribution from, (E), 20: 32512
deuteron reactions (d,p) at 1.5 to 2.5 Mev, (E), 20: 34571
deuteron reactions (d,p) at 2.5 to 4.6 Mev, (E/T), 20: 42163 (LA-DC-8082)
deuteron reactions (d,α), 20: 46580(R) (BMwF-FBK-66-05)
effects on carbon sulfide ultraviolet emission spectra, 20: 43209
effects with sulfur-34 in E2 and SN1-E1 reactions of *tert*-butyldimethylsulfonium iodide in ethanol, 18: 39202
electron elastic scattering from, 18: 14590(R) (NIRL/R/60)
electron elastic scattering at 187 Mev, differential cross sections for, (E), 19: 28962(R) (NIRL/R/81)
electron inelastic scattering at 120–180 Mev, reduced transition probabilities, parities, and spins of energy levels excited in, 17: 38262
electron inelastic scattering at 50 Mev, differential cross sections for, (T), 20: 21964 (AD-626684)
electron reactions (e,e'p) at 408 Mev, proton binding energies from, (E), 20: 38016
electron scattering at high energies, monopole elastic and inelastic, 17: 19283
electron scattering by, study of nuclear magnetic transitions by inelastic, 17: 19078
electron scattering at 120.63 to 177.85 Mev, cross sections for, 18: 40535
electron scattering by, energy levels and shell-model parameters from, (T), 19: 47677
energy level lifetimes, from resonance scattering of bremsstrahlung, 16: 26275
energy level spacings, 16: 6018
energy level structure of, (E/T), 19: 45275 (NP-15138)
energy levels, 16: 2535
energy levels, 16: 17090
energy levels, 17: 4090
energy levels, 17: 40033
energy levels, 18: 34924
energy levels, 18: 40535
energy levels, (E), 19: 21380
energy levels from phosphorus-31 (p,γ) reactions at 2 to 11.5 Mev, (E/T), 19: 12516
energy levels from chlorine-32 decay, T = 1 isobaric analog, (E), 20: 10020
energy levels from silicon (α,γ) reactions at 3.2 to 4.3 Mev, (E), 20: 11994
energy levels from chlorine-32 decay, (E), 20: 34640
energy levels in, excitation of alpha-cluster, (T), 20: 17802
energy levels of, energies, parities, and spins for, 17: 15290
energy levels of, spin assignments for, 17: 33012
energy levels of, shell model calculations for, 18: 32782
energy levels of, shell model calculations for, 18: 32783
energy levels of, in alpha-particle model, 19: 1619
energy levels of, shell model calculations of, (E/T), 19: 14512 (CONF-640301(p.1-12))
energy levels of, nucleon separation energy in 1p and 1s, 19: 21400
energy levels of, 0+, (T), 19: 25548
energy levels of, E1 photon absorption for, (T), 19: 37832(R) (TID-21940 (Paper I))
energy levels of, asymmetric-rotator model for rotational, (T), 20: 13849
energy levels of, parity and spin of, (T), 20: 19816 (INP-441/PL)
energy levels of, configuration splitting of giant dipole resonance for 1d-2s, 20: 36179 (UJV-1612)
energy-level positions and transitions in, calculations using particle-hole model, (T), 20: 42199
energy-level transitions from phosphorus-31 (p,γ) reactions at 0.8 to 1.16 Mev, (E), 20: 44822
exchange between carbon disulfide and a xanthogenate, 19: 18045(P)
exchange with sulfur-34 in sorbed sulfur dioxide on anion exchanger, 16: 29298
fractionation of, in reactions between sulfur dioxide and organic compounds or sulfurous acid ions, 18: 10442
gamma reactions (γ,n) with, neutron energy spectra from, 18: 21257
gamma reactions (γ,np) at 50 to 300 Mev, cross sections for, 18: 38198
gamma reactions (γ,p) with, cross sections, (E/T), 19: 14528 (LAL-1120)
gamma reactions (γ,n) at threshold to 22.1 Mev, cross sections for, (E), 19: 19170
gamma reactions at 10 to 27 Mev, cross sections, 16: 23057
gamma reactions (γ,d) to 45 Mev, deuteron spectra from, 16: 23068
gamma reactions (γ,np) at 30 to 80 Mev, 16: 24842
gamma reactions (γ,n) to 24 Mev, cross sections of, 17: 5342
gamma reactions (γ,n) at 30 Mev, cross sections of, 17: 5344
gamma transitions from excited states, 16: 19752 (SUI-61-5)
gamma transitions in, 16: 21497
helium-3 reactions (He-3,α) at 4.60 to 5.50 Mev, mechanisms of, 18: 36634
helium-3 reactions at 29 Mev, (E), 19: 21232 (JEN-141-DF/I-45)
helium-3 reactions (He-3,n) with, Q-value for, (E), 19: 31320
helium-3 reactions (He-3,p) at 12 Mev, Q value for, 20: 16331 (GA-6568)

helium-3 reactions (He-3,α) at 12.1 Mev, sulphur-31 levels from, (E), 20: 17780
neutron activation rates, calculation of neutron spectral distributions from, 16: 5500 (WAPD-T-1380)
neutron activation rates for threshold detectors, 17: 3541 (TID-17211)
neutron activation cross sections for threshold detectors, 17: 3541 (TID-17211)
neutron activation cross sections, 17: 10139
neutron activation rates for, fast, 17: 28221 (EUR-107.f)
neutron activation of foils of, fast, 17: 36347(R) (NARF-62-18P)
neutron capture, 18: 7696(R) (ORNL-TM-761)
neutron capture and transmission at 10 to 80 kev, resonance, 18: 24620(R) (ORNL-TM-874)
neutron capture and total cross sections of, resonances in, 19: 1636
neutron capture by, polarization of gamma rays from, (E), 19: 23633 (UJV-1211/64)
neutron capture cross sections of, energy dependence of, 17: 26521
neutron capture cross sections, 19: 32787(R) (NIRS-3(1-17))
neutron capture in, gamma energies from, 16: 28162
neutron capture, spectra of resonance and thermal, (E), 19: 35399 (ORNL-P-1307)
neutron cross sections of, fast, 17: 26038
neutron cross sections of, 17: 40046
neutron elastic and inelastic scattering at 4.6 Mev, 17: 5327
neutron elastic and inelastic scattering at 14.1 Mev, 18: 26600
neutron elastic and inelastic scattering at 2.45 to 5.80 Mev, cross sections for, (E), 20: 15811
neutron elastic scattering cross sections for, optical model calculations of, 18: 32726 (AERE-R-4649)
neutron elastic scattering at 13.8 to 14.7 Mev, energy dependence of backward, 18: 38136
neutron inelastic scattering by, 18: 11195(R) (EANDC(E)-49(L))
neutron inelastic scattering by, distributions from, 18: 16972
neutron reactions (n,d), transitions in, 16: 3668 (NYO-7864)
neutron reactions (n,np) and (n,p) at 14.4 Mev, nuclear temperature calculations, 16: 8205
neutron reactions (n,p), use in neutron flux measurements, 16: 8913(T) (CEA-tr-A-1025)
neutron reactions (n,p) at 2 to 5 Mev, cross sections, 16: 18499
neutron reactions at 2 to 5 Mev, cross section fluctuations, 16: 24845
neutron reactions (n,p) of, use in low intensity fast neutron measurements, 16: 33779 (AEEW-M-269)
neutron reactions (n,p), cross sections for, 17: 1176(R) (HW-70050 (p.78-142))
neutron reactions (n,d), (n,np), and (n,pγ) at 14 Mev, cross sections for, 17: 2242 (TID-16949)
neutron reactions (n,t) at 14 Mev, cross sections and Q values for, 17: 2242 (TID-16949)
neutron reactions (n,p), cross-sections of, 17: 4102
neutron reactions (n,p) on, yields from epithermal and fast, 17: 7306
neutron reactions (n,p) at 2 to 20 Mev, use of, as fast neutron flux monitor, 17: 9529
neutron reactions (n,p), cross section for fission, 17: 9542
neutron reactions (n,p), use in preparation of labeled drugs, 17: 10683
neutron reactions (n,d) at 14.1 Mev, angular distributions of, 17: 11716
neutron reactions (n,p) with, product half life for, 17: 25857(R) (PR-P-56(p.4-18))
neutron reactions (n,p) at threshold, cross sections for, 17: 26421 (EUR-10.e)
neutron reactions (n,p) at 14.6 Mev, proton angular distributions and energy for, 17: 29602
neutron reactions (n,p) on, yields from in-pile, 17: 29940
neutron reactions (n,p), production of phosphorus-32 by, 17: 30165
neutron reactions (n,p), use in neutron flux measurements, 17: 30165
neutron reactions (n,p) with, effective threshold energy for, 17: 38116
neutron reactions (n,p), neutron dosimetry by, 17: 41017 (CEA-2302)
neutron reactions (n,p) with, effects on thermal annealing of sulfur compounds, 18: 299
neutron reactions with, fast neutron in-pile detection by threshold, 18: 2020 (EUR-289.e)
neutron reactions (n,γ) with, angular correlations from, 18: 2403(R) (PR-P-58)
neutron reactions (n,p) with, for neutron flux measurements, 18: 23885 (NP-13930(p.178-80))
neutron reactions (n,γ) with, spectra from resonant, 18: 26542(R) (ORNL-3582(p.71-5))
neutron reactions (n,p)P-32, 18: 26590
neutron reactions (n,xγ) at 14.8 Mev, cross section and gamma spectrum for, 18: 30736(R) (TID-20658)
neutron reactions (n,α) with, 18: 34799
neutron reactions (n,d) at 14 Mev, 18: 34818
neutron reactions (n,p) with, absolute measurement of yields from, 18: 36751 (ANL-6912)
neutron reactions (n,d) at 14.1 Mev, cross section for, 18: 38083(T) (AEC-tr-6398(p.157-63))
neutron reactions (n,p) with, use as threshold detector for fast neutron spectra in iron, 18: 40531
neutron reactions (n,d), cross section for, 19: 14533(R) (NYO-1082-1)
neutron reactions (n,d), energy levels of phosphorus-31 from, 19: 14533(R) (NYO-1082-1)
neutron reactions with, in human hair, 19: 18195 (LA-DC-6646)
neutron reactions (n,p) and (n,t) at 14.8 Mev, cross sections for, (E), 19: 27516
neutron reactions (n,p), cross sections for, (E), 19: 31244 (ZfK-RN-23)
neutron reactions (n,p), use for neutron spectrometry, 19: 31245 (ZfK-RN-27)
neutron reactions (n,p), cross section for fast, (E), 19: 35378(R) (EANDC(E)-57(U))
neutron reactions (n,γ) with, gamma spectra from thermal, (E), 19: 43288
neutron reactions (n,α$_0$) at 3.6 Mev, angular distribution for, (E/T), 19: 43304
neutron reactions (n,p), use in determining fast fluxes, 19: 45679(R) (NYO-1859-11)
neutron reactions (n,α), cross sections and Q values of, 19: 45679(R) (NYO-1859-11)
neutron reactions (n,p) in soil, activity induced by, 19: 47569 (CEX-62-50)
neutron reactions (n,p) with, use in criticality dosimeter, 20: 647 (AERE-M-1631)
neutron reactions (n,p) with, cross sections for phosphorus-32 production in, (E), 20: 3020 (ORNL-TM-1065)
neutron reactions (n,α) at 14 Mev, compound-nucleus process in, (E/T), 20: 10010
neutron reactions (n,α) at 0.025 and 0.035 ev, cross sections and Q-values for, (E), 20: 11983
neutron reactions (n,α$_0$) at 3.2 Mev, angular and energy distributions from, (E), 20: 11993
neutron reactions (n,p) with, in cysteic acid, cysteine, and cystine, recoil atom retention in products from, 20: 14584(R) (TID-22444)
neutron reactions (n,2n) at 12 to 18 Mev, cross sections for, (E), 20: 15863
neutron reactions (n,p) at 0 to 20 Mev, cross sections for, 20: 19810 (EUR-119.e(Vol.2))
neutron reactions (n,p) at 2.9 Mev, cross section and threshold energy for, 20: 21427(R) (NASA-CR-54904)
neutron reactions (n,γ) with, sulfur-33 level spins from thermal, (E), 20: 22077
neutron reactions (n,α) at 2.5 to 3.2 Mev, angular distributions from, (E), 20: 28308
neutron reactions (n,d) at 14 Mev, (E), 20: 38150
neutron reactions (n,p) with, neutron dosimetry using, 20: 39228
neutron reactions (n,α$_0$) at 2.5 to 3.2 Mev, 20: 42375
neutron reactons (n,p) with, measurement of neutron fluxes with, 17: 29202 (NIRL/R/31)
neutron scattering at 14 Mev, differential cross sections for (E/T), 19: 3298
neutron scattering at 14.6 Mev, differential cross sections for (E), 19: 3320
neutron total cross sections of, 18: 26543(R) (ORNL-3582(p.75-82))
neutron transmission measurements on, 18: 7696(R) (ORNL-TM-761)
neutron transmission by, resonances in, 18: 24625 (WASH-1046)
nitrogen reactions (N^{14},2p) with, scandium-44 isomeric yield ratio for, 17: 24053(R) (ORNL-3432)
nitrogen-14 reactions (N^{14},O^{14}) on, 17: 19339
nitrogen-14 reactions at 27.5 Mev, scandium production in, 17: 38108
nitrogen-14 reactions (N-14,O-15) at 27.5 Mev, excitation functions for, 18: 24716
nitrogen-14 reactions at 30 to 42 Mev, scandium-44 isomer pair production in, (E), 19: 21392
nitrogen-14 reactions (N-14,2p) with, scandium-44 isomeric state from, (E), 19: 37823(R) (ORNL-3800(p.1-49))
nuclear dipole resonance in, 18: 40556
nuclear properties of, activation analysis of, 19: 10983(R) (TEES-2671-3)
nuclear properties in shell model, 20: 15730(R) (RHEL/R-112, pp 67-98)
nuclear surface oscillations in, calculation of, 17: 40019
nucleon separation energies for, adiabatic, (T), 19: 16844 (ISS-64/36)
nucleon spatial correlations in, 19: 19152
oxygen-16 reactions (O^{16},3pn) with, scandium-44 isomer pair production in, 17: 34877 (JINR-P-1277)
oxygen-16 reactions (O^{16},3pn) with, cross section for formation of scandium-44 and -44m in, 18: 6261
photon absorption by, E1, (T), 19: 19110
photon reactions (γ,n) at 22 Mev, cross sections for, 17: 28286
properties for use as threshold detector in shielding studies, 18: 32949(R) (EUR-534.d(Pt.II))

proton binding energy in, measurement of, 19: 41660 (ISS-65/3)
proton inelastic scattering at low energies, reaction mechanisms for, 16: 21393
proton inelastic scattering by, angular correlations for, 18: 7780
proton inelastic scattering by, excited states from, 18: 17042
proton inelastic scattering at 155 Mev, cross sections and energy levels from, (E), 20: 6354
proton reactions (p,α) at 14.5 Mev, energy levels from, 18: 42706
proton reactions (p,γ) at 1 to 2 Mev, resonances in, (E), 19: 6721
proton reactions (p,γ) at 1 to 2 Mev, resonances in, (E), 19: 14483 (AD-603601)
proton reactions (p,d) at 28 Mev, differential cross sections for, (E/T), 20: 9975 (PUC-937-174)
proton reactions (p,2p) at 460 Mev, (E/T), 20: 11948 (AD-624318)
proton reactions (p,p' γ) at 7.5 to 10.7 Mev, spin and decay modes of excited states from, (E), 20: 13823
proton reactions (p,2p) at 140 Mev, energy spectra and angular correlation distributions from, (E), 20: 17741
proton reactions (p,p'γ) at 8.5 Mev, angular correlations from, (E), 20: 22059
proton reactions (p,γ) at 0.3 to 2.1 Mev, resonance strengths for, (E), 20: 42182
proton reactions (p,n) with, chlorine-32 mass from threshold energy for, (E), 20: 44812
proton reactions at 150 Mev, gamma spectra from, 16: 31088
proton reactions (p,p' γ) at 5.7 to 6.34 Mev, angular correlations from, 16: 26327
proton reactions (p,γ), at 500 to 1900 kev, resonances for, 16: 32432
proton reactions (p,4p) and (p,5p), excitation functions for, 16: 33892
proton reactions (p,γ) at 350, 440, and 540 kev, angular distributions and spectra from, 17: 799 (TID-16950)
proton reactions (p,xp) at 100 to 400 Mev, cross sections for, 17: 5323 (NYO-8921)
proton reactions (p,d) with, nuclear structure studies using, 18: 1088
proton scattering at 6.2 Mev, elastic and inelastic, 16: 7024
proton scattering at 5.7 to 6.34 Mev, angular distributions from, 16: 26352
proton scattering at high-energies, spin-flip, 18: 38125
scattering of 28.5-Mev helium-3 ions, cross sections for elastic, 17: 15267
spectra in diatomic sulfur, uv rotational, (E/T), 19: 23307
spectra in diatomic sulfur, shifts in near infrared bands of, 20: 34098
spectra of sulfur dioxide containing, rotation, (T), 19: 22176
transitions to second excited state, 16: 5939
use as fast-neutron threshold detector, 17: 34268
use in determination of ore deposit genesis, 20: 37011
use in studying genesis of mineral deposits, 20: 41151
yields from radiolysis of thiourea by neutrons, 19: 46365

SULFUR ISOTOPES S-33

content in meteorites, variations in, (E), 19: 38847
content in meteorites, 20: 29893
deuteron reactions (d,p) at 6.0 Mev, ground-state Q value and proton groups from, 17: 7247
energy level spacings, 16: 6018
energy level transitions in, branching ratios for, (E), 20: 9981 (WASH-1064)
energy levels, 18: 28626
energy levels, 18: 34799
energy levels from deuteron beam reactions with light nuclei, 16: 11040
energy levels from proton capture by sulfur-32, 16: 32432
energy levels from sulfur-32 (n,γ) reactions, (E), 19: 43288
energy levels from thermal neutron reactions (n,γ) with sulfur-32, spins of, (E), 20: 22077
energy levels from deuteron reactions (d,p) with sulfur-32 at 2 to 3 Mev, spin of, (E), 20: 28389
energy levels from deuteron reactions (d,p) with sulfur-32 at 3.20 Mev, (E), 20: 30455
energy levels from sulfur-32 (d,p) reactions, (E), 20: 30518
energy levels from sulfur-32 (d,p) reactions, branching and mixing ratios, parities, and spins for low-lying, (E), 20: 32565
energy levels, gross-structure properties of, 16: 23123 (PR-P-57(p.37-43))
energy levels of, spins and transition correlations of, 17: 32725(R)
energy levels of, shell model calculations for, 18: 32782
energy levels of, shell model calculations for, 18: 32783
energy levels of, shell model calculations of, (E/T), 19: 14512 (CONF-640301(p.1-12))
energy levels of, parity and spin of, (E), 19: 23726
energy levels of, 1.34-Mev, (E), 19: 23815
energy levels of, parity and spin of, (E), 20: 9981 (WASH-1064)
energy levels of, spin of, (T), 20: 30360 (WASH-1068)
energy-level transition probabilities of, E2, (T), 20: 3115
gamma emission by, circular polarization in, (E), 19: 23633 (UJV-1211/64)
gamma spectra at 0 to 350 kev, 16: 28162
magnetic moments and M1 transition probabilities in $2s_{1/2}$ $1d_{1/2}$ shell, (T), 19: 47641
neutron capture by, resonances from, (E), 19: 45356
neutron compound inelastic scattering at 3 Mev, angular correlation functions for, 18: 9402
neutron reactions (n,p), separation energies for, 17: 2242 (TID-16949)
neutron reactions (n,αγ), (n,αn), (n,2n), (n,np), (n,2p), (n,pγ), and (n,pn) at 14.8 Mev, cross sections for, 17: 2242 (TID-16949)
neutron reactions (n,p), cross section for fast, (E), 19: 35378(R) (EANDC(E)-57(U))
neutron reactions (n,p) with, cross sections for phosphorus-33 production in, (E), 20: 3020 (ORNL-TM-1065)
neutron reactions (n,p) with, phosphorus-33 production in, (E), 20: 8178(P)
neutron reactions (n,α) at 0.025 and 0.035 ev, cross sections and Q-values for, (E), 20: 11983
neutron reactions (n,p), cross sections for, (E), 20: 14461(R) (ORNL-3889, (pp 48-70)
neutron reactions (n,p) with, effective cross sections for, (E), 20: 24424
neutron reactions (n,p), phosphorus-33 production in, (E), 20: 37166
neutron reactions, production of phosphorus-33 in, 20: 16914(R) (ORNL-3900, pp 182-93)
neutron total cross sections at 3–5 Mev, fast, 17: 28287
nuclear reactions of, cross section for, 19: 31788(R) (ORNL-3768 (p.33-57))
preparation as radiation target material, 18: 27811(R) (ORNL-TM-198)
production in iron meteorites by cosmic radiation, 19: 47195
proton reactions (p,p' γ) at 1.2 to 3.2 Mev, energy levels from, 18: 28626
proton reactions (p,γ) with, spectra from, 18: 42666
proton reactions (p,γ) at 1 to 2 Mev, resonances in, (E), 19: 6721
proton reactions (p,γ) at 1 to 2 Mev, resonances in, (E), 19: 14483 (AD-603601)
proton reactions (p,γ) at 300 to 1300 kev, gamma branching in, (E/T), 20: 6295 (NP-15647)
separation from other sulfur isotopes by anion exchange, 16: 15087
separation from phosphorus-33 in ORR, (E), 19: 28721
separation from sulfur, electromagnetic, (E), 19: 35510
spectra of isotopic shifts with fluorine, nuclear magnetic resonance, 18: 3745
spectra of sulfur dioxide containing, rotation, (T), 19: 22176

SULFUR ISOTOPES S-34

abundance in hypogene minerals of volcanic origin in New Zealand, 20: 45921
abundance in Mississippi River Valley galenas, 16: 29195
abundance in rocks of Sudbury district, Ontario, 16: 27440
abundance in sulfate and sulfide of meromictic lake, 17: 34134
abundance in Utah sulfides, 20: 45920
alpha reactions (α,p) with, 18: 18961
alpha reactions (α,γ) at 2.2 to 3.2 Mev, 18: 21264
alpha reactions (α,γ) with, 18: 44805
alpha reactions (α,γ) at 1.6 to 3.2 Mev, angular correlations and distributions from (E), 19: 1677
alpha reactions (α,γ) with, distributions from, (E), 19: 14517 (CONF-640301(p.109-42))
alpha reactions (α,n), threshold of, 17: 11715
content in central African sulfide deposits, 19: 36657
content in granites, meteorites, and basic rock strata, 17: 23523
content in hydrothermal fluids in New Zealand, 20: 45925
content in meteorites, ratio to sulfur-32, 18: 42281
content in meteorites, variations in, (E), 19: 38847
content in meteorites, 20: 29893
content in sulfides from copper–nickel deposits in Soviet Union, 18: 33767
content in sulfur dioxide gases from volcanoes, 19: 18152
content ratio to sulfur-32 in Orgueil meteorite, 19: 39351
determination of ratio with sulfur-32 in ores and rocks, 18: 33501
deuteron reactions (d,p) at 11 and 13 Mev, angular-momentum effects on angular distribution from, (E), 20: 32512
distribution in ancient oceans and evaporites, variations in, 20: 41135
distribution in lake waters, 17: 33598
effects on bacterial oxidation and reduction of sulfur, 19: 9112
effects on carbon sulfide ultraviolet emission spectra, 20: 43209
effects with sulfur-32 in E2 and SN1-E1 reactions of *tert*-butyldimethylsulfonium iodide in ethanol, 18: 39202
energy level lifetimes, from resonance scattering of bremsstrahlung, 16: 26275
energy levels, 16: 2535
energy levels, 17: 7247
energy levels excited by (α,p) reactions on phosphorus-31, 16: 21417
energy levels from silicon-30 (α,γ) reactions at 3.25 to 4.25 Mev, (E), 19: 43315

energy levels from silicon (α,γ) reactions at 3.2 to 4.3 Mev, (E), 20: 11994
energy levels of, spin assignments for, 17: 33012
energy levels of, decay modes, parities, spins, and strengths of, 18: 19055
energy levels of, shell model calculations for, 18: 32782
energy levels of, shell model calculations for, 18: 32783
enrichment in pyridine–water–sulfur dioxide, 19: 18371
exchange between carbon disulfide and a xanthogenate, 19: 18045(P)
exchange in phosphoric acid–pyridine–sulfur dioxide–water system, thermal phase reversal in, 20: 33298
exchange with sulfur-32 in sorbed sulfur dioxide on anion exchanger, 16: 29298
fractionation of, in reactions between sulfur dioxide and organic compounds or sulfurous acid ions, 18: 10442
neutron reactions (n,γ), sulfur-35 behavior in gaseous sulfur compounds following, 16: 28982 (UCRL-10360)
neutron reactions (n,γ), use in preparation of labeled drugs, 17: 10683
neutron reactions (n,γ) in gaseous sulfur compounds, chemical effects from, 17: 23386 (UCRL-10360(Rev.))
neutron reactions (n,d) at 14.1 Mev, cross section for, 18: 38083(T) (AEC-tr-6398(p.157-63))
neutron reactions (n,α) at 14.8 Mev, cross sections for, (E), 19: 27516
neutron reactions (n,γ) with, in cysteic acid, cysteine, and cystine, sulfur-35 recoil atom retention in products in, 20: 14584(R) (TID-22444)
neutron reactions (n,γ), hot atom effects from, in organic compounds, 20: 33336(R) (PRNC-86)
neutron reactions (n,p) at 14.8 Mev, cross sections for, (E), 20: 36212
neutron reactions (n,d) at 14 Mev, (E), 20: 38150
nucleon binding energies, 16: 11007
proton reaction (p,γ), angular distribution and spectra from, 18: 16945 (NP-13601)
proton reactions (p,γ) at 0.8 to 1.4 Mev, 18: 22910
proton reactions (p,γ) at 0.7 to 1.5 Mev, chlorine-35 energy levels from (E/T), 19: 1561 (NP-14430)
proton reactions (p,γ) at 1 to 2 Mev, resonances in, (E), 19: 6721
proton reactions (p,γ) at 1 to 2 Mev, resonances in, (E), 19: 14483 (AD-603601)
proton reactions (p,n) at 5 to 10 Mev, thresholds for, (E), 19: 14607
proton reactions (p,nγ) ($n \geq 2$) with, correlations from, (E), 20: 1146 (COO-1120-38)
proton reactions (p,γ) at 1.9 to 3.0 Mev, chlorine-35 resonance levels from, (E), 20: 19973
proton reactions (p,α) with, accelerator beam calibration from threshold energy for, 20: 28401
proton reactions (p,γ) at 1.214 Mev, chlorine-35 energy-level quantum numbers and transitions from, 20: 38071
proton reactions (p,γ) at 0.3 to 2.1 Mev, resonance strengths for, (E), 20: 42182
proton reactions (p,γ) with, chlorine-35 energy-level quantum numbers and transitions from, (E), 20: 44808
proton reactions (p,γ) with, chlorine-35 energy levels from, (E), 20: 46769
proton reactions (p,d) with, nuclear structure studies using, 18: 1088
separation from other sulfur isotopes, review of methods for, 19: 11642
spectra in diatomic sulfur, uv rotational, (E/T), 19: 23307
spectra in diatomic sulfur, shifts in near infrared bands of, 20: 34098
spectra of isotopic shifts with fluorine, nuclear magnetic resonance, 18: 3745
spectra of sulfur dioxide containing, rotation, (T), 19: 22176
use in determination of acid intrusive sources in ores, evaluation of, 19: 24735
use in determination of ore deposit genesis, 20: 37011
use in studying genesis of mineral deposits, 20: 41151

SULFUR ISOTOPES S-35

aberrant effects on jute leaves, 18: 43292
accumulation coefficients of, in marine organisms, 18: 21780(T) (JPRS-24227)
activity in irradiated chlorine compounds, chemical fate, 16: 11757
activity in yields from chlorine-35 (n,p) reactions in chlorobenzene, 16: 11758
activity of, specific, 18: 43994
annealing behavior of thermal neutron induced recoils of, in ferroelectric tri-glycine sulfate, 19: 42570
behavior in sewage waste disposal, 17: 36061
beta activity in sulfuric acid and lithium sulfate, scintillation counting using glass fiber paper for liquid, 19: 36527
beta activity of, comparison of international measurements of, 20: 25190
beta activity of, use of 4π proportional counters for measuring, 20: 31548
beta decay energy at liquid-nitrogen temperatures, 16: 2509
beta decay of, Coulomb corrections to internal bremsstrahlung in, 17: 26619
beta decay of, electromagnetic emission of atomic electrons in, 18: 6270
beta decay of, backward diffusion in aluminum from, (E), 20: 9982(T)
(MLM-1285(tr))
beta decay of, corrections for foil absorption in 4π counting of, (E), 19: 26654 (EUR-2248.e)
beta decay of, electron polarization in, (E), 19: 16894
beta decay of, internal bremsstrahlung spectra from, (T), 20: 19949
beta decay of, mean energies of, 18: 34785
beta decay of, shell model calculations of ft values in, (T), 20: 6393
beta self-absorption by barium sulfate on filter paper, 16: 28992
beta self-absorption in solutions of, effects of teflon on, 18: 12175
beta spectra and pulse-height distributions of, 18: 29988
beta spectra from, (E), 20: 23457 (CEA-R-2839)
beta spectra of, back-scattering and self-absorption of, 17: 36674
beta spectra of, Fermi plots of, 18: 20360
beta spectra, proportional counter efficiency study for, 16: 19076 (TID-15686)
beta spectra, effect of secondary electron emission on, 19: 23312
bremsstrahlung energy loss in, 17: 21015
chemical properties of recoil, in neutron-irradiated sulfur, 20: 31295
chemical state of, produced by chlorine-35 reaction (n,p) on potassium chloride, 18: 31598
contamination of man by accidental exposure, body burden and treatment in, 17: 36053
contamination of pig skin by, effect of acidity of soiling solution on, 20: 43010
content and production in exosphere, 19: 14120
content and properties of, in food, 19: 18218
content in blood of man, mice, and rats, after intravenous or intraperitoneal injection, 19: 27942
content in ground level air and precipitation, 18: 37865
content in seawater, 20: 43688
content in stratosphere, production mechanisms for, 18: 21080
core deformability and electric quadrupole moments, 16: 7026
counting techniques for, international comparison of proportional, 18: 31866 (AWRE-O-26/64)
decay of, continuous spectrum from internal bremsstrahlung in, (T), 20: 15801
decay of, transmission curves for beta particles from, 19: 10261
decay to chlorine-35 of, genetic effects, 19: 43816
deposition on magnesium of, from organic plating solutions, 18: 29594
deposition on surfaces for preparation of large-dimension beta sources, 18: 28064
detection and measurement, performance of liquid scintillation detectors, 17: 1185
detection and measurement of, by 4π-liquid scintillation counting, 19: 11595
detection and measurement in solution, use of 4π counter in absolute, 19: 19755 (KFK-252)
detection and measurement of, using scintillation ion exchange resin, 19: 32098
detection and measurement of, by 4π gas counter, 20: 666
detection and measurement in organic compounds, counting methods for, 20: 7421
determination by beta scintillation counting, effects of sample volume on efficiency of, 20: 5510
determination in atmospheric and precipitation samples, methods for radiochemical, 20: 14430 (AD-620219)
determination in biological samples by liquid scintillation counting, 16: 137
determination in biosynthetically labeled wool by direct liquid scintillation counting, 17: 14185
determination in biological materials by liquid-scintillation counting, 17: 18482
determination in bacteria, by liquid scintillation counting, 18: 36931
determination in biological materials using cryostat, method for, 19: 13244
determination in biological material by scintillation counting of beta decay, 19: 40425
determination in biological materials, method for, 20: 1758
determination in biological materials by liquid scintillation counting, combustion methods for, 20: 43128
determination in hydrogen sulfide by liquid scintillation counting, 19: 17818
determination in irradiated polyphenyls, 16: 7496
determination in labeled compounds by thin-layer and paper chromatography, 18: 29588
determination in labeled gases by proportional counters, 18: 37504 (A/CONF.28/P/855)
determination in labeled proteins after polyacrylamide disk electrophoretic separation, 19: 32067
determination in organic materials, 16: 10055
determination in organic compounds by liquid scintillation, 16: 16091
determination in organic sample by combustion and scintillation

counting, 20: 16387
determination in organic compounds by gas chromatography and scintillation counting, 20: 16371
determination in precipitates, glass filter paper suspension technique for liquid scintillation, 17: 40731
determination in presence of other radioisotopes, 19: 15689
determination in plant material by beta counting, 19: 46199
determination in radioisotope mixtures, microcalorimetric, 20: 3866 (CEA-R-2630)
determination in sea water, method for, 19: 40431
determination in variable quenching samples, method for, 18: 12005
determination, method for absolute, 16: 30339
determination of, by oxygen flask method, 17: 23263
determination of, international comparison of methods for, 18: 3676 (NP-13320)
determination of, in lacustrine organisms, 18: 6599(R) (TID-19930)
determination of internal, by radiochemical urine analysis, 18: 33519
determination of, in biological and organic materials, combustion method for, 20: 36721
determination of, instrumentation effects on quenching of energy spectrum in, 20: 36771
determination using liquid scintillation counters, 16: 24337
diffusion from irradiated sodium chloride on heating, 20: 25134
diffusion in iron, generalization of Gruzin method for studying, 19: 23042
distribution in mice of MEA-incorporated, 18: 43311
distribution of atmospheric, 16: 16589
distribution of atmospheric, 16: 16587
distribution of cysteine- and sodium sulfate-incorporated, in pigeon feathers, 20: 45317
distribution of inhaled, as $S^{35}O_2$, in dogs, 18: 5631(R) (NP-13382)
distribution of, in tissues of mammals, 18: 31168
effects of incorporated, on adenine-dependent yeast, mutagenic, 20: 33000
effects of phototaxic behavior in Euglena, 20: 24889
effects of sodium sulfate-incorporated, on skeletal growth in rats, 20: 16267
effects on bacteria, mutagenic, 18: 27121
effects on catalytic activity of magnesium and sodium sulfates, comparison with x radiation, 16: 227
effects on catalytic activity of magnesium and sodium sulfates, 18: 12188
effects on chemisorption and electric conductivity of cadmium sulfide, 19: 37183
effects on chick embryos, 18: 38775(R) (ORO-624)
effects on efficiency of activated sludge plants for sewage treatment, 20: 218(R) (STI/DOC/10/42, pp 1-22)
effects on hematopoietic system of massive doses of, 19: 36139
effects on lungs, carcinogenic, 18: 31349
effects on mice and rats, 17: 35515
effects on *Oenothera flavens*, mutagenic, 17: 23207
effects on polarization of alcohols in magnesium sulfate catalyst, 19: 28433
effects on rice seed, chlorophyll mutations from, 20: 40641
effects on sorptive properties of barium sulfates for dyes, 17: 20083
effects on specific surface of molybdenum disulfide, 18: 23696
effects on survival of rats and mice receiving subsequent lethal doses of x radiation, 16: 23443
effects on survival of mice and rats receiving subsequent lethal doses of x radiation, 16: 30223(T) (FTD-TT-62-501(p.9-16))
electron spin resonance spectra of, in irradiated 2,4,6-tri-*t*-butylthiophenol, 19: 30241
energy levels of, shell model calculations for, 18: 32782
energy levels of, shell model calculations for, 18: 32783
energy loss as beta source, spectra of linear, 19: 36062
exchange between barium sulfate crystals, rate of, 20: 12869
exchange between barium sulfate crystals and solutions, 20: 14572
exchange between carbon disulfide and liquid hydrogen sulfide in triethylamine solutions, kinetics of, 20: 27008
exchange between elemental sulfur and sulfur-containing compounds, 18: 15999 (TID-7689(p.93-5))
exchange between elemental sulfur and sulfur monochloride, 18: 35579
exchange between elementary sulfur or sulfides and thiophene, 20: 3976
exchange between hydrogen sulfide and sulfide crystals, 17: 32138
exchange between ions on surface of strontium sulfate crystals, 20: 26881
exchange between liquid hydrogen sulfides and sulfur compounds in basic and neutral solutions, rate of, 20: 27007
exchange between potassium sulfate and sulfite, 17: 39128
exchange between sulfates and sulfur trioxide, radiation effects, 16: 27099
exchange between sulfide and thiosulfate, kinetics of, 18: 39200
exchange between sulfuryl and thionyl chloride, 19: 24527
exchange between sulfur dioxide and sulfuric acid, effects of nitrous oxide on, 19: 26330
exchange between sulfuryl and thionyl chlorides, 20: 3965
exchange between strontium sulfate crystals and solutions, 20: 14572
exchange between sulfur and isothiocyanates, 20: 45769
exchange between 4,4'-dimethylbenzhydryl thiocyanate and sodium thiocyanate in acetonitrile, 19: 17945
exchange between 4-chlorobenzhydryl thiocyanate and sodium thiocyanate, 20: 29237
exchange equilibria on metal sulfides, 16: 13056
exchange in organic sulfur compounds, 18: 25460
exchange with organic compounds, paper chromatographic techniques for studying, 17: 1520
excretion in urine, 18: 41052
fallout of cosmic-ray-produced, 16: 16585
fallout of cosmic-ray-produced, 16: 16589
fallout of cosmic-ray-produced, 16: 16587
fixation to protein-polysaccharides of bovine cartilage, 20: 40544
half life, 16: 2541
half life of, determination by direct decay, (E), 19: 37847
incorporation from sulfate solutions in irradiated cornea tissue, 18: 19708
incorporation in amidazine and tebezone, 19: 15
incorporation in anhydride of *p*-toluenesulfonic acid, 19: 36439
incorporation in benzene derivatives, 17: 29952
incorporation in biological derivatives by biosynthesis in *E. coli* from labeled sulfates, 18: 43584
incorporation in barium sulfates and lead sulfates, effects of, on solubility, 19: 46274
incorporation in carbon disulfide by isotope exchange, 16: 3357(T) (AEC-tr-4497(p.465-72))
incorporation in cadmium, iron, potassium, and sodium sulfides, 18: 12228
incorporation in cellulose acetate matrix for use as beta source, 18: 27507
incorporation in catalysts used in dehydration of cyclohexanol, 19: 20013
incorporation in cystine by neutron irradiation, 19: 38747
incorporation in compounds, Boris Kidric Institute of Nuclear Sciences, Yugoslavia, 19: 42587
incorporation in carbon disulfide, 20: 25116
incorporation in ethyl and n-butyl xanthate, 18: 3829
incorporation in elemental sulfur and sulfides, 20: 12919
incorporation in heparin, 20: 6717 (BNL-9755)
incorporation in hypotaurine, enzymatic, 20: 23199
incorporation in isothiocyanates, 20: 45769
incorporation in methionine, method for, 19: 24597
incorporation in maleimides, method for, 20: 10937(T) (NP-tr-1323)
incorporation in methionine, 20: 20786
incorporation in Malathion, 20: 38931
incorporation in organic sulfur compounds, 18: 25460
incorporation in organic compounds by recoil techniques, 19: 32240
incorporation in organic compounds by recoil reactions, 20: 25114
incorporation in potassium thiocyanates and sodium thiosulfates, 18: 8417
incorporation in products of neutron reactions (n,p) with ethyl and methyl chloride and methane, 19: 13495
incorporation in pyridine complexes, 19: 32271
incorporation in polymers formed from reactions of carbon tetrachloride and cyclohexane, 20: 20784
incorporation in sodium *N*-methyldithiocarbamate, 18: 25461
incorporation in sulfuric acid aerosols, 19: 20027
incorporation in sodium sulfate, sinigrin uptake of, 19: 31670(R) (NIRS-3(p.19-56))
incorporation in sulfuric acid, 20: 8824 (CONF-727, pp 174-8)
incorporation in sulfur trichloride, 20: 25116
incorporation in steroids, 20: 38547(R) (NYO-918-15)
incorporation in tuberculin, 17: 30009
incorporation in *tris*(1-aziridinyl)phosphine sulfide by recoil reactions, 20: 5586
incorporation in 4-methyl-5-thiazoleethanol, 20: 20785
incorporation into inorganic compounds, review, 17: 8205
incorporation into organic sulfur compounds by isotopic exchange, 19: 17944(T) (CEA-tr-R-1797)
incorporation into mustard gas, 19: 32188 (UJV-1118/64)
incorporation with tritium in *sec*-butyl phenyl disulfide, method for, 20: 35575
labeled compounds, list of, 16: 28662 (STI/PUB/45)
labeled mercamine, uptake and activity of, in central nervous system, 18: 17663
magnetic moments and M1 transition probabilities in $2s_{1/2}$ $1d_{1/2}$ shell, (T), 19: 47641
metabolism in mice of mercapto group-incorporated, 18: 43312
metabolism in rat bone, effects of nerve supply on, 20: 5370
metabolism of, by irradiated growing bones, 17: 17894
metabolism of sodium sulfate-incorporated, in rat aorta, 20: 8590

neutron reactions (n,p), use in evaluation of neutron dose distribution in human phantom, 18: 37029 (A/CONF.28/P/812)
nuclear transformations in neutron irradiated alkali chlorides, chemical effects of, 19: 13504
preparation, 18: 13762
preparation as sulfide, method development for, 18: 27812(R) (ORNL-TM-415)
preparation by irradiating hexachlorobenzene in a reactor, 17: 34041
preparation for medical uses, 17: 7713
preparation for tracer uses, 19: 9572
preparation of carrier-free, 17: 28271
preparation of carrier-free, as sulfuric acid, 19: 36529
preparation of sources for use in removal of electrostatic charges from silk, 16: 13477(T) (AEC-tr-4492(p.337))
preparation, properties, and uses, 16: 7144
production at PRR, methods for, 20: 12545(R) (PAEC(A)AR651)
production by bombardment of ferric chloride, 16: 24082
production by (n,p) reactions on chlorine-35, in-pile, 17: 29942
production by neutron irradiation of potassium chloride, 17: 24437
production by neutron reactions (n,p), 17: 30165
production by neutron reactions (n,p) with chlorine-35, 19: 2701
production by reaction chlorine-35 (n,p) in TRIGA Mark II, 17: 35894
production in atmosphere, 16: 16585
production in Canada, 18: 14338
production in carbon tetrachloride by neutron reactions (n,p) with chlorine-35, 18: 22117(R) (RRL-133)
production in irradiated cysteic acid, cysteine, and cystine, 20: 16540
production in neutron reaction (n,γ) in gaseous sulfur compounds, chemical effects from, 17: 23386 (UCRL-10360(Rev.))
production in neutron reactions with chlorine-35 in various chlorides, 19: 20004
production in organic chlorine compounds by reaction of thermal neutrons with chlorine-35, 20: 25114
production in Spain, 19: 20432(T) (ORNL-tr-295)
production of carrier-free, 16: 22212
production of carrier-free, from pile-irradiated potassium chloride, 17: 14251
production of carrier-free, 20: 43398
production of, facility for, 18: 38550 (A/CONF.28/P/816)
production of, review of methods for, 18: 16398 (JAERI-4027)
production using fast neutron reactions, 20: 46102(R) (ORNL-4013)
production using Rossendorf Reactor in East Germany, 19: 20436
radiation effects on distribution of, in blood, kidneys, and liver in mice, 17: 33649
radiation effects on uptake by rat corneas, beta, 17: 38836
radiation effects on metabolism of, in chicks, 17: 38742(R) (NYO-10602)
radiation effects on human cells, 18: 5193
radiation effects on distribution of, in blood, kidneys, and liver in mice, 18: 9900
radiation effects on leukocytes, method for determining damage from, 18: 13496
radiation effects on chick metabolism of, gamma, 18: 17552
radiation effects on incorporation in sulfates of guinea pig eyes, strontium-90, 18: 38810
radiation effects on uptake by mouse knee joints of, x, 19: 2090
radiation effects on uptake by rat aorta, 19: 15028
radiation effects on uptake in methionine by rabbit marrow and spleen proteins, 19: 19604
radiation effects on uptake of, by soft tissues in mouse hind limb, 19: 21887
radiation effects on metabolism of, in rat bones, x, 20: 5370
radiation effects from, on physicochemical properties of solid systems, 20: 10936(T) (CEA-tr-A-1855)
radiation effects from, on sorption of aqueous organic dye solutions by barium sulfate, 20: 10936(T) (CEA-tr-A-1855)
radiation effects on uptake of sodium sulfate-incorporated, by rat liver, 20: 10542
radiation effects on metabolism of sodium sulfate-incorporated, in rat liver, x, 20: 20410
radiation effects on metabolism of taurine-incorporated, in rat liver, x, 20: 32944
radiation effects on uptake of vaccine-incorporated, by microsomes and mitochondria in rat spleen, x, 20: 42907
radiochemistry, 16: 20305(R) (UCRL-10023)
radioinduced mutations in rice, 20: 40640
reactions and valence state of recoil, in neutron-irradiated ammonium chloride, 20: 35545
reactions of recoil atoms of, with cyclic hydrocarbons, 16: 23550
reactions with gaseous sulfur compounds, 16: 28982 (UCRL-10360)
recoil chemistry in neutron-irradiated alkali metal chlorides, evidence for neutral species in, 19: 9166 (COO-32-106)
recoil chemistry in neutron reactions (n,γ) in cysteic acid, cysteine, and cystine, 20: 14584(R) (TID-22444)
recoil reactions with carbon dioxide and monoxide, labeled carbonyl sulfide yield in, 18: 12199
recoil reactions with biologically active compounds, yields of labeled products in, 19: 40619
recoil reactions with organic compounds, formation of polymeric products in, 19: 40628
removal from fabrics for protective clothing, 20: 9203
removal from glass, PVC films, and steel using detergents, 19: 4422
separation and measurement in air filters and rain in Heidelberg, 19: 18225
separation and purification for medical use, 18: 37581 (A/CONF.28/P/457)
separation from barium sulfate by ion exchange, 17: 1242(R) (TID-17178)
separation from chlorine-36 and phosphorus-32 by ion exchange, 16: 14822
separation from irradiated materials, 16: 4191
separation from irradiated potassium chloride by chromatography for preparation of labeled sulfuric acid, 18: 13929
separation from irradiated potassium chloride by solvent extraction using trichloroethylene, 19: 524
separation from neutron-irradiated potassium chloride by ion exchange and precipitation, 17: 40884
separation from organic reactor coolants, by adsorption, 17: 33280
separation from organic moderator-coolants, 19: 13520(P)
separation from organic reactor coolants, development of catalysts for, 17: 22795(R) (IDO-11221)
separation from steel surfaces by electrolysis, 18: 35946
separation method for, 20: 46102(R) (ORNL-4013)
separation of carrier-free, from irradiated potassium chloride, 16: 8756 (CNI-101)
separation of carrier-free, from neutron-irradiated potassium chloride, 16: 14823
separation of carrier-free, from neutron-irradiated potassium chloride by ion exchange, 18: 37100
sorption by hydrated barite, barium sulfate, aluminum, aluminum–zinc alloy, and iron oxides, 19: 9253 (UJV-1115/64)
sorption by PA-2 aluminum alloys and stainless steel, effects of pH on, 20: 25073
sorption from aqueous solutions by ionic precipitates or hydrated oxides, 19: 26478
sorption from aqueous solution on barium carbonate, ionic, 19: 36272
sorption from aqueous solutions on barites and barium sulfate, isotopic exchange in, 19: 36273
sorption from aqueous solutions on aluminum and iron oxides and aluminum-zinc oxides, 19: 36274
sorption of, by marine silts, 17: 37021(T) (JPRS-20795(p.1-6))
sorption of ionic, on aluminum surfaces, 19: 28427
sorption of ionic, by aluminum surfaces, 20: 7003 (INR-634/V/C)
stability and storage of organic compounds labeled with, review on, 20: 35574
standardization of pure, extension of efficiency tracing method for, 18: 37227
standards of, for diagnostic and therapeutic use, 17: 21744
toxic effects in mice and rats, 19: 29855(T) (JPRS-29411(p.1-7))
toxic effects on blood of mice and rats, 19: 17473
toxic effects on chick embryos, comparison of selenium and tellurium with, 19: 14999
tracer use in gross atmospheric circulation, 19: 16247
tracer use in ground-water flow measurements, 16: 17897
tracer use in polypeptide and protein pharmacodynamics, 18: 38762
tracer uses for atmospheric-circulation studies, 17: 18302
tracer uses in albumin and globulin studies in irradiated rabbits, 18: 37020
tracer uses in biology, 18: 36915
tracer uses in studying intestinal transport of methionine, 16: 14445
uptake and distribution in barley roots, radioautographic technique for study of, 16: 28686
uptake and distribution of, in rat tissues, effects of methionine sulfoximine and x radiation on, 17: 21437
uptake and excretion of, by dragonfly larvae, 17: 17738(T) (JPRS-18548 (Excerpt))
uptake and incorporation of, by radish seedlings, 17: 37048
uptake and retention of, by bones and tissues in chicks, effects of diet and vitamin B_{12} on, 17: 21446
uptake and retention by plant roots, 16: 1458
uptake by algae from water, 17: 28661
uptake by amino acids, tracer study of, 18: 13420
uptake by aquatic insects, coefficient of accumulation for, 19: 25857
uptake by barley roots, liquid scintillation determination of, 18: 41056
uptake by bones, effects of radioprotective compounds on, 20: 18479
uptake by irradiated rabbit cartilage, 16: 32769

uptake by liver and spleen proteins, 18: 31303
uptake by *Melanogrammus aeglefinus* developing spawn, 19: 17483
uptake by mice of AET labeled with, 18: 19774
uptake by rat liver, histologic fixation and release of, 19: 45800
uptake by rat teeth, tracer study to determine rat incisor dentin response to fluoride and strontium, 18: 29202
uptake by rice plants, effects of stage of growth on, 18: 41020
uptake by vibrissal hairs of mice, origin of, 19: 19479
uptake in bones of rats, 18: 13410(R) (ANL-6769(p.142-9))
uptake of, by bones in chicks, effects of vitamin B_{12} on, 17: 19800
uptake of, by uterine structures in guinea pigs, effects of estrogens on, 17: 27034
uptake of 2,3-dimercapto-1-propanol- incorporated, by acid mucopolysaccharides in rabbit cornea, 18: 38995
use as beta source for radiotherapy, 18: 41287
use as beta source for therapy, 20: 8799
use as film on aluminum oxide for radiotherapy, 19: 2884
use as tracer in diffusion studies for copper and copper alloys during annealing, 18: 37686(T) (AEC-tr-6398(p.322-7))
use as tracer in pulp and paper research, 17: 32328
use for body fluid measurements, 19: 43898
use for determination of thickness and uniformity of gelatin coatings on textile yarn, 19: 9561
use for study of composition of anodic film formation on niobium and tantalum, 17: 34335
use in blood volume measurements, 19: 17740
use in chondrosarcoma therapy, 19: 36139
use in hematology and radiodiagnosis, 18: 17695
use in labeling antibodies, technique for, 18: 9807
use in macroradiographic and radiometric analysis of steel, 19: 22833
use in placental permeability studies, review of, 18: 1345
use in protein sedimentation determinations, 18: 38756
use in rubber industry, 16: 15059
use in study of diffusion in selenium, 18: 37688(T) (AEC-tr-6398 (p.334-7))
use in testing autoradiographic images, 20: 22834
use in thiamine chloride determination by inverse isotope dilution, 20: 7040
use of methylene blue-incorporated, therapeutic, 19: 13134 (NP-14426)
use to determine optimum amount of material carried by viscose fibers, 19: 39063
uses of massive doses of, contamination control during therapeutic, 18: 37036
yields from chlorine-35 (n,p) reactions in chlorobenzene, 16: 23719(T) (AEC-tr-5093)
yields from thermal neutron reactions with chlorine-35 in sodium chloride, 20: 25134
yields in proton spallation of copper at 24 Bev, 16: 24859

SULFUR ISOTOPES S-36

content in meteorites, variations in, (E), 19: 38847
conversion bremsstrahlung spectra from chlorine-36 decay, (E), 20: 13758 (CONF-233(Vol.4), pp 609-13)
energy levels, (E), 19: 16956
energy levels from chlorine-36 decay, (E), 20: 22029
energy levels of, shell model calculations for, 18: 32782
energy levels of, shell model calculations for, 18: 32783
exchange between carbon disulfide and a xanthogenate, 19: 18045(P)
production in iron meteorites by cosmic radiation, 19: 47195
proton reactions (p,γ) at 1.4 to 2.1 Mev, excitation function for, (E), 20: 12005(T)
proton reactions (p,γ) at 0.80 to 1.90 Mev, chlorine-37 energy levels from, (E), 20: 38185

SULFUR ISOTOPES S-37

core deformability and electric quadrupole moments, 16: 7026
decay, 18: 13636(R) (ORNL-3537(p.71-105))
gamma decay, 18: 32277(R) (PR-P-61)
gamma dose constants for, 20: 46617
gamma spectra, 18: 1050
preparation and properties of, for use as neutron sources, 18: 16379

SULFUR ISOTOPES S-38

activity in irradiated chlorine compounds, chemical fate, 16: 11757
content in rain samples, 20: 8980(R) (BNWL-36, pp 3.1-122)
content in rain water, study by coincidence gamma spectra, 18: 43372 (HW-SA-3680)
contents of cosmic-ray-induced, in rain water, 19: 13626 (HW-SA-3742)
determination of cosmic-ray-produced, in rain water by gamma spectrometry, 19: 17829
yields in proton spallation of copper at 24 Bev, 16: 24859

SULFUR MINERALS

genesis of, determination by abundance of stable isotopes, 20: 37011
geochronology of hypogene sulfide deposits, 20: 18924(R) (NYO-1669-11)
isotope ratio variations in preparation and decomposition of melnikovite, 18: 29870
sulfur-32/-34 ratio in, of Bingham district Utah, 20: 45920

SULFUR NITRIDE CHLORIDES

preparation and reactions of S_4N_3Cl, 19: 43997(R) (UCRL-11889)

SULFUR NITRIDES

heat of formation of S_4N_4, 18: 6792(R) (TID-19898)
preparation by ammonia–sulfur chloride reaction, 18: 6797 (UCRL-11081)
reactions of S_4N_4, with dry hydrogen chloride, 18: 31431(R) (UCRL-11317(p.1-14))
spectra of nitrogen-15 in cationic thiotrithiazyl, NMR, 20: 31218(R) (UCRL-16658, pp 1-9)
spectra of radicals produced by reduction of S_4N_4, electron spin resonance, 19: 43997(R) (UCRL-11889)
spectrum of NS, new system in vibrational, 17: 14998
spectrum of NS, vibrational, 17: 14997

SULFUR OXIDES

see also Sulfur Dioxides
see also Sulfur Trioxides
dissociation energy of SO, 18: 19939 (WADD-TR-60-782(Pt.XXI))
effects as impurity on performance of carbon dioxide-filled proportional detectors, 18: 7068
effects on hydrogen yields in propane radiolysis, 19: 46396
effects on quenching of energy spectra in determination of carbon-14, sulfur-35, and tritium, 20: 36771
efficiency for clearing magnetic-field spark chambers, 17: 3311 (PPAD-454E)
helium ion energy-range relations in, 18: 14726 (UCRL-10647)
measurement in man, tracer method, 19: 43898
performance as coolant for gas-cooled fast reactors, 18: 2[illegible]973
reactions of, mass spectrometric study of, 18: 31418 (CEA-R-2398)
spectra and transitions of, rotational, 18: 13738
spectra of gaseous SO radicals, electron paramagnetic resonance, 18: 3746

SULFUR SYSTEMS

Al–Ce–S, thermoelectric properties at high temperatures, 17: 29854(R) (MND-2584-4)
As–Se–S, viscosity of, effects of sintering on, 20: 35886 (IS-T-80)
As–S–Se, sintering mechanism of, 20: 41064(R) (IS-1500(Sect.E))
Ba–rare earths–S, crystal structure, 19: 13298
benzene–S, radiolysis of, yields in, 18: 5366
Bi–Ag–S, crystal structure powder diffraction patterns of phases in, 19: 17795
Bi–Li–S, crystal structure powder diffraction patterns of phases in, 19: 17795
Bi–S, densities of liquid solutions of, 18: 6791 (SRIA-105)
Cd–Cu–S–Zn, radiation and temperature effects on luminescence of, 17: 37642(R) (ARF-1214-TR-3)
C–Mn–P–Si–S, crack growth testing of, 20: 28694(R) (GEAP-4964)
Co–Mo–S, catalytic effects on deuterium labeling of hydrocarbons, 18: 13802
CS_2–S–toluene, radiolysis of, formation of sulfur compounds in, 18: 25547
Cu–Fe–S–Sn, crystal structure powder diffraction patterns of phases in, 19: 17795
cyclohexane–S–toluene, radiolysis of, formation of sulfur compounds in, 18: 25547
Fe–S, sulfur evaporation from, at 1580 to 1680°C, 17: 37519(T) (AEC-tr-5983)
HF–S, radiolysis yields in, 19: 46324(R) (AGN-8132)
In–S, phase studies, 18: 8336 (UCRL-10857)
O–S–U, phase studies, 16: 30370 (TID-12048)
O–S–U, phase studies, 20: 42579(R) (ANL-7245, pp 29-47)
paraffin–S, radiation effects on polarization of, 18: 33622
P–S, analysis for phosphorus and sulfur, activation, 20: 18569 (NP-15887)
P–S, performance for absolute flux measurements on fast neutrons, 17: 30872
Pu–S, structure, 17: 3536
rare earths–Sr–S, crystal structure, 19: 13298
Se–S–Te–U, thermoelectric properties, 17: 14856 (WCAP-1866)
S–Te–U, preparation and thermoelectric properties, 17: 24058(R) (WCAP-1820)
S–toluene, radiolysis of, formation of sulfur compounds in, 18: 25547
S–U, phase studies, 20: 11224
S–U, thermochemistry of, research program on, 18: 1485(R) (ANL-6687(p.153-66))
S–UO_2SO_4, reactions in aqueous solutions of, 19: 7494
S–Zr, stability and thermodynamics of, 18: 26065

SULFUR TRIOXIDES

effects on densification during sintering of beryllium oxide, 19: 24963
oxygen-18 exchange with vanadium pentoxide, 19: 7439
photolysis and thermal decomposition to convert solar energy into power sources, 16: 7322 (ARL-60)
solubility in uranium(VI) oxide–water systems at 300°C, 16: 11636

vapor pressure of liquid, up to critical point, 18: 3722 (UCRL-7167)
vapor pressure up to critical point, 18: 41374 (UCRL-7167(Rev.I))
yields in gamma radiolysis of liquid sulfur dioxide, 18: 17896
$CuO–NiO–SO_3–UO_3–D_2O$, critical phenomena and liquid-liquid immiscibility at 260 to 410°C, 17: 33922
$CuO–NiO–SO_3–UO_3–H_2O$, phase studies, 19: 23163(R) (ORNL-3650 (p.111-86))
$CuO–NiO–SO_3–UO_3$–water-d_2, liquid-liquid immiscibility and phase studies of, 17: 25067(R) (ORNL-3417(p.77-98))
$CuO–SO_3–D_2O$, liquid immiscibility and critical phenomena at 320 to 430°C, 17: 8067
$CuO–SO_3–UO_3–D_2O$, critical phenomena and liquid-liquid immiscibility at 260 to 410°C, 17: 33922
$CuO–SO_3–UO_3$–water-d_2, liquid-liquid immiscibility and phase studies of, 17: 25067(R) (ORNL-3417(p.77-98))
$K_2SO_4–SO_3$, effects of sulfur-35 exchange on reactions in, 20: 10936(T) (CEA-tr-A-1855)
$Li_2O–SO_3–UO_3–D_2O$, critical phenomena and liquid-liquid immiscibility at 300 to 410°C in, 18: 12085
$Li_2O–SO_3–UO_3–D_2O$, critical phenomena and liquid-liquid immiscibility in, 18: 22014(R) (ORNL-3591(p.84-101))
$Li_2SO_4–SO_3–D_2O$, critical phenomena, 17: 25207
$Na_2SO_4–SO_3$, effects of sulfur-35 on exchange reactions in, 20: 10936(T) (CEA-tr-A-1855)
$Nb_2O_5–SO_3–H_2O$, preparation and solubility constants, 17: 28915
$NiO–SO_3–UO_3–D_2O$, critical phenomena and liquid-liquid immiscibility at 260 to 410°C, 17: 33922
$NiO–SO_3–UO_3–H_2O$, formation of $NiO·3UO_3$ at 300°C in, 18: 12084
$NiO–SO_3–UO_3$–water-d_2, liquid-liquid immiscibility and phase studies of, 17: 25067(R) (ORNL-3417(p.77-98))
$NO–SO_3–UO_3–H_2O$, uranyl sulfate liquid–liquid immiscibility in, above 300°C, 16: 10022
$SO_3–UO_3–D_2O$, liquid immiscibility and critical phenomena at 280 to 410°C, 17: 8067
$SO_3–UO_3–H_2O$, distribution of copper and nickel oxides between liquid phases in labeled and unlabeled, 16: 18896
$SO_3–UO_3–H_2O$, equilibrium compositions of heavy- and light-liquid phases in labeled and unlabeled, 16: 18895
$SO_3–UO_3–H_2O$, liquid immiscibility and critical phenomena at 298 to 380°C, 17: 8067
$SO_3–UO_3–H_2O$, pressure effects on liquid phase formation in, 17: 33923
$SO_3–UO_3$–water, fluid equilibria in, pressure effects on, 17: 25067(R) (ORNL-3417(p.77-98))

SULFURIC ACID
see also Peroxymonosulfuric Acid
see also Phenazine Dyes
activity of sulfur-35-labeled, liquid scintillation counting of, using glass fiber paper, 19: 36527
americium absorption spectra in, properties of, 18: 31460
analysis for acid assay, chlorides, iron, and residue, 16: 11518 (PG-Report-289)
analysis for deuterium by decomposition and gas chromatography, 20: 35441
analysis of aqueous, spectrophotometric, 18: 1614(R) (ORNL-3488 (p.65-90))
analytical use in separation of molybdenum and rhenium, 16: 14673
beryllium dissolution potentials in, 19: 11071
complexes with iron(III) ions, spectra, 16: 22164 (PAN-296/XVII)
corrosive effects on copper, effects of group VIII chlorides, 16: 484(R) (AD-256309)
corrosive effects on stainless steel, 16: 488(T) (AEC-tr-4683)
corrosive effects with radiation on metals, 16: 17976(R) (EURAEC-94)
corrosive effects on titanium alloys, inhibitors for, 16: 17989
corrosive effects on stainless steels under stress, mechanism of, 16: 30733 (ARF-2181-12)
corrosive effects on stainless steel (304-L) and titanium (A-55), 16: 30735 (HW-73378)
corrosive effects on titanium, zirconium, and their alloys, 16: 33440
corrosive effects on stainless steel, 17: 16594(T,R) (EURAEC-29)
corrosive effects of dilute, on Zircaloy-2, 17: 25066(R) (ORNL-3417 (p.69-76))
corrosive effects on chromium–iron and chromium–nickel stainless steel, potentiokinetic studies on, 17: 25729(T) (EURAEC-678)
corrosive effects on stainless steel, review on, 17: 25730(T) (EURAEC-679)
corrosive effects on surfaces of polystyrene, 17: 29983
corrosive effects of boiling, on stainless steel, 17: 39494
corrosive effects of aqueous solutions of, on uranium-bearing steels, 18: 2180 (NP-13261(p.207-34))
corrosive effects on aluminum and titanium, 18: 1614(R) (ORNL-3488(p.65-90))
corrosive effects on niobium and tantalum, 18: 10484
corrosive effects of solutions of, on stainless steels, 18: 12581 (HW-78186)
corrosive effects on niobium and vanadium, effects of acidity and current density on anodic, 18: 25929
corrosive effects on tantalum, tracer studies of, 19: 16021
corrosive effects on electrolytic cell materials, 19: 20484 (TID-19978 (Vol.I))
corrosive effects on carbon steel, protective effects of zirconium content against, 19: 22903
corrosive effects on molybdenum and vanadium, stress-, 20: 2254 (BM-RI-6680)
corrosive effects on stainless steel, effects of molybdenum and uranium on, 20: 4325 (TB-58)
corrosive effects on molybdenum, tungsten, and vanadium at 35, 60, and 100°C, 20: 11230 (BM-RI-6715)
corrosive effects on vanadium-base alloys at low temperatures, 20: 11230 (BM-RI-6715)
corrosive effects on types 416 and 430F stainless steels, effects of uranium on, 20: 14983 (NP-15875)
corrosive effects on niobium-base alloys, effects of alloy composition on, 20: 14997
corrosive effects of aqueous, on zirconium at high temperatures, 20: 23602(R) (ORNL-3913, pp 53-73)
corrosive effects on molybdenum-base alloys at high temperatures, 20: 46158
cyclopropane solvolysis in deuterium substituted, 18: 12127
determination in uranium solutions by potentiometric titration, 18: 15966
determination of, by backscattering of beta particles, 20: 36770
deuterium ESR spectra in frozen, shifts in, (E), 20: 33288
dissociation constant of deuterated, at 25 to 225°C, 17: 28868
dissociation constant of aqueous, at 25 to 35°C, 19: 30151(R) (ORNL-3789(p.139-63))
effects as leaching agent on recovery of thorium from thorium ores, 20: 41033 (INR-678/IV/C)
effects of concentration of, on yield of hydrogen peroxide in radiolysis of ethyl ether, 17: 207
effects of concentration of, on niobium, titanium, and tantalum hydrolysis, 17: 30461
effects of concentration of, on uranium peroxide solubility, 18: 16012
effects of concentration of, on isotopic exchange of hydrogen in isoxazole, 18: 31554
effects on cerium sulfate complexes with chloride ion, 17: 25204
effects on corrosion of rhenium at 25 and 100°C, 20: 21275
effects on electron spin resonance of boronated graphite, (E), 20: 44008
effects on ESR spectra of polycrystalline graphite, 20: 23785
effects on film growth on zirconium at 174 to 284°C, 20: 25501
effects on formaldehyde and hydrogen peroxide yields in gamma radiolysis of aerated methanol, 20: 14579(R) (NYO-2383-15)
effects on gamma radiolysis of 2-propanol, 20: 18766
effects on hydrogen yields in radiolysis of liquid ethanol, 18: 25589
effects on hydrogen reduction of plutonium(IV) to plutonium(III), 20: 26882
effects on hydrolytic properties of protactinium, 19: 15505
effects on hydroxylamine during radiolysis at pH 2 to 7, 16: 1811(T) (AEC-tr-4564)
effects on ion exchange properties of titanium and zirconium salts, 18: 33535
effects on ion exchange behavior of hafnium, molybdenum, niobium, tantalum, titanium, and zirconium, 20: 7039
effects on mutarotations of β-D-fructose and α-D-glucose, 20: 36577
effects on nitrogen-15 exchange between nitric acid and nitric oxide, 20: 9363(R) (NYO-755-2, Paper 3)
effects on nitrogen-15 concentration by nitric acid–nitric oxide exchange, 20: 31639(R) (NYO-755-1, pp 77-129)
effects on nitrogen-15 exchange between nitric acid and nitric oxide, 18: 2132(R) (TID-19592(Sect.IV))
effects on oxidation-reduction reactions of americium, 16: 3350(T) (AEC-tr-4497(p.411-28))
effects on peptization of solid thorium oxide, mechanism of, 20: 16419(T) (UCRL-Trans-1301(L))
effects on phosphorus-31 chemical shifts in triphenylphosphine oxide, 19: 2296
effects on radiolysis of methanol, 19: 13425(R) (NYO-2383-12)
effects on radiolysis of 2-propanol, 19: 13423 (KFK-243)
effects on radiolysis yields in deaerated methanol, 20: 14579(R) (NYO-2383-15)
effects on reactions between hydrogen peroxide and plutonium, 18: 25390
effects on self-diffusion of water at 23°C, 19: 32159
effects on separation of uranium from irradiated fuels, 17: 16145 (ORNL-3312)
effects on solubility of calcium sulfate in water, 19: 30156 (ORNL-tr-649)
effects on solvent extraction of hafnium and zirconium from potassium fluoride solutions using trioctylamine, 17: 14403

effects on solvent extraction of niobium, tantalum, and titanium by organic compounds, 18: 347
effects on solvent properties of hexone for iron, niobium, tantalum, tin, and titanium, 18: 39395
effects on solvent extraction of niobium and tantalum by TBP, 18: 39396
effects on solvent properties of butyl phosphates for hafnium, tantalum, and tungsten, 19: 24446
effects on spectra of uranium(III), 20: 18653
effects on uv photolysis of aqueous methanol solutions, 18: 43634
electric conductivity of aqueous, at 0 to 800°C and pressures to 4000 bars, 19: 30151(R) (ORNL-3789(p.139-63))
electrolysis of, luminescence of rare earth oxides during, 20: 45679
electron spin resonance spectra of, 20: 42433
europium absorption spectra in, properties of, 18: 31460
glass transformation temperature for, deuterium isotope effects on, 17: 33774
hydrogen ESR spectra in frozen, shifts in, (E), 20: 33288
labeling with sulfur-35 and aerosol preparation, 19: 20027
leaching nuclear test debris in copper ores, 20: 14662(R) (ORNL-TM-1394)
oxidation of cerium(IV) in, chronopotentiometry, 16: 2970
oxidation of niobium in, kinetics of, 17: 25246
oxidation of zirconium in, anodic current strength in, 17: 32528
oxidation potential of cerous-ceric electrode in, 18: 41422
oxidation-reduction potential of uranium(IV)–uranyl system in, effects of temperature on, 16: 16364
oxidation-reduction reactions in boiling, kinetics of, 17: 2707
oxidizing effects on molybdenum, passivation mechanisms in, 20: 37184
positron and positronium decay in aqueous solutions of, 19: 4899 (NRS-21)
preparation of carrier-free sulfur-35 labeled-, 18: 12186
preparation of carrier-free sulfur-35-labeled, from neutron-irradiated potassium chloride, 20: 36920
preparation of deuterated, method for, 18: 5247
preparation of sulfur-35-labeled, 18: 13929
preparation of sulfur-35-labeled, 19: 36529
processing and disposal of glass melter condensates containing, methods for, 20: 18159 (BNWL-SA-514)
production of, in processing of uranium ores, 17: 23428
production of, production of nitrogen-15 by NITROX method during, 20: 35569 (INR-674/XVI/J)
properties as eluant for inorganic ion chromatography on zirconium phosphate paper, 16: 23650
properties for use in elution of uranium from cation exchange resins, 19: 22410
proton paramagnetic resonance in aqueous solutions, 16: 20464
radiation chemistry of aqueous solutions, 16: 33048
radiation chemistry of aqueous solutions, 16: 33049
radiation chemistry of systems containing, 17: 10509(R) (ORNL-3320 (p.30-46))
radiation chemistry of glasses of, at 77 to 150°K, ESR studies of gamma and ultraviolet, 20: 45730
radiation effects on corrosive effects on copper, 18: 8899
radiation effects on, 18: 12165
radiation effects on reactions with uranium monocarbide, in-pile, 19: 7948
radiation effects on frozen aqueous, 19: 7574
radiation effects on human metabolism of indoxyl ester of, 19: 43852
radiation effects on oxidation of, dose rate effects on gamma and x-ray, 20: 412
radiation effects on glasses of, with sodium bromide, chloride, and iodide, 20: 16534
radiation effects on oxygenated aqueous solutions of, polarographic studies of 10-Mev pulsed electron, 20: 33337 (RISO-114)
radiation effects on frozen aqueous solutions of, EPR spectra of gamma, 20: 43290 (COO-1528-7)
radioinduced color center formation in frozen, ESR spectra of trapped holes on optical bleaching of, 19: 22330
radioinduced formation from sulfurous acid, 16: 4202
radioinduced formation from sulfurous acid, 19: 5967
radioinduced formation from sulfurous acid, effects of concentration and temperature on, 19: 5968
radioinduced hydrogen trapping in, electron-nuclear double resonance in x, 18: 41437
radiolysis in ferrous solutions, yields of products of, 20: 18745
radiolysis in light and heavy water, isotope effects in alpha and beta, 16: 10081
radiolysis in presence of ferrous sulfate, 17: 28956
radiolysis of aerated solutions of, hydrogen peroxide yields in alpha, 20: 7126 (LFEN-27)
radiolysis of aqueous solutions by beta particles, molecular and radical yields in, 16: 10080
radiolysis of aqueous solutions of, kinetics and recombination of radicals in, 17: 25336
radiolysis of aqueous solutions of, uv spectra of transients in, 18: 23683
radiolysis of aqueous solutions of, by alpha particles, 18: 23675
radiolysis of aqueous solutions of, kinetics of pulsed electron beam, 18: 25578
radiolysis of aqueous solutions of, 18: 37235
radiolysis of aqueous, products from gamma, 19: 46332(R) (ORNL-3832, pp, 50-65)
radiolysis of aqueous oxygenated solutions of, polarographic studies of 10 Mev-electron, 20: 10909
radiolysis of cerium and iron sulfate solutions of, 14-Mev neutron, 18: 22351
radiolysis of cerium(III) ions in, 19: 11188
radiolysis of deaerated, yields of molecular hydrogen from, 19: 42542
radiolysis of ferrous ammonium sulfate in, use for gamma dosimetry, 17: 36169
radiolysis of glasses of, at 77°K, reduction of metal ions in gamma, 20: 33378
radiolysis of iron-containing solutions of, performance of, for low-level gamma dosimetry, 20: 18793
radiolysis of, rate constants for hydrogen atom reactions with yields in, 18: 5378
radiolysis of solution containing nitrous oxide, G values for, 16: 20514
radiolysis of, effects of cerous ions on, 19: 429(R) (ORNL-3679(p.39-48))
radiolysis of, hydrated electron absorption spectrum and reaction constants for, 18: 23691
radiolysis with gold and platinum electrodes, gamma, 18: 37211(T) (AEC-tr-6398(p.462-71))
reactions with cerium(IV) ions, 18: 5303
reactions with neptunium-237, 17: 193 (LAMS-2756)
reactions with niobium and zirconium in organophosphorus solvents, 19: 13532(R) (ORNL-TM-1020)
reactions with ruthenium oxide, complex formation in, 20: 1853
reactions with sodium hydroxide, heat of, 17: 27323 (UCRL-7325-T)
reactions with uranium dioxide, effects of halides on, 18: 19943
reactions with uranium oxides, effects on composition and structure, 19: 38657
reactions with uranium trioxide, enthalpy of, 19: 24521
reduction of cerium sulfate by, catalytic effects of mercury and silver on, 18: 12086
separation by solvent extraction using trioctylamine, effects of diluent on equilibrium in, 18: 1799(R) (ORNL-3496)
separation by solvent extraction using *N*-alkylanilines, 19: 30139
separation from acid solutions and fission product waste streams by solvent extraction using Alamine-336, 18: 5418 (SRO-56)
separation from aqueous solutions containing metal values, method for, 20: 1578(P)
separation from aqueous solutions by solvent extraction using trioctylamine, 20: 9069
separation from fission products in waste condensates, methods for, 20: 18159 (BNWL-SA-514)
separation from Sulfex decladding wastes by solvent extraction using amines, 17: 3070(R) (ORNL-TM-265)
separation from uranium by solvent extraction using di-(2-ethylhexyl)-phosphoric acid, 17: 6196
separation from wastes by solvent extraction using alkylamines, 19: 23163(R) (ORNL-3650(p.111-86))
separation of group IV and V B elements from, by solvent extraction using *N*-benzoyl-*N*-phenylhydroxylaminates, 18: 5237
separation of niobium and titanium from solutions of, by solvent extraction, 17: 30629
separation of radiobarium and strontium from, 17: 18169 (AERE-AM-92)
separation of scandium from, by solvent extraction using alkyl phosphates, 19: 40689
separation of thorium from, by solvent extraction using *N*-cyclohexyl-*n*-alkylamines, 17: 20112
separation of titanium and zirconium from, by solvent extraction using organic solvents, 20: 4061
separation of uranium from, by ion exchange and solvent extraction, 17: 40747
separation of uranium(VI) from, by solvent extraction using cyclohexyl-alkylamines, 18: 10195
separation of uranium(VI) from, by solvent extraction using benzyl-alkylamines, 18: 10196
separation of uranium from, by anion exchange, 18: 23710
separation of uranium from, by ion exchange, 18: 31680
solubility in bis(2-chloroethyl) ether at 25°C in various electrolytes, 16: 8737
solubility in mixtures of alkyl esters of phosphoric acid and trioctylamine, 20: 5600
solvent effects in plutonium–trioctylamine systems, 16: 11806
solvent extraction from aqueous solutions by trioctylamine–benzene, 19: 32281 (HW-SA-3548)
solvent partition between aqueous and organic phases of aliphatic amines

in kerosene and xylene, 20: 223 (CEA-R-2760)
solvent properties for uranium, 16: 1861(T) (AEC-tr-4874)
solvent properties for thorium, titanium, and zirconium, 16: 1862(T) (AEC-tr-4875)
solvent properties for zirconium sulfates, 16: 5334
solvent properties for thorium oxide–uranium oxide systems (clad), 16: 7286 (BMI-1560)
solvent properties for uranium catalyzed by manganese dioxide, activation energy, 16: 7529
solvent properties for molybdenum, 16: 14667
solvent properties and spectral effects on protactinium(V), 16: 16365
solvent properties for zinc sulfides, 16: 17881(R) (MITS-47)
solvent properties for beryllium, attack and reactions, 16: 17663
solvent properties for plutonium(IV) and (VI), 16: 25480 (PAN-270/V)
solvent properties for thorium dicarbide at room temperature and 80°C, 16: 25365
solvent properties for thorium in monazites, 16: 31670
solvent properties for uranium, effects of oxidizing agents on, 16: 33059
solvent properties of, for beryllium, potentials of, 17: 19989 (AD-299972)
solvent properties for calcium sulfate, 17: 25089(R) (ORNL-3417(p.277-9))
solvent properties of deuterated and nondeuterated, for lithium sulfate at 200 to 350°C, 17: 25207
solvent properties of deuterated, for silver sulfate, 18: 1614(R) (ORNL-3488(p.65-90))
solvent properties for uranium tetrafluoride at 0, 25, and 50°C, 18: 8340
solvent properties in paper chromatographic separation of inorganic cations, 18: 39388
solvent properties in uranium ore leaching, 19: 4259
solvent properties for plutonium, 19: 5783
solvent properties for zirconium, zirconium carbide, and zirconium oxide, 19: 5905
solvent properties for uranium under anodic polarization conditions, 19: 13533 (RPI-2714-4)
solvent properties for aluminum and SAP using mercury catalyst, 19: 26474
solvent properties for thorium monocarbide at room temperature and 100°C, 19: 28247
solvent properties for uranium ore, 19: 28784
solvent properties of aqueous, for calcium sulfate at 25 to 350°C, 19: 30151(R) (ORNL-3789(p.139-63))
solvent properties of aqueous, for magnesium sulfate at 200 to 350°C, 19: 30151(R) (ORNL-3789(p.139-63))
solvent properties of heavy-water deutero-, for magnesium sulfate at 200 to 350°C, 19: 30151(R) (ORNL-3789(p.139-63))
solvent properties for scandium sulfate, 19: 30196
solvent properties for erbium and yttrium phosphates, 20: 1873
solvent properties for magnesium alloys and stainless steel, 20: 4048(R) (NP-15406)
solvent properties for uranium(IV-VI) oxide in presence of ferric ions, 20: 12863
solvent properties for thorium in uranium leach solutions, 20: 16573
solvent properties for organic salts, determination of cation activity coefficients from, 20: 23044(R) (MIT-905-52, pp 74-94)
solvent properties for lanthanum sulfate at 120 to 175°C, 20: 26859
solvent properties for iron meteorites, 20: 43550(R) (NYO-844-67)
solvent properties for protactinium, spectral studies on, 20: 45628(R) (ORNL-3945, pp 209-17)
solvent properties of, for uranium(IV-VI) oxide, 20: 45676
sorption of metals from solutions of, by anion exchange materials, 20: 40822
sorptive effects on ionic cobalt-60 by polystyrene surface, 17: 12239
spectra in tributyl phosphate solutions, infrared, 19: 17905
spectra of protactinium(IV) and protactinium(V) in, 20: 45694
spectra of vapors over deuterated and normal, infrared, 20: 16442
sulfur exchange between sulfur dioxide and, 20: 7112
sulfur-35 isotopic exchange with sulfur dioxide, effects of nitrous oxide on, 19: 26330
thermodynamic functions of undeuterated and deuterated, 17: 12252
tributyl phosphate solubility in, 18: 17719
tritium exchange between isoparaffins and, 19: 11101
uranium(VI) ion exchange equilibria on anion-exchange resins in, 20: 45818
use in destruction of radioactively contaminated celluloses, 20: 5208(P)
use in solvent extraction of uranium tetrachloride by kerosene–TBP system, 19: 38563
use in wet combustion of solid wastes at Risö, Denmark, 20: 26562
use of sulfur-35-labeled for radiochromatographic determinations in bone ash, 20: 8824 (CONF-727, pp 174-8)
uses of deuterium-labeled, as deuterating agent, 20: 38889
vapor partial pressures of aqueous solutions of, calculated, 17: 39028 (UCRL-10886)
vapor pressure behavior of aqueous, at 25°C, 18: 31362(R) (UCRL-11213(p.154-61))
voltammetry of cerium, chromium, manganese, and vanadium in, using pyrolytic graphite electrode, 18: 19967
alcohol–$Fe(NH_4)_2(SO_4)_2$–O–H_2SO_4–H_2O, effects of alcohol structure of radioinduced redox processes in, 18: 13877
benzene–H_2SO_4–trioctylamine, activity and dissociation coefficients for, 20: 45795(R) (ORNL-3945, pp 176-88)
benzene-H_2SO_4–trioctylamine–H_2O, solvent properties for uranyl sulfate, mass action and non-ideality in, 20: 43423 (ORNL-P-2354)
benzene–didecylamine–H_2SO_4–H_2O, solvent properties for uranyl sulfate, mass action and non-ideality in, 20: 43423 (ORNL-P-2354)
benzene–didecylamine–Na_2SO_4–H_2SO_4–H_2O, solvent properties for uranyl sulfate, interface and transferring species in, 20: 43424 (ORNL-P-2359)
butyl phosphate–H_2SO_4, solvent properties, 16: 17766
butyl phosphate–H_2SO_4, solvent properties of, for plutonium(IV) and (VI), 16: 25480 (PAN-270/V)
$CuSO_4$–D_2SO_4–UO_2SO_4–H_2O–D_2O, spectrophotometry of reactor fuel solutions of, 20: 20600
$CuSO_4$–H_2SO_4–UO_2SO_4, corrosive effects on stainless steel, 18: 20477
DEHPA–H_2SO_4–TBP, uranium solvent partition in, 18: 12262
dibutyl ester dibutyl phosphinic acid–H_2SO_4–H_2O, phase equilibria in, 18: 37122
ethanol–$FeSO_4$–O–H_2SO_4–H_2O, radioinduced oxidation of iron in, mechanism of electron and gamma, 19: 13426 (PAN-547/XVII)
ethanol–$FeSO_4$–H_2SO_4, radiolysis of aqueous solutions of, chain processes in gamma, 18: 5395
ethanol–naphthol–H_2SO_4, radiolysis in aqueous solutions, 20: 1920
ethanol–naphthalenesulfonic acid–H_2SO_4, radiolysis in aqueous solutions, 20: 1920
ethanol–H_2SO_4–tetramethyl-p-benzoquinone, radiolysis in aqueous solutions, 20: 1920
fatty acid–$Fe(NH_4)_2(SO_4)_2$–O–sulfuric acid, radioinduced redox processes in, 18: 13878
$Fe(NH_4)_2(SO_4)_2$–$CuCl_2$–H_2SO_4–H_2O, properties as gamma dosimeter, 19: 44372 (AFCRL-65-470)
$Fe(NH_4)_2(SO_4)_2$–isobutyl alcohol–O–H_2SO_4–H_2O, radioinduced oxidation and reduction of iron in, 18: 13875
$Fe_2(SO_4)_3$–H_2SO_4, corrosive effects on nickel–chromium–molybdenum alloys at 800 to 2375°F, 20: 21277
$FeSO_4$–H_2SO_4–H_2O, fast neutron dosimetry with, 18: 10372 (CONF-187-55)
Fe–2-methyl-1-propanol–O–H_2SO_4–H_2O, radioinduced oxidation and reduction reactions of iron ions in, 20: 388
HF–H_2SO_4, solvent properties for zirconium, 18: 37120
HF–H_2SO_4, solvent properties for zirconium, kinetics of, 19: 36341 (ORNL-P-862)
HF–H_2SO_4, solvent properties for zirconium, 20: 4055
$HgSO_4$–H_2SO_4, solvent properties for aluminum tubes, 19: 40655 (RT/CHI(65)-1)
HNO_3–H_2SO_4, catalytic effects on nitration of bis(trifluoromethyl)benzene, 18: 31362(R) (UCRL-11213(p.154-61))
HNO_3–H_2SO_4, reactions with bis(trifluoromethyl)benzene, 18: 9784 (UCRL-11069)
HNO_3–H_2SO_4, solvent properties for stainless steel, 19: 11301(P)
HNO_3–H_2SO_4–tridodecylamine, solvent properties for neptunium and plutonium, (E), 19: 15665 (CEA-R-2607)
HNO_3–H_2SO_4–UO_2, oxidation-reduction potentials in, 19: 19912
H_3PO_4–H_2SO_4, voltammetry of cerium, chromium, manganese, and vanadium in, 18: 19967
H_2SO_4–H_2O, pressure effects on temperature of liquid-liquid immiscibility in, 17: 33923
H_2SO_4–H_2O, radiolysis of oxygenated solutions of, 20: 14614
H_2SO_4–TBP, solvent properties for various elements, 20: 27037 (JAERI-1106)
H_2SO_4–tributyl phosphate, dielectric constants, 19: 7424
H_2SO_4–trioctylamine–H_2O, activity coefficient for equilibria in, 20: 45795(R) (ORNL-3945, pp 176-88)
H_2SO_4–$UO_2C_2O_4 \cdot 3H_2O$, radiolysis, 18: 37211(T) (AEC-tr-6398(p.462-71))
H_2SO_4–UO_2SO_4, density of, at 20 to 50°C, 16: 20435
$K_2Cr_2O_7$–H_2SO_4, properties for use in ultrasonic cleaning of cobalt-60 from Duralumin and steel-3, 20: 16767
$KMnO_4$–H_2SO_4, properties for use in ultrasonic cleaning of cobalt-60 from Duralumin and steel-3, 20: 16767
K_2SO_4–H_2SO_4, solvent properties for silver sulfate, 17: 2989
Li_2SO_4–H_2SO_4–water, critical phenomena and solubilities of, 17: 25067(R) (ORNL-3417(p.77-98))
Li_2SO_4–H_2SO_4–water-d_2, critical phenomena and solubilities of, 17: 25067(R) (ORNL-3417(p.77-98))
NaBr–H_2SO_4, radioinduced absorption spectra in, at 77°K, 20: 16534
NaCl–H_2SO_4, radioinduced absorption spectra in, at 77°K, 20: 16534
NaI–H_2SO_4, radioinduced absorption spectra in, at 77°K, 20: 16534
$NaNO_2$–H_2SO_4, in oxidation of iodides to molecular iodine, 20: 39103(R)

(BNWL-235-3, pp 51-69)
naphthalene–H_2SO_4, radiolysis in alcoholic, aqueous, and hydrocarbon solutions, 20: 1920
NH_4HSO_4–H_2SO_4, sulfur exchange between sulfur dioxide and, 20: 7112
$(NH_4)_2SO_4$–H_2SO_4, analysis for americium by controlled-potential coulometry, 20: 38854
oxalic acid–H_2SO_4, use as solvent in ion exchange processes, 20: 7039
sulfamic acid–sulfuric acid, properties as decontaminating solution for aluminum or zirconium, 20: 41214(P)

SULFUROUS ACID
effects on conductivity of hydrofluoric acid solutions, 16: 8738
radiation oxidation to sulfuric acid, 16: 4202
radioinduced oxidation to sulfuric acid, 19: 5967
radioinduced oxidation to sulfuric acid, effects of concentration and temperature on, 19: 5968
reactions with sulfur dioxide, sulfur isotope fractionation in ionic, 18: 10442

SULFURYL CHLORIDE
chlorine-36 exchange between antimony chloride and, 19: 24527
chlorine-36 exchange with antimony pentachloride, 20: 3965
chlorine-36 exchange between thionyl chloride and, 19: 24527
reactions with irradiated polypropene in carbon tetrachloride, 18: 25490(T) (AEC-tr-6372(p.197-205))
sulfur-35 exchange with thionyl chloride, 20: 3965
sulfur-35 exchange between thionyl chloride and, 19: 24527

SULFURYL FLUORIDE
preparation of fluorine-18-labeled, 20: 41020

SULTONES
radiolysis of unsaturated, yields from, 16: 16437

SUN
see also Stars
acoustic wave propagation in atmosphere of, temperature increase from, 18: 36149
acoustic wave propagation through chromosphere of, 18: 36144
active regions of, disturbances in the geomagnetic field from, 17: 13275(T)
active regions of, relation to high-velocity plasma streams of (E/T), 19: 2958
active regions of, radiation emission duration from, (T), 20: 27698(T)
activity and atmosphere of, 17: 37916
activity centers in, detection of persistent, 18: 40182
activity centers in, M-region, (E), 19: 18672
activity centers in, M-region relation to, (T), 19: 19012
activity centers in, relation to recurrent geomagnetic disturbances, (T), 19: 19016
activity centers in, geomagnetic field effects of, (E), 19: 19017
activity cycle of, cosmic-ray modulation by magnetic region from, 19: 25201
activity cycle of, correlations with primary cosmic-ray spectrum, (E), 19: 25207
activity cycle of, primary cosmic-ray spectral variation during, 19: 25214
activity cycle of, effects on cosmic-ray rigidity spectra variations, 19: 25217
activity cycle of, variations in primary cosmic-ray rigidity spectrum during, 19: 25230
activity cycle of, effects on neutral atmosphere properties at 90 to 10,000 km, (T), 19: 37711 (NP-15106)
activity cycle of, correlation with geomagnetic storms, (E), 19: 44921(T)
activity data for May, 1965, 19: 47468
activity data for June 1965, 20: 4750
activity data for July 1965, 20: 6206
activity data for Jan. to July 1965, 20: 28137
activity data from Jan. to Sept. 1965, 20: 19679
activity during first 14 months of International Years of the Quiet Sun, 19: 30935
activity during geomagnetic storms, (E), 19: 5076
activity during geomagnetic disturbance, plasma wind and, 19: 42988
activity during 1958 to 1962, effects on cosmic-ray intensity, 19: 25219
activity effects on geomagnetic storms, statistics of, 16: 15491
activity in August 1965, data for, 20: 11830
activity in facular regions of, model for, 17: 41702(T)
activity levels of, effects on upper atmosphere, 17: 5170
activity of, atmospheric density and temperature variations from, 18: 28463
activity of, correlation to wind velocity of, 18: 6083
activity of, criteria for predicting minimum and quiet, 18: 8994
activity of, corpuscular streams from 19th cycle, 19: 41216
activity of, correlations with cosmic ray 27-day recurrence tendency, 18: 44488
activity of, correlations with cosmic-ray intensity variations, 19: 25215
activity of, correlations with cosmic-ray intensity variations, 19: 25227
activity of, correlation of carbon-14 content in 18th- and 19th-century wood with, 19: 36675
activity of, correlation with solar-terrestrial events, (E), 20: 2855
activity of, correlations with cosmic ray rigidity spectrum, (E), 20: 37543
activity of, correlations with stability of reflections from sporadic E layer, 20: 46476
activity of, cosmic ray intensity effects of, 18: 32503
activity of, cosmic ray intensity variation with, (E), 19: 18725
activity of, cosmic-ray modulation by interplanetary magnetic field from, 19: 25212
activity of, data tabulation for July–Dec. 1964, 20: 1108
activity of, data for Nov. 1965, 20: 24221
activity of, distribution of burst, 20: 4521 (AD-618222)
activity of, east-west asymmetry of, 17: 13178(T)
activity of, effects on space environment, 19: 16365
activity of, effects on pressure distribution in Earth's atmosphere, (E), 19: 20780(T)
activity of, effects on cosmic-ray modulation, 19: 25202
activity of, effects on critical frequency of ionospheric F_2-layer, (T), 19: 27328(T)
activity of, effects on auroral forms, (E), 19: 27331(T)
activity of, effects on magnetic and ionospheric storms, 19: 47497
activity of, effects on cosmic-ray nuclear component, (E), 20: 23963
activity of, effects on zone of incidence of solar particles at Earth, 20: 23850
activity of, effects on ionospheric currents, 20: 27702
activity of, effects on cosmic-ray Forbush effects, (E), 20: 27773(T)
activity of, effects on tropospheric pressure variations, (E), 20: 30237(T)
activity of, effects on primary cosmic ray intensity, 20: 37509
activity of, effects on cosmic alpha flux, (E), 20: 37556
activity of, effects on cosmic particle intensities, 18: 44481 (EFINS-63-68)
activity of, geomagnetic disturbances for five cycles of, 17: 13177(T)
activity of, geomagnetic effects of sunspot, 18: 34387
activity of, geomagnetic field effects of, (T), 19: 19011
activity of, in 1964, 18: 40116
activity of, indices for measuring, 18: 28209
activity of, parameters for Mar. 1963, 17: 31256
activity of, parameters for June 1963, 17: 41680
activity of, parameters for July 1963, 18: 2736
activity of, parameters for Oct. 1963, 18: 15025
activity of, parameters for Dec. 1963, 18: 22817
activity of, parameters for, 18: 42539
activity of, parameters for 1963, 19: 5079
activity of, properties of 1954 to 1963 cycle of, 19: 41214
activity of, relation of solar plasma velocity to (E), 19: 2956
activity of, relation to cosmic-ray intensity in stratosphere, (E), 19: 12052(T)
activity of, relation of magnetic polarity to rise time for sunspot,
activity of, research program for minimum, 18: 2519 20: 35989
activity of, sudden ionospheric disturbances from, 19: 47494
activity of, uv radiation from, 18: 28210
activity on, variation of equatorial spread-F with, 18: 24535
activity parameters for March 1965, 19: 41589
activity parameters for Sept. 1963, 19: 41603
activity parameters for April 1965, 19: 45178
activity parameters for 1965, 20: 32259
activity regions of, effects on interplanetary magnetic field, 17: 24212
activity variations of, periodicity of parameters for diurnal, (E), 20: 37373
activity, chemical abundances, and sunspots, 19: 32852(R) (AD-608730)
Alfvén wave propagation from surface of, (T), 20: 7966
analysis for iron and silicon abundances and ratios, 18: 32347
analysis for technetium, spectral and theoretical, 16: 15484
analysis of corona of, for chemical composition, 18: 40109
analysis of, radiometric, 17: 35260(R) (TID-19135)
angular momentum exchange between planets and, 20: 41610
angular momentum of, effects of solar wind on, 20: 34024
argon content of atmosphere of, ratio to earth, 17: 25466
atmosphere near activity transients, motion of lower, 16: 16911
atmosphere of, magnetohydrodynamic properties of, 17: 9786
atmosphere of, structure in active and undisturbed regions, 18: 4389(T)
atmosphere of, structure of, 18: 4390(T)
atmosphere of, abundance of elements in, 20: 17229
atmosphere of, deuterium to hydrogen ratio measurements in, 20: 34007(R) (N-66-12863)
atmosphere of, dynamics of, 20: 37389
atmosphere of, gas-dynamic model of shock-heated, 18: 18541
atmosphere of, hyperthermal processes in, (E/T), 20: 34076
atmosphere of, theory of, 19: 30932
atmosphere of, transient behavior of heated, (T), 20: 7693
atmospheres of, equilibrium state of shock-heated, (T), 19: 34840
atmospheric motion of, velocity fields in, (E/T), 19: 4793

beryllium content ratio to meteorites, 17: 24202
beryllium content of atmosphere of, 18: 26202
book: *Astrophysics and Space Science*, 19: 20782
book: *Geo- and Heliophysical Effects in Cosmic Rays and Aurora Polaris*, 19: 14432
book: *Handbook of Geophysics and Space Environments*, 20: 25997
book: *Introduction to Solar Terrestrial Relations*, 20: 37916
book: *Physics of Solar Corona*, 18: 12827
book: *Reports of the Shemakhimski Astrophysical Observatory*, 19: 25142
book: *Research in Geophysics*. Vol. 1. *Sun, Upper Atmosphere, and Space*, 19: 16748
book: *Stellar and Solar Magnetic Fields*, 19: 44932
boron abundance in, photometric scan for determining, (E), 20: 19331
brightness fluctuations of, oscillatory component in granulation, (T), 20: 29886
calcium ion excitation and ionization in chromosphere, 16: 29603
carbon abundance in, computer programs for, 17: 24225
charged particle motion at surface of (T), 19: 1161
charged-particle acceleration in electromagnetic fields of, (T), 20: 955
charged-particle interactions with coronal plasma, 19: 41933
charged-particle motion near surface of, (T), 19: 9879
chromosphere heating by acoustic waves, (T), 20: 34770
chromosphere of, continuous emission beyond Balmer limit, 17: 13276(T)
chromosphere of, properties of radiation-producing eruptions in, 18: 5909
chromosphere of, hydrogen alpha spectra of, (E), 19: 16335
chromosphere of, models and observations of (E/T), 19: 1144
chromosphere of, review of theories on, 18: 14712
chromosphere of, structure of, 18: 36149
chromosphere of, spectral line profiles in, (T), 19: 41220
chromosphere of, spectra of spicules and fine structure of, 19: 44915(T)
chromosphere of, spicule models for, (T), 19: 44919(T)
chromosphere of, structure of, 20: 4528
chromosphere of, structure of, 20: 37912
chromosphere of, thermal instabilities in, 20: 39562
chromosphere structure, 17: 13182(T)
chromosphere-corona transition region of, electron density and temperature in, 18: 44366(T)
chromospheric oscillations in, hydrodynamic, 17: 24204
chromospheric structure and filaments in, geomagnetic activity prediction method using, 20: 30226
chromospheric velocity fields near quiescent filaments in, 18: 42268
comet ejection from solar system, 18: 2512 (LADC-5730)
conference on solar corona, Cloudcroft, New Mexico, August 28–30, 1961, 19: 18675
conference on solar-terrestrial relations, 19: 19010
core motion in, overshooting in convective, (T), 20: 15208
corona electron and ion temperatures for, measurement of, 20: 39572
corona electron temperatures, effect of corona expansion on, 18: 24278
corona expansion in, hydrodynamic (T), 19: 2955
corona of, condensations of, above active regions of, 17: 13281(T)
corona of, determination of electron density in, 17: 13280(T)
corona of, erroneous physical interpretations in hydrodynamic model of, 17: 16914
corona of, extent of, 18: 8982
corona of, extreme ultraviolet spectrum of, 17: 28105
corona of, hydrodynamic models of, 17: 5169
corona of, magnetic field damping effects on shock wave heating of, 18: 7387
corona of, magnetohydrodynamic heating of, 17: 13658(T)
corona of, overall structure of February 15, 1961, 17: 13284(T)
corona of, spatial structure of, 17: 13290(T)
corona of, thermoelectric phenomena in, 17: 13278(T)
corona of, diffusion effects on composition of, (T), 20: 31894
corona of, effects of radial diffusion on composition of, 20: 11437
corona of, electron temperature in, 18: 24281
corona of, electron density irregularities in, (E), 19: 18662
corona of, electron temperature in, 19: 25129
corona of, energy balance and temperature of, (T), 19: 28981
corona of, expansion and heating of, (T), 19: 20783
corona of, intensity and polarization of light from, 20: 13409
corona of, iron abundance in, (T), 20: 31867
corona of, iron emission lines in, (T), 19: 16336
corona of, iron, nickel, and silicon relative abundances in, (T), 20: 31865
corona of, motion of multiply charged ions in, 18: 10754
corona of, radiobursts for determining magnetic field intensity and physical properties of, 20: 19355
corona of, simulation device for, 20: 38335
corona of, spectrum from, 18: 14710
corona of, structure of outer, (E), 19: 12049(T)
corona of, sudden expansion of, 18: 5911
corona of, temperature models for expanding, 20: 27699
corona of, two-component model of, (T), 19: 14219(T)
corona of, velocity of corpuscular streams in, 19: 47189(T) (N64-31082)
corona rotation of, effects on, 20: 44073
corona structure determination using radio astronomy, 20: 31888
coronal condensation of, 18: 42270
coronal condensations, abundance of calcium and iron in, (E), 20: 37348
coronal emission lines of, origin of, (T), 19: 4796
coronal emission lines of, identification of, (T), 19: 4797
coronal emission line intensity of, geomagnetic index correlations with, 20: 25709(T)
coronal emission of, polarization of, 17: 13279(T)
coronal expansion of, corpuscular radiation from, 17: 34696
coronal heating by gravity waves, model for, 17: 24205
coronal heating mechanisms for, limitations on, 17: 19005
coronal heating mechanisms and acceleration of solar wind, 18: 7380
coronal intensity measurements during May 30, 1965 eclipse, 20: 8489 (SC-DC-65-1826)
coronal loop prominences following flares, 18: 44380
coronal loop prominences following flares, mass balance for, 18: 44381
coronal plasma, cross sections for ionization in, 17: 41688
coronal polar rays and polar magnetic fields, 19: 25132
coronal polar rays from, structure of, 20: 34038
coronal radio emission (type III) from, mechanisms of, 18: 30879 (ARL-64-111)
coronal self-emission effect on excited state of ions, limits on, 17: 24208
coronal spectra during eclipse, (E), 19: 47451 (SC-M-65-419)
coronal spectral line-profile shape of, distortion mechanisms of, 18: 18543
coronal streamers from, dynamics of, 18: 18542
coronal streamers from, stability of, (T), 19: 40000
coronal temperature from Lyman α profile width, (T), 19: 39341
corpuscular streams and corona above active regions of, 17: 13272(T)
corpuscular streams with force-free magnetic fields from, properties and structure of, 18: 7393
cosmic electron and positron modulation by, mechanism for, (T), 20: 34132
cosmic particle from solar winds in outer belts, physical model for trapping mechanism, 16: 18307
cosmic radiation intensity variations from, 16: 26053
cosmic-ray trapping by magnetic fields of earth and, electric fields from, (T), 20: 28539
cycle on, effects on inner Van Allen belt protons, 19: 37706 (N64-27250)
data during geomagnetic storm for Sept. 1963, 20: 28138
data on geomagnetic fields and activity of, for Sept., 1964, 19: 16737
density and mass for equilibrium state of, relativity theory for, 20: 7700
eclipse effects on geomagnetic micropulsations, (E), 20: 15617
eclipse effects on geomagnetic micropulsations, (E), 20: 15618
eclipse of, Feb. 1961, 17: 22282(T) (JPRS-18823)
eclipse of, airborne observation of, 19: 47451 (SC-M-65-419)
eclipse of, auroral activity during total, 19: 18973
eclipse of, effects on geomagnetic micropulsations, 18: 13001
eclipse of, effects on ionospheric vlf propagation, 18: 44644 (UAG-R-154)
eclipse of, high-altitude aircraft photographs of, 20: 44417 (LA-DC-7837)
eclipse of, ionospheric absorption of radio waves during, 20: 44426
eclipse of, ionospheric absorption of radio waves during, 20: 44427
eclipse of, ionospheric cosmic noise absorption variation during, 18: 2721 (AFCRL-62-312)
eclipse of, radio observations of, 19: 34856
eclipse of, sky brightness during, 20: 13409
effects on atmospheric density and temperature variations, (E), 20: 9866
effects on cosmic ray intensity, 18: 22703
effects on cosmic ray anisotropy, upper limiting primary rigidity for, 20: 4563
effects on cosmic ray daily intensity variation, absorption, (T), 20: 9689
effects on cosmic radiation intensity, determination from cosmic electron energy spectra, 20: 37499
effects on cosmic ray modulation, 20: 37545
effects on earth's radiation environment, 19: 14430
effects on galactic cosmic radiation intensity, 20: 29973
effects on geomagnetic field variations, 18: 42524
effects on geomagnetic activity variations, (E/T), 20: 39982
effects on low-energy cosmic rays, (E), 20: 11525
effects on primary cosmic ray spectra, modulation at low rigidities from, (E), 20: 37584
effects on radar reflection from planets for general relativity test, gravitational, (T), 20: 11433
effects on small daylight geomagnetic-field fluctuations, 19: 37712
effects on thickness of skin of negroid and white man, 18: 8167
electric charge on, alternate test of Bailey's hypothesis of, 17: 3909 (TID-13994)

electromagnetic radiation from solar corpuscular streams, 16: 4672
electron acceleration in corona of, 17: 12921
electron densities and temperatures in corona of, 18: 28215
electron density and temperature in corona, 17: 12917
electron density distributions in corona of, 18: 30380 (NP-14051)
electron density in corona of, limitations of optical methods for measuring, 17: 20810
electron density in corona of, radial distribution of, 17: 31248
electron distributions in, 18: 4390(T)
electron pressure of, method for determination of, 18: 6358
element abundance analysis of, (E), 20: 17237
element abundances in, deviations from thermodynamic equilibrium in, 18: 30387
element abundances in atmosphere of, (E), 19: 39345
element abundances in corona and photosphere, solar wind effects on, (T), 20: 15222
elements in, ionization equilibrium equation for, 17: 28112
energy balance between chromosphere and corona, (T), 19: 9876(T)
energy generation by, proton-proton chain and CNO-cycle contributions to, 20: 37366
energy losses in corona of, radiative, 18: 14702 (N63-14231)
energy transport in the corona, 18: 5911
envelope and interior of, calculation of, 17: 24198
eruptive regions, connection with absorption in ionosphere, 17: 13187(R)
evolution, 18: 26187 (BNL-837(p.193-233))
evolution and planetary formation of, 17: 24209
evolution from pure-hydrogen galaxie, 20: 37409
evolution of planetary system of, chemical evidence relative to, 20: 19346
evolution of, Brans-Dicke model for, 20: 34018
evolution of, contraction phase of, 20: 37397
evolution of, convection and luminosity in early, (T), 19: 23243
evolution of, effects of variation in gravitational constant on, 18: 18536
evolution of, with varying gravitation, (T), 20: 21493
flare distributions on, geomagnetically effective, 18: 44401
flare occurrence and sunspot acceleration on, correlations of, 19: 23239
flare-associated phenomena in solar atmosphere, transient, (E), 20: 46273 (AD-640661)
flow in a magnetic tube connected to, path of, 17: 13274(T)
formation of, physical processes in, 17: 5167
Fraunhofer line velocity displacements in atmosphere of, 16: 22823
gamma flux from, (E), 20: 34042
gas condensations from sunspot regions of, diamagnetic ejection of, (T), 19: 9875(T)
gas emission by, quasi-stationary, (E/T), 19: 4820
gas flow stability in corona and prominences of, dilute, (T), 20: 2573
gaseous emission to interplanetary regions, 17: 20808
granulation flow in, MHD equations for super-, (T), 19: 20764
gravitational contractions of, models for early phases of, 17: 36555
gravitational effects on light waves, test for, (T), 19: 8297
gravitational field of, equations for, 20: 21868
gravitational radiation from thermal collisions in, quantum electrodynamics for, 19: 47204
gravity variation of, (T), 19: 39665
gravity waves in chromosphere of, standing mode of compressional body, (T), 19: 39343
helium abundance in, 18: 10750
helium content in corona of, ortho- (E), 19: 1159(T)
helium content of, 19: 47193
helium content of, models for, 18: 42259
helium excitation in chromosphere of, electron density and temperature for, 17: 24206
helium isotope abundance ratios in the, 17: 6911
helium-3 abundance in, 19: 25131
hydrodynamic model of quiet-day corona and solar wind, 18: 5911
hydrogen content in chromosphere of, 20: 27716(T)
hydrogen convection zone of, unstable modes in, 17: 24203
hydrogen distribution in, 18: 4390(T)
hydrogen emission from, geomagnetic storm mechanism theory of, 20: 19687
hydrogen energy level populations in chromosphere of, atomic, 18: 42267
hydrogen excitation and ionization in prominences of (T), 19: 1160(T)
hydrogen ion transitions in, exchange effects on free-free, 18: 40133
hydromagnetic wave emission by, effect on geomagnetic fields, 17: 12878
hydromagnetic wave propagation and stability in convective zone of, (T), 20: 7969(T)
intensity of green coronal emission, solar wind velocity relation to (T), 19: 2957
interactions and properties of solar wind (T), 19: 2950
interstellar gas properties near, 16: 22820
ion densities and ionization mechanisms in corona of, 17: 15042
ion densities in corona of, 18: 28215
ion motion in plasma of, multiply charged, 18: 10754
ion recombination in corona of, rates for calcium and iron, (T), 20: 9636
ionization equilibria in, (T), 20: 19338
ionization in corona of, time-dependent, (T), 19: 4795
ionization of surrounding gas, size of H II region of, (T), 19: 39340
ionospheric effects of eclipses of, in F2 region, 18: 16643
iron autoionization in plasma of, collisional excitation in, (T), 19: 41244
iron content in photosphere of, 18: 42266
krypton content of atmosphere of, ratio to earth, 17: 25466
lead content of atmosphere of, 18: 26202
lithium content in, (E), 19: 39346
lithium content in atmosphere of, 18: 26202
lithium content ratio to meteorites, 17: 24202
loop prominence systems in, relation to flares, 18: 42269
loop prominence systems of, magnetic field strengths in, 18: 42275
magnesium content and ionization in chromosphere of, 20: 27716(T)
magnetic effects on flare phenomena, 18: 44383
magnetic energy dissipation during plages and flares, 18: 44409
magnetic energy storage and release in flares, 18: 44386
magnetic field and winds of, termination of, 17: 28111
magnetic field distributions and structures in outer atmosphere of, 17: 31245 (D1-82-0216)
magnetic field distributions in solar system (T), 19: 2948
magnetic field effects on shape of corona and supercorona of, inclined interplanetary, (T), 20: 7689
magnetic field energy storage and dissipation, 18: 44410
magnetic field measurements, (E), 20: 29885
magnetic field near, 16: 15516
magnetic field of, solar flare effects on, 17: 28109
magnetic field of, parameters for, 17: 32879
magnetic field of, interplanetary, 18: 5911
magnetic field of, 18: 10730
magnetic field of large sunspots, model for solar flare production by, (T), 19: 47188 (AD-613636)
magnetic field of, properties of, 18: 30671
magnetic field of, determination of components of total vector of, 18: 44367(T)
magnetic field of, evolution of, 19: 23537
magnetic field of, co-rotation of corona in model of, (T), 19: 41241
magnetic field of, evolution of, (T), 20: 15223
magnetic field of, sector structure of, 20: 23867
magnetic field of, solution of MHD equation for, 20: 34035
magnetic field of, connection of geomagnetic field to, 20: 39986
magnetic field of, effects of active regions on, 20: 39557
magnetic field of, effects of active regions on, 20: 39558
magnetic field of, expulsion of flux by eddies in, 20: 39567
magnetic field of, interaction of solar wind with, (T), 20: 39573
magnetic field properties, 16: 2385
magnetic field production in photosphere of, kinetic theory of, 17: 32854
magnetic field reversal with prominence filament motion, polar, (E), 19: 16334
magnetic field stability near flares, 18: 44414
magnetic field structural regularity in outer corona, 17: 2067(T) (JPRS-15517(p.423-30))
magnetic field structure in convection zone of, (T), 19: 25120
magnetic field strength above photosphere, (T), 20: 4524
magnetic field structure of, reconnection and annihilation in, (T), 20: 31895
magnetic field strength in corona of, above active regions, (T), 20: 34069(T)
magnetic field transport outward from spot and bipolar regions of, (T), 20: 29906(T)
magnetic field variation with time in sunspots, (T), 20: 25690
magnetic fields and motions in undisturbed photosphere of, 19: 41221
magnetic fields at flare positions, 18: 44385
magnetic fields in chromosphere of, force-free, 18: 28221
magnetic fields in prominences on, measurement of, 18: 44348
magnetic fields in photosphere of, random microscopic, 19: 30922
magnetic fields of, production from plasma thermal currents, 18: 4392(T)
magnetic fields of, effects on flare emission, 18: 42254 (TID-21105)
magnetic fields of, effects of convection on, 18: 44351
magnetic fields of, behavior during flares, 18: 44384
magnetic fields of chromosphere, 18: 44415
magnetic fields of arch structures in corona of, (T), 19: 12047
magnetic fields of, review of properties of, 19: 14221
magnetic fields of, model of, (T), 19: 27047
magnetic fields of, large-scale distribution of, (E), 19: 34844
magnetic fields of, solar activity from, (T), 19: 42978
magnetic fields of, relativistic effects on, 19: 42982
magnetic fields of, fine structure of, (T), 19: 44918(T)
magnetic fields of, review on measurement of, 19: 47208
magnetic fields of, interplanetary space extension of photospheric, (E), 20: 15215

magnetic fields of, kinematical hydromagnetic model for small-scale, 20: 21503
magnetic fields of, measurement of, 20: 29910
magnetic fields of, (E/T), 20: 41616
magnetic fields on, magnitude and orientation of, (E/T), 19: 12046
magnetic-field transport on, (T), 19: 9839
magnetohydrodynamic dynamo theory of, 19: 1067
mass losses through evaporation, 18: 37831
mass motions in corona of, radar evidence for, 18: 36146
mass variations of, (T), 19: 39665
microwave emission from, 18: 44393
microwave radiation sources, 17: 6906
model for, with solar neutrino spectrum, 18: 18548
model of chromosphere of, spicule, 18: 42284
model of M regions of, 18: 40105
models for atmospheric circulation and flares on surface of, (T), 19: 4805
modulation effects on primary cosmic radiation, (E), 19: 27113
modulation of cosmic-particle energy spectrum and intensity by, 19: 16435
molecular condensation and equilibria in nebula of, (T), 19: 39352
neon content of atmosphere of, ratio to earth, 17: 25466
neutrino emission, 17: 20803(T) (JPRS-18605)
neutrino emission by spectroscopy of, (T), 19: 8058
neutrino emission from, temperature of solar interior from, (T), 20: 23848
neutrino emission by, flux at earth from, (T), 20: 37366
neutrino flux from, (T), 20: 37377
neutrino production in, mechanism and rate of, 17: 15047
neutrino production in, 18: 28703
neutrino production in carbon-nitrogen and proton-proton cycles in, 18: 37835
neutrino production in helium-3 ($p,e^+\nu$) reactions in interior of, (T), 19: 32869
neutrino production in, (T), 20: 34058(T)
neutrino spectra of, (T), 20: 9646
neutron emission from, (T), 20: 9634 (D1-82-0484)
neutron outflow from, upper bounds of, 20: 21495
nickel abundance in atmosphere of, (T), 20: 19332
nuclear reactions on surface of, during 3+ flare, 18: 44400
nuclear reactions in, gamma and neutron production in, 18: 44416
nuclear reactions in flare regions of, (T), 20: 11438
nuclear reactions in, temperature dependence of rates of p-p-cycle, (T), 20: 23847
nucleosynthesis in early history, 16: 24658
optical phenomena for 1959, data compilation, 18: 7371
origin of solar system, 17: 26258
oxygen autoionization in plasma of, collisional excitation in, (T), 19: 41244
particle emission from, 18: 7390
particle emission from, propagation measurements from Explorer VII, 18: 7392
particle emission by, at high energies (E/T), 19: 2952
particle emission from, mechanisms of, (T), 20: 11438
particle emissions from, relations of terrestrial disturbances to, 19: 47495
photograph of, interpretation of April 19, 1960 x-ray, 17: 15040
photon flux from, variation with depth in photosphere, (T), 19: 39342
photosphere boundary conditions for, method for integration downward from, (T), 20: 2581
photosphere of, kinematical hydromagnetic theory of low, 17: 39822
photosphere of, gas thermodynamics in, (T), 19: 23249
photosphere of, kinetics and structure of hydrodynamic disturbances in, (T), 20: 2589
photosphere of, magnetic field structure in, (E), 20: 31892
photosphere spectra, inclined inhomogeneities in, 19: 37434
photospheric convection and granulation, 16: 16909
plage index spectra of, comparison with power spectra of artificial time series, 19: 41224
plages and sunspots on, development of, (E/T), 19: 34843
plasma clot motion during surges of, pressure distribution on surface of, (T), 20: 27697(T)
plasma cloud from, effects on solar cosmic particles, 18: 7443
plasma emission of, hydromagnetic wave propagation rise times in geomagnetic field interactions with, 17: 34666
plasma from, properties of, 19: 18668
plasma motion in, (T), 19: 27048
plasma streams from, electromagnetic properties of, 16: 19646
plasma streams from, evidence for interplanetary long-lived, 17: 34692
plasma streams from, on Feb. 12, 1961, 18: 7391
plasma streams from, radio evidence for, 18: 28211
plasma streams from, 27-day recurrence pattern of, 20: 29894
position relation to cosmic-neutron diurnal variations, 16: 6889
prediction of future sunspot cycles, 17: 34684
production of ozone, 16: 19162
prominence filaments, models for structure of, (T), 19: 16333
prominence of April 1963, associated activity and terrestrial effects of, 19: 30917
prominence spectral intensities of, quiescent, 19: 37433
prominences of, magnetic fields in, 17: 13285(T)
prominences of, activation by moving disturbances, 19: 30913
prominences of, classification and measurement of, 18: 44641(R) (AFCRL-64-275)
prominences of, coronal heating of, (T), 20: 27715(T)
prominences of, magnetic flux topological variations in, 20: 32656
prominences of, properties of, (E/T), 20: 9639
properties and structure of, 18: 32355
properties of corona of, hydrostatic and kinetic, 18: 5911
properties of, book on, 19: 1162
properties of, conference on, 20: 7717
properties of, from radio and radar studies, 18: 32356
properties of, review (E/T), 19: 2945
properties of, solar wind velocity correlations with, 20: 31882
proton emission and lifetime, 16: 15489
proton emission from, hydromagnetic model for, 19: 25144
proton emissions from, hypothesis on directivity of, 16: 27867 (D1-82-0189)
proton spectra from hydromagnetic shock waves in corona of, (T), 19: 25145
quiescent prominences, hydromagnetic model, 16: 18118 (NP-11463 (Pt.3)(p.473-80))
quiet-day coronal expansion, 18: 5911
radiations from, 16: 20231
radiative transfer between chromosphere and corona, stellar wind effects on, 20: 41618
radio bursts in corona of, frequency drift of type III, 17: 32855
radio bursts in corona of, properties of type III, 19: 41218
radio emission, 18: 14594(T) (JPRS-23436)
radio emission by, 17: 26276
radio emission by, relation of cosmic ray intensity to, 20: 7758(T) (NASA-TT-F-91, pp 164-8)
radio emission from, properties of peaks in type I, 17: 41703(T)
radio emission from, S-component of, 18: 44391
radio emission from, over spot groups, (T), 19: 25136(T)
radio emission from, weak disturbances of, (E), 19: 27050(T)
radio emission from, cosmic-ray intensity variations with type-IV, (E), 19: 27122
radio emission from, after chromospheric solar flare, (E), 19: 34850(T)
radio emission from, type-IV, 19: 37445
radio emission from, 1953 to 1963, 19: 41217
radio emission from active regions of, characteristics of, 20: 21506
radio emission from, correlations with chromospheric flares, (E), 20: 25711(T)
radio emission from shock propagation in corona of, type-II, (T), 20: 29903(T)
radio noise and sunspot observations, 18: 10727 (NP-13550)
radio storms on, origin of type-I, 18: 44356
radio wave bursts from, 17: 12921
radio wave emission from active regions of, 17: 41705(T)
radio wave emission (E), 19: 3006
radio wave emission by, model for (T), 19: 2936
radio wave emission by, 19: 14225
radio wave emission from, review on, 19: 23236
radio wave emission from type-V events, (E/T), 19: 23237
radio wave emission from type-II events, (T), 19: 23238
radio-wave emission from, mechanism for, (T), 20: 27712
radio-wave emission from, frequency spectrum of slowly varying component of, 20: 29908
radio wave pulse source propagation in corona of, (T), 19: 18656
radio waves from, frequency splitting of, 20: 41606
radio-wave emission from, variation with solar proton emission, 20: 23907 (N-66-15620)
radio-wave emission from, polarization of short-lived components in type II, (E), 20: 27694
radio-wave scattering in corona of, variation with solar activity, (E), 20: 23862
radiowave emission from plasma, mechanisms of, 18: 44914
radiowave production and polarization in corona of, 18: 44408
rare earth abundance in, spectral analysis for, 17: 34663
rare earth abundance analysis of, (E), 20: 17237
rare earth abundances in atmosphere of, determination of, 20: 46279
rare-gas content in, 18: 12345
research planned during IQSY, 19: 16761
research program for International Years of Quiet Sun, 18: 44360
rotation of, interior, 18: 24287
rotation of, nature of differential, 20: 9651

satellite orbits about, general relativity tests by precession of, (T), 20: 11883
shock propagation in exponentially decreasing atmospheres of, (T), 20: 15217
shock structure in M region disturbances of, correlation with geomagnetic impulse pairs, 20: 4758
shock-wave heating of corona of, magnetic-field effects in, (T), 19: 23252
sodium content in, Stark broadening effects on determinations of, (T), 20: 27706
sodium-22 decay in 1.28-Mev gamma flux from, (T), 20: 27695
solar and thermal radiation from, 16: 32252 (NASA-TN-D-1360)
solar and thermal radiation from, 16: 32253 (NASA-TN-D-1361)
solar wind detection and properties, (E/T), 19: 2949
solar wind direction and sudden commencement hydromagnetic waves, enhanced, 16: 19649
solar wind effects on geomagnetic field shape, 17: 37894 (NASA-TR-R-181)
solar wind, hydrodynamics of, 16: 3597
solar wind perturbation of geomagnetic fields, 17: 37903
spectra at 0 to 1500A, 20: 34060
spectra, electromagnetic emission, 16: 30991
spectra from, highly ionized atomic, 20: 341
spectra of carbon-12 and -13 in, 18: 740
spectra of, chemical composition of chromosphere and corona from ultraviolet, 17: 24207
spectra of chromospheric spicules of, absorption, 16: 29604
spectra of corona of, polarization of forbidden line λ 5303, (T), 20: 19329
spectra of corona of, polarization of forbidden lines in, 20: 19329
spectra of, dependence of line intensities on phase of activity, 17: 13277(T)
spectra of, information obtained from, 17: 21209
spectra of, intensity and velocity fluctuations of calcium K line in, 17: 32856
spectra of ions of lithium I sequence in, ultraviolet, 18: 7395
spectra of iron from, 19: 25564
spectra of prominences, hydrogen alpha line in, (T), 19: 20776(T)
spectra of Sp^4-configuration coronal ions in, ultraviolet, (T), 19: 9877(T)
spectra of, Brackett hydrogen gamma line in, (E/T), 19: 20778(T)
spectra of, conference on, 20: 15234
spectra of, Fraunhofer lines in, (E/T), 19: 20777(T)
spectra of, Fraunhofer lines and color temperature from, 19: 30915
spectra of, measurement using stabilized rockets, (E), 19: 28983
spectra of, photon energy loss mechanism for red shift of, (T), 19: 14205
spectra of, properties of uv and x-ray, 18: 32359
spectra of, review on u-v and x, 19: 27059
spectra of, saturation effects on lines in, (T), 19: 18660
spectra of, time variations of extreme uv, 18: 44377
spectral broadening in prominences on, Balmer-line, (E), 19: 9854
spectral line profiles at λ 10830, (E), 19: 4804
spectroscopy of, 18: 8978
spectroscopy of, rocket, 17: 26257
spot activity between Sept. 14 and 26, 1963, (E), 19: 16354
spot activity correlations with ionospheric electron density and uv and x radiation intensity, 20: 19647
spot activity effect on cosmic-ray nucleon component, 20: 44425
spot activity on, properties of, (T), 20: 37385(T)
spot activity, chemical test correlations with, 20: 46285
spot activity, ionospheric effects of, 20: 2848 (AD-615111)
spot activity, relations between space phenomena and physical-chemical and biological phenomena, 20: 46282
spot and faculae magnetic flux, variability of, 20: 39561(T)
spot area relation to major solar flares, 18: 7382
spot configuration and proton emission, (T), 20: 37346
spot content of lithium, 20: 9650
spot cycle effects on radio propagation, 18: 16843
spot cycle of, geomagnetic field variation with, 18: 2739
spot cycle of, neutron monitor pressure coefficient correlation with, 17: 37913
spot cycle of, events from, 20: 39563
spot cycle variation effects on midlatitude ionosphere, (E), 19: 39677
spot cycle variation in, geomagnetic activity correlation with double, (E), 20: 19678
spot data for February, 1966, 20: 34387
spot data for Sept. 1965, 20: 19679
spot formation cycle of, time variation of low rigidity cosmic rays during, 17: 28130
spot formation, isophotal contour maps and magnetic field configuration model for, 17: 22401
spot formation, multiple zonality, 16: 27418 (NP-11961)
spot formation of, prediction of activity of, 17: 25964
spot formation, model of cyclic, 19: 41215
spot formations in, magnetic field production in, 18: 4391(T)
spot formations on, data for Sept. 1963, 18: 11087
spot formations on, velocity field in, 18: 37832
spot formations on, radiative equilibrium in, 18: 42273
spot group area on, time variation in, (T), 19: 20779(T)
spot group magnetic field strength, secular variations in, (T), 20: 39559
spot magnetic effects on flare phenomena, 18: 44383
spot magnetic field strengths and polarities during IGY, 20: 2563
spot magnetic field structure, (T), 20: 27712
spot maximum of, x-ray emission during flare and non-flare, 18: 5910
spot model of, magnetic field effects on convective instability in, 20: 39939
spot model, statistical, 20: 46275
spot motion in photosphere of, parameters for large-scale, 17: 41704(T)
spot number correlations with cosmic neutron intensity variation, relative, (E), 20: 37524
spot number for Oct. 1965, 20: 21830
spot numbers for Aug. 1963, 18: 5902
spot numbers for Dec. 1964, 19: 27347
spot numbers for Feb. 1965, 19: 37730
spot numbers for June 1964, 19: 2939
spot numbers for July 1964, 19: 6600
spot numbers for Oct. 1964, 19: 18990
spot numbers for 1964 and January, 1965, 19: 33137
spot opacity properties, (T), 20: 37354
spot processes of, magnetohydrodynamic theory of, 19: 2938
spot structure on, intensity profiles for, (T), 20: 2576
spot structure on, mixing length damping for, (T), 20: 21489 (AD-623803)
spot temperature and pressure in magnetohydrostatic equilibrium, 19: 44897
spots on, structure of, 18: 8981
spots on, emission-line corona of, 18: 44641(R) (AFCRL-64-275)
spots on, gaseous pressure in, 20: 37343
spots on, structure of, and relations with flares, 18: 44641(R) (AFCRL-64-275)
spots on, umbra intensity of, 20: 37364
spots, phase anomaly in chemical test D on, 20: 46284
stability and wave propagation in corona and wind of, (T), 20: 15216
storm and wind effects on lunar surface, sputtering rates for, 17: 25870(R) (X62-11400)
storms and winds of, particle densities in, 17: 25870(R) (X62-11400)
structure of, ionization equilibrium equation of state for calculating, 19: 27046 (UCRL-7820(Rev.1) and (Suppl.))
structure parameters of, neutrino spectroscopy method for determining, 20: 37378
sunspot configurations during flares, 17: 13181(T)
sunspot correlation with sporadic E, 18: 26440
sunspot cycle effects on auroral activity, 19: 47472
sunspot cycle of, geomagnetic and ionospheric variations with, 18: 32680
sunspot cycle of, polar-cap absorption during, 19: 25123
sunspot effects on polar-aurora frequency, 18: 28205
sunspot effects, asymmetric ionospheric and magnetic, 18: 28204
sunspot group of high activity, 19: 30914
sunspot group of high surge activity, 19: 30918
Sunspot groups of, age-frequency distribution from 1888 to 1955, 19: 37437
sunspot groups on, magnetic field amplification in, (E), 19: 27060
sunspot magnetic field pattern, measurement of, 17: 39827
sunspot magnetic fields above flare regions, structure of, (T), 19: 34854
sunspot numbers for 1963, 18: 42293
sunspot numbers for August 1964, 19: 8332
sunspot numbers for 1957 to 1964, correlation of secular cosmic-ray variations with, 20: 23974
sunspot phenomenon of, gravitational quadrupole moment effect on, 20: 41610
sunspot relation to solar flare intensity, 17: 39826
sunspot structure, (T), 20: 25691
sunspot variations over one solar cycle, effects on cosmic nucleus intensities, 18: 42342
sunspot velocity field, micrometer and photometric observations of, 17: 39828
sunspot-number correlations with distribution of cosmic-neutron diurnal intensity variations, 19: 25228
sunspots of, magnetohydrostatic theory of, 19: 25126
sunspots of, photometric measurements of, 19: 30915
surface granulation of, 18: 10729
surface of, description, 18: 20721
temperature distribution in, 18: 4390(T)
temperature gradient of inner corona and effect of solar wind on coronal lines, 17: 15041
temperature measurement using a microwave radiometer at 2.04 mm, 17: 5175
temperature of interior of, methods using solar neutrino detection for

determining, 20: 37380
temperature of, method for determining, 18: 6358
temperature structure of chromosphere of, (T), 19: 4794
terrestrial accretion from solar wind, 16: 15009
thermodynamic equilibrium of calcium, magnesium, and oxygen in chromosphere, 16: 16898
thermodynamic equilibrium in atmosphere of, local deviations from, 18: 40108
ultraviolet emission from activity centers of, extreme, 18: 28215
ultraviolet radiation in upper atmosphere from, 18: 21089
ultraviolet radiation scattering by free electrons in corona of, profiles of Lyman-alpha, (T), 19: 39341
velocity fields in atmosphere of, detection and measurement, 16: 16897
wind emission to interplanetary regions, measurements of, 17: 31258
wind flux of, interpretations for geomagnetic storms by, 17: 28116
wind interactions with geomagnetic fields, interplanetary magnetic field effects on, 17: 27574
wind velocity from, consequences of nonuniform, 17: 16913
wind velocity from, correlations to cosmic-ray variations and geomagnetic and solar activity, 18: 6083
winds from, effects on lunar atmosphere of, 18: 6100
winds from, hydrodynamic model of, (T), 19: 25125
winds from, radar evidence for, 18: 36146
x radiation production and spectra of, 19: 41213
x ray emission from corona of, soft, 19: 41209(T) (N64-22932)
x-ray emission during subflare activity of, spectra of, 18: 28217
x-ray emission from, spectral anomalies of, 18: 28218
x-ray emission from, optical focusing systems for, 19: 14224
x-ray emission from, during quiet period, (E), 19: 18663
x-ray emission from, review on, 20: 9647
x-ray emission from, review and analysis of, 20: 17248
x-ray flux from 2 to 18 Å, (E), 19: 30927
x-ray flux from, variations in, 18: 28219
x-ray images of, soft, 19: 27054
x-ray images of, using grazing incidence optics, 20: 15203
x-ray spectra, (E), 20: 2585
x-ray spectra from, isothermal quiet-corona model for line intensities in soft, 20: 19338
x-ray spectra of, variability of, 18: 28216
xenon content in atmosphere of, ratio to earth, 17: 25466

SUNSHINE MINE (IDAHO)
ages of uranium minerals, 16: 29197

SUNSHINE PROJECT
see also Strontium Isotopes Sr-90

Super Kukla
see Critical Assemblies

SUPERCONDUCTIVITY
Abrikosov mixed state in, series solution of Ginzburg-Landau equations for, 19: 47519
analysis of, problems in experimental and theoretical, 18: 15119
appearance in crystals, effects of multiplicity of d or f shells on, (T), 19: 8031
appearance of high-magnetic-field, in alloys, 18: 6126
application to linear accelerators, 19: 12037
application to nuclear matter theory, 16: 2628
asymptotic behavior of perturbation series in, 17: 11416
bibliography, 18: 38016 (AD-438181)
bibliography, 18: 36425 (SRB-63-5)
bibliography on, 18: 6102 (AD-423735)
Bogoliubov quasiparticles in, criteria for, 20: 21839 (AD-627067)
book: *Perturbation Theory and the Nuclear Many Body Problem*, 16: 26023
book: *Phase Transitions*, 19: 18622
book: *Quantum Field Theoretical Methods in Statistical Physics*, 20: 11375(T)
book: *Superconductivity*, 17: 26252
book: *Superconductivity of Metals and Alloys*, 20: 19773(T)
book: *The Theory of Superconductivity*, 17: 39809
book: *Theory of Superconductivity*, 19: 19061
book: *Theory of Superconductivity*, 19: 23587
book: *Theory of Superconductivity*, 19: 23589
boundary effects in, 18: 15101
calculations of, using approximate many-fermion interactions, (T), 19: 20936 (TID-20558)
calorimetric study of, in alpha uranium, 20: 44504 (UCRL-17026)
canonical forms of antisymmetric tensors in, 17: 9821
collective excitations in, at nonzero temperature, 16: 32213
conference, 20: 19774
conference on, 18: 15062
correlation functions for fermions, theory, 16: 18360
criteria for, (T), 19: 12448
critical currents in surface, (T), 20: 34436
critical field in Ginzburg-Landau theory, lower, 17: 31108
critical field in alloys and compounds, theory of high, 18: 36515
critical field in cylindrical geometry, (T), 19: 19037
critical states of solenoids, (E), 20: 46545
critical temperature of, correlations with properties of metals, 17: 31230
critical temperature in films of, effects of thickness on, 20: 21891
critical temperatures of germanium and silicon under high pressure, (E), 20: 40039
critical temperatures of lead and tin up to 160 kbar, (E), 20: 40040
critical temperatures in, models for high, 20: 42129
crystal structure effects on, 18: 16878(R) (SSD-TDR-63-98)
crystallographic effects on, in niobium and vanadium, 18: 44688
current distribution in, 17: 12867
currents in surface layers of niobium–zirconium alloys, (E), 20: 40023
description of, 18: 7641
design of magnetic bottles, 20: 46544
destruction by a current, effects of Joule heat on, 17: 22388
destruction by direct current, (E), 19: 43236(T)
destruction by electric currents and magnetic fields, 19: 14449
destruction in tin films by current, resistance changes on, (E), 19: 47530
destruction in tin, magnetic induction distribution in, (E), 20: 4794
destruction of supercurrent in, by alpha particles, 17: 18951
detection by changes in inductance and losses of a resonant bridge, 20: 44508
detection in cobaltite- and pyrite-type compounds, 17: 34590
detection in crystal class-C16, 16: 22631
detection in gallium nitrides, (E), 19: 5095
detection in polar and nonpolar semiconductors, 16: 24332
detection of type II, magnetometer for, 18: 954 (NP-13274(p.40-6))
detection of type II, in rhenium, (E), 19: 43633(R) (NP-15354)
development and uses, 18: 21096 (NP-13809)
development of concepts in, and current problems, 18: 36440
development of surface, methods for, (T), 19: 14444
developments in, experimental and theoretical, 16: 30936
developments in, present and future, 17: 41636
developments in, review of experimental and theoretical, 16: 32243
developments in, for magnets and information storage, 18: 30686
dislocation effects on, 18: 15037 (DMS-63-10)
disruption of, in alloy with disperse superconducting phase, 20: 28181
effect of metallic contacts on gapless, (T), 20: 2910
effects of communal entropy of crystal structure on, 20: 19734
effects of impurities on, of metals, 20: 23715
effects of interstitial gases in niobium on, (E), 20: 40025
effects of orbital field on Fulde-Ferrell state in, 20: 40046
effects of structure on eutectic-alloy, 20: 13695
effects of superimposed copper and lead films on quartz on, 18: 36538
effects of surface, on magnetic hysteresis, (E), 20: 13679
electrodynamic theory of, 19: 1422 (NP-14404(p.245-54))
electron behavior in strong spin-exchange fields, 18: 24563
electron concentration and temperature conditions for, in thin nonmetallic films, (T), 19: 31179
electron-electron and electron-phonon interactions in, mathematical treatment of, 17: 11482 (NP-12435(Pt.II))
electron interaction in, 17: 11370
electron interaction effects on, conduction, (T), 19: 35341
electron spin paramagnetism effect on, (E), 19: 6610
electron tunneling effects in, 18: 15094
electron tunneling effects in, theory for, 18: 15095
electron tunneling in, boundary condition for Josephson, (T), 20: 44575
energetic stability of persistent currents in long hollow cylinders, 17: 658
energy-gap equation, *s*-wave solutions, 16: 19521
energy gap in, effects of paramagnetic atoms on, 18: 15102
energy gaps in, temperature effects on, 17: 18986
energy gaps in, theory for (E/T), 19: 1508
energy-gap anisotropy in, in single crystals, 18: 15107
energy-gap/transition-temperature ratio in, 18: 15106
enhancement of, chemical, 19: 40543
equilibrium theory of, self-consistency in quasi-chemical, 17: 31225
equipment developments for measuring, 18: 24544(R) (NBS-8253)
existence and properties of second-type, (E), 19: 23539 (CEA-R-2616)
existence of, in one-dimensional lattice, 18: 40456
existence of, in stellar matter at 10^8 to 10^9 °K, 18: 18549
ferromagnetic spin correlation effects on, 20: 44549
field theory for, Gorkov factorization in generalized, (T), 19: 8296
free path in, comparison with normal state, 17: 39744
grand partition function for Fermi system in, particle-hole representation for, 19: 43237
Hamiltonian role in field theory approximation methods, 16: 16850
hard superconductor effects in superimposed metals, 18: 36537
high field realization in ferromagnetic metals, 17: 6873
image properties of a superconducting ground plane, 18: 13013
impurity effects on critical temperatures for (E/T), 19: 3178
impurity-resonance effects on, 18: 15104

in bismuth-type metals, effects of electron excitation interactions on, 17: 41652
in ferromagnetic materials, 20: 26052(T)
in gapless doped materials, specific heat evidence for, 18: 40437 (IS-979)
in metals having spherical nuclei, theory, 17: 13133
in metals, mechanism of transition to, 17: 406 (ASD-TDR-62-269)
in rings interrupted by insulating junctions, 20: 19770
in semiconductor degenerate p-n junction, electron and hole, (T), 20: 9936(T)
in transition elements, similarity to ferromagnetism, 18: 36485
in transition metals under pressure, 18: 36482
in very thin films, measurement, 16: 24142 (AD-270673)
inducement in barium–gold alloys by variation of structural parameters, 18: 969
induction of currents in rings, using polarized electromagnetic waves, (T), 19: 45191 (LNF-65/15)
initiation of, effects in, 17: 27951(T) (AEC-tr-5850)
isotope effect in, 18: 36492
isotope effects on, 17: 31189
isotope effects on, 17: 34617
Josephson frequency-voltage relation, experimental test of, 20: 44540
Josephson tunneling effect in, many-body theory for, 19: 19027
losses in, a-c, 17: 11372
magnetic critical fields in, temperature effects on, 18: 15114
magnetic field effects on, in hollow cylinders and spheres, 17: 32809
magnetic field effects in hard, 18: 15063
magnetic field effects on, in rare-earth alloys, 18: 15089
magnetic field effects on, in films, 18: 15113
magnetic field effects on, in thin films, 18: 34682(R) (NBS-8407)
magnetic field effects on, in microscopic bridges, 18: 42566
magnetic field effects on, anisotropy of, 19: 1490
magnetic field effects on critical currents (E), 19: 1510
magnetic field effects on, in hollow rotating cylinders, (T), 19: 23540 (JPL-TR-32-650(Pt.I))
magnetic field effects on surface, (T), 20: 11891 (COO-264-224)
magnetic field penetration effects on breakdown of surface, (T), 20: 2900
magnetic flux penetration in cylinders of type-II superconductors, (E/T), 19: 41612
magnetic flux quantization in rings, 17: 6784 (CERN-62-30)
magnetic flux quantization in, 18: 15109
magnetic flux quantization and persistent currents in, 18: 15110
magnetic flux quantization in, theory for, 18: 15111
magnetic flux quantization in, 18: 36475
magnetic flux quantization in cylinders, apparatus to detect, 18: 36476
magnetic flux trapping by superconducting toroids, 16: 19535
magnetic moments in superconducting electron gases, 17: 37718
magnetic transitions in, theory for second-order, 18: 15088
magnetic transitions in, models and theory for (E/T), 19: 1509
mathematical structure of Bardeen-Cooper-Schrieffer theory, 16: 27801
mathematics of, 18: 9438
measurement in copper and platinum films, 18: 44685
measurement of, design of Hall probes for, 18: 32275(R) (ORNL-3652 (p.105-31))
measurements for transition metals, tables of, 20: 40047
measurements of, use of liquid helium-4 in low-temperature apparatus for, 20: 32336
mechanism for, instability against Cooper-pair formation in, (T), 19: 45208
mechanism of, effect of ion core in, (T), 19: 23559
mechanism of, lattice stability in electron-electron interaction, 20: 30264(T)
mechanisms for, in transition metals, 17: 34616
mechanisms for, in lanthanum and uranium, 18: 966
mechanisms for, in transition elements, 18: 36481
mechanisms in crystalline films, (T), 20: 9906(T)
mechanisms in metals and alloys, 20: 46966(R) (NAA-SR-12010)
mechanisms in non-transition and transition elements and their combinations, coexistence with ferromagnetism, 17: 37776
mechanisms of, model for, 20: 26033
metallurgical and technological aspects of hard, 18: 44681
microwave observation of surface, above the upper critical field, 18: 18838
model for, approximation methods in, 17: 31157
model for second kind, layer, 17: 41632
model for, new Fermi-surface, 20: 44542
model for, two-fluid, 20: 40037
model for, with exact solution, 20: 26056
model of, Josephson tunneling and persistent currents in charged Bose gas, 20: 13691
models for hard and soft, sponge, 18: 15067
models for, phase transitions in, 20: 21872 (AD-627189)
models for, with zero energy gap, (T), 19: 12429 (NP-14641)
nature and occurrence of, review on, 18: 11106
nucleation in wedge geometry, (T), 20: 1123
nucleation of, in wedge geometry, (T), 20: 36133
observation of surface, method for, 19: 5100
occurrence in decreasing fields, analysis of surface effects on, 18: 9271
occurrence of, prediction rules for, 18: 6101 (AD-402708)
of aluminum and tungsten films, 20: 25474(R) (BNL-954, pp 122-67)
of antiferromagnets, 18: 21103
of electron gas in homogeneous magnetic field, (T), 20: 21887
of fermions in inhomogeneous medium, equations for, 16: 31030
of ferromagnetic metals, 18: 24305
of ionic semiconductors, high-current, (T), 20: 21889
of lanthanum, effects of crystal imperfections on, 20: 41412(R) (IS-1500(Sect. M))
of metastable intermetallic compounds in gold and silver alloys, 18: 24142 (TID-20617)
of noble metals and their alloys, 18: 24179
of nondegenerate semiconducting films, factors affecting, (T), 20: 46525(T)
of solid solutions of noble metals, 17: 6860
of superimposed films of superconducting and normal metals, 18: 32704
of superimposed metallic films, 16: 27656
of tantalum–titanium wires, effects of crystal structure on, 20: 37268
of transition metal carbides and nitrides crystallizing in sodium chloride structure, 19: 20572
of transition metals and alloys down to 0.02°K, (E), 20: 30318
onset of, theory for, 18: 13011
ordering effects on, determination of long-range, 18: 42564
oxide-layer effects on surface, (T), 19: 33176
pairing in system with nonzero angular momentum, p- and d-wave, (T), 19: 19028
pairing interactions in, corrections to, 18: 971
paramagnetic-impurity and spin-orbit-coupling effects in, Abrikosov-Gor'kov theory for, 20: 2929
partition function in Bardeen-Cooper-Schrieffer theory, asymptotic properties, 16: 22770
penetration depths in, theory for (E/T), 19: 1507
performance of large magnet coils, 20: 46546
persistence at very high magnetic fields and current densities, 17: 9018
persistent currents in rotating cylinders, 18: 24549
phase transitions in, hysteresis of, 17: 13146
possible criterion for, 16: 6848
production in pure undoped semiconductors using laser illumination, (T), 20: 8026(T)
propagation in intermediate state of superconductors, (E), 19: 23578
properties in one-dimensional systems, monovalent metal model for, (T), 20: 9904(T)
properties in transition elements, Coulomb interaction effects on, (T), 19: 35332
properties of Bardeen–Cooper–Schrieffer distribution, 18: 26491
properties of degenerate fermion gas, suppression of Cooper pairing in, (T), 20: 11923
properties of ferromagnetic alloy, (T), 20: 15648
properties of organic macromolecules, model calculations for, (T), 19: 43241
properties of relativistic degenerated electron gases at 0°K, 16: 28273
properties of surface, in lead, (E), 19: 10193
properties of surface, 19: 37745
properties of surface, thermal conductivity measurements for, 20: 30294
pulse-induced transitions in thin films, 18: 28497
quantum interference from static vector potential in field-free region, 18: 14993
quantum vortices in a fermion system in, 17: 9286
radiation effect on, alpha, 17: 11291
refrigeration requirements for continuous-sheet computer memory, 20: 46536
relation to electron reactions with crystal structure, 16: 25987
relation to electron and lattice structure, 18: 9263(T) (JPRS-22588)
relation to metallurgy, 18: 6124
relations with electronic structure, 19: 12865(R) (NAA-SR-10501)
research at ORNL, 17: 34549(R) (ORNL-3480(p.41-5))
research in Japan on, 19: 23550
research on irreversible, 20: 25474(R) (BNL-954, pp 122-67)
research on, review of, 20: 17628
research on, ultrasonics in, 18: 13007(R) (NP-13592)
research program on, 19: 43997(R) (UCRL-11889)
research programs at UCRL on, 18: 31433(R) (UCRL-11317(p.18-31))
research programs on, at Siemens-Schuckertwerke laboratories, Erlangen, Germany, 19: 42228
research programs on, 20: 30735(R) (TID-22970, pp 331-73)
research programs on, review of, 20: 35841(R) (NAA-SR-11900)
resonator design for studying, 19: 5111

restoration in magnet coils, circuitry for, 20: 46548
review of type II, 18: 953 (CONF-301-3)
self-energy of Bogoliubov quasi-particle, 18: 34687
supercurrent dissipation in a-c magnetic fields, 17: 34619
supercurrents in junctions, theory for tunneling, 18: 15100
surface effects on magnetic properties in second-kind, 18: 42559
surface impedance of normal conducting films on superconducting substrates, 18: 13025
surface states correlation with high-temperature, review of, (T), 20: 2903
surface, above critical field in type I superconductors, 18: 26480
surface, types I and II, 18: 21101
symmetries in, dynamical rearrangement of, 20: 44518
theories, lectures on, 17: 13196
theories of, 18: 21106
theory, 16: 13780
theory, 16: 19887 (ANL-6527)
theory, 16: 27800
theory, 17: 17076
theory, 18: 5841(R) (AROD-2800.12)
theory, 18: 9261 (LNF-63/71)
theory, 18: 34694
theory, 18: 38019
theory, 19: 16765
theory, 20: 9911
theory, 20: 26053
theory, 20: 34446
theory, calculation of parameters using retarded electron-phonon interaction, 16: 13783
theory, collective behavior of boson systems, 16: 2662
theory for alloys, review of, (T), 20: 4791
theory for electron systems with singlet or triplet pairs, 18: 28520
theory for even and odd systems with two kinetic energies, 20: 13669
theory for, in transition alloys and metals, 17: 18830
theory for instability of Fermi state in one-dimensional system, 20: 26058
theory for long-chain organic macromolecules, 19: 8353
theory for many-fermion system, 19: 1497
theory for Mott insulator-metal transition, 19: 12074
theory for polyenes, 20: 30268
theory for type II, 18: 14638
theory for, in nonmetallic systems, (T), 20: 4781
theory for, in semiconductors, 18: 15103
theory for, microscopic, 20: 21874(T) (TT-62-23147)
theory for, strong electron-phonon coupling in pairing, 20: 37952
theory, functional derivative techniques in, 16: 21181
theory, ladder-diagram summation in, 16: 13811
theory of, 16: 29488(T) (AEC-tr-5267)
theory of, adiabatic approximations in, 17: 6867
theory of, application of statistical perturbation theory to, 17: 26747
theory of, applications to nuclear theory, 17: 28069
theory of, density matrix-pairing tensor equation solutions in, 17: 25947
theory of, effects in band-structure, 18: 9270
theory of electron interactions in transition metals, (T), 19: 8371
theory of, energy-gap function in, 17: 25937
theory of, equivalence of classical Wellenbild $\hbar \to 0$ limit and hydrodynamic, 17: 9023
theory of gapless, 18: 40440 (TID-21048)
theory of gapless, 19: 1481 (NYO-2391-2)
theory of hard, based on motion of quantized flux lines, 18: 15064
theory of hard, review on, 18: 44689
theory of high-current, 18: 2771
theory of high-current, 19: 27377
theory of high-current gapless, 20: 6241
theory of high-field, review of, 20: 21877
theory of hysteresis and low-frequency losses in, 20: 22520(R) (NAA-SR-11805)
theory of, in the case of overlapping bands, 17: 653
theory of magnetic critical fields and hysteresis in, 18: 15116
theory of, many-body Hamiltonian expectation value in quasi-chemical equilibrium, 16: 26012
theory of, nonlinear integral equations of Hammerstein type in, 18: 7547
theory of nonlocal extension of Ginzburg-Landau, 20: 21905
theory of nuclear pairing interaction, 19: 41843
theory of organic material, at room temperatures, 19: 12443
theory of phonon-induced, mechanism for, 19: 27382
theory of position-dependent, of superconducting-metal film on bulk normal metal and normal-metal film on bulk superconductor, 18: 2764
theory of, properties of the modified electron-lattice states of low energy in, 16: 30966
theory of, quantum field theory methods in, 18: 6107
theory of, review of developments in, 18: 955
theory of small superconducting region embedded in nonsuperconducting material, 18: 36491
theory of superconductive phase, 18: 4330(R) (TID-19744)
theory of surface, 20: 19273(R) (BNL-929, pp 3-43)
theory of surface, in strong magnetic fields, 18: 40462
theory of surface, at high temperatures, 20: 30302
theory of the energy gap function and transition temperature of, in superposed metal films, 18: 2762
theory of thin semiconductor film, 20: 32338(T)
theory of thin-film, 18: 38024
theory of thin-film, 18: 38029
theory of, transformation equations in, 17: 34584
theory of transition-metal, 18: 44697
theory of transition with Cooper pair formation, 20: 30311
theory of type II, developments in microscopic, 20: 21930
theory of, use of adiabatic approximations in, 16: 29477(R) (NP-11910)
theory of, with pairs in a relative p wave, 17: 31207
theory of, asymptotic exactness of BCS, (T), 19: 47509
theory of, asymptotic exact solution for Bardeen model in, (T), 20: 46528
theory of, based on electron-electron instead of electron-phonon interactions, 18: 36484
theory of, boundary conditions for equations near critical temperatures, 19: 37754
theory of, broken symmetries and massless particles in, 18: 15014
theory of, characteristic features of, 20: 37967
theory of, charged boson-gas statistical, (T), 19: 5089 (TID-21324)
theory of, criteria for Bogoliubov quasiparticles in, 20: 1126
theory of, de Gennes method of correlation functions in, 20: 40038
theory of, eigenstates and spectrum of BCS reduced hamiltonian in, 20: 13688
theory of, Einstein-Bose condensation in, (T), 20: 28182
theory of, electron-phonon interaction in, 18: 34722
theory of, electron-pair, 20: 28177
theory of, electrodynamical, 20: 46526
theory of, excitations in, 18: 21107
theory of, expansion of effective interaction in BCS, 20: 40017
theory of, experimental basis of, 18: 30678
theory of, field theoretical method in, 18: 24545
theory of, field-theoretical method in, 18: 28507
theory of, for thin films, 18: 36533
theory of, in alloys with unfilled d-bands, experimental test of, 18: 36486
theory of, in alloys, 19: 37752
theory of, in dilute magnetic alloys at low temperatures, (T), 19: 43240
theory of, inequivalent representations in, 18: 36428
theory of, inhibiting processes in, 20: 9891 (NP-15700)
theory of, integrodifferential equations of nonlocal, 18: 34692
theory of, microscopic, 19: 10213
theory of, nonlocal extension of Ginzburg-Landau equations in, 19: 47527
theory of, pairing correlations at nuclear surface layer in, 18: 24630
theory of, pairon, 20: 34466
theory of, paramagnetic effects in, 18: 26459(R) (AD-437194)
theory of, perturbation expansions and functional integrals in, 18: 18842
theory of, position- and time-dependent, (T), 19: 6614
theory of, review of, 20: 4789
theory of, S-matrix approach to, 20: 21879
theory of, structure of Bardeen, Cooper, and Schrieffer, 19: 27367 (ISS-64/29)
theory of, temperature dependence of Ginzburg-Landau parameters in, 20: 24266 (ORNL-P-1221)
theory of, time-dependent Ginzburg-Landau, 20: 21890
theory of, transformations of Fröhlich-Hamilton operators for, 19: 2908
theory of, using "inner field" concept, 18: 15105
theory of, with combined parallel and antiparallel spin pairing, 18: 36483
theory of, with pairs in triplet of spins, 20: 15644
theory on, effect of paramagnetic impurities in, 19: 37757
theory, review of Bardeen-Cooper-Schrieffer, 16: 2663
theory, spectrum of elementary excitations in, 16: 15292
theory, use of limit summation method, 16: 15266 (JINR-P-99)
time effects on, 18: 16881
transition interface propagation along strip transmission line structure, superconducting-to-normal, 18: 18835
transition point of, pressure effects on, 17: 32806
transition temperatures in films, in contact with superconducting films, 17: 16830
transition temperature for, in dilute alloys, effects of solute concentration on, 18: 6104
transition temperatures of, 18: 36493
transition temperature of thin films, (E), 19: 33175
transition temperature, quantum effects at, (E), 20: 46509(R) (COO-1569-1)
transition, propagation of normal region in niobium–zirconium solenoid during, 20: 42100
transitions in, phase boundary model for, 18: 36534
transitions of, alloy concentration limitations for ideal, 17: 11376
transport processes at low temperatures, 18: 36463

tunneling effect, Hamiltonian for, 16: 15336
tunneling in, Josephson currents in, 17: 34614
tunneling theory in, 18: 36499
use in cavities for accelerators, 18: 36517
use in electric cables, (T), 20: 46549
use in level sensor for slush hydrogen, 20: 46537
use in microwave frequency-mixing element design, 16: 3527 (AFCRL-75)
use in parallel cryotron switch, 18: 36522
use in resonant cavities at 280 Mc, 18: 36518
use in traveling-wave plasma accelerators, 17: 16771(R) (ASD-TDR-62-1105)
uses, 19: 39690
uses and potential, 17: 34451
uses in development of cryogenic power supplies, 18: 44678
uses of, 17: 4647
variational problems in, projection operators for, 17: 32738

SUPERCONDUCTORS

Abrikonov vortex lines in hard, driving force acting on, 17: 16805
acceleration to hypervelocities of Type-II, magnetic, 20: 41554
acoustic attenuation in type II, (T), 19: 45210
acoustic wave attenuation in type-II, near transition temperature, (T), 20: 37948
acoustic wave dispersion in, transverse, 20: 44536
acoustic wave reactions with Fermi surfaces in, transverse, 18: 40451
alternating current losses in, measurement of, 16: 26644(R) (NP-11755)
analysis for impurities, activation, 18: 31389
analysis for intermetallic compounds, method of, 20: 10767(T) (AD-620995)
analysis in lead–thallium films and foils, 20: 10272(R) (NAA-SR-9339)
analysis of a-c loss mechanisms in hard and soft, 18: 34683(R) (NP-14136)
angular momenta of Cooper pairs in, Green-function hierarchy impossibility in, 16: 18267
atomic energy levels of, containing magnetic impurities, triplet states of, (T), 20: 28230
Auger electron ejection, 17: 13134
bibliography on applications, properties, and theory of, 18: 36425 (SRB-63-5)
book: *Applied Superconductivity*, 18: 36438
boundary conditions for interfaces of, Ginzburg-Landau-Gorkov, 20: 30309
boundary effects between normal conductors and, 18: 36532
Brillouin zone effects and Fermi surface of indium–lead and indium–tin, 18: 970
calibration of magnets of, using NMR, 19: 29156 (NYO-2150-4)
charge polarization around impurities in, (T), 19: 37744
charged particle detection using cryotron, 16: 13314
colorimetry on type-II, isothermal, (E), 20: 40045
condensation energy of, expression for, 18: 15125
conductivity in, electric and thermal, (E), 20: 15656
conductivity, quasi-particles and transport phenomena in, 16: 10669 (EFINS-61-17)
conference on, New York, February 18, 1962, 18: 6123
conference on type II, 20: 21899
contact between niobium–zirconium and lead–tin, design and fabrication of, 20: 42124
cooling system for magnet coils of, design of cryostat for, 20: 19731
coupling constant range for coexistence of singlet and triplet pairs in anisotropic, 20: 17645
couplings in, properties of $l \pm 0$, 16: 27811
critical alternating currents in films of, 18: 9269
critical alternating currents in wire, density dependence on frequency of, 18: 13018
critical characteristic curves of, measurement of, 19: 41630
critical conditions for thin films of superconducting, application of Ginzberg-Landau theory to, 18: 36533
critical current and magnetization of, magnetic field rise-time dependence of, (E), 19: 8338
critical current behavior in longitudinal and transverse fields, 18: 16883
critical-current degradation in solenoids, model for, 17: 27944 (NP-12908)
critical current degradation and flux jumping in solenoids of heat-treated niobium–zirconium, 17: 36469
critical current density of, in pulsed magnetic field, 18: 18833
critical current density and specific heat of niobium–tin intermetallic compounds, (E), 19: 47508
critical current density in hard alloy, method for increasing, (E), 20: 1121(T) (AI-Trans-97)
critical current density in niobium–zirconium-alloy, magnetic field dependence of, (E), 20: 26031
critical current density of niobium–zirconium wires, (E), 20: 30267(T)
critical current density in niobium–zirconium–tantalum, effect of micro-heterogeneity on, 20: 40020
critical current density in niobium–zirconium, effect of alloy structure on, 20: 40021
critical current-field characteristics of short wire samples in solenoids of, 17: 37729
critical current in, with negative interphase surface energy, 17: 29453
critical current in rolled strip of niobium–zirconium, field-independent anisotropy of, 18: 6130
critical current in surface of type-II, asymmetry in, (T), 19: 41616
critical current in high-field, field dependence of, 20: 44520
critical current in indium–thallium, effects of field orientation on, 20: 44560
critical current measurement in, method for, 20: 4390(R) (ORNL-3870, pp 65-9)
critical current near transition field of bulk type-II, longitudinal, (T), 20: 28192
critical current of, critical field dependence of, 18: 11130
critical current oscillations in type II, field dependence of, 18: 28512
critical current of disperse phases in, 20: 9900
critical current of niobium–titanium, effect of precipitates on, 20: 32322
critical current training in solenoids of, (E), 19: 10215
critical currents of ternary-alloy, at 4.2°K, 17: 554
critical currents in hard, theory of flux creep at, 17: 6876
critical currents in, longitudinal, 17: 14961
critical currents in Nb_3Sn, 17: 16805
critical currents, 17: 24062 (UCRL-10402)
critical currents in niobium–tin, angular and field dependence of, 17: 39764
critical currents in niobium–zirconium, anomalous, 18: 6131
critical currents in type II, longitudinal field effects on, 18: 22833
critical currents of type-II, 18: 26472
critical currents in niobium and niobium–tin alloy, 18: 36434
critical currents in cold-rolled transition-metal alloys, anisotropy in, 18: 36524
critical currents and magnetization of type II, theory for, 18: 40444
critical currents of gallium–vanadium and niobium–tin, in transverse fields, 18: 44698
critical currents in tin film, edge-effect limitations on, (E), 19: 12433
critical currents in solenoids in passing through lambda point, a-c, (E), 19: 14438
critical currents in high-field, (E), 19: 16797
critical currents of high field, use of pulsed fields for measuring, (E), 19: 19056
critical currents of type-II, effect of circulating currents on, 19: 23551
critical currents of long wire, device for measuring, 19: 23554
critical currents in lead-thallium alloy, magnetic field dependence of, (E), 19: 14435(R) (NP-14676)
critical currents and fields in niobium–tin, (E), 19: 23541
critical currents in solenoids of, a-c, (E), 19: 25438
critical currents in, with pinned filament structure, (T), 19: 31173
critical currents in niobium strips, alternating, 19: 33169
critical currents in niobium carbide, (E), 19: 27371
critical currents in niobium carbide–niobium nitride systems, (E), 19: 39688
critical currents in indium film, (E), 19: 39724
critical currents of type II, effects of magnetic field rise times on, (E), 19: 43238
critical currents in, (T), 20: 4791
critical currents of alloy, method for increasing, 20: 4799(P)
critical currents in films of, applied magnetic field and temperature dependence of, (E), 20: 6232
critical currents in noninductive coils of niobium–zirconium alloy, anomalous, 20: 13674
critical currents in tin, temperature effects on, 20: 13693
critical currents in tin, effects of magnetic field and temperature on, 20: 15662
critical currents in, equipment for measuring, 20: 17602
critical currents in niobium diselenide single crystals, effects of stoichiometry on peak, (E), 20: 17609
critical currents in niobium-tin alloy, (E), 20: 21921
critical currents in niobium–tin and gallium–vanadium intermetallic compound, in high fields, (E), 20: 21922
critical currents and fields in flux-pump fed coils of, (E), 20: 21924
critical currents and magnetic hysteresis in mixed state, (T), 20: 21932
critical currents in niobium-tantalum alloy, effect of surface conditions on, (E), 20: 28185
critical currents in Nb_3Zr wires, magnetic field dependence of, (E), 20: 28175
critical currents in bismuth–indium and bismuth–tin film, magnetic field effects on, (E), 20: 32317
critical currents of antimony-lead, desolvation effects on, 20: 42099(T) (AD-636625)
critical currents in surface sheaths of, effects of copper, chromium, and nickel plating on, 20: 42114

critical currents in niobium–zirconium, effects of annealing and orientation on, (E), 20: 42569
critical field and energy gap of, relation between, (T), 19: 43244
critical field and vortex line structure in alloy, lower, (T), 20: 6251
critical field and transition temperature of rubidium, isotope effect on, (E), 20: 11913
critical field and energy gap of, relation between, 20: 28203
critical field and transition temperature of indium, in porous glass, (E), 20: 37949
critical field and magnetization of molybdenum–titanium alloy, Pauli spin and spin-orbit effects on, (E), 20: 37951
critical field and energy gap of, rules for, 20: 42119
critical field and surface current measurements for titanium–vanadium, 20: 44535
critical field calculations, integration of BCS expression for, 16: 15265 (IS-399)
critical field for surface conductivity in, 18: 11116
critical field for type II, temperature dependence of lower, (E/T), 19: 19031
critical field for indium–tin alloy film, (E), 20: 28223
critical field in thin, temperature and thickness dependence of limiting, 17: 25928
critical field in, temperature dependence of mixed-state upper, 17: 29456
critical field in cerium-doped lead, 20: 40050
critical field intensity of alloy wires of, pulse methods for measurement of, 20: 9899
critical field limits for hard, 17: 3635
critical field measurements in solenoids, 20: 44508
critical field measurements for niobium–zirconium, resistive effects on surface, 20: 44534
critical field of, maximum, 17: 8959
critical field of niobium, resistivity and temperature dependence of, 18: 2772
critical field of type II, temperature dependence of, 18: 11118
critical field of strong-coupling, 18: 36432
critical field of alloy, temperature dependence of upper, (T), 19: 23583
critical field of titanium alloy, spin-orbit effects on upper, (E), 20: 32330
critical field of gallium–vanadium, upper, (E), 20: 34434
critical fields and currents in, 17: 11421
critical fields and magnetic moments in thin films of, in magnetic field, 17: 31227
critical fields and transition temperatures of scandium–vanadium, (E), 19: 5108
critical fields and temperatures in multiple films, 19: 14447
critical fields and flux penetration pattern in anisotropic type II, (T), 19: 35344
critical fields and temperatures in indium, tin, and thallium, (E), 20: 26034
critical fields and temperatures of multiple, (E), 20: 30291
critical fields and magnetization of niobium-doped strontium titanate, (E), 20: 37953
critical fields for strong- and weak-coupling, two-fluid model for, 19: 39711
critical fields for plane films of, in longitudinal magnetic fields, (T), 20: 28191
critical fields in indium–lead, 18: 16884
critical fields in niobium and niobium-oxygen solutions, 18: 34704
critical fields in niobium-titanium alloy, Pauli paramagnetism effects on upper, (E), 20: 6236
critical fields in thin-films, angular dependence of upper, (T), 20: 13661
critical fields in thin films of, fluxoid quantization and Ginzburg-Landau theory for, 20: 13685
critical fields in type II, in presence of electron spin effects, (T), 20: 46516
critical fields of thin films of, thickness effects in, 16: 27826
critical fields of niobium–titanium and niobium–zirconium, expression for upper, 18: 11109
critical fields of niobium film, 18: 21114
critical fields of second-kind, lower, 18: 24562
critical fields of, purity and temperature dependence of upper, (T), 19: 5106
critical fields of strong and weak coupling, Ginzburg-Landau parameter for, (E), 19: 10195
critical fields of thin film, upper, (E), 19: 10206
critical fields of niobium nitride, measurements of, (E), 19: 12434
critical fields of thin film, (T), 19: 16781
critical fields of thin films of, (T), 19: 16802
critical fields of indium, isotope effects on, (E), 19: 19019 (UCRL-11901)
critical fields of type II, limiting, (T), 19: 19025
critical fields of alloy, (T), 19: 21192
critical fields of aluminum, 19: 27378
critical fields of alloy, temperature dependence of surface, (T), 19: 31178
critical fields of type II, angular dependence of upper, (T), 19: 35328
critical fields of type II, angular dependence of upper, (E), 19: 35329
critical fields of bismuth III, at high pressures, (E), 19: 45198
critical fields of thin films of, (T), 20: 2926
critical fields of niobium-, temperature dependence of Ginzberg-Landau parameter for, 20: 17585 (AD-627910)
critical fields of aluminum film, (E/T), 20: 17622
critical fields of vanadium film, (E/T), 20: 21915
critical fields of films and surfaces of, angular dependence of, (T), 20: 21917
critical fields of, angular dependence of surface, (T), 20: 28184
critical fields of niobium–zirconium alloy, angular dependence of upper, (E), 20: 30270
critical fields of type-II, temperature and purity dependence of, 20: 30295
critical fields of type-II, electron spin and spin-orbit effects on, 20: 30296
critical fields of thin-film, (T), 20: 44574
critical fields of bulk high-field, measurement of, 20: 46514
critical magnetic field of, theory of, 18: 15061
critical magnetic field strength of pure, pressure effects on, (T), 20: 17639
critical magnetic field of thin superposed films of, 20: 44543
critical persistent currents in hard, 17: 6875
critical persistent currents in cylindrical, 18: 36477
critical temperature of, Bethe-Salpeter equation for, 17: 22379
critical temperature of alloyed, impurity effects on, 17: 28044
critical temperature of transitionless, depression by transition metal impurities, 17: 29457
critical temperatures of, pressure effects on, 18: 15091
critical temperature of anisotropic, theory of impurity effects on, 18: 21116
critical temperature enhancement in titanium alloy, 18: 24553
critical temperature of, effect of electron mean free path on, (T), 19: 27376
critical temperature of impure, effect of resonance scattering on, 20: 1127
critical temperature of niobium-transition metal, 20: 1129
critical temperature of, with an impurity in the two-band model, (T), 20: 2925
critical temperature of, effect of electric impurities on, (T), 20: 8006
critical temperatures of carbide and nitride, correlation with valence electrons, (E), 20: 21911
critical temperature of, with paramagnetic impurity in two-band model, (T), 20: 24274
critical temperatures of, Froelich model calculations for, 20: 24297(T)
critical temperature of, transition-metal impurity effects on depression of, (E), 20: 37955
critical temperature in thin film, review of, 20: 37976
critical temperature of type-II, de Haas-van Alphen oscillations in, (T), 20: 42126
critical temperature of, with paramagnetic admixtures, (T), 20: 44513
critical temperature and critical field for pure gallium single crystals, 20: 44545
cryogenics system for, 18: 15042 (IDA/HQ-63-1412(Vol.I)(p.110-11))
cryostat design for solenoids of, with thermal working volume, 20: 32334
crystal lattice stiffness parameter of intermetallic Nb_3Sn, at 4.2 to 300°K, (E), 20: 28633
crystal phase transformations in, 18: 42568
crystal structure studies in transition metal alloys, 18: 34283 (UCRL-11390)
current and flux in, in filamentary and mesh-like paths, 16: 19406
current-carrying capacity of solenoid, 17: 11349
current-carrying ring, extension of Byers and Yang method to, 17: 22264(R) (ANL-6679)
current characteristics in lead tunnel junctions, (E), 20: 9918
current collective oscillations in second-type, hydrodynamic theory of eddy, 19: 31180
current decay propagation in niobium–zirconium alloy, persistent, (E), 19: 47507
current degradation in niobium–zirconium, 19: 37735(R) (N64-33921)
current degradation in solenoids of niobium–zirconium, mechanism of, 20: 8004
current degradation in solenoids of, flux pinning energy and temperature dependence of, 20: 21920
current degradation in niobium–zirconium, low-frequency alternating, (E), 20: 34449
current density and gap equation for local, in magnetic fields, 20: 21880
current density in, 17: 22381
current density in, electron-pair flow momentum dependent, 17: 24155
current density in contact points of oxidized niobium wires, (E), 20: 30277

current density in niobium–oxygen–titanium, effects of processing on, 20: 37267
current distribution in thin-film strip transmission-line, (T), 19: 39692
current distribution in thin film arrays of, (T), 20: 15643 (NASA-TN-D-3293)
current distribution in thin film transmission lines of, (T), 20: 19725 (NASA-TN-D-3344)
current distribution in sheets of type II, magnetic field effects on, (E), 20: 30273
current distribution in coils of, optimum, (T), 20: 37971
current distribution in cylindrical type II, 20: 40029
current distribution along vortex lines emerging from, (T), 20: 46513
current flow in, of the second kind, model for longitudinal force-free, 17: 32741
current flow in type-II, paramagnetic helical, (E), 19: 23576
current flow patterns in nonideal type II, in longitudinal fields, (E/T), 20: 17617
current fluctuations in circuits of, 18: 26484
current in hard, properties of surface, 20: 40014(R) (ORNL-3989, pp 109-27)
current losses and magnetic field aberrations from high-field wires of, in adiabatic demagnetization apparatus, 20: 37970
current losses in niobium, temperature dependence of surface, (E), 19: 14435(R) (NP-14676)
current losses in type II, 20: 28187
current losses in type II, calculation of a-c, 20: 37969
current losses in niobium–copper strip, 20: 46519
current losses in, a-c, 18: 28506
current motion in, in transverse magnetic fields, (E), 20: 11902
current phenomena in type II, surface, 20: 40015(R) (ORNL-TM-1598)
current propagation in composite, minimum, (T), 20: 2904
current quantization and stability in, 16: 9319
current quenching in thin lead films, (E/T), 19: 45193 (TID-21307)
current regulators for solenoids of, design of, 19: 38945
current stability at microwave frequencies in cavity resonators of, field-emission, (E/T), 20: 9895
current states in weakly coupled, stability of metastable, (E), 20: 46509(R) (COO-1569-1)
current transfer from power lead to, 18: 44675 (BSD-TDR-64-110)
current transmission through barriers in, long-range order effects from, (T), 20: 19726
current vortex motion in, effects of, (T), 20: 19746
current-carrying capacity of hard, degradation of, 18: 30308 (NASA-TN-D-2345)
current-carrying capacity of, measurement of temperature dependence of, 18: 34681 (BSD-TDR-64-87)
current-carrying capacity of hard, with zero external field, 20: 40015(R) (ORNL-TM-1598)
current-carrying states of weakly coupled, metastable, (E), 19: 45206
current-inductance characteristics of, 20: 30303
current-voltage characteristics of tunnel junctions of, second harmonic detection system for, 19: 38944
currents and magnetic fields close to surface of type-II, (T), 19: 35339
currents between deviation from single-particle tunneling, 17: 8948(R) (TID-17398)
currents between, in high magnetic fields, 20: 44531
currents in foil magnets of, flux pump for generation of high, 17: 24152
currents in foils, maximum of surface sheath, (T), 20: 44558
currents in Josephson junctions of, persistent, (E), 19: 47521
currents in rings of, energy of, (T), 20: 25646
currents in surface sheath of, persistent, (T), 20: 6243
currents in, magnetic hysteresis effects of surface, (E), 20: 13679
degradation and training in niobium-base alloy, metallurgy of, 19: 2816
degradation of ribbons of, in solenoids (E), 19: 1515
density modulation in fermion-system, 18: 38026
density of states of, effect of magnetic impurities on, (E), 19: 8349
density of states in, effect of paramagnetic impurities by magnetic field on, (T), 19: 12439
density of states from excitation in type II, (T), 19: 41623
design and construction of magnets of, for corpuscular ionography, 20: 21876
design and operation of magnetically supported rotors (E/T), 19: 3175 (NASA-CR-108)
design and performance of high voltage delay lines of, 20: 9889 (EGG-1183-1192)
design and performance of thin-film cryotron, 20: 13048
design and performance for MHD magnets, 20: 39643
design and testing of magnets of, 19: 39741
design economy optimization of coils of, for controlled fusion research, 20: 34708 (NASA-TM-X-1251)
design modification for energy-storage-system, 20: 17625
design of high-field, for compressing magnetic fields in apertures, 19: 14458(P)
design of high-field solenoid, 19: 14459(P)
design of high-field, with greater length than diameter, 19: 14460(P)
design of high-field, with stacked members, 19: 33186(P)
design of high-field split coil magnets of, with forced helium cooling, 20: 36125 (SLAC-PUB-182)
design of magnet with inductive excitation, 18: 16880
design of magnets of, for traveling-wave masers, 20: 17626
design of rotating cylindrical, for magnetic shielding, 18: 2768
design of 30 kG magnet coils of, 20: 19736
design of, magnets of, for plasma research, 19: 47533
design using niobium–zirconium alloy primary and copper secondary, 19: 23594(P)
design using titanium–vanadium alloy, 19: 39750(P)
development, 16: 16710(R) (AD-267028)
development, 17: 4886(R) (AD-275610)
development, 20: 20365
development, 19: 19265(R) (UCRL-12028(p.121-36))
development, 19: 31335(R) (UCRL-12303)
development and properties of refractory alloys, intermetallic compounds, and metals for use as, 18: 34179
development at ORNL for magnets, 17: 17336(R) (ORNL-3392(p.66-85))
development at ORNL, 17: 33158(R) (ORNL-3472(p.84-106))
development by crystallochemical methods, 20: 29623(R) (TID-22970, pp 121-256)
development for inductive energy storage, 19: 1489
development for magnetohydrodynamic cells, 18: 7459 (RTD-TDR-63-4170)
development for magnets, 19: 23163(R) (ORNL-3650(p.111-86))
development for magnet coils, 20: 40014(R) (ORNL-3989, pp 109-27)
development for power generation, review of, 18: 34499
development for power engineering, 20: 34450
development for use in magnets, 16: 28209 (TID-7636(p.299-308))
development for use in magnets, 19: 12428(R) (NBS-8481)
development of, for use in high-field magnets, 16: 32177(R) (UCRL-10349)
development of, for use in magnets, 17: 2339 (TID-16867)
development of instruments using, 19: 39690
development of magnets of, for MHD cells, 18: 36243
development of magnets of, 19: 1487
development of magnets of, (E/T), 19: 6607
development of magnets of, for thermonuclear research, 19: 12436
development of magnets of, 19: 33161
development of magnets of, 19: 45212
development of magnets of, for ultrahigh fields, 20: 32337
development of magnets of niobium–zirconium, 20: 34418(R) (N-66-16181)
development of magnets of, 20: 34422
development of niobium–tin and niobium–zirconium, 17: 6807 (UCRL-9819)
development of thin-film, for computer circuitry, 20: 30255(R) (ORO-2430-28)
development of 112 kgauss magnets of, 19: 19058
developments in uses of, 16: 30936
diamagnetism in type II, (E), 19: 5099
dielectric constant and phonon frequency of, 17: 39742
dielectric properties of, 17: 16840
differential paramagnetic effect and harmonic generation in enclosed, 20: 44544
diffusion in superimposed films of normal metals and, 17: 34594
dislocation damping in type II, 20: 20113(R) (NYO-3001-1)
dislocation effects in, mechanism for, 18: 965
dislocations in, review on role of, 17: 37664 (UCRL-10601)
domain structure instabilities in intermediate state of, 20: 4783
economics and properties of magnetic coil, 19: 12453
economics of magnets of, 18: 11104 (NIRL/R/53)
eddy currents in type-II, fast-pulsed magnetic field induced, 20: 30262
edge effects in films of, 18: 26482
effects of nonmagnetic impurities on anisotropic, 17: 20717
effects of nonmagnetic impurities on alloys of, 18: 39983
effects of Pauli paramagnetism on, 18: 44696
effects of Pauli paramagnetism on (T), 19: 1502
elastic constants of metallic, electron contribution to, (T), 19: 16772
elastic moduli of lead–thallium, as function of thallium content, 20: 46515
elastic modulus in type II, discontinuous variation of, (E/T), 20: 21912
elastic-wave attenuation in, mechanisms for, 17: 11400
electric and thermal conductivity of molybdenum–rhenium alloy, critical field measurements from, (E), 20: 13686
electric characteristics of tunnel junctions of, 18: 15096
electric conductivity of, fluctuations in, 17: 666
electric conductivity of, method for measuring, 17: 20538 (BSD-TDR-63-60)
electric conductivity of tin, disturbances in, 17: 30990
electric conductivity of non-ideal, a-c, 17: 41541 (BSD-TDR-63-147)

electric conductivity of tunnel junctions of, equipment for measuring, 18: 11127
electric conductivity at contacts between, effects of motion on, 18: 18844
electric conductivity of nonideal, a-c, 18: 18836
electric conductivity anomalies in, effects of s-d exchange interactions in, 18: 24555
electric conductivity of, electron-phonon interactions in, 18: 24557
electric conductivity and transition temperature of aluminum, dislocation effects on, (E), 19: 6611
electric conductivity of, surface, (E), 19: 11941
electric conductivity and transition temperature of indium–manganese alloy, (E), 19: 19046
electric conductivity of, Ginzburg-Landau equations for, (T), 19: 23574
electric conductivity fluctuations in intermediate state of, (E), 19: 23578
electric conductivity and Hall effect in type-II, 19: 25446
electric conductivity in the mixed state of type II, (T), 19: 33168
electric conductivity of type II, in mixed state, (T), 19: 39698
electric conductivity in type II, origin of, (T), 19: 39707
electric conductivity in intermediate state of, normal and superconducting layer motion from, (E), 20: 9910(T)
electric conductivity transitions in inhomogeneous antimony-lead alloy, anomalous, (E), 20: 9920
electric conductivity in intermediate state of type-I, vortex-motion mechanism for, (E), 20: 19743
electric conductivity of, current dependence of imaginary part of, (E/T), 20: 21919
electric conductivity and magnetization of titanium–vanadium alloy, at 4.2°K, (E), 20: 21928
electric conductivity in the mixed state of, r-f, (E/T), 20: 24286
electric conductivity of, technique for measuring, 20: 34421(T) (MATT-Trans-28)
electric conductivity of lead–indium, effect of transport-current polarity on, (E), 20: 37945
electric conductivity of type II, (T), 20: 37979
electric conductivity of niobium, from helicon-like resonances, (E/T), (E/T), 20: 40031
electric conductivity enhancement of niobium, through hydrogen treatment, 20: 46510 (NASA-TN-D-3638)
electric current and magnetic field distributions in sheets of, 18: 22827
electric current and magnetic field distribution in type II, 19: 41637
electric current behavior in, near breakdown, 18: 9264
electric current capacity in second-kind, 17: 24085
electric current decay in, theory of, 17: 652
electric current density and energy gap equation for, in slowly varying static magnetic field, 17: 39766
electric current density and resistive transition characteristics in niobium, 18: 22837
electric current density and energy gap for, in magnetic fields, 18: 30680
electric current distribution in, carrying quantized fluxoids, 18: 34688
electric current degradation in solenoids of, flux pinning dependence of, (E), 19: 6608
electric current degradation in solenoids of, 20: 26025(R) (N-65-35450)
electric current-field relation in non-ideal, critical, 17: 41542 (BSD-TDR-63-148)
electric current in, electron depairing effects on, 17: 32839
electric current in solenoid of, reduced, 17: 36375 (CONF-176-2)
electric current losses in high-field, alternating, 18: 9262(R) (NP-13492)
electric current persistence in, 17: 11404
electric current persistence in alloyed, 17: 18831
electric current through tunneling junction between identical, 17: 29458
electric current-voltage fine structure in tunneling junctions of, anomalous density of states in, 17: 34623
electric current vortices in strips of, quantized, 18: 2765
electric currents in, theory for non-transmission of alternating, 17: 29455
electric currents in wires of, 50-c critical, 17: 34595
electric currents in type II, theory for transport, 18: 11113
electric currents in, ohmic transport, 18: 18840
electric currents in hollow cylinder, off-diagonal long-range order for persistent, (T), 19: 10202
electric currents in lead–thallium alloy, surface, (E), 19: 10204
electric currents in, impurity effects on tunneling, (T), 19: 14436 (NYO-2391-1)
electric currents in, production means for, (E), 19: 14434 (LNF-64/50)
electric currents in, symmetry properties for spontaneous, 20: 24276
electric field effects on, accelerated energy and matter currents from long-wavelength, (T), 20: 11919
electric field penetration of surface-layer, 18: 44674 (BNL-8410)
electric fields in moving vortex cores in type-II, dissipation from, (T), 20: 19747
electric inductance of solenoids of niobium–zirconium alloy, 20: 26032
electric power losses in, at 50 cps, 18: 44677
electric properties, 17: 35260(R) (TID-19135)
electric properties of contacts to normal metals, 17: 36453 (TID-19310)
electric properties of thin films of, 18: 30185
electric properties, 19: 10675(R) (NAA-SR-9999)
electric properties of normal region of niobium–zirconium magnets, 20: 17610
electric properties of tunnel junctions in lead, 20: 44533
electric resistance states in intermediate region of, metastable, 18: 22826
electric resistivity and properties of pure and cadmium-doped tin, anisotropic, 20: 44546
electric surface impedance of, in kMc range, 18: 15093
electric surface resistivity at microwave frequencies (E), 19: 1511
electric-current and magnetic transitions in niobium stannide tubes (E), 19: 1513
electrodynamic response of local, microscopic-theory calculation of, 20: 21890
electrodynamics for small coherence distance in, nonlinear, 17: 24157
electrodynamics of, effects of collective excitations on, 18: 34720
electrodynamics of alloy, lower critical field and nonlinear effects in, 18: 36436
electrodynamics of type II, (T), 19: 35333
electrodynamics of alloy, in strong magnetic fields, (T), 20: 11907
electromagnetic forces in, device for measuring, 19: 10208
electromagnetic properties, 16: 10849
electromagnetic properties, material function dispersion relations, 16: 13817
electromagnetic wave propagation in mixed-state indium–lead, (E), 20: 24294
electron angular momentum pairing in, Cooper, (T), 19: 35327
electron band structure and transition temperature of cadmium–indium, 20: 19764
electron behavior in metals containing paramagnetic impurities causing spin-exchange fields, 18: 24563
electron capture rate, 17: 22345
electron collective excitations in, (T), 20: 8310
electron Compton wavelength in, measurement of, (E), 19: 33170
electron concentration and temperature in thin-film nonmetallic, (T), 19: 31179
electron decay rate in, injected, 20: 37984
electron density of states and phonon spectra in lead, (E/T), 19: 10207
electron diffraction at magnetic flux lines in, (T), 20: 34833
electron diffuse reflection from surface of, (T), 19: 5109
electron emission from, 17: 41553(R) (NP-13160)
electron emission by, analysis of enhanced, 18: 30166(R) (AD-439716)
electron energy spectra of tin, gap width of, 18: 11128
electron excitation spectra in type II, Kronig-Penney model for, 20: 21904
electron interactions in, virtual phonon exchange in, (T), 19: 12448
electron interactions in, isotropic model for coulombic, 19: 41627(T)
electron interaction effects in magnetic films superimposed on, (E), 20: 11918
electron-ion interactions in, conduction-paramagnetic, 17: 36458(T) (AEC-tr-5978)
electron-ion reactions in, mathematical analysis, 16: 18143 (AFOSR-1440)
electron mean free paths in, 18: 15079
electron motion on surface of, in gravitational field, (T), 20: 32325
electron-pair recombination periods in, 16: 13805
electron-pair recombination periods in, crystal structure effects on, 16: 13806
electron-pair tunnelling in, 18: 7651
electron pairing and flux quantization in cylindrical, (T), 19: 10205
electron pairing and flux quantization in cylindrical, (T), 20: 4784
electron pairing in small-dimension, (T), 20: 9907(T)
electron pairs in quasichemical equilibrium in, theory for, 18: 42569
electron scattering and thermal conductivity at interphase boundaries in, 17: 18969
electron scattering by alloy, anomalous, (T), 19: 8372
electron spectra of, 18: 9263(T) (JPRS-22588)
electron spectra of compounds formed from nonsuperconducting elements, 18: 32692(T) (JPRS-25289(p.1-13))
electron spectrum of intermediate state of, (T), 20: 2923
electron spin in, effects of uniform exchange field on conduction, 17: 36480
electron spin resonance in, model for conduction, (T), 20: 2899
electron spin-pairing in vanadium silicide, (E/T), 20: 30734(R) (TID-22970, pp 1-63)
electron states in, structure in density of, 17: 18968
electron tunneling in, 17: 643
electron tunneling through thin dielectric layers between, 17: 19

electron tunneling in, 17: 5138
electron tunneling current from, to normal metals, 17: 14941(R) (NBS-7608)
electron tunneling between, two-particle, 17: 28037
electron tunneling in, microwave effects on, 18: 4502
electron tunneling in, principle of, 18: 6125
electron tunneling in, phonon critical points in, 18: 9273
electron tunneling between, 18: 11098(R) (AD-407317)
electron tunneling in metal–insulator–superconductor sandwiches, 18: 15095
electron tunneling in junctions of, phonon effects on, 18: 15097
electron tunneling in junctions of, theory for multiple, 18: 15098
electron tunneling in, Josephson, 18: 15123
electron tunneling in mercury film, analysis of, 18: 28515
electron tunneling in, 18: 36155(R) (TID-20873)
electron tunneling in, use in r-f detection, 18: 36516
electron tunneling in, 18: 38030
electron tunneling between thin film, 18: 41710(R) (AL-TDR-64-46)
electron tunneling in junctions, d^2I/dV^2 circuit study of, 18: 42551 (ORNL-P-421)
electron tunneling in Nb–Nb_2O_5–In sandwich, Josephson and anomalous, 18: 44673 (AD-604097)
electron tunneling in mercury, (E), 19: 8365
electron tunneling through insulating barrier between, Josephson, (T), 19: 8373
electron tunneling density of states for, (T), 19: 10201
electron tunneling in hard, in mixed state, (T), 19: 12430 (NP-14644)
electron tunneling between layers of tin, Cooper pair, (E), 19: 12447
electron tunneling from hard, (T), 19: 21164
electron tunneling in junctions of, phonon effects on, 19: 23542
electron tunneling in, step structure in Josephson a-c, (E), 19: 23570
electron tunneling in, Ginzburg-Landau equations for Josephson, 19: 23572
electron tunneling between indium–lead, phonon impurity band from, 19: 23575
electron tunneling near upper critical fields, (E/T), 19: 23571
electron tunneling in tin, a-c Josephson, (E), 19: 33172
electron tunneling in, theoretical review for Josephson, 19: 41607 (LA-3342)
electron tunneling in, photon emission in Cooper-pair, (E), 19: 41631
electron tunneling between, Josephson effect in, (T), 19: 43247
electron tunneling in thin films of, quantum mechanical phase in Josephson, (T), 19: 45209
electron tunneling in junctions of, anomalous behavior of Josephson, 19: 47515
electron tunneling in, resonant mode interactions with a-c Josephson, (E/T), 20: 2895
electron tunneling in, entropy transport from, (T), 20: 6248
electron tunneling in, critical Josephson, (T), 20: 8032
electron tunneling in, step theory for current-voltage characteristic of Josephson, (T), 20: 9903(T)
electron tunneling in, singularities in electromagnetic radiation from Josephson, (E), 20: 9908(T)
electron tunneling from indium in aluminum–aluminum oxide–indium diodes, (E), 20: 9924
electron tunneling in thick films of, resonances in, (T), 20: 9927
electron tunneling in, macroscopic quantum interference in Josephson, (E), 20: 6235
electron tunneling in junctions of, electrodynamics of Josephson, (E), 20: 11910
electron tunneling in cylindrical junctions of, d-c Josephson currents and microwave resonances in, (T), 20: 13680
electron tunneling in normal aluminum film laminates with lead, (E), 20: 13687
electron tunneling in thick films of indium, geometrical resonances in, (E/T), 20: 15650
electron tunneling in junctions of lead, subharmonic structure in, (E/T), 20: 15651
electron tunneling excitation spectra in laminates of normal metals with, (T), 20: 15653
electron tunneling from films of, into normal metals, electron interference effects in, (E/T), 20: 17621
electron tunneling evidence for fluxon entry into thin type II, (E/T), 20: 17627
electron tunneling in tin-junction, structure of high-frequency Josephson, (E), 20: 17636
electron tunneling in lead junction, magnetic-field dependence of $2\Delta/n$ structure in, (E), 20: 19739
electron tunneling in aluminum–lead junction, structure from recombination effects on, (E), 20: 19744
electron tunneling in, effects of paramagnetic impurities on Josephson, 20: 26060
electron tunneling in, Josephson, (T), 20: 28219
electron tunneling in, spatial variation of order parameter effects on on density of states in, (T), 20: 32340
electron tunneling in superimposed layers of normal aluminum and lead, (E), 20: 32342
electron tunneling conductance in junctions of, model for zero-bias anomalies in, 20: 32714
electron tunneling in superimposed films of lead, (E), 20: 34442
electron tunneling in junctions of, design and performance of system for measuring small nonlinearities in, 20: 37973
electron tunneling in, review of Josephson, 20: 37975
electron tunneling in coupled, quantum effects of, 20: 37986
electron tunneling in junctions of, second derivatives for conductance in, (E), 20: 39470(R) (ORNL-3924)
electron tunneling in, radiation induced structure in d-c Josephson, 20: 40035
electron tunneling in, quantum coherence in, 20: 44551
electron tunneling in, theory for, 20: 44570
electron tunneling in, electrodynamics of Josephson, 20: 44571
electron tunneling in, transverse magnetic field effects on, 20: 44572
electron tunneling in, properties of, 20: 44573
electron tunneling density of states in type-II, energy and purity dependence of, 20: 44525
electron tunneling in Pb–PbO–Pb, fine structure of, 20: 46522
electron tunneling in films of tin, geometrical resonance effect on, (E), 20: 46518
electron-phonon coupling and energy gap in, (T), 19: 16787
electron-phonon interactions in, (T), 19: 18599
electron-phonon interactions in indium, (E), 19: 27384
electron–phonon systems in, coupled, 18: 15124
electron-spin pairing in single crystals of vanadium silicide, 20: 20152
electronic structure effects on transition-alloy and -metal, 18: 15083
electronic thermal conductivity of, theory of intrinsic, 17: 6869
electronic thermal conductivity of, with strong electron-phonon coupling, 18: 21100
electrostatic potential difference in, 20: 34432
electrostatic switching of organic macromolecular, 19: 18505
elementary particle models of, energy gap equivalence in, 17: 39936
energy conversion thermodynamics in, 16: 12247
energy conversion in cables of, direct, 19: 32930
energy gap above thermodynamic critical field, (E), 19: 6617
energy gap and critical field of, (T), 20: 40017
energy gap and microwave absorption in films of, magnetic field dependence of, 18: 40452
energy gap and thermal conductivity of, magnetic field effects on, 18: 22838
energy gap and ultrasonic attenuation in crystalline, 18: 15108
energy gap anisotropy in (E), 19: 3181
energy gap anisotropy in aluminum, in magnetic fields, determination using microwave absorption, 20: 32326
energy gap at finite temperatures, magnetic field dependence of, 18: 7650
energy gap effect of paramagnetic impurities in, 17: 6878
energy gap for niobium–tin, tunneling measurement of, 18: 15099
energy gap in, 18: 22728(R) (NP-13870)
energy gap in aluminum, microwave studies of, (E), 20: 15658
energy gap in, containing paramagnetic impurities, 17: 11405
energy gap in, disruption by paramagnetic impurities, 17: 13160
energy gap in, effects of magnetic fields on, 17: 9035
energy gap in lead alloy, infrared absorption data on, 18: 4510
energy gap in lead, 20: 4782
energy gap in lead, (T), 20: 6238
energy gap in rhenium, anisotropy of, (E), 20: 30281
energy gap in semiconductor film, lower temperature limit for, (T), 20: 8010
energy gap in single-crystal, anisotropy effects on, (T), 20: 40041
energy gap in thallium, ultrasonic determination of, 18: 34701
energy gap in thallium film, measurement to 0.804°K by electron tunneling, (E), 19: 12431
energy gap in thin films of, magnetic field dependence of, 18: 6110
energy gap in type II, magnetic field effect on, 18: 11114
energy gap in, dependence on transport current, (E), 19: 39735
energy gap in, effects of h-f phonon pulses on, 18: 15050
energy gap in, effects of magnetic field on, 18: 16885
energy gap in, magnetic-field dependence of, 18: 36502
energy gap in, temperature dependence of, (T), 19: 6615
energy gap in, theory of, 18: 44695
energy gap of anisotropic, Ginsburg-Landau equations for, 19: 41625
energy gap of film, temperature dependence of, 18: 26487
energy gap of film, magnetic-field dependence of, 18: 26488
energy gap of lanthanum, electron-tunneling measurements of, 20: 36130
energy gap of lead, temperature dependence of, (E), 20: 24295
energy gap of tin, (E), 20: 17619

energy gap of tin, anisotropy of, (E), 19: 29163
energy gap of, Bogoliubov equation for, (T), 19: 21190
energy gap of, dependence on critical field at critical temperature, (T), 20: 9933
energy gap of, magnetic field strength dependence of, 18: 34721
energy gap parameter of, nonmagnetic impurity effects on anisotropy of, (T), 20: 37958
energy gap relations for thin-film, 18: 1126(R) (NBS-7973)
energy gap resonances in, 17: 29452
energy gap resonances for cylindrical, at zero temperature, 19: 35323
energy gaps in hard, 18: 36495
energy gaps in, effects of magnetic fields on, (T), 19: 8368
energy gaps in, tunneling techniques for measuring, (E), 20: 21885
energy gaps of binary films of, (E), 20: 34425
energy gaps of niobium, tantalum, and vanadium, 19: 33180
energy gaps of, effects of electron-damped dislocations on determination of, (T), 20: 17618
energy levels in intermediate states of tin, specific heat decrease from quantization of, (E), 20: 9905(T)
energy losses from magnet coils of, (E), 20: 17630
energy losses in, h-f residual, 20: 30304
energy of rotating and stationary, free, (T), 19: 47504 (JPL-TR-32-650(Pt.2))
energy spectra in vicinity of normal metal contact with, 17: 20726
energy spectrum of mixed state, with low density of vortex lines, (T), 19: 41624
energy state density of, with paramagnetic impurities, (T), 19: 31177
energy state of V_3Ga, with paramagnetic impurities, 20: 28209
energy storage in inductive coils of, for high-power discharges, 17: 34574
energy storage in, 18: 15041 (IDA/HQ-63-1412(Vol.I)(p.106-9))
energy storage in magnet coils of, (T), 19: 27366 (IPP-4/13)
energy storage with coils of, magnetic, 18: 15038 (IDA/HQ-63-1412 (Vol.I)(p.53-75))
energy storage with, inductive, 18: 15039 (IDA/HQ-63-1412(Vol.I)(p.76-9))
energy-gap determination using low-resistance contacts, (E/T), 19: 37737 (TID-21947)
evaluation of β-titanium alloys as, 18: 21112
evaluation of materials as, 18: 44683
evaluation of niobium selenide as layer-like, 17: 39790
excitation spectra, collective, 16: 6883
excitation spectrum of type I and II, for situations of space-varying order parameter, 20: 46511
excitations in, (T), 19: 16283
excitations in strong-coupling alloy, Fermi-liquid theory for collective, 19: 47518
excitations in type-II, properties of fermion-type, 20: 42110
excitations in, Goldstone theory for, 20: 45042
excitations of, collective, 16: 33595
exciton modes in, effects of impurity scattering on, 17: 11412
excitons and plasmons in, 16: 10665 (AFOSR-2045)
fabrication and feasibility of thin film, for microwave and radiofrequency detection, 18: 41710(R) (AL-TDR-64-46)
fabrication from heat treated niobium–zirconium alloy, 20: 39372(P)
fabrication into cables, (E), 20: 3612 (CONF-651001-6)
fabrication of Nb_3Sn cylinder and ribbon, using diffusion layers, 20: 17649
fabrication of stranded niobium-tin wires, 20: 9897
fabrication of thin-film, 18: 26496(P)
fabrication of thin-film, elimination of edge effects in, 18: 28499
fabrication, properties, testing, and uses of wire and tape, 19: 16110
fabrication, properties, and theory of resonant-cavity, 19: 21186
Faraday unipolar induction in nonideal type II, 20: 40016
ferromagnetic film proximity effects on film, transition-temperature depression by, (T), 19: 45197
ferromagnetic particle acceleration by solenoidal, for nuclear fusion, 20: 36299
ferromagnetic particle effects on type-II, (E), 20: 40024
ferromagnetism in alloys of, 18: 24561
ferromagnetism of paramagnetic impurity-containing alloy, (T), 20: 28214
field penetration in, (E), 20: 46509(R) (COO-1569-1)
fluctuation compressibility theorem and its application to the pairing model of, 17: 11398
flux instabilities in hard, 18: 40445
flux jumping and degradation in, 18: 26463
flux jumping and training in solenoids of, 18: 26470
flux jumps in hard, (E/T), 19: 37750
flux penetration in, a-c susceptibility measurements of, 18: 44674 (BNL-8410)
flux penetration in cylindrical films of, 20: 1128
flux pinning in bulk type-II, (E/T), 20: 11911
flux precession in indium, (E), 19: 23564
flux quantization in, 16: 16877
flux quantization in cylinders of, 16: 27800
flux quantization and Knight shift in, theory of, 17: 24056 (TID-18658)
flux quantization in doubly connected, theory of, 18: 20667
flux quantization in (T), 19: 1422 (NP-14404(p.245-54))
flux quantization noise on hollow cylindrical, (E), 19: 12440
flux quantization in, gauge-invariant Hamiltonian formalism for, (T), 19: 21173
flux tube motion in type-I, precessional, (T), 19: 21167
fluxoid conservation in, 18: 15058
fluxoid conservation in thin-film ring, 20: 2927
fluxoid quantization in multiply connected, 18: 7652
fluxoid structure in films of, (T), 20: 4777
fluxoids in, inertial mass and relaxation time of, (T), 19: 19051
forces on thin films of tin, in magnetic fields, mechanical, (E), 20: 19765
free energy and energy gap equations for, fourth-order terms of, 18: 42573
free energy difference between normal states and (T), 19: 3183
galvanomagnetic effects in type II, (T), 20: 24290
gamma resonance absorption by tin, 16: 33895
Gibbs free energy of bulk type-II, (T), 20: 30287
Gibbs potential in variable magnetic field, Ginzburg-Landau equations for, (T), 19: 31170
Ginzburg-Landau equations for slabs of, in tangential external magnetic fields, 18: 4508
Ginzburg-Landau coefficient in type-I, temperature dependence of, (E/T), 19: 16778
Ginzburg-Landau equations for pure two-band, 18: 44691
Ginzburg-Landau equations for Abrikosov mixed state in, series solution of, 19: 47519
Ginzburg-Landau parameter in, temperature and mean-free-path dependence of, 18: 40448
Ginzburg-Landau parameters of type-II, (E/T), 20: 2906
Ginzburg-Landau parameter for type-I, 20: 20177(R) (BNL-929, pp 83-105)
Ginzburg-Landau parameters for niobium, temperature variation of, (E/T), 20: 26036
Hall coefficients, interplanar distance, and crystal structure, 16: 6848
Hall effect in indium and niobium, (E), 19: 27383
Hall effect in type-II, (E), 19: 19039
Hall effect measurements on niobium–zirconium magnets, 20: 17600(R) (ORNL-3908, pp 114-48)
heat absorption and emission by type II, Peltier effect in, (E), 20: 15649
heating at contacts with normal conductors, inhibition of, 17: 12830
heating effects on properties of coil, (E/T), 20: 13675
heating losses in second-kind, a-c, 17: 39754
high-frequency properties, 16: 13177(R) (NP-11413)
impurities in mean-free-path effects of, 17: 11418
impurity effects on niobium–tin, 18: 44679
inductive behavior of magnets of, 17: 41596
infrared absorption by lead films, effects of magnetic fields on, (E), 20: 40044
infrared radiation absorption by, threshold, 17: 2124
infrared radiation absorption in, collective excitations in, 18: 34720
interactions in, quantum-statistical Green-function method for many-body, 19: 23507(T)
interactions with magnetic fields, 17: 6784 (CERN-62-30)
interactions with Bose gases, 17: 20689
intermediate state of hard, 18: 6134
intermediate state in type II, (T), 19: 16804
joining of, using gallium mixtures, 19: 33185(P)
joints with normal-state leads, development of optimum, 18: 44147(R) (ORNL-3670(p.21-2))
Josephson current between, self-magnetic-field limitation of, 17: 31213
Josephson tunneling between ring, persistent currents and fluxoids in, (E), 19: 23592
Knight shift due to spin-orbit coupling in, magnetic field dependence of, (T), 19: 39739
Knight shift in transition metal, orbital contribution to, 18: 4505
Knight shift in, magnetic field dependence of, (T), 19: 39705
Knight shift in, theory of, 18: 11129
lattice effects on transition temperature in thallium, 20: 44566
lattice stability of Abrikosov vortex lines, energy and elastic moduli calculations of, 18: 24230
magnet coils of, size limitations on, 17: 39721 (NP-13148)
magnetic and resistive transitions of indium–lead alloy, (E), 19: 10216
magnetic behavior of niobium–zirconium wires, 18: 13019
magnetic behavior of semi-reversible type II, 18: 18841
magnetic behavior and I-H curve of anchored-filament-structure, 18: 24552
magnetic behavior of type-II, (T), 19: 25437
magnetic behavior of thin-film, 19: 31331(R) (NBS-8797)
magnetic behavior of, with pinned filament structure, (T), 19: 31172
magnetic behavior of dirty, (T), 20: 24292

magnetic coupling between adjacent type-II, (E), 20: 6244
magnetic critical fields in thin, hollow cylinders, 17: 34615
magnetic critical fields for London, 18: 2776
magnetic design with reduced winding space, 18: 9268
magnetic diffusivity in cylinder of niobium–zirconium alloy type-II, (E), 20: 24279
magnetic field attenuation by films, 16: 9308
magnetic field compression in, 19: 33184(P)
magnetic field distribution in annealed and plastically deformed niobium type-II, (E), 20: 13672
magnetic field effects on thin-film, 17: 22343
magnetic field effects on tantalum-film, 18: 15073
magnetic field effects on impure and pure tantalum, 18: 15074
magnetic field effects on lanthanum chalcogenides, (E), 19: 33177
magnetic field effects on spherical, force calculations for, (T), 20: 26023 (JPL-TR-32-806)
magnetic field effects on performance of type II, 20: 37942
magnetic field effect on type-II, Fulde-Ferrell, 20: 40046
magnetic field effects on order parameter of, (E/T), 20: 46520
magnetic field enhancement in tubes of, empirical formula for, (E/T), 20: 13678
magnetic field enhancement in tubes of, 20: 44532
magnetic field flux quantization in cylinders, 17: 2134
magnetic field force effects on, (E), 19: 31175
magnetic field generation by rotating, 18: 15057
magnetic field of small particles of, critical, (T), 19: 8360
magnetic field of type-II, critical, 19: 33181
magnetic field of rotating, (E/T), 20: 11911
magnetic field penetration in, noise propagation from, 17: 39746
magnetic field penetration depth and thermoelectric effect in anisotropic, 18: 32694
magnetic field penetration depth in, 18: 34721
magnetic field penetration depth in niobium, temperature dependence of, (E), 19: 14435(R) (NP-14676)
magnetic field penetration depth in niobium, (E/T), 19: 39726
magnetic field penetration of thick slabs of type-II, velocity of, (T), 20: 8011
magnetic field penetration in alloy, weak, (E), 20: 8030
magnetic field penetration depths for normal-metal-coated, (T), 20: 8024
magnetic field penetration at low field, (E), 20: 21908
magnetic field production by, 17: 27936 (AERE-M-1207)
magnetic field production by solenoid of niobium–tin, 101-kgauss, 18: 958
magnetic field production by solenoids of, 18: 36520
magnetic field production by flux compression in, 18: 36521
magnetic field reduction in expandable enclosures of, 19: 39742
magnetic field repulsion by split cylinders of, (E), 20: 30276
magnetic field reversal inside cylinders of, 16: 25997
magnetic field stabilization inside tubes of, 18: 11111
magnetic field structure in, 18: 22832
magnetic field strength at surface of niobium–zirconium alloy, EPR measurements for, (E), 20: 21898
magnetic field suspension of spherical, force calculations for, 20: 42130
magnetic field trapping in hollow soft cylinders of, length dependence of, 17: 36468
magnetic field trapping in, multiple-level memory cells from quantization of, 17: 37721
magnetic field transitions in type II, surface effects on a-c, (E), 20: 21918
magnetic field trapping by niobium–tin hollow cylinders, temperature dependence of, (E), 20: 32316
magnetic field variations in, NMR spectra of, 20: 44517(T)
magnetic fields inside cylindrical shells, 16: 22752
magnetic fields in type II, phase nucleation, 18: 11125
magnetic fields in solenoids of, probe for, 19: 9460
magnetic fields in dirty, anisotropic, temperature dependence of nucleation (T), 19: 47525
magnetic fields in thin film, Hall emf probe for measurement, 20: 24269
magnetic fields in, method of images for, (T), 20: 30310
magnetic fields in quadrupole lenses of, digital calculations of, 20: 39479 (BNL-10495)
magnetic fields in shorted coils of, method for reversing, 20: 44564
magnetic fields of, maximum critical, 17: 20774
magnetic fields of, effects of electron mean free path on, 18: 21109
magnetic fields of, devices for measuring, 18: 30683
magnetic fields of, design of magnetometer for, 20: 41228(R) (ORNL-3875, pp 15-20)
magnetic flux annihilation in hard, (E/T), 19: 43239
magnetic flux annihilation and instabilities in inhomogeneous, (E), 20: 1132
magnetic flux annihilation pulses in grossly inhomogeneous, reversed field, 20: 30261
magnetic flux compression and trapping in multiply connected, 17: 621
magnetic flux compression in cylinders and coils, 17: 13868
magnetic flux compression in hard, 18: 28509
magnetic flux conservation in multiply connected, 17: 9031
magnetic flux creep in hard, 17: 36489
magnetic flux creep and jumps in niobium–zirconium, effect of Joule heating on, (T), 20: 21884
magnetic flux degradation phenomenon in coils, (E), 19: 47512
magnetic flux density of bulk type-II, (T), 20: 30287
magnetic flux distribution in hard, under adiabatic field variations, (T), 19: 45192 (ORNL-TM-1266)
magnetic flux distribution in Type II, measurement of, 20: 8003(R) (MIT-3226-8)
magnetic flux entry into Meissner state of type-II, maximum field for delay of, (T), 20: 19748
magnetic flux flow in type-II, viscous drag coefficient in, (T), 19: 8357
magnetic flux flow resistance in type-II, (T), 19: 35338
magnetic flux flow in, with zero external field, 20: 40015(R) (ORNL-TM-1598)
magnetic flux in multiply connected network of indium, frozen-in, (E), 20: 26050
magnetic flux in macroscopic rings of, (E), 20: 30305
magnetic flux jumps in hard, 18: 34724
magnetic flux jumping and trapping in tubular samples of, 18: 42560
magnetic flux jumping in niobium–zirconium, (E), 19: 33164
magnetic flux jumping in niobium–tin, stability against, (T), 19: 35326
magnetic flux jumps in niobium, speed of, (E/T), 19: 45199
magnetic flux jumping in niobium-tin hollow cylinders, 19: 33159
magnetic flux jumps in hard, in pulsed magnetic fields, (E), 20: 2921
magnetic flux jumps and trapping in Nb_2Sn, (E), 20: 4793
magnetic flux jumps in hard, sample geometry effects on, (E), 20: 9916
magnetic flux jumps in niobium–zirconium alloy, training effects from, (E), 20: 11895
magnetic flux jumping in high-field indium-impregnated porous glass, field sweep-rate and temperature dependence of, (E), 20: 17604
magnetic flux jumping in niobium–tin hollow cylinders, (E), 20: 24272
magnetic flux jumping in high-field high-current, criterion for stability against, 20: 32320
magnetic flux jumping in high-field high-current niobium–tin intermetallic compound, stability against, (T), 20: 32320
magnetic flux lines in hard, collective motion of, 18: 15066
magnetic flux line motion in, quantized, (T), 19: 8352
magnetic flux line motion in type II, dissipative mechanism in, (E/T), 19: 8355
magnetic flux line motion in type II, (T), 19: 33168
magnetic flux line motion in type-II, (E/T), 20: 9929
magnetic flux line motion in, induced electromotive force from, (E), 20: 9930
magnetic flux lines in type-II, quantized, (E), 20: 9935
magnetic flux lines in type-II, motion of quantized, (T), 20: 24281
magnetic flux line motion in mixed state of type-II, (T), 20: 26040(T)
magnetic flux line lattices in, dislocations in, (T), 20: 34427
magnetic flux motion in type II, 18: 40446
magnetic flux motion in thin-walled tubes of hard, spatial variations of, (E), 20: 9917
magnetic flux motion in type I, coupled, (E), 20: 9926
magnetic flux motion in magnetically coupled films of, (E/T), 20: 17623
magnetic flux motion in type II, (E/T), 20: 21910
magnetic flux motion in lead and indium–lead, induced voltage from, (E/T), 20: 37966
magnetic flux movement through bulk, energy losses from, (E), 19: 6618
magnetic flux movement in type II, (T), 19: 39704
magnetic flux penetration and trapping in niobium–zirconium wires, (E), 19: 16795
magnetic flux penetration in, (T), 19: 39712
magnetic flux penetration in cylindrical type-II, (T), 20: 9886
magnetic flux penetration in niobium, ultrasonic attenuation for determination of, (E), 20: 13684
magnetic flux penetration in thin-walled cylinders of, (T), 20: 24265 (N-65-15147)
magnetic flux penetration and trapping in lead, geometrical dependence of, (E), 20: 28197
magnetic flux penetration into single-crystal, measurement of, (E), 20: 32343
magnetic flux penetration in Type-II, (E), 20: 42132
magnetic flux permeability and tunneling in superimposed layers of normal metal and, in magnetic fields, (T), 19: 39700
magnetic flux pinning in niobium, quantized, (E), 20: 21909
magnetic flux pinning in thin-film niobium, (E), 20: 30278
magnetic flux pinning by superconducting tin precipitate in indium–lead–tin and lead–tin alloys, (E), 20: 32313
magnetic flux pumping and trapping with solenoidal, 17: 14938 (LADC-5472)
magnetic flux pump for, design of, 20: 30274

magnetic flux pumps of, processes in, (T), 20: 37977
magnetic flux quantization in cylinders, 16: 12298
magnetic flux quantization and current-carrying state in cylinders of, 16: 18252
magnetic flux quantization in cylinders, 16: 19536
magnetic-flux quantization in, 16: 25982
magnetic flux quantization, gap energy, and pair symmetry of rings of, in the current-carrying Bardeen-Cooper-Schrieffer state, 17: 37845
magnetic flux quantization in multiply connected, 18: 6112
magnetic flux quantization and Meissner effect in, quasiparticle transformation for, 18: 6116
magnetic flux quantization in cylinders of, theory of, 18: 6121
magnetic flux quantization in films of, 18: 11134
magnetic flux quantization in hollow cylinders in magnetic field, 18: 34709
magnetic flux quantization in, 19: 12444
magnetic flux quantization in, microscopic theory of, 19: 14439
magnetic flux quantization in cylindrical, measurement of, 19: 21194
magnetic flux quantization in rings with Josephson tunneling, (E), 19: 23592
magnetic flux retention in hysteretic, 20: 44521
magnetic flux trapping in, temperature dependence of, 17: 11369
magnetic flux trapping in trained, measurement of, 18: 15070
magnetic flux trapping in ring of, 18: 21097 (UCRL-7308-T)
magnetic flux trapping in, quantized, 18: 42552 (SEL-63-128)
magnetic flux trapping and compression in niobium–tin compact, (E), 19: 6605
magnetic flux trapping in, r-f, 20: 11926
magnetic flux trapping threshold in niobium–tin alloy, (E), 20: 21926
magnetic flux trapping at 10 to 1000 Mc in, (E/T), 20: 37954
magnetic fluxoid annihilation instability in hard, (E/T), 19: 12441
magnetic fluxoid annihilation instability in hard, (E/T), 20: 21927
magnetic fluxoid conservation by thin film ring, 18: 34698
magnetic fluxoid transitions and loss in multiply connected niobium, (E/T), 20: 6246
magnetic hysteresis properties of hard and soft, 17: 13137
magnetic hysteresis losses from surface of, mechanism for, 18: 956
magnetic hysteresis in thin film, (E), 19: 6606
magnetic hysteresis in type II, intrinsic, (E), 19: 35334
magnetic hysteresis curves of, instruments for recording, (E), 20: 2913
magnetic hysteresis loops in, intrinsic properties of, (E), 20: 19741
magnetic hysteresis in mixed state of lead–thallium, effect of surface currents on, (E), 20: 21866
magnetic hysteresis losses of high-field niobium–zirconium alloy, (T), 20: 26044
magnetic hysteresis in niobium, effects of surface properties on, (E), 20: 28195
magnetic hysteresis of nonideal type II, surface contamination effects on, (T), 20: 28196
magnetic hysteresis in type II, surface current effects on, (E), 20: 30269
magnetic hysteresis in copper plated indium–lead, intrinsic, (E), 20: 34462
magnetic induction in transition metal alloys of, measurements of, 17: 37717
magnetic induction distribution with temperature in superconductivity destruction in tin, (E), 20: 4794
magnetic induction in hard vanadium–zirconium, remanent, (E), 20: 21893
magnetic moment of cylindrical tin, in transverse field, 18: 11105
magnetic moment of type II ellipsoidal, in mixed state, (T), 20: 32321(T)
magnetic moment produced by rotating, measurement of, 20: 19771
magnetic moments of small, formulas for calculation of, 18: 18834
magnetic moments of, magnetometer for measurement of, 19: 21486(R) (ORNL-3760(p.77-93))
magnetic moments of lead, niobium, and tin spheres, residual, (E), 19: 45195
magnetic ordering in thin films of, field strength dependence of, (T), 20: 34453
magnetic penetration depth in hard, 18: 28505
magnetic pinning in type II, (E), 20: 11894
magnetic properties of hard, in strong fields, 17: 619
magnetic properties of films, 17: 11399
magnetic properties of second-kind, 17: 13140
magnetic properties of lead-base, 17: 13150
magnetic properties of, theory, 17: 13197
magnetic properties of films of, quantum effects in, 17: 16838
magnetic properties of hard, a-c, 17: 28099
magnetic properties, 17: 32712 (LNF-63/26)
magnetic properties and phase transitions in thin-film, 17: 34618
magnetic properties of type II, 18: 15077
magnetic properties of transition metal alloy, 18: 15090
magnetic properties of bismuth–indium alloys as second kind, 18: 26495
magnetic properties of Nb_3Sn films, 18: 30687
magnetic properties of alloy, 18: 40458
magnetic properties (T), 19: 1480 (NP-14406)
magnetic properties of film (T), 19: 1495
magnetic properties of alloys of, (T), 19: 8361
magnetic properties of rod in cylindrical shell, (T), 19: 16805
magnetic properties of cylindrical enclosed, 19: 23555
magnetic properties of intrinsic London, near transition point, (T), 19: 39721
magnetic properties of gadolinium-lanthanum, antiferro-, (E), 20: 6247
magnetic properties of thin-film, in nonlocal regime, (T), 20: 6250
magnetic properties of, containing paramagnetic impurities, (T), 20: 9892 (NP-15817)
magnetic properties of type-II, (T), 20: 9912
magnetic properties of Abrikosov structures in alloy, (T), 20: 21906
magnetic properties of ideal type II, (T), 20: 21929
magnetic properties of type I, effects of lattice defects on, 20: 30253 (CEA-R-2808)
magnetic properties of niobium–tantalum type II, 20: 36359(R) (TID-22992)
magnetic properties of type-II, Pauli paramagnetism effects on, (T), 20: 37956
magnetic pulse transmission through plates of type II, (E), 19: 39733
magnetic, pump for flux accumulation in, 17: 16174 (LADC-5418)
magnetic quantized flux pinning in niobium, 18: 32698
magnetic resonances in niobium, low-frequency mixed-state, (E), 20: 21894
magnetic shielding by rotating cylindrical, 18: 2768
magnetic shielding of space vehicles by, 18: 26107 (ERR-FW-210)
magnetic shielding by plates of niobium–tin, 20: 26035
magnetic shielding properties of niobium–tin, for accelerator extraction systems, 20: 39523
magnetic support of spinning (E/T), 19: 3175 (NASA-CR-108)
magnetic susceptibility of alloys of, amplitude and frequency dependence of complex a-c, 17: 39747
magnetic susceptibility of thin-film, 18: 30674
magnetic susceptibility of tantalum, amplitude effects of alternating field, (T), 20: 8013
magnetic susceptibility dissipation in type II, in swept d-c fields, (E), 20: 9919
magnetic susceptibility of type II, complex, (T), 20: 34433
magnetic transitions in thin, verification of theory for, 17: 29454
magnetic transitions in alternating fields, 18: 15075
magnetic transitions of, pressure effects on, 18: 15078
magnetic transitions in niobium stannide disks, (E), 19: 1514
magnetic transitions of thin-film, hysteresis in, (E/T), 19: 5097
magnetic transitions of thin-film, 20: 4785
magnetic transitions in thin films and foils of lead, parallel and perpendicular, (E), 20: 24285
magnetic vortex line structure and behavior in, (T), 19: 12452
magnetic vortex properties in type II, (T), 19: 5098
magnetic-field penetration in, measurement of a-c (E), 19: 1494
magnetic-field readout for magnets of, inverse, (E), 20: 28215
magnetic-flux bundle penetration into indium, (E), 19: 33157
magnetism accumulation in, electric circuit for, 18: 43755(P)
magnetization and critical supercurrents in, 17: 6865
magnetization and resistance transitions of lead and lead alloys, (E), 20: 28183
magnetization curves in second-kind, 17: 13147
magnetization curve of alloyed, near second critical field, 17: 28068
magnetization curves for sheets of, 18: 22827
magnetization curves of indium–lead alloy, (E/T), 19: 5102
magnetization curve of niobium type II, (E), 19: 45200
magnetization discontinuities in type II, (E), 19: 37740
magnetization in mixed state of alloys of, temperature dependence of, (T), 20: 17633
magnetization instabilities in antimony-lead alloy, in reversed fields, (E), 20: 9921
magnetization of aluminum–magnesium, (E), 20: 37935 (CEA-R-2906)
magnetization of bismuth–lead, size effect in, (T), 19: 33166
magnetization of cylindrical hard, Kim-Anderson flux pinning model for, (T), 20: 8005
magnetization of cylindrical tin, by rotation, 20: 13690
magnetization of hard, validity of models for, 17: 9039
magnetization of hard, hysteresis in, 17: 27993
magnetization of hard, transport current effects on, 17: 34622
magnetization of high-field, irreversible, (E/T), 19: 16777
magnetization of hard, current-field paths in, (E/T), 19: 27372
magnetization of high-field type II molybdenum–titanium, mixed-state paramagnetism in, (E), 20: 8018
magnetization of high-field niobium–zirconium-alloy, a-c losses and hysteresis in, (E), 20: 26043
magnetization of indium–tin, 18: 15072
magnetization of irreversible, flux gradient instability in, (E), 20: 19745
magnetization of indium and indium–tin alloy thin film, Ginzburg-Landau

parameter from, (E), 20: 28193
magnetization of niobium–zirconium, effect of external current on, (E/T), 20: 19735
magnetization of niobium type-II, adiabatic, (E), 20: 24278
magnetization of niobium, peak effect in, 20: 44528
magnetization of second-type, 18: 4503
magnetization of type-II, 19: 41613
magnetization of Type-II, equilibrium, (E), 20: 42133
magnetization of wire, 18: 42563
magnetization of wires of nonideal type-II, Procopiu-effect analog in longitudinal, (E), 20: 24277
magnetization process of Type II, enthalpy from, (T), 20: 40036
magnetization properties of type II, hysteresis effects on, 20: 36126
magnetorestrictive properties of indium–manganese, (E), 19: 10197
magnetothermal effects in type II, (E), 19: 14433 (CONF-651-44)
magnets of, 18: 26478
magnets of, effects on economics of fusion power plants, 17: 15036
magnets of, for high fields, 17: 41592
magnets of long-wire, design of flux-pump fed, 18: 6108
magnets of niobium–tin, stabilization of, 18: 15045
magnets of niobium–zirconium, degradation of large, (E), 19: 25444
magnets of, performance as space-vehicle power supplies, 17: 9112
magnets of, applications, development, and properties of, 18: 13010
magnets of, design of, 18: 21118
materials for, data on, 17: 41604
materials for wire, properties of, 18: 34200
materials, preparation, and physics of high-field, 17: 18979
mechanical forces on type-I, in magnetic fields, (E), 20: 42134
Meissner effect and vortices in, (T), 20: 2914
Meissner effects in, analogy to photon self-energy, 18: 2767
metallurgical aspects of high-field materials, 18: 6127
metallurgical aspects of niobium–zirconium alloy as, 18: 6129
metallurgy and uses of high-field, 20: 21877
metallurgy of, 16: 30169(R) (ORNL-3313(p.133-78))
metallurgy of, research program on, 18: 44147(R) (ORNL-3670(p.21-2))
microstructure of niobium–zirconium, ultrasonic investigation of, 19: 25436(R) (RTD-TR-65)
microwave absorption by aluminum, effects of magnetic field on, (E), 19: 14450
microwave absorption by aluminum, effects of magnetic field on, (E), 19: 14456
microwave absorption in copper–tin and gold–tin, proximity effects on, (E), 20: 30289
microwave absorption in silver-doped aluminum, magnetic field effects on, (E), 20: 34438
microwave amplification using films of, 18: 34714
microwave amplification in films of, (T), 19: 25450
microwave effects and switching speed of tin, nonlinear, 17: 28045
microwave effects on critical currents in constricted films of tin, (E), 20: 32328
microwave emission by point contacts of, 20: 31482
microwave impedance of, dependence on direct current, 18: 36523
microwave interactions with, two-fluid model for, 19: 1498
microwave production by field-emission cathode in cavity resonators of, (E), 20: 9894
microwave properties of zinc, in energy-gap frequency region, (E), 20: 28204
microwave radiation from Josephson junctions of, (E/T), 19: 41614
microwave radiation from Josephson tunnel junctions of tin, 20: 40028
microwave reactions with Josephson junctions of, induced d-c voltages from, 20: 21882
microwave reflection and transmission coefficients of thin-film, 20: 19772
microwave residual losses in, temperature dependence of, (E), 19: 35335
microwave surface impedance of bismuth–indium, 18: 9276
microwave surface impedance of second kind, 18: 34705
microwave surface impedance of aluminum, effects of magnetic field on, (E), 19: 14457
microwave surface impedance of, magnetic field dependence of, (T), 19: 16786
microwave surface resistance in copper-plated lead–indium, intrinsic hysteresis in, (E/T), 20: 19752
microwave surface resistance in type II, (E), 20: 21916
microwave transmission nonlinearities in film, 18: 15115
microwave transmission in thin films of tin, nonlinear electrodynamics study using, (E), 20: 28189
model for alloys of type-I, (T), 19: 23566
model for organic polymer as, evaluation of Little, 20: 44541
model for polymers, (T), 20: 8012
model for type-II, Bose gas, (T), 20: 13677
model for, intermetallic high-field negative surface energy, 17: 9040
model for, quantum, (T), 19: 21163
model for, with two kinetic energies, (T), 19: 39687
models for high-field, 18: 13008(R) (ORNL-3564(p.100-25))
models for second-kind, corrections to layer, 18: 9280
models of, survey of theoretical, 19: 25436(R) (RTD-TR-65)
neutron diffraction by vortex lines in, cold, 20: 28256
neutron scattering by quantized magnetic flux lines in, (T), 19: 12450
neutron transmission through, in the mixed state, depolarization in, (T), 20: 2998
normal regions in mixed-state, 18: 26489
nuclear magnetic relaxation and resonance in, 18: 15092
nuclear magnetic resonance signals from, shape of, 18: 18848
nuclear magnetic resonance in nontransition-metal, spin-orbit coupling effects on Knight shift in, (T), 19: 39727
nuclear spin relaxation time in aluminum, size effects in, 18: 9275
nuclear spin relaxation in aluminum, phonon effects on, (T), 19: 21174
nuclear spin-lattice relaxation time in type II, (E), 20: 37941
nucleation magnetic field in, angular dependence of, 18: 26479
operation and use of high-current high-field, review of, 20: 28220
operation of bearings of, (E/T), 20: 28217
order parameter in homogeneous and zero fields, perturbation range of, (T), 19: 41622
ordering magnetic ions in, (E/T), 20: 4476(R) (IS-1200(Sect.P))
oscillation amplitude of magnetic field at interior of, measurement using Mössbauer effect, 18: 15046
oscillations in intermediate state of, (T), 20: 40026(T)
oxidation of, effects on surface superconductivity in, (T), 19: 33176
pair breaking effects in rotating cylindrical film, (T), 20: 34448
pair correlation functions in nonhomogeneous, spatial dependence of, 18: 9260 (CONF-301-24)
pair multiplicity of, Josephson method for finding, 20: 30265(T)
pair wave functions in the vicinity of plane boundaries for, Gor'kov equations for, 18: 962
pair-breaking mechanisms in, equivalence of, (T), 20: 6233
paramagnetic effect in type II, transverse, 18: 32695
paramagnetic limit in type II, (T), 20: 37936 (CLM-R-60)
paramagnetic resonance in type-II, (T), 20: 24296
paramagnetic susceptibility at 0°K, nonvanishing, 18: 9261 (LNF-63/71)
paramagnetic-impurity and spin-orbit-coupling effects in, Abrikosov-Gor'kov theory for, 20: 2929
partition functions for, perturbation expansions for, 18: 18842
peak effect in interstitial and substitutional solid solutions of, 18: 2778
penetration depth characteristics of indium-base, 17: 13152
penetration depth in niobium, temperature variation of, (E), 20: 1131
performance as electric generators for space vehicles, (E), 19: 13566(R) (AD-421061)
performance as magnetic mirror coils, (E), 19: 10449
performance in dynamic magnetic-field radiation shields for space vehicles, (T), 20: 3241 (NASA-SP-71, pp 199-209)
performance in electromagnets, 18: 30684
performance in electric generators for space vehicles, 20: 19424 (NASA-TN-D-3345)
performance in high-field magnets, 18: 42554
performance in high-field magnets, (E), 19: 19018 (ORNL-TM-1083)
performance in Josephson junctions used as high-sensitivity galvanometer, (E/T), 20: 25356
performance in large-volume solenoids, (E), 19: 10189 (RLE-TR-427)
performance in magnets up to 200 kgauss, review, 18: 11108
performance in magnets, 20: 1120(R) (ORNL-3836, pp 90-110)
performance in microwave mixers, 18: 33824(R) (AD-428788)
performance in rockets, engine vibration effects on, (E), 19: 8337
performance in solenoids for strong magnetic fields, 20: 4486
performance in thin-septum magnets for accelerators, 19: 44877 (UCRL-16346)
performance in 100-kOe electromagnet, 18: 30227
performance in 70-kG nested-solenoid magnets, (E), 19: 22474 (ANL-7002)
performance of, 18: 11100 (LNF-63/67)
performance of coaxial, 19: 1499
performance of coils of, in magnetic mirror system, 19: 33276
performance of copper–lead alloy, as low-inertia thermal resistor, 18: 959
performance of dynamo of, 20: 9898
performance of films as radiation detectors, 16: 25590
performance of films of, as charged-particle radiation detectors, (E), 19: 34465(R) (AD-603666)
performance of hollow cylindrical, as magnetic lens, 20: 17631
performance of magnets of, for bubble chambers, 19: 40869 (CONF-650510-14)
performance of magnets of, using aluminum stranded cables, (E/T), 20: 28218
performance of MHD generator magnets, (E), 20: 39733
performance of niobium–tin solenoid, in superfluid helium, (E), 20: 24268
performance of niobium–zirconium, for magnets, 20: 40015(R)

(ORNL-TM-1598)
performance of resonators of, 18: 24559
performance of resonant cavities of, for proton linacs, 19: 27012 (NURA-714(p.540-4))
performance of sandwiches of, for detecting microwaves and submillimeter waves, 18: 41875
performance of soils of, with composite stranded cables, 20: 21878
performance of stabilized magnet coils of, (E/T), 19: 27370 (NP-14995)
performance of thin film, as charged-particle detector, 20: 9893
performance of thin film, for threshold logic circuitry, 20: 32311 (ORO-2430-27)
performance of tunnel diodes of, as high-frequency sound detector, 19: 46739
peritectic decomposition of intermetallic compound Nb_3Sn, 19: 16167
permeability of, electromagnetic induction equipment and techniques for measuring, 18: 32149(R) (UCRL-11317(p.131-49))
phase studies on niobium–tin (E), 19: 1505
phase transformation in beta-tungsten, electric resistivity jump at, 18: 44687
phase transition in absence of external field, 18: 2756
phase transition in type-II, thermal nature of a-c, 20: 19753
phase transitions of cylindrical, magnetic-field induced, 17: 37681
phase transitions in thin-film, average energy density criterion for, 18: 15048
phase transitions in iridium–yttrium and rhodium–yttrium, 18: 15087
phase transitions in, theory of second-order, 18: 15126
phase transitions in, mechanisms of, 18: 34719
phonon attenuation in, L-band, 18: 2404(R) (TID-19651)
phonon effects in high-transition-temperature, strong, 18: 40449
phonon effects in, 20: 15664
phonon lifetimes in, at zero temperature, 16: 27825
phonon structure in energy gap function in, 17: 25951
photoelectric effect in, frequency and temperature for, 18: 26494(T)
pinning in mixed-state, by localized composition fluctuations, 18: 26469
polarization in vanadium silicide, electronic and nuclear, 20: 20109(R) (MIT-3031-3)
positron annihilation in lead, photon angular correlation from, (E), 20: 11912
potential differences in the mixed state of type II, (T), 19: 35331
power degradation phenomena in coils of niobium–zirconium, (E), 20: 17629
power losses by alternating current in, 19: 39695
power losses in bismuth–lead eutectic alloy, surface nature of a-c, 20: 19742
power losses in niobium–zirconium solenoid, 19: 16448(R) (TID-21380(p.85-111))
power losses in, measurement of a-c, (E), 19: 35324
power losses of surface sheath of, I-f, (T), 20: 17620
precipitation hardening effects on lead–cadmium and lead–tin, 18: 11110
preparation and properties of, review, 18: 4493
preparation and properties of ultrafine niobium–zirconium wire, 18: 6132
preparation and properties of thin-film hard, 18: 28501
preparation and properties of thin-film, 18: 42062
preparation and properties of bundles of Nb_3Sn filaments (E), 19: 1517
preparation by rapid quenching of molten alloys, 20: 15020
preparation of film, chemical-deposition, 18: 15040 (IDA/HQ-63-1412 (Vol.I)(p.80-4))
preparation of films of niobium alloy, 19: 33187(P)
preparation of hard films of, by exploding wires, 18: 2753
preparation of thin-film, by sputtering, 16: 22755
preparation of thin films of, getter sputtering technique for, 18: 13015
preparation of thin-film, by vapor codeposition, (E/T), 19: 4601
preparation of type II, 18: 954 (NP-13274(p.40-6))
preparation of, empiricism for guiding, 18: 14518
preparation, properties, and uses of thin-film, review on, 18: 26476
preparation, properties, and uses, bibliography on, 18: 38016 (AD-438181)
pressure contacts with normal metals, effects of, 20: 44526
principles of bearings of, 19: 11338
production of two-phase filaments, (E), 19: 5090
propagation of normal region in coils, electrical and thermal transients in, 17: 22267 (BSD-TDR-62-116)
properties, 18: 9281
properties, 18: 22845
properties and longrange order of tantalum–tin alloy, processing effects on, (E), 19: 47513
properties and size factors of, 17: 25927
properties and structure, 18: 4238 (63-RL-3252M)
properties and structure of rare earth compounds, 20: 24665
properties and structure of tin film, 20: 26030
properties and theory of type II, review of, 18: 953 (CONF-301-3)
properties and uses, survey, 16: 25881 (ASD-TN-61-160)
properties and uses, 19: 6616
properties and uses of, for producing high magnetic fields, 19: 16792
properties and uses of type-II, 20: 30257
properties and uses of, 20: 34445
properties as permanent magnets, 17: 5084
properties for aerospace uses, 19: 47068
properties in magnetic fields, 18: 5841(R) (AROD-2800.12)
properties in memory devices, 19: 21193
properties in sixth-order-compensated solenoids, 18: 20298
properties of, 20: 32339
properties of Abrikosov mixed state near second critical field, Ginzburg-Landau equations for, 20: 21902
properties of alkali tungsten bronzes, (E), 19: 23568
properties of alloy and hard transition-element, analysis of, 18: 36479
properties of alloy, containing paramagnetic impurities (T), 19: 3186
properties of aluminum–lead superconducting tunnel junctions, (E), 19: 5096
properties of aluminum–zinc Type II, 20: 8003(R) (MIT-3226-8)
properties of aluminum–nickel–niobium alloys, 20: 46512
properties of antimony, (E), 19: 10198
properties of antimony-gallium alloys, 19: 18519
properties of barium tungsten bronze, (E), 20: 2901
properties of beryllium–rhenium alloy, (E), 20: 2898
properties of cables and wires, homogeneity, 20: 34415 (IPP-4/31)
properties of cerium–gadolinium–ruthenium alloys, 18: 11133
properties of coated nickel, niobium, and platinum, 19: 28962(R) (NIRL/R/81))
properties of cold-worked niobium, heat-treatment effects on, (E), 20: 26029
properties of composite, of niobium fine wires in copper matrix, (E), 20: 13673
properties of copper–lead heterogeneous alloys, particle size effects on, (E), 19: 39747
properties of deformed and undeformed niobium, orientation dependence of, (E), 19: 6604
properties of ductile transition metal alloys as high-field, 18: 6128
properties of eutectic alloy, effects of structure on, (E), 20: 44514
properties of evaporated and sputtered films of niobium and tantalum and their compounds, 18: 34157
properties of ferromagnetic, (T), 19: 5110
properties of films of normal metals and, 17: 5140
properties of film, in magnetic fields, (T), 20: 9937
properties of gallium mixtures as, 19: 33185(P)
properties of germanium–niobium alloys, (E), 19: 39725
properties of hard and soft, effects of cold working and heat treatment on, 17: 41636
properties of hard and soft, 19: 19021
properties of hard, 19: 42884
properties of, high-frequency, 17: 36442(R) (NP-13084)
properties of high-field, 18: 44676 (ORNL-P-488)
properties of high-purity niobium, 20: 4774 (IS-T-22)
properties of high-field, review of, 20: 28172 (BNL-10147)
properties of high-purity niobium, (E), 20: 30315
properties of high transition-temperature interstitial compound, 20: 34444
properties of high-purity niobium, (E), 20: 42117
properties of homogeneous dirty, in high magnetic fields, (T), 19: 12442
properties of ideal type II, bulk, 20: 21931
properties of impure tantalum, (E), 20: 24267
properties of, in intermediate state, effect of imperfections on, 17: 16871
properties of indium alloys and compounds, 18: 34707
properties of indium as, effects of manganese on, 18: 40450
properties of indium–tin alloy, (E), 19: 23573
properties of indium and tin whiskers, 20: 4795
properties of indium–tin and tin, 20: 37271
properties of inhomogeneous tin alloy, nonideal, 20: 8008
properties of iron and vanadium films, 17: 28046
properties of laminar, 17: 19
properties of laminated copper–lead, proximity effects on, 20: 36128
properties of lanthanum–silver alloys, 20: 26022 (CALT-221-15)
properties of lanthanum telluride, type-II, (E), 20: 26041(T)
properties of large current carrying, 20: 26026(R) (NYO-3029-9)
properties of lead and mercury, electromagnetic, 20: 34441
properties of, macroscopic approach to, 17: 20689
properties of magnetic-impurity-doped, 18: 40437 (IS-979)
properties of magnetic-impurity containing, (E/T), 20: 4476(R) (IS-1200(Sect.P))
properties of manganese–titanium alloys and titanium as, 18: 967
properties of mercury single-crystal, (E), 20: 34437
properties of microgeometries in presence of high current densities, anomalous, (E), 19: 45207
properties of mixed niobium–tantalum–vanadium stannide (E), 19: 1504
properties of Mo_3Al_2C, 18: 32702
properties of molybdenum-technetium, 17: 11363
properties of molybdenum–niobium, 18: 15085

properties of molybdenum–rhenium alloy, (E/T), 20: 2890 (AFML-TR-65-154)
properties of molybdenum, (E), 20: 8031
properties of $Nb–Nb_2Sn$, sintered compacts, 17: 36470
properties of Nb_2Sn, and Nb_3Sn, as, 18: 6135
properties of Nb_3Sn coils, 17: 29386 (CEA-2239)
properties of Nb_3Sn, (T), 20: 1264 (NBS-8843)
properties of niobium–zirconium alloys at 9,250 Mcps, 17: 16722
properties of niobium–tin alloys with aluminum, antimony, germanium, and silicon, 17: 27861
properties of niobium–thorium eutectic alloys, 17: 32650
properties of niobium–titanium alloy, 18: 28524
properties of niobium, additive effects of oxygen on, (E), 19: 6609
properties of niobium, effects of fiber structure on, (E), 19: 8366
properties of niobium and niobium–zirconium alloy, (E), 19: 16764 (AROD-3473:2)
properties of niobium–zirconium alloys, (E), 20: 4792
properties of niobium stannide, effects of tensile stress on, 20: 8007
properties of niobium–zirconium alloy, (E), 20: 19722 (N-65-17099)
properties of niobium alloy, at elevated temperatures, 20: 34417(R) (N-65-34464)
properties of niobium–zirconium alloy, in strong d-c magnetic fields, (E), 20: 37950
properties of niobium–zirconium alloy, effects of oxygen on, 20: 42535
properties of nitrided niobium–zirconium wires, (E), 20: 2891
properties of nonmagnetic, in vicinity of transition point, 18: 21105
properties of normal-superconducting joints, 18: 952 (ANL-SBC-1)
properties of one-dimensional systems of, monovalent metal model for, (T), 20: 9904(T)
properties of paramagnetic-impurity-doped, 18: 40440 (TID-21048)
properties of platinum-metal chalcogenide, (E), 20: 11899
properties of porous niobium–tin, effects of metallic impregnants on, (E), 19: 41609
properties of protactinium, (E), 20: 8017
properties of, pulsed-magnetic-field studies of, 17: 18907 (TID-17310)
properties of pure, weak time dependence of, (T), 19: 8356
properties of pure, fourth order terms of Ginzburg–Landau–Gorkov equations for, 20: 21903
properties of quadrupole magnets of, for lens systems, 20: 31815 (BNL-10144)
properties of refractory carbide, high-field, (E), 19: 25449
properties of second kind, layer model for, 17: 41632
properties of sodium tungsten bronze, (E), 19: 8351
properties of solid solutions of indium–lead and indium–magnesium as, 17: 39789
properties of technetium, (E), 20: 9896
properties of thin hollow cylinders of, 17: 39762
properties of thin filamentary, 18: 30673(R) (SSD-TDR-63-311)
properties of thin-film, 19: 5091
properties of thin film, (E), 19: 37867
properties of thin film, Ginzburg-Landau theory for, 20: 1264 (NBS-8843)
properties of tin and zirconium alloys, 18: 9274
properties of tin alloys, nonideal, (E/T), 20: 21925
properties of titanium alloy, 18: 34700
properties of titanium iodide, compression and deformation effects on, (E), 20: 17634
properties of transition-alloy and -metal, 18: 15082
properties of transition-metal-alloy, 18: 15084
properties of transition metal carbides as, 18: 34684 (UCRL-11368)
properties of transition metal phosphides, (E), 20: 9901
properties of tungsten, (E), 20: 9931
properties of two-band, impurity scattering effects on, (T), 19: 34730
properties of type 2 in above-critical magnetic field, extension of Abrikosov's solution of Ginzburg-Landau equations for, 18: 32705
properties of type II, review of, 19: 47510
properties of type II, paramagnetic effects on, (T), 20: 21900
properties of type-II, 20: 28178
properties of type II, (T), 20: 30313
properties of type II, research on, 20: 32312(R) (UCRL-16658, pp 133-43)
properties of vanadium, (E), 20: 8014
properties of vanadium, Ginzburg-Landau parameters for, 20: 44537
properties of vortices in thin-film, 19: 32048(R) (NP-15073)
properties of weakly anisotropic, effects of nonmagnetic impurities on, 18: 6119
properties of, Brillouin zone effects on, 18: 15086
properties of, current and magnetic field effects on, (E), 19: 19060
properties of, data on, 19: 21187
properties of, double coil pulse device for studying, 20: 44512
properties of, effects of high pressures on, 18: 24560
properties of, effects of energy gap anisotropy on, 18: 30685(T)
properties of, effect of paramagnetic impurities on, (T), 19: 37757
properties of, effects of electron-phonon interactions on, (T), 19: 40073 (CONF-796(Paper 1))
properties of, effects of λ transition on, 20: 21875
properties of, effects of metallurgical variables on, 20: 31750
properties of, macroscopic quantum aspects of, 20: 46530
properties of, magnetic and thermal, 19: 40286(R) (NAA-SR-11200)
properties of, paramagnetic impurity effects on, (T), 19: 21191
properties of, relation of physical state to high-field, 18: 37729
properties of, relations with electronic structure, 19: 27735(R) (NAA-SR-10850)
properties of, review on effects of metallurgical variables on, 19: 37123
properties of, tables for calculating (T), 19: 1516
properties of, temperature-dependent, 20: 26028
pulse transmission by coaxial cables of high-field, (E), 19: 39740
pulse transmission properties of subminiature coaxial delay lines of, high-voltage, (E), 20: 37939
quantization in films of, macroscopic, 20: 32324
quantized superfluid vortices in, 20: 46529
quantum effects in thin film, (T), 20: 6242
quantum interference effects in point contacts of macroscopic, (E/T), 20: 11911
quantum interference in multiply connected, (E), 20: 32344
quasi-particle lifetime in, at finite temperatures, 16: 30957
quasi-particle lifetimes in, at zero temperature, 16: 27825
quasi-particles recombination time in, effect of mean free electron path on, 17: 22441
quenching characteristics of coils and solenoids, 16: 15396
radiation absorption in, spectral shape of infrared, 18: 28514
radiation absorption in lead-alloy, infrared, 18: 38027
radiation bulk absorption in, umklapp contribution to (T), 19: 1491
radiation effects on, neutron, 17: 18389 (TID-7652(p.808-18))
radiation effects on, alpha, 17: 21388(R) (LNF-63/11)
radiation effects on critical currents in, fast neutron, 18: 9265
radiation effects on magnetic properties and critical temperatures of type-II, fast-neutron, 18: 10583
radiation effects on, 18: 36052
radiation effects of fast neutrons on niobium stannide, (E), 19: 1023
radiation effects on niobium stannide, neutron, (E), 19: 1506
radiation effects on persistent current decay in soft, alpha, (E), 19: 10203
radiation effects on current density in uranium-vanadium silicide system, neutron, (E), 19: 14435(R) (NP-14676)
radiation effects on transitions in, thermal spikes from alpha, (E/T), 20: 9893
radiation effects on properties of indium and tin, neutron, 20: 30301
radiation effects on properties of boron- and uranium-doped aluminum–niobium alloy and vanadium silicides, (E), 20: 30260
radiation effects at low temperature, deuteron, 20: 33966
radiation effects on niobium–tin, neutron, 20: 34459
radiation effects on magnets of, 20: 36124 (RHEL-R-118)
radiofrequency effects in thin, 18: 34710
radiofrequency losses in, flux-trapping model for, (E/T), 20: 40042
representation of, reduced density matrices in coordinate space, 17: 11423
research on, 20: 32339
research programs on, 19: 23355(R) (BNL-867(p.1-117))
residual losses in, r-f, (E), 20: 42131
resistive behavior of second-kind, for viscous flux flow, 18: 24550
resistive states in hard, 18: 15065
resistive transition of thin film, effects of magnetic field, current, and surface on, (E), 20: 46517
resonance effects in slabs of, 17: 25950
resonances in plates of indium, helicon-like, (E), 20: 34429
review of intermetallic compounds, 19: 37027 (64-RL-3540M)
review on flux pumps and superconducting solenoids, 19: 37749
review on high-field, 18: 28525
review on type-II, 19: 21165
rotation of, magnetic field production from, 20: 44519
simulation of hard, by mercury filaments embedded in glass, 17: 3525
solid-solution, transition-metal and interstitial-element, 18: 22843
sound absorption in niobium–zirconium, u-h-f, 17: 39767
sound absorption in current-carrying, (T), 20: 28229
sound absorption in intermediate state of, (T), 20: 34456
sound attenuation in type II, formula for, 20: 15663
sound dispersion in, (T), 20: 42128(T)
sound-wave attenuation in cylindrical vanadium, energy gap from u-h-f, 17: 41622
sound-wave attenuation in tantalum, energy gap from u-h-f, 17: 41623
specific heat anomaly of, 17: 6893
specific heat anomaly in type II, lambda-type, 18: 40447
specific heat at transition point, (T), 20: 17612(T)
specific heat in Fermi system during second-order phase transition, (T), 19: 19041
specific heat of gapless, (E), 20: 4476(R) (IS-1200(Sect.P))

specific heat of mixed state in alloy, (T), 19: 39716
specific heat of pure niobium in magnetic field, 18: 2773
specific heat of transition metal, 17: 11380
specific heat of type-II, (T), 19: 19038
specific heat of unannealed niobium wire, in magnetic fields, 20: 46524
spectral shift at zero temperature, magnetic-field dependence of NMR Knight, (T), 19: 39719
spin ordering in ferromagnetic, 17: 20495
spin polarization around impurities in, (T), 19: 37744
spin scattering in manganese–zinc alloy, (E), 20: 34464
spin-lattice relaxation time of dirty type-II, in high fields, (T), 20: 42102
spin-orbit interaction with lattice in, Knight shift from, (T), 19: 37755
stability limits of type II, in magnetic fields, 20: 26057
stability of ideal film, with current, (T), 20: 37938
stabilization of magnets of, by incorporation of channels for liquid helium flow, 20: 36122 (LA-DC-7801)
state density in, effects of magnetic impurities on, 19: 47535
storage phenomena in thin-film, model for, 20: 13689
stress effects on critical temperatures of V_3Si (E), 19: 1496
stresses in multilayer solenoid of, (T), 19: 41632
structural transformation in V_3Si, vanadium-51 Knight shifts and field gradients during, 20: 42118
structure in, filamentary, 17: 18967
structure of hard, elastic energy of filaments in, 17: 9033
structure of hard, filamentary, 18: 2757
structure of hard, momentum vortices in, 18: 36478
structure of intermediate state of, (E), 19: 10191
structure of intermediate state and surface energy of indium, 20: 4778
structure of mixed-state in vanadium, NMR and relaxation studies of, 20: 37963
structure of type II, Josephson tunneling for detection of Abrikosov, 18: 28508
structure of type II, suggested experiments on, 20: 15663
structure of vanadium silicide, transformation in, (E), 20: 28194
superconducting transition temperature of thin films of, (E), 19: 47503 (BNL-9478)
superconducting transition of indium–lead alloy, effects of strain on, (E), 20: 21923
superconductivity in high magnetic fields, 17: 36440(R) (NP-13061)
superconductivity of, effects of composition fluctuations on, 18: 32149(R) (UCRL-11317(p.131-49))
superconductivity layers in, measurement of, 19: 36949(R) (BNL-900 (p.121-97))
supercooling and superheating in transition of indium, 20: 32331
supercooling in mercury and cadmium–mercury alloy, 18: 36430
supercurrent characteristics of niobium films, 18: 15117
supercurrent persistence and angular momentum in cylindrical, 18: 2758
supercurrent quantization and metastability, 17: 29468
supercurrents in tin films, measurement of critical, 18: 15112
surface barrier in type-II, study of interaction of supercurrent vortex with specimen surface causing, 18: 11121
surface barrier in type-II, 18: 22842
surface critical currents and a-c susceptibility transition in bismuth–lead, (E), 20: 30293
surface current effects in niobium–zirconium, 20: 30280
surface currents in type II, 18: 22828
surface currents in mixed state of niobium–tantalum, (E/T), 20: 26048
surface effects in, (E/T), 19: 31181
surface effects on metal, 19: 37745
surface impedance of thin films, 16: 3534 (NP-11091)
surface impedance of, 18: 26467
surface nucleation in normal-metal-coated, (T), 20: 21888
surface nucleation in magnetic-film-coated type II, 20: 44524
surface resistance of, 18: 38028
surface resistance of, (E/T), 20: 40042
surface sheath in type-II, removal by copper plating, (E), 20: 44530
surface sheath of type-II, below upper critical field, (T), 19: 21171
surface sheath of, (T), 20: 6240
surface sheath of, field distribution and magnetization for, (T), 19: 8339
surface sheaths of type II, 19: 40286(R) (NAA-SR-11200)
surface sheaths of type-II, responses to applied field, (E/T), 20: 42125
surface sheaths of, shielding properties of, (E), 20: 42127
surface superconductivity beyond H_{c_2} in type II, 18: 24548
surface superconductivity above critical field in type I, 18: 26480
surface superconducting in lead-based, angular dependence of, 18: 28510
surface superconductivity and supercooling in type I, 19: 16812
suspension of spherical, in magnetic fields, 18: 30677
suspension of spheres of, in magnetic fields, (E), 20: 19728
switching phenomenon in sheet, photon-induced, 17: 9020
switching properties of small-geometry thin-film, 20: 21012
systems of normal metals and, solution of Ginzburg-Landau equations for, 19: 23585
temperature effects on electronic stability and crystal structure of V_3Si-type, 20: 42531
temperature variation in type II, in changing magnetic field, (E), 19: 5105
testing for magnet coils, 20: 13666 (IPP-4/22)
testing of high-field magnets of, 19: 37736(R) (ORNL-TM-1173)
testing of large magnets of, facility for, 20: 40049
testing of wire, methods development for nondestructive, 18: 4250(R) (ORNL-3470(p.45-8))
theory, 19: 23590
theory, 20: 28211
theory of alloy, generalized Ginzburg-Landau, 19: 16776
theory of anisotropic, from Ginsburg-Landau equation, 18: 6122
theory of compound, 20: 40015(R) (ORNL-TM-1598)
theory of dissipative processes in mixed-state, 19: 31174
theory of electric conductivity and Meissner effect in, 19: 37738
theory of finite, infinite volume limit in, 18: 34703
theory of gapless, 19: 16793
theory of intermetallic compound, 18: 32699
theory of local, Ginzburg-Landau, 18: 40443
theory of organic, 18: 24554
theory of small, in strong magnetic field, 19: 16799
theory of type II, solution of Ginzburg-Landau equations in, 18: 11120
theory of type-I and -II, 19: 31171
theory of, containing singlet and triplet pairs, 19: 23579
theory of, Ginzburg-Landau-Abrikosov-Gor'kov parameters in, 18: 11119
theory of, Ginzburg-Landau equation in, 19: 12445
theory of, ground state in BCS, 19: 41629
theory of, Hartree-Fock solution in, 18: 16814
thermal capacity and transition temperature in the scandium–zirconium system of, 20: 42121
thermal capacity of tantalum–vanadium alloy, high-magnetic-field, 18: 7649
thermal capacity of, lattice contributions to, 18: 15081
thermal capacity of niobium, at 1.2 to 12°K, 18: 22841
thermal capacity of mercury and thallium, at 0.35 to 4.2°K, 18: 30675
thermal capacity of strong-coupling, 18: 36432
thermal capacity of type II, magnetic field effects on, 18: 40457
thermal capacity of niobium, in mixed state, (E), 19: 5094
thermal capacity of indium and tin, 19: 10200
thermal capacity of niobium, at 0.25 to 25°K, (E), 19: 19019 (UCRL-11901)
thermal capacity of niobium at lower critical field, λ-transition in, (E), 19: 33165
thermal capacity of niobium, tantalum, and vanadium at 0.35 to 25°K, (E), 19: 33180
thermal capacity of thin-film, in magnetic fields, (T), 20: 26059
thermal capacity of mixed state in vanadium, at 0.5 and 5.4°K, 20: 42116
thermal capacity of normal and superconducting vanadium, at 0.5 to 5.4°K, 20: 42115
theory for alloy, review of, (T), 20: 4791
theory of high-field, review of, 20: 21877
theory of nonhomogeneous, 20: 11908
theory of nonhomogeneous, 20: 15655
theory of, containing spherically symmetric nonmagnetic impurities, 20: 6239
theory of, containing magnetic impurities, 20: 11906
thermal capacity of mixed-state type II, 20: 26046
thermal capacity at low temperatures, (E), 20: 13692
thermal capacity of type II, in magnetic fields, 20: 4786
thermal capacity of, singularity at transition point in electronic, (T), 20: 8025(T)
thermal capacity of lanthanum- and yttrium-silicide, at transition temperature, (E), 20: 21883
thermal capacity of type II, in magnetic field, (E), 20: 21907
thermal conductivity, 17: 567
thermal conductivity of second-kind, 17: 11406
thermal conductivity of copper–lead sandwiches at 1.3–4.0°K, 17: 34456
thermal conductivity decrease in, in lattice scattering region, 17: 34629
thermal conductivity of niobium–30% tin, 18: 974
thermal conductivity of, magnetic field dependence, 18: 2774
thermal conductivity of, theory for lattice, 18: 4506
thermal conductivity of, model for electronic, 18: 26486
thermal conductivity of, in magnetic fields, 18: 30679
thermal conductivity of paramagnetic impurity-doped, 19: 1481 (NYO-2391-2)
thermal conductivity of intermediate state, (T), 19: 12449
thermal conductivity of paramagnetic-impurity containing, electronic, (T), 19: 16782
thermal conductivity of, with paramagnetic impurities, (T), 19: 19034
thermal conductivity of thermal switches of, at 0.3 to 2°K, (E), 19: 23584

thermal conductivity of lead, (T), 19: 27365 (AD-611439)
thermal conductivity of indium, lattice, (E), 19: 29159
thermal conductivity of pure lead, (T), 19: 39732
thermal conductivity of films of lead, (E), 19: 43248
thermal conductivity of lanthanum, (E), 20: 2893
thermal conductivity from impurity scattering for overlapping-band, (T), 20: 19763
thermal conductivity of type II, (E), 20: 21914
thermal conductivity of alloys of dirty type II, in high fields, (T), 20: 24283
thermal conductivity of tin, (T), 20: 30314
thermal conductivity of gapless, calculation of electronic, (T), 20: 30321
thermal conductivity of surface sheath of indium–lead, (E), 20: 32327
thermal conductivity of niobium–tantalum, (E/T), 20: 34428
thermal conductivity of type II bismuth–indium and niobium, (E), 20: 34465
thermal conductivity of indium–lead, temperature dependence of, (E), 20: 37940
thermal dissipation to liquid helium bath, 18: 28500
thermal equilibrium for, (T), 20: 4789
thermal expansion of, theory for, 18: 44219
thermal propagation of normal region in wires of niobium–zirconium, effect of copper plating on velocity of, 17: 37716
thermal propagation of normal transitons of niobium–zirconium alloy, 20: 24273
thermal resistance at boundaries between sapphire and indium at 1.1 and 2.1°K, 18: 34699
thermal resistivity maximum in the intermediate state and Peltier cooling below 4°K, 18: 2754
thermal resistivity in intermediate-state indium and lead, size effect in, (E), 20: 40022
thermal transport coefficients of (T), 19: 3182
thermodynamic properties, analysis of critical field curves, 16: 27788 (IS-303)
thermodynamic properties of composite-wire, 18: 15118
thermodynamic properties of type II bulk, 18: 15080
thermodynamic properties of molybdenum, (E), 19: 27381
thermodynamic properties of strong-coupling, 19: 47536
thermodynamic properties of tantalum–vanadium, 20: 10272(R) (NAA-SR-9339)
thermodynamic properties of alloy, approximation method for, 20: 15654
thermodynamic properties of ideal bulk type II, (T), 20: 21901
thermodynamic properties of, anisotropy effects on, (T), 20: 40041
thermodynamic properties of, use of effective interaction strength to predict, 20: 42120
thermodynamics of type-II, (T), 19: 19036
thermodynamics of, variational principle in, 18: 38018
thermodynamics of, in one and two dimensions, (T), 20: 2889 (AD-618203)
thermoelectricity in intermediate state of, 18: 21099
thermogalvanomagnetic effects in mixed state of type II, 20: 44538
thermomagnetic effects in type II, (T), 20: 24290
transfer characteristics of cryotron, 20: 8027
transformers of, layout for, 18: 26466
transients in unprotected coil of, normal-transition electric and thermal, 17: 28100
transition anomalies in h-c-p Ti alloy, (E), 19: 10214
transition behavior of local, in magnetic field, 17: 39769
transition effects in filamentary tin crystals, 20: 11924
transition field in rhenium single crystals, anisotropy of, 18: 6133
transition from superconducting to normal state, effects of uniform exchange field on, 17: 36480
transition in semiconductors, induction using field effect, (T), 20: 11901(T)
transition metal alloy, upper critical fields of, 17: 6874
transition of thin film, to normal state, 17: 36444 (NP-13090)
transition point in thallium, impurity effects on, (E), 19: 29164
transition points in single-crystal gallium, indium, and lead, (E), 20: 30734(R) (TID-22970, pp 1-63)
transition region determination by superfluid phase transition, (E), 19: 39691
transition temperatures in, 16: 15334
transition temperature maxima in, 16: 22632
transition temperature of superimposed films, 17: 5139
transition temperature of, effect of impurities on, 17: 9030
transition temperatures in indium–tin alloys, 17: 28047
transition temperature of tantalum, electron pair correlations in periodicity of, 17: 34624
transition temperature of aluminum–indium laminates, effect of bubble formation at metal interface on, 17: 37731
transition temperatures of elemental, law for, 18: 6103(T) (AI-Trans-18)
transition temperatures in Nb_3Sn and niobium–zirconium, pressure effects on, 18: 6120
transition temperature of thin films of, effects of tensile strain on, 18: 11107
transition temperature in thallium, impurity effects on, 18: 21113
transition temperatures of superimposed film, effects of intermetallic compound formation on, 18: 28511
transition temperature of niobium–tin alloy, pressure effects on, 18: 36429
transition temperature of, quantum periodicity in, 18: 36480
transition temperature of films of, with paramagnetic additions, 18: 36490
transition temperature in zero magnetic field, effects of coherence length on, 18: 39982
transition temperature of tin alloy, valence and volume dependence of, (T), 19: 8340
transition temperature in, effect of pressure on, (T), 19: 12438
transition temperature of lanthanum, pressure effects on, (E), 19: 19047
transition temperatures of indium and lead film, (E), 19: 21189
transition temperature of films on normal substrates, 19: 23553
transition temperature of zirconium, isotope effects on, (E), 19: 23569
transition temperature of, surface-charge effects on, (E), 19: 25452
transition temperatures in lead–tellurium compounds, (E), 19: 35325
transition temperatures of superposed films, (T), 19: 35330
transition temperature of thin films of tin, stress effects on, (E), 19: 37743
transition temperature of, pressure dependence of, (T), 19: 37753
transition temperature of, containing paramagnetic impurities, gap-anisotropy effects on, (T), 19: 39717
transition temperature in, magnetic impurity effect on, 19: 41608(R) (MIT-QPR-57, pp 59-65)
transition temperature of aluminum thin films, (E), 19: 47503 (BNL-9478)
transition temperature of superimposed films of iron and tin, 20: 2894
transition temperature of, effect of Suhl-Abrikosov resonance on, 20: 2911
transition temperature of lead films on superconducting substrates, (E), 20: 2917
transition temperatures of thin-film, effect of thin oxide layer on, 20: 2915
transition temperature of lead, effect of transition metals and transition metal oxides on, 20: 2916
transition temperature of uranium, pressure dependence of, (E), 20: 6234
transition temperatures of lead–gold, hafnium–vanadium and zirconium–molybdenum alloys, (E), 20: 8021
transition temperatures of dilute lead alloys, (E), 20: 9934
transition temperature of lanthanum sulfide, (E), 20: 11909
transition temperature of cadmium–mercury alloy, effects of ordering on, (E), 20: 11914
transition temperature of thin film, (T), 20: 13676(T)
transition temperature of pure, pressure effects on, (T), 20: 17639
transition temperature of, diamagnetic impurity effects on, (T), 20: 17637
transition temperature of niobium and vanadium, pressure dependence of, (E), 20: 19762
transition temperatures of mixed titanates, (E), 20: 19767
transition temperatures in epsilon-phase lead-bismuth alloys, (E), 20: 21892
transition temperature of indium antimonide, (E), 20: 28198
transition temperature of lanthanum, pressure dependence of, (E), 20: 28202
transition temperature of alpha-uranium, (E/T), 20: 28221
transition temperatures of superimposed copper and lead film, (E), 20: 28225
transition temperature of niobium, uniaxial stress effects on, (E), 20: 28228
transition temperature variation in magnetic impurity-containing, mechanism for, 20: 28205
transition temperature of niobium, at high pressures, (E), 20: 28227
transition temperature of indium and thallium, effects of lattice defects on, (E), 20: 28226
transition temperatures of, pressure dependence of, 20: 30259
transition temperatures of indium–lanthanum alloy, containing para-magnetic impurities, (E), 20: 30271
transition temperatures of niobium–tin intermetallic compound, 20: 30279
transition temperature of zirconium and zirconium isotopes, (E), 20: 30316
transition temperature in zinc, pressure dependence of, (E), 20: 34451
transition temperatures of tin, effects of uniaxial tension on, (E), 20: 34461
transition temperature of indium–lead, proximity effects of iron films on, 20: 34430
transition temperatures of lanthanum chalcogenides, 20: 36131
transition temperature of zinc, isotope effects on, (E), 20: 37959
transition temperatures for thin film, properties of, 20: 37980
transition temperature of indium films, thickness effects on, 20: 40043
transition temperatures of lead-alloy, 20: 44515
transition temperatures of, crystallite size effects on, 20: 44552

transition temperature of rhenium–technetium alloys, (E), 20: 44559
transition temperature of, effects of paramagnetic impurities on, 20: 44550
transition temperature of layers of silver and tin superimposed films, 20: 44567
transition to normal state in magnetic fields, 16: 22774
transition to normal state in variable fields, mechanisms of, (E), 20: 2902
transitions in barium–strontium titanates and calcium–strontium titanates, 20: 44506
transitions in bismuth–niobium alloys, (E), 19: 5092
transitions in cylinders of, second-order, (T), 19: 16770
transitions in fast-pulsed magnetic fields, (E), 19: 16779
transitions in filamentary, switching time of current-induced, 18: 28513
transitions in lead film, anomalies and surface effects in resistive, (E), 20: 19749
transitions in magnetic fields, angular dependence of, 18: 15076
transitions in, Mossbauer examination, 16: 1018(R) (AFOSR-1396)
transitions in niobium selenide and niobium sulfide, (E), 20: 13683
transitions in, normal-superconductive, 17: 36443 (NP-13089)
transitions in sintered niobium–tin alloy, (E), 20: 8029
transitions in solenoid, distribution of normal region after, (E), 20: 42103
transitions in strontium titanate, 18: 21102
transitions in strong magnetic fields, (T), 19: 37751
transitions in strontium titanates, 20: 44506
transitions in tellurium, (E), 19: 5103
transitions in thin-film strip transmission line structures, superconducting-to-normal, 18: 18835
transitions in thin-film, current-induced, 19: 14446
transitions in tin–zinc alloy, at 3.0 to 3.7°K, (E), 20: 28190
transitions in type-II, resistive, 18: 11124
transitions in type-II, nature of 50-cps phase, 20: 44522
transitions in, cell model for grain size and hysteresis effects in, (T), 19: 23563
transitions in, critical-current induced, 20: 24273
transitions in, current-induced, (E), 19: 43236(T)
transitions in, effects of nonmagnetic and paramagnetic impurities on, (T), 19: 21181
transitions in, effects of ordering-parameter fluctuations on, (T), 20: 26038(T)
transitions in, induced by current and magnetic-field pulses (E), 19: 1512
transitions in, magnetic and resistive, 18: 15071
transitions in, magnetic, (T), 19: 14443
transitions in, magnetic field effects on (T), 20: 28174
transitions in, method of plotting current- and field-induced, 20: 26051
transitions in, switching, (T), 19: 43234
transitions of indium–lead alloys, (E/T), 20: 21913
transitions to normal states, effects on Debye-Waller factors, 17: 13247
transitions to normal states, analytic properties of partition functions near, 17: 41619
transport equations for, (T), 19: 29158
tunneling between, supercurrents in, 17: 31214
tunneling between, review on, 19: 1500
tunneling between, quasi-spin method for Josephson, 19: 19022
tunneling by phonon assist in, theory of, 18: 2763
tunneling characteristics of aluminum–aluminum oxide–lead, geometrical resonance in, (E), 20: 2909
tunneling characteristics of contacts of normal metals and, (T), 20: 2910
tunnelling current between two, separated by potential barrier, 18: 21111
tunneling current in Josephson junction, electromagnetic radiation from, 20: 30292
tunneling density of states in, effective, 17: 25952
tunneling effect in barrier between, Josephson superconducting, 17: 18971
tunneling effect in barrier between, temperature and magnetic field dependence of Josephson, 18: 4509
tunneling in barrier between, quantum interference effects in Josephson, 18: 12789
tunneling in junctions of, microwave phonon effects on, (E), 19: 19052
tunneling in junctions of, in microwave field, (T), 19: 23582
tunneling in superimposed normal and conducting films, (E), 20: 42109
tunneling in superimposed, and normal films, 20: 44565
tunneling in, charged Bose gas model for Josephson, 20: 13691
tunneling in, microwave observation of quantum interference in, 18: 34696
tunneling in, theory for quasi-particle, 19: 41607 (LA-3342)
tunneling induced by microwave phonons in, (E), 19: 12437
tunneling junctions with normal metal, asymmetries in, 19: 7952
ultrasonic absorption in, theory of, 17: 6890
ultrasonic absorption in lanthanum, oscillations in temperature dependence of, 19: 16806
ultrasonic absorption in type-II, temperature dependence of, (T), 19: 19062
ultrasonic absorption in, device for measuring, 19: 23580
ultrasonic absorption in tin single-crystal, temperature dependence of, (E), 20: 17605
ultrasonic absorption in indium, nonlinear effects in, (E), 20: 17635
ultrasonic absorption in, 20: 40336(T)
ultrasonic attenuation in, for $ql < 1$, 17: 31203
ultrasonic attenuation in, 17: 35260(R) (TID-19135)
ultrasonic attenuation in, 18: 15711(R) (TID-20256)
ultrasonic attenuation in magnetic-impurity-containing (T), 19: 3179
ultrasonic attenuation in, in BCS theory (T), 19: 3187
ultrasonic attenuation in niobium, magnetic field effects on, (E), 19: 10192
ultrasonic attenuation in aluminum, 19: 14054
ultrasonic attenuation in niobium–zirconium alloy, in strong magnetic fields, (E), 19: 21188
ultrasonic attenuation in lead, longitudinal, (E), 19: 27379
ultrasonic attenuation in lead, amplitude dependence of, 20: 15657
ultrasonic attenuation in nonideal niobium–zirconium, flux jumping and magnetization effects on, (E), 20: 17606
ultrasonic attenuation in lead, anomalies of, (E), 20: 19766
ultrasonic attenuation in mixed state of niobium, (E), 20: 26045
ultrasonic attenuation by electromagnetic field in, 20: 28201
ultrasonic attenuation by, effects of magnetic fields on, (E/T), 20: 30735(R) (TID-22970, pp 331-73)
ultrasonic attenuation in pure strong-coupling, (T), 20: 30300
ultrasonic attenuation in, (T), 20: 32335
ultrasonic attenuation in mixed state of niobium, (E), 20: 34431
ultrasonic attenuation in gapless, coefficient for transverse, (T), 20: 37957
ultrasonic shear wave attenuation in tin, 17: 16729
ultrasonic shear wave attenuation in tin, 18: 6111
ultrasonic shear wave attenuation in aluminum (E), 19: 1492
ultrasonic wave attenuation in, effects of magnetic permeability on, (T), 20: 9890 (NP-15699)
ultrasonic wave attenuation in tin, frequency and temperature dependence of, (E/T), 20: 15659
ultrasonic wave attenuation in niobium, 20: 44529
ultrasonic-wave attenuation in thallium, (E/T), 20: 11915
ultrasonics attenuation in, 17: 21401(R) (TID-18585)
use as magnet coils for fields over 100 kgauss, feasibility, 16: 15460
use as magnet coils for magnetohydrodynamic power generation, 17: 9071
use as motor rotor and coils, 18: 22322
use as radiation detectors, theory of, 18: 38030
use for exciting electrical machines, 18: 42555
use for magnetic field generation and information storage, 18: 30686
use for producing strong magnetic fields (E), 19: 2897
use for producing high magnetic fields, 19: 37210
use for storage in memory devices, 18: 26490
use for strong magnetic field production and memory devices, review of, 20: 17628
use in a-c and d-c electric power transmission, 20: 24275
use in accelerators and storage rings, 18: 16602 (BNL-7534(p.417-47))
use in bolometer design, 20: 4229
use in bridge cell for memory devices, 20: 16797
use in cavities for proton linacs, 19: 26983 (MURA-714(p.108-9))
use in cavity resonators, 20: 9913
use in computer switches, 17: 37454
use in cryotron memory devices, (T), 20: 42108
use in d-c generators and motors, (T), 19: 12432
use in dynamo powered by a-c current, (E), 19: 10196
use in electron linacs, (E), 19: 11940
use in electron linac cavities, 19: 23232
use in electronic instruments, review, 18: 18149
use in electronic equipment, power-loss reduction from, 20: 17603
use in field windings of alternators, 20: 34458
use in field windings of alternators, 20: 34463
use in force-free magnet-coil design, 16: 12249
use in frequency-stabilized oscillators, 18: 27768
use in gating devices, 18: 16290(P)
use in high-field magnets, 17: 28074
use in high magnetic-field generation, review of, 18: 4492
use in high-field magnets, 20: 19724 (N-65-25286)
use in high-field electromagnetic lenses, 20: 42104
use in large high-field magnets, 20: 37934 (BNL-10380)
use in linear accelerators, 17: 7325 (BNL-6511(p.196-203))
use in linear accelerators, 18: 14590(R) (NIRL/R/60)
use in macroparticle acceleration for nuclear fusion, (T), 20: 30717
use in magnetic field shaping, 18: 16604 (BNL-7534(p.449-77))
use in magnetic shielding of space vehicles, 20: 30317
use in magnetics, economics of, 19: 1069
use in magnets, 18: 13012

use in magnets, 20: 28176
use in magnets, design engineering from, (T), 20: 42135
use in microwave cavities, 19: 23557
use in particle accelerators, 20: 11412
use in particle detection, 19: 34466(R) (AD-612677)
use in plasma containment, 19: 23938(P)
use in power cables and transformers, niobium, aluminum, and beryllium, 20: 44562
use in producing very strong magnetic fields, 18: 28498
use in solenoids for quantum paramagnetic amplifier, 20: 9228
use in space vehicle magnetic shielding systems, (E/T), 19: 8560
use in transformers, (T), 19: 14440
use in winding-type transformers, 20: 34447
use of bearings of, in three-phase induction motor, 19: 45196
use of coils of, for production of magnetic field, 17: 34438
use of cylindrical, in homogeneous magnetic field production, 18: 22831
use of films of, for microwave amplification, 20: 26027
use of gates of, for producing magnetic field pulses, 19: 19057
use of Josephson-type tunnel junctions of, for microwave and submillimeter-wave production, 20: 28212
use of magnet coils of, in NMR spectrometers, 20: 43685
use of magnet systems of, for MHD generators for, (T), 20: 25771
use of magnets of, in ESR studies, 18: 23524
use of magnets of, in thermonuclear propulsion systems, 19: 1810
use of magnets of, as junction shield in superconductive solenoid, 19: 35346(P)
use of niobium–zirconium, as magnet coils, 20: 5614
use of niobium–zirconium, in 40,000-gauss magnet, 20: 40018
use of niobium-25 zirconium, for magnetic bottle, 20: 40169 (NASA-TN-D-3595)
use of platinum metal compounds as, 17: 39594
use of, review of, 17: 37836
use of thin film, in fast storage devices, 20: 19720 (CEA-Bib-65)
use of thin film, for coupling ferromagnetic materials, 20: 45021
use of thin-film, in storage and switching devices, 18: 26477
use of thin-film, for adaptive logic networks, (E), 19: 16791
use of thin-film, in cryogenic devices, 20: 30258
use of titanium and its alloys as, 17: 37560
use of type II, in force-free infinite solenoid (T), 19: 1479 (NASA-TN-D-2156)
uses as level gages in liquid helium, 18: 40442
uses for high-field magnets, in USSR, (E/T), 19: 15700 (ATD-P-64-46)
uses for magnets, transition of solenoid windings to normal state in, (E), 20: 41760
uses for producing high uniform magnetic fields, 19: 6025 (CEA-R-2606)
uses in electrotechnics, 19: 25440
uses in magnets for measuring hyperon (Ξ^-) magnetic moment, (E), 20: 990 (BNL-9490)
uses in minimum-B magnets for plasma containment, (E), 20: 1279 (UCRL-14233)
uses in neuristors, 17: 37889
uses of hollow tubes of, for detecting Dirac magnetic monopoles, (E), 19: 41391
uses of, a-c equipment, 18: 34715
uses of, review, 18: 22846
uses of, review, 18: 24546
viscosity coefficient of type II, (T), 19: 16790
voltage along type-II, in mixed state, (T), 19: 21166
voltage in type II, transverse, (E), 20: 2897
voltages in, guided motion of vortices for transversal, 19: 39694
voltages in, longitudinal and transverse, (T), 20: 8009
vortex bound states in type II, one particle excitations of, (T), 19: 33163
vortex displacement in, losses from, (T), 20: 19738
vortex effects in thin, (E/T), 19: 16803
vortex lattices in type-II, hydrodynamic stability of, 20: 30286
vortex line bound fermion states in type-II, low-energy excitation of, 18: 24551
vortex lines in, lectures on, 20: 30783
vortex motion in alloy, (T), 20: 26037(T)
vortex motion in type II, guided, (E/T), 19: 8341
vortex motion in type-II, theory of, (T), 20: 2908
vortex motion in type II, effects of thermal forces on, (E), 20: 24284
vortex nucleation in type II, 20: 8023
vortex nuclei formation in type II, (T), 20: 34452
vortex pairs in, lifetime of, (T), 20: 37944
vortex wave spectrum of type II, 18: 24556
vortices in thin films of, (E/T), 19: 25453
vortices in thin-film, properties of quantized, (T), 19: 8370
wave amplification by films of, nonlinear reactance and frequency conversion at 1.8 to 2.2°K, 18: 16879

SUPERCRITICAL ONCE-THRU TUBE REACTOR

cost analysis for, 18: 26928 (WCAP-2294)
design and development, 20: 3485(R) (WCAP-2120)
design and development, 20: 40416 (WCAP-2222-P)
design and development of 1000-Mw(e), 18: 3197(R) (WCAP-2009)
design and development of 1000-Mw(e), 18: 3199(R) (WCAP-2070)
development and economic evaluation of 1000-Mw(e), 18: 1260(R) (WCAP-2361)
development and economic evaluation of 1000-Mw(e), 18: 11451(R) (WCAP-2525)
development and testing of 1000-Mw(e), 18: 19379(R) (WCAP-2564)
development of, heat transfer studies for (E), 19: 2515 (WCAP-2056 (Pt.III))
development of, status of, 20: 26499
development of, technological, 19: 29671
development, Jan.–June 1964, 18: 45035(R) (WCAP-2647)
stability analysis, 18: 19378 (WCAP-2258)

Supercritical Water Reactor (ANP)
see ANP Reactor (SCW)

SUPERFLUIDITY

behavior of quantized vortices in, 20: 46529
behavior of thin films and narrow channels of helium II, 17: 13132
book: *An Introduction to the Theory of Superfluidity*, 19: 41636(T)
book: *Theory of Interacting Fermi Systems*, 19: 3188
book: *Theory of Superconductivity*, 19: 19061
circulation at quantum level units in helium II, 19: 41620
circulation in liquid helium II, 18: 36462
conference, 20: 19774
critical velocities of liquid helium near λ transition, superfluid gyroscope for measuring, (E), 19: 23577
critical velocities in helium II, (T), 20: 30272
critical velocity in, wall roughness effect on (T), 19: 1503
density fluctuations in dilute Bose systems, correlation of, (T), 20: 19768
density of helium-4 near transition temperature, 20: 42122
density of liquid helium II, temperature dependence near λ point, (T), 20: 28206
description of, in helium II, 18: 7641
destruction, factors in, 16: 6881
destruction of helium-3, in magnetic fields, (T), 19: 23586
detection in helium-3, review, 20: 8002 (COO-1198-299)
detection of quantized vortex rings in (E/T), 19: 3180
dissipation and critical velocities in helium-II, 20: 44503 (LA-DC-8165)
dynamics in, quantum-statistical-mechanics studies of (T), 19: 1460
dynamics of, in helium-3 and -4, 17: 13198
dynamics of, in helium-filled capillary tubes, 18: 36460
dynamics of, in hydrodynamic and collisionless domains of stationary Bose system in thermal equilibrium, 18: 11123
effects in light nuclei, 18: 2951
energy difference between normal and superfluid nuclear matter, free-meson lattice model for free, 20: 28213
energy gap renormalization in Fermi system, 19: 27205
entropy principle and renormalization in systems of, stationary, 18: 7642
entropy principle and renormalization in systems of, stationary, 18: 7643
excitations in, Goldstone theory for, 20: 45042
Fermi system anisotropies, description of, 16: 18357
fermion interactions in, hamiltonian for strong, 18: 7748
films of helium II, thickness measurements on moving, 17: 31105
flow in oscillating geometries, laminar and turbulent, (E), 19: 8367
flow in Venturi tubes, (T), 19: 39696
flow in wide capillaries, 16: 2356
flow of helium II through porous partition, analogous Josephson effect for, (T), 19: 45202
flow of helium II, Helmholtz, (E), 19: 33174
flow of helium II, analog of a-c Josephson effect in, (T), 19: 33178
flow of helium II, dissipative normal fluid production in, gravitational, (E), 19: 45201
flow of helium II, stability between rotating cylinders, 20: 44555
flow of helium II, in an annulus, 20: 46523
flow of helium, thermomechanoelectrical effects for, (T), 19: 21176
flow of liquid helium II through narrow channels, (E), 20: 1119 (LA-DC-7357)
flow of nonequilibrium fluid in, relaxation times and vortex rings in, (T), 20: 13671
friction in rotating Bose gas, mutual, (T), 19: 19040
helium bulk transfer in, liquid, 18: 30682
helium flow, critical velocities and vortices in, 18: 44693
hydrodynamic equations for, in Fermi liquids, (T), 19: 21161 (JINR-P-1953)
hydrodynamical equations for Fermi liquid and two-particle Green functions, (T), 19: 19042
hydrodynamics, 17: 20688
hydrodynamics of, effects of Helmholz flows on, (T), 19: 8350
hydrodynamics of, thermodynamic Green functions for, 20: 11898

in Bose-Fermi isotopic mixtures, 16: 13809
ion motion in helium II, roton emission from negative, (T), 20: 28208
kinetics of Fermi gas, static equations at finite temperature for, (T), 20: 34454
mathematics of, 18: 9438
matter waves in, coherent, 19: 37741
nuclear level densities from, 17: 38215
nuclear, properties of, 17: 11735
of boson systems, effects of very dilute impurities, 16: 4687 (D1-82-0063)
operators for condensed Bose system, quasi-particle, (T), 20: 13670
particle motion in helium II, suspended, (E), 19: 33171
persistent currents in liquid helium II, experiments showing, 18: 36461
phase transition of helium-3, detection of, (E), 19: 29162
properties common to fluids, 19: 44842
properties of helium-3, 20: 4773 (COO-1198-306)
properties of helium, near λ line, 20: 30266(T)
properties of helium II, rotational, 20: 37987
properties of helium II, macroscopic quantum aspects of, 20: 46530
properties of liquid helium II, review of, 20: 37974
properties of, macroscopic approach to, 17: 20689
quantization of circulation, 20: 46509(R) (COO-1569-1)
quantum fluid master equations, sum of diagrams of, 17: 22331
quantum theory of energy spectrum in, 18: 944
rotation of Fermi systems, 20: 37473
rotation of helium II, quantization of, (T), 20: 44563
self-energy of Bogoliubov quasi-particle, 18: 34687
sound velocity in helium-3 and -4 mixtures, fourth, 18: 21115
stability of helium II flow down inclined planes, (T), 19: 5093
stability of helium II in narrow channels, phase coherence in, (E), 19: 33173
stability of rotatory flows in, 17: 32808
statistical behavior in, 17: 31218
statistical functions for, in terms of potentials, 17: 20691
statistical mechanics of, for Bose gases, 18: 36465
statistical theory of, in Bose gases, 16: 13812
surface excitation in helium, gapless, (E), 19: 39737
theory, 16: 29535
theory, 18: 44684
theory, 20: 4772
theory, 20: 4789
theory, 20: 34466
theory for degenerate Bose systems, quantum, 20: 46527
theory for neutron stars, (T), 19: 14226
theory of, applications to nuclear theory, 17: 28069
theory of Bose system, Green functions in, 18: 15043 (JINR-P-1517)
theory of Fermi liquid, 20: 6229
theory of Fermi liquid, (T), 20: 6237
theory of Fermi-liquid, collective oscillations in, 20: 30284
theory of helium, microscopic, 19: 47506
theory of, in nuclear thermodynamics, 17: 38214
theory of, Landau, 17: 20760
theory of, broken symmetries and massless particles in, 18: 15014
theory of, Einstein-Bose condensation in, (T), 20: 28182
theory of, in fermion systems, 18: 34864
theory of, lecture on, 18: 43151 (ISS-63/50)
theory of, two-particle excitation spectrum in Landau, 20: 17646
thermodynamic renormalization in equilibrium statistical mechanics, 19: 18601
torque exerted by pure superflow, 16: 10725
transition temperature of helium-3, effects of quasiparticle lifetime on, (T), 20: 28207
transition temperature of helium-3, effects of quasiparticle lifetimes on, 20: 34439
transition temperatures of helium-3, effect of quasiparticle lifetimes on, (T), 20: 34460
ultrasonic attenuation in helium, frequency and temperature dependence of, (E), 20: 30299
use in helium purification, 19: 36898(P)
vortex excitations in helium, transverse, (T), 19: 37746
vortex rings in helium, quantized, (E), 19: 5107
vortex rings in helium, quantized, (T), 19: 39723
wave function for stationary, in porous media, (T), 20: 9902(T)
zero sound in Fermi, absence of, 18: 26471

SUPERHEATERS

advantages of, in nuclear power plants, 16: 32587
burnout and heat transfer in once-through, 18: 27667
burnout in once-through, 18: 39461
corrosion of tubes by air and steam in, at 1100 to 1500°F, 16: 24125
corrosion of tubes by steam in, at 1200 to 1500°F, 16: 24126
corrosion of tubes by steam in, effects on heat-transfer properties, 16: 24127
description and performance of steam reheater for SELNI station, 16: 18675
design and development of sodium-heated, 19: 568(R) (TID-20894)
design and operation for nuclear power plant, 17: 34084
design and operation of separately fired, at Indian Point Power Station, 20: 22455
design concepts, 16: 9688
design for gas-cooled reactors, 16: 14329
design for pressurized water reactor power plant, 19: 45630(P)
design of bayonet, for molten-salt reactors, 17: 8373
design of conventional and nuclear, 17: 24707
design of, for heat recovery from pressurized fluid, 17: 4684(P)
design of sodium-heated, modular, steam generators, 19: 21611 (NAA-SR-9826)
design of sodium-heated, 19: 46478(R) (BAW-1280-25)
design of sodium, for steam generators, 19: 31474 (BAW-1280-23)
design of sodium, for steam generators, 19: 31475 (BAW-1280-24)
design of tubulous vapor generators, 17: 12446(P)
design of vapor generating and superheating apparatus, 17: 12443(P)
development, 19: 45572(R) (GEAP-4755)
development of fossil-fired, for use with heavy water reactors, 17: 15465(R) (SL-1974-3)
development of fossil-fueled, for nuclear power plants, 18: 38492 (A/CONF.28/P/672)
development of sodium-heated steam, 20: 16599(R) (BAW-1280-34)
development, testing of gravity steam separations, 16: 3938 (CEND-127)
materials development for, 18: 26946
materials for, failure of chromium–nickel–titanium steel as, 17: 37521(T) (TRG-Inf-Ser-191)
materials for sodium, 16: 25502 (NAA-SR-Memo-6849)
soot blower design, for, 17: 20146(P)

SUPERHEATERS (NUCLEAR)

boiler design for, 19: 38817(P)
characteristics of coupled fast-thermal steam superheating system, 16: 26553
characteristics, using secondary reheating methods, 16: 28583
chloride deposition from steam onto fuel clad materials in, tracer studies of, 18: 8751 (GNEC-295)
chloride-36 deposition from stream on, 17: 38461 (TID-7674(p.1-4))
conference, 19: 5486 (SAN-8003)
conference, Idaho Falls, Idaho, April 13 and 14, 1961, 16: 7295 (TID-7617)
conference on, Idaho Falls, Idaho, Mar. 1963, 17: 38460 (TID-7674)
conference on nuclear superheat projects, 16: 21817 (TID-7630)
conference on, Sioux Falls, S. D., Sept. 12 to 14, 1962, 17: 21225 (TID-7658)
control of boiling reactor containing internal, 16: 24531
conversion ratio in uranium-fueled, 19: 35756 (GEAP-3863)
cooling device for, emergency, 17: 22899(P)
corrosion in, design of facility for simulation, 16: 9647 (GEAP-3778)
corrosion in, facility for studying, 17: 3899
corrosion in, facility for studying, 17: 39496
criticality studies, 16: 24409
criticality studies, comparison of experiment and theory of uniform lattices, 16: 31203 (GEAP-3882)
criticality studies of annular multitube fuel elements for, 17: 3741
criticality studies, 17: 9835 (CEND-121)
criticality studies and physics calculations for, 18: 3096 (GNEC-282)
criticality studies for, in ZPR-7, 18: 3208
criticality studies of water-moderated uranium(IV) oxide, 18: 3210
description for Soviet 200-Mw power plant, 16: 9684
description of 200-Mw(e), 18: 3286
design, 16: 15852(P)
design, 16: 15854(P)
design, 17: 1146(P)
design, 17: 28549
design, 17: 42391(P)
design, 18: 4826(P)
design, 18: 24931(P)
design, 18: 43057(P)
design, 18: 45071(P)
design, 19: 3584(P)
design, 19: 5512(P)
design, 19: 17331(P)
design, 19: 19405(P)
design, 19: 21659(P)
design, 19: 29702(P)
design, 19: 29706(P)
design, 19: 35822(P)
design, 19: 38222(P)
design, 19: 38223(P)
design, 20: 1519(P)
design, 20: 1522(P)
design, 20: 1523(P)

design, 20: 16106(P)
design and development, 16: 14286(R) (GEAP-3785)
design and development of, 16: 30070(R) (GNEC-241)
design and development, 17: 7601(R) (GNEC-254)
design and development of radial-vane steam separators for, 17: 31729 (GEAP-4272)
design and development of, review, (E), 19: 43546
design and evaluation of Hanford Graphite Superheat Reactor, 18: 33104 (HW-73130)
design and operation of BORAX V, 18: 23052 (CONF-504-2)
design and operation of Vallecitos Superheat Reactor, 19: 3788
design development of Mixed Spectrum Superheater, 16: 1243 (GEAP-3590(Rev.1))
design development for 200-Mw(e) boiling superheating reactor, 16: 5022(R) (GNEC-202)
design evaluation, 16: 5011 (ANL-6437)
design evaluation for 100- and 300-Mw(e), 16: 9666 (PRWRA-GNEC-4)
design for boiling water reactor, 16: 6234(P)
design for boiling water reactor, 16: 17304(P)
design for boiling reactor, 19: 33647
design for boiling water reactors, 19: 45625
design for maritime use, 17: 7599(R) (GEMP-160)
design for nuclear power plant, 19: 38224(P)
design for passenger liner, 17: 40333 (ACNP-6125(Suppl.1))
design for use in 300-Mw(e) reactor, 16: 1242 (GEAP-3589(Rev.1))
design for use in multiple-reactor steam plants, 17: 15464 (SL-1812)
design of AEG, 19: 17285
design of Beloyarsk graphite-moderated, (E), 19: 43547
design of BONUS, effect of two-pass flow on, 20: 38509 (ORNL-TM-1449)
design of breeder-type, 17: 21352(P)
design of breeding, for boiling reactors, 20: 16105(P)
design of direct-cycle boiling 200-Mw(e), 16: 31256 (GNEC-212)
design of fuel elements, uranium thermal conductivity values for, 20: 39403 (ORNL-TM-1450)
design of graphite-moderated superheat power reactor, 17: 21256 (TID-7658(p.166-70))
design of Hanford Graphite Superheat Reactor, 17: 21242 (TID-7658 (p.99-100))
design of liquid-moderated vapor superheat reactor, 17: 40401(P)
design of mixed-spectrum, 16: 24473
design of mixed-spectrum, physics analysis of, 16: 24474
design of mixed spectrum 75-Mw(e), 16: 31255 (GEAP-4016)
design of pressurized, for boiling reactor, 17: 17536 (GEAP-4057)
design of prototype mixed spectrum, 18: 4795(R) (GEAP-3924)
design of reactor containing, 18: 6505(P)
design of Russian, 20: 1351 (WASH-1060)
design of steam-cooled heavy-water-moderated, 17: 29775(P)
design of VBWR in-pile loop E-SADE, 18: 45019 (GEAP-4617)
design of 300-Mw(e) Mixed Spectrum, 16: 2733(R) (GEAP-3581)
design of 300- and 1000-Mw(e) graphite, 20: 1515
design study of boiling, heavy-water-moderated, 16: 11273
design study of 607 Mw(e) boiling water-separate superheat reactor plant, 17: 21255 (TID-7658(p.162-6))
design without steam pumping, 16: 21835(P)
development, 16: 2734(R) (GEAP-3686)
development, 16: 3941(R) (GNEC-190)
development, 16: 21812(R) (GNEC-230)
development, 16: 31206(R) (GEAP-4024)
development, 16: 31302
development, 16: 33990 (TID-7634)
development, 18: 4795(R) (GEAP-3924)
development, 18: 9674
development, 18: 45051
development, 19: 1914
development, 20: 10393
development, 20: 26501
development, 19: 38178(R) (GEAP-4790)
development and use, review of, 19: 48012
development for boiling heavy-water reactors, 20: 26507
development in Germany, 18: 38465 (A/CONF.28/P/535)
development of, 16: 32573(R) (GEAP-3877)
development of corrosion-resistant materials for, 17: 493(R) (BMI-X-10003)
development of corrosion-resistant niobium alloys for, 19: 2758
development of design method for, 17: 15453(R) (GNEC-267)
development of EVESR, 20: 47056
development of, for maritime use, 16: 30068(R) (GEMP-130)
development of niobium-base alloys for use in, 16: 25695(R) (BMI-X-188)
development of once-through, 16: 1907 (GEAP-3703)
development of, quarterly summary of, 16: 28532(R) (GNEC-220)
development of steam-water separators for, 16: 11814 (GEAP-3787)
development of 300-Mw(e) Separate Superheat Reactor, 16: 2733(R) (GEAP-3581)
development of, summary, 18: 33083 (A/CONF.28/P/215)
development program for supercritical pressure-tube reactors, 17: 7624
development program for SCOTT-R, 17: 15486
development progress, April to June 1960, 16: 8361(R) (GEAP-3538)
development review, 20: 1513
economic and technological evaluation of steam-cooled power reactors, 16: 3945 (TID-8536)
economics, 20: 3508
engineering materials list, 18: 35661 (TID-4100(Suppl.23))
experiments on Borax-V PSH-1, 18: 35060(R) (ANL-6904)
fabrication of, problems in, 17: 21233 (TID-7658(p.57))
feasibility of mixed-spectrum steam-superheat power reactors, (T), 20: 3471(R) (GEAP-4861)
fuel assembly design for, 19: 35825(P)
fuel cladding behavior in, analysis of, 19: 28860
fuel cladding corrosion in, 19: 28769
fuel cladding failure in, effects of strain cycling on, 17: 33239 (GEAP-4244)
fuel cladding materials evaluation for, 18: 24080 (BMI-X-286)
fuel cladding materials testing for Marviken, 19: 28770
fuel development for, design of EVESR for, 17: 21236 (TID-7658(p.77-8))
fuel element assembly for, 19: 35821(P)
fuel element cladding and structures, alloy development for, 16: 27558(R) (BMI-X-195)
fuel element cladding for, survey of materials, 17: 12664 (GEAP-4060)
fuel element cladding materials, search for corrosion-resistant, 17: 42210
fuel element cladding materials for, analysis of, 18: 28025
fuel element cladding behavior in, 18: 34076 (TID-8540(p.213-330))
fuel element cladding corrosion in, 19: 4197 (SAN-8003(p.90-133))
fuel element cladding properties for, 19: 4597 (SAN-8003(p.13-89))
fuel element cladding for, properties of Incoloy 800 as, 20: 907
fuel element cladding materials for, 20: 35840 (KR-89, pp 131-52)
fuel element criticality studies for, 17: 15388 (CEND-167)
fuel element critical experiments, 17: 36862 (CEND-131)
fuel element design, fabrication, and irradiation, 16: 11223 (GEAP-3796)
fuel element design and testing in SADE loop in VBWR, 17: 40270 (GEAP-4240)
fuel element design for, 18: 11423(P)
fuel element design for, 20: 10363(P)
fuel element design for, 20: 36478 (KR-89, pp 238-64)
fuel element development for, 17: 21238 (TID-7658(p.82-9))
fuel element development for, 17: 35099 (GNEC-288)
fuel element development and testing for, 17: 38475 (TID-7674 (p.39-45))
fuel element fabrication, 16: 24635
fuel element fabrication for critical experiments in, 16: 30743 (CEND-119)
fuel element fabrication, 17: 26859 (GNEC-174)
fuel element fabrication for, 17: 38474 (TID-7674(p.36-9))
fuel element fabrication for BORAX-V, 18: 22453 (ANL-6649)
fuel element fabrication and design for, 20: 36477 (KR-89, pp 197-237)
fuel element failure in ESH-1, 18: 2274
fuel element for Pathfinder, corrosion tests of, 19: 16010 (ACNP-62024)
fuel element in-pile testing for, 17: 21237 (TID-7658(p.79-82))
fuel element testing for, 20: 14125 (GEAP-4898)
fuel element thermal shock tests, 19: 27772 (ACNP-64010)
fuel elements for, evaluation of stainless steel for cladding, 17: 12665 (GEAP-4095)
fuel elements for, neutron effective resonance integrals for, 17: 26036
fuel elements for advanced BONUS, development of, 19: 24081(R) (GNEC-361)
fuel elements for AEG, development of, 20: 18077
fuel elements for, design and testing of, (E), 19: 17285
fuel elements for, stresses in claddings of annular, 19: 38148
fuel elements for, testing in E-SADE loop of VBWR, 20: 5104 (ACNP-65006)
fuel fabrication and irradiation, 17: 21235 (TID-7658(p.59-77))
fuel materials for, development and testing of, 19: 35757(R) (GEAP-4810)
fuel-element failure in BONUS, 20: 35053
fuels and materials testing for, 18: 24886(R) (GEAP-4565)
fuels and materials testing for, 18: 24884(R) (GEAP-4419)
fuels and materials for, development and testing of, 18: 45020(R) (GEAP-4619)
heat exchanger support structure for, 20: 1525(P)
heat transfer analysis of forced-circulation, operating at subcritical pressure, 18: 26945
heat transfer and pressure drop testing in, 17: 28522 (ACNP-62030)
heat transfer in, (E), 19: 4329 (SAN-8003(p.134-62))
kinetics, 17: 38487 (TID-7674(p.63-4))

kinetics of mixed-spectrum steam-cooled, (E/T), 20: 3471(R) (GEAP-4861)
materials development for, review of, 17: 30930
materials for, development of niobium alloys as, 17: 23890(R) (BMI-X-10040)
materials, literature survey, 16: 24155 (GEAP-3875)
moderators in boiling reactors, evaluation of zirconium hydride for, 16: 15910 (NAA-SR-5943)
moisture control in, 17: 4323
neutron flux distribution in, thermal, 17: 26037
neutron resonance integrals for clustered pin lattices, 17: 38481 (TID-7674(p.54-5))
neutron thermal utilization in, 16: 24425
niobium-base alloy development for, 17: 1816(R) (BMI-X-10016)
operating experience with central-superheat core CSH-1 in Borax-V, (E), 19: 42149 (ANL-6961)
operation problems in BWR, 20: 20275
operations of Borax-V, summary, 18: 24951(R) (ANL-6880(p.1-5))
operations of MSSCEF, (E), 20: 3471(R) (GEAP-4861)
operations, survey of experience, 16: 5038
performance in sodium loop of HNPF, computer analysis of, 18: 38534 (NAA-SR-Memo-9474)
performance of boiling water reactors using, 19: 29670
physics analysis of, evaluation and review of, 17: 21244 (TID-7658 (p.112-14))
power and reactivity studies of boiling reactor, 16: 23285
power mapping of CSH-1 core, 18: 21698(R) (ANL-6860)
reactivity, flooding coefficient of, 16: 19978 (ACNP-6108)
reactor design for, 18: 38438 (A/CONF.28/P/309)
research program, 17: 13792
review of programs and concepts, 17: 33353
spacers in BONUS assemblies, temperature distribution under, 20: 42634 (ORNL-TM-1453)
stability of arrangements of, analysis of, (T), 19: 5498
steam contamination in, 18: 4805
steam flow control in large, 18: 4796(R) (GEAP-4153)
steam separation device development for, 16: 4238 (CEND-136)
steam separation requirements for large, 16: 24969 (CEND-116)
steam separator design and development for, 19: 6026(R) (GEAP-4728)
steam separator, mathematical analysis of Vane-type, 16: 24936 (GEAP-4012)
testing of, for stainless steel corrosion, 17: 21226 (TID-7658(p.1-14))
use in Rankine steam-cycle power plants for communications satellites, (T), 19: 10624

Superlattices
see Crystal Structure

SUPERSONIC FLOW
see also Subsonic Flow
see also Transonic Flow
around blunt bodies, 20: 4153(R) (UCRL-14360, pp 73-85)
around blunt magnetized bodies, inviscid, 17: 15016
atom concentrations in nonequilibrium, emerging from d-c glow discharge, 16: 1270 (AFOSR-1360)
calculations of stationary, in common cones, 20: 11767 (HMI-B-42)
characteristics of, in air passing cylindrically symmetric objects, 17: 18263 (LAMS-2826)
circumfluence of blunt bodies in magnetic field in conducting gas, numerical solution, 19: 44200(T) (SC-T-65-756)
density determination in, effects of shock waves on interferometric, 17: 20683
density measurement in low-density shock tunnels, 17: 30672
drag coefficients and heating ratios for right circular cylinders in free-molecular and continuum flow at Mach 10 to 30, 19: 24675 (SC-RR-64-2141)
effects on positive column of d-c electric arc under magnetic confinement, 18: 15412
electric arc stabilization in, 19: 25598
equilibrium of dissociated and ionized hydrogen in, 19: 20124
fluid dynamics of, 19: 30378(R) (SR-4-5)
heating of vehicle in compressible fluid, 19: 35874 (UCRL-7807)
heating rates for cylinders in laminar, 20: 20857 (SC-DC-65-1907)
interface stability between two fluids in, effects of compressibility on, 18: 24999 (RM-3953-AEC)
ionization nonequilibrium in expanding quasi one-dimensional, 16: 10686
ionization profiles in seeded, Mach 3, high-altitude rocket exhaust, mapping by microwave and probe techniques, 17: 40205
magnetogasdynamic viscous shock layers in hypersonic, 18: 30936
magnetohydrodynamics of, 17: 16855
MHD effects on stagnation-point heat transfer from plasmas, 17: 42143
missile flight through blast wave, transient base pressure study of, 19: 8008 (SC-DC-64-1595)
of nitrogen plasma, wave patterns in, 17: 42121
over cone models, 18: 20119 (ARL-64-5)
past a wedge, magnetohydrodynamics of, 17: 39457
past two-dimensional blunt body, numerical computation of, (T), 19: 5570 (NYO-1480-1)
past wedges, analysis of inviscid magnetohydrodynamic, 17: 6898
past wedges, shock-wave formation in magnetohydrodynamic, 17: 41576
plasma diagnostics of solid-propellant rocket exhaust plume containing cesium and potassium, 18: 21399
plasma jet interactions with magnetic field, 16: 20619
pressure distributions on sphere cones, 19: 12875 (SC-RR-64-1796)
pressure measurements on cone-cylinder probes, static, 19: 14919 (SC-RR-64-1689)
research programs on, 1964 Army Dept. summary, 19: 32048(R) (NP-15073)
shock-wave formation in, magnetohydrodynamic equations for, 17: 2105
shock wave interaction patterns for conical missiles, (T), 19: 43636 (SC-TM-65-217)
shock waves in, review of power-law for, 17: 9137
studies, 19: 28493 (ARL-65-18)
temperature variations in, of air, 18: 13365 (SC-4976(RR))
theory of, past a wedge, 17: 20597(T) (FTD-TT-62-958)
velocity distribution for compressible fluid, equation for stagnation-point, 19: 46956 (NP-15514(Vol.1))

Supersonic Inspection
see Sonic Inspection

Supo
see Los Alamos Water Boiler

SURFACE-ACTIVE AGENTS
(See also specific agents.)
see also Flotation Reagents
coalescence effects at planar interfaces, 16: 25956 (UCRL-10097)
decontamination of foliage, glass, and textiles using, 19: 22608
effectiveness in anionic and cationic decontamination, 19: 4051
effects of Pluronics F68 on excretion of inhaled plutonium, 17: 23055
effects on analytical procedures involving uranyl ions, 20: 20630
effects on coagulation and precipitation in waste solutions, 16: 2795 (AAEC/E-74)
effects on diffusion of hydrogen through iron, 16: 530(T) (AEC-tr-4856)
effects on mass transfer in two-phase flow, 20: 39050 (UCRL-16535)
effects on polarography of uranyl pyrophosphate complexes, 19: 19816
effects on polarographic determination of hexavalent uranium in nitric acid media, 20: 20631
effects on properties of nuclear emulsions, 18: 23495
evaluation of biodegradable, for foam separation treatment of wastes, 19: 40271(R) (RAI-350)
properties of Triton X-100 for formation of emulsions of aqueous solutions of beta emitters and toluene for liquid scintillation counting, 19: 30095
sorptive properties for polonium chloride ions, effect of adsorption bed of ionized molecules, 16: 27002
surface tension in bubbling water, dynamic, 18: 1861 (CONF-117-9)
synthesis and properties of fluorocarbon alcohol 3,5-dinitrobenzoates, 19: 21775 (UCRL-12307)
testing for foam removal of cerium, cesium, and strontium from aqueous solutions, 16: 14819(R) (RAI-100)
testing of, for thoria bead production, 18: 41305(R) (ORNL-TM-776)
use for concentrating water-d_2 in light water, 17: 1806(P)
use for preparation of 2,4-dinitrophenyl fluoroalkyl ethers, 20: 25110 (UCRL-14714)
use for surface decontamination of clothing, foliage, and glass, 19: 11427
wetting properties for construction materials, 16: 3292(T) (JPRS-9706 (p.81-6))

Surface-Barrier Detectors
see Semiconductor Detectors

Surface Bursts (Atomic)
see Atomic Explosions

SURFACE ENERGY
relation to critical temperatures and surface tension, 16: 25351
theory of interfacial, in corrosion of metals by liquid metals, 18: 27899 (NASA-SP-41(p.109-25))

SURFACE FRICTION
effects on heat transfer in parallel rod arrays, 20: 39084 (GEAP-5115)
for turbulent boundary-layer flow longitudinal to circular cylinder, 17: 16242
in concentric tubes with roughened inner tubes, 17: 273(T) (AAEC/Trans-13)
in turbulent boundary-layer flow longitudinal to a cylinder, 17: 8374
measurement between bearing materials, survey of, 17: 32208(R) (GDC-63-140)
measurement in gas-cooled and pebble-bed reactors, 17: 33326(R) (ORNL-3445(p.298-328))
of clean metals in sodium (liquid), 17: 2080
of refractory materials at high temperatures, radiation effects, 16: 10604 (APEX-671)

SURFACE PROPERTIES

see also Surface Energy
see also Surface Friction
see also Surface Tension
book: *Advances in Catalysis and Related Subjects*, 18: 33453
book: *Surface Phenomena in Metals and Alloys*, 16: 29434
chemistry of, review of, 17: 4516
measurement by charged-particle reactions, 16: 24568
measurement by charged particle reactions, 16: 24569
measurement using elliptically polarized light, 17: 23870 (TID-16871)
measurement using krypton-85, 18: 37566(R) (NYO-2757-3)
research on, at Ames laboratory, 20: 3863(R) (IS-1200(Sect. C))

SURFACE REACTIONS

book: *Interactions of Atomic Particles with the Surface of a Metal*, 18: 10769(T) (AEC-tr-6089)
of charge particles, use to determine composition of surfaces, 16: 24568
of charge particles, use to determine composition of surfaces, 16: 24569
research programs of U. S. Army on, 1962 summary, 17: 33413(R) (NP-12967)

SURFACE TENSION

calculation of dynamic, 19: 9046(R) (IS-900(Sect.C))
determination in metals from thermal conductivity, 16: 5726(T) (AEC-tr-4937)
effects on boiling heat transfer in, 19: 4336
measurement by pendant drop method, 19: 47065
measurement from photographed menisci, method for, 19: 34681 (LA-DC-6514)
measurement in liquid metals by pendant drop method, tables for, 19: 34682 (LA-DC-6515)
measurement of alkali metal, apparatus for, 19: 40409(R) (MSAR-65-95)
measurement of alkali metal, design of equipment for high-temperature, 20: 22965(R) (AGN-8177)
measurement of dynamic, in bubbling solutions, 18: 1861 (CONF-117-9)
measurement of interfacial, by falling-drop method, 16: 2926(R) (MLM-1117)
measurement of liquid metal, review on, 19: 47064
measurement of, survey of methods, 16: 29434
of metals and alloys, 16: 29434
relation to critical temperature and surface energy, 16: 25351
role of, in metallurgy, 17: 41472(T)
theory, 16: 29434
theory of, in ternary metal solutions, 17: 41474(T)
use in liquid storage, 20: 39091

SURFACE WATERS

(Limited to information on surface waters in general, including rivers, lakes, ponds, sloughs, etc. For information on specific rivers and bodies of water, see by name, e.g., Columbia River and White Oak Creek.)
age estimation of drainless Alpine lakes by determination of uranium-234: uranium-238 ratio, 18: 31762
age estimation of carbonates from Lake Bonneville and Lake Lahontan, Great Basin, 20: 546
age estimation of salt lakes using chlorine-36, 20: 25308
age estimation of, by tritium abundance variations, 20: 20894
alpha contamination of U. S., due to natural radioactivity or uranium processing, 18: 9816
alpha detection in, monitor for, 20: 21038 (K-1656)
analysis for alpha and beta activity in Hartbeespoort Dam, South Africa, 19: 11459
analysis for barium-140, radium-226, and strontium-90 by ion exchange, 18: 23421
analysis for beryllium, spectrophotometric, 18: 1546
analysis for carbon dioxide and residual gases in geothermal, in New Zealand, mass spectrometric, 16: 16581
analysis for carbon-13/12 ratio in geothermal, in New Zealand, 16: 16582
analysis for copper, activation, 18: 21986
analysis for fall-out radioactivity, 1962, 16: 30693
analysis for fallout fission products, 1963, 18: 6944(R) (HASL-142)
analysis for fallout fission products in, 19: 9367 (IAEA-R-1)
analysis for iodine, neutron activation, 19: 36313
analysis for lead-210, radiochemical, 20: 5505
analysis for pollution, activation, 20: 1739(R) (GA-4297)
analysis for radioactivity, 16: 30694
analysis for radioactivity, 1961, 17: 1677
analysis for radioisotopes, techniques for, 17: 25113 (DPSPU-63-30-6)
analysis for radioactivity from fallout fission products, 17: 30766
analysis for radioactivity, activation, 17: 30185
analysis for radioisotopes, 1956 to 1961, 18: 8525(T) (AEC-tr-6049 (p.233-57))
analysis for radioactivity in France, 18: 16204(R) (SCPRI(RM)-XII-1963)
analysis for radioactivity in Columbia River, 18: 37387
analysis for radioactivity in rivers in Washington, 18: 37385
analysis for radioactivity, methods for, 20: 20963
analysis for radium and strontium-90 in France, 16: 31966
analysis for radium, radiochemical, 18: 1574
analysis for radium-226, method of, 20: 45996
analysis for ruthenium-103 and ruthenium-106, radiochemical method, 16: 16309 (PG-Report-308)
analysis for sediments, using radiological gage, (E), 19: 29133(R) (NYO-10221)
analysis for strontium, spectrophotometric, 18: 27328
analysis for strontium-89 and -90, radiochemical, 18: 33769 (NP-14091)
analysis for strontium-90 in U. S., 1959 to 1964, 18: 37386
analysis for strontium-90, method for, 18: 39094
analysis for trace elements by neutron activation, 18: 37072 (A/CONF.28/P/854)
analysis for trace elements, activation, 20: 45880(R) (YALE-2912-12)
analysis for tritium in New Zealand, 1956 to 1960, 16: 16078
analysis for tritium, 16: 16077
analysis for uranium alpha activity by precipitation, 16: 23596 (AERE-R-3499)
analysis for uranium and radium, spring water from Cotes-du-Nord region, France, 16: 27455
analysis in uranium mining and milling area of Colorado Plateau, 16: 20815 (NYO-7831)
analysis of Arrone River Basin, Italy, 18: 41666
analysis of, for radioactive materials in Germany, 16: 32721
analysis of, for traces of hardness, continuous, 17: 33791 (HW-77538)
analysis of great basin, chlorine-36 and deuterium content, 16: 4378
bed load movements in Danube and Velika Morava Rivers, tracer study, 19: 18178(T) (OTS-64-11459/2(p.31-8))
bed load rate of streams, tracer measurements, 19: 601 (EUR-1837.f)
beta activity in, comparison of methods for measurement of, 20: 43601
beta activity of, in Italy, 1962, 18: 18040 (BIO/03/63)
book: *Advances in Water Pollution Research*, Vol. 1, 2, and 3, 20: 20982
carbon isotope distribution in lakes, 17: 33598
carbon-13 abundances in, 17: 34134
cerium-144 sorption by suspended matter in river, 20: 33501
cesium transport in, 18: 35726
cesium-137 and strontium-90 content in Meuse River, 1965, 20: 35644
cesium-137 content in Japanese, 19: 31672(R) (NIRS-3(p.65-77))
cesium-137 content in, Japan, 1964, 19: 42639 (NP-15278)
cesium-137 content in Finnish, 1964–1965, 20: 26604(R) (NP-16002, Paper 8)
cesium-137 content in, in Japan, 16: 26688(T) (AEC-tr-4642)
cesium-137 content in, at Ispra, Italy, 1960, 16: 4392 (CNI-95)
cesium-137 content of, Italy, 1961, 17: 27591 (EUR-223.i)
cesium-137 content in Japanese, calculation of river run-off from, 18: 4003
cesium-137 content of, effects on contamination of vegetables, 19: 18140 (CEA-R-2625)
cesium-137 in Japanese, contribution of meteoric water to, 18: 1932
characteristics of Niantic Estuary, Rhode Island, 18: 45192(R) (TID-21157)
cobalt-58 distribution in flowing and non-flowing, 20: 6716
concentration of sediment in, design of radiometric gage for monitoring, 20: 27229 (NYO-2983-1)
conference on radioactivity and water protection, Karlsruhe, Germany, June 26 to 28, 1963, 19: 2535
conference on transport of radionuclides in fresh water systems, 17: 40519 (TID-7664)
contamination by radioactive effluents, 18: 13352
contamination by radioactive waste, method for calculating, 19: 30408
contamination by waste solutions, sources of, 18: 6539
contamination control for, 19: 38290
contamination control of, 20: 7331
contamination of, by radioactive waste, 18: 14145
contamination of, effect of uranium mining on, 20: 45974
contents of minor elements in rivers, 17: 30687
current analysis, design of instrument using radioisotopes for, 16: 33340(R) (JLI-2748-0-5)
decontamination of, efficiency of rapid-filter plant for, 17: 18410
decontamination of Vistula River water by Warsaw filtration plant, 18: 20229 (CLOR-23)
decontamination of, rapid filtration installations for, 20: 45999
density-flow regime of Franklin D. Roosevelt Lake, Washington, 19: 26527 (BNWL-20)
deuterium content of, in Iceland, 17: 30689
deuterium content in Lake Vanda, Antarctica, 19: 26531
deuterium, oxygen-18, and tritium content in, in South Africa, 18: 1907
deuterium, oxygen-18, and tritium contents of, in Karst region, Turkey, 20: 538
diffusion into ground-water aquifers and bank storage of, 19: 606(R) (HW-81746(p.4.53-61))
diffusion pattern of radioisotopes in, 17: 28659
dilution and flow, use of activation analysis and radioisotopes for

measurement of, 18: 1933
discharge measurements of, use of radioisotopes for, 18: 1914
dispersion and movement in Cape Kennedy area, physical processes of, 20: 20359 (NYO-2973-1)
dispersion in Colorado River and Pierce Canal, dye tracer studies of, 18: 43741 (ORO-619)
dispersion of miscible materials in open channels in, model studies of, 17: 40535 (TID-7664(p.311-26))
dispersion of nuclides in, fluorescent-dye studies of, 17: 40534 (TID-7664(p.295-308))
distribution of radioisotopes in, 18: 1342(T) (JPRS-21816)
distribution of waste solutions in, use of iodine-131 for tracer studies on, 20: 29099
ecology of flowing stream, 20: 26607 (TID-22873)
ecology of, factors affecting cesium-137 uptake by fish, 20: 43512(R) (ANL-7136, pp 315-27)
effects of radioactive wastes on biological conditions in rivers, 18: 35238 (STI/DOC/10/28(p.9-20))
fall-out content in, procedures for estimation of, 16: 7771 (NP-11191)
fallout content of, 1962 to 1964, 19: 9370 (NP-14556(p.11-80))
fallout deposition and removal in drainage area of Vistula River, 17: 15617
fallout deposition and decontamination, 17: 41074
fallout distribution on, 19: 7755
fallout distribution in, at dam, effects of time of year and plankton on, 20: 11055
fallout distribution in, effects of planktological conditions and temperature on, 20: 27215
fallout monitoring in samples collected in 1962, 17: 21954
fallout monitoring in samples of, 1963, 18: 14090
fallout monitoring in Switzerland, 1956 to 1961, 18: 20218
fallout monitoring in U. S., 1964, 19: 637
fallout radioactivity in samples collected from 1960 through 1962, 17: 18454
fallout radioactivity in samples collected in 1962, 17: 18455
fallout radioactivity in samples collected in 1961 and 1962, 17: 18456
fallout radioactivity in samples of, collected in 1963, 18: 4047
fallout redistribution by, 18: 37368 (HNS-1229-46)
fission product behavior in, 16: 399(T) (CEA-tr-A-1012)
fission product distribution in, 16: 14371
fission product from, uptake by plants, 18: 33239
fission product metabolism by plants in, 19: 35939
fission product sorption by sediments in, 18: 1899 (TID-19559)
flood incidence and damage in United States, survey, 19: 11421 (RM-4238-TAB)
flow and element content of Spokane River, effects on Hanford reactor effluent radioactivity of, 19: 682(R) (HW-81746(p.3.25-8))
flow measurements, dispersion and persistence of radioisotope in tracer techniques for, 16: 20836
flow measurements in Magothy Estuary, Round Bay, and Severn Estuary using Deep Water Isotopic Current Analyzer, 17: 34195(R) (JLI-2748-0-7)
flow measurements, radioisotope methods for, 18: 1912
flow of, tracer measurements, 19: 32329
flow rate measurement in streams, radio-release method for volume, 19: 34326 (TID-21881)
flow rate measurements in rivers, tracer techniques for, 20: 20903 (AEET-Radiochem.-45)
flow rate of rivers, tracer measurements, 16: 31975
flow rate studies, maximum allowable radiotracer injections for, 18: 15905 (TID-7689(p.34-7))
flow rates of, analog simulation for, 19: 40282 (BNWL-SA-171)
flow velocities of, tracer techniques for measuring, 17: 10885
flow velocity measurements of Sorachi River in Japan, tracer techniques for river engineering study of, 18: 1916
geochemistry of Great Lakes and Hudson Bay, 20: 16711(R) (MIT-1381-13)
ground water exchange with fluctuating rivers, 18: 6945 (HW-SA-3198)
hydrogen isotope ratios in, effect of rain and spring water on, 20: 39127
hydrogeochemistry and hydrogeology of Arrone River Basin, Italy, 18: 41666
ion distributions in, effects of exchange capacity of sediments on, 17: 40523 (TID-7664(p.71-90))
isotope transport in soil by, 18: 35724
isotopic composition of, from Tarnobrzeg basin, 20: 43531
labeling lake water with tritium, method for, 17: 40998
lithium content in Egyptian, mass spectrometric determination of, 18: 43396
manganese content, 17: 33602
maximum permissible limits for beryllium in, 20: 42755
monitoring for beta activity and strontium-90 content in, in Poland, 1961, 17: 25474 (CLOR-13)
monitoring for beta activity in Austria, 1962, 19: 15804
monitoring for carbon-14 activity in organic contaminants in, 18: 14310
monitoring for radioactivity by analysis of biological materials, 16: 9003
monitoring for radioactivity in creeks and Ohio River at Paducah Plant, 1961, 16: 25653 (KY-419)
monitoring for radioactivity at Julich Nuclear Research Institute, Germany, 17: 307 (JUL-55-ST)
monitoring for radioactivity at Argonne, 1960 and 1961, 17: 36023(R) (ANL-6736)
monitoring for radium-226 near uranium mills, 17: 41137
monitoring of Bear Creek, for nitrogen compound content, 17: 26932(R) (ORNL-TM-516)
monitoring of lakes for radioactivity by analysis of mollusks, 16: 22428 (CNI-58)
monitoring of, methods of sampling for continuous, 20: 43624
monitoring, proportional sampler design for, 16: 10217
movement, tracer studies of, 19: 7715 (AECL-2005)
neutron flux over, 19: 7705
nitrogen cycle in lakes, tracer studies, 17: 33600
oxygen-18 content in Bracciano Lake in Italy, 17: 8395
phosphorus movement through ecosystem of cold-water West Branch of Sturgeon River, tracer studies, 16: 16172(R) (TID-15385)
phosphorus-32 distribution in, effects of biological cycling and transport on, 17: 40532 (TID-7664(p.247-59))
phosphorus-32 distribution in stream, by *E. coli*, 20: 40529
pollution in Great Britain, 16: 19207
pollution of, tracer study of, 16: 29292
pollution studies, development of low-level tracer technology for, 16: 30698(R) (JLI-650-9-1)
properties of, tracer studies of, 18: 43996
prospection of uranium in, hydrogeochemical, 17: 30728
radiation effects on fish and organisms in Nitelva River, Norway, 16: 6802(R) (KR-12)
radiation monitoring of small samples of, 17: 20343 (CEA-2236)
radiation monitoring of, equipment and methods, 19: 24766
radiation monitoring of, sample preparation for, 19: 26588
radiation monitoring at Argonne, Jan.-June 1965, 19: 44300 (TID-22171)
radiation monitoring of, at Savannah River Plant, January to June 1966, 20: 43577(R) (DPST-66-30-2)
radioactive contamination measurement, in Prague, 16: 7778
radioactive contamination of, sources of artificial and natural, 16: 27439
radioactive contamination from uranium processing plant, 17: 41147
radioactive contamination by dispersal of liquid wastes in, monitoring of, 19: 3800
radioactive contamination of, monitoring in EURATOM member states, 19: 2537
radioactive contamination of, site selection of reactors to protect against, 19: 2546
radioactive contamination of, review of conference on, 19: 20234
radioactive contamination dispersion in tidal estuaries, 19: 25780
radioactive contamination of, effects on Chironomus populations, 20: 12662
radioactive contamination of, 20: 18976
radioactive contamination concentration in, macroscopic flow analysis of, 20: 27193 (BNWL-SA-678)
radioactive contamination of, effects on hydrobionts, 20: 40527
radioactive contamination of organisms inhabiting, 20: 43596
radioactive contamination of, used for agricultural purposes, 20: 43598
radioactive contamination of, Japan, 1961–64, 20: 43615
radioactive contamination of, near uranium mines, 20: 45974
radioactive waste disposal in, economic evaluation of model for, 17: 40537 (TID-7664(p.353-89))
radioactive waste release to rivers and lakes at atomic energy sites, 18: 33160 (A/CONF.28/P/287)
radioactive waste disposal in, safety hazards from, 19: 12858
radioactive waste disposal in, hydrological problems in, 20: 2082 (CEA-Bib.-59)
radioactive waste disposal in, operations research on liquid, 20: 22513 (NYO-10447)
radioactivity and constituents of, BNL vicinity, Suffolk Co., New York, 19: 18169
radioactivity at Paducah Gaseous Diffusion Plant, Jan.-June 1965, 19: 44301 (TID-22172)
radioactivity content in, in Italy Jan.–June 1962, 17: 36024 (BIO/26/62)
radioactivity determinations in Czechoslovakian, beta, 19: 32477
radioactivity due to fallout in, 1964, 19: 22552
radioactivity due to fallout in Doe Run, Meade County, Ky., 1959 to 1965, 20: 20884(R) (TID-22815)
radioactivity due to fallout in Canadian, Nov. 1965, 20: 20883 (NP-15914)
radioactivity due to fallout in Canadian, Dec. 1965, 20: 20938 (NP-15921)
radioactivity from natural sources, 19: 13122(T) (JPRS-27535)
radioactivity from cesium-137 and strontium-90 in fallout in vicinity of

Canadian reactors, Feb. 1966, 20: 27204 (NP-16041, pp 14-24)
radioactivity from fallout in, 1965 and 1966, 20: 41131(R) (HASL-172)
radioactivity in Finland, 1965, 19: 46587(R) (NYO-3446-3)
radioactivity in Hungarian, 16: 4409(T) (JPRS-10595)
radioactivity in, in Ohio, 16: 27459
radioactivity in Monticello Project Area, Utah, 20: 16729 (IDO-12049)
radioactivity, in Prague, 16: 20878(T) (AECL-1498)
radioactivity in Poland, 1960, 16: 22400 (CLOR-10)
radioactivity in Poland, 1958 to 1962, statistical analysis of, 19: 15799
radioactivity in Ruhr area, 1961, 16: 9003
radioactivity in Soviet Union, 16: 22421
radioactivity in samples collected in U.S., 1962, 17: 14571
radioactivity in samples collected in U.S., 1962, 17: 14572
radioactivity in Texas, 1958 to 1961, 16: 9013
radioactivity in Taipei, 1957, 16: 10290
radioactivity in U. S., 1957 to 1962, 18: 8527
radioactivity in U. S., 1964, 19: 22557
radioactivity in U. S., 1965, 20: 18915
radioactivity in 1958, 1959, and 1960 at Ispra, 16: 4983 (NP-10731 (p.129-44))
radioactivity in, 1962 through 1964, 19: 22554
radioactivity in, control measures for, 20: 11021
radioactivity in, 1965, 20: 18914
radioactivity in, 1965, 20: 18918
radioactivity in, Jan. to July, 1965, 20: 18972
radioactivity in, 1965 fallout, 20: 29428
radioactivity in, near Canadian reactors, α and β, 20: 41136
radioactivity in, continuous sampling for, 20: 43523
radioactivity in, effect of mud and suspended matter on, 20: 43544
radioactivity levels in, factors affecting variations in, 20: 7265
radioactivity measurements in, design of gamma scintillation probe for, 18: 10403
radioactivity measurements in, of Columbia River and Pacific Ocean, 20: 25282 (RLO-1750-4)
radioactivity monitoring in, use of methane flow counters for, 18: 14095
radioactivity monitoring in Italy, 19: 42637 (BIO/32/63)
radioactivity monitoring of, at Portsmouth Gaseous Diffusion Plant, 1965, 20: 16726 (GAT-506)
radioactivity monitoring in Canadian, Sept. 1965, 20: 9177 (NP-15763, pp 26-38)
radioactivity monitoring of, near Canadian reactors, August, 1965, 20: 7311 (NP-15642, pp 33-45)
radioactivity of Colorado River, 19: 18163
radioactivity of Columbia River, 19: 36703 (HW-72229(Rev.))
radioactivity of Escaut River, Belgium, 20: 22515(T) (ORNL-tr-965)
radioactivity of Great Miami River near Mound Laboratory, Jan. to June 1963, 17: 41032(R) (TID-19492)
radioactivity of, hazards of natural, 17: 6341
radioactivity of Italian thermal, at Lurisia, Acqui Terme, and Ischia, 16: 6634
radioactivity of, in Switzerland, 1959 to 1961, 16: 31961
radioactivity of, in Lamalou and Bedarieux, 17: 6281
radioactivity of, in Austria, 17: 20216
radioactivity of, in Euratom countries, 18: 1947 (EUR-461.d,f,i,n)
radioactivity of Italian, network for monitoring, 19: 30467
radioactivity of Japanese, 18: 37428 (A/CONF.28/P/849)
radioactivity of Lake Maggiore, 1952 to 1961, 19: 11391(R) (NP-14658)
radioactivity of, measurements in Federal Republic of Germany, January to March 1962, 17: 15624
radioactivity of, measurements in Federal Republic of Germany, April to June 1962, 17: 15625
radioactivity of mineral waters at Covasna, 17: 21901
radioactivity of North American, 1964, 19: 22562
radioactivity of U. S., 1964, 19: 18162
radioactivity of water plants in Stechlin Lake in Germany, 1960 to 1962, 18: 5155
radioactivity of, in Germany, 3rd quarter 1962, 18: 12357
radioactivity of, sampled in U. S., 1963, 18: 12398
radioactivity of, in Federal Republic of Germany, 4th quarter, 1962, 18: 11898
radioactivity of, in Federal Republic of Germany, 3rd quarter 1962, 18: 14091
radioactivity of, in Poland, 1958 through 1962, 18: 20211 (CLOR-24)
radioactivity of, effects of fallout on, 18: 27714
radioactivity of, 1964, 19: 42677
radioactivity of, at Savannah River Plant, Jan. to June 1965, 19: 44288(R) (DPST-65-30-2)
radioactivity of, sources of errors in measurement of, 19: 46608
radioactivity of, bibliography on natural, 20: 5668 (WASH-1061)
radioactivity of, near Osaka, Japan, Sept. 1961–March 1962, 20: 7274
radioactivity of, near Canadian reactors, 20: 7306 (NP-15641, pp 22-9)
radioactivity of, in Savannah River Plant area, July through Dec. 1965, 20: 27195(R) (DPST-66-30-1)
radioactivity of, near Canadian reactor installations, March 1966, 20: 33556 (NP-16124)
radioecology of animal and plants in, bibliography, 19: 24237 (TID-3910(Suppl.3))
radioinduced neutralization of surface charges on suspensions in, 18: 12148(R) (TID-20067)
radioisotope contents of, methods of controlling, 19: 2536
radioisotope contents of, from Chariot site environment, 19: 25796 (PNE-445)
radioisotope contents of, from Chariot site environment, 19: 25799(R) (PNE-448)
radioisotope dispersion in open channel flow, 18: 35725
radioisotope distribution in, 17: 34137
radioisotope distributions in shallow fresh-water ponds, 17: 40521 (TID-7664(p.43-60))
radioisotope distribution on sediments in, 17: 40536 (TID-7664(p.327-52))
radioisotope distribution and uptake by organisms in Doe Run stream, Meade Co., Kentucky, 17: 40533 (TID-7664(p.261-7))
radioisotope separation from, by flocculation, 20: 8979(R) (BNWL-36)
radioisotope sorption and release by sediments in Guadalupe River drainage basin, 17: 40525 (TID-7664(p.113-25))
radioisotope sorption and release by sediments in Guadalupe River, Lake Falcon, and Lake Austin, 17: 40526 (TID-7664(p.127-48))
radioisotope transport in, in Wisconsin, 17: 4715
radiological monitoring of the Clinch and Tennessee Rivers below Oak Ridge, 16: 29272
radiological monitoring system for, 18: 7044 (HW-79186)
radiological monitoring at Indian Point Power Reactor, 18: 8530
radiological monitoring, 18: 41648 (NP-14254)
radionuclide metabolism by organisms, 16: 22456 (TID-7632(p.360-71))
radionuclide transport in river-estuary systems, 20: 39121
radionuclide uptake by biological organisms in fresh-water pond, 18: 25079
radiopollution of, standards for, 17: 29876
radium content in Nile River before, during, and after flood, 17: 8413
radium content of Japanese, 17: 30790
radium content of, methods for determining, 20: 31191
radium, radon, and uranium contents of Lake Techirghiol, 20: 10512
radon content in, measurement using gamma radiation, 20: 20959
radon-222 content in, MPC_N estimation, 16: 1338(R) (ORNL-3189 (p.191-7))
release rate of radioactive rare gases from, 20: 39103(R) (BNWL-235-3, pp 51-69)
river control and routing, analog-computer analysis of, (E), 19: 13859 (HW-84448-10)
ruthenium transport in, by microorganisms, 18: 1340 (TID-19529)
sampler design for, 17: 6398 (KY-423)
sampling of, and preparation for radiochemical analysis, 18: 8519(T) (AEC-tr-6049(p.1-10))
sampling of river, engineering drawings of equipment for, 20: 39185
sand movement in Yugoslav river, tracer studies, 19: 13618 (NP-14667)
sand movement in, use of chromium-51 tracer to study, 20: 43549 (NP-16200)
sand transport in, use of radioisotopes for measurement, 16: 16588
sediment concentration in, x-ray attenuation gage for measuring, 18: 16195 (TID-7689(p.142))
sediment content in, radioisotope technique for monitoring, 20: 23280
sediment content of river, radiometric instrument for measuring, 20: 37057
sediment density measurements in lakes and streams, use of radioisotopes in, 19: 13830
sediment movement in alluvial, tracer techniques for measuring, 18: 1918
sediment transport in, heterogeneous equilibria in, 17: 40522 (TID-7664 (p.61-70))
seepage, tritium tracer measurements, 16: 16082
separation of cesium-137 from, by solvent extraction using nitrobenzene, 17: 8455
separation of clay and plankton, density gradient method, 17: 8410
silt movement in Oxcars spoil ground, Firth and Forth, use of scandium-46 for, 20: 4166 (AERE-R-4980)
sorption and release of cesium-137 and strontium-89 by silts in Guadalupe River, 20: 24832 (TID-22872)
sorption of radionuclides by particulate material in, 18: 35761 (HW-79279)
storage of, in underground cavities formed by nuclear explosions, 17: 5658 (TID-16647)
strontium transport, 18: 35726
strontium-89 and -90 content in, in Japan from fallout, 18: 1931
strontium-89 removal from, by algae, 17: 8400
strontium-90 movement by, 16: 22452 (TID-7632(p.299-305))
strontium-90 uptake from, by rainbow trout, 16: 28698 (HW-SA-1997)
strontium-90 accumulation by plants growing in, 18: 35282(T) (AEC-tr-6447)

strontium-90 content, from fallout, 18: 31760
strontium-90 content in Don River basin, Russia, 18: 35776(T) (AEC-tr-6458)
strontium-90 content in Weser River, 18: 39536
strontium-90 content in USSR, 1961–62, 19: 20160 (NP-14728)
strontium-90 contents in rivers in Poland, 1962, 19: 24701 (CLOR-32)
strontium-90 content in Japanese, 19: 31672(R) (NIRS-3(p.65-77))
strontium-90 content in, Japan, 1964, 19: 42639 (NP-15278)
strontium-90 content in Soviet Union, 1961–1962, 20: 16705
strontium-90 content in, 1964 and 1965, 20: 18914
strontium-90 content and distribution in, Lake Haruna, Japan, 20: 24835
strontium-90 content in U. S., 1965, 20: 33589
strontium-90 content in, in Japan, 16: 26688(T) (AEC-tr-4642)
strontium-90 contents, Ispra, Italy, 1960, 16: 4392 (CNI-95)
strontium-90 content in, calculation of river run-off in Japan from, 18: 4003
strontium-90 content of, effects on contamination of cultivated vegetables, 19: 18140 (CEA-R-2625)
strontium-90 content in, equilibrium of, 17: 21940
strontium-90 deposition rates over, 20: 25296
strontium-90 in Japanese, contribution of meteoric water to, 18: 1932
strontium-90 levels in, in Italy, 1961, 17: 27591 (EUR-223.i)
sulfur isotopic composition, 16: 5569
sulfur isotopic distribution in lakes, 17: 33598
sulfur-34 abundances in, 17: 34134
temperature distribution in estuary from heated effluent discharge, prediction of excess, 19: 29809 (NYO-10508)
temperature reduction of, in rivers, 17: 6255 (HW-SA-2301)
thorium content in Nile River before, during, and after flood, 17: 8414
thorium content of Japanese, 17: 30790
tracer studies, 17: 3652
tracer studies, 18: 18052
tracer studies of, total-count flow measurements in, 17: 3653
tracer study of river basin hydrology using tritium, 18: 10293
tracer techniques for studying bed-load movement and transport in, 20: 20904 (STI-REP-101)
tracer techniques for studies on, review on, 20: 23321 (ORO-597)
transport in stratified lakes, tracer study of biological and physical, 17: 33597
transport of cesium-137 and strontium-85 in model, factors affecting, 20: 24833 (TID-22877)
transport of ruthenium chloride and nitrosyls in, effects of plants, sediments, and suspensions on, 20: 26606 (TID-22870)
transport of solids in, tracer studies, 16: 16070
transport of, tracer studies of, 20: 548
tritium content, 20: 14744
tritium content in, during nuclear test moratorium, 17: 32758
tritium content in Lake Leman, France, 20: 35647
tritium content of, in Japan, 1960 to 1964, 19: 30414
tritium content of, in New Zealand, 1956 to 1963, 20: 45926
tritium content variations in levels of Mont Cenis Lake, France, 1964 and 1965, 20: 16668
tritium distributions in Main and Rhine Rivers in Germany, 20: 5654
uptake of strontium-90 by man through drinking water and food chain, 20: 41142
uranium content in rivers of Japan, 17: 8413
waste disposal from Agesta Reactor in Lake Magelungen, Sweden, 19: 24193
waste disposal in, factors affecting, 20: 45224
water movement in an ice-covered lake, tracer study of, 18: 10270
wave production by travelling pressure in shallow, 20: 4153(R) (UCRL-14360, pp 73-85)
wind agitation of, recorder for wave patterns from, 19: 1030 (AECL-2051)
yttrium-90 content in, equilibrium of, 17: 21940
zinc cycle in, tracer study, 17: 33601
zinc distribution in water and silts of, 18: 38711 (NYO-10544)
zinc-65 distribution in flowing and non-flowing, 20: 6715
zinc-65 transport in, 20: 26608 (TID-22876)
zooplankton sampling in Ligurian Sea, 20: 42734

SURFACES

analysis by electron diffraction, use of ionic etching in, 18: 43363(T) (SC-T-64-1608)
analysis of lunar, instrumentation for radiometric, 17: 16894
analysis of metallic, for contaminants by rinse method, 19: 5775 (RFP-419)
analysis of remote, combination neutron technique for, 20: 31211
area measurement by continuous flow method, 16: 20525(R) (MCW-1472)
area measurement by krypton adsorption, effects of surface temperature on, 16: 32208
area measurement by rare-gas interactions with, 17: 20050
area measurement in porous materials by gas permeability method, effects of structure on, 19: 13286(T) (SC-T-65-706)
area measurement using radioactive indicator, 18: 30079
area measurements using krypton-85 adsorption, 20: 31353
area of fuel microspheres, values for calculation of, 20: 34994 (ORNL-TM-1513)
area of, from gas adsorption, 19: 2724 (NAA-SR-Memo-10209)
areas measurement by B.E.T. adsorption method using xenon-133, 19: 36410
areas of, determination by adsorption of xenon-133, 18: 30157(T,R) (EURAEC-933)
atom reactions with, energy transfer during recombination in, 18: 40157
beta recoil from solid, 16: 26009
biological cleanability of, tracer technique for, 20: 41218
centroids and inertias for surfaces of revolution, computer program for, 20: 16154 (Y-1420(Rev.1))
cleaning and passivation of, in atomic industry, 18: 25914(P)
cleaning beryllium alloy, for bonding and plating, 20: 43857 (NASA-TM-X-53453(Vol.4))
cleaning metallic, comparison of solvents for, 19: 6008 (RFP-469)
cleaning methods for, 20: 43599
conference on physics and chemistry of solid surfaces, Providence, Rhode Island, June 21 to 26, 1964, 19: 8036
contamination and decontamination of, literature survey, 17: 8460
contamination and decontamination properties of, 17: 30075
contamination and decontamination properties of, 19: 7210(R) (ORNL-3697(p.213-22))
contamination and decontamination of, mechanisms of, 20: 7316(R) (ORNL-3849, pp 215-29)
contamination by soft beta emitters, method for determining, 19: 7738 (TID-21400)
contamination of floors by plutonium, resuspension factors for, 19: 20191 (AERE-R-4635)
contamination of, hazards of alpha, 18: 5147(T) (JPRS-21975(Del.)(p.13-16))
contamination of, detection of alpha, 18: 12459 (HW-78268)
contamination of, evaluation of beta, 18: 27733
contamination of, monitoring beryllium, 18: 29876 (CEA-TP-472)
contamination of, equipment for measuring alpha, 19: 39045(P)
contamination of, radioactive process for detection of, 20: 9215(P)
contamination of, methods for testing for, 20: 23261
contamination of, tracer technique for detecting, 20: 29484(P)
contamination of, inhalation hazards from, 18: 22309
contour measurements on small samples, photogrammetric techniques for, 20: 2033
contour measurements on small irradiated, development of photogrammetry method for, 20: 11068 (WAPD-T-1815)
crack detection on, using diamond stylus and strain gage, 19: 44210 (KAPL-M-6484)
decontamination by removal of radioactive dust, 18: 6982
decontamination, evaluation of activated charcoal for, 16: 439
decontamination methods for, 19: 11449
decontamination methods for, 20: 23383(T) (JPRS-34927)
decontamination of, film-forming agents for, 17: 30781(P)
decontamination of, preparation of anion exchangers from amines and cellulose bases for, 18: 5421
decontamination of, evaluation of methods for, 18: 8538 (AHSB(S)R-57 (p.15-26))
decontamination of radioisotope-contaminated, 18: 25724
decontamination of metal, electrolytic, 18: 32069
decontamination of, agents for, 19: 11427
decontamination of, by washing using sodium dodecyl sulfate or water, 20: 5675
decontamination of, film method for, 20: 25337
decontamination, pastes for, 17: 30076
decontamination procedures, 16: 6653
decontamination under cold-weather and thawing conditions, 18: 31754 (NDL-TR-58(Pt.I))
decontamination using detergent-latex composition, 18: 8539 (AHSB(S)R-57(p.27-40))
decontamination using ultrasonics and cleaning solutions, 20: 43623
decontamination with detergents, 19: 42668
degasification of metal, by electron bombardment, 20: 915 (ORNL-TM-1166)
distribution of beta-active substances on, measurement by luminescent method, 17: 4757
effects of nuclear airblast, over desert, water, and asphalt, 16: 2825 (WT-1109)
effects of nuclear airblast over desert, water, and asphalt, 16: 2826 (WT-1110)
effects on preshock air temperature in vicinity of nuclear explosions, 16: 2833 (WT-1149)
effects on response of structures to blast loading, 16: 2829 (WT-1124)
effects on structure of superconductive vortices, (T), 20: 46513
electrohydrodynamics of dielectric liquid, with high-frequency fields, (E), 19: 30865

electromagnetic wave scattering from periodic, plane, (T), 19: 37209
electron and ion beam treatment of, sources for, 20: 41528
electron emission from, time dependence of Schottky effect in, 20: 46946
elemental composition of, alpha backscattering analysis of, 17: 5100
enthalpies of reactions on solid, instrumentation for, 20: 16153 (UCRL-16472)
fallout decontamination of paved, 19: 20207 (USNRDL-TR-797)
film adsorption on, thermodynamic theory for, 16: 33603
films on, radiometric apparatus for detection of, 20: 25372(P)
fission product deposition on, models for, 20: 8313 (CONF-651101-44)
fission product deposition on, method for determining, 20: 7573 (ORNL-TM-1330)
fission product deposition on standard, preparation for, 20: 20940(R) (ORNL-3915)
gages for plate, setups for, 20: 25346 (SC-R-66-871)
gas particle reactions with crystal, mechanical processes in, 18: 9045
gas reactions with, conference on rarefied, 20: 28090
gas-particle effects on, relativistic theory of, 20: 2841
heat conductance of aluminum-stainless steel contact interface during transient heating, 19: 30379 (UCRL-14227-T)
heat transfer across, in contact, effects of ambient pressure changes on, 17: 39251
heat transfer across contacting, analysis of resistance of, 18: 33735 (MIT-2079-2)
heat transfer by, effects of roughening on, 17: 8362
heat transfer by, effects of profile on, 20: 10993 (TID-22513)
heat transfer from, effects of roughness on, 18: 1878
heat transfer from flat, effects of surface inclination on boiling, 20: 9118
interface formation between film and substrate, 19: 13899 (SC-R-65-852)
ion beam effects on optical, controlled figuring in, 20: 9600
ion interactions with atoms of charge, energy, and mass balance for, 18: 37840(T) (AEC-tr-6398(p.271-87))
ion reactions at 30 to 300 ev, electron production in, 18: 10797
ion sorption at ionized, studies using recoil atoms, 18: 5278
ionization mechanism, (E/T), 20: 28495(R) (MATT-Q-22, pp 321-85)
kinetic parameters of, use of gas-solid chromatography for measurement of, 18: 31445
kinetic parameters of, chromatographic studies of, 19: 9046(R) (IS-900 (Sect.C))
measurement of small, use of xenon-133 in, 19: 4585 (EURAEC-1177)
measurement of specific, on radioactive sulfate catalysts, 18: 41308(T) (ORNL-tr-259)
microstructure of steel, microprobe determination of changes in, 20: 46204
moisture on, design of neutron device for measurement of, 17: 10925
molecular beam reactions with revolving, 18: 40154
molecular beam scattering from, decrease of frictional resistance in, 18: 40155
molecular beam scattering by, normal momentum transfer in, 18: 40156
molecule scattering by, misalignment effects in, 18: 8914 (K-1584)
monitoring for beryllium at Harwell, 20: 45945 (AERE-R-5106(Amended))
particle adhesion in gaseous and liquid environments to, decontamination methods for, 19: 46645 (ORNL-TM-1228)
particle adhesion to, mechanisms of, 20: 7316(R) (ORNL-3849, pp 215-29)
particle adhesion to, mechanisms of, 20: 33548 (CONF-650577-1)
particle deposits from air streams on, 18: 35260(R) (AERE-PR/HPM-5)
phase boundaries, optical techniques for study of, 20: 290 (UCRL-11997)
position determination of reflecting, optical system for, 19: 11343(P)
positional measurement of curved, alpha angle adjuster for, 19: 17425 (RFP-480)
preparation of nearly perfect metallic, 18: 10655
properties of, Mössbauer effect for studies of, 19: 40078 (NP-15111)
radiation dosimetry at interfaces of, γ and x, 20: 18952
radiation effects on structure and physico-chemical reactivity of metal, 19: 23140
radiation effects on molybdenum oxide, (E), 20: 44026(T)
radiation effects on, of radioactive salts, 16: 580
radiation monitoring of, using smear techniques, 17: 4743 (ORNL-TM-435)
radioactive contamination, methods of measuring and removing, 16: 2061(R) (ORNL-3189(p.230-2))
radioactive contamination of, use of polymers in control of, 18: 8537 (AHSB(S)R-57(p.1-14))
radioactive contamination of, protection against using stripping varnishes, 18: 10327
radioactive contamination of, study of methods for measurement of, 19: 17767 (ORNL-TM-1045)
radioactive contamination of, tolerance standards for, 19: 44311
radioactivity on, smear test for, 18: 18101
radioisotope transport to and from grass-like, vertical flux for gaseous, 20: 22539
reactions at fluid–solid, effects of ions on, 20: 29623(R) (TID-22970, pp 121-256)
reactions of gas molecules and photons with, 20: 29624(R) (TID-22970, pp 257-329)
reactions on metal, equipment for study of, 20: 3863(R) (IS-1200(Sect. C))
removal of contaminating gases from, using activated charcoal, 19: 6062
replication for hot-cell applications, development of methods for 16: 657
replication methods for hot-cell applications, 16: 3127
scanning with beam of charged particles, design of apparatus for, 18: 16628(P)
separation of hydroxyl groups and water from, by spectra of deuterium exchange with water-d_2, 17: 40759
shock wave reflection from plane rigid, analysis of, 18: 26123
site energy distributions of irradiated solid, 17: 3545
site energy distributions of irradiated solid, 17: 3546
sputtering by molecules, re-emission law for, 18: 40152
standard, for fission product deposition studies, 20: 5665 (ORNL-TM-1304)
temperature determination of radiation-shielded, 16: 10690
temperature measurement up to 1000°F, development of probe for, 18: 18138 (RTD-TDR-63-4015)
temperature of, thermocouple measurement of, 17: 3275 (WAPD-T-1270)
thermal conductivity across contacting metallic, 17: 22276 (NYO-9459)
thermal conductivity of contacting, in vacuum, (T), 20: 18867 (NP-15897)
thermal resistance of contacting, bibliography on, 19: 40744 (UCRL-14264)
treatment of entire, apparatus for chemical and electrolytic, 19: 16049(P)
tritium activity on, equipment for measuring, 20: 7323 (USNRDL-TR-913)
use of ionic bombardment for studying, 18: 28102
vibration modes from impurities adsorbed on, S-matrix method for, (T), 19: 40108

SURGERY

advantages of, compared with radiotherapy for treatment of laryngeal cancer, 20: 38782
anterolateral cordotomy, technique for, 18: 15734(R) (ACRH-20(p.37-46))
bone grafting technique, 19: 42788
combination of radiotherapy with, in treatment of cervical carcinoma, 19: 15294
combined with irradiation, effects on canine sciatic nerves, 19: 29954
control of infections during, use of ultraviolet radiation for, 19: 34090
cortical lesions induced in monkeys by, 19: 36034
effectiveness for cervical cancer in combination with drugs and radiotherapy, 20: 40778
effectiveness of prostate carcinoma, 20: 24955
effectiveness when combined with radiotherapy for cancer, review of, 20: 35363
effects combined with radiotherapy on cervical carcinomas in mice, 19: 31933
effects of irradiation combined with, on mouse and rat mortality, 20: 45498
effects of preirradiation on results of, for breast tumor, 20: 3861
effects of preirradiation on ovarian cancer, recovery rate of, 20: 5446
effects of preirradiation on pharyngo-larnyngectomy, 20: 5463
effects of preirradiation on cancer, 20: 5477
effects of preoperative irradiation on dissemination of cancer cells by, 20: 10735
effects of splenectomy in Thorotrast patients, 20: 45503
effects of unilateral nephrectomy on DNA content and weight of mouse kidneys, 20: 22726
effects of, combined with stilbestrol and x radiation on prostate carcinomas, 20: 8765
effects of, combined with hormones on prostate carcinomas, 20: 8765
effects of, combined with γ radiation on brain tumors, 20: 10575
effects of, combined with radium and x radiation on cervical carcinomas, complications from, 20: 14377
effects of, combined with radium and x radiation on cervical carcinomas, 20: 14409
effects of, combined with x radiation on cervical carcinomas, 20: 20526
effects of, combined with γ radiation on cervical carcinomas, 20: 20536
effects of, combined with gamma and x radiation on mammary carcinomas, 20: 22839
effects on cervical carcinomas, 20: 14409
effects on implanted ascites hepatoma in mice, 20: 45516
effects on lymphatic dynamics, 20: 42976
effects on radiosensitivity of patients, 20: 1717
effects on results of radiotherapy of tumors, 19: 19703
effects on urinary tract of liver carcinoma, 19: 35882
effects on wound healing after radical neck dissection, 20: 14303
efficiency of oophorectomy, for castration in human females, 20: 43044
for actinic enteritis from radiotherapy, 19: 31970
for nose cancer, effectiveness of, 18: 17712

for plutonium-239 removal from hands, 19: 33973
for radiation injury treatment, 18: 21916
for radionecrosis, 18: 17642
for repair of radiation injuries after radiotherapy of carcinomas of uterus, 19: 31938
for repair of radiation injuries of intestine induced by radiotherapy, 19: 34016
for repair of radioinduced bone lesions after radiotherapy of cancers, 19: 34026
for tumors of face and jaw, 19: 46074
hazards of dental, in irradiated patients, 20: 18308
hazards of post-irradiation, in the upper respiratory-digestive tract, 20: 22837
human cerebral, using high-energy protons, 18: 13580
method for strontium-90 neuro-, 19: 34063
methods for skin carcinomas, electro- and scalpel, 20: 6928
of breast cancer, adjuvant with chemotherapy and radiotherapy, 19: 22025
of carcinoma of bladder, effects on radiotherapy, 19: 22041
of carcinoma of the uterine cervix, 19: 7237
of carcinoma of uterus, 19: 32031
of carcinoma of uterus, 19: 34028
of carcinoma of uterus, combination of radiotherapy with, 19: 43884
of carcinoma of uterus, effects on urinary tract, 19: 46061
of carcinomas of esophagus, 19: 46051
of cervical cancer with radiotherapy, urologic complications in, 19: 17722
of cervical cancer, 19: 31934
of cervical cancer, 19: 31936
of cervical carcinomas, evaluation, 18: 5189
of cervical carcinoma, 19: 13138
of cervical carcinomas, comparison of radiotherapy with, 19: 31932
of cranial aneurysms, evaluation using radioisotope cerebrogram, 19: 22019(R) (UCLA-12-541(p.51-91))
of head in irradiated patients, 19: 46129
of lung cancer, radiotherapy during, 18: 35428
of malignant tumors of testis, advantages and limitations, 20: 43034
of neck in irradiated patients, 19: 46129
of neck, procedures for, 19: 27962
of neck, radiation effects on healing of, 19: 27962
of osteogenic sarcomas in children after radiotherapy, 19: 32007
of pelvic cancer, effects on lymphocyte chromosomes, 19: 36049
of radiation injuries, problems in, 19: 15236
of radioinduced necrosis of facial bones, 19: 31830
of radioinduced skin lesions after therapy, 19: 46085
of tumors of face and jaw, 19: 46075
of tumors, effect on skin homograft survival, 19: 13156
of tumors, preoperative irradiation, 19: 34069
on irradiated tissue, precautions for, 18: 15942
ovariectomy, effects on lifetime fertility in rabbits of, 18: 38775(R) (ORO-624)
pelvic exenteration for extensive visceral necrosis after radiotherapy of gynecologic cancer, 19: 46106
performance of combined radiotherapy and, for malignancies, review of, 20: 45547
postoperative parotitis from, use of γ and x radiotherapy for, 20: 45535
procedures for radiotherapeutic facial and maxillary injuries, 18: 11936
procedures for, for treatment of radioinduced osteomyelitis of mandible, 19: 33837
radiation as a pre-operative procedure in lung cancer, effectiveness of, 20: 38755
radiation effects on carotid arteries following head and neck tumors, 18: 11724
radiation effects on liver regeneration after partial hepatectomy, 19: 19512
radiation effects on recovery from tumor, 20: 12646
radiation effects on recovery from, gamma, 20: 12653
radiation pituitary, yttrium-90, 18: 13582
radiodermatitis of hands of surgeons and radiologists, 19: 33865
radioinduced chick thyroid, effects on glycogen content of iodine-131, 19: 15266
radioinduced, of human pituitary, gold-198 and yttrium-90, 19: 26207
radiological methods for, survey of, 20: 6951
radiosensitivity effects of spleen, in fetal mice, 20: 18436
radiosterilized homografts for neuro-, 18: 31176
radiotherapy combined with, effects on melanomas of, 20: 8714
radiotherapy of malignant tumors following, effectiveness of, 20: 22847
radiotherapy used with, 18: 29514
repair of fistulas induced by radiotherapy of pelvic cancers by, 19: 17713
repair of radiation injuries by, after radiotherapy of carcinomas, 19: 32037
repair of radiation injuries of larynx and trachea resulting from radiotherapy by, 19: 43897
repair of radioinduced skin lesions by, 19: 30021
repair of radioinduced skin lesions by, 19: 30022
repair of radioinduced fistulas by, 19: 36213
repair of thermal burn scars by plastic, for residents of Hiroshima exposed to atomic explosion, 19: 28007
role of radiotherapy in oral, 20: 22650
strontium-90 needle for nervous system, 18: 33436
techniques for repair of lesions resulting from radiotherapy of mouth cancers, 19: 34010
tissue reactions to radiosterilized sutures in, 20: 712
treatment for burn traumas in rabbits with radiation sickness, 19: 17642
use combined with radiotherapy of facial carcinomas, 19: 34044
use for breast cancers, evaluation of effects of radiotherapy after, 20: 16324
use for carcinomas of larynx, 20: 16313
use for lymphosarcoma extirpation, 20: 5485
use for metastatic cancers in lymph nodes, 20: 212
use for radioinduced ulcers of skin, 19: 38513
use for therapy of thyroid cancers, 20: 16307
use in lymphoma treatment, advantages of, 20: 6966
use in repair of radiation injuries resulting from therapy, 20: 6974
use in repairing radioinduced skin lesions, 20: 22774
use in treatment of hyperthyroidism, performance compared with iodine-131, 20: 40785
use of beta radiotherapy with, in treatment of glaucoma, 19: 46045
use of primary acrylate endoprostheses with radiotherapy for jaw tumors, 19: 15282
use of radical, for cervical carcinomas, 20: 8773
use of radiotherapy prior to, in treatment of breast cancer, 19: 46054
use of radiotherapy prior to, for lung cancer, efficiency of, 20: 33137
use of radiotherapy following orchiectomy, 20: 43038
use of, combined with radiotherapy in treatment of esophageal carcinomas, 19: 10952
use of, combined with radiotherapy for cancer of the bladder, 20: 35366
use of, in treatment of rectal complications resulting from radium therapy of cancer of uterus, 18: 29452
use with radiotherapy in uterine cervix carcinomas, complications in, 19: 34001
use with radiotherapy for malignancies of oral cavity, results of, 20: 45561
using radiation sources, review, 19: 43905

Survey Meters
see Radiation Detection Instruments (Ion Current Type)

SURVEYING
see also Aerial Surveying

Surveys
see Bomb Damage Surveys

Susie Reactor
see Shield Test Pool Reactor

SUSPENSIONS
(See also as main headings by name of material suspended.)
see also Colloids
see also Slurries
agglomeration and condensation of gas–solid, kinetics of, 18: 36837(R) (IITRI-C6007-12)
analysis by beta backscattering, equipment for, 20: 26784
analysis by neutron absorption, 20: 33183(T) (AEC-tr-6639, pp 114-17)
boiling burnout heat flux measurements in non-Newtonian, 17: 39258
circulation in heat exchange systems, power required for, 19: 42127(R) (TID-22009)
circulator design for gas–solid, 18: 27674
concentration in pipe lines, radiometric densitometer for measuring spatial, 20: 13049
convective heat exchange in gas-solid, 18: 29849(T) (NYO-2974-1 (p.D1-22))
density distribution in gaseous fluidized bed systems by x rays, 16: 7637(T) (AEC-tr-4976)
density profiles in turbulent flow, (E/T), 20: 16606(R) (TID-22621)
diffusion of helium in gas-solid, equipment for measuring, 19: 20098(R) (TID-21633)
droplets in, optical system for counting, 18: 2404(R) (TID-19651)
effects on heat transfer of fluids on, 19: 34336(P)
effects on statistical structure of turbulence in fluid flow, (T), 20: 16606(R) (TID-22621)
efficiency as working fluid in Brayton cycle, (T), 20: 16606(R) (TID-22621)
electric conductivity of gas-solid, from thermal electrification at high temperatures, 17: 37726
flocculation characteristics of, correlation with rheological properties, 17: 23484
flow and heat transfer of gas-solid, 18: 29845(R) (TID-20664)
flow and heat transfer in turbulent gas–solid, research program on, 20: 484(R) (TID-22282)
flow and stability of graphite, in carbon dioxide, 19: 22476 (CEA-R-2741)
flow measurement on gas-solid, design of flowmeter for, 18: 33123(R) (TID-20830)
flow measurement of gas-solid, design of flowmeter for, 19: 8650(R) (TID-21288)

flow measurements on gas-solid, 18: 15584(R) (TID-20319)
flow of gas-solid, in experimental loop, 17: 27541(P) (TID-18909)
flow of gas-solid, in experimental loop, 17: 27542(R) (TID-18910)
flow of gas-solid, 18: 16176 (NYO-2930-1)
flow of gas-solid, 18: 31720 (ILL-13-P)
flow of gas-solid, in experimental loop, 18: 14035(R) (TID-20377)
flow of gas-solid, turbulence in, 18: 25656 (NYO-2930-2)
flow of gas-solid, equipment and methods for measuring, 19: 17333(R) (TID-21596)
flow properties and densities in fluidized bed systems, 16: 8840(T) (AEC-tr-4974)
flow stability of gas-solid, in thermal gradient, 18: 29842 (NYO-2974-1)
fluid mechanics and heat transfer in turbulent gas–solid, research program on, 19: 40742(R) (TID-22002)
gas-solid, electric properties of, 17: 24027 (AD-282604)
heat transfer by, effects of thermal plate-out on, (T), 20: 16606(R) (TID-22621)
heat transfer characteristics of gas-solid, 18: 29841 (NYO-2930-4)
heat transfer coefficients in gas–solid, (E), 20: 16606(R) (TID-22621)
heat transfer from gas-solids, 19: 42127(R) (TID-22009)
heat transfer from coal, in closed-cycle gas turbines, 20: 33429(R) (TID-23117)
heat transfer in flowing gas-solid, in closed recycling loop, 17: 29068 (BM-RI-6255)
heat transfer to gas-solid, at Reynolds number of 130,000, 20: 35622 (NYO-2930-7)
isotopic exchange in, method for continuous recording of, 20: 36793
motion in turbulent gas-solid, 18: 8464(R) (TID-19924)
motion in turbulent gas-solid, 18: 8465(R) (TID-19925)
motion in turbulent gas-solid, equipment and techniques for measuring, 18: 8466(R) (TID-19963)
particle size measurement in, by centrifugation and gamma emission, 18: 13604(R) (MITS-51)
preparation using glass-water, conditions for, 16: 3102(R) (TID-14229)
properties of gas-solid, 20: 7231(R) (TID-22465)
radiation effects on, 17: 23587 (BNL-790)
radioactivity measurements in, scintillation method for, 20: 3870 (EUR-2459.f)
radiofrequency absorption by, measurement of, 19: 13278(R) (NYO-10995)
radioisotope distribution between Indian Ocean sea water and, 20: 41140
rheological properties of fluidized beds traversed by gases, 16: 7636(T) (AEC-tr-4973)
sedimentation, 17: 35617(R) (NYO-10329)
separation from uranium wastes solutions, methods for, 16: 23385 (TID-7616(p.223-34))
settling rates of, absorption of beta-excited x radiation for measuring, 20: 22914
stability of homogeneous fluidized beds, 17: 27325(T) (AERE-Trans-942)
thermal force effects in dense, (T), 20: 16606(R) (TID-22621)
thorium and thorium-230 contents in, from Indian Ocean, 18: 27713
transport characteristics, application of rheological models to flocculation data, 16: 18945
transport in conduits, minimum power requirements for, 17: 10809
turbulent transport characteristics of non-Newtonian, 18: 3962
use of radioisotope-containing, in cancer therapy, 16: 8551(T) (JPRS-11903)
viscosity of concentrated, lower bound of, 17: 33868 (CONF-154-1)
viscosity of unstable, method for measurement of, 16: 17881(R) (MITS-47)
x-ray fluorescence analysis of aqueous, instrument for automatic continuous, 20: 37152
zeta potential of aluminum powder, 18: 18294(R) (NP-13758)

SWAGING
design of die for high-temperature, of tungsten cylinders *in vacuo*, 20: 781 (AI-65-12)
equipment for hydrostatic, 18: 20134(R) (ORNL-TM-792)
equipment for tube, 19: 28796(P)
facility for, design of noise-reducing enclosure for four-die, 17: 23871 (TID-16897)
methods development for reactor materials, 18: 14446
methods development for reactor materials, 18: 32119
methods development for reactor materials, 18: 41987
methods for capillary tubes, 18: 17977(R) (ORNL-TM-793)
noise-reducing enclosure for four-die, engineering drawings for, 19: 6287
techniques for, development of, 17: 11130
use for fuel element fabrication, 17: 18712 (GEAP-3918)
use in fuel element fabrication, 19: 24968(P)
uses in reactor materials fabrication, 18: 18338

SWEDEN
atomic energy development in, 19: 8647
cesium-134 occurrence in Lapps, 16: 31469
cesium-137 body burden in North, 16: 5597 (A/AC.82/G/L.650)
cesium-137 burdens in Laplanders and reindeer, 16: 5126 (A/AC.82/G/L.652)
cesium-137 content in ground-level air and precipitation in 1958 to 1961, 16: 11945
cesium-137 body burden in, 19: 26605
cesium-137 content from fallout in man in, from 1961–1963, 19: 26608
cesium-137 content in lichens of, 20: 12578
cesium-137 content in residents of, 1961, 20: 7334
cesium-137 levels in people and reindeer in, 20: 42736
cesium-137 uptake by man in, hazards from, 20: 22795
civil defense program for fallout shelter construction in, 19: 18223
cobalt and radium therapy of uterine carcinomas, 20: 40769
cosmic-ray intensity monitoring during 1963 in, 18: 37863 (AFCRL-64-394)
davidite-thorite paragenesis on Björkö Island, 19: 30430
developments in atomic energy programs, summary of, 1963, 19: 626(R) (NP-14380)
ecology of phytoplankton from Lake Magelungen, 1960 through 1963, 20: 26595 (AE-219)
fall-out monitoring, 1961, 16: 22431 (NP-11704)
fall-out monitoring, 1961, 17: 1677
fallout levels and radioactivity of air in, 17: 39332
fallout monitoring, 1961, 17: 5763 (AE-80)
fallout monitoring in, 1958 to 1962, 17: 12497 (NP-12540)
fallout monitoring for beta activity in atmosphere in, Jan. to June 1963, 17: 37365 (NP-13078)
fallout monitoring, 1959, 1962, and 1963, 18: 20212 (NP-13846)
fallout monitoring, 1962, 18: 23790 (NP-13828)
fallout monitoring, 1963, 19: 626(R) (NP-14380)
fallout monitoring, 1958 to 1964, 19: 22558
fallout monitoring in, from Chinese nuclear weapons test, Oct. 1964, 19: 32436
fallout monitoring, 1961 to 1964, 19: 42249
fallout monitoring in upper atmosphere over, 1962 and 1963, 19: 42640 (NP-15326)
fallout monitoring, 1961 to 1964, 20: 2054
fallout monitoring in, after first Chinese nuclear test, 1964, 20: 27157
fallout radionuclide content in ecosystems of, 20: 31442 (BNWL-SA-661)
food irradiation research in, 19: 11624
geochronology of basement complex in, determination by uranium-lead isotopic ages, 19: 22567(R) (NYO-1669-10)
geochronology of rocks in, 20: 39126
geochronology of, from age measurements on radioactive minerals, 20: 39125
lead-bearing minerals in, isotopic composition of, 19: 30421
lithium emission in twilight at Uppsala during Nov. 1962, 17: 14980
nuclear fuel and reactor production in, 20: 35044
nuclear power development in, review on, 17: 22866
nuclear power development plans, 18: 45042
nuclear power development in, 20: 26477
nuclear power plants in, contribution of private industry to development of, 17: 22868
nuclear power plants in, construction and operation of, 17: 22867
nuclear power plant siting in, 18: 37393 (A/CONF.28/P/611)
nuclear power program, appraisal, 17: 22887
personnel monitoring at atomic energy plants in, 1962, 18: 6968 (AE-126)
personnel monitoring at AB Atomenergi, 1964, 20: 14782(R) (AE-211)
power system frequency regulation by nuclear power plants, 18: 38486 (A/CONF.28/P/606)
radiation dose to population of, diagnostic, 18: 33419
radiation processing of food in, review of, 20: 31628
radiation protection planning, 19: 46705
radioactivity distribution in minerals and rocks in Alno alkaline area, 19: 30406
radioactivity in food chain of lichen, reindeer, and man, 1961 to 1965, 20: 35705
radioisotope uses in, economics of industrial, 20: 27377
radon content in natural waters in, 19: 33746
reactor power plants in, design development of, 17: 22869
reactor site selection criteria in, 17: 19604
research of Swedish Atomic Research Council, 1963–64, budget for, 20: 24821(R) (NP-15948)
shelter design, construction, and cost in, deep-rock and normal, 16: 27486
survey of oral radiography practices in, 20: 3846
uranium disseminations and vein fillings in iron ores in Central, 18: 37417
uranium (IV-VI) oxide mining and processing in, 17: 27489
uranium resources in, 20: 28868
waste handling at Studsvik research station, 19: 27831 (AE-182)
x-ray standards in, 20: 37078

Swedish Reactors (Oskarshamn)
see Oskarshamn Power Reactor

SWEDISH REACTORS (R-0)
buckling measurements in, 18: 6454
control rod worths in, measurement of, (E), 19: 17200

description, 17: 22887
experimental facilities of, design and use of, 20: 1540
neutron buckling and diffusion in, void effects on, (E/T), 20: 8465 (RFX-316)
neutron spectra measurement in, activation techniques for epithermal, 20: 36524 (AE-230)
reactivity of, control-rod effects on, (E), 19: 17198
reactivity of, eccentric control rod theory for, 20: 10328 (RFX-70)
Swedish Reactors (R-1)
see SLEEP Reactor
SWEDISH REACTORS (R-2)
coolant beta monitor for, 20: 43688
description, 17: 22887
design, 18: 13335 (NP-13597)
design and operation, 18: 3324 (TID-7663(p.61-72))
experimental facilities of, design and use of, 20: 1540
fuel elements from, gamma irradiation facility using spent, 19: 18102
instrumentation in in-pile loop #2 of, 19: 24168 (CONF-640607(Vol.I) (Paper B-3))
instrumentation of, spectrometers for, 18: 11479 (ANL-6797(p.183-92))
neutron spectra in, foil-activation measurement of, 19: 3771 (AE-155)
SWEDISH REACTORS (R-3)
commissioning and criticality experiments, 18: 38493 (A/CONF.28/P/679)
control rod burnup, calculations, 17: 4259
control system development, 16: 1193(R) (NP-10915)
control-rod reactivity effects in, 20: 12362 (RFR-193)
description, 17: 22887
description, 18: 23083
description, 18: 45041
description, 19: 1911
description, 20: 12426
design and performance, 20: 1485
design and performance, 20: 6599 (AEE-5)
design description, 17: 33350
design of heavy water systems for, 18: 38483 (A/CONF.28/P/602)
design of 200-Mw(e) Marviken, 18: 15570
design, instrumentation, and operation of, 18: 40914
development of, survey, (E), 19: 43549
fuel consumption rate in, calculation of, 16: 33577(R) (AE-79)
fuel development, 18: 38487 (A/CONF.28/P/608)
fuel element assemblies, buckling measurements, 16: 932 (DP-613)
fuel element buckling, 16: 34008
fuel element design, 16: 2752
fuel element failures in, calibration of detection systems for, 20: 36450 (AE-231)
fuel element pressure drop, hydraulic instability, 17: 4312
fuel handling equipment for, 18: 38285 (A/CONF.28/P/808)
materials procurement aspects of, review, 20: 5110 (AES-4)
operation experience, 19: 43571
physics studies, 18: 38494 (A/CONF.28/P/682)
startup instrumentation for, description of in-core, (E), 19: 24073 (CONF-640607(Vol.II)(Paper G-1))
startup tests on, 18: 9675
startup using nuclear heating, (E), 19: 35784
survey, 17: 22888
waste disposal from Agesta, in Lake Magelungen, high-velocity jet release for, 19: 24193
SWEDISH REACTORS (R-4)
design, 18: 15570
design with nuclear superheat, 18: 38484 (A/CONF.28/P/603)
design with nuclear superheat, 18: 38484 (A/CONF.28/P/603)
development, 20: 35040
development, 19: 43459
fuel development, 18: 38487 (A/CONF.28/P/608)
fuel development for, 18: 38487 (A/CONF.28/P/608)
fuel element design for, 20: 36478 (KR-89, pp 238-64)
steam turbine for, performance of heavy-water, 20: 28795
SWEET POTATOES
radiation effects on propagation of root-knot nematodes in, 20: 28942
radioinduced mutations in, 16: 20178
radioinduced mutations in, review, 19: 43777
SWIMMING POOL REACTORS
see also Air Force Engineering Test Reactor
see also Bulk Shielding Facility
see also Fontenay-aux-Roses Reactors (Triton)
see also Grenoble Reactors (Melusine)
see also Livermore Pool Type Reactor
see also Michigan Research Reactor
see also NRL Research Reactor
see also ORNL Research Reactor
see also Pennsylvania Research Reactor
see also Philippine Research Reactor
see also South African Research Reactor
see also Spanish Reactors (JEN-1)
accidents at IRR-1, sea water contamination by, 19: 39265(R) (IA-1021)
argon-41 content and escape velocity, 16: 17312
book: *Two-Group Reactor Theory*, 19: 19341
characteristics and program of Puerto Rican L-77, 17: 10168
characteristics, installation, and uses of REBECCA at Indatom, 19: 5550
Cherenkov radiation in, spectral analysis of, 19: 3784
cobalt-60 irradiation facility in, 20: 43791
cofferdam design for, 19: 42190(P)
construction of Dutch 20-Mw high-flux, 17: 15507
construction, operation, and function of Geesthacht, survey, 16: 11282
control and safety systems of Siloe, 18: 24966
control and safety of Polish MARYLA, systems design for, 18: 38604 (A/CONF.28/P/500)
control by soluble-poison closed-loop automatic systems, 18: 3375
control of Japanese TTR-1, computer, 20: 32867
control rod behavior in Naval Research Laboratory Reactor during 1-Mw operation, 16: 4615(R) (NP-11098(p.30-4))
control rod drive mechanisms for, using watertight electromagnets, 16: 28484(P)
control rod drive system for, 18: 42900(P)
control rod drop times in Rolla Reactor, 19: 43622
control rod handling system for, design of watertight electromagnets for, 17: 31703(P)
control rod operations in Petten High-flux, (E), 19: 17385
control rod vibrations in Puerto Rico Nuclear Center 1-Mw, elimination of, 18: 3343 (TID-7663(p.859-63))
control rod worth, method for determining, (E), 19: 10657
control rods for high-flux, problems in design of, (E), 19: 17384
control system design for, 17: 9905(P)
control system design with soluble poison closed loop for Avogadro, 18: 15652
control system design for RTM, nonlinear, 19: 45682 (RT/ING(64)-15)
control system for safety rods of, design of improved electromagnetic, 19: 3796(P)
control system of SILOE, 18: 35227
control using gamma radiation, 17: 35081 (CONF-39-44)
coolant analysis for radioisotopes by gamma spectrometry, 17: 40702 (TID-7655(p.107-18))
coolant analysis for fission products in, design of monitor for, 20: 3909
coolant analysis for corrosives and solids in, activation and chemical, 20: 38800 (PAEC(C)TR-652)
coolant circulation system for, 18: 33159(P)
coolant circulation system for, 20: 14205(P)
coolant circulation system for, 20: 24807(P)
coolant contamination by fission gases in, 18: 38623 (A/CONF.28/P/790)
coolant electric conductivity in, circuit for continuous measurement of, 20: 10431
coolant flow by natural convection, activation flowmeter for measuring, 17: 3130
coolant purification in Polish EVA, system for, 16: 34120
coolant radioactivity and airborne radioactivity in Indian Apsara, 18: 24947 (AEET/AM/38)
coolant stratification in, process and equipment for, 20: 26547(P)
cooling system design for increased power in, 18: 17331(P)
cooling system design, 18: 21688
cooling system design to prevent rise of contaminated water to surface, 19: 34311(P)
cooling system for McMaster University reactor, control and maintenance, 16: 7314
cooling system for, design and operation of inexpensive, 18: 3366
core design for, 20: 24806(P)
core design for French SILOE, 18: 43076 (CEA-R-2534)
core design for 40-Mw Pressure Tube Reactor, 16: 7316
core-moving apparatus for, 18: 7978(P)
core supporting grid design, 17: 21365(P)
critical experiments of PTR core in IRL reactor, 16: 7318
critical experiments for Democritus, 18: 3340 (TID-7663(p.738-89))
critical mass measurements for water-reflected and graphite-reflected cores in Pool Test Reactor, 16: 9572 (CRRP-1064)
criticality studies of Advanced Pressure Tube Reactor, hazards evaluation for, 17: 33373 (NP-12998)
cryogenic irradiation system for German FRM, 17: 10138
description and characteristics of Checkerboard Pool Core, 17: 26917
description and operation of Battelle, 16: 11327
description and operation of GRR-1, 16: 11328
description and operation of McMaster Research Reactor, 16: 32610
description and operation of German FRM, 17: 10137
description and operation of ISPRA-2, 18: 24962 (RT/ING(63)-25)
description and performance of Shield Test and Irradiation Reactor, (E), 20: 6677 (NAA-SR-11528)
description and safeguard evaluation of 1-Mw, for Rhode Island and Providence Plantations AEC Nuclear Science Center, 16: 12775 (GEAP-3135)

description and use of FRM, 16: 11319 (JÜL-25-RX)
description and use of Union Carbide Nuclear Company 5-Mw, 16: 20028
description of ASTRA, 20: 16127
description of CABRI, for safety studies, 18: 38579 (A/CONF.28/P/103)
description of Dutch 20-Mw high-flux, 17: 15505
description of French SILOE and OSIRIS, 18: 38575 (A/CONF.28/P/47)
description of graphite-reflected Ispra-2, 16: 28609 (RT/ING(62)3)
description of Japanese JRR-4, 18: 19435
description of Japanese JRR-4, 19: 17372
description of JRR-4, 19: 3452 (JAERI-4029)
description of McMaster University, 16: 28615
description of McMaster University, 17: 13816
description of Pegase and Siloe, 18: 4875
description of SILOE, 17: 10147
description of SILOE, 18: 3314 (CEA-2307(Vol.1))
description of Swedish R2-0 research, 17: 4345
description of Univ. of Delft, 16: 2782
description of 5-Mw HERALD, 17: 24719
design, 16: 25028(P)
design, 17: 21366(P)
design and construction of Pégase, 18: 40953
design and hazards analysis of Portuguese 1-Mw RPI, 18: 15610 (LFEN-1)
design and operation at Industrial Reactor Laboratories, 5-Mw, 16: 7317
design and operation of Herald, 17: 10157
design and operation of Pakistan, training of personnel in U. S. for, 18: 3336 (TID-7663(p.436-51))
design and operation of Portuguese RPI, 18: 38605 (A/CONF.28/P/505)
design considerations, 18: 38347
design data and drawings for PTR, 16: 14344
design description of Japanese, 17: 2623
design for flexibility, 19: 33674(P)
design for high-flux neutron beams production, 18: 38577 (A/CONF.28/P/49)
design for irradiation studies, 18: 15653(P)
design for irradiation studies, 19: 29800(P)
design for irradiation studies, 19: 29802(P)
design for irradiation studies, 19: 33673(P)
design for large-scale irradiation tests, 20: 42685(P)
design for neutron irradiation experiments, 18: 7977(P)
design for producing short-lived radioisotopes, 17: 28571(P)
design for producing radioisotopes, 17: 29844(P)
design for reduced surface radioactivity, 20: 10433(P)
design for reduced radioactivity at pool surface, 20: 10435(P)
design for reduced radioactivity at pool surface, 20: 10434(P)
design for reduced radioactivity at pool surface, 20: 10436(P)
design for studying radiation effects on materials, 17: 21367(P)
design modifications to Avogadro RS1, at SORIN, 19: 48066
design of Biological Agricultural Reactor Netherlands, 18: 38620 (A/CONF.28/P/725)
design of Cabri, 19: 17370
design of compartmented, 19: 29798(P)
design of compartmented, 20: 12516(P)
design of facilities for 1-Mw research, 16: 11318 (JÜL-24-RX)
design of Hitachi Training Reactor, 18: 3331 (TID-7663(p.275-86))
design of Hitachi, 18: 35224
design of IRR-1, 16: 30133 (IA-680)
design of Ispra-2, 17: 22944
design of Osiris, for testing reactor structural materials, 19: 27824
design of pile unit for studying materials under irradiation, 19: 5556(P)
design of Siloe, 18: 24965
design of Siloe, 18: 31040
design of SILOETTE, 19: 3775 (CEA-R-2589)
design of South African, 17: 15511
design of Swiss SAPHIR, 18: 43086
design of THOR, in Republic of China, 18: 38601 (A/CONF.28/P/481)
design of VVR-Ts, 18: 13330 (AID-P-63-88)
design of 100-kw Consort Mark-2, 19: 48067
design of, to prevent radioactivity diffusion to surface, 20: 14204(P)
design of, with fuel in reflux pressure tube, 18: 43089(P)
design of, with improved cooling system, 20: 1370(P)
design with forced-convection primary cooling circuit, 19: 21744(P)
design with removable solid-moderator elements lining the tank, 17: 38521(P)
enclosure design for, 17: 28569(P)
experimental facilities, irradiation enclosure design, 18: 35230(P)
experimental facilities, self-contained loop for irradiations, 18: 38678(P)
experimental facilities for graphite research, 19: 5540 (CEA-R-2516)
experimental facilities in, cryogenic device design for, 19: 5554(P)
experimental facilities, oven for sample irradiations, 19: 10639 (CEA-R-2530)
experimental facilities for, self-contained gas-cooled loop design, 19: 29799(P)
experimental facilities for, design of loop, 19: 29801(P)
experimental facilities for, thermal-column pneumatic, 19: 43600
experimental facilities for hydraulic transfer of irradiated containers, 19: 45686(P)
experimental facilities for, design of irradiation capsule hydraulic transfer, 20: 24695(P)
experimental facilities of, for irradiation studies, 20: 23241
experimental loop design for, 18: 7975(P)
experimental program for Netherlands Research Center, 18: 3337 (TID-7663(p.531-84))
exposure chamber design for SAPHIR, gamma, 16: 1267
fission gas release in, collecting device for, 20: 1544(P)
fission product release monitoring in IRL 5-Mw, 17: 26918
frequency response of IRT-1000, oscillator method for determining, 18: 4855
fuel and reflector element positioning in, design of equipment for, 19: 38284(P)
fuel burnup calculations for ASTRA, 20: 6681 (SGAE-PH-18/1965)
fuel element arrangement in tank with variable pitch, device for, 18: 21690(P)
fuel element burnup analysis of Sorin, 16: 21734
fuel element cladding failure detection systems in Pegase, 18: 44945
fuel element design, 17: 22922 (TID-7642(p.197-243))
fuel element fabrication for, 18: 37645 (A/CONF.28/P/57)
fuel element failure in, method for detection, 16: 7265
fuel element failure in, detection apparatus for, 18: 3312 (CEA-2235)
fuel element failure in 5-Mw, monitoring and detection of, 18: 3382
fuel element flux distributions, 16: 3850(R) (ORNL-3193(p.100-2))
fuel-element removal and transfer from, design of liquid-filled carrier for, 17: 40316(P)
fuel element rupture in, radioactivity content in air from, 18: 11491
fuel elements for Puerto Rico Nuclear Center reactor, 16: 7315
fuel elements in, detection of fission product release from, 18: 3345 (TID-7663(p.1060-92))
fuel plate assembly with consumable poison, 18: 35231(P)
fuel plates of, equations for temperature distribution in, 19: 12764
fuel policies for refueling, 18: 33152(T) (CEA-R-2458)
fuel programming for intermediate power levels, 16: 1268
gamma and neutron attenuation in beryllium-reflected Pool Critical Assembly, 16: 3838(R) (ORNL-3193(p.4-9))
gamma flux calculations for power overrun in, 17: 40284(T) (AEC-tr-6060)
gamma fluxes near cores of, calorimetric measurement of high, 17: 29373 (CEA-2217)
gases released at surface of, device for trapping, 19: 14893(P)
hazards summary for Northrop, 16: 5608 (NB-61-349)
hazards summary for Purdue University Reactor I, 16: 9700 (NP-11333)
hazards summary for University of Cincinnati, 17: 28566 (NP-12915)
hazards summary for Western New York Nuclear Research Center, 18: 40951 (NP-14289)
hazards summary of, for Western New York Research Center, 17: 21360 (NP-12702)
health physics procedures at Brazilian IEAR-1, 17: 10163
heat exchanger design for, 18: 14013(P)
in-pile loop installation in, 17: 22802(T) (EURAEC-508)
in-pile loops for Melusine and Siloe (E), 19: 1824 (CEA-R-2537)
installation of PTR at Manhattan College, 18: 11495
instrumentation for Dutch 20-Mw high-flux, 17: 15506
instrumentation for, in-reactor radiometric calorimeter, 18: 2033 (UCRL-7489)
instrumentation for Austrian Astra, (E), 19: 24005 (CONF-640607 (Vol.I)(Paper A-1))
instrumentation for Swiss DIORIT and SAPHIR, (E), 19: 24165 (CONF-640607(Vol.I)(Paper A-12))
iodine-131 diffusion from carbon dioxide bubbles through water of Pegase, 18: 6528(T) (AEC-tr-6144)
irradiation capsule design for use in, 18: 23100 (SGAE-CH-2/1964)
irradiation enclosure design for, 20: 3602(P)
irradiation facility design and operation in SAPHIR, 17: 16074
irradiation facilities for German FRM, design of cryogenic, 18: 45142
irradiation facilities for, 18: 45145(P)
irradiation facilities for Siloe, description of cryogenic, 19: 5539 (CEA-R-2514)
irradiation rig for solid specimens, 20: 28844
isotope production in, 18: 35918
kinetic parameters from analysis of pile noise, 16: 3871(R) (ORNL-3193 (p.228-33))
kinetics of Philippine Research Reactor PRR-1, 18: 1307
kinetics of, use of pile noise analysis in measurement of, 17: 12775(R) (ORNL-3360(p.68-72))
loading device for, design of, 19: 35661(P)
loading device for, 19: 38283(P)
loading variable-pitch lattice, device for, 20: 14206(P)
lock chamber for transfer of objects from, design of water-air, 18: 9591(P)
loop design for, in-pile, 18: 4884(P)
loop design for irradiation studies in, 17: 29851(P)
loops for, design of trolley for displacement of, 19: 42189(P)

magnetic field device for irradiation studies in, 16: 26615 (CEA-2134)
materials testing in 20-Mw high-flux Dutch, 12: 14909
moderator-purity-determination in EWA, sensitivities, 16: 7311
neutron activation cross sections in, determination of, 17: 7100 (NP-12330(p.95-6))
neutron beam facilities at Dutch research, 17: 15508
neutron beams for spectrometers, core modification to enhance thermal, 19: 29797
neutron diffraction equipment for McMaster University reactor, 16: 8951
neutron energy effects in University of Maryland, 18: 37552
neutron flux distribution measurements and power calibration on Susie Reactor, 16: 15895 (DC 61-4-726)
neutron flux distribution in Susie at low power, 16: 24933 (DC-60-6-722)
neutron flux distributions in IRR-1 research, 18: 38612 (A/CONF.28/P/666)
neutron flux distributions and reactivity of Russian IRT-2000, 18: 38618 (A/CONF.28/P/718)
neutron flux distributions in, correlation with two-group diffusion theory, 20: 42600
neutron flux from fission plates in, transient-temperature method for measuring, 17: 38572
neutron flux in empty fuel element position in German FRM, 18: 23108
neutron flux in German FRM, measurements of fast, 16: 9703(T) (CEA-tr-A-1026)
neutron flux in University of Virginia, (E/T), 19: 25769
neutron flux in, beam port void effects on thermal, (E/T), 19: 17376
neutron generation time in, determination by pulsed neutron method, 17: 1024 (IDO-16791(p.151-56))
neutron lifetime in Portuguese, prompt, 18: 31035 (LFEN-16)
neutron multiplication in pulsed neutron injected cores, 16: 6122
neutron multiplication factor in Hitachi, effect of epithermal fission on, (E/T), 20: 30841
neutron spectra from split-core, 18: 4848 (EANDC(OR)-26U)
neutron spectra in Avogadro RS-I, fast, 17: 34268
neutron spectra in reflector of Melusine, (E), 19: 21729 (CEA-R-2442)
neutron spectral distribution, epithermal and thermal, 16: 7320
neutron spectral distributions in, activation analysis of, 17: 10139
neutron spectral distribution in core and reflector, 17: 17600(T) (CEA-tr-A-1194)
neutron transport in, 18: 38613 (A/CONF.28/P/670)
operating experience with APSARA, 18: 3363
operation and safeguards of Merlin, 17: 10159
operation and use of Herald Reactor, 18: 38584 (A/CONF.28/P/123)
operation and uses of THOR, 19: 24174 (NP-14832)
operation and utilization of Brazilian 5-Mw(t) IEAR-1, 16: 31327 (IEA-44)
operation experience of Avogadro, 18: 15652
operation of Battelle, five-year, 17: 10152
operation of Brazilian IEA-R1, 16: 2774(R) (IEA-43)
operation of FRM, organization for, 16: 11317 (JUL-23-RX)
operation of IRR-1, 19: 39265(R) (IA-1021)
operation of RPI, 20: 6675 (LFEN-26)
operation of Siloe, at 15 Mw, 18: 45140
operation of SILOE and SILOETTE, 19: 3773 (CEA-R-2532)
operation of University of Virginia, 18: 3330 (TID-7663(p.267-74))
operation of 2-Mw Avogadro RSI, 18: 3341 (TID-7663(p.842-54))
operation of, for activation analysis of trace metals in sea water, 20: 18576(R) (TID-22660)
operation, problems encountered in Avogadro RS1, 17: 13843
performance of IRT-2000, 18: 24960 (NP-13911)
physics measurements during operation of Indian APSARA, 18: 40940 (AEET/ROD/8)
poisoning in periodic operation, computer study of xenon, 19: 12755
poisoning of Pegase and Siloe, effects on shutdown behavior, 16: 21738
pool design, 16: 34121(P)
power calibration and regulation of Battelle Research Reactor, 16: 7312
power excursion testing for OSIRIS, simulated, 18: 42919 (CEA-R-2549)
power level monitoring using nitrogen-17, sensitivity of, 20: 30938
power of, technique for monitoring, 18: 19440
power output calibration as function of neutron flux, 18: 36755
radiation dosimetry in ASTRA, by calorimetric methods, 18: 23101 (SGAE-CH-3/1964)
radiation dosimetry in Siloe using Calvet calorimeter, 19: 26651 (CEA-R-2768)
radiation target cans for, use of anodized aluminum, 19: 28877
radioactivity problems with, 17: 35200
radioisotope production and handling at GRR-1, 20: 20339
radioprotection devices used near, review of, 20: 6670 (CEA-R-2864)
reactivity effects of moderator expulsion from enriched, 16: 28438
reactivity effects of fuel displacement, 16: 30678(R) (ORNL-3319)
reactivity effects and transients due to extraneous neutron source, (T), 19: 27823
reactivity in NORA, void, 19: 24040
reactivity measurements using kinetic techniques, subcritical, 17: 2470 (EIR-28)
reactivity measurement in Ispra 2, 18: 1305 (RT/ING(63)3)
reactivity measurements in IRR-1, pulsed-source technique for subcritical, (E), 20: 14200
reactivity measurements on TTR-1, using neutron noise analysis by two-detector correlation method, 20: 32868
reactivity noise analysis of Hitachi Training Reactor, 18: 43085
reactivity of Avogadro RS1, Italy, 16: 2776
reactivity of, effects of small fuel displacements on, 17: 16322(R) (ORNL-3401(p.3-4))
reactivity of, effects of small fuel displacements on, 17: 38437(R) (ORNL-3483)
reactivity of, effects of central and uniform voids on, 18: 4874
reactivity of, method for determining excess, (E), 19: 10657
reactivity of, modified pulsed-source techniques for measuring, (E), 20: 14199
reactivity of, temperature coefficient of, 18: 38313 (A/CONF.28/P/649)
reactivity oscillator for, 18: 38614 (A/CONF.28/P/671)
reactivity temperature coefficients of, method for measuring, (E/T), 20: 18145
reactivity transfer function of ASTRA, scintillator for measuring, 20: 6682 (SGAE-R-1/1965)
reactivity transfer function for SAPHIR, analyzer for measuring, 20: 20311 (EIR-87)
reactivity, void coefficients in Pool Critical Assembly, 16: 3837(R) (ORNL-3193(p.3-4))
reactivity, temperature coefficient of, 20: 47081
reflector element development for, uncanned graphite, 17: 40310
research and training at IRR-1, 18: 35219 (IA-894)
research program at McMaster Research Reactor, 16: 32609
research program at Merlin, 17: 10155
research program at IRR-1, 18: 35218 (IA-892)
research programs on neutron cross sections and scattering at FRM, 20: 20331
research progress at NORA, 20: 5060(R) (TID-22357)
rod lifting in, design of electromagnet for, 19: 5555(P)
safety analysis of SILOE, 18: 3316 (CEA-2307(Vol.3))
safety analysis of Sandia, 18: 9731 (SC-4966(RR))
safety aspects of, 17: 1087
safety of, analysis of maximum credible incident in, 18: 7974
safety of 1 to 5 Mw, 18: 3334 (TID-7663(p.353-67))
SAPIR, bulk shielding studies in, 16: 32604 (EIR-27)
shielding for, evaluation of, 19: 21739
shielding screens for, fabrication of lead, 20: 10314(P)
shutdown of IRT-2000, gamma dose level from sodium-24 and iron-59 activities after, 20: 36532
startup of Belorussian IRT-2000, 17: 7637(T) (JPRS-15345)
surface water activity control in, using hot water layer, 18: 35226
temperature distribution at coolant channel exit for 10-Mw SILOE, 18: 29836 (CEA-R-2422)
thermal-column loading in Israel (IRR-1), automatic equipment for, 18: 45084 (IA-919)
use as low-temperature irradiation facilities, design considerations for, 19: 3779 (ORNL-P-614)
use for radiochemistry research, 20: 12914 (IEA-100)
use of Avogadro RS-1, 18: 11494
use of Brazilian IEAR-1, 17: 10171
use of CNDC Triga Mark II in neutron physics studies, 16: 18426
use of FRM in neutron physics studies, 16: 18423
use of Greek GRR-1, for chemistry studies, 20: 20337
use of McMaster Univ., 18: 38567 (A/CONF.28/P/2)
uses of Brazilian IEA-R1, 18: 38581 (A/CONF.28/P/118)
uses of high-flux, for activation analyses, 17: 14171
uses of Indian Apsara, 18: 38621 (A/CONF.28/P/744)
uses of SAPHIR, 17: 10165
uses of Turkish Reactor-1, 18: 38622 (A/CONF.28/P/747)
ventilation systems of IRT-2000, efficiency of, 20: 5201
water radiolysis in, formation and distribution of gases and hydrogen peroxide from, 16: 26496(T) (TID-7622(p.310-15))

SWINE

analysis of, chemical, 20: 6750
analysis of, morphological, 20: 6750
bacterial infections and bacteremia in, after exposure to nuclear detonation, 18: 5019
calcium metabolism in bones of, effects of diet on, 17: 13940
calcium-45 metabolism by, 19: 3835(R) (ORO-625(p.64-9))
calcium-45 uptake by skeleton of miniature, effects of age on, 18: 19539
care and maintenance at Battelle-Northwest, facilities for, 20: 8504 (BNWL-SA-417)
care on Japtan Island for Operation Greenhouse, 16: 12805 (WT-2)
cerium-144 distribution in tissues of miniature, 17: 35294(R) (HW-76000(p.39-44))
cerium-144 absorption by, gastrointestinal, 20: 10525(R) (BNWL-122, pp 85-90)
cerium-144 toxicology in, 19: 45759(R) (ORO-631, pp 77-82)

cesium, potassium, and sodium content, 17: 30268
cesium-134 metabolism, 16: 17415
cesium-134 metabolism by, 20: 12588(R) (AD-626320)
cesium-137 distribution in tissues of, 16: 21882
contamination of skin of, by phosphorus-32, strontium-90, and yttrium-90, 18: 4953
contamination of skin of, using solutions of radioisotopes, 20: 40
contamination of skin of, by antimony-125, polonium-210, promethium-147, sulfur-35, thallium-204, effects of acidity of soiling solution on, 20: 43010
copper metabolism, tracer study, 17: 23010
decomposition of carrion of, effects of scavenger animals, insects, and microorganisms on, 20: 20941 (ORNL-TM-1432)
dietary effects of strontium-90 on miniature, 17: 13955
diets for miniature, development of, 20: 8505 (BNWL-SA-418)
diuretic action in, tracer study, 20: 12613
effect of calcium, zinc, and corn oil in diet on the in vitro uptake of various radioisotopes by blood cells of, 20: 40556
effects of aging on biochemical and hematological parameters in, 20: 1581 (BNWL-SA-341)
effects of chronic ingestion of strontium-90 in miniature, 17: 5700 (HW-74969)
effects of chronic, low-level ingestion of iodine-125 and iodine-131 in, 17: 35295(R) (HW-76000(p.45-55))
effects of ingested strontium-90 on miniature, pathological, 20: 10597(R) (BNWL-122, pp 37-45)
effects of ingested strontium-90 mixture in miniature, 17: 35299(R) (HW-76000(p.66-83))
effects of intradermally injected plutonium-239 in miniature, 17: 13920 (HW-SA-2626)
effects of irradiation of testes on weight of offspring, 17: 10414
effects of paternal irradiation on first generation, 20: 45362(R) (TID-23311)
effects of plutonium injected in skin, 16: 25122(R) (HW-72500(p.50-1))
effects of radiation-processed fruits on, 20: 37156
effects of strontium-90, radium-226, and plutonium-239 in miniature, 17: 13919 (HW-SA-2613)
effects of vitamin K deficiency in baby pigs, 16: 33344(R) (NP-12093)
effects on long-term ingestion of strontium-90 in miniature, 16: 25112(R) (HW-72500(p.1-12))
effects on radium-226 in kidneys of miniature, 18: 41032(R) (HW-80500 (p.79-82))
erythrocyte life span in, tracer study on, 20: 32907(R) (ORO-648, pp 62-70)
erythrokinetics in, effects of ingested strontium-90 on, tracer study of, 17: 35301(R) (HW-76000(p.89-92))
erythropoietin content of blood plasma in miniature, 17: 35302(R) (HW-76000(p.93-4))
fission product metabolism in, 18: 11645(R) (ORO-614)
fission product metabolism in, 20: 18188(R) (ORO-635)
function tests in miniature, use of iodine-131-hippuran renogram in, 18: 41274(R) (HW-80500(p.167-72))
genetics of blood group systems in, 18: 13393
hematological response to massive blood removal in miniature, effects of strontium-90 ingestion on, 18: 41087(R) (HW-80500(p.157-61))
hematological response to Pseudomonas endotoxin of miniature, effects of ingested strontium-90 on, 18: 41088(R) (HW-80500(p.162-6))
histological studies on species of, 20: 45352 (CEA-R-2978)
immune response to irradiated trichina larvae, 19: 13020
immunization against lung parasites, vaccine for, 20: 23570(P)
iodine metabolism, tracer study, 17: 23020
iodine toxicity in, dietary, 20: 45307
iodine-131 content in thyroid in, in Michigan, 1959 to 1963, 17: 34145 (CONF-66-6)
iodine-131 placental transfer, 19: 12942
iodine-131 uptake by thyroid gland of, from skin exposure, 20: 10518(R) (BNWL-122, pp 55-8)
iron-59 metabolism in fetal and growing, nutritional physiology of, 19: 15008
metabolism and skeletal retention of calcium-45 and strontium-90 in miniature, effect of age on, 17: 35300(R) (HW-76000(p.84-8))
metabolism of strontium-90 and calcium-45 in miniature, effects of age, 16: 25113(R) (HW-72500(p.13-14))
metabolism of strontium-85, strontium-90, promethium-147, and cerium-144 in miniature, 18: 23200 (HW-SA-3350)
molecular weight determination of blood factors VIII and IX in, using electron irradiation, 18: 29233
molybdenum metabolism in, tracer study, 19: 12928
molybdenum-99 metabolism in, 20: 32907(R) (ORO-648, pp 62-70)
mucopolysaccharide content in kidneys and intestinal mucosa cells of, 20: 32907(R) (ORO-648, pp 62-70)
neutron effects on skin of, 19: 32001
nutrition of, effects of vitamin A in foods on, 19: 17641
pancreatic juice from, collection of, 19: 43628 (BNL-8422)
placental transfer of glycine, urea, and water in, 19: 38344
plutonium metabolism and toxicity in miniature, 17: 7748 (HW-SA-2600)
plutonium-239 distribution in tissues of, 20: 10523(R) (BNWL-122, pp 81-2)
plutonium-239 effects in skin of, after intradermal injection, 18: 41077(R) (HW-80500(p.120-2))
potassium content in, effects of body composition on, 20: 6750
potassium-40 distribution in tissues, 16: 21882
potassium-40 measurements in, for use as growth index, 20: 42739(R) (COO-1339-3)
promethium-147 distribution in tissues of miniature, 17: 35294(R) (HW-76000(p.39-44))
promethium-147 absorption by, gastrointestinal, 20: 10525(R) (BNWL-122, pp 85-90)
protection against fallout, 19: 46700
radiation and maternal malnutrition effects on, prenatal, 18: 38775(R) (ORO-624)
radiation dosage determinations, 16: 11357 (WT-18)
radiation dosages for, lethal, 19: 7044
radiation dose determinations for, lethal, 19: 10799
radiation effects on skin of, fractionated and single fast neutron and x-ray, 17: 12146
radiation effects of plutonium-239, radium-226, and strontium-90 injected intravenously, 17: 15847
radiation effects on and interrelation of copper and vitamin A deposition in liver of, 17: 17729
radiation effects on glutathione content in lens of eyes in, 17: 17864
radiation effects, whole-body nuclear exposure, 17: 31816(R) (ORO-605)
radiation effects on serum proteins of, gamma and neutron, 17: 38752
radiation effects on, prolonged or single-exposure iodine-131, 18: 8159
radiation effects on frequency of bacteriological findings in, gamma, 18: 9903
radiation effects on reproduction of, 18: 11645(R) (ORO-614)
radiation effects on endotoxin immunity in, strontium-90, 18: 13518
radiation effects on oxidation and reduction in ears of, 18: 13524
radiation effects on microorganisms in, 18: 17534
radiation effects in, gamma, 18: 25188
radiation effects on thyroid functions, x, 18: 36975
radiation effects on sperm production in, 18: 38775(R) (ORO-624)
radiation effects on calcium-45 and strontium-89 absorption in intestine of, 18: 38775(R) (ORO-624)
radiation effects on, pathological, 18: 38775(R) (ORO-624)
radiation effects on mercapto groups in ears of, x, 18: 41204
radiation effects on, 19: 3891(R) (ORO-625(p.1-27))
radiation effects on reproductive system of, 19: 3892(R) (ORO-625 (p.28-37))
radiation effects on, pathological, 19: 3893(R) (ORO-625(p.38-55))
radiation effects on, physiological, 19: 3894(R) (ORO-625(p.56-63))
radiation effects on young, 19: 5699
radiation effects on, gamma, neutron, and x, 19: 5635
radiation effects on carcasses infected with trichinosis, gamma, 19: 7067
radiation effects on litter size of, 19: 7082
radiation effects on growth of ascaris eggs in, neutrons, 19: 7128
radiation effects on gonad function in, 19: 8875
radiation effects on, air and *in vivo* dosimetry of gamma and neutron, 19: 8951
radiation effects in, 19: 10799
radiation effects on limb development of fetuses of, exposed *in utero*, 19: 15096
radiation effects on skin of, fractionated, 19: 21888
radiation effects on skin of, dosimetry of fractionated, 19: 28153
radiation effects on skin of, x, 19: 32001
radiation effects on oogenesis in, x, 19: 36026
radiation effects on mercapto groups in blood, 19: 38427
radiation effects on, bibliography, 19: 43713 (BNWL-115)
radiation effects on properdin content of blood serum of, ultraviolet, 19: 45919
radiation effects on molybdenum-99 metabolism in, 19: 45759(R) (ORO-631, pp 77-82)
radiation effects on tungsten-185 metabolism in, 19: 45759(R) (ORO-631, pp 77-82)
radiation effects on, delayed pathological, 19: 45812(R) (ORO-631, pp 1-35)
radiation effects on reproduction of, 19: 45813(R) (ORO-631, pp 36-44)
radiation effects on, pathological, 19: 45814(R) (ORO-631, pp 45-66)
radiation effects on, physiological, 19: 45815(R) (ORO-631, pp 67-76)
radiation effects on weight gain of progeny of, x, 20: 1677
radiation effects on skin of, effects of dose fractionation on fast neutron and x, 20: 3735
radiation effects on behavior traits in, genetic analysis of, 20: 3784
radiation effects on, biological, 20: 10618
radiation effects on copper and zinc content and enzyme activity in blood serum of, 20: 16222 (AFWL-TR-65-112)
radiation effects on, pathological γ and neutron, 20: 18188(R) (ORO-635)
radiation effects, 20: 18198

radiation effects on, pathological γ, 20: 26692
radiation effects on, pathological γ, 20: 26693
radiation effects on blood picture of, γ, 20: 26694
radiation effects on development of Ascaris eggs in, gamma and neutron, 20: 33026
radiation effects on copper and zinc metabolism in, neutron, 20: 32907(R) (ORO-648, pp 62-70)
radiation effects on calcium-45 and strontium-89 metabolism in, whole-body, 20: 32907(R) (ORO-648, pp 62-70)
radiation effects on survival of, combined gamma and neutron, 20: 32965(R) (ORO-648, pp 1-25)
radiation effects on ovaries of, gamma, 20: 32966(R) (ORO-648, pp 26-35)
radiation effects on mortality of, patterns in, 20: 32967(R) (ORO-648, pp 36-55)
radiation effects on mortality of, from bilateral and unilateral neutron exposure, 20: 32965(R) (ORO-648, pp 1-25)
radiation effects on anatomy and pathology in, whole-body gamma, 20: 36657
radiation effects on Dische-positive material in blood and urine in, gamma, 20: 36604
radiation effects on, pathological γ, 20: 40608 (CEA-R-3001)
radiation effects on males, genetics 16: 31490
radiation hazards to, from fallout in event of nuclear war, 17: 34184
radiation injuries, pathology, 17: 15541(R) (ORO-598)
radiation injuries in, protective effects of aminoethylisothiuronium chloride-hydrochloride against, 17: 25048
radiation injuries of skin of, pathology, 20: 1609 (BNL-9477)
radiation lethal dose for gamma, 18: 25188
radiation sickness in, diagnosis of, 20: 128
radiation sickness in, anatomy and pathology of, 20: 36657
radiation syndrome in, compared to other large animals, 20: 8729
radiography of knuckle of, for estimation of ham composition in slaughtered animals, 20: 5224
radioinduced hematopoietic tumors in, effects of strontium-90 on, 20: 31031 (BNWL-SA-201)
radioinduced inactivation of foot and mouth disease virus in tissues of, γ, 20: 41392
radioinduced skeletal anomalies in, exposed *in utero*, γ, 20: 14337
radiosensitivity, effects of vitamin A, 16: 32788
radiosensitivity of skin, effects of dose fractionation, 17: 15662
radiosensitivity of germ-cells in, 19: 36026
radiosensitivity of, effects of conditioning exposure on x, 20: 40605 (AD-635735)
radium-226 distribution in skeleton of, 18: 29299
radium-226 distribution in tissues of, 20: 20385 (COO-1184-3)
radium-226 metabolism in normal and leukemic, 20: 45283(R) (COO-1184-4)
recovery from radiation injury as evaluated by split-dose technique, 20: 42996
Salmonella infections in, fed heat-treated or γ-irradiated meals, 20: 41394
secretion of injected cesium-134, potassium-42, and zinc-65 in pancreatic juice of, 19: 3835(R) (ORO-625(p.64-9))
selenium-75 metabolism in, 19: 45759(R) (ORO-631, pp 77-82)
skin lesions induced by plutonium-238, plutonium-239, or neptunium-237 in, pathology and treatment of, 17: 35312(R) (HW-76000(p.149-55))
strontium titanate metabolism in, tracer study of, 18: 41034(R) (HW-80500(p.100-1))
strontium-90 and calcium in milk of miniature, effects of diet, 17: 19796
strontium-90 effects, research program, 16: 7421 (HW-SA-2365)
strontium-85 metabolism by, 20: 12588(R) (AD-626320)
strontium-85 retention in, 20: 42739(R) (COO-1339-3)
strontium-89 metabolism in, 18: 38775(R) (ORO-624)
strontium-89 metabolism by, 19: 3835(R) (ORO-625(p.64-9))
strontium-90 content in bones of, 18: 33240
strontium-90 effects on miniature, dietary, 17: 13955
strontium-90 ingestion by miniature, biological effects of, 18: 41033(R) (HW-80500(p.83-99))
strontium-90 metabolism in, after chronic ingestion, effects of dietary calcium on, 19: 40328
strontium-90 metabolism as phytate or chloride in, 20: 35215
strontium-90 metabolism by bones in, dietary effects on, 17: 13940
strontium-90 uptake by, compared with calcium, 18: 31104
strontium-90 uptake by skeleton in miniature, age effects on, 18: 19539
tellurium-127 metabolism in, 19: 45759(R) (ORO-631, pp 77-82)
toxic effects of chronic ingestion of low levels of strontium-90 by, 17: 40482 (HW-SA-3085)
toxic effects of strontium, 16: 18752
toxic effects of strontium-90, radium-226, and plutonium-239 in miniature, 17: 35288(R) (HW-76000(p.1-10))
tumor incidence in newborn, 20: 32967(R) (ORO-648, pp 36-55)
tungsten-185 metabolism in, 20: 32907(R) (ORO-648, pp 62-70)
zinc-65 metabolism in blood cells of, effects of dietary calcium, zinc, and fats on, 19: 45759(R) (ORO-631, pp 77-82)
zinc-65 secretion by pancreas of, hormonal effects on, 18: 38775(R) (ORO-624)

SWITCHES

see also Relays

accuracy of strain-gage, 18: 35060(R) (ANL-6904)
breakdown of spark gaps, optical method for monitoring, 19: 22682
circuit analysis for, computer program for, 18: 6553 (LAMS-2986)
circuits for use as reactor safety devices, 16: 3816 (CEA-1858)
contact resistances in, current feedback amplifier for elimination of, 19: 2570 (BNL-7546)
contacts of rotary, wear characteristics of sliding, 19: 35871 (SC-DC-64-2086)
contamination in sealed, during fabrication, 19: 24647
description of fast-opening, using magnetically broken foils, 17: 36136(P)
description of fast high-current, with linear timer for heating graphite filament to high temperatures, 19: 30482 (BNL-9241)
description of transistorized fail-safe high-low trip, 18: 20292
description of triggered spark-gap type, 0.1 to 50 kv, 16: 19633
design and development of broadband ferrite, 17: 35260(R) (TID-19135)
design and development of a-c and d-c circuit breakers and d-c engine contactor for space nuclear electric systems, 18: 10346(R) (X64-11113)
design and development of radiation sensitive, 20: 9229
design and operation of stable electronic integrator, for use with monopolar signal, 16: 17169
design and operation of acceleration-responsive, 17: 30843(P)
design and performance for analyzing pulse-height distributions, 16: 17836
design and performance of parallel cryotron, 17: 10927
design and performance of simple air-gap, 17: 36122 (TID-17758)
design and performance of computer, using superconductive transitions, 17: 37454
design and performance of parallel cryotron, 18: 36522
design and performance of crowbar, for Pharos, 20: 10117 (CONF-650512, pp 57-62)
design and performance of ignitron, 20: 9216 (CONF-650512, pp 44-7)
design and performance of repetitive electronic, for pulse-type radiation counters, 20: 9259
design and performance of thin film superconducting cryotron, 20: 13048
design and performance of radiation-sensitive, 20: 37062
design and performance for Astron fast pulser, 20: 46830 (UCRL-70021)
design and properties at 0.15 to 0.5°K of lead thermal, 16: 8955
design and testing of, for fast 100,000-joule capacitor bank, 17: 19464(R) (TID-18439)
design for analog-to-digital converter, 18: 35811 (RISO-80)
design for capacitor banks, analog system for, 20: 34695 (IPP-4/29)
design for caulked cusp devices, (E/T), 19: 12637(R) (LA-3202-MS)
design for connecting thermocouples to measuring instrument, 16: 31952(P)
design for fast electric discharge, 19: 34459(P)
design for high-frequency tank circuit excitation, 18: 9447 (63-RL-3307E)
design for high-speed operation, 17: 12548(P)
design for high-current d-c systems, 18: 13981 (IDA/HQ-63-1412(Vol.I))
design for high-voltage spark gaps, 20: 13027 (IPP-4/24)
design for inductive energy storage devices, 18: 15039 (IDA/HQ-63-1412 (Vol.I)(p.76-9))
design for inductive energy storage system using ignitrons, 18: 31693 (MATT-264)
design for operation under weightlessness, 18: 35259(P)
design for power transfer to plasma devices, 17: 38376 (LRP-1-63)
design for precision trigger circuit, 18: 7339 (ISS-63/40)
design for pulsed magnet uses, 16: 27785
design for railway system using radioisotopes, 17: 30181
design for rapid discharge of high-energy capacitors, 17: 4782
design for rate meter emergency supply, 16: 4361(P)
design for space nuclear electric systems, 20: 20986(R) (N-65-29823)
design for space vehicles, relations with mission, 17: 29859(R) (NP-12888(Vol.3))
design for use near power plants of nuclear carriers, (E), 19: 6871 (RTD-TDR-63-3062)
design for 100-kjoule pulsers, 20: 27227 (BNL-10214)
design of actuator, for electrically operable device, 17: 29066(P)
design of automatic electronic, 16: 20773
design of bypass, for reactor scram relays, (E), 19: 38089 (DP-926)
design of circuit for high-speed, 17: 18586(P)
design of crowbar, with wide operating range, 20: 34694 (IPP-4/28)
design of cyclical, 17: 4657(P)
design of electronically operated, engineering drawings for, 19: 44359
design of exploding-wire-triggered solid dielectric, for crowbar and series operation, 18: 10343 (SIT-P78)
design of explosively actuated, for Astron fast-pulse system, 20: 46832 (UCRL-70030)
design of fast-acting high-current, 16: 17219(P)
design of fast and slow Mjoule, 17: 15038
design of fast-acting, with vaporizable wire, 20: 27255(P)
design of ferrite decoupled crowbar sparkgap, 20: 34697 (IPP-4/32)

design of fluid, for use in coolant-monitoring operations, engineering drawings for, 18: 6426
design of, for railway systems using radioisotopes, 17: 30182
design of gas-triggered pinch-discharge, 19: 6806
design of high current and voltage spark gap type, 16: 13368(P)
design of high-power gaseous-discharge duplexer, 17: 13626 (RADC-TDR-62-352)
design of high-voltage plasma, 17: 18239
design of high-current reversing, 20: 33616(P)
design of ignitron-capacitor assembly with low inductance, 18: 18162
design of light-activated semiconductor, (E), 19: 15827 (ORNL-TM-1032)
design of low-inductance and small jitter time, 20: 46815 (JUL-374-PP)
design of mercury-jet, for Levitron pinch devices, 20: 46827 (UCRL-70014)
design of multiplexers, for use with self-powered neutron flux detectors, 19: 40866 (AECL-2217)
design of omnidirectional, responsive to reduced gravimetric acceleration levels, 19: 6903(P)
design of rapid electronic, 16: 27395(P)
design of relay, connected with solenoid for electric energy storage, 19: 46475 (AD-612113)
design of rotary contact, 19: 31657(P)
design of sequential, 18: 7022(P)
design of shockproof magnetic reed, 16: 10144(P)
design of spark gap, for capacitor bank, 17: 3098
design of spark-gap, for minimized noise, 17: 20770
design of superconductive, 18: 37496(P)
design of thermal relay device, 17: 18248(P)
design of transistorized, for Kalousek polarography, 19: 24479 (AAEC/TM-279)
design of trigger system, for Stanford Linear Accelerator, 19: 30888 (SLAC-35)
design of vacuum spark gap, 18: 22947 (PAN-472/XVIII)
design of 30-channel PAM electronic commutator, 19: 10685 (SC-TM-64-58)
development and testing of, for space uses, 18: 33828(R) (NASA-CR-54059)
development for automation of physical experiments, control program for, 18: 18274 (ZFK-WF-7)
development for computer uses, summary, 18: 4156(R) (TID-19721)
development for computers, 20: 31645(R) (AD-627094)
development for ion engine electric systems, 18: 18135(R) (NP-13750)
development for magnetic mirror machines, 20: 8181(R) (LA-3434)
development for nanosecond circuits, 18: 29938
development for nuclear space power systems, 20: 18851(R) (N-65-26627)
development for nuclear-electric space power systems, 20: 25278(R) (N-66-15788)
development for reactor safety, 16: 7685(R) (GEMP-70)
development for Stanford linear accelerator modulators, 17: 42015(R) (SLAC-18)
development for thermonuclear reactors, (E), 19: 33420(R) (LA-3320 (p.104-7))
development of air-gap, 17: 22726(R) (SIT-P91)
development of circuitry for high-speed, 17: 10918 (UCRL-9035(Rev.))
development of decade tunnel diode, 18: 29940
development of electric, for space nuclear electrical systems, 19: 30487(R) (NASA-CR-54247)
development of electric switchgear for nuclear space power systems, 20: 25225(R) (N-65-35969)
development of fast transistorized, summary, 17: 36868(R) (GEMP-78)
development of fast 100-kv, 1-Mamp, solid dielectric, 20: 9219 (CONF-650512, pp 77-90)
development of high-speed transistor, 16: 25581 (UCRL-6012-T(Rev.1))
development of high-speed transistorized, 17: 24626(R) (GEMP-76)
development of high-power cyclotron resonance, 19: 46708(R) (AD-611560)
development of ignitron, 17: 19465(R) (UCRL-10607)
development of low-inductance, 17: 31568 (CONF-24-12)
development of slow expansion system for betatron, 18: 30361
development of solid-state static, 16: 11189(R) (APEX-666(Pt.1))
development of solid-state, 16: 30011(R) (GEMP-73)
development of spark-gap trigger system, 18: 37538
development of static circuit using solid-state devices, 19: 26630 (GEMP-300)
development of superconducting thin-film, 18: 26477
development of superconducting, for magnetic energy storage systems, 18: 26493
development of superconductive, book, 18: 36438
development of superconducting thin film cryotrons, 20: 30258
development of superconductive threshold, for logic circuits, 20: 32311 (ORO-2430-27)
development of transistorized, for reactor instrumentation, 17: 17411(R) (GEMP-177C)
development of trigatrons for electric discharge equipment, 18: 20147
development of 10-nsec semiconductor, 19: 44346(R) (N64-30522)
development of 50-kv, 50 kj capacitor-bank, 17: 22726(R) (SIT-P91)
discharge growth in ignitrons, 17: 24060 (UCRL-6635)
electric, development of high-speed transistorized, 17: 7542(R) (GEMP-75)
electric reliability of sealed, for nuclear weapons, 19: 28484
electron tube for high-power, development of deuterium-filled, 18: 16167
materials of rotary, wear characteristics of plated coatings as, 19: 42216 (SC-DR-65-269)
performance and stability of high-speed transistor, 20: 34887 (DP-MS-66-10)
performance in power crowbar banks of Scylla IV, (E), 19: 21474 (LA-3189)
performance in power crowbar banks of Scylla IV, 20: 8181(R) (LA-3434)
performance in radiation detection instrument, 19: 32602(P)
performance of coaxial superconducting, (E), 19: 30503
performance of high-speed-switching transistor Schmitt-trigger, 19: 38303 (TID-21898)
performance of ignitron in high-current pulsed applications, 17: 18236
performance of low-jitter trigatron, for use at 10 to 50 kv, 18: 14189
plasma stability in, 17: 42053 (PIBMRI-1025-62)
properties of cryotron, 20: 21012
properties of high-density plasma, 20: 6449 (AD-619370)
properties of spark-gap, 17: 34213
properties of spark gaps for condenser banks of 31 μf, 18: 32888 (EUR-1644.e)
properties of triggered spark-gap type, 17: 10455 (NP-12649)
properties of trigatrons for initial control of spark gaps, 18: 20151
radiation effects on digital circuits for, evaluation and compensation of, 17: 31044
radiation effects on micro-, 18: 8873 (NP-13505)
radiation effects on a-c and d-c circuit breakers and d-c engine contactor for space nuclear electric systems, 18: 10346(R) (X64-11113)
radiation effects on NERVA electronic components, neutron, 18: 30237 (NP-14069)
radiation effects on performance of, in telemetry electronics, 18: 33838 (RTD-TDR-63-4287(Vol.I))
radiation effects on performance of, in telemetry electronics, 18: 33839 (RTD-TDR-63-4287(Vol.II))
radiation effects on, review on, 18: 37788
radiation effects on electrical characteristics of temperature, 19: 7822 (NAA-SR-9634)
radiation effects on, fast-neutron, 19: 24880 (BMI-X-10120)
response of thermal, for magnet coil cooling system, 17: 33158(R) (ORNL-3472(p.84-106))
review of high-speed current-limiting, 18: 22208(T) (AERE-Trans-901)
sensitivity and speed of trigger circuits, 18: 10335 (EUR-430.i)
spark gap, for ringing circuit, 17: 31567 (CONF-24-11)
spark-gap for triggering intense-current, design of, 17: 30842(P)
stability of electrodeless plasma, hydromagnetic, 17: 36755 (PIBMRI-956-61)
status of silicon-controlled rectifier thyristor, 20: 16774 (CONF-650922, pp 788-96)
survey of, for Stanford linear accelerators, 17: 17317(R) (SLAC-8)
testing a-c interference effects in alarm, 18: 27755(R) (ORNL-3578 (p.78-95))
testing expansion compensator position, for SNAP-10A, 19: 2575 (NAA-SR-Memo-9883)
theory of electronic, 17: 22083(R) (TID-18478)
theory of electronic, 19: 43633(R) (NP-15354)
theory of low-level transistor, 18: 1989 (AE-121)
thermal conductivity of superconducting thermal, at 0.3 to 2°K, (E), 19: 23584
thresholds for tunnel-diode, operational definition of, (E), 20: 5700
transfer characteristics of cryotron, 20: 8027
transitions in superconducting, (T), 19: 43234
trigger design for thyratron, 17: 40164 (UCRL-6811)
trigger mechanism for snap-action, 20: 6693(P)
triggering mechanism for low-pressure spark-gap, 17: 6217
triggering of crowbar, steep voltage, 20: 34693 (IPP-4/27)
triggering of three-element high-voltage spark gap requiring zero energy, method for, 18: 8629
triggering of, timer for, 19: 2595(P)
use of rotary, in 2-Mev Cockcroft accelerator, 16: 9485
use of superconducting, energy losses in, (E), 20: 17630
use of transistorized circuit as linear gate, 18: 25798 (NAS-NRC-Pub-1184(p.121-3))
use of tunnel diodes in fast discriminating, 17: 16382 (IDO-16823)
voltage transients in capacitor, effects of, 20: 34700 (IPP-4/37)
Switchgear
see Switches

SWITZERLAND

atomic energy and radiation protection in, manual on, 19: 1986
atomic energy developments in, 18: 35082
atomic energy developments in, review of, 18: 43145
atomic energy law of 1960, review for claim of reactor insurer against the

supplier of nuclear equipment, 17: 7665
fallout monitoring in air, fish, plants, soil, and waters, 1956 to 1961, 18: 20218
fallout monitoring, 1963, 19: 44269
fallout monitoring, 1963, 19: 46612
fallout monitoring, 1963, 20: 43519
nuclear fuel and reactor production in, 20: 35044
nuclear power development in, 19: 48009
nuclear power development in, 20: 40441
nuclear power plant economic integration into existing electrical networks, 19: 24115
nuclear power use in, for electricity production, 20: 40442
nuclear reactors as source of electric energy for, economics of, 18: 31010
nuclear technology in, survey of, 17: 24650
power reactor development in, 20: 22421
radiation intensity variations at ground level in, 17: 7776
radiation monitoring, 1959 to 1961, 16: 31961
radiation monitoring of food in, 1963, 20: 7273
radiation processing of food in, review of, 20: 31628
radioactive waste disposal in, 19: 12860
radioactivity of rocks in, petrographic–microscopic study of, 20: 4157(T) (ORNL-tr-702)
radiography regulation in, 19: 32491
radioisotope applications in, 18: 41889
uranium occurrences in, 18: 1935

SYDNONES
complexes with metal chlorides, formation and properties, 18: 11528 (TID-20062)
spectra of substituted, infrared, 18: 11528 (TID-20062)

SYENITES
accessory minerals in alkaline, investigation of, 20: 45922
analysis for indium and thallium, quantitative spectrographic, 16: 18839
radioactivity of Swiss, petrographic–microscopic study of, 20: 4157(T) (ORNL-tr-702)
thorium content in Kola peninsula, geochemistry of, 18: 33797
uranites in nepheline, 20: 41173
uranium distribution in Soviet Union's Kyzyl-Ompul Mountain, 16: 2031

Sylphons
see Bellows

SYLVITES
age estimation of mineral deposits by radioargon diffusion in, 18: 6956

SYNCHROCYCLOTRONS
accelerating electrodes for, use of multiple, 19: 1120 (NASA-CR-56934(p.306-10))
accelerating system for Univ. Chicago (E), 19: 1105 (NASA-CR-56934(p.128-37))
accelerating voltage in JINR, determination of, 20: 35956 (JINR-P-2730)
acceleration cycle in, optimization of, 18: 20685
auxiliary multi-channel systems used for high-energy particle research, 16: 33248
beam acceleration at high harmonics in 10-Bev proton, 19: 11967
beam calculation for, computer program for, 18: 18503 (CERN-64-15)
beam capture efficiencies of, 20: 41533 (CERN-66-27)
beam characteristics of Harvard, 17: 18377 (TID-7652(p.523-94))
beam contamination by mesons (π^-), meson (μ^-), 16: 22889
beam control systems of 10-Bev, tuning of, 19: 11998
beam current in 680-Mev proton, increase of internal, 19: 11946
beam current of JINR, effect of electrostatic focusing on proton, 20: 37328
beam currents and space charge limit in, improvements for, 20: 15182
beam currents from JINR, electrostatic-field effects on, (E), 19: 18631 (JINR-P-1853)
beam debunching and extraction, 16: 28210 (TID-7636(p.311-14))
beam debunching in, 17: 19433
beam deflection system for CERN 600-Mev, 17: 7344 (CERN-62-25)
beam design for, meson (μ), 18: 12799 (CERN-63-35)
beam energy spread of, reduction of, 18: 26177
beam extraction from, 17: 19437
beam extraction from Carnegie, meson and proton (E), 19: 1103 (NASA-CR-56934(p.85-91))
beam extraction from Berkeley 184-in. (E), 19: 1104 (NASA-CR-56934(p.108-27))
beam extraction from 10-Bev, fast, 19: 23225
beam extraction from, regenerative, 20: 35973 (UCRL-16793)
beam extraction in, regenerative, 20: 39522
beam extraction systems for, design of modified regenerative, 17: 38320 (CERN-63-19(p.80-4))
beam extraction system for, peripheral C, 18: 36118
beam focusing in, by azimuthal asymmetric magnetic field, 17: 42024
beam for CERN, development of polarized proton, 20: 31835
beam frequencies and pulse control, 17: 11813
beam intensity and space charge limit of, method for increasing, 20: 37320 (CONF-660510-19)
beam intensity enhancement from, (E/T), 19: 4777
beam intensity in Harvard, measurement of, 18: 7362(R) (ORNL-3499 (Vol.II)(p.100-4))
beam intensity in Harvard, ionization chamber for measuring, 18: 18507 (ORNL-3505)
beam intensity of 110-in. Harwell, increase with auxiliary central dee, 17: 887 (NIRL/R/20)
beam intensity of, method for stabilizing, (E), 20: 2536 (JINR-P-2341)
beam intensity, study of increase by use of a centrally placed dee, 16: 14107 (NIRL/R/13)
beam of, proton energy distributions in internal, 18: 10707
beam orbits in, magnetic field effects on, 17: 42025
beam oscillations by peripheral cee of, excitation of, 19: 37389
beam phase oscillations in proton, stable, (T), 19: 11947
beam phase oscillations in strong focusing, effects of automatic control on, 19: 37259
beam production by proton, monoenergetic neutron (E), 19: 1108 (NASA-CR-56934(p.152-9))
beam pulse duration in JINR, method for increasing, (E/T), 20: 2548
beam pulse duration in proton, system for increasing, 20: 19298 (JINR-P-2281)
beam pulse stretcher for, design of, 18: 40101
beam separation in JINR, proton-antiproton, 20: 4496 (JINR-P-2375)
beam storage rings with nonlinear focusing for proton, 19: 11891
beam stretcher for, strong focusing ring as, 20: 39538
beam structure of JINR, measurement of, 20: 27644 (JINR-P-2657)
beams from Harvard, characteristics of proton, (E), 19: 14177 (ORNL-3722)
beams in Harvard, properties of, 18: 7361(R) (ORNL-3499(Vol.II) (p.95-100))
beams of 680-Mev, increase of pulse duration of, (E), 19: 26972 (JINR-P-1985)
characteristics and physical principles of annular, with radial sectors, 16: 23165(T) (FTD-TT-62-285)
charged-particle injection into, method for polarized, (T), 19: 28970
comparison with sector-focused, 17: 7379
construction of symmetrical, two-way, ring, 17: 11776 (BNL-767 (p.181-97))
control system for firing delay in Nevis, 17: 31077(R) (CU(PNPL)-228)
description of ring-shaped phasotron model with spiral magnetic field, 17: 15334
design and operation of CERN, 19: 35617
design and performance of annular, 16: 3756
design and performance of strong-focusing, 16: 29893
design features of, 19: 16323
design for NASA space radiation effects laboratory, 18: 1447
design modification of CERN 600-Mev, 20: 19307
design modifications of Nevis, 20: 23819 (AD-627351)
design modification for Uppsala 185-Mev, sector-focusing, 20: 39535
design modifications of NEVIS, 20: 39536
design modifications for beam improvement in Carnegie, 20: 39537
design of high-frequency free-oscillation excitation, 17: 24542
design of two-stage 300-Bev proton, with strong focusing, 17: 11768 (BNL-767(p.84-90))
design principles of relativistic, 16: 28241
detector arrangement in proton, 17: 12794(R) (ORNL-3360(p.272-80))
deuteron polarization in, resonance, 18: 10684 (JINR-P-1449)
development and focusing methods in, review of, 18: 8962
development and operation of, 17: 41555(R) (NP-13209)
development and operation of, 18: 42157(R) (NP-14228)
development of, 19: 42927(R) (NP-15281)
dosimetry at Orsay proton, 17: 22704
dosimetry of, methods for, 20: 10605(T) (NASA-TT-F-353, pp 21-54)
electric field distribution in, (T), 19: 37398
electron acceleration in annular, 16: 24866 (JINR-P-914)
electron acceleration by constant high-frequency and electric vortex fields in annular, 17: 24540
electron capture in annular, 17: 24541
hydrogen ion negative in, dissociation, 17: 7360
injector for protons, design of high-frequency, 18: 42245
ion beam extraction from, method for, 16: 1094(T) (UCRL-Trans-690)
ion injector for, design of, 19: 12031
ion orbit in, computer program for, 20: 39537
ion source design for, multicharged, 17: 2352
ion source design for, 17: 29653(P)
ion source for Carnegie (E), 19: 1103 (NASA-CR-56934(p.85-91))
ion sources for, hooded-arc, 18: 44327
magnet design for, 17: 36732
magnet parameters for, calculation of, 18: 10706
magnet pole profiles for, analytic determination of, 18: 34376
magnetic deflector system of Buenos Aires 180-cm, 16: 26373 (NP-11693)
magnetic field monitoring in 1000-Bev proton, auxiliary beam for, 19: 11889
magnetic median plane in, determination using Hall effect, 20: 17189

(CONF-650922, pp 421-7)
magnets for, pulsed, 19: 44888
materials activation and shielding in CERN, 17: 38332 (CERN-63-19 (p.157-64))
meson (μ) beam of JINR, properties of, 19: 14173 (JINR-P-1902)
mesons (μ⁻) elastic scattering in, detected by nuclear emulsion, 17: 31383
modifications to CERN, 18: 24255
operation of Columbia Univ. (E), 19: 1105 (NASA-CR-56934(p.138-42))
operation of symmetrical electron ring, 19: 11952
operation of 680-Mev, hygienic characterization of working conditions in, 16: 3284(T) (JPRS-9706(p.35-9))
operation synchronization with bubble chamber, design of system for, 16: 12581 (JINR-P-852)
operation synchronization with bubble chamber, design of system for, 16: 15708(T) (UCRL-Trans-811)
operations of University of Chicago, 16: 8760(R) (TID-14830)
oscillations in, proton capture in stable radial-phase, 18: 10683 (JINR-P-1448)
oscillator for, pulser circuit for, 17: 5418
particle accumulation in JINR 680-Mev, method for, 20: 39492 (JINR-P-2811)
particle injection into annular, 16: 26371 (JINR-P-930)
particle losses in, due to dissociation, 17: 11799 (TID-17617)
particle motion in annular, 17: 943
performance of Berkeley 184-in. (E), 19: 1104 (NASA-CR-56934 (p.108-27))
performance optimization of CERN 600-Mev, 20: 31830
properties as pulsed neutron source, 16: 14073
proton beam depolarization during initial acceleration, resonance effects on, 16: 17167
proton beam level increase in 6-m phasotron, 18: 18510
proton beam measurement in Russian 10-Bev, 16: 6033 (JINR-P-783)
proton beam properties in Russian 10-Bev, 16: 6034 (JINR-P-787)
proton beam properties in Russian 10-Bev, 16: 24871(T) (UCRL-Trans-843)
proton depolarization in, resonance, 18: 10684 (JINR-P-1449)
radiation dosimetry near, methods for mixed-field, 19: 22614
radiation dosimetry around high-energy, 20: 41206(T) (JPRS-36341, pp 10-17)
radiation hazards from, reduction of (E/T), 19: 1098 (NASA-CR-56934 (p.16-23))
radiation hazards in beam zones of, 19: 41171(T) (N64-33402)
radiation survey of heavy-particle, calculation of RBE dose from, 16: 29891
radio frequency system of proton phasotron, programming accelerating voltage amplitude of, 20: 39491 (JINR-P-2732-1)
radioactivity induced in CERN proton, buildup and decay of, 17: 22705
research program at CERN, during 1965, 20: 37308(R) (NP-16226)
research using 460-Mev, 20: 4577 (AD-618067)
review of CERN, 19: 14159
rotary condenser bearing design for, 17: 24536
rotating condenser performance for Carnegie (E), 19: 1116 (NASA-CR-56934(p.279-82))
shielding of JINR, neutron attenuation, 16: 3800
shielding of, neutron attenuation in, 17: 22700
shielding testing at Dubna proton, 18: 34374
target arrangement in proton, 17: 12794(R) (ORNL-3360(p.272-80))
theory of, with azimuthal variation of magnetic field, 17: 11772 (BNL-767(p.134-44))
use as pulsed neutron sources, 20: 46565
use for production of plutonium tracer, optimum conditions for, 18: 26169 (NP-13973)
use on-line with isotope separator for nuclear decay studies, 20: 19885

Synchrometers
see Mass Spectrometers

Synchrophasotron
see Synchrotrons

Synchroscopes
see Oscillographs

Synchrotron Radiation
see Cyclotron Radiation

SYNCHROTRONS
(Varying magnetic-field particle accelerators.)
see also Argonne Synchrotron
see also Bevatron
see also Brookhaven Alternating-Gradient Synchrotron
see also Brookhaven Synchrotron
see also Cambridge Synchrotron
see also Hamburg Electron Synchrotron
see also Harwell Synchrotron
see also Omnitron Synchrotron
see also Princeton Synchrotron
see also Saclay Proton Synchrotron
accelerating potential in, frequency modulation systems for, (E), 19: 20735 (UCRL-11807)
accelerating system for Harvard proton, design of stochastic (E/T), 19: 1107 (NASA-CR-56934(p.143-51))
acceleration and magnetic systems of electron, investigation by beam analysis, 19: 16303
achromatic inflector for, analytic investigation, 16: 4885 (CTSL-30)
background radiation near target in pulsed, 18: 42214
beam accelerating system for 70-Bev proton, 19: 11992
beam acceleration and control in 7-Bev proton, 17: 942
beam acceleration in alternating-gradient proton, voltage programming of r-f, 17: 35011
beam acceleration in Frascati, radiation from, 17: 42017
beam acceleration in, feedback networks for control of, (T), 19: 11977
beam acceleration in high-intensity cascade, stability of, (E), 19: 83211 (UCRL-11803)
beam acceleration in, design of ferrite-tuned resonators for, (E), 19: 25100 (UCRL-11801)
beam acceleration using multiple resonance frequencies in 10-Bev proton, 19: 32841
beam analysis in CERN proton, particle velocity measurements of secondary, 17: 21120
beam analyzing magnets for Frascati electron, (E), 19; 11864 (LNF-63/82)
beam behavior for increased efficiency in Saturne, 16: 28192 (TID-7636 (p.175-84))
beam betatron oscillations in, 16: 3752 (CERN-61-24)
beam bunching in strong-focusing, 18: 14680 (NP-13614)
beam calibration using incoherent visible electron radiation from, (E/T), 19: 9821
beam cluster stability in proton, (T), 19: 23221
beam collimators for, r-f separated, 20: 21468 (CERN-66-10)
beam construction at CERN, with two stages of separation, 17: 31551 (CERN-63-12)
beam contraction and current limitation in electron, 18: 726 (DESY-A2.104)
beam control design for external-injection, 17: 40151
beam control device for 7-Bev proton, 17: 913
beam control device for 7-Bev proton, 17: 914
beam control in JINR, 19: 32844
beam control in 7-Bev proton, model for analyzing, 17: 915
beam control in 7-Bev proton, equipment for, 17: 898
beam control in 7-Bev strong-focusing proton, 17: 11763 (BNL-767 (p.32-47))
beam control system for 7-Bev proton, automatic radial and phase, 17: 11764 (BNL-767(p.48-63))
beam control systems for proton, 19: 11994
beam control system for electron, development of, 19: 14172 (DESY-64/13)
beam current in 680-Mev electron, during betatron operation, (E), 19: 16319
beam current increases in electron, possibilities of, 18: 18523
beam current restrictions from limiting particle density in phase volume, (T), 20: 19302 (NP-15796)
beam currents of proton, (T), 19: 34818
beam deflection structures in CERN, waveguide coupler matching for r-f, 18: 20679 (CERN-64-14)
beam deflection system for, 18: 14667 (CEA-2342)
beam deflection system for electron, electromagnetic, 19: 30903
beam deflector design for Adone, 18: 16610 (LNF-63/72)
beam depolarization in proton, resonance, 17: 40143 (NP-13102)
beam design and performance in CERN, meson (K), 17: 23635
beam design layout for CERN, 18: 14694
beam deviation by geophysical forces on electromagnets of ITEF proton, (E), 19: 37255(T) (AEC-tr-6581)
beam distribution in 7-Bev proton, device for measuring, 17: 919
beam disturbances in alternating-gradient, control system for, (T), 19: 11981
beam ejection from CERN Proton, analysis of slow, 18: 30344 (CERN-64-25)
beam ejection from, internal, 18: 44323
beam ejection from 10-Bev proton, use of half-integral resonance for, 19: 11957
beam ejection from CERN proton, design and performance of septum magnets for fast and slow, 20: 13359 (CERN-65-36)
beam ejection from proton synchrophasotrons, slow, 20: 17208 (JINR-P-2537)
beam ejection schemes for CERN, 17: 4122 (BNL-6512(p.13-16))
beam ejection system of CERN, operation of, 17: 34901
beam ejection system for CERN proton, fast, 19: 11955
beam ejection system for JINR Synchrophasotron, (E), 20: 7671 (JINR-P-2387)
beam ejection system for CERN, description of external, 20: 7682
beam energy in, design of device for measuring, 17: 31553 (LNF-63/38)
beam energy meter for, calibration of, 20: 19291 (CALT-68-67)
beam expansion in German DESY, 16: 33913 (DESY-A2.94)

beam extraction and properties of Frascati, review, 16: 25903 (LNF-62/37(p.142-56))
beam extraction and transport from CERN, 18: 12800 (CERN-63-37 (p.83-95))
beam extraction from CERN proton, design of special magnets for secondary, 17: 9644 (CERN-62-24)
beam extraction from, design and development of aperture kickers for fast, 17: 34996 (CERN-63-24)
beam extraction from, theory of, 17: 35001 (UCRL-10807)
beam extraction from ITEF, 18: 5887 (NP-13331)
beam extraction from strong-focusing, 18: 5894
beam extraction from CERN proton (E/T), 19: 1101 (NASA-CR-56934 (p.59-68))
beam extraction from McGill Univ. 82-in. proton (E), 19: 1112 (NASA-CR-56934(p.192-7))
beam extraction from CERN, 19: 1133
beam extraction from 1-Bev Frascati electron, resonant, 19: 25111
beam extraction from Frascati electron, (E/T), 20: 15159 (LNF-65/36)
beam extraction from INS 750-Mev alternating-gradient electron, 20: 23826
beam extraction from Frascati electron, 20: 23833
beam extraction from properties of decatum, 20: 27643 (BNL-10236)
beam extraction from proton, field nonlinearily in lenses for, (T), 20: 31836
beam extraction in strong-focusing, resonance betatron oscillations for, (T), 19: 32845
beam extraction system (300-Mev) for NASA Space Radiation Effects Laboratory 600-Mev proton, (T), 19: 1122 (NASA-CR-56934(p.323-36))
beam extraction system for CERN proton, resonant, 19: 11956
beam focusing device for, design of meson, 17: 30854 (LNF-63/35)
beam focusing in Frascati electron, apparatus for, 20: 25654 (LNF-65/48)
beam focusing system of quadrupole magnets for long straight sections of alternating-gradient, 19: 18649(P)
beam formation and acceleration in, study of, using induction electrodes, 17: 24529
beam frequency and pulse duration, methods for changing, 16: 12580 (JINR-P-849)
beam frequency and pulse duration, methods for changing, 16: 18542(T) (UCRL-Trans-813)
beam geodetic measurements for German electron, 19: 28943 (DESY-65/1)
beam-handling equipment for CERN, 16: 31945
beam handling in 7-Bev Nimrod proton, 16: 28222 (TID-7636(p.422-32))
beam injection based on resonance priming in betatron radial oscillations, 18: 14677 (LNF-63/74)
beam injection by phase-grouping in JINR, 19: 37257
beam injection in strong-focusing, method of increasing pulse current for, 16: 33922
beam injection in, energy effects in, 17: 24550
beam injection in DESY electron, 19: 32837
beam injection, magnetic inflector for, 17: 7416
beam injection system for 7-Bev proton, 17: 906
beam injection system for 300-Bev proton, alternating-gradient, 19: 11888
beam injection system for, design of, 19: 16307
beam injection systems for 200-Bev proton, design, (E), 19: 20737 (UCRL-11955)
beam injector for 70-Bev proton, design of linac, 19: 11932
beam injector for CERN proton, performance of linac, 19: 11935
beam injector for 280-Mev, microtron, 19: 12012
beam injector linac for CERN proton, r-f cross-bar accelerating structure for, 19: 26978 (MURA-714(p.1-20))
beam injector linac for CERN proton, performance of, 19: 26996 (MURA-714(p.353-61))
beam injector linac for CERN proton, cavity tuning of, 19: 26969 (CERN-65-9)
beam injector synchronization for 300-Bev, for r-f systems, 18: 24240 (CERN-64-20)
beam injectors for proton, adjustment of linac, 19: 9832
beam injectors for proton, linear accelerator as, 19: 11934
beam injectors for, high-current linac, 19: 12015
beam instability thresholds in weak-focusing proton, longitudinal, (T), 20: 21471 (PPAD-577D)
beam intensity and quality from CERN proton, factors affecting external (E/T), 19: 1099 (NASA-CR-56934(p.24-34))
beam intensity enhancement from proton, injection regime for, 19: 42961 (JINR-P-2266)
beam intensity measuring system for 7-Bev, 17: 918
beam intensity of, program for increasing, 20: 21466 (CERN-65-32, pp 127-30)
beam intensity stabilization in, 19: 37404
beam layout and experimental buildings for 300-Bev proton, 19: 11958
beam loading of electron, dependence of shunt resistance on, (T), 19: 27043
beam losses from cross-mode oscillation in r-f acceleration of CERN 600-Mev proton (E), 19: 1097 (NASA-CR-56934(p.3-15))
beam losses in proton, nonlinear resonance effects on, 19: 11975
beam measurement in, proton-induced reactions used for, 18: 11224
beam momentum measurements in ITEP, proton, 20: 5941 (NP-15598)
beam monitoring system for CERN, design of, 20: 19292 (CERN-66-5)
beam motion in strongly focusing waveguide, (T), 19: 14188
beam optics of CERN, 17: 18514 (CERN-63-3(p.49-68))
beam orbit straight section for, design of, 20: 4512 (UCRL-16243)
beam oscillations in strong-focusing electron rings of CERN, damping of radial betatron, 16: 28199 (TID-7636(p.222-6))
beam oscillations in 7-Bev proton, 17: 941
beam oscillations in, mathematical analysis of, 17: 9630 (BNL-6420)
beam oscillations in, nonlinear resonance of radial betatron, 18: 727 (JINR-R-1331)
beam oscillations in alternating-gradient, 18: 4365 (NP-13345)
beam oscillations under space charge conditions, (T), 19: 11987
beam oscillations in, betatron, (T), 19: 30900
beam oscillations in AdA storage ring, damping of betatron, (T), 19: 34807 (LAL-1124)
beam phase stability in automatically controlled, (T), 19: 16305
beam polarization in, (T), 19: 11988
beam production at CERN, neutrino, 18: 26165 (BNL-837(p.91-113))
beam production at 0.6 to 1.2 Bev/c in CERN, (E), 19: 28940 (CERN-65-2)
beam production in CERN, secondary, 16: 28227 (TID-7636(p.459-67))
beam profile measurements using photographic plates, 20: 19289 (CALT-68-20)
beam profile monitoring system for CERN, (E), 19: 4518
beam resonance depolarization in proton, 19: 11989
beam screening of ITEP proton, effects on operation of, 19: 44879(T) (AEC-tr-6607)
beam separation in CERN, electrostatic, 19: 11962
beam separator for CERN proton, testing of r-f, (E), 19: 20748
beam separator for, servo correction of phase changes between deflectors in, 20: 21467 (CERN-66-8)
beam separators for, r-f, 19: 11968
beam separators for proton, high-voltage performance of, 20: 44045(T) (NP-tr-1419)
beam separators in Dubna proton, electrodynamic, 19: 11966
beam separators in CERN, electrostatic, 19: 11964
beam shifting to internal target in electron, 19: 12025
beam space-charge effects in proton, transverse, 18: 10723
beam space-charge compensation of proton, dynamic quadrupoles for, (T), 19: 34803 (CERN-65-18)
beam stability in, effect of space charge on, 17: 22673
beam stability in storage rings of, effect of space charge on, 17: 22675
beam storage in, 19: 11915
beam storage in electron, factors affecting, (E), 19: 14182(T) (SLAC-Trans-13)
beam storage rings for CERN proton, intersecting, 19: 11910
beam storage rings of CERN proton, r-f systems for, 19: 11911
beam storage rings for CERN, design of electron, 19: 11913
beam storage rings for CERN electron, ultrahigh vacuum for, 19: 11914
beam storage rings for, space-charge effects in electron-positron, 19: 11920
beam storage rings for, injection systems for electron-positron, (T), 19: 11922
beam stretching by excitation of radial oscillations in proton, internal meson (π) (E), 19: 1117 (NASA-CR-56934(p.283-9))
beam switching magnets for, design of nsec ferrite-core, (E), 20: 939 (UCRL-16364)
beam synchrotron light emission in NBS 180-Mev electron, (E), 19: 11871
beam systems in, obtention of two simultaneously stable, 16: 32455 (CERN-62-12)
beam tracking and matching, computer program for, 17: 15321 (NIRL/M/21)
beam transport arrangement for CERN, design and performance, 17: 23638
beam transport magnets of CERN proton, 20: 17183 (CONF-650922, pp 218-38)
beam transport systems in CERN, calculations for, 17: 18513 (CERN-63-3(p.27-47))
beam transport systems for, computer program to optimize magnets in, 17: 23636
beam transport system for CERN proton, 18: 40085 (CERN-64-35)
beam transport system for NASA 600-Mev proton, 19: 1121 (NASA-CR-56934(p.311-22))
beam transverse oscillations in, equations for, 19: 16306
beam-separator development at CERN, r-f, 19: 25109
beams from CERN, production of antiproton and meson (K^-), 19: 41184
beams of, design and performance of separated, 17: 9645 (CERN-62-26)
beams of, design of CERN d-c separators, 17: 4134 (BNL-6512(p.72-5))
beams of, efficient use of CERN, 17: 4123 (BNL-6512(p.17-23))
beams of, matching of external to targets, 17: 4125 (BNL-6512(p.29-31))
beams of, separation of mesons (K^+), 18: 2504

beams of, small production angles in, 17: 4124 (BNL-6512(p.24-8))
betatron oscillations in, measurement of, 17: 921
betatron oscillation resonances in, 20: 17221
betatron-injector synchronization with, 18: 16624
book: *The Electron Synchrotron of the Frascati Laboratory*, 17: 15341
bremsstrahlung beam production by inherent r-f bunching in electron, 16: 28225 (TID-7636(p.445-51))
bremsstrahlung beam from 700-Mev electron, alignment, 19: 23228
bremsstrahlung energy measurements, 16: 12595
bremsstrahlung production in, calorimeter for measuring energy of, 17: 41268
bremsstrahlung production in, 19: 9827
bremsstrahlung spectra of 500-Mev electron, 19: 30898
bubble chamber and data processing device for 12-Bev proton, 19: 24853
bubble chamber experiments at CERN proton, 18: 20400
bubble chambers for 10-Bev JINR, combination of, 19: 42970
cavity resonators for proton, r-f system for, 19: 11991
characteristics, construction, and design of Italy's 1100-Mev electron, 17: 15341
circuitry for Frascati electron, design, (E), 19: 11865 (LNF-64/45)
component handling systems for 200-Bev, design of shielded, (E), 20: 2542 (UCRL-16236)
computer datalink for CERN PS, 18: 32309 (CERN-64-30(p.245-9))
computer use on-line in photoproduction experiments for electron, 18: 32308 (CERN-64-30(p.31-9))
construction and operation of 30-Mev, at Institute of Physics USSR, 19: 9822
construction status of Frascati electron, 19: 39327
control and monitoring of Cornell 10-Bev electron, multiplex system for, 19: 37268
control of 200-Bev proton, computer, 20: 11401 (UCRL-16502)
control system, geodetic problems, magnet power supply, and vacuum systems of CERN proton, 16: 24865 (CERN-62-3)
coupling of h-f cavities to proton positions in, nonlinear technique for, 20: 41547
data analysis from CERN proton, using on-line Mercury computer, (E), 19: 26968 (CERN-65-5)
deflectors for Adone storage-ring, design and performance of, (E/T), 19: 34809 (LNF-64/68)
description and beam characteristics of Tokyo 24-Mev electron, 17: 19431
description of CERN proton, general, 17: 15336
description of CERN, and its targets, 17: 18512 (CERN-63-3(p.17-25))
description of large Russian proton, 18: 28193
description of 100-Mev linac injector for 70-Bev USSR, 18: 22623 (TID-7691(p.396-403))
description of 200-Bev proton, employing separate function magnet lattices, 20: 39480 (BNL-10508)
description of 7-Bev Nimrod proton, 16: 18546
design and development of 6-Bev electron, 19: 11902
design and development of 6-Bev electron, 19: 11904
design and development of 140-Mev PTB electron, 20: 25669
design and operational experiments at CERN proton, 16: 25917 (NP-11977(p.2-5))
design and operation of CERN, 16: 31928
design and operation of CERN proton, 19: 35617
design and operation of B-ZM, for storage ring injection, 20: 23825(T) (SLAC-Trans-34)
design and performance, 16: 2567(T) (AEC-tr-4141(p.33-78))
design and performance of Soviet 7-Bev proton, 16: 11062
design and performance of 660-Mev electron, 18: 4381
design and precision of CERN proton, 17: 15331
design and testing, 16: 26376(T) (FTD-TT-61-242)
design concepts for ultra-high energy, 16: 28189 (TID-7636(p.145-54))
design considerations for 300-Bev, use of storage rings, 17: 20587 (UCRL-10022(p.214-19))
design criteria for superconducting electron, 19: 37397
design features of, 19: 16323
design for acceleration of positive and negative ions to 10^9 ev, with subsequent collision, 19: 34830(P)
design modifications of 1.3-Bev electron, 20: 23818(R) (AD-627324)
design of alternating-gradient electron, with super-period structure, 16: 28198 (TID-7636(p.217-21))
design of alternating-gradient, to be constructed at Saclay, 17: 2351
design of beam transport system for CERN, 17: 4143 (BNL-6512 (p.162-9))
design of Cornell 10-Bev electron, 19: 11906
design of DESY electron, 19: 30893
design of drift tube arrangement, 16: 27181(P)
design of electron, 17: 19409 (BNL-772)
design of Frascati electron, 17: 5416
design of Frascati, 20: 27662
design of Italian Adone, 18: 28192
design of Omnitron, for light and heavy ions, 20: 29857 (UCRL-16839)
design of proton storage rings for CERN, 16: 25918 (NP-11977(p.5-20))
design of proton, for Space Radiation Effects Laboratory (E/T), 19: 1119 (NASA-CR-56934(p.300-5))
design of strong focussing magnets for, 16: 6031 (DESY-A2.82)
design of 4- to 6-Bev electron, 17: 11766 (BNL-767(p.66-74))
design of 5- to 25-Bev high-intensity alternating-gradient proton, 16: 28190 (TID-7636(p.155-9))
design of 7-Bev proton, 16: 24872
design of 7-Bev proton, 17: 895
design of 7-Bev proton, 19: 9810
design of 10-Bev, 16: 25929 (NP-11977(p.78-80))
design of 10-Bev electron, at Cornell, 20: 41568
design of 12-Bev proton, 16: 7179 (CEA-tr-X-398)
design of 12-Bev proton, 16: 28183 (TID-7636(p.65-9))
design of 15-Bev proton, 16: 25919 (NP-11977(p.20-31))
design of 15-Bev proton, for use as injector, 17: 11767 (BNL-767 (p.75-83))
design of 50- to 70-Bev proton, 17: 11765 (BNL-767(p.64-6))
design of 200-Bev proton, 19: 9775(R) (UCRL-11466)
design of 200-Bev proton, 19: 25265(R) (UCRL-11776)
design of 200-Bev strong-focusing proton, 19: 44873 (UCRL-16000 (Summ.))
design of 200-Bev proton, 20: 2543 (UCRL-16238)
design of 300-Bev proton, 19: 11887
design of 500-Bev proton, 17: 11767 (BNL-767(p.75-83))
design of 500-Bev, 18: 4366 (NP-13352)
design of 30-Mev electron, 18: 736
design of 100-Mev electron, 18: 30365
design of 192-Mev Uppsala proton (E), 19: 1102 (NASA-CR-56934 (p.69-74))
design of 680-Mev, for USSR Institute of Physics, 16: 33921
design of 1200-Mev electron, 18: 37822
design studies for 200-Bev, 19: 30889 (UCRL-16020)
design study of 200-Bev proton, 19: 37254 (UCRL-16000(Vols. I and II))
design study of 300-Bev proton, 18: 26170 (UCRL-10869)
design using iron-free magnet, 19: 37402
design using 450-Mev linac as injector, preliminary study of, 18: 10692 (LNF-63/47(p.239-47))
detector development for CERN proton, dE/dx plastic scintillation-type, 18: 23993
development and focusing methods in, review of, 18: 8962
development and improvement of CERN proton (E), 19: 1100 (NASA-CR-56934(p.35-58))
development and operation of Brookhaven AGS and CERN, conference on, 17: 4120 (BNL-6512)
development and operation of CERN proton, 17: 41555(R) (NP-13209)
development and operation of CERN proton, 18: 20693
development and operation of CERN proton, 18: 42157(R) (NP-14228)
development at CERN, 19: 27029
development in Britain, 18: 44334
development in Western Europe, 18: 20697
development of CERN, injection equilibrium orbit plans, 17: 4132 (BNL-6512(p.57-61))
development of CERN proton, status of, 19: 11892
development of CERN proton, 19: 42927(R) (NP-15281)
development of CERN proton, 20: 11404
development of Cornell 10-Bev strong-focusing electron, 19: 39327
development of electron, worldwide, 17: 32917 (TID-7668(Sect.IX))
development of electron, 19: 37395
development of French 60-Bev proton, 19: 11897
development of high-energy proton, 18: 20696
development of Lund 4-Bev strong-focusing electron, 19: 39327
development of NINA 4-Bev electron, 20: 41535 (DNPL-1)
development of NINA 4-Bev electron, 20: 41536(R) (DNPL-2)
development of proton, 17: 23627
development of pulsed, review of, 19: 47163 (BNL-9504)
development of r-f beam separators for CERN, 17: 4136 (BNL-6512 (p.94-8))
development of r-f system for 12-Bev Japanese proton AG, 18: 32318 (PPAD-512D)
development of Serpukhov (60 to 70)-Bev, status of, 19: 11896
development of University of Glasgow 4-Bev strong-focusing electron, 19: 39327
development of zero gradient, use of network analysis techniques in, 16: 19007 (ANL-6557)
development of 12-Bev proton, in Japan, 18: 18517
development of 300-Mev, 16: 32454 (60-RL-2345E)
development of 4-Bev electron, 17: 34998(R) (NP-13002)
development of 4-Bev electron, 18: 18506(R) (NP-13787)
development, survey, 16: 31126 (BNL-741)
efficiency of smooth decelerating systems in waveguide, (T), 19: 14187
electromagnet excitation in, stabilization of, 19: 12035
electromagnetic field control system for proton, automatic, 19: 12027
electromagnetic radiation emission by electrons in, 17: 6792(R) (ISS 62/14)
electron acceleration, capture theory, 16: 26384(T) (FTD-TT-61-242

(p.54-110))
electron acceleration in, noncoherent radiation from, 18: 735
electron beam injection in, design of 6.5-Mev microtron for, 17: 26649
electron beams separation from 30-Mev, 16: 28172 (AERE-Memo-G/M-117)
electron bunch size on magnetic cycle of C-25 FIAN, 16: 26395
electron capture in, mechanism of, 17: 26655
electron clusters in, dimension changes during acceleration, 16: 1097
electron energy stabilization in 30-Mev, 18: 738
electron injection in, time control of, 18: 42237
electron injection systems for, transistor integrator for, 18: 42238
electron losses in, effects of wall-coating resistance on, 17: 41290
electron, operation of Tokyo Bev, 16: 33923
electron oscillations, measurement by rapid photography, 16: 17171
electron oscillations in cluster in, 16: 18547
electron oscillation damping constants in, effect of nonlinear radiated energy expressions on, 17: 11787 (LNF-62/96)
electron oscillations in, electrodynamic, 18: 24264
electron oscillations in, 18: 24265
electron phase oscillations in high-current, 18: 42207 (DESY-64/4)
electron radiation in, study of coherent, 17: 11770 (BNL-767(p.100-5))
electron synchrotron radiation in Frascati, 18: 7339 (ISS-63/40)
electrostatic separator for CERN, 17: 23630
emulsion irradiation in CERN, general problems of, 17: 18517 (CERN-63-3(p.95-102))
emulsion irradiation in CERN, technical problems connected with, 17: 18518 (CERN-63-3(p.103-10))
energy stabilization circuit for measurement of yield curve, 16: 15710
equipment and techniques associated with, at ultra-high energies, 17: 23626
experimental facilities at Frascati, 20: 2521 (LNF-65/28)
experimental facilities of 200-Bev proton, for neutrino beam production, (T), 20: 11398 (UCID-1008)
experimental programs for 1000-Bev and high-intensity 30-Bev, 18: 16584 (BNL-7534(p.39-48))
experimental program at DESY, survey of, 19: 23216
experiments at CERN proton, use of spark chambers in, 18: 20401
experiments at CERN proton, with neutrinos, 18: 40375
frequency control in, equipment for, 17: 910
gamma production by, calibration of energy in, 17: 5347
general alarm system of CERN, 18: 16605 (CERN-64-7)
generator design for frequency modulation in 7-Bev proton, 17: 908
high-energy particle production, data from CERN, 16: 28179 (TID-7636 (p.15-22))
injection in 1-Bev, performance of linear betatrons for, 16: 2577
injection methods to get high beam intensity in 300-Bev, 17: 20586 (UCRL-10022(p.204-13))
injection system for CERN, slow-cycling synchrotron, 20: 27659
injection yield in Adone storage ring, (T), 19: 34810 (LNF-65/5)
injector design for 1-Bev, linac, 16: 7185
injector design for 7-Bev, electrostatic, 17: 901
injector design for, 40-Mev electron linear, 17: 5415
injector design for zero gradient proton, 17: 7310 (BNL-6511(p.7-18))
injector development for 1-Bev, 6-Mev linear accelerator, 16: 6038
injector for 100-Mev FFAG electron, at Berlin, 18: 30346 (NP-13982)
injector linac design for, 200-Mev proton, 18: 32315 (NIRL/R/55)
injector linac for CERN proton, failures of voltage generator in, 20: 7675 (MPS-INT.LIN-62-5)
injector vacuum system for ZGS, 17: 7339 (BNL-6511(p.318-22))
ion injector power supply for 7-Bev proton, 17: 907
leveling systems for 200-Bev, design of hydrostatic, (E), 19: 20733 (UCRL-11799)
linac injection in 1.3-Bev electron, 16: 28219 (TID-7636(p.401-5))
magnet alignment scheme for, 17: 11786 (CTSL-36)
magnet assembly and positioning in 1-Bev electron, 16: 9472 (INSJ-46)
magnet calibration and compensation for, 17: 929
magnet characteristics in, determination of, 17: 934
magnet characteristics in proton, assembly for measuring, 17: 927
magnet characteristics for NIMROD, effects of saturable fins on, 17: 31555 (NIRL/R/33)
magnet circuit design for 7-Bev proton, 17: 932
magnet coils for 4-Bev electron, design and fabrication of, 20: 17199 (CONF-650922, pp 686-99)
magnet computer codes for, 19: 28965 (UCRL-11798)
magnet costs for 200-Bev alternating-gradient, (T), 19: 20734 (UCRL-11800)
magnet current stabilizer for, design of multichannel, 20: 31837
magnet design for 7-Bev proton, 17: 897
magnet design for 7-Bev proton, 17: 924
magnet design for Cornell electron, 19: 39327
magnet designs for 200-Bev proton, quadrupole and sextupole, 19: 44878 (UCRL-16375)
magnet excitation stabilization, 17: 19434
magnet for Cornell electron, design of guide field, 19: 11905
magnet installation in 7-Bev proton, 17: 904
magnet parameters for 7-Bev proton, 17: 896
magnet pole face shape design for 300 Bev, 19: 37311
magnet pole face windings for German Electron Synchrotron (DESY), 16: 26370 (DESY-A1.9)
magnet pole face windings in Todai AG, 20: 5952
magnet pole shoe form and field exponents of, 17: 35010
magnet pole windings for U-7 ITEP proton, six-field compensating, (E/T), 19: 32829 (NP-15056)
magnet power supply for, use of ion inversion transformer as, 19: 37425
magnet power supplies for proton, 20: 17202 (CONF-650922, pp 755-68)
magnet power supplies for, flat topping of, 20: 19303 (PPAD-581D)
magnet power supply for BSB, design of, 20: 27648 (NP-16009)
magnet support for electron, design of pneumatic, 19: 23219
magnet testing for 10-Bev, 16: 24877
magnet testing, power supply system for, 17: 933
magnetic field asymmetry in 7-Bev proton, 17: 926
magnetic field changes in proton, measurement of, 17: 939
magnetic field compensation in 7-Bev proton, 17: 925
magnetic field configurations in 7-Bev proton, 17: 935
magnetic field configuration in, device for measuring, 17: 938
magnetic field corrections in proton, 17: 937
magnetic field distribution and pole face shape for 10^{12}-ev proton, (T), 19: 11986
magnetic field errors at low field, 16: 17164
magnetic field in 7-Bev proton, vacuum chamber effects on, 17: 936
magnetic field measurements for 48 magnets for, 16: 8247 (TID-13720)
magnetic field measurements using coil and integrator, 16: 14104 (DESY-A2.84)
magnetic field measurements in proton, assembly for, 17: 928
magnetic field measurements in 7-Bev proton, equipment for, 17: 909
magnetic field measurements in strong-focusing, (E), 19: 30901
magnetic field of, induction apparatus for measurements of, 17: 30817
magnetic field of 100-Mev FFAG electron, at Berlin, 18: 30348 (NP-13987)
magnetic field properties of BSB, measurement of, 20: 27649 (NP-16011)
magnetic field variations between cycles, 17: 931
magnetic fields for 1-Bev, 17: 883 (INSJ-50)
magnetic fields in elliptic vacuum chambers of, calculations for, 20: 37318 (BNL-10436)
magnetic guide field in, space and time dependence of, 17: 21127
magnetic screening in ITEF proton, effects on operation of, 19: 41168 (NP-15253)
magnets for CERN, excitation by short pulses, 20: 15157 (CERN-66-1)
magnets for strong-focusing 7-Bev, parameters, magnetic measurements, and field correction methods for, 17: 11762 (BNL-767(p.1-31))
magnets for 300-Bev, H-type, 19: 12005
magnets for, triggering parallel ion inverters for, 19: 37424
meson (μ) channel design for Univ. Chicago proton, (T), 19: 1114 (NASA-CR-56934(p.237-63))
meson (μ) channel performance for Univ. Chicago proton, (E), 19: 1115 (NASA-CR-56934(p.264-78))
meson (μ) production in, beam layout calculations for, 19: 28955 (LA-DC-6757)
meson (π) beam shaping in, electromagnetic lenses for, 19: 23223
meson (K^-) beam transport in CERN, 17: 18516 (CERN-63-3(p.81-93))
meson(μ) and meson(π) beams in, computer program for calculating, 18: 2496 (CERN-63-30)
meson (μ^-) beam production in CERN, 16: 31944
need for construction of 300-Bev proton, in Europe (CERN), 17: 40150
neutrino beam production in CERN, equipment for, 17: 23637
neutrino beam production in CERN, equipment for, 19: 1134
neutrino beams from 200-Bev proton, (T), 19: 20738 (UCRL-11983)
neutrino flux in CERN, focusing system for increasing, 19: 37244 (CERN-65-17)
neutrino production in CERN proton, (E/T), 19: 12003
neutrino yield from high-energy proton, estimate of, 18: 32320 (UCRL-10948)
neutron dosimetry on 10-Bev, 19: 39315 (JINR-P-2177)
neutron dosimetry methods for Nimrod, 20: 41543 (RPP-R-2)
neutron energy and flux around Frascati, skyshine, (E), 19: 20741
neutron energy spectrum in Frascati, 16: 19828
neutron spatial distribution around 10-Bev synchrophasotron, (E), 20: 11390 (JINR-P-2446)
nuclear stars in personnel photographic film detectors at CERN, 18: 16262
operation and experimental program at National Laboratories of Frascati, Italy, 16: 29877(R) (LNF-62/30)
operation of Cal. Tech. 1.5-Bev electron, developments for, 20: 4495 (CONF-650923-16)
operation of CERN, effects of neutrino experiments on scheduling of, 17: 4128 (BNL-6512(p.40-2))
operation of CERN, review of technical and human aspects of, 18: 5891
operation of electron, 17: 21388(R) (LNF-63/11)
operation of Frascati, 6-64 to 7-65, 20: 2521 (LNF-65/28)
operation of JINR, development of programming system for, 20: 31840
operation of Tokyo Univ. electron, 19: 16852(R) (NP-14647)
operation of Tokyo electron, 19: 39327

operation of 12-Mev, 20: 27646 (NP-115878)
operation of 7-Bev proton, 19: 11894
operation summary for Japanese electron, (E), 20: 13345(R) (NP-15772)
orbit characteristics of, effects of foundation shifting on, 17: 905
orbit control in alternating-gradient, by magnet structure displacement, (T), 19: 44875 (UCRL-16229)
orbital radiation from 750-Mev electron, measurement and uses of, 19: 16852(R) (NP-14647)
oscillations, derivation of canonical equations for, 16: 2558 (BNL-5752)
oscillations in high-energy, phase, (T), 19: 20745
oscillations in strong-focusing, calculation of damping constants of horizontal, 17: 33117 (LNF-63/18)
particle accelerators at CERN, 18: 24263
particle energy on target inside, imprecision in, 17: 22674
particle fluxes from high-energy, calculation of, 17: 20583 (UCRL-10022 (p.167-90))
particle injection into, technique for optimization of, 18: 2507
particle motion in, analog computer for studying, 17: 11773 (BNL-767(p.145-60))
particle motion in, phase-locked oscillator analog for studying, 17: 11774 (BNL-767(p.161-71))
particle motion in, stability of, 20: 39524
particle orbits in, effects of slow rotation of median plane on, 17: 17313 (LNF-62/95)
particle orbits in, solution of differential equations, 18: 41906 (CEA-R-2100)
particle oscillations in, calculation method for, 17: 922
particle production in CERN proton, low-energy, 16: 21645 (CERN-62-19)
particle production at 45 and 60° in CERN proton, 17: 795 (CERN-62-27)
particle storage system, 16: 11058
particle transverse oscillations in proton, equations for, 17: 923
performance as beam injector for 1000-Bev cybernetic accelerator, 19: 11899
performance of B-3M, as injector, 20: 33996
performance of CERN, 16: 28180 (TID-7636(p.25-38))
performance of CERN proton, 18: 28198
performance of Lund electron, 19: 39327
performance of mercury-arc rectifiers for proton, 17: 9665
performance of ring-shaped proton, 17: 9660
performance of 10-Mev electron, using dowel delaying systems, (E), 19: 25108
performance of 10-Mev waveguide, 19: 37258
personnel monitoring in environs of, performance of photographic film detectors for, 20: 4237 (BNL-9665)
phase-lock acceleration of proton, computer study of, 16: 28195 (TID-7636(p.201-5))
phase oscillations in, method for observing, 19: 6420
phase oscillations in, resonance of, (E/T), 20: 941
phase oscillations in, (T), 20: 17174 (CERN-66-6)
planning program for construction of 12-Bev proton, in Japan, 18: 18516
positioning 28-Bev CERN proton, precision surveying of ground changes in, 16: 19827
power supply and resonant magnet network for Nina 4-Bev electron, 19: 34826
power supply for CERN 28-Bev proton, 16: 26392
power supply for Italian 1000-Mev, 16: 32461
power supply for 7-Bev, 17: 899
power supply instability effects in proton, 17: 940
power supply performance in 7-Bev proton, 17: 900
power supply systems for 7-Bev proton, 17: 911
pre-injector linac for booster in 300-Bev, design of, 19: 28962(R) (NIRL/R/81)
proton beam characteristics of 10-Bev, 16: 23168
proton colliding-beam storage-ring developments for, 18: 16753 (BNL-7534(p.312-17))
proton injector linac for 300-Bev CERN, 18: 22624 (TID-7691(p.404-20))
proton source for, design of, 18: 20690
proton sources for, development of pulsed high-current, 16: 28217 (TID-7636(p.385-94))
proton storage rings for CERN, phase locking systems of, (E), 20: 2535 (CERN-65-31)
radiation control at Saturne, survey, 16: 7186
radiation control, safety, and shielding at Laboratori Nazionali de Frascati, 16: 17163
radiation dose from proton spallation in iron in high-energy, 16: 33847
radiation dosimetry near, methods for mixed-field, 19: 22614
radiation effects on interior targets in, 18: 20687
radiation emission by high-energy electrons in, polarization of, 17: 7418
radiation emission by electrons in, coherent, 18: 5888(T) (TG-230-T390)
radiation field around Saturne, reduction of, 17: 22706
radiation field outside shielded high-energy proton, 19: 42966 (UCRL-16267)
radiation from, angular distribution of, 16: 32456 (DESY-A2.90)
radiation from Frascati, lethal dose measurements on, 17: 22690
radiation from relativistic electron bunches in, coherent, 16: 29890
radiation from Saturne, simultaneous dose and dose rate measurements of, 17: 22707
radiation from, quality factor for pulsed, (E/T), 20: 9610 (JINR-P-2395)
radiation hazards from, reduction of (E/T), 19: 1098 (NASA-CR-56934 (p.16-23))
radiation hazards from material activation in proton (T), 19: 1118 (NASA-CR-56934(p.290-9))
radiation hazards to Brookhaven personnel from stray areas around proton, LET and quality factors in, 20: 4176 (BNL-9684)
radiation levels near JINR 10-Bev, 19: 44863 (JINR-P-2231)
radiation levels near CERN proton, 20: 17212(T) (UCRL-Trans-1305)
radiation monitoring and shielding studies, (E), 20: 13367 (UCRL-16445(Rev.))
radiation monitoring of Japanese, 20: 13345(R) (NP-15772)
radiation problems in 200-Bev proton, (T), 20: 5945 (UCRL-16464)
radiation safety at CERN, 16: 9043
radio frequency system for, design of 600-Mc, 20: 41532 (BNL-10559)
radioactivity distributions in 200-Bev AGS, (T), 19: 20732 (UCRL-11796)
radioactivity in CERN, induced, (E), 19: 12004
radioactivity induced in CERN proton, buildup and decay of, 17: 22705
radiofrequency control in 7-Bev proton, 17: 920
radiofrequency measuring device for, 17: 917
radiofrequency system in 7 Bev proton, 17: 912
radiofrequency system control for 7-Bev proton, design of automatic, 17: 916
rdiofrequency system for, 17: 22709(P)
radiofrequency system design for, 17: 33116 (LNF-63/10)
relativistic spin equation and depolarization in, 17: 2340 (TID-17059)
remodeling of Univ. Rochester proton (E), 19: 1111 (NASA-CR-56934 (p.177-91))
research above 3 Bev at CERN, review of, 17: 13374
research activity on Frascati electron, 19: 28917(R) (LNF-64/69)
research program at CERN proton, 1965, 20: 37308(R) (NP-16226)
research programs on CERN, data affecting neutrino experiments in, 17: 4129 (BNL-6512(p.43-5))
research using Frascati, 20: 27662
review of CERN, 19: 14159
review of recent developments in, 17: 24533
review of, of energy greater than 100 Bev, (T), 19: 12018
shielding for CERN, meson, 18: 26165 (BNL-837(p.91-113))
shielding of CERN, for neutrino experiments, 17: 4127 (BNL-6512 (p.37-9))
site selection for 300-Bev, geological analysis for, 20: 25302(T) (UCRL-Trans-1320)
site survey of 200-Bev for Berkeley, geological, 19: 41178
space-charge effects on proton, intensity limitations from transverse, 18: 16593 (BNL-7534(p.324-67))
space-charge forces in alternating-gradient, effects of gradient errors with, 18: 28191 (UCRL-10870)
storage-ring design and properties, 16: 15713
storage ring design for CERN, 18: 22586 (CERN-64-19)
storage ring design of Frascati, 20: 27680
storage ring design of CERN, 20: 27680
storage ring for CERN, design of intersecting, 20: 15158 (CERN-542)
storage ring for CERN, NMR field measuring equipment for, 20: 31817 (CERN-66-15)
storage ring for Frascati electron, 19: 28917(R) (LNF-64/69)
storage ring for Frascati, 20: 27662
storage-ring properties and advantages of colliding-beam techniques, 17: 20571 (UCRL-10022(p.74-82))
storage rings for CERN, feasibility study, 16: 28205 (TID-7636 (p.265-71))
storage rings for CERN, 17: 23708
storage rings for CERN proton, 18: 16585 (BNL-7534(p.128-70))
storage rings for electron, development of "AdA" and "Adone", 18: 16586 (BNL-7534(p.171-208))
storage rings for CERN, 18: 37823
storage rings for 28-Bev CERN, vacuum system for, 19: 16324
storage rings for CERN proton, intersecting, 19: 41176
storage rings for colliding-electron-beam studies, design of VEP-1, 20: 7680(T) (AEC-tr-6660)
storage rings for colliding-electron-beam studies, description of VEP-1, 20: 7681(T) (AEC-tr-6664)
storage rings for CERN, electron-proton interactions in, (T), 20: 23821 (CERN-66-12)
storage rings for CERN, design and development of intersecting, 20: 37325
storage rings for CERN, research on intersecting, 20: 37327
storage rings for CERN, design and development of intersecting, 20: 37326
storage rings of, electron–electron colliding-beam interactions in, (E), 20: 7803(T) (AEC-tr-6662)
synchrotron radiation from beam of Frascati, (E), 20: 11403

target for 1-Bev proton, design of liquid hydrogen-deuterium, 17: 22677
targets for CERN, efficiency of internal, 19: 11961
targets for, efficiency of multi-traversal, (T), 19: 28939 (CERN-65-1)
targets in, ionization chamber for monitoring particle incidence on, 18: 44320 (NP-14345)
theory of proton, 17: 20599(T) (FTD-TT-62-958(p.31-243))
timing pulse transmission system for CERN proton, description of multiplex, 20: 46253 (CERN-66-26)
trapping efficiency in proton, with phase lock, 16: 28194 (TID-7636 (p.194-200))
use as radiation source for cancer treatment, 19: 2197
use as radiation source for cancer treatment, 19: 2198
use for beam injection into electron-positron storage rings, 20: 27654
use in cancer therapy, neutron flux and spectrum in, 19: 38517
use in study of malignant tissue proton response, 18: 19812 (BNL-6966)
use of CERN proton, for elementary particle studies, 18: 20965
use of Frascati internal beam for (e,e'p) studies, proposed, 18: 24243 (ISS-63/42)
use of, in colliding proton beam experiments, 17: 11775 (BNL-767 (p.172-6))
use of pin-type moderating system, 16: 15712
use of pulsed reactor as neutron-gas target source for, 18: 16600 (BNL-7534(p.406-13))
use of 300-Bev, for production of high-energy neutrino beams, 17: 20589 (UCRL-10022(p.222-30))
uses of Harvard proton, biological and medical (E), 19: 1109 (NASA-CR-56934(p.160-5))
vacuum chamber for 6-Bev electron, design of, 19: 11903
vacuum chambers for proton, design of, 19: 12036
vacuum equipment for CERN 25-Gev, 16: 31778
vacuum system for 7-Bev proton, 17: 902
vacuum system of Tokyo electron, design and performance of, 19: 47175
vacuum systems performance in 7-Bev proton, 17: 903
waveguide theory for CERN, deflecting, 18: 5886 (CERN-63-33)
waveguides in pass-band region for, traveling, 18: 14672 (CERN-64-10)
x-ray spectra of orbital electrons in Frascati, 17: 36723

SYNERGISTIC ACTION
in separation of metals using mixture of organic solvents, 19: 30333
of gamma rays and triethylene benzoquinone on HeLa cell nuclei, 20: 40704
of heat treatments and γ radiation on yeasts, 20: 41387
of radiation and chemical mutagens on growth of wheat seedlings, 16: 25194 (CNEN-124)
of radiation and surgery on canine sciatic nerves, 19: 29954
of radiotherapy and chemotherapy on mouse sarcomas, 19: 10963
of x radiation and chemical mutagens on tobacco seeds, 16: 25193 (CNEN-118)
of x radiation and actinomycin D in tissue cultures, 16: 25232
radiation and magnetic field, on plant germination, x, 20: 18388
radiation–BUdR, in hamster cells, 20: 6862
radiation–vibration, in mice, 20: 28968
review of drug–radiotherapy, 20: 6967

Synkayvite
see 1,4-Naphthalenediol, 2-Methyl-Diphosphate, Sodium Salts

Syntheses
see Organic Syntheses

Synthetic Rubber
see Elastomers

Syntocinon
see Oxytocins

SYRIA
fall-out monitoring, 1961, 16: 5549 (A/AC.82/G/L.664)
monitoring of personnel of Atomic Energy Establishment, 16: 6637 (A/AC.82/G/L.663)

SYRINGES
see also Injections
radiosterilization of disposable hypodermic, effectiveness, 16: 13494
radiosterilization of disposable hypodermic, 17: 4764
radiosterilization of disposable hypodermic, commercial plant for, 17: 10266
radiosterilization of disposable hypodermic, economics of, 17: 27646
use in radiochemistry, septum cap technique for, 20: 1945

SYSTEMS FOR NUCLEAR AUXILIARY POWER
(Power systems developed for space, terrestrial, and marine uses. Odd-numbered systems are radioisotope-decay heated and even-numbered ones are fission heated.)
ablation during re-entry, safety aspects of suspended debris from, 18: 36837(R) (IITRI-C6007-12)
bearing materials compatibility for, 16: 12786 (NAA-SR-6476)
behavior on re-entry into earth's atmosphere following ICBM ballistic trajectory, 16: 23319(R) (MND-P-3018-I)
bibliography, 16: 6259 (TID-3561(Rev.1))
bibliography on, 16: 30151 (TID-3561(Rev.2))
bibliography on, 17: 15413 (TID-3561(Rev.3))
bibliography on, 20: 35128 (NP-16129)
book: *Radioisotopic Power Generation*, 19: 2692
braze joint experience on components for, review, 19: 20508 (NAA-SR-Memo-10625)
cladding material property data for hydride reactors, 19: 39166 (NAA-SR-Memo-11149)
component corrosion by mercury, 18: 21675 (NP-13795)
component irradiation studies for, techniques for, 18: 31028
congressional hearings, 1962, 17: 10216
control of SNAP reactors, static, 20: 3559
control of, SNAPTRAN program for, 18: 23107 (TID-7662(p.434-46))
coolant and power cycles for, review of liquid metal use in, 20: 20303
coolant and working fluids for SNAP-50/SPUR, analysis of, 20: 8447 (PWAC-491)
coolant corrosive effects, 16: 16681 (TID-7626(Pt.I)(p.87-91))
coolant, development of materials for containment of alkali metal, 16: 24165(R) (NP-11824)
coolant requirements for, vapor-cycle, 19: 1923 (ANL-6857)
cooling system, analysis of velocities in channels of, 17: 15460 (NAA-SR-Memo-7527)
cooling system design, 17: 20174(R) (TID-17707)
cooling system of, materials for, 16: 32079 (NAA-SR-6306)
criticality and shielding studies for, 20: 12475 (WANL-PR(B)-009)
criticality of, effects of water immersion on, 17: 26057
criticality of, effects of water immersion on, 17: 26058
description, 20: 2862
description of radioisotope and reactor, 19: 28714 (SC-DC-65-1131)
design, 17: 28576
design, 19: 7833
design and operation of zirconium hydride reactor—Mercury Rankine Power Conversion System for manned vehicles, 18: 29107 (NAA-SR-9715)
design and performance as thermoelectric generators, 20: 723 (NP-15531)
design and performance of MPRE, 20: 28823 (ORNL-P-1381)
design and performance of radioisotope-fueled Brayton cycle, 20: 35826
design and safety aspects of hydride-fuel reactors for, 18: 9712 (CONF-311-9)
design and use of isotope-fueled, review, 18: 32507 (A/CONF.28/P/217)
design concepts development, 16: 34123(R) (MND-1086(Del.))
design, economics, and testing of 710 reactor system, 18: 1283 (GEMP-245)
design of glowworm radiative heat transfer, 18: 4753 (LAMS-2427)
design of nuclear thermoelectric, computer program for, 20: 6660 (NAA-SR-Memo-11514)
design of reactors for, computer-programmed parameter study of, 18: 33129 (NP-14062)
design of SNAPSHOT Agena, 20: 14174 (TID-22417)
design of thermoelectric generator for unmanned lunar exploration, 16: 34137
design of, engineering drawings for, 20: 717
design reliability, 19: 25753
designs and status of, review on, 18: 7852 (HW-66666(Rev.2))
destruction of, shaped-charge technique for, 17: 22948(R) (AD-282977)
development, 16: 15947
development, 17: 10203
development, 17: 21368 (AD-282179)
development, 17: 22954 (TID-18558)
development, 18: 5980
development, 18: 43052
development, 19: 32655(R) (MND-P-3005)
development, 19: 32656(R) (MND-P-3006)
development and feasibility of radioisotopic-fueled, 18: 40935
development and materials testing, 17: 36477
development and safety aspects of radioisotopic, 17: 7643(R) (MND-P-3016-I)
development and technology for, 19: 17341(R) (NAA-SR-10496)
development and uses, 16: 15948
development and uses of radioisotope generator, 17: 26927
development and uses of radioisotope-fueled, 17: 35217 (CONF-17-7)
development for space vehicles, (E/T), 19: 38836 (NASA-SP-79)
development for space, terrestrial, and marine use, 20: 39305 (DP-1066 (Vol.1), pp V.3-16)
development for undersea uses, 20: 40362
development for undersea missions, 20: 45830
development in Russia and USA, for space, (E), 19: 35840
development of cesium-137 thermoelectric generator, June 22-Sept. 22, 1961, 17: 31766(R) (TID-17004)
development of fabrication techniques for, 17: 2662(R) (MLM-1135)
development of fuels and heat source containment capsules, 16: 7326(R) (MND-P-3014-III)
development of heat transfer components for, 17: 19690(R) (TID-15223)
development of radiator systems for, 17: 4358(R) (PWA-2100)
development of radioisotope-fueled, lecture on, UCLA, California, July 17 to 28, 1961, 17: 22277 (TID-18323)
development of radioisotope-fueled APU, Apr.–July 1957, 17: 29853(R)

(MND-1123)
development of radioisotope-fueled, 19: 4568
development of radioisotope, for manned space stations, 19: 9564
development of radioisotope power subsystem, 19: 44570
development of reactor-powered, 18: 14778(R) (GA-4071)
development of reactor-thermionic element combination, 18: 20837
development of reactor, high-temperature chemistry problems in, 20: 20870 (LA-DC-7703)
development of reactor-type, for oceanographic application, 20: 39313
development of semiconductors for, 16: 32116 (NAA-SR-Memo-6921)
development of, bibliography on, 18: 35204 (TID-3561(Rev.4))
development of, book on, 19: 1930
development of, for underwater uses, 20: 29607
development of, hearings before Joint Committee on Atomic Energy on, 20: 20305
development of, review of, 20: 7782
development of, review, 20: 16115
development of, review of, 20: 18182
development of, 1965 Report to Congress on, 20: 24825
development program for, 18: 15599 (TID-20103)
development progress, 16: 23319(R) (MND-P-3018-I)
development, review, 16: 21857
disposal after operation, methods for, 19: 42140 (NAA-SR-11353)
disposal of orbiting, techniques for ocean burial, 20: 20302 (SC-RR-65-472)
dissassembly of, remote operations in, 19: 46504 (CONF-641120, pp 86-97)
dynamic behavior of, bibliography on, 17: 17420 (NAA-SR-7786)
effects of electron injection from, on Van Allen belts, 18: 15029
entry into water, cavity generation in, 18: 15591 (NAA-SR-Memo-9105)
environmental problems for, 18: 13325
environmental testing of, laboratory and equipment for, 19: 4280 (NAA-SR-Memo-9438)
evaluation for space system applications, 17: 4359 (TID-17306)
evaluation of, AEC, 18: 40934
evaluation of, Jan. 1964, 18: 15598 (TID-20079)
fields generated by, torque developed in geomagnetic field interactions with electric and magnetic, 17: 24730
fuel element destruction during re-entry, analysis, 20: 8438(R) (AE-63-0011)
fuel element fabrication for, feasibility report on, 18: 14425 (NAA-SR-Memo-9299)
fuel elements for, radiographic measurement of rod spacing in, 17: 19620 (NAA-SR-Memo-7594)
fuel materials for, bibliography on zirconium–uranium, 18: 33128 (NAA-SR-9525(Vol.I))
fuel particles from, biological effects of ingestion or inhalation of, 20: 14785 (BNWL-182)
fuel performance in SNAPTRAN transient tests, uranium–zirconium hydride, 20: 35138
fuel rod analysis for uranium-235, nondestructive, 19: 30080 (NAA-SR-9600(Vol.III))
fuel rod re-entry burnup simulation in wind tunnel, 19: 3723 (NAA-SR-9779)
fuel technology development, 16: 3969(R) (MND-P-3015-III)
gas pressure buildup in thermoelectric, 18: 9065 (MND-3143-1)
hazards of curium-242 use in, 17: 21929 (MND-1963)
hearings before Eighty-seventh Congress on SNAP program, 16: 8437
heat and moments transfer in liquid-metal two-phase helical flows, (E/T), 20: 23255(R) (SAN-409-29)
heat sources for SNAP generators, characteristics and radioisotopic, 16: 2793
heat transfer, 18: 17322(R) (TID-19971)
heat transfer in, 17: 18273(R) (TID-18028)
heat transfer in, 17: 29076(R) (TID-18996)
heat transfer in reactors, model for simulating, (T), 20: 1529 (NAA-SR-Memo-10961)
heat transfer systems for, analysis of, 19: 20116(R) (SAN-409-12)
hot channel factors for compact reactors for, statistical treatment of, 17: 31730 (NAA-SR-8468)
insulation development for radioisotope, vacuum foil-type thermal, 20: 29606(R) (ALO-3634-1)
insulation development for radioisotope, vacuum-foil thermal, 20: 43798(R) (ALO-3634-2)
insulation for, development of fibrous-type, 20: 36983(R) (ALO-3633-1)
kinetics equations for, computer program for solving, 18: 21669 (NAA-SR-9190)
kinetics of, core transfer function models for, 17: 40415 (NAA-SR-Memo-8440)
launch success of isotope-fueled, probability of, (T), 20: 725
launching, lunar impact, and re-entry analyses of radioisotope generator, 16: 5082(R) (MND-P-3015-I)
materials development for, 18: 34046(R) (NASA-CR-54041)
materials development for Medium Power Reactor Experiment, 18: 45076(R) (ORNL-3670(p.225-7))
materials evaluation for, 18: 9713 (CONF-375-3)
materials for, reference manual on, 17: 20554 (DCAS-TDR-62-121)
materials for, corrosion testing of, 20: 18020(R) (ORNL-3900, pp 2-81)
materials for, properties of hydrided uranium–zirconium alloy at high temperatures as, 18: 12621 (ARF-A6003)
materials problems survey, 16: 7325 (MAB-177-M)
materials problems from high-temperature reactor operation, 18: 23093
mission integration of reactor, 19: 45661
neutron collimator design for core mapping, 20: 46928(R) (ORNL-3973(Vol.1), pp 26-47))
neutron scattering from radiator in, computer code for, 19: 31198 (TIM-799)
performance and safety, 19: 33704
performance of cobalt-60 fueled, 19: 46893 (DP-974)
performance of thermionic reactors, 20: 3547 (NAA-SR-Memo-7881)
performance of, computer programs for analysis of, 20: 9357 (NAA-SR-Memo-10913)
photographic exposures for density difference between reactor core and backlight, 19: 29735 (EGG-1183-1003)
power conditioning, distribution, and generation systems in, 18: 24942
power cycles for radioisotope-fueled, design and performance of mercury Rankine, 20: 36019
power cycles for, thermodynamic and turbomachinery concepts for, 19: 45654 (NASA-TN-D-2968)
power cycles for, evaluation of Rankine and Brayton, 20: 40452
power spectral density of reactor noise signals in SNAP Experimental Test Facility, 16: 12745 (NAA-SR-Memo-6662)
power supply for, factors affecting, 18: 13321
properties, 16: 27741 (NP-11716)
properties of radioisotope-fueled thermoelectric cells, 20: 35825
propulsion capabilities of, for lunar exploration, 17: 19692
pump for MPRE, fabrication of turbine-driven potassium boiler-feed, 20: 5184 (ORNL-P-1740)
pumps for Mercury-Rankine, performance of thermoelectric, (T), 19: 5522 (NAA-SR-Memo-9671)
radiation effects on electrical insulation in, in space flight environment, 17: 37636
radiation effects on telemetry electronics of, 18: 33838 (RTD-TDR-63-4287(Vol.I))
radiation effects on instrumentation of, gamma and neutron, 20: 14170 (EGG-1183-2019)
radiation effects on electric connectors and dielectrics for, at low pressure and high temperature, 20: 23524
radiation properties of plutonium-238 for, 19: 42789 (DP-984)
radiation testing of actuator and position-sensor assemblies for, (E), 19: 19407 (BMI-X-10109)
radiation tolerance of electronic equipment for, 20: 4262 (NP-15610)
radiator development tests for MPRE, 20: 5182 (ORNL-P-1721)
radiator-condenser structure R/C 6, low-level vibration testing of, 18: 43740 (NAA-SR-Memo-9963)
radiator-condenser testing for, aluminum-steel R/C-10, 19: 5523 (NAA-SR-Memo-9866)
radiator-condenser R/C-10 for, static structural tests of aluminum-steel, 19: 24146 (NAA-SR-Memo-10704)
radioactivity release from strontium titanate by dissolution in sea water, 18: 31363 (USNRDL-TR-745)
radioisotope evaluation for space, 20: 11188 (BLG-330)
radioisotope flight safety analyses and tests, 16: 3968(R) (MND-P-3014-I)
radioisotopes for, evaluation of, 20: 41397
re-entry ablation of molten droplets of strontium-90 fuel, analysis of, 19: 4400 (MND-3062-5)
re-entry ablation, calculation of vaporization losses from liquid droplets formed during, 19: 27813 (SC-RR-65-138)
re-entry behavior of zirconium hydride-uranium fuel elements in, (E), 19: 10628
re-entry burnup studies of reactor fuel elements, 18: 24933 (AFSWC-TDR-63-51)
re-entry destruction, 16: 5087 (RAD-TR-61-28)
re-entry disintegration of, oxidation properties of uranium–zirconium alloys in, 20: 14169 (AFWL-TDR-64-75)
re-entry flight demonstration (RFD-2) for, optical instrumentation for, 18: 36843 (SC-RR-64-968)
re-entry flight demonstration (RFD-2) for, heating data from, 20: 2207
re-entry flight test (RFD-2), stability analysis of vehicle for, 19: 34344 (SC-RR-65-129)
re-entry hazards to, development of tests for, 19: 4404 (TLW-1092)
re-entry heating rates for, methods for calculating, (T), 20: 12467 (NAA-SR-11704)
re-entry heating tests, 16: 31335(R) (MND-P-3019-I)
re-entry of cylinders in atmosphere, drag coefficients and heating ratios for supersonic, 19: 24675 (SC-RR-64-2141)
re-entry of radioisotope-powered, aerothermodynamic effects on, 17: 24728 (MND-P-2953)
re-entry of, analysis of burnup and dispersion of beryllium reflector during,

17: 36986 (AFSWC-TDR-62-119)
re-entry of, plutonium dioxide microsphere dispersion in, (T), 19: 31596 (MND-3169-47)
re-entry test analysis for RFD-2, (E), 19: 17352 (SC-RR-65-13)
re-entry trajectories for, computer programs for calculating, 20: 16113 (SC-RR-66-22)
reactivity and temperature coefficient for, effects of neutron thermalization on, 20: 22377 (GA-6930, App. B)
reactivity calculations for, effects of uncertainties in zirconium cross sections on, 20: 45192 (CONF-660303, pp 88-90)
reactivity control using prepoisons, effects of cross-section uncertainties, 20: 45193 (CONF-660303, pp 204-9)
reactivity feedback effects during power excursions in, using uranium–zirconium hydride fuel, 20: 36513 (CONF-650413, pp 437-56)
reactivity transients in, kinetics of uncontrolled, 18: 35201 (NAA-SR-9368)
reactivity transient tests in SNAPTRAN-1, step, 20: 42664(R) (IDO-17165)
reactivity worths of voids in reactor-type, (T), 19: 10619 (NAA-SR-Memo-10421)
reactor control and stability analysis for, computer program for, 20: 45196 (NAA-SR-Memo-11894)
reactor control-drum actuators for, 19: 29733
reactor dose rates and power level for, probability analysis of, (T), 20: 3549 (SC-RR-65-417)
reactor safety studies at Atomics International, 18: 31020 (NAA-SR-Memo-8215(Pt.8))
reactor shielding requirements for, effects of minimum-weight radial reflector on, 18: 21670 (NAA-SR-Memo-9117)
reactor shielding for, development of, 19: 23996(R) (ORNL-3650(p.1-110))
reactor temperature coefficients, 17: 7560 (NAA-SR-7140)
reentry ablation of reactor fuel elements for, 20: 24782 (NAA-SR-11502)
reentry and disposal phenomena for, (E/T), 19: 14878 (RTD-TDR-63-3003)
reentry burnup of, dose criteria for fallout from, 20: 20937 (NAA-SR-11761)
reflectors of reactor for, reactions of beryllium at reentry, 16: 33509 (AFSWC-TDR-62-15)
reliability and safety of radioisotopic, 17: 17607
review, 17: 16190
safety analysis for radioisotope generators, 16: 5082(R) (MND-P-3015-I)
safety analysis for, review of, 20: 3548 (SC-DC-65-1752)
safety analysis for SNAP reactor disposal systems, 20: 35140
safety aspects of, 20: 18949 (SC-DC-66-1369)
safety criteria for design and use of, in space, 20: 32855
safety hazards for, ground testing of, 18: 1955 (SC-DC-3248)
safety in uses in space vehicles, 18: 6513 (CONF-311-8)
safety in, problems in, 18: 31781 (A/CONF.28/P/286)
safety of, evaluation procedures for, 19: 10632
safety of, review of 1964 Geneva papers on, 19: 24779
safety problems in launch and reentry, 18: 4838
safety program at Sandia Corporation, 19: 27812 (SC-DC-65-1420)
safety program for, review of, 17: 23569
safety program for, review, 18: 43850
safety programs for radioisotope-powered, 16: 18696(R) (MND-P-3017-I)
safety programs for reactor-powered, 17: 19687(R) (NAA-SR-7797)
safety programs for reactor-powered, 17: 19688(R) (NAA-SR-8097)
safety testing of, program summary on, 19: 13671(R) (WASH-1052)
shaft-bearing system dynamics for MRP Combined Rotating Unit, analog study, 20: 39022 (NAA-SR-11943)
shield design for, for producing power, 17: 12039
shield optimization for manned, fast-neutron weighting factors for, 20: 43580 (NAA-SR-Memo-11901)
shield test facility for reactor, 18: 40736 (NAA-SR-9364)
shield weight scaling factors for reactors, 20: 45197 (NAA-SR-Memo-11971)
shielding, 16: 24594
shielding analysis for, RATRAP code for IBM 7094, 18: 28920 (NAA-SR-Memo-8968)
shielding, calculations using Monte Carlo method, 16: 24595
shielding data library for, 20: 34782 (NAA-SR-Memo-11718)
shielding design, (E), 20: 46928(R) (ORNL-3973(Vol.1), pp 26-47))
shielding design for, 18: 21676 (SSD-TDR-63-217)
shielding evaluation, design of facility for, 16: 32519 (NAA-SR-7432)
shielding experiments, physics tests on Shield Test Experiment Reactor for, 16: 28598 (NAA-SR-7368)
shielding from meteoroid penetration, Explorer XVI data on, 18: 741
shielding of, computer analysis for, 16: 27548 (MND-P-2726)
shielding of, research programs on, 17: 12778(R) (ORNL-3360(p.102-4))
shielding program on, review of, 20: 5183 (ORNL-P-1736)
shielding research for, 18: 6138(R) (ORNL-3499(Vol.I))
strontium-90-fueled thermoelectric generator development, 16: 3966(R) (MND-P-2483-2)
strontium-90-fueled thermoelectric generator development, 16: 3967(R) (MND-P-2483-3)
survey, 17: 26924
systems development for, material and temperature problems in, 17: 20149 (BNL-756(p.1-18))
technology handbook on, 19: 26818 (NAA-SR-8617(Vol.III))
technology of, review, 17: 30157
temperature reductions in computer analysis of, 18: 6515 (NAA-SR-Memo-9101)
testing in simulated environment, 20: 22475
testing of, design of ultrahigh vacuum chamber for, 17: 247 (NAA-SR-6490)
testing of, re-entry burnup, 17: 3855
testing of, reactor transient, 18: 9715 (SC-DC-3553(p.65-78))
testing of SNAPTRAN-2, destructive, 20: 42664(R) (IDO-17165)
testing RFD-2 re-entry vehicle, (E), 19: 21763 (SC-DR-64-1741)
thermal insulation for liquid metal components operating at 1000 to 1400°F in, 19: 24147 (NAA-SR-Memo-10730)
thermal models for core of, 18: 29115
transport of, shock and vibration tests during highway, 17: 24744 (NAA-SR-Memo-8074)
use in communications satellites, 16: 34126 (NAA-SR-7408)
use of, in electric propulsion, 16: 30150 (NAA-SR-7085)
use of radioisotope, for manned space laborstory, 19: 44571
use of Rankine liquid-metal cycle in, 18: 15601
use underwater, 20: 30929

SYSTEMS FOR NUCLEAR AUXILIARY POWER (SNAP-1)
development of, Apr.-July 1958, 17: 31763(R) (MND-P-3003)
development of, bibliography on, 18: 8700 (NYO-10689)
development of, Jan.-Apr. 1958, 17: 31762(R) (MND-P-3002)
development of, July–Sept. 1959, 17: 29855(R) (MND-P-3008)
development of, July-Sept. 1957, 17: 31760(R) (MND-P-1175)
development of, July-Sept. 1958, 17: 31764(R) (MND-P-3004)
development of, Oct. 1957-Jan. 1958, 17: 31761(R) (MND-P-3001)
development of, Sept.–Dec. 1959, 17: 29856(R) (MND-P-3009)
development status of SNAP-1A, 17: 35228
development status, 19: 32657(R) (MND-P-3007)
performance of SNAP-1A, 17: 31767
testing, results of 2500-hour endurance, 16: 12784 (NAA-SR-6308)

SYSTEMS FOR NUCLEAR AUXILIARY POWER (SNAP-2)
alternator design for, 16: 3972 (NAA-SR-6302)
boiler development, 16: 34142 (NAA-SR-6304)
boiler evaluation for, 17: 16227 (NAA-SR-Memo-7945)
characteristics, 18: 36846
characteristics of Rankine power plants in zero gravity, development of program for studying, 16: 3973 (NAA-SR-6303)
condenser, properties of mercury, 16: 3971 (NAA-SR-6301)
condenser-radiator of, aerodynamic heating effects on, 17: 21369 (NAA-SR-Memo-7573)
condenser-radiator design, fabrication, and testing for, (E), 19: 19408 (NAA-SR-9885)
control systems for, development of, 20: 22474
conversion system for, research program on, 17: 18264 (NAA-SR-6309)
coolant boiling research for, 17: 27535 (BNL-801)
coolant cross-flow distribution in, effects of "unfed" peripheral channels on, 18: 21673 (NAA-SR-Memo-9576)
coolant flow divider for thermoelectric pumps for, design of, 19: 29743 (NAA-SR-Memo-10694)
coolant flow patterns in SNAP 2/10A, model for studying, 18: 15592 (NAA-SR-Memo-9405)
coolant pump design and testing, 16: 3970 (NAA-SR-6300)
coolant pump development, 16: 11816 (NAA-SR-5244)
cooling system development, 16: 12785 (NAA-SR-6439)
cooling system testing, 16: 5084 (NAA-SR-Memo-6408)
core hydraulics for 10A/2, computer program for photographic analysis of, 18: 40931 (NAA-SR-Memo-9947)
criticality studies, 17: 28481 (TID-18880)
description of, 17: 2635
design, (E/T), 19: 31590 (AI-Memo-7585(Rev.2))
design and performance of, 17: 35224
design criteria for, dynamic analysis of, 18: 35199 (NAA-SR-9054)
design of multiple-unit, for manned space station, 18: 33136
destruct test SNAPTRAN-2, transducer evaluation for, 20: 24778 (IDO-17148)
destruct test SNAPTRAN-2, analytical models for energy release in, 20: 26517(R) (IDO-17126)
destructive test of SNAPTRAN 2/10A-3, analytical services in, 19: 32059(R) (IDO-14655)
destructive test SNAPTRAN 2/10A-3, fission product release and dispersion from, 20: 564 (CONF-650407, pp 512-36)
destructive test SNAPTRAN-2, 20: 3561
development, 17: 11986 (NAA-SR-6307)
development, 18: 15575
development, 19: 1922 (AI-Memo-7585(Rev.I))
development status, 18: 34001
energy release and reactivity feedback effects in SNAP-2/10A destruct,

19: 21719 (NAA-SR-9780)
energy release in SNAPTRAN 2/10A-2, destruct, 20: 22467(R) (IDO-17077)
examination and safety program for SNAPTRAN 2/10A-3, post-destruct, 19: 21718 (IDO-17071)
fission product release and reactor kinetics in SNAPTRAN 2/10A-3 destruct, (E), 19: 21717 (IDO-17019)
fission product release from irradiated uranium–zirconium hydride fuel for 2/10A, 20: 3562
flight instrumentation for, development of platinum resistance thermometer for, 18: 20283 (NAA-SR-Memo-8073)
flight-packaged speed control system for, 18: 40927 (NAA-SR-6319)
fuel element development for, 17: 6559
fuel elements for, strain and stress distributions in long, solid, cylindrical, (T), 20: 23796
gamma energy release following power transient in SNAPTRAN-1, 20: 24779 (IDO-17161)
gamma hazards from SNAPTRAN-1, (T), 20: 26517(R) (IDO-17126)
ground tests of SNAP 2/10A reactor assembly, 18: 13312 (AFSWC-TDR-62-144)
hazards evaluation in STEP project, 18: 24956(R) (IDO-16961)
hazards evaluation in STEP project, 19: 5542(R) (IDO-17012)
heat transfer components of, development of, 17: 20166 (BNL-756(p.294-325))
kinetic and thermal response of 2/10A, computer program for, 18: 26957 (NAA-SR-8414)
materials self-welding at 700 to 1300°F in environment of, facility for testing, 20: 7570 (NAA-SR-9643)
mercury boiling and condensing experiments at zero gravity, 17: 13679 (NAA-SR-6305)
mercury-Rankine system for, condenser analysis for, 18: 40929 (NAA-SR-9801)
neutron energy-density in 2/10A SNAPTRAN-3, during destruct (E), 19: 3739
neutron four group cross sections for SNAP 2 and 8 cores, 17: 17422 (NAA-SR-Memo-7789)
neutron scattering in, 18: 13051 (NAA-SR-Memo-9214)
operation and testing of, 20: 6655 (NAA-SR-7088)
performance, 19: 16444(R) (AFAPL-TR-64-135)
power conversion system for, development of rotational speed control for, 18: 17319 (NAA-SR-6310)
power systems of, development of turboalternator for, 20: 35116 (CONF-651026, pp 415-76)
power systems of, radiator condenser development for, 20: 35118 (CONF-651026, pp 582-640)
power systems of, boiler conditioning tests for, 20: 36517 (NAA-SR-6322)
radiation hazards from SNAPTRAN 2/10A-3 destruct, (E), 19: 17340 (IDO-17038)
radiator-condenser structural analysis for, R-C 14, 18: 38561 (NAA-SR-Memo-9375)
re-entry safety hazards evaluation for, 17: 38575 (NAA-SR-8303)
reactivity transients in 2/10A SNAPTRAN-3, super-prompt (E/T), 19: 3740
reactivity transient test SNAPTRAN-3, analysis of fuel element damage from, 19: 38233 (IDO-17065)
reactivity transient testing of SNAPTRAN 2/10A-1, step, 20: 22467(R) (IDO-17077)
reactivity transient testing in SNAPTRAN-1, 20: 26517(R) (IDO-17126)
reactivity transient testing in SNAPTRAN-1, 20: 26518(R) (IDO-17145)
reactivity transient tests using zirconium hydride–uranium fuel, SNAPTRAN-2, 20: 35139
reactivity transient testing of SNAPTRAN 2/10A-1, program sequence times for, 20: 12499(R) (IDO-17112, pp 52-80)
reactor vessel top head stress analysis, 18: 13316 (NAA-SR-Memo-9203)
reactor-reflector torque reactions for, harmonic analysis of, 18: 38562 (NAA-SR-Memo-9399)
reflector anodization in, thermal analysis of, 18: 19410 (NAA-SR-Memo-9539)
reliability of multiple CRU Rankine cycle systems for, 18: 38560 (NAA-SR-Memo-9361)
reliability program for, 18: 19407 (NAA-SR-8419)
rotational speed control system development, 16: 15964
rotordynamic analysis of, Combined Rotating Unit-V, 20: 36977 (NAA-SR-11944)
safety analysis for SNAP 2/10A, 18: 31019 (IDO-16825)
safety analysis of SNAPTRAN 2/10A-1 and -2 tests, 20: 6654 (IDO-17076)
safety testing of SNAPTRAN 2/10A-1 and 2/10A-3, (E), 19: 42134(R) (IDO-17070)
safety analysis of SNAPTRAN 2/10A-3 water immersion tests, 18: 29105 (IDO-16929(Rev.1))
stress analysis of reactor-vessel top head, experimental, 19: 31600 (NAA-SR-Memo-10695)
structural analysis of upper portion of sodium–potassium outlet pipe, 18: 3297 (NAA-SR-Memo-9043)
structural evaluation of prototype PSM-2, (E), 19: 6869 (NAA-SR-9906)
system heat balance, computer code for, 16: 5085 (NAA-SR-Memo-6531)
systems analysis of liquid metal cell power system for, 18: 3293 (EDR-3113)
temperature control coatings for, development of, 19: 48050 (NAA-SR-9903)
testing of, objectives of orbital, 17: 35225
testing of 2/10A SNAPTRAN-3, destruct (E), 19: 3738
testing of 2/10A, photography for SNAPTRAN-3, 19: 3715 (EGG-1183-1071)
testing of 2/10A, in STEP project, 19: 29739(R) (IDO-17058)
testing PSM-2, environmental, 19: 5529 (NAA-SR-Memo-10257)
tests of corrosion product separator in Haynes 25 Alloy loop containing mercury, 18: 21677 (TID-20552)
torque impulse calculations for squib firings in control drum actuator, 18: 43060 (NAA-SR-Memo-9750)
use in manned orbital space stations, 17: 24724 (AI-7950)
use of multiple-unit PCS of, for manned space stations, 18: 40928 (NAA-SR-9252)

SYSTEMS FOR NUCLEAR AUXILIARY POWER (SNAP-3)
design, 16: 5082(R) (MND-P-3015-I)
development of A, B, C, and D, July–Sept. 1959, 17: 29855(R) (MND-P-3008)
development of, Apr.-July 1958, 17: 31763(R) (MND-P-3003)
development of, bibliography on, 18: 8700 (NYO-10689)
development of, July-Sept. 1958, 17: 31764(R) (MND-P-3004)
development of, review of, 19: 11637
development status, 17: 35228
development status, 19: 32657(R) (MND-P-3007)
performance, 17: 31767
safety analysis, nuclear, 16: 6250
safety aspects of isotopic systems, 18: 9069 (SC-DC-3553(p.91-102))
safety tests of space version of thermoelectric generator, 19: 30625 (MND-P-2358)

SYSTEMS FOR NUCLEAR AUXILIARY POWER (SNAP-4)
coolant radiolytic decomposition in, hermetic sealing problems from, 18: 21672 (NAA-SR-Memo-9507)
core two-dimensional two-phase flow model and IBM 7090 code for, 18: 21557 (NAA-SR-Memo-9444)
fuel element geometries for, heat transfer and hydraulic studies of, 18: 10232 (TID-20046)
fuel element geometries of, heat transfer and hydraulic studies in, 19: 40249 (TID-22014)
fuel element structural analysis, 16: 34127 (NAA-SR-Memo-7456)
fuel rod bundle for, heat transfer and hydraulic studies of simulated, 17: 40345 (TID-19458)
heat transfer and hydraulic studies of fuel rod bundle for, 18: 1287 (TID-19563)
safety experiments on critical assembly of 4B, (E), 19: 6868 (NAA-SR-9871)

SYSTEMS FOR NUCLEAR AUXILIARY POWER (SNAP-7)
design and performance of 10-watt generator for light buoy, 16: 13695 (MND-P-2720)
design and performance of 7B, 17: 35221 (MND-P-2836)
design and testing, 17: 1685 (MND-P-2707)
design and testing of 60w strontium-90-fueled, for weather buoy, 17: 22273(R) (MND-P-2835)
development, 16: 21127(R) (MND-P-2483-5)
development, 17: 2627(R) (MND-P-2483-7)
development and testing of, 17: 4356(R) (MND-P-2483-4)
development of, bibliography on, 18: 8700 (NYO-10689)
development of, July–Sept. 1959, 17: 29855(R) (MND-P-3008)
development of 7A, 20: 39313
economic aspects of A and E, 17: 31088(R) (NYO-10462)
engineering drawings, 17: 16193
feasibility study of underwater 7E, acoustic beacon with fluid-mechanical energy conversion, 19: 20405 (MND-3180-1)
fuel processing for 7B, 18: 4142 (MND-P-2977)
heat transfer analysis of, 20: 4278 (MND-P-2229)
manual for handling, maintenance, operation limits, and safety, 17: 1684 (MND-P-2640)
modification and performance of 7A, (E), 19: 28713 (MND-3043-1)
operation of, instruction manual for, 19: 6226 (MND-P-2640(Rev.2))
performance and uses, 19: 855
performance of A and C, 18: 14793
radiological safety of, 20: 39307 (DP-1066(Vol.1), pp V.35-40)
safety analysis for 10-watt strontium-90-fueled generator, 16: 11997 (MND-P-2614)
safety evaluation for E model, 16: 27740 (MND-P-2761)
safety evaluation for 7B, 19: 4567 (MND-P-2762-A)
safety evaluation for 7B, 19: 4871 (MND-P-2762)
shielding calculations for, 20: 4278 (MND-P-2229)
strontium-90 preparation for, 18: 14334
thermoelectric generator development for, strontium-90 fueled,

16: 34125(R) (MND-P-2483-6)

SYSTEMS FOR NUCLEAR AUXILIARY POWER (SNAP-8)

alternator for, development of long-life, 20: 40453
boiler development and heat transfer properties, mercury, 20: 27102 (ANL-7100, pp 573-632)
compatibility of structural materials in, with potassium–sodium, 20: 9425 (ORNL-3898)
component development, 17: 27535 (BNL-801)
condenser and radiator development, 16: 14354 (NASA-TN-D-1188)
control system and instrumentation of, description of, 20: 35142
control systems for, development and testing of electromagnetic actuators of, (E), 19: 8654 (NAA-SR-9645)
control systems for, development of, 20: 22474
coolant chemistry of experimental reactor S8ER, 20: 3564
coolant circuit materials, corrosion loop experiments on, 19: 20475(R) (ORNL-3538)
coolant circuit materials, corrosion loop experiments on, 19: 20477(R) (ORNL-3604)
coolant circuit materials, corrosion loop experiments on, 19: 20479(R) (ORNL-3671)
coolant circuit materials, corrosion loop experiments on, 19: 20480(R) (ORNL-3730)
coolant circuit, corrosion loop experiments on matrials for primary, 19: 20478(R) (ORNL-3618)
coolant flow in tri-cusp channel in, salt velocity technique for, 18: 21671 (NAA-SR-Memo-9232)
coolant loops of, study of sodium–potassium corrosion of, 19: 24939(R) (ORNL-3784)
coolant velocity in, noise and analysis techniques for determining, 20: 20297 (NAA-SR-11193)
cooling system materials for, corrosion by liquid potassium–sodium, 20: 773(R) (ORNL-3859)
cooling system of SNAP-8 Experimental Reactor, argon-41 production in, (E), 20: 5178 (NAA-SR-11303)
description of, 17: 2635
design, (E/T), 19: 31590 (AI-Memo-7585(Rev.2))
design and performance of, 17: 35224
design for use in lunar base power plants, 19: 10631
design of electric generating system for, 18: 43062(R) (NASA-CR-54111)
development, 17: 35226
development, 18: 11477
development, 18: 15575
development, 19: 1922 (AI-Memo-7585(Rev.I))
development and evaluation, 19: 38245 (N64-29727)
development for Manned Orbiting Research Laboratory, 19: 21720 (NAA-SR-10318)
development of component materials for, 20: 11214(R) (NASA-CR-54717)
development of component materials for, 20: 11215(R) (NASA-CR-54718)
development of power conversion system for, 19: 29749(R) (NASA-CR-54310)
development of thermoelectric elements for, 17: 1124 (NAA-SR-7036)
development of, NASA Semiannual Report to Congress, Jan. 1 to June 30, 1964, 19: 19453
development status, 18: 34001
development status review, 18: 40932 (NP-14234)
electric insulation development for, 20: 10418(R) (NASA-CR-54716)
energy converter design for, computer program for calculating, 20: 45195 (NAA-SR-Memo-11819)
flight shield for, thermal radiative coatings for, 18: 39823 (NAA-SR-Memo-9749)
flight test facility, development of vault liners for, 17: 39461 (NAA-SR-Memo-8347)
flight testing of propulsion system for 70-kw(e) mission spacecraft, 16: 5079 (JPL-TR-32-190)
fuel burnup calculations for, 17: 40273 (NAA-SR-Memo-8675)
heat transfer in, 17: 20162 (BNL-756(p.262-75))
heat transfer model for, transient, 18: 15590 (NAA-SR-7938)
hydrogen diffusion from fuel elements through coolant in, 18: 23061(R) (ORNL-3591(p.217-22))
hydrogen diffusion through coolant system of, 19: 20475(R) (ORNL-3538)
hydrogen removal from primary coolant system of, studies of possible, 19: 20480(R) (ORNL-3730)
materials development and testing in boiling mercury, 17: 36200(R) (NP-13033)
materials development for, mercury corrosion-resistant, 18: 7152
materials for use in, radiation effects on electrical and structural, 20: 9563 (BMI-X-10152)
materials self-welding at 700 to 1300°F in environment of, facility for testing, 20: 7570 (NAA-SR-9643)
meteoroid effects on, 17: 22950 (NAA-SR-8127)
moderator testing, 19: 25749 (NP-15022(Vol.I))
operating capabilities and potential, 19: 29765
operation experience, 19: 45666
operation experience, 20: 38527
operation of S8ER, review, 18: 29113
operation of, continuous, 19: 43593
performance, 19: 16444(R) (AFAPL-TR-64-135)
performance as design model for manned-station electric power plant, (E), 19: 29730 (64SD-913)
performance in power systems for manned space stations, 19: 10633
performance of experimental reactor, 19: 6872
power conversion system performance, 18: 40932 (NP-14234)
power conversion system development, 19: 19410(R) (NASA-CR-54219)
power conversion system for, development of, 20: 36519(R) (NP-16166)
power cycles for, mercury pump development for, 20: 35113 (CONF-651026, pp 171-85)
power generation system for, development of, 20: 26521(R) (NASA-CR-54848)
power of, statistical hot-channel factors in, 18: 3243
power output of, 17: 10211
power systems for, development status of, 20: 35112 (CONF-651026, pp 103-38)
power systems for, potassium–sodium pump development for, 20: 35114 (CONF-651026, pp 186-200)
power systems of, boiler development for, 20: 35115 (CONF-651026, pp 285-306)
power systems of, turboalternator design for, 20: 35117 (CONF-651026, pp 477-97)
power systems of, condenser design and development for, 20: 35119 (CONF-651026, pp 641-68)
power transmission cables for, optimum weight of, 20: 32853 (NAA-SR-Memo-11925)
pressure vessels for, design and fabrication of, 19: 12836
propulsion potential of, 17: 22958
pump for seals-to-space development in, molecular, 19: 29746 (NASA-CR-54234(Vol.II))
pump for, development of electrodynamic mercury, 19: 44188 (NASA-TN-D-2965)
pumps for, cavitation damage to impellers in liquid-metal, 18: 3291(R) (CNLM-5202)
radiation effects on electric insulation materials for, 19: 25049 (NP-15022(Vol.II))
radiation effects on electrical components and subassemblies for, 19: 25750 (NP-15022(Vol.III))
radiation effects on electric insulator resistance in, 19: 39057 (NP-15022(Vol.II)(Add.))
radiation effects on electric components for, 20: 45194 (NAA-SR-11924)
radiator coating development, 16: 14358(R) (PWA-2043)
radiator development, 16: 25761(R) (PWA-2088)
radiator endurance tests, 18: 4257(R) (PWA-2279)
radiator segment coating endurance tests, 18: 5737(R) (PWA-2255)
reactivity coefficients of SNAP-8ER, dynamic measurement of, 20: 3557
reactivity of beryllium oxide reflected, 20: 5180 (NAA-SR-Memo-11604)
reactor and shield design for, 17: 33392
reactor vessel, welding tests of closure joint in Type 316 stainless steel, 19: 20509 (NAA-SR-Memo-10633)
reflector fabrication for, 16: 25734 (NAA-SR-7293)
seals development for mercury pump in, 19: 29745 (NASA-CR-54234(Vol.I))
seals development for mercury-vapor turbine in, 19: 29748 (NASA-CR-54234(Vol.IV))
seals-to-space development for, 19: 29747 (NASA-CR-54234(Vol.III))
semiconductor shielding weight optimization to minimize gamma and neutron damage, 19: 32615 (NAA-SR-10856)
shield design, 19: 45666
shielding design for, 20: 38527
shielding for, scattered gamma and neutron (T), 19: 3716 (FZK-154)
shielding of, neutron fluxes and heating in, (T), 20: 12468 (NAA-SR-Memo-9916)
simulation of, analog computers for, 19: 10622 (NAA-SR-Memo-10494)
startup of, analysis of automatic, 18: 29112
test facility for, high-vacuum ground, 20: 8451
test program for, summary of, 20: 22479
testing facilities, 19: 3741
testing facility for Flight Prototype of, design, (E), 20: 3550 (TID-21994)
testing of turbine for, 17: 1126 (NASA-TN-D-1529)
testing of, computer analysis of data from, (E), 19: 21721 (NAA-SR-Memo-10160)
thermal model for S8ER, three-dimensional transient, 20: 47065 (NAA-SR-Memo-11822)
thermocouple insertion in S8DS grid plate for measuring coolant temperature, 18: 3296 (NAA-SR-Memo-8817)
use in manned orbiting space station, integration studies for (E/T), 19: 3712 (64SD647)

SYSTEMS FOR NUCLEAR AUXILIARY POWER (SNAP-9)

cadmium-109 distribution in atmosphere from high-altitude burn-up of, predictions for, 20: 16662(R) (HASL-165)
debris from 9A, 19: 20154(R) (HASL-158)
development of, bibliography on, 18: 8700 (NYO-10689)
development of 9A, review of, 19: 11637

development status of SNAP-9A, 17: 35228
development status, 18: 34001
flight testing of isotope-fueled thermoelectric generators, re-entry, 18: 29108 (SC-DC-64-855)
plutonium-238 contamination from, 20: 521(R) (HASL-164)
plutonium-238 distribution in atmosphere from high-altitude burn-up of, predictions for, 20: 16662(R) (HASL-165)
reentry burnup of 9A, effects on plutonium-238 content in stratosphere, 20: 41131(R) (HASL-172)
review of 9A, 19: 20427 (TID-7698(Pt.I)(p.249-56))

SYSTEMS FOR NUCLEAR AUXILIARY POWER (SNAP-10)

ablation and stability of, during re-entry, 18: 35212
analysis and performance of 10A, (T), 19: 29763
compatibility tests of 10A FSEM-3, with Agena vehicle, 19: 31597 (NAA-SR-11129)
components for, testing fusistors, 18: 6514 (NAA-SR-Memo-8824)
components of 10A, testing program for, 20: 35126 (NAA-SR-Memo-11914)
containment thermal expansion compensator for 10A, performance of, 20: 35125 (NAA-SR-Memo-11865)
control and instrumentation circuits for 10FS-5, shock testing of, 20: 12469 (NAA-SR-Memo-11630)
control assembly for 10A, development of, 18: 29114
control system for 10A, irradiation testing of electric components of, 19: 38246 (NAA-SR-10717)
control system testing for 10A, in simulated environment, 20: 22475
control systems and instrumentation of 10A, development of, 20: 22476
control systems for, development of, 20: 22474
coolant loading cart acceptance test for 10A, 19: 3725 (NAA-SR-Memo-10169)
coolant pump acceptance testing for, PbSnTe S/N-026, 19: 5524 (NAA-SR-Memo-9877)
coolant pump acceptance testing for 10A, PbSnTe S/N-022, 19: 5525 (NAA-SR-Memo-10143)
coolant pump acceptance testing for 10A, PbSnTe S/N-028, 19: 5526 (NAA-SR-Memo-10144)
coolant pump acceptance test for 10A, PbSnTe S/N-022, 19: 5527 (NAA-SR-Memo-10199)
coolant pump acceptance testing for, PbSnTe S/N-029, 19: 5530 (NAA-SR-Memo-10300)
coolant pump acceptance testing for 10A, PbSnTe S/N-013, 19: 8656 (NAA-SR-Memo-9824)
coolant pump development for 10A, thermoelectric, (E), 19: 29764
coolant pump for 10A, development of thermoelectric, 20: 40446 (NAA-SR-11879)
coolant thermal expansion and pressurization compensator for SNAP-10A, development of, 19: 29760
cooling system pumps for 10A, testing, (E), 19: 8659 (NAA-SR-Memo-10317)
cooling system pumps for 10A, testing, (E), 19: 10618 (NAA-SR-Memo-10399)
cooling system pumps for 10A, testing, (E), 19: 10620 (NAA-SR-Memo-10464)
cooling system pumps for 10A, testing, (E), 19: 10621 (NAA-SR-Memo-10480)
core hydraulics for 10A/2, computer program for photographic analysis of, 18: 40931 (NAA-SR-Memo-9947)
criticality studies, 17: 28481 (TID-18880)
criticality studies on SNAPTRAN 10A/2-1, (E), 19: 17344 (NAA-SR-Memo-10660)
description of SNAP-10A, review, (E), 19: 43553
description of 10A, 17: 2635
design, 18: 24944
design and performance of prototype thermoelectric generator, 16: 34136
design and performance of SNAP-10A, 17: 35224
design and performance of 10A, in SNAPSHOT test, 20: 14177
design description for 10A system, 18: 32508 (A/CONF.28/P/218)
design of 10A, (E/T), 19: 31590 (AI-Memo-7585(Rev.2))
design, development, and flight test of SNAP-10A, 19: 45154
design, fabrication, and testing of 10A structure, 18: 36842 (NAA-SR-9899)
destruct test SNAPTRAN-2, transducer evaluation for, 20: 24778 (IDO-17148)
destruct test SNAPTRAN-2, analytical models for energy release in, 20: 26517(R) (IDO-17126)
destructive test of SNAPTRAN 2/10A-3, analytical services in, 19: 32059(R) (IDO-14655)
destructive test SNAPTRAN 2/10A-3, fission product release and dispersion from, 20: 564 (CONF-650407, pp 512-36)
destructive test SNAPTRAN-2, 20: 3561
development, 18: 15575
development and preflight testing of 10A, review on, 19: 33662
development of 10A, 19: 1922 (AI-Memo-7585(Rev.I))
development of 10A, 19: 6863
development of, hearings before Joint Committee on Atomic Energy on, 20: 20305
development status, 18: 34001
disposal of orbiting 10A, techniques for ocean burial, 20: 20302 (SC-RR-65-472)
disposal of orbiting 10A, techniques for ocean, 20: 20302 (SC-RR-65-472)
electric conductivity measurements on thermoelectric converter of, device for internal, 19: 4881
energy converter design for, computer program for calculating, 20: 45195 (NAA-SR-Memo-11819)
energy release and reactivity feedback effects in SNAP-2/10A destruct, 19: 21719 (NAA-SR-9780)
energy release in SNAPTRAN 2/10A-2, destruct, 20: 22467(R) (IDO-17077)
examination and safety program for SNAPTRAN 2/10A-3, post-destruct, 19: 21718 (IDO-17071)
expansion compensator position switch testing for 10A, 19: 2575 (NAA-SR-Memo-9883)
expansion compensator units for 10A, development, 20: 39023 (NAA-SR-11952)
fission product inventory for 10A orbit, 20: 12466 (NAA-SR-11642)
fission product release and reactor kinetics in SNAPTRAN 2/10A-3 destruct, (E), 19: 21717 (IDO-17019)
fission product release from irradiated uranium–zirconium hydride fuel for 2/10A, 20: 3562
flight data reduction and analysis of 10A, computer program for, 20: 6661 (NAA-SR-Memo-11603)
flight system 10FS-3 of, post-assembly electrical testing of, 20: 6658 (NAA-SR-Memo-11436)
flight test of 10A, performance of SNAPSHOT-1, 19: 45653 (NAA-SR-11430)
flight test of 10A, description of, 20: 47059
flight testing of 10A, computer programs for data reduction for, 18: 38563 (NAA-SR-Memo-9440)
flight testing of 10A, environmental testing of vehicle for, 18: 38564 (SC-DC-3409)
fuel element testing for, program evaluation using K-factors, 20: 40447 (NAA-SR-11913)
fuel elements for SNAP 10A, strain and stress distributions in long, solid, cylindrical, (T), 20: 23796
fuel for SNAP 10A/2, fission product release from irradiated, 18: 34045 (NAA-SR-9673)
fuel for 10A, hydrogen pressure measurements in, 20: 42664(R) (IDO-17165)
fuel for 10A, irradiation testing of, (E), 20: 6678 (NAA-SR-Memo-11374)
gamma energy release following power transient in SNAPTRAN-1, 20: 24779 (IDO-17161)
gamma hazards from SNAPTRAN-1, (T), 20: 26517(R) (IDO-17126)
hazards evaluation in STEP project, 18: 24956(R) (IDO-16961)
hazards evaluation in STEP project, 19: 5542(R) (IDO-17012)
heat radiation from 10A to Agena during flight system mockup test, 18: 40930 (NAA-SR-Memo-9337)
heat shield connectors for 10A, development testing of ejectable, 19: 8657 (NAA-SR-Memo-10176)
hydrogen redistribution in 10A, (T), 19: 29762
instrumentation for, design and testing of fixed resistors as, 17: 25549 (NAA-SR-Memo-8145)
instrumentation for monitoring liquid metal properties, 20: 27105 (ANL-7100, pp 641-65)
kinetic and thermal response of 2/10A, computer program for, 18: 26957 (NAA-SR-8414)
kinetics of SNAP-10A/2, with reactivity pulse excitation, 20: 3558
kinetics of 10A, 20: 12498(R) (IDO-17112, pp 1-51)
magnetic moments and vehicle torques in 10A, (T), 20: 1528 (NAA-SR-11207)
malfunction-detection systems for 10A, (E), 19: 21734 (NAA-SR-Memo-10666)
materials for, development of thermoelectric, 17: 23861(R) (AD-282505)
materials self-welding at 700 to 1300°F in environment of 10A, facility for testing, 20: 7570 (NAA-SR-9643)
mechanical resonances in, measurement of, (E), 19: 17342 (NAA-SR-Memo-8339)
neutron detector for 10A, development of semiconductor, 20: 20298 (NAA-SR-11762)
neutron energy-density in 2/10A SNAPTRAN-3, during destruct (E), 19: 3739
neutron kinetics of SNAPTRAN assembly, 18: 19408 (NAA-SR-Memo-9160)
neutron scattering in, 18: 13051 (NAA-SR-Memo-9214)
noise spectrum of, 19: 1956(R) (IDO-16994)
performance of 10A, in flight, 20: 1530
performance of 10A, in simulated space environment, 20: 35141
performance testing of 10A, FSM-4 mockup for, 20: 22471 (NAA-SR-11814)
performance tests of 10A-FSM-1 prototype thermoelectric converter, 19: 29742 (NAA-SR-10735)
piping system of 10A, stress analysis, 19: 31598 (NAA-SR-Memo-

9817)
prelaunch test facility safeguards, 18: 45075 (NAA-SR-Memo-8685)
pressure vessel stress analysis for 10A, under internal loading, 19: 8658 (NAA-SR-Memo-10248)
pressure vessels for 10A, design and fabrication of, 19: 12836
pumps for 10A, testing thermoelectric, (E), 19: 17345 (NAA-SR-Memo-10667)
radiation detection systems for 10A, calibration of, 20: 6656 (NAA-SR-Memo-11333)
radiation distributions and effects in SNAPSHOT vehicle, 20: 14175 (TID-22418)
radiation dosimeters for flight test of 10A, 20: 21105
radiation effects on thermal control materials for, gamma, neutron, and uv, 18: 20603
radiation effects on solid state tracking and command system for, hardening against, 19: 25754
radiation effects on electronic components for reactor control system, 19: 24883 (NAA-SR-10284)
radiation effects on electrical devices for, experiments on fast-neutron, 19: 24880 (BMI-X-10120)
radiation environment of 10A, equipment hardening against, 20: 31618
radiation hazards from SNAPTRAN 2/10A-3 destruct, (E), 19: 17340 (IDO-17038)
radiators of 10A, development and testing of thermal control coatings for, 20: 8454
re-entry destructive burnup, evaluation of, 17: 16310 (AFSWC-TDR-62-83)
re-entry safety hazards evaluation for, 17: 38575 (NAA-SR-8303)
re-entry ablation analysis for, 18: 36840 (NAA-SR-9723)
re-entry ablation and dispersion of beryllium in 10A, (E/T), 19: 10626
re-entry disintegration and dispersion of 10A, 19: 45651 (NAA-SR-11103)
re-entry flight demonstration testing of 10A, 18: 36839 (NAA-SR-9479)
re-entry flight demonstration, trajectory data of RFD-1 launch, 18: 43064 (SC-RR-64-510)
re-entry flight demonstration (RFD-1) data for 10A, 19: 1927 (SC-RR-64-502)
re-entry flight demonstration-1 for 10A, disassembly analysis (E/T), 19: 3730 (SC-RR-64-515)
re-entry flight demonstration (RFD-1) for 10A, atmospheric sciences support for, (E), 19: 5531 (SC-RR-64-517)
re-entry flight testing of 10A, re-entry vehicle design and performance for, 18: 31021 (SC-RR-64-511)
re-entry heating of fuel elements for 10A, 20: 3560
reactivity control of 10A using prepoisons, effects of cross-section uncertainties on, 20: 45193 (CONF-660303, pp 204-9)
reactivity transients in 2/10A SNAPTRAN-3, super-prompt (E/T), 19: 3740
reactivity transient test SNAPTRAN-3, analysis of fuel element damage from, 19: 38233 (IDO-17065)
reactivity transient testing of 10A, Snaptran machine for, 20: 8452
reactivity transient testing of SNAPTRAN 2/10A-1, step, 20: 22467(R) (IDO-17077)
reactivity transient testing in SNAPTRAN-1, 20: 26518(R) (IDO-17145)
reactivity transient testing in SNAPTRAN-1, 20: 26517(R) (IDO-17126)
reactivity transient testing of SNAPTRAN 2/10A-1, program sequence times for, 20: 12499(R) (IDO-17112, pp 52-80)
reactivity worths of fission products in 10A, computer analysis of, 20: 6659 (NAA-SR-Memo-11473)
recovery system for 10A-RFD-1 re-entry vehicle, design and tests, 19: 33655 (SC-DR-64-578)
reentry ablation of reactor fuel elements for 1DA, 20: 24782 (NAA-SR-11502)
reentry heating of 10A, intensity distribution of, 19: 14877 (NAA-SR-9781)
reflector assembly for 10A, development of, 18: 29114
relays for 10A, evaluation of DPDT, (E), 19: 21733 (NAA-SR-Memo-10532)
relays for 10A, testing, (E), 19: 10617 (NAA-SR-Memo-10286)
safety analysis for SNAP 2/10A, 18: 31019 (IDO-16825)
safety analysis of SNAPTRAN 2/10A-1 and -2 tests, 20: 6654 (IDO-17076)
safety flight test of, environmental testing of vehicle for, 18: 23085 (SC-DR-285-63)
safety hazards analyses during abort and re-entry, mechanical and thermochemical testing for, 17: 28573 (NAA-SR-8304)
separate-source pump optimization for SNAP-10A Follow-On, computer code for, 18: 10409 (NAA-SR-Memo-9332)
shield analysis for 10A flight system (E/T), 19: 3722 (NAA-SR-9647)
shield heat testing for 10A, ejectable, 19: 45650 (NAA-SR-10997)
shielding for 10A, stress analysis of short cylindrical, (T), 19: 17343 (NAA-SR-Memo-10293)
shutdown analysis of SNAP-10A/Agena satellite, 20: 10417 (NAA-SR-Memo-11635)
shutdown of 10A, electrically actuated band release device for, 20: 32852 (NAA-SR-Memo-11454)
startup and operation in simulated space environment, 19: 43594
startup controller for 10A, design of transistorized, 19: 28616
startup relays for 10A, overvoltage testing of, (E), 20: 8441 (NAA-SR-Memo-11435)
stress analysis of expansion compensator support structure, 18: 1285 (NAA-SR-Memo-8268)
structural analyses for 10A, static, vibration, and acoustic, 18: 35202 (NAA-SR-9655)
systems of 10A, performance of ground-test and flight, 20: 8453
temperature control coatings for 10A, development of, 19: 48050 (NAA-SR-9903)
temperature drift in reactivity in 10A, computer program for, 20: 45198 (NAA-SR-Memo-11977)
temperature sensors for 10A, development of, (E), 19: 5528 (NAA-SR-Memo-10211)
test plan for, re-entry, 18: 24941 (SC-RR-64-501)
testing electromagnetic interference generated by analog position-sensor demodulator in 10A, (E), 19: 12812 (NAA-SR-Memo-10499)
testing full-scale mockup of 10A, 19: 8655 (NAA-SR-Memo-9709)
testing of SNAP-10A, objectives of orbital, 17: 35225
testing of SNAP-10A/Agena, 20: 22477
testing of SNAP-10A/Agena, pre-launch operations in, 20: 22478
testing of SNAPSHOT vehicle equipment, 20: 14173 (TID-22416)
testing of vessels for 10A, 100-ft-drop accelerometer, 19: 3724 (NAA-SR-Memo-10165)
testing of 10A prototype (PSM-1A), structural, 18: 36841 (NAA-SR-9820)
testing of 10A-FSM-1 system, dynamic, 19: 31599 (NAA-SR-Memo-9897)
testing of 10A-PSM-1 prototype, structural, 18: 36838 (NAA-SR-8399)
testing of 10A, evaluation of prestartup orbital, 20: 35127 (NAA-SR-Memo-11927)
testing of 2/10A SNAPTRAN-3, destruct (E), 19: 3738
testing of 2/10A, photography for SNAPTRAN-3, 19: 3715 (EGG-1183-1071)
testing of 2/10A, in STEP project, 19: 29739(R) (IDO-17058)
testing 10A Development Reactor Mockup, nonnuclear, 18: 43061 (NAA-SR-Memo-9726)
testing 10A/2-3, destructive, 19: 6868 (NAA-SR-9871)
testing 10A, control devices for vibrational, (E), 19: 21722 (NAA-SR-Memo-10767)
testing 10A, development of high-temperature heaters for, (E), 19: 19409 (NAA-SR-9894)
thermal emittance and solar absorptance properties of 10A, 19: 38247 (NAA-SR-Memo-10676)
thermal expansion compensators for 10A, design and testing of, 20: 1527 (NAA-SR-9778)
thermal ground testing of SNAP-10A, high-flux radiant heaters for, 19: 29761
thermal testing 10A prototype (PSM-3), 18: 35200 (NAA-SR-9280)
thermoelectric arrangement of, 20: 40451
thermoelectric converter characteristics for 10A, silicon–germanium, 19: 45664
thermoelectric converter of 10A, effect of dimensional tolerances on power output of, 20: 5179 (NAA-SR-Memo-6484)
thermoelectric converter performance for 10A, leakage current effects on, 20: 6657 (NAA-SR-Memo-11417)
thermoelectric element performance tests, development of apparatus for, 16: 13696 (NAA-SR-Memo-6670)
thermoelectric element process development variables for, statistical analysis of, 17: 11314 (NAA-SR-7288)
thermoelectric generator for, design and performance of static, 17: 29861
thermoelectric pump for, microprobe study of brazed joint for, 18: 2199 (NAA-SR-Memo-9088)
thermoelectric pump for SNAP-10A, brazing and ultrasonic testing of throat-to-copper joint in, 18: 18332 (NAA-SR-Memo-9435)
thermoelectric pump tests for SNAP-10A, 19: 7662 (NAA-SR-Memo-10181)
thermometer tests in copper block attachment configuration, resistance, 18: 43890 (NAA-SR-Memo-10084)
transductor performance for, FS-4 differential current, 20: 8440 (NAA-SR-Memo-11418)
vibration testing of re-entry flight demonstration vehicle for SNAP-10A, 19: 18132 (SC-TM-65-31)

SYSTEMS FOR NUCLEAR AUXILIARY POWER (SNAP-11)
design and performance, 20: 13158
development of, bibliography on, 18: 8700 (NYO-10689)
development of, review of, 19: 11637
development status, 17: 35228
development status, 18: 34001
performance, 17: 31767

SYSTEMS FOR NUCLEAR AUXILIARY POWER (SNAP-13)
development status, 17: 35228
development status, 18: 34001

SYSTEMS FOR NUCLEAR AUXILIARY POWER (SNAP-15)
design and performance of 15A, 19: 46894 (GA-5296)
design and performance of 15A, 20: 35824
design, development, and performance of 15A, 20: 2204 (GA-6695)
generator test evaluations for 15A, 20: 39310 (GA-5781)

hazards analysis of 15A, 20: 722 (GA-4554(Rev.))
SYSTEMS FOR NUCLEAR AUXILIARY POWER (SNAP-19)
development of, review of, 19: 11637
ejection from NIMBUS-B, dynamic analysis of mechanism for, 19: 39071 (MND-3169-68)
electric converter-generator configurations for, integration conceptual study, 19: 30622 (MND-3169-21))
re-entry behavior of Nimbus satellite with, analysis, 19: 34342 (MND-3169-67)
re-entry destruction of, telemetry system for monitoring, 19: 42791 (SC-DR-65-205)
re-entry flight demonstration, RFD-2, 19: 24903 (SC-RR-65-43)
re-entry heating of, 20: 2207
re-entry heating of, flight test analysis of, 20: 4280 (SC-DC-65-1601)
review of, 19: 20427 (TID-7698(Pt.I)(p.249-56))
support structure for generator, dynamics analysis, 19: 30621 (MND-3169-18)
support structure design, development, and testing, 20: 2205 (MND-3169-52)
testing of fuel capsules for, plasma-arc, 19: 36886 (MND-3169-16)
tests of thermoelectric generator prototype, qualification, 19: 30623 (MND-3169-60)
vibration tests of generator and support structure assembly, 19: 30624 (MND-3169-61)
SYSTEMS FOR NUCLEAR AUXILIARY POWER (SNAP-21)
development, 20: 39313
SYSTEMS FOR NUCLEAR AUXILIARY POWER (SNAP-23)
development, 20: 39313
SYSTEMS FOR NUCLEAR AUXILIARY POWER (SNAP-27)
use on Apollo mission, 20: 33756
SYSTEMS FOR NUCLEAR AUXILIARY POWER(SNAP-50)
bearing tests for liquid metal pumps in, 19: 40703 (TIM-916)
boiler development for SNAP-50/SPUR, 20: 32857
boiler two-phase flow stability in SNAP-50/SPUR, simulation study of, 19: 4302 (APL-TDR-64-117)
coolant pump for SNAP-50/SPUR, development of electromagnetic, 20: 40450 (TIM-911)
coolant pumps for SNAP-50/SPUR, bearing analysis of, 20: 10419 (PWAC-468)
design and status, 19: 17354
development, 17: 26100
development, 17: 35218 (CONF-39-52)
development, 18: 15601
development, 18: 29103(R) (APS-5071-R)
development, 19: 1922 (AI-Memo-7585(Rev.I))
development, 19: 29732(R) (APS-5152-R2)
development, 19: 29734 (CONF-650416-1)
development for electric-propelled space vehicles, 19: 32402(R) (N64-18173)
development of boiler for SNAP-50/SPUR, 20: 3554
development of SNAP-50/SPUR for lunar bases and space propulsion, 20: 3553
development status, 18: 34001
electron flux from orbiting, trapped in radiation belts, (T), 19: 31589 (AFCRL-64-865)
frequency converter design for, 19: 29731(R) (APS-5152-R1(Suppl.1))
instrument development, 19: 44348 (PWAC-473)
mission capabilities of SNAP-50/SPUR electric propulsion, (T), 19: 8660 (PWAC-447)
neutron leakage from orbiting, trapped electron flux from, (E), 20: 7988
neutron shielding code MORTIMER for, (E), 19: 43587 (TIM-880)
performance of nuclear-electric space vehicles using, 18: 35211
power conversion system development for, 19: 27810(R) (APS-5152-R1)
power determination from barium-140 fission product measurements, 19: 45656 (PWAC-474)
protective environments for SNAP-50/SPUR, argon and helium uses for, 20: 10420 (TIM-824)
proton flux from orbiting, trapped in radiation belts, (T), 19: 31589 (AFCRL-64-865)
pump bearing development for, 19: 46458 (CNLM-6342)
pump motor development for SNAP-50/SPUR, materials and process specifications for, 20: 35110 (CNLM-5584(Vol.3))
pumps for SNAP-50/SPUR, design and development of, 20: 35111 (CNLM-6308)
pumps for, cavity evacuation study of, 19: 45660 (TIM-919)
radiators for, evaluation of direct and indirect, 20: 8446 (PWAC-456(Del.))
test facility for, evaluation of, (E), 19: 31591 (CNLM-5983)
testing, 18: 24945
testing facilities for, design of, 20: 3545 (CNLM-5729)
use in solar probe, 18: 33135
SZILARD-CHALMERS REACTIONS
chromium-51 enrichment by, 20: 18812
copper-64 enrichment by, using chelates, 18: 1752
distribution of cobalt-60 in neutron-irradiated dinitrotetramminecobalt(III) nitrate, 16: 28989
effect in isotopic exchange between alkyl iodide and iodine, 19: 30314
effect of defect centers on annealing in, 16: 27056
effects of, in solid xenon compounds, 20: 43373
effects on hafnium and zirconium phthalocyanines, 20: 26921 (BNL-10208)
effects on praseodymium complexes with β-diketones, 20: 16416(R) (NYO-906-68)
efficiency for preparation of iron-59, 18: 39321
efficiency in high neutron fluxes for producing bromine-82 and chlorine-36, 16: 15080
energy transfer in, review on theory of, 18: 33660
enrichment of recoil atoms by, 17: 30041
facility for radioisotope production at high specific activities, 16: 13080 (CEA-2072)
in ammonium and potassium chromates, 18: 12166
in ammonium dihydrogen phosphate, electrophoresis and ESR spectra of, 19: 26381 (RISO-95)
in ammonium, potassium, and tetramethylammonium dichromates, effects of thermal and uv annealing on, 18: 16115
in cobalt-amine complexes for production of cobalt-60, chemical constitution effects on, 18: 39291
in cobalt(III) complexes, 19: 9046(R) (IS-900(Sect.C))
in cyclohexane with and without iodide, free radical yields in, 18: 16112
in open-type cobalt complexes, effects of thermal annealing on, 16: 6494
in potassium chromate for production of chromium-51, 16: 33034
in potassium ferrocyanide, iron-55 and -59 distribution in products formed by, 20: 23073 (CEA-R-2873)
in potassium nitrosylopentacyanomanganate, 17: 32168
in potassium phosphate for production of phosphorus-32, 17: 30167
in praseodymium 1-phenyl-1,3-butanedione chelate, 19: 19445(R) (TID-21660)
in solid cobalt nitrate complexes, parent compound retention configuration in, 16: 6490
in solid xenon tetrafluoride, 18: 33666
in 8-quinolinolates of indium, molybdenum, and tungsten, 16: 8763(T) (CEA-tr-X-425)
isotope retention, comparative radiation, and condensation coefficients in, 20: 45720
isotopic retentions in, on metal complexes with $\alpha, \beta, \gamma, \delta$-tetraphenylporphines, 19: 40612
of diethylmercury and diphenylmercury, 19: 15587
of praseodymium chelates with β-diketones, 19: 36343(R) (TID-21847)
of trioxalatochromium ion on anion exchange resin under flow conditions, 19: 34245
on bromo- and chlorobenzene, 18: 12183
on gamma-irradiated copper and sodium phthalocyanines, 17: 28999
production of cobalt-60 and barium-139 by, in montmorillonite clay, 19: 18039 (IITRI-578P15-12)
production of enriched chromium-51 by neutron irradiation of ammonium and potassium chromates, 18: 10443
production of iodine-128 by neutron irradiation of ethyl iodide, 16: 29299 (RT/CH1(62)8)
recoil atom behavior in iridium and osmium halide complexes, 16: 6489
recoil atom behavior on hexamminecobalt(III) and trisethylenediaminecobalt(III) cation exchange resins, 17: 30168
recoil retention in, in $\alpha,\beta,\gamma,\delta$-tetraphenylporphine complexes, 19: 15647
recoils from, continuous extraction of, 20: 12897
retention and specific activity in, second-order rate law for, 20: 45727
retentions in neutron-irradiated arsenates, effects of variables, 17: 3031
review, 16: 242
targets for, pure and doped-crystal, 16: 17674
use for production of bismuth-210 from triphenylbismuth, 17: 23838
use for production of high-specific-activity radioisotopes, 19: 2704
use in activation analysis of biological materials, 19: 15335 (AE-172)
use in enrichment of cobalt-60 by neutron irradiation of cobalt(III) acetylacetonate, 17: 1533
use in enrichment of cobalt-60 by slow neutron irradiation of cobalt complexes, 18: 22143
use in in-pile radioisotope production, 17: 29944
use in preparation of high-activity chromium-51, 19: 42578 (JEN-144-DQ/I-45)
use in preparation of phosphorus-32, 19: 15582
use in preparation of chromium-51, 20: 27006
use in preparation of high-specific-activity chromium-51, 20: 38982 (PAEC(D)IS-652)
use in production of high-specific-activity radioisotopes, problems in, 19: 46332(R) (ORNL-3832, pp 50-65)
use of modified, for production of high-specific-activity isotopes, 17: 26212
uses in separation of radioisotopes from neutron-irradiated biological materials in activation analysis, 20: 18583

DEPOSITORIES OF USAEC REPORTS

In Countries Other than the U.S.

ARGENTINA
Buenos Aires, Comisión Nacional de Energía Atómica
AUSTRALIA
Canberra, Australian National Library
Sutherland, New South Wales, Australian Atomic Energy Commission
AUSTRIA
Vienna, Zentral Bibliothek der Physikalischen Institute der Universität
BELGIUM
Mol-Donk, Centre d'Etude de l'Energie Nucleaire
BOLIVIA
La Paz, Comisión Nacional de Energiá Nuclear
BRAZIL
Rio de Janeiro, Instituto Brasileiro de Bibliografia e Documentacao
São Paulo, Instituto de Energia Atomica, Cidade Universitaria São Paulo
BURMA
Rangoon, Union of Burma Applied Research Institute, Atomic Energy Center Library
CANADA
Hamilton, McMaster University
Ottawa, National Research Council Library
Vancouver, University of British Columbia
CHILE
Santiago, Departamento de Fisica, Universidad de Chile
CHINA
Hsinchu, Taiwan, Free China, National Tsing Hua University
COLOMBIA
Bogota, Instituto De Asuntos Nucleares
COSTA RICA
San Pedro, University of Costa Rica Library
DENMARK
Risö, Danish Atomic Energy Commission
ECUADOR
Quito, Escuela Politécnica Nacional
EL SALVADOR
San Salvador, Universidad de El Salvador, Biblioteca de Energia Nuclear
FINLAND
Helsinki, Teknillisen Korkeakoulun Kirjasto
FRANCE
Gif-sur-Yvette, Centre d'Etudes Nucléaires de Saclay
Paris, Académie des Sciences
GERMANY
Berlin, Hahn-Meitner-Institut für Kernforschung Berlin
Frankfurt/Main, Gmelin-Institut
Munich, Technische Hochschule, Bibliothek
GHANA
Accra, University College of Ghana
GREECE
Athens, Nuclear Research Center "Democritus"
GUATEMALA
Guatemala, Comisión Nacional de Energía Nuclear
INDIA
Bombay, Department of Atomic Energy
INDONESIA
Djogjakarta, Java, Science Faculty Gadjah Mada University
IRAN
Tehran, Tehran University Nuclear Centre
IRAQ
Baghdad, Iraqi Atomic Energy Commission
IRELAND
Dublin, University College
ISRAEL
Rehovoth, Israel Atomic Energy Commission
ITALY
Rome, Centro di Studi Nucleari della Casaccia
Rome, Comitato Nazionale per l'Energia Nucleare
JAPAN
Tokyo, National Diet Library
KOREA
Seoul, Office of Atomic Energy
LEBANON
Beirut, Lebanese National Council for Scientific Research
LUXEMBOURG
Luxembourg, Ministry of Transport and Electricity
MALAYSIA
Kuala Lumpur, University of Malaysia
MEXICO
Mexico, D.F., Comisión Nacional de Energía Nuclear
NETHERLANDS
The Hague, Reactor Centrum Nederland
NEW ZEALAND
Lower Hutt, Institute of Nuclear Sciences
NIGERIA
Ibadan, University of Ibadan
NORWAY
Lillestrøm, Institutt för Atomenergi
PAKISTAN
Islamabad, Pakistan Institute of Nuclear Science and Technology
PERU
Lima, Junta de Control de Energia Atomica
PHILIPPINE REPUBLIC
Manila, Philippine Atomic Energy Commission
POLAND
Warsaw, Biura Pelnomocnika Rzadu do Spraw Wykorzystania Energii Jadrowej
PORTUGAL
Sacavem, Junta de Energía Nuclear
REPUBLIC OF SOUTH AFRICA
Pretoria, Atomic Energy Board Library
REPUBLIC OF THE CONGO
Leopoldville, Université Lovanium
SPAIN
Madrid, Junta de Energía Nuclear, Biblioteca Documentación y Publicaciones, Ciudad Universitaria
SWEDEN
Nyköping, Aktiebolaget Atomenergi
SWITZERLAND
Zürich, Eidgenössische Technische Hochschule, Bibliothek
THAILAND
Bangkok, Office of the Thai Atomic Energy Commission, Department of Science
TURKEY
Ankara, Turkish Atomic Energy Commission, Atomic Energy Library
UNITED ARAB REPUBLIC
Cairo, Atomic Energy Commission
UNITED KINGDOM
Birmingham, Central Library
Boston Spa, National Lending Library for Science and Technology
Kingston upon Hull, Central Library
Liverpool, Central Library
London, Central Library, Acton
London, National Reference Library
London, Science Museum Library, South Kensington
Manchester, Central Library
Newcastle upon Tyne, Central Library
Nottingham, Central Library
Sheffield, Central Library
URUGUAY
Montevideo, Comision Nacional de Energia Atomica
VENEZUELA
Caracas, Instituto Venezolano de Investigaciones Científicas
VIET-NAM
Saigon, Atomic Energy Office
YUGOSLAVIA
Belgrade, Federal Commission for Nuclear Energy

In International Agencies

AUSTRIA
Vienna, International Atomic Energy Agency
BELGIUM
Brussels, La Bibliotheque EURATOM
FRANCE
Paris, European Nuclear Energy Agency, O.E.C.D.
ITALY
Ispra, EURATOM Research Center
SWITZERLAND
Geneva, United Nations Library

UNITED STATES
GOVERNMENT PRINTING OFFICE
DIVISION OF PUBLIC DOCUMENTS
WASHINGTON, D.C. 20402

OFFICIAL BUSINESS

POSTAGE AND FEES PAID
U.S. GOVERNMENT PRINTING OFFICE

TECHNICAL PROGRESS REVIEWS

The Di··ision of Technical Information, U. S. Atomic Energy Commission, also publishes the Technical Progress Reviews, a series of four quarterly journals on nuclear technology. These journals, compiled by specialists and recognized authorities, summarize, evaluate, and reference the progress of development in four important fields.

Isotopes and Radiation Technology P. S. Baker, A. F. Rupp, and associates, Oak Ridge National Laboratory. Reviews AEC-sponsored projects and related significant worldwide developments in radioisotopes and radiation technology.

Nuclear Safety Wm. B. Cottrell, W. H. Jordan, J. P. Blakely, and associates, Nuclear Safety Information Center, Oak Ridge National Laboratory. Covers topics relevant to the analysis and control of hazards associated with nuclear reactors and with operations involving fissionable materials and the products of nuclear fission.

Power Reactor Technology Argonne National Laboratory. Reviews research, development, design practices, and operating experiences associated with power reactors, including aerospace applications.

Reactor Materials E. M. Simons and associates, Battelle Memorial Institute. Covers the properties, behavior, and fabrication processes of materials used in nuclear reactors and associated equipment.

Availability

SUBSCRIPTION RATE: The Technical Progress Reviews may be purchased from the Superintendent of Documents, U. S. Government Printing Office, Washington, D. C. 20402. *Nuclear Safety* at $3.00 per year for each subscription or $1.00 per issue; each of the other journals at $2.50 per year or $0.70 per issue.

POSTAGE: Postpaid within the United States, Canada, Mexico, and all Central and South American countries except Argentina, Brazil, Guyana, French Guiana, Surinam, and British Honduras. For these Central and South American countries and all other countries, add $0.75 for each annual subscription or $0.20 for a single issue.

REMITTANCE: Payment should be by check, money order, or document coupons and MUST accompany order. Remittances from foreign countries should be made by international money order or draft on an American bank payable to the Superintendent of Documents or by UNESCO book coupons.